JOURNAL OF BONE AND MINERAL RESEARCH . . . . VOL. 19, SUPPL 1, OCTOBER 2004 S1-S543

JOURNAL OF BONE AND MINERAL RESEARCH

VOL. 19, SUPPL 1, OCTOBER 2004 PP. S1-S543

www.jbmronline.org

2004 Abstracts

Twenty-Sixth Annual Meeting of the American Society for Bone and Mineral Research

Washington State Convention & Trade Center
Seattle, Washington, USA
October 1-5, 2004

JBMR

ASBMR™

PUBLISHED MONTHLY BY
THE AMERICAN SOCIETY FOR BONE AND MINERAL RESEARCH

ADDENDUM
to the
2004 Abstracts

26th Annual Meeting of the
American Society for Bone and Mineral Research
Washington State Convention & Trade Center
Seattle, Washington, USA
October 1-5, 2004

On the following pages are five abstracts which were presented during the Late-Breaking Abstract Session on Monday, October 4, 2004, from 10:00 to 11:15 a.m., in Room 6E of the Washington State Convention & Trade Center.

We have provided these materials to afford our readership the information necessary to correctly cite these abstracts. To facilitate this, we have provided the citation under each abstract.

Also included is one abstract which was inadvertently left out of the *Abstracts* book. This abstract was presented on Monday, October 4, 2004, at Poster Session III in Exhibit Hall 4ABC of the Washington State Convention & Trade Center.

John A. Eisman, MBBS, PhD
JBMR Editor-in-Chief

2004 Late-Breaking Abstracts Session

LB1
Evidence that Fgf23 Is the Phosphatonin in Hyp Mice.
S. Liu, J. Zhou*, W. Tang*, L. D. Quarles. Internal Medicine, University of Kansas Medical Center, Kansas City, KS, USA.

X-linked hypophosphatemia (XLH) is caused by inactivating mutations of the endopeptidase, PHEX, which leads to the accumulation of an unknown circulating phosphaturic factor, called phosphatonin. FGF23 is a phosphaturic hormone produced by bone and is a candidate for phosphatonin. Inactivating PHEX mutations leads to increased serum levels of FGF23 in XLH and the Hyp mouse homologue of this disease. To determine if elevated fgf23 levels mediate the hypophosphatemia in Hyp mice, we generated fgf23 null mice and crossed them onto the Hyp background to create combined fgf23 and Phex deficient mice. We examined male mice with the following genotypes: $fgf23^{+/+}$, $fgf23^{+/-}$and $fgf23^{-/-}$, and $fgf23^{+/+}$/Hyp, $fgf23^{+/-}$/Hyp and $fgf23^{-/-}$/Hyp. Consistent with successful deletion of fgf23, we observed undetectable serum fgf23 levels in $fgf23^{-/-}$ mice compared to the normal levels in $fgf23^{+/+}$ mice (35.0 ± 4.9 pg/ml). The absence of circulating fgf23 levels in $fgf23^{-/-}$ mice resulted in higher mean serum phosphate levels compared to wild-type ($fgf23^{+/+}$) littermates (14.1 vs 11.0±0.3 mg/dL). In contrast, Phex deficient Hyp mice displayed markedly elevated serum fgf23 levels (2285.9 ± 377.8 pg/ml) that were associated with low mean serum phosphate concentrations (5.9±0.4 mg/dL). Superimposed fgf23 deficiency resulted in undetectable circulating fgf23 levels in combined $fgf23^{-/-}$/Hyp mice, and a 50% reduction in fgf23 levels (1241.0±396.7 pg/ml) in Hyp mice heterozygote for fgf23 null allele ($fgf23^{+/-}$/Hyp). The hypophosphatemia in Hyp mice was corrected in proportion to the degree of superimposed fgf23 deficiency. In $fgf23^{-/-}$/Hyp mice lacking any fgf23, the serum phosphate levels were indistinguishable from values in $fgf23^{-/-}$ mice (14.1±1.2 vs. 14.1 mg/dL). In combined heterozygous $fgf23^{+/-}$/Hyp mice, which had a partial reduction in fgf23 levels, the serum phosphate concentrations attained intermediate levels (7.5±0.5 mg/dL) that where greater than values in Hyp mice. These data confirm an essential role of fgf23 in the physiological regulation of serum phosphate and suggest that fgf23 is phosphatonin, the circulating factor causing hypophosphatemia in Hyp mice.

Citation:

LB2
Central Interleukin-1 Receptor Signaling Regulates Bone Mass.
I. Goshen*, A. Bajayo*, S. Feldman*, E. Shohami*, R. Yirmiya*, I. Bab. The Hebrew University of Jerusalem, Jerusalem, Israel.

The pro-inflammatory cytokine interleukin-1 (IL-1), acting via the hypothalamic IL-1 receptor type 1 (IL-1R1), activates pathways known for their association with the restrain of bone formation, such as the hypothalamo pituitary-adrenocortical (HPA) axis and the sympathetic nervous system. In addition, IL-1 has been implicated as a mediator of the bone loss induced by sex hormone depletion. To address more specifically the skeletal regulatory role of central IL-1R1 signaling, we characterized the bone phenotype of young $IL\text{-}1R1^{-/-}$ mice and mice with astrocyte-targeted overexpression of the human IL-1 receptor antagonist, under the control of the murine glial fibrillary acidic protein promoter (IL-1raTG mice). The genetically manipulated mice showed normal body weight and food consumption. Although a previous histomorphometric study reported a normal bone mass in the $IL\text{-}1R1^{-/-}$ mice, a present micro-computed tomographic (μCT) analysis demonstrated impaired femoral elongation and radial growth in these animals as well as in the IL-1raTG mice. Moreover, the trabecular bone density in the distal femoral metaphysis and lumbar vertebrae of both mouse lines was markedly lower as compared to their wild-type controls. Similar decreases were also seen in the trabecular thickness, number and connectivity. These data demonstrate a low bone mass (LBM) phenotype resulting from the absence of central IL-1R1 signaling. Whereas previously reported studies suggest a role for skeletal IL-1R1 signaling in bone loss, the present findings implicate the central IL-1R1 signaling as a positive regulator of bone mass accrual.

Citation:

LB3

The B6.C3H-4 Congenic Mouse Strain Carrying a Volumetric BMD Quantitative Trait Locus (QTL) Prevents Ovariectomy-Induced Bone Loss.

W. G. Beamer[1], K. L. Shultz[1], K. M. Delahunty*[1], C. J. Rosen[2], L. R. Donahue[1]. [1]The Jackson Laboratory, Bar Harbor, ME, USA, [2]Maine Ctr for Osteoporosis Research and Education, Bangor, ME, USA.

We have previously reported mapping 10 QTLs for femoral BMD utilizing F2 intercross progeny derived from progenitor inbred mouse strains C57BL/6J (B6, low BMD) and C3H/HeJ (C3H, high BMD). The strongest correlations for femoral BMD in F2 female mice were with regions on Chr 1, 4, and 18, each of which accounted for 5 to 10% of the variance in femoral BMD. Transfer of the individual BMD QTL regions from C3H to the B6 genetic background by backcrossing yielded congenic strains, B6.C3H, that recapitulated the BMD effects and the heritability properties predicted from the F2 data.

A remarkable feature of the progenitor strains, B6 and C3H, is the difference in responses of their bone mass to loss of gonadal steroid. Groups of 4 month old B6 and C3H females were treated by ovariectomy or sham surgery, held for six weeks, then necropsied for data on femoral dimensions, and femoral cortical and trabecular parameters by pQCT. Both progenitor strains showed subtle increases in the distal trabecular volume. The ovariectomized B6 mice lost femoral cortical bone mineral, mid-diaphyseal thickness, and volume when compared to sham controls. In contrast, similarly aged and ovariectomized C3H females fully maintained all cortical bone parameters when compared to sham controls. To determine whether the resistance of cortical bone in C3H mice to ovariectomy was a property associated with a specific BMD QTL, B6.C3H congenic strains carrying QTLs for Chrs 1, 4, 6, 8, and 18 were ovariectomized or sham treated at 4 months, held for 6 weeks, and pQCT data was obtained on isolated femurs. The B6.C3H-4T congenic females behaved like their C3H progenitor strain in that no loss of femoral cortical bone parameters was observed in response to ovariectomy. In contrast the B6.C3H-1T, -6T, -8T, and -18T mice behaved like their B6 progenitor and lost significant cortical bone mineral, volume, and mid-diaphyseal thickness. These results demonstrate: a) congenic strain sets carrying BMD QTLs on different chromosomes facilitate investigations defining function and regulation of bone; b) the cortical bone protective effect observed in C3H is associated with C3H alleles for the BMD QTL on Chr 4 and not with Chrs 1, 6, 8 or 18; and c) the protective effect appears limited to the cortical bone. Although nested subline mapping has reduced the Chr 4 BMD QTL from 39 to 7 cM in size (18.3 Mb; 433 known, 400 predicted genes), a smaller genetic segment will facilitate expression studies for candidate genes.

Citation:

LB4

Targeted Expression of BIG-3 Leads to Accelerated Osteoblast Differentiation During Embryonic Development.

F. Gori, C. P. Raftery*, M. M. Donohue*, M. B. Demay. Endocrine Unit, Massachusetts General Hospital, Harvard Medical School, Boston, MA, USA.

Skeletal development and growth occurs via two major processes, intramembranous and endochondral ossification, and requires coordinated activities of complex signaling pathways. Among the local signaling pathways that are known to play a role in these processes is the bone morphogenetic protein (BMP) pathway. We identified a novel BMP-2-induced gene named BIG-3 (BMP-2 Induced Gene 3kb) that dramatically accelerates the program of osteoblastic differentiation in MC3T3-E1 cells. BIG-3 encodes a novel protein belonging to the highly conserved family of WD-40 repeat proteins found in all eukaryotes. BIG-3 accelerates osteoblast differentiation *in vitro* and is developmentally expressed during embryogenesis being first detected at day 13.5 post coitus (pc) throughout the mesenchymal condensation. To identify a role for BIG-3 *in vivo*, a BIG-3 transgene was targeted to osteoblasts of mice using the 2.4-kb fragment of the mouse α (1) I collagen promoter. Two lines of transgenic mice were generated and qualitatively similar results were obtained with both transgenic lines. The expression of the BIG-3 transgene was confirmed by Northern analyses of calvarial RNA. *In situ* hybridization analyses of histological sections of newborn tibiae showed specific expression of the transgene in bone. Alizarin Red and Alcian blue staining of whole mount preparations at embryonic day 14.5, 15.5, and in newborn transgene positive and transgene negative littermates, showed that the expression of the transgene results in an accelerated mineralization and bigger skeleton compared to that of wild-type littermates. At embryonic day 15.5, the posterior and lateral processes of the lumbar vertebrae of transgenic mice were calcified while they were not in their wild-type littermates demonstrating accelerated skeletal maturation. Von kossa staining of forelimb sections of 14.5 dpc embryos showed mineral deposition in transgenic but not in wild-type embryos demonstrating that the presence of the transgene leads to accelerated mineral deposition. *In situ* hybridization analyses of histological sections of 14.5 dpc embryos demonstrated earlier and more extensive expression of type I collagen and osteopontin.

These data demonstrate that BIG-3 is developmentally expressed in osteoblasts during endochondral ossification, and that targeted overexpression of this novel protein to osteoblasts leads to an acceleration of differentiation during skeletal development.

Citation:

LB5

Large-scale Evidence for Differential Genetic Effects of ESR1 Gene Polymorphisms on Osteoporosis Outcomes: The GENOMOS Study.

J. Ioannidis*[1], S. Ralston[2], S. Bennett*[3], M. Brandi[4], D. Grinberg[5], F. Karassa*[1], B. Langdahl[6], J. van Meurs[7], L. Mosekilde[6], S. Scollen*[8], O. Albagha*[2], M. Bustamante*[5], A. Carey*[3], A. Dunning*[8], A. Enjuanes*[5], J. van Leeuwen[7], C. Mavilia*[4], L. Masi[4], F. McGuigan[2], X. Nogues[5], H. Pols[7], D. Reid[2], S. Schuit*[7], R. Sherlock*[3], A. Uitterlinden[7]. [1]University of Ioannina, Ioannina, Greece, [2]University of Aberdeen, Aberdeen, United Kingdom, [3]Oxagen Limited, Abingdon, United Kingdom, [4]University of Florence, Florence, Italy, [5]University of Barcelona, Barcelona, Spain, [6]Aarhus University, Aarhus, Denmark, [7]Internal Medicine, Erasmus MC, Rotterdam, Netherlands, [8]Cambridge University, Cambridge, United Kingdom.

Osteoporosis has a strong genetic component but the genes involved are ill-defined. Many candidate gene studies, however, have been hampered by small sample size, lack of standardization, and inconclusive results. We therefore started a program of prospective meta-analyses of polymorphisms involving standardized genotyping of 18,917 subjects (n=4,268 men), in 8 European centres, in relation to BMD of femoral neck and lumbar spine, fractures at any site (n=4944), and vertebral fractures (n=1067). We first studied 3 polymorphisms in the estrogen receptor alpha (*ESR1*) gene: the intron 1 polymorphisms *Xba*I and *Pvu*II, and the promoter TA-microsatellite, and haplotypes thereof.

No between-center heterogeneity was observed for any outcome in any genetic contrast. None of the 3 polymorphisms or haplotypes thereof had any statistically significant effect on BMD in adjusted or unadjusted analyses and estimated differences between genetic contrasts were <0.01 g/cm^2. Conversely, we found significant fracture risk reduction for the XbaI "X" allele. E.g., in XX homozygous women, the odds of fractures were reduced by 19% (p=0.002) and vertebral fractures by 35% (p=0.003). Genotype effects on fractures were independent of BMD, and remained similar in adjusted analyses. This study, which represents the largest gene-disease association study ever performed to-date with individual-level data, has shown that *ESR1* is a susceptibility gene for osteoporosis and that variation at the *Xba*I site determines fracture risk by mechanisms independent of BMD. The large sample size makes the study statistically robust, but the effects we observed were modest illustrating the limited contribution of single genetic markers to fracture risk. Our study demonstrates the value of adequately powered studies with standardized genotyping and clinical outcomes in defining effects of common genetic variants on complex diseases.

Citation:

POSTER SESSION III

M20

The Role of the Sodium/Calcium Exchanger Isoforms NCX-1 and NCX-3 in Osteoblasts.

F. S. Harman*[1], D. Sosnoski*[2], V. Gilman*[2], C. V. Gay[2]. [1]Intercollege Graduate Degree Program in Physiology, Penn State University, University Park, PA, USA, [2]Biochemistry and Molecular Biology, Penn State University, University Park, PA, USA.

Original characterization of calcium transport in bone from interstitial fluid for mineralization of a mature, extracellular matrix has been described as being a function of osteoblasts. The presence of the plasma membrane calcium ATPase (PMCA) calcium transporter as a unidirectional effector of calcium efflux from osteoblasts has been described. Cytochemical studies indicate that PMCA is differentially located on the lumenal side of the osteoblast facing bone marrow suggesting an unlikely role in calcium transport directly sent to the mineralizing extracellular matrix. The sodium-calcium exchanger (NCX) of osteoblasts has been characterized as an ion transporter that exchanges the influx of sodium ions for the efflux of calcium ions and has been established to be located on the apical or secretory side of the osteoblasts facing the extracellular matrix. Further, both NCX-1 and NCX-3 isoforms have been identified in osteoblasts. The purpose of this work is to determine the roles of NCX-1 and NCX-3 isoforms in calcium transport using MC3T3E1 osteoblasts, siRNA knock-down technology, and fluorescence changes in the marker calcium-green-1 (CG-1) following administration of a bolus of $CaCl_2$. Changes in calcium flux were detected using BioRad® timecourse software interfaced with a confocal microscope. Transfection studies have been completed with NCX-1 and NCX-3 siRNA that inhibit translation of the specific isoform allowing for a functional analysis of the opposite isoform during the timecourse. Transfection with the sequence 5'-AAAGATTCCGTGACTGCCGTT-3' blocks the synthesis of NCX-1 allowing for functional analysis NCX-3. Conversely, transfection with the sequence 5'-AATGCCGTCAATGTCTTCCTG-3' blocks the synthesis of NCX-3 allowing for functional analysis of NCX-1. Cells were also transfected with siRNA from Ambion™ to block glyceraldehyde phosphate dehydrogenase (GAPDH) synthesis as a transfection control which both NCX-1 and NCX-3 are functional. Inhibitors of PMCA and other calcium flux channels were used to isolate NCX-1 and NCX-3. With NCX-1, NCX-3, GAPDH individually inhibited, the slope of CG-1 fluorescence pixel intensity curve was -0.95±0.08, -0.45±0.12, and -0.53±0.13 respectively. These data suggest that NCX-3 clears the cytoplasm of calcium approximately two times faster than NCX-1 operating alone or in conjunction with NCX-3. Thus, NCX-3 may be located on the endoplasmic reticulum (ER) membrane as well as the plasma membrane, or it may represent a more efficient exchanger of calcium flux than NCX-1.

Citation:

ASBMR 26th ANNUAL MEETING OFFICIAL PROGRAM

Friday, October 1, 2004

Posters Open 5:15 pm - 7:00 pm
Exhibits Open 5:15 pm - 7:00 pm

9:30 am - 12:00 noon
Stem Cell Biology Symposium
Room 6ABC

12:30 pm - 1:30 pm
Meet-the-Professor Sessions
Rooms 601, 615-620

2:00 pm - 3:30 pm
Mini-Symposium A:
Craniofacial Development
Room 6ABC

Mini-Symposium B:
Paget's Disease
Room 6E

3:45 pm - 5:15 pm
Mini-Symposium C:
PTH/PTHrP Actions
Room 6E

Mini-Symposium D:
Pediatric Bone Biology: Disorders of Development and Growth
Room 6ABC

5:15 pm - 7:00 pm
Welcome Reception and Plenary Poster Session
Exhibit Hall 4ABC

Saturday, October 2, 2004

Posters Open 8:00 am - 6:00 pm
Exhibits Open 9:15 am - 4:30 pm

7:00 am - 8:00 am - *Room 4C-4*
New Investigator/New Member Breakfast

8:00 am - 8:10 am
Welcome & Announcements – *Room 6ABC*

8:10 am - 9:10 am - *Room 6ABC*
Gerald D. Aurbach Memorial Lecture

9:10 am - 9:25 am - *Room 6ABC*
(9:10) William F. Neuman Award Presentation
(9:15) Fuller Albright Award Presentation
(9:20) Gideon A. Rodan Excellence in Mentorship Award Presentation

9:30 am - 10:00 am
Break - *Exhibit Hall 4ABC*
ODD Posters Present

10:00 am - 11:30 am - Plenary Orals
I (Basic) - *Room 6E*
II (Clinical/Translational) - *Room 6ABC*

11:30 am - 2:30 pm
POSTER SESSION I - *Exhibit Hall 4ABC*
ODD: 11:30 am - 12:30 pm
EVEN: 1:30 pm - 2:30 pm

12:00 pm - 2:00 pm - *Rooms 606-607*
Special Session for Allied Health Professionals

12:30 pm - 1:30 pm - *Rooms 601, 615-620*
Meet-the-Professor Sessions

12:30 pm - 2:00 pm
Grant Writing Workshop - *Room 4C-4*

2:30 pm - 4:00 pm - Concurrent Oral Sessions
1) Osteoblasts I - *Room 6E*
2) Osteoporosis - Epidemiology I - *Room 6ABC*
3) Osteoclasts I - *Rooms 608-609*
4) Mechanical Loading: In Vitro - *Rooms 602-604*
5) BMPs and Other Growth Factors I - *Rooms 611-614*
6) Bone Acquisition & Pediatric Bone Disease - *Rooms 606-607*

4:00 pm - 4:30 pm
Break - *Exhibit Hall 4ABC*

4:30 pm - 6:00 pm
Concurrent State-of-the-Art Lectures
A: Hormone Action on Non-Traditional Targets - *Room 6ABC*
B: Collaborating with Industry: Issues for Individual Investigators - *Room 6E*

6:00 pm - 7:00 pm
ASBMR Annual Business Meeting

Sunday, October 3, 2004

Posters Open 8:00 am - 6:00 pm
Exhibits Open 9:30 am - 4:30 pm

8:00 am - 9:30 am
Plenary Symposium I: BMP Antagonists: Basic Science to Human Disease - *Room 6ABC*

9:30 am - 9:35 am - *Room 6ABC*
Frederic C. Bartter Award Presentation

9:35 am - 10:00 am
Break - *Exhibit Hall 4ABC*
ODD Posters Present

10:00 am - 11:30 am
Plenary Orals
I (Basic) - *Room 6E*
II (Clinical/Translational) - *Room 6ABC*

11:30 am - 2:30 pm
POSTER SESSION II - *Exhibit Hall 4ABC*
ODD: 11:30 am - 12:30 pm
EVEN: 1:30 pm - 2:30 pm

12:30 pm - 1:30 pm
Clinical Roundtable – *Rooms 606-607*

12:30 pm - 1:30 pm - *Rooms 601, 615-620*
Meet-the-Professor Sessions

12:30 pm - 2:00 pm
Biotechniques Workshop – *Rooms 611-614*

12:30 pm - 2:00 pm
Responsible Conduct in Bone and Mineral Research – *Rooms 602-604*

2:30 pm - 4:00 pm - Concurrent Oral Sessions
7) PTH Actions - *Room 6E*
8) Osteoporosis - Diagnosis & Treatment - *Room 6ABC*
9) Bone, Cartilage, Connective Tissue Matrix - *Rooms 611-614*
10) Genetics of Bone and Mineral Disorders I - *Rooms 606-607*
11) Steroids: Molecular - *Rooms 608-609*
12) Cancer and Bone - *Rooms 602-604*

4:00 pm - 4:30 pm
Break - *Exhibit Hall 4ABC*
EVEN Posters Present

4:30 pm - 6:00 pm
Concurrent State-of-the-Art Lectures
A: Osteoclast Biology - *Room 6ABC*
B: Research Methods in Skeletal Genetics - *Room 6E*

8:30 pm - 11:30 pm
ASBMR Social Event
Experience Music Project

Monday, October 4, 2004

Posters Open 8:00 am - 4:30 pm
Exhibits Open 9:30 am - 4:30 pm

8:00 am - 9:30 am
Plenary Symposium II: New Insights into Bone Strength - *Room 6ABC*

9:30 am - 9:35 am - *Room 6ABC*
Shirley Hohl Service Award Presentation

9:35 am - 10:00 am
Break - *Exhibit Hall 4ABC*
ODD Posters Present

10:00 am - 11:30 am
Plenary Orals - *Room 6ABC*
Late-Breaking Abstracts - *Room 6E*

11:30 am - 2:30 pm
POSTER SESSION III - *Exhibit Hall B*
ODD: 11:45 am - 1:15 pm
EVEN: 1:15 pm - 2:45 pm

12:30 pm - 1:30 pm - *Rooms 606-607*
Clinical Roundtable

12:30 pm - 1:30 pm - *Rooms 601, 615-620*
Meet-the-Professor Sessions

12:30 pm - 2:00 pm
Career Options for Scientists - *Rooms 611-614*

2:30 pm - 4:00 pm - Concurrent Oral Sessions
13) Osteoblasts II - *Room 6E*
14) Osteoporosis - Epidemiology II - *Room 6ABC*
15) Steroid Receptor Actions - *Rooms 602-604*
16) Osteoporosis - Pathophysiology I - *Rooms 608-609*
17) Chondrocyte Biology - *Rooms 606-607*
18) Bone Acquisition & Pediatric Bone Biology - *Rooms 611-614*

4:00 pm - 4:30 pm
Break - *Exhibit Hall 4ABC*
EVEN Posters Present

4:30 pm - 6:00 pm - Concurrent Oral Sessions
19) Osteoblasts III - *Room 6E*
20) Mechanical Loading: In Vivo - *Rooms 602-604*
21) Osteoporosis - Pathophysiology II - *Rooms 608-609*
22) Other Disorders of Bone and Mineral Metabolism I - *Rooms 606-607*
23) Peptide Hormones - *Rooms 611-614*
24) Osteoporosis - Treatment I - *Room 6ABC*

Tuesday, October 5, 2004

8:00 am - 9:00 am
Louis V. Avioli Memorial Lecture
Room 6ABC

9:00 am - 9:05 am
Louis V. Avioli Founders Award Presentation
Room 6ABC

9:05 am - 9:30 pm
Break - *East Lobby*

9:30 am - 11: 30 am - Concurrent Oral Sessions
25) BMPs and Other Growth Factors II - *Rooms 608-609*
26) Osteoporosis - Epidemiology III - *Room 6E*
27) Osteoclasts II - *Rooms 602-604*
28) Other Disorders of Bone and Mineral Metabolism II - *Rooms 606-607*
29) Osteoblasts IV - *Rooms 611-614*
30) Osteoporosis - Treatment II - *Room 6ABC*

11:30 am
Adjourn

2004 ANCILLARY PROGRAM

Friday, October 1, 2004

Working Groups

7:00 pm - 9:30 pm
Fluid Flow in Bone Working Group
Room 4C-4

7:00 pm - 9:30 pm
Nutrition and Bone Health Working Group
Rooms 602-604

7:00 pm - 9:30 pm
Working Group on Musculoskeletal Rehabilitation in Patients with Osteoporosis
Rooms 618-620

7:15 pm - 9:45 pm
In Vivo Working Group
Rooms 608-609

7:15 pm - 10:00 pm
Working Group on Biochemical Markers of Bone Turnover
Rooms 611-614

Industry-Supported Symposia

7:00 pm - 9:00 pm
Optimizing the Treatment of Osteoporosis: Evolutions and Solutions
Jointly sponsored by the University of Kentucky College of Medicine Continuing Education Office and Cerebrio
Jointly supported by an educational grant from Roche and GlaxoSmithKline
Grand Ballroom 1 and 2, The Westin Seattle

7:00 pm - 9:30 pm
Changes on the Horizon? The Future of Osteoporosis Diagnosis, Prevention and Management
Sponsored by the Center for Accredited Healthcare Education
Supported by an educational grant from Eli Lilly and Company
Grand Ballroom, Sheraton Seattle Hotel & Towers

Saturday, October 2, 2004

Working Groups

7:00 pm - 9:15 pm
Non-Invasive Assessment of Trabecular Bone Microarchitecture Working Group
Rooms 606-607

7:00 pm - 10:00 pm
Post Transplantation Bone Disease Working Group
Rooms 618-620

7:00 pm - 10:00 pm
Working Group on Hormone-Receptor Interactions
Rooms 608-609

7:15 pm - 9:30 pm
Bone Remodeling and Stress Fracture Working Group
Rooms 602-604

7:15 pm - 10:00 pm
Pediatric Bone and Mineral Working Group
Room 4C-4

Industry-Supported Symposia

7:00 pm - 9:30 pm
The Evolving Management of Bone Disease: Changes on the Horizon
Sponsored by Medical Education Resources
Sponsored by an educational grant from Novartis Pharmaceuticals Corporation
Room 6E

7:00 pm - 10:00 pm
The Role of Bone Strength in the Diagnosis and Treatment of Osteoporosis
Jointly sponsored by the Postgraduate Institute for Medicine and Photosound Communications, Inc.
Supported by an educational grant from the Alliance for Better Bone Health (a collaboration between Procter & Gamble Pharmaceuticals and Aventis Pharmaceuticals).
Grand Ballroom, Sheraton Seattle Hotel & Towers

Sunday, October 3, 2004

Industry-Supported Symposium

6:00 am - 8:00 am
Parathyroid Hormone: Meeting the Challenge of Osteoporosis
Sponsored by ApotheCom Associates LLC and Postgraduate Institute for Medicine
Supported by an educational grant from NPS Pharmaceuticals
Grand Ballroom, Sheraton Seattle Hotel & Towers

ASBMR Social Event

8:30 pm - 11:30 pm

Experience Music Project
Seattle Center
Seattle, Washington
(Tickets required.)

Monday, October 4, 2004

Working Groups

6:15 pm - 8:35 pm
Physical Activity Working Group
Rooms 608-609

6:30 pm - 9:30 pm
Adult Bone and Mineral Working Group
Room 4C-4

6:30 pm - 8:30 pm
Molecular Biology and Pathology of Bone Working Group
Rooms 611-614

6:30 pm - 9:30 pm
Vitamin D Working Group
Rooms 602-604

7:00 pm - 9:15 pm
Working Group on Aging and the Human Skeleton
Rooms 615-617

Industry-Supported Symposia

6:00 pm - 9:00 pm
The Clinical Outlook on RANKL: A Future Treatment Target for Osteoporosis and Cancer-Related Bone Diseases?
Sponsored by The Dannemiller Memorial Educational Foundation and The France Foundation
Supported by an educational grant from Amgen
Grand Ballroom, The Westin Seattle

7:00 pm - 10:00 pm
An Evidence-based Approach to the Clinical Management of Osteoporosis
Sponsored by the University of Pennsylvania School of Medicine
Supported by an educational grant from Merck & Co., Inc.
Grand Ballroom, Sheraton Seattle Hotel & Towers

American Society for Bone and Mineral Research

ASBMR Business Office
2025 M St, NW, Suite 800, Washington, DC 20036-3309 USA
Tel: (202) 367-1161 ◆ Fax: (202) 367-2161 ◆ E-mail: asbmr@smithbucklin.com ◆ Internet: www.asbmr.org

The *Journal of Bone and Mineral Research* (ISSN: 0884-0431) provides a forum for papers of the highest quality pertaining to all areas of the biology and physiology of bone, the hormones that regulate bone and mineral metabolism and the pathophysiology and treatment of disorders of bone and mineral metabolism. All authored papers and editorial news and comments, opinions, findings, conclusions or recommendations in the *Journal* are those of the author(s) and do not necessarily reflect the views of the *Journal* and its publisher, nor does their publication imply any endorsement. The *Journal of Bone and Mineral Research* is the official journal of the American Society for Bone and Mineral Research and is published monthly plus a special issue in September by the American Society for Bone and Mineral Research, 2025 M Street, N.W., Suite 800, Washington, DC 20036-3309, USA. Address reprint/offprint inquiries to Cadmus Journal Services Reprints at US (800) 407-9190 or (410) 819-3967. Periodicals postage paid in Washington, DC and additional offices. POSTMASTER SEND ADDRESS CHANGES TO: Journal of Bone and Mineral Research, P.O. Box 2759, Durham, NC 27715, USA. 2004 Subscription Rates: U.S. Personal $495.00, Institutional: $535.00; Canada/Mexico: Personal $515.00; Institutional $560.00; Overseas: Personal $570.00; Institutional: $575.00. Single issue $50.00. Subscription term is January – December.

Claims for missing issues will be serviced at no charge if received within six months of issue date {journal@jbmr.org, or fax (US) 919-620-8465}. Duplicate copies cannot be sent to replace issues not delivered because of failure to notify publisher of change of address. Please notify ASBMR of new address six (6) weeks in advance of moving date. All subscriptions are payable in advance in U.S. funds drawn on a U.S. bank. If not fully satisfied, notify publisher for a refund on all unmailed issues.

Address advertising and commercial reprint inquiries to Mr. Steve Kavalgian, Mill River Media LLC, 141 Boston Post Rd. Old Lyme, CT 06371-1303, USA; (860) 434-6889 (phone); (860) 434-9744 (fax); millrivermedia@aol.com (e-mail). Advertisements are subject to editorial approval.

The *Journal of Bone and Mineral Research* is a **Journal Club**™ selection. The *Journal* is indexed by *Index Medicus, Current Contents/Life Science, CABS (Current Awareness in Biological Sciences), Excerpta Medica, Cambridge Scientific Abstracts, Chemical Abstracts*, *Reference Update, Science Citation Index*, and *Nuclear Medicine Literature Updating and Indexing Service*.

TABLE OF CONTENTS

General Information xii

FRIDAY, OCTOBER 1, 2004

Day-at-a-Glance xxii

SATURDAY, OCTOBER 2, 2004

Day-at-a-Glance xxiii

SUNDAY, OCTOBER 3, 2004

Day-at-a-Glance xxv

MONDAY, OCTOBER 4, 2004

Day-at-a-Glance xxvi

TUESDAY, OCTOBER 5, 2004

Day-at-a-Glance xxviii

Abstracts Key xxix

Abstracts S2

Key Word Index S494

Author Index S518

JBMR Journal of Bone and Mineral Research

Official Journal of the American Society for Bone and Mineral Research

www.jbmronline.org

AMERICAN SOCIETY FOR BONE AND MINERAL RESEARCH (ASBMR)

OFFICERS

President: Robert A. Nissenson, Ph.D.
President-Elect: Sylvia Christakos, Ph.D.
Past-President: Clifford J. Rosen, M.D.
Secretary-Treasurer: Marc K. Drezner, M.D.

COUNCIL

Daniel Bikle, M.D., Ph.D.	*Term expires 2006*	Sundeep Khosla, M.D.	*Term expires 2005*
Dennis Black, Ph.D.	*Term expires 2004*	Barbara Lukert, M.D.	*Term expires 2004*
Jane Cauley, Ph.D.	*Term expires 2006*	Vicki Rosen, Ph.D.	*Term expires 2006*
John Eisman, M.B.B.S., Ph.D.	*Ex-officio*	Gary Stein, Ph.D.	*Term expires 2005*
Susan Greenspan, M.D.	*Term expires 2005*	Larry Suva, Ph.D.	*Term expires 2004*

PAST PRESIDENTS

Louis V. Avioli, M.D.	*1979-1980*	Mark R. Haussler, Ph.D.	*1991-1992*
Lawrence G. Raisz, M.D.	*1980-1981*	Steven L. Teitelbaum, M.D.	*1992-1993*
Claude D. Arnaud, M.D.	*1981-1982*	Henry M. Kronenberg, M.D.	*1993-1994*
Stephen M. Krane, M.D.	*1982-1983*	Ernesto Canalis, M.D.	*1994-1995*
William A. Peck, M.D.	*1983-1984*	John P. Bilezikian, M.D.	*1995-1996*
Paula H. Stern, Ph.D.	*1984-1985*	Gregory R. Mundy, M.D.	*1996-1997*
B. Lawrence Riggs, M.D.	*1985-1986*	Michael Rosenblatt, M.D.	*1997-1998*
Norman H. Bell, 4M.D.	*1986-1987*	Jane E. Aubin, Ph.D.	*1998-1999*
Gideon A. Rodan, M.D., Ph.D.	*1987-1988*	David Goltzman, M.D.	*1999-2000*
John G. Haddad, Jr., M.D.	*1988-1989*	Robert Marcus, M.D.	*2000-2001*
Armen H. Tashjian, Jr., M.D.	*1989-1990*	Robert R. Recker, M.D.	*2001-2002*
Frederick R. Singer, M.D.	*1990-1991*	Clifford J. Rosen, M.D.	*2002-2003*

PAST SECRETARY-TREASURERS

Norman H. Bell, M.D.	*1977-1985*	Steven R. Goldring, M.D.	*1997-2000*
Gregory R. Mundy, M.D.	*1985-1991*	Andrew F. Stewart, M.D.	*2000-2003*
Arnold J. Kahn, Ph.D.	*1991-1997*		

PAST COUNCILORS

Constantine Anast, M.D.	*1980-1982*	Marie Demay, M.D.	*2000-2003*
Claude D. Arnaud, M.D.	*1979-1980*	Richard Eastell, M.D., F.R.C.P.	*2000-2003*
Andrew Arnold, M.D.	*1999-2002*	John Eisman, MBBS, Ph.D.	*1994-1997*
Jane E. Aubin, Ph.D.	*1991-1994*	Murray J. Favus, M.D.	*1992-1995*
Roland Baron, D.D.S., Ph.D.	*1991-1994*	David Feldman, M.D.	*1982-1986*
John P. Bilezikian, M.D.	*1987-1990*	Lorraine A. Fitzpatrick, M.D.	*1998-2001*
Lynda F. Bonewald, Ph.D.	*1995-1998*	Francis Glorieux, M.D., Ph.D.	*1988-1991*
Arthur E. Broadus, M.D., Ph.D.	*1990-1993*	Julie Glowacki, Ph.D.	*1999-2002*
Ernesto Canalis, M.D.	*1989-1992*	Steven R. Goldring, M.D.	*1993-1996*
Janet M. Canterbury, M.D.	*1981-1984*	Ralph S. Goldsmith, M.D.	*1980-1983*
Sylvia Christakos, Ph.D.	*1989-1992*	David Goltzman, M.D.	*1984-1988*
Thomas L. Clemens, Ph.D.	*1998-2001*	Maxine Gowen, Ph.D.	*2000-2003*
Jack W. Coburn, M.D.	*1981-1984*	John G. Haddad, Jr., M.D.	*1982-1985*
David V. Cohn, Ph.D.	*1982-1985*	Mark R. Haussler, Ph.D.	*1982-1985*
Cary W. Cooper, Ph.D.	*1980-1981*	Hunter H. Heath III, M.D.	*1985-1988*
Steven R. Cummings, M.D.	*1996-1999*	Helen L. Henry, Ph.D.	*1985-1988*
Bess Dawson-Hughes, M.D.	*1996-1999*	Keith A. Hruska, M.D.	*1989-1992*
Hector F. DeLuca, Ph.D.	*1979-1980*	Arnold J. Kahn, Ph.D.	*1986-1989*

AMERICAN SOCIETY FOR BONE AND MINERAL RESEARCH (ASBMR)

PAST COUNCILORS (Continued)

Frederick S. Kaplan, M.D.	*1997-2000*
Stephen M. Krane, M.D.	*1979-1981*
Barbara E. Kream, M.D.	*1985-1988*
Henry M. Kronenberg, M.D.	*1986-1989*
Jane B. Lian, Ph.D.	*1991-1994*
Robert Marcus, M.D.	*1995-1998, 1999-2002*
T.J. Martin, M.D.	*1987-1990*
Stephen Marx, M.D.	*1983-1986*
Toshio Matsumoto, M.D.	*1999-2002*
Gregory R. Mundy, M.D.	*1983-1985*, *1995-1997*
Robert Nissenson, Ph.D.	*1993-1996*
Anthony W. Norman, Ph.D.	*1980-1982*
Philip A. Osdoby, Ph.D.	*1997-2000*
Susan M. Ott, M.D.	*1988-1991*
A. Michael Parfitt, M.D.	*1990-1993*
Nicola C. Partridge, Ph.D.	*1993-1996*
William A. Peck, M.D.	*1979-1981*
John T. Potts, Jr., M.D.	*1979-1981*
Paul A. Price, Ph.D.	*1986-1989*
Robert R. Recker, M.D.	*1995-1998*
Pamela Gehron Robey, Ph.D.	*1992-1995*
Gideon A. Rodan, M.D., Ph.D.	*1984-1986*
Sevgi B. Rodan, Ph.D.	*1990-1993*
Michael Rosenblatt, M.D.	*1988-1991*
Elizabeth Shane, M.D.	*1994-1997*
Dolores M. Shoback, M.D.	*1998-2001*
Ethel Siris, M.D.	*1996-1999*
Eduardo Slatopolsky, M.D.	*1980-1983*
Paula H. Stern, Ph.D.	*1980-1983*
Andrew F. Stewart, M.D.	*1994-1997*
Gordon J. Strewler, M.D.	*1992-1995*
Armen H. Tashjian, Jr., M.D.	*1979-1982*
John D. Termine, Ph.D.	*1984-1987*
Marian F. Young, Ph.D.	*1997-2000*
Robert Wasserman, Ph.D.	*1984-1987*
Glenda Wong, Ph.D.	*1984-1987*

ASBMR STAFF

Joan R. Goldberg, *Executive Director*
Karen R. Hasson, *Deputy Executive Director*
D. Douglas Fesler, *Project Manager*
Earline Marshall, *Executive Assistant*
Elizabeth Koenst, *Senior Program Coordinator*
Kimberly Seyran, *Membership/Project Coordinator*
Amy Werner, *Program Assistant*
Anna Camele, *Membership/Marketing Assistant*
Rebecca Boulos, *Association Assistant*
Bill Gaskill, *Accountant*
Melissa Huston, *Convention Manager*
Wayne Horton, *Registration Coordinator*
Kelly Marks, *Exhibits Coordinator*
Brooke Hirsch, *Convention Assistant*
Jann Teeple-Hewes, *Public Relations Director*
Kara Dress, *Public Relations Manager*
Adrienne Lea, *Director of Publications*
Heather Price, *JBMR Project Manager*
Amber Williams, *JBMR Managing Editor*
David Allen, *JBMR Publications Specialist*

ASBMR BUSINESS OFFICE

2025 M Street, NW
Suite 800
Washington, DC 20036-3309
USA
Tel: (202) 367-1161
Fax: (202) 367-2161
E-mail: ASBMR@smithbucklin.com
Internet: www.asbmr.org

The Fuller Albright Award

Supported by an unrestricted educational grant from Aventis Pharmaceuticals

Michael F. Holick, M.D., Ph.D.	*1980*	Andrew Arnold, M.D.	*1992*
Mark R. Haussler, Ph.D.	*1981*	Pamela G. Robey, Ph.D.	*1993*
Stephen Marx, M.D.	*1982*	Roberto Civitelli, M.D.	*1994*
Gregory R. Mundy, M.D.	*1982*	Roberto Pacifici, M.D.	*1995*
Edward M. Brown, M.D.	*1983*	Clinton T. Rubin, Ph.D.	*1996*
Helen L. Henry, Ph.D.	*1984*	René St-Arnaud, Ph.D.	*1997*
Henry M. Kronenberg, M.D.	*1985*	Shigeaki Kato, Ph.D.	*1998*
Michael Rosenblatt, M.D.	*1986*	Theresa A. Guise, M.D.	*1999*
Michael P. Whyte, M.D.	*1987*	Dwight Towler, M.D., Ph.D.	*2000*
Rajiv Kumar, M.D.	*1988*	Charles H. Turner, M.D.	*2001*
Timothy Chambers, M.D.	*1989*	Nobuyuki Udagawa, M.D.	*2002*
Michael A. Levine, M.D.	*1990*	Patricia Ducy, Ph.D.	*2003*
Dean T. Yamaguchi, M.D., Ph.D.	*1991*		

The Louis V. Avioli Founders Award

Supported by an unrestricted educational grant from Merck & Co., Inc.

Stavros Manolagas, M.D., Ph.D.	*2000*	Roland Baron, D.D.S., Ph.D.	*2002*
Gerard Karsenty, M.D.	*2001*	Edward Brown, M.D.	*2003*

The William F. Neuman Award

Supported by an unrestricted educational grant from Aventis Pharmaceuticals

Gerald D. Aurbach, M.D.	*1981*	Gideon A. Rodan, M.D., Ph.D.	*1993*
Paul L. Munson, Ph.D.	*1982*	Thomas John Martin, M.D., D.Sc.	*1994*
D. Harold Copp, M.D., Ph.D.	*1983*	Anthony W. Norman, Ph.D.	*1995*
Roy V. Talmage, Ph.D.	*1984*	Melvin Jacob Glimcher, M.D.	*1996*
Hector F. DeLuca, Ph.D.	*1985*	Tatsuo Suda, D.D.Sc., Ph.D.	*1997*
Lawrence G. Raisz, M.D.	*1986*	Steven L. Teitelbaum, M.D.	*1998*
John T. Potts, Jr., M.D.	*1987*	Gregory R. Mundy, M.D.	*1999*
Louis V. Avioli, M.D.	*1988*	R. Graham Russell, M.D.	*2000*
Stephen M. Krane, M.D.	*1989*	Harold M. Frost, M.D.	*2001*
Robert H. Wasserman, Ph.D.	*1990*	B. Lawrence Riggs, M.D.	*2002*
Claude D. Arnaud, M.D.	*1991*	Henry M. Kronenberg, M.D.	*2003*
Herbert A. Fleisch, M.D.	*1992*		

The Frederic C. Bartter Award

Supported by an unrestricted educational grant from NPS Pharmaceuticals

Jack Coburn, M.D.	*1986*	A. Michael Parfitt, M.D.	*1995*
Constantine Anast, M.D.	*1987*	C. Conrad Johnston, Jr., M.D.	*1996*
Charles Y.C. Pak, M.D.	*1988*	Robert Lindsay, MBChB, Ph.D.	*1997*
Arthur E. Broadus, M.D., Ph.D.	*1989*	B.E. Christopher Nordin, M.D., Ph.D.	*1998*
B. Lawrence Riggs, M.D.	*1990*	Pierre Meunier, M.D.	*1999*
Eduardo Slatopolsky, M.D.	*1991*	John P. Bilezikian, M.D.	*2000*
Norman H. Bell, M.D.	*1992*	Joseph Melton, III, M.D.	*2001*
Francis H. Glorieux, M.D., Ph.D.	*1993*	Ego Seeman, M.D., F.R.A.C.P.	*2002*
Robert P. Heaney, M.D.	*1994*	Robert R. Recker, M.D.	*2003*

The Shirley Hohl Service Award

Supported by an unrestricted educational grant from Aventis Pharmaceuticals

Louis V. Avioli, M.D.	*1997*	Lawrence G. Raisz, M.D.	*2001*
Norman H. Bell, M.D.	*1998*	Nicola C. Partridge, Ph.D.	*2002*
Murray J. Favus, M.D.	*1999*	Marc K. Drezner, M.D.	*2003*
Arnold J. Kahn, Ph.D.	*2000*		

The Gideon A. Rodan Excellence in Mentorship Award

Supported by an unrestricted educational grant from Merck & Co., Inc.

Gideon A. Rodan, M.D., Ph.D.	*2001*	Webster S. S. Jee, Ph.D.	*2003*
Sylvia Christakos, Ph.D.	*2002*		

AMERICAN SOCIETY FOR BONE AND MINERAL RESEARCH (ASBMR)

2004 ASBMR YOUNG INVESTIGATOR AWARD RECIPIENTS

Co-Supported by unrestricted educational grants from The Alliance for Better Bone Health (Procter &Gamble Pharmaceuticals and Aventis Pharmaceuticals), Amgen, Merck & Co., Inc., NPS Pharmaceuticals, Pfizer, Inc., Roche and GlaxoSmithKline and Wyeth Pharmaceuticals

Henrik G. Ahlborg, M.D., Ph.D.
Boucharaba Ahmed, M.Sc.
Imranul Alam, Ph.D.
Susan J. Allison, B.Sc.
Elisa Benasciutti, Ph.D.
Elizabeth A. Bowe, B.Sc., Ph.D.
Harveen Dhillon, Ph.D.
James R. Edwards, B.Sc.
Ghada N. Farhat, M.P.H.
Pierrick G. Fournier, M.Sc.
Chunxi Ge, M.D., Ph.D.
Luigi Gennari, M.D., Ph.D.
Robert Gensure, M.D., Ph.D.
Genevieve A. Gorny
Dayong Guo
Elizabeth Haney, M.D.
Julie R. Hens, Ph.D.
Matthew J. Hilton, Ph.D.
Kiyoshi Hiramatsu, M.D.
Shoji Ichikawa, Ph.D.
Satoru Kamekura, M.D.
Hidemi Kanazawa, M.D., Ph.D.
Stephen K. Kaptoge, B.Sc., M.Phil.
Isao Kii, Ph.D.
Takako Koga
Fumitaka Kugimiya, M.D.
Christopher J. Lengner
Christian Linden
Fei Liu, D.D.S.
Wei Liu, M.Sc., M.D.
Khalid S. Mohammed, M.D., Ph.D.
Yuko Nakamichi, Ph.D.
Charlene S. Noseworthy, B.Sc.
Despina Satara, Ph.D.
Kimihiko Sawakami, M.D.
Arndt F. Schilling, M.D.
Ann V. Schwartz, Ph.D.
Chan Soo Shin, M.D., Ph.D.
Michael L. Sohaskey, Ph.D.
Alexandra Soroceanu
Toshifumi Sugatani, D.D.S., Ph.D.
Nakamura Takashi
Amanda F. Taylor, Ph.D.
Katrien Venken
Makoto Watanuki, M.D., Ph.D.
Yoko Yamamoto, Ph.D.
Wuchen Yang, M.S., D.D.S.
Ling Ye, D.D.S., Ph.D.

2004 ASBMR MOST OUTSTANDING ABSTRACT AWARD

Supported by an unrestricted educational grant from NPS Pharmaceuticals

Bart Williams, Ph.D.

2004 ASBMR AWARD FOR OUTSTANDING RESEARCH IN THE PATHOPHYSIOLOGY OF OSTEOPOROSIS

Supported by an unrestricted educational grant from NPS Pharmaceuticals

Francesco Grassi

2004 ASBMR PRESIDENT'S BOOK AWARD

Supported by an unrestricted educational grant from Elsevier Science

Hector Rios, D.D.S.

AMERICAN SOCIETY FOR BONE AND MINERAL RESEARCH (ASBMR)

2004 SCIENTIFIC PROGRAM COMMITTEE

President: Robert A. Nissenson, Ph.D.
Program Co-Chair: Marie Demay M.D.
Program Co-Chair: Eric Orwoll, M.D.

John Adams, M.D.
Roy Altman, M.D.
Laura Bachrach, M.D.
Zvi Bar-Shavit, Ph.D.
Doug Bauer, M.D.
Teresita Bellido, Ph.D.
Craig Bentzen, Ph.D.
Daniel Bikle, M.D., Ph.D.
Neal Binkley, M.D.
Allesandro Bisello, Ph.D.
Robert Blank, M.D., Ph.D.
Michael Bliziotes, M.D.
Aubrey Blumsohn, M.D., Ph.D.
Peter Bodine, Ph.D.
J.J. Body, M.D., Ph.D.
Lynda Bonewald, Ph.D.
Jean-Philippe Bonjour, M.D.
Brendan Boyce, M.D.
Maria Luisa Brandi, M.D., Ph.D.
David Burr, Ph.D.
John Caminis, M.D.
Xu Cao, Ph.D.
Jane Cauley, Ph.D.
Timothy Chambers, M.D.
Wenhan Chang, Ph.D.
Roberto Civitelli, M.D.
Cyrus Cooper, D.M., F.R.C.P., F.Med.Sci.
Felicia Cosman, M.D.
Sarah Dallas, Ph.D.
Bess Dawson-Hughes, M.D.
Anne Delany, Ph.D.
Pierre Delmas, M.D., Ph.D.
Henry Donahue, Ph.D.
Patrick Doran, M.D.
Marc Drezner, M.D.
Hisham Drissi, Ph.D.
Patricia Ducy, Ph.D.
Colin Dunstan, Ph.D.
Richard Eastell, M.D.
Michael Econs, M.D.
Ghada El-Hajj Fuleihan, M.D.
David Eyre, Ph.D.
Kenneth Faulkner, Ph.D.
David Findlay, Ph.D.
Larry Fisher, Ph.D.
Lorraine Fitzpatrick, M.D.
Renny Franceschi, Ph.D.
Peter Friedman, Ph.D.
Dana Gaddy, Ph.D.
Robert Gagel, M.D.
Tom Gardella, Ph.D.
Edith Gardiner, Ph.D.
Marielle Gascon-Barre, Ph.D.
Louis Gerstenfeld, Ph.D.
Nandini Ghosh-Choudhury, Ph.D.
Matthew Gillespie, Ph.D.
Francis Glorieux, M.D., Ph.D.
Claus Glueer, Ph.D.
Steven Goldring, M.D.
Catherine Gordon, M.D.
Francesca Gori, Ph.D.
Jeffrey Gorski, Ph.D.
Gail Greendale, M.D.
Susan Greenspan, M.D.
Arg Grigoriadis, Ph.D.
Gloria Gronowicz, Ph.D.
Theresa Guise, M.D.
Kurt Hankenson, D.V.M., Ph.D.
Steven T. Harris, M.D.
Geoff Hendy, Ph.D.
Marc Hochberg, M.D.
Janet Hock, Ph.D.
Lorenz Hofbauer, M.D.
Mike Holick, M.D., Ph.D.
Ingrid Holm, M.D.
Marja Hurley, M.D.
Karl Jepsen, Ph.D.
Robert Jilka, Ph.D.
Olof Johnell, M.D.
Jean-Marc Kaufman, M.D., Ph.D.
Hiroshi Kawaguchi, M.D., Ph.D.
Sundeep Khosla, M.D.
Klaus Klaushofer, M.D.
Michael Kleerekoper, M.D.
Robert Klein, M.D.
Stravoula Kousteni, Ph.D.
Christopher Kovacs, M.D.
Elizabeth Krall, Ph.D., M.P.H.
Barbara Kream, Ph.D.
Subhash Kukreja, M.D.
Nancy Lane, M.D.
Craig Langman, M.D.
Meryl LeBoff, M.D.
Pheobe Leboy, Ph.D.
Michael Levine, M.D.
Nigel Loveridge, Ph.D.
Karen Lyons, Ph.D.
Paul MacDonald, Ph.D.
Luc Malaval, Ph.D.
Pierre Marie, Ph.D.
Lynn Marshall, Sc.D.
Thomas J. Martin, M.D.
Laurie McCauley, Ph.D.
Michael McClung, M.D.
L. Joseph Melton, M.D.
M.Z. Mughal, F.R.C.P.
Gregory Mundy, M.D.
Masaki Noda, M.D., Ph.D.
Philip Osdoby, Ph.D.
Merry Jo Oursler, Ph.D.
Roberto Pacifici, M.D.
Paola Pajevic, M.D., Ph.D
Munro Peacock, M.D.
Sara Peleg, Ph.D.
John Pettifor, Ph.D.
Peter Pietschmann, M.D.
Carol Pilbeam, M.D.,Ph.D.
Anthony Portale, M.D.
Charles Prince, Ph.D.
Darryl Quarles, M.D.
Lawrence Raisz, M.D.
Stuart Ralston, M.D.
Jonathan Reeve, D.M., D.Sc.
Ian Reid, M.D.
Johann Ringe, M.D.
Rene Rizzoli, M.D.
David Roodman, M.D., Ph.D.
Clifford J. Rosen, M.D.
Vicki Rosen, Ph.D.
Patrick Ross, Ph.D.
Clinton Rubin, Ph.D.
Janet Rubin, M.D.
Ego Seeman, M.D.
Peter Selby, M.D.
Elizabeth Shane, M.D.
Caroline Silve, M.D., Ph.D.
Timothy Skerry, Ph.D.
Thomas Spelsberg, Ph.D.
Rene St-Arnaud, Ph.D.
Andrew Stewart, M.D.
Larry Suva, Ph.D.
Pawel Szulc, M.D.
Rajesh Thakker, M.D.
Jon Tobias, M.D.
Dwight Towler, M.D., Ph.D.
Charles Turner, Ph.D.
Andre Uitterlinden, Ph.D.
Erwin Wagner, Ph.D.
Nelson Watts, M.D.
Connie Weaver, Ph.D.
Lee Weinstein, M.D.
Michael Whyte, M.D.
Andre van Wijnen, Ph.D.
Kristine Wiren, Ph.D.
John Wysolmerski, M.D.
Toshiyuki Yoneda, D.D.S., Ph.D.
Marian Young, Ph.D.
Babette Zemel, Ph.D.
Joseph Zmuda, Ph.D.

ADVOCACY COMMITTEE

Janet Rubin, *Acting Chairperson*
Jane E. Aubin, *Ex Officio*
Lorraine A. Fitzpatrick
Bernard P. Halloran
Gordon L. Klein
Laurie J. Moyer-Mileur
Nicola C. Partridge, *Ex Officio*
G. David Roodman
Diane L. Schneider
Paula Stern, *Ex Officio*

ARCHIVES COMMITTEE

Frederick R. Singer, *Chairperson*
Claude D. Arnaud
Norman H. Bell, *Ad Hoc*
John T. Potts, Jr.
Lawrence G. Raisz
Paula H. Stern
Armen H. Tashjian

EDUCATION COMMITTEE

Theresa Guise, *Chairperson*
Teresita M. Bellido
Brendan Boyce
Jan Bruder, *Ad Hoc*
Marja Marie Hurley
Susan M. Ott
Merry Jo Oursler, *Ad Hoc*
Margaret Seton
Marian F. Young

ETHICS ADVISORY COMMITTEE

Julie Glowacki, Ph.D., *Chairperson*
Barbara Lukert
Lawrence Raisz
Dolores Shoback
Clifford J. Rosen

FINANCE COMMITTEE

Marc K. Drezner, *Chairperson*
Sylvia J. Christakos, *Ex Officio*
Diane Cullen
Dolores Shoback
Robert A. Nissenson, *Ex Officio*
Timothy Skerry

LOCAL ARRANGEMENTS COMMITTEE

Susan M. Ott, *Chairperson*
Charles H. Chesnut
Andrea Z. LaCroix
Delia Scholes

MEMBERSHIP DEVELOPMENT COMMITTEE

Andre J. Van Wijnen, *Acting Chairperson*
Peter Bodine
Patricia Collin-Osdoby
Dana Gaddy
Ingrid Holm
Hiroshi Kawaguchi
Pamela G. Robey
Mone Zaidi

NOMINATING COMMITTEE

Clifford J. Rosen, *Chairperson*
Matthew Greenspan
Susan Greenspan
Theresa Guise
Rajiv Kumar
Gary Stein

PROFESSIONAL PRACTICE COMMITTEE

Stuart Silverman, *Chairperson*
Cyrus Cooper
Thomas Einhorn, *Ex Officio*
Ghada El-Hajj Fuleihan
Oscar Gluck
Gillian Hawker
Meryl LeBoff
Michael Lewiecki
Richard Prince
Shonni J. Silverberg

PUBLICATIONS COMMITTEE

Joseph Lorenzo, *Chairperson*
Lynda Bonewald
John A. Eisman, *Ex Officio*
Michael Econs
Murray Favus, *Ex Officio*
Renny T. Franceschi
Douglas Niel
Masaki Noda
L. Darryl Quarles
Anna Teti

PRIMER EDITORIAL BOARD

Murray J. Favus, *Chairperson*
Sylvia Christakos
Michael F. Holick
Michael Kleerekoper
Craig B. Langman
Pamela G. Robey
Elizabeth Shane
Dolores M. Shoback
Andrew F. Stewart
Michael P. Whyte

SCIENCE POLICY COMMITTEE

Philip Osdoby, *Chairperson*
Matthew Gillespie
Barbara Kream
Nancy Lane
Sylvia Christakos
Nicola Partridge, *Ex Officio*
Janet Rubin, *Ad Hoc*
Stuart Silverman, *Ad Hoc*

ASBMR REPRESENTATIVES TO FASEB

Jane E. Aubin
FASEB Board

Philip A. Osdoby
Science Policy Committee

Robert D. Blank
Research Conferences Advisory Committee

Jane B. Lian
Excellence in Science Award Committee

Dolores Shoback
Finance Committee

Paula Stern
FASEB Board and Finance Committee

Julie Glowacki
Federal Funding Consensus Conference

Janet Rubin
Federal Funding Consensus Conference

FASEB

Nicola C. Partridge
FASEB Vice-President for Science Policy

Steven L. Teitelbaum
FASEB Past-President

The ASBMR gratefully acknowledges the following companies and organizations for their support:

2004 SUPPORTERS

PLATINUM LEVEL SUPPORTERS

Alliance for Better Bone Health
(Procter & Gamble Pharmceuticals and Aventis Pharmaceuticals)
Eli Lilly and Company
Merck & Co., Inc.
NPS Pharmaceuticals
Roche and GlaxoSmithKline

SILVER LEVEL SUPPORTER

Amgen

OTHER SUPPORTERS

Abbott Pharmaceuticals
Aventis Pharmaceuticals
Elsevier Science
GlaxoSmithKline Consumer Healthcare
Mission Pharmacal Company
Novartis Pharmaceuticals
The Paget Foundation
Pfizer, Inc.
Procter & Gamble Pharmaceuticals
Wyeth Pharmaceuticals

2004 EXHIBITORS*

Alara, Inc.
ALPCO Diagnostics
The Alliance for Better Bone Health (A partnership between
Procter & Gamble Pharmaceuticals
and Aventis Pharmaceuticals)
Amgen
Bio-Imaging Technologies, Inc.
BIOQUANT Image Analysis Corp.
Biotrace, Inc.
Cambrex
CTBR (A Member of Inveresk Research Group)
DiaSorin, Inc.
Eli Lilly and Company
Elsevier
Elsevier/Saunders/Mosby/Churchill/Butternorth
Eskay Software LLC
Faxitron X-Ray Corporation
Food and Drug Administration
Office of Women's Health
GE Medical Systems Lunar
GlaxoSmithKline Consumer Healthcare
Hologic, Inc.
Humana Press Inc.
Hysitron, Inc.
Image Analysis, Inc.
Imaging Therapeutics, Inc.
Immuno Biological Laboratories (IBL-America)
Immunodiagnostic Systems (IDS)
Immutopics International, LLC
Ina Research
International Bone and Mineral Society (IBMS)
International Society for Clinical Densitometry (ISCD)
Inverness Medical Innovations, Inc.
Kamiya Biomedical Company
Lippincott Williams & Wilkins
Medi USA
Merck US Human Health
Micro Photonics Inc.
MicroMRI, Inc.
Mindways Software, Inc.
Mission Pharmacal Company
Nabi Biopharmaceuticals
National Osteoporosis Foundation (NOF)
Nichols Institute Diagnostics
NIDDK/NIAMS/NIA
NIH Osteoporosis and Related Bone Diseases –
National Resource Center
Nordic Bioscience Diagnostic A/S
Orthometrix, Inc.
Osteogenesis Imperfecta Foundation
Osteometrics, Inc.
Pacific Biometrics Laboratory
The Paget Foundation
Pharmatest Services Ltd.
Quidel Corporation
RATOC System Engineering Co., Ltd.
Roche and GlaxoSmithKline
Scanco USA, Inc.
Scantibodies
SkeleTech, Inc.
Springer
Synarc, Inc.
Wyeth Pharmaceuticals

*as of 08/19/04

GENERAL INFORMATION

ASBMR MEETING LOCATION

All ASBMR 26th Annual Meeting sessions will take place in the Washington State Convention & Trade Center, unless otherwise stated. The Washington State Convention & Trade Center is located at 800 Convention Place, Seattle, Washington, USA.

AUDIO- AND VIDEOTAPING

ASBMR expects that attendees will respect each presenter's willingness to provide free exchange of scientific information without the abridgement of his or her rights or privacy and without the unauthorized copying and use of the scientific data shared during his or her presentation. In addition, ASBMR expects that attendees will respect Exhibitors' desires not to have their products or booths photographed or videotaped. Cameras or recording devices will not be permitted in the Exhibit Halls, the Poster Sessions, or the Oral Scientific Sessions **without the prior written permission of the ASBMR Convention Management.**

The use of cameras, audiotaping devices, and videotaping equipment is strictly prohibited within all Oral Scientific Sessions, the Exhibit Halls, and the Poster Sessions without the express written permission of the ASBMR Convention Management. Unauthorized use of this taping equipment may result in the confiscation of the equipment or the individual may be asked to leave the Scientific Session or Exhibit Hall. These rules will be strictly enforced.

USE OF ASBMR NAME AND LOGO

ASBMR reserves the right to approve use of its name in all material disseminated to the media, public and professionals. ASBMR's name, meeting name, and meeting logo may not be used without permission. Use of the ASBMR logo is prohibited. Materials should be directed to ASBMR Executive Director Joan Goldberg. All ASBMR corporate supporters and exhibitors should share their media outreach plans with the ASBMR Executive Director before release.

No abstract presented at the ASBMR 26th Annual Meeting may be released to the press before its official presentation date and time. Press releases must be embargoed until one hour after the presentation.

ASBMR MEETING CONTENT AND EMBARGO POLICY

Abstracts submitted to the ASBMR 26th Annual Meeting are embargoed - that is, unavailable for public release in written, oral and electronic communications - until one hour *after* the abstract has been presented.

The ASBMR is sensitive to issues of commercial confidentiality and relevant aspects of the U.S. Securities and Exchange Commission (SEC) regulations. Therefore, the ASBMR reminds all readers that all must adhere to the U.S. Securities and Exchange Commission regulations and treat all scientific information as confidential until the embargo has been lifted – one hour after the abstract has been presented. Any reader of, or listener to, ASBMR Annual Meeting content may be viewed as an "insider" by the SEC due to knowledge of information included in abstracts, particularly clinical trial abstracts. SEC regulations may call for criminal penalties for using such information.

COPYRIGHT

DISCLAIMER

CONTINUING MEDICAL EDUCATION CREDITS

The Federation of American Societies for Experimental Biology (FASEB) is accredited by the Accreditation Council for Continuing Medical Education to sponsor continuing medical education for physicians. This activity has been planned and implemented in accordance with the Essential Areas and Policies of the Accreditation Council for Continuing Medical Education through the joint sponsorship of FASEB and the ASBMR.

Category I Continuing Medical Education (CME) credits toward the American Medical Association Physician's Recognition Award will be offered at this meeting. This meeting has been certified for CME Category I Credits on an hour-for-hour basis for up to 48 credit hours. CME application forms will be available in the *On-site Program* Book, which will be distributed at the meeting. There is a $45 application fee, payable to FASEB upon submission of the form. For more information, please contact:

FASEB Office of Scientific Meetings and Conferences
Tel: ..... (301) 530-7010
Fax: ..... (301) 530-7014
E-mail: ..... pmcgovern@faseb.org

Meeting Objective

The ASBMR 26th Annual Meeting is designed to allow members to present new developments in education, research and clinical practice related to bone and mineral metabolism. The program objectives include updating attendees on the recent advances in osteoporosis and other diseases of bone and mineral metabolism, vitamin D and other steroids, peptide calciotropic hormones, mechanical loading and exercise, bone acquisition and pediatric bone disease, cartilage and connective tissue matrix, and growth factors.

As a result of their attendance, participants should have enhanced their knowledge of osteoporosis, other diseases of bone, basic bone biology and its correlation to mineral metabolism, as well as their ability to treat and care for their patients. Attendees should have developed a clearer understanding of the interrelationship among basic research, clinical research and patient care through the discussions that are expected to take place. The ASBMR 26th Annual Meeting program should produce an enhanced appreciation of the investigative, diagnostic and therapeutic aspects of metabolic bone disorders.

Target Audience

The program is designed for researchers, physicians, clinicians, and other allied health professionals with interests in endocrinology, physiology, cell biology, pathology, molecular biology, genetics, epidemiology, internal medicine, rheumatology, orthopedics, dentistry, nephrology, and pharmacology.

DISCLOSURE/CONFLICT OF INTEREST

The Federation of American Societies for Experimental Biology (FASEB) requires that audiences at FASEB-sponsored educational programs be informed of a presenter's (speaker, faculty, author, or contributor) academic and professional affiliations, and the existence of any significant financial interest or other relationship a presenter has with the manufacturer(s) of any commercial product(s) discussed in an educational presentation. This policy allows the listener/attendee to be fully knowledgeable in evaluating the information being presented. The Program will note those speakers who have disclosed relationships, including the nature of the relationship and the associated commercial entity.

All authors of submitted abstracts completed the disclosure statement in the online submission program. Invited speakers who are not required to submit an abstract received a form in the mail that they completed and returned.

Disclosure may include any relationship that may bias one's presentation or which, if known, could give the perception of bias. These situations may include, but are not limited to:

DISCLOSURE KEY

1. stock options or bond holdings in a for-profit corporation or self-directed pension plan
2. research grants
3. employment (full or part-time)
4. ownership or partnership
5. consulting fees or other remuneration
6. non-remunerative positions of influence such as officer, board member, trustee, or public spokesperson
7. receipt of royalties
8. speaker's bureau

For full-time employees of industry or government, the affiliation listed in the *2004 Abstracts* will constitute full disclosure.

Disclosures for invited speakers and abstract presenters are provided at the end of the session listing for invited speakers (see *On-Site Program* book) and directly after the body of an abstract for abstract submissions. If there is no conflict of interest or disclosure listed, this means that the invited speaker and/or abstract presenter indicated no conflicts to disclose.

The disclosure information will correspond to the key above. If disclosures are given, the company name, along with the respective disclosure relationship number will be listed (for example: Company Name, 2, 8.).

2004 ABSTRACTS BOOK

Supported by an unrestricted educational grant from Roche and GlaxoSmithKline

This *2004 Abstracts* book is distributed on-site at the Annual Meeting to all ASBMR members and non-member attendees. Non-member subscribers to *JBMR* will receive the *2004 Abstracts* book by mail. ASBMR members who do not attend the Annual Meeting will receive their copy of the *2004 Abstracts* book by mail following the meeting. The entire ASBMR Scientific Program (invited speaker sessions, lectures, and abstract-based oral and poster presentation information), as well as the 2004 Ancillary Program (working groups and industry-supported symposia), are included in full detail in the *Onsite Program* book and on the ASBMR website at www.asbmr.org.

AWARD PRESENTATIONS

The following ASBMR Awards will be presented immediately following the morning Plenary Symposia and Plenary Lectures in the Room 6ABC of the Washington State Convention and Trade Center — the Gideon A. Rodan Excellence in Mentorship Award, the Fuller Albright Award, the Louis V. Avioli Founders Award, the Frederic C. Bartter Award, the William F. Neuman Award, and the Shirley Hohl Service Award. Please refer to the schedule found in the inside cover of this book for award presentation times.

ASBMR VIRTUAL EXHIBIT HALL

The ASBMR Virtual Exhibit Hall (www.asbmrexhibits.com) showcases exhibitors and their products, many of which are present at this year's ASBMR 26th Annual Meeting. Visitors to the ASBMR Virtual Exhibit Hall are able to learn more about exhibitor's products and services, easily contact them for further information, and enjoy an Exhibit Hall experience at their leisure year-round.

MEET-THE-NIH LOUNGE

Looking for another opportunity to ask U.S. National Institutes of Health and Center for Scientific Review staff about your grant proposal or idea? Plan to visit the Meet-the-NIH Lounge in Room 307 of the Washington State Convention & Trade Center, and get your questions answered. Program staff from the National Institute of Arthritis and Musculoskeletal and Skin Diseases, the National Institute of Diabetes and Digestive and Kidney Diseases, the Center for Scientific Review and more will be on-hand to meet with you.

YOUNG INVESTIGATOR LOUNGE

All Young Investigator Annual Meeting attendees are cordially invited to drop by the Young Investigator's Lounge located in Room 308 of the Washington State Convention & Trade Center. Expand your network of colleagues and make new friends.

ASBMR HALF-DAY SYMPOSIUM: STEM CELL BIOLOGY

This session will be held on Friday, October 1, 2004, from 9:30 am to 12:00 noon in Room 6ABC of the Washington State Convention & Trade Center. Several issues of critical importance to clinicians and researchers in the field will be discussed.

NEW INVESTIGATOR/NEW MEMBER BREAKFAST

Sponsored by the ASBMR Membership Development Committee

Supported by an unrestricted educational grant from Merck & Co., Inc.

The New Investigator/New Member Breakfast will be held on Saturday, October 2, 2004, from 7:00 am to 8:00 am in Room 4C-4 of the Washington State Convention & Trade Center. New Investigators (those early in their research careers) and new ASBMR members are invited to join the ASBMR Council, the Membership Development Committee and colleagues for an informational breakfast. Highlights will include opening remarks by the President of ASBMR, Dr. Robert Nissenson, an overview of the meeting and sessions of particular interest to new investigators and new members by the Program Chairs, Dr. Marie Demay and Dr. Eric Orwoll. Program Directors from US NIH Institutes and Centers, along with ASBMR member senior scientists will be available for discussion at specially marked tables. Attendees should look for table signs advertising a speciality or NIH Institute or Center of interest. Or attendees can make their own signs to join with colleagues who have similar interests. Breakfast will be provided.

SPECIAL SESSION FOR ALLIED HEALTH PROFESSIONALS

Sponsored by the ASBMR Membership Development Committee

Supported by an unrestricted educational grant from Merck & Co., Inc.

This session will be held on Saturday, October 2, 2004, from 12:00 noon to 2:00 pm in Rooms 606-607 of the Washington State Convention & Trade Center. This special session is designed for nurses, clinical research study coordinators, physical therapists, and other allied health professionals working in the area of clinical metabolic bone disease. An overview of the ASBMR 26th Annual Meeting will be given along with lectures on "Male Osteoporosis" and "Use of Bone Turnover Markers in the Evaluatioan of Osteoporosis." There is no additional fee or registration required for this session, nor will food and beverages be served. However, you are welcome to purchase lunch from the concession area of Hall 4ABC in the Washington State Convention & Trade Center.

GRANT WRITING WORKSHOP: TIPS ON GETTING FUNDED

Sponsored by the ASBMR Membership Development Committee

The Grant Writing Workshop will be held on Saturday, October 2, 2004, from 12:30 pm to 2:00 pm, in Room 4C-4 of the Washington State Convention & Trade Center. New investigators (those early in their research careers) and new members are invited to attend a workshop on the grant writing process, including advice on grantsmanship and the peer-review process. A panel discussion, based on questions and feedback from the audience, will be led by U.S. NIH represenatives and experienced ASBMR members from academia, including an international representative. Funding source information and opportunities will also be provided. This is a valuable opportunity for new investigators to gain helpful tips and information directly from these representatives and to become familiar with the different programs. There is no additional fee or registration required for this session, nor will food or beverages be served. However, attendees are welcome to purchase lunch from the concession area in the Hall 4ABC in the Washington State Convention & Trade Center.

BIOTECHNIQUES WORKSHOP: BIOLUMINESCENT IMAGING

Sponsored by the ASBMR Education Committee

This session will take place from 12:30 pm to 2:00 pm on Sunday, October 3, 2004, in Rooms 611-615 of the Washington State Convention & Trade Center. There is no additional fee or registration required for this session, nor will food and beverages be served. However, you are welcome to purchase lunch from the concession area in Hall 4ABC in the Washington State Convention & Trade Center.

RESPONSIBLE CONDUCT IN BONE AND MINERAL RESEARCH

Sponsored by the ASBMR Membership Development Committee

The session on Responsible Conduct in Bone and Mineral Research will be held on Sunday, October 3, 2004, from 12:30 pm to 2:00 pm in Rooms 602-604 of the Washington State Convention & Trade Center. This session, geared to new investigators, will begin with an overview of the various ethical issues that basic and clinical investigators encounter during their research careers. This will be followed by presentations that focus on: 1) the ethical issues of research publications, and 2) human subjects in research. There is no additional fee or registration required for this session, nor will food and beverages be served. However, you are welcome to purchase lunch from the concession area in Hall 4ABC in the Washington State Convention & Trade Center.

CAREER OPTIONS FOR SCIENTISTS

Sponsored by the ASBMR Education Committee

The Career Options for Scientists Workshop will be held on Monday, October 4, 2004, from 12:30 pm to 2:00 pm in Rooms 611-614 of the Washington State Convention & Trade Center. This year's Workshop will focus on "Private Choices – Professional Career Building: Navigating One's Career." Three speakers will give their perspectives on how they balance career and family choices. This workshop is organized for scientists at all levels in their careers, but particularly those who face challenging situations in their private lives, such as raising a family. There is no additional fee or registration required for this session, nor will food and beverages be served. However, you are welcome to purchase lunch from the concession area in Hall 4ABC in the Washington State Convention & Trade Center.

CLINICAL ROUNDTABLES

The Clinical Roundtable sessions are two informal sessions geared toward the practicing clinician, offering insight into treatment and diagnosis of bone diseases. These two special sessions will feature a focused discussion on topical issues of clinical relevance. Each session will feature two speakers and include ample time for discussion. The clinical roundtable on "Combination Therapy for Osteoporosis" will be held on Sunday, October 3, 2004, from 12:30 pm to 1:30 pm in Rooms 606-607 of the Washington State Convention & Trade Center. The session on "How Long Should We Treat with Anti-Resportive Drugs?" will be held on Monday, October 3, 2004, from 12:30 pm to 1:30 pm in Rooms 606-607 of the Washington State Convention & Trade Center. There is no additional fee or registration required for these sessions, nor will food and beverages be served. However, you are welcome to purchase lunch from the concession area in Hall 4ABC in the Washington State Convention & Trade Center.

MEET-THE-PROFESSOR SESSIONS

The Meet-the Professor Sessions are a series of informal sessions designed to provide an opportunity for meeting attendees to interact with experts in an intimate setting and discuss specific clinical and research topics. Interested individuals must sign up on-site for the sessions; tickets are extremely limited and are required for admission. These sessions are held from 12:30 pm to 1:30 pm on Friday, Saturday, Sunday, and Monday of the meeting. If you are interested in attending one of these sessions, we encourage you to sign up at your earliest convenience at the Registration Desk at the Washington State Convention & Trade Center. There is no additional fee required for this session, nor will food and beverages be served. However, you are welcome to purchase lunch from the concession area in Hall 4ABC in the Washington State Convention & Trade Center.

WELCOME RECEPTION AND PLENARY POSTER SESSION

Supported by an unrestricted educational grant from Merck & Co., Inc.

On Friday, October 1, 2004, from 5:15 pm to 7:00 pm, attendees and registered guests are invited to attend the ASBMR Welcome Reception and Plenary Poster Session in Exhibit/Poster Hall 4ABC of the Washington State Convention & Trade Center . Simply display your badge for admission. Guests may purchase a badge for $30 at registration, which will allow entrance to the Welcome Reception and Exhibit Hall.

ASBMR SOCIAL EVENT

Supported by Amgen

Experience Music Project (EMP) is a hands-on interactive museum that entertains and engages visitors of all ages as they discover and explore American popular music including rock, jazz, hip-hop, punk, soul, gospel, country and blues. EMP is the place to see amazing music-related artifacts including musical instruments like one of the first electric guitars, an extensive recorded sound archive, film, photographs, fanzines, stage costumes, hand-written song lyrics and rare song sheets. You can find your own rhythm and cut a CD in the museum's Sound Lab or jump up on stage with friends to start your own band and live out your rock'n roll fantasies. ASBMR guests will have exclusive access to the entire museum for this evening. Additionally, ASBMR will host a live dance band in the Sky Church - a room at the museum with a 70-foot high ceiling and the world's largest indoor video screen. So grab a quick dinner after the day's sessions and join us for drinks, desserts, dancing and a music experience you won't forget.

The EMP is located near Seattle's famous Space Needle at the Seattle Center. ASBMR guests can use their badges for a free ride on the monorail for the two-minute trip from downtown Seattle to the Seattle Center. Staff will direct you for the short walk from the monorail station to the museum. Please check for signs at the ASBMR registration desk regarding the monorail. At the time of this printing it is under repair. If the monorail is unavailable, shuttle buses will be provided.

Tickets are required for admission and must be purchased in advance for $30. You are encouraged to pre-register for this event. If available tickets remain, they will be sold on-site at the ASBMR Registration Counter in the South Lobby of the Washington State Convention & Trade Center.

REGISTRATION HOURS

All on-site registration will take place in the South Lobby of the Washington State Convention & Trade Center.

Thursday, September 30, 2004 ..... 9:00 am - 5:00 pm
Friday, October 1, 2004 ..... 7:00 am - 6:30 pm
Saturday, October 2, 2004 ..... 7:00 am - 5:30 pm
Sunday, October 3, 2004 ..... 7:00 am - 5:30 pm
Monday, October 4, 2004 ..... 7:30 am - 5:00 pm

EXHIBIT HALL HOURS

The Exhibit Hall is located in Hall 4ABC of the Washington State Convention & Trade Center. For meeting attendees, **lunch will be available for purchase in the hall** during Exhibit hours.

Friday, October 1, 2004 ..... 5:15 pm - 7:00 pm
Saturday, October 2, 2004 ..... 9:15 am - 4:30 pm
Sunday, October 3, 2004 ..... 9:30 am - 4:30 pm
Monday, October 4, 2004 ..... 9:30 am - 4:30 pm

SPEAKER READY ROOM

Supported by an unrestricted educational grant from Mission Pharmacal Company

Speakers must check into the Speaker Ready Room 24 hours in advance of their presentation. At that time, speakers may review their slides. The Speaker Ready Room is located in Room 304 of the Washington State Convention & Trade Center. Review of slides must occur at least 24 hours prior to your presentation. The Speaker Ready Room will be open during the following times:

Speaker Ready Room Hours

Thursday, September 30 ..... 12:00 noon – 5:00 pm
Friday, October 1 ..... 7:00 am – 5:30 pm
Saturday, October 2 ..... 7:00 am – 6:00 pm
Sunday, October 3 ..... 7:00 am – 5:30 pm
Monday, October 4 ..... 7:00 am – 5:30 pm
Tuesday, October 5 ..... 7:00 am – 11:00 am

SPEAKER LOUNGE

Supported by an unrestricted educational grant from the Alliance for Better Bone Health
(Procter & Gamble Pharmaceuticals and Aventis Pharmaceuticals)

The Speaker Lounge will be located in Room 305 of the Washington State Convention & Trade Center. The lounge provides a relaxing atmosphere for the oral presenters and invited speakers to rest, mingle with one another and to catch up on office work. The room will be equipped with computers, fax, copier, phone/modem lines, snacks and beverages, sofas and chairs. The Speaker Lounge will be available from Friday, October 1, to Monday, October 4, from 7:00 am to 4:00 pm, and on Tuesday, October 5, from 7:00 am to 11:00 am.

POSTER SESSIONS

All poster sessions will be held in Exhibit/Poster Hall 4ABC of the Washington State Convention & Trade Center. Authors must be at their posters for 1 hour of the designated poster sessions on Saturday through Monday and must be available to answer questions during this period, as well as during the designated morning or afternoon coffee breaks. Authors of odd-numbered posters should be present from 9:30 am to 10:00 am and from 11:45 am to 12:30 pm on their designated days. Authors of even-numbered posters should be present from 1:30 pm to 2:30 pm and from 4:00 pm to 4:30 pm

Poster numbers are listed in this *2004 Abstracts* book prefixed with a letter that denotes the day of presentation, i.e., F (Friday), SA (Saturday), SU (Sunday), M (Monday). These letters are not posted on the boards. **Presenters should mount their posters on the board bearing their assigned numbers, disregarding the letter prefix. ASBMR accepts no liability for posters or poster materials and will not adjudicate disputes between abstract presenters.**

Plenary Poster presenters and Young Investigator Award recipients presenting posters should mount their posters on Friday, October 1, 2004, between 3:00 pm and 5:00 pm. Plenary Poster presenters and Young Investigator Award recipients presenting posters are expected to be present during the Welcome Reception and Plenary Poster Session on Friday, October 1, from 5:15 pm to 7:00 pm. Plenary Poster presenters and Young Investigator Award recipients presenting posters will follow the odd/even hours for presenters during Poster Session I on Saturday, October 2, 2004. Plenary Posters will remain posted until Saturday, October 2, at 6:00 pm. Young Investigator Award posters will remain posted for the duration of the meeting.

Please note that children 12 years of age and under will not be permitted in the poster area or the Exhibit Hall at any time.

Presenter Check-in:
Since only poster presenters are allowed in the Exhibit/Poster Hall during the below poster set-up and dismantle hours, please go to the poster presenter check-in table to receive a security pass. The table will be located by the entrance to the Hall 4C. To speed the check-in process, please have your poster board number ready.

NOTE: Posters remaining after Poster Dismantling times will be discarded.

POSTER PRESENTATION SCHEDULE

	Poster Set-Up	Posters Open	Authors Present	Dismantle Posters
Friday, Oct. 1 **Welcome Reception/** **Plenary Poster Session**	3:00 - 5:00 pm	5:15 pm – 7:00 pm	5:15 - 7:00 pm Plenary Posters & YIA Award Posters	Do not dismantle.
Saturday, Oct. 2 **Poster Session I**	7:30 – 8:00 am	8:00 am – 6:00 pm	9:30 am - 10:00 am for Odd # 11:30 am - 12:30 pm for Odd# 1:30 pm - 2:30 pm for Even # 4:00 pm - 4:30 pm for Even #	6:00 – 6:30 pm Saturday Posters Plenary Posters
Sunday, Oct. 3 **Poster Session II**	7:30 – 8:00 am	8:00 am – 6:00 pm	9:30 am - 10:00 am for Odd # 11:30 am - 12:30 pm for Odd# 1:30 pm - 2:30 pm for Even # 4:00 pm - 4:30 pm for Even #	6:00 – 6:30 pm Sunday Posters
Monday, Oct. 4 **Poster Session III**	7:30 – 8:00 am	8:00 am – 4:30 pm	9:30 am - 10:00 am for Odd # 11:30 am - 12:30 pm for Odd# 1:30 pm - 2:30 pm for Even # 4:00 pm - 4:30 pm for Even #	4:30 – 5:00 pm Monday Posters YIA Award Posters

ASBMR MEMBERSHIP

The ASBMR Membership Booth will be located in booth 218 in Exhibit Hall 4ABC. Come by and meet the ASBMR staff, pick up information about the Society, and check out the on-line versions of the *Journal of Bone and Mineral Research* and 5th Edition of the *Primer on Metabolic Bone Diseases and Disorders of Mineral Metabolism*, as well as the ASBMR Bone Curriculum website. You will also be able to order copies of the 5th Edition of the *Primer.*

The ASBMR Membership Counter is located in the Registration Area in the South Lobby and will be prepared to accept 2005 ASBMR membership renewal payments.

ASBMR JOB PLACEMENT SERVICE

The ASBMR Job Placement Service is easily accessible year-round on-line. You can access the most up-to-date job and candidate listings using the ASBMR Job Placement Service Website. Simply submit your resume or job announcement using the on-line forms at **www.asbmr.org**. After your forms are submitted and payment is received, you will be able to use your self-assigned login name and password to access the On-line Placement Service database anytime you wish.

Employers enrolled in the service will be entitled to display unlimited job announcements on-line and on-site at the meeting on the bulletin board located in the Registration Area of the South Lobby of the Washington State Convention & Trade Center. In addition, employers will have access to candidates' Curricula Vitae.

Employers and candidates may request further information by accessing the ASBMR On-line Job Placement Service at www.asbmr.org.

ASBMR MEDIA OFFICE

The ASBMR Media Office will be in operation during the ASBMR 26th Annual Meeting to facilitate media-related activities during the meeting. The Media Office will be located in Room 306 of the Washington State Convention & Trade Center.

Hours of Operation

Friday, October 1, 2004	9:00 am - 5:00 pm
Saturday, October 2, 2004	8:00 am - 5:00 pm
Sunday, October 3, 2004	8:00 am - 5:00 pm
Monday, October 4, 2004	8:00 am - 5:00 pm
Tuesday, October 5, 2004	8:00 am - 11:00 am

SPECIAL NOTICES — SAFETY TIPS

- Remove your convention badge outside the meeting sites. Do not wear your badge outside or advertise that you're a visitor and not familiar with your surroundings.
- Walk with another person rather than alone. Avoid alleys, walkways between buildings, and deserted parking lots.
- Remain alert, be aware of your surroundings, and carry your handbag in front of you.
- While in your hotel room, always lock your door. Know where emergency exits are in your hotel.
- Place any valuables in a hotel safety deposit box rather than leaving them in your room or carrying them with you.
- Keep a copy of your passport and travel papers in a safe place.

DOES THE ASBMR HAVE YOUR EMAIL ADDRESS?

Next year all important ASBMR Annual Meeting materials will be found on the ASBMR Website… and we will broadcast email to everyone on our correspondence list early notice of the Call for Abstracts, Preliminary Program, Registration and Housing information, Abstracts Online, and more! **So you don't miss out** on early notices and regular updates, please send all your contact information to the ASBMR, including your email address.

American Society for Bone and Mineral Research
2025 M Street, NW, Suite 800
Washington, DC 20036-3309, USA
Tel: (202) 367-1161
Fax: (202) 367-2161
E-mail: ASBMR@smithbucklin.com
Internet: www.asbmr.org

ANNUAL MEETING EVALUATION

The 2004 Annual Meeting Evaluation will be accessible online following the 26th Annual Meeting. An email will be sent to all meeting attendees who provided their email addresses at the time of registration. The email will provide a hyperlink to the online evaluation site. It will also be accessible via the ASBMR home page at www.asbmr.org. We strongly encourage and welcome all attendees to provide us with feedback on the meeting. Your input is very important to us.

FUTURE ANNUAL MEETING DATES

September 23-27, 2005
ASBMR 27th Annual Meeting
Nashville, Tennessee, USA

September 15-19, 2006
ASBMR 28th Annual Meetinhg
Philadelphia, Pennsylvania, USA

September 16-20, 2007
ASBMR 29th Annual Meeting
Honolulu, Hawaii, USA

September 12-16, 2008
ASBMR 30th Annual Meeting
Montreal, Quebec, Canada

HOW THE PROGRAM WAS SELECTED

The 2004 ASBMR Program Co-Chairs and President began the process of program development well before the 2003 Annual Meeting in Minneapolis. We are grateful for the advice and suggestions from previous Program Co-Chairs. The overall structure of the 2004 meeting is similar to that of recent ASBMR meetings with an emphasis on short abstract presentations in oral and poster format. Each day opens with a plenary session: the Gerald D. Aurbach Memorial Lecture on Saturday, a Plenary Symposium on BMP Antagonists on Sunday and a second Plenary Symposium on New Insights into Bone Strength will be held on Monday, and the Louis V. Avioli Memorial Lecture closing the meeting on Tuesday. State-of-the-Art Sessions are scheduled for Saturday and Sunday afternoons. An effort was made to select State-of-the-Art topics that have not been covered in recent ASBMR Annual Meetings. A symposium on exciting advances in stem cell biology will be held on Friday morning. The four Mini-Symposia on Friday afternoon cover diverse clinical and basic science areas that were selected by the Program Co-Chairs with substantial input from the ASBMR membership via web based surveys and 2003 Annual Meeting online evaluations.

A major scientific focus of the meeting continues to be the presentation of abstracts in oral and poster formats. Each Program Co-Chair was responsible for approximately half of the abstract program (nearly 2000 abstracts were submitted). The same abstract categories were utilized as for the 2003 Annual Meeting. Program Co-Chairs, in consultation with the President, identified Chairs for each category. Nine additional reviewers were selected for each category, and these were chosen to reflect the diverse geographical distribution of our membership. Authors were asked to identify up to three categories into which their abstracts would fit, in order of priority. Program Co-Chairs then confirmed the most suitable category for review, re-assigning about 20% of abstracts to other categories based on content. Abstracts sent for review were blinded. Reviewers were instructed to abstain from reviewing any abstract with which they were in conflict. Abstracts were rated by reviewers on a 5-point scale, and the scores were tabulated by Coe-Truman Technologies, ASBMR's abstract processing vendor. The highest rated abstracts from each category were selected for the plenary oral sessions. The next highest rated abstracts were selected for concurrent oral sessions. Highly rated abstracts that were not selected for the oral program were assigned to the plenary poster session. Overall, approximately 11% of the submitted abstracts were assigned to the oral program. Each category had similar percentage representation on the oral program, with only minor variation due to differences in the spread of scoring between categories.

We have again included a Late-Breaking Abstract Session at the 2004 Annual Meeting. It will be held after the Plenary Symposium on Monday morning, and will run concurrently with a combined basic and clinical Plenary Oral Session. This session is for abstracts of broad interest where the findings were not available in time for submission at the regular abstract deadline. The procedure for selection of abstracts for the Late-Breaking Abstract Session is similar to that used for the other oral sessions and the merit of these abstracts must reach or exceed the level of those selected for the regular oral program.

As in previous years, the recipients of the ASBMR Young Investigator Awards, the ASBMR Outstanding Abstract Award, the ASBMR Award for Outstanding Research in the Pathophysiology of Osteoporosis, and the ASBMR President's Book Award were selected on the basis of abstract score and eligibility.

We are grateful to our many colleagues who provided suggestions and advice about topics and speakers for symposia and lectures. We also thank the abstract reviewers and the staff of the ASBMR Business Office, with special thanks to Lizzy Koenst and Amy Werner. Finally, we appreciate the valuable input of the staff of Coe-Truman Technologies. We believe that the hard work and dedication of everyone involved has again resulted in an outstanding scientific program for our annual meeting.

Sincerely,

Robert A. Nissenson, Ph.D., *President*
Marie Demay, M.D., *Program Co-Chair*
Eric Orwoll, M.D., *Program Co-Chair*

FRIDAY, OCTOBER 1, 2004
DAY-AT-A-GLANCE

Time/Event/Location
All events will be held at the Washington State Convention & Trade Center, unless otherwise noted.)

9:30 am - 12:00 noon
Stem Cell Biology Symposium
Room 6ABC

12:30 pm - 1:30 pm
Meet-the-Professor Sessions
Rooms 601, 615-620
Ticket required. See ticket for room assignment.

2:00 pm - 3:30 pm
Mini-Symposium A: Craniofacial Development
Room 6ABC

2:00 pm - 3:30 pm
Mini-Symposium B: Paget's Disease
Room 6E

3:45 pm - 5:15 pm
Mini-Symposium C: PTH/PTHrP Actions
Room 6E

3:45 pm - 5:15 pm
Mini-Symposium D: Pediatric Bone Biology: Disorders of Development and Growth
Room 6ABC

5:15 pm - 7:00 pm
Welcome Reception and Plenary Poster Session
Exhibit Hall 4ABC

Ancillary Program - Working Groups

7:00 pm - 9:30 pm
Fluid Flow in Bone Working Group
Room 4C-4

7:00 pm - 9:30 pm
Nutrition and Bone Health Working Group
Rooms 602-604

7:00 pm - 9:30 pm
Working Group on Musculoskeletal Rehabilitation for Patients with Osteoporosis
Rooms 618-620

7:15 pm - 9:45 pm
In Vivo Working Group
Rooms 608-609

7:15 pm - 10:00 pm
Working Group on Biochemical Markers of Bone Turnvover
Rooms 611-614

Ancillary Program - Industry-Supported Symposia (ISS)

7:00 pm - 9:30 pm
Changes on the Horizon? The Future of Osteoporosis Diagnosis, Prevention and Management
Grand Ballroom, Sheraton Seattle Hotel & Towers

7:00 pm - 9:00 pm
Optimizing the Treatment of Osteoporosis: Evolutions and Solutions
Grand Ballroom 1 and 2, The Westin Seattle

SATURDAY, OCTOBER 2, 2004
DAY-AT-A-GLANCE

Time/Event/Location
(All events will be held at the Washington State Convention & Trade Center, unless otherwise noted.)

7:00 am - 8:00 am
New Investigator/New Member Breakfast
Room 4C-4

8:00 am - 6:00 pm
Posters Open
Exhibit Hall 4ABC

8:00 am - 8:10 am
Welcome and Announcements
Room 6ABC

8:10 am - 9:10 am
Gerald D. Aurbach Memorial Lecture
Room 6ABC

9:10 am - 9:15 am
Presentation of William F. Neuman Award
Room 6ABC

9:15 am - 4:30 pm
Exhibits Open
Exhibit Hall 4ABC

9:15 am - 9:20 am
Presentation of Fuller Albright Award
Room 6ABC

9:20 am - 9:25 am
Presentation of Gideon A. Rodan Excellence in Mentorship Award
Room 6ABC

9:25 am - 9:30 am
Presentation of Gideon and Sevgi Rodan IBMS Fellowship Awards
Room 6ABC

9:30 am - 10:00 am
Coffee Break
Odd Posters Present
Exhibit Hall 4ABC

10:00 am - 11:30 am
Plenary Orals I - Basic (1001-1006)
Room 6E

Plenary Orals II - Clinical/Translational (1007-1012)
Room 6ABC

11:30 am - 2:30 pm
Poster Session I (Presentations SA001 - SA589)
11:30 am - 12:30 pm Odd numbers
1:30 pm - 2:30 pm Even numbers
Exhibit Hall 4ABC

12:00 noon - 2:00 pm
Special Session for Allied Health Professionals
Rooms 606-607

12:30 pm - 1:30 pm
Meet-the-Professor Sessions
Rooms 601, 615-620
Ticket required. See ticket for room assignment.

12:30 pm - 2:00 pm
Grant Writing Workshop: Tips on Getting Funded
Room 4C-4

2:30 pm - 4:00 pm
Concurrent Oral Sessions

1) Osteoblasts I (1013 - 1018)
Room 6E

2) Osteoporosis - Epidemiology I (1019 - 1024)
Room 6ABC

3) Osteoclasts I Rooms (1025 - 1030)
Rooms 608-609

4) Mechanical Loading: In Vitro (1031 - 1036)
Rooms 602-604

5) BMPs and Other Growth Factors I (1037-1042)
Rooms 611-614

6) Bone Acquisition and Pediatric Bone Disease I - (1043-1048)
Rooms 606-607

4:00 pm - 4:30 pm
Coffee Break
Even posters present
Exhibit Hall 4ABC

4:30 pm - 6:00 pm
State-of-the-Art Lectures A: Hormone Action on Non-Traditional Targets
Room 6ABC

4:30 pm - 6:00 pm
State-of-the-Art Lectures B: Collaborating with Industry: Issues for Individual Investigators
Room 6E

6:00 pm - 7:00 pm
ASBMR Annual Business Meeting
Rooms 611-614

Ancillary Program - Working Groups

7:00 pm - 9:15 pm
Non-Invasive Assessment of Trabecular Bone Microarchitecture Working Group
Room 606-607

7:00 pm - 10:00 pm
Post Transplantation Bone Disease Working Group
Rooms 618-620

7:00 pm - 10:00 pm
Working Group on Hormone-Receptor Interactions
Rooms 608-609

7:15 pm - 9:30 pm
Bone Remodeling and Stress Fracture Working Group
Rooms 602-604

7:15 pm - 10:00 pm
Pediatric Bone and Mineral Working Group
Room 4C-4

Ancillary Program - Industry-Supported Symposia (ISS)

7:00 pm - 9:30 pm
The Evolving Management of Bone Disease: Changes on the Horizon
Room 6E

7:00 pm - 10:00 pm
The Role of Bone Strength in the Diagnosis and Treatment of Osteoporosis
Grand Ballroom, Sheraton Seattle Hotel & Towers

SUNDAY, OCTOBER 3, 2004
DAY-AT-A-GLANCE

Time/Event/Location
(All events will be held at the Washington State Convention & Trade Center, unless otherwise noted.)

Ancillary Program - Industry-Supported Symposia (ISS)

6:00 am - 8:00 am
Parathyroid Hormone: Meeting the Challenge of Osteoporosis
Grand Ballroom, Sheraton Seattle Hotel &Towers

8:00 am - 6:00 pm
Posters Open
Exhibit Hall 4ABC

8:00 am - 9:30 am
Plenary Symposium I: BMP Antagonists: Basic Science to Human Disease
Room 6ABC

9:30 am - 4:30 pm
Exhibits Open
Exhibit Hall 4ABC

9:30 am - 9:35 am
Presentation of Frederic C. Bartter Award
Room 6ABC

9:35 am - 10:00 am
Coffee Break
Odd Posters Present
Exhibit Hall 4ABC

10:00 am - 11:30 am
Plenary Orals I - Basic (1049 - 1054)
Room 6E

Plenary Orals II - Clinical/Translational (1055 - 1060)
Room 6ABC

11:30 am - 2:30 pm
Poster Session II (Presentations SU001 - SU586)
11:30 am - 1:30 pm Odd numbers
1:30 pm - 2:30 pm Even numbers
Exhibit Hall 4ABC

12:30 pm - 1:30 pm
Clinical Roundtable: Combination Therapy for Osteoporosis
Rooms 606-607

12:30 pm - 1:30 pm
Meet-the-Professor Sessions
Rooms 601, 615-620
Ticket Required. See ticket for room assignment.

12:30 pm - 2:00 pm
Responsible Conduct in Bone and Mineral Research
Rooms 602-604

2:30 pm - 2:00 pm
Biotechniques Workshop: Molecular Bioluminescent Imaging
Rooms 611-614

2:30 pm - 4:00 pm
Concurrent Oral Sessions

7) PTH Actions (1061-1066)
Room 6E

8) Osteoporosis - Diagnosis and Treatment (1067-1072)
Room 6ABC

9) Bone, Cartilage, Connective Tissue Matrix (1073-1078)
Rooms 611-614

10) Genetics of Bone and Mineral Disorders (1079-1084)
Rooms 606-607

11) Steroids: Molecular (1085-1090)
Rooms 608-609

12) Cancer and Bone (1091-1096)
Rooms 602-604

4:00 pm - 4:30 pm
Coffee Break
Even Posters Present
Exhibit Hall 4ABC

4:30 pm - 6:00 pm
State-of-the-Art Lecture A: Osteoclast Biology
Room 6ABC

4:30 pm - 6:00 pm
State-of-the-Art Lecture B: Research Methods in Skeletal Genetics
Room 6E

8:30 pm - 11:30 pm
ASBMR Social Event
Experience Music Project at Seattle Center
Ticket required.

MONDAY, OCTOBER43, 2004
DAY-AT-A-GLANCE

Time/Event/Location
(All events will be held at the Washington State Convention & Trade Center, unless otherwise noted.)

8:00 am - 4:30 pm
Posters Open
Exhibit Hall 4ABC

8:00 am - 9:30 am
Plenary Symposium II: New Insights Into Bone Strength
Room 6ABC

9:30 am - 4:30 pm
Exhibits Open
Exhibit Hall 4ABC

9:30 am - 9:35 am
Presentation of Shirley Hohl Service Award
Room 6ABC

9:35 am - 10:00 am
Coffee Break
Odd Posters Present
Exhibit Hall 4ABC

10:00 am - 11:30 am
Plenary Oral Session (1097-1102)
Room 6ABC

10:00 am - 11:30 am
Late-Breaking Abstracts Session
Room 6E

11:30 am - 2:30 pm
Poster Session III (Presentations M001 - M585)
11:30 am - 12:30 pm Odd numbers
1:30 pm - 2:30 pm Even numbers
Exhibit Hall 4ABC

12:30 pm - 2:00 pm
Career Options for Scientists Workshop
Rooms 611-614

12:30 pm - 2:00 pm
Clinical Roundtable: How Long Should We Treat with Anti-Resorptive Drugs?
Rooms 606-607

12:30 noon - 1:30 pm
Meet-the-Professor Sessions
Rooms 601, 615-620
Ticket required. See ticket for room assignment.

2:30 pm - 4:00 pm
Concurrent Oral Sessions

13) Osteoblasts II - *(1103-1108)*
Room 6E

14) Osteoporosis - Epidemiology II - *(1109-1114)*
Room 6ABC

15) Steroid Receptor Actions - (1115-1120)
Rooms 602-604

16) Osteoporosis - Pathophysiology I - (1121-1126)
Rooms 608-609

17) Chondrocyte Biology - (1127-1132)
Rooms 606-607

18) Bone Acquisition and Pediatric Bone Disease - (1133-1138)
Rooms 611-614

4:00 pm - 4:30 pm
Coffee Break
Even Posters Present
Exhibit Hall 4ABC

4:30 pm - 6:00 pm
Concurrent Oral Sessions

19) Osteoblasts III - (1139-1144)
Room 6E

20) Mechanical Loading: In Vivo - (1145-1150)
Rooms 602-604

21) Osteoporosis - Pathophysiology II - *(1151-1156)*
Rooms 608-609

22) Other Disorders of Bone and Mineral Metabolism I- (1157-1162)
Rooms 606-607

23) Peptide Hormones - (1163-1168)
Rooms 611-614

24) Osteoporosis - Treatment I - (1169-1174)
Room 6ABC

Ancillary Program - Working Groups

6:15 pm - 8:35 pm
Physical Activity Working Group
Rooms 608-609

6:30 pm - 9:30 pm
Adult Bone and Mineral Working Group
Room 4C-4

6:30 pm - 8:30 pm
Molecular Biology and Pathology of Bone Working Group
Rooms 611-614

6:30 pm - 9:30 pm
Vitamin D Working Group
Rooms 602-604

7:00 pm - 9:15 pm
Working Group on Aging and the Human Skeleton
Rooms 615-617

Ancillary Program - Industry-Supported Symposia (ISS)

6:00 pm - 9:00 pm
The Clinical Outlook on RANKL: A Future Treatment Target for Osteoporosis and Cancer-Related Bone Diseases?
Grand Ballroom, The Westin Seattle

6:00 pm - 9:00 pm
An Evidence-Based Approach to the Clinical Management of Osteoporosis
Grand Ballroom, Sheraton Seattle Hotel & Towers

TUESDAY, OCTOBER 5, 2004
DAY-AT-A-GLANCE

Time/Event/Location
(All events will be held at the Washington State Convention & Trade Center, unless otherwise noted.)

8:00 am - 9:00 am
Louis V. Avioli Memorial Lecture
Room 6ABC

9:00 am - 9:05 am
Presentation of Louis V. Avioli Founders Award
Room 6ABC

9:05 am - 9:30 am
Coffee Break
East Lobby

9:30 am - 11:30 am
Concurrent Oral Sessions

25) BMPs and Other Growth Factors II - (1175-1182)
Rooms 608-609

26) Osteoporosis - Epidemiology III - (1183-1190)
Room 6E

27) Osteoclasts II - (1191-1198)
Rooms 602-604

28) Other Disorders of Bone and Mineral Metabolism II - (1199-1206)
Rooms 606-607

29) Osteoblasts IV - (1207-1214)
Rooms 611-614

30) Osteoporosis - Treatment II - (1215-1222)
Room 6ABC

11:30 am
Adjourn

ABSTRACT PRESENTATION KEY

Abstract Number	Session Type	Date	Presentation Time	Room
1000-1006	Plenary Oral I – Basic	Saturday, Oct. 2, 2004	10:00 – 11:30 am	Room 6E
1007-1012	Plenary Oral II – Clinical	Saturday, Oct. 2, 2004	10:00 – 11:30 am	Room 6ABC
1013-1018	Concurrent Oral 1: Osteoblasts I	Saturday, Oct. 2, 2004	2:30 – 4:00 pm	Room 6E
1019-1024	Concurrent Oral 2: Osteoporosis – Epidemiology I	Saturday, Oct. 2, 2004	2:30 – 4:00 pm	Room 6ABC
1025-1030	Concurrent Oral 3: Osteoclasts I	Saturday, Oct. 2, 2004	2:30 – 4:00 pm	Rooms 608-609
1031-1036	Concurrent Oral 4: Mechanical Loading – In Vitro	Saturday, Oct. 2, 2004	2:30 – 4:00 pm	Rooms 602-604
1037-1042	Concurrent Oral 5: BMPs and Other Growth Factors I	Saturday, Oct. 2, 2004	2:30 – 4:00 pm	Rooms 611-614
1043-1048	Concurrent Oral 6: Bone Acquisition and Pediatric Bone Disease I	Saturday, Oct. 2, 2004	2:30 – 4:00 pm	Rooms 606-607
1049-1054	Plenary Oral I – Basic	Sunday, Oct. 3, 2004	10:00 – 11:30 am	Room 6E
1055-1060	Plenary Oral II – Clinical	Sunday, Oct. 3, 2004	10:00 – 11:30 am	Room 6ABC
1061-1066	Concurrent Oral 7: PTH Actions	Sunday, Oct. 3, 2004	2:30 – 4:00 pm	Room 6E
1067-1072	Concurrent Oral 8: Osteoporosis – Diagnosis and Treatment	Sunday, Oct. 3, 2004	2:30 – 4:00 pm	Room 6ABC
1073-1078	Concurrent Oral 9: Bone, Cartilage, Connective Tissue Matrix	Sunday, Oct. 3, 2004	2:30 – 4:00 pm	Rooms 611-614
1079-1084	Concurrent Oral 10: Genetics of Bone and Mineral Disorders	Sunday, Oct. 3, 2004	2:30 – 4:00 pm	Rooms 606-607
1085-1090	Concurrent Oral 11: Steroids – Molecular	Sunday, Oct. 3, 2004	2:30 – 4:00 pm	Rooms 608-609
1091-1096	Concurrent Oral 12: Cancer and Bone	Sunday, Oct. 3, 2004	2:30 – 4:00 pm	Rooms 602-604
1097-1102	Plenary Oral – Basic and Clinical/ Translational	Monday, Oct. 4, 2004	10:00 – 11:30 am	Room 6ABC
1103-1108	Concurrent Oral 13: Osteoblasts II	Monday, Oct. 4, 2004	2:30 – 4:00 pm	Room 6E
1009-1114	Concurrent Oral 14: Osteoporosis – Epidemiology II	Monday, Oct. 4, 2004	2:30 – 4:00 pm	Room 6ABC
1115-1120	Concurrent Oral 15: Steroid Receptor Actions	Monday, Oct. 4, 2004	2:30 – 4:00 pm	Rooms 602-604
1121-1126	Concurrent Oral 16: Osteoporosis – Pathophysiology I	Monday, Oct. 4, 2004	2:30 – 4:00 pm	Rooms 608-609
1127-1132	Concurrent Oral 17: Chondrocyte Biology	Monday, Oct. 4, 2004	2:30 – 4:00 pm	Rooms 606-607
1133-1138	Concurrent Oral 18: Bone Acquisition and Pediatric Bone Disease II	Monday, Oct. 4, 2004	2:30 – 4:00 pm	Rooms 611-614
1139-1144	Concurrent Oral 19: Osteoblasts III	Monday, Oct. 4, 2004	4:30 – 6:00 pm	Room 6E
1145-1150	Concurrent Oral 20: Mechanical Loading – In Vivo	Monday, Oct. 4, 2004	4:30 – 6:00 pm	Rooms 602-604

Abstract Number	Session Type	Date	Presentation Time	Room
1151-1156	Concurrent Oral 21: Osteoporosis – Pathophysiology II	Monday, Oct. 4, 2004	4:30 – 6:00 pm	Rooms 608-609
1157-1162	Concurrent Oral 22: Other Disorders of Bone and Mineral Metabolism I	Monday, Oct. 4, 2004	4:30 – 6:00 pm	Rooms 606-607
1163-1168	Concurrent Oral 23: Peptide Hormones	Monday, Oct. 4, 2004	4:30 – 6:00 pm	Rooms 611-614
1169-1174	Concurrent Oral 24: Osteoporosis – Treatment I	Monday, Oct. 4, 2004	4:30 – 6:00 pm	Room 6ABC
1175-1182	Concurrent Oral 25: BMPs and Other Growth Factors II	Tuesday, Oct. 5, 2004	9:30 – 11:30 am	Rooms 608-609
1183-1190	Concurrent Oral 26: Osteoporosis – Epidemiology III	Tuesday, Oct. 5, 2004	9:30 – 11:30 am	Room 6E
1191-1198	Concurrent Oral 27: Osteoclasts II	Tuesday, Oct. 5, 2004	9:30 – 11:30 am	Rooms 602-604
1199-1206	Concurrent Oral 28: Other Disorders of Bone and Mineral Metabolism II	Tuesday, Oct. 5, 2004	9:30 – 11:30 am	Rooms 606-607
1207-1214	Concurrent Oral 29: Osteoblasts IV	Tuesday, Oct. 5, 2004	9:30 – 11:30 am	Rooms 611-614
1215-1222	Concurrent Oral 30: Osteoporosis – Treatment II	Tuesday, Oct. 5, 2004	9:30 – 11:30 am	Room 6ABC
F002-F581	Plenary Posters	Friday, Oct. 1, 2004, and Saturday, Oct. 2, 2004	Friday: 5:15 – 7:00 pm Saturday: Odd: 9:30 am – 10:00 am and 11:30 am – 12:30 pm Even: 1:30 pm - 2:30 pm and 4:00 pm - 4:30 pm	Exhibit Hall 4ABC
SA001-SA589	Poster Session I	Saturday, Oct. 2, 2004	Odd: 9:30 am – 10:00 am and 11:30 am – 12:30 pm Even: 1:30 pm - 2:30 pm and 4:00 pm - 4:30 pm	Exhibit Hall 4ABC
SU001-SU586	Poster Session II	Sunday, Oct. 3, 2004	Odd: 9:30 am – 10:00 am and 11:30 am – 12:30 pm Even: 1:30 pm - 2:30 pm and 4:00 pm - 4:30 pm	Exhibit Hall 4ABC
M001-M585	Poster Session III	Monday, Oct. 4, 2004	Odd: 9:30 am – 10:00 am and 11:30 am – 12:30 pm Even: 1:30 pm - 2:30 pm and 4:00 pm - 4:30 pm	Exhibit Hall 4ABC
WG1-WG6	Working Group on Musculoskeletal Rehabilitation in Patients with Osteoporosis	Friday, Oct. 1, 2004	7:00 pm – 9:30 pm	Rooms 618-620
WG7-WG11	Pediatric Bone and Mineral Working Group	Saturday, Oct. 2, 2004	7:15 pm – 10:00 pm	Room 4C-4
WG12-WG25	Adult Bone and Mineral Working Group	Monday, Oct. 4, 2004	6:30 pm – 9:30 pm	Room 4C-4
WG26-WG28	Physical Activity Working Group	Monday, Oct. 4, 2004	6:15 pm – 8:35 pm	Rooms 608-609
* (asterisk) by author's name denotes ASBMR non-membership				

DISCLOSURE/CONFLICT OF INTEREST

The Federation of American Societies for Experimental Biology (FASEB) requires that audiences at FASEB-sponsored educational programs be informed of a presenter's (speaker, faculty, author, or contributor) academic and professional affiliations, and the existence of any significant financial interest or other relationship a presenter has with the manufacturer(s) of any commercial product(s) discussed in an educational presentation. This policy allows the listener/attendee to be fully knowledgeable in evaluating the information being presented. The Program will note those speakers who have disclosed relationships, including the nature of the relationship and the associated commercial entity.

All authors of submitted abstracts completed the disclosure statement in the online submission program. Invited speakers who are not required to submit an abstract received a form in the mail that they completed and returned.

Disclosure may include any relationship that may bias one's presentation or which, if known, could give the perception of bias. These situations may include, but are not limited to:

DISCLOSURE KEY

1. stock options or bond holdings in a for-profit corporation or self-directed pension plan
2. research grants
3. employment (full or part-time)
4. ownership or partnership
5. consulting fees or other remuneration
6. non-remunerative positions of influence such as officer, board member, trustee, or public spokesperson
7. receipt of royalties
8. speaker’s bureau

For full-time employees of industry or government, the affiliation listed in the *2004 Abstracts* will constitute full disclosure.

Disclosures for invited speakers and abstract presenters are provided at the end of the session listing for invited speakers and directly after the body of an abstract for abstract submissions. If there is no conflict of interest or disclosure listed, this means that the invited speaker and/or abstract presenter indicated no conflicts to disclose.

The disclosure information will correspond to the key above. If disclosures are given, the company name, along with the respective disclosure relationship number will be listed (for example: Company Name, 2, 8.).

Key: 1000-1222 = Oral, F = Friday Plenary Poster, SA = Saturday Poster, SU = Sunday Poster, M = Monday Poster, WG = Working Group Abstract *(Asterisk) Denotes Non-ASBMR Membership

1001

Osteoblast-Specific Deletions of Apc and B-catenin Dramatically Alter Bone Development. S. L. Holmen*[1], C. R. Zylstra*[1], A. Mukherjee*[2], R. E. Sigler*[1], M. C. Faugere*[3], M. L. Bouxsein[4], T. L. Clemens[2], B. O. Williams[1]. [1]Van Andel Research Institute, Grand Rapids, MI, USA, [2]Department of Pathology, University of Alabama at Birmingham, Birmingham, AL, USA, [3]Department of Medicine, University of Kentucky, Lexington, KY, USA, [4]Orthopedic Biomechanics Laboratory, Beth Israel Deaconess Medical Center, Boston, MA, USA.

Mutations in the Wnt co-receptor Lrp5 produce striking alterations in bone mass in both humans and mice but the mechanisms responsible for Wnts actions in bone are unclear. Wnts activate several signaling cascades including the canonical pathway that inhibits APC-mediated degradation of ß-catenin with consequent activation of TCF/LEF transcription of target genes. We used Cre-mediated recombination to investigate the role of the canonical pathway in osteogenesis by selectively deleting the genes encoding ß-catenin and Apc. Mice carrying floxed ß-catenin and Apc alleles were mated to mice expressing the Cre recombinase driven by the human osteocalcin promoter (J Biol Chem. 277:44005). Mice deficient in ß-catenin were smaller than their littermates and died within five weeks with dramatic reductions in bone at all skeletal sites. MicroCT analysis of the femur showed severe cortical thinning and a complete absence of trabecular elements.Mice heterozygous for this mutation also had lower bone mass. By contrast, mice deficient in Apc exhibited a dramatic increase in bone acquisition. Metaphyseal bone was hypervascularized and poorly mineralized, whereas osteoid in the dyaphysis was more completely mineralized and entirely filled the marrow cavity. Interestingly, osteoclasts were virtually absent from these bones, possibly due to a decrease in the bone marrow precursor availability. Consistent with this, most Apc mutants died within two weeks of birth with evidence of anemia. To determine the effect of loss of ß-catenin and APC on osteoblast differentiation in vitro, primary calvaria osteoblasts isolated from mice homozygous for the floxed alleles were infected with adenoviral vectors expressing either Cre or GFP and allowed to differentiate in mineralizing medium. Osteoblasts lacking ß-catenin showed increased proliferation associated with a reduction in Runx-2 and osteocalcin expression and a delay in mineralization. By contrast, osteoblasts deficient in Apc demonstrated premature and upregulated expression of osteoblast marker genes. We conclude that canonical Wnt signaling is critically important in controlling normal bone acquisition in mice and likely accounts for how Lrp5 affects bone mass accrual in humans. Our results also suggest that this signaling pathway functions during development to control the pace of osteoblast differentiation.

Disclosures: ***B.O. Williams****, None.*

1002

Beta-catenin Is Essential for Normal Bone Development. M. J. Hilton*, F. Long. Department of Internal Medicine - Division of Bone and Mineral Diseases, Washington University School of Medicine, St. Louis, MO, USA.

Canonical Wnt signaling occurs through a receptor complex that includes the Frizzled family members and the Low Density Lipoprotein Receptor-Related Proteins 5 or 6 (LRP5/6), which leads to nuclear accumulation of Beta-catenin and activation of Wnt responsive genes. Recent genetic evidence analyzing mutations of LRP5 has indicated that canonical Wnt signaling positively regulates bone mass in the postnatal skeleton. Since Wnt signaling occurs normally during embryogenesis in the absence of LRP5, it is not known whether canonical Wnt signaling is required for osteoblast development in the embryo. Here we have addressed this issue by genetically removing Beta-catenin from all skeletogenic tissues by using the Cre-LoxP technology. Specifically, we have generated embryos of the *Dermo1*-Cre; *Beta-catenin* $^{c/c}$ genotype using the *Dermo1*-Cre "knock-in" line of mice which activates Cre expression in the mesenchymal condensations during early skeletogenesis. These mutant animals die at birth and analyses of embryonic skeletons clearly show a complete lack of bone formation throughout the body. Our results indicate that Beta-catenin is essential for osteoblast differentiation and molecular analysis has revealed an early arrest in the differentiation of the osteoblast lineage. Furthermore, consistent with previous studies, the Beta-catenin mutants also exhibit reduced chondrocyte proliferation and severely delayed chondrocyte maturation. The work presented here clearly demonstrates that Beta-catenin acts a positive regulator of osteoblast differentiation, chondrocyte proliferation, and chondrocyte maturation.

Disclosures: ***M.J. Hilton****, None.*

1003

Over-Expression of Activated NFATc1 plus RANKL Rescues the Osteoclastogenesis Defect of NF-κB p50/p52 Double Knockout Splenocytes. F. Li*[1], K. Matsuo[2], L. Xing[1], B. F. Boyce[1]. [1]Univeristy of Rochester, Rochester, NY, USA, [2]Keio University, Tokyo, Japan.

Expression of NF-κB p50 and p52, c-Fos, and NFATc1 is essential for RANKL- and TNF-mediated osteoclast (ocl) formation. NFATc1 is a downstream target for c-Fos in RANKL-induced osteoclast formation, but it is not known if it is a target of NF-κB. To examine this possibility, we used M-CSF-dependent splenocytes from NF-κB p50 and p52 double knockout (dKO) or control mice. NFATc1 expression, using real time PCR, was similar in splenocytes from dKO and control mice treated with M-CSF for 3d. In contrast, RANKL significantly increased NFATc1 expression in these M-CSF-dependent splenocytes (MDS) from wt, but not from dKO mice (fold induction over time 0 in control vs dKO: at 2 and 24 hr, 12+/-0 vs 3+/-0). To determine if retroviral expression of NFATc1 can rescue the ocl formation defect of dKO cells, we infected dKO MDS with a constitutively active nuclear form of NFATc4 (ΔNFAT), c-Fos or GFP in the presence or absence of RANKL. ΔNFAT plus RANKL induced ocl formation from dKO MDS (# Ocls/well: ΔNFAT/RANKL, 48+/-11; GFP/RANKL, 0+/-0; c-Fos/RANKL, 158+/-11). ΔNFAT overexpression alone did not induce ocl formation. IL-1 and TNF also induced some ocl formation from ΔNFAT-expressing dKO MDS, but less effectively than RANKL (#ocls/well: ΔNFAT/IL-1, 6+/-1; ΔNFAT/TNF, 10+/-2; ΔNFAT/PBS, 0+/-0; TNF alone, 0+/-0). We showed previously that c-Fos plus IL-1 induces ocl formation from wild-type MDS in the absence of RANKL. ΔNFAT plus IL-1 had a similar but less osteoclastogenic effect (# Ocls/well: c-Fos/IL-1, 58+/-6 vs ΔNFAT/IL-1, 31+/-3). To examine if c-Fos plus IL-1 stimulates NFATc1 expression or vice verse, the expression of NFATc1 or c-Fos was compared between IL-1-treated c-Fos-infected or ΔNFAT-infected wild-type spleen cells. c-Fos plus IL-1 increased NFATc1 expression by 4 fold, but c-Fos or IL-1 had no effect. In contrast, ΔNFAT plus IL-1 had no effect on c-Fos expression. Finally, We compared the expression of NFATc1 in wt and dKO MDS treated with RANKL or TNF and found that while RANKL increased NFATc1 expression in both wt and dKO cultures, TNF increased its expression only in the wt MDS. In summary, our results indicate that NFATc1 is a downstream target for NF-κB in RANKL-mediated osteoclastogenesis, but other cytokines such as IL-1 and TNF may also work through the NFAT pathway in the absence of NF-κB signaling.

Disclosures: ***F. Li****, None.*

1004

Dentin Matrix Protein-1 (DMP-1) Plays a Key Role in Osteocyte Function through Regulation of Mineralization and Response to Mechanical Strain. H. F. Rios*[1], Y. Xie*[1], S. Kotha*[1], D. Nicholella*[2], D. Nicholella*[2], L. Ye[1], L. Bonewald[1], J. Q. Feng[1]. [1]Oral Biology, UMKC, Kansas City, MO, USA, [2]Mech and Matls Engr, SW Res Ins., San Antonio, TX, USA.

Mechanical load determines bone architecture. Increased load yields increased bone, whereas decreased load leads to bone loss. Osteocytes appear to sense and translate mechanical strain into biochemical signals of formation or resorption. Dmp 1 is an extracellular matrix protein of unknown function, highly expressed and regulated by mechanical strain in osteocytes.

Dmp1 Knockout (KO) mice appear normal at birth suggesting that it does not play a role in embryonic bone development or mineralization. However, by 2-3 wks of age an increase in subchondral bone is observed, potentially a compensatory response to locomotion, which is rapidly reversed with age. Osteoid formation, not true bone formation, is accelerated in these mice. Histological analysis of Dmp1 KO mice at 1, 3 and 7.5 mos show highly expanded, irregular periosteal and endosteal osteoid. Using Raman microscopy, a decrease in mineral compared to matrix is also observed with age. Calcein/Alizarin red labeling is increased and extremely diffuse on both the endosteal and periosteal surfaces in the KO mice. Expression of non-collagenous matrix proteins such as biglycan, decorin, bone sialoprotein, osteopontin, osteocalcin are dramatically increased, whereas no differences were observed in collagen I by immunohistochemistry. By transmission and backscatter electromicroscopy, the mineral, when present is patchy and poorly organized. Osteocytes within osteoid have normal size and dendricity, but the morphology of the dendritic processes is abnormal with a 'buckling' of the membrane surface. In addition, there are clear differences in the osteocyte lacunae: those in the KO bone are larger than those in the WT bone. The long bones are less stiff, have greater total deformation, and yield at lower load levels compared to long bones from WT mice. Compressive loading at 60 Hz shows strains 1.7 times higher in *Dmp 1* KO mice than normal and heterozygous mice ($p<0.05$), indicating a significant change in the material (elastic moduli) and/or structural (stiffness) properties. These KO mice display multiple pathological fractures, likely a consequence of reduced bone mineral. Therefore, the osteocytes in these mice are constantly being subjected to higher strain levels than osteocytes in WT bone. These 'hyperstrained' osteocytes appear to signal increased bone formation that in the absence of Dmp1 results in increased osteoid, not bone. Together these data suggest that DMP 1 is critical for osteocyte function postnatally though its dual role in controlling mineralization and response to mechanical strain.

Disclosures: ***H.F. Rios****, None.*

1005

Cooperative Signaling of Fibroblast Growth Factor Receptors 1 and 2 in Skeletal Development. H. Kanazawa[1], K. Yu*[1], A. Jacob*[1], I. H. Hung*[1], J. M. Partanen*[2], D. M. Ornitz*[1]. [1]Molecular Biology and Pharmacology, Washington University Medical School in St. Louis, St. Louis, MO, USA, [2]Institute of Biotechnology, University of Helsinki, Helsinki, Finland.

Many craniosynostosis syndromes are caused by the mutations in fibroblast growth factor receptors (FGFRs) 1 and 2. In addition to craniofacial abnormalities, these patients often have short stature and malformations of the hands and feet. Although FGFR1 and FGFR2 each have important roles in skeletal development, redundancy between FGFR1 and FGFR2 is unknown. To address the combined affect of loss of function of both genes on skeletal development we have generated Fgfr1/Fgfr2 double conditional knockout (DCKO) mice using the mesenchymal osteoprogenitor-specific Dermo1 (Twist2)-cre gene. Taking advantage of Cre-loxP system, we mated Dermo1-Cre/Fgfr1delta/+;Fgfr2delta/+ mice with Fgfr1flox/flox;Fgfr2flox/flox mice to generate DCKO mice. The phenotype of DCKO mice was much more severe than deletion of either Fgfr1 or Fgfr2 alone. All DCKO mice died immediately after birth because of cleft palate. Compared to controls, sagittal sutures of DCKO mouse skulls were widely opened secondary to hypoplastic nasal and frontal bone growth. DCKO mice also had a hypoplastic squamous bone, missing tympanic rings, shortened or truncated zygomatic arch, and a shortened and malformed mandible. Costchondral gaps and the vertebral neuronal arch were severely deformed. In the limb, DCKO mice showed joint fusion at the elbow and knee. The hindlimb was more affected than the forelimb and proximal bones were more affected than distal bones. Long bones were shorter and wider compared to control mice. Osteopontin expression was examined in E16.5 and E.17.5 calvariae by whole mount in situ hybridization. The expression level of Osteopontin was elevated in DCKO in the frontal bone area compared to controls. These data demonstrate an essential and redundant role for both FGFR1 and FGFR2 in both axial and appendicular skeletal development. Moreover craniofacial abnormalities in DCKO mice suggested a potential role for FGFR signaling in neural crest cells that contribute to craniofacial skeletal development.

Disclosures: ***H. Kanazawa****, None.*

1006

Genetic Evidence of Androgen Receptor Function in Osteoclasts: Generation and Characterization of Osteoclast-specific Androgen Receptor Knockout Mice. T. Nakamura*[1], T. Watanabe*[1], Y. Nakamichi[1], T. Fukuda*[1], T. Matsumoto*[1], K. Yoshimura*[1], J. Miyamoto*[1], Y. Yamamoto*[1], H. Shiina*[1], S. Tanaka*[1], M. Sakari*[1], T. Sato*[1], D. Metzger*[2], P. Chambon*[2], S. Kato[1]. [1]Laboratory of Nuclear Signaling, Institute of Molecular and Cellular Biosciences, University of Tokyo, Tokyo, Japan, [2]Institut de Genetique et de Biologie Moleculaire et Cellulaire, CNRS/ INSERM/ ULP, College de France, Strasbourg, France.

Androgen actions appear essential for normal skeletal development and maintenance, particular in males. In fact, we have demonstrated by a gene disruption approach that AR function is essential for normal bone remodeling through suppression of bone resorption in male mice(Kawano.H et al *PNAS*, 2003). However, the primary bone cell-type for AR function remains to be established, though no clear expression of AR in mammalian osteoclasts was reported.

To directly examine AR function in osteoclasts, we used a Cre/*lox*P system to disrupt AR gene in mice osteoclasts. To drive Cre expression specifically in the osteoclasts, we carried out the targeted insertion of the Cre gene in the Cathepsin K gene (*Ctsk*) locus and generated Ctsk-Cre knock-in mice. Expression analysis of lacZ gene in CAG-CAT-Z reporter mice demonstrated that Cre-mediated recombination took place in a osteoclast-specific manner in Ctsk-Cre mice. Among the progeny of crosses betweeen Ctsk-Cre and floxed AR mice, males with $Ctsk^{Cre/+}$; AR^{flox}/Y genotype were selected as osteoclast-specific AR knockout (Oc-ARKO) mice for detailed analysis. Unexpectedly, histomorphometric analysis of the lumber spine from Oc-ARKO mice showed significantly increased number of osteoclasts and the other bone resorption parameters compared with control mice. This was further reflected in the increased levels of urinary deoxypyridinoline. The bone formation parameters were also increased in Oc-ARKO mice, with increased thickness of the region between two calcein-labeled layers. The Oc-ARKO mice bone phenotype suggests that AR serves as a critical regulator in osteoclasts.

Disclosures: ***T. Nakamura****, None.*

1007

Results of a 5 Year Double Blind, Placebo Controlled Trial of Calcium Supplementation (CAIFOS); Clinical Fracture Outcomes. R. L. Prince[1], A. Devine[1], S. S. Dhaliwal*[2], I. M. Dick[1]. [1]School of Medicine and Pharmacology, University of Western Australia, Western Australia, Australia, [2]School of Public Health, Curtin University of Technology, Western Australia, Australia.

Osteoporotic fracture is a major public health problem for elderly women. Prevention approaches can involve pharmacological treatment targeted at high risk individuals or a public health approach treating the whole population. We chose the latter approach to test the hypothesis that calcium supplementation (calcium carbonate 600mg twice per day) compared to identical placebo would reduce the clinical osteoporotic fracture rate by at least 27% over 5 years in women older than 70.

1460 women mean age 75 were recruited from the whole population using a recruitment letter strategy. Responders were excluded if they were on bone active treatment, calcium supplementation or had diseases that may have prevented them completing the 5 year study. Of the responders 18% were eligible and agreed to commence the study. Baseline calcium intake was determined from a food frequency questionnaire. Clinical osteoporotic fractures, verified by x-ray, were ascertained from diaries collected 4 monthly. All fractures, except those of the phalanges or skull, were included in the analysis. Study outcomes were examined using the Cox proportional hazard model to calculate hazards ratios and 95% confidence intervals (HR).

Baseline calcium intake was 970±354 mg/day. In all, 235 individuals (16.1%) sustained 296 fractures during the study. 67 patients died (4.6%), 165 (11.3%) withdrew completely and 305 (20.9%) ceased the medication but continued in the study. Thus 923 (63.2%) completed the study per protocol. The risks of death (HR 0.76: 0.47-1.23), withdrawal (HR 0.86: 0.63-1.16) or cessation of medication (HR 0.98: 0.80-1.21) was not different in the calcium versus the placebo group.

Calcium supplementation resulted in a 34% reduction in fracture in the per protocol patients (HR 0.66: 0.46-0.95). These results were not altered by age, BMI, hip BMD, baseline calcium intake or prevalent baseline fracture entered as covariates individually or in combination. The treatment effect was slightly stronger if vertebral fractures were not included (HR 0.63: 0.42-0.93). In an intention to treat analysis calcium supplementation did not reduce fractures significantly compared to placebo (HR 0.85:0.66-1.10, p=0.23).

These data demonstrate that elderly females who remain compliant with calcium supplementation of 1200 mg per day can reduce their 5 year risk of osteoporotic fracture from an average risk of 16% to an average risk of 10%. These data justify an increased emphasis on calcium supplementation as part of a public health approach to fracture prevention.

Disclosures: ***R.L. Prince****, None.*

1008

Deletion of the β2 Adrenergic Receptor Prevents Bone Loss Induced by Isoproterenol in Mice. H. Z. Ke, G. XU*, A. L. Brault*, H. Qi, D. T. Crawford*, H. A. Simmons, M. Li, T. A. Brown. Pfizer Global Research and Development, Groton, CT, USA.

Isoproterenol (Iso), a β-adrenergic receptor agonist, has been shown to reduce bone mass by decreasing bone formation. Since Iso interacts with all three β-adrenergic receptors (β1-β3), the receptor subtype responsible for its negative effects on bone is not completely understood. The purpose of this study was to determine the role of β2 in Iso-induced bone loss using the β2 knock-out (KO) mice. Male wild-type FVB/N (WT) or KO mice at 4 months of age were treated with vehicle or Iso at 30 mg/kg/d for 8 weeks by i.p. injection. PQCT analysis showed a significant decrease in total bone mineral content in both the distal femoral metaphysis (DFM, -15%) and femoral shaft (FS, -11%) in Iso-treated-WT mice compared with WT controls. Further, trabecular density in DFM and cortical thickness in FS were significantly decreased, while endocortical circumference in FS increased significantly in Iso-treated-WT mice compared with WT controls. A significant decrease in trabecular bone volume (-60%) was observed by micro-CT analysis of DFM in Iso-treated-WT mice compared with WT controls. These data indicate that Iso induced significant bone loss on endocortical and trabecular surfaces. Histomorphometric analysis of trabecular bone on the 4th lumbar vertebral body indicates that Iso treatment in WT mice increased bone turnover as evident by a significant increase in mineralizing surface (+99%), mineral apposition rate (+32%), bone formation rate/BS (+158%), osteoclast surface (+83%) and osteoclast number (+63%) as compared with WT controls. Unlike the findings in WT mice, treatment with Iso in β2 receptor KO mice did not induce significant changes in total bone mineral content, trabecular bone volume, osteoclast surface and osteoclast number compared with vehicle-treated KO controls. In mouse calvarial osteoblast culture, Iso dose-dependently increased cAMP production at concentrations between 60 nM and 5 uM with the maximal increase of 1441 folds at 5 uM in WT osteoblasts, but not in KO osteoblasts, indicating that β2 receptor directly regulates the stimulating effects of Iso on osteoblast. In summary, Iso induces bone loss by increasing both bone resorption and formation in WT mice *in vivo*. These data are in contrast with a previous report in which Iso induces bone loss by inhibiting osteoblastic bone formation. Deletion of the β2 receptor blocks high turnover bone loss induced by Iso, therefore, β2 adrenergic receptor mediates the negative bone effects of Iso. These data reveal that antagonizing β2 receptor provides therapeutic potentials for skeletal disorders such as osteoporosis.

Disclosures: ***H.Z. Ke****, Full Time Employee of Pfizer Inc. 3.*

1009

Hip and Spine BMD and Prediction of Hip and Other Fractures in Men. First Results from the Osteoporotic Fractures in Men (MrOS) Study. P. M. Cawthon[1], S. R. Cummings[1], B. K. S. Chan*[2], J. A. Cauley[3], K. E. Ensrud[4], D. C. Bauer[5], H. A. Fink[4], D. M. Black[5], E. S. Orwoll[2]. [1]Research Institute, California Pacific Medical Center, San Francisco, CA, USA, [2]Oregon Health Sciences University, Portland, OR, USA, [3]University of Pittsburgh, Pittsburgh, PA, USA, [4]University of Minnesota, Minneapolis, MN, USA, [5]University of California, San Francisco, CA, USA.

Background: The relationship between measurements of hip and spine bone mineral density (BMD) and the risk of hip and other fractures has not been established for men.
Methods: 5,989 men age ≥65 from six U.S. communities had BMD measured by DXA. 181 non-spine fractures (including 30 hip fractures) were validated during 2.6 years of >99% complete follow-up.
Results: Total hip BMD was a stronger predictor of hip fracture than was lumbar spine BMD (Table). All BMD measures (femoral neck, total hip and lumbar spine) were strongly and similarly predictive of non-spine fractures (Figure).

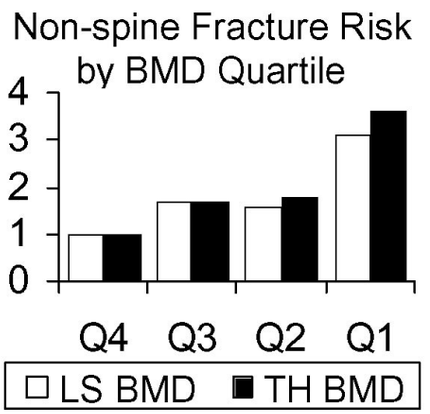

We estimate that among men aged ≥65, the annual risk of fractures for men with osteoporosis (N=103, total hip T score ≤ -2.5) is 3.7% (hip) and 7.4% (non-spine), versus 0.1% (hip) and 1.0% (non-spine) in men with higher BMD (N=5,886).
Conclusion: Measurements of hip and spine BMD in men strongly predict hip and non-spine fractures. Measurements at the hip are superior to measurements at the spine for predicting hip fracture. Men with 'osteoporosis' have a high yearly risk of fracture.

Age-Adjusted RR/SD by fracture type

BMD site	Hip Fracture	Non-spine Fracture
Total hip (TH)	3.6 (2.5,5.2)	1.8(1.5,2.1)
Lumbar spine (LS)	1.8 (1.2, 2.9)	1.7 (1.4, 2.0)

Disclosures: ***P.M. Cawthon****, None.*

1010

Measles Virus Nucleocapsid (MVNP) Gene Is Sufficient to Induce a Pagetic Bone Phenotype in Vivo. G. D. Roodman[1], S. V. Reddy[2], N. Kurihara[2], J. J. Windle[3], L. A. Ehrlich*[2], H. Zhou*[4], D. Dempster[4], M. Subler*[3]. [1]Univ of Pittsburgh & VA Med Ctr, Pittsburgh, PA, USA, [2]Univ of Pittsburgh, Pittsburgh, PA, USA, [3]VA Commonwealth Univ, Richmond, VA, USA, [4]Helen Hayes Hosp, W Haverstraw, NY, USA.

Paget's disease (PD) is the most exaggerated example of abnormal bone remodeling with increased bone resorption and excessive new bone formation. However, its etiology is unclear. A viral etiology for PD has been suggested based on the presence of paramyxoviral-like nuclear inclusions, detection of MVNP mRNA or protein in osteoclasts (OCL) from PD lesions, and in vitro studies showing that transfection of normal OCL precursors with the MVNP gene results in formation of OCL that express a pagetic phenotype (increased numbers of OCL; increased responsivity to 1,25-$(OH)_2D_3$, RANK ligand and TNF-α increased expression of the TAF_{II}-17 gene, and increased bone resorption capacity). A genetic component is also involved in PD and mutations in at least 2 genes have been linked to familial PD. It is our hypothesis that MVNP induces the abnormal OCL activity in PD, and the genetic factor enhances basal OCL activity to amplify this process. This suggests that MVNP should be sufficient to induce PD if expressed in large numbers of OCL. To test this hypothesis, we targeted MVNP to cells in the OCL lineage in transgenic mice using the tartrate resistant acid phosphatase promoter. The MVNP transgenic mice were viable and expressed low levels of MVNP in bone. Histomorphometric analysis, ex vivo studies of OCL formation, measurement of serum alkaline phosphatase and radiologic studies were then performed in 17 MVNP or 16 wild-type (WT) mice from 3-14 mths of age. Overall, there was a 64% increase in OCL perimeter (P = 6.0002) and 37% increase in osteoblast (OBL) perimeter in MVNP mice. In a mouse that was 14 mths of age, there was a 225% increase in OBL perimeter and 149% in OBL perimeter. This was accompanied by increased cancellous bone volume (83%), trabecular width (47%) and number (25%) with a marked increase in the amount of woven bone. In contrast, cancellous bone volume decreased between 3-12 mths in WT mice, while cancellous bone volume in MVNP mice increased over the same time period. Ex vivo studies showed that the numbers of OCL formed in marrow cultures from MVNP mice were increased, the OCL were hyper-responsive to 1,25-$(OH)_2D_3$, RANK ligand and TNF and had an increased bone resorbing capacity compared to WT cultures. Serum alkaline phosphatase levels were significantly increased in the MVNP mice by 8-12 mths of age compared to the WT mice [156 ± 24 units vs. 101 ± 20 (mean ± SD) $p < 0.04$]. These results demonstrate that expression of MVNP in OCL in vivo results in a bone phenotype that is characteristic of PD and support a pathophysiologic role for MVNP in PD.

Disclosures: ***G.D. Roodman****, Novartis 8; SCIOS, Inc. 5.*

1011

Role of Dickkopf 1 (Dkk) in Myeloma Bone Disease and Modulation by the Proteasome Inhibitor Velcade. B. O. Oyajobi[1], I. R. Garrett[2], A. Gupta*[1], M. Banerjee*[1], X. Esparza*[2], A. Flores*[2], J. Sterling[1], G. Rossini*[2], M. Zhao[1], G. R. Mundy[1]. [1]Cell & Structural Biology, Univ Texas Hlth Sci Ctr at San Antonio, San Antonio, TX, USA, [2]OsteoScreen, Inc., San Antonio, TX, USA.

Myeloma bone disease is characterized by increased osteoclastic bone resorption and impaired osteoblast activity. The secreted antagonist of Wnt signaling, Dkk1 has recently been implicated as a mediator of the osteoblast dysfunction in myeloma. In myeloma patients, Dkk1 was shown to be preferentially and abundantly expressed in tumor-infiltrated bone marrow (Tian et al., 2003). Since Dkk1 appears to play an important role in myeloma, we examined (i) its effects on bone; (ii) the cell source in myeloma; (iii) its modulation by proteasome inhibitors which have recently been shown to enhance bone formation in normal mice (Garrett et al., 2003). Excess Dkk1 reduced new bone formation induced by proteasome inhibitors in cultured neonatal mouse calvariae. Dkk1 was not detected in the Radl 5TGM1 and 5T33 murine myeloma cells nor in human myeloma (RPMI 8226, U266) and B lymphoblastoid (ARH-77, IM-9) cell lines. In contrast, Dkk1 was strongly expressed in all murine and human cell lines of mesenchymal origin tested (2T3, C2C12, C3H10T1/2, MC3T3-E1, 14M1, MG-63, HOBIT), with highest expression in 14M1, a marrow stromal cell line spontaneously derived from a 5T14 myeloma-bearing mouse. Dkk1 expression was even more markedly enhanced in co-cultures of 5TGM1 and bone marrow stromal ST2 cells in vitro. To determine the relationship in myeloma between osteoblast function, Dkk1 expression and its regulation by proteasome inhibitors, we used the Radl 5T model of myeloma bone disease. We found cancellous bone volumes and bone formation rates (assessed by fluorochrome-labeling) were significantly reduced in 5TGM1-bearing C57BL/KaLwRij mice and Dkk1 was detectable in whole marrow flushed from diseased bones of tumor-bearing mice suggesting osteogenic cells express Dkk1 in myeloma in vivo. Low nanomolar concentrations of Velcade™ the first-in-class proteasome inhibitor to be used in patients, stimulated new bone formation in neonatal mouse calvariae, inhibited IL-1-stimulated bone resorption, and induced apoptosis of 5TGM1, RPMI 8226 and U266 myeloma cells. We found Velcade at nanomolar concentrations inhibited Dkk1 expression in 14M1, 2T3, MG-63 cells and in the bone organ cultures dose- and time-dependently. Taken together, our data indicate that the strikingly beneficial effects of proteasome inhibition now being reported in myeloma patients likely results from its multiple effects on inducing tumor cell death whilst concomitantly promoting osteogenesis by reducing Dkk-1 expression and inhibiting osteoclastic bone resorption.

Disclosures: ***B.O. Oyajobi****, OsteoScreen 1.*

1012

Runx2 Contributes to Pathogenesis of Osteoarthritis through Chondrocyte Hypertrophy and Matrix Breakdown in Articular Cartilage under Mechanical Stress. S. Kamekura[1], K. Hoshi[1], U. Chung[1], Z. Maruyama*[2], T. Komori[2], K. Nakamura[1], H. Kawaguchi[1]. [1]Orthopaedic Surgery & Tissue Engineering, University of Tokyo, Tokyo, Japan, [2]Osaka University, Osaka, Japan.

Osteoarthritis (OA), one of the most common skeletal disorders, is induced by accumulated mechanical stress to joints; however, little is known about the molecular mechanisms by which the stress leads to cartilage degradation and osteophyte formation. To apply approaches from mouse genomics, we created experimental OA models in mice by producing instability in the knee joints using a microsurgical technique. Immunohistochemical and in situ hybridization analyses of these models revealed that the hypertrophic differentiation of chondrocytes with type X collagen expression and the matrix breakdown associated with MMP-13 expression were visible in the early stage of OA. Since both chondrocyte hypertrophy and MMP-13 expression are known to be positively regulated by a transcriptional activator Runx2, we compared the susceptibility of OA between heterozygous Runx2-deficient mice (Runx2+/-) and the wild-type (WT) littermates. Although homozygous Runx2-deficient mice died just after birth, Runx2+/- developed and grew normally without abnormalities of major organs except for cleidocranial dysplasia as previously reported. Both genotypes showed no abnormality in the articular cartilage under physiological conditions during observation periods up to 26 weeks of age. When OA was induced by medial ligament transection and menisectomy in the knee joints of 8-week-old male mice, the cartilage degradation assessed by Safranin-O staining and the cartilage destruction in superficial and middle layers were apparent in the WT joints within 8 weeks after surgery. The cartilage destruction reached the deep layer across the tidemark within 12 weeks. Contrarily, in the Runx2+/- joints the cartilage degradation was much milder and the destruction was confined within the superficial layer even after 12 weeks. Substantial osteophyte formation was seen in the WT knee 12 weeks after surgery, which was not seen in Runx2+/-. Mankin's score (0-14), a histological index of OA severity, at 12 weeks was 9.2±0.7 and 4.3±0.5 in WT and Runx2+/-, respectively (mean±SEM for n=8 / genotype, $p<0.01$). Immunohistochemistry and in situ hybridization revealed the expressions of type X collagen and MMP-13 within 8 weeks in the WT joints, both of which were rarely seen in Runx2+/-. We thus conclude that Runx2 haploinsufficiency prevented OA progression by suppressing chondrocyte hypertrophy and matrix breakdown under mechanical stress without affecting the physiological skeletal growth or turnover, suggesting that Runx2 could be a therapeutic target for OA.

Disclosures: ***S. Kamekura****, None.*

1013

Effects of Global or Targeted Deletion of the Ep4 Receptor on the Response of Cultured Osteoblasts to Prostaglandin E2. L. G. Raisz[1], C. A. Alander*[1], P. Zhan*[1], M. D. Breyer*[2], B. E. Kream[1], C. C. pilbeam[1]. [1]Department of Medicine, University of Connecticut Health Center, Farmington, CT, USA, [2]Department of Medicine, Vanderbilt University, Nashville, TN, USA.

Prostaglandin E2 (PGE2) is a potent stimulator of bone resorption and formation. These effects are attributed to stimulation of cAMP production through two receptors, EP2R and EP4R. Mice with global deletion of EP4R die at birth due to failure to close the ductus arteriosus. To circumvent this problem, we developed a targeted deletion of EP4R using combinations of mice heterozygous for global EP4R gene deletion, mice with exon 2 of EP4R flanked by Lox-P sites, and mice carrying an osteoblast-targeted 2.3 kb type I collagen promoter fused to Cre recombinase (Col 2.3-Cre). Males heterozygous for EP4R gene deletion and for Col 2.3-Cre were mated to females homozygous for floxed EP4R. This resulted in 4 genotypes: (A) wild type, (B) heterozygotes with a deletion of EP4R targeted to cells expressing Col 2.3-Cre, (C) heterozygotes with global deletion of EP4R, and (D) a combined knockout in which one EP4R allele was absent globally and the other deleted only in cells expressing Col 2.3-Cre. Calvarial cells were obtained from 5-8 week old mice by sequential collagenase digestion and cultured in a growth medium. Alkaline phosphatase (AP) activity, expressed as nM/mg protein, was measured at 12-14 days of culture. In group A control cultures (wild type) AP activity was 6.6 ± 0.7, which was significantly reduced to 3.6 ± 0.4 ($P<0.01$) in the presence of NS-398 (0.1 µM), a selective inhibitor of inducible cyclooxygenase (COX-2). NS-398 did not decrease AP activity in group D (combined knockout) cells. Since these data suggested that endogenous prostaglandins, acting through EP4R, have an effect on osteoblastic differentiation, studies of the effect of exogenous PGE2 were carried out in the presence of NS-398. Continuous treatment with PGE2 (1µM) significantly increased AP activity ($P<0.01$) in A cells (35.0 ± 3.1) as well as in heterozygous B (13.4 ± 2.0) and C cells (12.9 ± 2.3), but not in D cells (5.2 ± 1.0). The stimulated AP activities in B and C cells were significantly lower than in A cells ($P<0.01$). These results suggest that 1) targeted deletion of EP4R in cells of the osteoblastic lineage could be accomplished using the Col 2.3-Cre construct, 2) activation of EP4R is critical for the ability of PGE2 to enhance osteoblast differentiation, and 3) the level of expression of EP4R may be rate limiting, since EP4R heterozygotes had decreased PGE2 responses.

Disclosures: ***L.G. Raisz****, None.*

1014

TOPGAL Mice Demonstrate Wnt Signaling During Bone Development, Growth and Mechanical Loading. J. R. Hens*[1], K. Wilson*[1], P. Dann*[1], E. Fuchs*[2], M. C. Horowitz[1], J. Wysolmerski[1]. [1]Yale University, New Haven, CT, USA, [2]Rockefeller University, New York, NY, USA.

The canonical Wnt signaling pathway appears to control bone mass in both humans and mice. Activation of this pathway leads to the accumulation of β-catenin within the nucleus, where it combines with TCF-family transcription factors to regulate gene expression. We used TOPGAL mice, which harbor a TCF/β-catenin-responsive β-galactosidase (β-gal) transgene to determine which bone cells were targets of canonical Wnt signaling during bone development, bone growth and normal bone turnover *in vivo*.

Signaling was active in the cartilaginous skeleton in embryos, in clusters of chondrocytes within the growth plates of growing long bones and in the cartilaginous portions of the ribs. TOPGAL transgene expression was detected in chondroclasts at the chondro-osseous junction, but not in osteoclasts in mature bone. Wnt signaling was activated within forming joints and within cells surrounding the intervetebral discs of the spinal column. Signaling was active in some osteoblasts (OB) in embryos and neonatal mice, but not in OB in adult mice. In contrast, Wnt signaling was activated prominently in osteocytes and persisted in this cell type with age.

We also examined primary cultures of calvarial OB from TOPGAL mice for β-gal production. None was detected when these cells were cultured on plastic and only rare positive cells were seen when grown on Type I collagen. To confirm that cultured OB were competent to activate Wnt signaling, we used RT-PCR to score expression of Wnt related molecules. At the proliferating and post-confluent stages, 9FZs, 4TCFs, 5SFRPs, LRP5 and 6 and DKK1 and 2 were present. Wnts 1, 3, 3a, 7a, 8a, and 8b were not expressed, but all 12 other Wnts were detected.

Finally, we examined the consequences of mechanical load on Wnt signaling in OB. Cells were loaded for 2 h at 2.5-3% elongation at 0.3 Hz alternating with 1 h rest intervals using a Flexercell® device. In cells grown on Type I Collagen, this treatment led to clear activation of canonical Wnt signaling after 12 hours.

In summary, as detected by TOPGAL transgene expression, canonical Wnt signaling is active in many cell types within the developing and growing skeleton. Interestingly, the TOPGAL transgene is more prominently expressed in osteocytes than OB and expression is absent from OB in adult bone. These data suggest that canonical Wnt signaling may be a direct modulator of OB function during bone modeling but not during normal bone remodeling. Furthermore, the persistent activation of Wnt signaling in osteocytes *in vivo* and the ability of deformation to activate signaling *in vitro* suggest that canonical Wnt signaling participates in the regulation of bone mass in response to physical forces.

Disclosures: ***J.R. Hens****, None.*

1015

Activity of the Mdm2 Oncogene Supports Runx2 Expression and Osteoblast Differentiation during Embryonic Skeletogenesis. C. J. Lengner[1], H. A. Steinman*[1], J. Gagnon*[1], B. E. Kream[2], G. S. Stein[1], J. B. Lian[1], S. N. Jones*[3]. [1]Department of Cell Biology and Cancer Center, University of Massachusetts Medical School, Worcester, MA, USA, [2]Department of Medicine, University of Connecticut Health Center, Farmington, CT, USA, [3]Department of Cell Biology, University of Massachusetts Medical School, Worcester, MA, USA.

The Mdm2 oncogene can promote cell proliferation through its ability to negatively regulate the activity of the p53 tumor suppressor. Loss of Mdm2 results in p53 accumulation and ultimately results in exit from the cell cycle or apoptosis. Mdm2 null mice exhibit early embryonic lethality that can be rescued by deletion of p53. Mdm2/p53 null mice are phenotypically normal, indicating that the primary function of Mdm2 is p53 regulation. We have observed an increase in Mdm2 expression during the process of osteoblast differentiation that has led us to examine the role of Mdm2 during the process of skeletogenesis. To address this question, we have utilized a murine genetic system for tissue-specific Mdm2 ablation. In this system a conditional Mdm2 allele (Mdm2 flox) is excised during embryogenesis by Cre recombinase under control of the Type I Collagen promoter (Coll I-Cre). We find that deletion of Mdm2 in pre-osteoblasts upon activation of the Coll I-Cre transgene results in impaired skeletal formation. Bones of $Mdm2^{flox/flox}$ Coll I-Cre (Mutant) embryos are shorter, exhibit increased porosity, and have less mineral content than their $Mdm2^{flox/+}$ Coll I-Cre (Wildtype) littermates. To characterize the molecular basis for the decreased bone quality observed in these animals, we isolated calvarial pre-osteoblasts and induced them to differentiate *ex vivo*. In these cultures, mutant pre-osteoblasts proliferate identically to pre-osteoblasts isolated from wild type littermates and both cell types reach confluence concomitantly. In post-confluent cultures, however, the Coll I-Cre transgene becomes active in multilayering pre-osteoblasts resulting in Mdm2 excision and subsequently preventing the increase in Mdm2 expression observed in wild type cultures. The loss of Mdm2 in these cells prevented multilayered nodule formation *ex vivo* due to inhibition of post-confluent cell division. Further, mutant cultures that have ablated Mdm2 activity fail to activate the master osteogenic transcriptional regulator Runx2, and therefore fail to induce osteoblast associated phenotypic genes such as Alkaline Phosphatase and Osteocalcin. Thus, Mdm2 is genetically upstream of the mechanism mediating the bone-specific induction of Runx2. In addition, Mdm2 performs a novel osteogenic function that supports progression of osteoblast differentiation and post-confluent nodule formation.

Disclosures: ***C.J. Lengner****, None.*

1016

A Mutation in the *Osteoactivin/Gpnmb* Gene Alters Bone Remodeling in Mice. M. C. Rico[1], M. G. Anderson*[2], A. M. Virgen*[1], J. L. Castañeda*[1], S. W. M. John*[2], S. N. Popoff[1], F. F. Safadi[1]. [1]Anatomy and Cell Biology, Temple University School of Medicine, Philadelphia, PA, USA, [2]The Jackson Laboratory, Bar Harbor, ME, USA.

Osteoactivin/Gpnmb is a glycosylated protein implicated in osteoblast matrix production and mineralization. Previous studies from our laboratory have demonstrated that a synthetic osteoactivin peptide induces osteoblast differentiation associated with increased alkaline phosphatase activity, nodule formation, osteocalcin production and calcium deposition *in vitro*, and stimulates bone formation *in vivo.* A mutation on chromosome 6 of the *osteoactivin/Gpnmb* gene in mouse strains DBA/2J(D2) and Black 6 (B6) results in a premature stop codon leading to the production of a truncated osteoactivin/Gpnmb protein. Western blot and RT-PCR analyses confirmed the absence of osteoactivin/Gpnmb protein and message in the mutant when compared to control bones. Radiological analysis revealed an increase in bone size and radioopacity in the *osteoactivin/Gpnmb* mutant compared to control animals. Histological analysis also showed a decrease in adipocytes at the bone marrow cavity in *osteoactivin/Gpnmb* mutants compared to age- and gender-matched normal controls. Micro-CT measurements of femurs in the B6 mice revealed an increase in bone volume (BV/TV) (75%), trabecular number (Tb.N) (40%), and trabecular thickness (Tb.Th) (25%), and a decrease in trabecular space (Tb.Sp) (53%) in *osteoactivin/Gpnmb* mutants versus control. These data suggest that Osteoactivin/Gpnmb plays an important role in bone formation/remodeling. Total RNA isolated from long bones of *osteoactivin/Gpnmb* mutant and control animals were subjected to microarray analysis for differentially expressed genes using the mouse genome 430A GeneChip Array from Affymetrix. The expression of multiple bone-related genes was altered. These included sclerostin, an osteocyte-derived negative regulator of bone formation, which was increased (3.3-fold) in *osteoactivin/Gpnmb* mutants compared to controls. Wisp1 (Wnt-induced secreted proteins-1/CCN4), a novel CCN member that has been shown to mediate cell adhesion, extracellular matrix production and cell migration, was decreased (3.7-fold) in *osteoactivin/Gpnmb* mutants compared to controls. Further analysis of these genes may enhance our understanding of the mechanism(s) of action of osteoactivin/Gpnmb in bone formation/remodeling. These data support the hypothesis that osteoactivin/Gpnmb is a novel bone protein that regulates osteoblast differentiation and bone formation. Future studies using this mutation will help to elucidate the mechanism(s) of action and signaling pathways associated with osteoactivin/Gpnmb function in bone.

Disclosures: ***M.C. Rico****, None.*

1017

Transgenic Mice Over-Expressing Dkk-1 in Osteoblasts Develop Osteoporosis. J. Li, I. Sarosi*, S. E. Morony, D. Hill*, Y. Wang*, W. Qiu*, S. Adamu*, M. Grisanti*, K. Hoffmann*, T. Gyuris*, H. Nguyen*, R. Cattley*, P. J. Kostenuik, S. S. Simonet, D. L. Lacey. Amgen Inc., Thousand Oaks, CA, USA.

Skeletal homeostasis is maintained by a delicate balance between osteoclasts and osteoblasts. Imbalance can lead to skeletal pathologies with altered bone mineral density (BMD). Recently, strong human and murine molecular genetic data have pointed to the Wnt co-receptor LRP5 as a critical regulator of bone formation. Several loss-of-function mutations in the LRP5 gene cause osteoporosis-pseudoglioma (OPPG) syndrome in humans. Accordingly, LRP5 knockout mice have low BMD due to a defect in osteoblast proliferation and function, and these mice phenotypically resemble human OPPG patients. Conversely, gain-of-function mutations in LRP5 lead to high bone mass (HBM) in humans and transgenic mice. Dickkopf-1 (Dkk-1) is a secreted Wnt signaling inhibitor that directly binds to LRP5. In vitro signaling analysis of one of the HBM LRP5 mutation G171V demonstrated that the molecular defect in HBM LRP5 signal transduction may result from loss of Dkk inhibition to LRP5. To investigate the role of Dkk-1 in osteoblast biology, we have generated transgenic mice that over-express the murine Dkk-1 gene in the osteoblast lineage driven by rat Col1a1 promoter. RNA analysis confirms the over-expression of Dkk-1 transgene in transgenic bone tissue. Radiographically, decreased radiodensity was observed in the long bones and vertebral columns of high-expressor adult transgenic mice. Calvaria from the transgenics were very thin and flattened while also being discontinuous in places. BMD measurements of the tibial metaphysis by pQCT demonstrated that total, cortical and trabecular BMDs were significantly decreased when compared with wild-type littermate controls. In addition, serum concentration of osteocalcin, an osteoblast marker, is also significantly reduced in the Dkk-1 transgenics. Preliminary histologic analysis revealed that the transgenics had less trabecular bone present in the long bones and vertebrae. The transgenics also had very thin calvaria with some areas of bone being replaced by connective tissue. Moreover, bone histomorphometry analysis indicates that osteoblast cell number (NOb/TAr) and bone volume (BV/TV) are both decreased in the transgenics, while osteoclast parameters (NOc/TAr) remain unchanged. In summary, our current data demonstrates that transgenic over-expression of Dkk-1 in osteoblasts leads to a low bone mass phenotype. Therefore, these results not only confirm the critical function of Wnt signaling in bone biology, but also further support the important role that Dkk-1 may play in osteoblast biology and bone mass regulation.

Disclosures: ***J. Li****, Amgen Inc. 1, 3.*

1018

α1 Collagen Promoter-Directed Overexpression of Dkk1 in Mice Causes Dwarfism and Very Short Limbs. J. Guo, F. R. Bringhurst, H. M. Kronenberg. Endocrine Unit, Massachusetts General Hospital and Harvard Medical School, Boston, MA, USA.

Dickkopf1 (Dkk1) is a secreted protein that acts as a Wnt pathway inhibitor by binding to and antagonizing Lrp5/6. Using microarray technology, we observed a dramatic down-regulation of Dkk1 mRNA after PTH treatment of embryonic tibia ex vivo. The PTH/PTHrP receptor (PTHR) has been shown to play an important role not only in embryonic endochondral bone development but also in postnatal bone modeling and remodeling. To determine whether suppression of Dkk1 mediates PTHR actions during bone development, we first examined the effect of PTH on Dkk1 mRNA expression, using bone explants. Using in situ hybridization we found that Dkk1 is expressed early in the perichondral cells adjacent to prehypertrophic and hypertrophic regions in the tibia at E14.5. Treatment of cultured tibiae and femurs at E14.5 with hPTH (100 nM) for 6 hr led to a fall of Dkk1 mRNA, as shown by in situ hybridization and confirmed by real-time PCR. Similar inhibition of Dkk1 mRNA expression in osteoblastic cells was also observed in cultured rudiments at E15.5 and 16.5 in a time-dependent manner with a maximal effect at 8 hr of treatment. These observations suggest that PTH-induced down-regulation of Dkk1 might mediate some actions of PTHR on bone development and remodeling. To examine the role of Dkk1 in osteoblast differentiation and the role of suppression of Dkk1 in PTH action on bone, we generated a mouse model in which Dkk1 is overexpressed under the control of a 2.3 kb fragment of the mouse alpha1(I) collagen promoter. Mutant mice are small, with very short limbs and deletion of digits, suggesting that Dkk1 transgenic mice may phenocopy Lrp6-/- and perhaps Lrp5-/- abnormal bone development. Studies *in vivo* and *in vitro* will determine how non-suppressible Dkk1 expression affects PTH/PTHrP action.

Disclosures: ***J. Guo****, None.*

1019

A Tale of Two Steroids: Testosterone and Estradiol Are Related to Incident Fracture Risk in Older Men. E. S. Orwoll[1], L. Lambert[1], L. Marshall[1], J. Cauley[2], M. Nevitt[3], D. Bauer[3], E. Barrett-Connor[4], S. R. Cummings[5]. [1]Bone and Mineral Research Unit, Oregon Health & Science University, Portland, OR, USA, [2]U Pittsburgh, Pittsburgh, PA, USA, [3]U California, San Francisco, San Francisco, CA, USA, [4]U California, San Diego, San Diego, CA, USA, [5]San Francisco Coordinating Center at CPMC, San Francisco, CA, USA.

The effects of gonadal function on skeletal health in older men are controversial; no data exist concerning the influence of sex steroids on incident fracture risk. The relationships of serum estradiol (E) and testosterone (T) levels to fracture risk were studied in the MrOS cohort. 5995 community dwelling men ≥65 yrs recruited at 6 clinical sites in the US were extensively characterized, including measures of anthropometry, neuromuscular function and BMD. Sensitive methods were used to assay baseline AM total sex steroid, SHBG and albumin levels in archived serum from a randomly selected subset of 2618 men; bioavailable steroid levels (bE, bT) were derived from mass action equations. Incident non-vertebral fractures in that cohort were documented during an average follow-up of 2.7 yrs. Multivariate proportional hazards regression analysis was used to assess the independent relationships of variables to fracture risk. The overall fracture rate was 12.8 per 1000 person-years, and participant follow-up was ~98%. Baseline bE was positively related to baseline total hip BMD ($p<0.001$) but bT was not related to BMD ($p= 0.45$). However, in age adjusted analyses bT and bE were each inversely related to incident fracture risk (hazard ratio [HR] per SD decrease in bE= 1.4; CI 1.0-1.8, and in bT= 1.4; 1.1-1.7). BMD was also strongly related to fracture risk (HR 1.6; 1.3-2.1). The inclusion of bT, bE and BMD in the model attenuated the association of bE with fracture risk (HR 1.1; 0.8-1.5), but did not materially alter the bT-fracture risk relationship (HR 1.3; 1.0-1.6). After further adjustment for fall history, body composition, and race, lower levels of bT (HR 1.24; 1.0-1.6) were independently related to fracture risk, while the effect of estrogen remained insignificant (HR 1.1; 0.8-1.6). In sum, lower levels of bT and bE are both related to increased incident fracture risk in older men. The association of bE appears to be mediated to a large extent by BMD. In contrast, bT is not related to BMD and its effects on fracture risk are apparently the result of other pathways. These analyses indicate that gonadal function exerts important effects on fracture risk in older men via complex mechanisms. Moreover, they suggest that sex steroid measures may be useful in assessing fracture risk and that therapies based on sex steroid action could be effective in preventing fractures in older men.

Disclosures: ***E.S. Orwoll****, None.*

1020

Plasma Retinol and Retinyl Esters as Predictors of Incident Osteoporotic Fracture in Elderly Women. M. E. Barker*[1], E. V. McCloskey[2], S. Saha*[1], F. Gossiel*[2], H. J. Powers*[1], A. Blumsohn[2]. [1]Human Nutrition Unit Division of Clinical Science (North), University of Sheffield, Sheffield, United Kingdom, [2]Bone Metabolism Group Division of Clinical Science (North), University of Sheffield, Sheffield, United Kingdom.

Recent studies have suggested that higher Vitamin A intake may account for a component of fracture risk and lower BMD, and that supplemental Vitamin A may be harmful even within recommended limits. No studies have examined the relationship between biochemical retinol status and fracture in older women.

We examined plasma retinol, retinyl palmitate and β-carotene as predictors of incident fracture in a large prospective study of British women over age 75 (n=2790, 312 incident osteoporotic fractures, 92 incident hip fractures; mean follow-up duration 3.9 years). Fasting blood samples (09:00-11:00) were collected at baseline.

In a case control analysis (3 controls per case) using Cox proportional hazards regression, plasma retinol, retinyl palmitate and β-carotene were assessed as univariate predictors of all osteoporotic fractures and hip fracture in particular. Baseline BMD at the total hip (Hologic QDR4500), age, 25(OH)D, sβCTX, bone ALP, weight, height, and smoking were considered as covariates in a multivariate model.

Plasma retinol, retinyl palmitate and β-carotene were not significant univariate predictors of either hip fracture or any fracture (all $P>0.05$). For all osteoporotic fractures the hazard ratio was 0.95 (95% CI 0.86-1.06) for a 1SD increase in plasma retinol. There was a tendency for increased plasma retinol to predict benefit rather than harm in terms of fracture (Table) and BMD ($r=0.07$, $P=0.012$). Vitamin A supplementation was associated with a significantly lower risk of any fracture (hazard ratio 0.76, 95% CI 0.60-0.96). In multivariate analysis, only age, total hip BMD and weight were associated fracture risk ($P<0.05$). In conclusion, we have found no evidence to support any skeletal harm associated with higher dietary retinol intake or modest retinol supplementation in this population.

Unadjusted hazard ratios for incident osteoporotic fracture (95% CI)

Quartile of plasma retinol	Hazard ratio	P
Q1 (low)	1.00	
Q2	1.15 (0.96-1.38)	0.128
Q3	0.89 (0.73-1.09	0.273
Q4	0.85 (0.69-1.05)	0.132
Per 1 SD increase	0.95 (0.86-1.06)	0.371

Disclosures: ***M.E. Barker****, None.*

1021

Adipocyte Hormones and Fracture Risk in Older Men and Women. J. A. Cauley[1], A. Kanaya[2], F. Harris*[2], E. Strotmeyer[1], J. Lee*[2], J. M. Zmuda[1], D. Bauer[2], S. Cummings[3], F. Tylavsky*[4], T. Harris*[5], K. Ensrud*[6], A. Newman[1]. [1]U of Pittsburgh, Pittsburgh, PA, USA, [2]UCSF, San Francisco, CA, USA, [3]California Pacific Medical Center, Research Institute, San Francisco, CA, USA, [4]U of Memphis, Memphis, TN, USA, [5]NIA, Bethesda, MD, USA, [6]U of Minnesota, Minneapolis, MN, USA.

Men and women with higher body weight have higher bone mass and suffer fewer fractures. Biomechanical factors are important in mediating this association but biochemical factors secreted by adipose tissue may also contribute. Leptin regulates energy homeostasis and has direct action on bone but studies in humans are not consistent. Adiponectin has anti-inflammatory properties and may also contribute. Unlike leptin, adiponectin levels are lower in obese subjects. To test the hypothesis that leptin and adiponectin predict fractures independent of body weight, we analyzed data from the Health Aging and Body Composition Study of 3,075 white and black, well functioning men and women age 70-79 y. Leptin and adiponectin concentrations were measured in fasting serum at baseline by radioimmunoassay. Total hip BMD was measured by DXA (Hologic 4500A). 228 non-traumatic fractures were confirmed by x-ray report over a mean follow-up of 4.7 years. Cox proportional hazards models were used to estimate the Relative Hazard (RH) (95% Confidence Interval, CI) of fracture by quartile of adipocyte adjusting for age, gender, race and body weight. There was an inverse association between adiponectin and BMD even after adjusting for weight, but there was no association between leptin and BMD. Leptin was not associated with the risk of fracture (Table). Subjects with higher adiponectin levels tended to be at higher risk of fracture, but these results were not significant. The RH (95% CI) of fracture in subjects in Quartiles 2 through 4 compared to Quartile 1 was 1.44 (0.97, 2.14) (p=0.07). Models in which we substituted total body fat for body weight yielded similar results. In summary, circulating levels of leptin are not related to fractures. Subjects with higher adiponectin levels may be at increased risk of fracture, independent of body weight.

Table: Relative Hazard (95% CI) of Fracture by Quartile of Leptin and Adiponectin

	Leptin (ng/ml)		Adiponectin (µg/ml)	
Quartile	RH (95% CI)†	RH (95% CI)±	RH (95% CI)†	RH (95% CI)±
1 (Low)	Referent	Referent	Referent	Referent
2	1.02 (0.67, 1.55)	1.01 (0.67, 1.54)	1.31 (0.82, 2.08)	1.31 (0.82, 2.08)
3	1.20 (0.76, 1.88)	1.16 (0.72, 1.87)	1.59 (1.04, 2.43)	1.58 (1.03, 2.42)
4 (High)	0.97 (0.62, 1.52)	0.93 (0.57, 1.52)	1.43 (0.91, 2.23)	1.41 (0.89, 2.24)

†adjusted for age, race, gender

±adjusted for age, race, gender, and body weight

Disclosures: ***J.A. Cauley****, Merck 2, 8; Eli Lilly 2, 8; Pfizer 2; Novartis 2, 5.*

1022

Reduced Nerve Function Is Related to Lower Hip BMD and Heel QUS in Older White and Black Adults. E. S. Strotmeyer[1], J. A. Cauley[1], A. V. Schwartz[2], N. de Rekeneire*[3], H. E. Resnick*[4], B. Goodpaster*[1], R. Shorr*[5], F. A. Tylavsky[5], A. I. Vinik*[6], T. B. Harris*[3], A. B. Newman*[1]. [1]University of Pittsburgh, Pittsburgh, PA, USA, [2]University of California, San Francisco, CA, USA, [3]National Institute on Aging, Bethesda, MD, USA, [4]MedStar Research Institute, Hyattsville, MD, USA, [5]University of Tennessee Health Science Center, Memphis, TN, USA, [6]Eastern Virginia Medical School, Norfolk, VA, USA.

Bone tissue is innervated, yet little is known about the impact of nerve function on bone mineral density (BMD). Poor nerve function may contribute to lower BMD and higher fracture risk, particularly in those with diabetes complications of neuropathy. The Health, Aging, and Body Composition Study included yearly prospective exams in white and black men and women age 70-79 years and physically able at baseline from Pittsburgh and Memphis. Nerve function in legs/feet was assessed at year 4 by pain/numbness self-report, 1.4 and 10 g monofilament detection, vibration threshold, and peroneal motor nerve conduction velocity and amplitude. Total hip BMD, heel broadband ultrasound attenuation (BUA), total fat and lean mass were measured at year 5 (QDR 4500A, Sahara QUS; Hologic Inc, Bedford, MA). Participants with year 4-5 data (N=2200) were 48% men and 37% black. Poor nerve function (lower monofilament detection, higher vibration threshold, lower amplitude, lower velocity) was associated with lower BUA (Table 1). Results were similar for hip BMD and significant for monofilament and amplitude testing.

Table 1. BUA (dB/MHz)* by nerve test groups/quartiles

	1	2	3	4	p
Monofilament	70.4	71.0	73.2	-	0.007
Vibration threshold	72.9	73.2	71.3	71.5	0.11
Amplitude	69.6	70.9	72.8	74.1	<0.001
Velocity	70.3	70.7	71.8	74.1	0.002

*adjusted for gender, race, clinic site, age, diabetes, total lean and fat mass, lean and fat mass changes, strength, physical performance score

Lower monofilament detection and amplitude independently associated with lower heel BUA (p<0.01) and marginally associated with lower hip BMD in regression adjusted for Table 1 covariates and leg pain/numbness, falls, smoking, drinking, exercise, bone-active medications, and diabetes-related complications. Nerve function was thought to increase risk of fractures due to increased falls but may have a direct effect on bone, independent of falls and DM. Results suggest that for both diabetic and non-diabetic adults, those with poorer nerve function have lower heel BUA and BMD; although whether those with impaired nerve function are at higher risk for fracture is still unknown.

Disclosures: ***E.S. Strotmeyer****, None.*

1023

Quantitative Ultrasound Predicts Hip and Non-spine Fracture in Men: the MrOS Study. D. C. Bauer[1], J. A. Cauley[2], K. E. Ensrud[3], S. Ewing*[4], E. S. Orwoll[5]. [1]Medicine, UCSF, San Francisco, CA, USA, [2]Epidemiology, University of Pittsburgh, Pittsburgh, PA, USA, [3]Medicine, University of Minnesota, Minneapolis, MN, USA, [4]Epidemiology, UCSF, San Francisco, CA, USA, [5]Medicine, Oregon Health Sciences Univerity, Portland, OR, USA.

Quantitative ultrasound (QUS) predicts fracture risk among older women, but there are few prospective studies among older men. We studied the ability of QUS and BMD measurements to predict hip and other non-spine fractures in MrOS, a population-based study of older men.

Calcaneal QUS (Hologic Sahara) and femoral neck BMD (Hologic QDR 4500W) were measured in 5608 men >65 recruited from 6 US centers. At baseline duplicate QUS measurements with repositioning were obtained; if the first two BUA results differed by at least 10 dB/MHz, or if either was non-linear, a 3rd measurement was obtained. The mean of the two closest values was used. Subsequent hip and other non-spine fractures were documented by review of x-rays or x-ray reports. The relationships between QUS and fractures were examined with proportional hazard models adjusted for age and clinic, and results are presented as relative hazard (RH) with 95% confidence intervals (CI). Using logistic regression, receiver operator curves (ROC) were constructed and area under the curve (AUC) calculated to determine the overall ability of QUS, BMD or the combination of QUS+BMD to predict fracture outcomes. Analyses excluding non-linear measurements (one or more occurred in 16% of men) gave similar results and are not shown.

At baseline the mean (±SD) age was 73.6 ±5.8, BUA was 81.7±19.7 dB/Mz and BMDfn was 0.784±0.129 g/cm2. During a mean follow-up of 2.6 years with 99% complete follow-up, 164 men suffered a non-spine fracture, including 30 hip fractures. Lower BUA (per SD) was associated with an increased risk of hip (RH=1.97, CI: 1.32, 3.54) and non-spine fracture (RH=1.65, CI: 1.38, 1.96). The AUC were similar for BUA alone, BMDfn alone and the combination of BUA+BMD (Table), indicating that once BUA or BMD is known, the other measurement does not add useful information. Other QUS parameters (speed of sound and QUI) gave similar results.

We conclude that QUS measurements predict the risk of hip and other non-spine fracture in older men, and do so nearly as well as hip BMD measurements. Combined measurements of QUS and BMD are not superior to either measurement alone.

Table: AUC for BUA alone, BMDfn alone and the Combination of BUA+BMDfn

Fracture Type	AUC BUA	AUC BMD	AUC BUA+BMD
Non-spine	0.67	0.68	0.69
Hip	0.84	0.85	0.85

Disclosures: ***D.C. Bauer****, None.*

1024

SSRI Use Is Associated with Lower BMD among Men. E. M. Haney*[1], B. K. S. Chan[1], L. Lambert[1], J. Cauley[2], K. Ensrud[3], E. Orwoll[1], M. Blizniotes[1]. [1]Department of Medicine, Oregon Health & Science University, Portland, OR, USA, [2]University of Pittsburgh, Pittsburgh, PA, USA, [3]Univeristy of Minnesota, Minneapolis, MN, USA.

Functional serotonin transporters have recently been discovered in osteoblasts and osteocytes, and disruption of the serotonin transporter gene in mice results in osteopenia. Selective serotonin reuptake inhibitors (SSRIs) are a widely used class of anti-depressant medications that function by blocking the serotonin transporter and have been associated with hip fracture. We hypothesized that SSRI use would be associated with decreased bone mineral density (BMD).

5,995 men participating in the Osteoporotic Fractures in Men (MrOS) cohort had medications assessed and BMD at the femoral neck, greater trochanter, and lumbar spine measured by DXA (QDR4500W, Hologic, Inc). Other measures were obtained from self-reported questionnaires. We fit regression models on each BMD variable controlling for other covariates to assess the contribution of SSRI use to BMD.

158 men (2.7%) reported SSRI use. In multi-variate analyses, BMD among SSRI users was 3.2% lower at the femoral neck, 2.3% lower at the total hip, and 3.5% lower at the lumbar spine (see Table). These associations were not significantly different across SF-12 mental score quartiles. There was no significant interaction between SSRI use and trazodone and/or tricyclic use, nor did the use of these medications confound the relationship between SSRI use and BMD.

Adjusted BMD (g/cm2) for SSRI users vs. nonn-users (mean, s.d.)

	SSRI users	SSRI non-users	P value
Trochanter	0.752 (0.124)	0.766 (0.119)	0.162
Femoral Neck	0.760 (0.123)	0.785 (0.118)	0.011
Total Hip	0.936 (0.132)	0.958 (0.127)	0.034
Lumbar Spine	1.035 (0.187)	1.073 (0.180)	0.012

adjusted for age, site, use of trazodone and/or tricyclic anti-depressants, SF-12 mental and physical summary scores, average height, total lean mass, race, smoking, neuromuscular function (chair stands), medical history, multivitamin use, steroid and bisphosphonate use.

This cross-sectional study demonstrates that femoral neck and lumbar spine BMD are significantly lower among older men using SSRIs. If these results are confirmed in other populations, people using SSRIs might be targeted for osteoporosis screening.

Disclosures: ***E.M. Haney****, None.*

1025

Osteoclast Inhibitory Lectin (OCIL) Is Required for Normal Bone Remodelling *in vivo* and Inhibits Osteoblast Function *in vitro*. A. Nakamura*[1], J. M. W. Quinn[1], N. A. Sims[2], C. T. Gange*[1], H. Zhou[1], V. Kartsogiannis[1], E. H. Allan*[1], T. J. Martin[1], K. W. Ng[3], M. T. Gillespie[1]. [1]St. Vincent's Institute of Medical Research, Fitzroy, Australia, [2]Dept. Medicine, The University of Melbourne, Fitzroy, Australia, [3]Dept Diabetes and Endocrinology, The University of Melbourne, Fitzroy, Australia.

OCIL is a C-type lectin expressed by osteoblasts which binds sulphated glycosaminoglycans and NK cell receptors and was originally identified by its ability to inhibit osteoclast differentiation *in vitro*. To determine whether OCIL is required for normal bone metabolism, we generated OCIL null mice (*ocil*$^{-/-}$) and examined their bones by histomorphometry.

Ocil$^{-/-}$ mice were fertile and grossly normal, but tibial trabecular bone volume and cortical thickness were significantly lower (by 22% and 15% respectively) in 10 week old *ocil*$^{-/-}$ mice relative to age matched wild type mice. This osteopenia was associated with high bone turnover, showing a 153% increase in osteoclast surface (OcS/BS), consistent with previously described anti-osteoclastogenic action of OCIL. In addition, osteoblast surface (ObS/BS), and osteoid volume (OV/BV) were approximately treble that of control mice. We thus examined OCIL action on osteoblasts mineralisation and osteoblast marker gene expression by primary osteoblasts and pre-osteoblastic KUSA O cells *in vitro*. While OCIL did not affect proliferation or cell morphology in osteoblasts and KUSA O cells it profoundly inhibited mineralisation by these cells when treated with ascorbate and β-glycerophosphate for 21 days. Under these conditions, KUSA O mRNA expression of osteopontin, alkaline phosphatase, BSP and osterix were unaffected, but osteocalcin expression was strongly inhibited within the first 3 days, which occurred in a dose-dependent manner. This was also noted when cells were treated with ascorbate for 14 days prior to OCIL addition. Insulin/dexamethasone/IBMX-stimulated adipocyte differentiation of KUSA O cells was also inhibited by OCIL. Furthermore, OCIL expression was elevated in clonal sub-lines of KUSA O that could not mineralise, differentiate into adipocytes or express osteocalcin. In addition, BMP-2 treatment of KUSA O resulted in a decrease in OCIL mRNA expression.

Our data indicates *ocil*$^{-/-}$ mice show increased osteoblast numbers and function as well as increased osteoclast numbers. The finding that OCIL reduces osteoblast function *in vitro*, an effect that may be related to reduced osteocalcin production is consistent with the in vivo findings. The combined effects of OCIL to inhibit osteoclast and osteoblast formation, and studies from the *ocil*$^{-/-}$ mice, confirm that OCIL plays an important role in both bone resorption and formation.

Disclosures: ***A. Nakamura****, None.*

1026

In Vivo and in Vitro Evidence that Activation of NFAT1/NFATc2 Is Critical to Osteoclast Differentiation. F. Ikeda[1], T. Matsubara[1], K. Hata*[1], S. V. Reddy[2], R. Nishimura[1], T. Yoneda[1]. [1]Dept Biochem, Osaka Univ Grad Sch Dent, Osaka, Japan, [2]Div Hematol Oncol, Univ Pittsburgh Cancer Inst, Pittsburgh, PA, USA.

RANKL is a key cytokine in the regulation of osteoclast differentiation. Recently, a transcription factor NFAT2/NFATc1 has been identified as a target of RANKL by microarray profiling and is shown to play an important role in osteoclast differentiation in vitro. However, the role of NFAT family in the regulation of osteoclast development in vivo has not been clarified yet. NFAT2 deficient mice were embryonic lethal and mice deficient in each of other NFAT family members failed to show distinctive phenotype in bone presumably due to the compensation by other family members. To obtain compelling evidence for an important role of NFAT family in osteoclastogenesis in vivo, we generated transgenic mice in which constitutive-active NFAT1 was specifically expressed in osteoclast lineage under the control of TRAP gene promoter. These transgenic mice (TG) were fertile but much smaller than the wild-type (WT) mice. Radiograph and micro CT analyses demonstrated that bone mass was clearly reduced in TG compared with WT. Histological examinations revealed a significant reduction in trabecular bone volume in TG. Ex vivo experiments using M-CSF-dependent spleen macrophages isolated from TG or WT mice showed that the number of osteoclast-like cells formed was increased in TG compared with WT, suggesting that the decreased bone mass in TG is due to an increase in osteoclast formation. We then studied the mechanism underlying NFAT activation in vitro. Of interest, western analysis demonstrated that NFAT1/NFATc2 was expressed in un-stimulated osteoclast precursors derived from bone marrow macrophages, while NFAT2 expression was not detected, suggesting that NFAT1 is constitutive and NFAT2 may be inducible. Consistent with this notion, overexpression of NFAT1 in M-CSF-dependent spleen macrophages using retrovirus system induced NFAT2 expression. Furthermore, NFAT1 overexpression induced TRAP-positive multinucleated osteoclast-like cell formation and elevated TRAP gene promoter activity. Since activated NFAT1 exhibits nuclear translocation, sub-cellular localization of NFAT1 in the monocytic RAW264.7 cells was examined. Upon treatment with soluble RANKL, NFAT1 was translocated into the nucleus. In conclusion, our results for the first time demonstrate that NFAT1 activation is important to osteoclastogenesis both in vivo and in vitro. Our data suggest that the underlying mechanism is that RANKL-activated NFAT1 promotes osteoclast formation through inducing NFAT2 expression and upregulating the TRAP gene transcription following nuclear translocation.

Disclosures: ***F. Ikeda****, None.*

1027

IKKα Is Required for NFATc1 Upregulation during Osteoclastogenesis. M. L. Chaisson*, A. P. Armstrong*, M. E. Tometsko*, W. C. Dougall. Cancer Biology, Amgen, Inc., Seattle, WA, USA.

Signaling via the TNFR family member RANK is required for osteoclast differentiation. We have recently demonstrated a role for the IκB kinase α (IKKα) during RANK-mediated osteoclastogenesis, as IKKα $^{-/-}$ hematopoietic fetal liver cells fail to form large, multinucleated osteoclasts when cultured in the presence of RANKL. These defects occurred despite normal activation of NF-κB p65/p50 (as measured by IκBα degradation and resynthesis) and MAP kinases p38, JNK, and ERK. However, IKKα was required for activation of the non-canonical NF-κB pathway involving processing of p100 into p52. As recent studies have also implicated the transcription factor NFATc1 as a critical component of RANKL-mediated osteoclastogenesis, we wished to determine if NFATc1 activation was perturbed in the absence of IKKα. We analyzed mRNA from wild-type and IKKα$^{-/-}$ fetal liver cells treated for 6 days with CSF-1 +/- RANKL. In wild-type cells, RANKL treatment increased NFATc1 gene expression by >10-fold , but in IKKα$^{-/-}$ cells, no significant increases were observed in NFATc1 expression following RANKL treatment. To determine if a relationship existed between NFATc1 upregulation and p100 processing, we examined the timing of p100 processing and NFATc1 protein expression in both wild-type and IKKα$^{-/-}$ cells treated with RANKL. In wild-type cells, p100 processing was activated 24 hours after RANKL treatment and was followed by a dramatic increase in NFATc1 protein levels at 48 hours. However, in IKKα$^{-/-}$ cells, RANKL treatment failed to stimulate p100 processing or significantly increase NFATc1 protein levels. To determine if inhibition of p100 processing affected NFATc1 upregulation, we treated RAW264.7 cells with the proteasome inhibitor MG132 prior to RANKL treatment. MG132 blocked both p100 processing and NFATc1 upregulation, indicating that a proteasome-dependent event is required for NFATc1 upregulation in response to RANKL. As IκBα degradation is also dependent on proteasome activity, we next determined if TNFα, which activates IκBα degradation but not p100 processing, could increase expression of NFATc1 in osteoclast precursor cells. Treatment of either RAW264.7 cells or CSF-1 derived wild-type fetal liver cells with TNFα did not lead to increased NFATc1 protein. Interestingly, while TNFα treatment in combination with RANKL rescues osteoclast differentiation in IKKα$^{-/-}$ cells, we did not observe p100 processing or increased NFATc1 protein in IKKα$^{-/-}$ cells treated with TNFα + RANKL, suggesting that osteoclastogenesis can occur independently of IKKα and NFATc1. Taken together, these data indicate a novel regulatory role for IKKα and p100 processing in the upregulation of NFATc1 during osteoclastogenesis.

Disclosures: ***M.L. Chaisson****, Amgen, Inc. 1, 3.*

1028

The Alternative NF-κB Pathway, via RelB, Is Critical for Stimulated Osteoclastogenesis. D. V. Novack, T. Johnson*, M. Alhawagri*. Medicine, Washington University, St. Louis, MO, USA.

Osteoclasts (OCs) are derived from M-CSF-dependent myeloid bone marrow progenitors under the influence of RANKL. Like some other members of the TNF family (BAFF, CD40L, Lτβ), RANKL activates both the classical and alternative NF-κB pathways. The classical pathway is activated rapidly by the IKK complex, leading to nuclear translocation of p65/p50. The alternative pathway is controlled by NIK, whose activation leads to processing of p100, the precursor of p52 and the IκB for RelB. Over several hours, RelB/p52 complexes accumulate in the nucleus. Blockade of both classical and alternative NF-κB pathways, such as in p50$^{-/-}$/p52$^{-/-}$ mice, abolishes OC differentiation at a very early stage. We previously found that, in the absence of NIK, p100 is not processed, and accumulates in the cytoplasm where it can bind p65 and RelB, inhibiting their nuclear translocation, and resulting in decreased OC formation. Thus, although NIK is directly involved with the alternative pathway, removal of NIK perturbs the classical pathway as well.

To specifically assess the role of the alternative pathway in pathological bone loss, we analyzed the role of RelB in RANKL signaling and osteoclastogenesis. Like NIK$^{-/-}$ cultures, RelB$^{-/-}$ precursors generate few mature spread OCs when grown in M-CSF and RANKL. Classical NF-κB signaling based on p65 is similar to WT in both RelB$^{-/-}$ macrophages and preOCs, in contrast to NIK$^{-/-}$ preOC cultures which have diminished p65 signaling. These data suggest that RelB itself is important for optimal osteoclastogenesis, and we next investigated RANKL-mediated RelB signaling more fully. In WT cells, RelB mRNA and protein expression are induced by RANKL 3x within the first 24 hours. In this same time period, nuclear RelB levels rise 10x, indicating regulation beyond increased expression. In OC precursors lacking NIK, RelB is expressed at similar levels to WT, but is not found in the nucleus, due to its cytoplasmic retention by p100. We therefore asked if osteoclastogenesis could be rescued in NIK$^{-/-}$ cultures by retrovirus-mediated overexpression of RelB, which might overwhelm the binding capacity of p100. In contrast to NIK$^{-/-}$ cultures transduced with control empty pMX, NIK$^{-/-}$ cultures with pMX-RelB generate OCs similar to empty pMX-transduced WT controls. In summary, we show for the first time that RelB is required for optimal OC formation in vitro, and that overexpression of RelB can compensate for the absence of NIK. The alternative NF-κB pathway controlled by NIK and RelB regulates pathological induction of osteoclastogenesis, and represents a potential target for therapy of diseases mediated by OC overactivity, such as osteoporosis.

Disclosures: ***D.V. Novack****, None.*

1029

The LIM-Only Protein, FHL2, Suppresses TRAF6-Mediated Osteoclastogenesis. S. Bai[1], J. Chen*[2], F. P. Ross[1], S. L. Teitelbaum[1]. [1]Department of Pathology, Washington University School of Medicine, St. louis, MO, USA, [2]Medicine, University of California at San Diego, La Jolla, CA, USA.

TRAF6 associates with the cytoplasmic domain of RANK, an event central to normal osteoclastogenesis. We used the yeast two-hybrid system with a mouse embryo cDNA library to identify novel proteins which interact with TRAF proteins with the aim of determining their role in osteoclast recruitment and function. By this approach, and subsequent co-immunoprecipitation, we discovered TRAF6 interacts with FHL2, a LIM-only protein which functions, in a cell-dependent manner, as a transcriptional co-activator or co-repressor. We also find that full-length FHL2 is required for its interaction with TRAF6 and the TRAF domain of TRAF6 recognizes FHL2. Consistent with a role in modulating TRAF6 mediated osteoclastogenesis, FHL2 mRNA and protein are undetectable in marrow macrophages and increase *parri passu* with osteoclast differentiation. Furthermore, when overexpressed in different cell lines, FHL2 inhibits TRAF6-induced NF-κB activity, indicating FHL2 may act as a repressor in RANKL/RANK signaling. Supporting this contention, 1) IκB-α phosphorylation is enhanced in FHL2-/- osteoclasts and overexpression of FHL2 in WT macrophages inhibits RANKL induced IκB-α phosphorylation and osteoclastogenesis; 2) FHL2-/- macrophages differentiate into enlarged osteoclasts with highly developed actin rings earlier than WT osteoclasts; 3) resorption pits excavated on dentin by FHL2-/- osteoclasts are more numerous and deeper than WT. The interaction between RANK and TRAF6 is dose-dependently reduced by the presence of FHL2 in 293T cells overexpressing the proteins, indicating that the osteoclast suppressive properties of FHL2 reflects its impact on TRAF6-mediated RANK signaling. Finally, FHL2 interacts with HDAC-1 in the nucleus, again indicating FHL2 acts as a transcriptional co-repressor in RANKL/RANK signaling. FHL2 thus presents itself as a novel anti-resorptive target.

Disclosures: ***F. Chen****, None.*

1030

LIGHT (TNFSF14), A Novel Mediator of Normal and Pathological Bone Resorption. J. Edwards*[1], S. Sun*[2], C. Shipman*[1], N. Athanasou[1], A. Sabokbar[1]. [1]Botnar Research Centre, University of Oxford, Oxford, United Kingdom, [2]Xian Medical School, Military Hospital, China.

Members of the TNF super-family are involved in a broad range of biological functions such as cell proliferation and differentiation, apoptosis, lymphoid organogenesis and bone homeostasis. LIGHT, a recently identified TNF family member, is a type II transmembrane protein which is transiently expressed, and shed, from the surface of activated T cells and immature dendritic cells. LIGHT signals through two receptors, HVEM and LTβ receptor, which are found on the surface of T-cells and stromal cells respectively. As activated T-cells and T-cell products have been implicated in osteoclastogenesis, and a number of pathological bone disorders such as rheumatoid arthritis (RA), we sought to determine i) whether LIGHT can regulate RANKL/cytokine-induced murine/human osteoclast formation ii) the cellular mechanism by which LIGHT influences osteoclastogenesis and iii) if LIGHT is present in the serum of RA patients.

We found that LIGHT dose dependently (0-150 ng/ml) induces osteoclast formation and lacunar resorption in long-term cultures of murine RAW 264.7 cells and human CD14+ peripheral blood monocytes in the presence of M-CSF but in the absence of RANKL. Osteoclast formation was not inhibited by the addition of OPG and RANK:Fc. Neutralizing antibody studies showed that LIGHT-induced osteoclast formation was not mediated through other known promoters of osteoclastogenesis such as TNFα or IL-8. In addition, blocking of the HVEM receptor did not affect the process of osteoclast formation. However, addition of blocking antibodies to the p75 component of the TNF receptor resulted in 75.1% inhibition in LIGHT-induced osteoclast formation ($p<0.001$), suggesting that LIGHT may act via this receptor.

Combined treatment with LIGHT and RANKL induced 85.1% ± 2.2% mean resorption; this was significantly greater than treatment with LIGHT (19.1% ±2.3%) or RANKL (49.6% ±5.9%) alone ($p<0.0001$). In contrast, combined treatment with LIGHT and TNFα did not result in a significant increase in bone resorption compared to treatment with each factor alone. Serum analysis of LIGHT by ELISA demonstrated a significant increase ($p<0.05$) in RA samples (233.2 ± 31.1 pg/ml) when compared to age/gender matched controls (102.2 ± 21.1 pg/ml).

Our results suggest that LIGHT stimulation can induce osteoclast formation independent of RANKL; it also promotes RANKL-mediated osteoclastogenesis and may be a novel mediator of bone resorption in inflammatory (T-cell associated) conditions in which there is extensive osteolysis.

Disclosures: ***J. Edwards****, None.*

1031

Osteocytes Communicate Fluid-Flow Mediated Effects to Osteoblasts Altering Their Phenotype. A. F. Taylor*, M. Saunders*, Z. Zhou*, H. Donahue. Orthopaedics and Rehabilitation, Penn. State College of Medicine, Hershey, PA, USA.

A major tenet of bone cell biology is that *in vivo* the osteocyte network senses mechanical perturbations and coordinates the required osteogenic response via communication with osteoblasts. However, while it has been demonstrated *in vitro* that osteocytes can communicate with osteoblasts via both gap junctional intercellular communication (GJIC) and through the secretion of soluble factors there is, surprisingly, no direct evidence that osteocytic cells communicate physiologically relevant (i.e. osteogenic) information to osteoblastic cells. To address this issue we developed an *in vitro* system that models the osteocyte-osteoblast network *in vivo*.

Osteocytic MLO-Y4 and osteoblastic hFOB 1.19 cells were cultured on opposite sides of perforated membranes (tracer studies confirmed a migration rate through the membrane of less than 2%). This system enabled us to apply physiological levels of fluid shear to MLO-Y4 cells while permitting them to be in direct contact with hFOB 1.19 cells that are not themselves exposed to flow induced shear stress. Dye transfer analysis with calcein-AM showed that MLO-Y4 cells are coupled via gap junctions to hFOB 1.19 cells cultured on the opposite side of the membrane. GJIC between MLO-Y4 and hFOB 1.19 cells was completely blocked by the application 30μM α-GA to the culture system.

Fluid shear was applied to the system by a rotating disc placed 500μm above the membrane, resulting in the network of MLO-Y4 cells experiencing a defined gradient of fluid shear. The shear gradient ranges from 0 at the center of the membrane to a maximal rate of fluid shear (τ max) at the edge of the membrane, a system we believe is more physiologically relevant than the uniform field generated by parallel plate models.Using this model we exposed MLO-Y4 cells to a τ max of 5 dynes/cm^2 for 1 hour and post incubated the co-cultures for 2 hours at 37^{0}C. Under these conditions a highly significant increase in alkaline phosphatase activity was detected in the hFOB 1.19 cells in contact with flowed MLO-Y4, compared to un-flowed control co-cultures ($P<0.01$). Interestingly, when hFOB1.19 were exposed either to direct flow (via the rotating disc or parallel plate system) or to conditioned media from flowed MLO-Y4 they did not display an increased alkaline phosphatase activity. Thus, osteocytic cells not only detect and communicate flow-induced signals to osteoblasts but, remarkably, enhance the signal enabling osteoblasts to respond to a signal they cannot themselves detect.

Disclosures: ***A.F. Taylor****, None.*

1032

Osteogenesis after Mechanical Loading Requires the P2X$_7$ Nucleotide Receptor. J. Li[1], D. Liu[2], H. Z. Ke[3], R. L. Duncan[2], C. H. Turner[2]. [1]Anatomy and Cell Biology, Indiana University School of Medicine, Indianapolis, IN, USA, [2]Orthopedic Surgery, Indiana University School of Medicine, Indianapolis, IN, USA, [3]Groton Laboratories, Pfizer Global Research and Development, Groton, CT, USA.

The P2X$_7$ nucleotide receptor (P2X$_7$R) is an ATP-gated ion channel expressed in bone cells. Mice with a null mutation of the P2X$_7$R have reduced periosteal bone formation and increased trabecular bone resorption compared to wildtype (WT) controls. The observed phenotype resembles the effects of disuse on the skeleton, suggesting that the P2X$_7$R may be necessary for the proper skeletal response to mechanical loading. We measured the skeletal response to loading in P2X$_7$R knockout (KO) mice. Axial loading of the ulna (2 Hz for 120 cycles) for 3 days induced new lamellar bone formation on the periosteal surface at midshaft in WT mice, but this response was greatly attenuated in KO mice ($p < 0.01$ by ANCOVA). Sensitivity to mechanical loading, as shown by the bone formation rate per unit of mechanical strain (in μstrain), was reduced by 61% in female or 73% in male KO mice (Figure A). To further study the role of P2X$_7$R in osteoblastic response to mechanical loading, calvarial cells isolated from newborn KO and WT mice were subjected to a steady laminar fluid flow at 12 dynes/cm^2 fluid shear stress (FSS). FSS caused release of ATP from the bone cells of both KO and WT mice within one minute. Thirty minutes of FSS induced P2X$_7$R mediated pore formation, as determined by measuring cellular uptake of YO-PRO-1 (MW=630) in WT cells, but not in KO cells. Sixty minutes of FSS significantly increased prostaglandin (PG) E_2 release by 120% ($p=0.03$) in WT cells, but PGE_2 release in KO cells was not significantly increased by FSS ($p = 0.52$) (Figure B). These data suggest that ATP signaling through the P2X$_7$R is necessary for FSS-induced membrane pore formation and PGE_2 release in calvarial osteoblasts. We conclude that the P2X$_7$R is a key to mechanotransduction in osteoblasts. A functioning P2X$_7$R is necessary for mechanically induced release of prostaglandins by bone cells and subsequent osteogenesis.

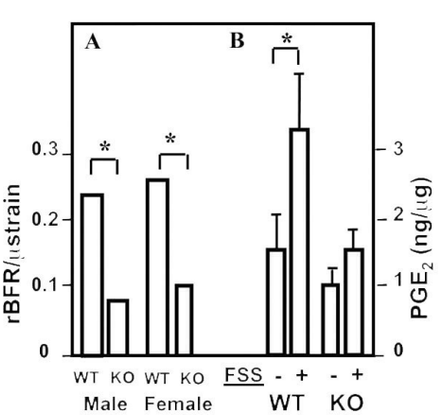

Disclosures: ***J. Li****, None.*

1033

Glutamate Signalling and LTP-like Mechanisms Account for Loading Memory in Osteoblasts. E. A. Bowe*, T. Notomi*, A. Horner*, T. Skerry. Royal Veterinary College, London, United Kingdom.

It is well known that the skeleton does not require long durations of exercise for maximal response to loading. This suggests either that cells are immediately and constantly sensitive to short durations of strain change, or that some cellular mechanism retains the information that a bone has been loaded. Since the discovery that glutamate functions in bone as an intercellular signalling agent, the possibility has been raised that the same long term potentiation (LTP) mechanisms that account for memory in the CNS could also occur in osteoblasts. NMDAR-dependent LTP occurs as a result of specific interactions of NMDA and AMPA type glutamate receptors with post-synaptic density proteins and in particular post-synaptic calcium calmodulin dependent kinase II (CaMKII).

To test the hypothesis that persistent loading responses are altered by interference with NMDAR-dependent LTP mechanisms in osteoblasts, we applied physiological strains (3400με at 1Hz) for 1,2,10, 20,40 and 80 minutes to ROS 17 2.8 cells plated onto coverslips (3 x10^5 cells/slip), using a 4 point bending device. 48 hours later, cell proliferation was assessed by Western blotting of lysates for PCNA corrected to β-actin. A dose dependent relationship was apparent between duration of loading and cell proliferation up to 10 minutes. After that time there was no further increase in proliferation, suggesting that 10 minutes of loading saturated the adaptive mechanism in these cells in vitro.

Further experiments were performed in which the same 10 minutes of loading of identical triplicate cultures had been preceded with treatments with either the NMDA receptor antagonist MK801 (100 μM), the AMPA receptor antagonist NBQX (50 μM) or the CaMKII antagonist KN93 (50 μM). In addition, plasmid based siRNA knockdown of either GluR2 or GluR3 subunits of the AMPA receptor were performed before loading. Control cultures were treated with vehicle, empty vector or GFP containing vector as appropriate.

Control cultures had a robust response to loading, with a 2 fold increase in proliferation. In contrast, MK801, NBQX and KN93 all abolished proliferative response to loading without affecting cell survival, as did GluR3 knockdown. Interestingly, GluR-2 knockdown induced apoptosis so no measurements of proliferation were possible, confirming previous data showing that glutamate signalling is essential for bone cell survival.

These results demonstrate that selective doses of agents that modulate processes involved in NMDAR-dependent LTP mechanisms remove the responsiveness of cells to what are saturating durations of loading, without affecting cells' viability. We interpret this to be evidence for strain memory in bone that resembles the mechanism in the brain.

Disclosures: ***E.A. Bowe****, None.*

1034

Specific Activation of the H-Ras Isoform Is Required for Mechanical Strain Inhibition of RANKL. J. Rubin, T. C. Murphy*, J. Rahnert*, M. S. Nanes, X. Fan. Medicine, Emory University and VAMC, Decatur, GA, USA.

Mechanical strain causes a magnitude dependent decrease in receptor activator of NFκB-ligand (RANKL) expression in murine stromal cells; this inhibition requires activation of the ERK1/2 kinase. To gain insight into the events leading to mechanical activation of ERK1/2, we examined proximal molecules in this MAPK signaling pathway. Ras proteins represent a family of GTPases that have variable location and specificity within the cell. At least 3 isoforms, H-, N- and K-Ras, are directly linked to ERK1/2 activation. We first asked whether mechanical strain caused Ras activation. For this study, strain was applied to primary murine stromal cells (2%, 0.2 Hz for 10 min, Flexcell Loading Station). Cell lysates were mixed with agarose immobilized Raf-1-GST which binds only activated Ras (i.e., Ras-GTP). Strained cells had measurable Ras-GTP while unstrained cells had little activated Ras unless treated with GTP. Post strain, activated Ras was easily measurable after capture by Raf-1-GST. The specificity of activated Ras was probed by western blot using Ras antibodies specific for H-, N- or K-Ras. The H-Ras isoform was activated by mechanical strain; N- and K-Ras isoforms were unaffected. We next wished to show that specific activation of the H-Ras isoform was necessary for downstream inhibition of RANKL expression. To this end we generated a silencing RNA for H-Ras using an Ambion "Silencer" siRNA Construction kit. Transduction with 40 nM siH-Ras caused a >70% decrease in H-Ras mRNA and protein 48h later; siH-Ras had no effect on K-Ras expression. Stromal cells were transduced with nothing (control), negative siRNA (siRNA-control) or the siH-Ras 24h prior to application of strain, which was continued overnight. Strain lowered RANKL expression to 76 ± 2% that of unstrained cells in both control and siRNA-control conditions (at 100 ± 5%). In those cells transduced with siH-Ras, the strain effect was completely abrogated. Interestingly, in both unstrained and strained cells treated with siH-Ras, expression levels of RANKL were significantly greater than in unstrained control and siRNA-control cells, ~135 ± 15% (no difference between unstrained and strain condition). This effect may indicate that H-Ras levels exert regulatory control over basal RANKL. In conclusion, mechanical strain downregulation of RANKL expression requires that the H-Ras isoform be activated, leading to downstream phosphorylation of ERK1/2. Our data suggests that the mechanotransducer sensitive to physiologic levels of strain may be identified through discrete associations with the H-Ras GTPase.

Disclosures: ***J. Rubin****, None.*

1035

Identification of an Osteocyte-specific, Mechanically Regulated Region of The Dentin Matrix Protein 1 Promoter. W. Yang[1], I. Kalajzic*[2], Y. Lu*[1], D. Guo[1], M. A. Harris[3], J. Gluhak-Heinrich*[3], L. F. Bonewald[1], J. Q. Feng[1], D. W. Rowe*[2], S. E. Harris[1]. [1]U. of Missouri at Kansas City, Kansas City, MO, USA, [2]U. of Connecticut Health Center, Farmington, CT, USA, [3]U. of Texas Health Science Center at San Antonio, San Antonio, TX, USA.

Dentin matrix protein 1 (DMP1) is selectively expressed in osteocytes, is activated in response to mechanical loading, and is thought to play a role in regulation of local mineralization within osteocyte lacunae and canaliculi. Finding enhancers specific to osteocytes and responsive to loading will lead to insights into how mechanical signals are transmitted to the genome in an osteocyte specific manner. The transcriptional activity of three cis-regulatory regions, -9624 to +1996, -7892 to +4439 and -2433 to +4439, of the DMP1 gene were studied using the 2T3 cell line in which endogenous DMP1 expression increases 20 fold with osteoblast-osteocyte differentiation. Constructs containing the mouse DMP1 gene regions, driving Green Fluorescent Protein (GFP) were stably transfected and GFP expression monitored over time. During the differentiation , GFP showed a localized increase within the early stages of mineralized matrix formation, with all three promoter constructs. Greatest GFP expression was observed with constructs containing at least 7.8 Kb of 5' flanking region. The GFP positive cells are dendritic in morphology representing early osteocytes in a mineralizing matrix. Subconfluent and mineralizing, stably transfected, 2T3/DMP1-GFP cells were subjected to fluid flow at defined levels of shear stress. In subconfluent cells, the three DMP1 cis-DNA regulatory regions are responsive to 1.6 Pascals with a lower response to 0.4 Pascals. At the highly dendritic mineralizing matrix stage, the -7892 to +4439 responded 7 to 8 fold to 1.6 Pascals of loading which is comparable to the endogenous DMP1 gene that is increased 5 fold. This DMP1 region, -7892 to +4439, driving GFP, was then used to generate a transgenic mouse model. GFP was shown to be highly selective for osteocytes and no expression was seen in osteoblasts. Differentiated bone marrow cells cultured from these mice showed GFP expression markedly increased in osteocytes within the mineralized matrix. Right ulnae from these mice were loaded for 1 bout of 60 cycles (2 Hz; peak force of 2.4 N) and the left ulna served as a control. After 24hrs, GFP expression was shown to increase in the loaded ulnae, distal to the mid-shaft. In summary, we have shown both *in vitro* and *in vivo* that the 12 Kb region (-7892 to +4439) of the DMP1 gene is capable of directing expression to osteocytes and that this region also responds to mechanical signals.

Disclosures: ***W. Yang****, None.*

1036

Deletion of Neuronal Nitric Oxide Synthase (NOS-1) α-isoform Induces a Higher Trabecular Peak Bone Mass and Modulates Bone Response to Unloading in Adult Male Mice. B. Boudignon*[1], L. Vico[1], N. Laroche*[1], D. Blottner*[2], M. Lafage-Proust[1]. [1]Lbto, INSERM 366, Saint-Etienne, France, [2]Anatomy, Benjamin Franklin University Hospital, Berlin, Germany.

In bone, mechanical strain signals through many second messengers including Nitric Oxyde (NO). NO is synthesized by 3 NO synthases (NOS) endothelial (3), inducible (2) and neuronal (1). NOS-2 knock-out inhibits osteogenic bone response to load after unloading. In this context, we studied the effects of NOS-1 alpha isoform knock-out on bone phenotype and response to unloading.

Twenty 4 month-old NOS I-alpha deficient male mice (NOS-$1^{-/-}$) (65.0 cM; AccID MGI:97368) and 20 wild type mice (WT, B6-129SF2/J) were divided into 2 groups: one control group (C) and one tail-suspended (Unload) for 21d. Cortical and trabecular bone mass and microarchitectural parameters were assessed with 3D microtomography (uCT40, Scanco), unloading effects were analysed on femur with sequential Bone Mineral Density measurements (BMD, Piximus, Lunar) and bone histomophometry of distal metaphysis made at the end of the experiment.

At baseline, NOS-$1^{-/-}$ mice displayed a trabecular bone mass 1.6 times higher (Figure) than WT ($p<0.01$), with plate-shaped trabeculae while WT's ones were more rod-like (SMI:1.58 +/- 0.15 vs 2.37 +/- 0.20, $p<0.05$). In contrast, cortical bone mass was similar between the 2 groups. After unloading, femoral BMD decreased by 14.5% in WT and by 17% in NOS-$1^{-/-}$ ($p< 0.01$). Trabecular bone mass was 30% and 38% lower in unloaded WT and NOS-$1^{-/-}$ compared to their respective C. Histomorphometric bone cell activities are shown in Table I.

	WT C	WT Unload	NOS-$1^{-/-}$ C	NOS-$1^{-/-}$ Unload
MAR, μm/d	1.4 +/- 0.2	1.2 +/- 0.2 [b]	1.3 +/- 0.1	1.3 +/- 0.1
MS/BS, %	63.0 +/- 6.8	50.5 +/- 8.1 [b]	38.4 +/- 8.6 [a]	62.5 +/- 4.1[b]
Oc.S/BS, %	20.6 +/- 3.9	27.4 +/- 8.0 [b]	15.6 +/- 3.1 [a]	25.1 +/- 3.2 [b]

a: significant vs WT-C, b significant vs respective C group, $p<0.05$.

In conclusion, these data show that NOS-1 alpha isoform plays a role in peak bone mass aquisition only in the trabecular envelope. Since it was shown that osteoclast resorption in NOS-$1^{-/-}$ mice is normal, the observed decrease in bone remodeling level is likely to involve the osteoblastic lineage which, moreover, responded to unloading with unexpected activity increase.

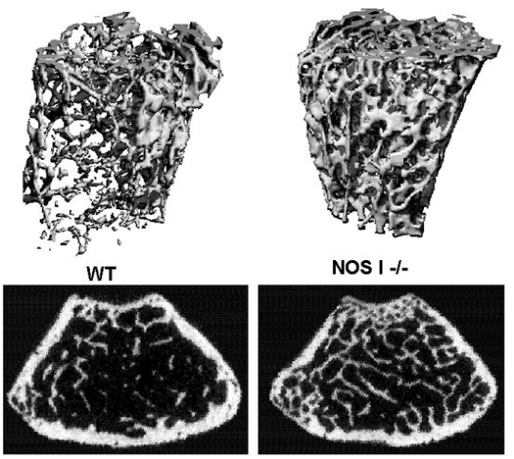

Disclosures: ***B. Boudignon****, None.*

1037

Absence of Both *BMP2* and *BMP4* during Skeletal Development Results in Severe Defects in Osteoblasts but not in Chondrocytes. K. Tsuji[1], A. Bandyopadhyay*[2], K. Cox[1], B. Harfe*[3], C. J. Tabin*[2], V. Rosen[1]. [1]Department of Tissue Growth and Repair, the Forsyth Institute, Boston, MA, USA, [2]Department of Genetics, Harvard Medical School, Boston, MA, USA, [3]Department of Molecular Genetics and Microbiology, University of Florida Colledge of Medicine, Gainesville, FL, USA.

BMP-2 and BMP-4 can induce both endochondral and membranous ossification when implanted into non-skeletal sites *in vivo* and are able to initiate the expression of osteoblast-related genes in undifferentiated mesenchymal cells *in vitro*. However, both *BMP2* and *BMP4* single knockout mice die before 11dpc, leaving the functions of these molecules during skeletal development to be established. In this study, we inactivated both *BMP2* and *BMP4* genes in the cranial and limb region by using double floxed mice with Cre recombinase driven by Prx-1 enhancer. X-ray and BMD (bone mineral density) data indicated that mineralized bone formation is severely decreased in homozygous conditional knockout *BMP2/BMP4* mice compared to control mice that do not carry the Cre recombinase at 1, 2 and 3 weeks after birth. Histological analyses of the long bones of these mice show abnormally thick perichondrium surrounding prehypertrophic- and hypertrophic-like chondrocytes, as well as the absence of osteoblasts and a bone marrow cavity. In addition to these defects, a large area of non-mineralized tissue occupies the posterior fontanel, indicating that membranous bone formation is also affected. These data demonstrate that *BMP2* and *BMP4* are required for osteoblastic differentiation and replacement of mineralized cartilage by bone but are less important for chondrocytic differentiation. They directly establish a link between these BMPs and bone formation.

Disclosures: ***K. Tsuji****, None.*

1038

Physiological Role of Combination of BMP2 and BMP6 in Bone Formation. F. Kugimiya*, S. Kamekura, H. Chikuda, K. Nakamura, H. Kawaguchi, U. Chung. Orthopaedic Surgery & Tissue Engineering, Univ. of Tokyo, Tokyo, Japan.

Pharmacologic actions of exogenously applied BMPs as potent bone anabolic agents have been demonstrated by a number of *in vitro* and *in vivo* studies. However, there is little evidence of the physiological roles of endogenous BMPs in bone formation, since mice deficient in BMPs and the receptors so far reported were normal or exhibited abnormalities in skeletal patterning or morphogenesis unless they died during embryonic development. During endochondral ossification, hypertrophic chondrocytes induce bone formation, and we have shown that BMP2 and BMP6 are the major BMPs expressed by the hypertrophic chondrocytes. Hence, to learn the physiological function of these BMPs, the present study investigated the skeletal abnormalities of mice deficient in BMP2 and/or BMP6. Since homozygous BMP2-deficient mice were embryonically lethal, heterozygous BMP2-deficient mice (BMP2+/-) and homozygous BMP6-deficient mice (BMP6-/-) were mated to create the double-deficient mice (BMP2+/-;BMP6-/-). Neither BMP2+/- nor BMP6-/- showed any skeletal abnormalities during observation periods up to 26 weeks of age. Alcian blue and alizarin red stainings showed no discernible difference in skeletal patterning or morphogenesis between BMP2+/-;BMP6-/- and wild-type (WT) embryos (E17.5); however, limbs and trunk of the mutant were 10-20% shorter than WT even after birth. Although BMP2+/-;BMP6-/- were healthy without major organ abnormalities, osteopenia developed postnatally and the bone volume determined by histomorphometric analysis of the proximal tibiae was decreased to 57% of the WT littermates at 8 weeks. Bone formation parameters (MAR & BFR/BS) of BMP2+/-;BMP6-/- were 40-50% lower than those of WT, while bone resorption parameters were comparable. When bone fracture was created at the midshaft of the tibia at 8 weeks, only BMP2+/-;BMP6-/-, but not BMP2+/- or BMP6-/- alone, showed impaired healing: both the volume and the mineral content of callus were about half those of WT littermates 3 weeks after the fracture. Histological analyses of the fracture site revealed that endochondral ossfication after chondrocyte hypertrophy was markedly impaired with intramembranous ossification unaffected. Finally, when hypertrophic chondrocytes derived from the rib cartilage were transplanted in the back muscle of nude mice, bone induction by BMP2+/-;BMP6-/- chondrocytes was markedly suppressed compared to that by WT chondrocytes. In summary, the double insufficiency of BMP2 and BMP6 impaired endochondral bone formation and osteoblast function without affecting skeletal morphogenesis. This is the first report clearly showing the physiological role of endogenous BMPs in bone formation.

Disclosures: ***F. Kugimiya****, None.*

1039

BMP Type IA Receptor Signaling in Osteoblasts Regulates Bone Resorption and Osteoclast Functions. S. Harada[1], V. Kasparcova*[1], N. Kamiya*[2], M. W. Starbuck*[3], M. A. Gentile[1], T. Fukuda*[2], R. R. Behringer*[3], Y. Mishina*[2]. [1]Molecular Endocrinology/Bone Biology, Merck Research Laboratories, West Point, PA, USA, [2]Reproductive and Developmental Toxicology, National Institute of Environmental Health Science, Research Triangle Park, NC, USA, [3]Molecular Genetics, The University of Texas, MD Anderson Cancer Center, Houston, TX, USA.

Bone morphogenetic proteins (BMPs) function in developmental processes including skeletogenesis. However, despite the powerful osteogenic action of BMPs, the role for BMP signaling in bone remodeling is not well understood. We previously generated mice with osteoblast-specific disruption of *Bmpr1a*, which encodes type IA BMP receptor, via Cre-recombinase under the *OG2* promoter. Mutant mice initially exhibited smaller body size and lower bone volume due to decreased bone formation (up to 3-month old). However, surprisingly, when animals were aged (> 10-month old), significantly higher bone mineral density was observed at femur of mutant mice compared to litter-mate controls. Dynamic histomorphometric analysis of distal femur confirmed increased bone volume and documented suppressed bone turnover (bone formation rate) in aged-mutant mice, indicating that increased bone mass in mutant mice results from suppression of bone resorption. Following ovariectomy (OVX), more significant bone loss was observed in mutant mice, likely due to decreased osteoblast function which failed to compensate for OVX-induced bone resorption. To gain insight into the role of Bmpr1a in bone resorption, the impact of *Bmpr1a* ablation on genes associated with osteoclasts and osteoblasts were evaluated using organ culture of calvaria and tibia from aged-mice with floxed *Bmpr1a* alleles. BMP-4 treatment increased the expression of cathepsin K, matrix metalloproteinase-9, tartrate-resistant acid phosphatase and CLC-7 chloride channel, evaluated by real-time PCR analysis of RNA isolated from cultured bone samples. Interstingly, in aged calvaria, BMP-4 treatment showed no effets on genes associated with osteoblasts, such as osteocalcin or osterix. Ablation of *Bmpr1a* gene by adenoviral Cre-recombinase *in vitro* in cultured calvaria and tibia abolished the stimulatory effects of BMP-4 on the expression of all these genes that play essential roles for osteoclastic bone resorption. BMP-4 treatment showed no effects on the expression of receptor activator of NFκB ligand (RANKL) or osteoprotegerin, suggesting that BMP-4 effects are independent of RANKL/RANK signaling pathway. Taken together, these *in vivo* and *in vitro* results demonstrate essential and age-dependent roles for BMP signaling mediated by type IA BMP receptor in bone resorption and osteoclast function.

Disclosures: ***S. Harada****, Merck & Co., Inc. 3.*

1040

Cartilage-Specific Over-Expression of Smurf2 Induces an Osteoarthritic Phenotype in Mice. Q. Wu, M. J. Zuscik, E. M. Schwarz, M. K. Mulcahey*, T. O'Brien*, H. Drissi, J. E. Puzas, R. J. O'Keefe, R. N. Rosier. Orthopaedics, University of Rochester, Rochester, NY, USA.

Cartilage within diarthroidal joints is maintained by articular chondrocytes (ACs) which produce matrix and are prevented from undergoing terminal maturation. During osteoarthritis (OA), maturational constraints are lost and ACs partially recapitulate the differentiation process that occurs during normal endochondral ossification. Evidence in the literature suggests that this inappropriate maturation may occur in situations where TGF-β signaling is reduced, correlating with the known function of this pathway in the inhibition of chondrocyte maturation. An endogenous mechanism for the inhibition of TGF-β signaling involves Smad ubiquitin regulatory factor-2 (Smurf2), an E3 ubiquitin ligase that targets Smad2 for the proteasome. Since we have observed strong expression of Smurf2 protein in osteoarthritic but not in normal human cartilage, we hypothesize that Smurf2-induced loss of TGF-β signaling in ACs represents an underlying cause of OA. To test this hypothesis, we generated transgenic mice over-expressing Smurf2 under control of the type II collagen promoter. Functional up-regulation of Smurf2 was verified in sternal chondrocytes from transgenic mice i) by detecting loss of TGF-β signaling on the P3TP promoter-luciferase reporter, and ii) by detecting enhanced ubiquitination of Smad2. While there were no gross abnormalities, the articular cartilage from the knees of transgenic mice showed evidence of degeneration that was mild at 2 months of age and that progressed to a severe stage by 7 months. Specifically, between 2 and 5 months, transgenic mice showed reduced proteoglycan content that was accompanied by cloning and hypertrophy of the ACs. Degeneration was progressive during this period, culminating with mild fibrillation of the articular surface. By 7 months, radiographic evidence of a reduced joint space and osteophyte formation correlated with significant loss of cartilage, severe fibrillation and clefting, and reduced cellularity of the remaining articular surfaces. These changes occurred without synovial inflammation. *In situ* mRNA analysis of type II and type X collagen was also performed in 2 month old mice. A reduction in type II and an increase in type X collagen was observed, suggesting that ACs undergo hypertrophic differentiation in this model. Thus, *in vivo* over-expression of Smurf2 in cartilage leads to inappropriate maturation of ACs that is followed by development of an OA-like phenotype. These findings suggest that the up-regulation of Smurf2 seen in human OA may represent a mechanism driving the cellular and tissue phenotypes that are seen in diseased cartilage.

Disclosures: ***M.J. Zuscik****, None.*

1041

A New Smad Anchor for Receptor Activation (SARA) for BMP Signaling. W. Shi*, C. Sun*, J. Wang*, X. Cao. Pathology, University of Alabama at Birmingham, Birmingham, AL, USA.

The cascade of phosphorylation is a pivotal event in TGFβ/BMP signaling. TGFβ specific Smads Anchor for Receptor Activation (SARA) binds to unphosphorylated R-Smads to facilitate their phosphorylation by activated TGFβ type I receptor (TβRI). Once Smad2/Smad3 are phosphorylated, phosphorylated TβRI can be dephosphorylated by Smad7 recruited GADD34/PP1c (catalytic subunit of the PP1 holoenzyme) complex. SARA facilitates the negative regulatory mechanism by controlling the subcellular localization of PP1c via its PP1c binding domain. However, SARA for BMP signaling remains to be identified and little is known of how phosphorylation of Smad1 by BMP receptors is controlled.

To characterize such a mechanism for BMP signaling, we screened a yeast two-hybrid human chondrocyte cDNA library, and identified a SARA-like molecule that controls subcellular localization of Smad1 and designated it as SARAb (SARA for BMP signaling). SARAb is another FYVE domain protein anchoring onto the cell membrane via PI3P-FYVE interaction. We examined whether it functions as a BMP specific SARA. Our co-immunoprecipitation assay demonstrated Smad1 was co-precipitated with SARAb. Mouse calvarial osteoblasts (MC-3T3 E1) were transfected with either HA-SARA or HA-SARAb, then stimulated with BMP for 5 hours. Cells were immunostained with either anti-HA or anti-phospho-Smad1. We found that SARAb, but not SARA, regulates phosphorylation and intracellular translocation of Smad1. PP1c was also co-precipitated with SARAb. Further mapping analysis of SARAb identifies a Smad binding domain (SBD), and a PP1c binding domain (PBD). Overexpression of mutant SARAb without PBD or knockdown of GADD34 by RNA interference causes hyperphosphorylation of BMPRI, enhanced BMP signaling, concomitant osteoblast differentiation, and mineralization nodule formation in culture of MC3T3-E1 cells, which can be inhibited by either overexpression mutant SARAb without SBD, or GADD34. Unlike in TGFβ signaling, the interaction between GADD34 and BMPRI is not mediated by inhibitory Smad6 or Smad7. Apparently, the extent of dephosphorylation of BMPRI largely depends on induction of GADD34 which is regulated by stresses such as hypoxia and starvation. This unique BMPRI dephosphorylation regulatory mechanism may be responsible for cell survival under stress conditions, like hypoxia in growth plate, by dampening BMP stimulation. In conclusion, we have identified SARAb for BMP signaling pathway. SARAb binds to Smad1 for its phosphorylation and to PP1c as a part of BMP negative feedback circuit. Identification of SARAb provides a mechanistic insight for BMP function in bone and cartilage, which could also potentially serve as a bone anabolic drug target for osteoporosis.

Disclosures: ***W. Shi****, None.*

1042

The Exported 18kDa Isoform of FGF2 Is a Critical Determinant of Bone Mass in Mice. L. Xiao[1], T. Naganawa[1], J. D. Coffin[2], T. Doetschman*[3], M. M. Hurley[1]. [1]Univ of Connecticut, Farmington, CT, USA, [2]Univ of Montana, Missoula, MT, USA, [3]Univ of Cincinnati, Cincinnati, OH, USA.

Fibroblast growth factor-2 (FGF2) has stimulatory effects on bone formation in vitro and in vivo. Although there are multiple nuclear isoforms of FGF2 and a low molecular weight (LMW, 18kDa) isoform that is exported from cells, the role of the individual isoforms in bone is not well defined. Previous studies showed that knockout of all isoforms of the Fgf2 gene (Fgf2 ALL-MW-/-) resulted in decreased bone mass in mice. Since the 18kDa isoform of FGF2 is exported, we tested its role in bone remodeling and the maintenance of bone mass by developing Col3.6-18kDaFgf2-IRES-GFPsaph mice in which a 3.6 kb fragment of type I collagen promoter (Col3.6) drives the expression of only the 18kDa isoform of FGF2 (18kDaFgf2) with green fluorescent protein-sapphire (GFPsaph). Vector mice (Col3.6-IRES-GFPsaph, VTg) were also developed. 18kDaTgFgf2 mice expressed high levels of Fgf2 mRNA and the 18kDa protein in type I collagen-producing tissues including bone, tendon and skin compared with VTg mice. Transgenic 18kDa FGF2 was not over-expressed in muscle, brain, heart, lung, liver, spleen or kidney. There was no difference in femur length, body weight, serum creatinine or hematocrit between 12-week-old 18kDaTgFgf2 and VTg mice. By DXA, tibial BMD and BMC were increased by 6.5 and 19 % respectively ($p< 0.01$), in 18kDaTgFgf2 compared with VTg mice. By micro-CT analysis, tibial cortical bone area, periosteal radius and endosteal radius were increased by 24, 17, and 29%, respectively ($p<0.001$), in 18kDaTgFgf2 mice. Histomorphometry revealed increased calvarial width of 18kDaTg Fgf2 mice vs. VTg (296±41 vs. 114±3, $p<0.01$). Marrow stromal cultures from 18kDaTgFgf2 mice produced more mineralized bone nodules than VTg marrow. Similar results were obtained in 2 independent lines of 18kDaTgFgf2 mice. To further examine the role of the 18kDa isoform in bone, Fgf2lmw-/- mice, which lacked only this isoform, were generated by targeted mutation of the ATG translational start site of 18kDa FGF2. DXA studies revealed a 10% reduction in femoral BMD in Fgf2lmw-/- mice and a marked reduction in mineralized nodules in marrow stromal cultures compared with wt littermates. These results are similar to the bone phenotype observed in Fgf2 ALL-MW-/- mice, and support an important functional role for the 18kDa isoform in bone. In summary, targeted over-expression of 18kDaFgf2 increased bone mass in vivo and increased mineralized bone nodule formation in vitro. Selective deletion of the 18kDa isoform resulted in decreased bone mass and ex vivo bone nodule formation. These results demonstrate that the exported 18kDa FGF2 isoform is a critical determinant of bone mass in mice.

Disclosures: ***L. Xiao****, None.*

1043

Alendronate in the Treatment of Pediatric Osteogenesis Imperfecta. F. H. Glorieux[1], F. Rauch[1], L. M. Ward[1], P. Smith*[2], N. Verbruggen*[3], N. Heyden[3], A. Lombardi[3]. [1]Genetics Unit, Shriners Hospital for Children, Montreal, PQ, Canada, [2]Shriners Hospital for Children, Chicago, IL, USA, [3]Merck & Co Inc, Whitehouse Station, NJ, USA.

Osteogenesis imperfecta (OI) is a group of heritable disorders characterized by osteoporosis and bone brittleness, leading to chronic bone pain, severe skeletal deformities, short stature, and functional limitation. Currently, no medical treatment is approved for the treatment of OI. Although pamidronate has shown beneficial effects, it requires intravenous administration. We conducted a multicenter, double-blind, randomized, placebo-controlled study to examine the efficacy and safety of oral alendronate (ALN; manufactured by Merck & Co. Inc) in pediatric patients with moderate to severe OI. Lumbar spine areal bone mineral density (BMD) was the primary endpoint. The study was not powered to examine fracture differences. A total of 139 children (age 4-19 years) with type I, III, or IV OI were enrolled and randomized to either placebo (PBO, N=30) or ALN (N=109) for 2 years. ALN doses were 5 mg/day in children weighing < 40 kg, and 10 mg/day in those weighing ≥ 40 kg. Seventy patients took calcium, and 59 took vitamin D supplements. After 2 years of treatment, ALN significantly decreased urinary NTx by 62%, compared with a 32% reduction with PBO ($p<0.001$). ALN increased spine BMD by 53% vs. a 16% increase with PBO ($p<0.001$). The mean spine BMD Z-score increased significantly from -4.6 to -3.3 with ALN, while the change in the PBO group (from -4.6 to -4.5) was not significant. Positive trends (albeit not significant) were observed in bone pain and physical activity in ALN-treated patients. ALN was generally well tolerated, and the incidence of clinical or laboratory adverse experiences was very similar among treatment groups. Upper gastrointestinal adverse experiences occurred in 52% of ALN and 53% of PBO patients. There was no significant difference in the incidence of fractures between treatment groups. Histomorphometric analysis of transiliac bone biopsies revealed a significant increase of cortical width in the ALN (median +162 µm) but not in PBO patients. No evidence of a mineralization defect was found in either group. In summary, oral ALN treatment for 2 years in pediatric patients with OI significantly decreased bone turnover, increased spine BMD and cortical width, and was generally well tolerated.

Disclosures: ***F.H. Glorieux****, None.*

1044

A Lifestyle Intervention for Teen Girls Enhances Bone Mineral Density over Two Years. C. Ritenbaugh[1], L. DeBar*[1], M. Aickin*[1], P. Elmer[1], D. Elliott*[2], E. Orwoll[2]. [1]Kaiser Permanente Center for Health Research, Portland, OR, USA, [2]Oregon Health & Science University, Portland, OR, USA.

YOUTH is a lifestyle intervention for increasing bone mineral density (BMD) among teen girls (14-17 years of age); the primary endpoint is change in BMD by DEXA at two years. Higher-risk female adolescents (BMI 16-23) and their parent(s) were individually recruited among members of a large HMO in the Pacific Northwest. Eligible teens (N=228) were randomized into a lifestyle intervention or to a general health education control group. The intervention targets were: (1) improving diet (increasing consumption of fruits, vegetables, and high calcium foods and decreasing soft drink consumption), and (2) increasing high-impact physical activity and spinal motion.

Interim (1 yr) and final (2 yr) results of the intervention on spine, trochanter, and total hip BMD (Hologic 4500) are shown below for the 179 girls who provided complete data at all three time points. At baseline (mean ± S.D.): overall age = 15.6 ± 0.6 yrs; overall BMI = 20.6 ± 1.9; months since menarche = 33.3 ± 15.6. In both groups, 76% of girls self-identified as white. There were significant 1-yr and 2-yr differences in diet changes from baseline between the intervention group and control group (intervention: more fruits, vegetables, calcium, vitamin D; less soda), but no significant differences in high-impact or total activity levels or spinal motion. The table below shows adjusted mean changes (± S.E.) from baseline BMD values by group at one and two years, and the p-values for the differences between groups. The adjusted mean differences are estimated by conditional change regression (ANCOVA), adjusting for family history, BMD, time since menarche at baseline; BMI, height at measurement. Total body, femoral neck, and Ward's triangle BMD showed no differences between groups.

Year 01 - baseline	Change (control)	Change (intervention)	p
Spine L1-L4	.0171±.0025	.0306±.0025	.0002
Trochanter	.0025±.0025	.0118±.0026	.0099
Total hip	.0078±.0026	.0161±.0026	.0245
Year 02 - baseline			
Spine L1-L4	.0331±.0031	.0448±.0031	.0081
Trochanter	.0024±.0034	.0138±.0034	.0184
Total hip	.0154±.0035	.0215±.0035	.2186

Our findings show that teenage girls can enhance bone mineral density at predominantly trabecular bone sites through lifestyle dietary changes sustained over two years.

Funded by NICHHD grant HD037744.

Disclosures: ***C. Ritenbaugh****, None.*

1045

PTH Can Improve the Disturbed Bone Growth in Achondroplastic Mice. K. Ueda*[1], Y. Yamanaka[1], D. Harada*[1], R. Nishimura[2], D. M. Ornitz*[3], Y. Seino[1], H. Tanaka[1]. [1]Pediatrics, Okayama University Graduate School of Medicine and Dentistry, Okayama, Japan, [2]Molecular and Cellular Biochemistry, Osaka University Graduate School of Dentistry, Osaka, Japan, [3]Molecular Biology and Pharmacology, Washington University Medical School, Saint Louis, MO, USA.

Achondroplasia (ACH) is caused by a constitutively activated mutation in FGFR3. The excessively activated FGFR3 inhibits the proliferation of chondrocytes, resulting in disturbing the growth of long bones. Recently, we have reported that the introduction of the mutated *FGFR3* into ATDC5, chondrogenic cell line, down-regulated PTHrP expression and induced apoptosis, and that replacement of PTHrP prevented the apoptotic changes.

To explore further mechanisms and new therapeutic applications, we performed organ culture experiments, using transgenic mice (AchTG) expressing ACH-type mutated *FGFR3* controlled by type II collagen gene. Wild-type (WT) female mice were mated with male AchTG.

At d.p.c.15, the fetal mouse femurs were dissected, transferred into serum-free medium and cultured for 4 days with/without 10^{-8}M PTH. AchTG femurs were significantly disturbed in longitudinal bone growth compared with WT ones after 4-day-culture (0.29 ± 0.10mm and 0.46 ± 0.06mm, respectively; $p<0.05$). PTH significantly increased bone growth of AchTG (0.50 ± 0.06mm; $p<0.01$ vs control), whereas WT did not show remarkable change of bone growth (0.55 ± 0.09mm; n.s.).

PTH is known to share its receptor with PTHrP, and increase chondrocyte proliferation and inhibit cell maturation. PTH widened proliferative zone but narrowed hypertrophic zone in the growth plate of AchTG.

In conclusion, constitutively active FGFR3 inhibited bone growth in organ culture experiments and that PTH rescued bone from the growth disturbance. PTH has a potential for the treatment of achondroplasia.

Disclosures: ***K. Ueda****, None.*

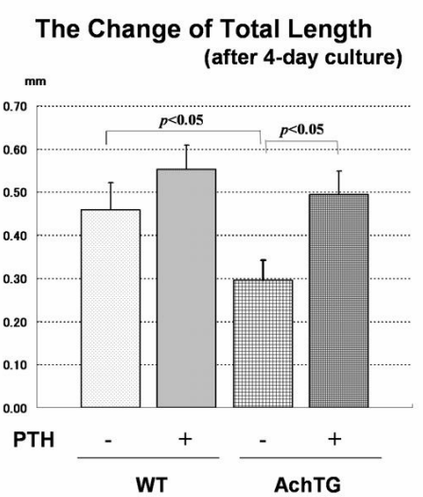

1046

Mechanical Adaptation to Weight Gain in Late Adolescence: Do Fat Kids Have Weaker Bones? T. Lloyd[1], M. Petit[1], H. Lin*[1], C. Bentley*[1], T. Beck[2]. [1]Health Evaluation Sciences, Penn State College of Medicine, Hershey, PA, USA, [2]Radiology, Johns Hopkins Medical Institute, Baltimore, MD, USA.

The United States is in the midst of an obesity epidemic. Chronic weight gain often begins in childhood and adolescence but little is known about the effect of obesity on young adult bone strength. Using 6 years of longitudinal data from The Penn State Young Women's Health Study we explored the effects of weight gain in late adolescence on proximal femur geometry and strength. 71 participants remaining in the study until at least age 21 were classified as either weight-gainers (WG, n = 23) or stable weight (SW, n = 48). Using a random coefficients model, groups were partitioned by whether the age trend in weight slope was significantly positive. Annual hip DXA scans (Hologic QDR 2000) during ages 17-22 were analyzed using a hip structure analysis program to assess areal BMD (g/cm^2), subperiosteal width, cortical thickness, bone cross-sectional area (CSA) and section modulus (Z), at the proximal femoral shaft. Total body lean and fat mass were measured from DXA total body scans. Over ages 17-22, height remained stable in both groups. Weight remained static in the SW group but increased 14% in the WG group ($p < 0.05$). After controlling for age 17 baseline values, section moduli values were similar at age 22 but the WG group had thicker cortices, greater CSA and greater BMD. The SW group achieved similar Z values by subperiosteal expansion from 17-22y. When the bone strength index (SI = section modulus / height) was normalized to body weight, the ratio (shown in Figure) remained stable in the SW group but decreased significantly in the WG group. In contrast, the SI normalized to lean mass did not change in either group. These data are consistent with the hypothesis that bone adapts its strength primarily to muscle force, and not to static weight. Interestingly the greater BMD in the WG group did not translate to stronger bones, indeed their bones were relatively weaker relative to their body weight. Under trauma conditions where injury-producing forces are weight dependent (e.g., falls) bone strength would be lower in the obese. Whether the effect is mitigated by greater fat padding or actually results in higher traumatic fracture incidence in the obese is unknown.

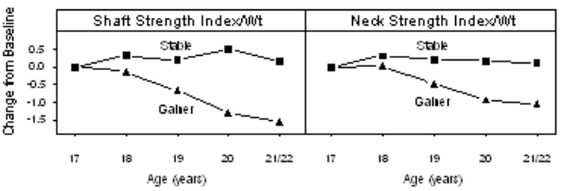

Disclosures: ***T. Lloyd****, None.*

1047

Impact of Vitamin D Supplementation on Musculoskeletal Parameters in Adolescents: A Randomized Trial. G. El-Hajj Fuleihan[1], M. Nabulsi*[2], H. Tamim*[3], J. Maalouf*[1], M. Salamoun*[1], M. Choucair*[1], R. Veith[4]. [1]Calcium Metabolism and Osteoporosis Program, American University of Beirut Medical Center, Beirut, Lebanon, [2]Pediatrics Department, American University of Beirut Medical Center, Beirut, Lebanon, [3]Epidemiology and Population Health Department, American University of Beirut, Beirut, Lebanon, [4]Mt Sinai University, Toronto, ON, Canada.

Despite the high prevalence of hypovitaminosis D in children and adolescents worldwide, the real impact of such insufficiency on skeletal health is unclear.

We conducted a randomized double-blind placebo controlled trial to evaluate the safety and efficacy of vitamin D supplementation on bone mineral density (BMD) and content (BMC) in 362 children ages 10-17 yrs , N= 168 girls (34 pre-menarcheal), and 172 boys. They received oral vitamin D (vigantol oil) 1400 IU/week, 14000 IU/week, or placebo for one year. BMD/ BMC of the lumbar spine, total body, hip, forearm, and body composition were measured at baseline and one year. At one year, vitamin D levels stayed in the 15-17 ng/ml range in the placebo arms, increased to 17-20 ng/ml in the low dose arm and to 35-38 ng/ml in the high dose arm.

At entry girls had lower vitamin D levels than boys and they showed significant correlations between BMD/BMC and vitamin D levels, R =0.17-0.24 depending on the skeletal site (spine, forearm, femoral neck, total body). In the overall group of girls, and in the subgroup of pre-menarcheal girls there were significant changes in musculoskeletal variables in response to vitamin D supplementation (Table).

% Changes in Musculoskeletal Parameters with Treatment in Girls at 12 Months

Overall	Placebo	Low dose	High dose	p
Hip BMC	8 (8)	11 (9)	13 (11)	0.02
Lean Mass	6 (7)	9 (8)	9 (8)	0.05
Pre-menarcheal				
Spine BMD	8 (4)	15 (7)	12 (8)	0.04
Trochanter BMC	13 (11)	32 (16)	26 (21)	0.05
Lean Mass	11 (5)	17 (7)	18 (7)	0.04

Trends for increments were noted at the spine and trochanter BMC in the overall group, and at the spine BMC, total hip BMC/BMD, and total body BMC in the premenarcheal group (p=NS). In post-menarcheal girls, in the overall group of boys, and in the subgroups of early pubertal boys (Tanners I and II) and mid late pubertal boys (Tanner III-V), there was no significant effect of intervention on lean mass, BMD or BMC. The treatment was safe and well tolerated.

Low vitamin D levels are prevalent in healthy children and adolescents, more so in girls. The positive impact of vitamin D supplementation on BMD/BMC in girls and not boys may be explained by the higher prevalence of hypovitaminosis D in that gender, and may be partially mediated by increments in lean mass.

Disclosures: ***G. El-Hajj Fuleihan****, Nestle Foundation Switzerland 2; Merck KGaA 2.*

1048

The Bone Mineral Density in Childhood Study (BMDCS): Baseline Results for 1554 Healthy Pediatric Volunteers. M. Horlick[1], J. M. Lappe[2], V. Gilsanz[3], H. J. Kalkwarf[4], B. S. Zemel[5], S. Mahboubi*[5], J. A. Shepherd[6], M. M. Frederick*[7], K. Winer[8]. [1]Pediatrics, Columbia University, New York, NY, USA, [2]Creighton University, Omaha, NE, USA, [3]Children's Hospital of Los Angeles, Los Angeles, CA, USA, [4]Children's Hospital Medical Center, Cincinnati, OH, USA, [5]Children's Hospital of Philadelphia, Philadelphia, PA, USA, [6]UCSF, San Francisco, CA, USA, [7]C-TASC, Baltimore, MD, USA, [8]NICHD, Rockville, MD, USA.

To establish reference standards for bone mineral density in children, 5 US clinical centers recruited 1554 healthy subjects (793 girls 6-15 y, 761 boys 6-16 y) for a longitudinal study with baseline and 3 annual follow-up visits. Height, weight, pubertal maturation and bone age were measured. BMD and BMC of total body (TB), lumbar spine (LS), total hip (TH), and forearm were obtained by dual energy x-ray absorptiometry (DXA, Hologic Delphi).

Preliminary sex-specific percentiles and z-scores for age for bone mineral density (BMD) and bone mineral content (BMC) for TB and LS were derived from the baseline data using LMS PRO software. Relationships between z-scores for BMD and BMC at different DXA sites were evaluated with Pearson correlation coefficients.

Curves from the cross-sectional data revealed earlier increase in BMD and BMC for girls than boys. In girls, TB BMD slope increased at about 10 y and leveled off at about 14 y. In boys, the slope increased at about 12 y and did not level off. LS BMD slope increased earlier, about 9 y in girls and 11 y in boys. The slope leveled at 13 - 14 y in girls, but not in boys. For both sexes, BMC slope increased slightly earlier than BMD, but the overall patterns were similar.

Correlations between z-scores for BMD and BMC at different sites were all significant (r: 0.53 - 0.93), and similar for girls and boys. The highest correlation for LS BMD z-score was with TB BMD, and the lowest was with ulna BMD. The highest correlation for TB BMC z-score was with LS BMC, and the lowest was with ulna BMC.

These are the first pediatric reference values for DXA bone results from a multiethnic population from across the US. Correlations between z-scores for different DXA sites could suggest appropriate combinations of scans for pediatric protocols. Use of uniform standards and protocols will link DXA values to pediatric clinical outcome, information that has been lacking to date. Follow-up visits will provide data on velocity of gain in BMC and on the effects of change in age, bone age, and pubertal status on bone measurements.

Disclosures: ***M. Horlick****, None.*

1049

BMP4 Is Necessary for Bone Formation: Conditional BMP4Knock-out Using the 3.6kb and 2.3kb Collagen 1a1 Promoter-Cre and BMP4 Floxed Mice. D. Guo[1], S. Harris[1], W. Yang[1], M. Harris[1], J. Zhang[1], J. Feng[1], C. Anderson[2], B. Kream[3], A. Lichtler[3], B. Hogan[4], H. Kulessa[5]. [1]Oral biology, U of Missouri, Kansas City, MO, USA, [2]Pathology, Kansas U Medical School, Kansas City, KS, USA, [3]Genetics and Developmental Biology, U of Connecticut, Farmington, CT, USA, [4]Genetics, Duke U, Durham, NC, USA, [5]U of Vanderbilt, Nashville, TN, USA.

Bone morphogenetic protein 4 (BMP4) has multiple functions during embryonic and post natal development. A specific role in bone formation and osteoblast function is not known. BMP4 is abundantly expression in osteoblasts, osteoclasts, and osteocytes. However, the embryonic lethality of BMP4 knock-out mice at 8.5 dpc precluded analysis of BMP4 role in bone formation. Specific deletion of BMP4 gene was achieved by crossing collagen 1a1-Cre transgenic mice with BMP4 flox mice. Using the 3.6kb Col1a1-Cre, first, we deleted BMP4 in early spindle shaped osteoblasts, tendon, and components of the heart, kidney and skin. Using the 2.3kb Col1a1-Cre, we are deleting BMP4 at later stages of osteoblast development but with higher specificity. After crossing BMP4 floxed mice with 3.6kb Col1a1-Cre mice, less than expected new born mice (only 29 out of expected 50) were genotyped as conditional knock-out, indicating embryonic lethality. As assayed by histology, BMD, and X-ray, BMP4 conditional knock-out mice are defined as three types. Type I are arrested at 13.5 to 15.5 dpc, with asymmetric limb buds, absence of calvarias or mandible, and open circulation system. Type II conditional knock-out mice survive after birth, but show 30~50% ($p<0.001$) decrease of body size, weight, polydactyly, kinky tail, polycystic kidney, and severe osteopenia. Figure 1 shows an X-ray of Type II mutants. Type II mice do not live beyond about 35 days. Type III mice (50% of the surviving mice with BMP4 conditional knock-out) show a similar phenotype but less severe than type II. These mice have a reduce BMD and BV/TV, primarily in the vertebrae and other flat bones as compared to the long bones. There was no change in osteoclasts activity, as demonstrated by TRAP staining in Type II or III mutants. Dynamic measurements of bone formation rates in these Type II and III are now underway as well as analysis of the conditional BMP4 knock-out using the 2.3kb Col1a1-Cre mice. In summary BMP4 is necessary but not sufficient for bone formation in adult life.

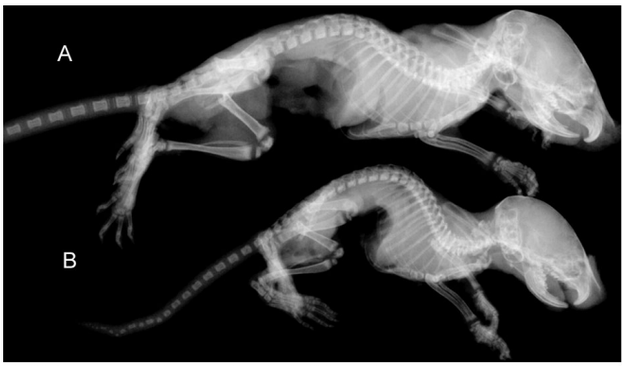

Fig.1 A. Heterozygous control mouse(BMP4flx/KO). B. BMP4 conditional knock-out(3.6Col1a1-Cre; BMP4flx/KO)

Disclosures: ***D. Guo****, None.*

1050

Cyclic GMP-Dependent Protein Kinase II Is a Molecular Switch from Proliferation to Hypertrophic Differentiation of Chondrocytes through Attenuation of Sox9 Function. F. Kugimiya*[1], H. Chikuda[1], T. Ikeda[1], K. Nakamura[1], K. Komeda*[2], U. Chung[1], H. Kawaguchi[1]. [1]Orthopaedic Surgery & Tissue Engineering, University of Tokyo, Tokyo, Japan, [2]Tokyo Medical College, Tokyo, Japan.

The Komeda miniature rat Ishikawa (KMI) is a naturally occurring mutant caused by an autosomal recessive mutation *mri*, which exhibits severe longitudinal growth retardation. Our positional cloning analysis identified the *mri* mutation as a 5 kb deletion in the rat gene encoding cGMP-dependent protein kinase type II (*cGKII*), which resulted in a truncated product that lacks the kinase domain. KMI showed an expanded growth plate and impaired bone healing with abnormal accumulation of postmitotic but non-hypertrophic chondrocytes, demonstrating that the cGKII dysfunction impairs the synchronized switching from proliferation to hypertrophic differentiation of chondrocytes. *Ex vivo* culture of KMI chondrocytes reproduced the differentiation impairment, which was restored by introducing the adenovirus-mediated *cGKII* gene. Immunohistochemical analysis revealed that the expression of Sox9, a transcription factor that induces chondrogenesis from mesenchymal cells and prevents the hypertrophic differentiation, was not detected in the hypertrophic zone of wild-type rats, but persisted in the nuclei of the abnormal postmitotic chondrocytes of KMI. The Sox9 transduction increased the type II collagen (COL2) mRNA level in the culture of human hepatoma HuH-7 cells, and decreased the type X collagen (COL10) level in the three-dimensional culture of mouse chondrogenic ATDC5 cells. Co-transduction with cGKII attenuated both the COL2 induction and the COL10 suppression by Sox9, neither of which was seen by cGKII with the KMI mutation or lacking the entire kinase domain. The cGKII co-transduction stimulated the Sox9 phosphorylation and inhibited the Sox9 nuclear entry. To learn the functional relevance, we created two Sox9 mutants: one is resistant to phosphorylation ($Sox9^{S181A}$) and the other is forced to be localized in the nucleus (Sox9-NLS). Although both mutants regulated COL2 and COL10 levels similarly to the wild-type Sox9, cGKII could suppress only the $Sox9^{S181A}$ function but not the Sox9-NLS function, indicating that cGKII attenuates the Sox9 function by interfering with its nuclear entry independently of its direct phosphorylation. Finally, the impaired differentiation of cultured KMI chondrocytes was confirmed to be restored by the silencing of Sox9 through RNA interference. Hence, the present study is the first to shed light on a novel role of cGKII as a molecular switch, coupling the cessation of proliferation and the start of hypertrophic differentiation of chondrocytes through attenuation of Sox9 function.

Disclosures: ***F. Kugimiya****, None.*

1051

Bidirectional Signaling by Ephrinb2-EphB4 Coordinates Osteoclast and Osteoblast Functions to Enhance Bone Formation. C. Zhao*[1], N. Irie*[1], K. Shimoda*[2], T. Miyamoto[3], T. Nishiwaki*[4], H. Ishikawa*[1], T. Suda*[3], K. Matsuo[1]. [1]Department of Microbiology and Immunology, School of Medicine, Keio University, Tokyo, Japan, [2]Laboratory Animal Center, School of Medicine, Keio University, Tokyo, Japan, [3]The Sakaguchi Laboratory of Developmental Biology, School of Medicine, Keio University, Tokyo, Japan, [4]Department of Orthopedic Surgery, School of Medicine, Keio University, Tokyo, Japan.

Bone homeostasis depends on the delicate balance between bone-forming osteoblasts and bone-resorbing osteoclasts. Several molecules are known to coordinate the function of osteoclasts with that of osteoblasts. However, no molecules that directly mediate osteoclast-osteoblast interactions by simultaneous signal transduction into both cell types have yet been identified. Interaction between ephrinB and EphB family proteins results in bidirectional signalling into both the ephrinB- and the EphB-expressing cells. Whereas activation of the receptor EphB by the ligand ephrinB is referred to as "forward signaling", activation of the ligand ephrinB by the receptor EphB is designated "reverse signaling". Here we show that ephrinB2 is expressed on differentiated osteoclasts, while its cognate receptor EphB4 is expressed on osteoblasts. Furthermore, using gain and loss-of-function experiments, we show that reverse signaling through ephrinB2 suppresses osteoclast differentiation, and forward signaling through EphB4 enhances osteoblast differentiation.

Reverse signaling down-regulates the essential osteoclastogenic transcription factors c-Fos and NFATc1, whereas forward signaling up-regulates osteoblastic transcription factors, such as *Runx2*, *Osterix* and *Dlx5* presumably through Erk1/2 activation. To further verify this interaction in vivo, we generated transgenic mice expressing EphB4 in osteoblasts. These mice show significantly increased bone mineral density compared to wild-type mice, suggesting that ephrinB2 and EphB4 interaction plays an important role in maintaining bone mass in vivo. In conclusion, our results demonstrate that bidirectional signaling by ephrinB2 and EphB4 functionally links osteoclasts and osteoblasts, suppressing bone resorption and simultaneously enhancing bone formation.

Disclosures: ***C. Zhao****, None.*

1052

FIAT, a Novel Leucine Zipper Repressor of ATF4-mediated Transcription that Regulates Bone Mass Accrual in Transgenic Mice. V. W. C. Yu*, G. Ambartsoumian*, J. Prud'homme*, J. M. Moir*, R. St-Arnaud. Genetics Unit, Shriners Hospital for Children, Montreal, PQ, Canada.

We report the cloning and characterization of FIAT (Factor Inhibiting ATF4-mediated Transcription), a 66 kDa leucine zipper nuclear protein. FIAT interacted with ATF4 in yeast and mammalian cells and inhibited ATF4-mediated transcriptional activation of the osteocalcin gene promoter in cultured cells. Considering the recently reported role of ATF4 in the regulation of osteoblast function (Yang, X., et al. 2004. Cell 117: 387), we investigated a putative role of FIAT in bone forming cells in vivo. Transgenic mice specifically overexpressing FIAT in osteoblasts had reduced bone mineral density (21%). Histomorphometric measurements demonstrated a dramatic decrease in bone volume (70%), mineralized volume (45%), trabecular thickness (38%), and trabecular number (55%). This phenotype translated into decreased rigidity (20%) of long bones. Mineral homeostasis, osteoclast number and activity, and osteoblast proliferation and apoptosis were unchanged in transgenic animals. Expression of osteoblastic differentiation markers was largely unaffected but reduced BSP expression was measured. Mineral apposition rate was reduced by 46% in transgenic mice, suggesting that the lowered bone mass was due to a decline in osteoblast activity. This cell-autonomous decrease in osteoblast activity was confirmed by measuring reduced alkaline phosphatase activity and mineralization in primary osteoblast cultures. These results show that FIAT regulates bone mass accrual and establish FIAT as a novel transcriptional regulator of osteoblastic function.

Disclosures: ***V.W.C. Yu****, None.*

1053

C/EBP Homologous Protein (CHOP, Ddit3) Is Essential for Osteoblastic Function. R. C. Pereira[1], S. J. Marciniak*[2], D. Ron*[2], E. Canalis[1]. [1]Research, Saint Francis Hospital and Medical Center, Hartford, CT, USA, [2]Skirball Institute, New York University School of Medicine, New York, NY, USA.

CCAAT/enhancer binding proteins (C/EBPs) are a family of transcription factors with important roles in cell differentiation and function. C/EBP homologous protein (CHOP, GADD153, Ddit3) was recently found to enhance BMP/Smad signaling, and as a consequence to induce osteoblast cell differentiation. But, the effects of CHOP on osteoblastic function are not known. To evaluate CHOP's role in skeletal cell function, we examined the skeletal phenotype of *chop* null mice and the function of *chop* null osteoblasts *in vitro.* Homozygous *chop* null mice back-crossed to a C57BL/6 genetic background five times were compared to wild type controls of identical genetic composition. *Chop* null mice exhibited a decrease in bone formation rate of 75%. The number of osteoblasts was not decreased, but the number of functional osteoblasts was, since the mineralizing surface was markedly reduced. *Chop* null mice exhibited a 30% reduction in eroded surface, indicating impaired osteoclastic/resorptive response and impaired bone remodeling. As CHOP has been implicated in the response of cells to client protein load in the endoplasmic reticulum (so-called ER stress), and as procollagen α_1 and α_2 chains are imported into the ER where they are post-translationally modified and then secreted, we hypothesized that impaired procollagen processing might be implicated in the bone phenotype of the *chop* mutant mice. We observed that whereas collagen synthesis rates were not decreased in cultured *chop* null osteoblasts, procollagen processing was severely affected compared with the wildtype cells. To estimate changes in procollagen processing, wild type and *chop* null osteoblasts were labeled with [^{3}H] proline and 'chased' in high proline containing medium. [^{3}H] hydroxyproline in the cell layer was separated by high performance liquid chromatography and measured by scintillation counting, and cell extracts were fractionated on 5% polyacrylamide/5M urea gels to visualize pro α1 and pro α2 type I collagen chains. This experiment demonstrated accumulation of newly synthesized procollagen in *chop* null osteoblasts. The half life of newly synthesized radiolabeled procollagen in the cell layer was extended from 14 min in wild type osteoblasts to ~60 min in *chop* null cells, confirming accumulation of newly synthesized procollagen in null cells and impaired export of procollagen from the cell to the extracellular space. In conclusion, CHOP is required for normal osteoblastic function and procollagen export from osteoblastic cells.

Disclosures: ***R.C. Pereira****, None.*

1054

Conditional Disruption of Hypoxia Inducible Factor 1 α in Mouse Osteoblasts Reduces Bone Volume. L. Deng*[1], N. Akeno[1], A. Mukherjee*[1], M. Bouxsein[2], M. Faugere[3], R. S. Johnson*[4], T. L. Clemens[1]. [1]Department of Pathology, University of Alabama at Birmingham, Birmingham, AL, USA, [2]Department of Orthopedic Surgery, Beth Israel Deaconess Medical Center, Boston, MA, USA, [3]Department of Medicine, University of Kentuky, Lexington, KY, USA, [4]Department of Biology, University of California at San Diego, San Diego, CA, USA.

The ability of cells to sense and respond to changes in oxygen tension is critical for many developmental, physiological, and pathological processes. Osteoblasts are ideally positioned in bone to sense and respond to fluctuations in oxygen and nutrient supply. Osteoblasts respond to hypoxia by elevating the level of the hypoxia-inducible factor 1α (HIF-1α), which transactivates expression of angiogenic and nutrient sensitive genes whose products act in concert to facilitate the supply of metabolic energy. To investigate the role of HIF-1α in skeletal acquisition we conditionally disrupted this transcription factor in bone osteoblasts by Cre-mediated recombination. Transgenic mice expressing the Cre recombinase from the human osteocalcin promoter were crossed with mice homozygous for the floxed HIF-1α allele to obtain mice lacking HIF-1α in osteoblasts. Eight week-old mutant mice (N=6) were of normal size and weight. Micro CT measurements at the mid shaft of the femur revealed a significant decrease in cross sectional area in both sexes. Consistent with these changes we observed that bones dissected from HIF-1α mutants were more susceptible to breaking than controls. Histomorphometric analysis revealed a reduction in osteoblasts (678 ± 57 vs 440 ± 25) and a decrease in osteoid volume (2.74 ± 0.57 vs 1.43 ± 0.8) consistent with a role for HIF-1α in bone formation. Osteoclast number and erosion surface were significantly increased suggesting a state of uncoupled bone formation and resorption. To begin to examine the cellular mechanisms responsible for the changes in bone architecture in the HIF-1α deficient mice we determined the effect of loss of HIF-1α in vitro on osteoblast differentiation and mineralization. Primary calvarial osteoblasts from mice homozygous for the floxed HIF-1α allele were infected with adenoviral vectors expressing either Cre or GFP and allowed to differentiate in mineralizing medium. Cells deficient in HIF-1α showed a marked developmental delay associated with reduced expression of Runx-2 and osteocalcin and a reduction in calcified nodule formation. These results suggest that HIF-1α can function independent of angiogenic signals during skeletal development to promote the differentiation program of the osteoblast.

Disclosures: ***T.L. Clemens****, None.*

1055

Osteoporosis as an Independent Risk Factor for Cardiovascular Events in Postmenopausal Women: Data from the Multiple Outcomes of Raloxifene Evaluation (MORE) Trial. C. Christiansen[1], L. Tanko*[1], D. A. Cox*[2], M. J. Geiger*[2], M. McNabb*[2], S. Cummings*[3]. [1]Center for Clinical and Basic Research, Ballerup, Denmark, [2]Eli Lilly and Company, Indianapolis, IN, USA, [3]University of California San Francisco, San Francisco, CA, USA.

Previous studies suggest an inverse association between bone mass and both cardiovascular (CV) mortality and the severity of peripheral atherosclerosis. The predictive value of osteoporosis for risk of CV events has not been addressed systematically. The objective of this analysis was to retrospectively assess the relationship between osteoporosis and CV risk in postmenopausal women in the MORE osteoporosis treatment trial assigned to placebo. MORE was a randomized, double-blind trial which enrolled 7705 postmenopausal women, 2576 taking placebo. For these analyses, osteoporosis (n=1289) was defined as having a baseline vertebral fracture or a total hip BMD t-score of -2.5 or less (based on Third National Health and Nutrition Examination Survey). Low bone density (n=1153) was defined as a t-score greater than -2.5 but less than or equal to -1 without baseline vertebral fracture. CV events (coronary events and stroke) were collected through 4-years as safety endpoints and subsequently adjudicated by a cardiologist. Proportional hazard models were unadjusted and adjusted for CV risk factors (age, smoking, diabetes, prior events, hypertension and hyperlipidemia) or for a composite CV risk score calculated for each woman. The incidence of CV events was significantly higher among women with osteoporosis [49 events (3.8%)] versus those with low bone density [10 events (0.9%)], both without and with adjustment for multiple CV risk factors or CV risk score (Figure). Coronary events and stroke were significantly higher in women with osteoporosis. Prevalent vertebral fracture [HR, 3.3; 95%CI, 1.5-7.1)] or low (t-score of -2.5 or less) total hip BMD [HR, 3.4; 95%CI, 1.4-8.0) were both associated with an increased incidence of CV events, independent of CV risk factors. We conclude that osteoporosis was a strong predictor of CV events independent of age and other traditional CV risk factors in postmenopausal women in the MORE trial, suggesting a possible pathophysiological link between these diseases that warrants further study.

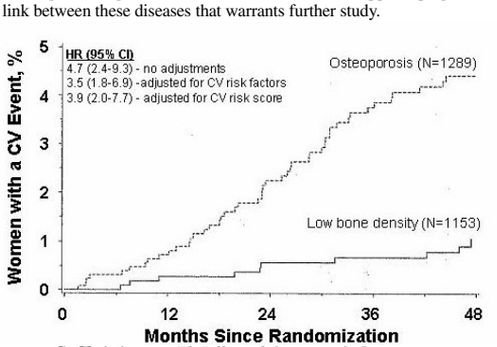

Disclosures: ***C. Christiansen****, Eli Lilly and Company 2, 5.*

1056

Bone Mineral Density Predicts Incident Non-Spine Fractures in African-American Women. The Study of Osteoporotic Fractures. J. A. Cauley[1], L. Y. Lui[2], K. Ensrud[3], J. M. Zmuda[1], K. Stone[2], M. C. Hochberg*[4], S. R. Cummings[5]. [1]University of Pittsburgh, Pittsburgh, PA, USA, [2]UCSF, San Francisco, CA, USA, [3]U Minnesota, Minneapolis, MN, USA, [4]U Maryland, Baltimore, MD, USA, [5]California Pacific Medical Center, San Francisco, CA, USA.

Bone mineral density (BMD) measurements are powerful predictors of fracture risk in Caucasian women. To date, there have been no prospective studies of BMD and incident fractures in African-American women. To test the hypothesis that BMD predicts non-spine fractures in African-American women, we enrolled 651 women, mean age 75.4 years and followed them for an average of 5.2 years. Fifty-three African -American women experienced an incident non-spine fracture; all were confirmed by radiographic report. Hip BMD was measured by DXA (Hologic 2000 Bedford, MA). Femoral neck bone mineral apparent density (BMAD) was calculated to estimate volumetric density (BMAD = BMD/area^2). African-American women who fractured had a lower BMI (kg/m^2) (28.6 vs. 30.5, p = 0.05); were less likely to walk for exercise (25% vs. 37%, p = 0.06); were more likely to report osteoarthritis (34% vs. 20%, p = 0.02) and were more likely to use their arms to stand from a chair (25% vs. 16%, p = 0.09) as compared to African-American women who did not fracture. In age adjusted proportional hazards models, one standard deviation (SD) decrease in femoral neck BMD was associated with a 49% increased risk of fracture. (Relative risk = 1.49; 95% CI, 1.09 - 2.05) Similar results were obtained after adjusting for body weight and other risk factors. A one SD decrease in BMAD was associated with a 60% increased risk of fracture. (RR= 1.60; 1.16-2.22) We compared the incidence of non-spine fracture across tertile of BMD after 5.2 years of follow-up in African-American women to Caucasian women enrolled in SOF. (Table).

Tertile Femoral Neck BMD (g/cm^2)	Incidence Rates (per 1000 Person Years)	
	African-American	Caucasian
Low (≤ 0.599)	31.1	59.2
Med (0.5991 - 0.693)	22.6	35.8
High (≥ 0.6931)	12.0	25.1

In conclusion, Low BMD and BMAD predict fracture in older African-American women. The magnitude of the association is similar to that observed in Caucasians. Nevertheless, at every BMD level, the incidence of fracture is 40 to 50% lower among African-American women suggesting that other skeletal e.g. bone turnover and non-skeletal factors contribute to the lower incidence of fracture in African-American women.

Disclosures: ***J.A. Cauley****, Merck 2; Eli Lilly 2; Pfizer 2.*

1057

Inhibition of GSK-3β by Lithium Chloride Reverses the Osteoporotic Phenotype Displayed by Lrp5 Deficient Mice and Increases Bone Density in Intact C57Bl6 and in Osteopenic SAMP6 Mice. P. Clément-Lacroix[1], M. Ai*[2], R. Chiusaroli*[3], F. Morvan*[3], S. Roman Roman[1], B. Vayssière*[1], C. Belleville*[1], M. Warman*[2], R. Baron[1], G. Rawadi*[1]. [1]Proskelia Pharmaceutical, Romainville, France, [2]Case Western Reserve University, Cleveland, OH, USA, [3]Yale University, Yale, CT, USA.

The importance of the Wnt signaling pathway in the regulation of bone mass has been recently underlined with the identification of mutations in the Wnt coreceptor low-density lipoprotein receptor-related protein 5 (Lrp5) gene causing either the osteoporosis-pseudoglioma (OPPG) or the hereditary high bone density (HBM) syndromes in human. The bone-related phenotypic modifications found in human and mice either lacking the LRP5 protein or displaying LRP5 gain-of-function mutations seem to be largely caused by an alteration of osteoblast function. A number of experimental data lead to speculate that pharmacological modulation of LRP5 signaling could positively affect bone mass and reduce the risk for developing clinically significant osteoporosis. In this study, we show that Primary calvarial osteoblasts derived from LRP5$^{-/-}$ mice display a delay in differentiation and exhibit a significant decrease in their responsiveness to BMP-2 compared to wild-type cells. Stimulation of LRP5$^{-/-}$ primary calvaria cells with Wnt3a fails to induce β-catenin nuclear translocation or TCF1-mediated transcriptional activity. In contrast, the GSK-3β inhibitor lithium chloride (LiCl) increases both β-catenin nuclear translocation and TCF1 activity. Since the inhibition of GSK-3β is a key event downstream of LRP5, we have examined whether LiCl treatment, acting downstream of the deleted receptor, could improve bone mass in LRP5$^{-/-}$ mice. We found that LiCl markedly increased bone volume, trabecular number, osteoblast number and bone formation rate in LRP5$^{-/-}$ animals. These data strongly suggest that the low bone mass in Lrp5-/- mice results from a defective canonical Wnt signalling. Furthermore, LiCl is able to significantly increase bone formation parameters in intact C57Bl6 and in osteopenic SAMP6 mice. Given that the serum levels of Li in treated animals are equivalent to the levels reported to inhibit GSK-3ß in humans, our results suggest that inhibiting this enzyme could constitute an efficient treatment for a number of osteopenic disorders including OPPG and senile osteoporosis.

Disclosures: ***G. Rawadi****, None.*

1058

Sex Steroid Hormones in Older Men: Cross-sectional and Longitudinal Associations with Bone Mineral Density (BMD). The Osteoporotic Fracture in Men Study (MrOS). J. Cauley[1], B. Taylor*[2], H. Fink*[2], K. Ensrud[2], D. Bauer[3], E. Barrett-Connor*[4], L. Marshall*[5], M. Nevitt[3], M. Stefanick*[6], E. Orwoll[5]. [1]U of Pitt, Pittsburgh, PA, USA, [2]U Minnesota, Minneapolis, MN, USA, [3]UCSF, San Francisco, CA, USA, [4]U California, San Diego, CA, USA, [5]Oregon Health & Science U, Portland, OR, USA, [6]Stanford U School of Medicine, Stanford, CA, USA.

Sex steroid hormones may be important determinants of BMD in older men, but there is limited information on whether they predict changes in BMD or whether declines in hormones are associated with faster rates of bone loss. To address this, we measured sex hormones in 2,619 randomly selected men aged 65+ enrolled in MrOS. A subset of 1,327 men returned for a follow-up clinic visit, an average of 1.8 years later. Estradiol, testosterone, SHBG, and albumin were measured in paired serum samples collected at baseline and follow-up visits using sensitive immunoassays; free steroid levels were calculated from mass action equations. BMD was measured by DXA (Hologic 4500 W). Linear regression models were used. Total hip and lumbar spine BMD were 5.3% and 7.0% higher, respectively, in men in the top quintile of total estradiol level compared to men in the lowest quintile, Table. The rate of hip bone loss was also higher in men with the lowest estradiol compared with men with the highest estradiol. During follow-up, estradiol levels declined in 65% of the men. Men who experienced the greatest declines in total estradiol lost more total hip BMD (-0.72%/yr) compared to men who experienced the greatest increase in estradiol (-0.22%/yr), p<0.002, independent of age, weight, baseline BMD, and baseline estradiol. Similar results were observed for free estradiol. Total and free testosterone were inversely related to hip BMD in age adjusted models, but this was not significant after adjusting for body weight. Men with the lowest (Quintile 1) free testosterone experienced greater rates of hip bone loss (-0.79%/yr) compared to men with the highest (Quintile 5) free testosterone (-0.41%/ yr) p=0.02. There was no relationship between change in testosterone and change in BMD. We conclude that estradiol is a major predictor of BMD and rates of bone loss in men. Higher serum estradiol levels in older men should preserve BMD and may prevent osteoporotic fractures.

	Baseline BMD g/cm^2		Change in
Estradiol Quintile (nmoL/L)	Total Hip[a]	Lumbar Spine[a]	Total Hip BMD[b] %/year
1 (low) (<0.0046)	0.94	1.15	-0.66
2	0.97	1.17	-0.51
3 (middle)	0.97	1.18	-0.75
4	0.98	1.19	-0.42
5 (high) (≥0.079)	1.00	1.23	-0.42
p value for trend	<0.0001	<0.0001	0.02

[a] adjusted for age, race, weight, and clinic

[b] adjusted for age, race, weight, clinic, and baseline BMD

Disclosures: ***J. Cauley****, Merck 2, 8; Eli Lilly 2, 8; Pfizer 2; Novartis 2, 5.*

1059

Bone Marrow Restricted Antigen Presentation by Dendritic Cells Induces T Cell Activation and T Cell TNF Production in Ovariectomized Mice. F. Grassi, J. K. Leavey, K. Dark*, W. Qian*, M. N. Weitzmann, R. Pacifici. Medicine, Emory University School of Medicine, Atlanta, GA, USA.

It has been reported that increased T cell TNF production resulting from enhanced T cell activation stimulates osteoclast (OC) formation and leads to bone loss in ovariectomized (ovx) mice. T cell activation is induced by ovx in all lymphoid organs through upregulation of antigen (Ag) presentation by macrophages, a population of antigen presenting cells (APC). However, since ovx increases OC formation only in the bone marrow (BM), a greater stimulation of Ag presentation and thus of T cell TNF production may specifically occur in the BM. Site-specific, Ag-dependent, T cell activation driven by dendritic cells (DC) is known to take place in the BM (Feuerer M et al. Nat Medicine 2003). DC are extremely powerful APC harbored in BM foci. The formation of foci of T cell activation through upregulation of DC Ag presentation may explain why osteoclasts form specifically in the BM but do not differentiate in the spleen or lymph nodes despite the presence of all the necessary precursors and cytokines. To investigate this hypothesis, BM DC (CD11c+ cells) were purified by positive immunomagnetic selection. Ovx increased by ~ 4 fold the antigen presentation activity of BM DC, as compared to BM DC from sham operated mice. This increased activity was further potentiated by a 20% increase in DC number. Attesting to specificity, ovx had no effect on the number or Ag presentation activity of splenic DC. Furthermore, ovx was found to increase the percentage of CD4+ T cells expressing the early activation marker CD25 in the BM but not in the spleen, demonstrating a local enrichment of activated T cells. Consistent with the fact that ovx upregulates Ag presentation by increasing MHCII expression, we found that ovx increased by 70 % the mRNA expression of the H-2b chain of the MHCII complex in BM DC, but not in splenic DC. Furthermore, the expression level of the key MHCII regulatory gene CIITA, which is known to be down-regulated when DC become activated, was 66% lower in BM DC from ovx than sham operated mice. In contrast sham and ovx splenic DC had similar CIITA mRNA levels. In summary, the data show that ovx is followed by a BM specific DC activation that leads to increased Ag presentation, T cell activation and T cell TNF production. These findings suggest that one of the mechanisms which restricts OC formation to the BM is the production of high levels of osteoclastogenic cytokines in discrete foci located in close proximity to osteoclast precursors and the endosteal bone surface. The data also demonstrate that DC represent a novel estrogen target that play a previously unrecognized role in the mechanism of ovx induced bone loss.

Disclosures: ***F. Grassi****, None.*

1060

Osteopenia and Reduced Bone Formation Due to a Mutation in the Indian Hedgehog (IHH) Gene. L. Gennari[1], D. Merlotti[1], N. Giordano*[1], V. De Paola*[1], A. Calabrò*[1], G. Martini[1], A. Renieri*[2], R. Nuti[1]. [1]Dept. of Internal Medicine Endocrine Metabolic Sciences and Biochemistry, University of Siena, Siena, Italy, [2]Dept. of Molecular Biology, University of Siena, Siena, Italy.

Indian hedgehog (IHH), a member of the vertebrate hedgehog morphogen family, is a key signaling molecule that controls chondrocyte proliferation and differentiation. Recent in vitro and in vivo evidences support a direct role of IHH in the regulation osteoblast differentiation and bone formation. However, the consequences of IHH inactivation in bone homeostasis in man remain unknown. We report the skeletal phenotype of a family affected by brachydactyly type I (BDA-1) due to a mutation in the IHH gene. The proband was a 34 years old men admitted to our institute because of increasing low back pain. He was 160 cm tall (below the 3rd centile) and 58 kg in weight. At age 10 yrs he had his first fracture of a wrist after a mild fall. At age 12 he had a fracture of the humerus. Physical examination showed an upper lower segment ratio of 1.4 and brachydactyly. Skeletal x-ray examination showed signs of brachydactyly of the hands and feet, in accordance of the clinical diagnosis of BDA-1. His 66 yrs old mother and 11 yrs old daughter showed similar radiological manifestations of BDA-1. Moreover, the proband's mother also reported non-traumatic fractures of the vertebrae and the wrist, and a hip fracture. Linkage analysis showed segregation compatible with a locus at 2q35-q36 and sequence analysis of the IHH gene demonstrated the presence of a heterozygous codon 298 G/A transition in exon I, resulting in a substitution of asparagine for aspartic acid at residue 100, in all the three affected subjects.The mutation was not detected in other relatives as well as in 100 unrelated controls. DXA analysis of the proband showed marked osteopenia and reduced bone volume at the lumbar spine, proximal femur and total body, with long bones being the most severely affected. Similarly, reduced ultrasound parameters were observed at the calcaneous and the phalanxes. DXA analysis of the mother showed osteoporosis at both the spine and the hip. A DXA study on the father and on 6 male cousins was normal. Interestingly, the three affected BDA-1 subjects showed serum levels of bone formation markers (bone alkaline phosphatase and osteocalcin) at the lower values of the normal range, significantly lower than those observed in non affected family members. The markers of bone resorption (serum and urinary CTX) were in the normal range in the proband and his daughter, and slightly elevated in the mother. In summary we report the first evidence that mutations in the IHH gene in man, causing BDA-1, may be associated with low bone formation, osteopenia and increased fracture risk.

Disclosures: ***L. Gennari****, None.*

1061

CREM/ICER Deficiency Blunts the Anabolic Effect of Intermittent PTH on Bone Mass. F. Liu*[1], S. Lee[1], D. J. Adams[2], G. A. Gronowicz[2], B. E. Kream[1]. [1]Endocrionology, University of Connecticut Health Center, Farmington, CT, USA, [2]Orthopaedic Surgery, University of Connecticut Health Center, Farmington, CT, USA.

The cAMP response element modulator (Crem) gene encodes a variety of transcriptional activators and inhibitors. We previously showed that osteoblasts express many Crem transcripts including the inducible cAMP early repressors (ICER), which are induced by PTH and act as potent transcriptional attenuators. To determine whether CREM/ICER factors play a role in the anabolic response of bone to intermittent PTH, Crem knockout (KO) mice, which are deficient in all CREM/ICER factors, and wild-type (WT) mice (11-12 week old males, n=20 per group) were given daily subcutaneous injections of vehicle or hPTH(1-34) (160 µg/kg) for 10 days. Skeletal parameters were assessed by DEXA, histomorphometry and microcomputed tomography (microCT). PTH significantly increased femoral bone mineral content and density by 12.5 and 7.6%, respectively, in WT mice but only by 2.3 and 3.5%, respectively, in KO mice. Similar results were seen in tibiae and vertebrae. MicroCT of femurs showed that PTH significantly increased cortical area by 11.5% in WT mice but only by 2.2% in KO mice. The increase in cortical area in WT mice was due to periosteal expansion. Histomorphometry showed that PTH significantly increased femoral trabecular bone volume and trabecular thickness by 28.3 and 27.3%, respectively, in WT mice but only by 11.9 and 14.0%, respectively, in KO mice. MicroCT corroborated these results. Interestingly, histomorphometry showed that PTH markedly increased the percent osteoblast surface (by about 2-fold) and the bone formation rate (by about 3-fold) in femurs of both WT and KO mice, indicating that the bone formation response to PTH was not altered by CREM/ICER deficiency. By contrast, PTH increased the percent osteoclast surface and osteoclast number by 88 and 71%, respectively, in WT mice but only by 49 and 21%, respectively, in KO mice. Moreover, PTH significantly increased calvarial porosity in KO but not WT mice. Since these data indicated that Crem KO mice might have a heightened osteoclastogenic response to PTH, ex vivo bone marrow cultures were established from WT and KO mice. PTH-induced (100 ng/ml) formation of TRAP-positive multinucleated cells (MNC) was about 2-fold greater in KO marrow, while MNC formation in response to M-CSF (30 ng/ml) and RANKL (30 ng/ml) was only 10-30% greater in KO marrow. There was no difference between WT and KO marrow in CFU-GM, the osteoclast precursor population. In conclusion, our data suggest that the Crem gene may specify anabolicity of intermittent PTH treatment by limiting PTH-induced osteoclastogenesis.

Disclosures: ***F. Liu****, None.*

1062

Elucidation of Osteoblastic versus Bone Marrow Cellular Compartments in the Anabolic Actions of PTH. A. J. Koh*[1], B. Demiralp*[2], E. L. Ealba*[1], A. Mattos*[1], L. K. McCauley[1]. [1]Perio/Prev/Geriatrics, University of Michigan, Ann Arbor, MI, USA, [2]Periodontology, Hacettepe University, Ankara, Turkey.

Mice with an ablation of c-*fos* do not respond to PTH in an anabolic manner whereas wildtype littermates do. It is difficult to conclude if the lack of PTH action is due to an osteoblast, c-*fos* transcriptional effect versus an osteoclast (OC) dependent effect associated with the osteopetrotic phenotype of c-*fos* knockout mice. The purpose of this study was to elucidate mechanisms for the altered PTH response in c-*fos* knockout mice. *In vitro* studies evaluated effects of PTH on osteoblast proliferation and differentiation in primary cells from c-*fos* wildtype (+/+), heterozygote (+/-) or null (-/-) mice. Primary cells induced to differentiate for 28d showed no difference in nodule formation (Von Kossa) or calcium incorporation amongst the genotypes, and all responded similarly to PTH which inhibited mineral formation. Interestingly, -/- cells exhibited increased cell viability over 8d compared to +/+ and +/- but responded similarly to PTH and to the induction of apoptosis. These *in vitro* data suggest knockout of c-*fos* may alter cell cycle regulation but there is no apparent alteration in the response to PTH. To focus on the dependence of OCs for the PTH anabolic response, an innovative model used transplanted vertebrae from test mice in recipient mice to rescue the hematopoietic component. Vertebral bodies (vossicles) were isolated from 4d -/-, +/- and +/+ mice, implanted into athymic mice, and vehicle or hPTH (1-34) (80µg/kg) administered s.c. daily for 3wks. Prior to sacrifice, a 2-4h BRdU injection was used to label proliferating cells. Vossicles were microradiographed and processed for histology. Qualitatively, PTH treated vossicles of all genotypes had thicker cortical bone and increased number and thickness of trabeculae. Quantitatively, bone mass was significantly increased by PTH compared to vehicle in mice from all genotypes. OCs (TRAP postive cells) were present in -/- vossicles after 3wks, confirming the rescue of OCs by host mice. BRdU staining revealed increased proliferation of bone marrow cells in PTH vossicles, while proliferation in vehicle-treated vossicles was limited to the lining of bony surfaces. Taken together, these results indicate that c-*fos* ablation is not critical for PTH effects in osteoblasts and while c-*fos* is necessary for OC formation *in vivo*, rescue of bone marrow cells containing OCs into c-*fos* deficient bones restores PTH's anabolic action. Therefore, cells in the bone marrow such as osteoclasts may be critical intermediaries of anabolic actions of PTH.

Disclosures: ***A.J. Koh****, None.*

1063

The Bone Anabolic Effects of Parathyroid Hormone (PTH) are Blunted by Deletion of the Wnt Antagonist Secreted Frizzled-Related Protein (sFRP)-1. P. V. N. Bodine, Y. P. Kharode, L. Seestaller-Wehr*, P. Green*, C. Milligan*, F. J. Bex. Women's Health Research Institute, Wyeth Research, Collegeville, PA, USA.

sFRP-1 is a secreted Wnt antagonist that when deleted in mice leads to increased trabecular bone formation in adult animals after 13 weeks of age. Treatment of mice with PTH also increases trabecular bone formation, and some of the anabolic actions of this hormone may result from altered expression of Wnt pathway components in bone. To test this hypothesis, we treated +/+ and -/- female sFRP-1 mice with 100 ug/kg/day, s.c., of hPTH 1-34 for 30 days and measured distal femur trabecular bone parameters by peripheral quantitative computed tomography and high-resolution microcomputed tomography. During the course of the 32-week study, volumetric bone mineral density (vBMD) declined 41% in vehicle treated +/+ mice, but increased 24% in vehicle treated -/- animals. At 8 weeks of age when vBMD was not altered by deletion of sFRP-1, treatment of +/+ and -/- mice with PTH increased vBMD by 147-163%, respectively. In contrast, at 24 weeks of age when vBMD was 75% higher in -/- mice, treatment with PTH increased vBMD 164% in +/+ animals, but only 58% in -/- mice. Moreover, at 36 weeks of age when vBMD was 117% higher in -/- mice, treatment with PTH increased vBMD 74% in +/+ animals, while no increase was observed in -/- mice. At each of these time points, PTH treatment increased vBMD to a similar level in +/+ and -/- mice, and this level declined with age. In addition, at 36 weeks of age, the vBMD level reached by PTH treatment of +/+ mice was the same as that achieved by deletion of sFRP-1. These results indicate that loss of sFRP-1 and PTH treatment increase vBMD to a similar extent in female mice, suggesting that there are overlapping mechanisms of action. As the effects of sFRP-1 deletion on vBMD increase, the ability of PTH to enhance vBMD declines. In contrast, PTH treatment of transgenic mice harboring the G171V gain-of-function mutation of human low-density lipoprotein receptor-related protein (LRP)-5, a Wnt co-receptor, leads to synergistic increases in trabecular vBMD when compared to non-transgenic control animals, suggesting that these mechanisms are complimentary. Thus, although these data support the concept that PTH and Wnt signaling may share common components to affect bone formation, they also suggest that the mechanisms of this signaling are complex and may extend beyond control of the canonical Wnt pathway.

Disclosures: ***P.V.N. Bodine****, Wyeth Research 3.*

1064

Lrp5 Is not Essential for the Stimulatory Effect of PTH on Bone Formation in Mice. U. T. Iwaniec[1], G. Liu*[2], R. R. Arzaga*[1], L. M. Donovan*[1], R. Brommage[2], T. J. Wronski[1]. [1]Physiological Sciences, University of Florida, Gainesville, FL, USA, [2]Endocrinology, Lexicon Genetics, The Woodlands, TX, USA.

Lrp5 (low-density lipoprotein receptor-related protein 5), a key component of the Wnt signaling pathway, is involved in the regulation of osteoblastic proliferation, differentiation, and function. The purpose of this study was to evaluate the role of Lrp5 in mediating the bone anabolic effects of parathyroid hormone (PTH). Mice homozygous for the Lrp5 knockout (KO) allele were generated using retrovirus-mediated gene trapping. Eighteen-week-old male wildtype (WT, n = 10) and Lrp5 KO (n = 19) mice were treated sc with vehicle or 80 µg/kg human PTH (1-34) on alternate days for 6 weeks. Lumbar vertebrae (LV) were collected and processed undecalcified for quantitative bone histomorphometry (LV 3-4). Bone architecture of LV5 and the femoral midshaft were analyzed by microCT (Scanco µCT40). Data are expressed as mean ± SD and analyzed using a 2-way (genotype, treatment) ANOVA.

Cancellous bone volume in LV was lower in KO than WT mice (4.9 ± 2.9% versus 9.6 ± 3.7%, respectively, P<0.001). This 50% decrease in bone volume in Lrp5 KO mice determined by histomorphometry was confirmed by a similar decline measured by microCT. Femur cortical thickness was reduced by 10% (P < 0.006) in KO mice in comparison to WT mice. Osteoclast surface, an index of bone resorption, was similar in both genotypes. However, osteoblast surface was approximately 50% lower in the KO than in WT mice (P < 0.004), indicating that bone formation is decreased with Lrp5 deficiency. Treatment of mice with PTH for 6 weeks resulted in a 3 to 4-fold increase in osteoblast surface (P < 0.0001), a relatively modest 30 to 70% increase in osteoclast surface (P = 0.054), and a 13% increase in femur cortical thickness (P < 0.001), regardless of genotype. PTH treatment did not augment cancellous bone volume in either genotype. Our data confirm previous findings that loss of function of Lrp5 results in decreased cancellous and cortical bone mass due to decreased bone formation. Furthermore, we show that Lrp5 does not appear to be essential for the stimulatory effect of PTH on cancellous bone formation.

Disclosures: ***U.T. Iwaniec****, None.*

1065

The Temporal Profile in Humans of the Subacute Skeletal Anabolic Response to Continuous Infusion of PTHrP and PTH. M. J. Horwitz[1], C. M. Gundberg[2], M. Tedesco*[1], S. Sereika*[1], A. Garcia-Ocana*[1], A. Bisello[1], G. Marshall*[1], C. J. Rosen[3], A. F. Stewart[1]. [1]U Pittsburgh, Pittsburgh, PA, USA, [2]Yale U, New Haven, CT, USA, [3]St. Joseph Hosp, Bangor, ME, USA.

While both PTH and PTHrP are skeletal anabolic agents in humans, the subacute (> 12-24 hours) temporal profile of the anabolic response is unknown. In young healthy adults, we explored the responses to continuous 46 hr infusions of either hPTH(1-34) or hPTHrP(1-36), in doses between 12 to 28 pmol/kg/hr. Plasma IGF-1, osteocalcin (OC), P1NP, and serum NTX were used to assess bone turnover.

Serum calcium increased over 48 hours from baseline (8.9 mg/dl) to a mean of 10.7 mg/dl for PTHrP and 11.5 mg/dl for PTH. There were no calcemic differences among individual doses of PTH or PTHrP.

As reported by others, sNTX, a resorption marker, increased following PTH, reaching a peak of +50% at 14 hours. In the PTHrP group, a group not previously studied with respect to resorption, sNTX increased by +20%, with a peak at 14 hours.

Plasma IGF-1, a putative mediator of PTH and PTHrP actions on osteoblasts and their precursors, rose rapidly (within 7 hours) and continued to increase over the 48 hours of the study, from a baseline of 188 ng/ml to a maximum of 232 ng/ml (p < 0.001). As observed previously in osteoblasts in vitro, as well as in 12-18 hour studies in humans, the formation marker OC initially decreased by approximately 20% (p < 0.001) in both the PTH and PTHrP groups in the first 14 hours. However, in contrast to prior 12-24 hour studies, OC then continuously rose (+40%, p < 0.0001) between 14 and 48 hours. The second formation marker, P1NP, declined continuously in both the PTH and PTHrP groups, reaching a nadir of -45% at 48 hours (p < 0.001). Interestingly, there was no dose response for either PTH or PTHrP for IGF-1, OC and P1NP, and there were no differences between the PTH and PTHrP groups.

In response to a two-day of infusion of PTH or PTHrP: 1) IGF-1 increases rapidly; 2) OC displays a biphasic response, initially declining, and then increasing continuously up to 48 hours; 3) P1NP, a marker of collagen-1 synthesis, declines continuously for 48 hours. While increases in P1NP and OC may reflect increases in bone formation under chronic, steady-state conditions, their acute responses to PTH and PTHrP in humans are negative. These human studies corroborate prior in vitro rodent osteoblast and calvariae studies with PTH causing acute declines in collagen and OC synthesis. The physiologic explanation for this apparent acute reduction in bone formation to PTH and PTHrP is uncertain, but we hypothesize that it may participate in the early calcemic response to acute increases in PTH. Finally, the suppression of bone formation in response to continuous PTH and PTHrP mirrors skeletal events in HHM.

Disclosures: ***C.M. Gundberg****, BiomedicalTechnologies Inc. 5.*

1066

Suppression of Runx2-Regulated Genes, but not Runx2 mRNA, Following Continuous but not Intermittent PTH Administration to Mice: *In Vivo* Evidence for PTH-stimulated Proteasomal Degradation of Runx2 and a Mechanistic Explanation for why Continuous PTH does not Attenuate Osteoblast Apoptosis. A. A. Ali, I. Gubrij, X. Liu*, Q. Fu, X. D. Chen, C. A. O'Brien, S. Manolagas, T. Bellido, R. L. Jilka. Center for Osteoporosis and Metabolic Bone Diseases, Central Arkansas Veterans Healthcare System, University of Arkansas for Medical Sciences, Little Rock, AR, USA.

Intermittent PTH causes bone anabolism at least in part by attenuation of osteoblast apoptosis, whereas continuous administration does not affect osteoblast lifespan. *In vitro* studies have indicated that PTH-induced survival signaling is short-lived because the hormone also stimulates Smurf1-mediated proteasomal proteolysis of Runx2 - a transcription factor needed for increased synthesis of survival genes like Bcl-2. Here, we sought evidence for a PTH-induced reduction in functional Runx2 by quantifying transcript levels of 4 osteoblast/osteocyte-specific genes that strongly depend on Runx2 for transcription: osteocalcin (OCN), bone sialoprotein (BSP), dentin matrix protein 1 (Dmp1) and sclerostin (SOST). Addition of PTH to osteoblastic OB-6 cells caused a reduction in all 4 transcripts (determined by TaqMan PCR), which was first significant at 3-6 hours, and reached <10% of basal levels by 24 hours. Runx2 transcripts did not change, but the decline in target gene transcripts coincided with a 50% reduction in Runx2 protein. More important, infusion of female adult Swiss Webster mice with PTH to raise the circulating level from 10 pg/ml to 500 pg/ml also caused a 2-3 fold reduction in the level of all 4 transcripts in tibia and vertebrae after 16 h of treatment. By 48 h, transcript levels had declined by 10-fold as compared to contemporaneous vehicle controls. Again, Runx2 transcripts were not affected. The reduction in OCN mRNA corresponded with a 50% reduction in circulating OCN protein. By 96 h however, OCN, BSP and Dmp1 transcripts returned to levels at or above vehicle controls, corresponding with an increase in osteoblast number. SOST transcripts remained low at 96 h, perhaps because it is highly expressed in osteocytes as compared to osteoblasts. In contrast to the strong suppressive effects of continuous PTH, an injection of 100 ng/g of PTH did not significantly decrease these Runx2-regulated transcripts at 1, 2, 4 or 16 h. These findings support the hypothesis that continuous elevation of PTH is unable to attenuate osteoblast apoptosis because of a sustained decrease in functional Runx2, whereas intermittent administration of PTH allows repeated bursts of anti-apoptosis signaling.

Disclosures: ***A.A. Ali****, None.*

1067

A Prospective Study of DXA and QCT at the Hip and Spine Predicting Clinical Fractures in Men: the MROS Study. D. M. Black[1], L. Palermo[1], T. F. Lang[1], B. Chan[2], S. R. Cummings[3], E. S. Orwoll[2]. [1]U of CA, SF, CA, USA, [2]OR Health Sci. U, Portland, OR, USA, [3]CA Pac. Med. Ctr., SF, CA, USA.

QCT can assess several characteristics of bone density and size but the relationship of QCT of the hip and spine to risk of fractures has not been prospectively studied nor compared to DXA BMD. Using data from the MROS study, we examined this question with the hypothesis that QCT would better predict non-spine fracture than DXA.

The MROS study is a prospective cohort study of 5995 men conducted at 6 clinical sites in the U.S. A total of 3486 men had either hip or spine QCT; for this analysis, 2959 had usable hip QCT data and 3250 had usable spine QCT. The baseline visit was conducted in 2000-2002 and at the time of this analysis the mean follow-up was 2.8 years. There were a total of 120 men (12 per 1000 person years) with one or more fully adjudicated clinical non-spine fractures. We analyzed the DXA BMD, QCT volumetric BMD in the cortical and trabecular compartments at the spine and total femur and cortical volume from QCT at the hip as predictors of non-spine fracture risk. We used age-adjusted proportional hazards models and report the relative risk per standard deviation decrease in BMD/volume (RR/SD). Variations in some QCT parameters across sites were adjusted for by including clinical center in all multivariable models.

Several QCT parameters of bone density along with cortical bone volume were significantly associated with risk of non-spine fractures:

QCT and DXA for the Prediction of Non-Spine Fractures

	Spine		Total Femur				
	DXA	QCT BMD (trabecular)	DXA	QCT BMD (integral)	QCT BMD (cortical)	QCT volume (cortical)	QCT BMD (trabecular)
RR/SD	1.6	1.6	1.8	1.7	1.4	2.0	1.6
95% CI	(1.3, 2.0)	(1.3,2.1)	(1.5,2.1)	(1.4,2.2)	(1.1,1.8)	(1.5,2.7)	(1.3,2.0)
p	<.0001	<.0001	<.0001	<.0001	.002	<.0001	<.0001

The results show that QCT measurements at the hip and spine are significant predictors of non-spine fractures. QCT had similar predictive value as corresponding DXA. QCT measurements in subregions of the hip were similarly or less predictive than QCT of the total femur. QCT parameters of bone size (cross sectional area of femoral neck and vertebra) were not significantly associated with risk of non-spine fractures. Multivariate analyses including both DXA BMD and QCT BMD or cortical volume showed that DXA dominated prediction and QCT parameters were greatly attenuated.

We conclude that QCT-assessed volumetric BMD of the hip and spine and QCT cortical volume significantly predict non-spine fracture risk in men. However, in this study QCT BMD was not a better predictor than DXA BMD and the addition of QCT BMD to DXA did not substantially improve prediction of non-spine fractures in men.

Disclosures: ***D.M. Black****, Novartis Pharmaceuticals 2, 5; Merck 2, 8; NPS 2.*

1068

Type I Collagen C-telopeptide Isomerization Predicts the Long-term Risk of Non-vertebral Facture in Postmenopausal Women, Independently of Bone Mineral Density and Bone Turnover: A Non Invasive Index of Bone Collagen Quality. P. Garnero[1], P. Qvist*[2], F. Munoz*[3], E. Sornay-Rendu*[3], C. Christiansen[2], P. Delmas[3]. [1]Synarc, Inserm Unit 403, Lyon, France, [2]Nordic Bioscience, Herlev, Denmark, [3]Inserm Unit 403, Lyon, France.

Bone strength depends on its mass and architecture, but also on the material properties of its matrix. In vitro studies have suggested that the extent of post-translational modifications of collagen is associated with mechanical properties of cortical bone.

Aim: To investigate the relationships between type I collagen C-telopeptide isomerization - an index of the overall extent of spontaneous post-translational modifications of bone collagen- and the risk of fracture in postmenopausal women.

Methods: We measured native (α CTX) and age-related β isomerized (β) type I collagen C-telopeptide fragments (CTX) in the baseline fasting second morning void urine of 283 healthy premenopausal (pre MP) women (mean age: 40 from 30-57 yr) and 671 postmenopausal women (mean age 62.2 ± 9 years) from the OFELY cohort using new highly specific two site ELISAs (α-α and β-β Crosslaps, Nordic Biosciences). During a median 9.1 (IQ:2.9) yr follow-up, 158 incident fractures including 50 vertebral and 108 non-vertebral fractures were recorded in 116 women among the postmenopausal cohort.

Results:

	Hazard ratio* (95% CI) for α/β CTX > upper limit of pre MP	
	All w. with Fractures (n=116)	W. with Non-Vertebral Fractures only(n=78)
Unadjusted	1.70 (1.05-2.75)	1.84 (1.07-3.14)
Adj. for bone turnover	1.57 (0.96-2.57)	2.09 (1.23-3.58)
Adj. for hip BMD	1.39 (0.85-2.30)	1.84 (1.07-3.14)
Adj. for turnover and BMD	1.34 (0.81-2.23)	1.75 (1.04-3.041)

* adjusted for age

After adjustment for age, postmenopausal women with a urinary α/β CTX ratio above the upper limit of the premenopausal range (97.5 percentile of pre MP; 20% of postmenopausal women) had an increased risk of fracture. For non-vertebral fractures, the odds-ratio remained significant after adjustment for the overall bone turnover (assessed by serum bone alkaline phosphatase) and hip BMD.

Conclusion: Abnormally high urinary ratio between native and β isomerized CTX predicts the long-term risk of non-vertebral fracture in postmenopausal women independently of BMD and bone turnover. The measurement of urinary α/β CTX may provide a non invasive biological index of bone collagen quality.

Disclosures: ***P. Garnero****, None.*

1069

In vivo **Monitoring of Local Bone Formation Activity by Quantitative Near-Infrared Fluorescence Imaging (NIRF).** H. Gremlich*, R. Kneuer*, S. Kerrad*, M. Merdes*, A. Suter*, M. Kneissel. Novartis Institutes for BioMedical Research, Basel, Switzerland.

Detection of bone formation rates by histomorphometric evaluation of fluorochrome markers in bone is slow. It takes months from the actual *in vivo* experiment to the final readout. We tested whether we can monitor local bone forming activity *in vivo* by near-infrared fluorescence imaging (NIRF), using a near-infrared fluorescent bisphosphonate derivative homing to bone and binding to hydroxyapatite, as suggested previously [1]. In the cited study, a specific uptake of near-infrared labeled bisphosphonate into skeletal structures was demonstrated. It was hypothesized, that the bisphosphonate is taken up preferentially at sites of active bone turnover, where matrix, laid down by osteoblasts, is mineralizing. If correct, the use of such a labeled bisphosphonate should make it possible to quantify bone formation activity by NIRF.

In a 1st experiment we treated 3-month-old OF1/IC mice (n=3/group) with 0.1 or 1 mg/kg of Cy5.5 labeled pamidronate or vehicle intravenously for 1 to 5 days. NIRF images of the calvaria of the anaesthetized mice were recorded 0.5, 1, 2, 4 and 24 hours after the last administration of the near-infrared fluorescent bisphosphonate derivative using a Siemens bonSAI small animal imager prototype. Fluorescent signals could be detected in the calvaria of mice treated with labeled bisphosphonate in a dose- and application number-dependent manner but not in vehicle treated controls. Standard deviation within groups was on the average 6% of the mean value. The fluorescent signals reached 4 hours after the bisphosphonate application a steady state level that remained constant over the 1 day monitoring period. Histological examination using fluorescence imaging confirmed the presence of Cy5.5 signal on calvaria microtome sections of animals treated with the labeled bisphosphonate. In a 2nd experiment 4-month-old OF1/IC mice (n=6/group) were administered hPTH (30, 100, 300 nM), BMP-2 (2400 ng/mL, 7200 ng/mL) or vehicle (PBS + 0.1 BSA) twice daily subcutaneously onto the calvaria for 5 or 7 days. The mice were administered intravenously 0.1 mg/kg of the Cy5.5 labeled bisphosphonate or control on day 7 and 8. A dose-dependent increase of NIRF signal was observed upon hPTH (5 days: 1.8-, 2.5-, 3.2-fold; 7 days: 1.9-, 2.7-, 5.7-fold) and BMP-2 (5 days: 2.6-, 2.8-fold; 7 days: 5.7-, 7-fold) treatment 4 and 24 hours after the last application of the labeled bisphosphonate.

These results confirm that homing of fluorescent bisphosphonate into skeletal structures can be monitored by NIRF. Furthermore they demonstrate that bone formation responses can be quantified rapidly *in vivo* by the use of this technology.

[1] Zaheer et al Nat Biotech 2001

Disclosures: ***M. Kneissel****, Novartis Institutes for BioMedical Research, Switzerland 3.*

1070

Teriparatide Prevents the Fracture Risk Associated With Increasing Number and Severity of Osteoporotic Fractures. J. H. Krege*[1], G. C. Crans*[1], J. C. Gallagher[2], H. K. Genant[3]. [1]Eli Lilly and Company, Indianapolis, IN, USA, [2]Bone Metabolism Section, Creighton University Medical Center, Omaha, NE, USA, [3]Osteoporosis and Arthritis Research Group, University of California, San Francisco, CA, USA.

The relationship between number and severity of prior fractures and risk of new fractures was evaluated in 931 postmenopausal women with prevalent vertebral fractures (VFx) who were randomized to daily placebo or teriparatide 20 μg in the Fracture Prevention Trial (Neer et al. NEJM 2001). Spine radiographs were evaluated using a visual semiquantitative scoring system (Genant et al. JBMR 1993) at baseline and after a median observation of 21 months. The number of prior nonvertebral fragility fractures (NVFx) was assessed at baseline and new nonvertebral fragility fractures were confirmed by radiographs or radiologic reports. For each treatment group, the relationship between each baseline covariate and fracture risk was assessed using the Cochran-Armitage trend test; treatment group slopes were compared using the bootstrap technique. In the placebo group, both increasing number and severity of prevalent vertebral fractures were associated with a significant increase in incident vertebral fracture risk. In the placebo group, increasing number of prior nonvertebral fragility fractures was associated with a significant increase in new nonvertebral fragility fracture risk. In the teriparatide group, neither increasing number nor severity of prevalent vertebral fractures was significantly associated with increased risk for new vertebral fractures. Additionally, increasing number of prior nonvertebral fragility fractures was not significantly associated with an increased risk for new nonvertebral fragility fractures. In conclusion, in placebo patients, the number and severity of prior fractures predicted risk for new fractures. This relationship was not observed in women treated with teriparatide.

	New VFx (%)	
Prevalent VFx number	Placebo	Teriparatide 20 μg
1	6.8*	3.4
2	15.7*	5.8
≥3	22.6*	7.2
Prevalent VFx severity		
Mild	9.6*	3.5
Moderate	12.9*	6.4
Severe	28.4*	5.8
	New NVFx (%)	
Prior NVFx number	Placebo	Teriparatide 20 μg
0	3.6*	2.7
1	8.2*	0
≥2	18.0*	3.9

*P<0.001 for association between increase in baseline variable and increasing new fracture risk; slope significantly greater than in teriparatide group. (bootstrap technique).

Disclosures: ***J.H. Krege****, Eli Lilly and Company 1, 3.*

1071

The RANKL Antagonist OPG-Fc Causes Significant Increases in Cortical Bone Mineral Area, Content and Density in Adult Cynomolgus Monkeys. P. J. Kostenuik[1], C. Paul*[2], S. Smith[3], F. Asuncion*[1], J. Atkinson[2]. [1]Metabolic Disorders, Amgen, Inc., Thousand Oaks, CA, USA, [2]Toxicology, Amgen, Inc., Thousand Oaks, CA, USA, [3]CTBR, Senneville, PQ, Canada.

OPG-Fc is a RANKL antagonist that blocks osteoclast differentiation, activation and survival. OPG-Fc leads to rapid, profound and sustained suppression of bone resorption and increased bone mineral density (BMD) in rodents, monkeys and humans. Cortical bone contributes significantly to overall skeletal strength, but this bone compartment tends to be less responsive to antiresorptive therapy compared to the more dynamic trabecular compartment. We therefore tested the effects of OPG-Fc on cortical bone area, bone mineral content (BMC), and density (BMD) in 2-3 year old intact female cynomolgus monkeys. OPG-Fc was administered once weekly for 6 months at 15 mg/kg SC (n = 8) or IV (n = 5). Vehicle (PBS) was administered weekly (SC) to control animals (n = 5). The distal radius and proximal tibia were analyzed at baseline and at 6 months by peripheral quantitative computed tomography (pQCT). Serum was obtained for biochemical markers of bone turnover. All measured pharmacologic responses to IV and SC administration of OPG-Fc were very similar, so data from these groups were merged for analyses.

Bone resorption was dramatically suppressed by OPG-Fc, as evidenced by a ~90% suppression of urine N-Telopeptide (NTx) versus PBS controls at month 6. This antiresorptive response was associated with significant improvements in total, trabecular and cortical BMC and BMD at the distal radius and at the proximal tibia. The following comparisons were all statistically significant ($p<0.05$) versus PBS controls after 6 months of treatment: OPG-Fc increased cortical thickness by 251% and 39% in the distal radius and proximal tibia, respectively. OPG-Fc increased cortical bone area by 223% and 49% in the distal radius and proximal tibia, respectively. The radius of OPG-treated animals had a 20% increase in periosteal circumference and a 40% reduction in endosteal circumference. Cortical BMC was increased by 269% in the distal radius, and by 67% at the proximal tibia. OPG-Fc treatment also significantly improved BMD at each of these sites, as well as at the midshaft of the radius and tibia. These data demonstrate that OPG-Fc treatment of intact female cynomolgus monkeys results in the significant expansion of cortical bone. Increases in cortical bone volume were associated with proportional increases in bone mineral content and improvements in BMD. The expansion of periosteal circumference at cortical sites suggests that osteoblast activity is maintained during OPG-Fc therapy despite the significant suppression of bone resorption.

Disclosures: ***P.J. Kostenuik****, None.*

1072

AMG 162 Increases Bone Mineral Density (BMD) within 1 Month in Postmenopausal Women with Low BMD. M. R. McClung[1], E. M. Lewiecki[2], M. A. Bolognese*[3], G. Woodson*[4], A. Moffett*[5], M. Peacock*[6], P. D. Miller*[7], S. Lederman*[8], C. H. Chesnut*[9], R. Murphy*[10], D. L. Holloway[10], P. J. Bekker[10]. [1]Oregon Osteo Ctr, Portland, OR, USA, [2]New Mexico Clin Research & Osteo Ctr, Albuquerque, NM, USA, [3]Bethesda Hlth Research Ctr, Bethesda, MD, USA, [4]Atlanta Research Ctr, Decatur, GA, USA, [5]OBGYN Associates of Mid Florida PA, Leesburg, FL, USA, [6]Indiana Univ School Medicine, Indianapolis, IN, USA, [7]Colorado Ctr for Bone Research, Lakewood, CO, USA, [8]Radiant Research, Lake Worth, FL, USA, [9]Univ Washington Med Ctr, Seattle, WA, USA, [10]Amgen Inc, Thousand Oaks, CA, USA.

AMG 162, a high-affinity, high-specificity, fully human monoclonal antibody to receptor activator of NF kappa B ligand (RANKL), inhibits osteoclastic bone resorption. The objectives of this randomized, dose-ranging study were to evaluate the efficacy and safety of AMG 162 in postmenopausal women with low lumbar spine BMD (T-score ≤-1.8). Four hundred eleven women were randomized to placebo or 6, 14, or 30 mg 3-monthly or 14, 60, 100, or 210 mg 6-monthly (q6mo) or 70 mg/wk alendronate. BMD (DXA), bone turnover markers, and safety measurements have been followed for 12 months.

Baseline age and lumbar spine BMD T-score (mean [SD]) were 63 (8) years and -2.2 (0.8), respectively. At month 12, AMG 162 increased lumbar spine BMD 4% to 7% in all groups (alendronate 5%). Total hip BMD change for the 60-mg, q6mo AMG 162 group was greater than alendronate ($p < 0.001$) (Figure). AMG 162 had a positive effect on mainly cortical bone sites, distal 1/3 radius and total body.

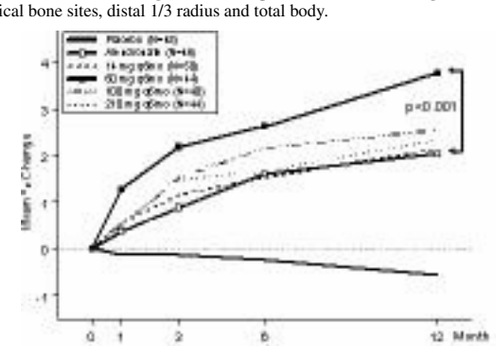

AMG 162 given 3-monthly also was effective. A rapid (72 hours), dose-dependent decrease of serum C-telopeptide and urine N-telopeptide/creatinine occurred with AMG 162. AMG 162 was well tolerated. The most common adverse event in any group was dyspepsia (4%, 5%, and 20% in the placebo, AMG 162, and alendronate groups, respectively). One (0.3%) subject (14 mg AMG 162) had a transient, asymptomatic decrease in albumin-adjusted serum calcium below 8 mg/dL (7.8 mg/dL at month 2). No other clinically meaningful laboratory changes occurred. Non-neutralizing anti-AMG 162 antibodies occurred at month 1 for 1 (0.3%) subject, but did not persist. Two fractures (traumatic vertebral and ankle) occurred in the AMG 162 groups.

In summary, AMG 162 increased BMD within 1 month in postmenopausal women and appeared to be more effective than alendronate at cortical bone sites.

Disclosures: ***M.R. McClung****, Amgen 5.*

1073

New Insights into Bone Extracellular Matrix Assembly from Dynamic Computational Imaging in Living Osteoblasts. P. Sivakumar[1], B. J. Rongish*[2], A. Czirok*[2], V. P. Divakara*[1], S. L. Dallas[1]. [1]Univ. of Missouri, Kansas City, MO, USA, [2]Univ. of Kansas Medical Center, Kansas City, KS, USA.

Bone extracellular matrix (ECM) has been classically viewed as a static scaffold that supports cells and tissues. However, using dynamic imaging in living osteoblast cultures we have shown that the ECM is highly elastic and undergoes large dynamic movements associated with cell motility. We have also shown that fibronectin is a key regulator for assembly of multiple bone ECM proteins. To gain further insights into the kinetics of bone ECM assembly and the role of fibronectin, we have performed time lapse imaging in living osteoblasts using fluorescent probes for fibronectin and other bone ECM proteins and have developed computational techniques to correlate cell and fibril movement. Time lapse imaging revealed that fibronectin was initially incorporated onto the cell surface as punctate spots, resembling focal adhesions, which then coalesced progressively to form fibrils. Individual fibrils received contributions from cells that could be quite distant (up to 100µm) from the forming fibril. Pulse-chase dynamic imaging using green followed by red fluorescent fibronectin showed that newly incorporated fibronectin did not assemble onto existing fibrils. Instead it was localized in focal spots on the cell surface which then redistributed over the next 24 hours to become colocalized with preexisting fibronectin fibrils. This reorganization was inhibited by jasplakinolide, an actin destabilizing agent, suggesting that cell motility is critical for reorganization of newly incorporated fibronectin. Next we performed dual imaging of fibronectin and latent TGF beta binding protein-1, an ECM glycoprotein responsible for storage of TGFβ in bone. Time lapse movies in living osteoblasts revealed a surprising amount of cell and fibril movement even after 12 days in culture, resulting in continual stretching and contracting of fibrils. Cells appeared to actively contribute to ECM assembly by adding "packets" of ECM material onto growing fibrils. In addition there were many examples where fibrillar material appeared to be exchanged between fibrils, suggesting a novel mechanism for ECM reorganization. Image analysis showed that individual fibrils could stretch up to twice their length and contract as much as 75%. Occasionally fibrils were seen to break and recoil, suggesting that they exist in a highly stretched state. Analysis of cell and fibril movement by vector displacement mapping showed that the movement of cells and fibrils was correlated in magnitude and direction. These data suggest a major role for cell motility in assembly of bone ECM proteins and suggest novel cell mediated mechanisms for ECM reorganization.

Disclosures: ***P. Sivakumar****, None.*

1074

Glucocorticoids Induce Osteocyte Death by Blocking Focal Adhesion Kinase Survival: Evidence for Inside-Out Signaling Leading to Cell Detachment-Induced Apoptosis (Anoikis). L. I. Plotkin, L. Dominguez, K. Vyas*, J. I. Aguirre, S. C. Manolagas, T. Bellido. Endocrinology, Center for Osteoporosis and Metabolic Bone Diseases, Central Arkansas Veterans Healthcare System, Univ. Arkansas for Med. Sci., Little Rock, AR, USA.

Premature apoptosis of osteocytes by direct actions on these cells contributes to the bone fragility syndrome that characterizes glucocorticoid (GC)-induced osteoporosis. However, the mechanism of this phenomenon remains unknown. The GC dexamethasone (dex) induces apoptosis of osteocytic MLO-Y4 cells, which is prevented by caspase 3 inhibitors. We now report that dex-induced apoptosis is abolished by the GC receptor antagonist RU486, it is not affected by inhibitors of protein or RNA synthesis and it is preceded by changes in cell shape leading to detachment. Thus, dex increased the percentage of cells exhibiting 3 or less cytoplasmic projections at expenses of a decrease in cells with more than 4 projections. Both cell survival and shape are controlled by the focal adhesions, sites at the plasma membrane in which integrins assemble with cytoskeletal and signaling molecules such as the focal adhesion kinase (FAK). FAK promotes attachment and survival, whereas the related protein proline-rich tyrosine kinase 2 (Pyk2) has the opposite effects. We found that cells overexpressing FAK were protected from dex-induced apoptosis. On the other hand, cells overexpressing Pyk2 were as responsive to dex as vector transfected cells. However, cells expressing either a kinase-deficient (Lys457Ala) or an authophosphorylation-defective (Tyr402Phe) Pyk2 were refractory to dex-induced apoptosis. Consistent with this, dex induced rapid Pyk2 phosphorylation in Tyr402; and knockdown Pyk2 expression with small interference RNA abolished the proapoptotic effect as well as the changes in cell shape induced by dex, whereas transfection with human Pyk2 rescued both responses. Furthermore, the proapoptotic effect of dex was abolished by inhibiting JNK activity - a known mediator of Pyk2 actions - with SP600125; but it was not affected by inhibiting other kinases involved in apoptosis regulation, such as p38, ERKs, Src, or PI3K. Moreover, inhibition of JNK activity also abolished the effect of dex on cell shape. In sharp contrast, although inhibition of caspase 3 with DEVD abolished dex-induced apoptosis, it did not reverse its effect on cell shape, indicating that changes in cellular morphology precede caspase 3 induction and apoptosis. We conclude that GC promote osteocyte apoptosis via a receptor-mediated mechanism that do not require gene transcription and that is mediated by Pyk2 and JNK, followed by inside-out signaling which favors cell detachment-induced apoptosis or anoikis.

Disclosures: ***L.I. Plotkin****, None.*

1075

Osteocrin, a Local Mediator of the Natriuretic System. G. P. Thomas, K. Sellin*, M. Bessette*, F. Lafreniere*, C. Lanctot*, P. Moffatt*. Phenogene Therapeutics, Montreal, PQ, Canada.

The natriuretic system, important in regulation of vascular tone and cardiovascular homeostasis, also acts on the skeleton. Control is exerted through 3 peptides, ANP, BNP and CNP, and 3 receptors, GC-A and GC-B which are guanylate cyclases producing cGMP, and NPR-C the clearance receptor. CNP- and BNP-transgenic mice and NPR-C knockout mice have elongated bones and marked kyphoses whereas CNP-knockout mice exhibit dwarfism. We previously identified an osteoblast lineage protein, osteocrin (Ostn) which has no clear homology with any other protein group except for limited C-terminal homology with the natriuretic peptides.

Thus, we hypothesised that Ostn could interact with members of the natriuretic receptor family thereby modulating natriuretic peptide actions on the skeleton. To investigate Ostn binding to the natriuretic receptors we generated a fusion protein consisting of an N-terminal secreted placental alkaline phosphatase moiety linked to mouse Ostn (PLAP-Ostn). Binding studies showed that PLAP-Ostn binds specifically and saturatably to the NPR-C receptor with no binding to the GC-A or GC-B receptors. Further, PLAP-Ostn can be competed off NPR-C with either cold ANP or cold mn306C, a synthetic C-terminal Ostn peptide. We then investigated the ability of Ostn to augment the activity of natriuretic peptides. Overexpression of NPR-C in HEK293 cells (which express endogenous GC-A) inhibited ANP-stimulated increases in intracellular cGMP production. However, when cells overexpressing NPR-C were co-treated with ANP and Ostn or mn306C, the effects of ANP activity were greatly increased. These results suggest that Ostn can modulate the hormonal response of cells to natriuretic peptides by limiting their clearance through NPR-C. To investigate the role of Ostn *in vivo* we generated transgenic mice overexpressing Ostn in osteoblastic cells using the collagen type I 3.6kb promoter. These mice displayed elongated bones and a marked kyphosis. Further, cGMP levels were elevated in the bones of the transgenic mice suggesting elevated natriuretic peptide activity contributed to the increased bone length.

Thus we have demonstrated that Ostn is a naturally occurring antagonist of the NPR-C clearance receptor and may act to locally modulate the actions of the natriuretic system in the skeletal compartment. Interestingly, we and another group have also observed Ostn expression in other mesenchymal tissues such as tendons, ligaments and muscle suggesting Ostn may play a more general role in mediating the local actions of the natriuretic system in mesenchyme tissue.

Disclosures: ***G.P. Thomas****, None.*

1076

Mechanical Stress Dependent Remodeling of the Periodontal Ligament Is Defective in Periostin Deficient Mice; Mechanotransduction through Periostin Protein. I. Kii*[1], N. Amizuka[2], S. Kitajima*[3], M. Li*[2], K. Takeuchi*[2], T. Maeda*[2], J. Kanno*[3], T. Inoue*[3], Y. Saga*[4], A. Kudo[1]. [1]Department of Biological Information, Tokyo Institute of Technology, Yokohama, Japan, [2]Department of Oral Biological Science, Niigata University Graduate School of Medical and Dental Science, Niigata, Japan, [3]Division of Toxicology, National Institute of Health Science, Tokyo, Japan, [4]National Institute of Genetics, Division of Mammalian Development, Mishima, Japan.

The secreted matricellular protein, periostin is specifically expressed in the periodontal ligament and the periosteum in adult mice, and is postulated as a cell spreading factor to matrix. The periodontal ligament is involved in the tooth eruption and the orthodontic tooth movement. To investigate the function of periostin in the periodontal ligament, we generated periostin-/- mice and found that -/- mice are born and grow normally, however, during aging from 6 to 12 weeks old -/- mice showed abnormal incisors, disorganized ameloblastic layer and deformed enamel matrix because of disappearance of the shear zone in the incisor periodontal ligament. Electron microscopic analysis of the periodontal ligament in -/- mice showed no matrix remodeling but accumulated matrix fiber with type I collagen. Excision of incisors demonstrated that in -/- mice, no tooth eruption was observed. Moreover, the experimental molar movement revealed that at the compressed side of the periodontal ligament in -/- mice, hyalinized extracellular matrix induced by compression largely remained, although it was removed from +/+ mice. The results suggested that periostin functions in remodeling of the periodontal ligament, specifically in matrix degradation and metabolism in response to compressive mechanical stress. In in-vitro analyses using the purified periostin protein, we revealed that periostin bound to type I collagen mediated with the cysteine-rich N-terminal region of periostin, and matrix-free periostin was endocytosed into 10T1/2 cells to give rise to phosphorylation of ERK. We speculate that mechanical stress unfasten the periostin cysteine-rich domain binding to collagen matrix, then periostin is endocytosed and acts on the hyalinized matrix degeneration through the MAPK activation. Taken together, periostin functions as a mechanosensor in the remodeling of periodontal ligament.

Disclosures: ***I. Kii****, None.*

1077

Insertional Mutagenesis of Osteopotentia, a Novel Transmembrane Protein Essential for Skeletal Integrity. M. L. Sohaskey*[1], Y. Jiang[2], J. Zhao[2], A. Mohr*[2], F. Roemer*[2], H. K. Genant[2], W. C. Skarnes*[1]. [1]Molecular and Cell Biology, University of California, Berkeley, CA, USA, [2]Osteoporosis and Arthritis Research Group, University of California, San Francisco, CA, USA.

Strict coordination of bone remodeling processes is essential for skeletal integrity and homeostasis. Deregulation of these processes leads to pathophysiological changes and metabolic bone disease. In an insertional mutagenesis screen for critical regulators of mammalian development and physiology, we identified *Osteopotentia* (*Opt*), a gene encoding a novel transmembrane protein. We have investigated the consequences of *Opt* mutation for postnatal skeletal development using a combination of genetic, biochemical, histological and radiological approaches. Mice homozygous for an insertional mutation in the *Opt* gene die predominantly at birth of undetermined causes. A subset of these mice, however, survive for up to twenty days and develop striking skeletal abnormalities similar to those seen in humans and genetically engineered mouse models having severe forms of the brittle bone disease osteogenesis imperfecta. Abnormalities include inflammation and hemorrhaging around limbs, bowing deformities of the long bones, and poorly healed fractures evidenced by the formation of hypertrophic calluses on long bones and ribs. Histological analyses reveal a marked decrease in the amount of trabecular and cortical bone in surviving *Opt* homozygous mutant mice relative to normal littermates. Likewise, quantitative dual-energy x-ray absorptiometry (DEXA) and micro-CT imaging demonstrate a significant reduction in total bone mineral density as well as 3D trabecular bone volume fraction, number and thickness, with an increase in 3D trabecular spacing. Biochemical assessment of serum and urine parameters reveals that *Opt* homozygous mutants are hypercalciuric and hypophosphaturic, despite having normal serum calcium and phosphate levels. Finally, decreased levels of osteocalcin mRNA and protein in bone and serum, respectively, suggest that *Opt* homozygous mutants may manifest a defect in osteoblast differentiation and/or activity. Overall, elucidation of the physiological role played by Opt will be important in determining how mutagenesis of this novel gene results in severely compromised skeletal integrity in the mouse. Our studies may thus provide mechanistic insight into the etiology of recessively inherited forms of osteogenesis imperfecta demonstrating no genetic linkage to either type I procollagen locus. Moreover, our results may have important therapeutic implications for the clinical understanding, prevention and treatment of idiopathic hypercalciuria.

Disclosures: ***M.L. Sohaskey****, None.*

1078

Biglycan and Decorin Are Essential for Post-Natal Fronto-Nasal Craniofacial Growth and Development. S. Wadhwa, M. Embree*, Y. Bi*, M. Young. Csdb, NIDCR/NIH, Bethesda, MD, USA.

Biglycan (BGN) and decorin (DCN) are members of a family of proteins known as SLRPs (Small leucine rich proteoglycans). They are believed to have similar physiologic roles important for growth factor binding and function. Thus, the absence of one SLRP may be compensated for by the presence of another. The objective of this study was to determine whether BGN and /or DCN play a role in craniofacial growth and development by characterizing their expression at various stages of development, and examining the phenotype of mice deficient in one or both small proteoglycan. At embryonic day (ED) 18.5 biglycan and decorin were found to be abuduntantly expressed in the craniofacial complex. ED 18.5 day embryos deficient for biglycan and decorin had no craniofacial abnormalities compared to wildtype (WT) littermates. However, ED 18.5 double knock out (DKO) embryos were severely hypomineralized in the frontal bone compared to the control littermates. In the adult mice, biglycan and decorin were also found to be expressed throughout the craniofacial complex. In particular, in the calvarial sutures, biglycan appeared in the fusing bone fronts while decorin was highly expressed in the dura underlying the fusing sutures. Adult 60 day-old mice deficient in either biglycan or decorin did not have a craniofacial phenotype. However, the DKO mice had a severe phenotype. The DKO skulls were 40 % smaller in the anterior-posterior direction compared to WT. In normal mice, the posterior frontal suture normally fuses within 25-45 days after birth. Analysis of 60 day-old DKO mice showed that the posterior frontal sutures were completely patent and lacked symmetry compared to WT controls. In addition there was also disorganization in the olfactory structures. In particular there was hypoplasia of the olfactory epithelia and irregular shape of the nasal bones. In order to determine the molecular basis for the craniofacial defects in the DKO mice, we examined the expression of several genes previously shown to control olfactory and/or calvarial suture development. In these experiments bone marrow stromal cells were isolated from normal and DKO mice, treated with TGF-beta and mRNA expression profiles measured by semi-quantitative RT PCR. One factor, DLX5, was significantly reduced and dysregulated by TGF-beta, a factor that is overactive in the DKO cells. We conclude that biglycan and decorin potentially control postnatal frontonasal craniofacial growth and organization through a molecular link to DLX5 signaling pathways.

Disclosures: ***S. wadhwa****, None.*

1079

Van Buchem Disease Mouse Models and Genomic Comparisons Reveal a Bone-specific Enhancer Regulating Sclerosteosis Causing Gene SOST. M. Kneissel[1], H. J. Keller*[1], M. Baptist*[1], E. M. Rubin*[2], G. G. Loots[3]. [1]Bone Metabolism, Novartis Institutes for BioMedical Research, Basel, Switzerland, [2]JGI, Walnut Creek, CA, USA, [3]Genomics Division, LLNL, Livermore, CA, USA.

Sclerosteosis is a generalized progressive bone overgrowth disorder due to the loss of function of the SOST gene product sclerostin (SOST). Affected patients display increased bone formation, while bone resorption is undisturbed. Van Buchem disease (VB) is a very similar skeletal abnormality associated with a ~52kb noncoding deletion downstream of the SOST transcript. It has been proposed that VB is caused by misregulating SOST transcriptional activity. We have tested this hypothesis by analyzing the expression pattern of human SOST in transgenic mice carrying either normal alleles (hSOSTwt) or genetically modified VB alleles (hSOSTvbd) cloned from human BACs. Several independent lines of transgenic hSOSTwt and hSOSTvbd animals were obtained and characterized. Similar to the endogenous murine SOST expression, human SOST transcripts were robustly expressed in bone of adult hSOSTwt but not of hSOSTvbd mice. DEXA, microCT and histomorphometric analysis of the skeleton of 5-month-old animals revealed that increased doses of human SOST resulted in osteopenia and reduced bone formation rates in the axial and appendicular skeleton in hSOSTwt but not in hSOSTvbd mice, whose bone mass and structure were indistinguishable from wild-type control mice. In contrast, elevated embryonic SOST expression resulted in dose-dependent digit abnormalities in both hSOSTwt and hSOSTvbd transgenic mice, suggesting the presence of different tissue specific enhancers. To search for regulatory elements within the 52kb VB deletion that drive bone-specific sost expression a cross-species human-mouse sequence comparison was performed for conserved sequences. The seven most highly conserved sequences (>200bp length; >80% identity; CNS2-8) were tested for the ability to stimulate the SV40 promoter in an osteoblastic and a control kidney cell line, both expressing high levels of endogenous SOST. Only CNS5 significantly activated transcription in the osteoblastic but not in the kidney cells. Furthermore, CNS5 was also able to stimulate the human SOST promoter (2kb upstream sequence) and to drive bone-specific reporter gene expression in transient transgenic mice. Thus, we have identified an enhancer element within the VB deletion that drives SOST expression in the mouse skeleton.

Disclosures: ***G.G. Loots****, None.*

1080

Congenic Mice with Low Serum IGF-I Have An Impaired Osteoblast Differentiation Program as well as Increased Body and Marrow Adiposity. C. Ackert-Bicknell[1], M. C. Horowitz[2], T. Nelson*[2], K. L. Shultz[1], V. E. Guido*[1], L. R. Donahue[1], M. L. Bouxsein[3], M. L. Adamo[4], W. G. Beamer[1], C. J. Rosen[1]. [1]The Jackson Laboratory, Bar Harbor, ME, USA, [2]Yale University School of Medicine, New Haven, CT, USA, [3]Beth Israel Medical Center, Boston, MA, USA, [4]University of Texas Health Center, San Antonio, TX, USA.

We previously reported 4 Quantitative Trait Loci (QTLs) for serum IGF-I on Chr 1, 6, 10 and 15. The B6.C3H-6T (6T) congenic strain is a C57BL/6J (B6) mouse carrying a portion of the C3H/HeJ (C3H) from Chr 6 (*D6Mit93* to *D6Mit150*). It has reduced serum IGF-I, a smaller periosteal circumference, shorter femurs and reduced BMD compared to B6. The 6T strain also has a lower bone formation rate and nearly a 50% reduction of IGF-I mRNA in adult bone ($p<0.05$). In order to further understand this skeletal phenotype, we investigated osteoblast (OB) precursor number and their differentiation in bone marrow stromal cell (BMSC) cultures from B6 and 6T mice as well performing candidate gene analysis. Adherent BMSC were cultured with guinea pig BM feeder cells in α-MEM with 10%FCS and ascorbate. OB progenitor colonies were stained with alkaline phosphatase (CFU-AP+) and counter stained with crystal violet (CFU-F). At 7, 10 and 15 days, 6T BM revealed there were less CFU-Fs ($p<0.007$) and less CFU-AP+ colonies ($p<0.0001$) than B6. We then assessed Runx2 expression, by Quantitative Real Time PCR (QPCR), using a Global Pattern Recognition algorithm to assess statistical significance. Runx2 mRNA was decreased in femur (-1.52 fold in 6T vs B6) from 8 wk old females as well as BMSC cultures (-1.32 fold in 6T vs B6). Co culture of stromal cells with BM or spleen cells reveal no strain differences in the generation of osteoclast-like cells (by TRAP). 6T females weigh less ($p=0.006$) than B6 at 16 weeks, but have higher percent body fat (B6:17.5 ± 0.50; 6T: 20.5±1.0 $p=0.02$). These mice also have significantly more marrow fat than B6 by Oil Red 0 staining ($p=0.05$). The 6T congenic region is very large (25cM) and contains > 500 genes. To quickly narrow this list, we used block haplotyping with SNPs and SSLPs makers to excluded genomic regions where B6 was identical to C3H. Further power was added to this analysis by adding the A/J strain, which does not have a serum IGF-1 phenotype mapped to Chr 6. We were able to narrow our region to two haplotype blocks (<2cM) on distal Chr 6, containing 11 known genes and 39 novel or predicted genes. By QPCR we have identified two potentially important candidate genes on Chr 6 involved in OB differentiation. In conclusion, 6T mice have increased body and marrow adiposity, along with impaired OB differentiation and reduced BMD due to allelic differences in a gene on Chr 6 that suppresses skeletal IGF-I and impacts OB differentiation.

Disclosures: ***C. Ackert-Bicknell****, AR45433 2.*

1081

Genetic Association Studies of the Human Arachidonate Lipoxygenase Genes, *ALOX12* and *ALOX15*, with Peak Bone Mineral Density. S. Ichikawa*[1], D. L. Koller[2], M. L. Johnson*[1], D. Lai*[2], R. F. Klein[3], E. S. Orwoll*[3], S. L. Hui[1], C. C. Johnston[1], T. M. Foroud[2], M. Peacock[1], M. J. Econs[1]. [1]Medicine, Indiana University School of Medicine, Indianapolis, IN, USA, [2]Medical and Molecular Genetics, Indiana University School of Medicine, Indianapolis, IN, USA, [3]Bone and Mineral Research Unit, Oregon Health & Science University, Portland, OR, USA.

The arachidonate 15-lipoxygenase (*Alox15*) gene was recently identified as a negative regulator of peak bone mineral density (BMD) in mice. At the protein level, mouse Alox15 has the highest identity to its human homolog ALOX15 (73%), followed by arachidonate 12-lipoxygenase (ALOX12) (57%). However, mouse Alox15 is functionally more similar to human ALOX12 as both enzymes preferentially oxygenate arachidonic acid at carbon-12, instead of carbon-15. To determine the contribution of the lipoxygenase genes to peak BMD variation in normal subjects, we performed population- and family-based genetic association studies in Caucasian sibpairs ascertained in Indiana. Analysis of genome screen marker data from this sample demonstrated minimal inflation of the false positive rate of association tests due to population stratification (JBMR, in press). BMD was measured at proximal femur and lumbar spine in 190 men, aged 20-61 and 588 women, aged 21-52. We tested five and seven single nucleotide polymorphisms (SNPs) distributed across *ALOX15* and *ALOX12*, respectively. SNP genotyping was performed using matrix-assisted laser disorption/ionization time-of-flight (MALDI-TOF) mass spectrometry of allele-specific primer extension products. No statistically significant association was found between the five *ALOX15* SNPs and peak BMD variation. In contrast, moderate evidence for association was found with six SNPs in the *ALOX12* gene. Five allelic variations in the 5' region were significantly associated with spine BMD in both men and women ($p=0.0041$-0.057). These genetic variations may account for 0.5-2.8% and 0.5% of BMD variation in men and women, respectively. The most common haplotype, composed of these 5 SNPs, was also associated with spine BMD in men ($p=0.019$). Of note, there were two nonsynonymous SNPs in exons 6 and 8 of *ALOX12*, which change encoded residues, Arg261Gln and Ser322Asn, respectively. Further, genetic variation with the highest association, accounting for 2.8% of the variation in men, was located within 300 bp upstream of the gene, suggesting that the regulatory element in the promoter region may influence *ALOX12* expression. In light of the recent finding in mice, association between *ALOX12* alleles and peak BMD variation suggests a role for this gene or another in linkage disequilibrium with *ALOX12*, in the development of peak BMD in men and women.

Disclosures: ***S. Ichikawa****, None.*

1082

Bone Formation Phenotype in Cathepsin K Null Mice. B. Pennypacker, D. B. Kimmel. Bone Biology and Osteoporosis, Merck Research Laboratories, West Point, PA, USA.

Cathepsin K (CatK), a cysteine protease that degrades Type I collagen, is highly and selectively expressed in osteoclasts. Adult CatK null mice have osteopetrosis with hypofunctional osteoclasts that appear to have reduced ability to degrade bone matrix. Bone strength of CatK null mice is increased in proportion to the increased bone mass. The purpose of this study is to evaluate bone formation in CatK null mice.

Fifty mice of both genders, including wild type homo- and heterozygotes, aged 4.5 months were necropsied after *in vivo* dual calcein labeling. Right femora were fixed in 70% ethanol. The distal femur was embedded non-decalcified in methyl methacrylate. Bone volume (BV/TV, %), trabecular thickness, trabecular number, mineral apposition rate (MAR, μm/d), mineralizing surface (MS/BS, %), and bone formation rate were determined in 6μm, unstained sections of cancellous bone. Data were analyzed by two-factor ANOVA (gender/genotype) plus Neuman-Keuls post-hoc testing within gender.

Bone volume, reflected as both increased thickness and number of trabeculae, was influenced positively by genotype ($P<.001$). Both osteoblast activity (MAR) and extent of formation surface (MS/BS) were also influenced positively by genotype ($P<.001$). Both were also increased in female as comapred to male mice.

The osteopetrosis seen in cancellous bone of adult CatK null mice was accompanied by an unexpectedly high rate of bone formation. Based on ultrastructure and the increased bone mass, it has previously been inferred that osteoclasts in CatK null mice are hypofunctional. Usually, when resorption is inhibited, bone formation is similarly reduced due to coupling. The CatK null mouse disobeys this paradigm, since bone resorption rate is decreased while bone formation rate remains high. This finding may suggest that CatK plays a role in the coupling of resorption and formation that is usually present in adult bone tissue.

Bone Formation and Bone Volume

Sex/Geno	BV/TV	MAR	MS/BS
M +/+	12.4±1.6	1.7±0.1	13±1
M +/-	16.6±3.0	1.9±0.1	23±3†
M -/-	21.1±1.8*	2.3±0.2*	25±3*
F +/+	5.2±0.7	2.1±0.1	20±1
F +/-	14.2±3.5*	2.6±0.2†	26±2*
F -/-	29.4±4.6*	3.4±0.2*	30±2*

Mean±SEM *Significantly different from +/+ of same sex (*P <0.01; † P<0.05)

Disclosures: ***D.B. Kimmel****, None.*

1083

Congenic Mice from Chromosome 1 Reveal Sex-Specific Differences in Vertebral Trabecular Bone Volume Fraction and Microarchitecture. J. Swenson*[1], K. L. Shultz[2], C. J. Rosen[2], L. Donahue[2], W. J. Beamer[2], M. L. Bouxsein[1]. [1]Beth Israel Deaconess Medical Center & Harvard Medical School, Boston, MA, USA, [2]The Jackson Laboratory, Bar Harbor, ME, USA.

Low BMD is among the strongest risk factors for osteoporotic fracture, and growing evidence indicates that a large portion of the variability in adult BMD is genetically determined. Identification of genes that regulate bone density may improve diagnosis and promote development of novel interventions. We and others have used inbred strains of mice to established heritability and identify quantitative trait loci (QTL) for several skeletal features. Specifically, we used genome-wide analysis of an F2 intercross of C57BL/6J (B6) and C3H/HeJ (C3H) mice to identify QTL associated with several traits (1), including two QTL on Chr 1 that were associated with vertebral trabecular bone volume fraction (BV/TV) (3). To further evaluate the influence of these QTL, we generated a congenic mouse strain wherein the initial QTL chromosomal region from C3H was introgressed into the B6 background for 10 generations, and then nested sublines were created by genetic decomposition of this region (2). To test the effect of the Chr1 QTL on vertebral trabecular bone, we used microCT to compare trabecular BV/TV and microarchitecture in L5 vertebrae from 4-month old B6 controls (n=24 F, 21 M) and 8 Chr1 congenic sublines (n=7-10 per subline and sex). Analysis of the congenic sublines revealed that compared to B6 controls, BV/TV was about 10% lower in M and F mice carrying a proximal portion of Chr 1 (25 to 62 centiMorgans (cM) distal to the centromere, $p=0.0008$ to 0.04). This decreased BV/TV was accompanied by a lower trabecular thickness in F (-6.5%, $p=0.01$), and a lower trabecular number in M (-7%, $p=0.003$). In comparison, F congenic mice carrying a distal portion of Chr 1 (71 to 109 cM) had 28% higher BV/TV than B6 controls ($p<0.0001$). This increased BV/TV was accompanied by an increased number of trabeculae (+24%, $p<0.0001$), but no change in the mean trabecular thickness, and persisted after adjusting for the higher body weight observed in mice from this subline. In contrast, male congenic mice carrying a distal portion of Chr 1 exhibited lower BV/TV than B6 controls (-15%, $p=0.007$), primarily attributable to a decline in trabecular thickness (-10%, $p=0.008$). In summary, decomposition of QTL regions by congenic sublines can be used to verify QTL, and to refine their genomic locations. Interestingly, male and female mice show different regulation of vertebral trabecular bone, providing strong rationale for further study of genetic and hormonal contributions to trabecular bone mass and microarchitecture.

Refs: 1) Beamer et al; JBMR 2001; 2) Bouxsein et al, JBMR 2004; 3) Shultz et al, JBMR 2003.

Disclosures: ***M.L. Bouxsein****, None.*

1084

Sex Differences in Skeletal Development Are Independent of the Complement of Sex Chromosomes. R. F. Klein[1], D. C. Dinulescu*[1], D. A. Olson*[1], E. A. Larson*[1], L. Lambert[1], T. Yang*[2], R. Bijlani*[2], A. P. Arnold*[2], E. S. Orwoll[1]. [1]Bone and Mineral Unit, Oregon Health & Science University, Portland, OR, USA, [2]Department of Physiological Science, University of California, Los Angeles, CA, USA.

Sex exerts a profound effect on the skeleton, especially peak bone size and mass. Since the male phenotype is associated with considerable fracture risk reduction, an understanding of the genetic basis for the male-female divergence in bone development is of significant interest. The aim of this study was to determine if sex differences in skeletal development are the result of gonadal hormones, or alternatively the result of an effect of genes encoded on the sex chromosomes. We examined 20-wk-old mice that were normal males or females, as well as mice in which the testis-determining gene (Sry) had been deleted from the Y chromosome and inserted as a transgene on an autosome to produce XX-Sry+ animals that possessed testes, or XY-Sry- animals that possessed ovaries. In addition, all animals in each group underwent gonadectomy (GDX) or sham operation at 4 weeks of age (n= 12-20 per group). Thus, this model allowed assessment of the role of sex chromosome genes, independent of gonadal hormones, in the ontogeny of sex differences in the mouse skeleton. Whole body bone density and body composition was assessed by DEXA, femoral bone geometry was determined with microCT, and biomechanical properties of the femoral shaft were determined by 3-point bending. As expected sex differences ($p < 0.05$) were observed in body weight, lean body mass (LBM), femoral shaft geometry (marrow area, cortical area and thickness) and bone strength parameters (ultimate failure load, stiffness and modulus). For each of these differences, mice possessing testes were invariably more masculine in their skeletal morphology, independent of their sex chromosome chromosomes (XX vs. XY), than mice with ovaries. In all 4 groups of mice, GDX resulted in greater femoral length, and reduced bone density and strength measures (failure load and modulus). There was no evidence that sex chromosomes affected the response to gonadectomy. These data strongly suggest that sex differences in skeletal development are under the control of gonadal steroids rather than genes located on sex chromosomes. The origins of sex differences in skeletal traits should be sought in physiological pathways related to gonadal hormone action.

Disclosures: ***R.F. Klein****, Eli Lilly & Co. 8; Merck & Co. 8; Procter & Gamble, Inc. 8; Aventis Pharmaceuticals 8.*

1085

cAMP/PKA Transactivation of Murine 1-hydroxylase in Renal Proximal Tubular Cells Requires Enhanced C/EBPβ Transcriptional Activity at a C/EBPβ Binding Site, a Process Antagonized by Ligand-activated VDR. T. Sato*, J. Yang*, L. Esteban*, A. Dusso. Internal Medicine/Renal, Washington University, St. Louis, MO, USA.

1-hydroxylase catalizes the main step in vitamin D activation to 1,25-dihydroxyvitamin D (1,25D), a potent calcitropic hormone. To maintain calcium homeostasis, renal 1-hydroxylase is induced by PTH and inhibited by 1,25D. PTH transactivates the1-hydroxylase gene through a cAMP/PKA mediated mechanism, which is inhibited by 1,25D. To delineate the mechanisms underlying the transactivation of 1-hydroxylase by cAMP and its inhibition by 1,25D, the murine renal proximal tubule cell line MCT was transfected with luciferase reporter contructs driven by the whole murine 1-hydroxylase promoter [-1652+22], which contains three putative cAMP responsive sequences (CRE), as well as 5'-deletion contructs. Surprinsingly, the response to 1mM dibutyryl cAMP in inducing 1-hydroxylase promoter activity mapped to a CRE-less minimal promoter [-85+22] that contains a putative C/EBPβ-binding site. Mutations of three base pairs in the core C/EBPβ binding site eliminated cAMP transactivation of the minimal promoter. Furthermore, neither ectopic CRE-binding protein (CREB) expression nor the expression of a dominant-negative CREB isoform affected cAMP induction of either whole or minimal [-85+22] promoter activity. Consistent with a C/EBPβ-mediated transactivation, ectopic C/EBPβ expression enhanced both basal- and cAMP-induced minimal promoter activity. Both C/EBPβ actions were inhibited by simultaneous co-expression of C/EBPβ and its dominant negative isoform, which lacks C/EBPβ transactivation domain. Studies using the specific inhibitors for PKA (H89) and MAPK (U0126) before cAMP treatment demonstrated that cAMP activation of PKA is mandatory for cAMP induction of de novo C/EBPβ expression, whereas both PKA and MAPK activate C/EBPβ nuclear translocation and transactivating potential in response to cAMP treatment. The finding that cAMP transactivation of 1-hydroxylase in MCT cells requires C/EBPβ activation and binding to a C/EBPβ site in the minimal promoter led us to examine whether 1,25D-inhibition of cAMP-transactivation of 1-hydroxylase involved a direct antagonism on C/EBPβ transactivating potential. Ectopic expression of VDR, in a ligand-dependent fashion, inhibited both cAMP induction of minimal promoter activity and the cooperative enhancement by ectopic C/EBPβ of the response to cAMP. These studies reveal a novel cross talk between C/EBPβ and the vitamin D endocrine system. cAMP/PKA transactivation of 1-hydroxylase requires enhanced C/EBPβ transcriptional activity at a C/EBPβ binding site, a process directly inhibited by ligand activated VDR.

Disclosures: ***T. Sato****, None.*

1086

Estrogenic Control of the MHC Class II Transactivator in Vivo through Chromatin Remodelling. E. Benasciutti*[1], L. Oliva*[1], W. Reith*[2], S. Cenci[1]. [1]Dibit, San Raffaele Scientific Institute, Milano, Italy, [2]University of Geneva Medical School, Geneva, Switzerland.

Estrogen (E) withdrawal has been reported to induce osteoclastic bone resorption and bone waste through enhanced MHC class II expression by bone marrow macrophages (BMM), resulting in enhanced T cell activation and production of inflammatory cytokines. An increased induction of the MHC class II transactivator (CIITA), the molecular switch of MHCII genes, has been proposed to underlie such effects. We thus investigated the nature of the suppressive effect of E on CIITA gene expression.

We adopted chromatin immunoprecipitation (ChIP) and real-time PCR on cross-linked samples from primary purified BMM from ovariectomized mice and sham-operated controls to analyze histone modifications and recruitment of cofactors at the CIITA regulatory region. The analysis of global post-translational modifications at the amino-terminal tails of histones H3 and H4 on CIITA promoter IV (pIV), the main promoter responsible for CIITA induction, revealed a selective and profound hyperacetylation of histone H3 in E deficiency. A wider analysis showed that histone acetylation is increased by E withdrawal in the whole CIITA regulatory region. The analysis of key modifications of single aminoacid residues within H3 tail revealed that E in vivo specifically represses acetylation of lysine 9 and methylation of lysine 4, two modifications known to potently activate transcription. ChIP analysis was also adopted to identify the cofactors involved in the observed modifications. We found that E deficiency greatly increases recruitment of the key histone acetyl transferase CREB binding protein (CBP) to the CIITA promoter.

Furthermore, we aimed at defining the in vivo role of pIV in mediating the suppressive effect of E on CIITA expression by utilizing CIITA pIV deficient mice. In primary wild-type BMM E suppressed by over 70% CIITA mRNA induction by IFNγ in vitro (as assessed by real time RT-PCR). Conversely, E failed to suppress CIITA induction in pIV deficient BMM, indicating a key role of pIV in mediating the suppressive effect of E in vivo on CIITA expression.

Taken together, our data describe a pattern of histone modifications and cofactor recruitment underlying the control exerted by E on CIITA transcription and MHCII expression. The data provide insights towards a better understanding of the molecular interplay between E, inflammation, and bone homeostasis.

Disclosures: ***E. Benasciutti****, None.*

1087

The Importance of Nuclear Localization in Ligand-Mediated Protection of the Vitamin D Receptor (VDR) from Ubiquitination and Proteasome-Mediated Degradation. S. Peleg[1], J. Hsieh[2], M. R. Haussler[2], C. V. Nguyen*[1]. [1]Endocrine Neoplasia & HD, M. D. Anderson Cancer Center, Houston, TX, USA, [2]Biochemistry, University of Arizona, Tucson, AZ, USA.

Recent studies from our laboratory have shown that susceptibility of the VDR to proteasome-mediated degradation depends on the cell type and on ligand structure. We found that in intestinal-derived Caco-2 cells the predominant form of VDR was resistant to proteasome degradation and shuttled between the chromatin and the cytoplasm in a ligand-independent fashion. In these cells, 1,25(OH)2D3 (1,25D3) but not the selective agonist Ro-26-9228 could induce the accumulation of a distinct proteasome-sensitive transcriptionally-active form of the VDR in the chromatin. In contrast, in the osteoblastic cells hFOB, the VDR was localized in the cytoplasm in the absence of ligand, but rapidly accumulated in the chromatin upon treatment with either 1,25D3 or the analog Ro-26-9228. Further studies suggested that ligand treatment caused the accumulation of a proteasome-sensitive VDR, which is the predominant form in hFOB cells. These results also suggested a linkage between nuclear import and ligand-dependent stabilization of the VDR against proteasome-mediated degradation. To further explore this possibility we used COS-1 cells transfected with hVDR and histidine-tagged ubiquitin expression vectors to determine which residues are necessary for VDR ubiquitination and what is the role of nuclear translocation in ligand-mediated protection of the VDR from degradation. We found that WT VDR was polyubiquitinated in the absence of ligand and that 1,25D3 diminished this modification. The analog Ro-26-9228 had no inhibitory effect on VDR ubiquitination. Deletion (410-427) or point mutations (V421M/F422A) in AF2 core diminished 1,25D3's ability to protect the VDR from ubiquitination. Deletion of residues 403-427 abolished VDR's ubiquitination, suggesting that ubiquitination signal may reside between residues 403-410. Mutations in the nuclear localization signal (R49W/R50G or K53Q/R54G/K55E) abolished the ability of 1,25D3 to protect the VDR from ubiquitination. Because neither the nuclear localization signal nor the AF-2 residues are required for high affinity binding of 1,25D3 to VDR, but both are necessary for ligand-dependent nuclear import of VDR, we concluded that C-terminal/AF-2 or DNA-binding domain mutations that diminish nuclear import of the VDR also cause a loss in the ability of 1,25D3 to prevent ubiquitination and proteasome-mediated degradation. These results also provide a foundation to the hypothesis that effective nuclear import machinery is essential to maintain transcriptionally active pool of the VDR.

Disclosures: ***S. Peleg****, None.*

1088

The Human TRPV6 Distal Promoter Contains Functional Vitamin D Receptor Binding Sites that Mediate 1,25-Dihydroxyvitamin D3 Response in Intestinal Cells. M. Watanuki, S. Kim, N. K. Shevde, J. W. Pike. Biochemistry, University of Wisconsin- Madison, Madison, WI, USA.

Transient receptor potential vanilloid type 5 and 6 (TRPV5 and TRPV6) are members of a large superfamily of non voltage-gated cation channels that function as sensory detectors for environmental stimuli. TRPV6 (CaT1/ECAC2) encodes an epithelial calcium channel that is highly expressed in calcium transporting tissues such as the intestine. In this tissue, TRPV6 is localized to the apical membranes of mucosal epithelia where it is believed to mediate the uptake of calcium from the gut lumen, the rate limiting step in trans-epithelial calcium absorption. Indeed, recent studies reveal that this channel protein is regulated physiologically by 1,25-dihydroxyvitamin D3. The molecular basis for this regulation has yet to be defined, however. To explore this, we first established a model system in which 1,25(OH)2D3 induced TRPF6 mRNA expression in a typical time- and dose-dependent manner using cultured human intestinal Caco-2 cells. Next, we scanned the TRPV6 promoter for functional, 1,25(OH)2D3-induced VDR/RXR binding sites in intact cells using chromatin immunoprecipitation (ChIP) methods. We identified at least two such sites or VDREs located approximately 2.1 kb and 4.3 kb upstream of the start site of transcription. Small 200-400 bp fragments encompassing these two regions were then amplified from human genomic DNA, cloned into the luciferase expression vector pTK-luc and shown to mediate 1,25(OH)2D3-response in transfected Caco2 cells. Sequence analysis of these DNA fragments together with point mutagenesis in the pTK-luc/TRPV6 gene chimeras that resulted in abrogation of hormonal response verified the location of the two VDREs. These sites also bound the VDR/RXR heterodimer with high affinity, as assessed using DNA bandshift analysis. To confirm the functional nature of these elements in intact cells, we utilized ChIP to show that 1,25(OH)2D3-induced localization of the VDR/RXR heterodimer to this region of the TRPV6 gene also coincided with the time-dependent recruitment of the p160 coactivators SRC-1, SRC-2 and SRC-3 as well as selective acetylation of histone 4. These studies define two regions within the TRPV6 gene that contain regulatory sequences capable of mediating 1,25(OH)2D3's actions on TRPV6 gene expression. Interaction of both VDR and RXR at these sites leads to chromatin remodeling processes that are directly associated with increases in gene expression.

Disclosures: ***M. Watanuki****, None.*

1089

Estrogen and Vitamin D Utilize Common Transcriptional Machinery to Exert Transcriptional Inhibition. T. Okazaki, T. Fujita*. Division of Endocrinology and Nephrology, University of Tokyo, School of Medicine, Tokyo, Japan.

Expression of PTHrP gene is repressed by $1,25(OH)_2$ vitaminD_3 (abbreviated as vit.D) in various cell lines. On the assumption that the mechanism of gene inhibition by the liganded nuclear hormone receptors is conserved, we examined whether other nuclear hormones affect PTHrP gene expression. Here, by using RT-PCR, we report that 17β estradiol, like vit.D, inhibits PTHrP gene transcription, while dexamethasone, triiodothyronine and dihydrotestosterone were all transcriptionally inert in human breast cancer MCF7 cells. Both types of inhibition were recognized as early as 1h after administration of 10 nM of each hormone, which lasted 40h. Chromatin immunoprecipitation (ChIP) assay revealed that each hormone, respectively, recruited HDAC2 (histone deacetylase2) as well as DNA-dependent protein kinase (DNA-PK) to the chromatinized nVDREm, a half site of DR-3 type DNA element in the PTHrP promoter region. In both, recruitment of HDAC2, which first emerged 15 min after each hormone treatment and exhibited a cyclic occupancy pattern thereafter, displayed mirror image of histone acetylation around the nVDREm during the same time course. On the other hand, DNA-PK remained linked to the nVDREm region for 40h since its first appearance 15min after hormone treatment. The behavior of p300 histone acetyltransferase resembled that of acetylated histone3, while mSin3A was recruited in a way similar to HDAC2. The DNA spanning more upstream region of the PTHrP gene did not produce these patterns. Further, we found that transcriptional repression of the PTHrP gene by each hormone was abrogated after treatment of the cells with inhibitors of either HDAC or DNA-PK. We also observed that the mechanism of transcriptional repression is quite different from that of stimulation; we employed oligonucleotides surrounding the positive VDRE region in the 24,25vitamin D hydroxylase promoter or positive ERE in the PS2 promoter in ChIP assay using MCF7 chromatin. In these experiments, only cyclic acetylation of the histone surrounding nVDREm was recognized; neither HDAC2 nor DNA-PK gathered around these DNA after the treatment of each hormone. Finally, while VDR was consistently recruited to the nVDREm region irrespective of the presence of vit.D, the initial absence of the estrogen receptor (ER)α around the nVDREm region was followed by the periodical recruitment after 17β estradiol administration to the cells. In agreement with this finding, gel shift assay using appropriate antibodies showed that nVDREm binds directly to VDR, but not ERα. Taken together, we raise a possibility that estrogen and vit.D utilize some transcriptional machinery in common to exert nVDREm-mediated gene inhibition.

Disclosures: ***T. Okazaki****, None.*

1090

Docking Genomic and Non-Genomic Agonists to the Vitamin D Receptor Ligand Binding Domain: Discovery of a Novel Alternative Ligand Binding Site and Functional Validation. M. T. Mizwicki*, C. M. Bula*, J. E. Bishop, L. P. Zanello, A. W. Norman. Dept. Biochem., Univ. California, Riverside, CA, USA.

$1\alpha,25(OH)_2$-vitamin D_3 (1,25D) is known to activate genomic and non-genomic cellular signaling. While novel membrane receptors may exist that serve to bind and initiate rapid, non-genomic responses (RR), increasing evidence in the vitamin D receptor (VDR) and estrogen receptor (ER) fields suggests that the traditional nuclear receptor (NR) may also function as a RR receptor. To elucidate a mechanism describing how the VDR can function in both genomic and RR signaling we developed a molecular modeling protocol designed around the sterol structural attributes shown to be required in rapid opening of osteoblast chloride channels; these include a 3β-OH, 25-OH, and 6-*s-cis* sterol configuration. Docking the 6-*s-cis* locked, chloride channel agonist, $1\alpha,25(OH)_2$-lumisterol (JN) to the VDR LBD resulted in the discovery of an alternative ligand binding site (A-pocket). Calculated interaction energies (I_E) for JN, $25(OH)D_3$ (25D), and 1,25D docked in the partially overlapping x-ray, genomic pocket (G-pocket), or the proposed A-pocket provide a plausible molecular mechanism consistent with 1,25D, JN, and 25D chloride channel agonism as well as antagonism of the 1,25D response by $1\beta,25(OH)_2D_3$. Similarly, docking the RR specific ER agonist, 4-estren-3α,17β-diol (EST), indicates that ERα may also contain an A-pocket that EST prefers, possibly explaining its ER dependent RR effects in bone. Functional validation of the VDR A-pocket was obtained from assaying three vitamin D sterols that have different A-ring chemistries [3-deoxy-1,25D, 25D, and 1,25D] with VDR point mutants made in the overlapping region of the two pockets: Y143A, S237A, R274A, S278A, and Y143F/ S278A. Results show the ligands genomic responses (EC_{50}s) and VDR affinities are affected in a differential manner, consistent with the existence of the A-pocket. Of 20 analogs docked in the VDRwt A-pocket, 23S,25R-$1\alpha,25(OH)_2D_3$-26,23-lactone (BS) and 21-(3'-hydroxy-3'-methylbutyl)-$1\alpha,25(OH)_2D_3$ (KH) have the best I_E, 10 kcal/mol better than any other vitamin D sterol tested. Since ligands in the A-pocket do not directly contact helix-12, the presence of an A-pocket provides the first molecular evidence that explains why BS and KH have different protease sensitivity profiles than 1,25D. In summary, we propose that VDR and 1,25D both exist in multiple conformations that follow the standard laws of statistical distribution. The differential ligand affinities for the G- and A-pocket provide an explanation for how the VDR can function as a RR receptor as well as explain puzzling VDR/ vitamin D sterol structure/ function results.

Disclosures: ***M.T. Mizwicki****, None.*

1091

Resveratrol Prevents Osteoclast Formation, Promotes Osteoblast Differentiation Markers and Inhibits Proliferation of Myeloma Cells. P. Boissy*[1], T. L. Andersen*[1], B. M. Abdallah*[2], M. Kassem[2], T. Plesner*[1], J. M. Delaisse[1]. [1]Clinical Research Unit (KFE) and Division of Hematology, Vejle Hospital, Vejle, Denmark, [2]Endocrinology and Metabolism, Odense University Hospital, Odense, Denmark.

A typical multiple myeloma patient shows proliferation of clonal plasma cells in the bone marrow, massive bone destruction, and reduced bone formation. It is a challenging task for the clinician to act simultaneously at each of these 3 different levels. We report here that each of these 3 processes are reversed by resveratrol (3, 4', 5 trihydroxystilbene), a natural compound that has recently drawn the attention because of its antitumor effects in various experimental systems.

First, resveratrol was tested on the proliferation of 2 human myeloma cell lines, RPMI 8226 and OPM2. After a 3-day culture, cell-numbers showed a 4- to 5-fold increase which was dose-dependently inhibited by resveratrol. Full inhibition was obtained at 100microM. Second, the effect of resveratrol on osteoclasts was investigated. CD14-positive cells isolated from human PBMCs differentiated into osteoclasts after a culture of 7 days in the presence of M-CSF and RANKL. Upon addition of resveratrol (1 to 100microM), the number of TRAP+ multinucleated cells and the level of TRAP activity released in the medium were strongly reduced, and instead, elongated mononucleated cells were seen. Almost full effects were obtained at 25 microM. Accordingly, pit formation was abrogated. When added at different time points before and during cell fusion (day 0-3 or day 3-6), resveratrol retained its inhibitory activity. When added for only 2 days to multinucleated osteoclasts cultured on dentine slices, pit formation was strongly impaired and osteoclast morphology was dramatically affected.

Finally, we analyzed the effect of resveratrol on the induction of osteoblast markers in telomerized human bone marrow stem cells (hMSC-TERT) known to differentiate into osteoblasts. A 3-day-culture in the presence of resveratrol led to an up-regulation of the expression level of osteocalcin and the nuclear receptor of calcitriol (VDR), as evaluated by Q-PCR. Moreover, resveratrol synergized the calcitriol-induced osteocalcin induction in hMSC-TERT.

In conclusion, we demonstrate that a single compound, resveratrol, inhibits bone resorption, promotes osteoblast differentiation markers, and prevents myeloma cell proliferation. We are presently elucidating its molecular mechanism of action, and thereby hope to understand why a single compound antagonizes 3 distinct processes that all cooperate in promoting myeloma development.

Disclosures: ***P. Boissy****, None.*

1092

Lysophosphatidic Acid: A New Link between Breast Cancer and Bone Metastasis. A. Boucharaba*[1], C. Serre*[1], J. Saulnier Blache*[2], J. Bordet*[3], J. Guglielmi*[1], P. Clezardin[1], O. Peyruchaud*[1]. [1]INSERM U-403, Lyon, France, [2]INSERM U-586, Toulouse, France, [3]EA3735, Lyon, France.

Bone is a very common metastatic site for breast cancer. Current treatments of bone metastatic patients with bone resorption inhibitors (*e.g.* bisphosphonates) are only palliative and do not provide a life-prolonging benefit. This indicates that in addition to the vicious circle established between tumor cells and osteoclats, there exists at the bone site unidentified factors that stimulate skeletal tumor growth independently of bone-derived growth factors released from the bone matrix. Lysophosphatidic acid (LPA) is a naturally occurring lipid which interacts with cell surface G-protein couple receptors (LPA1, 2 and 3). LPA exhibits growth factor-like activities for breast cancer cells *in vitro* but its role *in vivo* is unknown. To address this question we engineered human MDA-BO2 breast cancer cells (a bone metastatic cell line) to over-express LPA1 using the tet-Off expression-regulated system. We found that LPA1 over-expression (1) specifically sensitized these cells to the mitogenic action of LPA *in vitro*, (2) enhanced the subcutaneous tumor growth in animals, and (3) increased 2 to 3-fold the extent of osteolytic lesions and (4) skeletal tumor burden in an experimental model of bone metastasis. MDA-BO2 cells did not produce LPA nor did they express autotaxin (a LPA-producing enzyme). Instead, these cells induced platelet aggregation and the release of LPA from activated platelets. In turn, platelet-derived LPA stimulated both the proliferation of tumor cells *in vitro* and the production by these cells of IL-6 and IL-8, two potent bone resorption stimulators. *In vivo*, a specific platelet aggregation inhibitor (eptifibatide) inhibited by 50% both bone destruction and skeletal growth of parental MDA-BO2 cells. In addition, it abolished the increased extent of osteolytic lesions caused by LPA1 over-expressing cells. Overall, our data indicated that in addition to the vicious circle coming from the reciprocal interaction between breast cancer cells and osteoclasts, the development of bone metastasis is supported by a second vicious circle wherein bone-residing cells stimulate LPA production by blood platelets which, in turn, enhances tumor growth and cytokine-mediated bone resorption.

Disclosures: ***A. Boucharaba****, None.*

1093

Adrenomedullin Is Made by Prostate Cancers and Increases Both Osteolytic and Osteoblastic Bone Metastases. K. S. Mohammad[1], Z. Wang*[2], A. Martinez*[3], E. Corey*[4], R. L. Vessella[4], T. A. Guise[1], J. M. Chirgwin[1]. [1]U Virginia, Charlottesville, VA, USA, [2]Northwestern U, Chicago, IL, USA, [3]Natl Cancer Inst, Bethesda, MD, USA, [4]U Washington, Seattle, WA, USA.

Adrenomedullin (AM) is a polypeptide produced by many cancers. It stimulates angiogenesis and tumor cell growth. AM potently enhances osteoblast proliferation in vitro and new bone formation in vivo. We hypothesized that AM is secreted by prostate cancers and stimulates bone metastasis by enhancing osteoblast proliferation.

AM dose-dependently increased osteoblast number and new bone area ($p<0.05$) in ex vivo organ cultures of neonatal mouse calvariae, with significant effects at 10pM. To test the role of AM in bone metastases, we carried out a gain-of-function experiment in prostate cancer by stable expression of AM cDNA in PC-3 prostate cancer. Mice bearing PC-3 clones which overexpressed AM by 10-fold had accelerated bone metastases ($p<0.05$) and significantly reduced survival compared to mice bearing empty vector PC-3 cells. Mice bearing AM-overexpressing tumors showed extensive bone destruction but also many areas of new bone formation by x-ray and histology. The AM-overexpressing cells grew more slowly than control cells as subcutaneous tumors, indicating that the effect of AM was specific to bone.

To test whether prostate cancers generally express AM, we surveyed human prostate cancer cell lines for AM mRNA. LNCaP, C4-2B, and DU145 cells made moderate levels of message, while parental PC-3 cells made higher amounts. RNA was also isolated from LuCaP23.1 xenografts (established from a metastasis). It causes a strong osteoblastic response 15 weeks after inoculation into the tibiae of nude mice. When analyzed by RT-PCR, the LuCaP23.1 tumor expressed AM mRNA in substantially greater amount than the other prostate cancer lines, suggesting that AM may be responsible for the osteoblastic responses caused by these tumors.

We have also carried out a loss-of function experiment with AM in bone metastasis. In a mouse model of bone metastasis, clonal variant lung adenocarcinoma A549 cells with 50% decreased AM secretion caused fewer osteolytic metastases ($p<0.05$) and improved survival compared to animals receiving parental A549 cells.

Secretion of AM by tumor lines such as PC-3 and A549, which cause osteolysis, appears to increase the severity of osteolytic bone destruction, perhaps by stimulating osteoblast proliferation and the number of RANK ligand-positive cells. AM may also function as an osteoblastic factor, a role supported by its high expression in LuCaP23.1 tumors. The data identify AM as an important contributor to the pathophysiology of bone metastases.

Disclosures: ***K.S. Mohammad****, None.*

1094

Use of Bisphosphonate Analogs of Risedronate to Elucidate Antitumor Mechanisms of Bisphosphonates *In Vivo*. P. G. Fournier*[1], M. W. Lundy*[2], F. H. Ebetino*[2], P. Clézardin[1]. [1]INSERM U403, Lyon, France, [2]Procter & Gamble Pharmaceuticals, Mason, OH, USA.

Bisphosphonates (BPs) exhibit antitumor activity *in vitro* and reduce skeletal tumor growth in experimental models of bone metastasis. However, because of their high bone affinity and rapid uptake in bone, it is likely that the antitumor activity of BPs is mainly mediated through inhibition of bone resorption which, in turn, deprives tumor cells of bone-derived growth factors released from the bone matrix. Conversely, a BP having a lower bone affinity could act to a higher degree directly on tumor cells because of its more rapid release from bone mineral. To address this question, we compared the antitumor potency of risedronate (RIS) with that of NE-10790 and NE-58051. NE-10790 is a phosphonocarboxylate analog of RIS which had a 15-fold lower bone affinity compared to RIS. NE-58051 is a pyridyl BP which differs from RIS only in the length of the R2 chain but exhibited similar bone affinity compared to RIS. *In vitro*, RIS, NE-10790 and NE-58051 inhibited to a similar extent the proliferation of GFP-expressing B02 breast cancer cells. *In vivo*, a continuous treatment of mice with RIS (0.05 to 0.15 mg/kg/day) dose-dependently inhibited bone destruction caused by GFP-expressing B02 cells (as judged by radiography, microCT and histomorphometry). The highest dose of RIS (0.15 mg/kg/day) also substantially reduced skeletal tumor burden (as judged by external fluorescence imaging and histomorphometry). NE-58051 (0.15 mg/kg/day) and NE-10790 (0.15 mg/kg/day) did not inhibit bone destruction. This lack of inhibitory effect of NE-58051 and NE-10790 on bone destruction was consistent with the observation that these analogs were 8,000 to 10,000-fold less potent than RIS in preventing ovariectomy-induced bone loss in rats. However, as opposed to NE-58051, a daily dose (0.15 mg/kg) of NE-10790 that did not inhibit bone resorption did drastically reduce skeletal tumor burden (75% reduction). A higher dose (37,000 mg/kg/day) of NE-10790 reduced skeletal tumor burden similarly, but also decreased bone destruction. Moreover, using a daily dose of 0.15 mg/kg, RIS, NE-58051 and NE-10790 did not inhibit the subcutaneous growth of B02 cells nor did they inhibit B16F10 melanoma lung metastasis in animals. As exemplified with NE-10790, low bone affinity BPs are rapidly released from bone and act directly on tumor cells to inhibit their growth. Conversely, as exemplified with NE-58051, high bone affinity antiresorptive BPs mainly reduce skeletal tumor growth through inhibition of bone resorption. Overall, our findings strongly suggest that BPs exhibit *in vivo* antitumor activity in bone through two distinct mechanisms.

Disclosures: ***P.G. Fournier****, None.*

1095

RANK Ligand Directly Induces Osteoclastogenic, Angiogenic, Chemoattractive and Invasive Factors on RANK-expressing Human Cancer Cells MDA-MB-231 and PC3. M. Tometsko*[1], A. Armstrong*[1], R. Miller*[1], J. Jones*[1], M. Chaisson*[1], D. Branstetter*[2], W. Dougall[1]. [1]Cancer Biology, Amgen Washington, Seattle, WA, USA, [2]Pathology, Amgen Washington, Seattle, WA, USA.

RANK and RANKL are the key regulators of osteoclast differentiation, activation and survival. Blockade of RANKL in animal models of breast and prostate cancer metastases inhibits tumor-induced osteolysis and prevents the progression of skeletal tumor burden (Morony et al., 2001; Zhang et al., 2003). RANK and RANKL knockout mice also have a defect in mammary lobulo-alveolar formation during pregnancy suggesting that RANK and RANKL may function on breast carcinomas. In this study we have demonstrated that RANK is expressed on the breast cancer cell line MDA-231 and the prostate cancer cell line PC3. While neither cell line expresses RANKL in vitro, it is probable that the locally increased RANKL within the bone microenvironment could activate tumor cell-expressed RANK in a paracrine manner. RANKL treatment of both MDA-231 and PC3 cells led to the acute activation of signal transduction pathways including p38 MAPK, p42/44 MAPK, NF-kB, and this activation can be blocked by OPG. Global gene expression analysis indicates that RANKL treatment of MDA-231 cells leads to the upregulation of 194 mRNAs greater than 2-fold. The transcriptional profile induced by RANKL on human tumor cells includes osteotropic factors (IL-1, IL-6, CSF-1), angiogenic factors (IL-8, CXCL-2), metalloproteinases (MMP1, MMP9, MMP13), and chemoattractants (CXCL-1,2,3,5 and 6). In addition, RANKL treatment of MDA-231 significantly decreased the expression of thrombospondin-1 and TIMP-4. Interestingly, of all the mRNA changes induced by RANKL in MDA-231 cells, COX-2 mRNA was induced to the greatest extent; activation of this pathway in tumor cells by RANKL was confirmed by PGE2 ELISA.

Local increases of RANKL result from the interaction of tumor and bone. These studies suggest that the locally increased RANKL can activate RANK positive breast or prostate tumors within the bone and can influence tumor cell homing and invasion and result in the secretion of angiogenic and osteolytic factors. These data indicate that RANKL regulates the osteolytic tumor-bone "vicious cycle" in at least three different ways: 1). release of growth factors from bone matrix; 2). production of growth factors, chemokines and cytokines by the activated osteoclasts; and 3). direct RANKL-mediated induction of angiogenic, invasion, chemoattractant and osteotropic factors by RANK positive tumor cells. Current studies are underway using an experimental metastasis animal model to test whether RANKL inhibition will target tumor cells directly.

Disclosures: ***W. Dougall****, Amgen, Inc. 1, 3.*

1096

Targeting EGF-R, VEGF-R, and the Osteoclast in Renal Cell Carcinoma Bone Metastasis. M. Doucet*[1], R. Langley*[2], K. Weber[1]. [1]Orthopaedic Surgery, Johns Hopkins University School of Medicine, Baltimore, MD, USA, [2]Cancer Biology, University of Texas M.D. Anderson Cancer Center, Houston, TX, USA.

Metastatic renal cell carcinoma (RCC) to the skeleton is clinically challenging as there is no reliable, effective method of treatment. The tumors are relatively radio- and chemoresistant. The goal of our study was to find an effective combination of agents to decrease the growth of RCC in the bone and inhibit bone destruction. We hypothesized that a combination of pegylated interferon-*a* (PEG-IFN-*a*), Zometa, and blockade of the epidermal growth factor receptor (EGF-R) and vascular endothelial growth factor receptor (VEGF-R) pathways would be effective in an established animal model.

Proliferation studies and western blotting were performed using mouse-derived bone endothelial cells and human bone-derived metastatic RCC cells. The cells were stimulated by the addition of TGF-*a* (40 ng/ml) with or without the addition of various inhibitory agents. In a nude mouse intratibial injection model, mice were treated with AEE788, PEG-IFN-*a,* and Zometa in various combinations and compared with control mice. Tumor incidence, tumor weight, radiographic lysis, and immunohistochemical staining were evaluated at 12 weeks.

Proliferation studies revealed that AEE788, an EGF-R/VEGF-R inhibitor, was effective in inhibiting cell proliferation of both RBM1-IT4 and bone endothelial cells in a dose-response fashion ($p<0.01$). PEG-IFN-*a* was also effective, but comparatively higher doses were required. Zometa had no effect on cell proliferation. On western blotting, AEE788 effectively inhibited EGF-R phosphorylation of RBM1-IT4 cells (90%) more than bone endothelial cells (28%) at the same dose. Downstream signaling through AKT was also inhibited. There was a significant decrease in tumor incidence and tumor weight in the 4 groups of mice treated with AEE788 alone or in combination with Zometa or PEG-IFN-*a* ($p<0.05$). PEG-IFN-*a* was not effective alone but was synergistic with AEE788. Bone destruction was decreased in all groups except mice treated with PEG-IFN-*a* alone ($p<0.05$). Immunohistochemistry revealed decreased staining of activated EGF-R, activated VEGF-R, and TGF-*a* in all groups that included treatment with AEE788 ($p<0.001$). VEGF was decreased in all groups except Zometa alone ($p<0.001$). Basic fibroblast growth factor (bFGF) was decreased in mice treated with AEE788/Zometa and PEG-IFN-*a*/Zometa ($p<0.01$).

The targeting of multiple growth factor receptors and the inhibition of osteoclastic resorption is effective in the treatment of metastatic RCC to bone in a nude mouse model.

Disclosures: ***M. Doucet****, None.*

1097

Teriparatide Suppresses Activation of Aortic Msx2 /Wnt Gene Regulatory Programs *In Vitro* and *In Vivo*. J. S. Shao, S. L. Cheng, N. Charlton-Kachigian*, A. P. Loewy*, D. A. Towler. Dept. of Internal Medicine, Washington University School of Medicine, St. Louis, MO, USA.

In a murine model of diabetic vascular calcification, an aortic BMP2-Msx2 gene regulatory program is activated that recruits aortic adventitial and valvular myofibroblasts to the osteogenic lineage. In these LDLR receptor-deficient mice, male animals are susceptible, while females are resistant. Consistent with an active role for BMP2 in this process, BMP2 synergizes with Msx2 to re-program cell fate and drive mineralization in vitro. Moreover, mice transgenic for BMP2 driven by the vascular smooth muscle cell (VSMC) SM22 promoter exhibit more extensive cardiac valve calcification, and female SM22-BMP2tg+; LDLR+/- mice become susceptible to disease. To better understand the mechanisms controlling vascular osteogenic differentiation, we studied effects of BMP2 in cultured primary aortic myofibroblasts. Since PTHrP had been demonstrated to suppress VSMC calcification in vitro, we examined the response to teriparatide in this system as well. BMP2 treatment (100 ng/ml) markedly induced Msx2 expression (40-fold) in aortic myofibroblasts at 72 hours. By contrast, a 90 min exposure to teriparatide (100 nM) on day 1 suppressed basal Msx2 expression by 50% ($p < 0.05$) - with no effect on endogenous BMP2-- and teriparatide treatment completely abrogated Msx2 induction by BMP2. A downstream component of Msx2 actions in aortic myofibroblasts is upregulation of Wnt3a and Wnt7a with paracrine activation of Wnt signaling; recombinant Dkk1 inhibits Msx2 reprogramming of cell fate. Consistent with its effects on Msx2 expression, teriparatide significantly inhibited Wnt3a and Wnt7a by ca. 90% either in the presence or absence of BMP2, but had no effect on Dkk1 expression. To confirm the physiological relevance of this in vitro observation, we studied the effects of teriparatide on calcific vasculopathy and Msx2/Wnt activity in vivo. Male LDLR-/- mice (n= 5 to 6 animals per arm) were fed high fat diets and treated with either vehicle or teriparatide (400 ng/gm s.c. 5 days a week, 4 weeks). Teriparatide inhibited cardiac valve calcification in male LDLR-/- mice (area of valve calcification by Alizarin red decreased from 8.3 +/- 1.5% to 1.4 +/- 0.5%; $p < 0.001$). Fluorescence RT-PCR analysis of aortic mRNA accumulation revealed that teriparatide concomitantly reduced aortic expression of Msx2, Wnt3a, and Wnt7a by ca. 60% ($p < 0.05$), but did not alter BMP2 or Dkk1. Thus, in vitro and in vivo, teriparatide suppresses the Msx2/Wnt gene expression program that recruits aortic myofibroblasts to the osteogenic lineage. This activity may contribute to beneficial effects of teriparatide in prevention of diabetic vascular calcification in our murine model.

Disclosures: ***D.A. Towler****, Pfizer-Washington University Research Agreement 2; Amgen 5; Proctor and Gamble 8; Novartis 5.*

1098

The Effect of 1 year of Alendronate following 1 Year of PTH 1-84: Second Year Results from the PTH and Alendronate (PaTH) Trial. D. M. Black[1], C. J. Rosen[2], L. Palermo[1], T. Hue[1], K. E. Ensrud[3], S. L. Greenspan[4], T. F. Lang[1], J. A. McGowan[5], J. P. Bilezikian[6]. [1]U of CA, SF, CA, USA, [2]ME Ctr. for Osteo. Res., Bangor, ME, USA, [3]U of MN & MVAMC, Minn, MN, USA, [4]U of Pitt, Pitt, PA, USA, [5]NIAMS, NIH, Bethesda, MD, USA, [6]Columbia U, New York, NY, USA.

Since PTH use is limited to no more than two years, a key question to address is whether it should be followed by antiresorptive agent. We have previously reported the results of a trial comparing 1 year of therapy with either PTH(1-84) alone, alendronate alone or the two in combination. (Black et al., NEJM, 2004). This randomized trial was designed also to evaluate the results of a second year in which PTH(1-84) was discontinued and either followed by no therapy or with the antiresorptive alendronate (ALN). We tested the hypothesis that antiresorptive therapy is required to maintain the densitometric gains in bone mineral density after 1 year of PTH(1-84).

The 119 women who received PTH 1-84 (100 mcg) monotherapy in the first year were randomized to 1 additional year with either placebo (n=60) or alendronate (n=59)(10 mg/day) in a protocol that continued to be double-blinded. PTH was stopped in all subjects after the first year. The main endpoints were spine and hip BMD by DXA and by QCT, the latter in a subset (approximately 75%) of participants. Bone markers were measured but results are not yet available.

During the first year of study among those treated with PTH 1-84 alone, there was a 6.2% mean increase in DXA spine BMD and a 29% increase in trabecular spine BMD (QCT). Comparable increases at the (total) hip were 0.3% by DXA and 8.6% for trabecular hip BMD. The second year, post-PTH changes, in the ALN and placebo groups are described in the table below:

Mean Percent Changes: 1 year of PTH(1-84) followed by 1 year of ALN or PBO

	Changes within 2nd year Treatment in year 2			Changes over 2 years Treatment in year 2		
Endpoint	**ALN**	**PBO**	**Difference**	**ALN**	**PBO**	**Difference**
Spine BMD (DXA)	+4.9%*	-1.7%*	6.6%***	+12%^	+4.1%^	8.0%***
Trabec. spine BMD (QCT)	+2.7%	-9.9%*	12.6%***	+34%^	+13%^	21%***
Total. Hip BMD (DXA)	+3.6%*	0.03%	3.6%***	+4.5%^	-0.1%	4.6%***
Trabec hip BMD (QCT)	+6.4%*	-3.7%	10.1%***	+12%^	+5.4%	6.2%

*p<0.01 vs. year 1 value; ***p<0.01 between groups; ^p<0.01 vs. baseline value

Following PTH, there were significant gains in the group treated with ALN while there were losses in those on PBO. Changes in other QCT-assessed parameters such as cortical BMD showed similar trends as the results in the table but did not achieve significance.

There were striking differences following PTH in those on alendronate compared to those on placebo, particularly for trabecular bone. These data suggest that BMD gains after 1 year of PTH(1-84) are quickly lost in the next year if PTH is not followed by an antiresorptive agent. The results have clear implications for therapeutic choices after PTH therapy is stopped.

Disclosures: ***D.M. Black****, Novartis Pharmaceuticals 2, 5; Merck 2, 8; NPS 2.*

1099

A Genetic Evidence of Direct VDR function in Osteoblasts -Generation and Analysis of Osteoblast-specific VDRKO Mice. Y. Yamamoto*[1], T. Yoshizawa[2], T. Fukuda*[1], H. Kawano[3], T. Nakamura*[1], T. Yamada[3], G Karsenty[4], S. Kato[1]. [1]Institute of Molecular and Cellular Biosciences, The University of Tokyo, Tokyo, Japan, [2]Niigata University Graduate School of Medical and Dental Sciences, Niigata, Japan, [3]Department of Orthopedic Surgery, Faculty of Medicine, The University of Tokyo, Tokyo, Japan, [4]Department of Molecular and Human Genetics, Baylor College of Medicine, Houston, TX, USA.

1α,25-Dihydroxyvitamin D_3[V.D], an active form of vitamin D, is a primary regulator in many biological phenomena such as calcium homeostasis and bone formation. Such V.D actions are thought to be mediated through transcriptional controls by the V.D receptor (VDR), a member of the nuclear hormone receptor superfamily. To investigate the physiological roles of VDR, we had generated VDR deficient mice by a conventional gene targeting, and found that $VDR^{-/-}$ knockout (VDRKO) mice showed features typical of vitamin D-dependent type II rickets, but only after weaning (Yoshizawa *et al. Nature Genet.* 1997). However, it is impossible to account for all these phenotypes only by direct VDR functions, considering from the facts that the observed impaired bone formation in the VDRKO mice may be caused, at least in part, by secondary hyperparathyroidism. Taking possible parathyroid hormone (PTH) actions in VDR KO mice, the direct function of VDR in bone thus still remains to be defined. To assess such VDR function in bone formation and remodeling, a conditional gene inactivation scheme was undertaken using the Cre/loxP system.

Mice with loxP sites in both sides of the VDR gene exon2 ($VDR^{L2/L2}$) were generated, and crossed with transgenic mice with the Cre recombinase under the mouse α1(I)-collagen promoter (Dacquin *et al. Dev.Dyn.* 2002), which is presumed to be functional only in osteoblasts.

Serum calcium, phosphate, PTH and V.D levels were normal in osteoblast-spcific VDRKO (Ob-VDRKO) mice, and the growth curve appeared normal without any overt rachitic abnormality. However, to our surprise, clear increases in bone mass as well as bone mineral density were found in 16-week-old Ob-VDRKO mice. Reflecting such bone phenotypes, decreased trabecular bone formation and increased cortical bone formation were seen in Ob-VDRKO

mice. Trabecular bone resorption and the level of urinary deoxypyridinoline, a marker of bone resorption, were also decreased. Thus, the present study suggests that VDR directly functions in bone, at least in osteoblasts, to control bone remodeling and formation, without indirect VDR functions like secondary hyperparathyroidism. It also establishes that VDR is a global regulator for normal bone remodeling and formation though its direct function in bone and indirect functions in the other tissues.

Disclosures: ***Y. Yamamoto****, None.*

1100

Fracture Risk After Estrogen Plus Progestin Discontinuation: The Women's Health Initiative. R. D. Jackson, N. B. Watts, P. Caralis*, J. A. Cauley, Z. Chen, N. Greep, A. Z. LaCroix, C. E. Lewis, C. P. Mouton*, J. M. Neuner, M. J. O'Sullivan*, J. A. Robbins, A. Sato*, M. L. Stefanick. The Ohio State University, Columbus, OH, USA.

After publication of the Women's Health Initiative (WHI) results on the overall balance of risks and benefit of estrogen plus progestin (E+P), it was estimated that 56% of women taking E+P attempted to discontinue hormone therapy (HT). Previous observational studies and clinical trials (CT) suggested that there might be accelerated bone loss after HT discontinuation and recent epidemiologic data suggest that women have an increased risk of hip fracture within 5 years of stopping HT relative to women who never used HT. The purpose of this report of fracture data during the early follow-up of the WHI after study drug was stopped, is to prospectively determine the overall effect of discontinuation of E+P on fracture risk. Out of the 16,608 women who were initially randomized in the E+P trial, 15,694 women were in the post-treatment phase of WHI E+P. After exclusions for prior fracture and drop in/drop-out that had occurred during the CT, 10,095 women were included in the analyses (5166 women from the former placebo group, 4929 women from the former E+P group; mean age 63 yrs; 85% White). Six-month interval fracture history (hip and total fractures) was collected by standardized questionnaire and locally adjudicated based on review of radiology reports; all hip fractures were centrally confirmed. In the first 16.12 (SD 2.53) months after study medication was stopped, fractures occurred in 96 women in the former E+P group (1.33 fractures per 1000 pt-yrs) and 130 women in the former placebo group (1.76 fractures per 1000 pt-yrs) [hazard ratio (HR) 0.76; 95% CI 0.58-0.99]. During this interval, hip fractures occurred in 12 former E+P patients (0.15 fractures per 1,000 pt-years) and 20 former placebo patients (0.24 fractures per 1000 pt-yrs) (HR 0.63; 95% CI 0.31-1.29). These results did not differ after exclusion for use of defined osteoporosis medication during the follow up and exclusion of women who were non-adherent to study medication during the CT. In summary, through 16 months of follow up after discontinuation of combination E+P, there was maintenance of overall facture benefit and no increased risk of hip fracture. Longer follow up will be required to determine when loss of protection occurs.

Disclosures: ***R.D. Jackson****, None.*

1101

Distinct Y-Receptor Effects on Leptin Antiosteogenic and Adipogenic Pathways. S. J. Allison*[1], P. A. Baldock[1], A. Sainsbury*[2], R. F. Enriquez*[1], M. Couzens*[2], H. Herzog*[2], E. M. Gardiner[1]. [1]Bone and Mineral Research Program, Garvan Institute of Medical Research, Sydney, Australia, [2]Neurobiology Program, Garvan Institute of Medical Research, Sydney, Australia.

The neuropeptide Y (NPY) Y2 receptor and the adipocyte-derived hormone, leptin, regulate cancellous bone formation in the mouse by central mechanisms, with increased cancellous bone volume in Y2-deleted and in leptin-deficient obese (*ob/ob*) mice. Understanding the mechanisms involved is important for development of anabolic strategies using these pathways. Leptin and NPY are known to interact in the hypothalamus to regulate energy homeostasis, with deletion of Y1 or Y2 but not Y4 receptors reducing peripheral fat mass in *ob/ob* mice. We therefore proposed that these pathways also interact to regulate marrow fat content and bone formation. To this end, adipocyte and bone formation were determined in distal femora of Y1, Y2, Y4, *ob/ob*, Y1ob, Y2ob and Y4ob deleted and wildtype mice. Values are given: mean ± SEM.

BV/TV [%] was increased in Y1 KO (13.4 ± 1.8), Y2 KO (12.4 ± 1.7) and *ob/ob* (10.3 ± 1.0) mice relative to wildtype (5.3 ± 0.5) and Y4 KO (8.3 ± 1.1). Interestingly, double deficiency of leptin and Y2 in Y2ob did not change BV/TV from Y2 KO (12.4 ± 1.6 vs 12.4 ± 1.7 in Y2 KO). However, BV/TV was reduced in Y1ob (8.5 ± 1.4) compared to Y1 KO. BV/TV of Y4ob (10.2 ± 1.2) was not different from Y4 KO or *ob/ob*. The high bone mass in Y2ob was associated with a significant 43% elevation in mineral apposition rate above wildtype, not seen in Y1ob.

Marrow adipocyte number was increased 80-fold in *ob/ob* mice (268 ± 63 vs 3.3 ± 1.2 in wildtype). While marrow adipocyte number in Y1 KO, Y2 KO or Y4 KO was not significantly different from wildtype, deletion of either Y1 or Y2, but not Y4 receptors in *ob/ob* mice significantly decreased adipocyte number from *ob/ob*, with the effect most pronounced in Y2ob (76 ± 23 vs 268 ± 63 in *ob/ob*). Interestingly, while adipocyte size (μm^2) tended to be larger in genotypes lacking leptin compared with single Y KO and wildtype mice (787 ± 185), Y4 KO adipocytes were large and comparable to *ob/ob* (1176 ± 140 vs 1326 ± 50 in *ob/ob*).

Thus, deletion of Y1 attenuated the high bone phenotype of *ob/ob* mice, suggesting functional interaction between Y1 and leptin in their antiosteogenic responses. Roles for Y2 and Y4 in leptin antiosteogenic action were not evident in these models. Moreover, Y1 and Y2 but not Y4 receptors mediated the effects of leptin deficiency on marrow fat, to an even greater extent than effects seen in peripheral fat. Effects of Y4 on marrow fat appeared to be independent of leptin. These studies provide evidence that leptin and specific Y-receptor pathways interact by distinct mechanisms in the regulation of bone formation and marrow adipogenesis.

Disclosures: ***S.J. Allison****, None.*

1102

A Novel *COL1A1* Mutation Causes Autosomal Dominant Infantile Cortical Hyperostosis (Caffey Disease). R. C. Gensure[1], O. Mäkitie*[2], C. Barclay*[2], C. Chan*[2], S. DePalmer*[3], M. Bastepe[4], H. Abuzahra*[4], R. Couper*[5], J. Seidman*[3], W. G. Cole*[2], H. Jüppner[4]. [1]Department of Pediatrics, Tulane University, New Orleans, LA, USA, [2]Division of Orthopaedics, The Hospital for Sick Children, Toronto, ON, Canada, [3]Department of Genetics, Harvard Medical School and Howard Hughes Medical Institute, Boston, MA, USA, [4]Endocrine Unit, Department of Medicine, Massachusetts General Hospital and Harvard Medical School, Boston, MA, USA, [5]Department of Paediatrics, University of Adelaide, Women's & Children's Hospital, North Adelaide, Australia.

Infantile cortical hyperostosis (Caffey disease) is an autosomal dominant disorder characterized by episodes of localized rapid subperiosteal bone formation, which are usually limited to the first 2 years of life. We performed a genome-wide screen for genetic linkage in an affected family and mapped the genetic locus of Caffey disease to chromosome 17q21 (2-point LOD score: 6.78). Candidate genes within the linked region were sequenced after PCR amplification of genomic DNA. Affected individuals and obligate carriers were heterozygous for a missense mutation (3041C>T) in exon 42 of *COL1A1*, which was predicted to alter the amino acid sequence (R836C) of the triple helical domain of the α1(I) chain of type I collagen. The same mutation was identified in the affected members of an unrelated family with Caffey disease, and it occurred, most likely as a *de-novo* mutation, in identical twins each affected by this disorder. The mutation was not found in a single sporadic case, and it was not present in >300 chromosomes from healthy individuals. Dermal fibroblast cultures from an affected individual retained abnormal disulfide-bonded dimeric α1(I) chains, designated ß11', within the cell layer. Two-dimensional SDS-PAGE analysis showed that these ß11' dimers dissociated after reduction of disulfide bonds into a α1(I) chain and a α1(I)' chain that was likely to comprise the R836C mutation. Consistent with a change in collagen type I that impairs its secretion, electron microscopic analysis revealed a mildly dilated rough endoplasmic reticulum. Mutations in *COL1A1* have been previously shown to cause Ehlers-Danlos syndrome type III and osteogenesis imperfecta; we therefore re-examined our Caffey patients for features of these disorders. Individuals with R836C mutation showed increased joint laxity, noticeably soft skin, frequent inguinal hernias and increased fracture rates. Our findings extend the spectrum of *COL1A1*-related diseases to include a hyperostotic disorder. Further definition of the mechanisms leading to Caffey disease may provide new approaches for treating disorders associated with abnormal bone turnover.

Disclosures: ***R.C. Gensure****, None.*

1103

Sequential Roles of Hedgehog and Wnt Signaling in Osteoblast Development. F. Long, H. Hu*. Washington University, St. Louis, MO, USA.

Signals that govern development of the osteoblast lineage are not well understood. Indian hedgehog (Ihh), a member of the Hedgehog family of proteins, is essential for osteogenesis in the endochondral skeleton during embryogenesis. The canonical pathway of Wnt signaling has been previously implicated by studies of LRP5, a co-receptor for Wnt proteins, in postnatal bone mass homeostasis; our recent genetic studies in the mouse have demonstrated that β-catenin, a central player in the canonical Wnt pathway, is indispensable for osteoblast differentiation in the embryo (Hilton and Long, abstract submitted to 26th ASBMR). Here we present evidence that Hedgehog and Wnt signaling function sequentially in development of the osteoblast lineage. Tcf1, the predominant member of the Lef/Tcf family that mediates canonical Wnt signaling in the perichondrium of wild type long bones, is undetectable in the perichondrium of Ihh null embryos. Consistent with defective canonical Wnt signaling in the perichondrium, Dkk1, a transcriptional target of the pathway and normally expressed in the developing perichondrium, is absent in the Ihh null embryo. Furthermore, nuclear accumulation of β-catenin normally detected in cells within the osteogenic region of the perichondrium, is abolished in the Ihh mutant. Functional studies in the C3H10T1/2 cells demonstrate that osteogenesis induced by Hedgehog signaling is mediated at least in part by Wnt/Tcf signaling as Hh-induced expression of osteoblast markers is partially inhibited by either Dkk1 or a dominant negative form of Tcf4. Whereas Hh signaling induces expression of Osx, activation of the Wnt pathway by a dominant active form of β-catenin does not alter Osx expression. Finally Hh signaling induces expression of several Wnt molecules in C3H10T1/2 cells. These data support a model in which Hh signaling directs osteoprogenitors along the osteoblast lineage and subsequently induces either directly or indirectly expression of Wnts, which further promotes osteoblast development.

Disclosures: ***F. Long****, None.*

1104

An Evolutionarily Conserved CREB-binding Enhancer, in an Unusually Remote Location 74 kb Upstream from the Initiation Site, Confers the Stromal/Osteoblast-Specific Control of RANKL Transcription by PTH, 1,25(OH)$_2$D$_3$, and gp130 Cytokines. Q. Fu, I. P. Foote*, S. C. Manolagas, C. A. O'Brien. Div. of Endo/Metab, Center for Osteoporosis & Metabolic Bone Diseases, Central Arkansas Veterans Healthcare System, Univ. of Arkansas for Med. Sciences, Little Rock, AR, USA.

RANKL is highly expressed only in bone and lymphocyte-containing tissues, and stimulation of RANKL by PTH, 1,25(OH)$_2$D$_3$ and the gp130 cytokines seems to be limited to stromal/osteoblastic cells. Based on evidence that all these agents require protein kinase A (PKA)-mediated activation of the CREB transcription factor to elevate RANKL, we searched for the molecular basis of the cell type-specificity and hormonal responsiveness of this gene. Injections of dibutyryl-cAMP (db-cAMP) into mice elevated RANKL mRNA in bone, but not in spleen, kidney, liver, or lung, whereas a control mRNA, IL-6, was elevated in all these tissues. Therefore, restricted receptor expression alone does not account for cell type-specific regulation of RANKL by cAMP. Next, we sought evidence for cell type-specific transcription by determining the activity of RANKL promoter-reporter constructs in cell lines that express or do not express RANKL. Constructs containing up to 2 kb of the murine RANKL 5'-flanking region were not regulated by db-cAMP and had similar activity in stromal/osteoblastic and hepatocytic cell lines. However, a construct containing 120 kb of 5'-flanking region was stimulated by db-cAMP in the stromal/osteoblastic, but not a hepatocytic, cell line. Deletion analysis of this fragment revealed that an 8 kb region located 74 kb upstream of the transcription start site was required for full responsiveness to cAMP. Comparison of mouse, rat, chimp, and human genome sequences in this region identified a highly conserved non-coding sequence (CNS). Deletion of this CNS from the 120 kb construct significantly reduced cAMP-responsiveness, as well as responsiveness to PTH, 1,25(OH)$_2$D$_3$, or oncostatin M. Moreover, this CNS was sufficient to confer cAMP-responsiveness to a minimal RANKL promoter in a cell type-specific manner. Furthermore, the CNS contained 2 sequences resembling cAMP-response elements (CREs) that are evolutionarily conserved. CREB protein binding to the CNS was confirmed by chromatin immunoprecipitation assay, and mutation of the CRE-like sites abolished cAMP-regulation of RANKL promoter activity. These observations establish that the cAMP responsiveness of the RANKL gene is due to a distant regulatory region that responds to CREB activation in a cell type-specific manner and that this site plays a central role in the regulation of RANKL expression by all major hormones and cytokines that stimulate bone resorption.

Disclosures: ***Q. Fu****, None.*

1105

Mapping Expression Patterns of Mechanically Responsive Genes, DMP1 and MEPE, in Osteocytes Using the Mouse Ulnae: Correlation to Predicted Local Strain. S. E. Harris[1], J. Gluhak-Heinrich*[2], M. A. Harris[3], W. M. Yang[1], L. F. Bonewald[1], A. G. Robling*[4], C. H. Turner[5]. [1]Oral Biology, U. of Missouri at Kansas City, Kansas City, MO, USA, [2]Orthodontics, U. of Texas Health Science Center at San Antonio, San Antonio, TX, USA, [3]Periodontics, U. of Texas Health Science Center at San Antonio, San Antonio, TX, USA, [4]Orthopedics, Indiana University School of Medicine, Indianapolis, IN, USA, [5]Orthopedics, Indiana University School of Medicine, Indianapolis, IN, USA.

Axial loading of the mouse ulna is a useful model for studying bone formation in response to mechanical loading. New periosteal bone formation occurs in the ulna at 12-20days after a single 30 second bout of dynamic loading of 2.4N, 60 cycles, 2Hz. Ulnae from 4 month old loaded C57BL/6 mice were prepared for in situ hybridization and for total diaphyseal RNA at 1, 2, 4, and 24hrs after loading. From microarray analysis using 5K oligonucleotide arrays, combined with Northern analysis, we identified a series of matrix and cytoskeleton related genes thought to be involved in osteocyte function. These include cdc 42, CD44, OPN, DMP1, MEPE and others. From these data we built a pathway model (GenMapp.org) to describe this selective response. We have developed an efficient in situ hybridization procedure to evaluate expression of the osteocyte specific genes, DMP1 and MEPE, along the axis of the ulna using serial cross sections. We found dramatic increases in DMP1 and MEPE expression, specific to osteocytes 24hrs after loading. The expression of both of these genes was highest 2 mm distal to the mid-shaft and highest in osteocytes closer to the periosteal and endosteal surface. An example for DMP1 expression in the ulnae is shown in Figure 1. The expression patterns of DMP1 and MEPE were then mapped, both axially and laterally to develop a 3D model of expression within the ulna. These data were then compared with estimated mechanical strain maps. Gene expression in osteocytes consistently correlated with predicted local strains. Since both MEPE and DMP1 are thought to regulate mineralization processes within the lacunocanalicular system, we conclude that the osteocyte is altering it local environment in a spatially restricted manner that correlates to strain.

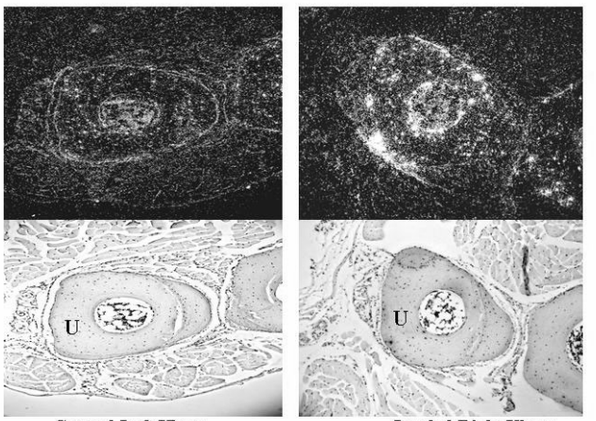

Control-Left Ulnae **Loaded-Right Ulnae**

Figure 1. DMP1 Expression at 2mm Distal to Mid-shaft assayed at 24hr after a 30 sec loading Bout of 2.4N at 60 cycles 2 Hz. Top –darkfield Bottom-lightfield, U =ulnae

Disclosures: ***S.E. Harris****, None.*

1106

Gap Junctions Regulate Extracellular Signal-Regulated Kinase (ERK) Signaling to Affect Osteoblast Gene Transcription. J. P. Stains, R. Civitelli. Bone and Mineral Diseases, Washington University in St. Louis, St. Louis, MO, USA.

ROS 17/2.8 cells are highly coupled by gap junctions formed by connexin43 (Cx43). Overexpression of connexin45 (Cx45), which has been shown to act in a dominant negative fashion with respect to Cx43 function, decreases chemical and electrical coupling in these cells. We have recently demonstrated that Cx45 overexpression reduces gene transcription by diminishing recruitment of the transactivator Sp1 to connexin response elements (CxREs) in the promoters of the osteocalcin and α1 (I) collagen genes. We now find that an identical mechanism accounts for the decreased osteocalcin gene transcription in Cx43 "knockout" calvaria cells, thus pointing to a direct role of Cx43 in gene transcriptional regulation. Furthermore, we demonstrate that transcription of a luciferase reporter driven by the osteocalcin CxRE is regulated by extracellular signal-regulated protein kinase (ERK) activity in ROS 17/2.8 cells. Overexpression of upstream activators of ERK, including constitutively active MEK, Raf, or Ras can increase transcriptional activity of the CxRE-luciferase reporter at least 2.5-fold in all cases. Accordingly, the MEK1/2 inhibitor, U0126 can decrease transcription 3-fold from the osteocalcin CxRE. Importantly, immunoblotting performed using phospho-Raf and -ERK antibodies reveal that overexpression of Cx45 in ROS 17/2.8 cells results in reduced amounts of active Raf and ERK. Cell exposure to the gap junction inhibitor, oleamide, mimics the effects of Cx45 overexpression on both CxRE-mediated transcription and ERK activation. We hypothesize that this attenuation of signal transduction is a consequence of decreased signal propagation caused by perturbation of intercellular communication via gap junctions. Consistent with this notion, disruption of ERK activation by either Cx45 overexpression or by treatment with U0126 results in decreased Sp1 phosphorylation, by immunoblotting, and diminished recruitment of Sp1 to CxREs, by chromatin immunoprecipitations. Therefore, Cx43 control of gene transcription is effected by modulation of Ras/Raf/MEK/ERK signaling and consequent regulation of Sp1 recruitment on CxREs. These data demonstrate that Ras/Raf/MEK/ERK signaling is required for the optimal elaboration of transcription from the osteocalcin CxRE and establish a paradigm by which intercellular communication via gap junctions composed of Cx43 can modulate nuclear function.

Disclosures: ***J.P. Stains****, None.*

1107

Expression of the Trps1 Transcription Factor and Its Regulation of Runx2. D. Napierala*[1], R. Morello*[2], G. Zhou[2], Q. Zheng*[2], T. Bertin*[2], R. Shivdasani*[3], B. Lee[1]. [1]Howard Hughes Medical Institute, Houston, TX, USA, [2]Molecular and Human Genetics, Baylor College of Medicine, Houston, TX, USA, [3]Dana-Farber Cancer Institute and Harvard Medical School, Boston, MA, USA.

Trps1 is a GATA-type transcription factor that contains nine zinc-finger domains. Unlike other GATA transcription factors, Trps1 acts as a transcriptional repressor and this activity maps to the C-terminal Ikaros-type zinc-finger domain. Mutations involving *Trps1* gene cause dominantly inherited craniofacial and skeletal dysplasia tricho-rhino-phalangeal syndrome (TRPS). Loss of function mutations in GATA and Ikaros domains cause milder type I TRPS phenotype, more severe type III TRPS is caused by missense mutations in GATA domain, while type II TRPS is caused by deletion of the gene as a part of a larger continuous gene deletion syndrome (Langer-Geideon syndrome). To analyze the expression pattern of *Trps1* during embryonic development, we performed RNA *in situ* hybridization on E12.5, 14.5 17.5 and P1 mouse sections. At E12.5, *Trps1* is highly expressed in mesenchymal condensations destined for chondrogenic lineages, then expression becomes intense in joint mesenchyme and perichondrial cells. After establishment of endochondral ossification, *Trps1* expression is restricted to prehypertrophic chondrocytes and perichondrium. Interestingly, *Trps1* high expression is observed in skeletal regions where *Runx2*

expression is not usually found. *Runx2* is a key transcription factor involved in osteoblast differentiation and chondrocyte maturation. To test the potential interaction of *Trps1* and *Runx2*, we performed cotransfection studies in ROS17 and COS7 cell lines. In COS7 cells, *Trps1* strongly represses *Runx2* transactivation of the target 6xOSE reporter derived from the osteocalcin promoter, which responds only to *Runx2* transactivation. The 6xOSE reporter is also down regulated in the presence of *Trps1* in ROS17 cells expressing high levels of endogenous *Runx2*. Analysis of transcriptional activity of *Runx2* deletion mutants as well as chimeric Runx2 runt domain-Vp16 fusion protein demonstrated that runt domain mediates the Trps1 repression effect on Runx2 activity. Moreover, the bone-related promoter of *Runx2* contains several potential GATA consensus sequences. *In vitro* analyses showed that *Trps1* forms complexes with each of these elements in COS7 but not in ROS17 cell lines. Our data suggest that *Trps1* can inhibit expression of the *Runx2* gene as well as *Runx2* protein function.

Disclosures: ***D. Napierala****, None.*

1108

Dlx5 Specifically Regulates Runx2-type II Expression by Binding with the Homeodomain Response Elements in the Distal Promoter. M. Lee*[1], H. Park*[1], S. Bae[2], J. Cho*[1], H. Ryoo[1]. [1]Dept. of Biochemistry, School of Dentistry, Kyungpook National University, Daegu, Republic of Korea, [2]Dept. of Biochemistry, School of Medicine, Chungbuk National University, Cheongju, Republic of Korea.

Dlx5 is a key mediator of BMP-2-induced osteoblast differentiation that triggers osteogenic master gene, Runx2, and ultimately results in the bone marker gene expression in BMP-induced osteogenic transdifferentiation. However, little is known about the molecular mechanisms by which Dlx5 regulates Runx2 expression in response to BMP-2 signaling. Two major isoforms of Runx2 have been reported, and are caused by different promoter usage. One of these isoforms, denoted as Runx2-typeI/p56 (starting with the sequence MRIPV), use the proximal promoter and the other, denoted as Runx2-type II/p57 (starting with the sequence MASNS), use the distal promoter. In this study, we found that Dlx5 overexpression strongly stimulated Runx2 expression and the bone specific Runx2-typeII expression was specifically stimulated either by BMP treatment or by Dlx5 overexpression. As Runx2 isoforms are distinctly regulated by two different promoters, we first tested Dlx5 responsiveness of each promoter-reporter constructs. The promoter activity of Runx2-typeII was strongly stimulated by Dlx5 overexpression while that of Runx2-type I by Dlx5 was marginally stimulated. The different responsiveness of the two promoters was highly correlated with the higher expression of Runx2-II by BMP-2 signalling. To identify Dlx5 response elements in Runx2-II promoter, serial promoter deletion constructs were generated. Cotransfection of the Dlx5 expression vector and the promoter deletion constructs indicated that Dlx5 response element is between -1kb and -0.45kb of Runx2-II transcription start site. There were 3 putative homeodomain binding consensus sequences between -1kb and -0.45kb in the Runx2-II promoter. We found that all 3 putative binding sites effectively interact with Dlx5 by gel mobility shift assay. The site-directed mutagenesis of each binding site or combinations of two or three of those sites indicated that all three elements are responsible for the regulation. These results indicate that Dlx5 is a key mediator of BMP-2-induced osteoblast differentiation that triggers osteogenic master gene, Runx2 (more specifically type-II isoform), and ultimately results in the BMP-induced osteogenic transdifferentiation.

Disclosures: ***M. Lee****, None.*

1109

Expedited Cataract Surgery can Reduce Recurrent Falls and Fractures - A Randomised Controlled Trial. T. Masud[1], R. Harwood*[1], A. Foss*[2], F. Osborn*[2], R. Gregson*[2], A. Zaman*[2]. [1]Medicine, Nottingham City Hospital, Nottingham, United Kingdom, [2]Opthalmology, Queens Medical Centre, Nottingham, United Kingdom.

Epidemiological evidence suggests that poor vision increases the risk of falls and fractures. Cataract is the commonest cause of visual impairment. We aimed to determine if expedited cataract surgery would reduce the risk of falling by more than 30% (primary outcome) and fractures (secondary outcome).

306 women over 70 years with bilateral cataracts were randomised to expedited (approximately 4 weeks) or routine (12 months wait) first eye cataract surgery by phakoemulsification with intra-ocular lens implantation. Falls and fractures were ascertained by diary, with follow-up by telephone at 3 and 9 months, and by interview at 6 and 12 months. Health status parameters were also measured at baseline and 6 months.

Visual function improved in the operated group (spectacle corrected binocular vision improved by 0.25 log MAR units and proportion with visual acuity worse than 6/12 decreased from 24% to 8%). Falls were recorded in 76 participants (49%) randomised to expedited surgery, with 28 (18%) falling more than once. 69 (45%) patients in the control group fell at least once, and 38 (25%) fell more than once. Hazard ratio for first falls was 0.95 (95%CI 0.69-1.35; p=0.77), and for second (recurrent) falls was 0.60 (95%CI 0.36-0.98; p=0.04). Measurements of activity, anxiety, depression, confidence, vuisual disability and handicap all improved in the operated group. Four particpants in the operated group had fractures (3%), compared with 12 (8%) in the control group (p=0.04).

In conclusion, first eye catarct surgery improves visual function and health status , and to our knowledge this is the first randomised controlled trial which has shown that recurrent falling (though not first fall) and fractures can be reduced by intervention to improve impaired visual function.

Disclosures: ***T. Masud****, None.*

1110

Falls and Physical Performance Changes in Older Adults with Diabetes and Pre-diabetes. A. V. Schwartz[1], E. Vittinghoff*[1], D. E. Sellmeyer*[1], N. De Rekeneire*[2], K. R. Feingold*[1], M. C. Nevitt[1], E. S. Strotmeyer[3], H. E. Resnick*[4], R. I. Shorr*[5], J. A. Cauley[3], S. R. Cummings[6], T. B. Harris*[2]. [1]University of California, San Francisco, CA, USA, [2]National Institute on Aging, Bethesda, MD, USA, [3]University of Pittsburgh, Pittsburgh, PA, USA, [4]Medstar Research Institute, Hyattsville, MD, USA, [5]University of Tennessee, Memphis, TN, USA, [6]California Pacific Medical Center, San Francisco, CA, USA.

Type 2 diabetes (DM) is associated with elevated fracture risk despite higher bone mineral density (BMD). Falls may be a contributing factor. To determine if falls and decline in physical performance are associated with DM or impaired glucose metabolism (IG), we analyzed data from the Health, Aging and Body Composition study of 3,075 white and black, well-functioning men and women age 70-79 years. Participants reported falls in the previous year at each annual clinic visit. Physical performance was measured at the baseline, year three and year five visits. Of 2940 participants with baseline data on diabetes, 719 (24%) participants had DM, defined by self-report, use of hypoglycemic medication, or an elevated fasting glucose (FG≥ 126 mg/dl) or 2-hour glucose (OGTT≥ 200 mg/dl); 658 (22%) had IG; and 1,563 had normal glucose homeostasis (NG), defined as FG<110 mg/dl and OGTT<140 mg/dl. At the year five visit, 862 (33%) had DM, 1,066 (41%) had IG, and 695 had NG.

Falling and performance measures were evaluated over five years of follow-up using ordinal logistic (falls), linear mixed (walks and chair stands), and gamma-frailty (standing balance) models adjusted for age, gender and race. Those with DM fell more frequently compared with NG participants (OR = 1.40; 95% CI 1.17, 1.67) but those with IG did not (OR = 0.95; 95% CI 0.81, 1.12). DM participants had poorer baseline performance on the 6m usual walk (longer time), chair stands (fewer per minute), and standing balance (shorter time held) compared with NG participants and had bigger declines over follow-up in the 6m usual and narrow walks (Table) and standing balance (RH = 1.27; 95% CI 1.06, 1.53, for decline in performance). IG and NG participants did not differ at baseline or in rate of decline.

Difference in change in performance over 5 years, adjusted for age, gender and race

Performance test	DM vs NG		IG vs NG	
	Coefficient	(95% CI)	Coefficient	(95% CI)
6m usual walk (sec)	0.16*	(0.04, 0.28)	0.03	(-0.08, 0.15)
6m narrow walk (sec)	0.35*	(0.15, 0.54)	0.16	(-0.02, 0.34)
Chair stands (per min)	-0.56	(-1.19, 0.07)	-0.21	(-0.82, 0.41)

* p<0.05

Older adults with diabetes have an increased risk of falls and of declines in gait and balance, factors that may contribute to their higher fracture rate.

Disclosures: ***A.V. Schwartz****, None.*

1111

Rib Fractures Predict Incident Limb Fracture: Results from the European Prospective Osteoporosis Study. A. A. Ismail*[1], A. J. Silman*[2], J. Reeve[3], S. Kaptoge*[3], T. W. O'Neill[2]. [1]Department of Rheumatology, Stepping Hill Hospital, Stockport, United Kingdom, [2]ARC Epidemiology Unit, University of Manchester, Manchester, United Kingdom, [3]University Department of Medicine, Strangeways Research Laboratory, Cambridge, United Kingdom.

Population studies suggest that rib fractures are associated with a reduction in bone mass. While much is known about the predictive risk of hip, spine and distal forearm fracture on the risk of future fracture, little is known about the impact of rib fracture. The aim of this study was to determine the predictive risk of rib fracture on future risk of limb fracture.

Men and women aged 50 years and over were recruited from population registers in 31 European centres for participation in a screening survey of osteoporosis (European Prospective Osteoporosis Study). Subjects were invited to complete an interview administered questionnaire which included questions about previous fractures including rib fracture, the age of their first fracture and the level of trauma. Lateral spine radiographs were performed and the presence of vertebral deformity was determined morphometrically. The subjects were followed prospectively by annual postal questionnaire to determine the occurrence of clinical fractures. Poisson regression was used to assess the predictive risk of recalled history of low trauma rib fracture on future limb fracture.

6,344 men, mean age 64.2 years, and 6,788 women, mean age 63.6 years were followed for a median of 3 years (range 0.4-5.9 years). 135 men (2.3%) and 101 women (1.6%) reported a previous low trauma rib fracture. In total, 138 men and 391 women sustained a limb fracture during follow-up. In women, after age adjustment, those with a recalled history of low trauma rib fracture had an increased risk of sustaining 'any' limb fracture (Relative Risk [RR]=2.3;95%Confidence Intervals [CI] 1.3, 4.0). When stratified by fracture type the predictive risk was more marked for hip (RR=7.8;95%CI 2.3, 25.9) and humerus fracture (RR=4.5;95%CI 1.4, 14.7). Additional adjustment for prevalent vertebral deformity and previous low trauma fractures slightly reduced the strength of the association between rib fracture and subsequent limb fracture. In men, after age adjustment, there was a small though not significant association between recalled history of rib fracture and future limb fracture.

Our data highlight the importance of rib fracture as a marker of bone fragility in women. Treatment of osteoporosis in women with low trauma rib fracture may help reduce the morbidity related to limb fracture in later life.

Disclosures: ***T.W. O'Neill****, None.*

1112

Asymptomatic Vertebral Deformity as Major Risk Factor for Subsequent Fractures and Mortality: A 14-year Prospective Study. C. Pongchaiyakul, N. D. Nguyen, J. R. Center, J. A. Eisman, T. V. Nguyen. Bone and Mineral Program, Garvan Institute of Medical Research, Sydney, Australia.

In the elderly, vertebral deformity silently affects at least 20% of the population and is associated with considerable disability and increased mortality. However, it is unclear how the three events of vertebral deformity, fracture, and mortality are linked with each other and with bone mineral density (BMD). The present study examined the association between asymptomatic vertebral deformity, osteoporotic fractures and risk of mortality in a sample of elderly men and women.

In 1992, radiographs (X-ray) at the lumbar spine were performed on 300 individuals (113 men and 187 women) aged 60 or above (as at mid-1989), who were randomly selected from the Dubbo Osteoporosis Epidemiology Study (DOES). The presence of vertebral deformity was defined as a reduction of at least 3 standard deviations (SD) from same-sex normals for each vertebrae. Baseline lumbar spine and femoral neck bone mineral density (BMD) was measured by dual energy x-ray absorptometry (GE Lunar DPX-L, WI, USA). Incidence of mortality and atraumatic fractures was ascertained during the study period of 1989 and 2003.

At baseline, the prevalence of asymptomatic vertebral deformity was 30.7% in men and 16.7% in women. During the follow-up period, subjects with vertebral deformity had a significantly higher risk of all types of osteoporotic fractures than those without vertebral deformity (44% vs. 29%; relative risk (*RR*), 2.1 [95%CI, 1.2 to 3.7]), particularly symptomatic vertebral fracture (*RR,* 7.4 [3.0 to 17.7]). Mortality rate was highest after a symptomatic fracture among those with vertebral deformity (*RR*, 9.6 [3.0 to 30.6]). These associations remained virtually unchanged after adjusting for age, BMD and gender. In conclusion, vertebral deformity was a strong predictor of subsequent risk of fractures, particularly symptomatic vertebral fracture, and of fracture-associated mortality in both elderly men and women. Vertebral deformity should be considered a primary risk factor for mortality as well as fracture.

Disclosures: ***C. Pongchaiyakul****, None.*

1113

The Near Absence of Osteoporosis Treatment in Older Men with Fractures. A. C. Feldstein*[1], G. Nichols*[1], E. Orwoll*[2], P. J. Elmer*[1], D. H. Smith*[1], M. Herson*[3], M. Aickin*[1]. [1]Center for Health Research, Kaiser Permanente Northwest, Portland, OR, USA, [2]Bone and Mineral Unit, Oregon Health & Sciences University, Portland, OR, USA, [3]Northwest Permanente, Portland, OR, USA.

Background; The burden of osteoporotic fractures in older men is significant, and treatment rates for secondary prevention are low. The study objectives were to 1) Characterize older men with fractures associated with osteoporosis, 2) Determine if treatment rates for osteoporosis are improving, and 3) Identify patient, healthcare benefit and utilization, and clinician characteristics that are significantly associated with treatment.

Methods: *Design*. Retrospective cohort study used multiple logistic regression to evaluate pre-fracture factors for their association with osteoporosis treatment in the 6-month post-fracture period.

Setting. A non-profit health maintenance organization in the United States.

Participants. 1,171 men aged 65 or older with any new fracture associated with osteoporosis between January 1, 1998, and June 30, 2001.

Main Outcome Measure. Pharmacologic treatment for osteoporosis in the 6 months after the index fracture.

Results: Average age was 76.7 years; 3.3% had a diagnosis of osteoporosis and 15.2% a diagnosis or medication associated with secondary osteoporosis. Only 7.1% of the study population received a medication for osteoporosis following the index fracture, and treatment rates did not improve over time. In the multivariate model, a higher value on the Charlson Comorbidity Index (odds ratio 1.26, 95% confidence interval 1.05-1.51), having an osteoporosis diagnosis (odds ratio 8.11, 95% confidence interval 3.08-21.3), chronic steroid use (odds ratio 5.37, 95% confidence interval 2.37-12.2), and a vertebral fracture (odds ratio 16.6, 95% confidence interval 7.8-31.4) were significantly associated with drug treatment. Bone mineral density measurement was rare (n=13, 1.1%).

Conclusions: There is under-ascertainment of osteoporosis and modifiable secondary causes in older men with fractures. Fracture does not prompt sufficient bone mineral density measurement or treatment. Information systems merging diagnostic and treatment information can help delineate gaps in patient management. Interventions showing promise in other conditions should be evaluated to improve care for osteoporosis.

Disclosures: ***A.C. Feldstein****, None.*

1114

Screening and Treatment of Glucocorticoid Induced Osteoporosis among 6517 Adults. J. R. Curtis*[1], J. Allison*[1], A. Becker*[1], L. Casebeer*[1], V. George*[1], S. H. Kovac*[2], C. Spettell*[3], A. Westfall*[1], N. Weissman*[1], S. Wilkie*[3], K. G. Saag[1]. [1]Division of Rheumatology, University of Alabama Birmingham, Birmingham, AL, USA, [2]Durham VA Medical Center, Durham, NC, USA, [3]Aetna Integrated Informatics, Inc., Blue Bell, PA, USA.

Aim: Despite a significant associated fracture risk, previous population-based studies document low screening and treatment rates for glucocorticoid induced osteoporosis (GIOP). We determined updated rates and predictors of BMD measurement and anti-osteoporotic prescriptions among chronic glucocorticoid (GC) users.

Methods: Using data from a national managed care organization (MCO), adults receiving 60+ days of GCs from Jul '01-Dec '02 were identified. Linked MCO databases identified both BMD tests and prescription medications used to prevent or treat GIOP, including hormone replacement therapy (HRT), testosterone (T), and GIOP-specific therapies. Multivariate logistic regression, adjusted for case mix, was employed to examine potential effects of physician specialty.

Results: 6,517 GC patients treated by 2,138 physicians were identified and were: 34% male, mean age = 50 (SD = 14) yrs, 16 (13) mg/day of prednisone for 9.8 (7.3) months. GC associated conditions included RA (37%), SLE (13%), COPD (11%), asthma (12%) and IBD (9%).

Overall rates of BMD testing and any GIOP prescription medication including HRT & T were 33% and 37%, respectively. HRT use was 12% among women < 50, 35% among women 50-70, and 23% among women >70. Testosterone was used by 3% of men. BMD testing and GIOP-specific medications (excluding HRT & T) were significantly greater among women ≥50 (50% & 42%) compared to men (18% & 15%) and women <50 (31% & 18%) [see Figure].

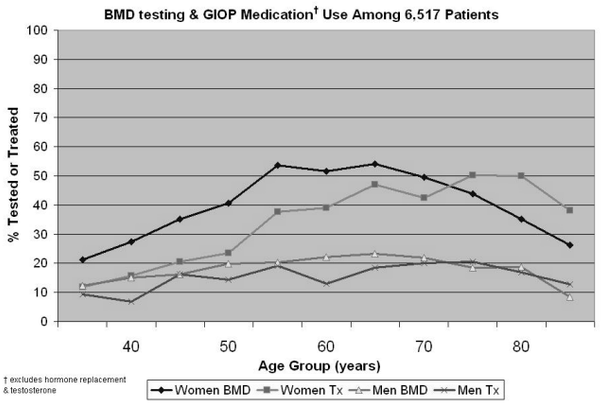

After adjusting for physician case mix, BMD testing differed significantly by specialty (internal medicine referent): nephrology (OR = 1.5; 95% CI 1.1-1.9), rheumatology (OR = 1.7; 1.4-2.0). GIOP medication use also differed by specialty (internal medicine referent): rheumatology (OR = 1.3; 1.1-1.5), gastroenterology (OR = 0.6; 0.4-0.8), and family medicine (OR = 0.7; 0.5-1.0).

Conclusions: Even among high risk patients, both BMD screening and GIOP treatment rates remain low, particularly for pre-menopausal women and men of all ages. Significant practice pattern variations among specialties persist. Developing interventions to improve GIOP management remains a high priority.

Disclosures: ***J.R. Curtis****, None.*

1115

Disruption of Endogenous Glucocorticoid Signaling in Col2.3-HSD2 Transgenic Mice Results in Decreased Cortical Bone Mass and Impaired Ex Vivo Osteogenic Differentiation. L. B. Sher[1], J. R. Harrison[2], D. J. Adams*[3], B. E. Kream[1]. [1]Medicine, UCONN Health Center, Farmington, CT, USA, [2]Orthodontics, UCONN Health Center, Farmington, CT, USA, [3]Orthopaedic Surgery, UCONN Health Center, Farmington, CT, USA.

In contrast to the well known catabolic effects of excess glucocorticoids (GC) on bone mass, disruption of GC signaling in mature osteoblasts in Col2.3-11ß-hydroxysteroid dehydrogenase (Col2.3-HSD2) transgenic mice revealed an anabolic role for endogenous GC on bone. We previously showed trabecular bone volume of vertebrae was reduced and mineralization was impaired in female Col2.3-HSD2 mice. In the present study, we compared femoral cortical bone morphometric parameters in Col2.3-HSD2 mice versus wild type (WT) controls and the differentiation of Col2.3-HSD2 versus WT osteoblasts ex vivo. Cortical bone morphometric parameters were measured in 7-week-old mice using X-ray microcomputed tomography. Cortical thickness and cross-sectional area were significantly reduced in Col2.3-HSD2 males and females, while femur length was unchanged. In females, this was due to a decrease in periosteal diameter. This cortical bone phenotype was seen in two Col2.3-HSD2 lines. For cell culture, hemizygous Col2.3-HSD2 mice were crossed to mice homozygous for a Col2.3-driven green fluorescent protein transgene (GFP) that serves as a marker of late-stage osteoblast differentiation. All progeny contained Col2.3-GFP; approximately half contained the Col2.3-HSD2 transgene (Col2.3-HSD2/GFP) while the remaining progeny (WT/GFP) served as controls. Primary calvarial osteoblasts and bone marrow stromal cells were isolated from 6- to 8-week-old male and female progeny and differentiated in culture with ascorbate and ß-glycerophosphate. At day 21 (calvarial osteoblasts) and day 28 (stromal cells), plates were imaged for GFP fluorescence, alkaline phosphatase and von Kossa (mineralization) staining. Bone markers were assessed by Northern blotting. Col1a1, bone sialoprotein, osteocalcin and GFP expression were reduced in Col2.3-HSD2/GFP cultures. The amount of alkaline phosphatase staining per well was unchanged in Col2.3-HSD2/GFP primary calvarial osteoblast cultures, but was significantly decreased in stromal cultures. Both primary calvarial osteoblasts and stromal cultures from male and female Col2.3-HSD2/GFP mice showed decreased mineralization compared to WT/GFP cultures. Overall, cortical bone parameters in females and female-derived cell cultures appeared more affected than males. These data show that disruption of glucocorticoid signaling *in vivo* leads to a decrease in cortical bone mass. This may be due at least in part to impairment of osteoblast differentiation.

Disclosures: ***L.B. Sher****, None.*

1116

Estrogen Represses Hematopoietic Stem Cell Proliferation, Thymopoiesis, Thymic Output, and T Cell Peripheral Expansion through IL-7. M. Ryan, F. Grassi, W. Qian, M. N. Weitzmann, R. Pacifici. Division of Endocrinology, Metabolism, and Lipids, Emory University, Atlanta, GA, USA.

Ovariectomy (ovx) leads to bone loss through an expansion of the pool of TNF producing T cells resulting in TNF potentiation of RANKL induced osteoclastogenesis. Bone loss following ovx is prevented by neutralization of IL-7, an estrogen regulated factor required for T lymphopoiesis and T cell homeostasis. To determine how ovx leads to the expansion of T cells critical for bone loss through IL-7, mice were ovx or sham operated and treated with neutralizing IL-7 antibody or irrelevant antibody for 2 weeks. Bone marrow (BM) hematopoietic stem cells (HSC) and common lymphoid progenitors (CLP), thymic T cell differentiation, thymic output, and T cell peripheral expansion was then measured. Ovx increased the proliferation of early T cell precursors and the number of naïve T cells in the thymus by ~ 2-fold while IL-7 neutralization in vivo completely prevented these effects, demonstrating that ovx upregulates thymopoiesis through IL-7. We then examined if increased seeding of BM lymphoid progenitors contributes to the ovx-induced stimulation of thymopoiesis. We found that ovx induced, and IL-7 neutralization prevented, a 2-fold increase in the number of HSC and CLP in the BM, thus unveiling a novel IL-7 mediated effect of ovx on progenitor expansion and differentiation. Measurements of T cell receptor excision circles (TREC), a specific marker of recent thymic emigrants, revealed that ovx decreases TREC by 2-fold in the thymus while it increased TREC in the spleen, suggesting increased export of naïve T cells into the periphery. In addition, in vivo FITC thymic labeling showed a 2-fold increase in the total number of FITC labeled naive T cells in the spleen following ovx, confirming enhanced thymic export of T cells induced by estrogen deficiency. The ovx induced changes in TREC expression and FITC labeling were prevented by IL-7 neutralization establishing that thymic output was regulated through IL-7. Furthermore, ovx also increases the proliferation of naïve and memory T cells in the spleen and the BM in an IL-7 dependent manner. In summary these findings demonstrate for the first time that ovx stimulates the proliferation of HSC, the influx of early lymphoid precursors to the thymus, thymopoiesis, thymic output and mature T cell peripheral expansion through an IL-7 dependent mechanism. Thus IL-7 is a newly recognized key "upstream" target through which estrogen regulates multiple aspects of T cell differentiation critical for bone homeostasis and ovx induced bone loss.

Disclosures: ***M. Ryan****, None.*

1117

Osteoblast-targeted Overexpression of ERRα Decreases Bone Formation in Transgenic Mice. B. Horard*[1], P. Clément-Lacroix[2], F. Morvan[3], R. Chiusaroli[3], C. Belleville*[2], R. Galien*[2], R. Baron[2], M. Resche-Rigon[2], J. Vanacker*[4]. [1]Lbmc, ENS, Lyon, France, [2]ProSkelia Pharmaceuticals, Romainville, France, [3]Orthopaedics and Cell Biology, Yale University School of Medicine, New Haven, CT, USA, [4]Crlc, INSERM, Montpellier, France.

Estrogen-Receptor Related receptors (ERRs) constitute a subfamily of orphan receptors closely related to the Estrogen Receptors (ER) that interfere with estrogen signaling though their activities are not regulated by natural estrogens. ERRα has been suggested to play a role in bone development and/or homeostasis. This receptor is indeed expressed in ossification zones during mouse development, but also in osteoblasts of adult long bones. In addition, ERRα stimulates osteoblastic proliferation and differentiation *ex vivo*, and upregulates the expression of osteopontin. To investigate the *in vivo* functions of ERRα in bone, we have established mouse transgenic lines overexpressing the receptor specifically in osteoblasts through the osteocalcin promoter. Detailed analysis of bone remodeling activity in these mice at various time points after birth including pQCT, μCT, dynamic histomorphometry, and bone markers, revealed a specific role of ERRα in bone formation. Overexpression of ERRα in osteoblasts did not affect longitudinal growth. In contrast, sexually immature mice overexpressing wild-type ERRα display significantly reduced trabecular bone mineral density, and trabecular bone volume (-12% and -16.7% respectively) compared to WT controls), associated with decreased trabecular thickness and number. Cortical thickness was significantly reduced as well. More importantly, while the osteoclast number was not affected in transgenic mice, the parameters of bone formation were all significantly decreased in ERRα tg mice (30%, 20%, and 22% decrease in osteoid surface, osteoblast surface and osteoblast number respectively). The phenotype was less markedly altered in adult (12 week-old) transgenic animals. The trabecular bone mass was still reduced in older tg mice (-9.8% and -7.5% for trabecular BMD and BV/TV, respectively) but the parameters of bone formation, as well as the bone turnover were normalized compared to control animals. Finally overexpression of ERRα in osteoblast did not prevent bone loss associated with gonadectomy. These data confirm that ERRα may affect bone homeostasis and suggest that it functions as an inhibitor of bone formation.

Disclosures: ***M. Resche-Rigon****, None.*

1118

Estrens Are Non-selective Ligands of the Androgen Receptor, Protecting Bone in Estrogen Receptor α-deleted Male Mice Whilst Also Affecting Reproductive Organs. S. H. Windahl[1], R. Chiusaroli[1], P. Clément-Lacroix[2], D. Minet*[2], R. Galien*[2], W. C. Horne[1], M. Resche-Rigon[2], R. Baron[1]. [1]Orthopaedics and Cell Biology, Yale University School of Medicine, New Haven, CT, USA, [2]ProSkelia Pharmaceuticals, Romainville, France.

Bone can be maintained in vivo by estrogens acting on the estrogen receptors (ERs) and by androgens acting on the androgen receptor (AR). Given a recent report that 4-estren-3α, 17β-diol (estren-α) acts via both receptors, the present study was designed to 1) compare the abilities of estren-α and its isomer estren-β (4-estren-3β, 17β-diol) to prevent orchidectomy (orx)-induced bone loss in adult male mice, 2) examine the safety profile of these compounds on reproductive organs and 3) determine which receptor/s was/were utilized by these compounds in vivo (ER vs. AR).

We and others have previously shown that ERα is the only receptor that can be activated by 17β-estradiol in the male mouse. In order to study the possible activation of AR and/or other steroid receptors by the estrens in vivo, we examined the response of bone and seminal vesicles in ERα-deficient ($ERα^{-/-}$) orx mice to hormone treatment with or without anti-androgen treatment. Twelve week-old orx male $ERα^{-/-}$ mice were implanted with slow-release pellets delivering either 1) vehicle, 2) estren-α (5mg/kg/d), 3) estren-β (5mg/kg/d) or 4) 5α-dihydrotestosterone (DHT, 2.5mg/kg/d), with or without daily injections with the pure anti-androgen RU58642 (30mg/kg/d) in all cases but vehicle.

After 4 weeks of treatment, detailed histomorphometric analysis showed that both of the estrens and DHT prevented orx-induced cancellous bone loss by affecting osteoblast and osteoclast numbers and bone formation rate. The effect could be reversed by simultaneous delivery of RU58642, indicating that in the absence of ERα, the estrens signal only through the AR in male rodent bone. Interestingly, both estrens had deleterious effects on the seminal vesicles, similar to DHT, suggesting that in the absence of ERα signaling, these compounds are not selective in their effect on bone versus reproductive organs. Again, these effects were totally abolished by co-administration of RU58642, showing that in the absence of ERα signaling, estrens exert their effects on the seminal vesicles, as on bone, via the AR. Both estrens were found to be ligands for the AR and to display full agonist activity on the AR, with strong stimulation of androgen response element-dependent transcription from the probasin promoter. In conclusion, estren-β and estren-α can activate both ERα and AR in vivo and are thereby capable of efficiently preventing bone loss in orx $ERα^{-/-}$ males. However, neither estren demonstrated a good safety profile on reproductive organs.

Disclosures: ***S.H. Windahl****, None.*

1119

Estren, but not Estradiol, DHT or 19-Nortestosterone, Induces Osteoblast Commitment and Differentiation by Stimulating Smad1/5/8 Phosphorylation and Transcription. S. Kousteni, L. Han, M. Almeida, A. D. Warren*, V. G. Lowe*, T. Bellido, S. C. Manolagas. Div. Endocrinol., Center for Osteoporosis and Metabolic Bone Diseases, Center for Osteoporosis and Metabolic Bone Diseases, Central Arkansas Veterans Healthcare System, Univ. Arkansas Med. Sci., Little Rock, AR, USA.

4-Estren-3α, 17β-diol (estren), a synthetic compound that mimics nongenotropic effects of both estrogen and androgen with minimal effects on classical transcription, exerts bone anabolic effects as opposed to the anti-remodeling/anti-catabolic effects of estrogens and androgens. We searched for mechanism(s) responsible for this unique biologic profile. Estren dose dependently (10^{-12} to 10^{-6} M) induced lineage commitment and differentiation towards osteoblasts in two bipotential cell lines, C2C12 and UAMS32, and in primary cultures of murine calvaria cells, as assessed by induction of alkaline phosphatase (AP) activity or osteocalcin. These effects were blocked by ICI 182,780 or flutamide, the BMP antagonist noggin, the Wnt antagonist Dkk1, the Src inhibitor PP1, the PI3K inhibitor wortmannin, and the JNK inhibitor SP600125. Estren also upregulated the expression of AP, osteocalcin, BMP-2 and Runx2, as assessed by real time PCR, in cultures of C2C12 cells and MC3T3-E1 pre-osteoblasts. Further, estren induced mineralization in MC3T3-E1 cells and the uncommitted mesenchymal progenitor cell line ST2. In addition, estren rapidly and transiently stimulated the phosphorylation of Smad1/5/8 in cultures of C2C12 and calvaria cells and this effect was blocked by ICI, flutamide, noggin, Dkk1, PD98059 (an inhibitor of MEK), wortmannin and SP600125; however, cycloheximide was ineffective. Moreover, estren upregulated the expression of Smad6, a Smad1/5/8-specific transcriptional target. Importantly, E_2, DHT or 19-nortestosterone, a potential androgenic metabolite of estren, at concentrations five orders of magnitude higher than estren did not exhibit these properties, perhaps because of counter-regulatory genotropic actions. Consistent with the abrogation of the effects of estren by Dkk1, estren stimulated Wnt/β-catenin-mediated transcription from a TCF-luciferase reporter in MC3T3-E1 cells. Finally, estren, but not E_2 or DHT, upregulated by at least 2-fold the expression of Wnt1, the Wnt receptor Frizzled 1 and the Wnt/β-catenin transcriptional target Axin2 in C2C12 cells. These results provide a mechanistic explanation for the bone anabolic effects of estren and suggest the existence of a large signalosome in which inputs from steroid receptors, BMPs, Wnt signaling and kinases converge. Activation of this signalosome is a property of ANGELS, but not of classical sex steroids or androgenic metabolites.

Disclosures: ***S. Kousteni****, Nuvios Inc 1, 2, 5.*

1120

Runx2-independent Stimulation of Osteoblastogenesis and PPARγ-Mediated Inhibition of Adipogenesis by the Homeobox Gene Msx2. F. Ichida*[1], K. Hata*[1], F. Ikeda[1], T. Matsubara[1], K. Hisada*[1], H. Yatani*[1], A. Yamaguchi[2], R. Nishimura[1], T. Yoneda[1]. [1]Dept Biochem Osaka Univ Grad Sch Dent, Osaka, Japan, [2]Dept Pathol Tokyo Medic and Dent Univ Grad Sch, Tokyo, Japan.

Increased adipose tissue and decreased bone mass in bone marrow are associated with osteoporosis and aging. Given that adipocytes and osteoblasts share the common precursors of mesenchymal origin, either stimulation of osteoblastogenesis or inhibition of adipogenesis is critical to maintain bone volume. Msx2 is a homeobox gene which regulates development, morphogenesis and cell differentiation. Recent observations that mice deficient in Msx2 gene showed a defect in skull ossification and reduction in bone formation with decreased osteoblast number and apparently increased adipocytes suggest that Msx2 is a potential regulator of osteoblastogenesis and adipogenesis in bone development. To study this, we used the multipotent mesenchymal cell line C3H10T1/2 that is capable to differentiate into osteoblasts and adipocytes by the treatment with BMP2. BMP2 induced osteoblastogenesis by elevating ALP activity in C3H10T1/2 cells with an induction of Msx2 and Runx2 expression. Overexpression of Msx2 in C3H10T1/2 cells using an adenovirus system induced osteoblast differentiation. This effect of Msx2 was enhanced in the presence of BMP2. To understand the molecular basis of these findings, the interactions of Msx2 with Runx2 in osteoblast differentiation were examined. Msx2 had no effects on BMP2-induced Runx2 expression. BMP2 induced Msx2 expression in Runx2-deficient calvarial mesenchymal cells. Furthermore, Msx2 overexpression induced osteoblast differentiation in Runx2-deficient mesenchymal cells. A dominant-negative Runx2 did not affect the stimulatory effect of Msx2 on osteoblast differentiation. We subsequently investigated the role of Msx2 in adipogenesis with a special focus on the interactions with C/EBP and PPARγ, both of which are well-characterized regulators of adipogenesis. Adipocyte differentiation of C3H10T1/2 cells upon treatment with BMP2 was abolished by Msx2 introduction. Msx2 profoundly impaired the stimulatory effects of C/EBP α, β and γ on adipogenesis. In addition, Msx2 markedly suppressed PPARγ promoter activity and PPARγ expression that were up-regulated by C/EBP β and γ. Msx2 inhibited adipogenic action and transcription activity of PPARγ. In conclusion, our results show that Msx2 stimulates osteoblast differentiation without the interactions with Runx2 and inhibits adipocyte differentiation by inhibiting C/EBP α, β and γ and PPARγ. Thus, Msx2 might contribute to increase bone mass by directing mesenchymal stem cell differentiation to osteoblasts and preventing adipogenesis.

Disclosures: ***F. Ichida****, None.*

1121

ß1ß2-Adrenergic Receptor KO Mice Have Decreased Total Body and Cortical Bone Mass Despite Increased Trabecular Number. D. D. Pierroz[1], P. Muzzin*[2], V. Glatt*[3], M. L. Bouxsein[3], R. Rizzoli[1], S. L. Ferrari[1]. [1]Div of Bone Diseases, University Hospital, Geneva, Switzerland, [2]Medical Biochemistry, University Medical Center, Geneva, Switzerland, [3]Orthopedic Biomechanics Laboratory, Harvard Med School, Boston, MA, USA.

Leptin is a central inhibitor of bone mass, whose negative effects on osteoblasts are reportedly mediated by the ß-adrenergic (adr) system, more specifically through the ß2-adr receptor. Accordingly, vertebral trabecular bone density, particularly trabecular number, is increased in leptin- and leptin receptor-deficient male mice (ob/ob and db/db, respectively) and in the dopamine ß-hydroxylase deficient mice. In contrast, the effect of leptin on cortical bone is controversial. To further elucidate the role of adr stimulation on trabecular (Tb) and cortical (Cort) bone compartments, we investigated bone mass (by pDXA) and microarchitecture (by µ-CT) in 8 and 20 wks old male mice null for ß1ß2-adr receptor (ß-AR KO) (n=4-7/group). Furthermore, we compared wild-type (WT) growing male mice treated for 8 weeks with a ß-adr agonist, isoproterenol (ISO, 10 mg/kg/d) or vehicle (VEH) (n=4-6/group).

In ß-AR KO mice, total body (TB) BMC was significantly decreased compared to WT mice at both 8 and 20wks (-18 to -28%), as were mid-femoral cross-sectional area (CSA) (-12 to -35%) and Cort thickness (Th) (-5 to -20%) (all P<0.0001 for ß-AR KO vs WT, by 2F-ANOVA). In marked contrast, vertebral Tb number (N) was higher (+9%, P=0.0004) and Tb spacing was consequently decreased (-10%, P=0.0001). Since Tb Th was decreased (-6 to -10%, P=0.0038) in ß-AR KO mice compared to WT, Tb bone density (BV/TV) was similar in both genotypes. ßAR-KO had increased percentage fat mass at 8 wks compared to WT (+18%, P=0.0326), with a persistent trend at 20 wks. In WT, ISO markedly decreased TB BMC gain (-33%, P<0.0001), as well as vertebral Tb BV/TV, Tb N, and Cort Th compared to VEH (-24 to -34%, p=0.031 to 0.0001). ISO significantly decreased the percentage fat mass (-77%, P=0.0067), lowered circulating leptin levels, and reduced seminal vesicles weight (-30%, P=0.0084), a marker of androgenic activity.

Altogether these data confirm that the adrenergic system is involved in the regulation of bone mass and architecture. Although activation of the leptin-adrenergic system consistently inhibits TbN, its effects on other Trab and Cort bone architectural parameters are more complex, as they involve alterations in fat mass and gonadal steroids that contribute to bone mass regulation. Hence, pharmacological modulation of the adrenergic system may not lead unequivocal and consistent effects on the various bone compartments.

Disclosures: ***D.D. Pierroz****, None.*

1122

β-Adrenergic Receptor KO Mice Have Increased Bone Mass and Strength But Are Not Protected from Ovariectomy-Induced Bone Loss. H. Dhillon*[1], V. Glatt*[1], S. L. Ferrari[2], M. L. Bouxsein[1]. [1]Beth Israel Deaconess Medical Center & Harvard Medical School, Boston, MA, USA, [2]Geneva University Hospital, Geneva, Switzerland.

Mice devoid of leptin (ob/ob) or the signaling form of its receptor (db/db) have markedly increased trabecular bone mass, despite reduced gonadal function (1). Recent evidence suggests that the inhibitory effects of leptin on bone may be mediated by the β-adrenergic system and that β-adrenergic antagonists inhibit bone loss after estrogen deficiency (2). Thus, we hypothesized absence of β-adrenergic signaling will lead to increased bone mass and strength, and will inhibit bone loss after ovariectomy (OVX). To test this, we evaluated mice that lack the three known β-adrenergic receptors (β-AR KO)(3) using in vivo bone densitometry, ex vivo microCT and femoral biomechanics. We studied 6- and 16-week old male β-AR KO and WT (n=7-9/gr), and female β-AR KO and WT mice 8 wks after OVX or sham-OVX (n=10-12/gr). Body weight and % fat were signficantly increased in β-AR KO, particularly at 16 wks. Leptin levels were 2-fold higher in β-AR KO than WT (7.63 ±; 0.94 vs 3.93 ±; 1.02 ng/ml). Total body bone mass was 14 to 22% higher (p<0.05) in β-AR KO than WT males. At 6 weeks male β-AR KO mice had 1.3 and 3.5-fold higher vertebral and distal femoral trabecular bone volume fraction (p<0.001 for both); these differences were less prominent at 16 wks. Mid-femoral cross-sectional area, bone area and cortical thickness were also significantly increased in 16 wk old β-AR KO, as was femoral failure load (+49%), stiffness (+28%) and energy to failure (+41%) (p<0.01 for all). OVX induced similar deficits in vertebral trabecular BV/TV in β-AR KO (-15.5%, p=0.11) and WT (-18.4%, p=0.05) compared to sham-OVX. Altogether these data support a role for β-AR signaling in the regulation of bone mass, but do not preclude direct positive effects of leptin on bone as well. Bone loss following estrogen-deficiency is not prevented by the absence of β-AR signaling. Additional studies are needed to delineate the relative roles of the different β-AR sub-types, as well as the independent contributions of increased fat mass and/or other hormonal and growth factor differences that may contribute to bone mass alterations in mice deficient in β-adrenergic signaling.

REFS: 1) Ducy, Cell 2000; 2) Takeda, Cell 2002; 3) Bachman, Science 2002

Disclosures: ***H. Dhillon****, None.*

1123

Pleiotropic Responses to Hypothalamic Neuropeptide Y1 Receptor Deletion are Associated with a High Bone Mass Phenotype. P. A. Baldock*[1], S. Allison*[1], A. Sainsbury*[2], D. Lin*[3], R. F. Enriquez*[1], M. During*[3], H. Herzog*[2], E. Gardiner[1]. [1]Bone and Mineral Program, Garvan Institute of Medical Research, Sydney, Australia, [2]Neurobiology Program, Garvan Institute of Medical Research, Sydney, Australia, [3]Department of Molecular Medicine & Pathology, University of Auckland, Auckland, New Zealand.

Recent studies have revealed pathways within the brain that regulate bone formation. Neuropeptide Y Y2 and leptin receptors of the hypothalamus are known to modulate such pathways. Y2 deletion results in few non-osteoblast effects, while loss of leptin signalling is associated with both metabolic and hormonal changes. Other Y receptors are expressed in the hypothalamus and interactions between these have produced unexpected results in bone. Gender specific changes in Y2Y4 delete mice have suggested pleiotropic effects on bone tissue as a result of central neural changes. This study investigated Y1 receptor deletion and its effects on bone homeostasis and interaction of Y1 deletion with Y2 and leptin. Germline and conditional hypothalamic Y1 delete mice were assessed for both cancellous and cortical phenotypes. Y1Y2 and Y1ob double mutant mice were assessed and Y1 delete mice following hyperleptinemia after weight gain induced by hypothalamic NPY over expression.

Y1 deletion resulted in a high bone mass phenotype in both germline (13.9% ± 1.9 vs 6.6 ± 1.4) and hypothalamic delete models (17.4% ± 3.0 vs 7.8 ± 0.4). Osteoblast function was increased with mineral apposition rate (MAR) elevated compared to wild type (1.9 um/d ± 0.2 vs 0.96 ± 0.03). Contrary to Y2 delete mice, osteoclast surface was also increased (16.3% ± 1.3 vs 8.0 ± 0.9) as was body weight (29.7g ± 1.0 vs 24.4 ± 0.8) due to greater fat mass. Again unlike Y2 delete mice, IGF-1 levels were reduced by around 50%. There was no effect on cortical bone size or length.

Y1Y2 double delete mice had increased bone volume (12.4% ± 0.9) but was not different to Y1 or Y2 (12.4% ± 1.7) alone, with no increase in osteoclast surface (7.0 % ± 0.7). There was no cortical phenotype and body weight was normal.

Y1ob mice had reduced bone volume (8.5% ± 1.3) compared to Y1, but not ob/ob (10.3% ± 1.0); this reduction was consistent with increased osteoclast surface. Hypothalamic over expression of NPY greatly increased leptin levels, and was associated with reduced bone in Y1 (10.0% ± 0.9 vs 6.6 ± 1.2), consistent with a reduced MAR (2.0 um/d ± 0.2 vs 1.1 ± 0.2).

Hypothalamic Y1 receptors are potent modulators of cancellous bone volume and bone cell function. As with ob/ob, Y1 receptor deletion results in pleiotropic effects with hormonal and metabolic effects in addition to osteoblastic and osteoclastic changes, in contrast to Y2 deletion.

Disclosures: ***P.A. Baldock****, None.*

1124

The Age-Related Increase in Bone Area Assessed by QCT Is Site- but not Sex-Specific: Age, Gene/Environment Susceptibility-Reykjavik Study. G. Sigurdsson[1], T. Aspelund*[1], B. Jonsdottir*[1], A. Gudmundsson*[1], T. B. Harris*[2], V. Gudnason*[1], T. F. Lang[3]. [1]Icelandic Heart Association, Kopavogur, Iceland, [2]National Institute on Ageing, San Francisco, CA, USA, [3]University of California, San Francisco, CA, USA.

Quantitative computerized tomography (QCT) is a novel technology that allows estimation of the trabecular and cortical bone but there are few data on this measurement in populations. We compared cross-sectional QCT measures of bone size by age and gender in the axial skeleton (lumbar spine) and appendicular skeleton (hip and mid-femur) in the Age, Gene/Environment Susceptibility-Reykjavik Study (AGERS). In AGERS, an ongoing population-based study in Icelandic men and women 67 years and older, we measured the cross-sectional area of L_1 and L_2 (VCSA) and mid-vertebral integral bone mineral density (BMD) to derive a figure for vertebral compression strength (g^2/cm^4=BMD^2xVCSA). We also measured the min. cross-sectional area in femoral neck (MINCSAFN), max. area through the intertrochanteric plane (MAXCSATR), total, medullary and cortical cross-sectional areas through mid-femur. Study population consists of 638 men and 568 women, 67-93 years old, and excludes 1036 persons with evidence of fracture in L_1 or L_2 or on medication affecting bone. We used regression models to assess the effects of age and gender adjusting for current and measured height in mid-life for cohort effects in height.
Average VCSA (L_1 and L_2) increased by 5%/10 years of age in men (trend for age, $p<0.001$) and 4% in women ($p<0.001$), with no significant difference by gender. Vertebral integral BMD decreased significantly more in women than men, 12% vs. 6%/10 years ($p<0.01$ for gender). Vertebral compressive strength decreased by 26% in women compared to 11% in men/10 years ($p<0.01$ for gender). The MINCSAFN did not change significantly with age or gender, whereas the MAXCSATR increased by 2%/10 years of age in both sexes (trend for age, $p<0.01$). Mid-femoral cross-sectional area (MFCSA) increased by 1.8% in men and 1.4%/10 years of age in women ($p<0.01$). While gender differences in MFCSA were not significant, the medullary area in mid-femur increased by 15%/10 years of age in women compared with 3% in men ($p<0.01$ for gender). The cortical area in mid-femur decreased by 2.8%/10 years in women with no change in men. In the lumbar vertebrae, the decline in compressive strength with age is accompanied by greater decline in BMD than in bone size with differences greater in women than men. In mid-femur, the main age-related change was an increase in medullary area, greater in women than men. Our cross-sectional data indicate that bone size changes with age differ by anatomic site but the differences are not consistently significant by gender.

Disclosures: ***G. Sigurdsson****, None.*

1125

GGT (gamma-glutamyltranspeptidase) as a Pathogenic Factor of Bone Loss. K. Hiramatsu*[1], S. Tatsumi*[1], Y. Nimura*[2], H. Takasu[1], S. Niida[1], M. Ito[3], K. Ikeda[1]. [1]Department of Bone and Joint Disease, National Center for Geriatrics and Gerontology (NCGG), Obu, Japan, [2]Department of Surgery, Nagoya University Graduate School of Medicine, Nagoya, Japan, [3]Department of Radiology, Nagasaki University Hospital, Nagasaki, Japan.

We have recently identified GGT (gamma-glutamyltranspeptidase) as an osteoclastogenic factor, in Xenopus oocyte expression screening of cRNA derived from T lymphoma cells that cause osteolysis when injected into nude mice (J Biol Chem 2004). GGT is an ectoenzyme that catalyzes cleavage of glutathione (GSH) and transfer of gamma-glutamyl moiety to acceptors. GGT is most abundantly expessed in proximal renal tubules, while its serum activity is widely used as a biochemical marker of alcoholic liver disease. We have demonstrated that purified GGT from rat kidney as well as recombinant human GGT induces the formation of multinucleated functional osteoclasts in murine bone marrow cultures. Interestingly, GGT's enzymatic activity is not required for its osteoclastogenic function, raising the possibility that GGT has a cytokine mode of action. In order to examine if GGT induces osteoclastogenesis in vivo and stimulates bone resorption, we have generated transgenic mice that over-express GGT using Cre-loxP system. Crossing of floxed eGFP-GGT mice with CAG-Cre gave rise to CAG-GGT mice that produce GGT systemically. They show markedly elevated serum GGT activity and significant increases in serum calcium concentrations (10.1 mg/dl vs. 8.8 mg/dl in WT) with relative decrease in urinary calcium excretion. Micro CT scanning of tibia of CAG-GGT mice revealed decreased 3D BV/TV with increased trabecular separation. Bone histomorphometry showed increased osteoclast number with tendency of suppressed bone formation. Bone marrow macrophages from CAG-GGT mice, when stimulated with M-CSF and sRANKL, generated 2 times more osteoclasts, compared with WT-derived cultures, suggesting increased sensitivity of osteoclast precursors by GGT. Thus, GGT may play a pathogenic role in bone diseases due to accelerated osteoclastic activity, including osteoporosis, arthritis and bone metastasis.

Disclosures: ***K. Hiramatsu****, None.*

1126

Increased Adipogenesis in Bone Marrow Associated with Decreased BMD in Mice Deficient in Thyroid Hormone Receptors. J. M. Kindblom[1], E. Gevers*[2], S. Movérare*[1], M. K. Lindberg*[1], S. Göthe*[3], B. Vennström*[3], C. Ohlsson[1]. [1]Internal Medicine, Sahlgrenska Academy, Gothenburg, Sweden, [2]National Institute for Medical Research, Division of Molecular Endocrinology, London, United Kingdom, [3]Karolinska Institute, Dept of Cell and Molecular Biology, Stockholm, Sweden.

Mice deficient in thyroid hormone receptor α1 and β (TRα1-/-β-/-) have a severe skeletal phenotype with growth retardation, delayed maturation of long bones and decreased trabecular and total bone mineral density (BMD). The aim of the present study was to investigate the molecular mechanisms behind the skeletal phenotype in TRα1-/-β-/- mice. Global gene expression analysis was performed on total vertebrae from wild type (WT) and TRα1-/-β-/- mice using DNA microarray and the results were verified by real-time PCR. The mRNA levels of six genes (AdipoQ, Adipsin, fat-specific protein 27 (FSP 27), lipoprotein lipase (LPL), retinol-binding protein (RBP) and phosphoenolpyruvate carboxykinase (PEPCK)) expressed by mature adipocytes were increased in TRα1-/-β-/- compared with WT mice. In contrast, markers of early adipocyte differentiation were unchanged in TRα1-/-β-/- mice. Quantitative image analysis revealed an increased amount of fat (225% over WT) due to an increased number but unchanged size of adipocytes in the bone marrow of TRα1-/-β-/- mice. The total BMD was inversely correlated to the expression of genes expressed by mature adipocytes and to the number of adipocytes in the bone marrow. Interestingly, the mRNA levels of the key regulator of osteoclastogenesis, receptor activator of NF-κb ligand (RANKL), were dramatically decreased in TRα1-/-β-/- mice, which might at least partly explain the reduced bone turnover observed in hypothyroidism. In conclusion, TRα1-/-β-/- mice have decreased BMD associated with an increased number of mature adipocytes. One may speculate that disrupted thyroid hormone receptor signalling causes an imbalance in the osteoblast-adipocyte differentiation, leading to a reduced amount of trabecular bone and an increased amount of fat in the bone marrow of TRα1-/-β-/- mice.

Disclosures: ***J.M. Kindblom****, None.*

1127

The Effects of Differentially Modified Forms of Shh on Endochondral Bone Formation. K. I. Larsen[1], D. J. Robbins*[2], R. Serra[1]. [1]Cell Biology, University of Alabama at Birmingham, Birmingham, AL, USA, [2]Pharmacology and Toxicology, Dartmouth Medical School, Hanover, NH, USA.

During endochondral bone formation, chondrocyte proliferation and differentiation are tightly regulated to achieve proper bone size. The morphogen, Indian hedgehog (Ihh), is secreted from prehypertrophic chondrocytes as they commit to terminal differentiation, inhibiting hypertrophic differentiation in a Pthrp-dependent manner. Ihh binds its receptor, Patched (Ptc), on target cells resulting in increased Ptc expression, which can be used as a read-out for signaling activity. Sonic Hedgehog (Shh), another member of this morphogen family, is highly homologous to Ihh and has comparable activity in several biological assays. Shh was used as a functional substitute for Ihh in these studies. Shh and Ihh are uniquely lipid modified with cholesterol and palmitate, which increase hydrophobicity. We hypothesized that lipid modification of Ihh alters its ability to move through the cartilage matrix and/or affect signaling in target cells. The purpose of this study was to characterize activity in response to differentially modified forms of Shh in the mouse metatarsal organ culture system. Conditioned medium from 293 cells that had been transfected with different Shh constructs was collected and Shh quantified by ELISA and Western analysis. Biological activity of the Shh-conditioned medias was measured by alkaline phosphatase activity in limb micromass cultures. Metatarsal rudiments from E15.5 $Ptc^{(LacZ/+)}$ mice, which contain a targeted knock-in of the β-gal gene into the *Ptc* locus, were incubated with the different Shh-conditioned medias or recombinant Shh (rShh-N), which lacks all lipid modification. Metatarsals were stained with X-gal and Ptc expression was determined by light microscopy of whole mount and cryosectioned bones. Metatarsals incubated with media containing native lipid modified Shh potently increased Ptc expression in prehypertrophic chondrocytes and in the perichondrium only adjacent to the hypertrophic zone, the physiologic Ptc expression zone. Pre-incubation of media with 5E1 neutralizing antibody blocked this increase demonstrating specificity of the Shh signal. Media containing Shh with only the palmitate modification gave the same activation pattern but at much reduced potency suggesting the cholesterol is critical for potency. rShh-N and conditioned media containing Shh without any lipid modification induced Ptc expression in round proliferating chondrocytes and perichondrium along the entire length of the bone. We conclude that lipid modification of Shh alters its potency and range of signaling during endochondral bone formation.

Disclosures: ***K.I. Larsen****, None.*

1128

Nkx3.2/Bapx1 Delays Chondrocyte Maturation by Repressing Runx2 Expression. S. Provot*[1], H. Kempf[2], L. C. Murtaugh*[2], U. Chung*[1], H. M. Kronenberg[1], A. B. Lassar*[2]. [1]Endocrine Unit, MGH - Harvard Medical School, Boston, MA, USA, [2]Bcmp, Harvard Medical School, Boston, MA, USA.

The proper formation and growth of limb bones requires tight control over the rate at which cartilage cells divide and mature. A feedback loop between Indian hedgehog (Ihh) and parathyroid hormone related protein (PTHrP) is essential to maintain a pool of dividing, immature chondrocytes at the epiphyses of growing long bones; in the absence of these signals, the proliferative cells are depleted by premature maturation. Conversely, the transcription factor Runx2 is required for chondrocyte maturation. Here we present evidence that the transcription factor Nkx3.2/Bapx1 acts as a key participant in the Ihh/PTHrP loop, at least partly by inhibiting *Runx2* expression, and therefore chondrocyte maturation. In chick and mouse, expression of *Nkx3.2/Bapx1* is restricted to the proliferative zone, and is down-regulated as maturation begins. Artificially preventing this down-regulation, by misexpression of chick *Nkx3.2* through retroviral infection of wing buds of 3.5 days chick embryos, inhibits maturation and traps the chondrocytes in an immature state. Nkx3.2 acts as a transcriptional repressor, and we show that its DNA binding activity as well as its repression activity is essential for its ability to inhibit maturation. Conversely, a "reverse function" mutant of Nkx3.2 that has been converted into a transcriptional activator hastens chondrocyte maturation. We also show that *Nkx3.2/Bapx1* appears to lie downstream of PTHrP, as its expression is lost in *PTHrP*$^{-/-}$ and *PTHrP-receptor*$^{-/-}$ mouse E18.5 growth plates, and is maintained by retroviral *PTHrP* misexpression in infected chick wings. Furthermore, we demonstrate that Nkx3.2 represses *Runx2* expression partially in infected chick embryos, and dramatically in cultures of chick somite explants, and that *Runx2* misexpression can rescue the Nkx3.2-induced delayed maturation, both *in vivo* and *in vitro*. Taken together, these results suggest that Nkx3.2 is a mediator of the effects of PTHrP signaling on chondrocytes, in which it acts to repress the expression of *Runx2*, normally required for the progression of chondrocyte maturation.

Disclosures: ***S. Provot****, None.*

1129

Nkx3.2 Repression of Runx2 Gene Activity Promotes Mesenchymal Chondrogenesis. C. J. Lengner, C. Lepper*, J. L. Stein*, A. J. van Wijnen, J. B. Lian, G. S. Stein. Department of Cell Biology and Cancer Center, University of Massachusetts Medical School, Worcester, MA, USA.

The DNA-binding transcription factor Runx2 has been shown to be required for osteoblast maturation. We and others have recently shown Runx2 gene activity in pre-cartilaginous condensing mesenchyme in the developing embryo. Here we examine the regulation of Runx2 gene activity in mesenchymal progenitor cells by pro-chondrogenic signaling molecules and transcription factors as well as examine the role of the Runx2 protein during entry of a mesenchymal progenitor cell into the chondrocytic lineage. We identify the homeodomain protein Nkx3.2 as a potent repressor of the Runx2 P1 promoter. We show that Nkx3.2 binds to the Runx2 promoter in a sequence-specific manner at a consensus sequence approximately 100 bp upstream from the transcriptional initiation site and that this binding results in a 5-fold repression of promoter activity. In order to understand the biological significance of this repression, we utilize the C3H10T1/2 pluripotent mesenchymal progenitor cell line as a model system for mesenchymal chondrogenesis. We find that upon induction of the chondrogenic phenotype there is an activation of Nkx3.2 and a concomitant repression of Runx2 gene activity in accordance with our *in vitro* findings. By infecting C3H10T1/2 cells with a Runx2-expressing adenovirus prior to initiation of chondrogenic differentiation, we can by-pass the observed Runx2 repression and prevent the induction of the chondrocytic phenotype, as assessed by Sox9 and Collagen Type II gene expression. If, however, Runx2 is introduced into C3H10T1/2 cultures after the induction of chondrogenesis, there is no effect on the expression of chondrocyte phenotypic genes. Taken together our results demonstrate that Runx2 is a direct target of Nkx3.2-mediated transcriptional repression, and that repression of Runx2 in mesenchymal progenitor cells prior to chondrogenic differentiation is a prerequisite for the activation of chondrocyte phenotypic gene expression. These findings establish a novel role for Runx2 in mesenchymal progenitor cells and identify Runx2 as the first bona fide target of the pro-chondrogenic transcriptional repressor Nkx3.2.

Disclosures: ***C.J. Lengner****, None.*

1130

Identification of the Tissue-specific Enhancer Element Responsible for Mouse Type X Collagen Gene Expression *In vivo*. Q. Zheng*[1], B. Keller*[1], G. Zhou[1], D. Napierala*[2], Y. Chen*[1], A. Parker*[3], B. Lee[2]. [1]Molecular and Human Genetics, Baylor College of Medicine, Houston, TX, USA, [2]Howard Hughes Medical Institute, Houston, TX, USA, [3]Respiratory and Inflammation Research Area, Astrazeneca, Cheshire, United Kingdom.

Type X collagen (*Col10a1*) gene is specifically expressed in hypertrophic chondrocytes of the growth plate during endochondral ossification. Its deficiency in human causes Schmid metaphyseal chondrodysplasia (SMCD). Multiple regulatory elements within human, murine and chicken *Col10a1* promoter regions have been reported to direct type X collagen gene expression at different levels by in vitro transfection studies. Our previous studies showed that 4 kb *Col10a1* promoter containing Runx2 elements can specifically drive weak reporter gene (*LacZ*) expression in the lower hypertrophic zone of transgenic mice. However, cis elements directing its high level expression throughout the hypertrophic chondrocyte-specific expression *in vivo* have not yet been described. In this study, we report identification of the tissue-specific enhancer element responsible for high level mouse *Col10a1* expression by generating additional transgenic mouse lines harboring various *Col10a1* promoter and intronic fragments driving *LacZ* as reporter. An 8 kb *Col10a1* regulatory region encompassing the same 4 kb proximal promoter and second intron can direct reporter gene expression throughout the zone of hypertrophy, albeit at low level. In another transgenic mouse line containing a 10 kb regulatory element, high level tissue-specific expression throughout the hypertrophic zone was observed. These in vivo data suggest the presence of enhancer elements in both *Col10a1* distal promoter and second intron that cooperate with the Runx2 binding elements in the proximal promoter to specify its tissue-specific expression. *In silico* cross species analysis of *Col10a1* shows highly conserved elements within both the *Col10a1* distal promoter and second intron. These elements contain putative AP-1 (Activator protein-1) and Cdx (mouse homologue of Drosophila homeobox gene, caudal) binding sites respectively. We found that transgenic mice using the 6 kb and 4.6 kb *Col10a1* element could direct *LacZ* expression within the hypertrophic zone. This suggests that the conserved *Col10a1* distal promoter element (-4.6 to -3.9 kb) acts as a critical tissue-specific enhancer for *Col10a1* (reporter) expression *in vivo*. Further characterization of this cis element and the putative transcriptional factors that confer its tissue specificity in hypertrophic chondrocytes is essential for understanding the molecular mechanisms that specify endochondral ossification and the pathogenesis of the metaphyseal chondrodysplasias.

Disclosures: ***Q. Zheng****, None.*

1131

Dishevelled Is Required for Chondrocyte Proliferation and Differentiation. N. Zhong*, R. Gersch*, M. Hadjiargyrou. Biomedical Engineering, SUNY, Stony Brook, Stony Brook, NY, USA.

Wnt signaling is crucial for regulating cell proliferation and differentiation leading to the development of many organisms, including Hydra, D. melanogaster, C. elegans and mammals. Previously, we have reported on the activation of Wnt signaling during the early stages of mammalian bone regeneration. In this study, we focused on Dishevelled (Dvl), the first intracellular molecule that is activated following binding of Wnt proteins to its receptors, Frizzled and LRP5/6. Subsequently, Dvl induces the dissociation of the GSK3/Axin/β-catenin complex which normally leads to phosphorylation of β-catenin followed by its polyubiquitination and proteosomal degradation. In the absence of this inhibitory complex, dephosphorylated β-catenin enters the nucleus where it binds to members of the LEF/TCF family of transcription factors and alters the activity of Wnt target genes. As such, Dvl represents a pivotal molecule in the Wnt signaling pathway. Herein, we show that Dvl1, 2, and 3 were upregulated during the early phases of fracture repair, more specifically in proliferating chondrocytes and osteoblasts. Similarly, Dvl 2 and 3 were upregulated during differentiation of chondroblast RCJ3.1(C5) cells. To directly study the functional contribution of Dvl in RCJ differentiation, we utilized RNA interference (RNAi) to specifically target each of the Dvl members. Results indicate significant suppression (19-33%) of cell proliferation following separate transient transfection of Dvl1, 2 and 3 RNAi (as compared to empty vector control). Additionally, following a 4 day transient trasfection of Dvl1, 2, and 3 RNAi, we observe a dramatic suppression of chondrocyte differentiation (as determined by quantitative alcian blue staining), with a 21%, 67%, and 63%, respectively. Similarly, following a 6 day Dvl RNAi transfection, we found a similar trend in suppression of chondrocyte differentiation. Lastly, we find that in the presence of Dvl 1, 2, and 3 RNAi, the expression of both early (Sox9, COL2A1) and late (COL10) chondrogenic differentiation markers, were also significantly suppressed. Taken together, the data indicates the expression and functional significance of Dvl in chondrocytes. It is interesting to note that Dvl2 -/- mice have vertebral and rib malformations and that these skeletal defects were more pronounced in mice deficient for both Dvl1 and Dvl2. Morover, our data strongly suggests that all Dvl1, 2 and 3 function as key components of Wnt signaling. Since the biochemical mechanism by which Dvl regulates Wnt signaling is not fully understood, further work is required to identify which of the many Dvl interacting proteins are also required specifically for chondrocyte proliferation and differentiation.

Disclosures: ***M. Hadjiargyrou****, None.*

1132

The Novel Collagen Triple Helix Repeat Containing Gene (Cthrc1) Indicates a Role in Cartilage and Bone Formation via Regulation of Collagen Matrix Production. V. Lindner, P. Pyagay*, Q. Wang*, L. Liaw*. Center for Molecular Medicine, Maine Medical Center Research Insitute, Scarborough, ME, USA.

The purpose of the present study was to understand the function of the novel gene Cthrc1 using both in vitro and in vivo approaches.

Transgenic mice overexpressing Cthrc1 were generated and analyzed using established methods. Routine cell transfection procedures were used to establish CTHRC1 overexpressing and CTHRC1 depleted cell lines. CTHRC1 is a secreted 26.5kDa protein that is glycosylated and highly conserved from lower chordates to mammals. The sequence contains a short collagen domain which prompted the name 'collagen triple helix repeat containing 1'. Cthrc1 mRNA expression is regulated by TGF-ß family members.

During mouse development at 8.5dpc, strong expression of Cthrc1 is observed in the caudal notochord and anterior ventral neural tube and prominent expression is seen at 9.5dpc in the somites and branchial arches. At later stages CTHRC1 was abundant in the developing heart, proliferating chondrocytes and in the surrounding periosteum. Expression of CTHRC1 protein was examined by immunohistochemistry and Western blotting with an antibody raised against recombinant CTHRC1. Expression of CTHRC1 was prominent in the adventitial matrix of injured but not normal blood vessels, distal tubules of the kidney, in the basal layer of the epidermis, airway epithelium, the chorioid plexus and Purkinje cells of the cerebellum. Immunoreactive CTHRC1 was abundant in the bone matrix of growing and adult bones and it was expressed by osteocytes and osteoblasts. In growing bones, CTHRC1 was expressed by chondrocytes of the resting and proliferating zone of

the growth plate but CTHRC1 immunoreactivity was absent from the hypertrophic cartilage. No CTHRC1 expression was seen in the cartilage of adult bones but expression persisted in the perichondrium and periosteum. Overexpression of Cthrc1 in transgenic mice caused severe skeletal abnormalities with disorganized mesenchymal condensations and markedly reduced cartilage proteoglycan as well as brittle bones and skull ossification defects with reduced amounts of bone matrix. The affected tissues revealed reduced levels of mature collagen type 1 while corresponding mRNA levels were markedly increased. Overexpression of Cthrc1 in vivo and in vitro was associated with decreased levels of the procollagen C-proteinase BMP-1. These data indicate that CTHRC1 may inhibit processing of procollagen by reducing BMP-1 expression levels.

Disclosures: ***V. Lindner****, None.*

1133

Physiological Role and Expression of Fgf-23 *in vivo*. D. Sitara[1], R. G. Erben[2], C. Carr*[3], H. Jüppner[4], B. Lanske[1]. [1]Oral and Developmental Biology, The Forsyth Institute and Harvard School of Dental Medicine, Boston, MA, USA, [2]Institute of Physiology, Physiological Chemistry and Animal Nutrition, Ludwig - Maximilians University, Munich, Germany, [3]Oral and Developmental Biology, The Forsyth Institute, Boston, MA, USA, [4]Endocrine Unit, Massachussetts General Hospital and Harvard School of Medicine, Boston, MA, USA.

FGF-23 has recently been recognized as the circulating phosphaturic factor associated with renal phosphate wasting. To study the expression of Fgf-23 *in vivo* and to determine its physiological role, we generated an animal model in which the entire coding region of mouse *Fgf-23* was replaced with *lacZ.* Heterozygous Fgf-23-ablated mice (Fgf-23$^{+/-}$) appeared to be normal and were fertile. *LacZ* staining of Fgf-23$^{+/-}$ animals showed expression in liver, heart, and somites as early as E11.5 suggesting a specific role during embryonic development. Homozygous Fgf-23-ablated mice (Fgf-23$^{-/-}$) were born according to Mendelian frequency and were macroscopically indistinguishable from their normal littermates at birth. Starting at 10 days postnatally, however, we observed remarkable growth retardation in Fgf-23$^{-/-}$ mice. Body weight and size were significantly reduced when compared to wild-type (WT) littermates (10 days: 6.1 ± 0.4 vs. 6.6 ± 0.5 g, 24 days: 6.2 ± 0.5 vs. 11.3 ± 0.9 g, 40 days: 7.1 ± 0.5 vs. 16.7 ± 1.2 g). The life span of Fgf-23$^{-/-}$ mice was markedly shortened with the longest survival of 9 weeks. Compared to WT mice, homozygous mutant animals exhibited significantly increased serum phosphate concentrations (16.3 ± 0.3 vs. 9.6 ± 0.5 mg/dl). Preliminary data furthermore suggest that serum PTH levels of Fgf-23$^{-/-}$ mice were indistinguishable from those of WT litter mattes at 3 weeks of age, but significantly decreased at 6 weeks of age. Full body skeleton staining using Alizarin Red S showed diminished mineralization in most bones, but more than normal mineralization in other parts of the skeleton. Bone mineral density as measured by pQCT and Piximus was reduced in extremities of Fgf-23$^{-/-}$ mice. Histological examination of bones from Fgf-23$^{-/-}$ revealed severe osteoidosis in the axial and appendicular skeleton, gross deformities and woven bone formation especially in ribs and vertebrae,and disorganized growth plates with reduction in hypertrophic chondrocytes, abnormal formation of secondary ossification center, and hypermineralisation of the primary spongiosa. Taken together, our data suggest that FGF-23 has a role beyond its involvement in the regulation of phosphate homeostasis.

Disclosures: ***D. Sitara****, None.*

1134

A Pro253Arg Mutation in Mouse FGFR2 Causes Craniosynostosis. L. Yin*[1], J. Wang*[1], X. Du*[1], L. Zhao*[1], N. Su*[1], L. Chen[1], C. Li*[2], C. Deng*[2]. [1]Daping Hospital, Chongqing, China, [2]NIH, Bethesda, MD, USA.

Apert syndrome (AS) is one of the most severe craniosynostosis and is characterized by premature fusion of coronal sutures, craniofacial anomalies, and syndactyly of the digits. Nearly all known cases of AS are caused by mutations of either Ser252Trp or Pro253Arg in fibroblast growth factor receptor 2 (FGFR2). Using knock-in strategy, recently we generated a mouse model which mimic human AS that caused by a Pro253Arg mutation in FGFR2. We showed here the mutant mice exhibit premature fusion of coronal sutures, brachycephaly and smaller body size but no syndactyly of the digits. Some of the mutant mice exhibit distorted skulls with proptosis too. The ossification of calvaria is accelerated in mutant embryo and accompanied by decreased, rather than increased, bone formation. Examination of the coronal sutures of postnatal mutant mice revealed premature fusion. The osteoblast proliferation is slightly decreased but the osteoblast differentiation is not obviously altered in the mutant coronal suture. We did not find premature fusion of the cranial base, but the mutant synchondroses had slightly shorter columns of proliferating chondrocytes. The abnormalities of mutant skull appear before the premature fusion of coronal suture. Thus, the retarded growth of cranial base may also play an important role in the early pathogenesis of skull deformation of AS, while the role of premature fusion of coronal suture is more important in later development stage.

Disclosures: ***L. Yin****, None.*

1135

Circulating Osteogenic Cells in Heterotopic Bone Formation. R. J. Pignolo[1], P. C. Billings*[2], R. K. Suda*[1], E. M. Shore[2], F. S. Kaplan[2]. [1]Department of Medicine, University of Pennsylvania, Philadelphia, PA, USA, [2]Orthopaedic Surgery, University of Pennsylvania, Philadelphia, PA, USA.

Cells with osteogenic potential, including mesenchymal precursors, can be found in a variety of tissues. Recently, osteogenic precursor cells have been identified in the circulation as a population of mononuclear blood-derived adherent cells (BdACs) that can produce bone in vivo. To test the hypothesis that BdACs are more abundant in patients who are predisposed to heterotopic bone formation, we used peripheral blood samples from patients with fibrodysplasia ossificans progressiva (FOP) and from unaffected individuals to determine relative circulating levels of these osteogenic precursor cells. BdACs were isolated from 22 subjects in a blinded fashion, 11 who were later identified as unaffected individuals and 11 individuals with FOP. The presence of BdACs was analyzed by direct visualization using light microscopy 72 hours after introduction of cells into culture. FOP patients with recent exacerbations (episodes of heterotopic ossification) had significantly higher numbers of BdACs compared to patients with stable disease or unaffected individuals. Using immunofluorescence, we characterized BdACs as a type I collagen+/CD34+ subpopulation that may be related to circulating fibrocytes, initially described in the context of wound repair, but subsequently found to participate in granuloma formation and various fibrosing disorders. We further demonstrated by assays of in vitro mineralization and in vivo bone formation that fibroblast-like BdACs from patients with FOP are osteogenic. These cells differ most notably from those derived from unaffected individuals by their ability to form polyclonal cultures with bone-forming capacity. The possibility that circulating fibroblast-like cells with osteogenic potential can seed sites of inflammation and tissue injury with resultant ectopic bone formation has tremendous clinical implications. The greater abundance and osteogenic potential of FOP BdACs may portend a possible pathophysiologic role for these cells as osteoprogenitor cells and, to our knowledge, would represent the first example of their involvement in heterotopic ossification.

Disclosures: ***R.J. Pignolo****, None.*

1136

Evidence that Osteoblast Lineage Cells are Present in the Peripheral Circulation and Increase Markedly During the Pubertal Growth Spurt. G. Z. Eghbali-Fatourechi, J. Lamsam*, D. Fraser*, B. L. Riggs, S. Khosla. Mayo Clinic, Rochester, MN, USA.

That osteoclast lineage cells circulate is well accepted. Using assays requiring adherence to plastic, rare concentrations [<1 in 10^8 mononuclear cells (MNC)] of osteoblast (OB) lineage cells have been detected in peripheral blood in humans, but larger numbers comparable to those reported for osteoclasts and correlations of these cells with bone turnover markers have not been reported. Since circulating OB lineage cells may lack the capacity to adhere to plastic (or to other matrices), we used flow cytometry with an anti-osteocalcin (OCN) antibody (Ab) to search for OB lineage cells and identified cells in the circulation of adult humans that express OCN (~1% of MNC). These cells have low forward/side-scatter, consistent with a small, mononuclear phenotype, and the majority do not express the myeloid/stromal marker, CD34. Under appropriate culture conditions [expansion of cell numbers in stem cell medium for 3 weeks (including isolation and re-addition of non-adherent cells with media changes) followed by OB differentiation medium for 3 weeks], sorted OCN+ form mineralized nodules in vitro. Moreover, as shown in panel A, when compared to adult male subjects (n = 11, mean age 38.7 yrs), the percentage of these OCN+ cells is markedly increased in the circulation of adolescent boys going through the pubertal growth spurt (n = 11, mean age 14.5 yrs), who also have increased bone formation indices [serum OCN (mean ± SE), 145 ± 17 vs 25 ± 1 ng/mL and bone alkaline phosphatase (BAP), 148 ± 19 vs 29 ± 2 U/L in the boys vs men, P < 0.001 for both). Panel B shows the flow cytometry profile of these cells in the circulation of an adolescent boy (OCN Ab and isotype control). Finally, we also found that in the two merged groups, the percent OCN+ cells correlated directly with serum OCN (R = 0.72) and BAP (R = 0.77, P < 0.001 for both).

We conclude that OB lineage cells circulate in significant numbers. Because they correlate directly with bone formation markers and are markedly increased during the pubertal growth spurt, they may represent a heretofore unrecognized circulatory component to the process of bone formation. Further, these methods potentially provide a powerful new tool for studying OB differentiation without bone or bone marrow sampling and for investigating the pathophysiology of osteoporosis and other metabolic bone diseases.

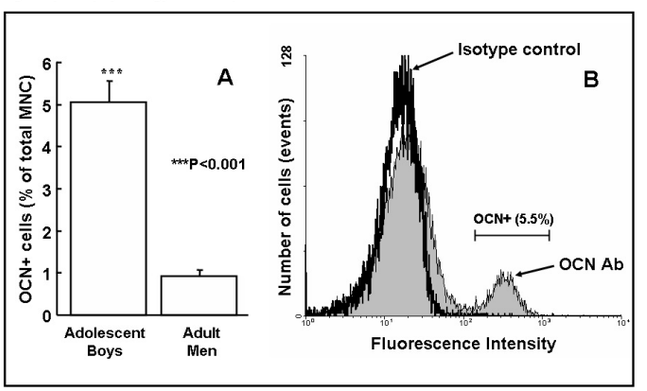

Disclosures: ***S. Khosla****, None.*

1137

Crohn's Disease in Childhood Is Associated with Decreased Trabecular Density, Cortical Dimensions and Muscle Mass. M. B. Leonard, R. M. Herskovitz*, K. M. Howard, R. N. Baldassano*, J. M. Burnham, B. S. Zemel. Pediatrics, The Children's Hospital of Philadelphia, Philadelphia, PA, USA.

Pediatric Crohn's disease (CD) is associated with decreased bone mass and increased risk of fracture; however, the effects of CD on muscle mass, trabecular density and cortical geometry have not been well-characterized. The objective of this longitudinal study was to identify bone deficits at the time of CD diagnosis, and to evaluate changes in bone measures over the subsequent 12 months.

Peripheral quantitative computed tomography (Stratec XCT 2000) measurements of the tibia were obtained in 68 incident CD subjects (36M/32F) and 159 healthy controls (73M/86F), ages 5 to 18 yr. To date, 31 CD subjects have completed the 12 month visit. Trabecular volumetric BMD (vBMD) was measured at the 3% distal site; cortical vBMD, cross-sectional area (CSA), and stress-strain index (SSI, density-weighted section modulus) at the 38% site; and muscle CSA at the 66% site.

Height and BMI were converted to age and gender specific Z-scores using national reference data. Multivariable linear regression models were developed to evaluate pQCT results in the baseline CD subjects, compared with controls. In order to examine changes over the 12 months, bone and muscle measures were expressed as gender-specific Z-scores derived from linear regression models in the controls.

At diagnosis, CD was associated with decreased height and BMI Z-score (both $p< 0.001$). Trabecular vBMD was significantly decreased ($p< 0.001$), adjusted for age, gender and race. Cortical vBMD did not differ between CD and controls. CD was associated with significant deficits in cortical CSA ($p < 0.001$), SSI ($p < 0.05$), and muscle CSA ($p < 0.001$), adjusted for gender, race and tibia length. When the models for bone outcomes were adjusted for muscle CSA, the deficits in cortical CSA and SSI were no longer statistically significant, and the deficits in trabecular vBMD were attenuated.

Baseline and 12 month Z-scores are summarized below for the CD subjects completing the 12 month visit. Z-scores for trabecular vBMD and muscle CSA Z-scores increased significantly; however, cortical CSA and SSI Z-scores decreased further.

This is the first prospective, longitudinal study using pQCT to evaluate bone health in a chronic childhood disease, demonstrating significant deficits in trabecular density, cortical geometry and muscle.

Gender-Specific Z-Scores (Mean ± SD) at Baseline and 12 Months in CD

VARIABLE	Baseline	12 Month	p
Height-Z	-0.42 ± 0.90	-0.34 ± 0.87	NS
BMI-Z	-0.81 ± 0.92	-0.35 ± 0.74	< 0.0001
Trabecular vBMD-Z*	-1.51 ± 1.51	-1.1 ± 1.32	< 0.01
Cortical CSA-Z**	-0.41 ± 1.23	-0.65 ± 1.11	0.05
Cortical SSI-Z**	-0.20 ± 1.00	-0.50 ± 0.88	< 0.001
Muscle CSA-Z**	- 0.75 ± 1.11	-0.41 ± 0.92	< 0.01

* Adjusted for age. ** Adjusted for tibia length.

Disclosures: ***M.B. Leonard****, None.*

1138

Bone Defects in NSE/hIL-6 Mice Overexpressing IL-6 Reminiscent of the Human Systemic Juvenile Idiopathic Arthritis. F. De Benedetti*[1], A. Funari*[2], S. Berni*[3], P. Ballanti*[3], C. Di Giacinto*[2], R. Paro*[2], E. Spica*[2], N. Rucci[2], A. Teti[2]. [1]Ospedale Bambino Gesù, Rome, Italy, [2]University of L'Aquila, L'Aquila, Italy, [3]University La Sapienza, Rome, Italy.

Stunted growth is a complication of childhood diseases characterized by chronic inflammation or infections. Systemic juvenile idiopathic arthritis (s-JIA) is an inflammatory disease characterized by prominent IL-6 production and elevated IL-6/sIL-6R complexes. We have generated the NSE/hIL-6 transgenic mice, over-expressing IL-6 under the control of the rat neurospecific enolase (NSE) promoter, and observed a bone phenotype reminiscent of the human s-JIA syndrome. NSE/hIL-6 mice expressed high circulating levels of IL-6 since birth and showed a marked decrease in growth rate leading to adult mice 50-70% the size of wild-type littermates. The growth defect was completely abolished by neutralization of IL-6. X-ray analysis showed significant reduced length of tibia and femurs, which persisted throughout life. Conventional histomorphometry of tibias showed decreased bone trabecular volume and number in the secondary spongiosa of the proximal and distal chondro-osseous junctions to the diaphysis in 5- to 20-d old mice, fully rescued in adult mice. Histochemical analysis revealed increased osteoclast and decreased osteoblast numbers and surfaces. Remarkable reduced cortical thickness characterized juvenile mice, with rescue in adult animals at the proximal and, to a lesser extend, distal ends of the diaphysal collar, but not in the mid-diaphysis. Dynamic measurements by calcein/alizarin red labelling showed no endosteal and 50% reduced periosteal apposition in the NSE/hIL-mice compared to controls. Consistently, increased osteoclast numbers and bone resorption was observed in the endosteal surface of the transgenic mice suggesting that endosteal erosion and reduced periosteal deposition contributed to cortical thinness. Clear-cut reduction of growth plate thickness was consistent with reduction of secondary spongiosa. In young mice, secondary ossification centers were delayed at both epiphyses, as they appeared less extended, showed less hyperthrophic chondrocytes, blood vessels, osteoclast and osteoblast precursors, and were not mineralised as indicated by negative von Kossa staining. NSE/hIL-6 mice showed normal serum growth hormone and low IGF-I, the latter due to marked decreased levels of IGFBP-3 and subsequent increased IGF-I clearance. In conclusion, NSE/hIL-6 mice mimic the systemic juvenile idiopathic arthritis, represent a faithful animal model of the growth impairment associated with chronic inflammatory diseases, and emphasize a role for IL-6 and/or for IGF-I catabolism in stunted skeletal growth.

Disclosures: ***A. Teti****, None.*

1139

Regulation of Runx2 Action during Osteoblast Development by a Novel Runx2-interacting Protein. G. Zhou[1], P. Hermann*[2], E. Munivez*[2], R. Morello*[1], Y. Chen*[2], Q. Zheng*[1], B. Lee[2]. [1]Dept. of Molecular and Human Genetics, Baylor College of Medicine, Houston, TX, USA, [2]Dept. of Molecular and Human Genetics/Howard Hughes Medical Institute, Baylor College of Medicine, Houston, TX, USA.

RUNX2 is one of three vertebrate members of the runt family of transcription factors which have in common an 128 amino acid motif that mediates both DNA binding and protein-protein interaction. Runx2 null mice have complete absence of osteoblast and bone but an intact cartilagenous skeleton and loss of function mutations of RUNX2 result in the human skeletal disorder-cleidocranial dysplasia (CCD). While Runx2 is essential for osteobalst differentiation and chondrocyte maturation, additional factors are likely required to regulate the differentiation program. To identify potential RUNX2-interacting proteins, we screened a human osteosarcoma cDNA library using a yeast two-hybrid approach with RUNX2 as bait and isolated a 500-bp partial cDNA which was termed RIP(Runx2-interacting protein). Multiple human tissue Northern blot analysis and in situ hybridization on mouse E15.5 embryos revealed ubiquitous expression including osteoblasts. RIP encodes a 297 amino acid polypeptide with no homology to known proteins in the database. Sequence analysis revealed a multidomain structure characterized by several protein-protein interaction domains and a nuclear localization signal. The physical interaction between RIP and RUNX2 was confirmed by GST pulldown experiment. In transient transfection RIP down-regulated the transactivation by RUNX2 in a dose-dependent manner in 10T1/2 cells and it also decreased the activity of an osteoblast-specific reporter in ROS17/2 cells by 50%. Furthermore immunofluorescent staining showed that RIP mainly localized in the nucleus. Both human and mouse RIP gene is encoded by 11 exons dispersed over 40kb of genomic DNA. FISH and radiation hybrid mapping studies showed that RIP localizes to chromosome 8q22 syntenic with a hypothesized second CCD-like locus. Interestingly RIP expression is upregulated in CCD-like patient cells with 8q22 rearrangements, supporting its function as a repressor of RUNX2. We would predict that upregulation of a putative repressor of Runx2 would cause loss of Runx2 transactivation and hence a CCD-like phenotype in vivo. To elucidate the potential effect of RIP on skeletogenesis, we are studying its action by generation RIP null mice and transgenic mice overexpressing RIP in osteoblasts.

Disclosures: ***G. Zhou****, None.*

1140

The High-Mobility-Group Transcription Factor Sox8 Regulates Osteoblast Differentiation in a Runx2-Dependent Manner. T. Schinke[1], K. Schmidt*[2], M. Haberland*[1], M. Priemel[1], A. F. Schilling[1], C. Mueldner*[1], J. M. Rueger*[1], E. Sock*[2], M. Wegner*[2], M. Amling[1]. [1]Trauma Surgery, Hamburg University, Hamburg, Germany, [2]Institute of Biochemistry, Friedrich-Alexander University Erlangen-Nuernberg, Erlangen, Germany.

Bone remodeling is an important physiologic process that is required to maintain a constant bone mass from the end of puberty until gonadal failure. This is achieved through a well-balanced activity of bone-resorbing osteoclasts and bone-forming osteoblasts that needs to be tightly regulated. In this study we have identified the high-mobility-group transcription factor Sox8 as a physiologic regulator of osteoblastic bone formation. Sox8-deficient mice show normal bone development, but display an osteopenic phenotype at the age of six months. This phenotype is caused by an impaired osteoblast differentiation, since the numbers of functional osteoblasts are largely reduced in Sox8-deficient mice compared to wildtype littermates (5.63 + 2.51 vs. 17.86 + 2.25 osteoblasts per bone perimeter, n=6, $p<0.005$). Surprisingly, primary osteoblasts derived from these mice show an accelerated mineralization ex vivo as well as a premature expression of Runx2, a key transcription factor involved in the regulation of bone formation. Taken together, these results suggested that Sox8 is a negative regulator of osteoblast differentiation acting in a Runx2-dependent manner. To confirm this hypothesis we have generated transgenic mice expressing Sox8 under the control of an osteoblast-specific Col1a1 promoter fragment. These Col1a1-Sox8-trangenic mice have a severely impaired bone formation and display a phenotype that is reminiscent of cleidocranial dysplasia. Accordingly, we observed a marked reduction of Runx2 expression in Col1a1-Sox8-trangenic mice compared to wildtype littermates, thereby suggesting an involvement of Sox8 in the regulation of Runx2 expression. This hypothesis is consistent with the finding that functional Sox8 binding sites overlap with the autoregulatory Runx2 binding sites in the promoter region of the Runx2 gene. Taken together, these data demonstrate that Sox8 is a physiologic regulator of postnatal bone formation, whose coordinated expression is critical for osteoblast differentiation.

Disclosures: ***T. Schinke****, None.*

1141

Msx2 Regulates Mesenchymal Cell Fate & Body Composition Via Paracrine Wnt-Dkk Signaling. S. Cheng, J. Shao*, N. Charlton-Kachigian*, A. Loewy*, D. A. Towler. Div. of Bone and Mineral Diseases, Dept. of Med, Washington University School of Medicine, St. Louis, MO, USA.

Msx2 promotes osteogenic differentiation of mesenchymal and vascular progenitors while suppressing adipogenic potential. Along with cell autonomous actions, conditioned medium (CM) from Msx2-transduced cells controls cell fate; Msx2 CM enhances alkaline phosphatase (ALP) activity of C3H10T1/2 cells by 50%, but inhibits adipogenesis by > 90%. Since Wnts exert similar activities, we studied effects of Msx2 on Wnt and Dkk signaling. Msx2-transduced 10T1/2 cells and myofibroblasts express significantly elevated Wnt1, Wnt3a, Wnt5a, and Wnt5b levels. In contrast, Dkk expression is decreased to <24% of control (Dkk1 in myofibroblasts, Dkk2 in 10T1/2 cells). Msx2 transduced cells exhibit

enhanced nuclear accumulation of beta-catenin, consistent with enhanced canonical Wnt signaling. Moroever, Msx2 CM stimulates canonical Wnt-regulated LEF-TCF transcription activity. Importantly, 1 µg/ml recombinant Dkk1 suppresses Msx2-dependent ALP induction; in addition, Dkk1 partially reverses Msx2 suppression of adipogenesis (by Oil Red O staining). To confirm these results, we generated CMV-Msx2 transgenic mice. Msx2 is significantly over-expressed in aorta, bone marrow cells, and osteoblasts isolated from transgenic mice (2.9, 1.6, and 2.6 fold, respectively) as compared to wild type littermates (WT). Wnt3a levels in aorta and osteoblasts are increased in Msx2 transgenics (2.7 and 3.8 fold), with a concomitant decrease in Dkk1 in aorta and Dkk2 in osteoblasts (27% and 64% of WT). Mineralization of cultured osteoblasts derived from these transgenic mice is enhanced as compared to cultures derived from non-transgenic WT littermates. DXA was used to assess body composition. The BMD of Msx2 transgenic mice is significantly higher than WT littermates after 4 and 8 weeks of a high fat diet challenge (2.7% and 3.5% increase), and persisted out to 16 weeks of dietary challenge. By contrast, total body fat is significantly decreased in Msx2 transgenic mice as compared to WT, and serum leptin levels are concomitantly lower (452.1+/- 174.4 vs. 1773.1+/- 383.6 pg/ml). Thus, Msx2 regulates mesenchymal cell fate and body composition in part via paracrine Wnt-Dkk signals.

Disclosures: ***S. Cheng****, None.*

1142

DeltaFosB Interacts with a Novel Zinc-finger Containing Protein (MC-33) which Downregulates Expression of Runx2 and Alkaline Phosphatase. M. Wu, F. Morvan, J. Zhang*, L. Neff*, W. Philbrick*, W. C. Horne, R. Baron. Cell Biology, Yale University, New Haven, CT, USA.

We have previously demonstrated that overexpression of ΔFosB in transgenic mice resulted in a severe and progressive, but reversible osteosclerotic phenotype that led to increased bone volume. *Ex vivo* and *in vitro* studies demonstrated that increased levels of Δ2ΔFosB, an N-terminally truncated isoform, mimicked most of the effects of ΔFosB, i.e. increased expression of osteoblast markers (collagen type 1, osteocalcin, osteopontin, and Runx2) as well as an increased rate and amount of bone nodule formation. This effect was shown to be cell autonomous to the osteoblast lineage. In an effort to identify the mechanism by which ΔFosB and Δ2ΔFosB regulate bone formation and osteoblast differentiation, we performed a yeast two-hybrid screen to identify Δ2ΔFosB binding partners. In addition to interacting with Runx2, we identified a novel clone (MC-33) as a Δ2ΔFosB binding partner. The 3.9 kb open reading frame of the full-length cDNA of MC-33 encodes a protein of approximately 180 kDa with multiple zinc fingers that localizes to the nucleus in transiently transfected cells. Northern blotting demonstrates that MC-33 is mostly expressed in brain, heart, lung, and skeletal muscle, but is also expressed at lower levels in spleen, kidney and liver as well as bone and fat. Primary osteoblasts cultured from calvarial preparations exhibit high levels of MC-33 expression. In-situ hybridization studies demonstrate that during bone development, MC-33 mRNA is expressed in mesenchymal condensations as early as embryonic day 12. Expression is maintained at high levels through embryonic day 18 and birth, with expression in the preosteoblastic layers and in the growth plate. *In vitro*, MC-33 mRNA is downregulated by stimulation with BMP-2 and adipogenic agents (indomethacin, hydrocortisone and IBMX). Further, transient transfection of MC-33 into C3H10T1/2 and MC3T3-E1 cells results in suppression of the Δ2ΔFosB-induced increase in Runx2 expression. Finally, MC-33 decreases alkaline phosphatase activity in transiently transfected primary osteoblasts. We propose that MC-33 modulates the control of osteoblast differentiation and that overexpressed Δ2ΔFosB binds MC-33, thereby disturbing the balance of transcriptional regulators.

Disclosures: ***M. Wu****, None.*

1143

Identification and Functional Characterization of a Novel Osteoclast-Derived Osteoblastic Factor (ODOF). T. Phan*, R. Han*, T. Davey*, V. Smuts*, M. H. Zheng, J. Xu*. Orthopaedic Surgery, The University of Western Australia, Nedlands WA, Australia.

Intercellular communication between osteoblasts and osteoclasts is the quintessential mechanism in bone remodelling. Here we report the identification and functional characterization of an Osteoclast-Derived Osteoblastic Factor (ODOF), which is expressed by osteoclasts, binds specifically to osteoblasts and elevates cytosolic calcium ($[Ca^{2+}]_i$) resulting in the proliferation of osteoblastic cells. The ODOF gene was identified in $RAW_{264.7}$ cell-derived osteoclasts utilising a PCR-selected subtractive hybridisation screening process. Further investigations using reverse transcriptase PCR, revealed that ODOF mRNA was up-regulated during RANKL-induced osteoclastogenesis but was not expressed in osteoblasts or osteoblast-like cells. Recombinant His-tagged ODOF was subsequently produced and labelled with ^{125}I to ascertain its binding profile. The protein exhibits highly specific binding to primary calvarial osteoblasts with a binding affinity of 1.7±0.4nM and $2.7x10^4$±306 receptors per cell but not with osteoclasts and their precursor cells. Functional studies demonstrated that ODOF stimulates an increase in the growth and proliferation of osteoblastic cells. In contrast, the protein did not promote osteoclastogenesis, osteoclast survival or bone resorption. Mechanistic analysis revealed that ODOF, alone, elevates intracellular $[Ca^{2+}]_i$ through the PLC-IP3 induced depletion of calcium stores. Moreover, western blot analysis reveals that ODOF induces the activation of the PI3K-Akt and ERK pathways in osteoblasts. Taken together, our results provide evidence for a novel cross-talk mechanism between the osteoclast and osteoblast and indicate that osteoclasts play a role in regulating osteoblastic growth and proliferation.

Disclosures: ***J. Xu****, None.*

1144

Dlx3 Is a Transcriptional Regulator of Osteoblast Differentiation and Increases Expression and Promoter Activity of Runx2. M. O. Hassan*[1], A. Javed[1], M. I. Morasso*[2], J. Karlin*[1], M. Montecino*[3], A. J. van Wijnen[1], G. S. Stein[1], J. L. Stein*[1], J. B. Lian[1]. [1]Department of Cell Biology and Cancer Center, University of Massachusetts Medical School, Worcester, MA, USA, [2]Developmental Skin Biology Unit, NIAMS, National Institutes of Health, Bethesda, MD, USA, [3]Departmento de Biologia Molecular, Universidad de Concepcion, Concepcion, Chile.

In response to the osteogenic BMP2 signal, multiple homeodomain HD) proteins are induced by BMP2 within 1-4 hrs and exhibit distinct temporal expression profiles during osteoblast differentiation. Among these are Msx and Dlx family members. While null mouse phenotypes indicate Msx2 and Dlx5 HD proteins support their roles in skeletal development, ablation of the closely related Dlx3 gene results in early embryonic lethality. Here we examined the role of Dlx3 in bone formation. In the mouse embryo, Dlx3 is expressed in periosteum and osteoblasts associated with sites of new bone formation. Dlx3 overexpression in osteoprogenitor cells promotes a 3-6 fold induction of bone markers, while RNAi knock-down of Dlx3 delays upregulation of these which include BSP, collagen I, osteopontin and osteocalcin (OC) during MC3T3 cell maturation. We characterized regulation of the bone specific OC gene by Dlx3 in relation to Dlx5 which is also reported to stimulate osteoblast differentiation and to the repressor HD protein Msx2. Interaction of these proteins with the OC gene during primary rat osteoblast differentiation was examined using chromatin immunoprecipitation assays. Two molecular switches in the association of HD proteins with the OC gene promoter were observed. In proliferating osteoblasts, the transcriptionally repressed OC gene is occupied by Msx2 at the homeodomain regulatory element; while Dlx3, Dlx5 and Runx2 are recruited post-proliferatively when transcription is initiated. A second switch occurs at the mineralization stage when Dlx5 occupancy increases and Dlx3 interaction declines. We also show that Dlx3 protein-DNA interactions stimulate Runx2 and OC promoter activity, while Dlx3 and Runx2 form a co-regulatory complex and this protein-protein interaction reduces OC transcription. Thus, our findings provide direct cellular and molecular evidence that Dlx3 contributes to regulating osteoprogenitor cell differentiation and supports both positive and negative regulation of gene transcription. Further our results show that distinct homeodomain proteins sequentially associate with promoter regulatory elements during progression of differentiation. We propose that multiple HD proteins in osteoblasts constitute a regulatory network which mediates development of the bone phenotype.

Disclosures: ***M.Q. Hassan****, None.*

1145

Resistive Vibration Exercise Prevents Bone Loss During 8 Weeks of Strict Bed Rest in Healthy Male Subjects: Results from the Berlin BedRest (BBR) Study. J. Rittweger*[1], D. Felsenberg[2]. [1]Institute for Biophysical and Clinical Research into Human Movement, Manchester Metropolitan University, Alsager, United Kingdom, [2]Center for Muscle and Bone Research, Charite - University Medicine Berlin, Campus Benjamin Franklin, Berlin, Germany.

Introduction: Muscle atrophy and bone loss pose problems in clinical immobilisation, but also during space flight. No effective countermeasure is available. For space flight, this restricts the possibility to perform long term missions. Bed rest studies are recognized as ground based models for microgravity. We hypothesized that vibration exercise (VbX), combined with progressive resistive training is an effective countermeasure to prevent bone loss from the lower body half during prolonged bed rest.

Method: 20 young healthy males were reqruited and randomly assigned to either the control group (Ctrl) or to the exercise group (Vbx). All subjects completed 8 weeks of strict bed (BR) rest under video surveillance. Bone mineral content (BMC) and muscle cross sectional area (mCSA) were measured by quantitative computed tomography in the calf and the forearm, and leg muscle volume by MRI. Jumping height and power were assessed along with peak isometric torque in knee extension and foot dorsiflexion and plantarflexion before and after BR. Exercise was performed in supine position in 4 bouts of 1 minute twice per day on 6 days/week. Vibration frequency was 19-23 Hz, and peak forces during squat exercise were around 2000 N.

Results: Since the last 4 subjects will be re-ambulated on 16/05/2004, this abstract is based on 16/20 subjects only. An interim analysis, however, shows that the final results will be very similar to these.

Percent Changes in the Left Calf; mean (SD); Different from Ctrl: * = p<0.05, *** = p<0.001

	Ctrl	VbX
Calf mCSA	-16.5 % (3.9 %)	-8.6 % (3.9 %) ***
BMC Tibia Epiphysis	- 4.0 % (1.7 %)	-0.5 % (0.9 %) ***
BMC Tibia Metaphysis	-1.2 % (1.0 %)	-0.2 % (.7 %) *
BMC Tibia Diaphysis	-1.3 % (0.4 %)	-0.4 % (0.5 %) *

Significant group differences were found in all BMC and mCSA variables, with the VbX group having smaller changes than the Ctrl group. Bone loss from the tibia was non-significant in the VbX group. Results in the right limbs were equivalent to those obtained in the left limbs. Immediately after reambulation, jumping height had decreased by 31.4% (SD 19.8%) in the Ctrl and by 13.1 % (SD 4.2%) in the VbX group (p<0.01), and peak power declined by 26.2 % (SD 11.6 %) in the Ctrl and by 10.5 % (SD 6.4 %) in the VbX group (p<0.01).

Conclusion: Resistive vibration exercise, as applied here, appears to completely prevent bone loss from the tibia during prolonged bed rest. It is thus the first effective countermeasure found.

Disclosures: ***J. Rittweger****, ESA Grant 14431/02/NL/SH 2.*

1146

Rest-Inserted Loading, When Supplemented with IGF-1, Enhances Bone Formation and Bone mass in the Aged Skeleton. S. Srinivasan, K. A. King*, N. A. Rabaia*, M. Sheafor*, S. Warner, T. S. Gross. Orthopaedics and Sports Medicine, University of Washington, Seattle, WA, USA.

Previously, we reported that inserting rest (10-s unloaded intervals) between low-magnitude load cycles was perceived by bone cells and tissues as a potently osteogenic regimen. More recently, we observed that aging substantially blunted the osteogenic response to rest-inserted loading, primarily via deficits in mineral apposition by osteoblastic cells. We proposed that explicitly countering this deficit via systemic IGF-1 administration (given the role of IGF-1 in modulating osteoblast function), might provide a means to enhance and sustain bone formation in the aged skeleton. Here, we tested this proposal by subjecting aged female C57BL/6 mice (23 Mo) to long-term rest-inserted loading protocols, with and without IGF-1 supplements. Animals (n = 12) were subject to 50 c/d of rest-inserted loading, 3 d/wk for 9-wk. Within this cohort, one group received rhIGF-1 on loading days (2 mg/Kg, n = 7). Adaptive responses were assayed via dynamic histomorphometry and microCT imaging. By 3-wk, the tissue responses in intact contralateral tibia of mice receiving IGF-1 were no different from that in animals that did not receive IGF-1. Rest-inserted loading alone significantly ($p < 0.05$) enhanced mineralizing surface (MS, 35% compared to control) but did not significantly elevate either mineral apposition (MAR) nor bone formation rates (BFR). In contrast, rest-inserted loading, when supplemented with IGF-1, significantly enhanced MS (70%), MAR (45%) and BFR (150%) compared to controls and MAR (45%) and BFR (70%) compared to animals receiving rest-inserted loading alone. As well, similar response trends were observed at 9-wk. Finally, over the longer-term, rest-inserted loading, when supplemented with IGF-1, significantly enhanced cortical bone volume in aged mice (by 6%, $p = 0.03$). As such, while rest-inserted loading initiated bone cell activity in aged animals (increased MS), it was not sufficient to sustain activity over the short (21-d) or longer-terms (63-d). In contrast, low-dose IGF-1, when utilized as a supplement with rest-inserted loading, augmented bone mass in senescent animals, via enhanced and sustained mineral apposition by osteoblastic cells. Given these promising observations, mechanisms via which rest-inserted loading and IGF-1 interact in the aged skeleton are being explored. More broadly, our observations serve as a model for how select pharmacological agents in concert with potent mechanical stimuli such as rest-inserted loading might provide a means to counteract mechanotransduction deficits precipitated by aging.

Disclosures: ***S. Srinivasan****, None.*

1147

A School Curriculum Based Exercise Program Increase Bone Mineral Accrual in Boys and Girls During Early Adolescence - Three Years data from the POP-study (Pediatric Osteoporosis Prevention Study) - a Prospective Controlled Intervention Study in 223 Children. C. Linden*, P. Gardsell*, O. Johnell, K. Obrant, M. Karlsson. Department of Orthopaedics, Malmö University Hospital, Malmö, Sweden.

The longest reported prospective controlled intervention study with exercise in growing children which evaluate the accrual of bone mineral density (BMD) span 20 months. The purpose of this study was to evaluate the effect of an exercise intervention program within the school curriculum during the first school years, to catch also children not specifically interested in exercise, and to present the so far longest controlled follow-up data of exercise during growth. A population based cohort including 76 healthy Caucasian boys (aged 7.8 ± 0.6 at baseline) and 48 girls (aged 7.6 ± 0.6) in the only school in the Bunkeflo society outside Malmo, Sweden, were included in a school curriculum with 40 minutes physical activity every school day. Ninety nine healthy age and gender matched children (55 boys and 44 girls) in three nearby schools, subjected to the general Swedish curriculum of physical activity (60-90 min/w), served as controls. Bone mineral density (BMD; g/cm2) were measured with dual X-ray absorbtiometry (DXA) at total body (TB), lumbar spine (LS), femoral neck (FN) and leg before initiation of the intervention and after 3 years. Data is presented as mean ± SD. There were no differences in height, weight, total lean body mass, total fat content or BMD at baseline when comparing the groups. In boys, the annual gain in BMD in the LS was greater in the intervention group in comparison with the controls during the 3 year follow-up, 0.028 ± 0.011 vs. 0.023 ± 0.009, $p<0.05$. In girls, a similar effect was seen at most sites; TB 0.031 ± 0.012 vs. 0.024 ± 0.009, LS 0.038 ± 0.023 vs. 0.023 ± 0.012, FN 0.051 ± 0.031 vs. 0.036 ± 0.027 and leg 0.059 ± 0.018 vs. 0.049 ± 0.015, all $p < 0.05$ respectively. The discrepancies remained after adjusting for differences in baseline age, weight gain and pubertal development during the study. A school based exercise program within the general curriculum during the first three school years seems to increase the accrual of BMD. This is the first published intervention study that is population based and include the intervention within the school curriculum. Furthermore, it is so far the only intervention study that exceeds 20 months. This is extremely important as it is only when we can show that exercise increase the accrual of BMD during several years, that we can draw conclusions that exercise may increase peak bone mass. Based on the data in this study it seems that increased time spent in physical education classes may increase peak bone mass and subsequently can be used as a prevention strategy for osteoporosis.

Disclosures: ***C. Linden****, None.*

1148

Sciatic Denervation Increases Load-induced Cortical New Bone Formation Independently of the Sympathetic Nervous System. C. C. Chenu, R. L. De Souza*, A. A. Pitsillides, L. E. Lanyon, T. M. Skerry. Veterinary Basic Sciences, Royal Veterinary College, London, United Kingdom.

Recent studies have shown evidence for neural regulation of bone remodelling involving the sympathetic nervous system (SNS). While the SNS mediates disuse bone loss, the contribution of innervation to bone's adaptative response to its strain environment is unclear. We therefore examined the effect of sciatic denervation, which induces limb immobilisation and decreased nerve fibers density in the tibiae, on cortical bone formation in response to loading and whether the SNS is directly involved in such load-induced responses. In a first experiment, 40 female C57Bl/J6 mice, aged 10 weeks, were divided randomly into 4 groups. Two groups were submitted to surgical sciatic neurectomy (N) with and without loading, while two groups were sham-operated with and without loading. The loaded regimen used was non-invasive axial loading of the tibiae that induced 2000 µstrain on the lateral midshaft cortex. Tibiae were cyclically loaded, 3 days after surgery, at a frequency of 1 Hz, for a period of 7min, 3days/week for 2 weeks, and received calcein on the third and last days of loading. The mice were killed 18 days after surgery. Tibiae were processed for histomorphometry, and transverse confocal images from 3 diaphyseal sites were analysed. N alone induced a decrease in both periosteal and endocortical bone formation in the tibial midshaft. Both sham and N groups had increased cortical bone formation after loading, but periosteal and endosteal bone formations at the midshaft were significantly higher (+183% and +203% respectively) in the N group compared to sham. To determine the effect of loading on long-term established bone loss, another 2 groups of mice (sham-operated and N) were loaded 100 days after surgery. Similarly, N mice showed significantly increased endosteal (+137%) and periosteal (+120%) new bone formation compared to the sham-loaded group. To establish the contribution made by the SNS to those responses, another 40 female C57Bl/J6 mice, aged 10 weeks were treated daily for 3 weeks either with vehicle (C) or with guanethidine sulphate (GS) (40mg/kg/day) which chemically inactivates the SNS. Half of the C and GS groups were loaded *in vivo*, 2 weeks after the start of injections. GS alone did not affect cortical new bone formation; C and GS-treated mice had similarly increased periosteal and endosteal new bone formation in response to mechanical loading. Our data indicate that sciatic neurectomy enhances loading-related new bone formation in the tibia in the absence of loading function, and that such response cannot be attributed to SNS blockade. This suggests that the SNS does not mediate the load-induced new cortical bone formation.

Disclosures: ***C.C. Chenu****, None.*

1149

Site-Specific Osteopenia and Decreased Mechanoreactivity in Lrp5-Mutant Mice. K. Sawakami*[1], A. G. Robling[1], N. D. Pitner*[1], S. J. Warden[1], J. Li[1], M. Ai*[2], M. L. Warman[2], C. H. Turner[1]. [1]Indiana University School of Medicine, Indianapolis, IN, USA, [2]Case Western Reserve University, Cleveland, OH, USA.

LRP5 has an important role in bone mass regulation. Loss-of-function mutations in LRP5 cause osteoporosis pseudoglioma syndrome (OPPG), an autosomal recessive disorder associated with low bone mass and increased bone fragility in humans. We have found that Lrp5-mutant mice (Lrp5-/-) exhibit site-specific osteopenia, especially in mechanically relevant sites, which suggests that LRP5 regulation of bone mass might involve mechanotransduction pathways. We hypothesize that the loss-of-function mutation in LRP5 decreases responsiveness to mechanical loading. We compared Lrp5-/- mice to wild-type controls (+/+) to investigate the impact of Lrp5 on site-specific bone mass regulation and trabecular bone microarchitecture. Further, we investigated the role of Lrp5 in mechanoreactivity by subjecting Lrp5-/- and +/+ mice to *in vivo* ulnar loading. Longitudinal *in vivo* pDXA scans of the whole body from Lrp5-/- mice showed significantly less BMD from 4-week-old compared to age-matched +/+ mice ($p<0.05$). Peak BMD in the femur and, spine from Lrp5-/- mice was ~22% lower than +/+ mice, whereas BMD in the skull, a non-loaded site, was only 15% lower in Lrp5-/- mice. Detailed analysis of the trabecular bone microarchitecture of the distal femur using micro-CT revealed significantly lower BV/TV (75.1%), Tb.N (47.0%), Tb.Th (20.0%), and connectivity (82.9%) in Lrp5-/- vs. +/+, whereas the spine revealed a milder disparity in BV/TV (43.1%), Tb.N (32.6%), Tb.Th (6.8%), and connectivity (40.1%). The right ulnae of 16-week-old mice of both genotypes were loaded at three different magnitudes, 2 Hz, 60 cycles/day for 3 consecutive days. The bone formation response was measured using histomorphometry, and the relative bone formation rate (rBFR/BS) was calculated. Lrp5-/- mice were significantly less responsive to mechanical loading than +/+ mice (Figure). Lrp5-/- mice required much more mechanical strain to initiate bone formation and, once initiated, the rBFR/BS per strain unit was much smaller indicating lower mechanoreactivity. We conclude that loss-of-function mutation in Lrp5 decreases the osteogenic response following mechanical loading. The mechanism by which Lrp5 participates in skeletal mechanoreactivity remains to be elucidated.

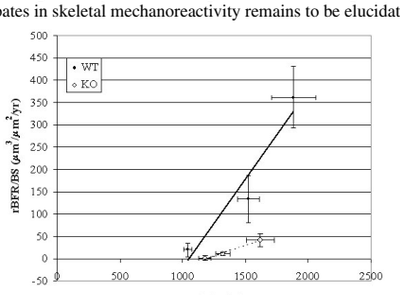

Disclosures: ***K. Sawakami****, None.*

1150

Skeletal Imaging of [^{18}F]Fluoride Ion with PET Reveals Damage- and Time-Dependent Responses to Fatigue Loading in Rats. B. A. Uthgenannt*, J. R. Rutlin*, J. S. Lewis*, M. J. Welch*, M. J. Silva. Orthopaedic Surgery, Washington University, St. Louis, MO, USA.

Fatigue damage of bone plays a critical role in stress fractures and may contribute to age-related skeletal fragility. Yet little is known about the *in vivo* bone response to fatigue damage. Our aims were to develop a model with controlled levels of bone fatigue damage, and to evaluate the *in vivo* response to a range of damage levels. Right forelimbs of anesthetized rats (4-5 mo) were fatigue loaded in axial compression (2 Hz, constant peak force); left (control) forelimbs were not loaded. During fatigue-to-fracture tests (n = 22), fracture consistently occurred after peak displacement increased 2 mm from its initial value. Subsequently, we performed sub-fracture fatigue loading to displacement increases of 0.6, 0.9, 1.3 or 1.7 mm. After loading, time-zero properties of ulnae were assessed by μCT and three-point bending. Bone damage increased with increasing fatigue displacement. No cracks were seen at the 0.6 mm displacement level, while increased cracking occurred at 0.9 to 1.7 mm ($p < 0.01$; Table). Accordingly, mechanical properties of the ulna were unchanged at 0.6 mm and decreased progressively at higher displacements ($p < 0.05$; Table). The *in vivo* damage response was assessed by quantifying uptake of a bone-binding isotope ([^{18}F]fluoride ion) using positron emission tomography (PET) 2, 4, 7, 9, 11, 14, 18, 24 and 30 days after loading. [^{18}F]fluoride uptake increased with damage level, with no change in the 0.6 mm displacement group and increases from 0.9 to 1.7 mm ($p < 0.05$; Figure). Uptake increased by day 2 and returned to normal by day 24. In conclusion: 1) we developed a model that allows modulation of the level of structural bone damage; 2) non-invasive *in vivo* monitoring using [^{18}F]fluoride PET reveals a damage-dependent response that peaks 4-11 days after loading, indicating the time of peak bone turnover. We hypothesize that the displacement-dependent increases in uptake reflect periosteal bone formation in proportion to the level of acute damage.

Displacement	0.6 mm	0.9 mm	1.3 mm	1.7 mm
Crack length per bone area (mm^{-1}) (n = 5)	0.0± 0.0	1.31± 1.53	3.09± 0.88	4.40± 0.87
Ultimate Force (Loaded/Control) (n = 7)	0.95± 0.08	0.82± 0.25	0.55± 0.11	0.39± 0.19

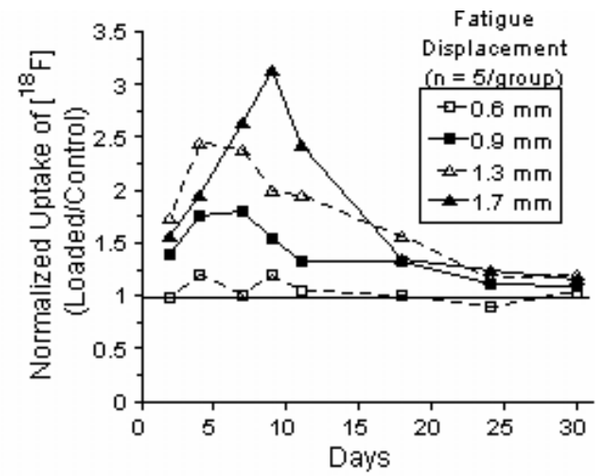

Disclosures: ***M.J. Silva****, None.*

1151

Sex-Hormone Status Is Related to Rate of Expansion of Proximal Femur Diameter in Women. S. Kaptoge[1], N. Dalzell*[1], K. Khaw*[1], T. Beck[2], N. Loveridge[1], M. Dowsett*[3], J. Reeve[1]. [1]Public Health and Medicine, U Cambridge, Cambridge, United Kingdom, [2]Radiology, JHU, Baltimore, MD, USA, [3]Biochemistry, U London, London, United Kingdom.

The femur gains structural rigidity as its subperiosteal diameter (PD) increases. Conversely cortical instability, measured as critical buckling stress, increases if the lateral cortex is located further away (d-lat) from the centre of gravity of the cross-section. The extent to which sex-hormone status determines the rates of increase in PD and d-lat is unknown. We studied the effect of sex-hormone status adjusting for key biochemical analytes, on the growth of proximal femur PD and d-lat in a random sample of 161 women aged 67-79 (mean 72y) at recruitment into the longitudinal EPIC-Norfolk study. Up to 4 hip DXA scans were performed within 8-years of follow up: 2 scans (n=152, 3.0y); 3 scans (n=134, 5.6y) and 4 scans (n=41, 7.5y). Hip structural analysis (HSA) software was used to measure PD and d-lat from the DXA scans on three narrow regions; narrow neck (NN), intertrochanter (IT) and shaft (S). The biochemical analytes measured in serum at baseline were: sex hormone binding globulin (SHBG, median=58nmol/l), estradiol (E2, median=22pmol/l), PTH, creatinine, albumin, calcium, phosphate, potassium, sodium, iron, 25(oh)vitD, 1,25(oh)vitD, Glu and Gla osteocalcin. A standard physical activity and lifestyle questionnaire was administered at baseline. A linear mixed model with random intercept and random slope for age was used to model longitudinal rates of change and associations with predictor variables. Continuous interactions with age at measurement were tested to determine if any of the predictors significantly modified the effect of aging. Aging was associated with increasing PD and d-lat and their rates of increase significantly differed ($P<0.0001$) by region: PD (NN=0.021cm/y, IT=0.014cm/y, S=0.005cm/y; all $P<0.006$); d-lat (NN=0.010cm/y, IT=0.011cm/y, S=0.002cm/y; all $P<0.027$). Baseline SHBG significantly modified the effect of aging on both PD and d-lat ($P<0.003$), with higher values being associated with faster rates of increase. Baseline SHBG values 2SD above the mean increased rates of change with age by 0.007cm/y for PD and 0.004cm/y for d-lat in all 3 regions. E2 had no significant additional effect. Higher baseline creatinine was independently associated with subsequent faster increase in d-lat with aging ($P=0.004$).

These results show large effects of SHBG on the regulation of proximal femur strength via subperiosteal expansion. Unless this is explained through an undescribed effect of SHBG acting through the SHBG receptor, it is likely that SHBG increases proximal femur expansion through reducing the bioavailability of E2.

Disclosures: ***S. Kaptoge****, None.*

1152

Volumetric Bone Mineral Density and Bone Size among Older Men in Relation to Endogenous Estradiol and Testosterone Levels. L. M. Marshall[1], L. C. Lambert[1], T. F. Lang[2], E. S. Orwoll[1]. [1]Oregon Health & Science University, Portland, OR, USA, [2]University of California, San Francisco, San Francisco, CA, USA.

Effects of androgens and estrogens on skeletal material and geometric properties among older men have yet to be clarified. We studied the associations femoral neck (FN) and lumbar spine volumetric bone mineral density (vBMD) and cross-sectional area (CSA) with bioavailable fractions of testosterone and estradiol among 1,256 US men ages ≥65 years sampled from the Osteoporotic Fractures in Men (MrOS) Study. Estradiol, testosterone, SHBG and albumin concentrations were measured with sensitive assays in serum stored from a fasting blood draw at baseline. Bioavalable fractions of testosterone (BioT) and estradiol (BioE) (nM/l) were derived from mass action equations. The skeletal measures were obtained from quantitative computed tomography scans of the FN and of the L1 vertebral body exclusive of the spinous and transverse processes. FN measures were: total and trabecular vBMD (g/cm^3) and CSA (cm^2). L1 vertebral body measures were: trabecular vBMD (g/cm^3) and CSA (cm^2). The relations of vBMD and CSA at each anatomic site with BioT and BioE were estimated with generalized linear models. Each model included terms for BioE, BioT, age, race, study site, height, lean body mass and fat mass. Total and trabecular vBMD in the FN and L1 vertebra were positively associated with BioE, but were unrelated to BioT (Table). In both the FN and L1 vertebra, CSA was inversely related to BioE. BioT was positively associated with FN CSA, but was unrelated to L1 vertebral body CSA. Notably, associations that were statistically significant explained a very small portion of variance in the skeletal measures (partial $r^2 \leq 0.012$). In summary, this cross-sectional study among older men demonstrated that BioE was consistently associated with skeletal measures in the FN and lumbar spine, but BioT was not. Specifically, BioE was strongly associated with the measures of trabecular vBMD, suggesting inhibition of trabecular bone loss. Possibly divergent effects of BioE and BioT on CSA were observed, especially in the FN. These effects, although small, are consistent with the hypothesis that BioT promotes, but BioE inhibits, periosteal apposition. The clinical importance of these small but statistically significant associations warrants further study with longitudinal data.

Table. Relation of femoral neck and lumbar spine vBMD and CSA with sex steroid hormones.

	Bioavailable Estradiol (nM/l)			Bioavailable Testosterone (nM/l)		
	β	p-value	partial r^2*	β	p-value	partial r^2*
vBMD (g/cm^3)						
FN Total	0.21	0.05	0.003	0.0001	0.91	0.00
FN Trabecular	0.22	0.01	0.006	-0.0002	0.76	0.00
L1 Trabecular	0.28	<0.0001	0.012	0.0001	0.96	0.00
CSA (cm^2)						
Femoral Neck	-5.04	0.08	0.002	0.04	0.03	0.003
L1 Vertebra	-6.62	0.05	0.002	0.02	0.26	0.001

* partial r^2 indicates the proportion of variance in the dependent variable explained by the sex hormone variable independent of other factors. Abbreviations: vBMD=volumetric BMD, CSA=cross-sectional area, FN=femoral neck, β=regression coefficient.

Disclosures: ***L.M. Marshall****, None.*

1153

Relationship of Bone Density, Geometry and Strength Indices to Patterns of Fragility Fractures in the Peripheral Skeleton. B. L. Riggs[1], L. J. Melton[2], E. J. Atkinson*[3], A. L. Oberg*[3], M. L. Bouxsein[4], S. Khosla[1]. [1]Endocrinology, Mayo Clinic, Rochester, MN, USA, [2]Clinical Epidemiology, Mayo Clinic, Rochester, MN, USA, [3]Biostatistics, Mayo Clinic, Rochester, MN, USA, [4]Orthopedic Biomechanics Laboratory, Beth Israel Deaconess Medical Center, Boston, MA, USA.

Although the relationship of decreases in volumetric bone mineral density (vBMD) to risk of fragility fractures (fx) is well established for the spine and hip, there is limited information about the distal radius (DR) and distal tibia (DT), the two common sites of fragility fx in the peripheral skeleton. We assessed vBMD (g/cm^3), geometry and indices of bone strength using peripheral quantitative computed tomography (Densiscan, Scanco, Inc.) at the sites of these fractures in age-stratified, population samples. The table gives mean±SEM for 75 young (20 - 40 yrs) females (YF), 75 young males (YM), 141 elderly (≥65 yrs) females (EF), and 121 elderly males (EM). MOI (cm^3) reflects the distribution of bone relative to a central axis whereas ΣEA (N) and ΣEI (N x cm) estimate the resistance of bone to compressive and bending forces, respectively, and incorporate both material and geometric properties. In this population, we previously found that the incidences of DR and DT fx were 10- to 20-fold higher in F than M, and, although estimated trauma was similar, that DR fx were 2- to 3-fold higher than DT fx.

Variable	Total vBMD	MOI	ΣEA	ΣEI
DR YF	0.58±.08	1.3±0.3	3.3±0.5	9.7±2.2
DR EF	0.47±.10	1.5±0.5	2.8±0.6	8.8±2.4
DR YM	0.64±.08	2.7±0.8	5.2±0.7	20.8±4.9
DR EM	0.52±.10	3.4±1.3	4.7±0.9	21.3±6.4
DT YF	0.53±.07	8.4±1.8	8.3±1.1	56.4±11.4
DT EF	0.43±.08	9.5±3.0	7.0±1.4	48.8±13.3
DT YM	0.58±.06	15.0±3.8	12.1±1.6	104.7±22.5
DT EM	0.50±.08	16.3±5.0	10.6±1.7	95.2±22.2

For M vs F, vBMD for DR or DT was only ~10% higher. However, except for ΣEI at DT, the indices of bone strength (MOI, ΣEA and ΣEI) were much higher (51% to 114%) in M vs F and were even higher (125% to 646%) for the DT vs DR scanning sites. Most of these indices declined by only 9% to 15% with aging. By ANOVA, all sex differences (except for DR at EI) and scanning site differences (except for ΣEI at DT) were significant (P<0.001). Conclusions: 1) Superior geometric properties achieved in pubertal growth, rather than large differences in vBMD, may explain why late in life that males have a lower incidence of fx at DT and DR than females and why fx at DT are less frequent than at DR; and 2) Biomechanical indices of bone strength, which now can be calculated from QCT scans, will play an increasingly important role in assessing fx risk in the future.

Disclosures: ***B.L. Riggs****, None.*

1154

Postmenopausal Hormone Therapy and Body Composition --- Results from the Women's Health Initiative E + P Trial. Z. Chen[1], T. Bassford*[1], S. B. Green*[2], M. Leboff[3], K. L. Margolis*[4], A. LaCroix[5], R. D. Jackson[6], J. Cauley[7], M. L. Stefanick*[8]. [1]University of Arizona, Tucson, AZ, USA, [2]Arizona Cancer Center, Tucson, AZ, USA, [3]Brigham and Women's Hospital, Boston, MA, USA, [4]Hennepin County Medical Center, Minneapolis, MN, USA, [5]Fred Hutchinson Cancer Research Center, Seattle, WA, USA, [6]The Ohio State University, Columbus, OH, USA, [7]University of Pittsburgh, Pittsburgh, PA, USA, [8]Stanford School of Medicine, Stanford, CA, USA.

The primary objective of this study is to test the hypothesis that treatment with estrogen plus progestin (E+P) alters body composition among postmenopausal women from the randomized, controlled clinical trial of E +P in the Women's Health Initiative (WHI). Only women with body composition measurements at baseline and year three were included in the analysis. Among them, 437 were women in the treatment group and 398 were in the placebo group. Body composition was assessed by dual-energy x-ray absorptiometry. The mean age at baseline was 62.9 and 63.4 years for the treatment and placebo group respectively. On average, women in this study were 13.8 years past menopause and approximately 82% of them were from a non-Hispanic white ethnic background. There was no difference in baseline measurements for the treatment and placebo groups respectively: 74 kg vs. 75 kg in body weight, 37.9 kg vs. 38.5 kg in total body lean mass, 32.7 kg vs. 33.0 kg in total body fat mass, 1.266 to 1.295 in trunk to leg fat mass ratio, 53.2% vs. 53.4% in percent lean mass, and 44% vs. 43.8% in percent fat mass.

Absolute Changes between Year Three and Baseline

Body Composition	E +P (N = 437)	Placebo (N = 398)	Difference	95% CI		p value
				Lower	Upper	
Weight (kg)	0.59	0.10	0.49	-0.48	1.46	0.320
BMI (kg/m^2)	0.43	0.14	0.29	-0.02	0.60	0.070
Lean Mass (g)	-39	-438	399	158	640	0.001
Fat Mass (g)	286	356	-70	-629	489	0.810
T/L Fat Ratio*	-0.025	0.004	-0.029	-0.047	-0.010	0.003
% Lean Mass	-0.16	-0.47	0.31	-0.14	0.76	0.180
% Fat Mass	0.04	0.44	-0.40	-0.85	0.06	0.090

* Trunk to Leg Fat Mass Ratio

In comparison to women on placebo, women in the treatment group had significantly less loss in lean tissue mass (p = 0.001) and a small but significant change in the distribution of body fat as indicated by the reduced trunk to leg fat mass ratio (p = 0.003). Previous results from this WHI E+P trial indicate that E+P treatment significantly prevents fractures. It is possible that the reduced loss of lean tissue mass by E+P treatment contributed to the lower fracture risk through maintaining bone mass and balance.

In conclusion, E+P treatment has significant positive effects on body composition by reducing both lean tissue mass loss and truck to leg fat mass ratio. Whether the reduced fracture risk by E+P is partially mediated through the effect of E+P on body soft tissue composition remains to be determined.

Disclosures: ***Z. Chen****, None.*

1155

Labyrinthectomy Decreases Bone Mineral Density in the Femoral Metaphysis in Rats. R. Levasseur[1], O. Etard*[2], J. P. Sabatier*[3], J. Corvisier*[2], C. Potrel-Burgot*[4], A. Réber*[5], P. Denise*[2]. [1]Rheumatology CHU, Caen, France, [2]Physiologie, Faculté de Médecine, Caen, France, [3]Nuclear Medicine CHU, Caen, France, [4]Cetor, Faculté de Médecine, Caen, France, [5]UFR Sciences, Rouen, France.

Recently, it has been shown that sympathetic nervous system regulates bone remodeling (Takeda et al. Cell 111:305, 2002. Levasseur et al. Joint Bone Spine 70:515, 2003). As it is well known that vestibular system influences the sympathetic system (Yates et al. Brain Res Rev 17:51, 1992) it might also affect bone remodeling. To answer this question, we started an experiment on 14 pigmented male adult rats (DA/HAN). Seven of them were bilaterally labyrinthectomized, the seven others were sham-operated. Bone mineral density (BMD, g/cm²) was measured by dual energy X-rays absortiometry (Hologic QDR 4500A) before and 30 days after vestibular lesions, in the distal femoral metaphysis (DFM), the femoral cortical diaphysis (CD), the lumbar spine (SP) and the whole body (WB). Body weight (BW, g), lean mass (LM, g) and fat mass (FM, g) were also measured in each rat. Comparatively to sham-operated rats, labyrinthectomized animals showed a significantly reduced BMD in distal femoral metaphysis (P=0.007) : the changes in BMD between day 0 (D0) and day 30 (D30) were +3% for controls and -13.9% for labyrinthectomized rats. BMD gain in femoral CD was also significantly decreased in labyrinthectomized rats compared to sham operated (+10.4 vs + 16.5, P=0.015). No significant difference between the 2 groups was observed in the whole body or in the lumbar spine BMD (P=0.12 an P=0.06, respectively). The body weight, the lean mass and the fat mass of control and bilaterally labyrinthectomized rats were not different at D0 nor at D30 (P=0.39, P=0.20, P=0.89, respectively). The major finding of the present study is that bilateral labyrinthectomy in rats decreases bone mineral density of the distal femoral metaphysis but not of the spine or of the whole body. These results suggest that the peripheral vestibular apparatus is a modulator of bone mass and more specifically in weight bearing bone. This bone loss is not due to reduced motor behavior since the evolution of lean mass is the same between the 2 groups during the experiment and it has been also recently demonstrated that the tonic muscular activity is not decreased after vestibular lesions (Kasri M et al, Exp Neurol. 185:143, 2004). We suggest that the vestibular system is involved in the control of bone remodeling via the sympathetic system and that the vestibular system could be implicated in the osteoporosis observed during space flight.

Disclosures: ***R. Levasseur****, None.*

1156

A Cellular Mechanism for Dietary Protein-induced Increases in Calcium Absorption. S. Busque*[1], J. Kerstetter[1], J. Geibel*[2], K. Insogna[2]. [1]School of Allied Health, U of CT, Storrs, CT, USA, [2]Yale University, New Haven, CT, USA.

Several studies indicate that increasing the level of dietary protein increases the efficiency of intestinal calcium (Ca) absorption. The basis for this is unclear but modulation of the calcium sensing receptor (CaSR) by amino acids in the stomach could potentially enhance gastric acid secretion, improving ionization and bioavailability of dietary Ca. When over-expressed in kidney cells, the CaSR is allosterically activated by amino acids at sub-stimulatory concentrations of extracellular Ca. It has recently been shown that Ca stimulates acid production in gastric parietal cells. To determine if the endogenously expressed parietal cell CaSR is also influenced by amino acids, we examined the effect of L-phenylalanine (phe) on luminal pH in isolated rat stomachs. Rats were fasted for 24h prior to experimentation to reduce basal acid secretion, anesthetized, and a total gastrectomy was performed. One cc of non-buffered isotonic saline was infused, and the stomach incubated for 60 min at 37ºC in oxygenated Ringers, pH 7.4. In 9 stomachs incubated in buffer alone, mean luminal pH was 4.07±0.37, and in 9 separate preparations in buffer plus 50 mM L-phe, the mean pH was significantly lower, 2.69±0.22 (p=0.003). In contrast, 50 mM D-phe had no effect on gastric pH. To monitor intracellular pH or calcium, individual rat gastric glands were hand-dissected and loaded with the pH sensitive dye BCECF or Fluo-3 respectively. Proton extrusion by parietal cells was monitored by measuring the recovery of cytosolic pH as an index of H,K-ATPase activity, following intracellular acidification with 20mM NH_4Cl and subsequent perfusion with a Na free buffer containing 2 mM Ca or 2 mM Ca plus 30 mM L-phe. The rate of cellular pH recovery, measured as the rise in cytosolic pH over time, was significantly more rapid in cells exposed to amino acids (0.08±0.03 pH units/min) than buffer alone (0.04±0.01; p<0.0001). The effect of amino acids was lost when the Ca concentration in the buffer was lowered to 0.5 mM. In contrast, blocking the H2 receptor with cimetidine did not attenuate the recovery of cytosolic pH (0.07±0.01). Furthermore, cytosolic calcium increased by 16% (p<0.0001) over baseline upon perfusion with amino acids. We conclude that L-phe directly stimulates parietal cell acid secretion by increasing H,K-ATPase activity in the absence of neuronal/hormonal stimulation. The sterio-specificity, dependence on extracellular calcium, and induced rise in cytosolic Ca are consistent with the conclusion that L-phe is an allosteric activator of the CaSR. These data identify a cellular mechanism by which dietary protein enhances Ca absorption via activation of the CaSR on parietal cells.

Disclosures: ***S. Busque****, None.*

1157

Gs-alpha Expression Is Biallelic in Normal and Fibrous Dysplastic Bone. M. Riminucci[1], N. Cherman*[2], K. Holmbeck*[2], S. Michienzi*[3], L. Travaglini*[3], P. Bianco[4], P. Gehron Robey[2]. [1]Experimental Medicine, University of L'Aquila, L'Aquila, Italy, [2]NIDCR, NIH, DHHS, Bethesda, MD, USA, [3]Parco Scientifico Roma San Raffaele, Rome, Italy, [4]Experimental Medicine and Pathology, University La Sapienza, Rome, Italy.

Activating mutations of the Gs-alpha gene (GNAS) cause a wide range of pathological phenotypes (McCune-Albright Syndrome (MAS), isolated fibrous dysplasia (FD) and endocrine lesions, Mazabraud's syndrome) each of which is characterized by a remarkable heterogeneity of clinical expression. Although the postzygotic nature of the mutation provides an immediate explanation for the clinical variability of Gs-alpha related diseases, the contribution of epigenetic mechanisms, such as imprinting, can not be excluded. Clinical evidence, in fact, suggests that Gs-alpha has a predominant maternal expression in some tissues such as pituitary and thyroid (although different studies have failed to show promoter methylation) and recently it has been shown that imprinting of Gs-alpha is lost during neoplastic growth of pituitary cells in some somatotroph adenomas.

FD is a skeletal disease that reflects the impact of activating Gs-alpha mutations in bone marrow stromal cells. Skeletal involvement in FD patients ranges from localized, clinically silent lesions to a diffuse severely crippling disorder. In this study, we asked whether Gs-alpha is imprinted in bone marrow stromal cells, and if imprinting affects the expression of the mutated allele in FD lesions. To address this issue, we took advantage of the polymorphism (ACT/ATT) within exon 5 of GNAS, which allows recognition of the allelic origin of the Gs-alpha transcript in heterozygous patients. FD patients (N=16) were analyzed by PCR amplification of the relevant gDNA fragment, followed by digestion with the restriction enzyme, FokI (which recognizes the ACT allele), and DNA sequencing. Gs-alpha mRNA was analyzed in stromal cells isolated from 3 informative (polymorphic) patients. Clonal populations of normal and mutant cells were grown in order to separately analyze the imprinting status of Gs-alpha in cells with the normal and disease genotype. Using FokI digestion followed by subcloning and DNA sequencing, we demonstrated that Gs-alpha mRNA is biallelic in all the samples analyzed, with no difference between normal and mutant cells. Our work shows for the first time the lack of imprinting of Gs-alpha in the stromal component of the bone microenvironment, which gives rise to bone, and excludes any major role for Gs-alpha imprinting in the clinical expression of FD.

Disclosures: ***M. Riminucci****, None.*

1158

PTH (1-34) Accelerates Osteoblast Differentiation via a PLC-Independent PKC Pathway. D. Yang, J. Guo, F. R. Bringhurst. Endocrine Unit, Massachusetts General Hospital and Harvard Medical School, Boston, MA, USA.

PTH regulates osteoblastic function by activating PTH/PTHrP receptors (PTH1Rs), which trigger several signaling pathways in parallel. In addition to adenylyl cyclase (AC)/PKA, PTH1Rs activate PKCs via both PLC-dependent and PLC-independent mechanisms. To probe the biological function of the PLC-independent PTH1R PKC pathway in osteoblasts, we employed mutant PTH peptide analogs that can selectively activate only subsets of these various signaling pathways .

An osteoblastic cell line ("wt9') stably expressing PTH1Rs (80,000-100,000 sites/cell) was generated by stable transfection of PTH1R cDNA into F1-14 PTH1R-null clonal osteoblasts. To control the pattern of PTH1R signaling, two PTH(1-34) analogs were employed: [G1,R19]hPTH(1-28) ("GR1-28"), which cannot activate PLC and also lacks the 29-34 domain of hPTH(1-34) required for PLC-independent PKC activation and [G1,R19]hPTH (1-34) ("GR1-34"), which lacks only PLC signaling but retains PLC-independent PKC activity. Both analogs stimulated cAMP accumulation comparably to hPTH(1-34) at a high concentration (100 nM) but neither GR1-28 nor GR1-34 could activate PLC, even at a concentration of 1000 nM (at which PTH(1-34) induced a 4-fold stimulation).

We observed that several PKC isoforms -beta I, gamma, delta, epsilon and zeta - were expressed by wt9 cells, of which PKC-delta and PKC-epsilon were phosphorylated within minutes in response to PTH(1-34). Isoform-specific western blots and pulldown kinase assays showed that both PTH(1-34) and GR1-34, but not GR1-28 , could increase the phosphorylation and activation of PKC-delta, suggesting that these were mediated by a PLC-independent receptor signaling event .

To investigate PTH1R signals involved in regulating osteoblast differentiation, PTH peptides (100 nM) were applied to wt9 cells every 48 hours. On day 16, von Kossa stain and calcium mass measurements showed that PTH(1-34) and GR1-34, but not GR1-28, could increase both the formation of calcified nodules and the total amount of calcium deposited in the cell cultures.

We conclude that PTH1R activation of AC (as by GR1-28) is not sufficient to phosphorylate and activate PKC-delta or to increase differentiation by intermittent peptide administration in osteoblasts. The ability of GR1-34 to mimic these actions of PTH(1-34) points to a key role for AC- and PLC-independent PTH1R signaling, possibly involving activation of PKC-delta, in control of osteoblast differentiation.

Disclosures: ***D. Yang****, None.*

1159

Measles Virus Nucleocapsid Protein (MVNP) Increases p62 and IKK-gamma Expression to Enhance TNF-α-induced Osteoclast (OCL) Differentiation and Activation in Paget's disease. M. Ito[1], N. Kurihara[1], S. V. Reddy[1], G. D. Roodman[2]. [1]Medicine-Hematology/Oncology, University of Pittsburgh, Pittsburgh, PA, USA, [2]Medicine-Hematology/Oncology, University of Pittsburgh and Dept. of Veterans Affairs Medical Center, Pittsburgh, PA, USA.

Osteoclasts (OCL) from Paget's patients (PD) are abnormal and contain MVNP transcripts. Furthermore, human OCL precursors transfected with MVNP demonstrate many features of pagetic OCL. We previously reported that OCL precursors from patients with Paget's disease are hyperresponsive to RANKL and 1,25-$(OH)_2D_3$ and that expression of MVNP in normal OCL precursors increases their responsivity to RANKL and 1,25-$(OH)_2D_3$. We recently found that OCL precursors from PD were also hyper-responsive to TNF-α. Since TNF-α does not induce RANKL, we determined if MVNP could also increase TNF- responsivity of OCL precursors. To test this hypothesis, NIH3T3 cells were used as surrogate for OCL precursors and transfected with MVNP or empty vector (EV). Western blot analysis showed that TNF-α treatment of empty vector (EV)-transfected NIH3T3 cells increased the expression of IKK-γ approximately 40% compared to media alone. Treatment of MVNP-transfected NIH3T3 cells with TNF-α increased both p62 and RIP expression levels approximately 50% but increased IKK-γ 5-fold compared to results with EV-transfected cells. IKK-γ is an important regulatory of NFκB signaling induced by TNF and is absolutely required for IKK activation by TNF. Consistent with these results in NIH3T3 cells, MVNP-transfected normal human CFU-GM showed increased responsivity to TNF-α and increased expression of p62 and IKK-γ approximately 2 fold. We then determined if these effects resulted in enhanced NF-κB signaling. We observed a 1.4-fold increase in basal NF-κB reporter gene activity in MVNP-transfected NIH3T3 cells compared to EV-transfected cells and this was increased 2.1- to 2.6-fold when MVNP-transfected cells were treated with TNF-α. Since TNF-α also stimulates the MAPK signaling pathway via TRAF2 to activate OCL, we then determined if TNF-α increased MAPK signaling in MVNP-transfected NIH3T3 cells, by Western blot analysis of phospho-MAPK (p42/44). TNF-α increased the phosphorylation of MAPK in MVNP-transfected NIH3T3 cells by 50% compared with EV-transfected cells within 15 minutes after addition of TNF-α. These results demonstrate that MVNP increases TNF-α induced OCL differentiation and activation by increasing NFκB signaling through increased expression of p62, and IKK-γ and increased MAPK signaling. These results suggest that MVNP's effects on TNF-a signaling may contribute to the increased OCL formation in PD.

Disclosures: ***M. Ito****, None.*

1160

A Mutation in FGF-23 Gene Enhances the Processing of FGF-23 Protein and Causes Tumoral Calcinosis. K. Araya*[1], S. Fukumoto[2], R. Backenroth*[3], Y. Takeuchi[2], K. Nakayama[2], N. Ito*[2], Y. Yamazaki*[4], T. Yamashita[4], J. Silver[3], T. Igarashi*[1], T. Fujita*[2]. [1]Department of Pediatrics, University of Tokyo Hospital, Tokyo, Japan, [2]Division of Nephrology & Endocrinology, Department of Medicine, University of Tokyo Hospital, Tokyo, Japan, [3]Minerva Center for Calcium and Bone Metabolism, Nephrology and Hypertension Services, Hebrew University Hadassah Medical Center, Jerusalem, Israel, [4]Pharmaceutical Research Laboratories, KIRIN Brewery, Takasaki, Japan.

Tumoral calcinosis is a disease characterized by high serum phosphate and 1,25-dihydroxyvitamin D (1,25D), and ectopic calcification. These clinical features are mirror images of several hypophosphatemic rickets/osteomalacia including autosomal dominant hypophosphatemic rickets/osteomalacia and tumor-induced osteomalacia. Recently, FGF-23 was shown to play important roles in the development of these hypophosphatemic diseases. It was also shown that full-length FGF-23 is processed between Arg^{179} and Ser^{180} and this processing abolishes its effect to cause hypophosphatemia. Two kinds of assay for FGF-23 have been developed. A full-length assay detects only biologically active full-length FGF-23 and a C-terminal assay measures both full-length and processed C-terminal fragment of FGF-23. We have examined the involvement of FGF-23 in tumoral calcinosis. A twenty-eight year old patient of consanguineous parents had had subcutaneous lumps. He presented with intermittent claudication and a plain film of his legs showed an angiogram-like picture. Laboratory tests showed hyperphosphatemia of 5-10 mg/dl (normal 3 - 5), hypophosphaturia with TRP of 96-100% (80 - 90) and high serum1,25D levels of 89 pg/ml (15-55). Serum calcium, alkaline phosphatase, pH and creatinine were all normal. Two brothers had a similar syndrome and he was diagnosed as having tumoral calcinosis. Serum level of FGF-23 was low normal (11.0 pg/ml: normal 10 - 50) by full-length assay, but extremely high (5874 RU/ml: < 150) by C-terminal assay. Direct sequencing of FGF-23 gene revealed a homozygous S129F mutation. Immunoprecipication followed by Western blotting detected both full-length and processed N- and C-terminal fragments of FGF-23 when wild-type FGF-23 was expressed in vitro. However, only the C-terminal fragment but not full-length and N-terminal fragment of FGF-23 was detected when this mutant FGF-23 was expressed. These results suggest that this mutation in FGF-23 gene enhances the processing of FGF-23 protein. The biochemical features of this patient are similar to those with FGF-23 knockout mice suggesting that activity of full length FGF-23 is essential for normal phosphate and vitamin D metabolism in man.

Disclosures: ***S. Fukumoto****, None.*

1161

Direct Binding of MEPE by PHEX via the ASARM-motif Is Confirmed by Surface Plasmon Resonance: Implications for Impairment of Mineralization in X-linked Rickets. P. S. N. Rowe[1], I. R. Garrett[2], P. M. Schwarz*[1], D. L. Carnes[1], E. M. Lafer*[1], G. R. Mundy[3], G. E. Gutierrez[2]. [1]Periodontics, University of Texas HSC, San Antonio, TX, USA, [2]Osteoscreen, San Antonio, TX, USA, [3]Cell & Struc, UTHSCSA, San Antonio, TX, USA.

Impaired mineralization is a key feature of X-linked rickets (HYP) but the mechanisms responsible remain unclear. MEPE and proteases are elevated and PHEX is defective. PHEX prevents proteolysis of MEPE and potentially the release of a protease-resistant MEPE-ASARM-peptide (mineralization inhibitor). We hypothesize that binding of MEPE by PHEX regulates mineralization and in HYP, mutated-PHEX increases ASARM-peptide release, thereby impairing mineralization. To test this, we examined 1. whether PHEX binds specifically to MEPE; 2. whether the binding involves the ASARM-motif; and 3. whether ASARM-peptide affects mineralization *in-vivo.*

ASARM-peptide and etidronate mediated mineralization-inhibition *in-vivo* and *in-vitro* were determined by quenched calcein-fluorescence in hind limbs and calvariae in mice and by histological Sanderson stain. Protein interactions between MEPE and soluble PHEX (secPHEX) were measured using Surface-Plasmon-Resonance (SPR) and SPR experiments were performed on a Biacore 3000 high performance system. Briefly, secPHEX, MEPE and control protein (IgG) were immobilized on a Biacore CM5 sensor-chip. Pure secPHEX was then injected at different concentrations and interactions with immobilized proteins measured. To determine MEPE sequences interacting with secPHEX the inhibitory effects of MEPE-ASARM-peptides (phosphorylated and nonphosphorylated), control peptides and MEPE-RGD-peptides on secPHEX binding to chip-immobilized MEPE were measured.

Subcutaneous administration of ASARM-peptide resulted in marked quenching of fluorescence in calvariae and hind-limbs relative to vehicle controls indicating impaired mineralization. Similar results were obtained with etidronate. Sanderson-stained calvariae also indicated a marked increase in unmineralized osteoid with ASARM-peptide and etidronate groups. A specific, dose-dependent and Zn-dependent protein-interaction between secPHEX and immobilized-MEPE occurs (EC_{50} of 553 nM). The MEPE PO4-ASARM-peptide inhibited the PHEX-MEPE interaction (K_{Dapp} = 15 uM and $B_{max/inhib}$ = 68%). In contrast, control and MEPE-RGD-peptides had no effect.

We conclude that the ASARM-peptide impairs mineralization *in vivo*, and that PHEX and MEPE binding involves the carboxy-terminal MEPE-ASARM-motif. The binding of MEPE and ASARM-peptide by PHEX and the finding that this peptide inhibits mineralization in-vivo, may explain why loss of functional PHEX results in defective mineralization in HYP.

Disclosures: ***P.S.N. Rowe****, None.*

1162

Genetic Dissection of Phosphate- and Vitamin D-Mediated Regulation of Circulating Fgf23 Concentrations. X. Yu*[1], Y. Sabbagh[2], S. I. Davis*[1], M. B. Demay[2], K. E. White[1]. [1]Department of Medical and Molecular Genetics, Indiana University School of Medicine, Indianapolis, IN, USA, [2]Endocrine Unit, Massachusetts General Hospital and Harvard Medical School, Boston, MA, USA.

The mechanisms that control serum phosphate are complex and our current models are incomplete. Fibroblast growth factor-23 (FGF23) is a phosphaturic factor that plays critical roles in phosphate and vitamin D metabolism. Previous studies demonstrated that serum Fgf23 increases in mice after treatment with 1,25-dihydroxy vitamin D, however potential concomitant changes in serum phosphate may contribute to this change in circulating Fgf23. The goal of the present studies was to examine the mechanisms that direct the vitamin D-phosphate-FGF23 homeostatic axis. To test the regulation of Fgf23, wild type (WT) mice were fed either standard (0.67% phosphorus) or low-phosphate (0.02%) diets, followed by determinations of serum phosphate, and intact Fgf23, measured by ELISA. WT mice on standard diet had a mean serum phosphate of 9.5±0.5 mg/dl and an Fgf23 concentration of 99±18 pg/ml, whereas mice on the low-phosphate diet had a serum phosphate of 3.0±0.3 mg/dl (P<0.01), and a markedly suppressed Fgf23 value of 11±5.0 pg/ml (P<0.01). We then examined vitamin D receptor knockout (VDR-/-) mice, a model for Hereditary Vitamin D Resistant Rickets, characterized by resistance to 1,25-dihydroxy vitamin D, hypocalcemia, hypophosphatemia, and hyperparathyroidism. After 35 days on standard diet, WT and VDR+/- mice had comparable Fgf23 values of 57±19 and 76±21, respectively, whereas Fgf23 was undetectable in VDR-/- mice. Following one year on standard diet, WT mice had an Fgf23 of 173±34 pg/ml and levels in VDR-/- mice remained low at 8.5±8.9 pg/ml (P<0.02). To determine the relative contributions of hypophosphatemia and 1,25-dihydroxy vitamin D resistance to the suppression of Fgf23 in the VDR -/- mice, Fgf23 levels were measured in VDR-/- mice placed on a diet that normalizes serum calcium and phosphorus levels (1.25% phosphorus, 2% calcium and 20% lactose). This supplemented diet increased the Fgf23 levels of the control VDR+/- mice to 465±264pg/ml, and increased the Fgf23 levels of VDR-/- mice to 484±182 pg/ml (P<0.9 vs VDR+/-). In summary, serum Fgf23 is suppressed in diet-induced hypophosphatemia, as well as in hypophosphatemia associated with hyperparathyroidism secondary to VDR ablation. Normalization of serum phosphate by diet in VDR-/- mice increases serum Fgf23. Thus, our results demonstrate that Fgf23 is suppressed during hypophosphatemia, protecting against renal phosphate loss. Finally, the regulation of serum Fgf23 levels by phosphate is independent of the genomic effects of vitamin D.

Disclosures: ***K.E. White****, Kirin Pharmaceutics 7.*

1163

Calcium Receptor Haploinsufficiency Increases Mammary PTHrP Secretion, Reduces Mammary Calcium Transport and Accelerates Bone Loss During Lactation. J. VanHouten[1], L. Ardeshirpour*[1], E. Brown[2], M. Pollak[2], J. Wysolmerski[1]. [1]Yale Medical School, New Haven, CT, USA, [2]Brigham and Women's Hospital, Boston, MA, USA.

Calcium-sensing receptor (CaR) expression is dramatically induced on mammary epithelial cells (MECs) at the start of lactation and extracellular calcium inhibits PTHrP production and stimulates transepithelial calcium transport by lactating MECs. In order to determine if these effects were mediated by the CaR, we studied the effects of CaR haploinsufficiency on PTHrP secretion and milk calcium content in lactating heterozygous CaR-null ($CaR^{+/-}$) mice.

$CaR^{+/-}$ mice lactated without difficulty and their mammary glands displayed normal histology and expression of milk protein genes. The growth curves of pups suckling $CaR^{+/-}$ mothers were indistinguishable from those suckling WT mothers suggesting that overall milk production was normal. As measured by real-time RT-PCR, CaR mRNA levels were reduced by 50% in the mammary glands of lactating $CaR^{+/-}$ mice as compared to WT littermates. This led to a doubling of PTHrP mRNA levels in the $CaR^{+/-}$ glands. PTHrP secretion was also elevated; the PTHrP concentration in milk from CaR $^{+/-}$ mice was 41.7±8.0 nM as compared to 20.5±4.3 nM in milk from WT mice. In contrast, milk calcium content was decreased in $CaR^{+/-}$ mice by 25%. Finally, $CaR^{+/-}$ mice lost more bone during lactation than control mice. At the onset of lactation spine, femur and total body bone mineral density (BMD) were similar in $CaR^{+/-}$ mice and controls. Both types of mice lost significant bone by day 12 of lactation. However, by this point BMD at all three sites was statistically lower in $CaR^{+/-}$ mice as compared to controls, suggesting higher rates of bone loss in these mice.

In summary, haploinsufficiency for the CaR results in a reduction of CaR mRNA expression within the lactating mammary gland. This is associated with an increase in PTHrP gene expression and protein secretion by MECs. CaR deficiency also leads to a reduction in milk calcium content and accelerated bone loss during lactation. These data provide genetic evidence that the mammary gland becomes a calcium-sensing organ during lactation and that CaR signaling regulates PTHrP production and transepithelial calcium transport by MECs. In response to a perceived calcium deficiency, the lactating mammary glands of $CaR^{+/-}$ mice reduce the transport of calcium into milk and produce more PTHrP. The accelerated loss of bone by the $CaR^{+/-}$ mice suggests that some of this excess PTHrP circulates and acts to mobilize more calcium from the skeleton. Expression of the CaR thus allows the lactating mammary gland to act as an "accessory parathyroid" and integrate systemic calcium and bone metabolism with milk production.

Disclosures: ***J. VanHouten****, None.*

1164

Modulation of Bone Remodeling by Osteoprotegerin in Mice Expressing a Constitutively Active PTH/PTHrP Receptor. R. Chiusaroli[1], M. C. Knight*[1], P. Kostenuik[2], E. Schipani[1]. [1]Medicine, MGH-Harvard Medical School, Boston, MA, USA, [2]Metabolic Disorders Research, Amgen Inc., Thousand Oaks, CA, USA.

A transgenic mouse model (CL2) in which a constitutively active PTH/PTHrP receptor (PPR) was expressed in cells of the osteoblast lineage has been recently reported. The Cl2 phenotype is characterized by exuberant increase in both bone formation and resorption, with the net result of increased trabecular bone and cortical porosity. To study whether bone resorption is a prerequisite for PPR-induced bone formation, we injected adult CL2 mutant mice and wild-type (wt) control littermates with recombinant human osteoprotegerin (OPG-Fc) for 10 days. Treatment of both wt and CL2 mice with OPG-Fc resulted in the significant reduction in osteoclast numbers. In situ hybridization also revealed significant reductions in TRAP and MMP9 mRNA with OPG-Fc treatment. These changes were also associated with suppression of osteoblastic markers such as osteocalcin, osteopontin and collagen type I mRNAs in both Cl2 and wt mice treated with cOPG. Histomorphometric analysis revealed significant reductions in osteoblast number and activity in the trabecular bone of both wt and CL2 animals treated with OPG-Fc. Despite the impairment of bone formation, trabecular bone volume was not reduced in mice treated with OPG-Fc in comparison to vehicle-treated mice. The suppression of bone formation was likely to be an indirect coupling response to the profound suppression of bone resorption upon OPG-Fc administration. In order to further study the role of bone resorption in mediating the PPR receptor-dependent increase of bone formation, and to rescue the cortical porosity of the CL2 mice, we cross-bred CL2 mice with transgenic mice overexpressing soluble OPG under the control of the ApoE promoter (ApoE-OPG). ApoE-OPG mice displayed significant suppression of osteoclast and osteoblast activity, along with the previously described osteopetrotic phenotype. Interestingly, however, the OPG transgene expressed in a CL2 background decreased osteoclast number without significantly affecting osteoblast number and activity. The net result of these actions was a further increase in trabecular bone volume and a rescue of the cortical bone porosity. Taken together, our findings suggest: 1) basal and PPR-stimulated bone formation are, at least in part, dependent on bone resorption; 2) OPG-dependent inhibition of bone resorption rescues the increased cortical porosity observed upon activation of PPR.

Disclosures: ***R. Chiusaroli****, None.*

1165

Sustained, but not Transient, Elevation of PTH Reduces SOST Gene Expression: Evidence That Osteocytes Participate in the Increase in Osteoblast Number that Occurs in Hyperparathyroidism. T. Bellido, A. A. Ali, L. I. Plotkin, Q. Fu, I. Gubrij, X. Liu*, R. A. Wynne*, C. A. O'Brien, S. C. Manolagas, R. L. Jilka. Center for Osteoporosis and Metabolic Bone Diseases, Central Arkansas Veterans Healthcare System, University of Arkansas for Medical Sciences, Little Rock, AR, USA.

Sclerostin, a product of the SOST gene, is produced mainly by osteocytes and it antagonizes the pro-differentiating actions of BMPs on osteoblasts. Genetic evidence in mice and humans indicates that sclerostin negatively regulates bone formation, suggesting that osteocytes can influence bone homeostasis by changes in SOST expression. PTH exerts potent effects on osteoblast number and bone formation. Because SOST is a Runx2-dependent gene, and PTH downregulates Runx2 levels via proteasomal degradation, we have examined here whether administration of PTH to mice alters SOST expression. We found that SOST expression in tibia, as measured by quantitative real-time PCR, was not affected at 1, 2, 4 or 16 hours following a single injection of 100 ng/g of PTH(1-84) to adult female Swiss Webster mice; or after 4 daily injections when osteoblast number had increased 3-fold. Therefore changes in SOST expression appear not to contribute to the anabolic effect of intermittent PTH. In contrast, continuous elevation of PTH(1-84) by infusion with an osmotic pump, which raised circulating PTH(1-84) levels from a basal level of 15 pg/ml to 500 pg/ml, decreased SOST expression in tibia and vertebrae to less than 20% of that in control mice, beginning as early as 18 h. After 96 h when osteoblast number had increased by 2-fold, SOST expression remained at 20% of basal values. Consistent with a direct effect of the hormone on SOST expression, addition of 50 nM PTH to osteoblastic OB-6, or osteocytic MLO-Y4 cells, reduced SOST expression by 50% within 3h, and to undetectable levels after 24 h. Because of the high level of SOST expression in osteocytes compared to osteoblasts, and the fact that osteocytes are the most abundant cell type in bone, the reduction in SOST expression caused by continuous PTH most likely reflects a direct effect of the hormone on osteocytes. We propose that the increase in osteoblast number that occurs as part of the increased remodeling caused by continuous elevation of PTH is due to down-regulation of sclerostin secretion by osteocytes, thereby permitting increased BMP action and increased osteoblast differentiation. Moreover, our findings reinforce the notion that intermittent and continuous PTH administration increase osteoblast number via distinct mechanisms: attenuation of apoptosis in the former and increased differentiation in the latter.

Disclosures: ***T. Bellido****, Nuvios, Inc. 1, 2, 5.*

1166

SOST Is a Target Gene For PTH Action During Bone Formation. H. Keller, H. Jeker*, A. Studer*, J. Wirsching*, M. Kneissel. Bone Metabolism, Novartis Institutes for BioMedical Research, Basel, Switzerland.

Intermittent application of parathyroid hormone (PTH) is a well established pharmacological principle to stimulate bone formation in animals and humans. However, the mechanisms responsible for the bone anabolic effects of PTH are still poorly understood. Recently, sclerostin (SOST), which is structurally most closely related to the DAN/cerberus family of BMP antagonists, was identified as a potent osteocyte expressed negative regulator of bone formation in vitro, in vivo and in patients with the bone overgrowth disorders Sclerosteosis and Van Buchem disease. Therefore, we have analyzed SOST expression during PTH-induced bone formation in a classical model of local bone formation. 8-month-old OF/IC female mice (n=7/group) were injected twice daily with 100 nM hPTH(1-34) or vehicle onto the calvaria for 5 days and were then sacrificed or left untreated for a week to allow for the full bone formation response. Bone formation was assessed by fluorochrome label based histomorphometry and gene expression was measured by real-time quantitative PCR at day 5 and day 12. As expected, PTH stimulated bone formation: bone formation rates were increased 2-fold at the 1st and 6-fold at the 2nd measurement time point. SOST expression was significantly reduced in calvaria of PTH-treated animals compared to controls at day 5 four hours after the last PTH administration, whereas expression of the house keeping gene GAPDH was unchanged. In addition, osteocalcin was also weakly reduced at day 5, but clearly increased at day 12 in PTH-treated animals. SOST expression was not significantly different in treated and control mice at day 12 seven days after cessation of PTH treatment, as well as GAPDH. Next, we analyzed the effect of PTH on SOST expression in calvaria organ cultures of newborn mice. 100 nM PTH(1-34) suppressed SOST expression within 6 hours by about 95%. A similar time-course and efficacy was observed in cell culture using an osteoblastic cell line with robust endogenous SOST expression. An IC_{50} of about 5 nM was determined by a dose-response curve. The effect of PTH was specific as 100 nM bovine PTH(7-34) was inactive. PTH inhibited SOST expression also in the presence of the protein synthesis inhibitor cycloheximide indicating a direct regulation of the SOST expression by PTH. Finally, PTH did not influence SOST mRNA stability in the presence of actinomycin D suggesting a regulation of SOST transcription by PTH. In summary, we have shown that PTH directly inhibits SOST expression in vivo and in vitro suggesting that SOST reduction may play an important role in PTH-induced bone formation.

Disclosures: ***H. Keller****, Novartis Pharma AG, Basel, Switzerland 1, 3, 4.*

1167

Growth without Growth Hormone Receptor: Estradiol Is a Major Growth-Hormone Independent Regulator of Hepatic Insulin-like Growth Factor-I Synthesis. K. Venken*[1], S. Boonen[1], J. Kopchick*[2], K. Coschigano*[2], S. Movérare*[3], R. Bouillon[1], C. Ohlsson[3], D. Vanderschueren[1]. [1]K.U. Leuven, Leuven, Belgium, [2]Ohio University, Athens, OH, USA, [3]Gothenburg University, Gothenburg, Sweden.

Growth hormone (GH) stimulates postnatal growth. Its action is mediated by GH-induced hepatic and local insulin-like growth factor-I (IGF-I) synthesis. Estrogens are also essential for pubertal growth and bone mineral accrual. These effects may reflect estrogen-induced GH secretion, providing a GH-dependent mechanism for the effects of estrogens on skeletal growth. It is presently unclear to what extent estrogens may be able to regulate pubertal growth and bone mineral acquisition independently of GH and its receptor. To this end, we examined the effects of estradiol (E_2) replacement (0.03 µg/day via subcutaneous silastic implants) in orchidectomized (orch) male mice with a disrupted GHR (GHRKO) and corresponding WT mice during late puberty (6-10 weeks). Results are expressed as % gain or loss compared to orch. E_2 stimulated growth of the appendicular skeleton as it significantly enhanced femur length (+ 9%), induced thickening of the growth plate (+ 16%) and fully rescued the longitudinal growth rate (+ 182%) to WT levels in orch GHRKO mice, while no changes were observed in WT. Growth of the axial skeleton, as assessed by crown-rump length, was accelerated by E_2 in both GHRKO and WT (+ 7% and + 8% respectively). E_2 also stimulated radial bone growth as reflected by a significant increase in cortical thickness (+ 27%) and periosteal perimeter (+ 11%) in orch GHRKO mice. In addition, the periosteal bone formation rate, which was severely impaired in GHRKO compared to WT (- 76%), was fully rescued to control WT levels, associated by an increase in osteoblast number (+ 127%) at the femoral periosteal site. Measurement of IGF-I mRNA levels in GHRKO mice revealed a pronounced E_2-induced increase in IGF-I synthesis in the liver from 1.4% to 53% of control WT levels, while IGF-I expression in bone was unaffected. This E_2-induced upregulation of hepatic IGF-I mRNA levels resulted in a 10-fold increase in serum IGF-I, which, in turn, correlated strongly with the rate of periosteal bone formation ($r = 0.86$, $P = 0.01$). Our data provide the first evidence for stimulation of skeletal growth through upregulation of hepatic IGF-I by a hormone other than GH and support the concept that E_2 rescues pubertal skeletal growth during GH resistance through a novel mechanism of GH-independent stimulation of IGF-I synthesis in the liver. Estrogen or estrogen-like compounds (e.g., SERMs) merit investigation as potential IGF-I secretagogues to restore serum IGF-I levels in disease-related or age-dependent GH/IGF-I deficient or resistant conditions.

Disclosures: ***K. Venken****, None.*

1168

Liver-Derived Insulin-Like Growth Factor I Is Permissive for Ovariectomy-Induced Bone Loss. N. Andersson[1], M. K. Lindberg[1], S. Movérare[1], J. Svensson*[1], T. Chavoshi*[2], K. Venken[3], D. Vanderschueren[3], H. Carlsten*[2], C. Ohlsson[1]. [1]Center for Bone Research at the Sahlgrenska Academy, Department of Internal Medicine, Göteborg University, Göteborg, Sweden, [2]Department of Rheumatology and Inflammation Research, Göteborg University, Göteborg, Sweden, [3]Laboratory for Experimental Medicine and Endocrinology, Katholieke Universiteit Leuven, Leuven, Belgium.

Estrogen deficiency as a result of ovariectomy (ovx) results in a pronounced trabecular bone loss. Insulin-like growth factor I (IGF-I) is involved in the regulation of bone metabolism and a major part of serum IGF-I is derived from the liver.

The aim of the present study was to investigate the role of liver-derived IGF-I for ovx-induced bone loss. Three-month-old mice with Cre-loxP induced liver specific IGF-I inactivation (LI-IGF-$I^{-/-}$) and wild type mice (WT) were either ovx or sham operated. As expected, five weeks after ovx, there was a pronounced reduction in trabecular bone mineral density (BMD) in WT mice as measured using pQCT (-52%, $p<0.001$). The decreased trabecular BMD was caused both by a reduced number (-45%, $p<0.01$) and thickness (-13%, $p<0.01$) of trabeculae compared with sham operated mice as measured using µCT. The trabecular bone mass in sham operated LI-IGF-$I^{-/-}$ mice was similar to that seen in sham operated WT mice. Interestingly, the trabecular bone parameters were not affected by ovx in LI-IGF-$I^{-/-}$ mice.

Recent studies indicate that skeletal homeostasis is influenced by several components of the immune system. Therefore, we measured the number of T cells in bone marrow of the femur using flow cytometric analysis. Ovx increased the number of T cells in the bone marrow of the femur in WT (193% over sham, $p<0.001$) but not in LI-IGF-$I^{-/-}$ mice. Interleukin 7 (IL-7) has been reported to stimulate the formation and function of osteoclasts by inducing the expression of receptor activator of NF-κB ligand (RANKL) on T-cells. The expression of IL-7 was increased by ovx in WT (26% over sham, $p<0.05$) but not in LI-IGF-$I^{-/-}$ mice as studied by real time PCR analysis. Similarly, ovx of WT mice resulted in an increase in the RANKL/ osteoprotegerin ratio (52% over sham, $p<0.05$), while this ratio was unaffected by ovx in LI-IGF-$I^{-/-}$ mice. In conclusion, liver-derived IGF-I is permissive both for ovx-induced trabecular bone loss and for the associated increase in number of T-cells in bone marrow. Our mechanistic studies indicate that the permissive effect of liver-derived IGF-I for ovx-induced trabecular bone loss involves modulation of the expression of IL-7 and a subsequent modulation of RANKL on T-cells in the bone marrow.

Disclosures: ***N. Andersson****, None.*

1169

Raloxifene In Combination with Teriparatide Reduces Teriparatide-Induced Stimulation of Bone Resorption but not Formation in Postmenopausal Women With Osteoporosis. C. Deal[1], M. Omizo*[2], E. N. Schwartz*[3], E. F. Eriksen[4], P. Cantor*[4], J. Wang*[4], E. V. Glass*[4], S. L. Myers*[4], J. H. Krege*[4]. [1]Cleveland Clinic Foundation, Cleveland, OH, USA, [2]Oregon Osteoporosis Center, Portland, OR, USA, [3]Foundation for Osteoporosis Research and Education, Oakland, CA, USA, [4]Eli Lilly & Co, Indianapolis, IN, USA.

Teriparatide (rDNA) injection [rhPTH(1-34)] increases bone turnover, stimulates new bone formation, and reduces fracture risk in postmenopausal women with osteoporosis. To assess the effects of combination teriparatide and raloxifene therapy in postmenopausal women with osteoporosis, we conducted a 6-month randomized, double-blind trial comparing combination teriparatide plus raloxifene (n=69) versus teriparatide plus placebo (n=68). Women were osteoporosis treatment naïve and received calcium and vitamin D. Fasting serum N-terminal propeptide of type 1 collagen (PINP) and C-terminal telopeptide of type I collagen (CTX) were monitored at baseline, and after 1, 3 and 6 months treatment. Bone mineral density was measured by DXA at baseline and 6 months.

TABLE: Results are mean +/- SE of percent change from baseline to endpoint.

	TPTD + placebo	TPTD + RLX	P-value*
Formation (PINP)	167±30†	148±31†	0.66
Resorption (serum CTX)	96±15†	44±15‡	0.01
DXA Lumbar Spine BMD	5.19±0.67†	6.19±0.65†	0.28
DXA Femoral Neck BMD	1.03±0.67	2.23±0.64†	0.19
DXA Total Hip BMD	0.68±0.59	2.31±0.56†	0.04

*P-value for between group comparisons, † P<0.001, ‡ P=0.005 for within group change from baseline. Results are ITT by last observation analysis.

Baseline demographics were similar between groups. Bone formation (PINP) increased similarly in both groups. However, the increase in bone resorption (CTX) was significantly reduced (-52%, P=.01) in the combination group. In the teriparatide-alone group, lumbar spine BMD increased significantly from baseline. In the combination group, lumbar spine, femoral neck, and total hip BMD increased significantly from baseline, and the increase in total hip BMD was significantly greater than in the teriparatide alone group. In the teriparatide-alone group, mean serum calcium levels increased from baseline to endpoint (0.30±0.06 mg/dl, P<.001) and mean serum phosphate was unchanged. In the combination group, mean serum calcium was unchanged, and mean serum phosphate decreased (-0.20±0.06 mg/dl, P<.001) from baseline to endpoint. Serum calcium (P<.001) and phosphate (P<.004) changes from baseline to endpoint were significantly different between the teriparatide-alone and combination groups. Therapy in both groups was well tolerated.

Compared to teriparatide alone, raloxifene plus teriparatide increased bone formation to a similar degree. However, compared to teriparatide alone, combination therapy induced a lesser increase in bone resorption and significantly increased total hip BMD.

Disclosures: ***C. Deal****, Eli Lilly and Company 2, 5, 8; Proctor and Gamble 5, 8; Merck 8.*

1170

Fracture Risk Reduction During Treatment with Teriparatide Is Independent of Pretreatment Bone Turnover. P. D. Delmas[1], A. A. Licata*[2], G. G. Crans*[3], P. Chen*[3], D. A. Misurski*[3], R. B. Wagman[3], B. H. Mitlak[3]. [1]INSERM Research Unit 403, Claude Bernard University of Lyon, Lyon, France, [2]Department of Endocrinology, Diabetes, and Metabolism, The Cleveland Clinic, Cleveland Clinic Foundation, Cleveland, OH, USA, [3]Lilly Research Laboratories, Indianapolis, IN, USA.

In the Fracture Prevention Trial, postmenopausal women with osteoporosis randomized to teriparatide 20 mcg/day or 40 mcg/day for a median of 19 months had a reduced risk of fracture compared to women on placebo (Neer, 2001). However, the relationship between baseline bone turnover and anti-fracture efficacy remains unclear. To assess this relationship, data from women enrolled in the Fracture Prevention Trial were examined using logistic regression analysis. A subset of 520 women had biochemical markers of bone turnover (serum bone-specific alkaline phosphatase [BSAP], serum carboxy-terminal extension peptide of procollagen type 1 [PICP], urinary N-terminal telopeptide [NTX], and urinary free deoxypyridinoline [DPD]) measured at baseline. A partially overlapping subset of 771 women also had serum amino-terminal extension peptide of procollagen type 1 [PINP] evaluated at baseline. A total of 45 osteoporotic fractures (vertebral and non-vertebral) occurred in the four-marker subset and 74 occurred in the partially overlapping PINP subset. The relationship between bone markers and fracture risk was modeled as a function of therapy (placebo or pooled teriparatide), baseline bone marker covariate, and therapy-by-baseline bone marker covariate interaction. Higher bone turnover was associated with increased fracture risk. For each bone marker, the main effect of therapy was statistically significant ($p < 0.05$); however, therapy-by-baseline bone marker covariate interaction was not significant, suggesting that the ability of teriparatide to reduce fracture risk is independent of baseline bone turnover. The effects of pretreatment biochemical marker concentrations are shown below. Women with the highest pretreatment bone turnover had the greatest risk of fracture. The anti-fracture efficacy of teriparatide was similar regardless of baseline bone turnover.

Table. Effect of different pretreatment biochemical marker concentrations on the estimated relative risk of new osteoporotic fracture in women receiving teriparatide therapy compared to women in placebo group.

Percentile	BSAP RR (95% CI)	PICP RR (95% CI)	PINP RR (95% CI)	NTX RR (95% CI)	DPD RR (95% CI)
25th	0.41 (0.11-0.71)	0.40 (0.15-0.65)	0.31 (0.15 - 0.47)	0.38 (0.13 – 0.63)	0.41 (0.13- 0.70)
50th	0.41 (0.16- 0.67)	0.40 (0.17 - 0.64)	0.31 (0.17 – 0.46)	0.38 (0.15 – 0.61)	0.42 (0.16- 0.67)
75th	0.43 (0.19 – 0.66)	0.41 (0.18- 0.64)	0.32 (0.18- 0.46)	0.39 (0.16- 0.61)	0.42 (0.18 – 0.67)

Disclosures: ***P.D. Delmas****, None.*

1171

Daily Nasal Spray of hPTH(1-34) for 3 Months Increases Bone Mass in Osteoporotic Subjects. T. Matsumoto[1], M. Shiraki[2], T. Nakamura[3], H. Hagino[4], H. Iinuma*[5]. [1]University of Tokushima, Tokushima, Japan, [2]Research Institute and Practice for Involutional Diseases, Nagano, Japan, [3]University of Occupational and Environmental Health, Fukuoka, Japan, [4]Tottori University, Tottori, Japan, [5]The Cardiovascular Institute, Tokyo, Japan.

Intermittent administration of PTH has been shown to develop strong anabolic effects on bone. However, invasiveness of currently available formulas given by daily subcutaneous (sc) injections has been a considerable disadvantage for patient acceptance. We, therefore, have developed a nasal spray formula of hPTH(1-34), and found that similar peak serum hPTH(1-34) concentrations to those obtained after sc injections of 20 µg hPTH(1-34) can be achieved by nasal spray of 1000 µg hPTH(1-34). Furthermore, hPTH(1-34) was absorbed from nasal mucosa much more quickly than by sc injections. In order to determine clinical efficacy as well as safety and tolerability of nasal hPTH(1-34) spray, a randomized, open-labeled clinical trial was conducted in subjects with osteoporosis.

Ninety-two osteoporotic subjects 52 to 84 years of age (mean age, 66.6 years) were enrolled in this study. The subjects were randomly assigned to receive either 250 µg (PTH250, n=31), 500 µg (PTH500, n=30), or 1000 µg (PTH1000, n=31) of daily nasal hPTH(1-34) spray for 3 months. All the participants received daily supplements of 300 mg Ca and 200 IU vitamin D_3.

Daily nasal hPTH(1-34) spray for 3 months increased lumbar bone mineral density (L-BMD) in a dose-dependent manner, and PTH250, PTH500 and PTH1000 groups showed 0.1 (p=0.817), 0.7 (p=0.165), and 2.4% (p=0.012) increase in L-BMD from the baseline, respectively. Among bone formation markers, serum PINP and osteocalcin increased in a dose-dependent manner at 3 months, and were significantly increased from the baseline in PTH1000 group by 16.7 and 20.6%, respectively. Interestingly, urinary CTX and NTX did not increase but were suppressed in PTH500 and PTH1000 groups after 3 months. At the baseline, 0.5, 1, 2, and 3 months, serum Ca was monitored before and 3 hours after nasal hPTH(1-34) spray. Two subjects in PTH250 group, and 5 in PTH1000 group developed hypercalcemia over 10.4 mg/dL but less than 11 mg/dL 3 hours after nasal hPTH(1-34) spray. None of the subjects developed hypercalcemia before nasal spray. There were no significant treatment differences in the number of subjects with at least one adverse event.

These results demonstrate that nasal hPTH(1-34) spray is safe, well-tolerated, and is associated with an early increase in L-BMD. Based upon the pharmacokinetics of nasal hPTH(1-34) spray with quick absorption and short half-life, the present results warrant further studies to examine its long-term efficacy on bone mass and fractures.

Disclosures: ***T. Matsumoto****, Chugai Pharmaceutical Co., Ltd 2, 5.*

1172

Effects of PTH, Alendronate, or Both on Bone Turnover in Osteoporotic Men. B. Z. Leder, J. J. Wyland*, R. M. Neer, A. Hayes*, J. Hunzelman*, K. Gibson*, J. S. Finkelstein. Endocrine Unit, Massachusetts General Hospital, Boston, MA, USA.

We recently reported that alendronate (AL) impairs the ability of PTH to increase spine and femoral neck BMD, but not total body BMD, in men. Here we report the effects of AL, PTH, or the combination (A+P) on bone turnover in the same population. 83 men age 46-85 with lumbar spine or femoral neck T-scores < -2 were randomized to receive AL 10 mg daily, hPTH-(1-34) 40 mcg sc daily, or both. AL was given for 30 months whereas PTH was begun at month 6. Serum osteocalcin (OC) and N-telopeptide (NTX) were measured at months 0, 1, 2, 3, 6, 7, 8, 9, 12, 18, 24, and 30 and between-group differences in the area under the curve (AUC) between month 6 and 30 were compared by ANOVA. To assess changes in the balance of bone formation and resorption, we also compared changes in an Uncoupling Index (UI) defined by the equation: Z-score OC - Z-score NTX. Only subjects who completed the study are included in this analysis (AL n=26, A+P n=20, PTH n=17). Changes in OC, NTX, and UI (+ SE) are shown below.

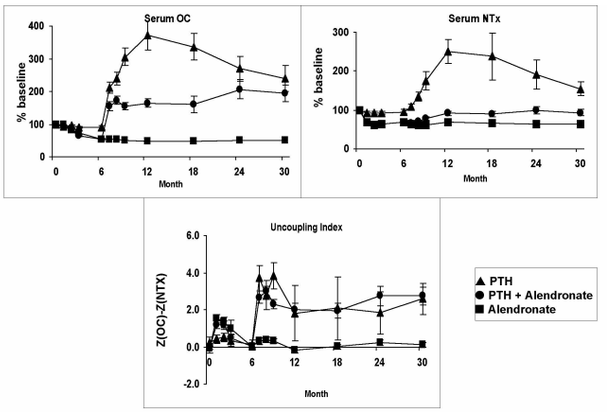

Differences were found for all between-group comparisons in OC and NTX (P<0.001). In the PTH group, markers peaked at month 12 (6 months after initiation of therapy) and then gradually fell during the remaining 18 months of treatment. Both NTX and OC decreased in the A+P group during the first 6 months of AL therapy. The addition of PTH at month 6, however, restored NTX to its pre-treatment level and increased OC to double its pre-treatment level. In contrast to the PTH alone group, markers in the A+P group continued to increase from month 12 through 30. UI increased significantly and similarly in the PTH and A+P groups. This increase was greatest 1-3 months after initiation of PTH. Changes in OC were associated with changes in NTX in all groups (PTH group: R=0.78, P<0.001; A+P group: R=0.86, P<0.001: AL group: R=0.42, P=0.03).

In conclusion, pre-treatment with AL diminished the ability of PTH to stimulate bone formation and resorption in men, eliminated the up-and-down pattern of stimulation, but did not alter the relationship between formation and resorption as assessed by UI. Individual changes in bone formation and resorption were strongly linked in both PTH-treated groups. The BMD effects of the sustained increase in bone turnover in the combination group may be best assessed in studies of even longer duration.

Disclosures: ***B.Z. Leder****, Merck 8.*

1173

Normal Bone Histomorphometry and 3D Microarchitecture After 10 Years Alendronate Treatment of Postmenopausal Women. R. Recker[1], K. Ensrud[2], S. Diem*[2], E. Cheng*[2], S. Bare*[1], P. Masarachia[3], P. Roschger*[4], P. Fratzl*[5], K. Klaushofer*[4], A. Lombardi[6], D. Kimmel[3]. [1]Creighton University, Omaha, NE, USA, [2]University of Minnesota, Minneapolis, MN, USA, [3]Merck Research Laboratories, West Point, PA, USA, [4]Ludwig Boltzmann Institute of Osteology, Vienna, Austria, [5]Max Planck Institute of Colloids and Interfaces, Potsdam, Germany, [6]Merck Research Laboratories, Rahway, NJ, USA.

FLEX (FIT Long-term EXtension) was a 5-year randomized, placebo (PBO)-controlled trial, designed to assess the efficacy and safety of long-term treatment with alendronate (ALN). 1099 postmenopausal women who had received 3-6 years treatment with ALN (5 mg/d during the first two years and 10 mg/d thereafter) in the Fracture Intervention Trial (FIT), were randomized to placebo (ALN/PBO) (N=437), ALN* 5 mg/d (N=329) or 10 mg/d (ALN/ALN) (N=333). Transilial bone biopsies were obtained following dual fluorochrome labeling from 31 women. Trabecular bone turnover, quantity, microarchitecture and mineralization were assessed. Twenty-nine specimens were suitable for quantitative back-scatter electron microscopy (qBEI; MCC and CAW), eighteen for histomorphometry (2D) and fourteen for micro-computed tomography (3D). Since there were no differences between the 5mg/d and 10mg/d ALN groups, the two groups were pooled. Results are shown in the table.

Abbrv	Mean (S.D.)	ALN/PBO (N=14)	ALN/ALN (N=15)
MCC	Mean Calcium Concentration (%)	22.1 (0.58)	22.4 (0.54)
CAW	Calcium Width	3.57 (0.38)	3.48 (0.45)
	2D Endpoints	**(N=9)**	**(N=9)**
BV/TV	Bone Volume (%)	18.3 (5.2)	19.5 (6.2)
OV/BV	Osteoid Volume (%)	1.1 (0.4)	0.9 (0.7)
Tb.N	Trabecular Number (#/mm)	1.3 (0.2)	1.3 (0.2)
Tb.Th	Trabecular Thickness (µm)	142 (27)	148 (35)
OS/BS	Osteoid Surface (%)	11.6 (4.7)	9.9 (6.3)
O.Th	Osteoid Thickness (µm)	4.8 (0.4)	5.1 (0.7)
MAR	Mineral Apposition Rate (µm/d)	0.6 (0.1)	0.5 (0.1)
MS/BS	Mineralizing Surface (%)	3.0 (3.4)	1.4 (1.6)
	3D Endpoints	**(N=6)**	**(N=8)**
BVF	Bone Volume Fraction (%)	16.5 (4.9)	16.6 (6.0)
BSD	Bone Surface Density mm^2/mm^3)	1.0 (0.4)	1.2 (0.5)
Tb.N	Trabecular Number (#/mm)	1.3 (0.2)	1.4 (0.3)
Tb.Th	Trabecular Thickness (µm)	130 (20)	121 (26)

In this study, all patients were initially treated with ALN for ~5 years, followed by an additional five years of PBO or ALN. All patients in both ALN/PBO and ALN/ALN groups displayed double fluorochrome label in trabecular bone. The cortical and trabecular bone tissue of both groups appeared normal, lacking qualitative abnormalities such as woven bone, osteitis fibrosa, defective mineralization, and non-lamellar bone. There were no differences between the groups for any quantitative endpoint (p=NS). These data, from a limited sampling, suggest that iliac trabecular bone tissue remains normal following use of ALN 5 or 10 mg/d for 5-10 years.

*Manufactured by Merck & Co., Inc, Whitehouse Station, NJ

Disclosures: ***R. Recker****, Merck and Co., Inc. 2, 5; Procter & Gamble 2, 5; Eli Lilly and Company 2, 5; Novartis 2, 5.*

1174

A 5 Year Randomized Trial of the Long-term Efficacy and Safety of Alendronate: The FIT Long-term EXtension (FLEX). D. Black[1], A. Schwartz[1], K. Ensrud[2], A. Rybak-Feiglin*[3], J. Gupta*[3], A. Lombardi[3], R. Wallace*[4], S. Levis[5], S. Quandt[6], S. Satterfield*[7], J. Cauley[8], S. Cummings[9]. [1]U CA, SF, CA, USA, [2]U MN, Minn, MN, USA, [3]Merck & Co., Rahway, NJ, USA, [4]U IA, Iowa City, IA, USA, [5]U Miami, Miami, FL, USA, [6]Wake Forest U, Winston-Salem, NC, USA, [7]U TN, Memphis, TN, USA, [8]U Pitt, Pitt, PA, USA, [9]CA Pac. Med. Ctr., SF, CA, USA.

Alendronate (ALN) has been shown to increase BMD and reduce fracture risk in trials up to 5 years but optimal longer term use remains an important clinical question. FLEX was a 5-year randomized, placebo-controlled trial to test the hypothesis that in women previously on ALN for 3-6 years, continued ALN would preserve or increase total hip BMD vs placebo (PBO). BMD at other sites and bone turnover were secondary endpoints; fractures were exploratory.

Women on ALN in the Fracture Intervention Trial (FIT) with T-scores > -3.5 were eligible. 1099 participants with a mean of 5 (range 3-6) years previous ALN (5 mg/d in yrs 1-2 & 10 mg/d thereafter) in FIT were randomized to 5 years of PBO (n=437) or ALN 5 mg/d (n=329) or 10 mg/d (n=333).

The mean age at FLEX baseline was 73 yrs; mean total hip BMD T-score was -1.77. As shown below, women switched to PBO had significant loss of hip BMD (p<0.001) and significant increases in bone turnover (p<0.001) relative to FLEX baseline. In contrast, spine and total body BMD were preserved in the PBO group.

Mean % Changes in BMD and Markers Among Women with 3-6 Years Prior ALN

Endpoint	PBO	ALN+	Difference (95% CI)
Total hip BMD	-3.4**	-1.0**	2.4% (1.8, 2.9)^
Femoral neck BMD	-1.5**	0.5	1.9% (1.2, 2.7)^
Lumbar spine BMD	1.5**	5.3**	3.8% (3.0, 4.4)^
Total body BMD	-0.3	1.0**	1.3% (0.7, 1.9)^
Urinary NTx	33.7**	1.2	-32% (-44, -21)^
Serum BSAP	27.7**	4.9**	-23% (-28, -17)^

**p<0.001 vs. BL; ^p<0.001 between groups; + =pooled doses of ALN

Compared to FIT baseline, women treated with ALN up to 11 years increased their spine BMD by 14.8%, total hip BMD by 2.4%, and total body by 3.6%. Women treated with PBO in the last 5 of 11 years had respective changes (vs. FIT baseline) of 11.0% (p<0.001 vs. continuous ALN), -0.2% (p<0.001), and 2.5% (p=0.005). During the 5 years of FLEX, clinical spine fracture risk was reduced in ALN vs PBO (RR=0.45, 95% CI (0.23,0.84)) but risks were similar for non-spine fractures (RR=1.0, 95% CI (0.76,1.32)) and morphometric spine fractures (0.87, 95% CI (0.61,1.25)). Adverse experiences were similar in both treatment groups.

We conclude that 4-6 years of ALN followed by continued treatment with ALN for up to 5 additional years increases spine BMD, maintains other BMD measures and preserves decreases in bone markers. Decreases in hip BMD and increases in bone turnover markers occurred among those who stopped ALN during FLEX; nevertheless, BMD levels were similar or higher and marker levels remained slightly lower than at FIT baseline 11 years earlier.

Disclosures: ***D. Black****, Novartis Pharmaceuticals 2, 5; Merck 2, 8; NPS 2.*

1175

Convergence of BMP2/TGFβ, MAPK and Runx2 Signaling in Subnuclear Foci During Osteogenic Lineage Induction. A. Javed, F. Afzal*, J. Pratap, A. J. van Wijnen, J. L. Stein*, J. B. Lian, G. S. Stein. Department of Cell Biology and Cancer Center, University of Massachusetts Medical School, Worcester, MA, USA.

The Runx2/Cbfa1 transcription factor is a scaffold protein that interacts with mediators of signal transduction pathways critical for bone formation. We have previously shown that a knock-in mutation in the mouse that ablates the Runx2 C-terminus results in absence of a mineralized skeleton (Choi et al, PNAS, 2001). The C-terminus contains a Runx family unique nuclear matrix targeting signal (NMTS) and a SMAD interacting domain. Although the coordinated activity of Runx2 and BMP/TGFβ-activated Smads are necessary for bone formation, the precise structural basis for the Runx2/Smad interaction and its requirement for osteoblast differentiation has not been resolved. Using a series of mutations, we have defined a sequence in Runx2 required for physical and functional interaction with Smads. Smad responsive transcriptional activity was retained upon deletion of the C-terminus to amino acid 432, but lost with deletion to amino acid 391. Deletion to 391 also abolished the in situ association of Runx2 and Smad at subnuclear sites. Thus the domain of Runx (391-432) required for Smad binding and function overlaps the well-defined nuclear matrix targeting signal (NMTS). We further established using heterologous Gal4 fusion proteins that the NMTS is necessary and sufficient for interaction with either BMP or TGFβ responsive SMADs. Moreover, formation of Runx2 and Smad complexes are dependent on Runx2 phosphorylation through the MAPK signaling pathway. Finally we demonstrate that the 391-432 Runx2- SMAD domain is essential for BMP2 mediated induction of C2C12 cells into the osteogenic lineage. Our findings demonstrate that the Runx-Smad interaction (i) is dependent on MAPK phosphorylation of Runx2, (ii) is required for osteogenic induction by TGFβ/BMP2, and (iii) supports Runx2 gene transcription in subnuclear domains. We propose the genetic requirement for the Runx2 C-terminus in bone formation in vivo is causally related to the integration of these three signaling pathways to promote osteogenic differentiation.

Disclosures: ***A. Javed****, None.*

1176

The Zinc Finger Transcription Factor Gli2 Enhances BMP-2 Gene Transcription, Osteoblast Differentiation and Bone Formation. M. Zhao[1], M. Qiao*[1], J. A. Sterling[1], D. Chen[1], B. O. Oyajobi[1], I. R. Garrett[2], G. Gutierrez[2], G. Rossini*[2], G. R. Mundy[1]. [1]Cellular and Structural Biology, UTHSCSA, San Antonio, TX, USA, [2]Osteoscreen, San Antonio, TX, USA.

BMP-2 is an important skeletal growth factor, but regulation of its transcription in osteoblasts is not well understood. Expression of BMP family members is mediated by hedgehog signaling, but the mechanism is unknown. The Gli family of zinc finger transcriptional factors mediate hedgehog signaling in other organ systems. Thus, we reasoned that the Gli family may directly regulate BMP-2 gene transcription and thereby subsequent skeletal development. We examined specifically Gli2 since Gli2 has been shown to be the major mediator of hedgehog signaling in other cells. Gli2 null mutant mice ($Gli2^{-/-}$) are embryonic lethal with severe skeletal abnormalities. Recently, we found the one third of two-month old $Gli2^{-/+}$ nulls were smaller and had profound osteopenia associated with impaired bone formation as shown by decreased bone mineral density, trabecular bone volume and cortical bone thickness. A similar osteopenic phenotype occurs in transgenic mice unresponsive to BMP-2 because of a dominant negative BMP type IB receptor targeted to osteoblasts. Culture of Gli2-deficient calvarial cells from $Gli2^{-/-}$ mice showed significant inhibition of BMP-2 gene expression, alkaline phosphatase (ALP) activity and mineralized bone nodule formation. Gli2 siRNA, which inhibited Gli2 expression by 90% in osteoblast precursor C2C12 and 2T3 cells, markedly decreased osteoblast differentiation and also decreased basal BMP2 promoter activity. In contrast, overexpression of Gli2 in these cells caused increases in BMP2 mRNA expression, ALP activity and mineralized nodule formation. Gli2-enhanced ALP activity was blocked by noggin. These results indicate that Gli2 stimulates osteoblast differentiation at least partially through up-regulation of BMP2 expression. Promoter studies showed that transfection of Gli2 in C2C12 cells increased BMP2 promoter activity by 10-fold and that two Gli2-responsive regions lie between -202/-312 and -1997/-2712. Three putative Gli response elements in these areas bound Gli2 protein as demonstrated by gel shift and supershift in EMSA. Co-transfection showed a synergistic effect of Gli2 with Smad1 on BMP-2 transcription, suggesting that Gli2 may directly interact with Smad1 and co-activate target genes. We have previously reported that truncated Gli3 is a repressor of BMP-2 gene and taken together with this new data, we propose that the Gli family of zinc finger proteins control BMP2 transcription in osteoblasts and subsequent osteoblast differentiation, in which Gli2 serves as a powerful stimulant for BMP-2 gene expression.

Disclosures: ***M. Zhao****, None.*

1177

Ectopic Bone Formation in Tooth Pulp, Absence of Cementum, Hyperplastic Periodontal Ligament and Reduced or no Dentin in Mice Lacking Bone Morphogenetic Protein Receptor Type 1A (BMPR1A). l. ye[1], Y. Mishina*[2], J. Zhang*[3], S. Zhang*[1], Y. Xie*[1], N. Kamiya*[2], V. Dusevich*[1], L. Li*[3], D. Eick*[1], L. Bonewald[1], J. Q. Feng[1]. [1]Oral Biology, University of Missouri-kansas city, School of Dentistry, Kansas City, MO, USA, [2]NIEHS/NIH, Research Triangle Park, NC, USA, [3]Stowers Institute, Kansas City, MO, USA.

Three type 1 receptors, BMPR1A, BMPR1B, and ActRI, are responsible for signaling of the Bone Morphogenetic proteins. It is known that recombinant BMP-2 or -4 can induce both *de novo* dentin and bone formation at the same induction site. It is unclear which receptors determine the fate of precursors for bone or dentin *in vivo*. Whereas, the *Bmpr1b* null mouse is viable and has a mild skeletal phenotype, the *Bmpr1a* null is lethal. To examine the function of BMP1A in mineralized tissue, a tissue specific null mouse was generated using the loxP/Cre approach. To delete the *Bmpr1a* gene specifically in osteoblasts, periodontal ligament (PDL) cells, cementoblasts and odontoblasts, *Col 1a1*-cre mice were crossed to floxed *Bmpr1a* mice. Histological analyses revealed a striking phenotype in the tooth as well as in bone. A dramatic reduction of alveolar and calvarial bone is observed in *Bmpr1a* null mice which maintains a woven bone character compared to compact bone in normal mice. A more dramatic phenotype was observed in the teeth as both the acellular and cellular layers of cementum are absent and the PDL is hyperplastic and replaced by loosely disorganized fibers. Dentin is extremely thin (one eighth of normal to missing) with few odontoblasts. The tooth pulp is replaced by poorly mineralized bone-like osteoid, and the remaining pulp cells appear degenerated. The dentin peritubules, equivalent to lacunae in bone, are ~1/2 normal size, Instead of forming secondary dentin in the normal response to the dentin fractures, a bone canus is formed. Immunohistochemistry of the ectopic bone in the tooth pulp shows higher expression of periostin and decorin compared to normal bone. This dental phenotype is similar to “shell teeth”, a genetic disease in humans. Based on these observations, we propose that BMPR1A is an essential signaling molecule in determining the cell fate of cementoblasts, odontoblasts, and PDL cells from mesenchymal precursors. In the absence of this receptor, the mesenchymal precursor cells by default differentiate into bone cells however, the bone fails to mature, but maintains the characteristics of immature woven bone, therefore BMPR1A is also critical for bone maturation.

Disclosures: ***L. ye****, None.*

1178

Twisted Gastrulation Is a Bone Morphogenetic Protein Agonist in Cartilage but not in Bone. E. Gazzerro[1], V. Deregowski[1], L. Stadmeyer*[1], A. N. Economides[2], E. Canalis[1]. [1]Research, Saint Francis Hospital and Medical Center, Hartford, CT, USA, [2]Functional Genomics, Regeneron Pharmaceuticals, Inc., Tarrytown, NY, USA.

Twisted gastrulation (Tsg) is a secreted glycoprotein that binds bone morphogenetic proteins (BMP) -2 and -4, and it is unique since it can display both BMP agonist and antagonist functions. Tsg can form a ternary complex with BMP and its antagonist chordin, enhancing chordin actions, or it can induce the cleavage of chordin by the metalloprotease BMP-1/tolloid, releasing BMP into the extracellular matrix. Tsg dual activities depend on the developmental stage, and on relative concentrations of BMP, chordin and BMP-1/tolloid in the target tissues. Tsg is expressed in chondrocytes and osteoblasts, and it acts as a BMP agonist in cells of the chondrocytic lineage. However, its actions in adult skeletal tissue *in vivo* are not known. A targeted deletion of the Tsg gene was created by replacing the first two Tsg coding exons with a LacZ cassette in frame with the first codon on a BAC clone containing Tsg genomic sequences. The LacZ reporter gene, with an associated neomycin selectable marker, were introduced by homologous recombination into the BAC clone. The deletion of the Tsg gene was confirmed by RT-PCR from calvarial mRNA. Tsg null mice were mostly viable, exhibited kinking of the tails, a 20% decrease of femoral length and a 40% decrease in body size when compared to age-sex matched wild type controls of equal genetic background. Dynamic histomorphometric analysis revealed no evidence of impaired BMP activity that would suggest an agonist role of Tsg since trabecular bone volume, mineral apposition rate, mineralizing surface and bone formation rate were not decreased in Tsg null mice compared to wild type controls. An increase in the percentage of osteoblast surface/bone surface was noted in Tsg null mice, and this is in accordance with the known effect of BMP on osteoblast cell differentiation. In an attempt to confirm a function of Tsg in bone, primary marrow stromal cells from Tsg null mice and wild type controls were cultured in osteoblastic differentiating conditions in the presence or absence of BMP-2. Cells from Tsg null mice were more susceptible to BMP-2 effects, forming mineralized nodules earlier than wild type controls, indicating an antagonist, and not an agonist role of Tsg. In conclusion, Tsg deletion in adult skeletal tissue reveals a modest BMP antagonist effect in bone, which is in contrast with the agonist effect of Tsg in cartilage.

Disclosures: ***E. Gazzerro****, None.*

1179

Antagonism between BMP and FGF Signaling Pathways in the Growth Plate Revealed by Analysis of BMPRIA and BMPRIB Mutant Mice. B. S. Yoon*[1], Y. Mishina*[2], I. Yoshii*[1], R. R. Behringer*[2], K. M. Lyons[1]. [1]Molecular, Cell, Developmental Biology, UCLA, Los Angeles, CA, USA, [2]Department of Molecular Genetics, M. D. Anderson Cancer Center, Houston, TX, USA.

During endochondral ossification, chondrocytes form a cartilaginous template for bone formation, known as the growth plate. Growth plate chondrocytes undergo a highly organized differentiation program. Cells at the ends of skeletal elements form the resting zone. Cells exiting the resting zone form the proliferative compartment. These cells eventually exit the cell cycle and differentiate into prehypertrophic chondrocytes, which terminally differentiate to form the hypertrophic zone.

Bone Morphogenetic Proteins (BMPs) are members of the Transforming Growth Factorβ (TGFβ) superfamily, and signal through receptor complexes that subsequently activate intracellular smad proteins. Although it is known BMPs are required for chondrogenesis, little is known about their roles in specific regions of the growth plate. In order to examine these roles, we generated mice null for BMPR1B (*Bmpr1b*$^{-/-}$) and conditionally null (CKO) for BMPR1A in cartilage (*Bmpr1a*^{CKO}). *Bmpr1a*^{CKO} mice die postnatally due to general chondrodysplasia with mild growth plate defects. This phenotype is exacerbated by the loss of one allele of *Bmpr1b*. *Bmpr1a*^{CKO} ;*Bmpr1b*$^{+/-}$mice have hypocellular proliferative zones and an abrupt transition to expanded hypertrophic zones. We demonstrate that the defects in proliferative zones are caused by increased apoptosis and severe defects in proliferation, as evidenced by decreased PCNA levels and increased production of cyclin inhibitors. Furthermore, *Bmpr1b*$^{+/-}$*; Bmpr1a*^{CKO} mice exhibit increased STAT and Erk1/2 MAPK signaling, both components of the Fibroblast Growth Factor (FGF) signaling pathway. Although the ability of FGFs to antagonize BMPs signals in the growth plate is established, our results provide *in vivo* evidence for this inhibition, and demonstrate that reciprocal inhibition of FGF pathways by BMPs is required for proliferation and differentiation of chondrocytes. Using the rat chondrosarcoma (RCS) cell line, we also show that smad-mediated BMP signaling is inhibited by FGFs, and demonstrate a direct mechanism for the antagonistic relationship. In summary, our results show that BMP signaling is required in the growth plate *in vivo*, in part to antagonize FGF signaling.

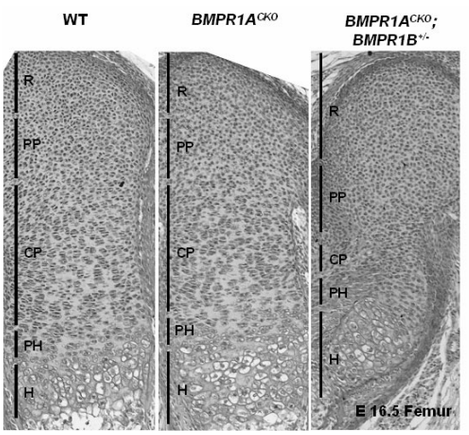

Disclosures: ***B.S. Yoon****, None.*

1180

Smad3 Deficient Chondrocytes Have Accelerated Differentiation and Enhanced BMP Signaling. T. Li*, M. J. Zuscik, D. Chen, E. M. Schwarz, R. N. Rosier, H. Drissi, R. J. O'Keefe. Orthopaedics, University of Rochester, Rochester, NY, USA.

Although TGF-β inhibits terminal differentiation of chondrocytes, the relative importance of various downstream signals as mediators of this effect remains unclear. Mice lacking Smad3 expression have accelerated chondrocyte maturation that results in post-natal dwarfism and premature osteoarthritis. We examined the rate of differentiation, responsiveness to TGF-β and BMP signaling, and expression of various signaling molecules in chondrocytes isolated from the sterna of neonatal wild type (Smad3$^{+/+}$) and knock out (Smad3$^{-/-}$) mice. In culture, wild type (wt) chondrocytes had abundant expression of *col2*, but had minimal spontaneous expression of *colX* over 8-days. *Col2* expression was even greater in knock out (ko) cells, and high levels of *colX* expression occurred in these cultures by 2-days and remained elevated for 8 days. Other markers of maturation, including *alkaline phosphatase*, *osteocalcin*, and *VEGF* were also elevated in ko cells. Experiments were performed to assess the responsiveness of the chondrocytes to TGF-β and BMP signaling. As anticipated, TGF-β failed to induce the Smad3 specific reporter, SBE-Luc in ko cells, and had reduced activation of P3TP-Luc, which is activated by TGF-β through Smad3 and other signals. In contrast, the BMP responsive reporter 9X GCG-Luc was more highly activated by BMP-2 in ko cells, suggesting an up-regulation of BMP responsiveness in cells lacking Smad3. Real time RT-PCR and Western blot was used to examine Smad expression. Similar levels of Smad2 and Smad4 were found in wt and ko chondrocytes, demonstrating the absence of a compensatory up-regulation of these factors. Furthermore, ko cells had reduced TGF-β1 and the type I TGF-β receptor expression (approximately 50% each), suggesting down-regulation of TGF-β signaling in chondrocytes lacking Smad 3. In contrast, components of the BMP signaling pathway were up-regulated in ko cells, including Smad1 (70%), Smad5 (80%), BMP-2 (2-fold), and BMP-6 (2.2-fold). BMP-2 markedly enhanced chondrocyte differentiation in both wt and ko cells, but the effect was much greater in ko cells**.** The maximal effect was 50-fold in ko cells and 5-fold in wt cells at 8-days. TGF-β continued to suppress maturation in ko cells (50%) suggesting that remaining components of the signaling pathway are functional. However, while TGF-β markedly suppressed alkaline phosphatase activity in wt cells (> 90%), the effect was much less in ko cells (50-75%). Thus, absence of Smad3 results in enhanced BMP signaling and responsiveness and is not associated with a compensatory increase in TGF-β signaling molecules. These changes account for the enhanced maturation observed in Smad3$^{-/-}$ chondrocytes.

Disclosures: ***T. Li****, None.*

1181

Transgenic Overexpression of IGFBP-5 in Mice Leads to Unexpected Decrease in Peak BMD in a Gender Specific Manner: Evidence for IGF-independent Mechanism of Action. D. A. Salih*[1], Y. Kasukawa[2], G. Tripathi*[1], F. A. Lovett*[1], N. F. Anderson*[1], E. J. Carter*[1], J. E. Wergedal[2], D. J. Baylink[2], J. M. Pell*[1], S. Mohan[2]. [1]The Babraham Inst, Cambridge, United Kingdom, [2]JLP VAMC / LLU, Loma Linda, CA, USA.

Past studies have shown that IGFBP-5 (BP-5) stimulates bone formation (BF) parameters *in vitro* and *in vivo* by mechanisms involving stimulation of IGF actions and IGF-independent action. To test the hypothesis that BP-5 overexpression promotes acquisition of peak BMD, we generated transgenic (Tg) mice overexpressing BP-5 using the CMV, a regulatory element shown to drive expression in chondrocytes, osteoblasts, lining cells and cells within the marrow. In Tg mice, BP-5 concentrations were increased by 8.8 fold (P<0.001) at 3 wks. We found two unexpected findings in BP-5 Tg mice. First, BP-5 Tg mice were 35% smaller compared to wild type (WT) mice at 8 wks. Second, BMD as measured in femora and tibiae at 3, 5 and 8 wks by DEXA was decreased and showed a gender specific effect. BMD in Tg females was reduced by 19% compared to WT siblings (P<0.001) at 8 wks. The BMD reduction in Tg males (31%) was significantly greater than that of females (P<0.001) at 8 wks. Femoral BMD was reduced by 17% in males from a second Tg line overexpressing BP-5 at an intermediate level. Total vBMD measured by pQCT at the mid diaphysis was significantly less in Tg males compared to females (76±1 vs 91±4% of WT, P<0.01). Serum osteocalcin levels were reduced (P<0.01) by 25-40% in BP-5 Tg mice compared to WT mice. Histomorphometric studies revealed that while BF rate and mineraling surface at the periosteum was significantly decreased (P<0.01) in the BP-5 Tg mice, they were increased (P<0.01) at the endosteum, suggesting opposite effects of BP-5 overexpression on periosteal and endosteal osteoblasts. If the observed inhibitory effects of BP-5 on the skeletal phenotype upon continuous exposure to high levels of BP-5 from early development are only due to sequestration of IGFs, then we would anticipate the skeletal phenotype of BP-5 transgenic mice to be similar to that of IGF-I/-II null mice. However, our findings in BP-5 Tg mice on the gender specific effects and the differential effects at the periosteum vs endosteum are different from what we observed for the skeletal phenotypes of IGF-I/-II null mice and support a model involving IGF-independent effects of BP-5. Conclusions: 1) BP-5 overexpression decreases peak BMD, periosteal BF and serum osteocalcin levels in mice; 2) BP-5 overexpression increases endosteal BF; 3) BP-5 effects in Tg mice are gender specific; and 4) The observed phenotype in BP-5 Tg mice cannot be explained solely on the basis of IGF sequestering effects of BP-5 and provide the first *in vivo* evidence for IGF-independent effects of BP-5 in bone.

Disclosures: ***S. Mohan****, None.*

1182

Functional Analysis of a 395-kilobase Region Surrounding the Mouse Bmp2 Gene: In Vivo BAC Transgenes and Comparative Analysis. R. L. Chandler*, K. J. McDermott*, D. P. Mortlock*. Molecular Physiology and Biophysics, Vanderbilt University, Nashville, TN, USA.

The Bmp2 gene is implicated as a key regulator of bone and articular cartilage maintenance and as a genetic risk factor for osteoporosis. However, little is known about the regulatory mechanisms that control Bmp2 transcription in vivo. To identify potentially distant cis-regulatory DNA elements that regulate Bmp2 transcription, we have performed in vivo functional analysis of a 395-kilobase genomic region flanking the mouse Bmp2 gene. Since other BMP family member genes are known to require distant cis-regulatory elements, we engineered Bmp2 bacterial artificial chromosomes (BAC) into reporter transgenes. Two overlapping BAC clones that extend far 5' and 3' to the Bmp2 promoter region were engineered to contain a LacZ reporter cassette inserted into the Bmp2 transcription unit using homologous recombination in bacteria. Modified BAC clones were injected into fertilized mouse eggs, and transgenic embryos were analyzed for LacZ expression at midgestation stages. The robust patterns of LacZ expression detected in our transgenic BAC embryos recapitulate many sites of endogenous Bmp2 expression in the developing skeleton. These included hypertrophic chondrocytes of the developing long bones, ribs and vertebrae, bone collar flanking ossifying regions, intervertebral joints, and incisor buds. Transgene expression was also detected in bone ossification centers, suggesting differentiating osteocytes. However, each BAC clone directed a different subset of normal Bmp2 expression patterns. Thus, a modular arrangement of distant 5' and 3' regulatory elements exist around the Bmp2 gene. Specifically, our data suggest that cis-regulatory sequences directing Bmp2 expression in hypertrophic chondrocytes are separate from those that control expression in the bone collar, intervertebral discs, and teeth, with the latter regulatory elements most likely located greater than 50 kilobases from the Bmp2 promoter. Although the Bmp2 gene resides in a large genomic region devoid of other genes, significant 'islands' of conserved sequence exist across this region. This is consistent with the presence of numerous Bmp2 cis-regulatory sequences in distant flanking regions. Our findings demonstrate that distant, complex regulatory elements direct Bmp2 expression in different locations within the developing skeletal system.

Disclosures: ***R.L. Chandler****, None.*

1183

Genetic and Environmental Contributions to Hip Strength: In Female Twins Aged 18 and Over. L. M. Paton*[1], T. J. Beck[2], L. Semanick*[3], S. Kantor*[1], R. Teh*[1], C. Nowson*[4], J. D. Wark[1]. [1]Department of Medicine, University of Melbourne, Parkville, Australia, [2]School of Radiology, Johns Hopkins University School of Medicine, Baltimore, MD, USA, [3]Department of Radiology, Johns Hopkins University School of Medicine, Baltimore, MD, USA, [4]School of Health Sciences, Deakin University, Burwood, Australia.

The technique of hip structural analysis (HSA) allows the mechanical properties of bone to be estimated from densitometric scans of the proximal femur. We postulated that, like BMD, the variation in HSA-derived biomechanical parameters may have a significant genetic component which may help explain the familial aggregation of fractures.

Proximal femur scans from 508 female twin pairs (238 monozygotic, 270 dizygotic) with a mean (SD) age of 42.2 (14.7), range 18 - 89 years, were analyzed. HSA provided measures of BMD (g/cm2), cross-sectional area (CSA, cm2), cross-sectional moment of inertia (CSMI, cm4), subperiosteal width (cm), section modulus (cm3), average cortical thickness (cm) and buckling ratio (BR) at the narrowest region of the femoral neck (NN), intertrochanteric (IT), and femoral shaft (FS) regions. [Mechanosensitivity index (MI) was calculated for the NN [((section modulus/moment arm of the NN)/lean body mass)), where the moment arm is the NN length*sin(180-neck shaft angle)]]. The intraclass correlations for rMZ and rDZ twin pairs were used to estimate the proportion of variance due to genetic (G = 2*(rMZ - rDZ), common environment (C = rMZ - G) and unique environmental effects (E = total variance - rMZ).

There was a moderate to strong genetic influence on almost all HSA-derived parameters which persisted after height and height-weight adjustment. Particularly at the NN, the strength of the genetic influence appeared to be less in the 45+ age group(section modulus G = 0.27) compared with 18 -45 years (section modulus G = 0.91) while the environmental component of variation appeared to be greater in the older group.

The finding suggest that environmental exposure may be more important than genes in determining hip fracture risk.

Table. The range in genetic variance for HSA parameters for the NN, IT and SF regions.

	Age		Age-height-weight	
	18 - 45 years	45+ years	18-45 years	45+ years
Section modulus	0.75 - 0.94	0.22 - 0.58	0.52 - 0.91	0.27 - 0.71
Cross-sectional area	0.79 - 0.90	0.48 - 0.73	0.72 - 0.88	0.45 - 0.74
Subperiosteal width	0.48 - 0.77	0.28 - 0.76	0.27 - 0.74	0.35 - 0.81
Endocortical diameter	0.33 - 0.63	0.22 - 0.90	0.30 - 0.60	0.37 - 0.84
Average cortical thickness	0.57 - 0.70	0.28 - 0.55	0.51 - 0.61	0.16 - 0.77

Disclosures: ***J.D. Wark****, None.*

1184

Prediction of Hip Fracture in the Elderly by Fall-related Factors. N. D. Nguyen, C. Pongchaiyakul, J. R. Center, J. A. Eisman, T. V. Nguyen. Bone and Mineral Program, Garvan Institute of Medical Research, Sydney, Australia.

Although bone mineral density (BMD) is a primary determinant of hip fracture risk, it cannot reliably discriminate individuals with fracture from those without. The aim of this study was to examine the contribution of fall-related factors to the prediction of hip fracture in the elderly.

The study included 960 female and 689 male participants in the Dubbo Osteoporosis Epidemiology Study (DOES), from whom measurements of femoral neck BMD, postural stability, and quadriceps strength were obtained at baseline in 1989 and every subsequent 2 years. Incidence of hip fractures was ascertained during the study period of 1989 and 2003. Apart from traditional proportional hazards analysis, postural instability, quadriceps weakness, fall history, fracture history and age were dichotomized in two categories: risk presence (1) and risk absence (0) that was based on the significant relative risks adjusted for FNBMD and gender. The sum of these risk factors was then derived for each individual and was termed "risk score" with range being 0 to 5. Incidence of hip fracture was analyzed according to the risk score.

During the 14-year follow-up period, 115 (86 women and 29 men) have sustained a hip fracture. Each standard deviation (0.12 g/cm^2) reduction in FNBMD was associated with a 3.8-fold (95% CI: 3.5 to 4.7) increased risk of hip fracture in women and a 3.3-fold (95% CI: 2.5 to 4.1) in men. Each 5-year increase in age was associated with a 1.6-fold (95% CI: 1.4 to 1.8) increased risk of hip fracture after adjusting for FNBMD and sex. Individuals with the highest tertile of postural sway (>16.2cm^2 for women and >14.5cm^2 for men) and lowest tertile of quadriceps strength (≤15kg for women and ≤28kg for men) had a relative risk of hip fracture of 2.7 (95% CI: 1.6 to 4.5) and 3.0 (95% CI: 1.3 to 6.8), respectively, after adjustment for FNBMD. In addition, a fall during the preceding 12 months and a prior low trauma fracture were independent predictors of hip fracture. For each level of BMD, the risk of hip fracture increased exponentially with the number of these risk factors. Individuals with risk score ≥ 3 had the highest risk of hip fracture (RR= 4.0, 95% CI: 2.5 to 6.0) compared to < 3 risk scores independent of BMD.These results suggest that postural instability, quadriceps weakness and a prior fall and a prior fracture are BMD-independent predictors of hip fracture in both men and women. These risk factors could be incorporated into an assessment model for prediction of hip fracture in the elderly population. The prevention of hip fracture should move beyond the "paradigm" of bone alone to include aspects of falls risk.

Disclosures: ***N.D. Nguyen****, None.*

1185

Secondary Causes of Osteoporosis in Older Men and Women. H. A. Fink[1], B. C. Taylor*[2], E. S. Orwoll[3], E. Barrett-Connor[4], J. M. Zmuda[5], D. C. Bauer[6], C. B. Lewis[7], D. Sellmeyer*[6], K. E. Ensrud[1]. [1]for the MrOS and SOF Research Groups, VAMC, Mpls, MN, USA, [2]U of MN, Mpls, MN, USA, [3]OHSU, Portland, OR, USA, [4]UC, SD, CA, USA, [5]U of Pitt, Pittsburgh, PA, USA, [6]UC, SF, CA, USA, [7]UA, Birmingham, AL, USA.

Secondary osteoporosis (OP) involves underlying risk factors (RF) other than aging or menopause. The relative importance of secondary RF for OP between men and women has not been directly studied.

We examined the cross-sectional association between putative, self-reported secondary RF and OP in community-dwelling men (MrOS, n=5994) and women (SOF, n=7959) aged ≥65y. RF were considered if comparably defined in MrOS and SOF and included self-reported medical conditions, current medications, current smoking and increased alcohol use (defined as >2 drinks/day). OP was defined as femoral neck BMD T-score <-2.5 (Hologic 4500 DXA) using sex-specific reference values (male cut-point 0.59 g/cm^2; female cut-point 0.57 g/cm^2). Prevalence of each individual RF and of ≥1 RF among subjects with OP (%), and age-adjusted odds of OP associated with each RF and with ≥1 RF (OR, 95% CI) were determined for each sex using logistic regression. Subjects were then pooled, and sex and an interaction term (sex*RF) added to each RF model to evaluate whether the strength of the association between RF and OP differed significantly by sex (p<0.10 for interaction term).

	Men		Women	
Risk factor (RF)	**OP men (n=290) with RF (%)**	**Age-adj OR of OP in men with RF (95%CI)**	**OP women (n=1993) with RF (%)**	**Age-adj OR of OP in women with RF (95%CI)**
Hyperthyroidism	2.4	1.4 (0.6-3.1)	10.8	1.1 (0.9-1.3)
Gastrectomy	11.7	1.5 (1.0-2.2)*	2.6	2.7 (1.8-4.0)
COPD	15.9	1.6 (1.1-2.2)	12.0	1.5 (1.3-1.8)
Parkinsonism	1.0	1.0 (0.3-3.3)	1.0	2.2 (1.2-4.0)
Stroke	8.3	1.2 (0.8-1.9)	3.0	1.0 (0.7-1.3)
Oral corticosteroid	5.3	2.0 (1.1-3.8)	3.6	2.1 (1.5-3.0)
Nonbenzodiazepine anticonvulsant	3.1	1.0 (0.5-2.3)	1.2	1.3 (0.8-2.1)
Current smoking	5.5	2.5 (1.5-4.4)	11.1	1.6 (1.4-1.9)
Increased alcohol use	2.8	0.6 (0.3-1.2)	0.8	0.8 (0.4-1.4)
≥1 RF	44.3	1.5 (1.1-1.9)	34.2	1.4 (1.3-1.6)

*p<0.10 for interaction term

There appeared to be no significant difference in overall prevalence of self-reported secondary RF in men and women with OP (44% vs. 34%). For most individual self-reported RF we found relationships with OP to be similar in men and women, though gastrectomy appears to be a stronger RF in women.

Disclosures: ***H.A. Fink****, None.*

1186

Hypovitaminosis D in a Sunny Country and its Relation to Musculoskeletal Health in the Elderly. A. Arabi[1], R. Baddoura[2], H. Awada*[2], M. Salamoun*[1], G. El-hajj Fuleihan[1]. [1]Internal Medicine, American University of Beirut, Beirut, Lebanon, [2]Rheumatology, Saint Joseph University, Beirut, Lebanon.

Osteoporosis is proposed as the long term latency disease for hypovitaminosis D. We have demonstrated a high prevalence of vitamin D deficiency among school children and young adults in Lebanon (1,2), but the prevalence of hypovitaminosis D in the elderly population is not clear. This is particularly important in view of the effect of vitamin D on muscle strength, fall risk, BMD, and therefore on fracture risk.

The aims of this study are to determine the prevalence of hypovitaminosis D and its effect on the musculoskeletal health in elderly subjects from a sunny country.

460 ambulatory, home-dwelling elderly subjects, aged 65-85 years, were randomly recruited from the Greater Beirut area, based on geographical maps. BMD and body composition were measured using Hologic QDR 4500A and Hologic QDR 4500W device in two centers. A cross-calibration formula was derived by having 30 subjects simultaneously measured BMD on both devices. Serum 25 hydroxy-vitamin D (25OHD) levels were measured between December and March.

The clinical characteristics of the study population are shown in the Table.

Variable	Females N=301	Males N=159	p-value[b]
Age (years)	73.4±5.2	74.1±5.2	NS
BMI (kg/m^2)	30.6 ± 6.5	27.3 ± 4	NS
25 (OH) vit D <10 ng/ml	56%	37%	<0.001
25 (OH) vit D 10-20 ng/ml	39%	57%	< 0.001
25 (OH) vit D >20 ng/ml	5%	5%	<0.001
Lumbar Spine Z-score	0.004±1.3	-0.6±1.4[a]	<0.001
Total hip Z-score	-0.1±1.0[a]	-0.5±1.0[a]	<0.001
1/3Radius Z-score	-0.5±1.3[a]	-1.2±1.6[a]	<0.001

a p< 0.05 compared with western databases
b p-value (t-test or chi-square)for difference between genders

In both genders, only 5% of the study participants had 25OHD levels >20 ng/ml. In both genders 25OHD levels correlated with BMD. In males, correlation coefficients were as follows: spine (r=0.21, p=0.01), total hip (r=0.25, p=0.001), femoral neck (r=0.21, p=0.008), trochanter (r=0.29, p=0.001) and forearm (r=0.20, p=0.01). In females, the coefficients were (r=0.17, p=0.002) at the total hip, (r=0.19, p=0.001) at the femoral neck, (r=0.18, p=0.002) at the trochanter and (r=0.12, p=0.03) at the forearm. There was no significant correlation between 25OHD and lean or fat mass. In a linear regression model, 25OHD was a significant independent predictor of BMD at multiple skeletal sites, after adjustment for age and BMI, in both genders.
This study refutes the erroneous assumption that hypovitaminosis D is non-existent in sunny Mediterranean countries. It documents a deleterious impact of vitamin D insufficiency on bone health in the elderly, and provides evidence for the institution of cheap and efficacious preventive health strategies to fight its latent manifestation, namely osteoporosis.
1-El-Hajj Fuleihan et al, Bone 2002
2-El-Hajj Fuleihan et al, Pediatrics 2001

Disclosures: ***A. Arabi****, None.*

1187

Increased Mortality Following Acute Hip Fracture: Secular Trends in California 1990-2001. S. L. Silverman[1], D. Zingmond*[2]. [1]Cedars-Sinai, Los Angeles, CA, USA, [2]UCLA, Los Angeles, CA, USA.

Purpose: The care of acute hip fracture has changed dramatically of the past two decades - lengths of stay have shortened, while patient illness has increased. Improvements in patient management may not translate into better patient outcomes. We studied in-hospital, 30-day, 60-day, 180-day and 365-day mortality, and length of stay following hip fracture.
Methods: Using inpatient discharge abstracts from the California Office of Statewide Health Planning and Development (OSHPD)'s inpatient discharge database (PDD), all patients hospitalized in California with acute hip fracture and repair were identified between 1990 and 2001. Out-of-hospital death was ascertained by linkage to the state death registry through 2001. Independent impact of temporal trends were estimated using multivariate logistic and Cox regressions controlling for patient characteristics.
Results: Between 1990 and 2001, 268,611 individuals were discharged from California hospitals with acute hip fracture repairs. Overall, 73% were female; 86% were White, 2.7% were Black, 6.5% Latino, and 3.4% Asian. During the period, the percent of Latinos admitted doubled. Medicare paid for 80% of hospitalizations. Ten percent of patients were admitted from nursing homes. Comorbidity, measured by Charlson Index, steadily increased from 0.8 to 1.3 over the decade. Mean hospital length of stay decreased from 9.2 to 5.8 days by 1997, but increased to 6.3 days by 2001. Similarly, in-hospital death decreased from 3.0 to 2.1% by 1997 and increased to 2.4% by 2001. Total mortality increased over the period: 30-day - 6.6 to 7.4%; 60-day - 9.0 to 11.0%; 180-day - 14 to 18%; and 365-day - 19 to 23%. In multivariate analyses, temporal trends regarding in-hospital and total mortality and length of stay were significant and were consistent with unadjusted analyses.
Conclusions: Improvements in the care of patients with hip fracture have not been consistent or maintained. Decreasing early mortality and hospital length of stay in the early 1990's were not been matched by decreases in intermediate mortality for these patients. Increasing in-hospital mortality and length of stay since 1997 implies that inpatient care is worsening or that improvements in patient care are insufficient for increasingly old and frail elderly. Future research should focus on identifying the cause of worsening outcomes and whether these outcomes are generalizable to other regions.
Acknowledgement: This study was supported by a grant from the SW Osteoporosis Council of the Alliance for Better Bone Health

Disclosures: ***S.L. Silverman****, None.*

1188

Prevalence of Low Bone Mass in Women - Secular Trends Over 30 Years. H. G. Ahlborg[1], O. Johnell[1], T. L. N. Järvinen[2], M. K. Karlsson[1]. [1]Department of Orthopaedics, Malmö University Hospital, Malmö, Sweden, [2]Department of Orthopaedics and Traumatology, Tampere University Hospital, Tampere, Finland.

The burden of hip fractures has during the last decades dramatically increased worldwide. In Malmö, Sweden, the incidence of hip fractures has increased by 100% in women aged 50 and above, and by 30% in women aged 80 and above between 1970 and 2001. However, whether also the prevalence of osteoporosis within this population has increased during the same period is unclear. This study was therefore designed to characterize the secular trends in bone mineral density (BMD) in women during the last three decades.
Between 1971 and 2001, normative bone densitometry data of the female population aged 40 and above was collected in Malmö, Sweden. BMD (mg/cm^2) in the distal forearm was measured both at a site 1 cm and 6 cm proximal to the styloid process of the ulna by single-photon absorptiometry. The same densitometer was used throughout the study, and no long-term drift, determined by measurements of a standardized phantom every other week, was observed during the study period. Altogether, the study population consisted of 1591 women; 516 were measured between 1971 and 1978 (cohort A), 625 between 1988 and 1993 (cohort B), and 450 between 1998 and 2001 (cohort C). We present data for the women divided into two age groups, 40 to 64 years (cohort A n=452; cohort B n=350; cohort C n=115) and 65 years and above (A n=64; B n=275; C n=335). A linear regression model with adjustment for age was used to compare BMD between the three cohorts.
In women aged 40 to 64, there was no difference in mean (±SD) age-adjusted BMD between the three cohorts, either at the 1 cm [A 308(70); B 303(69); C 308(69)] or the 6 cm [A 532(67); B 539(65); C 530(66)] measurement site. In women aged 65 and above, cohort C [250(68)] had a higher age-adjusted BMD compared to both cohort A [228(68), p<0.05] and cohort B [238(68), p<0.05] at the 1 cm measurement site. However, at the 6 cm site, cohort C [391(74)] had a lower age-adjusted BMD compared to cohort B [421(74), p<0.001] but not significant different compared to cohort A [398(73)]. Furthermore, there was no significant difference in the proportion of women with osteoporosis (i.e. lower than -2.5 SD of young women) between the three cohorts in either age group or measurement site. In women aged 65 and above, the proportion of women with osteoporosis at the 1 cm measurement site was 17% in cohort A, 17% in cohort B, and 16% in cohort C; and 25%, 22% and 28% in cohort A,B, and C respectively at the 6 cm measurement site.
These data suggests that within a population with increased incidence of hip fracture during the last three decades, the proportion of women with low BMD has not increased during the same period.

Disclosures: ***H.G. Ahlborg****, None.*

1189

Volumetric and Areal Bone Mineral Density Measures Are Associated with Cardiovascular Disease in Older Men and Women: The Health Aging and Body Composition Study (Health ABC). G. N. Farhat*[1], E. S. Strotmeyer[1], A. B. Newman*[1], K. Sutton-Tyrrell*[1], D. C. Bauer[2], T. Harris*[3], K. C. Johnson*[4], D. Taaffe[5], J. A. Cauley[1]. [1]U of Pittsburgh, Pittsburgh, PA, USA, [2]UCSF, San Francisco, CA, USA, [3]NIA, Bethesda, MD, USA, [4]U of Tenn., Memphis, TN, USA, [5]UQ, Queensland, Australia.

Low bone mass has been related to increased cardiovascular mortality, morbidity, and subclinical measures of cardiovascular disease (CVD). Studies that investigated these associations have focused mostly on white women; none have employed volumetric measures of bone mineral density (BMD). In this cross-sectional analysis, we tested the hypothesis that volumetric (vBMD) and areal (aBMD) BMD measures are inversely associated with clinical CVD and subclinical peripheral arterial disease (PAD) in men and women.
Data are from the baseline assessment of Health ABC which included 3075 well-functioning white and black men and women (42% Black; 51% women) between the ages of 70-79 years. Existing clinical CVD was defined as diagnosis of coronary heart disease, PAD, congestive heart failure, or cerebrovascular disease. Subclinical PAD was defined as a low ankle-arm index (≤0.9) in the absence of clinical CVD. Total hip aBMD was measured using DXA (Hologic 4500A). Trabecular and integral vBMD of the spine were measured using QCT (GE 9800 Advantage) in a subset (n=1489). Multiple logistic regression was used to assess the contribution of BMD measures (per SD) to clinical CVD and subclinical PAD after adjusting for age, race, gender, anthropometric measures, blood pressure, lipids, hypertension, diabetes, physical performance scores, and other important covariates. Models in women were additionally adjusted for time since menopause and hormone use.
The prevalence of clinical CVD in this population was 25%. Among participants without clinical CVD, 11% had subclinical PAD. Integral vBMD was inversely associated with clinical CVD in the whole group (OR=0.80, 95%CI 0.69-0.93), in men (OR=0.75, 95%CI 0.61-0.90), and in women (OR=0.72, 95%CI 0.56-0.94). Similar results were found for trabecular vBMD (OR for all participants= 0.85, 95% CI 0.73-0.99). aBMD was associated with subclinical PAD among all participants (OR=0.69, 95%CI 0.56-0.84) and in each gender separately. However, it was significantly correlated with clinical CVD only in women (OR=0.80, 95%CI 0.67-0.96).
In conclusion, both vBMD and aBMD measures were inversely related to clinical CVD and subclinical PAD in a biracial cohort of older men and women independent of shared risk factors between osteoporosis and CVD. These associations maybe mediated, in part, by endogenous sex hormones or cytokines, which are implicated in both atherogenesis and bone remodeling.

Disclosures: ***G.N. Farhat****, None.*

1190

Vascular Pressure in the Lower Limbs and Bone Mineral Density. K. J. McLeod, R. Spathis*. Bioengineering, Binghamton University, Binghamton, NY, USA.

Interstitial fluid flow is essential for the maintenance of bone mass. Interstitial flow refers to the extravasated fluid and nutrients which leave the vascular supply and are subsequently collected by the lymphatic system and returned to the circulatory system. This flow is dependent both on vascular pressure and the microfiltration coefficient of the capillaries. Correspondingly, vascular pressure is dependent on the blood pressure due to heart contraction and on the hydrostatic pressure column of blood above the site of interest. In the lower limbs of the body, the hydrostatic pressure component serves to significantly increase total vascular pressure. Here, we determined the association between vascular pressure in the lower limbs and bone mineral density of the femoral neck, using a dataset containing 31,000 subjects.

Data on age (range 20-90 years), sex, ethnicity, height, weight, systolic pressure, and femoral neck BMD were obtained from the Third National Health and Nutrition Examination Survey, 1988-1994. Subjects being treated for hypertension were excluded. BMI was calculated from height and weight data, and total vascular pressure in the lower limbs was calculated from systolic pressure, body height and blood density. Stepwise regression was performed on the BMD data using age, BMI, and total vascular pressure as independent variables, with all interaction terms included (SPlus 6.0). Significance was established at the p=0.01 level.

Stepwise regression modeling of the white women in this population (N=3240), showed that neither BMI nor age were significant predictors of femoral neck BMD, but total vascular pressure was a highly significant correlate (p=0.006). For black women (N=2120), age (p=0.001), BMI (p=0.009), and total vascular pressure (p=0.002) were all found to be significant predictors of femoral neck BMD. For Hispanic women (N=1805), only BMI (p=0.0001) and total vascular pressure (p=0.0002) were significant predictors of neck BMD. For males, age was a significant predictor for all three ethnic groups, and total vascular pressure was significant for the white male population (p=0.001).

These results lend support to the concept that adequate interstitial flow across bone tissue is essential to the maintenance or enhancement of bone tissue. While upright posture has long been known to be important in the prevention of bone loss, this observation is commonly interpreted as indicating that mechanical loading of the skeleton is responsible for bone tissue integrity. Instead, we suggest that upright stance plays an important role through its dramatic effect on vascular pressure in the lower limbs, thereby significantly enhancing interstitial fluid flow.

Disclosures: ***K.J. McLeod****, None.*

1191

Silencing of TGFbeta Signaling in T Cells Stimulates T Cell Production of Osteoclastogenic Cytokines and Abolishes the Bone Sparing Effect of Estrogen. Y. Gao[1], W. Qian*[1], K. Dark*[1], A. S. P. Lin*[2], R. E. Guldberg[2], R. A. Flavell[3], M. N. Weitzmann[1], R. Pacifici[1]. [1]Division of Endocrinology, Metabolism and Lipids, Emory University School of Medicine, Atlanta, GA, USA, [2]Woodruff School of Mechanical Engineering, Georgia Institute of Technology, Atlanta, GA, USA, [3]Section of Immunobiology, Yale University School of Medicine, New Haven, CT, USA.

A key mechanism by which ovariectomy (ovx) leads to bone loss is through an expansion of TNF producing T cells that results in TNF potentiation of RANKL induced osteoclastogenesis. Ovx increases T cell number by promoting T cell activation, but the responsible mechanism is poorly understood. One of the involved factors is TGFbeta, a cytokine stimulated by estrogen (E) and repressed by ovx. Overexpression of TGFbeta1 in vivo prevents ovx induced bone loss. Furthermore, transplantation of T cells insensitive to TGFbeta signaling into E replete T cell deficient nude mice is followed by significant bone loss, despite the presence of E. These data suggest that TGFbeta signaling in T cells is required for E to prevent bone loss. We have now examined transgenic mice containing T cells rendered insensitive to TGFbeta by the T cell specific overexpression of a dominant negative TGFbeta type II receptor (dnTGFbIIR). We found that dnTGFbIIR mice displayed significantly lower bone density than wild type (WT) littermates starting from the age of 8 weeks. After surgery, all groups of dnTGFbIIR mice (intact, sham operated, ovx and E treated ovx) lost as much bone as ovx WT mice. The finding that E replete dnTGFbIIR mice lost as much bone as ovx WT mice demonstrates that silencing of TGFβ signaling in T cells abolishes the bone sparing effect of E. T cells from both E replete and ovx dnTGFbIIR mice secreted ~3 fold higher levels of TNF and RANKL than T cells from E replete WT mice, thus demonstrating that T cells insensitive to TGFbeta produce maximal amounts of osteoclastogenic cytokines in spite of the presence of E. Ovx increases T cell activation through enhancement of macrophage antigen presenting cell (APC) activity and expression of the APC regulating gene CIITA. We found that T cells from all groups of dnTGFbIIR mice also produced high levels of IFNgamma, a cytokine which upregulates APC activity through CIITA. Macrophages from both E replete and ovx dnTGFbIIR mice expressed high levels of CIITA mRNA and exhibited increased APC activity. In contrast, only macrophages from ovx WT mice exhibited increased CIITA levels and APC activity. In summary, the data confirm that T cells play an essential role in ovx induced bone loss and suggest that TGFβ mediates the repressive effect of E on T cell activation thus preventing T cell production of bone wasting cytokines.

Disclosures: ***Y. Gao****, None.*

1192

Osteoprotegerin Tightly Regulates the Shedding of RANKL by Osteoblasts and Activated T Cells. Y. Nakamichi[1], N. Udagawa[2], M. Nakamura[2], Y. Kobayashi[1], M. Mogi*[3], N. Takahashi[1]. [1]Institute for Oral Science, Matsumoto Dental Univ., Shiojiri, Japan, [2]Biochemistry, Matsumoto Dental Univ., Shiojiri, Japan, [3]Pharmacology, Aichi Gakuin Univ., School of Dentistry, Nagoya, Japan.

OPG is a decoy receptor for RANKL. OPG-deficient ($OPG^{-/-}$) mice exhibit aberrant bone metabolism characterized by accelerated bone resorption and formation. Recent studies have shown that serum levels of RANKL are markedly elevated in patients with OPG-deficient juvenile Paget's disease and in $OPG^{-/-}$ mice. Using $OPG^{-/-}$ mice, we investigated (i) which organ is responsible for the elevated serum levels of RANKL; (ii) whether serum RANKL levels reflect the state of bone resorption; (iii) whether OPG and OPG-related proteins inhibit the shedding of RANKL; and (iv) which proteases are involved in the shedding of RANKL. When $1,25(OH)_2D_3$ was daily administered into $OPG^{-/-}$ mice for 4 days, serum levels of RANKL as well as calcium were increased. RANKL mRNA expression was increased in bone but not in thymus or spleen in the $1,25(OH)_2D_3$-treated mice. Treatment with $1,25(OH)_2D_3$ increased RANKL mRNA expression and the release of RANKL in cultures of calvarial cells and bone marrow-derived stromal cells but not T cells prepared from $OPG^{-/-}$ mice. In addition, serum RANKL levels in $OPG^{-/-}$ mice decreased in an age-dependent manner when the assay was performed at 1-18 weeks of age. The release of RANKL in cultures of $OPG^{-/-}$ osteoblasts as well as RANKL-induced osteoclast formation was dose-dependently inhibited by adding OPG and a soluble form of RANK but not other OPG-related proteins such as DR6 (death receptor 6) and DcR3 (decoy receptor 3). Normal $CD4^+$ T-cells activated with anti-mouse CD3 antibody produced a large amount of soluble RANKL but not OPG. Treatment of activated T cells with OPG or soluble RANK inhibited the release of soluble RANKL. OPG and T cell-double deficient mice produced by crossbreeding $OPG^{-/-}$ mice with athymic nude mice showed serum RANKL levels equivalent to those of $OPG^{-/-}$ mice. Among several protease inhibitors examined, inhibitors of membrane-type matrix metalloproteases (MT-MMPs) efficiently blocked the shedding of RANKL from $OPG^{-/-}$ osteoblasts in culture. These results suggest (i) that soluble RANKL in $OPG^{-/-}$ mice is derived from osteoblasts; (ii) that serum RANKL levels sharply reflect the bone resorption state; (iii) that OPG and soluble RANK inhibits the RANKL shedding, with a dosage similarity to their inhibitory action on osteoclastogenesis; and (iv) that MT-MMPs are involved in the shedding of RANKL in osteoblasts. Altogether these findings establish a key role for OPG in maintaining locally expressed RANKL which is essential for normal bone development and function.

Disclosures: ***Y. Nakamichi****, None.*

1193

Dominant Negative N-cadherin Inhibits Osteoclast Differentiation by Suppressing RANKL Expression through Wnt Pathway. C. S. Shin[1], S. J. Her*[1], J. A. Kim*[1], D. H. Kim*[1], S. W. Kim*[1], S. Y. Kim*[1], J. G. Kim[2], H. S. Kim*[1], R. Kitazawa*[3], S. Cheng[4], R. Civitelli[4]. [1]Department of Internal Medicine, Seoul National University College of Medicine, Seoul, Republic of Korea, [2]Department of Obstetrics and Gynecology, Seoul National University College of Medicine, Seoul, Republic of Korea, [3]Division of Molecular Pathology, Kobe University Graduate School of Medicine, Kobe, Japan, [4]Division of Bone and Mineral Diseases, Washington University School of Medicine, St. Louis, MO, USA.

Cadherin is a calcium dependent cell adhesion molecule, which plays major role during embryonic development. Classic cadherins interacts with β-catenin, which is also involved in the wnt signaling pathway. We have previously demonstrated that cadherin-mediated cell-cell adhesion is involved in maturation and function of osteoblasts both in vitro and in vivo. We tested whether disruption of N-cadherin function in stromal cells by dominant negative cadherin affects the ability to support osteoclastogenesis by altering heterotypic interaction with osteoclast precursors. Immunoblotting analysis showed that primary bone marrow stromal cells, and two stromal cell line, ST2 and MC3T3-G2/PA6, expressed N-cadherin. The expression of N-cadherin was also identified in bone marrow macrophages(BMM) and RAW 264.7 cell line by RT-PCR analysis. Retroviral expression of extracellular domain- truncated, dominant negative cadherin (NcadΔC) in ST2 cells resulted in slightly decreased cell-to cell adhesion but markedly impaired the formation of TRAP-positive osteoclasts (>40%) when cocultured with BMMs. However, the inhibition of osteoclatogenesis was not reproduced by neutralizing antibody against N-cadherin and addition of Ncad-Fc, a soluble cadherin, did not recover the decreased formation of osteoclasts by NcadΔC expression, suggesting that decreased cellular adhesion has only partly contributed to the decreased formation of osteoclasts by NcadΔC. Expression of NcadΔC, however, strongly suppressed β-catenin/Tcf transcriptional activity in ST2 cells, which was rescued by stably-active β-catenin adenovirus (Ad ΔN46 β-catenin). As a potential downstream target of wnt signaling, we have found that the expression of RANKL was decreased in ST2 cells expressing NcadΔC. Expression of OPG was not different. Moreover, Wnt-3A conditioned medium, Ad ΔN46 β-catenin, and lithium chloride increased the expression of RANKL and enhanced the transcriptional activity of mouse RANKL promoter in ST2 cells. In conclusion, these results suggest that expression of dominant negative cadherin in ST2 cells suppressed osteoclastogenesis by suppressing RANKL expression, which seems to be regulated by wnt signaling pathway.

Disclosures: ***C.S. Shin****, None.*

1194

Akt1/Akt2 and mTOR/Bim Play Critical Roles in Osteoclast Differentiation and cEll Survival, Respectively, while Akt Is Dispensable for Cell Survival in Isolated Osteoclast Precursors. T. Sugatani, K. A. HrUSKA. Pediatrics, Washington University, St.louis, MO, USA.

Akt, also known as protein kinase B, is a serine/threonine protein kinase with antiapoptotic activities. Akt is also a downstream target of phosphatidylinositol-3-kinase (PI3K), and recently, Akt has been implicated in cell differentiation. Here we show that Akt1/Akt2 play a critical role in osteoclast differentiation but not cell survival, while the mammalian target of rapamycin (mTOR) and Bim, a member of the BH3-only subfamily of cell death activators, are required for cell survival in isolated osteoclast precursors. To investigate the function of Akt1, Akt2, mTOR and Bim in osteoclast precursors, we employed a retroviral system for delivery of small interfering RNA (siRNA) into cells. Akt1 and/or Akt2 siRNA-induced post-transcriptional gene silencing abolished phosphorylation of IKK α/β and IκB-α during treatment of murine osteoclast precursors with RANKL, and loss of Akt1 and/or Akt2 protein suppressed nuclear translocation of NFκB p50. Moreover, depletion of Akt1 and/or Akt2 protein inhibited NFκB p50 DNA-binding activity. Consistent with these data, Akt1 and/or Akt2 siRNA gene silencing reduced TRAP-positive multinucleated osteoclast formation number. One possible explaination of the data is that TRAP-positive multinucleated osteoclast formation number was reduced by Akt1 and/or Akt2 siRNA-induced apoptosis. Therefore, we investigated whether Akt1 and/or Akt2 siRNA gene silencing promoted apoptosis in isolated osteoclast precursors. Surprisingly, loss of Akt1 and/or Akt2 protein did not stimulate cleaved caspase-3 activity and failed to induce apoptosis in the apoptosis detection in situ marker assay. Moreover, in a cell viability assay, there was no difference between control and infected cells after M-CSF withdrawal, strongly suggesting that Akt1/Akt2 are dispensable for cell survival in isolated osteoclast precursors. Conversely, mTOR siRNA gene silencing markedly stimulated cleaved caspase-3 activity and quickly induced apoptosis after M-CSF withdrawal in the cell viability assay. In contrast, Bim siRNA gene silencing did not stimulate cleaved caspase-3 activity, but induced precursors resistant to M-CSF withdrawal-induced apoptosis. In addition, we found that mTOR is downstream of PI3K but not Akt, and M-CSF down-regulates Bim expression through mTOR activation for cell survival in osteoclast precursors. Thus, we provide the first evidence that Akt1/Akt2 are among the key elements of osteoclast differentiation but not survival, and that the M-CSF-mediated mTOR/Bim axis is essential for cell survival in isolated osteoclast precursors.

Disclosures: ***T. Sugatani****, None.*

1195

TREM2, a DAP12-Associated Receptor, Functions During *In Vitro* Osteoclast Differentiation, Migration, and Resorption. M. B. Humphrey, E. C. Niemi*, M. C. Nakamura, M. R. Daws*. Medicine, VA Medical Center and University of California, San Francisco, CA, USA.

TREM2 (Triggering Receptor Expressed in Myeloid cells-2) associates with the signaling adapter DAP12 in myeloid lineage cells including osteoclasts. TREM2 mutations and deletions are associated with the human bone and brain disorder, Nasu-Hakola. We and others recently demonstrated the critical requirement for ITAM signals through DAP12 and/or the FcRγ chain during osteoclast development. In earlier studies we demonstrated that direct stimulation of TREM2 transfected into RAW264.7 enhanced *in vitro* osteoclastogenesis. To further define the role of TREM2, we generated anti-TREM2 antibodies, analyzed preosteoclasts and mature osteoclasts for TREM2 surface expression and determined the effect of antibody ligation on *in vitro* osteoclast differentiation, migration, and resorptive function. In addition, we utilized TREM2 RNAi introduced by lentivirus to disrupt expression of TREM2 in osteoclast precursors. Our studies reveal that by flow cytometry TREM2 is weakly expressed (4-5%) on C57BL/6 non-adherent bone marrow macrophages (BMM) maintained in MCSF and is upregulated during culture with RANKL (18% at 72 hours). Anti-TREM2 antibody treatment in addition to RANKL and MCSF enhances the formation of multinuclear, TRACP+ C57BL/6 osteoclasts compared to control antibody treatment, while antibody treatment of RAW264.7 treated with RANKL/TGFβ increases the formation of multinuclear, TRACP+ osteoclasts 3-fold. Anti-TREM2 antibody treatment inhibited migration of C57BL/6 BMM and RAW246.7 preosteoclasts (treated 3 days with RANKL/MCSF) in response to 100ng/ml MCSF ($p<0.05$). RAW264.7 osteoclasts (Day 4 RANKL/TGFβ) treated with anti-TREM2 antibody exhibit decreased resorption on artificial calcium-phosphate substrate, while isotype control antibody had no effect.

Following prolonged *in vitro* culture, we noted that RAW264.7 cells often lose capacity to form multinuclear, TRACP+ osteoclast-like cells in response to RANKL/TGFβ. Examination of these cells compared to highly osteoclastogenic RAW264.7 cells reveals that the level of expression of TREM2 correlates with osteoclastogenic capacity. Additionally, we designed aTREM2 RNAi that effectively decreases TREM2 surface expression in RAW264.7 cells and inhibits the formation of osteoclast-like cells with RANKL/TGFβ. TREM2 RNAi that did not reduce TREM2 expression had no effect on osteoclastogenesis. These data support a role for TREM2 in formation of multinucleated osteoclasts and also osteoclast migration and resorptive functions. The role for TREM2 may be of particular importance during *in vitro* osteoclastogenesis, particularly in RAW264.7 cells.

Disclosures: ***M.B. Humphrey****, Abbott Scholar Award in Rheumatology 2.*

1196

Mmp9 Plays a Critical Role in Bone Remodeling in the Absence of Cathepsin K. C. Li*[1], B. Gelb*[2], K. J. Jepsen[1], D. M. Laudier*[1], G. Bouyer*[1], R. Ni*[2], J. Zhang*[2], G. Opdenakker*[3], M. B. Schaffler[1]. [1]Orthopaedics, Mount Sinai School of Medicine, New York, NY, USA, [2]Human Genetics, Mount Sinai School of Medicine, New York, NY, USA, [3]Rega Institure, University of Leuven, Leuven, Belgium.

Cathepsin K (Ctsk) is a lysosomal cysteine protease expressed in osteoclasts and plays the major role in degradation of organic matrix during bone resorption. However, recent studies also show that bone resorption is still possible in the absence of Ctsk, suggesting that other enzymes play an essential role driving bone matrix solubilization. In the present study we examined whether Mmp9 plays a critical role in osteoclast-mediated bone remodeling when Ctsk is absent. Ctsk knockout mice (Ctsk-/-) and mice lacking both Ctsk and Mmp9 (Ctsk-/-/Mmp9-/-) were generated. Bone phenotypes were examined histomorphometrically in metaphyseal cancellous bone and diaphyses from 10-week-old mice. Ctsk-/-: Compared to wild type mice, Ctsk-/- mice showed normal femur length, mild osteopetrosis in metaphyses (Tb.Ar/T.Ar +85%), accumulation of calcified cartilage near the growth plate and evidence of increased osteoclastogenesis (osteoclast number and surface). Small regions of demineralized bone matrix within Howship's lacunae were occasionally noted, suggesting a qualitative change in osteoclast function. Long bone cortices were thicker (+42%), marrow cavities smaller (-28%) and intracortical porosity was increased. Ctsk-/-/Mmp9-/-: Combined Ctsk-/-/Mmp9-/- mice were profoundly affected, with shorter femurs, severe osteopetrosis (Tb.Ar/T.Ar +40% compared to Ctsk-/- alone) and large accumulations of calcified cartilage near the growth plate. Osteoclastogenesis was dramatically increased. The majority of Howship's lacunae contained areas of unresorbed demineralized matrix, overlaid by flattened, bone lining-type cells. Long bones had thicker cortices, marked reduction of marrow space (-53%) with extensive presence of unresorbed trabecular bone in the marrow cavity of the mid-diaphysis, and increased intracortical porosity (~3 fold) when compared to Ctsk-/-. Together, these data indicate that Mmp9 plays a critical role in the coupling of bone resorption and formation, allowing the required bone remodeling for the longitudinal and transversal growth of long bone in the absence of CatK.

Disclosures: ***C. Li****, None.*

1197

TIEG Expression Is a Key Factor in Osteoclast Differentiation and Osteoblast Support of Osteoclast Differentiation. G. A. Gorny*[1], M. Subramaniam[1], T. C. Spelsberg[1], M. J. Oursler[2]. [1]Biochemistry and Molecular Biology, Mayo Clinic, Rochester, MN, USA, [2]Endocrine Research Unit, Mayo Clinic, Rochester, MN, USA.

During pathological bone loss there are increased osteoclast (OC) numbers. Given the limited effective therapies for this bone loss, it is vital to investigate means of targeting OC differentiation. We have shown that TGF-β Inducible Early Gene 1 (TIEG) plays an important role in osteoblast (OB) differentiation and TIEG overexpression in human OBs mimics TGF-β effects on these cells. In order to study the effects of TIEG expression on OC differentiation, marrow- and spleen-derived OC precursors and calvarial OBs were harvested from $TIEG^{+/+}$ and $TIEG^{-/-}$ mice and their ability to function during OC differentiation *in vitro* was examined.

$TIEG^{-/-}$ OC precursors co-cultured with ST2 stromal support cells or $TIEG^{+/+}$ calvarial OBs exhibited less OC differentiation when compared to $TIEG^{+/+}$ OC precursors. There were significantly fewer multinucleated OCs when either $TIEG^{+/+}$ or $TIEG^{-/-}$ precursors were co-cultured with the $TIEG^{-/-}$ OBs compared to $TIEG^{+/+}$ OBs.

The RANKL/OPG expression ratio was lower in $TIEG^{-/-}$ OBs compared to $TIEG^{+/+}$ OBs. RANKL addition to $TIEG^{-/-}$ calvarial OBs co-cultured with $TIEG^{+/+}$ OC precursors resulted in partial restoration of differentiation, whereas M-CSF addition alone or in combination with RANKL had no impact of differentiation. There was no difference in RANK or c-fms receptor expression levels comparing $TIEG^{+/+}$ to $TIEG^{-/-}$ spleen cells. Flow cytometry detected no difference in $CD11b^+$ and/or $RANK^+$ and/or $c\text{-}fms^+$ OC precursors in either marrow or spleen. When equal numbers of $CD11b^+$ OC precursors were cultured with RANKL and M-CSF, differentiation was observed in the $TIEG^{+/+}$ cultures. Interestingly, less differentiation occurred in the $TIEG^{-/-}$ $CD11b^+$ cultures.

There was a dose dependent increase in OC differentiation of $TIEG^{+/+}$ cells when treated with TGF-β . In contrast, there was no TGF-β impact on $TIEG^{-/-}$ precursor differentiation. When spleen cells cultured with RANKL and M-CSF were treated with TGF-β , there was a significant increase in RANK and c-fms expression in $TIEG^{+/+}$ cells, but not in $TIEG^{-/-}$.

In summary, TIEG expression in OC precursors and OBs is important in OC differentiation. The RANKL/OPG ratio is one component of OB support of differentiation, but other factors must also contribute. The defect in OC precursors is not at the level of either precursor number or expression of RANK or c-fms. Moreover, TIEG-mediated increases in RANK and c-fms expression may be the mechanism by which TGF-β stimulates OC differentiation. We conclude from these data that TIEG expression in both OC precursors and OB support cells is important in normal OC differentiation.

Disclosures: ***G.A. Gorny****, None.*

1198

Cbl-b Deletion Increases RANK Expression, Cell-autonomous Increase in Bone Resorption and Osteopenia in Vivo. A. Sanjay, R. Chiusaroli, A. Nakajima, W. C. Horne, R. Baron. Orthopedics, Yale University school of Medicine, New Haven, CT, USA.

Cbl proteins (Cbl and Cbl-b) are both expressed in cells of hematopoietic origin including osteoclasts. Although Cbl is a critical substrate of Src in osteoclasts, deletion of cbl gene in mice leads only to a subtle bone phenotype with delay in osteoclast migration both in vivo and in vitro suggesting compensation by the other family member. To better understand the role of these two family members in bone resorption, we have compared the phenotypes of Cbl and Cbl-b knock out mice. In contrast to the mild phenotype of the Cbl-deficient mice, Cbl-b-deficient mice have a 30% decrease in trabecular bone volume in both vertebrae and long bones. Although no changes were detected in osteoblast or osteoclast surface or numbers, there was a significant increase in serum C-terminal collagen telopeptide (82 ng/ ml Cbl-b-/- vs. 51 ng/ml WT, $p<0.05$). In vitro, the pit formation capacity of the Cbl-b deficient osteoclasts was enhanced 2 to 2.5-folds as compared to the wild type counterparts, further substantiating the in vivo findings. Bone marrow cells derived from Cbl-b-deficient mice differentiated more rapidly, with 2-fold more mature osteoclasts present on days 4 and 6 than with WT precursors. Similarly the mRNA levels of c-Fos, one of the osteoclast differentiation marker, was upregulated during the differentiation of the Cbl-b deficient bone marrow cells. Given the role of Cbl proteins in the regulation of receptor degradation, we next looked at the surface expression of c-Fms and RANK, two proteins that are critical for osteoclast differentiation and function. The surface expression of c-Fms was not changed in the absence of Cbl-b. In contrast, the surface expression RANK and effectors of RANK signaling, (e.g. Jun kinase and Erk kinase) were enhanced in the Cbl-b deficient osteoclasts suggesting that RANK-mediated signaling maybe enhanced in the absence of Cbl-b. These results suggest that in spite of similarity in structural organization and function, some unique aspects of Cbl-b not being compensated by Cbl. One such unique function appears to involve the down-regulation of RANK and signaling.

Disclosures: ***A. Sanjay****, None.*

1199

Cinacalcet HCl Is an Effective Therapy for the Hypercalcemia of Primary Hyperparathyroidism across a Broad Range of Patients. M. Peacock[1], J. P. Bilezikian[2], S. Scumpia*[3], M. A. Bolognese*[4], M. A. Borofsky*[5], S. A. Turner*[6], M. D. Guo*[6], L. C. McCary*[6], D. M. Shoback[7]. [1]Indiana Univ Sch Med, Indianapolis, IN, USA, [2]Columbia Univ Med Ctr, New York, NY, USA, [3]Ctr for Clin Research, Austin, TX, USA, [4]Bethesda Health Research, Bethesda, MD, USA, [5]Clin Research Ctr of Reading, LLP, West Reading, PA, USA, [6]Amgen Inc., Thousand Oaks, CA, USA, [7]Dept of Veterans Affairs Med Ctr, Univ of California, San Francisco, San Francisco, CA, USA.

The calcimimetic, cinacalcet, is a potential therapy for primary hyperparathyroidism (PHPT) because it reduces parathyroid hormone and serum calcium by increasing the sensitivity of the calcium-sensing receptor to extracellular calcium. Although parathyroidectomy (PTX) can be curative, there are patients for whom a specific pharmacologic approach is needed. These patients include the following: those with recurrent PHPT after unsuccessful PTX, patients for whom PTX is contraindicated or who refuse PTX; and others who do not meet current guidelines for surgery but in whom reduction of the serum calcium is desired. For these patients, an unmet medical need exists.

For this analysis, 122 patients with PHPT who participated in clinical trials with cinacalcet were divided into 3 groups: 1) patients with recurrent PHPT post-PTX (n = 30); 2) patients who met ≥ 1 criteria for PTX, but had not had surgery (n = 66); and 3) other PHPT patients (n = 26). Three double-blind, placebo-controlled and two open-label, single arm studies were included in this analysis. The dose range of cinacalcet used was 30 mg twice daily to 90 mg four times daily for from 2 weeks to 3 years of therapy. A positive response to cinacalcet was defined as a decrease in serum calcium to ≤ 10.3 mg/dL. In all 3 groups, cinacalcet normalized serum calcium in more patients than placebo (Table). Reductions in serum calcium were sustained in the 18 patients who were treated for 3 years. Cinacalcet was generally well-tolerated in each group.

	Group 1		Group 2		Group 3	
	Cinacalcet n = 20	Placebo n =10	Cinacalcet n = 37	Placebo n = 29	Cinacalcet n = 18	Placebo n = 8
Mean (SE) Baseline Calcium (mg / dL)	11.2 (0.2)	10.6 (0.2)	11.1 (0.1)	10.6 (0.1)	11.0 (0.1)	10.7 (0.1)
Mean (SE) Baseline iPTH (pg / mL)	123 (23)	121 (14)	136 (12)	120 (11)	114 (12)	87 (8)
% Patients with Calcium ≤ 10.3 mg / dL after Rx	80%[a]	33%	81%[a]	24%	83%	38%
Mean (SE) % Change in Calcium	-13.0 (2.3)[b]	-0.8 (1.1)	-13.5 (1.0)[b]	-0.2 (1.0)	-12.6 (1.9)[b]	-0.7 (2.2)

[a]$P < 0.05$ using Fisher's exact test to compare between treatment groups.

[b]$P < 0.05$ using two sample t-test to compare between treatment groups.

This analysis of several clinical trials indicates that cinacalcet effectively normalized the serum calcium across a broad range of patients with PHPT, including those for whom PTX is not a treatment option. Cinacalcet has the potential to be an effective alternative to PTX in some patients with PHPT.

Disclosures: ***M. Peacock****, Amgen Inc. 5.*

1200

Lysyl Oxidase Is a Downstream Target Gene for PDGF-A Signaling in a Rat Model for Parathyroid Bone Disease. S. Lotinun[1], M. Zhang*[1], A. A. Leontovich*[2], R. T. Turner[1]. [1]Department of Orthopedics, Mayo Clinic, Rochester, MN, USA, [2]Department of Experimental Pathology, Mayo Clinic, Rochester, MN, USA.

Parathyroid hormone (PTH)-induced osteitis fibrosa is common in patients with renal osteodystrophy. The peritrabecular fibrosis in these patients contributes to the deterioration of bone quality and commensurate increase in fracture risk. The migration of fibroblasts to bone surfaces requires tissue remodeling to allow cellular infiltration. Targeting pathological tissue remodeling is a potential treatment for fibrosis. Histological changes identical to osteitis fibrosa can be induced in rats by continuous administration of PTH. Microarray analysis was used to identify candidate genes by comparing the skeletal response to intermittent (bone anabolic) and continuous (catabolic and fibrotic) PTH treatment. Continuous but not intermittent PTH upregulated mRNA levels for several genes associated with tissue remodeling (e.g., platelet-derived growth factor A, PDGF-A; secreted frizzled-related protein 4, Sfrp 4; matrix metalloproteinase 14, Mmp 14; decorin, Dcn; and lysyl oxidase, LOX). We investigated the hypothesis that these candidate genes are involved in the initiation of PTH-induced peritrabecular fibrosis. PTH (40 mg/kg/d) was continuously infused into 6-month-old female Sprague-Dawley rats for 1, 3, 5, 7, 14 and 28 d. Additionally, after 7 d PTH was withdrawn for 7 and 21 d. Total RNA from distal femur metaphysis was isolated and mRNA levels for PDGF-A, Sfrp 4, Mmp 14, Dcn and LOX were measured by RT-PCR. These analyses confirmed the upregulation of mRNA levels for Sfrp 4 within 3 d and PDGF-A, Mmp 14, Dcn and LOX within 5 d of initiation of PTH infusion, consistent with the appearance of peritrabecular fibroblasts on d 5. One week following termination of PTH, the mRNA levels were decreased to the control level and the peritrabecular fibroblasts disappeared. These data suggest a direct relationship between genes regulating tissue remodeling and peritrabecular fibrosis. Using cDNA microarray analysis we compared rats treated with continuous PTH to rats treated with PTH and trapidil. Trapidil, a PDGF-A signaling antagonist, antagonizes PTH-induced fibrosis. RT-PCR confirmed that trapidil prevented the increase in LOX mRNA level induced by PTH. In contrast, trapidil had no effect on Sfrp 4, Mmp 14 and Dcn. LOX which catalyzes the final step of collagen and elastin cross-linking required for the biosynthesis of mature functional extracellular matrices and is known to play an important role in tissue remodeling associated with cancer metastasis. These findings suggest that LOX is a downstream target gene of PDGF-A signaling induced peritrabecular fibrosis.

Disclosures: ***S. Lotinun****, None.*

1201

Generation and Therapeutic Potential of ABX10241, a Fully Human Neutralizing Monoclonal Antibody (mAb) to Human Parathyroid Hormone (huPTH). L. Roskos*[1], I. Foltz*[2], Q. Zhou*[1], R. H. Arends*[1], C. King*[2], M. Liang*[1], N. Raie*[1], S. Klakamp*[1], H. Lu*[1], G. M. Bell[1]. [1]Abgenix, Inc., Fremont, CA, USA, [2]Abgenix BioPharma, Inc., Burnaby, BC, Canada.

Current therapies often inadequately control primary and secondary hyperparathyroidism (HPT) and consequent bone disease. A fully human mAb to PTH has the potential to tightly regulate PTH levels while offering high specificity and a prolonged duration of action. To realize this potential, a neutralizing mAb (ABX10241) with very high affinity to huPTH was generated from transgenic IgG2κ XenoMouse® animals and was characterized in preclinical models.

Mice were immunized with huPTH(1-34) and B cells were analyzed with XenoMax™ technology. B cell cultures containing huPTH-specific antibodies were identified by ELISA and a mAb with the desired affinity was found. ABX10241 has picomolar affinity for huPTH(1-84), (1-34), (7-84), and cynomolgus (cyno) monkey PTH(1-84); nanomolar affinity for rat PTH(1-84); and no crossreactivity with PTHrp. ABX10241 neutralized huPTH(1-34) in a concentration-dependent manner, as measured by blockade of huPTH(1-34)-induced mobilization of intracellular calcium in UMR-106 cells.

Due to the low affinity of ABX10241 for rodent PTH (precluding the study of many HPT models), HPT was modeled in vivo by infusing huPTH into Sprague-Dawley rats or cyno PTH into cyno monkeys. Serum total (tCa) and ionized (iCa) calcium were monitored in rats (N=6/group) infused with subcutaneous huPTH(1-34) at 14.4 μg/day for 6 days and in cyno monkeys (N=4/group) infused with intravenous (iv) cyno PTH(1-84) at 24 μg/day for 17 days; animals received a single iv bolus of ABX10241 or an isotype control mAb on Day 3 of PTH infusion.

Control rats infused with huPTH(1-34) had a ≥ 20% elevation of iCa for 6 days; ABX10241 as a single 3 or 10 mg/kg iv bolus reversed iCa to the normal range for the 4 remaining days of the study. Control monkeys infused with cyno PTH(1-84) experienced stable hypercalcemia (iCa ≥ 20% over baseline) for 17 days; ABX10241 (single 1 or 4 mg/kg iv bolus) caused reversal of hypercalcemia lasting ≥ 4 days in the 1 mg/kg group and ≥ 12 days in the 4 mg/kg group (see figure).

ABX10241 exhibited potent, prolonged suppression of PTH-induced hypercalcemia in preclinical models after a single dose, suggesting that ABX10241 may have therapeutic value in the treatment of HPT.

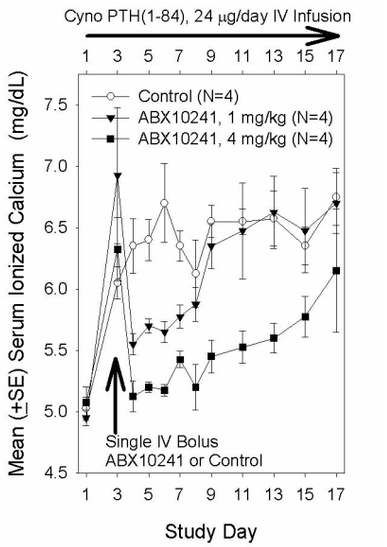

Disclosures: ***L. Roskos****, Abgenix, Inc. 1, 3.*

1202

Methylation of ABC Transporter Genes in Parathyroid Adenomas Affect Sestamibi Imaging. N. C. Greep, D. S. B. Hoon*, A. E. Giuliano*, N. M. Hansen*, H. Wang*, F. R. Singer. John Wayne Cancer Institute, Santa Monica, CA, USA.

Parathyroid ^{99m}Tc-sestamibi scans (^{99}MIBI) facilitate the surgical management of parathyroid adenomas (Ad) but are negative in about 20% of cases. To understand why some scans are negative, we studied adenoma size and the activity of two ATP-binding cassette (ABC) membrane transporter genes [Multiple Drug Resistance (MDR1) and MDR-associated Protein (MRP)] whose products (P-gp and MRP, respectively) are thought to extrude ^{99}MIBI from normal parathyroid glands (Nl). Paraffin-embedded tissue were obtained from 27 Ad (13 ^{99}MIBI + and 14 ^{99}MIBI- cases) and 16 normal (^{99}MIBI-) parathyroid glands. Polyclonal goat anti-human MDR1 and MRP antibodies were used to detect P-gp and MRP by immunohistochemistry (IHC), and Quantitative Real Time reverse transcriptase polymerase chain reaction (qPCR) was used to quantify transporter specific mRNA [with glyceraldehyde-3-phosphate dehydrogenase (GAPDH) as an internal reference for RNA integrity]. Hypermethylation (HM) of CpG islands in the promoter region of MDR1 and MRP was assessed with quantitative methylated PCR. Both P-gp and MRP proteins were present in 100% of Nl but in only 30% of Ad. Referenced to GAPDH, the mean±SE mRNA for each gene was higher in IHC+ compared to IHC- glands (P-gp 88±15 vs. 33±9, p=0.003; MRP 937±141 vs. 299±45, p<0.001). In Ad, HM of the ABC gene was more common for MDR1 than for MRP (70% vs. 30%), but in 11 Nl, none was hypermethylated in the MDR1 gene and only 1 in the MRP gene. Methylation status of the MDR1 (p<0.001) but not the MRP (p=ns) gene was associated with reduced presence, detected by IHC, of its transporter. HM of the MDR1 (100% vs. 43%) but not the MRP (15% vs. 14%) gene was greater in ^{99}MIBI+ than in ^{99}MIBI- Ad. Presence of P-gp and MRP by IHC were both lower in ^{99}MIBI+ than in ^{99}MIBI- Ad (P-gp 0% vs. 57%; MRP 8% vs. 50%). We compared the weight of 120 ^{99}MIBI+ and 33 ^{99}MIBI - adenomas from all cases operated on at our hospital over the past 2 years. ^{99}MIBI+ Ad were ~ 2X heavier than ^{99}MIBI- Ad (888 vs. 450 mg, p=0.009) and the smallest Ad which could be detected 80% of the time was 250 mg. Among all Ad, 13 of 13 ^{99}MIBI+ scans were accounted for by the absence of both P-gp and MRP (12) or absence of P-gp alone (1). Twelve of 14 ^{99}MIBI- scans were accounted for by either small size (2) or the presence of P-gp and/or MRP (10), leaving only 2 large Ad (>1000mg) whose failure to image with ^{99}MIBI was not explained by small size or presence of an ABC transporter. In conclusion, down regulation of the MDR gene by HM and the MRP gene by some other mechanism occurs in Ad and accounts for most ^{99}MIBI+ scans, whereas persistence of P-gp and/or MRP and small size accounts for most ^{99}MIBI- adenomas.

Disclosures: ***N.C. Greep****, None.*

1203

A Novel Deletion Upstream of GNAS Causes a Form of Autosomal Dominant Pseudohypoparathyroidism Ib and Delineates a Region Crucial for Maintaining Exon A/B Methylation. A. Linglart*, H. Jüppner, M. Bastepe. Endocrine Unit, Massachusetts General Hospital and Harvard Medical School, Boston, MA, USA.

Autosomal dominant pseudohypoparathyroidism Ib (AD-PHP-Ib) (OMIM#603233) is an imprinted disease characterized by isolated renal resistance to parathyroid hormone, which was mapped to a region centromeric of *GNAS*. This complex imprinted locus gives rise to transcripts that are paternally (antisense, XLαs, A/B), maternally (NESP55, Gsα in proximal renal tubules) or biallelically expressed (Gsα in most other tissues).

Recently, we identified in 16 different families with autosomal dominant PHP-Ib (AD-PHP-Ib) an identical 3-kb deletion, removing exons 4-6 of *Syntaxin16* (*STX-16*), a non-differentially methylated gene located about 280kb upstream of *GNAS*. In another large AD-PHP-Ib kindred (lod score at *D20S171* = 2.7, θ=0), we now identified an overlapping novel microdeletion. Southern blot analysis using three different restriction endonucleases and a probe telomeric of *GNAS*, revealed an approximately 4.3-kb deletion. This deletion was found in all affected individuals and obligate carriers, but was not found in the unaffected individuals by multiplex PCR using primers across both predicted breakpoints. Besides indistinguishable clinical findings, affected individuals in this latter family showed epigenetic abnormalities identical to those previously observed in kindreds with the 3-kb deletion, i.e. loss of exon A/B methylation, but no additional changes at other differentially methylated regions (DMRs) of *GNAS*. The novel deletion overlaps with the previously described 3-kb deletion by 899 nucleotides and, like the latter, it disrupts the *STX-16* gene. Using total RNA from a patient-derived lymphoblastoid cell line, the deleted and normal *STX-16* products were amplified by RT-PCR and sequenced directly. These studies revealed that nucleotides derived from *STX-16* exons 2, 3 and 4 were missing in the product derived from the mutant allele. Our results show that AD-PHP-Ib when associated with methylation abnormalities restricted to the exon A/B DMR is caused by a deletion in *STX-16* region. Since we found *STX-16* to be biallelically expressed, it appears likely that an as-of-yet undefined regulatory element within this 899-bp region, rather than haploinsufficiency of *STX-16*, is involved in the maintenance and/or establishment of downstream imprinting at exon A/B.

Disclosures: ***A. Linglart****, None.*

1204

The P392L Mutation in the Sequestasome-1 Gene (p62) that Is Linked to Paget's Disease (PD) Is not Sufficient to Induce a Pagetic Phenotype in Osteoclast (OCL) Precursors. N. Kurihara[1], S. Reddy[1], J. Windle*[2], F. Singer[3], D. Roodman[4], M. Subler*[2]. [1]Univ of Pittsburgh, Pittsburgh, PA, USA, [2]Virginia Commonwealth Univ, Richmond, VA, USA, [3]John Wayne Cancer Ctr, Santa Monica, CA, USA, [4]Univ of Pittsburgh & VA Med Ctr, Pittsburgh, PA, USA.

Pagetic OCL precursors are hyper-responsive to 1,25-$(OH)_2D_3$, RANKL, and TNF-α, and express high levels of TAF_{II}-17. However, the basis for these abnormalities is unclear. Both viral and genetic factors have been implicated in PD. OCL from PD patients express measles virus nucleocapsid (MVNP) transcripts, and up to 40% of patients have an affected 1st degree relative. In addition, there are families with PD with an autosomal dominant mode of inheritance. Recently, mutations in the p62 gene ($p62_{MUT}$) have been linked to 30% of patients with familial PD and 12% of sporadic PD. The p392L mutation is the most frequent mutation reported. However, the role of $p62_{MUT}$ in PD is unclear. Some patients with $p62_{MUT}$ do not have PD. p62 is involved in NF-κB activation. It is our hypothesis that $p62_{MUT}$ increases RANKL and TNF-α induced OCL formation but not 1,25-$(OH)_2D_3$ responsivity or TAF_{II}-17 expression, since RANKL and TNF-α signal via NF-κB. To test this hypothesis, we used OCL precursors from PD patients carrying the $p62_{MUT}$. Peripheral blood monocytes from PD patients formed OCL at much lower concentrations of RANKL, TNF-α, and 1,25-$(OH)_2D_3$ than normals, and had increased TAF_{II}-17 expression. However, $p62_{MUT}$ patient OCL precursors contained both MVNP and $p62_{MUT}$. To further dissect the role of $p62_{MUT}$ in PD we transfected normal OCL precursors with the $p62_{MUT}$ gene or empty vector (EV). $p62_{MUT}$ transfected OCL precursors had increased TNF-α and RANKL sensitivity, but had no increased 1,25-$(OH)_2D_3$ responsivity or increased expression of TAF_{II}-17. In addition, nuclear number per OCL was not increased in $p62_{MUT}$ cells. To confirm the effects of $p62_{MUT}$ in vivo, we targeted $p62_{MUT}$ to the OCL lineage in transgenic mice using the TRAP promoter. At four mths of age, the $p62_{MUT}$ mice had osteopenia. $p62_{MUT}$ and wild type mice marrow cells were cultured with 1,25-$(OH)_2D_3$, RANKL or TNF-α to induce OCL formation. OCL precursors from $p62_{MUT}$ mice were hyper-responsive to RANKL and TNF-α and formed increased numbers of OCL, but were not hyper-responsive to 1,25-$(OH)_2D_3$ nor expressed high levels of TAF_{II}-17. Furthermore, $p62_{MUT}$ marrow cultures did not form OCL with increased nuclei per OCL. These results show that the $p62_{MUT}$: a) increased NF-κB signaling and OCL formation in response to RANKL, TNF-α; b) does not increase 1,25-$(OH)_2D_3$ responsivity nor induce TAF_{II}-17. These data suggest that $p62_{MUT}$ increases basal OCL formation in PD patients but is not sufficient to induce the complete PD phenotype in OCL precursors.

Disclosures: ***N. Kurihara****, None.*

1205

Homozygosity for a Dominant Mutation in col1a1 Restores Pup Survival, Bone Mechanics and Histology and Collagen Fibril Diameter to Near-wt Values, in Comparison to the Moderately Severe Bone Disease (Type IV OI) Present in Heterozygous Brtl Mice. K. M. Kozloff*[1], C. Bergwitz*[2], T. E. Uveges*[2], T. Chen*[3], M. D. Morris*[3], G. Gronowicz*[4], F. Ledgard*[4], S. A. Goldstein[1], J. C. Marini[2]. [1]Ortho Res Labs, U Mich, Ann Arbor, MI, USA, [2]Bemb, NICHD/NIH, Bethesda, MD, USA, [3]Dept Chem, U Mich, Ann Arbor, MI, USA, [4]U Conn Heath Ctr, Farmington, CT, USA.

The Brtl mouse is a dominant-negative model for type IV osteogenesis imperfecta (OI). Brtl is heterozygous for a glycine substitution (G349C) in one col1a1 allele. Brtl pups have 30% perinatal lethality; surviving Brtl mice have reduced BFR and MAR and smaller, weaker, and more brittle bones than WT. Unexpectedly, mice homozygous for the G349C mutation are not lethal but have viability and size indistinguishable from WT. Only mutant α1(I) mRNA is detected and virtually all α1(I) chains form homodimers. This study characterizes the 1st mouse in which homozygosity for a dominant mutation (Brtl/Brtl) attenuates the phenotype of the heterozygous mouse. Femurs from 2 month Brtl, Brtl/Brtl, and WT mice were assessed for areal BMD by PIXImus, geometry and vBMD by μCT, load to failure in 4-pt bending, and histomorphometry. Tibial sections were imaged by Raman spectroscopy to measure collagen cross linking. Areal and vBMD are normal in the Brtl/Brtl. Femoral cross sectional area is intermediate between Brtl and WT. While Brtl femurs fail earlier in bending than WT, Brtl/Brtl femurs appear normal. Furthermore, Brtl/Brtl femurs do not demonstrate the reduced post-yield displacement characteristic of the Brtl mouse. Ultrastructural parameters suggest Brtl/Brtl appears to rescue hypermineralization and abnormal collagen cross linking in the Brtl matrix. On static histomorphometry, Brtl/Brtl TbN is equal to WT, and significantly higher than in Brtl. TbTh of Brtl/Brtl is intermediate between Brtl and WT, as is BV/TV. Percent ObS and OcS, MAR and BFR/BS were the same in all genotypes. Dermal fibril diameter was significantly larger in Brtl/Brtl than Brtl or WT. In Brtl, approximately 25% of α1(I) chains are linked as a homodimer by S-S bonds between mutant Cys 349 residues. The homodimers form efficiently in collagen heterotrimers and are well-secreted from the cells. Collagen triple helices containing a single mutant chain comprise 50% of the intracellular collagen of Brtl; these helices are not well secreted (30-50%) from cells but do occur in media and matrix. The moderately severe bone phenotype in Brtl may result from a combination of collagen matrix insufficiency and the dominant negative effect of the reactive cysteine moiety. Surprisingly, bone composed entirely of type I collagen containing an S-S dimer appears to be sufficient for supporting normal functional requirements.

Disclosures: ***J.C. Marini****, None.*

1206

Three Closely Mapped Genetic Loci in Chromosome 1 Acting via Different Mechanisms Contribute To BMD Phenotype. B. Edderkaoui[1], D. J. Baylink[1], J. Wergedal[1], N. Dunn*[1], K. Shultz*[2], W. G. Beamer[2], L. R. Donahue[2], S. Mohan[1]. [1]JLP VAMC / Loma Linda Univ, Loma Linda, CA, USA, [2]Jackson Laboratory, Bar Harbor, ME, USA.

In previous studies, using an F2 population from the intercross CASTt/EiJ (CAST) and C57BL/6J (B6) mouse strains, 4 quantitative trait loci (QTL) that contribute to bone mineral density (BMD), were identified (Beamer, et al 99). Our subsequent studies have focused on Chromosome 1 (Chr 1) QTL since it is the major QTL contributing to approximately 30% of the femur BMD variation between CAST and B6 strains. In order to fine map the location of the BMD QTL, we performed additional genotyping for 565 F2 mice using 29 markers mapped within the 30 cM QTL region. Linkage analysis using MAPQTL and MapMaker revealed evidence for the presence of 3 significant BMD QTL in this region.Three markers (D1mit453, D1mit354 and D1mit359) showed significant association with total vBMD with LOD scores of 12, 12.9 and 11 respectively using MAPQTL. In order to confirm and narrow the location of BMD QTL genes, we developed subcongenic lines that contain different regions of the 30 cM Chr 1 QTL region from CAST strain placed in a B6 background. Phenotypic analyses of the sub-congenic line 1.3 (Cong1.3) which carries markers at D1Mit354 and D1Mit359 but not D1Mit 453 from CAST revealed a 9.9% increase ($P<0.01$) in total vBMD in congenic mice compared to control B6 mice at 16 weeks of age. Cong 1.3 showed significant 4% increase in periosteal circumference but not endosteal circumference compared to control mice, and as a result both bone area (9%) and cortical thickness (9%) were significantly higher in Cong 1.3 compared to control mice. Histomorphometeric studies revealed 37% higher ($P<0.01$) periosteal bone formation rate in the Cong 1.3 mice compared to control mice. Sub-congenic line 1.6 (Cong 1.6) which carries marker at D1Mit 453 but not D1Mit354 or D1Mit359 exhibits 10.6% higher total vBMD. In contrast to Cong 1.3, Cong 1.6 did not show an increase in periosteal circumference but did show a 7% decrease in endosteal circumference. These data demonstrate that increased bone accretion at the periosteum (Cong 1.3) and endosteum (Cong 1.6) contributes to BMD change. This result suggests different mechanisms for BMD change in these two subcongenic lines. Conclusions: 1) The major BMD QTL in Chr 1 contains 3 genetic loci that show significant association with total vBMD; 2) Our data using congenic mice together with phenotypic analyses are consistent with the idea that genetic loci within chromosome 1 act via different mechanisms to regulate BMD.

Disclosures: ***B. Edderkaoui****, None.*

1207

P2X7 Nucleotide Receptors Induce Membrane Blebbing in Osteoblasts through a Pathway Involving Lysophosphatidic Acid. N. Panupinthu*[1], F. Possmayer*[2], S. M. Sims*[1], S. J. Dixon[1]. [1]CIHR Group in Skeletal Development and Remodeling, Department of Physiology & Pharmacology, The University of Western Ontario, London, ON, Canada, [2]Department of Biochemistry, The University of Western Ontario, London, ON, Canada.

Extracellular nucleotides, released in response to mechanical and inflammatory stimuli, signal through P2 nucleotide receptors in many cell types including osteoblasts. P2X7 receptors are ATP-gated ion channels that can induce formation of large membrane pores. We have shown previously that a subpopulation of osteoblasts expresses functional P2X7 receptors. Deletion of the gene encoding this receptor leads to decreased periosteal bone formation. Our purpose was to investigate the signaling pathways coupled to P2X7 receptor activation in osteoblasts. Cells were isolated from calvariae of newborn mice by sequential collagenase digestion. Live cell imaging techniques were used to monitor responses of osteoblasts to nucleotides. Within 4-6 min, benzoylbenzoyl-ATP (BzATP, a relatively potent P2X7 receptor agonist) induced dynamic membrane blebbing in 45 ± 3% of cells, an effect that was reversible upon removal of BzATP. Since BzATP activates a number of P2 receptors in addition to P2X7, we tested responses of osteoblasts from P2X7 receptor knockout (KO) mice. BzATP did not induce blebbing in osteoblasts from KO mice, consistent with involvement of P2X7 receptors. Treatment with phospholipase D (PLD) inhibitor 1-butanol, but not its inactive analog 3-butanol, suppressed BzATP-induced blebbing. Inhibition of phospholipase A_2 (PLA_2) by arachidonyltrifluoromethyl ketone or bromoenol lactone also suppressed BzATP-induced blebbing. Activation of PLD and PLA_2 leads to production of lysophosphatidic acid (LPA), which signals through G protein-coupled receptors of the endothelial differentiation gene (Edg) family. We found that LPA itself caused dynamic membrane blebbing similar to that induced by BzATP, but with faster onset (2-3 min). LPA-induced blebbing was not affected by inhibition of PLD or PLA_2, suggesting that these phospholipases function upstream of LPA. Interestingly, desensitization of LPA responses by prolonged incubation with LPA suppressed blebbing induced by both LPA and BzATP. Moreover, inhibition of Rho-kinase using Y27632 abolished blebbing induced by both ligands. Taken together, these findings indicate that activation of P2X7 receptors leads to synthesis of LPA, which in turn signals through Rho-kinase to induce membrane blebbing. Thus, we have identified a role for LPA in mediating downstream effects of P2X7 receptor activation on osteoblasts. This pathway may contribute to the stimulatory effect of P2X7 receptors on bone formation *in vivo*.

Disclosures: ***N. Panupinthu****, None.*

1208

Increased Bone Formation in Mice Lacking Apolipoprotein E. A. F. Schilling[1], T. Schinke[1], C. Münch*[1], M. Gebauer*[1], A. Niemeier*[2], M. Priemel[1], T. Streichert*[3], J. M. Ruegerr*[1], M. Amling[1]. [1]Trauma Surgery, Hamburg University, Hamburg, Germany, [2]Orthopaedic Surgery, Hamburg University, Hamburg, Germany, [3]Clinical Chemistry, Hamburg University, Hamburg, Germany.

Apolipoprotein E (ApoE) is a major protein component of very low-density lipoproteins and chylomicron remnants and facilitates their clearance from the circulation. This is confirmed by the phenoytpe of ApoE-deficient mice that have high plasma cholesterol levels and spontaneously develop atherosclerotic lesions. The bone phenotype of these mice has not been analyzed to date, although an association between certain ApoE alleles and bone density has been reported. Using a genome-wide expression analysis during the course of osteoblast differentiation we found that ApoE gene expression is strongly induced upon mineralization of the cultures. Since we did not observe expression of other apolipoprotein genes, we hypothesized that ApoE may have a specific function in bone remodeling. This was confirmed by the histomorphometric analysis of ApoE-deficient mice that display a high bone mass phenotype at the age of 3 and 8 months. This phenotype is caused by an increased bone formation rate (BFR(μm3/μm2/y): wt 85.08±12.98 vs ApoE-/- 131.91±30.15, n=6), whereas bone resorption is not affected. Since vitamin K, a cofactor required for γ-carboxylation of osteocalcin, is transported by ApoE-containing triglyceride-rich lipoproteins (TRL), we speculated that ApoE expression in differentiated osteoblasts could be required for the maximal uptake of vitamin K. Using primary osteoblasts from wildtype and ApoE-deficient mice we were able to demonstrate that TRL-uptake is indeed diminished in the absence of endogenous ApoE production. Furthermore, after separation on a hydroxyapatite column, we found that the amount of undercarboxylated osteocalcin is strongly elevated in the serum of ApoE-deficient mice, whereas carboxylated osteocalcin is barely detectable. Thus, the high bone mass phenotype observed in the ApoE-deficient mice is possibly due to a reduction of functional osteocalcin, since the targeted deletion of osteocalcin in mice leads to a similar phenotype. Taken together, these data provide the first evidence for a physiologic role of ApoE in the regulation of bone formation.

Disclosures: ***A.F. Schilling****, None.*

1209

A Structure Function Analysis of the Twist Box Reveals an Additional Function for Twist-1 During Skeletogenesis. P. E. Bialek*, M. Sage*, M. Justice*, G. Karsenty. Molecular and Human Genetics, Baylor College of Medicine, Houston, TX, USA.

Runx2 is both necessary and sufficient for osteoblast differentiation. Recently we showed using genetic and molecular means that the Twist proteins, acting via the Twist box, delay osteoblast differentiation by transiently inhibiting Runx2 function. In this work, we used as a tool, a hypomorphic allele of Twist-1, called Charlie Chaplin (CC) that harbors a Ser192Pro mutation in the Twist box. Through our continued analysis of CC/CC mice, we uncovered a novel function of Twist-1 during bone development. Indeed, CC/CC mice exhibit multiple skeletal patterning defects including radial and tibial aplasia as well as missing clavicles and cranial bones. A developmental study showed that the defects can be ascribed to a failure to form mesenchymal condensations. That Twist-2 null embryos do not have any skeletal patterning abnormalities raised the questions as to whether this is a specific function of Twist-1. To address this question, we generated CC/+; Twist-2+/- double heterozygotes. CC/+; Twist-2+/- mice do not show any patterning defects but do exhibit advanced osteoblast differentiation in both ribs and limbs. This indicates that while both Twist-1 and -2 are involved in controlling the onset of osteoblast differentiation during endochondral ossification, only Twist-1 is involved in skeletal patterning. That this function was uncovered in CC/CC embryos, indicate that it is also mediated by the Twist Box. This led us to pursue our analysis of the Twist box through biochemical and evolutionary means. While Ser192Pro, the CC mutation, binds the Runt domain poorly, Ser192Ala binds as strongly as wild type suggesting that the Ser192 does not play a critical role and that the phenotype of CC was secondary to a change in the Twist-1 tertiary structure caused by the introduction of a proline residue in the Twist box. This is important since Drosophila Twist, which can also inhibit Runx2 activity, does not have a serine at this location. Further deletion analysis identified residues187-200, a region highly conserved between Drosophila and mouse Twist-1, as the core of the Twist box. In summary, our analyses demonstrate that Twist-1 regulates skeletal patterning in addition to osteoblast differentiation through the Twist box and identifies a core sequence within the Twist box. Further in vivo analysis will determine the range of functions of the Twist box.

Disclosures: ***P.E. Bialek****, None.*

1210

Transgenic Modification of MAP Kinase Signaling in Osteoblasts Leads to Altered Bone Formation and Osteoblast Activity. C. Ge*, G. Xiao, D. Jiang*, R. T. Franceschi. Periodontics, Prevention, Geriatrics, University of Michigan School of Dentistry, Ann Arbor, MI, USA.

The Erk branch of the mitogen-activated protein kinase (MAPK) pathway plays an important role in osteoblast growth and differentiation. Short-term inhibition of MAPK activity in cell culture using either specific inhibitors or dominant negative MEK (MEK-DN) inhibited osteoblast specific gene expression and responsiveness to BMPs (Xiao et al, 2002 JBMR 17:101, 2002). Furthermore, activation of the MAPK pathway with constitutively active MEK (MEK-SP) stimulated phosphorylation and activation of Runx2 (Xiao et al, JBC 275:4453, 2000). Recently, RSK2, a kinase downstream of Erk, was also shown to stimulate osteoblast activity by activating ATF4 (Yang et al., Cell 117:387,2004). To elucidate the function of the MAPK pathway in osteoblasts in vivo, transgenic mice were developed in which the murine 0.6 kb mOG2 promotor was used to drive MEK-DN or MEK-SP synthesis. Bone-specific expression of both transgenes was confirmed by RT-PCR. Transgenic hemizygotes were viable and showed no gross abnormalities at birth except that the body weight of MEK-DN mice was slightly less than wildtype littermates. Analysis of embryos revealed no clear differences before E14.5. Beginning at E15.5, MEK-DN embryos were smaller while MEK-SP embryos were larger than non-transgenic littermates ($p<0.01$). Differences were also apparent when bone size and onset of mineralization were measured. Femurs and clavicles were longer in MEK-SP embryos and shorter with the MEK-DN transgene ($p<0.01$). Alcian blue and alizarin red staining revealed an overall delay in mineralization with MEK-DN and an acceleration with MEK-SP at multiple sites including the skull, vertebrae and long bones. In addition, initial vascular invasion and formation of ossification centers in long bones was delayed at E14.5 in MEK-DN and stimulated in MEK-SP embryos. Consistent with these results, calvarial osteoblasts isolated from 5 week old MEK-DN animals exhibited a clear differentiation defect as measured by reduced alkaline phosphatase activity, mineral formation and expression of osteoblast marker mRNAs (osteocalcin and BSP) although they proliferated at the same rate as cells from non-transgenic littermates. The differentiation defect was most obvious during the first 10 d of culture, suggesting an overall delay in cell maturation. These studies support our hypothesis that the Erk MAPK pathway plays a major role in the regulation of osteoblast differentiation and bone formation.

Disclosures: ***C. Ge****, None.*

1211

Heparanase Regulates Osteoblast Function and Bone Mass. V. Kram*[1], E. Zcharia*[2], O. Yacoby-Zeevi*[3], Y. Gabet[1], R. Müller[4], I. Vlodavsky*[2], I. Bab[1]. [1]Bone Laboratory, Hebrew University of Jerusalem, Jerusalem, Israel, [2]Oncology, Hadassah-Hebrew University Medical Center, Jerusalem, Israel, [3]Insight Biopharmaceuticals, Rehovot, Israel, [4]Institute for Biomedical Engineering, ETH and University Zürich, Zürich, Switzerland.

Heparan sulfate proteoglycans (HSPGs) are ubiquitous macromolecules associated with bone cell surfaces and extracellular matrix. Furthermore, heparan sulfate (HS) chains bind a multitude of bioactive molecules thereby controling diverse normal and pathological processes. The mammalian gene encoding HS-degrading endoglycosidase, heparanase (Hpa), has been cloned and implicated in important biological processes such as inflammation, vascularization and cancer metastasis. The present study aimed at assessing Hpa regulation of bone cell activity and bone mass. RT-PCR analysis in murine bone marrow derived stromal cells undergoing osteoblastic differentiation showed progressive expression of the *hpa* gene. Immunohistochemistry using anti-Hpa antibodies identified a particular distribution of Hpa which was spread throughout the bone marrow with increasing concentration in osteoblasts and preosteoblasts. Hpa was also found in occasional osteocytes but not in growth plate chondrocytes. A similar distribution of Hpa positive cells was also found in the metaphyseal compartment of *hpa*-transgenic (*hpa*-tg) mice, but here hypertrophic chondrocytes were also positive. Micro-computed tomographic analysis in male and female *hpa*-tg mice showed approximately 2-fold increase in trabecular bone volume and connectivity densities secondary to increases in trabecular number and thickness. The cortical thickness of the *hpa*-tg mice was increased and the diameter of the medullary cavity decreased. Dynamic histomorphometry revealed a vast increase in bone formation rate. The osteoclast number was unchanged. In line with these findings, recombinant mammalian heparanase stimulated bone cell proliferation, alkaline phosphatase activity and matrix mineralization in primary bone marrow-derived stromal cell and MC3T3 E1 osteoblast cultures. Collectively these data demonstrate a highly potent anabolic activity of Hpa in bone via the stimulation of bone marrow derived osteoblastic cells.

Disclosures: ***V. Kram****, None.*

1212

Transgenic Overexpression of WIF-1, a Secreted Wnt Antagonist Expressed in Bone, Causes Decreased Bone Mineral Density and Increased Susceptibility to Bone Fracture in Mice: A Role for WIF-1 in Bone Biology. J. Cao*, S. Morony, K. Warmington*, J. Pretorius*, K. McDorman*, C. Paszty. Metabolic Disorders, Amgen Inc, Thousand Oaks, CA, USA.

Genes that might play a role in adult bone biology were identified by computer-based gene expression pattern mining of an expressed sequence tag (EST) database. One such gene, Wnt-inhibitory Factor-1 (WIF-1), encodes a secreted protein with Wnt antagonistic activity. Previous studies have established a role for Wnts in skeletal development, and recent work has shown the importance of the Wnt pathway (LRP5) in postnatal bone formation.

In situ hybridization of WIF-1 revealed strong expression in murine embryonic skeletal tissues, specifically cartilage primordium and zones of hypertrophy. In adult mice, there is strong expression in osteoblasts, endosteal lining cells, articular chondrocytes, as well as in a number of other tissues. *In situ* analysis of knee samples from older humans (normal, arthritic, and osteoporotic; ages 48-78) shows consistent, low level expression of WIF-1 in osteoblasts and endosteal lining cells.

To explore the impact of WIF-1 on bone biology in an *in vivo* setting, transgenic mice were made using a rat a1(I) collagen promoter transgene for overexpressing mouse WIF-1 in cells of the osteoblast lineage. Peripheral quantitative computed tomography (pQCT) analysis of tibia harvested from female transgenics revealed that the lowest bone mineral density (BMD) was present in the mouse with the highest WIF-1 transgene expression levels. Histopathology showed chondrodysplasia and decreased endochondral ossification in long bones. Male transgenic founders were mated with wild-type females to establish individual lines of WIF-1 transgenic mice. On the following day, one male was observed to be dragging its hind legs. Radiography showed that both tibias were broken, suggesting that overexpression of WIF-1 can increase susceptibility to bone fracture. Subsequent analysis of adult male mice from a stable breeding line of WIF-1 transgenics included the collection of lumbar vertebrae and tibiae for pQCT measurement of BMD. Total, trabecular and cortical BMD in vertebrae and tibiae were decreased in transgenics as compared to non-transgenic littermates. Significant decreases in cortical BMD of the lumbar vertebrae and tibial diaphysis (3.5% and 10% respectively vs. control) were noted, as well as decreases in the total tibial metaphysis BMD (7% vs. control).

The gene expression data for WIF-1 in mice and humans, together with the low BMD phenotype of WIF-1 transgenics, suggests that WIF-1 plays a role in bone biology as a negative regulator of bone mass. As such, antagonism of WIF-1 may have therapeutic potential in the treatment of osteoporosis.

Disclosures: ***C. Paszty****, None.*

1213

Wnt Signaling Regulates Runx2 Expression In Vivo and Activates the Bone-Related Runx2 P1 Promoter. T. Gaur*[1], A. Javed[1], A. J. van Wijnen[1], J. L. Stein*[1], P. V. N. Bodine[2], B. S. Komm[2], G. S. Stein[1], J. B. Lian[1]. [1]Department of Cell Biology and Cancer Center, University of Massachusetts Medical School, Worcester, MA, USA, [2]Women's Health Research Institute, Wyeth Research, Collegeville, PA, USA.

Wnt signaling plays a vital role in a variety of biological processes, including skeletal development and related diseases. Increased Wnt signaling either by gain-of-function mutation in the Wnt co-receptor LRP5 or by null mutation of sFRP1, a Wnt antagonist has resulted in increased trabecular bone formation. Here we characterized the mechanism linking Wnt signaling to increased bone formation. We examined bone phenotypic genes in the sFRP1 null mouse and find elevated levels of Runx2, an indispensable transcription factor for skeletogenesis and osteoblastic differentiation. We further show that the bone promoting function of Wnt is attributable to transcriptional control of the Runx2 gene. A Wnt responsive element in the bone related P1 promoter which corresponds to a binding site for LEF/TCF proteins was delineated. Transient transfection studies in the osteoblast progenitor cell line, MC3T3-E1, reveal that activation of the Runx2 promoter by TCF1 requires co-expression with canonical Wnt proteins (Wnt1, Wnt3, Wnt3a and Wnt6). The combination of TCF1 with any of these Wnts could provide 2-3 fold induction of Runx2 promoter activity. However, this response was not observed in cells representing the mature osteoblast phenotype, such as ROS 17/2.8 cells which expression high levels of Runx2. We also find that sFRP proteins inhibit the activation caused by Wnt1 and TCF1, consistent with their antagonistic function of Wnt signaling. Additionally, in the combined presence of Wnt1 and TCF1, a significant induction (~7-fold) of endogenous Runx2 mRNA levels in MC3T3-E1 cells was observed. Our findings provide critical evidence for the concept that Wnt signaling activates the Runx2 gene which is an early regulator of commitment to the osteoblast lineage. Thus, we have uncovered a potential regulatory relay that may function during development to mediate bone cell specification.

Disclosures: ***J.B. Lian****, None.*

1214

Decreased Bone Density and Limb Deformities in Mice Carrying Mutations in Both Lrp5 and Lrp6. S. L. Holmen*[1], T. A. Giambernardi*[1], C. R. Zylstra*[1], B. D. Buckner-Berguis*[1], J. H. Resau*[1], J. F. Hess*[2], M. Ai*[3], M. A. Bouxsein[4], M. L. Warman[3], B. O. Williams[1]. [1]Van Andel Research Institute, Grand Rapids, MI, USA, [2]Department of Human Genetics, Merck Research Laboratories, West Point, PA, USA, [3]Department of Genetics and Center for Human Genetics, Case Western Reserve University, Cleveland, OH, USA, [4]Orthopedic Biomechanics Laboratory, Beth Israel Deaconess Medical Center, Boston, MA, USA.

The low-density lipoprotein receptor-related proteins 5 and 6 (LRP5 and LRP6) are co-receptors for Wnt ligands. Loss-of-function mutations in *LRP5* cause osteoporosis pseudoglioma syndrome(OPPG), an autosomal recessive disorder characterized by low bone mass and ocular pathology. *Lrp6*-deficient mice display phenotypes similar to, but not as severe as, those seen in several Wnt gene knockouts, and they die between e14.5 and birth (Pinson *et al*. 2000 *Nature* 407, 535-8). *Lrp5* is highly expressed in mouse embryos and may partially compensate for *Lrp6* loss. To better understand the role of Lrp5 and Lrp6 during development, mice deficient for *Lrp5* were generated and crossed to *Lrp6*-heterozygous mice. By DEXA and microCT, we demonstrate that loss of *Lrp5* and *6* affects normal limb development and bone mass accrual, in a dosage dependent manner. Mutant calvarial osteoblasts isolated from these mice and differentiated *in vitro* grew at a faster rate and had increased expression of an early differentiation marker compared to the normal cells. These results suggest that both Lrp5 and Lrp6 play roles in osteoblast proliferation and differentiation. From these data we conclude that *Lrp5* and *Lrp6* encode proteins with partially overlapping functions.

Disclosures: ***B.O. Williams****, None.*

1215

Increases in Bone Mineral Density Are Maintained after 7 Years of Raloxifene Therapy: Results from the Continuing Outcomes Relevant to Evista (CORE) Study. S. T. Harris[1], E. S. Siris[2], J. L. Stock[3], P. M. Kulkarni*[3], Y. Qu*[3], S. R. Siddhanti*[3], B. D. Mitchell*[3], S. R. Cummings[1]. [1]University of California San Francisco, San Francisco, CA, USA, [2]Columbia University, New York, NY, USA, [3]Lilly Research Laboratories, Indianapolis, IN, USA.

Postmenopausal women (N=4011) from the 4-year Multiple Outcomes of Raloxifene Evaluation (MORE) osteoporosis treatment trial were observed for an additional 4 years in the multicenter, double-blind, placebo (PL)-controlled CORE study to investigate the effects of raloxifene 60 mg/d on the incidence of invasive breast cancer. An addendum studied the effects of raloxifene treatment, at 7 years after randomization in MORE, on lumbar spine (LS) and femoral neck (FN) bone mineral density (BMD) in women enrolled at U.S. sites of CORE. All women received elemental calcium (500 mg/d) and vitamin D (400-600 IU/d). Women randomized to PL in MORE continued receiving PL in CORE, while those randomized to either raloxifene dose (60 or 120 mg/d) in MORE received raloxifene 60 mg/d (RLX) in CORE. BMD was measured by DXA at Years 1 and 3 in CORE. The primary analysis was based upon 386 women who did not take other bone-active agents from the fourth year of MORE through Year 3 of CORE, who were at least 80% compliant with study medication in CORE, and who had a BMD measurement at Year 3 of CORE. Baseline characteristics at enrollment in MORE were not different between women in the PL (n=127) and RLX (n=259) groups. At Year 3 of CORE, the difference in mean BMD was 1.7% at the LS (P=0.30) and 2.4% at the FN (P=0.045), in the RLX group compared with the PL group. A pre-specified time-trend analysis showed a 4.3% increase from baseline in LS BMD after 7 years of RLX, which was 2.2% greater than the change in PL, and a 1.9% increase from baseline in FN BMD, which was 3.0% greater than the change in PL (both P<0.01). For the RLX group, the LS and FN BMD measurements were significantly increased from the baseline of MORE at all time points (P<0.01). The percent change in LS BMD from baseline in the RLX group was significantly greater, compared with that in the PL group, at Years 1 to 4 in MORE and Year 7 (Year 3 of CORE), while for FN BMD, this comparison was significantly greater at all time points. In conclusion, increases in BMD are maintained after 7 years of therapy with raloxifene.

Disclosures: ***S.T. Harris****, Eli Lilly and Company 2.*

1216

A Novel, Nonsteroidal Selective Androgen Receptor Modulator (SARM) Increases Periosteal Bone Formation and Inhibits Trabecular Bone Turnover in Aged Intact and Orchidectomized Male Rats. H. Z. Ke, D. T. Crawford*, H. Qi, H. A. Simmons, M. Li, T. A. Brown, E. D. Salter*, J. P. O'Malley*, C. T. Salatto*, B. A. Lefker*, T. G. Gant*, R. J. Hill*, X. N. Wang*, D. D. Thompson*. Pfizer Global Research and Development, Groton, CT, USA.

SARMs have been investigated as a new approach for the treatment of osteoporosis. SARMs are hypothesized to have beneficial effects on bone without causing prostate hypertrophy in men or virilization in women. CMP1 is a newly identified nonsteroidal compound that selectively binds to androgen receptor (AR) with an IC50 of 5.7 nM, and acts as a receptor agonist with an EC50 of 0.012 nM in AR-transfected C2C12 cells. In animal study, male SD rats at 11 months of age were sham-operated or orchidectomized (ORX), and treated with CMP1 at an average daily dose of 3 or 10 mg/kg by s.c. injection for 8 weeks. ORX for 8 weeks induced significant decreases in weights of prostate and levator ani and trabecular and cortical bone mineral content. CMP1 significantly increased levator ani weight with minimal effects on prostate weight in both sham and ORX rats compared with their controls. Further, CMP1 at 10 mg/kg significantly decreased body weight by reducing fat body mass in both sham and ORX rats. In sham rats, CMP1 increased distal femoral metaphyseal (DFM) trabecular density by 11% and 10% at 3 and 10 mg/kg, respectively, compared with sham controls. Bone histomorphometric analysis showed that CMP1 in sham-operated rats at 10 mg/kg increased significantly mineral apposition rate (MAR), mineralizing surface (MS/BS) and bone formation rate (BFR/BS) on the periosteal surface of tibial shaft, while it significantly decreased these parameters on the endocortical surface of the tibial shaft and significantly decreased MS/BS, BFR/BS and osteoclast surface on trabecular bone of the proximal tibial metaphysis (PTM) compared with sham controls. In ORX rats, CMP1 at both doses completely prevented ORX-induced decreases in DFM trabecular density and trabecular bone volume. Trabecular MS/BS, BFR/BS and osteoclast surface of PTM decreased significantly in CMP1-treated ORX rats compared with ORX controls, indicating that CMP1 preserves trabecular bone mass by decreasing bone turnover. Histomorphometry of TS showed that CMP1 increased periosteal MS/BS and BFR/BS and decreased endocortical eroded surface, MS/BS and BFR/BS resulted in decreasing marrow cavity area and increasing cortical bone area in ORX rats as compared with ORX controls. These results indicate that this SARM stimulates bone formation on the periosteal surface and decreases bone turnover on endocortical and trabecular surfaces in intact and ORX aged male rats. Thus, SARMs have potentials for prevention and treatment of osteoporosis.

Disclosures: ***H.Z. Ke****, Full Time Employee of Pfizer Inc. 3.*

1217

Sclerostin Antagonism in Adult Rodents, via Monoclonal Antibody Mediated Blockade, Increases Bone Mineral Density and Implicates Sclerostin as a Key Regulator of Bone Mass During Adulthood. K. Warmington*[1], S. Morony[1], I. Sarosi*[1], J. Gong*[1], P. Stephens*[2], D. G Winkler[2], M. K. Sutherland[2], J. A. Latham[2], H. Kirby*[2], A. Moore*[2], M. Robinson*[2], P. J. Kostenuik[1], S. Simonet[1], D. L. Lacey[1], C. Paszty[1]. [1]Metabolic Disorders, Amgen Inc, Thousand Oaks, CA, USA, [2]Celltech Group plc, Slough, United Kingdom.

In humans, complete lack of the protein sclerostin due to homozygosity for null mutations in the SOST gene is responsible for causing sclerosteosis, a rare genetic disease characterized by an early onset (mid-childhood) increase in bone mineral density (BMD) throughout the skeleton. Similar to humans with sclerosteosis, knock-out mice homozygous for a deletion of the SOST gene have increased BMD throughout their skeleton, but are otherwise essentially normal. *In situ* analysis of bone harvested from older rats and humans (55-78 years old) reveals robust expression of sclerostin in osteocytes, suggesting a role for sclerostin in regulating bone mass throughout life.

To further explore the biology of sclerostin and its therapeutic potential as a target in the treatment of osteoporosis, sclerostin neutralizing monoclonal antibodies were tested in mice and rats. Statistically significant increases in BMD, as determined *in vivo* by Dual Energy X-ray Absorptiometry (DEXA), were found in tibial metaphysis (26-38% increase versus vehicle) and lumbar vertebrae (35-40% increase) in young mice (4-wk old BDF1 strain males; 3-wk study). Serum osteocalcin, a marker of bone anabolic activity, was also increased by 35%. In studies using skeletally mature mice (4 month old males and females, various strains) similar increases in BMD were found. *Ex vivo* analysis of the tibial metaphysis by peripheral quantitative computed tomography (pQCT) showed statistically significant increases in total BMD (18-42%), trabecular BMD (30-64%) and cortical BMD (7-14%).

In a postmenopausal osteoporosis disease model study, treatment of aged ovarectomied (OVX) rats (9 months old, 3 months post OVX) for 6 weeks caused statistically significant increases in BMD in lumbar vertebrae (18% increase versus vehicle), femoral metaphysis

(17% increase) and femoral diaphysis (9% increase). The bone had normal lamellar structure as assessed by polarization microscopy. Gross observation, serum clinical chemistry and hematological panel analysis indicated no systemic abnormalities associated with pharmacological inhibition of sclerostin.
The genetic, phenotypic and expression data, coupled with the above *in vivo* data, point towards sclerostin being a key regulator of bone mass throughout life, and furthermore, suggests that inhibition of sclerostin may have therapeutic potential for the anabolic treatment of osteoporosis.

Disclosures: ***C. Paszty****, None.*

1218

An Orally Bioavailable GSK3 α/β Dual Inhibitor Increases Markers of Cellular Differentiation *In Vitro* and Bone Mass *In Vivo*. N. H. Kulkarni*[1], M. Liu*[1], D. L. Halladay*[1], C. A. Frolik[1], T. A. Engler*[2], L. M. Helvering*[1], T. Wei*[3], A. Kriauciunas*[3], T. J. Martin[4], M. Sato[1], H. U. Bryant[1], J. E. Onyia[3], Y. L. Ma[1]. [1]Bone and Inflammation, Eli Lilly and Company, Indianapolis, IN, USA, [2]Discovery Chemistry, Eli Lilly and Company, Indianapolis, IN, USA, [3]Integrative Biology, Eli Lilly and Company, Indianapolis, IN, USA, [4]St. Vincent's Institute for Medical Research, Fitzroy, Victoria, Australia.

Glycogen synthase kinase 3 (GSK3) is a serine/threonine kinase that regulates β-catenin, a key component of the canonical Wnt signaling pathway which regulates bone mass in humans and rodents. Inactivation of GSK3 leads to the accumulation of cytosolic β-catenin which then enters the nucleus to activate Wnt target genes. To examine whether GSK3 directly regulates bone formation, we evaluated the effect of a small molecule GSK3 α/β dual inhibitor, 603281-31-8 in pre-osteoblasts *in vitro* and in osteopenic ovariectomized (Ovx) rats. C3H10T1/2 cells, were treated with 1 μM 603281-31-8 at different time points. β-Catenin stabilization (western blot), translocation (immunoflourescence), activation of canonical Wnt reporter gene and markers of bone formation (Northern/Real-Time PCR) were measured as indicated. In C3H10T1/2 cells, inactivation of GSK3 resulted in stabilization of β-catenin and activation of Wnt reporter gene. This was associated with ~2-fold increases in the expression of mRNA for collagen 1 and bone sialoprotein, markers of the osteoblast phenotype and bone formation activity. Furthermore, treatment with 603281-31-8 increased alkaline phosphatase activity by 2-fold in C3H10T1/2 cells. For *in vivo* studies, 6month old rats were Ovx, and permitted to lose bone for one month, followed by treatment with 603281-31-8 at 3mg/kg/d po for 60 days. The expression levels of bone formation genes were analyzed in the rat femur by Real-Time PCR. Gene expression analysis showed increases in the mRNA levels of collagen 1, collagen 5, alkaline phosphatase, biglycan, bone sialoprotein and osteonectin upon treatment with 603281-31-8 relative to ovariectomy controls in rat femur. DXA analysis of whole femora, midshaft and distal femora showed significant increases in BMD and BMC after 60 days treatment relative to Ovx, concordant with the increases in the gene expression levels of bone formation genes. These data showed that an orally active, small molecular weight, GSK3 α/β dual inhibitor increased bone mass in ovariectomized rats, induced osteoblast differentiation *in vitro* and increased markers of bone formation both *in vitro* and *in vivo*. These observations are consistent with the pronounced role played by the canonical Wnt pathway in osteogenesis.

Disclosures: ***N.H. Kulkarni****, None.*

1219

First Demonstration of the Efficacy of an Anti-Osteoporotic Treatment in Very Elderly Osteoporotic Women. E. Seeman[1], B. Vellas*[2], C. Roux[3], S. Adami[4], J. Aquino*[5], J. Semler*[6], J. Graham*[7], O. Sorensen[8], J. Padrino*[9], R. Rizzoli[10], T. Spector[11], J. Kaufman[12], S. Boonen[13], J. Reginster[14]. [1]Dept of Endocrinology, Austin and Repatriation Medical Centre, Melbourne, Australia, [2]CHU Purpan, Toulouse, France, [3]Hôpital Cochin, Paris, France, [4]University Hospital, Valeggio sul Mincio, Verona, Italy, [5]Clinique Médicale de la Porte Verte, Versailles, France, [6]Immanuel Krankenhaus Rheumaklinik, Berlin, Germany, [7]Ashford Specialist Centre, Ashford, Australia, [8]Hvidvre University Hospital, Hvidovre, Denmark, [9]Hospital 12 de Octubre, Madrid, Spain, [10]University Hospital, Geneva, Switzerland, [11]St Thomas' Hospital, London, United Kingdom, [12]U. Z. Gent Department of Internal Medicine, Gent, Belgium, [13]Center for Metabolic Bone Diseases, Leuven University, Leuven, Belgium, [14]University of Liège, Liège, Belgium.

The number and burden of fractures is increasing as age advances in relation with increased longevity. This is particularly the case in over eighty year-olds, a group at highest absolute risk for fracture and thus for whom the number needed to treat to prevent one event is the lowest. About 25 percent of all fragility fractures, and 50% of hip fractures, occur in this high risk group so prevention of fractures is likely to confer the highest benefit at a community level. Moreover, the burden of fractures will still increase as life-expectancy is increasing. Few, if any, drugs have proven anti-fracture efficacy in this high risk group**.** Strontium ranelate, a drug that allows continued production of bone while decreasing resorption at the cellular level, has been reported to reduce the risk of vertebral fracture by 41% (p<0.001) and hip fracture by 36% (p=0.046) over 3 years in the SOTI and TROPOS studies.
A pre-planned analysis was performed on the pooled data from these two phase III trials to evaluate the efficacy of strontium ranelate in patients aged 80 years and over (n=1488). Yearly spinal X- rays were performed in 895 patients, and assessed by grading (Genant method). Only documented non-vertebral fractures were considered. There was no difference between groups for baseline characteristics of age 83.5± 3.0 years; lumbar BMD T-score -2.7± 1.7; femoral neck BMD T-score -3.3± 0.7; 49% of the patients had at least one prevalent vertebral fracture and 36% had at least one prevalent osteoporosis-related non vertebral fracture. In the ITT population, strontium ranelate reduced the risk of vertebral fracture by 32% (p = 0.013) and of non vertebral fracture by 31% (p = 0.011) over 3 years compared to placebo. The drug had an excellent safety profile. To the best of our knowledge, this is the first experimental evidence of significant reduction of both vertebral and non-vertebral fractures of an anti-osteoporotic agent in osteoporotic women aged 80 years and over.

Disclosures: ***E. Seeman****, None.*

1220

Effect of Annual Intramuscular Vitamin D_3 Supplementation on Fracture Risk in 9440 Community-Living Older People: The Wessex Fracture Prevention Trial. F. H. Anderson[1], H. E. Smith*[2], H. M. Raphael*[2], S. R. Crozier*[3], C. Cooper[3]. [1]Geriatric Medicine Group, University of Southampton, Southampton, United Kingdom, [2]Primary Medical Care, University of Southampton, Southampton, United Kingdom, [3]MRC Environmental Epidemiology Unit, University of Southampton, Southampton, United Kingdom.

Vitamin D supplementation may reduce fracture risk in older people, although results from previous trials are not entirely consistent. Giving vitamin D as a single annual injection before the onset of each winter is operationally feasible if linked to an existing programme of influenza immunisation and might be economically viable as a public health measure in the low-risk elderly population. We set out to test the hypothesis that an annual intramuscular vitamin D_3 injection would reduce fracture rate among men and women aged >75 years who were living in the community - i.e. not in institutional care.
The study, which was approved by the Southampton & South West Hampshire Research Ethics Committee, was a randomised, double-blind placebo-controlled trial of 300,000 IU intramuscular vitamin D_3 (Cholecalciferol) injection or matching placebo administered every autumn (fall) over three years.
9,440 community-dwelling older people (4,354 men and 5,086 women) aged 75 to 100 years were recruited from primary care registers throughout Wessex, England. After three years of follow up, 609 subjects had incident fractures (hip 110, wrist 107, ankle 24). Hazard ratios in the vitamin D group compared with the placebo group were 1.10 (95% CI 0.94-1.29 p= 0.23) for any first fracture and 1.48 (95% CI 1.01-2.17, p=0.04) for first hip fracture; and 1.17 (95% CI 0.80-1.71, p=0.43) for first wrist fracture, controlling for age and sex. Although the findings were similar among men and women, the difference between treatment groups for hip fracture appeared more pronounced among those aged 80 years and over than among those without previous fractures. No apparent protective effect was observed when the cohort was stratified by age, previous fracture, or level of mobility. Analysis of serum PTH and 25-hydroxyvitamin D concentrations in a subset of subjects suggested that the intervention achieved a 20% suppression in peak winter PTH levels.
We conclude that an annual intramuscular injection of 300,000 IU vitamin D is not effective in preventing hip and other non-spine fractures among elderly men and women resident in the general population.

Disclosures: ***F.H. Anderson****, None.*

1221

Effect of Vitamin D_3 Plus Calcium on Fall Risk in Older Men and Women: a 3-year Randomized Controlled Trial. H. A. Bischoff-Ferrari[1], J. E. Orav*[2], B. Dawson-Hughes[3]. [1]Div. of Aging and Rheumatology, Brigham and Women's Hospital, Boston, MA, USA, [2]Div. of Biostatistics, Brigham and Women's Hospital, Brigham and Women's Hospital, MA, USA, [3]Jean Meyer USDA Human Nutrition Research Center on Aging, Tufts University, Boston, MA, USA.

Background: A recent meta-analysis suggested that vitamin D in any form should lower the risk of falling in older persons by more than 20%. However, there was limited evidence for vitamin D3 (cholecalciferol) and men. Furthermore, little is known about whether supplemental vitamin D3 plus calcium will lower risk of falling over the long term.
Aim: To assess the long-term effect of vitamin D3 plus calcium on the risk of falling in ambulatory older men and women, and active and inactive individuals.
Methods: This is a 3-year double-blind randomized controlled trial. We studied 176 men and 213 women living at home of age 65 or older. Individuals received either 700 IU of vitamin D3 plus 500 mg of calcium or placebo. The outcome of interest was the risk falling at least once during the 3-year follow-up. Falls were ascertained by postcards and by follow-up visits every 6 months. All analyses controlled for age, body mass index, calcium intake, baseline 25-hydroxyvitamin D, physical activity, smoking, alcohol intake and length of follow-up. Subjects were classified as less physically active if they were below the median of average physical activity measured across time.
Results: In 3 years 94 of 176 men (53%) and 125 of 213 women (59%) reported at least one fall. 53% of all first falls occurred in the first year, 27% in the second year and 21% in the third year. Mean baseline 25-hydroxyvitamin D levels were 33.1 ng/ml (SD±14.1) in men and 27.0 ng/ml in women (SD±12.9). Vitamin D3 plus calcium significantly reduced the odds of falling in women (OR = 0.55, 95% CI [0.30 , 0.996]), but not in men (OR = 0.92, 95% CI [0.50 , 1.72]). Independent of gender, vitamin D3 plus calcium significantly reduced the odds of falling in less active persons (OR = 0.54, 95% CI [0.29 , 0.993]). This effect was primarily found in less active women (OR = 0.34, 95% CI [0.14 , 0.79]) rather than in less active men (OR = 0.89, 95% CI [0.32 , 2.48]).
Conclusion: Within 3 years**,** dietary vitamin D3 plus calcium supplementation reduces the odds of falling in ambulatory older women by 45% and in less active subjects by 46%. Thus dietary vitamin D3 and calcium supplementation may be warranted in the long-term prevention of falls in ambulatory older persons, particularly in women and those who are less physically active.

Disclosures: ***H.A. Bischoff-Ferrari****, None.*

1222

Effects of Vitamin D and Calcium Supplementation on Falls and Parameters of Muscle Function - A Prospective, Randomized, Double-blind, Multi-center Study. M. Pfeifer[1], H. Dobnig*[2], B. Begerow*[1], K. Suppan*[2]. [1]Institute of Clinical Osteology, Bad Pyrmont, Germany, [2]Department of Endocrinology, Graz, Austria.

The effects of calcium and vitamin D supplements on falls, falls-related fractures and functional measures are well-known (Pfeifer et al. 2000, Bischoff et al. 2003, Dukas et al. 2004, Larsen et al. 2004). This prospective study was undertaken to test the influence of latitude, seasonal variations, possible threshold effects and duration of vitamin D efficacy after cessation of therapy. 242 healthy male and female subjects over 70 years of age and a 25-OH-D3 serum level below 78 nmol/l were recruited in Bad Pyrmont (52°N) and Graz (48°N) and were randomly assigned to two treatment groups: one receiving 1000 mg Calcium/day (Ca) and the other 1000 mg Calcium and 800 I.U. Vitamin D (Ca+D) over 12 months. This double blind intervention phase was followed by a treatment free observation phase over another 8 months. Falls as the primary efficacy parameter were recorded by diaries and phone calls every two months. Parameters of muscle function such as quadriceps strength, body sway and "timed up and go test" were measured every four months. Statistical evaluation was carried out using the statistics software of IDV, Gauting (Test + Estimation, Version 5.2, "CRO" Dr. Heinz, Vienna, Austria). Baseline parameters did not differ between groups.

TABLE 1 shows intention-to-treat analysis after 12 months of treatment and 8 months of follow-up:

Table 1

Parameter	Calcium mono	Calcium plus Vitamin D	P-Value
Mean number of falls per group	0.69	0.45	p<0.01
Number of falls per subject	1.61	0.95	p<0.01
Body sway frontal (mm)	12.9 +/- 9.1	9.2 +/- 7.9	p<0.01
Quadriceps strength left leg (Newton)	175 +/- 65	210 +/- 63	p<0.01
"Timed up and go"-test (seconds)	8.1 +/- 3.4	7.3 +/- 3.8	p<0.01
25-OH-Vit.D after follow-up (nmol/l)	38 +/- 13	48 +/- 16	p<0.01

Despite a relatively high inclusion criterion for vitamin D (78 nmol/l) and independent of latitude, we observed a significant reduction of falls and parameters of muscle function after supplementation with vitamin D and calcium (MaxiKalzD3). So far, we did not find any evidence for a threshold phenomenon or an effect of latitude.

Disclosures: ***M. Pfeifer****, None.*

F002

Is Peak Bone Mass Attained In Early Adulthood? A. D. G. Baxter-Jones*, R. L. Mirwald*, R. A. Faulkner, D. A. Bailey. College of Kinesiology, University of Saskatchewan, Saskatoon, SK, Canada.

Peak bone mass is defined as the highest bone mineral content during adulthood. However, the age of attainment of peak bone mass is still debatable. The purpose of this study was to determine if peak bone mass had been obtained by early adulthood in a longitudinal study of individuals followed from childhood through to early adulthood. Subjects were from the Saskatchewan Pediatric Bone Mineral Accrual Study (PBMAS), a mixed longitudinal study which ran from 1991 through to 1997. Subjects were aged between 8 and 14 years at study entry and were subsequently measured annually for 6 consecutive years. Between 2002 and 2004, 49 males and 59 females were reassessed on a further two occasions. During follow-up the age range of the subjects was 17 to 27 years. Total body bone mineral content (TBBMC) was assessed annually by dual energy X-ray absorptiometry (DXA) (Hologic 2000). The precision of the DXA in vivo, expressed as the coefficient of variation, was 0.6 %. A change of ± 1.7% (2.8 times the instrument precision) was deemed a biologically significant difference. Although, the average lines of TBBMC with age appears to plateau at 20 years of age (see figure), individual analysis suggests otherwise. In 64% and 56% of males and females respectively, the difference between the two adult measures was within the error of the measurement (± 1.7%). In 16% of the males and 22% of the females, TBBMC increased by more than 1.7% (range 1.8 to 4.9%). In 20% of the males and 22% of the females it decreased by more than -1.7% (range -1.9 to -4.9%). These results suggest that age of attainment of peak bone mass cannot yet been defined. A plateau in TBBMC has not been detected in 36% of males and 44% of females. In fact, TBBMC is fluctuating outside the error of measurement, in a number of individuals. For consistency in change to be confirmed, individuals must be reassessed on at least one more occasion.

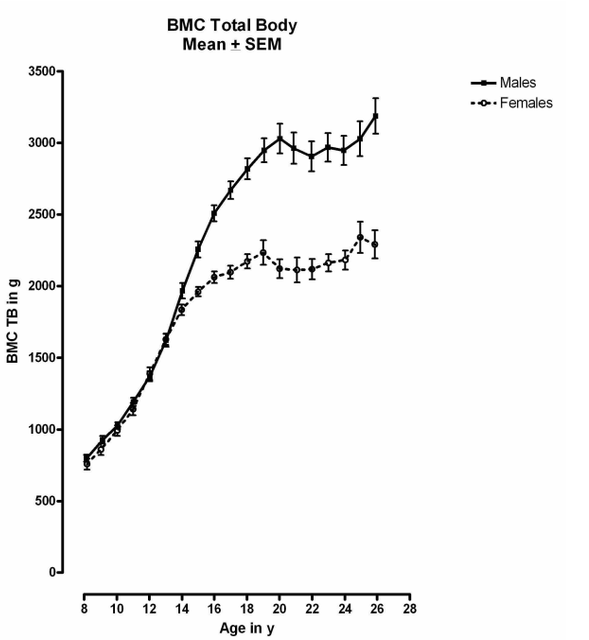

Disclosures: ***A.D.G. Baxter-Jones****, None.*

F005

The Kinase Inhibitory Protein, p27, Is a Likely Mediator of the Vascular Protective Effects of Parathyroid Hormone-related Protein Following Arterial Angioplasty. N. M. Fiaschi-Taesch, K. K. Takane*, I. Cozar-Castellano*, A. F. Stewart. U Pittsburgh, Pittsburgh, PA, USA.

PTHrP contains a nuclear localization signal (NLS). Arterial expression of PTHrP is markedly induced by angioplasty in rodents and humans. In vivo, adenoviral overexpression of PTHrP worsens the neointimal response to angioplasty. In contrast, PTHrP mutants in which the NLS has been removed (ΔNLS-PTHrP) are potent inhibitors of vascular smooth muscle cell (VSMC) proliferation, blocking the phosphorylation of the retinoblastoma protein (pRb), and arresting VSMC in G_1/G_0. This is of clinical relevance, for adenoviral delivery of ΔNLS-PTHrP at angioplasty completely inhibits arterial re-stenosis in rats. In this study, we explored the mechanisms through which ΔNLS-PTHrP arrests the cell cycle, using A-10 VSMC stably overexpressing ΔNLS-PTHrP, and untransfected A-10 cells as controls.

By immunoblot, p107and p130, the two "pocket protein family" homologues of pRb, were not affected by ΔNLS-PTHrP overexpression. Similarly, protein levels of all members of the cyclin D family and cdk-4 were unchanged by ΔNLS-PTHrP, as was cdk-2. There was a marginal decrease in cyclin E and cdk-4 kinase activity. In contrast to the minimal or absent changes in these cell cycle regulators, cdk-2 kinase activity was specifically and dramatically (70%) downregulated by ΔNLS-PTHrP. This suggests that the cdk-2/cyclin E-complex is a likely site of regulation of pRb phosphorylation by ΔNLS-PTHrP.

To examine the upstream regulators of cdk-2/cyclin E activity, VSMC INK/KIP family members were investigated. By immunoblotting, p16 and p21 were unchanged in ΔNLS-PTHrP-expressing cells. In contrast, p27, a potent cdk-2/cyclin E kinase inhibitor, was dramatically (~5-fold) increased in ΔNLS-PTHrP-A-10 cells. Unlike p27 protein, p27 mRNA levels were identical in control and ΔNLS-PTHrP A-10 cells, suggesting that p27 is upregulated by ΔNLS-PTHrP at the translational or posttranslational level. To determine whether p27 upregulation is the central regulator of ΔNLS-PTHrP inhibitory actions on VSMC, we prepared siRNA oligonucleotides and can reduce p27 protein levels to baseline in ΔNLS-PTHrP A-10 cells. Flow cytometry studies are in progress. To explore whether the reduction in p27 was a specific effect of ΔNLS-PTHrP, p27 was examined in VSM cells overexpressing wild-type PTHrP, in which pRb phosphorylation and in S and G2/M cell cycle phases are increased. p27 was dramatically decreased in these wild-type PTHrP A-10 cells. These studies suggest that p27 is a critical downstream regulator of both ΔNLS-PTHrP and wild-type PTHrP effects on VSMC proliferation. Whether this is a common pathway in other PTHrP target cells requires further study.

Disclosures: ***N.M. Fiaschi-Taesch****, None.*

F007

Maturity- and Sex-related Changes in Tibial Bone Geometry, Strength and Muscle-bone Indices during Growth: A 20-month pQCT Study. H. M. Macdonald*[1], S. A. Kontulainen[2], K. J. MacKelvie-O'Brien[3], K. M. Khan*[4], H. A. McKay[5]. [1]Human Kinetics, University of British Columbia, Vancouver, BC, Canada, [2]Orthopaedic Engineering Research, University of British Columbia, Vancouver, BC, Canada, [3]Endocrinology and Diabetes Unit, British Columbia's Children's Hospital, Vancouver, BC, Canada, [4]Orthopaedics/Family Practice, University of British Columbia, Vancouver, BC, Canada, [5]School of Human Kinetics/Orthopaedics/Family Practice, University of British Columbia, Vancouver, BC, Canada.

Structural changes in bone and muscle across stages of maturity have not been well characterized. Our aim was to describe sex and maturity differences for 20-month changes in bone geometry and strength and the muscle-bone relationship. We measured height and weight in 128 children (69 girls, 11.9 ± 0.6 years at baseline). Girls were categorized as EARLY, PERI- or POST-pubertal based on menarcheal status and boys were similarly categorized based on Tanner pubic hair stage. We used peripheral quantitative computed tomography (pQCT) to measure 20-month change in total bone cross-sectional area (*ToA*, mm^2), cortical area (*CoA*, mm^2), section modulus (*Z*, mm^3) and muscle area (*MA*, mm^2) at the tibial shaft (50% site). We calculated two muscle-bone indices (*MBI*); *CoA/MA* and relative bone strength (*RBS*, [*Z*/(leg length/2)]/*MA*). Both EARLY boys and girls had smaller *ToA* and *CoA* at baseline than more mature, same-sex groups. There were no baseline sex differences in *ToA, CoA* (Fig) and *Z*; however, boys increased significantly more than girls in each maturity group. Baseline *MBI* did not differ between sexes in EARLY and PERI groups, whereas they were significantly greater for POST boys compared to POST girls ($p < 0.05$). Over 20-months, *MBI* decreased significantly among EARLY and PERI girls compared to EARLY and PERI boys ($p< 0.05$). However, due to greater gains in *MA* among POST boys (Fig), there was a trend towards decreased *MBI* compared to POST girls. The present study provides novel longitudinal descriptions of change in bone geometry and strength at the tibial shaft in three maturity categories of girls and boys using pQCT. Further, this study highlights how sex differences in bone structure and muscle strength influence the muscle-bone relationship. The sexual dimorphism in musculoskeletal development may influence how bone responds to mechanical loading during puberty.

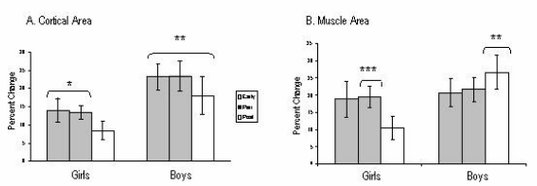

Figure. 20-month percent change in cortical area (A) and muscle area (B) for early, peri- and post-pubertal boys and girls. * EARLY & PERI > POST; ** Boys > Girls; *** PERI > POST. Bars indicate 95% confidence intervals. Noted differences significant at $p < 0.05$.

Disclosures: ***H.M. Macdonald****, None.*

F009

Bone Growth at the Distal Radius and Tibia Shaft in Pubertal Girls - A 2-year Longitudinal Study. Q. Wang*[1], M. Alén*[2], P. Nicholson*[1], A. Lyytikäinen[1], M. Suuriniemi[1], E. Helkala*[1], H. Suominen[1], S. Cheng[1]. [1]University of Jyväskylä, Jyväskylä, Finland, [2]PEURUNKA -Medical Rehabilitation Center, Jyväskylä, Finland.

We investigated growth trends in the distal radius and tibial shaft in 258 normal Finnish girls aged 10-13 years followed over two years in terms of geometric properties and bone density measured annually using peripheral quantitative computed tomography. Volumetric bone mineral density was assessed in the total bone (total vBMD) and, in the case of the tibia, also in the cortical compartment alone (cortical vBMD). A hierarchical linear statistical model with random effects was used to estimate polynomial functions representing the true longitudinal growth trends relative to menarche. The growth rates of distal radius cross-sectional area (CSA) and bone mineral content peaked at 16 and 9 months before menarche, respectively. This discrepancy between CSA and BMC trends was reflected in a decline in distal radius total vBMD up until 12 months before menarche. In contrast, in the tibial shaft both total and cortical vBMD increased steadily throughout puberty. Tibial cortical thickness increased linearly, and was accounted for mainly by bone formation at the periosteal surface before menarche, and at both the periosteal and endosteal surfaces after menarche. The ratio of cortical/total CSA increased, and the ratio of marrow/total CSA decreased, during puberty. Interestingly, for both radius and tibia, the growth rate in bone CSA peaked at the same time as the growth rate in body height (16-20 months before menarche), but the peak BMC growth rate occurred later, concurrent with the peak rate of increase in body weight (9-10 months before menarche). The results suggest that there is a transitional period of decreased distal radius total vBMD during puberty, and this may explain the increased forearm fracture incidence in puberty reported in previous epidemiological studies.

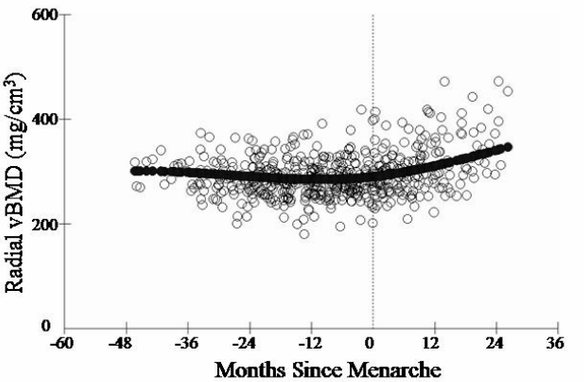

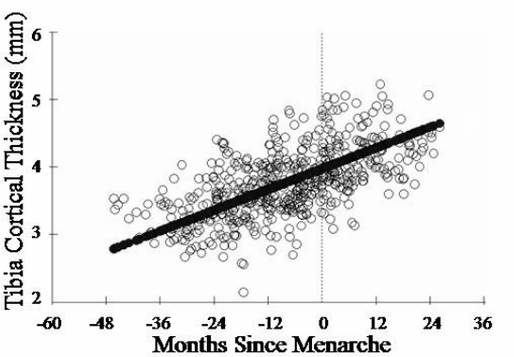

Disclosures: ***Q. Wang****, None.*

F012

Gender-specific Differences in the Functional Muscle-bone Unit at Different Skeletal Sites in Children Assessed by DXA and pQCT. R. Ashby*[1], Z. Mughal*[2], J. Adams[1], K. Ward[1]. [1]Clinical Radiology, University of Manchester, Manchester, United Kingdom, [2]Central Manchester and Manchester Children's Hospitals NHS Trust, Manchester, United Kingdom.

The functional muscle-bone unit may be important for the evaluation of musculoskeletal development and health in children. The relationship between muscle and bone may be expressed as a ratio, where bone mineral content (BMC)(g) or area (BA)(cm2) is divided by lean mass (LM) (g). The aim of this study was to determine whether there are gender differences in BMC:LM and BA:LM of the whole body (WB) and regional body segments of growing children. As height is a major determinant of the muscle-bone unit, gender differences at different skeletal sites may be more apparent when the muscle bone unit is interpreted according to height.

250 healthy children (114 male [M], 136 female [F]; age 10.6±3.4, range 5-18 years; height 141.1±17.3, range 110.1-179.9cm) were studied. BMC, BA and LM values for the WB and regional body segments (trunk, arms and legs) were determined from WB DXA scans (Hologic QDR-4500A). The XCT-2000 pQCT scanner (Stratec) was used to measure cortical BMC (CC) (mg/mm), cortical BA (CA) (mm2) and cross-sectional muscle area (CSMA) (mm2) of the non-dominant midshaft radius. Bone:muscle ratios (BMC:LM, BA:LM, CC:CSMA and CA:CSMA) were determined for each subject. Data were split into 10cm height group increments. The differences in each height group between and within genders were then analysed.

Arm, leg and WB BMC:LM ratios increased with successive height groups in both males and females. Females had significantly higher arm BMC:LM at 130-169cm ($p<0.001$-0.007), trunk BMC:LM at 130-139 and 150-159cm ($p<0.001$-0.020) and WB BMC:LM at 150-169cm ($p=0.011$ & $p=0.048$) compared to males. There was a trend for greater CC:CSMA ratios in females vs males.

Arm BA:LM ratios reached peak values at 150-159cm in females; these ratios were greater in females between 120-179cm ($p<0.001$-0.036). Leg BA:LM ratios reached maximum values in both genders between 130-139cm, then declined with sequential height; females being higher than males ($p=0.004$-0.039). WB BA:LM ratios were greatest at 120-120cm in males and 130-139cm in females, then decreased in both genders. At the radius, CA:CSMA ratios increased with height and were greater in females, but this did not reach significance.

These data show females have greater BMC and BA relative to muscle mass compared to males of comparative heights, and supports the work of Schiessl (1998). Increased bone deposition in females may be due to oestrogen lowering the mechanostat remodelling threshold. This may be an adaptive mechanism whereby extra bone is stored as a reservoir for the potential demands of pregnancy and lactation.

Disclosures: ***R. Ashby****, None.*

F017

Is Mechanical Homeostasis Faulty in Elderly Women Who Suffer Osteoporotic Fractures? M. M. Daphtary*[1], C. B. Ruff[2], K. L. Stone[3], S. R. Cummings[3], T. J. Beck[1]. [1]Radiology, Johns Hopkins University, Baltimore, MD, USA, [2]Cell Biology and Anatomy, Johns Hopkins University, Baltimore, MD, USA, [3]Department of Medicine, University of California San Francisco, San Francisco, CA, USA.

It is known that bones adapt strength to changing loading conditions, but does net bone loss in aging bones mean that homeostatic adaptation is less effective in those who fracture? To examine this question we evaluated load stresses in the proximal femurs of elderly women participating in the Study of Osteoporotic Fractures over two time points averaging 3.5 years apart. Theoretically, homeostatic adaptation should continually adapt bone strength to changing skeletal loading demands so that stresses remain constant. If homeostasis is defective, bone loss should cause stresses to increase over time. We computed magnitudes and rates of change in medial and lateral stresses at the femoral neck using body weight as load in an analytical model of a fall on the greater trochanter. BMD, BMC and structural dimensions including bone cross-sectional area (CSA) and section modulus (Z) were derived from dual energy x-ray absorptiometry scans of the hip using Hip Structure Analysis (HSA). Results were compared between 1079 women who remained free of all fractures at last follow-up (Fx-Free) and 1703 women who suffered incident or prevalent hip, vertebrae, rib, forearm or other fragility fractures (Fx). Group differences were assessed by ANCOVA and differences between time points by paired t-tests. Compared to Fx-Free at each time point, Fx women had ~2% lower body weights, but bone CSA and Z adjusted for differences in age, weight and knee height were ~7-8% lower hence stresses were ~7% higher (all differences $p<0.05$). Between time points, Z and CSA declined 0.5-0.6%/y in Fx women and skeletal load (weight) declined 0.3%/y (all changes $p<0.05$); neither strength nor weight changed in Fx-Free. Consequently, stresses did not change significantly in either group ($p > 0.05$). Interestingly BMD declined 0.8% and 1.07%/y in Fx-Free and Fx, respectively ($p<0.05$). BMC did not change in Fx-Free; the decline in BMD was entirely due to 0.5%/y expansion of diameter ($p<0.05$). In Fx, BMC declined 0.2%/y and diameter expanded 0.6%/y ($p<0.05$). These results indicate that whether or not women suffer osteoporotic fractures, their bones maintain the ability to adapt to changing mechanical loads and this is not reflected in the change in BMD. However, those who do fracture have bones apparently adapted to higher stress levels, i.e., of lower strength. Our findings suggest that, even in those who suffer osteoporotic fractures, bone loss in elderly women is not indicative of a defect in mechanical homeostasis that prevents adaptation to current loading conditions.

Disclosures: ***M.M. Daphtary****, None.*

F024

Twisted Gastrulation Inhibits Bone Morphogenetic Protein Actions and Prevents Osteoblast Cell Differentiation. E. Gazzerro, V. Deregowski, S. Vaira*, E. Canalis. Research, Saint Francis Hospital and Medical Center, Hartford, CT, USA.

Twisted gastrulation (Tsg), a secreted glycoprotein that binds bone morphogenetic protein (BMP)-2 and -4, can display both BMP agonist and antagonist functions. Tsg can complex with BMP and its antagonist chordin, enhancing chordin actions, or it can facilitate chordin cleavage by the metalloprotease BMP-1/tolloid, releasing active BMP. Consequently, Tsg dual activities depend on the relative concentrations of BMP, chordin and BMP-1 in target tissues. Tsg null mice have defective endochondral ossification, indicating an agonist effect in cartilage. But, the actions of Tsg in bone and cells of the osteoblastic lineage are not known. To investigate the role of Tsg in cells of the osteoblastic lineage, we examined its expression and activity in ST-2 stromal cells. Tsg and BMP-1, but not chordin, transcripts were detected under basal conditions. BMP-2 induced chordin, downregulated Tsg, and did not modify BMP-1 transcripts. To define the effects of Tsg on stromal cells, ST-2 cells were transduced with a retroviral vector where Tsg expression is under the control of the CMV promoter and compared them to cells transduced with parental vector. ST-2 cells were cultured in osteoblastic differentiating conditions with and without BMP-2. Tsg overexpression precluded the formation of mineralized nodules induced by BMP-2 in control cells, and delayed the expression of osteoblastic gene markers. BMP can signal by activating the Smad pathway or the mitogen activated protein (MAP) kinases, ERK, p38 and JNK. In ST-2 cells, BMP-2 induced Smad 1/5/8 phosphorylation and the transactivation of a transfected 12x-SBE-Oc-pGL3 construct containing 12 repeats of a Smad binding site directing luciferase expression. In accordance with the phenotypic changes, Tsg overexpression opposed BMP-2 effects on Smad 1/5/8 phosphorylation and on the transactivation of the 12x-SBE-Oc-pGL3 construct. BMP-2 had a modest effect on ERK and no effect on p38 or JNK phosphorylation. The effects of Tsg appeared to be selective to BMP-2/Smad signaling, since Tsg did not alter the activity of a transfected Wnt/ß-catenin responsive construct containing Tcf4/Lef1 recognition sequences upstream of the reporter luciferase. In conclusion, Tsg inhibits BMP signaling and actions, preventing its effects on the differentiation of stromal cells toward the osteoblastic pathway. These results contrast the Tsg agonist role in cartilage, and demonstrate an antagonist role in cells of the osteoblastic lineage.

Disclosures: ***E. Gazzerro****, None.*

F026

The Anabolic Response to Bone Morphogenetic Protein-2 Is Impaired in Fibroblast Growth Factor-2 Null Mice. T. Naganawa[1], L. Xiao[1], J. D. Coffin[2], T. Doetschman*[3], M. M. Hurley[1]. [1]Medicine, University of Connecticut Health Center, Farmington, CT, USA, [2]The University of Montana, Missoula, MT, USA, [3]University of Cincinnati, Cincinnati, OH, USA.

Bone Morphogenic Protein-2 (BMP2) is a member of the transforming growth factor beta (TGFb) super-family that plays an important role in the commitment and differentiation of osteoprogenitors to active osteoblasts. We made the novel observation that BMP2 stimulates fibroblast growth factor-2 (Fgf2) mRNA in osteoblast/stromal cells (OBs). FGF2 is a potent stimulator of osteoblast precursor proliferation and is anabolic in experimental animals. In addition, disruption of the Fgf2 gene resulted in reduced bone mass and bone formation in mice. To characterize the role of FGF2 in the BMP2 responses, we examined bone formation in vivo in response to BMP2 in Fgf2+/+ and Fgf2-/- mice. Three-month-old Fgf2+/+ and Fgf2-/- male mice were weighed and injected s.c. once daily with vehicle or BMP2 (20µg/kg body wt) for 5 days. Mice were injected with calcein (0.6 mg/kg) on day 7 and day12 to assess new bone formation. There were no significant differences in body wt pre- and post-BMP2 in either genotype. Histomorphometry of the calvaria showed that BMP2 significantly increased calvarial width by 13% (186.1±6.3 vs. 164.1±4.0, $p<0.05$) in Fgf2+/+ but caused only a 5% increase (161.5±10.9 vs. 153.3±6.1) in Fgf2-/- mice that was not significant. Bone formation rate (BFR/BS) was increased by 57% (0.74±0.07 vs. 0.47±0.06, $p<0.05$) in Fgf2+/+ mice but the changes were smaller 15% (0.53±0.12 vs. 0.46± 0.18) and not significant in Fgf2-/- mice. To assess the mechanism of reduced bone formation, bone marrow stromal cells from 3-month-old Fgf2+/+ and Fgf2-/- mice were cultured in differentiation medium in the absence or presence of BMP2 (30 ng/ml) or FGF2 (1 nM) for 7-21 days. In vehicle treated Fgf2-/- cultures, there were fewer alkaline phosphatase positive, mineralized nodules compared with Fgf2+/+ cultures. Treatment with FGF2 but not BMP2 rescued bone nodule formation in Fgf2-/- cultures. Since BMP2 signals via activation of Smad and p38MAPK, we examined the integrity of these pathways in OBs. Fgf2+/+ and Fgf2-/-OBs were treated with vehicle or BMP2 (50 ng/ml) for 30 to 120 mins and cellular proteins were analyzed by Western blot. BMP2 caused a marked induction of phospho-Smad1/5/8 and phospho-p38 within 30 mins in Obs from both Fgf2+/+ and Fgf2-/- mice. We conclude that FGF2 is crucial in the anabolic effect of BMP2 and that this may be independent of activation of Smad and MAPK signaling pathways.

Disclosures: ***T. Naganawa****, None.*

F037

Expression of PHOSPHO1 during Embryonic Development: Implications for Skeletal Mineralization. A. J. Stewart*, S. J. Roberts*, C. Farquharson. Roslin Institute, Midlothian, United Kingdom.

Matrix mineralization is a biphasic process that occurs within terminally differentiating chondrocytes, osteoblasts and ondontoblasts and is the mechanism by which cartilage, bone and tooth formation occurs by each of these cell types, respectively. The initial phase concerns the formation of Ca^{2+} ions and inorganic phosphate (P_i) within matrix vesicles (MVs). Accumulation of Ca^{2+} is controlled by calcium-binding molecules such as annexin I and phosphatidylserine. The accumulation of P_i is less clear. It has long been speculated that the generation of P_i results from the action of phosphatases, the most abundant being tissue non-specific alkaline phosphatase (TNAP). During skeletal development, the generation of P_i for mineralization does not appear to be due to the activity of TNAP. In newborn TNAP knockout mice, bone development and mineralization essentially appear normal, despite the subsequent observation of hypomineralization and other abnormalities. PHOSPHO1 is a novel phosphatase upregulated in mineralizing cells, which exhibits high specific phosphohydrolase activity toward phosphoethanolamine and phosphocholine and is localized to mineralizing regions of developing bone and cartilage. However, it is unclear if PHOSPHO1 is present in MVs. In this study we have investigated PHOSPHO1 mRNA expression during embryonic development in the chick by whole-mount *in-situ* hybridization. *In-situ* hybridization was done using digoxigenin labeled RNA probes. Cryosectioning of the whole mounts indicated that chondrification of the long bones occurred from day5/6 and von Kossa-positive staining was observed in both the femur and tibia from day 7. Mineralization was initially restricted to the bone collar within the mid-shaft of the diaphysis. At day-12 mineralization was observed over the entire length of the diaphysis. The localization of PHOSPHO1 mRNA was found in all long bones studied (femur, tibia, ulna, radius, metatarsals and phalanges). No hybridization was observed in any other tissues. Microscopically, its localization mirrored that of the von Kossa staining and was observed only at the developing bone collar. To determine the presence of PHOSPHO1 we isolated MVs from growth plates of juvenile (3-week-old) chicks by ultracentrifugation. High TNAP activity verified the identity of the MV-containing fraction. Immunoblotting using a PHOSPHO1 specific antiserum confirmed the presence of high levels of the enzyme. These studies provide further evidence that PHOSPHO1 is involved in the generation of P_i for matrix mineralisation during embryonic skeletal development.

Disclosures: ***A.J. Stewart****, None.*

F039

Hypomineralization of Tibia in Nucleoside Triphosphate Pyrophosphohydrolase (NPP1) Deficient Mice. H. Clarke Anderson[1], D. Harmey*[2], N. P. Camacho[3], R. Garimella[1], J. B. Sipe*[1], S. Tague*[1], R. Terkeltaub[4], J. L. Millan[2]. [1]Pathology, University of Kansas Medical Center, Kansas City, KS, USA, [2]The Burnham Institute, La Jolla, CA, USA, [3]Hospital for Special Surgery, New York, NY, USA, [4]VA/UCSD, San Diego, CA, USA.

A study was undertaken to characterize long bone mineralization in mice with a genetic deficiency of the enzyme nucleoside triphosphate pyrophosphohydrolase (NTPPase), also known as PC-1 or NPP1. NTPPase is present at sites of biomineralization, i.e., at the surfaces of growth plate chondrocytes, metaphyseal osteoblasts and matrix vesicles (MVs). NTPPase hydrolyzes ATP yielding pyrophosphate (PP_i). Depending on the local concentration, PP_i has dual functions: at concentrations above 2mM, PP_i inhibits bone mineralization, but when present at low (micromolar) concentrations in the extracellular fluid of cartilage and bone, PP_i can promote calcification. At skeletal mineralization sites, PP_i is hydrolyzed to orthophosphate (P_i) by tissue-nonspecific alkaline phosphatase (TNAP) thus increasing the local concentration of P_i for incorporation into nascent hydroxyapatite mineral. Previously, we found that double deletion of the NPP1 and TNAP genes lead to correction of soft tissue calcification in the vertebral apophyses of the double mutant mice. In this study, we aimed at evaluating the extent of the corrective changes by examining long bone mineralization in the NPP1 and NPP1/TNAP double mutant mice. We also performed a detailed immunohistochemical study of NPP1 expression. Single or double knockout 10 day-old mouse upper tibias were examined by non-decalcified histology, mineral estimation by Alizarin red, micro CT, Fourier-transform infrared spectroscopy (FTIRIS) and by transmission electron microscopy (TEM). Unexpectedly, we found that bone mineralization was slightly reduced in NPP-1 deficiency and moderately to severely deficient in TNAP/NPP-1 double knockout mouse tibias. Our data indicate that the hypermineralization state of NPP1-deficient mice and the degree of correction attained by simultaneously ablating the TNAP gene is restricted to certain sites, e.g. the vertebral apophysis, but was not seen in tibial growth plate or metaphysis. Our immunohistochemistry data reveal that the differential rescue with respect to bone sites correlates with the local expression pattern of the NPP-1 protein. We found that sites of mineralization correction (e.g. vertebrae) express high levels of NPP-1 while sites such as tibia have low to undetectable levels of NPP-1 expression.

Disclosures: ***H. Clarke Anderson****, None.*

F042

A Mouse Model of Jansen Metaphyseal Chondrodysplasia (JMC): Introduction of the H223R Mutation into the Murine PTH/PTHrP Receptor gene results in Delayed Endochondral Bone Formation. L. F. Fröhlich, U. I. Chung, J. Guo, H. Jüppner. Endocrine Unit, Massachusetts General Hospital/ Harvard Medical School, Boston, MA, USA.

JMC is a very rare form of short-limbed dwarfism associated with abnormalities in endochondral bone formation and mineral ion homeostasis. Four different heterozygous gain-of-function point mutations in the membrane spanning domains of the PTH/PTHrP type 1 receptor have been identified thus far as the cause of this autosomal dominant genetic disorder. These mutations lead to constitutive ligand-independent cAMP accumulation when tested in vitro.

We used gene targeting to introduce the human H2232R mutation into the murine PTH/PTHrP receptor (Pthr1) gene and to thereby generate a mouse model of JMC for functional analysis of a constitutively active Pthr1 in vivo.

At E12.5, 15.5, 16.5 and 18.5 homozygous fetuses were identified, however, no homozygous live neonates were thus far found, indicating that the H223R may be postnatally lethal. Mice heterozygous for the mutant receptor are viable and fertile, and exhibited no obvious abnormalities. However, one mouse was distinguished by its small size and developmental delay, while a few other animals showed lethal kyphosis possibly indicating that differences in the genetic background may affect the phenotype.

Histological analysis of the skeleton of neonatal and 5 week old heterozygotes was performed. A severe delay in endochondral bone formation was observed in sternum, vertebral column, femur and tibia of newborn mice. The growth plates of all investigated bones showed an obvious accumulation of proliferative as well as of hypertrophic chondrocytes at chondro-osseous junctions associated with a disturbance of regular columnar structures and a delay in vascular invasion. This finding was particularly pronounced in parts of sternum and vertebral column where different sternebrae and vertebrae completely lacked primary ossification centers and were smaller compared to those of wild-type littermates. By 5 weeks of age, the long bones of the H223R mutant mice appeared to have essentially normal histology, with the exception of some thickening in the growth plates. In comparison to wild-type controls, blood serum ionized calcium levels of heterozygous H223R-Pthr1 mice were slightly elevated (1.28 ± 0.05 mmol/l wt; n=8 vs. 1.34 ± 0.02 mmol/l het; n=8) at the age of 1 month.

Our results indicate that a mouse model of JMC has been generated and confirm that the H223R-Pthr1 mutation delays chondrocyte differentiation and leads to mild hypercalcemia. These mice will now be used to further explore the molecular mechanisms leading to the changes in endochondral bone formation and mineral ion homeostasis that are typically observed in JMC.

Disclosures: ***L.F. Fröhlich****, None.*

F044

PTH-rP Expression in Cartilage Cells Is Regulated by the Gli Family of Transcription Factors. J. A. Sterling, B. O. Oyajobi, M. Zhao, A. Gupta*, M. Banerjee*, G. R. Mundy. Cellular and Structural Biology, University of Texas Health Science Center at San Antonio, San Antonio, TX, USA.

Parathyroid hormone-related peptide (PTH-rP) has an important physiological role in the growth plate, where it regulates chondrocyte proliferation. Its expression is controlled by Indian hedgehog (Ihh), and both Ihh and PTH-rP null mutant mice have severe and similar growth plate abnormalities, with premature differentiation and decreased proliferation of growth plate chondrocytes resulting in small stature. Although these data suggest that Ihh controls PTH-rP expression in cartilage cells, the mediators responsible are unknown. In drosophila, hedgehog signaling is mediated by the transcriptional regulator cubitus interruptus (Ci), which is the ortholog of the Gli family of transcriptional activators in vertebrate cells. Gli2 null mice exhibit increased hypertrophic chondrocytes and decreased PTH-rP expression (Miao et al., 2004), suggesting similarities to deletion of Ihh and PTH-rP. Since the Gli family has been shown to mediate Hh signaling in other vertebrate cells, we reasoned that this same family may mediate Ihh effects on PTH-rP expression in cartilage cells. To examine this, we performed transfections of the growth plate chondrocyte cell line TMC-23 with PTH-rP promoter luciferase and Gli expression constructs. We found that Gli2 up-regulated the activity of a 1.1kb PTH-rP promoter luciferase construct by approximately 3-fold. This effect appears specific to Gli2 as transfections with the other family members, Gli3 or Gli1, had no effect on basal PTH-rP promoter activity. We and others have demonstrated that Gli3 is proteasomally processed to a truncated repressor form, similar to its ortholog Ci in drosophila . In TMC-23 this truncated repressor form of Gli3 blocked Gli2 mediated PTH-rP promoter activity. Furthermore, an siRNA for Gli2 that specifically decreases Gli2 expression by >90% dramatically blocked the Gli2 mediated PTH-rP promoter activity, suggesting that Gli2 is a physiologic regulator of PTH-rP expression in cartilage cells. Since the Gli family appears to be an important regulator of PTH-rP promoter activity, we analyzed the PTH-rP promoters for consensus Gli binding sites. The site with the closest homology was a 6/9 match, which by EMSA did not bind Gli2, indicating that the effects of Gli2 on the PTH-rP promoter are likely indirect. Taking all of these data together, we conclude that the Gli family of transcription factors mediates the effects of hedgehog proteins on PTH-rP expression and subsequent endochondral bone formation in the cartilage cells of the growth plate.

Disclosures: ***J.A. Sterling****, None.*

F047

Hypoxia Promotes Chondrocytic Differentiation *in vitro* and Cartilaginous Matrix Synthesis in Organ Culture via p38 Kinase Pathway. M. Hirao*, N. Tamai*, N. Tsumaki*, A. Myoui, H. Yoshikawa. Department of Orthopaedics, Osaka University Graduate School of Medicine, Suita, Japan.

Cartilage is an avascular tissue that functions at a lower oxygen tension than do most other tissues. On the other hand, ossification is always accompanied by vascularization, suggesting high oxygen requirement. Under the hypothesis that oxygen tension plays an important role in the commitment to chondrocyte of the cells in mesenchymal lineage, we investigated the role of oxygen tension on chondrocytic differentiation induced by recombinant human bone morphogenetic protein-2 (rhBMP-2) using pluripotent mesenchymal cell line C3H10T1/2. These cells were cultured in normoxia (O2 20%) and hypoxia (O2 5%) conditions in the presence of rhBMP-2 (500ng/ml). Alcian blue staining revealed more abundant glycosaminoglican (GAG) synthesis in the cells cultured in hypoxia than in normoxia. In parallel, type II collagen (*Col2a1*) gene expression by Northern blotting was elevated in hypoxic condition, while type X collagen (*Col10a1*) gene expression and alkaline phosphatase (ALP) staining were suppressed by hypoxia. Since p38 mitogen activated protein kinase (p38MAPK) has been suggested to regulate chondrocyte differentiation and to play a key role in hypoxia-induced signaling, we next examined the role of p38MAPK in hypoxia-induced chondrocytic differentiation. We found that hypoxia up-regulated phosphorylation of p38MAPK in C3H10T1/2 cell culture but down-regulated that of Smad 1/5/8. An inhibitor of p38MAPK, FR167653 partially suppressed hypoxia-induced GAG synthesis and *Col2a1* gene expression. Furthermore, dominant-negative MKK3 that specifically inhibits p38MAPK pathway abolished hypoxia-induced GAG synthesis. On the other hand, wild type Smad6 that down-regulates Smad signaling did not alter the hypoxia-induced GAG synthesis. To investigate the role of oxygen tension in cartilage tissue development we performed organ culture of neonatal mouse forearm and histologically evaluated. Although hypoxia did not alter the proportion of zonal structure of growth cartilage, the width of growth cartilage was increased by hypoxia both in the absence and in the presence of BMP-2, suggesting increased cartilaginous matrix production. Hypoxia-promoted widening of growth cartilage was clearly suppressed by FR167653. These findings suggest that hypoxia promote chondrocytic differentiation of the pluripotent mesenchymal cells as well as matrix production in cartilage tissue via p38 MAPK pathway.

Disclosures: ***M. Hirao****, None.*

F049

BMP Signaling Regulates Chondrocyte Differentiation and Maturation at Multiple Steps. T. Kobayashi[1], K. M. Lyons[2], A. P. McMahon*[3], H. M. Kronenberg[1]. [1]Endocrine Unit, Massachusetts General Hospital, Boston, MA, USA, [2]University of California, Los Angeles, Los Angeles, CA, USA, [3]Harvard University, Cambridge, MA, USA.

In order to investigate roles of BMP signaling in cartilage development, we overexpressed a constitutively active form of BMPR1A receptor (*caBmpr-1a*) in chondrocytes. First, *caBmpr-1a* was overexpressed directly by a rat collagen 2 promoter. Acute transgenic embryos (*Col2-caBmpr-1a*) were analyzed. Second, *caBmpr-1a* was overexpressed using the GAL4/UAS system to establish transgenic lines. GAL4 is misexpressed in chondrocytes using the same rat collagen 2 promoter in the driver mouse (*Col2-Gal4*). *Col2-Gal4* mice were crossed to mice carrying *caBmpr-1a* sequence downstream of GAL4 responsive UAS elements (*UAS-caBmpr-1a*). *Col2-Gal4:UAS-caBmpr-1a* embryos (bigenic mice) were analyzed. Lastly, BMPR1B (*Bmpr-1b*) null mice were crossed to bigenic mice to examine whether expression of *caBmpr-1a* in the chondrocytic lineage was able to rescue the phenotype. Acute overexpression of *caBmpr-1a* in the chondrocytic lineage caused enlargement of cartilage elements and a relative reduction in proliferating chondrocytes. Expression of *Sox9* and *Noggin*, of which expression is augmented during chondrocyte maturation, was upregulated in transgenic vertebral cartilage, suggesting acceleration of chondrocyte maturation. A reduction in proliferating chondrocytes was also observed in bigenic *caBmpr-1a* mice. However, unlike acute transgenic mice, bigenic mice showed no enlargement of the cartilage elements. This difference between the two phenotypes may result from subtle differences in timing of *Bmpr-1a* expression. Target gene expression in the bigenic system requires earlier GAL4 protein synthesis, which may delay expression *caBmpr*-1a compared with acute transgenic mice. This may have restricted the *caBmpr-1a* expression in chondrocytes to more advanced stages in bigenic mice. It is, therefore, possible that BMP signaling in immature cells of the chondrocytic lineage stimulates commitment to form chondrocytes, whereas BMP signaling in committed chondrocytes stimulates their maturation and terminal differentiation.

The first and second phalanges of *Bmpr-1b-/-* mice fail to form cartilage molds. Overexpression of *caBmpr-1a* in the cartilage of *Bmpr-1b-/-* mice rescued the defect in phalange development, demonstrating that the loss of BMP signaling in prospective phalangeal cells of the chondrocytic lineage is responsible for the digit defect of *Bmpr-1b-/-* mice. The rescue also suggests that BMPR-1A signaling can substitute for BMPR-1B signaling in this setting. These results suggest that BMP signaling regulates cartilage development at multiple steps.

Disclosures: ***T. Kobayashi****, None.*

F051

Mitogen-activated Protein Kinases Mediate Parathyroid Hormone Regulation of Indian Hedgehog Transcript in Chondrocytes. L. P. Lai*, J. Mitchell. Pharmacology, University of Toronto, Toronto, ON, Canada.

Endochondral ossification is the process by which long bones develop and grow. It is regulated by multiple paracrine factors including parathyroid hormone-related peptide (PTHrP) and Indian Hedgehog (Ihh). Pre-hypertrophic chondrocytes secrete Ihh, which stimulates PTHrP secretion from the perichondrium, and indirectly regulates chondrocyte terminal differentiation. Previous studies have shown that PTHrP can in turn inhibit the Ihh mRNA level in pre-hypertrophic chondrocytes, providing a negative feedback mechanism. In this study, we have examined the role of mitogen-activated protein (MAP) kinases in mediating the PTH regulation of Ihh mRNA levels in a chondrocytic cell line, CFK-2. Ihh mRNA levels were decreased in cells treated with U0126, a specific MEK1/2 inhibitor, as well as SB203580, a specific p38 MAP kinase inhibitor. Cells transiently transfected with constitutively active MEK1 or MKK3 had increased Ihh mRNA levels, while dominant-negative forms of MEK1, p38α or p38β all diminished the level of Ihh mRNA, implicating both ERK1/2 and p38 MAP kinase pathways in the regulation of Ihh expression. Activation of the common receptor for PTH and PTHrP with 10^{-8}M PTH (1-34) decreased the Ihh mRNA levels. PTH also caused a transient dephosphorylation of p38 MAP kinase that was maximal after 25 minutes, as well as dephosphorylation of ERK1/2 that was evident within 15 minutes and sustained for at least one hour. The PTH inhibition of MAP kinases was mimicked by 500nM forskolin, and was accompanied by the stimulation of MKP-1 expression, a specific MAP kinase phosphatase, within 30 minutes. The PTH down-regulation of Ihh mRNA levels was blocked by transfecting the cells with the constitutively active MEK1 but not by the constitutively active MKK3. Our data demonstrate the central role of MAP kinases in the regulation of Ihh expression in chondrocytes. Stimulation of the PTH/PTHrP receptor results in a sustained inhibition of ERK1/2 activity and subsequent down-regulation of Ihh mRNA levels, which is at least partially mediated by MKP-1. This study also suggests that a negative feedback loop between PTHrP and Ihh may extend to inhibition of Ihh gene transcription or mRNA stability.

Disclosures: ***L.P. Lai****, None.*

F053

Primary Chondrocytes from c-Fos Overexpressing and Knockout Mice Exhibit Altered BMP-Induced Differentiation and Chondrocyte Gene Expression. I. Anagnostopoulos*, J. Kan*, A. E. Grigoriadis. Craniofacial Development, King's College London, London, United Kingdom.

The c-Fos proto-oncogene, a member of the AP-1 transcription factor family plays an important role in bone and cartilage differentiation, as demonstrated in gain- and loss-of-function studies. We have generated a regulatable c-Fos inducible system *in vitro* in ATDC5 chondrocytes (clone DT12.4) and have shown that exogenous c-Fos expression inhibits chondrocyte differentiation and nodule formation. However, the mechanisms underlying this effect remain unknown.

We have now investigated whether altered c-Fos levels in chondrocytes affects their responsiveness to BMPs. Treatment of DT12.4 cells with BMP-2 or -4 rescued the c-Fos block in differentiation, and stimulated cartilage nodule formation to a greater extent in c-Fos-overexpressing cells compared with non-transgenic cells. The enhanced BMP effect in the presence of c-Fos was confirmed by RT-PCR analysis for types II and X collagen expression. It is unlikely that the BMP effects were caused by altered proliferation since preliminary BrdU assays suggested that induction of c-Fos had no effect on BMP-induced DNA synthesis. Northern blot analysis showed that induction of c-Fos decreased endogenous BMP-4 levels in DT12.4 cells, whereas there were no differences in BMP receptor expression.

We next investigated the role of c-Fos in modulating BMP signalling in primary chondrocytes isolated from c-Fos transgenic or knockout mice, both of which have cartilage phenotypes. BMP-2 treatment of chondrocytes from c-Fos-transgenic mice resulted in enhanced differentiation and a higher number of cartilage nodules compared to non-transgenic chondrocytes. Types II and X collagen expression were also enhanced in BMP-2-treated transgenic chondrocytes compared to wild-type cells. In addition, chondrocytes overexpressing c-Fos exhibited reduced levels of endogenous BMP-4. Thus, primary chondrocytes from c-Fos transgenic mice showed a similar phenotype to c-Fos-overexpressing DT12.4 cells. In contrast, the effects of BMP-2 and -4 on cartilage differentiation were suppressed in primary chondrocytes from c-Fos knockout mice, and this was paralleled by a decrease in types II and X collagen expression. Finally, preliminary BrdU experiments suggested that chondrocyte proliferation following BMP-2 and -4 treatment was enhanced in c-Fos null cells compared with wild-type cells.Taken together, these findings suggest that overexpression of c-Fos in chondrocytes results in enhanced BMP signalling, whereas inactivation of c-Fos results in suppressed BMP signalling. This altered BMP responsiveness may mediate the effects of altered c-Fos expression in chondrocytes *in vivo*.

Disclosures: ***I. Anagnostopoulos****, None.*

F056

Preservation of Bone Mass after Ovariectomy in Caf1-Deficient Mice through Activation of BMP Signaling in vivo. K. Oikawa[1], T. Nakamura*[2], M. Usui[1], K. Tsuji[1], I. Ishikawa*[3], A. Nifuji[1], T. Noda*[4], T. Yamamoto*[2], M. Noda[1]. [1]Molecular Pharmacology, Tokyo Medical and Dental University, Tokyo, Japan, [2]University of Tokyo, Tokyo, Japan, [3]Periodontology, Tokyo Medical and Dental University, Tokyo, Japan, [4]Cancer Institute, Tokyo, Japan.

Postmenopausal osteoporosis is caused by depletion of estrogen as well as low peak bone mass, though the molecular mechanisms involved in the osteopenia due to postmenopausal bone loss have not yet been fully understood. Recently, we reported that Tob is involved in the determination of bone mass after ovariectomy-induced bone loss (PNAS 2004). Tob associates with Caf1 (CCR4-associated factor 1), which is a component of CCR4-NOT complex, and is involved in gene transcription and mRNA modulation in yeast. Therefore, we examined whether Caf1 could be involved in the determination of bone mass after estrogen depletion. Caf1-deficient (CAFKO) mice were born normally. Ovariectomy reduced cancellous bone volume (BV/TV) in wild type (WT) mice. In contrast, even after ovariectomy, BV/TV levels in CAFKO mice were preserved and similar to those in sham-operated wild type. High bone mass trend was observed in CAFKO of both genders. 3D-microCT analyses revealed that basal BV/TV was more in CAFKO mice compared to wild type. Bone formation rate (BFR) and mineral apposition rate (MAR) were enhanced in CAFKO compared to WT while osteoclast number and surface were not altered in CAFKO bone, indicating that Caf1 specifically targets osteoblasts in vivo. As mineralized nodule formation in ex vivo bone marrow cultures was enhanced in CAFKO cells while osteoclast formation in vitro was similar between WT and CAFKO. Thus, CAFKO effect was cell autonomous. To address the mechanism of CAFKO enhancement of osteoblastic activity, bone marrow ablation was conducted. Bone formation on day 14 after ablation was observed in 3/4 CAFKO mice compared to 1/5 in WT or heterozygote mice. This was similar to the observation that BMP injection onto the calvariae of newborn CAFKO mice induced more new bone formation in vivo than WT and that BMP treatment induced higher alkaline phosphatase activity in CAFKO calvaria-derived cells cultured in vitro compared to WT. Finally, BMP treatment enhanced Caf1 gene expression in MC3T3E1 osteoblastic cell line suggesting that Caf1 is involved in a negative feed back signaling system in osteoblasts. This Caf1 gene activation is specific to BMP as TGF-beta did not alter Caf1 gene expression. These observations suggest that Caf1 deficiency preserved bone mass after ovariectomy via enhancement of osteoblastic bone formation through BMP actions in vivo.

Disclosures: ***K. Oikawa****, 21st Century Center of Excellence Program 2; Core to Core Program 2.*

F058

Runx1/Cbfa2 Induces Early Stages of Chondrogenesis in Mouse Limb Bud Cells. R. M. Belflower*, Y. Wang*, Y. Dong, J. E. Puzas, E. M. Schwarz, R. J. O'Keefe, H. Drissi. Orthopeadics, University of Rochester, Rochester, NY, USA.

Work to date has focused primarily on Runx2/cbfa1 since bone formation is abrogated in Runx2 null mice, while all cartilaginous structures are fully formed. Since Runx proteins share several structural and function features, we investigated the implication of Runx1 in chondrogenesis. Our in situ hybridization data shows that *Runx1* and *Runx2* expression overlaps during early stages of embryonic development in the cartilage primordia of various skeletal elements. *Runx* transcripts being expressed in mesenchymal condensations with the potential to form cartilage, we assessed their expression and regulation during chondrogenesis using limb bud mesenchymal progenitors from E11.5 embryos. Our real time RT-PCR data shows that both isoforms of *Runx1* and *Runx2* are regulated in these cells. The MASXS isoform of both Runx factors is up-regulated throughout chondrocyte maturation, as evidenced by expression of cartilage phenotypic genes. In contrast, the MRIPV isoform of both genes is more abundant during early stages of chondrocyte differentiation, and subsequently down regulated. This differential expression of the *Runx* isoforms predicts a distinct and sustained role for these proteins in chondrogenesis. The overall expression of *Runx1* mRNA remains significantly higher than *Runx2* mRNA levels throughout mesenchymal cell differentiation. We then treated limb bud cells for 4, 8 and 14 days with BMP-2 and PTHrP, which are known to respectively induce and delay chondrogenesis. Our gene expression analysis shows that BMP-2 induced both isoforms of *Runx1* and *Runx2*. However, a more potent and earlier induction of the MASXS isoform is observed for both factors. Interestingly the up-regulation of *Runx2* by BMP-2 is stronger than *Runx1*. In contrast, PTHrP inhibited both factors, with the most potent effect being on the *Runx1* transcripts. Our results clearly establish a potential role for Runx1 in early chondrogenesis while Runx2 may mediate later stages of chondrocyte maturation. In order to determine the function of Runx1 during chondrogenesis, we over-expressed both Runx1 isoforms using retroviral vectors to infect mouse embryonic limb bud cells. Our data show that *Runx1* over-expression results in a significant induction of the early chondrocyte differentiation markers, *type II collagen* and *alkaline phosphatase*, but not the marker for chondrocyte hypertrophy, *collagen X*.

In summary, our results strongly support a role for Runx1 in mediating the onset of the early stages of chondrocyte differentiation from mesenchymal stem cells. Thus our findings show for the first time, that the hematopoiesis related factor Runx1 acts as a novel mediator of cartilage development.

Disclosures: ***H. Drissi****, None.*

F061

Adipocyte-Directed Expression of GFP in Transgenic Mice. M. S. Kronenberg[1], X. Jiang*[1], H. Li*[1], I. Kalajzic*[1], L. C. Pan[2], D. W. Rowe[1]. [1]Genetics and Developmental Biology, University of Connecticut Health Center, Farmington, CT, USA, [2]Cardiovascular and Metabolic Diseases, Pfizer Global Research and Development, Groton, CT, USA.

Adipocytic and osteogenic cells are two of the primary lineages of the bone marrow stromal system and evidence suggests that they are both derived from a common multipotential mesenchymal progenitor. In order to investigate this interrelationship we used a 7.6 kb promoter fragment from the adipocyte specific marker gene adipocyte protein 2 (aP2/FABP4) to express the topaz variant of enhanced green fluorescent protein (aP2/Tpz). Initial validation of this construct was done by transiently transfecting the pluripotent C3H10T1/2 mesenchymal cell line and then encouraging adipocytic differentiation by treatment with insulin, 9-cis-retinoic acid and rosiglitazone. After 5 days of treatment, cells expressing aP2/Tpz exhibited a differentiated, adipocytic morphology characterized by an accumulation of refractile cytoplasmic vacuoles. Subsequent injection of the aP2/Tpz construct into fertilized C57BL/6 eggs yielded 4 transgenic lines of which 3 then transmitted the GFP reporter gene. In samples from freshly killed mice, cytoplasmic GFP protein expression was only seen in white adipose tissue (WAT) isolated from the abdomens of animals from 2 different lines. Cryosections of fixed WAT confirmed this observation and also showed the presence of GFP in brown adipose tissue and in a small subset of cells in the bone marrow. Marrow stromal cell (MSC) cultures were established from long bones of PCR positive F1 transgenic mice and treated after 8 days with either a vehicle control, an adipogenic cocktail consisting of isobutylmethylxanthine, hydrocortisone and indomethacin (MHI) or the peroxisome proliferator-activated receptor gamma agonist ciglitazone (CIG). Fluorescent cells were evident in cultures from the 2 WAT-positive lines after 48 hours in both the MHI and CIG treated groups and the number and intensity of GFP-expressing cells increased over a period of 6 days. Based on the number of fluorescent cells containing refractile droplets and the Oil Red O staining of similar appearing cells in fixed cultures, CIG appeared to be more effective in promoting adipocytic differentiation of cells derived from bone marrow of aP2/Tpz mice. These results indicate that we have produced a real-time reporter for cells of the adipocytic lineage that will enable us to track this branch of the MSC family in vitro and in vivo. In addition, crossing these lines with our osteoblastic GFP reporter mice should allow us to better dissect the interplay between bone and fat cells in the marrow as that microenvironment changes during development, aging and pharmacologic intervention.

Disclosures: ***M.S. Kronenberg****, None.*

F063

Missouri Variant of Human Spondyloepimetaphyseal Dysplasia (SEMDMO) due to Matrix Metalloproteinase 13 (MMP13) Mutation in the Pro-domain Results in Altered Secretion and Intracellular Auto-activation of MMP13. M. Inada*[1], M. H. Byrne*[1], A. M. Kennedy*[2], P. T. Christie*[2], M. P. Whyte[3], R. V. Thakker[2], S. M. Krane[1]. [1]CIID, Medicine, Mass General Hospital, Charlestown, MA, USA, [2]Nuffield Department of Clinical Medicine, University of Oxford, Oxford, United Kingdom, [3]Metabolic Research Unit, Shriners Hospital for Children, St. Louis, MO, USA.

Autosomal dominant SEMDMO (Patel et al. Medicine 72:326, 1993) is caused by a missense mutation encoding Phenylalanine56Serine (F56S) in the pro-domain of MMP13 (Kennedy et al. J. Bone. Miner. Res. 17[Suppl 1]:S175, 2002). Here, we examine possible mechanisms by which the F56S mutation could alter MMP13 function. Transformed human chondrocytes or HEK293 cells were transfected with mutant or wild type (wt) MMP13 cDNA inserts (± C-terminal fusion tags) in pcDNA3.1. Levels of wt and F56S mutant mRNAs in transfected cells were similar. Medium and cell lysates were harvested after 48 h and analyzed by Western blotting with antibodies directed towards the fusion tags or multiple epitopes in the pro-, catalytic or hinge domains of MMP13. These antibodies are useful for detection of proteolytic products that are formed after activation of the inactive zymogen. Whereas after transfection with wt cDNA, abundant intact MMP13 (~ 55kDa) was present in conditioned medium (CM), only traces of intact MMP-13 were found in CM after transfection with F56S cDNA; several lower Mr degradation fragments of F56S, however, were found in CM. Intact as well as degradation fragments of F56S were found in cell lysates. Addition to cell cultures of monensin, 2 mM, eliminated wt intact and F56S fragments in CM; wt intact and F56S intact and fragments were, however, retained in cell lysates. We constructed the catalytically inactive E204A wt MMP13 in pcDNA3.1 and it was expressed and secreted. The catalytically inactive compound mutant E204A /F56S MMP13 in pcDNA3.1 rescued the abnormal functioning F56S mutation since only pro-MMP13 compound mutant was found in CM or cell lysates. An engineered C77S mutant was also auto-activated and degraded intracellularly. F56S MMP13 in stable expressing clones intracellularly degraded transfected wt MMP13. Our results are consistent with misfolding of F56S MMP13 in which the downstream cysteine (C77) fails to contact the catalytic Zn and thus F56S MMP13 is auto-activated and it auto-degrades to low Mr fragments that lack collagenolytic activity. Thus, loss of collagenase activity could, in part, account for the dominant SEMDMO phenotype, since Mmp13-null mice also have chondrodysplasia.

Disclosures: ***M. Inada****, None.*

F066

RANKL and VEGF Signals Mediate Cortical Bone Healing Derived from Structural Autografts: Effective Transfer to Processed Allografts via Immobilized rAAV. H. Ito[1], M. Koefoed*[2], J. J. Goater*[2], R. J. O'Keefe[2], E. M. Schwarz[2]. [1]Orthopaedic Surgery, Kyoto University Graduate School, Kyoto, Japan, [2]University of Rochester, Rochester, NY, USA.

To the end of generating a remodeling structural allograft we developed a murine femoral model, which utilizes live autografts and processed allografts. The aim of this study was to characterize the role of RANKL and VEGF in autograft healing and to evaluate the effects of introducing these signals onto the cortical surface of femoral allografts via immobilized recombinant adeno-associated virus (rAAV). A 4 mm mid-diaphyseal segment was removed from 8-week-old C57BL/6 mice, and a segmental bone graft was secured with a intramedullary pin. The segment of bone graft was obtained from the same femoral shaft of the animal (autograft) or from that of a different stain of mouse: ICR mouse (allograft). For gene expression analysis, total RNA was extracted from the healing grafts and analyzed by real time RT-PCR and Affymetrix microarrays. Histomorphometry was performed on OrangeG/aclian blue, X-gal and tartrate resistant acid phosphatase (TRAP) stained sections. For loss of function studies, anti-mouse VEGF goat antibody, RANK:Fc fusion protein, or goat IgG was administered via intraperitoneal injection. *Ex vivo* gene transfer of β-galactosidase (LacZ), osteoprotegerin (OPG) and/or the soluble VEGF receptor (sFlt1) to live autografts were performed by harvesting the specimens, incubating them in rAAV/PBS solution for 10 min, and rapidly placing it back in the original donor. *In vivo* gene transfer of LacZ, RANKL and VEGF to processed allografts were performed by pipetting 1% sorbitol-PBS solution containing rAAV onto the cortical surface of the grafts. The allografts were then frozen, lyophilized, and stored at -80 ºC until they were transplanted. Gene expression analyses revealed that there is a significant decrease in *RANKL* and *VEGF* during allograft healing. Systemic inhibition with RANK:Fc & anti-VEGF, and local inhibition with rAAV-OPG & rAAV-sFlt1, demonstrated that both RANKL & VEGF are required for autograft healing. Using allografts containing freeze-dried rAAV-RANKL and rAAV-VEGF we demonstrate that both signals are sufficient to significantly increase new bone formation around the cortical surface of the allograft. We also noted that these factors induce allograft remodeling and vascularization, which leads to a new bone collar that spans the entire graft. Addition of either signal alone failed to yield significant effects. In conclusion we find that RANKL and VEGF are necessary and sufficient for efficient autograft healing and can be transferred via rAAV to revitalize structural allografts.

Disclosures: ***H. Ito****, None.*

F068

Role of the Serotonin Transporter (5-HTT) in Bone Metabolism. R. A. Battaglino[1], M. Joe*[1], U. Späte*[1], A. Sharma*[1], D. Graves*[2], T. Kohler*[3], R. Muller*[3], P. Stashenko*[1]. [1]Cytokine Biology, Forsyth Institute, Boston, MA, USA, [2]Boston University School of Dental Medicine, Boston, MA, USA, [3]ETH, Zurich, Switzerland.

Mounting evidence exists for the operation of a functional serotonin (5-HT) system in osteoclasts and osteoblasts, that involves both receptor activation and 5-HT reuptake. In previous work we demonstrated that the serotonin transporter (5-HTT) is expressed in osteoclasts and that its inhibition reduces osteoclast differentation *in vitro*. The purpose of the current study was to determine the effect of serotonin uptake on bone metabolism *in vivo*. To that end, we conducted histomorphometric and micro-computed tomographic imaging (micro-CT) analysis in 5-HTT deficient mice and in wild type (wt) mice treated with fluoxetine, a 5-HTT blocker. Mice homozygous for a deletion of the *5-htt* gene exhibited increased whole body bone mineral density (BMD) compared to age matched wild type (WT) controls. Micro-CT analysis revealed an increase in BV/TV in tibial cortical bone. This effect was confirmed by systemic administration of fluoxetine to Swiss-Webster mice for six weeks, which resulted in increased trabecular BV/TV in femurs, as a result of an increase in trabecular number and connectivity beta, and decreased trabecular spacing. The effect of blocking the 5-HTT on bone loss following challenge was also investigated. Subcutaneous injections of LPS over the calvariae of Swiss-Webster mice for 5 days resulted in increased numbers of osteoclasts and net bone loss, whereas new bone formation and a net gain in bone mass was seen when LPS was given with fluoxetine. In contrast, neither 5-HTT deficient mice nor WT mice given fluoxetine were protected against bone loss after ovariectomy. We conclude that inhibition of the 5-HTT *in vivo* leads to increased bone mass under normal physiologic or inflammatory conditions, but does not modulate bone loss associated with estrogen deficiency. These findings support the hypothesis that the serotonin system plays a crucial role in bone formation and remodeling, via effects on both osteoclast and osteoblast development and activity.

Disclosures: ***R.A. Battaglino****, None.*

F070

Nell-1, a Downstream Target of Cbfa1, in Bone Formation. K. Ting[1], X. Zhang*[2], T. Truong*[1], Y. Miao*[1], R. Chiu*[2], C. Soo*[3]. [1]Orthodontics, UCLA , Los Angeles, CA, USA, [2]Dental and Craniofacial Research Institute, UCLA , Los Angeles, CA, USA, [3]Plastic Surgery, UCLA , Los Angeles, CA, USA.

Nell-1 overexpression is associated with craniosynostosis in both human patients and transgenic mice. Initial promoter analysis of the *Nell-1* gene suggest that Cbfa1 may regulate human *Nell-1* transcription. The objective of the study is to examine the transcriptional regulation of *Nell-1* by Cbfa1. If Nell-1 is a downstream effector/target of Cbfa1, then we would expect Nell-1 to functionally compensate for some aspects of *Cbfa1* deficiency. A 2.2kb and 325bp fragment of the human *Nell-1* promoter was cloned into the pGL3 Basic luciferase reporter plasmid and used in transient transfection assays with Cbfa1. EMSA, supershift, and mutagenesis studies were conducted. *Nell-1* overexpression mice (*Nell-1*^{overexp}) were mated with heterozygous *Cbfa1* deficient mice (*Cbfa1*$^{+/-}$). Skeletal staining was performed using Alcian blue and Alizarin red. Micro-CT scans were also used. For the promoter analysis, Cbfa1 overexpression increased luciferase activity 6 fold from the 2.2 kb promoter construct, but had no effect on the 325 bp promoter construct. In cotransfection assays with increasing amounts of Cbfa1 plasmid, the 2.2 kb promoter construct, but not the 325 bp construct, exhibited a positive dose response of luciferase activity. Cbfa1 binds specifically to three OSE2 sites and induces luciferase activity. The Nell-1^{overexp},Cbfa1$^{+/-}$ mice confirmed the presence of significantly reduced fontanelle size and suture width and increased clavicle size. In conclusion, Cbfa1 positively regulates the human Nell-1 promoter. Nell-1 may partially compensate for Cbfa1 insufficiency and lend further support to the hypothesis that Nell-1 may be a central downstream target of Cbfa1.

Disclosures: ***K. Ting****, None.*

F072

Lack of the Tumor Suppressor Gene Vhlh Increases Trabecular Bone and Expands the Osteoblast/Stromal Cell Population. R. Chiusaroli, M. C. Knight*, E. Schipani. Medicine, MGH-Harvard Medical School, Boston, MA, USA.

The transcription factor Hypoxia-Inducible-Factor 1alpha(HIF-1alpha) is essential for chondrocyte growth arrest and survival. HIF-1alpha also inhibits adipocyte cell differentiation in vitro. The von Hippel Lindau tumor suppressor protein (pVHL) is a component of a ubiquitin ligase promoting proteolysis of HIF-1α. Conditional inactivation of Vhlh in the cartilaginous elements using the Cre-loxP strategy has demonstrated its critical role in endochondral bone development, at least in part through stabilization of HIF-1α protein. As previously reported, mice lacking Vhlh in cartilage are dwarf, and Vhlh null growth plates display a dramatic decrease of chondrocyte proliferation rate with an increased accumulation of extracellular matrix. In postnatal life, the Vhlh mutant mice developed a unique bone phenotype, very likely because the Cre recombinase driven by the rat collagen type II promoter is expressed in cells of the osteoblast lineage, as indicated through the use of reporter mice. As shown by histology and in situ hybridization analysis, this bone phenotype was already evident at two weeks of age, and was characterized by increased trabecular bone with significant expansion of the osteoblast/stromal cell population. HIF-1α transcriptional activity augments the expression of enzymes of the glycolytic pathway such as phosphoglycerokinase-1 (PGK-1) and angiogenetic factors such as vascular endothelial growth factor (VEGF). In adult long bones isolated from Vhlh mutant mice expression of both PGK-1 and VEGF mRNAs was clearly upregulated in osteoblasts in comparison to control littermates, as shown by in situ hybridization analysis. Notably, VEGF is an important autocrine/paracrine factor for osteoblast differentiation. Our current working hypothesis is that increased HIF-1a stability in the Vhlh null bone leads to expansion of the osteoblast/stromal cell population through up regulation of metabolic pathways and VEGF expression. Our data support the model that the VHL/HIF system is an important modulator of mesenchymal cell differentiation.

Disclosures: ***E. Schipani****, None.*

F075

Skeletal Overgrowth in Tight Skin (Tsk) Mice. T. Barisic*, S. H. Clark*. Deparment of Genetics and Developmental Biology, University of Connecticut Health Center, Farmington, CT, USA.

The tight skin (Tsk) mutation is an autosomal dominant mutation located on mouse chromosome 2. Mutant mice (Tsk/+) display a tightness of skin interscapular region, lung emphysema, myocardial hypertrophy, skeletal overgrowth and kyphosis. The Tsk mutation has been identified as a tandem duplication of the mouse fibrillin 1 gene. Fibrillin is a large extracellular matrix glycoprotein and is an important component of microfibrils. Several reports have suggested a role of fibrillin in the modulation of TGF-beta action on the regulation of the metabolism of matrix producing cells, i.e. fibroblasts and osteoblasts. It is hypothesized in this report that in the Tsk mice the presence of mutant fibrillin molecules in the matrix produced by mutant bone cells alter bone cell metabolism. In the present study we analyzed the phenotype of 2-month-old Tsk/+ mice and found that body length of the Tsk/+ and longitudinal femur length were significantly longer in Tsk male mice compared with control male littermates. These changes in the skeleton of Tsk/+ mice indicate that fibrillin 1 gene may regulate skeletal development and differentiation. In order to examine collagen expression in osteoblasts of Tsk mice we utilized the pOBCol2.3GFP transgene that has been documented to be expressed in mature osteoblasts. The pOBCol2.3GFP transgene was introduced by mating producing Tsk/+ and +/+ littermates carrying this transgene. The decalcified femur sections showed increased numbers of GFP expressing cells in Tsk/+ mice compared with +/+ littermates. In an effort to examine the potential impact of the mutant fibrillin molecule of the osteoprogenitor lineage, marrow stromal cell cultures were initiated from bone marrow isolated for one-month-old Tsk/+ and +/+ sibs. We examined the expression of osteoblast the specific genes, Col1a1, BSP and OC in these marrow stromal cell cultures at various time points. In the Tsk/+ cultures the pattern of gene expression was normal, however, a difference in the tempo of differentiation was observed. Specifically, there was a slowing in maturation of the Tsk cells indicated by delay in the appearance of OC expression. In summary the enlarged skeleton observed in the Tsk mouse is associated with an elevated number of osteoblasts actively producing collagen as well as an alteration in the tempo of osteoblast maturation. These initial experiments suggested the role of fibrillin 1 gene as important regulator of bone formation.

Disclosures: ***S.H. Clark****, None.*

F077

Integrin Ligands Arranged in Nanopatterns Modulate Focal Adhesion Assembly and Signaling in Osteoblasts. E. A. Cavalcanti-Adam[1], M. Bezler*[1], P. Tomakidi*[2], J. P. Spatz*[1]. [1]Biophysical Chemistry, Heidelberg University, Heidelberg, Germany, [2]Orthodontics, Heidelberg University, Heidelberg, Germany.

Integrin lateral clustering is a key event for the formation of focal adhesions and for the control of cell shape and mobility. The size and distribution of integrin clusters modulate extracellular matrix composition and organization, as well as cell growth and differentiation. To study the geometrical limits for single integrins in the assembly of focal adhesions and their effect on osteoblast function, we created regular patterns of adhesive nanodots coated with integrin ligands, separated by nonadhesive regions.

Surfaces were decorated with gold nanoparticles arranged in hexagonal pattern by using block-copolymer nanolithography. With this technique, nanoparticles are deposited on surfaces at defined, but variable distances (28, 58, 73 or 85nm), according to the molecular characteristics of the copolymers. The diameter of each nanodot is less than 8nm, so only one integrin binds per dot. The space between the nanodots is then passivated against cell adhesion and protein deposition by polyethylene glycols, and the nanodots are functionalized with c(RGDfK)-thiols to promote integrin binding.

Focal adhesion molecules were evaluated in primary human osteoblasts and in MC3T3E1 osteoblast-like cells cultured on nanopatterned substrates for 0-24hr.

On 28 and 58 nm patterns, cells presented elongated integrin clusters, colocalization of vinculin and organized actin stress fibers. A separation of >58nm between the nanodots resulted in limited cell spreading, and dramatically reduced formation of focal adhesions . We attributed these cellular responses to restricted integrin clustering rather than insufficient number of ligands, since micro-nanopatterned patches, with minimal local ligand density but optimal interdot distance, still supported osteoblast adhesion. Moreover, osteoblasts adhering to the 73nm pattern, exhibited characteristics of migrating cells, rich in focal complexes at the peripheral extensions. Since the maturation of focal complexes into focal adhesions is influenced by intracellular contractility and extracellular tension transmitted to the ECM, we evaluated the organization of ECM proteins secreted by osteoblasts. On the 58nm pattern, cells produced a matrix rich in collagen type I and fibronectin, organized in a network supporting and surrounding cells, while on the 73nm, the fibers were rather disorganized and packed under cell contacts.

Knowledge of these geometrical limits for integrin clustering is essential to elucidate the physical and molecular mechanisms by which integrins mediate bidirectional signal transduction in osteoblasts.

Disclosures: ***E.A. Cavalcanti-Adam****, None.*

F081

Myeloma Cells Suppress Osteoblast Differentiation by Secreting a Soluble Wnt Inhibitor, sFRP-2. T. Oshima*, M. Abe, E. Sekimoto*, Y. Tanaka*, H. Shibata*, T. Hashimoto*, S. Ozaki*, S. Kido, D. Inoue, T. Matsumoto. Department of Medicine and Bioregulatory Sciences, University of Tokushima, Tokushima, Japan.

Multiple myeloma (MM), a malignancy of plasma cells, develops in the bone marrow, and generates devastating bone destruction. Along with enhanced bone resorption, clinical evidence has also suggested suppression of bone formation as a contributing factor to a bone loss in MM. Despite recent advances in our understanding of the mechanisms of osteolysis enhanced in MM, little is known about factors responsible for impaired bone formation. A canonical Wingless-type (Wnt) signaling pathway has recently been shown to play a critical role in osteoblast differentiation. Therefore, in the present study, we aimed to clarify mechanisms of suppression of osteoblast differentiation by MM cells with a particular focus on a canonical Wnt signaling pathway. Because several secreted Frizzled related protein (sFRP) and DKK family members are known as soluble Wnt antagonists, we first examined the expression of sFRP-1, 2 and 3 and DKK-1 in MM cell lines including U266, RPMI8226 and ARH77. RT-PCR analysis revealed that all cell lines expressed sFRP-2 and sFRP-3 mRNA. However, sFRP-1 was not at all expressed, and DKK-1 was expressed only in U266 cells. By Western blot analyses for these factors, we were able to detect only sFRP-2 protein in immunoprecipitants of conditioned media (CM) as well as cell lysates of all these cell lines. No other factors were found at the protein level. Importantly, sFRP-2 mRNA and protein expression was detected in most MM cells from patients with advanced or terminal stages of MM (3/4 and 8/10, respectively). In order to examine a biological role for sFRP-2, we added recombinant sFRP-2 to MC3T3-E1 cell culture together with BMP-2. Exogenous sFRP-2 partially suppressed alkaline phosphatase activity but almost completely blocked mineralized nodule formation enhanced by BMP-2. Furthermore, sFRP-2 immunodepletion significantly restored mineralized nodule formation in MC3T3-E1 cells suppressed by ARH77 CM. These results suggest that sFRP-2 alone is able to suppress osteoblast differentiation induced by BMP-2 and that MM cell-derived sFRP-2 is among predominant factors responsible for defective bone formation in MM. Because MM cell-derived factors such as DKK-1, IGF-BP4 and IL-3 other than sFRP-2 have been implicated as an inhibitor of osteoblast differentiation, sFRP-2 may also act in concert with such other factors to potently suppress bone formation in MM. Thus, MM cells may cause an imbalance of bone turnover by enhancing osteoclastic bone resorption and at the same time suppressing bone formation, which leads to devastating destruction and a rapid loss of bone.

Disclosures: ***T. Oshima****, None.*

F084

Noggin Inhibition of BMP-2 Decreases the Formation of Osteoblastic Lesions in Prostate Cancer. B. T. Feeley*[1], S. C. Gamradt*[1], L. Krenek*[1], W. K. Hsu*[1], N. Liu*[1], P. Robbins*[2], J. Huard*[2], J. R. Lieberman*[1]. [1]Orthopaedic Surgery, University of California, Los Angeles, Los Angeles, CA, USA, [2]Orthopaedic Surgery, University of Pittsburgh, Pittsburgh, PA, USA.

Bone morphogenetic proteins (BMPs) are growth factors that have a vital role in the growth and development of the skeletal system, and have been shown to have altered expression in multiple types of cancer. We have previously demonstrated that osteoblastic lesions express multple BMPs including BMP-2, -4, and -7. We examined the role of BMP-2 in the formation of an osteoblastic lesion in a murine metastatic cancer model. RT-PCR and Western blot analysis demonstrated that the prostate cancer osteoblastic cell lines LAPC-4 and LAPC-9 expressed BMP receptor subtypes I, IIa, and IIb, suggesting these cells would be responsive to host bone expression of BMPs. To determine the effects of BMP-2 on these cells *in vitro*, we performed cellular migration and invasion assays. At BMP concentrations of 10 ng/ml, 100 ng/ml, and 500 ng/ml, LAPC-4 cells were stimulated to both migrate and invade through extracellular tumor matrix ($p<0.001$ vs NIH-3T3 control cells). In addition, the effects of BMP-2 were able to be inhibited by 10 ug/ml of its inhibitor, noggin in both the cellular migration and invasion assays ($p<0.001$ vs. BMP-2 alone). To determine the effects of BMP-2 expression *in vivo,* we performed tibial injections into SCID mice of either LAPC-9 cells alone or LAPC-9 cells infected with a retrovirus overexpressing noggin (RetroNog). Noggin expression was confirmed with Western blot and a BMP activity assay. All 9 mice treated with LAPC-9 alone had developed osteoblastic lesions at 8 weeks. In contrast, 8 of the 9 mice treated with LAPC-9+RetroNog showed only minimal new bone formation on radiographic examination. The area of bone present in the LAPC-9+RetroNog treatment group was significantly less compared to LAPC-9 alone in histomorphometric analysis ($p<0.01$). There was no difference in tumor size at 8 weeks between the groups. We concluded that BMPs have a vital role in the development of the osteoblastic prostate cancer lesion. BMPs stimulated cellular migration and invasion *in vitro*, and blockade of BMP activity with its inhibitor noggin was successfully able to block *in vitro* activity and *in vivo* bone formation. We believe that local blockade of BMP activity may allow for future therapeutic strategies in the treatment of osteoblastic prostate cancer lesions.

Disclosures: ***B.T. Feeley****, None.*

F085

Noggin Mediated Inhibition of Bone Morphogenetic Protein-2 Inhibits the Formation of Osteolytic Prostate Cancer Metastases. B. T. Feeley*[1], L. Krenek*[1], W. K. Hsu*[1], N. Liu*[1], J. Huard*[2], J. R. Lieberman[1]. [1]Orthopaedic Surgery, University of California, Los Angeles, Los Angeles, CA, USA, [2]Orthopaedic Surgery, University of Pittsburgh, Pittsburgh, PA, USA.

The majority of prostate cancer metastaseis to bone are osteoblastic in nature, but some lesions are mixed or purely lytic. The cytokine profiles of these different lesions have been shown to differ considerably. Bone morphogenetic proteins (BMPs) have been shown to have altered expression in multiple cancer cell lines. The purpose of this study was to identify the role of BMPs in the formation of an osteolytic lesion in a murine metastatic prostate cancer model. BMP receptor types Ia, Ib, and II were demonstrated to be present on the osteolytic prostate cancer cell line PC-3 with RT-PCR and Western blot analysis. Expression of these receptors suggested that PC-3 cells would be responsive to host bone expression of BMPs. Cell migration and invasion assays were performed to determine the effects of recombinant (Rh) BMP-2 on the oncogenic properties of PC-3 cells. At concentrations of 100 ng/ml and 500 ng/ml, BMP-2 stimulated a significant increase in PC-3 cell migration and invasion compared to controls ($p<0.001$). Addition of a BMP inhibitor, noggin, (50 ug/ml) inhibited the effects of BMP-2 on migration and invasion compared to BMP-2 alone ($p<0.01$). Addition of Rh-BMP-2 to PC-3 cells in serum free media resulted in a significant increase in cell growth ($p<0.01$ vs. control). Again, noggin inhibited the effects of BMP-2 on cell growth ($p<0.001$ vs. BMP-2 alone). Noggin was not cytotoxic to the cells. To determine the effects of BMP-2 expression on PC-3 cells *in vivo*, PC-3 cells were infected with a retrovirus overexpressing noggin (RetroNog) and injected into the proximal tibia of SCID mice. Noggin expression was confirmed with Western blot and a BMP activity assay. At 2, 4, 6, and 8 weeks, tumor size was significantly smaller in the PC-3+RetroNog group (n=20) compared to control PC-3 animals (n=20). Radiographic score was significantly less at each time point as well. Histologic analysis demonstrated no difference in the number of osteoclasts present between groups, suggesting that noggin had no effect on osteoclast activity. BMP-2 appears to play a key role in the cell growth, cell migration, and cell invasion of osteolytic prostate cancer PC-3 cells *in vitro*. The *in vivo* overexpression of noggin slows the rate of growth of osteolytic prostate cancer tumors in a murine metastatic model. This data suggests that BMP is a critical factor in the osteotropism of prostate cancer cells, and that it regulates cell growth in osteolytic prostate cancer cell lines.

Disclosures: ***B.T. Feeley****, None.*

F087

Cadherin-11-mediated Interactions between Metastatic Breast Cancer Cells and Bone Marrow Stromal/Osteoblastic Cells Enhance Bone Metastases. D. Tamura*[1], T. Hiraga[2], A. Myoui[1], H. Yoshikawa[1], T. Yoneda[2]. [1]Orthopaedics, Osaka Univ Grad Med, Suita, Japan, [2]Biochemistry, Osaka Univ Grad Dent, Suita, Japan.

Bone is one of the most preferential sites where breast cancer spreads. Although the precise molecular mechanism is yet to be elucidated, cell adhesion molecules have been proposed to contribute to bone-selective metastasis of breast cancer. Cadherin-11, which was originally isolated from MC3T3-E1 osteoblastic cells and is one of the classical type-2 cadherin family members, has been shown to be constitutively expressed in bone marrow stromal cells. Of note, cadherin-11 expression is also found in some human breast cancers and its expression level is correlated with their aggressiveness. These results led us to hypothesize that the homophilic interactions between breast cancer cells and bone marrow stromal/osteoblastic cells via cadherin-11 played a role in the development of bone metastases. To study this, we established MDA-MB-231 human breast cancer cells and 293T human embryonic kidney cells that were stably transfected with cadherin-11 cDNA (MDA/Cad11 and 293T/Cad11, respectively) and examined for the capacity of these cells to develop bone metastases following heart inoculation into female nude mice. Radiographic and histomorphometric examinations demonstrated that the number and size of osteolytic lesions and tumor burden in bone were markedly increased in both MDA/Cad11 and 293T/Cad11 with elevated numbers of osteoclasts compared with parental cells (MDA/pa and 293T/pa). Subsequently, we examined whether cadherin-11-overexpressing cells exhibit enhanced homing to bone. FACS analysis using fluorescent dye-labeled cancer cells showed that the number of cells arrested in bone marrow shortly after the heart inoculation was greater in 293T/Cad11 than 293/pa cells. Cell motility assay using Boyden chambers revealed that chemotactic migration of cadherin-11-overexpressing cancer cells was significantly increased when co-cultured with ST2 or MC3T3-E1 cells, both of which constitutively expressed cadherin-11. Moreover, the conditioned medium harvested from the co-cultures of 293T/cad-11 and MC3T3-E1 cells stimulated TRAP-positive osteoclast-like cell formation in mouse marrow cultures, whereas the conditioned medium of 293T/pa and MC3T3-E1 cell co-cultures had little effects. These data show that cadherin-11 expression in cancer cells enhances homing and osteoclastogenesis via homophilic interactions with bone marrow stromal/osteoblastic cells, thereby stimulates bone metastases. Our results suggest that cadherin-11 contributes to the preferential spread of breast cancer cells to bone and is a potential therapeutic target.

Disclosures: ***D. Tamura****, None.*

F090

A Nonpeptide Integrin avb3 Antagonist Inhibits Bone Metastasis Formation. J. Guglielmi*[1], I. Pecheur*[1], P. Pujuguet*[2], D. Minet*[2], R. Baron[2], P. Clement-Lacroix[2], P. Clezardin[1]. [1]U.403, INSERM, Lyon, France, [2]Proskelia, Paris, France.

Tumor cells expressing integrin avb3 have a greater propensity to metastasize to bone and subsequently stimulate osteoclast activity, leading to increased bone destruction. We have investigated here the effect of avb3 antagonist HMR1404 on bone metastasis caused by avb3-expressing tumor cells.

Because osteoclasts express avb3, the antiresorptive potency of HMR1404 was first studied in oophorectomized (ORX) mice. A continuous treatment of ORX animals with HMR1404 (2 x 10 mg/kg/day for 28 days) completely prevented castration-induced bone loss. Nude mice inoculated with CHO cells expressing avb3 (CHO b3wt) were then treated with HMR1404 using this dosing schedule. HMR1404 inhibited osteolytic lesions caused by tumor cells, as judged by radiography (HMR1404: 0.7 ± 0.8 mm2 vs placebo: 6.4 ± 4.5 mm2) and histomorphometry using the bone volume (BV) to tissue volume (TV) ratio (HMR1404: 12 ± 3.4 % vs placebo: 1.6 ± 0.3 %). Skeletal tumor burden was also reduced (HMR1404: 1% vs placebo: 92.3 ± 17.2 %). Thus, a continuous treatment with HMR1404 probably reduces bone metastasis formation through inhibition of osteoclast-mediated bone resorption. However, HMR1404 also dose-dependently inhibited CHO b3wt cell invasion and adhesion to vitronectin in vitro, suggesting that it could also directly act on tumor cells in vivo. CHO b3wt-bearing animals were therefore treated with HMR1404 using a dosing schedule (2 x 10mg/kg/day for 3 days) that did not inhibit bone resorption in ORX mice. Despite this, HMR1404 reduced osteolytic lesions (1.3 ± 0.4 mm2 vs placebo: 8 ± 1.2 mm2), increased the BV/TV ratio (11.3 ± 1.8 % vs placebo: 2.9 ± 0.6%), and decreased skeletal tumor burden (4.4 ± 0.4 % vs placebo: 100%). Similarly, a 3-day HMR1404 treatment inhibited osteolytic lesions caused by avb3-expressing B02 breast cancer cells that are stably transfected to express GFP (B02/GFP) (3.5 ± 4.2 mm2 vs placebo: 10.8 ± 4.7 mm2). It also increased the BV/TV ratio (12.7 ± 4.1 % vs placebo: 6.3 ± 1.3 %), and decreased tumor burden (6.4 ± 1.1 % vs placebo: 63.5 ± 11 %). Overall, these results suggested that a 3-day HMR1404 treatment could interfer with tumor cell trafficking in bone. To further address this question, animals receiving a 3-day treatment were sacrificed earlier than usual (7 days after tumor cell inoculation instead of 30 days), and bone marrow cells were analyzed by flow cytometry to detect fluorescent GFP-expressing B02 cells. HMR1404 inhibited by 80% the number of B02/GFP cells present in the bone marrow. In conclusion, our results indicate that avb3 antagonists may represent a novel therapeutic strategy for the treatment of patients with bone metastases.

Disclosures: ***P. Clezardin****, Proskelia Pharmaceuticals 2.*

F092

BMP Inhibits the Prostate Cancer Cell Growth by Inducing Smad1 Interaction with Androgen Receptor. T. Qiu*, X. Cao. Pathology, University of Alabama at Birmingham, Birminham, AL, USA.

Prostate cancer is the most commonly diagnosed malignancy in men and is often associated with bone metastases. Bone Morphorgenetic Proteins (BMPs), a subfamily of transforming growth factor-β, has been suggested playing roles in the prostate cancer proliferation, differentiation, and osteoblastic bone metastases.

Here we have examined the potential function of BMP in prostate cancer. We found that BMP regulates androgen receptor (AR) transcription activity through interaction between BMP specific signal transducer Smad1 and AR. Our experiments show that Smad1 endogenously co-immunoprecipitates with AR, and Smad1 suppresses 5α-dihydrotestosterone-induced AR transactivation in the LNCaP prostate cells. Constitutively active BMP type IB receptor induces the interaction between Smad1 and AR, but BMP-2 can not induce the interaction, suggesting BMP receptor deficiency present in LNCaP cells. Interestingly, Smad6 can reverse the suppression of Smad1 on AR transactivation since Smad6 inhibits BMP signaling by competitively binding to phosphorylated Smad1. These results suggest that phosphorylated Smad1 contributes to the Smad1-mediated suppression. Furthermore, Smad1 represses ligand-independent activation of AR by IL-6 and ligand-dependent activation by a transcription activator Tip60. In addition, Smad1 associates with the endogenous HDAC activity, suggesting the change of acetylation status of AR may contribute to the suppression. Gel-shift assay indicates that Smad1 and AR can form a complex on an androgen response DNA element. Chromatin immunoprecipitation analysis reveals recruitment of Smad1 to the endogenous PSA gene promoter in androgen-dependent manner. Thus, Smad1 functions as an AR corepressor.

We also analyzed the effects of BMP/smad1 on prostate cell growth. Overexpression of Smad1 down-regulates the expression of cyclin D1, and flow cytometric analysis reveals that LNCaP cell growth is arrested in G1 phase. Importantly, 5α-dihydrotestosterone enhanced the cell cycle arrest by Smad1, suggesting Smad1-induced cell growth inhibition via its interaction with AR. Smad1-induced growth inhibition was attenuated when endogenous AR expression was knocked down using AR siRNA. In addition, in AR negative prostate cancer PC3 cells, Smad1 does not inhibit cell growth and Smad1 retains the ability to inhibit cell growth in AR-stably expressed PC3-AR cells. Again, the interaction of Smad1 with AR is required in such growth inhibition. Our studies reveal a molecular mechanism of BMP/Smad1 in prostate cancer, which may enable development of a BMP/Smad1 based therapeutic strategy for the treatment of prostate cancer, and improve anti-androgen treatment for prostate patients.

Disclosures: ***T. Qiu****, None.*

F095

Novel Bisphosphonate Conjugates Decrease Metastatic Bone Tumor Burden in the 4T1/luc Mouse Model of Breast Cancer. M. M. Reinholz*[1], G. Reinholz[1], L. Jonart*[1], T. Yoneda[2], T. Spelsberg[1], W. Lingle*[1], M. Karpeisky*[3]. [1]Mayo Clinic College of Medicine, Rochester, MN, USA, [2]University of Texas Health Science Center at San Antonio, San Antonio, TX, USA, [3]MBC Research Inc., Boulder, CO, USA; Engelhardt Institute of Molecular Biology, Russian Academy of Sciences, Moscow, Russian Federation.

Metastatic bone disease is one of the major causes of morbidity and mortality in breast cancer patients. Bisphosphonates are currently used as effective bone-specific palliative treatments to reduce tumor-induced skeletal complications. We developed novel proprietary nucleotide-bisphosphonate conjugates, which were designed to bind bone with subsequent release of both drugs. We recently reported that the novel bisphosphonate analog, the anhydride formed between arabinocytidine (Ara-C) 5'-phosphate and etidronate, MBC-11, was the most potent inhibitor of in vitro MDA-MB-231 cell proliferation compared to Ara-C, etidronate, pamidronate and zoledronate alone. In this pilot study, we examined the in vivo effects of four conjugates, including MBC-11, the anhydride formed between medronate and Ara-C 5'-phosphate (MBC-29), and the anhydrides formed between 5-fluorouridine (5FU) 5'-phosphate and etidronate and medronate (MBC-1 and MBC-9, respectively) as well as zoledronate on bone tumor burden in mice orthotopically inoculated with 4T1/luc mouse tumor cells. These mice develop primary breast tumors, visceral organ metastases, as well as spontaneous bone metastases by 21 days after cell inoculation. Death typically occurs by day 28. Forty-four percent (8/18) of the mice treated daily with 0.04 μg of the novel conjugates did not have detectable bone metastases as measured by luciferase content in the tibiae and femurs of mice sacrificed at day 21 or 22. No luciferase activity was observed in the bones from 67% of these animals treated with MBC-11 (4/6) and MBC-29 (2/3). The bone luciferase content in the remaining three animals was below the average luciferase content in animals treated with zoledronate (0.04 μg, n = 2) and PBS (n = 6). In addition,we used histomorphometry to determine the percent bone volume in the femurs from endstage animals. Bone volume was approximately two-fold higher ($p < 0.001$) in animals treated with the 5FU conjugates (n = 14) and two-three-fold higher ($p < 0.001$) in animals treated with Ara-C conjugates (n = 11) compared to the animals treated with PBS (n = 9). As a positive control, bone volume was significantly increased (approximately 4-fold) in animals treated with zoledronate (0.04 μg; n = 3). In summary, our data suggest that these novel nucleotide-bisphosphonate conjugates are effective at decreasing metastatic bone tumor burden in mice inoculated with mouse breast cancer cells.

Disclosures: ***M.M. Reinholz****, None.*

F097

Smad4 Induced Apoptosis in Estrogen Receptor α Positive Cells. Q. N. Li, L. Wu*, Y. Wu*, N. Wang*, X. Shi, H. Chen*, X. Cao. Pathology, University of Alabama at Birmingham, Birmingham, AL, USA.

Estrogens regulate differentiation and maintenance of reproductive, skeletal and other tissues by activating their estrogen receptors (ER). Estrogens also act as mitogens to promote cell proliferation in both normal breast tissue and breast carcinomas. In contrast, TGFβ is an inhibitor of cell cycle progression in epithelial cells and antagonizes the effects of ERα mitogenic effect. We have identified that Smad4, a common TGFβ signal transducer, functions as an ER transcriptional corepressor. In this study we found that Smad4 induces apoptosis in ERα positive breast cancer cells, but not in ERα negative cells, suggesting an a potential function of the interaction between Smad4 and ERα. MCF-7 ERα positive and MDA-MB-231 ERα negative cells were infected with a retrovirus encoding Smad4. Hoechst 33342 staining and Flow Cytometry analysis showed that Smad4 induced significant apoptotic cells in MCF-7 , not in MDA-MB-231 cells, within 48h of infection. Furthermore, stable Smad4 expression induces proapoptosis marker protein expression including BIM and Bax in MCF-7, again not in MDA-MB-231 ERα negative cells. To confirm that ERa is required, we expressed ERα siRNA in MCF-7 cells, which significantly reduced Smad4-induced Bax expression, cytochrome-C release and apoptosis. For the same purpose, ERα was stably introduced in MDA-MB-231 cells with retrovirus, and Smad4 was able to induce apoptosis MDA-MB-231 cells with acquired ERα expression. These results indicate that ERα is required for Smad4-induced cell apoptosis.

We then examined whether Smad4 also induces apoptosis in ERα positive cells in nude mice. MCF-7 ERα positive and MDA-MB-231 ERα negative cells were stably transfected with Smad4 or Green Florence Protein (GFP), and were inoculated in nude mice. The tumor volumes were measured every two days. The tumor sizes of MCF-7 breast cancer cells stably transfected with Smad4 are only one tenth of those expressing GFP, and Tunnel assays showed apoptosis positive cells were significantly induced in Smad4 tumor xenograft compared with its GFP control. Whereas in MDA-MB-231, tumor sizes in Smad4 transfected cells are not significantly different from GFP transfected cells. These tumor xenografts were further analyzed Western blot and immunihistochemical stain for apoptotic biomarkers, which showed that MCF-7 with Smad4 expression induced proapoptosis protein expression including BIM and Bax, but induction of these proapoptotic markers was not observed in nude mice bearing MDA-MB-231 tumor xenografts. These results indicate that presence of ERα is required in Smad4 inducing apoptosis in breast cancer cells. Therefore, our findings may provide a potential therapeutic intervention for breast cancer.

Disclosures: ***Q.N. Li****, None.*

F099

Targeting Skeletal Metastases in Prostate Cancer with a Novel VEGF121 Fusion Toxin. A. T. Poblenz*, K. Mohamedali*, M. G. Rosenblum*, B. G Darnay*. Experimental Therapeutics, University of Texas M.D. Anderson Cancer Center, Houston, TX, USA.

Osteolysis that accompanies bone metastasis is a major cause of morbidity, often resulting in severe bone pain and susceptibility to fractures, and results in a significant decline in the quality of life of cancer patients with bone disease. Bone destruction is primarily mediated by osteoclastic bone resorption and cancer cells that have metastasized to bone stimulate the formation and activation of osteoclasts adjacent to metastatic foci. The progression of osteolytic metastases itself is a result of complex interaction between tumor cells, osteoclasts, osteoblasts, and the many factors in the bone microenvironment. There are numerous cytokines involved in tumor growth, neovascularization and bone resorption. Vascular endothelial growth factor-A (VEGF-A) and its cognate receptors Flt-1 and Flk-1/KDR have been identified as central mediators of tumor neovascularization. We previously developed a novel fusion construct designated VEGF121/rGel, composed of VEGF121 and the plant toxin gelonin, which targets the tumor neovasculature and exerts impressive cytotoxic effects by inhibiting cellular protein synthesis in target cells. We have previously shown that in vivo administration of this molecule inhibits tumor growth in melanoma, bladder, breast, and prostate tumor xenograft models. Treatment of mice (iv) bearing PC-3 intrafemoral tumor xenografts with VEGF121/rGel was shown to dramatically suppresses PC-3 skeletal metastases. All control mice were sacrificed by day 67. In contrast, 50% of the VEGF121/rGel-treated mice survived past day 140 without any sign of osteolysis. VEGF and its receptors participate in the complex process involved in tumor-directed bone resorption; however, their roles have not been identified. We have investigated the direct effect of VEGF121/rGel on differentiation of RAW cells and mouse bone marrow-derived monocytes (BMM). VEGF121/rGel was shown to inhibit RANKL-mediated osteoclastogenesis. The observed effect was not mediated by either VEGF121 or gelonin alone, but is a characteristic unique to the combined fusion protein. While immunofluorescence studies clearly show VEGF121/rGel penetration into RAW cells, the receptor responsible for mediating the cellular entry of VEGF121/rGel is unknown. Preliminary data indicate that VEGF121/rGel most likely inhibits the growth of mouse BMM through an unknown mechanism in vitro. These studies demonstrate the best combined therapy for prostate cancer metastases in which one agent provides both a multi-modal attack targeting the blood supply feeding the tumors and the osteoclast precursors which are instrumental in developing lytic bone lesions.

Disclosures: ***A.T. Poblenz****, None.*

F102

The Bone Mineral Density in Childhood Study (BMDCS): Substudy Comparing DXA and CT Vertebral Bone Measurements in Healthy Children and Adolescents. T. A. L. Wren[1], V. Gilsanz[1], P. Pitukcheewanont[1], X. Liu*[1], M. Horlick[2], J. M. Lappe[3], H. Kalkwarf[4], B. S. Zemel[5], S. Mahboubi[5], J. A. Shepherd[6], M. M. Frederick[7], K. Winer[8]. [1]Childrens Hosp Los Angeles, LA, CA, USA, [2]St. Luke's-Roosevelt Hosp, NY, NY, USA, [3]Creighton Univ, Omaha, NE, USA, [4]Childrens Hosp Med Ctr, Cincinnati, OH, USA, [5]Childrens Hosp of Philadelphia, Philadelphia, PA, USA, [6]University of Calif San Francisco, SF, CA, USA, [7]Clinical Trials & Surveys Corp, Baltimore, MD, USA, [8]NICHD, Rockville, MD, USA.

The BMDCS was designed to establish reference standards for bone mineral density (BMD) in healthy children in the U.S., and the purpose of this substudy was to optimize pediatric bone measurements using DXA. Comparisons were made between DXA and CT values for bone mineral content (BMC) and BMD in a subgroup of 64 boys and 60 girls, ages 6-17 yr, who participated in the BMDCS and had bone measurements using both techniques. Chronological age, height, weight, body mass index (BMI), skeletal age and Tanner stage of sexual development were recorded. DXA BMC (g) and areal aBMD (g/cm^2), CT volumetric vBMD (mg/cm^3), vertebral cross-sectional area, vertebral height and vertebral volume of the lumbar spine were obtained. CT-BMC was calculated by multiplying vertebral density and vertebral volume. Volumetric densities were estimated from DXA measurements using published correction factors [vBMD1=aBMD/sqrt(DXA-area); vBMD2=aBMD/bone height]. Linear regression was used to compare DXA-BMC vs. CT-BMC and CT-vBMD vs. DXA aBMD, vBMD1, and vBMD2. Multiple regression including the anthropometric measures was also performed. There was excellent agreement between DXA-BMC and CT-BMC (r^2=.94). There was only moderate agreement between DXA aBMD and CT vBMD (r^2=.39). Geometric corrections to calculate DXA volumetric densities resulted in only slight improvement in the correlations with CT density (r^2=.49 for vBMD1; r^2=.55 for vBMD2). Accounting for age, height, weight, BMI, Tanner stage, and skeletal age improved the agreement between DXA aBMD and CT vBMD to r^2=.91, lower than the agreement for BMC. In conclusion, measurements of DXA-BMC were very accurate when compared with CT-BMC. This suggests that inclusion of the posterior elements by DXA and the effects of soft tissue distribution were not significant for the healthy children in this study who were all in the 3rd to 97th percentiles for height, weight, and BMI. In children of more extreme body size, fat and soft tissue distribution may contribute to greater errors. Much greater variability occurred when BMDs were compared, even when corrections for the DXA beam direction were employed, suggesting that BMC may be a more accurate and reliable measure for assessing bone properties in pediatrics when using DXA.

Disclosures: ***T.A.L. Wren****, None.*

F104

Prediction of Non Vertebral Osteoporotic Fracture Risk by High Resolution Peripheral Quantitative Computerized Tomography (hrpQCT) of the Distal Radius or Tibia in a Sample of 953 Elderly Ambulatory Swiss Women. M. A. Dambacher[1], M. Neff[2], P. Pancaldi*[3], M. Krieg*[4], P. Burckhardt[4], J. Cornuz*[4], R. Kissling*[5]. [1]Rheumatology and Rehabilitation, University Clinic Balgrist, Zürich, Switzerland, [2]Center for Osteoporosis, Zürich, Switzerland, [3]Osteoporosis Center, Locarno, Switzerland, [4]CHUV Hospital Cantonal, Lausanne, Switzerland, [5]Dept. of Rheumatology and Rehabilitation, University Clinic Balgrist, Zürich, Switzerland.

As a part of the SEMOF (Swiss Evaluation of Methods of Osteoporotic Fracture Risk) study, 1'046 women aged 75.5 ± 3.2 years (mean ± SD) have been measured with the hrpQCT system (Densican 1000, Scanco Medical, Zürich, Switzerland).

From the 1'046 women included in the study, 953 women, have been prospectively followed by 6 monthly questionnaires during a mean follow-up of 2.9 years, which represents a global follow-up of 2'730 women-years.

The measurement site was the non dominant distal radius (n=942). The 2 centers of Zürich also measured the non dominant distal tibia (n=723). 3 regions of interest were considered: D50 (trabecular bone, central area), D100 (total area); D100-50 (cortical bone, peripheral area).

During the follow-up, non vertebral osteoporotic fractures were recorded. Were considered: low trauma hip fractures, and fractures of the forearm or of the humerus. Each reported fracture was confirmed by the family physician or the hospital in charge of the patient. During the whole follow-up, 44 low trauma non vertebral fractures were recorded. Statistical analysis were performed on Stata 7.0 software.

For the whole variables, the mean absolute values were significantly lower ($p<0.01$) in the group of women who reported an incident low trauma non vertebral fracture than in the group of women without any fracture.

All variables were predictive of low trauma non vertebral fracture risk

The prediction value was lower when measuring cortical site (D100-50) at the radius or at the tibia compared with the prediction value of D100 ($p<0.05$).

Mean baseline values. Comparison between non fractured and fractured women (Student's t-test).

	No incident fracture group		Incident fracture group	
	n	Mean ± SD	n	Mean ± SD
Radius				
D50 (g/cm^3)	898	195.3 ± 75.5	44	155.0 ± 63.3**
D100 (g/cm^3)	898	427.3 ± 98.0	44	378.2 ± 77.7**
D100-50 (g/cm^3)	898	659.2 ± 143.8	44	601.4 ± 114.0**
Tibia				
D50 (g/cm^3)	689	225.4 ± 75.6	34	177.8 ± 66.1**
D100 (g/cm^3)	689	418.9 ± 85.1	34	365.6 ± 77.1**
D100-50 (g/cm^3)	689	614.0 ± 119.2	34	553.5 ± 97.9**

** p<0.01 compared to non incident fracture group
p<0.05 compared to D100-50 radius
* p<0.05 compared to D100-50 tibia

Disclosures: ***P. Pancaldi****, None.*

F106

Utility of Densitometric Vertebral Fracture Assessment in Men. N. Vallarta-Ast, D. Krueger, N. Binkley. University of Wisconsin, Madison, WI, USA.

Vertebral fracture assessment (VFA) using bone densitometers is an excellent means to detect unappreciated vertebral compression fracture in women. However, little evaluation of VFA utility in men has been performed. This study evaluated applicability of VFA in a population of men referred for clinically indicated bone mineral density (BMD) measurement at the Wm. S. Middleton VAMC. Additionally, we explored potential VFA indications in men and, in those with no known prior low-trauma fracture, compared osteoporosis prevalence diagnosed by BMD alone and combined with VFA. In 139 men, mean age, weight and BMI of 68 years, 190 pounds and 27.9 kg/m^2, scans of the spine, hip, non-dominant forearm and lateral vertebral assessment images were obtained by one technologist using a GE Medical Systems Lunar Prodigy densitometer. Vertebral fractures were conservatively defined as being grade 2 or 3 (> 25% height reduction) using the Genant visual semi-quantitative method. We considered that height loss, BMD, age or standing occiput to wall distance (OWD) might be useful to define men in whom VFA is indicated. Of 1807 potentially evaluable vertebral bodies (T4-L4) 1436 (79%) were adequately visualized on VFA. Most non-evaluable vertebrae were from T4-T7; 91% of vertebral bodies from T8-L4 were adequately visualized. In these 139 men, grade 2 or 3 vertebral fractures were present in 47 (34%). Height loss of > 2 inches was associated with a greater ($p < 0.001$) likelihood of prevalent vertebral fracture on VFA. When reported height loss was 2.5 inches or greater, vertebral fracture was present in 52% (24/46). However, vertebral fractures were present in 26% (19/73) of men with height loss < 2 inches. Older men (age > 69 years) and those with low BMD (T-score < -1.5 at the spine or hip) were more likely ($p < 0.001$) to have fractures on VFA. Kyphosis was not a reliable predictor of vertebral fracture. Though 45% (13/29) of men with more than a 3 inch OWD had vertebral fractures, 25% (15/59) with no kyphosis (< 1 inch OWD) were found to have prevalent fracture on VFA. Fifty-two men reported having no prior fracture. In these men, VFA identified vertebral fracture in 23 increasing osteoporosis diagnosis from 39% with BMD alone to 78% using a T-score of < -1.5 plus VFA documented fracture.

In conclusion, VFA allows evaluation of the majority of vertebral bodies in men and identifies a substantial number with unappreciated fracture. As could be expected, older men (age > 69) and those with low BMD (T-score < -1.5) were more likely to have prior vertebral fracture. In this population, absence of height loss and kyphosis, defined by occiput to wall distance, do not preclude presence of vertebral fracture.

Disclosures: ***N. Vallarta-Ast****, None.*

F112

Fall Index Predicts Hip Fracture Independent of Bone Density and Hip Axis Length. K. G. Faulkner[1], W. K. Wacker*[1], C. Simonelli[2], P. K. Burke[3], S. Ragi[4], L. Del Rio[5]. [1]GE Healthcare, Madison, WI, USA, [2]HealthEast Clinics, Woodbury, MN, USA, [3]Osteoporosis Diagnostic and Treatment Center, Richmond, VA, USA, [4]4Centro de Diagnóstico e Pesquisa da Osteoporose do Espírito Santo, Vitoria, Brazil, [5]Densitometría Ósea, CETIR Centre Médic, Barcelona, Spain.

Femur BMD is a primary determinant of hip fracture risk. However, fracture risk also depends on patient age, height, weight, and factors such as bone structure and distribution. Femoral structural parameters, including hip axis length (HAL), cross sectional moment of inertia (CSMI) and cross sectional area (CSA) can be measured with newer bone densitometers. Fall Index (FI) combines density, structure (CSMI and CSA), age, height and weight to estimate the ability of a hip to withstand a fall on the greater trochanter. We compared femur BMD with CSMI, CSA and FI for assessing hip fracture risk.

DXA scans were obtained in 2406 women, 365 with prior hip fracture and 2041 controls using Lunar Prodigy (GE Healthcare) systems at 4 centers. The non-fractured femur was measured in fracture subjects. All scans were acquired and analyzed at the densitometry centers. Femur neck BMD and HAL were determined, as well as CSMI and CSA with the Lunar Hip Strength Analysis program. The FI is the ratio of a patient's estimated femoral strength (based on age, bone density and structure) and the expected force of a fall on the greater trochanter (based on height and weight). Larger FI values indicate greater femoral strength, corresponding to lower fracture risk. BMD, structure and FI measures were compared between fracture and control groups using an unpaired t-test, and logistic regression models were used to calculate odds ratios for hip fracture.

Age-adjusted femur neck BMD was significantly lower and HAL significantly higher in the fracture group vs. controls. After adjustment for BMD and HAL, neither CSMI nor CSA were significantly different between groups. However, FI was significantly lower in the fracture group, consistent with a reduced capacity to withstand a fall. Odds ratios by logistic regression were BMD 2.0, HAL 1.3, and FI 1.5 per standard deviation change in each measurement.

We conclude that the Fall Index and HAL are significant predictors of hip fracture, even after adjustment for BMD. Measurements of CSMI and CSA, which are based on BMD distribution, do not provide additional predictive power compared to BMD alone.

	Age	Height	Weight	Neck BMD	HAL	CSMI	CSA	FI
Fracture	71 yrs	156 cm	63.0 kg	0.722 g/cm^2*	103 mm*	8186	109 mm^2	1.34*
Controls	66 yrs	156 cm	64.0 kg	0. 812 g/cm^2	101 mm	8302	120 mm^2	1.56

*Significantly different than controls (p<0.0001)

Disclosures: ***K.G. Faulkner****, None.*

F118

Enzyme Immunoassay for Cathepsin K in Human Serum and Cell Culture Supernatants. G. Hawa*[1], N. Brinskelle-Schmal*[1], S. Maitzen*[1], M. Skoumal*[2], G. Kolarz*[2], W. Woloszczuk[1]. [1]Research & Development, Biomedica, Vienna, Austria, [2]Institut für Rheumatologie der Kurstadt Baden in Kooperation mit der Donauuniversität Krems & Rheumasonderkrankenanstalt der SVA der gewerblichen Wirtschaft, Baden, Austria.

Cathepsin K is a cysteine protease, which is highly expressed in Osteoclasts when they actively resorb bone. This enzyme has been shown to cleave a number of bone matrix proteins including collagen type I, II, and osteonectin. So it is widely accepted, that Cathepsin K plays an important role in bone remodelling, which is also supported by the finding, that Osteoclasts derived from Cathepsin K deficient mutant mice are predominantly mononuclear, do not form ruffled borders, and resorb bone poorly. Therefore Cathepsin K is an attractive target for the treatment of several diseases with pathologically elevated bone resorption like osteoporosis, rheumatoid arthritis and osteolytic bone metastasis. It also may become a new and highly specific biomarker of those diseases.

We have developed an ELISA for measuring Cathepsin K levels in human serum and cell culture supernatants. The calibration curve was set from 0-300pmol/l and the analytical detection limit was determined as 1.1pmol/l. The required sample volume was 50µl serum or cell culture supernatant. Intra- and Interassay CVs ranged from 4-6% and 6-8% respectively. Incubation was performed over night at room temperature. No cross-reactivity to the structurally related Cathepsins E,D,B and L was detected. The high homology of Cathepsin K across various species (mouse 86%, rat: 88%, pig: 97%, rabbit: 96%) should allow the use of this assay for studies in animal models for those diseases The assay was used to investigate serum samples from patients with rheumatoid arthritis and from a healthy control group. We found significantly elevated levels in rheumatoid arthritis (median 54.8 pmol/l). compared to the control group (median 8.7 pmol/l). We found no interference caused by rheumatoid factors. This data indicate, that as a specific marker enzyme for osteoclast activity, our Cathepsin K ELISA will be a valuable tool for bone research. Together with the determination of OPG and sRANKL it will add to our insights into the mechanism of bone resorption.

Disclosures: ***G. Hawa****, None.*

F123

Prediction of Fracture Risk in 5195 Postmenopausal Women from Spain by Quantitative Ultrasound of the Calcaneus: 18 Months Interim Results from the ECOSAP Prospective Study. J. González-Macías[1], F. Marín[2], J. Vila*[3], D. Martín*[4], C. Alfonso*[5], P. Benavides*[6], J. Pozuelos*[7], F. Chavida*[8], J. Pérez*[9], J. Granados*[10]. [1]Internal Medicine, H. U. Valdecilla, Santander, Spain, [2]Medical Research, Eli Lilly and Company, Madrid, Spain, [3]IMIM, Barcelona, Spain, [4]C.S. Torredelcampo, Jaén, Spain, [5]C.S. San Andrés, Murcia, Spain, [6]C.S. Pumarín, Oviedo, Spain, [7]C.S. de la Paz, Badajoz, Spain, [8]C.S. Brihuega, Guadalajara, Spain, [9]C.S. Estación, Talavera, Toledo, Spain, [10]C.S. Guayaba, Madrid, Spain.

Bone quantitative ultrasound (QUS) is known to discriminate subjects with fracture history. Several prospective studies have also shown that QUS are predictive of osteoporotic fractures with a similar magnitude to DXA. ECOSAP is a 3-year prospective study to evaluate the ability of calcaneus QUS and several clinical risk factors of osteoporosis and fractures, to predict the non-vertebral fracture risk in women ≥ 65 years recruited in 58 Primary Care Centers in Spain. 5195 women aged 72.3±5.3 years (mean±SD) were assessed with a Sahara® equipment. Women were selected using non-probabilistic sampling of consecutive cases regardless of the reason for consultation. At baseline, 1042 women (20.1%) presented a history of fragility fracture in adulthood (>35 years)**.** We report here the results after 4705 women have completed the 18-month follow-up visit. During the mean 17.8 months follow-up, 194 non-osteoporotic fractures in 170 women were reported. A logistic regression analysis with QUS parameters as the dependent variable was performed. Independent variables included were all those with a p value < 0.15. The final model consisted of age, history of falls, prevalent fractures, and chronic airway disease (COPD + asthma). The hazard rates (and 95% CI) per SD decrease of each QUS parameter after adjusting for them are shown in the Table.

Type of fracture (number)	All non-vertebral (n=170)	Forearm (n=65)	Hip (n=23)	Humerus (n=28)
BUA	1.32 (1.11 ; 1.56)	1.54 (1.16 ; 2.04)	1.50 (0.95 ; 2.36)	1.32 (0.87 ; 1.99)
SOS	1.19 (1.04 ; 1.36)	1.34 (1.13 ; 1.59)	1.08 (0.73 ; 1.62)	1.14 (0.81 ; 1.61)
QUI	1.33 (1.12 ; 1.58)	1.67 (1.24 ; 2.25)	1.24 (0.79 ; 1.96)	1.34 (0.88 ; 2.04)
Estimated heel BMD	1.32 (1.11 ; 1.57)	1.64 (1.22 ; 2.21)	1.25 (0.79 ; 1.97)	1.34 (0.88 ; 2.06)
Estimated heel BMD (T-score)	1.30 (1.10 ; 1.53)	1.64 (1.24 ; 2.16)	1.32 (0.83 ; 2.04)	1.34 (0.90 ; 2.00)

Values are Hazard Rate (95% CI)

The interim results of the ECOSAP study show that QUS of the heel is a predictor of non-vertebral osteoporotic fractures in a cohort of elderly Spanish women.

Disclosures: ***J. González-Macías****, None.*

F127

Bone Strength Is Regulated Predominantly by Genetic Loci that Regulate Bone Geometry. J. E. Wergedal[1], C. L. Ackert-Bicknell[2], S. Tsaih*[2], M. H. Sheng[1], W. G. Beamer[2], G. A. Churchill*[2], D. J. Baylink[1]. [1]JL Pettis VA Medical Center and Loma Linda Univ., Loma Linda, CA, USA, [2]Jackson Laboratory, Bar Harbor, ME, USA.

Bone strength is reduced in osteoporotic subjects to the extent that fractures begin to occur. Identifying the factors that can affect bone strength and potentially alter fracture incidence is very important. Previous studies have shown that bone geometry, bone density and bone quality are all important factors that affect bone strength. There is evidence that geometry and density are influenced by genetic mechanisms involving polygenic traits. We hypothesize that bone strength is regulated by genetic loci that influence bone geometry, density and quality. Inbred strains of mice are amenable to genetic analysis of these traits via the experimental design of quantitative trait loci (QTL) analysis. We have applied this approach to an F2 cross of the RF/J and NZB/B1nJ inbred mouse strains. These two strains differ widely in femur bending strength. The F2 progeny (737 mice) have been genotyped for 89 genome-wide markers and phenotyped for femur bending strength, cross sectional geometry, vBMD, material (m)BMD. QTL analysis was carried out with the Pseudomarker Package, version 1.02.

Table 1 Major QTL for bone strength, cross sectional geometry, and density.

Chrom.	Distance (cM)	Strength LOD	Geometry LOD	vBMD LOD	mBMD LOD
4	65	4.1	5.5	-	3.8
5	50	6.4	10.4	-	-
7	55	3.1	10.3	4.1	-
11	65	4.4	26.8	-	-
12	5	9.6	9.7	-	-

A total of 8 strength QTL were identified, and only one was not associated with a cross sectional geometry QTL. Four additional geometric QTL were found that were not associated with strength QTL. Of the strength QTL only 2 were associated with BMD QTL and those 2 were also associated with geometric QTL. There were 4 additional density QTL; and those were also associated with geometric QTL. Body weight QTL were also determined to test whether they were associated with strength QTL. Only 3 of the 8 strength QTL were associated with body weight QTL and only 2 of these 3 strength QTL had decreased significance when body weight was included as a covariate in the QTL analysis. Including body weight in the analysis did decrease 2 of the other strength QTL, but increased the significance of 2 of others. Conclusion: 1) Femur strength, cross sectional geometry and density are polygenic traits. 2) Bone Strength is regulated predominantly by genetic loci that regulate bone geometry. 3) Genetic regulation of bone strength is largely independent of body weight.

Disclosures: ***J.E. Wergedal****, None.*

F131

Whole-Genome Scan for Linkage to Bone Strength and Mineral Density in Inbred Rats. I. Alam[1], Q. Sun[1], L. Liu*[2], D. L. Koller[2], T. M. Fishburn*[3], M. J. Econs[3], T. Foroud[2], C. H. Turner[1]. [1]Orthopaedic Surgery, Indiana University School of Medicine, Indianapolis, IN, USA, [2]Medical and Molecular Genetics, Indiana University School of Medicine, Indianapolis, IN, USA, [3]Medicine, Indiana University School of Medicine, Indianapolis, IN, USA.

Bone mineral density (BMD) and bone biomechanical properties are major determinants of osteoporosis. Genetic analyses in inbred mice and humans have identified several chromosomal regions linked to BMD, bone structure and biomechanics. However, the key genes that influence these phenotypes have not yet been identified. Rats are the most commonly used animal model for skeletal research. One of these rat strains, the Fischer (F344) has been shown to develop osteopenia similar to humans. Previously, we reported that compared to Lewis (LEW) rats, Fischer (F344) rats have significantly lower ($p<0.001$) bone strength and BMD both at the femur and spine. In this study, we seek to identify chromosomal regions that contain quantitative trait loci (QTLs) underlying variation in BMD, bone geometry and biomechanical properties in a sample of 595 F344 X LEW F2 rats. A genome screen was performed using 100 microsatellite markers at an average density of 20 cM. Skeletal phenotypes were measured by peripheral quantitative computed tomography (pQCT) and dual energy x-ray absorptiometry (DXA). Femoral and spinal biomechanical tests were performed using an MTS machine. Genetic marker maps were estimated from our own data and compared with published maps. These maps were then used to detect QTLs using interval mapping methods (MAPMAKER/QTL). Our results indicate that several chromosomal regions harbor QTLs for bone strength and BMD. The main QTLs and their synteny to a known QTL region in mice and human are summarized in the following Table.

Marker	Phenotype	LOD score	Mouse Synteny	Human Synteny
D1Rat136	Lumbar BMD	8.7	17, Whole body BMD and femoral structure	5q, Femur BMD and structure
D1Rat256	Femur BMD	7.4	17, Whole body BMD and femoral structure	5q, Femur BMD and structure
D2Rat67	Femur BMD Polar moment of inertia (Ip)	7.2 7.5	3, Femur BMD	1p, Whole body and lumbar BMD
D4Rat193	Polar moment of inertia (Ip)	7.5	6, Femur BMD and strength	3p, Femoral structure and spinal BMD
D5Rat159	Polar moment of inertia (Ip) Ultimate Force	8.3 6.9	4, Femur and lumbar BMD	1p, Whole body and lumbar BMD
D7Rat64	Polar moment of inertia (Ip)	10.9	10, Femoral structure and biomechanics	19p, Femoral structure

Our results provide evidence of new QTLs for bone strength and biomechanical properties as well as several QTLs syntenic to those previously identified in other species. These studies provide essential data for identification of genes that affect bone density and strength.

Disclosures: ***I. Alam****, None.*

F136

Interaction Between Polymorphisms of the Low Density Lipoprotein Receptor-Related Protein 5 (LRP5) Gene and Physical Activity on Bone Mineral Density (BMD): The Framingham Offspring Study. D. P. Kiel[1], A. G. Herbert*[2], S. L. Ferrari[3], L. A. Cupples*[4], D. Karasik[1], A. Imamovic*[2], J. Dupuis*[4]. [1]Heb Rehab Ctr for Aged, Boston, MA, USA, [2]Framingham Heart Study Genetics Lab, Boston Univ, Boston, MA, USA, [3]Div of Bone Diseases, Geneva Univ Hosp, Geneva, Switzerland, [4]Dept Statistics, Boston Univ Sch Pub Health, Boston, MA, USA.

Mutations in the LRP5 gene result in different single gene disorders with either high or low BMD. In mice, the LRP5 gene may be involved in bone adaptation to mechanical load, yet little information exists regarding the contribution of the LRP5 gene to BMD in the general population, nor the possibility of interaction between variants in this gene, physical activity, and BMD. Therefore, we genotyped 9 single nucleotide polymorphisms (selected tag SNPs to account for at least 80% of the common haplotypes for each of three LRP5 blocks previously identified) in LRP5 and tested for their association with hip (neck, troch, wards) and spine BMD in unrelated women and men from the Framingham Offspring Study. There were 695 men (mean age 62±9) and 747 women (61±9) in the sample. We hypothesized a priori that SNPs in LRP5 would be associated with BMD, especially in younger men (≤ 60 yrs of age). We coded SNP genotypes as the number of minor alleles (0,1,2) and used an additive model for genotype effect in combined sexes as well as within sex, in younger (age ≤60) males, and in pre- and post-menopausal women. From the 9 SNPs examined, two exonic missense mutations in H-W equilibrium (G2047A in exon 9 and C4037T in exon 18) yielded significant associations with BMD in men ≤ 60 yrs of age when using linear regression, adjusting for age, age squared, sex, wt, physical activity (using the Physical Activity Scale for the Elderly (PASE)), and in women, use of estrogen. Femoral neck BMD was lower the greater the number of A alleles in G2047A ($p=0.07$) and T alleles in C4037T ($p=0.01$) in males aged ≤ 60 years. Similar findings were observed for Wards BMD ($p<0.02$ both SNPs) and for spine BMD ($p=0.06$ C4037T only) in these males). The rs312016 intronic SNP in haplotype block 1 was associated with BMD at all hip sites in premenopausal women, with TT homozygotes having greater BMD than CC. There was also a significant interaction between exon18 T-allele count and PASE on spine BMD in males ($p=0.002$) such that the benefit of higher PASE values on BMD decreased with the number of T alleles.

We conclude that variation in two exonic missense mutations in the LRP5 gene was associated with BMD in men ≤ 60 yrs of age, and that the effect of these variants modifies the influence of physical activity on BMD. These findings support a role for the LRP5 gene as a contributor to BMD in the general population and potentially in the adaptation of bone to mechanical load.

Disclosures: ***D.P. Kiel****, None.*

F139

Catechol-*O*-methyltransferase Is a Physiological Regulator of Longitudinal Bone Growth and Cortical Bone Dimensions both in Female Mice and in Pubertal Girls. A. Eriksson[1], M. Forsberg*[2], P. T. Männistö*[2], C. Ohlsson[3]. [1]Division of Clinical Pharmacology, Department of Internal Medicine, Göteborg University, Göteborg, Sweden, [2]Department of Pharmacology and Toxicology, University of Kuopio, Kuopio, Finland, [3]Center for Bone Research at the Sahlgrenska Academy, Department of Internal Medicine, Göteborg University, Göteborg, Sweden.

Estrogen is of vital importance for normal pubertal growth in humans as well as in mice. Catechol-*O*-methyltransferase (COMT) is a key enzyme in the degradation of estrogens. A functional polymorphism in the *Comt* gene (val158met) decreases the activity of the enzyme by 60-75%. We have previously shown that early pubertal girls who are homozygous for the low activity COMT genotype ($COMT^{LL}$) are taller and have an increased cortical thickness as well as an increased cortical BMC, and higher serum levels of bioavailable estrogens compared with girls homozygous for the high activity COMT genotype ($COMT^{HH}$). The aim of the present study was to investigate whether young female *Comt* gene disrupted ($COMT^{-/-}$) mice exhibit a similar bone phenotype as girls with the low activity $COMT^{LL}$ genotype.

Femurs of 70 days old female $COMT^{-/-}$ mice and wild type ($COMT^{+/+}$) littermates were analyzed using peripheral Quantitative Computerized Tomography. $COMT^{-/-}$ mice had longer femurs than wild type mice ($p<0.001$). Cortical thickness was increased by 7.0 % ($p<0.01$) in $COMT^{-/-}$ mice compared with wild type mice. This was due to a decreased endosteal circumference, while periosteal circumference did not differ between the two genotypes. Moreover, cortical volumetric BMD was increased by 3.7% in $COMT^{-/-}$ mice ($p<0.01$).

In conclusion, our results demonstrate that $COMT^{-/-}$ mice have a bone phenotype which is similar to that of young girls with the $COMT^{LL}$ genotype, characterized by an increased longitudinal bone growth and cortical thickness. Our findings indicate that in female mice as well as in early pubertal girls, COMT is an important regulator of growth velocity during puberty. However, further studies are needed to investigate the role of COMT genotype in adult stature and bone phenotype.

Disclosures: ***A. Eriksson****, None.*

F141

Osteoprotegerin Genetic Variants Are Associated with Both Susceptibility to Rheumatoid Arthritis and Rate of Joint Erosion. S. Steer*[1], L. J. Miles*[2], B. Lad*[1], J. Grumley*[1], a. National Repository*[3], M. A. Brown*[2]. [1]Kings College London, London, United Kingdom, [2]Botnar Research Centre, University of Oxford, Oxford, United Kingdom, [3]arc Epidemiology Unit, Manchester, United Kingdom.

Purpose: We have recently demonstrated that variation in the osteoprotegerin (OPG) gene influences bone density and serum OPG levels. OPG is known to have major effects on osteoclast activity and differentiation, as well as on T- and B-lymphocyte differentiation and activation. The aim of this study was to examine whether *OPG* sequence variation could influence either susceptibility to rheumatoid arthritis (RA) or the severity of erosive disease.

Methods: Eight haplotype-tag SNPs within *OPG* were genotyped in 295 RA affected sibling pair families from the arc National Repository, and in 300 Caucasian cases from London in whom Larsen scores and disease duration were available. Nonparametric linkage analysis was performed using MERLIN. TRANSMIT was used for single marker and two marker TDT analysis, with p-values calculated by bootstrap simulation. PHAMILY and PHASE were used to construct phase known/estimated haplotypes for the non-familial cases; only haplotypes with >90% certainty were analysed. ANOVA was used to test global association of markers and haplotypes with Larsen scores adjusted for gender and disease duration; Dunnett's post-hoc test was used to assess association of individual haplotypes where global association was observed.

Results: 'Nominal' linkage was detected across the locus with a multipoint LOD score of 1.3 ($P=0.007$). Association was noted with the single marker IVS2+4 ($P=0.003$), with over-transmission of the major allele (IVS2+4*1). Considering the haplotype of this marker with a neighbouring SNP, IVS2+1256, global association was observed $P=0.04$), with highly significant under-transmission of the haplotype IVS2+4*1/IVS2+1256*2 ($P=0.003$), and over-transmission of haplotype IVS2+4*1/IVS2+1256*1 ($P=0.02$). Association of a two-marker haplotype E1+9/E1-142 was also observed ($P=0.03$), with over-transmission of the major haplotype E1+9*1/E1-142*1 ($P=0.007$). The SNPs IVS2+4 and IVS2+1256 were also associated with disease severity as assessed by adjusted Larsen score. SNP IVS2+4 was globally associated with $P=0.02$, and the haplotype IVS2+4/IVS2+1256 with $P=0.05$. Posthoc tests showed that the under-transmitted haplotype IVS2+4*1/IVS2+1256*2 was associated with less erosive change than other haplotypes ($P<0.05$).

Conclusion: Genetic variation in *OPG* affects both susceptibility to and rate of erosive change in RA.

Disclosures: ***L.J. Miles****, None.*

F144

T Cells Suppress Physiological Bone Resorption In Vivo by Stimulating the B Cell Production of Osteoprotegerin. Y. Li*[1], G. Toraldo[2], H. Zhang[1], W. Qian*[1], R. Pacifici[1], M. N. Weitzmann[1]. [1]Division of Endocrinology & Metabolism & Lipids, Emory University School of Medicine, Atlanta, GA, USA, [2]Division of Bone & Mineral Diseases, Washington University School of Medicine, St. Louis, MO, USA.

Activated T cells secrete RANKL and TNF causing bone destruction in models of estrogen deficiency and rheumatoid arthritis. We have reported that nude mice, a model of T cell deficiency, are protected from ovariectomy induced bone destruction and that reconstitution of T cells restores bone loss. However, paradoxically nude mice also exhibit significantly decreased baseline bone mineral density (BMD), suggesting that the absence of T cells may also lead to bone destruction during physiological bone turnover. We have now examined physiological bone modeling in nude mice and elucidated a potential mechanism to explain the protective effects of T cells on bone mass under physiological conditions. Our data verifies decreased BMD and indices of bone mass in nude mice, and demonstrate the presence of enhanced numbers of osteoclasts in nude mouse tibias. Serum C-terminal telopeptide was significantly elevated in nude mice in the face of unchanged levels of serum osteocalcin. This data suggests that bone resorption is uncoupled from bone formation in nude mice leading to enhanced osteoclastic bone resorption. As T cells have been reported to stimulate the production of B cell osteoprotegerin (OPG), a potent inhibitor of osteoclastogenesis we investigated the production of OPG by bone marrow B cells. Our data shows that B cells are responsible for >40% of the total OPG produced by bone marrow under physiological conditions. Importantly, OPG production from purified B cells derived from nude mice was decreased by 3 fold relative to wild type mice. As T cells have been reported to stimulate OPG production by B cells, via T cell CD40 ligand interactions with the B cell CD40 receptor, we evaluated BMD in CD40 and CD40 ligand null mice. As expected, CD40 and CD40 ligand knock out mice displayed significantly decreased BMD and increased biochemical indices of bone resorption, concurrent with decreased B cell OPG secretion, although the magnitude of these changes was less than that observed in nude mice. Based on our data we hypothesize that B cells provide a critical reservoir of OPG in the bone marrow microenvironment and that this effect is upregulated by T cells, in part via a CD40-CD40 ligand dependent mechanism. This B cell derived OPG may serve to protect bone mass by neutralizing periodic increases in RANKL production in the bone marrow, a possible consequence of low grade T cell activation that occurs physiological in healthy humans and animals.

Disclosures: ***M.N. Weitzmann****, None.*

F147

Placental Growth Factor Is Essential for Normal Fracture Healing in Mice by Affecting Inflammation, Angiogenesis and Mesenchymal Cell Development. C. Maes*[1], I. Stockmans*[1], K. Moermans*[1], R. Van Looveren*[1], N. Smets*[1], P. Carmeliet*[2], R. Bouillon[1], G. Carmeliet[1]. [1]Laboratory of Experimental Medicine & Endocrinology, KUL, Leuven, Belgium, [2]Center of Transgene Technology & Gene Therapy VIB, KUL, Leuven, Belgium.

It is generally accepted that signaling pathways regulating bone development are reactivated during fracture healing. In agreement, VEGF is important in both processes. Yet, some aspects of bone repair markedly differ from bone development, including its initiation by inflammatory and angiogenic responses to trauma and the source of mesenchymal progenitors. Particularly these aspects may be involved in failing repair, such as delayed or non-unions. Placental growth factor (PlGF), a homologue of VEGF, has no obvious role in development but is important during pathology as a mediator of inflammation and angiogenesis. Here we studied its role during bone repair. Histological analysis and quantitative real-time (q)RT-PCR revealed striking differences in the repair process between WT and PlGF-deficient (-/-) mice.

At post-fracture day (PFD) 13 the callus of WT mice was already mainly composed of woven bone, whereas PlGF-/- calluses contained massive hypertrophic cartilage (cartilage area of the callus, measured on safranin O staining: 2.1% ± 0.7 in WT versus 8.4% ± 1.7 in PlGF-/- mice, P<0.05, n=6-8). This type of impaired healing resembles a clinical delayed union. Molecular analysis at various time points by in situ hybridization and qRT-PCR revealed that the cartilage accumulation in PlGF-/- mice was due to both increased cartilage formation (increased collagen 2 and 10 and Ihh expression) and impaired cartilage resorption (reduced expression of MMPs). To further understand the causing mechanism, we studied the initial events of the repair process at PFD 2-3. Evidently, PlGF-/- mice showed an inadequate inflammatory reaction, with strongly reduced accumulation of CD45+ leukocytes in the callus and reduced expression of inflammatory cytokines. Concomitantly, the angiogenic reaction (CD31+ endothelial cell recruitment) was reduced. Surprisingly, PlGF-/- mice completely lacked the periosteal thickening seen in WT mice at PFD 3, and BrdU labeling revealed reduced proliferation of these mesenchymal progenitors (46% ± 8 of WT, P<0.01). Together, these defects in PlGF-/- mice resulted in impaired endochondral ossification at later stages, marked by imbalanced cartilage and bone formation with reduced invasion of osteoclasts and blood vessels (H&E, Von Kossa, TRAP, CD31 staining at PFD 8, 13, 21).

In conclusion, this study provides new insights in the mechanisms of fracture repair and may contribute to the development of new treatments for delayed/non-union types of fractures.

Disclosures: ***C. Maes****, None.*

F152

FGF23 Uses Both VDR-Independent and Dependent Pathways in the Maintenance of Phosphate and Vitamin D Metabolism. T. Shimada*[1], H. Hasegawa*[1], M. Takahashi*[1], T. Oshima*[1], Y. Yamazaki*[1], I. Urakawa*[1], M. Kakitani*[1], K. Tomizuka*[1], Y. Takeuchi[2], T. Fujita[3], S. Fukumoto[3], T. Yamashita[1]. [1]Pharmaceutical Research Laboratories, Kirin Brewery Co.,Ltd., Takasaki, Japan, [2]Division of Endocrinology and Metabolism, Toranomon Hospital, Tokyo, Japan, [3]Division of Nephrology and Endocrinology, Department of Internal Medicine, University of Tokyo Hospital, Tokyo, Japan.

FGF23 plays crucial roles in maintaining phosphate and vitamin D metabolism in the physiological state, and enhanced action of FGF-23 was shown to cause several hypophosphatemic rickets/osteomalacia. The injection of recombinant FGF23 into mice lowered serum phosphate and 1,25-dihydroxyvitamin D [1,25D] levels, whereas treatment with anti-FGF23 neutralizing antibodies increased both serum concentrations of phosphate and 1,25D. In these experiments, serum 1,25D levels changed earlier than serum phosphate levels. Since 1,25D itself is known to be a potent regulator for phosphate metabolism, it has remained unclear whether FGF23 regulates serum phosphate by changing serum level of 1,25D. To address this issue, we established the vitamin D receptor (VDR) null mouse lacking exon 1 and evaluated the effect of recombinant FGF23 in those mice. Serum FGF23 levels in *Vdr* KO mice were not detectable at all, suggesting that the basal expression level of FGF23 appears to be regulated by a VDR dependent mechanism. Administration of recombinant FGF23 into 8-week-old *Vdr* KO mice further decreased serum phosphate and ameliorated the constitutionally elevated serum 1,25D level. These changes were accompanied by the reductions in sodium phosphate cotransporter type IIa (NaPi2a) protein in renal brush border membrane fractions and renal 25-hydroxyvitamin D-1alpha-hydroxylase (1aOHase) mRNA levels, as seen in the normal mice treated with FGF23. Thus, regulatory mechanisms for NaPi2a and 1aOHase by FGF23 are likely to be independent of the 1,25D/VDR system. On the other hand, the FGF23-induced increase in 24-hydroxylase (24OHase) mRNA levels already shown in normal mice was completely ablated in *Vdr* KO mice, indicating that the regulation of 24OHase mRNA by FGF23 depends on the 1,25D/VDR system. Therefore, these findings clearly indicate that FGF23 regulates phosphate and vitamin D metabolism by multiple signaling cascades involving VDR-dependent and -independent pathways.

Disclosures: ***T. Shimada****, KIRIN Brewery CO.,LTD. 3.*

F154

A Novel Splicing Variant Transcript of the Renal Type IIa Sodium-Dependent Phosphate Cotransporter (NPT2a) Gene Is Positively and Negatively Regulated by 1,25-dihydroxyvitamin D_3 and Phex Cleavable Humoral Factors. H. Yamamoto, Y. Taketani, M. Tsuji*, T. Sato*, H. Arai*, E. Takeda. Department of Clinical Nutrition, Institute of Health Biosciences, University of Tokushima, Tokushima, Japan.

Decreased expression of the renal type IIa sodium-dependent phosphate cotransporter (NPT2a) has been shown in X-linked hypophosphatemic rickets (XLH) caused by mutations in the Phosphate-regulating gene with homologies to endopeptidases on X chromosome (Phex) gene, autosomal dominant hypophosphatemic rickets (ADHR) caused by mutations in the Fibroblast growth factor 23 (FGF-23). However, the repression mechanism of renal NPT2a gene expression in these disorders is unknown. During our efforts to understand the molecular mechanisms involved in regulatory factors, such as vitamin D, Phex and FGF-23 for the NPT2a gene expression, we identified a novel splicing variant transcript of the mouse NPT2a gene, Npt2a variant transcript 1 (Npt2a-v1), in addition to the previously known Npt2a variant transcript 2 (Npt2a-v2), characterized by the presence of alternative first exons (either exon 1A or exon 1B) that are spliced to exon 2 of the known transcript. Analysis of the chromosomal gene structure revealed the Npt2a gene is comprised of two promoters and 14 exons that, together with the 13 intervening introns, span approximately 17 kb. Real-time PCR analysis revealed that both renal Npt2a-v1 and Npt2a-v2 mRNAs expression in X-linked Hyp (hypophosphatemic) mice is decreased by 50% and 70% respectively when compared with normal littermates. On the other hand, abnormal metabolism of vitamin D has been also shown in XLH, ADHR. Therefore, we next examined the effects of $1,25(OH)_2D_3$ on the renal Npt2a variants expression in normal mice. Interestingly, renal Npt2a-v1 mRNA abundance was increased up to 4-folds following 48 h treatment with $1,25(OH)_2D_3$ (0.125μg/10g of diet), while renal Npt2a-v2 mRNA abundance was not changed. Furthermore, luciferase reporter assay showed that $1,25(OH)_2D_3$ or vitamin D analogs increased the transcriptional activity of Npt2a promoter including exons 1A and 1B in renal cell line, OK cells. These data suggest that a novel Npt2a variant transcript, Npt2a-v1 is positively and negatively regulated by $1,25(OH)_2D_3$ and Phex cleavable humoral factors and the differential regulation of these Npt2a gene promoters and splicing variant transcripts may have implications for understanding the various actions of phosphate regulating factors.

Disclosures: ***H. Yamamoto****, None.*

F156

FGF-23 Mediated Internalization of the Type IIa Sodium Phosphate Co-Transporter (NaPi-2a) Requires the Scaffolding Protein, NHERF-1. M. D. Ruppe*, S. M. Jan de Beur. Endocrinology, Johns Hopkins Medical Institute, Baltimore, MD, USA.

FGF-23, a potent inhibitor of renal phosphate reabsorption, is central to several acquired and inherited renal phosphate wasting syndromes. FGF-23 exposure results in a down regulation of NaPi-2a RNA and protein expression in the proximal renal tubule. NaPi-2a co-localizes with PDZ containing proteins, including NHERF-1 (sodium-hydrogen exchange regulatory factor-1). This cytosolic scaffolding protein is thought to localize NaPi-2a to the apical membrane and mediate the rapid endocytic retrieval observed upon PTH stimulation. We hypothesized that FGF-23 inhibits phosphate reabsorption via internalization of NaPi-2a and that this is a NHERF-1 dependent process. To determine if FGF-23 promotes internalization of NaPi-2a from the membrane, we labeled OK cell surface proteins with biotin followed by incubation with PTH (10^{-7}M), FGF-23 (20 ng/mL) or untreated media for 30 minutes. Subsequently, cell surface biotin was removed with a membrane-stripping agent (TEPC). Whole cell lysates were prepared from both stripped and unstripped cells and immunoblotted with a NaPi-2a antibody. The signal intensity of the stripped versus the unstripped samples was compared to determine the proportion of internalized NaPi-2a cotransporters. Upon treatment with FGF-23, 86% of NaPi-2a was internalized compared to 67% in PTH treated cells and 5% in untreated cells. To investigate the role of NHERF-1 in FGF-23-mediated NaPi-2a internalization, we repeated the experiment with OKH cells, a subclone of OK cells known to have a markedly reduced level of NHERF-1. In these cells, NaPi-2a failed to internalize upon stimulation with neither FGF-23 nor PTH. To confirm the lysosomal processing of internalized NaPi-2a, OK and OKH cells were pre-treated with or without leupeptin (a lysosomal inhibitor) followed by 30 minutes of treatment with PTH (10^{-7}M), FGF-23 (20 ng/mL) or untreated media. After treatment, whole cell lysates were prepared and immunoblotted with a NaPi-2a antibody. Upon pretreatment with leupeptin, the decrement in NaPi-2a protein expression observed with PTH and FGF-23 was eliminated. In contrast, pretreatment with leupeptin had no effect on NaPi-2a expression in OKH cells suggesting that NaPi-2a does not undergo internalization and subsequent lysosomal degradation. Based on these observations, FGF-23 induces internalization of NaPi-2a from the renal apical membrane and subsequent lysosomal degradation in a process requiring NHERF-1. NHERF-1 may serve as the core for a multimolecular complex that integrates the receptors, ion transporters and signaling molecules important in FGF-23-mediated internalization of NaPi-2a.

Disclosures: ***M.D. Ruppe****, None.*

F160

Whole Genome Microarray Analysis of the *In Vivo* Effects of Single Effective Growth Hormone (GH) Dose on Gene Expression in Bones of GH-Deficient *lit/lit* Mice: Potential Involvement of Tbx3, a Novel Transcription Factor, in Mediating GH Effects in Bone. K. Govoni, S. Lee*, R. B. Chadwick*, H. Yu*, Y. Kasukawa, G. Linares*, D. J. Baylink, S. Mohan. JLP VAMC / Loma Linda Univ, Loma Linda, CA, USA.

The importance of GH in the development and maintenance of bone has been well established. GH effect on bone may be mediated via IGF-dependent and -independent mechanisms, however the molecular pathways remain to be established. To evaluate the major signaling pathways utilized by GH to mediate its effects on bone, we measured GH-induced changes in gene expression using Agilent microarray chips that contain 20,000 oligonucleotides. 4-wk old GH-deficient *lit/lit* mice were treated with GH (4 mg/kg body wt) or PBS (n = 6/group). 6 or 24 h after a single injection, bones were removed, RNA extracted and used for microarray. RNA from 2 animals was pooled and 3 pools per group were analyzed. After data normalization, analysis by Student's T-test determined that 393 and 633 genes showed significant changes in expression ($P < 0.01$) 6 and 24 h after GH treatment, of which over 50% represents cDNA clones with no assigned function. Approximately 75% of the genes up regulated by >2-fold at 6 h were also up regulated at 24 h. Consistent with the known effect of GH on the IGF axis, a number of GH responsive genes (IGF-I, IGF-II, BP-3 and BP-5) were significantly up regulated in the GH treated group, thus validating the microarray data. Of the known bone growth factor signaling pathways, IGF, BMP, and Wnt pathways are acutely regulated by GH treatment. For subsequent studies, we focused on Tbx3 because: 1) Tbx3 expression was increased more than 2-fold at both time points; 2) Tbx genes play an important role in limb development; and 3) Little is known about Tbx-3, a T-box containing transcription factor, except that mutations in Tbx3 result in human ulnar-mammary syndrome. After confirming microarray data with real time PCR (4.8 fold increase in Tbx3 expression at 24 h, $P < 0.01$), we found that GH treatment increased Tbx3 expression in MG63 and MC3T3-E1 cells ($P < 0.05$). Because GH effect on target gene expression is known to be mediated via stat5b, we pretreated MC3T3-E1 cells with TNFα which blocked GH-induced Tbx3 expression in MC3T3-E1 cells ($P < 0.05$). TNFα alone had no effect on Tbx3 expression. In conclusion, 1) GH caused acute change in the expression of signaling genes for IGF, BMP and Wnt signaling pathways. 2) Our findings that majority of the GH-induced genes in bone are not annotated suggest that many GH-induced signaling pathways and target genes remain to be discovered. 3) Our data demonstrate for the first time GH acutely regulates expression of Tbx3, which may act to mediate GH effects in bone.

Disclosures: ***K. Govoni****, None.*

F168

Hypoxia Inhibition of Adipogenesis in Human Bone Marrow Stromal Cells Requires TGFβ/Smad Signaling. S. Zhou[1], S. Lechpammer*[1], J. Greenberger[2], J. Glowacki[1]. [1]Orthopedic Surgery, Brigham & Women's Hospital, Harvard Medical School, Boston, MA, USA, [2]University of Pittsburgh Medical Center, Pittsburgh, PA, USA.

Hypoxia (Hy) inhibits differentiation of murine preadipocytes, but it is not known whether Hy affects human marrow stromal cell (hMSC) differentiation nor whether there is a relationship between Hy and TGFß signaling in cellular differentiation. We tested the hypothesis that TGFß/Smad signaling mediates Hy's effects in hMSCs.

Early passage hMSCs (42-year-old woman) were cultured with adipocytogenic medium (MEM-α, 1% FBS-HI with insulin, dexamethasone, and 1-methyl-3-isobutylxanthine). Murine MSCs were established from $Smad3^{+/+}$ and $Smad3^{-/-}$ mice.

First, Western blot showed that treatment (16 h) of hMSCs with Hypoxia (2% O_2) or 15 μM of the hypoxia-mimetic deferoximine mesylate (DFO) induced hypoxia-inducible factor-1α (HIF-1α) protein. Macroarray and Northern blot analyses showed that Hypoxia (2 d) stimulated (relative to control) HIF-target genes, e.g. *VEGF* (210%), *PKM2* (310%) and *p21/Waf1/Cip1*, and inhibited adipocyte genes, e.g. *PPARγ, Adipsin* (43%), *C/EBPβ, INSR* (84%), and *LDLR*. DFO blocked the development of adipocytes at 3 w (38.8%, 20.4%, 1.0% vs. control at 2.5, 5.0, 15.0 μM respectively), and it prevented expression of adipocyte genes *PPARγ2* and *LPL*. Second, Hy up-regulated *TGFβ1* expression and many TGFß/Smad target genes, e.g. *βig-h3/TGFBI* by 383%, *PAI-1* by 686% (Northern and macroarray). Third, the direct effects of TGFß1 on adipocytogenesis were compared with Hy or its mimetic DFO. TGFß1 (1 ng/ml) decreased adipocyte number (1.4% vs. control) and adipocyte *PPARγ2* and *LPL* gene expression, and did not induce HIF-1α protein in hMSCs. Changes in adipogenic genes, e.g. *PPARγ, Adipsin, LPL, INSR*, induced by TGFß were similar to Hy-induced changes (macroarray and RT-PCR). Fourth, because these findings suggest that Hy or DFO actions are mediated by TGFß /Smad signaling, we tested effect of DFO on adipocytogenesis with mouse $Smad3^{-/-}$ MSCs. There were two notable differences in adipocyte development in stromal cells from $Smad3^{-/-}$ and $Smad3^{+/+}$ mice. First, there was more extensive (37-fold) adipocyte differentiation in $Smad3^{-/-}$ than $Smad3^{+/+}$ MSCs. The data suggest that Smad3 is a critical inhibitor of adipocyte differentiation. Second, there was less DFO inhibition in $Smad3^{-/-}$ (67.7% inhibition of adipocytogenesis) compared to in $Smad3^{+/+}$ (32.9%) MSCs.

In summary, hypoxia inhibits adipocyte differentiation in marrow stromal cells via activation of the TGFß/Smad signaling pathway and Smad3 is required for inhibition of adipocyte differentiation.

Disclosures: ***S. Zhou****, None.*

F170

Loss of TIEG1 Results in Impaired TGFβ Regulated Gene Expression in Osteoblasts. M. Subramaniam[1], D. G. Monroe[1], G. Gorny*[1], K. Rasmussen*[1], M. Oursler[2], T. C. Spelsberg[1]. [1]Biochemistry and Molecular Biology, Mayo Clinic, Rochester, MN, USA, [2]Endocrinology, Mayo Clinic, Rochester, MN, USA.

TGFβ inducible early gene-1 (TIEG) is a Krüppel-like transcription factor which was originally cloned in our laboratory from human osteoblasts and plays an important role in mediating TGFβ effects in these cells. TIEG1 over expression in human osteosarcoma (MG63) cells mimics TGFβ treatment. Our laboratory has also demonstrated that TIEG over expression in human osteoblasts enhances Smad signaling by down-regulating negative feedback through inhibitory Smad7. In order to understand the biological functions of TIEG in bone development, we generated TIEG knockout mice. $TIEG^{-/-}$ mice appeared to be normal with typical breeding patterns. To examine the role of TIEG in osteoblast differentiation, we isolated neonatal calvarial osteoblasts from $TIEG^{+/+}$ and $TIEG^{-/-}$ mice and cultured them *in vitro*. Interestingly, osteoblasts derived from $TIEG^{-/-}$ mice display a retarded differentiation with the inability to produce mineralized nodules *in vitro*, and repressed expression of important osteoblast differentiation marker genes. To better understand the actions of TIEG in osteoblast cells, we performed Affymetrix microarray analysis on $TIEG^{+/+}$ and $TIEG^{-/-}$ calvarial osteoblasts treated with vehicle or $TGFβ_1$ for 24 hours to assess the full impact of the loss of TIEG on osteoblast function. When osteoblasts derived from $TIEG^{+/+}$ were treated with $TGFβ_1$, 403 genes were repressed compared to 149 genes repressed by $TGFβ_1$ treatment in $TIEG^{-/-}$ osteoblasts. Interestingly, the reverse pattern occurs with the induction of gene expression by $TGFβ_1$ with 138 induced in the $TIEG^{+/+}$ osteoblast and 260 in the $TIEG^{-/-}$ osteoblast. This change to the induction of more genes in the $TIEG^{-/-}$ mice is not unexpected, since TIEG is reported to be a general repressor of transcription with minor cases of gene induction. The results further demonstrate that 21% of the genes were commonly regulated by $TGFβ_1$ in osteoblast cells by both the genotypes, suggesting that $TIEG^{-/-}$ may not play a role in the modulation of all TGFβ regulated genes. Interestingly, 47% and 32% are regulated exclusively either in the $TIEG^{+/+}$ and $TIEG^{-/-}$ osteoblast cells respectively. Overall, the elimination of TIEG causes the loss of 126 genes that are regulated by $TGFβ_1$. In conclusion, we believe that loss of TIEG in osteoblasts results in perturbation of most (but not all) $TGFβ_1$ regulated genes which, in part, might explain the defective differentiation in osteoblasts involving mineralized nodule formation *in vitro* and reduced expression of important osteoblast-specific genes.

Disclosures: ***M. Subramaniam****, None.*

F173

The Osteocyte-specific Antigen, E11, Is Responsive to Mechanical Loading in vitro and in vivo in Bone Distant from Maximal Strain. K. Zhang, K. Shiva*, L. Ye*, M. Dallas*, J. Feng, L. F. Bonewald. University of Missouri at Kansas City, Kansas City, MO, USA.

The earliest osteocyte-specific antigen as compared to osteoblasts is a membrane glycoprotein, E11/gp38, that appears to play a role in dendrite formation as the cells become embedded in osteoid. Although E11 is expressed in other tissues, it appears to be specifically post-translationally modified in osteocytes. To determine if mechanical loading could potentially affect dendrite formation, the regulation of E11 expression was examined both *in vitro* and *in vivo*. MLO-Y4 osteocyte-like cells respond to fluid flow shear stress at 4 and 16 dynes/cm^2 with an increase in E11 gene expression as determined by both northern analysis and gene arrays. To validate these *in vitro* observations, normal mice were used for immunohistochemical staining for E11 protein and for E11 gene expression, a mouse model in which the endogenous E11 promoter drives β-galactosidase expression was used. Compressive mechanical loads (-3.5 N, 30 sec, 2Hz), which induce bone formation, were applied to the right forearm of 3-month-old male mice (n=4). The mice were sacrificed at 4, 24, and 48 hrs after loading for Lac Z staining and at 24, 48, and 96 hrs for E11 immunostaining. The ulnae were fixed and cross-sectioned at 7 equidistant sections. Both positive and total osteocytes were counted for each section. At 4 hours after loading, there were significantly more LacZ(+) osteocytes at 5.5mm from the tip of the olecranon process (the elbow end) of loaded ulna than unloaded (4.8%±3.4% vs 1.4%±1.6%, p=0.02). There was no significant difference in other sections, including those with maximal strain, nor at 24 or 48 hours after loading. A significant increase in protein was observed at 24 hrs in the normal mice, not only in the 5.5mm section, but also in the 4.5 and 6.5mm sections.
In summary, increased E11 expression was observed in a level of the ulna that was subjected to lower, not maximal levels of strain. No significant differences were observed in areas of maximal strain. The majority of the positive osteocytes were near the bone surface, but mature osteocytes deep in the bone matrix also responded. If E11 is responsible for dendrite formation, embedded osteocytes can increase dendricity in response to strain. This raises the question of whether the osteocyte can modify and generate canaliculi when embedded in mineralized matrix.

Disclosures: ***K. Zhang****, None.*

F175

Bone Matrix Strain Is Amplified at Osteocyte Lacunae in Cortical Bone. D. P. Nicolella[1], D. M. Moravits*[1], J. Lankford*[1], L. F. Bonewald[2]. [1]Materials Engineering, Southwest Research Institute, San Antonio, TX, USA, [2]Oral Biology, University of Missouri at Kansas City, Kansas City, MO, USA.

Mechanical factors affect bone remodeling such that increased mechanical demand results in net bone formation, whereas decreased demand results in net bone resorption. Previous studies suggest that osteocytes, due to their location within the bone matrix, are the best candidates for sensing mechanical stress. The most prominent of the proposed mechanical signals are stress-generated fluid flow forces acting on cells and bone matrix deformation itself. *In-vitro*, bone cells are more sensitive to fluid flow than to substrate stretch in terms of their production of NO, PGE_2, and osteopontin. Typical maximal *in-vivo* strains in humans have been measured, and found to range from around 1,200 μ (principal compressive strain) to about 1,900 μ (maximum shear strain). In these experiments, strains were measured on the surface of the bone using a strain gage that covered an area of several square mm, which encompasses thousands of bone cells. Therefore, the strains measured are averages over the total area covered by the gage and yield no information regarding local variations in the strain field that necessarily must result from naturally occurring microstructural inhomogeneities such as osteocyte lacunae. However, it is these average levels of mechanical strain that are typically used in cell culture experiments to investigate the effect of mechanical strain on bone cell function. Thus, the purpose of this study was to quantify osteocyte perilacunar strain relative to globally applied strain levels. We directly measured perilacunar bone matrix strain in bovine cortical bone using a digital stereoimaging technique. The bone specimens were loaded in a specially designed microscopy load frame to increasing levels of global mechanical strain while the microstructure was observed and digitally imaged at high magnification using an optical microscope. At all global strain levels, average perilacunar strains were significantly greater compared to the globally applied bone strain with strain concentration factors ranging from 1.5-4.5, which are consistent with both numerical and analytical estimates. Furthermore, local peak bone matrix strains reach up to ten times the globally applied strain indicating the possibility of local bone matrix damage. These results suggest that osteocytes embedded within lacuna in cortical bone may experience significantly higher strains due to matrix deformation than previously estimated from *in-vivo* strain gage studies and can be used to guide the application of substrate strain in *in-vitro* cell culture investigations.

Disclosures: ***D.P. Nicolella****, None.*

F178

The Mechanism for IGF-I Resistance Induced by Skeletal Unloading Is Specific for IGF-I and Mediated by Down Regulation of the Integrin Signaling Pathway. S. Nishida, Y. Wang, H. Z. ElAlieh*, B. P. Halloran, D. D. Bikle. Endocrine Unit, University of Calfornia, San Francisco and Veterans Affairs Medical Center, San Francisco, CA, USA.

Skeletal unloading leads to decreased bone formation and decreased bone mass. These results can be explained in part by a failure of IGF-I to activate its signaling pathways in unloaded bone. In previous studies we demonstrated that the resistance to IGF-I was caused by its failure to activate its receptor. To determine whether this resistance is specific for IGF-I or common to all skeletal growth factors acting through receptor tyrosine kinase mechanisms, we compared the effect of IGF-1 and PDGF in a rat model using hindlimb suspension. We evaluated the response of osteoprogenitor cells isolated from the tibia and femur of suspended and control rats to IGF-I and PDGF treatment in vitro with respect to activation to IGF-I and PDGF signaling pathways, respectively. IGF-I (10ng/ml) did not increase bone marrow osteoprogenitor (BMOp) cell proliferation in bone marrow stromal cells (BMSC) taken from unloaded bone, whereas PDGF (1ng/ml) was fully effective. The ability of IGF-I and Des-IGF-I, which has little affinity for IGFBPs, to stimulate IGF-I receptor phosphorylation was blocked in BMSC from unloaded bones but not the ability of PDGF to stimulate PDGF receptor phosphorylation. Integrins are likely to serve as mechanical sensors in bone, and integrin activation is known to augment growth factor signaling. In recent studies we found that unloading resulted in decreased integrin expression. In this study we found that skeletal unloading reduced the activation (phosphorylation) of focal adhesion kinase (FAK), an important mediator of integrin signaling, without affecting its protein level. Echistatin, an inhibitor of integrin signaling, blocked IGF-I stimulated BMOp cell proliferation and IGF-I receptor phosphorylation but was much less effective in blocking these actions of PDGF. Our results indicate that the mechanism by which skeletal unloading leads to IGF-I resistance is specific for IGF-I, involves integrin signaling, and has little impact on the anabolic response to PDGF. These results suggest that PDGF, and, possibly other growth factors may be of clinical use in preventing and /or treating bone loss during immobilization and other forms of skeletal unloading.

Disclosures: ***S. Nishida****, None.*

F180

Global Analysis of 22,000 Genes in the Bones Reveals Involvement of Several Novel Genes/ESTs and Pathways in Mediating the Anabolic Response of Mechanical Strain in Mice *In Vivo*. W. Xing, D. J. Baylink, C. Kesavan*, H. Yu*, R. B. Chadwick, Y. Hu*, R. Rajkumar*, S. Mohan. JLP VAMC / LLU, Loma Linda, CA, USA.

To clarify the mechanisms and identify the genes responsible for mediating the effects of mechanical loading on osteogenesis, we evaluated differential gene expression on a global basis in the tibias of 10-wk old C57BL/6J (B6) females after 4 days of 4-point bending. We chose 4 point bending as a loading regimen based on our findings that it produces a robust bone anabolic response (15% increase in BMD after 2 wks, P<0.001) compared to other forms of loading in B6 mice. The right tibias of the mice were loaded at 9N, 2Hz for 36 cycles per day and the left tibias of the same mice were used as unloaded controls. RNA from the tibias harvested 24 hrs after last stimulation was subjected to oligonucleotide microarray-based analysis of 22,000 mouse genes. In total, 1074 genes/ESTs were significantly up- or down-regulated (N=5, t-test: p<0.05), of which, 741 are known and can be characterized into 120 biological processes. As expected, genes related to biological processes such as extracellular matrix synthesis, cell growth, cell adhesion, immune response and proteolysis were increased, thus validating the microarray data. Functional annotation of known genes and unknown genes/ESTs based on functional motifs revealed several interesting and unique findings: 1) Of the known genes, 27 exhibit kinase activity (e.g.. CDK2,PTK2, CDC42) and 34 exhibit receptor activity (e.g. PDGF, BMP, toll-like). These findings suggest that multiple pathways are stimulated in this large response to loading in bone. In this regard, several growth factor genes (e.g. pleiotrophin, osteoclycin, PDGFα, inhibinβ, IL25, nephroblastoma overexpressed gene) that have not been previously implicated in mechanical loading pathway have been identified as mediators of mechanical stress; 2) Of the 1074 significantly expressed genes, 31% express EST clones, some of which contain functional domains such as LIM, cysteine-rich protein and leucine-rich repeats, which are characteristics of motifs found in transcription factors, suggesting that future studies on these ESTs are essential for complete understanding of the molecular pathways for mechanical loading; 3) Pathway analysis revealed involvement of both well known (Integrin, Wnt, Calcium channels) and less known (Orphan GPCR, small ligand GPCR, apoptosis) pathways in mediating the effects of loading in bone. Conclusions: 1) This is the first study to examine the in vivo effect of mechanical loading on differentially expressed genes in the whole genome; 2) We have identified a number of novel genes, ESTs and pathways that have not been previously implicated to play a role in mechanical loading.

Disclosures: ***W. Xing****, None.*

F182

In-vivo Site-Specific Correlation of Dentin Matrix Protein 1 (DMP1) and Matrix Extracellular Phosphoglycoprotein (MEPE) Gene Expression: Effect of Overload. J. Gluhak-Heinrich*[1], S. P. Kotha*[2], L. F. Bonewald*[2], M. B. Schaffler*[3], S. E. Harris*[4]. [1]Ortho., Univ. of TX Health Sci. Ctr at San Antonio, San Antonio, TX, USA, [2]Oral Biol., Univ. of MO at Kansas City, Kansas City, MO, USA, [3]Orthopedics, Mount Sinai School of Medicine, New York, NY, USA, [4]Perio., U of TX Health Sci Ctr at San Antonio, San Antonio, TX, USA.

Osteocytes are thought to play critical roles in translating mechanical stimuli into signals that regulate mineralization, bone formation and resorption. In response to mechanical loading, we have previously shown increased gene expression of an acidic glycoprotein, DMP1, which may function to modulate mineralization. Another sibling protein that modulates and organizes the mineralization process, MEPE, may also play a role in osteocyte function. We sought to determine if there is a site-specific correlation between DMP1 and MEPE gene expression in normal bone and in bone subjected to overload. We used the rat ulnae fatigue model to mechanically stimulate osteocytes and correlate the magnitude of DMP1 to that of MEPE gene expression. After loading, (20 N, 4 Hz, 30% stiffness loss), expression of DMP1 and MEPE mRNA was assessed at day 1 and day 2 by quantitative in situ hybridization using P32 labeled RNA probes. Transverse cross-sections of control and loaded bones were analyzed from the mid-shaft and both proximally and distally in 0.75mm sections. Each section was divided into 100-150 segments. Gene expression in each segment was normalized by the number of osteocytes in that area. DMP1 and MEPE gene expression in loaded bones were compared to an equivalent segment in control bone and with each other. The results indicate that maximum increases in DMP1 and MEPE gene expression occurred at a section that was about 2-3mm distal to the ulnar mid-shaft. In these sections, the in-plane magnitudes of DMP1 and MEPE gene expression per osteocyte in the loaded ulnae were 1.9 and 3.2 times higher than in the control ulnae. The magnitude of changes in DMP1 and MEPE expression per osteocyte due to loading were similar indicating the same number of increased mRNA molecules after loading ($r2 = 0.67$; $p<0.001$). There were numerous segments with differential expression, where there was a larger increase in expression of DMP1 than MEPE. When combining data of both the loaded and control bone, DMP1 expression was highly correlated with MEPE ($r2 = 0.56$; $p<0.001$). Our results suggest that in response to loading, osteocytes may alter their microenvironment by causing site-specific changes in mineralization through increases in DMP1 and MEPE expression. These modifications could then alter the dynamics of fluid flow through bone with important implications for osteocyte survival, bone formation and resorption.

Disclosures: ***J. Gluhak-Heinrich****, None.*

F185

Changes in Vigorous Physical Activity Predict Bone Mineral Content in Young Children: The Iowa Bone Development Study. K. F. Janz*[1], S. M. Levy[2], T. L. Burns*[3], J. C. Torner*[4], M. C. Willing[5], J. M. Gilmore*[2], T. A. Marshall*[2]. [1]Health and Sport Studies, University of Iowa, Iowa City, IA, USA, [2]Preventive and Community Dentistry, University of Iowa, Iowa City, IA, USA, [3]Program in Public Health Genetics, University of Iowa, Iowa City, IA, USA, [4]Epidemiology, University of Iowa, Iowa City, IA, USA, [5]Pediatrics, University of Iowa, Iowa City, IA, USA.

Longitudinal observational studies during childhood have the potential to define the natural history of bone development and may provide insight into the prediction of future bone health. To examine whether changes in everyday physical activity predict bone mineral content (BMC, g) and accrual, we assessed physical activity (PA, min/d) and BMC at age 5.3 yr (SD $\pm$ 0.4) and again at age 8.6 yr (SD $\pm$ 0.6) (3-yr interval) in a cohort of Iowa children. PA was measured using whole-day accelerometry (MTI uniaxial) and described as frequency of sedentary, moderate, and vigorous movement. BMC of the hip, spine, and whole body was measured with a Hologic 2000 DXA. Associations were examined using partial correlation coefficients, stepwise linear regression, and general linear models. Age, gender, and body size were included as covariates. Change in BMC analyses also included adjustment for baseline BMC.

Partial Correlation Coefficients

p<0.01 unless NS=not significant		Hip BMC	Spine BMC	Whole Body BMC
* Baseline n=430	Vigorous PA	0.29*	0.20*	0.17*
** Follow-up n=454	Vigorous PA	0.22*	0.12*	0.14*
***Change n=342	Vigorous PA	0.13*	NS	0.14*

* Baseline BMC and PA, controlling for sex and baseline age, weight, height.
** Follow-up BMC and PA, controlling for sex and follow-up age, weight, height.
***Follow-up BMC (adjusted for baseline BMC) and change in PA, controlling for sex and baseline age, weight, height, and change in age, weight, height.

Vigorous PA was consistently and positively associated with BMC, whereas sedentary and moderate PA were not. Vigorous PA explained 1.4 to 8.2% of the variance in BMC ($p<0.05$), except change in spine BMC ($p\geq0.05$). Children who increased their vigorous activity, on average, by 8 min/d between baseline and follow-up had a follow-up whole body BMC that was 2% greater than less active peers. Even without targeted bone loading or extraordinary amounts of PA, young children who engage in vigorous PA are likely to have more BMC and likely to accrue more BMC than peers. Results are potentially important since observational studies are needed for public health recommendations that set realistic levels of exercise for children based on potential benefits.

Disclosures: ***K.F. Janz****, None.*

F187

Estrogen Does Not Modulate the Sensitivity of the Bones to Mechanical Loading. I. Pajamaki*[1], H. Sievanen*[2], P. Kannus*[1], T. Vuohelainen*[1], T. L. N. Jarvinen[1]. [1]Department of Orthopaedics and Traumatology, University of Tampere, Tampere, Finland, [2]UKK Institute, Tampere, Finland.

Estrogen, the primary non-mechanical regulator of the female skeleton, is believed to have a permissive role on the osteogenic effects of mechanical loading. In essence, it has been proposed that the mechanical loading-induced osteogenic response is dependent either on oestrogen or ER-α. To determine whether estrogen and loading are indeed coupled in the regulation of skeletal integrity, we first subjected 30 three-week-old female rats either to sham-operation (E^+) or ovariectomy (E^-). We then removed loading from the left hind limb of each rat by cast immobilization (L^-), while the right limb served as a non-immobilized control (L^+). After an 8-week period of unloading, a comprehensive analysis of the femoral neck of both limbs was carried out using peripheral quantitative computed tomography and mechanical testing.

As readily evident in the figure below, the bone mineral content (BMC: -42% in E^+ and -35% in E^-, both $p<0.001$) and cross-sectional area (CSA: -46% in E^+ and -40% in E^-, both $p<0.001$) were significantly reduced in the immobilized legs in both estrogen-replete (E^+) and -deplete (E^-) rats (**A-B**). Similarly, a profound decrease was observed in the fracture load of the immobilized legs in the E^+ (Fmax: -25%, $p=0.002$) and the E^- (-35%, $p<0.001$) groups, respectively (**C**). Despite the apparent stimulatory effect of estrogen on BMC ($p=0.025$ for the interaction, **B**), there was no difference between the estrogen-replete (E^+) and -deplete (E^-) rats in the CSA or Fmax (**A** and **C**).

The results of this study show that despite an apparent modulatory effect of estrogen on the mechanical loading-induced bone mass accrual, estrogen had no effect on fracture load, and accordingly, the skeletal sensitivity to mechanical loading. This finding actually emphasizes the importance of choosing the most appropriate final outcome - bone strength - for analysis, instead of only measuring some surrogates or determinants of bone strength.

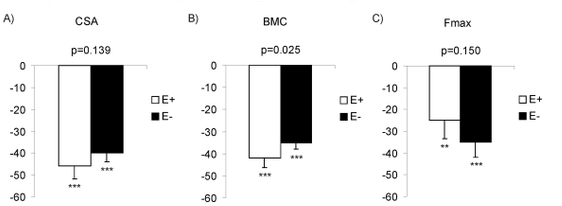

Figure: The unloading-induced reduction in the (A) total cross-sectional area (CSA), (B) the bone mineral content (BMC), and (C) the fracture load (Fmax) of femoral neck in estrogen-replete (E+, blank bars) and estrogen-deplete (E-, solid bars) rats. Bars represent percent (%) deficit of the unloaded group compared with the contralateral, normally loaded control group. Significant differences between unloaded and control limb are indicated: **p<0.01, ***p<0.001.

Disclosures: ***I. Pajamaki****, None.*

F191

Sympathetic Nervous System Is Involved in Both Unloading -Induced Suppression of Bone Formation Rate and Unloading-Induced Enhancement in Osteoclast Surface in Vivo. H. Kondo[1], K. Tsuji[1], K. Kitahara[1], S. R. Rittling[2], A. Nifuji[1], D. T. Denhardt[3], S. Takeda[1], G. Karsenty[4], M. Noda[1]. [1]Molecular Pharmacology, Tokyo Medical and Dental University Medical Research Institute, Tokyo, Japan, [2]Cell Biology and Neuroscience, Rutgers University, Piscataway, NJ, USA, [3]Cell Biology and Neuroscience, Rutger University, Piscataway, NJ, USA, [4]Molecular and Human Genetics, Baylor College of Medicine, Houston, TX, USA.

Unloading in bed ridden patients decreases bone mass and causes osteoporosis which is a major problem in the modern aging society. However, the mechanisms underlying such unloading-induced bone loss have not been yet fully understood. Sympathetic nervous system has been reported to suppress bone formation. This paper examines whether sympathetic nervous system is involved in alteration of the bone formation activity as well as bone resorption activity in mice subjected to tail suspension (TS). We conducted TS experiments using adult mice treated with vehicle or antagonist or agonist of β-adrenergic receptors. In vehicle treated control mice, TS reduced mineral apposition rate (MAR) as well as bone formation rate (BFR) as reported previously. Propranolol (PRO), a β-adrenergic blocker, treatment blocked the TS-inducded suppression of MAR and BFR, corresponding to the PRO blockage against TS-induced suppression on cancellous bone volume (BV/TV). Another β-adrenergic antagonist, Guanethidine sulfate (GS), which depletes storage of norepinephrine, also blocked the TS-induced suppression of MAR and BFR, again corresponding to the GS block of TS-induced bone loss. Isoproterenol (ISO), a β-agonist, treatment by itself reduced MAR and BFR in loaded group, similarly to the TS-induced suppression. In the presence of ISO, TS failed to further suppress BFR and MAR, corresponding to the failure of TS to further suppress BV/TV when ISO was administered. Bone marrow cells (BMCs) were taken after TS of mice treated with PRO in vivo and cultured. Nodule formation (NF) was suppressed by TS. In contrast, PRO treatment in vivo blocked the TS-induced suppression of NF levels. Osteoclast surface (OcS) in these mice was increased by TS in vehicle treated mice while this TS enhancement was blocked by the treatment with PRO during TS. GS treatment also blocked TS-induced increase in OCs. ISO treatment in vivo increased osteoclasts development in BMCs culture in loaded group, similarly to TS. After ISO treatment, there was no further increase in osteoclast development even after TS. These observations indicated that both TS suppression of osteoblastic activity as well as TS enhancement in osteoclastic activity in vivo are both mediated through β-adrenergic pathway.

Disclosures: ***H. Kondo****, 21st Century COE Program 2.*

F194

Insulin-like Growth Factor II (IGF-II) Induces Apoptosis in Osteoblasts. W. Zhang, M. McCarthy*, H. Zhang, G. Gronowicz. Orthopedic Surgery, Uconn Health Center, Farmington, CT, USA.

Insulin-like growth factor II (IGF-II) is an important growth factor produced in bone and is more prevalent in human osteoblasts than IGF-I, but its function in bone metabolism is not well known. In this study, the ability of IGF-II to modulate apoptosis was investigated in primary osteoblast cultures. At 72 h of culture, 0.01, 0.1 and 1.0 nM IGF-II produced a dose-dependent increase in apoptosis assayed by TdT-mediated dUTP-biotin nick end labeling (TUNEL) and was confirmed with acridine orange/ethidium bromide staining in primary murine osteoblast cultures. A maximal increase of 5.0-fold above control was found with 1 nM IGF-II. A time course of treatment with 0.1 nM IGF-II demonstrated a significant increase in apoptosis compared to vehicle-treated cells by 48 h. IGF-II-induced apoptosis could not be inhibited by a blocking antibody to the IGF-I receptor during 72h of treatment with 0.01, 0.1, or 1 nM of IGF-II. Primary human osteoblast cultures demonstrated a similar dose-dependent increase in apoptosis with IGF-II treatment, with a 4-5 fold maximal increase in apoptosis after 72h treatment with 1.0 nM IGF-II. No significant effect of IGF-II was found on proliferation in murine osteoblast cultures. Western blot analysis demonstrated that IGF-II decreased Bcl-2 protein levels but not Bax resulting in a significant reduction in the Bcl-2/Bax ratio. To determine if overexpression of Bcl-2 could block IGF-II-induced apoptosis, osteoblasts were isolated from a transgenic mouse that overexpresses human Bcl-2 in bone through a construct utilizing the 2.3 kb promoter region of the Type I collagen gene linked to a 1.8kb region of human Bcl-2 cDNA (Col2.3Bcl-2). At 72h, IGF-II significantly increased apoptosis in a dose-dependent manner in the osteoblast cultures from the wild type littermates. In osteoblasts from Col2.3Bcl-2 mice, no significant effect on apoptosis was found with 0.01, 0.1 or 1.0 nM IGF-II. Western blot analysis of Bcl-2 and Bax levels demonstrated a transient decrease in the Bcl-2/Bax ratio at 24 h with no decrease in the ratio at 48 h or 72 h. Thus, IGF-II appears to promote osteoblast apoptosis, and overexpression of Bcl-2 is able to block IGF-II-induced apoptosis.

Disclosures: ***W. Zhang****, None.*

F199

Identification of the Spliced Variant of CAPRI as a Critical Regulator of RANKL Shedding. A. Hikita*[1], H. Yasuda[2], K. Nakamura[1], H. Oda[1], S. Tanaka[1]. [1]Department of Orthopaedic Surgery, The University of Tokyo, Tokyo, Japan, [2]Institute of Medical Science, The University of Tokyo, Tokyo, Japan.

Accumulating evidence has demonstrated an essential role of RANKL (receptor activator of NF-kappa B ligand) in osteoclast differentiation and activation. RANKL is made as a membrane-anchored precursor, which is released from the plasma membrane by enzymatic shedding. However, the molecular mechanism and physiological/pathological importance of RANKL shedding have not been clarified yet.

To identify essential molecules for RANKL shedding, we constructed an assay system for expression screening. Plasmids encoding SEAP (secreted placental alkaline phosphatase) fused with partial cDNA of mouse RANKL containing stalk region was constructed, and co-transfected to 293T cells together with subpools of cDNA library of ST2 cells. RANKL-shedding activity was detected as AP activity in the supernatant, and positive subpools were partitioned into smaller subpools, and positive clones were sequenced.

One of the positive clones we identified was the splice variant of CAPRI (Ca^{2+}-promoted Ras inactivator), a novel member of RAS-GAP (GTPase-activating protein) which .is activated in response to Ca^{2+} stimuli and suppresses Ras activity. The splice variant (ΔCAPRI) lacks GAP-related domain, indicating that it works in a dominant negative fashion. ΔCAPRI expression was detected in primary osteoblasts, and overexpression of ΔCAPRI efficiently induced RANKL shedding as does activated mutant of Ras, while wild type CAPRI did not stimulate RANKL shedding. Stimulation with Ca ionophore induces the membrane translocation of wild type CAPRI, while ΔCAPRI remains at the cytoplasm. These results indicate the regulatory action of Ras pathways in RANKL shedding, and CAPRI-ΔCAPRI is a critical modulator of Ras activity.

In conclusion, we established an efficient assay system to identify the molecules involved in RANK shedding, and found that CAPRI-ΔCAPRI system is a critical regulator.

Disclosures: ***A. Hikita****, None.*

F202

Androgens Inhibit Osteoclast Activity In AR-Transgenic Mice Through Reductions In RANKL/OPG Ratio. K. Wiren[1], A. Toombs*[1], V. Kasparcova*[2], S. Harada[2], X. Zhang[1]. [1]VA Medical Center, Oregon Health & Science Univ, Portland, OR, USA, [2]Merck Research Laboratories, West Point, PA, USA.

Our appreciation of the physiological functions of androgens has been changing. We recently characterized transgenic mice with AR overexpression in the osteoblast lineage under control of type I collagen promoter (col3.6 AR-transgenic mice), demonstrating proof of principle for the specific importance of androgen transactivation of AR directly in bone. Static and dynamic histomorphometric analysis in male AR-tg mice revealed site-specific effects on bone formation consistent with an anti-resorptive response. Characterization of gene expression by quantitative RT-PCR (qRT-PCR) in RNA isolated from tibial mid-diaphysis demonstrated reduced expression for osteoclastic genes including cathepsin K, RANKL and TRAP, while OPG expression was increased in males. Increased OPG serum levels were also observed. Since these results suggest osteoblast lineage-mediated inhibition of osteoclast activity, we characterized androgen control of osteoclastogenesis using a coculture system with monocytic RAW 264.7 cells as osteoclast precursors and col3.6 AR-MC3T3 cultures as a model of enhanced androgen responsiveness for osteoblasts. Cultures were treated with vehicle, 10^{-8}M DHT or soluble recombinant RANKL (50 ng/ml) alone, or DHT and sRANKL in combination. TRAP+ multinucleated cells containing 3 or more nuclei were considered formation of osteoclast-like cells. After 7 days, DHT inhibited osteoclast formation over 50% (P<0.001). The effects of DHT were abrogated with coadministration of sRANKL. The response in coculture with control ß-gal MC3T3 (no AR overexpression) demonstrated the same pattern but with reduced androgen efficacy. To evaluate the stage of osteoblast differentiation mediating androgen inhibition of osteoclastogenesis, OPG and RANKL mRNA was assayed using qRT-PCR at day 5 (proliferating preosteoblasts) and day 25 (osteocytic) colAR-MC3T3 cells, and with the osteocyte-like cell line MLO-Y4 (transiently transfected with an AR expression construct). Consistent with the effects in vivo, DHT inhibited RANKL but stimulated OPG gene expression in MLO-Y4 cells and day 25 colAR-MC3T3 osteoblastic cells. In contrast, in day 5 proliferating osteoblasts RANKL expression was undetectable while OPG expression was inhibited. These results demonstrate that inhibition of osteoclastogenesis occurs primarily by suppression of RANKL and/or elevation of OPG in mature osteoblasts. Collectively, these findings demonstrate that androgen signaling through the AR in bone directly influences osteoblast-osteoclast signaling and offers valuable insight into the role of androgen in bone homeostasis.

Disclosures: ***K. Wiren****, None.*

F207

Transgenic Expression of Constitutively Active Mutant Estrogen Receptor-alpha (CAMERA) in Osteoblasts Leads to Increased Trabecular Bone Mass. N. Quibria*[1], R. Fajardo*[2], J. deSilva*[2], J. M. Alexander[3]. [1]ACCESS Program, University of California, Los Angeles, CA, USA, [2]Orthopedic Biomechanics Laboratory, Beth Israel Deaconess Medical Center, Boston, MA, USA, [3]Physiology Department, Tufts University, Boston, MA, USA.

This study examines targeted expression of a **c**onstitutively **a**ctive **m**utant **e**strogen **r**eceptor-**a**lpha [CAMERA] in osteoblasts and its developmental effects on bone formation and phenotype in transgenic Swiss-Webster mice. Using cell-based gene activity assays, we characterized human ERα point mutations that result in nearly 100% constitutive transcriptional activity of ERα in the absence of hormone. After *in vitro* characterization, the CAMERA structural gene was cloned downstream of a 1.3 kb 5' flanking region of the mouse osteocalcin (mOC) gene to target its expression to osteoblasts. Transgenic Swiss-Webster lines expressing the mOC/CAMERA transgene were established, and their bone mineral density and structure were investigated using Piximus and microCT analysis, respectively. Both analytical methods demonstrated that transgenic females have significantly higher bone densities than age-matched non-transgenic Swiss-Webster mice. Piximus scanning documented consistent increases in overall BMD compared with non-transgenic females at both the femur (mean 22% increase) and lumbar spine (mean 24% increase). A microCT analysis revealed that trabecular BV/TV was dramatically increased in transgenic females (mean, 93% Tb BV/TV) compared to non-transgenic females (mean, 27% Tb BV/TV). At the femoral diaphysis, transgenic animals had significantly greater cortical thickness (mean Ct.Th, 0.380mm) compared to wildtype controls (mean Ct.Th, 0.230mm). Furthermore, transgenic females exhibited endosteal trabecular bone formation at the mid-shaft that resulted in dramatic increases in endosteal bone volume (mean, 70% endosteal BV/TV) compared to wildtype females who have no trabecular bone at the mid-shaft. To investigate the ability of the CAMERA transgene to protect against hormone deficient bone loss, transgenic females were ovariectomized (OVX) at 12 weeks of age, and bone parameters were examined 4 weeks later at 16 weeks of age. Despite the obvious developmental effects of the CAMERA transgene on overall bone density and structure, transgenic animals were only partially protected against post-OVX bone loss. Trabecular BV/TV in transgenic females decreased 55% after 4 weeks post-OVX compared to a 73% trabecular bone loss in wildtype females. We continue to evaluate this transgenic line for new insights regarding the mechanisms of action of ERα on bone physiology and post-OVX bone loss.

Disclosures: ***J.M. Alexander****, None.*

F212

Wnt3a Regulates Induction of Id1 gene Expression by Bone Morphogenetic Protein 2 in Osteoblastic Differentiation. A. Nakashima*[1], T. Katagiri[2], M. Tamura[1]. [1]Department of Biochemistry and Moleculer Biology, Graduate School of Dental Medicine, Hokkaido University, Sapporo, Japan, [2]Division of Pathophysiology, Research Center for Genomic Medicine, Saitama Medical School, Hidaka, Japan.

It has been shown that loss of function of the Wnt corecepter, LRP5, in both humans and mice leads to decreased bone formation and bone mass, and a point mutation in this gene results in high bone mass, indicating the crucial role that Wnt/LRP5 signaling plays in bone formation. However, the exact signaling mechanisms by which Wnt members regulate bone formation remain to be elucidated. In this study, we examined a potential role for Wnt/LRP5 in osteoblast differentiation and functional cross-talk of bone morphogenetic protein (BMP) 2. To assess the functional contribution of Wnt, we generated a C2C12 cell line overexpressing Wnt3a, Wnt5a or the activated form of β-catenin and treated these cells with BMP2 for 24 h. The Id1 mRNA level induced by BMP2 decreased in the stable Wnt3a-expressing cells. In contrast, Wnt5a did not alter the Id1 mRNA level induced by BMP2. We show that this suppression is mediated by a 29-bp GC rich region of the BMP2-response element (BRE) of the human Id1 gene promoter. A novel interaction between Smad1, 4 and Tcf1 in the BRE was identified and found to be crucial for Wnt-mediated suppression of the BMP2 response in C2C12 cells. Overexpression of Dkk1 or the truncated secretary form of LRP5 inhibits this suppression, whereas Dkk2, Dkk3 or Dkk4 did

not alter the suppression. In contrast, neither Smad1, Smad4 nor BMP2 up-regulated activated β-catenin-induced Tcf-1-dependent transcriptional activity. Nevertheless, Smad4 lead to activation of Tcf-1 dependent transcriptional activity in C2C12 cells. These results identify a novel mechanism by which Wnt/LRP5 regulates the BMP2-response in osteoblastic differentiation, and is the first study linking Id1 expression to Wnt/β-catenin signaling. Thus, these results demonstrate the link between Wnt and BMP signaling in osteoblastic differentiation.

Disclosures: ***A. Nakashima****, None.*

F214

C/EBP Homologous Protein (CHOP, Ddit3) Interacts with Smads and Enhances Smad and Wnt Signaling. R. C. Pereira, V. Deregowski, S. Rydziel, E. Canalis. Research, Saint Francis Hospital and Medical Center, Hartford, CT, USA.

CCAAT/enhancer binding proteins (C/EBPs) play important roles in cell fate and gene regulation. C/EBP homologous protein (CHOP, Ddit3) forms heterodimers with classic C/EBPs, preventing their binding to target DNA sequences, but CHOP can also interact with additional transcription factors. We demonstrated that CHOP suppressed adipogenesis and induced osteoblastogenesis by enhancing the effect of bone morphogenetic protein (BMP)-2. To assess mechanisms involved in the induction of osteoblast differentiation by CHOP, we examined its effect on BMP and Wnt signaling pathways in permanently transduced ST-2 cell lines overexpressing CHOP under the control of the CMV promoter. CHOP overexpression did not modify the basal activity of a transiently transfected BMP-responsive 12xSBE-Oc-pGL3 construct, containing 12 repeats of a Smad binding site directing luciferase expression. However, CHOP amplified markedly the effect of BMP-2 on the activity of the construct and the effect of BMP was 6 fold greater in the presence than in the absence of CHOP. Transfections of mutant Smad 1 or 5 constructs with dominant negative properties, significantly decreased the effect of CHOP on BMP-2 induced transactivation of 12xSBE-Oc-pGL3 construct. BMP-2 induced Smad 1/5/8 phosphorylation, but CHOP overexpression did not modify the level of phosphorylated Smad 1/5/8 in control or BMP-2 treated cells. However, co-immunoprecipitation experiments in nuclear extracts from CHOP overexpressing cells transfected with Smad 1 and 5 expression constructs and treated with BMP-2 revealed that Smad 1/5 associated with CHOP. Although BMPs can activate mitogen activated protein (MAP) kinases in osteoblastic cells, BMP-2 had no significant effect on the phosphorylation of the MAP kinases ERK, p38 or JNK, and these were not modifed by CHOP. Furthermore, CHOP overexpression did not modify the transactivation of a construct in which seven AP-1 recognition sequences direct the expression of luciferase, confirming no involvement of the MAP kinase pathway. The results indicate that BMP modulates osteoblastic differentiation via the Smad signaling pathway and that CHOP associates with Smads enhancing their interactions with DNA recognition sequences. CHOP overexpression also increased the activity of the Wnt/ß-catenin pTOP-FLASH responsive construct, containing 3 copies of the Lef 1/Tcf4 binding sequences, by 3 fold. In conclusion, CHOP interacts with Smad 1/5 and enhances osteoblastic differentiation by sensitizing the BMP/Smad and the Wnt/ß-catenin signaling pathways, but not the MAP kinase pathway.

Disclosures: ***R.C. Pereira****, None.*

F216

Discovery of Genomic Sites Occupied by RUNX2 in Living Osteoblasts. A. Barski[1], S. K. Pregizer*[1], B. Frenkel[2]. [1]Biochemistry and Molecular Biology, University of Southern California, Los Angeles, CA, USA, [2]Orthopaedic Surgery, University of Southern California, Los Angeles, CA, USA.

The transcription factor Runx2 is considered a master gene for osteoblast differentiation. Although some transcriptional targets for Runx2 are known, it is believed that the osteogenic action of Runx2 requires additional target genes. However there is no established method for unbiased discovery of genomic sites directly occupied by transcription factors of interest. Therefore, we developed a novel approach, Chromatin Immunoprecipitation (ChIP) Display (CD), which allowed us to identify several novel Runx2 target genes. The CD technique was successfully employed with a robustly mineralizing MC3T3-E1 osteoblastic subclone. Cells were subjected to ChIP with Runx2 antibodies, resulting in a precipitate containing Runx2 targets, but also the inevitable vast excess of non-specifically co-precipitated DNA. This background makes problematic identification of Runx2 targets by direct cloning of immunoprecipitated fragments. To overcome this obstacle, fragments containing Runx2 targets were effectively concentrated using restriction digestion with *Ava*II, which brought all the fragments representing any one target to a unique size. Furthermore, following linker ligation, the immunoprecipitated DNA fragments were PCR amplified in distinct families, segregated based on the identity of two nucleotides in the vicinity of the *Ava*II sites at the ends of each fragment. This results in improved signal-to-background ratio for each target because all fragments containing any given target are amplified within its respective family, while all other DNA fragments, mostly background, are scattered between different families. Indeed, upon gel electrophoresis, fragments representing true Runx2 target genes formed distinct bands. In contrast, the non-specifically precipitated DNA resulted in a background smear formed by fragments of diverse sizes. Bands of interest were excised, and the DNA fragments were identified by sequencing and comparison to genomic databases. Our initial CD experiments identified several novel Runx2 targets, including both well known and novel genes i.e. the transcription factors Fli1 and Runx3 and less well-known genes ORP8 and a novel EST homologous to the DYRK1 kinase. These genes were confirmed as Runx2 targets using conventional ChIP assay. Promoter-reporter assays and RNA analysis of BMP-2-treated cells further establish ORP8, a member of the oxysterol-binding protein family, as a functional Runx2 target. In principle, CD can facilitate the discovery of novel target genes for any DNA binding protein.

Disclosures: ***A. Barski****, None.*

F218

Smad1 Binding to the Dlx5 Promoter Is Responsible for the BMP-2-Induced Dlx5 Expression. H. Park*[1], Y. Kim*[1], B. Kim*[1], H. Shin[2], J. Cho*[1], H. Ryoo[1]. [1]Department of Biochemistry, School of Dentistry and Skeletal Disease Genome Research Center, Kyungpook National University, Daegu, Republic of Korea, [2]Department of Oral Pathology, School of Dentistry, Kyungpook National University, Daegu, Republic of Korea.

Bone morphogenetic protein (BMP)-2, a member of transforming growth factor (TGF) β superfamily, is well known by its ability to induce ectopic bone formation *in vivo* and osteoblastic transdifferentiation from non-skeletal cells *in vitro*. Our previous results indicated that Dlx5 is an indispensable regulator of BMP-2-induced transdifferentiation in myoblastic C2C12 cells. However, little is known about the molecular mechanism by which BMP-2 regulates Dlx5 promoter. In this study, to identify BMP responsive elements (BRE), we established a series of 5' deletion constructs of the mouse Dlx5 promoter region; Dlx5P-3kb, Dlx5P-2kb, Dlx5P-1kb, Dlx5P-0.9kb, and Dlx5P-0.2kb which contain the -2935, -1928, -965, -774, and -94 to +123 region of the mouse Dlx5 promoter, respectively. BMP-2 treatment or cotransfection of the Smad1 expression vector with the promoter deletion constructs to C2C12 cells indicated that BMP response region is between +47 to +61 nucleotide of the Dlx5 transcription initiation site. By sequence analysis, we identified Smad1 binding consensus motifs (5'GCCGNCGC3') in the region. Site directed mutagenesis of the Smad1 binding consensus motifs in Dlx5P-1kb resulted in a complete abrogation of the BMP2- or Smad1- induced promoter activation. Furthermore, gel mobility shift assays indicated that the putative binding sites effectively interact with Smad1 as sequence specific manners. These results indicated that BMP-2 activated Smad1 mediates the transcription of Dlx5 through the direct binding to the cognate cis-acting element in Dlx5 promoter.

Disclosures: ***H. Ryoo****, None.*

F220

Selective *Runx*2-II Deficiency Differentially Affects Endochondral, Cortical and Intramembranous Bone Formation in Adult Mice. Z. Xiao[1], H. Awad*[2], S. Liu[1], F. Guilak*[2], L. D. Quarles[1]. [1]Internal Medicine/Kidney Institute, University of Kansas Medical Center, Kansas City, KS, USA, [2]Orthopaedic Surgery, Duke University Medical Center, Durham, NC, USA.

The *Runx*2 gene transcribes the "bone-related" *Runx*2-II and *Runx*2-I isoforms that differ only in their N-termini. *Runx*2 is essential for osteoblast differentiation. Homozygous mice lacking both isoforms die at birth and lack a mineralized skeleton. In contrast, selective deletion of the *Runx*2-II isoform results in a less severe skeletal phenotype in newborn mice characterized by a greater impairment of endochondral bone formation compared to the mild defects in intramembranous and cortical bone formation. In this study we determined the post-natal effects of selective *Runx*2-II deficiency. We performed bone mineral density (BMD), micro-computer tomography (μCT), and 3-point bending biomechanical testing of femurs as well assessed biochemical markers in wild-type (WT), *Runx*2-II heterozygous ($^{+/-}$) and null ($^{-/-}$) mice up to 24-weeks of age. WT mice exhibited an age-dependent increase in bone mass due to an increase in cortical bone (BV/TV% 21.2±1.4 vs 14.5±1.2, Ct.Th 0.18±0.01 vs 0.24±0.01 mm and BMD 0.061±0.001 vs 0.086±0.001 g/cm^2 at 6 and 24 weeks, respectively). These changes were associated with reduced osteoclastic and osteoblastic markers (deoxypyridinoline (DPD) 126±11 vs 34±3 ηmol/mmol creatinine, osteocalcin (Osc), 451±51 vs 114±10 ηg/ml at 6 and 24 weeks, respectively). There were also significant age-dependent increases in bending strength (Fmax) and flexural rigidity (EI) of femurs in WT mice (Fmax, 25.1±5.4 vs 37.8±6.4 N; EI, 125.2±32.2 vs 242.2±44.0 at 6- and 24-weeks, respectively). *Runx*2-II $^{-/-}$ mice did not survive past 8 weeks, whereas survival in *Runx*2-II$^{+/-}$ was identical to WT littermates. Compared to WT mice, 6-week-old *Runx*2-II $^{+/-}$ had reduced BV/TV% (14.8±1.4), Ct.Th (0.16±0.01mm) and BMD (0.057±0.001 g/cm^2), but no difference in DPD or Osc, whereas *Runx*2-II $^{-/-}$ had severe reductions in BV/TV% (7.1±1.7), Ct.Th (0.11±0.01), and BMD (0.037±0.002) associated with reduced Osc (107±56) but not DPD (121±24). These changes were associated with significant reductions in Fmax (18.7±3.3 and 8.1±2.7 N) and EI (89.2±16.1 and 27±8) in *Runx*2-II $^{+/-}$ and *Runx*2-II $^{-/-}$ mice, respectively. Although 24-week-old *Runx*2-II $^{+/-}$ mice had persistently reduced BV/TV%, Osc levels and impaired mechanical strength, these mice normalized both femoral Ct.Th and BMD. These studies suggest that *Runx*2-II has differential effects on trabecular and cortical bone formation, possibly reflecting a site-specific function of *Runx*2-II in osteoblasts derived from sites of endochondral ossification.

Disclosures: ***Z. Xiao****, None.*

F222

Increase of Bone Mass in Dominant-Negative Runx2 Transgenic Mice. T. Komori[1], T. Furuichi*[1], R. Fukuyama*[1], T. Fujita[2], S. Toyosawa*[3], K. Yamana*[4], N. Kanatani*[1]. [1]Department of Developmental and Reconstructive Medicine, Nagasaki University, Nagasaki, Japan, [2]Department of Pharmacology, Setsunan University, Hirakata, Japan, [3]Department of Oral Pathology, Osaka University, Osaka, Japan, [4]Teijin Institute for Biomedical Research, Teijin Ltd., Hino, Japan.

Runx2-deficient mice completely lack osteoblasts, demonstrating that Runx2 is an essential transcription factor for osteoblast differentiation. Further, previous in vitro and in vivo studies showed that Runx2 plays an important role in the expression of major bone matrix protein genes. As Runx2-deficient mice die after birth, the role of Runx2 in postnatal bone development remains to be clarified. We pursued this issue using dominant negative (dn)-Runx2 in vitro and in vivo. Adenoviral introduction of dn-Runx2 into primary calvarial cells and into C2C12 cells that were stimulated with BMP-2 inhibited early osteoblast differentiation. However, adenoviral introduction of dn-Runx2 into primary calvarial cells and MC3T3-E1 cells, both of which had been cultured for 10 days after confluence for their maturation, and into MLO-A5 cells did not inhibit Col1a1 and osteocalcin expression. We generated transgenic mice that expressed dn-Runx2 under the control of 2.3 kb mouse Col1a1 promoter. Further, the dn-Runx2 transgenic mice were mated with Runx2 transgenic mice under the control of Col1a1 promoter, which showed osteopenia with fractures and drastic reduction in osteocytes (J. Cell Biol. 155: 157, 2001). Runx2/dn-Runx2 double transgenic mice showed no fracture, and a large number of osteocytes were observed. In dn-Runx2 transgenic mice, the number of osteoblasts was reduced and the parameters for osteolysis were normal in bone morphometric analysis, and the osteoblasts expressed normal levels of major bone matrix protein genes. However, the trabecular bone gradually increased during aging. Further, the trabecular bone was highly mineralized and urinary deoxypyridinoline was significantly decreased. Moreover, the bone in dn-Runx2 transgenic mice was conserved after ovariectomy. These findings indicate that dn-Runx2 induces terminal differentiation of osteoblasts, decreases the number of osteoblasts, and suppresses osteolysis. Thus, Runx2 plays an important role in maintaining the number of osteoblasts, but Runx2 is not essential for the regulation of expression of major bone matrix protein genes. Further, our findings indicate that Runx2 is responsible for the high bone turnover in estrogen deficiency. All experiments were reviewed and approved by the Osaka University Medical School Animal Care and Use Committee.

Disclosures: ***T. Komori****, None.*

F224

Dissection of PTH-induced Signaling Network in Osteoblastic Cells Using a Novel Bioinformatics Approach. X. D. Chen, S. A. Stewart*, S. C. Manolagas, R. L. Jilka. Center for Osteoporosis and Metabolic Bone Diseases, Central Arkansas Veterans Healthcare System, University of Arkansas for Medical Sciences, Little Rock, AR, USA.

The anabolic effect of intermittent PTH is due at least in part to attenuation of osteoblast apoptosis. As little as 1h of PTH is sufficient to induce survival signaling in cultured osteoblastic cells, which is abolished by inhibition of RNA and protein synthesis. Earlier work demonstrated that PTH inhibition of apoptosis requires an increase in the synthesis of the anti-apoptotic protein Bcl-2. Here, we used global gene expression profiling to more fully appreciate the changes in gene expression underlying the anti-apoptotic effect of PTH. The level of 12,488 transcripts in osteoblastic OB-6 cells was quantified with Affymetrix U74A chips under basal conditions (0 time), and after addition of 50 nM PTH for 30 or 60 minutes. Triplicate cultures were analyzed. Significance Analysis of Microarray, and t-test comparison of changes in single transcripts (0 vs 30, 0 vs 60, 30 vs 60), indicated significant changes in the expression of 1984 genes with a false discovery rate of <5%. Using PathwayAssistant, a database of several thousand proteins and information on the relationships among them, we conducted an unbiased search for those PTH-regulated genes that have a biological relationship with at least one other PTH-regulated gene in an effort to visualize components of the interconnected signaling cascade affected by the hormone. We identified 440 such genes, which were then mapped onto 44 established signaling cascades. We found that the pathways most affected by PTH are highly interconnected and are involved in the control of cell cycle and apoptosis. They include FAS/death domain, MAPK-ERK, p53, caspase, integrin signaling, mitochondrial control of apoptosis, G-protein, PI3/PI4-kinase, Rb, SAP-JNK, Cx43, Rb, PTEN, p38. The PTH-regulated genes that most frequently appear in the 44 pathways were *Jun*, *MAPKK3*, *AKT1*, *c-fos*, *p53*, and *ADPRT,* which were up-regulated; *Fyn* and *FADD* were down-regulated. These 8 genes have direct links to 144 of the 440 PTH-regulated genes. These 144 genes thus represent highly connected co-regulated factors, some of which are potentially involved in the anti-apoptotic effect of PTH. Among these genes are the anti-apoptosis factor survivin and integrin-linked kinase. This unbiased bioinformatics approach has thus identified new candidates for the key PTH-regulated pro-survival genes. Moreover, hierarchical clustering revealed unique dynamic expression patterns of PTH-regulated genes, and provided an outline of the interconnected signaling cascade involved in control of cell behavior by short-term exposure to the hormone.

Disclosures: ***X.D. Chen****, None.*

F226

Interactions between Twist and Fibroblast Growth Factor Receptor 2 Controls Osteoblast Gene Expression in the Saethre-Chotzen Syndrome. H. Guénou*, K. Kaabeche*, S. Le Mée*, P. J. Marie. Laboratory of Osteoblast Biology and Pathology, Inserm U606, Paris, France.

Genetic mutations of the Twist gene, a bHLH transcription factor, induce premature fusion of cranial sutures in the Saethre-Chotzen syndrome (SCS). We previously showed that Twist haploinsufficiency in SCS induces marked alterations in osteoblast differentiation and survival. In this study, we investigated the role of fibroblast growth factor receptor 2 (FGFR2) in the abnormal expression of osteoblast differentiation genes induced by bHLH deletion in Twist. Cranial osteoblasts from a SCS patient with a Y103X mutation in Twist showed decreased Twist dosage associated with decreased Runx2, osteocalcin (OC) and bone sialoprotein (BSP) mRNA, compared to normal osteoblasts. This phenotype in Twist mutant osteoblasts was associated with decreased FGFR2 mRNA levels (C-terminal, N-terminal and intramembranous domains). EMSA analysis in nuclear extracts from Twist mutant osteoblasts showed specific reduction of Runx2 binding to the FGFR2 promoter, suggesting that the reduced Runx2 expression in mutant osteoblasts results in decreased FGFR2 levels. Transfection of Twist mutant osteoblasts with a dominant-negative (DN) FGFR2 vector decreased Runx2, OC and BSP expression compared to empty vector, indicating that FGFR2 signaling upregulates Runx2 and downstream targets in mutant cells. Transfection of Twist mutant osteoblasts with Twist cDNA rescued FGFR2 mRNA levels, and corrected Runx2, OC and BSP mRNA expression. We conclude that 1) Twist haploinsufficiency induced by bHLH deletion causes reduced FGFR2 mRNA; 2) this effect may contribute to the reduced Runx2, OC and BSP mRNA expression in Twist mutant osteoblasts; 3) the reduced Runx2 expression induced by Twist haploinsufficiency may conversely contribute to downregulate FGFR2 in Twist mutant cells.This provides novel genetic evidence for positive interactions between Twist and FGFR2, and for reciprocal interactions between Runx2 and FGFR2 in human osteoblasts. This indicates that Twist haploinsufficiency can alter osteoblast differentiation gene expression by multiple mechanisms in the Saethre-Chotzen Syndrome.

Disclosures: ***P.J. Marie****, None.*

F228

Characterization of Stromal/Preosteoblast Cells from Heat Shock Factor-2 (HSF-2) Null Mice. H. Kajiya[1], M. Ito[1], H. Ohshima*[2], S. Kenmotsu*[2], I. J. Benjamin*[3], W. L. Ries[4], S. V. Reddy[1]. [1]Medicine/Hematology, University of Pittsburgh, Pittsburgh, PA, USA, [2]Division of Anatomy and Cell Biology of the Hard Tissue, Niigata University, Niigata, Japan, [3]Internal Medicine, University of Texas Southwestern Medical Center at Dallas, Dallas, TX, USA, [4]Pediatrics, Medical University of South Carolina, Charleston, SC, USA.

RANK Ligand (RANKL) is a critical osteoclastogenic factor that is expressed on marrow stromal/osteoblast cells. We previously cloned a 2 Kb hRANKL promoter region and identified functional heat shock factor-2 (HSF-2) responsive motifs (HSE) in the promoter. We also demonstrated that b-FGF induced HSF-2 nuclear localization and binding to the RANKL promoter region in stromal/preosteoblast cells. These data suggested that HSF-2 is a down-stream target of b-FGF to induce RANKL expression in stromal/osteoblast cells, and that HSF may play an important role in modulating RANKL gene expression in the bone microenvironment. In the present study, we characterized HSF-2 null mice bone marrow derived stromal/preosteoblast cells for RANKL expression and their capacity to support osteoclastogenesis. Western blot analysis demonstrated that b-FGF (4 ng/ml) treatment (3 days) of HSF-2 (-/-) stromal/preosteoblast cells did not induce RANKL expression. In contrast, b-FGF induced a 10-fold increase in RANKL expression in cells derived from wild type littermates. Furthermore, basal RANKL expression was decreased three fold in HSF-2 -/- stromal/preosteoblast cells compared to wild type littermates. Wild type mouse bone marrow derived spleen cells cocultured with HSF-2 -/- mice stromal/preosteoblast cells in the presence of dexamethasone (10^{-9} M) and b-FGF (40 ng/ml) did not form osteoclasts. In contrast, cocultures using wild type stromal/preosteoblast cells formed significant numbers of osteoclasts. Interestingly, micro CT analysis of HSF-2 null mice long bones demonstrated that the trabecular bone was thin and decreased. Electron microscopic studies showed that although osteoclasts of HSF2-/- mice were in direct contact with the bone surface, ruffled borders are poorly developed compared to osteoclasts from wild type littermates. These data further suggests that HSF-2 modulates osteoblast and osteoclast function in the bone microenvironment and thus plays an important role in bone remodeling.

Disclosures: ***S.V. Reddy****, None.*

F230

Runx2 Acts as a Negative Regulator of the Repressive Activity of the Basic Helix Loop Helix Factor Hes-1 on $1,25(OH)_2D_3$ Induced Osteopontin Transcription. Q. Shen*, S. Christakos. Biochemistry, Graduate School of Biomedical Science-New Jersey Medical School, Newark, NJ, USA.

Osteopontin (OPN), a glycosylated phosphoprotein that binds calcium, is present in bone extracellular matrix. OPN deficient mice are resistant to PTH induced bone resorption, indicating a requirement for OPN in bone remodeling. In osteoblastic cells the transcription of OPN is stimulated in response to $1,25(OH)_2D_3$ and we previously reported functional cooperation between Runx2 and the vitamin D receptor (VDR) in the regulation of OPN transcription. We now report that the helix loop helix factor Hes-1, a mammalian counterpart of the Drosophila Hairy and Enhancer of split proteins, which is expressed in osteoblastic cells, is involved in $1,25(OH)_2D_3$ and Runx2 mediated regulation of osteopontin transcription. Studies were initially done in COS-7 cells transfected with the mouse OPN promoter (-777/+79) and Hes-1 and VDR expression vectors. With increasing amounts of Hes-1 DNA transfected (10 -200 ng), the $1,25(OH)_2D_3$ dependent induction of OPN transcription was steadily repressed to control levels. In COS-7 cells these concentrations of Hes-1 did not significantly affect the basal level of OPN promoter activity. Cotransfection of Runx2 in COS-7 cells reversed the inhibition by Hes-1. In ROS 17/2.8 cells, that contain endogenous Runx2, transfection of Hes-1 (10 - 100 ng) resulted in a dose dependent enhancement of both basal and $1,25(OH)_2D_3$ induced transcription (the maximal enhancement was 4.7 ± 0.1 fold). The enhancement of the induction of OPN transcription by Hes-1 in ROS cells was inhibited in a dose dependent manner by AML-1/ETO, which acts as an inhibitor of Runx2 and has also been reported to recruit histone deacetylase.

Sodium butyrate (2mM), which acts in part as a histone deacetylase inhibitor, was able to partially rescue the inhibition by AML-1/ETO of Hes-1 induced OPN transcription, suggesting the involvement of both histone deacetylase dependent and independent mechanisms. Immunoprecipitation assays using ROS 17/2.8 cells coexpressing Hes-1 and Runx2 indicated that Hes-1 and Runx2 interact and that $1,25(OH)_2D_3$ (10^{-8} M, treatment for 24h) can enhance this interaction. Taken together, our studies show that Hes-1 can potentiate both basal and VDR mediated OPN transcription in the presence of Runx2 and Runx2 can act as a negative regulator of the inhibitory activity of Hes-1. These findings define new mechanisms and functional interactions that are involved in the regulation of OPN and may therefore affect the process of bone remodeling.

Disclosures: ***Q. Shen****, None.*

F232

Expression of MINT, the Msx2 Interacting Nuclear Matrix Target Protein, Is Upregulated with Osteogenic Commitment of Murine Mesenchymal Progenitors. O. L. Sierra, S. L. Cheng, J. S. Shao*, A. P. Loewy*, D. A. Towler. Bone & Mineral Diseases, Washington University School of Medicine, St Louis, MO, USA.

The transcription factor Msx2 is required for craniofacial bone formation and normal cerebellar development. The gain - of - function Msx2 variant, Msx2(P148H), causes Boston-type craniosynostosis, and enhances the osteogenic differentiation of mesenchymal progenitors -- exhibiting markedly enhanced synergy with BMP2. Detailed mechanistic studies indicate that Msx2 promotes early osteogenic commitment by augmenting paracrine Wnt/Dkk signals; stable expression of Msx2 in uncommitted mesenchymal progenitors enhances Wnt3a and Wnt7a expression, but suppresses Dkk1 expression. However, also Msx2 suppresses late phenotypic markers such as osteocalcin by targeting a specific nuclear matrix protein, MINT, that organizes a multiprotein osteocalcin promoter complex containing Runx2. In situ hybridization studies confirm expression of MINT in neonatal craniofacial bone and in cerebellar Purkinje cells, two tissues dependent upon Msx2 action. RNAi directed towards MINT selectively inhibits osteocalcin gene expression in MC3T3E1 calvarial osteoblasts.. Since *spen* -the Drosophilan ortholog of MINT- is required for *wingless* (Wg) signaling in fly eye development, we studied the expression and regulation of MINT during the osteogenic commitment of C3H10T1/2 mesenchymal progenitors -- a process regulated by paracrine Wnt signals. Uncommitted C3H10T1/2 cells grown in vitro for 5 days in the presence of beta-glycerolphosphate and ascorbic acid led to a 260-fold increase of alkaline phosphatase mRNA abundance. This osteogenic commitment C3H10T1/2 is dependent upon endogenous Wnt signaling; treatment with recombinant Dkk-1 (1 ug/mL) for 5 days decreased alkaline phosphatase by 50% ($p < 0.05$). We next studied the expression of MINT over this same time frame. With osteogenic commitment of C3H10T1/2 cells, MINT mRNA was increased 3-fold ($p < 0.05$) as quantified by fluorescence RT-PCR. By contrast, no significant change in Msx2 expression was noted. Unlike committed MC3TE1 cells, MINT siRNA had little effect on basal OC expression. However, MINT siRNA significantly enhanced the antagonistic actions of Dkk1 on OC expression in during commitment of C3H10T1/2 cells to the osteogenic lineage ($p < 0.05$). Dkk1 treatment had no effect on endogenous MINT mRNA accumulation. Thus, these data suggest that MINT participates in the control of osteoblast gene expression, potentially regulating stage-specific responses to paracrine Wnt/Dkk signaling.

Disclosures: ***O.L. Sierra****, None.*

F234

1,25-Dihydroxyvitamin D Downregulates PHEX Gene Expression in Osteoblasts via Repression of a 110 kDa Positive Transfactor that Binds to a Polyadenine Element in the Promoter. E. R. Hines*[1], O. I. Kolek*[1], M. D. Jones*[2], S. H. Serey*[1], N. B. Sirjani*[1], P. R. Kiela*[1], P. W. Jurutka[3], M. R. Haussler[3], J. F. Collins*[1], F. K. Ghishan*[1]. [1]Pediatrics and Steele Memorial Children's Research Center, University of Arizona College of Medicine, Tucson, AZ, USA, [2]Orthopedic Surgery, University of Arizona College of Medicine, Tucson, AZ, USA, [3]Biochemistry & Molecular Biophysics, University of Arizona College of Medicine, Tucson, AZ, USA.

The PHEX gene, mutated in X-linked hypophosphatemic rickets, encodes an endopeptidase expressed in osteoblasts that inactivates an uncharacterized peptide hormone, phosphatonin, which suppresses bone mineralization as well as renal phosphate reabsorption and vitamin D bioactivation. We demonstrate that 1alpha,25-dihydroxyvitamin D (1,25D), the active renal vitamin D metabolite, decreases both mineralization (measured by calcein staining of calcium phosphate) and PHEX mRNA (monitored by real time PCR) in the rat osteoblastic cell line, UMR-106. 1,25D also represses PHEX expression in mouse calvaria, in vivo. Promoter/reporter construct analysis of the murine PHEX gene in transfected UMR-106 cells localized the repressive effect of 1,25D to the -133 to -74 region, and gel mobility shift experiments revealed that 1,25D treatment of the cells diminished the binding of a nuclear protein(s) to a stretch of 17 adenines from -116 to -100 in the proximal PHEX promoter. Either overexpression of a dominant negative vitamin D receptor (VDR) or deletion of this sequence of 17 A-T base pairs abolished the repressive effect of 1,25D by attenuating basal promoter activity, indicating that this region mediates the 1,25D response and is involved in basal transcription. Southwestern blot analysis and DNA affinity purification show that an unidentified 110 kDa nuclear protein recognizes the poly A element. Because 1,25D-liganded VDR neither binds to the polyadenine region of the PHEX promoter nor directly influences the association of the 110 kDa transfactor, we propose that 1,25D indirectly decreases PHEX expression via VDR-mediated repression of this novel transactivator. Thus, we have identified a cis-element required for PHEX gene transcription that participates in negative feedback control of PHEX expression and thereby potentiates the actions of phosphatonin. We conclude that although 1,25D-VDR indirectly promotes bone mineralization by inducing intestinal calcium and phosphate absorption, the direct action of the hormone-receptor complex on bone is to limit osteoblastic mineralization. One mechanism whereby 1,25D suppresses mineralization appears to involve amplification of the autocrine effect of phosphatonin as a result of PHEX repression.

Disclosures: ***E.R. Hines****, None.*

F244

Notch1 Overexpression Impairs Osteoblastogenesis Exclusively by Downregulating Wnt Signaling. V. Deregowski, E. Gazzerro, L. Priest*, E. Canalis. Research, Saint Francis Hospital and Medical Center, Hartford, CT, USA.

Notch is a family of transmembrane receptors that mediate signaling mechanisms controlling cell fate decisions. Notch activation requires a regulated intramembranous proteolytic cascade leading to the release of Notch intracellular domain (NotchIC) and its nuclear translocation. Overexpression of NotchIC in ST-2 stromal cells depresses osteoblastogenesis and the response to bone morphogenetic protein 2 (BMP) and enhances adipogenesis. The mechanisms involved are not known, but interactions between Notch1 and Wnt/β-catenin may explain the effects observed, since they have opposite effects on cell differentiation and fate. NotchIC overexpression in stromal cells opposes Wnt/β-catenin signaling, decreasing the activity of the Wnt/β-catenin responsive construct, pTOPFLASH, containing Tcf4/Lef1 binding sequences upstream of the luciferase gene, by 50%. NotchIC overexpression induced low density lipoprotein receptor (LRP) 1 mRNA, providing a mechanism for Wnt downregulation since LRP-1 interacts with the Wnt receptor Frizzled to repress Wnt binding and signaling. Moreover, NotchIC overexpressing cells expressed lower β-catenin levels by Western blot analysis. In accordance, transfection of a stable mutant β-catenin expression construct rescued the inhibitory effect of NotchIC on transfected pTOPFLASH constructs. To exclude additional mechanisms involved in the inhibition of osteoblastogenesis by NotchIC, we explored whether Notch1 modified the BMP dependent Smad or mitogen activated protein (MAP) kinase signaling pathways. BMP-2 induced phosphorylation of Smad 1/5/8 and enhanced the transactivation of a transiently transfected BMP-responsive 12xSBE-Oc-pGL3 construct, containing 12 repeats of a Smad binding site directing luciferase expression, but NotchIC overexpression did not modify the level of phosphorylated Smad 1/5/8 or the transactivation of the 12xSBE construct in control or BMP-2 treated cells. BMPs had no significant effect on the phosphorylation of the MAP kinases ERK, p38 or JNK, or on the transactivation of a transfected construct containing seven AP-1 binding site repeats directing luciferase expression, in either control or NotchIC overexpressing cultures. These results indicate that whereas NotchIC overexpression prevents BMP-2 induced osteoblastogenesis, it does not inhibit Smad or MAP kinase signaling pathways, but it impairs Wnt/β-catenin signaling, possibly by inducing LRP-1. This also suggests that maintaining Smad/MAP kinase signaling is not sufficient for BMP-2 dependent osteoblastogenesis.

Disclosures: ***V. Deregowski****, None.*

F246

Mesenchymal Cells Derived from Human Embryonic Stem Cells Differentiate into Bone Forming Osteoblasts. N. K. Shevde[1], J. A. Fretz*[1], L. Crandall*[2], J. A. Thomson*[3], J. W. Pike[1]. [1]Biochemistry, University of Wisconsin- Madison, Madison, WI, USA, [2]WiCell Research Institute, Madison, WI, USA, [3]NPRC/Anatomy, University of Wisconsin- Madison, Madison, WI, USA.

Self-renewing mesenchymal stem cells (MSCs) give rise to a variety of differentiated cell types including adipocytes, chondrocytes, myoblasts, and bone-forming osteoblasts. Thus, MSCs have an enormous therapeutic potential for restoring tissues damaged through injury or disease, and, in the context of bone, may be particularly useful in orthopedic/dental transplants, fracture healing, and skeletal regeneration and repair. Accordingly, isolated bone marrow-derived MSCs have been developed for these applications and have been shown to restore bone *in vivo* in a variety of animal models. We describe here the production of MSCs from human embryonic stem cells (hES) that are capable of forming bone *in vitro*. Totipotent hES cells (H9 and H11 cell lines) routinely maintained in the undifferentiated state on feeder layers of mouse embryonic fibroblasts (MEFs) were allowed to undergo progression and differentiation over a period of 10 to 12 days to form embryoid bodies (EBs). EBs were then disaggregated using trypsin and the isolated cells cultured for an additional 10-14 days in Mesencult medium containing 15% pre-tested FBS. Cells produced in this manner exhibited a sustained high proliferative capacity and a spindle-shaped morphology typical of MSCs. RT-PCR analysis of RNA derived from hES, EBs, and MSC populations revealed a dramatic suppression of Oct4 and BMP7 expression during the progression of hES cells to EBs, and an upregulation of the transcription factor genes Runx2, Msx2 and Dlx5 during the progression of EBs to MSCs. Osteocalcin RNA was undetectable in each of these cell culture populations. To assess the ability of these MSCs to differentiate into bone forming osteoblasts, cells were cultured in DMEM/F12 containing 10% FBS, 50μg/ml fresh ascorbic acid, 5mM β-glycerophosphate and steroids for periods up to 21 days, and then evaluated for the presence of calcified bone nodules using von Kossa staining. Almost all of the cultures showed significant bone nodule formation. RT-PCR analysis of phenotypic markers for authentic osteoblasts confirmed the expression of both osteopontin and osteocalcin. Current experiments are focused on evaluating the bone forming ability of these cells *in vivo*. Our studies demonstrate that hES cells can be induced to produce MSCs capable of further differentiation into functional bone-forming osteoblasts. Thus, hES cells may represent an inexhaustible source of MSCs with therapeutic potential for specific skeletal indications.

Disclosures: ***N.K. Shevde****, None.*

F248

Inhibitory Action of N-Cadherin on Osteoblast Differentiation. C. Lai-Huang, C. Liu*, S. Cheng, G. Mbalaviele, R. Civitelli. Bone and Mineral Diseases, Washington University in St. Louis, St. Louis, MO, USA.

We have previously shown that targeted expression of a dominant negative truncated form of N-cadherin (Ncad) delays acquisition of peak bone mass in mice and retards osteoblast differentiation, most likely by interfering with β-catenin signaling. To gain insights on the specific role of Ncad in bone, we used heterozygous Ncad null mice (homozygous loss of Ncad is embryonically lethal), since $Ncad^{+/-}$ calvarial cells express lower abundance of Ncad protein relative to wild type ($Ncad^{+/+}$) cells. Whole body bone mineral density (BMD) by DEXA was not significantly different between $Ncad^{+/-}$ and $Ncad^{+/+}$ littermates up to 8 months of age, implying that a single allele of Ncad is sufficient for bone mass development and maintenance. However, while 4-month-old $Ncad^{+/+}$ mice rapidly (within 3-4 weeks) lost about 8% of baseline BMD following ovariectomy (OVX), bone loss was surprisingly far slower and less pronounced (about -2% at 3 weeks and -4% at 6 weeks post-OVX) in $Ncad^{+/-}$ mice. Since Ncad is expressed in osteoblasts but not in osteoclasts, we characterized the function of $Ncad^{+/-}$ osteoblasts in vitro. Intriguingly, development of calcified nodules was faster and more intense in calvarial cells isolated from $Ncad^{+/-}$ mice relative to $Ncad^{+/+}$ cells, in the presence of ascorbic acid and β-glycerophosphate. Similarly, bone marrow stromal cells from heterozygous mice developed ~40% more alizarin red positive colony forming units than cells from wild type mice, although the difference disappeared after 4 weeks of culture. In 2-week calvarial cultures, alkaline phosphatase activity was 5-fold higher in $Ncad^{+/-}$ relative to $Ncad^{+/+}$ cells. Consistent with an inhibitory role on osteoblast differentiation, Ncad expression (mRNA and protein) was progressively down regulated with differentiation in $Ncad^{+/+}$ calvarial cells. Ncad protein was barely detectable after 3 weeks in mineralizing medium, while cadherin-11 abundance remained unchanged. Interestingly, cell-cell adhesion (tested immediately after reaching confluence) was decreased >30% among heterozygous calvaria cells, as was cell proliferation (pre-confluence), relative to wild type cells. However, the abundance of whole cell β-catenin was not different between $Ncad^{+/+}$ and $Ncad^{+/-}$ cells. These data suggest that Ncad functions as an inhibitor of osteogenic differentiation by preventing cells from progressing through the late stages of osteoblast development, presumably via stabilization of cell-cell adhesion and perhaps reduction of the osteoprogenitor pool. Partial release from this inhibition may be involved in the attenuated bone loss following OVX in $Ncad^{+/-}$ mice.

Disclosures: ***R. Civitelli****, None.*

F251

The Transcription Factor C/EBPα Isoform p30 Promotes Osteoblastogenesis but Inhibits Adipogenesis Contrary to C/EBPα. M. Ueda*, K. Hata*, F. Ikeda, T. Matsubara, S. Ebisu*, R. Nishimura, T. Yoneda. Osaka Univ Grad Sch Dent, Suita, Japan.

Evidence has accumulated that the undifferentiated mesenchymal progenitor cells in bone marrow give rise to both adipocytes and osteoblasts. The transcription factor CCAAT/enhancer-binding protein α (C/EBPα) is known to play a crucial role in adipogenesis. Formation of mature adipocytes was profoundly diminished in C/EBPα-deficient mice. However, little is known about its role in the mesenchymal cell differentiation to osteoblasts. Here, we investigated the role of C/EBPα in osteoblastogenesis as well as adipogenesis using the multipotent mesenchymal cell line C3H10T1/2. Treatment of C3H10T1/2 cells with BMP2 induced C/EBPα expression along with osteoblast differentiation. Of note, we also observed strong expression of C/EBPα isoform p30, which lacks the transcription activation domain, in BMP2-treated C3H10T1/2 cells. These results suggest that C/EBPα and its isoform p30 are involved in osteoblastogenesis. To clarify the role of C/EBPα and p30 in osteoblastogenesis, C/EBPα or p30 were overexpressed in C3H10T1/2 cells using an adenovirus system. Overexpression of C/EBPα induced osteoblast differentiation and enhanced osteoblastogenic effects of BMP2. On the other hand, overexpression of p30 showed marginal induction of osteoblast differentiation. However, p30 markedly augmented BMP2-promoted osteoblastogenesis as C/EBPα did. To understand the molecular mechanism underlying the osteoblastogenic activity of C/EBPα and p30, interactions of C/EBPα or p30 with Runx2 were examined. Overexpression of C/EBPα or p30 stimulated the osteoblastogenic effects and transcriptional activity on the osteocalcin gene promoter of Runx2. Moreover, co-immunoprecipitation experiments revealed a physical association of C/EBPα or p30 with Runx2. Next, the role of C/EBPα and p30 in adipogenesis was examined. Overexpression of C/EBPα induced adipogenesis and PPARγ expression and enhanced BMP2-promoted adipogenesis in C3H10T1/2 cells. Of interest, p30 alone exhibited no effects on adipogenesis. However, it markedly inhibited adipogenesis induced by BMP2 or C/EBPα and suppressed C/EBPα-induced PPARγ expression in a dominant-negative fashion. In conclusion, our results suggest that C/EBPα and its isoform p30 promote osteoblastogenesis through physical and functional association with Runx2. However, p30 exhibits inhibitory effects on adipogenesis contrary to C/EBPα which stimulates adipogenesis. P30 isoform may be a key transcriptional regulator that promotes osteoblastogenesis and inhibits adipogenesis and a potential molecular target in design of therapeutic agents for osteopenia and obesity.

Disclosures: ***M. Ueda****, None.*

F253

Inhibition of Wnt Signaling by DKK-1 Decreases Osteoblast Differentiation via Mechanisms Dependent on Transcriptional Repression of FRA-1. A. K. Chesterfield*, J. Rohrbach*, V. Easwaran*, D. Ebert*, P. Stevens*, D. Cody*, Y. O. Taiwo, A. Houghton, G. Sabatakos. Skeletal Research, Procter and Gamble Pharmaceuticals, Mason, OH, USA.

Signaling through the canonical Wnt pathway has a dramatic effect on bone mass as has been demonstrated by the low and high bone mass phenotypes of LRP5 mutations. Dkk-1 is an inhibitor of the Wnt pathway by antagonizing LRP5/6 activity. The aim of this study was to explore the mechanism by which Dkk-1 regulates Wnt target gene function that is essential for osteoblast differentiation. For this we generated stable transfectants of Dkk-1 and of a mutant Dkk-1 C220A in C2C12 cells. Cells overexpressing Dkk-1 demonstrated a significant reduction in alkaline phosphatase activity in response to BMP-2. Unexpectedly, overexpression of the C220A mutant inhibited BMP-2-induced differentiation to a greater extent than wild type Dkk-1. In addition, the mRNA levels of the osteoblast markers osterix and alkaline phosphatase were also significantly decreased by both Dkk-1 and C220A overexpression, and these effects were Runx2 independent. Using co-immunoprecipitation studies with the C-terminal of LRP5 we showed that these effects could be due to interactions with LRP5. In the absence of BMP-2 only wild type Dkk-1 interacted with the C-terminal domain of LRP5, whereas, in the presence of BMP-2 both wild type and C220A interacted with LRP5. Having demonstrated the regulatory role of Dkk-1 in BMP-2 induced osteoblast differentiation we investigated whether these events could be mediated through Fra-1. Using EMSA analysis with a Lef/TCF site from the Fra-1 promoter we confirmed that in the presence of BMP-2 complex formation was increased in cells overexpressing both Dkk-1 and the C220A mutant, thus indicating that the inhibitory effect of Dkk-1 or the C220A mutant could be mediated by interactions on the Lef/TCF site of the Fra-1 promoter. However, western blot analysis revealed no change in Fra-1 protein levels in cells overexpressing either Dkk-1 or the C220A mutant, suggesting that Dkk-1 signaling affects transcriptional activity but not abundance of Fra-1. To determine the mechanism of transcriptional regulation of the Fra-1 promoter by Dkk-1, we performed co-tranfections of Dkk-1 with a Fra-1 luciferase reporter containing a trimerized TCF-binding site. Dkk-1 inhibited the Wnt3a-induced luciferase activity demonstrating that the inhibitory effect of Dkk-1 on osteoblast differentiation could be mediated by transcriptional repression of Fra-1. In conclusion, our data demonstrate that Dkk-1 and the C220A mutant are inhibitors of osteoblast differentiation and that the inhibitory effect is mediated by repression of Fra-1 activity at the transcriptional level.

Disclosures: ***G. Sabatakos****, None.*

F256

Genomic Occupancy and Chromatin Organization of the Runx2/Cbfa1 Gene P1 Promoter, Which Regulates Its Bone-Specific Expression in Osteoblasts. H. Hovhannisyan*, C. J. Lengner, J. Shen*, J. B. Lian, G. S. Stein, J. L. Stein*, A. J. van Wijnen. Department of Cell Biology and Cancer Center, University of Massachusetts Medical School, Worcester, MA, USA.

The essential biological function of the Runx2 transcription factor in skeletal development and the physiological responsiveness of Runx2 gene expression to osteoblast-related anabolic and catabolic factors have become conclusively established concepts in bone cell biology. However, the exact molecular mechanisms that control transcription of Runx2 in mesenchymal cells to support its skeletal gene regulatory function remain to be established. To characterize bona fide promoter elements, we analyzed the regulatory organization of the P1 promoter in intact cells using DNaseI hypersensitivity and chromatin immuno-precipitation (ChIP) assays, as well as LM-PCR assisted genomic DNaseI footprinting. We find that there is only a single DNaseI hypersensitive region (DHS) within 15 kB of the P1 transcriptional start site. At higher resolution this region resolves into several discrete sites located between -0.4 and 0.0 kB which contain the key elements required for basal Runx2 transcription in osteoblasts (as defined by transient transfections with reporter genes). ChIP assays reveal that the DHS of the basal promoter interacts with acetylated histones H3 and H4, reflecting its open chromatin conformation, and the Runx2 protein itself, which we have shown auto-regulates its own promoter. Genomic DNase I footprinting with a panel of mesenchymal cell lines indicates that the DHS region encompasses several in vivo protein/DNA interaction sites (e.g., AP1 binding site at -0.4 kB, an HLH/E-box at -0.1 kB, and Runx2 motifs in the 5'UTR), which are occupied in the endogenous Runx2 P1 promoter within the intact cell. Occupancy of the HLH/E-box, which overlaps with a Runx2 motif, is also observed in Runx2 null cells, as well as in non-osseous cells where Runx2 gene expression is virtually undetectable. We propose a model in which the DHS region (i.e., the first 0.4 kB of the P1 promoter) interacts with HLH factors to repress Runx2 transcription prior to osteoblast lineage commitment. This model invokes putative long-distance control elements (beyond the 15 kB region we examined here) for the BMP2 responsive and bone-tissue specific induction of Runx2.

Disclosures: ***A.J. van Wijnen****, None.*

F260

Structure-Function Analysis of SFRP-1 for its Wnt Antagonist Function. R. A. Bhat, B. Stauffer*, P. V. Bodine. Women's Health and Bone, Wyeth Research, Collegeville, PA, USA.

Wnts are secreted glycoproteins that mediate fundamental biological processes like embryogenesis, organogenesis and tumorigenesis. Many extracellular proteins control Wnt signaling including Wnt inhibitory factor, secreted frizzled related proteins, cerberus and dickkopfs. These proteins either bind to Wnt directly or interact with frizzled receptor or with low-density lipoprotein-receptor related protein (LRP) to modulate Wnt signaling. Recent studies from our group have shown that secreted frizzled related protein-1 (SFRP-1) is an important regulator of osteoblast survival, and the targeted disruption of SFRP-1 in mice led to decreased osteoblast and osteocyte apoptosis and increased trabecular bone formation. SFRP-1 is a secreted glycoprotein of ~35 KD and contains two cysteine rich domains. The amino-terminal Cysteine Rich Domain (CRD) contains 10 cysteines involved in 5 disulphide bridges and is homologous to the CRD domain of Frizzled receptors (FZD). The CRD domain can bind to both the Wnt and the FZD receptor and interfere with Wnt signaling. The carboxyl half of the SFRP-1 contains 6 cysteine residues and is homologous to netrin domains and also contains a hyaluronan-binding region. The present study was focused on identifying the functional domains of SFRP-1 and the structural requirements that are necessary for its Wnt inhibitory function. Several mutants of SFRP-1 were generated and tested by transient transfection in human osteosacrcoma cell line, U2OS, for their ability to inhibit Wnt -3 mediated upregulation of an optimized TCF-Luciferase reporter. Chimeras of SFRP-1 and SFRP-3 were generated by switching their netrin domains and tested for their ability to antagonize Wnt function. Deletion mutants of CRD domain showed reduced Wnt inhibitory activity and deletion of amino acids 71-163 resulted in total loss of Wnt antagonist function. These results indicate that the CRD domain of SFRP-1 is critical for its Wnt inhibitory function. The SFRP-1/SFRP-3 chimera showed a loss of about 30% Wnt inhibitory activity compared to SFRP-1, and SFRP-3/SFRP-1 chimera gained about 40% of the Wnt inhibitory function compared to SFRP-3. These studies from the chimeras have indicated that the netrin domain is necessary for optimal Wnt inhibitory function and may be involved in proper folding of the molecule. Mutation of the hyaluronan binding region of SFRP-1 resulted in about 35% loss of Wnt antagonistic function, suggesting that the SFRP-1 protein may interact with the matrix that results in efficient Wnt inhibition, probably by increasing the local concentration of SFRP-1. The mutational studies clearly demonstrate the interaction of several functional domains in SFRP-1 for the optimal Wnt antagonist function.

Disclosures: ***R.A. Bhat****, None.*

F262

Importance of Human Dkk1 C-terminal 21 Amino Acids and Glycosylation for Its Function as an Antagonist of LRP5/6-Wnt-TCF-Signaling. B. M. Bhat[1], H. Lam*[1], V. E. Coleburn*[1], A. Anisowicz*[2], K. M. Allen*[2], P. Yaworsky*[3], F. J. Bex[1]. [1]Women's Health & Bone, Osteoporosis Group, Wyeth Research, Collegeville, PA, USA, [2]Human Genetics, Oscient Pharmaceuticals Corporation, Waltham, MA, USA, [3]Genomics, Wyeth Research, Cambridge, MA, USA.

Human Dickkopf 1 (Dkk1) is an inhibitor of canonical Wnt signaling by interacting with trans-membrane receptors LRP5/6 and Kremens. Members of the Dkk family contain two conserved cysteine-rich (Cys-1 & Cys-2) domains separated by variable-length spacer regions and show greater than 50% aa homology at the C-terminal region. The importance of Cys-2 to functional activity was shown when expression of this region alone retained Wnt signaling inhibitory activity and by the ability of a single C220A mutation in the Cys-2 region of the full-length protein to abolish its inhibitory activity. Opposing activity between the N-terminal Cys-1 domain region and the C-terminal Cys-2 region on Wnt signaling has been reported. To further investigate the structural requirements for Dkk1 activity, we tested the functional consequences in a Wnt3a TCF reporter assay of deletion constructs of Dkk1 that retained either one or both Cys-domains, but had the N-terminal 97aa or C-terminal 21aa removed. Most interestingly, the construct lacking C-terminal 21 aa lost TCF inhibitory activity even though it contained both Cys-domains. Moreover, expression of Kremen-2 enhances wild type Dkk1-mediated inhibition, but cannot reverse the lost functionality of Dkk1 that lacks the C-terminal 21aa. Since this 21 aa region contains a putative N-glycosylation site, it was hypothesized that the glycosylation of Dkk1 could also be necessary for its inhibitory function. When Dkk1-transfected 293A cells were treated with tunicamycin (N-glycosylation inhibitor), Western blot analysis of the conditioned medium (CM) showed a downward mobility shift of Dkk1 (~45kD to ~35kD) suggesting a loss of glycosylation. Importantly, the tunicamycin treated CM showed significantly reduced Wnt-TCF-inhibitory activity as compared to that of the control CM. The importance of Dkk1 glycosylation to its function was further substantiated when we observed 5-10 fold lower Wnt-TCF inhibitory activity in insect cell-derived Dkk1, which lacked proper glycosylation, as compared to that produced by mammalian cells (293A). These results indicate that in addition to conserved Cys-2 domain, the C-terminal 21 aa are essential for the inhibitory function of Dkk1. They also suggest that only properly glycosylated Dkk1 can fully inhibit the Wnt-TCF signal, presumably as a result of improved interaction with LRP5/6 and Kremen-2.

Disclosures: ***B.M. Bhat****, None.*

F264

Global Application of Expression Profiling Reveals Potential Involvement of the Wnt, IGF-I, Estrogen Receptor (ER), and BMP/TGFβ Pathways in C57BL/6J (B6) but not C3H/HeJ (C3H) Mouse Osteoblasts in Response to Fluid Shear Stress. K. H. W. Lau, S. Kapur, D. J. Baylink. Musculoskeletal Disease Center, Jerry L. Pettis Mem VAMC, Loma Linda, CA, USA.

Our previous studies indicate that, while B6 inbred mice responded to in vivo mechanical loading with an increase in bone formation; C3H mice showed no such response. In this study, we tested the hypothesis that this inbred mouse differential response would be present in vitro in response to shear stress. We found that a steady fluid shear stress of 20 dynes/cm^2 for 30 min, while significantly increased (by 2-fold, $p<0.001$) thymidine incorporation and ALP specific activity in B6 osteoblasts (ob), had no effects on either parameter in C3H ob, confirming that osteogenic responses to mechanical strains are genetically regulated. We next applied global gene expression profiling 4 hr after the 30-min shear stress in an attempt to identify signaling pathways to account for the differential shear stress response in ob from these 2 inbred strains of mice. RNAs isolated from C3H and B6 ob (4 replicates each) were analyzed by microarray with our in-house chips (containing 5,500 gene fragments). Paired t-test and Lowess normalization were performed with Genespring software and gene expression changes defined as significant if $p<0.05$. The expression of 672 genes in B6 ob and 477 genes in C3H ob was altered in response to the shear stress. 515 genes were affected only in B6 ob. Preliminary grouping (according to gene functions or pathways) of known mouse genes that were affected only in B6 ob revealed that (consistent with an anabolic response) genes involved in proliferation and energy metabolism were upregulated. Several genes of the IGF-I (IGFBP-5, IGF-IR, MKK3, Big MAPK1, c-Fos, c-Jun) and ER (ERα, NCOA1) pathways were upregulated only in B6 ob. Moreover, several genes of the BMP/TGFβ pathways (BMP-4, TGFβ1, TGFβ2, BMP2/4 receptor, Mef2, Dlx-1, Necdin) and the Wnt pathway (Wnt-5a, Lef-1, β-catenin) were also upregulated in B6 but not C3H ob. Regarding the Wnt pathway, the upregulation of gene expression of Wnt-5a, Lef-1, LRP-5, and β-catenin in B6 but not C3H ob was confirmed by real-time PCR and western blots. Importantly, endostatin (a potent inhibitor of wnt pathway) abolished the upregulation of β-catenin gene expression and blocked the shear stress-induced proliferation in B6 ob. In summary, the robust mitogenic response to steady shear stress in B6 but not C3H ob was associated with significant increased gene expression in the IGF, ER, BMP/TGFβ, and Wnt pathways. The differential regulation in these anabolic pathways could contribute to the good and poor response, respectively, in the B6 and C3H mice to fluid shear stress.

Disclosures: ***K.H.W. Lau****, None.*

F266

Essential Role for Siah1a, but not Siah2, Ubiquitin Ligase in Bone Growth and Remodeling. N. A. Sims[1], I. J. Frew*[2], J. M. W. Quinn[3], C. R. Walkley*[2], R. A. Dickins*[2], L. E. Purton*[2], D. D. L. Bowtell*[2], M. T. Gillespie[3]. [1]Department of Medicine at St. Vincent's Hospital, The University of Melbourne, Melbourne, Australia, [2]Peter MacCallum Cancer Institute, Melbourne, Australia, [3]St. Vincent's Institute, Melbourne, Australia.

The seven in absentia homolog (Siah) proteins function as E3 ubiquitin ligases to target degradation of diverse protein substrates. Mice have three homologous Siah proteins: Siah1a, 1b and Siah2. Siah1a and b differ by only 6 of their 282 amino acids, while Siah2 contains an extended N-terminal region. Given the tightly controlled process of proteasomal degradation of proteins in the Wnt pathway, we predicted that deficiencies in Siah (Siah1a and Siah2 null mice) may reveal physiological roles of these proteins in bone metabolism in vivo, and have analyzed adult Siah1a and Siah2 null (KO) mice by histomorphometry and ex vivo cell cultures.

Siah2KO mice are largely phenotypically normal, and while trabecular and cortical structure and bone turnover are normal, Siah2KO bone marrow produced more osteoclasts in vitro than wild-type bone marrow when stimulated with RANKL, indicating a role for Siah2 in regulating osteoclastogenesis, which is corrected by compensatory mechanisms in vivo.

Siah1aKO mice, however, are growth-retarded and exhibit early lethality. These mice also exhibit a striking osteopenia: trabecular bone volume was half that of wild type mice in both males and females. This osteopenia was associated not only with a low level of bone formation, including low osteoblast numbers and osteoid volume, but also a high level of bone resorption (osteoclast numbers were more than double wild type levels). While ex vivo osteoblast colony formation from Siah1aKO mice was normal, mineralization from these cells was elevated, and may explain the reduction in osteoid volume seen in vivo. In contrast, haematopoietic osteoclast progenitor numbers were normal in Siah1aKO mice and ex vivo osteoclast formation occurred at wild type levels. Furthermore, adoptive transfer of Siah1aKO bone marrow into wild type mice failed to generate osteopenia or elevated osteoclast numbers.

These findings suggest that, unlike Siah2, Siah1a is clearly essential for normal bone metabolism in vivo, yet the bone defect in Siah1a mutant mice is not the result of cell-autonomous requirements for Siah1a in either osteoblast or osteoclast formation.

Disclosures: ***N.A. Sims****, None.*

F268

OPPG and HBM Disease-causing Missense Mutations in LRP5 Have Opposite Effects on Wnt Signaling. M. Ai*, D. Schelling*, M. L. Warman*. Genetics, Case Western Reserve University, Cleveland, OH, USA.

Low-density-lipoprotein receptor Related Protein 5 (LRP5) plays a critical role in regulating bone mass. Nonsense, frameshift, and missense mutations in the gene cause the autosomal recessive disease osteoporosis-pseudoglioma syndrome (OPPG), which is characterized by reduced bone mass. Other missense mutations have been associated with dominantly inherited high bone mass (HBM) phenotypes. How missense mutations in the same gene cause opposite skeletal phenotypes is the subject of this study.

At least one function of LRP5 is as a co-receptor of Wnt ligand in the canonical signaling cascade. We tested 6 OPPG-causing missense muteins (S356L, T390K, G404R, D434N, G520V, G610R) and 7 HBM-causing missense muteins (D111Y, G171R, G171V, A214T, A214V, A242T, T253I) for their ability to transduce Wnt signaling in 293T cells using the TopFlash reporter assay. Wild-type LPR5, when co-transfected with v5-tagged Wnt1 (Wnt1-v5) yielded a 4-fold increase in luciferase activity compared to transfection with Wnt1-v5 alone. The OPPG-causing muteins S356L, T390K, and G520V completely abolished the response to Wnt1-v5, while G404R, D434N, and G610R reduced the response by >50%. Cell surface labeling studies suggest that some of the OPPG-muteins affect protein folding and transport to the cell surface, whereas others may affect Wnt1 binding or interaction with frizzled co-receptors. None of the 7 HBM-causing muteins demonstrated constitutive activity in the absence of Wnt1-v5 ligand. When compared to wild-type LRP5, each of the individual HBM-causing muteins caused modestly or moderately higher (5-35%) luciferase induction in the presence of Wnt1-v5. Also, we found that exogenously applied DKK1 was >50% less effective in inhibiting Wnt1-v5 signaling via the HBM-causing muteins compared to wild type LRP5. This result supports a similar observation made by Boyden et al (N Engl J Med, 2002, 346(20), 1513-1521) for the mutein G171V. Surprisingly, despite the ability of DKK1 to inhibit Wnt1-v5 signaling via LRP5, we could not detect a direct interaction between DKK1 and LRP5 by either co-immunoprecipitation or cell surface labeling. This suggests either that the mechanism of inhibition is more complex than a simple two-protein interaction or that another DKK family member with higher affinity for LRP5 is the primary regulator of signaling in bone. In conclusion, we find that OPPG-causing LRP5 missense muteins have completely or markedly reduced ability to transduce Wnt1-v5 signaling in 293T cells. HBM-causing muteins are not constitutively active, but have slightly increased responsiveness to Wnt1-v5, and are less inhibited by DKK1 compared to wild-type LRP5.

Disclosures: ***M. Ai****, None.*

F270

Characterization of Protein-Protein Interactions of Lrp5/6 with Dkk-, Sclerostin- and Kremen-Proteins. H. Glantschnig*[1], P. D. Zuck*[1], V. Kasparcova*[1], H. Zhang*[1], F. J. Hess*[2], L. P. Freedman*[1], S. Harada[1]. [1]Molecular Endocrinology & Bone Biology, Merck & Co.,Inc., West Point, PA, USA, [2]Molecular Neurology, Merck & Co.,Inc., West Point, PA, USA.

Gain of function mutations of LRP5 have defined Wnt/LRP signaling as regulator of bone mass accrual throughout life. LRP5 and LRP6 are cell surface co-receptors for Wnt and Dickkopf (Dkk) proteins, and ligand binding to LRP5/6 modulates the Wnt-signaling pathway. We have found earlier that Dkk-1, like Sclerostin, is expressed predominantly in adult bone. Internalization of LRP5/6 receptors, triggered by Kremen proteins and Dkk, has been proposed as a mechanism to down-regulate Wnt/LRP mediated signaling.

To further define the mechanism of ligand binding to LRP/Kremen receptors, we have established a cell-based ligand-binding assay. Dkk-1, Dkk-4, Soggy, and Sclerostin-proteins were fused to GFP and binding was observed to cells over-expressing LRP5/6 or Kremen2 proteins. Protein-interaction of LRPs and Kremen2 protein were studied by chemical cross-linking and co-immuno-precipitation. Taqman analysis was performed to measure Kremen transcripts in bone.

We find that, in the cell system used, ectopic Dkk-1, Dkk-4, and Sclerostin but not Soggy, bind to LRP5/6. We find that Kremen2 transcripts are highly expressed in bone tissue, and although Kremen2 showed little specific in-vitro binding of Dkk on its own, Kremen2 effectively cooperates with over-expressed LRP5/6 for Dkk binding. LRPs and Kremen2 were found to be associated on the cell surface of double-transfected cells. Interestingly, the complex containing LRP5/6 and Kremen2 on the cell surface was preformed, independently of ectopically added Dkk-1. Further, LRP/Kremen2 complex formation was not affected by LRP5G171V or LRP6G158V substitutions. More importantly, Dkk-1 as well as Sclerostin binding to LRP6G158V is diminished, and this defect extends to functionally affect the cooperativity seen for LRP/Kremen2.

HBM-mutations in LRPs result in reduced cell surface binding of ligands in vitro. This might result in a failure of LRPs to cooperatively interact with Kremen2 for ligand binding and a failure to efficiently remove the LRP/Kremen complex from the cell surface

Disclosures: ***H. Glantschnig****, None.*

F272

Hypoxia Inducible Factor-1 and Inducible Nitric Oxide Synthase are Involved in the Inhibition of Osteoblast Differentiation during Modeled Microgravity. M. Zayzafoon, V. E. Meyers, T. L. Clemens, J. M. McDonald. Department of Pathology, University of Alabama at Birmingham, Birmingham, AL, USA.

Spaceflight, prolonged disuse and aging are known to induce bone loss due, in part, to decreased osteoblastic differentiation. We have previously shown that osteoblastic differentiation of human mesenchymal stem cells (hMSC) is suppressed after 7 days of culture in modeled microgravity (MMG) while adipocytic differentiation is induced (*Endocrinology* 145:2421-2432). We are also showing at this meeting that MMG alters the actin cytoskeleton in hMSC. The purpose of this study is to examine the effects of MMG on the expression of inducible nitric oxide synthase (NOS2) in order to elucidate the mechanism by which MMG suppresses osteoblastogenesis. It is known that the expression of NOS2 is modulated in response to changes in the actin cytoskeleton. Here we show that exposure of hMSC to MMG for 3 hours increases NOS2 protein expression with plateau at 24 hours. NOS2 is known to be regulated by several transcription factors including the hypoxia inducible factor-1 alpha (HIF-1 alpha). Using Western blotting we show that HIF-1 alpha is acutely increased after 30 minutes of MMG and remains elevated for 7 days. In addition, EMSA demonstrated that MMG increases the DNA binding activity of the hypoxia response element (HRE). Surprisingly, this increase in HIF-1 expression and binding activity were not due to hypoxia. The use of the rotary cell culture system (RCCS), used to simulate microgravity, does not alter pCO2, pO2 or pH. MMG does not alter oxygenation parameters; pO2 (140.8 ± 4.9 mmHg in gravity and 150.4 ± 3.6 mmHg in MMG) and pCO2 (26.9 ± 1.3 mmHg in gravity and 25.3 ± 0.6 in MMG). In addition, MMG using the RCCS did not cause acidosis, as the medium's pH remained constant throughout the study (7.61 ± 0.02). Based upon our previous and recent findings, we propose a novel mechanism by which disruption of the actin cytoskeleton, as seen in microgravity or prolonged disuse, induces normoxic upregulation of HIF-1 alpha and NOS2. The resulting increase in nitric oxide inhibits osteoblastogenesis and induces adipogenesis. These findings may ultimately assist in developing novel anabolic therapy for various forms of osteoporosis.

Disclosures: ***M. Zayzafoon****, None.*

F275

Leptin Treatment Decreases Bone Marrow Adipocyte Number and Increases Endosteal Bone Formation in Leptin-Deficient Ob/Ob Mice. M. Hamrick[1], H. Choi*[2], D. Hartzell*[2], C. Pennington*[1], M. A. Della-Fera*[2], C. A. Baile*[2]. [1]Cellular Biology & Anatomy, Medical College of Georgia, Augusta, GA, USA, [2]Animal & Dairy Science, University of Georgia, Athens, GA, USA.

The limb bones of leptin-deficient ob/ob mice are known to show lower bone mass, density, and cortical thickness than the limb bones of normal mice. The low bone mass observed in the appendicular skeleton of ob/ob mice is also associated with a marked increase in marrow adipocyte number. Increased marrow adipogenesis has been implicated in the pathogenesis of osteoporosis because mesenchymal progenitor cell populations are directed towards the adipocyte lineage rather than the osteoblast lineage. We tested the hypothesis that leptin treatment increases osteogenesis and decreases marrow adipogenesis by treating leptin-deficient, ob/ob mice with leptin using two different doses of leptin: 2.5μg leptin per day and 10 μg leptin per day. One group of normal mice and one group of ob/ob mice were treated with saline (vehicle) as controls. At the age of 15 weeks mice were implanted with Alzet osmotic pumps for subcutaneous delivery of treatment solutions for 14 days at a delivery rate of 0.25 μl/h. Mice were injected with tetracycline (20 mg per kg body weight) 6 days before the end of the experiment and then with demeclocycline (same dosage as above) one day before the end of the experiment to label bone forming surfaces. The right femur was decalcified, embedded in paraffin, sectioned, and stained with hematoxylin and eosin to visualize adipocytes. The left femur was embedded in methyl-methacrylate and sectioned for visualization of fluorochrome labels. Results indicate that both doses of leptin decreased the number marrow adipocytes by more than 20% (P<.05) compared to PBS-treated ob/ob mice. Both doses also significantly (P<.05) increased the percentage of labeled bone forming endosteal surface by more than 30% compared to PBS-treated ob/ob mice. We conclude that leptin treatment can eliminate bone marrow adipocytes in leptin-sensitive animals and, furthermore, that elimination of marrow adipocytes has positive effects on bone formation.

Disclosures: ***M. Hamrick****, None.*

F277

Structure/Activity Analyses of β-catenin in Osteoblast Differentiation. V. S. Salazar*, J. P. Stains, G. Mbalaviele, R. Civitelli. Bone and Mineral Diseases, Washington University in St. Louis, St. Louis, MO, USA.

Although the Wnt/β-catenin signaling system is now recongnized as a critical regulator of bone formation, the mechanisms by which β-catenin, a ubiquitous transcription factor, provides tissue-specific cues remain unknown. We have previously reported that a transcriptionally active N-terminal truncated β-catenin (ΔN151) enhances osteoblast differentiation induced by BMP-2 in mesenchymal stem cells, but it is inactive by itself. Since endogenous β-catenin has functions beyond transcriptional activity (e.g. modulating cell structure and cell-cell adhesion), and since ΔN151 lacks many important protein-interaction sites (e.g. α-catenin), we asked whether alternative mutants could have different activity. Using retroviral vectors (pLNCX2), we expressed two other transcriptionally active β-catenin mutants, *mut*GSK3β (full length β-catenin with S33A, S37A, T41A, S45A mutations) and ΔN90, with >90% transduction efficiency in multipotent mesenchymal C3H10T1/2 or C2C12 cells. Similar to ΔN151, *mut*GSK3β and ΔN90 had negligible effects on osteogenic differentiation, but all mutants synergized with BMP-2 (100 ng/ml) to stimulate alkaline phosphatase activity (1.8-, 1.6-, 2.5- fold above BMP-2 alone in C3H10T1/2; 1.8-, 1.3-, 2.5-fold in C2C12 cells, respectively). Thus, interference with cell-cell adhesion or with α-catenin binding is not responsible for the osteogenic action of β-catenin. While all 3 mutants stimulated Tcf/Lef transcriptional activity, their relative potency did not correlate with their ability to stimulate cellular differentiation: *mut*GSK3b was the most powerful in activating a Tcf/Lef-luciferase reporter system (2.5-fold), whereas ΔN90 induced the highest degree of synergism with BMP-2 on alkaline phosphatase activity in both cell lines. Although Tcf/Lef transcriptional activity is not sufficient to drive differentiation, in C3H10T1/2 lysates both Tcf-4 and β-catenin co-immunoprecipitate with Smad4, suggesting that Tcf/Lef factors may participate in β-catenin osteogenic signaling. Interestingly, exposure to BMP-2 results in a rapid (within 10 min.) dephosphorylation of endogenous β-catenin, an event required for β-catenin transcriptional activity,

and this correlates to increased β-catenin/Smad4 interaction, as evidenced by co-immunoprecipitation analysis. Collectively, these data support the notion that β-catenin is not sufficient to induce osteogenesis (insufficient activator). Rather, it is direct interactions between β-catenin, downstream components of the canonical β-catenin system, and tissue-specific transcription factors, which drives mesenchymal cell differentiation towards the osteogenic lineage.

Disclosures: ***V.S. Salazar****, None.*

F283

Functional Interaction of Dynamin with the Cbl-Src-Pyk2 Signaling Complex in Osteoclasts Regulates Podosome Turnover and Bone Resorption. A. Bruzzaniti, L. Neff*, A. Sanjay, O. Destaing, P. De Camilli*, R. Baron. Yale University School of Medicine, New Haven, CT, USA.

Podosomes are highly dynamic actin-rich structures that mediate osteoclast (OC) attachment and migration. Following integrin engagement, Src forms a tri-molecular signaling complex with c-Cbl and Pyk2. Signaling from this complex is essential for cell migration, and deletion of either molecule leads to disruption of the podosome ring and decreased OC migration and/or resorption. Dynamin, a GTPase essential for endocytosis, is also involved in actin cytoskeleton remodeling. We previously showed that dynamin and dynK44A (a dynamin GTP-binding mutant) are localized to podosomes and that dynK44A slows actin turnover in podosomes relative to wild type dynamin (Ochoa, JCB, 2000). Thus, we hypothesized that dynamin regulates podosome turnover by modulating signaling downstream of integrins, possibly by interacting with the Cbl-Src-Pyk2 complex. Our results show that dynamin is enriched in the podosome ring of OCs and at steady state, is often restricted to the inner edge of the actin ring where podosomes may disassemble. Phosphorylation by Src is known to increase dynamin's basal GTPase activity and in Src-/- osteoclasts, which exhibit disrupted actin ring formation and decreased podosome turnover (Sanjay, JCB, 2001), dynamin failed to localize to podosomes, suggesting that Src-catalyzed phosphorylation of dynamin may promote podosome disassembly. OCs infected with dynamin adenovirus resorbed more when plated on dentin, while resorption was decreased in dynK44A-infected OCs, revealing a GTP-dependent role of dynamin in bone resorption, consistent with the reduced podosome turnover observed in dynK44A over-expressing cells. Immunoprecipitation studies demonstrated a GTPase-independent association of dynamin with both Cbl and Pyk2. Activated Src destabilized the association of dynamin with Cbl, while kinase-inactive Src stabilized dynamin-Cbl binding. Furthermore, a Cbl mutant that binds poorly to Src was constitutively bound to dynamin, confirming that the kinase activity of Src regulates the stability of the dynamin-Cbl complex. In contrast to Src, Pyk2 enhanced dynamin-Cbl association. Moreover, dynamin, but not dynK44A, decreased Pyk2 autophosphorylation at Tyr402, the docking site for the Src SH2 domain, potentially disrupting Src-Pyk2 interaction and negatively affecting recruitment and signaling from this integrin-induced complex at adhesion sites. These studies demonstrate a functional role for dynamin in actin remodeling in osteoclast podosomes and bone resorption, and suggest that this regulation occurs through dynamin's interaction with the Cbl-Src-Pyk2 signaling complex.

Disclosures: ***A. Bruzzaniti****, None.*

F285

c-Fms Y559 Is Required, but not Essential, for Formation of a Multimeric Complex which Controls M-CSF-dependent Motility in OCs. R. Faccio[1], S. Takeshita[2], J. Chappel*[2], G. Colaianni*[1], S. L. Teitelbaum[2], F. P. Ross[2]. [1]University of Bari, Italy and Washington University, St Louis, MO, USA, [2]Washington University, St Louis, MO, USA.

While M-CSF is known to induce cytoskeletal reorganization in macrophages and osteoclasts (OCs) by activation of PI3K and c-Src, the detailed mechanisms remain unclear. We have established a system to identify the role of individual tyrosine (Y) residues in signal transmission by the M-CSF receptor, c-Fms. Despite the fact that wortmannin, a potent inhibitor of PI3K activity, blocks M-CSF-induced OC motility, we find that mutation of Y721, the PI3K binding site of c-Fms, to phenylalanine (F) fails to affect cytoskeletal remodeling or actin ring formation, raising the question of how PI3K modulates the OC cytoskeleton. Surprisingly, mutation of c-Fms-Y559, which we show binds Src, to phenylalanine (F), blocks all the above actin-dependent processes and also fails to activate the Rho-GTPases. We find that PI3K binds c-Fms not only through the canonical c-Fms-Y721, but also indirectly at the level of c-Fms-Y559, via association with Cbl and Src, in a Src kinase dependent manner. Interestingly, several members of the Src Family bind directly c-Fms-Y559 and form a complex with Cbl and PI3K, even in Src-/- OCs, explaining the mechanism by which M-CSF rescues motility in these mutant cells. To better understand how c-Fms-Y559 controls actin reorganization and cell motility, we generated mutants in which selected Y residues are added back to a c-Fms receptor where the existing 7Ys are all mutated to F. While the single add-back mutant c-Fms-Y559 has no effect, the double add-back mutant Y559/Y697, the latter a putative binding site for Grb2, promotes 50% increase in cell migration compared to WT c-Fms, and induces formation of the Src/Cbl/PI3K complex. Grb2 is also recruited to this complex, via binding to Cbl, in a process dependent on M-CSF and blocked by the Src Family kinase inhibitor PP2. Finally, the add-back mutant Y721, in combination with Y559 and Y697, but not alone, maximally rescues osteoclast migration. The mechanism of this event involves recruitment of a second complex between PI3K and Src to Y721. In summary, we have dissected initial steps in a signaling cascade involved in M-CSF induced-actin dynamics. M-CSF, by binding its receptor c-Fms, initiates a series of phosphorylation events resulting in formation of multimeric complexes with Src/Cbl/PI3K/Grb2 via Y559 and Y697, and between PI3K and Src at the level of Y721, which are required for osteoclast motility.

Disclosures: ***R. Faccio****, None.*

F287

Bone Morphology of the Super *op/op* Mice, M-CSF and VEGFR-1 Tyrosine Kinase Domain Deficient Mice. S. Niida[1], K. Ikeda[1], M. Shibuya*[2]. [1]Bone and Joint Disease, National Center for Geriatrics and Gerontology, Obu, Japan, [2]Institute of Medical Science, University of Tokyo, Tokyo, Japan.

Vascular endothelial growth factor receptor-1 (flt-1/VEGFR-1) is a high-affinity tyrosine kinase (TK) receptor for VEGF, and regulates angiogenesis and functions of monocyte/macrophage lineage cells including osteoclasts. We demonstrated that VEGF and placenta growth factor (PlGF) can substitute for macrophage colony-stimulating factor (M-CSF), an essential cytokine for osteoclastogenesis, to recruit osteoclasts in CSF-1-deficient osteopetrotic (*op/op*) mice. In order to clarify how M-CSF and VEGF signalings interact in bone morphogenesis and to determine which VEGF receptor, VEGFR-1 or VEGFR-2, is responsible for osteoclast formation, we introduced VEGFR-1-signaling deficient mutation (*flt-1TK-/-*) into *op/op* mice. The double mutant (*op/opflt-1TK-/-*) mice, we call them super *op/op* mice in this abstract, show severe osteopetrosis due to a lack of osteoclasts. However, super *op/op* mice could not recruit enough osteoclasts in the bone, whereas in the *op/op* mice osteoclasts were progressively increased in an endogenous VEGF-dependent manner. Administration of VEGF-E, a VEGFR-2-specific ligand, efficiently rescued osteoclastogensis in the super *op/op* mice, whereas PlGF, a VEGFR-1-specific ligand, did not. Administration of VEGF-A, which binds to both VEGFR-1 and -2, induced osteoclast formation in the super *op/op* mice. These results were confirmed in osteoclast formation assays *in vitro* of spleen cells cocultured with OP9 cells (established from *op/op* mice and used as a feeder). These results indicate that osteoclast precursors alos express VEGFR-2 in the super *op/op* mice. Furthermore, the super *op/op* mice exhibited deformation of cartilage structure in the growth plate. Taken together with the previous report that VEGF is involved in cartilage remodeling at growth plate, it was suggested that signaling through VEGFR-1 tyrosine kinase plays a predominant role with M-CSF function for osteoclast formation and cartilage growth.

Disclosures: ***S. Niida****, None.*

F290

CSF-1-Dependent Rac-1 Interaction With the Coatomer Protein, Delta-COP in Osteoclasts: A Novel Cellular Role for Rac. K. Yu*, X. Zhao*, K. Insogna. Internal Medicine, Yale University School of Medicine, New Haven, CT, USA.

Rac-1 is a member of the family of small GTPases with prominent effects on the actin cytoskeleton. In osteoclasts, Rac-1 is required for CSF-1-induced cytoskeletal remodeling. To explore other metabolic pathways in osteoclasts where Rac plays a role, we undertook a yeast two-hybrid screen using the Clontec Matchmaker-3 system with wild-type Rac-1 as bait and a cDNA library prepared from osteoclast-like cells (OCLs) as prey. OCLs were prepared by co-culturing murine bone marrow and calvarial osteoblasts. RNA isolated from these cells was highly enriched for c-src, cathepsin K and calcitonin receptor transcripts. Five clones were identified in an initial mating assay screen of the OCL library, which contained 8.6X105 transformants. A Y2H assay using co-transformation confirmed that 3 of the five clones expressed Rac-interacting proteins. One of these encoded delta-COP, a member of the coatomer-I (COP I) family of proteins that coat transport vesicles involved in retrograde transport of proteins from Golgi to endoplasmic reticulum (ER). These retrograde transport vesicles recycle resident ER proteins back to the ER that have arrived at the Golgi as part of COP II-coated cargo vesicles. Deletion of delta COP is lethal in yeast. By RT-PCR we found that the transcript for delta-COP is highly expressed in OCLs. The cDNA for delta-COP was translated and radiolabeled using rabbit reticulocyte lysates and 35S-methionine, and the radiolabeled protein used in an in vitro pull down assay with GST-Rac. This experiment confirmed direct interaction of delta-COP and Rac. Immunoprecipitates of delta-COP prepared from lysates of p-zen cells (mouse fibroblasts expressing the CSF-1 receptor, c-fms) demonstrated CSF-1-dependent co-immunoprecipitation of Rac-1 and delta-COP that was maximal at 2 minutes. We repeated this experiment in lysates prepared from OCLs treated either with vehicle or CSF-1 for 2 minutes. As in p-zen cells, Rac co-immunoprecipitated with delta-COP after 2 min. of treatment with CSF-1. Confocal microscopy demonstrated co-localization of Rac-1 with TGN38, a trans-Golgi-specific protein. As far as we are aware, this is the first report to describe a potential role for Rac in early vesicular transport. It is also the first evidence that Rac can interact with a COP I protein, in this case delta-COP, and that this interaction is regulated by a growth factor. Given the known importance of Rac in regulating the osteoclast cytoskeleton and the importance of the cytoskeleton for Golgi function, it is possible that co-ordination of vesicular transport and actin dynamics in these cells is achieved, in part, through the interaction of Rac-1 and COP I proteins such as delta COP.

Disclosures: ***K. Yu****, None.*

F293

NF-kappa B and p38 MAPK Cross-talk Is Critical for Osteoclast Differentiation. C. Menaa[1], M. Corr*[2], C. Froelich*[1], S. Sprague[1]. [1]Evanston Northwestern Healthcare, Northwestern University, Evanston, IL, USA, [2]Evanston Northwestern Healthcare, Evanston, IL, USA.

RANKL is the key cytokine that regulates osteoclast (OC) differentiation. RANKL binds to its receptor, RANK, which then mediates the activation of NF-κB and various MAP kinases, in particular, p38 MAPK and JNK. The role of NF-κB and JNK in OC biology have been demonstrated by *in vivo* studies using knock-out mice. In, *in vitro* studies utilizing specific inhibitors, a regulatory role of the p38 MAPK has been demonstrated. Additional *in vitro* studies have demonstrated that NF-κB and p38 are regulated by both activators and inhibitors of OC formation suggesting cross-talk between these two signal pathways. However, at what step of OC formation and whether the activation of these signaling pathways is synchronized are not known. In order to differentiate the role of the p38 MAPK, we first developed stable cell lines of an OC precursor (RAW 264.7) which over-express dominant negatives (DN) of the upstream kinases regulating p38 MAPK, KK6 and KK3. While the *in vitro* assay demonstrated that the DNs block the effect of immuno-precipitated KK6 or KK3 on p38 MAPK, OC formation was not affected. Moreover, CFU-GM isolated from knock-out mice (KK3 -/- and KK6 -/-) show no difference to response to RANKL compared to the wild type. Equally important, double transfected cells, which over-expressed both the DN of KK6 and KK3, were still capable to form OC in response to RANKL. These findings suggest that an alternative pathway might account for the critical role of p38 MAPK during OC formation. However, the inhibition of NF-κB activity by over-expression of the super-repressor IκB mutant, totally blocked OC formation in response to RANKL. This effect was due to a shift in RAW cell differentiation pathway, rather than to an absolute reduction in numbers of OC precursors, which could be related to either an inhibition in their proliferation or an increase cell death. More importantly, this effect was not due to an impaired RANK receptor but rather to a specific effect of NF-κB, because the IκB super-repressor does not block RANKL stimulating NF-ATc1. Further analysis demonstrated that the p38 MAPK activation was impaired suggesting that the inhibitory effect of NF-κB on OC formation might be due to the inhibition of p38 MAPK. In summary, these data demonstrated that NF-κB is critical for OC differentiation even during the over-expression of NF-ATc1 and that p38 MAPK may mediate this effect. In conclusion, these results collectively suggest that the cross-talk between NF-κB and p38 MAPK is essential for osteoclastogenesis. Thus, our data provide new insight on how multiple signaling pathways of RANKL are synchronized.

Disclosures: ***C. Menaa****, None.*

F295

Modulation of NFAT2 by TLR Signaling in RANKL-Stimulated RAW264 Cells. T. Ogawa*[1], T. Hirouchi*[1], N. Ishida*[1], K. Yogo*[1], T. Kimura*[2], M. Matsumoto*[3], T. Seya*[3], T. Takeya*[1]. [1]Graduate School of Biological Sciences, Nara Institute of Science and Technology, Ikoma, Nara, Japan, [2]Research Division, Sumitomo Pharmaceuticals Co., Ltd., Konohana, Osaka, Japan, [3]Department of Immunology, Osaka Medical Center for Cancer and Cardiovascular Diseases, Higashinari, Osaka, Japan.

Osteoclasts are formed by fusion of mononuclear precursor cells derived from colony-forming unit granulocyte macrophages (CFU-GM) and branch from the monocyte-macrophage lineage during an early stage of the differentiation process. We previously elucidated the key role of a transcription factor, NFAT2, in the progression to multinucelated cell formation using an *in vitro* differentiation system consisting of the murine monocytic cell line RAW264 and recombinant RANKL. Toll-like receptors (TLRs) have been shown to affect bone metabolism, besides affecting the activation of macrophages and monocytes. Here we report that signaling through TLR 2, 3 and 4 downregulates *NFAT2* at the transcriptional level and suppresses the progression to multinucleated cell formation.

LPS and poly (I:C), triggers of TLR4 and TLR3 activation, respectively, induced *IFN*-ß in RAW264 cells, and conversely, ectopic administration of *IFN*-ß mimicked the effects of LPS and poly (I:C). Neutralizing antibody against IFN-ß suppressed the inhibitory effect of ectopically expressed IFN-ß, but did not cancel the effects of LPS, suggesting the existence of *IFN*-ß-dependent and -independent signaling cascades. In fact, MALP2, a TLR2 ligand, caused the same effects as LPS and poly (I:C), but its activity could be exerted without inducing *IFN*-ß. We found that c-Fos is a component of the AP-1 complex that binds to the *NFAT2* promoter in RANKL-stimulated RAW264 cells, and that IFN-ß as well as the TLR ligands downregulated c-*fos* mRNA. Furthermore, sustained activation of ERK was observed in the TLR ligand- and IFN-ß-treated cells, and PD98059, a specific inhibitor of MEK, restored c-Fos and NFTA2 expression and diminished the inhibitory effects of TLR ligands and IFN-ß.

Together, these results suggest that signaling cascades lying downstream of TLR2, 3 and 4 convergently activate ERK through IFN-ß-dependent and -independent pathways in RAW264 cells and downregulate the signaling from RANK to c-*fos* and *NFAT2*. TLRs, therefore, seem to regulate the balance of immune responses and bone metabolism during acute attacks of vertebrate hosts by various microbes by activating monocyte/macrophages on one hand and suppressing osteoclastogenesis on the other hand.

Disclosures: ***T. Ogawa****, None.*

F297

ITAM-mediated Costimulatory Signals Cooperate with RANKL for Osteoclastogenesis. T. Koga*[1], M. Inui*[2], A. Suematsu*[1], T. Taniguchi*[3], T. Takai*[2], H. Takayanagi[1]. [1]Department of Cellular Physiological Chemistry, Tokyo Medical and Dental University, Tokyo, Japan, [2]Department of Experimental Immunology, Institute of Development, Aging and Cancer, Tohoku University, Sendai, Japan, [3]Department of Immunology, Tokyo University, Tokyo, Japan.

We previously reported that RANKL-induced NFATc1 is a master transcription factor for regulating terminal differentiation of osteoclasts. However, it remains unclear how RANKL activates Ca^{2+} signals that lead to induction of NFATc1. In the immune system, DAP12 and FcRγ, which bear immunoreceptor tyrosine-based activation motif (ITAM), are shown to be important for Ca^{2+} signaling. This prompted us to analyze the role of ITAM in osteoclast differentiation. In the osteoblast-free culture system, osteoclastogenesis induced by RANKL/M-CSF in the bone marrow monocyte/macrophage lineage cells (BMMs) derived from DAP12-deficient mice was severely blocked. However, in coculture system with osteoblasts, the impairment of osteoclastogenesis in DAP12-deficient BMMs was efficiently recovered. In addition, DAP12-deficient mice contained a normal number of osteoclasts *in vivo*. These results suggest that osteoblasts can stimulate the pathway that compensates for the loss of DAP12-mediated ITAM signal. Among ITAM-harbouring adaptors, we found that FcRγ was also abundantly expressed in osteoclast precursor cells. Considering the possibility that DAP12 and FcRγ compensate for each other, we generated the double knock out (DKO) mice of DAP12 and FcRγ. *In vitro* osteoclastogenesis in precursor cells derived from DKO mice was completely blocked in both systems of RANKL/M-CSF and coculture with osteoblasts. Importantly, DKO mice exhibited severe osteopetrosis due to impaired osteoclast differentiation, indicating that DAP12 and FcRγ are essential for osteoclast differentiation *in vivo*. We analyzed DAP12- or FcRγ-associating immunoreceptors in osteoclast precursor cells and identified TREM-2 and SIRP-β1; OSCAR and PIR-A, which associated with DAP12 and FcRγ, respectively. Stimulation of these receptors accelerated RANKL-induced osteoclast differentiation. We found that Ca^{2+} oscillation and NFATc1 expression was impaired in RANKL-stimulated DKO cells, and that osteoclastogenesis in these cells was rescued by the ectopic expression of NFATc1, suggesting that ITAM signaling through these receptors is critical for Ca^{2+} signals and NFATc1 induction during osteoclastogenesis. Thus, ITAM-dependent costimulatory signals activated by multiple immunoreceptors are indispensable for the maintenance of bone homeostasis. This indicates that RANKL and M-CSF are not sufficient to activate signals required for osteoclastogenesis.

Disclosures: ***T. Koga****, None.*

F299

CD44 Intracellular Domain Stimulates Osteoclastogenesis in a Presenilin-dependent Manner. W. Cui*[1], C. Chalouni*[2], J. Zhang*[1], H. Ke[3], A. Vignery[1]. [1]Orthopaedics, Yale School of Medicine, New Haven, CT, USA, [2]Cell Biology, Yale School of Medicine, New Haven, CT, USA, [3]Metabolism, Pfizer Global Research and Development, Groton, CT, USA.

Presenilins (PS1 and 2) belong to an enzymatic complex that cleaves the intracellular domain of Alzheimer Precursor Protein (APP) after its extracellular domain has shed. Mutations in PS have been associated with Alzheimer Disease. While PS1 and PS2 share over 60% identity, only PS2 expression is regulated. In addition, PS1 deletion is associated with major skeletal defects. We identified PS2 as a transcript transiently induced in fusing macrophages using oligonucleotide microarray. As we previously reported, CD44 is a transmembrane protein the expression of which is highly but transiently induced in macrophages at the onset of fusion. CD44, like APP, sheds its extracellular domain. We therefore set out to investigate whether PS plays a role in osteoclastogenesis, and if so, whether it targets CD44. DAPT and DupE, two potent inhibitors of PS, dose-dependently inhibited fusion of pre-osteoclasts without affecting PS expression. To next investigate whether PS targets CD44, we engineered fusion proteins lacking CD44 extracellular domain (DE-CD44) tagged with myc or GFP inserted in the retroviral vector MigR1. Using confocal microscopy, we found DE-CD44-GFP transiently expressed in pre-osteoclasts localized in both the plasma membrane and the nucleus. This was confirmed by subcellular fractionation studies that revealed the presence of a lower molecular weight form of CD44 in the nuclear fraction. In contrast, DAPT and DupE treatment of these cells confined DE-CD44 localization to the plasma membrane. To investigate the role of CD44 intracellular domain (ICD), we engineered a fusion protein containing CD44-ICD tagged with myc. CD44-ICD-myc transiently expressed in pre-osteoclasts potentiated their fusion into TRAP+ multinucleated osteoclasts. In addition, CD44-ICD-myc rescued fusion in cells treated with DAPT. MigR1 containing myc alone had no effect. To initiate an investigation on the mechanism by which CD44-ICD promotes fusion, pre-osteoclasts were transiently transfected with CD44-ICD together with promoter-linked luciferase reporter genes. CD44-ICD strongly activated NFkB and SRE, and modestly AP-1, but not NFAT. We next subjected 8 month old female mice deficient in CD44 and age-sex matched wild types to pQCT analysis. CD44-/- demonstrated a 1.5 fold higher total bone density, and 2 fold higher trabecular bone density than controls. Together, our data suggest that the intracellular domain of CD44 stimulates osteoclastogenesis by virtue of altering gene transcription in a presenilin-dependent manner.

Disclosures: ***W. Cui****, None.*

F301

Multiple RANK Cytoplasmic Motifs Play Distinct Roles in Osteoclast Differentiation, Function and Survival. W. Liu*, D. Xu*, X. Feng. Pathology, Univ. of alabama at birmingham, Birmingham, AL, USA.

Osteoclasts differentiate from mononuclear cells of monocyte/macrophage lineage upon the stimulation of two critical factors: M-CSF and RANKL. RANKL, a member of the TNF superfamily, exerts its effects through its receptor RANK which is expressed on osteoclast precursors and mature osteoclasts. Since the unraveling of the RANKL/RANK system, it has been established that the RANKL/RANK system plays an important role in osteoclast differentiation, function and survival. As a member of the TNF receptor superfamily, RANK mediates intracellular signaling by recruiting signaling molecules such as TRAFs. The previous data have shown that the RANK possesses three functional RANK motifs (Motif 1: PFQEP$^{369-373}$; Motif 2: PVQEET$^{559-564}$ and Motif 3: PVQEQG$^{604-609}$ in its cytoplasmic domain that are capable of promoting osteoclast formation. In addition, Motif 1 is less potent than Motif 2 and Motif 3 in stimulating osteoclast formation. In the present study, we investigated the role of the three RANK cytoplasmic motifs in osteoclast function and survival. The bone resorption assays demonstrated that all these motifs are able to mediate bone resorption. However, our data indicated that Motif 1 plays a predominant role in modulating the survival of mature osteoclasts. Notably, while Motif 1 is not very potent in promoting osteoclast formation, it plays an important role in osteoclast survival. Thus, these three RANK motifs play distinct roles in osteoclast differentiation and survival. RANK has been shown to activate NF-κB/IκB and three MAPK (JNK, ERK and p38) pathways in osteoclasts. So, we examined the role of the RANK motifs in the activation of these signaling pathways. Our signaling studies demonstrated that these functional RANK motifs activate different intracellular signaling in osteoclasts. All three RANK motifs were able to activate IκB/NF-κB pathway. Moreover, our data showed that Motif 1 could also significantly activate all three MAPK pathways: JNK, ERK and p38. In contrast, Motif 2 only induced p38 activation and Motif 3 did not activate any of MAPK pathways. In summary, the identification of these functional RANK cytoplasmic motifs not only revealed the complexity of the RANK signaling in osteoclast formation, function and survival but also laid a foundation for further delineating downstream RANK signaling pathways in osteoclasts. Moreover, these RANK motifs themselves represent potential therapeutic targets for bone disorders such as osteoporosis.

Disclosures: ***W. Liu****, None.*

F304

In Vivo Characterization of β_3 Integrin $S^{752}P$ and $Y^{747}F/Y^{759}F$ Mutants in Ovariectomy-induced Bone Loss. H. Zhao, F. P. Ross, S. L. Teitelbaum, D. V. Novack. Departments of Pathology and Medicine, Washington University School of Medicine, St. Louis, MO, USA.

$\alpha_v\beta_3$ integrin, the most abundant integrin expressed in osteoclasts, plays a fundamental role in osteoclastic bone resorption. We have previously performed an in vitro structural-functional analysis of the β_3 integrin cytoplasmic domain mediating osteoclast function, using retroviral transduction of $\beta_3^{-/-}$ osteoclast precursors . Of a series of human β_3 integrin constructs bearing point mutations known to effect β integrin function, only one, $S^{752}P$, representing a mutation seen in Glanzmann's thrombasthenia, failed to rescue $\beta_3^{-/-}$ osteoclast function. Although Y^{747} and Y^{759} are essential for platelet function, the $Y^{747}F/Y^{759}F$ mutant behaved like β_3^{WT}. We previously demonstrated that $\beta_3^{-/-}$ mice are protected from ovariectomy-induced bone loss. In the current experiments we characterize the role of these β_3 mutants, in vivo, using the ovariectomy model, combined with transplantation of lentiviral-transduced bone marrow. Whole bone marrow cells were collected from $\beta_3^{-/-}$ female donor mice and transduced overnight with lentiviral vectors harboring human β_3^{WT}, β_3^{S752P}, or $\beta_3^{Y747F/Y759F}$, then tail-vein injected into irradiated $\beta_3^{-/-}$ female recipient mice. Five weeks later, baseline measurement of bone mineral density (BMD) was performed by DEXA, and the mice were ovariectomized. One-month after the operation BMD was again measured by DEXA, at the time of sacrifice. At this point, two months post-transplantation, approximately 40%-50% of bone marrow cells expressed the human β_3 constructs, as demonstrated by flow cytometry, with equivalent levels of surface expression. Bone marrow macrophages were also isolated and incubated with MCSF and RANKL for 5 days to generate osteoclasts. β_3^{WT} and $\beta_3^{Y747F/Y759F}$ but not β_3^{S752P} expressing osteoclasts had normal cell spreading and formed actin-rings on dentin. Most importantly, β_3^{S752P} transplanted mice, like $\beta_3^{-/-}$ mice, were protected from bone loss induced by estrogen deficiency, compared to β_3^{WT} and $\beta_3^{Y747F/Y759F}$ transplanted mice. Specifically, ovariectomy resulted in a 4% or 2.5% loss in whole body BMD in $\beta_3^{-/-}$ mice transduced with β_3^{WT} and $\beta_3^{Y747F/Y759F}$, respectively, while $\beta_3^{-/-}$ mice transduced with β_3^{S752P} showed a 2% gain ($p<0.01$). BMD loss was 10% in the lumbar vertebrae with β_3^{WT} and $\beta_3^{Y747F/Y759F}$, but only 2% with β_3^{S752P} ($p<0.01$). Isolated tibial BMD was 0.049 g/cm^2 for β_3^{WT}, 0.052 g/cm^2 for $\beta_3^{Y747F/Y759F}$, and 0.058 g/cm^2 for β_3^{S752P} ($p<0.01$). In summary, we have used a lentiviral transduction strategy to introduce various human β_3 integrin constructs into $\beta_3^{-/-}$ mice, demonstrating that S^{752}, and not $Y^{747/759}$, is critical for osteoclast function in vivo.

Disclosures: ***H. Zhao****, None.*

F306

Further Characterization of Human Osteoclast Inhibitory Peptide-1 (OIP-1/hSca) Gene Expression. M. Ito[1], H. Kajiya[1], N. Kawanabe*[1], N. Kurihara[1], T. L. Johnson-Pais*[2], J. J. Windle*[3], S. V. Reddy[1]. [1]Medicine-Hematology/Oncology, University of Pittsburgh, Pittsburgh, PA, USA, [2]Pediatrics, University of Texas Health Science Center at San Antonio, San Antonio, TX, USA, [3]Human Genetics, Virginia Commonwealth University, Richmond, VA, USA.

We have previously identified and characterized osteoclast inhibitory peptide-1 (OIP-1), a member of Ly-6 gene family. Although previous studies have determined the chromosomal localization and partial characterization of the OIP-1 gene 5'-flanking region, the promoter activity and mechanisms of gene regulation remain to be elucidated. Therefore, in the present study we isolated a human BAC genomic clone containing the OIP-1 gene and sequence analyzed 2 Kb 5'-flanking region for transcriptional factor binding motifs and promoter activity. We identified motifs with significant identity (>85%) for transcription factors SP-1, SRY, c-Myc, c-Myb, GATA-2, AP-2, AP-4 and ADR1 in the OIP-1 gene promoter region. IFN-gamma treatment of RAW264.7 cells transfected with OIP-1 gene promoter-luciferase reporter plasmids demonstrated a significant (4 fold) enhancement of OIP-1 gene promoter activity. In order to assess the effects of constitutive over-expression of OIP-1 on osteoclast differentiation, we stably expressed OIP-1 in RAW264.7 cells and clonal cell lines were established. OIP-1 expression in RAW264.7 cells significantly inhibited osteoclast differentiation compared to mock transfected cells stimulated with RANKL. We further examined OIP-1 binding to RAW 264.7 cells using FACS analysis. Fluorescein conjugated OIP-1 c-peptide demonstrate a low affinity binding (<30%) to these cells. These data may suggest presence of a low affinity binding surface receptor or membrane protein partner. To further determine the in vivo effects of OIP-1, we have developed transgenic mice in which OIP-1 expression was targeted to cells of osteoclast lineage using the mouse TRAP gene promoter and identified three founder mice (two males and one female), which express OIP-1. RANKL stimulation of OIP-1 mice derived bone marrow cells resulted in significantly decreased osteoclast formation compared to wild type littermates. Furthermore, OIP-1 transgenic mice bones demonstrated an osteopetrotic phenotype. These data suggest that OIP-1 is an important physiologic regulator of osteoclast development and bone resorption in vivo.

Disclosures: ***M. Ito****, None.*

F309

Recruitment of Csk to Lipid Rafts by Cbp/PAG Is Critical to the Regulation of c-Src Activity in Osteoclasts. T. Matsubara[1], F. Ikeda[1], K. Hata*[1], F. Ichida*[1], M. Okada*[2], R. Nishimura[1], T. Yoneda[1]. [1]Dept Biochem, Osaka Univ Grad Sch Dent, Osaka, Japan, [2]Oncogene Res, Res Inst for Microbial Diseases, Osaka, Japan.

A tyrosine kinase c-Src is essential for the formation of actin rings and ruffled borders and subsequent bone resorption in osteoclasts. c-Src activity is negatively regulated by Csk. Despite that Csk is ubiquitously expressed, c-Src activity is characteristically increased in osteoclasts compared with other cells, suggesting the presence of yet-unidentified specific mechanism for elevated c-Src activity in osteoclasts. Recently, Csk binding protein Cbp/PAG has been identified and found to recruit Csk to lipid rafts on cell membrane where c-Src and Csk harmoniously control actin organization. However, it is currently unexplored whether Cbp/PAG plays a role in the regulation of c-Src and Csk function and ultimately bone resorption in osteoclasts. To determine subcellular localization of c-Src and Csk in osteoclasts, lipid rafts were isolated from osteoclast-like cells formed in RAKL-treated spleen cultures by successive fractionation by Triton X-100 and n-octyle-D-glucoside treatment. Western analysis demonstrated that c-Src was localized in lipid rafts and highly activated. In contrast, Csk expression in lipid rafts was not detected, although its expression in unfractionated osteoclasts was equivalent to other tissues or cells including lung, liver and macrophages. To examine whether Cbp is involved in decreased Csk expression in lipid rafts, we determined Cbp expression in osteoclasts. Interestingly, Cbp expression in osteoclasts was much lower than other tissues or cells. In addition, co-immunoprecipitation experiments showed that the amount of Csk bound to Cbp was profoundly decreased in osteoclasts. Consistent with these observations, Cbp expression was markedly down-regulated in osteoclast-like cells formed in soluble RANKL-treated spleen macrophages or RAW-D cells, while c-Src activity was up-regulated. To validate the relationship between Cbp expression and Csk recruitment to lipid rafts, we introduced Cbp in osteoclasts using adenovirus technology. Cbp introduction caused physical association between Csk and Cbp and recruitment of Csk to lipid rafts in a Cbp concentration-dependent manner and profoundly suppressed c-Src activity. More importantly, Cbp markedly inhibited actin ring formation in osteoclasts and blocked pit formation on dentine slices by these osteoclasts. In conclusion, our results suggest that increased c-Src activity in osteoclasts is attributable to decreased Cbp expression, leading to impaired recruitment of Csk to lipid rafts. Cbp/Csk/c-Src cascade may be a critical signaling pathway involved in osteoclastic bone resorption.

Disclosures: ***T. Matsubara****, None.*

F311

Osteopetrosis in Pyk2 -/- Mice Is Due to an Autophosphorylation-dependent Cell Autonomous Defect in Actin Organization and Bone Resorption. A. Sanjay[1], H. Henn*[2], L. Neff*[1], N. Sims[1], K. Aoki[1], T. Miyazaki[1], J. Schlessinger*[2], R. Baron[1]. [1]Orthopaedics & Rehabilitation, Yale University School of Medicine, New Haven, CT, USA, [2]Pharmacology, Yale University School of Medicine, New Haven, CT, USA.

Pyk2 is a member of the focal adhesion kinase (FAK) family of non-receptor tyrosine kinases and like Src, it is highly expressed in podosomes in osteoclasts. Like Src, Pyk2 is phosphorylated in response to adhesion-induced integrin stimulation, but in a calcium-dependent manner. Pyk2 is characterized by a centrally located kinase domain which autophosphorylates tyrosine 402. The Src SH2 domain binds to the autophosphorylated tyrosine 402 of Pyk2, and we have previously established that this recruitment of Src to the activated integrin complex is necessary for osteoclastic bone resorption. Pyk2$^{-/-}$ mice are osteopetrotic and the osteopetrotic effects of deleting Pyk2 and Src are additive. The present study aimed to identify the molecular mechanisms by which Pyk2 regulates bone resorption. Mix-and-match experiments co-culturing bone marrow and osteoblasts from wild type and Pyk2$^{-/-}$ mice demonstrated that the defect is cell autonomous to the osteoclast lineage. Analysis of the cytoskeleton demonstrated that Pyk2$^{-/-}$ osteoclasts failed to form an actin ring. The podosomes were instead organized as dense clusters or in multiple small rings. In addition, the cells failed to form a proper ruffled border and the localization of the proton pump was altered. In vitro, osteoclasts derived from Pyk2$^{-/-}$ cultures showed decreased bone resorption activity with shallow pits. To determine the molecular mechanisms of Pyk2 function in osteoclasts, we then examined the effects of adenovirus-driven expression of wild type Pyk2 and kinase-dead and Y402F mutants of Pyk2 on the actin cytoskeleton and bone resorption. Reconstitution of Pyk2-deficient cells with wild type Pyk2 or kinase-dead Pyk2 resulted in full rescue of the altered actin phenotype, while in wild type osteoclasts they did not affect bone resorption. In contrast, expression of the Y402F mutant failed to rescue Pyk2$^{-/-}$ osteoclasts while its expression in wild type cells resulted in smaller cells with disrupted actin rings and decreased bone resorption. Thus, the osteopetrotic phenotype of Pyk2$^{-/-}$ mice is due to a cell autonomous defect in osteoclasts that affects the organization of podosomes, the actin ring and bone resorption and is due at least in part to the lack of Src recruitment to adhesion sites by Pyk2 autophosphorylation at Y402.

Disclosures: ***A. Sanjay****, None.*

F313

The IKK Inhibitor, NEMO-binding Domain Peptide, Blocks Osteoclastogenesis and Bone Erosion in Inflammatory Arthritis. S. Dai*, T. Hirayama*, S. Abbas*, Y. Abu-Amer. Orthopaedics and Cell Biology & Physiology, Washington University School of Medicine, Saint Louis, MO, USA.

Activation of the transcription factor NF-kB leads to expression of ample genes that regulate inflammatory and osteoclastogenic responses. In this regard, gene targeting studies have shown that members of the NF-kB family are obligatory for osteoclastogenesis, and mediate inflammatory processes. Activation of NF-kB requires induction of IkB kinase (IKK) complex that phosphorylates the NF-kB inhibitory protein IkB and leads to its dissociation form the NF-kB complex, thus permitting nuclear translocation of NF-kB. The IKK complex contains several factors primarily IKK-alpha, IKK-beta, and the regulatory kinase IKK-gamma, also known as NEMO. IKK activity is utterly dependent on the integrity of NEMO and entails recruitment of this kinase through its binding to carboxyl-terminal region of the IKK-alpha and IKK-beta, termed NEMO-binding domain (NBD). In this regard, recent studies have shown that a cell-permeable NBD peptide blocks association of NEMO with the IKK complex, inhibits cytokine-induced activation of NF-kB, and ameliorates inflammatory responses. Given the pivotal role of cytokine-induced NF-kB in osteoclastogenesis and inflammatory bone loss, we deduced that cell-permeable TAT-NBD peptide may hinder osteoclastogenesis and bone erosion in inflammatory arthritis. Using NBD peptides, we show that wild type, but not mutant, NBD blocks recruitment of NEMO to IKK-alpha and IKK-beta as reflected by diminished TNF activation of IKK-alpha and by comprehensive inhibition of IKK-beta activation measured by in vitro kinase activity assays. Consistent with the crucial role of IKKs as activators of NF-kB, and the pivotal role of NF-kB in osteoclastogenesis, wild type NBD inhibition of IKK-alpha and IKK-beta led to reduced TNF-induced promoter and DNA-binding activities of NF-kB and to inhibition of cytokine-induced osteoclast formation by macrophages. NF-kB is considered a key regulator of osteolytic and inflammatory responses. To test their effect in vivo, wild type and mutant TAT-NBD peptides were administered into mice prior to induction of inflammatory arthritis. Our findings indicate that wild type NBD efficiently blocks in vivo osteoclast recruitment, inhibits focal bone erosion, and ameliorates inflammatory responses in the joints of arthritic mice. The mutant NBD failed to execute these functions. These results provide strong evidence that IKKs are potent regulators of cytokine-induced osteoclastogenesis and inflammatory arthritis. More importantly, blockade of NEMO assembly with the IKK complex is a viable strategy to avert inflammatory osteolysis.

Disclosures: ***Y. Abu-Amer****, None.*

F316

Calcineurin Is Necessary for Osteoclastogenesis. L. Sun[1], Y. Peng*[1], J. Iqbal*[1], G. Rajendren*[1], B. Moonga[1], O. Adebanjo*[1], E. Abe[1], H. C. Blair[2], A. Zallone[3], S. Epstein[1], M. Zaidi[1]. [1]Medicine, Mt. Sinai School of Medicine and the Bronx VA GRECC, New York, NY, USA, [2]University of Pittsburgh, Pittsburgh, PA, USA, [3]University of Bari, Bari, Italy.

We demonstrate that dephosphorylation of the transcription factor NFATc1 by the Ca^{2+}-activated phosphatase calcineurin is required for osteoclast formation. Specifically, we show that (a) calcineurin A$\alpha^{-/-}$ progenitors display reduced osteoclastogenesis, (b) the calcineurin inhibitors cyclosporine A (CsA) and tacrolimus (FK506) inhibit osteoclast differentiation, (c) calcineurin over-expression, as a TAT fusion protein, stimulates NFATc1 expression, (d) calcineurin dephosphorylates NFATc1, and (e) dominant-negative and constitutively-active NFATs, respectively, inhibit and enhance osteoclast differentiation. Immune labeling localized calcineurin to osteoclasts both *in vivo* and *in vitro*. Real time PCR showed that the calcineurins Aα, Aβ, Aγ, B1, and B2 remained constant during osteoclastogenesis. However, NFATc1 expression increased up to 10-fold at days 3 and 5, while NFATc2 showed a 5-fold decrease at day 5. NFATs c3 and c4 showed no change. Parallel cross-linking, immunoprecipitation, and phosphatase assays determined that NFATc1 bound to, and was dephosphorylated by calcineurin Aα. That calcineurin was required for osteoclastogenesis was established by the 50% reduction in osteoclast formation noted in calcineurin A$\alpha^{-/-}$ bone marrow cell cultures and in cultures treated with CsA or FK506. In separate experiments, TAT-calcineurin Aα over-expression in RAW-C3 cells enhanced NFATc1, and to a lesser extent NFATc2 expression. Inhibiting the expression of specific calcineurin isoforms through anti-target (Aα, Aβ, Aγ or B1) U1 vectors resulted, in every case, in a marked reduction in NFATc1 expression. TAT-calcineurin Aα increased osteoclast differentiation markers, notably TRAP and β3. Co-expression of TAT-calcineurin Aα with dominant-negative NFAT significantly attenuated this induction, establishing that NFAT was downstream of calcineurin. Finally, constitutively active NFAT stimulated TRAP and β3 expression by up to 8-fold, confirming a direct effect of NFAT on osteoclast differentiation. Taken together, the results demonstrate that an intact calcineurin-NFAT axis is a requirement for full osteoclastogenesis.

Disclosures: ***L. Sun****, None.*

F318

An Osteoclastic Protein-Tyrosine Phosphatase (PTP-oc) Regulates Osteoclast Activity In Part By Decreasing Osteoclast Apoptosis Through c-Src-Dependent Activation of NFκB. K. H. W. Lau, M. Amoui, D. J. Baylink. Jerry L. Pettis Mem VAMC, Loma Linda, CA, USA.

Our previous studies have indicated that PTP-oc plays an important regulatory role in osteoclast (Oc) activity. The present study sought to determine the mechanism whereby PTP-oc regulates Oc activity by evaluating the effects of overexpression of wild-type (WT) or phosphatase-dead (PD) PTP-oc on Oc or precursors. We have shown that Oc-like cells derived from RAW264.7 clones stably overexpressing WT-PTP-oc showed 2- to 3-fold increases, while Oc-like cells derived from stable clones expressing PD-PTP-oc had a significant > 50% reduction in resorption activity, suggesting that these clones can be used to investigate the mechanism whereby PTP-oc regulates Oc activity. Since c-src has an essential role in Oc activity and since c-src is regulated negatively by tyr-527 phosphorylation (PY527), we tested the hypothesis that PTP-oc acts to dephosphorylate c-src PY-527, leading to c-src activation and increased Oc activity. The rationale for this hypothesis was that we had previously shown that WT-PTP-oc overexpressing clones showed significant reduction, whereas PD-PTP-oc expressing clones had elevation, in c-src PY527. The Oc-like cells derived from WT-PTP-oc overexpressing clones appeared to have a longer life span than control Oc-like cells. Because an increase in the life span of Oc could increase their overall resorption activity, we sought to test the hypothesis that PTP-oc regulates Oc activity in part by reducing the apoptosis of Oc. Because the NFκB pathway (activated by phosphorylation and degradation of IκB) has anti-apoptotic functions in Oc, and because IκB can be phosphorylated by c-src in Oc, we tested the effects of PTP-oc overexpression on NFκB activation. We found that WT-PTP-oc overexpressing clones showed a significant decrease (30-70%) in cellular IκB level with a corresponding increase (50-100%, $p<0.01$) in NFκB activation. Conversely, PD-PTP-oc expressing clones exhibited a 50-75% ($p<0.01$) increase in cellular IκB and a 25-50% reduction in NFκB activation. Moreover, WT-PTP-oc overexpressing clones showed a 2- to 4-fold ($p<0.001$) decrease, whereas PD-PTP-oc expressing clones had an increase (50% to 2-fold, $p<0.001$), in apoptosis. Consistent with the premise that the increased IκB degradation was mediated through PTP-oc-induced c-src activation, we found that overexpression of the K295S-inactive c-src mutant in PTP-oc overexpressing clones led to several-fold increases in cellular IκB level. In conclusion, these findings are entirely consistent with the position that PTP-oc activates Oc activity in part by decreasing Oc apoptosis through the PTP-oc-mediated c-src-dependent activation of the NFκB pathway.

Disclosures: ***K.H.W. Lau****, None.*

F320

SHIP Negatively Regulates M-CSF Stimulated Proliferation of Osteoclast Precursors via Altering the Akt-GSK-3β - cyclin D Pathway. P. Zhou[1], S. L. Teitelbaum[1], N. Namba*[2], C. D. Helgason*[3], R. K. Humphries*[3], G. Krystal*[3], F. P. Ross[1], S. Takeshita[1]. [1]Pathology, Washington University, St. Louis, MO, USA, [2]Padiatrics, Okayama University, Okayama, Japan, [3]Terry Fox Laboratory, BC Cancer Agency, Vancouver, BC, Canada.

SHIP, an SH2-containing inositol-5-phosphatase, negatively regulates phosphatidylinositol-3-kinase (PI3-K)-initiated signaling by dephosphorylating phosphatidylinositol-3, 4, 5-triphosphate. SHIP is essential for normal bone homeostasis as knock out mice contain increased numbers of hyper-resorptive osteoclasts leading to osteoporosis. SHIP null osteoclast precursors, in the form of bone marrow macrophages, undergo robust osteoclastogenesis in response to both macrophage colony-stimulating factor (M-CSF) and receptor activator of nuclear factor-κ B ligand (RANKL) *in vitro*. Here we characterize the mechanism involved in the negative regulation of osteoclast differentiation by SHIP. We find that inhibition of M-CSF dependent osteoclast precursor proliferation by SHIP contributes to the ability of the lipid phosphatase to suppress osteoclastogenesis. We show that *SHIP*$^{-/-}$ osteoclast precursors exhibit a hyperproliferative response to M-CSF. This accelerated proliferation correlates with advanced and elevated accumulation of D-type cyclins and subsequently hyperphosphorylation of the retinoblastoma (Rb) protein in *SHIP*$^{-/-}$ osteoclast precursors compared to wild type cells. Analysis of M-CSF signaling reveals that SHIP suppresses activation of Akt but not ERK. Consistent with elevated active Akt in *SHIP*$^{-/-}$ osteoclast precursors, inactivation of GSK-3β , a process primarily regulated by Akt-induced phosphorylation, is also enhanced in these cells. Inhibition of PI3-K activity by the specific inhibitor, LY294002, abrogates M-CSF induced Akt activation, GSK-3β phosphorylation and D-type cyclin expression, and also dose dependently blocks osteoclast precursor proliferation at doses that have no affect on cell viability. Reconstitution of SHIP expression in *SHIP*$^{-/-}$ osteoclast precursors via retrovirus corrects their enhanced Akt activation, proliferation and osteoclastogenesis. Retroviral expression of SHIP mutants lacking phosphatase activity, or the N-terminal SH2 domain or the C-terminal 163 amino acids in *SHIP*$^{-/-}$ osteoclast precursors fails to rescue enhanced osteoclastogenesis, documenting the requirement of these domains in SHIP-regulated osteoclast precursor proliferation and osteoclastogenesis. These studies establish a critical role of the PI3-K->SHIP->Akt->GSK-3β pathway in M-CSF induced osteoclastogenesis.

Disclosures: ***P. Zhou****, None.*

F323

Clinically-Defined Frailty Is Associated with Lower Hip Bone Mineral Density and a Greater Rate of Decline in Hip Bone Mineral Density in Older Women: Data from the Study of Osteoporotic Fractures. J. K. Tracy*[1], M. C. Hochberg[2], J. Cauley[3], K. Ensrud[4], T. Hillier*[5]. [1]Epidemiology, University of Maryland, Baltimore, MD, USA, [2]Medicine and Epidemiology, University of Maryland, Baltimore, MD, USA, [3]Epidemiology, University of Pittsburgh, Pittsburgh, PA, USA, [4]Medicine, University of Minnesota, Minneapolis, MN, USA, [5]Medicine, Kaiser Permanente, Portland, OR, USA.

To determine whether the clinical syndrome of frailty is associated with lower bone mineral density (BMD) in older women, we evaluated data from 7809 white women aged 67 years and above (mean [SD] 73.6 [5.1] years) who completed their second clinic visit (V2) between 1988-1989 and had BMD measured by DXA (Hologic QDR-1000, Waltham, MA). Women were categorized into three groups (frail, pre-frail, not frail) based on a phenotypic definition that includes the elements of weight loss, weakness, poor endurance and energy, slowness and low physical activity (J Gerontol 2001;56A:M146-56). 629 (8.1%) women were categorized as frail (3 or more features), 4987 were pre-frail (1 or 2 features) and 2193 were not frail (no features). Frail women were significantly older, shorter and lighter and more likely to have had a prior fracture than both pre-frail and not frail women. Frail women had lower total hip and femoral neck BMD (P < .001); however, lumbar spine BMD did not differ by frailty group (Table 1). These results were unchanged after adjustment for age. To determine whether frail women had a greater rate of decline in total hip BMD, we evaluated data from the subgroup of 5657 women who had BMD measured by DXA at both V2 and V4, a mean of 3.5 years apart. Frail women had a greater rate of decline in total hip BMD, even after adjustment for age and weight (P = .001) (Table 2). These results demonstrate that the clinical syndrome of frailty is associated with both lower hip BMD and a greater rate of decline in hip BMD in older women. Further analyses will explore whether frailty is an independent risk factor for hip fracture among older women.

Table 1. Mean (SD) BMD (gm/cm2) by frailty group

Site of BMD	Frail	Pre-frail	Not frail
Total Hip	0.73 (.14)	0.75 (.13)	0.77 (.13)
Femoral Neck	0.62 (.11)	0.65 (.11)	0.66 (.11)
Lumbar Spine	0.85 (.17)	0.86 (.17)	0.86 (.17)

Adjusted rate of change (%/year) in Total Hip BMD by Frailty Group (mean [95% confidence intervals])

Frail	Pre-frail	Not frail
-0.79 (-0.93, -0.64)	-0.59 (-0.63, -0.54)	-0.52 (-0.58, -0.49)

Disclosures: ***M.C. Hochberg****, None.*

F328

The Relation between Dietary Vitamin A and Bone Mineral Density in a Multi-ethnic Cohort of Midlife Women. M. Huang*[1], A. Karlamangla*[1], C. Crandall[2], B. Sternfeld*[3], C. Luetters*[1], G. Block[4], G. A. Greendale[1]. [1]Department of Medicine/Division of Geriatrics, University of California, Los Angeles, Los Angeles, CA, USA, [2]Div of Gen Int Med and Health Svcs Res, University of California, Los Angeles, Los Angeles, CA, USA, [3]Dept of Epidemiology and Biostatistics/Div of Research, Kaiser Permanente, Oakland, CA, USA, [4]Division of PH Biology & Epidemiology, University of California, Berkeley, Berkeley, CA, USA.

In animals, high levels of vitamin A stimulate bone resorption and inhibit bone formation. In humans, observational studies suggest a detrimental effect of Vitamin A on bone, but these studies have largely been cross-sectional and have not focused on midlife women.

To study the association between vitamin A intake and longitudinal change in bone mineral density (BMD), we analyzed data from the Study of Women's Health Across the Nation (SWAN), a multi-ethnic, community based, cohort study of women aged 42 to 52 years at entry. Dietary and supplement vitamin A intakes were estimated at baseline from an interviewer-administered food frequency questionnaire. This analysis includes African-American (N =287), Caucasian (N = 645), Chinese (N =162) and Japanese (N =183) participants. The mean total daily vitamin A (diet + supplement) and dietary vitamin A (from food only) intakes were 2731 and 993 RE/day, respectively. BMD were measured at lumbar spine, hip and femoral neck (FN) sites, both at baseline and follow up visits. Energy-adjusted Vitamin A intakes were calculated using the residual method. Linear regression models were run separately for each site (spine, FN, and total hip); change in BMD between baseline and the 4th annual follow up visit were the outcome variables. Separate regression models considered 2 primary vitamin A exposure variables: quartiles of energy-adjusted total vitamin A intake (diet + supplements) and quartiles of energy-adjusted dietary vitamin A intake (food sources only). All models controlled for age, ethnicity, study site, smoking history, physical activity, dietary calcium, body mass index, duration of hormone use during the study, duration in different menopause transition status, and site-specific BMD at baseline.

Dietary vitamin A and total vitamin A were not associated with change in spine or FN BMD. Higher dietary vitamin A was associated with a longitudinal decline in hip BMD. Compared to the lowest quartile of dietary vitamin A intake, the beta coefficients for 2nd to 4th quartiles were -0.0036, -0.0017 and -0.0071 (p = 0.03). In contrast, total vitamin A (diet + supplement) was not associated with longitudinal change in hip BMD.

Our data provide some support for the detrimental effect of high vitamin A from dietary sources on hip BMD. The effect of total vitamin A intake (diet + supplement) on BMD may be confounded by other constituents in the supplements (e.g. vitamin D).

Disclosures: ***M. Huang****, None.*

F330

Beer Intake in Men, and Wine Intake In Post-Menopausal Women, Is Associated With Higher Bone Mineral Density. K. L. Tucker*[1], J. Powell*[2], N. Qiao*[1], L. A. Cupples*[3], D. P. Kiel[4]. [1]USDAHuman Nutrition Research Center, Tufts University, Boston, MA, USA, [2]Human Nutrition Res Lab, Med Research Council, Cambridge, United Kingdom, [3]Epidemiology, Boston University, Boston, MA, USA, [4]Hebrew Rehab Ctr for Aged, Harvard Med Sch, Boston, MA, USA.

Although alcoholism is associated with osteoporosis, positive associations between moderate alcohol intake and BMD have been noted. However, it is not known if this is due to alcohol per se, or to components in alcoholic beverages, such as silicon (si) in beer or phytochemicals in wine. We examined intake of total alcohol and of wine, beer and liquor with BMD in the Framingham Offspring cohort. BMD was measured at the spine and hip using a Lunar® DPX-L. Dietary intake was assessed by food frequency questionnaire. We regressed each BMD measure onto alcohol intake, as g/d, for men, post-menopausal and pre-menopausal women, adjusting BMI, height, age, physical activity, smoking, osteoporosis medication, calcium or vitamin D supplements, dietary intake of energy, protein, magnesium, calcium and vitamin D, season of measurement and for women, menopause status and estrogen. We repeated analyses replacing total alcohol with beer, wine and liquor. Finally, we categorized intakes as none, moderate (up to 1 drink/d women; 2/d men), and heavy, and compared adjusted LS means for BMD. Linear results follow with coefficients for the trochanter, as example, and # (of 5) BMD sites where p <.05:

	Men		Post-menopausal Women		Pre-menopausal Women	
	b	#	b	#	b	#
Alcohol	.00064**	1	.00100***	5	.00028 (0)	0
Beer	.00102**	2	.00023	0	-.00080 ()	0
Wine	.00105+	0	.00177***	0	.00059 ()	0
Liquor	.00004	0	.00128	2	.00308 (ns)	0

+p<.1, *<.05, ** <.01, *** <.001

In men, beer was significantly associated with BMD at the femoral neck and trochanter, and approached significance for total BMD and spine. Adjustment for si intake attenuated results with beer, but not wine, suggesting that si in beer could partially explain this association. For post-menopausal women, wine was significant at all 5 sites, and liquor at the trochanter and spine. No form of alcohol was associated with BMD in pre-menopausal women, but power was low in this group. Comparison of LS means by intake category confirmed a tendency to linear trend, except for liquor in men, where heavy drinkers had lowest BMD at all sites. These results reinforce the idea that moderate alcohol use is protective for bone, but suggest that wine and beer may contain additional protective components.

Disclosures: ***K.L. Tucker****, None.*

F333

The Relationship Between Historical Height Loss and Multiple Vertebral Fractures. K. Siminoski[1], K. Lee*[2], H. Jen*[2], R. Warshawski*[2]. [1]Radiology and Medicine, University of Alberta, Edmonton, AB, Canada, [2]Radiology, University of Alberta, Edmonton, AB, Canada.

We have analyzed the relationship between historical height loss (HHL) and the presence of multiple prevalent vertebral fractures Subjects were women referred for specialist assessment of osteoporosis (n=490; average age 56 yrs; range: 18-92 years). HHL was determined as the difference between the tallest recalled height and height measured using a stadiometer. Vertebral morphometry was performed on all subjects from T4 to L4. Prevalent vertebral fracture was defined as a vertebral height ratio < 0.80. One or more fractures were present in 34.3%; the average number of fractures among those with fractures was 2.3±0.3.

The areas under the receiver operating characteristics curves (AUC) increased for the ability of HHL to detect greater numbers of fractures. For detection of 1 or more fractures, the AUC was 0.69; for 2+ fractures AUC = 0.74; for 3+ fractures AUC = 0.79; for 4+ fractures AUC = 0.81; and for 5+ fractures AUC = 0.90.

The odds ratios (OR) for detecting 1 or more fractures increased with the amount of height loss, as shown in the figure. The rate of increase was modest until HHL = 6-8 cm, where OR = 9, and only increased sharply when HHL >8 cm, where OR = 20. The same relationship was seen for detecting higher numbers of fractures, with the OR rising sharply after HHL >6 cm. For detecting 5 or more fractures, HHL = 6-8 cm produced an OR of 9, while HHL >8 cm produced OR = 64.

Two relationships were revealed by these analyses. First, the greater the number of prevalent vertebral fractures to be detected, the better HHL performed as a clinical test. Second, for a specific number of predicted vertebral fractures, the OR remained relatively flat until HHL >6 cm, and only rose substantially when HHL >8 cm. We conclude that there is a moderate relationship between historical height loss and prevalent vertebral fractures, and that the relationship is even stronger with multiple vertebral fractures. This is further evidence of the utility of using historical height loss in the assessment of osteoporotic patients or those at risk for osteoporosis.

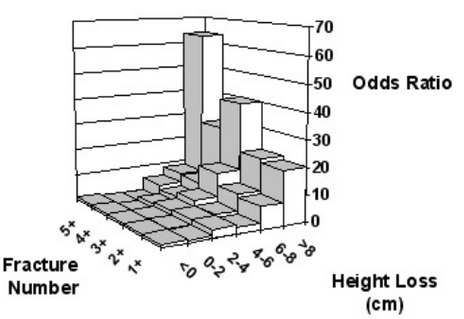

Disclosures: ***K. Siminoski****, None.*

F335

Knee Pain, Knee Osteoarthritis and the Risk of Fracture. N. K. Arden*[1], S. Crozier*[1], H. Smith*[1], F. Anderson*[1], P. Maslin*[2], H. Raphael*[1], C. Cooper[1]. [1]Southampton University Hospitals, MRC Epidemiology Resource Centre, Southampton, United Kingdom, [2]Department of Academic Primary Care, Southampton, United Kingdom.

Patients with knee osteoarthritis have increased BMD but whether this is translated into a reduced risk of fracture is uncertain. The relevance of knee pain (KP) versus a clinician diagnosis of knee OA (COA) is also uncertain. We studied 6,641 elderly men and women who participated in a three year RCT of intramuscular vitamin D. Patients were randomised to 300,000 units of ergocalciferol or placebo annually for three years and completed fracture and fall diaries every 6 months.All subjects were asked if they suffered from knee pain or had COA.

The median age was 78.8 (IQR 76.7, 81.7) and 54% were female. There was no effect of vitamin D on non-vertebral fractures and so the two groups were combined and treatment group added into the statistical model.

2,186 subjects reported knee pain at study entry (PKP)and 581 during follow up (IKP). 277 reported COA at entry (PCOA) and 82 during follow up (ICOA). Both KP ((HR 95% CI)1.27 (1.19, 1.36)) and COA (1.14 (1.01, 1.29)) were associated with an increased risk of falls. There was no significnt difference between the incident and prevalent groups. The risk of fracture (table) were increased for both KP and COA, but with greater HR's for COA. When falls were added into the statisitical model, the hazard ratios were substantially reduced for knee pain, remaining significant only for hip fracture and PKP (1.86 (1.10, 3.16)). The addition of falls had less of an effect on the association with COA, the association with PCOA still 1.53 (1.04, 2.24). The computed 5 year risk of a non-vertebral fracture for a 75 year old man without KP, with KP and with COA are 4.7%, 6.0% and 7.0% respectively.

Despite an increase in BMD, patients with KP and COA have an increased risk of non-vertebral and hip fracture, which is partially explained by an increased risk of falls. When assessing a patients risk of fracture, KP and COA should be included as important risk factors .

Hazard ratio of fracture in knee pain and knee osteoarthritis

	PKP	IKP	PCOA	ICOA
Non-vertebral	1.17 (0.93, 1.48)	1.37 (1.01, 1.87)	1.60 (1.10, 2.36)	1.72 (0.89, 3.33)
Hip	2.00 (1.18, 3.37)	1.01 (0.39, 2.58)	2.21 (0.95, 5.13)	2.46 (0.60,10.1)
Wrist	0.92 (0.55, 1.55)	1.42 (0.76, 2.64)	0.76 (0.24, 2.42)	2.57 (0.81, 8.13)

Disclosures: ***N.K. Arden****, None.*

F336

Changes in Hip Geometry from Medieval to Modern Times. A. Chumley*[1], G. Petley*[1], C. J. Edwards*[2], P. Taylor*[1], S. Mays*[3], J. Sofaer Derevenski*[4], P. Mahon*[5], C. Cooper[5], N. K. Arden*[5]. [1]Medical Physics, Southampton, United Kingdom, [2]Department of Rheumatology, Southampton, United Kingdom, [3]English Heritage, Brighton, United Kingdom, [4]Department of archaeology, University of Southampton, United Kingdom, [5]MRC Epidemiology Resource Centre, Southampton, United Kingdom.

The age and sex adjusted rates of hip fracture are increasing in many countries. Femoral neck geometry, especially femoral neck axis length (FNAL) has increased over the last 40 years and may partially explain this association. Here we extend these observations to femurs dating from the 10th-16th Centuries.

Sixty two adult female femora from the medieval archaeological site of Wharram Percy, England were scanned using pencil beam DXA. FNAL and the femoral neck width (FNW) were evaluated.. These measurements were compared with age and sex matched femoral scans from randomly selected volunteers in Southampton, England collected in the 1990's using the same densitometer.The use of pencil beam, as opposed to fan beam DXA, ensured that there were no magnification errors in comparing the two sets of results. Identical scan modes and settings were used to acquire both sets of femoral scans. Rigorous theoretical modelling, showed that there may be errors in the results, if femurs from the different eras were not positioned identically. To account for this, a positioning rig for the medieval femora was constructed. This allowed each femur to be positioned with the correct amount of rotation and abduction, ensuring that the femoral neck was parallel to the surface of the scanner. The scans were analysed by one operator (A-C). Measurement of the FNAL and the FNW were assessed using the DXA software, and the ratio FNAL/FNW was calculated. These results were then adjusted for the difference in height between the two groups.

FNAL and the FNAL/FNW ratio were found to be significantly greater in modern femurs ($p<0.001$) compared with medieval femurs after adjustment for height. No significant change in FNW was found.

These findings indicate that the proximal femur has undergone a change in shape, as opposed to an overall increase in size. An increase in the FNAL/FNW ratio of modern women, suggests that the femoral neck is now narrower for a given length and this may offer a partial explanation for the increase in fracture incidence in this group.

Mean (SD) femoral neck dimensions (values adjusted for height)

	Medieval	Modern	p value
Femoral neck length (mm)	85.8 (5.0)	92.4 (5.3)	<0.001
Femoral neck width (mm)	28.8 (2.1)	28.6 (1.9)	0.38
Femoral neck length / Femoral neck width	3.0 (0.2)	3.2 (0.2)	<0.001
Height (cm)	154.6 (20.5)	162.6 (6.6)	0.006

Disclosures: ***A. Chumley****, None.*

F339

Effect of Age and Bone Mineral Density (BMD) on Short-term Fracture Risk in Postmenopausal Women Age 50 - 99. E. S. Siris[1], S. K. Brenneman[2], Y. Chen[2], P. D. Miller[3], S. Sajjan*[2], E. Barrett-Connor[4]. [1]Columbia University, New York, NY, USA, [2]Merck & Co., Inc., West Point, PA, USA, [3]Colorado Center for Bone Research, Lakewood, CO, USA, [4]University of California, San Diego, La Jolla, CA, USA.

The relationship between bone mineral density (BMD) and fracture risk has been reported mostly in women age 65 years and older. Less is known about the risk of fracture for younger women. Using the National Osteoporosis Risk Assessment (N.O.R.A.) data, we report fracture events during 3 years of follow-up and their associations with baseline peripheral BMD measures by age in decades for women age 50 - 99 years. Women were eligible for N.O.R.A. if they were ≥ 50 years old, postmenopausal, had no diagnosis of osteoporosis and were not currently taking bone-specific medication (HT use was allowed); 170,090 women who had a baseline BMD measurement at one peripheral site (forearm, heel, finger) and who responded to either the first or second follow-up survey (median: 37 months; 99% range: 11- 46 months) after testing were included in the analysis. New fractures at the hip, spine, rib, wrist and forearm were identified by self-report. T-scores were categorized into three groups: T > -1.0; -2.0 < T ≤ -1.0; and T ≤ -2.0. Ages were categorized into 4 groups: 50-59, 60-69, 70-79 and 80-99. Fracture rates per person were calculated for the first fracture occurring since baseline weighted for time of follow-up. Relative risk (RR) and 95 % confidence interval (CI) of fracture was calculated for each age group and T-score group by Cox proportional hazards model adjusting forage, prior fracture, HT usage, ethnicity, health status maternal history of fracture, education level, and smoking status. A total of 5312 women reported 5676 fractures (868 hip, 2420 wrist/forearm, 1531 rib and 857 spine). Fracture rate per 1000 person-years and relative risk (RR) for any fracture are shown; absolute fracture rates increased with age, but relative risks by BMD did not (p = 0.07)

	50 - 59		60 - 69		70 - 79		80 - 99	
	Fx Rate (95% CI)	RR (95% CI)	Fx Rate (95% CI)	RR (95% CI)	Fx Rate (95% CI)	RR (95% CI)	Fx Rate (95% CI)	RR (95% CI)
>-1.0	6.7 (6, 7)	Ref	7.3(7,8)	Ref	11.7(11,13)	ref	19.0(15,23)	Ref
-1.0 to -2.0	13.0(12,14)	1.8(1.6,2.1)	13.2(12,14)	1.7(1.5,1.9)	19.1(18,20)	1.5(1.3,1.7)	27.1(23,31)	1.4(1.0,1.8)
≤ -2.0	21.1(18,25)	2.6(2.2,3.2)	23.7(21,26)	2.8(2.4,3.2)	32.0(30,34)	2.4(2.1,2.7)	42.8(39,47)	2.0(1.5,2.5)

Although fracture rates increase with increasing age, rates are similar in women aged 50-59 and 60-69 within each T-score category. Greater relative risk for fracture associated

with lower BMD T-score is observed regardless of age and the risk levels are not substantially different across age groups. BMD is an important risk factor in all ages for identifying women who have increased risk for fracture.

Disclosures: ***E.S. Siris****, Merck & Co., Inc. 5, 8; Proctor & Gamble 8; Lilly 8.*

F340

Prevalence of Vertebral Fractures in Brazil, Puerto Rico and Mexico. Preliminary Report of the Latin American Vertebral Osteoporosis Study (LAVOS). P. Clark[1], S. Ragi[2], L. Haddock[3], E. Suarez*[3], C. Pérez*[3], F. Cons Molina[4], M. Deleze[5], J. Salmeron*[6], L. Palermo*[7], S. R. Cummings and the LAVOS Group[7]. [1]Faculty of Medicine UNAM, IMSS, Mexico City, Mexico, [2]CEDOES, Vitoria, Brazil, [3]Universidad de Puerto Rico, San Juan, Puerto Rico, [4]Unidad de Diagnostico de Osteoporosis, Mexicali, Mexico, [5]Clinica de Osteoporosis, Puebla, Mexico, [6]Unidad de Epidemiologia y Sistemas, IMSS, Morelos, Mexico, [7]Coordinating Center, UCSF, San Francisco, CA, USA.

The risk of fractures in women in Latin America is assumed to be much lower than the United States and Northen Europe. However, there has been no population-based study of the rates of vertebral fracture in Latin America.

To determine the rates of vertebral fracture in varios regions of Latin-America, we undertook the Latin American Vertebral Osteoporosis Study (LAVOS), the first multi-country population based study of vertebral fractures in Latin America.

Using an identical design, we selected age-stratified (50-59, 60-69, 70-79 and 80+) and truly random samples of 400 women in Vitoria Brasil, 400 in San Juan, Puerto Rico and 400 in Puebla, Mexico. Over 80% of the women contacted participated in a face to face interview and questionnaire. We measured BMD of the hip and and spine and took lateral spine X-rays on all women. Vertebral fractures were assessed centrally in Mexicali, Mexico using morphometry and compared with independent reading at the San Francisco Coordinating Center with very good agreement (kappa=0.75). Fractures were defined according to a modified Eastell method as used in the comparative US study.

The overall prevalence of vertebral fractures was 14.8 in Brazil, 12.1 in Puerto Rico and 19.5 in Mexico and increases with age. The oveall rates of fracture in these 3 LA countries Brazil, Puerto Rico and Mexico were lower than SOF rates although Mexico presented the highest rate of these countries, similar to SOF rates in women over 70 years (table)

We conclude that the rate of vertebral fractures in Latin American women is high. Vertebral fractures are a substantial problem in Latin America and should be the focus of research, clinical and public health measures to prevent them.

Age-Stratified Prevalence

Age	Brazil PV 95% IC	Puerto Rico PV 95% IC	Mexico PV 95% IC	White USA* SOF Study 95% IC
50-59	6.7 2.7-13.2	5.4 1.9-11.3	8.3 2.7-13.8	-
60-69	8.0 3.5-15.1	8.3 3.8-15.1	12.6 6.1-19.1	14.5 13.4-15.5
70-79	19.4 12.3-28.4	17.0 10.5-25.2	18.6 10.7-26.4	22.0 20.8-23.3
80+	26.8 17.5-36.3	21.5 12.3-33.4	37.9 28.3-47.4	33.9 30.9-36.9

*includes 65>

Disclosures: ***P. Clark****, None.*

F341

Does 'ORACLE' Provide Good Risk Assessment for Osteoporotic Fracture? A. Stewart*[1], M. Garton*[2], S. Ogston*[3], G. Leese*[4], D. Reid[1]. [1]Osteoporosis Research Unit, University of Aberdeen, Aberdeen, United Kingdom, [2]Perth Royal Infirmary, Perth, United Kingdom, [3]Department of Epidemiology and Public Health, University of Dundee, Dundee, United Kingdom, [4]Department of Medicine, Ninewells Hospital, Dundee, United Kingdom.

A new osteoporosis risk assessment tool (ORACLE) has been developed based on age, bone mineral density (BMD) Z-scores and historical incidence figures for fracture. A 10-year absolute risk for hip, vertebral, wrist and other type of fracture is then computed. We have applied these risk estimates to a population-based sample of women who have been followed up for over 10 years with incident fracture data collected. At baseline women aged 45 to 54 years attended for BMD of spine and hip as part of the Aberdeen Prospective Osteoporosis Screening Study (APOSS). Over a period of approx. 10 years the women were followed up on 2 occasions and incident factures noted and validated by examining x-ray reports. We have compared the ORACLE calculated risk for these women, according to BMD decile, with the actual fracture rate noted over the follow-up period (mean = 9.7 years, SD 1.1 years, range 7.49 to 12.2 years). As these women have now only reached the mean age of 58.4 years the most common type of fracture to have occurred is wrist fracture. We have therefore used the ORACLE calculated risk for wrist fracture only. ORACLE risks were calculated using both spine and hip Z-scores. The baseline BMD at both spine and hip were divided into deciles and the average ORACLE risk was calculated per decile. We then calculated the actual percentage of women in each decile who had an incident fracture of the wrist. In Table 1 we show the results.

Decile of BMD measurement	Deciles of Spine BMD		Deciles of neck of femur BMD	
	ORACLE risk (%) based on spine BMD	Actual % with incident wrist fractures	ORACLE risk (%) based on hip BMD	Actual % with incident wrist fractures
1	4.96	6.3	5.95	6.0
2	3.12	2.7	3.83	4.0
3	2.59	4.7	2.98	3.2
4	2.20	1.3	2.48	3.5
5	1.95	2.5	2.12	2.9
6	1.74	4.0	1.78	2.2
7	1.53	3.1	1.48	1.3
8	1.33	0.9	1.16	0.9
9	1.13	0.9	0.86	1.3
10	0.82	0.7	0.50	1.6

Using a Chi-square test comparing the predicted and actual risk there were no significant difference in the actual % of incident wrist fracture and the ORACLE risk based on spine BMD (p = 0.599) or for hip BMD (p = 0.939). This simple risk assessment tool performs very well when applied to our population based random sample for which we have incident fracture data. The 10-year risk assessment tools such as this are likely to become essential tools in clinical practice in the near future.

Disclosures: ***A. Stewart****, None.*

F343

Children With Bone Fragility Fractures Have Reduced Volumetric Bone Mineral Density of the Radius. J. D. Landoll*[1], S. L. Mobley*[1], E. Ha*[1], N. E. Badenhop-Stevens*[1], T. N. Hangartner*[2], V. Matkovic[1]. [1]Bone and Mineral Metabolism Laboratory, The Ohio State Univ., Columbus, OH, USA, [2]BioMedical Imaging Laboratory, Wright State Univ., Dayton, OH, USA.

Bone fragility fractures in children are very common during the pubertal growth spurt. Two underlying causes may be a reduced bone mineral density at this time, or physically smaller bones. Peripheral quantitative computed tomography (pQCT) is able to evaluate separately bone geometry and true (volumetric) bone mineral density (BMD).

This study measured volumetric BMD of 613 male and female children aged 7-17 y (mean 10.9 +/- 2.2 y) as part of a case-controlled study evaluating the risk factors for bone fragility fractures. Case subjects (n=307; age = 10.8 +/- 2.2 y) had a forearm fracture caused by low to moderate trauma. Control subjects (n=306; age = 10.9 +/- 2.2 y) were free from previous fracture and were matched for age, gender and socio-economic status (from either the same class/school or a similar school). BMD of the proximal (33%) and distal (4%) radius was measured by pQCT using a Norland-Stratec XCT 2000. For case subjects, measurements were made on the non-fractured arm. For control subjects, measurements were made on the matching (dominant vs. non-dominant) arm.

There were significant differences in bone mineral density between the fracture group as a whole and the paired control group. Fracture cases had significant reduction in volumetric bone density at both the distal ($p<0.0001$) and proximal ($p< 0.0001$) radial sites. In addition, volumetric bone mineral density of the trabecular bone at the distal radius was significantly ($p< 0.0001$) reduced in the fracture cases. The cross-sectional bone areas at the two radial sites in both groups were the same. This indicates that bone geometry was not an important contributing factor for the pathogenesis of fractures in the cohort. The deficiency of bone tissue within the volume of an anatomical bone seems to be a single reason for the fracture, besides trauma itself.

Results of this study show that low BMD (not small bones) is one of the most powerful determinant of bone fragility fracture in children. This emphasizes the importance of adequate calcium intake during this critical time of growth. The results also underscore the importance of volumetric bone mass measurements in growing individuals.

Disclosures: ***V. Matkovic****, None.*

F345

Inhaled Steroid Induced Risk of Osteoporotic Fractures Confounded by Disease Severity in Obstructive Airway Disease. F. de Vries*[1], T. van Staa[1], H. Leufkens*[1], M. Bracke*[1], J. Lammers*[2], C. Cooper[3]. [1]Dept. of Pharmacoepidemiology and Pharmacotherapy, Utrecht Institute for Pharmaceutical Sciences - Utrecht University, Utrecht, Netherlands, [2]Dept. of pulmonary diseases, Utrecht Medical Center, Utrecht, Netherlands, [3]MRC Environmental Epidemiology Unit, Southampton General Hospital, Southampton, United Kingdom.

Background: an earlier study conducted in the UK General Practice Research Database (GPRD) found a dose response with use of inhaled corticosteroids and hip fracture risk, and concluded that this was related to corticosteroid intake. However, severe obstructive airway disease (OAD) has been associated with a decreased bone mineral density of the hip and spine, and it has yet to be established whether this effect is related to the disease itself or to extensive use of respiratory medication. ***Objective*:** to evaluate the relation between OAD severity and osteoporotic fracture risk. ***Methods*:** a large case-control study (n=108.754) was conducted among adults using data from the GPRD. Cases were defined as patients with a first record for a fracture of the radius/ulna, hip, distal femur, unspecified femur, ribs, humerus, vertebrae and clavicle. For each case, one patient without a history of a fracture was randomly selected as control patient. They were matched to cases by age, gender, and practice. Control patients were assigned the index date of their matched case. Indicators of severe OAD included exacerbations, use of oxygen, and oral steroids prior to index date. Current exposure was defined as at least one prescription 6 months prior. ***Results:*** we found a dose response relationship between the use of inhaled steroids and he risk of osteoporotic fractures. Current users of high dose inhaled steroids (>1600 mcg beclomethasone equivalent per day) with a history of OAD had increased risk of osteoporotic fractures (crude OR 1.95, 95% CI: 1.68-2.27), hip fractures (crude OR 1.78, 95% CI: 1.21-2.62) and vertebral fractures (crude OR 6.11, 95% CI: 3.73-10.01). After adjustment for general risk factors, specific OAD disease severity markers and daily dose of bronchodilators, the dose response relationship disappeared. Current users of high dose inhaled steroids (>1600 mcg per day) with a history of OAD had the following risks of osteoporotic fractures (adj. OR 1.19, 95% CI: 1.01-1.41), hip fractures (adj. OR 1.18, 95% CI: 0.75-1.85), and vertebral fractures (adj. OR 1.85, 95% CI: 1.01-3.38). ***Conclusions:*** patients with severe OAD and using high dose inhaled steroids are at increased risk of osteoporotic fractures. Adjustment for disease severity is essential when the association between use of inhaled corticosteroids and risk of osteoporotic fractures is studied in observational research.

Disclosures: ***F. de Vries****, None.*

F349

The Effect of Recent Fracture on Quality of Life in Postmenopausal Women. S. K. Brenneman[1], E. Barrett-Connor[2], P. D. Miller[3], Y. Chen[1], S. Sajjan*[1], L. E. Markson*[1], E. S. Siris[4]. [1]Merck & Co., Inc., West Point, PA, USA, [2]University of California, San Diego, La Jolla, CA, USA, [3]Colorado Center for Bone Research, Lakewood, CO, USA, [4]Columbia University, New York, NY, USA.

Health-related quality of life (HRQoL) has been well-studied after vertebral and hip fractures. Less is known about HRQoL following clinical fractures at peripheral sites. We studied the impact of clinical fractures on HRQoL in participants in the National Osteoporosis Risk Assessment (NORA). 86,010 postmenopausal women who completed both the first and the second follow-up surveys (median 11 and 37 months after baseline) were included in the analyses. At both follow-up surveys, information on HRQoL was assessed by Short Form-12 (SF-12: an instrument standardized to have a mean of 50, SD 10) and new fractures (hip, vertebral, wrist/forearm and rib) were collected by self-report. Means for the SF-12 physical component scores (PCS) and mental component scores (MCS) were calculated for each survey. The effect of recent fracture on HRQoL was assessed by comparing PCS and MCS for women with and without new fractures at the 2nd survey by fracture type and by age and adjusted for PCS and MCS at the 1st survey. Age-specific means and standard deviations of PCS and MCS in NORA overall and among those who did not fracture were similar to the reported norms for the US population. New fractures (364 hip, 478 vertebral, 694 rib, 1078 wrist/forearm) occurring during the 2nd survey interval were reported by 2,477 women. Regardless of age, women with new fractures had poorer PCS compared to those who had not fractured for hip, vertebral and rib fractures ($p \leq 0.001$). The greatest observed differences in PCS between women with and without fractures across age cohorts were for hip (range -4.7 to -3.7) and spine (range -7.1 to -4.8) fractures. These differences are similar to those found for patients with comorbidities such as asthma, COPD, osteoarthritis, and hip impairment compared to patients without the comorbidity. Wrist/forearm fractures had an impact on PCS only in women ≤ 65 of age ($p<0.0001$), but not > 65 of age ($p > 0.10$). MCS was less affected by fracture status, but women with vertebral fracture at all ages ($p< 0.05$) and women with rib or hip fractures age > 75 years ($p<0.001$) had poorer MCS compared to those who did not fracture within their age cohort. Recent fractures of the hip, vertebrae, rib and wrist/forearm have significant impact on HRQoL physical domain as measured by SF-12. The impact of all fracture types should be considered in estimations of the burden osteoporosis.

Disclosures: ***S.K. Brenneman****, None.*

F354

Bone Resorption and Osteoporotic Fractures in Elderly Men: The Dubbo Osteoporosis Epidemiology Study. C. Meier[1], T. V. Nguyen[2], J. R. Center[2], M. J. Seibel[1], J. A. Eisman[2]. [1]Bone Research Program, ANZAC Research Institute, University of Sydney, Concord NSW, Australia, [2]Bone and Mineral Research Program, Garvan Institute of Medical Research, St. Vincent's Hospital and University of NSW, Sydney NSW, Australia.

Approximately one third of osteoporotic fractures occur in men. Among the potential risk factors for fragility fractures, bone turnover is considered an important determinant. The association between fracture risk and rates of bone turnover has not been well established in men. We examined this relationship in elderly community-dwelling men.

This case-cohort control study included 50 men with incident low-trauma fractures (cases) and 101 men without fracture (controls), aged 71±5.2 yrs (mean±SD) who have been prospectively followed in the Dubbo Osteoporosis Epidemiology Study for a median of 6.3 yrs (range, 2-13 yrs). Bone mineral density at the lumbar spine (LSBMD) and at the femoral neck (FNBMD), and markers of bone turnover were measured at baseline. Bone resorption was assessed by serum carboxyterminal cross-linked telopeptides of type I collagen (S-ICTP, S-CTX). Bone formation was assessed by serum aminoterminal propeptide of type I procollagen (S-PINP).

At baseline and compared to controls, cases had lower BMD, both at the femoral neck and the spine, lower dietary calcium intake, and higher S-ICTP levels. Age, BMI, ΔFNBMD/yr, smoking habits, S-CTX and S-PINP did not differ between groups. Based upon univariate regression analysis, S-ICTP (RR 2.2, 95% CI, 1.5-3.2), FNBMD (RR 1.5, 95% CI, 1.0-2.1), LSBMD (RR 1.5, 95% CI, 1.1-2.2), and age (RR 1.4, 95% CI, 1.0-1.9) were all associated with increased risk of fracture. In multivariate logistic regression analyses, only S-ICTP (RR 2.3, 95% CI, 1.4-3.5) and FNBMD (RR 1.8, 95% CI, 1.2-2.9) remained independent predictors of fracture risk in men. Men within the highest quartile of S-ICTP had a 2.8-fold (95%CI 1.4-5.4) increased risk of fracture compared with men with levels in the lowest quartile. The incidence of osteoporotic fractures was 10 times higher in men with high S-ICTP and low FNBMD as compared to men with low S-ICTP and high FNBMD. Of the fracture risk in the population, 31% was attributable to high S-ICTP and/or low FNBMD, and S-ICTP contributed 24% to the estimated risk.

In conclusion, high bone resorption is associated with an increased risk of osteoporotic fracture in elderly men, independent of BMD. Combining measurements of BMD and bone turnover improved fracture prediction in this cohort. In populations and studies were biological variability (i.e. fasting state, diurnal variation) can not be controlled, S-ICTP appears to be a more robust marker of future fracture risk than S-CTX.

Disclosures: ***C. Meier****, None.*

F356

Relationship of Volumetric Density, Size, Geometry and Bone Structure at Different Skeletal Sites to Sex Steroid Levels in Men. S. Khosla, L. J. Melton, E. J. Atkinson*, A. E. Oberg*, R. Robb*, J. Camp*, B. L. Riggs. Mayo Clinic, Rochester, MN, USA.

Serum sex steroids, particularly estrogen (E) levels, are known to be associated with bone mass in men. However, previous studies addressing this issue have exclusively used DXA, which cannot separate cancellous from cortical bone or provide information on bone geometry or structure. We assessed bone geometry and volumetric bone mineral density (vBMD) by QCT at the lumbar spine (LS), femoral neck (FN), and distal radius (DR) and related these to circulating estrone (E_1), bioavailable estradiol (bio E_2) and testosterone (bio T) levels in an age-stratified population sample of 314 men (ages 22 to 91 yrs). Using stepwise regression models that included age and the sex steroid levels (transformed where appropriate), none of the sex steroid variables were related to the vBMD/structural parameters in young men (age 20-39 yrs). However, there were significant associations between many of these variables and sex steroid levels in middle-aged men (age 40-59 yrs) and even more so in elderly men (age 60+ yrs) (Table below, asterisks indicate level of significance: *P < 0.05; **P < 0.01; ***P < 0.001; sign indicates positive or negative correlation.)

Variable	Age	E_1	Bio E_2	Bio T	Model R^2 (%)
LS Total bone area (middle-aged)	--	--	--	--	--
LS Total bone area (elderly)	--	(-)***	--	--	7.4
LS Trabecular vBMD (middle-aged)	--	--	--	(+)***	14.0
LS Trabecular vBMD (elderly)	(-)***	(+)**	--	--	18.4
FN Cortical area (middle-aged)	--	(+)*	--	--	4.2
FN Cortical area (elderly)	(-)**	--	(+)*	--	10.8
FN Total vBMD (middle-aged)	--	--	--	--	--
FN Total vBMD (elderly)	(-)*	--	(+)**	--	11.4
FN Trabecular vBMD (middle-aged)	--	(+)**	--	--	6.0
FN Trabecular vBMD (elderly)	(-)**	--	(+)**	--	14.7
FN Cortical vBMD (middle-aged)	--	--	--	--	--
FN Cortical vBMD (elderly)	--	--	(+)*	--	3.7
DR Total bone area (middle-aged)	--	--	--	--	--
DR Total bone area (elderly)	--	--	--	(-)*	2.7
DR Trabecular vBMD (middle-aged)	--	(+)*	--	(+)*	10.3
DR Trabecular vBMD (elderly)	--	--	(+)*	--	2.8
DR Cortical vBMD (middle-aged)	--	--	--	--	--
DR Cortical vBMD (elderly)	(-)***	--	--	--	20.9

In summary, (1) the lack of association between vBMD/structural parameters and sex steroid levels in young men suggests that these men are largely sex steroid sufficient, and variations in their relatively high sex steroid levels do not impact bone mass/structure; (2) the association between these parameters in middle-aged, and particularly elderly, men suggests that the declining bio E and T levels with age become increasingly important in

determining vBMD/structural variables in these men; and (3) other than a negative association between DR bone area and bio T levels, all of the other vBMD/structural variables were independently associated solely with serum E (E_1 or bio E_2) levels in the elderly men, consistent with a more important role for declining bio E levels (as compared to bio T levels) in determining these vBMD/structural parameters in aging men.

Disclosures: ***S. Khosla****, None.*

F358

Endogenous Sex Steroids, Weight Change and Rates of Hip Bone Loss in Older Men: The MrOS Study. K. Ensrud[1], L. Lambert[2], B. Taylor[1], H. Fink[1], E. Barret-Connor[3], C. Lewis[4], J. Cauley[5], E. Orwoll[2]. [1]VAMC & U of MN, Mpls, MN, USA, [2]OHSU, Portland, OR, USA, [3]UCSD, SD, CA, USA, [4]U of AL, Birmingham, AL, USA, [5]U of Pittsburgh, Pittsburgh, PA, USA.

Weight loss in older men may be associated with higher rates of bone loss for several reasons, including lower levels of endogenous sex steroids (ESS) produced in adipose tissue & muscle. To test whether ESS levels modify the association between weight loss & hip bone loss in older men, we measured body weight, ESS (total, bioavailable and free estradiol and testosterone in paired serum samples using sensitive immunoassay) & total hip bone mineral density (THBMD) at a baseline and subsequent exam (mean 1.8 yrs between exams) in a cohort of 1263 men aged ≥65 yrs at baseline. During this period, 10% of participants lost ≥5% of their baseline weight (weight loss), 81% had a <5% change from their baseline weight (stable weight) & 8% gained ≥5% or more of their baseline weight (weight gain). The effect of baseline ESS & change in ESS was much smaller in magnitude than the effect of weight change on % change in THBMD/yr; men with weight loss had higher rates of hip bone loss compared to those with stable weight and those with weight gain, irrespective of baseline ESS or change in ESS. However, among men with weight loss, the rate of decline in THBMD steadily increased with decreasing level of baseline bioavailable estradiol (test for trend p <0.02) and greater decreases in bioavailable testosterone from baseline (test for trend p <0.001). The test for interaction between weight change and ESS for prediction of change in THBMD almost reached significance for change in bioavailable testosterone (p=0.052), but not for baseline bioavailable estradiol (p=0.242).

Category of Weight Change	Mean Annual % Change in THBMD (95% CI)† Quartile of Baseline Bioavailable Estradiol*			
	Q1 (Lowest)	Q2	Q3	Q4 (Highest)
Weight Loss (N = 131)	-1.8 (-2.2, -1.4)	-1.4 (-1.8, -0.9)	-1.1 (-1.6, -0.6)	-1.0 (-1.6, -0.5)
Stable Weight (N = 1027)	-0.5 (-0.6, -0.3)	-0.5 (-0.6, -0.3)	-0.3 (-0.5, -0.2)	-0.2 (-0.4, -0.1)
Weight Gain (N = 105)	0.4 (-0.1, 1.0)	-0.1 (-0.6, 0.4)	0.0 (-0.5, 0.4)	0.2 (-0.4, 0.8)

†Adj. for baseline age and weight; *Quartile cutpoints: 9.6 pg/ml, 11.9 pg/ml, 14.6 pg/ml

Among older men, weight change is a stronger predictor of change in THBMD than ESS. However, our finding that the effect of weight loss on hip bone loss is most pronounced in men with the lowest estradiol or greatest decline in testosterone supports the hypothesis that the relationship between weight loss and hip bone loss is in part mediated by sex steroid insufficiency.

Disclosures: ***K. Ensrud****, None.*

F360

Vertebral Deformities in Older Black and White Men: Data from the Baltimore Men's Osteoporosis Study. J. K. Tracy*[1], R. H. Flores*[2], M. Grigoryan*[3], B. Fan[3], H. Genant[3], M. C. Hochberg[2]. [1]Epidemiology, University of Maryland, Baltimore, MD, USA, [2]Medicine, University of Maryland, Baltimore, MD, USA, [3]Radiology, University of California, San Francisco, CA, USA.

Data from participants in the Baltimore Men's Osteoporosis Study (MOST) were examined 1) to estimate the prevalence of vertebral deformities (VFx) in older men, 2) to determine whether there were differences in prevalence of VFx by race, and 3) to examine factors associated with the presence of VFx in older men. Baseline data on the 694 men age 65 and above enrolled in MOST have been published (J Bone Miner Res 2003;18:2238-44). 542 men (415 white and 127 black) completed a second clinic visit after a mean (SD) follow-up of 1.5 (0.5) years. At this visit, lateral radiographs of the thoracic and lumbar spine were taken using standard protocols. Films were digitized using standardized methods and morphometry was performed. In addition, all films were read by an expert radiologist and each vertebra was scored for presence and severity of deformity using the technique of semiquantitative grading. VFx were defined using the Eastell method (a height ratio [h(a)/h(p), h(m)/h(p), or h(p)/h(p+1)] that was >3 SDs below the normative mean ratio for a particular vertebra). 514 men (398 white and 116 black) with a mean (SD) age of 75.8 (5.6) years had complete data for analysis. 30 men had 1 or more VFx (25 had 1 and 5 had 2 or more); the overall prevalence of VFx in this sample was 5.8% (95% CI: 4.0%, 8.3%). VFx were significantly more common in white (29 [7.3%]) than black (1 [0.9%]) men (Fishers' exact P = 0.01): age-adjusted odds ratio (95% CI) = 8.33 (1.10, 62.5). Further analyses were limited to the white men. Men with VFx were shorter than men without VFx (P < .05); there were no significant differences in age, weight, body mass index, knee height, proportion of current smokers or drinkers, grip strength or femoral neck, total hip or lumbar spine bone mineral density between groups (Table). These data demonstrate that, in this cohort of older healthy volunteers, white men have a higher prevalence of VFx than black men. The results extend our prior observations that older black men have higher BMD and a lower rate of decline in total hip BMD than older white men.

Factors associated with vertebral deformities in older white men

Variable (mean [SD])	VFx present	VFx absent
Age, years	77.0 (6.0)	76.4 (5.5)
Height, cm	170.0 (6.1)	172.6 (6.6)
Weight, kg	80.9 (15.3)	82.5 (13.0)
Femoral neck BMD, g/cm2	0.78 (0.17)	0.78 (0.13)
Total hip BMD, g/cm2	0.91 (0.15)	0.94 (0.14)
Lumbar spine BMD, g/cm2	1.16 (0.22)	1.13 (0.21)
Grip strength	26.8 (6.8)	29.3 (7.3)

Disclosures: ***M.C. Hochberg****, None.*

F362

'Viva le Difference!' Bone Mass and Fractures in Men versus Women from SOF (Study of Osteoporotic Fractures) and MrOS (Osteoporotic Fractures in Men). S. R. Cummings[1], P. M. Cawthon[1], J. A. Cauley[2], K. E. Ensrud[3], D. C. Bauer[4], H. A. Fink[3], D. M. Black[4], E. S. Orwoll[5]. [1]Research Institute, California Pacific Medical Center, San Francisco, CA, USA, [2]University of Pittsburgh, Pittsburgh, PA, USA, [3]University of Minnesota, Minneapolis, MN, USA, [4]University of California, San Francisco, CA, USA, [5]Oregon Health Sciences University, Portland, OR, USA.

We measured femoral neck (FN) and total hip (Hip) BMD in 5,119 men and 6,583 women aged ≥65. During 2.7 years, 850 non-spine (101 hip) fractures occurred in women, 200 (29 hip) in men.

Non-spine fractures: Compared with men, women had a 3.4 (2.8, 4.2) age-adjusted RR of fracture, unchanged (3.2; 2.7, 3.9) by adjustment for estimated volumetric bone density (FN BMAD) but largely attenuated by adjustment for FN BMC (1.7; 1.3, 2.1).

The age-adjusted relationship of Hip BMD to fracture risk (1.9 RR/SD; 1.7, 2.1) was not significantly different (P=0.3) in women and men. However, women had a 1.6-fold (1.3, 2.1) greater risk at all Hip BMD levels (Figure) and appaer to have a greater risk at equivalent gender-specific T-scores (Table)

Hip fracture: The association between Hip BMD and hip fracture risk was significantly (P=0.008) stronger in men (4.3 RR/SD) than women (2.6 RR/SD).

Conclusions: The male-female difference in risk of non-spine fracture is mostly attributable to the difference in bone mass not density. Women and men share a similarly strong relationship between BMD and non-spine fracture, but at any BMD or T-score, women have a higher risk than men. The relationship between Hip BMD and hip fracture is stronger for men than for women.

Total Hip T-score	Non-spine fx (%/yr)	
	Men	Women
Above -1	0.9%	2.7%
-1 to -2.5	1.7%	4.2%
< -2.5	9.5%	7.9%

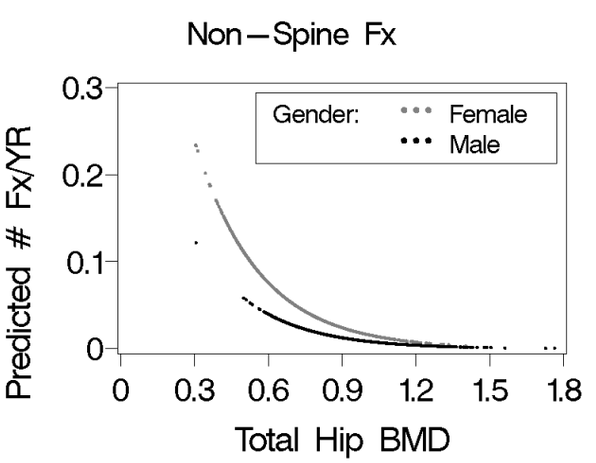

Disclosures: ***S.R. Cummings****, None.*

F364

Circadian Activity Rhythms and Bone Density in Men. D. R. Miller*, L. Silva*, S. Rich*, E. Krall. Chqoer, Boston University, Bedford, MA, USA.

Regular daily activity patterns may be considered a measure of health and well-being, and irregular patterns have been associated with a number of medical and psychiatric conditions. Circadian activity rhythms have not been well studied in relation to bone even though physical activity and circadian patterns in other measures (e.g. cortisol) are related to bone density. We studied circadian activity rhythms in the VALOR study, a longitudinal, observational study of bone in older men (mean age of 70 years). Femur and radius BMD were measured by dual energy x-ray absorptiometry and bone strength of the calcaneus by quantitative ultrasound up to 3 times over a mean follow-up of 2 years. Activity patterns were measured in 426 men who wore wrist actigraphs for at least one 7 day period, recording activity counts at one minute intervals. We calculated four summary statistics of circadian rhythms: goodness-of-fit to the 24 hour cosinor model, a measure of circadian rhythmicity; acrophase (time of day of the cosinor model peak); amplitude (height of the peak); and autocorrelation coefficient, a measure of the consistency of activity levels at each time of day across the seven days measured. Goodness-of-fit was related directly to BMD at the forearm and femoral neck and to bone strength ($p<0.01$), even with adjustment by linear modeling for age, body mass index, disability, physical activity (by self-report or actigraphy), sleep time, depression, and other factors. Adjusted BMD was lower and rates of osteopenia (<1 SD below norm in femoral neck BMD) were higher in the lowest quartile (mean BMD= 0.916 g/cm2, 66.5%) relative to the highest quartile (0.964, 56.1%) ($P<0.05$) of goodness-of-fit (mean r=0.502+/-0.096). Comparable results were found for autocorrelation coefficient (mean r=0.319+/-0.107) and the other circadian activity measures. A significant interaction was observed with physical activity in that the associations were absent in those who exercised regularly and were strongest in those with little or no exercise. These findings suggest that circadian rhythms of physical activity are a marker for bone density and strength independent of total activity, sleep time, and mental conditions and they may be an important new marker of modifiable risk of fracture.

Disclosures: ***D.R. Miller****, None.*

F367

The Association Between Bone Mineral Density and Neurologically Active Medications: Results from NHANES III. M. Kinjo*[1], S. Setoguchi*[2], S. Schneeweiss*[2], D. H. Solomon[2]. [1]Internal Medicine, Teine Keijinkai Hospital, Teine-ku Sapporo, Japan, [2]Division of Pharmacoepidemiology, Brigham and Women's Hospital, Boston, MA, USA.

Background: Decreased bone mineral density (BMD) defines osteoporosis and is an important predictor of future fractures. The use of several types of CNS active drugs, including benzodiazepines, anti-depressants, narcotics and anticonvulsants, have all been associated with an increased risk of fracture. It is unclear whether this is related to an effect on BMD or other mechanisms, such as an increased risk of falls.

Objective: To examine the relationship between BMD and the use of benzodiazepines, anti-depressants, narcotics and anticonvulsants in a representative US population-based sample.

Method: We analyzed data on adults aged 17 and older from The Third National Health and Nutrition Examination Survey (NHANES III: 1988-1994). Total femoral BMD of 7,114 male and 7,532 female participants was measured by dual-energy x-ray absorptiometry. Multivariable linear regression models were examined that considered total femoral BMD as the dependent variable and the CNS medications as the exposures of interest. All models controlled for age, gender, race, tobacco use, alcohol, history of hip and wrist fracture, cognitive impairment, menopausal status, chronic disease, BMI, exercise, fall, self-reported health, hormone replacement therapy, calcium intake, steroid and thiazide use, and serum vitamin D level.

Results: We included 14646 persons in these analyses. 4.8% of the study sample had femoral neck BMD measurements with t-scores < -2.5. The percentage of subjects with osteoporosis taking benzodiazepines was 6.1%, anti-depressants was 5.2%, narcotics was 3.2%, and anticonvulsants was 14.1%. In linear regression models, subjects taking anticonvulsants had significantly lower femoral neck BMD,0.915 g/cm2, compared to nonusers,0.952 g/cm2 (difference = 3.9%, p = 0.017). None of the other CNS active drugs -- benzodiazepines, antidepressants, or narcotics - were associated with significantly lower BMDs. Among anticonvulsants, the mean BMDs of users of carbamazepine, phenytoin and phenobarbital were consistently lower than nonusers.

Conclusions: The use of anticonvulsants is associated with significantly lower BMD. None of the other CNS active agents studied were associated with lower BMD. These findings have implications for fracture prevention strategies.

Disclosures: ***D.H. Solomon****, Merck 2; Pfizer 2.*

F369

Use of Selective Serotonin Receptor Inhibitors Increases the Rate of Hip Bone Loss. S. Diem*[1], T. Blackwell[2], K. Yaffe[3], D. Bauer[4], K. Ensrud[5]. [1]Medicine, University of Minnesota, Minneapolis, MN, USA, [2]California Pacific Medical Center Research Center, San Francisco, CA, USA, [3]Psychiatry, Neurology, & Epidemiology, University of California, San Francisco, CA, USA, [4]Medicine, University of California, San Francisco, CA, USA, [5]Medicine & Epidemiology, VA Medical Center &University of Minnesota, Minneapolis, MN, USA.

Depression is associated with low bone mineral density (BMD) in some studies but the biologic mechanisms underlying this association are unknown. Serotonin transporters have been documented in bone and the use of antidepressant medications, which often block the serotonin transporter, are associated with an increased risk of fractures in older women. To test the hypothesis that elderly women who use selective serotonin receptor inhibitors (SSRIs) have increased rates of hip bone loss, we assessed current use of SSRIs using an interviewer-administered questionnaire and serial BMD measurements in a cohort of 2556 elderly women (mean age 78.5 yrs) participating in the Study of Osteoporotic Fractures. Hip BMD was measured at the 6th exam and an average of 4.9 years later at the 8th exam. We verified current antidepressant use (defined as daily or almost daily use in the preceeding 30 days) by inspection of medication containers and classified type of medication from product brand or generic names using a computerized medication dictionary. We categorized women according to their reported SSRI use as users (use at either exam or both) or non-users (use at neither exam). Individual drug use within the user category included fluoxetine, paroxetine, sertraline, citalopram, escitalopram, and fluvoxamine. Users of other classes of antidepressants at either visit were excluded. The mean annual % change in total hip BMD (THBMD) and 3 subregions were calculated by category of SSRI use. Depressive symptoms were identified using a cutoff score of >= 6 on the Geriatric Depression Scale as measured at the 6th exam. All results were adjusted for the following characteristics measured at the 6th exam: age, race, health status, functional status, walking speed, cognitive function, calcium supplement use, vitamin D supplement use, estrogen use, thiazide use, weight change, THBMD at the 6th visit, and depressive symptoms.

THBMD at the 6th visit did not differ among users and non-users (p= .33), but mean TH bone loss was -.47%/yr among non-users vs. -.81%/yr among the SSRI users (p=.0008). Findings were similar at the subregions of the hip and when women with depressive symptoms were excluded from the analysis.

Use of SSRIs in elderly women in this cohort is associated with increased rates of hip bone loss. Further work is needed to determine if this widely-used class of drugs has a direct effect on bone metabolism.

Disclosures: ***S. Diem****, None.*

F371

Evaluation of Easily Measured Risk Factors in the Prediction of Osteoporotic Fractures. R. Bensen*[1], A. Papaioannou[2], J. D. Adachi[2], G Ioannidis[2], W. Olszynski*[3], R. Sebaldt*[2], T. Murray*[4], R. Josse*[4], J. Brown*[5], D. Hanley*[6], A. Petrie*[2], C. Goldsmith*[2]. [1]Medical Sciences, McMaster University, Hamilton, ON, Canada, [2]McMaster University, Hamilton, ON, Canada, [3]University of Saskatchewan, Saskatoon, SK, Canada, [4]University of Toronto, Toronto, ON, Canada, [5]Laval University, Ste-Foy, PQ, Canada, [6]University of Calgary, Calgary, ON, Canada.

The purpose of this study was to examine the effectiveness of easily measurable risk factors for new hip, vertebral, wrist and rib fractures in postmenopausal women registered in CANDOO.

The CANDOO registry is a multi-site clinical dataset related to osteoporosis. A total of 3653 postmenopausal women with a baseline and follow-up visit were considered. Of these, a total of 40, 158, 99, and 64 women respectively developed a new hip, vertebral, wrist or rib fractures. The mean (SD) weight for those with a fracture was 63.6 (12.9) kg while age was 68.0 (7.5) years. We examined seven risk factors predictive of fracture in research trials including: age (<65, 65-69, 70-74, 75-79, 80+ years), rising from a chair with arms (yes, no), weight (< 57, ≥ 57 kg), maternal history of a hip facture (yes, no), a prior fracture after the age of 50 years (yes, no), total hip t-score (>-1, -1 to >-2.5, ≤-2.5), and current smoking status (yes, no). Multivariable logistic regression analysis was used to examine each risk factors ability to independently predict new fracture.

The inability to rise from a chair without the use of arms (3.58; 95% CI: 1.173, 10.927) was the most significant risk factor for new hip fracture. New wrist fractures were significantly identified by low body weight (1.71, 95% CI: 1.007, 2.897) and prior fracture after 50 years (1.96; 95% CI: 1.191, 3.223). Predictors of new rib fractures include a maternal history of a hip facture (2.89; 95% CI: 1.035, 8.081) and a prior fracture after 50 years (2.16; 95% CI: 1.201, 3.874). Notable risk factors for predicting new vertebral fractures were: low body weight (1.57; 95% CI: 1.035, 2.373), current smoking (1.95; 95% CI: 1.199, 3.184) ages 75-79 years (1.96; 95% CI: 1.096, 3.508). Fracture represents the most important clinical event in patients with osteoporosis, yet few if any premonitory symptoms are present. It is critical that physicians at all levels of care be able to effectively and efficiently identify those individuals at increased risk of fracture. This study has shown that there exists many predictors of future fracture, besides BMD, that can be easily assessed by a physician. Of greatest interest is the fact that decreased mobility/strength, as represented by an inability to rise from a chair, is perhaps the most identifiable significant risk factor for hip fracture and can be easily incorporated into clinical practice.

Disclosures: ***R. Bensen****, None.*

F373

Use of Clinical Risk Factors to Select Elderly Women for Treatment or Bone Densitometry. P. Dargent-Molina, S. Piault*, G. Breart*. Unite 149, INSERM, Villejuif, France.

It has been suggested that a strategy of triage, based on the calculation of a clinical fracture risk score, could be used to stratify individuals in three groups : a group at high risk for whom a treatment is indicated, an intermediate group for whom further assessment by DXA is indicated, and a group at low risk.

We used prospective data from the EPIDOS study (7512 women 75+ followed for an average of 3.9 yrs) to assess the potential value of such a strategy to identify elderly women who have a risk of hip fracture two times higher than the average risk in the cohort (ie greater than 20 per 1000 women-years). To construct the score, we selected factors that were associated both with the risk of hip fracture and with low BMD. We used the final risk function (Cox model) to calculate an individual fracture risk score based on each woman's characteristics. We compared this strategy to systematic BMD measurement and to current recommendations in Europe (ie, selection of women for bone densitometry based on specific risk factors, followed by treatment of women with T-score below -2.5). The main criteria used for comparison were the number of high risk women identified, their average level of risk, the sensitivity for hip fracture, and the number needed to screen to prevent one hip fracture (hypotheses: all identified women are treated; treatment reduces fracture risk by 35%).

The set of osteoporosis-related risk factors that are most predictive of the risk of hip fracture includes age, history of fracture since the age of 40, BMI, number of IADL for which assistance is needed, grip strength, and visual acuity. A strategy of triage based on these factors allows the identification of a large number of women at high risk of hip fracture (20% of the cohort). About 75% of the identified women have been selected based on clinical factors only. The rest have been identified after BMD measurement (with a threshold at -2.5 T-score). The results are summarized below:

	Triage based on clinical score	Systematic BMD measurement	Current recommendations
Sensitivity (%)	51.0 (45.3 - 56.8)	34.9 (29.5 - 40.3)	46.9 (41.2 - 52.5)
High risk group:	20	15	27
% women	29.8 (25.0 - 34.6)	26.8 (21.7 - 31.9)	19.6 (16.4 - 22.9)
average risk of hip fx (p. 1000 women-yrs)			
No. needed to screen to prevent one hip fx	29	30	41
BMD examinations (%)	10	100	52

A major issue with the triage strategy concerns the efficacy of treatments in women identified solely on the basis of clinical factors since 37% of them are not osteoporotic. However, most of these non-osteoporotic women have osteopenia and a risk of hip fracture close to our high risk threshold. We conclude that the proposed strategy of triage could be a useful clinical tool to select elderly women for treatment or bone densitometry.

Disclosures: ***P. Dargent-Molina****, None.*

F375

A Family History of Fracture and Fracture Risk: A Meta-Analysis. O. Johnell, J. A. Kanis, H. Johansson*, A. Oden*, C. De Laet*, J. A. Eisman, E. V. McCloskey, E. V. McCloskey, D. Mellstrom*, L. J. Melton, H. A. P. Pols*, J. Reeve, A. J. Silman, A. Tenenhouse. Centre for Metabolic Bone Diseases, University of Sheffield, Sheffield, United Kingdom.

The aims of the present study were to determine whether a parental history of any fracture, or hip fracture specifically, are significant risk factors for future fracture in an international setting, and to explore the effects of age, sex and bone mineral density (BMD) on this risk. We studied 34,928 men and women from 7 prospectively studied cohorts followed for 134,374 person-years. The cohorts comprised the EPOS/EVOS study, CaMos, the Rotterdam Study, DOES and cohorts at Sheffield, Rochester and Gothenburg. The effect of family history of osteoporotic fracture (or hip fracture) in first degree relatives, BMD and age on all fracture, osteoporotic fracture and hip fracture risk alone was examined using Poisson regression in each cohort and for each sex. The results of the different studies were merged from the weighted β coefficients.

A parental history of fracture was associated with a modest but significantly increased risk of any fracture, osteoporotic fracture and hip fracture in men and women combined. The risk ratio (RR) for any fracture was 1.17 (95% CI = 1.07-1.28), for any osteoporotic fracture was 1.18 (95% CI = 1.06-1.31), and for hip fracture alone was 1.49 (95% CI = 1.17-1.89). The risk ratio was higher at younger ages but not significantly so. No significant difference in risk was seen between men and women with a parental history for any fracture (RR = 1.17 and 1.17, respectively) or for an osteoporotic fracture (RR = 1.17 and 1.18, respectively). For hip fracture, the risk ratios were somewhat higher, but not significantly higher, in men than in women (RR = 2.02 and 1.38, respectively). A family history of hip fracture in parents was associated with a significant risk both of all osteoporotic fracture (RR 1.54; 95% CI = 1.25-1.88) and of hip fracture (RR = 2.27; 95% CI = 1.47-3.49). The risk was not significantly changed when BMD was added to the model.

We conclude that a parental history of fracture confers an increased risk of fracture that is independent of BMD. Its identification on an international basis supports the use of this risk factor in case-finding strategies.

Disclosures: ***O. Johnell****, None.*

F377

Osteoporosis and Cardiovascular Disease are Highly Associated Comorbidities in Elderly Women. L. B. Tankó, Y. Z. Bagger, P. Alexandersen, C. Christiansen. Center for Clinical and Basic Research, Ballerup, Denmark.

The purpose of the study was to investigate associations between bone and cardiovascular status in a large population-based sample of 5409 elderly women participating in the Prospective Epidemiological Risk Factors (PERF) study. Age of participants was between 60 and 85 years (mean 71 years). Main study parameters on the bone side were bone mineral density (BMD) at the hip, lumbar spine, and forearm measured by DEXA, radiographic vertebral fracture(s), and self-reported non-vertebral fractures. Cardiovascular status was characterized by a surrogate of atherosclerosis, aorta calcification (AC) visualized and graded on lateral X-rays using validated scoring system, and self-reported cardiovascular diseases (angina pectoris, myocardial infarct, stroke, intermittent claudicatio) verified by hospital discharge summaries. There was 2118 (39.1%) fractures registered, of which 1064 (19.7%) was vertebral fracture verified by X-ray. The number of women with manifest cardiovascular disease was 558 (10.3%). Table 1 summarizes the main findings of the analysis. After adjustment for age, the risk of CVD was 2.30-fold higher in women in the highest compared with the lowest quartile of AC. Age-adjusted BMD showed a significant inverse association with the severity score of AC at the hip and the forearm, but not at the lumbar spine. However, the frequency of osteoporotic vertebral fractures was significantly higher in the largest compared with the lowest quartile of AC (35.1% vs. 15.7%, $p<0.001$) and the age-adjusted relative risk of having an osteoporotic vertebral fracture was 29% higher in the highest compared with the lowest quartile of AC. Associations with the frequency of non-vertebral fractures was weaker and statistically non-significant. Finally, those with manifest CVD had a 22% increased risk for having at least one vertebral fracture compared with controls without CVD. These observations provide strong support for the coexistence of osteoporosis with cardiovascular disease in elderly women suggesting potential causal links. The results also emphasize that elderly women with severe osteoporosis at the hip and forearms should be referred to proper cardiovascular diagnostics to reveal or exclude the presence of subclinical CVD.

	Quartiles of Aortic Calcification			
Age-adjusted	1	2	3	4
Odds ratio for CVD (95% CI)	1.0	1.11 (0.8-1.6)	1.54 (1.2-2.0)*	2.30 (1.8-2.9)*
Forearm BMD (g/cm2)	0.367	0.364	0.361	0.355*
Hip BMD (g/cm2)	0.793	0.795	0.783*	0.764*
Spine BMD (g/cm2)	0.910	0.908	0.900	0.904
Odd ratio for vertebral fracture (95% CI)	1.0	1.24 (0.9-1.6)	1.19 (1.0-1.4)	1.29 (1.1-1.6)*

Disclosures: ***L.B. Tankó****, None.*

F380

The Rate of Bone Loss Is associated with an Increased Risk of Fracture in Postmenopausal Women. The OFELY Study. E. Sornay-Rendu*, F. Munoz*, F. Duboeuf*, P. D. Delmas. Unit 403, INSERM, Lyon, France.

A low bone mineral density (BMD) is a major determinant of fragility fractures but the role of the rate of postmenopausal bone loss is still unclear. In the OFELY study, we analyzed the risk of fracture in postmenopausal women according to the rate of bone loss. BMD was measured annually by dual-energy X-ray absorptiometry (DXA) at the forearm in 671 postmenopausal women (mean age 62.2 ± 9 years), for up to 11 years. Peripheral fractures, all confirmed by radiographs, were prospectively registered and vertebral fractures were evaluated with spine radiographs every four years. During a median 9.1 yr (IQ :2.3) of follow-up, 158 incident fragility fractures including 50 vertebral and 108 non-vertebral fractures were recorded in 116 women. The annual mean rate of bone loss, calculated from the slope (mean ± SD), was -0.30 ± 0.3 at the mid radius, -0.28 ± 0.3 at the distal radius and -0.15 ± 0.3 at the ultradistal radius. Bone loss was associated with a significant increased risk of fracture. A 1 SD increase of bone loss at the mid, distal and ultradistal forearm was associated with an odds ratio (95% CI) of 2.62 (1.02-6.8), 1.98 (1.02-3.5) and 2.70 (1.03-7.1) respectively, after adjusting for age, prior fractures and baseline BMD. In that multivariate model, baseline BMD (T score <-2.5) and prevalent fractures were also predictor (1.74 [1.35-2.24] and 2.93 [1.37-6.25] respectively) and age >65 yrs was borderline significant (1.82 [0.99-3.36]). In summary, the rate of bone loss in postmenopausal women is significantly associated with fracture risk independently of other well known predictors such as BMD and history of fractures. Our data suggest that BMD and the rate of bone loss contribute to a similar extent to the risk of fractures.

Disclosures: ***E. Sornay-Rendu****, None.*

F383

Baseline Buckling Ratio Derived from Hip Structure Analysis Predicts the Risk of Nonvertebral Fracture. G. G. Crans*[1], T. J. Beck*[2], L. M. Semanick*[2], K. D. Harper[1], K. V. Pinette[1], E. F. Eriksen[1]. [1]Lilly Research Laboratories, Eli Lilly and Company, Indianapolis, IN, USA, [2]The John's Hopkins University School of Medicine, Baltimore, MD, USA.

The purpose of this study was to determine if buckling ratio (BR), an index of cortical bone stability derived from Hip Structural Analysis (HSA) (Beck et al. 1990 and 2000), is able to predict nonvertebral fracture (NVFx) risk. The HSA program analyzes 5mm cross-sectional regions traversing the proximal femur across the intertrochanter (IT), femoral neck and femoral shaft. HSA has the ability to measure BMD, cross-sectional area, cross-sectional moment of inertia, section modulus, subperiosteal width and estimated mean cortical thickness. BR is derived as the ratio of the maximum distance from the region center of mass to the outer cortex divided by the estimated mean cortical thickness. A decrease in BR suggests an improvement of local cortical stability (Beck et al. 2001). We investigated the relationship between three-year NVFx risk and baseline BR in the placebo group of the MORE study (Ettinger et al.1999). Two analyses were conducted on the three HSA regions of the proximal femur. First, we used an Armitage trend test to determine if NVFx risk was associated with baseline BR tertiles. Second, logistic regression was used to help understand the quantitative nature of the relationship; we modeled three-year NVFx risk as a function of BR (up to cubic terms). The same analysis strategy was repeated using three-year hip fracture data. There was a strong relationship between NVFx risk and baseline BR, Table 1. The test for trend was significant ($p < 0.05$) for the IT and shaft BR, and near significant for the neck ($p = 0.07$). The results from the logistic regression analyses confirmed these results, as the main effect of BR was significant for each location. The relationship was linear (on the logit scale), as neither quadratic nor cubic effects were statistically significant. The trend for hip fracture risk was only significant for the IT BR, Table 2. Although the numeric trend of the hip data suggests an increased fracture risk with increasing baseline BR, there were, unfortunately, too few hip fractures in MORE to adequately address this very interesting question. In conclusion, despite the limitations of the estimate, BR derived from HSA may be able to predict the risk of NVFx in postmenopausal women with osteoporosis.

Table 1. Any Nonvertebral Fracture	**First Tertile**	**Second Tertile**	**Third Tertile**	**p-value**
Intertrochanter	23/442 (5.20)	47/444 (10.59)	49/443 (11.06)	0.0023
Femoral Neck	35/456 (7.68)	41/461 (8.89)	51/455 (11.21)	0.0658
Femoral Shaft	31/443 (7.00)	37/444 (8.33)	51/443 (11.51)	0.0186
Table 2. Hip Fracture	**First Tertile**	**Second Tertile**	**Third Tertile**	**p-value**
Intertrochanter	0/442 (0.00)	2/444 (0.45)	6/443 (1.35)	0.0092
Femoral Neck	2/456 (0.44)	1/461 (0.22)	5/455 (1.10)	0.1909
Femoral Shaft	2/443 (0.45)	1/444 (0.23)	5/443 (1.13)	0.1924

Disclosures: ***G.G. Crans****, Eli Lilly and Company 1, 3.*

F388

How Carolic Restriction Affects Bone Mass and Trabecular Structure. S. Tatsumi*[1], M. Ito[2], K. Tsutsumi*[3], H. Takasu[3], K. Ikeda[3]. [1]Pharmaceuticals and Medical Device Agency (Pmda), Tokyo, Japan, [2]Nagasaki University Hospital, Nagasaki, Japan, [3]Department of Bone and Joint Disease, National Center for Geriatrics and Gerontology (NCGG), Obu, Japan.

Caloric restriction (CR) is the only and evolutionally conserved remedy that has been demonstrated to extend life-span of various organisms, as diverse as yeast, worms, flies and mammals, although the underlying mechanism is not fully understood. CR is also known to slow or block the onset of age-related disorders, including neurodegenerative disease, cancer, atherosclerosis and renal disease. With respect to CR and bone metabolism, conflicting results have been reported, from acceleration of bone loss to preventive effect through counteraction of age-related development of secondary hyperparathyroidism, and underlying mechanisms are not clear. In the present study, we have examined the effect of long-term CR (by alternate day feeding) vs. AD (ad libitum feeding) on bone remodeling in male C57B6 mice and F344 rats, focusing on its relation to energy balance. CR was started at the age of 3 months to minimize its effect on bone growth and was continued for up to 13 months. CR by 40% for 6 months (i.e. at the age of 9 months) caused decreased adipose tissue and body weight, in association with decreased serum leptin and insulin concentrations but comparable albumin levels, assuring that animals are not in malnutirition state. Micro CT scanning revealed that CR causes a substantial decrease in 3D BV/TV, both in mice and rats, with significant decreases in connectivity density and trabecular (Tb) number and increases in SMI (structure model index) and Tb separation, compared with AD group, while Tb thickness did not differ. Bone histomorphometry showed that reduction in BV was due to suppressed bone formation with elevated bone resorption. Ex vivo cultures revealed increases in both osteoclastogenesis and osteoblastogenesis in CR mice-derived marrow cultures, suggesting a feedback mechanism for osteoblast recruitment. In control AD mice, BV decreased between 9 and 16 months of age, whereas this age-related decline of bone mass did not occur in CR group, suggesting that CR may have biphasic effect on bone. In db/db mice with defective leptin receptor, CR failed to decrease bone mass. Also, reduced bone mass by CR was restored to AD level by administration of a beta adrenergic blocker, propranorol. Thus, CR may regulate bone formation through leptin signaling in the hypothalamus and elevated tone of sympathetic nervous system.

Disclosures: ***S. Tatsumi****, None.*

F390

The Postprandial Bone Resorption Process Is Regulated by Gastrointestinal Signal. D. B. Henriksen[1], B. Hartmann*[2], P. B. Jeppesen*[3], J. Miholic*[4], C. Christiansen[5], J. J. Holst*[2]. [1]Sanos Bioscience A/S, Herlev, Denmark, [2]Department of Medical Physiology, University of Copenhagen, Copenhagen, Denmark, [3]Department of Medicine CA, National University Hospital, Copenhagen, Denmark, [4]Department of Surgery, University of Vienna, Vienna, Austria, [5]Center for Clinical & Basic Research, Ballerup, Denmark.

The circadian pattern of bone resorption as assessed by s-CTX is tightly regulated to respond to food intake and the process is significantly dampened by meal ingestion. In contrast, the bone formation process is seemingly unaffected by ingestion of nutrients.

We conducted two studies, one in patients with short bowl (SB) syndrome and one in patients with total gastrectomy. The objective was to elucidate whether the signal for the acute reduction of bone resorption after a meal was initiated from the stomach or the intestine.

SB patients with a preserved colon (n=5) and patients with SB and colectomy (n=7) and healthy controls (n=8) were admitted for a breakfast test meal (936 kcal) after an overnight fast. Blood samples were collected 15 minutes before and at 30, 60, 120, and 180 minutes after the meal. Patients who had total gastrectomy (n=8) were studied after an oral glucose (75g in 150ml). Blood samples were collected at 0, 30, 60, 90, 120, 150, and 180 minutes after ingestion.

We found that the normal reduction in bone resorption (s-CTX) after a meal was completely abolished in SB patients without colon. SB patients with a preserved colon had an intermediate response with a 27% ($p<0.05$) reduction of s-CTX after 120 minutes as compared to 66% ($p<0.001$) for normal controls. A significant reduction of 53% ($p<0.001$) was seen in individuals with total gastrectomy after oral glucose, which is comparable to published data for OGTT in healthy subjects (50% reduction over 120 min). Bone formation was unchanged for both SB and gastrectomy patients after ingestion of nutrients.

These data imply that the signal regulating the acute postprandial reduction in bone resorption arises from the intestine. Several hormones are released in response to the ingestion of nutrients. In particular the gastrointestinal hormone glucagon like peptide-2 (GLP-2) is thought to serve, together with the other proglucagon-derived peptides, in the regulation of absorption and disposal of ingested nutrients. The acute postprandial reduction of bone resorption coincides with the release of GLP-2 from the intestine. Furthermore, a subcutaneous injection of GLP-2 have been shown to result in a significant and acute reduction of the bone resorption in a dose dependent manner and with an apparent positive effect on bone formation as assessed by osteocalcin.

Disclosures: ***D.B. Henriksen****, Sanos Bioscience 3.*

F394

Mice Failing to Undergo Puberty Due to Targeted Inactivation of the GPR54 Gene Exhibit Alterations in Body Composition and Reduced Bone Mass. R. Brommage[1], N. Qian*[2], P. Vogel*[3], G. Liu*[1], M. Kelly*[4], D. R. Powell*[1]. [1]Endocrinology, Lexicon Genetics, The Woodlands, TX, USA, [2]Target Validation, Lexicon Genetics, The Woodlands, TX, USA, [3]Pathology, Lexicon Genetics, The Woodlands, TX, USA, [4]Molecular Genetics, Lexicon Genetics, The Woodlands, TX, USA.

GPR54 has recently been identified as a critical receptor involved in the initiation of puberty, as humans and mice with loss of GPR54 function have hypogonadotropic hypogonadism (de Roux et al., PNAS USA 100:10972-10976; 2003, Seminara et al., New Engl J Med 349:1614-1627; 2003, and Funes et al., Biochem Biophys Res Commun 312:1357-1363; 2003). The natural ligand for GPR54 is metastin (also known as KiSS-1), a 54 amino acid peptide containing an amidated carboxy-terminal phenylalanine. As part of Lexicon Genetics' efforts to examine phenotypes of knockout (KO) mice with targeted inactivations of novel genes that are potential pharmaceutical targets, KO mice with deletion of all 5 exons of the GPR54 gene were generated using homologous recombination. Both male (N = 3) and female (N = 4) KO mice are infertile. KO males (N = 3) have hypoplastic testes, epididymidies, seminal vesicles and prostates whereas KO females (N = 3) have hypoplastic uteri and ovaries. PIXImus DEXA measurements were performed at ~14 weeks of age in 7 KO males, 11 KO females, 5 male and 8 female wild-type littermates. Male KO mice have reduced body weight (↓22%) and lean body mass (LBM, ↓26%) but normal fat content, and therefore have an increased body fat percentage (↑18%). Female KO mice have normal body weight and LBM, but elevated body fat content (↑65%), and therefore have an increased body fat percentage (↑50%). Total body volumetric bone mineral density (vBMD) is reduced in both male (↓12%) and female (↓7%) KOs, with the BMC/LBM ratio being normal in males but low in females (↓26%). Femur and spine BMD are reduced in KOs of both genders (↓14% to ↓29%). Bone architecture was determined at ~16 weeks of age by microCT (Scanco μCT40) in 7 KO males, 6 KO females, 5 male and 6 female wild-type littermates. KO mice exhibit reduced LV5 trabecular bone volume (↓58% in males and ↓47% in females) and reduced femur midshaft cortical thickness (↓22% in males and ↓12% in females) and total cross-sectional area (↓29% in males and ↓23% in females) in both genders. All reported differences are statistically significant at $P < 0.05$. In summary, male and female mice with developmental hypogonadotropic hypogonadism have low bone mass. Male mice have low LBM whereas female mice have excess body fat. These alterations in body composition and bone mass are consistent with sex hormone deficiency throughout life.

Disclosures: ***R. Brommage****, Lexicon Genetics 3.*

F396

A Two-year Study of Bone Mineral Density in Adolescent Girls using either Depot Medroxyprogesterone Acetate or Oral Contraceptives. B. Cromer*[1], A. Bonny*[1], J. Ziegler*[2], R. Lazebnik*[3], E. Rome*[4], S. M. Debanne*[2]. [1]Pediatrics, MetroHealth Medical Center/Case Western Reserve University, Cleveland, OH, USA, [2]Case Western Reserve University, Cleveland, OH, USA, [3]Pediatrics, University Hospitals of Cleveland/Case Western Reserve University, Cleveland, OH, USA, [4]Pediatrics, The Cleveland Clinic/Case Western Reserve University, Cleveland, OH, USA.

There are mixed results on the effects of hormonal contraception on adolescent bone mineral density (BMD). In question are the effects of depot medroyxprogesterone acetate (DMPA) and oral contraceptives (OC) containing 20mcg ethinyl estradiol on BMD. The purpose of this study was to compare BMD over 24 months in adolescents who selected either DMPA (n=58) or OC (n=181), and girls who received no treatment with hormonal contraception [control group (N=161)]. The study population comprised 400 healthy, post-menarcheal girls aged 12 - 18 years recruited from four primary care clinics in a large, urban area. At baseline, 6, 12, 18, and 24 months, BMD of the lumbar spine (L1-L4) and femoral neck were obtained with dual x-ray absorptiometry (DXA). Data were also obtained on tobacco use, calcium intake, physical exercise, and menstrual history.

Mean chronologic age in years at baseline was as follows: DMPA (15.8±1.6 SD), OC (16.0±1.4 SD), and control (14.9±1.6 SD). The control group was significantly younger than the other two groups (p<.001). Approximately 60% of each group self-reported race as black. Mean weight in kilograms was as follows: DMPA 60.4(±12.8 SD), OC 69.1(±17.2 SD), and control 63.3(±16.8 SD). The OC group weighed significantly more than the other two groups (p<.001). To date, a total of 130 girls have completed the study: DMPA (n=17), OC (n=44), and control (n=69). Using analysis of covariance, after adjusting for age, race, and body weight, the results were as follows: percent change in BMD at femoral neck over 24 months was as follows: DMPA -5.2%, OC 3.0%, and control 3.8% (p< .001). Post hoc testing showed significance for DMPA vs. OC (p<.001) and DMPA vs. control (p<.005). Percent change in BMD at L1 - L4 spine over 24 months was as follows: DMPA -1.4%, OC 4.2%, and control 6.2% (p<.001). Post hoc testing showed significance for DMPA vs.OC (p<.001) and DMPA vs. control (p<.001).

Conclusion: Over a 24 month period, adolescent girls receiving DMPA had significant bone loss in both the femoral neck and lumbar spine compared to bone gain in these areas in the other two groups. The clinical implication of these results is whether use of DMPA reduces peak bone mass during a crucial period of bone development in adolescent girls.

Disclosures: ***B. Cromer****, None.*

F400

Increases in Femoral Neck Strength Indices with Alendronate versus Placebo. A. Karlamangla[1], D. Black[2], E. Barrett-Connor[3], J. Liu*[1], D. Kado[1], G. Greendale[1]. [1]Division of Geriatrics, UCLA, Los Angeles, CA, USA, [2]UCSF, San Francisco, CA, USA, [3]UCSD, La Jolla, CA, USA.

The fracture risk reduction achieved with alendronate therapy in clinical trials is greater than would be expected from the increases seen in bone mineral density. This discordance may be a consequence of the effects of the therapy on bone size. We therefore set out to study the effects of alendronate therapy on composite indices of femoral neck strength, which integrate bone mineral density, bone size, and body size:

Compression Strength Index = BMD * FNW / Weight,

Bending Strength Index = BMD * $(FNW)^2$ / (HAL * Weight),

Impact Strength Index = BMD * FNW * HAL / (Height * Weight).

Here, BMD refers to projected (areal) bone mineral density of the femoral neck, FNW is femoral neck width, and HAL is hip axis length. These indices have previously been shown to predict hip fracture risk in older women.

In all participants from 2 sites of the Fracture Intervention Trial (post- menopausal women, N=573), we measured BMD, HAL, and FNW from archived DXA hip scans and calculated the 3 strength indices at baseline and final follow up (3-4 years later).

At baseline, mean values of FNW and strength indices were similar in the 2 arms of the trial (p>0.3). By final follow up, FNW had increased in both groups (p=.0008 for placebo, p<.0001 for alendronate), but since BMD decreased in the placebo group (p=.0003) and increased in the alendronate group (p<.0001), the composite strength indices remained essentially unchanged in the placebo arm (p=.08 for compression index, p=.14 for bending index, and p=.79 for impact index), while they increased significantly in the alendronate arm (p<.0001 for all 3 indices).

Femoral Neck Variables	**Mean Change (%)**		*p value for comparison of 2 groups*
	Alendronate (N=288)	*Placebo* (N=285)	
Femoral Neck Width	+ 0.9	+ 0.6	0.25
Femoral Neck BMD	+ 3.1	- 0.9	< .0001
Compression Strength Index	+ 4.1	- 0.2	< .0001
Bending Strength Index	+ 4.4	+ 0.0	< .0001
Impact Strength Index	+ 5.1	+ 0.5	< .0001

As BMD declined with aging in the placebo group, there was a compensatory increase in FNW, which minimized the effect on bone strength. However, in the alendronate group, the increase in BMD was still accompanied by an increase in FNW similar to that seen in the placebo group. Thus increases in femoral neck strength in the alendronate group were substantially larger than the increases in the placebo group. In future studies, we will investigate how much of the fracture risk reduction in the alendronate group is explained by these increases in strength indices.

Disclosures: ***A. Karlamangla****, None.*

F402

Drug Therapy For Early Post-menopausal Osteopenic Women in the Absence of Prior Fracture Is NOT Cost-Effective. J. T. Schousboe[1], K. E. Ensrud[2], J. A. Nyman*[3], R. L. Kane*[3], L. J. Melton[4]. [1]Park Nicollet Health Services, Minneapolis, MN, USA, [2]Univ of Minnesota & MVAMC, Minneapolis, MN, USA, [3]Univ of Minnesota, Minneapolis, MN, USA, [4]Mayo Clinic, Rochester, MN, USA.

Some drugs are FDA approved to prevent bone loss in osteopenic (spine or hip T-score between -1.0 and -2.5) post-menopausal women, and are currently being marketed for that indication by industry. In the absence of prior fracture, osteopenic women are not at high risk of fracture. Targeting healthy women at the menopause may be especially problematic. To evaluate this issue, we used a Markov model with seven health states (No Fracture, Wrist, Clinical Vertebral, Hip, Vertebral and Hip, Other Fractures, & Death) to estimate the incremental lifetime costs & health benefits of a strategy of alendronate therapy for five years compared to no drug therapy in osteopenic early post-menopausal women. "Other" fractures included distal femur, humerus, proximal radius, pelvis, rib, and fibula/tibial fractures. Fracture rates, direct medical costs of fracture, & long-term care costs after hip fracture were derived from comprehensive population-based data of Rochester, MN. We assumed 1) the worst estimates for loss of quality of life from fracture published in the medical literature, 2) a 50% reduction in vertebral and 34% reduction in non-vertebral fractures with alendronate therapy in the no fracture state, 3) a 50% reduction in all fractures with alendronate therapy after any incident fracture, 4) discount rates of 3% for costs & health benefits, 5) alendronate cost equal to U.S. average wholesale price for 2001, and 6) gradual offset of fracture reduction benefit over 5 years after alendronate discontinuation. The table below shows the incremental cost (in 2001 US $) per quality adjusted life-year saved with this strategy compared to no drug therapy, from Monte Carlo simulations (20,000 trials each) of the model.

Age	**Femoral Neck T-Score**		
	-1.0	-1.5	-2.0
50	$258,609	$196,138	$135,161
55	$211,178	$150,896	$100,379
60	$183,161	$129,756	$85,676

These results are insensitive to varying fracture rates or costs by 30%. Even assuming a very high societal willingness to pay of $100,000 per QALY saved & best case scenario regarding drug efficacy, alendronate therapy for healthy osteopenic early post-menopausal women who have not had a fracture is not cost-effective. These results are highly likely to be applicable to other anti-resorptive drugs, since they are similar in cost to & no more efficacious in preventing fracture than alendronate.

Disclosures: ***J.T. Schousboe****, Hologic, Inc 2.*

F404

Reduction of Osteoporotic Fractures with Risedronate in Osteopenic Postmenopausal Women. E. S. Siris[1], I. P. Barton*[2], M. R. McClung[3], A. Grauer[4]. [1]Columbia University, New York, NY, USA, [2]Procter & Gamble Pharmaceuticals, Egham, United Kingdom, [3]Oregon Osteoporosis Center, Portland, OR, USA, [4]Procter & Gamble Pharmaceuticals, Mason, OH, USA.

There is increasing evidence that a significant number of vertebral and non-vertebral osteoporotic fractures occur in patients with BMD values in the osteopenic range. Using data obtained from the VERT and BMD studies, we investigated the efficacy of risedronate in reducing osteoporotic fractures in postmenopausal women who had a baseline femoral neck BMD T-Score above -2.5 SD (NHANES-III) and no prevalent vertebral fracture (VFx). We studied the effect of 3 years of risedronate 5mg vs. placebo daily on reducing the combined risk of vertebral and non-vertebral fractures. Patients were stratified per trial and data were analysed using a time-to-first fracture analysis. All patients received 1000mg calcium and, if needed, 500IU vitamin D/day. There were 707 patients with a femoral neck T-score higher than -2.5 SD without prevalent VFx at baseline (355 on placebo, 352 on risedronate). They were well matched for mean age (64 vs 64 years) and mean femoral neck T-score (-1.68 vs. -1.71). The fracture incidence in the placebo group over three years was 8.3%, compared to 2.1% in the risedronate treated patients (RR 0.25, CI 0.09-0.67, p<0.006). The results were similar when only the 371 patients who had a BMD T-score above -2.5 at both femoral neck and lumbar spine were included (placebo 7.0%, risedronate 1.1%, RR 0.24 (CI 0.05-1.11, p=0.068). Risedronate significantly reduced the risk for vertebral and non-vertebral osteoporotic fractures over 3 years in patients with a femoral neck T-score higher than -2.5 and no prevalent VFx by 75%. In addition to its established fracture risk reduction in osteoporotic patients, these data demonstrate that risedronate also significantly reduces the risk of both spine and non-spine fractures in patients without prevalent VFx and femoral neck-BMD values in the osteopenic range.

Disclosures: ***E.S. Siris****, Procter & Gamble Pharmaceuticals 5; Aventis Pharmaceuticals 5.*

F406

Monthly Oral Ibandronate Significantly Reduces Bone Resorption in Postmenopausal Osteoporosis: 1-Year Results from MOBILE. R. R. Recker[1], D. L. Kendler[2], S. Adami[3], C. Hughes*[4], E. Dumont*[5], R. C. Schimmer[4], C. Cooper[6]. [1]Creighton University, Omaha, NE, USA, [2]University of British Columbia, Vancouver, BC, Canada, [3]University of Verona, Verona, Italy, [4]F. Hoffmann-La Roche Ltd, Basel, Switzerland, [5]GlaxoSmithKline, Collegeville, PA, USA, [6]University of Southampton, Southampton, United Kingdom.

Bisphosphonate therapies are effective in normalizing the elevated rate of bone turnover associated with postmenopausal osteoporosis (PMO). Ibandronate (Boniva®) is a potent, nitrogen-containing bisphosphonate with proven antifracture efficacy when administered daily or intermittently in postmenopausal women with osteoporosis (3-year vertebral fracture risk reduction: 52% and 50%, respectively).[1] An ongoing, randomized, double-blind, phase III, non-inferiority study (MOBILE) is comparing the efficacy and safety of monthly oral 50/50mg (single doses on consecutive days), 100mg (single day) and 150mg (single day) ibandronate regimens with the proven oral daily (2.5mg) regimen in 1,609 women with PMO. In MOBILE, relative change (%) in the biochemical marker of bone resorption, sCTX, is a secondary efficacy endpoint, measured immediately prior to the scheduled ibandronate doses at 3, 6, 12 and 24 months. After 1 year, the magnitude of median sCTX suppression in the oral daily arm was 67.3% (**Table**). A comparable magnitude of sCTX suppression was reported in each of the monthly oral arms after 1 year (one month after dosing): 62.8%, 66.7% and 75.8% in the 50/50mg, 100mg and 150mg arms, respectively (**Table**). Substantial decreases in sCTX were also observed after 3 and 6 months (**Table**). At all assessment points, the 150mg regimen provided the greatest magnitude of sCTX suppression. In summary, monthly oral ibandronate rapidly suppresses bone resorption to normal levels within 3 months of initiation, and maintains this magnitude of suppression with continued therapy. Monthly oral ibandronate also provides a comparable magnitude of sCTX suppression to that observed with an oral daily ibandronate regimen of proven antifracture efficacy (3-year vertebral fracture risk reduction: 52%). These findings indicate that monthly oral ibandronate is a highly effective alternative to more frequently administered bisphosphonates in PMO.

1. Chesnut CH, et al. J Bone Miner Res (In press).

Table. Median relative change (%) from baseline in sCTX

	Daily ibandronate	Monthly ibandronate		
Month	2.5mg (n=318)	50/50mg (n=330)	100mg (n=315)	150mg (n=327)
3	-53.6	-50.0	-53.2	-66.1
6	-63.5	-60.7	-63.2	-73.4
12	-67.3	-62.8	-66.7	-75.8

Disclosures: ***R.R. Recker****, F. Hoffmann-La Roche Ltd 2, 5.*

F408

Monthly Oral Ibandronate Is at Least as Effective as Oral Daily Ibandronate in Postmenopausal Osteoporosis: 1-Year Results from MOBILE. P. D. Miller[1], M. K. Drezner[2], P. D. Delmas[3], J. A. Stakkestad*[4], C. Hughes*[5], B. Bonvoisin[5], J. Y. Reginster[6]. [1]Colorado Center for Bone Research, Lakewood, CO, USA, [2]University of Wisconsin, Madison, WI, USA, [3]Claude Bernard University and INSERM Research Unit 403, Lyon, France, [4]CECOR AS, Haugesund, Norway, [5]F. Hoffmann-La Roche Ltd, Basel, Switzerland, [6]University of Liège, Liège, Belgium.

Adherence to oral daily and weekly bisphosphonates in postmenopausal osteoporosis (PMO) is suboptimal. Less frequent dosing regimens, such as once monthly, are expected to enhance long-term compliance and persistence with therapy, optimizing therapeutic outcomes. Ibandronate (Boniva®) is a potent, nitrogen-containing bisphosphonate with proven antifracture efficacy in PMO when administered daily or intermittently with a between-dose interval >2 months (3-year vertebral fracture risk reduction: 52% and 50%, respectively). A 2-year, randomized, double-blind, phase III, non-inferiority study (MOBILE) is comparing the efficacy and safety of 2 years' treatment with 50/50mg (single doses on consecutive days), 100mg (single day) and 150mg (single day) monthly oral ibandronate regimens versus the proven oral daily (2.5mg) regimen. A total of 1,609 postmenopausal women (aged 55-80 years; YSM: ≥5 years) with osteoporosis (lumbar spine BMD T-score <-2.5 and ≥-5) were enrolled into the study. Calcium (500-1,500mg) and vitamin D (400 IU) supplements are provided. The primary endpoint is mean relative change (%) from baseline in lumbar spine (L2-L4) BMD after 1 year. Relative changes (%) in total hip, femoral neck and trochanter BMD after 1 year are secondary efficacy endpoints. After 1 year, lumbar spine BMD increased by 3.9%, 4.3%, 4.1% and 4.9% in the daily (n=318), 50/50mg (n=330), 100mg (n=315) and 150mg (n=327) treatment arms, respectively (per-protocol population). Non-inferiority to the oral daily regimen was proven for all monthly oral regimens (margin of non-inferiority: 1%). In addition, superiority of the 150mg regimen to the oral daily regimen was prospectively demonstrated as part of the primary analysis. Significant and substantial increases in hip (all sites) BMD were also reported with all regimens. In post-hoc analyses, non-inferiority to the daily regimen was demonstrated for all monthly oral regimens in terms of total hip and trochanter BMD and the 100mg and 150mg regimens with respect to femoral neck BMD. Superiority of the 100mg and 150mg regimens to the oral daily regimen for total hip and trochanter BMD was also demonstrated. These findings confirm that the unique monthly oral ibandronate regimens evaluated in MOBILE provide efficacy that is at least equivalent to an oral daily ibandronate regimen of proven antifracture efficacy in PMO.

Disclosures: ***P.D. Miller****, F. Hoffmann-La Roche Ltd 2.*

F410

Effects of Bisphosphonates on Hip Fracture Risk Reduction: A Bayesian Analysis of Clinical Trials. N. D. Nguyen, J. A. Eisman, T. V. Nguyen. Bone and Mineral Program, Garvan Institute of Medical Research, Sydney, Australia.

Following 7 randomized clinical trials (RCTs) with 16557 patients since 1995, the evidence of anti-hip fracture efficacy of alendronate and risedronate is conflicting. Two trials (one each with alendronate and risedronate) suggested a beneficial effect, but the rest found no significant effect on hip fracture risk. Meta-analysis for each drug also yielded no statistically significant effect.

The discrepancy in results is partly related to "conventional" statistical analyses of RCTs, including meta-analysis, and p-values derived from those analyses that do not take into account pre-existing data about therapeutic effect. To address this issue and to assess the effects of bisphosphonates on hip fracture risk, the Bayesian concept of probability was utilized to systematically review past RCT data. In this analysis, three basic elements were considered: prior distribution, likelihood of present RCT data, and posterior distribution. The prior distribution describes a clinical belief *a priori,* or in this case, previously observed effect of bisphosphonates; the likelihood function captures how the present data modify the prior knowledge of the therapeutic effect; and the posterior distribution synthesizes both prior knowledge and likelihood function to provide the ultimate answer, e.g., the probability that bisphosphonates reduce hip fracture risk by a minimal magnitude of effect and its *credible interval*.

Data from a previous RCT involved alendronate treatment showed that the RR of hip fracture was 0.22 (95% confidence interval: 0.02, 2.13, p = 0.90). By incorporating these prior data to the sequential data from 3 subsequent RCTs, the average posterior RR of hip fracture was estimated at 0.60 (95% credible interval: 0.39, 0.92). Moreover, the probability that alendronate reduces hip fracture risk by at least 30% was 76%. A similar analysis of 3 risedronate trials yielded an RR of 0.61 (95% credible interval: 0.45, 0.85), with the probability that risedronate reduces hip fracture risk by at least 30% (ie, RR<0.3) was 80%. Furthermore, the probability that alendronate and risedronate reduce hip fracture by at least 50% (ie, RR<0.5) was 23% and 12%, respectively. These Bayesian analyses indicated that relative to placebo, alendronate or risedronate treatment reduces hip fracture risk at a clinically significant and public health relevant magnitude.

Disclosures: ***N.D. Nguyen****, None.*

F412

Alendronate Produces Greater Gains in BMD and Greater Reduction in Markers of Bone Turnover than Risedronate with Similar Tolerability. C. Rosen*[1], M. Hochberg*[2], S. Bonnick*[3], M. McClung*[4], P. Miller*[5], S. Broy*[6], R. Kagan*[7], E. Chen*[8], R. A. Petruschke*[8], A. E. de Papp[8]. [1]Maine Center of Osteoporosis Research and Education and Saint Joseph Hospital, Bangor, ME, USA, [2]University of Maryland Division of Rheumatology, Baltimore, MD, USA, [3]Institute for Women's Health-Texas Woman's University, Denton, TX, USA, [4]Oregon Osteoporosis Research Center, Portland, OR, USA, [5]Colorado Center for Bone Research, Lakewood, CO, USA, [6]Illinois Bone and Joint Institute, Morton Grove, IL, USA, [7]Foundation for Osteoporosis Reseach and Education, Oakland, CA, USA, [8]Merck & Co., Inc., West Point, PA, USA.

We performed a 12 month, double-blind trial of once weekly (OW) alendronate (ALN) 70 mg and OW risedronate (RIS) 35 mg at 78 US sites. 1053 postmenopausal women with low bone mineral density (BMD) (T-score ≤-2.0 at hip trochanter, total hip, femoral neck or spine) were randomly assigned to OW ALN 70 mg and OW RIS placebo, or OW RIS 35 mg and OW ALN placebo. Treatment was administered fasting, in the morning, and patients were instructed to remain fasting for 30 minutes post dosing. The primary endpoint was the hip trochanter BMD at 12 months. Secondary endpoints included total hip, femoral neck and spine BMD, markers of bone turnover (uNTx/Cr, serum CTxI, serum BSAP, and serum P1NP), and tolerability as assessed by adverse experience (AE) reporting.

The mean age of subjects was 64 years, with a mean time since menopause of 18.4 years. ALN produced significantly greater increases in BMD at all sites measured, than did RIS (P<0.001 for hip trochanter, total hip, lumbar spine, and P=0.005 for femoral neck). Significant differences were seen at all BMD sites as early as 6 months.

Significantly greater reduction in all markers of bone turnover was seen with ALN compared to RIS at 12 months; treatment differences were significant as early as 3 months.

76.5% of ALN patients and 76.1% of RIS patients reported any clinical AE during the study. There was no significant difference in the percent of patients reporting any upper GI AE (22.5% ALN, 20.1% RIS, p=0.364) or discontinuation due to an upper GI AE (2.5% ALN, 3% RIS, p=0.708).

In this one year head-to-head study, ALN produced significantly greater gains in BMD and greater reductions in markers of bone turnover than RIS, with no differences in overall and upper GI tolerability. The greater antiresorptive efficacy of ALN was seen as early as 3 months.

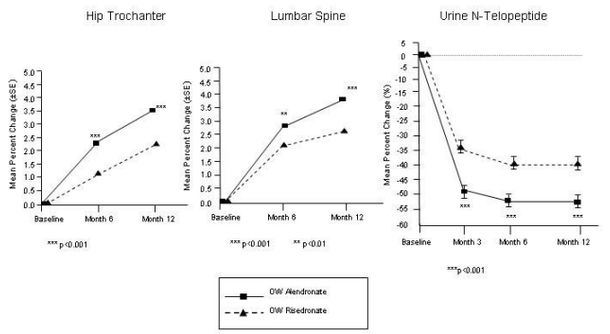

Disclosures: ***A.E. de Papp****, Merck & Co., Inc. 1, 3.*

F415

The Low Creatinine Clearance Associated High Risk of Falls Can Significantly Be Treated With Alfacalcidol. L. C. Dukas*[1], E. Schacht[2], Z. Mazor[3], H. B. Stähelin*[4]. [1]Acute Geriatric University Clinic, Kantonsspital, Basel, Switzerland, [2]Metabolic Bone Disease Unit, Universitätsklinik Balgrist, Zürich, Switzerland, [3]Bone Metabolism Unit, TEVA Pharmaceutical Industries, Jerusalem, Israel, [4]Acute Geriatric University Clinic, Kantonsspital Basel, Basel, Switzerland.

In elderly a treatment with D-hormone analogues can significantly reduce the number of fallers and falls. The synthesis of D-hormone is dependent on renal function. We determined the cutoff level of creatinine clearance (CrCl) at which D-hormone serum levels decline and using the cutoff, we further investigated in a post hoc analysis of a double-blind randomized study, if CrCl is associated with the risk of falls and whether treatment with Alfacalcidol can reduce this risk.

For 36 weeks 378 community-dwelling elderly men and women received randomly 1µg Alfacalcidol (Alpha-D_3® TEVA) or placebo daily. Using radioimmunoassay we measured regularly serum calcitropic hormones and assessed falls by a questionnaire. In multivariate-controlled logistic regression models we assessed, according to treatment groups and according to a CrCl cutoff at 65ml/min, the risk of becoming a faller and the risk of falling. Results are from ITT analyses.

In multivariate-controlled analyses D-hormone serum levels were significantly associated with CrCl ($p<0.0001$) and steadily declined below a CrCl of 65ml/min. A CrCl of <65ml/min was in multivariate controlled analyses associated with significantly lower D-hormone serum levels ($p=0.0008$). In the Placebo group participants with a CrCl of <65ml/min. were found to be, compared to participants with a CrCl of ≥65ml/min, 4 times significantly more prone to become fallers (OR 4.01, 95%CI 1.48-10.98, $p=0.006$). 36 weeks of treatment with Alfacalcidol were, compared to placebo, in participants with a CrCl of <65ml/min associated with a significant 74% reduction in the number of fallers (95% CI 20-92%, $p=0.019$), and a significant 71% reduction in the number of falls (95% CI 12-91%, $p=0.028$). The difference in number of fallers and falls between treatment groups was already significant after a 24 week treatment with Alfacalcidol ($p=0.022$ for number of fallers, $p=0.039$ for number of falls). No clinically relevant hypercalcemia was observed.

A reduced CrCl of <65ml/min is associated with a significant 4 times increased risk of falls. Treatment with Alfacalcidol is safe and is, compared to placebo, in a community-dwelling elderly population with a CrCl of <65ml/min, associated with a significant 74% decrease in number of fallers and a significant 71% decrease in number of falls.

Disclosures: ***L.C. Dukas****, TEVA Pharmaceuticals Industries ltd.; Israel 2; 2. Scientific grant, University Hospital Basel, Switzerland 2.*

F417

Results of a 5 year Double Blind, Placebo Controlled Trial of Calcium Supplementation (CAIFOS); Vertebral Deformity and Clinical Vertebral Fracture Outcomes. I. M. Dick[1], A. Devine[1], S. S. Dhaliwal*[2], R. L. Prince[1]. [1]School of Medicine and Pharmacology, University of Western Australia, Western Australia, Australia, [2]School of Public Health, Curtin University of Technology, Western Australia, Australia.

Vertebral fracture is a major public health problem in elderly women. We chose to test the hypothesis that calcium supplementation (calcium carbonate 600mg twice per day) offered to unselected individuals would reduce vertebral deformities and clinical spine fracture events compared to identical placebo tablets over 4 years.

1460 women mean age 75 were recruited from the whole population using a recruitment letter strategy. Responders were excluded if they were on bone active treatment, calcium supplementation or had diseases that may have prevented them completing the study. Of the responders 18% were eligible and agreed to participate. Vertebral deformities were assessed using morphometric X-ray absorptiometry (MXA) software version MXA 9.1 on a Hologic 4500A densitometer at years 1 and 5. The cv error varied from 5.8% at T6 to 3.1% at L4. A local reference range for vertebral deformities was developed using the McCloskey Kanis algorithm in 120 elderly women. Incident vertebral deformities were defined as vertebral deformities not present at baseline, with a reduction in posterior, mid or anterior heights of 20%. Clinical vertebral fractures were recorded from diaries reviewed 4 monthly and verified from spinal x-ray reports. The study outcomes were examined using logistic regression for MXA and Hazards Ratios (HR) were calculated using Cox Proportional Hazards Model for clinical vertebral fracture.

The prevalence of vertebral deformities was the same in the calcium compared to the placebo group (calcium 33%; placebo 36%, $p=0.42$). The incident vertebral deformity rate in those subjects who had a second MXA scan (n=883) was similar in the calcium and placebo group (calcium 10.2%; placebo 11.1%, RR 0.90: 0.59-1.39). Inclusion of BMI or prevalent vertebral deformity did not modify these results. In the per protocol subjects (n=706), the incident deformity rate was similar in the calcium compared to the placebo group (calcium 7.8%; placebo 11.1%, RR 0.67: 0.40-1.12).

Clinical spine fracture occurred in 76 subjects overall and in 17 subjects who finished the study per protocol. No difference in vertebral fracture between calcium and placebo groups in the whole study (HR 0.90: 0.57-1.41) or those who finished per protocol (HR 0.82: 0.32-2.14) was observed.

These data show that there were no detectable effects of calcium supplementation on incident vertebral fracture or deformity over the four years of this study.

Disclosures: ***R.L. Prince****, None.*

F421

Bone Loss and Lower Extremity Loading During Long-Duration Space Flight. A. J. Rice*[1], C. C. Maender*[2], K. O. Genc*[1], R. S. Ochia*[3], J. G. Snedeker*[4], P. R. Cavanagh[1]. [1]The Cleveland Clinic Foundation, Cleveland, OH, USA, [2]NASA - Johnson Space Center, Houston, TX, USA, [3]Rush Presbyterian-St. Luke's Medical Center, Chicago, IL, USA, [4]ETH, Zurich, Switzerland.

Bone loss in the lower extremities is an established consequence of long-duration human space flight, whereas bone mass in the upper extremities appears to be maintained. These changes may be the result of selective disuse atrophy of bone in the lower extremities. Reduction in load bearing on the feet may play a key role in these changes, but no quantitative data showing loads on-orbit currently exist. The purpose of the present experiment was to measure loads on the feet over an entire day in the same subject during daily life on the ground and on the International Space Station (ISS). In-shoe forces were monitored with modified Pedar insoles (Novel Gmbh, Munich, Germany) placed inside the shoes of a single astronaut on a 161-day ISS mission. DXA scans were also performed pre- and post-flight. All instrumentation was built into a Lower Extremity Monitoring Suit custom made for the subject, who gave informed consent to participate in the IRB-approved experiment. The force data were analyzed by a custom routine written in MATLAB (Mathworks Inc., Natick, MA). Daily load stimulus (DLS), a mathematical model used to relate changes in bone mineral density to daily loading histories, was calculated from the in-shoe force data. Average monthly BMD losses in the proximal femur, total hip, and lumbar spine regions were 0.64%, 0.72% and 2.31%, respectively. There was a net BMD gain of 0.32% per month in the arms. Peak force histograms from sample days in 0g and 1g (Fig. 1) show a marked shift in the two main modes of loading (walking and running from 260% and 120% BW in 1g to 160% and 90% BW in 0g). The total number of peaks above 5% BW was greatly reduced (10,112 peaks in 1g vs. 2,569 peaks in 0g) and force peaks greater than 200% BW were absent in 0g. The ratio of mean DLS in 0g to that in 1g varied from 0.44 to 0.55. Thus, exercise in space over an entire work day provided only approximately half the stimulus to bone experienced during a typical work day on Earth. These data suggest that in-flight exercise countermeasures for loss in bone mass should be augmented to restore key regions of the 1g daily loading profile in space.

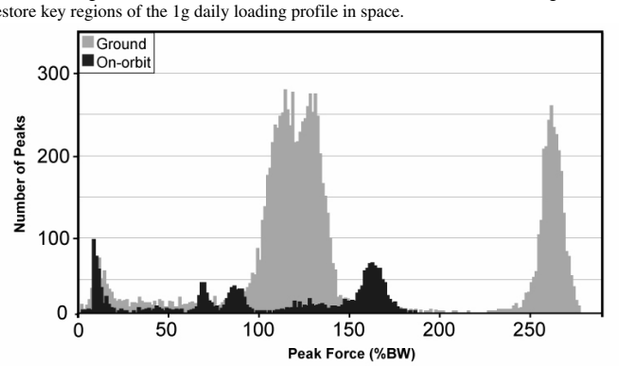

Figure 1: Peak force histograms in percent body weight (%BW) units for typical days on earth (light) and on the ISS (dark).

Disclosures: ***A.J. Rice****, None.*

F424

Comparison of Lasofoxifene and Raloxifene for the Prevention of Bone Loss in Postmenopausal Women. M. McClung[1], M. Omizo*[1], S. Weiss*[2], A. Moffett[3], M. Bolognese*[4], R. Civitelli*[5], V. Somayaji*[6], A. Lee[6]. [1]Oregon Osteoporosis Center, Portland, OR, USA, [2]Center on Drugs and Public Policy, University of Maryland School of Pharmacy, Baltimore, MD, USA, [3]OB-Gyn Associates of Mid-Florida, Leesburg, FL, USA, [4]The Bethesda Health Research Center, Bethesda, MD, USA, [5]Washington University School of Medicine and Barnes-Jewish Hospital, St Louis, MO, USA, [6]Global Research and Development, Pfizer, New London, CT, USA.

Bone loss in early menopause is an important determinant of fracture risk in older women. Estrogen therapy (ET) is effective in preventing bone loss but has recently been shown to have adverse extraskeletal effects. Selective estrogen receptor modulators (SERMs) may be attractive alternatives to ET. In this 2-yr, phase 2 study, the effects on skeletal health of lasofoxifene, a next generation SERM, were compared to placebo and raloxifene.

410 postmenopausal women were randomized: 82 each to receive lasofoxifene 0.25 mg/d and 1.0 mg/d, 163 to raloxifene 60 mg/d, and 83 to placebo. All women also received daily calcium 1000 mg and vitamin D 250 IU. Bone mineral density (BMD) at the lumbar spine (LS) and hip by DXA and biochemical markers of bone turnover (urinary N-telopeptide and deoxypyridinoline crosslinks; serum bone-specific alkaline phosphatase and osteocalcin) were measured at different time points over the treatment period.

At baseline, treatment groups were comparable for age (mean age 58-59 yrs), weight (mean weight 68-69 kg), years post menopause (8-10 yrs) and lumbar spine BMD (mean T-score -1.0). Statistically significant improvement in BMD in lumbar spine and total hip and reduction of biochemical markers of bone turnover occurred after 2 years of lasofoxifene treatment compared to placebo. Overall lasofoxifene was well tolerated, with an adverse event profile similar to raloxifene.

In conclusion, lasofoxifene significantly reduced indices of bone turnover and increased BMD in younger postmenopausal women. The responses were similar to or greater than those observed with raloxifene. These results support the use of lasofoxifene in postmenopausal women at risk for osteoporosis.

Mean Percent Changes from Baseline to Month 24

	Lasofoxifene 0.25 mg/d	Lasofoxifene 1.0 mg/d	Raloxifene 60 mg/d	Placebo
Lumbar spine BMD@	1.8%*	2.2%*†	-0.1%‡	-1.7%
Total hip BMD@	1.9%‡	1.3%	1.5%‡	-0.1%
N-telopeptide	-35.5%*†	-28.7%*	-15.6%‡	-7.0%
Deoxypyridinoline	-15.9%*†	-15.4%*	-3.3%‡	7.6%
Bone specific alk phos	-18.8%*	-20.7%*†	-6.6%*	5.4%
Osteocalcin	-39.7%*†	-36.3%*	-28.0%*	-13.1%

*p<0.001 vs placebo; †p<0.05 vs raloxifene; ‡0.001≤p<0.05 vs placebo; @ least squares means.

Disclosures: ***M. McClung****, Michael McClung, Molly Omizo, Stuart Weiss, Alfred Moffett, Michael Bolognese, and Roberto Civitelli 5; Veena Somayaji and Andy Lee 3.*

F426

Lasofoxifene, a Next Generation SERM, Is Effective in Preventing Loss of BMD and Reducing LDL-C in Postmenopausal Women. A. H. Moffett, Jr.[1], M. Ettinger[2], M. Bolognese*[3], S. Weiss*[4], V. Somayaji*[5], R. Brunell*[5], A. Lee[5]. [1]OB-GYN Associates of Mid-Florida, P.A., Leesburg, FL, USA, [2]Radiant Research, Stuart, FL, USA, [3]The Bethesda Health Research Center, Bethesda, MD, USA, [4]School of Pharmacy, Uni. of Maryland, Baltimore, MD, USA, [5]Global Research and Development, Pfizer, New London, CT, USA.

This study investigated the efficacy and safety of lasofoxifene, a next generation SERM, on BMD and LDL-C in early postmenopausal non-osteoporotic women.

Healthy postmenopausal women (n=394) with a mean age of 58 yrs (50-74 yrs) and mean duration since menopause of 9 yrs with a mean lumbar spine BMD T-score of -1.0 and mean LDL-C of 135 mg/dL were randomized to lasofoxifene 0.017 mg/d, 0.05 mg/d, 0.15 mg/d, 0.5 mg/d, or control groups for 1 yr; all patients received daily calcium and vitamin D. The primary endpoint was % change in BMD of lumbar spine and hip at 1 yr. Secondary analyses included changes in markers of bone turnover and lipid metabolism. BMD response was analyzed using a least significant change approach with 3% as the criterion for a significant change.

For lumbar spine at 6 months, the proportion of women who gained or did not significantly lose BMD was 92%, 95%, 93%, 97% and 91% for 0.017 mg/d, 0.05 mg/d, 0.15 mg/d, 0.5 mg/d and calcium + Vit D treated control groups, respectively with response on lasofoxifene 0.15 and 0.5 mg/d superior to control (p≤0.008). At 1 yr, response was 97%, 97%, 94%, 98% and 85% for 0.017 mg/d, 0.05 mg/d, 0.15 mg/d, 0.5 mg/d and control groups, respectively with response on all lasofoxifene groups superior to control (p≤0.001). For total hip at 6 months, proportion of subjects who gained or did not significantly lose BMD was 90%, 97%, 95%, 98% and 96% for 0.017 mg/d, 0.05 mg/d, 0.15 mg/d, 0.5 mg/d and control groups, respectively with response on lasofoxifene 0.15 mg/d superior to control (p=0.008). At 1 yr, response was 95%, 92%, 98%, 98% and 90% for 0.017 mg/d, 0.05 mg/d, 0.15 mg/d, 0.5 mg/d and control groups, respectively with response on lasofoxifene 0.05 and 0.15 mg/d superior to control (p<0.05). For LDL-C at 6 months, lasofoxifene therapy resulted in dose dependent decreases of 12.8%, 16.3%*, 20.6%*, 21.1%* and 6.1% for 0.017 mg/d, 0.05 mg/d, 0.15 mg/d, 0.5 mg/d doses and control group, respectively (*p<0.001 vs control). Lasofoxifene was well tolerated and no dose response was seen for AEs. Vasodilatation, leg cramps, and increased vaginal moisture were most frequently reported AEs attributed to lasofoxifene. No clinically meaningful effect on endometrium was observed with lasofoxifene and no breast cancer cases were reported.

Lasofoxifene effectively prevented loss of BMD, with a very high percent of responders, and reduced LDL-C in healthy non-osteoporotic postmenopausal women.

Disclosures: ***A.H. Moffett, Jr.****, Moffett A Jr., Ettinger M, Bolognese M, Weiss S 5; Somayaji V, Brunell R, Lee A 3.*

F428

Effects of Raloxifene on the Risk of Nonvertebral Fractures After 8 Years: Results from the Continuing Outcomes Relevant to Evista (CORE) Study. E. S. Siris[1], S. T. Harris[2], R. Eastell[3], J. Zanchetta[4], S. Goemaere[5], A. Diez-Perez[6], J. Song*[6], G. Crans*[6], S. R. Cummings[2]. [1]Columbia University, New York, NY, USA, [2]University of California San Francisco, San Francisco, CA, USA, [3]University of Sheffield, Sheffield, United Kingdom, [4]Universidad del Salvador, Buenos Aires, Argentina, [5]University of Ghent, Ghent, Belgium, [6]Lilly Research Laboratories, Indianapolis, IN, USA.

The multicenter, double-blind, placebo (PL)-controlled CORE study assessed the effects of raloxifene on invasive breast cancer for an additional 4 years from the 4-year MORE trial, with new nonvertebral fractures (NVF) studied as a secondary endpoint. In the 4011 postmenopausal women from MORE, those receiving PL in MORE (n=1286) continued with PL in CORE, whereas those treated with raloxifene (60 or 120 mg/d) in MORE received raloxifene 60 mg/d (RLX, n=2725) in CORE. Analyses were based on the time-to-first-event. The incidence of any new NVF was similar in the PL (22.9%) and RLX (22.8%) groups [hazard ratio (HR)(Bonferroni-adjusted confidence interval (CI)); 1.00 (0.82, 1.21)]. The incidence of NVF6 (clavicle, humerus, wrist, pelvis, hip, leg) was 17.5% in both groups [HR 1.01 (Bonferroni-adjusted CI 0.81, 1.26)]. No significant effect was found at individual fracture sites. Pre-specified subgroup analyses of age and BMD tertiles, prevalent NVF and vertebral fractures (VF), VF severity (SQ grade) at baseline of MORE, and study drug compliance did not reach statistical significance in the CORE population (n=4011). Post hoc Poisson analyses, to account for event rate (number of fractures/ time on therapy), showed neutral NVF and NVF6 effects in the overall populations. However, NVF6 risk was reduced in women with prevalent VF [HR 0.78 (95% CI 0.63, 0.96)], but did not reach statistical significance in those with severe (SQ grade 3) baseline VF [HR 0.66 (95% CI 0.43, 1.02)]. In the combined MORE and CORE cohort (N=7705), NVF6 risks were also decreased in women with SQ grade 3 baseline VF [HR 0.64 (95% CI 0.44, 0.92)], with an unchanged risk in the corresponding low-risk subgroups. Interaction effects were significant (P<0.10) for the subgroup analyses. Limitations in assessing NVF efficacy in CORE were due to selection bias, as women who enrolled in CORE had less severe osteoporosis than those who did not enroll. Also, 20% of those enrolled never took study drug and more women in the PL group (P=0.026) used other bone-active agents, as permitted in this breast cancer prevention study protocol. In conclusion, raloxifene had overall neutral effects on NVF after 8 years, with NVF6 efficacy in some high-risk subgroups shown by exploratory analyses, consistent with results of MORE.

Disclosures: ***E.S. Siris****, Eli Lilly and Company 2.*

F429

Hetereogeneity in Skeletal Response to Full-length Parathyroid Hormone (PTH). D. E. Sellmeyer[1], L. Palermo[2], M. L. Bouxsein*[3], J. Bilezikian[4], S. Greenspan[5], K. Ensrud[6], D. M. Black[2], C. J. Rosen[7]. [1]Medicine/Endocrine, Univ. CA San Francisco, San Francisco, CA, USA, [2]Epidemiology & Biostatistics, Univ. CA San Francisco, San Francisco, CA, USA, [3]Beth Israel Deaconess Medical Center, Boston, MA, USA, [4]Columbia Univ., New York, NY, USA, [5]Univ. of Pittsburgh, Pittsburgh, PA, USA, [6]Univ. of Minnesota, Minneapolis, MN, USA, [7]Maine Center for Osteo Research & Education, St. Joseph's Hospital, Bangor, ME, USA.

To examine variation in response to PTH (1-84) therapy, we examined the first year changes in BMD and bone markers from two arms of the PTH and Alendronate (PaTH) trial in which 119 women were randomized to PTH 1-84 (100mcg rhPTH/day, NPS) and 60 to alendronate (ALN, 10 mg/day, Merck). We also examined the data for subgroups with larger responses to PTH.

We found much greater variation in response to PTH compared to ALN for both BMD and bone markers. For example, the standard deviation (SD) of 12 month % change in cancellous spine BMD (by QCT) was 32% among those on PTH compared to 15% on ALN (p<0.0001, test for equality of standard deviations). We also found that substantial numbers of women on PTH had large increases in BMD. For example, as shown in the table below, 39% of the women on PTH had an increase of more than 30% in cancellous spine BMD compared to 6% on alendronate. In addition, despite the large mean increase in cancellous BMD (29%) among those on PTH, 17% of the women on PTH had no increase in cancellous BMD, a value similar to the 21% on alendronate. Results were similar, although less extreme, for DXA spine BMD.

For biochemical markers we found similarly high variation in response to PTH. The SD of 3 month change in bone alkaline phosphatase (BAP) was 72% in PTH compared to 15% in ALN (p<0.0001). The SD of 3 month change in serum type I collagen C-telopeptides (CTX) was 170% in PTH compared to 25% in ALN (p<0.0001).

Distribution of participants (ppts) by categories of change in bone density and bone turnover markers during therapy with PTH or alendronate.

	PTH (n=109)	Alendronate (n=57)	p-value (2x3 chi squared)
	% of ppts in category	% of ppts in category	
% change in cancellous spine BMD by QCT (baseline to 12 month)			
<=0	17%	21%	<0.001
0-30	44%	72%	
>30	39%	6%	
Total	100%	100%	
% change in spine BMD by DXA (baseline to 12 month)			
<=0	15%	11%	0.17
0-10	65%	79%	
>10	20%	11%	
Total	100%	100%	
% change in BAP (baseline to 3 month)			
<=0	13%	95%	<0.001
0-100	67%	5%	
>100	20%	0%	
Total	100%	100%	
% change in CTX (baseline to 3 month)			
<=0	25%	95%	<0.001
0-100	38%	5%	
>100	37%	0%	
Total	100%	100%	

None of the baseline factors we examined including age, BMI, BMD or bone markers explained this heterogeneity among PTH users. Analyses restricted to PTH adherers (per protocol analysis) did not substantially change these results.

In conclusion, there is significant individual variability in the skeletal response to PTH which exceeds that observed with alendronate. It is not known whether this heterogeneity is a characteristic feature of PTH therapy or anabolic therapy in general. Further investigation is needed to clarify which patients maximally respond to PTH.

Disclosures: ***D.E. Sellmeyer****, Proctor and Gamble 5; Aventis 5; Metabolex, Inc 5; Novartis 2.*

F431

Treatment of Osteoporotic Women with Parathyroid Hormone 1-84 for 18 Months Improves Cancellous Bone Formation and Structure: A Bone Biopsy Study. R. R. Recker[1], S. P. Bare*[1], M. A. Miller[2], M. K. Newman[2], J. Fox[2]. [1]Creighton University, Omaha, NE, USA, [2]NPS Pharmaceuticals, Salt Lake City, UT, USA.

Histomorphometry studies in rhesus monkeys have shown that daily treatment with full-length parathyroid hormone 1-84 (PTH) increases new bone formation and bone volume. However, there is no information on the effects of PTH treatment on bone microarchitecture in humans. We obtained iliac crest biopsies from postmenopausal osteoporotic women given daily injections of placebo or 100 μg PTH for 18 months to assess the effects of treatment on cancellous and cortical bone formation and structure. All subjects received background treatment with Ca (700 mg) and vitamin D (400 IU). At baseline there were no significant differences between groups in age, weight, bone turnover markers, and spine and hip bone mineral density. The histomorphometry results are summarized in the table.

Parameter	Placebo	PTH	P-value*
BV/TV (%)	15.5 ± 1.6	22.8 ± 2.5	0.036
Tb.N (/mm)	1.19 ± 0.09	1.47 ± 0.09	0.046
Tb.Th (μm)	130 ± 10	152 ± 9	0.172
Tb.Sp (μm)	858 ± 59	678 ± 39	0.046
MS/BS (%)	5.9 ± 1.3	12.1 ± 3.4	0.046
MAR (μm/day)	0.48 ± 0.04	0.53 ± 0.02	0.208
BFR/TV (mm3/mm3/yr)	0.027 ± 0.007	0.079 ± 0.031	0.021
OS/BS (%)	11.9 ± 2.5	16.1 ± 3.6	0.294
Ac.F (/yr)	0.39 ± 0.10	0.69 ± 0.18	0.074
ES/BS (%)	1.67 ± 0.48	1.75 ± 0.35	0.674
Ct.Po (%)	4.2 ± 0.8	5.6 ± 0.8	0.294

Values are mean ± SE, n=8/group. *Mann-Whitney U-test

Trabecular bone volume was 48% higher in subjects treated with PTH; this increase was the combined effect of 24 and 17% higher trabecular number and thickness, respectively, and resulted in a 21% lower trabecular separation. Treatment with PTH significantly increased bone formation rate (BFR) primarily by increasing mineralizing surface; mineral appositional rate was not increased significantly. Osteoblast and osteoid surfaces were 58 and 35%, respectively, higher in the PTH-treated group, but the increases were not significant. No index of bone resorption was significantly affected by PTH treatment, although a trend towards increased activation frequency was noted. No significant effects of PTH treatment were observed on periosteal or endocortical BFR, or on cortical thickness or porosity. The new bone produced by PTH treatment had normal lamellar structure and mineralization; there were no abnormal histological findings, including marrow fibrosis or osteomalacia. In conclusion, treatment of osteoporotic women for 18 months with PTH was generally safe and resulted in marked increases in cancellous bone formation and bone volume in the iliac crest without significantly affecting bone resorption.

Disclosures: ***R.R. Recker****, NPS 2; Lilly 2, 5; Procter & Gamble 2, 5; Roche, Merck, Novartis, Wyeth 2, 5.*

F433

Pthrp **Haploinsufficiency Impairs Bone Formation but Potentiates the Bone Anabolic Effects of PTH (1-34).** M. A. Sorocéanu*[1], D. S. Miao[1], Y. Jiang[2], J. J. Zhao[2], X. Y. Bai[1], H. Su*[1], H. K. Genant[2], N. Amizuka[3], D. Goltzman[1], A. C. Karaplis[1]. [1]Medicine, McGill University, Montreal, PQ, Canada, [2]Osteoporosis and Arthritis Research Group, University of California, San Francisco, CA, USA, [3]Department of Oral Biological Sciences, Niigata University, Niigata, Japan.

Despite normal serum PTH levels, *Pthrp*$^{+/-}$ mice exhibit decreased *Pthrp* expression in bone and an inappropriate, early (3-month-old) low trabecular bone content with increased marrow adipocity. This inverse relationship suggests that these animals are afflicted by a genetic form of osteoporosis.

To determine the etiology of these skeletal changes, histomorphometric analysis of long bones was undertaken. In *Pthrp*$^{+/-}$ specimens, osteoclast number and surface area were diminished but there was an even more marked decrease in osteoblast number and in mineral apposition rate (MAR) (36%) following calcein/tetracycline labeling. The number of apoptotic osteoblasts and osteocytes was also increased. Moreover, *ex vivo* bone marrow cell cultures from these mice exhibited a profound reduction in their capacity to give rise to ALP positive staining colonies.

Next, we sought to examine how the anabolic action of daily administered PTH 1-34 is influenced in the setting of PTHrP haploinsufficiency. Three-month-old *Pthrp*$^{+/-}$ male mice and wild type (WT) male litter mates were injected with either vehicle or PTH 1-34 (40 μg/kg/d) for three months and μCT and dynamic histomorphometric analysis of the skeleton was undertaken. In WT bones, PTH 1-34 had modest positive effects whereas profound anabolic changes were observed in bone specimens from treated *Pth*$^{+/-}$ mice. BV/TV increased 178% from baseline compared to 19% in WT mice. Similarly, Tb.N (25% vs. -4%), Tb.Th (55% vs. 14%), connectivity (306% vs. 38%) and DA (9% vs. -6%) increased while Tb.Sp (-22% vs. 3%) and SMI (-32% vs. -1%) decreased in specimens from *Pthrp*$^{+/-}$ mice. MAR also increased compared to treated control litter mates (260% vs. 44%). Cortical thickness increased by 25% in bone specimens from treated *Pth*$^{+/-}$ mice compared to 18% in WT mice, while cortical porosity decreased (72% vs. 1%).

These findings demonstrate that: (i) impaired bone formation is the basis of the osteoporotic phenotype in *Pthrp*$^{+/-}$ mice; these animals would therefore serve as useful model for testing new anabolic agents, (ii) that normal levels of PTHrP within the skeletal microenvironment are critical for healthy postnatal bone development and maintenance by promoting recruitment and survival of osteogenic cells, and (iii) the anabolic action of exogenous PTH is potentiated in the *Pthrp*$^{+/-}$ background, alluding to a pivotal interaction of these related proteins on the mechanism that promotes bone formation.

Disclosures: ***A.C. Karaplis****, None.*

F435

A No Observable Carcinogenic Effect Dose Level Identified in Fischer 344 Rats Following Daily Treatment with PTH(1-84) for 2 Years: Role of the C-Terminal PTH Receptor? C. E. Wilker*[1], J. Jolette*[2], S. Y. Smith[2], N. Doyle*[2], J. F. Hardisty*[3], A. J. Metcalfe*[1], T. B. Marriott[1], J. Fox[1], D. S. Wells*[1]. [1]NPS Pharmaceuticals, Salt Lake City, UT, USA, [2]CTBR, Senneville, PQ, Canada, [3]EPL, Research Triangle Park, NC, USA.

Administration of teriparatide, the N-terminal 1-34 fragment of parathyroid hormone, induces osteosarcoma in Fischer 344 rats. The carcinogenic potential of full-length parathyroid hormone 1-84 (PTH) was assessed by daily sc injection (0, 10, 50, 150 µg/kg/day) for 2 years in the same rat strain. Histopathological analyses were conducted on the standard set of soft tissues, selected bones (femur, tibia, lumbar spine, sternum), and all tissues with macroscopic abnormalities. In addition, whole body radiographs were also taken at term on all surviving rats to better ensure that all bone abnormalities were examined. All PTH doses caused widespread osteosclerosis and increased femoral and vertebral BMD in both sexes. The incidence of bone proliferative changes was comparable in control and low dose groups providing a no-carcinogenic effect dose of 10 µg/kg/day for PTH. In the mid and high dose groups, proliferative changes were dose dependent; osteosarcoma was most common, followed by focal osteoblast hyperplasia, osteoblastoma, osteoma and skeletal fibrosarcoma. Increased mortality, attributed to skeletal tumors, occurred only in high-dose males.

Number of animals with skeletal neoplasia (treated for up to 2 years)

Gender (N=60/sex/group)	Findings	PTH (µg/kg/day)				
		0	0	10	50	150
Males	Osteosarcoma	0	0	1	13	27
	All bone neoplasms	0	0	1	17	30
Females	Osteosarcoma	2	0	0	5	13
	All bone neoplasms	2	0	0	10	21

In contrast to PTH, teriparatide induced osteosarcoma at all doses tested. The rat-to-human exposure ratio (3- to 4-fold) was comparable for the lowest doses of the two peptides. Moreover, the incidence of osteosarcoma was lower with PTH than teriparatide at all doses. We propose that structural differences between PTH and teriparatide provide a mechanism for these observations. Both peptides contain the N-terminal region that activates the PTH-1 receptor, leading to their anabolic effects, e.g., bone cell anti-apoptosis. PTH, however, contains the C-terminal region that activates a different receptor with distinct biological activities, e.g., pro-apoptosis. Balancing the effects of the N- and C-terminal regions may lead to the lesser proliferative response of PTH vs. teriparatide. In conclusion, a safety margin between the pharmacological and carcinogenic effects of PTH was demonstrated in this study.

Disclosures: ***C.E. Wilker****, None.*

F437

Parathyroid Hormone Added to Raloxifene and Subsequent Maintenance of BMD Gain with Raloxifene Alone. F. Cosman, J. Nieves, N. Barbuto*, M. Zion*, R. Lindsay. Clinical Research Center, Regional Bone Center, Helen Hayes Hospital, West Haverstraw, NY, USA.

Many women treated with anti-resorptive medications remain at high risk for fracture as a result of their prior fracture history, very low starting BMD or suboptimal response to anti-resorptive treatment. The influence of prior anti-resorptive agents on PTH treatment effect may differ by medication used, and the ability of antiresorptive agents to maintain BMD after stopping treatment with PTH might also vary. We performed a study of 40 postmenopausal women (mean age 67, range 47-82) already treated with raloxifene (60 mg/day) for at least 1 year (mean 2.7 years) who had recent fractures or persistent osteoporosis by BMD criteria at the spine or hip. Women were randomly assigned to stay on raloxifene alone or to receive (1-34)hPTH 25 mcg/day subcutaneously for 12 months while continuing raloxifene, and were then followed for 1 subsequent year on raloxifene alone. Bone turnover markers [Serum aminoterminal propeptide of Type 1 Procollagen (P1NP), osteocalcin (OC), and urinary N-telopeptide (NTX)] and bone density by DXA were measured at baseline and every 3 months. Data are presented for the first 28 completers of the 12-month treatment study and for 15 women who completed the subsequent 12-month follow-up. Biochemical indices of formation increased rapidly, reaching a peak within 6 months of initiating PTH treatment, whereas NTX continued to drift upward between 6 and 12 months. At 6 months, P1NP levels increased to 567% above baseline and OC to 111% above baseline. At 12 months, urinary NTX increased to 222% above baseline. There were no significant biochemical marker changes in the raloxifene alone group. Mean BMD after 1 year of PTH treatment increased 10.9% at the spine and 3% at the total hip in the PTH plus raloxifene group (both p<0.008), with no significant BMD change in the raloxifene alone group. In the subgroup of patients followed for 1 year after completing PTH, spine BMD declined 2.6% (from a peak of 13.6% above baseline) and total hip BMD declined 1.1% (from a peak of 3.6% above baseline) after one year of follow-up off PTH, while continuing raloxifene (both NS). We conclude that substantial BMD gain occurs with PTH treatment in people on prior and ongoing raloxifene. Although a slight drift downward in BMD after PTH withdrawal was seen, there was no significant BMD loss in patients maintained on raloxifene after PTH withdrawal. PTH-induced BMD benefits remain 1 year after stopping PTH when raloxifene is continued.

Disclosures: ***F. Cosman****, Eli Lilly 2, 5, 8.*

F439

Effects of Parathyroid Hormone, Alendronate, or Both on Bone Density in Osteoporotic Postmenopausal Women. R. Neer, A. Hayes*, J. Wyland*, J. Finkelstein. Endocrine Unit, Mass General Hospital, Boston, MA, USA.

We recently reported that alendronate blunts parathyroid hormone (PTH)-induced increases in serum alkaline phosphatase and spine and hip bone mineral density (BMD) in osteoporotic men. We now report final results of a companion study, testing how alendronate affects skeletal responses to PTH in osteoporotic postmenopausal women. We randomly assigned 93 such women with a spine and/or femoral neck BMD T-score ≤ minus 2.0 to 30 months treatment with oral alendronate 10 mg/day (ALN, n=31), sc PTH 37 ug/day (PTH, n=31), or BOTH (n=31). PTH treatment started at month 6. All women had normal serum PTH, 25-OH D, and TSH levels at entry. None had other disorders that (or took medications that) affect bone metabolism or BMD. We maintained calcium intake at 500-1500 mg/day and serum 25-OH vitamin D >15 ng/mL. We measured BMD by DXA in the lumbar spine, proximal femur, radius diaphysis, and total body (without head) every 6 months, vertebral trabecular BMD at month 0 and 30 by QCT, and serum alkaline phosphatase at months 0,1,2,3,6,7,8,9,12,18,24, and 30.

ALN blunted PTH-induced increases in serum alkaline phosphatase and vertebral trabecular BMD, total vertebral BMD, femoral neck BMD, and total hip BMD, reduced PTH-induced decreases in radius shaft BMD (each $p < 0.01$-0.05), and did not alter PTH effects on total body BMD. BOTH increased serum alkaline phosphatase, vertebral trabecular BMD, and total vertebral BMD more than ALN, and decreased radius shaft BMD (each $p < 0.01$-0.05), but increased femoral neck, total hip, and total body BMD no more than ALN. Tabulated below are mean (±SEM) percent changes in BMD at month 30 and serum alkaline phosphatase at month 18, calculated on an intention-to-treat basis:

Rx/ months	QCT Spine	DXA Spine	Femoral Neck	Total Hip	Radius Shaft	Total Body	Alkaline P'tase
PTH/24	57 ± 7	18.5 ± 2.3	10 ± 1.3	6.4 ± 1.0	- 6.9 ± 1.0	4.2 ± 0.7	79 ± 14
BOTH	23 ± 5	14.8 ± 1.4	4.8 ± 1.2	5.3 ± 1.1	- 2.2 ± 0.9	5.4 ± 0.6	4 ± 5
ALN/30	0 ± 1	6.8 ± 0.8	3.8 ± 0.8	3.1 ± 0.8	0.3 ± 0.6	4.7 ± 0.4	- 15 ± 4

Our data suggest that PTH effects on bone formation depend partly on its ability to increase bone resorption, or that ALN directly inhibits bone formation or PTH effects thereon. Studies of other anti-resorptive drug-PTH interactions can discriminate among these possibilities and clarify bone formation-resorption coupling.

Disclosures: ***R. Neer****, Eli Lilly 5, 8; Merck 8.*

F441

Early BMD Response to Teriparatide (rhPTH 1-34) in Patients with and without Prior Antiresorptive Treatment: Interim Results from the EUROFORS Study. J. Farrerons[1], R. Eastell[2], H. Minne[3], M. Audran[4], G. Lyritis[5], E. Simoes*[6], F. Marin*[7], T. Nicholson*[7], P. Ochs*[7], R. Alonso*[7], T. N. Nickelsen[7]. [1]Hospital Santa Creu i Sant Pau, Barcelona, Spain, [2]University of Sheffield, Sheffield, United Kingdom, [3]Klinik Der Fuerstenhof, Bad Pyrmont, Germany, [4]Centre Hospitalier Universitaire, Angers, France, [5]University of Athens, Athens, Greece, [6]Instituto Portugues de Reumatologia, Lisbon, Portugal, [7]Eli Lilly & Company, Indianapolis, IN, USA.

EUROFORS is a prospective randomized trial of 24 months duration, designed to investigate various sequential treatments of teriparatide over two years in postmenopausal women with established osteoporosis. We divided participants into three subgroups: osteoporosis treatment-naïve patients (group 1), and patients with adequate (group 2) or inadequate (group 3) clinical outcome to prior antiresorptive (AR) therapy. For the purpose of this study, inadequate clinical outcome to prior AR therapy was predefined as: (a) sustaining ≥1 new clinical fragility fracture(s) despite prescription of AR therapy during the 12 months prior to fracture; (b) a T-score of at least -3,0 SD or (c) a BMD decrease of ≥3.5% at the lumbar spine (LS), total hip or femoral neck ≥ 2 years after initiating AR therapy. In the first year, all patients (n=863) receive an open-label treatment with teriparatide 20 µg/d and supplements of 500 mg/d of calcium and 400-800 IU/d of vitamin D. Here we report the 6-month interim BMD results for the first 201 patients (mean age, 69.8±7.2 years) who obtained a follow-up BMD measurement.

At baseline, mean lumbar spine and total hip BMD were comparable among the groups. The BMD changes from baseline to month 6 (mean±SD) were as follows:

Group (n)	Lumbar spine (%)	*p-value*	Total hip (%)	*p-value*
1 (31)	+6.9 ± 4.8	<.001	+0.7 ± 3.2	.219
2 (40)	+4.5 ± 4.7	<.001	-0.1 ± 3.1	.826
3 (130)	+4.0 ± 5.5	<.001	-0.9 ± 4.0	.010

While the changes in total hip BMD are in agreement with previous results from the teriparatide after antiresorptive drugs (AAA) study (Ettinger et al., JBMR 2003; 18 Suppl 2:S15), the increases in LS BMD seen in our patients who used prior ARs (mostly bisphosphonates; groups 2 and 3) are more pronounced than those in prior alendronate users from that trial. As the requirements for treatment duration and compliance with prior AR use were less strict in our study than in the AAA trial, this difference in results may be interpreted as a more robust BMD response to teriparatide in AR-pretreated patients when ARs were given in the less controlled, naturalistic conditions of routine care.

Disclosures: ***T.N. Nickelsen****, Eli Lilly & Company 3.*

F445

Small Molecule GSK3 Inhibitor Stimulates Bone Formation and Restores Bone Mass in Osteopenic, Ovariectomized Rats. Q. Zeng*[1], M. Sato[1], A. Schmidt*[1], J. Hoover*[1], S. Malhotra*[1], T. A. Engler*[1], Q. Zhang*[2], W. S. Jee*[2], C. E. Ruegg*[1], B. R. Berridge*[1], C. A. Frolik*[1], H. U. Bryant[1], Y. L. Ma[1]. [1]Bone and Inflammation, Eli Lilly and Company, Indianapolis, IN, USA, [2]Radiobiology, University of Utah, Salt Lake City, UT, USA.

In the canonical Wnt pathway, glycogen synthase kinase-3β (GSK3β) activity is critical for phosphorylation and degradation of cytosolic β-catenin. Inactivation of GSK3β allows β-catenin to accumulate and migrate to the nucleus where it can interact with DNA-binding protein to activate the expression of target genes. We examined the skeletal effects of 603281-31-8, a GSK3 α and β dual-inhibitor in osteopenic, ovariectomized (Ovx) rats. 603281-31-8, 0.5 or 3 mg/kg/d po or PTH (1-38) 10 ug/kg/d sc were given for 2 months to 7-month old ovx rats which had been permitted to lose bone for 1 month. Most of the bone effects for 603281-31-8 at 0.5 mg/kg/d were not significant, but 603281-31-8 at 3 mg/kg/d completely restored Ovx-induced loss of bone mineral content (BMC) and density (BMD) in the 4th lumbar vertebra and significantly increased mid-femur BMC over both Sham (8%) and Ovx controls (13%). When compared to Ovx controls, trabecular area in the proximal tibial metaphyses was 70% higher, and it was accompanied by a thickening of the trabeculae and improved trabecular connectivity. In the tibial shaft, 603281-31-8 significantly increased cross sectional area (3%), cortical area (12%) and decreased the marrow cavity area (-26%) compared to Ovx controls. The cortical effects were comparable to PTH treatment. Furthermore, bone formation rate tended to increase on trabecular and endocortical surfaces and significantly increased on the periosteal surface (506%). Endocortical eroded surface was decreased (-35%) when compared to Ovx controls. These data show that the orally active, small molecular weight, GSK3 inhibitor 603281-31-8 increases bone mass by stimulating bone formation activity in osteopenic, ovariectomized rats.

Disclosures: ***Q. Zeng****, Eli Lilly Company 3.*

F450

Effect of MRL123, an Orally Administered alphaVbeta3 Integrin Antagonist, on Markers of Bone Turnover and Bone Mineral Density in Postmenopausal Osteoporotic Women. M. Murphy*[1], K. Cerchio*[1], S. Stoch[1], K. Gottesdiener*[1], M. Wu*[1], R. Recker[2]. [1]Department of Clinical Pharmacology, Merck Research Laboratories, Rahway, NJ, USA, [2]Osteoporosis Research Center, Creighton University, Omaha, NE, USA.

The $\alpha_v\beta_3$ integrin (vitronectin receptor) has been shown to play a pivotal role in mediating bone resorption. We hypothesized that administration of MRL123, an orally administered $\alpha_v\beta_3$ integrin antagonist, would be a potent inhibitor of bone resorption, thereby increasing bone mass as assessed by bone mineral density (BMD) in women with postmenopausal osteoporosis. We determined the effects of MRL123 administration on BMD and biochemical markers of bone turnover including urinary N-telopeptide crosslinks [NTx] for 12 months. In a multicenter, randomized, double-blind, placebo-controlled, 12-month study, 227 women (mean ± SD 63.4 ± 8.1 years) with low lumbar spine or femoral neck BMD and no history of osteoporosis or fractures were randomly assigned (1:1:1:1 ratio) to one of four treatment groups for 12 months: MRL123 100 mg once daily (q.d.), MRL123 400 mg q.d.; MRL123 200 mg twice daily (b.i.d.); or placebo. All patients received 500 mg calcium plus 250 IU Vitamin D daily. Administration of MRL123 for 12 months significantly increased lumbar spine BMD (2.1, 3.1 and 3.5% for the 100 mg q.d., 400 mg q.d. and 200 mg b.i.d. treatment groups, respectively, vs -0.1% for placebo; $P < 0.01$ for all treatments vs placebo). Administration of MRL123 200 mg b.i.d significantly increased BMD at the hip (1.7% vs 0.3% for placebo; $P < 0.03$) and femoral neck (2.4% vs 0.7% for placebo; $P < 0.05$) as well and maintained an upward trend over the 12 months of the study. Effects on total body BMD, however, were similar among the MRL123 groups and not significantly different from placebo. Administration of MRL123 for 12 months significantly decreased NTx from baseline. The net treatment effects were similar, approximately -42%, for all active treatment groups vs placebo ($P < 0.001$). MRL123 was generally well tolerated and adverse events resulting in discontinuation from the study were relatively infrequent. In conclusion, the antiresorptive effect of the $\alpha_v\beta_3$ integrin antagonist MRL123 translated into significant increases in bone mineral density of the lumbar spine. Furthermore, administration of 200 mg MRL123 twice daily consistently provided efficacy at the hip sites. These data suggest that the $\alpha_v\beta_3$ integrin antagonist MRL123 could be developed as an effective therapeutic agent for osteoporosis.

Disclosures: ***S. Stoch****, None.*

F459

Should all Older People in Residential Care Receive Vitamin D to Prevent Falls? Results of a Randomised Trial. L. Flicker[1], R. J. MacInnis*[2], M. S. Stein*[3], S. C. Scherer*[4], K. E. Mead*[5], C. A. Nowson*[6], J. Thomas*[1], C. Lowndes*[5], J. L. Hopper*[5], J. D. Wark[5]. [1]University of Western Australia, Perth, Australia, [2]The Cancer Council Victoria, Melbourne, Australia, [3]Royal Melbourne Hospital, Melbourne, Australia, [4]Royal Freemasons' Homes, Melbourne, Australia, [5]University of Melbourne, Melbourne, Australia, [6]Deakin University, Melbourne, Australia.

We found previously that a 25-hydroxyvitamin D (25D) level of less than 25nmol/l was present in 22% of residents in 60 assisted living facilities (ALF) and 45% of residents in 89 nursing homes (NH) located in urban and rural centers across three states of Australia. Serum 25D level was independently associated with time to first fall. The aim of this study was to test whether vitamin D supplementation could reduce the risk of falls and fractures in this setting.

2454 NH and 1797 ALF residents were approached, and 952 NH and 667 ALF residents consented to participate in screening. Subjects with 25D levels less than 25 nmol/l or greater than 90 nmol/l were excluded. Subjects were randomised to ergocalciferol (initially 10, 000 IU per week, then 1000 IU per day) or matching placebo. All subjects received 600 mg of elemental calcium as calcium carbonate. Residents, institutional staff and study staff were blinded to treatment allocation. Institutional staff recorded falls and fractures prospectively in diaries for a 2 year intervention period. Compliance with ergocalciferol was monitored by pill counts and categorised as $< 50\%$ and $\geq 50\%$. Logistic regression, Cox proportional hazard and negative binomial models were used to estimate the effect of vitamin D supplementation on the outcomes of falls and fractures, both before and after excluding non-compliant subjects.

601 subjects entered the intervention phase. The two randomised groups had similar baseline characteristics. The Odds Ratio (OR) [95% CI] for the effect of vitamin D supplementation on the risk of ever falling was 0.85 [0.61-1.17] and was 0.72 [0.42-1.25] on the risk of ever fracturing. The incident rate ratio between groups for falls was 0.78 [0.60-1.00] and the hazard ratio for time to first fall was 0.86 [0.70-1.06]. Restricting the analyses to the 534 subjects whose compliance was $\geq 50\%$ produced an OR of 0.71 [0.50-1.00] for ever falling and of 0.68 [0.42-1.25] for ever fracturing. The incident rate ratio between groups for falls was 0.67 [0.52-0.88] and the hazard ratio for time to first fall was 0.80 [0.64-1.00]. We conclude that vitamin D supplementation reduces the risk of falls and possibly of fractures in older people in residential care, whose vitamin D level is greater than 25 nmol/l. This effect was apparently additional to any effect of calcium supplementation but may depend on calcium.

Disclosures: ***L. Flicker****, None.*

F462

Pamidronate Therapy in Children with Osteogenesis Imperfecta: Effect on the Bone Material Level. M. Weber*[1], P. Roschger[1], F. Rauch[2], T. Schoeberl*[3], N. Fratzl-Zelman*[1], F. H. Glorieux[2], P. Fratzl*[4], K. Klaushofer[1]. [1]Ludwig Boltzmann Institute of Osteology, 4th Med. Dept., Hanusch Hospital and UKH-Meidling, Vienna, Austria, [2]Genetics Unit, Shriners Hospital for Children, and McGill University, Montreal, PQ, Canada, [3]Erich Schmid Institute of Material Science, Austrian Academy of Sciences and Institute of Metal Physics, University Leoben,, Leoben, Austria, [4]Max Planck Institute of Colloids and Interfaces, Dept. Biomaterials, Potsdam, Germany.

Treatment with cyclical intravenous pamidronate has been reported to increase bone mass and to decrease fracture incidence in children with osteogenesis imperfecta (OI). This beneficial effect may be partly explained by increasing cortical width and trabecular bone volume, but possibly pamidronate treatment also influences material bone properties. This is an important issue, because disturbed material properties conceivably might negate the beneficial effects of increasing bone mass during therapy. We therefore studied paired iliac bone biopsies from patients (age 10-15 y) with OI types III and IV (n=6) before and after pamidronate treatment, in comparison to an age-matched control group (n=6). Quantitative backscattered electron imaging was applied to determine the typical bone calcium content (Ca_{Peak}) and its variation (Ca_{Width}). Nanoindentation was employed to determine hardness and stiffness (E-modulus). One-way ANOVA revealed a significant increase in baseline Ca_{Peak}, hardness and E-modulus for OI patients as compared to controls (+10 % at $P<0.0001$, +18 % at $P<0.05$ and +9 %, $P<0.05$, respectively). However, paired t-test between OI before and after treatment showed no treatment specific change on the bone matrix for any of the parameters measured. This is in contrast to the effect of bisphosphonate treatments in osteoporosis, where the calcium content is known to increase. In conclusion, our data show that stiffness, hardness and calcium content are elevated in OI patients with respect to controls, but that these matrix characteristics are not influenced any further by pamidronate treatment. Thus, the beneficial effect of the antiresorptive treatment on trabecular bone volume and cortical width does not seem to be accompanied by any alterations at material level.

Disclosures: ***P. Roschger****, None.*

F464

***Col1a2^{oim}* Mice Express Dentinogenesis Imperfecta.** G. E. Lopez Franco[1], A. Huang*[2], N. P. Camacho[2], R. D. Blank[3]. [1]Medicine, University of Wisconsin-Madison, Madison, WI, USA, [2]Research Division, Hospital for Special Surgery, New York, NY, USA, [3]Geriatrics Research, Education, and Clinical Center, William S. Middleton Veterans' Hospital, Madison, WI, USA.

Dentinogenesis imperfecta (DI) is an inconstant feature of osteogenesis imperfecta (OI), an inherited disorder resulting from mutations of the genes encoding type I collagen, the major structural protein in bone and dentin. Whether the apparent absence of dental abnormalities in some OI cases reflects biology or insensitivity of the diagnostic methods applied to teeth remains an open question. We therefore studied the dental phenotype of mice harboring the *Col1a2^{oim}* mutation (*oim*), a well-studied mouse model of α2(I) chain deficiency. There is no gross dental phenotype in *oim*/+ mice, while *oim*/*oim* teeth are fragile. To further define the phenotype, we examined teeth by light and scanning electron microscopy (SEM). Both *oim*/*oim* and *oim*/+ mice demonstrate reduced pulp chamber size, with nearly complete obliteration in *oim*/*oim* and reduction to about ½ normal size in *oim*/+. SEM of teeth fractured at the level of the junctional epithelium reveals several notable features. First, there is a clear difference of surface roughness among the +/+, *oim*/+ and *oim*/*oim* teeth. Second, there is a reduction in the number and regularity of spacing of the dentin tubules in *oim*/+ and *oim*/*oim* teeth. Third, the images suggest an impairment of matrix mineralization and ultrastructural ordering of the tissue in *oim*/+ and *oim*/*oim* teeth. These abnormalities are more severe in *oim*/*oim* than *oim*/+ animals, indicating dose-dependence of the mutant phenotype. In *oim*/+ heterozygotes, abnormalities are more pronounced in incisors than in molars. These findings demonstrate that both *oim*/*oim* and *oim*/+ mice suffer from DI. DI features are, as expected, more severe in the *oim*/*oim* than *oim*/+ animals. The more severe *oim*/+ incisor phenotype may be a reflection of incisors' continuous growth throughout the life of the animal. The presence of microscopic abnormalities in clinically normal *oim*/+ teeth suggests that reliance on insensitive diagnostic criteria may have resulted in underestimation of the prevalence of human DI in OI patients.

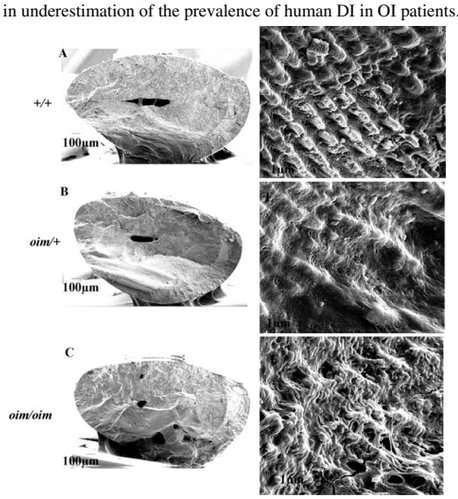

Disclosures: ***G.E. Lopez Franco****, None.*

F466

A Randomized, Controlled Study of Oral Alendronate vs. IV Pamidronate Therapy for Children with Osteogenesis Imperfecta. L. A. DiMeglio[1], L. Ford*[2], C. McClintock*[2], R. McClintock*[2], M. Peacock[2]. [1]Pediatrics, Indiana University, Indianapolis, IN, USA, [2]Endocrinology, Indiana University, Indianapolis, IN, USA.

Bone mineral density (BMD) increases in children with osteogenesis imperfecta (OI) treated with intravenous (iv) bisphosphonate. The efficacy and safety of oral alendronate have not been established. We have conducted an open-label, prospective, 2 year, randomized clinical trial of oral alendronate compared to iv pamidronate in 15 children with OI. Children were stratified according to bone age, pubertal stage, and type of OI and randomized to receive iv pamidronate, 3 mg/kg over 3 days every 4 months or oral alendronate 1 mg/kg daily. Primary efficacy outcome was change in BMD. Secondary outcomes included change in growth rate, biomarkers of bone turnover, and fracture incidence.

14 children were randomized, 7 to oral and 7 to iv. One was assigned to iv treatment because of chronic abdominal pain. In the iv group, 3 patients had type III/IV OI, while 5 had type I. In the oral group, 3 had type III/IV, while 4 had type I. The mean age of the oral group was 9.1 years (range 3.8-12.7); the iv group was also 9.1 years (range 3.5-13.7).

On treatment, both groups had a sustained and significant increase in total body and L2-L4 BMD (see table), above that expected from normal accrual for age. Although the response at L2-4 was greater at all times measured with oral treatment the differences in BMD between oral and intravenous treatment were not significant.

Growth showed moderate improvement with treatment, with length/height SDS for age going from -3.1 to -2.8 ($p<0.01$). All children had a decrease in biochemical markers of bone turnover, with significant changes over time ($p<0.05$ by RM ANOVA) in the serum bone formation markers, total alkaline phosphatase and osteocalcin and in the urine bone resorption markers, NTX/Cr, and DPD/Cr. Urine Ca/Cr decreased significantly but serum Calcium, TRAP, and PTH did not change significantly. There was a trend toward decreased fracture incidence in the two groups combined (from a mean of 2.0 ± 1.5 to 1.3 ± 1.5 fractures/year, $p=0.05$). Other than transient fevers following the first dose of iv pamidronate, no adverse effects of treatment were noted. These data suggest that oral and iv bisphosphonate therapy are equally safe and effective for children with OI. Supported by NIH K23 RR15538-01

BMD Responses	Oral	Sig	iv	Sig
24 month change in total body BMD (g/cm^2)	0.132 +/- 0.080	0.005	0.126 +/- 0.075	0.002
24 month change in total body BMD z-score	+0.9 +/- 0.7	0.019	0.9 +/- 0.9	0.031
24 month change in L2-L4 BMD (g/cm^2)	0.312+/- 0.163	0.002	0.284 +/- 0.127	<0.001
24 month change in L2-L4 z-score	+2.1+/- 1.1	0.002	+2.0 +/- 1.3	0.003

Disclosures: ***L.A. DiMeglio****, None.*

F468

LRP5 and High Bone Mass Disease. S. Mumm[1], X. Zhang*[1], M. Rickels*[2], A. Burshell[3], W. R. Reinus*[4], F. E. McKiernan[5], M. P. Whyte[6]. [1]Division of Bone and Mineral Diseases, Washington University School of Medicine, St. Louis, MO, USA, [2]Division of Endocrinology, Diabetes, and Metabolism, University of Pennsylvania School of Medicine, Philadelphia, PA, USA, [3]Bone Mineral Density Facility, Ochsner Clinic Foundation, New Orleans, LA, USA, [4]Mallinckrodt Institute of Radiology, Washington University School of Medicine, St. Louis, MO, USA, [5]Center for Bone Diseases, Marshfield Clinic, Marshfield, WI, USA, [6]Center for Metabolic Bone Disease and Molecular Research, Shriners Hospitals for Children, St. Louis, MO, USA.

Gain-of-function mutation (*Gly171Val*) of the gene encoding LDL receptor-related protein 5 (LRP5) was first discovered in 2002 in two American kindreds (AJHG 70:11, 2002; NEJM 346:1513, 2002). Both had uncomplicated high bone density and one also featured asymptomatic torus palatinus and a wide jaw. In 2003, however, 6 novel *LRP5* missense mutations affecting the same LRP5 protein domain were reported in individuals from the Americas and Europe, some with clinically significant dense bone disease (AJHG 72:763, 2003).

We have studied, clinically and molecularly, 3 patients with a high bone mass phenotype consistent with LRP5 activation. PCR amplification and sequencing of *LRP5* exons 2-4 and adjacent splice sites revealed heterozygosity for 3 *LRP5* missense mutations, *Arg154Met*, *Gly171Val*, and *Ala214Thr* (molecular study of a fourth patient is underway). These LRP5 changes affect the same first "-propeller" module as the 7 previously reported gain-of-function missense mutations. Notably, one patient with high bone mass and the same mutation (*Gly171Val*) as the original 2 families with benign high bone mass has significant skeletal disease including cranial nerve palsies, Chiari malfunction, and extensive maxillary and mandibular exostoses surrounding her teeth. She also has diffuse bone pain. Another patient has a previously reported LRP5 mutation (*Ala214Thr*) and lost vision in childhood and later had craniectomy for a small skull. The third patient has a novel mutation (*Arg154Met*) and has undergone surgical removal of mandibular exostoses for recurrent infections.

Because our patients' LRP5 mutations alter the region responsible for the receptor's antagonism by dickkopf (Dkk), their clinical features and high bone mass likely reflect increased Wnt signaling through LRP5. As yet uncertain nutritional, environmental, or more likely genetic factors condition *Gly171Val* effects so that LRP5 gain-of-function and increased Wnt signaling in bone may not always be benign.

Disclosures: ***S. Mumm****, None.*

F471

PTHrP Appears Selectively Less Effective than PTH in Stimulating 1,25(OH)$_2$D Production in Humans. M. J. Horwitz[1], M. Tedesco*[1], S. Sereika*[1], A. Bisello[1], A. Garcia-Ocana*[1], P. Dann*[2], J. J. Wysolmerski[2], G. Marshall*[1], B. Hollis[3], A. F. Stewart[1]. [1]U of Pittsburgh, Pittsburgh, PA, USA, [2]Yale U, New Haven, CT, USA, [3]U. South Carolina, Charleston, SC, USA.

Humans with humoral hypercalcemia of malignancy display reductions in plasma 1,25(OH)$_2$D, whereas those with primary hyperparathyroidism show increases. Long-term (46 hour) continuous steady-state infusions of both hPTH(1-34) and hPTHrP(1-36) using a single dose (8 pmol/kg/hr) in humans suggest that PTHrP may be slightly less calcemic than PTH, and may have an attenuated effect on circulating 1,25(OH)$_2$D. To confirm and quantitate the magnitude of the differences between the two peptides, we employed continuous, 46 hour steady-state infusions of hPTH(1-34) or hPTHrP(1-36) in multiple doses ranging from 8 to 28 pmol/kg/hr to 50 healthy normals. The composition and potency of the peptides was confirmed by mass spectroscopy, amino acid analysis, and adenylyl cyclase assay in SaOS-2 cells.

Serum total and ionized calcium increased significantly for both peptides at all doses ($p < 0.0001$). The PTHrP group displayed slightly milder hypercalcemia (mean = 10.7 mg/dl), than those receiving PTH (11.5 mg/dl) ($p = 0.0016$), but, surprisingly, the degree of hypercalcemia did not depend on PTH or PTHrP dose ($p = 0.96$). The percentage of individuals reaching the safety limit (serum calcium ≥ 12.0 mg/dl) was greater, and occurred at a lower dose, in those receiving PTH vs. PTHrP (12 vs. 28 pmol/kg/hr). Both peptides had predicable effects on serum phosphorus ($SP0_4$), TmP/GFR, fractional excretion of calcium (FECa) and suppression of endogenous PTH(1-84), and no differences between the two peptide groups were observed.

In striking contrast, subjects receiving PTH displayed markedly higher plasma 1,25(OH)$_2$D responses at every dose studied. For example, at the PTH 12 pmol/kg/hr dose, plasma

$1,25(OH)_2D$ rose from 33 pg/ml to 100 pg/ml. For the same PTHrP dose, the mean plasma 1,25 rose to only 48 pg/ml. For even the highest PTHrP dose, 28 pmol/kg/hr, $1,25(OH)_2D$ rose to only 85 pg/ml.

Thus, PTH may be marginally more calcemic than PTHrP in humans, but the two peptides have comparable effects on $SP0_4$, TmP, FECa and suppression of endogenous PTH(1-84). In contrast, PTH produces markedly greater increments than PTHrP in $1,25(OH)_2D$ in humans. The differential calcemic effect could reflect: 1) relative instability of PTHrP as compared to PTH in the human circulation; 2) the higher $1,25(OH)_2D$ levels that result from PTH infusion, and/or 3) differences in intrinsic ability to stimulate bone resorption. The differences in $1,25(OH)_2D$ may reflect differential effects on renal tubular signal transduction pathways associated with 1-alpha hydroxylase activation in humans.

Disclosures: ***A.F. Stewart****, Osteotrophin Inc. 4; Eli Lilly Inc 5.*

F474

Tissue-nonspecific Alkaline Phosphatase: A Novel Therapeutic Target for Arterial Calcification. D. Harmey, J. L. Millan. The Burnham Institute, La Jolla, CA, USA.

Abnormalities in the production or degradation of inorganic pyrophosphate (PP_i), a potent inhibitor of mineralization, leads to defects in mineral deposition. Tissue-nonspecific alkaline phosphatase (TNAP) hydrolyzes PP_i, and deletion of the TNAP gene (*Akp2*) in mice results in hypophosphatasia, characterized by elevated levels of PP_i and poorly mineralized bones. In contrast, genetic ablation of the molecules that produce and transport PP_i, *i.e.* nucleosidetriphosphate pyrophosphohydrolase (NPP1) and ANK, causes soft tissue ossification and hyperostosis. Abnormalities in NPP1- (*Enpp1*$^{-/-}$) and ANK- (*ank/ank*) deficient mice are ameliorated by deletion of *Akp2*, thus mice lacking both TNAP and either NPP1 or ANK displayed normalized skeletal mineralization in comparison to mice lacking either gene alone. In addition to bone abnormalities, *Enpp1*$^{-/-}$ mice develop arterial calcification and are a model of the human disease, idiopathic infantile arterial calcification (IIAC), characterized by hydroxyapatite deposition and smooth muscle proliferation in the internal elastic lamina. We hypothesized that arterial calcification would also be observed in ANK-deficient mice, and moreover, that the arterial calcification in *Enpp1*$^{-/-}$ and *ank/ank* mice would be normalized by the genetic or pharmacological ablation of TNAP function.

To establish if *ank/ank* mice display arterial calcification, hydroxyapatite deposition was examined using von Kossa and Alizarin Red staining. These analyses confirmed that *ank/ank* arteries have phosphate and calcium deposits. Also, H&E and van Giesson's staining of the arterial wall and elastic fibers revealed abnormalities in arterial wall morphology in comparison to wild-type (WT) mice, including thickening of the wall and disrupted elastic fiber organization. In order to assess the mineralizing capacity of aorta-derived cells from the mutant mice, *in vitro* studies were performed using primary vascular smooth muscle cells (VSMCs) which form mineralized nodules when cultured in the presence of β-glycerophosphate. We found that the number of mineralized nodules formed in cultures of *Enpp1*$^{-/-}$ and *ank/ank* VSMCs was increased compared to WT controls. Importantly, TNAP activity in mutant cells was significantly higher than in WT cells. Interestingly, treatment of these VSMC cultures with tetramisole, a specific uncompetitive inhibitor of TNAP, normalized TNAP activity in the mutant cells.

Our data support the hypothesis that TNAP is a potential therapeutic target for treatment of arterial calcification, and suggest that increased TNAP activity may contribute to the ossification abnormalities in both the skeleton and aortas of *Enpp1*$^{-/-}$ and *ank/ank* mice.

Disclosures: ***D. Harmey****, None.*

F477

Early Lethality in FGF23(R176Q) Transgenic Mice with Targeted Deletion of the *Pth* Gene. X. Bai, D. S. Miao, H. Fu*, J. R. Li*, Q. W. Xia*, D. Goltzman, A. C. Karaplis. Medicine, McGill University, Montreal, PQ, Canada.

Mutations in *FGF23* cause ADHR. Transgenic mice that express human FGF-23 (R176Q) (m*FGF23*^{Tr}) recapitulate the biochemical and skeletal alterations associated with ADHR. Unexpectedly, the transgenic mice also exhibit low-normal serum calcium levels with increased urinary calcium excretion and circulating PTH levels, consistent with secondary hyperparathyroidism. While its cause is not entirely clear, high PTH may contribute to the observed renal phosphate wasting and associated hypophosphatemia.

To examine the role of PTH in the pathophysiology of the observed phenotype, mice homozygous for the *Pth*-null allele carrying the FGF-23 (R176Q) transgene were generated. The *Pth*$^{-/-}$/m*FGF23*^{Tr} genotype was observed at the expected frequency but these mice were much smaller and very few of them were alive longer than 10 weeks after birth when maintained on regular rodent chow (0.61% Pi, 1.0% calcium and 4.5 IU/kg vitamin D_3). Analysis of serum biochemistry was performed in the four genotypes (wild-type (WT), *Pth*$^{-/-}$, m*FGF23*^{Tr}, *Pth*$^{-/-}$/m*FGF23*^{Tr}) at 50 days after birth. In the *Pth*$^{-/-}$/m*FGF23*^{Tr} mice, serum Pi levels were comparable to those in the WT mice, while in m*FGF23*^{Tr} mice the serum concentration was significantly decreased. Serum calcium levels were reduced in the *Pth*$^{-/-}$/m*FGF23*^{Tr} mice, more profoundly so than those in *Pth*$^{-/-}$ animals, while in m*FGF23*^{Tr} mice they were slightly decreased. Circulating levels of $1,25(OH)_2D_3$ were progressively lower in the *Pth*$^{-/-}$ and m*FGF23*^{Tr} mice and undetectable in the *Pth*$^{-/-}$/m*FGF23*^{Tr} mutants, reflecting the combined effect of increased FGF23 and lack of PTH activity on renal 1-alpha (Cyp27b1) and 24-hydroxylase (Cyp24) activity. Serum PTH levels in m*FGF23*^{Tr} mice were elevated compared to WT, but were undetectable in the *Pth*$^{-/-}$ groups. Interestingly, the renal threshold for phosphate, and urine calcium concentration were increased in *Pth*$^{-/-}$/m*FGF23*^{Tr} mutants but were significantly suppressed in the m*FGF23*^{Tr} mice. Introduction of rescue diet (0.5% Pi, 2.0% calcium, lactose 20%) improved survival as well as the biochemical and skeletal abnormalities associated with transgene overexpression.

The present findings indicate that the likely cause of death in the *Pth*$^{-/-}$/m*FGF23*^{Tr} mice is hypocalcemia. A potential role for FGF-23 in promoting secondary hyperparathyroidism by suppressing renal Cyp27b1 activity while activating Cyp24 is proposed. Hence, the combined effect of very low $1,25(OH)_2D_3$ levels and absence of circulating PTH leads to hypocalcemia and early lethality. Hyperparathyroidism, therefore, is an integral component of the pathophysiology of ADHR that also contributes to the renal phosphate transport defect in this disorder.

Disclosures: ***X. Bai****, None.*

F479

Matrix Extracellular Phosphoglycoprotein (MEPE) Fragments Circulate in Excess in Patients with Tumor-Induced Osteomalacia (TIO) and X Linked Hypophosphatemic Rickets (XLH). S. M. Jan de Beur[1], A. Jain*[2], M. Khan*[1], N. S. Fedarko[2]. [1]Endocrinology, Johns Hopkins Medical Institute, Baltimore, MD, USA, [2]Geriatrics, Johns Hopkins Medical Institute, Baltimore, MD, USA.

MEPE, an extracellular matrix protein first discovered in and highly expressed in mesenchymal tumors associated with tumor-induced osteomalacia (TIO), is a regulator of bone mineralization and formation. MEPE was initially considered a candidate for phosphatonin, the circulating inhibitor of renal phosphate reabsorption elaborated in TIO, but evidence of its phosphaturic effect has been inconsistent. Recent studies suggests that proteolytic fragments of MEPE have disparate actions on bone mineralization and formation. MEPE (507-525) inhibits mineralization in a mouse osteoblastic cell line; whereas, MEPE (242-264) stimulates new bone formation in neonatal mouse calvariae. MEPE excess has been implicated in the pathophysiology of XLH as *mepe* expression is markedly upregulated in osteoblast from *hyp* mice. Furthermore, MEPE may serve as a substrate for PHEX, the metalloprotease that is defective in XLH. Since MEPE has been implicated in the aberrant renal phosphate handling and bone mineralization in TIO and XLH, we hypothesized that MEPE and/or MEPE fragments would be elevated in the serum of patients with XLH and TIO. We developed competitive ELISAs that measure intact MEPE (~60 kD) and a C terminal fragment of MEPE (~ 30 kD) and measured fasting serum samples from patients with XLH (N =13), TIO (N=13) and age-matched controls (N=11 for C terminal and N=28 for intact). Serum C terminal MEPE was elevated in TIO (579.0+/-280.0 ng/ml) and XLH (768.5+/-641.0 ng/ml) and was significantly different than age-matched controls (212.2 +/- 80.0 ng/ml). In contrast, intact MEPE was not significantly different in TIO (561.0+/-135.0 ng/ml) or XLH (589.0+/-116.5 ng/ml) than in age-matched controls (674.7 +/-284.5 ng/ml). In two TIO patients with pre and post surgical serum samples available, serum C terminal MEPE levels dropped but intact MEPE levels remained unchanged. In TIO and XLH, the correlation between intact MEPE and MEPE fragment ($r=0.2$, $p<0.5$) was much weaker than in age-matched controls ($r=0.45$, $p<.005$). These data suggest that although intact MEPE is not elevated, MEPE fragments circulate in excess and may mediate the profound mineralization defects observed in TIO and XLH. Defining the precise bioactive MEPE peptides that circulate in XLH and TIO will elucidate the role of MEPE in the pathogenesis of the renal phosphate wasting and bone demineralization observed in these disorders and yield important information about the normal physiological function of MEPE in mineral ion homeostasis, bone formation and mineralization.

Disclosures: ***S.M. Jan de Beur****, None.*

F482

Zoledronic Acid Produces Greater Clinically Relevant Reductions in Biochemical Markers in Patients with Paget's Disease Versus Risedronate. D. J. Hosking[1], P. Miller*[2], J. Brown[3], W. Fraser[4], K. Lyles[5], I. Reid[6], P. Mesenbrink*[7]. [1]General Medicine and Metabolic Bone Disease, Nottingham City Hospital, Nottingham, United Kingdom, [2]Colorado Center for Bone Research, Lakewood, CO, USA, [3]Le Centre Hospitalier Universitaire de Quebec, Quebec, PQ, Canada, [4]Liverpool University Hospital, Liverpool, United Kingdom, [5]Duke University Medical Center, Durham, NC, USA, [6]University of Auckland, Auckland, New Zealand, [7]Novartis Pharmaceuticals Corporation, East Hanover, NJ, USA.

Bisphosphonates have revolutionised the treatment of Paget's disease. However, the need remains for therapies that achieve clinically meaningful reductions in serum alkaline phosphatase (SAP) and other biochemical markers to increase the likelihood of long-term remission. Zoledronic acid (ZA), a nitrogen-containing bisphosphonate, offers a single intravenous infusion with the possibility of achieving prolonged remissions. This randomised controlled trial assessed the efficacy and safety of a single 15-minute infusion of ZA 5 mg (n=88) in patients with confirmed Paget's disease over 6 months compared with oral risedronate (RIS) 30 mg/day for 60 days (n=90). The primary efficacy end point was defined as a ≥75% reduction in SAP excess or its normalisation at 6 months. Secondary efficacy end points included changes in serum CTx, urine α-CTx, and serum P1NP. These have previously been reported. More stringent and clinically relevant responses (percentage of patients who achieve a turnover below the midpoint of the normal range and above the lower limit of the normal range for each marker) have also been evaluated and are reported here. For each biochemical marker, ZA demonstrated a consistent, statistically greater response at 6 months relative to RIS (all $P<.001$). At 6 months, the percentage of ZA patients below the midpoint of normal ranged from 54.6% for SAP and urine α-CTx to 67.0% for P1NP. In comparison, RIS patients ranged from 23.6% for SAP to 32.6% for urine α-CTx . These differences were equal to or greater than those observed for the original definition of response. Within 3 days of drug administration, influenza-like symptoms occurred in 14% of ZA and 6% of RIS patients. Other symptoms, mostly transient, such as fever, myalgia, arthralgia, and bone pain occurred less commonly. Adverse events, including gastrointestinal and renal, were similar between groups. We conclude that, compared with RIS, ZA achieves more profound reduction in biochemical markers that are reflective of a true clinically relevant response.

Disclosures: ***D.J. Hosking****, Novartis, MSD, P&G, Lilly 5.*

F484

Wildtype SQSTM1 Protein Co-Localizes and Aggregates In Vivo with SQSTM1 Proteins Carrying Mutations in the UBA Domain. T. L. Johnson-Pais[1], Y. M. Ench*[2], J. H. Wisdom*[2], F. R. Singer[3], R. J. Leach[2]. [1]Pediatrics, Univ. of TX Health Science Center-San Antonio, San Antonio, TX, USA, [2]Cellular and Structural Biology, Univ. of TX Health Science Center-San Antonio, San Antonio, TX, USA, [3]John Wayne Cancer Institute, Santa Monica, CA, USA.

Six unique sequestosome 1 (SQSTM1) mutations clustered within the ubiquitin-associated (UBA) domain have been reported to predispose an individual to Paget's disease of bone (PDB). The P387L and P392L mutant proteins contain single amino acid substitutions within the UBA domain, while the other 4 mutant proteins are prematurely truncated near the start of the UBA domain. Since some of these mutant proteins bind ubiquitin and some do not, alterations in ubiquitin-binding may not be the cause of the abnormal osteoclast activity found in PDB. To understand the mechanism by which these different mutant proteins predispose an individual to PDB, we wanted to determine if mutant SQSTM1 proteins, differing in the UBA domain, can interact with wildtype SQSTM1 protein *in vivo.*

Wildtype and mutant SQSTM1 cDNAs were synthesized by RT-PCR using mRNA isolated from lymphocytes of control and PDB patients. The cDNAs were cloned into expression vectors to create N-terminus fluorescently-labeled proteins corresponding to wildtype SQSTM1, and the P392L, P387L and D391fsX394 mutant proteins. These constructs were transiently transfected into HEK293, HepG2 and RAW264.7 cells and analyzed by confocal microscopy.

In all three cell lines, wildtype SQSTM1 was localized in a punctate cytoplasmic pattern. The P392L and P387L proteins both formed much larger aggregates within the cytoplasm, while the truncated protein was localized in a very diffuse cytoplasmic pattern, as compared to the wildtype protein. Interestingly, co-transfection of wildtype and either P392L or P387L proteins resulted in co-localization of the wildtype and mutant protein in a large aggregate, very similar to the aggregate formed by either P387L or P392L alone. Co-transfection of the D391fsX394 truncated protein with the wildtype protein resulted in co-localization of the mutant and wildtype proteins in a punctate cytoplasmic pattern that was identical to the pattern of the wild-type protein alone.

The SQSTM1 protein contains an N-terminal dimerization domain that mediates the formation of homotypic arrays. Since the wildtype protein co-localizes in the cytoplasm with each of the mutant proteins, we assume the proteins are interacting through the N-terminal domain. Our results suggest that in PDB the function of wild-type SQSTM1 may be disrupted in a dominant-negative mechanism by interaction with the mutant protein, irregardless of the ubiquitin-binding capability of the mutant protein.

Disclosures: ***T.L. Johnson-Pais****, None.*

F486

Interaction of LIMD1 with p62/Sequestosome1 Is Required for Maximal Osteoclastogenesis in vivo. H. Zhao[1], Y. Feng*[2], S. L. Teitelbaum[1], F. P. Ross[1], G. Longmore*[2]. [1]Department of Pathology and Immunology, Washington University School of Medicine, St. Louis, MO, USA, [2]Departments of Medicine and Cell Biology, Washington University School of Medicine, St. Louis, MO, USA.

Paget's disease of bone (PDB) is a common bone disorder of aging characterized by foci of increased osteoclastic bone resorption followed by increased and chaotic new bone formation. Several potential susceptibility loci for familial PDB have been identified by genome-wide screen, including one on chromosome 5q35, coding for p62/sequestosome1. Importantly, genetic inactivation of p62 in mice leads to impaired osteoclastogenesis. We have performed studies to establish how p62 regulates osteoclast differentiation and function. In a yeast two-hybrid screen we find that p62 specifically interacts with LIMD1, a novel LIM domain-containing protein. By co-expression of Myc-tagged LIMD1 and a series of FLAG tagged p62 deletion mutants in 293 cells we establish that 50 amino acids between the RIP and TRAF6 binding domains of p62 are required for LIMD1 binding. To characterize further the role of LIMD1 in vivo, we generated knockout (KO) mice by homologous recombination. The KO mice are viable and appear healthy. Histological analysis of sections from tibia demonstrated similar bone volume and the number of osteoclasts as compared to wildtype (WT). Initially, we examined the role of LIMD1 in osteoclast differentiation by culturing bone marrow macrophages from WT and KO mice with MCSF and RANKL for 5 days. Osteoclast differentiation is dramatically decreased in LIMD1-deficient cells, a phenotype rescued completely by retroviral transduction of full-length of LIMD1 into KO macrophages. Consistent with the essential role of NFκB and AP-1 in osteoclasttogenesis, the activation of these two transcription factors in KO pre-osteoclasts is aberrant compared with that in WT cells. Finally, when LIMD1 null mice are injected subcutaneously with 100μg of recombinant RANKL for 7 days, the number of $TRAP^+$ osteoclasts in the calvaria of KO mice is reduced significantly compared to WT controls. These data indicate that, like the NIK and p62 knockouts, basal osteoclast differentiation is not affected by the loss of LIMD1, whereas the molecule is required for maximal stimulated osteoclastogenesis. Thus, LIMD1 is a new mediator of p62 signaling in response to RANKL/RANK activation.

Disclosures: ***H. Zhao****, None.*

F489

Mild Primary Hyperparathyroidism Is Associated with Low BMD but not Fracture Risk, Quality of Life or Mortality in Community Dwelling Elderly Women. E. McCloskey[1], D. deTakats*[1], M. Beneton*[1], J. Cliffe*[1], L. Reaney*[1], C. McGurk*[1], D. Charlesworth*[1], T. Jalava*[2], J. Kanis[1]. [1]University of Sheffield, Sheffield, United Kingdom, [2]Schering Oy, Helsinki, Finland.

Conservative management of mild primary hyperparathyroidism is recommended in patients without a history of complications. We wished to examine the impact of mild hyperparathyroidism (serum calcium <0.4mmol above the upper reference range) on fracture risk, mortality and quality of life in elderly community-dweeeling women.

Albumin-adjusted serum calcium and serum phosphate were measured in 5212 women aged at least 75 years at entry to the MRC Hip Fracture Study. Serum PTH was measured if adjusted serum calcium was greater than 2.60mmol/l to confirm the diagnosis as women with non-parathyroid hypercalcaemia were excluded from the study. Other assessments included measurements of total hip BMD (Hologic QDR4500), quality of life (Euroqol), incident fractures and mortality.

The mean age in the population was 79.5±3.8 years at entry to the study. A total of 126 (2.4%) women fulfilled the above criteria for primary hyperparathyroidism (cases). There were no significant differences in mean age, height or weight compared to the rest of the population (controls). Quality of life as measured by Euroqol was similar in cases and controls (P=0.75). Serum phosphate and serum creatinine were significantly lower (mean difference -0.12±0.01mmol/l) or higher (+3.7±1.7μmol/l) respectively in the cases. Bone mineral densities at the total hip (0.70±0.14 vs. 0.76±0.14g/cm2, P<0.001) and all hip subregions (P<0.003) were significantly lower in mild primary hyperparathyroidism. There was no significant interaction between the presence of mild primary hyperparathyroidism and the ability of clodronate to prevent fractures (20% reduction). Over a median follow-up of 4 years, the incidence of all clinical fractures was similar in the cases compared to controls (17.5 vs. 14.3%, OR 1.27, 95%CI 0.80-2.02, P=0.31) though the trend was stronger for peripheral fractures (OR 1.53, 0.83-2.80). The incidence of hip fracture was similar in both groups (3.2 vs. 3.6% in controls, OR 0.88, 0.32-2.42, P=0.81). The mortality rate in the cases was slightly but not significantly lower than in the controls (12.7 vs. 14.5%, OR 0.86, 0.50-1.45, P=0.7).

Mild primary hyperparathyroidism appears to have no major consequences for elderly women living in the community. Conservative management appears to be an appropriate management strategy.

Disclosures: ***E. McCloskey****, None.*

F493

Parafibromin, Product of the Hyperparathyroidism-Jaw Tumor Gene *HRPT2,* Is a Nucleocytoplasmic Protein that Regulates Cyclin D1 Expression. G. E. Woodard*, L. Lin*, S. K. Agarwal*, S. J. Marx, W. F. Simonds. Metabolic Diseases Branch, National Institutes of Health, Bethesda, MD, USA.

Parafibromin is the 531-amino acid protein product encoded by the recently identified *HRPT2* gene, a putative tumor suppressor gene implicated in the hyperparathyroidism-jaw tumor syndrome (HPT-JT) and sporadic parathyroid cancer. HPT-JT is an autosomal dominant familial cancer syndrome with high but incomplete penetrance. The major features are primary hyperparathyroidism (90%) including 15% of all affected by HPT-JT with parathyroid cancer, fibro-osseous jaw tumors (30%), bilateral renal cysts (10%), and less commonly solid renal tumors. Parafibromin contains no identified functional domains though it has weak homology to a protein in *S. cerevisiae*, Cdc73p, which participates as a cofactor in an alternative complex with RNA polymerase II. This study was undertaken to understand the expression, subcellular distribution, and functional properties of endogenous and recombinant human parafibromin.

Polyclonal antibodies were raised in rabbits to a purified recombinant protein consisting of glutathione S-transferase fused to amino acids 2 -135 of human parafibromin and the IgG fraction of this antiserum (NC190) was isolated by Protein A affinity chromatography. For transient transfection studies human parafibromin cDNA was modified with two copies of an in-frame N-terminal AU5 epitope and the construct placed downstream of the CMV promoter in the mammalian expression vector pcDNA3 (AU5-parafibromin). COS-7 cells transfected with AU5-parafibromin, but not empty vector, expressed a single band of 61 kD reactive with both AU5 monoclonal antibody and NC190. A survey of human tissues analyzed by immunoblotting showed NC190-reactivity with a 61 kD band in adrenal and parathyroid glands, kidney and heart, and a ~42 kDa NC190-reactive band also present in heart and skeletal muscle. The reactivity of all NC190-positive bands was blocked by preabsorption with purified His6-parafibromin (2-135) fusion protein. Subcellular fractionation of normal human parathyroid gland homogenate demonstrated expression of a 61 kD NC190-immunorective band in the cytoplasmic and nuclear fractions. Transient transfection of AU5-parafibromin, but not empty vector, strongly inhibited expression of cyclin D1/ PRAD1, a key cell cycle regulator previously implicated in parathyroid neoplasia. These results demonstrate that endogenous human parafibromin is a nucleocytoplasmic protein and demonstrate a potent biologic effect of parafibromin on a key cell cycle regulator consistent with its postulated role as a tumor suppressor protein.

Disclosures: ***W.F. Simonds****, None.*

F495

Cinacalcet HCl Effectively Treats Hypercalcemia in Patients with Parathyroid Carcinoma. S. J. Silverberg[1], C. Faiman*[2], J. P. Bilezikian[1], D. M. Shoback[3], M. R. Rubin*[1], R. Smallridge[4], L. E. Schwanauer*[5], K. A. Olson*[5], S. A. Turner*[5], M. Peacock[6]. [1]Columbia Univ Med Ctr, New York, NY, USA, [2]Cleveland Clin Found, Cleveland, OH, USA, [3]Dept of Veterans Affairs Med Ctr, Univ California, San Francisco, San Francisco, CA, USA, [4]Mayo Clin Jacksonville, Jacksonville, FL, USA, [5]Amgen Inc., Thousand Oaks, CA, USA, [6]Indiana Univ Sch Med, Indianapolis, IN, USA.

Cinacalcet HCl reduces serum calcium by effects mediated through the calcium-sensing receptor. In parathyroid carcinoma, a rare but important cause of severe hypercalcemia, the cancer retains PTH-secreting function. Most patients suffer with significant sequelae, including renal and skeletal complications. Although surgical removal can be curative, local seeding of functional parathyroid carcinoma cells in the neck and recurrence with metastases do occur. The cancer is commonly resistant to chemotherapy and radiotherapy, making medical management a challenge. We evaluated cinacalcet in a single-arm, dose-titration trial in 21 patients with parathyroid carcinoma. The cinacalcet dose was adjusted sequentially (30 mg twice daily to 90 mg four times daily) in a titration phase to achieve a ≥1 mg/dL reduction in serum calcium. The end of the titration phase occurred when serum calcium was ≤10.0 mg/dL or after 16 weeks, whichever came first.

All 21 patients had prior parathyroid surgery and one or more symptoms of hypercalcemia (somnolence, nausea and vomiting, decreased appetite, fatigue, and depression). Evaluation also revealed kidney stones (48%), acute renal failure/renal insufficiency (19%), and pathological bone fractures (14%). In 8 patients, parathyroid surgery had been performed multiple times, including 1 patient who had 6 operations. 81% of patients had been treated previously with bisphosphonates. The baseline mean (range) serum calcium was 14.5 (9.4 to 20.2) mg/dL and the baseline iPTH (nl range: 10-65 pg/mL) was markedly elevated, 856 (232 to 2106) pg/mL. At the end of the titration phase, cinacalcet reduced serum calcium to 12.4 (9.0 to 17.0) mg/dL; 71% (15/21) of patients achieved a target reduction in serum calcium of ≥1 mg/dL. In one patient, the calcium fell from 17.9 to 11.4 mg/dL. Pre-dose iPTH levels were reduced modestly (719; range 191 to 1130 pg/mL); even lower levels of iPTH were observed at 2 and 4 hours post-dose (mean of 630 and 610 pg/mL, respectively). Serum calcium reductions have been maintained for up to 3 years. Cinacalcet was generally well-tolerated in this study; the most common adverse events were nausea and vomiting.

Cinacalcet effectively reduced the extent of severe hypercalcemia in these patients with parathyroid carcinoma and can fulfill an unmet medical need in this critically ill patient population.

Disclosures: ***S.J. Silverberg****, Amgen Inc. 5.*

F497

Clinical Course of 10 Patients with Inoperable Parathyroid Carcinoma Treated with the Calcimimetic Cinacalcet HCl. M. R. Rubin, J. Sliney*, S. J. Silverberg, J. P. Bilezikian. Columbia University College of Physicians & Surgeons, New York, NY, USA.

Management of inoperable parathyroid carcinoma (PTHCa) presents a challenge because effective medical therapy has not been available. Morbidity and eventual mortality are consequences of severe hypercalcemia. The calcimimetic, cinacalcet HCl, reduces PTH secretion by binding to the calcium receptor and increasing its affinity for calcium. The resulting increase in intracellular calcium inhibits PTH with consequent reductions in the serum calcium. In primary hyperparathyroidism, cinacalcet normalized serum calcium levels for up to 3 years. We examined the clinical course of 10 patients with inoperable PTHCa treated with cinacalcet.

4 women and 6 men (52 ± 5 yr) underwent parathyroidectomy 6.8 ± 2 yrs prior to study. Metastatic disease had been resected in 9 patients: lung (n=6), neck (n=2) or esophagus (n=1). Hypercalcemia had not resolved with bisphosphonate use in 8; 7 had kidney stones and 4 had fractures. All had symptoms of hypercalcemia. Baseline biochemistries included marked elevations in the serum calcium (15.4 ± 1 mg/dl), PTH (mean: 914 pg/ml; range: 232-2106), urinary calcium excretion (503 ± 134 mg per 24 hrs; n=4), total alkaline phosphatase(AP, 203 ± 41 U/L; nl: <100), Bone-specificAP (BSAP, 60 ± 19 ng/ml; nl: 3.0-20.9), and serum NTX (178 ± 56 nM BCE; nl: 5.4-24.2). Cinacalcet was started at 30 mg twice daily and titrated over 16 weeks to a maximum of 90 mg four times daily. 8 patients required the maximal dose. The serum calcium fell to 11.8 ± 0.5 mg/dl and PTH to 700 pg/ml (range 191-984). The reduction in serum calcium was maintained for up to 1.5 yr, although PTH levels actually rose 42% from baseline values. Urinary calcium excretion decreased by 46% to 295 ± 107 mg 24 hrs (n=3) while bone turnover markers increased (serum NTX by 29%, BSAP by 110%).

Marked improvement in symptoms of hypercalcemia occurred in all, including increases in appetite, energy and strength. Nausea and vomiting occurred in 6 patients, necessitating discontinuation of cincacalcet in 1, but resolving fully in the others over time. Effects on tumor burden by sequential sestamibi scanning did not reveal a change in metastatic lesions (n=4). 4 patients sustained hip fractures and 1 patient died from acute congestive heart failure.

Cinacalcet was effective in reducing serum calcium in patients with inoperable PTHCa and is associated with symptomatic improvement. It represents an important treatment option in this patient population in which morbidity and mortality are high. Effects on the natural history of PTHCa, including tumor burden, fracture rate and mortality are unknown.

Disclosures: ***M.R. Rubin****, None.*

F500

Recombinant Osteoprotegerin Treatment Potently Inhibits Bone Resorption in Subjects with Osteoprotegerin Deficiency. T. Cundy[1], J. Davidson*[1], C. Stewart*[2], A. De Paoli[3]. [1]Department of Medicine, University of Auckland, Auckland, New Zealand, [2]Amgen Inc., Thousand oaks, CA, USA, [3]Amgen Inc., Thousand Oaks, CA, USA.

The autosomal recessive syndrome of Juvenile Paget's Disease/Familial Hyperphosphatasia (MIM239000) arises most commonly from inactivating mutations in the *TNFRSF11B* gene that encodes osteoprotegerin. Osteoprotegerin (OPG) is a critical regulator of bone resorption, and in its absence a high turnover deforming bone disease develops in infancy or childhood, that is relatively resistant to calcitonin and bisphosphonate treatment. In two siblings, aged 31 and 26, with OPG deficiency resulting from a 3bp deletion in the ligand-binding domain of OPG (delAsp182) we have studied the effect of synthetic OPG replacement treatment. OPG was produced as a recombinant Fc-OPG fusion molecule (AMGN 0007; 30mg/ml solution), and administered by subcutaneous injection. Sequential measurements were made of plasma total calcium, phosphate, and alkaline phosphatase (ALP) activity, and the bone resorption markers of deoxypyridinoline (DPD) and N-telopeptide (NTX) excretion. Bone resorption was rapidly inhibited at doses of 0.1 and 0.3 mg/kg body weight, with an obvious dose effect on intensity and duration of action. 0.3 mg/kg recombinant OPG suppressed uDPD to ~65% of basal values; in normal subjects uDPD is suppressed by ~40%, suggesting increased sensitivity in OPG-deficient subjects.

With continued treatment it was possible to suppress completely uNTX excretion with once weekly injections of 0.4 mg/kg. Over 6 months elevated plasma ALP also suppressed to within the normal range in both subjects. Apart from moderate hypocalcemia and hypophosphatemia there were no adverse events. Hematologic, renal, hepatic and thyroid function were unaffected. Replacement treatment with subcutaneous injections of recombinant OPG, or another means of inhibiting RANK-ligand, could be an effective long term treatment for OPG deficiency.

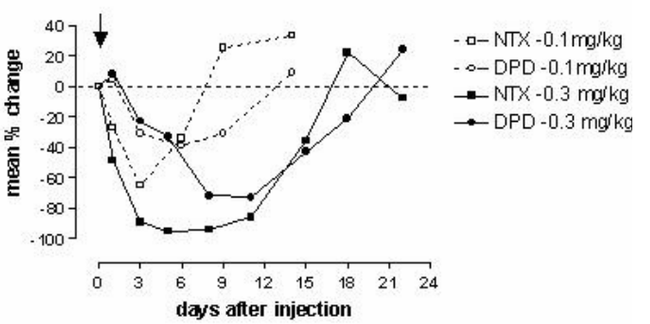

Disclosures: ***T. Cundy****, None.*

F503

Withdrawn

F507

The Results of a Study to Assess the Effects of Lanthanum Carbonate versus Calcium Carbonate on Bone Histomorphormetry in Patients with End-Stage Renal Disease. A. J. Freemont[1], J. Denton[1], C. Jones*[2], M. Gill*[2]. [1]Osteoarticular Pathology, University of Manchester, Manchester, United Kingdom, [2]Shire Pharmaceuticals Development Ltd, Basingstoke, United Kingdom.

In this study (LAM-IV-303), the effect of treatment with lanthanum carbonate, a new non-aluminium-, non-calcium-based phosphate binder, on bone in patients with end-stage renal disease (ESRD) was compared with the effect of treatment with calcium carbonate.
The trial was an open-label, multicentre, parallel-group study involving patients with ESRD initiated onto dialysis within 12 weeks of recruitment. Phosphate binder treatment was stopped, tetracycline labelling administered, and a transiliac bone biopsy taken. After randomization to treatment with lanthanum carbonate or calcium carbonate, patients were titrated to an optimum dose of elemental lanthanum (maximum: 3750 mg/day) or elemental calcium (maximum: 9000 mg/day) for 8 weeks, and maintained at this dose or titrated further as required for 44 weeks. Phosphate binders were then stopped, the bone was again labelled with tetracycline, and a second biopsy taken. Biopsies were analysed histomorphometrically and the data compared with normal values. Primary parameters included mineralization lag time (Mlt), % osteoid surface (%OS), % osteoid volume (%OV), % osteoblast surface (%ObS), bone formation rate (BFR), % osteoclast surface (%OcS) and mean erosion depth. Secondary parameters included activation frequency (AcF) and %OcS *vs.* BFR.
Paired biopsies from 63 patients were suitable for analysis; 33 from lanthanum carbonate-treated patients, and 30 from calcium carbonate-treated patients. The treatment groups were well balanced in terms of age, sex and race. Medical and surgical histories were typical of patients with ESRD. An analysis of the incidence of adynamic bone and hyperparathyroidism (%OcS *vs.* BFR) showed that 55% of lanthanum carbonate-treated patients moved towards normal bone, whereas 33% of patients receiving calcium carbonate treatment improved. A change towards normal %ObS in the lanthanum carbonate-treated group supported this finding. Lanthanum carbonate was also found to improve global bone cell activity (AcF) in 52% of patients, compared with improvement in 23% of calcium carbonate-treated patients. Osteoclast and osteoblast activity and bone matrix parameters indicated that lanthanum carbonate had no toxic effect on bone. In particular, it had none of the toxic effects associated with the use of aluminium-based phosphate binding agents.In conclusion, this study indicates that, compared with calcium carbonate, lanthanum carbonate treatment for 1 year may improve bone and bone cell activity in patients with ESRD.

Disclosures: ***J. Denton****, None.*

F511

Dysfunction of Membrane-Bound Prostaglandin E Synthase-1 (mPGES-1) Reduces Inflammatory Bone Resorption. K. Yamakawa*[1], M. Saegusa[1], D. Kamei*[2], Y. Takegoshi*[2], S. Uematsu*[3], S. Akira*[3], M. Murakami*[2], I. Kudo*[2], K. Nakamura[1], H. Kawaguchi[1]. [1]Univ. of Tokyo, Tokyo, Japan, [2]Showa Univ., Tokyo, Japan, [3]Osaka Univ., Osaka, Japan.

Prostaglandin E_2 synthase (PGES) is the terminal and specific enzyme following phospholipase A_2 and cyclooxygenase in the biosynthetic pathway of PGE_2 that induces various catabolic disorders including bone resorption. Among three isozymes of PGES: membrane-bound PGES-1 (mPGES-1), mPGES-2, and cytosolic PGES (cPGES), only the mPGES-1 mRNA level was upregulated in cultured mouse calvariae by proinflammatory cytokines TNF-α and IL-1. When an antisense oligonucleotide against mPGES-1 was added to the coculture of mouse bone marrow cells and osteoblasts on a dentine slice, it not only suppressed mPGES-1 expression and PGE_2 production, but also reduced by 80-90% the osteoclastogenesis and resorbed pit formation stimulated by the cytokines, which was restored by addition of exogenous PGE_2. To further examine the role of endogenous mPGES-1 *in vivo*, we created mice lacking the *mPGES-1* gene (*mPGES-1* KO) by homologous recombination in mouse ES cells. The KO mice developed and grew normally without abnormalities of major organs. Radiological and histomorphometric analyses also showed no difference in long bones and vertebrae between KO and wild-type (WT) littermates under physiological conditions during observation periods up to 26 weeks of age. However, pain nociception determined by the acetic acid writhing response was about 80% reduced, and inflammatory granulation tissue formation in the dorsum induced by subcutaneous implantation of a cotton thread was about 50% reduced in KO relative to WT. When arthritis was induced by the intraperitoneal injection of anti-type II collagen antibody, PGE_2 production and mPGES-1 mRNA level were markedly increased in paws of WT, which was rarely seen in KO. mPGES-2 and cPGES mRNA levels were not affected by the arthritis induction in either WT or KO. Histological analysis revealed that synovial hypertrophy, pannus formation and cartilage destruction were much milder in KO joints, and the arthritis score of the KO paws was about 40% of WT. The decrease of bone density and the histomorphometric parameters for bone resorption (N.Oc/B.Pm & ES/BS) around the KO knee joint were about half those of WT (all $p<0.01$). In contrast to the arthritis induction, bone decreases after ovariectomy or unloading by tail-suspension were similarly seen in KO and WT littermates. We conclude that mPGES-1 contributes to pain sensitivity, inflammation, and inflammatory bone resorption without affecting physiological conditions, implying that an inhibitor of mPGES-1 could be a highly selective treatment for these disorders such as rheumatoid arthritis.

Disclosures: ***K. Yamakawa****, None.*

F513

Increased Expression of ADAM8 in Rheumatoid Pannus. J. Mandelin[1], T. F. Li*[2], M. Hukkanen*[1], M. Ainola*[1], S. J. Choi[3], Y. T. Konttinen*[4]. [1]Institute of Biomedicine/anatomy, University of Helsinki, Finland, [2]Department of Orthopedics, University of Rochester Medical Center, Rochester, NY, USA, [3]Medicine-Hematology/Oncology, University of Pittsburg, Pittsburg, PA, USA, [4]Medicine/Invärtes medicin, Helsinki University Hospital, Helsinki, Finland.

A disintegrin and a metalloproteinase (ADAM)8, a recently identified osteoclast-activating factor, may promote tissue destruction in rheumatoid arthritis (RA). The presence of ADAM8 in RA characterized by bone erosions was compared to that of osteoarthritis (OA) characterized by subchondral bony sclerosis.
RA pannus (n=10), RA synovitis (n=10) and OA synovial membrane (n=10) samples were studied using tissue extraction and Western blotting, immunostaining and morphometry, tartrate-resistant acid phosphatase staining, in situ hybridization and quantitative reverse transcriptase-polymerase chain reaction (RT-PCR).
Western blots of tissue extracts showed the typical 65 kDa ADAM8 band in all samples prepared from RA pannus, RA synovitis tissue and OA synovial membrane. Immunostaining, confirmed with *in situ* hybridization, disclosed high ADAM8 expression in RA compared to OA (60.0 ± 2.2 % in RA pannus and 47.1 ± 2.1 % in RA synovial membrane compared to 9.8 ± 1.1 % in OA, $p < 0.001$), in particular in the pannus-cartilage junction, often close to tartrate-resistant acid phosphatase positive multinucleate cells. Pannus contained 23 ± 7 ADAM8 mRNA copies per 10,000 β-actin copies compared to 1.7 ± 0.3 in OA ($p<0.001$).
ADAM8, upregulated in RA pannus overlying developing erosions, may be actively involved in joint destruction through its role in monocyte-macrophage adhesion, direct cartilage degradation by its protease-like property and bone destruction by its osteoclast-activating effect.

Disclosures: ***J. Mandelin****, None.*

F521

The Mechanism Used by Parathyroid Hormone to Arrest the Cell Cycle Progression of Osteoblastic Cells from G1 to S Phase. L. Qin, X. Li*, J. Ko*, N. C. Partridge. Physiology and Biophysics, University of Medicine and Dentistry of NJ, Piscataway, NJ, USA.

Parathyroid hormone (PTH) plays a major role in bone remodeling. Current interest has focused on its ability to increase bone mass after intermittent administration. High concentrations of PTH inhibit the growth of UMR 106-01 cells, a rat osteosarcoma cell line, arresting them in G1 phase. Here we demonstrate that PTH employs at least three mechanisms to do this: inducing expression of MAP kinase phosphatase 1 (MKP-1) and $p21^{Cip1}$, and decreasing expression of cyclin D1. The induction of MKP-1 by PTH is a rapid primary response, with mRNA increasing 14-fold induction after 1 h. This was confirmed by Western blot analysis. Phosphorylated extracellular signal-regulated kinase 1/2 (ERKs1/2) are substrates for MKP-1 activity. We observed a coincident ERK dephosphorylation and MKP-1 induction after PTH (10^{-8} M) treatment of UMR cells. Inhibition of *de novo* protein synthesis by cycloheximide abolished both effects of PTH on dephosphorylation of ERK and increase in MKP-1 protein suggesting the new synthesis of MKP-1 may be required for ERK1/2 dephosphorylation. Orthovanadate, a tyrosine phosphatase inhibitor, also eliminates PTH's effect on ERK dephosphorylation. Moreover, overexpression of MKP-1 arrested UMR cells in G1. Since phosphorylated ERKs are important for cell growth, these data strongly suggest that the induction of MKP-1 by PTH affects cell cycle progression possibly by dephosphorylation of active ERKs. Phosphorylated ERKs stimulate cell growth by increasing the expression of cyclin D1, which is critical for G1 to S phase transition. We found PTH indeed decreases cyclin D1 protein level by 3-fold in UMR cells after 8 h of treatment and this is a secondary response. Orthovanadate abolished this decrease, suggesting MKP-1 may play a role in inhibiting the expression of cyclin D1. Furthermore, we identified $p21^{Cip1}$, a potent cyclin-dependent kinase inhibitor preventing G1 to S phase progression, but not $p27^{kip1}$, is an immediate response gene for PTH in UMR cells. More importantly, PTH injection (80 μg/kg) produces similar effects on expression of MKP-1, cyclin D1 and $p21^{Cip1}$ in rat femoral metaphyseal primary spongiosa. While 1 injection of PTH in rats only increases $p21^{Cip1}$ mRNA 2-fold 1 h later, intermittent daily injections of PTH for 14 days significantly increase $p21^{Cip1}$ mRNA 8-fold 1 h after the last injection. We propose that repeated PTH injections make the osteoblast more sensitive to successive PTH treatments and this feature is important for PTH's anabolic functions. Our data also suggest that one important mechanism for PTH's anabolic effect is to arrest the cell cycle progression of osteoblast and hence increase its differentiation.

Disclosures: ***L. Qin****, None.*

F523

Parathyroid Hormone (PTH) Regulates Placental Calcium Transfer Independently of PTH-related Protein (PTHrP). C. S. Noseworthy[1], N. J. Fudge*[1], G. Karsenty[2], A. C. Karaplis[3], C. S. Kovacs[1]. [1]Memorial University of Newfoundland, St. John's, NF, Canada, [2]Baylor College of Medicine, Houston, TX, USA, [3]McGill University, Montreal, PQ, Canada.

PTH and PTHrP regulate fetal blood calcium (Ca) and skeletal mineralization, while only PTHrP has been shown to regulate placental Ca transfer. Evidence against a role for PTH includes the fact that *Pthrp* null fetuses increased placental Ca transfer in response to PTHrP treatment while PTH was without effect. However, exogenous PTH treatment may have been ineffective because *Pthrp* null fetuses have a 3 to 4-fold increase in endogenous PTH.

To determine if PTH regulates placental Ca transfer, we examined fetal mice that are either partly deficient in PTH (*Gcm2* null) or which lack PTH altogether (*Pth* null).

Fetal serum PTH was 41.9 pg/ml in wt, but was reduced to 5.03 pg/ml in *Gcm2* null fetuses, and was reduced to the limit of detection (1.6 pg/ml) in *Pth* null fetuses ($p<0.001$). Both *Gcm2* and *Pth* null fetuses exhibited evidence of hypoparathyroidism. In *Pth* null fetuses, mean ionized Ca was reduced to 1.31 mmol/l (wt: 1.75 mmol/l), serum P was increased to 3.5 mmol/l (wt: 3.00 mmol/l), and serum Mg was reduced to 1.11 mmol/l (wt: 1.17 mmol/l) ($p<0.001$ for all vs. wt). *Gcm2* null fetuses similarly had low Ca, high P and low Mg. *Gcm2* null and *Pth* null fetuses differed with respect to the net skeletal mineralization and rate of placental 45Ca transfer. *Gcm2* null fetuses had normal ash weight and normal von Kossa staining of tibial sections, indicating normal mineral content of the fetal skeleton. *Pth* null fetuses had an ash weight reduced to 90% of wt value ($p<0.001$) and reduced staining of mineral by von Kossa. Placental 45Ca transfer was significantly increased to 119% of normal in *Gcm2* null fetuses ($p<0.02$) but was not increased in *Pth* null fetuses (104% versus 105% in wt and 100% in het). Finally, in preliminary experiments, fetuses were injected *in utero* with 1 nmol PTH 1-84 or vehicle 70 minutes prior to measuring placental 45Ca transfer. Compared to 3 saline injected *Pth* nulls, placental 45Ca transfer increased to 120% in 3 *Pth* null fetuses treated with PTH 1-84.

In summary, hypocalcemic *Gcm2* null mice upregulated placental Ca transfer and maintained skeletal mineralization. Despite equivalent hypocalcemia, *Pth* null mice did not upregulate placental Ca transfer and had a deficit in skeletal mineral content. Preliminary experiments indicate that *Pth* null fetuses upregulated placental Ca transfer in response to PTH 1-84.

In conclusion, PTH can regulate placental Ca transfer, because *Gcm2* null mice (which produce PTH) were able to upregulate placental Ca transfer in response to modest hypocalcemia, while *Pth* null mice (which do not produce PTH) did not until treated with PTH injections.

Disclosures: ***C.S. Noseworthy****, None.*

F525

Bone Anabolic Effects of PTH in LRP5 (G171V) Transgenic High Bone Mass Mice. Y. Kharode[1], P. Bodine[1], P. Green*[1], C. Milligan*[1], J. Li[2], E. Smith-Adaline[2], P. Yaworsky*[3], F. Bex[1]. [1]Women's Health Research Institute, Wyeth Reserach, Collegeville, PA, USA, [2]Women's Health Research Institute, Wyeth Reserach, Cambridge, MA, USA, [3]Genomics Division, Wyeth Reserach, Cambridge, MA, USA.

Transgenic mice expressing a G171V mutation in the low density lipoprotein receptor related protein 5 (LRP5) have a high bone mass phenotype (HBM), an increased response to skeletal loading and a resistance to bone loss due to skeletal unloading. LRP5 is a co-receptor in the Wnt β-catenin pathway and the mutation results in a gain in function in this pathway. PTH, in addition to its osteogenic activity, also has been reported to affect skeletal loading responses as well as act on components of the Wnt β-catenin pathway. To evaluate the interrelation of the skeletal effects of HBM and PTH, groups of 9, 26, 36 and 52 week-old HBM transgenic and age-matched non-transgenic (NTG) male mice were treated with 100 μg/kg/day, sc hPTH 1-34 or vehicle for 30 days. Total vBMD of the distal femur measured by pQCT was significantly increased ($p< 0.01$) by PTH treatment in both HBM and NTG mice at all of the ages tested. However the magnitude of the increase in the HBM groups (16-29%) was consistently greater than NTG (6-14%) despite the fact that total vBMD in HBM vehicle controls was already 46-63% greater than in the NTG controls. The PTH-induced increase in vBMD in HBM mice was almost entirely due to trabecular changes, with little or no effect on cortical vBMD. In contrast, increases in cortical vBMD appeared to be primarily responsible for the PTH anabolic effect in NTG. Analysis of the trabecular bone by μCT indicates that the increased bone volume in HBM is associated with increased trabecular thickness although increases in trabecular number are evident in the older age groups. Like the femur, the L_5 vertebrae of HBM showed a greater PTH-induced increase in BV/TV than NTG, primarily due to effects on trabecular thickness.

Recent studies suggest that the magnitude of the anabolic response to PTH is dependent on the amount of trabecular bone template available. The markedly greater response of axial and appendicular trabecular bone in HBM would support this concept. This is in contrast with results in the sFRP-1 KO animal where there appeared to be an inverse relationship between the existing skeletal phenotype and the magnitude of the PTH response. Since sFRP-1 KO exerts skeletal effects, at least in part, through the Wnt β-catenin pathway, the results suggest shared components with the anabolic action of PTH. However, the ability of PTH to increase BMD in HBM suggests a complementary rather than common pathway for Wnt β-catenin and PTH skeletal activity.

Disclosures: ***Y. Kharode****, Wyeth 1, 3.*

F527

Ablation of Osteoblasts, but not Lining Cells, in 3.6Col1a1-tk Transgenic Mice Prevents the Anabolic Effect of Intermittent PTH: Evidence Against the Lining Cell Activation Hypothesis. R. L. Jilka, I. Gubrij, A. A. Ali, R. A. Wynne*, R. S. Weinstein, C. A. O'Brien, S. C. Manolagas. Center for Osteoporosis and Metabolic Bone Diseases, Central Arkansas Veterans Healthcare System, University of Arkansas for Medical Sciences, Little Rock, AR, USA.

The anabolic effect of intermittent PTH is due at least in part to attenuation of osteoblast apoptosis. However, the possibility that PTH activates lining cells to become matrix synthesizing osteoblasts has not been ruled out. To address this issue, we made mice expressing herpes thymidine kinase (tk) under the control of a 3.6-kb fragment of the rat collagen1a1 promoter (3.6Col1a1-tk mice). Previous studies had established that this promoter is active in the early stages of osteoblast differentiation. Because the nucleoside analog ganciclovir is toxic in the presence of tk, daily administration of ganciclovir to these mice will deplete bone of osteoblasts because osteoblast production ceases and the existing mature osteoblasts either die, become incorporated into bone as osteocytes, or become lining cells. At this point only the lining cells should remain, permitting unambiguous ascertainment of lining cell activation upon administration of PTH. After establishing that PTH did not interfere with ganciclovir-induced cytotoxicity of cultured osteoblastic cells expressing tk, transgenic mice were made in the FVB strain. TaqMan PCR demonstrated tk expression in calvaria, femurs and vertebrae of transgenic mice but not in soft tissues. Daily administration of 8 mg/kg ganciclovir caused a time dependent decrease in serum osteocalcin that was <10% of vehicle-injected mice after 17 days, whereas wild-type littermates were unaffected by ganciclovir. Examination of vertebral bone from ganciclovir-treated 3.6Col1a1-tk mice revealed the absence of osteoblasts and osteoid perimeter, as well as depletion of marrow elements. Nevertheless, osteocyte and lining cell morphology was normal, and neither cell type was labeled by ISEL staining to detect apoptotic cells. Daily injection of both ganciclovir and PTH for 8 days to 3.6Col1a1-tk mice pretreated with ganciclovir for 17 days failed to increase osteoblast number or osteoid perimeter, whereas 8 days of PTH administration to 3.6Col1a1tk mice not pretreated with ganciclovir increased osteoblast number and osteoid perimeter by 3-fold. We conclude that intermittent PTH administration does not directly activate lining cells to become matrix synthesizing osteoblasts. However, it remains possible that osteoblasts, their progenitors, or hematopoietic cells are required for PTH-induced lining cell activation.

Disclosures: ***R.L. Jilka****, Nuvios, Inc. 1, 2, 5.*

F529

Synergistic Actions of Parathyroid Hormone and Beta-Catenin in the Canonical Wnt Signaling Pathway in Osteoblastic Cells. E. S. Leman*[1], M. Bencsik*[1], P. Nguyen*[2], U. Marvi*[1], R. A. Nissenson[3]. [1]Endocrine Research Unit - VA Medical Center, Univ California San Francisco, San Francisco, CA, USA, [2]Endocrine Research Unit - VA Medical Center, Univ California San Francisco, San Francisco, CA, USA, [3]Endocrine Research Unit - VA Medical Center, Departments of Medicine and Physiology, Univ California San Francisco, San Francisco, CA, USA.

Parathyroid hormone (PTH) produces an anabolic effect on the skeleton, but the mechanism of this action is poorly understood. Low-density lipoprotein receptor-related protein (LRP) 5 and 6 serve as co-receptors for canonical wnt signaling in many tissues. A critical role for this pathway in bone is evidenced by the low bone mass phenotype in individuals with loss of function mutation in LRP5, and the high bone mass present in patients with gain of function mutation in LRP5. In this study, we assessed whether signaling by the G protein-coupled PTH receptor converges with the wnt/LRP pathway. UMR 106 osteoblastic cells were transfected with an expression vector for the transcription factor LEF/TCF together with a LEF/TCF-responsive luciferase reporter (pTOP). Addition of PTH for 5 hours produced a dose-dependent increase in reporter activity in UMR 106 cells. Treatment with LiCl (to inhibit degradation of beta-catenin) or expression of a stable form of beta-catenin produced an increased in pTOP luciferase reporter activity that was synergistic with that produced by PTH administration. Treatment of UMR 106 cells with recombinant wnt-3A slightly increased the reporter activity, whereas treatment with both PTH and wnt-3A further increased LEF/TCF activity. Both LiCl and recombinant wnt-3A increased endogenous levels of beta-catenin, whereas PTH treatment produced little if any increase in beta-catenin levels. Treatment with either forskolin or 8-Br-cAMP resulted in a small increase in pTOP luciferase reporter activity, but failed to fully reproduce the effect of PTH, indicating that signaling via pathway(s) other than cAMP/PKA was responsible for activation of LEF/TCF signaling by PTH. An inhibitor of phospholipase C (U 73122) blunted the ability of PTH to promote LEF/TCF signaling by more than 50 %, indicating that this signaling pathway contributes to the effect of PTH. Thus, PTH treatment activates a LEF/TCF-responsive reporter and does so by a mechanism distinct from that utilized by wnt-3A. Synergism between PTH action and the canonical wnt signaling pathway in osteoblasts may contribute to the anabolic effect of PTH in bone.

Disclosures: ***E.S. Leman****, None.*

F531

The IGF-I Receptor Is Required for the Anabolic Actions of Parathyroid Hormone on Bone. Y. Wang[1], S. Nishida[1], A. Burghardt*[2], H. Z. ElAlieh*[1], S. Majumdar[2], B. P. Halloran[1], T. L. Clemens[3], D. D. Bikle[1]. [1]Endocrine Unit, University of California, San Francisco/VAMCSF, San Francisco, CA, USA, [2]Radiology, University of California, San Francisco, San Francisco, CA, USA, [3]Medicine, University of Cincinnati, Cincinnati, OH, USA.

Although the ability of parathyroid hormone (PTH) to stimulate bone formation is well known, the mechanism is not clear. To examine the role of insulin-like growth factor I (IGF-I) signaling in mediating the actions of PTH on bone, we investigated the bone response to PTH in 3 month old male and female and mice with a bone specific IGF-I receptor null mutation (bIGF-IR$^{-/-}$) (floxed IGF-IR x osteocalcin promoter driven Cre recombination) and their normal littermates treated with vehicle or PTH (80 µg/kg bw/day for 2 weeks).Structural measurements of the proximal and mid-shaft of the tibia were made by micro-CT. Cortical bone formation at the tibiofibular junction (TFJ) was made by bone histomorphometry. Bone marrow stromal cells (BMSCs) were obtained to assess the effects of PTH on osteoprogenitor number and differentiation. The fat free weight of bone normalized to body weight (FFB/BW), bone volume (BV), and cortical thickness (C.Th) in both proximal tibia and shaft were all less in the bIGF-IR$^{-/-}$ mice compared to controls. PTH decreased FFB/BW, total volume (TV), and BV of the proximal tibia more substantially in controls than in bIGF-IR$^{-/-}$ mice, although the increase in C.Th after PTH in the proximal tibia was comparable in both control and bIGF-IR$^{-/-}$ mice. Periosteal bone formation at the TFJ was markedly lower in the bIGF-IR$^{-/-}$ mice than in the control mice, as was the response to PTH. Endosteal bone formation was comparable in control and bIGF-IR$^{-/-}$ mice, but PTH stimulated endosteal bone formation only in the control animals. Compared with BMSCs from control mice, BMSCs from bIGF-IR$^{-/-}$ mice showed far fewer alkaline phosphatase (ALP) positive colonies on day 14 and essentially no mineralization on day 28. Administration of PTH increased the number of ALP positive colonies and mineralization on day 14 and 28 in BMSCs from control mice, but not in BMSCs from bIGF-IR$^{-/-}$ mice. Our results indicate that the IGF-IR null mutation in mature osteoblasts leads to less bone and decreased periostеal bone formation in part due to the requirement for the IGF-IR in mature osteoblasts to enable PTH to stimulate osteoprogenitor cell proliferation and differentiation.

Disclosures: ***Y. Wang****, None.*

F533

Calcium-Mediated PTH mRNA Destabilization In Parathyroid Cells Requires Gene Transcription. C. S. Ritter*, S. Pande*, I. Krits*, E. Slatopolsky, A. J. Brown. Renal Division, Washington University, Saint Louis, MO, USA.

Extracellular calcium suppresses PTH release by inhibiting secretion, promoting peptide degradation and destabilizing PTH mRNA. Calcium-regulated PTH mRNA stability has not been investigated directly in parathyroid cells due to the unavailability of a suitable cell model. We have recently reported a culture system for bovine parathyroid cells that promotes the formation of small organoids (termed pseudoglands) that retain a stable response to calcium over several weeks (J Bone Min Res 19:491, 2004). Using this model, we confirmed that calcium directly regulates PTH mRNA levels. Time course studies showed that switching the medium from 0.4 mM calcium to 3.0 mM calcium reduced PTH linearly over 16 hours to a nadir of 20 to 30% basal. Switching from 3.0 mM to 0.4 mM calcium medium gradually increased PTH to a maximum by 48 h. Addition of the transcription inhibitor 5,6-dichloro-1-beta-D-ribofuranosylbenzimidazole (DRB) to pseudoglands pre-incubated for 24 hours in 0.4 mM Ca did not alter PTH mRNA over the ensuing 24 hours, indicating that PTH mRNA is completely stable when parathyroid cells are exposed to low calcium. In contrast, addition of DRB to pseudoglands 2 hours after addition of 3.0 mM calcium medium produced a 62% decrease in PTH mRNA over a 24-hour period (estimated half-life = 20 hours). The decrease with DRB treatment was slower than when DRB was absent, suggesting a requirement for transcription in calcium-mediated decay of PTH mRNA. This was confirmed by pre-incubating the pseudoglands with DRB 30 minutes prior addition of the 3.0 mM calcium medium, a maneuver that almost completely blocked the destabilization of PTH mRNA by calcium. Our results demonstrate for the first time that calcium directly accelerates the turnover of PTH in parathyroid cells, confirming earlier studies by Naveh-Many and co-workers using an in vitro degradation assay. Furthermore, using this novel parathyroid cell culture model, we have documented the requirement for calcium-dependent gene transcription in the destabilization of PTH mRNA.

Disclosures: ***A.J. Brown****, None.*

F537

Exogenous PTHrP Administration Rescues Double Knockout Mice Which Are Homozygous for Both the 1α-Hydroxylase and PTH Null Alleles. Y. B. Xue, Z. L. Zhang*, A. C. Karaplis, G. N. Hendy, D. Goltzman, D. S. Miao. Medicine, McGill University, Montreal, PQ, Canada.

Double mutant mice which are homozygous for both the 1α-hydroxylase and PTH null alleles (1α-(OH)ase$^{-/-}$PTH$^{-/-}$) die with tetany 1-3 weeks after birth. We examined the effect of PTHrP on calcium homeostasis and bone remodelling in these animals by administering PTHrP (1-86), 0.2 µg per mouse per day subcutaneously from day 4 to 2 weeks of age. Serum calcium rose from 1.25±0.2 mmol/L (48% of wild-type) in vehicle-treated 1α-(OH)ase$^{-/-}$PTH$^{-/-}$ mice to 1.8±0.1 mmol/L (70% of wild-type) in PTHrP-treated 1α-(OH)ase$^{-/-}$PTH$^{-/-}$mice. Renal levels of mRNA encoding calbindin-D_{28K} and calbindin-D_{9K} rose by 2.6 fold and by 2.1 fold, respectively, after PTHrP treatment and protein levels of calbindin-D_{28K} and calbindin-D_{9K} rose by 1.4 fold and by 1.5 fold, respectively. The treatment of PTHrP also up-regulated both mRNA and protein expression levels of calbindin-D_{28K} in a dose dependent manner in primary renal cell cultures from wild-type and 1α-(OH)ase$^{-/-}$ mice. Osteoclast numbers in bone did not increase significantly in the PTHrP-treated double mutants compared to either vehicle-treated wild-type or vehicle-treated double mutants. In contrast, alkaline phosphatase-positive osteoblasts were increased in PTHrP-treated double mutants compared to vehicle-treated double mutants, although they did not reach the levels observed in wild-type mice. In association with increased osteoblast number, Cbfa1 expression and matrix deposition of type I collagen and osteocalcin were significantly increased and mineralized trabecular and cortical bone were increased compared to vehicle-treated double mutants. The width of the cartilaginous growth plate was also augmented by PTHrP treatment, and long bone length was increased. With continued treatment, in contrast to vehicle-treated mutants which died at 1-3 weeks of age, PTHrP-treated mice remained viable for at least 1 month and continued to increase their bone mineral density and cortical and trabecular bone volume. These parameters even exceeded levels in vehicle-treated wild-type animals at 1 month of age. These results indicate that increases in systemic PTHrP in the post-natal state can increase serum calcium by renal mechanisms, which can maintain viability, and promote bone growth. In the early post-natal period, the major effect of NH_2-terminal PTHrP is to increase bone anabolism and not bone resorption.

Disclosures: ***Y.B. Xue****, None.*

F553

Importin 4, not Importin Beta, Is Responsible for the Ligand-Independent Nuclear Translocation of Vitamin D Receptor. Y. Miyauchi*[1], T. Michigami[1], T. Sekimoto*[2], Y. Yoneda*[2], M. Yamagata*[1], K. Ozono[3]. [1]Department of Environmental Medicine, Osaka Medical Center and Research Institute for Maternal and Child Health, Izumi, Osaka, Japan, [2]Department of Frontier Biosciences, Osaka University Graduate School of Frontier Biosciences, Suita, Osaka, Japan, [3]Department of Pediatrics, Osaka University Graduate School of Medicine, Suita, Osaka, Japan.

Vitamin D receptor (VDR) is localized in nuclei and acts as a ligand-dependent transcription factor. Although several nuclear localization signals (NLSs) have been identified, the molecular mechanisms underlying the nuclear translocation of VDR remain unclear. To address this issue, we utilized an in vitro nuclear transport assay where nuclear translocation of molecules of interest can be reconstructed using semi-intact cells consisting of permeabilized plasma membrane and intact nuclear envelope. This assay can dissect the nuclear import event from nuclear accumulation and nuclear export which also determine nuclear localization. When subjected to this assay, recombinant full-length VDR was imported to nuclei even in the absence of ligand. A truncated mutant, VDR[DBD-Hinge] lacking the ligand-binding domain, was also imported to nuclei regardless of the presence or absence of ligand. In contrast, VDR[LBD] possessing only the ligand-binding domain failed to be imported both in the presence and absence of ligand. Interestingly, another mutant VDR[Hinge-LBD], which carries the hinge region and the ligand-binding domain but lacks DNA-binding domain, was not imported to nuclei in the absence ligand, but was efficiently imported in the liganded form. The data suggest that there are two distinct mechanisms underlying the nuclear translocation of VDR; the ligand-dependent and -independent pathways in which the responsible NLSs are likely to be localized in the hinge and DNA-binding domain, respectively. Next, we attempted to identify the molecules which confer the nuclear translocation of VDR. In the yeast two-hybrid screening using DBD-Hinge as the bait, importin 4, a member of importin beta-like family, was identified as an interacting protein. To examine whether importin 4 confers the nuclear translocation of VDR, recombinant importin 4 was subjected to the nuclear transport assay where all the required molecules were supplied as recombinant proteins. As the result, importin 4 transported VDR even in the absence of ligand. In contrast, importin beta, which is the classical member of importin family, failed to transport VDR. In conclusion, 1) VDR has two distinct mechanisms of nuclear translocation; ligand-dependent and -independent pathways, and 2) importin 4 is responsible for the ligand-independent nuclear translocation of VDR.

Disclosures: ***Y. Miyauchi****, None.*

F555

Characterization of the Hairless Protein as a Vitamin D Receptor Corepressor: Mapping the Physical and Functional Interaction between Two Proteins Required for the Mammalian Hair Cycle. S. A. Slater*[1], J. C. Hsieh[1], J. L. Dawson*[1], J. M. Sisk*[2], T. K. Barthel[1], M. L. Thatcher*[1], C. A. Haussler[1], P. W. Jurutka[1], G. K. Whitfield[1], C. C. Thompson*[2], M. R. Haussler[1]. [1]Biochemistry & Molecular Biophysics, University of Arizona, Tucson, AZ, USA, [2]Neuroscience, Johns Hopkins University School of Medicine & Kennedy Krieger Institute, Baltimore, MD, USA.

The hairless gene product (Hr), vitamin D receptor (VDR) and retinoid X receptor (RXR) are all essential for mammalian hair cycling. VDR and RXR signal as a heterodimeric complex bound to vitamin D responsive elements (VDREs) in target gene promoters. Transcriptional activation is achieved by 1,25-dihydroxyvitamin D_3 (1,25D) liganding of VDR-RXR and recruitment of coactivators, whereas the mechanism of gene repression by VDR is uncharacterized. We demonstrate that rat Hr (rHr), a protein expressed primarily in skin and brain that functions as a corepressor of the thyroid hormone receptor (TR) and orphan nuclear receptor ROR, is a potent repressor of VDR-mediated transcription driven by both natural and synthetic VDREs. Utilizing both in vitro pulldown and coimmunoprecipitation, rHr was found to interact significantly with VDR irrespective of 1,25D, but only minimally with nuclear receptors not functionally repressed by Hr. The rHr contact site(s) in human VDR is independent of the C-terminal activation function-2 domain that recruits coactivators, and is located instead in the ligand binding domain in a region (helices 3-6) that attracts corepressors in other nuclear receptors. Con-

versely, VDR binding to rHr, assessed by deletion and point mutant analyses, is absent in an N-terminal fragment (residues 31-568) and occurs strongly with the C-terminal half of rHr (residues 568-1207). The C-terminal half of rHr acts as a potent VDR corepressor and contains two TR repressive domains that partially overlap two LXXLL and two ΦXXΦΦ (Φ = hydrophobic) motifs required for respective ROR and TR binding by rHr. Generation of smaller rHr deletants and point mutation of the hydrophobic interaction motifs revealed that rHr utilizes all four nuclear receptor interaction domains (residues 586-590, 778-782, 817-821 and 1028-1032) in contacting and maximally repressing VDR. Therefore, rHr represses VDR signaling by employing a combination of ROR and TR interaction sites that contact the helix 3-6 region of VDR, with repressive domains in the C-terminal half of rHr presumably attracting histone deacetylases (HDACs) that modify chromatin architecture to silence target gene transcription. We propose that RXR-VDR-Hr-HDAC repression of an unknown target gene(s) triggers the telogen to anagen phase transition of the hair cycle.

Disclosures: ***S.A. Slater****, None.*

F558

Cell-Specific Crosstalk between the Vitamin D Receptor and beta-Catenin Signal Transduction Pathways in $1,25(OH)_2D_3$ Target Tissues. P. W. Jurutka[1], N. Hall*[2], G. K. Whitfield[2], M. Gurevich*[2], T. K. Barthel[2], J. C. Hsieh[2], C. A. Haussler[2], M. R. Haussler[2]. [1]Life Sciences, Arizona State University West, Phoenix, AZ, USA, [2]Biochemistry & Molecular Biophysics, University of Arizona, Tucson, AZ, USA.

β-catenin, a mediator of canonical Wnt signaling, is dysregulated in many cancers and has been implicated in hair growth as well as bone development, maintenance and repair. Previous work suggests that the vitamin D receptor (VDR) inhibits β-catenin activity in colonic cells. We evaluated the physical and functional association between VDR and β-catenin in colon cancer cells as well as in keratinocytes and osteoblasts. Human colon cancer cells (Caco-2) were transfected with a luciferase reporter vector containing TCF/LEF binding sites (TOPFLASH) to monitor β-catenin-mediated transactivation. Cotransfection of VDR resulted in a 50% decrease in reporter activity. GST pulldown assays demonstrated an association between GST-VDR and labeled β-catenin or GST-β-catenin and labeled VDR, an interaction independent of 1,25-dihydroxyvitamin D_3 (1,25D) or the VDR AF-2, but partially disrupted by the carcinogenic VDR ligand, lithocholate (LCA). Mammalian two hybrid assays confirmed the β-catenin-VDR association in Caco-2, and revealed that this interaction also occurs in human keratinocytes (KERTr-1106) and osteoblasts (TE85). Therefore, we tested the effect of VDR overexpression on β-catenin transactivity in these cells and, unlike the results in Caco-2, β-catenin-driven TOPFLASH transcription was stimulated up to 2-fold with increasing amounts of transfected VDR expression vector, but not empty vector. Thus, when VDR interacts with β-catenin, distinct functional effects are observed depending on the cellular milieu. In colon cells, downregulation of Wnt/β-catenin signaling provides a molecular basis for the known anticancer action of VDR, and could also explain why exposure of colonic cells to LCA, which disrupts the association between VDR and β-catenin, may lead to tumorigenesis. In contrast, VDR-β-catenin interaction in keratinocytes or osteoblasts results in stimulation of β-catenin transactivity. Hair cycling is initiated by a surge of β-catenin in keratinocytes, and we propose that VDR collaborates with β-catenin to regulate the expression of genes required for hair growth. Finally, Wnt/β-catenin signaling is crucial for bone formation, as loss of function mutations in the Wnt coreceptor, LRP5, reduce bone mass, whereas gain of function mutations elevate bone mineral density (BMD). Thus, promotion of β-catenin activity by VDR in osteoblasts represents a potential crosstalk mechanism whereby VDR could impact the Wnt signaling pathway to enhance osteoblastogenesis and BMD.

Disclosures: ***P.W. Jurutka****, None.*

F565

Glucocorticoid Enhances the Expression of Dickkopf-1 in Cultured Human Osteoblasts: Novel Mechanism of Glucocorticoid-Induced Osteoporosis. K. Ohnaka*[1], H. Taniguchi*[1], H. Kawate*[1], H. Nawata*[2], R. Takayanagi*[1]. [1]Department of Geriatric Medicine, Kyushu University, Fukuoka, Japan, [2]Department of Medicine and Bioregulatory Science, Kyushu University, Fukuoka, Japan.

Glucocorticoid-induced osteoporosis (GIO) is a serious problem during glucocorticoid therapy. Although the major cause of GIO is considered to be impairment of bone formation, detailed mechanism underlying GIO remains to be fully elucidated. Recently, the Wnt signal emerged as a novel regulator of bone formation. The aim of this study is to determine whether glucocorticoid would affect the Wnt signal of bone formation in human osteoblasts. We examined the effect of glucocorticoid on the expression of the Wnt signal-related molecules in primary cultured human osteoblasts. Dexamethasone markedly induced the expression of mRNA for dickkopf-1(Dkk-1), an antagonist of Wnt, in a dose- and time-dependent manner. The expression of Kremen1, a receptor for Dkk, did not change by the treatment with dexamethasone, while that of low-density lipoprotein receptor-related protein 5 (LRP5), a Wnt coreceptor, slightly decreased by the treatment with dexamethasone. Dexamethasone increased the transcriptional activity of the human Dkk-1 gene promoter in cultured human osteoblasts. Serial deletion and mutation analyses of the Dkk-1 promoter showed that one putative glucocorticoid responsive element-like sequence located from -788 to -774 bp is essential for the enhancement of Dkk-1 promoter activity by dexamethasone in human osteoblasts. Since the Wnt signal is now recognized as a crucial regulator for bone formation, the Dkk-1 enhanced by glucocorticoid may inhibit the Wnt signal in osteoblasts, which may be involved in the pathogenesis of GIO.

Disclosures: ***K. Ohnaka****, None.*

F573

MNAR Regulates the Non-genotropic Action of the Vitamin D_3 Receptor. F. Barletta*, G. O'Donnell*, B. S. Komm, B. J. Cheskis*. Women's Health Research, Wyeth Research, Collegeville, PA, USA.

The vitamin D receptor (VDR) is a member of the nuclear hormone receptor superfamily of ligand-activated transcription factors that regulate target gene expression. The actions of 1,25 dihydroxyvitamin D_3 (1,25D3), the active form of vitamin D, are mediated through the VDR, and have been shown to be essential for maintaining calcium homeostasis and proper bone health. Recently, there has been a dramatic increase in evidence supporting rapid signaling actions of 1,25D3. This rapid action of 1,25D3 has been linked to activation of c-Src, phospholipase C, PKCI, and the MAPK signaling cascade. Previously, we have identified a novel scaffolding protein, MNAR, which integrates the interaction of the estrogen receptor (ER) with Src tyrosine kinase, and has been shown to be required for the rapid activation of the Src/MAPK pathway by estrogens. To gain insight into the rapid actions of 1,25D3, we investigated the role of MNAR in VDR mediated signaling and osteoblast function. We have shown that endogenous MNAR, c-Src, and VDR interact in a ligand-dependent manner. Further analysis using GST pulldown experiments reveal that the ligand-dependent interactions between VDR/MNAR and VDR/c-Src are direct, and require the receptor's ligand binding domain (LBD). The SH2 domain of Src is sufficient for the VDR/Src interaction, while the VDR/MNAR interaction requires one of MNAR's LXXLL motifs. We have previously reported that MNAR interacts with the SH3 domain of Src through an N-terminal PXXP motif (Barletta *et. al*., Molecular Endocrinology, 18:1096-1108,2004). We propose that VDR, MNAR, and c-Src form a ligand-inducible ternary complex through these interactions, similar to the formation of the ER/MNAR/Src complex. We show that MNAR can modulate the ability of 1,25D3 to activate the MAPK pathway, resulting in the phosphorylation of Erk 1/2. Overexpression of MNAR in UMR-106 cells results in a 4-fold increase of the 1,25D3 induced levels of phosphorylated Erk 1/2 at 5 min with a 20 min treatment resulting in a 9-fold enhancement. Additionally, the 1,25D3 induced expression of two markers of osteoblast differentiation, osteocalcin (OC) and alkaline phosphatase (AP), are also enhanced by MNAR overexpression. The 1,25D3 induction of alkaline phosphatase activity is blocked by co-treatment with both Src kinase and PI3K inhibitors, PP2 and LY294002, respectively. However, co-treatment with the PKC inhibitor, Go6983, was unable to block the induction of AP. These results suggest the involvement of both Src and PI3K activation in osteoblast differentiation and indicate that MNAR may play an important role in VDR-mediated signaling and osteoblast development.

Disclosures: ***B.S. Komm****, Wyeth 1, 3.*

F586

Alternative Splicing of Human Vitamin D 24-Hydroxylase (CYP24) Gene. S. Ren[1], L. Nguyen*[1], M. Hewison[2], J. S. Adams[1]. [1]Endocrinology, Cedars-Sinai Medical Center, Los Angeles, CA, USA, [2]Endocrinology, The University of Birmingham, Birmingham, United Kingdom.

Alternative splicing of genes is more the rule than the exception. 40-60% of the human genes are alternatively spliced. Alternative splicing in cytochrome P450 genes has been reported to cause changes in functional activity, substrate preference, tissue-specific expression and subcellular localization of the P450 proteins. However, the functional consequences of alternative splicing have not been reported with vitamin D metabolizing P450s. We have previously reported that alternative splicing of avian CYP24 gene produced a cytoplasmically-localized (i.e. exo-mitochodrial), truncated protein in chick macrophage HD-11 cells. This splice variant, which retains its promoter-driven 1,25-dihydroxyvitamin D (1,25-D) responsiveness but lacks a mitochondria targeting domain, functions to down-regulate 1,25-D production by acting as a catabolically-inactive decoy acceptor of substrate 25-hydroxyvitamin D (25-D). We hypothesized that this mode of altering 1,25-D catabolism by creation of a non-metabolically-active CYP24 gene product was not unique to avian species. We now report that similar alternative splicing events exist in human cells. Using total RNA from the human monocytic cell line THP-1 post-exposure to 1,25-D as template and a series of nested, bridging primers derived from adjacent exons and introns of the human CYP24 gene to perform RT-PCR, four splice variants (SVs) of the human CYP24 gene have been identified and cloned. One of the SVs, the CYP24-SV1, recapitulated the splicing pattern of the chick CYP24 gene and encoded an N-terminally-truncated protein. The human CYP24-SV1 1] lacked the mitochondria targeting domain, missing the N-terminal 139 amino acids of the holo protein, but 2] retained an intact sterol-binding domain. This structure permitted the CYP24-SV1 product to be capable of capturing substrate 25-D but unable to be inserted in the mitochondria membrane and function to catabolize 1,25-D. As a consequence, transient transfection of antisense CYP24-SV1 cDNA in THP-1 cells increased the 1,25-D production by 40% ($p = 0.03$) compared to the control, vector-alone-transfected cells. A screen of human tissue-specific expression of the CYP24-SV1 revealed its presence in decidual cells of the placenta, epidermal keratinoncytes, as well as in other macrophage-like cells, all recognized extra-renal sites for 1,25-D hormone synthesis. In summary, alternative splicing of the human CYP24 gene appears to be a means of regulating 1,25-D production at extra-renal sites by securing substrate 25-D in the cell cytoplasm and away from the mitochondrial hydroxylation machinery.

Disclosures: ***S. Ren****, None.*

SA001

Change in Maternal Calcaneal QUS during Pregnancy and Intrauterine Bone Mineral Accrual in the Offspring. M. K. Javaid[1], S. Crozier*[1], P. Taylor*[2], N. Harvey*[1], E. Dennison*[1], H. M. Inskip*[1], K. Godfrey*[1], N. Arden*[1], C. Cooper*[1]. [1]Medical Research Council Environmental Epidemiology Unit, Southampton, United Kingdom, [2]Southampton University Hospitals NHS Trust, Southampton, United Kingdom.

During pregnancy, the fetus acquires 30g of calcium for skeletal growth and to meet this demand the mother undergoes several adaptations including increased bone resorption. We have previously demonstrated that lower maternal milk intake and nulliparity are associated with accelerated loss in maternal calcaneal QUS measurements during pregnancy; however, it is not known whether measured changes in maternal skeletal status influence fetal bone mineral accrual. We have therefore investigated the relationship between change in maternal calcaneal QUS during pregnancy, as measured by an Hologic Sahara instrument, and neonatal whole body BMC, measured using a Lunar DPX-L, in a sample of 106 pregnancies from the Southampton Women's Survey, a longitudinal study of healthy mothers whose lifestyle and anthropometry was assessed during early and late pregnancy. The QUS measurements were performed at 11 and 34 weeks and the neonatal DXA scans performed within 2 weeks of birth.

During pregnancy, there were significant reductions in maternal calcaneal SOS (-0.34 SD, p<0.001) and BUA (-0.22 SD, p<0.001). Mothers with larger reductions in calcaneal SOS during pregnancy had babies with greater whole body bone mineral content and bone area (r=-0.22, p=0.04 and r=-0.23,p=0.02, respectively, adjsuting for maternal size) This relationship was not weakened by adjustment for changes in maternal heel width, parity, milk intake or season during early pregnancy. Change in maternal QUS was weakly negatively associated with neonatal lean mass but there was little association with neonatal fat mass.

These findings suggest the maternal skeletal response to pregnancy is an important determinant of linear foetal growth. The mechanism is likely to involve the capacity of maternal skeleton to deliver mineral balanced with the fetal demand. Further investigation of the mechanisms involved may lead to strategies to optimize peak bone mass accrual.

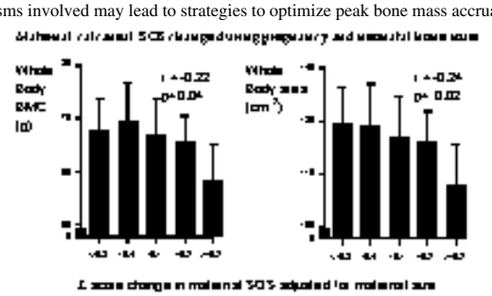

Disclosures: ***M.K. Javaid****, None.*

SA002

See Friday Plenary number F002

SA003

Impact of Parathyroid Status and Ca and Vitamin-D Supplementation on bone Mass and Muscle-Bone Relationships in 208 Belarussian Children after Thyroidectomy because of Thyroid Carcinoma. P. Schneider[1], J. Biko*[1], C. Reiners*[1], Y. Demidchik*[2], V. Drozd*[2], R. Capozza*[3], G. Cointry*[3], J. Ferretti[3]. [1]Clinic for Nuclear Medicine, University of Wuerzburg, Wuerzburg, Germany, [2]Endocrinology, University of Minsk, Wuerzburg, Belarus, [3]Cemfoc, University of Rosario, Rosario, Argentina.

This observational study analyses Ca-P metabolism and its impact on bone mass accrual and density and the muscle-bone mass/mass relationship in male and female children and adolescents who were parathyroidectomized because of thyroid carcinoma.

208 children and adolescents (119 girls and 89 boys) from Gomel city (Belarus) and its rural surroundings were referred to our institution after having undergone total thyroidectomy for the treatment of advanced papillary thyroid cancer. A subgroup of children with demonstrated primary hypoparathyroidism received dihydrotachysterol (AT-10) and / or Ca supplementation. Among routine procedures over a maximum follow-up period of 5 years (average 3.7 years, maximum 8 visits), whole- body scans were taken using dual energy X-ray absorptiometry (DXA) at each visit in order to determine whole-body bone mineral content (TBMC), projected "areal" bone mineral density (TBMD), total lean mass (TLM) and total fat mass (TFM).

The average serum Ca, P and AP concentrations over the whole observation period were significantly different between the groups; however, TBMC z-scores for all studied children were statistically similar in all visits. In girls, no between-group differences in height- and weight-controlled TBMC and TBMD or the TBMC/TLM ratio were observed and supplementation exerted no effect on these data, suggesting that the total bone mass accrual was not impaired by PTH deficiency in the studied conditions. However, non-supplemented boys showed lower values of the TBMC/TLM ratio than girls, and supplementation normalized these values in direct correlation with the induced improvement in serum P availability to bone.

Results indicate that the primary impairment in parathyroid function and bone metabolism indicators in the thyroidectomized children was unrelated to any measurable change in crude bone mass values. However, in boys this condition impaired the TBMC/TLM ratio in such a way that the administered supplementation could normalize it as a function of improved P availability. Girls´ skeleton seemed to have been naturally protected against the negative metabolic effect of the studied condition. An estrogen-induced enhancement of the biomechanical impact of muscle contractions on bone mass and structure could not be excluded in this group.

Disclosures: ***P. Schneider****, None.*

SA004

Body Composition of Newborn Twins Versus Singletons. S. DeMarini*[1], W. W. K. Koo[2], E. M. Hockman*[3]. [1]Neonatology, Istituto per l'Infanzia, Trieste, Italy, [2]Pediatrics, Wayne State University, Detroit, MI, USA, [3]Computing and Information Technology, University of Tennessee, Memphis, TN, USA.

At birth, infants from multiple gestations frequently weighed less than gestation matched singletons. However, there are no data to indicate whether normally grown twins have same bone mass and body composition as normal singletons. Anthropometric and dual energy X ray absorptiometry (DXA) measurements were performed in 76 infants from twin gestations with appropriate birth weights (between the 10th and 90th percentile) for gestational age (AGA), and same number of AGA singleton neonates matched as closely as possible for birth weight. Studies were performed at a mean of 3.8 ± 3.2 days after birth. Clinical details of study subjects are shown in Table 1. The absolute and percentage of each component of bone mass and body composition are shown in Table 2.

We conclude that for normally grown neonates, the body composition, with respect to bone, fat and lean mass components, is similar regardless of whether they are products of singleton or twin pregnancies.

Table 1. Clinical details of twins with appropriate birth weight for gestation (AGA) matched for birth weight of AGA singletons*

	AGA Twin	Matched Singleton
n	76	76
Birth weight (g)	2191 ± 50	2200 ± 51
Gestational age (weeks)	34.5 ± 0.3	34.4 ± 0.3
White/Black/Asian	14/61/1	26/50/0
Male/Female	44/32	44/32
Naked weight (g) at study	2128 ± 49	2119 ± 52
Study length (cm)	43.9 ± 0.2	44.1 ± 0.3
Study head circumference (cm)	31.5 ± 0.2	31.1 ± 0.2

* Measure of agreement for race and sex, kappa coefficient = 0.642 and 1.000 respectively, p <0.001 for both. Independent samples t-test for other comparisons, no significant difference between groups. Values are expressed as mean ± SE.

Table 2. Dual energy X ray absorptiometry (DXA) measurements of appropriate birthweight for gestation twins versus matched singletons (n = 76 per group)

	Bone mineral content	Fat mass	Lean mass
Absolute Values			
Twin	38.2 ± 1.1	243 ± 11	1926 ± 41
Singleton	39.5 ± 1.2	235 ± 10	1939 ± 44
As percentage of total weights			
Twin	1.71 ± 0.02	10.7 ± 0.3	87.5 ± 0.3
Singleton	1.76 ± 0.02	10.4 ± 0.2	87.9 ± 0.2

AGA = appropriate for gestation. Profile analysis using repeated measure analysis of variance showed that there were no significant differences in bone, fat and lean mass either as absolute values or as percentage of total weight. Values are expressed as mean ± SE.

Disclosures: ***S. DeMarini****, None.*

SA005

See Friday Plenary number F005

SA006

Site-specificity in Differential Rates of Bone Mineral Accrual from Adolescence into Adulthood. D. A. Bailey, A. D. G. Baxter-Jones*, R. L. Mirwald*, R. A. Faulkner. College of Kinesiology, University of Saskatchewan, Saskatoon, SK, Canada.

The tempo of bone mineral accrual during the growing years may have implications in terms of adolescent fracture risk and fracture prediction as an adult. In this study 51 boys and 56 girls were measured annually for six consecutive years across the adolescent growth spurt and again five years later when all the subjects had reached skeletal maturity with a mean age of 22.2 ± 1.9 y and 21.0 ± 1.9 y for the boys and girls respectively. Bone mineral content of the lumbar spine (L1 to L4), femoral neck and total body was measured by DXA (Hologic 2000 QDR in the array mode). The purpose of the study was to determine the percentage of adult status attained at similar developmental ages during adolescence for the total body, lumbar spine and the femoral neck compared to linear growth. The developmental age points chosen for comparison were the age of peak height velocity

(PHV), mean age for girls 11.8 ± .85 y and for boys 13.4 ± 1.0, and two years beyond the age of peak height velocity (PHV +2). As shown in the following table, at the ages of PHV and PHV +2, BMC of the femoral neck is much more advanced (closer to adult status) than BMC for the lumbar spine or total body. In terms of percentage of adult status, BMC for all sites in both sexes lags behind linear growth in height, indicating a possible transient period of relative skeletal weakness during adolescence. No gender-specific differences in percent adult values were observed.

Percent Adult Bone Mineral Content

	Males		Females	
	At Age of PHV	At Age PHV+2	At Age of PHV	At Age PHV+2
Height	91%	99%	92%	99%
BMC Fem. Nk.	74%	95%	75%	94%
BMC Tot Body	57%	81%	60%	80%
BMC PA Spine	52%	82%	52%	81%

Disclosures: ***D.A. Bailey****, None.*

SA007

See Friday Plenary number F007

SA008

Sexual Dimorphism in Cortical Bone Characteristics across Puberty: 20-month pQCT Study of the Tibial Shaft. S. Kontulainen[1], S. Manske*[2], K. Khan*[3], H. McKay[4], H. Macdonald*[5]. [1]Department of Orthopaedics, University of British Columbia, Faculty of Medicine, Vancouver, BC, Canada, [2]University of British Columbia, School of Human Kinetics, Vancouver, BC, Canada, [3]University of British Columbia, Faculty of Medicine, Vancouver, BC, Canada, [4]Department of Orthopaedic Engineering Research, University of British Columbia, Faculty of Medicine, Vancouver, BC, Canada, [5]School of Human Kinetics, University of British Columbia, Vancouver, BC, Canada.

Greater fracture risk in women compared with men can be attributed to a smaller female skeleton that experiences greater cortical thinning after menopause. Sex differences in bone size and density are evident at puberty. However, there are no longitudinal data that describe sex-differences in cortical bone cross-sectional geometry, density and its distribution across puberty. We assessed 20-month bone structural and material changes by peripheral quantitative computed tomography (pQCT) at the 30 and 50% sites of the tibial shaft across EARLY-, PERI- and POST -puberty in boys (N=60) and girls (N=68). pQCT scans were analysed using Bonalyse 2.1 software (BonAlyse Oy, Jyväskylä). Outcome variables were total, and cortical bone cross-sectional areas (*ToA, CoA,* mm^2 respectively), *CoA/ToA,* area of marrow cavity (*CavA,* mm^2), average cortical bone mineral density (*CoD,* mg/cm^3) and radial distribution of cortical density.

ToA and CoA did not differ between sexes within maturity groups at baseline. ToA and CoA increased more for boys (p<0.05) than girls in all maturity group. We observed no endosteal contraction for girls across maturity although marrow cavity increased less for girls compared with boys. Changes in the *CoA/ToA*-ratio did not differ between sexes. *Cortical density* was greater for girls in each maturity group at baseline, and EARLY- and PERI-pubertal girls also increased CoD significantly more (p<0.001) than boys (Fig 1). An examination of radial distribution showed that increased CoD was explained by increased CoD throughout the midcortex. Increase in bone size is greater for boys than girls at puberty. In contrast, girls increase cortical density more than boys. This sexual dimorphism of CoD is consistent with the hypothesis that rising estrogen levels in girls induce consolidation of bone mineral as maturity progresses.

Figure 1. Change in the average cortical density between sexes and maturity categories.

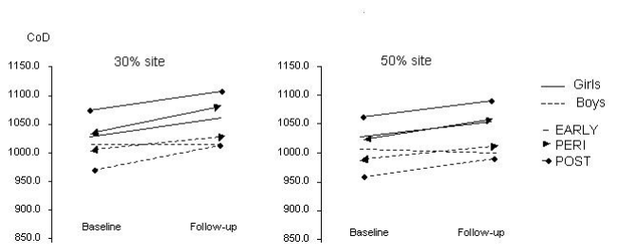

Disclosures: ***S. Kontulainen****, None.*

SA009

See Friday Plenary number F009

SA010

What Factors Contribute Toward Maximizing Peak Bone Mass in Japanese Young Women? Y. Onoe[1], Y. Miyabara*[1], R. Yoshikata*[1], A. Harada*[2], H. Okano[1], S. Sasaki*[3], T. Kuroda*[4], M. Shiraki[5], H. Ohta[1]. [1]Obstetrics and Gynecology, Tokyo Wemen's University, Tokyo, Japan, [2]Biostatistics, University of Tokyo, Tokyo, Japan, [3]National Institute of Health and Nutrition, Tokyo, Japan, [4]Public Health Research Foundation, Tokyo, Japan, [5]Research Institute and Practice for Involutional Diseases, Nagano, Japan.

Lifestyle management, including moderate physical activity and nutritional intake required for bone health, is assumed to play a key role in maximizing peak bone mass. However, these factors remain to be prioritized, as well as weighed for their relative impact on bone mass accumulation. This cross-sectional study was designed to establish a methodology for maximizing peak bone mass in young Japanese women by investigating the impact of intake of various nutrients, as well as physical activity, on BMD values in these women.

The study subjects (n = 139) comprised healthy women aged between 19 to 25 years of age. Subject background data surveyed included age, weight at birth, age at menarche, and current menstrual status. Measurements included height, body weight, lumbar vertebrae 2-4 BMD (L 2-4 BMD), and total BMD of the proximal femur (QDR 4500). To evaluate physical activity in these subjects, we used the number of steps taken per week as measured by using Suzuken Lifecorder EX. Nutritional intake by these subjects was evaluated by means of a self-administered Diet History Questionnaire (DHQ), and physical activity by the Physical Activity Questionnaire (PAQ) developed by the JALS Physical Activity Working Group.

Mean weight at birth was 3,101 g; mean age at menarche was 12.0 years of age; and L 2-4 BMD and total BMD of the proximal femur were 0.90 g/cm^2 and 0.99 g/cm^2, respectively. Based on the interquartile analysis of their L 2-4 values, study subjects were divided into a low-BMD group (L 2-4 BMD < 0.92 g/cm^2), or a high-BMD group (L 2-4 BMD > 0.92 g/cm^2). The variables for which statistically significant differences were noted between these groups were height, body weight, body mass index (BMI), weight at birth, total energy on the PAQ, energy expenditure as measured by using Lifecorder EX, cholesterol and P on the DHQ. Thus, height was shown to be significantly (p < 0.01) shorter, body weight significantly (p <0.01) lighter, and weight at birth significantly (p < 0.05) lighter in the low-BMD group, compared to the high-BMD group.

Disclosures: ***Y. Onoe****, None.*

SA011

Bone Mass Status of the School-Aged Children in Taiwan Assessed by Quantitative Ultrasound - Preliminary Results of the Nutrition and Health Survey in Taiwan, 2001-2002. Y. Lin[1], S. Tu*[2], W. Pan*[1]. [1]Institute fo Biomedical Sciences, Academia Sinica, Taipei, Taiwan Republic of China, [2]Center for Survey Research, Academia Sinica, Taipei, Taiwan Republic of China.

Bone health status in childhood and adolescence may be important factors influencing the attainment of peak bone mass. The Children Nutrition and Health Survey in Taiwan, 2001-2002 was carried out to evaluate the overall nutrition and health status of school children aged between 6 and 13 years. The survey was conducted using a multi-stage complex sampling scheme. Townships and city districts in Taiwan were classified into 13 strata. Bone mass measured as broadband ultrasound attenuation (BUA, in dB/MHz) was taken at heel by quantitative ultrasound (QUS) bone densitometry (CUBA Clinical, McCue), and the corresponding Z-score was calculated. 1164 boys and 1016 girls who had complete physical examination data with ultrasound bone scan were included in the current analysis. Statistical analyses were performed using SAS v8.1 and SUDAAN v8.0. All variables were weighted to represent the children population in Taiwan.

Subjects were grouped by gender and/or age. The overall mean BUA Z-score was -0.55±0.02 for boys and -0.25±0.03 for girls, respectively, and girls had significantly higher mean BUA Z-score than boys. Most boys and girls had BUA Z-score in between 0 and -1 (45.8% of the boys and 49.3% of the girls, respectively), and 36.3% of the boys and 22.2% of the girls had BUA Z-score below -1. There were no apparent differences in BUA across all strata for both genders. Results of univariate regression analyses showed that in both genders, age (r^2=0.29 for boys and r^2=0.26 for girls), height (r^2=0.36 for boys and r^2=0.35 for girls), body weight (r^2=0.36 for boys and r^2=0.37 for girls) and BMI (r^2=0.18 for boys and r^2=0.19 for girls) were significant predictors of BUA (p<0.0001 for all the variables above in boys and girls, respectively). In boys, there was a significant inverse relationship between age and BUA Z-score (β=-0.11, p<0.0001). Similar inverse association was also observed in girls with less significance (β=-0.04, p=0.0236).

This is the first island-wide survey with the attempt of using QUS bone densitometry as the screening tool to investigate the bone health status of the children in Taiwan. The inverse association between age and BUA Z-score as shown in the results suggested that the strategies enhancing the accrual of bone mass may be considered to prevent suboptimal development of bone mass in children in Taiwan

Disclosures: ***Y. Lin****, None.*

SA012

See Friday Plenary number F012

SA013

Seasonal Variation of BMC in Lumbar Spine and Hip in Early-puberty Girls. H. T. Viljakainen*[1], A. Palssa*[1], A. Natri*[1], J. Jakobsen*[2], K. D. Cashman*[3], C. Mølgaard*[4], C. Lamberg-Allardt[1]. [1]Department of Applied Chemistry and Microbiology, division Nutrition, University of Helsinki, Helsinki, Finland, [2]Danish Institute for Food and Veterinary Research, Söborg, Denmark, [3]Department of Food and Nutritional Sciences, University College Cork, Ireland, [4]Research Department of Human Nutrition, The Royal Veterinary and Agricultural University, Frederiksberg C, Denmark.

The seasonal variation of serum 25-hydroxy-vitamin D (25-OHD) and calciotrophic hormones is thought to determine the seasonal variation of bone mass. In healthy adults it is shown to compromise a 2%-variation, but in adolescent girls it has not been reported. Furthermore, the impact the seasonal variation has on growing bones has not been fully investigated.

The aim of this study was to define the existence of a seasonal variation in serum 25-OHD, parathyroid hormone (PTH), bone markers and site-specific bone mineral content (BMC) in early-puberty Finnish girls.

Subjects (N=196) were healthy Finnish early-puberty Caucasian girls, mean (sd) age 11.4 (0.4) y, recruited from the Helsinki area from September 2001 to March 2002. Of the subjects 77.4% scored in Tanner 2 (T2) and 32.6% in Tanner 3 (T3). Their median daily dietary intakes of calcium and vitamin D were 1240 (700) mg and 4.7 (4.1) µg, respectively.

Serum 25-OHD was measured from fasting samples by a HPLC method, intact PTH by OSTEIA assay and osteocalcin by ELISA. Bone mineral densities were measured by DXA Hologic 4500 at the lumbar spine (L1-L4) and the left femoral neck. In the analysis BMC was adjusted for bone area and age.

We found a seasonal variation in serum 25-OHD, which was higher in autumn (September-October) than in winter (November-March) ($p<0.0001$), but PTH did not differ between season. A seasonal variation in BMC in lumbar spine and at the femoral neck was observed in the T2-girls: in autumn the BMC was 5.35% higher in the lumbar spine ($p=0.007$) and 4.81% higher BMC in hip ($p=0.03$) than girls measured in the winter, after adjustment for bone area and age. Moreover, the osteocalcin concentration was higher in autumn than in winter ($p=0.04$) in T2. No variation was observed in the BMC or osteocalcin in girls in T3. In conclusion, a seasonal variation in both 25-OHD and in site-specific BMC was observed, even though no correlation was found. However, the results differed between puberty development stages 2 and 3. Whether this variation is of clinical importance remains to be evaluated.

Disclosures: ***H.T. Viljakainen****, None.*

SA014

A Transgenic Dwarf Rat Strain as an Experimental Model for the Study of Senile Osteoporosis. M. Tomita[1], I. Shimokawa*[2], S. Motokawa*[3]. [1]Medicine, Orthopaedic Surgery, Kitakyushu City Yahata Hospital, Kitakyushu, Fukuoka, Japan, [2]Medicine, Pathology & Gerontology, Nagasaki University Graduate School of Biomedical Sciences, Nagasaki, Japan, [3]Medicine, Orthopaedic Surgery, National Nagasaki Medical Center, Omura, Nagasaki, Japan.

Introduction: Bone mineral density (BMD) is known to decrease with advancing age, a condition of senile osteoporosis. Secretion of growth hormone (GH) and insulin like growth factor-1 (IGF-1) are also known to decrease with age. In order to elucidate the effect of GH-IGF-1 axis on age-dependent changes in BMD, we analyzed the femoral bone in the transgenic dwarf rat strain in which GH-IGF-1 axis is selectively suppressed by over-expression of antisense GH-gene. Materials and Methods: Transgenic male rats (mini), control Wistar (WT) rats, and their F1 hybrid rats (F1) were used. At 6, 15, and 24 months of age, rats were sacrificed and femoral bones were removed to measure the length and BMD with peripheral quantitative CT (pQCT). On sacrifice at 6 months of age, we also collected trunk blood to measure the plasma IGF-1 concentration by radioimmunoassay (RIA). Results: Mean plasma concentrations of IGF-1 were 1058.3 ng/ml in WT, 626.5 ng/ml in F1, and 265.8 ng/ml in mini. The length of femoral bones was significantly shorter in mini and F1 than WT, but there were no significant differences between mini and F1. BMD of the cortical and cancellous bones of femoral bone significantly decreased in mini, and F1 rats, as compared with WT rats; BMD in F1 was greater than mini. BMD of the cancellous bone, but not of the cortical bone, was decreased with age. The age-dependent decrease of cancerous bone BMD was suppressed in mini. Discussion: In human, BMD decreases with age, and this change is obviously seen in the cancellous bone but not in the cortical bone. WT rats showed a similar age-dependent decrease of BMD. In mini and F1 rats, BMD in the cancellous bone was decreased even at the young age. The present results suggest that selective suppression of GH-IGF-1 axis alone produces a condition similar to that of senile osteoporosis in the young age; thus the transgenic rat strain is a useful animal model to study human osteoporosis.

Disclosures: ***M. Tomita****, None.*

SA015

Increased Osteonal Degree of Mineralization Was Associated with Deteriorated Cortical Structure in the Fibular Shaft of Aged Women. T. Mashiba, S. Mori, N. Gomi*, Y. Kaji*, T. Manabe*, H. Norimatsu. Dept. of Orthopedic Surgery, Faculty of Medicine, Kagawa University, Kagawa, Japan.

Age related changes in bone quality have not been clarified yet. This study was designed to evaluate the effects of aging on the cross-sectional structure and degree of mineralization in the cortical bone of human fibular diaphyses.

Specimens for this study came from fibular mid-shafts of nineteen women (50-78 y.o.) who underwent high tibial osteotomy for medial type osteoarthritis or osteonecrosis of the knee. The protocol of this study has been checked and approved by the clinical research institute of Kagawa University. The collected bones were stored frozen at -80°C until specimens were made. After thawing at room temperature, they were stained en-bloc with 1% basic fuchsin dissolved in ascending concentration of ethanol, defatted with xylene, and embedded in methyl methacrylate. A 125 µm-thick transverse ground section was made for the static histomorphometry and measurement of degree of mineralization of bone (DMB). For DMB measurement, quantitative contact microradiograph was taken and DMB at each osteon was calculated using a computerized microdensitometric method. Measured DMB parameters include mean osteonal DMB and the distribution of osteon based on DMB. Age related changes in static cortical histomorphometric parameters and DMB parameters were evaluated.

Percent cortical area and cortical thickness decreased with age whereas total cross sectional area was not significantly changed. Medullary area and cortical porosity increased with age. Mean osteonal DMB significantly increased with age. Especially in the patients over 70 years old, the range of distribution of osteonal DMB was higher and narrowed in association with the decrease in the number of osteons with lower DMB when compared with younger patients.

As previously reported, cross sectional geometrical evaluation in this study demonstrated the age related structural deterioration of cortical bone, characterized by the bone marrow expansion, cortical thinning and increased cortical porosity. Because older osteon should have higher DMB, narrow and higher distribution of DMB in aged patients also suggests that replacement of old into new osteon was suppressed by lower osteonal remodeling activity. However, increased mean osteonal DMB shown in aged patients changes bone quality and this may be a compensative mechanism for the structural deterioration to maintain the mechanical strength of cortical bone.

Disclosures: ***T. Mashiba****, None.*

SA016

Kudzu Isoflavones Reduce Bone Loss in Ovariectomized Rats. J. Yong*. Foods & Nutrition, Purdue University, West Lafayette, IN, USA.

Isoflavones have been proposed as an alternative to steroid hormone replacement therapy to prevent postmenopausal bone loss. Soy isoflavones have been the most studied. Kudzu is another rich source of isoflavones. Puerarin, the main isoflavone from Kudzu root, is more effective at binding to ER-β than any other legume isoflavones. The objective of the present study was to determine whether Kudzu isoflavones reduce postmenopausal bone loss in an older ovariectomized rat model. Kudzu powder was given as a dietary supplement to 6-month-old ovariectimized Sprague Dawley rats for 8 weeks with an isoflavone concentration of 5g/kg diet in the high dose group, 0.05 g/kg diet in the low dose group and 0g/kg diet in the control group (n = 15/group). BMD and BMC of cortical and trabecular bone were analyzed by pQCT. By the end of the treatment, uterine weight in the high dose group was significantly ($P < 0.05$) higher than in the low dose and control groups. At the intertrochanteric site, total BMC, trabecular area, BMD, cortical area, BMC were significantly ($P < 0.05$) higher in the high dose group than in control and low dose groups. At the midshaft site, cortical area and cortical BMC were significantly ($P < 0.05$) higher in the high dose group than in low dose and control groups; At the distal site, total BMD and trabecular BMD were significantly ($P < 0.05$) higher in the high dose group than in low dose and control groups. This study indicates that Kudzu isoflavones have an estrogenic effect on the uterus. Kudzu isoflavones can reduce bone loss caused by estrogen deficiency in both trabecular and cortical bone, but the effect is site specific.

Disclosures: ***J. Yong****, None.*

SA017

See Friday Plenary number F017

SA018

Young-Elderly Differences In Medullary Compartment Size, Bone Mass, And Density At The Femoral Neck And Trochanteric Region In Caucasian Women. M. Meta[1], Y. Lu[1], K. Joyce[2], T. Lang[1]. [1]Radiology, University of California San Francisco, San Francisco, CA, USA, [2]Orthopedic Surgery, University of California Irvine, Irvine, CA, USA.

At the proximal femur, aging is characterized by cortical thinning, periosteal apposition, and decreased bone mass. However, differences in size and bone distribution in the tissue adjacent to the cortical compartment (subcortical) and in the center of the medullary compartment (central trabecular) have not been examined. To address this issue 28 young (41±3 years) and 129 elderly (74 ±3 years) healthy Caucasian-American women underwent volumetric quantitative computed tomography (vQCT) at the hip. We estimated medullary (m), subcortical (sc) and central trabecular (ct) volume (VOL), bone mineral content (BMC) and bone mineral density (BMD) at the femoral neck (FN) and trochanteric (TR) regions. The F-test was used to compare mean differences between young and elderly after adjusting for height and body mass

index in an ANOCOVA model. Mean values (SD) are tabulated below. The F-test for interaction compared logarithmic young/elderly differences between FN and TR after adjusting for height and body mass index in an ANOCOVA model. P-values are tabulated below.

	mVOL cm^3	scVOL cm^3	ctVOL cm^3	mBMC g	scBMC g	ctBMC g	mBMD g/cm^3	scBMD g/cm^3	ctBMD g/cm^3
Femoral Neck									
Young	6.30 [a] (2.07)	3.65 [a] (1.21)	2.65 [a] (1.08)	0.81 [ns] (0.26)	0.47 [c] (0.14)	0.35 [a] (0.15)	0.132 [a] (0.03)	0.133 [a] (0.02)	0.130 [a] (0.04)
Elderly	8.76 (2.86)	5.75 (1.66)	3.06 (1.35)	0.75 (0.39)	0.58 (0.23)	0.17 (0.20)	0.085 (0.03)	0.102 (0.02)	0.049 (0.04)
Trochanteric									
Young	35.30 [a] (7.86)	13.77 [a] (2.91)	21.53 [a] (5.33)	4.80 [ns] (0.87)	2.08 [a] (0.33)	2.72 [a] (0.69)	0.140 [a] (0.04)	0.155 [a] (0.03)	0.130 [a] (0.03)
Elderly	43.40 (10.05)	19.01 (4.22)	24.78 (5.54)	4.50 (1.44)	2.45 (0.66)	2.08 0.84	0.105 (0.03)	0.130 (0.03)	0.086 (0.03)
p-value FN/TR	0.044	0.029	0.719	0.967	0.420	0.001	0.069	0.132	0.0001

p value (young vs elderly) [a] $p<0.001$, [b] $p<0.01$, [c] $p<0.05$, [ns] $p>0.05$.

In the elderly medullary size is larger, ct bone mass is lower and interestingly, subcortical bone mass is larger with no inter-site difference. The FN showed a larger cross-sectional age-related decrease in trabecular BMD and increase in sc and medullary spaces than the TR. The larger young-old differences in BMD and volume at the FN may be due to differences in modes of mechanical loading between these two anatomic sites.

Disclosures: ***M. Meta****, None.*

SA019

Aging Is Associated with Up-Regulation of Insulin-like Growth Factor Receptor Type I (IGF-I) and Down-Regulation of IGF-I Signaling Pathways. J. J. Cao, P. S. Kurimoto*, B. P. Halloran. Medicine, UCSF, San Francisco, CA, USA.

Osteoblast activity and bone formation decrease with aging, as does the serum concentration of IGF-I. That IGF-I is abundant in bone, and can stimulate osteoblast formation and activity suggests that decrease in serum IGF-I, alterations in IGF-I signaling or both may contribute to age-related bone loss. To determine whether aging affects IGF-I intra-cellular signaling in osteoblasts, we examined the effect of IGF-I on bone *in vivo* and bone marrow stromal cells (BMSCs) cultured *in vitro* from 6 week (young), 6 month (adult), and 24 month (old) old mice. We evaluated the response of BMSCs to IGF-I administration with respect to activation of two IGF-I signaling pathways *in vitro* i.e. the Ras/MAPK pathway and the phosphatidy inositol 3 kinase (PI3K)/Akt pathway. With aging, IGF-I receptor expression increased at both the message and protein levels. Treatment with IGF-I for two hours had no effect on its receptor expression. Total ERK and the basal level of phosphorylated MEK and ERK did not change with age. IGF-I stimulated the activation of MEK and ERK 1/2 (p44/42 MAPK) in cultured BMSCs from young mice, but these effects were blunted in cells from mice of increasing age. These data suggest that the responsiveness of BMSCs to IGF-I treatment decreases with age and is in part due to down-regulation of IGF-I signaling.

Disclosures: ***J.J. Cao****, None.*

SA020

Subcellular Trafficking and Potential Functions of Klotho Proteins. J. Barsony[1], Y. Nabeshima*[2], J. G. Verbalis*[1]. [1]Division of Endocrinology and Metabolism, Georgetown University, Washington, DC, USA, [2]Department of Pathology and Tumor Biology, Kyoto University, Kyoto, Japan.

The recently discovered klotho gene products are thought to be negative regulators of the ageing process by protecting mammals against of ageing-related diseases including osteoporosis. Disruption of the klotho gene in mice decreased the number of osteoblast progenitors in the bone marrow and decreased the activities of osteoblastic cells. The klotho gene is predominantly expressed in the kidney and encodes a type I membrane protein with a large N-terminal extracellular domain. The effects of Klotho in bone and other tissues were presumed to be due to a humoral factor. Interestingly, the 130 kD Klotho protein has also been recently detected in human and mouse sera and cerebrospinal fluid, and appeared to be generated by proteolytic cleavage from the membrane-bound Klotho. To gain initial insight into the mechanisms of klotho functions, we generated fluorescent protein fusions of Klotho: a C-terminal fusion for the detection of the membrane-bound protein (Kl-GFP) and an N-terminal fusion (GFP-Kl) for the detection of the circulating form. Fusion proteins were stably expressed in kidney-derived cells (COS, LNCaP). Confocal laser scanning microscopy in living cells demonstrated for the first time distinct subcellular distribution and functions of klotho proteins in the kidney and in a target cell population (SaOS-2 human osteoblastic cells). Under steady-state conditions, Kl-GFP was predominantly at the plasma membrane (PM) of kidney-derived cells and underwent rapid endocytosis following treatment with insulin. The Kl-GFP containing endocytic vesicles fused with the Golgi after 15 minutes and returned to the PM by 30-60 min. This finding, in conjunction with reported effect of klotho decreasing insulin sensitivity, strongly suggests that klotho plays a role in insulin signaling in the kidney. The second fusion protein, GFP-Kl, was detected intracellularly and in the culture media. GFP-Kl colocalized with markers of endoplasmic reticulum (rhodamine B) and mitochondria (red MitoTracker CMX) in kidney-derived cells. GFP-Kl was also secreted into the culture media. Culture media was collected from COS-7 cells expressing GFP-Kl for 6 hours and was added to SaOS-2 cells. The GFP-Kl taken up from the media was readily detectable in vesicles and in the mitochondria of SaOS-2 cells. GFP-Kl protected mitochondrial morphology and membrane potential from hydrogen peroxide or tobacco extract induced oxidative stress in SaOS-2 cells. These findings suggest that protection of mitochondrial integrity and modulation of energy production in osteoblasts may contribute to the bone-protective effect of klotho.

Disclosures: ***J. Barsony****, None.*

SA021

β-Adrenergic Receptor Antagonist Enhances Ectopic Bone Formation Induced by Bone Morphogenetic Protein 2 and Fibroblast Growth Factor 2 in Rodent. T. Suzuki*[1], H. Takita*[2], A. Yokoyama*[1], M. Tamura[2]. [1]Oral Functional Science, Graduate School of Dental Medicine, Hokkaido University, Sapporo, Japan, [2]Department of Biochemistry and Molecular Biology, Graduate School of Dental Medicine, Hokkaido University, Sapporo, Japan.

The existence of systemic control of osteoblast activity and bone formation has been the subject of speculation for some time. Leptin has been identified as a powerful inhibitor of bone formation. Subsequent studies have led to the identification of hypothalamic neurons involved in this anti-osteogenic function of leptin and the sympathetic nervous system has been identified as its peripheral mediator. Takeda et al. (2002) also showed that catecholamine-deficient mice have a high bone mass and beta-blockers increase bone formation and bone mass. However, it is not clear how local bone formation is controlled by the sympathetic nervous system or what molecular mechanisms are involved. Here, we examined whether local application of the β-adrenergic receptor antagonist, propranolol, modulated ectopic bone formation induced by bone morphogenetic protein (BMP) 2 and fibroblast growth factor (FGF) 2 in the rat. Propranolol or vehicle together with 0.8 μg of BMP2 and 0.1 μg of FGF2 were mixed with fibrous glass membrane as a carrier and implanted subcutaneously into the back of male rats weighting 60-70g. After 2 weeks, soft X-ray radiographs showed a trabecular pattern indicating that formation of calcified trabeculae was increased by application of propranolol compared with vehicle. Calcium content, ALP activity and mRNA expression of α1(I) collagen, osteocalcin and Runx2 of implants also increased with application of propranolol, indicating that local application of propranolol enhanced ectopic bone inductive activity in our experimental system. However, when intraperitoneal injections of propranolol were administered daily for 21 consecutive days, we could not detect enhancement of ectopic bone formation by BMP2 and FGF2. These results suggest that osteoblasts in ectopic bone formation might express β-adrenergic receptors and regulate bone formation via synaptic interaction with the central nervous system.

Disclosures: ***T. Suzuki****, None.*

SA022

Lentivirus-Mediated BMP-2 Transduction Induced Long-Term Protein Expression In Vitro and New Bone Formation In Vivo. O. Sugiyama*[1], D. An*[2], S. Gamradt*[1], B. T. Feeley*[1], N. Q. Liu*[1], I. S. Y. Chen*[2], J. R. Lieberman*[1]. [1]Orthopaedic Surgery, UCLA David Geffen School of Medicine, Los Angeles, CA, USA, [2]AIDS Institute, UCLA David Geffen School of Medicine, Los Angeles, CA, USA.

Ex vivo gene therapy has the potential to be used to treat difficult bone repair problems. Selection of an appropriate vector is critical to determine the duration of protein expression. Lentiviral vectors are attractive vectors for gene therapy because of the potential for long-term expression and because both dividing and non-dividing cells can be transduced. The objective of this study was to examine the potential for ex vivo gene therapy using a lentiviral vector to enhance bone repair. W-20-17 cells (murine bone marrow stromal cell line) or primary rat bone marrow stromal cells (BMSCs) were transduced with the lentiviral vector encoding enhanced green fluorescent protein (EGFP) under the control of the RhMLV or the CMV promoter (Lenti-RhMLV-EGFP or Lenti-CMV-EGFP). The mean fluorescent intensity (MFI) of EGFP expression was determined in cells by flow cytometry. Lenti-RhMLV-EGFP-transduced cells showed significantly higher MFI than Lenti-CMV-EGFP-transduced cells at 1, 2, 4, 6 and 8 weeks after transduction. Next, we constructed the lentiviral vector encoding human bone morphogenetic protein-2 (BMP-2) cDNA instead of EGFP (Lenti-RhMLV-BMP-2 or Lenti-CMV-BMP-2). W-20-17 cells or rat BMSCs were transduced with these vectors and BMP-2 protein production was detected in media by ELISA. Lenti-RhMLV-BMP-2-transduced cells secreted significantly greater BMP-2 than Lenti-CMV-BMP-2-transduced cells at 2, 4, 6 and 8 weeks. Finally, 2.5 million of rat BMSCs transduced with Lenti-RhMLV-BMP-2 or Lenti-CMV-BMP-2 were implanted into a muscle pouch in hindlimbs of severe combined immune deficient (SCID) mice with a collagen sponge. Three weeks after implantation, ectopic new bone formation was noted on plain radiographs in the hindlimbs of mice implanted with BMP-2 transduced cells. Increased bone formation was noted with implantation of Lenti-RhMLV-BMP-2-transduced cells in comparison to Lenti-CMV-BMP-2-transduced cells. Histological examination revealed woven bone with reconstitution of the bone marrow cavity with implantation of the Lenti-RhMLV-BMP-2-transduced cells. These results demonstrate that lentiviral vectors expressing BMP-2 can induce long-term gene expression in vitro and new bone formation in vivo under the control of the RhMLV promoter. This may be advantageous for developing tissue-engineering strategies to repair large bone defects.

Disclosures: ***O. Sugiyama****, None.*

SA023

Alendronate Promotes Increased Ossicle Mineralization in a Rat Vascularized Bone Formation Model. M. E. Cunningham*[1], E. A. Tomin[1], S. B. Doty*[2], E. R. Myers*[2], J. M. Lane[1]. [1]Orthopaedics, The Hospital for Special Surgery, New York, NY, USA, [2]Research, The Hospital for Special Surgery, New York, NY, USA.

Vascularized bone grafts are optimal in orthopaedics, providing immediate structural support and accelerated healing, but have unacceptable morbidity. Using a rat model for production of rhBMP-2 induced vascularized neo-ossicles, we previously found rapid early bone production, followed by aggressive late bone resorption. The purpose of the current experiment using osteogenic protein-1 (OP-1/BMP-7) for osteoinduction and alendronate (Fosamax) to limit late bone resorption, was to test the hypotheses: (1) OP-1/bone marrow would form neo-ossicles, (2) OP-1 would have more bone present at late time points than historical controls, and (3) bisphosphonate would prevent late neo-ossicle mineral resorption. Silastic chambers containing isogenic bone marrow and 20 mcg OP-1 were implanted around the inferior epigastric pedicle of male Lewis rats, and neo-ossicles produced were assessed at 1, 2 4 and 8 week time points. Using micro-CT analysis, a significant increase in total mineral content was found between 4 and 8 week samples ($p<0.001$, n=6,9), with alendronate significantly increasing total mineral content in the 8 week samples ($p=0.009$, n=9,8), but not at 4 weeks ($p=0.226$, n=6,8). Histological and histomorphometrical analysis of decalcified sections revealed sparse bone production (1 to 5%) at one week, and a plateau of bone production at 2, 4 and 8 week time points (7 to 12%) that did not trend with time, and did not demonstrate alendronate effects. Maturation of tissues through time was also observed (early red marrow production vs. late fatty marrow, and transition from woven to lamellar bone). We conclude that OP-1 induced neo-ossicle production in this model is comparable to historical controls, that OP-1 does not predispose ossicles to late osteolysis, and that alendronate can be utilized to augment mineralization of neo-ossicles.

Disclosures: ***M.E. Cunningham****, Stryker Biotech 2.*

SA024

See Friday Plenary number F024

SA025

Enhanced Osteoblastic Cell Differentiation by Co-transfection with the OP-1 Gene and the IGF-I Gene. L. C. Yeh*, J. C. Lee. Biochemistry (MC7760), Univ. Texas Health Sci. Ctr. at San Antonio, San Antonio, TX, USA.

Osteogenic Protein-1 (OP-1, BMP-7), a member of the bone morphogenetic protein (BMP) family that belongs to the transforming growth factor-β superfamily, induces formation of new bone and cartilage *in vivo*. OP-1 stimulates IGF-I expression in a variety of osteoblastic cells. Previous studies from this laboratory showed that the action of OP-1 on osteoblastic cell differentiation could be enhanced by protein factors, such as IGF-I. In the present study, we examined the effects of gene transfer of osteoblastic cells with an OP-1 expressing plasmid in combination with an IGF-I-expressing plasmid. Fetal rat calvaria (FRC) cells were transfected with pW24, a plasmid that contains the OP-1 gene under the control of the CMV promoter. Transfected cells showed substantial production of OP-1 proteins by Western blot analysis and a maximum 4-fold increase in alkaline phosphatase (AP) activity in a DNA concentration-dependent manner. Mineralized bone nodules were observed in the transfected cells after 26 days in culture, whereas control cells did not exhibit bone nodules under similar experimental conditions. These transfected cells also showed a dose-dependent enhancement in AP activity when treated with exogenous IGF-I. Moreover, the effects of co-transfection of FRC cells with pW24 and pI, a plasmid containing the IGF-I gene under the control of the CMV promoter were examined. FRC cells transfected with a constant amount of pW24 and varying concentrations of pI showed increased AP activity. The increase in AP activity was pI DNA concentration dependent. Control FRC cells transfected with pI alone or co-transfected with both empty plasmids did not exhibit an enhanced AP activity. The observations suggested that the stimulation of AP activity in these co-transfected FRC cells was the result of the synergistic action of OP-1 and IGF-I produced intracellularly under the direction of the plasmid-borne genes. In conclusion, the current data show that transfection of OP-1 gene to osteoblastic cells increases cell differentiation *in vitro*. The present results also extend the previous observation that a synergy between OP-1 and IGF-I exists in stimulating biochemical and morphological markers characteristic of bone cell differentiation when FRC cells were treated with OP-1 and IGF-I proteins. This study demonstrates the feasibility of employing gene transfer of a second gene in combination with an OP-1 vector to produce enhanced OP-1 activity.

Disclosures: ***J.C. Lee****, Stryker Biotech 2.*

SA026

See Friday Plenary number F026

SA027

Expression of Two Morphogenic Families During Distraction Osteogenesis in Mouse Tibia. K. Jacobsen*, E. Tsiridis*, T. A. Einhorn, L. C. Gerstenfeld, R. S. Carvalho. Orthopaedic Surgery Research Laboratory, Boston University Medical Center, Boston, MA, USA.

Clinical correction of limb length discrepancies has been made possible with the advent of distraction osteogenesis (DO) techniques. Many therapeutic applications have been established to accomplish elongation of long bones which were abnormally short as a result of injury, disease or malformation. A simple and reproducible model of murine tibia DO was developed using a monolateral external fixator. The aim was this study was to assess the expression of two classes of morhphogens; Wnts and bone morphogenetic proteins (BMPs) following DO in the mouse tibia. DO was carried out on the tibia of Balb-c mice using the monolateral fixator with three distinct phases; a latency phase of 7 days following surgery; an active distraction phase of 10 days (0.15 mm distraction/day) and a consolidation phase of 14 days after the end of active DO. Time course used for analysis was: a) 0 days (no surgery), b) 7 days (no DO), c) 10 days (3 d after DO), d) 17 days (end of DO), e) 20 days (3 days into consolidation) and f) 31 days (end of consolidation). RNA expression of Wnts and BMPs was assessed using ribonuclease protection assays. VEGF activity was blocked on some animals by selectively inhibiting its receptors VEGFR-1 (Flt1) and VEGFR2 (Flk-1). Standard histology was also performed for all time periods. DO promoted new bone formation through an intramembranous process with maximum osteogenesis during the active distraction phase. The analysis of the steady state mRNA expression levels suggests that the major BMPs are upregulated by DO, particularly at day 17. When VEGF blocking antibodies were used, all BMPs appeared to be equally upregulated across the time course, except for BMP7 which peaked at 17 days and returned to control levels by day 31. BMPs 4 and 5 peaked earlier during DO with VEGF blocking. DO also enhanced the expression of Wnts 1, 3, 3a, 4, 5b and 6. These were upregulated at day 7, peaking at day 17 and returned to lower levels at day 31. Wnt 4 showed the highest expression. These results suggest that these two families of morphogens contribute to the process of bone formation induced by DO. Additional study is required to test the precise role of individual genes from these families as mediators of this unique type of bone formation.

Disclosures: ***K. Jacobsen****, None.*

SA028

Overexpression of Human Bone Morphogenetic Protein-4 (BMP4) Driven by the 1.1kb Murine Bmp4 Promoter Results in Smaller Size and Reduced Bone Mineral Density in Transgenic Mice. J. Zhang*, S. Harris, V. Dousevich*, X. Tan*, D. Guo*, D. Eick, L. Bonewald, J. Feng. Oral Biology, University of Missouri-Kansas City, Kansas City, MO, USA.

Clearly, Bmp4 will induce ectopic bone formation. The Bmp4 null is an early embryonic lethal clearly showing that Bmp4 is essential for development. Our original hypothesis was that overexpression of Bmp4 would lead to new dentin and new bone formation. We generated mice using a 1.1kb Bmp4 promoter that had shown expression specificity in the ameloblast in order to increase enamel. We have shown endogenous Bmp4 gene expression in osteoblasts, osteocytes, and osteoclasts using a Bmp4 Lac Z reporter model. We also performed *in situ* hybridization of normal mice which also showed high expression in osteoblasts, osteocytes and osteoclasts. Unlike the endogenous promoter, Lac Z expression driven by the 1.1kb Bmp4 promoter was highly observed in osteoclast lineage, but was reduced in osteoblasts, and not detectable in osteocytes as revealed by both LacZ staining and LacZ mRNA *in situ* hybridization.Overexpression of human Bmp4 driven by the 1.1 kb Bmp4 promoter resulted in smaller mice with lower bone mineral density at 5 weeks, 4 months and up to 20 months as compared with wild type control. The bones appeared morphologically normal but there was a decrease trabecular bone. The numbers of osteoclasts per bone surface in these mice were similar to normal mice, but the sizes were larger and had more nuclei and more intensely stained for TRAP, suggesting elevated enzyme activity. Homozygote mice showed severe hypomineralized enamel. These findings suggest the 1.1kb region of the Bmp4 promoter may be more highly expressed in ameloblasts and osteoclasts and that continuous expression of Bmp4 in the osteoclast may induce or maintain osteoclast activation resulting in greater bone resorption that is unaccompanied by or not balanced with increased bone formation. This work is supported by NIH/NIDCR F32 DE015465-01(ZJ).

Disclosures: ***J. Zhang****, None.*

SA029

Three Dimensional Characterization of Cortical Bone Porosity on Microcomputed Tomography Images: A New Method of Evaluation. A. Basillais*[1], C. Chappard[1], S. Bensamoun*[2], B. Brunet-Imbault*[1], M. Ho Ba Tho*[2], C. Benhamou[1]. [1]Ipros, Université d'Orléans, Orleans, France, [2]Laboratoire de Biomécanique et Génie Biomédical, Université de Technologie de Compiègne, Compiègne, France.

Evaluation of cortical images mainly involves geometry measurements such as cortical thickness and pores diameter, or two dimensions (2D) porosity quantification. On microcomputerized tomography (μCT) images, cortical bone appears as a compact structure which is difficult to characterize (Fig. A). An inversion of the image leads, after reconstruction, to volumes prone to be analyzed by the same algorithms as trabecular bone (Fig. B).

Nineteen parallelepipedic cortical samples were prepared from 3 cadaveric human male femurs. The femur diaphysis was divided into three segments : top (16 to 40 %), middle (40 to 55%) and bottom (55 to 70%). Four samples of femur I were extracted from the top of the diaphysis (I/T), 6 samples of femur II from the middle diaphysis (II/M), 4 samples of femur II from the bottom diaphysis (II/B) and 5 samples of femur III from bottom diaphysis (III/B). They have been scanned with a μCT (Skyscan ®1072) with an isotropic resolution of 7.81

µm. After reconstruction and thresholding (a unique threshold for the whole dataset), images similar to figure B were analysed. The pore volume represented the equivalent of BV/TV in the trabecular bone, it was labelled PoV/TV for pore volume / total volume expressed in %. The porosity was also evaluated from 2D femoral sections at the same levels observed by Scanning Electron Microscopy. Mean PoV/TV ± SD were measured : 3.8 ± 3.11 % (femur I/T), 9.3 ± 5.7 % (Femur II/M), 51.3 ± 7.7 % (Femur II/B) and 53.7 ± 19 % (femur III/B). Correlation coefficient with porosity measured on sections was : r = 0.98 ($p<10^{-4}$). These data suggest that 3D cortical porosity can be efficiently evaluated on µCT images, with a good degree of validation using a direct evaluation by scanning electron microscopy of 2D sections.

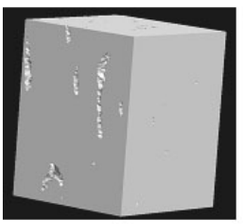
(A)

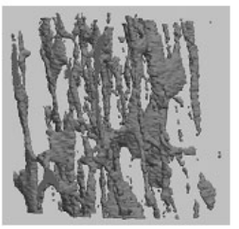
(B)

Disclosures: ***A. Basillais****, None.*

SA030

Rat CIA Model: Evaluation of Markers of Bone and Cartilage Turnover and Juxta-Articular Changes. J. Mayer*, N. Doyle*, I. Moreau*, A. Varela, L. Chouinard, M. Boyer*, S. Y. Smith. CTBR Bio-Research Inc., Montreal, PQ, Canada.

The rat collagen-induced arthritis (CIA) model is used to evaluate the efficacy of potential disease modifiers for the treatment of rheumatoid arthritis (RA). The purpose of this study was to evaluate several biochemical markers of bone and cartilage turnover as well as juxta-articular morphological changes. Osteoclast-derived tartrate-resistant acid phosphatase form 5b (TRAP 5b, SBA Sciences), C-terminal peptide of collagen type I (CTx), osteocalcin (OC), collagen type II cleavage (C2C), procollagen II C-propeptide (CPII), and aggrecan chondroitin sulfate 846 epitope (CS846) (Ibex Diagnostics) were measured. Disease progression was monitored using limb circumference measurements, radiographic scoring and micro-CT images using a Scanco VivaCT40. *Ex vivo* bone densitometry was performed by pQCT and joints were scored histologically.

Female Lewis rats were randomly assigned into the following groups at the onset of arthritis: CIA Vehicle controls (saline), CIA treated with Dexamethosone (Dex) at 0.025 mg/kg/day for 6 days, CIA treated with Methotrexate (MTX) 0.1 mg/kg/day for 12 days. Additional rats were assigned as Non-disease (ND) controls.

With the exception of OC, all markers evaluated were increased 6 days post-onset of arthritis compared to ND controls, significant for TRAP 5b and CTx. Increases were also noted 12 days post-onset, significant for CPII. Increases in CTx were positively and significantly correlated with radiographic scoring and limb circumference. Micro-CT imaging showed clear evidence of disease progression *in vivo*. Bone density (BMD) at the proximal tibia metaphysis was significantly decreased. At the dose level selected, Dex partially inhibited the increases in markers, reduced limb circumference, radiographic and histologic scores. MTX at the dose level selected failed to consistently modify the CIA-induced response, although C2C, CPII and CS846 were notably lower than CIA vehicle controls.

These data support the use of bone and cartilage biochemical markers, radiographic scoring, micro-CT scanning, densitometry and histology to provide a comprehensive assessment of disease progression in bone and cartilage, and to assess potential disease modifiers in this rat model of RA.

Disclosures: ***S.Y. Smith****, None.*

SA031

Relationship Between Structure Analysis Based on the 3D Scaling Index Method and DXA in Postmenopausal Women with Osteoporotic Spine Fractures. D. Mueller*[1], R. Monetti*[2], S. Majumdar[3], D. C. Newitt[3], H. Boehm*[1], C. Raeth*[2], E. J. Rummeny*[1], T. M. Link[3]. [1]Department of Radiology, Technische Universitaet Muenchen, Muenchen, Germany, [2]Max Planck Institute for Extraterrestrial Physics, Garching, Germany, [3]Department of Radiology, UCSF, San Francisco, CA, USA.

The scaling index method (SIM) is a recently proposed non-linear technique to extract texture measures for the quantitative characterisation of the trabecular bone structure in high resolution magnetic resonance imaging (HR-MRI). This new non-linear method, which demonstrated to improve the diagnostic performance in differentiating postmenopausal women with and without osteoporotic spine fractures, was applied to high resolution magnetic resonance images of the distal radius in patients with osteoporotic spine fractures. The purpose of this study was to investigate the relationship between the SIM and dual energy x-ray absorptiometry (DXA) at different sides of the body of postmenopausal women with osteoporotic spine fractures.

Axial HR-MR images of the distal radius were obtained at 1.5 T in 66 women with osteoporotic spine fractures. A three-dimensional gradient-echo sequence was used with a voxel size of 500x195x195 µm³. After normalization and segmentation of each MR-image trabecular structure analysis was performed using algorithms based on our new local 3D scaling index method. In addition BMD measurements of the distal radius, the spine and the proximal femur using dual energy X-ray absorptiometry (DXA) were obtained in all patients. Linear regression was applied to the data to describe the relationship between the SIM and BMD using DXA at different sides of the body. However, there was no significant ($p>0.05$) correlation found for any of the BMD values versus the 3D structure measure based on the local scaling index method (radius BMD vs. SIM: r=.09, spine BMD vs. SIM: r=.17, femur BMD vs. SIM: r=.14)

The results of this study suggest that our recently developed algorithm based on a local 3D scaling index method, which showed a high diagnostic performance in differentiating postmenopausal patients with and without osteoporotic fractures, determines different entities of trabecular bone that are important for the prediction of individual fracture risk and are not reflected by BMD.

Disclosures: ***D. Mueller****, None.*

SA032

A Scanning Small Angle X-Ray Scattering (SAXS) Study of the Nanometer Length Scale Bone Structure in Connection with Implants. M. H. Bünger*[1], K. Erlacher[1], M. Foss*[1], H. Li*[2], Z. Xuenong*[2], B. Langdahl[3], F. Besenbacher*[1], J. Pedersen*[1]. [1]Interdisciplinary Nanoscience Center (iNANO), University of Aarhus, Aarhus, Denmark, [2]Department of Ortopedics, Aarhus University Hospital, Aarhus, Denmark, [3]Dept of Endocrinology and Metabolism C, Aarhus University Hospital, Aarhus, Denmark.

The understanding of the interaction between bone and orthopedic implants is important for the development of biomaterials with improved biocompatibility. The SAXS technique has previously been applied to offer structural information on mean crystal thickness, predominant orientation and degree of orientation of mineral particles in bone. Therefore, one possible application of SAXS is to investigate the nanostructure of bone in connection with ingrowth on implants, which is not possible with conventional optical techniques.

Three 190µm thick sections of vertebrae bone from three 6 month old Danish Landrace pigs were examined. One sample included the neurocentral growth zone, while the other two were sections with bone and either titanium or tantalum implants from pigs that 3 month previously had undergone spinal surgery.

At predefined regions, Scanning SAXS were done with a step width of 50µm and a diameter of the X-ray beam slightly larger than 100µm. The number of recorded SAXS-2d frames was approximately 1000 frames for each of the implant samples and 299 frames in the region of the growth zone.

The mean crystal thickness in the titanium implant sample was 2.40nm (σ =0.251nm) and 2.47nm (σ =0.288nm) in the titanium sample ($P<0.01$). Bone provided a strong SAXS signal and relatively low transmission intensity, whereas regions within the neurocentral growth zones showed a high transmission as well as a high SAXS signal. Combining the transmission and the SAXS data, it was clearly possible to differentiate between areas of fibrous tissue and bone. This was supported by elemental analysis performed by SEM-EDAX. The mineral particles in the cancellous bone were aligned along the trabeculae, with less orientation close to the growth zone. Also, the mineral particles tended to be aligned along the implant surfaces. Within the individual bone samples, a large variation in all SAXS parameters was observed depending on the bone position relative to the implant. Furthermore, larger particle thicknesses were found in areas of bone formation, which matches our growth zone data.

In conclusions, scanning SAXS offers unique information of the bone structure on a nanometer length scale. The data suggests that the parameters obtained by SAXS can be used to assay the local mineral particle growth. This indicates that SAXS is a powerful tool for the characterization of the detailed mineral structure of bone in the vicinity of implants.

Disclosures: ***M.H. Bünger****, None.*

SA033

Identification of the Elemental Composition of Metal Particles from a Failed Joint Prosthesis by Laser Ablation Inductively Coupled Plasma Mass Spectrometry. A. G. Cox*[1], M. Holt*[2], J. Denton*[3]. [1]Centre for Analytical Sciences, University of Sheffield, Sheffield, United Kingdom, [2]Orthopaedic Surgery, Wythenshawe Hospital, Manchester, United Kingdom, [3]Osteoarticular Pathology, University of Manchester, Manchester, United Kingdom.

The purpose of this study was to investigate the potential of Laser Ablation Inductively Coupled Plasma Mass Spectrometry (LA-ICP-MS) to identify metal particles in connective tissues from a failed surgical implant. Samples of connective tissues obtained at open operation from the area surrounding a painful, failing, shoulder prosthesis were obtained. The shoulder prosthesis was composed of a HDPE glenoid component with a cobalt-chromium alloy stem and head. In order to enhance osteo-intigration, the metal stem component had been coated with titanium by plasma deposition. At operation the tissues surrounding the prosthesis were clearly abnormal, of a grey colour and contained necrotic tissue debris. The samples were LR White (Hard Grade) embedded and sections taken for histological examination. On section and staining a macrophage response with giant cell formation was evident. The macrophages contained numerous intracellular black particles. On the surface of the block it was apparent that there were also larger (>50 micron) pieces, of what appeared from their shiny surface, to be metal. The surface of this block was used for the investigation without further treatment. The technique of LA-ICP-MS is an analytical beam technique whereby a 4 micron diameter laser beam (213nm) is used to vaporise the surface of any material in a controlled, precise manner. The vaporisation takes place inside a sample chamber which has a controlled argon gas flow passing through it. The entrained vaporised sample is then carried to the argon plasma (8000K) where it is ionised. The ions are resolved and analysed using a quadrapole mass spectrometer. Single line scans through the intracellular black particles show their composition to be chromium-cobalt alloy, identical to the metal composition of the implant. The elemental composition of the larger particles seen in the block surface was shown to be titanium, different to the intracellular debris composition. These findings demonstrate the ability of LA-ICP-MS to spatially resolve the elemental composition of connective tissues and to give a precise indication of metal composition.

Disclosures: ***A.G. Cox****, None.*

SA034

Direct Measurement of Bone Turnover Using ^{41}Ca. R. L. Fitzgerald*[1], T. L. Griffin*[1], D. J. Hillegonds*[2], D. W. Burton[3], L. J. Deftos[3], S. Mullaney*[3], J. Vogel*[2], D. A. Herold*[1]. [1]Pathology, University of California and SDVAMC, San Diego, CA, USA, [2]Center for Accelerator Mass Spectometry, Lawrence Livermore National Laboratory, Livermore, CA, USA, [3]Medicine, University of California and SDVAMC, San Diego, CA, USA.

Currently most of the laboratory methods for determining the status of bone health are indirect. The ideal measure of bone health would be a direct measurement of the amount of calcium that is being resorbed from the bone matrix. This can be accomplished using accelerator mass spectrometry (AMS) to measure attomole concentrations of calcium isotopes. Small quantities of the radioactive ^{41}Ca isotope (10 nCi) are administered to volunteers and the ratio of ^{41}Ca to naturally occurring calcium (^{41}Ca/Ca) in urine or serum is monitored as the tracer reaches equilibration with deep bone compartments. In healthy patients the terminal elimination half-life of ^{41}Ca is expected to be significantly longer than that of patients with resorptive bone disease. The ^{41}Ca solutions were prepared for IV administration under sterile conditions. Each 9 mL ^{41}Ca dosing solution contains: 10 nCi ^{41}Ca (the isotope that will be monitored); 1 mg Ca (to prevent loss of ^{41}Ca due to nonspecific binding); 0.6 mg of $NaHCO_3$ (buffering agent); and 9 mL of 0.9 % NaCl (diluent). Individual 9 mL prepared doses passed sterility and endotoxin tests according to the USP protocol. To ensure that the solution does not trigger an immunologic response a Limulus Amebocyte Lysate assay gave a result of < 0.27 EU/9 mL (acceptable limit is 175 EU/9 mL dose). USP Bacteriostasis and Fungistasis assay showed no growth at 14 days. We use ICP-MS to demonstrate that only Ca was present above 1 ppm in the $NaHCO_3$ / NaCl solution. Five normal controls and seven end-stage renal disease patients on hemodialysis have been dosed. Urine and serum samples have been collected for AMS measurements and subsequent characterization of absorption and elimination kinetics. The samples are acid digested, precipitated as calcium oxalate, re-dissolved in nitric acid for purification over cation exchange resin and then re-precipitated as CaF_2. This sample is mixed with silver powder and analyzed by AMS. The method is linear over 5 orders of magnitude, from background concentrations (approximately 5.6 x 10^{-14}) to 1 x 10^{-9} ratios of ^{41}Ca/Ca. The precision at concentrations expected in serum samples ranged from 1 to 8% with errors ranging from 1 to 14%. These results demonstrate that ^{41}Ca has potential to be used to directly monitor bone turnover in health and disease allowing for better clinical management of bone disorders caused by end-stage renal disease.

Disclosures: ***D.W. Burton****, None.*

SA035

Loading Direction Affects Mechanical Property Results in Bending of Rat Tibia Specimens. H. A. Hogan[1], D. Older*[1], M. Rose*[1], S. Vaculik*[1], M. R. Allen[2]. [1]Mechanical Engineering, Texas A&M University, College Station, TX, USA, [2]Anatomy & Cell Biology, Indiana University School of Medicine, Indianapolis, IN, USA.

Mechanical properties from biomechanical tests are important outcome measures in skeletal research. A common and effective way to assess cortical bone in rodents animal models is to conduct bending tests on one of the long bones of the appendicular skeleton. The objective of the current study was to determine whether loading direction affects mechanical properties measured from 3-point bending tests of the tibia. Both left and right tibiae were harvested from 21 animals acquired through a tissue sharing program. Animals were not involved in skeletal studies and were all male Sprague-Dawley rats varying in age and size (body mass 230g to 885g). Left and right bones were randomly assigned to two groups and tested by loading in the medial-lateral plane with opposite loading directions. One group was placed with the medial side down and the loader contacting the lateral surface to load in a "lateral-to-medial" direction (designated LM). The other group was loaded "medial-to-lateral" (designated ML). Cross-sectional moment of inertia at mid-diaphysis was assessed by pQCT. Despite the wide range in size of the animals, statistical differences (one-way ANOVA) were found between the two groups for many variables. Values in the table are mean(SE). Stiffness and strength properties (both extrinsic and intrinsic) were generally higher for the LM group. Post-yield displacement was dramatically lower for the LM group. Two-way ANOVA was also conducted to test for effects due to the size (body mass) of the animals. Differences for load direction were the same as for the one-way ANOVA for all variables except yield load, which did not show a load direction effect in the two-way ANOVA (P=0.098). These findings suggest that care should be taken in choosing a loading direction for bending tests of rat tibae. Caution should also be exercised in comparing numerical values of properties from different studies since both loading directions are commonly used. Post-yield displacement is a measure of ductility, which is the opposite of brittleness, and the ML test direction produces a much more progressive failure response (as evidenced by higher values). This direction is thus better for investigating differences in brittleness.

One-Way ANOVA

	LM	ML	different?	P-value
Stiffness (N/mm)	250(20)	235(17)	N	0.154
Ultimate Load (N)	125(10)	103(7)	Y	0.001
Yield Load (N)	113(10)	93(6)	Y	0.020
Post-Yield Disp. (mm)	0.11(0.03)	0.45(0.10)	Y	0.015
Elastic Modulus (GPa)	8.1(0.5)	7.6(0.5)	N	0.311
Ultimate Stress (MPa)	208(8)	177(6)	Y	0.002
Yield Stress (MPa)	187(10)	161(6)	N	0.058

Disclosures: ***H.A. Hogan****, None.*

SA036

Vasopressin Enhanced Na-dependent Pi Transport Activity and the Mineralization in Vascular Smooth Muscle Cells. A. Suzuki[1], K. Nishiwaki-Yasuda*[1], Y. Ono*[1], A. Kakita*[2], Y. Ishiwata*[1], T. Matsumoto*[1], S. Imamura*[1], T. Kato*[1], N. Hayakawa*[1], N. Oda*[1], Y. Oiso*[3], M. Itoh*[1]. [1]Department of Internal Medicine, Fujita Health University, Aichi, Japan, [2]Hekinan Municipal Hospital, Aichi, Japan, [3]Division of Metabolic Diseases, Nagoya University Graduate School of Medicine, Aichi, Japan.

We have previously reported that A-10 rat aortic vascular smooth muscle cells (VSMCs)expressed type III sodium-dependent inorganic phosphate (Pi) transporter, Pit-1 (Glvr-1), and that platelet-derived growth factor enhanced its expression and Pi transport activity in these cells. In the present study, we investigated the effect of arginine vasopressin (AVP) on Pi transport activity, which has been reported to be involved in the mechanism of atherosclerosis, in VSMCs. AVP dose-dependently (1 pM to 100 nM)stimulated Pi transport in A-10 cells. The effect was time-dependent and sustained for up to 24 h. Protein kinase C (PKC) inhibitor calphostin C suppressed the stimulatory effect of AVP on Pi transport. On the other hand, inhibition of mitogen-activated protein (MAP) kinases by selective inhibitors did not affect Pi transport. Furthermore, the long-term treatment with AVP (100 nM) stimulated the calcification of VSMCs. In summary, these results indicated that AVP selectively enhanced the Pi transport activity in VSMCs, resulting in the calcification of these cells. The mechanism responsible for this effect is not mediated by MAP kinase, but involves activation of PKC.

Disclosures: ***A. Suzuki****, None.*

SA037

See Friday Plenary number F037

SA038

Inter-individual Heterogeneity Index of Mineralization Is an Important Determinant of the Quality of Bone. G. Boivin, P. J. Meunier. Faculté de Médecine R. Laennec, INSERM Unité 403, Lyon, France.

Bone quality determinants include the degree of mineralization of bone (DMB) mainly measured by quantitative microradiography (Boivin & Meunier Calcif Tissue Int 2002, 70:503-11). Mean DMB and intra-individual Heterogeneity Index of the distribution of DMB (mean full width at half-maximum of the individual DMB curve) reflect the DMB known to vary over basic structure units with their secondary mineralization. The intra-individual Heterogeneity Index depends on the rate of remodeling, a high turnover leading to a large heterogeneity of DMB and conversely a low one leading to a decreased heterogeneity. From the individual data, a mean Inter-individual Heterogeneity Index (Inter HI) is calculated. In control women who were divided into pre- and post-menopausal groups, on the basis of age, mean DMB is not different between the two groups while Inter HI is significantly higher (p=0.038) in pre- than in post-menopausal group, and reflects a significant homogeneization of DMB with age (p<=0.01). In post-menopausal group only, DMB and Inter HI were correlated (p=0.05).

Changes in bone remodeling rate influence not only the DMB but also the Inter HI. When antiresorptive agents cause a decrease of the remodeling rate - this is well documented in osteoporotic women treated for 2-3 yrs with alendronate (10mg/day) - mean DMB is significantly increased after alendronate (Boivin et al. Bone 2000, 27:687-94) with a shift of DMB values towards highest values. In parallel, and specially after 3 yrs, the Inter HI is decreased concomitantly to the shift of DMB. If such a high DMB combined with a low Inter HI was maintained after long-term treatments, the mechanical properties of bone tissue could be changed. Zoledronic acid given for only 1 yr (Boivin et al. J Bone Miner Res 2003, 18 Suppl. 2:S261) provoked a small increase of DMB (+4-5%) associated with a normal Inter HI. When less potent antiresorptive agents as raloxifene (Boivin et al. J Clin Endocrinol Metab 2003, 88:4199-205) and estrogen (Boivin et al. Osteoporos Int 2004, 15 Suppl. 1:abstract P338SU) are used, mean DMB increased but the shift of DMB is not accompanied by significant changes in Inter HI except after high doses of estrogen. Conversely, in case of accelerated remodeling activity, for example in 11 patients with primary hyperparathyroidism, mean DMB is decreased with a shift of the distribution of DMB towards the lowest values but Inter HI does not change. In 9 patients with skeletal fluorosis mean DMB is decreased but Inter HI remains normal.

Beside DMB, this new approach leads to consider also Inter HI as a determinant of bone quality. It remains to evaluate the properties of bone at the tissue (micro-indentation) and crystal (infrared spectroscopy) levels.

Disclosures: ***G. Boivin****, None.*

SA039

See Friday Plenary number F039

SA040

Association Between Hand and Lumbar Exostoses and Abdominal Aortic Calcification: The Framingham Study. D. Karasik[1], D. K. Kiely*[1], L. A. Cupples*[2], P. W. F. Wilson*[3], C. J. O'Donnell*[4], D. P. Kiel[1], D. T. Felson[5]. [1]Research, Hebrew Rehab Center for Aged, Boston, MA, USA, [2]Biostat, BU Sch Pub Health, Boston, MA, USA, [3]Endocrin, Med Uni S. Carolina, Charleston, SC, USA, [4]NHLBI Framingham Heart Study, Framingham, MA, USA, [5]Clin Epid, BU Sch Med, Boston, MA, USA.

Bone proliferation (exostoses) and vascular calcification are common in elderly men and women. It is unclear whether the increased prevalence of both exostoses and aortic calcification with aging is due to a common etiology.

In this cross-sectional study, lateral lumbar and hand radiographs were obtained in 715 men and 1004 mostly postmenopausal women (mean age 61, range 47-80 yrs), from the Framingham Heart Study Original Cohort (1967-1970). Each group of hand exostoses, specifically apiostoses (tufting), enthesophytes, and nodes (osteophytes), were graded on a scale 0-3 (absent to severe) and summed across phalanges of digits II-V. Anterior lumbar osteophytes (OPH) were graded on a scale 0-3 for each vertebra and summed across L1-L5. Abdominal aortic calcification (AAC) was graded 0-3 for the anterior and posterior aortic walls in each lumbar segment (L1 to L4) and then summed. Information on known risk factors (age, sex, BMI, smoking, alcohol consumption, physical activity, systolic blood pressure, total cholesterol levels, diabetes, and estrogen replacement therapy in women) was obtained at the time of radiography. We excluded participants with diffuse idiopathic skeletal hyperostosis (7.6% of the sample) who have bony proliferation and a high prevalence of diabetes.

After initial correlation analysis, we used logistic regression models to assess multivariate-adjusted relations between dichotomized AAC score (0 or 1+) and exostoses, in each gender.

Prevalence and severity of hand exostoses, anterior lumbar OPH, and AAC positively correlated with age in both genders. Spearman age-adjusted partial correlations between exostoses ranged from -0.06 (hand apiostoses and anterior lumbar OPH) to 0.33 (enthesophytes and apiostoses).

Multivariate adjusted logistic regression analysis revealed a significant association between AAC and anterior lumbar OPH (per increase in summary score) in men (OR 1.2, 95%CI 1.1-1.3) and women (OR 1.3, 1.2-1.4, both P<0.0001). Additionally, a significant association was found between apiostoses and AAC in men (OR 1.1, 1.0-1.2, P=0.02), and enthesophytes and AAC in women (OR 0.8, 0.7-0.9, P<0.001). Nodes were not significantly associated with AAC.

In conclusion, AAC was associated with anterior lumbar osteophytes in both men and women. Sex-specific factors are involved in association between abdominal aortic calcification and hand exostoses.

Disclosures: ***D. Karasik****, None.*

SA041

Galectin-3 in Osteoarthritis: from the Protection to the Destruction Role. C. Boileau*[1], J. Martel-Pelletier*[1], M. Guévremont*[1], J. Pelletier*[1], F. Poirier*[2], P. Reboul[1]. [1]Arthritis Unit, University of Montreal, Montreal, PQ, Canada, [2]Laboratoire de Génétique et de Développement des Mammifères, Institut Jacques Monod, Paris, France.

Osteoarthritic (OA) chondrocytes are able to re-express numerous genes normally activated in the growth plate. Among these genes, we are interested in studying galectin-3 (gal-3) since we have recently demonstrated that its expression was increased in OA cartilage. Gal-3 is a mammalian lectin and is involved in numerous functions such as adhesion, splicing activity, cell cycle regulation and apoptosis. These functions are related to the galectin-3 cellular localization. In the present study, we investigated the role(s) of gal-3 by using both mono-iodoacetate-induced OA model and in vitro experiments.

OA was induced with an injection of iodoacetate into each knee joint of four month-old mice (WT) or galectin-3 null mice (KO). Mice were sacrified 7, 14 and 21 days after the injection. Histologic evaluation was performed on sagittal sections knee joint. OA lesions were graded using a modified histologic/histochemical scale of Mankin. Intracellular and extracellular roles of gal-3 were investigated in both human chondrocytes and chondrogenic ATDC5 cells.

Intra-articular injection of MIA up-regulated the expression of gal-3 in WT mice 7 days post injection, reaching a statistical significance 14 days post injection (p<0.05). Histologic grading score indicated that KO mice (control group) had a poorer quality of cartilage compared to WT mice (control group). Moreover, the induction of OA in KO mice showed a marked decreased of bone surface (p<0.05).

Therefore, it seemed that gal-3 was important for the cartilage homeostasis. As it was suggested that gal-3 could be implicated in chondrocyte survival, we treated human OA chondrocytes with SNP, which is known to generate chondrocyte cell death. Our results showed that gal-3 was much further decreased than was Bcl2 in the same conditions. Moreover, SNP decreased the gal-3 phosphorylation, which is a key process in the capacity of gal-3 to prevent cell death. Finally, ATDC5 cells transfected with a gal-3-expressing vector, were more resistant to SNP-induced cell death compared to those transfected with the empty vector. On the other hand, gal-3 was found in synovial fluid, particularly during inflammation. Therefore, we investigated the potential role of exogenous gal-3 in chondrocyte cultures. Surprisingly, we found that exogenous gal-3 induced chondrocyte death.

In that study, we demonstrated the role of gal-3 in cartilage homeostasis in gal-3 KO model and the importance of gal-3 for bone by inducing OA in KO mice. Moreover, we showed different effects of gal-3 on chondrocytes depending its localization.

Disclosures: ***C. Boileau****, None.*

SA042

See Friday Plenary number F042

SA043

Expression of Mouse Receptor Activator of NF-κB Ligand (RANKL) in Growth Plate and Articular Cartilage. K. Kishimoto*[1], R. Kitazawa[1], A. Darwanto*[1], T. Kondo[1], S. Maeda*[1], M. Kurosaka*[2], S. Kitazawa[1]. [1]Division of Molecular Pathology, Kobe University Graduate School of Medicine, Kobe, Japan, [2]Division of Orthopaedic Surgery, Kobe, Japan.

Based on developmental fate and function, cartilage tissue is broadly classifiable into transient cartilage (embryonic or growth plate: GP) and permanent cartilage (articular cartilage: AC). The former eventually disappears and is replaced by bone (endochondral ossification). RANKL is expressed in not only osteoblasts but also prehypertrophic chondrocytes to recruit chondroclasts at endochondral ossification sites, indicating that RANKL is an essential factor defining the fate of transient and permanent cartilage. We investigated the expression pattern of factors regulating differentiation and function of osteo(chondro)clasts as well as of Runx2 and its putative upstream genes in GP and AC. Knee joints of male BALB/c mice aged 8 weeks were dissected, fixed with 4% paraformaldehyde in 0.1 M phosphate buffer (PB) at 4 C for 3 days, decalcified with 20% EDTA in 0.1M PB for 4 days, and then subjected to tartrate-resistant acid phosphatase (TRAP) staining to detect osteo(chondro)clasts. BMP-2, -4, -6 and type X collagen mRNA were detected by in situ hybridization (ISH). Immunostaining was conducted using anti-RANKL, Runx2, Dlx5 and Msx2 antibodies. The methylation status of the mouse RANKL gene promoter in both GP and AC was analyzed by sodium bisulfite mapping using microdissected mouse bone tissue. Besides showing osteoblasts positive for Runx2 and RANKL lining the trabecular bone surface, RANKL expression was observed in hypertrophic chondrocytes in GP, where numerous TRAP-positive osteo(chondro)clasts were observed, but barely in chondrocytes in the deep zone of AC. At the boundary between the calcifying and the hypertrophic chondrocytes of GP, RANKL-expressing chondrocytes overlapped those expressing Runx2, Dlx5 and Msx2. Although similar BMP-2 and -4 expression was observed in chondrocytes in both GP and AC as well as in maturing osteoblasts, a rather restricted BMP-6 expression pattern was observed in chondrocytes in GP. On the other hand, sodium bisulfite mapping showed that mainly non-CpG methylation was similarly scattered in a non-specific manner in chondrocytes in GP and AC. Taken together with the fact that putative Runx2 binding elements are located in the RANKL promoter, our data suggested that Runx2, an essential transcription factor for skeletal development, may also be a key regulator of RANKL expression in chondrocytes that promotes endochondral ossification. Furthermore, a selective expression of a subset of BMP, as an upstream factor of Runx2, may play an important role in defining the fate of chondrocytes.

Disclosures: ***K. Kishimoto****, None.*

SA044

See Friday Plenary number F044

SA045

Extracellular Calcium and Parathyroid Hormone-related Protein (PTHrP) Signaling Determines the Pace of Cell Differentiation of Mouse Growth Plate Chondrocytes (mGPCs). L. Rodriguez*, T. H. Chen*, C. Tu*, D. Shoback, W. Chang. Endocrine Unit, VAMC, UC San Francisco, San Francisco, CA, USA.

Raising the extracellular $[Ca^{2+}]$ ($[Ca^{2+}]_e$) promotes the differentiation of chondrogenic RCJ3.1C5.18 cells and mGPCs by inhibiting the expression of early chondrogenic markers and increasing the expression of markers of terminal differentiation. These effects are opposite to those of the PTHrP/Indian hedgehog (Ihh) feedback mechanism that delays chondrocyte maturation. To assess the interactions between extracellular Ca^{2+} and PTHrP/Ihh-mediated signaling, we tested the ability of PTHrP to alter the effects of Ca^{2+} and vice versa on proteoglycan (PG) synthesis by alcian green staining, matrix mineralization by alizarin red staining, and gene expression by quantitative real-time PCR in mGPCs. In the absence of PTHrP, raising $[Ca^{2+}]_e$ from 0.5 to 3.0 mM dose-dependently suppressed PG accumulation and the expression of early markers of chondrocyte differentiation (type II collagen and aggrecan) and increased signs of terminal differentiation -- matrix mineral deposition and the expression of osteopontin and osteocalcin -- with ED_{50}'s ≈ 1-2 mM Ca^{2+}. Incubation of cells with PTHrP (10^{-7} M), in contrast, blunted the effects of high $[Ca^{2+}]_e$ on PG synthesis, matrix mineralization, and gene expression as indicated by right-shifted Ca^{2+} dose-response curves. Although with reduced potency, high $[Ca^{2+}]_e$ (3 mM) continued to influence the above biochemical pathways in the presence of maximal doses of PTHrP (10^{-7} M). High $[Ca^{2+}]_e$ did not change PTHrP-induced cyclic AMP formation but did decrease RNA levels for both PTH/PTHrP receptors and Ihh by ≈75% and 95%, respectively. High $[Ca^{2+}]_e$ also affected the expression of several components of the insulin-like growth factor-1 (IGF-1) signaling pathway that is known to promote GPC differentiation. Raising $[Ca^{2+}]_e$ from 0.5 to 3.0 mM increased RNA levels for IGF-1 and the IGF-1 receptors by 4- and 2-fold, respectively, and decreased RNA levels for IGF-1 binding proteins (IGF1BP 2, 3, and 4) by 50-85%. The effects on these binding proteins should raise free IGF-1 levels. These effects of high $[Ca^{2+}]_e$ were blocked (80-90%) by co-incubating the cells with PTHrP (10^{-7} M). Taken together, these studies support the idea that signaling by extracellular Ca^{2+} and PTHrP/Ihh determines the pace of differentiation in cultured chondrocytes either by direct interactions between the two pathways or indirect interactions with other regulators of chondrocyte differentiation such as IGF-1, its receptor, and associated proteins.

Disclosures: ***W. Chang****, None.*

SA046

Disease Modifying Effects of a Selective COX-2 Inhibitor in the Rat Anterior-cruciate Ligament Transection (ACLT) Model of Osteoarthritis. T. Hayami*[1], Y. Zhuo*[1], G. Wesolowski*[1], M. Pickarski*[1], S. Lerger*[2], G. A. Rodan[1], L. T. Duong[1]. [1]Merck Res. Labs., West Point, PA, USA, [2]Merck Frosst Centre for Therapeutic Res., Montreal, PQ, Canada.

Osteoarthritis (OA) is a degenerative joint disease characterized by articular cartilage degradation, subchondral bone sclerosis, and osteophyte formation. To investigate the potential contribution of inflammation and bone turnover to OA progression, we examined the effects of MF tricyclic, a potent and selective inhibitor of cyclooxygenase (COX)-2, in combination with Alendronate (ALN), on the disease progression in the rat surgically induced OA model. Male rats received sham- or ACLT-surgery in the right knee; the study duration was 10 wk post-surgery. By comparison to sham using real time quantitative PCR, we found that COX-2 expression was up-regulated 2-fold in the articular cartilage of ACLT-joints. Using immunohistochemistry, we also detected the increase in COX-2 protein in articular cartilage derived from both rat and human OA joint tissues. Next, sham- and ACLT-rats were dosed with vehicle, MF tricyclic (3 mg/kg, daily p.o.), or ALN (120 μg/kg/wk, s.c.), or with a combination of both drugs. Similar to ALN, the COX-2 inhibitor had significant chondroprotective effects on the ACLT-joints. MF tricyclic and ALN partially reduced the histological Mankin score ($p<0.05$ and <0.001, respectively) of cartilage damage during OA progression, and suppressed the elevated levels of urinary Col2CTx, a cartilage degradation marker, 2-wk post-surgery. While MF tricyclic did not inhibit generalized bone resorption, as determined by urinary Col1CTx, this compound ($p<0.0001$) significantly inhibited local subchondral bone sclerosis in the ACLT-joints as evaluated by histomorphometry, by comparison to ALN ($p<0.001$). Osteophyte formation was also suppressed by both COX-2 inhibitor and ALN. Interestingly, there was no additive effects observed in chondroprotection and osteophyte formation in the ACLT-joints treated with the combination of both drugs. Immunohistochemical analysis revealed that protein levels of COX-2 and mPGES in articular chondrocytes were inhibited in the ALN-treated ACLT-joints. Moreover, we observed that ALN (30 μM) reduced COX-2 mRNA levels and PGE2 production in IL-1-treated primary culture of human articular chondrocytes. Taken together, this study suggests that COX-2-mediated pathway is up-regulated in both human and rat OA tissues, and inhibition of this enzyme results in structure-modifying effects in the rat OA model. In addition, the lack of additivity of the two compounds *in vivo*, together with the inhibition of COX-2 activity by ALN *in vitro,* suggest that ALN may directly modulate the COX-2/PGE2 pathway.

Disclosures: ***L.T. Duong****, Merck & Co. 3.*

SA047

See Friday Plenary number F047

SA048

Overexpression of CDK6 and CCND1 in Chondrocytes Induces Chondrocyte Proliferation and Apoptosis and Causes Dwarfism. Z. Maruyama[1], N. Kanatani*[2], C. Yoshida*[2], K. Nakamura[1], H. Kawaguchi[1], T. Komori[2]. [1]Orthopaedic Surgery, Surgical Science, Sensory and Motor System Science, Graduate School of Medicine and Faculty of Medicine,the University of Tokyo, Tokyo, Japan, [2]Division of Oral Cytology and Cell Biology, Department of Developmental and Reconstructive Medicine, Nagasaki University Graduate School of Biomedical Sciences, Nagasaki, Japan.

In endochondral bone formation, chondrocytes develop through sequential processes, including initiation, proliferation, and maturation, and finally undergo apoptosis. G1 cyclins play a fundamental role in cell cycle entry, and growth arrest is required for cell differentiation and maturation. To assess the function of G1 cyclins during skeletogenesis, we generated transgenic (Tg) mice that overexpress cyclin dependent kinase 6 (CDK6) or cyclin D1 (CCND1) under the control of Col2a1 promoter/enhancer. Several lines of Tg mice with different levels of transgene expression were established in each gene. Both CDK6 Tg lines and CCND1 Tg lines showed grossly normal skeletal development. We further generated CDK6/CCND1 double Tg mice. The double Tg mice displayed dwarfism and died at birth from respiratory failure. In the growth plate of double Tg mice, chondrocyte maturation was mildly delayed at embryonic day (E) 15.5, as shown by the delayed vascular invasion and the absence of osteopontin-positive terminal hypertrophic chondrocytes. The frequency of BrdU labeling was increased in double Tg mice (27.7 ± 2.6 %) as compared with wild-type mice (14.3 ± 2.8 %) ($P < 0.005$, $n = 3$) at E 15.5. In wild-type mice, TUNEL-positive cells were restricted to the terminal hypertrophic chondrocytes. In double Tg mice, however, many TUNEL-positive cells, which have apoptotic bodies and fragmented nuclei, were observed in immature chondrocytes that expressed Col2a1. The TUNEL-positive cells were most frequently observed in the epiphises at E15.5. These apoptotic cells were accumulated in the cartilage, because they escaped phagocytosis. It is considered that the dwarfism of double Tg mice was caused by apoptosis, because chondrocyte proliferation was increased and the delay in chondrocyte maturation was not severe in double Tg mice. These findings demonstrate that overexpression of both CDK6 and CCND1 in chondrocytes promotes cell cycle progression but also induces chondrocyte apoptosis in vivo.

Disclosures: ***Z. Maruyama****, None.*

SA049

See Friday Plenary number F049

SA050

Osteopontin-Deficiency Suppresses TNF-alpha Induced Cytotoxicity in Chondrocytes. K. Yumoto[1], M. Ishijima[1], S. R. Rittling[2], K. Tsuji[1], Y. Tsuchiya[3], S. Kon[4], A. Nifuji[1], T. Uede[4], D. T. Denhardt[2], M. Noda[1]. [1]Molecular Pharmacology, Tokyo Medical and Dental University, Tokyo, Japan, [2]Rutgers University, Piscataway, NJ, USA, [3]IBL, Gumma, Japan, [4]Hokkaido University, Sapporo, Japan.

Apoptosis of chondrocytes in articular cartilage has been observed in rheumatoid arthritis patients. However, the mechanisms underlying chondrocyte apoptosis in arthritic joints have not been fully understood. We previously reported that apoptosis of chondrocytes was enhanced in anti-type II collagen antibodies and lipopolysaccharide (mAbs/LPS)-induced arthritis in mice and osteopontin (OPN)-deficiency suppressed chondrocyte apoptosis in this arthritis model (*PNAS* **99**:4556, 2002). To understand the mechanisms of OPN-deficiency-induced resistance against chondrocyte apoptosis, we examined the cellular basis for such protection. Chondrocytes were prepared from mouse ribs and the release of lactate dehydrogenase (LDH), a cytotoxic marker, from wild-type chondrocytes in culture, was induced by LPS or TNF-alpha. In contrast to wild-type, LDH release by LPS or TNF-alpha was significantly suppressed in chondrocytes derived from OPN-deficient mice. Furthermore, OPN-overexpression using adenovirus vector in OPN-deficient chondrocytes enhanced the levels of LDH release induced by TNF-alpha. These data indicated that the presence of OPN in chondrocytes is involved in the apoptosis susceptibility of these cells to TNF-alpha. It was reported that p38 MAPK was activated by recombinant OPN fragments in osteoblastic cells (*Biomaterials* **24**:1059, 2003). To understand the pathway involved in the TNF-alpha induced intra-cellular signals leading to cytotoxicity in chondrocytes, we examined the effects of the MAPK inhibitors on TNF-alpha induced cytotoxicity. MEK inhibitor U0126 did not alter the TNF-alpha induced LDH release. On the other hand, p38 inhibitor SB203580 significantly suppressed TNF-alpha induced LDH release. These observations suggest that TNF-alpha induced cell death in chondrocytes is mediated by OPN and p38 MAPK.

Disclosures: ***K. Yumoto****, 21th Century COE 2.*

SA051

See Friday Plenary number F041

SA052

The RhoA/ROCK Signaling Pathway Coordinates Cell Shape, Cytoskeletal Organization and Tissue-Specific Gene Expression During Chondrogenesis. A. Woods*, G. Wang*, F. Beier. Physiology and Pharmacology, University of Western Ontario, London, ON, Canada.

Rho GTPases have been identified as regulators of cytoskeletal organization and control of gene expression in several cell types. Because of the well-documented direct correlation between chondrocyte shape, gene expression and stage of differentiation, we hypothesized that RhoA and its effector kinases ROCK1/2 regulate expression of chondrocyte-specific genes through modulation of the actin cytoskeleton. RhoA and ROCK1/2 are expressed throughout chondrogenic differentiation of primary mouse limb bud cells. Inhibition of ROCK activity with the pharmacological compound Y27632 results in rounding of cells and cortical actin organization, characteristic features of chondroyctes. In contrast, overexpression of RhoA in the chondrogenic cell line ATDC5 causes the opposite phentoype of increased stress fibre formation. Real-time PCR and western blotting demonstrated that ROCK inhibition induces expression of the chondrogenic transcription factor Sox9. Sox9 induction is accompanied by increased alcian blue staining, a marker of chondrogenesis, in Y27632-treated cultures. In contrast, RhoA overexpression in ATDC5 cells suppresses Sox9 mRNA and protein levels. All effects of RhoA overexpression can be reversed by Y27632. Inhibition of actin polymerization by cytochalasin D induces Sox9 gene expression in a similar fashion as Y27632, whereas inhibition of microtubule polymerization by colchicine completely blocks Sox9 expression. Surprisingly, stabilization of the actin cytoskeleton by jasplakinolide also induces Sox9 expression and activity. In summary, we demonstrate that RhoA inhibits Sox9 expression and chondrogenesis through ROCK1/2 signaling and modification of the actin cytoskeleton. These data suggest that the RhoA pathway plays a crucial role in the coordination of the long-known, but poorly understood interdependence of cell shape, cytoskeletal organization and chondrocyte-specific gene expression during skeletal development.

Disclosures: ***A. Woods****, None.*

SA053

See Friday Plenary number F053

SA054

TGF-β1 Regulates ATDC5 Differentiation, and Fibronectin Isoform and SRp40 Expression. F. Han*[1], Z. Tao*[1], C. J. Williams*[2], R. Zaka*[3], R. S. Tuan*[4], P. A. Norton*[5], N. J. Hickok*[1]. [1]Orthopaedic Surgery, Thomas Jefferson University, Philadelphia, PA, USA, [2]Div. Rheumatology, Dept. Medicine, Thomas Jefferson University, Philadelphia, PA, USA, [3]Div. Rheumatology, Dept. Medicine, Thomas Jefferson University, Philadelphia, PA, USA, [4]Cartilage Biol. Orthop Branch, NIAMS, NIH, Bethesda, MD, USA, [5]Biochem.Mol.Pharm, Thomas Jefferson University, Philadelphia, PA, USA.

Chondrogenesis is dependent on cellular condensation and a regulated program of gene expression. During chondrogenesis, regulated splicing of the fibronectin (FN) pre-mRNA results in differential FN isoform expression. Transforming growth factor (TGF)-β alters FN splicing in other systems and induces chondrogenesis. We have asked, using mouse pre-chondrogenic ATDC5 cells, if TGF-β1 affects chondrogenesis in parallel with FN isoform expression. We first assessed if TGF-β1 altered production of a sulfated extracellular matrix,characteristic of cartilage. To prevent chondrocyte maturation, cells were maintained without insulin. By day 5, TGF-β1-treated cultures exhibited more Alcian blue staining than controls. To assess chondrogenesis, we measured by RT-PCR collagen type I and type II mRNA expression. In these first 5 days of culture, representative of the condensation phase, TGF-β1 treatment decreased col α1(I) and increased col α1(II) mRNA expression, suggesting that TGF-β1 accelerated initial stages of chondrogenesis. We next examined inclusion of the EDIIIA (A) and EDIIIB (B) exons in FN mRNA. Inclusion of the A and B exons (A+B+) is characteristic of the pre-chondrocyte, whereas A-B+ form is characteristic of the maturing chondrocyte. TGF-β1 treatment decreased exon A inclusion and increased exon B inclusion, in parallel to effects of TGF-β1 on chondrogenesis. Expression of the short-form of the pre-mRNA splicing protein, SRp40, also correlates with the onset of chondrogenesis. Exclusion of the FN A exon has been directly linked to expression of this short-form. TGF-β1 treatment increased expression of the short-form of SRp40, as assessed by RT-PCR, suggesting a mechanism for the effect of TGF-β1 on FN splicing events. These data indicate that TGF-β1, which increases the commitment of the pre-chondrogenic ATDC5 cells to chondrocytes, decreases inclusion of the FN-EDIIIA exon and increases inclusion of the FN-EDIIIB exon in a time- and dose-dependent manner. These splicing events directly correlate with the increased expression of the splicing factor SRp40. Other extracellular matrix proteins, i.e., collagen type II, undergo regulated splicing during chondrogenesis. Our data suggest that an important effect of TGF-β1 during chondrogenesis involves the regulation of alternative splicing.

Disclosures: ***F. Han****, None.*

SA055

The Effect of Pamidronate on Intervertebral Disc and Endplate. S. Moon, H. Kim*, U. Kwon*, K. Lee*, H. Kim*, K. Yang*, J. Jahng, S. Park*, J. Jeon*, H. Lee*. Department of Orthopaedic Surgery, Yonsei Univesity College of Medicine, Seoul, Republic of Korea.

As potent inhibitors of bone resorption, bisphosphonates (BPs) are widely used for the treatment of bone disorders that are due to increased osteoclast activity. BPs also exhibit partial chondroprotective effect, inhibiting breakdown of collagen type II. Nutritional deprivation caused by sclerosis of vertebral end plate provides, in part, a mechanism of intervertebral disc (IVD) degeneration. The fact that BPs have a powerful antiresorptive effect and chondroprotective effect prompts a research for the sum effect of BPs on IVDs, since antiresorptive action can cause hypertrophy of endplate while chondroprotective effect can maintain chondrogenic phenotype of IVDs. Accordingly, the purposes of this experimental study were, firstly, demonstrate the effect of pamidronate, second generation N-containing BPs on in vitro metabolism of IVD cells and secondly, the effect of pamidronate on histologic changes of endplate and IVD. Human lumbar IVD cells were cultured in alginate beads for in vitro test. Pamidronate (10^{-9}, 10^{-6}, 10^{-3} M) was administered to cultures. ^{3}H-Thymidine for DNA synthesis and ^{35}S-Sulfate incorporation for proteoglycan synthesis were performed. RT-PCR for mRNA expression of collagen type I, collagen type II, and aggrecan was also performed. For in vivo test, pamidronate was injected intravenously (30ug/kg, 90ug/kg) to mice (C57BL/6) weekly for 5 and 12 weeks. H-E, Safranin-O stain, and TUNEL assay were done. Histomorphometric data were also collected. Human IVD cell cultures with pamidronate showed significant increase in proteoglycan synthesis, 40% increase with a dose of 10^{-9} M pamidronate ($p<0.05$). In densitometric assay of RT-PCR, cultures showed no significant changes in mRNA expression of type I collagen, type II collagen, and aggrecan. Mice with pamidronate injection showed significant increase in thickness of endplate without evidence of IVD degeneration. Furthermore, Mice with pamidronate demonstrated no significant increase in TUNEL positive cells in endplate and IVD. In conclusion, these in vitro and vivo data confirm that pamidronate, N-containing second generation BPs, is safe to IVD metabolism without causing apoptosis and IVD degeneration.

Disclosures: ***S. Moon****, Brain Korea 21 Project 2.*

SA056

See Friday Plenary number F056

SA057

Osteoprotegerin and Receptor Activator of NF-kB Ligand Were Regulated by Retinoic Acid and Bone Morphogenetic Protein-2 during Chondrogenesis or Osteogenesis of USAC. K. Yagami. Oral and Maxillofacial Surgery, Showa University, Tokyo, Japan.

[Introduction] Several cytokines affect on bone and cartilage resorption at the invasive site of bone tumors. Receptor activator of NF-κB ligand (RANKL) and osteoprotegerin (OPG) are potent regulator of osteoclasts in bone metabolism. At present, however the effect of RANKL and OPG on the differentiation of chondrocyte is unclear. Retionic acid (RA) increases alkaline phosphatase activity and type X collagen synthesis. These stimulatory effects of RA imply the enhancement of chondrocyte maturation. We have newly established a human chondrocytic cell line (USAC) expressing chondrocytic phenotypes. USAC also shows osteogenic differentiation by rhBMP-2 in vivo. In the present study, we examined changes in the expression of RANKL and OPG by RA or rhBMP-2 in the process of maturation and differentiation of USAC.

[Materials and Methods] USAC cells were cultured at a density of 1x106/ml in 2.5%FBS/a-MEM, and were treated with RA (30-300 nM) or rhBMP-2 (10-1000 ng/ml) for several days. RT-PCR was performed with the specific DNA probe for h-RANKL and h-OPG. Cell extracts of parallel culture, containing equal protein concentrations, were electrophoresed on 10% sodium dodecyl sulfate-polyacrylamide gels (SDS-PAGE) for Western blot analysis with anti-human antibody for RANKL and OPG. USAC cells were transplanted into peritoneal cavities of 6-week-old athymic mice using diffusion chambers with or without rhBMP-2. In some chambers, 1000 nM of RA or 5 mg of rhBMP-2 was coated on the inner surface of the membrane filter. The chambers were removed from mice 1-4 weeks after implantation, then fixed and embedded in plastic for undecalcified sections. These sections were stained with anti-human antibody for RANKL and OPG.

[Results] RANKL and OPG mRNAs were expressed in USAC. RANKL mRNA was up regulated and OPG mRNA was down regulated both by the treatment with RA and rhBMP-2. Moreover, the cartilage like tissue formed in DC was mostly stained with OPG. However, RANKL was strongly stained in the calcification portion and the osteoid in DC. These results suggested that RANKL and OPG were regulated by RA and BMP-2 during chondrogenesis or osteogenesis on USAC.

Disclosures: ***K. Yagami****, None.*

SA058

See Friday Plenary number F058

SA059

PERK eIF2 Alpha Kinase Regulates Neonatal Bone Development. D. Cavener, J. Wei*, X. Sheng*, B. McGrath*, A. Frank*, M. Teta*. Biology, Penn State University, University Park, PA, USA.

Genetic deficiencies of the PERK eIF2 alpha kinase result in severe neonatal growth retardation, osteopenia, and infantile diabetes in the human Wolcott-Rallison syndrome (WRS) and in mice. Through phosphorylation of the translation initiation factor eIF2 alpha, PERK can regulate either global protein synthesis or translation of specific regulatory genes depending upon the physiological and developmental status of a specific tissue or organ. As an endoplasmic reticulum (ER) transmembrane kinase, we have proposed that PERK acts as multipurpose sensor of secretory activity and modulator of secretory capacity in highly secretory cells such as osteoblasts, chondrocytes, hepatocytes, and insulin-secreting beta cells. Previously we showed that the growth defect in PERK KO mice is caused by an early neonatal deficiency in circulating IGF-1 derived from the liver, whereas the osteopenia is caused by deficiencies in both cortical and trabecular bone formation. To elucidate the underlying molecular and cellular defects associated with the skeletal anomalies in PERK KO mice, we have performed a detailed developmental examination of the skeletal and cellular structure of the axial and appendicular skeleton. In addition we have examined the expression of genes and proteins known to be critically involved in late embryonic and postnatal bone development as well as performed gene profiling experiments comparing wild-type and mutant osteoblasts and fibroblasts. These studies have indicated that PERK plays a crucial role in postnatal synthesis, assembly, and secretion of type I collagen, particularly in osteoblasts.

Disclosures: ***D. Cavener****, None.*

SA060

Gene Expression Microarray-based Hypothesis for Cadmium-Induced Bone Loss. M. H. Bhattacharyya, A. Regunathan*, D. A. Glesne*, A. Ebert-McNeill*. Biosciences Division, Argonne National Laboratory, Argonne, IL, USA.

To identify a mechanism of cadmium-induced bone loss that did not rely on guessing the pathways involved, a whole-mouse genome c-DNA microarray was used to determine changes in bone cell gene expression after a single cadmium gavage to mice. To identify early pathways, time points were 2h and 4h after gavage, for a dose (200 ug Cd/mouse) at which calcium release from bone starts at 8h. Three mouse strains [CF1, metallothionein-normal (MTN), and MT1,2-deficient (MT1,2KO)] were studied to identify a robust mechanism that applied across mouse strains. Results showed that ~18 genes increased significantly in mRNA level in bone cells after Cd gavage in all 4 or in 3 of the 4 microarrays. High to low in Cd responsiveness, these were: cysteine-rich protein 61 (Cyr61), metallothionein 2 (MT2), transferrin receptor (TfR), glutamine synthetase pseudogene 1, MT1, acidic chitinase, RIKEN cDNA 3930401B19, src-like adaptor protein, vacuolar proton pump ATPase, integrin alpha v, aquaporin 1, and p38 MAP Kinase. No genes showed analogous decreases. Concentration increases were small but were validated by Northern analyses. Gene changes fit into the following hypothesis: Cadmium could, by currently unknown mechanisms, increase expression of cysteine-rich protein 61 (Cyr61) in osteoblasts. Cyr61 has been shown to be high in osteoblasts. It is a secreted extracellular matrix-associated protein that binds the integrin dimer, alpha-v beta-3. Cyr-61 secretion from osteoblasts could attract osteoclasts or their precursors and bind to their surface integrin molecules, thus stimulating cell migration, adhesion and osteoclast activation. Activation would stimulate expression of other osteoclast genes, including integrin alpha-v (signaling molecule involved in activation), vacuolar proton pump ATPase (provides acid to dissolve bone calcium and to activate acid proteases that degrade bone matrix), transferrin receptor (provides needed iron), acid chitinase (acidic polyglucosamine hydrolase, maybe involved in degradation of bone matrix glycoproteins, such as osteonectin, decorin, biglycan?), and aquaporin (water pore that enables solute movement to resorption pit?). Osteoclast precursor cells contain high concentrations of p38 MAP kinase compared to other bone cells, and this kinase is required for osteoclast formation. The latter pathways could explain existing evidence that cadmium stimulates bone loss by increasing both osteoclast formation and activation.

Disclosures: ***M.H. Bhattacharyya****, None.*

SA061

See Friday Plenary number F061

SA062

Enhanced Bone Regeneration in HIF-1α +/- Mice. D. E. Komatsu[1], D. J. Manalo*[2], G. L. Semenza*[2], M. Hadjiargyrou[1]. [1]Biomedical Engineering, SUNY, Stony Brook, Stony Brook, NY, USA, [2]Pediatrics, Medicine, Oncology, Radiation Oncology, Johns Hopkins University, Baltimore, MD, USA.

Previous work in our laboratory has demonstrated that regional hypoxia subsequent to bone fracture activates hypoxia- inducible factor 1α (HIF-1α) and initiates HIF-1 mediated up-regulation of numerous genes involved in bone regeneration. This study was designed to test the hypothesis that HIF-1α has a functional role in bone regeneration. Fixed femoral fractures were generated unilaterally in 10 female mice heterozygous for HIF-1α (HIF-1α+/-) and 10 wild-type littermates (HIF-1α+/+). The animals were euthanized on post-fracture day 21 and the fractured and unfractured (contralateral control) femurs were harvested and scanned by micro computed tomography (μCT) to determine volumetric and areal properties. In addition, 4-point bending to failure was conducted on the specimens in order to determine stiffness and ultimate strength, quantitative measures of healing. All 10 intact femurs from each group of mice were analyzed, while only 5 fractured femurs from each genotype were analyzed (sample losses due to pin removal and mechanical testing). The μCT scans of the intact femurs revealed no significant differences in femur length or periosteal, cortical and endosteal areas between HIF-1α+/- and HIF-1α+/+ mice. However, mechanical testing demonstrated a significant increase in ultimate strength (17%) in the HIF-1α+/- mice. The μCT scans of the fractured femurs were used to quantify callus volume (including soft tissue, mineralized callus and cortical bone) and mineralization (mineralized callus only) in proximal, central and distal callus regions. These analyses yielded significant increases in mineralization in both proximal (70%) and central regions (57%) as well as callus volume in distal regions (81%) in the HIF-1α+/- mice, as compared to HIF-1α+/+. Since the intact femurs showed significant differences in strength between genotypes, the mechanical testing results for the calluses were normalized to their respective contralateral controls. The results from this analysis identified a significant increase in stiffness (142%) in the HIF-1α+/- mice but no significant differences in ultimate strength. Contrary to our expectation that partial HIF-1α deficiency would lead to impaired bone regeneration, our data surprisingly indicate the reverse. Further experiments are ongoing to verify these data and identify the underlying molecular mechanisms responsible for these observations.

Disclosures: ***D.E. Komatsu****, None.*

SA063

See Friday Plenary number F063

SA064

Alterations in Osteoblast-specific Gene Products by Isoflavones in the Context of Soy- and Casein-based Protein in a Rat Model of Male Osteoporosis. D. Y. Soung[1], L. Devareddy*[1], D. A. Khalil[1], E. A. Lucas[1], B. J. Smith[1], S. Juma[2], B. H. Arjmandi[1]. [1]Nutritional Sciences Department, Oklahoma State University, Stillwater, OK, USA, [2]Department of Nutritional Sciences, University of Cincinnati Medical Center, Cincinnati, OH, USA.

Soy and its isoflavones have been shown to increase bone formation. The purpose of this study was to examine the effect of isoflavones on bone matrix protein synthesis and osteoblast activity (i.e. collagen type I, COL: osteocalcin, OC; osteonectin, ON; osteopontin, OP; alkaline phosphatase, ALP) at the mRNA level in male rats. Twenty-four male F344 rats, aged 13 months were either sham-operated (Sham; 1 group) or orchidectomized (ORX; 5 groups). Rats in the Sham and one ORX group were fed a casein-based control diet (AIN-93M) and the remaining four ORX groups were fed one of the two doses of isoflavones in the context of either casein (Iso1 = 600 or Iso2 = 1200 mg isoflavones/kg diet) or soy protein (Soy = 600 or Soy+ = 1200 mg isoflavones/kg diet) for 180 days. Total RNA was extracted from distal femur and Northern blot analysis was used to measure mRNA levels. cDNA of 18S ribosomal RNA was used as an internal control to normalize gene expression. The table below shows the effect of treatments on osteoblast-specific gene products.

Group	COL/18S	OC/18S	ON/18S	OP/18S	ALP/18S
Sham	1.38 ± 0.33^{c}	0.66 ± 0.11^{c}	0.63 ± 0.11^{c}	0.90 ± 0.26	0.68 ± 0.11^{c}
ORX	2.56 ± 0.33^{b}	1.07 ± 0.11^{ab}	1.04 ± 0.11^{ab}	0.99 ± 0.16	0.96 ± 0.11^{bc}
Iso1	2.97 ± 0.38^{b}	1.10 ± 0.12^{ab}	1.01 ± 0.13^{ab}	0.87 ± 0.19	1.08 ± 0.13^{ab}
Iso2	4.13 ± 0.38^{a}	1.32 ± 0.12^{a}	1.31 ± 0.13^{a}	1.06 ± 0.19	1.25 ± 0.13^{ab}
Soy	2.47 ± 0.38^{b}	0.80 ± 0.12^{bc}	0.83 ± 0.13^{bc}	1.17 ± 0.19	0.90 ± 0.13^{bc}
Soy+	3.41 ± 0.38^{ab}	1.29 ± 0.12^{a}	1.11 ± 0.13^{ab}	1.00 ± 0.19	1.41 ± 0.13^{a}

Data are mean ± SE (n=4). Values in a column that do not share the same superscript letters are significantly (P<0.05) different from each other.

Our findings suggest that high dose of isoflavones, irrespective of protein source, have a more pronounced effect on certain osteoblast-specific genes products involved in bone formation.

Disclosures: ***D.Y. Soung****, None.*

SA065

Orally Administered N-Butyrylated Glucosamine (GlcNBu) Decreases Inflammation in the Streptococcal Cell Wall Rat Arthritis Model and Increases the Bone Mineral Density and Content of the Subchondral Regions of the Femur and Tibia. T. P. Anastassiades[1], M. Grynpas[2], S. Wang*[3], J. R. Carran*[1], D. S. Wainman*[1]. [1]Medicine, Rheumatology, Queen's University, Kingston, ON, Canada, [2]Laboratory Medicine and Pathobiology, Samuel Lunenfeld Research Institute, Mount Sinai Hospital, Toronto, ON, Canada, [3]Samuel Lunenfeld Research Institute, Mount Sinai Hospital,, Toronto, ON, Canada.

Purpose. Determine the effects of feeding a novel N-acyl glucosamine, GlcNBu, on (i) the inflammatory arthritis in the rat, and (ii) on the bone mineral density in a region of interest (ROI) comprising of the distal part of femur and proximal part of the tibia.

Methods. Female Lewis rats, 150 g, on were injected intra-peritoneally with streptococcal cell wall antigen (15 μg/g) and ankle swelling was measured daily by a standard caliper method. Standard chow was supplemented as follows (mg/kg/day) : Group I - GlcNBu, 200; II - glucose, 200; III - GlcNBu 20; IV - no arthritis induced, no supplementation. At the end of 4 weeks the animals were sacrificed and the dissected femurs and tibias (70 bones of each) were scanned with a micro-DXA technique, standardized at the ROI, to provide normalized bone mineral denisty (BMD) and content (BMC). Statistics were done with SPSS.

Results. Group I, high dose GlcNBu, demonstrated significant reductions in inflammation compared to glucose controls (bottom and top lines, respectively, Fig 1). A smaller reduction in inflammation was seen at 20mg/kg/day (not shown). In Fig 2 the bars show ROI BMDs in the order of I to IV. Group I had the highest BMD and BMC, compared to all other Groups, with statistically significant differences. Group III (low dose GlcNBu) demonstrated the next highest BMD/BMCs, followed by Groups IV and II.

Conclusions. Orally administered GlcNBu at 200mg/kg/day, to rats with inflammatory arthritis significantly reduced the inflammatory response and increased the BMD/BMC in subhondral areas, over controls including normals. The mechaism of these effects has not been elucidated.

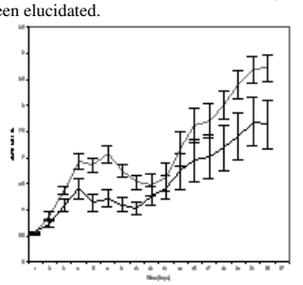

Fig 1

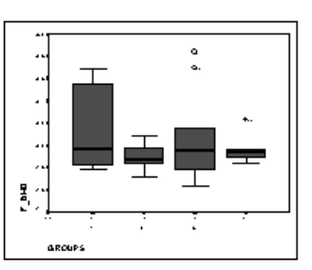

Fig 2

Disclosures: ***T.P. Anastassiades****, Anacoti Ltd. 4; Canadian Arthritis Network (Federal Center of Excellence) 2, 7.*

SA066

See Friday Plenary number F066

SA067

A New Technique Using Calcium Phosphate Precipitate Enhances Efficiency of In Vivo Plasmid Gene Transfer. S. Kuroda[1], H. Kondo[1], K. Ohya[2], S. Kasugai[1]. [1]Oral Implantology and Regenerative Dental Medicine, Tokyo Medical and Dental University, Tokyo, Japan, [2]Pharmacology, Tokyo Medical and Dental University, Tokyo, Japan.

Currently, in vivo gene transfer with expression plasmid vector is one of the emerging remedies because gene transfer with plasmid vector is simple and clinically safe compared to the other transfer systems with virus vectors. An expression plasmid vector encoding hBMP-2 was combined with collagen and transplanted to a segmental bone defect of experimental animals, consequently regenerating the bone defect. However, large amounts of plasmid vectors (1 mg or more) have been used in these studies, suggesting the low efficiency of gene transfer. On the other hand, calcium-phosphate (CaP) precipitate, in which plasmid vector is incorporated, has been used for in vitro gene transfer. Since CaP particles stabilize nucleic acid, we speculated that CaP precipitate would be also useful for in vivo gene transfer. In the present study, we combined CaP precipitate with expression plasmid vector encoding BMP-2 and examined whether this formula becomes more effective on gene transfer and bone formation. Twenty μg of pEGFP plasmid vector encoding hBMP-2 was served as several formulas in 1% collagen base in combination with CaP or CaP plus 5% of hyaluronic acid in 400 μl, freeze-dried, and then transplanted on rat calvarias subcutaneously. The animals were killed at 1, 2 and 3 weeks post operation and the calvarias were subjected for EGFP detection and histology. At 2 weeks, fluorescence was observed in "pEGFP-collagen", "pEGFP-CaP-collagen" and "pEGFP-CaP-collagen-hyaluronic acid" groups. Notably, the fluorescence of "pEGFP-CaP-collagen" and "pEGFP-CaP-collagen-hyaluronic acid" groups were much extensive compared to "pEGFP-collagen". Corresponding to these CLSM images, fluorescence measurement of the tissue homogenates revealed intense fluorescence of the "pEGFP-CaP-collagen" and "pEGFP-CaP-collagen-hyaluronic acid" groups. Histological sections from "pEGFP-CaP-collagen" and "pEGFP-CaP-collagen-hyaluronic acid" groups elucidated osteoblast cohesion at 1 to 3 weeks. However, the sections from "pEGFP-collagen"Group suggested that entries of osteoblasts into the matrix area were not as clear as in the other two groups. Additionally, the formula incubation in PBS released more the plasmid from "pEGFP-CaP-collagen" and "pEGFP-CaP-collagen-hyaluronic acid" than from "pEGFP-collagen". Although the safety of the plasmid DNA administration has been speculated, decrease in plasmid DNA dose is obviously ideal. Our formula would reduce the dose of plasmid DNA and impact on experimental and therapeutic fields employing plasmid DNA transfer.

Disclosures: ***S. Kuroda****, None.*

SA068

See Friday Plenary number F068

SA069

Signal-Dependent and Developmentally Regulated Transcription Factors are Activated During Chondrocyte Differentiation Induced by Demineralized Bone. K. E. Yates. Orthopedic Surgery, Brigham and Women's Hospital, Boston, MA, USA.

The mechanisms that regulate chondrocyte differentiation post-natally are not well understood. In this study, an *in vitro* model of induced chondrocyte differentiation was used to identify changes in transcriptional networks. Human dermal fibroblasts (hDFs) were cultured in three-dimensional, porous collagen sponges with or without chondroinductive demineralized bone powder (DBP). Nuclear extracts were prepared on day 3, before the chondroblast phenotype is evident (i.e., matrix containing collagen type II and aggrecan). Nuclear protein binding to transcriptional enhancer sites (TranSignal Protein/DNA Arrays, Panomics Inc) was measured as a surrogate of transcription factor activity. DBP-induced changes were classified according to transcription factors' roles in cellular regulatory circuits [Science 295: 813, 2002].

1) No changes in activity were found at serum inducible or thyroid hormone receptor binding sites, validating the assay and the specificity of hDFs' response to DBP. 2) Among constitutively active factors, DBP increased activity at TFIID sites (180% of control) and decreased activity at CCAAT-box sites CBF (30%) and C/EBPalpha (30%). 3) Among regulated factors, DBP greatly increased activity at targets of cell surface receptor-ligand activated signaling pathways (Figure). Immunoblotting showed increased (180%) active CREB protein (phospho-CREB) in DBP/collagen sponges, and immunocytochemistry showed intense nuclear staining of phospho-CREB in hDFs in contact with DBP. Quantification of AP-1 proteins by ELISA showed increased JunB (200%) and phospho-Jun (130%). cDNA array analysis documented increased mRNA levels of *NFkB* (290%) and *RelA* (160%). 4) Among developmentally regulated factors, increased or decreased activity was found for several GATA, homeobox, and forkhead binding sites (Figure). Increased expression of *RUNX2* mRNA (200%) in DBP/collagen sponges was detected by real-time PCR.

These changes in transcriptional networks imply upstream activation of cell signaling pathways, including calcium 2nd messengers and serine kinases, in hDFs cultured with DBP for 3 days. Concomitant changes in developmentally regulated factors suggest co-ordination between extracellular and intracellular signals during chondroinduction of post-natal fibroblasts.

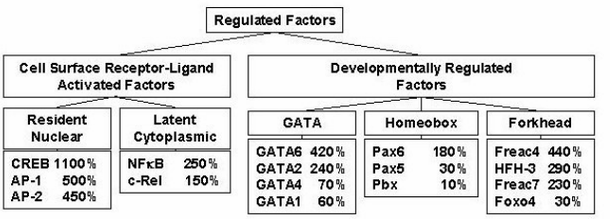

Figure. Classification of DBP-induced changes (% of control) in nuclear extract protein binding activity to enhancer elements.

Disclosures: ***K.E. Yates****, None.*

SA070

See Friday Plenary number F070

SA071

Multiple Potential of Rat Mandible Marrow Mesenchymal Stem Cells: Isolation, Cultivation, and Induction of Differentiation. C. Shih, J. Shyu. Biology and Anatomy, National Defense Medical Center, Taipei, Taiwan Republic of China.

The regeneration of periodontal tissue apparently depends on differentiation of mesenchymal stem cells migrating into wound which have the potential for osteogenesis, cementogenesis, and formation of periodontal tissues. In addition, successful implant therapy may also be dependent on the differentiation of stem cells arising from the surrounding bone marrow. It is important to establish an in vitro animal study model which deals with cellular aspect of periodontal tissue engineering, regeneration or repair using bone marrow MSCs of mandibular origin. The purpose of this study was to isolate, characterize, and induce cell differentiation into different lineage cells by density gradient separation method, cell culture, CD marker selection, alkaline phosphatase activity(ALP), bone colony formation, light and phase contrast inverted microscopy, H&E stain, oil red O stain, MAP-2 , GFAP and flow cytometry. Rat bone marrow cells were harvested from mandible and MSCs isolated by density gradient separation, cultivation and CD markers (e.g. CD 90 and etc.) selection. Isolated bone marrow MSCs were cultured to semiconfluent and treated with osteogenic differentiation medium(DMEM-LG supplemented with 10% FBS, ascorbic acid, 100 nM dexamethasone, with or without 10 mM beta-GP) or adipogenic differentiation medium (100 nM dexamethasone, indomethacin and insulin) or neurogenic differentiation factor. Appearance of cuboid-shaped osteoblastic cells, unmineralized or mineralized colony was noted approximately 10, 15 and 21 days after osteogenic induction. With adipogenic induction, small sized lipid droplets began to appear within cytoplasm 7 days. More and larger lipid droplets accumulation were noted 10-14 days after induction. We also noted that lipid droplets-containing adipocytes terminally differentiated into round shaped adipocyte and finally became unadherent and floating within the medium. In addition, MAP-2-positive neurons and GFAP-positive glial cells were noted after induction. The results of this study indicated that rat mandible bone marrow MSCs could be isolated, cultured, and induced to become osteogenic, adipogenic and neurogenic cells/tissues.

Disclosures: ***C. Shih****, None.*

SA072

See Friday Plenary number F072

SA073

Changes in Permeability of Osteocyte Lacunar Wall After Ischemia and Reperfusion Injury. S. Qiu[1], D. Rao[1], S. Palnitkar*[1], A. Parfitt[2]. [1]Bone & Mineral Research Lab, Henry Ford Health System, Detroit, MI, USA, [2]Division of Endocrinology and Center for Osteoporosis and Metabolic Bone Disease, University of Arkansas for Medical Sciences, Little Rock, AR, USA.

Our objective was to determine the effects of ischemia/reperfusion (I/R) on the permeability of the lacunar wall. Basic fuchsin is able to stain microcracks, unmineralized osteoid and osteocyte lacunae and canaliculi, but unable to penetrate into the mineralized bone matrix. Penetration of basic fuchsin through the lacunar wall indicates that the material property of perilacunar matrix has been changed.

A rubber band tourniquet was applied at the right thigh in 5 rats for 3 hours and then released. The animals were sacrificed 7 days after surgery. Five normal rats were used as controls. The diaphyseal segments were placed in 70% ethanol containing 1% basic fuchsin, embedded in methylmethacrylate, sectioned into 100 µm and examined using fluorescence and confocal microscopy.

In normal bone, 97.6% of osteocyte lacunae were impermeable to basic fuchsin. The thickness of perilacunar labeling was < 1 µm (mean ± SD for 100 normal osteocyte occupied lacunae: *0.43 ± 0.15 µm*) under confocal microscopy. Based on this, a band thicker than 0.8 µm, > 2 SD greater than the mean value for normal lacunae, was taken to define fuchsin permeability. There were many fuchsin permeable lacunae in I/R bone (Fig 1A). However, the small scanning field makes confocal microscopy unsuitable for a large-scale measurement of osteocyte lacunae. Since the fluorescence intensity of basic fuchsin is very strong, the perilacunar band can also be viewed using fluorescence microscopy (Fig 1B). The fluorescence band was not clear around normal osteocyte lacunae. Approximately 98% of the permeable lacunae had a band thicker than 0.8 µm (mean ± SD: *1.71 ± 0.63 µm*). This number was consistent with the value derived from confocal microscopy. There was no significant difference in total lacunar density between I/R and normal bones (1319 ± 98/mm² vs 1384 ± 83/mm²). However, the density of permeable lacunae was about 5 times higher in I/R bone than in normal control (150 ± 24/mm² vs 33 ± 17/mm², $p < 0.001$).

The results show that very few osteocyte lacunae in normal bone are permeable to basic fuchsin. A significant increase in permeable lacunae at 7 days of I/R suggests that the perilacunar matrix may be damaged under certain extreme pathological conditions.

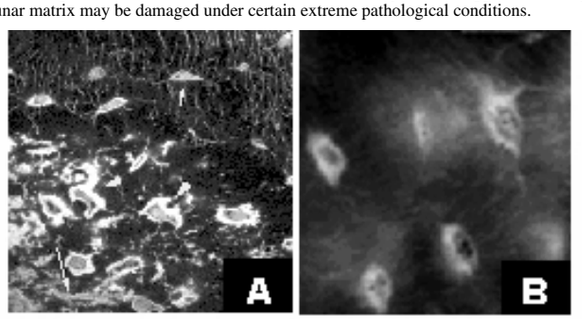

Fig 1. Osteocyte lacunae in bone with I/R injury. A) normal (short arrow) and permeable lacunae (arrowheads) under confocal microscopy, B) permeable lacunae under fluorescence microscopy.

Disclosures: ***S. Qiu****, None.*

SA074

Secreted Phosphoprotein-24 (SPP-24) Reduces Bone Mass in Transgenic Mice Whereas BMP Binding Peptide (BBP), a Polypeptide Deduced from the Sequence of SPP-24, Enhances the Activity of rhBMP-2 In Vivo. S. S. Murray*[1], K. Behnam[2], J. D. P. Silva*[3], M. E. L. Duarte[3], E. J. B. Murray[1]. [1]GRECC/Medicine, VAGLAHS/University of California, Sepulveda/Los Angeles, CA, USA, [2]Physiological Sciences, University of California, Los Angeles, CA, USA, [3]Histology and Embryology, Universidade Federal do Rio de Janeiro, Rio de Janeiro, Brazil.

We have determined by chromatographic separation, MALDI/ToF MS, and peptide fingerprinting analysis that the protein that Marshall Urist referred to as "bone morphogenic protein" is an 18.5 kD acidic fragment of the previously described secreted phosphoprotein-24 (SPP-24). The 18.5 kD protein contains a cystatin- or cysteine-protease inhibitor-like domain similar to that of fetuin. As with fetuin, within this sequence there is a region with sequence similarity to the TGF-beta receptor II called the TRH1 (TGF-beta receptor II homology 1) domain. BMP binding peptide (BBP) is a synthetic 19 amino acid polypeptide deduced from the sequence of Urist's BMP which is similar to the cystatin/TRH1 domain of fetuin. We have investigated the effects of SPP-24 and BBP on bone formation. Transgenic mice expressing full-length SPP-24 under the control of the osteocalcin promoter were created. Five independent strains were generated, though expression could not be quantitated. Femoral, but not vertebral, BMD was 5.7% lower in female, but not male, transgenic mice at 8 months of age. Similarly, quantitative histomorphometric analysis demonstrated reduced bone volume, trabecular thickness, and trabecular separation in female transgenic animals. On the other hand, surface plasmon resonance demonstrated that BBP, like fetuin, binds rhBMP-2. BBP enhanced the activity of rhBMP-2 in the 3-week mouse hindquarter heterotopic bone forming assay. In this assay, 500 ug of BBP increased the activity of 5 ug of rhBMP-2. The area of ectopic bone formed increased by 62%, and bone mineral content increased by 74%. In time-course studies, cartilage was detected earlier in mice who received BBP in addition to rhBMP-2. We conclude that Urist's BMP is an 18.5 kD fragment of SPP-24 and hypothesize that its activity is related to binding BMPs and increasing their residence time at the site of action.

Disclosures: ***S.S. Murray****, None.*

SA075

See Friday Plenary number F075

SA076

Involvement of the Urokinase Receptor in Bone Homeostasis. F. Furlan[1], N. Jorgensen*[2], J. Jensen*[2], A. Rubinacci*[3], E. Mrak*[3], I. Villa*[3], F. Blasi*[1]. [1]Molecular Gentics, Vita-Salute University, HSR, Milano, Italy, [2]Endocrinology, Osteoporosis Unit, Copenhagen, Denmark, [3]Bone Metabolic Unit, HSR, Milano, Italy.

The plasminogen activator system (PAS) is an intricate system of serine proteases, protease inhibitors, and protease receptors that governs the conversion of the abundant plasma protease zymogen, plasminogen, to the active protease, plasmin. Plasmin directly or indirectly, via the activation of latent matrix metalloproteases, degrades components of the extracellular matrix in the context of tissue homeostasis, tissue remodeling, and tissue repair. In particular, urokinase receptor (uPAR) is actively involved in the regulation of important cell functions like adhesion and migration and it has been shown to interact with integrins.

PAS is also implicated in the pathogenesis of a remarkable array of important human degenerative diseases, tumor dissemination, vessel wall diseases, and rheumatoid arthritis. The skeleton is particularly rich in extracellular matrix, and remodeling is central to skeletal physiology throughout life. Furthermore, it has been previously shown that the major players of bone remodeling, osteoblasts (Obs) and osteoclasts (Ocs), produce urokinase (uPA) and express its receptor (uPAR).

The purpose of this study was to investigate the role of uPAR in bone remodeling. To achieve this aim we analyzed the bone phenotype in uPAR-null female mice. Morphological analysis of the skeleton showed a significant decrease in tibia length in mutant mice as compared to Wt. Bone mass analysis by peripheral quantitative computed tomography (pQCT), reveals that the absence of uPAR determines an increase in bone mass as compared to normal mice ($p<0.02$). Moreover, mechanical test showed a reduction in the capability to sustain a given load in uPAR Ko tibias as compared to normal tibias from female animals ($p<0.02$).

To explore the cellular bases of the bone defect in uPAR Ko mice, we cultured Obs in vitro. The results confirmed these findings showing a proliferative advantage and a higher susceptibility of the matrix to be mineralized as compared to Wt cells. The production of important proteins involved in the mineralization process, like alkaline phosphatase (ALP), is increased only during the first weeks of Ob maturation. After 4 weeks ALP is similar in both genotypes.

Together our preliminary data indicate that uPAR may play an important role in bone physiology.

Disclosures: ***F. Furlan****, None.*

SA077

See Friday Plenary number F077

SA078

Regulation of Osteoactivin (OA) Expression by Osteotrophic Factors and its Role in Mediating BMP-2 Effects on Osteoblast Differentiation and Function. S. A. Abdelmagid*[1], E. Nuglozeh*[1], M. F. Barbe[2], S. N. Popoff[1], F. F. Safadi[1]. [1]Anatomy and Cell Biology, Temple University, Philadelphia, PA, USA, [2]Physical Therapy, Temple University, Philadelphia, PA, USA.

Osteoactivin (OA) is a novel osteoblast-related glycoprotein that plays an important role in osteoblast differentiation and function. TGF-β1, BMP-2 and calcitriol are important osteotrophic factors that regulate osteoblast proliferation and differentiation. In this study we first examined the effects TGF-β1, BMP-2 and calcitriol on OA expression. Primary osteoblast cultures treated with TGF-β1 (5 ng/ml), BMP-2 (50 ng/ml) and calcitriol (10^{-8} M) were terminated at different time points and examined for OA expression using Western blot analysis. TGF-β1 treatment showed minimal effect on OA expression, while BMP-2 and calcitriol showed an up-regulate of OA expression especially during the matrix maturation and mineralization stages in culture. BMP-2 maximally induced OA expression (5-fold) during the matrix mineralization stage in culture. Next, we treated primary osteoblast cultures with different doses of BMP-2 (10-200 ng/ml) for 24 hours under serum free conditions. OA protein expression levels reached a maximum at 50 ng/ml. In order to examine whether OA is a downstream mediator of BMP-2 effect on osteoblast differentiation, OA anti-sense oligonucleotide was used to inhibit OA expression in cultures treated with BMP-2. Primary osteoblast cultures treated with BMP-2 (50 ng/ml) stimulated nodule formation and matrix mineralization when compared to non-treated cultures. Cultures treated with OA anti-sense oligonucleotide (0.5 µM) showed a reduction of OA expression associated with decreased nodule formation and calcium deposition. BMP-2 (50 ng/ml) treatment rescued OA expression associated with an increase in nodule formation and matrix mineralization, when compared to OA anti-sense treated cultures. BMP-2 is known to stimulate osteoblast differentiation mainly through the phospho-Smad 1, 5 and 8 path-

way. Cultures treated with BMP-2 showed an up-regulation of phospho-Smad 1 when compared to non-treated cultures. In OA anti-sense treated cultures, phospho-Smad 1 was down-regulated when compared to non-treated cultures, while BMP-2 rescued phospho-Smad 1 expression. These data suggest that OA might be a downstream mediator of BMP-2 in osteoblasts. Future studies are designed to use phospho-Smad 1 inhibitors, to examine whether OA expression is altered. We conclude that OA is regulated by different osteotrophic factors and may act as downstream mediator of BMP-2 effects on osteoblast differentiation.

Disclosures: ***S.A. Abdelmagid****, None.*

SA079

IL-3 Stimulates Osteoclast (OCL) Formation and Inhibits Osteoblast (OBL) Differentiation in Myeloma. L. A. Ehrlich*[1], M. Ito[1], S. J. Choi[1], G. D. Roodman[2]. [1]Medicine-Hematology/Oncology, University of Pittsburgh, Pittsburgh, PA, USA, [2]Medicine-Hematology/Oncology, University of Pittsburgh and Dept. of Veterans Affairs Medical Center, Pittsburgh, PA, USA.

Normally, bone resorption is coupled to an increase in osteoblast activity. In Multiple Myeloma (MM), bone remodeling is uncoupled, and bone destruction occurs both by markedly increased osteoclastic bone destruction and severely impaired osteoblastic bone formation. Although several reports have shown that conditioned media from MM cell lines suppress OBL differentiation, the identity of the OBL inhibitor(s) is unknown. A recent report by Tian et al (NEJM 2003) has identified DKK1, an inhibitor of the WNT signaling pathway, as a putative OBL inhibitor in MM. However, it is likely that other inhibitors of OBL differentiation are present in the myeloma microenvironment, just as there are several potent stimulators of OCL formation produced or induced by myeloma cells. We recently reported that IL-3 levels in bone marrow plasma of patients with MM are increased compared to normal controls and that IL-3 in MM marrow plasma stimulates osteoclast formation. We also demonstrated that IL-3 is produced by primary myeloma cells and that it increased MM cell growth in vitro. However the effects of IL-3 on OBL are unknown. Therefore, to determine if IL-3 could affect OBL growth and differentiation, we tested if primary marrow stromal cells and OBL-like C2C12 cells differentiated with BMP2 expressed IL-3 receptor α (IL-3R). Both cells types expressed IL-3R by RT-PCR. Immunostaining for IL-3R in murine marrow stromal cell cultures showed that the IL-3R was present on thirty percent of the cells after treatment with IL-3, confirming the PCR results. Importantly, treatment of primary murine stromal cell cultures with IL-3 (0.01-10 ng/mL) inhibited basal and BMP-2 stimulated osteoblast formation in a dose dependent manner, without affecting cell growth. At 10 ng/mL IL-3 inhibited OBL differentiation by 80%. Time course studies demonstrated that IL-3 affected the later stages of osteoblast differentiation. Further, the inhibitory effects of IL-3 were not due to induction of TNFα. TNFα levels were very low (0-20 pg/ml) in the conditioned media of these cultures, and treating the cultures with anti-mouse TNFα did not block the IL-3 effect. This data suggests that IL-3 may be an important mediator of the bone destruction in MM by both inducing osteoclast formation and inhibiting bone formation.

Disclosures: ***L.A. Ehrlich****, None.*

SA080

A New Method for Early *in vivo* Detection of Bone Metastases Using Green Fluorescence Protein (GFP) Expressing A375 Human Melanoma Cells. D. C. Huang[1], G. Ma*[2], A. Belenkov*[2], X. F. Yang*[1], A. Kremer*[1], L. McIntosh*[2], R. Kremer[1]. [1]Medicine, Royal Victoria Hospital and McGill University, Montreal, PQ, Canada, [2]ART Advanced Research Technologies Inc., Saint-Laurent, PQ, Canada.

Nude mice injected into the left cardiac ventricle with A375 human melanoma cells usually develop osteolytic lesions within 2-3 weeks. X-ray analysis is a routine but insensitive method to detect metastatic bone destruction. Histomorphometric analysis is a specific and sensitive method to detect bone metastasis but is labour intensive and consequently not suitable for large scale analysis. A system that would allow early detection of tumor cells colonization within bone prior to detectable bone destruction by X-ray analysis would greatly facilitate research in this area. In the present study, we used a new *in vivo* small animal molecular imager fluorescence scanning system (eXplore Optix) to study the cancer cell dissemination to the skeleton in nude mice injected into the left cardiac ventricle with A375 human melanoma cells expressing green fluorescent protein (GFP). A375 human melanoma cells expressing GFP were established following stable transfection of GFP driven by a CMV promoter. Preliminary quantitative analysis of GFP by eXplore Optix indicated that the minimal detectable specific signal was $3x10^3$ cells. eXplore Optix eliminates non specific fluorescence signals by performing time resolved fluorescence measurements *in vivo*. As a result, the system analyzes fluorescence lifetime, which permits to distinguish fluorophores with similar emission spectra according to their fluorescence lifetime. Fluorescence analysis by eXplore Optix and X-ray detection by Faxitron were done at timed intervals following intracardiac administration of cancer cells. Our analysis indicated that GFP-labeled cancer cells could be detected at 9 days in bone of live animals in the absence of any detectable osteolytic lesions by X-ray. At 3 weeks all animal had detectable lesions by X-ray at the locations previously identified by fluorescence. As predicted, the size of the lesions determined by the intensity of the signals increased progressively with time and correlated with histomorphometric analysis of tumor volume. Taken together these results indicate that fluorescence detection of tumor cells within bone by eXplore Optix is both specific and sensitive and that the signals correlate well with tumor volumes making it a powerful tool for longitudinal analysis of bone metastasis.

Disclosures: ***D.C. Huang****, None.*

SA081

See Friday Plenary number F081

SA082

Elevated Serum Fibroblast Growth Factor 23 in Patients with Small Cell and Squamous Cell Lung Cancer with Normal Serum Phosphorus. P. Tebben[1], R. J. Singh*[2], A. O. Bungum*[3], R. Kumar[4]. [1]Endocrinology, Mayo Clinic, Rochester, MN, USA, [2]Laboratory Medicine, Mayo Clinic, Rochester, MN, USA, [3]Pulmonary Research, Division of Pulmonary Medicine, Mayo Clinic, Rochester, MN, USA, [4]Nephrology Research, Mayo Clinic, Rochester, MN, USA.

Serum or tissue concentrations of the fibroblast growth factor family of proteins have been studied in relation to several human malignancies including lung cancer. Fibroblast growth factor 23 (FGF23) is a recently discovered member of the FGF family with a distinct carboxy-terminal region that is elevated in the serum of patients with oncogenic osteomalacia and humoral hypercalcemia of malignancy. In order to determine whether FGF23 physiology is altered in malignancies not associated with abnormal phosphate metabolism we measured serum FGF23 concentration in 23 patients with small cell lung cancer and 26 patients with squamous cell lung cancer. Serum samples were collected prior to treatment of their disease. FGF23 values were also determined in 80 healthy controls (41 male and 39 female) to determine a normal range. Patients with elevated serum creatinine were excluded. The mean±SEM serum phosphorus was 3.7±0.1 mg/dL and 3.6±0.2 mg/dL in the small cell and squamous cell groups, respectively. Patients with small cell lung cancer had significantly higher serum FGF23 concentrations compared to the healthy controls (p=0.03). (Figure 1) The patients with squamous cell lung cancer tended to have higher FGF23 concentrations but this failed to meet statistical significance (p=0.1). There was no correlation between serum FGF23 concentrations and serum phosphorus, calcium, creatinine, parathyroid hormone, or 1,25 dihydroxyvitamin D_3. There was no correlation between FGF23 and age in the patients with lung cancer or healthy controls. Serum FGF23 concentrations are elevated in patients with small cell lung cancer and this elevation does not cause hypophosphatemia.

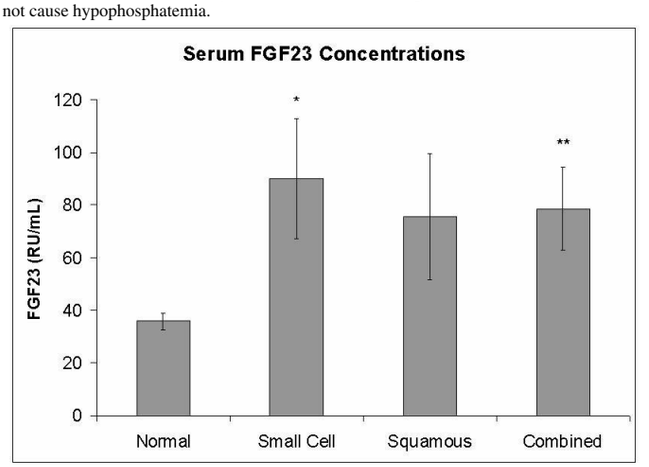

Disclosures: ***P. Tebben****, None.*

SA083

Elevated Serum Fibroblast Growth Factor 23 without Changes in Phosphorus in Women with Advanced Stage Malignant Ovarian Tumors. P. Tebben[1], K. R. Kalli*[2], W. A. Cliby*[3], L. C. Hartmann*[2], R. J. Singh*[4], R. Kumar[5]. [1]Endocrinology, Mayo Clinic, Rochester, MN, USA, [2]Oncology, Mayo Clinic, Rochester, MN, USA, [3]Gynecologic Surgery, Mayo Clinic, Rochester, MN, USA, [4]Laboratory Medicine, Mayo Clinic, Rochester, MN, USA, [5]Nephrology Research, Mayo Clinic, Rochester, MN, USA.

Serum or tissue concentrations of the fibroblast growth factor family of proteins have been studied in relation to human ovarian cancer. Concentrations of fibroblast growth factor 23 (FGF23), a recently discovered member of the FGF family with a distinct carboxy-terminal region, are elevated in some patients with oncogenic osteomalacia and in some patients with humoral hypercalcemia of malignancy. In order to determine whether FGF23 plays a role in other cancers in which fibroblast growth factor physiology is altered such as ovarian cancer, we measured serum FGF23 concentrations in patients with benign and malignant ovarian tumors. Forty patients presenting with an ovarian mass were studied. Twelve patients had stage III or IV ovarian cancer, fourteen had stage I or II ovarian cancer, and fourteen were found to have benign masses. Serum collected preoperatively was analyzed for FGF23, calcium, phosphorus, and creatinine concentrations. FGF23 concentrations were compared between groups and to thirty-nine healthy women. Patients with elevated serum creatinine were excluded from the study. The mean±SEM serum FGF23 concentrations were 31.3±2.7 RU/mL, 30.5±4.2 RU/mL, 16.2±3.7 RU/mL, and 245±115 RU/mL for the healthy, benign, stage I-II, and stage III-IV groups, respectively. Six of twelve women with stage III-IV disease had elevated serum FGF23 concentrations (Figure 1). None of the women with benign masses or stage I-II ovarian cancer had elevated FGF23 concentrations. There was a significant positive correlation between the serum FGF23 concentration and stage of disease ($p<0.02$). FGF23 concentrations also positively correlated with serum phosphorus across all women with ovarian masses ($p<0.001$). There were no differences in serum phosphorus, calcium or creatinine among the three groups of women with ovarian masses. In this series, half of the women with stage III-IV ovarian cancer have elevated serum FGF23 concentrations. These elevations in FGF23 are not associated with hypophosphatemia as is seen in other disorders with abnormal FGF23 physiology.

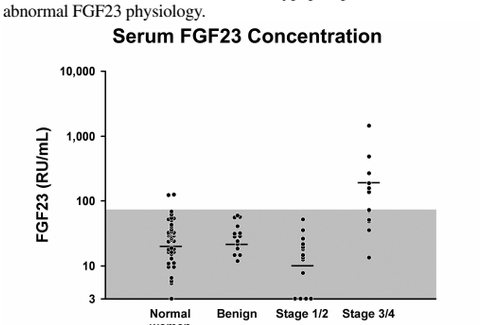

Disclosures: ***P. Tebben****, None.*

SA084

See Friday Plenary number F084

SA085

See Friday Plenary number F085

SA086

Breast Cancer Skeletal Metastases affect Osteoblast Function. R. R. Mercer*[1], D. Welch[2], C. V. Gay[1], A. M. Mastro*[1]. [1]Biochemistry, Pennsylvania State University, University Park, PA, USA, [2]Pathology, University of Alabama-Birmingham, Birmingham, AL, USA.

Breast cancer frequently metastasizes to bone, resulting in osteolytic lesions. These lesions, formed by stimulated osteoclasts, cause an increased susceptibility to fractures, pain, and hypercalcemia. It has been shown that breast cancer cells communicate with osteoblasts and subsequently stimulate osteoclast activity; however, little research has focused on understanding the interaction between the breast cancer cells and osteoblasts. To study how cancer cells affect osteoblasts, MC3T3-E1 cells, an immature osteoblast cell line that differentiates *in vitro*, were cultured with conditioned medium from MDA-MB-231 cells, a bone-metastatic breast cancer cell line. We determined that alkaline phosphatase activity and mineralization, two defining characteristics of a mature osteoblast, were completely blocked. Moreover, mRNA expression for both bone sialoprotein and osteocalcin, two genes upregulated during osteoblast differentiation, were not expressed even after 25 days of culture. Together, these data suggested that when cultured with MDA-MB-231 conditioned medium, MC3T3-E1 cells did not differentiate into mature osteoblasts. We speculated that the conditioned medium factor causing this inhibition in differentiation was transforming growth factor β (TGFβ). To test this, MDA-MB-231 conditioned medium was pretreated with a neutralizing antibody to TGFβ. The neutralized conditioned medium was then added to MC3T3-E1 osteoblasts. mRNA expression of alkaline phosphatase, bone sialoprotein, and osteocalcin were all completely restored in the presence of TGFβ-neutralized conditioned medium. While trying to understand how breast cancer conditioned medium affected osteoblast differentiation, we made another key observation: MDA-MB-231 conditioned medium altered MC3T3-E1 morphology and adhesion. Examination with interference reflection microscopy revealed that MC3T3-E1 osteoblasts had fewer focal adhesion plaques when cultured with MDA-MB-231 conditioned medium. Further scrutiny revealed a substantial alteration in actin stress fibers. Instead of forming normal stress fibers, cells cultured with MDA-MB-231 conditioned medium demonstrated thick cortical filaments, as well as areas of large, punctate staining. We determined that the changes in adhesion were not due to TGFβ; thus, another factor present in MDA-MB-231 conditioned medium must be responsible for these effects. These data suggest that osteoblasts are also affected during skeletal metastasis and should be considered as important targets for drug intervention.

Disclosures: ***R.R. Mercer****, None.*

SA087

See Friday Plenary number F087

SA088

Comparison of the Osteolytic Potential of Two Breast Carcinoma Cell Lines MDA-MB-231 and T47D. M. Gallet*, M. Chasseraud*, I. El Hajj Dib*, M. Brazier*, S. Kamel. Faculté de Pharmacie, Amiens, France.

Malignant breast carcinoma metastasizes to the bone and enhances osteoclast bone resorption. It is now well established that breast tumor cell release growth factors and cytokines which stimulate osteoclastogenesis and thus bone resorption. Moreover, we have recently shown that breast cancer cells could also increase osteoclast survival contributing to osteolysis. Herein, we determined the osteolytic potential of two breast carcinoma cell lines T47D and MDA-MB-231, with respectively low and high metastatic potential. The osteolytic potential was defined as the ability of breast cancer to (i) express gene known to target bone resorption, (ii) to induced osteoclastogenesis, (iii) to increase osteoclast survival and (iiii) to up-regulate hyper-resorptive genes in osteoblastic cell.

First, we established that MDA-MB-231 cells transcriptionnally expressed detectable levels of TGFβ1, IL-6, IL-1α, IL-1β, M-CSF, IGF2, GM-CSF, VEGF compared to T47D cells which expressed only TGFβ1, TNFα, IGF2 and VEGF mRNA. None of the two cell lines expressed RANKL mRNA. Then, we demonstrated that conditioned media (CM) prepared from the two cell lines exerted direct and dose dependent effect on osteoclast like cells generation from the monocytic cells RAW264.7. When soluble RANKL was added in the culture media in presence of CM of both cell lines, the effect on osteoclastogenesis was synergistic. Moreover, MDA-MB-231 and T47D CM greatly up-regulated IL-1α, IL-1β and IL-6 mRNA expression in osteoblastic cells MG63. Finally, we studied the effect of CM on mature osteoclasts which were isolated from 10-day-old New Zealand rabbit long bones. Our results showed that 20% MDA-MB-231 CM stimulate significantly bone resorption while 20% T47D CM had no effect. Because osteoclast have a short life span and could undergo apoptosis after bone resorption, we evaluated the effects of MDA-MB-231 and T47D CM on osteoclast apoptosis. We demonstrated that 20% MDA-MB-231 CM inhibited significantly osteoclast apoptosis (-52%) while 20% T47D CM had much less pronounced effect (-15%).Taken together, these results suggest that both breast cancer cell CM could directly induce osteoclast formation with or without RANKL. Furthermore, CM could also stimulate release of osteoblastic factors which are potent enhancers of osteoclastogenesis. In contrast, only the high metastatic cell line could influence the activity of fully differentiated osteoclasts. In conclusion, osteolytic potential of breast cancer cells may be correlated to their gene expression patterns of hyper-resorbing factors. Such studies could be of great interest to predict the aggressive behaviour of breast carcinomas.

Disclosures: ***M. Gallet****, None.*

SA089

Heterogeneous Bone Response to Systemic Therapy (Bisphosphonates and/or Chemotherapy) in Patients with Metastatic Prostate Cancer. M. P. Roudier[1], L. D. True*[2], C. S. Higano*[3], S. M. Ott[4], R. L. Vessella*[1]. [1]GU Cancer Research Lab, University of Washington, Seattle, WA, USA, [2]Pathology Department, University of Washington, Seattle, WA, USA, [3]Oncology Department, University of Washington, Seattle, WA, USA, [4]Medicine and Endocrinology, University of Washington, Seattle, WA, USA.

Effects of cancer on the bone are the major sources of morbidity in prostate cancer patients. To better understand tumor effects and dynamics, we studied a series of 14 patients who died of prostate cancer and underwent a Rapid Autopsy, which involved systematic biopsy, histologic and histomorphometric analysis of 19 separate bones.

Bone biopsies showed a wide variability of tumor-induced bone volume/tissue volume (BV/TV, range from 3.72% [osteopenic pattern] to 73.6% [osteodense pattern], median = 39.4%). New bone was mostly woven with tumor-induced woven bone volume/tissue volume ranging from 0% [osteolytic pattern] to 70.30% [osteoblastic pattern], median = 20%. Qualitative analysis of bone biopsies revealed in 86% of all metastases the presence of an osteoblastic response as defined by the increased presence of osteoid and woven bone. This could occur with a BV/TV as low as 10% [osteopenic pattern with osteoblastic response].

We addressed the following questions, with these respective findings:

Does bisphosphonate therapy, administered for at least 2 months, enhance an osteoblastic state by reducing osteolytic events? In general, we found that bisphosphonate therapy was associated with osteoblastic bone, although some sites in a patient with predominantly blastic changes still had evidence of osteolysis.

Does cancer in a bone have a predictable influence on the response of bone? In general, tumor was associated mostly with osteoblastic bone changes and rarely with osteolytic bone changes. However, there were exceptions, where tumor either had no apparent effect on bone, or where bone was blastic or lytic without identifiable residual tumor.

Does chemotherapy have a predictable response on tumor? Although recent chemotherapy

"caused" tumor necrosis in some patients, the tumor in other patients who did not receive chemotherapy was extensively necrotic.
Do the peripheral bones become sites of hematopoiesis in patients whose central/axial bones are completely replaced by tumor? Ribs, femoral and humeral heads were bones showing hematopoietic bone marrow.
In summary, the effects of end-stage prostate cancer on bone and the effects of systemic therapy on the cancer and on bone vary both between patients and in different bones of each patient. These findings raise the possibility that tumor cells in a given patient may produce a different balance of osteoblastic and osteolytic factors at different sites.

Disclosures: ***M.P. Roudier****, None.*

SA090

See Friday Plenary number F090

SA091

Runx2 Regulates Transcription of Gelatinases (MMP9) in Metastatic Cancer Cell Lines and Functionally Related to Cell Migration. J. Pratap[1], S. Vashi*[1], J. Zhang*[2], L. Languino*[2], A. J. van Wijnen[1], J. L. Stein*[1], J. B. Lian[1], G. S. Stein[1]. [1]Department of Cell Biology and Cancer Center, University of Massachusetts Medical School, Worcester, MA, USA, [2]Department of Cancer Biology, University of Massachusetts Medical School, Worcester, MA, USA.

The transcription factor runt-related gene 2, RUNX2 (CBFA1/AML3), regulates osteoblast differentiation and bone formation. We identified matrix metalloproteinase-9 (MMP9) as a novel downstream target of Runx2 using total RNA from Runx2 $^{-/-}$ and Runx2 ΔC mutant mouse on cDNA expression array. MMP9 expression, like MMP13 but not MMP2, is nearly depleted in Runx2 deficient mice. In vivo analysis by chromatin immunoprecipitation assay and in vitro by EMSA revealed recruitment of Runx2 to the MMP9 promoter. A Runx2 motif present in the proximal promoter region of the MMP9 gene was functionally characterized by creating point mutants. We show that Runx2 site mediates transactivation of the MMP9 promoter activity in both osteoblastic cells (MC3T3 E1) and non-osseous (HeLa) cells. Upregulation of MMP9 expression has been implicated in invasion and metastasis of breast and prostate tumors, and Runx2 is ectopically expressed in breast (MDA-MB-231) and prostate (PC3) cancer cells that metastasize to bone. We find that over-expression of Runx2 by adenovirus delivery in both primary and bone metastatic cancer cell lines significantly increase endogenous levels of MMP9. Furthermore knockdown of Runx2 by RNA interference results in decreased MMP9 expression. Importantly, we have demonstrated using a cell migration assay that the Runx2 regulated MMP9 levels are functionally related to the invasion properties of the cancer cell. In conclusion, our findings demonstrate the role of Runx2 in transcriptional regulation of MMP9 and that modulation of MMP9 expression by Runx2 influences cell migration. We suggests that Runx2 is a primary initiator for expression of genes that contribute to the metastatic related properties of cancer cells and their activity in the bone environment.

Disclosures: ***J. Pratap****, None.*

SA092

See Friday Plenary number F092

SA093

SELDI-TOF Mass Spectrometry Discriminates PSA-Stable and PSA-Rising Hormone-sensitive Advanced Prostate Cancer. S. Bhattacharyya[1], M. Kohli*[2], E. Siegel*[3], R. Shah*[2], L. J. Suva[1]. [1]Orthopaedic Surgery, UAMS, Little Rock, AR, USA, [2]Pathology, UAMS, Little Rock, AR, USA, [3]Biometry, UAMS, Little Rock, AR, USA.

Prostate cancer is one of the most commonly diagnosed malignancies in the US and is the second leading cause of cancer deaths in males, with bone metastases a common occurance. Protein profiling of clinical specimens to discriminate protein patterns indicative of cancer or non-cancer conditions is a rapidly evolving field. In this study, we collected serum from patients undergoing androgen deprivation therapy (ADT) for hormone-sensitive prostate cancer and determined their respective protein expression fingerprints utilizing surface enhanced laser desorption/ionization time-of-flight mass spectroscopy (SELDI-TOF MS). Group I (n=15), constituted of patients with a stable-PSA response and Group II (n=16) with a rising PSA during ADT. Group II patients had serially rising PSA measurements. Survival data were also collected for all patients. The collected serum samples were fractionated via ion-exchange batch elution into 6 different fractions based on isoelectric point (pI). 1.4 µL aliquots from the most basic fraction (pI≥9) were applied in duplicate to IMAC 30 ProteinChip arrays, and adsorbed material was subjected to SELDI-TOF MS. The resulting spectra were compiled, normalized to total ion current, and mass peaks with mass-to-charge ratios (m/z) ≤20,000 were detected. For each patient, the average intensity per peak was calculated and tested for univariately significant differences between the two groups via the Kruskal-Wallis test. Of 119 peaks having m/z between 2000 and 20,000, seven were statistically significant (P<0.05), with Group II median intensities higher for three peaks and lower for four. An additional eight peaks were marginally significant (0.05=P<0.10), with Group II median intensities higher for five peaks and lower for three. Using SELDI-TOF MS we have identified significantly different serum protein expression profiles in the sequential stages of prostate cancer progression that discriminate between the cancer groups. Additional studies with expanded sample sets are currently ongoing. These data suggest that SELDI profiling may provide critical insights into the rapid diagnosis of prostate cancer progression, and provide a mechanism for evaluating efficacy of treatment regimens. Identification of the specific proteins expressed during relapse may be used to target enhancement of the therapeutic response.

Disclosures: ***S. Bhattacharyya****, None.*

SA094

Expression of 25-hydroxyvitamin D_3-1α-hydroxylase (CYP27B1) Is Increased in Breast Tumors Compared to Paired Normals. K. Townsend*[1], M. Guy*[2], M. J. Campbell*[1], J. L. Mansi*[2], K. W. Colston*[2], M. Hewison[1]. [1]Medical Sciences, The University of Birmingham, Birmingham, United Kingdom, [2]St George's Hospital Medical School, London, United Kingdom.

Recent studies have highlighted a role for vitamin D in the prevention and treatment of breast cancer. The active form of vitamin D, 1,25-dihydroxyvitamin D3 ($1,25(OH)_2D_3$), is a potent antiproliferative agent and the vitamin D receptor (VDR) is well expressed in breast tissue. We have investigated whether VDR signaling in breast tumors is due to systemic (renal) $1,25(OH)_2D_3$ or whether there is autocrine/paracrine synthesis of the hormone. Initial analyses using normal breast cells and a panel of breast cancer cell lines showed expression of the vitamin D-activating cytochrome P450 1α-hydroxylase (CYP27B1), highlighting a potential autocrine mechanism by which environmental/dietary vitamin D status can affect breast tumors. Expression of CYP27B1 and other components of vitamin D signalling such as VDR and the inactivating enzyme 24-hydroxylase (CYP24) was then assessed using a panel of 41 matched tumor/normal breast biopsies. Quantitative RT-PCR analyses showed that CYP27B1 mRNA expression was 27-fold ($p<0.001$) higher in tumors compared to controls, which was confirmed by immunohistochemical analyses. Increased expression of the enzyme was accompanied by upregulation of VDR (7-fold, $p<0.001$) and CYP24 (4-fold, $p<0.02$, n=34). These data indicate that breast tumors are able to synthesize and actively respond to $1,25(OH)_2D_3$. However, the resulting sensitive induction of CYP24 may abrogate the anticancer effects of $1,25(OH)_2D_3$ via the generation of inactive vitamin D metabolites. This was demonstrated by in vitro manipulation of CYP24 using antisense cDNA which increased the sensitivity of MDA-MB-231 cells to the antiproliferative effects of $1,25(OH)_2D_3$. Paradoxically, breast cancer cell lines showed lower levels of CYP27B1 and VDR than non-transformed cells highlighting the divergence in vitamin D metabolism and signaling between cell lines and tumor tissue. Further studies suggest that this may be due to immunological responses in the tumors as expression CYP27B1 and VDR correlated with mRNA levels for toll-like receptor 4, an endotoxin receptor and inflammatory marker. These data provide a potential mechanism by which dietary/environmental vitamin D status can influence breast tissue responses via local conversion to active $1,25(OH)_2D_3$ and enhanced VDR expression. The mechanisms involved in upregulation of CYP27B1 and VDR are currently under investigation and appear to be linked to innate immune responses within the breast tumors.

Disclosures: ***M. Hewison****, None.*

SA095

See Friday Plenary number F095

SA096

Radiation Therapy Inhibits Tumor-Mediated Bone Destruction and Preserves Bone Mass in a Pre-Clinical Model of Breast Cancer Metastasis to Bone. M. J. Allen, S. A. Arrington*, B. S. Margulies*, J. E. Schoonmaker*, K. A. Mann*, T. A. Damron*. Orthopedic Surgery, SUNY Upstate Medical University, Syracuse, NY, USA.

Pathological fracture is a devastating complication of benign and malignant tumors of the skeleton. It is generally accepted that radiation therapy, which is widely used to palliate bone pain in patients with skeletal metastases, inhibits bone formation and fracture repair. However, in many patients with bone metastases from breast cancer radiation therapy leads to partial or even complete re-mineralization of the lesion. The specific aims of this study were to determine whether (a) radiation is effective in inhibiting tumor-mediated bone loss and (b) whether normal bone and osteolytic bone display different responses to radiation. In a series of IACUC-approved experiments, human breast cancer cells were injected into the right distal femur of female nude mice (n=54); vehicle (medium only) was injected into the left femur as a sham control. Radiation therapy (0 Gy or single dose 20 Gy) was given 3 weeks post-surgery, at which time there is histological evidence of early tumor growth. Radiography and bone density analysis (DEXA) were performed at the start of the study and 3, 6 and 9 weeks later. Groups of animals were euthanized at each time point and their femora were mechanically tested using a novel test method that applies torsional forces through the intact knee. In untreated limbs (0 Gy) tumor was found to cause a statistically significant decrease in bone strength ($p<0.001$ for peak torque, stiffness and energy to failure). Radiation provided moderate but statistically significant protection from the adverse effects of tumor ($p<0.001$ for all parameters) such that 12 of 14 mice (81%) that were irradiated completed the study to 9 weeks as planned compared with only 50% of the untreated mice. Interestingly, radiation had no significant effect on either BMD or mechanical indices in normal bone. These data indicate that radiation *per* se does not stimulate an increase in bone mass in the mouse. We did not observe clinically significant re-mineralization of lesions in this model, probably because irradiation was performed prior to the development of advanced lytic lesions and the follow-up in these animals was relatively short (6 weeks post-radiation). However, our data indicate that radiation therapy is not effective in completely restoring bone mass in bones that have been damaged by tumor. This is consistent with the clinical observation that up to 23% of metastatic lesions may develop pathological fractures after irradiation. New therapies are now needed to try to enhance bone healing after irradiation. The mouse model appears to be a clinically relevant model for evaluating these therapies.

Disclosures: ***M.J. Allen****, None.*

SA097

See Friday Plenary number F097

SA098

Effects of Osteolytic Bone Metastases on Bone Mass and Bone Strength in the Mouse: Validation of a Pre-Clinical Model of Breast Cancer Metastasis to Bone. M. J. Allen, S. A. Arrington*, B. S. Margulies, J. E. Schoonmaker*, K. A. Mann*, T. A. Damron*. Orthopedic Surgery, SUNY Upstate Medical University, Syracuse, NY, USA.

Skeletal metastases are a common cause of morbidity in patients with malignant disease. The primary goals of therapy for symptomatic osteolytic bone metastases are palliation of bone pain and preservation of skeletal integrity. Although radiation therapy is highly effective in alleviating bone pain, its effects on bone mass and bone strength are less well understood. The specific aim of this study was to determine the temporal pattern of bone loss in a mouse model of tumor osteolysis. Human breast cancer cells were injected into the right distal femur of female nude mice (n=53); vehicle (culture medium) was injected into the left femur as a sham control. All of the experimental procedures in this study were reviewed and approved by the local IACUC. Radiography and bone density analysis (DEXA) were performed at the start of the study and at 3, 6 and 9 weeks post-tumor inoculation. Groups of animals were euthanized at each time point and their left and right femora were mechanically tested using a novel test method that applies torsional forces through the intact knee joint. As expected, DEXA analysis indicated time-dependent increases in BMD in the control (left) femur. Injection of tumor into the femur negated normal bone accrual such that there was no net increase in BMD over time. Analysis of the mechanical test data revealed that there was no significant time-dependent increase in peak torque, stiffness or energy to failure in control femora. However, femora that had been injected with tumor demonstrated a significant time-dependent pattern of decreasing mechanical integrity ($p<0.001$ for all three mechanical test parameters). The clinical significance of this loss of skeletal integrity was underscored by the fact that 10 of 20 mice (50%) that had been injected with tumor developed lameness and/or pathological fractures that necessitated their removal from the study prior to the original scheduled time point of 9 weeks. Taken as a whole, these results confirm the clinical relevance of the mouse model of tumor osteolysis and the utility of DEXA and torsional testing as sensitive indicators of tumor-mediated bone loss. Ongoing studies in this laboratory are now using this model to develop improved therapies for isolated bone metastases from breast and other solid cancers.

Disclosures: ***S.A. Arrington****, None.*

SA099

See Friday Plenary number F099

SA100

High Bone Mineral Density Is a Risk Factor For Prostate Cancer in Older Men of African Descent. C. H. Bunker[1], J. M. Zmuda[2], A. L. Patrick*[3], V. W. Wheeler*[3], J. A. Cauley[2]. [1]Epidemiology, University of Pittsburgh, Pittsburgh, PA, USA, [2]University of Pittsburgh, Pittsburgh, PA, USA, [3]Tobago Prostate Survey, Scarborough, Trinidad and Tobago.

Endogenous steroid hormones and growth factors have been linked to prostate cancer but results are not consistent. Bone mass, as a surrogate indicator of lifetime hormone and growth factor exposure, has been associated with prostate cancer risk in Caucasian men but nothing is known about bone mass and prostate cancer risk in men of African descent, a group at high risk of prostate cancer. To test this hypothesis, cases were ascertained in a population-based screening for prostate cancer among Afro-Caribbean men, aged 45-79, on the island of Tobago. Serum prostate specific antigen (PSA) $\geq$ 4 ng/ml, or abnormal digital rectal exam, were the criteria for referral for ultrasound guided sextant biopsy. Hip bone mineral density (BMD) was measured by dual X-ray absorptiometry (Hologic QDR 4500W). Men with body mass index (BMI, kg/m^2) more than 3 standard deviations above the mean (>40 kg/m^2) or prior androgen ablation therapy were excluded. To reduce the likelihood of including men with skeletal metastases, which may modulate BMD, men with PSA >20 ng/ml or highly undifferentiated tumors (Gleason score 8, 9, 10) were also excluded. Analysis of variance was used to estimate age and BMI adjusted BMD between cases and non-cases. Logistic regression, adjusted for age and BMI within each age group, was used to estimate prostate cancer risk in younger (45-59 years) and in older (60-79 years) men categorized by quartile of BMD based on the BMD distribution in each age group.

Over all age groups, adjusted mean hip BMD was higher in 222 cases (1.157g/cm^2, 95%CI 1.138-1.175) than in 1503 non-cases (1.134 g/cm^2 , 95%CI 1.127-1.141) (p=0.02). However, there was an interaction (p=0.055) between BMD and age (Figure). In men aged 60-79, prostate cancer risk was two-fold higher (OR, 2.12; 95%CI: 1.21 - 3.71) in the highest BMD quartile compared to the lowest quartile**.** There was no association in younger men. (Figure).

We conclude that high bone density is a risk factor for prostate cancer among older Afro-Caribbean men, supporting an etiological role for hormone and growth factors. However, other etiologies may be stronger determinants of prostate cancer risk among younger men of African descent.

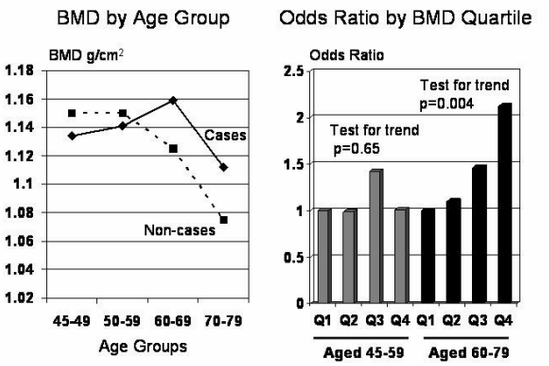

Disclosures: ***C.H. Bunker****, None.*

SA101

Reference Data for BMD in the Calcaneus for Healthy Children 4-years of Age by Dual Energy X-ray Absorptiometry and Laser (DXL). A. Söderpalm*[1], R. Kullenberg[2], K. Albertsson-Wikland*[3], D. Swolin-Eide[3]. [1]Dept of Orthopaedics, Sahlgren University Hospital, Inst. for Surgical Sciences, Göteborg, Sweden, [2]Dept of Radiology, Inst. for Radiation Physics, Halmstad, Sweden, [3]Dept of Pediatrics the Queen Silvia Children´s Hospital, Inst. for the Health of Women and Children, Göteborg, Sweden.

There is a growing demand for studying and evaluating pediatric bone status. A debated issue in bone research is the optimal techniques to determine bone mass in growing children. Dual X-ray and Laser (DXL) Calscan measures areal bone mineral density (BMD) by using dual X-ray absorptiometry in combination with laser measurement of the total heel thickness. This technology reduces the uncertainty related to variable composition of soft tissue in adults. The DXL Calscan is portable, easy to use, has a short measurement time and gives a low absorbed dose (<0.12μSv).

The aim of this cross-sectional study was to investigate: if the device was tolerated by young children, if BMD could be measured with good precision, if BMD was related to height, weight and body mass index (BMI) and further to create reference data in healthy 4y old children.

The DXL Calscan was modified for children with a lower absorbed dose and adapted software. 110 strictly healthy Swedish children (49% boys, 51% girls, mean age 4.3y) were included. The left foot was scanned, the actual height, weight and foot length was measured.

The intra-individual CV measured by 2 repeated measurements on 26 subjects was 6.53% for BMD and 8.12 % for bone mineral content (BMC). The mean BMD in the subjects was 0.22 ± 0.003 g/cm^2 (0.14-0.34) and BMC 0.16 ± 0.003 g (0.11-0.25). No significant difference was found in BMD between girls and boys. BMD was significantly correlated to weight ($p=0.007$, $r=0.26$), weight SDS ($p=0.015$, $r=0.24$) and to height ($p=0.03$, $r=0.21$). BMD was not correlated to BMI or foot length.

In conclusion, the measurements were easily performed and well tolerated by these young children. This is the first study to present normative data for BMD and BMC in the calcaneus in 4y old children by DXL. Further studies are required to evaluate this method. The study was approved by the local Ethical Committee of the Medical Faculty Sahlgren Academy at Göteborg University.

Disclosures: ***A. Söderpalm****, None.*

SA102

See Friday Plenary number F102

SA103

Bone Density in Healthy Spanish Children and Adolescents. L. Del Rio[1], S. Di Gregorio*[1], L. Ibañez*[2], S. Artigas*[2]. [1]Densitometría Ósea, CETIR Centre Médic, Barcelona, Spain, [2]Endocrinología, Hospital de San Juan de Dios, Barcelona, Spain.

Dual energy x-ray absorptiometry (DXA) is the method of choice to measure bone mineral density (BMD) in children, because of low radiation dose, and excellent precision and accuracy. BMD increases during childhood and reaches a peak in early adulthood before declining gradually in later life. Acquisition of adequate bone mass during childhood may influence the risk of fracture in adulthood. Reference data allow comparison of an individual's BMD with the BMD of healthy peers.

We measured BMD using DXA (Lunar Prodigy and DPX-IQ, GE Healthcare) at the spine in 576 children (367 females and 209 males) and at the total body in 537 children (404 females and 133 males) from urban Barcelona. All children were defined as normal based on health history and questionnaire.

Total body BMD showed remarkable similarity between males and females, with BMD nearly congruent throughout most of the age range. Total body BMD was about 5% higher in females than males during the female adolescent growth spurt (ages 11-13 years). Female spine BMD was about 10% higher than males from ages 10 to 16 years, with male BMD catching up at about 17 years of age.

We conclude that total body BMD from age of 4 to 19 years was similar in males and

females, except for differences related to the earlier timing of the female adolescent growth spurt. Spine BMD was generally higher in females during childhood and early teen years, with male BMD approaching female values in the middle to late teen years. These BMD differences demonstrate the need for sepaate gender-based reference data.

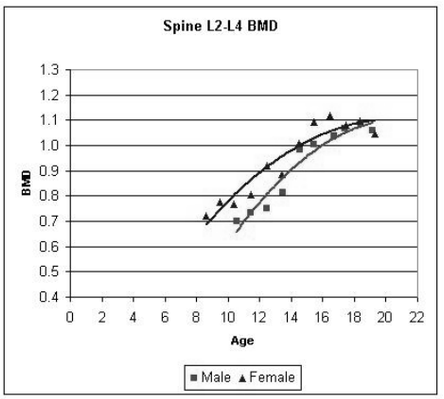

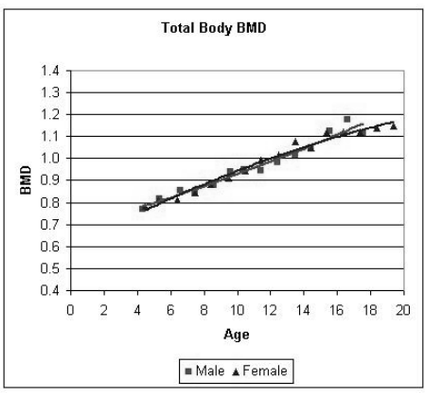

Disclosures: ***L. Del Rio****, None.*

SA104

See Friday Plenary number F104

SA105

Calcaneal BMD with DXL Technique Discriminates Between Postmenopausal Females With and Without a History of Fracture - the CALCOS Study (Calcaneal Osteoporosis Study). T. B. Brismar*[1], C. Nyberg*[2], H. Salminen*[3]. [1]Centre of Surgical Sciences, Division of Radiology, Karolinska Institutet, Stockholm, Sweden, [2]Läkarhuset Hötorget, Stockholm, Sweden, [3]Centre for Family Medicine, Karolinska Instutet, Stockholm, Sweden.

A recently developed technique for assessing calcaneal BMD called dual X-ray and laser (DXL), combines two X-ray energies with a laser measurement of heel thickness. It is theoretically appealing as it allows separation of bone mineral, lean tissue and adipose tissue (a three-component model) instead of using the traditional two-component model (bone mineral and soft tissue). The advantage of this technique does, however, require further evaluation.

We have evaluated whether calcaneal BMD, measured using DXL (Demetech AB, Stockholm, Sweden) can discriminate between females with and without osteoporosis-related fracture. 30 health-care units and outpatient clinics in Sweden participated and 1677 consecutive females over the age of 55 were studied. A standardised questionnaire was used to obtain previous fractures and risk factors. In total 894 fractures were reported by 753 individuals. The mean calcaneal BMD of those with a history of fracture was 313 mg/cm^2 (SD 83), compared with 365 mg/cm^2 (SD 79) in those without a fracture. The best discrimination was observed for hip fractures (area under curve (AUC) 0.72, sensitivity 0.73, specificity 0.58). After correction for age group and other risk factors, the following risk factors were associated with lower BMD: previous fracture (-35 mg/cm^2), significant height decrease (-26 mg/cm^2), low body weight (-2.3 mg/cm^2 and kg), smoking (-12 mg/cm^2) and early menopause (-12 mg/cm^2). Steroid use, gastro-intestinal disease/hormonal disease, weight loss or heredity did not significantly lead to lower BMD. Decrease in height was associated with a 0.42 SD decrease in T-score, and we therefore suggest that this risk factor should be regarded as a strong indication for BMD measurements.

We conclude that calcaneal BMD obtained by the DXL technique has potential to predict osteoporosis-related fractures.

Disclosures: ***T.B. Brismar****, None.*

SA106

See Friday Plenary number F106

SA107

Radiographic Absorptiometry (RA) Assessment of Bone Mineral Density Using a CR-based System Compared to the Film-based System. M. Greenwald[1], L. Al-Dayeh*[2], X. Bi*[2], S. L. Silverman[3]. [1]Desert Medical Advances, Palm Desert, CA, USA, [2]CompuMed, Los Angeles, CA, USA, [3]UCLA, Los Angeles, CA, USA.

Phalangeal BMD assessment using Radiographic Absorptiometry (RA) by means of scanning standard hand radiographs has been in use for years. It is a reliable and inexpensive method for assessing peripheral BMD with high predictability of future fracture risk of the hip and spine. With the recent development and availability of digital radiography platforms, i.e., Computed Radiography (CR), Direct Radiography (DR) and Picture Archiving and Communications Systems (PACS), there exists a need for a reliable Digital Imaging and Communications in Medicine (DICOM) compliant BMD method, such as a DICOM-based RA p study reports the comparison of BMD results between a DICOM-based RA system that utilizes a CR device (ACLxy, Orex, Yokneam, Israel) and a standard film-based RA system.

The 45 Caucasian and Asian volunteers between the ages of 50 to 81 participated in this study. Two consecutive x-rays of the non-dominant hand were acquired for each volunteer, one using a standard film and another using a CR cassette. The standard films were scanned using a flatbed scanner at the resolution of 254 dpi matching the CR resolution. The CR cassette was read at its native resolution of 254 dpi. The images of both x-ray platforms were analyzed for RA results using the OsteoGram® (CompuMed, Inc., Los Angeles, CA) software which performs automated RA analysis.

Regression analysis of the results showed a significant ($p<0.001$) Pearson correlation coefficient of 0.98, between a DICOM-based RA system and a film-based RA system.

We conclude that BMD may be measured using RA on a digital x-ray platform. The availability of DICOM-compliant RA may help improve access to BMD testing in settings where central DXA is not available.

Disclosures: ***L. Al-Dayeh****, CompuMed 3.*

SA108

Bone Mineral Density, Vertebral Fracture and Related Factors in Patients with Ankylosing Spondylitis. B. Kuran*, A. Caglilyan*, N. Kotevoglu*, S. Ergan*. Department of Physical Medicine and Rehabilitation, Sisli Etfal Research and Teaching Hospital, Istanbul, Turkey.

PURPOSE : To determine bone mineral density, factors related with bone density and osteoporosis and observe the relation of osteoporosis with depression, fatigue, quality of life and fracture in patients with ankylosing spondylitis (AS).

MATERIAL AND METHOD : 38 men, diagnosed as AS according to Modified New York criteria (Group1) and 30 healthy controls (Group2) were included in this prospective, controlled study.Bone mineral density of proximal femur,tibia and lateral lumbar vertebrae were evaluated in with DEXA. Calcaneal bone assessment was done with quantitative calceneal ultrasound.Results were interpreted according to WHO Study Group recommendations. Dorsal radiographs centered at T7 and lumbar radiographs centered over L3 were obtained for vertebral morphometric measurements. BASFI,BASMI,BASDAI and multidimensional assesment fatigue scale (MAF), Beck Depression Scale (BDS) and SF-36 for quality of life were used to evaluate the impact of AS. Erytrocyte sedimentation rate (ESR), CRP, calcium, phospor,1,25 dihydroxy Vitamin D, parathyroid hormone,follicule stimulating hormone (FSH), Luteinizing hormone (LH) and testosterone levels were analyzed.

RESULTS : Mean age of the patients was 36,8 years and mean disease duration was 7.6 years.L3 t values were significantly lower than controls($p<0,05$).Femur neck and total BMD values (g/cm2,t) were significantly lower in Group I($p<0,01$). In both of the groups tibia measurements were similar ($p>0,05$). Lumbar BMD values were osteopenic in 44,7% and at osteoporotic in 31,6% of the cases. Among the controls, 46,7% of them had osteopenia. Femoral and tibial BMD had good correlation ($r =0.648$; $p<0,01$) with each other. Calceneal QUS was moderately correlated ($r =0.427$; $p<0,05$) with total femoral values. Osteoporosis was strongly associated with CRP,BASMI, duration of disease, age and ESR . 21% of the patients had vertebral fracture but the presence of vertebral fractures was not correlated with BMD. Physical role difficulty subgroup of SF-36 was correlated with BMD of femoral neck ($p<0,05$). There wasn't any correlation between BMD, FSH,LH,testosterone and BDS.

Osteoporosis and vertebral fracture are frequent complications of AS. Calcaneal QUS and tibial BMD values also inform us about femoral bone mass. Vertebral fracture can develope independently from BMD. CRP levels and limitation in movement play significant roles in the development of osteoporosis in AS patients.

Disclosures: ***B. Kuran****, None.*

SA109

Ethnic Differences in Bending Stiffness of the Ulna and Tibia. S. B. Arnaud[1], M. T. C. Liang*[2], S. Bassin*[2], W. Braun*[2], D. Dutto*[2], K. Plesums*[2], H. T. Huynh*[2], D. Cooper*[3], N. Wong*[4]. [1]Life Sciences Division, NASA Ames Research Center, Moffett Field, CA, USA, [2]Kinesiology and Health Promotion, California State Polytechnic University, Pomona, CA, USA, [3]Dept. Pediatrics and GCRC, Univ. of California, Irvine, CA, USA, [4]Dept of Cardiology, University of California, Irvine, CA, USA.

There is considerable information about the variations in bone mass associated with different ethnicity, but little on the structural differences in bones from different ethnic groups. We had the opportunity to compare a mechanical property of bone in young college women of Caucasian, Hispanic and Asian descent who gave informed consent to participate in an exercise study. The subjects were sedentary, in good health, eumenorrheic, non-smokers and had body mass indices (BMI) less than 30. Measurements acquired were body weight, kg, and height, cm, calcaneal and wrist bone density, g/cm^2 (PIXI, Lunar GE) and bending stiffness (EI, Nm^2) in the ulna and tibia. EI was determined non-invasively with an instrument called the Mechanical Response Tissue Analyzer (MRTA) that delivers a vibratory stimulus to the center of the ulna or tibia and analyzes the response curve based on the equation EI = k_b L^3/48 where k_b is lateral bending stiffness, L is the length of the bone, E is Young's modulus of elasticity and I, the bending moment of inertia. The error of the test (CV) based on measurements of an aluminum rod with a known EI was 4.8%, of calcaneal BMD, 0.54%, and of wrist bone density, 3.45%.

Averages from each ethnic group

Group	n...BW	Ht.. BMI	WBMD.... HBMD	U EI... T EI
Cauc	19... 63	162.. 24	0.457.... 0.524	31.4...168
Hisp	25... 59	157.. 24	0.472.... 0.538	26.8 ...151
Asn	22... 53*	157.. 21*	0.466.... 0.519	23.7*..123*

Differences (*) were from p<0.001 to p<0.02, ANOVA and Student-Newman-Keuls. For all 3 groups combined, ulnar EI was related to height (r = 0.274, p<0.03) and tibial EI, to HBMD (r = 0.245, p<0.045). Wrist and heel bone densities were similar in all groups. BW, BMI and EI in both the ulna and tibia were lower in Asians than in either Hispanics or Caucasians. Ethnic differences in the tibias and ulnas of young Asian women are revealed as differences in structure, not bone density of the heel or wrist.

Disclosures: ***S.B. Arnaud****, None.*

SA110

Assessment of Trabecular Bone Microarchitecture from Conventional X-ray Micro Computed Tomography: Quantification of Effects of Thresholding and Decrease Signal to Noise Ratio. C. Chappard, A. Basillais, B. Brunet-Imbault*, N. Bonnet*, C. Benhamou. Atosep, Université d'Orleans, Orleans, France.

Desktop microcomputed tomography (micro-CT) is available to acquire trabecular bone 3D images. The optimal protocole to analyse bone micro-architecture is not well known. Fourteen subchondral bone samples from femoral heads were obtained in 5 osteoarthritis and 4 osteoporosis patients. All samples were defatted. The micro-CT images (Skyscan® 1072) were acquired at 80keV (voxel size=10.77µm). Two different angular rotation steps were tested 0.23°, 0.9° corresponding respectively to 800, 200 radiographic projections. The increase of rotation step leads to a decrease in signal to noise ratio (S/N) of the image. In all sections of specimens, bimodal histograms were obtained the first peak (low gray levels) corresponding to the background and the second one to bone. In all cases, the two peaks were well identified at 0.23° rotation step and moved very close together at 0.9° rotation step. In the last case, differences between the two peaks were so reduced that it became difficult to use a unique threshold for the whole data set. We tested at 0.9° rotation step to binarize images, a global threshold for the whole data corresponding to the average gray level value between the two peaks and an adapted threshold for each sample located at the minimum between both peaks. Usual morphological bone parameters are measured: Bone Volume/Tissue Volume (BV/TV), Trabecular Number (TbN) derived from the 3D Mean Intercept Length method and Trabecular Thickness (TbTh) from the Hildebrand method.

For each parameter, two types of measurement errors were evaluated by the average absolute percentage deviation: threshold effect (at 0.9° with an adapted or global threshold) and/or S/N effect (by comparison between 0.23° and 0.9° rotation step). The error due to a slice matching variation (visual matching±10 slices) was assessed by the Root Mean Square Coef. of Variation (RMSCV%).

	RMSCV%	*<Δboneparameter$_i$>*		
	slice matching	*threshold*	*decrease S/N*	*threshold + decrease S/N*
BV/TV (%)	1.4%	3.0%	4.7%	5.7%
Tb.Th (µm)	1.0%	3.2%	9.2%	11.5%
Tb.N (1/mm)	1.1%	0.7%	10.5%	11.0%

The error of measurements due to a decrease in S/N is more critical than threshold and slice matching effects for all parameters in particular for TbN likely due to artifactual disconnections of few trabeculae at 0.9° rotation step. Errors of measurements are increased with combination of two effects. Fast scan set at 0.9° rotation steps is not recommendable for trabecular bone assessment.

Disclosures: ***C. Chappard****, None.*

SA111

Transiliac Bone Biopsy in Osteoporosis: Indications, Consequences and Complications. P. H. Kann*[1], G. Delling*[2], S. Meyer*[1]. [1]Endocrinology & Diabetology, Philipps University Hospital, Marburg, Germany, [2]Osteopathology, Eppendorf University Hospital, Hamburg, Germany.

Bone biopsy is a diagnostic procedure restricted to untypical, unclear and complicated cases in evidence based guidelines on diagnosis and treatment of osteoporosis. Its relevance has been a topic of recent controverse discussion. This study was performed to evaluate its role and relevance in routine use. A total of 99 horizontal transiliac bone biopsies performed over a time period of 14 years because of an osteological indication in one single centre were analysed, which reflects that bone biopsy followed about 0.003% of patients' consultations. Indications for bone biopsy were osteoporotic males (n = 63) and premenopausal osteoporotic females (n = 18) without endocrine abnormality and normal immunofixation, suspected systemic/malignant disease such as mastocytosis, osteogenesis imperfecta, non secreting plasmocytoma, metastatic infiltration (n = 16) and decreasing bone mineral density under anti-osteoporotic treatment (n = 2). Most frequent diagnoses besides osteoporosis were normal histology, borderline finding towards mild osteoporosis, and osteoporomalacia with relevant osteoidosis. In some cases, pathological findings in bone marrow were detected. In most cases (82/99), bone biopsy led to consequences in medical treatment. Following histopathological diagnosis, sixteen patients did not receive any anti-osteoporotic treatment. In six patients, further diagnostic procedures were initiated because of bone histology. Bone biopsy was well tolerated, complications were rare and mild. In conclusion, despite all progress of non invasive diagnostic procedures in metabolic bone diseases such as osteoporosis, there remains a small but significant subset of patients who may benefit from inclusion of bone biopsy into the diagnostic procedure.

Disclosures: ***P.H. Kann****, None.*

SA112

See Friday Plenary number F112

SA113

Characterization of Trabecular Micro-Architecture Improvement under Teriparatide by a Fractal Analysis of Texture on Calcaneus Radiographs. C. Benhamou[1], C. Chappard[1], C. Gadois*[1], G. Lemineur*[2], E. Lespessailles[1], M. De Vernejoul[3], P. Fardellone[4], P. Delmas[5], G. Weryha[6], R. Harba*[2]. [1]Atosep, Université d'Orleans, Orleans, France, [2]Lesi, Université d'Orleans, Orleans, France, [3]Rhumatologie, Hôpital Lariboisière, Paris, France, [4]Rhumatologie, Hopital, Amiens, France, [5]Rhumatologie, Hopital, Lyon, France, [6]Rhumatologie, Hopital, Nancy, France.

Teriparatide (parathormone 1-34) is a bone forming drug able to reduce fractures and to increase bone mass. It has been shown to improve trabecular micro-architecture on histomorphometry and micro-computerized tomography. We have developed and validated a fractal analysis of texture on radiographs which is able to distinguish osteoporosis (OP) fracture from control groups. This analysis was performed on a region of interest of the calcaneus after digitizing the radiographs, using a previously described algorithm based on the Maximum Likelihood Estimator of the fractional Brownian Motion. This analysis is correlated with 3D micro-architecture. It has not yet shown in a prospective study its ability to characterize effects of drugs on micro-architecture. We have compared 18 OP women treated by teriparatide plus calcium and vitamin D to 22 OP women under other therapies (7 hormone replacement therapy, 8 calcium vitamin D, 6 bisphosphonates). Patients were post-menopausal women 65.6±5.0 years old for the PTH group and 65.2±7.5 for the control group. They were included on the basis of a T score of BMD at the spine or femoral neck <-2.5 SD. There were no vertebral fracture in the PTH group and 2/22 in the control group. This multicenter study involved 4 centers in France for the PTH therapy (subset of an ongoing open label PTH study, Eli Lilly) and one center for the control group. A calcaneus radiograph was performed at following a very standardized procedure at day 0 (before starting the treatment) then at 1 year. The results were expressed by the Hmean value for each image (H=2-fractal dimension). The average Hmean±SD was measured at 0.790±0.06 at day 0 and 0.826±0.03 at 1 year in the PTH group (p=0.02) versus 0.841±0.02 and 0.839±0.02 in the control group (p=0.38). When the evolution was expressed in % of the initial value of Hmean, it was measured at +5.1 % (PTH) p=0.02 versus -0.3% (controls) p=0.3.

Osteoporosis and aging are characterized by a lower Hmean value. The significant Hmean increase observed under PTH indicates an improvement in the texture analysis corresponding to the micro-architecture improvement described with the other techniques. These data suggest that the fractal analysis of texture on radiographs could be a convenient tool to characterize not only OP changes but also changes induced by bone forming agents such as teriparatide.

Disclosures: ***C. Benhamou****, None.*

SA114

Structure Analysis of High Resolution Magnetic Resonance Images of the Calcaneus using the Anisotropic 3D Scaling Vector Method. D. Mueller*[1], R. Monetti*[2], S. Majumdar[3], H. Boehm*[1], C. Raeth*[2], E. J. Rummeny*[1], T. M. Link[3]. [1]Department of Radiology, Technische Universitaet Muenchen, Muenchen, Germany, [2]Max Planck Institute for Extraterrestrial Physics, Garching, Germany, [3]Department of Radiology, UCSF, San Francisco, CA, USA.

The purpose of this study was to use the scaling vector method (SVM) to analyze the trabecular bone structure of high resolution magnetic resonance (HR-MR) images of the calcaneus. The 3D SVM is a non-linear texture measure which takes into account the anisotropic nature of the trabeculae. This new structure analysis technique was compared with BMD in its diagnostic performance to differentiate postmenopausal patients with and without osteoporotic spine fractures.

HR-MR imaging of the calcaneus was performed at 1.5 T in 75 women (35 postmenopausal women with osteoporotic spine fractures and 30 postmenopausal controls) using a receive-only phased-array coil. A three-dimensional gradient-echo sequence was applied with an axial orientation, a slice thickness of 0.5 mm, a TE of 5.7 ms, a TR of 28.1 ms, a flip angle of 30° and in plane spatial resolution of 195x195 µm². After normalization of the images and selection of the region of interest (ROI) structure analysis was performed using algorithms based on the new anisotropic SVM, which is respecting the orientation of the trabeculae of the analyzed bone. In addition BMD measurements of the calcaneus and proximal femur using dual energy X-ray absorptiometry (DXA) were obtained in all patients.

Significant differences between both patient groups were obtained using structure analysis and BMD ($p<0.01$). Receiver operating characteristics (ROC) analyses were used to determine the diagnostic performance in differentiating both groups. In comparison with BMD of the calcaneus (AUC = 0.73) and BMD of the proximal femur (AUC = 0.83) the best results were found for the 3D scaling vector method (AUC = 0.88). By combining structure analysis and BMD a moderate improvement for the diagnostic performance could be achieved (AUC = 0.90), which was, however, not significant ($p>0.01$).

The results of this study suggest that the new anisotropic algorithm based on a local 3D SVM which is respecting the orientation of the trabeculae may improve the diagnostic performance in differentiating postmenopausal women with and without osteoporotic spine fractures.

Disclosures: ***D. Mueller****, None.*

SA115

Age-related Changes in Bone Mineral Density and Trabecular Bone Structure Evaluated by DEXA Imaging. L. Pothuaud*[1], V. Boudouscq*[2], N. Barthe*[3], B. Basse-Cathalinat*[3], J. Leroux[4], P. Kotzki*[2]. [1]A2IOS, Bordeaux, France, [2]CHU - Médecine Nucléaire, Nîmes, France, [3]INSERM U577, Bordeaux, France, [4]CHU - Rhumatologie, Nîmes, France.

The in vivo evaluation of Trabecular Bone Structure (TBS) is a major challenge in bone study. The modern definition of osteoporosis involves low Bone Mineral Density (BMD) and TBS alterations, but TBS cannot be measured in routine at the present time. The aim of the present study is to exploit a new process of analysis of DEXA images for the evaluation of TBS, and to explore the BMD and TBS age-related changes in normal women.

Seventy-eigth normal women from 22 to 83 years were examined on a LEXXOS system (DMS, France), and BMD was evaluated in the standardized neck area of the femoral site. The gray level DEXA images were exported onto a workstation for the evaluation of TBS in the same area. Mean values and standard deviations were evaluated in each ten-year interval. In the two-dimensional (BTS, BMD) representation, mean age-related changes were linked as a continuous variation of both BMD and BTS parameters (see figure). In order to check the complementarity of these two parameters, we have consituted several subgroups with paired BMD values and different ages. The first pairing was constituted of two subgroups of 11 subjects each with mean age of 29.6+/-4.1 years (G_1) and 50.5+/-6.9 years (G_2) and matched neck-BMD: 0.857+/-0.128 g/cm^2 (G_1) versus 0.856+/-0.129 g/cm^2 (G_2). The second pairing was constituted of two subgroups of 7 subjects each with mean age of 33.7+/-3.8 years (G_3) and 65.7+/-4.7 years (G_4) and matched neck-BMD: 0.729+/-0.058 g/cm^2 (G_3) versus 0.726+/-0.058 g/cm^2 (G_4). Significant differences of BTS parameter were obtained in each pairing: 0.501+/-0.101 (G_1) versus 0.632+/-0.089 (G_2), p=0.004 (t-test); 0.466+/-0.079 (G_3) versus 0.631+/-0.080 (G_4), p=0.002 (t-test). At present only BMD is used to evaluate the quality of bone. The prevention strategy then consists into comparing the BMD value of a subject to two "age-matched " and "young normal" standards. Nevertheless, it is well recognized that BMD alone is not sufficient to accurately predict the risk of fracture in individual subject. More accurate normative references of age-related changes including both BMD and TBS parameters, evaluated from the same DEXA exam, would permit to increase the prediction of the risk of fracture.

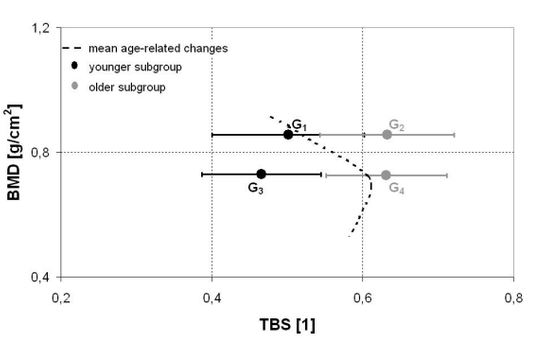

Disclosures: ***L. pothuaud****, None.*

SA116

Change of Biochemical Bone Markers in Korean Postmenopausal Women According to Their Menopausal Period. B. M. Kang*[1], H. Choi*[2], H. M. Park*[3], S. H. Seo*[4]. [1]Obstet & Gynecol, Ulsan University Medical School, Seoul, Republic of Korea, [2]Obstet & Gynecol, Inje University Medical School, Seoul, Republic of Korea, [3]Obstet & Gynecol, ChoongAng University Medical School, Seoul, Republic of Korea, [4]Obstet & Gynecol, Hanlim University Medical School, Seoul, Republic of Korea.

Changes of bone turnover with aging are responsible for bone loss and play a major role in osteoporosis. To investigate the bone turnover pattern in old menopausal women, 674 healthy women including 451 postmenopausal women were classified, according to their menopausal period(less than 5 years, 5-10 years, more than 10 years). Bone formation were assessed by serum osteocalcin(OC) and bone-specific alkaline phosphatase(BSAP). Bone resorption were assessed by the urinary deoxypyridinoline(DPD) and cross-linked N-telopeptide of type I collagen(NTX). All biochemical bone markers, except OC, significantly increased after menopause($p < 0.05$). DPD, NTX and BSAP remained elevated after 10 years of menopause(Table 1). These data indicated that the overall rates of both bone formation and bone resorption increased after menopause and remained high in elderly women.

Table 1. Bone turnover in pre- and postmenopausal women

Bone markers	Premenopause	Postmenopause (n=451)		
	(n=223)	< 5years	5-10 years	> 10 years
DPD(nM/mM)*	4.8±1.3	6.4± 3.1	6.9± 7.3	6.4 ±3.9
NTX(nM BCE/mM)*	31.5±14.0	52.7±26.6	57.8±30.3	57.9±44.3
BSAP(U/L)*	13.2±30.3	19.0± 7.9	19.2 ±9.3	21.8±10.5
OC(ng/ml)	24.1±17.5	24.4 ±9.3	27.2±14.0	27.5±11.1

*$p < 0.05$ vs. premenopause

Disclosures: ***B.M. Kang****, None.*

SA117

Interactions of Parathyroid Hormone (PTH) with Markers of Bone Health in a Prospective Study of Perimenopausal Scottish Women. A. J. Black[1], H. M. Macdonald[2], W. D. Fraser[3], D. M. Reid[2]. [1]Department of Rheumatology, Osteoporosis Research Unit, Aberdeen, United Kingdom, [2]Department of Medicine and Therapeutics, University of Aberdeen, Aberdeen, United Kingdom, [3]Department of Chemical Pathology, University of Liverpool, Liverpool, United Kingdom.

While the role of PTH in bone turnover in the elderly is well established, there is little knowledge of the interactions of PTH with bone turnover and bone loss at the time of the menopause.

The Aberdeen Prospective Osteoporosis Screening Study commenced in 1992. All results median ± SD. At the second visit in 1998(6.41±0.9 years later), 3886 subjects had a repeat DXA scan of lumbar spine (LS) and femoral neck (FN), blood and urine samples and risk factor questionnaires performed. The median calcium intake for the group was 1044(+/-257) mg and 4% were pre, 7% peri and 89%postmenopausal.

PTH, P1NP, 25(OH) Vit D_3 and adjusted calcium (Aca) were measured in 2338(75%) and urinary pyridinoline crosslinks in 2771(90%).

Analyte	A Ca Mmol/L	Vit D_3 ug/l	PTH pmol/L	P1NP ug/L	fDPD nmol/ mmol	fPYR nmol/ mmol	Age (yrs)	Height (cm)	Weight (Kg)
Median ±SD	2.35±0.122	0.0±8.7	2.90±2.083	2.0±19.3	5.0±1.96	181±6.4	54.5±2.24	161.1±7.4	67±12.9

Significant but weak correlations with PTH were seen with Vitamin D ,bone turnover markers, height and weight. PTH also negatively correlated with bone loss in the preceding 6 years. These correlations remained significant after adjusting for weight and physical activity. No significant correlations were seen with age or serum Aca.

Pearson correlations with PTH	P1NP	$VitD_3$	fPYR/ creat	Weig ht	LS %change	FN %change
unadjusted	0.11**	0.05*	0.084**	0.11**	-0.08*	-0.06*
adjusted for wt and physical activity.	0.11**	0.05*	0.05*	N/A	-0.063*	-0.07**

*P<0.05**p<0.001, after log transformation of variables

PTH was lower in smokers (2.7±1.9) than non-smokers 2.9±2.12, as was 25(OH) D3 (18.0±7.9, 21.0±8.8 respectively, P<0.05)

The postmenopausal group who had never taken HRT (32%) had the highest bone turnover and PTH when compared to the premenopausal and the oestrogen replete group (premenopausal or on HRT). In none of the menopausal groups nor in the whole group did PTH predict the bone density or bone loss.

PTH has major bone influences in elderly women but only shows minor effects on bone metabolism in women at the menopause. This may be due to the major effects of oestrogen loss at the menopause and the fact that these women are free living with good calcium intakes

Disclosures: ***A.J. Black****, None.*

SA118

See Friday Plenary number F118

SA119

Low Performance of Circulating RANKL to Identify Postmenopausal Women with Osteoporosis and Pre-existing Vertebral Fractures. P. Mezquita-Raya*[1], M. de la Higuera*[1], D. Fernandez*[1], G. Alonso*[1], M. Ruiz-Requena*[2], F. Escobar-Jimenez[1], M. Muñoz-Torres[1]. [1]Bone Metabolic Unit. Department of Endocrinology, University Hospital San Cecilio, Granada, Spain, [2]Biochemistry Division, University Hospital San Cecilio, Granada, Spain.

Regulation of osteoclastic activity is critical for understanding bone loss associated with the postmenopausal period. In vitro and animal studies have revealed the role of RANKL on the differentiation and activation of osteoclasts. However, the relationship between serum concentrations of RANKL and bone mass is uncertain, with different studies yielding different results. AIMS: To examine the relationship among circulating levels of RANKL, bone mineral density (BMD) and vertebral fractures in healthy postmenopausal women. SUBJECTS AND METHODS: We determined anthropometric parameters, serum RANKL (Biomedica Gruppe, Vienna, Austria), BMD by dual X ray absorptiometry at lumbar spine and femoral neck (Hologic QDR4500, Waltham, MA), and pre-existing vertebral fractures in 206 ambulatory postmenopausal women. RESULTS: The mean circulating RANKL levels was 3.9±10.7 pg/ml. Serum RANKL concentrations were undetectable in a high percentage of women (n=113, 54,9%). There were no significant differences in clinical variables or prevalent vertebral fractures among women with detectable vs. undetectable RANKL. RANKL were not correlated to clinical variables or BMD. The percentage of women with detectable circulating RANKL was significantly different according to bone status (osteoporosis: 54%, osteopenic 25%; normal bone mass: 14%; p=0.029). However, the association between RANKL and BMD was lost in the multivariate analysis. CONCLUSION: These preliminary results indicate that serum RANKL measurement is of limited practical value at present in the study of bone metabolism.

Disclosures: ***P. Mezquita-Raya****, Eli Lilly & Co (Spain) 2; Fondo de Investigación Sanitaria (FIS: PI02/1089) 2.*

SA120

Serum Gla-type Osteocalcin, Osteoprotegerin, and Urinary Cross-linked N-telopeptide as Markers in Glucocorticoid-Induced Osteoporosis. I. Tanaka, H. Oshima. Department of Laboratory Medicine, Fujita Health University School of Medicine, Toyoake, Japan.

[Objective] Glucocorticoid-induced osteoporosis (GIO) has been increasingly paied attension as a secondary osteoporosis, but valuable markers for outcome such as bone mineral densities and incidental fractures in GIO have not yet available. In this study, we try to clarify a clinical role of serum Gla-type osteocalcin (GlaOC), serum osteoprotegerin (OPG), and urinary Cross-linked N-telopeptide (NTX) levels in GIO.[Subjects & Methods] One hundred patients (75 females and 25 males) with connective tissue diseases under glucocorticoid therapy were enrolled in this study. The mean of age, daily glucocorticoid dosage (prednisolone equivalent), and total glucocorticoid dosage were 46 years old, 19 mg/day, and 7.9 g, respectively. Serum OPG, urinary NTX and serum GlaOC were measured by ELISA, respectively. [Results] 1) Among patients who started to take glucocorticoids (an average dosage of 37 mg/day) but not anti-osteoporosis agents, OPG levels decreased after four weeks significantly (from 3.7+/-1.2 to 2.6+/-1.1 pmol/ml,p<0.05). Anti-osteoporotic agents did not change this decrease. NTX values increased after four weeks (an average of 158% of pre-value, p<0.02). On the other hand, there was no significant change in GlaOC levels. 2) A significant positive correlation was found between OPG and NTX (p< 0.01) before the start of glucocorticoid treatment. In patients under glucocorticoids, however, there was no correlation between these markers. 3) OPG was positively correlated with a change in bone mineral densities of the lumbar spine after 1 year (p<0.02). 4) Among patients (n=12) treated with menatetrenone, a vitamin K analog, GlaOC showed higher values (15.5+/-3.1ng/ml) in 3 cases who had new vertebral fractures in the following 2 years than in 9 cases (7.0+/-4.1) having no fracture in thatpriod (p<0.03).[Conclusion] These results suggest that 1) bone absorption is increased, at least in part, with suppression of OPG by glucocorticoids in the early stage of glucocorticoid treatment, 2) serum OPG level is a predictive marker of change in bone mineral densities, and 3) menatetrenone effectively prevents vertebral fractures in patients with low serum GlaOC values.

Disclosures: ***I. Tanaka****, None.*

SA121

Gender and Age Related Changes in Calcaneal Speed of Sound (SOS) in 9,146 Japanese Pediatric Population. T. Yamamoto[1], K. Mimura*[2], H. Morii[3], K. Yoh[4], K. Nonaka*[5], T. Arai*[6]. [1]Pediatrics, Minoh City Hospital, Minoh, Japan, [2]Department of Physical Education, Osaka University of Education, Kashihara, Japan, [3]Emeritus Professor, Osaka City University, Osaka, Japan, [4]Orthopedic Surgery, Hyogo College of Medicine, Nishinomiya, Japan, [5]Department of Health Care, Elk Corporation, Tokyo, Japan, [6]Department of Development, Furuno Electric Co., Ltd., Nishinomiya, Japan.

It seems that the maximum bone quantity in young people will influence a future osteoporosis in the aged. To prevent osteoporosis, it is important for assessment of bone quantity in young people. Previous study was reported to measure calcaneal speed of sound SOS in the elementary school children by using special foot adapter to give more reliable results in ASBMR 2003 by us. The purpose of this study was to assess gender and age related changes for right calcaneal SOS in Japanese pediatric population by using quantitative ultrasound (QUS). A total of 9,146 Japanese children and adolescents (4,352 females and 4,794 males, age range: 6-20 years) at 6 elementary schools, 7 junior high schools, 4 high schools and 4 colleges in 6 provinces from various parts of Japan were , after signing an informed consent, assessed by using QUS device (CM-100, Furuno Electric,Co., Ltd., Japan). To minimize impact of skin temperature, all the measurements in this study were performed in the period during July to October closing to summer season in Japan by the exclusive operators. The age related changes in male: the SOS value increased with age from 12 to 18 years old and showed a peak at age 18. Then it decreased gradually. In contrast, the age changes in female: the SOS values increased with age 12 to 14 years old and showed a peak at age 14. The peak value remained in a plateau until age 18, and then decrease gradually. The SOS value in female was higher than that in male until 16 years old. A significant difference was found between male and female aged 13 and 14. However, the SOS value was becoming similar value in male and female aged 17 to 20. These differences are probably attributed to a different pubertal development.
A detailed reference database for SOS at the calcaneus in Japanese children and adolescents were established. The CM-100 is a useful tool for assessment of pediatric bone quantity.

Disclosures: ***T. Yamamoto****, None.*

SA122

Inhaled Steroids do not Produce Bone Mass Loss in Asmathic Women. M. Sosa[1], P. Saavedra*[2], and The GIUMO Study Group*[3]. [1]Medicine, University of Las Palmas de Gran Canaria, Las Palmas de Gran Canaria, Spain, [2]Mathematics, University of Las Palmas de Gran Canaria, Las Palmas de Gran Canaria, Spain, [3]Medicine, Multicentre Cooperative, Study Group, Spain.

Background: Systemic corticosteroid therapy leads to bone loss and increases fracture risk especially with high doses and prolonged use. However it is unclear to what extent inhaled corticosteroids produce detrimental effects on bone mineral metabolism.
Main objective: To study the effect of inhaled steroids on bone mineral density measured by quantitative ultrasound at the heel. To assess the possible influence of menopause as an etiological cofactor on bone mineral loss
Secondary objectives: To study the influence of inhaled steroids on bone mineral density measured by dual X-ray absorptiometry (DXA) at the lumbar spine and the proximal hip.
Subjects and Methods: Cross-sectional study performed on pre and postmenopausal Caucasian women. Group I (patients with oral steroids) was composed by 176 women suffering from asthma and using inhaled steroids for years. They did not use oral steroids. Group II (controls) was composed by 197 women of similar age, height and weight who did not use inhaled steroids. Group III (asmathic) was composed by 72 patients, suffering from asthma and not using any kind of oral or inhaled steroids.
Results: Are shown in tables. We did not find statistical differences in QUS andDXA parameters between the groups.
Conclusions: The chronic use of inhaled steroid in asthmatic pre and postmenopausal Caucasian women, does not produce significative changes in BMD, measured either by QUS at the heel or by DXA at the lumbar spine or the proximal hip.

	Group I Asmathics with inhaled steroids	Group II. Controls	Group III. Asmathic with no steroids	p value
L2-L4 (g/cm^2)	0.936 ± 0.160	0.945 ± 0.152	0.985 ± 0.162	NS
Femoral neck (g/cm^2)	0.760 ± 0.135	0.753 ± 0.119	0.802 ± 0.127	NS
BUA (dB/MHz)	73.6 ± 18.3	69.0 ± 17.7	70.0 ± 15.1	0.03
SOS (m/sg)	1548 ± 31.7	1544 ± 33.3	1545 ± 24.5	NS
QUI	94.2 ± 21.1	90.5 ± 20.1	90.7 ± 15.5	NS

Disclosures: ***M. Sosa****, GIUMO group received an investigation grant from Italfármaco Laboratories. Spain. 2.*

SA123

See Friday Plenary number F123

SA124

Radiographic Absorptiometry and Quantitative Ultrasound Techniques Are Associated with Vertebral Deformity, but Not with Prior Nonspine Fracture in Japanese Women. Y. Abe*, K. Aoyagi*. Department of Public Health, Nagasaki University Graduate School of Biomedical Sciences, Nagasaki, Japan.

The purpose of this cross-sectional study was to evaluate the association of radiographic absorptiometry (RA) and quantitative ultrasound (QUS) with fractures among 586 Japanese women ages 40 to 89 years (mean age = 64.3, SD = 9.6 years). Bone measurements were performed using RA for metacarpal bone and QUS for calcaneus (stiffness index). Lateral spine radiographs were obtained and radiographic vertebral deformities were assessed by quantitative morphometry, defined as vertebral heights more than 3 SD below the normal mean. Information on previous nonspine fractures after age 45 (due to minor or moderate trauma) was obtained using a questionnaire. The associations of vertebral deformity, previous nonspine fracture, and any (spine or nonspine) fractures with bone measurements were examined using logistic regression analysis, adjusting for age. Both metacarpal bone mineral density (BMD) and stiffness index of calcaneus had significant associations with vertebral deformity. The age-adjusted odds ratio (per 1 SD decrease in bone mass) for vertebral deformity was 1.90 (95% confidence interval [CI]: 1.33-2.71) for metacarpal BMD and 4.03 (95% CI: 2.61-6.22) for stiffness index. However, neither metacarpal BMD nor stiffness index was significantly associated with nonspine fractures; the respective age-adjusted odds ratios were 1.41 (95% CI: 0.99-2.01) and 1.28 (95% CI: 0.89-1.84). Our results suggest that both RA and QUS are significantly associated with existing vertebral deformity, suggesting that peripheral low bone mass contributes to

greater risk of vertebral fracture among Japanese women. Vertebral fractures are rare before age 50, and are typical of osteoporosis in older women. The lack of association of prior nonspine fractures with bone measurements in our study may be partly related to the fact that some fractures occurred much earlier in life, prior to the development of low bone mass or osteoporosis. In addition to bone mass, other factors such as extrinsic energy due to falls may be also important for the occurrence of nonspine fractures. These convenient methods, with portability and relatively low cost, could be in part useful alternatives to conventional bone measurement techniques used for the assessment of fracture risk.

Disclosures: ***Y. Abe****, None.*

SA125

A Family with Osteoporosis-Pseudoglioma Syndrome (OPG) due to Compound Heterozygous Mutation of the LRP5 Gene. L. Y. Jin*[1], H. H. L. Lau[1], D. K. Smith*[2], K. S. Lau*[1], P. T. Cheung*[3], E. Y. W. Kwan*[3], L. Low*[3], V. Chan*[1], A. W. C. Kung[1]. [1]Medicine, The University of Hong Kong, Hong Kong, China, [2]Biochemistry, The University of Hong Kong, Hong Kong, China, [3]Paediatrics, The University of Hong Kong, Hong Kong, China.

Osteoporosis-pseudoglioma syndrome (OPG) is an autosomal recessive disorder due to mutations in the low-density lipoprotein receptor-related protein 5 (LRP5) gene. Here we report two novel missense mutations found in a southern Chinese family from a non-consanguineous marriage. 3 out 4 children had blindness, low bone mineral density (BMD) and multiple fractures in their childhood. The affected subjects were compound heterozygous for W478R and W504C mutations. The father with heterozygous mutation for W478R had low spine BMD while the mother and the unaffected child with heterozygous mutation for W504C had normal BMD. W478R is immediately C-terminal of the third YWTD repeat of the second YWTD/EGF domain in LRP5, while W504C is located between the third and the fourth YWTD repeat of the second YWTD/EGF domain in LRP5. In a model of the LRP5 second YWTD β-propeller domain both W478 and W504 are in close proximity. The two corresponding residues, W515 and W541 in the low-density lipoprotein receptor (LDLR), are involved in contacts with domain R4 of LDLR at endosomal pH. In nidogen W1053 and L1080, which are part of the contact surface with laminin, are the corresponding residues. The observed mutations in LRP5 may affect molecular interactions leading to the observed phenotype. Probable structural perturbation of the β-propeller domain by the charge change of mutation W478R affecting interactions with nearby charged residues may give rise to its apparent greater individual effect.

Disclosures: ***L.Y. Jin****, None.*

SA126

Spontaneous and Familial Progressive Osseous Heteroplasia (POH), a Human Disorder of Ectopic Bone Formation, Is Dependent on Mutations in the Paternally-Inherited Allele of GNAS. M. Xu*[1], F. S. Kaplan[1], E. M. Shore[2]. [1]Orthopaedics, University of Pennsylvania, Philadelphia, PA, USA, [2]Orthopaedics and Genetics, University of Pennsylvania, Philadelphia, PA, USA.

Progressive osseous heteroplasia (POH) is an autosomal dominant disorder of infantile dermal ossification followed by progressive bone formation within skeletal muscle and deep connective tissue. We previously reported heterozygous inactivating GNAS mutations as a cause of POH. The GNAS gene is transcriptionally complex, initiating mRNA synthesis from multiple promoters and unique first exons that splice into common exons 2-13. Expression of GNAS transcripts is regulated through genomic imprinting. Imprinted genes show a preferential expression of one of the two alleles, dependent on the parent of origin of the allele. The GNAS-Nesp55 transcript is synthesized from the maternally-inherited allele, and the GNAS-XLαs and -1A transcripts from the paternally-inherited allele. The GNAS-$G_s\alpha$ transcript, which encodes a G protein alpha subunit, is bi-allelically expressed in most cells, however, shows preferential expression of the maternal allele and silencing of the paternal allele in some tissues. This tissue-specific imprinting of GNAS-$G_s\alpha$ explains the hormone resistance in patients with pseudohypoparathyroidism type Ia (PHPIa) who have heterozygous inactivating GNAS mutations in their maternally-inherited alleles. POH is a rare condition, with most cases arising as a spontaneous (new) mutation within a family. However, in each of the few families that show inheritance of POH, transmission from fathers to affected children is observed. In this study, we investigated whether POH is dependent on mutations in the paternally-inherited GNAS allele in spontaneous as well as familial cases of POH. To determine whether identified GNAS mutations in POH patients (n= 13; samples obtained following an IRB approved protocol) occurred on the maternally- or paternally-inherited allele, RT-PCR amplification was used to specifically detect the Nesp55 and 1A transcripts followed by DNA sequencing of the cDNAs. If a mutation occurred on the maternal allele, then the mutation would be found in the Nesp55 cDNA but not the 1A cDNA; if a mutation occurred on the paternal allele, the complementary pattern would be observed. In all spontaneous and familial cases of POH examined, GNAS mutations were found to consistently occur on the paternally-inherited allele. These data support that, in contrast to mutations in PHPIa, which occur on the maternally-inherited GNAS allele, POH is dependent on mutations in the paternally-inherited allele of GNAS.

Disclosures: ***E.M. Shore****, None.*

SA127

See Friday Plenary number F127

SA128

Polymorphisms Within the Osteoprotegerin (OPG) Gene are Associated with both Serum OPG levels and Bone Mineral Density. L. J. Miles*[1], O. Beynon*[1], P. Y. Woon*[1], A. Blumsohn*[2], R. Eastell[2], E. L. Duncan[1], J. A. Wass*[1], M. A. Brown*[1]. [1]Botnar Research Centre, University of Oxford, Oxford, United Kingdom, [2]Bone Metabolism Group, University of Sheffield, Sheffield, United Kingdom.

Osteoprotegerin (OPG), a member of the tumour necrosis factor receptor family, plays a key role in the physiological regulation of osteoclastic bone resorption. By virtue of its decoy function, OPG inhibits the binding of RANKL to RANK with a resultant suppression of mature osteoclast activation and inhibition of the terminal stages of osteoclastogenesis. We sought to determine whether polymorphisms within the OPG gene influence bone density (BMD), bone turnover as assessed by serum P1NP, and serum levels of OPG.

This study involved 814 family members (330 men, 484 women) belonging to 164 extended Caucasian pedigrees recruited with probands with extreme low BMD (T-score <-2.5, Z-score <-2.0 at either the lumbar spine (LS) or femoral neck (FN)). Serum OPG was measured by ELISA and P1NP by RIA.

Eleven common single nucleotide polymorphisms (SNPs) spanning the OPG gene were identified from public databases, and previous publications, and confirmed by direct sequencing. SNPs were genotyped by a combination of SNaPshot™, MALDI-TOF mass spectrometry and PCR-RFLP approaches. Two-point linkage disequilibrium was determined using SIMWALK/GOLD, and haplotype estimates using MERLIN/FUGUE. Association was tested between individual polymorphisms and raw BMD using the program QTDT. Proband, age, gender, height and weight were used as covariates.

Significant association was noted between a SNP at the intron2-exon3 boundary (IVS2-4C/T) and LS BMD (p=0.024). Borderline association was found for a SNP within the promoter region (T-847G), and intron 1 (IVS1-865IT/C), with LS BMD (p=0.049 and 0.055, respectively). SNP IVS1-865IT/C was also correlated with OPG levels in serum (p=0.027). No association was found with FN BMD.

Our results suggest that polymorphisms in the OPG gene appear to be important markers for low bone mass and influence serum OPG levels. Further mapping and functional studies will be required to identify the specific variants involved.

Disclosures: ***L.J. Miles****, None.*

SA129

High Heritability of Bone Mineral Density in Pedigrees of Men with Idiopathic Osteoporosis. I. Van Pottelbergh*[1], C. Wang*[2], M. Cohen-Solal[3], M. Martinez*[2], A. Ostertag*[3], J. Kaufman[1], M. de Vernejoul[3]. [1]Endocrinology, Ghent University Hospital, Ghent, Belgium, [2]INSERM EMI 00-06, Evry, France, [3]Inserm U606, Hôpital Lariboisière, Paris, France.

Keeping in mind the finding of a high familial resemblance characterising male idiopathic osteoporosis (IO) as observed in 2 independent study groups (1,2), we checked whether pooling of the data was justified. Subsequently we estimated the heritability (h^2) of bone mineral density (BMD) in order to evaluate whether genetic factors influence the familial resemblance for BMD in an extended group of pedigrees ascertained through a male subject with IO, arbitrarily defined as a *Z*-score at the lumbar spine (Z-LS) or at the femoral neck (Z-FN) <= -2, aged 19 to 67. LS- and FN-BMD was measured in IO men (n=89), their first- & second-degree relatives and in their spouses, aged 19 to 85 (n=403). BMD distribution in both the group of IO men and in first-degree relatives was not different for Z-LS and Z-FN between the 2 caucasian study populations (Wilcoxon-testing, P>0.05) indicating that the 2 groups can be pooled. Estimates of h^2 for Z-LS and Z-FN were obtained using the variance component approach taking into account covariate effects as implemented in the Sequential Oligogenic Linkage Analysis Routines (Solar, Version 1.7.3.). The h^2 estimates for Z-LS and Z-FN were highly significant (Table 1). As to covariate effects, BMI had a significant effect on both Z-LS and Z-FN whereas gender significantly affected the variability of Z-LS but not Z-FN (Table 1). Overall, the proportion of phenotypic variance in Z-LS and Z-FN explained by covariates was 18% and 14%, respectively. When the pedigrees were divided in 2 groups according to the probands'age (cut-off 48 yrs), the estimates for covariate effects remained essentially unchanged with slightly higher h^2 estimates for Z-FN in younger probands. In conclusion, our findings confirm that a significant proportion of BMD variability is attributable to additive effects of multiple genes. Considering our findings on BMD h^2 and covariate estimates, a genome-wide search will be performed using non-parametric linkage analyses with adjustment for the identified covariates in this homogeneous group of pedigrees ascertained through men with IO.

1)JBoneMinerRes,13:1909,1998;2)JBoneMinerRes,18:303,2003; Supported by the European Commission: NEMO: QL6-CT-2002-00491.

Table 1. Heritability +/-SD and covariate effect estimates (*P<0.001)

	h^2	Beta Gender	Beta Age	Beta BMI
Z-LS	0.82+/-0.07*	0.77*	0.005*	0.05*
Z-FN	0.76+/-0.08*	0.13	0.004	0.07*

Disclosures: ***I. Van Pottelbergh****, None.*

SA130

Quantitative Genetic Analysis of Hand Skeleton Aging and Biochemical Indices of Bone and Cartilage Metabolism. G. Livshits, I. Malkin*, S. Trofimov*, I. Pantsulaia*, E. Kobyliansky*. Anatomy and Anthropology, Tel Aviv University, Tel Aviv, Israel.

The present study was driven by a clinical problem of chronic degenerative disease of skeleton that includes osteoporosis (OP) and osteoarthritis (OA) related phenotypes. The skeletal phenotypes were assessed from hand radiographs. Our research was carried out on about 150 nuclear and complex three-generational families randomly collected in ethnically homogeneous European pedigrees. The obtained results can be divided into 3 sections: 1.Genetic analysis of bone mass and size characteristics (OP) and traits related to hand OA. 2.Pedigree based investigation of circulating levels of calciotropic hormones, growth factors, cytokines, and biochemical indices of bone and cartilage remodeling. 3.Linkage disequilibrium study of several candidate genes polymorphisms and OP/OA related phenotypes. Model fitting techniques of the genetic analysis were implemented to reveal effects of age, sex, sex hormones, latent environmental, and genetic factors on variation of each of the studied variables and covariation between them. The results indicated strong involvement of the putative genetic factors in determination of variation of the majority of the studied phenotypes. Thus, narrow sense heritability estimates for OP and OA phenotypes, and for biochemical indices such as Leptin, PTH, 25(OH)D, Osteocalcin, PICP, IGFBP-3, TGFb, TNFa, M-CSF, OPG, and TIMPs ranged between 0.30 and 0.80, but were virtually zero for IL6 and soluble RANKL. Genetic relationships between the studied biochemical indices, as well as between them and bone aging traits were complex. Note for example, significant correlations between the OA and OPG (r=0.52, P<0.001) and IGFBP-3 (r=0.46, P0.35, P<0.01) between circulating leptin levels and hand bones size. The search for possible candidate genes revealed that statistically significant portion of OA and OP phenotypes could be attributed to some of these genes. For example, BMD variation, in particular in postmenopausal women maybe accounted for combined effect of ER_a and COLIA1 genes. These effects are likely to be mediated through PTH levels that were significantly related to ER_a polymorphism. Of special interest were results obtained in collaboration with P. Nurnberg's group (Berlin) analyzing ANKH and ENPP1 genes, involved in the control of extra cellular pyrophosphate levels. Each of these genes and in combination was significantly associated (P<0.03-0.006) with hand bone size and proportion. Further extensive research is needed in this field to clarify the situation.

Disclosures: ***G. Livshits****, None.*

SA131

See Friday Plenary number F131

SA132

Genome-wide Linkage Analyses of Femoral Neck Density and Strength in Inbred Rats. I. Alam[1], Q. Sun[1], L. Liu*[2], D. L. Koller[2], T. M. Fishburn*[3], M. J. Econs[3], T. Foroud[2], C. H. Turner[1]. [1]Orthopaedic Surgery, Indiana University School of Medicine, Indianapolis, IN, USA, [2]Medical and Molecular Genetics, Indiana University School of Medicine, Indianapolis, IN, USA, [3]Medicine, Indiana University School of Medicine, Indianapolis, IN, USA.

The laboratory rats are the most commonly used animal model for skeletal and aging research. Rats have been used extensively for biomechanical analyses of bone fragility and compared to mice they offer much lower measurement variability, particularly at the femoral neck. Recent progress in mapping of the rat genome and syntenic mapping among different species makes the inbred rats a potentially useful genetic model for skeletal fragility. One of these rat strains, Fischer 344 (F344), has been shown to develop osteopenia similar to humans. Previously, we reported that compared to Lewis (LEW) rats, Fischer (F344) rats have significantly lower (p<0.001) BMD in the femur. In this study, we identified chromosomal regions that contain quantitative trait loci (QTLs) influencing femoral neck density as well as geometric and biomechanical properties in a 595 adult female F2 rats from F344 and LEW progenitors. We performed a whole-genome screen using 100 microsatellite markers at an average density of 20 cM. Skeletal phenotypes were measured by peripheral quantitative computed tomography (pQCT) and femoral neck biomechanical testing. Genetic marker maps were estimated from our own data and compared with published maps. These maps were then used to detect QTLs using interval mapping methods (MAPMAKER/QTL). Our results indicate that a number of different chromosomal linkage regions are linked to femoral neck strength and density. The main QTLs and their synteny to a known QTL region in mice and human are summarized in the following Table.

Marker	Phenotype	LOD score	Mouse Synteny	Human Synteny
D1Rat250	Femur neck BMD	11.6		
D4Rat231	Femur neck BMD	12.3	6, Femur BMD and structure	4q, Hip BMD
	Polar moment of inertia (Ip)	6.8		
	Femur neck width	18.9		
D6Rat39	Femur neck BMD	3.8		
D5Rat159	Ultimate force	3.5	4, Femur and lumbar BMD	1p, Whole body and lumbar BMD
D7Rat64	Ultimate force	6.1	10, Femoral structure and biomechanics	19p, Femoral structure

The results of our study demonstrate novel QTLs for femur neck density and strength and also prove the importance of inbred rat model for genetic linkage analyses for hip fragility.

Disclosures: ***I. Alam****, None.*

SA133

A QTL with Pleiotropic Effects on Radius Cortical and Trabecular Bone Density in Baboons Maps to a Region Corresponding to Human Chromosome 11q12-13. L. M. Havill, M. C. Mahaney, J. Rogers*. Genetics, Southwest Foundation for Biomedical Research, San Antonio, TX, USA.

We conducted a bivariate statistical genetic analysis of radius bone mineral density (BMD) at two sites, one primarily cortical (dyaphyseal radius (Rad-1/3)) and one primarily trabecular (ultradistal radius (Rad-UD)), to search for genes with pleiotropic effects on both types of bone. BMD was obtained via DXA for 667 pedigreed baboons aged 4.6-30.0 years. We used a maximum likelihood variance decomposition approach to estimate the following parameters simultaneously for both traits: population mean; mean effects of age, age^2, sex, age-by-sex, age^2-by-sex, height, weight, and osteophytosis score; the proportion of the residual phenotypic variance due to the additive effects of genes (heritability (h^2)); unmeasured environmental factors; and the correlations between both traits due to shared genetic effects (ρ_G) and shared environmental factors. Rad-1/3 and Rad-UD BMD showed residual h^2 of 0.42±0.07 (p<0.0001) and 0.35±0.07 (p<0.0001), respectively. The genetic correlation between the two phenotypes (ρ_G=0.63±0.09, p<0.0001) provides strong evidence that 40% of the additive genetic variance in the two traits is attributable to the same gene(s). Initial univariate linkage screens localized QTL for genes influencing Rad-1/3 BMD (LOD=3.00) and Rad-UD BMD (LOD=3.11), to a 20 cM region of baboon chromosome 14 (homologous to human chromosome 11). Maximization of a multivariate multipoint linkage model, parameterized according to the bivariate model (above) and allowing for an additive genetic correlation due to the QTL, improved evidence for linkage (LOD=3.92) in this same region, localizing the QTL to human microsatellite marker D11S916. This region corresponds to human chromosome 11q12-13. Likelihood ratio tests reject the hypothesis of coincident linkage, supporting the pleiotropic effect of a single QTL on both cortical and trabecular BMD in the baboon forearm. This QTL accounts for 31% and 29% of the residual h^2 for Rad-1/3 and Rad-UD, respectively. 11q12-13 harbors the LRP5 gene, known to be influential in Mendelian disorders of BMD and in normal BMD variation in some human populations. The apparent conservation of function to the same genomic region across these two primate species is likely due the effects of the same gene. These results not only provide cross species replication of a BMD QTL on 11q12-13, but also support results of studies in mice and humans showing both pleiotropic and unique gene effects on trabecular and cortical bone. Given the close genetic and physiological similarity of baboons to humans, these results should be highly informative in our search for genes affecting skeletal maintenance and repair.

Disclosures: ***L.M. Havill****, None.*

SA134

A Pleiotropic Relationship between Bone Mineral Density and Circulating Leptin Levels in Pedigreed Baboons. L. M. Havill, A. G. Comuzzie*, G. Cai*, J. Rogers*, M. C. Mahaney. Genetics, Southwest Foundation for Biomedical Research, San Antonio, TX, USA.

We conducted preliminary statistical genetic analyses of fasting plasma concentrations of leptin, an adipocyte-derived hormone with known antiosteogenic effects, and dyaphyseal radius bone mineral density (BMD) to search for evidence of shared genetic effects on these two phenotypes. Leptin levels were assayed in frozen plasma samples obtained from 331 pedigreed baboons (*Papio hamadryas*) (231 females, 100 males) aged 6 to 27 years. Radius BMD was obtained via DXA at a point 33% proximal to the styloid process. In initial univariate analyses, we used a maximum likelihood-based variance decomposition approach to estimate heritability and screen for potential covariate effects on each trait. In the subsequent bivariate analysis, we estimated the following parameters simultaneously: population (male) mean; mean effects of significant covariates sex (leptin only), age (BMD), age-by-sex (BMD), weight and osteophytosis score (BMD); the proportion of the residual phenotypic variance due to the additive effects of genes (heritability (h^2)) and unmeasured environmental factors (e^2); and the correlations between both traits due to shared genetic effects (ρ_G) and shared unmeasured environmental factors (ρ_E). Variation in plasma leptin levels and radius BMD showed residual heritabilities of 0.36±0.09 (p<0.0001) and 0.42 ±0.07 (p<0.0001), respectively. We observed a significant positive genetic correlation between these two traits (ρ_G=0.88±0.59, p=0.045), indicating that a significant percentage of the additive genetic variance in plasma leptin levels and BMD is attributable to the effects of the same gene or suite of genes. We estimate (albeit tentatively, given the small sample size in these analyses) that this pleiotropic effect accounts for a minimum of 8% of the additive genetic variance in forearm BMD and a powerful inhibitor of bone formation in this animal model for bone maintenance and turnover. Given the close genetic and physiological similarity of baboons to humans, these results may provide new insights into the role of leptin in regulation of bone mass in our own species.

Disclosures: ***L.M. Havill****, None.*

SA135

Macrophage Migration Inhibitory Factor (MIF)Gene Promoter Region Polymorphism and Femoral Neck Bone Density. C. Joseph*[1], K. M. Prestwood*[1], J. A. Burleson*[2], P. K. Gregersen*[3], A. Lee*[3], R. Bucala*[4], G. A. Kuchel*[1], A. M. Kenny[1]. [1]Geriatrics, University of Connecticut, Farmington, CT, USA, [2]Community Medicine & Health Care, University of Connecticut, Farmington, CT, USA, [3]North Shore / Long Island Jewish Research Institute, Long Island, NY, USA, [4]Rheumatology, Yale School of Medicine, New Haven, CT, USA.

Macrophage migration inhibitory factor (MIF), a potent pro-inflammatory cytokine, is elevated in inflammatory conditions like rheumatoid arthritis and sepsis. Polymorphism in numbers of tetranucleotide CATT (cytosine, adenine, thymine, thymine) repeats in the

human *Mif* promoter (5 versus 6,7 or 8) has been linked to lesser MIF expression and lower rheumatoid arthritis disease severity. MIF protein is expressed in osteoblasts and induces metalloproteinase activity. We undertook a pilot study to explore an association between *Mif* CATT polymorphism and bone mineral density.
Methods: Eighty six community dwelling men and women aged 65 and older, with previously determined bone mineral density (BMD), body mass index, and sex hormone levels were recruited. Secondary causes of osteoporosis, hip replacement and high dose corticosteroid use was excluded. Individuals were dichotomized according to CATT alleles into a "low-expressing" genotype (presence of any 5 allele) and a "high-expressing" genotype (no 5 allele). Femoral neck BMD (dependent variable) was compared between the two groups using 2-tail *t* test. Logistic regression was also used to analyze the contribution of *Mif* genotype to femoral neck BMD controlling for age, gender, height and weight.
Results: The distribution of *Mif* genotype was as follows: 5,5 genotype in 5/86 (5.81%); 5,non-5 genotype in 26 (30.2%); and non-5, non-5 in 55 (63.9%) participants. The mean femoral neck BMD for those with any 5 allele (low expressing genotype) was 0.89 ± SD 0.13 and for group with no 5 allele (high expressing genotype) was 0.84 ± SD 0.13 (p= 0.063). There was no significant contribution of CATT genotype to femoral neck bone density (F = 1.64, P=0.204.) when adjusted for age, gender, and Body Mass Index.
Conclusions: In this preliminary pilot study, no difference was seen in femoral neck bone density between individuals with low- and high-expressing *Mif* alleles once potentially confounding variables were controlled. A larger sample cohort will be required to adequately address the study hypothesis

Disclosures: ***C. Joseph****, None.*

SA136

See Friday Plenary number F136

SA137

Withdrawn

SA138

The Effect of *Bsm*I and *Fok*I Genotypes on BMD and Bone Turnover Response to Raloxifene Therapy. A. Rogers, J. A. Clowes, F. Gossiel*, N. F. A. Peel, R. Eastell. Academic Unit of Bone Metabolism, University of Sheffield, Sheffield, United Kingdom.

The vitamin D receptor polymorphism, *Bsm*I, has previously been associated with the efficacy of raloxifene therapy. The aim of this study was to determine the presence of an association between the *Bsm*I and *Fok*I polymorphisms of the vitamin D receptor (VDR) gene and bone density and bone turnover response to raloxifene.
One hundred osteopenic postmenopausal women (ages 52 to 80 years, mean 64 years) were prescribed raloxifene (60mg/day) and calcium carbonate (500mg/day) for 48 weeks. Bone density at the lumbar spine (LSBMD) and total hip (THBMD) was measured in duplicate by DXA (Hologic, QDR 1000W) at baseline and 48 weeks. Urinary N-telopeptides of type I collagen (UNTX), a marker of bone resorption, was measured in quadruplicate at baseline and at 48 weeks using an autoanalyser (Vitros Eci). The *Bsm*I and *Fok*I polymorphisms were assayed using an ABI Prism™ 7200 Sequence Detection System (Taqman®). Adherence to treatment was assessed using electronic monitoring devices. 18 women either withdrew from the study or discontinued treatment before the end of the 48-week study period and were not included in this analysis.
The frequency of genotypes was BB 31%, Bb 47%, bb 22% and FF 31%, Ff 52%, ff 17%. The mean percentage changes in LSBMD, THBMD and UNTX in the whole group bone were +1.5%, +0.83% and -24% respectively. Women who were homozygous for the f allele had a significantly higher increase in THBMD than those who were F homozygous (table, values are % change (SEM)). Women who were homozygous for the b allele had a slightly higher increase in LSBMD than those who were B homozygous, but this borderline association was in the opposite direction to that reported previously.

	BB	Bb	bb	P (ANOVA)	P (BB vs bb)
LSBMD	+1.25 (0.35)	+1.50 (0.37)	+2.41 (0.47)	0.14	0.06
THBMD	+0.97 (0.38)	+0.77 (0.33)	+0.79 (0.50)	0.93	0.82
UNTX	-28.36 (6.78)	-21.41 (4.75)	-28.16 (6.78)	0.61	0.87
	FF	Ff	ff	P (ANOVA)	P (FF vs ff)
LSBMD	+1.83 (0.45)	+1.48 (0.31)	+1.34 (0.66)	0.75	0.59
THBMD	+0.39 (0.34)	+0.84 (0.34)	+1.66 (0.42)	0.16	0.03
UNTX	-30.47 (8.30)	-21.76 (5.25)	-24.78 (5.02)	0.62	0.56

There were no other significant differences in BMD or UNTX response to therapy by *Bsm*I and *Fok*I genotype.
We conclude that in this group of postmenopausal women there is a significant difference between the FF and ff VDR genotypes and THBMD response to raloxifene. However, unlike a previous report, we saw no significant associations between *Bsm*I genotypes and BMD response.

Disclosures: ***A. Rogers****, None.*

SA139

See Friday Plenary number F139

SA140

The Catechol-O-Methyltransferase val158met Polymorphism Is Associated with Bone Mineral Density in Young Adult Men. A. Eriksson[1], M. Lorentzon[1], N. Andersson[1], D. Mellström[2], C. Ohlsson[1]. [1]Center for Bone Research at the Sahlgrenska Academy, Department of Internal Medicine, Göteborg University, Göteborg, Sweden, [2]Department of Geriatric Medicine, Göteborg University, Göteborg, Sweden.

Peak bone mineral density (peak BMD) is an important predictor of future risk of osteoporosis. Estrogens influence the accretion of bone mass during puberty. Catechol-O-Methyltransferase (COMT) is involved in the degradation of estrogens. There is a functional polymorphism in the COMT gene (val158met), resulting in a 60-75% difference in enzyme activity between the val (high activity = H) and met (low activity = L) variants. The aim of the present study was to investigate the associations between this polymorphism and peak BMD in young men. 458 healthy men (age 19, SD 0.6) were genotyped and classified as $COMT^{LL}$, $COMT^{HL}$ or $COMT^{HH}$. Bone parameters were measured using both DXA and pQCT.
Regression models using physical activity, height, weight, age and COMT genotype as covariates showed that COMT genotype was an independent predictor of areal BMD in the total body, total femur and trochanter ($p<0.01$) but not in the spine. Areal BMD of the femur was 3.7% lower in $COMT^{LL}$ than in $COMT^{HL}$, while the values for $COMT^{HL}$ and $COMT^{HH}$ were very similar. pQCT analyses demonstrated that COMT genotype was an independent predictor of trabecular vBMD in the tibia, radius and fibula ($p<0.05$). Trabecular vBMD of the radius in $COMT^{LL}$ was 5.4% and 5.1% lower than that of $COMT^{HL}$ and $COMT^{HH}$ respectively. COMT genotype was associated with cortical volumetric BMD ($p<0.05$) but not with cortical cross sectional area in the tibia. These findings demonstrate that the COMT polymorphism is associated with BMD in young adult men.

Disclosures: ***A. Eriksson****, None.*

SA141

See Friday Plenary number F141

SA142

An Intron 2 Polymorphism at the Serotonin Transporter Is Associated with Reduced Hip Bone Mineral Density. E. M. Haney*[1], L. Marshall[1], L. Lambert[1], J. Zmuda[2], K. Stone[3], E. Orwoll[1], M. Bliziotes[1]. [1]Department of Medicine, Oregon Health Sciences University, Portland, OR, USA, [2]University of Pittsburgh, Pittsburgh, PA, USA, [3]University of California, San Francisco, CA, USA.

Functional serotonin transporters have recently been discovered in osteoblasts and osteocytes, and disruption of the serotonin transporter gene in mice results in osteopenia. We investigated whether genetic variation within the serotonin transporter influences BMD in humans. The serotonin transporter has two well-characterized variations: one at the promoter, with 14 or 16 repeats of a 22 base pair unit designated S (14 repeats) and L (16 repeats), and one at intron 2 with 9, 10, or 12 repeats of a 16-17 base pair unit.
We genotyped the serotonin transporter of 431 white men enrolled at the Portland, OR site of the Osteoporotic Fractures in Men (MrOS) study, a longitudinal cohort study of fractures in men. BMD was measured at baseline by DXA (QDR4500W, Hologic, Inc). Genotyping was performed with PCR analysis of DNA from peripheral blood samples using published primer sequences for the polymorphisms of interest.
Table. Frequency of Serotonin Transporter gene polymorphisms at the promoter and intron 2 alleles and mean BMD in the proximal femur according to genotype among 431 US men. BMD=g/cm2 (mean, s.d.).

Promoter Region	**S/S**	**S/L**	**L/L**	
Genotype Prevalence	79 (19.0%)	211 (50.8%)	125 (30.1%)	
Total hip BMD	0.965 (0.151)	0.945 (0.150)	0.967 (0.145)	
FN BMD	0.800 (0.148)	0.771 (0.139)	0.790 (0.132)	
Trochanter BMD	0.764 (0.139)	0.752 (0.137)	0.766 (0.131)	
Intron 2	**9/12**	**10/10**	**10/12**	**12/12**
Genotype Prevalence	6 (1.4%)	90 (21.7%)	164 (39.5%)	155 (37.3)
Total hip BMD	1.05 (0.140)	0.944 (0.152)	0.960 (0.158)	0.955 (0.138)
FN BMD	0.844 (0.142)	0.782 (0.149)	0.784 (0.137)	0.780 (0.137)
Trochanter BMD	0.879 (0.142)	0.749 (0.139)	0.760 (0.139)	0.758 (0.130)

After adjusting for age and lean body mass, the 9-repeat allele was associated with a 12% higher BMD at the trochanter (adjusted means: 0.759 vs. 0.880, P=0.019) and a 10% higher BMD at the total hip (adjusted means: 1.050 vs. 0.955, P=0.08). The L-allele was associated with a 4% lower BMD at the femoral neck (0.777 vs. 0.811, P=0.032). There were no significant differences in BMD noted at the lumbar spine for the other polymorphisms.
These results demonstrate an association between allelic variation at the serotonin transporter locus and BMD in white men. The mechanism for this is unknown, however the association between increased BMD and the 9-repeat allele is consistent with in vitro observations that the 9-repeat allele increases transporter promoter activity, which may lead to increased transporter expression. Additional studies of serotonin transporter polymorphisms and other populations will be required.

Disclosures: ***E.M. Haney****, None.*

SA143

Combination of Platelet-Rich Plasma (PRP) and COX-2 Inhibitor Potently Stimulates Mesenchymal Stem Cell Proliferation. D. Chikazu, S. Ohba, T. Ogasawara, M. Katagiri, H. Kawaguchi, T. Takato*. Oral-maxillofacial Surgery & Orthopaedic Surgery, University of Tokyo, Tokyo, Japan.

Platelet-rich plasma (PRP) is a component of blood in which the platelets are concentrated in a limited volume of plasma. PRP contains many growth factors such as PDGF, TGF-β and IGF-I, which are known to show potent osteogenic actions. Although the clinical application of PRP has become prevalent in oral and maxillofacial surgeries, little is known about the mechanism by which PRP leads to bone formation. The present study therefore investigated the effects of PRP on cultured mouse bone marrow mesenchymal stem cells (BMSC) using a double chamber dish separated by a porous membrane with the PRP on the top and cells on the bottom in the absence of serum. Although PRP inhibited mRNA levels of type I collagen, ALP and Runx2 as determined by real-time RT-PCR analysis, it stimulated cell proliferation about 4 fold that of the control culture. Interestingly, PRP potently stimulated cyclooxygenase-2 (COX-2) mRNA level and medium prostaglandin (PG) E_2 accumulation, and endogenous PGE_2 treatment inhibited the proliferation of BMSC. To know the involvement of the COX-2 / PGE_2 induction in the PRP osteogenic action, we added a COX-2 inhibitor, celecoxib, to the BMSC culture. Although celecoxib did not influence the inhibitory action of PRP on osteoblastic markers, it stimulated the mitogenic action of PRP about 2-fold. Moreover, when PRP was added to the culture of BMSC derived from COX-2-deficient mice (KO) or the wild-type (WT) littermates, its mitogenic action in the KO cell culture was about double that in the WT culture. We therefore conclude that PRP induces bone formation from BMSC by stimulating the proliferation, but not the differentiation. Since COX-2 induction by PRP blunts its mitogenic action, the combination with COX-2 inhibitors may reinforce the osteogenic activity of PRP.

Disclosures: ***D. Chikazu****, None.*

SA144

See Friday Plenary number F144

SA145

ELR^+ CXC Chemokine Production by and Action in Human Mesenchymal Stem Cells. D. S. Bischoff*, N. Makhijani*, J. Zhu*, K. Tachiki*, D. T. Yamaguchi. Research Service, VA Greater Los Angeles Healthcare System, Los Angeles, CA, USA.

Inflammation is the initial phase of bone repair, and recruitment of mesenchymal stem cells (MSCs) to the region of repair has been suggested to occur via a number of growth factors released by injured bone. CXC chemokines bearing the glu-leu-arg (ELR^+) motif have been shown to be released by inflammatory cells and serve as angiogenic factors by stimulating chemotaxis and proliferation of endothelial cells. The potential role of ELR^+ CXC chemokines in early events in bone repair was studied using human MSCs (hMSCs). hMSCs cultured in osteogenic medium (OGM) (containing ascorbate, β-glycerophosphate, dexamethasone) showed a 255-fold and 45-fold increase in mRNA for the ELR^+ CXC chemokines, IL-8 and GROα, respectively, as determined by real-time RT-PCR, compared to hMSCs grown in medium without osteogenic components. OGM also induced an increase in alkaline phosphatase activity, a marker of osteoblastic differentiation, in hMSCs. IL-8 alone but not GROα stimulated alkaline phosphatase activity in the absence of OGM in a dose-dependent manner, with 200 ng/ml (highest concentration of IL-8 tested) showing maximal stimulation. hMSCs exhibited chemotaxis to 10 nM IL-8 but not to lower doses. MC3T3-E1 cells, representative of committed mouse osteoblastic cells were not chemotactically stimulated by KC, the GROα equivalent in mice. Experiments were also conducted to examine CXC receptors on hMSCs. While IL-8 can bind to both CXC receptors (CXCR1 and CXCR2), GROα binds with higher affinity to CXCR2 and much less affinity to CXCR1. Real-time RT-PCR demonstrated that both CXCR1 and CXCR2 mRNA are detected in hMSCs with CXCR1 at much higher levels than CXCR2. FACS analysis showed that CXCR1 and CXCR2 protein levels followed a similar pattern to that shown by the mRNA levels. Preliminary experiments to define signal transduction pathways in hMSCs activated by IL-8 demonstrated that IL-8 treatment induced an increase in cytosolic calcium levels. Additionally, IL-8 stimulated the phosphorylated forms of ERK1/2 (p44/p42) in a pertussis toxin-sensitive manner. Conclusions: 1) hMSCs express ELR^+ CXC chemokines when grown in OGM; 2) hMSCs show significantly more CXCR1 than CXCR2 mRNA and protein expression; 3) hMSCs can respond to ELR^+ CXC chemokines by chemotaxis; 4) IL-8 but not GROα stimulates osteoblastic differentiation in hMSCs, and stimulation of osteogenic differentiation of hMSCs may be related to expression of CXCR1 and not CXCR2; 5) intracellular signaling stimulated by IL-8 include cytosolic calcium and MAPK pathway activation.

Disclosures: ***D.T. Yamaguchi****, None.*

SA146

Adiponectin Deficiency Partially Protects against Age-related Trabecular Bone Loss in Male Mice. A. Nampei*[1], J. Hashimoto[1], K. Maeda*[2], T. Ono*[1], N. Nakamura*[1], W. Ando*[1], K. Tateishi*[1], H. Tsuboi*[1], K. Shi*[1], K. Hayashida*[1], T. Funahashi*[2], H. Yoshikawa[1]. [1]Orthopaedics, Osaka University Graduate School of Medicine, Suita, Japan, [2]Internal Medicine and Molecular Science, Osaka University Graduate School of Medicine, Suita, Japan.

It is well established that body weight and body mass index are positively associated with bone mineral density (BMD). Obesity also protects against osteoporosis related fracture. Recent studies revealed that adipose tissue secretes various bioactive substances including leptin, tumor necrosis factor-alpha and adiponectin. These adipocyte-derived cytokines shed some light on the relationship between metabolic syndrome and bone metabolism. Many studies focused on leptin to explain the association between fat mass and BMD, however few studies dealt with adiponectin. Adiponectin is known to be associated with type 2 diabetes mellitus and atherosclerosis, but the relation with bone metabolism is still unknown. To investigate the contribution of adiponectin to the positive relationship between obesity and BMD or bone metabolism, we evaluated the morphometrical changes of bone in adiponectin deficient mice radiologically. Radiographs, bone mineral density (BMD), 3-dimensional bone structural architecture of lower extremity of male adiponectin knockout (KO) mice and wild type (WT) mice were analyzed and evaluated at 3 and 9 months old, using dual-energy X-ray absorptiometry (DEXA) and micro-computed tomography (micro-CT). There were no radiographical changes in skeletal frame, i.e. length, and diameter of bone. There were no significant differences of femoral and tibial BMD evaluated with DEXA between WT and KO mice both at 3 and 9 months old. For micro- CT, there were no differences of trabecular bone volume of proximal tibia between WT and KO mice at 3 months old (WT 22.63 ± 0.85 % vs. KO 21.50 ± 1.24 %), but at 9 months old, trabecular bone volume of KO was significantly higher than that of WT (WT 11.66 ± 1.05 % vs. KO 17.48 ± 0.84 % ; $p < 0.005$). Other parameters evaluated with micro-CT also showed the high bone mass and high connectivity of trabecular bone in KO mice than wild mice at 9 months old, although there were no significant differences at 3 month old. Our results revealed that adiponectin is associated with age-related trabecular bone loss and its deficiency protects the age-related trabecular bone loss in male mice, despite the fact that there were no influences upon developmental peak bone mass. These data suggest that adiponectin is one of the biochemical factors to explain the relation between obesity and bone mass.

Disclosures: ***A. Nampei****, None.*

SA147

See Friday Plenary number F147

SA148

Regulation of Dickkopf Homolog 1 (Dkk1) Expression by Endothelin-1 (ET-1): Implications in the Pathogenesis of Osteoblastic Metastases. G. A. Clines, K. S. Mohammad, J. M. Chirgwin, T. A. Guise. Internal Medicine, University of Virginia, Charlottesville, VA, USA.

Tumor-produced endothelin-1 (ET-1) is a causal agent in osteoblastic metastases. It stimulates osteoblasts via the endothelin A (ETA) receptor. ET-1 stimulates osteoblast proliferation and new bone formation in neonatal mouse calvariae, effects that are blocked by ETA receptor antagonists. However, the molecular mechanisms through which ET-1 stimulates osteoblasts are unclear.

Downstream targets of ET-1 in osteoblasts were identified by gene array analysis. Calvariae were excised from four-day-old mouse pups and treated with or without 100 nM of ET-1 for 6 hours, 1, 4 and 7 days. Total RNA was isolated and hybridized to mouse Affymetrix GeneChips representing 22,600 genes. Upregulated genes with putative or established roles in osteoblast function included four secreted factors [interleukin 6 (p=.023), Wnt5a (p=.042), tissue inhibitor of metalloproteinase-3 (p=.026), cysteine-rich protein 61 (p=.002)], two signaling molecules [serum/glucocorticoid regulated kinase (p=.016), TGIF (p=.016)] and three transcription factors [TSC-22 (p=.023), C/EBP delta (p=.049) and Twist homolog 2 (p=.039)]. ET-1 significantly downregulated Dickkopf homolog 1 (Dkk1) (p=.019), a secreted inhibitor of the Wnt signaling pathway recently implicated in suppressed bone formation of multiple myeloma. We hypothesized that ET-1 activates osteoblasts by decreasing the tonic negative regulation exerted by autocrine Dkk1. In validation of the gene array data, ET-1 decreased Dkk1 mRNA in calvarial organ cultures and primary osteoblasts.

To test the role of Dkk1 in ET-1-stimulated new bone formation, we utilized the mouse calvarial assay for new bone formation. Recombinant Dkk1 (50 ng/ml) abrogated ET-1-induced osteoblast proliferation and new bone formation in calvarial organ cultures ($p<.05$) but did not inhibit basal osteoblast activity. Dkk1 did not inhibit the osteoblast stimulatory actions of FGF2 or BMP2. These data suggest that Dkk1 may be specific for the ET-1-stimulated pathway rather than a general regulator of new bone formation.

Our data demonstrate that Dkk1 is an abundant product of osteoblasts; and activation of the ETA receptor by ET-1 decreases Dkk1 expression, thereby relieving tonic negative regulation of osteoblast activity. In multiple myeloma bone disease Dkk1 may depress bone formation. The opposite may occur in osteoblastic disease, where ET-1 stimulates osteoblast activity by decreasing autocrine production of the negative regulator Dkk1.

Disclosures: ***G.A. Clines****, None.*

SA149

Possible Mechanisms Of TP508, A Synthetic Thrombin Peptide, In Promoting Fracture Healing. H. Wang[1], X. Li*[2], E. Tomin[3], J. Convery*[1], E. Rousseau*[1], S. Doty[3], D. Carney*[4], J. Lane[3], J. T. Ryaby[1]. [1]OrthoLogic Corp., Tempe, AZ, USA, [2]University of Chicago, Chicago, IL, USA, [3]Hospital for Special Surgery, New York, NY, USA, [4]Chrysalis Biotechnology, Inc., Galveston, TX, USA.

TP508, a synthetic 23 amino acid peptide, represents a receptor-binding domain of human thrombin, an important growth factor and immunoregulator of tissue injury. TP508 has been shown to accelerate wound and bone fracture healing, and to promote cartilage repair. In this study, we aim to elucidate the molecular mechanisms of TP508 action using Affymetrix profiling. Closed fractures of the femoral midshaft were created in 10-month-old male Sprague-Dawley rats (3-12 animals/group/time point). TP508 at a dose of 0 (saline control), 1 and 10μg in 100 μl saline was injected percutaneously into the fracture

site one hour post-fracture. For torsion testing, the femurs were collected at 4 weeks post-fracture. For histology, the femurs were collected at week 3. For microarray analysis, the femurs were collected at days 1, 2, and 4. At 4 weeks post-fracture, 1μg TP508 treatment increased mechanical strength 21% relative to the control group, while 10μg caused a 36% increase ($p<0.05$). Histological analysis showed a 41% increase of newly formed blood vessels in 1μg TP508 treated groups in comparison with control. Microarray data showed that major genes involved in the early immune response, including several MHC Class II genes, IL-1β, and IL-1β receptor type 2, were significantly increased in 1μg TP508 treated group relative to controls. The expression of early response factor genes regulating angiogenesis, such as Egr-1, c-Jun and c-Fos, were also significantly increased. In addition, a set of Egr-1 target genes including FGF2 was also positively affected by TP508. This study suggests that TP508 promotes fracture healing through a mechanism that involves an increased induction of a number of growth factors, and enhanced expression of inflammatory mediators and angiogenesis-related genes.

Disclosures: ***H. Wang****, OrthoLogic 3.*

SA150

Induction of Bone Repair During Distraction Osteogenesis Requires VEGF Receptor Signaling. R. S. Carvalho, K. Jacobsen*, E. Tsiridis*, T. A. Einhorn, L. C. Gerstenfeld. Orthopaedic Surgery Research Laboratory, Boston University Medical Center, Boston, MA, USA.

The technique of distraction osteogenesis (DO) was developed to correct limb length discrepancies that occur as a result of injury, disease or malformation. Clinically and in animal this is one of the most dramatic means of regeneration of large amounts of osseous tissue and is capable of lengthening a long bone up to ~20% of its length. Despite its wide spread clinical application, very little is understood about the basic biology of bone repair and regeneration induced by DO. Though not mechanistically well understood, the primary descriptive features of DO are that it induces new bone formation through an intramembranous process devoid of extensive cartilage, and the repair tissue is highly vascularized. Due to these observations, we hypothesized that an angiogenic process drives bone regeneration during distraction osteogenesis. In order to test what the role of vascularization was during DO, we examined the functional role of vascular endothelial growth factor (VEGF). VEGF has previously been shown to be responsible for the migration and proliferation of endothelial cells that are essential for the development of new blood vessels. DO was carried out using a monlateral fixator that was applied to the tibia of male mice. The time course of DO was for 35 days. VEGF activity was selectively inhibited by antibody blockade of both receptors, VEGFR1 (Flt-1) and VEGFR2 (Flk-1). Loss of VEGF receptor function lead a failure of bone repair as confirmed by x-ray and histological analysis. Analysis of mRNA expression within the DO regeneration gaps demonstrated a ~50 % reduction in the expression of osteogenic mRNAs (collagen type I, OC and BSP)expression while chondrogenic mRNAs (collagen- type II and X) expression were elevated in the tissues from VEGFR antibody blockaded mice when compared to control DO mice. These results demonstrate that VEGFR signaling is essential for new bone formation during DO, and in the absence of VEGFR signaling a chondrogenic phenotype develops in the regenerating tissues.

Disclosures: ***R.S. Carvalho****, None.*

SA151

The Stimulatory G Protein Signaling Indirectly Increases FGF-23 mRNA Level. M. Takaiwa*[1], K. Aya[1], Y. Yamanaka[1], Y. Seino[2], H. Tanaka[1]. [1]Pediatrics, Okayama Univresity Postgraduate School of Medicine and Dentistry, Okayama, Japan, [2]Pediatrics, Osaka Kousei Nennkinn Hospital, Osaka, Japan.

Background: Fibrobalst growth factor 23 (FGF-23) has been identified as a causative factor in several hypophosphatemia; tumor induced osteomalacia, autosomal dominant hypophosphatemic rickets and X-linked hypophosphatemic rickets. Since the elevation of serum FGF-23 level was also reported among patients with McCune Albright syndrome (MAS)/fibrous dysplasia of bone (FD) and secondary hyperparathyroidism, we hypothesized that the stimulatory G-protein(Gs) - adenylyl cyclase(AC)- cyclic AMP(cAMP) signaling system may positively regulate FGF-23 mRNA expression.
Method: We first measured the serum FGF-23 levels of 3 MAS/FD patients using ELISA in order to confirmed the relationship between serum FGF-23 level and clinical manifestations of MAS/FD. We next investigated the effect of PTH(1-34),forskolin (FSK) and 8Br-cAMP on FGF-23 mRNA abundance in the primary mouse thymic cell culture. We also tested mouse mesenchymal cell line culured with or without the protein kinase A inhibitor H-89. FGF-23 mRNA was quantified using real-time PCR method. To explore molecular regulatory mechanism, 2174bp genomic DNA fragment upstream of FGF-23 gene were cloned into pGL3 basic plasmid (Promega) and transfected to a mouse mesenchymal cell line in order to perform luciferase assay. Transfected mesenchymal cells were cultured for 12 hours with or without PTH(1-34) or FSK and the luciferase activity were measured.
Result: Serum FGF-23 levels were increased in all MAS/FD patients (92-593RU/ml). Serum FGF-23 levels were correlated to serum phosphorus level, the renal threshold phosphate concentration (TmP/GFR), and alkaline phosphatase.
12 hours exposure to PTH(1-34), FSK, 8Br-cAMP increased FGF-23 mRNA abundance of wild type derived thymic cells (2.0-2.2 fold of control ($p<0.05$)) and Hyp mouse derived thymic cells (1.6-2.8 fold of control ($p<0.05$)). Though it required prolonged treatment (20-30 hours), similar effects were observed in a mouse mesenchymal cell line and were suppressed by H-89. Luciferase assay of FGF-23 upstream clone did not show significant change by the treatment of PTH(1-34) or FSK.
<Discussion>
Serum FGF-23 levels indicated that FGF-23 induces hypophosphatemia of MAS/FD patients, and may be produced in FD lesion. The results from the experiment with mouse thymic cells and mesenchymal cell lines suggested that prolonged stimulation of Gs-AC-cAMP signaling may increase FGF-23 mRNA abundance. But, the long duration of cell treatment and the poor results of luciferase assay may indicate that Gs-AC-cAMP signaling sysytem does not directly regulate FGF-23 mRNA expression.

Disclosures: ***M. Takaiwa****, None.*

SA152

See Friday Plenary number F152

SA153

Elevated Expression of *fgf23* in Bone in Primary Hyperparathyroidism *in vivo*. Y. Imanishi[1], T. Kawata*[1], K. Kobayashi*[1], E. Ishimura*[2], T. Miki[3], A. Arnold[4], M. Inaba[1], Y. Nishizawa[1]. [1]Department of Metabolism, Endocrinology and Molecular Medicine, Osaka City University Graduate School of Medicine, Osaka, Japan, [2]Department of Nephrology, Osaka City University Graduate School of Medicine, Osaka, Japan, [3]Department of Geriatrics and Neurology, Osaka City University Graduate School of Medicine, Osaka, Japan, [4]Center for Molecular Medicine, University of Connecticut Health Center, Farmington, CT, USA.

While the importance of FGF-23 is established in the pathogenesis of phosphate wasting disorders, little is known about the mechanisms regulating its circulating level. To investigate the role of calcium metabolism in FGF-23 homeostasis, we investigated the regulation of FGF-23 *in vivo* on PTH-*cyclin D1* transgenic mice (PC2 mice), a model of primary hyperparathyroidism. Studies were approved by the appropriate institutional animal care committees. Serum FGF-23 level was elevated in PC2 mice (PC2: 761 ± 101 vs. WT: 244 ± 51 pg/mL), and the level was significantly correlated with serum PTH ($P= 0.004$), Ca ($P< 0.001$), and P ($P= 0.002$) levels. Expression profile of *fgf23* revealed abundant expression in bone, especially in calvaria by quantitative real-time RT-PCR. The *fgf23* expression in calvaria, significantly increased in PC2 mice compared to WT mice (about 20 times), was well correlated with serum FGF-23 levels ($P<0.001$). Alkaline phosphatase and osteocalcin expression were also significantly correlated with the expression of *fgf23* ($P<0.001$), suggesting the importance of osteoblastic activity in FGF-23 regulation. Serum FGF-23 level was suppressed by parathyroidectomy in PC2 mice, and increased by continuous 1-34 PTH infusion in WT mice. In conclusion, our observations indicate that PTH has a role in the regulation of serum FGF-23 level, likely via osteoblast activation in bone.

Disclosures: ***Y. Imanishi****, None.*

SA154

See Friday Plenary number F154

SA155

FGF-2 Induces Osteoblast Survival Through a PI3-Kinase-Dependent, -Beta-Catenin-Independent Pathway. F. Debiais[1], G. Lefevre*[2], J. Lemonnier*[1], S. Le Mée*[1], F. Lasmoles*[1], F. Mascarelli*[2], P. J. Marie[1]. [1]Laboratory of Osteoblast Biology and Pathology, Inserm U606, Paris, France, [2]Institut Biomedical des Cordeliers, Inserm U450, Paris, France.

Fibroblast growth factor-2 (FGF-2) is an important molecule that controls bone formation through activation of osteoblastic cell replication and differentiation. The role of FGF-2 on human osteoblast survival and the signaling pathway that mediates its effect are not known. We studied the effect of FGF-2 on apoptosis induced by low serum concentration and the signal transduction pathway involved in this effect. Treatment of human primary calvaria osteoblasts or immortalized human immortalized calvaria osteoblastic cells with FGF-2 (10-100 ng/ml) for 24-48 h protected against osteoblast apoptosis induced by low serum concentration. This effect occured through specific inhibition of caspase-2 and caspase-3 activity. Pharmacological inhibition of MEK-1 or p38 MAPK had no effect on the inhibition of caspases-2 and -3 induced by FGF-2. In contrast, inhibition of phosphatidylinositol-3 Kinase (PI3K) with LY294002 abolished the FGF-2-induced inhibition of caspases-2 and -3 in human osteoblastic cells. Using a kinase assay, we found that FGF-2 increased PI3K activity. However, this effect did not induce phosphorylation of the downstream effectors PKB/Akt or p70 S6 kinase. Treatment with FGF-2 induced GSK-3 alpha and beta phosphorylation in osteoblastic cells. However, this effect did not result in beta-catenin accumulation or Lef/Tcf transcriptional activity. In contrast, lithium induced beta-catenin accumulation, Lef/Tcf transcriptional activation and increased caspase-2 and -3 activity. The results indicate that the immediate protective effect of FGF-2 on human osteoblastic cell apoptosis involves PI3K and inhibition of downstream caspases, independently of GSK-3 and beta-catenin-Lef/Tcf-mediated transcription.

Disclosures: ***P.J. Marie****, None.*

SA156

See Friday Plenary number F156

SA157

Incomplete Glycosylation of Crouzon Mutant FGFR2 Diminishes Protein Stability and Alters Subcellular Localization and Signaling. N. E. Hatch[1], M. Seto*[2], M. Bothwell*[1]. [1]Physiology and Biophysics, University of Washington, Seattle, WA, USA, [2]Pediatrics, University of Washington, Seattle, WA, USA.

Craniosynostosis is a debilitating clinical condition characterized by premature fusion of one or more of the cranial sutures. Mutations in three members of the fibroblast growth factor receptor (FGFR) gene family have been genetically linked to several of the craniosynostosis syndromes and have been shown to be gain of function mutations in terms of ligand binding, dimerization and auto-phosphorylation of the receptor. A commonly accepted hypothesis is that craniosynostosis results from excess mineralization that occurs downstream of overactive FGF/FGFR signaling in the cranial suture environment. Contrary to this idea, we show that a Crouzon mutation of FGFR2 (FGFR2/c278f) diminishes receptor cell surface expression and ligand induced signaling, and that this an effect of inadequate mutant receptor glycosylation. To determine levels of receptor expression/degradation, glycosylation, cell surface expression, and signaling, mammalian expression vectors expressing normal or Crouzon mutant (c278f) FGFR2 were transfected into COS7, NIH3T3 and MC3T3E1C4 cells. Protein expression and degradation was assessed with the use of specific protease inhibitors. FGFR2 cell surface expression was monitored through the use of an N-glycosylation inhibitor followed by streptavidin precipitation of biotinylated cell surface proteins. FGFR2 signaling was induced by treatment of cells with 50 ng/ml FGF2 and 100 mg/ml heparin and monitored through the use of activation-state specific antibodies. Crouzon mutant FGFR2 was found to be degraded to a significantly greater extent than normal FGFR2 protein. Degradation was lysosome and calpain, but not proteasome dependent. FGFR2/c278f was expressed predominantly as the partially glycosylated, 110 kDa form while normal FGFR2 was expressed predominantly as the fully glycosylated, 120 kDa form. Glycosylation of FGFR2 was shown to be essential for cell surface expression. MAPK signaling upon FGF2 treatment was lower in cells expressing the mutant, as opposed to the normal, receptor. The c278f Crouzon mutation in FGFR2 results in diminished glycosylation, increased degradation and dramatically lower levels of cell surface expression. These observations suggest that, although these mutations may induce dimerization and autophosphorylation, it is likely the mutated receptors are trafficked to the lysosome for degradation as opposed to the cell surface for expression, ligand binding and signaling.

Disclosures: ***N.E. Hatch****, None.*

SA158

Identification and Characterization of a Novel IGFBP-5 Interacting Protein (IGFBP5-IP) by Yeast Two Hybrid Screen of U2 Osteosarcoma cDNA Library: Evidence that IGFBP5-IP Is an Important Regulator of Osteoblast Proliferation and Differentiation. Y. Amaar, D. J. Baylink, B. Tapia*, S. Mohan. JLP VAMC / Loma Linda Univ Dept Med, Loma Linda, CA, USA.

IGFBP-5 (BP-5) is an important bone formation regulator and a multifunctional protein that acts not only as a traditional binding protein but also as a growth factor independent of IGFs. To identify the potential molecular signals that mediate BP-5 effects, we sought to identify proteins that bind BP-5 using BP-5 as bait in a yeast two hybrid screen of U2 human osteosarcoma cell cDNA library. We identified a 0.875 kb partial cDNA clone (clone A) displaying a strong interaction with the bait under high stringency conditions. The Clone A sequence did not match with any known genes in the Genebank, but did show partial sequence identity with a mouse Riken cDNA clone (Accession # BC057304.1) which encodes an ORF of 7 exons. The first segment of the clone A sequence is identical to part of exon 4 and the entire exon 5 sequence of Riken cDNA encoding an ORF of 143 amino acids. The second segment of clone A sequence falls within intron #5 of Riken cDNA clone genomic sequence on mouse chromosome10, suggesting that clone A and Riken cDNA most likely represent alternatively spliced forms of the same gene. Because clone A encodes a previously unidentified novel protein, we termed this protein BP5-IP. If BP5-IP is an important intracellular mediator of BP-5 actions, we expected BP5-IP to be expressed in a variety of osteoblast (OB) cell types that produce BP-5. Accordingly, we found that a number of OB cell types, including normal human OBs, osteosarcoma (U2 and MG63) and MC3T3-E1 mouse OBs, express BP5-IP transcript by Northern blot and RT-PCR analyses. We next determined the role of endogenously produced BP-5-IP on proliferation and differentiation of OBs using small siRNA technology. Treatment of MG63, SaOS-2 and MC3T3-E1 cells with siRNA duplex sequence specific to BP5-IP reduced expression of BP5-IP by >70% and decreased cell number by 20-35% (P<0.01) compared to plasmid control. Furthermore, treatment of high ALP expressing SaOS-2 cells (HSaOS) with siRNA duplex specific to BP5-IP caused a significant reduction in ALP activity compared to plasmid control (65% of control, P<0.01). Conclusions: 1) We identified a novel protein that interacts with BP-5 (BP5-IP) in our yeast two hybrid screen of U2 cell cDNA library; 2) BP5-IP and Riken cDNA clone, BC057304, represent alternatively spliced products of a novel gene located in chromosome 10; 3) BP5-IP is expressed in many cell types that produce BP-5; 4) The findings that inhibition of expression of BP5-IP decreased cell proliferation and ALP activity are consistent with an important role for this novel protein in regulating OB cell functions.

Disclosures: ***Y. Amaar****, None.*

SA159

Local IGF-II Expression in Human Bone Is Greater in Women Treated with Teriparatide than with Placebo: A Quantitative Immunohistochemical Study of Bone Biopsies from the Fracture Prevention Trial. E. F. Eriksen, Q. Q. Zeng*, D. W. Donley*, Y. L. Ma*. Eli Lilly and Company, Indianapolis, IN, USA.

Insulin-like growth factors play important roles in the regulation of skeletal remodeling and have been implicated in the anabolic action of teriparatide [rhPTH(1-34)] on bone. PTH induces IGF-1 synthesis in rat calvariae, but the effects on IGF-I or II in humans have not been elucidated. We studied 39 biopsy samples obtained from the Fracture Prevention Trial to quantitatively assess the expression of IGF-I and II in situ (median treatment 18 months, range 12-24 months; 13 posttreatment samples from each group: placebo, teriparatide (TPTD) 20 µg/d & 40 µg/d). Biopsies were embedded at -20ºC in methacrylate to maintain immunoreactivity (Erben 1997). Seven µm sections were stained with specific antibodies against IGF-I and II after pretreatment with 0.1% acetic acid. Immunoreactivity for IGF-I was sparse, while expression of IGF-II on cement lines and bone surfaces was intense, in accordance with previous studies demonstrating higher levels of IGF- II vs. IGF- I in human bone matrix (Mohan and Baylink 1991). The total length of IGF-II positive stained cement lines was measured at the cancellous and cortical envelopes, then normalized to bone area and surface perimeter. There was a dose-dependent relationship in IGF-II immunoreactive expression at all bone envelopes studied. The IGF-II positive cement line length per unit bone surface or area was more than 2 fold greater in the 20 µg group compared with placebo (Table). In conclusion, this study suggests that in situ expression of IGF-II in human cancellous and cortical bone was greater with teriparatide treatment than with placebo. This apparent greater local IGF-II production with teriparatide compared with placebo may play a key role in the positive bone balance and improved cancellous and cortical bone architecture previously demonstrated in these biopsies (Ma et al. 2003).

Quantitative Local IGF-II Expression

IGF-II Expression per unit:	Placebo	TPTD20	TPTD40
Cancellous bone surface (%)	7.2 ± 4.5	15.7 ± 10.8*	18.8 ± 11.8*
Cancellous bone area (mm/mm^2)	1.3 ± 0.8	2.4 ± 1.4	2.8 ± 2.0*
Cortical area (mm/mm^2)	0.38 ± 0.35	1.06 ± 0.64†	1.46 ± 1.14†
Endocortical surface (%)	11.1 ± 5.4	25.1 ± 15.7*	18.5 ± 8.5*
Periosteal surface (%)	13.6 ± 7.3	28.7 ± 10.9†	28.9 ± 11.8†

Mean ± SD *P<0.05; †P<0.005 (Pairwise TPTD vs. Placebo using two-sided exact test)

Disclosures: ***E.F. Eriksen****, Eli Lilly and Company 1, 3.*

SA160

See Friday Plenary number F160

SA161

High IGFBP-2 Levels Predict Increased Bone Turnover in Aging Men and Women. S. Amin, L. J. Melton, S. Achenbach*, A. L. Oberg*, B. L. Riggs, S. Khosla. Mayo Clinic, Rochester, MN, USA.

Among the insulin-like growth factors (IGF-I, IGF-II) and their binding proteins (IGFBP-1, -2, and -3), we previously found that IGFBP-2, which increases with age, was the strongest predictor of bone density in men and women, with higher age-adjusted levels associated with lower bone density. How IGFBP-2, or other IGF/IGFBPs, affect bone metabolism in aging men and women is unclear.

In an age-stratified, random sample of the adult community population, we assessed serum levels of IGF-I, IGF-II, IGFBP-1, -2 and -3 as well as markers of bone formation (serum osteocalcin (OC)) and resorption (urine & serum NTX). We had measures of serum CTX for women only. We measured body mass index (BMI); serum bioavailable estradiol ($BioE_2$) and testosterone (BioT); and sex hormone binding globulin (SHBG). Associations between IGF/IGFBPs and bone turnover markers were assessed using Pearson correlations, before and after adjustment for covariates. Analyses were stratified by gender and by menopausal status. We studied 344 men (age 23-90) and 276 women, not on any hormones, (age 21-93; 166 postmenopausal). OC, urine & serum NTX in men and women, and serum CTX in women, tended to be greater with age. Adjusted for age, IGF-I was associated with greater OC, as well as urine & serum NTX, in men only (r=0.12, 0.12. 0.14; p<0.05). Higher age-adjusted IGFBP-1 was associated with greater OC in premenopausal women only (r=0.21; p<0.05). No other associations were seen between IGF-I, IGF-II, IGFBP-1 or IGFBP-3 with turnover markers in men or women. In contrast, higher IGFBP-2 was associated with greater OC, urine & serum NTX in men (r=0.30, 0.29, 0.29, respectively; p < 0.001), premenopausal (r=0.20, 0.21, 0.16; p <0.05, but NS for serum NTX) and postmenopausal (r=0.28, 0.37, 0.25; p<0.01) women. Similar results were seen with serum CTX in premenopausal (r=0.29; p<0.01) and postmenopausal (r=0.28; p < 0.001) women. After adjusting for age, BMI, $BioE_2$, BioT and SHBG in multivariate models, IGFBP-2 remained associated with OC, urine & serum NTX in men (r=0.20, 0.25, 0.23, respectively; p<0.001) and postmenopausal women (r=0.23, 0.33, 0.14; p<0.01, except serum NTX (p=0.08)). In similar models, IGFBP-2 was associated with serum CTX in pre- (r=0.29; p<0.01) and post- (r=0.20; p<0.05) menopausal women.

Among the IGF/IGFBPs studied, IGFBP-2 was the strongest predictor of bone turnover. Higher IGFBP-2, which is associated with lower bone density, appears to increase bone resorption in aging men and women independent of sex steroids and body mass. The increased bone formation observed likely occurs from coupling of bone turnover, but does not seem to be adequate to maintain bone density. Results suggest a direct negative influence of IGFBP-2 on bone metabolism.

Disclosures: ***S. Amin****, None.*

SA162

Localization of Insulin-Like Growth Factor I Gene-Expression in Rat Tibiae. C. M. A. Reijnders*[1], N. Bravenboer[1], M. A. Blankenstein*[2], P. Lips[1]. [1]Endocrinology, VU Medical Center, Amsterdam, Netherlands, [2]Clinical Chemistry, VU Medical Center, Amsterdam, Netherlands.

Growth factors, especially insulin-like growth factor I (IGF-I), have a key role in maintaining skeletal integrity. IGF-I can regulate specific bone cell function. In this study we developed a non-radioactive in situ hybridization (ISH) method in order to localize the mRNA expression pattern of IGF-I in rat bone.

Tibiae of 12-week-old female Wistar rats were dissected, fixed, decalcified and embedded in paraffin. Rat brain tissue was used as positive control. Sections of 5 µm were mounted on aminoalkylsilane-coated glass-slides and hybridized with the IGF-I or the ribosomal RNA probe. As control for degradation of RNA by RNAses the ribosomal RNA probe was used. Hybridization with sense probes was used to investigate the level of non-specific binding.

In the tibiae IGF-I mRNA is expressed in osteoblasts, which are situated against the surface of trabecular and cortical bone, in some osteocytes in the first lamella of the endosteal shaft and in the periosteum. Within the shaft the endosteal osteocytes, which are located within the other lamellae, and the periosteal osteocytes did not express IGF-I mRNA. In the growth plate IGF-I mRNA is located in chondrocytes of the hypertrophic and proliferative zone. The bone marrow cells i.e. megakaryocytes, macrophages and myeloid cells also expressed IGF-I mRNA. The brain showed IGF-I mRNA expression in Purkinje cells of the cerebellum and in neurons of the medulla oblongata. The ribosomal RNA probe exhibited cytoplasmatic expression in every cell type of the tibiae and the brain.

In conclusion, this non-radioactive ISH is a powerful and sensitive method to localize gene-expression within decalcified rat tibiae. During the whole decalcification procedure the RNA is not broken down by RNAses, because all the bone cells, including the osteocytes in the shaft, show ribosomal RNA expression. The osteoblasts and the osteocytes, within the first lamella of the endosteal side of the shaft, synthesize IGF-I mRNA. These bone cells might play a role during bone remodelling. This ISH technique is a useful method to detect acute changes of growth factor mRNA expression levels in bone after stimulation by mechanical stress.

Disclosures: ***C.M.A. Reijnders****, None.*

SA163

Ghrelin Levels in Osteoporotic Patients. Z. Valkusz*[1], J. Gardi*[1], T. Nyári*[2], J. Julesz*[1]. [1]Dept. of Endocrinology, University of Szeged, Szeged, Hungary, [2]Dept. of Medical Informatics, University of Szeged, Szeged, Hungary.

Ghrelin an endogenous ligand for the growth hormone secretagogue (GHS) receptor, has been reported to stimulate GH secretion and food intake in both humans and animals. Studies have been shown that GH or GHS treatments increase bone mass in rodents and in adult GH-deficient humans, suggesting a stimulatory effect of GH and GHS on bone mass in humans. Objective: To investigate whether a relationship exist between serum ghrelin levels and bone mineral density (BMD) in postmenopausal women and in men with osteoporosis. Methods: 18 women and 6 men with osteoporosis and 22 healthy individuals (17 women and 5 men) were included in the study. Serum ghrelin concentrations were determined by radioimmunoassay (Phoenix Pharmaceuticals, Belmont, CA, USA) Spine and femur BMDs were measured by dual energy X-ray absorptiometry Serum ghrelin concentration in the osteoporotic group was not significantly different from that of the control group (292 ± 36.6 pg/ml and 308 ± 30.2 pg/ml, respectively). Summarized data of all the investigated subjects (osteoporotic plus control groups, serum ghrelin levels correlated with body mass index (BMI) but not with spinal or femoral BMD. However relations were observed between BMI and spinal or femoral BMD. Conclusion: Our results indicate that ghrelin content of the blood serum does not have a direct influence on bone mass in osteoporotic patients.

Disclosures: ***Z. Valkusz****, None.*

SA164

Genetic Regulation of IGFBP-2 Is Independent of GH and Is Gender Specific. L. R. Donahue, W. G. Beamer, J. Hurd*, V. Guido, C. J. Rosen. The Jackson Laboratory, Bar Harbor, ME, USA.

The importance of the insulin like growth factor (IGF) system in skeletal growth and development is well known, and the genetic determinants of IGF-I and its binding proteins is an active area of study in our lab. We have discovered 3 strong quantitative trait loci (QTL) for serum IGF-I in F2 mice from a cross between 2 inbred strains with normal growth hormone (GH) levels (Rosen, et al 2000). To alleviate the GH influence on genetic regulation of the IGF system, we are using a spontaneous mutation in the mouse growth hormone releasing hormone receptor *Ghrhr^{lit}* that results in smaller mice with disproportionate low bone density and low serum IGF-I, compared to littermates, due to the lack of circulating GH. By transferring the *Ghrhr^{lit}* mutation from its original C57BL/6J (B6) background to the higher density, higher IGF-I, C3H/HeJ (C3H) background, we have produced C3.B6-*lit/lit* mice with higher BMD and increased IGF-I in the presence of GHD. The two GH deficient strains have now been intercrossed and a population of F2 mice, all GH deficient, but with the high and low alleles for BMD and IGF segregating, is being produced. The intention is to find QTLs in these F2 mice that determine a variety of skeletal and IGF phenotypes that are independent of GH influence. IGFBP-2 is of particular interest because serum levels are not affected by the genotype of mice; that is serum IGFBP-2 in *lit/lit* vs *lit/+* mice do not differ on either the C3H or B6 background. However, strain differences within genotype are seen, but only in females. Thus, C57BL/6J-*lit/+* females have lower IGFBP-2 than C3.B6-*lit/+* females, as do C57BL/6J-*lit/lit* females compared to C3.B6-*lit/lit* females. No strain or genotype differences are seen in males. Using this genetic model we will discover chromosomal loci that represent important regulatory genes for IGFBP-2. These loci will give new insight into the pathway through with IGFBP-2 has its biological effect. Data for serum IGFPB-2 in 8 week old male and female mice are shown in the table below (mean ± SEM, n=7-10; p<0.002; * within *lit/+;* @within *lit/lit*).

Serum IGFBP-2 in 8 week old male and female mice

	MALE	FEMALE
C57BL/6J-*lit/+*	854.5 ± 126.0	696.0 ± 33.6*
C57BL/6J-*lit/lit*	769.0 ± 91.1	690.4 ± 50.4@
C3.B6-*lit/+*	898.6 ± 114.2	983.0 ± 52.5*
C3.B6-*lit/lit*	797.4 ± 57.8	956.2 ± 51.9@

Disclosures: ***L.R. Donahue****, None.*

SA165

Long Term Caloric Restriction Does Not Deleteriously Impact Bone Characteristics or Body Composition in Wildtype and Long-Lived Growth Hormone Receptor/Binding Protein Null Mice. M. S. Bonkowski*[1], R. Pamenter*[2], J. S. Rocha*[2], K. Al-Regaiey*[2], M. M. Masternak*[2], J. A. Panici*[2], A. Bartke*[2]. [1]Pharmacology and Internal Medicine, Southern Illinois University - School of Medicine, Springfield, IL, USA, [2]Internal Medicine, Southern Illinois University - School of Medicine, Springfield, IL, USA.

Caloric restriction (CR) increases lifespan in many species ranging from yeast to dogs. While CR is beneficial in delaying the onset of disease and prolonging life, it is not well known if CR regimens that prolong life detrimentally affect bone health. Growth hormone receptor/binding protein knock out (GHR-KO) mice are long-lived (~50%) compared wildtype (WT) littermates and are GH resistant. GHR-KO mice are smaller, with decreases in bone mineral density (BMD) compared to WT. This research explores the effects of feeding a long term mild CR regimen on body composition and bone characteristics in GHR-KO mice and WT littermates. Starting at 8 weeks of age, WT and GHR-KO mice were placed on either Ad Libitum (AL) feeding or CR (70% of AL). This regiman is previously reported to extend lifespan in rodents. At 30±2 months of age, the mice were mildly anesthetized and body composition and bone characteristics were measured using dual-energy x-ray absorptiometry (DEXA) with a PIXIMUS instrument (LUNAR). Using three-way ANOVA to reveal effects of phenotype, sex, and treatment, CR caused an expected reduction in BW ($P<0.004$) compared to AL. In addition, GHR-KO mice weighed less ($P<0.0001$) than their WT siblings, with females weighing less than males across treatments and phenotypes ($P<0.0001$). CR did not effect % fat or the inversely correlated % lean ($P<0.8415$). In addition, whole animal bone mineral density (BMD), bone area, or bone mineral content did not differ between AL and CR regimen ($P<0.9295$, $P<0.166$, and $P<0.5478$, respectively). Analysis of femur revealed there were no significant effects of CR treatment on femur length ($P<0.9536$) and femur BMD ($P<0.9280$), but femur length and femur BMD were significantly less in GHR-KO mice compared to WT ($P<0.0001$). Surprisingly, lower lumbar (LL) measurements showed that CR treatment increased LL BMD benificially, but results showed an interaction between treatment and phenotype ($P<0.013$). Fisher's post hoc analysis revealed GHR-KO phenotype and CR treatment positively increased femur BMD ($P<0.0001$ and $P<0.011$, respectively), with the exception of GHR-KO female mice which showed overlapping LL BMD results (AL 0.052±0.002, CR 0.049±0.001). These findings suggest that in addition to delaying the onset of disease and prolonging longevity, the employed relatively mild (30%) CR regimen has no deleterious effects on bone health and may even provide a bone health benefit.

Disclosures: ***M.S. Bonkowski****, None.*

SA166

Targeted Disruption of IGF-I Gene in Mature Osteoblasts Using Human Osteocalcin Promoter Driven Cre in Mice. S. K. Lee[1], K. Govoni[1], Y. Chung*[1], C. Kesavan*[1], D. J. Baylink[1], D. LeRoith[2], T. Clemens[3], S. Mohan[1]. [1]JLP VAMC / LLU, Loma Linda, CA, USA, [2]NIH, Bethesda, MD, USA, [3]Univ of Alabama, Birmingham, AL, USA.

It is now well established that IGF-I is an important regulator of peak BMD. Accordingly, femur BMD is decreased by 65% in mice lacking functional IGF-I. The anabolic effects of IGF-I on bone are known to be mediated via liver-derived IGF-I which acts as an endocrine hormone and bone-derived IGF-I which acts as an autocrine/paracrine growth factor. Based on the findings that little or no deficit in BMD occurs in mice with disruption of liver-derived IGF-I gene, we predicted that locally produced IGF-I exerts a significantly greater role than circulating IGF-I in regulating BMD. To evaluate the role of mature osteoblast (OB)-derived IGF-I in regulating bone accretion, we used Cre/loxP recombination technology to conditionally disrupt IGF-I gene in mature osteoblasts (OBs). Human osteocalcin (hOC) promoter driven transgenic Cre mice were bred with loxP IGF-I mice to generate mice homozygous for loxP and cre positive (knockout, KO) and cre negative loxP mice (control) for the experiments. Cre expression was verified in the bones of Cre positive mice by real time PCR. Surprisingly, neither total body BMC nor total body BMD measured by DEXA was significantly different in the KO mice compared to control mice at 8 or 16 weeks of age. Furthermore, there were also no significant differences in the total vBMD (717 vs 711 mg/cm^3) or periosteal circumference (4.35 vs 4.45 mm) in the femur of KO mice compared to control mice. One possibility for the lack of phenotypic change in KO mice is that IGF-I is produced by different bone cell types (e.g. stromal cells, pre OBs etc.) and that disruption of IGF-I in mature OBs is not sufficient to reduce IGF-I levels below a thresh hold level that is required to produce an effect on BMD. We, therefore, compared the expression of IGF-I, Cre, osteocalcin and PPIA (control gene) at different time points (days 0, 6, 12, 18 and 24) in bone marrow stromal cells that were induced to differentiate into mature OBs in vitro. We found IGF-I was expressed at high levels throughout OB cell lineage but at much higher levels in pre-OBs (produce no or very low osteocalcin) compared to mature OBs. Accordingly, IGF-I expression was not significantly reduced in the bones of KO mice compared to control mice (30.8±0.9 vs 30.6±0.5, Ct values, Mean±SD). Conclusions: 1) Transgenic disruption of IGF-I gene in mature OBs using hOC promoter driven Cre did not reduce either bone IGF-I expression nor peak BMD. 2) Although hOC driven Cre has been used successfully to disrupt a number of trasngenes, in the case of IGF-I, it appears to be not effective since multiple bone cell types besides mature OBs produce IGF-I.

Disclosures: ***S.K. Lee****, None.*

SA167

Determining the Time-Point when TGF-β acts to Promote Lineage Diversion Towards the Osteoclastic Phenotype. S. W. Fox*, A. C. Lovibond*. Cellular and Molecular Medicine, St George's Hospital Medical School, London, United Kingdom.

Transforming growth factor-β (TGF-β) is a multifunctional cytokine that is an essential co-factor for osteoclastogenesis. Exposure to TGF-β within the first few days of culture significantly increases the proportion of uncommitted precursors that form osteoclasts in the presence of receptor activator of nuclear factor-κB ligand (RANKL). However, its actions appear to be bi-phasic since TGF-β may have suppressive effects later on in the culture period. Therefore, the effect of TGF-β is clearly dependent on the time and length of administration.

We have previously shown that TGF-β is able to suppress interferon-γ (IFN-γ) mediated inhibition of osteoclast formation *in vitro*. This finding supports the hypothesis that TGF-β may promote lineage diversion to the osteoclastic phenotype through suppression of pro-inflammatory stimuli. Therefore, to determine the critical time-point at which TGF-β primes non-committed precursors towards the osteoclastic fate, we examined the duration of exposure to TGF-β that was required to overcome the inhibitory effect of IFN-γ.

Murine non-adherent M-CSF dependent precursors were pre-treated with TGF-β for various time-periods (1, 6, 24, 48, 72 hours). After washing thoroughly, cells were incubated with M-CSF and RANKL with or without IFN-γ for 5 days. Alternatively, precursors were cultured with combinations of M-CSF, RANKL, IFN-γ, concurrently with TGF-β for up to 5 days. Osteoclast formation was assessed by staining for tartrate-resistant acid phosphatase (TRAP).

As previously demonstrated, IFN-γ significantly inhibited osteoclast formation compared to RANKL-treated controls. Pre-treatment with TGF-β for 24 hours was able to prevent the suppressive effects of IFN-γ, suggesting that TGF-β acts within this time period to irreversibly commit precursors to the osteoclastic lineage. Longer incubation with TGF-β for 48 and 72 hours did not further enhance osteoclast formation from precursors. In addition to these findings, we found that co-incubation with TGF-β was not able to overcome the inhibitory effect of IFN-γ. This is to be expected since the physiological effects of IFN-γ during an inflammatory response are more pertinent to an organism's survival, than the effect of TGF-β on osteoclasts.

Therefore, our data clearly shows that signalling mechanisms by which TGF-β acts to promote lineage diversion are fully activated within 24 hours. This finding can be used to determine the order and nature of genes up-regulated by TGF-β at this time-point and therefore clarify the mechanism by which TGF-β enables RANKL-induced osteoclast formation.

Disclosures: ***S.W. Fox****, None.*

SA168

See Friday Plenary number F168

SA169

TGF-β Regulation of Intrinsic Mechanical Properties of Bone. G. Balooch*[1], M. Balooch*[1], G. W. Marshall*[1], S. J. Marshall*[1], R. Derynck*[2], T. N. Alliston[2]. [1]Preventative and Restorative Dental Sciences, University of California San Francisco, San Francisco, CA, USA, [2]Growth and Development, University of California San Francisco, San Francisco, CA, USA.

TGF-β has a vital and complex role in bone. TGF-β binds its cell-surface receptor to activate Smad3, a transcription factor that regulates the expression of defined genes. While TGF-β regulates osteoblast differentiation and gene expression, the effect of TGF-β on bone matrix quality is less clear. To study the effect of TGF-β on bone matrix quality, this study evaluated the intrinsic mechanical properties of bone from mice with altered TGF-β signaling. Intrinsic mechanical properties, including hardness and elastic modulus, are measured using atomic force microscopy with nanoindentation and are independent of bone size or geometry. Previously developed transgenic mouse models show altered TGF-β signaling, ranging from 16-fold (D4 mice) and 2.5-fold (D5 mice) overexpression of TGF-β in bone, to decreased TGF-β signaling due to expression of a dominant negative TGF-β receptor in bone (E1 mice) or deletion of the Smad3 gene (Smad3 +/- or -/- mice). Age- and sex-matched tibias of each mouse model were evaluated. Mice with increased TGF-β signaling (D4, D5) had up to 23% reduced elastic modulus and hardness relative to wild-type littermates ($p<0.05$). However, mice in which TGF-β signaling was impaired (E1, Smad3 +/-, Smad3 -/-) had up to 54% increased elastic modulus and hardness ($p<0.05$). Though both have decreased TGF-β signaling, E1 mice are osteopetrotic whereas Smad3 -/- mice are osteopenic. The similarity in E1 and Smad3 -/- intrinsic mechanical properties suggests that bone matrix quality is independent of other osteoblast-intrinsic effects of TGF-β. Though no phenotype had previously been described for Smad3 +/- mice, these bones also had increased intrinsic mechanical properties. Therefore, partial reduction of TGF-β signaling in bone, either by expression of a dominant negative TGF-β receptor or by heterozygous loss of Smad3, is sufficient to produce bone with increased intrinsic mechanical properties. We are further investigating the Smad3 +/- mouse bone phenotype. We are also employing 3-point bending to determine the relative contribution of bone morphometry and intrinsic mechanical properties to bone resistance to fracture. The current study shows that intrinsic mechanical property testing is a useful tool for the analysis of bone phenotype. We provide the first evidence that growth factor signaling defines bone intrinsic mechanical properties. Finally, the effect of TGF-β on bone matrix quality appears to be independent of other TGF-β effects on osteoblast differentiation and function.

Disclosures: ***T.N. Alliston****, None.*

SA170

See Friday Plenary number F170

SA171

Glitazones, the Anti-Diabetic PPAR-γ Agonists, Suppress Osteoblast Differentiation and the Activity of TGF-β/BMP Signaling Pathways. B. Lecka-Czernik, K. Teng*, O. P. Lazarenko*. Geriatrics, UAMS, Little Rock, AR, USA.

Glitazones, a new class of oral anti-diabetic agents, sensitize cells to insulin through a specific activation of PPAR-γ nuclear receptor. PPAR-γ2 isoform is expressed in marrow mesenchymal stem cells and controls development of both, osteoblasts and adipocytes. As previously demonstrated *in vitro* and *in vivo,* PPAR-γ2 inhibits osteoblast and promotes adipocyte differentiation. In this study, the effects of three different glitazones (rosiglitazone, pioglitazone, and troglitazone) on osteoblast and adipocyte differentiation, phenotype-specific gene expression, and TGF-β/BMP signaling pathways were evaluated. Glitazones activities were tested in U-33/γ2 cells, an *in vitro* model of PPAR-γ2-controled differentiation of marrow mesenchymal cells, and the results were validated in murine primary bone marrow cultures. All tested glitazones simultaneously inhibited osteoblast differentiation and stimulated adipocyte development in a rank order corresponding their binding affinity for PPAR-γ (rosiglitazone>pioglitazone> troglitazone). Glitazones suppressed the expression of osteoblast-specific transcription factors, Dlx5 and Runx2, and phenotype-specific gene markers, osteocalcin and collagen I. Since TGF-β and BMP2/4 cytokines are essential for osteoblast differentiation and bone formation, we assessed the effects of tested glitazones on the expression of components of these signaling pathways using real-time RT-PCR. Glitazones decreased the expression of TGF-β1 and TGF-β3, TβR-II, Smad3, Smad4 and Smad7, as well as BMP4, Smad1 and Smad6. They did not affect the expression of Smad2 and Smad5, TGF-β1 and BMP2 cytokines, and their receptors, TβR-I, BMP-RII, BMPR-IA and BMPR-IB. Decreased expression of components of the TGF-β/BMP pathways resulted in a decreased cell responsiveness to these cytokines as measured by the effects on the expression of genes that are under their control. For example, in a presence of rosiglitazone the BMP4 cytokine effectiveness to stimulate Dlx5 gene expression was reduced by 85%, whereas stimulatory effect of TGF-β on Smad7 and PAI-1 gene expression was reduced by 50%. In conclusion, glitazones affect an activity of TGF-β/BMP signaling pathways which may account for their inhibitory effect on osteoblast differentiation and bone formation.

Disclosures: ***B. Lecka-Czernik****, None.*

SA172

Increased Prevalence of Osteocyte Apoptosis Precedes Osteoclastic Bone Resorption and the Loss of Bone Mineral and Strength Induced by Lack of Mechanical Forces in a Murine Model of Unloading. J. I. Aguirre, L. I. Plotkin, S. B. Berryhill*, R. S. Shelton*, S. A. Steward*, K. Vyas*, R. S. Weinstein, A. M. Parfitt, S. C. Manolagas, T. Bellido. Endocrinology, University of Arkansas for Medical Sciences, Little Rock, AR, USA.

Bone responds to mechanical strains through osteocytes, which detect the need for adaptation and transmit signals to the executive cells of remodeling, the osteoblasts and osteoclasts. Whereas physiological strains sustain bone formation, mechanical unloading causes bone loss. Based on earlier evidence that mechanical stimulation prevents apoptosis of osteocytic cells *in vitro*, we investigated here whether, conversely, reduced mechanical forces increase the prevalence of osteocyte apoptosis *in vivo* and whether this event is linked to bone loss. Adult (5 month-old) Swiss Webster female mice were tail suspended for 1, 3, 7 or 18 days (n=10/group). Global and spinal bone mineral density (BMD) measured by DEXA, and vertebral (L5) compression strength were significantly reduced after 18 days but not at earlier time points compared to fully ambulatory control mice. No differences in BMD or strength, as determined by 3-point-bending, were found in the hind limbs at any time, indicating that the axial skeleton is more sensitive to reduced load than the appendicular skeleton in this mouse strain. Increased prevalence of apoptotic cancellous and cortical osteocytes was found at day 3 and was sustained to day 18, as detected by *in situ* nick-end labeling of undecalcified bone sections. Histomorphometric analysis of vertebral bone indicated that the early increase in osteocyte apoptosis was followed by an increase in the cancellous osteoclast perimeter and number at day 18; and by decreased cortical width at days 7 and 18 with increased cortical porosity at day 18. The vertebral width did not change during the course of the experiment but the width of the bone marrow cavity increased significantly at days 7 and 18, indicating that the decreased cortical width was due to endosteal, rather than periosteal, bone resorption. Indeed, whereas apoptotic osteocytes were randomly distributed in controls, they were preferentially located in the endosteal cortical bone of unloaded animals at day 3 before cortical width was decreased. These findings indicate that reduced mechanical loading leads to osteocyte apoptosis that precedes the removal of bone in the same location by osteoclasts, followed by loss of bone mineral and strength. Furthermore, these results confirm that physiologic levels of strain provide survival signals for osteocytes which maintain the mechanosensory function of the osteocyte network.

Disclosures: ***J.I. Aguirre****, None.*

SA173

See Friday Plenary number F173

SA174

Effects of Oscillatory Fluid Flow on RANKL and OPG Expression. C. H. Kim*, C. R. Jacobs. Mechanical Engineering, Stanford University, Stanford, CA, USA.

Physical activity creates bending in the bone which leads to localized pressure gradients that drive interstitial fluid flow, which is oscillatory by nature, within the bone tissue. Oscillatory fluid flow (OFF) may lead to positive bone remodeling through effects on both the osteoblasts and osteoclasts but its effect on the osteoclastogenesis is especially poorly understood. In this study, the effects of OFF on expression of receptor activator of nuclear κB ligand (RANKL) and osteoprotegerin (OPG), two important regulators of osteoclast differentiation, were investigated.

ST-2 murine bone marrow stromal cells (Riken, Japan) were plated on glass slides and cultured with 10 nM 1,25 dihydroxyvitamin D_3 (Sigma, MO) to express RANKL. Two days after plating, cells were exposed to either 1 hour of no flow or OFF resulting in a shear stress of 10 dynes/cm^2. Total RNA was isolated immediately (0 hour) after, 1.5 hours after, or 24 hours after end of treatment. Real-time PCR was used to quantify levels of RANKL, OPG, and 18S mRNA (Applied Biosystems, CA).

Immediately after end of 1 hour OFF, RANKL/OPG ratio was significantly decreased by 60% (p=0.013) compared to no flow controls (Fig. 1). The decline in RANKL/OPG ratio due to OFF weakened after 1.5 hours and even further after 24 hours where the ratio was no longer significantly different (p>0.05).

These results confirm that OFF is a potent regulator of bone remodeling and suggest its effect on RANKL/OPG is maximal immediately after flow. Since RANKL is necessary in osteoclast differentiation, these results also suggest that an OFF induced positive bone remodeling can be achieved via suppression of the formation of osteoclasts.

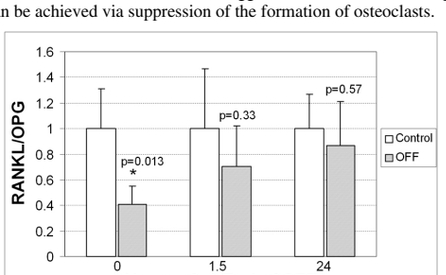

Figure 1. Temporal change in RANKL/OPG ratio after OFF. RANKL/OPG value is normalized to corresponding control values. N=4 for each group.

Disclosures: ***C.H. Kim****, None.*

SA175

See Friday Plenary number F175

SA176

Five Minutes of Fluid Shear Stress Is Sufficient to Induce Cyclooxygenase-2 in MC3T3-E1 Cells. S. Masatomo, M. Mehrotra, L. G. Raisz, C. Pilbeam. Department of Medicine, University of Connecticut Health Center, Farmington, CT, USA.

Mechanical loading of bone is transmitted to osteocytes and osteoblasts via the flow of interstitial fluid. Cyclooxygenase-2 (COX-2), an enzyme shown to mediate some of the anabolic effects of mechanical loading on bone, has been shown to be transcriptionally induced via a mitogen activated protein (MAP) kinase ERK signaling pathway in MC3T3-E1 and primary murine calvarial osteoblasts by continuous fluid shear stress (FSS), with peak effects at 4-8 h of flow. However, it seems unlikely that cells *in vivo* will see the physiologic equivalent of 4 h of continuous fluid flow. Hence, we examined the response of osteoblasts to short exposure of FSS. MC3T3-E1 cells were subjected to 5-30 min of laminar fluid flow, equivalent to a FSS of 10 dynes/cm^2, in serum free medium (0.1% BSA) and then returned to static culture (post-FSS) in the same medium. All experiments were performed in the presence of NS-398 (0.1 μM) to avoid the auto-amplification of COX-2 by endogenously produced prostaglandins. The induction of COX-2 mRNA following 5, 10 or 30 min of FSS peaked at 30-60 min in post-FSS culture and mRNA levels declined thereafter but remained elevated 4-8 h post-FSS. The induction of COX-2 mRNA by 5 min of FSS followed by 30 min of static culture was greater than or equal to the induction of COX-2 mRNA by 4 h of continuous FSS. Luciferase activity was measured in MC3T3-E1 cells stably transfected with 371 bp of the murine COX-2 promoter fused to a luciferase reporter. Although COX-2 mRNA expression peaked at 30 min post 5 min of FSS, luciferase activity in post-FSS cultures peaked at 2.5 h post-FSS, suggesting that the early COX-2 induction occurs in part by a non-transcriptional mechanism. Bioarray analysis (GenUs Biosystems, Chicago, IL) performed on 2 independent experiments (5 min FSS, 30 min post culture) showed 14 genes that were increased > 2-fold consistently in both experiments. In addition to COX-2, these included IL-6, zinc finger protein 36, a member of nuclear receptor subfamily 4, histone 1, and c-Jun. In other experiments, we have also shown that 5 min of FSS induces MMP-13 and RANKL expression at 4-6 h of post culture. Hence, 5 min of FSS is sufficient to initiate a signaling cascade in osteoblasts that leads to new expression of genes important in the regulation of bone turnover.

Disclosures: ***S. Masatomo****, None.*

SA177

Fluid Shear Stress Induces MMP-13 in Murine Osteoblastic Cells. S. Masatomo[1], M. Mehrotra[1], K. Nakamura*[2], H. Kawaguchi[2], C. Pilbeam[1]. [1]Department of Medicine, University of Connecticut Health Center, Farmington, CT, USA, [2]Orthopaedic Surgery, University of Tokyo, Tokyo, Japan.

Murine matrix metalloproteinase-13 (MMP-13) degrades interstitial collagen and plays an important role in physiologic and pathologic bone remodeling. A recent study reported that biaxial strain applied to MC3T3-E1 cells increased MMP-13 expression as an early response gene via the MEK-ERK signaling pathway (C-M Yang et al, J Biol Chem, in press 2004). Since mechanical loading may be mediated via shear stresses at cell surfaces generated by the fluid flow, we investigated the regulation of MMP-13 by fluid shear stress (FSS). We used a laminar flow apparatus to apply FSS of 10 dynes/cm^2 to MC3T3-E1 cells or to primary osteoblasts derived from neonatal mouse calvariae. By Northern blot analysis, MMP-13 mRNA levels were low or undetectable in control (no flow) cultures but were strongly induced by various flow regimens, including 4 h of continuous flow or 10 min of flow followed by 4 h in static culture. We subjected MC3T3-E1 cells to FSS for 30 min or primary calvarial osteoblasts to FSS for 60 min, replaced the cells in static culture (post-FSS) for 0-24 h, and measured the expression of MMP-13 mRNA by Northern analysis. In both types of cells, MMP-13 mRNA was increased at 2 h post-FSS; levels peaked at 8-16 h post-FSS and remained elevated at 24 h. In MC3T3-E1 cells subjected to 30 min of FSS and then placed in static culture for 8 h, the protein synthesis inhibitor cycloheximide (CHX) blocked the FSS induction of MMP-13 mRNA, indicating that *de novo* protein synthesis was required for the induction. Since FSS induces both cyclooxygenase-2 (COX-2) and c-Fos by 30-60 min in these cells, these proteins are candidates for mediating the FSS induction of MMP-13. Treatment of cultures with an inhibitor of COX-2 activity, NS398, did not affect the FSS induction of MMP-13. However, preliminary studies indicate that the FSS stimulation of MMP-13 mRNA was reduced 40-50% in primary calvarial cells from *c-fos* knockout mice compared to cells from mice carrying at least one allele for *c-fos*. To examine the role of the MEK-ERK pathway in the FSS stimulation of MMP-13, we used a specific inhibitor of MEK-ERK activation (PD98059, 50 μM). At 6 h post-FSS, PD98059 did not decrease the induction of MMP-13. We conclude that FSS induces MMP-13 mRNA as a delayed response gene, that this induction may depend on the FSS induction of c-Fos, and that the pathway for FSS induction of MMP-13 in osteoblastic cells differs from that for the biaxial strain induction of MMP-13.

Disclosures: ***S. Masatomo****, None.*

SA178

See Friday Plenary number F178

SA179

Role of TREK Stretch-Activated Potassium Channels in Mechanically-Induced PTHrP Gene Expression in Osteoblasts. X. Chen[1], K. W. Ng[2], L. F. Bonewald[3], A. E. Broadus[1]. [1]Internal Medicine, Yale University School of Medicine, New Haven, CT, USA, [2]University of Melbourne, Melbourne, Australia, [3]School of Dentistry, University of Missouri, Kansas City, MO, USA.

The PTHrP gene is normally expressed in cells of the osteoblastic lineage and is mechanically inducible in smooth muscle cells. N-terminal PTHrP species are equipotent with PTH in bone systems and PTHrP has recently been shown to have an anabolic function in bone in vivo based on conditional knockout of PTHrP in osteoblastic cells (J Bone Min Res 17, S138, 2002). We therefore decided to see whether PTHrP might be mechanically induced in osteoblast-like cells.

Reduction of osmolality from 317 to 240 mosm produced a 3-fold increase in PTHrP mRNA in UMR-201 cells, which have an early osteoblastic phenotype. Addition of either gadolinium or nifedipine had no effect, and removal of extracellular calcium or depletion of intracellular calcium with thapsigargin also had no effect. These findings indicate that neither stretch-activated cation channels, L-type calcium channels, nor intracellular calcium is involved in the induction of PTHrP in response to hypotonicity. TREK family members (two-pore domain potassium channels) are novel stretch-activated channels that can be activated by both stretch and intracellular acidosis. By RT- PCR and direct sequencing, we identified the TREK-2 gene expression in UMR-201cells. We found that intracellular acidification markedly increased PTHrP mRNA expression. Furthermore, we found that siRNA targeted against the TREK-2 gene reduced endogenous TREK-2 expression by 80% and hypotonic induction of PTHrP mRNA by 30% compared with control siRNA transfected cells.

Cell swelling may activate ion channels other than those opened by mechanical force, so we studied UMR-201 cells with Flexercell 4000 apparatus, we found cells exposed to 2% magnitude mechanical strain increased PTHrP mRNA by 2-fold at 24 hours. We also studied MLO-A5 cells, which are phenotypically similar to late osteoblasts-early osteocytes, thought by many to be key targets for mechanical force in vivo, and found a 3-fold Flexercell-induced increase in PTHrP

We propose PTHrP as a candidate mediator of the anabolic effects of mechanical force on bone and that TREK channels maybe involved in the induction of PTHrP.

Disclosures: ***X. Chen****, None.*

SA180

See Friday Plenary number F180

SA181

Increase in Osteoblast-Like Cell Number by Cyclic Strain Is Augmented by Rest-Insertion *In Vitro*. V. J. Armstrong*, D. B. Ong*, G. Zaman*, R. F. L. Suswillo*, J. S. Price, L. E. Lanyon. Veterinary Basic Sciences, The Royal Veterinary College, London, United Kingdom.

In vivo, insertion of a rest period after each load cycle enhances a bone's osteogenic response to cyclic loading [1]. This raises the question as to whether this is an inherent property of the cells, or a feature of the mixed stimulus arising from strain, fluid flow and pressure change to which osteocytes are exposed when bone tissue is cyclically loaded. To investigate this we exposed sub-confluent cultures of ROS 17/2.8 cells to a single short period of cyclic strain by four-point bending of the plastic slides onto which they were seeded (60,000/slide). The cells were then incubated for a further 24 hours before being fixed and counted. Three different straining regimens were used, in each of which the peak strain on the surface of the plastic was 3,400μ. 40 strain cycles at 1 Hz lasting 40 seconds and 600 strain cycles at 1 Hz lasting 10 minutes stimulated a similar statistically significant increase in cell number compared with static (non-strained) controls ($p<0.01$). Insertion of a 14.9 second rest period after each of the 40 strain cycles (0.06 Hz over 10 minutes) stimulated a greater increase in cell number ($p<0.01$) than either 40 strain cycles or 600 strain cycles at 1 Hz. These *in vitro* data confirm that relatively few cycles of strain are needed to stimulate osteoblasts' increase in number. This is consistent with *in vivo* data on the osteogenic effects of loading from mice, rats and birds and from human exercise studies. These data also suggest that the increased osteogenic response to rest insertion [1] is an inherent feature of bone cells' response to cyclic mechanical stimulation (in this case strain and associated fluid perturbation), rather than any effect on fluid flow arising from cyclic strain in bone tissue.

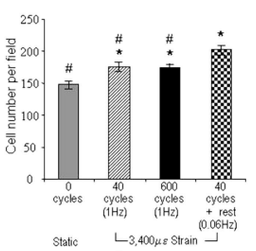

Fig 1. Effect of rest-inserted strain on osteoblast-like cell number. Values = mean +/- SEM; n=6; *P<0.01 vs Static; #P<0.01 vs 40 cycles + rest

1. Srinivasan, S., Weimer, D. A., Agans, S. C., Bain, S. D., and Gross, T. S. (2002) *J Bone Miner Res 17*, 1613-20.

Disclosures: ***V.J. Armstrong****, None.*

SA182

See Friday Plenary number F182

SA183

Pressure Modulation During Loading of a Trabecular Bone Core in an Ex Vivo Model. E. L. Smith[1], A. Gerson*[1], H. Ploeg*[2], D. B. Jones[3]. [1]Population Sciences, University Of Wisconsin, Madison, WI, USA, [2]Mechanical Engineering, University Of Wisconsin, Madison, WI, USA, [3]Exp. Othopädie & Biomechanik, Phillips- Universität, Marburg, Germany.

It has been hypothesized that bone cell response to mechanical loading is not due to the bending of the bone matrix but to the shear fluid flow. The purpose of this experiment was to determine the degree of deformation on a trabecular bone core that will induce pressure shifts within the morrow cavity. It is difficult to measure shear fluid flow within trabecular bone, however it is possible to measure pressure shifts of fluid within the bone morrow during loading and use this pressure shift as an indicator of changes at the cellular level. Bovine trabecular bone cores 5 mm thick and 10 mm in diameter were prepared using an Exakt diamond band saw and diamond tipped drill. A confocal microscope showed rough surfaces from the saw varying 5 to 10 micrometers. Hemodynamic measurements of pressure shifts were determined using a 1.4 Fr high-fidelity pressure catheter from Millar Instruments in the center of the morrow cavity. The catheter has a pressure range from -50 to +300 mmHg, and a standardized sensitivity of 5 μV/V/mmHg. A hole was drilled through the bioreactor chamber and into the center of the bone cores. The Millar catheter was then placed either just outside the bone core or into the center of the bone core. After stabilization and calibration of the catheter, bone pressure tracings were recorded. Pressure changes were determined while using a 1 Hz loading jump, to induced deformations of 5, 10, 20 and 30 micrometers. Thirty measurements were made at each deformation both with the catheter just outside the bone core and with the catheter resting in the center of the morrow cavity. Pressure changes at the lower deformations were difficult to distinguish from the resting pressure values of about 0.5 mmHg. Figure 1 shows the rise in pressure in the center and outside the bone core bone from 5 to 30 micrometers of deformation (± SD). Pressure modulation was directly related to deformation, with an R^2 value of 0.95 from regression analysis of the inside pressures. Ref. Jones DB, Broeckmann E., Pohl T and Smith EL. Development of a mechanical testing and loading system for trabecular bone studies for long term culture, European Cells and Materials, 5(2003):48-60

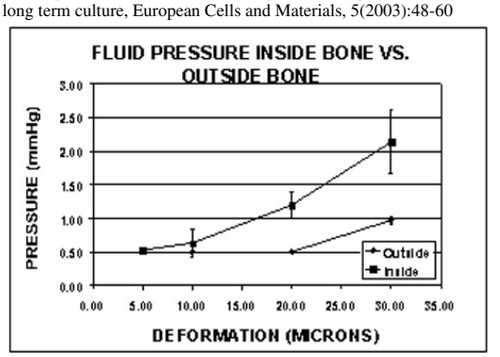

Disclosures: ***E.L. Smith****, None.*

SA184

Physical Activity Is Associated with the Size but not with the Volumetric Mineral Density of the Cortical Bone in Young Adult Men. M. Lorentzon[1], D. Mellström[2], C. Ohlsson[1]. [1]Department of Internal Medicine, Center for Bone Research at the Sahlgrenska Academy (CBS), Gothenburg University, Gothenburg, Sweden, [2]Department of Geriatric Medicine, Gothenburg University, Gothenburg, Sweden.

Physical activity has been reported to enhance bone mass accretion but little is known about its differential influence on the separate bone compartments, i.e. trabecular and cortical bone.

The *G*othenburg *O*steoporosis and *O*besity *D*eterminants (*GOOD*) study consists of 1075 Swedish men, age 18.9±0.6 yrs, and was initiated with the aim to find both environmental and genetic determinants for bone and fat mass. Questionnaires were used to collect information about current and previous physical activity (hours/week and duration in years), dairy product intake and smoking. 670 men (63%) were currently physically active and 761 (71%) had previously participated in any sports. Bone parameters were measured using both DXA and pQCT.

Both current and previous physical activity were independent predictors (multivariate analysis including age, height, weight, dairy product intake and smoking) of areal BMD of the total body, femoral neck, and lumbar spine as measured by DXA. To determine the associations between physical activity and the different bone compartments pQCT was utilized, demonstrating that current physical activity was an independent predictor of cortical bone mineral content (radius β=0.14, $p<0.001$; tibia β=0.22, $p<0.001$), cortical bone area (radius β=0.15, $p<0.001$; tibia β=0.22, $p<0.001$), and periosteal circumference (radius β=0.16, $p<0.001$ tibia β=0.17, $p<0.001$), but not of cortical volumetric BMD in the long bones. These results demonstrate that physical activity is associated with the size but not with the volumetric mineral density of the cortical bone in young adult men, suggesting that physical activity increases the amount but not the material quality of the cortical bone.

Disclosures: ***M. Lorentzon****, None.*

SA185

See Friday Plenary number F185

SA186

The Effect of Reloading on Osteoprogenitor Number, Osteoprogenitor Proliferation, and Bone Histomorphometry: Studies in Hind Limb Unloaded Rats. N. Basso*, C. G. Bellows*, J. N. M. Heersche. Faculty of Dentistry, University of Toronto, Toronto, ON, Canada.

Skeletal unloading associated with space flight results in bone loss. In astronauts the extent to which bone is lost varies greatly between different bones of the skeleton as well as between different individuals. Following return to earth, recovery of bone mass during reloading also varies between different bones and different individuals. Due to this variability between subjects it is difficult to study the effects of unloading/reloading on bone in humans. A viable alternative is to use the rat model of hind limb unloading developed at NASA. We have previously demonstrated that in 6 week old male rats, 14 days of unloading results in a decrease in osteoprogenitor number in cell populations isolated from the proximal femur. The goal of the current study was to determine the numbers of osteoprogenitor cells present in cell populations derived from the proximal femur of young rats after 14 days of unloading followed by 14 days of reloading and to characterize their proliferative capacity. To establish whether the effects of unloading and reloading were specific for cells of the osteoblast lineage, we determined the number of fibroblastic colony forming units (CFU-F), alkaline phosphatase positive CFU (CFU-AP), and osteoblast CFU (CFU-O). Effects of unloading and subsequent reloading on proliferation were evaluated by measuring the size of CFU-O. Neither unloading nor reloading had an effect on the total number of progenitors (CFU-F) in femoral cell populations. Unloading resulted in a 66% reduction in CFU-AP. CFU-O was decreased by 76% and mean colony size was 33% less than controls. The decrease in osteogenic and osteoprogenitor cells in vitro paralleled the decrease in bone volume, trabecular thickness, and trabecular number (which were decreased by 49%, 23%, and 35%, respectively) observed in the proximal tibial metaphysis of unloaded rats. Subsequent reloading restored CFU-AP. CFU-O numbers were only partially restored at 14 days (83% of controls) but nodule size was fully restored to control levels. Serum osteocalcin was unchanged by loading status, however, serum undercarboxylated osteocalcin, levels of which are possibly related to bone quality, was elevated 1.3-fold in unloaded rats and was still elevated following reloading. An assessment of static and dynamic histomorphometric parameters in reloaded animals is currently in progress. Our results indicate that in the 6-week old male rat 14 days of unloading results in a decrease in osteoprogenitor number and that reloading for 14 subsequent days is sufficient to restore osteogenic cell number, if not bone quality, to control levels.

Disclosures: ***N. Basso****, None.*

SA187

See Friday Plenary number F187

SA188

Expression of Insulin-like Growth Factors and Estrogen Receptor Alpha in the Tibia of Ovariectomized Rats after a Single Loading Bout. A. M. Tromp, H. W. van Essen*, M. Koesoebjono*, N. Bravenboer, P. Lips. Department of Endocrinology, Amsterdam, Netherlands.

We examined the influence of a single loading stimulus on mRNA expression of the insulin-like growth factors (IGF-I, IGF-II) and on the expression of type-I IGF-receptor (IGFR) and estrogen receptor alpha (ERα), in the tibia of ovariectomized rats.

Forty female rats, 12 weeks old, were randomly assigned to one of 4 experimental groups (n=10), consisting of sham-loading (SHM-LD), loading (LD), loading and ovariectomy (LD+OVX) or loading and ovariectomy with estrogen replacement (LD+OVX+E2).

Two days after surgery, estrogen replacement was started in the LD+OVX+E2 group and 5 weeks after surgery, rats were subjected to a single loading bout exerted through a four-point bending device. Loading consisted of either bending (LD groups) or compressing the right tibia (SHM-LD group) with 60N, 2Hz, during 300 cycles. The left tibia served as an unloaded internal control (NON-LD). Rats were sacrificed 6 hours after loading. Left and right tibiae were dissected and the diaphyses were prepared for RNA isolation and real-time PCR quantification. Threshold cycles (Ct) of IGF-I, IGF-II, IGFR and ERα were calculated and corrected for the expression of the housekeeping gene PBGD. The Kruskal-Wallis test was used to determine differences between the four groups, analyzed for the right (LD and SHM-LD) and left (NON-LD) tibiae separately. The Wilcoxon test was used to examine differences between the right and left tibiae within the same group. P≤ 0.05 was considered significant. The University Committee on Animal Experiments approved the protocol.

In the left (non-loaded) tibiae, IGF-I mRNA expression differed significantly (p=0.007) between the groups but IGF-II, IGFR and ERa did not. In the right tibiae, both IGF-I (p=0.049) and ERα (p=0.005) mRNA expression differed significantly between the groups, whereas IGF-II and IGFR did not. IGF-I mRNA expression was significantly decreased after loading in the LD+OVX group (p=0.028). IGFR mRNA expression was significantly decreased after loading in the LD+OVX+E2 group (p=0.046). ERα mRNA expression was significantly decreased after loading in the LD group (p=0.043).

We conclude that IGF-I mRNA expression in the tibia was up regulated after ovariectomy; mechanical loading partly counteracted this process. Mechanical loading down-regulated the type-I IGF receptor in the ovariectomized rats with estrogen replacement and the estrogen receptor alpha in the LD group. Since we were not able to detect any effects of IGF-II in this study, we suggest that IGF-I is more sensitive to the effects of mechanical loading and estrogen deficiency than IGF-II in rats.

Disclosures: ***A.M. Tromp****, None.*

SA189

Disuse-Induced Transcriptional Changes Differ From Morphologic Changes in the Male Skeleton. M. E. Squire[1], L. R. Donahue[2], C. Rubin[1], S. Judex[1]. [1]Biomedical Engineering, SUNY Stony Brook, Stony Brook, NY, USA, [2]The Jackson Laboratory, Bar Harbor, ME, USA.

The loss of functional weight bearing has detrimental consequences on trabecular bone morphology and identifying the molecular basis of disuse-induced skeletal changes will be important for developing effective countermeasures on Earth and in space. Using genetically distinct strains of mice, we recently demonstrated that both male BALB/cByJ (BALB) and C3H/H3J (C3H) suffered moderate losses of trabecular bone averaged across the distal femoral metaphysis and epiphysis with skeletal unloading (-10% and -15% respectively, p<0.05 each). Here, we tested the hypothesis that transcription levels of bone formation-related and bone resorption-related genes will be similarly suppressed by unloading in both mouse strains. Adult (16 wk) *male* BALB and C3H were randomly assigned to control (n=8 BALB and n=4 C3H) and disuse (tail suspension) (n=6 each) groups. After 4d, total RNA was extracted from the whole proximal tibia (including bone marrow and cartilage) and real time RT-PCR assessed expression levels of bone formation-related genes including collagen type Iα1 (col Iα1), core binding factor α1 (CBFA1), alkaline phosphatase, osteocalcin, and osteonectin as well as resorption-related genes including cathepsin K and osteopontin (relative to GAPDH, a housekeeping gene). In disuse BALB, transcription levels of col Iα1, alkaline phosphatase, osteocalcin, and osteonectin were significantly suppressed (-60%, -36%, -65%, and -45%, respectively, p<0.05 each) relative to control. In C3H mice, the extent by which weightlessness suppressed expression levels of col Iα1, alkaline phosphatase, osteocalcin, and osteonectin was much less than in BALB (-23%, -13%, -32%, and -11%, respectively), and only the suppression of osteocalcin was statistically significant (p<0.05). The expression levels of formation-related genes affected by disuse in C3H correlated well (r^2=0.88, p<0.01) with changes in disuse BALB when considering all formation-related genes whose expression levels were suppressed by at least 10%. Transcription levels of CBFA1, cathepsin K, and osteopontin were not affected by disuse in either strain of mice. Relating the molecular level response to disuse to the induced morphologic changes in male BALB and C3H suggests that even though the molecular pathways underlying disuse-induced suppression of bone formation may be similar across different genotypes, similar changes in bone morphology may be accompanied by drastically different changes in the expression levels of some genes. The future development of effective pharmacological and/or biomechanical countermeasures of osteoporosis may need to consider genetic variations.

Disclosures: ***M.E. Squire****, None.*

SA190

Gender Influences the Skeletal Sensitivity of F1 BALBxC3H Crossbreds to Mechanical Unloading. M. E. Squire[1], S. Xu*[1], R. A. Garman[1], L. Xie*[1], C. Rubin[1], L. R. Donahue[2], S. Judex[1]. [1]Biomedical Engineering, SUNY Stony Brook, Stony Brook, NY, USA, [2]The Jackson Laboratory, Bar Harbor, ME, USA.

Skeletal morphology as well as sensitivity of the skeleton to the loss of functional weight bearing is under the influence of the genome. Using genetically distinct inbred strains of mice, we have previously demonstrated that the skeleton of female BALB/cByJ (BALB) mice was highly sensitive to the loss of functional weight bearing (-60% loss of metaphyseal trabecular bone) while the skeleton of genetically distinct male C3H/HeJ (C3H) mice was much less responsive (-20% loss of metaphyseal trabecular bone). Here, we subjected F1 crossbreds (BALBxC3H) to hindlimb suspension and hypothesized that the degree of the skeleton's sensitivity to disuse would be intermediate to that of the parental strains. Further, we tested the hypothesis that gender would influence bone morphology and skeletal sensitivity to disuse in these F1 mice. Adult (16 wk) male and female F1 mice (n=20 each) were randomly assigned to control and disuse (tail suspension) groups (n=10 each). After 21d, right femurs were extracted and high-resolution micro-computed tomography (12μm) scanning (μCT) was used to assess indices of trabecular bone quantity and morphology in the distal femoral metaphysis and epiphysis. Comparisons of bone morphology between male and female F1 mice revealed that males had less metaphyseal BV/TV than females (-22%, p<0.01), yet epiphyseal BV/TV was not different across gender. The catabolic effects of hindlimb unloading were seen in both male and female F1 mice, yet female F1 suffered from greater loss of trabecular bone (-29%) averaged across the metaphysis and epiphysis as compared to male F1 (-8%) (p<0.01). Separated into the metaphysis and epiphysis, female F1 mice lost 36% of metaphyseal BV/TV and 15% of epiphyseal BV/TV (p<0.01 each), yet male F1 mice only lost significant amounts of BV/TV from the distal femoral metaphysis (-11%, p< 0.05). These findings demonstrate that male C3H mice/female BALB crossbred mice produce female F1 offspring whose skeletal sensitivity to unloading is intermediate to that of the parental strains. Consistent with data from the female and BALB skeletons, the female F1 mice was more responsive to disuse than the male F1 skeleton. Further, the relatively small response of the male F1 skeleton to disuse more closely corresponds to the responsivity of the skeletons of female and male C3H mice. Taken together, these results suggest that genetics modulates the influence of gender on the sensitivity of the skeleton to altered mechanical loading environments.

Disclosures: ***M.E. Squire****, None.*

SA191

See Friday Plenary number F191

SA192

Quantitation of an Osteogenic Response to Isometric Mechanical Loading. J. D. Delaney*, D. W. Rowe. Genetics and Developmental Biology, University of Connecticut Health Center, Farmington, CT, USA.

Net bone formation is dependent on remodeling and hence the stimulation and differentiation of multipotent progenitor cells towards an osteogenic lineage. We have been evaluating a strategy to provide a controlled physiologically relevant stress without the volition of the subject sufficent to stimulate osteoblastic activity. A New Brunswick orbital shaker (Model C10) was modified to house up to 16 animals for mechanical loading. Mice transgenic for pOBCol2.3GFP, a visual marker of osteoblasts and osteocytes, were loaded 30 minutes every other day in subsequent three-week intervals of 180, 210 and 240 RPM. Xylenol orange injections were administered to the animals ten and two days prior to sacrifice. Animals were sacrificed at one-week intervals. During sacrifice animals were cardiac perfused with a normal saline solution and then cold 4% paraformaldehyde (PFA). Decalcified and non-decalcified femur and spine were embedded in OCT matrix and cryosectioned. Full-length femurs were viewed on an inverted Zeiss Axiovert 200M and imaged with a digital Axiocam CCD camera. Using Improvision thresholding software we identified and quantitated select sub-populations of high expressing GFP cells (osteoblasts) and low expressing GFP cells (osteocytes) in whole femur sections. GFP expression patterns demonstrated a statistically significant increase in both high expressing and low expressing osteoblast activity at 21, 27 and later at 57 days of loading. Non-decalcified sections revealed marked xylenol orange labeling in the whole femur as the experiment progressed. Extensive xylenol orange labeling was evidenced in the femoral head region as compared to control sections. Results from this study indicate that this mechanical loading protocol is providing an increased stress level particularly in the proximal femur and to a lesser extent along the diaphyseal shaft and metaphysis. Isometric loading protocols should focus examination of boney responses in proximal femur where peak stresses are highest and there is the greatest osteoblastic activity.

Disclosures: ***J.D. Delaney****, None.*

SA193

Design and Evaluation of an Apoptosis-Sensitive GFP Reporter Construct. M. B. McKinstry*, Q. F. Yang*, D. W. Rowe. Genetics and Developmental Biology, University of CT Health Center, Farmington, CT, USA.

Apoptosis plays a central role in controlling the number of osteoblasts making and maintaining bone mass. Our goal is to design a reporter system that would initiate a green fluorescent protein (GFP) signal early in the apoptotic process either in histological sections of bone or in real time in primary osteogenic cultures.

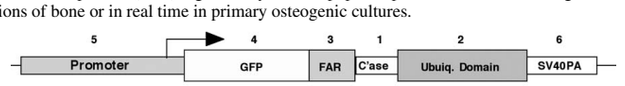

Central to our design is a caspase-3 recognition sequence (1) followed by a ubiquitination target (2) downstream of a GFP reporter (4) so that in the absence of apoptosis, GFP is targeted to the proteasome and the cell is "off." Conversely, an apoptotic cell is "GFP on" when caspase 3 is activated and cleaves off the ubiquitination target. Ubiquitination and proteosomal degradation are coordinated within a cell to rapidly prevent expression of intracellular proteins. Two examples of highly regulated and rapidly degraded proteins via the ubiquitination pathway are the hypoxia-inducible factor 1 alpha transcription factor (HIF) and the PRAJA1 protein (PRAJA). Cloning of this construct began with the pEGFP-F1 vector (Clontech), which contains a CMV promoter (5) driving eGFP (4) with a farnyslational domain (FAR, 3) to localize the signal to the cell membrane, followed by a multiple cloning site (MCS), and SV40 polyadenylation signal (6). The farnyslation linker and MCS were modified with an in-frame linker containing the caspase-3 cleavage recognition sequence of DEVD as well as restriction sites for insertion of either HIF or PRAJA. The completed constructs are identified as CMV-EGFP-FAR-DEVD-HIF and CMV-EGFP-FAR-DEVD-PRAJA. Stable cell lines expressing these constructs were generated by LipofectAMINE transfection and selected with G418. Apoptosis was induced with etoposide treatment or by transient transfection with a caspase-3 cDNA. Incubation with etoposide versus vehicle with both HIF and PRAJA clonal lines resulted in GFP-positive cells only with etoposide treatment. Furthermore, overexpression of caspase-3 cDNA resulted in GFP detection in clonal lines expressing the caspase-3 substrate sequence DEVD but not in a line containing a caspase resistant (DEVG) linker sequence. Thus the concept of a visual reporter for a protein cleavage (caspase-3) process appears to be validated by these constructs and justifies further studies on its application as a marker for apoptosis in primary cells and intact animals.

Disclosures: ***M.B. McKinstry****, None.*

SA194

See Friday Plenary number F194

SA195

Endogenous COX-2 Gene Expression Does Not Alter Apoptosis in Murine Osteoblastic Cells. S. Choudhary, Z. Xu, L. G. Raisz, C. C. Pilbeam. Dept. of Medicine, Univ. of Connecticut Health Center, Farmington, CT, USA.

Primary calvarial osteoblasts from cyclooxygenase (COX)-2 knockout (KO) and wild type (WT) mice can be used to examine the effects of endogenous COX-2 expression on osteoblastic function. We previously found that cell number and proliferation were significantly increased in primary calvarial osteoblasts cultures from COX-2 KO mice relative to cultures from COX-2 WT mice. The goal of this study was to determine if apoptosis was also affected by the absence of endogenous COX-2. Calvariae from 5-8 wk old mice were sequentially digested, and cell populations 2-5 were pooled, grown to confluence and replated for experiments at 5000/cm^2. We used the same culture conditions that were previously used to study proliferation. Under normal culture conditions, each addition of fresh serum induces COX-2 expression and COX-2 associated PGE_2 production. Little PGE_2 is produced in COX-2 KO cultures. To measure apoptosis and cell death, we used flow cytometry after staining of cells with annexin-V-FITC and propidium iodide, as well as TUNEL staining of fixed cells. Cells were grown for 3 d before measurement. Six independent flow cytometry experiments showed no differences between COX-2 WT and KO cells in percent early (annexin only staining) apoptotic cells (2.7 ± 1.0% vs 2.0 ± 0.8%), late (annexin + PI staining) apoptotic cells (1.0 ± 0.1% vs 0.9 ± 0.2%), or dead (PI only staining) cells (1.0 ± 0.2% vs 1.5 ± 0.1%). On TUNEL staining, there was no significant difference between apoptotic cells in COX-2 WT cultures (14.5 ± 0.9%) and COX-2 KO cultures (16.1 ± 0.5%). Moreover, addition of NS-398 (1 μM) to COX-2 WT cultures, to block prostaglandin synthesis, or of PGE_2 (1 μM) to COX-2 KO cultures had no effect on apoptosis. In order to induce apoptosis, we treated cultures with calcium and phosphate (3 mM each), which also induces COX-2 expression and PGE_2 production in COX-2 WT cells. Cells were grown for 5 days and treated with calcium and phosphate for 6 h. In 3 independent experiments using flow cytometry, calcium and phosphate significantly ($P<0.05$) increased the percent apoptotic cells (early + late) similarly in COX-2 WT cultures (from 2.9 ± 0.3% to 6.3 ± 0.7%) and in COX-2 KO cultures (from 3.3 ± 0.2% to 8.0 ± 0.7%). We conclude that endogenous COX-2 expression has little effect on apoptosis in cultured calvarial osteoblasts. Hence, the increased cell proliferation seen in cultured COX-2 KO calvarial osteoblasts compared to WT cells accounts for the increased cell numbers in KO cultures.

Disclosures: ***S. Choudhary****, None.*

SA196

Overexpression of COX-2 in Saos-2 Human Osteosarcoma Cells Increases Apoptosis Via Oxidative Stress. S. Choudhary, Z. Xu, O. S. Voznesensky*, C. C. Pilbeam. Dept. of Medicine, University of Connecticut Health Center, Farmington, CT, USA.

Overexpression of cyclooxygenase (COX)-2 promotes tumor growth in many tissue types, primarily by increasing resistance to apoptosis. To examine the role of COX-2 in osteosarcoma cells, we overexpressed murine COX-2 in human Saos-2 cells, which normally express very low levels of COX-2 mRNA. COX-2 overexpression in Saos-2 cells has previously been shown to reduce cell number and proliferation via cell cycle arrest at G2/M. The goal of this study was to examine effects of overexpressed COX-2 on apoptosis. Two methods of overexpression were used. In the first, we compared cells derived from a single clone stably transfected with neomycin resistance (Neo) and type I Col 3.6-driven murine COX-2 cDNA with cells from a clone expressing only Neo. In the second method, cells were retrovirally transduced with a construct expressing green fluorescent protein (eGFP) and murine COX-2 (CMV-COX-2/eGFP) or with empty vector (CMV-GFP). Expression of COX-2 was confirmed by Northern blot, by Western blot and immunostaining, and by PGE_2 production. Apoptosis was examined by TUNEL staining and by flow cytometry after annexin-V-FITC / propidium iodide (PI) staining. In stably transfected cells examined by flow cytometry, early apoptosis (cells stained only by annexin) increased from 6.6 ± 3.0% in cells with Neo alone to 25.7 ± 4.7% in cells overexpressing COX-2 ($P<0.01$). In retrovirally transduced cells, early apoptosis increased from 14.6 ± 0.4% in cells carrying empty vector to 24.8 ± 0.5% in cells overexpressing COX-2 ($P<0.01$). By TUNEL staining, COX-2 overexpression in retrovirally transduced cells increased apoptosis from 4.0 ± 0.8% to 13.9 ± 3.1 % ($P<0.05$). Effects of COX-2 overexpression could not be reversed by inhibitors of COX activity or mimicked by exogenous PGE_2, indicating that effects were not mediated by prostaglandins. Reactive oxygen species (ROS) may be formed during the catalysis of arachidonate by COX-2 and can potentiate apoptosis. Flow cytometric measurement of intracellular ROS using the fluorescent dye hydroethidine, a marker of superoxide anion, showed increased ROS formation in COX-2 overexpressing cells. Treatment of cells with the antioxidant N-acetyl-cysteine (NAC, 5 mM) for 24 h inhibited both ROS accumulation and apoptosis in COX-2 overexpressing cells. Hence, the increased apoptosis seen with overexpression of COX-2 is likely to be the result of increased ROS. Since overexpression of COX-2 decreases cell proliferation and increases apoptosis in Saos-2 cells, it is unlikely to promote tumor progression in these osteosarcoma cells, in contrast to the findings in other types of malignancies.

Disclosures: ***S. Choudhary****, None.*

SA197

The Mechanism of Calcium and Phosphate induced Osteoblast Apoptosis. R. Saunders*, K. H. Szymczyk*, I. M. Shapiro, C. S. Adams. Orthopaedic Surgery, Thomas Jefferson University, Philadelphia, PA, USA.

Our previous work has demonstrated that the $Ca^{2+}$and Pi ion pair is a potent osteoblast apoptogen. The underlying mechanisms by which it activates apoptosis remain unclear. We hypothesize that release of intracellular Ca^{2+} stores causes loss of mitochondrial membrane potential and, subsequently, apoptosis. To establish the mechanism of Ca^{2+}·Pi ion pair induced apoptosis in osteoblasts, MC3T3-E1 osteoblast-like cells were used. Cell death was activated by incubation with 5 or 3 mM Pi and 2.4 or 2.9 mM Ca^{2+}, and measured using the MTT assay. Apoptosome formation was confirmed using Western blot analysis for cytochrome c and Smac/Diablo release. Inhibitors of numerous mitochondrial and endoplasmic reticulum (ER) functions were used to block apoptosis. In addition, neomycin, an inhibitor of phosphoinositide (PI) hydrolysis was also used. Western blot analysis showed that cells treated with the Ca^{2+}·Pi ion pair released cytochrome c and Smac/Diablo from their mitochondria, confirming our previous observation that the ion pair caused a mitochondrial membrane permeability transition (MMPT), and activated an apoptosome in osteoblasts. Blockade of either the electron transfer chain, or induction of the MMPT, inhibits Ca^{2+}·Pi apoptosis in a dose-dependent manner. Pretreating osteoblasts with ruthenium red, a uniporter inhibitor in both mitochondria and the endoplasmic reticulum, also completely abolished Ca^{2+}·Pi -induced programmed cell death. As the endoplasmic reticulum (ER) participates in the propagation of calcium waves and an increase in intracellular Ca^{2+} has previously been observed prior to the MMPT, calcium mobilization from ER stores was examined. Modulation of apoptosis was observed with Dantrolene, a specific inhibitor of the ryanodine receptors in the ER, but not cyclopiazonic acid, an ER Ca^{2+}-ATPase inhibitor. This indicated involvement of calcium stores regulated by ryanodine-receptor channels. Pretreatment with 200 μM neomycin, a general inhibitor of phosphoinositide (PI) hydrolysis also inhibited Ca^{2+}·Pi induced osteoblast cell death while treatment with carbamylcholine chloride, an activator of PI hydrolysis, activated apoptosis in osteoblasts. As calcium sensing receptors utilize PI hydrolysis, these results are consistent with the involvement of those receptors in Ca^{2+}·Pi induced apoptosis. Together, these data demonstrate that Ca^{2+}·Pi induced osteoblasts apoptosis is characterized by the generation of a true apoptosome. Secondarily, calcium release from ER stores may play a major role in the activation of osteoblast apoptosis by the Ca^{2+}·Pi ion pair. Furthermore, such Ca^{2+} release may implicate the involvement of calcium sensing receptors.

Disclosures: ***C.S. Adams****, None.*

SA198

Tartrate Resistant Acid Phosphatase (TRACP) in Osteoblasts: Endogenous Expression and Endocytosis of the Enzyme. S. G. Perez*[1], I. Vogels*[2], T. Schoenmaker*[3], S. Alatalo*[4], H. Jussi[5], W. Beertsen[6], V. Everts[7]. [1]Experimental Periodontology, Academic Centre for Dentistry, Universiteit van Amsterdam and Vrije Universiteit, Amsterdam, Netherlands, [2]Cell Biology and Histology, Universiteit van Amsterdam, Amsterdam, Netherlands, [3]Experimental Periodontology, Academic Centre for Dentistry Amsterdam, Universiteit van Amsterdam and Vrije Universiteit, Amsterdam, Netherlands, [4]Finish Red Cross, Helsinki, Finland, [5]Department of Anatomy, University of Turku, Turku, Finland, [6]Periodontology, Academic Centre for Dentistry Amsterdam, Universiteit van Amsterdam and Vrije Universiteit, Amsterdam, Netherlands, [7]Oral Cell Biology, Academic Centre for Dentistry Amsterdam, Universiteit van Amsterdam and Vrije Universiteit, Amsterdam, Netherlands.

TRACP is generally considered as a selective histochemical and biochemical marker of osteoclasts. Yet, several data suggest that other cell types, such as osteocytes and osteoblasts, may also produce the enzyme. Expression of TRACP activity in osteoblasts is particularly obvious at sites were osteoclasts resorb bone. This could suggest that osteoclasts (or their precursors) somehow induce TRACP expression by osteoblasts. In the present study we investigated this by using medium conditioned by osteoclast precursors (monocytes).

Human osteoblasts were obtained from bone samples and cultured with or without medium conditioned by cultured monocytes (MCM). Analysis of TRACP included activity assays, immunolocalization and real time PCR.

Osteoblasts cultured in control medium proved to express TRACP. However, the enzyme was present in an inactive form. Upon culturing with MCM a high level of active TRACP was found. Since this activity could have been due to activation of the inactive enzyme fraction or to endocytosis of TRACP present in the conditioned medium, osteoblasts were cultured in MCM in which the enzyme was depleted by immunoprecipitation. Data obtained from cells cultured with this medium or with non-depleted MCM revealed that (1) a relatively large fraction of TRACP is endocytosed (approximately 80 % of the total level of TRACP activity), (2) endogenous expression of TRACP is stimulated by -yet unidentified- compounds present in MCM, and (3) that this endogenous fraction is activated in the presence of MCM.

The present data show that osteoblasts not only have the capacity to synthesize TRACP, but also to endocytose this enzyme. We propose that osteoblasts endocytose TRACP released by osteoclasts at sites were osteoclastic bone resorption occurs. In the mean time, endogenous TRACP is expressed by the osteoblasts. Osteoblastic TRACP may be used for helping to clean the Howship's lacuna left by the osteoclast.

Disclosures: ***S.G. Perez****, None.*

SA199

See Friday Plenary number F199

SA200

Paradoxical Regulation of RANKL by Runx-2 in Mature Versus Less Mature Osteoblasts. H. A. Bullock*[1], B. C. Yaden*[1], D. L. Halladay*[1], P. Ducy*[2], V. Krishnan[1]. [1]Bone and Inflammation, Eli Lilly and Company, Indianapolis, IN, USA, [2]Cell Biology, Baylor College of Medicine, Houston, TX, USA.

In an attempt to elucidate the role of runx-2 in mature versus less mature osteoblasts we transfected Saos (mature) and U2OS (less mature) cells with an adenoviral CMV-runx-2 construct. RNA was isolated and hybridized to a human array (SuperArray Bioscience). U2OS cells transfected with adeno-runx-2 showed a 3-fold increase in TNSF11, a 3-fold decrease in MCL-1, and an absence of Nip-3 compared with adeno-CMV-GFP transfected controls. TNFSF11 (RANKL) is a key factor in osteoclast differentiation and is essential in bone remodeling (Fata et al., 2000). Mice deficient in RANKL show severe osteoporosis with a complete absence of osteoclasts and marrow spaces and growth retardation of the skull, limbs, and vertebrae (Kim et al., 2000). RT-PCR analysis was performed using RANKL primers on both U2OS-adeno-runx-2 and Saos-adeno-runx-2 RNA. Runx-2 transfected Saos cells showed an inhibition of RANKL, while runx-2 transfected U20S cells showed an induction of RANKL compared with adeno-CMV-GFP transfected controls. To further explore these differences we utilized a 4.6 kb fragment containing the human RANKL promoter in a βGAL reporter plasmid. This construct contained the TATAA and CAAT boxes as well as several proximal and distal OSE (runx-2 responsive) elements. These striking differences in RANKL regulation can be attributed to the mature versus less mature phenotypes between Saos and U2OS cells, respectively.

Disclosures: ***H.A. Bullock****, None.*

SA201

Specific Domains of TRAP Control Bone Formation at Sites of Remodeling. M. Matsuzawa*, T. J. Sheu*, R. J. O'Keefe, R. N. Rosier, E. M. Schwarz, M. J. Zuscik, H. Drissi, J. E. Puzas. Orthopaedics, University of Rochester, Rochester, NY, USA.

Purpose: The mechanism by which osteoblasts recognize sites of prior resorption for targeting new bone formation involves a local activation of the TGFbeta and BMP signaling pathways. This occurs through a protein-protein interaction between type 5 tartrate resistant acid phosphatase (TRAP) in the lacuna and TGFbeta receptor interacting protein (TRIP) in the cells. We now show that specific regions of the TRAP molecule are responsible for activating the pathways and describe further characterization of the effect.

Methods: Six domains of human TRAP spanning the signal peptide, catalytic and glycosylation domains were expressed in a Gateway expression system. They were then used in a mammalian two-hybrid system with TRIP to identify the regions of TRAP-TRIP interactions. Immunoprecipitation, Smad reporter assays and RT-PCR experiments for Runx2 and BMP6 further refined the interactions.

Results: Fragment 4, representing overlapping regions in the catalytic and glycosylation domains of TRAP, appears to have the highest affinity for TRIP. It also, i) stimulated TGF-beta/Smad reporter signaling, ii) demonstrated a high specificity for TRIP and iii) induced Runx2 and BMP6 expression by approximately 8 fold over control treatments. These are all features that are consistent with the stimulation of proliferation and differentiation in osteoblasts.

Conclusion: TRAP contains protein recognition domains for TRIP. Upon binding of these fragments to TRIP in osteoblasts, a cascade of signaling pathways is activated involving TGFbeta, Runx2 and BMP6. These effects contribute to the expansion and differentiation of osteoblasts exactly within osteoclast lacunae containing TRAP. This signaling mechanism is a means by which the site-specific formation of bone can be directed to osteoclast lacunae during normal remodeling. It is also identifies another anabolic pathway for the stimulation of osteoblastic activity.

From a clinical perspective, removal of the TRAP signal would be expected to disrupt normal remodeling and may explain the disrupted bone formation that occurs at sites of inflammation and tumor metastasis.

Disclosures: ***J.E. Puzas****, Merck Pharmaceuticals 8; Proctor and Gamble Pharmaceuticals 8; Lilly Pharmaceuticals 8.*

SA202

See Friday Plenary number F202

SA203

Divergent Effects of Androstene Immune Regulation Hormones (IRH) on RANKL/OPG Ratio and Cell Viability in Osteoblast Cells. N. H. Urban*[1], R. M. Loria*[2], M. J. Beckman[3]. [1]Orthopedic Surgery, Virginia Commonwealth University, Richmond, VA, USA, [2]Microbiology and Immunology, Virginia Commonwealth University, Richmond, VA, USA, [3]Biochemistry, Virginia Commonwealth University, Richmond, VA, USA.

Immune Regulating Hormones (IRH) α androstenediol (5-androstene-3 beta-17 alpha diol, αAED)and β androstenediol (5-androstene-3 beta-17 beta-diol, βAED) have profound effects on the immune system. αAED inhibits tumor cell proliferation and mediates apoptosis via TH_1-type immune pathways. βAED stimulates myelopoesis, strengthens host resistance and counteracts the immuno-suppressive effects of glucorticoids. The emerging concept of osteoimmunity links immune function via T-cell activation to associated bone loss diseases. Recent data suggests that T-cells activate receptor activator of NFκB ligand (RANKL), one of the primary signaling molecules responsible for mediating bone remodeling. RANKL mediates osteoclastogenesis by binding to RANK receptors on osteoclast progenitors, and RANKL potency is balanced by the antagonist (decoy receptor) osteoprotegrin (OPG). We hypothesize that α or β positioning of the C-17 hydroxyl on AED is crucial to the divergent functions of these hormones and their effects on osteoblast signaling and osteoclast recruitment and survival. Using RealTime RT-PCR we determined that αAED significantly increased the RANKL/OPG expression ratio 2-fold in osteoblasts (FOB-9 cells). Confocal immunofluorescence microscopy revealed that αAED altered the morphology and RANKL localization in osteoblasts. Moreover, αAED significantly decreased cell viability (3 fold) as determined in a fluorescent Live/Dead cell assay suggesting a potential for αAED to cause osteoblast apoptosis. However, βAED had no effect on RANKL expression, localization or cell viability. Whereas αAED has recently been shown to increase peroxisome proliferator-activated receptor γ (PPARγ), βAED decreases PPARγ and its genomic effects. In this study, we determined that an increase in PPARγ, via incubation of cells with the known peroxisome proliferator, WY14643, resulted in a significant decrease (4 fold) in viable cells. There was no effect on cell viability upon incubation of osteoblast cells with the PPARγ antagonist GW9662. Co-incubation of cells with αAED and WY14643 also resulted in a decrease in cell viability (6 fold), but co-incubation with αAED and GW9662 had no effect. It is known that a loss of function mutation in CYP17 gene results in decreased growth and osteoporosis which suggests a link between the 17-hydroxylase and bone remodeling. In conclusion, the C-17α hydroxylation on AED regulates both an increase in RANKL and activation of a cell death pathway in osteoblasts.

Disclosures: ***N.H. Urban****, None.*

SA204

Oxytocin: an Estrogen-Controlled Autocrine-Paracrine Enhancer of Bone Cell Activity. S. Colucci*, G. Colaianni*, R. Tamma*, A. Di Benedetto*, C. Camerino*, G. Mori*, N. Patano*, M. Grano*, A. Zallone. Human Anatomy and Histology, University of Bari, Bari, Italy.

Oxytocin (OT) is a well known hypothalamic hormone, whose effects in recent years have been demonstrated to be more widespread than previously believed. We recently demonstrated oxytocin receptor expression on both osteoblasts and on mature osteoclasts and their precursors. Here we show that oxytocin is an estrogen-controlled autocrine-paracrine short life peptide that turns on cell activity in bone, stimulating pulses of bone resorption and formation. In fact we demonstrated by immunofluorescence, western blot and RT-PCR that a 6 hours pre-treatment with estradiol up-modulated the receptor both in osteoblasts and in osteoclasts. Simultaneously RNA expression for oxytocin became strongly evident in osteoblasts, as demonstrated by RT-PCR and Northern blot analyses, while with antibodies raised against oxytocin we demonstrated by immunofluorescence that the peptide expression was strongly enhanced in the cells after 6-12 hours and was back to control levels after 24 hours. The presence of OT caused receptor endocytosis within 12hours. OTR stimulation elicited in both cell kinds an intracellular calcium increase, but with different patterns; ERK activation, inhibited by Pertussis toxin, followed after 5' OT treatment and was back to basal levels after 20'. OT stimulated proliferation in growing osteoblast cultures. In more differentiated osteoblasts OT, as seen by Western Blot and RT-PCR, reduced the expression of osteoprotegerin and induced a RANK-L increase. OT on human blood monocytes in the presence of MCSF strongly increased cell proliferation and RANK expression. Osteoclast precursors, cultured in the presence of MCSF and RANK-L, gave rise to a higher number of TRAP-positive cells when OT was added to the medium. In differentiated osteoclasts OT treatment was also followed by AKT phosphorylation. Bone resorption activity was, however, decreased by 40% in the first 48 hour after OT stimulation, but was thereafter back to control levels. All together these results indicate that the Oxytocin acts as an estrogen-mediated switch that keeps up bone cell activity.The increased osteoclastogenesis coupled to decreased bone resorption, considering the cyclic activity of the hormone due to the down regulation of receptors, alternates period of bone formation with resorption performed by the newly differentiate osteoclasts. This fact is particularly important during the final period of pregnancy and during lactation when a high level of circulating calcium is necessary, but can also explain at least part of the protective action of estrogens on the skeleton.

Disclosures: ***A. Zallone****, None.*

SA205

Tibolone Effects on Human Osteoblast Cells in Culture Require Estrogen Receptor. K. L. Shogren*[1], A. Maran[1], M. Zhang*[1], T. C. Spelsberg[2], H. J. Kloosterboer*[3], R. T. Turner[1]. [1]Orthopedics, Mayo Clinic, Rochester, MN, USA, [2]Biochemistry and Molecular Biology, Mayo Clinic, Rochester, MN, USA, [3]Research and Development Laboratories, NV Organon, 5340 BH Oss, Netherlands.

Tibolone is a Selective Tissue Estrogenic Activity Regulator (STEAR), which expresses estrogenic activity on bone, vagina and brain without stimulating the breast and the endometrium. Clinical studies have proven that postmenopausal loss of bone from the spine and proximal hip can be prevented by tibolone. Animal studies have shown that tibolone can prevent bone loss following ovariectomy and the protective effect of tibolone can be blocked by antiestrogens, suggesting that the effect is estrogen receptor (ER)-dependent. However, direct effects of tibolone on normal human bone cells have not been reported. The effects of two major metabolites of tibolone, 3α-hydroxy tibolone and 3β-hydroxy tibolone were determined on human fetal osteoblast (hFOB) cells that have been stably transfected with ERα cDNA . The effects of these compounds compared to the vehicle control were investigated on bone genes at the level of RNA (alkaline phosphatase, type 1 collagen and osteonectin), protein (type 1 collagen) and enzyme activity (alkaline phosphatase). Both metabolites of tibolone (3α-hydroxy and 3β-hydroxy tibolone) upregulated RNA and protein levels for bone proteins. At 20 μM, 3α-hydroxy tibolone increased mRNA levels for alkaline phosphatase, type 1 collagen and osteonectin by 2.5-fold, 4-fold and 2-fold, respectively, whereas 3β-hydroxy tibolone increased the mRNA levels for the three genes by 2.5-fold, 6-fold and 2-fold, respectively. 3α-Hydroxy and 3β-hydroxy tibolone each increased Type 1 collagen protein levels by 5-fold. When a wide range of doses was used (2-20 μM), tibolone metabolites increased alkaline phosphatase enzyme activity in a dose dependent manner. At 2 μM concentrations, a 4-fold stimulation of alkaline phosphatase activity was observed with both 3α-hydroxy and 3β-hydroxytibolone. A maximum of 6-fold and 7.5-fold stimulation of alkaline phosphatase activity occurred with 20 μM concentrations of 3α-hydroxy and 3β-hydroxy metabolites respectively. In contrast to these results, neither tibolone metabolite had an effect on RNA levels nor protein levels for bone proteins expressed by ER negative hFOB cells. Thus, these results suggest that the direct actions of tibolone metabolites on bone proteins in cultured human osteoblasts are mediated through ER.

Disclosures: ***A. Maran****, NV Organon 2.*

SA206

Regulation of OPG, RANKL, IL-6 and Growth Factor Expression by Androstenedione, DHEA and Dexamethasone: Potential Usefulness of the Adrenal Androgens in the Prevention of Corticosteroid-induced Osteoporosis. G. Harding*[1], Y. Mak*[1], J. Cheung*[1], B. A. J. Evans[2], I. Fogelman[3], G. Hampson[1]. [1]Chemical Pathology, St Thomas' Hospital, London, United Kingdom, [2]Child Health, University Hospital of Wales, Cardiff, United Kingdom, [3]Osteoporosis Screening Unit, Guy's Hospital, London, United Kingdom.

The adrenal androgens ; dehydroepiandrosterone (DHEA) and androstenedione (ANDI) may have anti-resorptive as well as anabolic effects on bone. The aim was to assess the regulation of cytokines involved in bone remodelling by DHEA, ANDI and Dexamethasone (DEX) in a human osteoblastic cell line (HCC1). Expression of osteoprotegerin (OPG), RANKL, IL-6 was measured following treatment of the cells with DHEA, ANDI (10^{-12} -10^{-6} M) and DEX. The expression of a variety of cytokines and their receptors was assessed using a human cytokine/receptor gene array consisting of 268 cytokine-related cDNAs. An intensity ratio of the cDNA spots between the treated array and control array was set at >1.5 or < 0.66. DEX treatment (10^{-9}-10^{-7}M) reduced OPG (10^{-7}M: 33.7% [4.7] $p < 0.001$). OPG production also decreased with DHEA and ANDI (10^{-7}M) (DHEA 52.5% [7.8] $p < 0.001$, ANDI 51.2% [4.5] $p<0.001$). This was not inhibited by co-treatment with the androgen receptor antagonist, flutamide (10^{-7} M). Co-treatment of ANDI (10^{-8}, 10^{-6} M) with the aromatase inhibitor, ketoconazole (10^{-5} M) reversed the inhibition in OPG production. DEX led to an increase in RANKL production (185% [87.7]) which was abolished by co-treatment with ANDI (77.3 % [12.1] p=0.08) and DHEA (47.4% [8.8] p=0.08). A significant reduction in IL-6 was observed with DEX (14.1[5.4] %, $p < 0.01$), ANDI (28% [9.7], $p <0.02$) and DHEA (10-7 M) (14% [9.8] $p <0.05$). OPG mRNA decreased with DEX (33.3% [1.3], $p <0.001$), ANDI (36% [1.3] $p <0.001$) and DHEA (48% [1], $p<0.02$). DEX increased RANKL mRNA (391.1% [147], p=0.14). DHEA alone or with DEX resulted in a significant reduction in RANKL mRNA (76% [3] p=0.02, 46% [3] $p<0.001$). DHEA and ANDI reversed the DEX-induced increase in RANKL/OPG ratio. In contrast to DEX, DHEA up-regulated over 30 genes; fibroblast growth factor 5 (4.4 -fold), Pleiotrophin (2.5-fold) , Macrophage inhibitory factor (2.0-fold), vascular endothelial growth factor (VEGF 1.7-fold). VEGF up-regulation by DHEA (10^{-7} M) was confirmed by ELISA (133% [9.5] p = 0.1). Our data suggest that the adrenal androgens may slow bone resorption through their conversion to oestrogens. DHEA may also stimulate bone formation through up-regulation of growth factors and may counteract some of the catabolic effects of glucocorticoids on the skeleton.

Disclosures: ***G. Harding****, None.*

SA207

See Friday Plenary number F207

SA208

Anabolic Effects of the Phytoestrogens Genistein, Daidzein, and Resveratrol in Human Osteoblastic MG-63 Cells. A. de Gortázar*, V. Alonso*, P. Esbrit. Bone and Mineral Metabolism Laboratory, Fundación Jiménez Díaz-UTE, Madrid, Spain.

Estrogen deficiency is an important cause of osteoporosis after menopause. The pharmacological effects of soy isoflavones such as genistein and daidzein are of current interest because of their potencial role in the management of osteoporosis. However, there only a few studies so far aimed at evaluating the direct effects of these agents on osteoblastic cells *in vitro*. We assessed here the effects of genistein, daidzein, and resveratrol (another natural phytoestrogen), compared to those of 17β-estradiol (E2), on several osteoblastic markers in human osteoblastic osteosarcoma MG-63 cells. Subconfluent cells were grown in medium with charcoal-treated FBS, with or without the agonists, added every other day for 6 days, and then alkaline phosphatase (ALP) activity and bone nodule formation were determined. In experiments to assess the other markers studied, agonists were added to confluent cells without FBS for 3 days, and then total cell RNA and protein were isolated. We found that genistein, daidzein, and resveratrol, in a similar manner than 17β-estradiol, at 100 nM, inhibited (by 30%) both ALP activity and mineralization in these cells. However, the tested phytoestrogens, at 100 nM, failed to affect either core binding factor-alpha 1 or the PTH1 receptor in MG-63 cells. In contrast, these agonists, within 0.1-100 nM, similarly stimulated (maximal, 2-fold over control, at 100 nM) osteocalcin mRNA and osteoprotegerin (OPG) expression (mRNA and protein; by RT-PCR and western blot, respectively) in these cells. On the other hand, these agents either inhibited (E2) or did not affect receptor activator of nuclear factor (NF)-kappaB ligand (RANKL) protein expression in MG-63 cells. However, in these cells, these agents similarly inhibited (by 50%) basal interleukin (IL)-6 mRNA levels; although daidzein and resveratrol were less efficient than the other agonists in inhibiting PTHrP (1-36)-induced IL-6 gene expression. This inhibitory effect appear to occur by interaction with NF-kappaB activation in MG-63 cells. The stimulatory and inhibitory effects of these agents on OPG and IL-6 expression, respectively, were abolished by raloxifen and ICI182,780, two estrogen receptor antagonists, in these cells.

These findings indicate that genistein, daidzein, and resveratrol can exert similar estrogen-like osteogenic actions on human osteoblastic cells *in vitro*.

Disclosures: ***P. Esbrit****, None.*

SA209

Selective Expression of The Soluble or Membrane-Bound Colony Stimulating Factor-1 (CSF-1) Isoform in Osteoblasts Accelerates Estrogen-Deficiency Bone Loss. G. Yao[1], J. Wu*[2], S. Ovadia*[1], N. Troiano*[3], K. Karl. Insogna[2]. [1]Comparative Medicine, Yale University, New Haven, CT, USA, [2]Internal Medicine, Yale University, New Haven, CT, USA, [3]Orthopaedics, Yale University, New Haven, CT, USA.

Osteoblasts express biologically-active soluble (sCSF-1) and membrane-bound (mCSF-1) isoforms of CSF-1. To explore the role of CSF-1 isoforms in estrogen-deficiency bone loss, transgenic mice, selectively expressing either human sCSF-1 or human mCSF-1 in osteoblasts, were engineered using the 2.4 kb rat alpha I collagen promoter. Bone density determined by pQCT at three months was significantly reduced in both mCSF-1 and in sCSF-1 transgenic mice as compared to wild-type animals. For both isoforms, the decrement in bone density in female transgenic animals was greater than the decrement in male transgenic animals when compared to their respective wild-type counterparts (-19.6% vs. -10% for sCSF-1 $p<0.05$ and -11% vs. -3% for mCSF-1 $p<0.05$). Since it has been reported that the relative expression of CSF-1 isoforms changes following estrogen withdrawal, we examined the effect of individual CSF-1 isoforms on rates of bone loss following ovariectomy (OVX). For this purpose, we engineered mice expressing a single CSF-1 isoform on an *op/op* background (e.g. no endogenous CSF-1). This was accomplished by breeding mCSF-1 or sCSF-1 transgenic mice with *op*/+ mice and back crossing the offspring to an *op*/+ genotype to yield mice with an *op/op*-mCSF-1/+ or *op/op*-sCSF-1/+ genotype. Five month-old female mice with these genotypes and their wild-type female littermates underwent OVX or sham-ovariectomy (Sham). One month after surgery, bone density determined by pQCT was reduced by 9% in OVX-wild-type as compared to Sham-wild-type mice. Sham-*op/op* mCSF-1 and Sham-*op/op* sCSF-1 mice showed 6.8% and 7% bone loss respectively compared to Sham-wild-type mice. OVX further reduced the bone density in these two groups such that, compared to Sham-wild type animals, OVX-*op/op* mCSF-1 and OVX-*op/op* sCSF-1 mice showed 20% and 16% reductions in BMD respectively. We conclude that expression of CSF-1 in osteoblasts significantly augments the bone loss associated with estrogen-withdrawal. This effect is not isoform dependent. Therefore, the overall level of CSF-1 expression, rather than the ratio of the two isoforms, seems more important in accelerating estrogen-deficiency bone loss. Since the effects of estrogen withdrawal and CSF-1 expression are additive in this experimental model, it is possible that estrogen and CSF-1 act at different steps in the osteoclast formation/survival pathway. Finally, OVX-*op/op* sCSF-1 and OVX-*op/op* mCSF-1 mice are useful animal models for postmenopausal osteoporosis.

Disclosures: ***G. Yao****, None.*

SA210

An Isopropanolic Extract of Cimicifuga Racemosa (black cohosh) Stimulates Osteoprotegerin Production by Primary Human Osteoblasts. V. Viereck[1], C. Grundker*[1], S. Blaschke*[2], K. Frosch*[3], M. Schoppet*[4], G. Emons*[1], L. C. Hofbauer[4]. [1]Gynecology and Obstetrics, Georg-August-University, Goettingen, Germany, [2]Nephrology and Rheumatology, Georg-August-University, Goettingen, Germany, [3]Trauma Surgery, Georg-August-University, Goettingen, Germany, [4]Medicine, Philipps-University, Marburg, Germany.

Despite its positive effects on the skeleton, estrogen replacement therapy is no longer recommended for the prevention of postmenopausal osteoporosis because of increased cardiovascular, thromboembolic and breast cancer risks. Recently, certain herbal therapeutics have been shown to exert selective estrogen receptor modulator (SERM)-like effects with positive effects against menopausal symptoms and bone loss, but without adverse effects on the uterus or on breast tissue. Isopropanolic extracts from the rhizomes of *Cimicifuga racemosa* (black cohosh; iCR) have gained acceptance as a herbal alternative in the treatment of menopausal symptoms, although their effect on bone metabolism is unclear. Receptor activator of nuclear factor-κB ligand (RANKL) is essential for osteoclast formation and activation, while osteoprotegerin (OPG) neutralizes RANKL. 17β-estradiol and genistein have been demonstrated to modulate osteoblastic production of RANKL and OPG. In this study, we assessed the effects of iCR on OPG and RANKL mRNA steady-state levels (by semiquantitative RT-PCR) and protein production (by ELISA) in primary human osteoblasts (hOB). Under serum-free conditions, treatment with iCR increased OPG mRNA levels and protein secretion of hOB by 2- to 3-fold in a dose-dependent manner with a maximum effect at 10^6-fold dilution of iCR (0.075 µg/ml) ($P < 0.001$) after 24 - 48 hrs. Time course experiments indicated a stimulatory effect of iCR on osteoblastic OPG protein secretion by 3- to 5-fold ($P < 0.001$) as early as 12 hrs. RANKL expression was very low, and was not found to be modulated by iCR. Moreover, iCR enhanced osteoblastic differentiation markers, alkaline phosphatase activity and osteocalcin expression by up to 4- and 3-fold, respectively ($P < 0.001$). In conclusion, our data suggest that an isopropanolic extract of CR modulates OPG and RANKL production by normal human osteoblasts, which may contribute to the inhibition of osteoclastic bone resorption. Since, OPG production increases with osteoblastic cell maturation, enhancement of OPG by iCR could be related to its stimulatory effects on osteoblastic differentiation.

Disclosures: ***V. Viereck****, None.*

SA211

Osx, an Osteoblast-specific Transcription Factor, Is Mediated by Multiple Signaling Pathways. A. B. Celil*[1], P. G. Campbell*[2], J. O. Hollinger[3]. [1]Biological Sciences, Carnegie Mellon University, Pittsburgh, PA, USA, [2]Institute for Complex Engineered Systems, Carnegie Mellon University, Pittsburgh, PA, USA, [3]Bone Tissue Engineering Center, Carnegie Mellon University, Pittsburgh, PA, USA.

Recent discoveries have revealed the presence of a nuclear transcription factor, Osx, implicated in bone formation. Osx deficient mice lack the formation of cortical bone and bone trabeculae (Nakashima *et al*., 2002). The purpose of this study was to determine the possible mediators of *Osx* expression. Using quantitative real-time PCR, we showed that *Osx* was induced in response to rhBMP-2 and AdBMP-2 in human mesenchymal stem cells (hMSCs) and in NIH3T3 mouse fibroblasts. BMP-2 induced *Osx* expression in a time- and dose-dependent manner in hMSCs. We tested the effect of several different growth factors implicated in osteoblast differentiation and among these factors IGF-I showed a synergistic interaction with BMP-2 in inducing *Osx*. Further, from our studies in Runx2 stably-transfected cells, we showed that Runx2 overexpression is not sufficient to induce *Osx*. BMP-2 and Runx2 display synergistic interactions in upregulating *Osx*. The BMP-2 mediated effect is not direct since it requires *de novo* protein synthesis. These results suggest that *Osx* is not entirely dependent on Runx2 and that a new protein mediator needs to be synthesized downstream of BMP-2 signaling pathway.

We also investigated the possible involvement of MAPK pathway in mediating *Osx* expression. Through our studies, we have determined that the expression of osteoblast marker gene *Alkaline phosphatase* in addition to alkaline phosphatase enzymatic activity is inhibited in response to a block in MAPK signaling pathway in hMSCs. While the inhibition of ERK1/2 seems to have no effect on *Runx2* gene expression, *Osx* expression is inhibited. hMSCs showed an inhibition of BMP-2 mediated *Osx* expression in the presence of p38 inhibitor. We confirmed the results of our MAPK inhibition experiments using chemical inhibitors as well as adenoviral MAPK constructs. As they progress into osteoblastic lineage, hMSCs may utilize MAPK signaling both via ERK1/2 and p38, but in the presence of BMP-2, p38 mediated signaling may be activated for *Osx* regulation.

Disclosures: ***A.B. Celil****, None.*

SA212

See Friday Plenary number F212

SA213

The αNAC Coactivator must Bind the Promoter to Potentiate the AP-1-Dependent Transcription of the Osteocalcin Gene. O. Akhouayri*, I. Quélo*, R. St-Arnaud. Genetics Unit, Shriners Hospital for Children, Montreal, PQ, Canada.

Tissue-specific gene activation is regulated by a combination of sequence-specific DNA-binding transcriptional activators, general transcription factors, and associated coactivators. The αNAC coactivator was identified in a differential screen for genes expressed in differentiated osteoblasts, and shown to function as a coactivator for the homodimeric c-Jun AP-1 transcription factor. In the course of these studies, it was shown that αNAC can specifically bind DNA in vitro, but it remained unclear whether the DNA binding function of αNAC is expressed in vivo or is required for its coactivating activity. We have identified an αNAC binding site within the murine osteocalcin gene proximal promoter region and demonstrated that recombinant αNAC or αNAC from ROS17/2.8 nuclear extracts can specifically bind this element. Using transient transfection assays, we have shown that αNAC specifically potentiated the c-Jun-dependent transcription of the osteocalcin promoter, and that this activity required the DNA binding domain of αNAC. Our results show that the osteocalcin gene is a target for the αNAC coactivating function and that αNAC is specifically targeted to the osteocalcin promoter as a means to achieve increased specificity in gene transcription.

Disclosures: ***O. Akhouayri****, None.*

SA214

See Friday Plenary number F214

SA215

The Dual Role of Hoxc8 as Transcription Repressor and Activator. N. Wang*[1], M. Wan[1], S. Bai*[2], X. Li*[1], X. Cao[1]. [1]Pathology, The University of Alabama at Birmingham, Birmingham, AL, USA, [2]Pathology, Washington University, St. Louis, MO, USA.

BMPs are potent osteotropic agents that induce osteoblast differentiation and bone development. BMPs transduce their signals into cells through Smad proteins. We have shown that Hoxc8 is a BMP downstream factor by functioning as a transcription repressor to stimulate bone marrow mesenchymal proliferation for their self renewal. Interestingly, Hoxc8 acts as a transcription activator in terminally differentiated cells. There are 39 members within the Hox gene family arranged into four clusters whose activities are essential for tissue patterning and bone development. Our previous data suggest that all of the 39 Hox proteins interact with Smad1, Smad4 and Smad6, not TGF-β specific R-Smads, as major BMP downstream transcription factors. To understand the molecular mechanism that Hoxc8 acts a transcription repressor in stem cells and an activator in differentiated cells, we attempted to characterize the role of Hoxc8 in osteoprotegerin (OPG) and osteopontin (OPN) transcription. We have identified Hoxc8 DNA binding elements in both OPG and OPN promoters and Hoxc8 acts as a transcription repressor in both promoters in C3H10T1/2 mesenchymal cell. Hoxc8 inhibits OPG and OPN expression to prevent C3H10T1/2 mesenchymal cells from differentiation. However, Hoxc8 activates OPN and OPG transcription in 2T3 osteoblastic cells, LNCap prostate cells, MCF-7, MDA-MB-231 breast cells, functioning as a transcription activator. These observation suggests that Hoxc8 contain both activation and repression domains.

To identify such dual function domains, we truncated Hoxc8 into a series of expression plasmids that fused with GAL4 DNA binding domain. The activities of these truncated expression plasmids were examined in C3H10T1/2 cells by using GAL4 reporter plasmid. The results showed that the highly conserved domains in Hoxc8 (Hoxc8PHC) including hexapeptide motif, the homeodomain, and C-terminus mediate its repression and N-terminus of Hoxc8 (Hoxc8N) exhibits transactivation ability. Furthermore, Hoxc8PHC motif only interacts with all class I HDACs, including HDAC1, HDAC2 and HDAC3 in coimmunoprecipitation assay. These data suggests the repressive activity of Hoxc8PHC is mediated by recruiting HDACs. Our data first time demonstrated that Hoxc8 functions as either transcription activator or repressor depending on promoter contexts and the stage of cell differentiation. Based on the conservative nature of Hox transcription factors, these results also imply that dual domains may exist in all of the 39 Hox transcription factors. Thus, this Hox fundamental transcription mechanism may help to understand the mechanisms of BMPs in bone development and remodeling.

Disclosures: ***N. Wang****, None.*

SA216

See Friday Plenary number F216

SA217

Establishment of a Mechanistic Link Between the Osteogenic Function of Runx2 and Its Subnuclear Organization by Intranuclear Informatics. D. Young, S. K. Zaidi*, A. Javed, J. L. Stein*, J. B. Lian, A. J. van Wijnen, G. S. Stein. Department of Cell Biology and Cancer Center, University of Massachusetts Medical School, Worcester, MA, USA.

Osteogenesis is controlled by the Runx2 transcription factor through the integration of complex signaling pathways that influence growth and differentiation of mesenchymal progenitor cells. Runx2 is localized in punctate subnuclear domains (foci) and organizes the assembly of supramolecular regulatory complexes that mediate the activation and repression of target genes. A conserved intranuclear targeting signal (NMTS) within the C-terminus of Runx2 directs the protein to matrix-associated subnuclear sites that support transcriptional control during osteoblast differentiation. To understand the relationship between Runx2 subnuclear organization and its physiological roles, we have developed "intranuclear informatics," a multivariate quantitative approach that combines image-processing and statistical tools. This strategy was used to quantify the spatial organization of nuclear protein domains from immunofluorescence microscopic images and provides a framework that establishes a mechanistic connection between nuclear architecture and biological function. We find that Runx2 foci have a distinct non-random organization within the nucleus. Using site-directed mutagenesis, we show that the C-terminal NMTS is a critical molecular determinant for the spatial organization of Runx proteins. Collectively, our results establish that the NMTS contributes to fidelity of Runx subnuclear organization. NMTS mutations affect the number, size and spatial randomness of foci, but not radial position. Further, our experimental strategy has enabled us to discriminate between functional and non-functional Runx proteins based, only, upon their domain organization within the nucleus. Finally, we establish that there is a direct link between Runx2 domain organization and its biological function. We conclude that the architectural organization of the Runx2 transcription factor within the nucleus is obligatory for its osteogenic regulatory function.

Disclosures: ***D. Young****, None.*

SA218

See Friday Plenary number F218

SA219

Expression of Extracellular WNT Pathway Components in Adult Human Trabecular Bone Cells. V. Trendelenburg*[1], M. Schaeublin*[1], C. Halleux[1], J. A. Gasser[1], S. Guth*[1], J. Porter*[2], D. Curtis*[2], K. Seuwen*[3], M. R. John[1]. [1]Bone Metabolism, Novartis Institutes for Biomedical Research, Basel, Switzerland, [2]Developmental and Molecular Pathways, Novartis Institutes for Biomedical Research, Inc., Cambridge, MA, USA, [3]GPCR Expertise Program, Novartis Institutes for Biomedical Research, Basel, Switzerland.

LRP5 is an important coreceptor in the WNT signaling cascade and has been shown to play a key role in early bone formation. Distinct mutations in the human LRP5 gene can lead to three different diseases: high-bone-mass syndrome, osteoporosis-pseudoglioma syndrome and familial exsudative vitreoretinopathy. Additionally, recent human genetic association studies suggest that LRP5 allelic variation contributes significantly to vertebral bone mass and size determination in males.

To get a comprehensive overview of extracellular human WNT pathway components we have examined the expression of all LRP5/6, WNT, Frizzled (Fzd), sFRP, DKK and Kremen family members in cultured adult trabecular bone cells by RT-PCR and partially by realtime-PCR. As a control, RNA from multiple normal control tissues was included.

Both LRP5 and LRP6 were ubiquitously expressed at comparable levels. Of the 19 Wnt genes, Wnt 1, 2b, 3, 4, 5a, 5b, 9a, 11, and 16 were expressed in trabecular bone as judged by RT-PCR and we could also demonstrate expression of Norrin. Realtime-PCR confirmed particularly strong expression relative to normal tissues for Wnt 2b, 3, 5b and 16 with the highest expression relative to other tissues for Wnt 5b. All Fzd receptors except Fzd 10 were expressed in trabecular bone, but only Fzd 3, 4, 5, 8 and 9 showed some preference for bone. Members of the sFRP and DKK family mainly act as secreted antagonists of Wnt signaling. Expression of these genes in trabecular bone could be shown for sFRP3 and 4, as well as DKK1, 2 and 3 while DKK1 seemed to be most highly expressed in trabecular bone compared to control tissues. Only weak expression of DKK4 and Soggy could be detected in bone tissue. Furthermore, we could demonstrate expression of Kremen1 in human trabecular bone cells.

In conclusion, simultaneous expression of a large number of extracellular WNT signaling components with synergistic but also opposite effects and the capability to activate multiple signaling pathways demonstrates the existence of a complex equilibrium of partially functionally redundant molecules in cultured adult human trabecular bone cells. These data suggest persistent important physiological functions of the WNT pathway(s) in the maintenance of adult human trabecular bone in addition to its demonstrated role during early development.

Disclosures: ***M.R. John****, None.*

SA220

See Friday Plenary number F220

SA221

Evidence For A Role For CCAAT Enhancer Binding Protein β As A Nuclear Coupling Factor For Coordinated Regulation of Osteopontin by 1,25Dihydroxyvitamin D_3 and Parathyroid Hormone. P. Dhawan*, X. Peng*, S. Christakos. Biochemistry, University of Medicine and Dentistry of New Jersey, Newark, NJ, USA.

Osteopontin (OPN), induced in response to $1,25(OH)_2D_3$ in osteoblasts, has been reported to modulate both resorption and mineralization. Parathyroid hormone (PTH) and/or activation of protein kinase A can enhance the $1,25(OH)_2D_3$ induction of OPN expression and transcription in osteoblasts. To understand regulatory mechanisms involved we asked whether C/EBPβ, which is induced by $1,25(OH)_2D_3$ and PTH, may play a role in the regulation of OPN transcription. Northern analysis using UMR 106 osteoblastic cells indi-

cated that PTH (25 nM) potentiates the induction of C/EBPβ, vitamin D receptor (VDR) and OPN mRNAs by $1,25(OH)_2D_3$ (10^{-8}M) as well as the rapidity of the response. In the presence of both PTH and $1,25(OH)_2D_3$ the first significant induction of C/EBPβ mRNA (at 30 min.) precedes the response of VDR mRNA (3h) and OPN mRNA (6h). In UMR 106 osteoblastic cells co-transfected with a C/EBP dominant negative expression construct (DN-CEBP) and the mouse OPN promoter (-777/+79), the cAMP or PTH enhancement of $1,25(OH)_2D_3$ induced OPN transcription was inhibited, suggesting the involvement of C/EBP in PTH enhanced OPN transcription. The OPN vitamin D response element was found to be sufficient to observe the inhibitory effect of DN-C/EBP, indicating that C/EBP is not acting through a site in the OPN promoter. VDR mRNA levels, induced after cAMP treatment in UMR cells (1 mM 8 bromo cAMP, 9h), were inhibited by prior transfection of DN-C/EBP, suggesting that C/EBP may mediate an effect on the PTH and cAMP mediated enhancement of OPN transcription through up-regulation of VDR. Data using the hVDR promoter (-1500/+60) indicate that expression of PKA results in a 3.5 ± 0.5 fold induction of hVDR promoter activity that is further enhanced two fold in the presence of C/EBPβ. DN-C/EBP (100 ng) inhibited the C/EBP enhancement and at higher concentrations (250 ng) DN-C/EBP inhibited the PKA induction of VDR transcription. Basal levels of hVDR transcription were unaffected at these concentrations of DN-C/EBP. 5'Deletion mapping studies indicated that the putative C/EBP sites at -1490/-1480 and at -919/-911are not involved in the response to C/EBP. C/EBPβ, in the presence of PKA, induced transcription from the VDR promoter within -580 and +60 (two CREs at -579/-558 and -367/-347), indicating that the interaction between the effects of PKA and C/EBP β occurs within this region of the hVDR promoter. In summary, the findings presented provide evidence that C/EBP β is a nuclear coupling factor that coordinates regulation of osteoblast function by $1,25(OH)_2D_3$ and PTH, at least in part, by enhancing PKA induced VDR transcription.

Disclosures: ***P. Dhawan****, None.*

SA222

See Friday Plenary number F222

SA223

Osteogenic Differentiation of Marrow Stromal Cells Induced by Oxysterols Is Associated With the Induction of Cbfa1 Expression and Activity. J. A. Richardson*[1], S. Tetradis[2], C. M. Amantea*[1], T. J. Hahn[1], F. Parhami[1]. [1]Medicine, UCLA, Los Angeles, CA, USA, [2]Dental School, UCLA, Los Angeles, CA, USA.

Identification of anabolic agents that induce osteogenic differentiation and inhibit adipogenic differentiation of osteoprogenitor cells and enhance bone formation is of great importance for improved prevention and management of osteoporosis. Oxysterols are naturally occurring products of cholesterol oxidation, have multiple biologic activities, and are made in part by cellular cytochrome P450 enzymes. We previously reported that specific combinations of oxysterols, namely 22(R)- or 22(S)-hydroxycholesterol with 20(S)-hydroxycholesterol have novel pro-osteogenic and anti-adipogenic effects when applied to osteoprogenitor cells including the pluripotent M2-10B4 (M2) mouse marrow stromal cells (MSC) *in vitro*. In the present report we demonstrate that these osteogenic oxysterol combinations positively regulate Cbfa1, a transcription factor that is a master regulator of osteoblastic differentiation. Treatment of M2 cells with 1-5 μM oxysterol combination 22S+20S (SS) for 4 days caused a dose-dependent increase in Cbfa1 mRNA expression. Treatment of M2 cells for 4 days with 1-5 μM SS also induced a dose-dependent increase in DNA-binding activity of Cbfa1 to mouse OSE2 sequence 5'-AGCTGCAATCACCAACCACAGCA-3', but not to mouse NFκB DNA binding sequence. Antibody specific to Cbfa1, but not irrelevant antibody specific to the nuclear transcription factor Nurr1, caused a supershift in EMSA using nuclear extracts from SS treated M2 cells. Excess unlabelled OSE2 oligo, but not unlabelled NFκB oligo, successfully competed for binding to SS-induced Cbfa1 in M2 nuclear extracts. Other oxysterols and oxidized lipids without osteogenic properties did not induce Cbfa1 expression or DNA binding. Inhibitors of cyclooxygenase 1 and MAPK, SC-560 and PD98059, respectively, partially inhibited SS-induced Cbfa1 DNA binding. We previously demonstrated that osteogenic oxysterols act synergistically with BMP2 and BMP7 to induce osteogenic differentiation of osteoprogenitor cells. This synergy in induction of osteogenic differentiation is associated with synergistic induction of Cbfa1 expression. Altogether these data demonstrate that osteogenic differentiation of cells in response to oxysterols is associated with the induction of previously characterized factors including Cbfa1 that drive osteoblastic differentiation.

Disclosures: ***F. Parhami****, None.*

SA224

See Friday Plenary number F224

SA225

Molecular Mechanisms of Bisphosphonate Action on Osteoblasts. G. Tell*[1], A. Pines*[2], A. Costessi*[1], M. Romanello*[2], D. de Feo[3], L. Moro*[2]. [1]Biomedical Science and Technology, Udine University, Udine, Italy, [2]Biochemistry, Center for the Study of Metabolic Bone Diseases, Trieste University, Trieste, Italy, [3]Procter & Gamble, Rome, Italy.

Bisphosphonates prevent osteoblast apoptosis by a mechanism involving extracellular signal-regulated kinase (ERK) activation. However, information regarding molecular targets and mechanisms of bisphosphonate actions are still scanty. ERKs are a family of kinases which play a central role in regulating several biological functions through modulation of the gene expression profile by acting on different transcription factors such as AP-1, Egr-1 and Cbfa-1/Runx-2. With this in mind, we tested the hypothesis that alendronate and risedronate could also act at the genomic level by controlling the activity of those transcription factors acting downstream of ERKs. We recently characterized a signalling pathway in a differentiated human osteoblast cell line (i.e. HOBIT), responsible for the activation of collagen a2 (I) gene expression through activation of Egr-1 transcription factor after mechanical stimuli (Pines et al. *Biochem. J.* 2003 373, 815-824). By using this cellular system, our data suggest that alendronate and risedronate play a role at the transcriptional level, by activating Egr-1 transcription factor itself. Interestingly, the functional activity of risedronate seems more effective and prolonged than alendronate in activating ERKs and Egr-1 and Cbfa-1/Runx-2. To more deeply understand the mechanism of bisphosphonate action at the molecular level, we are using a global approach based on differential proteomics by using hightroughput technologies based on 2-D gel analysis coupled to MALDI-Mass protein identification.These data confirm that bisphosphonate modulate osteoblast function by acting at the genomic level and open new pharmacological perspectives in the treatment of osteoporosis.

Disclosures: ***L. Moro****, None.*

SA226

See Friday Plenary number F226

SA227

Hypoxia Suppresses runx 2 Transcription in Osteoblasts and Osteocytes. R. Irwin*[1], S. Botolin*[1], J. LaPres*[2], L. R. McCabe[1]. [1]Departments of Physiology and Radiology, Michigan State University, East Lansing, MI, USA, [2]Department of Biochemistry, Michigan State University, East Lansing, MI, USA.

Mechanical loading is known to be a major regulator in the promotion and maintenance of normal bone homeostasis. Increasing mechanical load increases bone formation and correspondingly decreasing load decreases bone formation. It remains unclear as to exactly how a bone cell senses load, however interstitial fluid flow (increased with loading and decreased with unloading) is thought to be involved either through direct mechanical stresses on the cell (via shear stress, movement of actin microvilli, etc…) or possibly through its ability to deliver oxygen and nutrients to bone cells in areas of use. We hypothesize that decreased oxygen delivery could contribute to altered osteoblast and osteocyte gene expression, phenotype and function. Previously we identified hypoxia as a key suppressor of runx2 mRNA levels in osteoblasts grown in suspension in a rotating wall vessel. Similarly, when cultured in standard tissue culture dishes under hypoxic (2% oxygen) compared to normoxic (21% oxygen) conditions, osteoblast runx2 mRNA levels are suppressed by 50%. In contrast, VEGF and GAPDH mRNAs (hypoxia responsive genes) are induced 4-10 fold by hypoxic conditions. Live/dead and apoptosis assays indicate that osteoblasts and osteocytes are viable even after greater than 96 hours of hypoxic conditions. Consistent with a transcriptional regulatory component, runx2 promoter-luciferase assays demonstrate, under hypoxic conditions, a 50 and 90% decrease in activity in osteoblasts and osteocytes, respectively. Interestingly, osteocytes were significantly more responsive than osteoblasts. Furthermore, promoter deletion assays indicate that the proximal promoter region of runx2 is critical for this response. Taken together, our data indicate that hypoxia is a key regulator of runx2 expression and could contribute to altered osteoblast and osteocyte function and ultimately bone loss under conditions of decreased oxygenation, interstitial flow and loading.

Disclosures: ***L.R. McCabe****, None.*

SA228

See Friday Plenary number F228

SA229

mSin3a and Multiple HDACs Regulate Runx2 Transcriptional Activity. T. M. Schroeder*[1], J. J. Westendorf[2]. [1]Graduate Program in Biochemistry, Molecular Biology and Biophysics, University of Minnesota, Minneapolis, MN, USA, [2]Orthopaedic Surgery and The Cancer Center, University of Minnesota, Minneapolis, MN, USA.

Runx2 (Cbfa1, AML3) is an essential regulator of osteoblast differentiation and bone development. Runx2 activates or represses osteoblast specific genes through interactions with multiple cofactors. Runx2-mediated transcriptional repression is at least partially dependent on the recruitment of histone deacetylases (HDACs) and associated corepressors (e.g. mSin3A). We previously showed that HDAC3 and HDAC6 interact with amino- and carboxy-terminal Runx2 repression domains, respectively, but mSin3A contact regions have not been defined. Identification of these interaction domains will be important in understanding the regulatory mechanisms that control Runx2 transcriptional activity. Here we show that mSin3A interacts with an amino-terminal portion of Runx2 and represses Runx2-dependent activation of the osteocalcin promoter. The Runx2-mSin3a interacting region contains two serine residues (S286 and S304) that are conserved with Runx1. When these residues are phosphorylated in Runx1, mSin3a interactions are relieved. We have mutated the corresponding serines in Runx2 to alanine (to abolish the phosphorylation site) or to glutamic acid (to structurally mimic a phosphorylated residue). The S>A mutations hinder Runx2's ability to activate transcription, whereas the S>E mutations increase Runx2-dependent transactivation. Unexpectedly, neither set of mutations affected mSin3A or HDAC3 interactions with Runx2. These results suggest that mechanisms regulating Runx2-mediated repression differ from those controlling Runx1 activity. To identify candidate corepressors whose interactions may be dependent on phosphorylation of S286 and S304, we recently found that HDAC7, 9 and 10 form contacts with both the amino and carboxy termini of Runx2. These interactions may be functionally relevant as HDAC7, 9 and 10 messages were detected in osteoblast cell lines. Together these data demonstrate that Runx2 interacts with multiple co-repressors. Identifying the mechanisms regulating these interactions will increase our understanding of how Runx2 regulates gene expression.

Disclosures: ***T.M. Schroeder****, None.*

SA230

See Friday Plenary number F230

SA231

Osteopenia in Col3.6-p20C/EBPß Transgenic Mice Is Associated with Reduced Expression of Col2.3-GFP in Vivo and in a Heterotopic Bone Formation Model. L. M. Moranda*[1], P. L. Kelly*[1], J. Delaney*[2], J. He*[3], J. R. Harrison[1]. [1]Orthodontics, University of Connecticut Health Center, Farmington, CT, USA, [2]Genetics and Developmental Biology, University of Connecticut Health Center, Farmington, CT, USA, [3]Medicine, University of Connecticut Health Center, Farmington, CT, USA.

We reported previously that Col3.6 promoter-targeted overexpression of p20C/EBPß, a dominant negative C/EBP isoform, results in osteopenia in transgenic (TG) mice. Stromal cells derived from TG mice in a Col2.3-green fluorescent protein (GFP) genetic background showed a decrease in intensity of GFP expression associated with reduced osteocalcin expression. This suggests that p20C/EBPß overexpression interferes with late osteoblast differentiation or function. To further test this hypothesis, we analyzed Col2.3-GFP expression in vivo and in heterotopic implants seeded with bone marrow stromal cells derived from WT or TG mice. For in vivo analysis, femurs were harvested, fixed, subjected to micro-computed tomography (CT) and frozen sectioned. For heterotopic implantation, WT and TG marrow was flushed from the femur and tibia and cultured in serum-supplemented MEM. After two passages, cells were seeded into Gelfoam sponges and implanted s.c. into athymic nude CD-1 mice. Implants were harvested after 8 weeks, analyzed by micro-CT, and frozen sectioned. GFP was visualized using a fluorescent microscope equipped with a motorized stage, allowing a series of contiguous high-resolution images to be obtained and concatenated into a single image. Heterotopic TG implants showed a 3-fold decrease in bone volume relative to WT controls by micro-CT. This was accompanied by a significant decrease in the area within the implant occupied by GFP-positive cells. Some TG implants were noted to contain skeletal muscle, but the origin of muscle tissue from donor versus host has not been established. In vivo, femurs showed reduced cortical thickness and decreased trabecular bone volume, accompanied by a decrease in the total GFP positive area within the trabecular bone compartment. To determine whether the intensity of GFP expression was altered, Improvision Openlab software was used to threshold GFP-expressing cells into high- and low-expressing populations. In WT femurs, 35% of GFP expressing cells were found to be high expressors, compared to only 15% of TG GFP-expressing cells. These studies demonstrate that TG mice with Col3.6 targeted expression of a dominant negative C/EBP show a cell autonomous decrease in osteogenic capacity that is associated with reduced expression of Col2.3-GFP in vivo. These findings suggest that C/EBP transcription factors may be important determinants of osteoblast differentiation and bone formation.

Disclosures: ***J.R. Harrison****, None.*

SA232

See Friday Plenary number F232

SA233

Transgenic Mice Expressing a Ligand-Inducible Cre Recombinase in Osteoblasts and Odontoblasts: ***A New Tool to Examine Physiology and Disease of Postnatal Bone and Tooth*****.** J. Kim*, K. Nakashima*, B. de Crombrugghe. Molecular Genetics, UT M. D. Anderson Cancer Center, Houston, TX, USA.

Disruption of genes involved in mammalian bone formation often causes embryonic lethality, hence preventing study of these genes's role in adult animals. To develop a usable tool for such study, we generated transgenic mice in which a 2.3-kb mouse *Col1a1* proximal promoter, which is active in all osteoblasts, drives a transgene coding for a polypeptide consisting of Cre recombinase fused to a mutated ligand-binding domain of the estrogen receptor. Cre-mediated DNA recombination was analyzed in the offspring of crosses between these *Col1a1-CreERT2* mouse lines and *ROSA26* reporter mice. Administration of 4-hydroxytamoxifen induced Cre-mediated recombination detected by X-gal staining in osteoblasts in all bones and in odontoblasts in teeth of postnatal mice. Hence, these transgenic mice provide a useful tool with which to study the function of specific genes in bone and tooth in intact animals after birth. We are now using these *Col1a1-CreERT2* mice to study the role of the transcription factor *Osterix* (*Osx*) in bone physiology after birth. *Osx* is needed for bone formation and osteoblast differentiation but *Osx*-null mice die in the immediate perinatal period. We, therefore, generated mice with a conditional allele of *Osx* in which detection of the *Osx* gene is linked to *EGFP* expression. In mice heterozygous for this *Osx* allele, *EGFP* expression recapitulates the expression of *Osx* after Cre-mediated deletion of the *Osx* gene. The characterization of mice in which *Osx* is deleted after birth will be discussed.

Disclosures: ***J. Kim****, None.*

SA234

See Friday Plenary number F234

SA235

Expression of Nitric Oxide Synthase Isoforms in Human Dental Pulp Cells. P. D. Damoulis[1], L. Suri*[2], E. Gagari*[3]. [1]Periodontology, Tufts University, Boston, MA, USA, [2]Orthodontics, Tufts University, Boston, MA, USA, [3]Oral and Maxillofiacial Pathology, Tufts University, Boston, MA, USA.

Cells derived from human dental pulp (HDP) exhibit phenotypic characteristics similar to multipotent bone marrow-derived stromal cells, including the capacity to form mineralized nodules (Gronthos, S. et al, PNAS 97:13625-13630, 2000). Given the recent evidence implicating nitric oxide (NO) as an important mediator in osteoblast differentiation, the goal of this study was to compare the patterns of expression of type III (endothelial) and type II (inducible) NO synthase (NOS) in mineralizing and non-mineralizing (control) HDP cultures. Cells were cultured in αMEM for 44 days with medium changes every 3 days, starting at d2. Mineralization was induced by ascorbic acid and β glycerol phosphate supplementation at every medium change. Assays were performed every 6 days, starting with d14. Since expression of type II NOS requires cytokine stimulation, a cocktail of TNFα (25 ng/mL) + IL-1β (25 ng/mL) + IFNγ (50 ng/mL) was added to the respective groups 48 hours before each assay time point. NOS expression was assessed through Western analysis (for types II and III) and nitrite content in the conditioned media (Griess assay, sensitive for type II activity only). Cell number was evaluated through total protein content. Alkaline phosphatase (AlP) activity was also monitored, whereas mineralization was assessed through alizarin red staining. Control cultures showed relatively stable protein content with low AlP activity and no evidence of mineralization. Expression of type III NOS was constant throughout the culture period with minor fluctuations. Cytokine stimulation in the control cultures did not result in type II NOS expression or any measurable nitrite in conditioned media. Interestingly, cytokines appeared to down-regulate type III NOS expression at d14 and d20 only. In contrast, mineralizing cultures showed a sharp drop in protein content on d32, which coincided with peak AlP activity and the onset of mineralization. At the same time point, type II NOS expression was abrogated. Cytokine stimulation did elicit nitrite release in conditioned media and concomitant type II NOS expression but only after mineralization had been initiated. These results indicate an inverse correlation between type II and type III NOS expression in HDP cultures. This is particularly evident under mineralizing conditions, where the cells appear to be primed for cytokine-mediated type II NOS induction. This interplay in the expression of the two NOS isoforms at various stages of osteoprogenitor cell maturation is a novel finding that could provide significant insight in the role of nitric oxide during bone development and healing.

Disclosures: ***P.D. Damoulis****, None.*

SA236

Plasticity in Adipogenic and Osteogenic Differentiation Pathways using Human Bone Marrow Derived Mesenchymal Stem Cells. T. Schilling*, U. Noeth*, J. Schneidereit*, F. Jakob*, N. Schuetze. Molecular Orthopaedics, Orthopaedic Institute, Wuerzburg, Germany.

Expansion of adipose tissue in bone marrow at the expense of osteogenesis is age-related and may contribute to osteoporosis and osteonecrosis. The molecular basis for this phenomenon is largely unknown. We aimed to establish a cell culture system which allows for reprogramming (transdifferentiation) of osteoblasts into adipocytes and vice versa during differentiation pathways originating from human mesenchymal stem cells (hMSCs). Cells were isolated from the femoral head of patients undergoing total hip arthroplasty. For transdifferentiation of osteoblasts into adipocytes hMSCs were cultured in osteogenic medium for 2 weeks. Alkaline phosphatase (AP) staining revealed a homogenous increase

in expression. Osteocalcin and AP were highly expressed by RT-PCR analysis. These committed osteoblasts were then cultured in the adipogenic medium for 2 weeks resulting in a homogenous oil-red O staining. Direct adipogenic differentiation of hMSCs performed in parallel displayed the same homogenous staining. After adipogenic transdifferentiation of the committed osteoblasts no RNA markers for osteoblasts remained detectable whereas the lipid markers (lipoprotein lipase and peroxisome proliferator activated receptor gamma2) were highly expressed. For transdifferentiation of adipocytes into osteoblasts the hMSCs were cultured in adipogenic medium for up to 2 weeks in which differentiation into adipocytes was controlled by RT-PCR analyses and stainings. Thereafter cells received the osteogenic medium for 4 weeks resulting in marked deposition of mineral (alizarin red staining) and expression of osteoblast markers in RT-PCR analysis. Some adipocytes however, did not respond to the osteogenic medium since residual lipid markers were still detectable. Our results indicate that the plasticity between osteogenesis and adipogenesis extends into the differentiation pathways of osteoblasts and adipocytes . The transdifferentiation process of committed osteoblasts into adipocytes was as efficient and followed the same kinetics as the direct differentiation of adipocytes from hMSCs. Since the molecular mechanisms of this reprogramming phenomenon are unknown, cell culture systems could provide the basis for the elucidation of the underlying molecular pathways. Thereby, novel targets could be detected for therapeutic interventions in order to stimulate osteogenesis.

Disclosures: ***T. Schilling****, None.*

SA237

Low Passage MC3T3-E1 Cells: Proliferation, Alkaline Phosphatase Production And Regulation By Prostaglandins During Osteogenesis In Vitro. W. J. Peterson[1], D. T. Yamaguchi[2]. [1]Grecc 691/11g, Greater Los Angeles Healthcare System and UCLA School of Medicine, Los Angeles, CA, USA, [2]Research Service 691/11g, Greater Los Angeles Healthcare System and UCLA School of Medicine, Los Angeles, CA, USA.

The MC3T3-E1 cell line is a well-known model for studying bone formation in vitro. Since these cells are immortalized but non-transformed, it is commonly assumed that their capacity for proliferation and differentiation is unlimited. However, recent studies revealed that high passage cells show decreased proliferation and differentiation suggesting that MC3T3-E1 cells may go through a form of replicative senescence. It is conceivable that each time these cells are passaged, small changes occur that make them different from their ancestors of previous passages. Thus, even low passage cells would be expected to reveal evidence of small changes during serial passage and assessment of proliferation and differentiation. To test this hypothesis, we initiated experiments to assess passage-related change in cell proliferation and differentiation and to compare the activity and function of 2 selected subpopulations of low passage cells separated by 8-9 passages. In the latter study, we assess the importance of kinetics and seeding density on proliferation and alkaline phosphatase production during osteogenesis in vitro. Also, co-cultures were established to assess suppression and the role of prostaglandins in the suppression. Data are expressed as the mean ±SE. The results show that once MC3T3-E1 cells are placed into culture, decreased proliferation and alkaline phosphatase production are observed in 11-12 passages and 5 passages, respectively. Comparison of p23 and p30-31 cells reveal that: (1) Day 9 is the optimal time for maximal cell number and alkaline phosphatase production in cultures where the seeding density ranged from $0.25 \times 10^4/cm^2$ to $2 \times 10^4/cm^2$; (2) Seeding density does not affect maximal cell number; (3) A direct relationship exists between seeding density and alkaline phosphatase production; (4) P30-31 cells do not suppress proliferation and alkaline phosphatase production by p23 cells in co-culture; (5) The number of cells per cm^2 in cultures of p23 and p31 cells treated with indomethacin reached 78% and 79% of control, respectively; (6) nM of alkaline phosphatase per 10^6 cells in cultures of p23 and p31 cells treated with indomethacin reached 133%and 236% of control, respectively. These results suggest that (a) replicative senescence begins early in the life history of MC3T3-E1 preosteogenic cells; and that (b) the diminishing ability of low passage cells to undergo proliferation and alkaline phosphatase production is mediated by prostaglandins acting through intracellular pathways.

Disclosures: ***W.J. Peterson****, None.*

SA238

Local Release of a Prostanoid Receptor EP4 Agonist with rhBMP-2 Enhances Bone Morphogenetic Protein-Induced Bone Formation. H. Toyoda*[1], H. Terai[1], R. Sasaoka*[1], K. Oda*[2], K. Takaoka[1]. [1]Orthopaedic Surgery, Osaka City University Graduate School of Medicine, Osaka, Japan, [2]Ono Pharmaceutical Co., Ltd., Osaka, Japan.

Recombinant human bone morphogenetic protein (rhBMP), will tend to be utilized widely to repair damaged bones or bone defects in the fields of orthopedic surgery. However, one major problem is the large amount of rhBMP required for clinical use in human. In order to improve the performance of rhBMP, we have sought agents to enhance the bone-inducing activity of BMP. We have reported the mass of ossicles induced by BMP was significantly augmented by systemic administration of prostaglandin E EP4 agonist, especially administrated in the initial phase of bone formation. We postulated the local release of EP4 agonist with BMP might enhance bone formation without adverse events induced by systemic administration. In this study, we investigated the effects of EP4 agonist when released locally with rhBMP.

As a drug delivery system, a block co-polymer composed of poly-D,L-lactic acid with random insertion of p-dioxanone and polyethylene glycol (PLA-DX-PEG, Taki Chemical Co., Ltd.) was used. The polymer is biodegradable and absorbed within 2 weeks. Polymer disks containing several amounts of rhBMP-2 (Yamanouchi Pharmaceutical Co., Ltd.) and EP4 agonist were prepared and implanted into the left dorsal muscle pouch of the respective mouse. To examine the dose dependent effects of EP4 agonist, total 20 mice were divided into 4 groups (1. BMP 5µg, EP4 0µg, 2. BMP 5µg, EP4 3µg, 3. BMP 5µg, EP4 30µg, 4. BMP 5µg, EP4 300µg). To examine the effect of EP4 agonist alone, 300µg of EP4 agonist was added to the polymer without rhBMP-2 (group 5). One, 2 and 3 weeks after surgery, body weight was measured. Implants were harvested and served for following morphological, radiological and histological analyses at 3 weeks after surgery.

No significant difference in body weight was noted among the groups. Ectopic ossicles induced by BMP were harvested from the implanted site at 3 weeks. However, no bone formation was recognized in the group 5. On DXA analysis, bone mineral contents (BMC) of ossicles were dose-dependently higher in the group 2, 3 and 4 (9.36 ± 1.89 mg, 14.21 ± 1.27 mg, 18.75 ± 2.31 mg respectively) than those in the group 1 (6.52 ± 0.80 mg). The mean BMC value of the group 4 was approximately 3-fold higher than that of the group 1. Conclusively, EP4 agonist can enhance bone-inducing activity of rhBMP-2 without apparent systemic adverse effect when added to the rhBMP delivery system. This approach might be useful tool to improve the performance of the rhBMP-2 in the clinical practice.

Disclosures: ***H. Toyoda****, None.*

SA239

High Affinity Leptin Receptors Are Present In Human Mesenchymal Stem Cells (MSCs) Derived From Control And Osteoporotic Donors. J. P. Rodriguez, R. Hess*, A. M. Pino*, S. Ríos*, M. Fernández*. Laboratory of Cell Biology, INTA - University of Chile, Santiago, Chile.

There are disparate observations on central and peripheral effects of leptin, but several studies consistently support its role as a link between fat and bone. Bone marrow stroma contains mesenchymal stem cells (MSCs), which differentiate into osteoblasts and adipocytes, among others cell phenotypes. In this study we assessed the expression of leptin receptors protein in MSCs obtained from control and osteoporotic postmenopausal donors and their change during osteogenic and adipogenic differentiation. Also we assessed the effects of leptin on osteogenic and adipogenic differentiation of these cells. For this, MSCs were isolated from bone marrow obtained from both type of donors and maintained in culture in DMEM suplemented with 10% fetal bovine serum, at 37ºC in an humidified atmosphere of 5% CO_2. Specific binding of ^{125}I-leptin by cells was measured by competition studies using increasing amounts of recombinant human leptin. To determine the effect of leptin on osteogenic and adipogenic differentiation, MSCs were cultured in the presence or absence of 1 µg/ml of leptin in osteogenic and adipogenic culture conditions. In this study, we demonstrated high affinity leptin binding (IC_{50} = 0.4 +/- 0.09 nM) in both types of cells. Binding was very low under basal, but increased significantly (2-3 times) through osteogenic and adipogenic differentiation. Osteoporotic MSCs showed lower leptin binding capacity than control cells at an early osteogenic and adipogenic differentiation time, which could restrict cell sensitivity to the protective action of leptin. In this regard, we observed that leptin significantly inhibited (60%) the adipocyte differentiation in control but not in osteoporotic MSCs, while it exerted a low stimulatory effect on calcium deposition (10-20%) in both types of MCSs. In summary, we report the presence of high affinity leptin receptors on control and osteoporotic MSCs which were modified distinctly by osteogenic and adipogenic stimulation. Also we demonstrated a direct and distinct effect of leptin on both type of cells.

Disclosures: ***J.P. Rodriguez****, None.*

SA240

Induction of Multipotent Stem Cells through Dedifferentiation of Mesenchymal Cells by Msx2 Protein Transduction. C. Shinotsuka*[1], A. Hishiya*[1], K. Mizuno*[1], H. Aburatani*[2], K. Ikeda[1], K. Watanabe[1]. [1]Department of Bone & Joint Disease, National Center for Geriatrics & Gerontology, Obu, Japan, [2]Research Center for Advanced Science and Technology, The University of Tokyo, Tokyo, Japan.

Limited availability of stem cells poses a major problem in regenerative medicine and tissue engineering. It has recently been reported that ectopic expression of homeoprotein Msx induces dedifferentiation of terminally differentiated cells (Cell 2000) as well as suppression of adipogenesis (JBC 2003). In the present study we have attempted to generate multipotent stem cells from terminally differentiated cells, such as adipocytes, using Msx protein transduction technology. First, to clarify the underlying mechanism of Msx2-induced dedifferentiation, we employed Msx2-ER (estrogen receptor) system whose activity is controlled by tamoxifen. We generated osteoblastic KUSA-A1 cell lines that express Msx2-ER, and confirmed nuclear import of Msx2-ER fusion protein in response to tamoxifen treatment. Alkaline phosphatase activity was decreased in tamoxifen-treated KUSA/A1 cells expressing Msx2-ER, but not in mock-transfected cells. Total RNA was extracted from Msx2-ER- or mock-transfectants treated either by tamoxifen or ethanol vehicle, and analyzed by GeneChip (Affymetrix). Genes whose expression was decreased after induction of Msx2 function included periostin, sFRP2, osteoglycin and natriuretic receptor 3, whereas mRNA expression of cyclinD1 GADD45 and serpin 6 was upregulated. For application of Msx2, protein transduction (PTD) technique was employed. Msx2 protein with a protein transduction peptide (TAT) was produced as GST fusion protein in bacteria, and GST portion was removed by Precision protease treatment and GSH-Sepharose. Purified TAT-Msx2 protein was added to culture media, and protein transduction was confirmed by indirect immunocytochemistry and western blotting. Within 2 hr of application, TAT-Msx2 protein was readily detected in the nucleus of ~70% of cells. To determine whether TAT-Msx2 possesses dedifferentiation-inducing activity, PTD was applied to myotubes terminally differentiated from C2C12 cells. As a result, the morphology of myotubes changed and some population started proliferating. The PTD of TAT-Msx2 was also effective in inhibiting adipogenesis in vitro. Thus, Msx2-mediated dedifferentiation may be useful for generating multipotent stem cells that can then be diverted to osteogenic or chondrogenic lineages.

Disclosures: ***K. Watanabe****, None.*

SA241

Comparison of Bone Marrow Aspiration and Bone Core Biopsy as Methods for Harvest and Assay of Human Connective Tissue Progenitor. C. Nakamoto*, C. Boehm*, J. H. Tao*, K. Powell*, G. F. Muschler. Biomedical Engineering, Lerner Research Institute, The Cleveland Clinic Foundation, Cleveland, OH, USA.

Adult bone marrow and bone tissue contain connective tissue progenitors (CTPs), which can differentiate into a variety of connective tissues. The design and selection of optimal clinical methods for harvest and assay of CTPs has general relevance. Bone or bone marrow harvested from the iliac crest is currently the most commonly utilized tissue source for CTPs. However, little is known about the variation in CTP localization or concentration within human bone and marrow tissue. This study was designed to characterize the location of CTPs within human cancellous bone from the iliac crest.

Bone marrow aspirates (BM fraction) and 7 mm diameter transcortical iliac crest bone core were obtained from 10 human subjects undergoing elective hip arthroplasty procedures. Cells contained within the cancellous bone core samples were separated into those cells that could be easily suspended from the marrow space using mechanical agitation (MS fraction) and those cells that could only be liberated from the remaining trabecular bone surface by collagenase digestion (TS fraction). The number and concentration of cells in the BM, MS, and TS fractions were counted. Cells in each fraction were also assayed to determine the prevalence of CTPs in an established CTP colony formation assay.

Significant variation was seen between subjects, both in the cellularity of bone and marrow tissue and in the prevalence of CTPs among liberated cells. The MS fraction contained roughly six fold more nucleated cells than the TS fraction (MS, $1.3 \pm 0.81 \times 10^8$; TS, $0.18 \pm 0.81 \times 10^8$). However, as the prevalence of CTPs was over 25 fold greater in the TS fraction (TS 306 ± 344 CTPs/10^6 nucleated cells, MS 12 ± 12 CTPs/10^6 nucleated cells), the overall distribution of CTPs was significantly greater in the TS fraction (TS, 3512 ± 2059 /ml sample; MS, 1745 ± 1891 /ml sample). Quantitative analysis of CTP colonies in the three fractions showed no significant difference in proliferation rate, however the TS fraction produced colonies with less density and larger area than the BM and MS fraction.These data suggest that more than 67 % of CTPs within bone reside on or near the trabecular surface. The number of cells and CTPs harvested by aspiration (BM fraction) was poorly correlated with the actual number of cells and CTPs in bone. This suggests that marrow aspiration may be poorly suited as a sampling strategy designed to assess the effect of age, gender, and other clinical variables on the CTP population in human bone, and that a combination of assays applied to transcortical iliac crest biopsies may be better suited to provide quantitative tissue specific information.

Disclosures: ***C. Nakamoto****, None.*

SA242

Withdrawn

SA243

Mutations of *TWIST1* Lead to Decreased Proliferation of Calvarial Osteoblasts Derived from Patients with Saethre-Chotzen Syndrome. C. Ratisoontorn[1], M. L. Seto*[2], K. M. Broughton*[2], M. L. Cunningham*[3]. [1]Oral Biology, University of Washington, Seattle, WA, USA, [2]Pediatrics, University of Washington, Seattle, WA, USA, [3]Children's Craniofacial Center, CHRMC, Pediatrics & Oral Biology, University of Washington, Seattle, WA, USA.

Seathre-Chotzen syndrome (SCS) is an autosomal-dominant craniosynostosis syndrome, associated with loss-of-function mutations in *TWIST1*. Naturally occurring mutations in humans and the heterozygous null *Twist* mouse are suggestive of haploinsufficiency as the disease-causing mechanism. *TWIST1* has been implicated in the inhibition of differentiation of multiple cell lineages. Therefore, premature fusion of cranial sutures in SCS might be mediated by altered differentiation of calvarial osteoblasts. To test this hypothesis, we evaluated cells derived from calvarial bone of three patients with SCS compared with those derived from three unaffected individuals as controls to investigate the three principle stages of osteoblast differentiation: 1) proliferation, 2) matrix maturation, 3) mineralization. Using a BrdU-Hoechst flow cytometry assay, we found that the percent of proliferating cells is significantly less in cells derived from patients with SCS compared with those derived from controls ($P \leq 0.05$). In the matrix maturation stage, alkaline phosphatase (ALP) activity, and expression of extracellular matrix genes, collagen I alpha 2 (COL1A2), osteopontin (OPN) and osteocalcin (OCN), were examined by real-time quantitative RT-PCR. The ALP assay revealed that the ALP activity of cells both from SCS and controls are highest at day 3, and continually declined at days 7 and 14. However, the ALP activity of cells derived from SCS patients is significantly lower than controls at days 3 and 7($P \leq 0.05$), and declined to an insignificant difference by day 14, suggesting that cells derived from SCS patients are in a later differentiation stage. There is no significant difference in levels of expression of COL1A2, OPN, or OCN between cells derived from patients with SCS and controls at 3, 7, 14, 21, and 28 days in culture. To evaluate the third stage of differentiation, a quantitative alizarin red-S mineralization assay was performed. Although not statistically significant, we found that osteoblasts derived from patients with SCS have higher levels of alizarin red-S staining at days 21 and 28. Taken together, these results suggest that loss-of-function mutations of *TWIST1* lead to reduced proliferation and increased differentiation of calvarial osteoblasts derived from patients with SCS.

Disclosures: ***C. Ratisoontorn****, None.*

SA244

See Friday Plenary number F244

SA245

In Vitro and in Vivo Osteogenic Differentiation of FAT Cells Induced by Cbfa1 Overexpression. H. Kojima, T. Uemura. ADRC(Age Dimension Research Center), AIST (National Institute of Advanced Industrial Science and Technology), Tsukuba, Ibaraki, Japan.

As a methodology for bone tissue engineering, a technique for the transplantation of cultured bone has been developed to overcome the disadvantages of autologous bone grafts or the simple implantation of biomaterial into bone defects such as a limited bone supply for bone graft, risk of infection, insuitability for large bone defects etc. The procedure essentially involves the in vivo transplantation of MSC-derived osteoprogenitor cells/ porous ceramic composite, to form bone-like tissue, which can provide applications of tissue engineering to patients with skeletal defects. However, autologous bone marrow cells have potential limitations in the amounts of MSCs and transplantation of cultured bone is difficult for large bone defects. In this study, we examined that a population of stem cells in adipose tissue can be useful as an alternate source of MSCs. Adipose tissue is an abundant, expendable, and easily obtained tissue that may prove to be an ideal source of autologous stem cells for tissue engineering. To accelerate the process of differentiation into osteoblastic cells, we overexpressed the Cbfa1 (Core binding factor alpha-1) gene with adenovirus vector in a population of rat fibroblast like cells obtained from adipose tissue (FAT cell). Cbfa1 is known to be a key osteogenic transcription factor and was found to be indispensable for osteoblast differentiation by the finding that Cbfa1- knockout mice completely lacked osteoblasts. The in vitro results of northern blot analysis revealed that the expression of osteocalcin was induced in Cbfa1 overexpressed FAT cells. Markers of osteoblast differentiation, such as alkaline phosphatase activity, the expression of osteocalcin, and calcium content, in Cbfa1 overexpressed FAT cells were markedly greater than those of uninfected normal FAT cells. Alizarin red staining of the Cbfa1 overexpressed FAT cells showed marked mineralization compared to the infected cells. A subcutaneous implantation of porous scaffolds / Cbfa1 overexpressed cells composite resulted in rich bone formation compared to uninfected composite. These findings suggested that the overexpression of the Cbfa1 gene induced a remarkable and rapid differentiation of FAT cells into osteogenic cells in vitro and in vivo.. Our results implied that Cbfa1 overexpressed FAT cells may become an alternative stem cell source of bone marrow-derived MSCs, and these cells present a potential to provide a practical and instantaneous application for bone tissue engineering.

Disclosures: ***T. Uemura****, None.*

SA246

See Friday Plenary number F246

SA247

Calvarial Osteoblasts Transdifferentiate into Adipocytes when Treated with a Combination of PPARγ and α Activators. T. Hasegawa*[1], H. Hatano*[2], K. Tanne*[1], N. Maeda*[2], J. E. Aubin[3], Y. Yoshiko[2]. [1]Orthodontics and Craniofacial Developmental Biology, Hiroshima University, Hiroshima, Japan, [2]Oral Growth and Developmental Biology, Hiroshima University, Hiroshima, Japan, [3]Molecular and Medical Genetics, University of Toronto, Toronto, ON, Canada.

While pluripotent mesenchymal stem cells differentiate into osteoblasts, adipocytes and others, considerable evidence also supports the notion that osteoblasts and adipocytes are closely related through a common bipotential progenitor and/or transdifferentiation capacity. The PPARγ nuclear receptor regulates osteoblast-adipocyte fate choice (inducing adipocytic while inhibiting osteoblastic differentiation). However, activation of PPARγ alone appears to be insufficient to convert relatively mature osteoprogenitors such as fetal rat calvaria (RC) cells into adipocytes. To assess whether such cells can convert into adipocytes and, if they do, to determine the cellular events at single cell colony level, RC cells were cultured at very low density in osteogenic medium. Cells from developing and mature single cell colonies were subcultured (secondary cultures) and treated with a combination of PPARγ (BRL-49653) and PPARα (fenofibrate) activators or used for total RNA extraction. Amongst 112 colonies selected, 99 colonies were successfully adapted to secondary cultures and classified into four groups by double staining for osteoblasts (alkaline phosphatase) and adipocytes (oil red O). Single lineage colonies comprised 47% of colonies (osteoblasts 29%; adipocytes 18%), 21% (20 colonies) were bipotential and 32% failed to differentiate into either osteoblasts or adipocytes. To characterize the colonies with adipogenic potential, total RNA from all groups classified by staining (total 44 colonies) was amplified by cRNA synthesis and adaptor primer PCR and then subjected to semiquantitative or real time PCR. Unexpectedly, some colonies expressing osteoblast markers also expressed not only adipocytic markers (LPL and adipsin) but also markers of other lineages (*e.g.*, the chondrocyte marker sox 9), but expression profiles did not correlate with capacity for adipogenesis and osteogenesis in secondary cultures. Adipocyte differentiation was seen in 8 colonies expressing osteoblast markers (osteocalcin and/or bone sialoprotein), but these colonies also expressed high levels of either $PPAR\gamma_1$, PPARα or C/EBPα. Thus, calvarial osteoblasts express considerable potential for transdifferentiation into adipocytes in the presence of PPARγ and α activators, a lineage conversion that may be determined by whether the osteoblasts express relatively high levels of $PPAR\gamma_1$, PPARα or C/EBPα.

Disclosures: ***T. Hasegawa****, None.*

SA248

See Friday Plenary number F248

SA249

Combination of BMP and Runx2 Signalings Constitute the Minimum and Sufficient Unit for Osteogenic Differentiation through Regulation of Cbfb. S. Ohba*[1], T. Ikeda[1], S. Kamekura[1], F. Kugimiya*[1], F. Yano*[1], A. Lichtler[2], T. Ogasawara[1], K. Hoshi[1], K. Nakamura[1], T. Takato*[1], H. Kawaguchi[1], U. Chung[1]. [1]Univ. of Tokyo, Tokyo, Japan, [2]Univ. of Connecticut Health Ctr., Farmington, CT, USA.

Among signaling pathways that have been implicated in the control of osteogenic differentiation from precursor cells, determination of the minimum signaling unit is the most important issue to realize an ideal bone regeneration. We recently established a monitoring system for osteogenic differentiation with EGFP gene driven by bone-specific 2.3 kb rat Col1a1 promoter fragment (COL1A1GFP). Using this system, in the present study we made a comprehensive search for the minimum osteogenic unit among adenovirus-mediated putative signaling pathways: BMP signaling by constitutively active (ca) ALK6, Runx2 signaling by wild-type Runx2, Hedgehog signaling by caSmoothened, Wnt signaling by caTCF/LEF, and IGF-I signaling by wild-type IRS-1. Although no single pathway could induce GFP fluorescence in COL1A1GFP-embryonic stem (ES) cells cultured in a serum-free medium, stimulation of all pathways strongly induced it within a week. When random combinations of all pathways were exhaustively examined, only the co-transduction of caALK6+Runx2 induced GFP fluorescence as strongly as that of all stimulations, indicating that this combination is the minimum and sufficient unit for osteogenic differentiation. The expressions of osteocalcin, BSP and ALP mRNA, and matrix calcification were induced by the caALK6+Runx2 to levels similar to all stimulations in various cells including mouse ES cells, human mesenchymal stem cells, human dermal fibroblasts (DFB), and non-osteoblastic cell lines such as NIH3T3 and HeLa. In addition, transplantation of DFB transduced with caALK6+Runx2 to non-healing critical-sized defects in mouse calvariae induced bone formation *in vivo*. To further investigate the mechanism underlying the synergism of the two pathways, we transduced NIH3T3 cells with caALK6 or Runx2 or both. caALK6 did not affect the expression of endogenous Runx2, or subcellular localization or the DNA binding ability of overexpressed Runx2. Either caALK6 or Runx2 alone moderately stimulated the expression of Cbfb, a heterodimer partner of Runx2, which was not enhanced by the co-transduction. However, chromatin immunoprecipitation analysis revealed that both together, but neither of them alone, recruited Cbfb to OSE2 element in the osteocalcin promoter. These results demonstrate that BMP and Runx2 signalings constitute the minimum and sufficient unit to induce osteogenesis from various cell sources through regulation of Cbfb, suggesting a possible application to bone regenerative medicine.

Disclosures: ***S. Ohba****, None.*

SA250

Correlation Between Bone Mineral Density (BMD) and Gene Expression of OPG-RANKL of Human Osteoblast Cultures from Postmenopausal Women. S. Ruiz-Gaspà*, A. Enjuanes*, J. C. Monllau*, E. Cáceres*, M. Payes*, J. Vila*, L. Mellibovsky*, J. Blanch, I. Aymar*, A. Diez-Perez, X. Nogués. Urfoa, IMIM-Hospital del Mar, Barcelona, Spain.

Postmenopausal osteoporosis is produced by an unbalanced bone remodeling between resorption and formation. OPG-RANK-RANKL is an important regulation system of the process. There are few studies of this regulatory system trying to find a relationship between clinical and in vitro data.

Study of proliferation and OPG-RANKL gene expression in human osteoblast cultures from postmenopausal women and influence of Vitamin D3, 17-beta estradiol in this expression.

22 postmenopausal women (50 to 80 year-old) were included from orthopedic material removed during knee replacement surgery. BMD was measured by HOLOGIC QDR 4500 SL in lumbar spine and femoral neck and patients were classified according to WHO criteria in normal (six cases), osteopenic (six cases) and osteoporotic (ten cases). Human bone cells were obtained from 1 to 2 mm explants of trabecular bone of surgical specimens. Cells were grown in Dulbecco´s modified Eagle medium and 10% fetal calf serum (FCS). Cells were isolated using 0.25% trypsin and then subcultured. Osteoblasts were characterized by alkaline phosphatase activity and osteocalcin synthesis. Confluent culture were treated with: 1) 10% FCS, 2) 10-8M Vitamin D3 (Vit D), 3) 367nM 17-beta estradiol, and a culture without FCS was used as control. OPG and RANKL expression were quantified by real time PCR. Statistical analysis was performed using the SSPS 11.5 software.

Osteoblast proliferation was not different between normal, osteopenic and osteoporotic groups. OPG and RANKL expression levels in human osteoblasts of osteoporotic women were lower than normal and osteopenic women ($p<0.0001$, $p=0.01$). When cultures were supplemented with FCS, OPG expression levels were lower in all cultures ($p=0.012$). After adding Vit D3 and 17-beta estradiol expression levels of OPG were lower but not reached statistically significance whereas expression levels of RANKL were not influenced.

We confirm in vitro the relevance of OPG-RANK-RANKL regulation system since osteoblasts in culture, from osteopenic and osteoporotic postmenopausal women, express decreased levels of OPG and RANKL. Addition of Vitamin D3 and 17-beta estradiol seem not to affect the expression of OPG and RANKL in this experiment.

Disclosures: ***S. Ruiz-Gaspà****, None.*

SA251

See Friday Plenary number F251

SA252

Subchondral Osteoblasts from Osteoarthritic Patients Show Abnormal Expression and Production of Leptin: Possible Role in Cartilage Degradation. D. Lajeunesse[1], A. Delalandre*[1], J. C. Fernandes*[2]. [1]Medicine, CRCHUM, Hôpital Notre-Dame, Montréal, PQ, Canada, [2]Surgery, Hôpital Sacré-Coeur, Montréal, PQ, Canada.

Leptin is a peptide hormone with a role in body weight regulation, immune response, bone metabolism and possibly in rheumatic diseases. Osteoarthritis (OA) is characterized by cartilage damage and loss, synovial membrane inflammation and bone sclerosis and the formation of osteophytes. It is now evident that the subchondral bone tissue plays a prominent role in the pathophysiology of osteoarthritis (OA), a situation that is related to abnormal osteoblast (Ob) differentiation. Leptin can promote the differentiation of osteoblasts (Ob), however, a direct role for leptin in human OA has yet to be demonstrated. We prepared primay cultures of normal and OA Ob from subchondral bone and OA chondrocytes from articular cartilage from tibial plateaus removed for knee replacement surgery of OA patients or at autopsy. We determined the expression and production of leptin using RT-PCR and ELISA. Our results indicated using two different sets of primers for RT-PCR experiments, that leptin was expressed only in Ob not in chondrocytes. The expression of leptin was also higher in OA Ob compared to normal using real-time PCR and was responsible for the increase in leptin levels noted in conditioned-media from OA Ob. Although leptin was not expressed by chondrocytes, it was present in articular cartilage suggesting that leptin produced in bone tissue reached the overlaying cartilage. The long-form leptin receptor mRNA levels were similar between normal and OA Ob. Since leptin can promote the differentiation of Ob, we next questionned if the observed increase in alkaline phosphatase activity (ALP) and osteocalcin release (OC) observed in OA Ob was linked with their endogenous leptin production. Inactivating antibodies against the leptin receptor reduced both ALP and OC in OA Ob about 35%. Leptin expression was regulated in OA Ob by $1,25(OH)_2D_3$, transforming growth factor-beta 1 (TGF-beta 1) and hepatocyte growth factor (HGF). Indeed, TGF-beta 1 reduced leptin expression whereas both $1,25(OH)_2D_3$ and HGF increased leptin expression. These results indicate that OA Ob produce more leptin than normal, and that leptin found in articular cartilage is derived from bone tissue. The increase in leptin in OA bone tissue is responsible for increased ALP and OC of Ob. Since leptin can promote inflammation and cartilage loss in combination with cytokines, this suggests that subchondral bone production of leptin may be responsible, at least in part, of cartilage loss in OA.

Disclosures: ***D. Lajeunesse****, None.*

SA253

See Friday Plenary number F253

SA254

Expression of Voltage Sensitive Calcium Channel (VSCCs) L-type α_{1C} ($Ca_v1.2$) and T-type α_{1H} ($Ca_v3.2$) Subunits during Mouse Bone Development. Y. Shao*, M. Alicknavitch*, M. C. Farach-Carson. Department of Biological Sciences, University of Delaware, Newark, DE, USA.

Plasma membrane VSCCs serve as key regulators of Ca^{2+} permeability including regulation of secretion of paracrine activators of osteoclastogenesis. In osteoblasts, L-type VSCCs consist of a pore forming α_1 subunit, a disulfide-linked $\alpha_2\delta$ dimer, and an intracellular β subunit. Subunit composition plays an important role in fine-tuning of VSCC expression and function. Osteoblasts express as the major L-type channel α_{1C} ($Ca_v1.2$), and two T-type channels α_{1G} ($Ca_v3.1$) and α_{1H} ($Ca_v3.2$). However, only α_{1C} and α_{1H} are regulated by treatment of osteoblasts with 1,25-dihydroxyvitamin D_3. We used a combination of approaches to investigate the α_{1C} and α_{1H} subunit expression in both developing mouse long bones, and in differentiating *in vitro* models of osteogenesis and chondrogenesis, the MC3T3-E1 and ATDC5 cells, respectively. Immunohistochemical studies showed α_{1C} subunits were present in regions of rapid growth, including in the perichondrium, periosteum, chondro-osseous junction and along the surfaces of newly formed trabecular bones throughout various mouse bone developmental stages. Interestingly, α_{1H} subunit expression followed a similar distribution pattern as seen for the α_{1C} subunits, suggesting the coordination of L-type α_{1C} and T-type α_{1H} VSCCs in regulating osteoblastic functions. Western Blot analysis also identified the expression of α_{1C} and α_{1H} subunits in total protein extracts from MC3T3-E1 cells, and the protein level decreased during osteoblastic differentiation. Immunostaining of these cells during growth and differentiated phases confirmed these findings and suggested that subunit assembly is also important. Co-immunoprecipitation and subsequent Western Blot analysis indicated β_2 and β_3 subunits, but not β_1 and β_4, assembled with α_{1C} subunits in growth phase MC3T3-E1 cells. Similar studies are underway with differentiating ATDC5 cells. Our findings support the conclusion that VSCCs in osteoblasts are critical components of growth and development of new bones. Ongoing studies utilize fluorescent resonance energy transfer (FRET) to further investigate the interaction between α_1 subunit and the accessory subunits in functional VSCC complexes in intact bone, as well as in both MC3T3-E1 and ATDC5 cells.

Disclosures: ***Y. Shao****, None.*

SA255

Responses of MC3T3-E1 Osteoblast Cells to Parathyroid Hormone Are Dependent on Differentiation Stage and Duration of Treatment. R. J. Arends*, P. E. J. Langerwerf*, T. M. C. van de Klundert*, M. van Beuningen*, M. van Duin*, A. G. H. Ederveen. Pharmacology, N.V. Organon, Oss, Netherlands.

To select new anabolic drugs for the treatment of osteoporosis, a functional assay is required to predict anabolic effects *in vitro*. Parathyroid hormone (PTH) exerts an anabolic effect *in vivo* when administered intermittently. However, the effect of PTH on mineralization of osteoblasts *in vitro* is less consistent. We studied the effects of different treatments of PTH to various differentiation stages of MC3T3-E1 cells on cAMP signaling and mineralization of extra-cellular matrix in long-term (25 days) cultures, in order to build a functional anabolic assay *in vitro*.

The mRNA expression of the PTH receptor-1 (PTH1R) was quantified using real time PCR. Moderate PTH1R mRNA levels were detected during the culture period and the levels start to increase 3 days after stimulation with 50 μg/ml ascorbic acid (AA) and 10 mM β-glycerol phosphate (βGP) up to 15 times basal levels (day 25). Under these culture conditions MC3T3-E1 cells differentiate and mineralization starts around day 14. Changes in intracellular cAMP levels were found in response to PTH treatment indicating that a functional PTH-induced signaling mechanism is present in differentiating MC3T3-E1 cells.

To study the effects of PTH (10-13 to 10-6M) on mineralization of MC3T3-E1 cells, we exposed long-term cultures for various time periods to different treatments. Cells were cultured in the presence of AA and βGP and exposed to PTH during 1-25, 11-25, 14-25, 17-25 or 21-25 days. The cultures were performed in triplicate and in parallel treated; (a) for 6 h with PTH followed by 42 h fresh medium, (b) 24 h PTH followed by 24 h fresh medium or (c) 48 h PTH. Culture medium was refreshed every 48 h. Mineralization on day 25 was quantified using a calcein method.

A 6 h PTH pulse (a) given from day 1-25 inhibited mineralization around 50%, whereas (a) given from day 11, 14, 17 or 21 had little (<20%) or no effect on mineralization (day 25). A 24 h PTH pulse (b) from day 1-25, 11-25 or 14-25 inhibited mineralization more than 35%. On the other hand, when (b) started on day 17 or 21 no effects were found (day 25). Continuous exposure (c) of MC3T3-E1 cells to PTH from 1-25 days did not change mineralization, whereas when (c) started at day 11 (just before mineralization starts) a 25% inhibition of mineralization was measured. When (c) started on day 14 or 17 it had no effect, whereas when PTH was given on day 21-25 a 20% increase in mineralization was found.

These data indicate that it is unclear how to predict anabolic effects *in vitro* on mineralization by MC3T3-E1 cells. The effect of PTH on mineralization by MC3T3-E1 cell is dependent on the differentiation stage of the cells and on the duration of treatment.

Disclosures: ***R.J. Arends****, N.V. Organon 3.*

SA256

See Friday Plenary number F256

SA257

Mice Lacking Phosphatidylinositol Transfer Protein-alpha (PITP-alpha) Display Bone Formation Defect. Z. Zhou*, H. Yang*, X. Feng, W. Xiong. Pathology, University of Alabama at Birmingham, Birmingham, AL, USA.

Phosphatidylinositol transfer proteins alpha (PITPa) is a protein essential for phosphatidylinositol signaling. Reduction of PITPa expression in mice leads to aponecrotic spinocerebellar disease, hypoglycemia, and intestinal and hepatic steatosis. The role of PITPa and PITPa dependent phosphatidylinositol signaling in bone remodeling is unclear. We have characterized the potential role of PITPa in regulating bone metabolism by using PITPa -/- mice. The reduced bone density and decreased cortical and trabecular bone areas and volumes have been observed in PITPa mutant mice. While osteoclasts derived from PITPa mutant mice show normal bone resorptive function, osteoblasts isolated from the mutant mice exhibit reduced cell proliferation and differentiation. We are in the process to further characterize the phenotype and to understand the underlying mechanism.

Disclosures: ***Z. Zhou****, None.*

SA258

Transfer of 128-kb BMP-2 Genomic Locus by HSV-Based Infectious BAC Stimulates Osteoblast Differentiation: A Platform for Functional Genomic Studies. W. Xing, D. J. Baylink, C. Kesavan*, S. Mohan. JLP VAMC/LLU, Loma Linda, CA, USA.

In order to localize chromosomal regions and subsequently identify the genes responsible for musculoskeletal diseases, we previously developed mouse genetic models and discovered quantitative trait loci (QTL) in a number of mouse chromosomes that contribute to phenotypes such as bone density, size and strength. Subsequent analyses of the congenic mice further confirmed and narrowed two predominant QTLs that regulate BMD to < 5 cM regions in mouse chromosome 1. However, these regions contain dozens of genes and are still difficult to clone by time-consuming, expensive positional cloning strategies. A feasible and efficient approach for identifying candidate genes is to transfer the genomic loci of overlapping bacterial artificial chromosomes (BACs) or P1 artificial chromosomes (PACs) encompassing the QTL regions into bone cells in vitro for a high throughput functional screening. In this study, we retrofitted a BAC construct into herpes simplex virus-1 (HSV-1) amplicon and packaged it into an infectious BAC (iBAC) to test gene function in a cell-based system, using a 128-kb clone containing the complete bone morphogenetic protein-2 (BMP-2) gene. We transduced MC3T3-E1 cells with the iBAC bearing BMP-2 and examined transduction efficiency, transgene expression and function. Our experiments revealed that approximately 84% of MC3T3-E1 cells were transduced by the iBAC at a multiplicity of infection (MOI) of 5. The amount of BMP-2 protein was estimated to be 10 ng per 10^6 cells 24 hours after infection of HSV amplicon containing BMP-2 genomic locus. Like the cells treated with 200 ng/ml recombinant human BMP-2, about 20% of the osteoblast cells were differentiated and exhibited positive ALP-staining 9 days post-infection. No ALP-positive cells were seen in the control cells infected with HSV-1 mock amplicon without BMP-2 genomic locus. Our results have indicated that an iBAC can efficiently deliver a BMP-2 genomic locus into preosteoblast cells and express functional BMP-2 protein, stimulating a phenotype of cell differentiation. Therefore, this experimental system provides a rapid, efficient cell-based model of high-throughput phenotypic screening to identify the BAC clones from physically mapped regions that are important for osteoblast differentiation. Because multiple copies of BAC clones can be transferred into the target cells depending on the amount of HSV used, the BAC clone approach also provides a sensitive platform for studies on gene function, gene expression and for identification of gene regulatory elements that are located in the intronic regions.

Disclosures: ***W. Xing****, None.*

SA259

Osteoblast Differentiation Is Regulated by CaMKII and Mediated by *c-fos* Expression. M. Zayzafoon, J. M. McDonald. Department of Pathology, University of Alabama at Birmingham, Birmingham, AL, USA.

CaMKII (Ca^{2+}/calmodulin-dependent protein kinase II) was previously thought to be exclusively expressed in neuronal tissue. However, it has been recently shown that the expression of CaMKII is not limited to the brain and that it plays a critical role in regulating various signaling pathways leading to modulation in several aspects of different cellular functions, including cytoskeleton structure, cell shape and gene expression. The purpose of this study was to examine the expression of CaMKII in osteoblast-like cells (MC3T3-E1) and to elucidate its role in osteoblast differentiation. Here we demonstrate by RT-PCR, Western blotting and immunofluorescence that the alpha-CaMKII gene and protein are expressed in osteoblasts both *in vitro* and *in vivo*. Inhibition of CaMKII by calmodulin or CaMK inhibitors (TFP or KN-93 respectively) resulted in inhibition of osteoblast differentiation, demonstrated by decreased alkaline phosphatase (ALP) activity and mineralization, as well as a 5- and 2-fold decreases in ALP and osteocalcin gene expression, respectively. Incorporation of [^{3}H]-Thymidine was not affected by this treatment, suggesting that the inhibition of differentiation is not due to a decrease in proliferation. We also demonstrate, using the newborn mouse calvaria *in vivo* model, that treatment with TFP and KN-93 causes a 41% and 31% decrease in osteoblast number and mineralization, respectively. In order to elucidate the potential mechanism by which CaMKII regulates osteoblast differentiation, we examined signaling pathways and their downstream transcription factors known to play a role in osteoblast differentiation. TFP and KN-93 decrease the phosphorylation of alpha-CaMKII, ERK and CREB leading to a 31% and 48% decrease in the transactivation of SRE and CRE, downstream response elements of ERK and CREB respectively. The promoter of *c-fos*, a member of the family of activating protein-1 (AP-1), is regulated by SRE and CRE. Inhibition of CaMKII by TFP or KN-93 decreases the expression of *c-fos* and AP-1 transactivation. In addition, EMSA results show that TFP and KN-93 decrease both CRE and AP-1 DNA binding. Supershift analyses confirm that the decrease in AP-1 DNA binding is a result of decrease in c-Fos. Our findings demonstrate that CaMKII is expressed in osteoblasts and is involved in *c-fos* expression through regulation of SRE and CRE. Inhibition of CaMKII results in decrease in *c-fos* expression and AP-1 activation leading to inhibition of osteoblast differentiation.

Disclosures: ***M. Zayzafoon****, None.*

SA260

See Friday Plenary number F260

SA261

Diosgenin Stimulates Angiogenesis via Up-regulation of Osteoblast-Derived Vascular Endothelial Growth Factor-A. M. Yen[1], J. Su*[2], W. Chen*[2], M. Kuo*[2]. [1]Departments of Obstetrics and Gynecology , Departments of Primary care Medicine, College of Medicine, National Taiwan University, Taipei,, Taiwan Republic of China, [2]Institute of Toxicology, College of Medicine, National Taiwan University, Taipei,, Taiwan Republic of China.

Diosgenin, a steroidal saponin that is extracted from the root of Wild Yam (Dioscorea villosa), has been reported to have tremendous medical applications. Angiogenesis is a critical process during bone formation and fracture healing and vascular endothelial growth factor-A (VEGF-A) is an important angiogenic factor produced in a regular manner by many cell types, including osteoblasts. The aim of the present study was to examine whether diosgenin modulates VEGF-A expression in osteoblasts and promote angiogenesis. In murine MC3T3-E1 preosteoblast-like cells, we found that VEGF-A expression was significantly elevated in response to diosgenin. Conditioned media of MC3T3-E1 cells treated with diosgenin also induced a strong angiogenic activity in either *in vitro* nor *ex vivo* assay, which were blocked by VEGF-A specific neutralizing antibody. At the mechanistic level, we found that diosgenin treatment activated the Akt and p38 MAPK. The use of pharmacological inhibitors or genetic inhibition by transfection with the dominant-negative (DN)-Akt or DN-p38 plasmids revealed that both Akt and p38 MAPK signalings are involved in diosgenin-mediated VEGF-A up-regulation. Furthermore, we found that diosgenin-treated MC3T3-E1 cells showed an increased hypoxia-inducible factor-1α(HIF-1α) protein in the nucleus. Blockage of HIF-1α activity by transfection with a DN-HIF-1αexpression vector significantly abolished diosgenin-induced VEGF-A up-regulation, suggesting that diosgenin-induced VEGF-A expression was HIF-1α-dependent. Taken together, our results provided evidence that diosgenin up-regulates VEGF-A and promotes angiogenesis in preosteoblast-like cells by a HIF-1α-dependent mechanism involving the activation of Akt and p38 MAPK signaling pathways.

Disclosures: ***M. Yen****, None.*

SA262

See Friday Plenary number F262

SA263

Fluid Shear Stress Synergizes with IGF-I on Osteoblast Proliferation Through Integrin-Dependent Activation of IGF-I Receptor. K. H. W. Lau, S. Kapur, D. J. Baylink. Musculoskeletal Disease Center, Jerry L. Pettis Mem VAMC, Loma Linda, CA, USA.

Mechanical strain increases osteoblast proliferation. Recent studies suggested that mechanical strain has a permissive role in the IGF-I mitogenic action in osteoblasts. The present study tested the hypothesis that mechanical strain interacts with the IGF-I pathway in the stimulation of osteoblast proliferation ([^{3}H]Thymidine incorporation, TdR). Human TE85 osteosarcoma cells were subjected to steady shear stress of 20 dynes/cm^2 for 30 min followed by 24-hr incubation with IGF-I (0 to 50 ng/ml). IGF-I increased TdR (1.5- to 2.5-fold, $p<0.01$) in a dose-dependent manner. Shear stress alone increased TdR by 70% ($p<0.01$). The combination of shear stress and IGF-I stimulated TdR (3.5- to 5.5-fold) much greater than the additive effects of each treatment alone (ANOVA), suggesting a synergistic interaction. IGF-I dose-dependently increased the phosphorylation level of Erk1/2 (1.2- to 5.3-fold) and IGF-I receptor (IGF-IR) (2- to 4-fold). Shear stress alone also increased the phosphorylation Erk1/2 and IGF-IR (2-fold each). The combination treatment resulted in synergistic enhancements in both Erk1/2 and IGF-IR phosphorylation (up to 12-fold for Erk1/2 and 8-fold for IGF-IR). Shear stress did not alter the binding affinity or number of IGF-IR, indicating that the synergy occurred at the post-ligand binding level. Recent studies have implicated a role for integrin in the regulation of IGF-IR phosphorylation and activation of IGF-I signaling mechanism (i.e., integrin activation recruits away SHP-2 from the IGF-IR, allowing sustained IGF-IR phosphorylation and activation). To test the hypothesis that the synergy between IGF-I and shear stress involve integrin-dependent mechanisms, we measured the effect of echistatin (an inhibitor of integrin) on TdR in response to shear stress ± IGF-I. Echistatin reduced basal TdR by 60%, and slightly but not significantly reduced the mitogenic response to the shear stress (173±16% vs. 157±20% of control). However, echistatin completely abolished the mitogenic effect of IGF-I and that of the combination treatment, indicating that the IGF-I action and the synergy between shear stress and IGF-I involves integrin activation. Shear stress also significantly ($p<0.05$ for each) reduced the amounts of SHP-1 and SHP-2 co-immunoprecipitated with IGF-IR, supporting that the synergy involves the integrin-dependent recruitment of SHP-1 or -2 away from IGF-IR. In conclusion, shear stress interacts synergistically with the IGF-I signaling pathway in osteoblast proliferation and this interaction involves integrin-dependent upregulation of IGF-IR phosphorylation and activation

Disclosures: ***K.H.W. Lau****, None.*

SA264

See Friday Plenary number F264

SA265

A Novel Target For Calcimimetics In Osteoblasts Lacking CASR. M. Pi[1], D. Martin[2], L. D. Quarles[1]. [1]Internal Medicine, University of Kansas Medical Center, Kansas City, KS, USA, [2]Amgen, Inc, Thousand Oaks, CA, USA.

The phenylalkylamine NPS-568 is an allosteric modulator of the G-protein coupled calcium sensing receptor, CASR. NPS-568R binds to CASR and increases its sensitivity to extracellular calcium, whereas NPS-568S is the less active stereoisomer of this calcimimetic that is often used as a negative control in experiments testing CASR function. There is controversy regarding whether a functional CASR is present in osteoblasts. To determine the response of osteoblasts to calcimimetics, we compared the activation potential of NPS-568R and NPS-568S in MC3T3-E1 osteoblasts and immortalized osteoblasts derived from CASR null mice. Negative and positive controls for CASR activation respectively consisted of non-transfected HEK-293 cells and HEK-293 cells transfected with CASR. NPS-568R at doses of 1 μM stimulated the activity of a serum response element luciferase reporter construct (SRE-luc) in HEK-293 cells transfected with CASR, but not in HEK-293 cells lacking CASR, indicating the requirement of CASR for NPS-568 activation of SRE signaling pathways. NPS-568S failed to stimulate SRE activity in HEK-293 cells with and without CASR overexpression. In contrast, neither NPS-568R nor NPS-568S activated the SRE-luciferase reporter construct in either MC3T3-E1 osteoblasts or immortalized osteoblasts derived from CASR null mice. Consistent with the absence of a functional CASR in osteoblasts, we also failed to detect CASR transcripts by RT-PCR in these osteoblasts cell lines. However, both NPS-568R and NPS-568S caused a dose-dependent activation of ERK1/2 in MC3T3-E1 osteoblasts as well as immortalized osteoblasts derived from CASR null mice, consistent with activation of a non-CASR dependent signaling pathway. The calcium channel blocker, nifedipine, failed to block NPS-568-mediated ERK activation in osteoblasts. These results suggest the presence of a novel target for NPS-568R and its stereoisomer NPS-568S in osteoblasts. Stimulation of this target is not dependent on the configuration of the calcimimetic and is coupled to ERK activation in a manner that does not lead to downstream induction of SRE.

Disclosures: ***M. Pi****, None.*

SA266

See Friday Plenary number F266

SA267

Withdrawn

SA268

See Friday Plenary number F268

SA269

P2 Receptors Are Involved in the Regulation of Proliferation of Human Osteoblastic Cells. M. Solgaard*, Z. Henriksen*, N. R. Jorgensen. Bone Metabolic Unit, Dep.s of Endocrinology and Clinical Biochemistry, Copenhagen University Hospital Hvidovre, Hvidovre, Denmark.

Extracellular nucleotides acting through P2 receptors could be an important factor in the remodeling of bone, affecting the activity of both bone-forming osteoblasts and bone-resorbing osteoclasts. The aim of this study was to investigate the expression of different P2 receptors in human osteoblasts (hOB) and in the osteoblastic cell line SaOS-2, as well as the effect of stimulation with adenosine 5'-triphosphate (ATP) on cell proliferation. Osteoblasts were obtained as stromal cells derived from human bone marrow. Marrow material was collected by puncture of the posterior iliac spine of healthy young volunteers, aged 20-32. Osteoblasts were isolated and cultured in MEM supplemented with 10% fetal calf serum and penicillin/streptomycin for approximately 6 weeks after which reverse transcriptation-linked polymerase chain reactions (RT-PCR) were performed with specific primers in order to detect the expression of different P2 receptors. Cell proliferation was measured by analyzing the number of viable cells, expressed by the cleavage of a tetrazolium salt by a mitochondrial dehydrogenase. Cells were seeded in 96-well plates and assays ran for 5 days. Each day the cells were stimulated with ATP in concentrations ranging from 0,1 μM to 1000 μM. Measurements of cell proliferation were made daily in order to follow proliferation after respectively no, one, two and three stimulations. RT-PCR revealed that hOB expressed mRNA for the following P2 receptors; P2Y 1,2,4,6 and P2X 1,4,6,7 while SaOS-2 cells expressed P2Y 1,2 and P2X 1,4,6,7. Results concerning cell proliferation showed no statistically significant difference in cell proliferation after 2 days stimulation with ATP. However stimulation with ATP each day for 3 days induced an almost significant ($p=0,07$) decrease in cell proliferation for the hOB cells. Only a few assays have been done with SaOS-2 cells so far, but initial results indicate that ATP also acts on osteoblastic proliferation in an inhibitory manner, like in the hOB cells. Thus we have identified, which subclasses of P2 receptors are expressed in human osteoblasts and in SaOS-2 cells. Further, we have shown, that repeated ATP stimulation decreases proliferation of osteoblasts, suggesting an inhibitory function of one or more of the P2 receptors on bone formation. This may be a future target for pharmaceutical modulation of osteoblast numbers and activity in vivo by using specific agonists or antagonists.

Disclosures: ***N.R. Jorgensen****, None.*

SA270

See Friday Plenary number F270

SA271

Involvement of MAPK Pathways in Phosphorylation of Cbfa1 in Human OsteoProgenitor Cells (HOP) Cultured onto Cyclo-RGD Peptide. S. Pallu*[1], M. Dard*[2], R. Bareille*[1], A. Sewing*[2], A. Jonczyk*[3], M. Vernizeau*[4], J. Amedee[1]. [1]INSERM U 577, Bordeaux, France, [2]Biomet-Merck Biomaterials, Darmstadt, Germany, [3]Merck KgaA Preclinical Research, Darmstadt, Germany, [4]Biomet-Merck France, Valence, France.

Osseointegration of bone substitute materials can be improved by grafting RGD-containing peptides able to stimulate adhesive properties of biomaterials towards osteogenic cells. Modification of materials by grafting a cyclo-DfKRG peptide is based on the affinity of αvβ3-αvβ5 integrins expressed by HOP. Our previous results have shown that cyclo-DfKRG peptide coating stimulates osteoblastic differentiation and provokes early phosphorylation of p^{125}FAK / Erk 1 followed by activation of p38 / Erk 2 / JNK 2 MAPKs after 30 min of cell seeding. As described in the literature, MAPK pathways play a crucial role in cbfa1 activity. The aim of this work is to study phosphorylation of Cbfa1 in HOP cultured onto this cyclo- peptide and furthermore to identify the role of JNK 1/2 and p38 MAPK pathways using specific inhibitors.

HOP were seeded onto different coatings (poly-L-Lysine (PLL), cyclo-DfKRG peptide and plastic culture dishes) and then were treated (or not) for 24 hours with 10 μM SP600125 (JNK 1/2 inhibitor) or with 25μM SB 203580 (p38 inhibitor). Cellular proteins were extracted after 30 to 90 min of culture and phosphorylation of Cbfa1 was investigated by immunoprecipitation using a polyclonal antibody against Phospho-Ser/Thr/Tyr (Cliniscience) and then by Western blot using a monoclonal antibody against Cbfa1 (Tebu-Bio).

The results of these experiments have shown that the cyclo-DfKRG peptide induces a 3 fold increase of phosphorylation of Cbfa1 after 60 min of cell seeding when compared to plastic culture or to PLL coating. JNK 1/2 inhibitor treatment (n =3) did not affected its activity, while a p38 MAPK inhibitor (n=2) seems to inhibit partly Cbfa1 phosphorylation in HOP cultured onto cyclo-DfKRG peptide.

In conclusion, adhesion of HOP onto cyclo-DfKRG peptide promotes cell differentiation (Al-P and cbfa1 mRNA expression), activates MAPK pathways and stimulates phosphorylation of Cbfa1 after 60 min of cell seeding. However, inhibitors of JNK1/2 MAPK pathway fail to inhibit the Cbfa1 phosphorylation induced by cyclo DfKRG, while this last process seems to be dependent of the p38 MAPK pathways.

Disclosures: ***S. Pallu****, None.*

SA272

See Friday Plenary number F272

SA273

PTH Regulates IGFBP-5 Transcription through AP-2. M. S. Erclik*, J. A. Mitchell. Pharmacology, University of Toronto, Toronto, ON, Canada.

Parathyroid hormone (PTH) regulates bone remodeling and calcium homeostasis by binding to its G protein-coupled receptor, PTH1R in osteoblastic cells. PTH has divergent effects on bone metabolism; intermittent injections of PTH have an anabolic effect on bone while prolonged PTH exposure causes increased bone resorption. The molecular mechanisms regulating these events remain largely uncharacterized. Previously, we have shown that PTH increases insulin-like growth factor binding protein-5 (IGFBP-5) mRNA levels, a process that occurs through transcriptional mechanisms and that requires PKC-δ activation. IGFBP-5 is secreted by osteoblasts and is thought to bind IGF within the extracellular environment, a process that may favor the anabolic effects of IGFs in bone. We have investigated the molecular mechanisms by which PTH mediates the increase in IGFBP-5 transcription in UMR106-01 osteoblastic cells. To identify specific PTH responsive elements within the IGFBP-5 proximal 5'-flanking region deletion analyses was undertaken by fusing deletion fragments upstream of the luciferase reporter gene. Our studies identified a PTH-dependent regulatory element, 20 base pairs in length, that exists within 40 base pairs of the transcription start site. This 20 base pair region contains a recognition sequence of the transcription factor AP-2 and mutational analysis indicated that AP-2 binding is required to achieve full PTH response. Gel-mobility shift assays demonstrated PTH-induced binding to a DNA segment containing the regulatory region. To investigate the mechanisms by which PTH regulates IGFBP-5 gene transcription, we have examined the effect of PTH on the activity of members of the mitogen activated protein kinase (MAPK) family. PTH stimulates p38 but inhibits JNK and Erk1/2 activity in UMR cells. Luciferase reporter assays demonstrated that activation of p38 was functionally involved in PTH-stimulated transcription of the IGFBP-5 gene. The p38 selective inhibitor, SB203580 and dominant negative mutants of p38, were able to partially block the PTH stimulation of luciferase activity. These findings are the first to demonstrate the involvement of the transcription factor AP-2 in the effects of PTH in the regulation of IGFBP-5.

Disclosures: ***M.S. Erclik****, None.*

SA274

Osteogenic Effect of Danshensu (D(+)β-3,4-Dihydroxyphenyl-lactic acid) on Bone Marrow Stromal Cells of Intact and Glucocorticoid -treated Rats. L. Cui[1], Y. Y. Liu*[1], L. Y. Zou*[1], C. M. Ai*[2], T. Wu*[1]. [1]Department of Pharmacology, Guangdong Medical College, Zhanjiang, China, [2]Guangdong Key Laboratory for research and development of Natrual Drugs, Guangdong Medical College, Zhanjiang, China.

Our previous study had showed that the danshensu (TSU) had anabolic effects on glucocorticoid(GC)-induced osteoporosis in rats by analyzing bone histomorphometry. The current study was further to investigate the mechanism of molecular biology of danshensu on the abilities of osteogenesis and adipogenesis of bone marrow stromal cells in intact and in GC-treated rats by using cytochemistry and RT-PCT technique. Three-months old SD male rats were received either distilled water, 2.7mg/kg/d of prednisone oral gavage, or prednisone plus danshensu at dose of 25mg/kg/d for 45 days. At the endpoint the bone marrow stromal cells of the rats (rMSCs) was isolated by density-gradient centrifugation and cultured. Compared with intact rats group, the type I collagen (Coll-I) mRNA expression was decreased and the lipoprotein lipase (LPL) mRNA was increased in the first generation of rMSCs from GC-treated group, danshensu treatment group showed a increase in Coll-I mRNA expression and a decrease in LPL mRNA expression when compared with the GC-treated rats. Danshensu at concentration of 0.5μg/ml *in vitro* induced ALP expression, increased ALP activity and Coll-I mRNA expression of rMSCs both in intact and in GC-treated rats, danshensu at concentration of 0.5μg/ml decreased LPL mRNA expression of rMSCs in GC-treated rats (figure shows bellow). Our results illustrate that the increase of osteogenic ability and decreased of adipogenesis in the bone marrow is likely the mechanism of danshensu for protecting bone from glucocorticoid-induced osteoporosis.

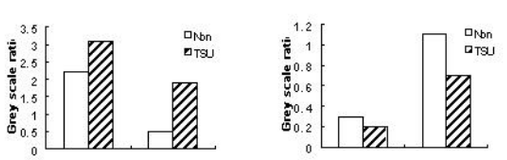

Fig. Effect of TSU on Coll-I (left) and LPL (right) mRNA expression of rMSCs in intact rtas (Cont.) and in glucocorticoid-treated rats (GC).

Disclosures: ***L. Cui****, L.Cui 2.*

SA275

See Friday Plenary number F275

SA276

Successful Engraftment by Donor-derived Osteoblasts Delivered as an Intramarrow but not Systemic Transplantation. L. Wang, Y. Liu*, X. Jiang*, Z. Kalajzic*, P. Liu, D. W. Rowe. Department of Genetics and Developmental Biology, University of Connecticut Health Center, Farmington, CT, USA.

Providing evidence for engraftment of host bone by donor derived osteoprogenitor cells has confounded the interpretation of adult stem cell transplantation studies. We have developed a series of bone specific promoter-GFP reporter transgenic mice to provide a rapid and sensitive method for judging the success of transplantation. The pOBCol3.6GFPtpz and pOBCol3.6GFPcyan construct is expressed in preosteoblasts and early osteoblasts (only a portion of which co-label with injected xylenol orange, XO) while the pOBCol2.3GFPemd construct is active in osteoblasts (that uniformly co-localize with XO) and osteocytes. Marrow stromal fibroblasts (MSFs) derived from any of these transgenic mice and delivered by venous or intracardiac injection fail to show evidence of engraftment in total body irradiated (TBI) and non-transgenic total bone marrow (TBM) rescued mice. However when TBM was derived from pOBCol3.6GFPcyan donor mice, cyan positive cells were located on the trabecular and endosteal bone surface. These cyan positive cells did not prove to be osteoblasts. They never migrated into the bone matrix, failed to co-localize with XO labeling and did not generate bone nodules in MSF cultures derived from the transplanted mice.

When MSFs derived from the pOBCol3.6GFPtpz or pOBCol2.3GFPemd were directly injected into the marrow space of the lethally irradiated non-transgenic mouse along with TBM from a pOBCol3.6GFPcyan donor, clear evidence of local osteoblast differentiation and engraftment were found. GFPtpz and GFPemd positive cells were incorporated into trabecular and endosteal bone and positive cells on the bone surface co-localized with XO. GFPcyan positive cells derived from the TBM co-transplant were found both within the injected bone and at distal bone sites. Again, these cells did not become osteocytes and did not co-label with XO. Further studies indicate that the osteoprogenitors capable of engraftment can be derived from freshly isolated calvarial cells and from primary calvarial or bone marrow stromal cultures. They are capable of making new bone at many sites within the marrow space but lack evidence for osteoblast engraftment other than the bone of injection. The use of the osteoblast lineage restricted GFP markers, coupled with co-localization with a fluorescent label of new matrix formation and recovery of donor osteogenic nodules from the transplanted mice indicate that local osteoblast engraftment with stromal derived progenitors is a feasible strategy for cell therapy at defined sites of the skeleton.

Disclosures: ***L. Wang****, None.*

SA277

See Friday Plenary number F277

SA278

Effect of Raloxifene on the Proliferation and Differentiation of Bone Marrow Stromal Stem Cells in Ovariectomized Rats. S. Hong[1], M. Nam*[1], W. Park*[1], B. Lee*[2], Y. Kim*[1]. [1]Internal Medicine, Inha University, Inchon, Republic of Korea, [2]Obstetrics and Gynecology, Inha university, Inchon, Republic of Korea.

Since osteoblast and adipocytes originate from a common mesencymal precursor cell, it has been proposed that osteoporosis might in part result from a switch of cell differentiation favoring adipogenesis. Raloxifene, selective estrogen receptor modulator, prevent bone loss. Although it is largely used for the treatment of osteoporosis, the mechanisms by which this compound modulate bone cells are poorly understood. So, We used a rat model in which estrogen depletion was established for a period of 1 months before the treatment. After this period the animals were divided into three experimental groups consisting of sham operated(CON), Ovariectomy(OVX) and OVX-Raloxifene-treated rats(OVX-Ral). All animals received daily treatment of raloxifene 1 mg/kg or placebo for 12 weeks. OVX and OVX-Ral were compared with the CON group and were assessed for the alteration of these cell's proliferation and differentiation. The proliferation of stromal stem cells was measured by CFU-F assay. CFU-F count were not different among 3 groups. But Alkaline phosphatase(ALP)- positive colony count was decreased in bone marrow stromal cells derived from OVX group, was increased in OVX-Ral group. Differentiation of bone marrow stromal cell were assessed in vitro. Marrow stromal cells underwent differentiation in a osteogenic medium containing dexamethasone, ascorbic acid, β-glycerophsphate. In cells of OVX-Ral group, alkaline phosphatase activity and nodule formation were increased compared with one of OVX. The mRNA expression of ALP, osteocalcin were decreased in OVX , but maintained in OVX-Ral. During the adipogenic differentiation, mRNA expresssion of PPAR gamma, FAS of OVX-Ral were decreased than those of OVX group. Oil-red O stains showed similar findings. In conclusion, osteogenic differentiation of bone marrow stromal cells was enhanced after raloxifene treatment. Adipogenic differentiation was negatively regulated in the OVX-Ral group compared to OVX group. Our result might explain the clinical observation that raloxifene treatment decrease fracture incidence.

Disclosures: ***S. Hong****, None.*

SA279

Osteoclast AlphaVbeta3 Integrin-induced ERK1/2 Activation Is Intracellular Ca2+ and c-Src-Dependent, Shc/Ras/Raf-1-Independent, and Is Triggered by Engagement of PKCalpha. N. Rucci[1], C. Di Giacinto*[1], L. Orrù*[1], R. Baron[2], A. Teti[1]. [1]Department of Experimental Medicine, University of L'Aquila, L'Aquila, Italy, [2]Department of Cell Biology and Orthopaedics, Yale University School of Medicine, New Haven, CT, USA.

The alphaVbeta3 integrin is central to osteoclast function, is engaged by adhesion to bone matrix proteins and activates cytoskeletal reorganization and intracellular signaling. The role of protein kinases C (PKC) in these pathways is still unknown and, to clarify it, mouse primary osteoclast-like cells and beta3-stably transfected CHO cells (CHOalphaVbeta3) were allowed to adhere to immobilized alphaVbeta3-monoclonal antibody, LM609. We observed subcellular redistribution of PKCalpha, with translocation (i.e. activation) of the isoenzyme from the cytosol to the membrane and/or triton-X-insoluble compartments, independent of PLCgamma and PI3-K. Immunoprecipitation assays revealed that alphaVbeta3 integrin was engaged in a complex with PKCalpha and Grb2, as well as with the tyrosine kinases FAK in CHOalphaVbeta3 cells and PYK2 in osteoclasts. AlphaVbeta3 ligation induced ERK1/2 activation, while the JNK and p38 MAPKs were unaffected. Association between ERK1/2 and alphaVbeta3 or PKCalpha was not detectable, suggesting indirect interaction among these molecules. Moreover, the adaptor protein Shc and the canonical Ras/Raf-1/MEK-1/2 signal were not involved in ERK1/2 activation. AlphaVbeta3-dependent ERK1/2 phosphorylation was blunted by pre-treatment with the PKCalpha inhibitor Gö6976 and by downregulation of PKCalpha by long-term treatment with the phorbol ester, TPA. Ligand-induced alphaVbeta3 integrin-dependent ERK1/2 activation was also blocked by c-Src inhibition. However, c-Src and PKCalpha did not appear to interact nor to cooperate to the signal pathway leading to ERK1/2 phosphorylation. Pre-treatment with the intracellular calcium chelator BAPTA inhibited PKCalpha translocation, its recruitment by alphaVbeta3 and ERK1/2 activation, demonstrating intracellular calcium dependence of these events. PKCalpha inhibition did not impair cell adhesion and survival, but significantly reduced migration and osteoclast bone resorption. In conclusion, ERK1/2 activation is central to alphaVbeta3 signaling, and intracellular calcium, c-Src and PKCalpha are key regulators affecting events downstream of the integrin, associated with ERK1/2 activity, cell motility and bone resorption.

Disclosures: ***N. Rucci****, None.*

SA280

Disruption of the Actin-binding Domain of Vacuolar H^+-ATPase Subunit B1 Prevents its Transport to Ruffled Membranes of Osteoclasts. J. Zuo*[1], S. Chen*[1], J. Jiang*[2], M. Kaku*[3], J. Xue*[1], L. S. Holliday[1]. [1]Orthodontics, University of Florida College of Dentistry, Gainesville, FL, USA, [2]Endodontics, University of Florida College of Dentistry, Gainesville, FL, USA, [3]Orthodontics & Craniofacial Development, Hiroshima University, Hiroshima, Japan.

In mammals, two isoforms isoforms of subunit B of vacuolar H^+-ATPase (V-ATPase) exist and both contain F-actin binding sites that can be disabled by minimal alterations[1]. Isoform B1 is normally expressed in kidneys, and isoform B2 is expressed ubiquitously and at high levels in osteoclasts. LLC-PK_1 cells express both B1 and B2, but the two do not co-assemble into the same holoenzyme. In the present study, to test the physiologic relevance of the actin binding domain, we introduced wild type B1 (wtB1) and B1 with the actin binding site disrupted (mutB1) into primary mouse marrow osteoclasts using adeno-associated virus vectors. WtB1 and mutB1 were detected by immunoblotting with anti-B1 antibodies. Both constructs were expressed at similar levels to endogenous B2. Pelleting analysis indicated that wtB1, but not mutB1, associated with the detergent-insoluble cytoskeleton. Localization of B1 in osteoclasts was determined by immunocytochemistry and confocal microscopy. Like B2, wtB1 was targeted to ruffled membranes of resorbing osteoclasts. In contrast, mutB1 was not transported to ruffled membranes, remaining diffusely distributed in the cytosol. In summary, these data show that although the B1 isoform is not normally expressed in osteoclasts, wtB1 has the necessary elements required for proper targeting and transport to ruffled membranes of osteoclasts. Minimal disruption of the actin-binding domain perturbs this transport.

1. Chen,S.H. *et al.* Vacuolar H+-ATPase binding to microfilaments: regulation in response to phosphatidylinositol 3-kinase activity and detailed characterization of the actin-binding site in subunit B. *J. Biol. Chem.* **279**, 7988-7998 (2004).

Disclosures: ***L.S. Holliday****, None.*

SA281

$\alpha_9\beta_1$ Integrin Is Expressed on Osteoclast Precursors and Mediates Osteoclast Formation Though Its Interaction With ADAM8. H. Rao[1], H. Kajiya[1], K. Safran*[1], S. J. Choi*[1], N. Kurihara[1], J. Anderson*[1], G. D. Roodman[2]. [1]Medicine/Hematology, University of Pittsburgh, Pittsburgh, PA, USA, [2]Medicine/Hematology, University of Pittsburgh and VA Pittsburgh Healthcare System, Pittsburgh, PA, USA.

Integrins play an important role in OCL formation. In particular, $\__v\beta_3$ is expressed on OCL, binds osteopontin and is required for normal osteoclastic bone resorption. During OCL precursor differentiation, $\__v\beta_5$ is expressed initially and then is replaced by $\__v\beta_3$ as OCL precursors differentiate to mature OCL. However, the role of other integrins in OCL formation and OCL activity has not been clearly defined. We recently identified ADAM8, a disintegrin and metalloproteinase, as a novel stimulator of OCL formation. Structure-function studies demonstrated that the disintegrin domain of ADAM8 mediated its effects on OCL formation. Since the disintegrin domain of ADAM8 does not bind RGD sequences, we determined which integrin bound ADAM8. Plastic petri dishes were coated with a GST-fusion protein containing the disintegrin domain of ADAM8. CHOK1 cells transfected with various integrin cDNAs were tested for their capacity to bind the disintegrin domain of ADAM8. We found that the $\alpha_9\beta_1$ integrin and not $\alpha_v\beta_3$ bound the disintegrin of ADAM8. Western blot analysis confirmed that the α_9 integrin was present in normal human marrow cultures and was specifically expressed on early human OCL precursors, CFU-GM. The levels of α_9 mRNA expression decreased with progressive OCL precursor differentiation. In addition, α_9 mRNA expression was detectable in mouse bone marrow cultures by immunocytochemistry. Importantly, a blocking monoclonal antibody to α_9 (0.1 and 1 μg/ml) inhibited human OCL formation stimulated by 1,25-$(OH)_2D_3$ in a dose dependent fashion. The antibody also blocked RANKL induced OCL formation by a highly purified CFU-GM. We also found that RAW264.7 cells also expressed α_9 mRNA and that α_9 mRNA expression decreased with subsequent OCL differentiation in the presence of RANKL. Taken together, these data demonstrate that early OCL precursors express $\alpha_9\beta_1$ integrin and that expression of $\alpha_9\beta_1$ integrin decreases with subsequent differentiation. Furthermore, $\alpha_9\beta_1$ integrin appears to be the receptor for ADAM8 and mediates its effects on osteoclastogenesis. These data support an important role for $\alpha_9\beta_1$ integrin in OCL formation.

Disclosures: ***H. Rao****, None.*

SA282

Osteoclast Podosome Organization Is Dependant of the Maturation of Microtubules under Control of a New Rho/mDIA2/HDAC6 Pathway. O. Destaing[1], F. Saltel*[1], O. Destaing[2], S. Ory*[3], B. Gilquin*[4], S. Khochbin*[5], P. Jurdic[1]. [1]Lbmc, ENS-Lyon, Lyon, France, [2]Cell Biology, School of Medicine, New Haven, CT, USA, [3]Upr 1086, CRBM, Montpellier, France, [4]Inserm U309, Institu Albert Bonniot, Grenoble, France, [5]Inserm U309, Institut Albert Bonniot, Grenoble, France.

By using confocal videomicroscopy, we have previously shown that immature osteoclasts present clusters of podosomes which will evolve later into dynamic, internal and unstable podosome rings (life-span under 30 min). At the end of the differentiation and under controlled of the microtubules network, podosomes rings are stabilized into the classical and peripherical podosome belts, which are reminiscent of the sealing zone in bone resorbing osteoclasts, (*Destaing et al. 2003*, Mol Biol Cell).

However, microtubules are present during all the osteoclastogenesis. To try to understand how microtubules could act only at the end of the differentiation process, we have looked at the post-translationnal modifications of α-tubulin monomers along osteoclast differentiation. Indeed, multiple post-translationnal modifications (phosphorylation, acetylation, detyrosination…) of microtubules are linked with them stabilization and in some specific differentiation process such as myogenesis. We have found that sealing zones and podosome belts are specifically associated with an increase of acetylation of microtubules. In parallel by using TAT-C3 peptide, we have found that Rho inhibition induces a strong stabilization of microtubules which.

It has been shown recently that acetylation is controlled by the histone deacetylase 6, HDAC6. This point lead us to investigate the relationship between Rho and HDAC6 in the context of osteoclast. The expression of constituvely activated form of Rho, RhoA V14, induced deacetylation of microtubules, effect which is blocked by the specific inhibitor of HADC6, trichostatine A. In the osteoclasts, Rho can activate the adaptator mDIA2 which co-immunoprecipitates and activates HDAC6 in an in vitro deacetylase assay. We then defined a new pathway where Rho activation stimulates mDIA2 which is able to interact and activate HDAC6, leading to a decrease of microtubule acetylation. By using differential treatment of trichostatineA and the stabilizing microtubule agent taxol, we have shown that the podosome belt formation is dependant upon microtubule stabilization and acetylation.

Our data suggests the existence of a new pathway leading to decrease Rho activity along osteoclast maturation necessary to allow hyperacetylation and then podosome belt formation. This point opens up new potential strategies to control podosomes and sealing zone properties in bone resorbing osteoclasts.

Disclosures: ***O. Destaing****, None.*

SA283

See Friday Plenary number F283

SA284

Vitaxin®, an Alphav Beta3 Blocking Antibody, Inhibits Osteoclastic Resorption by Decreasing the Number of Attached Osteoclasts. A. Gramoun*[1], M. F. manolson[1], J. N. M. Heersche[1], D. P. Trebec*[2], S. Y. Mao*[3]. [1]University of Toronto, Faculty of Dentistry, Toronto, ON, Canada, [2]University of Toronto, Department of Biochemistry, Toronto, ON, Canada, [3]MedImmune, Inc., Gaithersburg, MD, USA.

The integrin $\alpha_v\beta_3$ is an abundant osteoclast surface receptor mediating both cell to matrix and cell-to-cell interactions and is thought to be involved in osteoclast differentiation, attachment and resorption. Vitaxin® is an anti-human $\alpha_v\beta_3$ antibody that blocks the conformational epitope of this integrin. Vitaxin also binds rabbit $\alpha_v\beta_3$, therefore, effects of Vitaxin on osteoclast differentiation, adhesion and resorption using rabbit osteoclasts cultured on plastic surfaces and osteologic discs were studied. After an 18 hour attachment period, osteoclasts were incubated with different concentrations of Vitaxin for an additional 24 or 48 hours. Vitaxin at 30 ng/ml, 100 ng/ml and 300 ng/ml decreased the number of osteoclasts attached to plastic in a dose dependent fashion by an average of 6%, 25% and 35% respectively. This paralleled a decrease in the total number of nuclei in osteoclasts indicating that the decrease in the number of attached osteoclasts was not due to cell fusion. Activation of $\alpha_v\beta_3$ using 2.5 mM $MgCl_2$ in culture did not alter Vitaxin's inhibitory effect on attachment demonstrating that the epitope is not sensitive to activation state of the integrin. Initial attachment (measured at 2 hours) was reduced by 30% when osteoclasts were incubated with 300 ng/ml Vitaxin for 25 minutes prior to plating. However the rate of differentiation of both Vitaxin treated and control groups was equal, indicating that Vitaxin did not interfere with differentiation. Approximately a 50% decrease in the total area of resorption on osteologic slides was seen with Vitaxin at 100 ng/ml and 300 ng/ml. The percentage of large osteoclasts (>10 nuclei) was increased by an average of 1.88 fold in the groups incubated with 300 ng/ml Vitaxin suggesting that it has a greater effect on small osteoclasts (<10 nuclei). The differential sensitivity of large and small osteoclasts to Vitaxin is partially explained by the observation that there was a 4.5 and 2.8 fold increase in the levels of expression of β_3 and α_v respectively on the surface of large osteoclasts compared to small osteoclasts. Our results suggest that in a primary osteoclast culture, the decrease in resorption is a result of Vitaxin impairing osteoclast attachment rather than osteoclast differentiation.

Disclosures: ***A. Gramoun****, None.*

SA285

See Friday Plenary number F285

SA286

CXCL12 Chemokine Up-regulates Bone Resorption and MMP-9 Release by Human Osteoclasts: CXCL12 Levels Are Increased in Synovial and Bone Tissue of Rheumatoid Arthritis Patients. G. Lisignoli*, F. Grassi, S. Cristino*, S. Toneguzzi*, A. Piacentini*, A. Facchini*. Laboratorio di Immunologia e Genetica, Istituti Ortopedici Rizzoli, Bologna, Italy.

Chemokines has recently emerged as important modulators of osteoclasts recruitment and function. In addition to their chemotactic function, some chemokines have been shown to be able to modulate osteoclasts differentiation and ability to resorb bone. CXCL12 is a chemokine involved in T cells activation during rheumatoid arthritis, but recent findings have revealed that human osteoclasts express high levels of this chemokines at the final stages of differentiation. We hypothesized that CXCL12 may play a role in osteoclasts differentiation and function. Therefore, we evaluated in vitro CXCL12 modulation of osteoclasts development and ability to resorb bone; also, we analysed its expression on synovial and bone tissue biopsies from rheumatoid arthritis (RA) patients. Osteoclasts were obtained by 7 days in vitro differentiation with RANKL and M-CSF of CD11b positive cells in the presence or absence of CXCL12. The total number of osteoclast was analyzed by TRAP staining and bone resorbing activity was assessed by pit assay. MMP-9 and TIMP-1 release were evaluated by ELISA. CXCL12 expression on biopsies from RA patients was analyzed by immunohistochemistry. Osteoclasts obtained in the presence of CXCL12 at 10 nM concentration displayed a highly significant increase in bone-resorbing activity (~ 90% increase relative to control sample) as measured by pit resorption assay, while the total number of mature osteoclasts was not affected. The increased resorption was associated with significant overexpression of MMP-9. Addition of anti-CXCL12 antibody to the culture media suppressed both MMP-9 overexpression and increased resorbtion by osteoclasts. Immunostaining for CXCL12 on synovial and bone tissue biopsies from both rheumatoid arthritis (RA) and osteoarthritis (OA) samples revealed a strong increase in the expression levels under inflammatory conditions.
In summary, CXCL12 chemokine showed a clear activating role on mature osteoclast by inducing bone-resorbing activity and specific MMP-9 enzymatic release. These findings may provide new insights into osteoclasts activation in inflammatory diseases of bone.

Disclosures: ***G. Lisignoli****, None.*

SA287

See Friday Plenary number F287

SA288

TSH Negatively Regulates the TNF Axis During Osteoclast Formation. L. Eldeiry*, Y. Peng*, J. Iqbal*, T. Ando*, T. Davies*, M. Zaidi, E. Abe. Endocrinology, Mt. Sinai School of Medicine and VA Medical Center, New York, NY, USA.

We have shown that the anterior pituitary-derived hormone, thyrotropin (TSH), is a negative regulator of bone remodeling. Even heterozygote mice with 50% TSH receptor (TSHR) deleted display osteopenia due to increased osteoclast formation, function and survival. Here, we establish that the enhanced osteoclastogenesis in the TSHR null mouse results from an up-regulated TNF axis. Real time PCR showed a ~20-fold increase in the expression of both TNF receptors, TNFRI and TNFRII, in $TSHR^{-/-}$ hematopoetic stem cell cultures. Immunoblotting demonstrated a significant increase in the phosphorylated (degradable) form of IκBα, a key TNF signaling inhibitor. In addition to elevated TNF signaling, TNFα levels were increased ~3-fold in $TSHR^{-/-}$ bone marrow supernatants and hematopoetic stem cell cultures. A neutralizing TNFα antibody abrogated the osteoclastogenic response to TSHR deletion, providing direct evidence that the increased osteoclast formation in the $TSHR^{-/-}$ mice resulted from elevated TNF signaling. We next examined the regulation of TNFα expression by TSH in TSHR-positive RAW-C3 osteoclast precursors and bone marrow-derived $CD11b^+$ cells. TSH potently inhibited TNFα expression when cells were co-stimulated by IL-1 and TNFα. Lipopolysaccharide- (LPS-) stimulated TNFα expression was, however, TSH-resistant. To obtain mechanistic insights, we PCR amplified a 1.2 kb murine TNFα promoter sequence containing 3 NFκB binding sites. Exposure to IL-1 and TNFα concomitantly, or to LPS alone enhanced TNFα promoter activity in RAW-C3 cells, by ~3-fold. TSH neither affected basal nor stimulated promoter activity, indicating that the effect of TSH in suppressing TNFα expression was post-transcriptional. Parallel real time PCR studies indicated that TSH reduced basal expression of both TNFRI and TNFRII mRNA by ~30%. Finally, immunoblotting showed that pIκBα and nuclear p65 (but not p50) were inhibited strongly by TSH in RAW-C3 cells. Taken together, the results establish the negative regulation of the TNF axis by TSH during osteoclast formation. The hormone may thus play a more global role in controlling TNF expression and action in tissues other than bone.

Disclosures: ***E. Abe****, None.*

SA289

The Role of Marrow Stromal Cells in TNF-alpha Induced Inflammatory Arthritis and Osteoclastogenesis In Vivo. H. Kitaura[1], S. Wei[1], P. Zhou[1], K. Aya[1], S. Takeshita[1], Y. Abu-Amer[2], F. P. Ross[1], S. L. Teitelbaum[1]. [1]Department of Pathology, Washington University School of Medicine, St.Louis, MO, USA, [2]Department of Orthopedic Surgery, Washington University School of Medicine, St.Louis, MO, USA.

The marrow stromal cell is the principal source of RANKL and M-CSF and is thus central to physiological osteoclastogenesis. Stromal cells also express receptors for TNF, but the contribution these cells make to the osteolysis associated with excess levels of the cytokine is unknown. To define the role of marrow stromal cells in varying states of TNF-driven osteoclast formation, *in vivo*, we generated chimeric mice using wild type (WT) or TNF receptor deficient (KO) marrow, immunodepleted of T-cells and stromal cells. The samples were reciprocally transplanted into KO or WT mice (i.e. WT→KO; KO→WT) following lethal irradiation to eliminate native marrow. As controls, similarly-treated WT marrow was transplanted into WT mice and KO marrow transplanted into KO mice. Each group was administered increasing doses of TNF and marrow was obtained after five days. Exposure to high dose cytokine, *ex vivo*, induces exuberant osteoclastogenesis irrespective of *in vivo* TNF treatment, or whether the recipient animals possess TNF-responsive stromal cells. In contrast, the osteoclastogenic capacity of marrow treated ex vivo with lower dose TNF requires priming by TNF receptor-bearing stromal cells, *in vivo*. TNF increases the number of marrow macrophages in KO to WT and WT to WT but not WT to KO marrow transfer, suggesting that TNF responsive stromal cells are an essential component of osteoclast precursor proliferation. On the other hand, the osteoclastogenic contribution of cytokine responsive stromal cells *in vivo* diminishes as the dose of TNF increases. At all doses of the cytokine tested, the increase in OC number, *in vivo*, is blunted in mice whose marrow cells are TNF non-responsive. In keeping with a diminishing role of stromal cells as ambient TNF increases, mice with severe inflammatory arthritis accompanied by exuberant TNF production develop profound osteoclastogenesis and bone erosion independent of stromal cell expression of TNF receptors. The direct induction of osteoclast precursor differentiation by TNF is accompanied by their enhanced RANK expression and sensitization to RANKL. These data suggest osteolysis attending relatively modest elevations in ambient TNF depend upon responsive stromal cells. On the other hand, in states of severe periarticular inflammation, such as active rheumatoid arthritis, TNF may exert its bone erosive effects fully by directly promoting the differentiation of osteoclast precursors independent of cytokine-responsive stromal cells and T-lymphocytes.

Disclosures: ***H. Kitaura****, None.*

SA290

See Friday Plenary number F290

SA291

Regulation of Ca^{2+}-Regulating Enzymes, CD38 and CD157, by TNF-α During Osteoclastogenesis. J. Iqbal*, L. Sun, E. Abe, M. Zaidi. Medicine, Mt. Sinai School of Medicine and the Bronx VA GRECC, New York, NY, USA.

CD38 and CD157 are evolutionary conserved ecto-enzymes that catalyze the conversion of NAD^+ to the Ca^{2+}-releasing molecules, ADP-ribose and cyclic ADP-ribose. We have shown that CD38 is a negative regulator of osteoclast formation. The expression of both CD38 and CD157 is enhanced in severe rheumatoid arthritis, the osteolysis associated with which is TNF-mediated. We therefore examined whether CD38 and CD157 were positively regulated by TNF as a means to control excessive osteoclastogenesis. TNF-α stimulated, by >30- and >8-fold respectively, the expression of CD38 and CD157 mRNA in ficoll-purified bone marrow cells for up to 48 hrs. This was expectedly not seen with $CD38^{-/-}$ cells, confirming specificity. Likewise, FACS analysis showed a ~30-fold increase in CD38 fluorescence of osteoclast progenitors in the presence of TNF-α. Again, $CD38^{-/-}$ progenitors showed no such up-regulation, but did elevate CD157 in response to TNF-α. RANK-L treatment failed to elevate CD38, but did cause a modest increase in CD157. We next investigated the cell-specificity of the CD38 induction by TNF-α. Cells up-regulating CD38 in response to TNF-α were of macrophage/dendritic cell origin, defined as $CD11b^{Hi}$ after ficoll-purification. Double-labeling experiments showed that both CD38 and CD157 were up-regulated in the same cells. This was associated with a TNF-α-induced decrease in proliferation of $CD11b^+/RANK^+$ cells in BrdU incorporation studies. Finally, to understand the mechanism of the TNF-α effect, we carried out (a) half-life experiments and (b) DNA binding assays. Both CD38 and CD157 mRNAs in TNF-α treated cells displayed half-lives at about 3 hrs, excluding effects on mRNA stabilization. Consistent with this, we detected specific binding of a NF-κB responsive element in the murine CD38 promoter to the NF-κB subunit, p50. This binding was abrogated when a G->C point mutation was introduced within the CD38 promoter, confirming specificity. As CD38 negatively regulates osteoclast formation, its up-modulation may provide a primary mechanism for controlling the TNF-α-driven osteoclastogenesis in rheumatoid arthritis.

Disclosures: ***J. Iqbal****, None.*

SA292

Ca^{2+}-sensing by Cell Populations in Murine Bone Marrow: Effects on Osteoclast Formation and Gene Expression. T. Chen*, L. Rodriguez*, W. Chang, D. Shoback. San Francisco VA Medical Center, University of California, San Francisco, CA, USA.

Bone formation and resorption are regulated by systemic hormones and local signals including growth factors and ions released from bone matrix. During active resorption, the free $[Ca^{2+}]$ in the bone microenvironment can rise to levels as high as 40 mM. Cells within the marrow, therefore, are exposed to extracellular $[Ca^{2+}]$ ($[Ca^{2+}]_e$) that are many times higher than those of serum. These studies were designed to test the hypothesis that changes in $[Ca^{2+}]_e$ act as a signal in mediating the functions of diverse cell populations in bone marrow (BM). Cells from BM were harvested from 6-week-old male Black Swiss mice and cultured at different $[Ca^{2+}]_e$ (0.5 to 6 mM) for up to 28 days. Alkaline phosphatase activity (APA) and alizarin red (AR) staining for minerals were determined during culture. Osteoclast (OC) formation was assessed by examining cultures after staining for tartrate-resistant acid phosphatase (TRAP) and by measuring TRAP activity. Gene expression was assessed by quantitative real-time PCR (qPCR). In unfractionated BM cells, there was no significant effect of $[Ca^{2+}]_e$ on APA, however, AR staining was 24 +/- 6 fold greater in cells grown at 4 vs 0.5 mM Ca^{2+} (N=4, $p < 0.001$). High $[Ca^{2+}]_e$ promoted (4-6 mM) the development of multinucleated TRAP+ cells in BM cultures. TRAP activity increased by ≈5-fold after culture at 6 mM Ca^{2+} (vs 1.0 mM Ca^{2+}). This effect of high $[Ca^{2+}]_e$ was inhibited (50-90%) by exogenous osteoprotegerin in a dose-dependent manner. Expression of the receptor activator of nuclear factor kappa B ligand (RANKL) was also increased by culturing BM cells at high $[Ca^{2+}]_e$ by qPCR and western blotting. This suggested that high $[Ca^{2+}]_e$ enhanced the formation of OC's in BM by increasing RANKL expression by osteoblastic cells. To define the populations involved in the response to Ca^{2+}, BM cells were separated into macrophages/monocytes and osteoblastic/stromal cells by magnetic cell sorting (MACS) using CD11b/Mac 1 and vascular cell adhesion molecule-1 (VCAM-1, CD106) antibodies, respectively. VCAM+ cells grown at 6 mM Ca^{2+} expressed ≈15-fold more RNA for RANKL vs cells at 1 mM Ca^{2+} (N=2) -- confirming the findings from whole BM. In contrast, in highly purified (>95%) CD11b+ cells, high $[Ca^{2+}]_e$ inhibited RANKL- and macrophage colony stimulating factor-induced TRAP activity in a dose-dependent manner. These findings indicate that the effects of high $[Ca^{2+}]_e$ in bone likely represent a balance between the actions of Ca^{2+} on distinct cell populations. The membrane mechanism(s) responsible for Ca^{2+}-sensing in these populations remain to be identified and offer potential targets for interrupting pathologic bone remodeling.

Disclosures: ***D. Shoback****, None.*

SA293

See Friday Plenary number F293

SA294

A Novel Role for Megakaryocytes in the Inhibition of Osteoclast Formation. M. A. Kacena, C. M. Gundberg, M. C. Horowitz. Orthopaedics and Rehabilitation, Yale University School of Medicine, New Haven, CT, USA.

A growing body of evidence suggests that megakaryocytes (MK) or their growth factors may play a role in skeletal homeostasis. We have previously identified a novel regulatory pathway that controls bone formation which is mediated by MK. The co-culture of MK with osteoblasts resulted in increased osteoblast proliferation in vitro, by a mechanism that required direct cell-to-cell contact. Here we examine a second, heretofore unrecognized, MK mediated pathway that regulates osteoclast (OC) generation.

We have begun examining the unique inhibitory effect of MK on OC formation. Spleen or bone marrow cells ($2x10^6$ cells/ml) from C57BL/6 mice, as a source of OC precursors, were cultured with M-CSF (30 ng/ml) and RANKL (50 ng/ml) to induce OC formation. MK were prepared by culturing fetal liver cells with thrombopoietin for 3-5 days which were then separated into MK and non-MK populations by a 1g BSA sedimentation gradient. The MK fraction was 95% pure, whereas the non-MK fraction was comprised of non-MK, MK precursors, and a small number of MK. MK were titrated into the spleen cells and OC were identified as tartrate resistant acid phosphatase positive giant cells with >3 nuclei. There was a significant, dose-dependent reduction (up to 15-fold) in OC formed when MK (0-0.5%) were added to the spleen cell cultures. To rule out the possibility that the inhibition was non-specific, we cultured spleen cells with either thymocytes or the non-MK fraction. We demonstrated that from 0-0.15%, thymocytes and non-MK did not inhibit OC development, whereas comparable numbers of MK inhibited OC formation by up to 5-fold. We determined that MK conditioned media (CM) inhibited OC formation ($ED_{50} \approx 2\%$) in a dose-dependent manner (up to 10-fold), indicating that a soluble factor(s) is responsible, at least in part, for the inhibition. Next, we examined MK CM for known inhibitors of OC formation, using ELISAs. IL-4 was undetectable in both MK and non-MK CM, whereas IL-10 levels were similar in MK and non-MK CM (21±9 and 21±5 pg/ml), respectively. Interestingly, we found a significant increase in the levels of OPG in MK CM compared to the non-MK CM (450±62 and 10±8 pg/ml), respectively, suggesting that OPG could be responsible for the reduction in OC formation in these cultures. Furthermore, the potential of MKs as a heretofore, unrecognized OPG source, implicates a potential physiologic role for MKs in regulating OPG levels. These studies indicate that MK may play a dual role in skeletal homeostasis by stimulating osteoblast proliferation and simultaneously inhibiting OC formation.

Disclosures: ***M.A. Kacena****, None.*

SA295

See Friday Plenary number F295

SA296

In Vitro **Interaction Between Nacre and Mature Osteoclasts and Effects of Nacre Water Soluble Matrix in Osteoclastogenesis Cell Culture Models.** D. Duplat*[1], M. Gallet*[2], L. Bédouet*[1], C. Milet*[1], M. Brasier[2], S. Kamel[2], E. Lopez*[1]. [1]Milieux et Peuplement Aquatique, Muséum National d'Histoire Naturelle, Paris, France, [2]Laboratoire de Pharmacie Clinique (UMRO), Faculté de Pharmacie, Amiens, France.

Nacre is the mother-of-pearl inner layer of the shell of the pearly oyster *Pinctada margaritifera*. It is composed of calcium carbonate crystallized in aragonite form on an organic matrix scaffold. Previously, it has been demonstrated *in vivo* that the nacre implanted in the femur of a sheep is accepted and stimulates bone remodelling at the interface between bone and nacre suggesting that nacre represents a potential newly biomaterial. Furthermore, several *in vitro* studies have confirmed that the nacre water soluble matrix (WSM) stimulates the osteoblasts differentiation but no information is available on the osteoclast lineage.

The objective of our study was to assess the ability of mature osteoclasts to degrade nacre and to evaluate the effect of the nacre diffusible molecules on the osteoclasts differentiation and activity. Two mammalian cell models were used: a murine monocytic cell line RAW263.7 and osteoclasts isolated from long bones from 10-day-old rabbits.

The RAW263.7 cells were cultured during 5 days with RANKL in presence of WSM or fractions of WSM obtained by SE-HPLC. The number of osteoclast-like TRAP positive cells is a measure of the differentiation. On the other hand, rabbit osteoclasts were cultured on bovine cortical bone and nacre slices for 48 hr and 72 hr in presence of WSM. The resorption activity was determined by quantification of the resorption pit area.

Firstly we found that, nacre can be resorbed by rabbit osteoclasts indicating that it exists a bio-interactivity between bone resorbing cells and nacre.

Then we showed that WSM decreases the number of osteoclast-like TRAP positive cells as well as the number of resorption pit area. On RAW264.7 cells, a low molecular weight fraction increases the number of osteoclast-like TRAP positive cells whereas the high molecular weight fractions have a reverse activity.

This nacre matrix can be compared to the bone matrix that contains signal molecules with opposite effects according to the cell type targeted. The opposite effect of the high and low molecular WSM fractions on both osteoblasts and osteoclasts suggested that they contain signal molecules that are involved in a non specific manner in the bone cell differentiation pathway.

This study confirms the previous results obtained *in vivo* and *in vitro* with other bone cell lineage: the nacre organic matrix is the source for the signal molecules responsible for bone cell stimulation in mammals.

Disclosures: ***D. Duplat****, None.*

SA297

See Friday Plenary number F297

SA298

Human Microvascular Endothelial Cells (HMVEC) Activated by IL-1 and TNF alpha Selectively Recruit Circulating Human CD14+ Monocytes That Develop Into Functional Osteoclasts. L. Kindle, M. Kriss*, L. Rothe, P. A. Osdoby, P. A. Collin-Osdoby. Department of Biology, Washington University, St. Louis, MO, USA.

Inflammatory diseases such as rheumatoid arthritis and periodontal disease exhibit elevated local cytokine production, monocyte (MN)/macrophage infiltration, and pathological bone erosion due to increases in resorptive osteoclasts (OCs). OC precursors derive from the MN/macrophage lineage and reside in the bone marrow and peripheral circulation, from which they may be recruited to inflammatory sites, develop into OCs, and contribute to localized osteolysis. However, little is known about how pre-OCs may be recruited from the circulation or are influenced by the microvasculature in inflammation. Previously, we showed that IL-1 and TNF alpha upregulate RANKL in HMVEC and thereby promote the co-culture formation and bone resorption of OCs from human peripheral blood mononuclear cells (hPBMC). Here, we analyzed if cytokine-activated HMVEC directly interact with hPBMC to promote adhesion or transendothelial migration (TEM) of precursors that can form bone-resorptive OCs after M-CSF/RANKL culture. Pretreatment of HMVEC with IL-1 and TNF alpha (1 nM, 24h) increased hPBMC adhesion to HMVEC (2-fold in 30 min). Moreover, hPBMC underwent increased TEM (3h) through confluent HMVEC monolayers that were cytokine pre-activated. The majority of hPBMC with OC potential remained attached to the transwell filter after TEM, but were released in 24-48 h of culture with M-CSF/RANKL to form TRAP+ multinucleated OCs by day 7. Antibody neutralization revealed that ICAM-1, VCAM-1, and PECAM-1 cell adhesion molecules were involved in hPBMC TEM through HMVEC. Because pre-OCs are reported to derive from the CD14+ human MN (hMN), but not CD14- lymphocyte, fraction of hPBMC, we isolated and analyzed these fractions. CD14+ hMN displayed increased adhesion to cytokine activated HMVEC, attaining full capture of all CD14+ hMN by 2h, and adherent cells could develop into OCs with M-CSF/RANKL. Cytokine activated HMVEC also caused an increased TEM by CD14+ hMN, which could subsequently be developed into resorptive OCs with M-CSF/RANKL. In contrast, cytokine activation of HMVEC had no effect on CD14- cell adhesion, nor did CD14- cells that had (or had not) undergone TEM through cytokine-activated HMVEC develop into OCs. We conclude that inflammatory cytokine activation of microvascular cells causes the selective adhesion, recruitment and TEM of precursors capable of forming bone-resorptive OCs. Coupled with locally raised levels of pro-resorptive cytokines and RANKL expression by vascular and other cells, such mechanisms may significantly contribute to the bone loss associated with inflammatory diseases.

Disclosures: ***L. Kindle****, None.*

SA299

See Friday Plenary number F299

SA300

Synovial Fluid Macrophages Are Capable Of Osteoclast Differentiation. I. Adamopoulos*[1], A. Sabokbar[1], P. Wordsworth*[2], D. Ferguson*[3], N. Athanasou[1]. [1]Department of Pathology, Nuffield Department of Orthopaedic Surgery, University of Oxford, Oxford, United Kingdom, [2]Department of Medicine, Nuffield Department of Orthopaedic Surgery, University of Oxford, Oxford, United Kingdom, [3]Department of Clinical Medicine, University of Oxford, Oxford, United Kingdom.

Bone destruction is controlled by a number of cytokines including RANKL, OPG, M-CSF, TNFα and IL-1α, all of which influence osteoclast differentiation. The balance of these factors is disturbed in pathological joint conditions such as rheumatoid arthritis (RA) where there is formation of marginal erosions and an increase in inflammatory cells and cytokines such as RANKL, M-CSF, TNFα in synovial fluid. In RA, increased numbers of macrophages are present in the synovial membrane and these cells are capable of osteoclast differentiation. In this study we have determined whether synovial fluid macrophages in inflammatory arthritis are similarly capable of osteoclast differentiation. We isolated macrophages from the knee joint synovial fluid of RA, OA, gout and chondrocalcinosis patients and cultured them for 14 days in RANKL (30ng/ml) and M-CSF (25ng/ml) or M-CSF/TNFα (30ng/ml), and IL-1 (20ng/ml). Both RANKL and TNFα/IL-1 treated cultures resulted in the formation of numerous small (10μ) mononuclear and multinucleated $TRAP^+$ and VNR^+ cells capable of lacunar resorption. Many of the mononuclear cells formed small resorption pits (<10μ) when cultured on dentine slices in the presence of RANKL and M-CSF. In TNFα/IL-1-treated cultures, osteoclast formation was also noted, although lacunar resorption was not as extensive as in RANKL-treated cultures. Significantly more resorption was noted in macrophage cultures of RA/Crystal arthritis than OA. Our studies indicate that synovial fluid macrophages in inflammatory arthritic conditions are capable of osteoclast formation and extensive lacunar resorption. RANKL, TNFα and IL-1 are increased in RA synovial fluid and these factors may promote bone loss in inflammatory (RA/crystal) arthritis by enhancing synovial macrophage/osteoclast differentiation.

Disclosures: ***I. Adamopoulos****, None.*

SA301

See Friday Plenary number F301

SA302

Strontium Ranelate Decreases *In Vitro* Osteoclastic Differentiation and Bone Resorption. A. Wattel*[1], A. Hurtel-Lemaire*[1], C. Godin*[1], R. Mentaverri*[1], A. Blesius*[2], I. Dupin-Roger*[2], S. Kamel[1], M. Brazier[1]. [1]Laboratoire de Biologie et Pharmacie Cliniques, Faculté de Pharmacie, Amiens, France, [2]Institut de Recherches Internationales SERVIER, Courbevoie, France.

Strontium ranelate dissociates bone remodelling by increasing bone formation and decreasing bone resorption and it has been shown to reduce the risk of vertebral, nonvertebral fractures including the hip-fractures and to increase Bone Mineral Density in postmenopausal osteoporosis. Several studies have already demonstrated strontium ranelate's inhibitory effect on osteoclastic bone resorption.

The aim of the present study was to investigate the effect of strontium ranelate on *in vitro* osteoclastic differentiation. For this purpose, two cellular models were used: a human model using PBMC (Peripheral Blood Monocytic Cells) in the presence of RANKL and M-CSF and secondly, a murine model of RAW 264.7 cells in the presence of RANKL. Strontium ranelate was tested in conditions close to the *in vivo* situation *i.e.* by reproducing the same proportion of strontium ions and ranelic acid present in the plasma of patients. Strontium and ranelic acid were tested simultaneously from 0.1 to 24 mM and from 0.001 to 0.24 mM, respectively. Osteoclastic differentiation was assessed by measuring TRAP activity, by counting the TRAP-positive multinuclear cells or osteoclasts-like (OCLs) and by the assessment of the bone resorption activity. Our results indicate that strontium ranelate inhibits the osteoclastic differentiation in both models. TRAP activity, OCLs counting and bone resorption activity decrease in a dose-dependent manner. Significant differences occur at concentration levels from 6 mM of strontium in the human model: OCLs number was evaluated to 60% of the control, TRAP activity to 60% of the control and bone resorption decreases to 70% ($p < 0.05$). In the murine model, significant results are obtained at lower concentrations (i.e. 2 mM of strontium), TRAP activity decreases to 50% and OCLs number represents 70% of the control ($p < 0.05$). Taken together, these data show that strontium ranelate decreases production of bone resorbing cells. Therefore, osteoclastic precursors are probably important cellular targets of strontium ranelate when given as a treatment for osteoporosis.

Disclosures: ***A. Wattel****, None.*

SA303

Etanercept Suppresses the Number of Circulating Osteoclast Precursors in Psoriatic Arthritis. A. P. Anandarajah*[1], E. Schwarz[2], C. T. Ritchlin*[1]. [1]Rheumatology, University of Rochester Medical Center, Rochester, NY, USA, [2]Orthopedics, University of Rochester Medical Center, Rochester, NY, USA.

Background: Erosive bone lesions occur in up to a third of patients with psoriatic arthritis (PsA). We previously demonstrated osteoclasts at the bone-pannus junction in psoriatic joints. We also found an increased frequency of circulating osteoclast precursors (OCP) in these patients. TNF-blockade rapidly lowered the level of circulating OCP. Thus, we hypothesized that etanercept inhibits bone erosions, in part, by lowering the number of circulating OCP.

Methods: 20 patients with erosive PsA (>1 erosion on plain x-ray) were given 25mg twice a week of etanercept for 24 weeks. Gadolinium enhanced, fat suppressed MRIs (using T1 and T2 weighted spin echo and gradient recall echo sequences) were performed at baseline and after 24 weeks of etanercept. 3 radiologists working independently scored the images for bone erosions and bone marrow edema (BME) on a 6 and 9-point scale respectively. Scoring was based on size/extent, the intensity of T2 signal and contrast enhancement. The circulating osteoclast precursor (OCP) frequency was measured at 0, 2, 12 and 24 weeks. OCP numbers were obtained by counting the number of TRAP positive cells with >3 nuclei present in unstimulated peripheral blood mononuclear cells after 2 weeks in culture.

Results: MRI data was available in 13 patients. BME was present in 81% of patients and the BME score improved from a mean of 5.92 +/- 2.72 to 3.92 +/- 2.69 (p=0.004) at 24 weeks. The erosion score also improved from a mean of 2.54 +/- 0.97 to 2.08 +/- 1.44 but was not significant. The OCP numbers decreased from a mean of 55.45 +/- 73.4 to 11.4 +/- 13.8 cells/ 10^6 ($p<0.01$) at 24 weeks. A significant decrease was noted as early as 2 weeks after starting etanercept. A significant correlation was noted between the erosion scores and the OCP frequency (Spearmans r^2 0.591; p=0.034).

Conclusions: The decrease in BME coupled with the dramatic decrease in OCP frequency following etanercept therapy may provide an additional mechanism to explain how TNF blockade limits joint destruction in PsA. The significant correlation between the OCP frequency and erosion scores supports the concept that the OCP frequency may be used as a biomarker to help determine which PsA patients are at greater risk for bone resorption.

Disclosures: ***A.P. Anandarajah****, None.*

SA304

See Friday Plenary number F304

SA305

Differentiation of Hydroxyapatite Affinity of Bisphosphonate Analogs For Mechanism of Action Studies. F. H. Ebetino[1], P. Emmerling*[2], B. Barnett*[1], G. H. Nancollas*[2]. [1]New Drug Development, Procter & Gamble Pharmaceuticals, Mason, OH, USA, [2]Department of Chemistry, University at Buffalo, SUNY, Buffalo, NY, USA.

The mechanism of action of bisphosphonates continues to receive attention in models of disease states including osteoporosis, oncology, and arthritis. As these studies progress, it is becoming clear that significant variation in properties can stem from very small structural changes. Thus, no two bisphosphonates possess exactly the same balance of mineral affinity and intrinsic biochemical antiresorptive potency. In vivo, BP's act against osteoclasts, disrupting key biochemical processes within the cell. However, the binding affinity of BP's to bone surfaces may also play an important role in their effectiveness in modulating their loading and release from bone surfaces. Precise methodology is required to completely understand each of these properties. Constant Composition (CC) enables quantitative comparison of BP's at very low concentrations that may be more relevant to clinical studies than in vitro saturation binding data previously reported. (CC) crystal growth kinetic studies were performed at sustained relative supersaturation (9.0 with respect to HAP, pH 7.4) on a wide range of affinity analogs. In the higher affinity series of hydroxybisphosphonates, a surprisingly wide variation of affinity was noted. Risedronate (LED=0.0003 mg P/kg, in vivo growing rat) and structurally similar pyridyl BP's of varying antiresorptive potency including NE-58018 (A) (0.001), and NE58051 (B) (1.0) were studied. Kinetic affinity constants ($X10^{-6}$), K_L= 2.00 (Risedronate), 3.82 (A), ~1.1 (B)] were calculated based on a Langmuir adsorption model. Thus, a key factor influencing the binding of BP's to bone surfaces may be the orientation of the pyridine nitrogen relative to the P-C-P backbone. NE-58018 demonstrated the highest affinity, more similar to pamidronate (K_L =3.3) and alendronate (K_L = 2.93) yet was not the most antiresorptive potent. NE-58051 exhibited lower affinity more similar to risedronate but exhibited a 3,000 fold difference in potency. Two low affinity comparative benchmarks, demonstrate how this property can be even more dramatically modified with studies on phosphonocarboxylate analog NE10790 (LED = 3.0, K_L=0.03) and phosphonophosphinate analog NE-58029 (LED = 1.0, K_L=0.004). Thus, it is more clear that antiresorptive potency stems from both bone affinity and an intrinsic biochemical potency, and that a different structure activity relationship is required for hydroxyapaptite binding than that elucidated for the biochemical target FPPS. This suggests that the clinical consequences should continue to be examined.

Disclosures: ***F.H. Ebetino****, Procter & Gamble Pharmaceuticals 3.*

SA306

See Friday Plenary number F306

SA307

Validation of *In Vitro* Human Osteoclast Differentiation Assay and Osteoclast Activity Assay with Antiresorptive Agents: Potential Use for Preclinical Testing of the Effects of Antiresorptive Agents on Human Osteoclasts. J. Rissanen[1], H. Ylipahkala*[2], S. Suutari*[1], J. M. Halleen[1]. [1]Pharmatest Services Ltd, Turku, Finland, [2]Institute of Biomedicine, Department of Anatomy, University of Turku, Turku, Finland.

Despite of the recent development of new techniques allowing culturing of human osteoclasts (OCs) *in vitro*, such culture models for testing antiresorptive effects of drug candidates are not available commercially. Here we have studied the effects of various antiresorptive agents on human OCs in an *in vitro* culture system. We cultured commercially available OC precursor-cells (Poietics™, Cambrex, East Rutherford, NJ, USA) on bovine bone slices in the presence of M-CSF, RANKL and TGF-β_1. Two different assay conditions were validated, a 7-day OC differentiation assay and a 9-day OC activity assay. In the OC differentiation assay, the cells were cultured without added compounds and with osteoprotegerin (OPG) and sodium azide (AZ). After the culture period, the number of TRACP-positive multinucleated OCs formed during the culture period was counted under microscope, and the amount of tartrate-resistant acid phosphatase isoform 5b (TRACP 5b) released into the culture medium was determined with a commercial assay (BoneTRAP®, SBA-Sciences, Oulu, Finland). In the OC activity assay, culture medium was replaced with fresh medium at day 7, and the formed OCs were allowed to resorb bone for an additional 2 days. Cultures without added compounds and with the cysteine protease inhibitor E64 and AZ were included. At day 9, formed resorption pits were visualized with rhodamine-conjugated Wheat Germ Agglutinin lectin, and the amount of C-terminal cross-linked telopeptides of type I collagen (CTX) released into the culture medium was determined with a commercial assay (CrossLaps® for culture, Nordic Bioscience, Herlev, Denmark). Cytotoxicity was determined in both assays after the culture period using a commercial ToxiLight® assay (Cambrex). Both OPG and AZ decreased dose-dependently OC number in the OC differentiation assay, and both E64 and AZ decreased bone resorption in the OC activity assay. As expected, the effects of AZ were caused by toxic effects leading to cell death. OPG and E64 did not show toxic effects. In the OC differentiation assay, TRACP 5b was not released from dying cells and was therefore a reliable index of the number of OCs formed. In the OC activity assay, medium CTX was a reliable index of the amount of bone resorbed. We conclude that we have developed and validated fast and reliable *in vitro* methods for preclinical testing of the effects of new antiresorptive agents on differentiation and activity of human OCs.

Disclosures: ***J. Rissanen****, None.*

SA308

Oligomeric RANK Induces the Receptor Signals Ligand-independently. K. Kiyoshi*, A. Kudo. Tokyo Institute of Technology, Yokohama, Japan.

RANK, a member of the TNF receptor family, is essential for osteoclast differentiation. Recently, TNF type I and type II receptors were shown to form a trimer even before ligand binding. Here, we investigated self-assembly of RANK. First, self-assembly was examined by immunoprecipitation assay in 293T cells, which were transfected with mouse RANK tagged FLAG or HA, resulting that the interaction was detected between RANK-FLAG and RANK-HA without RANKL. Next, we generated various RANK constructs to find a domain that mediates ligand-independent self-assembly. RANK-HA was interacted with ΔECD-FLAG that lacks the extracellular domain of RANK, indicating that RANK is self-assembled through the cytoplasmic domain. These results inspired us to investigate whether osteoclast progenitors from mouse bone marrow could differentiate into TRAP positive multinucleated cells (MNCs) when RANK or ΔECD is overexpressed. RANK overexpression induced differentiation of progenitors into TRAP-positive MNCs, demonstrating that self-assembled RANK induces signals for osteoclast differentiation. Moreover, overexpression of ΔECD also induced differentiation, suggesting that RANK, specifically the cytoplasmic domain of RANK, could induce the receptor signals when RANKs themselves assemble on intracellular vesicles. Previously, it was reported that heterozygous insersional mutation in the signal peptide of RANK caused familial expansile osteolysis (FEO), suggesting the mechanism; lack of cleavage of a proper RANK signal peptide results in higher intracellular accumulation of the mutant RANK in compartments of the secretion pathway, leading to receptor-association and increase of constitutive RANK signals. Thus osteoclastogenesis by ΔECD overexpression will help to find the cause of FEO. Therefore, the further analysis of additional RANK mutations may lead to better understanding of the function of RANK and the mechanism of FEO.

Disclosures: ***K. Kiyoshi****, None.*

SA309

See Friday Plenary number F309

SA310

Generation and Characterization of Transgenic Mice that Express Cre Recombinase in Osteoclasts. J. D. Zajac[1], W. S. M. Chiu*[1], J. F. McManus*[1], A. J. Notini*[1], A. I. Cassady*[2], R. A. Davey*[1]. [1]Department of Medicine, Austin Health, University of Melbourne, Victoria, Australia, [2]Department of Biochemistry and Molecular Biology, The Institute for Molecular and Bioscience and The University of Queensland, Queensland, Australia.

To aid the study of the physiological control of osteoclasts, we have generated two transgenic mouse lines that express Cre recombinase in osteoclasts under the control of tartrate-resistant acid phosphatase (TRAP) or cathepsin K (Ctsk) promoter.

The suitability of TRAP and Ctsk promoters to drive the expression of Cre recombinase in osteoclasts was determined by the examination of their mRNA levels in normal C57BL/6 mouse tissues by Northern blot analysis. TRAP mRNA was expressed in a number of tissues, however, it was significantly higher in bone compared with brain (14 fold), colon (4 fold), heart (25 fold), kidney (5 fold), liver (4 fold), lung (13 fold), muscle (15 fold) and stomach (11 fold) (P<0.05). Ctsk mRNA was also expressed at significantly higher levels in bone and at lower levels in heart (55 fold), lung (12 fold) and muscle (60 fold) but was undetectable in brain, colon, kidney, liver and stomach ($P < 0.05$).

Two constructs, namely TRAP-Cre and Ctsk-Cre, were generated. Transient transfection of the constructs into RAW 264.7 cells showed that both the TRAP and Ctsk promoters were capable of driving the expression of Cre recombinase *in vitro*. These two constructs were then used to generate transgenic mice. TRAP-Cre and Ctsk-Cre transgenic mouse lines were characterized by breeding with *lacZ* ROSA 26 (R26R) reporter mice and immunohistochemistry for Cre recombinase. Function of Cre was assessed in the mice by the presence of β-Galactosidase activity resulting in blue coloration. Cre recombinase was functional in all lines tested with Cre-mediated recombination occurring primarily in the long bones, vertebrae, ribs and calvaria. Histological analyses of the long bones demonstrated that functional Cre recombinase protein was present in osteoclasts in both TRAP-Cre and Ctsk-Cre mouse lines. In addition in two of the TRAP-Cre lines, functional Cre protein was also detected in proliferating and hypertrophic chondrocytes (Line 4) and round proliferating chondrocytes (Line 3).

In conclusion, we have generated transgenic mouse lines that will enable the deletion of *floxed* target genes in osteoclasts using the Cre/*loxP* system. These genetically modified mouse lines will be valuable tools for studying the regulation of osteoclast function.

Disclosures: ***J.D. Zajac****, None.*

SA311

See Friday Plenary number F311

SA312

Active STAT6 Is a Potent Inhibitor of JNK-mediated Osteoclastogenesis and Bone Erosion. S. Dai*, S. Abbas*, T. Hirayama*, Y. Abu-Amer. Orthopaedics and Cell Biology & Physiology, Washington University School of Medicine, Saint Louis, MO, USA.

Signal transduction pathways transmitted by pro-inflammatory cytokines play a key role in the pathogenesis of inflammatory arthritis. Among these pathways, NF-kB and MAP kinases have been identified as fundamental mediators of inflammatory responses that govern various forms of inflammatory arthritis. The c-Jun N-terminal kinase (JNK) group of MAP kinases are activated by pro-inflammatory cytokines and other stresses. Evidence in recent studies implicates JNK as a potent kinase in the synovium. The kinase is constitutively expressed and activated in synoviocytes and is required for joint destruction in inflammatory arthritis. Destruction of the bony component of the joint is facilitated by recruitment of osteoclasts, cells that necessitate several genes for their formation and tissue destructive function. In this regard, JNK1 was portrayed to be indispensable for osteoclast differentiation and survival. JNK is also activated in response to osteoclastogenic factors, such as RANKL and TNF, and cohorts with c-fos to form the AP-1 complex which is crucial for osteoclastogenesis. It was also noted that inflammatory arthritis concurs with expression of anti-inflammatory cytokines such as IL-4, a component of the response aimed at inhibiting inflammation and tissue destruction. Indeed, recent evidence points out that IL-4 inhibits osteoclastogenesis through blockade of NF-kB and JNK pathways in a STAT6-dependent fashion. Therefore, we reasoned that STAT6 may inhibit JNK and bone erosion in inflammatory arthritis. Using a serum-transfer model of arthritis, we show that JNK phosphorylation/activation is increased in extracts of cells retrieved from joints of arthritic mice. This activation/phosphorylation coincides with activation of the AP-1 complex as shown by electrophoretic mobility shift assay. Because previous observations point out that IL-4-induced STAT6 is required to block JNK activation, we generated a constitutively active form of STAT6, termed STAT6-VT, which does not require activation by IL-4/JAK pathway. Cell-permeable TAT-fusion form of STAT6-VT was effective in blocking JNK phosphorylation/activation in RANKL and TNF-treated osteoclast progenitors. More importantly, while the fusion protein moderately blocks joint swelling, it significantly inhibits in vivo activation of JNK, attenuates osteoclast recruitment to the inflamed joints and leads to a significant decline in bone and cartilage destruction. Therefore, active STAT6-VT presents itself as a novel approach to ameliorate inflammatory arthritis.

Disclosures: ***Y. Abu-Amer,*** *None.*

SA313

See Friday Plenary number F313

SA314

Nox4 Participates in Superoxide Production During Osteoclast Differentiation and Bone Resorption. S. Yang[1], Y. Zhang*[1], S. Reddy[2], W. Ries[1], L. Key[1]. [1]Pediatrics, Medical University of South Carolina, Charleston, SC, USA, [2]Dept. of Medicine/Hematology-Oncology,, University of Pittsburgh, Pittsburgh, PA, USA.

Osteoclasts generate superoxide that is involved in osteoclastic bone resorption activity. NADPH oxidase is the enzyme system responsible for osteoclastic superoxide production. Based on the fact that osteoclasts from $p91^{-/-}$ mutants (absence of the catalytic subunit of NADPH oxidase) generate normal amounts of superoxide, we have previously cloned an alternative form of p91 sub-unit, Nox4, which exhibits 58% similarity with the amino acid sequence of p91 subunit of the NADPH oxidase complex. This observation undermined that Nox4 oxidase derived superoxide is essential for osteoclastic function and activity.

We have previously demonstrated that Nox4 is expressed in osteoclasts. Antisense oligos of Nox4 reduced superoxide generation and inhibited bone resorption in p91 knockout mice (Yang et al, 2001). To further study the physiological role of Nox4 in osteoclasts, we have generated RAW 264.7 cells that over express Nox4. A stable transfection technique was applied using the linear Nox4 expression cassette driven by the CMV promoter. After G418 selection, we have established four clonal cell lines (Nox4 RAW cells), which over express Nox4. RANKL stimulation induced osteoclast differentiation of Nox4 RAW cells similar to parental RAW cells. However, Nox4 RAW cells derived osteoclasts demonstrated two fold increase in superoxide production compared to osteoclasts derived from the parental RAW cells. Furthermore, Nox4 over-expression resulted in increased tartrate resistant acid phosphatase (TRAP) activity in osteoclasts compared to osteoclasts formed from control RAW cells. These data suggest Nox4 response to RANKL stimulation and its participation in superoxide production during osteoclast differentiation. Therefore, NADPH oxidase complex sub-unit, Nox4 play important role in osteoclast differentiation and bone resorption activity.

Disclosures: ***S. Yang****, None.*

SA315

Rac1 Interacts Directly With Rab7. Y. Sun*, K. G. Buki*, J. Vääräniemi*, H. K. Väänänen*. Department of Anatomy, Institute of Biomedicine, University of Turku, Turku, Finland.

Rabs are small GTPase proteins that control many membrane fusion and vesicular trafficking events in various mammalian cells. Most likely each Rab protein functions through multiple effectors thus allowing cell and compartment specific actions. Rab7 has been shown to regulate the late steps of the endocytic pathway from early endosomes to late endosomes or from late endosomes to lysosomes. We have shown earlier that in resorbing osteoclasts, Rab7 is involved in formation of the ruffled border which is a late endosomal-like compartment at the plasma membrane. In order to reveal the molecular mechanisms which are important in the ruffled border formation, we used bacterial two hybrid system and rat trabecular bone derived cDNA library to identify specific effectors for Rab7. We used constantly active form of Rab7 as a bait. We identified P21 Ras-related C3 botulinum toxin substrate 1 (Rac1), another small GTPase protein as a new Rab7 interacting protein. Rac1 is known principally for its regulatory role on actin cytoskeleton, cell polarization, and microtubule dynamics. Rac1 has no homology with RILP or Rabring7, which have been reported earlier as other Rab7 effectors in other cellular system. Our pull down results show that wild type and active GTPase deficient mutant form of Rab7 specifically bind to Rac1. Moreover, we show that this specific interaction doesn't occur with another Small GTPase Rab9 which is also located in late endosomal compartment. More importantly, confocal microscopy images showed that Rab7 colocalises with Rac1 at ruffled border in the resorbing osteoclasts, however, in non resorbing cells, Rab7 and Rac1 colocalises at perinuclear area where the late endosomes and lysosomes are located. These results suggest that Rac1 could act as a downsteam effector of Rab7, thus regulating the late endosomal trafficking in general, and specifically the formation of ruffled border in osteoclasts. As far as we know, this is the first evidence that two small GTPase proteins directly interact with each other. Since Rac1 is known to control actin cytoskeleton directly through its effectors, Rab7-Rac1 interaction may mediate late endosomal trafficking along actin microfilaments to ruffled border.

Disclosures: ***Y. Sun****, None.*

SA316

See Friday Plenary number F316

SA317

Normal Human Osteoclasts Formed From Peripheral Blood Monocytes Express PTH Type 1 Receptors and Are Stimulated by PTH in the Absence of Osteoblasts. D. W. Dempster[1], C. Hughes-Begos[1], A. Brandao-Burch*[2], K. Plavetic-Chee*[1], F. Cosman[1], J. Nieves[1], S. Neubort*[1], S. Lu[1], A. Iida-Klein[1], T. Arnett[2], R. Lindsay[1]. [1]Regional Bone Center, Helen Hayes Hopital, West Haverstraw, NY, USA, [2]Department of Anatomy and Developmental Biology, University College London, London, United Kingdom.

The prevailing view for many years has been that osteoclasts (OC) do not express PTH receptors and that PTH effects on OC are mediated indirectly via osteoblasts. However, several recent reports suggest that osteoclasts express PTH receptors. This study tested the hypothesis that human OC formed in vitro express functional PTH Type 1 receptors (PTH1R).

Peripheral monocytes were obtained from healthy donors and were selected for the CD14-positive population (CD14+Mo) by immunomagnetic separation. Cells were cultured on bone slices or plastic culture dishes with RANKL and M-CSF for 16-21 d. At 21 d there was a mixed population of mono-and multi-nucleated cells, all of which stained positively for the human calcitonin receptor. The cells actively resorbed bone, assessed by release of C-terminal telopeptide of type I collagen and the formation of abundant resorption pits.

We obtained evidence for the presence of PTH1R by 4 independent techniques. First, CD14+Mo cultured with M-CSF and RANKL for 21 d were immunocytochemically stained for PTH1R using a goat polyclonal antibody to the human PTH/PTHrP receptor. Positive staining was observed in both mono- and multinucleated cells intimately associated with resorption cavities, whereas staining was markedly reduced in control samples incubated with blocking peptide. Second, Western blot analysis was performed on protein lysates extracted from 4 different samples: 21 d OC cultures, Cos-7 cells transfected with pcDNA1 vector (negative control), Cos-7 cells transfected with the PTH1R and SaOS2 cells (positive controls). PTH1R was detected only in the lysate of OC cultures and positive controls. The band for PTH1R was diminished in the presence of blocking peptide. Third, OC cultures clearly expressed PTH1R mRNA at 21 d and treatment with 10^{-7}M hPTH(1-34) reduced PTH1R mRNA expression by 35%, as detected by RT-PCR. Finally, we tested the effects of PTH(1-34) on unfractionated monocytes, which were cultured with RANKL and M-CSF for 14 d and then exposed to 50 or 100 ng/ml rat PTH(1-34) or vehicle for a further 2 days. Bone resorption was reproducibly increased by 2-3 fold in the presence of PTH(1-34).

These findings provide strong support for a direct stimulatory action of PTH on human OC mediated by PTH1R. This suggests a dual regulatory mechanism, whereby PTH acts both directly on osteoclasts and also, indirectly, via osteoblasts.

Disclosures: ***D.W. Dempster****, None.*

SA318

See Friday Plenary number F318

SA319

Estrogen-Induced Apoptosis Of Osteoclasts Is Delayed By Low-Level Cadmium Exposure. J. Rink*, A. K. Wilson. Biological Sciences, Benedictine University, Lisle, IL, USA.

Low-level cadmium exposure has been demonstrated to induce bone loss *in vitro* and *in vivo* by increasing the bone resorbing activity of osteoclasts. Since osteoclasts undergo apoptosis shortly after they are activated, one possible mechanism is that cadmium may influence the timecourse of apoptosis, allowing the osteoclast more time to resorb bone. To test whether cadmium affects the timecourse of apoptosis, osteoclasts were differentiated from mouse spleen cell cultures in the presence of M-CSF and RANKL. Apoptosis was induced in osteoclasts by the addition of estrogen, mevastatin or etoposide in the presence or absence of cadmium. After incubation for 24 hours, the osteoclasts were stained with DAPI and phalloidin and the percentage of apoptotic cells present was determined by morphometric analysis using fluorescent microscopy. Estrogen, mevastatin and etoposide increased percent apoptosis up to two-fold above control groups. Cadmium alone (100 nM) did not prevent control (baseline) apoptosis. However, when cadmium was added in combination with any of the three inducers of apoptosis, the percent apoptosis values remained constant with control values, indicating that cadmium inhibits induced apoptosis in osteoclasts at 24 hours. A time course indicated that cadmium completely rescued estrogen-induced apoptosis at 12 and 24 hours, with diminishing effects at 36 and 48 hours. These data suggest that cadmium delays the onset of apoptosis for at least 24 hours, giving the osteoclasts more time to resorb bone. Incubation of ICI, an estrogen receptor antagonist, at concentrations that diminish estrogen-induced apoptosis approximately 50% can be further rescued by cadmium to control apoptosis levels. Cadmium could not rescue mevastatin-induced apoptosis when incubated with ICI. These data suggest that cadmium's effect on delaying the onset of apoptosis is via the estrogen receptor.

Disclosures: ***A.K. Wilson****, None.*

SA320

See Friday Plenary number F320

SA321

Syk Is Critical for $\alpha_v\beta_3$ Integrin-Mediated Signal Transduction in Osteoclast. W. Zou, R. Faccio, F. P. Ross, S. L. Teitelbaum. Pathology, Washington University, St. Louis, MO, USA.

Osteoclast $\alpha_v\beta_3$ integrin engagement leads to cytoskeletal reorganization and activates a signaling cascade critical for bone resorption and cell survival. Several downstream pathways, such as c-Src and Pyk2, are known to transduce $\alpha_v\beta_3$ signaling, but the potential role of non-receptor tyrosine kinase, Syk, has not been elucidated. We find Syk-/- macrophage fail to differentiate into mature osteoclasts in the presence of M-CSF and RANKL. Attachment of Syk-/- pre-osteoclasts to the $\alpha_v\beta_3$ ligand, osteopontin, is delayed, and those cells which do adhere, fail to spread properly. These findings suggest that Syk participates in osteoclast differentiation and cytoskeletal organization perhaps by participating in $\alpha_v\beta_3$ integrin-dependent recruitment of signaling and cytoskeletal molecules. In keeping with this hypothesis, adhesion to the $\alpha_v\beta_3$ ligand vitronectin, but not collagen, induces tyrosine phosphorylation of Syk, suggesting that Syk is involved in $\alpha_v\beta_3$ integrin signaling pathway in osteoclasts. In co-immunoprecipitation experiments, Syk, as well as c-Src and Pyk2 bind the cytoplasmic tail of β3 integrin subunit in a matrix adhesion-dependent manner. In this circumstance, Syk forms a complex with c-Src, Pyk2 and Vav3. Consistent with integrin modulation of this complex, association between Syk and c-Src or Pyk2 in β3 integrin deficient osteoclasts is dramatically reduced as compared to wild type although expression of these tyrosine kinases is unaltered. These findings document that syk is critical for $\alpha_v\beta_3$ integrin-mediated signals which prompt cytoskeletal organization in the osteoclast.

Disclosures: ***W. Zou****, None.*

SA322

Reduced Bone Mineral Density in Men Who were Prescribed Short-term High Dose Steroid Therapy. F. Chan*[1], E. Lau[1], D. Hui*[2], A. Wu*[2], P. Leung*[3]. [1]Jockey Club Center for Osteoporosis Care and Control, The Chinese University of Hong Kong, Hong Kong, Hong Kong Special Administrative Region of China, [2]Department of Medicine & Therapeutics, The Chinese University of Hong Kong, Hong Kong, Hong Kong Special Administrative Region of China, [3]Department of Orthopaedics and Traumatology, The Chinese University of Hong Kong, Hong Kong, Hong Kong Special Administrative Region of China.

During the Severe Acute Respiratory Syndrome (SARS) outbreak in Hong Kong in 2003, patients were treated with very high doses of corticosteroid and ribavirin. The detrimental effects of such treatment on bone mineral density (BMD) are unknown. To test the hypothesis that the combination therapy may lower the bone mass, a cross-sectional study was conducted to compare the BMD of SARS patients with normal range data. Two hundred and twenty-four patients with SARS were recruited from the teaching hospital in shatin, where SARS originated. Bone Mineral Density (BMD) at the total hip and spine was measured at around 6 months post SARS by DEXA (Hologic, Inc). Subjects were treated with an average of 2,753mg (SD=2,152mg) prednisolone and 29,344 mg (SD=15,849mg) of ribarivin. When compared to normal range data, 6% of men of had a hip BMD Z-score ≤-2 (P=0.057 for testing the hypothesis that >2.5% of subjects should have a Z-score of ≤-2). The results of BMD at the spine in men, or of the total hip and spine in women, were statistically non-significant. We conclude that high doses of corticosteroid and ribavirin may result in low BMD in male SARS patients.

Disclosures: ***F. Chan****, None.*

SA323

See Friday Plenary number F323

SA324

Bone Mineral Density in Ethnic Norwegians and Pakistani Immigrants - The Oslo Health Study. K. Alver*[1], H. E. Meyer*[2], J. A. Falch*[3], A. J. Sogaard*[1]. [1]Division of Epidemiology, Norwegian Institute of Public Health, Oslo, Norway, [2]University of Oslo, Oslo, Norway, [3]Aker University Hospital, Oslo, Norway.

Bone mineral density (BMD, g/cm^2) is scarcely studied in immigrants from the Sub-Indian continent. In Oslo, Norway, random samples of the participants in the Oslo Health Study, including also those of Pakistani origin, were invited to a forearm BMD measurement by single x-ray absorptiometry. We have previously shown that Pakistani immigrants in this population have a very high prevalence of vitamin D deficiency. The aim of this study was to compare bone density with and without adjustment for bone size and height among Pakistani immigrants and ethnic Norwegians in Oslo.

BMD was measured at the distal and ultradistal forearm site in 173 Pakistani-born (73 women, 102 men) and 1386 Norwegian-born subjects (678 women, 711 men) aged 30, 40, 45 and 59/60 years, living in Oslo. To account for variation in skeletal size, we computed height-adjusted BMD, BMD/height (g/cm^3) and volumetric bone mineral apparent density (BMAD, g/cm^3). Comparisons were made by both age-specific t-tests and one-way analysis of covariance adjusted for age.

We did not find any differences in distal or ultradistal forearm BMD between Pakistanis and Norwegians in either women or men. We found, however, statistically significant higher values in Pakistani men when BMD was height-adjusted (2% higher at the distal and 5% at the ultradistal site). We also found statistically significant higher bone density values (both distal and ultradistal) in Pakistani women and men compared to their Norwegian counterparts when volumetric measures as BMD/height (7-8% higher in women, 6-7% in men) and BMAD (6% higher in women, 8% in men) were used.

We conclude that Pakistanis living in Oslo have similar BMD as ethnic Norwegians, but they have higher volumetric bone density.

Disclosures: ***K. Alver****, None.*

SA325

Bone Mineral Density, Muscle Mass and Fat Mass of the Lower Extremities in Independent Ambulators with Chronic Stroke. M. Y. C. Pang*, J. J. Eng*. School of Rehabilitation Sciences, University of British Columbia, Vancouver, BC, Canada.

Community-dwelling individuals with chronic stroke have a high incidence of falls. The loss of bone mass and muscle atrophy, particularly on the paretic side, may be important contributing factors to the much higher risk of fractures resulting from a fall. The purpose of this study was (1) to evaluate the bone mineral density and soft tissue composition of the lower extremities and (2) to identify the stroke-specific impairments that are important determinants of bone mineral density of the lower extremities of fifty-eight community-dwelling individuals with chronic stroke. The bone mineral density, lean mass and fat mass of the lower extremities were measured by dual energy X-ray absorptiometry (DEXA). The results showed that the bone mineral density of the paretic lower extremity was significantly lower than that of the non-paretic lower extremity. The lean mass of the paretic lower extremity was also significantly reduced when compared to the non-paretic leg. The bone mineral density in the paretic leg was positively correlated with the lean mass (r=0.565) and negatively correlated with the fat mass (r=-0.537). Multiple regression analyses revealed that ambulatory capacity and leg strength were significant determinants of the bone mineral density of the paretic lower extremity. The results point to the importance of enhancing mobility and muscle strength to promote bone health of the lower extremities in the chronic stroke population.

Disclosures: ***M.Y.C. Pang****, None.*

SA326

Vitamin D Insufficiency in a Racially Diverse Population of Men: Results from BACH/BONE. S. S. Harris[1], T. C. Chen[2], A. B. Araujo[1], M. F. Holick[2], J. B. McKinlay*[1]. [1]New England Research Institutes, Watertown, MA, USA, [2]School of Medicine, Boston University, Boston, MA, USA.

Our aims are 1) to report race and season-specific prevalences of vitamin D insufficiency in a population-based sample of men and 2) to determine whether a 25-hydroxyvitamin D (25OHD) level of 50 nmol/l maximally suppresses parathyroid hormone (PTH) in this group. This information contributes to the current debate about optimal blood levels of vitamin D and the need to reexamine recommended dietary intakes.

We report preliminary, unweighted findings from the Boston Area Community Health Bone Study (BACH/BONE), a study of skeletal health in Boston men aged 30-79 yrs. The platform-based automated Nichols Advantage Specialty System (San Clemente, CA) was used for determinations of 25OHD and PTH. The method uses acridinium ester as the label in its protein binding assay (for 25OHD) or chemiluminescence immunoassay (for PTH).

Age and BMI did not differ by race, and 25OHD was not correlated with age. 25OHD values < 25 nmol/l were more common in Blacks than in others (Table 1). Values < 50 nmol/l were most common in Blacks, intermediate in Hispanics, and least common in Whites. Hispanics and Whites had much lower prevalence of values < 50 nmol/l in summer than winter, but no seasonal difference was seen in Blacks.

Table 1. Prevalence (%) of 25OHD values < 25 and <50 nmol/l

	N	Winter (Nov-Apr)		Summer (May-Oct)	
		< 25	< 50	< 25	<50
Black	106	8.8	43.9	8.2	44.9
Hispanic	128	1.7	30.0	0.0	14.7
White	151	2.1	16.8	1.8	5.4

PTH concentrations were 13% to 29% lower in men with 25OHD values ≥ 50 nmol/l compared with values < 50 (Table 2).

Table 2. Median PTH (pmol/l) by 25OHD (nmol/l)

	25OHD < 50	25OHD ≥ 50	Diff.
Black	3.72	2.65	-29%
Hispanic	2.77	2.41	-13%
White	3.29	2.60	-21%

Over 40% of Black men had low 25OHD levels in both winter and summer. The percentage was lower in Hispanic and even lower in White men, particularly in the summer. A 25OHD level of 50 nmol/l is not associated with maximal PTH suppression in Black, Hispanic or White men, suggesting that a higher 25OHD target may be desirable.

Disclosures: ***S.S. Harris****, None.*

SA327

Variation in Bone Turnover within the Normal PTH Range: Results from BACH/BONE. S. S. Harris[1], T. C. Chen[2], A. B. Araujo[1], M. F. Holick[2], J. B. McKinlay*[1]. [1]New England Research Institutes, Watertown, MA, USA, [2]School of Medicine, Boston University, Boston, MA, USA.

A frequently proposed indicator of optimal vitamin D status is the 25-hydroxyvitamin D (25OHD) level at which parathyroid hormone (PTH) is maximally suppressed. However, although there is clear evidence that above normal PTH is harmful to the skeleton, there is much less evidence, especially in racially/ethnically diverse populations, that suppressing PTH within the normal range is beneficial. We examine the association of serum osteocalcin values (a marker of bone turnover) with normal PTH values in Black, Hispanic and White men. Since reduced bone turnover is generally associated with reduced bone loss, an association of osteocalcin with PTH in the normal range would provide support for maximal PTH suppression as a desirable goal in determining 25OHD targets for skeletal health.

We report preliminary, unweighted findings from the Boston Area Community Health Bone Study (BACH/BONE), a population-based study of skeletal health in a racially/ethnically diverse sample of Boston men aged 30-79 yrs. The platform-based automated Nichols Advantage Specialty System (San Clemente, CA) was used for determinations of serum PTH and osteocalcin. The method uses acridinium ester as the label in its chemiluminescence immunoassays. The normal range and midpoint for the PTH assay are 0.85-5.31 and 3.08 nmol/l, respectively. Primary analyses were restricted to the 346 of 385 men who had PTH values within the normal range (median osteocalcin was 0.97 nmol/l in the excluded men compared with 0.72 in the included men).

Mean age in the six race/ethnic (Black, Hispanic, White) by PTH (low-normal:0.85-3.08, high-normal: 3.08-5.31) groups was 49-54 yrs, and mean BMI was 28-29 kg/m^2. Median serum osteocalcin was higher in the 107 men with high-normal PTH than in the 239 men with low-normal PTH (Figure). Differences in the medians were similar across race/ethnic groups: 22% in Blacks, 22% in Hispanics and 20% in Whites. These data provide preliminary evidence that reducing PTH within the normal range may benefit the skeleton by reducing bone turnover. In addition, they suggest that the benefit may be similar across race/ethnic groups.

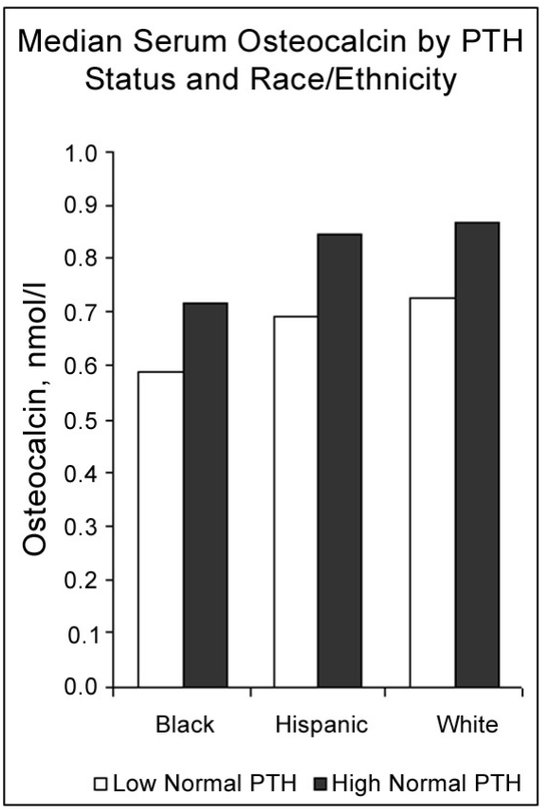

Disclosures: ***S.S. Harris****, None.*

SA328

See Friday Plenary number F328

SA329

Withdrawn

SA330

See Friday Plenary number F330

SA331

Increased Risk of Fractures Is Associated with Acidogenic Food Intake among Post-Menopausal Women Enrolled in the Observational Study of the Women's Health Initiative. U. S. Barzel[1], A. Aragaki*[2], C. Ritenbaugh*[3], J. Wylie-Rosett*[4], M. S. LeBoff[5], J. A. McGowan[6]. [1]Montefiore Medical Center & Albert Einstein College of Medicine, Bronx, NY, USA, [2]Women's Health Initiative, Seattle, WA, USA, [3]Kaiser Permanente Center for Health Research, Portland, OR, USA, [4]Albert Einstein College of Medicine, Bronx, NY, USA, [5]Brigham and Women's Hospital & Harvard Medical School, Boston, MA, USA, [6]Musculoskeletal Diseases Branch, NIAMS/NIH, DHHS, Bethesda, MD, USA.

Human and animal studies demonstrate that an acidogenic diet can cause a negative calcium balance and a reduction in bone mass. The purpose of this study was to test the hypothesis that acidogenic food intake increases fracture risk. Dietary data were collected by a food frequency questionnaire from 93,676 post-menopausal women, ages 50 to 79 years, at baseline. From these data we assessed the consumption by each woman of total animal protein, as surrogate for acid intake (P), and of total potassium as surrogate for alkali intake (K). Fracture data was collected prospectively over an average of 5.5 years. There were 10,875 total fractures, including 616 hip fractures.

In lieu of assessment of actual potential renal acid load, we calculated the ratio of K/P (Frassetto 1998)and arranged the data in quintiles. Statistical models were adjusted for age, ethnicity, education, body mass index, physical activity, hormone replacement therapy, smoking, relevant medications (thiazides, thyroid hormone, corticosteroids, antiestrogens and bisphosphonates), personal and family fracture history, and falls in the past 12 months. Dietary variables included calcium, retinol, vitamin D, vitamin K, alcohol and coffee consumption. All dietary variables, including K/P, were adjusted for total energy intake.

Since our hypothesis was that a very high animal protein diet affects bone metabolism negatively, and it has been shown that a very low protein diet also affects it negatively, we used the middle quintile of K/P as basis for comparison. The lowest K/P was associated with a significant risk for all fractures - hazard ratio (HR) 1.14 (95% 1.05,1.25) p=0.0031. The risk for the lowest half of this quintile was 1.21 (1.08,1.35) p=0.0009. Risk at the highest quintile approached but did not reach significance - HR 1.08 (0.99,1.18) p=0.07. There was a similar, but not statistically significant, trend for hip fractures with lower and upper quintiles of K/P that had HR 1.28 (0.86,1.90) and 1.11 (0.75,1.63), respectively.
This prospective study, with a fracture end point, demonstrates that a relatively high intake of animal protein, unbalanced by alkali supplying foods such as vegetables and fruits, significantly increases the risk of all fractures in post-menopausal women.

Disclosures: ***U.S. Barzel****, None.*

SA332

Detection of Prevalent Vertebral Fractures Using Historical Height Loss: Comparison of Different Height Measurement Methods. K. Siminoski[1], J. D. Adachi[2], G. Ioannidis, and the CaMOS Research Group[2]. [1]Radiology and Medicine, University of Alberta, Edmonton, AB, Canada, [2]Medicine, McMaster University, Hamilton, ON, Canada.

Previous studies have shown that historical height loss (HHL) >6 cm increases the likelihood of a prevalent vertebral fracture and may serve as a clinically useful diagnostic threshold. Those data were derived from a specialist patient population and employed a stadiometer. In this study we have evaluated HHL in a randomly chosen population to assess the generalizability of a 6 cm HHL threshold, and have compared different methods of height measurement.
We have analyzed HHL for 3,732 women from the Canadian Multicentre Osteoporosis Study (CaMOS), a randomly chosen study population from 9 sites across Canada. Average age was 65.5 years (range: 49 - 93 years). HHL was determined as the difference between the tallest recalled height and current measured height. Four different methods were used to determine height: Method 1 = stadiometer (1 site, n = 320); Method 2 = weight scale attachment (6 sites, n = 2,482); Method 3 = wall-mounted pull-down device (1 site, n = 496); Method 4 = ruler on head with tape measure on wall (1 site, n = 434). Vertebral morphometry was performed on all subjects from T4 to L4, with prevalent fracture defined as any vertebral height ratio >3 SD below the population mean.
The area under the receiver operating characteristics curve (AUC) for the entire population was 0.63 (95% confidence interval [CI], 0.61-0.65; p<0.001). The AUC was similar for the four different height measurement methods (see table). At HHL > 6 cm, sensitivity for the entire group was 30%, ranging from 17% for Method 4 to 33% for Method 2. Specificity for the entire population was 90%, ranging from 88% for Method 2 to 97% for Method 4.
These results confirm previous data that were derived from a specialist referral population and show that HHL >6 cm can be a useful threshold for detecting prevalent vertebral fractures among the general population. The findings also show that different height measurement methods function comparably for determination of HHL, and that the weight scale attachment is acceptable.

Comparison of Height Measurement Methods

METHOD	AUC (95% CI)	Sens for HHL >6 cm (%) (CI)	Spec for HHL > 6 cm (%) (CI)
ALL	0.63 (0.61-0.65)	30 (27-33)	90 (89-91)
1	0.62 (0.57-0.67)	19 (12-29)	96 (92-98)
2	0.63 (0.61-0.66)	33 (29-37)	88 (86-89)
3	0.67 (0.63-0.71)	32 (25-40)	92 (89-95)
4	0.62 (0.57-0.67)	17 (11-25)	97 (94-98)

Meth 1 = stadiometer; Meth 2 = weight scale; Meth 3 = wall-mounted; Meth 4 = ruler

Disclosures: ***K. Siminoski****, None.*

SA333

See Friday Plenary number F333

SA334

The Use of Height Measurement in Primary Care. K. Siminoski. Radiology and Medicine, University of Alberta, Edmonton, AB, Canada.

Measurement of total body stature is recommended in a number of clinical practice guidelines for two main purposes. The first is to determine body mass index (wt/ht^2) for monitoring obesity and cardiovascular risk. The other is to assess height loss as a means of detecting subclinical vertebral fractures in people with osteoporosis. Since there is no data on current clinical practice in regards to height measurement, we conducted a telephone survey of primary care practitioners.
One hundred primary care physicians randomly chosen from across Canada were questioned on current height measurement perceptions and practice. Physicians (82% male) had been in practice for 20.3±6.3 years (±SD) and saw 185±65 patients per week. Most patients in their practices were female (58.2±11.4%) and 41.0±17.3% were over age 65. Of their patients with osteoporosis, 82.7±14.2% were female.
These physicians regarded height as a useful parameter: it was rated 7.4±2.5 on a 10-point scale. The most commonly used height measurement device was the office weight scale attachment (79%), followed by a flat beam on the head with a tape on the wall (13%), and a wall-mounted sliding arm (6%). Two percent recorded height based on history from the patient. Adequacy of the current height method was rated 7.7±1.8 on a 10-point scale.
Physicians reported that among all female patients, 64.0±36.1% had at least one height measurement on the chart and 47.4 ±35.2% had height recorded on an annual basis (see table). The principle reason for measuring height among all patients was to assess BMI, obesity, or cardiovascular risk. Among females diagnosed with osteoporosis, 76.7±34.8% had at least one height on the chart, and 62.9±37.4% had annual heights. The main reason for doing height in osteoporotics was to detect vertebral fractures. Values were slightly lower in men for both having at least one height on the chart and for having annual heights, but confidence levels overlapped those of women. The reasons for doing height were also similar in men.
These results show that primary care physicians recognize the value of height measurement in clinical practice and do it for the recommended reasons, and that the majority of patients reportedly have at least one height recorded in their medical records. There is room for improvement among both the general patient population and in those patients diagnosed with osteoporosis.

Height Measurements in Different Patient Groups

PATIENT GROUP	At Least One Height On Chart (%) (95% CI)	Annual Height On Chart (%) (95% CI)	Main Reason for Height
All Females	64 (54-73)	47 (37-57)	BMI
Females With Osteoporosis	77 (68-85)	63 (53-72)	Fractures
All Males	61 (51-71)	45 (35-55)	BMI
Males With Osteoporosis	69 (59-78)	58 (48-68)	Fractures

BMI = body mass index

Disclosures: ***K. Siminoski****, Procter & Gamble Pharmaceuticals 5, 8.*

SA335

See Friday Plenary number F335

SA336

See Friday Plenary number F336

SA337

Seasonal Presentation of Osteoporotic Hip Fracture. M. Larrosa*[1], E. Casado*[1], A. Gómez*[1], J. Gratacòs*[1], E. Fernández*[1], E. Berlanga*[2]. [1]Rheumatology, Hospital Sabadell. University Institute Parc Taulí, Sabadell, Spain, [2]Laboratory, UDIAT, Sabadell, Spain.

Objectives: To analyze if the osteoporotic hip fractures have a seasonal incidence in our area and its relation with serum 25-OHD3 and PTH levels. To evaluate the relation between sunlight exposure and 25-OHD3 serum levels.
Methods: Patients older than 65 years with osteoporotic hip fractures admitted into hospital between March 2002-February 2003. The following data was recorded: date of fracture, degree of sunlight exposure [semiquantitative questionnaire: nil (patients confined to home or institutionalized), poor (1-2 weekly outings), medium (3 or more weekly outings) or high (active sunlight exposure)] and serum 25-OHD3 (25-95 ng/mL, RIA) and PTH levels (10-65 pg/mL, RIA).
Results: 321 patients were included, 258 women (80.4%), age 83+/-7 years old (65-100). The mean 25-OHD3 concentrations were 22.5+/-17.9 ng/mL and PTH 85.0 +/- 59.4 pg/mL. 54 p. (17.0%) had a nil degree of sunlight exposure, 102 p. (32.1%) poor, 151 p. (47.5%) medium and 11 p.(3.5%) high.
During summer we observed a significant reduction of hip fracture incidence, along with an increase of 25-OHD3 levels (Table). 25-OHD3 levels were significantly increased in patients with higher sunlight exposure (p<0.000). Hypovitaminosis D was observed among 85% patients with nil, 74% with poor, 57 with medium and 30% with active sunlight exposure (p<0.000).
Table:

	Number fractures	25-OH-D3 ng/ml (mean+/-SD)	PTH pg/ml (mean+/- SD)
Winter	91	19.7+/-17.0	93.0+/-61.1
Spring	88	20.0+/-16.4	84.6+/-67.7
Summer	54	28.7+/-20.1	73.2+/-37.8
Autum	92	24.1+/-17.9	84.2+/-59.1
P	0.006	0.013	NS

Conclusion: Hip fractures have a seasonal incidence with a reduction during summer and along with higher serum 25-OHD3 levels. Serum 25-OHD3 levels increase with the degree of patients' sunlight exposure.

Disclosures: ***E. Casado****, None.*

SA338

Sunlight Irradiation, 25-OH-D3 Serum Levels and Osteoporotic Hip Fracture. E. Casado*[1], M. Larrosa*[1], A. Gómez*[1], J. Gratacòs*[1], E. Fernández*[1], E. Berlanga*[2]. [1]Rheumatology, Hospital Sabadell. University Institute Parc Taulí, Sabadell, Spain, [2]Laboratory. UDIAT, University Institute Parc Taulí, Sabadell, Spain.

Background: In a recent study we have observed that hip fracture have a seasonal incidence in our area. In medical literature it has been frequently related to poor weather conditions (snow, ice, rain or minimum daily temperatures), which are not frequent in our area (Barcelona; latitude 41º N)
Objectives: To analyze if osteoporotic hip fracture incidence correlates with mean local sunlight irradiation and serum 25-OH-D3 levels.
Methods: Patients older than 65 years with osteoporotic hip fractures, admitted into hospital between March 2002-February 2003 were included. Patients with vitamin D supplementation and patients without sunlight exposure (confined to home or institutionalized) were excluded. 25-OH-D3 (23-95 ng/ml, RIA) was determined at admission. The number of hip fractures, mean 25-OH-D3 and sunlight irradiation (MJ/m2) (official data of 'Centre meteorologic de Catalunya') were analyzed on monthly basis.
Results: 243 patients, 189 women (77.8%) and 54 men were included in the study, mean age 81.8+/-7.4 years (65-100 years). The mean 25-OH D3 values were 22.8+/-16.0 ng/ml. A significant inverse correlation among fractures incidence and 25-OH-D3 level was observed r= - 0.65 (p=0.02). Every month, serum 25-OH-D3 concentrations correlated with the mean sunlight irradiation recorded two and three months before the fracture r= 0.63 (p=0.02) whereas the monthly incidence of fractures correlated with the mean sunlight irradiation recorded three months before the fracture r= - 0.59 (p=0.04) A tendency to statistical significance with the recorded irradiation 2 months before was observed.
Conclusion: The monthly incidence of hip fracture, among individuals with sunlight exposure, inversely correlates with 25-OH-D3 serum levels and mean sunlight irradiation recorded between 2 and 3 months before the fracture. This data could help to better understanding the seasonal incidence of hip fracture.

Disclosures: ***E. Casado****, None.*

SA339

See Friday Plenary number F339

SA340

See Friday Plenary number F340

SA341

See Friday Plenary number F341

SA342

Despite Low Bone Mass, Fracture Prevalence Is Low in Post-Menopausal Mayan Women. E. Brudzinski*, N. Binkley. University of Wisconsin, Madison, WI, USA.

Kyphosis and fracture are reputed to be rare in post-menopausal Mayan women. This community-based study investigated self-reported fracture prevalence, known fracture risk factors, physical examination findings of kyphosis and calcaneal bone mass by ultrasonometry.
Thirty-one women age 50 and older were evaluated at a temporary clinic in the Mayan village of Yaxchecu, Mexico. All presented for other health concerns and were directed to the investigator. Language barriers were addressed by both Spanish and Mayan translators. Height, weight, diet, physical activity, fracture and medication history were obtained. Kyphosis was subjectively assessed by physical examination and calcaneal ultrasonometry performed using an Achilles Express (GE Medical Systems, Lunar).
Patient mean age was 69.3 ± 8.7 with menarche at 13.4 ± 1.6 and menopause at 46.2 ± 5.7 years. Age at first childbirth was 18.6 ± 3.7 years and these women were pregnant 8.4 ± 4.3 times. Their mean height, weight and BMI was 4.6 ± 0.2 feet, 116 ± 19.5 pounds and 26.3 ± 3.7 kg/m^2 respectively. None took estrogen, smoked or drank alcohol. They had essentially no dairy intake. All participated in physical labor centered around the home and field, e.g., carrying water from wells and farming in their younger years, and maintained activity by walking around the village. Sun exposure occurred on an almost daily basis and sunscreens are not used in this population. About half (48%) had fallen within the last year, both standing and from heights. Only four women (13%) reported fractures during their adult life: one clavicle, two wrist and one with bilateral humerus fractures. Notably none sustained a hip fracture. Kyphosis was present on examination in none of these women. Their mean calcaneal stiffness T-score was -2.2 ± 1.0, range -4.1 to -0.1. T-scores were lower by 0.04 per year since menopause. There was no effect of BMI or parity on T-score.
In conclusion, despite low calcaneal bone mass and falls, low-trauma fractures are rare, hip fractures absent and kyphosis not observed in this population of Mayan women. Possible explanations for this include maintained physical activity, bone geometry, vitamin D replete status and alterations of bone turnover. Future study in Mayans is necessary and may identify factors contributing to bone strength and fracture resistance.

Disclosures: ***E. Brudzinski****, None.*

SA343

See Friday Plenary number F343

SA344

Quality of Life in Postmenopausal Women: Effects of Bone Mineral Density (BMD) and Subclinical Vertebral Fractures. E. Romagnoli*[1], V. Carnevale*[2], E. D'Erasmo*[1], F. Paglia*[1], S. De Geronimo*[1], J. Pepe*[1], N. Raejntroph*[1], M. Maranghi*[1], S. Minisola[1]. [1]Dpt of Clinical Sciences, "La Sapienza" University, Rome, Italy, [2]Dpt of Internal Medicine, CSS IRCCS, S. Giovanni Rotondo, Italy.

Quality of life (QOL) in postmenopausal osteoporosis has been mainly assessed in patients with clinically recognized vertebral fractures. We investigated the reliability and validity of the Italian version of the quality of life questionnaire of the European Foundation for Osteoporosis (QUALEFFO) in subjects with subclinical vertebral fractures. We also tested its validity in discriminating patients with reduced BMD from normal subjects, independently of vertebral fractures.
We studied 361 healthy ambulant asymptomatic postmenopausal women, sent by their general practitioners to our Mineral Metabolism Center as part of an osteoporosis screening program on healthy postmenopausal women. The QUALEFFO consists of 41 questions divided into five domains, which explore pain, physical function, social function, general health perception and mental function, respectively. All participants underwent BMD measurement by DXA of either the lumbar spine and/or the femoral neck. as well as x-ray examination of the thoraco-lumbar spine. Vertebral deformity was defined when anterior, middle, or posterior height loss was more than 20% in respect to the adjacent vertebra
According to the WHO criteria, when subjects were subdivided by BMD values into three groups (normal BMD, osteopenia, and osteoporosis), a significant difference was found only for the domains exploring general health perception ($p<0.01$) and mental function ($p<0.001$ by ANOVA). Among osteopenic patients, no difference was found between fractured (30) and non-fractured (120) ones for each domain considered. A significant difference was instead found between fractured (52) and nonfractured (93) osteoporotic patients for the domains exploring physical function ($p=0.002$), social function ($p<0.001$), general health perception ($p=0.011$) and total QUALEFFO score ($p=0.008$). Stepwise multiple logistic regression analysis of the whole sample showed that both vertebral fractures and a low femoral BMD impairs QOL perception, while age did not exert a significant influence. ROC curves analysis demonstrated a low discriminating capacity of individual domains and total QUALEFFO score for both vertebral deformities and BMD categorization.
Our results showed that QUALEFFO is not able to discriminate between patients with or without subclinical vertebral fractures. However, some aspects of QOL appear to be impaired in patients with silent vertebral fractures or reduced BMD.

Disclosures: ***S. Minisola****, None.*

SA345

See Friday Plenary number F345

SA346

"Occult" Osteoporotic Vertebral Fractures: Vertebral Body Fractures without Radiological Collapse. T. Pham*[1], J. Azulay-Parrado*[1], P. Champsaur*[2], C. Chagnaud*[3], P. Lafforgue[1]. [1]Service de Rhumatologie, la Conception, Marseille, France, [2]Service de Radiololgie, Hôpital la Timone, Marseille, France, [3]Service de Radiologie, Hôpital la Conception, Marseille, France.

Summary of background data: Osteoporotic vertebral fractures are usually diagnosed on plain radiographs on the basis of vertebral deformation, *i.e.* vertebral collapse. There are no data on either the possibility or the features of osteoporotic vertebral fractures without significant vertebral body deformation.
Methods: We retrospectively analyzed cases which presented with acute back pain with initially no vertebral deformity on plain radiographs, and which later proved to be fresh osteoporotic vertebral body fractures. All cases met each of the following criteria: 1) The incriminated vertebra appeared normal (Genant's grade 0 deformation) on initial radiographs. 2) The diagnosis of fresh vertebral body fracture was confirmed by MRI (band-like homogenous bone marrow edema feature , a horizontal linear fracture line parallel to a vertebral plateau or both, and the absence of signs of tumor). 3) The diagnosis of osteoporosis was made by the combination of established osteoporosis, exclusion of another underlying disease, and follow-up.
Results: We observed 21 such fractures in 16 patients (11F/5M, mean age 72 years). Most of these fractures affected the lumbar spine (14/21 occurred at L2 to L5). Osteoporosis was previously known in 9 patients, newly diagnosed in 7. At follow-up, the vertebral fracture worsened in 15 of 19 cases towards a classical vertebral collapse (Genant's grade = 0.5) in a mean of 12.5 weeks (4-24 weeks). In 4 of 19 cases, the vertebra remained normal. All cases have had a clinically favorable outcome.
Conclusion: True osteoporotic vertebral fractures without collapse at presentation exist. They are the equivalent in the spine of occult stress fractures well known in other skeletal sites. They must not be misdiagnosed as malignant lesions.

Disclosures: ***P. Lafforgue****, None.*

SA347

The Burden and Management of Osteoporosis: A Missed Opportunity. C. J. Metge*[1], W. D. Leslie[2], L. Manness*[3], B. Kvern*[4], M. Yogendran*[5], C. K. Yuen[4]. [1]Faculty of Pharmacy, University of Manitoba, Winnipeg, MB, Canada, [2]Medicine, St. Boniface General Hospital, Winnipeg, MB, Canada, [3]Patient Health Management, Merck Frosst Canada Ltd., Winnipeg, MB, Canada, [4]Faculty of Medicine, University of Manitoba, Winnipeg, MB, Canada, [5]Faculty of Medicine, MB Centre for Health Policy, University of Manitoba, Winnipeg, MB, Canada.

The difference between 'best care' or use of proven interventions and 'usual care' is often large. The Maximizing Osteoporosis Management in Manitoba (MOMM) project is a public/private partnership and includes the province of Manitoba; its sole purpose is to identify gaps in the delivery of osteoporosis care and to promote 'best care'. Using administrative claims data, we performed a panel study (1997-2002) of women aged ≥ 50 years who were residents of Manitoba and had experienced a hip or spine or a non-spine/non-hip fracture. Fracture events were used to identify women at high risk of osteoporosis and fracture. To examine the kinds of care women received 1-year post-fracture we used two data sources and calculated rates of bone mineral density (BMD) testing and pharmacological intervention for each panel. BMD testing is indicated after a non-spine/non-hip fracture in women over 50; the availability of a province-wide BMD database allowed us to identify when BMD investigation was done post-fracture. The use of pharmacological treatment post-spine or hip fracture was determined by examining dispensations of recognized osteoporosis therapies. All years of data show similar results. For example, among the 1802 women fracturing a hip or spine vertebra in 2001/2002, < 18% (n=317)were dispensed a known pharmacological treatment for osteoporosis and < 5% (n=83) had BMD testing in the year post-fracture. The same low patterns of intervention were found in the 4673 women with a non-spine/non-hip fracture in 2001/2002; 15.5% (n=723) were dispensed pharmacological treatment and only 7.0% (n=328) had BMD testing in the year post-fracture. Gaps in the treatment and prevention of osteoporosis in Manitoba women ≥ 50 years old have been identified. Data responsive interventions are currently being implemented in a rural health region of Manitoba.

Disclosures: ***C.J. Metge****, Merck Frosst Canada Ltd. 2, 5.*

SA348

Development of a Model of Integrated Post-Fracture Care. S. Jaglal[1], G. Hawker[2], E. Bogoch*[3], S. Cadarette[4], J. Carroll*[5], D. Davis*[3], L. Jaakkimainen*[5], H. Kreder*[3], W. McIsaac*[5]. [1]Rehabilitation Science, University of Toronto, Toronto, ON, Canada, [2]Medicine, University of Toronto, Toronto, ON, Canada, [3]Surgery, University of Toronto, Toronto, ON, Canada, [4]Health Policy Management and Evaluation, University of Toronto, Toronto, ON, Canada, [5]Family and Community Medicine, University of Toronto, Toronto, ON, Canada.

The objective of this study was to develop a model for integrated post-fracture care in the province of Ontario, Canada. Both qualitative and quantitative research methodology were utilized to identify barriers and opportunities for post-fracture care interventions. A literature review was first conducted. A provincial telephone survey of all 178 hospitals in Ontario was also conducted to describe the current processes and patterns of post-fracture care in hospitals. Four focus groups were conducted with 26 family physicians to determine the factors influencing post-fracture care, including the diagnosis, treatment and management of osteoporosis. Four focus groups were also conducted with 21 fragility fracture patients to examine their experiences with fracture care, awareness of osteoporosis and information needs. Thirty-four key informant interviews were conducted to validate the findings from the hospital survey, to identify community-based services and programs, to explore roles and responsibilities of various organizations and health care professionals and to identify barriers and facilitators for post-fracture care. Finally, a stakeholder consultation workshop was held to obtain feedback on the feasibility of a proposed model of integrated post-fracture care. Findings suggest that there are gaps in investigation and treatment and a lack of integration between health care professionals who provide fracture care and those who provide osteoporosis management and falls prevention. The development of a model for integrated post-fracture care resulted from triangulating the information. The model reflects the complexity of post-fracture care, from the acute management of the fracture and the role of in-hospital health services (e.g. emergency departments, rehabilitation services, orthopaedic services), through follow-up in the primary care setting (e.g. family physicians, nurse practitioners, pharmacists), and with services and programs provided by community-based organizations. There is an additional telemedicine multidisciplinary osteoporosis clinic component. Interventions were identified for each of the model components. These need to be evaluated for feasibility and outcome effectiveness. A demonstration project is currently underway to implement and evaluate this model in four communities in Ontario, Canada.

Disclosures: ***S. Jaglal****, Ontario Women's Health Council 2.*

SA349

See Friday Plenary number F349

SA350

Impact of Vertebral Deformities, Osteoarthritis and Other Chronic Diseases on Quality of Life: A Population-based Study. N. M. Van Schoor*[1], J. H. Smit*[2], P. Lips[3]. [1]EMGO Institute, VU University Medical Center, Amsterdam, Netherlands, [2]Department of Sociology and Social Gerontology/ Department of Psychiatry, VU University Medical Center, Amsterdam, Netherlands, [3]EMGO Institute/Department of Endocrinology, VU University Medical Center, Amsterdam, Netherlands.

Vertebral deformities and spinal osteoarthritis are common disorders in elderly persons and are associated with back pain, impaired physical functioning, and loss of quality of life. The objectives of this study were to assess the impact of vertebral deformities and spinal osteoarthritis on quality of life in a population-based sample, and to compare this to the impact of six other important chronic diseases on quality of life.

The study was performed as a substudy of the Longitudinal Aging Study Amsterdam. Vertebral deformities and osteoarthritis were assessed by spinal radiographs in 1998/1999; chronic diseases were assessed by self-report; quality of life was estimated by the physical and mental component summary scales of the SF-12 (PCS-12 and MCS-12) in 1998/1999, and by the EQ-5D (EuroQol) and Qualeffo-41 in 2001/2002 (n=336).

The prevalence of the different diseases was 21.4% for severe osteoporosis of the vertebrae, 42.3% for spinal osteoarthritis, 18.2% for chronic obstructive pulmonary disease (COPD), 26.2% for cardiac disease (CD), 11.0% for peripheral arterial disease (PAD), 8.3% for diabetes mellitus (DM), 7.1% for cerebrovascular accident (CVA) and 15.2% for cancer. Most persons suffered from 2 chronic diseases. In univariate analyses, severe osteoporosis of the vertebrae significantly worsened quality of life as assessed by the PCS-12 (-3.5 points difference in median score; p=0.02) and the total score of Qualeffo-41 (+6.5 points; p=0.04). The impact of osteoarthritis on quality of life was less pronounced and not statistically significant. The other chronic diseases reduced quality of life, although not all changes reached statistical significance. In multivariate analyses, the largest decrease in quality of life, as measured by the PCS-12, was seen for DM (standardized Beta=-1.21), closely followed by PAD (-1.17) and CD (-1.12). Severe osteoporosis of the vertebrae showed a similar worsening of quality of life when assessed by the Qualeffo-41 (+1.12). In conclusion, most persons in an elderly population suffer from one or more chronic diseases, and therefore experience loss of quality of life. After adjustment for age, sex and other chronic diseases, DM, PAD, CD and severe osteoporosis of the vertebrae showed the largest decrease in quality of life. Although the degree of quality of life loss is largest for DM and PAD, the burden of CD and osteoporosis might be higher because of their higher prevalence.

Disclosures: ***N.M. Van Schoor****, Wyeth Research, Collegeville, Pennsylvania 2.*

SA351

Gender Affects Presentation and Outcome in Osteoporosis and Myeloma Patients Who Undergo Kyphoplasty. S. V. Bukata, J. Koob*, J. M. Lane. Orthopaedics, Hospital for Special Surgery, New York, NY, USA.

Patients with osteoporosis or multiple myeloma suffer vertebral compression fractures with resulting pain and functional disability from biomechanical changes in the spine and residual kyphosis. 45 (36 female/6 male) consecutive osteoporosis patients and 17 (10 female/ 7 male) consecutive myeloma patients with vertebral compression fractures underwent unipedicular balloon kyphoplasty with PMMA stabilization to restore as much normal height and angulation as possible to their fracture site. Patients were evaluated preoperatively and post-operatively with the validated general Oswestry back questionnaire. In the entire population of age, gender, and fracture number matched individuals we found equivalent pain relief and functional improvement between the myeloma and osteoporosis groups. Gender specific analysis within the groups revealed a few important differences. Average pre-operative and post-operative Oswestry scores were greater amongst the female osteoporotic patients (Female 52.9/Male 37.7 pre-operative, and Females 39.1/ Male 22.7 post-operative), but change in the score following surgery was not different (Female 13.8/Male 15.0). With myeloma, male average pre-operative scores were greater than female (Male 53.1/ Female 41.2) but the average post-operative scores were almost identical (Males 32.0 / Females 32.2). Vertebral height restoration was equivalent between all groups, and men and women in both groups experienced good results. In this instance, caution must be used in setting a minimal pre-operative score for consideration for kyphoplasty since osteoporotic men tend to score lower, yet experience equivalent improvement with the procedure. Due to the differences in both presentation and final outcome, gender specific analysis is critical in evaluating outcome data for orthopaedic procedures, including kyphoplasty.

Disclosures: ***S.V. Bukata****, None.*

SA352

Bone Mass Measurements Are Associated with Cardiovascular Mortality: A 5-year Analysis. M. M. Pinheiro*, C. H. M. Castro, R. E. Heymann*, K. R. B. Oliveira*, C. Ohashi*, V. L. Szejnfeld. Rheumatology, Unifesp, Escola Paulista de Medicina, Sao Paulo, Brazil.

Previous studies suggest that osteoporotic fracture is associated with increased risk of mortality, however the relationship between bone mineral density (BMD), quantitative ultrasound (QUS) and mortality is still controversial. Our aim was to evaluate the ability of BMD and QUS measurements to predict new osteoporotic fracture and mortality. Two-hundred seventy five women were invited to participate in this study. Risk factors for osteoporosis and fracture were evaluated by a questionnaire that included details concerning lifestyle habits, diet, hormonal factors and drug use. Patients with suspected secondary osteoporosis were excluded. Spine and femur BMD (DPX-L, Lunar) and calcaneus QUS (Achilles +, Lunar) were performed in all patients at baseline. Lateral thoracic and lumbar X-ray was taken at baseline and 5-year later to confirm the presence of vertebral fractures. Five-year after baseline visit, all reported deaths were confirmed by review of hospital records and classified according to ICD-10 code. Two-hundred eight (75.6%) women completed the study and 25 (9.1%) lost follow-up. Mean age and weight were 75.2 ± 6.5 years and 60.3 ± 10.2 kg, respectively. Forty-two (15.3%) women died (incidence rate = 36.2/ 1.000 person-years) and 41 patients (19.7%) had new osteoporotic fracture (incidence rate = 41.7/ 1.000 person-years). After adjustments for age, weight, previous fracture, smoking, physical activity, drugs and comorbities, femoral neck BMD, trochanter BMD and stiffness index (SI) were associated with new osteoporotic fracture [standardized HR = 2.0 (95% CI 1.26-3.18), 1.62 (95% CI 1.08-2.42) and 2.2 (95% CI 1.30-3.82), respectively]. Trochanter BMD, SI and femoral neck BMD were the most significant predictors of death in this population [standardized HR = 1.59 (95% CI 1.07-2.36), 1.57 (95% CI 1.10- 2.46) and 1.43 (95% CI 1.06-2.22), respectively]. Cardiovascular mortality was also associated with low femoral neck BMD [RH = 1.28 (95% CI 1.07-2.62)], trochanter BMD [RH = 1.30 (95% CI 1.08-2.18)] and SI [RH = 1.54 (95% CI 1.08-2.79)]. Mortality due to cancer, infectious or pulmonary diseases had no statistically significant association with BMD or QUS measurements. Spine BMD was not related to the risk of new fracture or death. In conclusion, low SI and femur BMD were able to predict the risk of new osteoporotic fracture and were associated with total and cardiovascular mortality, independently of age, health status and other diseases in Brazilian elderly women. These results reinforce epidemiological and biological recent evidence supporting common physiopathological aspects between osteoporosis and atherosclerosis.

Disclosures: ***M.M. Pinheiro****, None.*

SA353

Low Bone Mineral Density of Distal Forearm Predicts the Mortality in Elderly Men - the MINOS Study. P. M. Szulc[1], F. Munoz*[1], F. Marchand*[2], P. D. Delmas[1]. [1]Epidemiology of Osteoporosis, INSERM 403 Research Unit, Lyon, France, [2]SSMB, Montceau les Mines, France.

Only limited data on the association between areal bone mineral density (aBMD) and mortality are available in men. We evaluated if cross-sectional area (CSA), aBMD, volumetric BMD (vBMD) and morphologic parameters (external diameter, cortical thickness) predict the risk of death in 792 men aged 50 to 85 belonging to the MINOS cohort. During the follow-up of 7.5 yrs, 134 men died. After adjustment for age, co-morbidity, medication, hormonal levels and professional physical activity, decreased aBMD of distal forearm and ultradistal radius was associated with higher mortality (O.R. = 1.25-1.30 per 1 SD decrease, p < 0.02-0.002). In analyses performed separately for radius and ulna, decreased CSA, aBMD, vBMD and cortical thickness of each bone were associated with increased mortality (O.R. = 1.20 - 1.34 per 1 SD decrease, p < 0.04-0.02) whereas the external diameter was not (p>0.6). In similar multiple adjusted models, hip and lumbar spine BMD were not associated with the increased mortality (p>0.15).

In summary, our data indicate that in elderly men decreased CSA, aBMD, vBMD and cortical thickness of distal radius and ulna, but not of lumbar spine and hip, are associated with a higher mortality. Bone mineral of distal forearm, which is neither a weight-bearing site nor influenced by osteoarthritis, may reflect the deterioration of general health status better than other sites of measurement.

Disclosures: ***P.M. Szulc****, None.*

SA354

See Friday Plenary number F354

SA355

Relationship of Diabetes and Falls in Older Men. T. L. Dam[1], R. Fullman[2], P. M. Cawthon[2], J. Cauley[3], E. Orwoll[4], E. Barrett-Connor[5]. [1]Medicine, UCSD, San Diego, CA, USA, [2]Prevention Studies Group, UCSF, San Francisco, CA, USA, [3]U. of Pittsburgh, Pittsburgh, PA, USA, [4]Medicine, OHSU, Portland, OR, USA, [5]Family and Preventive Medicine, UCSD, San Diego, CA, USA.

Patients with diabetes have increased bone mineral density. Nevertheless, several studies have shown that diabetics also have increased rates of fracture possibly due to an increased risk of falls that may contribute to their increased fracture rates.

We evaluated 5,995 community dwelling men ages 65 years and older enrolled in the prospective cohort study of Osteoporotic Fractures in Men. Self reported diabetes status and multiple covariates were collected at a baseline visit via questionnaire in 2000-2002. Physical, cognitive, visual and neuromuscular functions were measured at the baseline visit. Incidence of falls was ascertained every 4 months by a mailed questionnaire for 2 years (response rate >95%). We compared the prevalence of risk factors for falls and incidence of falls by diabetes status.

The 653 (10.9%) men who reported diabetes had significantly higher BMD scores (at the total spine, total hip, femoral neck, trochanter and intertrochanter) compared to nondiabetics. During each year of follow up, a higher percentage of men with diabetes fell compared to men without diabetes. By the end of year 2, 40% of men without diabetes and 47.4% of men with diabetes had reported at least 1 fall (p=.0003), with an age-adjusted 36% increased fall risk (OR 1.36 (1.15-1.61), p<.0001). More than 10 previously described risk factors for falls were significantly (p <.0001) more prevalent in men with diabetes. After adjusting by logistic regression models for selected covariates (age, weight, history of cataracts or stroke, dizziness, use of benzodiazepine, loop diuretic and tricyclic antidepressant, depth perception and grip strength), the risk of falling associated with diabetes decreased and was no longer statistically significant (OR 1.15 (0.97-1.38), p=.11).

Diabetes was associated with better BMD and an increased risk of falls in these older men. Diabetes co-morbidities and associated medications may explain the higher fall risk, as evidenced by the attenuation of the diabetes fall association in multiply adjusted analyses. These results suggest a multifactorial etiology for the increased risk of fracture despite higher BMD levels observed in diabetics.

Disclosures: ***T.L. Dam****, None.*

SA356

See Friday Plenary number F356

SA357

Comparison of the OST Versus a Typical Risk-Factor Questionnaire for Evaluating Osteoporosis in Men. C. L. Sybrowsky*, J. G. Skedros. Utah Bone and Joint Center, Salt Lake City, UT, USA.

Although dual-energy x-ray absorptiometry (DXA) is an effective means of determining low bone mineral density (BMD), identifying the appropriate population to screen remains a topic of controversy. This is especially problematic in males, since the majority of osteoporosis risk-assessment models have focused on females. Previous studies have shown that the osteoporosis self-assessment screening tool (OST) is highly sensitive for identifying males at risk for osteoporosis (Adler et al., 2003 Mayo Clin Proc). This value is determined as: [(weight in kg - age in years) × 0.2, truncated to an integer]. The purpose of this study was to determine if the OST more strongly correlated with BMD than responses to a 'typical' risk-factor questionnaire that assessed 30 known or suspected risk factors for osteoporosis or osteoporosis-related fracture in men. This questionnaire has been used in our orthopaedic surgery specialty clinic to determine candidates for DXA and to provide documentation of risk to insurance companies for payment authorization. A population of 158 American Caucasian men with a mean age of 67.5 ± 13.1 years and weight of 85.3 ± 16.0 kg completed the risk-assessment questionnaire and underwent central DXA (total hip, femoral neck, and lumbar spine). T-scores for the population were then correlated with questionnaire responses and OST risk indices. 16.5% of the men had T-scores lower than -2.5 at one or more of the scanned sites. OST indices ranged from -6 to 16 (mean 4 ± 5). Total number of reported risk factors ranged from 0 to 13 (mean 4 ± 2). When defining osteoporosis as a T-score of ≤ -2.5, an OST index of ≤ 3 yielded sensitivity of 92%, specificity of 55%, positive predictive value of 29%, and negative predictive value of 97%. Questionnaire assessment of 3 or more risk factors yielded sensitivity of 65%, specificity of 42%, positive predictive value of 18%, and negative predictive value of 86%. These data confirm the high sensitivity of the OST for detecting osteoporosis in men and demonstrate that it more accurately predicts low BMD than gross quantification of standardized risk factors. However, since the risk-assessment questionnaire assigns equal importance to each of the 30 risk factors, differential weighting of risk factors may improve sensitivity/specificity.

Osteoporosis prevalence determined by OST index and standardized risk-assessment questionnaire

Category	T-score ≤ -2.5	T-score ≤ -2.0
OST ≥ 4	2.7% (2/75)	8.0% (6/75)
OST -1 to 3	26.6% (16/60)	38.3% (23/60)
OST ≤ -2	34.8% (8/23)	56.5% (13/23)
3 or more risk factors	18.1% (17/94)	28.7% (27/94)
5 or more risk factors	22.7% (10/44)	40.9% (18/44)

Disclosures: ***C.L. Sybrowsky****, None.*

SA358

See Friday Plenary number F358

SA359

Predictors of Femoral Neck Geometry in Caribbean Men: The Tobago Bone Health Study. L. M. Semanick*[1], T. Beck[1], J. A. Cauley[2], V. Wheeler*[3], A. Patrick*[3], C. Bunker*[2], J. M. Zmuda[2]. [1]Radiology, Johns Hopkins University, Baltimore, MD, USA, [2]University of Pittsburgh, Pittsburgh, PA, USA, [3]Tobago Hospital, Trinidad, Trinidad and Tobago.

Osteoporotic fracture is less prevalent in African Americans than Caucasians suggesting a difference in bone structural strength. Studies of bone differences in African Americans are confounded by their heterogeneity due to their admixture of African, European and other origins. We analyzed the associations between anthropometry, lifestyle factors

and bone cross sectional geometry in 1,886 men of African descent on the Caribbean island of Tobago (age > 39 y; mean 56 y). Femur neck geometry was assessed with Hip Structure Analysis on hip DXA scans. In multiple linear regression models using forward selection, age, body size and composition, indirect measures of physical activity, fracture history, and presence of several health related conditions including coronary heart disease, high blood pressure (HBP), arthritis and diabetes were considered as independent predictors of section modulus (Z), cross sectional area (CSA), BMD and neck width. Standardized beta coefficients for significant predictors ($p<0.05$) of these parameters after adjusting for neck shaft angle, age and neck length are listed in the Table. Multivariate models accounted for over 40% of the variance in Z and CSA. Ever being a farmer was positively associated with CSA and BMD but not Z unless appendicular lean mass (ALM) is taken out of the model indicating that the bone strength effect was mediated through muscle size. Diabetes was associated with all skeletal parameters and requires further investigation. Arthritis was negatively associated with BMD, but not with strength properties or width. Sustaining a fracture after the age of 35 had a significant negative association with BMD apparently due to a positive effect on width but not on the amount of bone (CSA) or Z. Minutes walked per week, smoking, coronary heart disease, or a family history of fracture were not independent predictors of Z, CSA, BMD and width. Offsetting the negative association of age with BMD are opposing trends in femoral neck width and the amount of bone it encloses (CSA); the net effect is that age has no significant association with bending strength (Z). These associations are consistent with a model whereby periosteal expansion might compensate for the loss of bone mass with aging.

	Z	CSA	BMD	Width
Age	-	-0.143	-0.181	0.204
Height	0.239	0.156	-	0.383
ALM	0.441	0.464	0.400	0.133
% Body Fat	-0.049		-	-0.047
Ever farm	-	0.038	0.056	-.0.047
Grip strength	0.055	-	-	0.079
Fx after 35	-	-	-0.041	0.051
Arthritis	-	-	-0.045	-
Diabetes	0.052	0.073	0.101	-0.052
HBP	-	-	-	-0.046
Model R^2	0.427	0.403	0.283	0.221

Disclosures: ***L.M. Semanick****, None.*

SA360

See Friday Plenary number F360

SA361

Risk Factors Associated To Low-Impact Fractures In Men With Ankylosing Spondylitis. R. E. Heymann*, L. Nappo*, R. Vilela*, K. Luz*, M. M. Pinheiro*, V. L. Szejnfeld*. Rheumatology, UNIFESP, São Paulo, Brazil.

Ankylosing spondylitis (AS) is associated with low bone mineral density (BMD). Whether low bone mass in this patients leads to increased fracture rate is still not clear.

The purpose of this study was to determine fracture rate and investigate risk factors associated with low-impact fracture in men with AS.

Eight-Five men were enrolled in this cross-sectional study (40 age matched healthy controls). Clinical risk factors were evaluated by a questionnaire that included details about aspects of lifestyle, diet, drug use and previous fracture. Spine and femur BMD (DPX-L, Lunar) and heel QUS (Achilles +, Lunar) measurements were performed in all the subjects. Lateral thoracic and lumbar radiographs were taken to check for the presence of vertebral fractures, according to Genant's method.

AS patients were thinner and shorter than healthy controls (HC).The mean age, weight and height are 42.6 ± 10.6 vs. 38.4 ± 10 years, 71.7 ± 8.5 vs. 67 ± 17,1 kg, and 1.68 ± 0.08 vs. 1.64 ± 0.08 m, respectively (HC vs. AS). Vertebral deformity (grades II and III) had a significantly 2 fold increase in AS paients compared to HC (identified in 21 AS patients and 12 HC). Patients with AS also had more non vertebral fractures. Spine and femur BMD and QUS measurements were not singnificantly different between AS patients and HC. The mean spine BMD and stiffness index were 1.170 ± 0.17 vs. 1.180 ± 0.24 g/ cm2 and 96,1 ± 17,2 vs. 91,5 ± 19,3, respectively (HC vs. AS) (NS).The most relevant risk factors to discriminate AS patients with low-impact fractures from non-fracture were race and previous history fracture.

In conclusion, the clinical risk factors for fractures were more important than bone mass measurements to discriminate AS patients with low-impact fracture from those without. Interestingly, AS patients had a higher rate of fractures even with BMD and QUS values similar to that observed in the healthy population.

Disclosures: ***R.E. Heymann****, None.*

SA362

See Friday Plenary number F362

SA363

Race/Ethnic Differences in Bone Mineral Density in Men: Preliminary Results from BACH/BONE. A. B. Araujo[1], S. S. Harris[1], M. F. Holick[2], A. Turner*[2], J. B. McKinlay*[1]. [1]New England Research Institutes, Watertown, MA, USA, [2]School of Medicine, Boston University, Boston, MA, USA.

While there are a number of studies on bone mineral density (BMD) in men, few present racial/ethnic differences by skeletal site. Our objective was to estimate racial/ethnic differences in areal BMD in men at the femoral neck, total radius and ulna (forearm), L2-L4 lumbar spine (spine), and whole body. We report preliminary, unweighted BMD data from the Boston Area Community Health/Bone (BACH/BONE) Survey, a population-based study of skeletal health in a racially/ethnically diverse sample of Boston men aged 30-79 y. Data are available for N=538 men. Race/ethnicity was determined by self-report. BMD (g/cm^2) was measured at the hip, forearm, spine, and whole body with a Hologic QDR 4500W, which was calibrated daily with a spine phantom supplied by the manufacturer. Mean age was 50.7±12.7 y. Means for each skeletal site were as follows: 0.867±0.142 g/cm^2 (femoral neck), 0.610±0.063 g/cm^2 (forearm), 1.056±0.159 g/cm^2 (spine), and 1.201±0.129 g/cm^2 (whole body). Compared with Whites, Blacks had 12.6%, 5.9%, 8.6%, and 6.8% higher age-adjusted femoral neck, forearm, spine, and whole body BMD, respectively. None of the Black-White differences were dependent on age. Race/ethnic differences in forearm BMD (Whites and Blacks 1.3% and 7.3% higher, respectively, than Hispanics) and whole body BMD (Whites and Blacks 2.4% and 9.4% higher, respectively, than Hispanics) were constant across age. However, race/ethnic comparisons in femoral neck and spine BMD varied by age, as shown in Table 1. In this population-based study of men, Black/White differences in BMD at various skeletal sites range from 5.9-12.6%. The difference at the hip is of similar magnitude to that reported in previous studies, but few studies provide estimates of Black-White differences at other skeletal sites. Observed Black/White differences suggest a parallel age decline in BMD in the two groups. Comparisons involving Hispanic men are more complex. Forearm and whole body BMD are higher in Whites and Blacks compared with Hispanics. Not noted in previous studies is the age-dependent race difference in femoral neck and spine BMD. Thus, Hispanic men may have steeper age declines in these parameters than observed in White or Black men, suggesting the possibility of a greater increase in fracture risk with age among this group.

Table 1. Whites and Blacks compared with Hispanics in femoral neck and lumbar spine BMD by age.

	White vs. Hispanic (%)		Black vs. Hispanic (%)	
Age	Femoral neck BMD	Spine BMD	Femoral neck BMD	Spine BMD
35 y	-7.8	-1.2	3.8	7.3
45 y	-5.6	1.7	6.3	10.4
55 y	-3.3	4.6	8.8	13.7
65 y	-1.0	7.7	11.3	17.0
75 y	1.4	10.8	14.1	20.4

Disclosures: ***A.B. Araujo****, None.*

SA364

See Friday Plenary number F364

SA365

Osteoporosis: A Silent Epidemic in Male Veterans. R. A. Adler[1], C. A. Hertel*[2], M. I. Williams*[3], V. I. Petkov*[1]. [1]Endocrinology, McGuire Veterans Affairs Medical Center/Virginia Commonwealth University School of Medicine, Richmond, VA, USA, [2]Primary Care, Veterans Affairs Western New York Health Care System - Batavia Division, Batavia, NY, USA, [3]Endocrinology, McGuire Veterans Affairs Medical Center/Virginia Commonwealth University School of Pharmacy, Richmond, VA, USA.

Osteoporosis (OP) is considered a disorder of older women, but we and others have found osteoporosis to be common among male veterans. We used data from screening studies in two Veterans Affairs Medical Centers (VAMC) to estimate the frequency of osteoporosis in men receiving medical care from the Department of Veterans Affairs. At the Richmond VAMC and the VA Western New York Healthcare System, we used the Osteoporosis Self-Assessment Tool (OST), a simple screening method (based on weight and age only) to determine which men in primary care clinics were at moderate or high risk for osteoporosis. The men who were referred by their primary care providers underwent DXA testing. From the DXA data and the distribution of men according to OST, we estimated the total number of male veterans with undiagnosed osteoporosis.

At the Batavia site, spine and hip DXA (Lunar DPX-L) of 612 men revealed 138 (22.5%) with osteoporosis and 265 (43.3%) with osteopenia. In Richmond, DXA testing (Hologic Delphi) of 441 men showed 109 (24.7%) with osteoporosis and 239 (54.1%) with osteopenia. We concluded that 23.5% of men at moderate or high risk by OST have silent osteoporosis.

In the Richmond primary care clinics, 5,645 out of 15,027 men (37.6%) were at moderate or high risk for OP according to OST. There are 4.5 million veterans receiving care from the Department of Veterans Affairs, and we estimated that 3.8 million are men. Using the above data, we calculated that there are 335,768 veteran men with silent osteoporosis. From our studies adding forearm DXA to spine and hip, the estimate would be 475,790.

In conclusion, we estimate that 12.5% of male veterans have osteoporosis and don't know it. It is likely that men followed in the community have a similar prevalence of osteoporosis. We conclude that screening methods such as OST should be used widely to uncover osteoporosis in men.

Disclosures: ***R.A. Adler****, None.*

SA366

Family Physician Awareness of Risk Factors For Fracture and the Appropriate Use of Bone Mineral Density Screening in Accordance With The Canadian Osteoporosis Guidelines: Canadian Quality Circles (CQC) Project. A. Papaioannou[1], G. Ioannidis[1], M. Doupe*[2], A. Katz*[2], B. Kvern*[2], A. Hodsman[3], A. Baldwin*[4], D. Johnstone*[5], M. Baranci*[6], J. D. Adachi[1]. [1]McMaster University, Hamilton, ON, Canada, [2]University of Manitoba, Winnipeg, MB, Canada, [3]University of Western Ontario, London, ON, Canada, [4]St. Boniface Hospital, Winnipeg, MB, Canada, [5]Procter & Gamble Pharmaceuticals Inc, Toronto, ON, Canada, [6]Aventis Pharma, Laval, PQ, Canada.

The CQC Pilot Project is a one year, integrated disease management project to disseminate the OSC 2002 guidelines and to improve family physicians (FP) adherence to the guidelines. Fifty-two FP participated in the study and formed 7 quality circles. The FP enrolled a total of 1505 patients. These patients were women age 55 years and over and had attended at least 2 visits in the past 24 months. Data were gathered using the project data collection form.

Our baseline analysis examined the physicians' awareness of thirteen risk factors for fracture (9 major and 4 minor) and the appropriate use of bone mineral density (BMD) screening in accordance with the Canadian Osteoporosis guidelines. The major risk factors included age (>65 yr), prior hip fracture after age 40, prior wrist fracture after age 40, prior vertebral fracture after age 40, family history of fragility fracture, a fall in the previous 12 months, oral prednisone therapy (>3 months), menopause before age 45, and historical height loss (2-4 cm). The minor risk factors included caffeine intake (>4/day), alcohol intake (>9/week), current smoking, and weight (< 57 kg). Patients highly recommended for BMD screening were defined as those with one or more major risk factor, or two or more minor risk factors. Patients with one minor or no risk factors were not recommended for BMD screening in accordance with the guidelines.

Results indicated that 9 of 13 risk factors were identified by over 90% of FP. Four risk factors were identified by only 46-72% of the physicians. Of these, 3 risk factors were major (a family history of fragility fracture [46%], menopause before the age of 45 years [72%] and historical height loss [57%]; and 1 was minor (caffeine intake [57%]). FP reported prevalent hip, wrist, and vertebral fractures in approximately 5% of their patients. BMD screening was conducted in 65% of those highly recommended as compared with 57% for those not recommended.

In conclusion, most risk factors were identified by FP; however, the awareness of a few major risk factors should be strengthened. Given the low prevalence rates of prior fractures (much lower than reported in other studies), it is possible that many prior fractures were not recognized by the FP. Risk factor evaluation did not appear to have an important role in BMD assessment.

Disclosures: ***A. Papaioannou****, None.*

SA367

See Friday Plenary number F367

SA368

High Prevalence of 25(OH)D Deficiency and Secondary Hyperparathyroidism (sHPT) Suggesting "Osteomalacia in Immigrants" in a Turkish Population in Germany (TG) with Diffuse Skeletal Pain. M. Z. Erkal*[1], J. Wilde*[2], Y. Bilgin*[3], C. Algan[3], E. Demir*[3], R. Bretzel*[1], H. Stracke[1]. [1]Medizinische Klinik und Poliklinik III der JLU, Giessen, Germany, [2]Nichols Institute Diagnostika GmbH, Bad Vilbel, Germany, [3]Turkish-German Health Foundation, Giessen, Germany.

Background: the expression "osteomalacia in immigrants" has been used in England during the early 70th to describe a phenomenon observed in Pakistani and Indian immigrants. In 1978 Offermann used the same term in a study including 97 Turkish people living in Germany. During the last years the number of patients in TG complaining of diffuse skeletal pain has constantly increased. Therefore we studied parameters of bone metabolism in TG in comparison to matched groups of Germans (G) and Turks living in Turkey (T).

Methods: 994 apparently healthy volunteers (age 16-70, median 37 years, BMI 16-47, median 23 kg/m^2) were included and divided into 3 groups: (T) 242 female (f) and 85 male (m) Turkish individuals living in Turkey; (TG) 296 f and 270 m Turkish individuals living in Germany and (G): 51 f and 50 m German individuals living in Germany. EDTA blood samples were collected during March to measure 25(OH)D, BioPTH (1-84) and Calcium. Additionally clinical data were obtained by standard questionnaires, including the items age, sex, country, city, BMI, veiled/not veiled, smoking habits, nutritional habits, sun exposure, diffuse skeletal pain, number of children and duration of stay in Germany (TG).

An unconditional logistic regression model was used to calculate relations between different parameters.

Results: Despite similar low 25(OH)D values (75-80% with <20 ng/mL) in all Turkish volunteers only the immigrants in Germany showed elevated PTH values indicating high prevalence of sHPT. Especially veiled female Turkish immigrants were at high risk. In individuals with low 25(OH)D levels the risk of diffuse skeletal pain was increased (x1.8).

Nichols Advantage® 25(OH)D (ng/mL)	Females Median [95% CI]	Males Median [95% CI]	P (females / males)
G	28,7 [20,3; 37,1]	23,4 [17,4; 29,5]	n.s.
T	14,3 [10,7; 18,7]	18,6 [15,6; 22,6]	<0,0001
TG	12,5 [9,5; 17,1]	15,8 [12,6; 19,2]	0,0005
Nichols Advantage® BioPTH (pg/mL)			
G	25,6 [22,8; 28,5]	27,8 [25,1; 30,6]	n.s
T	27,4 [25,8; 29,0]	27,6 [25,4; 29,8]	n.s
TG	37,1 [34,2; 39,9]	34,0 [31,9; 36,1]	n.s

25(OH)D level < 20 ng/mL = deficiency, Bio-PTH reference range: 6-40 pg/mL

Discussion: sHPT due to 25(OH)D deficiency bears the risk of osteomalacia/osteoporosis. Therefore Turkish immigrants in Germany should be regarded as a risk population. In case of diffuse skeletal pains 25(OH)D and PTH levels should be controlled. If "osteomalacia in immigrants" is diagnosed calcium and vitamin D should be substituted.

Disclosures: ***M.Z. Erkal****, None.*

SA369

See Friday Plenary number F369

SA370

Gender Differences in Relationships between Body Composition Components, Their Distribution and Bone Mineral Density: An Opposite Sex Twin Study. J. Makovey*[1], P. Sambrook[1], V. Naganathan[2]. [1]Department of Rheumatology, Institute of Bone and Joint Research, Royal North Shore Hospital, University of Sydney, Sydney, Australia, [2]Centre for Education and Research on Ageing, Centre for Education and Research on Ageing,Concord Hospital, University of Sydney, Sydney, Australia.

Background: Numerous studies indicate that bone mineral density (BMD) is closely related to body mass and its components. Most studies have examined these relationships in women with little attention given to how these relationships differ by gender.

Aims: The aims of the present study were to use the opposite sex twin model to determine if there were gender differences in the relationship between body composition and its relation to BMD and how any such differences were influenced by age.

Methods: We measured body composition and bone mass by dual energy x-ray absorptiometry in 93 pairs of opposite sex twins. To examine the effect of age, they were divided into two age groups: under 50 years old (45 pairs) and over 50 years old (48 pairs).

Results: Lean mass (LM) had stronger positive relationships with bone variables in both genders at all ages than fat mass. Fat mass (FM) had positive relationships with total body, lumbar and hip BMD in women under age 50, but not over 50. In general, use of volumetric regional BMD did not improve associations with fat mass or lean mass. There was no significant relationship between FM and total or regional BMD in men under age 50, but men over 50 showed positive relationships between FM measures and total and some regional BMD measures. Central adiposity showed a positive relationship with BMD in men over 50 and women under 50.

Conclusion: Fat mass (FM) and lean mass (LM) and their distribution in the body have different relations with BMD in men and women with ageing.

Key words: Bone mineral density, body composition, fat mass, lean mass

Disclosures: ***J. Makovey****, None.*

SA371

See Friday Plenary number F371

SA372

Increased Circulating hsCRP Levels Associated with Low Bone Mineral Density in Healthy Pre- and Postmenopausal Women: Evidence for Links between Systemic Inflammation and Osteoporosis. J. Koh[1], Y. Khang*[2], S. Bae*[1], Y. Chung*[3], G. S. Kim[1]. [1]Division of Endocrinology and Metabolism, Asan Medical Center, University of Ulsan College of Medicine, Seoul, Republic of Korea, [2]Department of Preventive Medicine, Asan Medical Center, Seoul, Republic of Korea, [3]Department of Internal Medicine, Seoul Veterans Hospital, Seoul, Republic of Korea.

Factors involved in inflammation have been associated with bone remodeling. We therefore investigated the association between serum concentrations of high sensitivity C-reactive protein (hsCRP) and bone mineral density (BMD) in 3,662 healthy premenopausal and 1,031 postmenopausal Korean women. At the femoral neck, there was a significant association between the highest hsCRP quintile and low BMD after adjustment for confounding variables in pre- (p=0.0026) and post- (p=0.0006) menopausal women, when compared with the lowest quintile. At the lumbar spine, however, this association was marginal in both groups (p=0.0602 for premenopausal; p=0.0711 for postmenopausal). In premenopausal women with the highest hsCRP quintile, the odds ratio (OR) for osteopenia/osteoporosis was 1.354 (CI=1.018-1.801) at the lumbar spine and 1.377 (CI=1.099-1.726) at the femoral neck. In postmenopausal women, the OR for osteoporosis was high at the femoral neck (OR=3.260, CI=1.546-6.873), but not at the lumbar spine (OR=1.269, CI=0.750-2.149), suggesting a difference that may be due to osteophyte or aortic calcifica-

tion with aging at the spine. These results indicate that hsCRP may be a useful marker in the risk assessment of osteoporosis. In addition, our findings suggest a role of subtle systemic inflammatory processes in the determination of bone mass.

Disclosures: ***J. Koh****, None.*

SA373

See Friday Plenary number F373

SA374

Rapid Weight Loss Related To Gastric Lap-Banding Is Associated With Loss Of Femoral Neck Bone Mass, Predicted By Baseline Truncal Fat. K. M. Sanders*[1], G. K. Kiroff*[2], G. C. Nicholson[1]. [1]Clinical and Biomedical Sciences, The University of Melbourne, Geelong, Australia, [2]St John of God Hospital, Geelong, Australia.

There is evidence that rapid or marked weight loss in the obese also results in bone loss. This study aimed to identify the sites of most significant bone loss accompanying large decreases in body weight following lap-band gastric surgery and to identify the best predictors of bone loss. Subjects (20 women, 4 men) undergoing surgery for morbid obesity had baseline and serial six-monthly DEXA scans for two years (Lunar DPX-L; total body, L2-L4, hip and forearm sites). Biochemistry was measured at baseline. The characteristics of the group were (median, range): age 44, 25-60 years; initial weight 264, 200-387 lbs; initial BMI 42, 34-56; weight loss 51, 16-113 lbs; decrease in BMI 8, 2-20. The median baseline FN T score was +1.1 (range -0.7 to +2.6). The largest bone loss occurred at the femoral neck (FN) BMC -3.0% (-0.17g, -0.89 55to +0.55g) and BMD -2.7%, equivalent to 0.25 SD change. One woman shifted from normal to osteopenic range BMD at this site. Loss of FN BMC was best predicted by baseline truncal fat (R^2 adj 23%, p=0.012). This relationship was not strengthened when males were excluded (p=0.03). Baseline total body fat, and serum SHBG in females, were less strong predictors (R^2 adj 7.2%, p=0.12, 10.4%, p=0.12 respectively). Serum estradiol, PTH, 25-OH vitamin D and C-peptide levels were not significant. Adjusting for age, gender and time between scans (median 12mths) did not change the results. Changes in weight, total body or truncal fat and lean mass were not significant predictors of FN bone loss. BMD changes at other sites were -0.3% L2-L4 and +0.5% UD forearm and +0.8% at mid forearm.

Losses of bone mass associated with lap-band surgery are sufficient to significantly increase risk of fracture, particularly hip fracture, but in this study appear to be more strongly related to baseline measures than change in body composition. Although methodological problems in the serial analysis of body composition using DEXA may influence results, initial BMI was a better predictor of the decrease in FN BMC than change in BMI (p=0.16 and p=0.56, respectively). The amount of FN bone loss accompanying significant weight loss may be partially determined by factors such as common genetic determinants of fat and bone mass and/or dietary changes.

Disclosures: ***K.M. Sanders****, None.*

SA375

See Friday Plenary number F375

SA376

The Oslo Health Study: Biochemical Markers of Bone Turnover and Their Relation to Parathyroid Hormone Levels in Persons of Pakistani and Norwegian Origin Living in Oslo. K. Holvik*[1], H. E. Meyer*[1], J. A. Falch*[2], A. J. Søgaard*[3], E. Haug*[4]. [1]Department of General Practice and Community Medicine, University of Oslo, Oslo, Norway, [2]Department of Internal Medicine, Aker University Hospital, Oslo, Norway, [3]Division of Epidemiology, Norwegian Institute of Public Health, Oslo, Norway, [4]Hormone Laboratory, Aker University Hospital, Oslo, Norway.

We have shown that the prevalence of secondary hyperparathyroidism (i.e. low serum 25-hydroxy vitamin D and elevated parathyroid hormone levels) was much higher in Pakistan-born than in Norwegian-born persons attending the Oslo Health Study. In spite of this, bone density in the Pakistanis was at least as high as that in Norwegians. We wanted to explore possible ethnic differences in bone turnover in these groups.

The aim was to study the levels of biochemical markers of bone turnover and the correlation between parathyroid hormone levels and bone marker levels in Pakistanis and Norwegians living in Oslo.

Serum levels of intact parathyroid hormone (s-iPTH), osteoblast markers osteocalcin (s-OC) and bone specific alkaline phosphatase (s-bALP), and osteoclast marker tartrate resistant acid phosphatase (s-TRAP) were measured in a subgroup of Pakistanis and Norwegians participating in the large population-based Oslo Health Study 2000-2001. We here present results for 141 Pakistani men and women aged 30-45 years, and 167 Norwegian men and women aged 45 years.

Mean age-adjusted s-OC was 1.23 nmol/l in Pakistanis and 1.45 nmol/l in Norwegians (p=0.006), a difference corresponding to nearly 1/2 SD. Norwegian women had s-OC levels 0.32 nmol/l higher than Pakistani women (p=0.010), whereas Norwegian men had s-OC levels 0.15 nmol/l higher than Pakistani men (ns). Mean age-adjusted s-bALP was 19.1 U/l in Pakistanis and 17.6 U/l in Norwegians (ns). Mean age-adjusted s-TRAP was 2.30 U/l in Pakistanis and 2.43 U/l in Norwegians (ns).

In Norwegian women there was a positive correlation between s-iPTH and s-bALP (r=0.30, p=0.004), and between s-iPTH and s-OC (r=0.25, p=0.017). In Pakistani women there was a positive correlation between s-iPTH and s-bALP (r=0.29, p=0.020), and a tendency to a positive correlation between s-iPTH and s-OC (r=0.23, p=0.065). S-iPTH was not correlated to s-TRAP in any of the groups. There were no correlations between s-iPTH and bone marker levels in men.

In conclusion, there were no striking ethnic differences in levels of bone turnover markers, although the levels tended to be higher in Norwegians. Although bone marker levels were correlated to parathyroid hormone levels also in Pakistani women, the widespread secondary hyperparathyroidism in Pakistanis does not seem to influence bone turnover adversely at this age.

Disclosures: ***K. Holvik****, None.*

SA377

See Friday Plenary number F377

SA378

Osteoporosis Risk Factor Assessment: Comparison of Interviewer-assisted, Patient Self-report and Physician-supplied Data Sources. C. K. Yuen[1], W. D. Leslie[2], C. Metge*[3], B. Kvern*[4], L. Manness*[5]. [1]Obstetrics and Gynecology, Manitoba Clinic, Winnipeg, MB, Canada, [2]Internal Medicine, Nuclear Medicine, University of Manitoba, Winnipeg, MB, Canada, [3]Faculty of Pharmacy, University of Manitoba, Winnipeg, MB, Canada, [4]Family Medicine, University of Manitoba, Winnipeg, MB, Canada, [5]Merck Frosst Canada, Montreal, PQ, Canada.

Clinical risk factor (CRF) and medical risk factor (MRF) assessment has been shown to predict low BMD and fracture when derived from an interviewer-assisted (IA) survey. Our objective was to determine if survey instrument could be adapted to give valid results from patient self-report (SR). We evaluated twelve CRFs (JCD 5(2):117-130, 2002: overall health, physical activity, mobility, current smoking, current weight, height at age 25, height loss, any fracture after age 50, osteoporotic fx in parents/siblings, fall in previous 12 months, previous hyperthyroidism, age) and four MRFs (abnormal menstrual cycling, premature menopause, surgical menopause, steroid use > 3 months). A convenience sample of 63 menopausal women referred for BMD testing was mailed a SR assessment tool three weeks prior to BMD testing. The same tool was completed using IA on the day of BMD testing. Physician supplied (PS) CRF information was extracted from the BMD test requisition which assesses the same items (PS MRF information not available). Agreement between individual items (kappa) and total scores (corr coeff) was determined. Mean total CRF and total MRF were similar for SR and IA (P>0.2) while PS gave a significantly greater total CRF than SA (P=.002) or IA (P=.001). There was excellent agreement between SA and IA for both total CRF (R=0.90, P<.001) and total MRF (R=0.89, P<.001), and also for the individual items (all P<.001). In contrast, only a modest correlation was found between total CRF scores for PS and IA (R=0.39, P=.002) and the individual items. We conclude that interviewer-assisted and patient self-report can provide equivalent CRF and MRF information. Routine physician-supplied CRF information shows a weak agreement and is unlikely to be useful for research purposes.

	SA versus IA	PS versus IA
Total CRF (mean ± SD)	2.8 ± 0.2 versus 2.7 ± 0.2	3.1 ± 0.2 versus 2.7 ± 0.2
Total CRF Correlation (R)	0.90	0.39
Individual CRFs (mean kappa)	0.79 (range 0.49-0.97)	0.37 (range 0.22-0.68)
Total MRF (mean ± SD)	1.0 ± 0.1 versus 1.0 ± 0.1	--
Total MRF Correlation (R)	0.89	--
Individual MRFs (mean kappa)	0.78 (range 0.47-0.96)	--

Disclosures: ***C.K. Yuen****, Merck Frosst Canada 2.*

SA379

Differences in Hip Bone Mineral Density and Strength between Glucocorticoid-treated and Glucocorticoid-naïve Postmenopausal Women. K. Lian*[1], T. F. Lang[1], J. H. Keyak[2], G. W. Modin*[1], Q. Rehman*[1], N. E. Lane[1]. [1]University of California, San Francisco, San Francisco, CA, USA, [2]University of California Irvine Medical Center, Orange, CA, USA.

Chronic treatment with glucocorticoids (GC) leads to significant bone loss, osteoporosis, and often results in bone fractures. In GC treated subjects, bone mineral density (BMD) has typically been evaluated by dual-energy X-ray absorptiometry (DXA) to assess fracture risk. However, since GC induce significant trabecular bone loss, DXA may underestimate fracture risk. The purpose of this investigation was to determine if there are differences in trabecular BMD, cortical BMD, volume, and bone strength of the hip between GC treated osteoporotic patients and controls.

Study subjects were GC treated osteoporotic postmenopausal women (PMO) and controls were PMO recruited for separate clinical trials. QCT and DXA of the hip were obtained in all subjects. QCT outcome variables measured included total, cortical, and trabecular BMD of hip subregions (femoral neck, trochanter) and total hip. In addition, finite element modeling (FEM) was performed on a subset of 19 cases and 38 controls, matched on age (± 5yrs), weight (± 5kg), and history of hormone replacement (>1yr use) to assess failure load in stance and fall loading conditions.

Compared with controls subjects, GC treated subjects were significantly ($p<0.05$) younger, weighed less, and had more years of hormone replacement. QCT of the hip in GC treated subjects for total femoral integral, cortical, and trabecular BMD averaged 4.9-23.2% ($p<0.002$) less than controls, and similar results were seen by hip subregion including the trochanter and femoral neck. DXA of the total hip was 17% lower in GC subjects than controls ($p<0.05$).

Compared with controls, FEM failure load in GC subjects was 15% and 16% lower for the stance and fall loading conditions, respectively. Multiple regression analysis demonstrated that a combination of QCT measures was correlated with bone strength as measured by FEM.

Chronic GC treatment in PMO resulted in significantly decreased BMD of the hip, measured by QCT, with loss of both trabecular and cortical bone. In addition, GC treatment also decreased bone strength as determined by FEM. The reduced cortical and trabecular bone mass in the hip may contribute to the disproportionately high hip fracture rates observed in GC treated subjects.

FEM results for stance and fall loading conditions

Failure Load (kN)	Cases (n = 19)	Controls (n = 38)	*p* value
Stance	6.264 (0.942)	7.334 (1.057)	0.004
Fall	1.186 (0.338)	1.410 (0.339)	0.073

Mean ± SD, *p* values unadjusted

Disclosures: ***K. Lian****, None.*

SA380

See Friday Plenary number F380

SA381

The Fat Endocrine Axis And Bone Metabolism In Obese Premenopausal Women. L. Dib*[1], R. Abou Samra*[2], N. Hwalla*[2], N. Torbay*[2], G. El-Hajj Fuleihan[1]. [1]Internal Medicine, American University of Beirut, Beirut, Lebanon, [2]Nutrition and Food Sciences, American University of Beirut, Beirut, Lebanon.

Obesity's protective effect on bone density may be mediated through increased muscle mass, fat mass, increased estrogen, and possibly insulin, and leptin levels. Furthermore, in vitro data suggests a direct role for leptin and the PPARϒ pathway in osteogenesis. The associations between circulating leptin levels and BMD are however debatable and confounded by body composition, insulin levels, and possibly insulin resistance.

48 obese normally cycling premenopausal women were studied: 28 were considered insulin resistant and 20 normoinsulinemic by McAuley index; ISI= exp[2.63-0.28ln(insulin in mU/l)-0.31 ln(triglycerides in mmol/l)], insulin resistance defined as an ISI< 5.8 [1]. Anthropometric, body composition, BMD measurements, serum leptin, insulin, free testosterone, IGF1, bone remodeling markers and calciotropic hormones were obtained.

Subjects were 31± 10 years (mean ± SD), and had a BMI of 35.7± 5 kg/m^2. The baseline characteristics, including age, calcium intake, number of menstrual cycles, BMI, lean mass, fat mass, were comparable between the two study groups. Both groups had comparable serum levels of IGF1, free testosterone, calciotropic hormones, osteocalcin, bony alkaline phosphatase and crosslaps. Hyperinsulinemic subjects had significantly wider waist circumference [101 (10) cm], and higher insulin and leptin levels 31(9) U/L and 69 (26) ng/ml than normoinsulinemic subjects, 95(5) cm, 18.6(3.5) U/L, and 2(26) ng/ml respectively. Despite higher circulating insulin and leptin levels, hyperinsulinemics had mean values of biochemical markers of bone remodeling and BMD at all skeletal sites that were comparable to the normoinsulinemic group. In the hyperinsulinemic group, fat mass but not lean mass, serum leptin, insulin, testosterone, and IGF1 levels correlated positively with hip, and/or total body BMD/BMC, R=0.2-0.61, P< 0.05, depending on the hormone and skeletal site. Conversely, in the normoinsulinemic group, lean mass but not fat mass, and only IGF1 correlated with hip BMD/total body BMC, R= 0.49-0.69, p< 0.05.

In conclusion, there is a dichotomy in the impact of body composition parameters, insulin and leptin levels on bone parameters in obese individuals. The interaction between the fat related endocrine system and bone seems to be complex and may be modulated by local resistance to the putative protective effect of insulin and leptin on bone.

1. Ascaso J., Pardo S., Real J., Lorente R., Priego A., Carmena R. Diagnosing Insulin Resistance by Simple Quantitative Methods in Subjects with Normal Glucose Metabolism. Diabetes Care 2003; 26:3320-3325.

Disclosures: ***G. El-Hajj Fuleihan****, None.*

SA382

Similar Trunk Length but Shorter Leg Length in Chinese than Caucasians: Implication for Racial Differences in Hip Fracture Rates. X. Wang*, Y. Duan, E. Seeman. Endocrinology and Medicine, the University of Melbourne, Heidelberg, VIC 3084, Australia.

The basis for the lower hip fracture rate in Chinese than Caucasians is unknown. We asked: (i) are there racial differences in trunk length or leg length? (ii) Do Chinese have shorter femoral neck axis length (FNAL) after adjustment for femur length? We measured standing and sitting height, leg length, femur length and FNAL in 239 healthy Chinese (162 females) and 542 Caucasians (403 females) aged 18-45 years living in Melbourne, Australia. In both women and men, Chinese had a 5.8-6.3cm (~3.5%) shorter stature than Caucasians due to their shorter leg length (~85%) not sitting height. There was a lower ratio of leg length/standing height in Chinese than Caucasians in both sexes. In a subgroup of Chinese and Caucasians matched by standing height, Chinese had shorter leg length but greater sitting height than Caucasians. FNAL was shorter in Chinese than Caucasians before (~7.4%) and after (~3.8%) adjusted for their shorter femur length in both sexes. In a subgroup of Chinese and Caucasians matched by femur length, Chinese had 3.5% shorter FNAL than Caucasians in both sexes. Racial differences in standing height is predominantly on the leg, not trunk, length. Chinese have a shorter FNAL relative to their femur length. We infer that the lower body segment length and shorter FNAL in Chinese may contribute to the lower hip fracture rates in Chinese than Caucasians.

Disclosures: ***Y. Duan****, None.*

SA383

See Friday Plenary number F383

SA384

Bone Tissue Quality Is Differently Altered by PTH and Bisphosphonates. P. Ammann[1], S. Barrauld*[1], P. Zysset[2], R. Rizzoli[1]. [1]Department of Rehabilitation and Geriatrics, Division of Bone Diseases, Geneva, Switzerland, [2]Swiss Federal Institute of Technology, Laboratory of Bone Biomechanics, Lausanne, Switzerland.

Treatment with inhibitors of bone resorption or stimulators of bone formation reduces fracture risk. Bone strength, hence the resistance to fracture, depends on bone mineral density, bone geometry, micro-architecture, bone turnover rate and intrinsic bone tissue quality. Despite comparable antifracture efficacy, bone resorption inhibitors and bone formation stimulators are likely to modify quite differently these various determinants of bone strength. To address this issue, we treated 8-month old osteoporotic ovariectomized (OVX) rats with either pamidronate (APD, 0.6 mg/kg 5 days/month s.c.), PTH(1-34) (10microg/day s.c.) or the vehicle for 16 weeks, and measured proximal tibia areal BMD (g/cm2), ultimate strength (N), stifness (N/mm) and energy (N*mm) with an axial compression test, micro-architecture by microCT, and bone intrinsic quality by nanoindentation. This latter test allows the calculation of the elastic modulus and tissue hardness (mPa). The markers of bone turnover deoxypyridinoline (Dpd) and osteocalcine were also determined. Values are tabulated as means± SEM, * P<0.05 vs OVX, ° P<0.05 vs OVX/APD.

	SHAM	OVX	OVX/APD	OVX/PTH
Ultimate Stength	303.5±27.3*	215.8±11.3	321.1±18.1*	404.9±25.0 *°
Stiffness	662.6±54.5	563.8±29.6	825.2±43.9*	720.8±53.5*
Energy	108.7±21.8	68.1±12.9	78.3±8.8	170.6±19.0*°
BMD	187.1±4.2*	153.5±3.8	177.3±3.3*	201.4±2.8 *°
Hardness	975±22*	878±15	921±20	872±18
Dpd	29.1±4.3	34.4±2.9	16.2±1.26*	46.2±3.2 *°
Osteocalcine	11.1±0.7	14.9±1.3	8.2±0.5*	23.4±1.2*°

The higher bone strength induced by PTH as compared with APD was associated with a greater absorbed energy, BMD, and bone turnover markers. Furthermore, PTH, but not APD markedly increased trabecular bone volume and connectivity. Tissue hardness was identical in PTH-treated and OVX untreated controls. In contrast, the correction of bone strength by APD was accompanied by reduced bone turnover, and increased hardness. Elastic modulus was similar in all groups. These results illuminate the different mechanisms by which inhibitors of bone resorption and stimulators of bone formation reduce fracture risk. PTH influences micro-architecture and bisphosphonate intrinsic bone tissue quality, with probable opposite effects on remodeling space.

Disclosures: ***P. Ammann****, None.*

SA385

The Relationship Between Bone Morphology and Bone Quality: Implications for Stress Fracture Risk in Young Adult Male Tibiae. S. M. Tommasini[1], P. Nasser*[2], K. J. Jepsen[2]. [1]CUNY Graduate School, New York, NY, USA, [2]Mt Sinai School of Medicine, New York, NY, USA.

Stress fractures occur among persons with normal bones, no acute injury, and are most common among elite runners and military recruits [1]. Having a narrow or slender tibia has been shown to be a major predictor of stress fracture risk and fragility [2]. Previous studies revealed that inbred mice with slender bones had increased mineral content. Although increased mineral content may have compensated for the smaller morphology by increasing tissue stiffness and strength, the increased mineral had the adverse effect of increased bone brittleness and tissue damageability under fatigue loading [3]. It is unknown whether a similar reciprocal relationship between bone geometry and bone tissue level mechanical

properties also exists in the human skeleton. We assessed the biomechanical properties of tibiae from young adult males in order to determine whether whole bone geometry is a predictor of tissue fragility. Tibiae from 17 male donors (age 17-46 yrs) were measured for bone geometry [length, cortical area (CtAr), AP and ML width, moments of inertia (I_{AP}, I_{ML}, J)]. A slenderness index was defined as the inverse ratio of the section modulus to tibia length and body weight [4]: S=1/[(J/width)/(L*BW)]. The diaphyses were cut into rectangular beams and tested for monotonic properties in 4-point bending [modulus (E), strength, post-yield strain (PYε), work] and tissue damageability (*D*) in 4-point bending using the methods of Jepsen and Davy [5]. Partial correlation coefficients were determined between each geometrical parameter (CtAr, width, I_{AP}, I_{ML}, J, S) and each tissue level mechanical property (E, strength, PYε, work, *D*) while taking age into consideration.
Significant correlations ($p < 0.05$) were observed between AP width and two mechanical properties related to tissue brittleness (PYε, work) indicating that the tissue of individuals with narrow tibiae was less ductile. Further, there was a significant correlation between tissue damageability and tibia slenderness ($p = 0.05$) consistent with the mouse model suggesting that slender bones may have more damageable tissue. This data indicated that not all bone is made the same way. Having a more slender tibia was associated with tissue that was less ductile and more susceptible to damage accumulation. Thus, under extreme loading conditions (e.g., military training), variation in bone quality may be a contributing factor for increased stress fracture risk in individuals with a more slender bone. [1] Milgrom et al, 1989 J Biomech 22 [2] Beck et al, 2000 Bone 27 [3] Jepsen et al, 2001 JBMR 16 [4] Selker and Carter, 1989 J Biomech 22 [5] Jepsen and Davy, 1997 J Biomech 30.

Disclosures: ***S.M. Tommasini****, None.*

SA386

High Resolution Spiral-CT for the Assessment of Osteoporosis: Which Site of the Spine and Region of the Vertebra Is Best Suited to Obtain Trabecular Bone Structural Parameters? J. S. Bauer*[1], D. Mueller*[2], M. Fischbeck*[3], F. Eckstein*[4], E. J. Rummeny*[2], T. M. Link[1]. [1]Radiology, University of California, San Francisco, CA, USA, [2]Radiology, Technical University, Munich, Germany, [3]Anatomy, Ludwig-Maximilian-Universität, Munich, Germany, [4]Anatomy, Paracelsus Private Medical University, Salzburg, Austria.

Objectives: In osteoporosis, bone demineralization is heterogeneous: There may be major differences between different skeletal sites, as well as between different regions within one bone. The purpose of this experimental study was to investigate which site of the spine and region of the vertebral body is best suited for analysis of trabecular bone structure in the assessment of osteoporosis resp. biomechanical strength.
Material and Methods: 133 vertebrae (63 thoracic vertebrae, 70 lumbar vertebrae, all with adjacent intervertebral discs and vertebrae as motion segments) were harvested from 73 human spines. All specimens were examined with Spiral-CT using a slice thickness of 1 mm and an in plane spatial resolution of 0.4 mm. Quantitative structure parameters, analogous to bone histomorphometry, were determined in those specimens for a superior (below the endplate), mid-vertebral and inferior (superior to the endplate) region of interest (ROI). Additionally BMD was measured using quantitative CT (QCT) with a standard protocol. In all specimens maximum compressive strength (MCS) was determined using axial loading.
Results: The standard BMD measurement correlated significantly with the MCS ($r^2 = 0.55$, $p < 0.01$). For the structural parameters the highest correlation with the MCS was obtained using the structure parameter app. (apparent) BV/TV (bone volume/ total volume) in the inferior region of the lumbar vertebrae ($r^2 = 0.72$, $p < 0.01$). It could be improved using a multi regression model with app. BV/TV, app. trabecular separation and cortical BMD (r^2=0.77, $p < 0.01$). This correlation was significantly higher than the correlation between MCS and BMD ($p < 0.05$).
Conclusion: Compared to clinical BMD measurements the prediction of MCS was significantly improved using a structure parameter measured in the inferior region of excised vertebral bodies. This indicates that histomorphologic parameters measured at skeletal sites with higher bone turn-over, such as the part near the endplate of the vertebral body, may improve the assessment of biomechanical strength of bone.

Disclosures: ***J.S. Bauer****, None.*

SA387

Idiopathic Inflammatory Bowe Disease and Decreased Bone Mineral Density in Children and Adolescents. S. Kutilek[1], J. Sykora*[2], V. Vyskocil[1]. [1]Bone disease center, Charles University Hospital, Plzen, Czech Republic, [2]Department of Pediatric, Charles University Hospital, Plzen, Czech Republic.

Idiopathic inflammatory bowel diseases (IBD) are characterised by weight loss, abdominal pain and diarrhea, often mixed with blood. Skeletal changes, in particular osteopenia, osteoporosis or osteomalacia, have been observed in almost 70% of adult patients with IBD. We evaluated 13 patients (9 girls and 4 boys) with IBD, aged 5-22 years (mean age 13.6 ± 4.5 SD). Calcium and vitamin D intake was maintained as adequate according to the recommended daily allowance. The mean values of body height and weight (expressed as Z-scores) didn´t differ from age- and sex-related reference values ($p = 0.8$ and 0.7, respectively), however the body mass index (BMI) was decreased ($p< 0.02$). The spinal (L1-L4) bone mineral density (BMD, g/cm^2; expressed as Z-score) was low in comparison to reference values ($p< 0.02$). When calculated as volumometric BMD (BMDvol, g/cm^3), and expressed as Z-scores, we observed even higher difference in comparison to age- and sex related reference values ($p< 0.0001$). We found high and significant correlation between BMD and body height ($r = 0.67$, $p< 0.01$). There was no significant relationship between BMD and body weight or BMI. The estimation of areal BMD is influenced by bone size and can be underestimated in smaller individuals. However, our results of low BMDvol further confirm the low bone mass in patients with IBD, as volumometric bone density gives more reliable information than areal data. Low bone mass and consequent risk of developing osteoporosis must be taken into consideration in pediatric patients with IBD.

Disclosures: ***S. Kutilek****, None.*

SA388

See Friday Plenary number F388

SA389

Nutritional Assessment in a Sample of Brazilian Post-Menopausal Osteoporotic Women. T. M. Aniteli*[1], C. M. Z. Carnevalli*[1], R. M. Pereira[2], M. M. Madureira*[3], L. A. Martini[1]. [1]Nutrition, Sao Paulo University, Sao Paulo, Brazil, [2]Medicine, Sao Paulo University, Sao Paulo, Brazil, [3]Rheumatology, Sao Paulo University, Sao Paulo, Brazil.

Diet is one of the main approach therapeutic in the Osteoporosis. The relationship of calcium deficiency and osteoporosis is the most studied one and it is well known that women affected by this illness need an adequate diet in calcium for preservation and maintenance of bone mass. The objective of the present study was to evaluate the dietary intake of calcium, phosphorus, energy and percentile distribution of protein, carbohydrates and lipids using the 24 hour diet recall and body composition by DEXA of osteoporotic women. Twenty-nine women, mean age 75 ± 5 years old (X ± SD), body mass index 24 ± 6.3 kg/m^2 were evaluated. The mean fat mass percentage measured by DEXA was 38 ± 8%. The mean calcium intake was of 875 ± 374 mg/day. From these, 83% of patients had an intake lesser than the proposed intake (AI) of 1200mg/d. However, it is a value of intake bigger that the average for the Brazilian population (633 ± 320 mg/d). The mean phosphorus intake was 993 ± 307 mg/d and 21% of them had lower intakes than the RDA recommendation (700 mg/d). None of the patients reached the upper limit levels (UL) for both nutrients. The percentile distribution of carbohydrates, protein and lipids was of 53.2 ± 8.6 %, 18.5 ± 4.8 % and 28.1 ± 8.2 %, respectively. All the women were in according to the recommended standards of protein intake (10-35%), 80% adequate for carbohydrate (45-60%), and 21% presented higher values of fat intake (20-35%). Multiple linear regression analysis showed that calcium intake and percentage of fat mass are responsible for 36% of the BMD in lumbar spine L1-L4 [L1-L4 = 6.104 + 0.001 (calcium intake) + 0.065 (% FM) R^2=0.358]. This study demonstrate the importance of an adequate calcium intake in bone mass of postmenopausal women, exerting an important role in calcium retention and therefore prevention loss of bone mass and fractures.

Disclosures: ***T.M. Aniteli****, None.*

SA390

See Friday Plenary number F390

SA391

Effect of Pinealectomy on Bone Remodeling in Sheep. M. Egermann*[1], C. Gerhardt*[1], A. Barth*[2], E. Schneider[1], M. Alini*[1]. [1]AO Research Institute, Davos, Switzerland, [2]Neurosurgery, University of Berne, Berne, Switzerland.

Osteoporosis and associated fractures are a major public health burden. Osteoporosis is a multifactorial disease and the causes are yet not fully understood. New literature data have shown, that melatonin, the hormone of the pineal gland, seems to influence the bone metabolism. This study aims to evaluate whether absence of melatonin due to pinealectomy (Px) affects the bone microarchitecture and remodeling comparable to the absence of sex hormones subsequent to ovariectomy (Ovx) using an ovine animal model.
Following approval of the appropiate ethical committee, 26 female sheep (3.1±0.5 yrs) were arranged into four groups: Control (C) (n=8), Ovx (n=6), Px (n=6), Ovx+Px (n=6) and surgically pinealectomized or ovariectomized respectively. Pinealectomy was confirmed by absence of nocturnal melatonin secretion. Before and 6 months after surgery, bicortical iliac crest biopsies (∅8.4mm) were harvested and structural parameters (BV/TV, Tb.Sp, Tb.Th, Tb.N) were determined using µCT. Deoxypyridinoline (DPD) was determined from urine samples three times before surgery as baseline level and at 6 month. All parameters are expressed relative to baseline. Statistical analysis tested for difference to control group (*= $p<0.05$).
The complete removal of the pineal gland and the ovaries was tolerated well by all animals without drop out or notable side effects. The changes of the structural parameter in cancellous bone after 6 months are shown in the table. Compared to baseline, increased levels of DPD were found in all treated groups, with significant differences for the combined Ovx+Px group only (C: +1±63%, Ovx: +8±55%, Px: +10±36%, Ovx+Px: +69±47%*).

Group	BV/TV	Tb.Sp	Tb.Th	Tb.N
C	7 ±14%	-11 ±12%	26 ±18%	7 ±13%
Ovx	-4 ±22%*	3 ±21%	-6 ±13%	1 ±14%
Px	-13 ±9%*	12 ±8%*	-6 ±7%*	-8 ±6%*
Ovx+Px	-18±14%*	21±22% *	-7 ±9% *	-11±17%*

The changes of structural parameters in the treatment groups are indicative of bone loss, although these data could have been influenced by several factors like site of biopsy, short term follow up or seasonal variation, particularly in penealectomized sheep. However, a similar trend is observed for the biochemical resorption marker, DPD. This also suggests that in the treated groups there is an increased bone resorption activity. Overall, these preliminary findings suggest that the pineal gland may influence bone metabolism, although, large number of animals and long term follow up are needed to draw final conclusions.

Disclosures: ***M. Egermann****, AO Foundation 3.*

SA392

Is the Effect of Raloxifene and Estrogen on Bone Mediated by a Differential Expression of Estrogen Receptors? M. Naves*, A. Rodríguez-Rodríguez*, C. Gómez, A. González-Carcedo*, N. Carrillo-López*, J. B. Cannata-Andía. Bone and Mineral Research Unit, Hospital Universitario Central de Asturias, Oviedo, Spain.

The protective effect of estrogen and raloxifene on bone metabolism is well established. However, the cellular and molecular mechanisms of their actions are still not fully understood.

The aim of this study was to measure changes in bone histomorphometric parameters and the expression of estrogen receptors on proximal tibial segment in rats with mild kidney insufficiency and ovariectomy treated with raloxifene and estrogen, alone or combined with calcitriol.

Six-month old female Sprague-Dawley rats (n=48) were ovariectomized and nephrectomized (7/8). One week after surgery, the rats were divided into 6 groups and treated with: 1) Placebo, 2) 17-β-estradiol 10 µg/kg/day, 3) raloxifene 1 mg/kg/day 4) calcitriol 10 ng/Kg/day, 5) 17-β-estradiol plus calcitriol and 6) raloxifene plus calcitriol. A group of non-treated animals with normal ovarian and kidney function was used as the control group (n=8). The rats were sacrificed after 8 weeks of treatment.

Total RNA was extracted from bones and mRNA levels of alpha (ERα) and beta (ERβ) estrogen receptors were measured by quantitative RT-PCR. The relative amount of ERα and ERβ mRNA adjusted for 18s rRNA was calculated.

Bone loss, measured by densitometry and histomorphometry, was partially prevented in the groups treated with 17-β-estradiol, raloxifene and calcitriol (table). However, the best response was observed in the groups treated with raloxifene plus calcitriol and 17-β-estradiol plus calcitriol, achieving a similar bone mineral density and trabecular bone volume to the control group (0.40±0.03 g/cm^2 and 32.5±8.6 % respectively).

Compared with the placebo group, the ERα expression decreased significantly in those rats treated with raloxifene alone or combined with calcitriol and in the rats treated with 17-β-estradiol plus calcitriol. Although the treatments either 17-β-estradiol or calcitriol also decreased the ERα expression, the changes were not significant. No statistical differences in ERβ expression were found in either group (table).

* p<0.05 compared with placebo

Groups	Proximal tibia BMD (g/cm2)	Trabecular bone volume (%)	Relative quantity of ER a mRNA	Relative quantity of ER b mRNA
Placebo (n=7)	0.33±0.01	16.9±3.5	21.0±6.6	14.0±7.1
17-b-estradiol (n=8)	0.35±0.01*	28.8±6.4*	14.3±3.4	6.9±4.1
Raloxifene (n=9)	0.35±0.03*	29.8±12.2*	5.7±2.2*	18.8±27.9
Calcitriol (n=8)	0.36±0.02*	26.7±4.6*	14.9±4.5	7.9±4.8
17-b-estradiol+Calcitriol (n=8)	0.40±0.05*	32.8±10.7*	11.8±2.2*	6.5±3.7
Raloxifene+Calcitriol (n=8)	0.42±0.02*	46.8±12.7*	12.5±3.2*	11.9±9.7

In conclusion, the best response to treatment was always accompanied by a significant decrease in the ERα expression, suggesting a down-regulation of the estrogen receptor. By contrast, there was no relationship with the ERβ expression.

Disclosures: ***M. Naves****, None.*

SA393

Estrogen Deficiency Causes Bone Loss through Induction of TNF-alpha by Hydrogen Peroxide. C. J. Jagger*, J. M. Lean*, J. T. Davies*, T. J. Chambers. Cellular Pathology, St George's Hospital Medical School, London, United Kingdom.

We recently found that antioxidant defenses fall substantially in rodent bone marrow after ovariectomy, and are rapidly normalised by exogenous estradiol. Moreover, administration of N-acetyl cysteine or ascorbate, antioxidants that increase tissue antioxidant levels, abolish ovariectomy-induced bone loss, while buthionine-(S,R)-sulfoximine (BSO), a specific inhibitor of the synthesis of glutathione, the major intracellular antioxidant, cause substantial bone loss. These results suggest that estrogen deficiency causes bone loss by lowering antioxidant defenses in bone marrow.

How does lowering of antioxidant defenses cause bone loss? All cells generate reactive oxygen species (ROS), and osteoclasts in particular produce them in large amounts. If thiol antioxidant defenses are lowered, this will increase the half-life of ROS. Amongst ROS, hydrogen peroxide is sufficiently stable and membrane-permeant to transmit both intra- and inter-cellular ROS signals. Hydrogen peroxide also increases expression of TNF-alpha in many cell types, including osteoclasts. Blockade of TNF-alpha signaling has been reported to prevent estrogen-deficiency bone loss in mice.

We therefore tested the role of hydrogen peroxide in estrogen-deficiency bone loss. We found that catalase, which destroys hydrogen peroxide, prevented osteopenia in ovariectomised mice. This shows that hydrogen peroxide is essential for bone loss in response to estrogen deficiency, and is consistent with the notion that the lowering of antioxidant defenses observed after ovariectomy cause bone loss through an increase in hydrogen peroxide. We also found that the bone loss caused by both BSO and ovariectomy was reduced by administration of TNF-alpha, and abrogated in mice deleted for TNF-alpha gene expression. Furthermore, in mice treated with soluble receptors, antioxidant defenses remained low, despite inhibition of bone loss.

These experiments are consistent with a model for bone loss in which estrogen deficiency lowers antioxidant defenses in bone marrow and thereby increases hydrogen peroxide levels, which in turn induces expression of TNF-alpha, which causes bone loss.

Disclosures: ***C.J. Jagger****, None.*

SA394

See Friday Plenary number F394

SA395

Oral Contraceptive Users Have Lower Bone Density than Nonusers. H. C. Almstedt*, C. M. Snow. Exercise and Sport Science, Oregon State University, Corvallis, OR, USA.

Osteoporosis is a skeletal disease affecting 44 million Americans. A primary strategy to prevent osteoporosis is to develop a high peak bone mass in youth. Oral Contraceptives (OCs) alter hormones in women and could affect bone mass development. Forty percent of American women between the ages of 18 and 24 use OCs. However, the interaction between OCs and skeletal mineralization is poorly understood. Our aims were to 1) compare bone mass (BMD) of young women who have a history of OC use with eumenorrheic controls and 2) evaluate whether years on oral contraceptives predict BMD among those with a history of use. We recruited 98 women who were 18 to 25 years of age and had a history of OC use (n=44, 3.4 + 1.9 years of OC use) and controls (n=54). BMD at the hip, whole-body, and spine (AP, g/cm^2 and width-adjusted lateral, g/cm^3) was measured by dual-energy x-ray absorptiometry (DXA). Physical activity (METs) was measured via questionnaire and grip strength was evaluated using an isometric dynamometer. Groups were similar in body mass index (BMI), fat mass, grip strength, and physical activity but controls were older than OC users (21.3 ± 1.9 vs. 20.3 [[Unsupported Character - Codename]]± 1.6, $p < .05$). In analysis of covariance, controlling for age and BMI, controls had significantly greater BMD than OC users at the AP and lateral spine, femoral neck, greater trochanter, total hip, and whole-body ($p < .05$). We conducted stepwise regression of the OC users that included the following independent variables: 1) years on oral contraceptives, 2) BMI, 3) calcium intake, 4) grip strength, and 5) physical activity. Results indicated that history of oral contraceptive use was a negative independent predictor only at the femoral neck BMD. Specifically, physical activity (β=.47), BMI (β=.34), and years of OC use (β= -.28) predicted 32% of the variance in femoral neck BMD. At the trochanter, BMI (β=.31) and physical activity (β=.30) predicted 15% of the variance in BMD, while, at the total hip, physical activity (β=.40) and BMI (β=.37) accounted for 26% of the variance in BMD. Twenty-eight percent of the variance in total body BMC was predicted by BMI (β=.42) and grip strength (β=.34). At the spine, BMI was the only independent predictor of BMD and accounted for 9-30% of the variance in volumetric, lateral and AP areal BMD. We conclude that, in this cross-sectional analysis, oral contraceptive use by young women may compromise bone health during a time when mineral is still accruing. Further longitudinal analysis will corroborate these findings.

Disclosures: ***H.C. Almstedt****, None.*

SA396

See Friday Plenary number F396

SA397

Additive Stimulatory Effects of Estrogen and Androgen Receptor Activation on Trabecular Bone in Ovariectomized Rats. S. Moverare[1], Å. Tivesten*[2], A. Chagin*[3], K. Venken[4], P. Salmon*[5], D. Vanderschueren[4], L. Sävendahl*[3], A. Holmäng*[2], C. Ohlsson[1]. [1]Internal Medicine, Center for Bone Research at the Sahlgrenska Academy, Gothenburg, Sweden, [2]Cardiovascular Institute at the Sahlgrenska Academy, Wallenberg Laboratory for Cardiovascular Research, Gothenburg, Sweden, [3]Karolinska Institute, Pediatric Endocrinology Unit, Stockholm, Sweden, [4]Katholieke Universiteit Leuven, Laboratory for Experimental Medicine and Endocrinology, Leuven, Belgium, [5]Skyscan N. V., Aartselaar, Belgium.

Sex steroids are important regulators of trabecular bone mass. Both estrogen receptor (ER) and androgen receptor (AR) activation results in increased trabecular bone mass. The aim of the present study was to investigate if combined ER and AR activation might be beneficial in the treatment of trabecular bone loss. Twelve-week-old female rats were ovariectomized (ovx) and treated with vehicle (V), 17β-estradiol (E2; ER activation), dihydrotestosterone (DHT; AR activation) or the combination (E2+DHT) for six weeks. The skeletal phenotype was analyzed by peripheral quantitative computerized tomography (pQCT), micro-computerized tomography (micro-CT), histomorphometry of growth plates and serum levels of biochemical bone markers. Both E2 (+121% over V) and DHT (+34%) increased the trabecular volumetric bone mineral density (tvBMD) in ovx rats. The effect of E2 and DHT was additive, resulting in a 182% increase in tvBMD of the rats given E2+DHT. Micro-CT analyses of the trabecular bone microstructure revealed that the effect of E2 and DHT was additive onboth the number and the thickness of trabeculae. E2 treatment reduced serum markers of both bone resorption (collagen C-terminal telopeptide) and bone formation (osteocalcin), indicating a reduced bone turnover. Addition of DHT to E2 treatment did not modulate the effects of E2 on the marker of bone resorption while it attenuated the inhibitory effect of E2 on the bone formation marker, which might explain the additive stimulatory effect of E2 and DHT on trabecular bone mass. In contrast, DHT partially counteracted the suppressive effect of E2 on longitudinal bone growth and the E2-induced alterations in growth plate morphology. These findings demonstrate that a combined ER and AR activation results in additive stimulatory effects on trabecular bone in ovx rats. Our data suggest that a combined treatment with selective ER and AR modulators might be beneficial in the treatment of osteoporosis.

Disclosures: ***S. Moverare****, None.*

SA398

The Effect of Ovariectomy on Aromatase Bone Expression in Rat. C. Potrel-Burgot*[1], H. Mittre*[2], J. Sabatier*[3], R. Levasseur[1], M. Kottler*[2], C. Marcelli[1]. [1]Medicine/Rheumatology, University of Caen, Caen, France, [2]Ea 2608 usc inra, University of Caen, Caen, France, [3]Nuclear Medicine, University of Caen, Caen, France.

The origin of the decrease in bone loss observed in woman a few years after the menopause remains unknown at yet. Aromatase is the enzyme responsible for the peripheral conversion of androgens into estrogens. The aim of this study was to analyse the aromatase bone expression in rats after ovariectomy with or without estrogen replacement therapy.

45 female wistar rats 12-week-old were randomized into 3 groups : bilateral ovariectomy plus subcutaneous injection of 20 µg/kg estradiol three times per week (OVX+E2), ovariectomy plus vehicle injection (OVX+VH) and the sham-operated control group (SHAM). BMD was measured on day 0 and day 30 at both distal femurs in all rats using dual X-ray absorptiometry. Transcripts for aromatase were measured in the right distal femur of all animals using competitive and quantitative RT-PCR. Immunohistochemistry was also performed at the left femur in order to localize aromatase in bone. Vaginal smears were performed daily in SHAM during the 10 days before the end of the study. Bones were also sampled from five 8-week-old male rats.

At day 30, a 9 % decrease in BMD was observed in OVX+VH (p=0.0012), a 10 % increase in SHAM (p=0.0010) and a non significant 2 % increase in OVX+E2. At day 30, the aromatase mRNA level (mean ± SE) was significantly lower in OVX+VH (0.11 ± 0.07 fg) than in OVX+E2 (0.49 ± 0.26 fg, p=0.0004) and SHAM (0.29 ± 0.24 fg, p=0.014). In SHAM, the mRNA level was low on the day of proestrus (0.16 ± 0.03 fg, n=3), an increase was observed on the day of estrus (0.29 ± 0.04 fg, n=5) and the highest mRNA level was measured on the day of diestrus (0.42 ± 0.25 fg, n=3). In male rats mRNA level was 0.49 ± 0.20 fg. Aromatase immunoreactivity was localized in osteocytes and in some bone lining cells.

In rats, ovariectomy results in a fast decrease in BMD as well as a decrease in aromatase mRNA bone expression, both being prevented by estrogen replacement therapy. The decrease of aromatase mRNA expression seems to be related to the important bone loss induced by ovariectomy. The variable mRNA levels observed in control rats and the high levels observed in males suggest a negative control of aromatase bone expression by circulating estradiol levels which could modulate ovariectomy-induced bone loss.

Disclosures: ***C. Potrel-Burgot****, None.*

SA399

Vitamin D Status, Risedronate and Bone Turnover in Nursing Home Residents. D. Krueger[1], L. Nest*[2], P. Krause*[2], P. Drinka*[2], N. Binkley[1]. [1]University of Wisconsin, Madison, WI, USA, [2]Wisconsin Veterans Home, King, WI, USA.

Though osteoporotic fractures and hypovitaminosis D are extremely common among nursing home (NH) residents, studies of optimal vitamin D (D) repletion approaches and/or antiresorptive therapy in this population are quite limited. The purpose of this study was to assess the effect of supplementation with a commonly used D dose (400 IU daily) and risedronate (RIS) administered once weekly using a flexible dosing schedule on serum bone turnover markers. This randomized double-blind placebo-controlled trial involved 60 skilled nursing home residents (46 men/14 women) who received RIS 30 mg or matching placebo (PBO) once weekly for 12 weeks. All participants received calcium and D (315 mg/200 IU) twice daily. Participant mean age and weight (SD) were 76 (6) years and 190 (40) pounds respectively; 68% were independently ambulatory and 57% had sustained a prior fracture. Serum was obtained following an overnight fast between 0600-1000 at baseline, after 6 and 12 weeks of therapy. Research nurses administered study preparation at least 2 hours from any food or drink. Fifty-three participants completed the study, discontinuations were evenly divided (4 PBO/3 RIS). As expected in NH residents, adverse events (AE's) were extremely common, but there was no difference in AE occurrence between RIS and PBO groups. Compared to PBO, RIS reduced BSAP by 8% ($p < 0.05$) at 6, but not 12 twelve weeks; no effect on serum NTx was observed. If hypovitaminosis D were defined as a serum 25OHD concentration below 32 ng/ml, 50/53 (94%) of study participants had D insufficiency at baseline with the mean serum 25OHD concentration being 19 ng/ml. Though 12 weeks of supplementation increased mean 25OHD concentration to 25 ng/ml, D status remained insufficient in 74% of participants.

In conclusion, hypovitaminosis D was extremely common and not reliably corrected by daily administration of 400 IU cholecalciferol in this population of NH residents. Weekly RIS administered using a flexible dosing schedule reduced serum BSAP at six, but not 12, weeks of treatment. These results differ from previously reported studies demonstrating RIS efficacy in older adults. Potential explanations for this discordance include the high prevalence of hypovitaminosis D, inadequate correction of this deficiency despite supplementation, the flexible dosing schedule chosen where RIS absorption may have been impaired by delayed gastric emptying, or other unidentified factors specific to this NH population. Additional study is required to evaluate approaches to optimally diagnose and subsequently conduct D repletion in NH residents and determine under which conditions bisphosphonate treatment is efficacious in this population.

Disclosures: ***D. Krueger****, None.*

SA400

See Friday Plenary number F400

SA401

Oral Risedronate at High Doses Demonstrates Upper Gastrointestinal Tolerance in an NSAID-using Population. W. Benson*[1], G. Cline*[2], M. Hosterman*[2], S. Adami[3]. [1]St. Joseph's Hospital/McMaster University, Hamilton, ON, Canada, [2]Procter & Gamble Pharmaceuticals, Mason, OH, USA, [3]Rheumatologic Rehabilitation, University of Verona, Verona, Italy.

Five (5) mg daily oral risedronate, used in the treatment of osteoporosis, has demonstrated favorable gastrointestinal (GI) tolerance in a clinical database involving over 10,000 patients. Approximately two-thirds of patients in this database had either a history of GI tract disease, or prospectively received non-steroidal anti-inflammatory drugs (NSAIDs). We now have experience on the GI tolerance of risedronate from an osteoarthritis patient population receiving 3 times the dose used in the treatment of osteoporosis. Two, Phase III placebo-controlled studies in 2483 patients with a diagnosis of medial compartment knee osteoarthritis have been completed. Patients received orally placebo, daily risedronate at doses of 5 mg or 15 mg, or weekly risedronate at doses of 35 mg (in Europe) or 50 mg (in North America) for 24 months. This report will focus on adverse event profile of placebo, 5 mg risedronate, and 15 mg risedronate, since these were the common doses across both studies. The average age of the study population was 62 years with the majority (60%) being postmenopausal women. Forty-one percent of patients had a history of GI disease. The incidence of NSAID use during the study period was 87%. Approximately 87% (2154) of the patients completed the month 24 visit. Withdrawals due to AEs were low and comparable for the placebo (12%), 5 mg (9%), and 15 mg (11%) groups. Upper GI adverse event (AE) data are presented in the table for the placebo, 5 mg, and 15 mg groups.

Treatment (n)	Placebo (622)	Ris 5 mg daily (628)	Ris 15 mg daily (609)
Upper GI AEs	18%	20%	17%
Moderate to Severe Upper GI AEs	8%	10%	7%

The GI tolerability of risedronate was comparable to placebo with regard to incidence of upper GI AEs and severity of upper GI AEs. Weekly doses of 35 and 50 mg were also similar when compared to their respective placebo groups (data not shown). In summary, risedronate, even when given at higher doses, is well-tolerated in a population at risk for increased GI side effects. In addition, this study confirms previous observations of the favorable tolerability of 5 mg daily and 35 mg weekly risedronate used in the treatment of osteoporosis.

Disclosures: ***W. Benson****, Procter & Gamble Pharmaceuticals 5.*

SA402

See Friday Plenary number F402

SA403

TNF Protects Osteoclasts from Alendronate-Induced Apoptosis by Stimulating Bcl-xL Expression through the Transcription Factor, Ets 2. Q. Zhang*, I. Badell*, E. M. Schwarz, B. F. Boyce, L. Xing. University of Rochester, Rochester, NY, USA.

Bisphosphonates prevent bone resorption in osteoporosis, but clinical trials have reported that they fail to prevent bone loss around joints in patients with rheumatoid arthritis, suggesting that they may be less effective for inflammation-induced osteolysis. Based on the known functions of TNF in inflammatory arthritis and osteoclast (ocl) survival, we hypothesized that TNF protects ocls in inflamed joints from bisphosphonate-induced apoptosis by inducing the expression of cell survival genes. We previously found that: TNF stimulates Bcl-xL expression in ocls; ocls at the erosion front in joints of TNF-Tg mice express high levels of Bcl-xL and are resistant to high doses of alendronate (ALN); and Bcl-xL protects ocls from ALN-induced cell death. Here, we attempted to identify the molecules that mediate TNF-induced Bcl-xL expression and have focused on NF-κB (p65), c-Fos and Ets members because they are known to regulate Bcl-xL transcription. We also studied if RANK signaling is required for TNF-mediated ocl survival. By real time PCR, we found that TNF significantly increased the expression of NF-κB, c-Fos and Ets 2, but not PU.1 and Ets 1 (fold increase at 8 hr over 0 hr: NF-κB, 7+/-0.1; c-Fos, 8+/-2; Ets2, 14+/-1; PU.1, 1+/-0.1; Ets1, 0.2+/-0.1) in M-CSF-treated bone marrow cells. To examine if over-expression of these proteins could protect ocls from ALN-induced apoptosis, we infected bone marrow cells with NF-κB, c-Fos, Ets2, Bcl-xL or GFP retroviral supernatant and cultured with M-CSF/RANKL to form ocls. The mature ocls that formed were treated with ALN for 24 hr and the % apoptotic ocls was counted. Only Bcl-xL and Ets2 over-expressing ocls had a 50% reduction in ALN-induced cell death (% apoptotic ocls: GFP, 76+/-5; Bcl-xL, 36+/-2; Ets 2, 39+/-5; c-Fos 75+/-1; NF-κB 80+/-2). Ets2 infected ocls had 1.6 fold increased Bcl-xL expression. To study if RANK mediates TNF's survival effect, we treated RANK-/- mature ocls (generated from RANK-/- splenocytes with TNF/M-CSF) with TNF for 24 hr and counted ocl numbers. TNF supported RANK-/- ocl survival. Accordingly, Etanercept, but not RANK:Fc, blocked TNF's survival effect on wt ocls. In summary, we found that: TNF increases the expression of Ets 2 in ocl precursors; over-expression of Ets2, but not NF-κB or c-Fos, protects mature ocls from ALN-induced cell death; Ets2 increases Bcl-xL expression in ocls; the survival effect of TNF on ocls is RANK independent. In conclusion, in inflammatory bone disease where TNF levels are high, local TNF triggers survival signals that render ocls more resistant to bisphosphonate-induced cell death by up-regulating Bcl-xL and Ets2 expression, thus reducing bisphosphonate efficacy.

Disclosures: ***Q. Zhang****, None.*

SA404

See Friday Plenary number F404

SA405

Efficacy and Safety of Long-Term Alendronate in Male Solid Organ Transplant Recipients. R. C. Christian[1], M. E. Elliott[1], N. Vallarta-Ast[2], K. Hansen[1]. [1]University of Wisconsin, Madison, WI, USA, [2]Radiology, Wm. S. Middleton VAMC, Madison, WI, USA.

Background: Solid organ transplant recipients are at high risk for osteoporosis and fragility fractures. Many clinicians are reluctant to prescribe bisphosphonates, as reduced renal function is common in transplant patients. Outcomes data on bisphosphonate use in transplant patients is limited to short term (≤12 month) trials.

Objective: This retrospective study compared efficacy and tolerability of long- term alendronate therapy in male solid organ recipients and a comparable group of non-transplanted men (controls).

Methods: Among 900 veterans filling at least one alendronate prescription between 1997 and 2002, 17 male transplant recipients and 44 male controls had bone density studies bracketing use of alendronate. Demographic and anthropometric data, fracture incidence, adverse events and therapy duration were obtained from medical and pharmacy records. We calculated annualized BMD change by dividing total change in BMD by days between DXA scans, and multiplying by 365.25 days.

Results: Mean duration of alendronate therapy was 34 months in both groups, with a notable average delay of 36 months between organ transplant and onset of alendronate therapy. Glucocorticoid use was more common (100% vs. 41%, $p < 0.001$), and creatinine clearance was lower (32 vs. 48 cc/minute, $p = 0.004$) in transplanted than in control men. Transplanted men were younger (59 vs. 72 years, $p < 0.001$), and no more likely to experience adverse events (12% vs 27%, NS) than controls. Fracture rates, hypogonadism, alcohol abuse and smoking did not differ between groups. Neither initial BMD nor change in BMD differed significantly between groups at either site ($p > 0.05$).

Conclusions: Alendronate increased spine BMD and stabilized hip BMD in transplanted men comparable to non-transplanted men, despite delayed therapy initiation. Transplanted men were no more likely to experience adverse effects, despite compromised renal function and ongoing glucocorticoid therapy. This retrospective study suggests that chronic alendronate therapy is both safe and effective at stabilizing or increasing bone mass in male veterans following solid organ transplant.

Bone Mineral Density Results

BMD (gm/cm2)	Transplant (mean BMD ± SD)	Non-transplant (mean BMD ± SD)
Initial Lumbar Spine	1.032 ± 0.144	1.044 ± 0.212
Initial Total Hip	0.859 ± 0.135	0.828 ± 0.134
Annualized Spine Change	0.028 ± 0.074	0.030 ± 0.061
Annualized Hip Change	0.005 ± 0.013	0.006 ± 0.041

Disclosures: ***R.C. Christian****, None.*

SA406

See Friday Plenary number F406

SA407

Medication Persistence Is Better With Weekly Bisphosphonates, but It Remains Suboptimal. R. Recker[1], R. Gallagher*[2], M. Amonkar*[3], J. Smith*[3], P. MacCosbe*[3]. [1]Creighton University, Omaha, NE, USA, [2]NDCHealth, Pheonix, AZ, USA, [3]GlaxoSmithKline, Durham, NC, USA.

Persistence on bisphosphonates (BPs) for the treatment of osteoporosis is necessary to prevent bone fractures. An indicator of treatment persistence is medication possession ratio (MPR). It has been reported that the risk of bone fractures increases significantly among osteoporosis patients with MPR <80% (Caro et al. *Osteoporosis Int.* 2003:14 (Suppl 7);S2). The objective of this study was to compare MPR between women receiving daily BPs vs. women receiving weekly BPs.

A HIPAA-compliant, longitudinal patient database of prescriptions dispensed from ~25% of US retail pharmacies was used to assess MPR in women at least 50 years old receiving risedronate (5, 35mg) or alendronate (5, 10, 35 or 70mg). Data were assessed for a 12 month study period (10/02-9/03). MPR was defined as the total days of supply from all prescriptions for a brand and strength filled or refilled during the study, divided by 365 potential days of therapy. Adequate persistence was defined as MPR at least 80% and inadequate persistence was defined as MPR less than 80%. Pre-study data (10/01-9/02) were used to classify patients as new to therapy (no osteoporosis prescription in the pre-study) or receiving existing therapy (at least one prescription in the pre-study for the same brand and strength as in 10/02).

A total of 33,767 patients were receiving daily BPs and 177,552 were receiving weekly BPs. Most patients were classified as receiving existing therapy; 91% of patients receiving daily BPs and 84% receiving weekly BPs. The percent of patients with adequate persistence vs. inadequate persistence were as follows:

	New Patients*		Existing Patients*		All Patients*	
MPR Category	Daily	Weekly	Daily	Weekly	Daily	Weekly
Adequate Persistence	13.2%	25.2%	35.2%	48.1%	33.3%	44.8%
Inadequate Persistence	86.8%	74.8%	64.8%	51.9%	68.7%	55.2%

*daily vs. weekly, P<0.0001, Cochran-Mantel-Haenszel test; data source: NDCHealth

In all patient groups, less frequent dosing of BPs was associated with a higher percent of patients who had adequate persistence (MPR at least 80%). The highest percent of patients with adequate persistence was among those classified as receiving existing therapy with weekly BPs. However, only ~48% of these patients had adequate persistence. Thus, medication persistence and fracture protection with weekly BPs appear to be suboptimal.

Disclosures: ***R. Recker****, Merck, P&G/Aventis 2, 5; Roche, Lilly 2, 5; NPS, Novartis, Amgen 2, 5.*

SA408

See Friday Plenary number F408

SA409

Cost-Effectiveness Of Alendronate In The Treatment Of Postmenopausal Women In Spain- An Economic Evaluation Based On The Fracture Intervention Trial. F. Borgström*[1], Å. Carlsson*[1], O. Johnell*[2], G. Nocea*[3], S. S. Sen*[4], B. Jönsson*[5]. [1]Stockholm Health Economics AB, Stockholm, Sweden, [2]Department of orthopaedics, Malmö General Hospital, Malmö, Sweden, [3]Merck Sharp & Dohme, Madrid, Spain, [4]Outcomes Research, Merck&Co., Inc., Whitehouse Station, NJ, USA, [5]Centre for Health Economics, Stockholm School of Economics, Stockholm, Sweden.

The Fracture Intervention Trial (FIT) showed that the bisphosphonate alendronate reduces the risk of fractures in women with low bone mass, with and without prior fractures. The objective of this study was to estimate the cost-effectiveness (cost per quality-adjusted life-year, QALY, gained and cost per life-year gained) of treating women with vertebral fracture in Spain with alendronate, compared with no treatment.

A further development of a Markov model earlier used in the economic evaluation for Sweden, Denmark and the UK was adapted to fit a Spanish setting. This Markov model depicted patients progressing through healthy (with existing vertebral fracture) state, spine fracture state, post spine fracture state, wrist fracture state, hip fracture state and post hip fracture state over time until the patient reached 100 years of age or died with a cycle length of 1-year. In the base-case scenario alendronate was assumed to have a fracture-risk reducing effect as shown in the vertebral fracture arm of FIT. Patients were assumed to receive treatment for 5 years as it was in the FIT population, followed by 2 years with maintained full effect and thereafter a 3-year period where the effect declined linearly to zero.

The cost-effectiveness ratios of treating a 71-year old (the mean age in the vertebral fracture arm of the FIT) woman with one prior vertebral fracture with alendronate were found to be associated with a cost of €4 341 per life year gained and €3,147 per QALY gained, well below the threshold of €30,000/QALY gained generally accepted as bench mark for cost-effective interventions in Spain.

The results of this study indicate that treating post-menopausal women with vertebral fracture with alendronate in Spain is projected to be cost-effective.

Disclosures: ***S.S. Sen****, Shuvayu S. Sen 3.*

SA410

See Friday Plenary number F410

SA411

Is Alendronate Effective on BMD and Metabolic Markers of Postmenopausal Osteoporotic Patients with Normal to Mildly High Turnover? Comparison with High Turnover Bone. T. Miki[1], H. Naka*[1], H. Masaki*[1], T. Koumo*[2], Y. Imanishi[2], M. Inaba[2], Y. Nishizawa[2]. [1]Geriatrics, Osaka City Univerisy Graduate School of Medicine, Osaka, Japan, [2]Department of Metabolism, Endcrinology, and Molecular Medicine, Osaka City Univerisy Graduate School of Medicine, Osaka, Japan.

Aim: We investigate whether basal bone metabolism influences on the effectiveness of alendronate on lumbar BMD (L-BMD) increase and suppression of metabolic markers of bone.

Methods: Postmenopausal osteoporotic patients (n=58, mean age=69 years old) were divided in to two groups depending on median basal urinary NTX. High turnover group (H group, mean u-NTX=79.3nmolBCE/mmol.cre) consists of 30 patients and normal to moderately high turnover group (N group, mean u-NTX=40.6, $p<0.01$ vs. H-group) consists of 28 patients. These patients were treated with alendronate for 18 months. L-BMDs were followed every 6 months, and metabolic markers of bone (u-NTX, serum NTX, u-βCTX, BAP) were evaluated before, 1, 3, 6, 12 months after initiation of the treatment.

Results: L-BMD in H-group was 7.3% lower than that of L-group ($p<0.04$), although mean age was not different between these groups. The % suppressions at 3rd, 6th, and 12th month of u-NTX were significantly higher in H-group than that of N-group ($p<0.03$), but the absolute difference between these groups was decreased. The initial BAP in H-group was significantly higher than that of N-group ($p<0.05$), but significant differences between these groups were not found in % suppression at 6th and 12th month. The similar findings were also observed in both serum NTX and u-βCTX. The increment of L-BMD was 4.9% in H-group and 5.2% in N-group at 6th month, and 6.6% and 7.3% at 12th month respectively, and the differences between H and L-group were not significant. The differences of absolute increases($\Delta g/cm^2$) of every 6th month between these groups were not significant.

Summary and Conclusion: The ffectiveness of alendronate on the L-BMD and bone metabolism is similar in both u-NTX high group and normal to moderately high turnover group, This suggests alendronate is not contra-indication to postmenopausal osteoporosis without high turnover bone metabolism up to 18 months.

Disclosures: ***T. Miki****, None.*

SA412

See Friday Plenary number F412

SA413

Intravenous Pamidronate Therapy for Treatment of Osteoporosis. What Is the Optimum Dose? S. J. Wimalawansa. Dept. Medicine, Div. Endocrinology, Robert Wood Johnson Medical School, New Brunswick, NJ, USA.

Rationale: Oral bisphosphonate therapy is highly effective in prevention and treatment of osteoporosis, but the compliance is poor due to the inconvenience, and the responses take a year or so. These issues including compliance and upper gastrointestinal problems are overcome by administering a bisphosphonate intravenously. This is particularly true for patients who cannot adhere to, or tolerate oral bisphosphonates, or patients with severe osteoporosis. However, the optimum dose or the frequency of administration of this agent is not known.

Method: A dose-response study was carried out using bone mineral density (BMD) and biochemical markers (BCM) as the end points. Doses of pamidronate between 30 and 120 mg were compared over a 3-year duration. Pamidronate was administered 10 mg/30 min as infusion in normal saline. Two separate infusions of pamidronate were administered a week apart at the onset (loading dose), and single doses were repeated at 6-monthly intervals. BCM were checked prior to each administration of pamidronate.

Results*:* Doses of 90 and 120 mg pamidronate administered at 6 monthly intervals were able to keep the BCM (hydroxyproline/creatinine) suppressed (Table 1), while significantly increasing BMD over the three-year period (Fig 1).

Table 1	Months				
Dose	6	12	24	36	n
30 mg	-18%	-9%	-5%	10%	21
60 mg	-22%	-12%	-10%	-13%	25
90 mg	-40%	-38%	-36%	-39%	29
120 mg	-46%	-44%	-40%	-42%	21

Discussion: Evaluating the BCM and BMD changes, it is concluded that the optimum doses of pamidronate for the treatment of osteoporosis is 90 mg given at 6 monthly intervals. Due to the inability of keeping the BCM suppressed, doses below 90 mg are recognized as sub-therapeutic and unlikely to have beneficial effects on fracture reduction. There was no serious drug-related adverse effect noted in any of these patients. Conclusion: Intravenous pamidronate therapy is a practical and highly effective way of administering a bisphosphonate to improve BMD and fracture reduction, provided that the appropriate doses are used

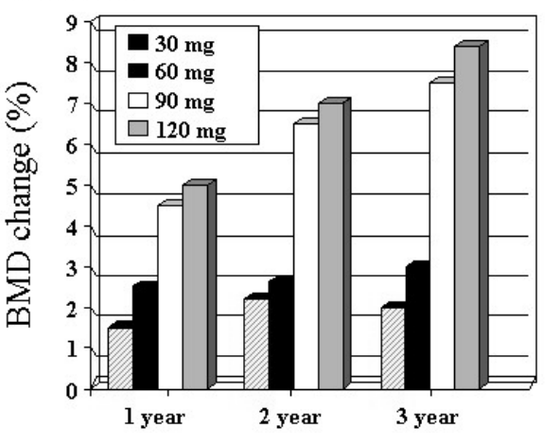

Disclosures: ***S.J. Wimalawansa****, Alliance of Better Bone Health 5; Norvatis 5; Lilly 8.*

SA414

Dose Response Study of Soy Isoflavones on Bone Resorption in Postmenopausal Women. J. M. K. Cheong*[1], J. R. Nolan*[2], G. S. Jackson*[3], B. R. Martin[1], D. Elmore*[3], G. P. McCabe*[2], S. Barnes*[4], M. Peacock[5], C. M. Weaver[1]. [1]Foods and Nutrition, Purdue University, West Lafayette, IN, USA, [2]Statistics, Purdue University, West Lafayette, IN, USA, [3]PRIME Lab, Purdue University, West Lafayette, IN, USA, [4]Pharmacology, University of Alabama, Birmingham, AL, USA, [5]School of Medicine, Indiana University, Indianapolis, IN, USA.

The purpose of this 3-way crossover study was to identify the effective dose of soy protein isolate enriched with isoflavones for suppressing bone resorption in postmenopausal women. Thirteen postmenopausal women (≥ 6 years since menopause) were pre-dosed with ^{41}Ca intravenously. After a 100-day baseline period, subjects were given 40 grams of soy protein per day that contained either 0, 97.5, or 135.5 mg of total isoflavones in randomized order. The soy protein isolate powder was incorporated into baked products and beverages. Each 50-day treatment phase was followed by a 50-day recovery phase. Serum isoflavone levels and biochemical markers were measured at the end of each phase. Twenty-four hour urine collections were performed every ~10 days during each phase for ^{41}Ca/Ca analysis by Accelerator Mass Spectrometry. Serum isoflavone levels reflected the amount of isoflavones consumed in a dose-dependent manner. None of the isoflavone levels had a significant effect on biochemical markers of bone turnover, urinary cross-linked N-teleopeptides of type I collagen (NTx) and serum osteocalcin (OC), or bone turnover as assessed by urinary ^{41}Ca/Ca. In conclusion, soy isoflavone doses of up to 135.5 mg per day did not suppress bone resorption in postmenopausal women.

Disclosures: ***J.M.K. Cheong****, None.*

SA415

See Friday Plenary number F415

SA416

Results of a 5 year Double Blind, Placebo Controlled Trial of Calcium Supplementation (CAIFOS); Bone Density Outcomes. A. Devine[1], R. L. Prince[1], S. S. Dhaliwal*[2], I. M. Dick[1]. [1]School of Medicine and Pharmacology, University of Western Australia, Western Australia, Australia, [2]School of Public Health, Curtin University of Technology, Western Australia, Australia.

Osteoporotic fracture is a major public health problem in elderly women. Another presentation demonstrates a 34 % reduction in clinical non vertebral fractures in patients receiving calcium supplementation (calcium carbonate 600mg b.d.) compared to identical placebo in women over 70. In this presentation we examine the hypothesis that calcium supplementation prevents fractures by reducing bone mass loss.

1460 women mean age 75 were recruited from the whole population using a recruitment letter strategy. Responders were excluded if they were on bone active treatment, calcium supplementation or if they had diseases that may have prevented them completing the study. Bone mineral content (BMC), area and BMD were measured using an Hologic 4500A at years 1 and 5. The BMD cv was 1.4 % for the femoral neck and 0.82% for the whole body. Outcomes for those patients completing the per-protocol study were assess using GLM procedures in SPSS version 11.

194 patients had whole body BMD measured at 1 and 5 years. There was no significant treatment group difference in the 1 year BMC (1851 ± 260 g), area (1871 ± 134 cm^2) or BMD (986 ± 90 mg/cm^2). At 5 years the age and BMI adjusted changes in BMC for calcium vs placebo was -19 ± 6 vs -42 ± 6 g (P=0.01); area -18 ± 5 vs -34 ± 5 cm^2 (P=0.025); BMD -0.60 ± 2.6 vs -5.4 ± 6 gm/cm^2 (P=0.20).

In a cross sectional analysis of 692 patients measured at 5 years, the whole body BMC for calcium vs placebo was 1855 ± 15 vs 1782 ± 15 g (P < 0.001); area was 1864 ± 8 vs 1829 ± 8 cm^2 (P < 0.001) and BMD was 990 ± 5 vs 970 ± 5 mg/cm^2 (P=0.007), after adjustment for age and BMI.

741 patients had femoral neck BMD measured at 1 and 5 years. There was no significant treatment group difference in the 1 year BMC (3.56 ± 0.59 g), area (5.13 ± 0.34 cm^2) or BMD (694 ± 103 mg/cm^2). At 5 years the age and BMI adjusted changes in the femoral neck BMC for calcium vs placebo was -49 ± 14 vs -111 ± 14 mg (P =0.002); area 0.008 ± 0.014 vs -0.034 ± 0.014 cm^2 (P=0.027); BMD -10.7 ± 2.0 vs -17.9 ± 2.0 mg/cm^2 (P =0.01). No effects at other hip DXA sites were detectable.

In a cross sectional analysis of 812 patients measured at 5 years, the femoral neck BMC for calcium vs placebo was 3.53 ± 0.03 vs 3.42 ± 0.29 g (P=0.009); area was 5.13 ± 0.02 vs 5.09 ± 0.02 cm^2 (P = 0.094) and BMD was 688 ± 5 vs 672 ± 5 mg/cm^2 (P=0.025) after adjustment for age and BMI. No effects at other hip DXA sites were detectable.

Therefore calcium supplementation reduces the loss of bone mass and area occurring with aging. This effect may explain at least in part the reduction in clinical osteoporotic fracture outlined described in this study.

Disclosures: ***R.L. Prince****, None.*

SA417

See Friday Plenary number F417

SA418

Racial Differences in Calcium Retention in Adolescent Girls on a Range of Controlled Calcium Intakes. M. Braun[1], Z. Jiang*[2], C. Palacios*[1], K. Wigertz*[1], L. A. Jackman*[1], R. J. Bryant*[1], B. R. Martin[1], G. P. McCabe*[2], M. Peacock[3], C. M. Weaver[1]. [1]Foods & Nutrition, Purdue University, West Lafayette, IN, USA, [2]Statistics, Purdue University, West Lafayette, IN, USA, [3]Indiana University School of Medicine, Indianapolis, IN, USA.

Calcium balance studies were conducted in adolescent females aged 11-13, matched for weight and post-menarchal age. A range of calcium intakes (760-2195 mg Ca/day) were tested in the 3-week controlled feeding studies. Some subjects were studied repeatedly; total observations were sixty-eight for whites and eighty-two for blacks. Diet composites and all urine and feces were collected during each 3-week period in 24-hour pools and analyzed for calcium. All procedures were approved by the Purdue University and Indiana University School of Medicine Institutional Review Boards. Non-linear regression analysis indicated that blacks had higher calcium retention than whites at all intakes. Higher calcium retention during adolescence may play a role in the development of higher bone mineral content observed in blacks compared to whites in adulthood.

Disclosures: ***M. Braun****, None.*

SA419

Significant Reduction of Risk of Fall in Osteoporotic Women: A Four-Week Proprioceptive Dynamic Program. M. Sinaki[1], R. Brey*[2], C. Hughes*[3], D. Larson*[4], K. Kaufman*[5]. [1]Physical Medicine and Rehabilitation, Mayo Clinic, Rochester, MN, USA, [2]Vestibular Laboratory, Mayo Clinic, Rochester, MN, USA, [3]Motion Analysis Laboratory, Mayo Clinic, Rochester, MN, USA, [4]Biostatistics, Mayo Clinic, Rochester, MN, USA, [5]Biomechanics Laboratory, Mayo Clinic, Rochester, MN, USA.

Twenty-six women ages 60 and older, 13 osteoporotic/kyphotic (O/K) women with thoracic kyphosis of 50 to 65 degrees (Cobb angle) and 13 healthy controls without hyperkyphosis (C) were enrolled in a study to assess risk of falls. Measured parameters included kyphosis, balance, muscle strength, gait, and height.

Computerized Dynamic Posturography (CDP) testing of the two groups at baseline demonstrated a significant balance disorder in the O/K group as compared with the C group ($p < 0.001$). Isometric strength testing of the lower extremities revealed that the O/K group had significantly lower strength ($p < 0.05$) than the C group in all muscle groups except for the right plantar flexors. Objective gait evaluation showed significant differences in various temporal-distance parameters between the O/K and C groups including right and left step length, stride length, forward velocity and average cadence ($p < 0.03$).

Following baseline evaluations, a specific 4-week proprioceptive dynamic program (PDP) was initiated for the 13 O/K subjects. This program consisted of application of a specially designed weighted back support while performing prescribed balance exercises. Twelve subjects completed the program.

At follow-up, balance improved significantly ($p = 0.003$) on CDP testing. Height also improved significantly ($p < 0.001$). Gait parameters showed statistically significant improvement relative to the baseline evaluations. The average increase for forward velocity was 5.7 cm/s ($p = 0.04$) and anteroposterior maximum velocity of the center of mass during level walking improved 0.1 m/s ($p = 0.02$). Cadence improved 3.9 steps/min ($p = 0.02$). Total support time decreased an average of 1.2% on the left and 1.7% on the right ($p = 0.02$, $p = 0.001$, respectively). Swing phase increased for both left (1.2%) and right (1.7%) ($p = 0.02$, $p = 0.001$, respectively). The double support time decreased 1.2% on the right side ($p = 0.04$). Lower extremity strength was not significantly changed from baseline.

Risk of falls in O/K individuals can be successfully reduced with a specific proprioceptive dynamic program without increasing muscle strength. This is the first controlled proprioceptive trial for reduction of risk of falls (in addition to our pilot study) that has been significantly effective without increasing muscle strength in the lower extremities. These results indicate that balance can be improved without strenuous strengthening exercises.

Disclosures: ***M. Sinaki****, None.*

SA420

Yaktrax® Walker Reduces Outdoor Winter Falls and Injurious Falls in Fall-Prone Elderly. F. E. McKiernan. Center for Bone Diseases, Marshfield Clinic, Marshfield, WI, USA.

Falling is an oft-overlooked target for fracture reduction strategy. In elders (>65y) 5-10% falls result in soft tissue injury, 3-5% in fracture, 1-2% in hip fracture. An expert panel on fall prevention recently identified 12 high priority research questions including "What is the safest footwear for people who have fallen or are at risk for falling?"

The objective of this IRB approved study was to determine whether Yaktrax® Walker (YW; a non-medical, gait stabilizing device) reduced outdoor winter slips, falls or injurious falls in the fall-prone elderly. Ambulatory, community dwelling elders who had fallen at least once during the previous year were randomized by independent numerical assignment to wear either YW or usual winter footwear (UWF) during the winter of 2003-4 under appropriate environmental conditions. Both groups maintained daily diaries of all indoor/outdoor slips/falls and injurious falls. Injurious falls were rated mild (no medical attention), moderate (medical attention) or serious (hospitalization). Indoor slip/fall occurrences served as the control for fall tendency.

113 subjects (46 M/67F) were randomized. 2 UWF subjects met tests for exclusion (indoor slip/fall rate >3 SD group mean) and were not analyzed. 2 YW subjects were excluded from analysis; 1 withdrew consent, 1 completed only 10 diary days. Mean subject age was 74.2 yrs (range 65-96). Throughout 10,724 observation-days there were 93 indoor slips, 13 indoor falls, 714 outdoor slips and 62 outdoor falls. The YW group RR for indoor slip was 1.46 (p=0.45) and for indoor fall was 1.17 (p=0.78). Thus the tendency for YW and UWF groups to slip or fall appeared comparable. By intention to treat analysis the RR of outdoor slip for YW was 0.50 (p<0.04) when all diary days was the exposure variable and 0.62 (p=0.14) when only days walked on snow and ice was the exposure variable. By intention to treat analysis the RR of outdoor fall for YW was 0.44 (p<0.02) when all diary days was the exposure variable and 0.49 (p<0.03) when only days walked on snow and ice was the exposure variable. About 1/3 of outdoor slips and 2/3 outdoor falls occurred when YW were not wearing their assigned device. Falls resulted in 10 injuries (8 mild, 2 moderate) in UFW and 1 mild injury in YW. No serious injury or fracture occurred in either group. RR of injurious fall for YW was 0.10 (p=0.004). RR of injurious fall per day walked on snow and ice for YW was 0.12 (p<0.02). NNT for the Yaktrax Walker® to prevent 1 injurious fall per winter was 6.

Under appropriate environmental conditions YW prevents falls and injurious falls in fall-prone elderly. Fewer falls should result in fewer serious injuries, fractures and fatalities.

Disclosures: ***F.E. McKiernan****, None.*

SA421

See Friday Plenary number F421

SA422

Effects of Reducing Intensity of Back-Strengthening Exercise on Strength of Back Extensors in Healthy Young Women: A Preliminary Study. M. Hongo*[1], E. Itoi*[1], N. Miyakoshi[1], M. Sinaki[2], Y. Shimada*[1]. [1]Orthopedic Surgery, Akita University School of Medicine, Akita, Japan, [2]Mayo Clinic, Rochester, MN, USA.

We reported that back-strengthening muscle exercise using a specific backpack was effective in increasing back extensor strength (BES) and decreasing risk of vertebral fractures. The same intensity of exercise, when performed by patients with osteoporosis, may cause back pain or even vertebral fractures. A reduction in intensity of the exercise may thus be beneficial for osteoporotic patients. We have shown that reduction in intensity from 30% of BES to 15% had similar effect in terms of increasing the back extensor strength. However, we do not know how much reduction in intensity of back exercise would still be effective in increasing the BES. The purpose of the present study was to determine the least effective intensity of back exercise in increasing the BES in healthy young volunteers. Fifty-four healthy young female volunteers with a mean age of 21 years were enrolled in this study. Participants were instructed to lift the upper trunk in prone position with or without a backpack. The protocol was to perform the exercise 10 repetitions per day, 5 days per week. Subjects were randomly assigned to one of the following five groups: control group (Control; n=11) without exercise prescription; 30% of the BES weighted group (30%-W:average weight=9.0kg; n=11) with a standard protocol that has been shown to increase BES and decreasing the risk of vertebral fractures; 15% weighted group (15%-W:average weight=4.4kg; n=13); 2kg weighted group (2kg-W; n=9); and no-weighted exercise group (No-W; n=9). The isometric BES was measured at baseline, 4, 8 and 12 weeks using a dynamometer. Of the original 54 subjects, 47 completed the study. Two subjects in the 30%-W group and one in the No-W group dropped out because they experienced low back pain. The BES increased significantly in all groups except in the Control by 12 weeks. The maximum increase in the BES at 12 weeks was observed in the 30%-W group (39%), followed by the 15%-W (22%), 2 kg-W (32%), No-W (17%), and Control (5%). The increase in BES of the 30%-W was greater than that of Control (p=0.0001), No-W (p=0.0176), and 15%-W (p=0.0337). The percent change of Control was smaller than that of 2 kg-W (p=0.0017) and 15%-W (p=0.0026). There was no significant difference in the change of BES between 30%-W and 2 kg-W. We conclude that either a load of 2 kg or 15% of maximum back extensor strength is effective in increasing the back extensor strength when this amount of load is used during back strengthening exercise.

Disclosures: ***M. Hongo****, None.*

SA423

Comparison of the Extraskeletal Effects of Lasofoxifene and Raloxifene. M. McClung[1], D. Portman*[2], R. Emkey*[3], J. McKenny*[4], M. Ettinger[5], V. Somayaji*[6], A. Lee[6]. [1]Oregon Osteoporosis Center, Portland, OR, USA, [2]Columbus Center for Women's Health Research, Columbus, OH, USA, [3]Radiant Research, Wyomissing, PA, USA, [4]National Clinical Research Inc, Richmond, PA, USA, [5]5Regional Osteoporosis Center of South Florida and Radiant Research, Stuart, FL, USA, [6]Global Research and Development, Pfizer, New London, CT, USA.

Estrogen effectively prevents bone loss after menopause but has recently been shown to have adverse extraskeletal effects. SERMs bind to estrogen receptors to display a variety of estrogen-like and antiestrogen effects in different tissues. Evaluating the extraskeletal effects of new SERMs such as lasofoxifene that prevents bone loss is important.

This 2-yr, phase 2 study was compared the bone density responses to lasofoxifene, a next generation SERM with raloxifene and placebo. 410 women (mean age 58 y and 9 y post-menopausal) were randomized: 82 each to 0.25 mg/d and 1.0 mg/d lasofoxifene, 83 to placebo, and 163 to raloxifene 60 mg/d. All women received daily calcium 1000 mg and vitamin D 250IU. BMD and biochemical markers of bone turnover (data presented in another abstract), markers of lipid metabolism, selected coagulation factors, and gonadotropins were measured.

Both doses of lasofoxifene resulted in greater reductions ($p \leq 0.05$) in LDL-C when compared to raloxifene and placebo. At month 24, median LDL-C reductions of 20.6% and 19.7% were observed for the lasofoxifene 0.25 mg/d and 1mg/d dose groups, respectively, compared to 12.1% and 3.2% reductions observed for raloxifene and placebo, respectively. Lasofoxifene-treated women had significantly ($p \leq 0.0049$) greater decreases as compared to raloxifene in TC (11.3% vs 6.7%), Apo B100 (11.7% vs 5.0%), and Lp(a) (37.7% vs 25.6%), and a significantly ($p<0.05$) greater increase in Apo A1 (5.5% vs 1.6%).There were no consistent treatment effects on HDL-C and TGs. Lasofoxifene was effective in reducing levels of coagulation factors (fibrinogen, PAI-1, and antithrombin III activity), and in reducing serum LH and FSH, compared to placebo ($p<0.05$).

Overall, lasofoxifene was well tolerated. Similar adverse events, including hot flushes and leg cramps, were reported more often with lasofoxifene and raloxifene than placebo. More urogenital symptoms were observed with lasofoxifene compared to raloxifene. This finding was driven largely by leukorrhea (increased vaginal lubrication) - which was considered a beneficial effect by some women.Lasofoxifene was efficacious as compared to raloxifene not only in preventing bone loss, but also showed positive effects on LDL-C and other lipid parameters, no deleterious effects on coagulation markers, and was well tolerated, supporting its use in the management of the postmenopausal woman.

Disclosures: ***M. McClung****, Michael McClung, David Portman, Ronald Emkey, James McKenney, Mark Ettinger, 5; Veena Somayaji and Andy Lee 3.*

SA424

See Friday Plenary number F424

SA425

Short-Term Changes in the Hormonal Profile and OPG-RANKL System in Osteoporotic Patients Treated with Raloxifene. D. Fernandez*[1], P. Mezquita-Raya*[1], M. de la Higuera*[1], R. Reyes*[1], G. Alonso*[1], M. Ruiz-Requena*[2], F. Escobar-Jimenez*[1], M. Muñoz-Torres[1]. [1]Bone Metabolic Unit. Department of Endocrinology, University Hospital San Cecilio, Granada, Spain, [2]Biochemistry Division, University Hospital San Cecilio, Granada, Spain.

Several *in vitro* studies suggests that the antiresorptive effect of raloxifene (a selective estrogen receptor modulator) might be produced by changes in several cytokines involved in the bone remodelling process. In this context, the OPG-RANKL system is considered a key component in the osteoclastogenesis regulation. In addition, the treatment with raloxifene leads to changes in hormonal profile that can be related with its extra-osseous effects. However, these effects are not adequately established in osteoporotic patients. Objectives: To determine the effects of raloxifene administration on serum concentrations of OPG, RANKL, IGF system and biochemical markers of bone turnover in women with postmenopausal osteoporosis. Subjects and methods: We selected 48 postmenopausal women (mean age 63±7 years) with densitometric criteria of osteoporosis (T-score ≤ -2.5 SD). We determined anthropometric parameters, biochemical markers of bone turnover, serum levels of IGF-I, IGFBP-3, OPG (OPG ELISA, BIO-MEDICA-GRUPPE Wien, Austria) and RANKL (sRANKL ELISA BIO-MEDICA-GRUPPE Wien, Austria), before and after three months of raloxifene-HCL (60 mg/day) treatment. Results: OPG (84 ± 35 vs. 73 ± 32 pg/ml; p = 0.001), IGF-I (131 ± 60 vs. 99 ± 39 ng/ml; p = 0.001) and biochemical markers of bone turnover (ALP: 87 ± 41 vs 67 ± 18 UI/L; p = 0,001, TRAP: 3.1 ± 0.4 vs 2.7 ± 0.6 UI/L; p = 0.002, urinary CTX: 616 ± 356 vs 499 ± 410 ugr/pmol ; p = 0.04) significantly diminished to 3 months. A high percentage of serum RANKL determinations were undetectable (basal: 68%, 3 months: 63%). RANKL was neither affected by treatment and nor related to OPG or IGF-I variations. The changes in the IGF-I/IGFBP-3 ratio were positively related with variations in OPG (r = 0.347; p= 0.018). Conclusions: The treatment with raloxifene in osteoporotic postmenopausal women leads to a decrease in serum levels of OPG that it might be attributed to the inhibitor effect on bone remodelling. The changes in IGF-I could be related to the extra-osseous effects of this drug. The determination of serum RANKL does not contribute any additional information.

Disclosures: ***M. Muñoz-Torres****, Eli Lilly & Co (Spain) 2; Fondo de Investigación Sanitaria (FIS: PI02/1089) 2.*

SA426

See Friday Plenary number F426

SA427

The Decrease in Bone Strength induced by Ovariectomy in Adult Rats Is corrected by the New Selective Estrogen Receptor Modulator PSK3471. P. Ammann[1], P. Clément-Lacroix[2], N. Bruynick*[2], R. Baron[2], R. Rizzoli[1]. [1]Department of Rehabilitation and Geriatrics, Division of Bone Diseases, Geneva, Switzerland, [2]ProSkelia Pharmaceuticals, Romainville, France.

Prevention of bone loss after menopause with estrogens affect not only bone but also the uterus and breast. There is therefore a need for alternative therapy like selective estrogen receptor modulators (SERMs), which can prevent bone loss and decrease bone fragility, while preventing breast cancer and lacking side effects on the genital tract. PSK3471 is such a new compound and displays good safety profile on breast and uterus. We investigated the effects of this new steroidal SERM, on bone mineral density (BMD; mg/cm2) and bone strength (U St; N) at the level of the proximal tibia (PT), and midshaft femur (MF) in ovariectomized (OVX) osteoporotic rats, and compared these effects to those of Raloxifene and the bisphosphonate Pamidronate (APD). Eight weeks after OVX, 8-month old rats were allocated to 6 groups (n=8) and given orally PSK3471 at 0.03/0.1/0.3 mg/Kg, or RAL at 3.0 mg/kg BW x day, APD (0.6 mg/kg 5 days/month) or the vehicle for 16 weeks. Values are means±SEM; * indicates p<0.05 vs OVX and by ANOVA.

	PT BMD	PT U St	MF BMD t	MF U S
SHAM	259.6±4.4	220.0±11.8	261.2±4.6	155.9±7.3
OVX	229.5±3.1	164.8±8.3	247.3±2.7	155.8±2.8
OVXPSK 0.03	239.3±2.7	187.4±8.3	246.6±2.2	152.1±6.6
OVXPSK 0.1	241.5±3.7	195.2±8.3*	244.2±4.5	150.2±5.6
OVXPSK 0.3	241.5±5.2	197.9±10.7*	243.0±4.5	158.1±6.9
OVX RAL 3.0	239.0±4.4	190.3±8.3	252.0±4.1	165.7±8.0
OVX APD	255.0±5.*	197.0±4.6*	256.7±3.9	169.7±5.4

In OVX rats, moderate increment of BMD was observed in rats treated with PSK3471 and raloxifen but a full recovery in pamidronate treated rats. Interestingly at the optimal doses PSK 3471 and pamidronate resulted in similar increment of ultimate strength despite different effects on BMD. These results suggest a different mechanism of action between bisphosphonate and PSK 3471 (action on bone turnover, trabecular bone volume or level of mineralisation). Similar trends were observed at the level of the midshaft femur. In conclusion, similar to Raloxifene, PSK3471 increased moderately BMD but was very efficient in restoring bone mechanical strength in aged osteoporotic rats, while displaying good safety profile on breast and uterus. PSK3471 may therefore be an improved second generation SERM molecule, preventing bone loss while maintaining good biomechanical properties.

Disclosures: ***P. Ammann****, proskelia 5.*

SA428

See Friday Plenary number F428

SA429

See Friday Plenary number F429

SA430

Insulin Receptor Substrate-1 (IRS-1) Is Essential for Bone Anabolic Function of Parathyroid Hormone (1-34). M. Yamaguchi*[1], Y. Shinoda*[1], S. Kamekura[1], N. Ogata[1], T. Kadowaki*[2], Y. Terauchi*[2], K. Nakamura[1], H. Kawaguchi[1]. [1]Orthopaedic Surgery, University of Tokyo, Tokyo, Japan, [2]Metabolic Diseases, University of Tokyo, Tokyo, Japan.

Bone anabolic function of the recombinant human parathyroid hormone (PTH 1-34), which has attracted considerable clinical attention, has been suggested to be mediated by induction of insulin-like growth factor-I (IGF-I) in osteoblasts; however, little is known about the molecular mechanism by which IGF-I leads to bone formation under the PTH stimulation. For the intracellular signaling of IGF-I, insulin receptor substrates (IRS-1 and -2) are known to be essential adaptor molecules. Our analyses of the deficient mice under physiological conditions revealed that these molecules play different roles in the anabolic action of IGF-I: IRS-1 is essential to maintain bone turnover by stimulating both anabolic and catabolic functions of osteoblasts, while IRS-2 is needed to keep the predominance of the anabolic function over the catabolic function. Hence, this study investigated the involvements of IRS-1 and IRS-2 in the bone anabolic function of recombinant human PTH (1-34). PTH treatment (100 nM) increased alkaline phosphatase activity and IGF-I mRNA level to about 2 and 4 fold, respectively, in the mouse primary osteoblast culture. Western blotting revealed that these stimulations were accompanied by phosphorylations of IGF-I receptor and IRS-1, but not IRS-2. For the *in vivo* analysis, we subcutaneously injected PTH (0.08 mg/kg BW) or the vehicle solution 5 times / week for 4 weeks to IRS-1- or IRS-2-deficient mice (IRS-1-/- or IRS-2-/-), and compared the effects with that on wild-type (WT) mice (all 8-week-old male mice of the same strain). In the WT mice, the average bone densities of the PTH-applied group were 12.1, 11.1, and 9.0% higher than the vehicle group in the femur, tibia, and vertebrae (L2-L5), respectively (n=9-10 / group, all p<0.01 between PTH vs. vehicle). On the contrary, the differences were markedly suppressed in IRS-1-/-: 4.2, 1.6, and 0.5 %, respectively (n=10 / group, all p>0.40), while they were similar to WT in IRS-2-/-: 12.4, 11.2, and 5.7% (n=8 / group, all p<0.01). Since the serum IGF-I levels were not different between PTH and vehicle-treated mice in all genotypes, IGF-I was shown to act locally as an autocrine/paracrine factor. These lines of evidence demonstrate that the bone anabolic function of PTH is mediated by the induction of IGF-I expression in osteoblasts, which acts locally to activate IGF-I receptor and IRS-I, but not IRS-2. Further studies on the downstream pathway of IRS-I in osteoblasts will elucidate the molecular mechanism of PTH anabolic function.

Disclosures: ***M. Yamaguchi****, None.*

SA431

See Friday Plenary number F431

SA432

Vulnerability of the Post-OVX Skeleton: Is Additional Bone Loss Caused by Alcohol? F. H. Wezeman, D. Juknelis*, J. J. Callaci*. Orthopaedic Surgery, Loyola University Medical School, Maywood, IL, USA.

Peak bone mass in women occurs by the third decade followed by a plateau before its precipitous decline following menopause. The postmenopausal osteoporotic skeleton is at higher risk for fracture. As BMD declines with age and decreased ovarian function, additional factors may accelerate skeletal mass reduction. Disuse decreases BMD beyond levels associated with ovariectomy (OVX) alone indicating that the post-ovariectomized skeleton can still lose additional bone mass. We tested the hypothesis that binge alcohol administration in OVX rats increases osteopenia but that the loss can be compensated by PTH. Female Sprague Dawley rats (400 gms, n=6/group) were experimentally divided as: control non-OVX, binge alcohol-treated, PTH-treated, and PTH + alcohol-treated. Other rats were surgically bilaterally ovariectomized, briefly recovered, and divided into the same groups (n=6). Weight-matched non-OVX and OVX animals were maintained on standard rat chow ad libitum. A binge alcohol administration model used intraperitoneal injection of 20% (vol/vol) alcohol/saline. A one time/day injection of 3g/kg/day was made for 3 consecutive days followed by 4 non-alcohol days; binge cycles continued for 2 and 4 weeks. Rats received PTH (1-34), (80 ug/kg, s.c.) 5 times per week for 2 or 4 weeks. On the morning after completion of the 2nd and 4th binge cycle animals were sacrificed and the lumbar spine removed. Each 3rd lumbar vertebra was cleaned and imaged using a Scanco Medical Micro-CT 40 scanner at 16x16x16 microns/voxel. The cancellous compartment was contoured and morphometrically analyzed for BV/TV, TbN, TbTh, TbS, and trabecular connectivity density. BMD was determined using pQCT, biomechanical properties were quantified using an Instron materials testing machine, and serum osteocalcin and CTX were measured. Treatment of non-OVX rats with alcohol decreased BV/TV at 2 and 4 weeks (11.1% and 13.1%, respectively). BV/TV in OVX rats treated with alcohol decreased by 14.5% and 10.4% at 2 and 4 weeks, respectively. Intermittent PTH raised BV/TV in all groups. Two weeks of PTH compensated for alcohol-induced bone loss in non-OVX rats (BV/TV, 102.5% of control non-OVX) while 4 weeks of PTH was required in OVX + alcohol rats (BV/TV, 107.4% of control non-OVX). Statistical analysis using GLM showed no interaction between OVX, alcohol and time, while both OVX and alcohol main effects were significant ($p<.05$). Indices of remodeling (CTX, osteocalcin), microanatomical, and biomechanical parameters affected by OVX were also altered by alcohol and PTH. These findings suggest that binge alcohol administration in OVX rats results in aggressive bone loss and that intermittent PTH attenuates this bone loss.

Disclosures: ***F.H. Wezeman****, None.*

SA433

See Friday Plenary number F433

SA434

Identification of Responders to Teriparatide Therapy by Procollagen Type I N-Propeptide (PINP) Using the Least Significant Change Approach. R. Eastell[1], P. Chen*[2], J. H. Krege*[2]. [1]University of Sheffield, Sheffield, United Kingdom, [2]Lilly Research Laboratories, Indianapolis, IN, USA.

The response to a bone-forming therapy is best monitored using a biochemical marker of bone formation. We describe the use of procollagen type I N-terminal propeptide (PINP), which has the best signal-to-noise ratio, to monitor response to teriparatide, a bone-forming agent, using the least significant change approach expressed in absolute units. The long-term coefficient of variation of PINP in phase III clinical trials of women with osteoporosis was 16-17% (equivalent to 6.5 µg/L). Thus, the least significant change at p=0.05, for a one-tailed test was 2.36 (1.44*1.64)*6.5=15 µg/L. We also applied the method of Garnero et al. (Bone 1999) to identify 18-month spine bone mineral density (BMD) change of >3%, and a PINP increase of 15 µg/L, with a sensitivity of 70% and a specificity of 85%. “Response” was an increase of ³15 µg/L. We examined results from women with osteoporosis who were treated with teriparatide 20 µg/day once-daily in the Fracture Prevention Trial (Neer et al., NEJM 2001) and the teriparatide-alendronate comparator trial (McClung et al. JBMR abstract 2003). In the Prevention Trial 70% of 254 women, and in the comparator trial, 84% of 86 women, had an increase of ³15 µg/L by 3 months. In the Prevention Trial, 85% of patients with PINP <15 µg/L at 3 months had an increase of ³3% in spine BMD at 18 months. Thus, these response figures may be underestimates and a strategy to better investigate responders is needed. In the comparator study, the 14 nonresponders were further examined. The mean changes in procollagen I C-terminal propeptide, bone specific alkaline phosphatase, and N-telopeptide were -27 (µg/l), -2 (µg/l), and -7 (nmolBCE/mmol Cr), respectively, so the measurement of a second marker did not provide additional information. In the comparator study, PINP change was <15 µg/L at 3 months in 14 subjects (compliance was good in 9 of the 14) and by 6 months, 3 became responders and 2 were no longer responders. Thus, a second PINP measurement at 6 months is unlikely to be a helpful strategy. However, in this same population, a spine BMD measurement at 6 months identified responders in 6 out of 13 subjects. A strategy to identify responders to teriparatide is to measure PINP at 3 months, and if the change is more than 15 µg/L, consider the patient a responder; this is likely to be found in more than 75% of patients. In the rest, consider a spine BMD measurement at 6 months. This teriparatide PINP responder algorithm should not be used in patients receiving concomitant bisphosphonate therapy (Black et al. NEJM 2003).

Disclosures: ***R. Eastell****, Eli Lilly and Company 2, 5.*

SA435

See Friday Plenary number F435

SA436

Anabolic Effects of PTH on Cortical and Cancellous Bone when Given in Combination with Glucocorticoid. T. T. Andreassen[1], C. Ejersted*[2], G. Ortoft*[1], H. Oxlund[1]. [1]Department of Connective Tissue Biology, University of Aarhus, Aarhus C, Denmark, [2]Department of Endocrinology, University Hospital of Odense, Odense C, Denmark.

Glucocorticoid(GC)-induced osteoporosis is the most common secondary cause of osteoporosis. We therefore have investigated the effects of parathyroid hormone (PTH) treatment when given in combination with GC with reference to bone BMC, BMD, and mechanical strength. Because GC treatment hampers linear growth, twenty-seven-month-old female Wistar rats with ceased linear growth were used. The animals were divided into the following groups: baseline; vehicle-injected (Veh); PTH-treated; GC-treated; PTH+GC-treated. Doses: PTH (1-34) 25 µg/kg b.w. daily, GC (methylprednisolone) 2.5 mg/kg b.w. daily. Treatment period was 8 weeks. The animals were labeled with fluorochromes twice during the experiment. BMC and BMD were measured in whole vertebra (L5) and femur. The vertebral body (L4) and the femoral diaphysis were tested mechanically and analyzed using static and dynamic histomorphometry (mean values with SEM are given; * = significantly different from Veh, # = significantly different from PTH).
Vertebra BMC (mg) and BMD (mg/mm^3): Veh (125±3; 1.03±0.04), PTH (163±6*; 1.31±0.03*), GC (121±4#; 1.05±2#), PTH+GC (148±5*#; 1.22±0.03*#). Femur BMC (mg) and BMD (mg/mm^3): Veh (489±13; 0.86±0.02), PTH (582±19*; 1.00±0.02*), GC (479±4#; 0.84±0.02#), PTH+GC (531±11*#; 0.93±0.01*#). Vertebral body mechanical strength (Ultimate load (newton)): Veh (190±22), PTH (368±19*), GC (213±12#), PTH+GC (327±21*). Femur diaphysial mechanical strength (Ultimate load (newton)): Veh (176±4), PTH (194±8), GC (173±7), PTH+GC (185±6). Only PTH and PTH+GC induced bone formation at the endocortical femoral diaphysis (MAR (µm/day)): PTH (1.1±0.10), PTH+GC (0.5±0.03#).
Conclusion: Combined treatment with PTH+GC enhances femoral and vertebral BMC and BMD, but not to the same extent as treating with PTH alone. Treatments with PTH+GC and PTH alone both increase mechanical strength of the vertebral body. Treatments with PTH+GC and PTH alone both induce bone formation at the endocortical femoral diaphysis; however, this response is not sufficient to increase the diaphysial mechanical strength significantly.

Disclosures: ***T.T. Andreassen****, None.*

SA437

See Friday Plenary number F437

SA438

Serum Protein Profiling for Discovery of Early Biomarkers to Distinguish PTH Responders from Non Responders. A. K. Prahalad*[1], R. J. Hickey*[1], J. Huang*[2], S. Murthy*[1], T. Winata*[1], L. E. Dobrolecki*[1], J. M. Hock[1]. [1]Indiana University School of Medicine, Indianapolis, IN, USA, [2]Computer Science, Indiana University, Indianapolis, IN, USA.

Parathyroid hormone [hPTH(1-34)] (PTH) is an anabolic agent which stimulates bone formation and reduces risk of osteoporotic fractures. We speculate that distinctive serum protein profiles will define patients most likely to benefit from PTH therapy. Our goal was to determine if SELDI (surface enhanced laser desorption/ionization) proteinchip® array technology reliably detects changes in serum protein expression profiles in mice showing skeletal responses to PTH. To create a PTH-responder profile, 5-week old C57/BL6 male mice were given once daily sc injection of PTH (40 µg/kg bw) or vehicle control for 3 or 11 days. At 6 h after the last dose, sera were sampled for protein analysis by SELDI time-of-flight mass spectrometry. Serum protein profiling was done on a SAX2 proteinchip array surface to capture anionic proteins. Mass spectral data were corrected by baseline subtraction; peaks with high signal-to-noise ratios were selected and grouped into bins with various intervals along m/z (mass-to-charge) axis from treated and control mice. Two-sample t-test was utilized to identify candidate biomarkers in PTH spectral patterns that differed from control spectral patterns. Significant changes were observed in two proteins with molecular masses 14.8 and 15.4 kD, and their peptides 7.4 and 7.7 kD respectively, in PTH-treated mice at both 3 and 11 days. The magnitude of change was greater in serum from mice treated with PTH for 11 days. Peak intensities of albumin, an abundant serum protein, did not change with PTH treatment relative to controls, indicating that we can use albumin as a surrogate internal standard. After 3 days of PTH treatment, Kit^W/Kit^{W-v} C57/BL6 mice, whose bones fail to respond to PTH, showed a spectral pattern similar to vehicle-treated controls, and with none of the markers seen in PTH-responsive wildtype littermates. Validation of PTH responder proteins was carried out on proteinchips (WCX2, IMAC-Cu, SAX2) that captures cationic, metal binding and anionic proteins. As expected, serum albumin, pI 4.9 bound more strongly to SAX2 surface than to IMAC-Cu, and only weakly to WCX2. In contrast, PTH responder proteins and their peptides (14.8, 15.4, 7.4, 7.8 kD) bound more strongly to WCX2 than to either IMAC-Cu and SAX2. Based on comparative binding capacity of these proteins to different proteinchips, we suggest PTH responder proteins are weakly basic, with pI above 7.4. Our data demonstrate the feasibility of using serum protein biomarkers to detect a patient’s responsiveness to PTH shortly after starting anabolic therapy for osteoporosis.

Disclosures: ***A.K. Prahalad****, None.*

SA439

See Friday Plenary number F439

SA440

Osteoblast Specific Ablation of Connexin43 (Cx43) Attenuates the Anabolic Response to Intermittent PTH (1-34) in Aged Mice. D. Chung, J. Screen, J. P. Stains, C. Liu*, R. Civitelli. Bone and Mineral Diseases, Washington University in St. Louis, St. Louis, MO, USA.

Interference with Cx43 mediated gap junctional communication alters osteoblast gene expression and inhibits PTH induced cAMP accumulation and osteoblasts differentiation, whereas PTH up-regulates Cx43. Here, we have tested the anabolic response to PTH in a model of selective Cx43 deficiency in bone forming cell using a Cre/loxP approach. Under the control of a 2.3 kb fragment of the Colα1 promoter, Cre mediated recombination of a $Cx43^{flox}$ allele replaces the entire Cx43 reading frame with the LacZ reporter cassette. A total of 101 mature, 5- to 8-month-old C57BL mice (52 males and 49 females) of three genotypes, $Cx43^{+/flox}$ (wild type equivalent), $Cx43^{-/flox}$ (heterozygous equivalent) and ColIα1Cre;$Cx43^{-/flox}$ (knockout equivalent) were injected subcutaneously (5 days a week for 4 weeks) with either vehicle (saline; n=12) or PTH (1-34) (teriparatide, Eli-Lilly) at doses of 10 (n=19), 20 (n=18), 40 (n=18), and 80 μg/kg (n=23). Whole body bone mineral content (BMC) was measured at baseline and at 2-week intervals by DEXA (PIXImus, Lunar-GE). With the exception of at the lowest dose PTH induced significant percent increments (*p<0.05, ANOVA) in BMC at 4 weeks in the $Cx43^{+/flox}$ group (8.1±2.4, 10.1±2.2*, 13.2±3.2*, and 11.4±3.9*, respectively), and in $Cx43^{-/flox}$ mice (9.2±4.9, 7.1±3.3, 9.8±3.9*, and 13.4±3.7*, respectively). However, in the conditionally deleted Colα1(I)2.3-Cre;$Cx43^{-/flox}$ mice, only the intermediate doses of PTH resulted in statistically significant BMC increments (6.9±3.2, 9.4±2.8*, 9.9±3.0*, and 8.6±4.5, respectively). Although the BMC response to PTH was dose-related in the $Cx43^{+/flox}$ and $Cx43^{-/flox}$ groups, no significant differences among doses were detected in the Colα1(I)2.3-Cre;$Cx43^{-/flox}$ group, and the effect of PTH was overall diminished in these mice relative to the other groups. Since after 4 weeks untreated animals also experienced significant BMC increases (4.8±2.1%), and since we found the BMC changes in treated mice to be inversely related to age, we extended the study to older mice (7.5-8-month-old; n=11). In this aged group, 4 weeks of 40 μg/kg PTH induced significant changes only in $Cx43^{+/flox}$ (10.6±3.5%*; n=5) and $Cx43^{-/flox}$ (9.5%*; n=2), but not in Colα1(I)2.3-Cre;$Cx43^{-/flox}$ mice (2.5±1.4%; n=4). Therefore, the anabolic response to intermittent PTH administration is attenuated in conditions of Cx43 deficiency, an effect that becomes more severe with age. These results demonstrate that osteoblast Cx43 is necessary for development of a full bone anabolic response to PTH.

Disclosures: ***D. Chung****, None.*

SA441

See Friday Plenary number F441

SA442

Effects of Anabolic Peptide BCSP-7 (Bone and Cartilage Stimulating Peptide) Treatment in Ovariectomized Rats. D. R. Sindrey[1], J. A. Swafford*[2], M. W. Lundy*[2], E. Plawinski*[1], C. A. Blanton*[2], F. H. Ebetino[2], A. Houghton*[2], J. Auluck*[1], Y. O. Taiwo*[2]. [1]Millenium Biologix Inc., Mississauga, ON, Canada, [2]Procter & Gamble Pharmaceuticals, Manson, OH, USA.

Originally isolated from an extract of the epiphyseal of calf bone, synthetic BCSP (Bone and Cartilage Stimulating Peptides) are capable of stimulating localized increases in BMD in rat tibia by 7-12% in 7 days with one injection. A 5mer sub fragment of this peptide has shown improved local activity and may be suitable for development as a bone anabolic systemic pharmaceutical. A small molecule synthetic peptide could prove to be a promising pharmaceutical for the treatment of osteoporosis. This study was conducted to determine if the systemic administration of BCSP-7 could significantly increase bone volume compared to bisphosphonates in osteopenic rats compared to vehicle treated OVX controls. Briefly, female Sprague-Dawley rats were ovariectomized (OVX, or sham surgery) at 6 months of age, allowed to loose bone for 60 days, then treated for 57 consecutive days by subcutaneous injection with vehicle, BCSP-7 0.01, 0.03, 0.1, 0.3, 1.0, & 10 mg/kg. Positive control groups were treated with sodium Alendronate, another bisphosphonate NE-58018 or human PTH(1-34). In vivo densitometry (DXA) was used to assess changes to skeletal sites over the dosing period as well as ex-vivo micro CT measurements of vertebral and femoral bone volume. In-life bone mineral density of the vertebrae, tibia and whole body was increased with NE-58018 during the course of treatment. NE-58018 also significantly increased ex-vivo vertebral bone volume and distal femur BMD. Alendronate significantly increased in-life bone mineral density of the vertebrae, tibia and whole body compared to final OVX toward the end of treatment with significant increases also seen in ex-vivo vertebral bone volume. Alendronate did not significantly change femoral BMD compared to OVX control. In-life DXA measurements indicated that BCSP-7 (0.03 and 0.1 mg/kg) significantly increased vertebral BMD from day 14 to the end of the treatment period compared to final OVX. Although the changes seen with BCSP-7 were significantly lower than PTH(1-34), BCSP-7 demonstrated equivalent results to Alendronate. BCSP-7 did not significantly change ex-vivo vertebral bone volume or femoral BMD measurements. These results indicate that systemic administration of the 5mer peptide BCSP-7 increases bone mass equivalent to Alendronate at lower doses and in the early phase of bone resorption in an OVX model. Further studies are required to study the mode of action, pharmacokinetics and dosing paradigms to optimize the systemic bone anabolic activity to the levels achieved with local administration.

Disclosures: ***D.R. Sindrey****, Millenium Biologix 1, 3.*

SA443

Effect of Mushroom *pleurotus eryngii* Extracts on Bone Metabolism. S. Kim[1], H. Kim*[2], B. Lee*[3], S. Chang*[3], H. Hwang*[3], D. Jung*[3], D. Baek*[4], S. Ko[5]. [1]OCT Inc., Dept. of Dental Pharmacology, Dankook University, Chonan-si, Republic of Korea, [2]OCT Inc., Dept.of Pharmacology, Dankook University, Chonan-si, Republic of Korea, [3]OCT Inc., Chonan-si, Republic of Korea, [4]Dept.of Oral Microbiology and Immunology, Dankook University, Chonan-si, Republic of Korea, [5]Dept.of Oral Biochemistry, Dankook University, Chonan-si, Republic of Korea.

The present study was performed to investigate whether *Pleurotus eryngii* extracts (PEX) play roles in the bone metabolism. We examined cellular activities of osteoblasts by measurement of cell proliferation rate, alkaline phosphatase (ALP) activity, and osteoprotegerin (OPG) secretion. Expression levels of osteopontin (OPN), ALP and collagen (COL), Runx2 were also measured. Osteoclast activity was assayed by measuring TRAP activity, and the area of resorption pits after culture of osteoclast precursor cells on the calcium-phosphate coated culture dish (OAAS™, OCT Inc.). Bone Mineral Density (BMD) measurements and histological observations were also carried out.

Results: PEX treatment showed a significant increase ALP activity of osteoblasts. PEX increased the COL, ALP and OPN mRNA expression from rat calvarial primary cells. Also PEX increased the expression of the Rnux2 gene, which was detected by p6xOSE2-Luc-transient transfected C2C12 cells. Secretion of OPG, which was detected from MG63 cell supernatant by western blot analysis, showed marked increases after treatment of PEX. In addition, PEX treatment decreased the number of TRAP (+) MNCs and the resorption areas. *In vivo* studies using ovariectomy-induced osteoporotic rats revealed that PEX alleviated the decrease in the trabecular BMD, and increased the thickness of cortical bone and trabecules of tibia.Taken together, PEX stimulates the activities of osteoblasts, while inhibiting the generation and resorptive activities of osteoclasts. It also shows preventive effects on osteoporotic bone loss induced by an ovariectomy. It is believed that the PEX seems to contain active components that have a potential to overcome osteoporosis.

Disclosures: ***S. Kim****, None.*

SA444

Differences in Bone Response to hGH According to Sex and Age at the Manifestation of GH-Deficiency in Adults with Hypopituitarism. M. F. Farias[1], M. E. L. Duarte[2], E. M. C. Silva*[1], D. V. Soares*[1], F. L. Conceição*[1], L. D. C. Spina*[1], R. R. O. Brasil*[1], M. Vaisman*[1]. [1]Endocrinology, Federal University of Rio de Janeiro, Rio de Janeiro, Brazil, [2]Pathology, Federal University of Rio de Janeiro, Rio de Janeiro, Brazil.

Growth hormone deficiency has a negative impact on bone mineral density, limiting the attainment of peak bone mass during youth and favoring bone loss in adult life. We studied the effect of two-years hGH replacement on bone markers and bone density in twenty-eight patients with hypopituitarism, 20-62 yrs.old. GH-deficiency was confirmed by a peak GH<3 ng/mL on ITT. All sixteen female and seven male patients developed GH-deficiency during adult life, while other five males manifested the deficiency during childhood (men AD and men IN, respectively). Gonadal steroids, L-T4 and prednisone were administered as needed. The mean dose of hGH was 0.83+/-0.2 mg/day. Serum insulin growth factor-1 (IGF-1), bone-specific alkaline phosphatase (BSAP) and urinary N-telopeptide of type 1 collagen (NTX) were measured at 0, 3,6,9,12,18 and 24mo. BMD was evaluated at lumbar spine (LS) and femoral neck (FN) by DEX, Lunar Corp., at baseline, 12 and 24months. Serum IGF-1 remained above baseline values during the whole period. BSAP and NTX increased significantly during the first year (p=0.014 and p=0.000 respectively), decreasing progressively during the second year. Before treatment, the absolute values of BMD did not differ between sexes, but the expected bone density (Z score) was lower in men, mostly in the IN group, which also had the lowest values of IGF-1 before treatment . During GH-replacement, only male patients had a significant increase in BMD either at lumbar spine (p=0.01) and femoral neck (p=0.02).The differences between sexes were significant at the LS at 12 mo (p=0.006) and 24mo (p=0.002). The % variation in LS BMD at 24mo tended to be higher in men IN (7.57+/-4.7%) than men AD (4.0+/-6.3%) and women (-0.15+/-3.8%). We concluded that the negative impact of GH-deficiency on bone is greater in patients who manifest hypopituitarism before the attainment of peak of bone mass, and also greater in men than in women. On the other hand, men have a better bone response to hGH than females. Further studies are needed to explain these differences and to identify antecipately which patient will not gain bone with hGH-replacement.

Disclosures: ***M.F. Farias****, None.*

SA445

See Friday Plenary number F445

SA446

Additive Effects of EP4 Agonist and Risedronate on Bone Strength due to Maintaining Individual Actions on Microarchitecture. M. Ito[1], K. Nakayama*[2], Y. Shinagawa*[2], A. Konaka*[2], K. Sakata*[2], T. Maruyama*[2]. [1]Radiology, Nagasaki University, Nagasaki, Japan, [2]Discovery Res. Lab., ONO pharmaceutical Co., Ltd., Osaka, Japan.

Bone anabolic effect of EP4 agonist (ONO-4819·CD (48CD)) has been reported to inhibit the reduction of vertebral strength by gaining bone mass in ovariectomized (OVX) rats. The purpose of this study was to investigate the outcome in combination with 48CD (as bone-formative agent) and risedronate (RIS) (as anti-resorptive agent). Thirty three-week-old female SD rats were divided into 4 groups: baseline (n=10), sham (n=10), OVX (n=10), OVX with treatment (n=90). The treatments in detail were 1) monotherapy with 48CD (1,3,10mcg/kg, twice a day), 2) that with RIS (1,5mcg/kg, twice a week), 3) four combination therapies with these agents(48CD 3mcg/kg+RIS 1,5mcg/kg, 48CD 10mcg/kg+RIS 1,5mcg/kg) for 11 weeks (n=10 in all groups). Bone mineral density (BMD) values were measured in L5 and tibiae using pQCT. Trabecular microacrchitecture on cancellous bone in L6 and proximal tibiae, and cortical bone in tibiae were measured using microCT, and after these measurements, biomechanical test was performed on L6. 48CD increased the level of serum osteocalcin and urinary deoxypyridinoline, while RIS reduced them dose-dependently. Furthermore, the combination therapy maintained their does-dependent actions on bone metabolism. 48CD increased BMD both in spine and tibia, and RIS in tibia, dose-dependently. 48CD increased Tb.Th and changed rod-like structure into plate-like structure, whereas RIS showed a strong effect on connectivity density. Such independent effects on bone microarchitecture were maintained when the both agents were administered simultaneously. Combined 48CD and RIS had independent and additive effects on the strength (239.1N in OVX, 419.5N in 48CD (10mcg/kg), 288.7N in RIS (5), 445.4N in 48CD (10)+RIS (5)) as well as BMD, where the interactions of the two treatments were not significant (P>0.10) using a two-way ANOVA model. The additive effects were shown in cortical area and thickness. Although 48CD and RIS significantly independently increased the cortical density measured using microCT in comparison wth the OVX, the additive effect was not shown. Taken together, combination of 48CD and RIS could produce an additive effect on bone strength, which was considered due to maintaining individual actions on trabecular microarchitecture, as well as due to additive effects on cortical area.

Disclosures: ***M. Ito****, None.*

SA447

Glucose-dependent Insulinotropic Peptide Potentiates Parathyroid Hormone-Induced Increases In Bone Strength. F. Puentes*[1], D. Xie[2], K. H. Ding[1], M. Hamrick[3], A. L. Mulloy[1], C. M. Isales[1]. [1]Medicine, Medical College of Georgia and the Augusta VA Hospital, Augusta, GA, USA, [2]Institute of Molecular Medicine and Genetics, Medical College of Georgia, Augusta, GA, USA, [3]Cellular Biology and Anatomy, Medical College of Georgia, Augusta, GA, USA.

Parathyroid hormone (PTH) is known to stimulate bone formation when injected in a daily fashion. Similarly, we have demonstrated that Glucose-dependent insulinotropic peptide (GIP), an incretin hormone released from the small intestine in response to nutrient ingestion, also increases bone mass in vivo (see abstract by D. Xie et al). PTH acts predominantly to stimulate bone formation while GIP increases bone formation and inhibits bone breakdown. In view of recent data demonstrating a lack of synergism between daily PTH injections and the bisphosphonate alendronate on bone density, we decided to examine possible synergistic interactions between daily low-dose (25 µM) injections of PTH with or without daily GIP injections (10 nM). For these experiments we utilized three-month old female C57/Bl6 mice. Age and weight matched mice (ten animals/group) received daily subcutaneous injections of either: saline control, PTH (25µM) with or without GIP (10nM) for one month.

At the end of the four-week experimental period there was no statistically significant difference between the weights, fat or lean mass of the animals in the four different groups.

Bone density measurements by PIXImus demonstrated a significant increase in bone density in the animals receiving PTH (Control: 0.0477 vs. PTH: 0.0511 g/cm2, p<0.003). However, there was no significant change in bone density in animals receiving either GIP alone (Control: 0.0484 vs. PTH: 0.0486 g/cm2, p=NS) or any additive effect on bone mass in those animals receiving both GIP+PTH (PTH alone: 0.0510 vs. GIP+PTH: 0.0510 g/cm2, p=NS).

Despite a lack of a synergistic effect of GIP and PTH on bone density, biomechanical measurements involving three point bending revealed that GIP and PTH injections together did in fact further increase bone strength (Force at failure: Control: 16.7 N; GIP: 18.0 N; PTH: 19.6 N; GIP+PTH: 20.6 N; Control vs. PTH; p<0.0001 Control vs. GIP+PTH; Stress: Control: 7.4MPa; GIP: 7.9 MPa; PTH: 8.3 MPa; GIP+PTH: 9.2 MPa, p<0.05 PTH vs. GIP+PTH; p<0.05 GIP vs. GIP+PTH, p<0.001 Control vs. GIP+PTH).

These data are consistent with the conclusion that: 1. PTH even at lower concentrations than commonly reported has an anabolic effect on bone mass and strength. 2. GIP injection can potentiate PTH's effect on increasing bone strength.

Disclosures: ***F. Puentes****, None.*

SA448

Strontium Ranelate Increases Bone Quality in Rats: Improvement of the Microarchitecture and Preservation of the Intrinsic Bone Tissue Quality. P. Ammann*, S. Barrauld*, R. Dayer*, R. Rizzoli*. Division of Bone Diseases, Department of Internal Medicine, University Hospital, Geneva, Switzerland.

Recent clinical studies have demonstrated that strontium ranelate reduces the risk of vertebral and non-vertebral fracture in women with postmenopausal osteoporosis. We previously reported that strontium ranelate treatment increased maximal load (N) without affecting stiffness in adult female rats. We investigated the specific role of various determinants of strength in bone specimens of rats fed *ad libitum* a diet containing strontium ranelate at a daily dose of 0 (control) or 900 mg/kg/day (n=5/group), for 26 months. Microarchitecture was investigated using 3D-microCT analysis. Trabecular bone volume (BV/TV, %), trabecular number (Tb.N, /mm3), trabecular thickness (Tb.Th, mm), trabecular spacing (Tb.Sp, mm) and cortical thickness (Cort.Th, /mm) were determined.

	BV/TV	Tb.N	Tb.Th	Tb.Sp	Cort.Th
Control	48.4±3.2	4.10±0.19	0.122±0.006	0.212±0.014	3.52±0.02
Treated	70.2±1.5**	4.44±0.09*	0.173±0.006**	0.154±0.005**	4.25±0.02*

From the load deflection curve, obtained by axial compression of vertebral body, total and plastic energy (N*mm) were measured. Intrinsic bone tissue quality (Elastic Modulus, GPa, Hardness, GPa and Dissipated Energy, mN*nm) was evaluated by nanoindentation test performed on the vertebral body at the level of the trabecular nodes of dry bone tissue. Maximal load was 271.3±9.7 and 327.4±17.2* in controls and treated rats respectively. Energy was 101.8±7.9 and 157.3±15.0*, and plastic energy 30.0±3.3 and 70.7±10.0**. The elastic modulus was 17.8±1.04 and 17.7±0.71, hardness 0.818±0.061 and 0.855±0.054, dissipated energy 4294±128 and 4268±96 (means ± SEM, * : p<0.05, ** : p<0.01 vs control by Student-t test).

The increased energy to failure achieved with 900 mg/kg/d strontium ranelate treatment, was mainly due to an increment of plastic energy suggesting that bone formed under strontium ranelate treatment is able to withstand greater deformation before fracture while possessing similar elastic properties than non treated animal bone. The present results of 3D-microCT analysis and nanoindentation tests show that strontium ranelate treatment improves the trabecular and cortical microarchitecture respectively, without affecting the intrinsic quality of the formed bone material. These improvements in microarchitecture and the preserved quality of the bone tissue help to explain the antifracture efficacy of strontium ranelate in osteoporotic patients.

Disclosures: ***P. Ammann****, None.*

SA449

Comparative Uptake, Metabolism and Utilization of Menaquinone-4 and Phylloquinone in Human Cultured Cell Lines. Y. Suhara*, A. Murakami*, T. Okano. Department of Hygienic Sciences, Kobe Pharmaceutical University, Kobe, Japan.

It is generally accepted that availability of vitamin K in vivo depends on the homologues and their biological activities would be different from organ to organ. To evaluate this hypothesis, we examined the uptake, metabolism and utilization of menaquinone-4 (MK-4) and phylloquinone (PK) using their ^{18}O-labeled compounds in several kinds of human cultured cell lines (Hep G2, MG-63, and HUVEC). Lipid extracts were prepared from the cells and media collected at the time interval (1, 3, 6, 9, 12, 24h after incubation). The detection of the vitamin K analogues (^{18}O-, ^{16}O-quinone and epoxide forms) was carried out with LC-APCI-MS/MS method that we had previously reported. In this method, the ^{18}O of vitamin K was exchanged by atmospheric $^{16}O_2$ during the formation of vitamin K epoxide with carboxylative catalytic reaction. As the results, significant difference was observed between MK-4 and PK in the amounts uptaken into the cells. The ^{18}O-labeled MK-4 was extremely and rapidly absorbed into the cells and metabolized to the epoxide form via a hydroquinone form when compared to the ^{18}O-labeled PK. Rapid cellular uptake of the ^{18}O-labeled MK-4 continued by the end of culture (24 h) even after its conversion into the analogues was saturated. The differential uptake of MK-4 and PK was not affected by the treatment with Warfarin although the metabolism of both compounds was extremely inhibited. These findings suggest that a specific transporter(s) in the membrane and another metabolic pathway except for vitamin K cycle would exist in the cells and unknown metabolites might be produced. We conclude that these results should provide useful information to clarify some aspects of vitamin K action in the target cells and to develop new vitamin K drugs.

Disclosures: ***Y. Suhara****, None.*

SA450

See Friday Plenary number F450

SA451

Bone-protective Effects of Antidiabetic Thiazolidinediones in rat Adjuvant Polyarthritis: In Vivo DEXA Analysis. M. M. Muresan*[1], M. Koufany*[2], T. Maire*[1], D. Chappard*[3], P. Netter*[2], J. Y. Jouzeau*[2], G. Weryha[1]. [1]Endocrinology, CHU Brabois Adultes, Vandoeuvre, France, [2]Inserm, Faculte de Medecine, Vandoeuvre, France, [3]Inserm emi 335, Faculte de Medecine, Angers, France.

Adjuvant-arthritis in rats is characterized by synovial hyperplasia, inflammatory infiltration, cartilage destruction and generalized demineralization resulting both from reduced bone formation and increased bone resorption. We investigated the ability of 2 marketed TZDs to affect the severity of polyarthritis and corresponding bone changes in Wistar male rats (n=27). Polyarthritis was induced on day 0 by intradermal injection of 1 mg heat-inactivated Mycobacterium tuberculosis into the basis of the tail. Animals were randomly assigned to four groups: controls, arthritic untreated (ACF), arthritic treated with 10 mg/kg/day rosiglitazone (Rosi 10) or 30 mg/kg/day pioglitazone (Pio 30), from day of sensitization until necropsy (day 21) once/day by gastric gavage as suspension in 0.5 % carboxymethylcellulose. Arthritis severity was evaluated by a clinical score ranging from 0 (no sign) to 4 (severe) for each paw, yielding a maximum score of 16 per animal. DEXA analysis was performed in vivo the day before arthritis induction (D-1) and the day before necropsy (D20) using a Hologic fan beam QDR-4500A densitometer. Rats were anesthetized with isoflurane, positioned and scanned five times consecutively. Bone mineral density BMD, g/cm2 and bone mineral content BMC, g were determined on the whole body (total BMD & BMD) and on 3 regions of interest (ROI): lumbar spine (L2-L4), left femur and right femur. DEXA scan showed good precision and reproducibility for both whole body and ROIs. Arthritis severity was reduced by TZDs with Pio30 being more effective than Rosi 10 and loss in body weight gain corrected in a similar way. ACF rats had a less gain in total and ROIs BMD & BMC when compared to controls. TZDs prevented bone loss whatever the DEXA parameter used, with Pio30 being the most effective drug. TZD have controversial effects on normal bone since they could inhibit osteoblastogenesis by promoting stem cells differentiation into adipocytes while leaving resorption unaffected. However, they have antiproliferative, anti-inflammatory and immunomodulatory potencies which could have therapeutical relevance in the setting of inflammation-induced bone changes. The present work demonstrates that PPARg agonists prevent bone loss in experimental polyarthritis thereby suggesting that their anti-inflammatory properties account for the reduction of bone resorption. DEXA analysis in vivo is very reliable in terms of precision and reproducibility and suitable for longitudinal studies of rat skeleton in experimental models.

Disclosures: ***M.M. Muresan****, None.*

SA452

Outcome of Hip Fracture in the Elderly Aged 90 Years and Over. Y. Ishida. Department of Orthopaedic Surgery, Yamaguchi University School of Medicine, Yamaguchi, Japan.

This longitudinal study was conducted to investigate survival prognoses and functional results in the elderly aged 90 years and over with hip fracture. Seventy-four patients aged 90 years and over with hip fracture admitted to Tsushimi hospital between 1996 and 1999 were analyzed and followed until death or for at least 4 years. The age of the patients ranged between 90 and 99 years (65 women and 9 men, mean age 92.8 years) and all patients were surgically managed. All patients had severe osteoporosis (mean BMD at distal 1/3 radius, 0.33±0.01 mg/cm^2; T-score, 48.0±0.8%). Seventy-one of 74 patients (95.9%) presented at least one prevalent vertebral fracture on admission and the mean number of prevalent vertebral fractures was 2.48±0.19 per person. Overall, mortality was 27.0% during the first year. The significant predictors of survival prognoses were the pre-operative American Society of Anesthesiologists (ASA) score (relative risk of survival rate, RR= 2.82, 95% CI 1.57-5.08), pre-fracture walking ability (RR= 1.56, 95% CI 1.03-2.34), type of fracture (RR= 2.08, 95% CI 1.05-4.12), type of surgery (RR= 1.98, 95% CI 1.01-3.91), and the number of prevalent vertebral fractures on admission (RR= 1.38, 95% CI 1.11-1.72). Dementia was the significant predictor of the recovery of walking ability (on admission, odds ratio, OR=28.6, 95% CI 3.73-200.0; after surgery, OR=22.7, 95% CI 3.03-166.7): the recovery rate of walking was lower in patients with severe dementia. The number of prevalent vertebral fractures on admission was also the significant predictor of the recovery of walking ability (OR=1.64, 95% CI 1.04-2.59). Results of this study suggest that the type of surgery is the factor that can be chosen after injury among factors related to survival prognosis. In addition, the prevalent vertebral fracture is the significant predictor of both functional and survival prognosis, indicating the importance of treatment of osteoporosis for preventing vertebral fractures as well hip fractures.

Disclosures: ***Y. Ishida****, None.*

SA453

Does Vertebral Height Restoration Achieved at Vertebroplasty Matter? F. E. McKiernan, T. Faciszewski, R. Jensen*. Center for Bone Diseases, Marshfield Clinic, Marshfield, WI, USA.

Many vertebral compression fracture (VCF) sequelae are thought to result from loss of normal vertebral height and sagittal alignment. Percutaneous vertebroplasty (PV) can result in vertebral height restoration (VHR) and sagittal realignment but the assumption that this results in improved clinical outcomes is untested. The objective of this study was to determine whether VHR achieved at PV resulted in additional improvements in pain or functional outcome compared to no VHR.

This is an IRB approved, prospective study of consecutive patients undergoing PV. All subjects completed the OQLQ, a validated, 30-item, 5-domain (symptoms (Sx), physical function (Pf), activities of daily living (ADL), leisure (Le), emotional function (Ef)), 7-point response option instrument that measures health related quality of life (HRQOL) in osteoporotic women with back pain due to VCF. 2 wks, 2 mos and 6 mos postoperatively subjects completed the mini-OQLQ, a validated extraction of OQLQ. Pain was rated using a standard visual analogue scale (VAS) pre-op, 1 d post-op and each evaluation point thereafter. X-rays were manually digitized using centralized PACS system software and evaluated for the presence of dynamic mobility (DM) and VHR. DM is change in anterior vertebral height (ΔHa) between preoperative standing and supine X-rays that exceeds our in vivo precision error for Ha by 2 SD (thus, DM ≥ +/- 0.8 mm). VHR was ΔHa between pre- and post-operative standing lateral X-rays centered on the treated VCF after correction for magnification error.

46 subjects (32F/14M) underwent 49 PVs to treat 66 painful VCFs. Mean age was 74.3 ±10.9 years. 50% of treated VCFs were at T11-L1. Mean fracture age was 2.5 ± 2.1 mos. 59% had sustained previous fragility fracture. 26% were current steroid users. 1d after PV pain rating fell from 7.7 to 2.8 ± 1.8 ($p<0.001$) and remained improved through mo 6 ($p<0.001$). 2 wks post-PV all 5 OQLQ domains improved substantially (Sx, ADL and Le ($p\leq0.001$), Pf ($p=0.003$) and Ef ($p<0.02$)) and remained improved through mo 6 ($p\leq0.001$, except Ef; $p=0.007$). Average DM for all treated VCFs = +3.7 mm. Average DM in mobile VCFs = +5.5 mm (-2.9 to 19.9 mm). Average postoperative VHR in mobile VCFs = +2.9 mm (-2.1 to +9.6mm). Correlation between DM and postoperative VHR was excellent ($r=0.9$, $p<0.001$). Multivariate analysis showed that VHR achieved at PV did not correlate with superior postoperative pain relief or consistent additional improvement in any OQLQ domain compared with failure to achieve VHR.

The rationale and desire to restore vertebral height and sagittal alignment during PV are compelling but these initial data do not demonstrate additional benefit to pain relief or QOL over 6 months when incomplete VHR is achieved.

Disclosures: ***F.E. McKiernan****, None.*

SA454

The Cost-effectiveness of Bone Protection in Patients Using Oral Glucocorticoids. T. P. van Staa[1], P. Geusens[2], H. Leufkens*[3], H. Pols[4], C. Cooper[5]. [1]Procter&Gamble Pharmaceuticals, Egham, United Kingdom, [2]Limburg University Center, Diepenbeek, Belgium, [3]Utrecht University, Utrecht, Netherlands, [4]Erasmus University Medical Center, Rotterdam, Netherlands, [5]University of Southampton, Southampton, United Kingdom.

There are few data on the cost-effectiveness of bone protection in patients using oral glucocorticoids (GC). An individual patient-based pharmaco-economic model was developed using data from a large cohort of oral GC users aged 40+ (N=190,000) in the UK General Practice Research Database.

Mortality and hip, vertebral, and other osteoporotic fracture risks for each individual were estimated by age, sex, daily and cumulative GC dose, indication and other clinical risk factors (using Cox regression). The vertebral risks were standardised to those of the EPOS study (1/3 of the vertebral fractures were considered to be clinically symptomatic). UK costs on medication (the middle cost of a bisphosphonate) and direct costs of fracture were obtained from a UK national report (NICE) and discounted annually by 6% (£1=US$1.75). The fracture reduction by bisphosphonates was taken as 50%. The excess mortality in the 1 year after a fracture was based on a comparison of fracture cases to controls matched by age, sex, and GC indication and adjusted for GC dose and clinical risk factors. Using the individual mortality and fracture risks, the outcomes were simulated over a 5-year period, comparing presence and absence of bone protection. Bootstrapping techniques were used to calculate 95% confidence intervals (CI).

It was found that mortality and fracture risks were related to GC dose, indication and clinical risk factors. With use of 5 mg GC daily, the cost to avoid one fracture with a bisphosphonate was $49,023 (95% CI $46,765-51,066) in women aged 45 [men $80,841 (76,377-84,771)] and $6410 (5861-6877) in women aged 85 [men $17,163 (16,088-17,889)]. With 15 mg GC, these figures were $28,348 (27,328-29,131) and $5840 (5394-6259) in women and $46,120 (43,979-47,775) and $13,766 (13,109-14,558) in men, respectively. The cost-effectiveness improved in patients at high risk of fracture. With 5 mg GC daily, the cost to avoid one fracture was $54,800 in women aged 45 at low risk of fracture (15 mg GC: $32,313) and $28,102 at high risk (with 15 mg GC: $15,231). For men, these figures were $94,819 and 43,173 for 5 mg GC and $53,766 and $24,908 for 15 mg GC, respectively.

These data support the cost-effectiveness of bisphosphonates in oral GC users, improving with higher GC dose and targeting of high risk patients.

Disclosures: ***T.P. van Staa****, None.*

SA455

Health Utilities Index 3 Scores in Osteoporosis Compared to other Chronic Medical Conditions: A Population-Based Study from the Canadian Multicentre Osteoporosis Study (CaMos). A. M. Sawka[1], L. Thabane*[2], A. Papaioannou[3], A. Gafni*[2], G. Ioannidis[4], E. Papadimitropoulos[5], W. Hopman[6], A. Cranney[7], D. A. Hanley[8], L. Pickard[4], J. D. Adachi[4], C. Investigators*[9]. [1]Endocrinology, McMaster University, Hamilton, ON, Canada, [2]Clinical Epidemiology and Biostatistics, McMaster University, Hamilton, ON, Canada, [3]Medicine, McMaster University, Hamilton, ON, Canada, [4]Rheumatology, McMaster University, Hamilton, ON, Canada, [5]Eli Lilly, Toronto, ON, Canada, [6]Queens University, Kingston, ON, Canada, [7]Rheumatology, University of Ottawa, Ottawa, ON, Canada, [8]Endocrinology, University of Calgary, Calgary, AB, Canada, [9]Canadian Multicentre Osteoporosis Study, Hamilton, ON, Canada.

The Health Utilities Index 3 (HUI3) is a generic health status classification system. Data from the Canadian National Population Health Survey (NPHS) of 1996/97 have been used to compare relative decrements in HUI3 measurements between chronic conditions. HUI3 results were not reported for osteoporosis in the NPHS. We aimed to determine the relative decrement in HUI3 score attributed to osteoporosis compared to other chronic medical conditions using CaMos data. CaMos is a national cohort study in which regional participants were randomly recruited. We studied participants aged 65 years and older who completed a Health Utilities Index 3 (HUI3) questionnaire. An age- and gender-adjusted linear regression analysis was performed predicting mean decrement in HUI3 score for the following self-reported medical conditions: arthritis (osteoarthritis or rheumatoid arthritis), chronic obstructive pulmonary disease (COPD), diabetes mellitus (DM), heart disease (heart attack), and hypertension. Of the 4550 participants age ≥65 years recruited in CaMos, 1226 men and 3269 women completed a baseline HUI3 questionnaire, and 3712 participants provided information on presence of chronic medical conditions. The mean changes in HUI3 adjusted for age and gender (with 95% confidence intervals) were as follows: arthritis -0.10 (-0.11, -0.08), COPD -0.07 (-0.09, -0.05), DM -0.06 (-0.08, -0.03), heart disease -0.06 (-0.08, -0.03), hypertension -0.02 (-0.03, -0.01), and osteoporosis -0.09 (-0.11, -0.06), respectively. The mean changes in HUI3 for chronic conditions adjusted for age and gender for patients ≥65 years in the NPHS were similar to those seen in CaMos: arthritis -0.08, COPD -0.09, DM -0.06, heart disease -0.06, and high blood pressure 0.0. In conclusion, the decrement in HUI3 score seen in patients with self-reported osteoporosis was similar to that observed with other self-reported chronic medical conditions such as arthritis, COPD, diabetes mellitus, or heart disease.

Disclosures: ***A.M. Sawka****, Hoffmann-LaRoche 2.*

SA456

Quality of Life Measures in Canadian Aboriginal Women: The First Nations Bone Health Study. C. J. Metge*[1], W. D. Leslie[2], H. A. Weiler*[3], C. K. Yuen[2], M. Doupe*[2], E. A. Salamon[4], P. Wood Steiman*[5], J. D. O'Neil*[2], C. R. Greenberg*[2], L. M. Lix*[2], L. L. Roos*[2], A. Tenenhouse[6]. [1]Faculty of Pharmacy, University of Manitoba, Winnipeg, MB, Canada, [2]Faculty of Medicine, University of Manitoba, Winnipeg, MB, Canada, [3]Human Nutritional Sciences, University of Manitoba, Winnipeg, MB, Canada, [4]Department of Medicine, University of Manitoba, Winnipeg, MB, Canada, [5]Assembly of Manitoba Chiefs, Winnipeg, MB, Canada, [6]Department of Medicine, McGill University, Montreal, PQ, Canada.

Canadian Aboriginal women are at increased fracture risk compared with the general population (JBMR 18:S151,2003) but little is known about the burden of osteoporosis in this population. The First Nations Bone Health Study (FNBHS) is assessing indicators of bone health in Aboriginal and non-Aboriginal adult women and has relied on the Canadian Multicentre Osteoporosis Study (Ca*Mos*) for many of its measures and for Canadian normative data. Included in the baseline measurements was a health status measure, the Rand Health Science Program SF-36. The physical dimensions of this measure have been reported by Ca*Mos* to be sensitive to osteoporotic fractures (Osteoporos Int 2001;12:903). There have been no previous reports of use of the SF-36 measure in Canadian Aboriginal women. The FNBHS recruited a random age-stratified (25-39, 40-59 and 60-75) sample of Aboriginal women (n=267) and age-matched White women (n=184). The SF-36 survey was administered by trained interviewers as part of a detailed baseline survey. Aboriginal women had lower scores than White women on both the SF-36 physical health summary (PCS) and mental health summary (MCS) quality of life (QOL) components [PCS: 44.1±12.2 vs. 48.1±10.8, P=0.0004; MCS: 46.8±12.7 vs. 51.0±10.5, P=0.0050]. Fracture cases had lower PCS scores than non-fracture cases while MCS was similar [PCS: 44.4±12.3 vs. 47.2±11.1, P=0.0119; MCS: 47.5±12.7 vs. 48.6±11.3, P>0.2]. A 2-way ANOVA tested the independent effects of self-reported fracture and Aboriginal ethnicity on QOL. For PCS, there were significant main effects of fracture [F(1,440)=5.38, P=0.0208] and ethnicity [F(1,440)=12.11, P=0.0005] but no significant interaction [F(1,440)=0.64, P=0.4224]. For MCS, there was a main effect of ethnicity [F(1,440)=8.48, P=0.0038] but no significant fracture effect or interaction. In summary, the FNBHS provides the first comprehensive assessment of health status using the SF-36 in Canadian Aboriginal women. Our findings justify further work to validate the use of the SF-36 physical dimensions as a specific indicator of fracture-related QOL in Aboriginal women.

Disclosures: ***C.J. Metge****, None.*

SA457

Combination Therapy with Alfacalcidol and Risedronate at Their Subtherapeutic Doses Can Additively Improve Bone Dynamics in Ovariectomized Rat Model of Osteoporosis. A. Shiraishi*[1], M. Ito[2], N. Hayakawa*[1], N. Kubota[1], N. Imai*[1]. [1]Product Research Dept., Chugai Pharmaceutical Co., Ltd., Gotemba, Japan, [2]University of Nagasaki, Nagasaki, Japan.

Both alfacalcidol (ALF) and risedronate (RIS) have been reported to prevent estrogen deficiency-induced bone loss by an anti-resorptive effect. The aim of this study was to clarify the additive effect of simultaneous administration with ALF and RIS on the bone dynamics in ovariectomized (OVX) rats. Female wistar rats were OVX- or sham-operated at 40 weeks of age. Twelve weeks post-surgery, rats were randomized into 7 groups (n=7-8): 1) sham+vehicle, 2) OVX+vehicle, 3) OVX+ALF 0.025 μg/kg/day, 4) OVX+ALF 0.05 μg, 5) OVX+RIS 0.3 mg, 6) OVX+RIS 3.0 mg, 7) OVX+ALF 0.025 μg+RIS 0.3 mg. Each drug was administered orally 5 times a week for 12 weeks. The combined administration with ALF and RIS increased the mechanical strength in lumbar vertebra and femoral midshaft ($p<0.01$, $p<0.001$ vs. OVX group, respectively). The vertebral strength in ALF+RIS group (423N) was higher than the 371 and 296N in the ALF 0.025- and RIS 0.3-treated groups (n.s., $p<0.01$, respectively). To evaluate whether the site-specific improvement by combination therapy influenced the spinal strength, micro-CT and pQCT analyses were performed. As analyzed by pQCT, of particular interest, the additive effect of ALF and RIS on bone density was produced in cortical and sub-cortical regions more than trabecular region, whereas the BV/TV, Tb.Sp. and BS/BV in the ALF+RIS group were significantly higher than those in the OVX group. This indicated that the combined therapy affected not only trabecular bone but also cortical site, resulting in marked increment of spinal strength. Combined ALF and RIS had independent and additive effects on the strength as well as BMD in both spine and femur, where the interactions of the two treatments were not significant ($P>0.10$) using a two-way ANOVA model. Additionally, the combination therapy reduced urinary deoxypyridinoline excretion more than either drug alone (76.2% reduction vs. 42.2% for ALF, 14.5% for RIS, from OVX group). In conclusion, ALF and RIS can additively improve bone dynamics through the beneficial effect on both cortical and trabecular regions, and exert the additive anti-resorptive activity in rats, although the histomorphometrical analysis has been proceeding to clarify the exact mechanisms. Taken together, it is suggested that the combination of ALF and RIS therapy has a therapeutic advantage over each monotherapy for the treatment of osteoporosis.

Disclosures: ***A. Shiraishi****, None.*

SA458

Identification of Fast Bone Losers and Treatment with Alfacalcidol. M. A. Dambacher[1], M. Neff*[2], M. Ito*[3], E. Schacht*[1], R. Kissling*[1]. [1]Rheumatology and Rehabilitation, University Clinic Balgrist, Zürich, Switzerland, [2]Center for Osteoporosis, University Clinic Balgrist, Zürich, Switzerland, [3]Department of Radiology, School of Medicine, Nagasaki, Japan.

For the individualisation of prophylaxis and treatment of osteoporosis we use the high resolution peripheral quantitative computed tomography (hrpQCT system). We could show that postmenopausal patients with high bone turnover evaluated by biochemical parameters are identical to fast bone losers as determined by the hrpQCT system. As a consequence, we prefer agents that inhibit bone resorption in fast bone loser patients and agents that stimulate bone formation in slow bone loser patients.

For evaluation of the rate of bone loss, we use a high resolution pQCT system (DENSISCAN 1000), reproducibility of 0.2-0.4% in mixed population of normal individuals and patients with osteopenia or osteoporosis. This system enables us to assess trabecular and cortical bone density separately in the radius and differentiate between fast and slow bone losers within 6 to 9 months (threshold: >3 % loss of trabecular bone density in the radius per year).

In this study we examined fast bone losers with osteoporosis and osteopenia (N = 33) and could show with this high precise system that Alfacalcidol can halt fast bone loss (see graph).

In an animal study (Ito) with OVX rats, the results can be summarized: max. load, trabecular volume, trabecular thickness, trabecular number are increased, inter-trabecular space decreased with Alfacalcidol. The loss of bone mass and quality in these ovarectomized animals could be stopped with Alfacalcidol.

We can conclude that Alfacalcidol has an excellent effect especially on the trabecular bone in fast losers and that we can adapt the treatment for different forms of osteoporosis and bone turnover by the highly sensitive hrpQCT system. The result is not only a reduction of the number of nonrespondens but also a better compliance of the patients. Because our treatment was based on precise objective measurements, treatment modifications - especially in those patients who change from a slow to a fast bone-loser-state - can easily be justified.

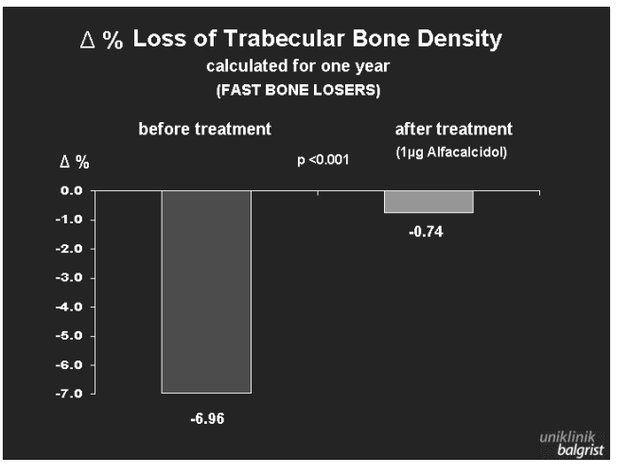

Disclosures: ***M.A. Dambacher****, None.*

SA459

See Friday Plenary number F459

SA460

A New Active Vitamin D, ED-71, Increases Bone Mass in Osteoporotic Subjects under Vitamin D Supply. T. Matsumoto[1], M. Shiraki[2], T. Nakamura[2], T. Hashimoto*[2], H. Itakura*[2], K. Suzuki*[2], T. Miki[2], N. Hamada*[2], T. Sugimoto[2], Y. Kuroki*[2], Y. Fujii[2], H. Hagino[2], S. Takata[2], S. Ikeda*[2], T. Nakano*[2], S. Okamoto[2], T. Hirota[2], Y. Tanigawara[2], M. Fukunaga[2], Y. Hayashi[2]. [1]University of Tokushima, Tokushima, Japan, [2]The ED-71 Clinical Study Group, Tokyo, Japan.

ED-71 [1α,25-dihydroxy-2ß-(3-hydroxypropoxy)vitamin D_3] is an analog of 1α,25-dihydroxyvitamin D_3 [1α,25$(OH)_2D_3$] with potent effects on bone. An earlier clinical study in osteoporotic subjects demonstrated that treatment with 0.25 to 1.0 µg/day ED-71 for 6 months increased lumbar bone mineral density (L-BMD) in a dose-dependent manner without causing sustained hypercalcemia or hypercalciuria. However, because many patients showed serum 25(OH)D levels below 20 ng/mL, there was a possibility that the effect of ED-71 on bone mass may be observed due to a nutritional vitamin D insufficiency of these patients.

The present study was undertaken to clarify whether the effect of ED-71 on bone is different from that of native vitamin D, and whether ED-71 can effectively increase bone mass in osteoporotic subjects under vitamin D supply with normal serum 25(OH)D.

Osteoporotic subjects with 49 to 87 years of age (mean 67.2 years, 218 subjects) were enrolled in the study. They were stratified by serum 25(OH)D levels, and for subjects with serum 25(OH)D below 20 ng/mL, 400 IU/day vitamin D_3, and for subjects with serum 25(OH)D over 20 ng/mL, 200 IU/day vitamin D_3 was supplemented throughout the study. In each stratum, the subjects were randomly assigned to placebo, 0.5, 0.75 or 1.0 µg/day ED-71, and treated for 12 months. L-BMD was measured as a primary end point, along with total hip BMD (H-BMD) and bone markers.

In 162 subjects (74%), serum 25(OH)D levels were below 20 ng/mL at the entry. Serum 25(OH)D became over 20 ng/mL in 93% of subjects by vitamin D_3 supplement at 3 months. After 12 months, L-BMD decreased slightly in placebo group (-0.72%), whereas ED-71 treatment increased L-BMD in a dose-dependent manner (2.16, 2.64 and 3.19, in 0.5, 0.75 and 1.0 µg/day groups, respectively. $p<0.01$ vs placebo in all three groups). H-BMD also increased significantly by 0.75 and 1.0 µg ED-71 treatment (0.6 and 0.9%, respectively). ED-71 was well tolerated at all doses examined, and only 2 patients developed transient hypercalcemia over 11 mg/dL.

These results demonstrate that ED-71 treatment can effectively increase bone mass in patients with sufficient vitamin D supply without causing sustained hypercalcemia. It is suggested that ED-71 may serve as a tissue-selective vitamin D agonist with stronger effects on bone.

Disclosures: ***T. Matsumoto****, Chugai Pharmaceutical Co., Ltd. 2, 5.*

SA461

Hearing Impairment in Familial X-Linked Hypophosphatemic Rickets. G. Fishman*[1], D. Miller-Hansen*[2], C. Jacobsen*[2], V. K. Singhal*[1], U. S. Alon*[3]. [1]Plastic and Craniofacial Surgery, Children's Mercy Hospital, Kansas City, MO, USA, [2]Hearing and Speech Department, Children's Mercy Hospital, Kansas City, MO, USA, [3]Pediatric Nephrology, Bone and Mineral Disorders Clinic, Children's Mercy Hospital, Kansas City, MO, USA.

Objective: The aim of the study was to assess hearing in patients with familial X-linked hypophosphatemic rickets (XLH) in order to better understand the association between the disease and hearing status, thus providing information regarding patients management. **Material and Methods:** Hearing evaluations including audiometry, tympanometry and stapedial reflex thresholds recording were prospectively performed in 16 children with XLH (aged: 1-18 years, mean: 8.5, median: 9.0, 6 males, 10 females) and all their 10 afflicted parents (aged 22-55 years, 3 male, 7 female). Further investigations were conducted when indicated. Related literature was searched and reviewed. **Results:** None of the individuals had a history of receiving treatment with ototoxic drugs, noise exposure, previous ear surgery or chronic ear disease. Fifteen of 16 children demonstrated normal hearing. One with bilateral profound hearing loss was found to have a congenital inner ear malformation (Mondini malformation). Among the adults, 2 males and 1 female (30%) ages 34-52 demonstrated sensorineural hearing loss, which was attributed to the disease process since other etiologies were ruled out. All three had severe XLH-related orthopedic manifestations. Analysis of three previously published articles studying a total of 66 XLH patients revealed hearing impairment in 1/14 children (7.1%) and 26/52 adults (50.0%) (Chi-square, $p<0.01$). **Conclusions:** We conclude that hearing impairment in XLH is likely part of the natural history of the disease, developing during adulthood. Therefore, whereas close follow-up and hearing monitoring is recommended in adults, serial audiograms in children with XLH are not justified. Furthermore, in a child with XLH and hearing impairment other etiologies should be explored.

Disclosures: ***U.S. Alon****, None.*

SA462

See Friday Plenary number F462

SA463

Cementum and Dentin in Childhood Hypohosphatasia Teeth. T. VandenBos*[1], G. Handoko*[1], A. Niehof*[1], M. Whyte[2], W. Beertsen[1]. [1]Periodontology, ACTA, Amsterdam, Netherlands, [2]Center for Metabolic Bone Disease and Molecular Research, Shriners Hospitals for Children, St. Louis, MO, USA.

Hypophosphatasia (HPP) is characterized biochemically by reduced activity of the tissue-nonspecific isoenzyme of alkaline phosphatase (TNSALP). Consequently, skeletal mineralization can be impaired causing rickets in affected children. Additionally, HPP almost invariably leads to premature loss of deciduous teeth due to defective formation of cementum. It was the objective to determine whether acellular and cellular cementum and various compartments of dentin are equally affected in HPP.

31 teeth from 7 children with the odonto- (n=2) or childhood (n=5) forms of HPP were compared with matched teeth from 21 healthy children. In addition to light and electron microscopy, mineral content was determined biochemically and by quantitative microradiography.

In all but 3 of the HPP teeth, acellular cementum layers were absent. Cellular cementum were present in 7 of 22 HPP teeth (9 not assessed due to root resorption). In the various dentin compartments (crown, root, circumpulpal, mantle), significant variations in mineral content were detected in both controls and HPP -highest density coronally, and lowest apically. However, no statistically significant differences were found between HPP and controls in any dentin compartment. To determine whether the dissimilar effects concerning cementum and dentin in HPP were related to pyrophosphate (PP_i) metabolism, we quantitated the PP_i concentrations and the expression and activity of TNSALP and other enzymes related to PP_i metabolism (e.g., PC-1 and ANK) in the periodontal ligament (PDL) and pulp of healthy teeth. Compared to the PDL, expression of TNSALP and PC-1 (per GAPDH) in pulp was about 50% and 10%, respectively. Also, the activity of PC-1 was significantly lower in pulp, as was the concentration of PP_i. ANK expression, however, was similar in the two tissues.

In HPP teeth, formation of cementum is severely diminished whereas the mineralization of dentin is unaffected. Differences in gene expression and activity of enzymes involved in PP_i metabolism are in keeping with the dissimilar impact on cementum and dentin of childhood and odonto-HPP.

Disclosures: ***T. VandenBos****, None.*

SA464

See Friday Plenary number F464

SA465

Osteoporosis Pseudoglioma Syndrome: 4 Siblings With a Compound Heterozygote LPR5 Mutation. E. A. Streeten[1], E. Puffenberger*[2], H. Morton*[2], D. McBride*[1]. [1]Endocrinology, Diabetes and Nutrition, University of Maryland School of Medicine, Baltimore,, MD, USA, [2]The Clinic for Special Children, Strasburg, PA, USA.

Osteoporosis-pseudoglioma syndrome (OPPG) is a rare autosomal recessive disorder of severe juvenile osteoporosis and congenital blindness, due to mutations in the LRP5 gene. Approximately 35 cases of OPPG are known worldwide. One year ago at this meeting, we reported 3 siblings with OPPG (Family 1), members of a conservative Mennonite church in PA, with an exon 6 (Trp-425-X) LRP5 mutation. We now report 4 additional siblings with OPPG (Family 2) who are cousins to Family 1. The 4 siblings in Family 2 are boys aged 15 and 5 and girls aged 10 and 4 years. All have been blind from birth, similar to Family 1, but have a more mild bone phenytype. The spine Z scores of the affected children in Family 2 are -3.5, -2.8, -1,7 and -2.3, compared to -6.1, -5.0 and -3.4 in Family 1. All OPPG children in both families appear intellectually normal. Unlike Family 1, only 1 affected (10 yo girl) in Family 2 had typical OPPG facies and joint hyperextensibility.

In Family 2, only one affected child (10 yo girl) has had a fragility fracture (wrist). The parents have osteopenia with spine T scores of -1.5 (mother) and -1.6 (father); both had normal hip T scores. There are 4 unaffected siblings. To study the LRP5 gene in Family 2, genomic DNA for PCR was obtained from the oldest (15 yo) boy's leukocytes in order to confirm the LRP5 exon 6 mutation found in Family 1. Sequence analysis demonstrated he was heterozygous for the exon 6 LRP5 mutation found in Family 1 (W-425-X) and a second exon 6 mutation (T-409-A). This compound heterozygote mutation appears to be sufficient to cause congenital blindness and osteoporosis but the bone phenotype is more mild than was seen in Family 1. DNA analyses of the 3 other OPPG children and the parents in Family 2 are in progress.

In summary, we report 4 siblings with OPPG and a novel compound heterozygote LRP5 mutation with a more mild bone phenotype than their cousins who are homozygous for one of the same mutations

Disclosures: E.A. Streeten, Merck 2.

SA466

See Friday Plenary number F466

SA467

Analysis of Variation in Expression of ADO2: Searching for the Modifier Genes. K. Chu*[1], D. L. Koller[2], R. Snyder*[1], D. Lai*[2], T. Fishburn*[1], T. Foroud[2], M. J. Econs[1]. [1]Medicine, Medical School of IUPUI, Indianapolis, IN, USA, [2]Medical and Molecular Genetics, Medical School of IUPUI, Indianapolis, IN, USA.

Autosomal Dominant Osteopetrosis type II (ADO2) is an osteosclerotic disorder due to heterozygous mutations in the ClCN7 gene. Analysis of ADO2 in our pedigrees indicates that the penetrance is 66%, with a highly variable phenotype even between family members with the same mutation. To identify genes that modify disease severity, we performed a 10cM genome-wide scan using 400 microsatellite markers in 8 ADO2 families. Parametric linkage analysis was conducted with the MLINK program, using both dominant and recessive models. Using the recessive model, evidence of linkage was detected with marker D9S283 (LOD=2.03) and with D2S347 (LOD=1.52). Additional microsatellite markers were then genotyped on chromosomes 9 and 2 to better delineate the position of the putative modifier locus. Based on the key recombinants in the families, a candidate 4.6 cM region was identified on chromosome 9q22. Of note, candidate genes in this region include cathepsin L, which is secreted by osteoclasts and processed to an active enzyme by acid, surface activation, or proteolysis. We are currently analyzing cathepsin L as well as other genes on chromosomes 9q22 and 2q14 to identify genes that modify phenotypic expression.

Since the linkage search strategy pursued above would be invalid in the chromosome 16pter region due to confounding of the disease mutation and putative modifier effects, we have also considered the hypothesis that genetic variation at other sites within the ClCN7 gene might influence disease expression. DNA sequence data has shown that at position 418 of the ClCN7 protein sequence there is a missence polymorphism resulting in an amino acid change from valine to methionine (V418M). To test the hypothesis that this polymorphism affects disease severity we genotyped this polymorphism in our ADO2 families. We found that, on the chromosome with the WT-ClCN7 allele, 94.54% (52/55) of affected and 75% (24/32) of carriers had the M allele while 5.45% (3/55) of the affected and 25% (8/32) of carriers had the V allele (p=0.016). Further analysis indicated that most of the evidence of association came from the 4 families with the G215R mutation. In these families, 100% (16/16) of affected and 42.86% (3/7) of carriers had the V allele on the non-disease carrying chromosome, while none of the affected and 57.14% (4/7) of the carriers had the M allele.

In conclusion, regions of chromosome 9 and 2 may harbor genes that affect disease severity. Additionally, we find statistical support for the hypothesis that the V418M polymorphism, on the non-mutant ClCN7 gene allele, influences the tendency to become an asymptomatic carrier.

*Disclosures: **K. Chu**, None.*

SA468

See Friday Plenary number F468

SA469

Tumoral Calcinosis: Resolution With Nasal Calcitonin Therapy / Dietary Mineral Reduction. D. Wenkert[1], W. H. McAlister*[2], M. P. Whyte[1]. [1]Shriners Hospitals for Children, St. Louis, MO, USA, [2]Washington University School of Medicine, St. Louis, MO, USA.

Tumoral calcinosis features painless mineral deposits involving periarticular bursae on the extensor surfaces of major joints. Hyperphosphatemia and increased TmP/GFR (phosphate transport maximum/glomerular filtration rate) occur in some patients. Treatment by phosphate (Pi)-binding with aluminum hydroxide (together with dietary Ca and Pi deprivation) as well as surgical excision has had some success. We document complete resolution of tumoral calcinosis after treatment with salmon calcitonin given by nasal spray together with dietary mineral reduction.

Our patient, a 15-7/12 year old Mexican-American girl, presented with a 3-4 year history of periarticular calcifications. She was healthy until age 12 or 13 years when she noticed pain and a mass overlying her right hip. Xrays revealed calcific deposits surrounding both hips. Serum calcium, Pi, 25-hydroxyvitamin D, aldolase, AST, ALT, CK, and alkaline phosphatase activity were normal. At age 14 years, xrays showed persisting calcific masses surrounding her hips. Bone scan revealed uptake on the right. Her masses continued to grow. She complained of discomfort and decreased range of motion of her right hip, although physical activities continued. Family history and review of systems were unremarkable for signs of autoimmune disease or calcinosis. Physical exam disclosed mild dermatographism, lividoreticularis (without Raynaud's phenomenon), 3-4 small café-au-lait spots, vitiligo, and stretch marks overlying her hips, but no facial or shawl rash, Gottron's papules, telangiectasias, or periungual changes. The palpable mass overlying her lateral right hip was somewhat mobile. Hip flexion there was decreased as compared to the left. Laboratory evaluation was remarkable only for an elevated sedimentation rate (40). Renal tubular reabsorption of phosphate was 95%. Nasal calcitonin therapy was begun (200u q day). During this time, our patient electively decreased her calcium intake by 50% and her phosphate intake by 25%. Within the first few months of therapy, her parents reported disappearance of the lump under her jeans. Complete radiographic resolution had occurred when first re-radiographed after 10 months of therapy. Nasal calcitonin was then stopped. Eight months later, physical examination revealed no re-emergence of the mass, and a return of her right hip range of motion. Xrays showed no recurrence. A single dose of calcitonin given at that time decreased her TRP from 97% to 94%.

Dietary mineral restriction with nasal calcitonin therapy to enhance mineral excretion should be evaluated in additional cases of tumoral calcinosis.

*Disclosures: **D. Wenkert**, None.*

SA470

Cinacalcet HCl Attenuates Hypercalcemia Observed in Mice with Either a Rice H-500 Leydig Cell or C26-DCT Tumor. M. Colloton*, E. Shatzen*, B. Wiemann*, C. Starnes*, D. Martin. Departments of Metabolic Disorders and Oncology, Amgen, Thousand Oaks, CA, USA.

Excessive secretion of PTHrP from certain tumor cells produces hypercalcemia by stimulating bone resorption and increasing renal tubular reabsorption of calcium. Hypercalcemia is associated with substantial morbidity and mortality. The calcium-sensing receptor (CaR) plays a key role in systemic calcium homeostasis by regulating parathyroid hormone (PTH) secretion in response to changes in extracellular calcium. The calcimimetic cinacalcet HCl binds to and allosterically modulates the CaR to increase its sensitivity to extracellular calcium. We investigated the ability of cinacalcet HCl to attenuate hypercalcemia in mice bearing either a Rice H-500 Leydig cell (Leydig tumor) or C26-DCT tumor and determined the effects of cinacalcet HCl on serum PTHrP levels in mice bearing a Leydig tumor.

Rice H-500 Leydig cells or C26-DCT cells were implanted subcutaneously into the proximal dorsal midflank of female CB17/SCID or male CDF-1 mice, respectively. Implanted mice in each group were divided into 8 subgroups and treated with cinacalcet HCl (3 or/and 30 mg/kg p.o.), its less active enantiomer S-AMG 073 (30 mg/kg p.o.), or vehicle, starting from day one after inoculation until sacrifice on day 10 (Leydig tumor), as a single dose on day ten (Leydig tumor), or as a single dose on day 17 (C26-DCT tumor). Animals were sacrificed 4 hrs after final drug treatment, and blood was removed for determination of calcium, phosphorus and PTHrP levels.

Vehicle-treated mice bearing either tumor had significantly higher baseline serum ionized calcium and/or total calcium levels than control mice without tumors. Cinacalcet HCl given daily or as a single dose significantly reduced serum ionized calcium and total calcium in both tumor models when compared to vehicle-treated animals (Table illustrates single dose studies). Furthermore, cinacalcet HCl normalized serum phosphorus levels but had no effect on elevated serum PTHrP levels. The less active enantiomer S-AMG 073 had no effect on serum calcium or phosphorus levels or on PTHrP levels in either tumor model.

Biochemistry in Mice (4 hours after a single treatment dose)

		C26-DCT Tumor			Rice H-500 Leydig Tumor	
Group	Tumor	Ca^{2+} (mmol/L)	Calcium (mg/dL)	Phosphorus (mg/dL)	Ca^{2+} (mmol/L)	PTHrP (pg/ml)
Control	No	1.4 ± 0.01	10.3 ± 0.5	10.1 ± 4.5	1.2 ± 0.2	0.1 ± 0.04
Vehicle	Yes	1.8 ± 0.03[a]	13.1 ± 0.3[a]	6.7 ± 0.5	1.7 ± 0.07[a]	6.6 ± 0.9[a]
Cinacalcet 30mg/kg	Yes	1.3 ± 0.05[*]	10.2 ± 0.9[*]	10.6 ± 1.1[**]	1.2 ± 0.08[**]	9.9 ± 3.4[a]
Cinacalcet 3 mg/kg	Yes				1.4 ± 0.07*	6.1 ± 1.1[a]
S-AMG073 30mg/kg	Yes	1.7 ± 0.05[a]	13.2 ± 0.4[a]	8.3 ± 0.6	1.53 ± 0.05[a]	6.1 ± 1.0[a]

Control vs Tumor [a]$p < 0.05$

Vehicle vs Drug Treatment [**]$p < 0.01$; [*]$p < 0.05$

These data support the potential use of cinacalcet HCl to reduce serum calcium in conditions of humoral hypercalcemia of malignancy.

*Disclosures: **D. Martin**, Amgen 1, 3.*

SA471

See Friday Plenary number F471

SA472

Bone Tissue Effects of Combined Dioxin and Sucrose Exposure Are Gender Related in Rats. P. M. Lind[1], H. M. Miettinen*[2], J. Örberg*[3], I. Pettersson*[3], M. Viluksela*[2]. [1]Institute of Environmental Medicine, Karolinska Institutet, Stockholm, Sweden, [2]Department of Environmental Health, National Public Health Institute, Kuopio, Finland, [3]Department of Environmental Toxicology, Uppsala University, Uppsala, Sweden.

Our previous experimental studies have demonstrated that high affinity aryl hydrocarbon receptor ligands such as 2,3,7,8-tetrachlorodibenzo-p-dioxin (TCDD) and the dioxin-like PCB congener, 3,3',4,4',5-pentachlorobiphenyl (PCB126), impair bone tissue composition and function. The effects of PCB126 on bone tissue in rats are related to endogenous estrogen status and estrogen supplementation modulates PCB126 induced effects on bone tissue. The aim of the present study was to investigate possible gender differences in effects on rat bone tissue caused by co-exposure to TCDD and sugar. Pregnant dams were exposed to a single oral dose of 1 ug/kg b.w. at gestation day (GD15). Control rats received the vehicle (corn oil). After weaning the rats were given either sucrose-rich diet (15% sucrose) and tap water containing 7 % sucrose or normal rat powder feed and tap water. Pups were killed at the age of 77 days. Peripheral quantitative computed tomography (pQCT) analyses were performed on the excised tibia. Trabecular volumetric BM D (trab BMD) was determined by metaphyseal scans of the proximal tibiae. Cortical parameters, including total and cortical volumetric bone mineral density (total and cortical BMD), total and cortical cross-sectional area (tot and cort CSA), medullary area, cortical thickness and polar moment, were determined by mid-diaphyseal scans.

In male rats the effect of TCDD alone was seen only as a reduced cortical BMD at the diaphysis whereas in the female rats a significant reduction of bone growth manifested as reduced total BMD, total and cortical CSA, and also reduced medullary area and polar moment. Adding sucrose to the diet ameliorated the toxic effects of TCDD. This sucrose-effect might be related to an increased stimulation of the bone tissue as a result of a higher body weight in the female rats. In conclusion, our results suggest that TCDD affected bone tissue in a gender dependent manner; the female rats being more sensitive.

Disclosures: ***P.M. Lind****, None.*

SA473

Recommendations for Management of Heterotopic Ossification Based on 12-Year Experience. K. Banovac, A. Sherman*, I. Estores*. Rehabilitation Medicine, Univ. of Miami, Miami, FL, USA.

Heterotopic ossification (HO) is one of the most common and irreversible complications after spinal cord injury (SCI). The purpose of this study was to develop an algorithm for management of HO after SCI based on our 12-year experience. This is a retrospective analysis of our results published over a period of 12 years. All studies were performed at the rehabilitation center of a university teaching hospital and were approved by the institutional review board. A total of 344 SCI patients with HO were included in the studies we reviewed. Prevention of HO was conducted by using selective and nonselective COX-2 inhibitors during the first 2 months after SCI. Diagnosis of HO was based on clinical findings and was confirmed by three-phase bone scintigraphy. The extent of muscle involvement by HO was followed by determination of serum creatine phosphokinase (CPK). Treatment of HO was initiated with intravenous and continued with oral etidronate for a period of 3 or 6 months. Serum C-reactive protein (CRP) was used to monitor inflammatory activity of HO. Our results showed an incidence of HO in approximately 50% of patients by using bone scintigraphy as a diagnostic test. Prophylactic administration of indomethacin and rofecoxib reduced the incidence of HO 2.7 and 2.5-fold respectively. Early treatment of HO with etidronate resulted in a 5-fold decrease of radiographic findings of HO. The elevation of CPK correlated with severity of HO in majority of patients. CRP declined during the first 3 to 4 weeks of etidronate therapy. In conclusion, our data suggest that the incidence of HO and subsequent progression to advanced HO can be significantly decreased by using the following algorithm: (1) Preventive use of NSAIDs early after SCI, (2) Use of bone scintigraphy for early diagnosis of HO prior to positive radiographic findings, (3) More aggressive treatment with etidronate when patients have elevated CPK levels, and (4) Use of NSAIDs with etidronate in the acute stage of HO until normalization of serum CRP.

Disclosures: ***K. Banovac****, None.*

SA474

See Friday Plenary number F474

SA475

Bone Mineral Density Changes After One Year of Antiepileptic Drug Treatment in Women with Epilepsy. A. M. Pack[1], E. Shane[2], L. Holloway*[3], E. Flaster*[1], M. Morrell*[1]. [1]Neurology, Columbia University, New York, NY, USA, [2]Medicine, Columbia University, New York, NY, USA, [3]VA Palo Alto Health Care System, Stanford University, Palo Alto, CA, USA.

Rationale: Antiepileptic drugs (AEDs), particularly those that induce the hepatic cytochrome P450 system, have been associated with abnormal vitamin D metabolism and osteoporosis. Recent studies have reported that low bone mineral density (BMD) in adults on AEDs is common and associated with multidrug regimens, generalized seizures, longer disease duration, and increased bone turnover markers. We therefore examined the effects of individual AEDs on healthy premenopausal women with epilepsy (WWE), hypothesizing that those receiving enzyme inducing AEDs, particularly phenytoin (PHT) and carbamazepine (CBZ), would have more bone loss than those receiving valproate (VPA), an enzyme inhibitor, or lamotrigine (LTG) which has no effect on the cytochrome P450 system.

Methods: Community-dwelling WWE aged 18-40 receiving AED monotherapy for at least 6 months were recruited. BMD was measured at the lumbar spine (LS), total hip (TH) and femoral neck (FN) hip by dual energy X-ray densitometry at baseline and one year, if they remained on the originally prescribed AED. Serum calcium, 25-(OH) vitamin D (25-OHD), parathyroid hormone (PTH), bone specific alkaline phosphatase (BAP, marker of bone formation) and urine N-telopeptide of type I collagen (NTX, marker of bone resorption) were measured at baseline and examined with respect to percent change in BMD.

Results: Of 71 women, 11 were on PHT, 26 on CBZ, 14 on VPA and 18 on LTG. Average age was 32 +/- 5.9 years and BMI was 26.5 +/- 6.3 kg/m^2 with no significant between-groups differences. Baseline Z scores were normal at all sites and did not differ among AED groups (range: -0.42 - 0.34). BMD was stable at the LS and TH in all groups after 1 year of treatment. In women on PHT, FN BMD declined by -2.75% +/- 2.76, p=0.05 compared to the other groups (CBZ, +0.49% +/- 4.03; VPA, +1.09% +/- 3.73; LTG, -0.005% +/- 0.02). In the group overall, bone loss correlated with serum calcium levels, but not other markers of bone function.

Conclusion: In general, BMD is stable in premenopausal WWE on AED monotherapy. We observed significant bone loss at the FN in those taking PHT. The bone loss was associated with lower serum calcium levels but not with serum 25-OHD or PTH levels, nor with markers of bone turnover. Although the mechanism of the bone loss is uncertain, our results suggest that premenopausal women receiving PHT are at significant risk for considerable bone loss and warrant BMD monitoring.

Disclosures: ***A.M. Pack****, GlaxoSmithKline 2, 5; Novartis 2, 8; UCB Pharma 2; Ortho-McNeil 5.*

SA476

Primary Aldosteronism and the Secondary Hyperparathyroidism of the Vitamin D Deficiency. D. N. Nguyen*[1], L. T. Nguyen*[2], K. V. Luong[2]. [1]Metropolitan State Hospital & Vietnamese American Medical Research Foundation, Norwalk, CA, USA, [2]Vietnamese American Medical Research Foundation, Westminster, CA, USA.

Objective: The purported originality of this case report is that the biochemical stigmata of hyperaldosteronism disappeared after vitamin D deficiency treatment.

Methods: We describe the clinical presentation, laboratory findings and clinical course in a vitamin D-deficient patient with primary aldosteronism and discuss underlying factors potentially contributing to the condition.

Result: A 62-year-old Caucasian male with history of type 1 diabetes mellitus presented with hypertension and persistent hypokalemia. Laboratory examination revealed hypokalemia, metabolic alkalosis, low level of renin activity, and an elevation of plasma aldosterone level. He also had low levels of serum ionized calcium, 25-hydroxyvitamin D, and an elevated level of intact PTH. The ultrasound of the adrenal revealed a normal size of the adrenal gland. Of interested, his serum levels of PTH and aldosterone were decreased with 1,25 hydroxyvitamin D_3 (1,25OHD) treatment in one month. Serum potassium level was normalized without potassium supplement or aldosterone antagonism treatment.

Discussion: 1,25OHD has been known to suppress PTH secretion. PTH-binding sites have been autoradiographically localized in the rat adrenal cortex. It was demonstrated that PTH and PTH-related peptide concentration dependently enhanced basal aldosterone and cortisol secretion from dispersed human adrenocortical cells.

Conclusion: The presence of the primary aldosteronism in the secondary hyperparathyroidism of the vitamin D deficiency suggested that hyperparathyroidism might have a role in the inducing primary aldosteronism. However, a coindental presence of two diseases cannot be excluded.

Disclosures: ***K.V. Luong****, None.*

SA477

See Friday Plenary number F477

SA478

Intraperitoneal Administration of Recombinant Receptor-Associated Protein Impairs Megalin Function and Increases Renal Phosphate Excretion. M. Yamagata*[1], K. Ozono[2], Y. Hashimoto*[1], H. Kondou*[1], T. Michigami[1]. [1]Department of Environmental Medicine, Osaka Medical Center and Research Institute for Maternal and Child Health, Izumi, Osaka, Japan, [2]Department of Pediatrics, Osaka University Graduate School of Medicine, Suita, Osaka, Japan.

Megalin is a multifunctional endocytic receptor expressed in apical membrane of renal proximal tubules, and plays critical roles in vitamin D metabolism through renal reabsorption of vitamin D binding protein (DBP) complexed with 25-hydroxyvitamin D. In the present study, to examine the acute effects of impairment of megalin function in kidney, we utilized a recombinant protein for soluble form of 39-kD receptor-associated protein (RAP), which binds to megalin and inhibits the binding of all other ligands. His-tagged soluble form of recombinant murine RAP [a.a.38-356] lacking the N-terminal signal peptide and the C-terminal ER retention signal was prepared by expression in E.coli (designated His-sRAP). After confirming the direct interaction between the purified His-sRAP and megalin by a ligand blot analysis, male ICR mice were given a single intraperitoneal administration of His-sRAP (3.5 mg/dose). Immunostaining using an antibody against His-tag demonstrated the subapical localization of His-sRAP in the proximal tubular cells after the administration, suggesting that His-sRAP interacted with megalin expressed in the brush border membrane and was taken up via megalin-dependent endocytosis. Using the same specimen, we performed immunohistochemical examination for type II Na/Pi co-transporter. Interestingly, it was observed that type II Na/Pi co-transporter was also internalized after the injection of His-sRAP. When the three administrations of His-sRAP were given to mice with 4-hour intervals, urinary excretion of low-molecular-weight proteins including vitamin D binding protein (DBP) was increased, confirming the impairment of megalin function. Consistent with the increased urinary loss of DBP, serum concentration of 25-hydroxyvitamin D was decreased after the administration. As to the urinary excreation of phosphate, it was increased by the treatment with His-sRAP, suggesting the involvement of megalin function in renal phosphate reabsorption. The plasma level of intact PTH was not altered by the administration of His-sRAP. Taken together, megalin might be involved in renal phosphate excretion via type II Na/Pi co-transporter independently of plastma PTH levels. These findings suggest the possibility that there might be a physiological or pathological ligand of megalin which exerts the similar effects to those of His-sRAP.

Disclosures: ***M. Yamagata****, None.*

SA479

See Friday Plenary number F479

SA480

Time-evolution and Reversibility of Strontium-Induced Osteomalacia (OM) in Chronic Renal Failure (CRF) Rats. L. Oste*[1], P. C. D'Haese*[1], A. R. Bervoets*[1], G. J. Behets*[1], G. Dams*[1], S. C. Verberckmoes[1], V. O. Van Hoof[2], M. E. De Broe*[1]. [1]Nephrology - Hypertension, University of Antwerp, Wilrijk, Belgium, [2]Biochemistry, University Hospital Antwerp, Edegem, Belgium.

In dialysis patients we showed an association between increased bone Sr levels and OM. Evidence for a causal role of the element in the development of the disease was presented in CRF rats. Sr-ranelate has been put forward as a therapeutic agent in the treatment of osteoporosis. Since the target population for Sr-treatment consists mainly in post-menopausal osteoporotic women, who may have a reduced renal function, the risk for OM should be considered.

We studied the time evolution and reversibility of the Sr-induced mineralization defect by oral loading of CRF rats with Sr (2g/l in the drinking water) during 2, 6 and 12 weeks, followed by a withdrawal period of 2, 4 or 8 weeks.

Histological examination revealed clear signs of OM already after 2 weeks of Sr treatment. Animals that received Sr during 6 and 12 weeks had significantly higher osteoid perimeter (68±12 vs 22±19% p=0.008 and 69±20 vs 36±17% p=0.044), osteoid area (31±15 vs 3±3% p=0.006 and 31±17 vs 7±7% p=0.008) and osteoid thickness (17.5±8.9 vs 4.2±1.1µm p=0.006 and 18.2±5.8 vs 5.9±2.4µm p=0.006) compared to controls. After 12 weeks of Sr administration, the mineralization was significantly affected, as evidenced by lower double-labelled surface (0±0 vs 10±10% p=0.008), lower mineral apposition rate (0.0±0.0 vs 1.9±1.1µm/day p=0.008), higher osteoid maturation time (>12 vs 4.1±4.4 days p=0.008), lower bone formation rate (0±0 vs 1054±1233µm²/mm²/day p=0.008) and higher mineralization lag time (>1000 vs 137±432 days p=0.008). After 6 and 12 weeks of loading the osteoblast perimeter was significantly lower in the Sr treated animals (3±5 vs 26±15% p=0.038 and 10±9 vs 14±15% p=0.05. A significant rise in serum total alkaline phosphatase (ALP) activity in the Sr-treated animals compared to controls was apparent after 2, 6 and 12 weeks of loading (81±7 vs 44±10U/l p=0.006; 92±16 vs 28±13U/l p=0.006 and 75±8 vs 42±8U/l p=0.006). Measurement of the ALP isoenzymes indicated that Sr loading not only stimulates the bone-ALP, but the intestinal and liver ALP iso-enzymes as well. In animals treated with Sr, at all time points a decrease of serum iPTH was found, suggesting a calcimimetic effect of Sr on PTH secretion.

After cessation of Sr treatment, the effects of Sr on ALP and PTH were reversed and the histological and histodynamical parameters evolved to control levels during the wash-out period of 2, 4 or 8 weeks.

In conclusion, in this study evidence is provided for a fast development of a Sr-induced mineralization defect in CRF rats, that is rapidly reversed after withdrawal of the compound.

Disclosures: ***L. Oste****, None.*

SA481

Canine Distemper Virus Dose-Dependently Increases Human Osteoclast Formation and Function. A. P. Mee*. Medicine, University of Manchester, Manchester, United Kingdom.

Paget's disease is characterised by a dramatic increase in size and number of osteoclasts, leading to uncontrolled bone resorption. Previously we have shown that canine distemper virus (CDV) RNA is present in Pagetic bone samples. However, the effects of CDV on human osteoclast formation in vitro have not been previously studied.

Replicate cultures (n=3) of purified human osteoclast precursors (Poietics Osteoclast Precursors, Cambrex, UK) were infected with increasing doses of CDV (50, 500 and 5,000 pfu/ml) and cultured on dentine slices for 14 days. Control cells were incubated in the absence of virus. Osteoclasts were stained for tartrate-resistant acid phosphatase and the dentine slices were examined for evidence of resorption. Ten high-power microscopy fields were analysed for each sample.

CDV dose-dependently increased osteoclast number and size ($p<0.0001$, ANOVA), and there was a corresponding increase in resorption on the dentine slices ($p<0.0001$, ANOVA). The maximum effect was seen with 500 pfu/ml CDV (20.3±4.4 osteoclasts/high power field cf. 9.8±1.3 osteoclasts in control culture; 14.3±5.5 cf. 5.5±0.7 nuclei/osteoclast; 54.0±5.2 cf. 25.0±4.6 percent of dentine slices covered by resorption pits).

These results provide the first conclusive evidence that CDV can infect human osteoclast precursors. The resulting increase in size and number of osteoclasts, and increased resorption, provide further evidence for the possible role of Paramyxoviruses in the pathogenesis of Paget's disease.

Disclosures: ***A.P. Mee****, None.*

SA482

See Friday Plenary number F482

SA483

Characteristics and Familial Aggregation of Paget's Disease of Bone in Italy. R. Nuti, D. Merlotti, B. Galli*, G. Martini, A. Calabrò*, V. De Paola*, E. Ceccarelli*, S. Salvadori*, A. Avanzati*, L. Gennari. Dept. of Internal Medicine Endocrine Metabolic Sciences and Biochemistry, University of Siena, Siena, Italy.

The aetiology of Paget's disease of bone (PDB) remains unknown. Current evidence suggests that interactions among genetic or exogenous factors, appear to be necessary for disease expression. Major epidemiological studies were performed in United Kingdom as well as in other populations of British descent. To date there are no reliable data on PDB characteristics among the Italian population, and its frequency in different areas of the country remains unknown. In attempt to evaluate clinical characteristics, the proportion of familial cases and the influence of environmental features on the occurrence of the disease we studied 147 consecutive PDB patients. For all subjects a detailed medical history was obtained, and constitutional features were recorded. Characteristics of PDB patients were compared to those obtained from 323 consecutive non PDB outpatient subjects. Among PDB cases, there was a slight male predominance, with a male to female ratio of 1.5:1. Of the 147 PDB patients, 22 (15%) had at least one other family member affected, 19 (13%) referred one family member with suspected features of PDB and 106 (72%) were classified as sporadic PDB. No significant differences between familial and sporadic cases were observed concerning skeletal extent, male to female ratio, age of onset, somatic features like hair and eyes color. A trend approaching statistical significance was observed for age of diagnosis that was lower in familial than in sporadic cases (59.0±12.3 vs. 53.6±14.6; p=0.06 ANOVA). Even though we observed a reduced clinical severity of PDB with respect to other populations (mean number of affected sites 2.2±1.6), we did not found any evidence of a decreased severity of the disease through years. We also found an association of PDB with animal-related factors (OR 2.22, $p<0.0005$) and a significant prevalence of PDB in rural vs urban districts (OR 2.42, $p<0.0005$). Osteoarthritis (40%), fractures (14%), hearing loss (14%), and valvular calcifications (15%) were the most observed complications. Interestingly, the geographical distribution of PDB showed a concentration of cases in rural areas of Campania and Tuscany. PDB characteristics differed significantly in PDB subjects from these high prevalence areas. In particular, age of diagnosis was significantly lower (48.15±13.1 yrs vs. 60.6±11.6; p=0.0005 ANOVA) and the number of involved sites was higher (3.15±2.3 vs. 2.07±1.4; p=0.019, ANOVA) in PDB subjects from the high prevalence areas than in the other PDB cases. These areas may indicate local clustering of PDB cases in Italy, similar to what observed in other countries.

Disclosures: ***R. Nuti****, None.*

SA484

See Friday Plenary number F484

SA485

Different Responses Of Bone Turnover Markers To Bisphosphonate Therapy In Pagetic Patients With Skull Involvement. L. Alvarez[1], P. Peris[2], N. Guañabens[2], S. Vidal-Sicart*[3], H. Solberg*[4], P. Cloos*[4], A. Monegal*[2], J. Bedini*[1], F. Pons*[3], A. Ballesta*[1]. [1]Biochemistry, Hospital Clinic, Barcelona, Spain, [2]Rheumatology, Hospital Clinic, Barcelona, Spain, [3]Nuclear Medicine, Hospital Clinic, Barcelona, Spain, [4]Nordic Bioscience, Herlev, Denmark.

Aims: The aims of this study were to evaluate response to therapy in disease activity in pagetic patients with and without skull involvement and to compare the usefulness of new bone markers in the evaluation of these patients.

Patients and Methods: 37 patients with Paget's disease (9 with skull involvement) treated with tiludronate (400 mg/d x 3 months) and 26 healthy controls were included in the study. Serum total alkaline phosphatase (TAP), bone alkaline phosphatase (BAP), PINP and urinary α-α CTX, β-β CTX and NTX were measured at baseline and at 1 and 6 months after discontinuation of therapy. Quantitative bone scintingraphy was performed at baseline and at 6 months, and an index of disease activity (SAI) was obtained. Patients were classified into three groups: patients with skull involvement (Sk group), patients without skull involvement and patients without skull involvement but with similar disease activity to those of the Sk group (based on SAI).

Results: All groups of patients showed higher baseline values in all markers compared to controls. At baseline patients with skull involvement showed significantly higher values in all markers when compared to the rest of the pagetic patients. In addition, there were no significant differences between the group of patients with similar SAI and those with skull involvement except for NTX, which was higher in the latter group. The α-α CTX was the marker with the highest values in this group of patients (46 times higher than normal values in Sk group vs 20 times higher in the rest of patients). Six months after discontinuation of therapy the percentage of patients with markers within the normal range in patients without skull involvement were: 71% for TAP, 71% for BAP, 63% for PINP, 54% for NTX, 48% for α-α CTX and 52% for β-β CTX; in patients with similar SAI to Sk group the values were 60% for TAP, 60% for BAP, 50% for PINP, 33% for NTX, 31% for α-α CTX and 38% for β-β CTX, whereas in patients with skull involvement they were: 33% for TAP, 22% for BAP, 0% for PINP, 13% for NTX, 17% for α-α CTX and 17% for β-β CTX.

Conclusion: Pagetic patients with skull involvement showed a marked increase in bone turnover and a lower response to bisphosphonate therapy. Moreover, α-α CTX is the marker with the highest increased values in these patients. The results suggest that these patients probably need to be treated with higher doses or more potent bisphosphonates.

Disclosures: ***L. Alvarez****, None.*

SA486

See Friday Plenary number F486

SA487

Paget's Disease Of Bone In A Younger Cohort: A More Subtle Disease. M. Seton. Allergy, Immunology & Rheumatology, Mass General Hospital, Boston, MA, USA.

Purpose: This study was designed to examine the skeletal distribution of Paget's disease of bone (PD) in persons enrolled in the New England Registry for Paget's Disease of Bone (NERPD) born after 1940. Studies in the prevalence of Paget's disease of bone (PD) have suggested that the number of bones involved has diminished as an inverse correlate with date of birth. This pattern is different in individuals with a positive family history of PD in whom there is a tendency towards polyostotic disease. Methods: The NERPD is a database designed to examine the distribution and determinants of disease frequency. Diagnosis is confirmed by bone scan and x-ray report; the highest alkaline phosphatase (AP) is noted. Of the 295 persons now entered into the database, all persons were selected with birth dates from 1940 forward, N= 35 (12%). This was an arbitrary cut off, chosen to include enough histories for an observational study. Results: Birth dates ranged from 1940 - 1961. Three of the 35 persons did not have PD after medical record review. Of the remaining 32 persons, 29 (91 %) had PD confirmed by radiographic studies. They are the subjects of this review. Of these persons, 17 were men, 12 women. One man was born in Haiti, and was the only person of color; 28 persons were born in the USA, as were most of their parents. Only 3 noted both grandparents from this country. The birth lands otherwise included Italy, Central Europe and Russia, followed in frequency by Ireland, Canada, Scotland, and Greece. One pair of grandparents was identified as American Indian. Of the 29 persons with PD born after 1940, 23 (79%) had monostotic disease, 7 involving the thoracolumbar spine, 8 the pelvis, 4 the skull, 2 the humerus, 1 a hip, 1 a tibia. Four persons (14%) had 2 sites involved; in all cases the pelvis was one of these. The two persons in the Registry with a positive family history of PD, had polyostotic disease, a female with 5 pagetic bones, and a male with 4. Nearly half of the persons in this cohort had a normal serum AP. Conclusions: The study corroborates what other scientists are reporting, that there may be a trend towards less extensive skeletal involvement in younger persons with PD. The individual histories suggest that cultural diversity will continue to appear in persons with PD. The environmental determinants of disease - whether those of the microenvironment of aging bone or the macroenvironment of our world- remain poorly understood. Epidemiological methods for determining disease frequency of PD may need to change. Screening with plain radiographs of the abdomen would have missed a full 25% of persons with PD. Elevations in AP may not prevail in persons with monostotic disease. In the clinical care of patients with PD, new guidelines on early diagnosis and effective treatment are needed.

Disclosures: ***M. Seton****, None.*

SA488

Fibroblast Growth Factor 23, Parathyroid Hormone, and 1α,25 Dihydroxyvitamin D in Surgically Treated Primary Hyperparathyroidism. P. Tebben[1], B. L. Clarke[1], R. J. Singh*[2], R. Kumar[3]. [1]Endocrinology, Mayo Clinic, Rochester, MN, USA, [2]Laboratory Medicine, Mayo Clinic, Rochester, MN, USA, [3]Nephrology Research, Mayo Clinic, Rochester, MN, USA.

Hypophosphatemia and suppressed renal phosphate reabsorption are observed in primary hyperparathyroidism. As fibroblast growth factor 23 (FGF23) has been implicated in the hypophosphatemia of several hypophosphatemic syndromes, we measured serum FGF23 to determine whether it contributes to the hypophosphatemia of primary hyperparathyroidism. In thirteen patients with primary hyperparathyroidism we measured serum inorganic phosphorus (Pi), calcium (Ca), 1α,25-dihydroxyvitamin D_3 ($1\alpha,25(OH)_2D_3$), parathyroid hormone (PTH), FGF23 (Immutopics, San Clemente, CA), creatinine, and bone specific alkaline phosphatase (BSAP) prior to, one day after, and at least 6 weeks after surgical cure of their disease. Normal serum FGF23 concentrations were derived from 80 healthy controls. Prior to surgery, patients had elevated serum Ca and PTH concentrations (Table 1). Serum Pi concentrations were in the low normal range. FGF23 concentrations were not elevated in patients with primary hyperparathyroidism compared to normal controls ($p>0.05$). Within 24 hours of surgery, serum Ca, PTH, $1\alpha,25(OH)_2D$, and BSAP concentrations were lower ($p<0.001$) and Pi concentrations were higher ($p<0.001$) than in the pre-operative state. FGF23 concentrations were similar prior to, one day after and six weeks following surgery. FGF23 concentrations did not correlate with serum Pi, Ca, PTH, $1\alpha,25(OH)_2D$, or BSAP concentrations in the pre- or post-operative state.

Parathyroid hormone is the major regulator of Pi, Ca and vitamin D metabolism in patients with primary hyperparathyroidism. FGF23 does not appear to play a role in Pi homeostasis in this group of patients with surgically treated primary hyperparathyroidism.

Table 1. Concentrations of serum analytes in patients with primary hyperparathyroidism before and after surgical excision of parathyroid adenomas or hyperplastic parathyroid glands.

	Pre Surgery	1 Day Post Surgery	6 Weeks Post Surgery
PTH (pmol/L)	10.9 ± 2.2	0.9 ± 0.2*	5.2 ± 0.7***
Calcium (mg/dL)	11.0 ± 0.2	9.4 ± 0.2*	8.7 ± 0.2*
Phosphorus (mg/dL)	3.0 ± 0.1	3.6 ± 0.2*	3.2 ± 0.3
$1\alpha,25\ (OH)_2D$ (pg/mL)	56.8 ± 7.3	34.9 ± 5.1*	42.5 ± 8.6
BSAP (μg/L)	19.5 ± 2.1	16.7 ± 2.0*	13.9 ± 1.7**
FGF23 (RU/mL)	167 ± 117	118 ± 47	130 ± 72
Creatinine (mg/dL)	1.0 ± 0.0	1.0 ± 0.0	1.0 ± 0.1

(Mean ± SEM) A paired t-test was used to compare pre surgical to 1 day and 6 week post-surgical values. *p<0.001; **p<0.01; ***p<0.03

Disclosures: ***P. Tebben****, None.*

SA489

See Friday Plenary number F489

SA490

Increased Body Weight in Primary Hyperparathyroidism: Implications for Disease Associations. M. J. Bolland*, A. B. Grey, G. G. Gamble*, I. R. Reid. Department of Medicine, Auckland University, Auckland, New Zealand.

Although primary hyperparathyroidism (PHPT) is frequently asymptomatic, it has been associated with an increased prevalence of hypertension, insulin resistance, dyslipidemia, cardiovascular mortality, and cancer. Previously, we reported that patients with PHPT are heavier than age-matched controls, but further studies addressing this important question have not been undertaken. Increased body weight potentially could explain the association between PHPT and these complications, and impact upon the effects of PHPT on bone density. We have carried out a meta-analysis of all available data to determine whether patients with PHPT are heavier than age- and sex-comparable eucalcemic controls.

MEDLINE was searched for English-language studies published between 1975 and 2003. 17 studies met pre-determined eligibility criteria. Data regarding weight, body mass index (BMI), serum calcium and PTH were extracted from each study. Data were pooled and meta-analyzed using weighted and standard mean difference analyses.

Subjects with PHPT were on average 3.34kg (95% CI 1.97 to 4.71, $P < 0.00001$) heavier than controls in 13 studies reporting body weight. In 4 studies reporting BMI, subjects with PHPT had an increased BMI of 1.13kg/m^2 (-0.29 to 2.55, $P = 0.12$) compared to the controls. Standard mean difference analysis showed that patients with PHPT have an increased weight or BMI of 0.3 standard deviations (0.19 to 0.40, $P < 0.00001$) compared to the controls.

A weight difference of this magnitude is likely to be of clinical significance. Data from published prospective studies indicate that an increased BMI of 1.1kg/m^2 would predict an increase in the risk of diabetes by 155%, hypertension by 15%, ischemic heart disease by 6%, overall mortality by 6-10%, and an increased risk of a variety of cancers. These predictions are consistent with published data on the prevalence of these diseases in PHPT.

We hypothesize that increased body weight predisposes to the development of PHPT. Body weight is positively associated with PTH and inversely correlated with 25(OH)-Vitamin D in eucalcemic populations. Thus, increased body weight may promote vitamin D deficiency, resulting in secondary hyperparathyroidism that in the long term increases the risk of the development of parathyroid adenomata.

Since no evidence exists that parathyroidectomy reduces body weight, our findings suggest that surgical intervention in an attempt to reduce the risk of cardiovascular or neoplastic disease is not justified.

Disclosures: ***M.J. Bolland****, None.*

SA491

Effect of Bone Growth in Juvenile Dogs Administered Cinacalcet for 28-Days. S. F. Greene*[1], A. Coluci*[1], B. B. Smith*[1], R. C. Mandella*[2], J. Bussiere*[1], M. E. Cosenza,*[1], H. E. Davis*[1]. [1]Toxicology, Amgen, Inc., Thousand Oaks, CA, USA, [2]Toxicology, Huntingdon Life Sciences Inc, East Millstone, NJ, USA.

Cinacalcet is a potent calcimimetic agent that lowers serum parathyroid hormone (PTH), ionized calcium, and calcium x phosphorus product in nonclinical and clinical studies and is used in the treatment of secondary hyperparathyroidism. Potential effects of cinacalcet on growing bone were evaluated in juvenile dogs treated with cinacalcet. At the start of the study, dogs were 10 weeks old (post weaning), or the human equivalent of 2 to 12 years (prepuberty). The dogs were administered 0, 0.5, 1.5, or 5.0 mg/kg/day cinacalcet for 28 consecutive days (n = 7/sex/group), with reversibility of effects evaluated in 3 animals/sex/group in a 28-day treatment-free recovery period. Analyses for bone biomarkers in serum (bone-specific alkaline phosphatase, C-telopeptide, and osteocalcin) were done pretest and at the end of the dosing and recovery periods. Urine deoxypyridinoline and creatinine were measured at the termination of dosing and recovery periods. The right femur was collected from all animals at the terminal and recovery sacrifice for bone density measurements using peripheral quantitative computerized tomograph (pQCT). Bone density measurements were made at 2 sites in the femur, the diaphysis and the metaphysis. Cortical, subcortical, trabecular, and total area, content and density were measured at the metaphyseal site. Total content and density as well as cortical area, content, density and thickness were measured at the diaphyseal site. Histopathologic evaluations of hematoxylin and eosin-stained left femur also were done.

Cinacalcet was well tolerated at oral doses up to 5.0 mg/kg/day. As expected, serum ionized calcium and PTH levels were reduced in a dose-dependent manner. Serum parameters for bone formation (alkaline phosphatase and osteocalcin) or bone resorption (C-telopeptide) were not altered at dosing termination or after the treatment-free recovery period. No effects on urine parameters for bone resorption (deoxypyridinoline) or creatinine concentrations were observed. No effects of cinacalcet on bone densitometry measurements in the mid-shaft (diaphysis) or metaphysis of the femur were observed at any dose. No microscopic changes related to cinacalcet administration were observed in the bone.

Cinacalcet did not alter serum or urinary bone biomarkers, bone densitometry measurements, or histopathologic evaluations in juvenile dogs. Oral administration of cinacalcet to juvenile dogs for 28 days was well tolerated with no effect on bone or the growth plate.

Disclosures: ***S.F. Greene****, Amgen, Inc. 3.*

SA492

Effect of Mild Asymptomatic Primary Hyperparathyroidism (PHPT) on Bone Geometry and Strength. T. S. H. Khairalla*[1], V. Reddy*[2], E. Phillips*[2], G. B. Talpos*[3], G. W. Divine*[4], G. Jacobson*[4], D. Rao[2]. [1]Internal medicine, Henry Ford Hospital, Detroit, MI, USA, [2]Bone and Mineral Metabolism, Henry Ford Hospital, Detroit, MI, USA, [3]Surgery, Henry Ford Hospital, Detroit, MI, USA, [4]Biostatistics and Research Epidemiology, Henry Ford Hospital, Detroit, MI, USA.

Moderate to severe PHPT is associated with decreased bone mineral density (BMD) and cortical thinning. However, whether the decrease in BMD leads to decreased bone strength and increased fracture risk is not known. Furthermore, the effects of mild PHPT on bone strength have not been previously reported. In this study we assessed the effect of mild PHPT on bone strength using indices of second metacarpal bone dimensions to calculate physical strength of the bone and compared the results to historical controls.

Forearm BMD was measured by DEXA. Metacarpal cortical thickness (MCT) was measured on the second metacarpal in 65 postmenopausal women with mild PHPT. Bone strength was assessed by cross sectional moment of inertia (CSMI), section modulus (SM), and bending breaking resistance index (BBRI). The results were compared to 60 healthy women.

The mean BMD was 0.638 ± 0.093 g/cm^2 and correlated significantly with MCT ($p<0.001$). As in patients with more severe PHPT, MCT was lower in mild PHPT compared to normals (4.2 ± 0.78 versus 5.53 ± 0.634; $p<0.001$). Both periosteal and endosteal diameters increased in PHPT patients compared to normals (8.5 ± 0.61 versus 7.86 ± 0.676; $p<0.001$ and 4.3 ± 1.05 versus 2.33 ± 0.865; $p<0.001$ respectively). Consequently, bone strength as assessed by CSMI (246 ± 66.3 versus 193 ± 68; $p=0.004$), SM (56.9 ± 11.3 versus 48.1 ± 12.4; $p=0.007$), and BBRI (579 ± 115 versus 490 ± 126; $p=0.007$), was greater in PHPT.

BMD and MCT are decreased in PHPT, but the changes in bone geometry appear to compensate for any adverse effects of decreased BMD and MCT on bone strength. Our results are consistent with the decreased prevalence of vertebral fracture in mild PHPT and for the anabolic role of PTH in osteoporosis.

Disclosures: ***T.S.H. Khairalla****, None.*

SA493

See Friday Plenary number F493

SA494

Correction of Extracellular Calcium Reduces Parathyroid Gland Size in a Model of Secondary Hyperparathyroidism Using Mice with a Nonfunctioning Vitamin D Receptor. K. Weber*, U. Zeitz*, C. Bergow*, R. G. Erben. Institute of Animal Physiology, University of Munich, Munich, Germany.

Cell proliferation and parathyroid hormone (PTH) secretion in the parathyroid gland is known to be regulated by the vitamin D hormone via the vitamin D receptor (VDR) and by extracellular calcium via the calcium-sensing receptor. In this study, we sought to separate the effects of extracellular calcium from the effects of vitamin D on parathyroid gland function and size using mice with a nonfunctioning VDR. Beginning from 16 days of age, wild-type and homozygous VDR mutant mice were kept on a rescue diet containing 2% calcium (Ca), 1.25% phosphorus (P), and 20% lactose until they were 4 - 5 months of age. Subsequently, all mice were switched to a challenge diet containing 0.5% Ca, 0.4% P, and 0% lactose. After 2 months on the challenge diet, groups of VDR mutant mice were either fed the challenge diet, a normal diet with 0.9% Ca, 0.7% P, and 0% lactose, or the rescue diet for another 3 months. All diets had the same energy, fat, protein, and carbohydrate content. At baseline, blood ionized calcium, PTH serum levels, PTH mRNA levels, parathyroid gland size, biochemical markers of bone turnover, femoral bone mineral density (BMD) and bone histology were normal or only slightly altered in VDR mutants. The 2-month challenge diet phase induced severe secondary hyperparathyroidism (sHPT) with PTH serum levels of 1444 ± 779 pg/ml (mean ± SD), a 2.3-fold increase in parathyroid gland area, increased expression of the PTH mRNA, profoundly reduced femoral BMD, and a dramatic increase in bone turnover in VDR mutant animals, but only mild increases in serum PTH and unchanged femoral BMD in wild-type mice. Interestingly, the increase in parathyroid gland area in VDR mutants was mainly caused by enlargement of existing chief cells, not by cell proliferation. Feeding of the normal diet during the 3-month therapy period stabilized the existing degree of sHPT, while the challenge diet further aggravated it. However, the rescue diet fully corrected serum PTH, femoral BMD, and bone turnover to baseline control levels in hyperparathyroid VDR mutants, but not the increased PTH mRNA levels. The normalization of PTH secretion was associated with a significant 25% reduction in parathyroid gland area, which was mainly caused by a decrease in cell size, not by cell apoptosis. We conclude 1) that vitamin D has no essential function in the control of parathyroid cell proliferation, 2) that correction of extracellular calcium in this model of sHPT fully normalizes PTH secretion and reduces parathyroid gland size, and 3) that functional adaptation in the parathyroid glands of mature mice occurs mainly by regulation of cell size.

Disclosures: ***R.G. Erben****, None.*

SA495

See Friday Plenary number F495

SA496

Apoptosis of Osteoblasts Is Increased in Patients with Mild Primary Hyperparathyroidism and Preserved Cancellous Bone. H. Zhou[1], D. W. Dempster[1], R. Lindsay[1], S. J. Silverberg[2], J. P. Bilezikian[2]. [1]Regional Bone Center, Helen Hayes Hospital, West Haverstraw, NY, USA, [2]Department of Medicine, Columbia University, New York, NY, USA.

We have previously demonstrated that cancellous bone microarchitecture is preserved in patients with mild primary hyperparathyroidism (PHPT) and that this is due, in part, to an anabolic effect of PTH, resulting in increased thickness of bone packets formed in each remodeling cycle. One hypothesis proposed to account for the anabolic action of exogenous PTH is that the life span of osteoblasts is prolonged due to suppression of osteoblast apoptosis. We tested this hypothesis in 2 groups of patients with PHPT.

In Group I, 9 women with PHPT underwent tetracycline-labeled transiliac bone biopsy before (age=52 yrs) and after (age=62 yrs) parathyroid surgery (n=6) or medical management (n=3). In Group II, 6 premenopausal women with PHPT (age =35 yrs) were biopsied and compared with 12 age-matched controls. Apoptotic osteoblasts and osteocytes were detected in bone biopsy sections using the TUNEL method. Apoptotic osteoblasts were expressed as the number of TUNEL-positive osteoblasts over the total osteoblast-covered perimeter (A.Ob/Ob.Pm #/mm) on cancellous, endocortical or intracortical envelopes. Apoptotic osteocytes were expressed as the number of TUNEL-positive osteocytes over the total number of osteocyte lacunae (empty plus occupied) (A.Cty/Lac, %) in cancellous and cortical bone.

In Group II, A.Ob/Ob.Pm was 596, 2104 and 486% higher in PHPT than control on cancellous, endocortical, and intracortical surfaces ($0.05> p< 0.01$) respectively. This was accompanied by a 110% higher mineralized perimeter (Md.Pm) ($p< 0.01$) and a trend towards a higher bone formation rate (BFR)(58%) and activation frequency (Act.F)(55%). Treatment (Group I) resulted in a 74 and 80% decrease ($p<0.05$) in A.Ob/Ob.Pm on cancellous and endocortical surfaces, respectively, accompanied by a 45% decrease ($p< 0.05$) in Md.Pm and a trend towards a decrease in BFR (-43%) and Act.F (-25%). A similar trend was seen on the intracortical surface. There was no significant change in the A.Cty/Lac in PHPT compared to controls or after treatment, although the trend was in the same direction as for osteoblasts.

We conclude that the anabolic action of continuous PTH excess in mild PHPT does not appear to be associated with increased osteoblast life span due to suppressed osteoblast apoptosis. On the contrary, osteoblast apoptosis was increased in PHPT and this was reversed by treatment. These observations are consistent with the hypothesis that enhanced osteoblast number and/or activity seen with continuously elevated PTH in PHPT is associated with enhanced osteoblast attrition.

Disclosures: ***H. Zhou****, None.*

SA497

See Friday Plenary number F497

SA498

Treatment of Parathyroid Carcinoma with ABX10241, a Monoclonal Antibody to Parathyroid Hormone. D. M. Shoback[1], R. H. Arends*[2], L. Roskos*[2], S. Shetty*[2], M. Wyres*[2], S. Huang*[2], N. Raie*[2], G. M. Bell[2]. [1]Endocrinology, San Francisco VA Medical Center, University of California, San Francisco, San Francisco, CA, USA, [2]Abgenix, Inc, Fremont, CA, USA.

ABX10241 is a fully human, high-affinity, monoclonal antibody directed against the 1-34 amino acid region of parathyroid hormone (PTH) that neutralizes the activity of PTH in vitro and in vivo. This report describes the use of ABX10241 to treat a 38 year-old male with a 14-year history of inoperable parathyroid carcinoma. The patient had been treated with calcitonin (severe allergic reaction), bisphosphonates (pamidronate and zoledronic acid) and cinacalcet without control of his disease. In February 2004, hemodialysis was initiated to treat progressive renal insufficiency. Following atraumatic, bilateral femoral neck fractures, treatment with ABX10241 was initiated under an emergency use IND. ABX10241 was administered by intravenous bolus at increasing doses over a two-week period to normalize plasma unbound PTH or serum iCa, whichever occurred first. ABX10241 was administered in doses of 25 mg (Day 1), 50 mg (Day 4), 100 mg (Day 8), and 200 mg (Day 11, Day 22, Day 32, and approximately weekly thereafter). Plasma unbound PTH (measured using the Nichols Intact Assay), collagen N-telopeptides (NTx), and 1,25 $(OH)_2$ vitamin D (vit D) and pharmacokinetic samples were obtained before each dose, 24 hours post-dose and approximately 24 hours prior to the next dose during the dose-escalation phase. Serum iCa was obtained every 8 hours during the dose-escalation phase. The patient continued to receive 3-4 times weekly hemodialysis and intermittent doses of zoledronic acid. Treatment with ABX10241 resulted in a profound, dose- and exposure-dependent reduction in plasma unbound PTH from a pre-dose level of 1196 pg/ml to the normal range (range 30 pg/ml - 100 pg/ml) at a final dose of 200 mg per week. Plasma NTx levels were reduced following each dose of ABX10241 suggesting bone turnover was impacted by the treatment (see graph). In addition, vit D levels were reduced by the treatment. Serum iCa fluctuated with hemodialysis but remained elevated. No drug related toxicities were observed during or after the administration of ABX10241 and the patient reported improvement of his bone pain. These findings support the potential benefit of ABX10241 in the treatment of hyperparathyroidism secondary to parathyroid carcinoma.

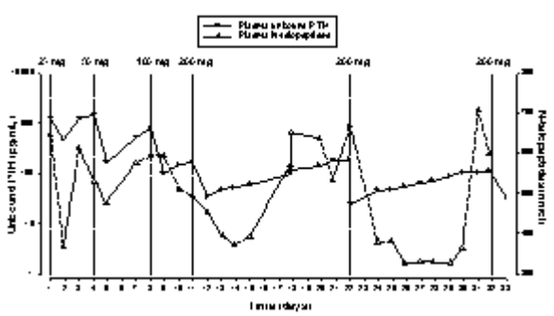

Disclosures: ***D.M. Shoback****, Abgenix, Inc. 5; Amgen 2, 5.*

SA499

Altered Geometry of the Proximal Femur Reduces Cortical Bone Strength in Pediatric Crohn Disease. J. M. Burnham*[1], J. Shults*[2], E. Semeao*[1], M. A. Petit*[3], T. J. Beck*[4], B. S. Zemel[1], M. B. Leonard[1]. [1]Pediatrics, The Children's Hospital of Philadelphia, Philadelphia, PA, USA, [2]Epidemiology, The University of Pennsylvania School of Medicine, Philadelphia, PA, USA, [3]Department of Health Evaluation Sciences, Penn State University, Hershey, PA, USA, [4]Radiology, Johns Hopkins University, Baltimore, MD, USA.

Crohn disease (CD) is associated with decreased DXA bone mineral density and increased risk of fracture. Our objective was to characterize cortical bone geometry relative to body size and lean mass in children and young adults with CD.

DXA proximal femur scans (Hologic QDR 2000) were obtained in 89 subjects with CD (55 M, 34 F) and 130 healthy controls (52 M, 78 F), ages 4-26 years. Subperiosteal and endosteal diameter, cortical cross-sectional area (CSA), cross-sectional moment of inertia (CSMI), and section modulus (Z) of the proximal femoral shaft were estimated using hip structural analysis software. Lean mass was assessed using whole body DXA. Bone measures and lean mass are strongly influenced by growth, so these variables were expressed as sex-specific standard deviation scores (SDS) relative to subject height derived from linear regression models in the controls. SDS results in CD were compared with controls, adjusted for age, race and Tanner stage. Bone outcomes were then adjusted for lean mass SDS to determine if deficits in bone strength were associated with decreased biomechanical loading.

CD was associated with decreased height and body mass index for age ($p < 0.001$). Lean mass SDS in CD was significantly decreased ($p < 0.001$), compared with controls. Bone geometry SDS in CD are summarized in the Table. CD was associated with significantly decreased subperiosteal diameter, endosteal diameter, and CSMI; Z was marginally decreased. Adjustment for lean mass SDS attenuated the deficits in CSMI and Z; however, CSMI remained significantly decreased in CD ($p = 0.04$), compared with controls.

After adjustment for decreased stature, CD was associated with altered cortical bone geometry, which may result in decreased resistance to bending and torsion. Reduced endosteal expansion counteracted the decreased periosteal dimensions and preserved cortical CSA. However, these structural changes resulted in decreased CSMI and marginally decreased Z. Bone strength deficits may be associated with decreased biomechanical loading in CD.

Proximal Femoral Shaft SDS Relative to Height in CD

Variable	SDS*	95% CI	p
Subperiosteal Diameter	-0.85	-1.20, -0.49	< 0.001
Endosteal Diameter	-1.00	-1.45, -0.55	< 0.001
Cortical CSA	-0.20	-0.53, 0.13	> 0.2
CSMI	-0.53	-0.86, -0.20	0.002
Z	-0.30	-0.63, 0.04	0.08

* Adjusted for age, race, and Tanner stage

Disclosures: ***J.M. Burnham****, None.*

SA500

See Friday Plenary number F500

SA501

Vitamin D Status and Measurements of Bone in Perinatally HIV-Infected Children and Adolescents in New York City. S. Arpadi[1], M. Horlick[1], D. McMahon*[2], E. Abrams*[3], S. Bakshi*[4], M. Bamji*[5], R. Lazell*[6], E. Engelson*[7], E. Shane[2]. [1]Pediatrics, Columbia University, New York, NY, USA, [2]Medicine, Columbia University, New York, NY, USA, [3]Pediatrics, Harlem Hospital, New York, NY, USA, [4]Pediatrics, Bronx-Lebanon Hospital Center, New York, NY, USA, [5]Pediatrics, Metropolitan Hospital Center, New York, NY, USA, [6]Pediatrics, St. Lukes-Roosevelt Hospital Center, New York, NY, USA, [7]Medicine, St. Lukes-Roosevelt Hospital Center, New York, NY, USA.

Alterations in bone and mineral metabolism and bone mass accrual are reported in children and adolescents with HIV infection. The purpose of this study is to evaluate Vitamin D status and its relationship to bone mass measurements in HIV infected children and adolescents.

Fifty-six HIV-infected subjects ages 6-16 yr (mean 10.8) were enrolled from 4 New York City outpatient treatment programs. Serum 25-hydroxyvitamin D (25-OHD), total body (TB) and spine (S) bone mineral content (BMC), bone area (BA) and bone mineral density (BMD) by dual x-ray absorptiometry (DXA, Hologic Delphi A) were measured in a cross-sectional study performed between August 2003-March 2004. HIV viral load and CD4+lymphocytes were also measured. No subjects receiving systemic corticosteroids, tenofovir, or with clinically evident bone disease were included. Separate multiple regression analyses were used to test whether BMC, BA, or BMD were significantly associated with serum 25-OHD concentration while adjusting for known or suspected effect modifiers.

Thirty female and 26 males were enrolled including 37 (66%) African-Americans and 19 (34%) Hispanics. All subjects had prior treatment with antiretroviral medication (ARVs) and 51/56 (91%) were receiving ARVs at enrollment. Mean CD4 count and CD4% were 720 ± 349 and 29 ± 10 respectively. Viral load was non-detectable in 14 (25%) with a mean of $13{,}386 \pm 45{,}725$ copies/ml in those with measurable HIV. Median serum 25-OHD concentration was 24 ng/ml (normal: 20-65 ng/ml); 18 (32%) were below normal, including 13 (23 %) with insufficiency (25-OHD > 12 and < 20 ng/ml) and 5 (9%) with frank deficiency (25-OHD < 12 ng/ml). Multiple regression analyses found that serum 25-OHD was significantly associated with TBBMC ($p = 0.05$) and TBBA ($p = 0.04$), but not with SBMC, SBA or SBMD in models that included age, sex, height, weight, race/ethnicity, Tanner stage, HIV viral load, and CD4%.

In conclusion, vitamin D deficiency and insufficiency are highly prevalent in a sample of perinatally HIV-infected children and adolescents living in New York City. Moreover, vitamin D status was a significant predictor of TBBMC and TBBA. Studies of vitamin D supplementation to enhance bone accrual in children and adolescents infected with HIV are warranted.

Disclosures: ***S. Arpadi****, None.*

SA502

Whole Body Bone Deficits in Children with Sickle Cell Disease. A. Buison[1], D. Kawchak*[1], J. I. Schall*[1], K. Ohene-Frempong*[2], V. A. Stallings*[1], M. B. Leonard[3], B. S. Zemel[1]. [1]Gastroenterology and Nutrition, Children's Hospital of Philadelphia, Philadelphia, PA, USA, [2]Hematology, Children's Hospital of Philadelphia, Philadelphia, PA, USA, [3]Nephrology, Children's Hospital of Philadelphia, Philadelphia, PA, USA.

Children with sickle cell disease (SCD) experience impaired growth and delayed skeletal and sexual maturation. Deficits in bone mineral content (BMC) have not been well characterized in this population. Our primary objective was to assess whole body BMC (WBBMC) in children with SCD, type SS (SCD-SS) compared to healthy controls with adjustments for height. The secondary objective was to examine the relationship between WBBMC and growth, nutrition, body composition and hematological measures in children with SCD.

WBBMC and body composition were measured using the Hologic QDR 2000 DXA (Bedford, MA) in 90 children with SCD-SS and 198 healthy controls, ages 4 to 19 years old. Skeletal maturation (bone age - chronological age) was determined in children with SCD-SS only. Z-scores for weight (WAZ), height (HAZ), and body mass index (BMIZ) were generated using national reference data. WBBMC and whole body bone area (WBBA) results in the controls were used to generate gender-specific WBBMC z-scores relative to age (WBBMC-age-z) and height (WBBMC-ht-z and WBBA-ht-z). Growth and bone status were compared by Student t-tests. Associations between growth status and hematological measures and WBBMC-ht-z and WBBA-ht-z were assessed by Pearson's correlation coefficient. Multiple linear regression models were developed using log-transformed WBBMC and WBBA and height.

Children with SCD-SS had significantly lower HAZ (-0.5 ± 1.0 vs. 0.3 ± 1.1, $p<0.01$), WAZ (-0.8 ± 1.1 vs. 0.39 ± 1.2, $p<0.01$), and BMIZ (-0.77 ± 1.19 vs 0.29 ± 1.15, $p<0.01$) compared with healthy controls. SCD-SS was associated with significant deficits in WBBMC ($p< 0.001$), adjusted for height, age, pubertal status, and lean body mass. WBBMC-age-z and WBBMC-ht-z were -2.7 ± 7.6 and -0.5 ± 1.0, respectively. They also had deficits in WBBA-ht (mean z-score of -0.6 ± 0.9). Among the children with SCD-SS, WBBMC-ht-z was significantly associated with skeletal maturation ($r=0.53$, $p<0.001$), total hemoglobin ($r=0.23$, $p<0.05$) and hematocrit levels ($r=0.30$, $p<0.001$). After accounting for height, these children have narrow bones (low WBBA-ht) and reduced bone mass (low WBBMC-ht), indicating that they have less cortical bone strength. This suggests that children with SCD-SS achieve suboptimal peak bone mass and may be subject to future bone fractures.

Disclosures: ***A. Buison****, None.*

SA503

Withdrawn

SA504

Low Bone Mass by DXA and QCT in Children with Sickle Cell Disease. E. B. Fung[1], A. Lal*[1], B. Kammen*[2], Z. Pakbaz*[1], E. Vichinsky*[1]. [1]Hematology/Oncology, Children's Hospital Oakland, Oakland, CA, USA, [2]Radiology, Children's Hospital Oakland, Oakland, CA, USA.

Multiple factors compromise bone mineralization in patients with sickle cell disease (SCD) including growth and pubertal delay, decreased vitamin D, reduced physical activity, inflammation, and bone marrow expansion. A pilot project was initiated to determine the prevalence of low bone mass in children (9 to19 years) with severe manifestations of sickle cell disease (Hb SS) and to compare dual-energy x-ray absorptiometry (DXA) with quantitative computerized tomography (QCT) in assessing bone mineral density (BMD). All subjects had one or more severe manifestations including multiple hospitalizations, chronic transfusion therapy, growth failure, and/or avascular necrosis. BMD was evaluated by DXA of lumbar spine (L2-4) and hip, and age, gender and ethnic specific Z-scores calculated. Bone mineral apparent density (BMAD) was calculated using published equations. L2-4 BMD was also measured by QCT, and Z-score estimated independently. Dietary calcium intake was evaluated by a standardized questionnaire. Twenty-five children have been recruited of which n=11 are on chronic transfusion therapy. Over 50% of subjects consumed less than the recommendation for calcium intake (diet + supplements). DXA L2-4 BMD Z-score was reduced in 80% of subjects (< -2.0 in n=13; -1.0 to -2.0 in n=7), whereas BMAD Z-score was reduced in 68% of subjects (<-2.0 in n=12; -1.0 to -2.0 in n=5). The total hip BMD Z-score was reduced in 63% (< -2.0 in n=11; -1.0 to -2.0 in n=4). The L2-4 BMD Z-score assessed by QCT was reduced in only 20% of subjects (< -2.0 in n=4; -1.0 to -2.0 in n=1). The BMAD Z-score values obtained by DXA were significantly different from QCT ($p=0.002$, Wilcoxon rank test), but discordant results were more common in subjects receiving transfusion therapy for >6 months ($p =0.028$, chi square). Further analysis of the DXA L2-4 spine BMAD showed reduced values in 77% of girls vs. 58% of boys; 75% of subjects under 14 years of age; 70% of those with poor dietary calcium intake and 82% of the chronically transfused patients. In summary, the majority of children with severe manifestations of SCD evaluated by DXA in this study had low bone mass (Z-score < -1.0). Z-scores measured by QCT were higher than BMAD Z-scores measured by DXA, however discordant results were observed mostly in patients on red cell transfusions for >6 months. BMAD values derived from DXA might prove more appropriate in assessing BMD in children with SCD. Screening for low bone mass in patients with SCD should take place by second decade of life, particularly for patients with severe manifestations of SCD.

Disclosures: ***E.B. Fung****, None.*

SA505

Decreased Acid-Induced Bone Resorption in COX-2 Knockout Mice. K. K. Frick, N. S. Krieger, K. LaPlante*, S. B. Smith*, D. A. Bushinsky. Medicine/Nephrology Unit, University of Rochester School of Medicine, Rochester, NY, USA.

Metabolic acidosis initially stimulates physico-chemical bone mineral dissolution, which is followed by cell-mediated bone resorption. Prostaglandin biosynthesis is central to this acid-induced, cell-mediated bone resorption as inhibition of cyclooxygenase activity, the rate limiting step for prostaglandin production, with indomethacin suppresses both the acid-induced stimulation of PGE_2 and consequent calcium (Ca) release. Cyclooxygenase is present in both a constitutive (COX-1) and an inducible (COX-2) form. We utilized two model systems to determine the contribution of COX-2 to cell-mediated, acid-induced bone resorption: mice engineered to have a null mutation in COX-2 and cultured calvariae from normal mice treated with a specific inhibitor (NS398) of this enzyme. To assess the role of COX-2 in acid-induced bone resorption in knockout mice, heterozygotic parents were mated, genotypes of resulting pups were determined by PCR and individual calvariae were incubated in either neutral medium (NTL, pH ~ 7.4, $[HCO_3^-]$ ~ 24 mM) or medium made acidic by a primary reduction in $[HCO_3^-]$ (ACID, pH ~ 7.1, $[HCO_3^-]$ ~ 12 mM) to model metabolic acidosis. Medium was changed at 24 and 48 hr for determination of Ca flux. At 24 hr, Ca efflux in NTL from heterozygotes (+/-) was less than that from wild type (+/+) and efflux from knockouts (-/-) was less than either +/+ or +/-. This graded response in unstimulated calcium release from bone indicates that COX-2 is instrumental in setting the baseline level of bone resorption. In ACID, there was a significant stimulation of net Ca efflux from all genotypes at 24 hr, a time in which acid-induced physico-chemical dissolution predominates. After 48 and after 51 hr, again Ca efflux in NTL from +/- was less than that from +/+ and flux from -/- was less than either +/+ or +/-. In ACID at 48 and 51 hr, when cell-mediated bone resorption predominates, while there was a significant stimulation of net Ca efflux from +/+ and +/- compared to NTL, there was less efflux from -/-. The graded response of acid-induced net Ca efflux to genotype indicates the essential role of COX-2 in this response to acidosis. We then determined the effects of incubating calvariae from normal mice in NTL or ACID, with or without 1 μM NS398. After 48 hr and after 51 hr, ACID induced a significant increase in both medium PGE_2 levels and net Ca flux compared to NTL. NS398 significantly inhibited both the acid-induced increase in PGE_2 and net Ca efflux. Thus genetic deficiency of COX-2 or its specific pharmacologic inhibition significantly decreases the net Ca efflux induced by metabolic acidosis, demonstrating the central role of this enzyme in acid-induced, cell-mediated bone resorption.

Disclosures: ***K.K. Frick****, None.*

SA506

Ultrastructural Localisation of Lanthanum in Bone of Chronic Renal Failure Rats Loaded with Lanthanum Carbonate. G. J. Behets*[1], S. C. Verberckmoes[1], L. Oste*[1], A. R. Bervoets*[1], M. Salome*[2], M. E. De Broe*[1], P. C. D'Haese*[1]. [1]Nephrology - Hypertension, University of Antwerp, Wilrijk, Belgium, [2]Id21, European Synchrotron Radiation Facility, Grenoble, France.

We have shown that administration of $La_2(CO_3)_3$ at high doses to CRF rats can induce a mineralisation defect, secondary to an important phosphate depletion due to the pharmacological action of the phosphate binder, rather than being a direct effect of La on bone. In order to further elucidate this finding localisation of La deposited in bone is necessary.

The scanning X-Ray fluorescence microscopy set-up at beamline ID21 of the European Synchrotron Radiation Facility achieves the necessary resolution and sensitivity to localise La that is present at relatively low levels (< 5 μg/g) in bone. A fixed energy X-Ray beam (6.3 keV) was focussed using a Fresnel zone plate to a 1μm probe. X-Ray fluorescence was detected using a solid state Ge detector placed at a 90° angle to the incident beam. Ca and La could be mapped simultaneously using energy windows of 3.52 to 4.12 keV (Ca $K\alpha$ and K_β) and 4.92 to 5.93 keV (La $L_{\beta1}$ and $L_{\beta2}$). Serial Goldner stained sections were used to visualise the scanned area using conventional light microscopy.

In CRF rats loaded orally with $La_2(CO_3)_3$ (12 weeks, 2000 mg/kg/day), bulk bone La concentrations reached values up to 5 μg/g wet weight. La could be demonstrated at the edge of the mineralised bone, at both actively mineralising and quiescent sites. No correlation with the presence of unmineralised osteoid, or the underlying bone pathology (mineralisation defect, hyperparathyroid bone disease or normal bone) could be found. In the presence of hyperparathyroid bone disease, La was also distributed homogeneously throughout the mineralised trabecular bone, and occasionally in resorption areas. Preliminary data in biopsies of patients treated with $La_2(CO_3)_3$ up to 4 years show a similar pattern.

These results suggest no direct correlation between the localisation of La in bone and the presence of either a mineralisation defect or other type of renal osteodystrophy, thereby further strengthening our hypothesis that La does not exert a direct effect on bone metabolism in CRF.

Disclosures: ***G.J. Behets****, None.*

SA507

See Friday Plenary number F507

SA508

Reversibility of Impaired Mineralisation Associated with Lanthanum Carbonate Induced Phosphate Depletion in Chronic Renal Failure (CRF) Rats. A. R. Bervoets*, L. Oste*, G. J. Behets*, P. C. D'Haese*, M. E. De Broe*. Nephrology - Hypertension, University of Antwerp, Wilrijk, Belgium.

Lanthanum (La) carbonate has recently been introduced as a new phosphate-binding agent. We have previously shown that oral administration of La carbonate at high doses (1000 mg/kg/day) during 12 weeks can induce phosphate depletion accompanied by a mineralisation defect in CRF rats. Treatment with sevelamer, a non metal-containing, non absorbed phosphate binder induced a similar effect on bone. This strongly suggests that the mineralisation defect occurred secondary to the phosphate depletion, and was not due to a direct effect of La accumulation in bone.

To further substantiate this hypothesis, male CRF rats (5/6th nephrectomy) received La carbonate for 2 or 6 weeks at a dose of 2000 mg/kg/day. Animals were sacrificed and bone samples for histomorphometry and measurement of the bone La content were taken immediately at the end of the treatment period, and after a washout period of 2 and 8 weeks. Control animals received vehicle only. After 2 weeks of treatment, the bone La level was 1.05 ± 0.11 µg/g (vs. 1.00 ± 1.13 µg/g in controls) and 5 out of 6 animals (83 %) showed signs of impaired mineralisation compared to chronic renal failure controls (1 out 7 animals). After a 2 week washout period, 7 out of 8 animals (87 %) showed normal bone histology in the presence of unchanged bone La levels (1.32 ± 0.35 µg/g); after an 8 week washout period, La levels still remained unchanged, yet 5 out of 6 animals (83 %) had normal bone. A similar evolution was noted in the animals treated with oral La for 6 weeks. Here bone La levels were even slightly increased up to 1.87 ± 0.40 µg/g at 6 weeks (vs. 0.51 ± 0.14 µg/g in controls), and after a 2 week washout period remained at the same level (1.89 ± 0.61 µg/g at 6 weeks). Bone histology, however, showed a reduction in the number of animals with an impaired mineralisation from 4 out of 7 (57 %) at 6 weeks to 1 out of 4 (25 %) after 2 weeks washout, and 2 out of 7 (28 %) after 8 weeks washout. La loading went along with a substantial hypophosphaturia in all animals. These results show that bone histology in CRF animals improved after a 2 and 8 weeks washout period, despite the fact that La remains present in the bone. This provides further support for our hypothesis that the impaired mineralisation is secondary to a phosphate depletion, and is not the direct consequence of La accumulation in bone.

Disclosures: ***A.R. Bervoets****, None.*

SA509

Treatment of a Rat Model of High-turnover Renal Osteodystrophy by Systemic Administration of BMP-7. R. A. Dodds, Y. Wang-Fischer*, A. C. Hughes, D. L. Xu, J. A. Tullai*, F. X. Farrell*. Growth Factors, Johnson&Johnson PRD, Raritan, NJ, USA.

BMP-7 (OP-1) is highly expressed in the kidney during development and in adult life. However, if the kidney experiences an acute injury, e.g., ischemia, BMP-7 mRNA levels decline in parallel with loss of renal.function. Chronic renal failure (CKF) is a progressive disorder leading to end stage renal disease. Present treatments (ACE inhibitors) do not impact the deleterious effects of CKF, including renal osteodystrophy (RO). Skeletal abnormalities in patients with CKF include high bone turnover, fracture and pain. This study evaluated the efficacy of BMP-7 in preserving renal function as well as preventing RO in the rat CKF 5/6 nephrectomy model. Rats (250g) were nephrectomized (NPX): a right contra-lateral NPX was followed in 10 days by left total NPX. Sham surgery was the same procedure minus NPX. The rats received BMP-7 (100 ug/kg), or vehicle i.v, weekly, 10 days after the 2nd surgery, for 6 weeks. Ten and three days before sacrifice, rats were injected (sc) with demeclocycline and calcein, and the proximal tibia processed for histomorphometry. BMP-7 improved renal function (increased GFR, elimination of hematuria, leucocyturia and proteinuria). PTH levels (pg/ml ± SD) were increased in the CKF group v sham (254.7 ± 74 v 405.1 ± 38). The levels were normalized in the BMP-7 group (272.8 ± 43). % Tb.Ar was 18% higher in CKF v sham*, and further increased (34% v sham) in the BMP-7 group. This resulted from an increase in Tb.N, and caused a 26% decrease (CKF-BMP-7 v sham) in Tb.Sp. There was a significant increase in %O.Pm (56%*) which was reduced in the BMP-7 group (-22%) to sham levels. There was an increase (22%) in % Er.Pm in the CKF v sham, that was normalized in the BMP-7 group. Oc.No. was the same in all groups. There was a 15%* increase in MAR in the CKF group v sham that was maintained in the BMP-7 group. BFR/BV/BPm were significantly increased* in the CKF group v sham. These parameters were lowered in the BMP-7 group (to sham level). Elevation of BFR/TV reflects de novo modeling, a feature of PTH action; there was a 47 and 45% increase* in BFR/TV in the CKF and BMP-7 treated group respectively (v sham). There was an 83%* increase in Ac.F in the CKF group v sham, which was reduced by 32% in the BMP-7 group. Wall width (W.Wi) was unchanged in the CKF groups v sham, but was significantly increased v sham in the BMP-7 group (6%*). In summary, CKF resulted in an increase in trabecular bone mass, attributed to an increase in bone turnover (2^0 hyperparathyroidism), with bone formation exceeding bone resorption. With BMP-7 treatment, bone turnover decreased (reduced PTH), but de novo bone formation and an increase in mean W.Wi resulted in the maintenance of increased bone mass (BMP-7 effects). *p<0.02 v sham

Disclosures: ***R.A. Dodds****, None.*

SA510

RANKL and TRAP-5b Are Markers of Bone Destruction in Two Rat Models of Inflammatory Arthritis. P. J. Kostenuik[1], M. Stolina*[2], B. Bolon*[3], S. Adamu*[1], F. Asuncion*[1], S. Morony[1], G. Schett*[4], S. Middleton*[2], U. Feige*[2], D. Zack*[2]. [1]Metabolic Disorders, Amgen, Inc., Thousand Oaks, CA, USA, [2]Inflammation, Amgen, Inc., Thousand Oaks, CA, USA, [3]Pathology, Amgen, Inc., Thousand Oaks, CA, USA, [4]Rheumatology, Medical University of Vienna, Vienna, Austria.

Inflammatory arthritis is associated with local bone erosions and systemic bone loss. We hypothesize that RANKL is an important and common mediator for both forms of bone loss. RANKL is elevated in the serum of arthritic patients, and serum RANKL levels correlate with joint destruction. RANKL mRNA is also highly expressed within the inflamed joints of arthritic rats and mice. We measured RANKL in the serum and joint extracts of rats, using two distinct models of inflammatory arthritis that are associated with bone erosions and systemic osteopenia.

Adjuvant arthritis (AdA) was induced in male Lewis rats using heat-killed mycobacteria in paraffin oil, while CIA was induced in female Lewis rats with collagen II in incomplete Freund's adjuvant. Rats (n = 8 arthritic and 2 healthy control/day) were necropsied intermittently from 5 days before disease onset to onset + 27 days. Inflammation (paw swelling) and skeletal destruction (bone erosions and osteoclasts) were quantified, and RANKL and TRAP-5b (an osteoclast-specific enzyme) were measured in sera and in joint extracts throughout disease progression.

RANKL was increased by 2-3 fold in the serum and by more than 10 fold in arthritic joint extracts of AdA and CIA rats. The induction of RANKL preceded the onset of bone erosions and the appearance of newly activated osteoclasts in arthritic joints. TRAP-5b, a novel bone resorption marker, increased by more than 10 fold in paws of both AdA and CIA. Concomitantly, progressive and significant bone loss was observed locally (in arthritic joints) and systemically (lumbar vertebrae) in both models. The AdA model was typically associated with more dramatic changes in each of these endpoints compared to the CIA model.

RANKL levels are increased significantly in both serum and joint extracts during early disease progression in two distinct rat models of rheumatoid arthritis. TRAP-5b, a novel osteoclast marker, was also significantly elevated in arthritic joints. These data suggest that bone resorption is elevated locally and systemically during the early stages of inflammatory arthritis. Time course analysis of biochemical markers and bone histomorphometry suggest that RANKL plays a pathogenic role in these processes.

Disclosures: ***P.J. Kostenuik****, None.*

SA511

See Friday Plenary number F511

SA512

Bone Mass Changes and Bone Turnover in Children with Early Juvenile Idiopathic Arthritis and Healthy Controls. G. Lien*[1], A. M. Selvaag*[1], B. Flatø*[1], M. Haugen*[2], O. Vinje*[1], D. Sørskaar*[1], K. Dale*[1], T. Egeland*[1], Ø. Førre*[1]. [1]Department of Rheumatology, Rikshospitalet University Hospital, Oslo, Norway, [2]Norwegian Institute of Public Health, Oslo, Norway.

The aim of this study was to explore early changes and predictors of bone mass in children with juvenile idiopathic arthritis (JIA) in order to identify patients who will develop bone mass reductions.

We conducted a prospective, cohort study of 108 children with early JIA (ages 6 to18, mean disease duration 19.3 months), and 108 healthy children randomly selected from the National Population Register, individually matched for age, gender, race, and county of residence. Bone mass and changes in total body, spine, femur and forearm bone mineral density (BMD), bone mineral content (BMC), and body composition were measured with DXA scanner (Lunar Expert) at base-line and follow-up a mean of 24 months later. Disease activity, growth, nutrition, physical activity and biochemical parameters of bone turnover were examined as possible predictors for the bone mass changes. Low bone mass was defined as z score <1SD below the age-specific mean for healthy individuals.

Among the 200 children participating at follow-up, the 100 healthy children had accelerated gains in total body BMC (P=0.035), distal radius BMC (P<0.001) and total body lean mass (P=<0.001), compared to the 100 JIA children by paired sample T-test. Low total body BMC was observed in 24% of the patients, and in 12% of the healthy children (P=0.045). Bone formation, bone resorption and weight-bearing activities were decreased in the patients compared to the healthy children (P<0.001, P<0.001 and P=0.013 respectively). The presence of JIA, serum bone-specific alkaline phosphatase, serum C-telopeptide-1, and weight-bearing activities were statistical significant predictors for the change in total body BMC by multiple regression analysis. Age-and sex adjusted total body BMC were lower in patients with polyarticular than with oligoarticular disease onset (P=0.023). JIA patients had moderate, but clinically important reductions in bone mass, bone turnover and lean mass early in the disease course. The most important independent predictors of bone mass changes were markers of bone turnover and weight-bearing physical activities.

Disclosures: ***G. Lien****, None.*

SA513

See Friday Plenary number F513

SA514

A 2-Year Prospective Study of the Relationship between Bone Biochemical Markers (BBM) and Change in Bone Mineral Density (BMD) in Systemic Lupus Erythematosus (SLE). C. Lee*[1], A. B. Chadha*[1], D. D. Dunlop*[2], O. Almagor*[2], C. B. Langman[3], H. Price*[3], S. Spies*[4], R. Ramsey-Goldman[1]. [1]Division of Rheumatology, Northwestern University, Chicago, IL, USA, [2]Institute for Health Services Research & Policy Studies, Northwestern University, Chicago, IL, USA, [3]Pediatrics, Children's Memorial Hospital, Chicago, IL, USA, [4]Radiology, Northwestern University, Chicago, IL, USA.

The purpose of this study was to determine the relationship between BBM and changes in BMD in women with SLE. 91 women with SLE had BMD measured (hip, spine, distal forearm) at baseline and at 2-years. 3 BBM were measured at baseline: 1) osteocalcin (OC), 2) bone alkaline phosphatase (BAP), and 3) urine N-telopeptide (NTX). Women completed a self-administered lifestyle questionnaire and medication survey. Data on disease features, including disease duration, renal involvement, the American College of Rheumatology/Systemic Lupus International Collaborative Clinics Damage Index (ACR/SLICC-DI) excluding osteoporosis, were collected. Pearson correlations coefficients were determined to assess the strength of the relationship between individual BBM and change in BMD. Women with SLE had a mean age at study visit of 43.9 ±11.4 years, 16.5% were African-American, and had a mean BMI of 26.8 ±7.3 kg/m^2. The mean age at SLE diagnosis was 34.7 ±12.4 years with a mean ACR/SLICC-DI of 1.2 ±1.8. 44% reported currently taking corticosteroids (CS) (mean dose 11.0 ±11.3 mg/day), mean duration of use was 6.7 ±6.9 years, mean daily calcium intake was 1289.8 ±752.9 mg/day, 9.9% were currently smoking, 52.7% reported drinking alcohol and 82.0% reported drinking caffeine. Baseline values for all BBM were near normal limits: 1) OC (8.3 ±8.0 ng/ml), 2) BAP (17.0 ±7.7 U/L), and 3) NTX (36.7 ±38.9 nM/mM). Higher baseline values of OC and NTX were significantly associated with less change in BMD over 2 years at the distal forearm irrespective of menopause status, current CS or plaquenil (PLQ) use. However, only higher baseline value of BAP was significantly related to less change in distal forearm BMD in post-menopausal women (r = -0.36, p=0.04) and in those taking PLQ (r = -0.54, p < 0.0001).

BMD Site	Baseline BMD* (SD)	Mean change in BMD* (SD)	Correlation coefficients for BBM and Change in BMD over 2-years for women with SLE					
			OC		BAP		U-NTX	
			r	p	R	p	r	p
Hip	0.901 (±0.15)	-0.007 (±0.04)	0.10	0.35	0.09	0.39	0.10	0.37
Spine	0.983 (±0.14)	0.009 (±0.05)	0.13	0.24	0.12	0.26	0.06	0.60
Distal forearm	0.680 (±0.07)	-0.012 (±0.03)	-0.37	**0.006**	-0.14	0.20	-0.43	**<0.0001**

*g/cm^2

BBMs at baseline were near normal. A limited relationship between baseline OC, BAP, and NTX with change in BMD at hip and spine was noted, however, higher levels of BBM maybe associated with increased change in distal forearm BMD.

Disclosures: ***C. Lee****, None.*

SA515

A 2-Year Prospective Study of the Relationship between Measures of Calcium Homeostasis (MCH) and Change in Bone Mineral Density (BMD) in Systemic Lupus Erythematosus (SLE). C. Lee*[1], A. B. Chadha*[1], D. D. Dunlop*[2], O. Almagor*[2], C. B. Langman[3], H. Price*[3], S. Spies*[4], R. Ramsey-Goldman[1]. [1]Division of Rheumatology, Northwestern University, Chicago, IL, USA, [2]Institute for Health Services Research & Policy Studies, Northwestern University, Chicago, IL, USA, [3]Pediatrics, Children's Memorial Hospital, Chicago, IL, USA, [4]Radiology, Northwestern University, Chicago, IL, USA.

The utility of MCH to assess bone health in SLE is not known. The purpose of this was to determine the relationship between MCH and changes in BMD in women with SLE. 91 women with SLE had BMD measured (hip, spine, distal forearm) at baseline and at 2-years. Two MCH measured at baseline included: 1) 25-hydroxyvitamin-D (25-OH-D) and 2) intact parathyroid hormone (PTH). All women completed a self-administered lifestyle questionnaire and medication survey, including use of plaquenil (PLQ). Data on disease features, including disease duration, renal involvement, and the American College of Rheumatology/Systemic Lupus International Collaborative Clinics Damage Index (ACR/SLICC-DI) excluding osteoporosis, were collected. Pearson correlations coefficients were determined to assess the strength of the relationship between individual MCH and change in BMD. Women with SLE had a mean age at study visit ±SD of 43.9 ±11.4 years, 16.5% were African-American (AA), and had a mean BMI of 26.8 ±7.3 kg/m^2. The mean age at SLE diagnosis was 34.7 ±12.4 years with a mean ACR/SLICC-DI of 1.2 ±1.8. 44.0% of women reported currently taking corticosteroids (CS) with a mean dose of 11.0 ±11.3 mg/day and the mean duration of use was 6.7 ±6.9 years. For all women, the mean daily calcium intake was 1289.8 ±752.9 mg/day, 9.9% were currently smoking, 52.7% reported drinking alcohol, and 82.0% reported drinking caffeine. The mean baseline value for 25-OH-D (13.3 ±6.3 ng/mL) was low, but PTH (29.1 ±20.9 pg/ml) value was normal. Baseline values of 25-OH-D and PTH demonstrated no significant correlation with mean changes in BMD at the hip, spine or distal forearm over 2-years. Mean baseline values for 25-OH-D and PTH were not significantly related to mean changes in BMD at any of the three anatomical sites regardless of current (PLQ) use.

BMD Site	Baseline BMD* (SD)	Mean change in BMD* (SD)	Correlation coefficients for MCH and change in BMD at 2-years for women with SLE			
			25 (OH)-D		PTH	
			r	p	r	p
Hip	0.901 (±0.15)	-0.007 (±0.04)	0.09	0.43	0.08	0.47
Spine	0.983 (±0.14)	0.009 (±0.05)	0.05	0.66	0.09	0.40
Distal forearm	0.680 (±0.07)	-0.012 (±0.03)	-0.06	0.56	-0.14	0.22

*g/cm^2

In summary, there appears to be no significant relationship between MCH at baseline with change in BMD over 2 years in women with SLE.

Disclosures: ***C. Lee****, None.*

SA516

Longitudinal Analysis of Change in Bone Mineral Density (BMD) in Women with Systemic Lupus Erythematosus (SLE). C. Lee*[1], A. B. Chadha*[1], D. D. Dunlop*[2], O. Almagor*[2], C. B. Langman[3], H. Price*[3], S. Spies*[4], R. Ramsey-Goldman[1]. [1]Division of Rheumatology, Northwestern University, Chicago, IL, USA, [2]Institute for Health Services Research & Policy Studies, Northwestern University, Chicago, IL, USA, [3]Pediatrics, Children's Memorial Hospital, Chicago, IL, USA, [4]Radiology, Northwestern University, Chicago, IL, USA.

There is limited prospective data on change in BMD in SLE. The purpose of this study was to compare change in BMD over a 2-year period at the hip, lumbar spine and distal forearm between SLE (LW) and control women (CW). LW (n=97) and CW (n=97) matched on age, race, and menopause status underwent BMD measurements (hip, spine, distal forearm) at baseline and at 2-years. All women completed a self-administered lifestyle questionnaire and medication survey. Data on disease features, including disease duration, renal involvement, and the American College of Rheumatology/Systemic Lupus International Collaborative Clinics Damage Index (ACR/SLICC-DI) excluding osteoporosis, were assessed. 2-year changes in BMD from baseline values were compared for LW and CW using generalized estimating equations (GEE) to account for the matched case/control design. Case/control differences in 2-year change and 95% confidence intervals (CI) from GEE were calculated. LW and CW were similar in their mean current age (46.6 ±11.5 vs. 47.0 ±11.2 years) and proportion of women who were: African-American (AA) (17.5% vs. 17.5%), menopause status (40.2% vs. 38.1%), and current smoking (9.3% vs. 13.3%). For LW, mean age at SLE diagnosis was 34.6 ±12.6 years with a mean ACR/SLICC-DI of 1.2 ±1.8, 54.6% had disease duration ≥5 years, and 25.8% had renal disease. LW compared with CW reported more corticosteroid (CS) use (75.3% vs. 1.0%) and mean daily calcium intake of (1269.1 ±756.8 vs. 1015.8 ±639.1 mg/day). Mean duration of CS use in LW was 7.05 ±7.0 years with an average CS dose of 14.8 ±11.7 mg/day. LW and CW experienced minimal change in BMD at all sites over 2 years. Similar findings for mean change in BMD were observed for pre-/post-menopausal, Caucasian and AA women with and without SLE.

	Mean change in BMD* measurements over 2-years ±SD		Case/Control Difference in 2-Year Change in BMD* (95% CI)
	LW (Cases)	CW (Controls)	
Hip			
All women	-0.005 ±0.04	-0.002 ±0.03	0.0029 (-0.0082, 0.0140)
Pre-menopausal	-0.002 ±0.04	-0.002 ±0.03	0.0002 (-0.0151, 0.0155)
Post-menopausal	-0.009 ±0.04	-0.002 ±0.03	0.0070 (-0.0080, 0.0219)
Caucasian	-0.003 ±0.04	-0.002 ±0.03	0.0006 (-0.0116, 0.0128)
AA	-0.015 ±0.04	-0.002 ±0.03	**
Spine			
All women	0.009 ±0.05	0.001 ±0.03	-0.0077 (-0.0184, 0.0030)
Pre-menopausal	0.007 ±0.05	0.001 ±0.03	-0.0059 (-0.0109, 0.0072)
Post-menopausal	0.011 ±0.05	0.001 ±0.04	-0.0104 (-0.0288, 0.0081)
Caucasian	-0.011 ±0.04	0.001 ±0.03	-0.0094 (-0.0213, 0.0025)
AA	-0.0004 ±0.05	0.001 ±0.03	**
Distal forearm			
All women	-0.012 ±0.03	-0.005 ±0.05	0.0066 (-0.0058, 0.0190)
Pre-menopausal	-0.011 ±0.02	-0.005 ±0.05	0.0057 (-0.0117, 0.0231)
Post-menopausal	-0.013 ±0.04	-0.005 ±0.03	0.0080 (-0.0071, 0.0230)
Caucasian	-0.011 ±0.03	-0.004 ±0.03	0.0067 (-0.0013, 0.0146)
AA	0.005 ±0.04	-0.004 ±0.03	**

* **g/cm^2**

** **Insufficient number of subjects for analysis**

Women with and without SLE matched on age, race and menopause status experience comparable changes in BMD at the hip, spine and distal forearm over a 2-year period. Longer prospective studies may help determine if such similarities for changes in BMD persist between these two groups of women.

Disclosures: ***C. Lee****, None.*

SA517

Effects of Neurotrophic Factors on Osteoblast Growth and Mineralization. C. Moran*[1], J. Farley[2], T. Linkhart[3]. [1]Anatomy, Loma Linda University, Loma Linda, CA, USA, [2]Biochemistry, Loma Linda University, Loma Linda, CA, USA, [3]Pediatrics, Loma Linda University, Loma Linda, CA, USA.

Numerous clinical and experimental studies indicate that the nervous system influences the regulation of bone growth, remodeling, and repair. Intact neural innervation appears to be essential for proper bone maintenance; bone deprived of neural innervation demonstrates significantly altered growth, repair, and remodeling. Bone receives innervation from both sensory and autonomic nerves. Neuropeptides found commonly in sensory nerves in bone include calcitonin gene-related peptide (CGRP) and Substance P. We investigated the effects of these neuropeptides on mouse osteoblast growth and differentiation in vitro. Murine calvarial osteoblasts were isolated and cultured using standard techniques. Osteoblasts were randomly plated in multi-well plates and grown with and without neuropeptides. Experimental wells received either CGRP or Substance P at concentrations of 0.1-10 micrograms/ml. Cellular alkaline phosphatase and total cell protein levels were measured after 24-hours and 48-hours of treatment. CGRP induced a dose-dependent increase in alkaline phosphatase levels (71%, $p< 0.017$) and total cell protein levels (65%, $p< 0.0004$) in calvarial osteoblasts. Alkaline phosphatase and cell protein were modestly but not significantly increased in calvarial osteoblasts treated with Substance P. MC3T3-E1 cells were used to determine the effect of CGRP and Substance P on osteoblastic mineralization. MC3T3-E1 cells were grown in mineralization media with and without addition of neuropeptides. After 1-3 weeks of treatment, cells were fixed and stained with alizarin red. Both CGRP and Substance P reproducibly increased the rate and extent of mineralization in MC3T3-E1 cells as shown by increased staining with alizarin red (Figure 1). These findings suggest that neuropeptides released from neurons in bone are involved with the regulation of osteoblast growth and mineralization.

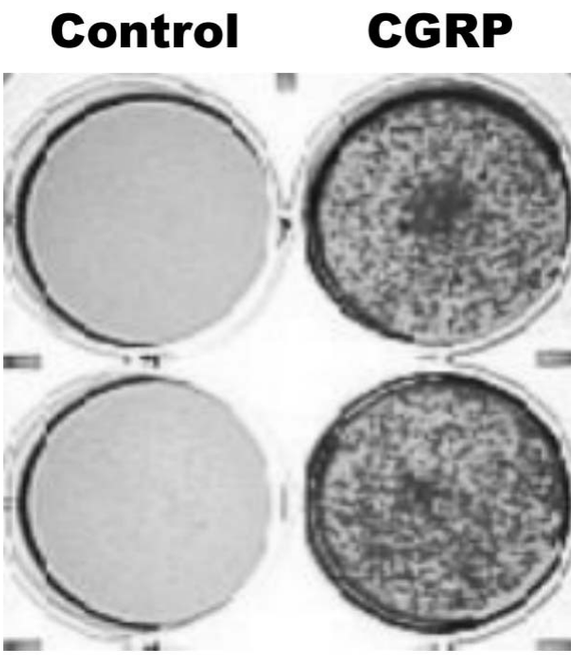

Disclosures: ***C. Moran****, None.*

SA518

Calcitonin Treatment Rescues Calcitonin-null Mice from Excessive Bone Resorption during Lactation. J. P. Woodrow[1], A. O. Hoff[2], R. F. Gagel[2], C. S. Kovacs[1]. [1]Memorial University of Newfoundland, St. John's, NF, Canada, [2]University of Texas MD Anderson Cancer Center, Houston, TX, USA.

We are exploring the role of calcitonin (CT) and calcitonin gene-related peptide (CGRP) in regulating maternal bone metabolism during lactation. Using CT/CGRP gene ablated (*Ct*-null) mice and PIXIMUS bone densitometer, we have reported that *Ct*-null mice lose more trabecular bone mineral content (BMC) during lactation than wt siblings, and recover fully after weaning. Expressed as percent of peak total spine BMC at term, *Ct*-null mice dropped during lactation to 49.3% while wt mice dropped to 70.5% of BMC ($p<0.0002$ by ANOVA).

We now present further studies designed to elucidate the mechanism of the loss and to determine if it can be prevented by treatment with calcitonin.

Urinary excretion of deoxypyridinoline (corrected for creatinine) was no different between *Ct*-null and wt at baseline or during pregnancy, but was increased during lactation in *Ct*-null versus wt (11.9 ± 1.4 versus 2.6 ± 1.8, $p<0.004$ by ANOVA on all time points). Serum osteocalcin increased slightly in lactation but was no different between genotypes. Compared to pre-pregnancy, serum PTH was suppressed normally during pregnancy in both *Ct*-null and wt, but was increased only in *Ct*-null during lactation (55.6 pg/ml ± 11.9 versus 8.9 ± 12.4 pg/ml, $p =0.069$). Micro-CT demonstrated increased trabecular thinning and spacing during lactation which was even greater in *Ct*-null than in wt ($p<0.01$).

Further experiments have used salmon calcitonin versus saline versus CGRP administered once daily intramuscularly to pregnant mice beginning at delivery and throughout 21 days of lactation. Implantable pumps were not used due to the inhibitory effect on lactation that surgery would impose. A mean dose of 10 IU of calcitonin was determined in preliminary experiments to be effective in reducing lactational bone mineral content losses. To date 6 *Ct*-null mice have received a full course of calcitonin treatment and 3 have received a full course of saline injections; none have yet completed a full course of CGRP treatment. Compared to peak of pregnancy, *Ct*-null mice treated with saline dropped to $59.5 \pm 2.1\%$ of BMC while *Ct*-null mice treated with calcitonin dropped to 70.1 ± 1.5 % ($p<0.005$).

In summary, *Ct*-null mice lose more trabecular BMC during lactation through a mechanism that involves increased bone resorption and possibly increased PTH secretion. This excess bone resorption appears to be specific to loss of calcitonin since treatment with calcitonin reduced the lactational loss to a value that was no different than the normal wt value.

We conclude that one role of calcitonin is to regulate the losses in BMC that occur during lactation; in its absence, the losses are more severe.

Disclosures: ***J.P. Woodrow****, None.*

SA519

CGRP Decreases Osteoprotegerin Expression in Human Osteoblast-Like Cells. E. Mrak*[1], I. Villa*[2], A. Rubinacci[2], F. Guidobono*[1]. [1]Dept. of Pharmacology Chemotherapy and Medical Toxicology, University of Milano, Milano, Italy, [2]Bone Metabolic Unit, Scientific Institute H San Raffaele, Milano, Italy.

Among the neuropeptides described in bone, calcitonin gene-related peptide (CGRP) was shown to exert an effect on bone metabolism. In our previous study we have demonstrated that CGRP induces cell proliferation and cAMP accumulation in human osteoblast-like cells (hOB). cAMP is one of the second messenger systems that modulates osteoprotegerin (OPG) production, an endogenous inhibitor of osteoclastogenesis produced by hOB. We therefore studied if CGRP anabolic action on bone could be exerted by regulating the OPG/RANKL/RANK system through the stimulation of cAMP production. First we demonstrated by Reverse Transcriptase PCR that hOB express the CGRP receptor, formed of the calcitonin receptor like receptor (CRLR) and its accessory protein, the receptor activity modifying protein-1 (RAMP-1). Then we treated the cells with human CGRP at different concentrations (0.1nM-10nM), and we determined OPG in the conditioned media of the cells by Elisa immunoassay after 24h and 48h treatment. While after 24h treatment there is no evidence of a change in the OPG secretion, after 48h treatment CGRP inhibited OPG secretion in a dose dependent manner with a maximal effect at the concentration of 10nM. To assess whether or not the effect of CGRP on OPG secretion was on the protein expression we analysed OPG mRNA levels after 6h and 24h of CGRP treatment by Real-Time PCR. OPG mRNA decreased in a significant manner ($p<0.05$) after 6h and remained suppressed for 24h after CGRP (10nM) treatment, thus indicating that the peptide acts on OPG protein expression.

In conclusion CGRP seems to have a potential pro-osteoclastogenic effect, reducing the hOB expression of OPG, the decoy receptor of RANKL. It is therefore likely that the bone anabolic action of CGRP also involves the regulation of bone formation/resorption coupling by inducing a shift of the enhanced bone remodeling to a positive balance.

Disclosures: ***E. Mrak****, None.*

SA520

PTH Regulates Akt/PKB Activity in Opossum Kidney (OK) Cells. P. Sarkar*, E. Dillard*, J. A. Cole. Microbiology and Mol Cell Sciences, University of Memphis, Memphis, TN, USA.

The G protein-coupled receptor (GPCR) agonist PTH activates receptors (PTH1R) coupled to adenylyl cyclase (AC) and phospholipase C (PLC) with cAMP/PKA and/or Ca^{2+}/PKC mediating PTH responses in target tissues. ERK1/2 (ERK) represents a point of signaling convergence for growth factor- and GPCR-dependent regulation of proliferation and differentiation. Several studies have shown that PTH increases ERK activity in kidney and bone. In addition, EGF receptor (EGFR) transactivation plays a role in PTH-induced ERK stimulation in proximal tubule-like OK cells (*Endocrinol 140: 5571-5579)* and TMOb osteoblasts (*Mol Endocrinol 17:1607*). GPCRs agonists also converge on growth factor signaling by activating the pro-survival ser/thr kinase Akt and inhibiting apoptosis. In this study we assessed Akt activation by PTH and the role of AC, PLC and the EGFR in mediating PTH responses. Changes in Akt activity were determined by Western analysis with an activation-specific anti-phosphoSer^{473}Akt antibody. ERK activity was also monitored with an activation-specific anti-phosphoThr^{203}-phosphoTyr^{204} antibody. PTH-stimulated Akt activity increased within 1min and persisted for at least 60 min. PTH doses as low as 10^{-11} M increased Akt activity and maximal responses occurred at 10^{-7} M. ERK activation by PTH displayed a similar time- and dose-dependency. EGF also caused dose-dependent Akt activation with a time course similar to that of PTH. Treatment with the AC activator forskolin or the PKC activator PMA stimulated Akt phosphorylation, suggesting cAMP and/or PKC mediate the PTH response. The Ca^{2+} ionophore ionomycin increased Akt activity while chelation of intracellular Ca^{2+} with EGTA-AM reduced Akt activation by ionomycin and PTH. These data suggest Ca^{2+} mediates at least part of PTH-dependent Akt and ERK activation. ERK activation was similarly affected by ionomycin and EGTA-AM. The PI 3-kinase (PI3K) inhibitors wortmannin and LY294002 and the EGFR-selective inhibitor AG1478 reduced both PTH- and EGF-dependent Akt and ERK activation. Thus PI3K and the EGFR appear to lie downstream of the PTH1R and upstream of Akt and ERK. These results indicate that PTH activates Akt through multiple signals including cAMP, PKC, Ca^{2+} , PI3K and the EGFR. In addition, these data may indicate a role for PTH in protecting kidney cells from apoptosis by activating cell survival pathways.

Disclosures: ***J.A. Cole****, None.*

SA521

See Friday Plenary number F521

SA522

Endogenous PKI$_\gamma$ Regulates PTH-induced Immediate Early Gene Expression. X. Chen[1], J. C. Dai[1], S. A. Orellana*[2], E. M. Greenfield[1]. [1]Orthopaedics, Case Western Reserve University, CLeveland, OH, USA, [2]Pediatrics, Case Western Reserve University, CLeveland, OH, USA.

Parathyroid hormone (PTH) stimulates both bone resorption and bone formation primarily by activating cAMP/protein kinase A (PKA) signaling and affecting the expression of immediate-early genes, such as IL-6 and *c-fos*. Our previous results showed that the primary mechanism responsible for termination of PKA activity, CREB phosphorylation, and immediate-early gene expression following PTH stimulation acts downstream of receptor desensitization, adenylyl cyclase activation, and cAMP degradation (Am J Physiol Cell Physiol 283:1432-40, 2002). We hypothesized that inhibition of PKA activity by the protein kinase inhibitor (PKI) family terminates transcription factor phosphorylation and gene expression. We found that PKI$_\gamma$ mRNA and protein are constitutively expressed in osteoblasts and fibroblasts at high levels, while PKIα and PKI$_\beta$ are weakly expressed. Therefore, to test our hypothesis, *in vitro* transcribed siRNA duplexes directed against the PKI$_\gamma$ coding region were transfected into ROS17/2.8 cells. Knock down of PKI$_\gamma$ mRNA and protein was virtually complete after 24 hours. Knock down resulted in increased levels of IL-6 and *c-fos* mRNAs induced by PTH at early time periods (≤ 1 hour). Knock down also extended the duration of mRNA induction (≥ 6 hours vs. 2 hours in mock-transfected cells). The effects of PKI$_\gamma$ knock down were confirmed using ROS17/2.8 clones stably transfected with PKI$_\gamma$ antisense constructs in the Tet-Off expression system. After 48 hours of tetracycline withdrawal, two independent antisense clones exhibited effects similar to those observed with siRNA. Controls included antisense clones with tetracycline as well as sense and irrelevant clones + tetracycline. PKI$_\gamma$ contains a potent nuclear export signal (NES) and likely inhibits PKA activity to terminate its effects on PTH-induced gene expression and then transports PKA out of the nucleus since we found that (1) PKI$_\gamma$ and all three isoforms of the catalytic subunit of PKA are rapidly re-exported to the cytoplasm following PTH-induced nuclear translocation, (2) PKI$_\gamma$ knock down blocks nuclear export of PKA, and (3) although PKA catalytic subunits lack a NES, the NES inhibitor, Leptomycin B, blocks nuclear export of both PKI$_\gamma$ and PKA. However, Leptomycin B has no effect on nuclear PKA activity, CREB phosphorylation, or immediate-early gene expression. Nuclear export is therefore not required and PKI$_\gamma$ binding is sufficient to terminate nuclear PKA signaling. These findings are the first in any cell type showing that endogenous PKI$_\gamma$ regulates PKA signaling.

Disclosures: ***X. Chen****, None.*

SA523

See Friday Plenary number F523

SA524

Parathyroid Hormone (PTH) Is Not Required to Restore Skeletal Mineral that was Lost During Lactation. K. L. Buckle[1], N. J. Fudge*[1], A. C. Karaplis[2], C. S. Kovacs[1]. [1]Memorial University of Newfoundland, St. John's, NF, Canada, [2]McGill University, Montreal, PQ, Canada.

During lactation, the maternal skeleton temporarily demineralizes to provide calcium to milk, and then the mineral is fully restored after weaning. The demineralization occurs due to the effects of PTH-related protein (PTHrP), produced by mammary tissue, which acts in concert with lower estrogen levels during lactation to stimulate bone resorption. In contrast, the mechanism controlling the restoration of mineral after weaning is not established. Limited data from humans has shown increases in serum PTH after weaning, which has led to speculation that PTH may regulate restoration of mineral to the maternal skeleton during that time frame.

To determine if PTH is required for normal mineral homeostasis during pregnancy and lactation, and in particular, for restoration of mineral after weaning, we studied mice that lack PTH (*Pth* null) and compared them to their wt and *Pth*+/- sisters.

Pth mice were backcrossed into Black Swiss for at least 4 generations and maintained by mating *Pth*+/- mice together. All mice consumed a standard chow containing 1% calcium. First degree relatives were chosen for study beginning at 12 weeks of age, after sexual maturity and the attainment of peak bone mass in mice. Total body and regional (spine, femur) bone mineral content (BMC) was measured by DXA (PIXImus, Lunar) every other day during 70 day reproductive cycles (baseline, pregnancy, lactation, post-weaning). Blood and urine were collected for serial assessment of minerals and hormones.

Pth null mice were hypocalcemic with ionized calcium of 0.89 ± 0.04 mmol/l versus 1.28 ± 0.04 mmol/l in wt. The ionized calcium did not change significantly during pregnancy, lactation and post-weaning in *Pth* null mice or siblings. Compared to their respective pre-pregnancy BMC values, total body BMC rose during pregnancy to a peak of 112 ± 3% in *Pth* nulls (112 ± 3% in wt and 114 ± 2% in *Pth*+/-, p=NS), and fell during lactation to a trough value of 91 ± 5% in *Pth* nulls (83 ± 3% in wt and 86 ±3% in *Pth*+/-, p=NS). Regional BMC values were also no different among genotypes. All BMC values returned to baseline within three weeks, with no significant differences among the time to recovery by genotype.

In summary, *Pth* null mice were hypocalcemic and this did not change during pregnancy or lactation. As compared to their siblings, *Pth* null mice achieved a similar increment in BMC during pregnancy, lost a comparable amount of BMC during lactation, and recovered fully to baseline without any delay.

In conclusion, PTH is not required to maintain mineral homeostasis in the pregnant or lactating mouse, and in particular, is not required to restore skeletal mineral content that was lost during lactation.

Disclosures: ***K.L. Buckle****, None.*

SA525

See Friday Plenary number F525

SA526

The Skeletal Anabolic Effect Of Parathyroid Hormone Is Not Dependant On Nitric Oxide. J. Davies*, C. J. Jagger*, J. W. Chow. Cellular Pathology, St George's Hospital Medical School, London, United Kingdom.

Parathyroid hormone (PTH) is currently the only anabolic agent licenced for treatment of osteoporosis. It is considered to act via the cAMP-protein kinase A and protein kinase C pathways, as well as calcium-signalling pathways. Nitric oxide (NO) is a well-recognised signal transduction molecule. Although no effect has been observed with PTH on bone cells *in-vitro*, NO release has been demonstrated in PTH-treated endothelial cells. To investigate whether the anabolic action of PTH is mediated by NO, we analysed the bone formation response to intermittent administration of PTH in eNOS $^{-/-}$ mice .

PTH (40 ugram/kg sc) was given once daily to 19 week old eNOS $^{-/-}$ and wild-type mice for 6 days. Animals were killed after 8 days, following two spaced fluorochrome lables. Bone histomorphometry was performed on the tibial metaphysis. We found a 4 fold increase in cancellous bone formation rate in PTH-treated wild-type mice compared with vehicle-treated animals. eNOS $^{-/-}$ mice showed a similar increase in bone formation rate as wild-type animals. There was no difference in response between males and females. There was no significant increase in cancellous bone volume after this short period of PTH administration.

The lack of blunted osteogenesis in eNOS $^{-/-}$ animals suggests that the anabolic effect of PTH is not dependant on nitric oxide.

Disclosures: ***J.W. Chow****, None.*

SA527

See Friday Plenary number F527

SA528

Arrestin Mobilization Is Facultative for PTH Receptor Endocytosis. W. B. Sneddon[1], P. A. Friedman[2]. [1]Dept. of Pharmacology, University of Pittsburgh School of Medicine, Pittsburgh, PA, USA, [2]Depts. of Pharmacology and of Medicine, University of Pittsburgh School of Medicine, Pittsburgh, PA, USA.

Arrestins are adaptor proteins that play a critical role in desensitizing and internalizing G protein coupled receptors. Agonist occupied receptors activate cognate G proteins, which in turn activate various downstream effectors, propagating the signal. The transduction cascade is terminated, i.e., desensitized, by receptor phosphorylation followed by arrestin binding. High affinity arrestin binding not only uncouples the receptor from its G protein as part of the desensitization process, but also targets the receptor for endocytosis in clathrin-coated pits. The role of arrestin mobilization in G protein coupled receptor signal termination varies depending on the receptor and the cell in which it is expressed. The parathyroid hormone type I receptor (PTH1R) is found primarily in kidneys and bone. In recent work we showed that PTH(7-34), which doesn't activate or desensitize the PTH1R but efficiently promotes its endocytosis. This raised the question of whether arrestins are required for the internalization of PTH1Rs that are not activated or desensitized. We examined the role of arrestin mobilization in ligand-induced PTH1R internalization and desensitization in mouse kidney distal convoluted tubule (DCT) cells, where PTH regulates calcium absorption. PTH(1-34), which activates, desensitizes, and internalizes the PTH1R promoted ßarrestin2 movement from the cytoplasm to the plasma membrane within 2 minutes. After 15 minutes, arrestin appeared in a punctate fashion in the cytoplasm. PTH(7-34) which does not activate the PTH1R but promotes its endocytosis did not induce arrestin trafficking. Furthermore, PTH(1-34) but not PTH(7-34) enhanced coimmunoprecipitation of ßarrestin1 with the PTH1R. Deletion of the C terminus of the PTH1R reduced the interaction between arrestin and the PTH1R but did not interfere with PTH(1-34) or PTH(7-34)-induced PTH1R endocytosis. Thus, PTH1R interacts directly with ß-arrestin by its intracellular C terminal tail. The clathrin-binding domain of ßarrestin1 acts as a dominant negative (dnArr) preventing trafficking of arrestin-associated proteins to clathrin-coated vesicles for endocytosis. dnArr did not inhibit PTH1R internalization by PTH(1-34) in DCT cells but blocked isoproterenol-induced ß-adrenergic receptor internalization. Furthermore, dnArr inhibited PTH1R internalization in HEK293 cells. We conclude that arrestin mobilization is facultative and not obligatory for PTH1R internalization. Arrestin trafficking, in response to activating PTH peptides, is consistent with a role in mediating PTH1R desensitization.

Disclosures: ***W.B. Sneddon****, None.*

SA529

See Friday Plenary number F529

SA530

Amino-terminal Structure of Non-(1-84) PTH Fragments Secreted by Parathyroid Glands of Patients with 1^{ary} and 2^{ary} Hyperparathyroidism. P. D'Amour[1], J. Brossard[1], L. Rousseau*[1], C. Lazure*[2], J. R. Lavigne[3], R. J. Zahradnik[3]. [1]Hôpital Saint-Luc, Centre de recherche du CHUM, Montreal, PQ, Canada, [2]Institut de recherches cliniques de Montréal, Montreal, PQ, Canada, [3]Immutopics Inc., San Clemente, CA, USA.

Non-(1-84) parathyroid hormone (PTH) are large circulating carboxyl-terminal (C) fragments with a partially preserved amino-terminal (N) structure. hPTH(7-84), a synthetic surrogate, has been demonstrated to exert biological effects in vivo and in vitro through a C-PTH receptor which are opposite to those of hPTH(1-34) on the PTH/PTHrP type I receptor. To determine the N- structure of non-(1-84) PTH fragments, we have incubated parathyroid cells isolated from glands obtained at surgery from 3 patients with 1^{ary} hyperparathyroidism (HP) and 3 patients with 2^{ary} HP with ^{35}S-Methionine and ^{3}H-Leucine to internally labeled their secretion products. Incubations were performed for 8 hr at the patient ionized calcium concentration and in the presence of various protease inhibitors (Roche Diagnostic). The supernatant was fractionated by HPLC and fractions were analyzed with a (1-4) and (13-34) PTH assay from Immutopic (San Clemente, CA). The serum of each patient was similarly analyzed. Peaks of immunoreactivity identified were submitted to sequence analysis (Procise model 494, Applied Biosystem) to recover the ^{35}S-Methionine residues in position 8 and 18 and the ^{3}H-Leucine residues in positions 7, 11 and 15. Four regions of interest were identified with PTH assays corresponding to non-(1-84) PTH fragments (regions 3 and 4), a peak of N-PTH reacting mainly in the (1-4) PTH assay (region 2) and a peak of immunoreactivity corresponding to the elution position of standard hPTH(1-84) (region 1). The last corresponded to a single sequence starting at position 1. Region 2 gave similar results most of the time (a sequence starting at position 1) but also sometimes a small amount of a sequence starting at position 4. Region 3 and 4 always identified major sequences starting at positions 7 and 15 and sometimes at positions 8 and 10 also. Surprisingly a sequence starting at position 1 was also present in region 3. The HPLC profile obtained from of a given patient parathyroid cells was similar to the one obtained from serum in each case. These results indicate that non-(1-84) PTH is composed of a family of fragments which are generated by progressive cleavage at their N-region, starting at position 4 and progressing to position 15. This is a process similar to the one described for smaller C-PTH fragments a number of years ago, suggesting a similar generation process and source for all PTH fragments. This work was granted by CIHR and NPS Pharmaceuticals.

Disclosures: ***P. D'Amour****, NPS Pharmaceuticals 2; Immutopics Inc. 5.*

SA531

See Friday Plenary number F531

SA532

Identification of the Response Element That Controls Transcriptional Activation of CCAAT Enhancer Binding Protein Beta by PTH In Osteoblastic Cells. P. Dhawan*[1], X. Peng*[1], Y. Liu*[1], S. Williams*[2], S. Christakos[1]. [1]Biochemistry, University of Medicine and Dentistry of New Jersey, Newark, NJ, USA, [2]Dept. of Cell Biology and Biochemistry, Texas Tech University Health Sciences Center, Lubbock, TX, USA.

We earlier reported that CCAAT enhancer binding protein β (C/EBPβ) is a $1,25(OH)_2D_3$ target in osteoblastic cells and also that C/EBPβ enhances vitamin D receptor (VDR) mediated 24(OH)ase transcription. Our findings indicated that not only $1,25(OH)_2D_3$ but also PTH can induce C/EBPβ in osteoblastic cells and suggested a role for C/EBPβ in the cross talk between PTH and $1,25(OH)_2D_3$ that involves enhancement of PKA induced VDR transcription. To examine the mechanisms involved in induction of C/EBPβ by $1,25(OH)_2D_3$ and PTH, UMR osteoblastic cells were transfected with different deletion constructs of the C/EBPβ promoter -1,400/+16. These constructs were unresponsive to $1,25(OH)_2D_3$ (10^{-9} - 10^{-7}M), suggesting possible post transcriptional regulation of C/EBPβ by $1,25(OH)_2D_3$. However a region located at -120/-60 was found to be required for the activation of the C/EBPβ promoter by PTH (1 - 25 nM; maximal induction at 25 nM, 10 ± 1.5 fold). The protein kinase A inhibitor H89, a dominant negative CREB as well as the inducible cAMP early repressor (ICER) blocked the PTH dependent effect on the C/EBPβ promoter activity, suggesting that PTH activation occurs via a PKA dependent pathway. The PKC inhibitor Go-6983 did not affect PTH dependent induction of C/EBPβ transcription. Mutation constructs of the C/EBPβ promoter demonstrated that the activation of the C/EBPβ promoter by PTH is mediated through a CREB binding site at -111/-107. Gel mobility shift assays indicate that both control and PTH treated (10 nM, 1h) nuclear extracts bind to this site. Significantly more protein-DNA complex was produced when extracts from PTH treated cells were used. An anti-CREB specific antibody markedly reduced protein binding indicating that this complex contains CREB. Thus we conclude that PKA dependent CREB activation mediates the PTH dependent effect on C/EBPβ transcription. In addition, studies using immunocytochemistry and fluorescence microscopy suggest that PTH can also stimulate the nuclear accumulation of C/EBPβ. Under control conditions C/EBPβ was diffusely distributed within the cell but after 2 h of PTH treatment (10 nM) the protein was predominantly nuclear. These findings provide a mechanism for the first time for PTH induction of C/EBPβ and suggest that stimulation of C/EBPβ transcription and C/EBPβ nuclear translocation may be important for other actions of PTH than can affect osteoblast function.

Disclosures: ***P. Dhawan****, None.*

SA533

See Friday Plenary number F533

SA534

The Anabolic Bone Response to Low Dose PTH Is Attenuated by Reduced Physical Activity. T. E. Hefferan[1], G. L. Evans*[1], M. Zhang*[1], E. Morey-Holton[2], R. T. Turner[1]. [1]Orthopedics, Mayo Clinic College of Medicine, Rochester, MN, USA, [2]Ames Research Center, NASA, Moffett Field, CA, USA.

Bone loss is a widespread problem facing the aging population and can be influenced by lifestyle factors such as reduced physical activity. Disuse results in uncoupled bone turnover where bone resorption is increased and bone formation decreased. Intermittent parathyroid hormone (PTH) increases bone formation, and is an approved treatment for osteoporosis. Thus, we examined the effectiveness of PTH in preventing bone loss that occurs with disuse. A 2-week dose response study was performed using 6 month old male Fisher rats that were hindlimb unloaded (HLU) and injected subcutaneously with PTH 0, 5, 20, or 80 ug/kg/d. The bone response was measured by dynamic histomorphometry and Northern blot analysis of bone matrix genes. All doses of PTH significantly increased bone formation rates (BFR/BS) ranging from a 2 fold increase, $p<0.01$, with the lowest dose (5 ug/kg/d) to a 6.5 fold increase, $p<0.0001$, with the highest dose (80 ug/kg/d) compared to normal loaded control. The 80 ug/kg/d dose significantly increased mRNA levels for type I collagen 10 fold ($p<0.0001$), osteonectin 4 fold ($p<0.001$) and osteocalcin 7 fold ($p<0.0001$). These findings indicate that the daily doses for PTH typically administered to rats are greatly in excess of that necessary to maintain normal bone formation in HLU rats. Therefore, a second study was conducted using a lower dose of PTH 1 ug/kg/d. Six month old intact male Fisher rats were assigned to HLU or normal weight bearing groups and treated for 2 weeks with 1 ug/kg/d PTH or vehicle. PTH treatment of normal weight bearing rats resulted in a significant increase in bone volume ($p<0.01$), trabecular thickness ($p<0.05$) and trabecular number ($p<0.05$), and a significant decrease in trabecular separation ($p<0.01$). HLU significantly decreased mineral apposition rate ($p<0.05$) and bone formation rate ($p<0.0001$), while PTH treatment of the HLU animals maintained mineral apposition and bone formation rates at the same level as the normal weight bearing control. Mineral apposition and bone formation rates were significantly increased (31%, $p<0.05$ and 230% $p<0.0001$) in the PTH treated normal weight bearing animals compared to vehicle control. Two-way ANOVA demonstrated that PTH had significant stimulatory effects while unloading had significant inhibitory effects on bone formation. In addition, there was a strong interaction term demonstrating that normal weight bearing potentiates the stimulatory effects of PTH. These studies suggest that while PTH therapy is beneficial, it may be less effective in patients with impaired physical activity.

Disclosures: ***T.E. Hefferan****, None.*

SA535

HSP-70 Expressed on the Surface of Cancer Cells Binds Specific PTHrP Peptides In Vitro. J. J. Grzesiak*[1], D. W. Burton[2], L. J. Deftos[2], M. Bouvet[1]. [1]Department of Surgery, University of California, San Diego and Veterans Affairs San Diego Healthcare System, San Diego, CA, USA, [2]Department of Medicine (Endocrinology), University of California, San Diego and Veterans Affairs San Diego Healthcare System, San Diego, CA, USA.

Recent studies confirm that the functions of parathyroid hormone-related protein (PTHrP) and its derived peptides cannot be attributed solely to binding of the classical 7 membrane-spanning and G protein coupled PTH/PTHrP receptor. The present study focused on elucidation of other proteins that might be involved in PTHrP binding and signal transduction at the cell surface. Using affinity chromatography techniques, we coupled different PTHrP-derived peptides to Sepharose 4B, including 1-34, 37-86 and 140-173; and applied octyl-ß-D-glucopyranoside solubilized extracts of cell-surface biotinylated Mia-PaCa-2 pancreatic adenocarcinoma, Saos-2 osteosarcoma and DU-145 prostate cancer cell lines over the affinity columns. After washing, the columns were sequentially eluted with 1 mg/ml of the corresponding free peptide, 10 mM EDTA, 1 M NaCl and 8 M Urea. Fractions analyzed by electrophoretic techniques revealed the presence of a major band of about 70 kDa that was elutable with the corresponding free peptide, along with other PTHrP binding proteins. MALDI analyses and immunoblotting revealed that the major PTHrP-binding protein was heat shock protein-70 (HSP-70). Other binding proteins identified by MALDI included HSP-90. Immunoprecipitation binding assays with radiolabled PTHrP peptides confirmed the binding of HSP-70 to specific fragments of PTHrP but not to others and not to control peptides. HSP-70 as well as other molecular chaperones normally expressed exclusively inside the cell are expressed on the cell surface in cancer. Taken together, these data suggest that PTHrP interacts with the proteins identified by these studies, and that these novel PTHrP-protein interactions may be involved in the transmission of PTHrP signals not currently attributable to the PTH/PTHrP receptor.

Disclosures: J.J. Grzesiak*, None.*

SA536

Role of Voltage Dependent Calcium Channels in Carboxyl-Terminal Parathyroid Hormone Receptor Signaling. A. Selim*, M. J. Mahon, H. Jueppner, F. R. Bringhurst, P. Divieti. Endocrine Unit, Massachusetts General Hospital and Harvard Medical School, Boston, MA, USA.

Parathyroid hormone (PTH), an 84-amino-acid polypeptide, is a major systemic regulator of calcium homeostasis and bone remodeling and elicits its classical functions by activating PTH/PTHrP receptors (PTHRs) on target cells. Carboxyl (C) fragments of PTH, secreted by the parathyroids in a calcium-dependent manner or generated by PTH proteolysis in the liver, circulate in blood at concentrations much higher than intact PTH(1-84) but cannot activate PTHRs. Receptors specific for C-PTH fragments (CPTHRs), distinct from PTHRs, are expressed by bone cells, especially osteocytes, in which they may regulate intercellular communication and cell survival. Activation of CPTHRs previously was reported to modify intracellular calcium within chondrocytes.

To further investigate the mechanism of action of CPTHRs in osteocytes, cytosolic free calcium, (Ca_i^{++}) was measured in the PTHR-null osteocytic cell line OC 59, which expresses abundant CPTHRs but no PTHRs. Ca_i^{++} was assessed by single-cell ratiometric microfluorimetry in Fura -2 loaded OC 59 cells that were pretreated for 16 h with 0.3 mM 8Br-cAMP, which increases CPTHR expression in these cells A rapid and transient increase in Ca_i^{++} was observed in OC59 cells in response to the CPTH fragment hPTH(53-84) (250 nM). Similar results were obtained using analogs of longer CPTH fragments, such as hPTH(13-84) and hPTH(23-84). No Ca_i^{++} signal was observed in COS-7 cells, in which CPTHR binding also cannot be detected. A mutant CPTH analog, [Ala^{55-57}]hPTH(53-84), which does not to bind to CPTHRs, also failed to elicit an increase in Ca_i^{++} in OC59 cells, as did hPTH(1-34).

The Ca_i^{++} response to hPTH(53-84) required the presence of extracellular calcium and was blocked by inhibitors of voltage-dependent calcium channels (VDCC), including nifedipine (100 nM), ω-agatoxin IVA (10 nM) and ω-conotoxin GVIA (100 nM). Interestingly, VDCC inhibitors also decreased specific binding of the radioligand ^{125}I-[Tyr^{34}]hPTH(19-84) to CPTHRs on OC59 cells.

We conclude that activation of CPTHRs in OC59 osteocytic cells leads to a rapid increase in influx of extracellular calcium, most likely through opening of VDCCs. VDCCs could interact directly with CPTH ligands or with CPTHRs. Alternatively, they may be required to maintain Ca_i^{++} levels necessary for CPTHR binding to extracellular CPTH ligands. Calcium influx through VDCCs may play a critical role in CPTH receptor signaling in bone cells.

Disclosures: ***A. Selim****, None.*

SA537

See Friday Plenary number F537

SA538

Creation of lacZ-PTHrP Knock-in Allele in the Mouse. X. Chen[1], B. E. Dreyer*[1], V. Hammond*[2], W. M. Philbrick*[1], A. E. Broadus[1]. [1]Department of Medicine, Endocrine Division, Yale University, New Haven, CT, USA, [2]Howard Florey Institute, University of Melbourne, Parkville, Australia.

PTHrP gene expression is tightly regulated by a combination of transcriptional and post-transcriptional mechanisms, as befits its cytokine-like function in many locations. The transcriptional mechanism is due to a variety of positive and negative regulatory elements operating on one or more promoters and the post-transcriptional regulation to multiple instability elements in PTHrP mRNA 3' UTRs. These mechanisms account for the generally low level of PTHrP products, which are frequently at the limit of detection of in situ hybridization histochemistry (ISHH) and immunohistochemistry (IH).

We have created mice with an allelic PTHrP-lacZ insertion. We targeted exon 3 of the mouse gene, comprising the bulk of the PTHrP coding region, and worked with 12kb of strain 129/Sv DNA flanking this exon. After extensive mapping, we settled on a 5.8-kb KpnI-SacI fragment from intron 2 and a 3.6-kb Sac1-BamHI fragment from intron3 as the long and short arms of homology, respectively. The B-galactosidase (gal) coding region was preceeded by stop codons in all three reading frames and a picornaviral internal ribosomal entry site. A nuclear localization sequence was not included. SV40 small t polyadenylation/termination sequences were used in place of the PTHrP 3' UTR, providing the transcription product with the t ½ of B-gal (estimated at 8 hr) rather than the 30-to 120-min t ½ of PTHrP mRNA. The combination of enhanced stability and the sensitivity of X-gal staining should increase detection sensitivity by 10-to 100-fold as compared to PTHrP ISHH or IH.

Some 200 W9.5 (129/Sv (S1)) ES clones resistant to G418 and gangcyclovir were selected and homologous integrants confirmed by PCR and Southern blotting. Two of these were karyotyped and injected into C57BL/6J blastocycts and the line with the highest percentage chimerism in F_0 mice bred to BL/6 mice to produce allelic F_1 mice at a 50% frequency (27/54).

We plan to use the PTHrP-lacZ allele for three principal purposes: 1) to localize PTHrP expression in previously difficult-to-detect locations such as keratinocytes, bone cells and the CNS/PNS, 2) to substitute for a null PTHrP allele in gene-replacement studies, enabling detection of PTHrP-expressing cells in such experiments, and 3) as readout in mouse experiments designed to study PTHrP gene responsiveness to physiological and pathophysiological stimuli. The mice will be made available to other investigators.

Disclosures: ***A.E. Broadus****, None.*

SA539

Anabolic Effects of Intermittent Parathyroid Hormone-Related Protein (107-139) (Osteostatin) on Human Osteoblastic Cells in Vitro. A. R. de Gortázar*, V. Alonso*, P. Esbrit. Bone and Mineral Metabolism Laboratory, Fundación Jiménez Díaz-UTE, Madrid, Spain.

The C-terminal fragment of parathyroid hormone-related protein (PTHrP) 107-139, referred to as *osteostatin*, has been shown to directly iinhibit osteoclastic-mediated bone resorption. Recent data suggest that this fragment also affects osteoblastic cell function. We performed an *in vitro* study to an assess the influence of exposure time on the effects of this fragment -compared with those of PTHrP (1-36)- on different osteoblastic markers. Subconfluent human osteoblastic osteosarcoma MG-63 cells were treated with PTHrP (107-139), or PTHrP (1-36), for several hours during several consecutive 48-h incubation cycles. Transient exposure of MG-63 cells to PTHrP (107-139), or PTHrP (1-36), at 100 nM, for the first 6-24 h of only one cycle stimulated alkaline phosphatase activity (1.5-fold over control) in these cells. Using a similar intermittent treatment for 3 cycles, both peptides failed to significantly affect core binding factor-α1 (Cbfa1) activity, but stimulated bone nodule formation, and also osteocalcin mRNA and osteoprotegerin (mRNA and protein) expression (maximal 2-fold over control, at 100 nM) in MG-63 cells. Moreover, transient exposure to PTHrP (107-139) during cell growth increased the PTH1 receptor (PTH1R) protein expression. These anabolic effects of this peptide were abolished by the PKC inhibitor bisindolylmaleimide I (25 nM) but not by a neutralizing anti-IGF-I antibody in these cells. In contrast, this antibody abolished these effects induced by PTHrP (1-36) in MG-63 cells. Both PTHrP peptides, within 0.1-100 nM, when added transiently to MG-63 cells, inbited (by 50%) receptor activator of NF-kappaB ligand (RANKL) protein levels in MG-63 cell membrane extracts. Thus, intermittent treatment with these PTHrP peptides significantly increased the OPG/RANKL ratio in these cells. Continuous treatment of MG-63 cells with each peptide for 3 cycles failed to induce these effects; and did not affect those triggered by the transient exposure to the other peptide.

These results indicate that intermittent exposure of human osteoblastic cells to *osteostatin* induces anabolic effects through a PTH1R-independent mechanism.

Disclosures: ***P. Esbrit****, None.*

SA540

PTHrP as a Mediator of DNA Repair in Cancer. N. Ilievska*, S. Bouralexis*, R. J. Thomas-Mudge*, T. J. Martin, M. T. Gillespie. Bone, Joint and Cancer, St. Vincent's Institute of Medical Research, Fitzroy, Australia.

Parathyroid hormone-related protein (PTHrP) is widely expressed in many tumors and its production by cancer metastases in bone promotes osteolysis. In addition, PTHrP affects cellular functions including differentiation, proliferation and apoptosis. To determine the potential roles of PTHrP within the progression of breast and other cancers, we have examined the effect of PTHrP expression by and upon breast, prostate and osteosarcoma cell lines. As a consequence of PTHrP overexpressing in the breast cancer cell lines (MCF-7, MDA-MB-231 and MCF-10A), several DNA repair (XPG, BRCA1, BRCA2 and Rad51), cell cycle (p21 and p53), and apoptosis-related genes such as Bcl-2 were determined to be regulated, both at the mRNA and protein level: the DNA repair genes were elevated. To determine whether this was a result of an intracrine or autocrine action of PTHrP, a range of PTHrP peptides were assessed for their ability to alter gene expression in breast (MCF-7, MDA-MB-231, MCF-10A), osteosarcoma (MG63, Saos, U-2 OS) and prostate (DU145, PC3) cells. PTHrP peptides 1-34, 1-108, 106-139 or 122-139 did not affect mRNA or protein levels for these target genes, whilst PTHrP peptides (107-139 or 107-111 at 100 nM) encompassing osteostatin (TRSAW: 107-111) upregulated the expression of mRNA levels for these genes, as well as for PTHrP, within 4 to 24 hrs: changes were also noted in protein levels. Mutant peptides of osteostatin (TRSPW, TRGAW, PRSAW, YRSAW, TKSAW and TASAW) identified a requirement for Thr107 and Ser 109 for activity on DNA repair genes in MCF-10A cells.

To determine the signal transduction pathway(s) involved in osteostatin-induced regulation of DNA repair genes, MCF-10A cells were treated with the NFkB inhibitor (N-acetyl-L-cystine), PKA inhibitor (H89) or PKC inhibitor (chelerythrine chloride) with and without TRSAW (100nM). These inhibitors indicated involvement of the PKA and PKC pathways for TRSAW effects on DNA repair genes.

Finally, to determine if PTHrP was indeed responsible for DNA repair, the ability of osteostatin or mutants peptides to protect against etoposide induced DNA damage was assessed by COMET assays. TRSAW and peptides that elevated DNA repair gene expression protected against etoposide-induced DNA damage, whilst peptides that had no effect upon DNA repair gene expression did not induce DNA repair.

Combined, these data indicate a new function for PTHrP to protect against as well as mediate DNA damage repair, and this activity may well account for the widespread distribution of PTHrP, and its association as a prognostic indicator of survival in patients with breast cancer.

Disclosures: ***M.T. Gillespie****, None.*

SA541

Regulation of Parathyroid Hormone Secretion: Putative Role of the Multiligand Endocytic Receptor Megalin. L. Cianferotti[1], S. Lisi*[1], T. Giacomelli*[1], R. Botta*[1], F. Cetani*[1], P. Miccoli*[2], A. Pinchera*[1], C. Marcocci[1], M. Marinò*[1]. [1]Endocrinology, University of Pisa, Pisa, Italy, [2]Surgery, University of Pisa, Pisa, Italy.

Megalin, a multiligand endocytic receptor belonging to the low density lipoprotein receptor superfamily, is expressed by several epithelial tissues, including parathyroid cells. The role of megalin in the parathyroids has not been established, although it was proposed that megalin may be involved in the regulation of parathyroid hormone (PTH) secretion. Here we investigated the possible role of megalin in PTH secretion, using primary cultures of human parathyroid cells. Cells were prepared from parathyroid tissue specimens collected at surgery from patients with sporadic primary hyperparathyroidism. Parathyroid cells in culture were found to maintain features of differentiation for at least 5 days, as shown by their ability to secrete intact PTH. Cells expressed full length megalin, as observed in cell extracts by Western blotting. To investigate the role of megalin in PTH secretion, cells were cultured in 96 well plates and then incubated with two known megalin ligands, namely the human receptor associated protein (hRAP) and human thyroglobulin (hTg). In addition, cells were incubated with three rabbit anti-megalin antibodies, namely A55 (against full length megalin), anti-megalin-GST (against an extracellular epitope in the second cluster of ligand binding repeats), and Rb4 (against the cytoplasmic tail). Normal rabbit IgG and ovalbumin were used as negative controls. After 6 hours of incubation at 37°C, cell media were collected and PTH was measured by immunoradiometric assay. Mean PTH values in the absence of competitors or controls ranged from 619 to 654 pg/well. PTH values were markedly reduced when cells were incubated with A55 (47% inhibition) or hTg (52.7% inhibition), whereas a slight degree of reduction was observed in the presence of hRAP (7% inhibition) or anti-megalin-GST (16% inhibition). No reduction of PTH values was observed with negative controls as well as with Rb4, as expected from the fact that the latter antibody is directed against an intracellular epitope of megalin, and thus should not affect its functions if applied extracellularly. The results suggest that megalin may be indeed involved in PTH secretion by parathyroid cells in a favoring manner, because its inhibition results in a reduction of PTH secretion. The molecular mechanisms underlying megalin function in the parathyroid remain to be investigated.

Disclosures: ***L. Cianferotti****, None.*

SA542

A Novel Mutation in the Calcium-Sensing Receptor in Familiar Hypocalciuric Hypercalcemia and Neonatal Severe Hyperparathyroidism. S. C. Andrade*, S. K. Kohara*, L. F. D´Souza-Li. Center for Investigation in Pediatrics, State University of Campinas, Campinas, Brazil.

Extracellular calcium concentration is regulated by the calcium sensing receptor (CASR). It belongs to the superfamily of G protein-coupled receptors and has a large amino terminal extracellular domain, seven transmembrane domains and a cytoplasmic carboxyl C-teminal tail. Cloning of the CASR provided insights into the molecular basis of several inherited disorders of Ca^{+2} homeostasis in humans. Inactivating mutations of calcium-sensing receptor are associated to Familial Hypocalciuric Hypercalcemia (FHH) when individuals have one defective copy of the gene and Neonatal Severe Hyperparathyroidism (NSHPT) when individuals have usually two defective copies. The aim of this study was to analyze the molecular genetics of a consanguineous family where the proband presented as a neonatal severe hyperparathyroidism and to correlate the fenotype (clinical findings) with the genotype. We report a boy who presented hypoactivity and poor feeding during the neonatal period. The biochemical profile showed serum Ca^{++} 21.0 mg/dL, phosphorus 1.3 mg/dL, alkaline phosphatase 1107 UI/L, Mg^{++} 2.18 mg/dL and PTH 1550pg/mL. He underwent total parathyroidectomy on the 30th day of life with significant improvement of the symptoms. The PTH level fell to 28 pg/dL and the serum Ca^{++} to 9.8 mg/dL. The serum calcium in the parents was normal in the mother (8.8 mg/dl) and on the higher limit of reference value in the father (10.5 mg/dl). Genomic DNA was isolated from peripheral blood leucocytes and used as a template to amplify the coding region of the *CASR* gene using nine pairs of primers. After purification, the PCR products were directly sequenced. We identified an inactivating mutation at nucleotide 2 of the cDNA (c.2T>G) changing the conserved Methionine of the first protein codon to Arginine (M1R). The proband was homozygous and parents were heterozygous for this mutation. We confirmed the mutation by restriction enzyme digestions since this mutation destroy a Nco I restriction site. Since this mutation disrupt the original Kozak sequence, a cryptic initiation start site will probably be used resulting in a non-functional protein.

Disclosures: ***L.F. D´Souza-Li****, None.*

SA543

Impaired Translocation of Calcium-sensing Receptor Nascent Chains into Endoplasmic Reticulum due to Signal Peptide Missense Mutations in Familial Hypocalciuric Hypercalcemia. S. Pidasheva*[1], W. F. Simonds[2], S. J. Marx[2], G. N. Hendy[1]. [1]Medicine, McGill University, Montreal, PQ, Canada, [2]Metabolic Diseases, NIH, Bethesda, MD, USA.

Inherited disorders of calcium homeostasis, familial hypocalciuric hypercalcemia (FHH) and neonatal severe hyperparathyroidism (NSHPT) are caused by inactivating mutations in the calcium-sensing receptor (CASR). This cell-surface glycoprotein plays a key role in calcium homeostasis. Here, we report that a CASR allele from a patient with FHH had a point mutation in the s ignal sequence replacing Leu (TTG) with Ser (TCG) at position 11 (L11S). The proband is a 43-yr-old male who underwent 2 unsuccessful neck explorations. A third parathyroidectomy significantly improved his condition. Pre-operative clinical data were: ionized calcium 1.59 mmol/l (ref:1.17-1.31); iPTH 120 pg/ml (10-65); total calcium 2.7 mmol/l (2.05-2.5); urinary calcium/creatinine clearance ratio, 0.022. Previously, an L13P mutation was found in a family with FHH/NSHPT. We engineered both mutants into a c-Myc tagged CASR cDNA and transfected them into human embryonic kidney (HEK293) cells. Wild type and mutant CASR proteins were analyzed by western blot, showing the mutants were much less well expressed than the wild type. Neither mutant was expressed at the cell surface as evaluated by immunofluorescence and confocal microscopy. Both mutants were transcribed and translated comparable to the wild type in an in vitro assay. Insertion into the endoplasmic reticulum (ER) and glycosylation status of wild type and mutants were analysed. Transcribed sense RNA strands were translated in a rabbit reticulocyte lysate cell-free system in the absence or presence of increasing concentrations of canine pancreatic microsomal membranes. Proper glycosylation of wild type receptor was confirmed by digestion with endoglycosidase H. However, both mutants failed to be glycosylated. We next used a co-translational translocation assay in which CASR RNAs were translated with microsomal membranes followed by incubation with proteinase K alone or in combination with Triton X-100. Wild type CASR was protected from protease digestion as it had translocated to the ER, but neither mutant CASR was protected. These results indicated that the mutant receptors' nascent chains do not translocate into the ER. The mutations occur in the CASR hydrophobic signal peptide core which is highly conserved among species. Thus, both mutations resulted in markedly impaired processing of the CASR, accounting for parathyroid dysfunction, and emphasizing the key role of the signal peptide in preprotein targeting.

Disclosures: ***S. Pidasheva****, None.*

SA544

Interleukin-1beta Stimulated Increase in Parathyroid, Thyroid and Kidney CASR Expression in Vivo Is Mediated by NF-kappaB Elements in the CASR Gene Promoters. L. Canaff*, G. N. Hendy. Medicine, McGill University, Montreal, PQ, Canada.

The calcium-sensing receptor (CASR), expressed in parathyroid gland, thyroid C-cells and kidney tubule, is essential for maintenance of calcium homeostasis. Hypocalcemia is common in critically ill patients in whom circulating pro-inflammatory cytokines are increased. We have investigated whether pro-inflammatory cytokines, via NF-κB activation upregulate transcription of the CASR gene. This would reduce the set-point for PTH suppression by extracellular calcium likely leading to the observed hypocalcemia and hypoparathyroidism. We show that after a single intraperitoneal injection of IL-1β in rats, parathyroid and thyroid CASR mRNA levels rose 2-2.5 fold and kidney CASR mRNA levels rose 1.5 fold over basal levels at 15 hours. Thyroid CASR mRNA levels had not returned to base line at 24 hours. Western blot analysis showed that kidney and thyroid CASR protein levels were also increased at 15 and 24 hours. Serum calcium and PTH levels were decreased significantly at 15 and 24 hours. Transcription of the human CASR gene is driven by two promoters (P1 and P2) yielding transcripts having alternative 5' untranslated regions (1A and 1B), but encoding the same receptor protein. Nuclear run-on assays performed on extracts of human proximal tubule kidney (HKC) cells and thyroid C-cells (TT) cultured with and without IL-1β for 8 hours showed that CASR exons 1A, 1B and 2 transcripts were all stimulated >2-fold, as was cyclooxygenase-2 gene transcription in both cell types. GAPDH was unaffected by IL-1β treatment. Previously, we showed that when human CASR promoter reporter gene constructs were transfected into HKC cells, IL-1β stimulated transcriptional activity of both P1 and P2 promoters 2-fold over basal. The CASR gene promoters have 4 potential NF-κB elements and the responsiveness to IL-1β was reduced or lost when the P1, exon 1A or P2, but not exon 2, NF-κB elements were mutated. P1, exon 1A and P2 NF-κB elements conferred IL-1β responsiveness to a heterologous promoter. Cotransfection of CASR reporter gene constructs with NF-κB proteins in HKC cells led to increased transcriptional activity with p65 only and the p50/p65 combination. Cotransfection with I-κB or pretreatment of HKC cells with a cell-permeable peptide containing the NF-κB nuclear localization sequence abrogated the responsiveness of P1 and P2 to IL-1β. In electrophoretic mobility shift assays, complexes comprising p65/p65, p65/p50 or p50/p50 dimers, formed on three of the four NF-κB elements. In conclusion, NF-κB elements in the CASR gene promoter mediate transcriptional up-regulation by pro-inflammatory cytokines, contributing to the hypocalcemia of the critically ill.

Disclosures: ***L. Canaff****, None.*

SA545

Ca^{2+}-sensing Receptor of Mozambique Tilapia (tCaR): cDNA Expression, Signal Transduction, and Salinity-Dependent mRNA Expression in Vivo.
D. M. Shoback[1], C. Pollina*[2], W. Chang[1], S. Pratt*[1], S. Hyodo*[3], Y. Takei*[3], C. A. Loretz*[2]. [1]San Francisco VA Medical Center, University of California, San Francisco, CA, USA, [2]National Science Foundation Tokyo Regional Office, Minato, Tokyo, Japan, [3]Ocean Research Institute, University of Tokyo, Nakano, Tokyo, Japan.

A CaR cDNA from the kidney of the euryhaline Mozambique tilapia was identified through PCR cloning. The cDNA of tCaR, with 5' and 3' UTRs, is an ≈3.3 kb transcript predicted to encode a 940 amino acid protein with 84% and 93% similarity to mammalian and teleost CaRs. tCaR lacks two stretches of amino acids present in mammalian CaRs -- comparable to residues 367-377 in the extracellular domain (ECD) and 923-1085 in the intracellular (IC) tail of bovine parathyroid (bp) CaR. By RT-PCR, expression of tCaR was strong in brain, gill, and kidney and less in heart, stomach, intestine and urinary bladder; this suggested a physiological role in barrier epithelia. Since tilapia adapts to fresh (FW) and seawater (SW), we considered the hypothesis that tCaR might be involved in responses to salinity change. Tissues from FW-adapted (< 10 mosmol/L, 0.4 mM Ca^{2+}) and SW-adapted (1000-1020 mosmol/L, 10 mM Ca^{2+}) tilapia were harvested. Changes in tCaR mRNA were assessed in kidney and intestine by PCR. Kidney and intestine demonstrated opposite expression patterns as a function of acclimation to salinity. In FW tilapia, kidney tCaR mRNA was 3-fold greater than that in SW fish (N=6-7; $p < 0.001$). In contrast, tCaR mRNA in intestine was elevated ≈3-fold in SW tilapia ($p < 0.01$). Because one of the regions missing in tCaR is in the ECD, which mediates Ca^{2+}-sensing, and the other is in the C-terminal IC tail, which is important in activation of phospholipase C (PLC), we tested tCaR signaling in response to changes in the extracellular $[Ca^{2+}]$ ($[Ca^{2+}]_e$). cDNAs encoding the bpCaR and tCaR were transfected into HEK-293 cells. PLC activation was assessed by ^{3}H-InsP accumulation after raising $[Ca^{2+}]_e$ from 0.5 mM to levels shown (see Table). ^{3}H-InsP increased less in tCaR- vs bpCaR-expressing cells ($p < 0.001$). ED_{50} values were 6 vs 3 mM Ca^{2+} for tCaR and bpCaR, respectively ($p < 0.001$). This suggests that tCaR may have a physiological role in responding to salinity change and that changes in the ECD of tCaR may alter its conformational changes in response to high $[Ca^{2+}]_e$.

TABLE. Fold-Increase in ^{3}H-InsP at $[Ca^{2+}]$ Shown vs 0.5 mM Ca^{2+} (N=3)

[Ca2+] mM	bpCaR	tCaR
2.5	7.2+/-0.6	1+/-0.1
5.0	15.8+/-0.6	5.6+/-0.4
7.5	18.3+/-0.8	10.4+/-0.9
10	17.1+/-1.4	10.9+/-1.2
30	18.5+/-0.3	13.3+/-0.6
50	15.3+/-0.6	12.4+/-0.7

Disclosures: ***D.M. Shoback****, None.*

SA546

Expression Levels of the Calcium Receptor Affect Responses to Calcimimetics.
W. L. Heaton*[1], P. S. Jacobson*[1], N. Lloyd*[1], T. Le-Capling*[2], B. T. Brinton*[2], E. F. Nemeth[2], K. J. Krapcho*[1]. [1]NPS Pharmaceuticals, Salt Lake City, UT, USA, [2]NPS Pharmaceuticals, Mississauga, ON, Canada.

The type II calcimimetic compound cinacalcet (Sensipar™) is the first FDA approved allosteric modulator of any G protein-coupled receptor. This compound acts preferentially on the parathyroid cell Ca^{2+} receptor (CaR) to rapidly lower circulating levels of parathyroid hormone (PTH). A seemingly identical CaR regulates calcitonin secretion from thyroid C-cells, yet in rodents and humans, type II calcimimetics are at least 40-fold more potent at regulating PTH secretion than calcitonin secretion. To determine if receptor density affects the potency and efficacy of calcimimetics, CaR expression levels were varied in a heterologous expression system using a tetracycline inducible promoter (TRex-HEK293). Characterization by Western and Northern analysis showed that addition of tetracycline (5 to 100 ng/ml; 24 h) to CaR TRex-HEK293 cultures resulted in concentration-dependent increases in CaR mRNA and protein expression. CaR activation was monitored by fluorimetric measurements of cytoplasmic Ca^{2+}. The potencies and efficacies of type I (Ca^{2+}, Mg^{2+}, Gd^{3+}, spermine) and type II calcimimetics (NPS R-568, NPS 1377, NPS R-467) were dependent on the level of CaR expression, with greater induction levels corresponding to increased potency and efficacy. Increasing levels of CaR expression increased the Hill coefficient of type I, but not type II, calcimimetics. In contrast, the potency and efficacy of carbachol, acting on natively expressed muscarinic receptors, was unaffected by treatment with tetracycline (Table). Increases in cytoplasmic Ca^{2+} evoked by extracellular Ca^{2+} in the absence of induction appear to be CaR mediated because the responses were potentiated by NPS R-467 but not by equimolar concentrations of its less potent stereoisomer NPS S-467. Extracellular Ca^{2+} at concentrations up to 5 mM had no effect in untransfected TRex-HEK293 cells. In conclusion, the density of CaRs profoundly affects the potencies and efficacies of calcimimetic ligands. The relatively high levels of CaR expression in parathyroid glands, compared to other tissues, might explain or contribute to the preferential effects of cinacalcet on PTH secretion.

	No Induction	10 ng/ml tetracycline	100 ng/ml tetracycline
Agonist	EC_{50} / Relative Efficacy	EC_{50} / Relative Efficacy	EC_{50} / Relative Efficacy
Ca^{2+}	2.78 mM / 37.0%	1.86 mM / 86.3%	1.08 mM / 100%
Mg^{2+}	>50 mM / 4.8%	3.6 mM / 66.5%	1.6 mM / 103%
Gd^{3+}	45.5 uM / 10.3%	15.6 uM / 61.0%	10.5 uM / 94.5%
Spermine	>5 mM / 4.5%	151 uM / 62.0%	24.3 uM / 103.2%
NPS 1377	>10 uM / 3.3%	191 nM / 51.5%	24.2 nM / 107.5%
Carbachol	2.1 uM / 31.0%	1.7 uM / 38.6%	1.5 uM / 27.6%

Relative Efficacy is the magnitude of the response as a percent of the maximal Ca^{2+} response with 100 ng/ml tetracycline.

Disclosures: ***W.L. Heaton****, None.*

SA547

A New Class of Non-competitive Antagonists of the Human Calcium-sensing Receptor Releasing Parathyroid Hormone (PTH) from Parathyroid Glands.
K. Seuwen*[1], C. Halleux[2], R. Bouhelal*[3], M. Kneissel[2], R. Gamse[2], T. Buhl*[2], R. M. Wolf*[1], G. Breitwieser*[4], R. Beerli*[2], S. Weiler*[2], L. Widler*[2]. [1]Gpcr ep, Novartis Institutes for Biomedical Research, Basel, Switzerland, [2]Bone Metabolism, Novartis Institutes for Biomedical Research, Basel, Switzerland, [3]Discovery Technologies, Novartis Institutes for Biomedical Research, Basel, Switzerland, [4]Dep. of Biology, Syracuse University, Syracuse, NY, USA.

Parathyroid glands express a calcium-sensing receptor (PCaR) which acts as the principal regulator of plasma calcium concentration. Lower than normal calcium levels lead to reduced signalling of the receptor, which is translated into increased release of the calcium-mobilising hormone PTH. This effect can be mimicked by PCaR antagonists (calcilytics). As pulsatile administration of PTH has anabolic effects on the skeleton, calcilytics may become useful for the treatment of osteoporosis. Known calcilytics are structurally related to ligands of adrenergic receptors, and molecules of this class are undergoing clinical trials. Their clinical usefulness will strongly depend on pharmacokinetic parameters.

We have used a sensitive high throughput screening approach to find new chemical structures inhibiting PCaR function. One class of molecules identified is related to biarison, a compound which is in clinical use as an anti-inflammatory agent. Chemical derivatisation resulted in highly potent, specific, and efficaceous compounds active at the human and rat receptor. Using receptor modelling and site-directed mutagenesis we identified a specific binding site for biarison-type calcilytics in a hydrophobic pocket within the seven transmembrane domaine of the receptor molecule. This site is different from the site employed by the calcilytics described before.

Compound NVP-AEB032 inhibited calcium-induced inositol phosphate production and mobilisation of intracellular calcium mediated by human PCaR non-competitively with an IC50 of 160 nM and 410 nM, respectively.

Upon i.v. administration to female Sprague Dawley rats, NVP-AEB032 transiently increased plasma PTH dependent on dose. Applied at 3 mg/kg, the compound increased PTH levels from < 50 pg/ml to 480 pg/ml, peaking at 5 minutes and declining back to baseline within 40 minutes. This profile is similar to that produced by i.v. administration of low doses of PTH.

Thus, biarison-type calcilytic molecules have the potential to generate pulsatile PTH release profiles required for anabolic action on the skeleton.

Disclosures: ***K. Seuwen****, Novartis Pharma AG 3.*

SA548

The Calcimimetic Cinacalcet Suppresses Parathyroid Hormone Secretion in Primary Hyperparathyroidism *in vitro* and *in vivo*.
T. Kawata*[1], Y. Imanishi[1], K. Kobayashi*[1], T. Kenko*[2], M. Wada*[3], N. Onoda*[4], H. Tahara[1], E. Ishimura*[5], T. Miki[6], N. Nagano[3], T. Ishikawa*[7], A. Arnold[8], M. Inaba[1], Y. Nishizawa[1]. [1]Department of Metabolism, Endocrinology and Molecular Medicine, Osaka City University Graduate School of Medicine, Osaka, Japan, [2]Osaka City University Medical School for Technical Assistance, Osaka, Japan, [3]Kirin Brewery Co., Ltd., Takasaki, Japan, [4]Department of Oncology, Osaka City University Graduate School of Medicine, Osaka, Japan, [5]Department of Nephrology, Osaka City University Graduate School of Medicine, Osaka, Japan, [6]Department of Geriatrics and Neurology, Osaka City University Graduate School of Medicine, Osaka, Japan, [7]Department of Surgical Oncology, Osaka City University Graduate School of Medicine, Osaka, Japan, [8]Center for Molecular Medicine, University of Connecticut Health Center, Farmington, CT, USA.

Cinacalcet HCl (cinacalcet), calcium-sensing receptor (CaR) agonist (calcimimetic), is a promising agent for the treatment of hyperparathyroidism secondary to uremia that acts by suppressing parathyroid hormone (PTH) secretion. To investigate cinacalcet's suppressive effect on PTH secretion in primary hyperparathyroidism both *in vitro* and *in vivo*, we investigated its effects on primary cultured human parathyroid cells obtained from 3 PHPT patients, and PTH-*cyclin D1* transgenic mice (PC2) as models of primary hyperparathyroidism. Studies were approved by the institutional ethics and animal care committees. Cinacalcet dose-dependently suppressed PTH secretion from cultured parathyroid cells. The IC_{50} of this compound in the cells was almost the same as that of cells prepared from normal bovine parathyroid glands. CaR expression determined by immunohistochemistry was reduced in the PHPT parathyroid glands compared with the normal glands obtained from thyroid carcinoma patients.

A single administration of 30 mg/kg BW cinacalcet significantly suppressed serum calcium levels by 2 h after administration in 65-85 week-old PC2 mice with chronic biochemical hyperparathyroidism. The percent reduction in serum PTH was significantly correlated with CaR hypo-expression. In older PC2 mice (93-99 weeks old) with advanced hyperparathyroidism, serum calcium and PTH levels were not suppressed by 30 mg/kg BW cinacalcet. However, serum calcium and PTH levels were significantly suppressed by 100 mg/kg BW cinacalcet, suggesting that higher doses of this compound could overcome the resistance developed in severe hyperparathyroidism.
To conclude, cinacalcet has efficacy in models of primary hyperparathyroidism, both *in vitro* and *in vivo*, in spite of any presumed endogenous CaR activation by hypercalcemia and hypo-expression of CaR in the parathyroid glands.

Disclosures: ***T. Kawata****, None.*

SA549

Chondrocyte Calcium-Sensing Receptor and PTHrP are Up-Regulated in Osteoarthritis and Promote Matrix Catabolism. D. W. Burton, M. Foster*, K. Johnson*, L. J. Deftos, R. Terkeltaub. Medicine, University of California and SDVAMC, San Diego, CA, USA.

Growth plate chondrocytes up-regulate calcium-sensing receptor (CaR) expression as they mature to hypertrophy. In cells other than chondrocytes, calcium-sensing via the CaR functions partly to promote expression of parathyroid hormone-related protein (PTHrP). Moreover, PTHrP, which is up-regulated in human OA cartilages, is a critical regulator of growth plate development and is believed to promote both chondrocyte proliferation and osteophyte formation in OA. Hence, our objective was to examine the potential role in the pathogenesis of osteoarthritis (OA) of CaR-mediated calcium-sensing in the chondrocyte. Studying spontaneous knee OA in aging Hartley guinea pigs, we observed that PTHrP and CaR immunostaining *in situ* concurrently increased between 2 and 12 months age as cartilage degeneration developed in the medial tibial plateau. Furthermore, PTHrP secretion by cultured chondrocytes from the guinea pig knees increased 3-fold over this period. Thus, we analyzed functional activities of calcium-sensing including modulation of the effects of PTHrP, using primary bovine knee chondrocytes and clonal immortalized human knee articular chondrocytes (Ch-8 cells) that expressed expressed PTH/PTHrP receptor and CaR. We incubated the primary chondrocytes and Ch-8 cells with the CaR calcimimetic agonist NPS R-467, or with physiologic (1.8 mM) or lesser or greater extracellular calcium concentrations. Firstly, NPS R-467 increased PTHrP expression dose-dependently. NPS R-467 also increased levels of MMP-13, and these effects were shared by treatment alone with elevated extracellular calcium (3 mM). Secondly, progressive elevation of extracellular calcium (from 1.8 mM to an excess level of 3.0 mM) extinguished basal expression of the broad matrix metalloproteinase inhibitor TIMP-3. NPS R-467 directly exerted the same attenuating effect on TIMP-3 expression. Lastly, the PTH/PTHrP receptor-binding peptide PTHrP 1-34 markedly suppressed TIMP-3 expression, but only did so under conditions where calcium-sensing was stimulated by either elevated ambient calcium or directly by the calcimimetic CaR agonist. Our results demonstrate that CaR and PTHrP expression increase *in situ* in spontaneous knee OA. Furthermore, calcium-sensing via the CaR promotes MMP-13 expression and tissue insufficiency of TIMP-3 and modulates the expression and biologic activities of PTHrP. Our results identify heightened calcium-sensing via the CaR as a novel mediator of cartilage catabolism in OA.

Disclosures: ***D.W. Burton****, None.*

SA550

1,25D3-MARRS: Molecular Identity and Functional Link to Phosphate Uptake in Intestinal Cells. I. Nemere[1], M. C. Farach-Carson[2], B. Rohe*[2], T. M. Sterling*[1], S. E. Safford*[3]. [1]Nutrition and Food Sciences, Utah State University, Logan, UT, USA, [2]Biological Sciences, University of Delaware, Newark, DE, USA, [3]Biology, Lincoln University, Lincoln University, PA, USA.

We used a ribozyme loss-of-function approach to demonstrate that the protein product of a cDNA encoding a multifunctional membrane-associated protein binds the seco-steroid $1,25(OH)_2D_3$ and transduces its stimulatory effects on phosphate uptake. These results are paralleled by studies in which the ability of the hormone to stimulate phosphate uptake in isolated chick intestinal epithelial cells is abolished by preincubation with Ab099 directed against the amino terminus of the protein. We now report the complete sequence of the cloned chicken cDNA for the $1,25D_3$-MARRS (membrane associated, rapid response steroid-binding) protein and reveal it to be identical to the multifunctional protein ERp57. Functional studies showed that active ribozyme, but not a scrambled control, decreased specific membrane-associated $1,25(OH)_2D_3$ binding, but did not affect binding to the nuclear receptor for $1,25(OH)_2D_3$. Seco-steroid dependent stimulation of protein kinase C activity was diminished as $1,25D_3$-MARRS protein levels were reduced in the presence of the ribozyme, as judged by Western blot analyses. Phosphate uptake in isolated cells is an index of intestinal phosphate transport that occurs during growth and maturation. While cells and perfused duodena robustly responded to $1,25(OH)_2D_3$ in preparations from young birds, older animals no longer responded with stimulated phosphate uptake or transport. The age related decline was accompanied by a decrease in $1,25D_3$-MARRS mRNA that was apparent up to 1 yr of age. Together, these studies functionally link phosphate transport in the chick duodenum with the $1,25D_3$-MARRS protein, and point to a new role for this multifunctional protein class.

Disclosures: ***I. Nemere****, None.*

SA551

The Hairless Gene Product (Hr) Is a Vitamin D Receptor Corepressor, and Several Mutations in Hr that Cause Alopecia in Humans Compromise this Function. J. L. Dawson*[1], J. C. Hsieh[1], S. A. Slater*[1], J. M. Sisk*[2], P. W. Jurutka[1], G. K. Whitfield[1], G. Hsieh*[1], M. L. Thatcher*[1], T. K. Barthel[1], C. A. Haussler[1], C. M. Thompson*[2], M. R. Haussler[1]. [1]Biochemistry & Molecular Biophysics, University of Arizona, Tucson, AZ, USA, [2]Neuroscience, Johns Hopkins University School of Medicine & Kennedy Krieger Institute, Baltimore, MD, USA.

The vitamin D receptor (VDR) and retinoid X receptor (RXR) are both required for hair cycling, and signal by forming a heterodimeric complex that binds to vitamin D responsive elements (VDREs) in the upstream promoter region of genes regulated transcriptionally by 1,25-dihydroxyvitamin D_3 (1,25D). We show that the hairless gene product (Hr), a nuclear protein expressed primarily in skin and brain which is known to interact with the thyroid hormone receptor (TR) and orphan nuclear receptor ROR, also associates physically with VDR in GST pulldown and immunoprecipitation experiments. Both rat Hr (rHr) and human Hr (hHr) function as repressors of basal and 1,25D-VDR-stimulated transcription of a VDRE-containing, natural human CYP24 promoter-reporter construct in cotransfected COS-7 and human keratinocyte cells. Thus, similar to its role with TR and ROR, Hr acts as a VDR corepressor, possibly cooperating with VDR-RXR to silence a gene encoding a tonic inhibitor of the hair cycle. Naturally occurring mutations in hHr cause alopecia in humans, and we probed the impact of several of these mutations on the ability of Hr to repress VDR. Twelve of the hHr point mutations known to elicit alopecia were introduced into the positionally conserved codons of the rHr cDNA, namely P95S, C422Y, A596V, E603V, E611G, R640Q, C642G, N988S, D1030N, A1040T, V1074M and V1154D. The rHr point mutants sort into 3 classes: equivalent to wild type (P95S, C422Y, E611G, R640Q, A1040T, V1074M), markedly reduced in ability to repress 1,25D-VDR-mediated transcription (C642G, N988S, D1030N, V1154D), or proteolyzed (A596V, E603V). The four functionally compromised rHr mutants interact normally with VDR in GST pulldown and coimmunoprecipitation studies. Therefore, the C642G, N988S, D1030N, and V1154D mutations that abolish the ability of Hr to repress VDR appear to blunt downstream signaling by the RXR-VDR-Hr complex to drive the hair cycle. Since histone deacetylases (HDACs) are likely downstream effectors of Hr mediated repression, we postulate that the compromised Hr mutants are defective in their interaction with an HDAC(s). This characterization of naturally occurring Hr mutants that cause alopecia provides evidence for the pathobiologic significance of Hr-VDR corepressive signaling in the mammalian hair cycle, and reveals the importance of downstream factors that execute gene repression.

Disclosures: ***J.L. Dawson****, None.*

SA552

Combined Impact of Two Common Vitamin D Receptor Gene Polymorphisms on Transcriptional Signaling by $1,25(OH)_2D_3$. M. J. Kaczmarska*[1], G. K. Whitfield[1], C. A. Haussler[1], M. L. Thatcher*[1], P. W. Jurutka[1], M. L. Brandi[2], P. J. Malloy*[3], D. Feldman[3], M. R. Haussler[1]. [1]Biochemistry & Molecular Biophysics, University of Arizona, Tucson, AZ, USA, [2]Clinical Physiopathology, University of Florence, Florence, Italy, [3]Medicine, Stanford University, Stanford, CA, USA.

The vitamin D receptor (VDR) is a transcriptional regulator that, with its 1,25-dihydroxyvitamin D_3 (1,25D) ligand, signals calcium and phosphate absorption, cell differentiation, detoxification and hair cycling. The human (h)VDR gene has common polymorphic variants, two of which are relevant to this study. The first, in exon II, creates two alternative translation start sites, designated *F* and *f*. Data suggest that the *F* hVDR isoform is intrinsically more active in stimulating gene expression, likely as a result of enhanced binding to basal transcription factor IIB. A second, unlinked exon IX polymorphism generates varying lengths of a singlet (A) repeat in the 3' UTR of the hVDR mRNA, classified according to the number of A's in the repeat (≤15 A's designated "short" (*S*) and ≥17 A's considered "long" (*L*)). Although *L/S* alleles do not affect the VDR protein sequence, results indicate that human fibroblasts with the *L* allele have higher VDR activity. To understand the mechanism whereby the *L/S* variation affects activity, saturation binding assays were performed using [^{3}H]1,25D to quantitate the endogenous VDR. Pairs of fibroblast lines were chosen that possessed the same *F/f* genotype, but opposite *LL* vs. *SS* genotypes. Binding plots yielded values for B_{max} which indicated that *LL* lines consistently expressed higher amounts of hVDR than did *SS* lines. We conclude that the *L/S* polymorphism affects the quantity of receptor, rather than its intrinsic activity. To assess the combined effect of *F/f* and *L/S* variations, 19 human fibroblast lines with various VDR genotypes were tested for endogenous VDR activity using a reporter construct containing the 1,25D-responsive natural promoter from the human CYP24 gene. To integrate the combined impact of these polymorphic alleles, the fibroblast genotypes were expressed as an "allele score" of 0-4, with *F* and *L* alleles each scored as 1, and *f* and *S* alleles each scored as 0. The results support previous data that cell lines with a higher allele score exhibit greater VDR potency. Analysis of the results using an ordered logistic regression model yielded a statistically significant P-trend of 0.005 for escalating VDR transcriptional activity with increasing allele score. We propose that the combined influence of these two unlinked hVDR polymorphisms is additive, and significantly affects the ability of 1,25D to elicit bioresponses crucial to the prevention of osteoporosis as well as various epithelial cell cancers.

Disclosures: ***M.J. Kaczmarska****, None.*

SA553

See Friday Plenary number F553

SA554

A Novel Model System Useful for Dissection of Vitamin D Receptor Functional Domains. M. E. Valrance*, J. E. Welsh. Biological Sciences, University of Notre Dame, Notre Dame, IN, USA.

The active form of vitamin D, 1,25-dihydroxyvitamin D3 (1,25D) exerts anti-proliferative and pro-differentiating actions on both stromal and epithelial derived cells, but the exact mechanisms underlying these effects have yet to be defined. The goal of this project is to identify the functional domains of the vitamin D receptor (VDR) that are necessary for the regulation of cancer cell proliferation, invasion, and apoptosis. Towards this goal, we have developed a novel model system consisting of epithelial cell lines that were established from mammary tumors generated in VDR knock-out (KO) mice and their wild-type (WT) littermates. Two of these cell lines, WT145 and KO240 have been characterized with respect to morphology, growth, and apoptosis in relation to VDR function. Both cell lines are estrogen receptor positive, invasive in vitro, and tumorigenic in vivo. The WT145 cells were shown to express the nuclear VDR, and exhibit 1,25D-mediated induction of 24-hydroxylase promoter luciferase activity in transient transfection assays. WT145 cells are also dose-dependently growth inhibited by 1,25D and synthetic vitamin D analogs. 1,25D induces apoptotic morphology, caspase activation, and PARP cleavage in WT145 cells. KO240 cells, as expected, do not express the nuclear VDR, and 1,25D does not induce 24-hydroxylase promoter luciferase activity in these cells. KO240 cells do not exhibit growth inhibition or apoptosis in response to 1,25D or analogs at concentrations up to 1 μM. No apoptotic morphology, caspase activation or PARP cleavage is seen in KO240 cells following vitamin D treatment. At doses of 5-10 μM, 1,25D and the synthetic analogs CB1093, EB1089, KH1230, and MC1288 do inhibit growth of KO240 cells, indicating non VDR-dependent growth inhibitory pathways can be triggered by vitamin D compounds at micromolar doses. These tumorigenic cell lines that differentially express VDR will be exploited to further define the role of VDR in cancer cell regulation. We show that transient transfection of a human VDR into the KO240 cells restores 24-hydroxylase induction, indicating that 1,25D-mediated signaling pathways can be recapitulated. Reconstitution of 1,25D-mediated signaling in VDRKO cells using VDRs with specific point mutations will enable assessment of functional domains that impact on proliferation, apoptosis, invasion, and tumorigenesis. The above data indicate that the WT145 and KO240 cell lines comprise a unique model system, useful for clarification of the impact of VDR ablation and mutation on breast cancer biology both in vitro and in vivo.

Disclosures: ***M.E. Valrance****, None.*

SA555

See Friday Plenary number F555

SA556

GATA-1 Mediates Strong Repression of Both VDR and 1-OHase Promoter Activities in Kidney Proximal Cells and Blocks 1-OHase Gene Expression by PTH. D. Iyer*, A. Bajwa*, M. J. Beckman. Biochemistry, Virginia Commonwealth University, Richmond, VA, USA.

Renal vitamin D activation results in a temporary decrease in gene expression for the $1,25(OH)_2D_3$ receptor (VDR) as the 1α-hydroxylase (1α-OHase) transcript increases. VDR transcriptional repression is relieved after serum calcium levels are restored to normal. Down-regulation of VDR has been found to be specific to the proximal convoluted tubule (PCT) and is proposed to be regulated by PTH. In this study, the globin activator of transcription (GATA-1) was found by GeneChip microarray and promoter analyses to be a candidate transcriptional regulator of VDR and 1α-OHase promoters. Quantitative Real-Time RT-PCR analysis showed the degree of differential regulation for GATA-1 gene expression in rat kidney cortex was 4-fold higher in low Ca compared to high Ca status ($p<0.01$). Two separate human proximal kidney cell lines, HK-2 and HKC-8, were positively identified for the presence of PTH receptors (PTHR1) using confocal immunofluorescence. Gel shift analysis confirmed the presence of GATA-1 protein in the proximal kidney cells. Using a transient transfection procedure GATA-1 was overexpressed in both cell types with luciferase constructs of null and either the VDR or the 1α-OHase promoter, respectively, and in the presence or absence of PTH (50 nM). To ensure there was no influence of extracellular Ca, the media was reduced to 0.1 mM Ca. The VDR and 1α-OHase gene expressions, were analyzed separately. The significant interaction effects demonstrated that: (1) GATA-1 forcefully down regulated both VDR and 1α-OHase, and (2) In the presence of PTH, 1α-OHase was up regulated, while VDR was even more forcefully down regulated. This was highly significant in the HKC-8 cell type, which to date is utilized more in scientific research concerning the vitamin D endocrine system than the HK-2 cell type. Furthermore, it was found that GATA-1 forcefully decreased VDR expression and blocked full activation of 1α-OHase gene expression in response to PTH. The differences were also statistically significant for comparisons between null constructs and GATA-1 constructs when transfected in the absence of PTH. In conclusion, GATA-1 is capable of forcefully down regulating renal proximal VDR and 1α-OHase, however, it is questionable whether the experiment accurately mimicked the real actions that occur on the organismic level, where additional co-regulators may exert a role. Future studies will concentrate on putative GATA-1 binding sites on the VDR and 1α-OHase promoters and work towards determining the specific binding sites and factors that are utilized in the PCT regulation of VDR and 1α-OHase.

Disclosures: ***M.J. Beckman****, None.*

SA557

The Vitamin D Receptor Is a Low Affinity Sensor of Dietarily Essential Unsaturated Fatty Acids. P. W. Jurutka[1], N. Hall*[2], K. Eichhorst*[2], G. K. Whitfield[2], M. Gurevich*[2], T. K. Barthel[2], J. C. Hsieh[2], C. A. Haussler[2], M. R. Haussler[2]. [1]Life Sciences, Arizona State University West, Phoenix, AZ, USA, [2]Biochemistry & Molecular Biophysics, University of Arizona, Tucson, AZ, USA.

The nuclear vitamin D receptor (VDR) mediates the actions of 1,25-dihydroxyvitamin D_3 (1,25D) to alter gene transcription, thereby effecting bone mineral homeostasis, hair cycling, xenobiotic detoxification and epithelial cell differentiation. Recently, lithocholate was found to be a novel VDR ligand, and also the retinoid X receptor (RXR) heterodimeric partner of VDR was shown to bind oleic and docosahexaenoic acid (DHA). We therefore tested a panel of steroidal and nonsteroid compounds as potential new ligands for VDR, using reporter gene and mammalian two hybrid systems. DHA (10^{-4} M) and 1,25D (10^{-9} M) activated transcription similarly via endogenous VDR in ROS 17/2.8 osteoblast-like cells transfected with a luciferase reporter vector containing the human CYP24 gene promoter. In mammalian two hybrid assays, human embryonic kidney cells (293) were transfected with expression vectors for VDR and RXR fusion proteins and a GAL4 response element-luciferase plasmid. Modest activation was observed with ω3 fatty acids such as α-linolenic acid, eicosapentaenoic acid (EPA) and DHA at dosages ranging from 10^{-4} to 10^{-5} M. Similar results were obtained with ω6 fatty acids including linoleic acid and arachidonic acid, as well as conjugated derivatives of linoleic acid (CLAs). Competition binding with radiolabeled 1,25D confirmed that these ω3 and ω6 fatty acids bind directly to VDR, obviating the possibility that these fatty acids are acting only via RXR. In contrast, several other compounds, such as 8S-hydroxyeicosatetraenoic acid, pregnenolone, lanosterol, α-tocopherol, and the PXR ligands, vitamin K_2 and hyperforin, did not activate VDR. A dietary requirement for polyunsaturated fatty acids (PUFAs) is well known, and deficiency of these fatty acids in VDR target tissues leads to clinical manifestations, including decreased bone mineralization and calcium absorption, cessation of growth, dermatitis, and hair loss. Some of these effects have been attributed to the role of PUFAs in maintaining cell membrane integrity/fluidity, and also to the fact that PUFAs are precursors of prostaglandins (PGs). However, administration of PGs in PUFA-deficient animals does not relieve the associated symptoms. The present results support a novel hypothesis that implicates VDR as a nutritional sensor of circulating essential fatty acids. Thus, PUFA binding to, and activation of, VDR may elicit unique, 1,25D-independent signaling pathways to orchestrate the pleiotropic effects of the ω3 and ω6 fatty acids in bone, skin and hair.

Disclosures: ***P.W. Jurutka****, None.*

SA558

See Friday Plenary number F558

SA559

Cell-, Promoter- and Ligand-specific Transactivation Responses of the VDRB1 Isoform. L. M. Esteban, C. Fong*, T. Cock*, S. J. Allison, J. L. Flanagan*, D. Amr*, C. Liddle*, J. A. Eisman, E. M. Gardiner. Bone and Mineral Research Program, Garvan Institute of Medical Research, Sydney, Australia.

The vitamin D receptor (VDR) mediates the effects of 1,25 dihydroxyvitamin D3, the active form of vitamin D, of which in humans there are two protein isoforms. The VDRB1 isoform differs from the originally described VDR (VDRA) by an N-terminal extension of 50 amino acids. Here we investigate cell-, promoter- and ligand-specific transactivation by the VDRB1 isoform. Transactivation was studied in response to the VDR natural ligand 1,25(OH)2D3 and the secondary bile acid, lithocholic acid (LCA), a cholesterol derivative like vitamin D, recently reported as a VDR activator. Transactivation of cytochrome P450 genes rat CYP24 and human CYP3A4 promoters was studied by transient transfection in COS1 and HEK293 cell lines. On the CYP24, the VDRB1 response to 1,25(OH)2D3 was greater (130%) than that of VDRA in COS1 cells, but similar in response to LCA. In HEK293 cells, the isoforms had similar activity in response to 1,25(OH)2D3, but with LCA VDRB1 was less active (68%) than VDRA. On the CYP3A4 promoter the activity of VDRB1 was lower (60-75%) than that of VDRA in response to either ligand in both COS1 and HEK293 cell lines. The interaction of both isoforms, VDRA and VDRB1, with the vitamin D responsive elements (VDRE) of CYP24 and CYP3A4 were analyzed by gel shift assays in the presence of the heterodimerization partner RXR and 32P-labeled oligonucleotides. The VDR:DNA complex formation was enhanced by the addition of both ligands, and was stronger in the presence of 1,25(OH)2D3 than with LCA. VDRB1 binding to the VDRE1 (proximal DR3) of CYP24 was maximal at a lower concentration of 1,25(OH)2D3 than for VDRA. The reverse-dependence of ligand-receptor binding pattern was evident on the distal DR3 of the CYP3A4 promoter. Increasing concentration of LCA appeared not to have any effect on the VDR:DNA complex formation in either promoter. Transactivation was completely abolished by AF-2 mutations L417S and E420Q in either VDR isoform, on the CYP24 promoter after 1,25(OH)2D3 and LCA treatment. Thus, despite ligand structural differences, VDR mediated transactivation by 1,25(OH)2D3, and LCA shared an AF-2 functional requirement. The present data thus provide new evidence for functional differences between the two VDR isoforms and indicate that these are determined by the promoter and cellular context possibly via differential cofactor interactions, and by the activating ligand.

Disclosures: ***L.M. Esteban****, None.*

SA560

Low Vitamin D Receptor Level Blunts 1,25 Dihydroxyvitamin D-Mediated Events in Mouse Intestine. Y. Song*[1], C. Gliniak*[1], S. Kato[2], J. C. Fleet[1]. [1]Interdepartmental Program in Nutrition, Purdue University, West Lafayette, IN, USA, [2]Institute of Molecular and Cellular Biosciences, University of Tokyo, Tokyo, Japan.

We tested the hypothesis that low vitamin D receptor (VDR) level causes intestinal calcium (Ca) malabsorption and intestinal vitamin D resistance using wild type (WT) mice and mice with reduced tissue VDR levels (VDR knockout heterozygotes, HT). Duodenal Ca absorption efficiency was upregulated by elevated plasma 1,25 dihydroxyvitamin D ($1,25(OH)_2$ D) caused by feeding 2.0% Ca (0.1%±0.5% absorption), 0.5% Ca (19.8±1.9% absorption), or 0.02% Ca (57.6±3.0% absorption) diets for 7-days (plasma $1,25(OH)_2$ D = 38±5, 134±11, and 244±19 pg/ml, respectively). However, HT mice required higher plasma $1,25(OH)_2$ D levels on the 0.5% Ca (27% higher) and 0.02% Ca (45% higher) diets to maintain calcium absorption at WT levels. This was also reflected in renal 1α hydroxylase mRNA levels (1αOHase) in HT mice on the 0.5% (63% > WT) or 0.02% Ca diets (56% > WT). Regression analysis confirmed that HT mice had lower calcium absorption in response to increasing $1,25(OH)_2$ D levels (slope = 0.31 for WT vs 0.19 HT). The relationship of calbindin D_{9k} (CaBP) protein levels to plasma $1,25(OH)_2$ D was also influenced by VDR level (e.g. CaBP protein slope = 0.045 for WT vs. 0.026 HT). While TRPV6 and CaBP mRNA levels increased significantly after a single $1,25(OH)_2$ D injection (TRPV6 = 22-fold increase at 6 h, CaBP = 5-fold increase at 16 h), there was no difference in response between WT and HT mice. In contrast, $1,25(OH)_2$ D induced 24-hydroxyase (CYP24) mRNA levels were 26-41% lower at 6 h in the duodenum of HT mice depending on dose used. Our data demonstrate that low VDR levels differentially influence $1,25(OH)_2$ D regulated events in mice and suggest that VDR is critical for classical transcriptional regulation (e.g. CYP24), non-classical transcription regulation (e.g. TRPV6), and post-transcriptional regulation (e.g. CaBP) of calcium metabolism. In addition, low VDR level causes resistance of intestinal Ca absorption to $1,25(OH)_2$ D and this may be manifested through post-transcriptional influences of $1,25(OH)_2$ D on CaBP production. Supported by NIH award DK54111-06 to JCF.

Disclosures: ***J.C. Fleet****, None.*

SA561

PTH and Ca Cause Differential Regulation of the Vitamin D Receptor (VDR) in Mouse Proximal Versus Distal Renal Cells. A. Bajwa*[1], P. A. Friedman[2], M. J. Beckman[1]. [1]Biochemistry, Virginia Commonwealth University, Richmond, VA, USA, [2]Pharmacology, University of Pittsburgh, Pittsburgh, PA, USA.

The $1,25(OH)_2D_3$ receptor (VDR) promoter was characterized in mouse and human species as a TATA-less, GC-rich promoter with Sp1-dependent activation. However, very little is known about the tissue-specific and cell-specific regulation of VDR. The renal nephron offers a unique model for gene expression study of VDR because both proximal and distal tubules are central targets of parathyroid hormone (PTH), calcium (Ca) and $1,25(OH)_2D_3$ activities. The regulation of VDR in response to PTH and Ca was examined in human proximal (HK-2 and HKC-8), mouse proximal (MPCT) and mouse distal (DKC-8) cell lines. Where PTH treatment was used, MPCT cells were transiently transfected with the human type 1 PTH receptor ($PTHR_1$). DKC-8 cells were stably transfected with $PTHR_1$ prior to our experiments. In experiments below, serum free media with calcium (+Ca) or without calcium (-Ca) was used. In cases of additional calcium (Ca^{++}) treatment, (0 - 8 mM) of $CaCl_2$ solution was added to -Ca media. VDR and 1α-OHase gene expressions and promoter activities were measured and analyzed in proximal and distal cells. In DKC-8 cells, PTH_{1-34} treatment (50 nM) significantly increased ($p<0.03$) the relative gene expression of VDR by 6.5-fold while 1α-OHase gene expression was unchanged. Conversely, Ca^{++} concentrations of 2, 4 and 8 mM, decreased VDR gene expression of DKC-8 cells within 2 hours. In MPCT cells, VDR gene expression was suppressed, whereas 1α-OHase gene expression was increased in response to PTH treatment. Ca^{++} exposure of MPCT cells stimulated VDR gene expression and repressed 1α-OHase gene expression in both dose and time-dependent fashion. PTH treatments in human HK-2 and HKC-8 cells demonstrated that PTH is involved in significant ($p<0.05$) down-regulation of VDR. The analysis of promoter activities corresponded with the gene expression data. Additionally, VDR promoter activation was increased in the DKC-8 cells in response to PTH in the absence of a change in 1α-OHase promoter activity. VDR promoter activity in the MPCT cells was decreased with treatment of PTH. In contrast, 1α-OHase promoter activity was increased by PTH in MPCT cells. The differential regulation of VDR in proximal *versus* distal cells suggests several possibilities: (1) distinct promoter usage in the two cell types, (2) an alternative splice pattern of VDR transcription, or (3) the presence of differentially regulated transcription factors in proximal *versus* distal cells. In conclusion, proximal cell VDR is down-regulated by PTH and counterbalanced by opposite effects of extracellular Ca, and in distal cells, PTH potently increases VDR transcription.

Disclosures: ***A. Bajwa****, None.*

SA562

Dexamethasone Suppresses Smad3 Pathway in Mouse Osteoblastic Cells. M. Iu*, H. Kaji, H. Sowa, J. Naito*, T. Sugimoto, K. Chihara*. Division of Endocrinology/Metabolism, Neurology and Hematology/Oncology, Department of Clinical Mole, Kobe University Graduate School of Medicine, Kobe city, Japan.

The central to the pathogenesis of glucocorticoid-induced osteoporosis (GC) is the effect of GC on bone formation. However, the mechanism of GC-inhibited bone formation is not well known. The proliferation and differentiation of osteoblasts are included in these events and are controlled by various local growth factors and cytokines produced in bone as well as by systemic hormones. Among them, insulin-like growth factor (IGF) and transforming growth factor (TGF)- β are included in the most important targets of GC in bone formation. We recently reported that Smad3 , a TGF-βsignaling molecule, promotes the production of type I collagen (COLI), alkaline phosphatase (ALP) activity, and mineralization in mouse osteoblastic MC3T3-E1 cells and that PTH-Smad3-axis exerts anti-apoptotic action in osteoblasts (JBC 2002, JBC 2003), suggesting that Smad3 is important for promoting bone formation. However, no reports have been available about the effects of GC on Smad3 in osteoblasts. In the present study, we investigated whether dexamethasone (Dex), an active GC analogue, would affect the expression and activity of Smad3 in mouse osteoblastic cell-line, MC3T3-E1 cells. Dex significantly suppressed Smad3-stimulated ALP activity, although it did not affect TGF-β-inhibited ALP activity in MC3T3-E1 cells. Moreover, pretreatment with Dex suppressed TGF-β-enhanced expression of COLI in these cells. In the luciferase assay using p3TP-Lux with a Smad3-specific response element, Dex significantly suppressed transcriptional activity induced by TGF-β as well as Smad3 in MC3T3-E1 cells. However, Dex did not affect the expression of Smad3 in these cells at both mRNA and protein levels. In conculusion, the present study indicated that Dex inhibits ALP activity and type I collagen expression presumably through suppressing Smad3-induced transcriptional activity, but not through modulating Smad3 expression in mouse osteoblastic cells.

Disclosures: ***M. Iu****, None.*

SA563

Regulation of Mouse Osteoprotegerin Gene Expression by Steroid Hormones. T. Kondo, R. Kitazawa, S. Maeda*, S. Kitazawa. Division of Molecular Pathology, Kobe University Graduate School of Medicine, Kobe, Japan.

Glucocorticoid-induced osteoporosis is a serious complication of the systemic use of glucocorticoid. It is generally accepted that bone loss is primarily induced by altered osteoblast differentiation, function and by accelerated apoptosis. At the same time, an increase in bone resorption markers is observed during glucocorticoid therapy, indicating that accelerated bone resorption also contributes to glucocorticoid-induced bone loss. To explore the precise mechanism whereby dexamethasone (Dex) stimulates osteoclastogenesis, we analysed the effect of Dex on cis-acting elements of mouse osteoprotegerin (OPG) and of the receptor activator of NF-κB ligand (RANKL) gene. A series of deletion constructs of the mouse OPG promoter (Luc-116, Luc-697, Luc-1125, Luc-1487, Luc-3261) was transfected into ST2 cells and subjected to luciferase assay. Transfected cells were treated with Dex to assess its effect on OPG promoter activity. Mirroring Northern blot analysis, Dex reduced the promoter activity of Luc-1487 to 50%. Transient transfection studies and gel shift assay showed that the c-Jun homodimer bound to the AP-1 binding site (-293/-287) and maintained steady-state transcription of the OPG gene. Furthermore, the mutation of the AP-1 site negated Dex-driven OPG suppression. To assess the effect of Dex on OPG at the protein level, the amount of OPG protein secreted by ST2 cells was measured. Dex downregulated the OPG gene at both mRNA and protein levels. In agreement with the transient transfection studies, the amount of phosphorylated c-Jun protein (p-c-Jun) decreased 1hr after treatment of ST2 cells with Dex, whereas the total amount of c-Jun protein decreased after 12hr. Corresponding to the decrease of p-c-Jun, the amount of phosphorylated p46 isoform of Jun N-terminal kinase (JNK) decreased significantly 30 min after Dex treatment, whereas that of phosphorylated p54 isoform decreased after 12 hr. These data suggest that Dex negatively regulates OPG by transrepressing the OPG gene through the AP-1 site by a reduction in the proportion of the p-c-Jun protein in a JNK-dependent manner and that the reduction was mediated mainly by the decrease in the p46 isoform of JNK. On the other hand, Dex slightly increased the expression of RANKL mRNA. Deletion mutant studies suggested that Dex upregulated RANKL through the putative GRE half sites (-642/-628) or the AP-1 sites in the promoter. We speculate therefore that glucocorticoids per se promote osteoclastogenesis mostly by inhibiting OPG as the main target and partly by concurrently stimulating RANKL reciprocally, thereby enhancing bone resorption.

Disclosures: ***T. Kondo****, None.*

SA564

Glucocorticoids Inhibit Osteocalcin Transcription in Osteoblasts by Suppressing an Egr-binding Cell Type-Specific Enhancer. N. Leclerc*[1], T. Noh*[1], A. Khokhar*[1], E. Smith*[2], B. Frenkel[2]. [1]Biochemistry and Molecular Biology, University of Southern California, Keck School of Medicine, Los Angeles, CA, USA, [2]Orthopaedic Surgery, University of Southern California, Keck School of Medicine, Los Angeles, CA, USA.

Glucocorticoids (GCs) are widely used for the management of rheumatoid arthritis and other autoimmune and inflammatory diseases. A major side effect of GC treatment is osteoporosis, due to the inhibition of bone formation, but the underlying molecular mechanisms are poorly understood. We refined culture conditions, under which the synthetic GC dexamethasone (DEX) strongly inhibits MC3T3-E1 osteoblast differentiation and osteocalcin (*OC*) gene expression. Although OC itself does not play a critical role in osteoblast differentiation and bone formation, *OC* promoter studies contributed to milestone steps made towards our current understanding of transcriptional control mechanisms in osteoblasts. Standard (short-term) transient transfection assays of *OC* promoter-reporter constructs did not recapitulate the strong DEX-mediated repression. Therefore, mapping of negative GC-response elements (nGREs) was performed initially by stable transfections. These assays mapped a nGRE to a 0.1 kb fragment upstream of the binding site for Runx2 (position -138), which itself was not substantially inhibited. Further mapping was achievable by "long-term transient transfection assays", in which transfected cells were allowed to progress to a commitment stage where DEX has been shown to inhibit the osteoblast phenotype. These assays mapped a nGRE to a -161/-147 G:C-rich element and EMSA with this element demonstrated the formation of a protein-DNA complex, which contained an Egr/Krox family member(s). Three copies of the Egr/Krox site conferred 100-fold transcriptional activation on the 147-bp basal *OC* promoter in osteoblasts. Enhancer activity was not observed in 10T1/2 fibroblasts, unless these cells were co-transfected with Runx2. Thus, an Egr/Krox-binding site located immediately upstream of the *OC* Runx2 element was identified as a cell type-specific enhancer, whose activity is inhibited by GCs. Since an additional experimental approach, which employed microarray hybridization, led to the identification of an Egr member, Egr2/Krox20, as the gene most strongly inhibited by GCs in MC3T3-E1 cultures, we suggest that the inhibition of Egr-regulated enhancers in osteoblasts likely contributes to GC-induced osteoporosis.

Disclosures: ***N. Leclerc****, None.*

SA565

See Friday Plenary number F565

SA566

Glucocorticoid Regulation of Receptor Activator of NF-κB (RANK), Osteoprotegerin (OPG) and RANK Ligand (RANKL) in Mouse Calvarial Bone. C. Swanson*[1], M. Lorentzon[1], H. Conaway[2], U. H. Lerner[3]. [1]Center for Bone Research at the Sahlgrenska Academy (CBI), Department of Internal Medicine, Göteborg University, Göteborg, Sweden, [2]University of Arkansas for Medical Sciences, Department of Physiology and Biophysics, Little Rock, AR, USA, [3]Umeå University, Department of Oral Cell Biology, Umeå, Sweden.

Treatment with glucocorticoids results in a rapid decrease of bone mass in humans. A significant portion of this loss is thought to be due to increased bone resorption. We used a mouse bone resorption model to investigate the effects of glucocorticoids on the expression of RANKL, OPG and RANK. Enhanced release by the glucocorticoid dexamethasone (DEX) of ^{45}Ca from cultured neonatal mouse calvariae was blocked by OPG. Using semi-quantitative RT-PCR, it was found that DEX increased mRNA expression of RANKL, OPG and RANK in calvarial bones. This was at variance from D3, which increased mRNA expression of RANKL and RANK, but decreased that of OPG. DEX also increased mRNA expression of numerous osteoclast markers: tartrate resistant acid phosphatase (TRAP), calcitonin receptor (CTR), cathepsin K and carbonic anhydrase II, enhanced the mRNA expression of the osteoblast marker, alkaline phosphatase, but decreased expression of the osteoblast marker, osteocalcin. Using quantitative realtime PCR, it was found that DEX time- and concentration-dependently stimulated mRNA expression of RANKL, OPG, RANK, calcitonin receptor, cathepsin K and TRAP. When calvariae were stimulated with both D3 and DEX, a supra-additive potentiation of RANKL and CTR mRNA was observed. The stimulation of RANKL, OPG, RANK and CTR mRNA by DEX was blocked by the glucocorticoid receptor antagonist, RU 38486 (mifepristone). These data show that DEX enhances, via a glucocorticoid-receptor mediated mechanism, the expression of two molecules that promote osteoclastogenesis, RANKL and RANK. The observation that OPG, an inhibitor of osteoclast formation, was also increased by DEX may explain why bone resorption caused by glucocorticoids is not as great as that seen with resorptive agents like PTH or D3. Furthermore, the synergistic stimulation of RANKL by DEX and D3 may also explain why there are such significant enhancements of osteoclast formation and bone resorption when these two agents are combined.

Disclosures: ***C. Swanson****, None.*

SA567

Development of a Rapid Assay to Assess the Effects of Glucocorticoid Analogs on the Differentiation of Human Osteoblasts. M. L. Millham*, L. Buckbinder. Cardiovascular and Metabolic Diseases, Pfizer Inc., Groton, CT, USA.

Glucocorticoids (GC) are used to treat inflammatory diseases, however, many serious side effects limit chronic use. The osteoblast (Ob) is a major target for bone side effects. One hypothesis is that GC stimulate differentiation and deplete the precursor Ob pool, leading to osteoporosis. To better describe this phenomenon we have studied effect of GC on the differentiation of cultured primary human Obs. Nodule formation and mineral deposition were assessed after 28 days of GC treatment in confluent Ob cultures by micrographic analysis with von Kossa or alkaline phosphatase staining. Cells treated with GC showed marked dose-dependent increase in mineral deposition. To facilitate assessment of GCs and new analogs, we developed a novel 96-well colorimetric assay to detect alkaline phosphatase activity in cultures after only 7 to 10 days of treatment and demonstrated correlation with the 28 day micrographic results. We have established a facile method predictive for Ob differentiation and, we propose, bone safety.

Disclosures: ***L. Buckbinder****, None.*

SA568

Transgenic Mice Over-expressing 11beta-Hydroxysteroid Dehydrogenase Type 2 (11betaHSD2) Under the Col 1 alpha (I) Promoter Provide a Model to Test Direct Effects of Exogenous Corticosteroids on Osteoblasts. K. J. Brennan*, H. Zhou, J. de Winter*, C. R. Dunstan, M. J. Seibel. Bone Biology Unit, ANZAC Research Institute, Sydney, Australia.

Endogenous Glucocorticoid (GC) levels are systemically regulated via the hypothalamic-pituitary-adrenal axis. However, cytokines, growth factors and certain enzymes are able to modulate this control at the local level. Within specific tissues, two isoforms of 11beta-hydroxysteroid dehydrogenase (11betaHSD) control cytoplasmic GC levels independent of circulating GC concentrations. 11betaHSD type 1 predominantly converts inactive cortisone to active cortisol. In contrast, 11betaHSD2 unidirectionally catalyses the conversion of active GCs to their inactive metabolites. The relative activities of 11betaHSD1 and 11betaHSD2 determine the availability of active ligand (i.e. cortisol or corticosterone) for the GC receptor. The aim of this study was to determine if mice over-expressing 11betaHSD2 in osteoblasts are relatively protected from direct bone effects when treated with corticosterone (the rodent analogue of cortisol). Four week old transgenic male mice or wild type littermates over-expressing 11betaHSD2 under the regulation of the Col1alpha(I) 2.3 kb promoter were treated with vehicle or corticosterone (0,5, 2, or 10mg/kg/d, n = 4 - 5) for 14 days. At the end of this time bones were removed for assessment of endogenous 11betaHSD 1 and 2 and 11betaHSD2-transgene expression in bone, and histological assessment of bone volume and osteoclast and osteoblast lined surfaces in the lumbar vertebrae and proximal tibia. Endogenous 11betaHSD2 expression was not detectable in the bones of wild type mice. The 11betaHSD2 transgene was abundantly expressed in tibia of the transgenic mice with no changes seen over the duration of the study or with corticosterone treatment. 11betaHSD1 was constitutively expressed in the bones of mice and was not altered by transgene expression or corticosterone dosing. 11betaHSD2 transgenic mice tended to have a lower bone volume compared to transgenic in both the vertebral bodies and proximal tibia though this did not reach significance. Wild type mice appeared to lose proportionally more bone in the proximal tibia than transgenic mice at the 2mg/kg dose, though this effect was lost at the highest dose. Osteoclast and osteoblast surfaces were similar at all doses as were bone formation and bone resorption markers. 11betaHSD2 transgenic mice provide a potential model for evaluating the osteoblast specific actions of both endogenous and exogenous glucocorticoids.

Disclosures: ***C.R. Dunstan****, None.*

SA569

Inhibition of Interleukin-11 Gene Transcription by Glucocorticoid. Y. Ito, S. Kido, D. Inoue, T. Matsumoto. Department of Medicine and Bioregulatory Sciences, University of Tokushima Graduate School of Medicine, Tokushima, Japan.

Glucocorticoid (GC) excess causes osteoporosis (GIO: glucocorticoid-induced osteoporosis) in part through suppression of bone formation, but the mechanism is still largely unknown. We have reported that GC inhibits expression of an osteogenic cytokine, interleukin (IL)-11, which has been shown to stimulate bone formation and thereby increase bone mass in vivo. Moreover, IL-11 inhibits apoptosis of osteoblasts induced by GC. Therefore, decreased IL-11 expression may be involved in the pathogenesis of GIO. In the present study, we aimed to clarify the mechanism by which GC inhibits IL-11 gene expression. Deletion analysis with mouse IL-11 promoter revealed that both FSS (fluid shear stress) and PTH promoted IL-11 gene transcription in a manner dependent on the AP-1 binding site, which we previously identified as a key element for serum and TGF-β-stimulated transcription, following induction of fos family members such as δosB. We found that dexamethasone (DEX) strongly inhibited IL-11 gene transcription induced by PTH and FSS also in an AP-1-dependent manner. DEX had no effect on induction of fosB/δfosB or upstream signals including ERK activation. Inhibitory effects of DEX on IL-11 gene transcription appeared steroid-specific, because no inhibition was observed with other steroid hormones such as progesterone, 17 β -estradiol and dihydrotestosterone. DNA precipitation experiments with AP-1 binding sequences on the mouse IL-11 promoter demonstrated that JunD and ΔFosB were actually bound to the AP-1 site. We found that GR (glucocorticoid receptor) was also co-precipitated with the DNA/AP-1 complex in a ligand-dependent manner. However, GC treatment did not cause any appreciable changes in the amount of the other transcription factors bound to the AP-1 site. We therefore con-

clude that GR inhibits IL-11 gene transcription in an AP-1-dependent manner probably by direct interaction with AP-1 and recruitment of co-repressors. Further elucidation of the molecular mechanism by which GC inhibits AP-1-dependent transcription in osteoblasts will help us better understand tissue-specific actions of GC, and may contribute to the development of SGRM (selective GR modulator).

Disclosures: ***Y. Ito****, None.*

SA570

1αOH Vitamin D_2: Primary Functions in Energy Metabolism. N. J. Fleming*[1], C. Corley-Mastick*[2], R. S. Fredericks[1]. [1]Endocrine Associates, Reno, NV, USA, [2]Biochemistry, University of Nevada Reno, Reno, NV, USA.

The role of calcitropic hormones to influence mineral metabolism is widely recognized. Concomitant effects on energy metabolism have received less attention. Vitamin D in particular appears to participate in both mineral and energy modulation. As an ancient signal, recognition of novel actions of Vitamin D should shed light on the origins of receptor-ligand function. We have found 1αOH Vitamin D to have unexpected actions when administered to patients with normally function kidneys. These effects appear to be associated with increases in circulating leptin, while both 1-25 D and PTH are reduced. In developing models of signaling structure to explain these findings, the possibility that $1\alpha D_2$ could have direct effects on adipocyte function has been considered. Primary rat epidydimal adipocyte cultures utilizing exposure to 1-25 D and $1\alpha D_2$ in the presence and absence of a PPARγ agonist, rosiglitazone, demonstrate discordant actions of $1\alpha D_2$ and 1-25 D, where the effects of $1\alpha D_2$ are only seen in the presence of rosiglitazone. Liganded VDR has been demonstrated to interact with PPARγ in the cytoplasm. We propose that $1\alpha D_2$ is able to induce a similar action, but does not act as a functional ligand for nuclear expression regulating gene transcription. Such a mechanism could be primitive and account for the natural selection of 1αhydroxylation of Vitamin D in adaptive behavior in response to inadequate environmental phosphate, as well as selection of receptors as a means to mediate these actions through non-nuclear mechanisms. This concept for Vitamin D as a regulator of energy metabolism as well as mineral metabolism is likely to resolve clinical questions related to thermogenesis, behavior, and phenotypic expression of disease, including diabetes and coronary artery disease.

Leptin secretion over 96 hours (pg/ml)

Rosiglitazone	35.9
1αOH Vitamin D	32.1
1,25 Vitamin D	63.4
Rosiglitazone + 1αOH D	65.0
Rosiglitazone + 1,25D	61.3
Control	64.5

Disclosures: ***N.J. Fleming****, Endocrine Associates 3.*

SA571

Effects of Noncalcemic Vitamin D Analogues on PTHrP Production in Prostate and Lung Cancer Cells. S. Tu*[1], D. Burton[1], R. H. Hastings[2], P. Clopton*[3], L. J. Deftos[1]. [1]Medicine, University of California and SDVAMC, San Diego, CA, USA, [2]Anesthesiology, University of California and SDVAMC, San Diego, CA, USA, [3]Research, SDVAMC, San Diego, CA, USA.

We and other investigators have shown that parathyroid hormone-related protein (PTHrP) can directly stimulate tumor cell growth and promote metastases to the skeleton. Therefore, down-regulation of PTHrP expression may provide therapeutic benefits for cancer patients. 1α,25-dihydroxyvitamin D_3 (1,25 D), the active form of vitamin D, decreases PTHrP expression in prostate cancer cells, and it also inhibits proliferation of breast, lung and prostate cancer cells. To reduce the development of hypercalcemia and hyperphosphatemia, the major side effects of vitamin D treatment, synthetic vitamin D receptor ligands are being developed for various medical applications. In an attempt to evaluate even more effective vitamin D analogues for application in selected cancers, we used human prostate cancer (PC-3) and squamous lung cancer cells (BEN) to evaluate the effects of 11 different vitamin D analogues (generously provided by BioXell, Inc. and Leo Pharma) on PTHrP secretion. These cell lines were selected because they robustly express PTHrP. The cells were cultured in the presence or absence of the vitamin D analogues (0-10 nM) for 48 hrs in triplicate dishes in 4 separate experiments. Conditioned media were collected and secreted PTHrP 1-34 was determined by radioimmunoassay. Of the analogues analyzed, the most effective vitamin D analogues in suppressing PTHrP secretion were EB 1089, RO 27-2094, and RO 27-2310. In PC-3 cells these vitamin D analogues suppressed PTHrP by 24-42% and in BEN cells they decreased PTHrP levels by 61-64% compared to vehicle control. In contrast, the 1,25 D was less effective in suppressing PTHrP, reducing PTHrP levels in PC-3 and BEN cells by 3% and 33%, respectively, compared to vehicle controls. From these results, we found that EB 1089, RO 27-2094, and RO 27-2310 were more effective than 1,25 D in down-regulating PTHrP expression in PC-3 and BEN cells. Some of these compounds may prove useful for the management of selected human cancers.

Disclosures: ***D. Burton****, None.*

SA572

Rapid Responses to 1,25-Dihydroxyvitamin D3 Require Phospholipase A2 Activating Protein for Functional Activation of ERp60 Signaling. B. D. Boyan[1], L. Wang[1], E. A. Graham*[2], V. Sylvia[3], Z. Schwartz[1]. [1]Biomedical Engineering, Georgia Institute of Technology, Atlanta, GA, USA, [2]Periodontics, University of Texas Health Science Center at San Antonio, San Antonio, TX, USA, [3]Orthopaedics, University of Texas Health Science Center at San Antonio, San Antonio, TX, USA.

$1,25(OH)_2D_3$ acts through two main pathways: via nuclear vitamin D receptors (VDR) and through rapid membrane-associated signaling pathways, including activation of PLA_2, PLC, PKC and MAP kinase. The membrane-associated $1,25(OH)_2D_3$ binding protein ERp60 (also called 1,25-MARRSbp) is present in growth plate chondrocytes but is functional only in cells from the prehypertrophic and upper hypertrophic zones (growth zone, GC). Here we used antibodies directed to the N- and C-terminals of rat ERp60 and verified that it mediates the effect of $1,25(OH)_2D_3$ on this signaling pathway. We evaluated the role of PLA_2 activating protein (PLAA) in the cell-maturation specific response. RT-PCR and Western blots confirmed that PLAA mRNA and protein were present in confluent cultures of rat costochondral GC cells; Northern blot analysis showed that PLAA expression was not regulated by $1,25(OH)_2D_3$ at 10 min, 12 hours, or 24 hours. PLAA levels in vivo were assessed by in situ hybridization and by immunolocalization of costochondral cartilage from rats as well as from wild-type and nuclear VDR knockout mice. In situ hybridization showed that PLAA was expressed in undifferentiated chondrocytes in 16-day rat fetuses. However, in adult rats PLAA mRNA and protein were found only in the prehypertrophic and upper hypertrophic cartilage. Moreover, both wild type and VDR knockout mice showed the same pattern of expression. PLAA increased PLA_2 specific activity in both plasma membranes and the matrix vesicles and regulated arachidonic acid turnover in a manner similar to $1,25(OH)_2D_3$. Effects of PLAA on alkaline phosphatase and PKC specific activities and proteoglycan production ($[^{35}S]$-sulfate incorporation) were also like those of $1,25(OH)_2D_3$. Inhibitor studies showed that both PLAA and $1,25(OH)_2D_3$ acted through PLA_2, PLC-beta, and PKC-alpha, and that PGE_2 mediated the response through its EP1 receptor and Gq. These results show that PLAA is a critical link between ERp60 and downstream cell-maturation specific signaling in growth plate chondrocytes.

Disclosures: ***B.D. Boyan****, None.*

SA573

See Friday Plenary number F573

SA574

Protein Partners in the Intracelluar Binding and Transport of Vitamin D. R. F. Chun, M. A. Gacad, L. Nguyen, J. S. Adams. Division of Endocrinology, Burns and Allen Research Institute, Cedars-Sinai Medical Center, UCLA School of Medicine, Los Angeles, CA, USA.

In proximal kidney tubular epithelium, vitamin D is internalized by LDL- receptor (megalin)-mediated endocytosis. However, the proteins involved in the post-endocytotic intracellular traffic of vitamin D are less well studied. In previous findings (JBMR 17:S292; 2002) we observed increased uptake of a fluorescently labeled 1,25-dihydroxyvitamin D (1,25D) in HKC-8 cells transfected with plasmid expressing human hsc70 (member of hsp70 family of chaperones) and reduced uptake with ATPase domain-mutated hsc70 compared to HKC-8 transfected with vector alone. This result is consistent with the known role of hsc70 in clatherin uncoating of endocytic vesicles. Besides assisting internalization, hsc70 may also serve to bind and transport vitamin D intracellularly. Suggestive evidence of this includes: hsc70 can be detected in pull-downs with GST-C terminal megalin but not with GST alone and specific binding of 25-hydroxylated vitamin D metabolites (25D and 1,25D) to hsc70 can be measured. To further confirm and characterize hsc70's specific vitamin D binding ability and the role of ATP, binding assays were performed in the presence and absence of ATP. A several-fold, significant increase ($p<0.05$) in specific binding for 25D and 1,25D was observed when 2 μM ATP was included in the reaction mixture; interestingly, specific binding of cholesterol to hsc70 was also enhanced by ATP ($p<0.05$) indicating that cholesterol may share hsc70 as a trafficking chaperone. Vitamin D metabolic activity occurs in mitochondria; thus, an hsc70-like protein residing in mitochondria would be a candidate for involvement in subcellular vitamin D trafficking. The mitochondrial hsc70 equivalent, grp75, fits this description. We synthesized holo-grp75 and various domain-deletion mutants in *e. coli* and purified them with HIS-tag/Ni affinity chromatography. An expression construct of grp75 missing the first 63 amino acids (i.e. minus the mitochondrial targeting sequence) produced a protein that retained specific binding for 25D and 1,25D, while a C-terminal fragment of grp75 did not. We also detected grp75 in GST-C-terminal 1-hydroxylase pull-down assays of whole cell protein extracts suggesting a protein-protein interaction between grp75 and vitamin D-1-hydroxylase. Taken together, our current working model for vitamin D traffic holds that it enters the cell via LDL-receptor mediated endocytosis and is picked up by cytoplasmic hsc70. Vitamin D metabolite can then be passed to VDR (nuclear destined transcription factor) or grp75 that may facilitate transfer to mitochondria-localized vitamin D hydroxylases for hormone metabolism or catabolism or both.

Disclosures: ***R.F. Chun****, None.*

SA575

1,25-dihydroxyvitamin D_3 Increases Hypoxia Inducible Factor-1alpha and Vascular Endothelial Growth Factor mRNA Expression and Release via Phosphatidylinositol-3-Kinase. M. J. Levine*, J. Noll*, D. Teegarden. Foods and Nutrition, Purdue University, West Lafayette, IN, USA.

Previously we reported phosphatidylinositol 3-kinase (PI3K) plays a role in 1,25 dihydroxyvitamin D_3 (1,25D) induced vascular endothelial growth factor (VEGF) release, in part by activating the VEGF promoter at 24 hrs in C3H10T½ cells. Here, we examine the role of PI3K in 1,25D stimulation of VEGF release (ELISA) and mRNA expression (RT-PCR). 1,25D significantly increased VEGF release 2-fold by 8 hrs and remained elevated at 24 hrs. 1,25D-induced VEGF release involves transcription, as it was blocked by actinomycin D. 1,25D stimulation of VEGF mRNA levels and release are abrogated by PI3K inhibition at 8 hrs. Since no known vitamin D response element exists on the VEGF promoter, we investigated if transcription factors nuclear factor κB (NFκB) and hypoxia inducible factor-1α (HIF-1α), a subunit of HIF-1, which may regulate VEGF via PI3K, mediate the effect of 1,25D. While PI3K mediated 1,25D induction of NFκB activity, NFκB did not mediate 1,25D-induced VEGF release since it was unaffected by a constitutively active mutant construct of IκB that impedes NFκB activity. 1,25D increased levels of a protein immunoreactive with the HIF-1α antibody 2.6-, 1.6-, and 3.2-fold at 0.5, 2, and 4 hours. Further, PI3K inhibition modestly suppressed 1,25D's increase of HIF-1α. In conclusion, PI3K is involved in 1,25D induction of HIF-1α and is required for 1,25D to increase VEGF mRNA and release. Supported by ACS RPG-00-038-01-CNE

Disclosures: ***D. Teegarden****, None.*

SA576

The Coordinated Action of Parathyroid Hormone and 1,25-Dihydroxyvitamin D_3 Is Essential for Endochondral Bone Formation and Postnatal Survival. Y. B. Xue, A. C. Karaplis, G. N. Hendy, D. Goltzman, D. S. Miao. Medicine, McGill University, Montreal, PQ, Canada.

We previously generated, by targeted gene ablation, mouse models homozygous for either the PTH ($PTH^{-/-}$) or 1α-hydroxylase (1α-$(OH)ase^{-/-}$) null alleles. Although both animal models developed post-weaning hypocalcemia on a normal calcium diet, they were viable. In the current study, we generated double "knockout" mice which are homozygous for both the 1α-hydroxylase and PTH null alleles (1α-$(OH)ase^{-/-}PTH^{-/-}$). Double knockout mice appeared normal at birth but died 1-3 weeks postnatally, prior to the end of weaning with severe tetany. Serum calcium concentrations at two weeks of age, were 2.5±0.02, 1.7±0.07, 2.2±0.08 and 1.2±0.05 mmol/L in wild-type, $PTH^{-/-}$, 1α-$(OH)ase^{-/-}$ and 1α-$(OH)ase^{-/-}PTH^{-/-}$ mice, respectively. mRNA and protein expression levels of epithelial calcium channel 1 (EcaC1), calbindin-D_{9K}, calbindin-D_{28K} and Na^+/Ca^{2+} exchanger 1 (NCX1) in kidney and calbindin-D_{9K} gene expression in intestine were decreased in $PTH^{-/-}$ mice, more markedly reduced in 1α-$(OH)ase^{-/-}$ mice and dramatically diminished in 1α-$(OH)ase^{-/-}PTH^{-/-}$ mice. Overall body and long bone size were reduced in all three mutant mice at 2 weeks of age, compared to wild-type controls, however, the reductions were most severe in the double mutants. Epiphyseal cartilaginous growth plates were widened in 1α-$(OH)ase^{-/-}$ mice and double mutants had reduced secondary ossification centers. Double mutants, with the lowest serum calcium/phosphate product, showed diminished mineralization of cartilage and bone. Trabecular bone volume was moderately diminished in $PTH^{-/-}$ mice and 1α-$(OH)ase^{-/-}$ mice, but markedly decreased in 1α-$(OH)ase^{-/-}PTH^{-/-}$ mice in association with reduced osteoblast number and diminished expression levels of alkaline phosphatase, type I collagen and osteocalcin. Osteoclast number and RANKL levels were also decreased. The results demonstrate that alteration in PTH and 1,25-$(OH)_2D_3$ levels in PTH and 1α-(OH)ase deficiency can modulate the expression of critical genes in the transcellular calcium transport system that contribute to severe hypocalcemia and reduced survival. The results also demonstrate: that 1,25-$(OH)_2D_3$ regulates epiphyseal growth plate development, that a low calcium/phosphate product can impede cartilage and bone mineralization, that PTH and 1,25-$(OH)_2D_3$ together regulate trabecular bone formation, and that combined deficiency of these modulators leads to severe defects in endochondral bone formation.

Disclosures: ***Y.B. Xue****, None.*

SA577

Candidate Genes for Novel Vitamin D-Dependent Proteins in the Mouse Kidney. R. A. Meyer, M. H. Meyer. Department of Orthopaedic Surgery, Carolinas Medical Center, Charlotte, NC, USA.

The mammalian kidney is known to express three vitamin D-dependent proteins: calbindin D_{9K}, calbindin D_{28K}, and C/EBPβ (Christakos *et al.*, J Cell. Biochem. 88: 238, 2003). To search for novel vitamin D-dependent transcripts, we have examined the Affymetrix MOE 430A and 430B whole-genome microarrays (>40,000 transcripts). The experimental model was to find transcripts which were down-regulated in response to the acute deprivation of 1,25-dihydroxyvitamin D_3 which occurs when X-linked hypophosphatemic (*Hyp*) mice are fed a low phosphate diet. Normal and *Hyp* mice at 10 weeks of age were fed control or low phosphate diet for 3 days. Three mice were pooled for each of six microarrays per treatment group. Normal mice showed a significant rise in 25-hydroxyvitamin D-1α-hydroxylase mRNA transcript levels when fed a low phosphate diet. In contrast, the 25-hydroxyvitamin D-1α-hydroxylase transcript level fell in *Hyp* mice fed the low phosphate diet ($P = 0.02$) to 0.044 times that of *Hyp* mice fed the control diet. This was the largest proportional decrease among all genes examined. The transcript level for calbindin D_{9K} had the second largest fall in *Hyp* mice on low phosphate diet to 0.17 times the level of *Hyp* mice fed the control diet ($P < 0.001$). Seven other genes also had stable or increased transcript levels in normal mice fed the low phosphate diet, while, in *Hyp* mice fed the low phosphate diet, their transcript levels decreased to 0.25 to 0.33 times that of *Hyp* mice fed the control diet (all decreases were significant at $P < 0.05$). These seven genes (GenBank entries: AV369309, BB660640, BM194786, BB046307, AW913782, BB732233, and AK016112) are all relatively weak expressors, are unnamed, and are of unknown function. In conclusion, a whole genome search of transcript levels of genes expressed in the mouse kidney has revealed seven candidate genes for novel vitamin D-dependent proteins.

Disclosures: ***R.A. Meyer****, None.*

SA578

Vitamin D Status: Long-Term Variability in Postmenopausal Women. A Follow Up Study. L. Rejnmark[1], A. L. Lauridsen*[2], P. Vestergaard[1], C. Brot*[3], L. Heickendorff*[2], L. Mosekilde[1]. [1]Dept of endocrinology and metabolism C, Aarhus Amtssygehus, Aarhus, Denmark, [2]Dept of Clinical Biochemistry, Aarhus Sygehus, Aarhus, Denmark, [3]The Osteoporosis Research Centre, Hvidovre Hospital, Hvidovre, Denmark.

Measurements of plasma 25-hydroxyvitamin D (25OHD) levels are often used in patients to determine vitamin D status. Our aim was to investigate whether individual plasma 25OHD- and vitamin D-binding protein (DBP) levels are stable over a period of 5 years in healthy postmenopausal women. We followed 187 women who were perimenopausal at baseline for five-year. At baseline, 89 women were allocated to treatment with Hormone replacement therapy (HRT). Measurements were performed at baseline and after one-, two-, and five-years of follow up. Use of HRT increased plasma levels of DBP (+8%) but did not affect 25OHD levels. At baseline, 25OHD levels were higher in women who reported that they often went sunbathing and in those using vitamin D supplements, whereas smoking was inversely associated with 25OHD levels. Analyses on within-patient variability revealed a high coefficient of variation (CV) on 25OHD measurements (app. 20%); mostly due to a large biological variation (18.9%). Among those classified in the lowest tertile at baseline, only 40% remained in the lowest tertile during all subsequent time-points of measurements. Similarly, only 32% of those classified in the highest baseline tertile remained in the highest tertile during all following measurements. Use of the free vitamin D index (molar ratio of 25OHD- to DBP-levels) showed similar results. No independent predictors of changes in vitamin D tertiles during follow up were identified. Thus, in healthy postmenopausal women, individual measurement of a single plasma 25OHD level is not a reliable predictor of vitamin D status during the following five-year. Measurements of 25OHD levels should be restricted to patients with symptoms and signs of hypovitaminosis D. Our results do not exclude the use of 25OHD measurements in groups of patients. In the general population, 25OHD levels may be useful to identify factors influencing vitamin D status in order to determine how to improve vitamin D status.

Disclosures: ***L. Rejnmark****, None.*

SA579

The Effect of Calcium Intake on the Vitamin D Requirement. R. Y. Goussous*[1], L. Song*[2], G. Dallal*[3], B. Dawson-Hughes[2]. [1]Division of Endocrinology, Tufts-New England Medical Center, Boston, MA, USA, [2]Bone Metabolism Laboratory, JM USDA HNRCA at Tufts University, Boston, MA, USA, [3]Biostatistics Department, JM USDA HNRCA at Tufts University, Boston, MA, USA.

It has been postulated that a low calcium intake may increase the vitamin D requirement. This study was conducted to examine the effect of increasing calcium intake on the rise in serum 25-hydroxyvitamin D [25(OH)D] levels in response to supplemental vitamin D3.

The subjects were 52 healthy men and postmenopausal women with a mean age of 61.7 ± 8.5 (SD) years, and with screening 25(OH)D levels restricted to the range of 22.5 to 63.0 nmol/l. They were randomly assigned to either calcium (500 mg twice daily with meals) or placebo tablets for 90 days. All participants were placed on 800 IU per day of vitamin D3. Serum 25(OH)D measurements were made at baseline and on days 30, 60 and 90. The study was approved by the Investigation Review Board.

The basal mean calcium intake was 521 ± 341 mg/day in the calcium group and 634 ± 352 mg/day in the placebo group (P=0.251). The mean baseline 25(OH)D values were 48.0 ± 15.8 nmol/l in the calcium group and 49.0 ± 16.8 nmol/l in the placebo group (P=0.808). The change in 25(OH)D during the study didn't differ significantly in the two groups (ANOVA P = 0.700). The mean change from day 1 to day 90 was 16.2 ± 14.8 nmol/l in the calcium group and 16.6 ± 17.4 nmol/l in the placebo group (P=0.923 for difference, 95% CI (calcium-placebo) = (-9.5, 8.7) nmol/l). Both groups increased significantly over time (P< 0.001). We conclude that in healthy older men and women, the level of calcium intake, within the range of 550 to 1500 mg per day, doesn't affect the rise in serum 25(OH)D that occurs in response to the frequently recommended dose of 800 IU per day of vitamin D3.

Disclosures: ***B. Dawson-Hughes****, National Dairy Council 2; GlaxoSmithKline 5.*

SA580

Post-Translational Means of Regulating 25-Hydroxyvitamin D-1-Hydroxylase Activity. S. Wu, L. Nguyen*, R. F. Chun, J. S. Adams. Endocrinology, Cedars-Sinai Medical Center, Los Angeles, CA, USA.

The vitamin D-1-hydroxylase is a mitochondrial-based cytochrome P450 enzyme. It is the product of the CYP-1α gene and preferentially catalyzes the conversion of 25-hydroxylated vitamin D substrates to their cognate 1α-hydroxylated metabolite. Expression of 1-hydroxylase enzyme activity in both renal and extrarenal sites is regulated at the level of CYP-1α transcription and post-translationally based on 1] the cellular site of residence of the enzyme and its access to required accessory proteins, 2] the presence and amount of competitive CYP-24 (24-hydroxylase) gene product and 3] the delivery of substrate to the 1-hydroxylase. With regard to the latter, we have recently shown that cellular uptake of a 25-hydroxylated vitamin D metabolite and expression of 1-hydroxylase enzymatic activity is enhanced in cells

overexpressing the cytoplasmically-based intracellular vitamin D trafficking protein, hsc70. Because hsc70-bound vitamin D metabolite does not enter the mitochondrial compartment, we theorized that 1] substrate 25-hydroxyvitamin D (25-D) may be passed from hsc70, bearing a relatively low affinity for 25-D, to the relatively high-affinity substrate binding domain of the 1-hydroxylase in the cell cytoplasm and 2] it is the substrate-"preloaded", inner membrane-targeted 1-hydroxylase that determines the yield of product 1,25-dihydroxyvitamin D (1,25-D). Using gst-pulldown, a protein-protein interaction between the C-terminal domain of hsc70 and the 1-hydroxylase was demonstrated in the human kidney cell line HKC-8, confirming the potential for hsc70 to pass substrate 25-D to the 1-hydroxylase. In order to support the hypothesis that it is 1-hydroxylase "preloaded" with substrate-in the cell cytoplasm that determines 1-hydroxylating potential of the cell, the holo human 1-hydroxylase (1-522) and truncated, but substrate binding competent, 1-hydroxylase (94-522) missing the N-terminal mitochondrial-targeting domain were transiently over-expressed in HKC-8 cells. Compared to vector-alone-transfected cells, specific 25-D uptake was increased significantly, 61% (p=0.03) and 75% (p=0.02), in holo and N-terminally-truncated 1-hydroxylase-transfected cells, respectively. However, transient overexpression of the N-terminally-truncated 1-hydroxylase significantly squelched endogenous 1-hydroxylase activity in either 24-hydroxylase-competent HKC (p=0.006) or 24-hydroxylase-incompetent, macrophage-like HD11 cells (p=0.01). Contrary to current dogma, these data suggest that the 25-D substrate-1-hydroxylase interaction may occur in the cell cytoplasm prior to enzyme trafficking to the inner mitochondrial membrane.

Disclosures: ***S. Wu****, None.*

SA581

Characterization of Recombinant CYP2C11: A Vitamin D 25-Hydroxylase and 24-Hydroxylase. M. Rahmaniyan*[1], K. Patrick*[2], N. H. Bell[1]. [1]Medicine, Medical University of South Carolina, Charleston, SC, USA, [2]Medical University of South Carolina, Charleston, SC, USA.

Studies were performed to further characterize rat male-specific hepatic recombinant microsomal vitamin D-25-hydroxlase CYP2C11 expressed in baculovirus-infected insect cells and whether it also is a vitamin D-24-hydroxylase, a physiologically significant alternative pathway of vitamin D_2 metabolism. CYP2C11 is not expressed in livers of female rats. 25- and 24-hydroxylase activities were compared to those of ten other rat recombinant hepatic microsomal cytochrome P-450 enzymes expressed in baculovirus-infected insect cells. Each of them 25-hydroxylated vitamin D_2, vitamin D_3, 1α-hydroxyvitamin D_2 [1αOHD_2] and 1α-hydroxyvitamin D_3 [1αOHD_3]. CYP2C11 had the greatest activity except for vitamin D_3 where it had the same activity as 4 of the other enzymes. CYP2C11 25-hydroxylated 1αOHD_3, 1αOHD_2, vitamin D_2, and vitamin D_3 in declining order. Each of the recombinant cytohrome P-450 enzymes 24-hydroxylated 1αOHD_2 and CYP2C11 had the greatest activity. 24-Hydroxylation of 1αOHD_3 was very low and there was none with vitamin D_3. Only CYP2C11 24-hydroxylated vitamin D_2. Rat liver microsomes and CYP2C11 also 26-hydroxylated 1αOHD_2 and 1αOHD_3. K_m and V_{max} values for 24-, 25- and 26-hydroxylation of 1αOHD_2 and 1αOHD_3 by recombinant CYP2C11 were determined. Structures of vitamin D metabolites including 24-hydroxyvitamin D_2, 1,24*(S)*-dihydroxyvitamin D_2, 1,24-dihydroxyvitamin D_3, 1,26-dihydroxyvitamin D_2, and 1,26-dihydroxyvitamin D_3 were confirmed by HPLC and gas chromatography retention times, and characteristic mass spectrometric fragmentation patterns. In male rats, hypophysectomy significantly reduced body weight, liver weight, hepatic CYP2C11 mRNA expression and 24- and 25-hydroxylation of 1αOHD_2. It is concluded that CYP2C11 is male-specific hepatic microsomal vitamin D-25-hydroxylase that hydroxylates vitamin D_2, vitamin D_3, 1αOHD_2, and 1αOHD_3. CYP2C11 also is a vitamin D 24-hydroxylase.

Disclosures: ***N.H. Bell****, None.*

SA582

Evidence for a Gastrointestinal-Kidney Axis Modulating Phosphate Effects on Vitamin D Metabolism. B. Yuan*[1], Y. Xing*[1], R. Achyutharao*[1], J. F. Collins*[2], F. K. Ghishan*[2], M. K. Drezner[1]. [1]Medicine, University of Wisconsin, Madison, WI, USA, [2]Pediatrics, University of Arizona Health Sciences Center, Tucson, AZ, USA.

Alteration of the serum phosphorus (P) concentration, due to dietary phosphate loading or depletion, modulates renal 25(OH)D-1α-hydroxylase activity, suggesting that circulating P levels regulate vitamin D metabolism. However, when aberrant Na^+-dependent phosphate transport underlies hyperphosphatemia (Tumoral Calcinosis) or hypophosphatemia (X-Linked Hypophosphatemia), the disease phenotype does not include expected changes in calcitriol production. Thus, it remains unclear if serum P directly influences renal 25(OH)D-1α-hydroxylase activity. Therefore, we compared 25(OH)D-1α-hydroxylase mRNA (RT-PCR), protein (Western) and enzyme activity in male 8-12 week old C57BL/6J normal and phosphate loaded mice with that in similarly aged male C57BL/6J transgenic (*KAP* [**K**idney **A**ndrogen-responsive **P**rotein]-*Npt2*) mice with hyperphosphatemia, due to *Npt2* over-expression and consequent enhanced renal Na^+-dependent phosphate transport. Mice were fed a similar diet (0.8% P) until 10 days before study when phosphate loaded mice received a P (1.5%) enriched ration. The serum P level in transgenic (8.9±0.3 mg/dl) and phosphate loaded mice (8.9±0.1 mg/dl) was similar and significantly elevated (p<0.001) above that in normal mice (6.1±0.2 mg/dl). In contrast, compared to normal mice, phosphate loaded mice exhibited a 2.5-fold suppression (p<0.001) of 25(OH)D-1α-hydroxylase mRNA while transgenic mice displayed normal mRNA levels (fold change: 1.0±0.04 vs 0.4±0.03 vs 1.1±0.08). Similarly, 25(OH)D-1α-hydroxylase protein was selectively decreased (p<0.001) in the phosphate loaded mice (fold change: 1.0±0.1 vs 0.4±0.1 vs 1.0±0.2) as was the enzyme activity (5.6±0.2 vs 3.8±0.4 vs 5.6±0.7 fmoles/mg/min; p<0.002). These data indicate 25(OH)D-1α-hydroxylase activity is not uniformly influenced by the serum P level, possibly due to hyperphosphatemia of variable cause impacting differently on proximal tubule cell cytosolic events or to a direct effect of the GI system on kidney function. We excluded the former possibility by discovering that hyperphosphatemia in phosphate loaded and transgenic mice equally stimulates mRNA transcripts of renal PEX19 (fold change: 1.0±0.1 vs 1.3±0.1 vs 1.2±0.2; p<0.05), a peroxisomal farnesylated protein, which initiates a cascade of cytosolic events regulating Npt2 endocytosis. These observations establish that circulating P levels do not directly modulate renal 25(OH)D-1α-hydroxylase activity and suggest that regulation of vitamin D metabolism may depend on unique modulating effects of the Gastrointestinal-Kidney axis.

Disclosures: ***B. Yuan****, None.*

SA583

C-3 Epimerization of Vitamin D_3 Metabolites in Osteoblast like cells. M. Kamao*[1], S. Hatakeyama*[2], N. Kubodera[3], T. Okano[1]. [1]Department of Hygienic Sciences, Kobe Pharmaceutical University, Kobe, Japan, [2]Graduate School of Biomedical Sciences, Nagasaki University, Nagasaki, Japan, [3]Chugai Pharmaceutical Co. Ltd., Tokyo, Japan.

Purpose: We have demonstrated that 25-hydroxyvitamin D_3 [25(OH)D_3] and 1α,25-dihydroxyvitamin D_3 [1α,25$(OH)_2D_3$] are metabolized into their epimers of hydroxyl group at C-3 of the A-ring in hepatoblastoma and osteosarcoma cell lines. In the present study, we examined the C-3 epimerization during differentiation in osteoblast-like cells and the basic properties of the enzyme responsible for the C-3 epimerization of vitamin D_3.

Materials and Methods: UMR-106 [rat, osteosarcoma] and MC3T3-E1 [mouse, calvaria] cells were cultured for 28 days with 50 μg/mL ascorbic acid and 10 mM β-glycerophosphate. Amounts of 25(OH)D_3 metabolites were determined by HPLC and the mRNA levels of alkaline phosphatase (ALP) and osteopontin (OP) were measured by real time RT-PCR. The degree of mineralization was assessed by Arizarin Red S staining. The microsome fraction of UMR-106 cells was incubated with vitamin D_3 compounds in the presence of NADPH-generating substrates.

Results: In UMR-106 cells, C-3 epimerization activity was increased until day 15 and maintained its level throughout the period. On the other hand, C-24 hydroxylation activity was increased for 28 days. The mRNA level of ALP reached the maximal level at day 15. Mineralization was observed after 10 days. In MC3T3-E1 cells, maximal level of C-3 epimerization activity was observed at day 5. The expression of ALP was gradually decreased until day 28 and mineralization was observed after 15 days. In both cell lines, C-3 epimerization activity was not related to the expression level of OP and the production ratio of C-3 epimer to C-24 hydroxide at day 5 was the highest. Vmax values for 1α,25$(OH)_2D_3$, 25(OH)D_3, 24,25-dihydroxyvitamin D_3 [24,25$(OH)_2D_3$] and 22-oxacalcitriol (OCT) were 1.52, 2.34, 0.51 and 0.03 pmol/min/mg protein, respectively and Km values for 1α,25$(OH)_2D_3$, 25(OH)D_3, 24,25$(OH)_2D_3$ and OCT were 98.9, 73.7, 200.1 and 24.2 μM, respectively. These results indicate that 25(OH)D_3 has the highest specificity for C-3 epimerization among the four compounds. In addition, C-3 epimerization activity was not inhibited by various cytochrome P450 inhibitors or anti serum of NADPH cytochrome P450 reductase. C-3 epimerization activity was not induced by 1α,25$(OH)_2D_3$ in UMR-106 cells.

Conclusion: C-3 epimerization activity may be altered during osteoblast differentiation. The enzyme responsible for the C-3 epimerization of vitamin D_3 are thought to differ from already-known cytochrome P450 related vitamin D metabolic enzymes and not induced by 1α,25$(OH)_2D_3$.

Disclosures: ***M. Kamao****, None.*

SA584

The Microsomal Vitamin D_3-25 Hydroxylase, *CYP2R1*, Is Expressed in the Normal Human Liver and Kidney and its Hepatic mRNA Levels are Negatively Correlated with the Circulating 1,25$(OH)_2$D Concentrations. M. Gascon-Barré, C. Demers*. Hopital Saint-Luc, Centre de recherche du CHUM, Montreal, PQ, Canada.

Vitamin D (D) must be hydroxylated in the liver at C-25 before acquiring its full hormonal potential in the kidney. A mitochondrial D_3 C-25-hydroxylase (CYP27A1) has been described and shown to play a substantial role in human. Lately, the orphan microsomal *CYP2R1* has been proposed as a potential D-25-hydroxylase. The purpose of our study was to evaluate the *CYP2R1* gene expression levels in adult and foetal human livers and kidneys. In addition, to probe the role of 1,25$(OH)_2D_3$ in its regulation, *CYP2R1* mRNA levels were evaluated in two human hepatoma cell lines following exposure to vehicle or 1,25$(OH)_2D_3$. Adult subjects referred for hepatic or renal surgery were recruited. In addition, 5 normal foetuses (16-20 wks of gestation) were obtained following voluntary termination of pregnancy. All mRNA levels are presented as *CYP2R1/GAPDH* ratios. The *CYP2R1* gene transcript was found to be clearly expressed in liver and kidney of both adult and foetal specimens. However, mean *CYP2R1* mRNA levels were found to be 2.3 times higher in liver than in kidney of adult specimens (p<0.05), and no correlation was observed between the expression of *CYP2R1* and *CYP27A1*. *CYP2R1* mRNA levels were also found to be twice as high in adult than in foetal livers. In adult subjects, hepatic *CYP2R1* mRNA levels were shown to decrease logarithmetically as serum 25OHD increased (n=12, r^2 = 0.392, p<0.05) which resulted in a significant difference between patients presenting low serum 25OHD (<37 pmol/L) and those with normal D status (*CYP2R1* levels 1.2±0.1 vs 0.4±0.1, p<0.001). In patients with serum 1,25$(OH)_2$D concentrations above 50 pmol/L, a significant negative linear correlation was observed between circulation 1,25$(OH)_2$D concentrations and hepatic *CYP2R1* mRNA levels (n=9, r^2 = 0.567, p<0.05). In addition, the hepatoma cell line HEP3B which expresses very low *CYP27A1* mRNA levels exhibited a 3 times higher *CYP2R1* expression levels than the HEPG2 cell line which expresses normal levels of the *CYP27A1* gene transcript. Moreover, 1,25$(OH)_2D_3$ but not D_3 was shown to negatively regulate the expression of the *CYP2R1* gene transcript in HEP3B (p<0.05) while it had no effect in the HEPG2 cell line. Our findings illustrate that the microsomal *CYP2R1* is expressed in the human adult and foetal liver and kidney and that a negative relationship between *CYP2R1* mRNA levels and 1,25$(OH)_2D_3$ is present in both *in vitro* and *in vivo* conditions.

Disclosures: ***M. Gascon-Barré****, None.*

SA585

Prostate Cells Express Vitamin D-25-Hydroxylases and Can Synthesize 1α,25-Dihydroxyvitamin D_3 from Vitamin D_3. J. N. Flanagan*, M. V. Young*, L. W. Whitlatch*, J. S. Mathieu*, K. S. Persons*, M. F. Holick, T. C. Chen. Department of Medicine, Boston University School of Medicine, Boston, MA, USA.

The biologically active form of vitamin D, 1α,25-dihydroxyvitamin D (1,25D), plays essential roles in calcium homeostasis, and regulates proliferation and differentiation of a variety of cells, including prostate cells. Two hydroxylation steps catalyzed by vitamin D-25-hydroxylase (25-OHase) in the liver and 25-hydroxyvitamin D (25D)-1α-hydroxylase (1α-OHase) in the kidneys are required for the activation of vitamin D to 1,25D. Previously, we reported that 1α-OHase is also expressed in extra-renal tissues, including prostate cells, suggesting that local production of 1,25D could provide an important cell growth regulatory mechanism. Now, we present evidence that prostate cells also possess 25-OHase and are capable of metabolizing vitamin D_3 to $1,25D_3$ in the immortalized PZ-HPV-7 cells derived from normal prostate tissue. Three types of 25-OHase, one mitochondrial (CYP27A1) and two microsomal (CYP3A4 and CYP2R1), have been described. Using real-time PCR we found that CYP2R1 was expressed two-fold greater in normal human prostate tissue, 3-fold greater in PZ-HPV-7 cells and 6-fold greater in LNCaP prostate cancer cells than in normal liver tissue, whereas CYP27A1 was expressed 10-fold greater in normal liver tissue than in normal prostate tissue. Very little or no expression of CYP27A1 was found in PZ-HPV-7, LNCaP and PC-3 cells. PC-3 cells also expressed very little or no CYP2R1. The presence of 25-OHase in PZ-HPV-7 cells was further supported by the use of functional assays: (1) the addition of vitamin D_3 caused a dose-dependent up-regulation of 24-hydroxylase (CYP24A1) and IGF-BP3 mRNA, two genes known to be sensitive to 1,25D regulation in prostate cells, (2) vitamin D_3 at 10^{-6} M caused a 40% inhibition of ^{3}H-thymidine incorporation into DNA. These data suggest that vitamin D_3 was converted to $25D_3$, which in turn was further converted to $1,25D_3$ before exerting biological actions in prostate cells. The higher expression of CYP2R1 in prostate cells than in liver cells may have chemo-preventive relevance in prostate cancer, since CYP2R1 has been recently identified by a gene mutation analysis of a vitamin D deficient patient as a biologically relevant 25-OHase. Our results suggest that maintaining adequate levels of serum vitamin D or 25D by oral supplementation or sun exposure can be a safe and effective chemo-preventive measure to decrease the risk of prostate cancer.

Disclosures: ***J.N. Flanagan****, None.*

SA586

See Friday Plenary number F586

SA587

Vitamin D Metabolism in Human Osteoblasts. G. J. Atkins[1], P. H. Anderson*[2], K. Welldon*[1], A. C. W. Zannettino*[3], H. A. Morris*[4], D. M. Findlay[1]. [1]Orthopaedics and Trauma, University of Adelaide, Adelaide, Australia, [2]Div. of Endocrinology, Institute of Medical and Veterinary Science, Adelaide, Australia, [3]Div. of Haematology, Institute of Medical and Veterinary Science, Adelaide, Australia, [4]Hanson Institute, Adelaide, Australia.

Circulating 1α ,25-dihydroxyvitamin D_3 (1,25D) derives from conversion of 25-hydroxyvitamin D_3 (25D) by the kidney 1α -hydroxylase (CYP27B1). 1,25D exerts a number of effects on human osteoblasts, including inhibition of proliferation and differentiation, and effects on gene expression, including stimulation of RANKL, osteocalcin (OCN) and bone sialoprotein (BSP). We have examined vitamin D_3 metabolism in human osteoblastic cells, and found that primary normal human osteoblasts (NHBC) and human osteosarcoma cell lines, including MG-63, SaOS-2, HOS, G-292, all up-regulate the negative regulator of 1,25D, the 24-hydroxylase (CYP24), in response to 1,25D exposure. Additionally, all of these cell types expressed CYP27B1 mRNA, implying that human osteoblasts are capable of metabolising 25D into 1,25D. We have investigated this possibility and found that NHBC exposed to physiological concentrations of 25D (10 - 100 nM) in the absence of serum, exhibit up-regulated transcription of the downstream genes RANKL and OCN. Unlike 1,25D, 25D did not elicit a vigorous CYP24 response except at high concentrations (10^{-7} - 10^{-6} M). Consistent with this, NHBC treated with high concentrations of 25D secreted detectable 1,25D into the culture supernatant. We also found that NHBC express the 25-hydroxylase, and treatment with 1-hydroxyvitamin D_3 (1D), resulted in a gene expression response qualitatively similar to 25D. Inhibition of CYP activity using ketoconazole (10 μ M) resulted in an elevated response to 1,25D, probably due to inhibition of the catabolic activity of CYP24. Results to date indicate that the activity of 1D is CYP-dependent, since ketoconazole abolished its effects. However, 25D effects at low concentrations were unaffected by ketoconazole, indicating that 25D may have direct effects in osteoblasts independent of its conversion to 1,25D. Our results suggest that vitamin D_3 metabolism represents an intrinsic autocrine/paracrine pathway in these cells. Thus, vitamin D metabolites may regulate key functions in human osteoblasts independently of circulating levels of 1,25D.

Disclosures: ***G.J. Atkins****, None.*

SA588

Auto/Paracrine Action of Vitamin D in Bone: Evidence for 1alpha-Hydroxylase Expression and Activity in Human Osteoblasts. M. van Driel*[1], C. J. Buurman*[1], M. Koedam*[1], H. Chiba*[2], H. A. P. Pols[1], J. P. T. van Leeuwen[1]. [1]Internal Medicine, Erasmus MC, Rotterdam, Netherlands, [2]Pathology, Sapporo Medical University School of Medicine, Sapporo, Japan.

Vitamin D is metabolised by sequential hydroxylations in liver and kidney. 25-Hydroxyvitamin D_3 ($25\text{-}(OH)D_3$) formed in the liver is metabolised to the active metabolite $1\alpha,25\text{-}(OH)_2D_3$ ($1\alpha,25\text{-}(OH)_2D_3$) in the kidney by the enzyme 1α-hydroxylase. However, 1α-hydroxylase expression or activity has also been reported at several extrarenal sites like skin, lymph nodes, and colon at which local synthesis of $1\alpha,25\text{-}(OH)_2D_3$ appears to fulfil autocrine or paracrine functions. Over 20 years ago also $1,25\text{-}(OH)_2D_3$ production by osteoblasts was reported but this was never further explored and functionally tested. Recently, we observed a significant increase in osteocalcin mRNA expression after short-term incubations of human osteoblasts with $25\text{-}(OH)D_3$. Aim of the current study was to extend the data on $25\text{-}(OH)D_3$ effects on human osteoblast differentiation and to study 1α-hydroxylase expression and $1\alpha,25\text{-}(OH)_2D_3$ production in human osteoblasts. Moreover, to assess expression of cubilin and megalin, mediators of cellular uptake of the $25\text{-}(OH)D_3$-vitamin D-binding protein (DBP) complex, in human osteoblasts.

Short-term treatment of differentiating human osteoblasts (SV-HFO) with $25\text{-}(OH)D_3$ (1 μM) increased alkaline phosphatase activity and 24-hydroxylase mRNA expression throughout the three weeks osteoblast differentiation process.

We found 1α-hydroxylase mRNA expression in human osteoblasts and human bone biopsies. Incubation of SV-HFO cells for 48 hrs with $25\text{-}(OH)D_3$ (1 μM) resulted in the production of about 600 pM $1,25\text{-}(OH)_2D_3$ (assayed using radioimmunoassay). The $1,25\text{-}(OH)_2D_3$ formed from $25\text{-}(OH)D_3$ exerted comparable effects as equimolar concentrations freshly added $1,25\text{-}(OH)_2D_3$. Time-course studies showed that already after one hour $25\text{-}(OH)D_3$ incubation 50 pM $1,25\text{-}(OH)_2D_3$ could be detected. Production of $1,25\text{-}(OH)_2D_3$ showed a clear substrate-concentration dependency. 1α-Hydroxylase activity decreased during osteoblast differentiation. $1\alpha,25\text{-}(OH)_2D_3$ did not change 1α-hydroxylase mRNA expression nor did 24 hours $1,25\text{-}(OH)_2D_3$ pre-incubation affect 1α-hydroxylase activity in human osteoblasts. Finally, cubilin and megalin mRNAs were expressed in human osteoblasts.

In conclusion, we show that human osteoblasts express 1α-hydroxylase and $25\text{-}(OH)D_3$-DBP receptors and are capable to produce $1\alpha,25\text{-}(OH)_2D_3$ concentrations that regulate osteoblast activity. Thereby, these data provide evidence for an autocrine and/or paracrine vitamin D endocrine system in human osteoblasts and bone.

Disclosures: ***M. van Driel****, None.*

SA589

Regulation of the Renal Vitamin D 1alpha-Hydroxylase Cytochrome P450 (CYP27B1) mRNA and Protein by Dietary Phosphorus in Young and Adult Rats. H. J. Armbrecht, M. A. Boltz*. Geriatric Center, St. Louis VA Medical Center, Saint Louis, MO, USA.

Previous studies have shown that the capacity of rats to adapt to low dietary phosphorus declines with age. Young rats adapt to a low phosphorus diet by increasing plasma levels of 1,25-dihydroxyvitamin D (1,25D), which increase intestinal phosphate and calcium absorption, but adult and old animals do not. The purpose of this study was to determine whether this decreased adaptation was due to decreased expression of the renal 1alpha-hydroxylase (1-OHase), which synthesizes 1,25D. Young (2 month) and adult (12 month) male F344 rats were placed on a low phosphorus (0.1%) or high phosphorus (1.0%) diet for 2 weeks. Plasma 1,25D was markedly increased by the low phosphorus diet in young animals but not in adults. To determine whether this difference was due to decreased 1-OHase expression, mRNA levels of the terminal cytochrome P450 (CYP27B1) of the 1-OHase were measured by ribonuclease protection assay. In young animals, the low phosphorus diet increased renal CYP27B1 mRNA levels 8-fold compared to the high phosphorus diet, but there was no increase in adults. Protein levels of renal CYP27B1 were measured by Western blotting, using a specific anti-peptide polyclonal antibody. Interestingly, CYP27B1 protein levels were not increased by the low phosphorus diet in either age group in these experiments. In parallel experiments, feeding a low calcium diet markedly increased CYP27B1 protein levels in young rats but not in adult rats. The effect of low dietary phosphorus on plasma calcium, phosphate, and parathyroid hormone levels was similar in both age groups. These results demonstrate that the decreased adaptation to low dietary phosphorus in adult rats can be accounted for by decreased CYP27B1 mRNA levels. The results also demonstrate that the decreased adaptation in the adult is not due to changes in the major regulators of 1-OHase activity. Finally, they suggest that adaptation to low dietary phosphorus is fundamentally different than adaptation to low dietary calcium with regard to CYP27B1 expression.

Disclosures: ***H.J. Armbrecht****, None.*

SU001

Early Screening and Characterization of Osteopenia in Middle-Aged Women. P. G. Masse[1], J. Jougleux*[1], J. Dosy*[1], S. M. Donovan[2]. [1]Nutrition, Université de Moncton, Moncton, NB, Canada, [2]Nutrition, University of Illinois, Urbana, IL, USA.

Fifty-eight healthy, active, Caucasian women living at latitude 46º 7'North were recruited based on the following criteria: BMI <30 kg/m2, non-smoker, not using estrogen, drugs, nutritive supplements, vegetarian or special diet and with no history of bone fracture. BMD (g/cm2) was measured by Lunar DXA at 13 different lumbar and femoral sites. Subjects were then classified into two groups: **A**) control: normal BMD; **B**) osteopenic on the basis of clinical WHO criterion (BMD between 1.1 and 2.5 SD below the average value

(T-score) of the peak bone of healthy young adults for one lumbar site or more. Osteopenic subjects (68.9%) were further divided into two subgroups **B** and **B-** according to reference absolute values used in bone research, **B-** subjects being more osteopenic with BMD <0.9 g/cm2 for one lumbar spine site or more combined to 0.795 g/cm2 for at least one femur site. Fasting morning plasma and urinary double markers of bone formation and resorption (expressed per mmol **Cr**eatinine) were used to assess bone metabolism in addition to IGF-1. The 3 groups were well-matched in terms of: age, serum estradiol, height, body weight and frame, dietary protein, vitamin D, Ca and P intakes and their ratio (as assessed from 3-d records). IGF-1 was significantly lower in both osteopenic groups. There was no difference between the two B groups. Osteocalcin (OC) was significantly higher only in the most severe osteopenic group. All other bone markers, calciotropic hormones [PTH, $1,25(OH)_2D_3$] and plasma minerals showed no significant differences. The present study confirmed that bone loss declined in middle age. It also demonstrated that: 1) IGF-1 was the most sensitive biochemical indicator of bone metabolism; 2) OC was the earliest specific biochemical marker to vary, a finding indicating that osteoblasts increased this protein synthesis at an early stage of bone mineral loss; 3) absolute BMD values (g/cm2) for lumbar site combined to femur are more sensitive criteria for the diagnosis of osteopenia than WHO criterion.

	A (n = 18)		B (n = 18)			B- (n = 22)		
Age, years	44,6	(6,9)	49,0	(5,6)		49,9	(8,2)	
Weight, kg	69,8	(11,7)	68,3	(9,3)		63,8	(9,1)	
bALP, µg/mL	6,06	(3,47)	7,14	(3,13)		7,3	(2,6)	
IGF-1, ng/mL	86,3	(26,6)	63,2	(16,8)	(1)	60,2	(20,1)	(2)
OC, ng/mL	36,8	(8,2)	38,0	(8,7)		44,3	(6,0)	(3)
Helical peptide, µg/mmol Cr	43,2	(28,8)	44,9	(21,5)		54,7	(26,3)	
fDpd, nmol/mmol Cr	4,30	(1,44)	4,89	(2,05)		4,65	(1,5)	
iPTH, pmol/L	2,93	(1,49)	3,72	(1,45)		3,11	(1,02)	
$25(OH)D_3$, ng/mL	31,9	(18,1)	30,0	(11,9)		28,6	(13,2)	
$1,25(OH)_2D_3$, pg/mL	28,1	(14,4)	30,3	(13,7)		28,1	(10,3)	
Ca, mmol/L	2,32	(0,11)	2,30	(0,09)		2,35	(0,13)	
Pi, mmol/L	1,05	(0,15)	1,07	(0,13)		1,06	(0,13)	

Mean (SD): (1) P<0.01 A vs B ; (2) P<0.001 A vs B- ; (3) P<0.01 A vs B

Disclosures: ***P.G. Masse****, None.*

SU002

Lifetime Recreational Gymnastics and Selected Risk Factors for Osteoporotic Fractures, Prospective 6-year Follow-up Study. K. Uusi-Rasi, H. Sievänen*, A. Heinonen, I. Vuori*, P. Kannus*. UKK Institute, Tampere, Finland.

High bone mass and good physical fitness are important factors in prevention of fragility fractures. We studied effects of lifelong recreational gymnastics (at least 20 years of recreational gymnastics ≥ 2 times a week) on maintenance of bone mass and physical performance.

Initially 223 postmenopausal women were enrolled in the study. Six years later, 217 of them (107 gymnasts and 110 sedentary referents) with mean age of 68 years (SD 5) participated in the follow-up measurements. Mean height and weight were 161 (5) cm and 67 (10) kg at baseline with no differences in changes.

Bone mineral content (BMC) of the femur was measured with DXA, and cortical density (CoD) and cortical area (CoA) of the tibial midshaft, and trabecular density (TrD) of the distal tibia with pQCT. Physical performance was estimated by measuring maximal isometric strength, dynamic power, agility and 2-km walking time. Analyses of covariance were used to analyze the between-group differences and changes by time.

Bone mass decreased at a similar rate in both study groups. The overall decline (95% CI) in the femoral neck BMC was 3.4% (2.2% to 4.7%) for the gymnasts and 3.8% (2.6% to 5.0%) for the referents. In the tibia, the changes were small. TrD of the distal tibia declined by 0.6% (0.1% to 1.2%) and 1.0% (0.4% to1.6%) among the gymnasts and referents, respectively. CoD declined by about 2% in both groups and CoA did not change significantly. However, the gymnasts had greater bone mass both in the femur and tibia, although the intergroup difference did not reach statistical significance in all bone sites. The mean BMC differences were 3.4% (0.0% to 6.9%) in the femoral neck and 3.2 (-0.3% to 6.8%) in the trochanter, and in the tibia 3.7% (-0.2% to 7.8%) for the TrD, 0.4% (-0.3% to 1.1%) for CoD and 3.6% (0.8% to 6.4%) for CoA.

Compared to the referents, the gymnasts were in better physical condition, but the mean decline in physical ability was similar in both groups. Leg extensor power decreased 11% (8% to 14%) and 10% (7% to 13%) among the gymnasts and referents, respectively, while the decline in isometric muscle strength was insignificant. Agility decreased 3% (2% to 5%) in both groups, and the 2 km-walking time increased by 1 minute.

In conclusion, despite the similar rate of decline in bone mass and physical performance, the gymnasts had maintained the benefits achieved with lifelong gymnastics. In consequence of their greater bone mass and better physical ability, their risk of falling and fragility fracture is likely to be lower compared to their sedentary counterparts.

Disclosures: ***K. Uusi-Rasi****, None.*

SU003

Dietary Fish Oil Mitigates Aging-induced Bone Loss in Middle-Aged Male Rats. C. Shen*[1], D. M. Dunn*[1], J. K. Yeh[2]. [1]Pathology, Texas Tech University Health Sciences Center, Lubbock, TX, USA, [2]Medicine, Winthrop-University Hospital, Mineola, NY, USA.

Recent studies indicated that n-3 polyunsaturated fatty acids (PUFA) prevented bone loss in ovariectomized rats and postmenopausal women. The present study investigated the effects of dietary n-3 PUFA on bone mineral density (BMD) and bone histomorphometry in middle-aged male rats (n=21, 12 mo) fed diets containing either 20% menhaden oil (M diet, rich in n-3 PUFA) or 20% safflower oil (S diet, rich in n-6 PUFA) for 20 wks. Another 7 rats were euthanized at the beginning of the study as baseline (B group). Aging was found to decrease total bone mineral contents and BMD in femur, but did not affect DEXA-total area of femur. Compared to the S diet, rats fed the M diet had higher bone mineral contents in femur, but lower osteoclastic activity in lumber vertebra. The results of pQCT scans in the metaphyseal region of rat femoral bones were similar to those of DEXA scans in terms of the following: (i) aging caused a significant decrease in the total density, and (ii) rats given the n-3 PUFA tended to result in higher values of cortical + subcortical than those fed the n-6 PUFA (P = 0.088). Based on the results of bone histomorphometry, aging resulted in a significant decrease in the trabecular bone volume (Tb Ar) and the cortical bone area (%Ct Ar) of all the dietary groups. Compared to the S group, M group had a significant higher Tb Ar. The higher Tb Ar was because M diet resulted in a decreased bone formation rate/bone periosteal perimeter (BFR/B.Pm) (11.19 mcm/d) compared to the S diet (17.55 mcm/d). Our study also demonstrated that M diet had a significant higher %Ct Ar (80.8%) compared to the S group (78.9%). It seemed that M diet resulted in an increase in the periosteal bone formation as well as a decrease in the endosteal bone turnover rate. The present data suggest that n-3 PUFA mitigate aging-induced bone loss in middle-aged male rats through modulating both periosteal and endosteal bone turnover rate.

Disclosures: ***C. Shen****, None.*

SU004

Decreased Self Renewal of Mesenchymal Stem Cells Underlies the Senescence-Associated Bone Loss in Two Independent Murine Models: p53 +/m (Activating Mutation) and SAMP6. R. L. Jilka[1], M. Dumble*[2], R. A. Wynne*[1], A. M. Parfitt[1], L. Donehower*[2], S. C. Manolagas[1]. [1]Center for Osteoporosis and Metabolic Bone Diseases, Central Arkansas Veterans Healthcare System, University of Arkansas for Medical Sciences, Little Rock, AR, USA, [2]Depts. Of Molecular Virology and Microbiology, and Molecular and Cellular Biology, Baylor College of Medicine, Houston, TX, USA.

Mesenchymal stem cells (MSC) serve as a reservoir of osteoblasts in the bone marrow by virtue of their ability to both self-renew (i.e. produce identical daughter cells) and differentiate into osteoblasts. Age-related bone loss is characterized by a deficit in the number of osteoblasts needed to refill resorption cavities created during bone remodeling. Earlier work in rodents and humans had shown an age-related decline in the number of MSCs, as measured by colony forming osteoblast progenitors (CFU-OB) in *ex-vivo* cultures. Here, we have investigated whether the decline in MSC number is due to a reduction in their self-renewal capacity using two murine models of premature aging that exhibit a decrease in skeletal mass. In the p53 +/m mouse, early senescence is caused by an activating mutation of the transcription factor p53. This protein plays a key role in the induction of replicative senescence or apoptosis in response to cell stress and DNA damage, which may contribute to the aging phenotype. Femoral marrow cell cultures were established from 4-6 month old p53 +/m mice, and wild type littermates, and used to determine the number of CFU-OB, as well as their ability to produce identical daughter cells. We found that CFU-OB number in p53 +/m mice was significantly decreased as compared to wild type littermates (34.8 ± 12 vs 47.5 ± 11 per 10^6 marrow cells, respectively, P<0.05 by Students t-test). CFU-OB from p53 +/m mice increased only 3.3 ± 0.6-fold during 6 days of culture, whereas wild type CFU-OB increased 6.5 ± 0.6 fold (P<0.05). Moreover, the hindlimb and vertebral BMD of p53 +/m mice was significantly reduced by 17 ± 1% and 12 ± 1%, respectively, as compared to wild-type mice. In the second model, SAMP6, earlier studies had linked a reduction in CFU-OB number to a decrease in bone mass, which is associated with 7 genetic loci as determined by QTL mapping. CFU-OB from SAMP6 mice increased by 2.3 ± 0.5 fold during 6 days of culture, whereas CFU-OB from SAMR1 controls increased 8.7 ± 1.3-fold (P<0.05). These findings, obtained with two independent murine models of premature aging, strongly support the hypothesis that diminished MSC replication, perhaps secondary to p53-mediated replication arrest or apoptosis, can lead to exhaustion of the osteoblast reservoir needed for orderly bone remodeling, thereby contributing to age-related bone loss.

Disclosures: ***R.L. Jilka****, Nuvios, Inc. 1, 2, 5.*

SU005

Walking tall Is Poor Long-term Protection against Hip Fracture. P. Mayhew*[1], D. Thomas*[2], J. Clement*[2], N. Loveridge[1], W. Bonfield*[1], T. Beck[3], J. Reeve[1]. [1]Medicine & Materials Science, University of Cambridge, Cambridge, United Kingdom, [2]Dental Science, University of Melbourne, Melbourne, Australia, [3]Radiology, Johns Hopkins, Baltimore, MD, USA.

Background: Hip fractures rise 10 fold every 20 years but this is only partly accounted for by reduced BMD (aBMD). Bone can fracture by buckling under compression, when Critical Buckling Stress (CBS) is exceeded. We wondered if CBS declines markedly with ageing in the supero-lateral cortex (SLC) of the femoral neck that takes the compressive load in a sideways fall.

Methods: We measured ex vivo with high-resolution CT (Densiscan, 0.25mm res.) the distribution of bone in the mid-femoral neck of 77 proximal femurs from unselected cases of sudden death aged 20-95 (35 F). We calculated CBS around the cortex of each femoral neck at its pre-defined mid point, in 16 cortical sectors using the conventional equation CBS=E*t/{R*sqrt(3*[1-u2])} where t=the thickness of each cortical sector (adjusted for the partial volume effect by Hangartner's method), E=the elastic modulus of bone tissue (estimated from the bone density in the inferior sector using the Carter & Hayes equation), R=the sector's distance from the centre of gravity of the cross section and u=the usual Poisson's ratio of 0.3. The CBS data were modelled by MANOVA for all 16 sectors with age as the independent variable.

Results: aBMD decreased by 27% from age 20 to 80 in women. However, the thin SLC thinned more still and lost 60-75% of its CBS in women, slightly less in men over the same time frame. Meanwhile the CBS in the inferior cortex increased about 30% on average (fig). Comparing femoral neck bone from 22 hip fracture patients with 24 age matched controls, the cases had levels of critical buckling stress that were symmetrically reduced by 20-30% around the whole mid-femoral neck.

Interpretation: As we age, risk of buckling-type failure upon a sideways fall increases greatly in the SLC. This might result from the limited variety of western physical activity (80+% walking), during which gluteal contraction locally neutralises ground reaction forces in the SLC predictably leading to underloading. The fragile zones in healthy bones might be kept stronger with mechanical loading targeted to the SLC, as occurs when extending the flexed femur under load. A targeted lifelong physical activity intervention might substantially reduce hip fractures.

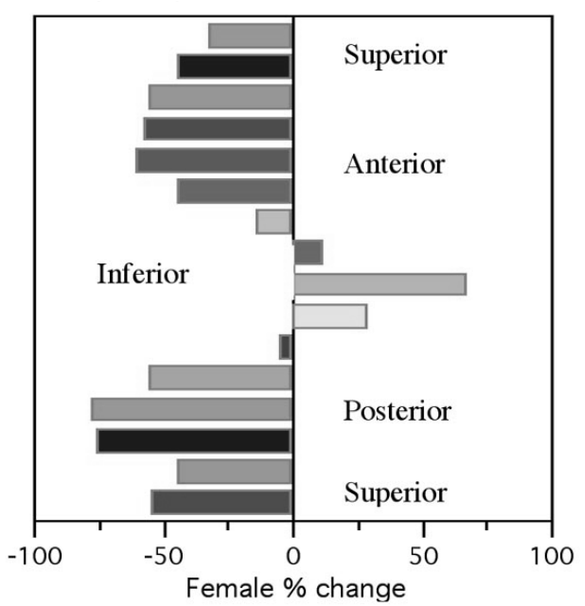

Change in CBS between 20-80y

Disclosures: ***P. Mayhew****, None.*

SU006

3D Volumetric Analysis of Age-Related Change in Cortical Porosity at the Human Anterior Femoral Mid-shaft. D. M. L. Cooper*[1], J. G. Clement*[2], C. D. L. Thomas*[2], B. Hallgrímsson[3]. [1]Archaeology, University of Calgary, Calgary, AB, Canada, [2]School of Dental Science, University of Melbourne, Melbourne, Australia, [3]Cell Biology & Anatomy, University of Calgary, Calgary, AB, Canada.

Relatively little is known about age dependent variation in the 3D structure of porosity within cortical bone. Accordingly, this study examines 3D volumetric age-related change in cortical porosity (on the level of osteonal canals) in the human anterior femoral mid-shaft. The sample included 42 individuals, 18 females and 24 males, spanning 20 to 85 years of age. The mean (+/- SD) ages for the males and females were 56.7 (+/- 18.5) years and 50.4 (+/- 21.4) years, respectively. Cortical blocks, 5 mm wide and 8 mm long were micro-CT (SkyScan 1072) scanned at 7 μm isotropic resolution. Cylindrical volumes of interest, 3 mm in diameter and 3 mm long, adjacent to the periosteal surface, were isolated from the scan data for quantitative analysis. Cortical porosity (%), mean canal diameter (μm), and mean canal separation (μm) were measured using model independent 3D stereological methods. Cortical porosity averaged 7.7 (+/-5.0) % for the males while females were relatively more porous at 14.4 (+/-14.0) %. Linear regression revealed significant positive relationships between age and cortical porosity for both males $R^2 = 0.243$ ($p = 0.014$) and females $R^2 = 0.718$ ($p < 0.001$). The average mean canal diameter followed a similar pattern, with males at 96 (+/- 47) μm and females at 161 (+/-137) μm. A significant positive linear relationship was found between mean canal diameter and age in females $R^2 = 0.686$ ($p < 0.001$) while this relationship was not significant $R^2 = 0.156$ ($p = 0.056$) for males. The average mean canal separation was 337 (+/- 38) μm for males and 328 (+/-55) μm for females. Significant negative linear relationships were found between age and mean canal separation for both males $R^2 = 0.365$ ($p = 0.002$) and females $R^2 = 0.447$ ($p = 0.002$). The results revealed two distinct trajectories for 3D age-related change in cortical porosity for the sexes. Females exhibited a dramatic increase in cortical porosity with age which occurred through the coalescence of larger canals with progressively less bone between them. For males, cortical porosity increased only slightly with age, canal separation decreased, and canal diameter did not change. From these findings we infer that the increase in porosity in males was a result of an increase in the number of canals (transverse and longitudinal) with age. 3D reconstructions of the canal networks provided qualitative evidence for this conclusion which is in contrast with previous 2D studies that have found that greater porosity in older specimens is due to greater canal size rather than a larger number of canals.

Disclosures: ***D.M.L. Cooper****, None.*

SU007

Growth Hormone Receptor/Binding Protein-Null Mice Indicate That Growth Hormone Plays a Role in Normal Bone Function in Young, Adult, and Aged Mice. R. W. Pamenter, M. S. Bonkowski*, J. S. Rocha*, M. M. Masternak*, K. AlRegaiey*, A. Bartke*. Internal Medicine, Southern Illinois University, School of Medicine, Springfield, IL, USA.

Growth hormone receptor/binding protein knock out (GHR-KO) mice are deficient in growth hormone signaling, have reduced insulin-like growth factor I levels, and are long-lived (~50%) compared to wildtype (WT) siblings. This study investigated the body composition and bone characteristics using dual-energy x-ray absorptiometry (DEXA) (PIXIMUS, Lunar GE, Madison, WI) in young (6-8 weeks), adult (7-10 months), and aged (28-32 months) GHR-KO and WT mice. Three-way ANOVA and post hoc testing was used to determine significant differences. Body weight was significantly different ($P<0.0001$) comparing WT and GHR-KO phenotypes, as previously reported. Percent fat across age groups was significantly higher in GHR-KO mice compared to WT ($P<0.0001$). Whole animal bone mineral density (BMD) increased with age ($P<0.0001$) and GHR-KO mice had reduced BMD ($P<0.0001$) compared to WT. Femur length increased across age groups in WT mice while GHR-KO mice had a numerical but not significant reduction in femur length at old age. Femur BMD was increased with age ($P<0.0001$) regardless of sex or phenotype, but reduced ($P<0.0001$) in GHR-KO compared to WT mice. Lower lumbar BMD was reduced ($P<0.0001$) in GHR-KO mice compared to WT. Lower lumbar BMD increased from young to adult regardless of phenotype or sex ($P<0.0001$). There was a decrease ($P<0.0006$) in lower lumbar BMD when comparing aged with adult WT male mice (0.061±.003 vs. 0.075±0.003, respectively). The decreased femur length linear growth in GHR-KO mice with advancing age indicates that growth hormone influences bone metabolism throughout the lifespan. In addition, bone characteristics and body composition of aged GHR-KO mice more closely matches values measured in young WT mice consistent with previous results of delayed growth and aging in GHR-KO animals.

Males

Age	WT Femur length	KO Femur length	BMD WT g/cm^2	BMD KO g/cm^2
Young	11.8±0.2	9.6±0.2	0.035±0.001	0.030±0.002
Adult	17.5±0.2	13.1±0.5	0.060±0.005	0.040±0.007
Aged	18.1±0.2	12.6±0.1	0.061±0.008	0.044±0.003

Females (mean±SD)

Age	WT Femur Length	KO Femur Length	BMD WT g/cm^2	BMD KO g/cm^2
Young	11.9±0.4	10.0±0.4	0.036±0.002	0.031±0.002
Adult	16.2±0.3	12.8±0.3	0.056±0.006	0.043±0.002
Aged	18.2±0.2	12.3±0.2	0.062±0.004	0.044±0.003

Disclosures: ***R.W. Pamenter****, None.*

SU008

Geometric Effects that Occur with Ageing and Osteoporosis Have an Impact on the Local Buckling Capacity of Bone at the Femoral Neck. T. Lee*[1], B. W. Schafer*[2], M. M. Daphtary*[1], T. J. Beck[1]. [1]Radiology, Johns Hopkins University, Baltimore, MD, USA, [2]Civil Engineering, Johns Hopkins University, Baltimore, MD, USA.

Osteoporotic fragility is ascribed to structural change in the amount and distribution of essentially normal bone material in ways that reduce density. But density declines with age by net bone loss and by expansion of volume due to periosteal apposition with opposing effects on mechanical strength. If declining bone density is actually homeostatic, why do bones become fragile? Since an expanding bone requires less material to achieve the same bending strength, it is conceivable that certain skeletal sites become locally unstable when expansion/thinning proceeds beyond stability thresholds. While it is known that Euler buckling does occur in the failure of individual trabeculae it is less obvious that whole bones may become unstable since they do not meet slenderness criteria. However, if one considers the possibility of local buckling of the bone cross-section then variations in the cross-section geometry become of primary importance. Local buckling is a phenomenon whereby the cross-section undergoes bending deformation as it destabilizes. Combinations of compressive bending and axial compression applied to the thinnest cortical region are potentially the most damaging. These conditions are likely at the thin lateral femoral neck in a fall on the greater trochanter. Using a tool specifically developed for investigating the local buckling of thin-walled members, i.e., elastic buckling analysis by classical finite strip method (CUFSM, Schafer 2003) we examined the local buckling characteristics of simulated femoral necks. Published cortical dimensions were used to simulate, femoral necks of young (20-29y), and old (80-89y) women with and without femoral neck fracture. Results indicate a strong sensitivity to the local geometry change that occurs with aging - the stress at which local buckling occurs decreases by a factor of 2.4 from a 20 year old to an 80 year old woman in those who do not fracture and a factor of 2.9 in those who fracture at the femoral neck. Geometric effects that occur with ageing clearly have a significant impact on the local buckling capacity of osteoporotic bones. However, the magnitude of the predicted local buckling stresses still remains relatively high in these crude simulations- and whether or not these large reductions trigger instabilities leading to fracture or are a secondary contributor remains unknown. Modeling sensitivity to material and geometric assumptions is being investigated, as are more realistic three-dimensional models of the proximal femur over a range of geometries observed in aging subjects.

Disclosures: ***T. Lee****, None.*

SU009

Increased Bone Loss During Disuse in Aged Animals May Be Due to Impaired BMP Responsiveness. D. S. Perrien, N. S. Akel, F. L. Swain*, R. A. Skinner*, L. J. Suva, E. E. Dupont-Versteegden*, D. Gaddy. Physiology and Biophysics, Orthopaedic Surgery, and Geriatrics, University of Arkansas for Medical Sciences, Little Rock, AR, USA.

Aging is associated with functional changes in many tissues, such as a decline in muscle mass and strength, and reduced bone density. We previously reported that 4 weeks of hindlimb suspension decreases BMD in the long bones of 6 month old Sprague Dawley rats, as measured by DEXA. To determine if aging enhances the rate of bone loss associated with disuse, and to examine the cellular basis of any age-related effects, a well-characterized model of musculoskeletal aging (Brown Norway/Fisher 344 rat) was utilized. Young adult 6 mo. old and aged 32 mo. old rats were hindlimb suspended (HS) for 2 weeks. Serial DEXA measurements of the hindlimb were obtained before HS and at sacrifice. Bone marrow cells were harvested from the femurs and cultured in osteogenic medium in the presence or absence of 100 ng/ml BMP2 or 200 ng/ml Noggin for 10 days. Recruitment of stromal cells to the osteoblastic lineage was assessed by alkaline phosphatase (AP) staining of CFU-F and determination of AP+ colony number. Unsuspended control young (CONY) and old (CONO) animals demonstrated similar increases in BMD in the proximal tibiae by DEXA analysis (P>0.05). However, rapid and significant decreases were observed in the BMD of proximal tibiae of old rats during 2 weeks of HS (HSO), compared with unsuspended control rats (p<.05) (CONO). However, HS did not have a significant effect on BMD in young adult animals (HSY) compared to CONY animals. As expected, osteoblastogenesis in bone marrow cells from CONO animals is under endogenous BMP control *in vitro*, since Noggin significantly suppressed the formation of AP+ colonies (P<0.05). Similarly, HS reduced the number of AP+ colonies in marrow cultures established from both old (HSO) and HSY animals, indicating decreased osteoblastogenesis as a consequence of disuse. Bone marrow cells from HSY animals maintained their responsiveness to exogenous BMP2, as indicated by increased numbers of AP+ colonies. In contrast, bone marrow cells from HSO animals were not responsive to either exogenous BMP2 or Noggin. These data suggest that, unlike younger animals, recruitment of HSO marrow cells into the osteoblast lineage is not under endogenous BMP control *in vitro*. Together, these data indicate that aging increases the rate of bone loss during disuse, and that this may be due to impaired response of marrow cells to the osteogenic effects of BMPs.

Disclosures: ***D.S. Perrien****, Immunogen 1.*

SU010

Age-Related Trabecular and Cortical Bone Loss in the Proximal Femur. C. E. Cann, J. K. Brown*. Mindways Software Inc, San Francisco, CA, USA.

Bone loss in the proximal femur with aging is well described as measured by dual x-ray absorptiometry (DXA), but no in vivo data are available about the age-related loss of trabecular versus cortical bone within specific regions such as the femoral neck. Such information could be useful in interpreting the role of age-related femoral bone loss in the increased risk of hip fracture. We have used 3D quantitative computed tomography scans projected as a DXA-like analysis to determine the fraction of trabecular versus cortical bone in the femoral neck and total hip regions of interest as a function of age in normal US women.

Six hundred sixteen normal women age 20-80 were recruited from 11 centers across the US. All were scanned using a standard 3D QCT proximal femur protocol. Quality control phantoms were used at each center to normalize all results to a common reference. QCT data were projected to a DXA-like 2D image using commercial software (CTXA Hip, Mindways Software, Inc, San Francisco, CA), and the area BMD measurements for Total Hip and Femoral Neck were segmented into "trabecular" and "cortical" compartments using a fixed threshold of 350 mg/cm3 as the upper limit for the trabecular bone. Area BMD in g/cm2 was calculated for each compartment with their sum equal to the standard DXA-like total bone BMD.A linear model was used to fit age-related bone loss for all compartments.

Age-related loss in the total bone for Total Hip and Femoral Neck regions of interest was -0.042 and -0.045 g/cm2/decade respectively. Cortical loss was -0.033 and -0.036 g/cm2/decade, and trabecular loss was -0.009 and -0.009 g/cm2/decade respectively. There were no significant differences between rates of loss in Total Hip vs. Femoral Neck regions, and cortical loss was significantly greater than trabecular loss ($p<0.01$). The cortical fraction of the total hip decreased from 66.8% at age 20 to 62.6% at age 80 and from 69.3% to 62.1% in the femoral neck ($p<0.02$).

Bone loss with age in the proximal femur is primarily due to loss from the "cortical" compartment comprised of the cortex and endocortical bone. While trabecular loss does occur with aging, it is relatively less. Use of this compartmental analysis in fracture rather than normal populations as done here may provide useful insight into the pathophysiology of hip fracture independent of simple total BMD measurements.

Disclosures: ***C.E. Cann****, Mindways Software Inc 3.*

SU011

Revitalization of Structural Allografts via Immobilized Recombinant Adeno-Associated Virus. M. Koefoed*[1], H. Ito[1], J. J. Goater*[1], R. E. Guldberg*[2], A. Lin*[2], R. J. O'Keefe[1], X. Zhang[1], E. M. Schwarz[1]. [1]Orthopaedics, University of Rochester, Rochester, NY, USA, [2]Georgia Institute of Technology, Atlanta, GA, USA.

Introduction: Due to their lack of osteogenic potential, structural allografts often result in catastrophic failure. To the end of generating a remodeling structural allograft we developed a murine femoral model, and a novel approach in which recombinant adeno-associated virus (rAAV) can be freeze-dried onto the cortical surface to mediate in vivo gene transfer. The aim of this study was to evaluate the transduction efficiency of immobilized rAAV in vitro and in vivo, and determine the effects of BMP gene therapy on allograft healing using this approach.

Methods: *In vitro* transduction of rAAV-LacZ was determined by freeze-drying 5 x 10^7 particles onto the surface of a stainless steel pin, which was incubated on a monolayer of 293 cells for 72hr. *In vivo* gene transfer to processed allografts was assessed by freeze-drying rAAV-LacZ onto the cortical surface, and transplantion into 8 week-old C57BL/6 mice. The mice were sacrificed at 2-weeks and transduction was assessed from X-gal staining. The effects of BMP gene therapy was evaluated by coating allografts with rAAV expressing a constitutively active Alk2 receptor (caAlk2) vs rAAV-LacZ controls, via X-ray, histomorphometry and micro-CT.

Results & Discussion. *In vitro* analysis of freeze-dried rAAV-LacZ revealed that storage of the vector at -80^{0}C had no effect on infectivity as determined by ß-gal assay. X-gal staining of the cultures demonstrated a mosaic transduction pattern both proximal and distal to the coated pin, indicating that the virus rehydrates and infects cells following passive diffusion in the culture media. X-gal staining of rAAV-LacZ coated allografts 2-weeks after transplantation revealed that the vector transduces ~5% of the cells in the immediate proximity of the allograft, as well as stromal cells in the fracture callus. To formally evaluate the efficacy of transferring BMP signals to the cortical surface of processed allografts we coated femoral allografts with rAAV-LacZ and rAAV-caAlk2 and evaluated their healing at 2, 4 and 6-weeks. Several remarkable features of rAAV-caAlk2 coated allograft healing were observed including: i) the absence of a foreign body reaction that normally encases the allograft in inflammatory tissue, ii) endochondral bone formation directly on the allograft surface, iii) a new bone collar that extends the entire length of the allograft, and iv) osteoclastic resorption of the allograft. Micro-CT analysis of the allografts at 6-weeks revealed the significant effects of the rAAV-caAlk2 vs rAAV-LacZ on bone formation around the allograft ($2.25 + 0.54mm^3$ vs $0.90 + 0.32mm^3$; $p<0.005$).

Disclosures: ***E.M. Schwarz****, LAGeT Inc. 4, 6.*

SU012

Regulation TGF-b/BMP Signaling by Smurfs and Arkadia. T. Imamura*, S. Maeda, M. Hayashi*. Department of Biochemistry, The JFCR Cancer Institute, Tokyo, Tokyo, Japan.

Smurf1, a HECT type E3 ubiquitin ligase, interacts with Smad1 and Smad5, and induces their poly-ubiquitination, with subsequent enhancement of turnover of Smads1 and 5. In addition, Smurf1 associates with type I receptors for TGF-b and BMP via inhibitory Smads (I-Smads), and induces poly-ubiquitination and degradation of the receptors. Thus, Smurf1 inhibits TGF-b superfamily signaling in cooperation with I-Smads. Here we show that Arkadia, a RING type E3 ubiquitin ligase, physically interacts with I-Smads and induces their poly-ubiquitination and degradation, but fails to associate with receptors. Overexpressed Arkadia enhances transcriptional activities induced by TGF-b and BMP. Silencing of the Arkadia gene by siRNA results in repression of TGF-b/BMP signaling. Arkadia may thus play an important role as an amplifier of TGF-b superfamily signaling.

Disclosures: ***T. Imamura****, None.*

SU013

Interferon-γ Inhibits Smad Signaling and Osteoblast Differentiation. F. A. Sylvester[1], N. Wyzga*[1], S. Varghese[2], E. Canalis[2]. [1]Digestive Diseases & Nutrition, Connecticut Children's Medical Center, Hartford, CT, USA, [2]Research, Saint Francis Hospital & Medical Center, Hartford, CT, USA.

Factors secreted by activated T cells regulate bone cell function and differentiation. We have shown that interferon (INF)-γ, a factor synthesized by activated $CD4^+Th_1$ T cells, inhibits the differentiation of primary bone marrow stromal cells into mature osteoblasts. However, the mechanisms involved are not known. We hypothesized that INF-γ blocks osteoblast differentiation by interfering with bone morphogenetic protein (BMP)-2 activity and signaling. For this purpose, we used ST-2 cells, a mouse bone marrow stromal cell line that is responsive to BMP-2. ST-2 cells were treated with BMP-2 at 1 nm in the presence and absence of INF-γ at 5 ng/mL under osteoblastogenic conditions. Cells treated with BMP-2 formed calcified nodules, whereas those treated with INF-γ did not. Furthermore, INF-γ altered the effect of BMP-2 so that the cultures did not develop discrete mineralized nodules, exhibited a reticular pattern of calcium precipitation, and did not express osteocalcin transcripts. INF-γ did not alter the number of viable cells and cell number was not different in cultures treated with BMP-2 with or without INF-γ. To test mechanisms responsible for the inhibitory effect of INF-γ on ST-2 cell differentiation, we examined whether it modified BMP-2 signaling. BMP-2 induced the phosphorylation of Smads 1/5/8, and this effect was decreased by INF-γ. Furthermore, transient transfection experiments with the BMP-responsive 12xSBE-OC-pGL3 plasmid, containing 12 repeats of Smad recognition sequences directing luciferase expression, revealed that its transactivation was significantly decreased in cells treated with INF-γ. BMP-2 induced luciferase β-gal activity was reduced from (means ± SEM) 43.5 ± 7 to 12.7 ± 2 ($p < 0.01$) by INF-γ. The expression of the inhibitory Smads 6/7 was not increased in INF-γ-treated cells, as determined by Western immunoblots. To investigate the possibility that INF-γ inhibits BMP-2 Smad-independent signaling, we studied the activation of MAP kinases p38, ERK, and JNK by BMP-2, in the presence and absence of INF-γ. BMP-2 did not enhance p38, ERK, and JNK phosphorylation, and INF-γ had no effect either. In conclusion, INF-γ inhibits the differentiation of ST-2 stromal cells into mature osteoblasts by a mechanism involving the inhibition of BMP-2 Smad-dependent signaling. INF-γ inhibits the differentiation of ST-2 stromal cells into mature osteoblasts. This effect is explained by an inhibition of BMP Smad signaling, although other mechanisms may also be operational.

Disclosures: ***F.A. Sylvester,*** *None.*

SU014

Quantitative in Vitro Assay for Osteoinductivity of Human Demineralized Bone Correlates with in Vivo Assay. S. Honsawek*[1], R. M. Powers*[2], L. Wolfinbarger[2]. [1]Biochemistry, Faculty of Medicine, Chulalongkorn University, Bangkok, Thailand, [2]Research & Development, LifeNet, Virginia Beach, VA, USA.

Demineralized bone matrix (DBM) has been extensively utilized in orthopaedic, periodontal, and maxillofacial applications and widely investigated as a material to promote new bone formation. Many studies have demonstrated that DBM comprises bone morphogenetic proteins (BMPs) that are substantial regulators for endochondral bone formation. The purposes of the present study were to quantitate BMP-4 in protein extracts of DBM and assess the osteoinductive potential of DBM preparations using in vitro and in vivo assays. Bone samples of 40 donors were ground and demineralized by exposure to 0.5 N HCl and then extracted by collagenase digestion. BMP-4 in protein extracts from DBM could be detected by Western blot analysis and measured using enzyme-linked immunosorbent assay (ELISA). The extractable BMP-4 levels were variable and averaged 3.70 ± 0.21 ng BMP-4/g of DBM. In the study of the effect of residual calcium on extractability of BMP-4, we found that the less residual calcium left in DBM increased the extractability of BMP-4. In the donor age and gender study, the extractable BMP-4 content appears to be age-dependent, with DBM from younger donors being most likely to have greater BMP-4 quantity. In contrast, no difference in the quantity of extractable BMP-4 was observed between male and female donors. In the in vitro dose-response studies, DBM protein extracts enhanced alkaline phosphatase activities of human periosteal cells in a dose-dependent fashion. Morphologic and histochemical analysis revealed osteoblast-like cells in the DBM protein extracts treated cells. Additionally, the osteoinductivity of DBM from the same donors quantitated by BMP-4 ELISA were assessed by histomorphometric analysis of new bone formation in an in vivo athymic mouse bioassay. The results revealed that DBM exhibiting high osteoinductivity in the nude mouse assay contained higher amounts of extractable BMP-4 than DBM samples possessing low levels of osteoinductivity. There was a good positive correlation between the quantitative BMP-4 in vitro assay and osteoinduction determined by the implantation of DBM in the in vivo nude mouse bioassay with a correlation coefficient of 0.7397 ($p < 0.001$).

Disclosures: ***S. Honsawek****, None.*

SU015

Evaluation of New Drug Delivery System for rhBMP-2 in a Rabbit Lumbar Spine Fusion Model. T. Namikawa*, H. Terai, E. Suzuki*, M. Hoshino*, H. Toyoda*, H. Nakamura*, S. Miyamoto*, K. Takaoka. Orthopaedic Surgery, Osaka City University Graduate School of Medicine, Osaka, Japan.

The purpose of this study is to achieve solid posterolateral intertransverse process lumbar fusion with use of an artificial osteoinductive implant without using autologous bone grafting. In this study, we use beta-tricalcium phosphate (β-TCP, Olympus. Co., Ltd.) and poly-D,L-lactic acid with random insertion of p-dioxanone and polyethylene (PLA-DX-PEG, Taki Chemical Co., Ltd.) composite paste implant added with low dose of an osteoinductive cytokine rhBMP-2 (Yamanouchi Pharmaceutical Co., Ltd.) as a potential bone graft substitute in a rabbit model. Thirty-six New Zealand white rabbits were used for this study. The rabbits were divided into six groups and underwent L5-L6 posterolateral intertransverse process lumbar fusion by using β-TCP and PLA-DX-PEG composite containing rhBMP-2 implants indicated in Table. The animals were examined for bone formation at the operated site every two weeks by radiographs, and evaluated by manual palpation, biomechanical testing and histological examination at 6 weeks after surgery. Radiographs demonstrated homogeneous calcified shadow between the transverse processes in all animals of group 1, 2 and in part of group 3 at 6 weeks. However, radiographs at 2 and 4 weeks, it was hard to assess fusion mass because of the β-TCP radiopacity. Fusion rate evaluated by manual palpation was 100% in the group 1and 2, 40% in the group 3 and 5. None (0%) had solid fusion in the group 4. Results of biomechanical testing correlated well with those of manual palpation. Histological section of L5-L6 intertransverse region of achieved solid fusion showed new bone formation between the L5-L6 transverse process and cortical rim around fusion mass. These results showed the efficacy of β-TCP powder and PLA-DX-PEG as a carrier of rhBMP-2 compared with those of reported previously (e.g., bovine type I collagen) from the standpoint of reducing the dose of rhBMP-2. We concluded that, with use of β-TCP powder and PLA-DX-PEG as a carrier of rhBMP-2, 15μg per each side of rhBMP-2 was enough to achieve posterolateral intertransverse process lumbar fusion at 6 weeks in a rabbit model. This artificial biomaterial containing rhBMP-2 can be useful as a autologous bone graft substitute.

Table: Summary of composition of implants per each side and fusion ratio

Group	rhBMP-2(μg)	β-TCP(mg)	PLA-DX-PEG(mg)	Fusion ratio
1	30	300	300	5/5
2	15	300	300	5/5
3	7.5	300	300	2/5
4	0	300	300	0/5
5	Autologous iliac bone graft (1-1.5g)			2/5

Disclosures: ***T. Namikawa****, None.*

SU016

Defective Trafficking of BMP Receptor in Fibrodysplasia Ossificans Progressiva. P. C. Billings*[1], J. L. Fiori*[1], L. Serrano de la Pena*[2], R. Caron*[1], E. M. Shore[1], F. S. Kaplan[1]. [1]Orthopaedic Surgery, University of Pennsylvania, Philadelphia, PA, USA, [2]Genetics, Rutgers University, Piscataway, NJ, USA.

Fibrodysplasia ossificans progressiva (FOP) is a devastating genetic disease characterized by congenital malformations of the great toes and progressive heterotopic ossification of connective tissues. There is no cure for this condition and only limited palliative treatment options are currently available. Although the molecular mechanisms giving rise to this disorder have not been elucidated, we have hypothesized that defects in the BMP signaling pathway play an important role in the pathophysiology of FOP. Previously, we demonstrated that BMP receptor IA (BMPRIA) is elevated 6-10 fold on the surface of FOP cells compared with control cells. Further, in the presence of BMP4 ligand, BMPRIA is rapidly degraded in control cells, but not in FOP cells. In this study, we used immunofluorescence to analyze BMPRIA in response to BMP4. All human cells were obtained from patients following IRB approved protocols. We found that treatment of normal cells with BMP4 induces BMPRIA clustering and internalization. However, under the same conditions, BMPRIA remains on the surface of FOP cells. Control and FOP cells bind transferrin protein and internalize transferrin receptor, indicting that this receptor internalizes similarly in both cell types. Our results suggest that the molecular defect in FOP is closely linked with BMP-receptor trafficking and supports the hypothesis that promiscuous BMP signaling in FOP cells results from increased BMPRIA density on the cell surface, thus giving rise to bone formation. Analysis of the molecular pathology of the human BMP4 pathway in FOP will elucidate the molecular mechanisms leading to abnormal ossification in these patients.

Disclosures: ***P.C. Billings****, None.*

SU017

rhBMP-2/CPM Accelerates Metaphyseal Trabecular Bone Formation in a Non-Human Primate Core Defect Model. X. Li, D. Gavin*, C. Wallace*, L. Li*, J. M. Wozney, H. J. Seeherman. Women's Health & Bone, Wyeth Research, Cambridge, MA, USA.

The efficacy of rhBMP-2/calcium phosphate matrix (CPM, ETEX Corporation, Cambridge, MA) (BMP/CPM) to accelerate trabecular bone formation was evaluated using a metaphyseal core defect model in 12 adult male cynomolgus monkeys. One core defect (n = 6) was treated with 1.5 mg/mL BMP/CPM in the distal radii, proximal tibiae and proximal femora. The contralateral core defects were treated with 4.5mg/mL BMP/CPM. Core defects in the remaining 6 animals were treated with CPM on one side and were untreated on the contralateral side (SXCT). Four weeks prior to the 8 week study termination, bilateral core defects created in the distal femora were injected with corresponding treatments. Histomorphometry was used to evaluate the regions surrounding and within the core defects. Values were significant ($p<0.05$) unless stated otherwise.

Results were equivalent for both BMP concentrations and for the CPM and SXCT groups except for mineral apposition rate (MAR). At 4 weeks, there was no difference in Tb.V between BMP/CPM and the CPM and SXCT groups in the region surrounding the core defects. However, O.V (osteoid volume) was increased by 25.6 fold and O.S (osteoid surface) by 14.4 fold (80.6 ± 18.6% vs. 5.69 ± 2.27%) in the BMP/CPM group compared to controls. The MS (mineralized surface) was 7.4 times greater in the surrounding region in the BMP/CPM compared to CPM and SXCT animals (64.1 ± 13.1% vs. 8.6 ± 3.4%). MAR also increased by 1.6 fold in the BMP/CPM-treated animals compared to SXCT. MAR of the CPM animals was 1.2 times greater than SXCT. Residual CPM was 88% vs. 60% in the CPM vs. BMP/CPM groups.

At 8 weeks, Tb.V for all anatomic locations treated with BMP/CPM was 1.7 times greater in the region surrounding the core defects compared to the combined CPM and SXCT groups. Increased Tb.V resulted from increased Tb.Th (trabecular thickness) and O.V on existing trabeculae, as well as new trabecular bone formation. O.S was increased from 12.8 ± 8.6% in the control groups to 61.0 ± 18.0% in the BMP/CPM animals. The increase in Tb.Th was due to a 5.2 fold increase in MS (70.8 ± 14.3% vs. 13.9 ± 6.7%) and a 1.6 fold increase in MAR in the BMP/CPM group compared to SXCT. MAR of the CPM group was 1.2 times greater than SXCT. Residual CPM was 67% vs. 26% in the CPM vs. BMP/CPM groups.

These results indicate that BMP/CPM induces rapid increases in O.V, O.S, MS and MAR in the region surrounding the core defects as early as 4 weeks. These increases were sustained at 8 weeks leading to increased Tb.Th and Tb.V. There was also considerable new trabecular bone formation within the core defects and the surrounding region. This study provides support for evaluating BMP/CPM to accelerate metaphyseal fracture repair and increase bone density.

Disclosures: ***X. Li****, Wyeth Discovery Research 3.*

SU018

NF-kB, p65 Represses BMP2 Signaling by Interfering with the Interaction of Smad and CBP. E. Jimi[1], T. Katagiri[2], F. Okamoto*[1], H. Fukushima[1], T. Tada[1], H. Kajiya[1], K. Okabe[1]. [1]Physiological Science and Molecular Biology, Fukuoka Dental College, Fukuoka, Japan, [2]Biochemistry, Showa University, Tokyo, Japan.

Bone morophogenetic proteins (BMPs) are members of the transforming growth factor-b (TGF- b) superfamily and control proliferation, differentiation and apoptosis of various cell types. Previous studies have shown that BMPs induce not only bone formation in vivo but also osteoblast differentiation of mesenchymal cells in vitro. On the other hand, transcription factor NF-kB is critical for the expression of inducible genes involved in immune reactions and inflammation, and BMPs and NF-kB have opposite biological functions during inflammatory processes and apoptosis. To clarify the regulatory mechanisms of NF-kB on BMP signaling pathway during osteoblast differentiation, we examined the effect of p65 (a subunit of NF-kB) expression on BMP2-induced osteoblast differentiation using p65 deficient (p65-/-) mouse embryonic fibroblasts (MEF). BMP2 induced more alkaline phosphatase (ALP) positive cells in p65-/- MEF than in wild-type MEF. BMP2-induced expression of osteoblast differentiation markers, such as ALP or osteocalcin was also enhanced in p65-/- MEF. Expression of p65 failed to affect receptor-dependent formation of heteromers containing Smad proteins (intracellular signaling molecules in the BMP signal transduction pathway) as well as the DNA-binding activity of Smad proteins. Overexpression of p65 in p65-/- MEF inhibited BMP2-responsive promoter activity despite a lack of direct interactions between p65 and Smad proteins. Furthermore, this p65-mediated inhibition of BMP2- and Smad-responsive promoter activity was restored after inhibition of NF-kB by overexpression of the dominant negative form of IkB. Overexpression of the transcriptional coactivator CBP suppressed the inhibitory effect of p65 on the BMP2-responsive promoter. Overexpression of p65 interfered with the interaction of Smad and CBP. These results suggest that NF-kB represses the BMP2 signaling through at transcriptional level by competing for transcriptional coactivators.

Disclosures: ***E. Jimi****, None.*

SU019

Withdrawn

SU020

Transcriptional Profiling of Murine Marrow Stromal Fibroblast Cultures Treated with Noggin. S. P. Suriyapperuma*, I. Kalajzic*, J. Glynn*, N. Boucher*, A. Kaur*, W. Krueger*, D. Rowe. Genetics and Developmental Biology, Univ. of Connecticut Health Center, Farmington, CT, USA.

Bone morphogenetic proteins (BMPs) have an important role in controlling mesenchymal differentiation. Important mechanisms of regulation of BMP action are BMP antagonists that prevent BMP's from binding to its receptors and therefore control BMP signaling. Previous studies described the biological effects of BMP antagonists on osteoblast lineage differentiation, but did not provide the broad spectrum of the modulation of gene expression induced by these agents. We have previously shown that primary marrow stromal cell (MSC) cultures grown under osteoblast inductive conditions, in the presence of continuous with 250ng/ml of noggin for 9 or 20 days fail to achieve full osteoblast differentiation (J. Cell Biochem. 88:1168, 2003). To identify the gene regulation triggered by noggin, we performed cDNA transcriptional profiling of noggin treated cultures. Total RNA from untreated and treated cultures was extracted on day 9 (N9 Vs C9) and day 20 (N20 Vs C20). RNA was amplified to make antisense RNA and hybridized to four UCHC Mouse 6K Chip each consisting of transcripts in quadruplicate. Noggin treated and control RNA was comparatively hybridized to provide comparisons in a loop design (N9 Vs C9), (N20 Vs C20), (N20 Vs N9), and (C20 Vs C9). The data was statistically validated by Confidence Analysis (CA-95%) and Significance Analysis of Microarrays (SAM-5%).

Comparison of N9 with C9 generated 13 and 22 up regulated genes and 3 and 2 down regulated genes by CA and SAM respectively. N9 showed down regulation of early markers of bone lineage (Akp2 and fibromodulin) and inhibition of Col2a1, a chondrocyte specific gene. N20 Vs C20 revealed more pronounced regulation of genes with 135 and 239 (up to 33 fold) up regulated genes and 131 and 812 down regulated genes by CA and SAM. Cartilage directed (Col2a1, Col11a1and FGFr3) and bone associated genes (Bmp1, Wnt4, Col1a1 and Dkk1) were down regulated. Among up regulated genes were myogenic genes i.e., Foxk1, Fhl2 and Spnb2. Preliminary data on C20 Vs C9 showed 76 up regulated and 86 down regulated genes by CA. Increased levels of Wnt1, Wnt4, Col1a1 and decreased levels of Myh11, Tmp2, Spnb2 and other skeletal genes validated the control cell cultures. Comparison of N20 Vs N9 identified 43 up and 79 down regulated transcripts. Longer exposure to noggin had stronger inhibitory effects on osteoblast and chrondocyte differentiation and accentuation of myogenic precursor cells. Our data validates the multi-lineage potential of MSCs and suggests that noggin inhibits mesenchymal lineage differentiation at the stage prior to bifurcation of progenitor cells into the chondrocyte and osteoblast lineage.

Disclosures: ***S.P. Suriyapperuma****, None.*

SU021

Modulation of BMP2-Induced Osteoblast Differentiation by Heparin and Heparin Sulfate Proteoglycans (HSPGs). X. Jiao*[1], E. M. Shore[2], F. S. Kaplan[3], D. L. Glaser*[1]. [1]Orthopedic Surgery, University of Pennsylvania, Philadelphia, PA, USA, [2]Orthopedic Surgery ,Genetics, University of Pennsylvania, Philadelphia, PA, USA, [3]Orthopedic Surgery, Medicine, University of Pennsylvania, Philadelphia, PA, USA.

Heparin and heparan sulfate proteoglycans (HSPGs) may interact with bone morphogenetic proteins (BMPs) during bone formation. However, the precise mechanisms remain unknown. This study examined the effects of both cell surface HSPGs and exogenous heparin on BMP2-induced osteoblast differentiation.

To examine the effects of exogenous heparin, C2C12 cells were cultured for 6 days with 0-300 ng/ml BMP2 and 0-2 mg/ml heparin added simultaneously. Osteoblast differentiation was assessed at day 7 by the expression of alkaline phosphatase (ALP), collagen type I, Cbfa1/Runx2 and osteocalcin. Messenger RNA levels of these markers were detected by semi-quantitative RT-PCR, and ALP activity was measured histochemically. Heparin at concentrations up to 2 µg/ml increased while at higher concentrations significantly inhibited BMP2 signaling as demonstrated by phosphorylated SMAD1 levels and ALP activity. At 2 mg/ml, heparin blocked the BMP2 mediated increase of mRNAs of osteoblast markers including osteocalcin, Cbfa1/Runx2, collagen type I and ALP. To study effects of cell surface HSPGs on BMP2 signaling, C2C12 cells were pretreated with either 0-80 mM sodium chlorate for 48 h or 0-6 SU Heparinase III for 2 h to deplete HSPGs and then cells were incubated with BMP2 for 6 days. Depletion of cell surface HSPGs by both methods enhanced BMP2 signaling in a dose-dependent manner indicated by increased ALP activity and pSMAD1. To investigate HSPGs' effects on BMP2 internalization, cells treated either with sodium chlorate and/or antibodies against BMPRIA were incubated with labeled BMP2. The internalization of BMP2 was monitored by fluorescence microscopy. In the presence of intact BMPRIA, ALP was induced but the cell surface BMP2 binding capacity was significantly reduced when HSPGs were depleted. When cells were treated with antibodies against BMPRIA, ALP induction was blocked; however, BMP2 still could be internalized through HSPGs. These results suggested that cell surface HSPGs mediated BMP2 internalization without signaling and thus competitively inhibited BMP2 signaling. With cell surface HSPGs intact, free heparin has a biphasic effect on BMP2 signaling, being stimulatory at low concentration and inhibitory at high concentration. Since BMPs play an important role in ectopic bone formation, exogenous heparin or alteration of endogenous HSPGs has a potential to block debilitating ectopic bone formation, as in fibrodysplasia ossificans progressiva (FOP).

Disclosures: ***X. Jiao****, None.*

SU022

The Relation of Medial Minimum Joint Space Width to Age in the Knees of Healthy and Osteoarthritic Women. K. A. Beattie[1], P. Boulos*[1], J. Duryea*[2], J. O'Neill*[1], M. Pui*[1], C. L. Gordon[1], J. D. Adachi[1], C. E. Webber[3]. [1]McMaster University, Hamilton, ON, Canada, [2]Dept. of Radiology, Brigham & Women's Hospital, Boston, MA, USA, [3]Hamilton Health Sciences, Hamilton, ON, Canada.

The purpose of this study was to evaluate medial minimum joint space width (mJSW) in the knees of healthy women of various age groups and compare these values with osteoarthritic women.

The group of healthy women included 20-69 year olds with no knee pain, bone/joint disease or knee injury. Women in the osteoarthritis (OA) group had been clinically diagnosed with OA by a rheumatologist. All volunteers underwent a single, fixed-flexion knee radiograph. Radiographs were graded using the Kellgren-Lawrence (K-L) scale and digital films were analyzed using a computer algorithm.

The 2 groups consisted of 62 healthy and 25 osteoarthritic females. Age distribution of healthy females included 21 aged 20-29, 11 aged 30-39, 12 aged 40-49, 13 aged 50-59 and 5 aged 60-69 with a mean (SD) age of 39.1 (13.6) years and a mean (SD) BMI of 24.2 (4.3) kg/m^2. K-L grading of healthy knees revealed 43 grade 0 and 19 grade 1 films with no differences in mJSW between grades 0 and 1. Analyses for age groups revealed the following mean (SD) mJSWs: 5.00 (0.54) mm for 20-29, 4.49 (0.69) mm for 30-39, 4.82 (0.74) mm for 40-49, 4.57 (0.76) for 50-59 and 4.61 (0.44) mm for 60-69.

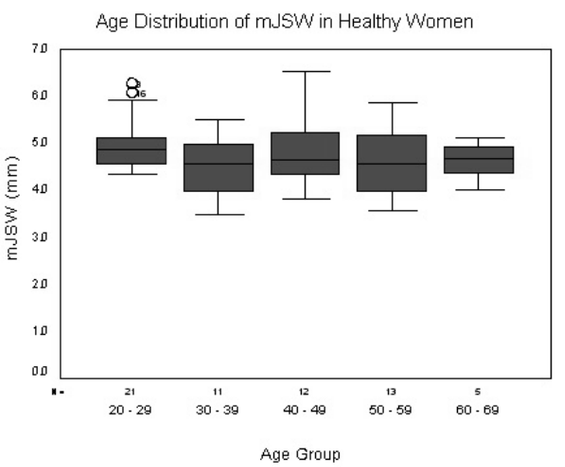

Age distribution in the OA group included 1 aged 30-39, 2 aged 40-49, 9 aged 50-59, 6 aged 60-69, 5 aged 70-79 and 2 aged 80-89. The mean (SD) age was 62.2 (11.7) years and mean (SD) BMI was 28.0 (5.8) kg/m^2. K-L grading yielded 3 grade 0, 4 grade 1, 9 grade 2, 3 grade 3 and 4 grade 4. mJSW decreased significantly as K-L grade increased. Analyses revealed the following mean (SD) mJSWs: 5.75 mm for 30-39, 4.43 (0.28) mm for 40-49, 4.12 (1.22) for 50-59, 3.07 (2.18) mm for 60-69 group, 1.85 (1.83) mm for 70-79 group and 0 mm for 80-89 group.

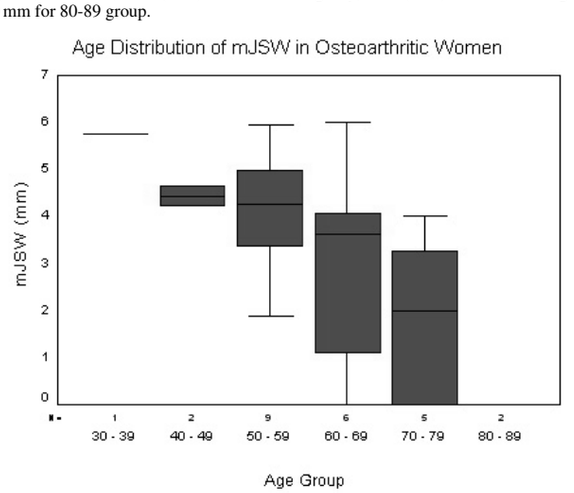

These data suggest that a "normal" range of mJSW for a healthy women lies between 4.55 and 5.00 mm. In OA patients, mJSW decreases with age and these values are smaller than healthy women in the same age group.

Disclosures: ***K.A. Beattie****, None.*

SU023

An Automated High-Resolution Technique for Volumetric Fluorescence Imaging of Large Bone Specimens. G. J. Kazakia*[1], J. J. Lee*[1], T. M. Keaveny[2]. [1]Mechanical Engineering, University of California, Berkeley, CA, USA, [2]Mechanical Engineering & Bioengineering, University of California, Berkeley, CA, USA.

Three-dimensional reconstruction of fluorescent labels is often crucial in the detailed study of biological structures and processes. Currently available techniques for fluorescence imaging cannot provide high-resolution volumetric reconstructions of large specimens. We describe a new system, based on the CNC milling technique, for generating high-resolution, 3D reconstructions of fluorescent signals within bone tissue specimens. This method produces images with resolution independent of specimen size, and with fluorescent signals segmented by emission spectra such that components labeled with different fluorochromes may be visualized individually (a single wavelength band) or as a unit. Biological specimens are stained in bulk with fluorescent dyes to reveal various matrix and cellular components, and are then embedded in an opaque resin. The specimen surface is then milled away at very small increments by a computer-controlled moveable specimen stage and milling machine. After each milling pass, a computer-controlled imaging station excites the exposed fluorochromes and captures the emitted fluorescence through a series of filters chosen specifically for the specimen. Through post-processing the 3D volume is reconstructed, allowing the researcher to visualize the stained components at a very high resolution (on the order of a few microns). To investigate both the qualitative and quantitative capabilities of this fluorescence imaging technique, we imaged damage within an 8 mm x 10 mm cylinder of bovine trabecular bone stained with the chelator xylenol orange. Autofluorescence was exploited to capture the geometry of the bone tissue; a UV excitation filter was coupled with a DAPI emission filter to image bone. Xylenol orange fluorescence was imaged using a TRITC filter set. Two 5x6 arrays of 30 images each were captured for each exposed surface - one array using the UV-DAPI filter set and one using the TRITC filter set. Using a 4x objective an in-plane resolution of 3 microns/pixel was achieved. An out-of-plane resolution of 7 microns was obtained by removing 7 microns of material during each pass of the milling tool. The volume representing xylenol orange-stained regions was superimposed onto the volume representing the bone, and then rendered to create a 3D map of damage throughout the volume. Our volumetric reconstruction of this specimen provides a visual map of the volume of damage present through the entire cylinder. These data also provide quantitative measures of damage distribution, which greatly add to the information derived from traditional 2D analysis.

Disclosures: ***G.J. Kazakia****, None.*

SU024

Structural Characterization of Cortical Bone Microarchitecture on Microcomputed Tomography Images: Correlation with Mechanical Analysis. C. Chappard[1], A. Basillais*[1], S. Bensamoun*[2], B. Brunet-Imbault*[1], M. Ho Ba Tho*[2], G. Lemineur*[3], C. Benhamou[1]. [1]Ipros, Université d'Orléans, Orleans, France, [2]Laboratoire de Biomécanique et Génie Biomédical, Université de Technologie de Compiègne, Compiègne, France, [3]Lesi, Université d'Orléans, Orleans, France.

Microcomputed tomography (µCT) is largely used to analyze trabecular bone. Cortical bone is made of compact bone including a network of pores (canals and resorption spaces). Its porosity is a major parameter conditioning bone strength. The morphological and topological arrangement of this network remains to be evaluated.

Nineteen cortical samples from 3 human femurs were scanned by a µCT (Skyscan ® 1072) with an isotropic 7.81 µm resolution. After reconstruction and thresholding, three dimensional (3D) cortical bone volumes were available. After inversion of the image, the algorithms developed for trabecular bone analysis were applied in order to characterize the network of pores.

The pore volume (BV/TV equivalent) was labelled PoV/TV. PoN (pore number, TbN equivalent) and DA (degree of anisotropy) were measured by the Mean Intercept Length method. PoDm (pore diameter, TbTh equivalent) and PoSp (pore spacing, TbSp equivalent) were derived from the Hildebrand method, PoS/PoV (pore surface on volume, BS/BV equivalent) from triangulation method, and FD (fractal dimension) by box counting analysis. Ultrasound measurements were performed by contact transmission technique to measure longitudinal velocities. Elastic coefficient C_{33} and Young modulus E_{33} were derived from ultrasound measurement at 2.25 MHz and 75 kHz respectively and apparent densities calculated from the ratio of bone mass to bone volume.

The morphological parameters showed a wide range of values especially for the mean CaDm 44 to 493 µm, the lowest values corresponding to Haversian and Volkman canals and the highest to resorption spaces. All the structural parameters were significantly correlated to the mechanical parameters (Spearman coefficients are given in the table below).

The 3D rendered volume revealed the porosity structure in details, and the parametric analyses quantitatively describe the microstructural organization of the porosity. This structural analysis of cortical bone is related to mechanical values. This analysis could bring new and pertinent insight on cortical bone evaluation.

r values	PoV/TV (%)	PoS/PoV (mm^{-1})	PoDm (µm)	PoSp (µm)	PoN (mm^{-1})	DA	FD
C_{33}	-0.94 [a]	0.78 [a]	-0.80 [a]	0.76 [b]	0.88 [a]	-0.53 [b]	0.79 [a]
E_{33}	-0.92 [a]	0.80 [a]	-0.77 [b]	0.74 [b]	-0.86 [a]	-0.54 [b]	0.78 [b]

[a]$p<10^{-4}$, [b]$p<5.10^{-2}$

Disclosures: ***C. Chappard****, None.*

SU025

NanoSIMS as an Analytical Tool for Trace Metal Detection in Bone and Liver from Haemodialysis Patients. J. Denton*[1], F. Hillion*[2], F. Horreard*[2], A. G. Cox*[3]. [1]Osteoarticular Pathology, University of Manchester, Manchester, United Kingdom, [2]CAMECA, Paris, France, [3]University of Sheffield, Centre Analytical Sciences, Sheffield, United Kingdom.

The purpose of this study is to investigate the potential of the NanoSIMS instrument in the identification of metals in bone and soft tissues at an ultrastructural level coupled with high sensitivity to PPB levels. It is the intention of this submission to demonstrate the capabilities of the instrument and not to demonstrate the presence of aluminium in bone as this has been described earlier. The technique of NanoSIMS was developed by CAMECA Paris and the first instrument installed in St Louis USA in 1999. There are 10 instruments in the world to date. The ability to extend the SIMS analysis to extremely small areas or volumes (50 nm beam diameter cesium, 150 nm oxygen) while maintaining extremely high sensitivity at High Mass Resolution is possible. Five masses or elements can be collected simultaneously by the instrument allowing true superimposition of ion maps.

Bone and liver specimens from an end stage renal failure patient treated by haemodialysis and receiving aluminium containing oral phosphate binders and whole blood transfusion were used as test specimens. They were formalin fixed and Araldite embedded. A block 10mm diameter and 100micron thick was taken, polished by diamond abrasion techniques and gold coated.

Using a 200nm diameter primary negative oxygen beam areas 40x40micron were examined by raster mapping.

There was significant deposition of iron and moderate deposition of aluminium in the liver specimen, however there was limited co-localisation of the two metals.

In contrast to the intracellular deposition of the metals in liver the accumulation of the metals in the bone was concentrated in the matrix of bone in a lamellar or banded pattern. The metal accumulation was mainly within bone concentrating at the cement or reversal lines.

The NanoSIMS instrument offers the ability to map ions in mineralised and non-mineralised tissues at extremely low concentrations <1 ppm with a spatial resolution of between 50 (Cs) and 150 nm (O)depending on the ion beam, no other instrument has this capability

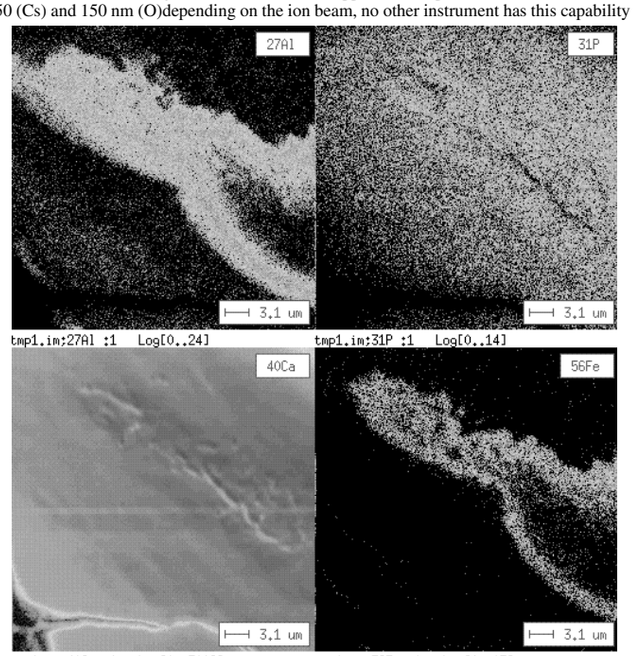

Disclosures: ***J. Denton****, None.*

SU026

Mathematical Modeling of ^{3}H-tetracycline and ^{45}Ca Metabolism as Bone Resorption Markers in Rats. Y. D. Zhao, J. M. K. Cheong*, B. R. Martin, C. M. Weaver. Department of Foods and Nutrition, Purdue University, West lafayette, IN, USA.

Urinary ^{3}H-tetracycline has been used as a bone resorption marker in pre-labeled animals. Changes in urinary ^{3}H-tetracycline are used to evaluate effectiveness of interventions to reduce bone loss. We used mathematical modeling to explore ^{3}H-tetracyline metabolism and to determine bone resorption rates from urinary ^{3}H-tetracycline data. Furthermore, the labeling efficiencies of ^{3}H-tetracyline and ^{45}Ca in cortical and trabecular bones were investigated. In our first study, 4-month-old female rats were injected with ^{3}H-tetracycline intravenously followed by 4-day serum kinetics at 13 time points and 4-day urine and fecal collection. Serum, urinary, fecal, and whole skeletal ^{3}H data revealed two exchangeable compartments (rapid and slow) between serum and bone ^{3}H-tetracycline pools. Using the ^{3}H-tetracylcine transfer rates derived from the modeling we were able to determine the bone resorption rates from urinary ^{3}H data of other rats. In another study, twelve 9-month-old OVX rats were injected subcutaneously with both 50 µCi ^{45}Ca and 20 µCi ^{3}H-tetracycline by single injection or multiple injections (twice a week for 6 weeks). Rats were sacrificed either 1 week or 6 weeks after single injection or after the last dose of multiple injections. Proximal tibia, femur midshaft, lumbar vertebrae (L1-L4), and the remaining skeleton were analyzed for ^{3}H, ^{45}Ca and calcium content. The total skeletal retention of ^{3}H-tetracycline in the multiple injection group (6.19±0.92%) was significantly higher than the single injection group (4.74±0.86%), whereas ^{45}Ca skeletal retention did not differ between the two injection groups. Among the bone sites, the labeling efficiencies (% dose/g Ca) of ^{45}Ca and ^{3}H were significantly higher in proximal tibia than those of femur midshaft. The ratio of ^{45}Ca to ^{3}H in bones varies by bone site, thus indicating that ^{3}H-tetracycline labels the skeleton differently from ^{45}Ca. In conclusion, kinetic modeling of ^{3}H-tetracycline enabled us to quantify the bone resorption rate from urinary ^{3}H-tetracycline data. Trabecular bones were labeled much more efficiently than cortical bones for both ^{45}Ca and ^{3}H.

Disclosures: ***Y.D. Zhao****, None.*

SU027

New Nano-CT Technology Allows Ultrastructural Study of Bone Quality Including Microcracks and Osteocyte Lacunae. P. L. Salmon, A. Y. Sasov. Skyscan, Aartselaar, Belgium.

A nano-CT scanner has been developed which promises new capabilities relevant to the study of bone ultrastructural quality, such as 3d imaging of osteocytes and micro-cracks. The device employs advanced x-ray technologies and new physical phenomena for signal detection. The highest nominal resolution (lowest isotropic voxel size) is about 140 nm, superior to synchrotron tomography. The instrument uses an x-ray source with a spot size of 300-400 nm. At these scanning parameters, small-angle x-ray scattering plays a significant role in the image formation, accentuating structure edges to sharpen image detail (a desirable "artefact") while on the other hand making density measurement based on x-ray absorption less accurate. This is analogous to phase contrast in optical microscopy. Detail detectability is 150-200 nm. An object manipulator allows positioning and rotation with an accuracy of 100 nm, and the intensified CCD x-ray detector has photon-counting sensitivity. Images obtained from the current prototype (figure 1, 530 nm voxel) show clearly osteocyte lacunae and cracks in a mouse fibula. Inspection of cracks in 3d suggests that they may propagate along paths between osteocytes.

Disclosures: ***P.L. Salmon****, Skyscan 3.*

SU028

Evaluation of Mineralization During Fetal Development in the IGF-I Deficient Mouse. A. Burghardt*[1], Y. Wang*[2], H. Z. ElAlieh*[2], X. Thibault*[3], D. D. Bikle[2], F. Peyrin[3], S. Majumdar[1]. [1]Radiology, University of California, San Francisco, San Francisco, CA, USA, [2]University of California, San Francisco and Veterans Affairs Medical Center, San Francisco, CA, USA, [3]ESRF/CREATIS, Grenoble, France.

Insulin-like growth factor I (IGF-I) has previously been established as an important regulator of skeletal metabolism. However the role of IGF-I during embryonic bone development has not been evaluated in detail. Here we investigate the role of IGF-I during embryonic mineral formation in the spinal ossification center and proximal metaphysis of the tibia using the von Kossa stain method and synchrotron based micro-computed tomography (SR μCT).

Lumbar spine and tibia were harvested from 6 IGF-I deficient (IGF-I -/-) mouse embryos (18 days gestational age) along with their wild type controls. SR μCT images were obtained in a 3D parallel beam geometry with an isotropic voxel size of 0.97μm and a 1mm field of view. A two phase model for x-ray attenuation in bone was used to relate the mean bone linear attenuation to mineral density (DMB). Histological sections (5μm) were obtained from a second group of animals and prepared using the standard von Kossa staining procedure.

Von Kossa staining of the proximal metaphysis of the tibia showed a comparable degree of silver nitrate substitution in control and knockout animals. In contrast, virtually no stain precipitation was observed in the lumbar ossification center of knockout animals while controls were found to have considerable staining. Surprisingly, DMB as determined by SR μCT, was found to have only a minor reduction (6.8%, $p < 0.0001$) in the knockout lumbar spine. In the tibia, DMB was determined to be slightly higher (8.2%, $p < 0.001$) in IGF-I -/- animals.

At 18 days, IGF-I deficient embryos were found to have significant material differences from their controls in both the lumbar spine and proximal tibia. However, the degree of differentiation was dependent on anatomic site and method used to assess mineralization. Specifically, we were surprised by the disparity between von Kossa staining and densitometric SR μCT seen in the spinal ossification center. Subtle differences in mineral chemistry or structure during embryonic mineral formation might explain this result. Implications for the interpretation of von Kossa specificity as well as the role of IGF-I during fetal development should be investigated further. Fourier transform infrared imaging and electron microscopy could help characterize the state of calcium phosphate crystallinity in this model. Additionally, experiments at different gestational time points will be an important next step in better understanding the role of IGF-I during fetal development.

Disclosures: ***A. Burghardt****, None.*

SU029

Mineralization in the Mouse Calvarial Cell-seeded Nano-fibrous Scaffolds. K. Woo*[1], J. Jun*[1], V. Chen*[2], J. Baek[1], S. Seo*[1], G. Kim*[1], S. Ko[3], P. X. Ma[4]. [1]Dept. of Craniofacial Cell and Developmental Biology, Seoul National University, College of Dentistry, Seoul, Republic of Korea, [2]Dept. of Biomedical Engineering, Univ. of Michigan, Ann Arbor, MI, USA, [3]Kangnung National University, College of Dentistry, Kangnung, Republic of Korea, [4]Dept. of Biologic and Materials Sciences, Univ. of Michigan, Ann Arbor, MI, USA.

Poly(L-lactic acid) nano-fibrous scaffolds with interconnected pores were developed under the hypothesis that synthetic nano-fibers, mimicking the structure of natural collagen fibers, could create a more favorable microenvironment for cells. In this work, the biological properties of the nano-fibrous scaffolds were evaluated in vitro in terms of the potential use for bone tissue engineering. Under electromicroscopic examination, mouse calvarial cells seeded on nano-fibrous scaffolds were found to connect to each other by forming a network of slender cell processes that were intermingled with the nanofibers of the scaffolds. Biomineralization was enhanced in the nano-fibrous scaffolds as revealed by transmission electromicroscopy and von Kossa staining. Consistent with histological results, the expression of bone sialoprotein transcripts in nano-fibrous scaffolds was much higher than that in solid-walled scaffolds. We inhibited collagen fibril formation by adding 3,5-dehydroproline to culture and examined the expressions of alpha 2 integrin and osteogenic markers in the nano-fibrous scaffolds and control (solid-walled) scaffolds. Nano-fibrous scaffolds supported the expressions of alpha 2 integrin and osteogenic markers (osteocalcin and bone sialoprotein), while the solid-walled scaffolds suppressed the expressions of the alpha 2 integrin and the osteogenic markers. These results indicate that the nano-fibrous architecture serves as superior scaffolding for biomineralization, and suggest that the synthetic nanofibers may function similarly to natural collagen fibers to osteoblasts.

Disclosures: ***J. Jun****, None.*

SU030

Fourier Transformed Infra-red Imaging Spectroscopic Analysis of the Mineral Phase Generated during *in Vitro* Matrix Vesicle Mineralization. R. Garimella[1], N. Camacho*[2], J. Sipe*[1], H. Clarke Anderson[1]. [1]Pathology and Laboratory Medicine, University of Kansas Medical Center, Kansas City, KS, USA, [2]Research Division, Hospital for Special Surgery, New York, NY, USA.

The process of skeletal mineralization is tightly regulated and displays unique spatial relation to the underlying organic matrix. Membrane-bound extracellular matrix vesicles (MVs) play an important role in the *de novo* initiation and propagation of biological mineral in calcifying cartilage, bone, dentin, and in pathologic calcification. Phosphatases of MVs including alkaline phosphatase (ALP), ATPase, 5' AMPase and inorganic pyrophosphatase (PPiase) promote MV-initiated mineralization. Phosphoester substrates such as ATP, AMP and PPi are hydrolyzed by MV phosphatases, thereby increasing the local concentration of orthophosphate (Pi) and thus initiating calcification. Characterization of the phase, composition, and crystal size and perfection provides valuable insight into the mechanism of bone mineral deposition. The hypothesis tested here, was that hydrolysis of AMP or β-GP, monophosphoester substrates of MV-5' AMPase (substrate: AMP) and ALP (substrates: AMP, β-GP), yields orthophosphate (Pi) which leads to the formation of mature crystalline, apatite mineral while the hydrolysis of ATP, a substrate for MV-ALP, ATPase or nucleoside triphosphate pyrophosphohydrolase (NTPPase) leads to the formation of immature mineral and not crystalline hydroxyapatite. MVs were isolated from collagenase-digested rachitic rat growth plate cartilage by differential ultra-centrifugation thus separating MVs from intact chondrocytes and larger cell fragments, e.g. nuclei, mitochondria and lysosomes. *In vitro* calcification was initiated by incubating 30 μg samples of MV protein in a calcifying solution (pH 7.65) containing 2.2 mM Ca^{+2} and 1.6 mM PO_4^{-2}, in the presence of 1 to 3 mM phosphoester substrate, e.g. 1 mM ATP, 3 mM AMP or 3mM β-GP, at 37°C for 5.5h. The calcified MV precipitates were pelleted by centrifugation at 8800g for 30 min. To identify the mineral phase formed, Fourier transform infrared imaging spectroscopy (FT-IRIS) was carried out on 1 μm sections of spurr-embedded MV after exposure to calcifying solution. FT-IRIS showed the presence of a hydroxyapatite-like phase associated with matrix vesicles when AMP or β-GP was used as a phosphatase substrate, while with ATP no identifiable crystalline mineral phase was present. The production of a hydroxyapatite-like mineral phase by the monophosphate substrates of alkaline phosphatase or AMPase supports earlier data indicating a significant role for these monophosphoesterases in biological mineralization.

Disclosures: ***R. Garimella****, None.*

SU031

Evidence for a Serum Factor that Initiates the Re-calcification of Demineralized Bone. P. A. Price, H. H. June*, N. J. Hamlin*, M. K. Williamson. Biology, University of California, La Jolla, CA, USA.

The present studies show for the first time that demineralized bone re-calcifies rapidly when incubated at 37°C in rat serum: Re-calcification can be demonstrated by Alizarin red and von Kossa stains, by depletion of serum calcium, and by uptake of calcium and phosphate by bone matrix. Bone re-calcification does not occur in a carbonate buffer that maintains the ionic milieu of serum, however, which indicates that re-calcification is driven by specific agent(s) in serum.

Re-calcification is specific for the type I collagen matrix structures that were calcified in the original bone, with no evidence for calcification in periosteum or cartilage. Re-calcification ceases when the amount of calcium and phosphate introduced into the bone matrix is comparable to that present in the original bone prior to demineralization, and the re-calcified bone is comparable in weight to the original bone and is palpably hard. Radiographs of fully re-calcified rat tibias are indistinguishable from radiographs of control tibias, and re-calcified bone mineral is comparable to the original bone mineral in calcium to phosphate ratio and in FTIR and XRD spectra.

The serum activity responsible for re-calcification is sufficiently potent that the addition of only 1.5% serum to DMEM causes bone re-calcification. This putative serum calcification factor has an apparent molecular mass of 55 to 150kDa and is inactivated by trypsin or chymotrypsin. The serum calcification factor must act on bone for 12h before re-calcification can be detected by Alizarin red or von Kossa staining, and before the subsequent growth of calcification will occur in the absence of serum. The first observable effect of the serum factor is the formation of numerous, discrete mineral foci within the collagenous bone matrix.

The speed, matrix-type specificity, and extent of the serum-induced re-calcification of demineralized bone suggest that the serum calcification factor identified in these studies may participate in the normal calcification of bone.

Disclosures: ***P.A. Price****, None.*

SU032

Glutamate Signalling Regulates Skeletogenesis and Bone Growth. J. H. Burford[1], D. S. Perrien[2], A. Horner*[1], E. A. Bowe*[1], T. Notomi*[1], L. J. Suva[2], T. M. Skerry[1]. [1]Royal Veterinary College (VBS), London, United Kingdom, [2]Center for Orth. Res., University of Arkansas for Medical Sciences, Little Rock, AR, USA.

Intercellular communication in the bone microenvironment controls cell function, regulating bone mass and strength. Evidence has emerged for a role in this communication for the excitatory amino acid glutamate, acting via cell membrane receptors on osteoblasts, osteoclasts and precursors. Here we show that skeletogenesis and bone growth in vitro and in vivo are regulated by AMPA gated glutamate receptors.

In fetal mouse limb buds, immunocytochemistry was used to demonstrate expression of AMPA receptors in cells within mesenchymal condensations that precede the formation of skeletal elements and in the apical ectodermal ridge. Treatment of explanted limb buds from 10.5 d.p.c fetuses with the non-competitive AMPA type glutamate receptor antagonist CFM-2 led to 70% and 90% inhibition of expression mRNA for the chondrogenic markers Sox-9 and aggrecan respectively. There was no effect on 12.5 d.p.c. explants. In micromass cultures of 10.5 d.p.c limb bud cells, cartilage nodule formation, aggrecan and collagen II expression were significantly inhibited by CFM-2, but at 12.5 d.p.c the same treatment was associated with a significant increased cartilage formation. Similar dose-dependent inhibition was also observed with the competitive AMPA antagonist, NBQX.

CFM-2 treatment of adult murine bone marrow cells cultured under osteogenic conditions was associated with a reduction in colony formation. Similarly siRNA knockdown of the AMPA receptors iGluR2 and iGluR3 of these cells resulted in a 100% and 90% inhibition respectively of AP-positive colony formation.

To test these findings in vivo, two groups of female CD1 mice (bw 22g +/- 2g) received

NBQX (approximately 20ug/kg/h), or saline via subcutaneous osmotic pumps for 9 days. NBQX was chosen on the basis of solubility, and its demonstrated inability to cross the blood-brain barrier.
Micro CT analysis of the proximal tibiae showed a highly significant increase in trabecular thickness (p=0.002), while Bone Surface/Bone Volume (p=0.007), and SMI (p=0.021) were significantly decreased. These data are indicative of thicker, more plate-like metaphyseal trabeculae, with reduced trabecular spacing and improved mechanical competence. BV/TV, trabecular number, and connectivity density were not significantly altered.
These effects demonstrate a direct influence of glutamate mediated signalling on bone cells, rather than effects mediated by the central and peripheral nervous systems. Collectively, these data demonstrate that glutamate regulates skeletogenesis, osteoblast progenitor differentiation and bone formation in vivo.

Disclosures: ***J.H. Burford****, None.*

SU033

Cardiovascular Risk Factors in Osteoporotic Women: Association between Fractures and Aortic Calcifications. G. Rajzbaum*[1], Y. Bézie*[2], M. Chauffert*[3], P. Bréville*[1], F. Roux*[1], M. Safar*[4], J. Blacher*[4]. [1]Rheumatology, Fondation hôpital Saint-Joseph, Paris, France, [2]Pharmacie, Fondation hôpital Saint-Joseph, Paris, France, [3]Biochimie, Fondation hôpital Saint-Joseph, Paris, France, [4]Hôpital Hôtel-Dieu, Paris, France.

Association between aortic calcifications (AC) and osteoporosis has been described but remains controversial. There is no data about the relation between osteoporotic fractures and CV diseases after adjustment on all potential cofounders. Our aim was to examine the multiadjusted relation between previous osteoporotic fractures and abdominal AC, an established CV risk factor.
We investigated correlation between AC, evaluated on lateral lumbar spine X-rays, and osseous parameters in 221 consecutive postmenopausal out patients consulting for osteoporosis between January 2000 and June 2003 in a French general hospital. Multiple linear regression with forward and backward selection of variable was used to assess the independent determinants of AC. Adjusted odds-ratio with Wald confidence intervals were estimated from multiple logistic regression.
Compared with women without AC (n=137), women with AC (n=84) were on the average almost 7-year older (69 $\pm$ 8.8 versus 61.6 $\pm$ 7.8 years ; $p< 10^{-6}$) . They presented a more deleterious CV risk profile : premature menopause (38% versus 24%, $p\leq0.05$), higher dyslipidemia (27 ± 32% vs 20 ± 15% ; p=0.002) and higher pulse pressure (58.3 ± 14.9 mmHg vs 52.9 ± 15.1 mmHg ; p=0.001), and a more severe osteoporosis : increased osteoporotic fractures (49% versus 27% p<0.001), lower lumbar T score and femoral BMD (respectively -2.44 $\pm$ 1.17 versus -2.06 + 1.39 SD, p<0.05, and 0.728 $\pm$ 0.12 versus 0.761 + 0.11 g/cm², p<0.05). Women with AC were smaller (154.2 cm $\pm$ 18.4 versus 158.1 cm $\pm$ 6.3, p<0.05), with a significant height loss (4.28 cm versus 2.27, p<0.001). Free desoxypyridinoline but not cross-laps were higher in women with AC (9.4 $\pm$ 3.73 versus 8.01 $\pm$ 3.14, p<0.05). No difference has been found for the osteoprotegerin concentration (6.45$\pm$3.1 vs 6.9$\pm$2.9 pmol/L, p=0.6). Concerning the AC, adjusted odds-ratio (OR) is 2 for previous osteoporotic fracture (95% IC 1.1-3.6), and 2.4 for the age, for a 1-SD increase (95% IC 1.7-3.4).
In this study, osteoporotic fractures are statistically correlated with the presence of AC, independently of the age and all other cofounders. The relationship between osteoporosis and atherosclerosis has not yet been clarified. Additional research is needed to further characterise the relationship between these two common illnesses of elderly. Prevention strategies would entirely differ.

Disclosures: ***G. Rajzbaum****, None.*

SU034

Up-regulation of Alkaline Phosphatase Activity and Bone Sialoprotein Gene Expression in PC-1 Mutant Periodontal Cells, in vitro. S. Sato[1], M. Kitagawa*[2], M. Miyauchi*[2], B. Foster[1], M. Somerman[1], T. Takata*[2]. [1]Department of Periodontics, University of Washington, Seattle, WA, USA, [2]Department of Oral Maxillofacial Pathobiology, Hiroshima University, Hiroshima, Japan.

Abnormal hypermineralization has been reported in mutant mice exhibiting mutations in genes regulating the level of extracellular pyrophosphate, e.g., plasma cell membrane glycoprotein-1 (PC-1), tissue-nonspecific alkaline phosphatase (TNAP) and the multiple-pass transmembrane protein ankylosis (ANK). However, while most of these studies have focused on cartilage/bone, effects on cells within the periodontal region have only begun to be examined. Teeth obtained from PC-1 mutant mice show a marked increase in cementum thickness on root surfaces of teeth as compared to wild-type. In this study, cultured periodontal cells established from PC-1 and wild-type mice were compared for cell proliferation rate, alkaline phosphatase activity and osteocalcin (OCN) and bone sialoprotein (BSP) gene expression. Primary cultures of PC-1 mutant and congenic wild-type periodontal cells, isolated from 8-week-old mice, were cultured in α-MEM supplemented with 20% FBS. For the cell proliferation assay, cells were plated at a density of 5 x 10^3 cells per well of 24 well-plates, and were counted every two days for 10 days. Alkaline phosphatase activity was determined after 4, 8 and 10 days by a p-nitro phenyl-phosphate method. Osteocalcin (OCN) and bone sialoprotein (BSP) mRNA expression were measured by RT-PCR at day 7. Results demonstrated that PC-1 mutant cells proliferated at a 1.5 fold greater rate when compared with wild type cells and this difference was apparent by day 6, a trend that continued through out the 10 day period. Further, PC-1 cells exhibited markedly higher alkaline phosphatase activity and BSP expression, as compared to wild-type controls. These findings suggest that the PC-1 gene mutation may affect mineralization through alteration of alkaline phosphatase activity and BSP mRNA expression, in addition to altering the phosphate (Pi) and pyrophosphate (PPi) levels. It has been reported that PC-1 mutant mice have decreased levels of extracellular PPi, and alkaline phosphatase hydrolyzes the mineralization inhibitor PPi. Currently, we do not know if phosphate has a direct role in the observed up-regulation of alkaline phosphatase activity and BSP expression, but BSP itself, consider to promote mineralization, may play a role in the enhanced mineralization noted in cementum of PC-1 mutant teeth.

Disclosures: ***S. Sato****, None.*

SU035

Low Phosphate Intake Induces Hypertrophic Chondrocytes Survival and Transdifferentiation in Normocalcemic Rats with Hypophosphatemic Rickets. V. Lascau-Coman*[1], G. Mailhot*[1], F. Moldovan*[2], N. Dion[1], M. Gascon-Barré[1], L. G. Ste-Marie[1]. [1]Hopital Saint-Luc, CHUM Research Centre, Montreal, PQ, Canada, [2]Faculty of Dentistry, Université de Montréal, Montreal, PQ, Canada.

Calcium (Ca) and phosphorus (P) play important roles in endochondral ossification and bone development. It was previously observed that young rats fed a low Ca diet depleted in D (Ca-D-) exhibit growth retardation. However, we showed that young rats fed a D depleted diet but high in Ca (Ca/P ratio: 4/1) developed rickets due to hypophosphatemia which partially inhibited chondrocytes apoptosis and impaired terminal differentiation (J Bone Miner Res 2003; 18 Suppl. 2: S189). In this study, we investigated the effect of dietary P on the fate of hypertrophic chondrocytes (HC) in the growth plate. Ca-D- rats were repleted for 14 days with diets presenting various Ca/P ratios. Three groups were studied with Ca/P ratios of: 4/1 (Ca++); 4/1.5 (P+); 4/3 (P++). Rats paired for age and fed a regular rat chow diet served as controls. In the Ca++ animals, chondrocytes were found in doublets or triplets (clones) in intact lacunae. This zone of clones was separated from the late HCs by a transitional zone with elongated chondrocyte-like cells (ECLC). These findings were not observed in the controls. Using immunohistochemistry, some clones were shown to be in division (expressing PCNA). In addition, some clones showed asymmetric cell division with one cell positive for Tunel while the other expressed type I collagen. Endothelin-1 which has been shown to be involved in the control of proliferation and probably in the differentiation of chondroprogenitors into chondroblasts or osteoblasts, was highly expressed in ECLCs. Safranin O staining demonstrated a loss of proteoglycans in the transitional zone. Goldner's trichrome was suggestive of osteoid tissue surrounding the clones indicating osteoid production by these cells. Compared to the controls, HCs of the Ca++ rats acquired osteogenic potential by switching from a maturational step to cell division and transdifferentiated into bone-forming cells. In the P+ group, partial onset of rickets was demonstrated without clones, while the P++ diet completely prevented the rachitic phenotype and HC division and transdifferentiation. Taken together, these data suggest that dietary P plays a role as an important metabolic mediator that contributes to the modulation of the fate of hypertrophic chondrocytes in the rat growth plate.

Disclosures: ***V. Lascau-Coman****, None.*

SU036

Regeneration of Cartilage Tissue from Bone Marrow Cells using an RWV Bioreactor System. N. Kida*[1], H. Kojima[1], T. Taguchi*[2], J. Tanaka*[2], T. Uemura[1]. [1]ADRC(Age Dimension Research Center), AIST (National Institute of Advanced Industrial Science and Technology), Tsukuba, Ibaraki, Japan, [2]BMC(Biomaterials Center), NIMS(National Institute of Materials Sciences), Tsukuba, Ibaraki, Japan.

Cartilage tissue regeneration attracted much attention not only in bone biologists but also clinicians having interests in treating bone diseases such as osteoarthritis. However, problems such as necrosis of cells due to high-density cell culture and shear stress by gravity have not yet been solved. Thus, we examined an RWV (Rotating Wall Vessel) bioreactor that simulates a micro-gravity environment with low shear stress for cartilage tissue regeneration. An RWV bioreactor generates stress by horizontal rotation of a cylindrical vessel equipped with gas exchange membrane to compensate the effect of gravity, resulting in homogenous cell growth and differentiation without sinking, and cells aggregate and form a three dimensional tissue. In this study, we established a three-dimensional culture technique for construction of large and homogenous cartilage tissues without necrosis by culture of bone marrow mesenchymal stem cells using RWV bioreactor.
Bone marrow cells were collected from rabbit long bones. The cells were cultured for 3 weeks in DMEM with 10% FBS. The cells were subcultured by trypsinization, and resuspended in DMEM supplemented with TGF-beta etc. The cell suspension was seeded in the cylindrical vessel of an RWV reactor, and rotatory culture was performed for 4 weeks. Cartilage function of the cultured tissues was examined by quantitative RT-PCR of aggrecan and type II collagen mRNA, safranin-O staining of paraffin-embedded sections, immunostaining, and measurement of the marker of matured cartilage, ALP activity. In addition, the elastic modulus of the formed cartilage tissue was measured.
Large cell aggregate with a longer diameter of about 1.4 cm was formed by rotatory culture of bone marrow cells in an RWV bioreactor, and the size of aggregates was maintained throughout 4 weeks.
The mRNA expression of aggrecan and type II collagen was detected, and homogenous production of the two proteins was confirmed in whole tissue by immunostaining. The tissue formed a cartilage cavity, differentiated into matured cartilage cells. Furthermore, no necrotic cell was observed in the formed tissue. Large and homogenous three-dimensional cartilage tissues were successfully generated by culture of bone marrow cells in a pseudo micro-gravity environment in an RWV bioreactor.

Disclosures: ***T. Uemura****, None.*

SU037

Distinct Roles of Smad Pathways and p38 Pathways in Cartilage-specific Gene Expression in Synovial Fibroblasts. H. Seto*[1], S. Kamekura*[1], H. Chikuda[1], H. Hiraoka*[1], T. Imamura[2], K. Miyazono[3], H. Oda*[1], H. Kurosawa*[4], K. Nakamura*[1], H. Kawaguchi[1], S. Tanaka[1]. [1]Orthopaedic Surgery, Faculty of Medicine, The University of Tokyo, Tokyo, Japan, [2]Department of Biochemistry, The Cancer Institute of the Japanese Foundation for Cancer Research, Tokyo, Japan, [3]Molecular Pathology, Graduate School of Medicine, The University of Tokyo, Tokyo, Japan, [4]Orthopaedic Surgery, Juntendo university, Tokyo, Japan.

Synovium is a thin tissue, which lines the nonarticular surfaces of diarthrodial joints. There is accumulating evidence that synovial tissues(STs) contain multipotent cells with chondrogenic potential that might be involved in the repair process of articular cartilage defects and therefore might provide a good source for engineering articular cartilage. In the present study, we analyzed downstream cascades of TGF-ß/BMP signaling in synovial fibroblasts (SFs) using the adenovirus vector-mediated gene transduction system. STs were obtained from the knee joints of patients at the time of operation under written informed consents, and SFs were isolated from STs by enzymatic digestion. After 3 - 5 passages, SFs were infected with adenovirus vectors , and chondrogenic phenotypes of the cells were examined by Northern blotting or real time-PCR of chondrocytic marker genes as well as histological staining. Overexpression of constitutively active activin receptor-like kinase 3 ($ALK3^{CA}$) dramatically increased type II collagen and aggrecan expression in SFs, while LacZ or $ALK5^{CA}$ expression had no effects. Chondrogenic differentiation via $ALK3^{CA}$ expression was also observed in SFs subcutaneously transplanted into nude mice. To analyze downstream cascades of ALK3 signaling, we utilized adenovirus vectors carrying either Smad1 to stimulate Smad pathways or constitutively active MKK6 ($MKK6^{CA}$) to activate p38 pathways. Smad1 expression had a synergistic effect on $ALK3^{CA}$, while activation of p38 MAP kinase pathways alone by transduction of $MKK6^{CA}$ accelerated terminal chondrocytic differentiation, leading to type X collagen expression and enhanced mineralization such as positive Alizarin Red staining. Overexpression of Smad1 prevented $MKK6^{CA}$-induced type X collagen expression and maintained type II collagen expression. In model mouse of osteoarthritis, activated p38 expression as well as type X collagen staining was detected in osteochondrophytes and marginal synovial cells. These results suggest that SFs can be differentiated into chondrocytes via ALK3 activation and that stimulating Smad pathways and controlling p38 activation at the proper level can be a good therapeutic strategy for maintaining the healthy joint homeostasis and treating degenerative joint disorders.

Disclosures: ***H. Seto****, None.*

SU038

Effects of Irradiation Therapy on Primary Rat Chondrocytes *In Vitro*. B. S. Margulies*, J. A. Horton*, Y. Wang*, M. J. Allen, T. A. Damron*. Orthopedic Surgery, S.U.N.Y. Upstate Medical University, Syracuse, NY, USA.

Introduction: Radiation therapy in pediatric patients may negatively impact the growth plate resulting in crippling therapy-related growth arrest and deformity. Negative irradiation effects on the growth plate observed in our Sprague-Dawley rat model suggest an acute chondrocyte irradiation sensitivity. The chondrocyte response to specific irradiation doses remains unknown. To address negative radiation therapy effects in the clinically relevant range below 20 Gy, we employed our cell culture model system to evaluate the acute irradiation effects on chondrocyte proliferation and cytotoxicity; while examining terminal differentiation, the induction of apoptosis, alterations in cell synthetic activity, and changes in the expression of PTHrP, PTHrP-receptor, Ihh, collagens II & X, VEGF, FGF 2, TGF-β, Bax and Bcl-2. We hypothesized that irradiation alters growth plate chondrocyte synthetic activity resulting in decreased mineral formation, while preferentially increasing the incidence of terminal differentiation over cell death. **Methods:** Primary rat chondrocytes were exposed to a series of single fraction irradiation doses using a clinical radiotherapy unit. Standard colorometric assays and flow cytometry were used to assess proliferation, cytotoxicity, terminal differentiation and apoptosis. RT-PCR and western blotting were used to demonstrate changes in mRNA and protein expression. **Results:** Radiation therapy reduced cell proliferation and increased cytotoxicity (Fig. 1); while increasing the induction of apoptosis and G_0/G_1 cell cycle arrest (Fig. 2). Irradiation decreased mineralization and expression of collagen II & X (Fig. 3), while increasing the expression of Ihh, TGF-β and FGF 2. **Discussion:** The irradiation doses employed in this study inhibited chondrocyte proliferation and increased cytotoxicity; except at the 1 Gy dose were there was no significant cytotoxicity. Evidence of terminal differenatiation was observed through dose and time dependent increases in alkaline phosphatase, TGF-β, FGF 2, Ihh and G_0/G_1 arrest. Decreases in collagen expression and mineral formation following irradiation suggest an alteration in synthetic activity when compared to the non irradiated chondrocytes and in contrast to the markers of terminal differeniation observed to increase in the irradiated chondrocytes.

Fig. 1

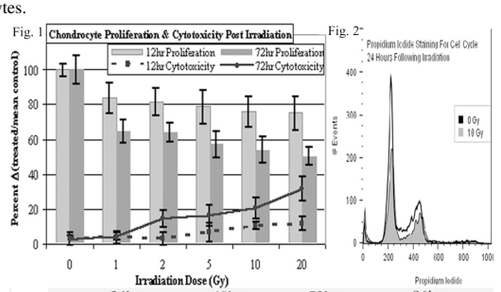

Fig. 2

Disclosures: ***B.S. Margulies****, None.*

SU039

Lack of Indian Hedgehog Disrupts Pre- and Post-natal Development of Murine Craniofacial Skeleton. B. Young*[1], N. Minugh-Purvis*[2], M. Iwamoto*[1], E. Koyama*[1], M. Pacifici[1]. [1]Orthopaedic Surgery, Thomas Jefferson University, Philadelphia, PA, USA, [2]Anatomy and Cell Biology, University of Pennsylvania, Philadelphia, PA, USA.

Incontrovertible evidence shows that Indian hedgehog (Ihh) has major roles in development of long bones, where it regulates chondrocyte proliferation in growth plates and ossification in intramembranous bone collar and endochondral shaft. Surprisingly little is known about potential roles of Ihh in craniofacial skeletal development. Here we carried out an extensive analysis of embryonic and neonatal mice homozygous- or heterozygous-null for Ihh (St. Jacques, et al., 1999), focusing on cranial vault and base. Litter analyses revealed that Ihh-/- embryos were identifiable not only by their dwarf limbs, but also by a foreshortened snout starting around E15.5. Alizarin red/alcian blue staining showed little effect on frontal bones of null embryos, whereas more posterior cranial vault regions showed growth delays. By far, the most dramatic defects were seen in cranial base, a largely endochondral structure. In wild-type E17.5 and E18.5 specimens, spheno-occipital and mid-sphenoidal synchondroses displayed their normal, striking and bipolar organization consisting of back to back growth plates with typical zones of chondrocyte maturation. The cells expressed characteristic molecular markers, including Ihh in pre-hypertrophic zone and collagen X and osteopontin in hypertrophic zone. By E18.5, wild-type synchondroses displayed abundant endochondral bone and marrow, with extensive vascularization. In Ihh-null littermates, the cranial base did form, but the synchondroses were completely disorganized. Presumptive growth plates lacked obvious zones of maturation before E16.5 but displayed collagen X-and osteopontin-positive hypertrophic chondrocytes scattered randomly by E17.5, and failed to undergo endochondral ossification thereafter. In addition, the growth plates were essentially devoid of proliferating chondrocytes, as indicated by histone C4 in situ analyses. Similar analyses of heterozygous Ihh+/- animals showed fairly normal embryonic craniofacial development. However, postnatal follow-up revealed defects in cranial base which became more pronounced with age, consistent with importance of spheno-occipital synchondrosis in postnatal growth. In sum, this is the first report showing that Ihh clearly plays major roles in craniofacial skeletal growth and development, and targets of its direct or indirect action appear to include the largely intramembranous bones of cranial vault as well as endochondral elements of cranial base. Supported by: NIH RO1AR47543.

Disclosures: ***B. Young****, None.*

SU040

Identification of PTHrP Target Genes in Chondrocytes Using cDNA Microarray. J. Hoogendam[1], E. Parlevliet*[1], R. Miclea*[1], C. Löwik[2], J. Wit*[1], M. Karperien[3]. [1]Pediatrics, LUMC, Leiden, Netherlands, [2]Endocrinology, LUMC, Leiden, Netherlands, [3]Pediatrics and Endocrinology, LUMC, Leiden, Netherlands.

Parathyroid Hormone related Peptide (PTHrP) is an essential regulator of the pace of chondrocyte differentiation. To gain more insight into the molecular mechanisms of action of PTHrP, we performed microarray analysis using the chondrogenic ATDC5 cell line to identify PTHrP target genes.

ATDC5 cells were cultured in micromasses to stimulate chondrocyte differentiation. During this process the PTHrP Receptor becomes expressed. The responsiveness of cells to PTHrP increases with differentiation as shown by a dose and time dependent increase in the generation of cAMP after a challenge with PTHrP. At day 8 of culture the cells have deposited an alcian blue positive matrix and express collagen type II and type IX mRNA as well as low levels of collagen type X mRNA. This time point represents cells in the transition zone of the growth plate, the main target cells for PTHrP, and was chosen for identification of PTHrP target genes. ATDC5 cells were stimulated with 10^{-7} M PTHrP, and RNA was extracted at 0h, 1h, 2h, 4h and 8h after stimulation. Samples were reverse transcribed, amplified and labelled with Cy5 and Cy3. All samples were hybridized against 0h in three, four or five fold using competition hybridization on a mouse 15k cDNA array. A list of approximately 50 genes ($p< 10^{-3}$), which were significantly regulated by PTHrP was generated. About 30% of the genes were up- and 70% were downregulated. Cluster analysis identified several patterns of response to PTHrP, including immediate early up- and downregulated genes (peak of regulation between 1-4 hours) and intermediate up- and downregulated genes (peak of regulation at 8 hours). Most of the identified genes were implicated in signal transduction and transcription regulation. Among the targets was RGS2, which was upregulated by PTHrP and is implicated in turning off PTHrP receptor signalling. Among the regulated genes were various proteins known to be involved in regulation of hormonal responsiveness, suggesting that PTHrP may influence the responsiveness of growth plate chondrocytes to hormones like GH and sex steroids.

Disclosures: ***J. Hoogendam****, None.*

SU041

Peroxisome Proliferator Activated Receptor-gamma Represses Thyroid Hormone Signaling in Growth Plate Chondrocytes. L. Wang*, Y. Shao*, R. T. Ballock. Orthopaedic Research Center, Department of Biomedical Engineering, The Cleveland Clinic Foundation, Cleveland, OH, USA.

Peroxisome proliferator activated receptors (PPARs) are DNA-binding nuclear hormone receptors and are upregulated in response to high fat diets. PPARs may compete with thyroid hormone receptors (TRs) for binding to the preferred heterodimerization partner, the retinoid X receptor (RXR). The purpose of this study was to investigate if PPARs are inducible repressors of thyroid hormone signaling in growth plate chondrocytes.

Epiphyseal chondrocytes were isolated from distal femoral growth cartilage of neonatal

rats. Chondrocytes were transiently transfected with a reporter plasmid containing a single copy of a thyroid hormone response element (DR+4) inserted upstream of a thymidine kinase promoter fused to a luciferase cDNA. Overexpression of a PPARγ cDNA or addition of the PPARγ activator ciglitazone each resulted in a decrease in TRα1-mediated transcriptional activation in the presence of T3. These inhibitory effects of PPARγ stimulated by ciglitazone or its endogenous ligands were attenuated by BADGE, an antagonist for PPARγ. Co-transfection of a RXRα expression vector in the growth plate cells partially restored the inhibition of transcriptional activation by PPARγ. The T3-induced increases in alkaline phosphatase activity associated with terminal differentiation of growth plate chondrocytes were suppressed by forced overexpression of a PPARγ cDNA in the cells. Electrophoretic mobility shift assay (EMSA) with nuclear extracts of growth plate chondrocytes demonstrated retarded bands of TR/RXR heterodimers and TR/TR homodimers binding to DR+4 probes. The formation of TR/RXR complexes was disrupted when chondrocytes were transfected with PPARγ plasmid before nuclear protein extraction.
In conclusion, PPARγ activation in growth plate chondrocytes represses TR-mediated gene transcription and inhibits the biological effects of thyroid hormone. This cross-talk between the peroxisome proliferator and T3 signaling pathways most likely occurs via competition for available heterodimeric partner RXRs. These findings may have important implications for development of an obesity-related hip disorder in children known as slipped capital femoral epiphysis.

Disclosures: ***L. Wang****, None.*

SU042

Heparanase Expression in Cartilage: A Novel Regulator of Heparin Binding Growth Factor (HBGF) Delivery. A. J. Brown*[1], C. Kirn-Safran*[1], M. C. Roy*[2], D. Marchetti*[2], M. C. Farach-Carson*[1], D. D. Carson*[1]. [1]Department of Biological Sciences, University of Delaware, Newark, DE, USA, [2]Department of Comparative Biomedical Sciences - SVM, LSU-Baton Rouge, Baton Rouge, LA, USA.

Heparanase, an endoglucuronidase that cleaves heparan sulfate (HS) chains from various proteoglycans, has been identified in a wide variety of tissues. Despite the ability of heparanase to release active heparan sulfate binding growth factors (HBGFs) in various tissues, the role that heparanase plays in chondrogenesis has not been determined. We developed an antibody to a synthetic peptide corresponding to a conserved sequence in mouse and human heparanase. The antibody recognized partially purified heparanase and heparanase in crude cell extracts. The antibody was used to localize heparanase in growth plate and articular cartilage. Following immunohistochemistry, heparanase was predominantly detected in the perichondrium and periosteum and in the growth plate. The location of heparanase in actively growing regions of bone suggests a functional relationship between growth factors such as (basic) fibroblast growth factor-2 (FGF-2) and heparanase. To examine the normal function of heparanase in the growth plate, we have begun to investigate the role of heparanase in HBGF delivery. Western blots, quantitative PCR (Q-PCR) and activity assays were used to monitor changes in heparanase expression and activity during *in vitro* chondrogenic differentiation of mouse ATDC5 cells. Q-PCR showed that heparanase transcript expression is transiently increased 60-fold in maturing chondrocytes. Western blot analysis confirms the presence of heparanase in total protein extracts, but the changes are of lower magnitude than seen by Q-PCR. Heparanase activity assays show robust heparanase activity throughout the differentiation period. Surprisingly, during the mid-point of chondrogenic differentiation in this system (day 15), overall heparanase activity was decreased although protein expression was still evident. The mechanism for this functional decrease has not been elucidated. Collectively, our data indicate that chondrogenic differentiation may be, in part, regulated by changes in heparanase expression and activity. Taken together, our results support the notion that heparanase is a regulated enzyme in the growth plate likely to be involved in HBGF delivery. Perturbing normal patterns of heparanase expression is expected to impact HS-dependent processes during cartilage differentiation.

Disclosures: ***A.J. Brown****, None.*

SU043

Wnt9a BAC Transgenes Drive Reporter Gene Expression in Developing Synovial Joint Articular Cartilage In Vivo. K. J. McDermott*, R. L. Chandler*, D. P. Mortlock*. Molecular Physiology and Biophysics, Vanderbilt University, Nashville, TN, USA.

More insight into the molecular events that regulate synovial joint development could help further the understanding of arthritis etiology, or lead to novel therapeutic approaches to modify cartilage differentiation. Surprisingly, little is known about the molecular regulation of joint development. The Wnt gene family encodes secreted glycoproteins utilized in many developmental processes. In both mouse and chick embryonic limb buds, Wnt9a is expressed in stripes of mesenchyme that mark interzones, the presumptive synovial joint-forming regions. Recently, retroviral expression of Wnt9a was reported to upregulate synovial joint markers in chick, implying a functional role for the Wnt pathway in joint induction. However, the upstream signaling components regulating Wnt9a expression have yet to be identified. To identify Wnt9a cis-regulatory sequences that could interact with key transcription factors or signaling pathways involved in joint specification, we used bacterial "recombineering" to insert LacZ reporter cassettes into Wnt9a bacterial artificial chromosome (BAC) transgenes. The resulting BACs were used to generate transgenic mouse embryos by pronuclear injection. Of the two BAC constructs tested, one clone that contains extensive Wnt9a 3' flanking sequence was able to drive LacZ expression in digit, carpal/tarsal and elbow/knee joints specifically in differentiating articular cartilage at 15.5 days post-coitus and in connective tissue adjacent to tendons. A BAC that carried much less 3' sequence failed to drive digit joint expression, suggesting that some key cis-regulatory sequences required for proper joint expression may lie in the 108 kb genomic region 3' to Wnt9a. Although this segment overlaps at least two adjacent genes, several noncoding stretches in this region are highly conserved across species. rVISTA analysis was used to identify conserved transcription factor binding sites in the Wnt9a BAC sequences. This revealed binding sites for several factors implicated in cartilage patterning, such as Hox, DeltaEF1, Gli, Smad, and Lef/TCF. Our data suggest long-range cis-regulatory sequences may control Wnt9a expression in developing joints. These results demonstrate new joint-specific transgene vectors and indicate Wnt9a BAC constructs should be useful for refining critical Wnt9a cis-regulatory sequences. Also, Wnt9a BACs can be engineered for future experiments that require targeted expression of desired gene products to developing joint cartilage, which will be useful for studies to determine whether Wnt ligand inhibitors (such as Sfrp/Frzb) can regulate interzone formation or differentiation.

Disclosures: ***K.J. McDermott****, None.*

SU044

Chondrogenic, Osteogenic and Adipogenic Differentiation of Pluripotent Adipose-derived Stem Cells from Type II Collagen Promoter-driven GFP Mice. Z. Huang[1], J. Bryan*[1], W. Horton[2], L. Sandell[1]. [1]Orthopaedic Surgery, Washington University, St Louis, MO, USA, [2]Oregon Health Sciences University, Portland, OR, USA.

Pluripotent adult stem cells such as bone marrow-derived stem cells and adipose-derived stem cells have been successfully isolated from human and other large mammals. Due to limited quantity of bone marrow in mice, it is impractical to obtain sufficient quantities of stem cells from mouse bone marrow. The aim of this study is to isolate pluripotent stem cells from mouse fat tissues and verify pluripotency of these adipose-derived stem cells. To expand fat stem cells in vivo, we fed mice with regular diet (9% fat) and high fat diet (42%) for two and half months. Mice were paired by ages from 2 months to 16 months and by gender. Significant weight gains were found in male mice that were placed on high fat diet at the age between 4 and 8 months. Visceral and inguinal fat tissues were excised, minced, and digested with collagenase for 2 hours as 37 °C. After brief centrifugation, cell pellet were resuspended in DMEM medium with 10% fetal bovine serum. After filtered through 70 um cell strainer, cell suspension was then placed in 10 cm dishes overnight. The suspended cells were removed in the following day and fresh medium were added. The attached cells were expanded for two to four passages before used in experiments or frozen down for storage. To test chondrogenic potential of the fat stem cells, cells were cultured in TGF-β containing medium for 28 days. Progression of differentiation was monitored by the appearance of fluorescence of the micro-spheres that were formed and by alcian blue staining. Adipogenic differentiation was induced by a cocktail of reagents including insulin, IBMX, indomethacin and dexamethasone, and was monitored by appearance of oily droplets in the cytoplasm and by oil-red staining. Osteogenic differentiation were induced by a cocktail of reagents including ascorbic acid, β-glycerophosphate, and dexamethasone, and monitored by nodule formation and von Kossa staining. Our data indicate that the cells that we isolated were pluripotent and capable of differentiate into multiple differentiation pathways under inducing reagents. Successful isolation of large amount of mouse stem cells provides a useful tool to explore increasing pools of transgenic mice available.

Disclosures: ***Z. Huang****, None.*

SU045

Intervertebral Disk Degeneration due to Aging and Oxidative Stress. N. Fujita*[1], T. Miyamoto[1], N. Hosogane*[2], M. Yagi*[1], Y. Toyama*[2], T. Suda*[1]. [1]Cell Differentiation, Keio University School of Medicine, Shinjuku, Japan, [2]Orthopaedics, Keio University School of Medicine, Shinjuku, Japan.

Low back pain is one of the most common deseases and constitutes a devastating economic burden on the individual and society. Degeneration of the intervertebral disk (IVD) based on aging is considered as a cause of low back pain, however, the pathophysiologic process of IVD degeneration is still unclear. In this study, we have analyzed the mechanisms of IVD degeneration using rabbit IVD cells. First, to investigate the disk degeneration in 4W, 14W and 160W rabbits, magnetic resonance imaging and histological analysis were performed. The IVD degeneration was obvious in 160W rabbit IVD as observed aged human disk degeneration. The IVD is composed of two distinct tissues: a gelatinous center, known as the nucleus pulposus (NP), and several surrounding lamellae known as the annulus fibrosus (AF). Each cell was separated by blunt dissection and isolated by pronase following collagenase treatment. Subsequently, the number of each AF and NP cell was examined, then RNA was extracted and cDNA was synthesized to analyze the expression pattern of various molecules by RT-PCR. The numbers of both AF and NP cells were reduced in 160W rabbit compared with other young rabbits such as 4W and 14W. The expression of typeI collagen, typeII collagen and aggrecan were also reduced in 160W rabbit, while decorin and lumican were up-regulated. These observations show a characteristic feature of degenerative change in IVD based on aging.
Next, we have examined the effect of oxidative stress as aging stress on the cells from 14W rabbit IVD in vitro whether the radical oxigen stress (ROS) mediate the degenerative changes in cultured cells as observed in vivo. AF cells were isolated from 14W rabbit and cultured for 24 hours with various concentration of hydrogen peroxide. ROS down-regulated the expression of typeIcollagen, typeIIcollagen and aggrecan dose-dependently as observed in aging rabbit and up-regulated the expression of typeX collagen, a marker of terminally differentiated chondrocyte. These results indicate that IVD degeneration based on aging is mediated via ROS. Moreover, we will discuss the possibility of the therapeutic effect of anti-oxidant on the IVD degeneration.

Disclosures: ***N. Fujita****, None.*

SU046

Regeneration of Defects in the Articular Cartilage in Rat Knee Joints by Connective Tissue Growth Factor/Hypertrophic Chondrocyte-Specific Gene Product 24/CCN Family Member 2 (CTGF/Hcs24/CCN2). T. Nishida*[1], S. Kubota*[1], T. Kuboki*[1], K. Nakao*[1], T. Kushibiki*[2], Y. Tabata*[2], M. Takigawa[1]. [1]Biochem. & Mol. Dent., Okayama Univ. Grad. Sch. Med. & Dent., Okayama, Japan, [2]Frontier Medical Sciences, Kyoto University Grad. Sch. Medicine, Kyoto, Japan.

CTGF/Hcs24/CCN2 is a unique growth factor that stimulates the proliferation and differentiation, but not hypertrophy, of articular chondrocytes in vitro. The objective of this study was to investigate the therapeutic use of CTGF/Hcs24/CCN2. The effects of recombinant CTGF/Hcs24/CCN2 (rCTGF/Hcs24/CCN2) on repair of damaged cartilage were evaluated by using both the monoiodoacetic acid (MIA)-induced experimental rat osteoarthritis (OA) model and full-thickness defects of rat articular cartilage in vivo. In the MIA-induced OA model, quantitative real-time reverse-transcription polymerase chain reaction (RT-PCR) assays showed a significant increase in the level of CTGF/Hcs24/CCN2 mRNA; and immunohistochemical analysis and in situ hybridization revealed that the clustered chondrocytes, which clustering indicates an attempt to repair the damaged cartilage, produced CTGF/Hcs24/CCN2. Therefore, CTGF/Hcs24/CCN2 was suspected to play critical roles in cartilage repair. In fact, a single injection of rCTGF/Hcs24/CCN2 incorporated in gelatin hydrogel (rCTGF/Hcs24/CCN2-hydrogel) into the joint cavity of MIA-induced OA model rats repaired their articular cartilage to the extent that it became histologically similar to normal articular cartilage. Next, to examine the effect of rCTGF/Hcs24/CCN2 on the repair of articular cartilage, we created defects (2 mm in diameter) on the surface of articular cartilage in situ and then implanted rCTGF/Hcs24/CCN2-hydrogel or PBS-hydrogel therein with collagen sponge. In the group implanted with rCTGF/Hcs24/CCN2-hydrogel-collagen, new cartilage filled the defect 4 weeks postoperatively. In contrast, only soft tissue repair occurred when the PBS-hydrogel-collagen was implanted. Consistent with these in vivo effects, rCTGF/Hcs24/CCN2 enhanced type II collagen and aggrecan mRNA expression in mouse bone marrow-derived stromal cells, and induced chondrogenesis in vitro. These findings suggest the utility of CTGF/Hcs24/CCN2 in the regeneration of articular cartilage.

Disclosures: ***M. Takigawa****, None.*

SU047

MMP13 Is a Component of the Large Latent TGF-β2 Complex Produced by Hypertrophic Chondrocytes. P. M. Mattioli*, R. K. Scott*, M. D'Angelo. Anatomy, Philadelphia College of Osteopathic Medicine, Philadelphia, PA, USA.

Chondrocytes produce transforming growth factor-beta 2 (TGF-β2) and store it in their matrix in a large latent complex (LLC) that includes latent TGF-β binding protein 1 (LTBP1). Large quantities of activated TGF-β2 are produced as a result of hypertrophy in chondrocytes and MMP-13 is involved in the activation of TGF-β2 from its latent complexes produced by these cells. In this study, our lab has made the novel observation that the LLC for TGF-β2 produced by hypertrophic chondrocytes also includes MMP-13. We isolated resting, early stage hypertrophic and late stage hypertrophic sternal chondrocytes and cultured them in serum-free alginate bead cultures as previously described. Conditioned media was collected at day 8 in culture and cells were extracted with 0.5% 3-([3-chlomadipropyl]dimethylammonio)-1-propane-sulfonate (CHAPS) buffer [10mM Tris, 100mM NaCl, 2mM EDTA, pH7.6]. Western blot analysis with antiserum to MMP-13 produced the previously described 59 kDa band and an additional band at approximately 250 kDa. Antisera to LTBP1 and TGF-β2 revealed the same immunoreactive band at approximately 250kDa, corresponding to the LLC. To further investigate whether MMP-13 is present in the hypertrophic chondrocyte-produced LLC, tibial hypertrophic chondrocytes were isolated from day 19 chicks, extracted and immunoprecipitated with antiserum to LTBP1 and MMP-13 and immunoblotted with antiserum to TGF-β2. These blots contained bands of immunoreactivity corresponding to the 250 kDa LLC, the 60kDa b-LAP N-terminus fragment of TGF-β2 and the 25kDa homodimer of TGF-β2. Furthermore, addition of 2.5ng/ml TGF-β2 to hypertrophic chondrocytes grown in serum-free alginate cultures resulted in an increase in mRNA for tissue transglutaminase and MMP-13 as measured by reverse-transcription polymerase chain reaction. These data suggest that the large latent complex for TGF-β2 produced by hypertrophic chondrocytes may include cross-linked MMP-13. The presence of covalently linked MMP-13 in the large latent complex would point to a novel storage process for TGF-β2 produced by hypertrophic chondrocytes. In addition, association of an activating protease with the LLC produced by these cells, suggests a mechanism to regulate the quantity and timing of activated TGF-β2 released from matrix storage by hypertrophic chondrocytes.

Disclosures: ***M. D'Angelo****, None.*

SU048

Impact of Small Collagen Fragments on Cartilage Cells. S. Oesser*[1], J. Seifert*[2]. [1]Collagen Research Institute, Kiel, Germany, [2]Surgical Research University of Kiel, Kiel, Germany.

The integrity of articular cartilage is dependent on the maintenance of the extracellular matrix (ECM), which is controlled by chondrocytes (Kuettner et al. 1991). Over the past years various degradation products of the ECM have been identified to influence the metabolism of cartilage cells (Huber et al. 2000). The aim of the present study was to investigate the effect of small collagen fragments on the biosynthesis of mature chondrocytes.

For the investigation, a primary cell culture model was used. Porcine chondrocytes were cultured under oxygen reduction and, after a 3-day lag phase, collagen hydrolysate (CH) with a mean MW of 3.3 kDa was supplemented to the culture medium. Type II collagen biosynthesis of the chondrocytes was quantified by means of ELISA technique. Moreover, pericellular proteoglycans were determined by colorimetric assay and immunoassay, respectively. In additional experiments, porcine articular cartilage explants were cultured in the presence of CH and protease activity in the culture media was assayed by gelatin-substrate zymography.

It was shown that the presence of CH in the culture medium led to a significant ($p<0.01$),dose-dependent increase in type II collagen biosynthesis, whereas native collagen and collagen-free hydrolysate failed to stimulate the production of type II collagen in cartilage cells. The amount of pericellular proteoglycans was also significantly ($p<0.05$) increased after CH treatment, indicating that the stimulated cells produce a complete ECM. In contrast, the presence of the CH in the cell medium had no effect on the protease activity of chondrocytes.

These results clearly indicate a stimulatory effect of CH on the type II collagen biosynthesis of chondrocytes and suggest a regulatory mechanism for the regulation of collagen turnover in cartilage tissue. Moreover, the cells seem to synthesize enhanced amounts of a complete ECM after CH treatment. Protease activity was not affected by the administration of such small collagen fragments.

Based on these results CH might be of particular importance for the regulation of chondrocyte metabolism and might help to reduce degenerative alterations in the ECM.

Huber M, Tratting S, Lintner F (2000) Invest Radiol 35, 573-580
Kuettner KE, Adylotte MB, Thonar EJMA (1991) J Rheumatol 18, 46-48

Disclosures: ***S. Oesser****, Gelita Health Initiative 2.*

SU049

FGF Signaling Inhibits Hypertrophic Differentiation of Chondrocytes by Suppressing Expression of the CDK Inhibitor, $p57^{Kip2}$. M. Stewart, Y. Geng*. Veterinary Clinical Medicine, University of Illinois at Urbana-Champaign, Urbana, IL, USA.

Fibroblast growth factor (FGF) signaling inhibits hypertrophic differentiation of chondrocytes *in vitro,* while constitutively activating point mutations of the type 3 FGF receptor are responsible for several inherited chondrodysplasias. The cyclin-dependent kinase inhibitor (CDKI) $p21^{Cip1}$ is up regulated by FGF signaling in chondrocytes and has been implicated in the molecular pathogenesis of the FGFR3-mediated chondrodysplasias. The closely related CDKI, $p57^{Kip2}$ has also been implicated in the regulation of hypertrophic differentiation. Both *in vitro* and murine gene deletion studies suggest that p57 is required for collagen type X (Coll X) expression by differentiating chondrocytes. This study was carried out to determine whether FGF signaling influences p57 expression in chondrocytes undergoing hypertrophic differentiation.

Prehypertrophic chondrocytes were collected from the distal femoral epiphyses of neonatal rat pups and isolated by sequential trypsin/EDTA and collagenase digestion. Isolated chondrocytes were cultured as non-adherent aggregates in defined, serum-free medium supplemented with ascorbic acid and antibiotics. Hypertrophic differentiation, induced by 100 ng rhBMP-2/ml, was monitored by expression of Coll X and alkaline phosphatase (ALP), and by ALP bioactivity. FGF-2 and FGF-18 were administered at 10 ng/ml. Gene expression was assessed by Northern and Western blot analyses. Adenoviral vectors were used to exogenously express p57 and p21.

Both FGF-2 and FGF-18 inhibited Coll X and ALP expression in epiphyseal chondrocytes with near-equal potency. Inhibition persisted despite co- or pre-treatment with BMP-2. Concurrently, FGFs suppressed p57 mRNA and protein expression to below-detectable levels. In contrast, both FGFs and BMP-2 up regulated p21 expression. Exogenous adenoviral p57 expression dose-dependently antagonized the effects of FGF on expression of ALP and Coll X in differentiating chondrocytes, whereas parallel expression of p21 had no such effect.

This study demonstrates that FGF signaling inhibits p57 expression in differentiating chondrocytes. This suppression is functionally significant since exogenous expression of p57 abrogates the inhibitory effects of FGF on expression of Coll X and ALP, both markers of the hypertrophic phenotype. These findings are of direct relevance to the molecular basis of the FGFR3-linked chondrodysplasias and suggest a novel mechanism by which excessive FGF signaling, through constitutive receptor activity, interferes with normal chondrocyte differentiation and associated skeletal growth.

Disclosures: ***M. Stewart****, None.*

SU050

***Ror2^{W749X}*, a Mutation Carried by Brachydactyly B Patients, Causes Brachydactyly in the Mouse and Altered Early Cartilage Development.** R. Raz[1], E. Gazzerro[2], J. L. Clor*[1], H. Nistala*[1], R. C. Pereira[2], L. Stadmeyer*[2], X. Wang*[1], W. T. Poueymirou*[1], T. M. DeChiara*[1], G. D. Yancopoulos*[1], E. Canalis[2], D. M. Valenzuela*[1], A. N. Economides[1]. [1]Regeneron Pharmaceuticals, Tarrytown, NY, USA, [2]Department of Research, Saint Francis Hospital and Medical Center, Hartford, CT, USA.

Mutations in *ror2*, a gene encoding a transmembrane tyrosine kinase (TK) related to MuSK and Trk receptors, can cause two different human disorders: recessive Robinow syndrome (RRS), a mesomelic short-limbed dwarfism, and brachydactyly B (BDB). BDB, associated with dominant mutations, is characterized by short or absent middle and terminal phalanges. To examine the molecular mechanisms underlying the two phenotypes associated with dominant and recessive mutations in *ror2*, we generated *knock-in* mice expressing a W749X mutation, predicted to remove the distal Ser-Thr- and Pro-rich domains of ROR2 and found in severe BDB cases.

In contrast to humans, $ror2^{W749X}$ has no effect in heterozygosis in the mouse and causes in homozygosis a mild skeletal phenotype reminiscent to that of $ror2^{V487lacZ/V487lacZ}$, in which the TK domain is also eliminated. Both mutations result in missing middle phalanges, indicating that the TK domain of ROR2 is not sufficient for normal phalanx specification. $Ror2^{W749X/W749X}$ mice are viable, although males exhibit variable degrees of infertility and

germ cell deficiency. Mutant testes can have up to 40% reduction in size, and display focal areas of tubular degeneration.

Ror2$^{W749X/W749X}$ mice exhibit delayed specification and decreased length of all cartilage anlagens, detectable at embryonic day 13, which result in limb shortening, brachyrrhiny and reduced spine length. Despite a delay in the onset of bone development, growth plate architecture is normal and there is no change in the proliferation of growth plate chondrocytes, suggesting that the bone length phenotype stems from defects in early cartilage specification. Confirming that the effects of ROR2 are specific to bone development, bone mineral density measurements and static and dynamic histomorphometry of post-natal and adult femurs do not reveal any abnormality in the mutants. Overall, the phenotype of *ror2*^{W749X} is markedly less severe than that of *ror2*^{V487lacZ}, indicating that the TK domain is an essential mediator of ROR2 function in proliferating chondrocytes. The Ser-Thr- and Pro-rich carboxy-terminal domain of ROR2 may be required for specification of the middle phalanx and for maintenance of spermatogenesis.

Disclosures: ***R. Raz****, Regeneron Pharmaceuticals 1, 3.*

SU051

Spring Growth in the Vertebrae of Atlantic Salmon (*Salmo salar*) Is Characterized by a Gradual Increase in *ihh* Expression, while a Certain Photoperiod Triggers *shh* Induction. A. S. Wargelius*, U. Nordgarden*, P. Fjelldal*, A. Berg*, T. Hansen*. Institute of Marine Research, Bergen, Norway.

Vertebral column defects are a common problem in salmon aquaculture. To acquire better understanding for how these defects are induced we studied natural and light simulated spring growth in the adult vertebral column. Osteoblast activity was measured following gene expression of proteins involved in bone morphogenesis namely Sonic hedgehog (Shh), Indian hedgehog (Ihh) and Collagen I (ColI). While hedgehog signalling is involved in osteoblast recruitment and differentiation, ColI is a bone matrix protein representing mature osteoblasts. Gene expression was monitored during a growth activation phase from January- to June 2003 in postsmolt Atlantic salmon, where one fish group was kept under constant light (LL) while another group was kept under natural light (NL). The vertebral bodies (n=10) were measured at three time points (Jan, Apr and Jun.) and the size increased with about 55% (length) and 65%(width). The LL group increased 10% more in size compared to the NL group from April-June. To monitor gene expression, vertebrae 40 was sampled monthly from January-June (n=6 group) and expressional level of *shh*, *ihh* and *colI* was measured at each time point. The expression of *ihh* gradually increased throughout the growth phase while the *ihh* expression in June was 8 times higher compared to that of January. Shh expression was induced in February (NL) and March (LL) after which the expression stayed high throughout the experiment. Interestingly, fish exposed to NL have a peak expression of *shh* in February while LL fish lack this expressional peak. Col I expression was essentially at the same level throughout the season, which indicates that osteoblasts produce a constant level of Collagen I. However, since bone volume significantly increased the expressional induction of *shh*, *ihh* may reflect osteoblast recruitment rather than an increased matrix production by individual osteoblasts. In conclusion expression of *shh* and *ihh* is significantly induced during natural bone growth. In addition *shh* expression was triggered by photoperiod in the beginning of the growth phase, however, the biological significance of this photoperiodic induction needs to be further investigated.

Disclosures: ***A.S. Wargelius****, None.*

SU052

Up-regulation of Bone Morphogenetic Protein Receptors Induced by Hepatocyte Growth Factor in the Early Phase of Fracture Repair. Y. Imai*[1], H. Terai*[1], C. Nomura-Furuwatari*[1], K. Matsumoto*[2], T. Nakamura*[2], K. Takaoka[1]. [1]Orthopaedic Surgery, Osaka City University Graduate Shool of Medicine, Osaka, Japan, [2]Division of Biochemistry, Department of Oncology, Biomedical Research Center B7, Osaka University Graduate School of Medicine, Osaka, Japan.

Introduction: The precise mechanisms of the up-regulation of the BMP, BMPRs or other molecules involved in the bone repair remain to be elucidated. In this study, we investigated effects of HGF to facilitate the BMP action through potential local induction of BMP or BMPRs by HGF which could be activated through thrombin-mediated activation of HGF activator (HGFA).

Materials and Methods: Fracture models of ICR mice tibia were produced. Samples were harvested for real time RT-PCR of HGF and BMPRs, for immunohistochemistry of c-Met (receptor for HGF) and for situ hybridization of BMPRs. To investigate the changes in expressions of BMPRs in response to HGF, C3H10T1/2 cells were cultured with or without recombinant human HGF and harvested for real time RT-PCR of BMP4 and BMPRs and for western blot analysis. To detect the contributions of HGF to biological action of BMP2, cells were pre-cultured with rhHGF, then cultured recombinant human BMP2. And alkaline phosphatase (ALP) activity and expression of luciferase gene linked to *Id1* promoter containing BMP responsive element were assayed.

Results: Positive immuno-staining of c-Met and elevation of HGF mRNA expression in the early phase of fracture repair indicated indirect evidence of activation of HGF at the fracture site. Messenger-RNA expressions of BMPRs were increased at day 1 after fracture and were localized in mesenchymal cells at the fracture site. On real time RT-PCR, the expressions of mRNA of BMPRs were elevated by treatment with HGF, but the expression of BMP4 was not altered. Western blot analysis also showed the BMPR2 up-regulation by HGF treatment. The results from luciferase and ALP assays indicated increased responsiveness to BMPs in the group treated by HGF.

Conclusion: This study indicated that HGF was activated and expressed in the fracture site and induced up-regulation of BMPRs in mesenchymal cells and subsequently might facilitate BMP signaling without affecting expression of BMP molecules.

Disclosures: ***Y. Imai****, None.*

SU053

Retroviral Infection of Osteoactivin Induces Osteoblast Differentiation and Function. M. C. Rico[1], M. P. Hurley*[1], E. Nuglozeh*[1], T. A. Owen[2], S. N. Popoff[1], F. F. Safadi[1]. [1]Anatomy and Cell Biology, Temple University School of Medicine, Philadelphia, PA, USA, [2]Pfizer Global Research and Development, Groton, CT, USA.

Osteoactivin (OA) is a novel protein expressed by osteoblasts and plays an important role in osteoblast differentiation and bone formation. Previously, our laboratory demonstrated that primary osteoblast cultures treated with OA antisense oligonucleotide exhibited a dramatic decrease in their differentiation. In this study, we utilized a retroviral system to over-express osteoactivin protein in osteoblasts. Retroviruses produced by co-transfection of a packaging retroviral vector pCL-10A1 (IMGENEX®) and a mammalian expression vector (pBabe) provide an effective mechanism to transiently and stably introduce cDNA into dividing cells. These viral particles were used to generate large recombinant retrovirus titers by co-transfection of pCL-10A1 and OA/pBabe in a 293 packaging cell line using a $CaCl_2$ method. A construct containing an osteoactivin DNA insert (1.4 Kb) was ligated into a BamH1 site in the multiple cloning region of the mammalian expression vector pBabe (5.4 Kb). Control retrovirus was produced by co-transfecting 293 cells with the pCL-10A1 and pBabe. We transiently infected the mouse osteoblast cell line, MC3T3-E1, with the media obtained from the 293 cells. Osteoactivin protein was over-expressed (4-fold) in MC3T3-E1 cells infected with OA/pBabe when compared to control cells infected with pBabe as determined by Western blot analysis. MC3T3-E1 cells infected with OA/pBabe showed a significant (2-fold) increase in nodule formation when compared to control cells infected with pBabe. Matrix mineralization, assessed by calcium deposition into the cell-matrix layer, was significantly increased in OA/pBabe infected MC3T3-E1 cells when compared to control cells infected with pBabe. These results confirm an important role of osteoactivin in osteoblast differentiation and function. Future studies will evaluate the potential clinical uses of osteoactivin in the treatment of bone diseases where increased osteoblast differentiation and bone formation are desired.

Disclosures: ***M.C. Rico****, None.*

SU054

TRAP Regulates Expression of Osteocalcin and Osteopontin in Cementoblasts, *in Vitro*. E. C. Swanson*[1], B. L. Foster*[1], M. L. Snead[2], M. L. Paine*[2], C. W. Gibson*[3], M. J. Somerman[1]. [1]Department of Periodontics, University of Washington School of Dentistry, Seattle, WA, USA, [2]Center for Craniofacial Molecular Biology, University of Southern California School of Dentistry, Los Angeles, CA, USA, [3]Department of Anatomy and Cell Biology, University of Pennsylvania School of Dental Medicine, Philadelphia, PA, USA.

Recent studies provide evidence that, in addition to their important role in the formation of enamel, amelogenins also act as signaling molecules during formation of dentin and cementum. Moreover, certain mutations in amelogenin protein sequence associated with mineral defects in human enamel have been reported. These single amino acid changes can be found in the tyrosine-rich amelogenin peptide (TRAP), a specific proteolytic cleavage product of the amelogenin N-terminus. This study focused on the role of TRAP and mutated forms of TRAP in regulating cementoblast gene expression in vitro. Two amelogenin TRAP peptides were selected because they are known to be found in patients affected with amelogenesis imperfecta (AI): (a) a single amino acid change that results in Thr^{21} to Ile (T^{21}TRAP) and (b) a protein engineered double amino acid substitution that results in Thr^{21} to Ile and Pro^{41} to Thr change ($T^{21}P^{41}$TRAP).

Clonal populations of immortalized murine cementoblasts (OCCM) were exposed in vitro to wild-type TRAP (wtTRAP), T^{21}TRAP, or $T^{21}P^{41}$TRAP at doses of 0.1, 1, and 10 μg/mL. Total RNA was isolated at 1, 6, 12, and 24 hours after treatment. Quantitative RT-PCR was used to evaluate change in transcripts for osteocalcin (OCN) and osteopontin (OPN).

It was shown that wtTRAP, T^{21}TRAP, and $T^{21}P^{41}$TRAP down-regulated OCN and up-regulated OPN in a time- and dose-dependent fashion. The aforementioned changes of OCN and OPN transcripts can be detected as early as 6 hours after treatment with proteins. After 24 hours of treatment at the highest concentration (10 μg/mL), OCN was down-regulated by wtTRAP (50%), T^{21}TRAP (85%) and $T^{21}P^{41}$TRAP (70%). Conversely, OPN was up-regulated after 24 hours of treatment by wtTRAP (60%), T^{21}TRAP (200%) and $T^{21}P^{41}$TRAP (150%) when compared to vehicle-treated controls.

TRAP appears to have a direct effect on genes associated with cementoblast function, where the cementoblasts seem to be more responsive to the mutated forms of TRAP. Interestingly in earlier studies, leucine-rich amelogenin peptide (LRAP), which has the first 33 amino acid residues in common with TRAP, was shown to regulate cementoblast gene expression in the same fashion, suggesting that the N-terminus is critical for the signaling events in cementoblasts.

Disclosures: ***E.C. Swanson****, None.*

SU055

Identification of a New Immunoglobulin-like Domain Containing Protein in Bone. Y. Jung*[1], M. Han*[1], J. Jeong*[1], M. Jung*[1], S. Kim*[2], H. Shin[3], S. Kim[3], T. Kwon*[1], I. Kim*[1], J. Choi[1]. [1]Dept.of Biochemistry, Kyungpook Natl. Univ. School of Medicine, Daegu, Republic of Korea, [2]Dept.of Oral and Maxillofacial Surgery, Hallym University, Sacred Heart Hospital, Kyoungkido, Republic of Korea, [3]Skeletal Diseases Genome Research Center, Daegu, Republic of Korea.

We identified a new immunoglobulin (Ig)-like domain containing gene from human chondrosarcoma cell line, HCS-2/8 cDNA library EST database and cloned its full-length cDNAs from both human and mouse chondrocytes HCS-2/8 and ATDC5 cells, respectively. Mouse gene is located in chromosome 4, and consists of 10 exons. We analyzed the structure and domain composition of this protein after in silico translation, and it belongs to Ig superfamily and composed of 442 amino acid residues which containing two Ig-like loops, one transmembrane region and relatively short cytoplasmic tail of 80 amino acid residues. It also has PDZ-domain binding motif in the end of cytoplasmic tail. In multi-alignment analysis, it is similar to CTX family proteins especially in two Ig domains and transmembrane region. This protein is ubiquitously expressed in various tissues including in brain, kidney, liver, cartilage and bone. Originally, the EST clone has been known as adipocyte specific protein 3 without functional study. Based on structural characteristics and its expression pattern, we called it as dual IgG domain containing cell adhesion family molecule (DICAM). The expression of DICAM was increased during chondrocytes and osteoblasts differentiation in ATDC5 and MC3T3-E1 cell culture systems, respectively. In immunohistochemical staining, DICAM was detected in chondrocytes and osteoblasts of growth plates. These results indicate that DICAM is one of Ig-like domain containing molecules which express in chondrocytes and osteoblasts.

Disclosures: ***J. Choi****, None.*

SU056

Whole Genome Expression Profiling of Fracture Healing Under Rigorous Experimental Design Reveals Novel Pathways: Pleiotrophin and Meox2 in Fracture Healing. C. H. Rundle[1], H. Wang[2], H. Yu*[1], R. B. Chadwick*[1], J. Tesfai*[1], K. H. W. Lau[1], S. Mohan[1], J. T. Ryaby[2], D. J. Baylink[1]. [1]Mdc, J.L. Pettis VAMC, Loma Linda, CA, USA, [2]Research, Orthologic Corporation, Phoenix, AZ, USA.

To better understand the molecular mechanism of fracture healing, we performed whole genome expression profiling by applying rigorous control design to the Agilent low-input labeling system and the large 20K rat oligomer microarray chip. This approach applied the stabilizing K-wire to fractured and unfractured control femurs to: 1) control for bone formation produced by the K-wire in the marrow, and 2) ablate the marrow equally in fractures and controls. The low-input system allowed us to use the low RNA recoveries and avoided pooling samples that can conceal individual variations. RNA was obtained from Sprague-Dawley femur diaphyses at 3 days (n=5), the inflammation and intramembranous bone formation stages, and at 11 days (n=4), the endochondral bone formation stage.

Cluster analysis identified 3398 genes with significant changes in expression ($p<0.05$), 33% of which were unidentified. A large number of Gene Ontology categories were represented, including cell growth/maintenance, apoptosis, adhesion, development, neurogenesis, transcription factors and angiogenesis. In agreement with previous studies, several growth factor gene families were represented, including the IGF1 ($p<0.004$), TGFB ($p<0.027$), FGF ($p<0.016$) and PDGF ($p<0.002$) families. Our study revealed fewer inflammatory and erythrocyte-related genes than previous studies, probably because we minimized the marrow RNA. Genes not previously described in fracture healing were also identified. Meox2, a homeobox gene expressed during embryonic chondrocyte differentiation, was up-regulated 2-fold at 3 days, suggesting that bone repair can indeed recapitulate development. Pleiotrophin was up-regulated 2-fold at 3 days, and possible pleiotrophin pathway genes (PIP3, Akt, ILK, paxillin and Rac/cdc42) were up-regulated at 3 and 11 days. Pleiotrophin shares several genes with the VEGFR3 pathway, suggesting that fracture angiogenesis is initiated early. As a modulator of neurogenic, osteogenic and angiogenic processes, pleiotrophin could also coordinate repair. In conclusion: 1) using a 20K gene chip and controls that normalized marrow RNA input among multiple replicates at two healing times, we identified 3398 genes with significant changes in expression in fracture tissue; 2) two new fracture healing pathways (pleiotrophin and Meox2) were discovered, with one (pleiotrophin) interfacing with a VEGFR pathway. Characterization of such gene expression pathways should facilitate the molecular understanding of normal and impaired fracture repair.

Disclosures: ***C.H. Rundle****, None.*

SU057

Transcriptional Activation of Collagenase-3 by PTH: Changes in Chromatin Structure in the Proximal Promoter Region. C. E. Boumah*, N. Selvamurugan, N. C. Partridge. Physiology and Biophysics, University of Medicine and Dentistry of NJ, Robert Wood Johnson Medical School, Piscataway, NJ, USA.

PTH induces collagenase-3 gene transcription in the rat osteoblastic cell line, UMR 106-01, through the protein kinase A pathway and is a secondary effect. The minimal promoter region for PTH responsiveness, identified in the first 148 bp upstream of the transcription start site, contains a conserved AP-1 binding site (-51/-44) as well as a runt domain (RD) binding site (-135/-129). Here, we have investigated the chromatin structure of the collagenase-3 gene and how PTH alters this to induce transcription. Using high resolution indirect end labeling of DNase I digested chromatin, we have mapped DNase I hypersensitive sites (DHS) at three locations in the proximal promoter region: one with very strong hybridization intensity, at -10/-2, a second DHS was found in a small AT-rich section at -166/-154 and the third DHS, of much weaker intensity, was found at -200/-191. PTH (10^{-8}M) activation, however, had no effect on the location of the DHS but rather caused significant increases in signal intensities. These data suggest that the proximal promoter of the collagenase-3 gene in UMR cells exists in a nucleosome structure between -154 and -10. Next, histone acetylation status was monitored using chromatin immunoprecipitation (ChIP) assays combined with quantitative real-time PCR. Two to 3-fold increases in amounts of acetylated histone H4 associated with the proximal promoter, specifically around the RD binding site (-176/-68), were detected as early as 5 min after PTH addition; maximal changes (20-fold) were reached by 60 min. There were no PTH-induced changes in acetylated histone H4 levels in the proximal promoter region containing the AP-1 site, in the distal promoter region (-1237/-970) or within exon 10. We detected no changes in acetylated histone H3 levels until after 120 min of PTH treatment and these were uniform throughout the proximal promoter region. Endogenous histone acetyl transferase (HAT) activity was elevated in UMR 106-01 cell lysates; treatment with PTH caused rapid and transient increases in HAT activity: high within 15 min, remaining so until approximately 60 min but returning to control levels by 90 min. We propose that PTH induces transcription of the collagenase-3 gene by altering the nucleosome structure of its proximal promoter, first by stimulating HAT activity, secondly by initiating histone H4 acetylation at the RD site, thirdly, by increasing histone H3 acetylation throughout the proximal promoter.

Disclosures: ***C.E. Boumah****, None.*

SU058

Soy Isoflavones May Increase Bone Formation as Seen by Enhanced Osteoblast-Specific Gene Products in Ovariectomized Rat Model of Postmenopausal Osteoporosis. L. Devareddy*, D. Y. Soung, D. A. Khalil, E. A. Lucas, B. J. Smith, A. B. Arquitt*, B. H. Arjmandi. Nutritional Sciences Department, Oklahoma State University, Stillwater, OK, USA.

It is generally believed that soy and its isoflavones improve bone mass, in part, by stimulating bone formation. The aim of the present study was to evaluate the effect of isoflavones on osteoblast-specific gene products including collagen type I, COL: osteocalcin, OC; osteonectin, ON; osteopontin, OP; and alkaline phosphatase, ALP. Sixty 9-month old female Sprague-Dawley rats were either sham-operated (Sham; 1 group) or ovariectomized (Ovx; 5 groups) and fed a semi-purified casein-based diet. After 90 days the occurrence of bone loss was confirmed using dual energy x-ray absorptiometry. Thereafter, rats were assigned to following treatments: Sham, Ovx (control), Ovx + 17β-estradiol (E_2; 10 μg E_2/kg body wt. twice per wk), Ovx + soy protein with normal isoflavone content (Soy; 3.55 mg isoflavones/g protein), and Ovx + soy protein enriched isoflavones (Soy+; 7.10 mg isoflavones/g protein). After 125 days of treatment, rats were sacrificed and bone specimens were collected. Total RNA was extracted from distal femurs and Northern blot analysis was used to measure mRNA levels of interest. cDNA of 18S ribosomal RNA was used as an internal control to normalize gene expression. Data are presented below:

	Sham	Ovx	Soy	Soy+	E_2
AP	0.676 ± 0.120^{c}	0.9247 ± 0.120^{abc}	0.8675 ± 0.120^{bc}	1.239 ± 0.120^{a}	1.133 ± 0.138^{ab}
COL (4.7kb)	0.421 ± 0.065^{b}	0.472 ± 0.065^{b}	0.507 ± 0.065^{b}	0.729 ± 0.065^{a}	0.546 ± 0.065^{ab}
COL (5.7kb)	0.301 ± 0.046^{b}	0.334 ± 0.046^{b}	0.355 ± 0.046^{b}	0.548 ± 0.046^{a}	0.373 ± 0.046^{b}
OC	0.468 ± 0.107^{c}	1.0687 ± 0.107^{ab}	0.958 ± 0.107^{b}	1.320 ± 0.107^{a}	0.601 ± 0.107^{c}
ON	0.596 ± 0.116^{c}	1.008 ± 0.116^{ab}	0.982 ± 0.116^{ab}	1.313 ± 0.116^{a}	0.782 ± 0.116^{bc}
OP	0.799±0.108	0.967±0.108	1.036±0.108	1.147±0.108	0.881±0.108

Data are means ± SE (n=4). Values in a row that do not share the same superscript letters are significantly (P<0.05) different.

The results of our study demonstrate that soy isoflavones may enhance the synthesis of bone matrix proteins and osteoblast activity as indicated by high mRNA levels of osteoblast-specific gene products. Since we have shown that soy isoflavones increase both circulating and bone levels of insulin-like growth factor-1 (IGF-1), we speculate that this upregulation of gene expression is, in part, mediated through IGF-1-dependent pathway.

Disclosures: ***E.A. Lucas****, None.*

SU059

Gene Expression Within Discrete Compartments in the Growth Plate Using Microarray Analysis. S. Nishimori[1], N. Elmessadi*[2], J. F. Burke*[2], D. Park*[2], G. F. Short*[2], H. M. Kronenberg[1]. [1]Endocrine Unit, MGH, Boston, MA, USA, [2]Microarray Facility, MGH, Boston, MA, USA.

To investigate the molecular underpinnings of the conversion of round chondrocytes to flat columnar and then hypertrophic chondrocytes, microarray analysis provides a powerful tool. We attempted manual microdissection of fresh-frozen tissues under an inverted microscope rather than Laser Capture Microdissection, to obtain as much RNA as possible. After isolating the tibiae of newborn mice, we compared three different treatments: quick freezing, freezing after Zincfix (Scheidl et al. 2002.*Am. J. Pathol.*) treatment, or freezing after RNAlater™ (Qiagen) treatment. Thick cryo-sections of proximal tibiae were used to dissect cells from the three distinct chondrocyte layers, and total RNA was isolated. The Bioanalyzer (Agilent) showed total RNAs with little degradation with the first two methods. We extracted 1.7-2.1 μg of total RNA from 115-147 sections from each layer by the quick freezing method.

We compared conventional RNA amplification of mouse liver and kidney total RNAs, using a T7dT primer (Eberwine et al, 1992.*PNAS*) with a new protocol using T3N9 random primers (Xiang et al, 2003. *Nucleic Acids Res*). We obtained sufficient antisense RNA (aRNA) with one round of the T3N9 protocol (from 1 μg to 56 μg). We evaluated both pro-

tocols by comparing the order of the genes expressed more in one tissue than another using both unamplified and amplified RNA. We evaluated the number of genes not detected at all and measures of slide quality (signal-to-noise ratio and % of detected genes), using two different amounts of aRNA (2 or 5 μg) on an oligo array (15,500 murine genes). The T3N9 protocol and higher amounts of aRNA yielded a higher gene matching ratio and a lower number of missing genes, but with higher backgrounds than ideal.
After optimizing microarray conditions to reduce backgrounds, we screened the genes differentially expressed in round vs. hypertrophic layer, using 8 μg of T3N9-amplified RNA. 221 genes were specific to the hypertrophic layer (fold ratio>2.0), and 211 genes were specific to the round layer (fold ratio<0.5). Success in separating the cell layers was suggested by the identification of genes known to be enriched in the hypertrophic layer, such as Type X collagen (fold ratio 0.06), Mmp13(0.14), Spp1(0.16), Alkphos 2(0.27), TGF-β1 (0.33), and PTH receptor 1(0.38). To validate the candidate genes, we perform real time (RT)-PCR and in situ hybridization. We found that signal intensities are as important as fold ratios, because genes with low signal intensities led to predictions sometimes not verified by RT-PCR. In summary, these procedures should prove useful for studying chondrocyte differentiation.

Disclosures: ***S. Nishimori****, None.*

SU060

Targeted Deletion of the SPARC Gene Accelerates Disc Degeneration in the Aging Mouse. H. E. Gruber*[1], E. H. Sage*[2], S. Funk*[2], E. N. Hanley*[1]. [1]Orthopaedic Surgery, Carolinas Medical Center, Charlotte, NC, USA, [2]Division of Basic Science, Hope Heart Institute, Seattle, WA, USA.

Interaction is needed between cells and the extracellular matrix (ECM) in order to maintain the structural integrity of the intervertebral disc. We have recently shown that SPARC (Secreted Protein, Acidic, and Rich in Cysteine) is present in human disc ECM and that it decreases with aging and degeneration. The objective of the present study was to assess whether the targeted deletion of the SPARC gene is deleterious for disc health in the aging mouse. Methods of investigation included quantitative histomorphometry, radiology, electron microscopy and immunohistochemistry. SPARC null and wild-type (WT) control mice were studied at 2-3 and 14-19 months of age. Radiologic examination of spines from 2 month old SPARC null mice showed wedging, endplate calcification and sclerosis, features absent in age-matched WT spines. At age 3 months, the SPARC null disc had a greater number annulus cells than did the WT control (1884.6 ± 397.9 (mean ± S.D.) vs 1500.2 ± 188.2, p=0.031). By age 19 months, however, SPARC null discs contained fewer cells than did the WT (1383.6 ± 363.3 vs 1466.8 ± 148.0, p=0.033; 3 mice/group/time and 5-7 discs/group). Histologic evaluation of mid-sagittal spines showed herniations of lower lumbar discs of SPARC null mice aged 14-19 months (see figure); no herniations were seen in WT age-matched controls. Ultrastructural studies showed that collagen fibril diameters were uniform in the WT annulus but in SPARC null discs fibrils were of variable size and had irregular margins. Immunohistochemistry showed decreased type I collagen in the null vs WT.
In summary, the absence of SPARC adversely affects the number of disc cells in the annulus of older animals, ultrastructural features of collagen fibrils, type I collagen content of the annulus, and spinal structure as reflected in radiologic wedging and endplate changes. Histologic evidence of disc herniations was also present in older null animals. These findings support the heretofore unrecognized role of SPARC in the structural integrity of the disc ECM.

Disclosures: ***H.E. Gruber****, None.*

SU061

Bone and Cartilage Stimulating Peptide BCSP-1 Induces Collagen Type I Expression in Osteoblasts. D. R. Sindrey[1], J. W. Terryberry*[1], F. Fulde*[2], A. Brunner*[2], V. Ciolfi*[1], E. Plawinski*[1], R. Tommasini*[2]. [1]Millenium Biologix Inc., Mississauga, ON, Canada, [2]Millenium Biologix AG, Zurich, Switzerland.

Decreasing bone and cartilage collagen levels are hallmarks of osteoporotic and osteoarthritic diseases. Increased turnover and excretion of collagen telopeptides are validated as diagnostic markers for osteoporosis and other bone disorders. Investigators have postulated that a drug able to enhance collagen production would facilitate recovery from or slow the development of connective tissue diseases, as well as promote bone repair. Bone and Cartilage Stimulating Peptides (BCSP™) are herein shown to induce the expression of the collagen type I gene in human or rat primary osteoblasts, which is accompanied by an increased production of immunoreactive collagen I. Collagen type I up-regulation was established by genomic arrays using CART-CHIP™ and a lucifierase reporter construct for collagen type I. Briefly, gene expression analysis was performed using CART-CHIP™ 300 microarray (Millenium Biologix) comprising 338 human skeletal tissue relevant oligonucleotides printed on glass substrate. RNA amplification was performed using two micrograms of total RNA from cultures treated with BCSP-1 for 4hrs or 24hrs. Amplified RNA was labeled with fluorescent dye, and hybridized onto CART-CHIP™ followed by fluorescence scanning. Further, human primary osteoblasts were transiently co-transfected with a firefly luciferase reporter construct for collagen type I alpha 2 (COL1A2). Plasmid (pGL3) containing firefly luciferase that integrates a 450 bp fragment of the promoter region COL1A2 and 0.1 μg phRG-TK were used for transfection. Cells were dosed with BCSP-1 17hrs after transfection followed by bioluminescence measurements at 4 and 24 hours post treatment using a Dual-Luciferase reporter assay system. Results showed a 2.5-fold increase in the COL1A2 gene expression in rat osteoblasts 4hrs post treatment with BCSP-1. Human primary osteoblast cells transfected with the luciferase construct for COL1A2 demonstrated a dose dependent increase in bioluminescence with BCSP-1 at 4hrs and 24hrs post treatment. Thus, we have shown specific and pronounced up-regulation of collagen I subunit in primary osteoblast cultures using BCSP-1. This result was confirmed by immunoblots of cell lysates with various anti-collagen I antibodies. Results demonstrated a qualitative increase in total collagen I isoforms, as well as the specific production of a unique collagen I monomer at 90kD. This isoform was detectable only in osteoblast cell cultures receiving BCSP-1. This mechanism may promote the recovery from or delay the onset of connective tissue trauma and disease.

Disclosures: ***D.R. Sindrey****, Millenium Biologix 1.*

SU062

SOX9-Dependent and SOX9-Independent Transcriptional Regulation of Human Cartilage Link Protein. I. Kou*, S. Ikegawa*. SNP Research Center, RIKEN, Tokyo, Japan.

Cartilage link protein is a key component of the extracellular macromolecular environment in cartilage. Transcriptional regulation of the gene encoding cartilage link protein (*CRTL1*) is largely unknown, however. Here, we investigate the regulation of *CRTL1* by SOX9, a key regulator of cartilage matrix genes and chondrogenesis. First, we expressed SOX9 in human non-chondrocytic immortalized cell lines, mesenchymal stem cell and adult dermal fibroblast by mammalian expression vectors or adenovirus vectors. *CRTL1* mRNA was significantly induced by SOX9 in these cells, suggesting SOX9 is also a key regulator of *CRTL1*. Then, we expressed SOX9 with its known transcriptional co-activators, L-SOX5 and SOX6 in these cells. The effect of L-SOX5 and SOX6 to the SOX9-induction of *CRTL1* was cell-type dependent. Next, we performed luciferase assays in several non-chondrocytic cell lines using pCRT1 that contains approximately 1.2-kb of the 5'-flanking region of *CRTL1*. Co-transfection of SOX9 significantly increased transcriptional activity from pCRT1, suggesting the presence of the SOX9-responsive element in the fragment. To localize the cis-acting element(s) in the fragment, we constructed several deletion plasmids of pCRT1. Luciferase assays with the 5'-deletion constructs showed 5'-untranslated region (5'-UTR) of *CRTL1* contained a cis-element that is regulated by SOX9. Electrophoretic mobility shift assays (EMSA) with *in vitro*-translated SOX9 showed that this element bound to SOX9. The element contains the consensus SOX-binding motif and substituting mutations for the motif abolished both enhancer activity and SOX9 binding. These results indicated that this element is critical for SOX9 binding and transcriptional activity, and SOX9 could directly regulate *CRTL1* expression. Interestingly, luciferase assays with 3'-deletion constructs of pCRT1 showed 5'-UTR of *CRTL1* contained another cis-acting element. This element was, however, not regulated by SOX9 and responded in a cell-type-specific manner. EMSA with *in vitro*-translated SOX9 and several cell extracts showed that this element bound to some proteins other than SOX9. These findings suggest the presence of the SOX9-independent enhancer element in *CRTL1*. We further examined whether these enhancer elements were functional in chondrocytes. Luciferase assays in a human chondrosarcoma cell line showed both elements could enhance *CRTL1* transcription. Our results suggest that there are two pathways for the regulation of *CRTL1* transcription; one is SOX9-dependent and the other is SOX9-independent. They might play important roles in mediating differential expression of *CRTL1* during chondrocyte differentiation and maturation.

Disclosures: ***I. Kou****, None.*

SU063

Fibronectin Is Required for BMP2-Induced Osteoblast Mineralization Through its Role as a Regulator of Assembly of Multiple Bone ECM Proteins. Q. Chen[1], P. Sivakumar[1], D. M. Peters*[2], D. F. Mosher*[2], S. L. Dallas[1]. [1]Univ. of Missouri, Kansas City, MO, USA, [2]Univ. of Wisconsin, Madison, WI, USA.

Fibronectin is an extracellular matrix (ECM) glycoprotein that is important for cell adhesion, migration and angiogenesis. Inhibition of fibronectin signaling via integrins has been shown to block mineralization in primary osteoblast cultures. Mice lacking the gene for fibronectin die at embryonic stage E8.5, prior to the formation of skeletal structures. Therefore, to gain further insights into the role of fibronectin in mineralization, we have used fibroblasts derived from E6.5 fibronectin null (FN-null) embryos and treated them with exogenous fibronectin at defined times to rescue fibronectin fibril assembly. Upon treatment with BMP2, these FN-null fibroblasts differentiate into osteoblasts as determined by induction of alkaline phosphatase and expression of terminal differentiation markers such as osteocalcin. However, these cultures fail to mineralize unless fibronectin is present in addition to BMP2. Time course studies showed that when fibronectin was present for only week 1, week 2 or week 3, mineralization did not occur. Only when fibronectin was present for the entire culture period did mineralization occur. Fibronectin has recently been shown to be critical for assembly of several ECM proteins. We therefore examined whether assembly of bone ECM proteins was compromised in FN-null cells. By immunostaining, we found that assembly of type I collagen, decorin, biglycan, perlecan, fibrillin-1 and latent TGF beta binding protein-1 (LTBP1) were impaired in FN-null cells. Western blotting confirmed that this was not due to a failure in synthesis or secretion. Assembly of ECM proteins was rescued by addition of exogenous fibronectin, but not by fibronectin fragments that were incapable of assembly into fibrils, including an RGD containing fragment that activates integrin signaling. As fibronectin may also be important for stability of ECM proteins, we examined the effect of addition of fibronectin to FN-null cells for 2 days, followed by withdrawal for 3 days. When fibronectin was withdrawn, the fibronectin fibrillar network disassembled. Assembly of other ECM molecules was halted and no further incorportation of collagen I, fibrillin-1, perlecan, biglycan and LTBP1 occurred. In contrast, when fibronectin treatment was continued these ECM proteins continued to assemble into the ECM. These studies suggest that osteoblast differentiation can occur in the absence of fibronectin. However, the continual presence of fibronectin is required for mineralization to proceed. This may be mediated through the function of fibronectin as a key regulator of assembly of multiple bone ECM proteins.

Disclosures: ***Q. Chen****, None.*

SU064

Collagen and Proteoglycan Perturbations in Cartilage of Patients with Morquio A Disease. R. Bank*[1], K. A. Hoeben*[2], J. E. Groener*[3], P. Maaswinkel*[4], H. A. Schut*[5], V. Everts[6]. [1]TNO, Leiden, Netherlands, [2]Cell Biology, AMC, Amsterdam, Netherlands, [3]Biochemistry, AMC, Amsterdam, Netherlands, [4]Pediatrics, Ootmarsum, Netherlands, [5]Physician, Eindhoven, Netherlands, [6]Oral Cell Biology, Academic Centre of Dentistry Amsterdam, Amsterdam, Netherlands.

Morquio A disease, mucopolysaccharidosis type IVA, is a lysosomal storage disease caused by a deficiency of *N*-acetylgalactosamine-6-sulfate sulfatase (GALNS; E.C. 3.1.6.4). This lysosomal enzyme is involved in the digestion of keratan sulfate and chondroitin-6-sulfate and its deficiency gives rise to a lysosomal accumulation of partially digested glycosaminoglycans (GAGs); a phenomenon seen particularly in bone and cartilage. Although Morquio disease is a disorder of connective tissue no reports have appeared on effects of the extracellular matrix. In the present study we analyzed the biochemical properties of collagen of both bone and cartilage of Morquio A patients and the ultrastructure of the cartilage matrix.

Bone and cartilage samples were obtained from two non-related Morquio A patients. The biochemical analyses included (i) the cross-links hydroxylysylpyridinoline (HP) and lysylpyridinoline (LP), and (ii) hydroxylysine (Hyl) and hydroxyproline (Hyp). Bone and cartilage samples of normal individuals (n=41 and 34, respectively) served as controls. For microscopy tissues were fixed in 1% glutaraldehyde and 4% formaldehyde, embedded in plastic and further processed.

Biochemical analyses revealed that in bone samples hydroxylation and cross-linking of collagen did not differ from the controls. Analyses of the cartilage, however, showed remarkable differences. The amount of Hyl residues in the triple helix of cartilage collagen was decreased by approximately 50% and the ratio of HP/LP was strongly increased due to a decreased level of HP and a concomitant increase in LP. Electron microscopy showed, in addition to a high number of vacuoles in the chondrocytes, a wide rim of extremely well ordered layers of proteoglycans surrounding the cells. In this pericellular area collagen fibrils were absent. The fibrils found interchondrally proved to be relatively thin. Our data demonstrate that in Morquio patients the hydroxylation and cross-linking of cartilage collagen, but not of bone collagen, is severely disturbed. In addition we show that the extracellular arrangement of proteoglycans is affected. So it seems that deficiency of GALNS not only disturbs intracellular digestion of GAGs but also affects processing of various extracellular matrix components.

Disclosures: ***V. Everts****, None.*

SU065

Increased Notch 1 in Osteonectin-null Osteoblasts: A Potential Mechanism for Aberrant Maturation. C. Kessler*, A. M. Delany. Center for Molecular Medicine, University of Connecticut Health Center, Farmington, CT, USA.

Osteonectin (SPARC, BM-40) is a matricellular protein supporting osteoblast formation, maturation and survival. Osteonectin-null mice develop low turnover osteopenia, and in culture, osteonectin-null osteoblasts are less mature and develop more adipocytic characteristics, suggesting that osteonectin could regulate cell fate. We found that, compared to control cells, osteonectin-null osteoblasts have increased levels of Notch 1, a regulator of cell fate determination in multiple systems. A 2-3 fold increase in Notch 1 mRNA and protein was detected at confluence and was maintained throughout in vitro osteoblast differentiation. Moreover, Notch 1 transcripts were increased at the level of gene transcription. The increase in Notch 1 was cell type specific, as it was not observed in confluent cultures of fibroblasts from osteonectin-null mice. Transcripts for Notch 2 and the Notch ligands Jagged 1 and Delta 1 were detectable and equivalent in both control and osteonectin-null osteoblastic cells, indicating the presence of both Notch receptors and ligands in the system. Our laboratory and others have shown that constitutive Notch signaling inhibits osteoblastic differentiation and stimulates adipogenesis. To define the impact of increased Notch 1 on the osteonectin-null osteoblast phenotype, we cultured cells with a gamma secretase inhibitor known to block Notch signaling. Surprisingly, this inhibitor blunted osteoblastic differentiation of the control cells and decreased the adipocytic and osteoblastic markers in the osteonectin-null cells. These data suggest a dual role for Notch signaling in osteoblast differentiation, similar to that recently observed for adipogenesis. In an effort to understand the mechanisms underlying Notch 1 over expression in osteonectin-null osteoblasts, we considered the cAMP pathway. In response to PTH stimulation, osteonectin-null osteoblastic cells exhibit a blunted cAMP response. Further, elevation of cAMP levels using a phosphodiesterase inhibitor decreased Notch 1 mRNA in control and osteonectin-null osteoblasts and fibroblasts, indicating that cAMP decreases Notch 1 expression in both cell types. We hypothesize that osteonectin-null osteoblasts generate less cAMP in response to stimuli, possibly due to decreased adenyl cyclase activity or increased activity of phosphodiesterases. This theory can explain the increased Notch 1 expression in osteonectin-null osteoblasts and could provide a more global mechanism for their diminished osteoblastic maturation.

Disclosures: ***A.M. Delany****, None.*

SU066

Osteopontin Regulates TNFα-Dependent Metalloproteinase Activity and NFkB-Dependent Transcription in Aortic Vascular Smooth Muscle Cells. C. F. Lai*[1], J. S. Shao[1], A. P. Loewy*[1], N. Charlton-Kachigian*[1], S. R. Rittling*[2], D. A. Towler[1]. [1]Dept. of Internal Medicine, Washington University School of Medicine, St. Louis, MO, USA, [2]Genetics, Rutgers Univ., Piscataway, NJ, USA.

Osteopontin (OPN) is a phosphorylated cytokine that exists in at least three forms: a calcified matrix-bound form; a circulating, soluble form entrained to the skeletal osteoanabolic response to teriparatide; and a form secreted by epithelia of breast and renal tubule. In aortic vascular smooth muscle cells (VSMCs) OPN gene expression is markedly upregulated in response to diabetes, induced in part via a glucose-activated, SP600125 - sensitive transactivation function in USF1. We wished to characterize the role of OPN in the activity and expression of TNF-α dependent gelatinases that control vascular matrix remodeling. In gelatin zymography, TNF-α upregulated the activity of MMP9 in aortic VSMCs isolated from wild-type male C57Bl/6 (B6.OPN+/+) mice ca. 2-fold. Modest induction of MMP3 (casein zymogram) was also observed, but little regulation of MMP2 was noted. By contrast, TNF-α induction of MMP9 was almost completely abrogated in aortic VSMCs from B6.OPN-/- mice, while upregulation of MMP3 was not affected. To better understand the potential mechanisms whereby OPN modulates MMP9, we examined the effects of purified bovine OPN (bOPN) on MMP9. At 50 nM, bOPN enhanced MMP9 induction by TNF-α ca. 2 fold. Moreover, addition of exogenous bOPN to cultures of B6.OPN-/- VSMCs re-constituted MMP9 activation by TNF-α. Since NFkB signaling mediates many intracellular actions of TNF-α, we examined the effects of OPN deficiency on the regulation of NFkB responsive promoter - luciferase reporter (NFkB-LUC). In transfected B6.OPN+/+ VSMCs, TNF-α enhanced NFkB-LUC activity 3-fold. However, NFkB-LUC induction was completely abrogated in B6.OPN-/- VSMCs. In A7r5 rat aortic VSMCs, the induction of MMP9 activity was highly dependent upon glucose concentration - a key stimulus for endogenous OPN expression. Hyperglycemia - glucose at 30.5 mM -- permits TNFα-dependent MMP9 activation; by contrast, TNF-α. treatment in 5.5 mM glucose/25 mM mannitol exerts little if any effect on MMP9. bOPN also enhances TNF-α upregulation of MMP9 activity, and neutralizing antibody against OPN can inhibit this TNF-α effect. Thus, OPN functions as a co-regulator of TNF-α signaling in primary and A7r5 aortic VSMCs. In A7r5 cells, the JNK pathway inhibitor SP600125 antagonizes MMP9 production and NFkB signaling, while ERK1/2 and p38 MAPK inhibitors have no effect. Hyperglycemia-induced aortic OPN expression may enhance vascular matrix remodeling, sensitizing aortic myofibroblasts to the low-grade macrovascular inflammation induced by diabetes.

Disclosures: ***D.A. Towler****, American Diabetes Association 2; Amgen 5; Procter & Gamble 8; Novartis 5.*

SU067

The Degree of Posttranslational Modifications of Collagen Is an Important Determinant of the Toughness of Cortical Bone. P. Garnero[1], O. Borel*[2], E. Gineyts*[2], F. Duboeuf*[2], C. Christiansen[3], P. Delmas[2]. [1]Synarc, Inserm Unit 403, Lyon, France, [2]Inserm Unit 403, Lyon, France, [3]CCBR & Nordic Bioscience, Herlev, Denmark.

Bone strength depends on its mass and architecture, but also on the material properties of its matrix. Mineral accounts mainly for pre-yield properties of bone including stiffness and yield strength, and collagen is believed to influence its toughness.

Aim: To analyze the role of posttranslational modifications of collagen on the compressive mechanical properties of cortical bone using an in vitro model where the extent of crosslinking can be modified, keeping constant the size and the mineral content of bone. In this model, we previously showed that collagen crosslinks are associated with bending mechanical properties.

Methods: Calibrated fetal bovine cortical bone specimens (11 animals, 41 samples in total) with a low degree of collagen modifications were incubated for 0, 60, 90 and 120 days at 37°C to increase crosslinking. At each time, compressive mechanical test was performed. The concentration of enzymatic (PYD, DPD) and non-enzymatic (pentosidine) crosslinks of bone matrix was measured by HPLC and the extent of C-telopeptide (CTX) isomerisation was evaluated by ELISA of native (α CTX) and isomerised (β CTX) forms.
Results: After 60 days, there was a significant increase of PYD (+98%, p=0.005), DPD (+42%, p=0.013), pentosidine (+55 fold, p=0.005) and β/α CTX ratio (+4.9 fold, p=0.005), levels reaching those of young adult bone, but remaining lower than levels of old bone. The increase of crosslink concentration was associated with a 2 fold (p=0.005) increase in toughness (energy absorbed after yield). After 60 days of incubation, no significant change of BMD, stiffness (young modulus), yield strength, and maximal strength was observed. As expected, BMD significantly correlated with pre-yield properties (young modulus, yield strength) and maximal strength (p=0.02-0.001), but not with post-yield toughness. In contrast, PYD (r=0.45, p=0.002), DPD (r=+0.35, p=0.02), pentosidine (r=0.46, p=0.002) and the β/α CTX ratio (r=044, p=0.005) were associated with toughness.
Conclusion: These data indicate that the degree of post-translational modifications of collagen plays a significant role in explaining the toughness of cortical bone, an important determinant of bone fragility.

Disclosures: ***P. Garnero****, None.*

SU068

Effect of Adrenalectomy and Glucocorticoid Replacement On Rat Osteocalcin and Lumbar Bone. P. Buckendahl[1], B. Mravec*[2], R. Kvetnansky*[2]. [1]Center of Alcohol Studies, Rutgers University, Piscataway, NJ, USA, [2]Institute of Experimental Endocrinology, Slovak Academy of Sciences, Bratislava, Slovakia.

Glucocorticoid (GC) deficiency and excess both alter skeletal physiology. We previously reported that 2 hr acute foot restraint immobilization of rats (Immo, a mental stressor) rapidly increased plasma osteocalcin (pOC), as well as the stress hormones corticosterone, epinephrine and norepinephrine within 5 minutes of onset of Immo. Daily repetition of this stimulus over a period of 8 weeks blunted pOC response, decreased bone growth and vertebral OC. Here we compare the pOC and on lumbar 3 bone weight and OC concentration in adrenalectomized (ADX) and sham operated rats with and without supplementation of cortisol (cort) at levels physiologically equivalent to corticosterone, the native rodent glucocorticoid. Rats were supplemented for 7 days following ADX or sham ADX (1) with 25 mg/kg/day cort via Alzet minipump, or (2) 15 mg/kg/day in two doses administered i.p.. Controls received isotonic saline. In expt. 1, plasma was obtained during Immo via cannulae implanted in the tail artery. ADX increased basal pOC more than 2.5 fold over sham controls, and was significantly further elevated during 120 min Immo. Basal pOC in cort supplemented ADX or sham rats did not differ from sham control, nor did Immo induced elevations differ among these groups. In expt 2, Non-Immo rats were compared with rats that were Immo for 120 min, and killed after 3 hr recovery. Plasma and L3 vertebrae were harvested. Normal plasma responses to Immo were eliminated by cort. After 3 hr recovery from Immo, pOC in ADXcort control and Immo did not differ from sham control or from each other, while sham Immo rats' pOC was lower than non-Immo controls. Both ADX control and Immo rats' pOC were significantly higher than sham control. Plasma Ca+2 in control or Immo ADXcort rats did not differ from unstressed sham or ADX rats, but was decreased by Immo in sham and ADX rats. Body wt was lower at sacrifice in ADXcort compared with ADX and sham rats; however, L3 dry wt was significantly lower in ADX compared with ADXcort and sham rats. Bone OC concentration was decreased in ADXcort, but not in ADX compared with sham, reflecting the expected decrease in OC synthesis due to cort down-regulation. Cortisol treatment preserved L3 bone wt, consistent with previous reports of prevention of bone loss in ADX rats by supplementation with corticosterone pellets. Plasma data from both experiments support previous reports of increased bone turnover in ADX rats. Cort also returned stress response of pOC in ADX rats to that of sham rats, confirming our previous data suggesting that glucocorticoids are required for return of pOC to normal levels following Immo.

Disclosures: ***P. Buckendahl****, None.*

SU069

Mice Lacking the Extracellular Matrix Protein Thrombospondin 3 (TSP3) Show Accelerated Skeletal Development. J. A. Meganck*[1], S. Hormuzdi*[2], K. D. Hankenson[3], P. Bornstein*[4]. [1]Mechanical Engineering, University of Michigan, Ann Arbor, MI, USA, [2]Biochemistry, University of Washington, Seattle, WA, USA, [3]Orthopedic Surgery, University of Michigan, Ann Arbor, MI, USA, [4]Medicine, University of Washington, Seattle, WA, USA.

TSP3 is a pentameric protein that is structurally similar to cartilage oligomeric matrix protein (COMP), also known as TSP5. Like TSP5, TSP3 is localized to bone and cartilage, but its role in the skeleton has not been previously examined. Mice with a targeted disruption of *Thbs3* were created to examine its functional significance. The mice were viable and fertile and showed normal skeletal patterning by alcian blue/alizarin red staining. To examine the effect of TSP3 disruption on post-natal bone modeling, femoral specimens were obtained from male and female TSP3-null and wild-type (WT) mice at 9, 15, and 26 weeks. Body weight was measured and femora were harvested into either PBS or ethanol and scanned using micro-computed tomography (μCT). Bone length, the moment of inertia (I), cortical thickness, endosteal and periosteal radii and cross-sectional area were calculated from the resulting images. Histological analysis was also performed using either hematoxylin and eosin (paraffin embedded specimens) or Von Kossa (undecalcified plastic sections). Mechanical properties of the bone tissue were investigated using 4-point bending, and predicted yield stress, σ_y, and predicted Young's modulus, E, were calculated. Results were considered to be significant if $p<0.05$ using the Mann-Whitney U test.
Female 9-w TSP3-null mice showed an increase in weight, I, endosteal and periostal radii, cross-sectional area, yield and failure load, and a decrease in modulus. Similarly, 15-w TSP3-null females had increased I, periosteal radius, cross-sectional area, stiffness, failure load, and post-yield and total work. Higher values for weight, I, endosteal and periosteal radii, stiffness and failure load were also seen in 9-w TSP3-null male mice, but there were no differences by 26-w.
When evaluating μCT scans, we noted that TSP3-null mice developed trabecular bone proximal to the femoral head growth plate earlier than WT mice. In TSP3-null mice trabecular bone was present at 9-w and ossification was completed by 15-w, whereas in WT mice trabeculation was only beginning at 26-w. Histological analysis showed that the WT femoral head was composed of hypertrophic chondroctyes in a calcified matrix until 26-w, while TSP3-null femoral heads showed vascular invasion and ossification beginning at 9-w. Overall, these results show that adolescent male and female TSP3-null mice have greater femoral bone volume and strength and accelerated endochondral ossification of the femoral head.

Disclosures: ***J.A. Meganck****, None.*

SU070

Biglycan and Fibromodulin Potentially Inhibit Ectopic Ossification in Tendon by Inhibiting the Differentiation of Osteogenic Stem Cells. Y. Bi*, T. Kilts*, M. F. Young. National Institute of Dental and Craniofacial Research, National Institutes of Health, Bethesda, MD, USA.

Biglycan (BGN) and fibromodulin (FM), two members of Small Leucine-rich Proteoglycans (SLRPs) are co-expressed in tendons. It was previously shown that BGN and FM double deficient mice (DKO) develop ectopic ossification in the tendon. It is also known that SLRPs bind to cytokines and growth factors to modulate their activities in regulating the growth and differentiation of osteogenic stem cells. In the absence of BGN, the differentiation of bone marrow stromal cells (BMSCs) is impaired due to the alteration of BMP-2/4 activity. We therefore hypothesized that BGN and FM inhibit osteogenesis in the tendon by regulating the activity of BMP-2. To test this hypothesis we used bone marrow stromal cells that are of mesenchymal origin and believed to be developmentally related to tendon cells. In this study we compared the osteogenic ability of BMSCs in the presence or absence of BGN and FM. First, we compared the colony forming efficiency (CFU-F) in bone marrow cells from DKO mice to cells from wild type (WT) mice. We found that the number of CFU-F formed from DKO bone marrow cells was increased by 88 ± 4 % (n = 3) compared to WT cells. The size of colonies formed in DKO cultures was bigger than that in WT cultures, suggesting the proliferation and/or survival of BMSCs are increased. Next, we determined the differentiation of BMSCs in response to BMP-2. The expression of alkaline phosphatase was significantly higher (29 ± 3 vs. 18 ± 1 Units/ml, $p<0.05$) in the cultures of DKO BMSCs compared to WT BMSCs. The expression of alkaline phosphatase was up-regulated in both DKO and WT cultures after treatment of BMP-2 for 20 hours. However, the BMSCs from DKO mice were more sensitive to BMP-2 (60 ± 2 vs. 28 ± 2 Units/ml, $p<0.005$) than WT cells. In addition, Western blotting analysis showed that the expression of cbfa1 in DKO cultures is higher compared to WT cultures in the presence or absence of BMP-2. Both experiments demonstrate that the differentiation of BMSCs increased in the absence of both BGN and FM. Based on our findings that BMP-2 activity is increased in BMSCs due to a loss of BGN and FM, we postulate that the SLRPs, BGN and FM, inhibit ossification in tendon by modulating BMP induced osteogenesis.

Disclosures: ***Y. Bi****, None.*

SU071

Bone Sialoprotein Elicits Biomineralization and Ossification in a Bone Defect Model. J. Wang*, H. Zhou, E. Salih*, J. G. Hofstaetter*, M. J. Glimcher. Orthopaedic Research, Children's Hospital, Boston,, MA, USA.

Bone sialoprotein (BSP) is one of the major non-collagenous glycosylated phosphoproteins of the extracellular matrix in bone. Previous *in vitro* precipitation and cell culture studies have suggested that BSP may play a significant positive role in the initiation of calcification. Here, we report for the first time that implantation of BSP-collagen complex into critical sized rat cranial defects, which do not heal spontaneously, elicits mineral deposition followed by osteoblast differentiation and ossification. To explore the biological functions of BSP *in vivo*, especially in a bone defect model. Highly purified bovine BSP linked to type I collagen (prepared from rat-tail tendons) was implanted into surgically created cranial defects (8-mm in diameter) and subcutaneous pouches in the thoracic region of 6-8 weeks old rats. Collagen alone was implanted as a control. All animal procedures were approved by the Animal Care and Use Committee at the Children's Hospital, Boston, MA. The molecular and cellular responses to the implants were evaluated by *in situ* hybridization, quantitative real-time RT-PCR, histochemical, immunocytochemical and histomorphometric analyses. BSP-collagen complex first induced the proliferation of cells in the dura and small mineral deposits at the junction areas between the dura and the BSP implant, which progressed further into the interior of the BSP implant at days 6-7. At this time there was no morphological evidence that the proliferating cells were either chondroblasts or osteoblasts. The proliferating cells in the BSP implants differentiated to osteoblasts at ~ 9-10 days followed by synthesis of bone. Collagen alone implanted into 8 mm rat cranial defects did not stimulate the mineral deposition or ossification in the mid-defect within the same experimental period. At days 10-21, expression levels of bone marker genes in the retrieved cranial BSP-collagen implants were significantly higher than that in the cranial control implants (collagen alone). By day 30, the total mass of new bone formed in the BSP-treated cranial defects was significantly greater than that occurred in the defects filled with collagen alone ($p<0.01$, N=8, Student t-test). BSP-collagen complex implanted into rat subcutaneous tissues did not induce mineralization or bone formation. These results demonstrate that BSP facilitates biomineralization and bone formation in cranial defects, but not in subcutaneous tissues. The site-specific responses to BSP implants suggest that the specificities of local responding cells and/or environment may play important roles in BSP-mediated biomineralization and ossification.

Disclosures: ***J. Wang****, None.*

SU072

Pressure Modulates OPG, RANK and RANKL in Macrophage/osteoblast Co-cultures. C. E. Evans[1], S. Lewis*[1], A. P. Mee*[2], J. L. Berry*[2], J. G. Andrew*[3]. [1]L.m.a.g., University of Manchester, Manchester, United Kingdom, [2]Medicine, University of Manchester, Manchester, United Kingdom, [3]Salford Royal Hospitals Trust, Salford, United Kingdom.

Mechanical load is crucial to maintenance of skeletal homeostasis, but the mechanism involved is still unclear. Recent research has implicated the OPG/RANK/RANKL triumvirate in bone homeostasis, by modulation of osteoclast activity. We have previously shown that cyclical hydrostatic pressure influenced synthesis by human macrophages of various molecules important in osteoclast activity and bone resorption (1-3). This study further examines this concept, looking at how pressure affects synthesis of OPG/RANK/RANKL.

Co-cultures of human osteoblasts and macrophages were subjected to pressure (5.0psi) for 5 consecutive days; static controls from the same cell population were included for all experiemnts. Cells were immunostained for RANK and culture media assayed using specific ELISAs for sRANKL and OPG.

Cultures subjected to pressure synthesised more RANK than controls (Fig 1a.) and this was further modulated by supplementation with 1,25 dihydroxy cholecalciferol (Fig 1b). A reciprocal relationship between OPG and sRANKL was seen in co-cultures exposed to pressure. Where pressure increased synthesis of sRANKL, OPG was decreased (Table 1); decreased [sRANKL] corresponded to increased [OPG].

In common with our previous findings, samples from different individuals responded differently to pressure (Table1). Comparison with non-poresurised controls showed that 66% of samples showed increased synthesis of OPG in response to pressure.

These data show that cyclical hydrostatic pressure increases RANK synthesis in pre-osteoclasts and modulates the ratio of sRANKL:OPG in co-cultures of osteoblasts and pre-osteoclasts. Our other studies have shown that pressure also stimulates differentiation of macrophages to osteoclasts (In press). These findings suggest a possible transduction mechanism for mechanical load in the skeleton, which has implications for future therapies for skeletal abnormalities such as osteoporosis.

Sample	SRANKL (pg/ml): -P	SRANKL (pg/ml): +P	OPG (ng/ml): -P	OPG (ng/ml): +P
AF	13	35	1.96	0.89
LM	>2000	1641	11	33
AH	339	609	22	11
JR	>2000	599	6	11
MI	743	558	9.6	17
DH	311	294	4.8	5.7

Disclosures: ***C.E. Evans****, None.*

SU073

RhoA and Cytoskeletal Disruption Contribute to Altered Differentiation of Human Mesenchymal Stem Cells in Modeled Microgravity. V. E. Meyers*, M. Zayzafoon, J. M. McDonald. Pathology, University of Alabama at Birmingham, Birmingham, AL, USA.

Bone loss during spaceflight, disuse, and aging is due, in part, to reduced osteoblastic differentiation. We have previously described reduced osteoblastic and enhanced adipocytic differentiation of human mesenchymal stem cells (hMSC) following 7 days of culture in modeled microgravity (MMG). The lineage 'decision' of hMSC is influenced by the small G protein, RhoA, which regulates cytoskeletal organization and stress fiber formation in fibroblastic cells. Cell shape and cytoskeletal organization are disrupted in many cell types during spaceflight and in MMG. Therefore, the purpose of our study is to determine the effects of MMG on cytoskeletal organization and Rho activation in hMSC.

To explore the effects of MMG on actin cytoskeletal arrangement, we stained cells with rhodamine-conjugated phalloidin to visualize f-actin. Stress fibers, present in normal gravity, are completely eliminated following 7 days of culture in MMG. There was a concomitant increase in monomeric G-actin in cells cultured in MMG, as determined by Alexa Fluor 488-conjugated deoxyribonuclease I. In addition, Western blot analysis demonstrates reduced total actin in cells cultured in MMG. Interestingly, this disruption in the actin cytoskeleton begins as early as 36 hours after initiation of MMG and is irreversible following return to normal gravity for 7 days. Due to the lack of stress fibers in MMG, we analyzed the activation of RhoA. We demonstrate an 88 $\pm$ 2% reduction in Rho activation in hMSC cultured in MMG. Reduced activation of Rho is known to be associated with adipocytic differentiation of hMSC. Therefore, we examined the lipid content of cells cultured in normal or MMG conditions, using a fluorescent dye, Nile Red. Cells cultured in MMG display a marked increase in lipid staining, compared to hMSC cultured in normal gravity. This is consistent with our previous data demonstrating increased expression of adipocytic genes in MMG, including PPARγ, leptin, and GLUT4 (*Endocrinology* 145:2421-2432). In summary, the data presented here provide a novel mechanism for decreased osteoblastic and increased adipocytic differentiation of hMSC in MMG, namely disruption of the actin cytoskeleton and reduced Rho activity.

Disclosures: ***V.E. Meyers****, None.*

SU074

Evidence of Anabolic Effects of Physiological Strain Regimen in a New Cancellous Bone Explants Tissue Culture-Loading System. V. David*[1], S. Peyroche*[1], A. Guignandon*[1], N. Laroche*[1], D. Jones*[2], E. L. Smith[3], L. Vico[1]. [1]Lbto, Inserm, St Etienne, France, [2]Exp. Orthopaed. Biomechan., Philipps-Universitat Marburg, Marburg, Germany, [3]Preventive Med, Wisconsin Univ, Madison, WI, USA.

To study coordinated bone cellular responses and the resulting tissue response while avoiding complexity of in vivo situation, as well as live animal experiments, we used a new organ culture model (named "Zetos"; Jones et al., ECM 2003). It provides the ability to culture cancellous bone cores over long periods (until now difficult due to rapid degeneration inside the organ) and to apply specific compressive strains to bone cylinders. We chose a regimen that mimics a jump pattern (4000µS, 1Hz, 300 cycles/d.). Cylindrical bovine biopsies (10mm diameter, 5mm height) from sternum were precisely machined, fitted in chambers and feeded with culture medium in conditions ensuring uniform double fluorochrome labelings within the whole sample. Biomechanical (through Zetos itself), tomographic (µCT40, Scanco Medical), and cellular evaluations were performed on basal control (BC) samples immediately processed, loaded (L), and non loaded (NL) 3-wk cultivated samples.

	BC	NL	L
Young Modulus (MPa)	159.53 ± 57.90	157.72 + 40.95	184.1 + 66.80[a]
Plate/Rod Index	1.25 ± 0.2	1.37 + 0.22	0.87 + 0.20[a]
Tb.Th (µm)	84 ± 16	84 ± 10	104 ± 16[a]
OS/BS (%)	7.05 ± 1.64	9.72 ± 3.67	14.37 ± 2.98[a]
O.Th (µm)	11.43 ± 1.93	10.38 ± 2.85	13.6 ± 3.70[a]
MAR (µm/day)	/	0.71 ± 0.17	0.94 ± 0.17[c]
BFR ($\mu m^2/\mu m^3$/day)	/	0.79 ± 0.30	1.16 ± 0.42[c]
Resorption lacunae. N/BS (%)	15.23 ± 2.50[d]	7.35 ± 2.95	8.52 ± 3.00

Means ± SD, [a]significant vs. NL and BC; [b]vs. L and BC; [c]vs. NL; [d]vs. NL and L. Assessment of bone alkaline phosphatase activity (ALP) in culture medium increased by 30 and 35% in L vs. NL after 5 and 8d., respectively, and no longer differed afterward. Sandwich ELISA for Runx2, osteocalcin, and ALP were performed in harvested bone samples. In L, Runx2 and osteocalcin showed increased levels after 7 and 14d. (Runx2: 322 and 285%; osteocalcin: 90 and 27%, respectively), which normalized thereafter. ALP activity increased (47%) only after 7d. in L. Meanwhile we showed that marrow stromal cells from bovine sternum plated on type I collagen-coated-silicon membranes and submitted to cyclic strain (6000 µS, 1Hz, 10 min/d., FLEXCELL FX-3000 unit) over 14d. showed an increased proliferation the first 3d. of stretch, increased levels of ALP and osteocalcin (147 and 76%, respectively) at 14d. and enhanced Runx2 level (67%) at 3d. In conclusion, mechanosensitive bovine osteoblast lineage cells retain their sensitivity in the Zetos organ culture loading system. Such cellular adaptation results in tissue response evidenced by thicker trabeculae arranged in a more plate-like pattern.

Disclosures: ***L. Vico****, None.*

SU075

Oxygen, Mechanical Compression and Inflammation in Articular Cartilage. B. Fermor[1], D. S. Pisetsky*[2], J. B. Weinberg*[2], F. Guilak*[1]. [1]Surgery, Division of Orthopaedics, Duke University Medical Center, Durham, NC, USA, [2]Medicine, VA and Duke University Medical Center, Durham, NC, USA.

Articular cartilage is avascular and exists at a reduced oxygen tension which can alter the level of inflammatory mediators such as nitric oxide (NO) and prostaglandin E2 (PGE_2) induced by interleukin 1 (IL-1). Mechanical stress influences cartilage metabolism and can increase the production of PGE_2 and NO. Increased NO production has been observed clinically in arthritis, and the severity of the disease is significantly decreased *in vivo* using nitric oxide synthase (NOS) inhibitors. The aim of this study was to determine how the oxidative state of cartilage affects mechanically induced NO and PGE_2 in the presence and absence of IL-1.

Articular cartilage explants from the femoral condyles of 2 yr old female pigs were cultured in DMEM with 10% FBS, non-essential amino acids, HEPES, penicillin and streptomycin. After 72 hrs in culture at 37ºC, 5% CO_2, 95 % air, explants were incubated in the presence and absence of 10 ng/ml IL-1, and incubated at 37^0C at either 5% CO_2, 95% air, or at 5% CO_2, 5% O_2, 90 N_2, or at 5% CO_2, 1% O_2, 94% N_2. Explants were allowed to equilibrate under a 10 gf tare load for 8 hrs. Intermittent compressive loads were applied at 0.05 MPa, 0.5 Hz for 24 hrs using a modified version of the Biopress system™ (Flexcell International). All controls were cultured in an unloaded state at either 20% O_2, 5% O_2 or 1% O_2 respectively. The effect of the selective NOS2 inhibitor 1400W (2 mM, Alexis) was tested. PGE_2 production was measured with the PGE_2 ELISA kit (R&D Systems), and NO production measured by the Griess reaction. Statistical analysis was performed by ANOVA with Duncan's multiple range test.

Incubating mature articular cartilage at 5% O_2 caused a significant increase ($p < 0.001$) in baseline NO production compared with incubation at 1% or 20% O_2. Mechanical compression caused a significant increase ($p < 0.001$) in NO at 20% O_2 but not at 5% or 1% O_2, and significantly increased ($p<0.001$) PGE_2 production at 20% (50 fold) and 5% (4 fold) but not at 1% O_2. Mechanical compression in the presence of IL-1 caused a significant increase ($p< 0.01$) in PGE_2 production at 5% O_2 only. Application of mechanical compression in the presence of 1400W caused a significant further increase in PGE_2 production at all oxygen tensions.

Our data show the oxidative state of articular cartilage is important in determining the effect of mechanical compression on production of inflammatory mediators. Therefore it is important to consider the avascularity and hence low oxygen tension, characteristic of articular cartilage, in our understanding of inflammation and mechanical loading of cartilage.

Disclosures: ***B. Fermor****, NIH AR47920 2; NIH AR48182 2; NIH AG15768 2; VA Research 2.*

SU076

Gender Differences in Long Bone Fatigue using a Rat Model. L. D. Moreno*[1], A. M. Cheung[2], M. D. Grynpas[1]. [1]Samuel Lunenfeld Institute, Mount Sinai Hospital, Toronto, ON, Canada, [2]Osteoporosis program, University Health Network and Mount Sinai Hospital, University of Toronto, Toronto, ON, Canada.

Stress fractures can occur because of prolonged exercise and are associated to cyclic loading. This is of special concern for athletes and army recruits. Understanding bone fatigue behavior may give insight into the mechanisms of bone fragility. Existing literature shows that the rates of stress fracture for female athletes and army recruits are higher than for their male counterparts. The objective of this work was to perform a comparative study of the fatigue response of female and male rat tibia. Young 16 weeks Sprague-Dawley rats were used for this study. Excised tibias were loaded at different strains from 0.5% to 1% ε to determine the strain versus cycles to failure curve (S/N curve) at physiological frequency of 2Hz. A set of tibias from male and female rats were monotonically loaded at different stages of the fatigue life (N_f) and the mechanical properties (stiffness, work to fracture and ultimate strength) were determined to assess bone mechanical properties deterioration. A set of tibias that were not fatigued were used as controls. The secant modulus of the tibias was fairly constant throughout the fatigue test; loss of stiffness and cyclic softening was reported only in the later stages of the fatigue life (>90%N_f). Male tibias undergo loss of stiffness for longer periods before fracture. From the S/N curves we inferred the endurance limit. We found that the tibias of the male rats have a higher endurance - about 17% higher. From the cumulative creep data, i.e. from the strain-time curve we found that ε_f (strain-to-failure) of both female and male are not significantly different ($p>0.05$), but for a given non-dimensional stress _/E_o the female bones deteriorate at higher rate than the males (e.g. for an initial peak strain of 0.007_ the steady-state strain rate was 0.035 μ/s and 0.18μ/s for male and females respectively). The results of this rat model suggest that extensive training session with high intensity, even if scaled down to female strength levels would have a detrimental effect on their bones, hence shorter training sessions for females might help to reduce the rates of stress fractures in female athletes.

Disclosures: ***L.D. Moreno****, None.*

SU077

Young's Modulus of C57BL/6J Cortical Bone Is Less Than That of Outbred *Col1a1^{oim}* Heterozygotes or Their Wild-Type Littermates. G. E. Lopez Franco[1], D. S. Stone*[2], R. D. Blank[3]. [1]Medicine, University of Wisconsin-Madison, Madison, WI, USA, [2]Materials Science and Engineering, University of Wisconsin-Madison, Madison, WI, USA, [3]Geriatrics Research, Education, and Clinical Center, William S. Middleton Veterans' Hosptital, Madison, WI, USA.

One must distinguish the inherent mechanical properties of the bone tissue from the contributions of bone mass and bone architecture to bone strength in order to understand bone's mechanical performance fully. Nanoindentation provides a means of calculating hardness and Young's modulus independently of the sample's geometry.

Mice harboring the *Col1a2^{oim}* mutation (*oim*) are a well-studied mouse model of osteogenesis imperfecta arising from α2(I) chain deficiency. Mice homozygous for the mutation produce type I collagen composed of α1 homotrimers and suffer from marked skeletal fragility. Mice heterozygous for the mutation suffer reduced type I collagen synthesis and have a much more subtle biomechanical defect.

We performed nanoindentation to compare the hardness and Young's modulus of cortical bone from animals heterozygous for the *oim* mutation, wild-type littermate control, and C57BL/6J, an inbred mouse strain with low bone mineral density and low Young's modulus. Cortical bone from either the tibia or femur was polished from the periosteal surface prior to testing. We performed nanoindentation in conjunction with atomic force microscopy using a Hysitron TriboScope and a diamond Berkovich tip at loads between 3000 and 8000 μN. Comparison among genotypes was performed by ANOVA and Tukey's test.

Cortical Bone Nanoindentation

	C57BL/6J	*oim*/+	+/+
Young's Modulus (GPa, Mean ± SEM)	20.6 ± 0.8	29.0 ± 1.8*	30.6 ± 1.8**
Hardness (GPa, Mean ± SEM)	1.06 ± 0.08	1.45 ± 0.13	1.48 ± 0.18

*P =0.00309 *v* C57BL/6J, **P = 0.00053 *v* C57BL/6J, *oim*/+ *v* +/+ = NS

The results are summarized in the table. C57BL/6J bone had a lower Young's modulus than either *oim*/+ or +/+ littermates. The 3 genotypes did not differ significantly in hardness.

It therefore appears that neither decreased bone modulus nor decreased bone hardness is the source of skeletal fragility in *oim*/+ mice. It is worth noting that the *oim* mutation is maintained on an outbred B6C3 background. Our data suggest that the collective influence of the segregating background genes has a greater impact on Young's modulus of cortical bone than does heterozygosity for the *oim* allele of *Col1a2*.

Disclosures: ***G.E. Lopez Franco****, None.*

SU078

QTL Mapping of Bone Quality Measured Using Nanoindentation Technology. Y. Jiao*[1], Z. Fan*[2], H. Chiu*[3], H. Yang*[1], E. C. C. Eckstein*[3], J. Rho*[3], W. G. Beamer[4], W. Gu[1]. [1]Department of Orthopedic Surgery-Campbell Clinic, Univ. of Tennessee Health Science Center, Memphis, TN, USA, [2]Orthopedic and Rehabilitation Engineering Center, Marquette University, Marquette, WI, USA, [3]Department of Biomedical Engineering, University of Memphis, Memphis, TN, USA, [4]The Jackson Laboratory, Bar Harbor, ME, USA.

Using nanoindentation technology to identify QTLs that regulate bone quality represents a novel approach to improving our understanding of molecular mechanisms that control bone matrix properties. So far, nanoindentation appears to be the superb technology for measurement of bone quality. In this study, we investigate the use of nanoindentation measurements in identification of QTLs that regulate bone quality.

Mouse tibiae for comparison of different ages were from C57BL/6J and C3H/HeJ and for QTL mapping were from a F2 population derived from C57BL/6J and C3H/HeJ (provided by WGB at Jax). Those tibiae were from the same population used for the analysis of QTLs of bone mineral density. All tibiae were embedded in epoxy resin without infiltration at room temperature. After using silicon carbide abrasive papers with progressively finer grit sizes, they were polished on micro cloths with a 0.05 μm aluminum suspension. A Triboindenter (Hysitron, Inc. Minneapolis, MN) was used to conduct all indentation tests. The Oliver-Pharr method was used to determine the elastic modulus. Genome scan was performed in The Jackson Laboratory. QTL mapping was conducted using Map Manager QTX software. The analysis procedure followed the instructions in the text at (http://mapmgr.roswellpark.org/mmQTX.html; http://webqtl.roswellpark.org)

We obtained the following results: 1) Mice at 4, 8, 16, 32, and 40 weeks were used for the nanoindentation tests. The data at 16 weeks of age shows a moderated variation among mice within a strain compared with older ages. The data suggest that 16 weeks is sufficient time for mouse tibia to mature; 2) We examined 800 tibiae from F2 mice and compared the data to the two progenitors. Data shows that both Er (stiffness) and Hr (hardness) modulus appears normal distributions, suggesting that multiple genetic factors control the bone quality; and 3) Four QTLs for hardness (chr. 9, 12, 13, and 16) and three for stiffness (two on chr. 12 and one on chr. 16) have been identified. Among the QTLs detected from nanoindentation, the one on chromosome 13 has a similar location with the QTL of bone density. The others are new QTLs that have not been detected.

Our study suggests that using nanoindentation technology to identify QTLs that regulate bone quality represents a novel approach to improving our understanding of molecular mechanisms that control the matrix properties of bone.

Disclosures: ***Y. Jiao****, None.*

SU079

Prevalence of Atypical Osteon Characteristics May Reflect Adaptations in Bending Environments and During Growth. S. M. Sorenson*, N. H. Jenson*, J. G. Skedros. University of Utah, Utah, UT, USA.

Basic multicellular units (BMUs) produce 2nd osteons, which mediate microdamage repair, mineral mobilization, and the introduction of interfaces. Since fatigue behavior of cortical bone is significantly different in tension, compression, and shear strain *modes*, histologic adaptations are expected since many limb bones receive consistent tension/compression/shear distributions. BMU-mediated adaptations include variations in 2nd osteon densities and collagen fiber orientation (CFO). Additional important BMU characteristics might include 'atypical' secondary osteons (zonal, connected canal, mature and active drifting, elongated, dumbbell, and multiple canal). If these characteristics correlate with strain-related parameters, then regional variations in these not-often-quantified osteon characteristics (O.C.) may reveal mechanisms (e.g., increasing microstructural complexity/interfaces) that serve to "toughen" bone for relatively more deleterious loading environments (e.g., prevalent tension and shear). O.C. were examined in bones loaded habitually in bending for strain-mode-related correlations. Specimens included mid-third diaphyseal sections of a growth series of calcanei of wild mule deer (older fawns to adults). This model is useful for examining strain-related relationships with microstructural adaptation since the cranial (Cr) cortex receives prevalent compression, the caudal (Cd) cortex receives tension, and the medial/lateral (M/L) cortices receive prevalent shear since they are in proximity of the neutral axis. Regional variations in O.C. were evaluated in backscattered electron images and expressed as "osteon heterogeneity index" (OHI = O.C./total 2nd osteons). Kruskal-Wallis analyses of spatial OHI variations revealed no significant differences among the four cortices in fawns. Sub-adults *and* adults showed these significant differences: Cd vs. L, Cr vs. L, and M vs. L. Although OHI in the whole section (i.e., all cortices) vs. bone length was poorly correlated, the total no.of O.C./area increased with age ($r = 0.538$, $p=0.005$). The increase in these atypical osteon characteristics occurs during the phase of development when osteons may generally serve to enhance toughness and fatigue resistance. The differences between the M cortex and other locations may reflect the fact that the neutral axis is oblique, placing the M cortex in prevalent/predominant shear *and* compression. CFO in this region is also known to be highly oblique, consistent with adaptation for shear/compression. These observations may help understand the mechanisms mediating regional and age-related cortical histologic changes in the complexly loaded human femoral neck.

Disclosures: ***S.M. Sorenson****, None.*

SU080

Trabecular Bone Strength with Virtual Osteoporotic Simulation and Finite Element Analysis. S. Ferreri*, E. Mittra*, B. Gruber, Y. Qin. Biomedical Engineering, Stony Brook University, Stony Brook, NY, USA.

Osteoporosis is a disease that is characterized by low bone density and chronic erosion of the microstructure. As a result, the structural integrity of the affected tissue is compromised and individuals suffering from the disease are at greater risk to develop bone fractures. Clinically, osteoporosis & osteopenia are characterized by decreased apparent bone mineral density (BMD). However, apparent BMD alone does neither explain all variation of the mechanical properties nor does it account for the structural anisotropy of trabecular bone, which might not be sufficient to accurately predict the quality of bone. The ultimate bone strength is directly dependent on bone's quality rather than quantity. In this study osteoporotic conditions are created virtually by decreasing the overall trabecular thickness and maintaining the characteristic microstructure using μCT technology. The response to mechanical loading for both samples is then evaluated using the finite element method.

Four human cadaveric, calcaneus samples with an average age of 76 years (SD ±10.25) were scanned using a μCT-20 scanner (SCANCO Medical) with a resolution of 34 μm. A SCANCO image processing package was used to reconstruct and threshold the scanned images. A ~4 mm cube near the center of the sample was selected for analysis. One third of a voxel was removed from the trabeculae surface using applications available in the SCANCO software. A finite element analysis was then conducted for both the original and simulated diseased samples. The analysis was implemented using ABAQUS (HKS INC.) version 6.3. A 1% compressive strain is applied to nodes on the medial surface with a non-friction boundary condition while nodes on the lateral surface are restricted from motion in the mediolateral direction. Additionally, nodes on the remaining four sides are restricted from moving in the direction of the unit normal to the side.

The ~4 mm cubes of human calcaneus bone had an average bone volume fraction (BVF) of 17.41 % (SD±3.46). For the case of simulated osteoporosis average BVF was 11.20% (SD±1.86). The effect of simulating osteoporosis removes on average 35.56% of bone from the original model. The apparent stress was defined as $\sigma_{33} = (F_{z,max} - F_{z,min})/2*A$, where $F_{z,max}$ and $F_{z,min}$ are the sum of the nodal forces on the top and bottom surfaces of the cube. The average apparent stress for the healthy bone is found to be 55.64 ±24.52MPa. However, under the same loading conditions, the case of simulated osteoporosis experiences an apparent stress of 90.2 ±14.15MPa, nearly 38% greater than that of the original bone. The results of this study suggest that decreasing BVF 35% severely compromises the structural integrity of calcanean trabecular bone.

Disclosures: ***S. Ferreri****, None.*

SU081

Repeatability of the Ex-Vivo Bioreactor Bone Organ Culture Chamber and Loading System. H. Ploeg*[1], E. Smith*[2], A. Gerson*[2], S. Garcia*[1], E. Broeckmann*[3], D. B. Jones*[3]. [1]Mechanical Engineering, University of Wisconsin, Madison, WI, USA, [2]Population Health, University of Wisconsin, Madison, WI, USA, [3]Exp. Orthopaedie & Biomechanik, Phillips Universitaet, Marburg, Germany.

The purpose of this study was to determine the repeatability of the Ex-vivo bioreactor Bone organ culture chamber and Loading System (EBLS) over the period of time of at least that of a 30 to 50 day experiment. Three standards were obtained from the Dr. David Jones' Laboratory in Marburg Germany. The standards are closed hollow cylinders open at one end. The apparent elastic moduli ($E=Kh/pi/r^2$, where E is apparent elastic modulus, K is apparent stiffness, h is cylinder height, r is cylinder radius), chosen to cover the expected range of ex-vivo trabecular bone samples, were a result of varying the material modulus and the thickness of the cylinder's end plate. The apparent elastic moduli of the three standards were 325 MPa, 495 MPa and 1590 MPa for the 500 μm thick aluminum, 800 μm thick steel, and 1200 μm thick steel standards, respectively. Thirteen sets of ten repeat measurements were made on three standards over a 90 day period. The coefficient of variation of the apparent elastic modulus was 1.4%, 1.3% and 2.3% for the three standards, in order of increasing apparent stiffness, over a period of 90 days. It is clear from this data that the reliability of the loading system is excellent and will not induce large variations into the ex-vivo bone core data set. Further testing is being carried out to determine the effects of the bone chamber, loading characteristics and specimen characteristics on the apparent elastic modulus measured using the EBLS.

Table 1. Reliability Testing Results for Three Standards (n=130 per standard)

	Force (N)	Displacement (μm)	Apparent Elastic Modulus (MPa)
Aluminum - 500 μm thick endplate			
Mean	148.9	29.62	325.0
Standard Deviation	2.375	0.04883	4.581
Coefficient of Variation	1.595%	0.1649%	1.409%
Steel - 800 μm thick endplate			
Mean	223.7	29.61	494.9
Standard Deviation	4.426	0.07139	6.540
Coefficient of Variation	1.978%	0.2411%	1.321%
Steel -1200 μm thick endplate			
Mean	719.5	29.63	1591
Standard Deviation	16.34	0.05167	0.03592
Coefficient of Variation	2.271%	0.1744%	2.257%

Reference: Jones D.B. et al., European Cells and Materials **5**:48-60, 2003.

Disclosures: ***H. Ploeg****, None.*

SU082

Correlation of Serum TRAcP 5b and Bone Mineral Density with Osteolytic Bone Cancer Pain. A. Gordon[1], J. Boulet*[1], J. Miller*[2], D. Bristol*[2], G. Crumley*[3], S. Gottshall*[1], S. Chaffer*[1], K. Walker*[1], J. Pomonis*[1]. [1]Neuropharmacology, Purdue Pharma, Cranbury, NJ, USA, [2]Biostatistics, Purdue Pharma, Cranbury, NJ, USA, [3]Molecular Pharmacology, Purdue Pharma, Cranbury, NJ, USA.

In patients with malignant disease, bone cancer pain is the most common kind of pain. Upon increased bone tumor burden, a patient's discomfort worsens with clinical presentation of mechanical allodynia, a pain response that occurs when a normal, nonpainful stimulus is perceived as painful. Increased serum tartrate-resistant acid phosphatase 5b (TRAcP 5b) and decreased bone mineral density (BMD) have been shown clinically to correlate to advanced states of osteolytic tumor burden. Moreover, clinical studies suggest both decreased serum TRAcP 5b and increased BMD can signify pharmacologic or analgesic activity and predict pain relief in these cancers.

To confirm the utility of serum TRAcP 5b and BMD as quantifiable correlates of mechanical allodynia, we used an established pre-clinical rat model of bone cancer pain. 3000 MRMT-1 rat mammary gland carcinoma cells were implanted in the tibiae of female Sprague Dawley rats and monitored for progression of osteolytic tumor burden over a 21-day period. Naïve, Hank's Balanced Salt Solution (HBSS) sham and MRMT-1 tumor-bearing rats were tested for von Frey paw withdrawal threshold (VWT) as a measure of mechanical allodynia, immunoassayed for serum TRAcP 5b, and radiographed for BMD prior to surgery and after 7, 10, 14, and 21 days. Increased serum TRAcP 5b levels were seen in MRMT-1 rats as compared to sham rats at 14 and 21 days after surgery. BMD and VWT significantly decreased in MRMT-1 rats as compared to sham rats, beginning 10 days after surgery. A repeated measures analysis of covariance was performed, regressing VWT on BMD, with covariate adjustment for baseline VWT. This analysis demonstrated that the concomitant decrease in BMD and VWT in MRMT-1 rats was statistically significant ($n=8$, $p<0.01$). Furthermore, multiple regression analysis over days 7-21, regressing VWT on serum TRAcP 5b, verified statistical significance of the simultaneous rise in serum TRAcP 5b and fall of VWT in MRMT-1 rats ($n=8$, $p<0.04$). Therefore, our statistical analysis establishes both BMD and serum TRAcP 5b as correlates of VWT.

This is the first study to demonstrate statistical correlation of serum TRAcP 5b levels with quantitative measures of mechanical allodynia in a pre-clinical bone cancer model. Increased serum TRAcP 5b and decreased BMD, known clinical correlates of osteolytic tumor burden, are statistically associated with and may predict more pronounced states of bone cancer pain. Our results will lead to greater understanding of the utility of potential analgesics in this regard.

Disclosures: ***A. Gordon****, Purdue Pharma 3.*

SU083

Bone Mineral Density in Long-term Survivors of Acute Lymphoblastic Leukemia (ALL). V. Vyskocil[1], Z. Cerna*[2], S. Kutilek[1]. [1]Bone Disease Center, Charles University Hospital, Plzen, Czech Republic, [2]Department of PediatricBone Disease Center, Charles University Hospital, Plzen, Czech Republic.

The childhood leukemia has an increasing number of survivors and therefore, more attention is being paid to the long-term side-effects of this disease and its treatment. In patients with ALL, the leukemic process itself together with the treatment are likely to undermine the achievement of peak bone mass 12 children (10 boys and 2 girls) with history of ALL were enrolled in the study. The ALL was diagnosed at the age of 6.1±3.7 years, treated for 2.1±0.3 y (ALL protocol BFM 83, n=2; BFM 90, n=6; BFM 95,n=4). The ALL remmission occurred at mean age 8.2±3.7 years. The first DXA (Hologic Delphi W S/N 70220, CV 1%, LSC 2.7 %) measurement was performed 3.83± 2.89 y after completion of chemotherapy (at mean age 12.0±3.4 y) and after additional 1.22 ± 0.34 y (mean age 13.5±3.6 y). Volumometric bone density (BMD_{vol}) was calculated: BMD_{vol}=BMC/Volume = BMD_{areal} [4/(π Width)],where Width = mean width of vertebral body. The obtained results of BMD_{areal} and BMD_{vol} were expressed as Z-scores. The BMD_{areal} didn´t differ significantly from the reference values at both time points ($p = 0.11$ and 0.25, respectively), neither was there any difference between the results of the two measurements ($p=0.33$). The BMD_{vol} was significantly lower in comparison to the reference data at the respective time-points ($p< 0.001$ and 0.006, respectively), and there was no difference between the results of the two measurements ($p=0.25$) There were no correlations between the basic anthropometric parameters and either BMD_{areal} or BMD_{vol}. Neither were there any correlations between cummulative doses of prednisone and cytostatic drugs (methotrexate, cyclophosphamide) and BMD_{areal} or BMD_{vol}, nor between number of hospital admissions or duration of hospitalisation and BMD. Our results further confirm that ALL survivors have decreased BMD. The estimation of BMD_{areal} is influenced by bone size and can be underestimated in smaller individuals. However, the absence of correlations between normal BMD_{areal} and normal anthropometric parameters suggests that this wasn´t the case in our patients. Furthermore, low BMD_{vol} values confirm the low bone mass in ALL survivors, as volumometric bone density gives more reliable information than the areal data There were no significant changes in BMD Z-scores between the two measurements in a mean time span of 1.22 ± 0.34 years. In conclusion, childhood survivors of ALL are at risk of decreased bone mass. Volumometric bone density gives more reliable information than the areal data

Disclosures: ***V. Vyskocil****, None.*

SU084

Differential Expression Profile of Haematopoietic Markers in the Giant Cell Tumor Stromal Cells (GCTSCs). E. A. Kaiser[1], A. Jeske*[1], M. Wuelling*[2], G. Delling*[2]. [1]Bone Pathology, Center of Biomechanics, Hamburg, Germany, [2]Bone Pathology, Hamburg, Germany.

Among the giant cell tumor of bone's (GCT) three cellular components, multinucleated giant cells, CD68 positive monocytes and mononucleated fibroblast-like stromal cells (GCTSCs), only the GCTSCs survive in cell cultures thus assuming that they are the neoplastic component of GCTs. In earlier studies the development of GCTs from monocytic/osteoclastic cells was proposed and a GCT cell line (GCT23) with osteoclast-like properties has been presented. Recent papers have suggested a mesenchymal cell as the origin of the GCTSCs. The present study sought to address this controversy. The hypothesis of the existence of pluripotent stem cells that can differentiate into haematopoietic as well as mesenchymal cell types may offer an explanation for the divergent results. The lack of definitive antibodies allowing recognition of pluripotent cells let us to the quantification of the relative gene expression of early haematopoietic (GATA1, 2, 3, 6) and mesenchymal (CD73, CD105, CD166) markers in eight GCTSCs, one primary human mesenchymal stem cell (MSC) population, the giant cell tumor cell line GCT23 and the pluripotent stem cell line V54/2 by Real Time PCR. Comparing the expression profiles of the control cells (MSC, GCT23 and V54/2) revealed that the mesenchymal markers did not differ appreciably between the control cell types. However, the haematopoietic markers displayed a differential expression profile. Matching up control cell expression profiles of the haematopoietic markers with the expression profiles of the GCTSCs identified three GCTSCs that demonstrated a similar expression profile as the GCT23, four GCTSCs that corresponded to the expression profile of MSCs and one GCTSC that related to the expression profile of V54/2. The presented results suggest that GCTs could comprise different entities, but further marker expression profiling, in addition to in vivo and in vitro differentiation studies need to be conducted to assume a pluripotency of GCTSCs.

Supported by Rudolf Bartling Stiftung, GCT23 were provided by Dr. Grano, Bari, Italy and V54/2 were provided by Dr. Huss, Munich, Germany

Disclosures: ***E.A. Kaiser****, None.*

SU085

Estrogen in the Establishment of Peak Bone Mass among Childhood Cancer Survivors. J. E. Mulder[1], C. A. Sklar*[2], A. C. Mertens*[3], L. L. Robison*[3], L. Diller*[4], A. Klibanski*[5], J. P. Bilezikian[1]. [1]Columbia University, NY, NY, USA, [2]Memorial Sloan-Kettering Cancer Center, NY, NY, USA, [3]University of Minnesota, Mpls, MN, USA, [4]Dana Farber Cancer Institute, Boston, MA, USA, [5]Massachusetts General Hospital, Boston, MA, USA.

Advances in multimodality therapy for the treatment of childhood cancers have resulted in markedly improved survival rates for many children. In young adults who have survived cancer, however, therapy and its complications place them at risk for suboptimal acquisition of peak bone mass. In addition to chronic illness, nutritional deficiencies, limited physical activity, and treatment with glucocorticoids, multiagent chemotherapy and radiation; the long-term adverse effects of cancer therapies on endocrine systems, specifically sex steroid and growth hormone deficiencies, are important risk factors for low bone mass in adult survivors of childhood cancer. As part of a study to assess the effects of estrogen dose on bone mineral acquisition in survivors of childhood cancer with premature ovarian failure, we evaluated bone mineral density and markers of bone remodeling in a group of childhood cancer survivors with normal menses. We hypothesized that estrogen status would have the greatest influence on BMD in cancer survivors, and therefore, cancer survivors with normal menses would have normal BMD. Six childhood cancer survivors (mean age 26.5, range 21-30) with normal menarche (mean age 11.8) and regular menses have been studied thus far. No subject had received growth hormone replacement therapy. BMD (DXA) was measured at the lumbar spine (LS), total hip (TH), femoral neck (FN), and 1/3 radial site (R). Markers of bone remodeling, vit D, PTH, androgens, estradiol and progesterone were measured during the luteal phase of the menstrual cycle. Mean height was 158.2 cm (148.6-175.2) Z-score -0.7, mean BMI was 22.7 (20.9-24.3). Mean Z-scores of the LS, TH, FN, and R were -0.87, -0.87, -0.82, and -0.08, respectively. Mean T-scores were -0.92, -0.88, -0.87, and -0.15, respectively. Despite having normal menses, 3 of 6 patients had BMD Z-scores below -1.0 at one or more sites. L-S and TH BMD Z-scores were at or below -2.0 in 2 patients. Markers of bone remodeling, PTH, gonadotropins, and estradiol were normal in all subjects. Serum progesterone levels confirmed ovulation in 4 of 6 patients. Two patients had vit D levels below 20 ng/ml. IGF-1 was normal in all subjects, although the 3 patients with the lowest BMD had lower IGF-1 levels. These 3 patients had received cranial or cranial-spinal irradiation. In summary, the continued presence of regular menses after cancer therapy was not always protective of acquisition of normal bone density in this small sample of childhood cancer survivors.

Disclosures: ***J.E. Mulder****, None.*

SU086

Oral Squamous Cell Carcinoma Cells Enhance Osteoclast Differentiation and Bone Resorbing Activity. T. Tada[1], E. Jimi[2], S. Ozeki*[1], K. Okabe[2]. [1]Oral and Maxillofacial Surgery, Fukuoka Dental College, Fukuoka, Japan, [2]Physiological Science and Molecular Biology, Fukuoka Dental College, Fukuoka, Japan.

The invasion of oral squamous cell carcinoma (SCC) into maxillary and mandibular bone is a common clinical problem. It is well known that bone destruction by SCC invasion is mediated by osteoclasts. We therefore investigated how SCC cells affect osteoclast differentiation and function. We injected BHY (human oral squamous carcinoma cell line) cells mixed with human gingival fibroblasts into the masseter muscle of nude mice and observed an increased number of osteoclasts and bone destruction on the surface of the mandibular bone. When BHY cells were co-cultured with mouse bone marrow cells, few osteoclasts were formed even though BHY cells express receptor activator of NF-kB ligand (RANKL). However, adding BHY cells to the co-culture of mouse osteoblasts and bone marrow cells markedly increased osteoclastogenesis in the absence of osteotropic factors. This effect was completely abolished by addition of osteoprotegerin (OPG). When co-cultures were separated from BHY cells using transwell culture system and conditioned media collected from BHY cell cultures were added to the co-cultures without any osteotropic factors, osteoclastogenesis was suppressed (up to 20-30%) but we still observed osteoclasts in both culture system. Paraformaldehyde-fixed BHY cells added to co-cultures of mouse osteoblasts and bone marrow cells still could induce small (mostly mono and binuclear) osteoclasts. These results indicate that soluble factors released from BHY cells as well as cell-to-cell contact between BHY cells and osteoblasts cooperatively induce osteoclastogenesis. When purified osteoclasts were cultured for longer than 24 h, most died spontaneously. The addition of either BHY cells or conditioned media from BHY cells markedly increased the survival of osteoclasts. We previously reported that enriched osteoclasts placed on dentin slices form few resorption pits and that their pit-forming activity is greatly increased by adding osteoblasts or BHY cells. Therefore, alteration of both osteoclast differentiation and function is a major factor of bone invasion by SCC.

Disclosures: ***T. Tada****, None.*

SU087

Risedronate, and its Phosphonocarboxylate Analogue NE10790, both Induce Apoptosis, but have Differential Effects on the Cell Cycle and Protein Prenylation in Human Myeloma Cells. A. J. Roelofs*[1], P. A. Hulley*[1], R. G. G. Russell[1], F. H. Ebetino[2], M. J. Rogers[3], C. M. Shipman*[1]. [1]Nuffield Department of Orthopaedic Surgery, University of Oxford, Oxford, United Kingdom, [2]Procter & Gamble Pharmaceuticals, Cincinnati, OH, USA, [3]University of Aberdeen, Aberdeen, United Kingdom.

Bisphosphonates (BPs) are widely used in the treatment of osteolytic bone disease associated with multiple myeloma (MM). In addition to their beneficial effects on bone disease in MM, BPs have recently been demonstrated to exert anti-tumour effects both *in vitro* and *in vivo*. NE10790 is a phosphonocarboxylate analogue of the potent BP risedronate (RIS), which has a lower affinity for bone mineral and is a weak inhibitor of bone resorption. NE10790 has been shown to specifically inhibit the prenylation of small Rab GTPases in macrophages and osteoclasts. Both RIS and NE10790 strongly reduce skeletal tumour burden in a murine model of breast cancer.

The aim of this study was to determine whether RIS, and its phosphonocarboxylate analogue NE10790, induce apoptosis in human MM cells *in vitro*, and to compare their anti-tumour mechanisms of action.

Both NE10790 and RIS significantly increased apoptosis in NCI H929, JJN-3, and RPMI 8226 MM cells in a dose-dependent manner ($p<0.001$), as determined by characteristic changes in nuclear morphology and by a fluorescence *in situ* nick translation assay. A significant increase in apoptosis was detected following treatment with 1 mM NE10790 ($p<0.01$) and 50 μM RIS ($p<0.05$) in JJN-3 cells. For both RIS and NE10790, induction of apoptosis was found not to be due to calcium chelation.

Flow cytometric analysis of propidium iodide (PI)-stained cells demonstrated that RIS induced an increase in the proportion of cells in S-phase of the cell cycle, before an increase in apoptosis could be detected. In contrast, NE10790 did not cause accumulation of cells in S-phase. Double labelling with BrdU and PI confirmed that DNA replication was partially inhibited after treatment with 10 μM RIS, and completely after treatment with 100 μM RIS.

Western blot analysis showed that RIS dose-dependently inhibited prenylation of both Rap1a (geranylgeranylated by GGTase I) and Rab6 (geranylgeranylated by GGTase II/Rab GGTase) proteins. In contrast, NE10790 only inhibited the prenylation of Rab6. These results demonstrate that RIS, and its phosphonocarboxylate analogue, NE10790, both induce apoptosis in human MM cell lines *in vitro* in a dose-dependent manner. However, effects of RIS are associated with cell cycle arrest in S-phase and general inhibition of protein prenylation, whereas our results suggest that NE10790 may have distinct mechanisms of action involving specific inhibition of prenylation of small Rab GTPases.

Disclosures: ***A.J. Roelofs****, None.*

SU088

Soluble RANK Ligand (sRANKL) and Osteoprotegerin (OPG) in Multiple Myeloma and in Monoclonal Gammopathy of Undetermined Significance. D. Beke*[1], G. Hawa*[2], P. Kudlacek*[3], G. Pohl*[1], K. Brenner*[1], L. Hofbauer*[4], M. Pecherstorfer[1]. [1]1. Department of Medicine and Medical Oncology, Wilhelminenspital der Stadt Wien, Vienna, Austria, [2]Biomedica Group, Vienna, Austria, [3]Department of Medicine, Hospital Barmherzige Brüder, Vienna, Austria, [4]Division of Gastroenterology, Endocrinology and Metabolism, Phillips University of Marburg, Marburg, Germany.

Background: Osteolytic bone disease is a major cause of morbidity in patients with multiple myeloma. The identification of the OPG/RANKL/RANK system as the apparently most important regulator of osteoclastogenesis and osteoclast activity represents a major advantage in bone biology.

Purpose: To evaluate the role of soluble receptor activator of nuclear factor kappa B ligand (sRANKL) and osteoprotegerin (OPG) in patients with plasma cell dyscrasias, we measured the serum concentrations of these parameters in 43 patients with monoclonal gammopathy of undetermined significance (MGUS), 46 patients with newly diagnosed, untreated myeloma (MM) and 90 healthy adults. We used commercially available immuno assays (Biomedica Group, Vienna, Austria). The OPG assay determined the total amount of circulating OPG in serum by measuring free and sRANKL bound OPG.

Results: Serum levels of OPG and sRANKL did not differ between patients with MM or MGUS. OPG levels and sRANKL levels were significantly higher in MM and MGUS patients than in healthy controls.

Conclusion: Patients with MGUS and MM did not differ with regard to serum levels of OPG and serum levels of sRANKL. Therefore, OPG and sRANKL levels were not useful in discriminating MM from MGUS patients in our study population. In patients with MGUS, serum concentrations of OPG and sRANKL were raised when compared to healthy controls. This finding might indicate the presence of already enhanced osteoclast activity in MGUS patients who per definition do not have overt neoplastic bone involvement.

	Multiple Myeloma (n=46)	MGUS (n= 43)	Healthy controls (n= 90)
Osteoprotegerin (pmol/L)	4.94* (1.00 - 17.36)	4.47* (1.00 - 10.99)	2.15 (0.85 -8.55)
sRankl (pmol/L)	0.27* (0.06 - 1.08)	0.24* (0.11 - 3.22)	0.18 (0.01 - 2.67)
Ratio sRankl/osteoprotegerin	0.06 (0.01 - 1.80)	0.06 (0.01 - 0.90)	0.06 (0.01- 1.52)

* p< 0.05 compared to healthy controls

Disclosures: ***D. Beke****, None.*

SU089

E1A Oncogene Repression of Parathyroid Hormone-related Protein Gene Expression in Human Prostate Cancer Cell Lines. F. Asadi*[1], B. Boyer*[2], A. Valles*[2], S. C. Kukreja[1], J. L. Cook*[3]. [1]Medicine, University of Illinois at Chicago & West Side VA Medical Center, Chicago, IL, USA, [2]Regulations Cellulaires et Oncogeneses, UMR 146 du CNRS, Institute Curie, Paris, France, [3]Medicine, University of Illinois at Chicago, Chicago, IL, USA.

Previous studies have demonstrated that PTHrP levels are high in prostate cancer and that PTHrP expression is greater in poorly differentiated tumors as compared to that in well differentiated tumors. In the advanced stages, prostate cancer cells become androgen-independent and resist apoptosis. Overexpression of parathyroid hormone-related protein (PTHrP) has been shown to result in resistance to apoptotic injuries in various cells including prostate cancer. In another study, we evaluated the effects of addition of PTHrP (1-34) and its neutralization on cell survival following exposure to trans-retinoic acid (tRA) in LNCaP and C42 and C42b prostate cancer cell lines. Cell survival was assessed by trypan blue exclusion and MTS proliferation assay and apoptosis was examined by intracellular DNA fragmentation analysis, caspase-3 activity assay, and TUNEL assay. In these cell lines, tRA (5μM) treatment reduced cell viability and PTHrP (1-34) (100nM) protected against the tRA-induced loss in cell viability. Similarly, PTHrP had a protective effect against tRA-induced DNA fragmentation and caspase-3 activation in these cell lines. On the other hand, addition of PTHrP (1-36) neutralizing antibodies to the tRA-treated cells further reduced cell survival and increased apoptosis.

Human adenoviruses are common human pathogens. Adenovirus early region 1A (E1A) proteins were originally described as immortalizing oncoproteins in rodent cells. Subsequent studies have shown that a '12 S' form of the E1A induces suscepitibilty to killer cell apoptosis. In a previous study, overexpression of E1A into an immortalized keratinocyte cell line PAM 212K has been shown to inhibit PTHrP expression via interaction with the the P3 promoter (Foley et al. Mol Cell Endocrino. 156:13-23, 1999). In the present study, we evaluated the effects of transient adenovirus type 5 early region 1A (E1A) gene transfection on PTHrP expression in PC-3 prostate cancer, a human breast carcinoma (MB 231), and a rat bladder carcinoma (NBT II) cell lines. Transfection with the '12 S' E1A gene resulted in a decrease in PTHrP mRNA levels in all three cell lines. We speculate that a part of the apoptosis-promoting effect of E1A may be mediated via repression of PTHrP expression. Further studies to evaluate the effects of E1A on cell apoptosis in these cell lines and the role of PTHrP in this process are warranted.

Disclosures: ***F. Asadi****, None.*

SU090

Influence of Chemotherapy(AC)on Bone Mineral Density (BMD) and Bone Ultrasonometry (QUS) in Women with Breast Cancer. M. Gottschalk*, P. Hadji*, C. Maskow*, V. Ziller*, C. Heitmann*, U. Wagner*. Endocrinology and Osteoporosis, Clinic of Gynokology and Obstretics of Philipps- University, Marburg, Germany.

Introduction: The aim of this prospective, case-control pilot study was to evaluate the influence of chemotherapy (Adriamycin/Cyclophosphamid) on BMD and QUS in premenopausal women with breast cancer.

Material and Methods: We included 53 premenopausal patients, mean age 47 ± 9,6 years with an incident diagnose of breast cancer who received a chemotherapy (4 cycles of AC) and 53 age- and BMI-matched controls. Women with metastases, a history of osteoporosis with or without fracture, diseases or treatments known to effect bone metabolism were excluded from the study. BMD was measured by DXA (DPX-L, GE/Lunar) at spine and hip. QUS was performed at the os calcaneus using the Achilles device (GE/Lunar) and at the phalanges using the Bone-Profiler (IGEA). Measurements were performed at baseline (before chemotherapy), after 6 and 12 months and were compared with measurement results of the age- and BMI-matched control group.

Results: DXA results of the spine and hip showed a significant decrease of T- and Z-score in patients with chemotherapy compared controls (p= 0,001). In accordance to QUS results, measurement at the os calcaneus as well as at the phalanges showed a similar significant, linear decrease of T- and Z-score (p= 0,001), with the largest difference between baseline and 12 months T-score (AD-SOS; p= 0,001).

Conclusion: The result of our prospective, case controlled pilot study confirms the deleterious influence of chemotherapy on BMD in women with breast cancer. This effect could equally be observed by DXA and QUS for the first time in this regard. Further, large scale longitudinal studies are needed to improve our understanding of the mechanism of bone changes during chemotherapy.

Disclosures: ***M. Gottschalk****, None.*

SU091

c-Src Inhibition as a Possible Therapy against Human Breast Cancer and Bone Metastases. D. Fortunati[1], C. Di Giacinto*[1], I. Recchia*[1], M. Susa*[2], D. Fabbro*[2], A. Teti[1], N. Rucci[1]. [1]Department of Experimental Medicine, University of L'Aquila, L'Aquila, Italy, [2]Novartis Pharma, Basel, Switzerland.

The proto-oncogene c-Src plays a role in breast tumors, which are prone to metastasize to bone. We investigated whether c-Src inhibition could affect survival and bone metastasis incidence in vivo. Intracardiac injection of human breast cancer cell line MDA-MB231 treated with c-Src inhibitor CGP76030 into Balb-c nu/nu mice resulted in a delayed cachexia and lethality, relative to mice injected with untreated cells. A delay was more prominent in mice injected with MDA-MB231 cells followed by in vivo oral gavage treatment with 100 mg/Kg/day of CGP76030. In untreated mice, osteolytic bone metastases progressively increased, reaching 12.5% incidence at day 31 and 40% at day 36 post-injection. In treated mice no bone metastases were detacted until day 36, while at day 45 bone lesions reached 40% incidence. When mouse bone marrow cells were cultured with conditioned media (CM) from MDA-MB231 cells, a significant increase of TRAP-positive multinucleated osteoclasts and resorption pits was measured, suggesting a stimulation of osteoclast activity by paracrine factors from breast cancer cells, such as IL-6 and IL-1beta, whose mRNAs were expressed in MDA-MB231 cells. Osteoblast cultures treatment with MDA-MB231 CM resulted in a up-regulation of IL-6, IL-1beta and RANKL mRNAs, suggesting an indirect stimulation of osteoclastogenesis and bone resorption via the osteoblast lineage. Similar results were observed using CM from a MDA-MB231 clone stably transfected with c-SrcWT construct (MDA-SrcWT), which also induced down-regulation of the osteoclastogenesis inhibitory cytokine IL-12 in osteoblasts. c-Src inhibitor caused a concentration- and time- dependent reduction of MDA-MB231 cell proliferation, adhesion, spreading and migration through gelatin. Consistently, MDA-SrcWT cells showed increased migration and invasion vs. parental cells. This increase was not observed in MDA-MB231 transfected with c-SrcK296R/Y528F kinase-dead and dominant negative construct (MDA-SrcK296R/Y528F). Treatment with CM from MDA-SrcWT cells significantly increased proliferation of the human endothelial cell line EAHy926, relative to treatment with CM from MDA-MB231 and MDA-SrcK296R/Y528F cells, while migration and invasion were unaffected by all types of CM. In conclusion, we demonstrated a role for c-Src in (i) development of in vivo bone metastases, (ii) breast cancer cell growth, motility and osteoclastogenesis ability, and (iii) paracrine stimulation of endothelial cell activity. We, therefore, identify c-Src as a pharmacological target for treatment of breast cancer-induced bone metastases.

Disclosures: ***D. Fortunati****, None.*

SU092

Osteonecrosis of the Maxilla and Mandible in Patients with Metastatic Breast Cancer. C. H. Van Poznak[1], C. L. Estilo*[2], T. Williams*[2], N. Sauter[1], C. Hudis*[1], S. Tunick*[2], J. M. Huryn*[2], J. Halpern*[2]. [1]Medicine, Memorial Sloan-Kettering Cancer Center, New York, NY, USA, [2]Dental Service, Memorial Sloan-Kettering Cancer Center, New York, NY, USA.

Background: Intravenous bisphosphonates (IVBP) are potent inhibitors of osteoclast activity, and have been shown to decrease skeletal morbidity rate in patients (pts) with metastatic bone disease by approximately one third. IVBPs have become standard therapy for pts with skeletal metastases from various solid tumors and multiple myeloma. Osteonecrosis (ON) of the jaw has been reported in pts treated with IVBPs. It is postulated that bisphophonates cause avascular necrosis of the jaw due to an antiangiogenic effect. To estimate the incidence and define the clinical sequelae of ON of the jaw in pts with metastatic breast cancer (MBC) receiving therapy with either pamidronate or zoledronic acid (IVBP), we preformed a retrospective chart review.

Patients and Methods: The medical and dental records of all pts with MBC who were treated in the Dental Service of Memorial Sloan-Kettering Cancer Center (MSKCC) between 1/1/00 and 9/14/03 were reviewed. Pts who presented with exposed bone or ON of the maxilla or mandible and were previously treated with IVBP were further evaluated for clinical and pathological characteristics of cancer, duration of IVBP therapy, dental history and symptomatology as well as dental intervention rendered.

Results: During the study period, 13,143 doses of IVBP were administered to 934 pts. 64 pts with MBC treated IVBP were evaluated by the MSKCC Dental Service and 6 pts (0.6%) were found to have ON of the maxilla or mandible. The median age of pts with ON was 53.5 years (range: 27-66), median duration of IVBP therapy was 52.5 months (range: 6-94). 4 of 6 pts presented with symptoms. ON was noted in the maxilla in 2 and mandible in 4. 4 pts had a history of dental extraction in the region of ON. 2 pts presented with spontaneous ON. All pts were prescribed chlorhexidine rinse & 4 pts received antibiotics. Conservative treatment consisting of local debridement and sequestrectomy was performed in 4 pts; resolution was achieved in 1 patient.

Conclusions: IVBPs are an important and effective treatment for many pts with MBC; however, it may be associated with ON, as a rare complication. Our retrospective review identified 6 cases among 943 pts. The true incidence may be greater and the specific causes may be multifactorial. Contributing factors may include advanced cancer, chemotherapy, IVBP and steroid use, as well as comorbid conditions and lifestyle behaviors. Clinicians involved in the care of pts with MBC treated with IVBPs should be aware of the possibility of ON. The etiology and optimal management of ON of the jaw in MBC pts warrants study.

Disclosures: ***C.H. Van Poznak****, Novartis 5.*

SU093

Comparison of Bone-derived Osteonectin and Breast Cancer-secreted Osteonectin; Reducing and Non-reducing Conditions Reveal Distinct Differences. D. A. Campo*[1], D. Sosnoski*[2], C. V. Gay[2]. [1]Intercollege Graduate Degree in Physiology, Penn State University, University Park, PA, USA, [2]Biochemistry and Molecular Biology, Penn State University, University Park, PA, USA.

Osteonectin has been described as a chemoattractant directing breast cancer cell and prostate cancer cell migration toward bone. In order for a substance to act as a chemoattractant, a diffusible gradient must form, thus luring a responsive cell toward higher concentrations. A paradox exists in that not only do osteoblasts secrete osteonectin, but so do vascular endothelial cells and breast cancer cells which colonize bone, potentially negating the formation of a gradient of osteonectin to which breast cancer cells could respond. We hypothesize that there are tissue dependent configurations of osteonectin such that the bone-derived form can exist as a gradient. Osteonectin was initially isolated by collection of conditioned media from two breast cancer cell lines (MDA-MB-435 and MDA-MB-468), from an osteoblast cell line (hFOB1.1) and from a bone-derived vascular endothelial cell line (HBME-1). Osteonectin was removed from conditioned media by affinity column purification using an anti-human osteonectin mouse monoclonal IgG (Haematologic Technologies, Essex Junction, VT) and a Pierce Aminolink® Immobilization kit. Immunoblots were prepared under reducing and non-reducing conditions. Under non-reducing conditions, osteonectin from the cancer cell lines appeared as doublets, ~ 41 and 38 kDa from the MDA-MB-435 cells and ~41 and 36 kDa from the MDA-MB-468 cells whereas under reducing conditions only a single band (~57 or 54 kDa, respectively) was evident. This phenomenon was not observed in osteonectin from bone and endothelial cells both of which display a single band under both non-reducing (~38 kDa) and reducing conditions (~53 kDa). These results suggest that breast cancer cells secrete two forms of osteonectin with different configurations of disulfide linkages whereas bone and endothelial cells secrete osteonectin with a single arrangement of disulfide links. Because disulfide bonds influence protein folding, at least one of the breast cancer-secreted types of osteonectin will have a different three-dimensional structure from the bone or endothelial-derived osteonectin. We conclude that there is structural variation due to the arrangement of disulfide links between bone-derived and breast cancer-derived osteonectin. The structural variation between osteonectin from indigenous and foreign cells at the site of bone metastasis supports the hypothesis that bone-derived osteonectin could form an attraction gradient and act as a chemoattractant even in the presence of breast cancer-derived osteonectin.

Disclosures: ***D.A. Campo****, None.*

SU094

Interleukin-1 Expression in Human Breast Cancer Bone Metastasis: A Newly Recognized Pathway in Breast Cancer-induced Osteolysis. A. G. Pantschenko*[1], R. Naujoks*[1], R. H. Quinn*[2], M. Sanders*[3], G. Gronowicz*[1]. [1]Dept. of Orthopaedic Surgery, University of Connecticut Health Center, Farmington, CT, USA, [2]Combined Hartford Hospital and CT Children's Hospital Orthopaedic Oncology Service, Hartford, CT, USA, [3]Dept. of Pathology, University of Connecticut Health Center, Farmington, CT, USA.

Bone metastasis in human breast carcinoma (HBC) occurs in 83% of patients with advanced disease. The pathophysiology of human breast carcinoma-induced osteolysis (HBC-IO) involves an increase in the number and activity of osteoclasts within the HBC metastatic lesion. These observations strongly support the involvement of cell-to-cell interactions and cytokine networks. We have recently demonstrated that the expression of the pro-inflammatory IL-1 family of cytokines and receptors correlates with disease severity and induction of pro-angiogenic and mitogenic cytokines (*e.g.* IL-8) in HBC primary tumor. Furthermore, IL-8, a product of HBC IL-1 stimulation, has recently been shown to have a greater correlation with HBC bone metastatic potential than PTHrP in the nude mouse.

Since IL-1 expression has been correlated with HBC aggressiveness and IL-1 is a known activator of osteoclasts, we examined the expression of the IL-1 family of cytokines and receptors in HBC-IO using archival human samples and immunohistochemistry. Samples from pathological fracture resection or biopsy of HBC metastasis from 16 patients (mean age, 52yrs; age range, 34-83yrs; no prior radiation to site; 14 samples from proximal femur) were obtained from the Dept. of Pathology, Hartford Hospital, Hartford, CT. and analyzed using the following antibodies; IL-1α, IL-1β, IL-1R1, IL-1R2, IL-8, CXC-R2, PTHrP, and anti-osteoclast antigen.

Thirteen of sixteen samples (81%) showed positive IL-1β tumor cell staining. Among these samples, the majority of tumor cells stained (82%). These thirteen samples were also positive for tumor cell staining of IL1-R1. Fifteen out of sixteen samples (94%) showed osteoclasts IL-1R1 staining. 14/16 showed positive staining of more than 50% of osteoclasts. 1/16 showed staining in 20-50% of cells and 1/16 sample showed no evidence of IL-1R1 staining of osteoclasts. This study supports the hypothesis that HBC tumor cell-induced osteolysis can be mediated through the HBC expression of IL-1 and the subsequent activation of osteoclasts via IL-1R1.

	IL-1β			**IL-1R1**		
	Number of (+) Samples	**Percent (+) Cells**	**Staining Intensity (0-3)**	**Number of (+) Samples**	**Percent (+) Cells**	**Staining Intensity (0-3)**
Tumor Cells	13/16 (81%)	82%	2.3	13/16 (81%)	62%	2.0
Osteoclasts	0/16 (0%)	0%	0	15/16 (94%)	74%	2.8

Disclosures: ***A.G. Pantschenko****, None.*

SU095

Smad3 Interacts with JunB and Cbfa1/Runx2 for Transforming Growth Factor-beta1-Stimulated Collagenase-3 Expression in Human Breast Cancer Cells. N. Selvamurugan, S. Kwok*, N. C. Partridge. Physiology and Biophysics, UMDNJ-Robert Wood Johnson Medical School, Piscataway, NJ, USA.

The specific characteristics of breast cancer cells and the unique properties of the bone/bone marrow microenvironment are largely responsible for the observed high frequency of skeletal metastases from breast cancer. A series of recent studies have indicated that collagenase-3 (matrix metalloproteinase-13) is overexpressed in a variety of tumors from diverse sources. Collagenase-3 is characterized by its ability to degrade the extracellular matrix (ECM) and is stimulated by TGF-β1 (which is enriched in bone matrix) in the human breast cancer cell line, MDA-MB231. Collagenase-3-driven extracellular matrix proteolysis may support cancer cell growth by exposing the cells to growth factors and cytokines, resulting in bone degradation (osteolysis). A greater understanding of the regulatory mechanisms that control collagenase-3 expression may provide several new avenues for therapeutic intervention. To understand the molecular mechanisms responsible for TGF-β1 regulation of the collagenase-3 promoter, a functional analysis of the promoter region of the collagenase-3 gene was carried out and we identified the distal RD (runt domain) and proximal RD/AP-1 (activator protein-1) sites as necessary for full TGF-β1-stimulated collagenase-3 promoter activity. Gel shift, real time RT-PCR and Western blot analyses showed increased levels of c-Jun, JunB, and Cbfa1/Runx2 upon TGF-β1 treatment in MDA-MB231 cells. Co-immunoprecipitation *in vitro* studies identified no physical interaction between JunB and Cbfa1/Runx2; whereas Smad3 interacted with both. Chromatin immunoprecipitation experiments confirmed interaction of Smad3 with JunB and Cbfa1/Runx2. Under basal conditions, Cbfa1/Runx2 bound to both the proximal RD/AP-1 and distal RD sites. In response to TGF-β1, Cbfa1/Runx2 was seen only at the distal RD site; whereas JunB occupied the proximal RD/AP-1 site. An assemblage of Smad3, JunB, and Cbfa1/Runx2 at the distal RD site of the collagenase-3 promoter occurred in response to TGF-β1 in MDA-MB231 cells. Co-transfection of Smad3, JunB, and Cbfa1/Runx2 constructs along with a constitutively active TGF-β type I receptor construct identified functional interaction of these proteins and transcriptional activation of the collagenase-3 gene by TGF-β1. Taken together, our results suggest that TGF-β1 stimulated JunB and Cbfa1/Runx2 to bind to their respective DNA consensus sites and Smad3 is likely to stabilize their interaction to confer functional TGF-β1-stimulation of collagenase-3 expression in MDA-MB231 cells.

Disclosures: ***N. Selvamurugan****, None.*

SU096

Role of VEGF in the Prostate Cancer Bone Microenvironment. C. Muir*[1], D. Carson[1], L. W. K. Chung*[2], M. C. Farach-Carson[1]. [1]Department of Biological Sciences, University of Delaware, Newark, DE, USA, [2]Department of Urology, Emory University, Atlanta, GA, USA.

Prostate cancer preferentially metastasizes to bone where it exhibits osteoblastic features. Angiogenesis is important for tumor growth, and vascular endothelial growth factor (VEGF) family members, including VEGF-A and VEGF-C, play an important role in this process. Hypoxia exists at tumor sites as a consequence of poorly organized or absent vasculature. Our purpose was to examine the effect of culturing bone-targeted, metastatic C4-2B prostate cancer cells and HS27a bone stromal cells in hypoxic conditions on expression of VEGF family members. A sealed growth chamber infused with 1% or 20% O_2 and 5% CO_2 was used to culture cells in hypoxic or normoxic conditions. RT-PCR and commercially available ELISA kits were used to determine growth factor and growth factor receptor expression at both mRNA and protein levels. The bone stromal cells and the prostate cancer cells both produced high endogenous levels of VEGF-A, but little to no detectable levels of HB-EGF and HGF were measured using ELISA. HS27a bone stromal cells expressed high amounts of VEGF-C, whereas the C42B cells made none, and no change was observed after hypoxic culture. Under hypoxic conditions, the cells upregulated secreted isoforms of VEGF-A ($VEGF_{121}$ and $VEGF_{165}$), but levels of heparin binding isoforms ($VEGF_{189}$) did not change. A greater than 2-fold change in secreted VEGF-A was observed in both the HS27a and C42B cells when cultured in 1% oxygen compared to 20% oxygen. Similar changes in VEGF-A were seen at the mRNA level detected by RT-PCR, though the change was more significant in the C42B cells. The mRNA was increased before day two during culture in 1% oxygen, but secreted protein began to change at day two and increased through day six. Treatment with 30ng/ml of $VEGF_{165}$ did not change mRNA levels of VEGF-A by C42B in either normoxic or hypoxic conditions, though C4-2B cells made low levels of VEGFR2, flk-1, and showed a moderate growth response to 30ng/ml of $VEGF_{165}$. Receptor expression levels were not changed during culture in 1% O_2. HBME, human bone marrow endothelial cells, express very high levels of flk-1 and are recruited for neovascularization of the hypoxic growing tumor within the bone environment. We conclude that culture in 1% O_2 causes a physiologically relevant increase in VEGF at mRNA and protein levels by prostate cancer and bone marrow stromal cells, and that this involves a paracrine loop that is likely to recruit bone marrow endothelial cells and support neovascularization.

Disclosures: ***C. Muir****, None.*

SU097

Bisphosphonates Suppress the Mitogenic Effects of Bone-derived Growth Factors on Prostate Cancer Cells. N. Kheddoumi*[1], F. Journé*[1], L. Lagneaux*[2], J. C. Dumon*[1], J. J. Body[1]. [1]Laboratory of Endocrinology and Bone Diseases, Institut Jules Bordet, Brussels, Belgium, [2]Laboratory of Hematology, Institut Jules Bordet, Brussels, Belgium.

Insulin-like growth factor-1 (IGF-1) is a principal growth factor released from the bone matrix resulting from tumor-induced osteolysis, and IGF-1 is a powerful mitogen for prostate carcinoma cells. Bisphosphonates are potent inhibitors of osteoclast-induced osteolysis and are being evaluated as adjunctive therapy for the prevention of bone metastasis. Moreover, they were recently shown to induce prostate cancer cell apoptosis in vitro. In the present study, we have investigated the effects of bisphosphonates on the in vitro proliferation of PC-3 prostate cancer cells in the presence of IGF-1. PC-3 cells were cultured for 1 to 6 days in growth factor-free media with 1 to 100 µM zoledronic acid (Zol) or clodronate (Clod) with or without 100 ng/mL IGF-1. Cell growth was evaluated by crystal violet staining. Apoptotic cell death was assessed using annexin V / propidium iodide double staining. IGF-1 increased PC-3 cell growth by 23 ± 7% (mean ± SEM) at day 6 ($P < 0.001$). At 1 µM, Zol alone did not affect cell growth but completely abolished the mitogenic effects of IGF-1. At 10 µM, Zol inhibited cell proliferation whether IGF-1 was present or not, and 100 µM Zol induced a marked decrease in cell number (to 15% of baseline at day 6). Moreover, 100 µM Zol induced apoptosis in PC-3 cells whether IGF-1 was present or not. In contrast, 1 µM Clod did not inhibit cell growth nor abolish the stimulatory effects of IGF-1. At 10 µM, Clod did not affect cell growth alone but inhibited the mitogenic actions of IGF-1, and 100 µM Clod weakly inhibited cell proliferation with or without IGF-1. Clod did not induce apoptosis even at the highest concentrations. In conclusion, bisphosphonates inhibit the mitogenic effects of IGF-1 on prostate cancer cells, at 1 µM for Zol and 10 µM for Clod. At these concentrations, they had no effect on cell proliferation. At higher concentrations, bisphosphonates inhibit PC-3 cell growth in the presence or absence of IGF-1. Zol was more potent than Clod, and induced apoptosis of prostate cancer cells at the highest concentration. The growth inhibition achieved by Zol in the presence of IGF-1 may contribute to beneficial effects in the treatment of prostate cancer-induced bone disease. We are currently evaluating the effects of other bone-derived growth factors, such as basic Fibroblast Growth Factor, under similar conditions.

Disclosures: ***F. Journé****, None.*

SU098

Inhibition of Growth of Breast Cancer Cells by Low-Dose Risedronate. F. H. Ebetino[1], L. Witters*[2], A. Lipton*[2]. [1]New Drug Development, Procter & Gamble Pharmaceuticals, Mason, OH, USA, [2]The Milton S. Hershey Medical Center, Pennsylvania State University, Hershey, PA, USA.

Risedronate (RIS) is a third generation nitrogen containing bisphosphonate (N-BP) used to prevent and treat postmenopausal and steroid-induced osteoporosis. Treatment of human breast cancer cell lines with RIS (1-20 µM) resulted in dose-dependent growth inhibition (MCF-7: IC50 = 6 µM; HER-2/neu transfected MCF-7: IC50 = 11 µM) These levels of RIS are not achievable in the plasma of patients receiving RIS. Bisphosphonates bind avidly to hydroxyapatite (HA), the major inorganic constituent of bone. The purpose of this study was to assess the effects of RIS bound to hydroxyapatite on the growth of breast cancer cells. MCF-7 cells were grown on HA wafers pretreated with 0.5 µM or 20 µM of RIS. Cells were also grown on HA wafers not pretreated with RIS but where RIS was added after attachment. Growth effects under these conditions were compared to the effects of RIS in culture media in 24 well plates. Cell number was determined by the colorimetric MTT tetrazolium dye assay after a 3 day exposure to RIS. MCF-7 cells grown in culture media were inhibited by 20 µM RIS (78%) or conditioned media from HA wafers pretreated with 20 µM RIS (71%). HA wafers pretreated with 20 µM RIS also inhibited cell growth but to a lesser extent (41%). MCF-7 cells were not inhibited by 0.5 µM RIS in culture media (7%) nor conditioned media from HA wafers pretreated with 0.5 µM RIS (4%). HA wafers pretreated with 0.5 µM RIS, however, inhibited MCF-7 cell growth by 29%. Also, when 0.5 µM RIS was added after cell attachment to the non pretreated HAP wafers, similar inhibition of proliferation was noted as with the pretreatment conditions. Thus, high doses (20 µM) of the N-BP, risedronate, produced antiproliferation of MCF-7 breast cancer cells in culture media, in conditioned media from HA wafers pretreated with 20 µM RIS, and to a lesser extent on the HA wafers pretreated with 20 µM RIS. Low doses (0.5 µM) of RIS caused negligible growth inhibition when added to culture media or in the conditioned media from HA wafers pretreated with 0.5 µM RIS. The 0.5 µM RIS pretreated HA wafers, however, had the ability to inhibit MCF-7 cells suggesting that interactions of tumor cells with bone may magnify the effectiveness of N-BPs beyond what may be expected from their serum concentrations.

Disclosures: ***F.H. Ebetino****, Procter & Gamble Pharmaceuticals 3.*

SU099

Cell-surface Carbohydrate Expression Supports Breast Cancer Colonization of Bone. J. Stanley*, M. Bendre, J. Cárcel Trullols*, S. Shaaf,*, R. Saha*, T. Kieber-Emmons*, L. J. Suva. Orthopaedic Surgery, Pathology and Arkansas Cancer Research Center, UAMS, Little Rock, AR, USA.

It has been suggested that distinct tumor cell phenotypes are required for the establishment of metastatic lesions in different organs. These metastatic phenotypes include changes in carbohydrate expression profiles that have been postulated to improve survival of the tumor cell in the circulation, allow adhesion of tumor cells to target organs and facilitate positive interactions within the microenvironment of the target organ. The variability of carbohydrate sequences, which cell surfaces can present to endogenous lectins, adhesion molecules, and other receptors, creates a refined pattern of potential sites for interactions between a tumor cell and its surrounding microenvironment. In an effort to identify patterns of carbohydrate expression that correlate with bone-specific tumor growth, the cell surface carbohydrate profile displayed by osteotrophic MDA-MET cells was compared with parental MDA-231 cells. The differences in cell surface glycosylation between MDA-MET and parental MDA-231 cells were identified using 14 plant lectins and 4 carbohydrate specific mAb's by flow cytometry and lectin blots. By FACS, MDA-MET cells demonstrated increased binding of SNA, ECL and PHA lectins as well as 19-9 mAb, relative to MDA-231, demonstrating that MDA-MET cells display increased alpha 2,6 sialylation prodcucts. There was also an increase in unsubstituted terminal N-acetyllactosamine structures (ECL) and complex branched structures (PHA) in MDA-MET. FACS analyses were confirmed by Western blot. Microarray analysis (Affymetrix) indicated that the expression of several galactosyltransferase genes responsible for these carbohydrate modifications also correlated with lectin and antibody binding profiles. PCR amplification of human specific DNA from several tissues confirmed the bone-selective distribution of the MDA-MET cell micrometastasis in mice *in vivo*; MDA-MET "seed" but do not produce tumors within non-bone sites. The incubation of MDA-231 or MDA-MET cells with bone marrow-derived cells *in vitro* demonstrated a selective advantage for MDA-MET cell proliferation. This marrow-enhanced tumor cell proliferation was also seen *in vivo*, where unlike MDA-231 cells, MDA-MET form large tumors following tibial implantation. These data suggest that the differences observed in the carbohydrate signatures of MDA-MET cells play a role in the bone-specific colonization and growth in the marrow of this aggressive cell line. Further studies are ongoing to identify the roles of individual proteoglycans that may participate in the formation of secondary tumor growths of breast cancer in bone.

Disclosures: ***L.J. Suva****, GlaxoSmithKline 1; Procter and Gamble 5; Wright Medical 2.*

SU100

NF-kB and not p38 MAPK Is Essential for Bone Resorbing Factor Production by Breast Cancer Cells. C. Menaa, M. Corr*, C. Froelich*, S. Sprague. Medicine, Evanston Northwestern Healthcare Northwestern University, Evanston, IL, USA.

Bone metastases are a frequent complication in patients with advanced breast cancer (BC). This is related to the process by which tumor cells metastasize; that involves adhesion, migration, and induction of osteoclast (OC) formation. How tumor cells acquire these capacities and the mechanisms involved are not yet identified. However, it is known that tumor cells are the source for expression and secretion of factors involved in bone metastasis, such as MMP9, uPA, and more importantly bone resorbing factors (BF).

Previous studies have highlighted the role of NF-κB and p38 MAPK (p38) as potential signaling pathways critical for BC cell viability. Specifically, NF-κB has been reported to be responsible for cell transformation, death resistance, and motility. However, p38 has been linked to the expression of factors critical for cell invasiveness and PTHrP production. In addition, constitutive activity of both signaling pathways has been recorded in BC cells, and the degree of activation positively correlates with cell`s aggressiveness, suggesting that NF-κB and p38 could be responsible for induction and progression of BC. Since stimulation of OC formation is critical for bone metastasis, the role of NF-κB and p38 in BF production by BC cells was examined. Initially stable BC cell lines which over-express the inactive kinase (DN) p38 MAPK (T189/A-Y191/F) were established and demonstrated

that the DN suppresses p38 MAPK activation even following TNF-α stimulation. MDA-MB-231 or MCF-7 cells deficient in p38 activity are still able to support OC formation in RAW 264.7 cells and mouse bone marrow suggesting that p38 activity is not involved in BF production by BC cells. However, the inhibition of NF-κB activity following the over-expression of the super-repressor IκB (S32/A-S34/A) in BC cells totally blocks NF-κB and the capacity of these cells to support OC formation. Further analysis demonstrated that IκB-kinase (IkK) complex is critical for NF-κB activity and expression of BF as well. While the inhibition of IkK-α or β alone has no effect, the overexpression of the regulatory subunit, the IkKγ, totally abolishes NF-kB activity of BC cells, and subsequently their capacity to support OC formation. In summary, we found that while p38 might be critical for some fundamental aspects of BC cells, its constitutive activity is not responsible for BF production. In contrast, NF-κB signaling pathway, specifically the IκK complex, is essential for both constitutive activation of NF-κB and expression and secretion of BF in BC cells. In conclusion, these data establish the role of NF-κB in bone metastasis in BC. Thus, NF-κB could be a suitable therapeutic target for bone destruction in BC.

Disclosures: ***S. Sprague****, None.*

SU101

Bone Loss after Chemotherapy in Women with Early Breast Cancer. M. M. Pinheiro*[1], A. R. Siniscalchi*[2], S. M. T. Carvalho*[3], H. J. Rigon*[2], M. Mourao Netto*[3], V. L. Szejnfeld[1]. [1]Rheumatology, Unifesp, Escola Paulista de Medicina, Sao Paulo, Brazil, [2]Medicine Interne, Hospital do Cancer A C Camargo, Sao Paulo, Brazil, [3]Breast's surgery, Hospital do Cancer A C Camargo, Sao Paulo, Brazil.

Our aim was evaluate the impact of the chemotherapy (CT) on bone mineral density (BMD) and quantitative ultrasound (QUS) parameters in patients with early breast cancer (EBC). One-hundred sixty two women were enrolled in this study (62 with EBC and 100 healthy controls matched for age, body mass index and menopausal status). Patients with history of other cancers, previous CT or metastatic disease were excluded. Spine and femur BMD were performed using DXA (Lunar, DPX) and calcaneus QUS was done using Achilles plus (Lunar). Fifty-four (87.1%) EBC patients and 83 (83%) healthy controls completed a 10-month follow-up. Mean age, height, weight and BMI for EBC patients were 52.1 ± 10 years, 68.2 ± 14.3 kg, 1.57 ± 0.7 m and 27.6 ± 5.4 kg/ m2, respectively. Twenty (43.5%) EBC patients were pre-menopausal and six (13%) had previous atraumatic fracture. CT protocols used were [fluorouracil, doxorubicin, cyclophosphamide] (71.7%) or [cyclophosphamide, methotrexate, fluorouracil] (28.3%) with mean cycles of 5.8 ± 1.8 and 7.7 ± 2.1, respectively. At baseline, EBC patients had BMD and QUS measurements 5% higher than healthy controls. After CT (8.5 ± 2.7 months), EBC patients had significantly lower BMD (2%) and QUS (3.2%) measurements as compared to healthy controls. No new fractures were detected during the follow-up. In conclusion, CT affects negatively bone mass and can be a potential risk factor for fracture in EBC patients.

Disclosures: ***M.M. Pinheiro****, None.*

SU102

MRI Mapping of the Degree of Bone Mineralization. Y. Wu*[1], J. L. Ackerman*[2], L. Graham*[1], M. Glimcher[1]. [1]Orthopaedic Surgery, Children's Hospital, Boston, Boston, MA, USA, [2]Radiology Department, Massachusetts General Hospital, Boston, MA, USA.

The degree of bone mineralization (DM), is defined as the weight of bone mineral in a unit volume of bone matrix. It can be expressed as the ratio of bone mineral density (BMD) divided by the bone matrix fraction factor. DM is a crucial parameter for bone quality, because it modifies the elastic modulus of the matrix material.

The ^{31}P NMR signals of bone mineral and some fraction of the ^{1}H NMR signals of bone matrix can be imaged by solid state projection magnetic resonance imaging (SMRI). Our previous study has shown that ^{31}P solid state MRI (SMRI) measurement of BMD was feasible. In this current study, quantitative water and fat suppressed ^{1}H projection MRI (WASPI) measurement of bone matrix fraction factor was performed in a Bruker 4.7T scanner. Combined ^{31}P/^{1}H MRI was performed using a double tuned coil in the Bruker 4.7T scanner.

Table 1 shows the bone matrix fraction factor measured by ^{1}H WASPI and gravimetry. Comparing the data of MRI and gravimetry, these results look very promising.

Figure 1A and B show corresponding slices of ^{31}P SMRI and ^{1}H WASPI of a bovine cortical bone specimen. A preliminary mapping of the degree of bone mineralization is obtained by dividing the ^{31}P image intensity by the proton image intensity pixel by pixel (Figure 1C).

Our study results demonstrate that measurement of matched ^{31}P SMRI and ^{1}H WASPI images of bone specimens is feasible, which would lead to the measurement of bone mineralization if ^{31}P and ^{1}H intensity are converted to BMD and bone matrix fractor respectively.

Table 1 Bone matrix fraction factor determined by ^{1}H WASPI and gravimetry (*all specimens were from the same bone)

	Bovine trabecular 1*	Bovine trabecular 2*	Bovine trabecular 3*	Bovine trabecular 4*
^{1}H WASPI (%)	21	18		
Gravimetry (%)			17	16

Figure 1 MRI slices in longitudinal and axial views (A, B), and mapping of a bovine cortical bone specimen

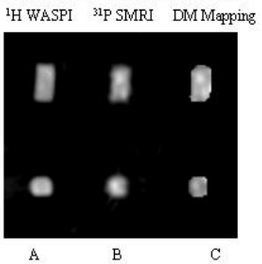

Disclosures: ***Y. Wu****, None.*

SU103

Comparison of Radiographic Absorptiometry (RA) and DXA in a Postmenopausal Middle Eastern Population. A. Ghasemzadeh*[1], N. Bayat*[2], G. Ali Shiri*[3], S. Hosseini M.*[4], E. P. Boling[5]. [1]Medical Physics, Research Center for Sciences and Technology in Medicine, Tehran, Iran (Islamic Republic of), [2]Rheumatology Dept, Baghayatallah Hosp.Baghayatallah Medical scineces University, Tehran, Iran (Islamic Republic of), [3]Rhumatolgy Dept., Baghiaitallah Hospital,Baghiaitallah Medical Science university, Tehran, Iran (Islamic Republic of), [4]Baghayatallah Medical scineces University, Baghayatallah Hosp., Tehran, Iran (Islamic Republic of), [5]Loma Linda University, Loma Linda, CA, USA.

Limited availability of DXA can delay or prevent diagnosis of osteoporosis in Middle Eastern women. A correlation study was therefore conducted in post-menopausal Middle Eastern females comparing peripheral bone mineral density (BMD) measured by RA to axial BMD measured by DXA. Data analysis showed good correlation between peripheral and axial BMD measurements.

33 postmenopausal Iranian women aged 45 to 74 years were seen at the BMD center of Baghayatallah Hospital, Tehran, Iran from November 2003 to January 2004 and were considered for this study. Those with secondary causes of osteoporosis were excluded. The mean age of the study participant was 57.9 + 7.7 years.

Peripheral BMD was measured by automated Osteogram (CompuMed, Inc; Los Angeles, CA) using radiographic absorptiometry (RA), a technique which measures BMD of 3 middle phalanges using 2 view, non-dominant hand X-rays taken with an adjacent aluminum reference wedge. Axial BMD of hip and L2-L4 spine was performed using a Norland XR-36 densitometer (Fort Atkinson, WI).

Pearson correlation coefficients between RA BMD of the middle phalanges and DXA BMD of the spine and femoral neck were 0.77 and 0.80 respectively. In comparison, Pearson between DXA BMD of the spine and DXA BMD of the femoral neck was 0.84. The correlation between RA BMD and the two DXA BMD assessments is considered statistically significant per kappa score definitions. In addition, it is comparable to the correlation between the two DXA BMD assessments at 0.84.

Osteogram measured BMD may be a cost effective and more readily available alternative to axial BMD for the diagnosis of osteoporosis in postmenopausal Middle Eastern women.

Disclosures: ***A. Ghasemzadeh****, None.*

SU104

Effect of Urbanization on Bone Mineral Density; A Comparative Study. C. Pongchaiyakul*[1], T. V. Nguyen[2], V. Kosulwat*[3], R. Rajatanavin*[4]. [1]Department of Medicine, Division of Endocrinology, Khon Kaen, Thailand, [2]Department of Medicine, Garvan Institute of Medical Research, Sydney, Australia, [3]Institute of Nutrition, Salaya campus, Division of Endocrinology, Nakonprathom, Thailand, [4]Department of Medicine, Division of Endocrinology, Bangkok, Thailand.

A cross-sectional study was designed to examine the difference in bone mineral density (BMD) between urban and rural Thai populations. Femoral neck and lumbar spine BMD was measured by DXA in 411 urban and 436 rural subjects (340 men and 507 women), age between 20 and 84 years. After adjusting for age and body weight, femoral neck BMD in rural men and women was significantly higher than those in urban men and women ($P <$ 0.001), but the difference was not observed at the lumbar spine. In the entire sample, rural subjects had a higher cross-sectional "rate of bone loss" than urban subjects, particularly at the femoral neck. As a result, among those aged 50^{+} years, BMD in rural subjects tended to be lower than (or converged to) BMD in urban subjects. After stratified by sex, age group, and BMI category, the urban-rural difference in femoral neck BMD became more pronounced in the younger age group (< 50 years old) and higher BMI (≥ 25 kg/m^2) in both men and women. This data suggest that femoral neck BMD in rural men and women was higher than their counterparts in urban areas. This difference could potentially explain the urban-rural difference in fracture incidence.

Disclosures: ***C. Pongchaiyakul****, None.*

SU105

Contribution of Lean Tissue Mass to the Urban-Rural Difference in Bone Mineral Density. C. Pongchaiyakul*[1], T. V. Nguyen[2], J. A. Eisman[2], R. Rajatanavin[3]. [1]Division of Endocrinology, Department of Medicine, Faculty of Medicine, Khon Kaen University, Thailand, [2]Bone and Mineral Research Program, Garvan Institute of Medical Research, Sydney, Australia, [3]Division of Endocrinology, Department of Medicine, Mahidol University, Thailand.

While the urban-rural difference in bone mineral density (BMD) has been well established, the reason for the difference is largely unknown, particularly in developing countries. This cross-sectional, epidemiologic study was designed to examine the hypothesis that measures of body composition such as lean mass (LM) and fat mass (FM) contribute to the urban-rural difference in BMD. The setting was in Bangkok city and Khon Kaen province. Lumbar spine and femoral neck BMD, LM and FM were measured by dual-energy X-ray absorptiometry in 411 urban and 436 rural Thai subjects, aged 20-84 years. The results showed that rural subjects had significantly higher BMD, higher LM and lower FM than urban subjects. In multiple linear regression analysis, LM, but not FM, was an independent predictor of BMD in both men and women. When the two groups were matched for FM, rural subjects with higher LM were associated with a 4.4percent to 7.2percent higher BMD than urban subjects. However, when the two groups were matched for LM, rural subjects with higher FM did not have higher BMD than those in urban areas. In match-pair regression analysis, the urban-rural difference in LM explained approximately 23percent and 5percent of the urban-rural difference in femoral neck BMD in men and women, respectively. These data are consistent with the hypothesis that the association between BMD and body composition is mediated mainly through lean mass, and that the urban-rural difference in BMD could be explained in part by the urban-rural difference in lean mass.

Disclosures: ***C. Pongchaiyakul****, None.*

SU106

Assessment of Cortical Bone Mineral Density by Peripheral Quantitative Computed Tomography in Children: Impact of Partial Volume Effects. L. W. Kibe*, B. S. Zemel, M. B. Leonard. Pediatrics, The Children's Hospital of Philadelphia, Philadelphia, PA, USA.

DXA measures of areal-bone mineral density (aBMD) are confounded by bone size. Peripheral quantitative computed tomography (pQCT) is purported to estimate volumetric BMD (vBMD) independent of bone size. However, as a consequence of incomplete filling of voxels at the bone edges (partial volume effects), cortical vBMD is underestimated in thinner bones, potentially confounding results in children with poor growth or thin bones. The objective of this study was to evaluate pQCT estimates of cortical vBMD as a function of bone thickness in healthy children and adolescents.

Methods: PQCT (Stratec XCT-2000; voxel size 0.4 mm) scans of the left tibia were obtained at the 38% site in 140 subjects, at the 20% site in 147 subjects and at both sites in 15 subjects, ages 5 to 19 yr. Cortical bone was identified at a threshold of 710 mg/cm^3, and cortical vBMD (CORT-vBMD) was determined as the mean vBMD over the entire cortical bone in the slice. In order to isolate a region of cortex with completely filled voxels, a 2 x 2 voxel region of interest (ROI) was manually centered between the endosteal and periosteal envelope at the thickest region of the cortex, and vBMD was measured (ROI-vBMD). Test-retest precision for ROI-vBMD was performed in 30 subjects: the CV was 2.6%.

Results: The mean ($\pm$ SD) cortical thicknesses (mm) at the 38% and 20% sites were 5.1 $\pm$ 0.9 (range 3.1 - 7.8) and 3.1 $\pm$ 0.7 (range 1.6 - 5.4), respectively. In the 15 subjects with both 20% and 38% scans, CORT-vBMD was significantly greater at the 38% compared with 20% site (1098 $\pm$ 52 vs. 1075 $\pm$ 63 mg/cm^2, p=0.001) but ROI-vBMD did not differ between sites (1176 $\pm$ 60 vs. 1180 $\pm$ 70, p=0.79). In the 140 subjects with 38% scans, CORT-BMD was significantly less than ROI-vBMD (1097 $\pm$ 54 vs. 1176 $\pm$ 81, p< 0.0001), consistent with partial volume effects. The difference between CORT-vBMD and ROI-vBMD did not vary as a function of cortical thickness. In contrast, in the 147 subjects with scans at the 20% site, the differences between CORT-vBMD and ROI-vBMD were more pronounced (1065 $\pm$ 55 vs. 1180 $\pm$ 59, p< 0.0001), and the difference (ROI-vBMD - CORT-vBMD) was negatively correlated with cortical thickness (p< 0.0001). That is, CORT-vBMD underestimated vBMD to an even greater degree in thinner bones.

Conclusion: pQCT measures of vBMD are subject to greater partial volume effects at the thinner 20% site. The partial volume effects are minimized through application of a discrete ROI which provides a measure of vBMD comparable to values obtained at the thicker 38% site. These effects are likely even greater in the thinner radius, another site commonly studied in pediatric pQCT applications.

Disclosures: ***M.B. Leonard****, None.*

SU107

An Evaluation of DXL Calscan Reproducibility. L. I. M. Toft[1], T. B. Brismar*[2]. [1]Merck, Sollentuna, Sweden, [2]Center for Surgical Sciences, Division of Radiology, Karolinska Institutet, Stockholm, Sweden.

The standard technique to measure spine and hip is rather expensive and requires skilled staff to provide accurate measurements. Techniques cheaper and easier to use have therefore been developed. Such a technique is dual X-ray and laser of calcaneus (DXL). The method combines DXA with laser technology. Theoretically the technique will obtain a more accurate BMD value as the laser enables a measurement of heel thickness making it possible to base the calculations on a three-compartment-model (fat, lean and bone).

We have evaluated short and long term reproducibility of DXL Calscan as well as the agreement between 4 individual units. The variation in BMD and T-score between the right and the left foot in a clinical material has also been studied retrospectively.

Short term reproducibility and agreement between individual units;

19 individuals aged 46 +/- 12 years were scanned twice on each of four DXL Calscan (Demetech, Stockholm, Sweden) units. All individuals were measured 8 times resulting in a total of 152 measurements. The difference between all 4 scanners was significant. The short term CV% for all measurements on all scanners was 2.1% and the average CV% per scanner ranged from 1.1% to 1.8%.

Long term reproducibility

The left foot was measured in one female volunteer aged 32 years at 13 occasions during 13 months. The average BMD was 400 mg/cm^2 with a CV% of 1.3%.

Variation in BMD and T-score between the right and left foot:

The right and left calcaneus was measured in 334 individuals (18 males and 316 females) under clinical suspicion of osteoporosis. There was no statistical difference in average BMD of the right and left foot (309 mg/cm^2 and 313 mg/cm^2 respectively). The squared correlation coefficient (r^2) between the right and left side was 0.92.

Conclusion

The observed difference between the units emphasis the importance of always using the same unit for follow-up studies. The observed average difference between individual units was however small (equivalent to 0.13 T-score) and should only be of minor importance in the epidemiological perspective. Both short and long term reproducibility of the equipment was good. We conclude that the Demetech DXL Calscan has a good potential for epidemiological studies.

Disclosures: ***L.I.M. Toft****, None.*

SU108

Osteoporosis in Chinese American Women: Development of a Bone Densitometry Database. M. A. Donovan[1], A. Opotowsky*[1], R. Babbar*[2], F. Nabizadeh*[2], M. Della Badia*[1], D. McMahon*[1], G. Liu*[2], J. P. Bilezikian[1]. [1]Medicine, College of Physicians and Surgeons, Columbia University, New York, NY, USA, [2]Medicine, NYU Downtown Hospital, New York, NY, USA.

Asian women have been shown to have lower bone mineral density (BMD) than Caucasian women. Despite this, studies in Asia and the USA suggest that Chinese women have a lower hip fracture rate than Caucasian women. The relationship between BMD and fracture risk, therefore, may differ for Caucasian and Asian women, an observation that may have implications for diagnosis and treatment of osteoporosis. The purpose of this study is threefold: (1) to develop a referent BMD database among Chinese American women; (2) to establish a relationship between BMD and fracture risk in this population; (3) and to compare these data to information for Caucasian women in the USA and Chinese women in China. Four hundred Chinese American women, living in New York City, ages 20 to 90, are being recruited. Along with DXA of the total hip (TH) and lumbar spine (LS), demographic, familial, nutritional, behavioral, and attitudinal features are being obtained using a bilingual questionnaire. The project also includes a case-control comparison of patients who will have sustained a hip fracture. To date, 356 women have been recruited. Preliminary data in this Chinese American population suggest that mean BMD values are lower at the TH for the decades beginning at ages 20 (.899±.109 *vs* .942± .122g/cm^2, p=.02), 30 (.897±.103 *vs* .939±.122g/cm^2, p=.06), 40 (.906±.129 *vs* .922±.122 g/cm^2, p=.02) and 50 (.809±.120 *vs* .886±.122 g/cm^2, p=.02), but not for those at 60, 70, or 80 compared to NHANES III values for Caucasian women. Similar findings are apparent for mean LS BMD values compared to the Hologic Caucasian female BMD database. In addition, peak BMD in Chinese American women is lower at the TH (.906±.129 *vs* .942±.122g/cm^2, p<.0001) and LS (1.013±.126 *vs* 1.047±.11g/cm^2, p<.0001) compared to Caucasian women and was not achieved until the fifth decade (ages 40-49). When we used this newly established Chinese American database, the osteoporosis detection rate in our Chinese American cohort ≥ age 50 was 51% lower than when we used the Hologic Caucasian database (p<.001). If fracture risk is considered in relation to peak BMD for a specific population, and not BMD in absolute terms (g/cm^2), then use of a Caucasian reference for diagnosis of osteoporosis would lead to an overestimate of fracture risk among Chinese Americans. These observations may explain apparent discrepancies between T-scores and fracture incidence among Chinese Americans. This study provides, for the first time, a race and geographically-specific BMD database that has direct clinical relevance to a Chinese American population.

Disclosures: ***M.A. Donovan****, None.*

SU109

DXA Bone Mineral Density (BMD) Measurements of the Proximal Femur: Clinical Value of Bilateral Hip Determinations and in the Location of the Region of Interest of the Femoral Neck. M. T. DiMuzio. The North Shore Osteoporosis Center, Deerfield, IL, USA.

Hip fracture is the most critical skeletal site in which to monitor fracture risk. DXA, is the gold standard for determining BMD and its sensitivity and accuracy have long been established as the principal risk factor for ranking a patient's skeletal health. However, the differences in skeletal structure and organization as well as location leads to differences in a given patients BMD values throughout the skeleton. This skeletal discordance must be taken into account when evaluating a patient for fracture risk and osteoporosis.

This study uses DXA to measure the BMD of the hip and shows: 1) the BMD of the femoral neck region is critically sensitive to location, and 2) the bilateral measurement of hip BMD is essential in determining a patients risk for hip fracture.

Patients were referred for a bone density test. Of the 350 subjects in the study, no preference for age, weight or WHO category of fracture risk was used to select patients for inclusion. 95% of the group were caucasian women, 5% were caucasian men. Each bone density test was performed using a Hologic QDR4500A.

Regions of Interest (ROI): BMD measurements of the femoral neck ROI were made along the neck beginning at greater trochanter and moving toward the head of the femur. BMD was determined at equal increments along the neck and showed a consistent increase for all patients. For the 350 patients examined, the average change in BMD from the edge of the greater trochanter to the central neck region was a 7.6% increase in BMD.

Bilateral Hip BMD: There were no patients found with identical BMD measurements of the right and left femur. The differences between right and left hips and the Total Hip and Femoral Neck BMD measurements were between 0.5% and 12% and 1% and 8%, respectively.

CONCLUSIONS: In all patients examined, the BMD increased as one moved from the edge of the greater trochanter toward the head of the femur. Since fracture risk increases with decreasing BMD, it is critical to measure to where the BMD is lowest in the femoral neck: along the edge of the greater trochanter. The use of handedness or other patient specific factors to assume hip dominance proved to be an insensitive means to monitor BMD of the hip. It is suggested and apparent from these results that both hips should be monitored and that the lowest valued hip (the hip at highest fracture risk) be used to follow future changes in BMD.

Disclosures: ***M.T. DiMuzio****, Proctor and Gamble 2.*

SU110

An Evaluation of the Revised United Kingdom National Osteoporosis Society Position Statement on the use of Peripheral X-ray Absorptiometry. R. Patel, E. Panayiotou*, G. Blake, I. Fogelman. Osteoporosis Research Unit, Guy's King's and St Thomas' School of Medicine, London, United Kingdom.

In a recent revision of its position statement on the clinical use of peripheral X-ray absorptiometry (pDXA), the United Kingdom National Osteoporosis Society (NOS) recommended a triage approach to the interpretation of peripheral measurements based on setting device specific upper and lower thresholds with 90% sensitivity and 90% specificity for identifying patients with osteoporosis at the hip or spine. For patients with a pDXA measurement either below the lower threshold or above the upper threshold, the decision whether or not to offer treatment is made without reference to an axial DXA examination. However, patients with a pDXA result between the two thresholds are recommended to have an axial DXA measurement to obtain a definitive diagnosis of osteoporosis. In this study we examined the practical implications of the NOS triage algorithm based on theoretical calculations using a bivariant Gaussian model. The predictions were compared with data from clinical studies using the Osteometer DTX200 and Schick AccuDEXA devices. The calculations predict that for a population of white women with a mean age of 60 y and for peripheral versus axial BMD correlation coefficients of $r = 0.2$, 0.4, 0.6 and 0.8 the percentages of patients requiring an axial DXA examination are 72%, 60%, 41% and 17% respectively. These predictions were compared with data from a study of 393 white women aged 55 to 70 y (mean age 62.5 y) who had spine and hip DXA followed by a forearm pDXA measurement on the DTX200. The device specific upper and lower thresholds were DTX200 T-scores of -1.4 and -2.6 respectively. Application of the NOS pDXA triage algorithm would result in 39% of women being sent for axial DXA, while for the observed correlation coefficient between hip and forearm BMD ($r = 0.65$) the model predicted 36%. In the second clinical study 300 white women aged 55 to 70 y (mean age 62.6 y) had spine and hip DXA followed by a finger pDXA measurement on AccuDEXA. The device specific upper and lower thresholds were AccuDEXA T-scores of +0.1 and -1.6 respectively. Application of the NOS pDXA triage algorithm would result in 44% of women being sent for axial DXA, while for the observed correlation coefficient between hip and finger BMD ($r = 0.58$) the model predicted 43%. We conclude that in practice for correlation coefficients around $r \approx 0.6$, the NOS pDXA triage algorithm requires sending about 40% of patients for hip and spine DXA.

Disclosures: ***R. Patel****, None.*

SU111

Gender Differences in Areal Bone Mineral Density (aBMD) Represents the Difference in Bone Size rather than in True Volumetric Bone Mineral Density (vBMD). B. Kim[1], J. Son*[2], G. Kim*[1], S. Kim*[3], D. Lee*[3]. [1]Family medicine and Community health, Ajou University College of Medicine, Suwon, Republic of Korea, [2]Family medicine, Eulji hospital, Seoul, Republic of Korea, [3]Family medicine, Samsung cheil hospital, Seoul, Republic of Korea.

We investigated how bone structure influences gender difference in aBMD in Korean adults. 183 men and 183 women, who attended periodic health examination program at the health promotion center at Ajou university hospital from Jan. 2001 to Dec. 2002, were enrolled for this study. We measured bone width, height, bone mineral content (BMC) and aBMD by dual energy absorptiometry (DEXA) and calculated bone volume and vBMD by Carter's method at the third lumbar vertebra. Height, width and volume of L3 vertebra were larger in men than in women, respectively (3.62±0.202cm vs 3.39±0.176cm, 5.02±0.336cm vs 4.42±0.271cm, 77.67±11.009cm^3 vs 58.34±7.733cm^3, all $p<0.001$). BMC and aBMD of the vertebra were also larger in men than in women, respectively (20.50±3.822g vs 15.68±3.178g, 1.13±0.173g/m^2 vs 1.05±0.197g/m^2, all $p<0.001$). However, BMC adjusted by bone volume, true BMD (vBMD) shows no difference between both genders (men; 0.27±0.042cm^3/g, women; 0.27±0.054cm^3/g, P=0.31). Bone mass and Bone size are larger in men than in women while true BMD in men is in consistency with that in women. Higher aBMD in men accounts for bigger bone size in men rather than true BMD.

Disclosures: ***B. Kim****, None.*

SU112

Reference Data for the Whole Body, Lumbar Spine and Proximal Femur for American Children Relative to Age, Gender and Body Size. B. S. Zemel[1], M. B. Leonard[2], H. J. Kalkwarf[3], B. L. Specker[4], L. J. Moyer-Mileur[5], J. A. Shepherd[6], T. J. Cole*[7], H. Pan*[7], T. L. Kelly[8]. [1]GI and Nutrition, Children's Hospital of Philadelphia, Philadelphia, PA, USA, [2]Nephrology, Children's Hospital of Philadelphia, Philadelphia, PA, USA, [3]General and Community Pediatrics, Cincinnati Children's Hospital Medical Center, Cincinnati, OH, USA, [4]Nutrition Center, South Dakota State University, Brookings, SD, USA, [5]Center for Pediatric Nutrition Research, University of Utah, Salt Lake City, UT, USA, [6]Radiology, University of San Francisco, San Francisco, CA, USA, [7]Institute of Child Health, University College London, London, United Kingdom, [8]Research and Development, Hologic, Inc, Bedford, MA, USA.

Assessment of bone mineral accrual abnormalities in children is dependent on reference data that capture the range of variability in healthy children relative to age, gender and body size. Childhood bone mineral disorders are often associated with growth abnormalities, so assessment relative to body size is essential. We report age and gender-specific reference data for bone mineral content (BMC) and density (BMD) of the whole body (WB), spine and proximal femur, and size-specific spine and WB BMC reference values in White children from a large U.S. multi-center sample.

Healthy children were evaluated at five centers in numerous IRB approved research protocols. DXA spine (n=1444), hip (n=1047) and whole body (n=1948) exams were acquired on Hologic, Inc. QDR 4500 fan beam systems and analyzed with the automatic low density analysis methods using the latest generation of software (version 12.1). Scan images were analyzed centrally by a single operator (TLK) to assure consistency. Gender-specific reference curves were generated using the LMS Pro software relative to age (WB, spine and proximal femur) and size (WB BMC-for-ht and spine BMC-for-bone area).

Children ages 5 to 20 years were evaluated for the spine and proximal femur; WB reference data extend from age 3 to 20 years. Several reference curves are shown.

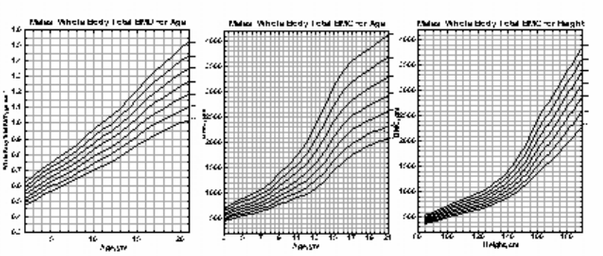

These reference curves are based on a large multi-center convenience sample of healthy children using state-of-the-art scan analysis and statistical approaches for reference curve generation. They allow for age, gender and size-specific comparisons with healthy children for the detection of abnormal bone mineral values in children in both research and clinical care.

Disclosures: ***B.S. Zemel****, None.*

SU113

Precision of Peripheral Quantitative Computed Tomography Measures of the Tibia in Children. B. S. Zemel[1], D. Paulhamus*[1], C. Dilzer*[1], V. A. Stallings*[1], M. Shabbout*[2], M. B. Leonard[3]. [1]GI and Nutrition, Children's Hospital of Philadelphia, Philadelphia, PA, USA, [2]Biostatistics, Children's Hospital of Philadelphia, Philadelphia, PA, USA, [3]Nephrology, Children's Hospital of Philadelphia, Philadelphia, PA, USA.

Peripheral quantitative computed tomography (pQCT) is increasingly available as a research tool in studies of pediatric bone disorders. In adults, the radius is the usual measurement site. For children, the tibia is a more optimal site because it has a larger diameter, greater thickness, and is a weight bearing site. Because of modeling of the tibia during growth, and maturational changes in the epiphysis, use of pQCT in children presents unique challenges. Here, we report the precision of pQCT measures of the tibia in children to aid in the interpretation of these measures.

Healthy children, ages 6 to 18 yrs were recruited from pediatric practices and the general community. Subjects were free of chronic disease and medication use that would affect growth or dietary intake. Tibia length was measured anthropometrically. pQCT measurements of the distal left tibia were obtained at the 3%, 8mm and 38% sites using a Stratec XCT 2000 (Orthometrix, White Plains, NY) 12-detector unit. The proximal edge of the medial physis was used as the reference point (voxel size = 0.4mm, scan speed = 25mm/sec). Duplicate measurements were obtained with repositioning, and repeated scout view scans. Within-subject coefficient of variation (CV) was estimated using the method of Bland and Altman (BMJ, 1996;313:106).

Sixty children enrolled in the study. Paired usable scans were available for 56, 51 and 55 children at the 3%, 8mm and 38% sites, respectively. Subjects were approximately evenly divided between younger (6 to 10 yrs) and older (11 to 18 yrs) children. The CVs of selected measures are shown in the table. Values for younger children are slightly higher than for older children. Trabecular density at the 3% site has a lower CV than at the 8mm site suggesting that a relative distance is more reproducible than a fixed distance.

Site	Measure	All Ages	6 to 10 yrs	11 to 18 yrs
3 Percent	Trabecular Density	1.4	1.5	1.3
8 mm	Trabecular Density	2.6	2.7	2.4
38 Percent	Cortical Density	0.7	0.9	0.5
38 Percent	Cortical Thickness	1.4	1.4	1.5
38 Percent	Endosteal Circumference	1.7	1.8	1.5
38 Percent	Periosteal Circumference	0.4	0.5	0.3
38 Percent	Strain Strength Index	2.1	2.2	2.0

In sum, measures of trabecular and cortical density, and cortical geometry of the tibia can be obtained with excellent precision in children. Reproducible measures can be obtained in both younger and older children. Use of a fixed distance at the distal site is not quite as reproducible as at a percentage distance from the reference point.

Disclosures: ***B.S. Zemel****, None.*

SU114

Total Lymphocyte Count and Lumbar Bone Mineral Density in Korean Postmenopausal Women. Y. Moon*, Y. K. Kim*. Family Medicine, Hallym University College of Medicine, Chunchon, Republic of Korea.

In vitro and vivo studies showed that several hormones and cytokines produced by immune system can affect in bone metabolism. Our aim was to evaluate the association between total lymphocyte count (TLC) and lumbar bone mineral density (BMD) in Korean postmenopausal women. We included 143 healthy women out of 423, who were after at least 2 years of menopause and not being diagnosed and treated for any chronic diseases including osteoporosis. Lumbar BMD was measured by dual-energy X-ray absorptiometry at lumbar (L)1-4. A positive correlation was observed in lumbar BMD (L1, r=0.294, P < 0.01; L2, r=0.249, P < 0.001; L3, r=0.260, P < 0.001; L4, r=0.222, P < 0.001; total r=0.286, P < 0.001) after adjusting for age and body mass index (BMI). Our data showed a positive association between TLC and lumbar BMD in a sample of apparently healthy, postmenopausal women, suggesting possible connection between the immune system and bone metabolism.

Disclosures: ***Y. Moon****, None.*

SU115

Determinants of Bone Mineral Density in Asian Men. J. Gu*[1], K. K. Lee*[1], E. Y. N. Cheung*[1], K. F. Lam*[2], A. Y. Y. Ho[1], S. Tam*[3], A. W. C. Kung[1]. [1]Medicine, The University of HongKong, HongKong, Hong Kong Special Administrative Region of China, [2]Statistics & Actuarial Science, The University of HongKong, HongKong, Hong Kong Special Administrative Region of China, [3]Clinical Biochemistry Unit, Queen Mary Hospital, HongKong, Hong Kong Special Administrative Region of China.

Osteoporotic fractures are increasing among Asian populations in both sex but the risk factors for low bone mineral density (BMD) in Asian men is unknown. To determine the hormonal and lifestyle risk factors for low BMD in Asian men, 407 community dwelling southern Chinese men aged 50 years and above were studied. Medical history and lifestyle habits were obtained using a structured questionnaire. Dietary calcium and phytoestrogen intake was assessed by a semi-quantitative questionnaire. BMD at the spine and hip were measured by DXA. Fasting blood was analyzed for 25(OH)D, PTH, total and bioavailable estradiol (bio-E) and testosterone (bio-T). The mean age of the cohort was 68.42±10.4 (50-96) yrs. In the linear regression model, weight, age, bio-E, cigarette smoking and weight bearing exercise were significant determinants of total hip BMD. Together they explained 46.4% of the total variance of hip BMD with body weight being the most important determining factor (r^2=0.39). With age and weight adjustment, height, bio-T and flavonoid intake were identified as additional determinants of total hip BMD. Strategy to prevent bone loss and osteoporosis in Asian men should include lifestyle modification and maintenance of hormonal sufficiency.

Disclosures: ***J. Gu****, None.*

SU116

Total Skeleton Is a Useful Tool to Study Bone Mineral Density and Body Composition in Healthy Postmenopausal Women. A. Bagur[1], S. Mastaglia*[1], M. Royer*[2], B. Oliveri[1]. [1]Sección Osteopatías Médicas, Hospital de Clínicas, Universidad de Buenos Aires, Buenos Aires, Argentina, [2]Sección Climaterio, Divisiòn Ginecologìa, Hospital de Clínicas, Universidad de Buenos Aires, Buenos Aires, Argentina.

Total skeleton (TS) is a useful tool to study simultaneously bone mineral density (BMD) and body composition (BC) in different diseases. Endogenous estradiol (EE2) over 10 pg/ml may play a role in the protection of BMD in healthy postmenopausal women (PMPW). The aim of this study was to evaluate the usefulness of TS to distinguish the effect of different EE2 levels on BMD in healthy PMPW, and to analyze its relationship with BC. Ninety-seven PMPW aged 55 to 75 years were studied. TS was measured by DXA (Lunar Prodigy). Serum calcium, bone alkaline phosphatase (BAP), serum crosslaps (sCTX), E2 (a sensitive assay that detects up to 5 pg/ml), estrone and urine calcium were measured. The general characteristics of the population were (mean ± DS): weight 65 ± 11 kg, height 1.55 ± 0.05 m, BMI 27 ± 4, TS BMD 0.985 ± 0.18 g/cm2, % fat 40.4 ± 6.3, fat mass 26.5 ± 7.3 kg, lean 37.6 ± 4.5 kg, EE2 10.1 ± 4.9 pg/ml, estrone 20.7 ± 10.2 pg/ml, SHBG 42.5 ± 17 nmol/l, scalcium 9.3 ± 0.5 mg/dl, phosphate 3.6 ± 0.5 mg/dl, BAP 74.7 ± 18.1 UI/L, sCTX 542 ± 254 ng/ml and urine calcium 157 ± 78.3 mg/24 hs. The population was divided according to EE2 levels: <10 and ≥10 pg/ml. Women with EE2 ≥10 pg/ml had higher BMD and BC values compared with women with EE2 <10 pg/ml: fat mass 28.2 ± 7.3 vs 25.1 ± 7.1 kg (p<0.04), lean 38.6 ± 4.8 vs 36.8 ± 4.1 kg (p<0.05), weight 68.4 ± 11.3 vs 63.8 ± 9.8 kg (p<0.03), TS BMD 1.028 ± 0.09 vs 0996 ± 0.08 g/cm2 (pns, 0.09) and EE2 14.3 ± 4.5 vs 6.8 ± 1.8 pg/ml (p<0.0001). Obese women with BMI values over 30 (n=17) were compared with women with BMI between 20 and 30 (n=78). Only two women had BMI values below 20. As expected, obese women had higher weight, fat, lean, and BMI values as well as higher EE2 (12.2 ± 6.3 vs 9.7 ± 4.5 pg/ml, p<0.05) and TS BMD (1.030 ± 0.11 vs 1.007 ± 0.09 g/cm2, p<0.02) and lower BAP values (72.8 ± 18.8 vs 83.2 ± 17.5, p<0.04) than PMPW with normal weight. No significant data were found with estrone. The following significant correlations were found: EE2 correlated with weight (r=0.2, p<0.05), fat mass (r=0.2, p<0.03 and estrone (r=0.4, p<0.0001); fat mass correlated with weight (r=0.9, p<0.0001), lean (r=0.5, p<0.001), TS BMD (r=0.4, p<0.0001), calcium (r=-0.2, p<0.03) and SHBG (r=-0.3, p<0.001). No correlations were found with estrone.

In conclusion, TS is a useful tool to evaluate the relation between levels of EE2 and BMD as well as to study differences in BC in healthy PMPW. Obese women had higher EE2 levels and TS BMD than PMPW with normal BMI.

Disclosures: ***A. Bagur****, None.*

SU117

Bone Mineral Density Reference Values in Males and Females 10 to 21 Years of Age in Venezuelan Subjects. G. S. Riera, R. Carvajal*, G. Velasquez*, M. Naressi*, J. Ramos*. Medicine, UNILIME.Universidad de Carabobo, Valencia, Venezuela.

Bone Mineral Density reference values for Latin American populations are scarce. However, comparison for diagnosis of low bone mineral density in adults requires normal reference values of 20 - 40 years-old control population. In contrast, in young individuals, matched by sex and age. The aim of this study is to show BMD values in normal young Venezuelan males and females subjects between ages 10 and 21.

191 healthy subjects with at least one Venezuelan progenitor, ages between 10 and 21, without any systemic disease of drug use which affects bone metabolism were recruited for Bone Mineral Density assessment. None of the subjects were under heavy physical therapy or training nor had previous fracture. BMD was measured by DEXA (LUNAR DPX. Variation Coefficient: 1.5%) at femoral neck and lumbar spine (L1-L4),

Subjects were divided into two groups: 89 males and 102 females. BMD results are presented in the 2 tables as follow.

Males. Age	Mean value (SD) Troch Femoral Neck	Mean value (SD) L1 - L4	Mean value (SD)
10 - 11	0.867 ± 0.13	0.755 ± 0.09	0.779 ± 0.11
12 - 13	0.956 ± 0.11	0.830 ± 0.08	0.846 ± 0.11
14 - 15	1.032 ± 0.18	0.911 ± 0.16	0.986 ± 0.16
16 - 17	1.086 ± 0.10	0.913 ± 0.10	1.103 ± 0.16
18 - 19	1.135 ± 0.10	0.845 ± 0.04	1.243 ± 0.05
20 - 21	0.956 ± 0.11	0.752 ± 0.12	1.092 ± 0.03

Females. Age	Mean value (SD) Troch	Mean value (SD)	Mean value (SD)
Femoral Neck		L1 - L4	
10 - 11	0.754 ± 0.15	0.655 ± 0.11	0.815 ± 0.10
12 - 13	0.913 ± 0.11	0.782 ± 0.11	0.981 ± 0.14
14 - 15	0.965 ± 0.12	0.775 ± 0.10	1.037 ± 0.13
16 - 17	0.995 ± 0.07	0.816 ± 0.07	1.094 ± 0.11
18 - 19	1.001 ± 0.11	0.759 ± 0.08	1.116 ± 0.07
20 - 21	0.959 ± 0.11	0.785 ± 0.11	1.156 ± 0.13

This study presents normal reference BMD values for young Venezuelan males and females subjects, 10-21 years of age, obtained with Lunar densitometer

Disclosures: ***G.S. Riera****, None.*

SU118

Recalculation of the NHANES Database Standard Deviation Improves T-score Agreement and Reduces Osteoporosis Prevalence. N. Binkley[1], M. K. Drezner[1], D. Krueger[1], E. M. Lewiecki[2], P. D. Miller[3], J. A. Shepherd[4], G. M. Kiebzak[5]. [1]University of Wisconsin, Madison, WI, USA, [2]New Mexico Clinical Research & Osteoporosis Center, Albuquerque, NM, USA, [3]Colorado Center for Bone Research, Lakewood, CO, USA, [4]University of California, San Francisco, CA, USA, [5]St. Luke's Episcopal Hospital, Houston, TX, USA.

The International Committee for Standards in Bone Measurement recommended the NHANES database for femur T-score derivation. Acquired on Hologic (Hol) instruments, this database requires conversion equations for application to other DXA systems. Total femur (TF) conversions have previously been available, femur neck (FN) and trochanter (TR) equations were reported recently. Appropriately, GE Lunar (GE) incorporated NHANES values into their female database. This should produce T-score and diagnostic agreement between Hol and GE instruments, however, this has not been evaluated. Thus, we compared T-scores from femur scans using GE Prodigy and Hol Delphi densitometers in 89 postmenopausal women.

The TF GE Hol T-score difference ($p < 0.01$) was < 0.1 with equal diagnoses of osteoporosis. FN and TR differences were larger, with mean GE T-scores lower than Hol ($p < 0.001$) by 0.17 and 0.50 respectively, thereby introducing osteoporosis diagnostic disagreement (13 [GE] vs 9 [Hol]). Our evaluation suggested that this disparity resulted from direct application of Hol standard deviations (SD) at the FN and TR. As such, we applied the conversion formulae to the NHANES young-normal female raw data and found the FN and TR SDs were greater than assumed by GE (0.138 vs 0.120 and 0.114 vs 0.099). Using these calculated SDs to derive new T-scores reduced the mean GE/Hol T-score difference to .03 at the FN and .34 at the TR and resolved osteoporosis diagnostic disagreement (n = 9). To validate utility of our calculated SDs, we compared GE femur scans in 115 additional postmenopausal women analyzed with software prior to and after the NHANES update. A FN and TR T-score difference ($p < 0.001$) was present with lower values found using post NHANES software, leading to increased osteoporosis prevalence from 7.8% to 18.3%. Using our calculated SDs to derive T-scores reduced osteoporosis prevalence to 9.6%.

These data reveal that the GE NHANES database update leads to lower FN and TR T-scores than obtained with Hol or prior GE software. An updated SD reduces this difference, but TR discrepancy remains raising questions regarding conversion equation accuracy at this site. Use of updated SD values at the femur subregions for GE densitometers is recommended. Difficulties with the T-score based diagnostic system, such as noted here, should further prompt development of diagnostic criteria that include absolute fracture risk estimates.

Disclosures: ***N. Binkley****, Merck 2, 5, 8; Novartis 2, 5; Aventis 2; Eli Lilly 2.*

SU119

Vertebral Fracture: A Difficult Diagnosis? The Act'os Study. J. Fechtenbaum[1], F. Bugnard*[2], S. Kolta[1], R. Said*[1], O. Madi*[3], P. Orcel[4], C. Roux[1]. [1]Rheumatology, Cochin hospital, Paris, France, [2]MAPI - CRO, Lyon, France, [3]Aventis, Paris, France, [4]Rheumatology, Lariboisière hospital, Paris, France.

Introduction: osteoporotic vertebral fractures are responsible of chronic back pain, impaired function and alteration of quality of life. Their secondary prevention is possible through several effective treatments. Their diagnosis is therefore necessary for an optimal management of osteoporosis.

Aim of the study: to evaluate the concordance in the diagnosis of radiologic vertebral fractures between rheumatologists.

Patients and methods: we have evaluated X-rays of dorsal and lumbar spines as well as the thoraco-lumbar junction of 629 menopausal patients taken in standardized conditions. The inclusion criterion was the presence of at least one vertebral fracture according to the investigator. The X-rays have been analyzed by a central reader, blind to the diagnosis of the investigator, according to a semi-quantitative method (grades 0 to 3). The concordance has been evaluated on the patient and on the vertebral levels.

Results: in the centralized reading, a diagnosis of the presence or absence of fracture could be done in 588 patients (in 41 cases, the diagnosis was not possible due to the presence of some non legible or missing vertebrae with the remaining vertebrae being non fractured). Diagnosis was confirmed in 548 cases (6.8% false positive). At the vertebral level (from T4 to L5, 7 878 vertebras), the kappa score varied from 0.20 to 0.77. It increased linearly from T4 to be greater than 0.6 for the 9 vertebrae from T8 to L4.

According to the centralized analysis, 1 536 vertebrae were fractured. Among these, 396 were considered as non fractured by the investigator (25.8% false negative). Fractures concerned all the vertebrae and 268 were grade 1, 74 grade 2 and 54 grade 3.

Among the 6 342 non fractured vertebrae according to the centralized analysis, 397 were considered as fractured by the investigator (6.3% false positive). The majority of these discrepancies was situated from T4 to T6. Among the 588 evaluable patients, 51.3% had at least one false negative and 52.4% one false positive vertebra.

Conclusion: the concordance of the diagnosis of vertebral fracture between specialists is not optimal. Some of these discrepancies could be explained by the difference in labeling of the vertebrae, others by the differences in the evaluation of the deformations of the vertebral bodies.

Disclosures: ***S. Kolta****, None.*

SU120

Bone Mineral Density In Pre- and Postmenopausal Women on L-thyroxine Suppressive Therapy. J. Payer*, L. Baqi*, Z. Killinger*, P. Hruzikova*, E. Stenova*. 1st Internal Clinic, Comenius Universtity Hospital, Bratislava, Slovakia.

Patients with long- term L-thyroxine suppressive therapy have high bone turnover, which could be associated with bone loss. The aim of our investigation was to examine effect of long- term L-thyroxine suppressive therapy on bone in relation to menopausal status. METHODS: 30 (aged 37±7yrs) premenopausal (PrSUPP) and 32 (aged 60±6yrs)postmenopausal (PoSUPP)with T4 suppresive therapy, 40 (aged 32±5yrs)premenopausal (PrEUTH), and 39 (aged 59±7yrs) postmenopausal control euthyroid (PrEUTH) women were studied. Bone mineral density (BMD) was assessed by dual X-rays absorptimetry (DXA) at lumbar spine(LS), and at the proximal femur (PF). BMD was expressed as g/cm2. Bone markers used were serum osteocalcin (S-OC) and serum NTx (S-NTx). RESULTS: At all sites, BMD findings were significantly lower ($p<0,05$) in PrSUPP and PoSUPP as compared to both EUTH controls groups. In comparing (PrSUPP) and (PoSUPP) BMD was significantly lower ($p<0,05$}only in LS region. There was no correlation between BMD and TSH and fT4 levels. S-OC, S-NTx and duration of L-thyroxine suppressive therapy negatively correlated with BMD. CONCLUSION: Women who are using L-thyroxine suppressive therapy are regardless to the age at higher risk of osteoporosis. This study suggests that L-thyroxine suppressive therapy affects bone mineralization and that is common with high bone turnover in pre- and postmenopausal women at the cortical and trabecular bone.

Disclosures: ***J. Payer****, None.*

SU121

Long-term Bone Loss in Men and Women: Effects of Quadriceps Strength and Body Weight. T. V. Nguyen, N. D. Nguyen, J. R. Center, J. A. Eisman. Bone and Mineral Program, Garvan Institute of Medical Research, Sydney, Australia.

Although femoral neck bone mineral density (FNBMD) is known to progressively decline with advancing age, the rate of loss in past longitudinal studies was based on a relatively short duration of follow-up with mostly two measurements per subject. Also, little is known about the underlying factors for the decline. This study was designed to estimate the rate of change in FNBMD and risk factors for the change in the elderly population.

Femoral neck BMD (g/cm^2) was measred in 866 female and 516 male participants in the Dubbo Osteoporosis Epidemiology Study, who had had at least 3 visits since 1989 at intervals of approximately 2 years between any two consecutive visits. The average number of BMD measurements was 4 for each subject. At each visit, quadriceps strength (maximum isometric contraction) (QS, kg), body weight and lifestyle factors, such as dietary calcium intake, smoking and alcohol intake, were also obtained. The relationships between FNBMD, weight and quadriceps strength across visits were analyzed for *each* individual in a mixed-effects model with the assumption that the change in BMD and the magnitude of association between a risk factor and BMD varied randomly among subjects.

On average FNBMD decreased by 0.57±1.28% and 0.30±1.05% (mean±SD) per year for women and men, respectively. However, the rate of decline increased with advancing age in women such that by the age of 80 yr, their rate of loss was equivalent to that in men (0.69±1.18%). The rate of change in BMD for *a given individual* was negatively correlated with both change in weight and change in quadriceps strength, such that increasing weight and quadriceps strength was associated with lesser bone loss. These two factors accounted for 13% and 12% of the variance of bone loss in men and women, respectively. There was no significant association between dietary calcium intake, smoking or alcohol use and the loss in FNBMD. These results indicate that the rate of loss in FNBMD is lower than previously reported (which was about 1% per year) and that change in quadriceps strength and change in body weight were significant determinants. Enhancement of physical fitness may have a protective effect against bone loss in the elderly.

Disclosures: ***T.V. Nguyen****, None.*

SU122

Precision of Spine BMD Measurement with and without Leg Elevation. S. Yang, T. Jeon*. Radiology, Eulji University Hospital, Daejeon, Republic of Korea.

There are some report that BMD measurement with the legs down shows no significant change on spine BMD accuracy and precision. We also studied to see the impact of leg elevation from DXA in our country.

Forty volunteers were scanned four times at the lumbar spine using Hologic QDR 4500A. Two scans were done with the leg elevated (E scan) by the spine positioning device supplied by manufacture. The other two scans were done with the legs lying flat (F scan) neutrally without femur positioner. Subjects were repositioned between all four scans. The precision error and linear regression were determined for the BMD obtained in each position.

Mean age of the subjects was 52 (range; 40 ~ 71). BMD was higher in the F scan (mean: 0.922 g/cm^2) compared with E scan (0.907 g/cm^2) except in two volunteers. T-scores at L1-4 were 0.13 higher for F scan. Only two volunteers had different diagnosis using T-scores from normal to osteopenia and vice versa from the two methods. Precisions (%CV) of the E scan were 1.50, 1.52, 1.96, 1.50, and 0.97% for the L1, L2, L3, L4, and L1-4 respectively. Precisions of the F scan were 1.46, 1.88, 1.63, 1.83, and 1.09% for the L1, L2, L3, L4, and L1-4 respectively. Correlation between two scans was high (r=0.99).Diagnostic differences from E and F scan are very small (0.13 T scores).

There is no significant statistical difference in spine BMD between with the legs elevated and with the legs flat on the scan table. One step scan with the leg flat with the dual femur positioner can expedite the examination without jeopardizing diagnostic value.

Disclosures: ***S. Yang****, None.*

SU123

Bone Mineral Density in Male Osteoporotics with Vertebral Fractures. P. Ryan[1], D. Doyle*[2], V. Thompson*[2], J. Griffin*[3], J. Day*[4], C. Kelsey*[5], G. Cambell*[6], G. Cambell*[6], N. Saunders*[7]. [1]Osteoporosis Unit, Medway Maritime Hospital, Gillingham, Kent, United Kingdom, [2]Chingford Osteoporosis Unit, Chingford, Essex, United Kingdom, [3]Rheumatology, Chase Fram Hospital, London, United Kingdom, [4]Elderly Care Unit, Luton and Dunstable Hospital, Luton, Herts, United Kingdom, [5]Rheumatology, Oldchurch Hospital, Romford, Essex, United Kingdom, [6]Elderly Care, Addenbrookes Hospital, Cambridge, United Kingdom, [7]Procter and Gamble plc, Staines, Middx, United Kingdom.

Interpretation of Bone Mineral Densitometry (BMD) in male vertebral fracture is complex. The same relationship between bone density and fracture occurs in males as in females and absolute fracture risk is similar at the same BMD. However, because BMD levels are higher and BMD changes with age differently the same T and Z scores imply different fracture risks in the 2 genders. In clinical practice there is sometimes difficulty in attributing vertebral fractures to osteoporosis or whether to infer other causes. This study retrospectively examined BMD data on 76 male vertebral fracture patients (average age 67 years) selected from clinical databases from 6 centres, which were matched by a randomly selected group of 104 females (average age 71 years) with vertebral fractures. For inclusion patients had to have a BMD and spinal x-rays within 1 year of the scan. Patient data was collected on BMD at the spine and hip, numbers and severity of vertebral fracture (Genant scale) and clinical risk factors. A single investigator read all the x-rays blinded to other results. 23 patients had BMD measurements on Lunar and 157 on Hologic devices. There were 190 male and 202 female fractures, (Wedge male 161, female 170, Mid male 29, female 32). Average T scores were similar in the spine (Male -2.55, Female -2.70) and slightly lower in females at the femoral neck and total hip (Male Total Hip -2.08, Female Total Hip -2.71). Average Z scores were markedly lower in males at spine (Male -1.86, Female -0.58) but similar at the femoral neck and total hip (Male Total Hip -1.19, Female -0.94) In the Hologic subgroup Male BMD was higher at all sites, more obviously at the hip (Male BMD Spine 0.794 g/cm2, Total Hip 0.758 g/cm2, Female BMD Spine 0.761 g/cm2, Total hip 0.644 g/cm2). Fracture thresholds derived from Hologic data suggest greater differences in hip compared to spine BMD (90 % threshold Male Spine 1.028 g/cm2, Total Hip 0.957 g/cm2, Female Spine 1.006 g/cm2, 0.796 g/cm2). Study findings suggest that when considering male vertebral fractures T scores in the spine can be used in a similar way to females, whereas Z scores in men are much lower, but the converse applies for the hip. Absolute BMD thresholds for vertebral fracture are higher in men than in women, particularly at the hip.

Disclosures: ***P. Ryan****, None.*

SU124

Pediatric DXA Precision Varies with Age. J. A. Shepherd[1], B. Fan[1], M. Sherman*[1], V. Gilsanz[2], M. Horlick[3], H. Kalkwarf[4], J. Lappe*[5], S. Mahboubi*[6], B. Zemel[7], M. Fredrick*[8], K. Winer[9]. [1]Radiology, University of California at San Francisco, San Francisco, CA, USA, [2]Radiology, Children's Hospital of Los Angeles, Los Angeles, CA, USA, [3]Pediatric, Columbia University, New York, NY, USA, [4]Pediatrics, Children's Hospital of Cincinnati, Cincinnati , OH, USA, [5]Pediatrics, Creighton University, Omaha, NE, USA, [6]Radiology, Children's Hospital of Philadelphia, Philadelphia, PA, USA, [7]GI and Nutrition, Children's Hospital of Philidelphia, Philadelphia, PA, USA, [8]Clinical Trials, Clinical Trials & Surveys Corp, Baltimore, MD, USA, [9]Center for Research for Mothers and Children, National Institute of Child Health and Human Development, Bethesda, MD, USA.

When assessing the suitability of a technique for follow up purposes, one of the most important parameters is precision. Constant adult precision values are commonly applied to pediatric patients or populations with little evidence that they are valid. The purpose of our study was to access the repeatability of four bone densitometry regions of interest (ROIs) in children as a function of age. We recruited 155 children of mixed sex and ethnicity, 30 children each from 5 clinical sites across the country. The subjects were recruited in three age groups of 10 children (Group C (6 to 9), B (10 to 13), and A (14 to 16 years)). These participants were all part of the larger reference data study, the NICHD BMD in Children Study. Each participant had duplicate scans with repositioning of the following DXA ROIs: PA spine, proximal femur, whole body, and forearm. Each clinical site used the same densitometer (Hologic Delphi, Hologic, Inc. Bedford, MA) and all scans were centrally analyzed by one trained research assistant using the Discovery software (version 12.1). The coefficient of variation (CV) is shown for each group and ROI in the graph. The Discovery analysis algorithms identified bone well for all age groups and measurement sites. Age-related changes were evident for the spine, hip, and whole body, but less so for the radius. Adolescent CVs were in general similar to adult values from the literature. We conclude that precision in DXA scans of children varies with age. These unique precision measures should be taken into account when determining if actual change has occurred between baseline and follow-up examinations.

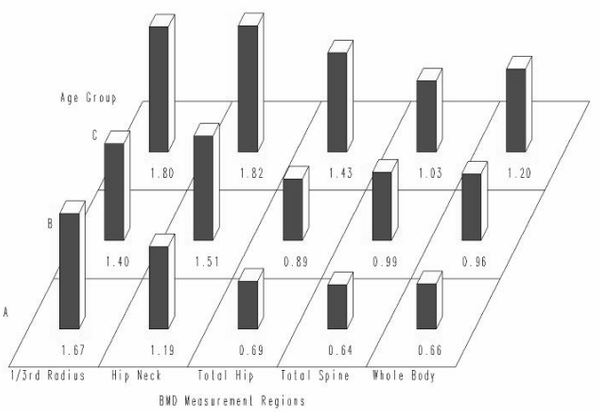

Disclosures: ***J.A. Shepherd****, None.*

SU125

Dual Energy X-ray Absorptiometry (DXA) of the Forearm in Men: Radius versus Total. V. I. Petkov*[1], M. I. Williams*[2], P. S. Via*[3], T. Hodson*[3], R. A. Adler[1]. [1]Endocrinology, McGuire Veterans Affairs Medical Center/Virginia Commonwealth University School of Medicine, Richmond, VA, USA, [2]Endocrinology, McGuire Veterans Affairs Medical Center/Virginia Commonwealth University School of Pharmacy, Richmond, VA, USA, [3]Endocrinology, McGuire Veterans Affairs Medical Center, Richmond, VA, USA.

The role of the dual energy X-ray absorptiometry (DXA) of the forearm for the diagnosis of osteoporosis (OP) is not well defined, especially in men. ISCD recommends using only 1/3 radius (Lunar densitometers default) when DXA of the spine is not acceptable. However, Hologic densitometers report total distal forearm by default. From observational cohort studies of fractures in men, central DXA predicts fractures modestly, at best. Adding forearm (FA) to spine and hip DXA, especially in older men, may improve the predictability of fractures. We decided to test if the addition of FA to spine and hip BMD will increase significantly the proportion of men identified to have OP. Additionally, we explored the sensitivity of different FA sites for diagnosis of OP.

Veteran men who had a BMD test as a result of an interventional study for improving diagnosis and treatment of OP in primary care clinics were included in the analysis. All patients had DXA of the spine, hip and forearm (Hologic Delphi). OP was defined as a T-score $\leq$ -2.5. The proportions of male patients with OP identified by spine plus hip and spine, hip plus various distal forearm regions were compared using the McNemar test for paired categorical data.

The mean age of the study group (N=355) was 71.5 (9.3) years and the mean weight was 75.9 (10.7) kg. Using ISCD recommendations for the diagnosis of OP (the lowest of T-scores at L1-L4 spine, femoral neck, trochanter or total hip) 25.9 % had osteoporosis and 53.5% osteopenia. Adding total distal forearm (or total radius) significantly increased the number of men with OP to 36.1% (36.9%). Replacing total FA/radius with 1/3 radius decreased the number of osteoporotic men to 32.7%, while adding ultradistal radius to 1/3 radius significantly increased the proportion of osteoporotic men (41.4%). Currently we are evaluating fracture data on the study patients.

Adding FA DXA in the diagnosis of OP in older men would identify a greater number of men with osteoporosis, in whom treatment should decrease fracture incidence.

Disclosures: ***V.I. Petkov****, None.*

SU126

Precision of Fan-Beam Densitometers in Clinical Practice. L. S. Weynand*, H. S. Barden, K. G. Faulkner. GE Healthcare, Madison, WI, USA.

Precision error determines the ability of a DXA system to detect small changes in patient bone mineral density (BMD). Factors affecting precision include the scan region, consistency of scan acquisition and analysis, operator training, densitometry equipment and software, and short- and long-term variations in densitometer performance. Recently, several studies have reported BMD precision at leading centers considered experts in the field of densitometry research and clinical osteoporosis (1). We evaluated precision errors at non-research centers to compare with precision obtained by densitometry experts.

Twenty clinics with fan-beam densitometers participated in the study; 10 Lunar Prodigy systems, and 10 Hologic 4500 or Delphi systems. Each center determined their precision error using clinic patients. Each clinic measured either 30 subjects twice or 15 subjects three times, with repositioning between scans. Standard 30-second scan mode was used for all systems. Acquisition and analysis was performed by trained technologists at each center. BMD precision error was calculated as the root-mean-square standard deviation (RMS-SD) and coefficient of variation (RMS-%CV) for the repeated measurements using a standardized spreadsheet program.

Average precision error at the non-research centers was approximately 50% higher than published precision values from research centers (1) at all scan regions. Hologic precision errors were 50% to 120% higher than Prodigy precision errors, depending on the region. Precision errors at individual centers ranged from a low of 1.0% at the spine to a high of 9.7% at the femur neck for the Hologic systems, and from a low of 0.6 % for total femur to a high of 8.2 % for femur neck for the Prodigy.

We conclude that non-expert densitometry providers had, on average, a 50% higher precision error than expert centers. These results, coupled with the wide range of precision errors found in the study, emphasize the need for every densitometry center to conduct their own precision study and understand the effect their precision has on patient care. Centers with precision errors grossly out of line with established standards should attempt to eliminate possible errors due to malfunctioning equipment, outdated software, inconsistent operator intervention, or insufficient operator training.

1. J Bone Miner Res 2003; 18 (Suppl 2): S205

Densitometer Model	Number of Clinics	Number of Subjects	Age (years) Mean ± SD	Spine L1-L4 % CV	Total Femur % CV	Femur Neck %CV
Prodigy	10	300	62 ± 9.8	**1.2**	**1.2**	**2.8**
Hologic	10	285	61 ± 12.2	**1.7**	**2.6**	**4.8**
Delphi	4	120	59 ± 12.3	1.6	2.2	6.8
4500	6	165	63 ± 12.0	1.9	2.8	3.2

Disclosures: ***L.S. Weynand****, None.*

SU127

Use of Anthropomorphic Phantoms to Cross-Calibrate DXA Scanners. L. Cole*, N. C. Grinnell*, T. M. DeFrancisco*, S. M. Strot*, E. A. Mossman, M. R. McClung. Oregon Osteoporosis Center, Portland, OR, USA.

Dual-energy X-ray absorptiometry (DXA) is widely used for the assessment of skeletal status in clinical or research settings. Differences in BMD measurement between DXA scanners from different manufacturers have been well established. Because of differences in calibration standards, even DXA scanners from the same manufacturer sometimes produce clinically significant differences in BMD. With equipment upgrades or when comparing clinical results from different laboratories, it is often desirable to cross-calibrate two or more DXA scanners. Because it is often not practical to use subjects for the cross-calibration, anthropomorphic phantoms are frequently used instead. The purpose of this study was to determine how well cross-calibration with phantoms predicts in vivo performance.

Two GE-Lunar Prodigy densitometers were cross-calibrated using both subjects and three anthropomorphic phantoms (GE Lunar Aluminum Step Wedge [LUN], Bona Fide Anthropomorphic Spine Phantom [BF], and Hologic Anthropomorphic Hip Phantom [HOLH]). The total hip (TH) and lumbar spine 1-4 (LS) regions were measured on each of 20 subjects on both DXA machines. Each phantom was measured 20 times on both scanners. Mean BMD values and regression equations were calculated to standardize the table results for the patients and for each phantom.

Table 1. Regression slopes and intercepts for phantom and patient cross-calibration data.

Phantom/ROI	Mean BMD Scanner1	Mean BMD Scanner 2	Slope	Slope p	Intercept	Intercept p
LUN	1.182	1.195	1.0261	<0.0001	-0.0179	0.0005
BF	1.074	1.082	1.0222	<0.0001	-0.0157	0.0077
Patient LS	1.099	1.090	1.0057	<0.0001	-0.0158	0.5773
HOLH	0.810	0.814	0.9318	0.0006	0.0594	0.3156
Patient TH	0.920	0.907	0.9573	<0.0001	0.0264	0.2109

The LUN and BF anthropomorphic phantoms, which simulate the spine region, both match the patient regression equation at LS fairly well, but neither matches well with the patient TH equation. In contrast, the HOLH hip phantom is similar to the patient TH equation, but does not correspond well with the LS equation.

These data suggest that the use of site-specific anthropomorphic phantoms is required for cross-calibrating densitometers where in vivo cross-calibration is impractical.

Disclosures: ***L. Cole****, None.*

SU128

Utility of Measuring Both Hips in Patients with Discordant Hip and Spine DXA Measurements. T. M. DeFrancisco*, S. M. Strot*, L. Cole*, N. C. Grinnell*, E. A. Mossman, M. R. McClung. Oregon Osteoporosis Center, Portland, OR, USA.

Dual energy x-ray absorptiometry (DXA) is generally agreed to be the best method for measuring bone mineral density (BMD) in order to diagnose osteoporosis, establish fracture risk, and monitor the effects of therapy, with the spine and hip the most commonly measured regions. When measuring the spine and one hip there can often be discordance between the two sites, where one site has BMD values consistent with osteoporosis (OP) and the other does not. In these cases, due to the potential for measurement artifact and/or disparity between the two hips, the opposing hip is often measured. However, it is unclear if there is a diagnostic advantage to measuring the second hip when a discordance exists between the spine and initial hip measurement.

The purpose of this study was to determine if there is a significant difference between DXA measurements of opposite hips in patients with discordance at the spine and the first measured hip, and to determine if such a difference would systematically affect diagnostic categorization in these patients.

We examined data from the electronic medical records of patients referred to the Oregon Osteoporosis Center for DXA testing from January 2000 through March 2004. 1374 patients had record of a DXA measurement at the spine and both hips on a single Lunar Prodigy densitometer (GE Lunar, Madison, WI). 206 of these had discordant first total hip (TH) and L1-4 lumbar spine (LS) measurements, with LS higher (T > -2.5) in 113 of these records.

Paired samples T-testing showed no significant difference in opposite hip TH BMDs among these patients, with a mean difference of only -0.004 g/cm^2 from first to second hip scanned (95% CI, -0.023 to 0.015, p=0.66). 113 patients (55%) of discordant records had a first measured TH value consistent with OP, while 126 (61%) had values consistent with OP at either TH. These percentages were identical using the femoral neck (FN) region instead of TH, and FN BMDs were not significantly different in the 228 patients discordant at LS and first measured FN (p=0.19). We conclude that there is not sufficient diagnostic or clinical advantage in including the second hip to justify its measurement when a discordance exists between the spine and initial hip measurement.

Disclosures: ***T.M. DeFrancisco****, None.*

SU129

Structure Analysis of High Resolution MRI of the Proximal Femur Using a 3D Anisotropic Method for the Prediction of Mechanical Strength In Vitro. R. A. Monetti*[1], H. Boehm*[2], D. Mueller*[2], E. Rummeny*[2], G. Morfill*[1], S. Majumdar[3], D. Newitt[3], T. Link[3], C. Raeth*[1]. [1]Cips, Max-Planck-Institut fuer extraterrestrische Physik, Garching, Germany, [2]Department of Radiology, TU-Munich, Munich, Germany, [3]Department of Radiology, UCSF, San Francisco, CA, USA.

In this study the so called scaling vector method (SVM) was applied to analyze the trabecular bone structure of high resolution magnetic resonance (HR-MR) images of the proximal femur. Using the SVM a 3D non-linear texture measure which takes into account the anisotropic nature of the trabeculae was extracted. The performance of this new structure analysis technique for the prediction of the biomechanical properties of the bone was compared with BMD and the standard 2D histomorphometric parameters.

25 human proximal femur specimens from 10 female and 15 male donors aged 39 to 91 years were obtained 1 to 2 days postmortem. Coronal HR MR images of the proximal femur were obtained using a 1.5 T MR scanner equipped with 22 mT/m gradients and a prototype 2 element phased array coil. A 3D-spin-echo sequence with an echo time (TE) of 13.0 ms, repetition time (TR) of 50 ms, and 3 acquisitions was used. A matrix of 384 x 512 was applied with a field of view (FOV) of 75 x 100 mm, yielding a pixel size of 0.195 × 0.195 mm^2. Sections with a slice thickness of 0.9 mm were obtained. The acquisition time was 27:19 min. Nineteen 0.9 mm thick sections were acquired. DXA of the proximal femur was performed using a DPX-L scanner and areal BMD (g/cm^2) of the femoral neck was determined.

The maximum compressive strength (MCS) was obtained in an electro-mechanical materials testing machine. Compressive force on the femur head was increased stepwise (0.5 kN). MCS was calculated from the first local maximum of the stress-strain curve. MCS ranged from 3.20 to 16.95 kN. After selecting the region of interest (ROI) and normalization of the images the structure analysis was performed using algorithms able to account for the orientation of the mineralized trabeculae of the proximal femur, i.e. the new anisotropic SVM.

In order to predict the mechanical strength of the bone, we performed a correlation analysis. The correlation coefficient obtained using the SVM versus MCS was 0.83 ($p < 0.001$) which should be compared with 0.74 and 0.68 obtained for BMD-neck and Apparent Bone volume versus MCS, respectively.

We conclude that local 3D non-linear structural anisotropic texture measures extracted from HRMRI applying the scaling vector method can successfully predict the mechanical properties of femoral specimens.This suggests that anisotropic texture measures have a superior performance in cases where directional properties play a relevant role.

Disclosures: ***R.A. Monetti****, None.*

SU130

Map of Heel BUA Values May Provide New Information on Skeletal Integrity. R. K. Bhattacharya[1], J. H. Goll*[2], D. L. Medich[1], K. T. Vujevich*[1], M. E. Shoup*[1], J. M. Wagner[1], S. M. Sereika*[3], S. L. Greenspan[1]. [1]Medicine, University of Pittsburgh, Pittsburgh, PA, USA, [2]Quidel Corp., Mountainview, CA, USA, [3]Epidemiology, University of Pittsburgh, Pittsburgh, PA, USA.

Bone mineral density (BMD) explains 50-70% of the variance of fracture risk, but other factors, such as bone geometry, bone turnover and fall biomechanics, contribute to fracture risk. Traditionally calcaneal ultrasound measures bone strength by broadband ultrasound attenuation (BUA). We have examined graphical presentations, which we call maps, of the BUA values measured over areas of 10 cm^2 of the calcaneus. These maps show substantial heterogeneity and biological diversity. We have assigned the maps to 4 groups, based on certain topological features or shapes observed. Our objective was to explore correlations between shapes and BUA, BMD, bone markers (osteocalcin, NTx), height, weight, and body mass index (BMI).

We enrolled 67 newly postmenopausal women from a study on osteoporosis prevention. At screening, women taking hormone replacement therapy, other antiresorptive agents, or anabolic therapies were excluded. We assessed BMD of the hip and spine (QDR-4500A; Hologic, Inc.), heel ultrasound by broadband ultrasound attenuation ([BUA] QUS-2; Quidel Corp.), height, weight, BMI, and markers of bone turnover. The BUA maps were separated into four distinct shapes by a blinded reviewer. (See table; *p<0.05, **p<0.01)

As expected, BUA was associated with hip and spine BMD, weight, and BMI, but not with markers of bone turnover. Furthermore, the topographical maps were associated with hip BMD, weight, BMI, and BUA. Using univariate multinomial logistic regression, we observed significant univariate effects on shape for BUA; BMI; weight; and total hip, trochanter, and intertrochanter BMD (all p<0.05). When multivariate multinomial logistic regression was done, the only statistically significant relationship we found was between BUA and the maps.

We conclude that ultrasound-derived topographical maps of the heel are associated with hip BMD, standard ultrasound, and weight, a relationship that may prove useful in the assessment of skeletal integrity. Future studies are needed to examine how maps may change with time or treatment and whether they can be used to enhance fracture prediction using quantitative ultrasound.

Measures of Association

	BUA (r)	Shapes (r^2)
Total hip	.47**	.14*
Femoral neck	.29*	.09
Trochanter	.47**	.16
Spine	.38**	.07
Weight	.48**	.16*
BMI	.45**	.14
BUA	--	.32*

Disclosures: ***R.K. Bhattacharya****, None.*

SU131

Side-to-Side Differences in Bone Strength in a Chronic Stoke Population: a pQCT Study. P. C. Fehling[1], M. C. Ashe[1], J. J. Eng*[2], H. A. McKay[1]. [1]Departments of Orthopaedics/ Family Practice; Division of Orthopaedic. Engineering Research, University of British Columbia, Vancouver, BC, Canada, [2]School of Rehabilitation Sciences, University of British Columbia, Vancouver, BC, Canada.

Following a stroke individuals have increased risk of fracture. Previous studies of this population have shown that BMD, measured by DXA, is significantly reduced in the affected limb compared with the nonaffected limb. There have however, been few pQCT studies of this population. Thus, we investigated the side-to-side difference in bone mass and structure by DXA and pQCT in ambulating chronic stroke patients. We recruited 42 participants (mean age 67.8 ± 7.3) who were at least 12 months post stroke (mean 45.0 ± 22.3 mo) and independently ambulating with or without an assistive device. Based on the American Heart Association Functional Classification (range from 1= complete independence to 5 = complete dependence) subjects had an average score of 2.4 ± 0.9 (mode = 3). We used dual energy X-ray absorptiometry (DXA: Hologic 4500W, software version 11.2) to assess total body and bilateral proximal femoral BMC (g) and aBMD (g/cm^2). We used peripheral quantitative tomography (pQCT:Stratec XCT 2000; 2.5 mm slice, scan speed 25 mm/second, 0.5 mm voxel) to assess cross sectional area (CSA, cm^2),vBMD (g/cm^3), and polar moment of inertia (Ipolar) for bilateral tibiae at 5 and 30% of bone length. Scans were analyzed with BonAlyse 1.3 software (BonAlyse Oy, Jyväskylä, Finland). Participants were 80.4 ± 16.5 kg, 169.2 ± 9.5 cm. Fifty per cent of subjects met the criteria of osteopenia and 10% met the criteria of osteoporosis. At the total proximal femur aBMD was 5.2% lower and BMC was 6.6% lower in the affected vs. non-affected side (P=0.001). Results were similar for all proximal femur subregions of interest. There were no statistically significant bilateral differences in any bone structural parameter (by pQCT) at either the 5 or 30% sites of the tibia. At 30%, CSA was 452.6 ± 80.1 vs. 449.3 ± 86.2, vBMD (g/cm^3) was 720.2 ± 106.6 vs. 716.9 ± 104.8, and Ipolar was 2951.8 ± 1121.0 versus 2908.5 ± 1181.9 (affected limb vs. non-affected limb, respectively). This is one of the first studies to use pQCT technology in stroke patients - a population at increased risk of fracture. Our novel data do not reveal any bilateral differences in measures of bone material or geometric properties using pQCT. These findings are not consistent with past studies that used DXA measurement alone in this population. Further studies are needed to determine if the discrepancy observed in this study between technologies (DXA vs. pQCT) are the result of measurement site limitations (hip vs. tibia), technology or represent true regional bone biology differences.

Disclosures: ***P.C. Fehling****, None.*

SU132

3D-Evaluation of Bone Microarchitecture in Humans using High Resolution pQCT; A New in vivo, Non Invasive and Time Saving Procedure. M. Neff[1], M. Dambacher[2], S. Haemmerle*[3], R. Rizzoli[4], P. Delmas[5], R. Kissling*[6]. [1]Center for Osteoporosis, Zürich, Switzerland, [2]University Clinik Balgrist, Zürich, Switzerland, [3]Federal Institute of Technology ETH, Zürich, Switzerland, [4]University Hospital Geneva, Geneva, Switzerland, [5]Hopital E. Herriot Lyon, Lyon, France, [6]University Clinic Balgrist, Zürich, Switzerland.

In contrast to animals (e.g. mice, rats) the in vivo, non invasive and quantitative evaluation of 3D-bone microarchitecture, which play an important role in the fracture risk prediction of the skeleton, was not directly possible in humans. But lately the quantitative and non-invasive 3D structure analysis in vivo became also available in humans with the help of high resolution pQCT (Densiscan-3D/XtremeCT, Scanco Medical Ltd).

The new high resolution pQCT has a 2-dimensional detector array combined with a 100µm focus x-ray tube (effective energy 42keV), enabling the simultaneous acquisition of a stack of 100 tomograms perpendicular to the bone axis with a maximal diameter of 126mm. The isotropic resolution is 120µm (10% MTF, isotropic voxel size 82µm). The tomograms are taken 7mm proximal from the endplate of the distal radius and/or 20mm from the endplate of the distal tibia respectively delivering a coverage of a region of about 8mm. The data acquisition time is about 3 minutes and the effective radiation dose for a standard examination (scout view included) below 3µSv (CTDIw = 6.1mSv). With automatic repositioning the reproducibility is <±1% (for structure elements) in mixed collectives.

In praxi it is now routinely possible (see graph) to quantify in vivo in humans the microarchitectural features as number of trabeculae, trabecular and cortical thickness, trabecular spacing and endosteal surface in addition to the volumetric BMD of trabecular and cortical bone.

Such quantitative characterizations will give better insight in pathogenesis, prevention and in treatment of primary and secondary osteoporosis. It also improves the individual skeletal fracture risk prediction; e.g. with the help of finite element analysis.

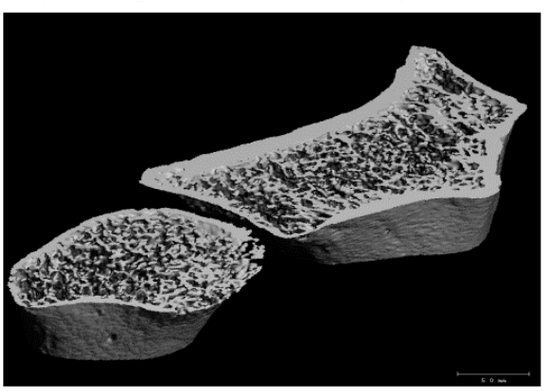

Distal Forearm in vivo
XtremeCT^R

Disclosures: ***M. Neff****, None.*

SU133

A Novel Approach For Monitoring and Predicting Bone Microstructure in Osteoporosis. S. K. Boyd[1], C. Mattmann*[1], A. Kuhn*[1], R. Müller[2], J. A. Gasser*[3]. [1]Calgary Centre for Innovative Technology, University of Calgary, Calgary, AB, Canada, [2]Institute for Biomedical Engineering, ETH and University Zürich, Zürich, Switzerland, [3]Novartis Institutes for Biomedical Research, Basel, Switzerland.

In vivo measurements of bone microstructure allow novel insight into the process of bone loss in diseases such as osteoporosis. Currently, histomorphologic information can be extracted from these temporal series of 3D data using standard techniques developed for micro-computed tomography (micro-CT) data. However, to fully realize the potential of newly available in vivo data, temporal trends at a trabecular level need to be identified, and these data may allow projection of future bone architectures.

The purpose of this research is to establish a new method to track temporal changes of bone micro-architecture based on in vivo measurements, and to use that information to extrapolate future bone architecture in a disease process.

The method was developed using data from simulated atrophy of canine femoral trabecular bone, and then applied to in vivo measurements in a rat model of osteoporosis (Novartis, Switzerland). A group of 10 ovariectomized (OVX) virgin, 8 mo old Wistar rats were in vivo micro-CT scanned (Scanco Medical, Switzerland) at 0, 4, 8 and 12 wk post-OVX in the proximal tibia. A second group of 10 sham-operated rats served as controls. In each rat, temporal data series were registered to superimpose 3D architecture from different time points. Deformable registration between each time point provided a 3D deformation field, and the trend of these fields between times 0, 4 and 8 wk was linearly extrapolated to predict the 3D micro-architecture at 12 wk. The prediction was directly compared to measured architecture at 12 wk.

The OVX rats, as expected, had decreased bone volume ratio (N=5, 40% decrease), and the sham-operated rats exhibited a minimal decrease (N=7, <2% decrease). The extrapolated 3D architecture from the canine data resulted in maximum local errors of 5 um (relative to

34 um isotropic resolution). Predicted 12 wk OVX rat bone architecture matched well with structural parameters (BV/TV, Tb.Th) of the measured 12 wk post-OVX data, and captured the dominant changes in architecture at the individual trabecular level. Complete resorption of trabeculae was problematic to predict, however the four week time interval may have been too large considering the significant architectural changes in the OVX rat.
In conclusion, this method based on measured trajectories of in vivo data provides novel insight into changes in 3D bone microstructure in the OVX model for osteoporosis, and introduces the ability to track individual trabeculae and predict future micro-architecture in a disease process.

Disclosures: ***S.K. Boyd****, None.*

SU134

The Spinal Curvature Irregularity Index (SCII) for the Thoracolumbar Spine Identifies Vertebral Fractures. G. Maalouf[1], R. Zezabe[2], N. Maalouf*[3], J. Wehbe*[1], E. Seeman[2]. [1]Orthopaedic Dept, St. Georgia Hospital, Beirut, Lebanon, [2]Austin & Repatriation MC University of Melbourne, Melbourne, Australia, [3]Southwestern MC, University of Texas, Dallas, TX, USA.

Differences in anterior and posterior vertebral heights (VHs) form the thoracolumbar curvature needed for stability in bipedal gait. Modest differences in VHs within and between adjacent vertebrae allow the spinal curve to change its trajectory gently. Large differences in VHs, as occurs following a fracture, produce abrupt changes in the curve direction producing a departure from regularity (i.e. irregularity). In this study we wished to determine if irregularity in the spinal curvature, quantified as the Spinal Curvature Irregularity Index (SCII), was correlated with the number of fractures and could identify women with vertebral fractures.
VHs and bone mineral density (BMD) were measured using DXA (Lunar Prodigy, GE Healthcare) in 470 Lebanese women aged 20-88 yrs. Vertebral heights (T4-L4) were obtained from a lateral spine scan while the BMD (L1-L4) was obtained from an AP-spine scan. Regularity of the curvature of the spine was measured by comparing the ratio of the anterior to the posterior vertebral height of one vertebra to that of the adjacent one (calculated in caudocephalic direction). The SCII in % for adjacent vertebrae *i* and *i+1* is given by

$$SCII_{i,i+1} = [(1 - I_{i,i+1})^2]^{1/2}$$

with

$$I_{i,i+1} = Ha_i/Hp_i * Hp_{i+1}/Ha_{i+1}$$

(Ha_i , Hp_i anterior and posterior heights of vertebra *i*; Ha_{i+1}, Hp_{i+1} anterior and posterior heights of vertebra *i+1*). Irregularity was measured at each pair of adjacent vertebrae and expressed as the SCII for the entire thoracolumbar spine. The average SCII in an individual is given by the sum of all $SCII_{i,i+1}$ devided by the number of adjacent vertebrae in the individual. Vertebral fractures were classified as wedge and as crush deformities using cutoffs of 3 SD (moderate) or 4 SD (severe).
A total of 74 deformities (43 moderate, 31 severe) were identified in the lateral scans of 56 of the 470 women. In all women younger than 50 mean SCII was 6.1% while for all women older than 50 mean SCII was 7.1%. To obtain a normal distribution of the SCII, the SCII was transformed ($SCII^{0.25}$). There were statistically significant differences between mean values for subjects with and without deformities for SCII (transformed) and age- and weight-adjusted BMD, but not age-adjusted height. Binary logistic regression calculations show that SCII is a good predictor of the presence of deformities, while age-adjusted height and age & weight-adjusted BMD are not. The probability of having a deformity increases about 1.75 times for every SD increase in transformed SCII.
We conclude that SCII provides a valuable measure to identify women with vertebral fractures.

Disclosures: ***G. Maalouf****, None.*

SU135

Treatment with Tibolone Partially Protects 3-D Microarchitecture of Lumbar Vertebral Bone Tissues and Prevents Ovariectomy-induced Reduction in Mechanical Properties. M. Ding*[1], M. Dalstra*[1], H. Weinans[2], A. G. Ederveen[3], I. Hvid*[1]. [1]Orthopaedic Research Laboratory, Aarhus University Hospital, Aarhuc C, Denmark, [2]Orthopaedic Research Lab, Erasmus University Rotterdam, Rotterdam, Netherlands, [3]Dept of Pharmacology, N.V. Organon, Oss, Netherlands.

Tibolone (Org OD14) is a tissue selective steroid with estrogenic effects on the brain, bone and vagina, without stimulating the breast and endometrium. A previous study has shown that long-term treatment with tibolone prevents ovariectomy (OVX) induced bone loss in rats. The aim of this study was to investigate the effects of tibolone on three-dimensional (3-D) microarchitecture and mechanical properties of rat lumbar vertebra. We hypothesized that tibolone might have significant effects on 3-D microarchitecture of vertebra, thus to preserve OVX-induced reduction in mechanical properties.
One hundred and sixty-six female 10-month-old rats were randomly allocated into one of the 13 groups. These groups included a baseline control group at experiment start-up and three groups (SHAM, OVX and OVX+tibolone) at each termination point - 4, 14, 34, or 54 weeks. The treated groups received tibolone 2 mg/kg/day, orally. After sacrifice, rat third lumbar vertebrae were removed and micro-CT scanned. Microarchitectural properties of the cancellous and cortical bones were quantified and the mechanical properties of the lumbar cancellous and cortical bones were determined separately.
Our data demonstrated that OVX lead to pronounced reduction in mechanical properties and bone mass. Treatment with tibolone increased mechanical properties and improved 3-D microarchitecture of both cancellous and cortical bone as compared to placebo treatment. Long-term treatment with tibolone for 54 weeks prevented OVX-induced reduction in the mechanical properties of both cancellous and cortical bone. Tibolone was shown to have relatively stronger microarchitectural compensation effect on trabecular bone than on cortical bone. Tibolone treatment did not prevent OVX-induced microarchitectural deterioration over the entire experimental period; there was only a statistically significant difference in microarchitectural parameters between OVX and tibolone groups after 34 weeks of tibolone treatment. This partially improved microarchitecture resulted in full recovery of mechanical properties to normal level, suggesting increased bone quality after long-term tibolone treatment. We concluded that long-term tibolone treatment completely preserved bone's mechanical properties and partially protects OVX-induced microarchitectural deterioration.

Disclosures: ***M. Ding****, None.*

SU136

Fluid Flow-induced ATP Release Occurs by a Vesicular Mechanism and Mediates Prostaglandin Release. D. C. Genetos[1], H. J. Donahue[2], R. L. Duncan[3]. [1]Cellular and Molecular Physiology, Pennsylvania State University College of Medicine, Hershey, PA, USA, [2]Orthopaedics and Rehabilitation, Pennsylvania State University College of Medicine, Hershey, PA, USA, [3]Orthopaedic Surgery, Indiana University College of Medicine, Indianapolis, IN, USA.

Emerging data suggests an important role for ATP-activated purinergic (P2) receptors in osteoblast and osteoclast function. In this study, we examined the mechanisms mediating fluid flow-induced ATP release. We found that fluid flow induced a rapid yet transient increase in ATP release compared to static MC3T3-E1 cells (59.8±15.7nM vs. 6.2±1.8nM), peaking within 1 minute of flow onset. While other authors have found a role for gap junctional communication and hemichannels in ATP release in astrocytes and chondrocytes, we found that inhibition of gap junctional communication with 18α-glycyrrhetinic acid had no effect on ATP release in the static or flowed state. We next examined what role vesicle formation and function played had in flow-induced ATP release. Inhibition of vesicle formation with monensin and, brefeldin A significantly attenuated flow-induced ATP release without affecting static ATP release. Inhibition of vesicle fusion at the plasmalemma in the presence of *N*-ethylmaleimide also significantly attenuated ATP release from flowed cells, suggesting that flow-induced ATP release was mediated through vesicular fusion and was dependent on Ca^{2+} entry into the cell via L-type voltage-sensitive Ca^{2+} channels. Activation of P2 receptors with the addition of exogenous ATP to static cells significantly increased prostaglandin E_2 (PGE_2) and I_2 (PGI_2) release, while hydrolysis of secreted ATP with apyrase prevented flow-induced increases in PGE_2 and PGI_2 release. These data suggest a time line of mechanotransduction where fluid shear results in Ca^{2+} entry through activation of L-VSCC's that, in turn, stimulates vesicular ATP release. Further, these data suggest that P2 receptors must be activated to complete the anabolic response of bone to mechanical load.

Disclosures: ***D.C. Genetos****, None.*

SU137

Normal Bone Geometry but Reduced Bone Mineral at the Femoral Neck with Cystic Fibrosis. J. H. Cole*[1], K. Kent*[2], G. S. Bhudhikanok*[3], L. K. Bachrach[3], M. C. van der Meulen[1]. [1]Sibley School of Mechanical and Aerospace Engineering, Cornell University, Ithaca, NY, USA, [2]Department of Medicine, Stanford University, Stanford, CA, USA, [3]Department of Pediatrics, Stanford University, Stanford, CA, USA.

Low bone mineral density at various anatomic sites is common among patients with cystic fibrosis (CF) (Bhudhikanok *et al.* 1996). Normal bone geometry and reduced bone mineral were reported previously in the femoral cortex of CF patients (Cole *et al.* 2003). The purpose of this study was to examine a primarily cancellous bone site in a population of CF patients and to correlate a bone strength indicator with measures of bone mineral. Bone mineral was assessed for 42 CF patients (15 male, 27 female, ages 8-48) using pencil-beam dual energy X-ray absorptiometry (QDR 1000W, Hologic Corp). Bone mineral content (BMC, g) and areal bone mineral density (BMD, g/cm^2) at the left femoral neck (FN) were recorded at baseline and at a 1.5-year follow-up visit. Bone mineral apparent density (BMAD, g/cm^3) was used as an estimate of volumetric bone density (Katzman *et al.* 1991). Geometric strength at the FN was assessed using the section modulus (Z, cm^3), an indicator of cross-sectional bone strength calculated from the cross-sectional moment of inertia (I, cm^4) and the bone diameter (D, cm). Both I and D were computed directly using the X-ray absorption curve from a single scan line at the mid-neck (Myers *et al.* 1993), requiring no geometric assumptions. Linear regressions were used to assess the correlation of Z with bone mineral measures (BMC, BMD, BMAD). Z increased linearly with BMC ($p<0.0001$, r^2=0.84-0.86) and BMD ($p<0.0001$, r^2=0.52-0.60) but not with BMAD at both baseline and follow-up. Similarly, changes in Z increased linearly with changes in BMC ($p<0.0001$, r^2=0.72) and BMD ($p<0.0001$, r^2=0.49) but not BMAD. As expected, Z was linearly related to body mass at baseline and follow-up ($p<0.0001$, r^2=0.68-0.72). Surprisingly, however, this relationship was identical between CF patients and a normal Caucasian population (48 male, 53 female, ages 9-26). Therefore, as was seen in the analysis at the mid-diaphysis, the geometry of the FN for CF patients is comparable to that of normal subjects for a given body size. This, along with a reduced BMAD, suggests that their skeleton does not compensate in size for the reduction in bone mineral density. This lack of adaptation is present for both cortical and cancellous bone sites. For CF patients, the cancellous bone of the FN is not more responsive to its mechanical environment than the femoral cortex, and this may account for the high incidence of fragility fractures across all sites.

Disclosures: ***J.H. Cole****, None.*

SU138

Radiographic Image Resolution of Fan-Beam Bone Densitometers Performing Vertebral Fracture Assessment. L. G. Jankowski*[1], G. Avery*[2], S. B. Broy[1]. [1]Center for Arthritis and Osteoporosis, Illinois Bone and Joint Institute, Morton Grove, IL, USA, [2]Nuclear Medicine, Methodist Hospital, Indianapolis, IN, USA.

We measure the radiographic resolution of the vertebral fracture assessment imaging modes on two different bone densitometers.

Bone densitometers have been approved for radiographic imaging of the lumbar and thoracic spine for vertebral fracture assessment (VFA), to identify vertebral deformities and measuring vertebral heights. One limitation often cited for these devices is their inherently poorer resolution compared to conventional radiographs. We acquired images of a standard radiographic line pair phantom (Nuclear Associates Part No. 07-538) using the recommended acquisition and image processing modes for VFA, on a GE-Lunar Prodigy Advance system with ClearView software, and a Hologic QDR 4500 SL, with Image-Pro software. We determined the inherent system resolution in units of line-pairs per millimeter (lp/mm).

The phantom was orientated with the lines in the transverse plane (horizontal lines on screen), as well as in the sagittal plane. The Prodigy scanner exhibited detector saturation when the phantom was scanned in air, so the phantom was placed between acrylic plates, each 4 cm thick, and maintained this configuration on the 4500SL. Two readers, using all available imaging tools provided by the respective manufacturers, obtained the best possible image resolution of the phantom line sets on the image display. The resolution was recorded as the highest grouping of lines that can be clearly resolved as three separate lines. When the readers disagreed, the average of their readings were used.

The best resolution on the QDR4500 was 0.9 lp/mm in the transverse plane, and 0.6 lp/mm in the sagittal plane. The best resolution on the Prodigy in the transverse plane was less than 0.6 lp/mm, the coarsest line spacing in the phantom, as only one of the two readers was able to visualize this grouping. Neither reader could visualize the line sets of the phantom in the sagittal plane on the Prodigy. The ability to identify compression deformities using a bone densitometer is limited by the inherent imaging resolution. The Hologic systems provided consistently better resolution than the Prodigy system in both the transverse and sagittal planes. The radiographic phantom used did not have sufficiently coarse gradations to accurately quantify the resolution on the Prodigy. A resolution phantom of suitable design may have value in assessing and monitoring system performance, or in selecting systems suitable for VFA.

Disclosures: ***L.G. Jankowski****, Proctor & Gamble Pharmaceuticals 8.*

SU139

Assessment of Femoral Neck Torsional Strength Indices. M. Sode*[1], J. Keyak*[2], M. Bouxsein*[3], T. Lang[1]. [1]Radiology, University of California, San Francisco, CA, USA, [2]Orthopaedic Surgery, University of California, Irvine, CA, USA, [3]Orthopedic Research Laboratories, Beth Israel Deaconess Medical Center, Boston, MA, USA.

Torsional strength indices (TSI), computed from QCT scan data may be predictive of bone strength. The goal of our study was to evaluate three TSI at femoral neck for their repeatability and correlations with femoral neck strength by a 3D finite element model (FEM).

To evaluate repeatability, nine subjects (60±10 years) underwent QCT imaging of the hip (GE 9800Q, 3mm slices) twice with repositioning between scans. Polar moment of inertia (CSMI) in a 4-mm thick transverse section at minimum cross-sectional area (CSA) of the left femoral neck was calculated. TSI were derived by dividing CSMI by a calculated bone width derived from CSA. Three TSI were computed: 1) TSI_E in which the image voxels were mapped to elastic modulus prior to CSMI calculation, 2) TSD in which the images had units of bone density and 3) TSC in which only voxels inside the cortex were included. Precision of TSI was computed from the nine repeat scans as the root-mean square coefficient of variation in %.

We obtained QCT scans of the left hip in 30 women (74±4 years) and computed TSI_E, TSD and TSC. The FEM of the left hip of each subject was generated and loaded simulating single-limb stance, giving failure load (FL) in kN. Agreement between TSI and FL was determined using linear regression and root mean square error (RMSE) was computed for the regression equation. The effects of trabecular BMD (tBMD), cortical BMD (cBMD), cortical volume (cVOL), and CSA on TSI were determined by multi-linear regression and given as standardized β, which represented the effect in units of SD on TSI of a 1SD change in each predictor variable.

Precisions for TSI_E, TSD and TSC were 6%, 5% and 3% respectively. Correlations of TSI with FL and β values for tBMD, cBMD and CSA are tabulated below.

Modest agreement of TSI with FL may be due to the fact that only torsion is taken into account and that they represent (unlike FEM) a thin section of the femoral neck. Also, FEM tends to predict fractures near the femoral head rather than at the minimum CSA. Because the cortical elements have high density and are situated at the bone periphery, TSI_E and TSD measures were strong functions of cBMD and CSA.

Only the TSI were addressed here; strength indices in other loading conditions will be explored.

[a] p<0.001, [b] p<0.01, [c] p<0.05, [ns] p>0.05.

	vs FL	Standardized β			
	R *RMSE(kN)*	tBMD	cBMD	cVol	CSA
TSI_E	0.65 *1.8*	0.20[c]	0.60[a]	0.18[ns]	0.56[a]
TSD	0.60 *1.9*	0.14[ns]	0.41[a]	0.21[b]	0.73[a]
TSC	0.3 *2.3*	n/a	n/a	0.02[ns]	0.94[a]

Disclosures: ***M. Sode****, None.*

SU140

Calcium Absorption in Hip Fracture Subjects. A. G. Need*[1], M. Metz*[1], P. D. O'Loughlin*[1], M. Horowitz*[2], B. E. C. Nordin*[1]. [1]Clinical Biochemistry, Institute of Medical and Veterinary Science, Adelaide, Australia, [2]Department of Medicine, Royal Adelaide Hospital, Adelaide, Australia.

Impaired intestinal calcium absorption has been reported in hip fracture cases [1] and claimed to increase the risk of hip fractures prospectively [2] but the relation between this impairment and circulating vitamin D metabolites has not been examined. We have measured fractional radiocalcium absorption (α)[3] and serum 25 hydroxyvitamin D (25D) and 1,25 dihydroxyvitamin D (1,25D) in 56 ambulant outpatients (48 female, 8 male) of mean age 67(SD11) yr with prevalent hip fracture, and in the same number of age and sex matched controls.

Mean α was significantly lower in the fracture subjects (0.46(0.18) vs 0.63(0.22):P<0.001) as was serum 1,25D (89(46) vs 106(36) pmol/L:P=0.036), but 25D did not differ significantly between the groups (54(27) vs 61(23) nmol/L:P=0.17). α was significantly related to 1,25D in both groups but not related to 25D in either group. Using the relation between α and 1,25D in the controls (α=0.36+0.0026x1,25D: r=0.41,P=0.002) as the reference line we calculated that the lower 1,25D in the fracture cases (17 pmol/L) could only account for 20% of their calcium absorption deficit.

The results suggest that the calcium absorption deficit in cases of hip fracture is largely due to a diminished intestinal response to circulating 1,25D.

1.Nordin et al, Osteoporos Int 2004;15:27-31
2.Ensrud KE et al, Ann Intern Med 2000;132:345-353
3.Nordin BEC et al, J Nucl Med 1998;39:108-113

Disclosures: ***A.G. Need****, None.*

SU141

Quantitative Analysis of Messenger RNA Expression of Lysyl Hydroxylases in Mandibular and Femoral Bone Marrows of Senescence-Accelerated Mice. T. Matsuura, K. Yamamoto*, Y. Nagashima*, Y. Daigo*, M. Katafuchi*, H. Sato*. Oral Rehabilitation, Fukuoka Dental College, Fukuoka, Japan.

Messenger RNA analysis of bone marrow is a potential examination to diagnose the quality of maxillofacial bone. Lysyl hydroxylases (LHs) are responsible for collagen cross-linking, determining bone quality. To investigate mRNA expression patterns of LHs in bone marrows with potentially different bone quality, we quantified the mRNA expression of LH isoforms (LH1, LH2, and LH3), type I collagen (COLI), and alkaline phosphatase (ALP) in the mandibular and femoral bone marrows of three senescence-accelerated mouse (SAM) strains; osteoporosis model SAMP6, mandibular osteoarthritis model SAMP8, and their control SAMR1. Total RNAs directly isolated from the bone marrow were used for reverse transcription and the products were then used to quantify mRNA expressions of the molecules using a real-time PCR assay. The experimental protocol was approved by the Ethical Committee for Animal Experiments in our institute. The expression levels of any molecule were varied in the mandibular and femoral bone marrows. The expression levels of COLI, ALP, and LH2 were higher in the mandibular than in the femoral bone marrows. In the mandibular bone marrow, the expression levels of COLI of 3 SAM strains was significantly different from one another. In both the bone marrows, the expressions between COLI and LH1 and between ALP and LH2 were associated with each other. This study indicates that gene expression patterns of LH1 and LH2 in bone marrows are associated with those of developmental bone markers and those of LH2 and the bone markers are differential between mandible and femur. Quantitative mRNA analysis of LHs in combination with developmental bone markers in bone marrows may be useful to investigate their relationship with quality of maxillofacial bone.

Disclosures: ***T. Matsuura****, None.*

SU142

Markers of Bone Remodeling Predict Rate of Bone Loss in Multiple Sclerosis Patients Treated with Low Dose Glucocorticoids. J. J. Stepan[1], E. Havrdova*[2], M. Tyblova*[2], D. Horakova*[2], V. Ticha*[2], V. Zikan*[1], I. Novakova*[2]. [1]3rd Dept. of Internal Medicine, Charles University Faculty of Medicine, Prague, Czech Republic, [2]Dept. of Neurology, Charles University Faculty of Medicine, Prague, Czech Republic.

The contribution of the underlying disease, for which glucocorticoids are used, confounds the assessment of glucocorticoid effects on bone. Multiple sclerosis (MS) is a gait disorder characterized by acute episodes of neurological defect leading to progressive immobilization. Long-term glucocorticoid use and progressive immobilization, along with vitamin D deficiency, are likely to be determinants for osteoporosis and skeletal muscle atrophy, and the increased risk of fracture in patients with multiple sclerosis. The aim of this study was to evaluate the clinical value of markers of bone remodeling in assessment of rate of bone loss in patients with MS long term treated with low dose glucocorticoids. The study involved 70 patients with MS. Thirty one women were premenopausal (mean age, 35.1 ± 8.1 yrs), 16 postmenopausal women (mean age, 50.3 ± 5.0 yrs) were on regular hormone replacement therapy. Mean age of men was 42.4 ± 12.1 yrs. The patients received the daily recommended dose of calcium (500 mg) and vitamin D (400 IU). Motor function of the patients was evaluated using the Kurtzke Expanded Disability Status Scale (KEDSS). Bone mineral density (Hologic QDR 4500) was determined at the lumbar spine and proximal femur at baseline and after 1.8 ± 0.8 years. Bone remodeling was assessed using circulating concentrations of type 1 collagen cross-linked C-telopeptide (beta CTX), aminoterminal propeptide of type I procollagen, and N-MID osteocalcin (OC). A control group of 140 age-matched healthy subjects was used to compare bone-turnover markers. The plasma CTX concentration was the most significant parameter of bone remodeling which correlated with the rate of bone loss and with the KEDSS. After adjustment for BMI, the plasma CTX concentration remained the most significant predictor of the rate of bone loss ($p<0.05$). The rate of bone loss at the proximal femur was not significantly different between tertiles of plasma OC concentrations. In physically disabled patients, plasma OC was not significantly increased despite evidence of increased bone resorption, indicating an impaired coupling between bone resorption and bone formation in GC treated patients. In conclusion, in physically active patients with MS treated with low-dose GC, the bone-turnover markers were not different from controls. Patients having plasma CTX but markers of bone formation higher as compared to controls were confirmed 2 years later as bone losers.

Disclosures: ***J.J. Stepan****, None.*

SU143

Urine Osteocalcin as a Marker of Bone Metabolism. K. K. Ivaska*[1], S. Käkönen*[1], P. Gerdhem[2], K. Akesson[2], K. J. Obrant[2], A. Nenonen*[3], A. Heinonen[3], P. Kannus*[3], K. Uusi-Rasi[3], H. K. Väänänen*[1]. [1]Institute of Biomedicine, Department of Anatomy, University of Turku, Turku, Finland, [2]Department of Orthopaedics, Malmö University Hospital, Malmö, Sweden, [3]UKK Institute for Health Promotion Research, Tampere, Finland.

Osteocalcin (OC) is produced by osteoblasts and although most of OC is adsorbed to bone hydroxyapatite, some OC leaks into blood stream where it can be detected. Part of OC found in blood is also thought to originate from degradation of bone matrix during bone resorption. Levels of circulating OC have been widely used in clinical investigations as a marker of bone turnover. In addition to circulation, OC can be found in urine as mid-molecule fragments and these fragments (U-OC) can be classified into two main categories according to their size.

We developed three immunoassays for the detection of various molecular forms of U-OC. Competitive U-TotalOC assay recognized OC fragments from both U-OC categories whereas two-site assays U-MidOC and U-LongOC were unable to detect more truncated fragments in the second category. U-OC was studied in healthy premenopausal women (n=58) and postmenopausal women with or without hormone replacement therapy (HRT) (n=13 and n=20, respectively). The association of U-OC and bone mineral density (BMD) was evaluated in 1040 randomly recruited 75-year-old women. Furthermore, U-OC was studied in a one-year double-blinded placebo-controlled alendronate intervention trial (n=76 for both placebo and alendronate) in which U-OC levels were measured at baseline and after 3, 6 and 12 months. All U-OC values were corrected for urine creatinine.

U-OC measured with any of the three assays had a significant correlation to BMD measured at various body sites ($p<0.0001$, Spearman's correlation coefficients from -0.15 to -0.29). Total concentration of U-OC (U-TotalOC) was significantly higher in postmenopausal women compared to premenopausals ($p<0.05$) and U-MidOC and U-TotalOC assays were also able to distinguish between postmenopausal women with and without HRT ($p<0.05$ and $p<0.01$). Furthermore, all U-OCs were significantly reduced after three months treatment with alendronate ($p<0.001$) and did not alter during the remaining follow-up period. Previously we have also demonstrated that U-MidOC and U-LongOC were able to predict fractures, particularly fractures engaging trabecular bone.

In conclusion, urine osteocalcin offers an alternative method for monitoring bone metabolism and may have potential applications in diagnostics related to disorders of bone metabolism.

Disclosures: ***K.K. Ivaska****, None.*

SU144

Differences in Baseline NTX Levels in Treatment-Naïve Patients and Patients Previously Treated with Alendronate, Etidronate, or Hormone Replacement Therapy. W. G. Bensen*[1], W. P. Olszynski[2], A. Jovaisas*[3], S. Morin[4], J. Stewart*[5], C. Crowley[6], K. S. Davison[1]. [1]Med., McMaster Univ., Hamilton, ON, Canada, [2]Med., Univ. of Saskatchewan, Saskatoon, SK, Canada, [3]Med., Univ. of Ottawa, Ottawa, ON, Canada, [4]Int. Med., McGill Univ. Health Centre, Montreal, PQ, Canada, [5]Aventis Pharma Inc., Laval, PQ, Canada, [6]P&G Pharmaceuticals, Toronto, ON, Canada.

Anti-resorptive therapies differ in the rate and extent of bone turnover suppression, as well as the rate and extent of resolution of bone turnover after their discontinuation. The Point-of-Care device and Actonel® Once-a-Week Dosing Satisfaction Trial (POWER) is a 24-week, multi-centre, prospective, open-label, randomized, controlled community practice-based study designed to determine whether feedback on response to therapy, assessed by bone turnover, will improve subject satisfaction with therapy. Eligible patients included postmenopausal women diagnosed with osteoporosis who were untreated or previously treated for osteoporosis, but discontinued prior to enrolment due to lack of effect or intolerance. All patients were assigned Actonel® 35 mg Once-a-Week treatment. The levels of urinary cross-linked N-telopeptides of type I collagen (NTX) were measured at baseline in half the cohort using the Osteomark® NTX Point-of-Care device.

Baseline Characteristics of Bone Turnover Marker Group (mean±SD)

Characteristic	Treatment naïve	Previously treated		
		Hormone	Etidronate	Alendronate
Sample size	641	66	269	74
Age in years (y)	67±11	66±10	71±10	68±11
Uncorrected NTX (nM BCE/ mM creatinine)	71±45	67±44	58±38	39±25
Time on therapy (mo)	NA	49±73	34±27	22±30
Time since therapy discontinued (mo)	NA	4.5±8.3	2.9±6.4	4.0±5.6

Baseline NTX (95% CI), corrected for time on and time since discontinuation of therapy, was 41 (32-50) for the alendronate group, 59 (54-63) for the etidronate group and 64 (55-73) for the hormone replacement therapy group. Baseline NTX was significantly lower in the alendronate group compared to either the etidronate ($p=0.0004$) or hormone replacement therapy ($p<0.001$) groups. The untreated group had significantly ($p<0.0001$) higher baseline NTX than both bisphosphonate groups. No significant NTX differences existed between etidronate and hormone replacement therapy groups. Baseline NTX levels with previous alendronate therapy were the lowest of all therapies investigated, independent of time on and time since discontinuation of therapy. These results may have important implications for individuals who discontinue anti-resorptive therapy and plan to begin anabolic therapy, as decreased levels of bone turnover may attenuate the anabolic effects.

Disclosures: ***W.G. Bensen****, Alliance for Better Bone Health, a collaboration agreement between Procter & Gamble Pharmaceuticals and Aventis Pharma 5.*

SU145

Pharmacokinetics of ^{41}Ca Distribution in Mice. D. W. Burton[1], D. J. Hillegonds*[2], R. L. Fitzgerald*[3], D. A. Herold*[3], L. J. Deftos[1]. [1]Medicine, University of California and SDVAMC, San Diego, CA, USA, [2]Center for Accelerator Mass Spectrometry, Lawrence Livermore National Laboratory, Livermore, CA, USA, [3]Pathology, University of California and SDVAMC, San Diego, CA, USA.

Previous studies have shown the value of ^{41}Ca, a rare isotope with a half-life of 10^5 years, in tracking bone health, primarily related to osteoporosis. Accelerator mass spectrometric quantitation of ^{41}Ca offers advantages over ^{45}Ca decay counting because of the elimination of radiation hazards in both handling and waste disposal, while retaining the advantages of high tracer selectivity and sensitivity. This novel ^{41}Ca tracer technique promises to provide a direct measure of net bone calcium balance in both humans and in animal models. Our goal is to use ^{41}Ca technology to develop a minimally invasive method to detect the transition from the primary cancer site of prostate, breast or lung cancers to the skeleton and to assess the efficacy of treatments on the bone lesions. To demonstrate the feasibility of using the ^{41}Ca assay in mouse models for lytic and/or osteoblastic bone cancer lesions, we established a baseline for the pharmacokinetic distribution of the ^{41}Ca material in mice. In this study, normal, immunocompromised SCID mice were injected IP with 0.55 nCi ^{41}Ca / 0. 5 ml PBS. After 4 weeks, to allow the mice to equilibrate with a stable pool of ^{41}Ca, they were exanguinated and various organs harvested. The tissues were weighted, and microwave digested with nitric acid. Carrier ^{40}Ca was added to the samples and they were analyzed for ^{41}Ca/Ca ratios by accelerator mass spectrometry (AMS). The ^{41}Ca dosed mice specimens had ^{41}Ca/Ca ratios >100-fold above non-^{41}Ca dosed tissue controls. As expected, the majority of the ^{41}Ca that was retained by the mice was in the skeleton. The tibiae and femurs demonstrated >5000-fold higher levels of ^{41}Ca/^{40}Ca /g wet weight compared to the other soft tissues specimens evaluated (heart, kidney, muscle, spleen, liver, and RBCs). The serum ^{41}Ca/Ca ratios were also readily measurable above background. Ongoing studies using the ^{41}Ca assay in a SCID mouse model for prostate cancer that produces lytic bone lesions are currently underway. If the ^{41}Ca assay demonstrates an excess loss of ^{41}Ca in the sera or feces from mice that have overall lytic bone lesions compared to control mice, this ^{41}Ca method could be applied clinically to patients for monitoring skeletal changes.

Disclosures: ***D.W. Burton****, None.*

SU146

Urinary Gamma-glutamyl Transpeptidase (GGT) Activity Measurement Is Useful as a Novel Biochemical Marker for Bone Metabolism. I. Kodama[1], M. Sanada*[1], M. Tsuda*[1], K. Ohama*[2]. [1]Obstetrics and Gynecology, Hiroshima University, Hiroshima City, Japan, [2]Hiroshima Prefectural Hospital, Hiroshima City, Japan.

The purpose of this study is to investigate the measurement of urinary gamma-glutamyl transpeptidase (GGT) activity is useful as a biochemical marker for bone metabolism in postmenopausal women.

A total of 80 postmenopausal Japanese women, aged 48 to 74 years, were admitted to study. Each subject had experienced natural menopause for at least 1 year but not longer than 5 years. All participants were followed up without any lifestyle modification. A total of 30 women (mean age 52.5±1.3) received conjugated equine estrogen, 0.625 mg daily each morning for 12 months (HRT group). A total of 25 women (mean age 64.2±1.6) received alendronate sodium 35mg daily each morning for three months (ALN group). Urinary cross-linked N-telopeptides (NTX), GGT activity and serum GGT activity were measured on all HRT group subjects before the start of therapy and for 3, 6 and 12 months after therapy. Urinary NTX and GGT activity were measured on all ALN group subjects before the start of therapy and three months after therapy. Lumber spine (L2-L4) bone mineral density (BMD) and femoral neck BMD were measured using a dual X-ray absorptiometer (DPX-alpha, Lunar Co). These parameters were measured on all HRT group subjects before the start of therapy and for 6 and 12 months after therapy.

Correlation between urinary GGT activity and NTX were significant at before the start of therapy, and those relations were being maintained within the period of therapy (HRT group and ALN group) .

L2-L4 BMD was increased after the start of the HRT, averaging +3.24% and +5.91%, at the 6 months and 12 months, respectively.

Femoral neck BMD was slightly increased compared with baseline value, averaging +0.97% and +1.97 %, at the 6 months and 12 months after HRT.

In conclusion, we now report that urinary GGT activity measurement is useful as a novel biochemical marker for bone metabolism.

Disclosures: ***I. Kodama****, None.*

SU147

Technical and Clinical Evaluation of a Point of Care Device for Measurement of N-Telopeptide Fragment of Type I Collagen in Urine. R. A. Hannon, J. V. Boreham*, J. A. Porter*, K. Karnik*, A. C. Eagleton*, R. Eastell, A. Blumsohn. Academic Unit of Bone Metabolism, University of Sheffield, Sheffield, United Kingdom.

Assessment of bone turnover using point-of-care technology may facilitate therapeutic monitoring in osteoporosis. We examined the detailed technical and clinical performance of a point of care device (POCD) for measurement of NTX and creatinine (Cr) in urine (OSTEOMARK® NTX Point-of-Care) in comparison with laboratory methods (automated chemiluminescent immunoassay, Ortho ECI NTX; manual immunoassay, Osteomark ELISA NTX; enzymatic Cr).

Between device analytical imprecision was 20.4% (CV) over 12 weeks at 17.5nmolBCE/mmol. The effect of in-vivo dilution on Cr correction was assessed by measuring NTX/Cr in fasting second morning void urine on two occasions in 19 healthy adults with a) fluid restriction, b) 500ml oral water at first morning void. POCD NTX/Cr was not significantly affected by fluid intake (ratio hydrated/dehydrated 1.22±0.12) despite a 3-fold difference in urine concentration. Within-subject imprecision of POCD NTX/Cr was 26.7% (CVa+i) at an interval of 1 day, and 41.7% at an interval of 1 week. The circadian rhythm of POCD NTX/Cr was similar to that for ECI NTX/Cr. POCD NTX/Cr was 37.4±4% higher for samples collected at 07h30 vs 13h30 in 15 healthy volunteers. In healthy adults POCD NTX/Cr decreased by 20.0±3.8% following milk supplementation (n=20, 500mL bd x 1wk) and by 24.6±4.8% following calcium supplementation (n=25, 500mg bd x 1wk). In postmenopausal women with osteoporosis POCD NTX/Cr decreased by 60.9±7.4% following alendronate (n=15, 10mg + 500mg Ca x 24wks), and by 50.0±4.8% following risedronate (n=14, 5mg x 13wks). All based on SMV urine collection. The apparent response to risedronate depended on the timing of sample collection (24.3±6.9% at 13h13, vs 50.0±4.8% at 07h30 P<0.01). Responses were similar in all respects to ECI NTXC/Cr and ELISA NTX/Cr. Calibration was similar to ECI NTX/Cr (slope of Deming comparison 1.14, r=78, n=60 over the reference range). POCD NTX/Cr was higher in postmenopausal women (geometric mean 55.3nmol/mmol [95% CL 46.4-65.8] n=30) vs premenopausal women (35.6nmol/mmol [30.9-41.0] n=30, P<0.01), and the estimated premenopausal reference interval (95% limits 16.6-76.5nmol/mmol) was similar to ECI NTX/Cr.

Data were obtained under controlled laboratory conditions. POCD may perform differently under other conditions. Although the technical imprecision of POCD NTX/Cr may be greater than laboratory NTX/Cr, data obtained by the POCD is clinically plausible, unaffected by urine flow rate, comparable to that obtained using ELISA NTX and ECI NTX, and is likely to be useful for therapeutic monitoring.

Disclosures: ***R.A. Hannon****, Unipath Limited 2.*

SU148

Serum Osteocalcin Assay by the Elecsys 2010 Is Robust and Suitable for Monitoring Bone Turnover. E. T. Leary, T. K. Aggoune*, T. H. Carlson*. Pacific Biometrics, Inc., Seattle, WA, USA.

Serum osteocalcin (OC) has demonstrated clinical utility as a biomarker of bone formation. However, OC is commonly believed to be unstable and to require special sample handling. OC fragments especially produced in some disease states may interfere with many existing assays. Therefore, we evaluated the long-term performance of the N-MID Osteocalcin assay on the automated Elecsys 2010 analyzer (Roche Diagnostics) and the stability of different sample types under a variety of conditions. The Elecsys OC is specific for intact OC (amino acids 1-49) and the main N-terminal fragment (amino acids 1-43) resulting from proteolytic cleavage after blood collection.

OC assay precision was evaluated by commercial and in-house quality control samples. To evaluate the stability of OC by Elecsys, matched serum, K_3 EDTA plasma (EDTA) and Li heparin plasma (Heparin) were collected from volunteers. Sample stability was evaluated at room temperature, at 4 ° C for 7 days and at -70°C for 2 yr. To measure OC in a specimen matrix likely to accumulate fragments, matched serum, EDTA, and Heparin samples were collected from 44 subjects on kidney hemodialysis. OC analyzed within one month of collection and again after 4 yr of storage at -70°C were compared. To demonstrate that samples stored long-term were suitable for monitoring clinical response, OC was measured in 103 osteoporotic postmenopausal women on antiresorptive therapy, at baseline and after 12 weeks of treatment. Values determined immediately after the treatment period were compared with those after 3 yr of storage at -70°C.

Within-run precision of OC was 1.4 -3.6 % CV at 72 - 7.9 ng/mL. Among-run precision was 3.7-5.9% CV at 21.3 - 110 ng/mL. OC concentrations in serum, EDTA and Heparin did not differ significantly. EDTA was a more stable matrix at room temperature and at 4 deg C than either serum or Heparin (3-4 days versus 24 hr or less). Change in OC at 24 mo at -70°C was less than 10% for all three sample types, with no trend. Assays of samples from subjects on renal dialysis with greatly elevated values (17-1133 ng/mL, SD = 300 ng/mL) recovered well in dilution studies. OC values agreed after 4 yr of storage in serum, EDTA, and Heparin and correlated well with the initial results (all r > 0.99, slopes 0.92 - 1.01 and intercepts -7.2 - +1.3 ng/mL). Initial OC results for 103 osteoporotic women on antiresorptive therapy exhibited a mean decrease of 20.2% from baseline (baseline mean = 30.4 ng/ml) compared to -21.1 % (baseline mean = 32.2 ng/mL) measured in samples following 3 yr of storage.

We conclude the N-MID Osteocalcin assay on the Elecsys 2010 is stable and robust, and may be included in clinical trials with usual precautions.

Disclosures: ***E.T. Leary****, None.*

SU149

Unexplained Increase in Parathyroidectomies in the U.S. T. Cantor. President, Scantibodies Laboratory, Inc., Santee, CA, USA.

With the increased use of vitamin D analogs for "medical parathyroidectomy" for ESRD (end stage renal disease) patients it was expected that the number of parathyroidectomies would decrease. Therefore, the USRDS (US Renal Data Services) database on parathyroidectomies was examined to see if this expectation was, indeed, realized. From 1995 through 1998 the number of parathyroidectomies declined steadily among the Medicare ESRD patients in the US as expected. However, in 1999 the trend changed, with an increasing number of parathyroidectomies. This trend has persisted through 2001 (the latest data available). From 1999 to 2000 there was a 17% increase in parathyroidectomies and from 2000 to 2001 there was a 29% increase in parathyroidectomies. K/DOQI (National Kidney Foundation's Kidney Disease Outcome Quality Inititative) guideline 14 states that "parathyroidectomy should be recommended in patients with severe hyperparathyroidism (serum levels of intact PTH >800 pgm/ml)." Therefore, the predominant intact PTH assay used should be examined for any changes that might explain this increase in parathyroidectomies. Meanwhile, this data indicates a reason for caution before prescribing a parathyroidectomy.

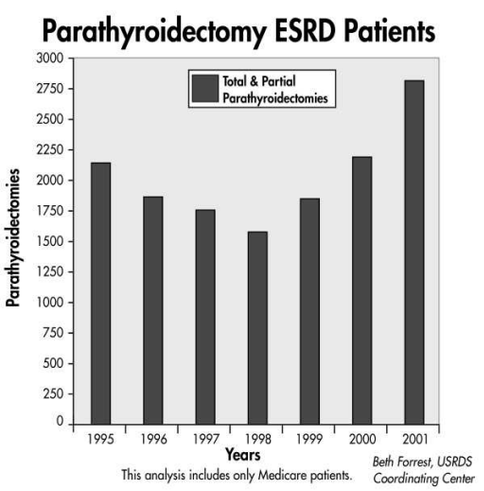

Disclosures: ***T. Cantor****, Scantibodies Laboratory, Inc. 4; Scantibodies Clinical Laboratory 4.*

SU150

Microarray Study of Circulating Monocytes in Search for Functional Genes for Osteoporosis. Y. Z. Liu*, V. Dvornyk*, Y. Lu*, H. Shen*, J. Wilde*, T. Conway*, R. R. Recker, H. W. Deng. Osteoprosis Research Ctr. and Dept. of Biomedical Sciences, Creighton Univ., Omaha, NE, USA.

Circulating monocytes are major target cells for hormones in bone metabolism and actively participate in osteoclastogenesis by either serving as the early precursors of osteo-

clasts or producing cytokines important to osteoclast differentiation, activation, and apoptosis.
Gene expression studies of blood monocytes in high vs. low BMD subjects may identify genes functionally relevant to osteoclastogenesis and thus to bone mass variation and pathogenesis of osteoporosis.
In this study, we analyzed gene expression of blood monocytes using Affymetrix HG-U133A GeneChip®, containing probes for 14,500 genes. The monocytes came from 14 perimenopausal women aged 47-55. The subject distribution and BMD Z score for the L1-4 (mean±SD) are listed in Table 1A.
Comparison of low vs. high BMD women has identified 42 differentially expressed genes (p<0.001). Since menopause has dramatic effects on bone loss, we also compared 4 postmenopausal low vs. 4 postmenopausal high BMD women in order to identify genes relevant to postmenopausal BMD variation. This revealed 69 differentially expressed genes (p<0.001). Their biological functions are listed in Table 1B (↑,↓: up or downregulated).

Table 1A	Pre-		Post-menopausal	
	N	Z_{BMD}	*N*	Z_{BMD}
High BMD	4	2.74±1.04	4	2.03±0.95
Low BMD	2	-0.83±0.21	4	-1.67±0.17

Table 1B	Low vs. high BMD		Post-M low vs. high BMD	
	↑	↓	↑	↓
Cell signaling	6	1	4	2
Transcription regulation	2	-	3	2
Proteolysis	1	1	1	3
Apoptosis	1	1	2	1
Other (e.g., immune response)	21	8	35	16
Total	31	11	45	24

Among the genes differentially expressed, several ones are of potential importance. The FOLR2 gene is upregulated in low BMD subjects and its upregulation has been associated with monocyte activation in inflammatory conditions. JAK2, GPR44, and GPS1 are members of two important pathways for monocyte differentiation and proliferation, i.e., JAK/STAT and MAPK. The first two genes are up- and the last downregulated in low BMD subjects. Two genes related to bone metabolism, caldecrin and P2RX5, are down and upregulated respectively in postmenopausal low vs. high BMD subjects. The caldecrin gene can inhibit PTH's bone resorption and the P2RX5 gene is involved in interleukin processing and release as well as activation of NF-κB and p38 MAP kinase. Importantly, the chromosome regions of these two genes have also been found linked to BMD.
This is the first *in vivo* gene-expression profiling study of osteoporosis in humans. By confirming important genes relevant to bone metabolism and identifying novel genes for further study, it demonstrates the power and prospect of microarray in genetic dissection of osteoporosis.

Disclosures: ***Y.Z. Liu****, None.*

SU151

Genetic Liability to Fracture in Elderly. K. Michaëlsson[1], H. Melhus[2], H. Ferm*[1], A. Ahlbom*[3], N. Pedersen*[4]. [1]Dept. of Orthopaedics, University Hospital, Uppsala, Sweden, [2]Dept. of Clin. Pharmacol, University Hospital, Uppsala, Sweden, [3]IMM, Karolinska Institutet, Stockholm, Sweden, [4]Dept. of Epidemiol. and Biostat, Karolinska Institutet, Stockholm, Sweden.

The extent of genetic influence on fracture risk is unclear. Twins offer a natural study population for evaluating genetic risk. The authors of the only previous fracture twin study concluded that the heritability of osteoporotic fracture risk was low. On the contrary, genetic influence on variation in BMD has been determined as substantial and a low BMD has become the most established risk factor for osteoporotic fractures. The extent to which BMD is the primary risk factor for osteoporotic fractures ought to be reflected in genetic liability to these fractures. On the other hand, if concomitant diseases, balance disorders or lifestyle habits not directly related to BMD but to fracture risk have a low genetic impact, these may modulate and counterbalance the strong genetic impact of BMD when estimating the influence of genetic propensity to fractures. A low genetic impact on fracture risk should encourage life style intervention approaches but a high genetic influence should focus research and primary prevention efforts to families with high risk of fractures.
In order to evaluate the genetic liability of fractures in the elderly we used a cohort, within the Swedish Twin Registry, of all 33,432 twins born 1896-1944 who were alive in 1972. The Swedish Inpatient Registry and computer assisted telephone interviews enabled us to identify twins with fractures. There was 6,520 twins with any fracture, 3,681 with any osteoporotic fracture and 1,097 with a hip fracture after the age of 50 years.
Genetic variation in liability to fracture differed considerably by type of fracture and age. Less than 20% of the overall age-adjusted fracture variance was explained by genetic variation. The age-adjusted heritability of any osteoporotic fracture was, however, somewhat greater (0.27, 95% CI 0.09-0.28), and for hip fracture alone, 0.48 (95% CI 0.28-0.57). The genetic influence was not attenuated after further adjustment for several known osteoporotic covariates. Genetic influences were considerably greater for first hip fractures before the age of 69 years (0.68, 95% CI 0.41-0.78) and between 69-79 years (0.47, 95% CI 0.04-0.62) than for hip fractures after 79 years of age (0.03, 95% CI 0.00-0.26).
These findings can be important to effectively target interventions and research efforts to prevent fractures. The search for susceptibility genes and environmental factors that may modulate expression of these genes in young patients with hip fracture should be encouraged. Prevention of fractures in the oldest can be focused on life-style interventions.

Disclosures: ***K. Michaëlsson****, None.*

SU152

Variability in Bone Status among Inbred Strains of Mice. S. Syberg*, S. D. Ohlendorff*, Z. Henriksen*, J. Teilmann*, N. R. Jørgensen. Dep. of Endocrinology and Clinical Biochemistry, Copenhagen University Hospital Hvidovre, Hvidovre, Denmark.

More than 70% of the variability in human bone density has been attributed to genetic factors. For experimentally defining the genetic influence on bone status, animal models are important. The purinergic P2X7 receptor mediates intercellular signaling between osteoblasts and osteoclasts, and it is involved in the regulation of osteoclast activity. Knockout models for this receptor have been established, but conflicting results have been reported for the different models. However, the knockouts are based on inbred strains of mice housing a natural mutation in the P2X7 gene, which may account for some of the conflicting results. The purpose of this study was to compare adult peak bone density with bone strength measurements in 5 inbred strains of mice and to relate them to the P451L mutation in P2X7.
Fifteen females from each strains were DEXA scanned to determine bone mineral density (BMD) and bone mineral content (BMC). The ability of the femurs to resist mechanical forces was quantified, by a three-point bending test ex vivo (Maxload/N). Finally, the distribution of the P451L mutation in the strains was determined by sequencing exon 13 of P2X7.
BMD and BMC varied significantly among the strains (see table below). AKR had the higher BMD and BMC, whereas C57BL and BALB had the lower. In bone strength measurements femurs from the C57BL strain were significantly weaker than from the other strains, while femurs from C3H were significantly stronger that the others. The P451L mutation is very frequent in the inbred strains. Between BALB and C57BL, where the latter is housing the P451L mutation of P2X7, there was no significant difference in BMC or BMD, however there was a significant difference in bone strength. BALB mice had significantly stronger femurs than C57BL. However between 129X1 and C3H there was no difference in BMC or BMD, and again a significant difference in bone strength, but in this case the P451L mutation is in the mice with the strongest femur.
In conclusion the P451L mutation in P2X7 is not associated with the difference in bone density of different strains. Thus no correlation between the mutation in P2X7 and bone strength have been found at the age of 4 months. When choosing a strain as background for an animal model of osteoporosis it is important to be aware of the differences in bone status between the strains.

Strain	Mean ± SD			
	BMD (g/cm2)*	BMC (g)*	Maxload (N)*	P451L mutation
AKR/J	0,0576 ± 0,0021	0,599 ± 0,04	30,2 ± 2,4	+
C3H/HeJ	0,0563 ± 0,0018	0,558 ± 0,04	34,2 ± 3,0	+
129X1/SvJ	0,0561 ± 0,0020	0,535 ± 0.05	31,5 ± 3,2	-
BALB/cJ	0,0512 ± 0,0017	0,471 ± 0,03	24,6 ± 1,6	-
C57BL/6J	0,0497 ± 0,0016	0,455 ± 0,03	17,3 ± 1,5	+

* *p<0,01*

Disclosures: ***S. Syberg****, None.*

SU153

Bone Vasculature as a New Marker for Bone Quality Varies within the Femoral Diaphysis of Two Genetically Distinct Mouse Strains. P. Schneider*[1], M. Stampanoni*[2], L. R. Donahue[3], R. Müller[1]. [1]Institute for Biomedical Engineering, ETH and University Zürich, Zürich, Switzerland, [2]Swiss Light Source (SLS), Paul Scherrer Institute (PSI), Villigen, Switzerland, [3]The Jackson Laboratory, Bar Harbor, ME, USA.

In clinical orthopaedics fractures often occur in bones exposed to chronic overload. On the microstructural level bone density and architecture are the dominant parameters determining bone strength. However, to determine tissue strength, cellular effects such as tissue mineralization or cell lacunae variations must be investigated. More recently, it was found that bone vasculature is a major contributor to local tissue porosity and therefore is linked directly to the mechanical tissue properties. With the advent of synchrotron radiation sources, micro-computed tomography (SRμCT) with resolution on the order of 1 μm becomes feasible. Moreover, new features such as bone vasculature and even single osteocytes inside the bone tissue are now detectable in a fully nondestructive and three-dimensional fashion. In this study, inbred strains of growth hormone deficient mice B6-*lit/lit* (B6*lit*) and C3.B6-*lit/lit* (C3*lit*) were used to quantify ultrastructural bone tissue properties. Here we report of vascular alterations in the two strains as assessed from SRμCT. Measurement of the mid-diaphyses of ten B6*lit* and C3*lit* femoral specimens was performed (1 mm section, 1.75 μm voxel size). Morphometric indices for vasculature and bone were determined including cortical thickness (Ct.Th), vessel thickness (Vs.Th), number (Vs.N), and orientation. Results showed that local Vs.N was higher in C3*lit* where Ct.Th was larger along the cortical circumference. This feature was less pronounced in B6*lit* where Ct.Th varied only mildly in the different regions. Additionally, vessel orientation was mainly radial for all B6*lit* specimens as well as for those regions in C3*lit* bones with low Ct.Th. This behavior changed when Ct.Th increased locally such that vessels started to be oriented along the longitudinal axis. This was not the case in B6*lit* with a more uniform, rather thin cortex. In this study, for the first time, we described a method to assess 3D bone vasculature in a fully non-destructive way and with micrometer resolution. First results indicate that vasculature varies in different genetic backgrounds. From this we hypothesize that better understanding of bone vasculature will provide new insight in the assessment of bone quality and its contribution to bone strength and fracture risk.

Disclosures: ***R. Müller****, None.*

SU154

A New Recurrent Mutation for Paget's Disease of Bone. L. Michou*[1], C. Collet*[2], S. Varin*[3], Y. Maugars*[3], J. Laplanche*[2], P. Orcel[4], F. Cornélis*[1]. [1]Unité de génétique clinique, Hôpital Lariboisière, Paris cedex 10, France, [2]Service de Biochimie, Hôpital Lariboisière, Paris cedex 10, France, [3]Service de rhumatologie, Hôpital Hôtel Dieu, Nantes, France, [4]Fédération de rhumatologie, Hôpital Lariboisière, Paris cedex 10, France.

Purpose : Paget's disease of bone (PDB) has often an autosomal dominant pattern of inheritance, with high penetrance. Genetic heterogeneity has been demonstrated and a first PDB gene was discovered, Sequestosome 1 (5q35). All mutations reported were located at exon 7 and 8, which encode the ubiquitin protein-binding domain. The P392L mutation was the only mutation reported in France, with a frequency of 11% in the French population affected by PDB. The aim of this study was to search for other recurrent mutations in the French population.

Methods: DNA sequencing of Sequestosome 1 gene, exons 7 and 8 (with adjacent intron sequences), was performed in 52 patients without P392L mutation.

Results: The IVS7+1 G-A mutation affecting the splice donor site in intron 7, previously described only in one Australian family, was found in a patient of French Caucasian origin.

Conclusions : The discovery of this new recurrent mutation in PDB supports the hypothesis of its direct pathophysiological involvement and validates the DNA test strategy, for patients who do not carry the P392L mutation, of exon 7 and 8 sequencing.

Disclosures: ***L. Michou****, None.*

SU155

Functional Networks of Structure-Function Interactions Determined for Bone Using Multigenic Perturbations in Recombinant Inbred Mice. K. J. Jepsen[1], J. H. Nadeau*[2]. [1]Mt Sinai School of Medicine, New York, NY, USA, [2]Case Western Reserve University, Cleveland, OH, USA.

Correlation metrics have proven successful in defining functional relationships among cardiovascular traits [1]. This approach used Recombinant Inbred (RI) mouse strains to test multiple genetic perturbations that occur in a natural, non-pathological manner. The analytical method measures the tendency of traits to correlate after genetic randomization of the parental genomes in the RI panel. In this study, we tested whether this network analysis would correctly identify known structure-function relationships for bone [2].

Femurs from 20 AXB/BXA RI mouse strains (16 wks, n=1-6/strain) were phenotyped for mechanical properties [stiffness, max load, post-yield deflection (PYD), work-to-failure] and physical traits [area, moment of inertia (J), mineral content]. Using the mean values of each RI strain, a correlation matrix was established that related each physical trait with each mechanical property. Correlations exceeding a threshold of 0.66 were considered significant ($p<0.05$).

Genetic randomization was associated with significant variation in all physical traits and mechanical properties among the RI panel, as expected. The correlation matrix, which revealed significant and non-significant correlations, identified the physical traits and mechanical properties that cosegregated (i.e., remained functionally related) after randomization of AJ and B6 genes in the RI panel. To visualize these interactions, a hierarchical network was constructed by linking the physical traits and mechanical properties that correlated significantly (Fig 1). This preliminary network correctly identified the functional interactions among the physical traits and the mechanical properties that were determined by independent means [2]. Thus, this network method is a powerful, multivariate approach for identifying physical traits that are deterministic of genetic variation in adult bone strength and fragility. Further, this approach can be extended to the next hierarchical level to identify the cellular processes that define adult bone size, shape, and quality. [1] Nadeau et al, 2003 Genome Res 13. [2] Jepsen et al, 2003 Mamm Genome 14.

Fig 1 Network of functional interactions. Solid line = significant positive correlation. Dashed line = significant negative correlation.

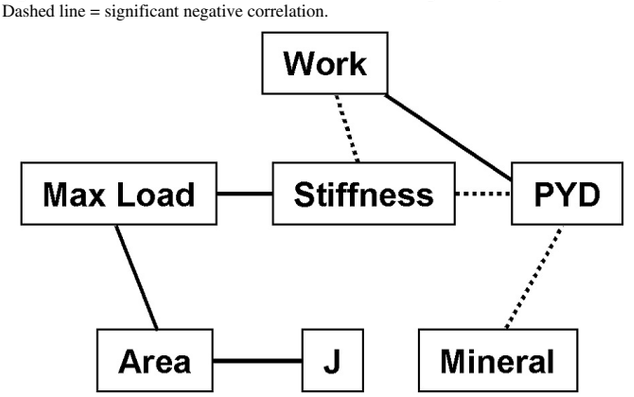

Disclosures: ***K.J. Jepsen****, None.*

SU156

Gene Expression in Femoral Bone from Two Divergent Chicken Populations, Differing Markedly in Bone Phenotypes. C. Rubin*[1], R. Fredriksson*[2], P. Savolainen*[3], U. Gunnarsson*[2], J. Lundeberg*[3], L. Andersson*[2], A. Kindmark[1]. [1]Dep. Medical Sciences, Uppsala University, Sweden, [2]Dep. of Animal Breeding and Genetics, Swedish Univ. of Agricultural Sciences, Uppsala, Sweden, [3]Dep. of Biotechnology, Royal Institute of Technology (RIT), Stockholm, Sweden.

Domestic animals are excellent models for evolution by natural selection since the selection for growth traits over a long period of time has introduced a multitude of genetic changes. The domestic White Leghorn (WL) chicken and the wild ancestor, the Red Junglefowl (RJF) are separated by several thousand years of evolution. The selection in the WL for growth traits and egg production has resulted in profound differences in bone phenotypes between the populations, with bone mineral content (BMC) differing as much as 40%. As a part of a large-scale functional genomics project (FunChick) aimed at elucidating the genetic explanations of several multifactorial traits, we have previously performed a Quantitative Trait Loci- (QTL) analysis of a WL and RJF intercross. Results reveal five regions with significant QTLs affecting BMC and/or bone biomechanical strength (manuscript in preparation).

To identify candidate genes responsible for the phenotypic heterogeneity of the two founder populations, we analysed gene expression in femoral bones from 20 WL and RJF founders using cDNA microarrays developed at RIT, comprising 13000 putatively unique chicken clones.

Twenty individuals, (5 male and 5 female from each population) were sacrificed at 250 days of age (approved by local ethics committee). Femoral bones were snap frozen in liquid nitrogen and stored at -70°C. 20 µg of purified RNA from each individual and 20 µg reference RNA were subjected to cDNA synthesis and were labelled with either Cy3 or Cy5 in a dye swap manner, and were then hybridised onto the microarray. The raw fluorescence data was subjected to filtration, normalization and statistical tests in the software R, where all individuals representing the same sex and population were treated as biological replicates.

In total, 2753 transcripts displayed differential expression, as measured by an empirical Bayesian approach, the B-test. Fifty genes showed significant ($P < 0.05$) differential expression between (1.3-2.4 fold change), but not within populations.

Altogether, the expression data, the results from our QTL-analysis and the newly released chicken genome assembly will greatly facilitate the future identification of genes affecting bone metabolism and bone biomechanical strength. The human orthologues of candidate genes thus identified in chicken will be characterized and screened for association to bone metabolic phenotypes in our population based human cohorts.

Disclosures: ***C. Rubin****, None.*

SU157

Association of Peak Bone Mineral Density and Related Factors with Osteoporosis in Chinese Women: A Case Control Study for Daughter to Mother. Y. Qin*, Z. Zhang, Q. Huang*, J. He*, Y. Hu*, Q. Zhou*, M. Li*, Y. Liu*. Center for preventing and treating osteoporosis, affiliated sixth people`s hospital,Shanghai Jiaotong university, Shanghai, China.

To determine whether premenopausal daughters of women with postmenopausal osteoporosis have lower bone mineral density (BMD) than other women of the same age, and to analyses the related risk factors affecting BMD variation. We recruited aged 20 ~ 40 healthy Han nationality premenopausal women and their healthy parents. The lumber spine (L_{1-4}) and proximal femur (femoral neck, trochanter, ward's striangle) were measured by dual-energy X-ray aborptionmetry in each subject. The study subjects were 126 mothers with osteoporosis,126 of their premenopausal daughters, 136 normal postmenopausal mothers and 149 their premenopausal daughters(in which 123 and 13 families have 1 and 2children, respectively). In the study, daughters were excluded if their fathers were osteoporosis or osteopenia. All subjects completed a questionnaire to obtain information on lifestyle. The VDR *Apa* I genotype and ER-α *Pvu* II, *Xba* I genotype were determined by PCR-restriction fragment length polymorphism. As compared with daughters of normal mothers, daughters of mothers with osteoporosis were weight less ($P<0.05$). The daughters of the mothers with osteoporosis did not differ in age, height, menarche age, milk consumption, activity and occupation. The daughters of mothers with osteoporosis had lower BMD in L_{1-4} ,femoral neck, trochanter and Ward's triangle than the daughters of normal mothers, by 6.2%, 7.9%, 7.1% and 9.6% , respectively ($P<0.001$). Multivariate regression analysis demonstrated that weight was most highly associated with BMD at all measurement sites, which contributed to 14.7%, 18.3%, 16.2% and 8.0% of BMD variation at L_{1-4} ,femoral neck, trochanter and Ward's triangle, respectively. Secondly is a family history, which explained 3.2%, 2.9%, 1.8% and 2.2% of BMD variation, respectively. Age of menarche was less to weight and family history in contributing BMD variation. When weight was excluded in the analysis, family history became the most important factors affect BMD variation and contributed to 5.1%,5.3%,4.2% and 4.1% of BMD variation , respectively. We did not detected age, height, milk consumption, activity, occupation, VDR *Apa* I genotype and ER-α *Pvu* II, *Xba* I genotype contributed to BMD variation in the study. We conclude that daughters of women with osteoporosis have reduced bone in the lumber spine and proximal femur. Weight was the most important factor affecting BMD variation. Secondly was family history.

Disclosures: ***Y. Qin****, None.*

SU158

Novel DEXA-based Osteoporosis Phenotypes for Genetic Studies. F. Rivadeneira[1], M. C. Zillikens*[1], J. J. Houwing-Duistermaat*[2], T. J. Beck[3], Y. Aulchenko*[4], B. Oostra*[4], A. G. Uitterlinden[1], C. M. van Duijn*[4], H. A. P. Pols[1]. [1]Internal Medicine, Erasmus Medical Center, Rotterdam, Netherlands, [2]Medical Statistics & Bioinformatics, Leiden University Medical Center, Leiden, Netherlands, [3]Radiology, Johns Hopkins University, Baltimore, MD, USA, [4]Genetic Epidemiology, Erasmus Medical Center, Rotterdam, Netherlands.

BMD is a highly heritable surrogate phenotype for fracture. Its use in genetic linkage and association studies is complicated by its ambiguous relation to mechanical properties and its dependence on size and age. This study explored alternative bone phenotypes based on DEXA and hip geometry measured with the *Hip Structural Analysis* (HSA) software.

We estimated heritabilities ($\mathbf{h^2}$) and genetic correlations (**GC**) in 374 men and 545 women (age 18-85 years) from the ERF study, an extended-pedigree study designed to map disease-related QTL. Age and sex adjusted traits included BMD of the hip, spine and total body (including composition) and HSA measurements. Statistically independent phenotypes were identified using principal components analysis (**PCA**). An index of mechanosensitivity (**IM**) was estimated as the ratio of section modulus (Z)/moment arm to lean mass.

Total body, hip and spine BMD $\mathbf{h^2}$ ranged from 50-70%. Height, fat and lean mass indexes (FMI, LMI) $\mathbf{h^2}$ were 60, 31 and 28%. **GC** between BMD sites ranged from 70 to 99% (same regions) and was 20%, 15% and 30% with height, FMI, and LMI. Bone geometry $\mathbf{h^2}$ was 40% for BMD, buckling ratio (BR, index of cortical instability) and cortical thickness (T); 30% for cross-sectional area (CSA); 50% for inner (ED) and outer (W) bone diameters; and 25% for strength indexes including Z and CSMI.

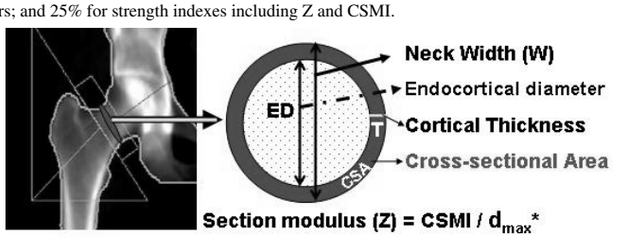

*$\mathbf{d_{max}}$: maximum distance from center of mass to medial or lateral cortex

Table. Genetic correlations narrow neck (NN) phenotypes

	NN-BMD	NN-Z	NN-BR
LUNAR-BMD	0.83 (0.05)	0.56 (0.12)	-0.76 (0.06)
W	-0.26 (0.14)	0.55 (0.12)	0.54 (0.11)
CSA	0.88 (0.03)	0.94 (0.03)	-0.67 (0.09)
ED	-0.46 (0.12)	0.36 (0.15)	0.71 (0.07)
T	1.00 (0.00)	0.67 (0.10)	-0.96 (0.02)
Z	0.69 (0.09)	-	-0.41 (0.15)
CSMI	0.39 (0.14)	0.91 (0.03)	-0.09 (0.17)
BR	-0.95 (0.03)	-0.41 (0.15)	-
Height	0.07 (0.11)	0.48 (0.13)	0.12 (0.11)
FMI	-0.15 (0.16)	-0.17 (0.20)	0.23 (0.17)
LMI	0.03 (0.17)	0.04 (0.20)	0.08 (0.19)

Data are correlations (SE) adjusted for sex and age

Table shows **GC** of the HSA. **PCA** of HSA measurements identified two independent components explaining 95% of the variance in all traits: a component highly correlated with BMD, BR, and T (stability) with $\mathbf{h^2}$ of 45% and a component highly correlated with W, ED, CSMI and Z (dimensions and strength) with $\mathbf{h^2}$ of 39%. **IM** had an $\mathbf{h^2}$ of 27% and a higher **GC** with the stability component (42%) than with the strength-related component (3.5%).

We identified two heritable and genetically independent components of hip bone geometry. A conceptually biomechanical trait like **IM**, reflects genetically-determined predisposition to weak bones that reach instability faster with age. Gene identification studies should be targeted on these phenotypes.

Disclosures: ***F. Rivadeneira****, None.*

SU159

Test of Linkage and/or Association of Genes and Bone Mineral Density in Chinese. A. W. C. Kung[1], H. H. L. Lau[1], A. D. Paterson*[2], W. M. W. Cheung*[1], K. D. K. Luk*[3], V. Chan*[1]. [1]Medicine, The University Of Hong Kong, Hong Kong, Hong Kong Special Administrative Region of China, [2]Program in Genetics and Genome Biology, The University of Toronto, Toronto, ON, Canada, [3]Orthopaedic Surgery, The University Of Hong Kong, Hong Kong, Hong Kong Special Administrative Region of China.

Bone mineral density (BMD), one of the major determinants of osteoporosis and fracture risk, is a complex trait with a heritability estimate that ranges from 50% to 90%. Linkage and/or association of 14 loci of 8 candidate genes were evaluated in 177 southern Chinese pedigrees with 674 subjects (each pedigree was identified through a proband having BMD Z score $\leq$-1.28 at the hip or spine) by the quantitative trait locus transmission disequilibrium test (QTDT). The candidate genes studied include estrogen receptor alpha (ERα) and beta (ERβ), calcium sensing receptor (CASR), vitamin D receptor (VDR), collagen type Iα1 (COLIA1), LDL receptor-related protein 5 (LRP5), transforming growth factor β1 (TGFβ1) and parathyroid hormone receptor (PTHR). Nucleotide (nt) Ivs1-397T/C (Pvu II genotype) and Ivs1-351G/A (Xba I genotype) of ERα; 1082A/G (Rsa I genotype), 1730G/A (Alu I genotype) and CA repeat polymorphism (D14s1026) of ERβ; CA repeat polymorphism of CASR; 2T/C (Fok I genotype) of VDR; -1363 C/G and -1997 T/G of COLIA1; 266 A/G, 2220 C/T and 3989 C/T of LRP5; 29 T/C of TGFβ1 and D3S1289 (which is closely related to the PTHR gene) were analyzed. BMD values were adjusted for sex, age, height and weight. For the total association, D14s1026 genotypes of ERβ were associated with femoral neck and total hip BMD (both $p<0.05$); D3S1289 (which is closely related to the PTHR gene) was associated with trochanter BMD ($p<0.02$) and total hip BMD ($p<0.03$). For within-family association, D14s1026 genotypes of ERβ were associated with femoral neck and total hip BMD (both $p<0.05$); D3S1289 was associated with trochanter BMD ($p<0.02$) and total hip BMD ($p<0.03$). For linkage analysis of all pedigree, Ivs1-351G/A genotype of ERα was in linkage with L1-4 BMD ($p<0.05$); 1082A/G, 1730G/A and D14s1026 genotypes of ERβ were linkage with L1-4 ($p<0.05$) and femoral neck BMD ($p<0.03$); ERβ 1082A/G and D14s1026 genotypes of ERβ were linkage with total hip BMD ($p<0.05$). These data suggested that ERα and ER beta gene might play a modulatory role in determining bone mineral density in our population. Further mapping studies are required to determine the genetic association of D3S1289 with BMD.

Disclosures: ***A.W.C. Kung****, None.*

SU160

Familial Aggregation of BMD and Osteoporosis. Y. Feng*[1], X. Xu*[1], Y. H. Hsu*[1], H. Terwedow*[1], T. Zang*[2], Z. Li*[2], X. Hong*[2], B. Wang*[1], M. L. Bouxsein[3], J. Brain*[1], S. R. Cummings[4], C. Rosen[5], X. Xu*[1]. [1]Program for Population Genetics, Harvard School of Public Health, Boston, MA, USA, [2]Institute of Biomedicine, Anhui Medical University, Hefei, China, [3]Beth Israel Deaconess Medical Center, Boston, MA, USA, [4]San Francisco Coordinating Center, UCSF, San Francisco, CA, USA, [5]Maine Center for Osteoporosis Research and Education, St. Joseph Hospital, Bangor, ME, USA.

Data from a cross-sectional study in Anhui, China were used to examine the familiar aggregation of BMD and osteoporosis. A total of 6760 subjects aged 25-65 years from 1843 families were available for the analysis. Whole body and hip BMD was assessed for each subject by DXA. Pearson's correlation coefficients of BMD were calculated for each sibling pair and multiple regression models were used to test the family aggregation with adjustment for potential confounders. The correlation coefficients of BMD varied among different skeletal sites and between men and women and their ranges were from 0.17 to 0.57. The estimated regression coefficients were 0.313 (SE=0.027) and 0.207 (SE=0.025), respectively for total body BMD and total hip BMD, in men; 0.230 (SE=0.032) and 0.298 (SE=0.037) in premenopause women; and 0.319 (SE=0.059) and 0.193 (SE=0.063) in postmenopause women. If the first sibling had osteoporosis, defined as BMD <-2.5 using young individuals from a population as a reference database, then his/her same sex siblings had a significantly higher chance of being diagnosed as having osteoporosis. Specificlly, the OR for osteoporosis in the younger sibling when the older sibling had osteoporosis was 10.1 (95% CI: 3.5-29.4) in males and 3.8 (95% CI: 1.8-8.1) in females.

This analysis demonstrated a significant familiar aggression for both BMD and osteoporosis in our population.

Supported by NIAMS grant R01 AR045651.

Disclosures: ***Y. Feng****, None.*

SU161

Chromosomal Regions Influencing Femoral Shaft Failure Load in Laboratory Mice: Concordance with Regions Associated with Intrinsic Strength, Density, and Geometry. R. F. Klein[1], J. N. Kansagor*[1], W. J. Wagoner*[1], A. S. Carlos*[1], J. K. Belknap*[2], M. Shea[3], E. S. Orwoll[1]. [1]Bone and Mineral Unit, Oregon Health & Science University, Portland, OR, USA, [2]Department of Behavioral Neuroscience, Oregon Health & Science University, Portland, OR, USA, [3]Department of Orthopaedics, Oregon Health & Science University, Portland, OR, USA.

Bone strength and thus, the likelihood of fracture, is a complex trait likely influenced by a number of different genes. The number, locations and effects of the individual genes contributing to natural variation in skeletal fragility are all unknowns. To complement previous genetic analyses of bone density and bone geometry (determinants of skeletal fragility) in laboratory mice, we examined femoral shaft failure load (FL) in a genetically heterogeneous F_2 population of mice (N=994) derived from C57BL/6 (B6) and DBA/2 (D2) inbred mouse strains. Femora were harvested from 16-week-old mice and bone mineral density (BMD) was measured by DEXA, femoral geometry (cortical area, CtAr; cortical thickness, CtTh) was measured by microCT and FL was determined by 3-point bending. Femoral bending strength (FBS) was calculated from the load deflection curve and the cross-sectional areal measurements. FL values were normally distributed, suggesting polygenic control of this trait. Analysis of 18 RI strains derived from the same progenitors (B6 & D2) provided a narrow-sense heritability estimate of 0.53 for FL. To identify genetic loci influencing FL, a whole genome scan was carried out using 154 polymorphic microsatellite markers distributed across 19 autosomes and X chromosome. Quantitative trait locus (QTL) analysis of the B6D2F_2 population revealed 8 chromosomal regions (QTLs 1-8; see table) that were very strongly linked to FL (peak logarithm of the likelihood for linkage (LOD) score ≥ 3.6). Interestingly, no unique FL QTLs were identified. Instead, all of the FL QTLs were concordant with femoral bone density, bone geometry and/or intrinsic bone strength loci. Thus, a substantial genetic contribution to femoral breaking strength appears to be exerted by effects on multiple skeletal traits (pleiotropism) to coordinately regulate overall skeletal integrity. These results suggest that the genetic determinants of the complex phenotype of skeletal fracture can be effectively studied by analysis of primary skeletal characteristics.

	QTL 1	QTL 2	QTL 3	QTL 4	QTL 5	QTL 6	QTL 7	QTL 8
Location (Chr:cM)	3:38	7:05	8:46	12:02	13:43	14:44	17:40	20:20
FL LOD	5.4	5.6	3.6	11.7	4.4	4.1	3.6	3.9
BMD LOD		5.3	5.1					4
CtTh LOD	5.8	13.3	13.7	4		4.1	7.7	
CtAr LOD		5.8		10.5	4.7	4.5		3.6
FBS LOD		3.8	5.2					

Disclosures: ***R.F. Klein****, Eli Lilly & Co. 8; Merck & Co. 8; Procter & Gamble Pharmaceuticals, Inc. 8; Aventis Pharmacewuticals, inc. 8.*

SU162

The Muscle-Bone Relationship in The Lower Skeleton Is Gender- Specific: The Age, Gene/Environment Susceptibility Study. T. F. Lang[1], G. Sigurdsson[2], B. Jonsdottir[2], K. Siggeirsdottir*[2], G. Eiriksdottir*[2], S. Sigurdsson*[2], M. Garcia*[3], M. Meta[1], T. Harris*[3]. [1]Radiology, University of California, San Francisco, San Francisco, CA, USA, [2]Icelandic Heart Association, Reykjavik, Iceland, [3]Epidemiology and Biometry, National Institute of Aging, Bethesda, MD, USA.

Muscles exert among the strongest mechanical loads on bone, and studies have found a relationship between bone density and muscle mass. Because of sex differences in muscle size, muscle strength, and body habitus, we hypothesized that the relationship between muscle mass, muscle strength and bone density would differ between genders. Thus, we have performed analyses of 1,146 subjects (466 male and 680 female) enrolled in the Age, Gene/Environment Susceptibility-Reykjavik Study (AGERS) cohort, a group aged 67 years or older participating in an ongoing research study in Iceland. To assess muscle mass and attenuation, we used computed tomography to measure the area (QAR) and mean hounsfield unit (QHU) of the quadriceps muscle group at the mid-thigh (a measure of fat infiltration into muscle). We also measured the quadriceps strength (QSTR). Trabecular bone mineral density (BMD) was measured in g/cm^3 at the femoral neck (ftBMD) and trochanteric (trtBMD) regions using quantitative computed tomography. We performed gender-specific multivariate linear regressions relating BMD to QAR, QHU and QSTR, adjusting for body mass index (BMI) and age. To determine the statistical significance of gender differences in muscle-BMD relationships, data from men and women were pooled in another regression model incldluing interactions for muscle parameters and gender.

	Men	Women
Variable	Mean (SD)	Mean(SD)
ftBMD (g/cm^3)	0.042 (0.055)	0.021 (0.040)
trtBMD (g/cm^3)	0.081 (0.042)	0.057 (0.032)
QHU (HU)	47.6 (3.9)	46.7 (3.47)
QAR (cm^2)	64.1 (15.4)	43.4 (7.1)
QSTR (newton)	404.2 (101.7)	254.1 (71.2)
BMI	26.4 (3.7)	27.0 (4.9)
Age	75.9 (5.6)	75.6 (5.7)

Age- and BMI-adjusted means for the key variables are shown below. Age was inversely correlated with BMD and BMI was positively correlated with BMD in both genders. In gender-specific models, QSTR, but not QAR or QHU, was significantly associated with ftBMD ($p<0.01$) and trtBMD ($p<0.05$) in men, but only QHU was associated with trtBMD ($p<0.05$) in women. In the pooled model, there was a statistically significant interaction term ($p<0.05$) between gender and QHU only, indicating a sex difference in the effect of QHU on bone density.

Our data support sex differences in the bone-muscle relationship in the lower skeleton. We conclude that strategies aimed at modifying bone density by changing muscle mass or strength should take gender into account.

Disclosures: ***T.F. Lang****, None.*

SU163

Effects of Gender on Genetic Regulation of Trabecular and Cortical Bone in Congenic Strains of Mice. W. G. Beamer, K. L. Shultz, K. M. Delahunty*, L. R. Donahue, C. J. Rosen. The Jackson Laboratory, Bar Harbor, ME, USA.

Genetic analyses of crosses among inbred strains of mice have defined heritability, enumerated major and minor effect loci, and established chromosomal locations for genes underlying many bone properties. Further genetic manipulations (congenic and consomic strains, chemical mutagenesis, spontaneous mutations) have confirmed genome wide screen data for quantitative trait loci (QTL), as well as facilitated functional and molecular studies aimed at gene identification. A critical theme that needs further experimental attention is the role of gender in relation to understanding and interpreting QTL effects on bone. Orwoll and Klein (2001) first reported differences in QTL between females and males associated with areal BMD observed in BXD Recombinant Inbred strains and in (B6xDBA/2)F2 progeny. Both shared and unique QTL were indicated as participants in sex specific pathways regulating peak bone mass.

To further examine sex specific effects, we tested isolated 4 mo old femurs by pQCT from 11congenic strains carrying individual QTL for strong or weak effects on total bone volumetric (v)BMD. Each congenic strain was made by introgressing chromosomal segments carrying QTL from C3H/HeJ (high vBMD; C3H) into C57BL/6J (low vBMD; B6) background strain by repeated backcrossing. Data were gathered on trabecular bone (metaphyseal mineral, volume) and on mid-diapyseal cortical bone (mineral, volume, cortical thickness, periosteal circumference). The resultant data yielded clues about which bone compartment and gender showed effects associated with each of the QTL on bone. QTL on Chrs 1, 4 and 9 markedly influenced male trabecular bone, while having little if any effect on female trabecular bone. Chrs 10 and 11 QTL did not affect trabecular bone in either gender. Six remaining QTL (Chrs 6, 8, 13, 15, 17, and 18) significantly affected trabecular bone in both males and females. None of the 11 congenics significantly changed only female trabecular bone. All 11 QTL affected cortical bone. QTL on Chrs 4, 9, and 10 primarily affected male cortical bone, with little if any effect in females. Conversely, QTLs on Chrs 13, 15, and 18 primarily affected female cortical bone with little or no effect on male cortical bone. Five remaining QTLs (Chrs 1, 6, 8, 11, and 17) significantly affected cortical bone in both sexes. Surprisingly, the majority of QTL from C3H reduced bone in the congenic strains. These data confirm sex specific pathways for acquisition of peak bone mass, reveal compartment specific effects, and imply caution is warranted when generalizing findings across gender.

Disclosures: ***W.G. Beamer****, AR43618 2.*

SU164

Unique and Common Genetic Effects between Bone Mineral Density and Calcaneal Quantitative Ultrasound Measures among Healthy Adults: The Fels Longitudinal Study. M. Lee, S. A. Czerwinski*, A. C. Choh*, E. W. Demerath*, W. C. Chumlea*, S. S. Sun*, R. M. Siervogel, B. Towne*. Lifespan Health Research Center, Wright State University School of Medicine, Dayton, OH, USA.

Areal bone mineral density (BMD) measures and calcaneal quantitative ultrasound (QUS) measures are correlated, and both traits predict the osteoporotic fracture risk independently. However, few studies have examined the common genetic effects (i.e., pleiotropy) between these traits in extended families. In this study, we estimate the additive genetic correlation (ρ_G) and random environmental correlation (ρ_E) between BMD measured at various skeletal sites and calcaneal QUS measures in a sample of healthy adults. The study population includes 537 adults (251 men and 286 women) aged 18 to 91 years (mean ± SD: 45 ± 16 yrs) who belong to 110 nuclear and extended families participating in the Fels Longitudinal Study. Total body, lumbar spine (L1-L4), and femoral neck BMD were measured using dual energy X-ray absorptiometry (DXA: QDR4500, Hologic, Inc., Waltham, MA). Three measures of calcaneal structure, speed of sound (SOS), broadband ultrasound attenuation (BUA), and quantitative ultrasound index (QUI) were collected from the non-dominant heel using the Sahara ® bone sonometer (Hologic, Inc., Waltham, MA). Using a variance components-based maximum likelihood method (SOLAR), we estimated the heritability of the different BMD and QUS measures while simulateously adjusting for age, sex, age^2, age-by-sex, age^2-by-sex, physical activty, smoking, alcohol use and menopausal status. Genetic and enviromental correlations between the different BMD and QUS measures were also estimated.

Heritability estimates were significant for all traits ($p < 0.000001$), and ranged from 0.64 to 0.68 for the BMD measures, and from 0.55 to 0.78 for the QUS measures. Significant nonzero genetic correlations were found between the different BMD and QUS measures. For total body BMD, $\rho_G \pm$ SE was 0.53 ± 0.11 with BUA, 0.52 ± 0.10 with SOS, and 0.53 ± 0.10 with QUI. For lumbar spine BMD, $\rho_G \pm$ SE was 0.37 ± 0.12 with BUA, 0.34 ± 0.10 with SOS, and 0.35 ± 0.11 with QUI. For femoral neck BMD, $\rho_G \pm$ SE was 0.60 ± 0.11 with BUA, 0.40 ± 0.11 with SOS, and 0.48 ± 0.10 with QUI. Tests for complete pleiotropy (i.e., $\rho_G = 1$) revealed incomplete pleiotropy between the different BMD and QUS measures ($p < 0.00001$). All random environmental correlations were not significantly different from zero.

This study demonstrates that BMD and calcaneal QUS measures among healthy men and

women are heritable, and are, in part, jointly influenced by a common set of underlying genes. Additionally, this study also shows evidence for a different set of genes independently influencing each trait.

Disclosures: ***M. Lee****, None.*

SU165

Relationship between Vitamin D Receptor Gene Polymorphism and Trabecular Bone Pattern of the Mandible in Japanese Postmenopausal Women. A. Taguchi[1], S. C. White*[2], J. Kobayashi*[3], S. K. Survice*[4], T. Nakamoto*[1], M. Ohtsuka*[3], M. Sanada*[5], M. Tsuda*[5], K. Ohama*[5], Y. Suei*[1], K. Tanimoto*[3]. [1]Oral & Maxillofacial Radiology, Hiroshima University Hospital, Hiroshima, Japan, [2]Oral & Maxillofacial Radiology, UCLA School of Dentistry, Los Angels, CA, USA, [3]Oral & Maxillofacial Radiology, Graduate School of Biomedical Sciences, Hiroshima University, Hiroshima, Japan, [4]Biomathematics, The David Geffen School of Medicine at UCLA, Los Angels, CA, USA, [5]Obstetrics and Gynecology, Graduate School of Biomedical Sciences, Hiroshima University, Hiroshima, Japan.

Tooth loss and oral bone loss may be partly influenced by genetic factors in postmenopausal women (JAMA, 2001; Menopause, 2003); however, little is known about whether mandibular trabecular bone pattern is also influenced by genetic factors. In this study, we investigated the associations between vitamin D receptor (VDR) gene polymorphism and several parameters that characterize trabecular bone pattern of the mandible in 96 Japanese postmenopausal women (mean age [SD], 54.3 [6.9] years). Strut analyses and run-length analysis were used to evaluate trabecular bone pattern of the mandibular ramus on digitized dental panoramic radiographs scanned at 600 dpi. Patients' DNA was amplified with the polymerase chain reaction and Bsm I restriction enzyme was used to analyze VDR gene allele. Patients who were homozygous for the presence of this restriction site were designated as genotype bb. BMD of the femoral neck was measured by dual energy x-ray absorptiometry. Bsm I polymorphism was in Hardy-Weinberg equilibrium. There was no significant association between VDR gene polymorphism and any 30 parameters obtained by strut analyses. However, subjects with bb allele had significantly smaller run-length analysis parameters (gray level non-uniformity, run length non-uniformity and run percentage measured both horizontally and vertically) than did those with B allele. After adjustment of age, years since menopause and body mass index, significant differences still remained in horizontal run percentage (P=0.035), vertical gray level non-uniformity (P=0.025) and vertical run percentage (P=0.016) between subjects with and without B allele. There was no significant difference in low BMD status at the femoral neck between them. These results suggest that VDR gene polymorphism may be associated with mandibular trabecular bone pattern in postmenopausal women.

Disclosures: ***A. Taguchi****, None.*

SU166

Relationship among Calcium Sensing Receptor Gene (CA) Polymorphism, Bone Mineral Density and Bone Responsiveness to Hormone Replacement Therapy in Postmenopausal Korean Women. J. Kim, S. Ku*, C. Suh*, S. Kim*, Y. Choi*, S. Moon*. Obstetrics & Gynecology, Seoul National University Hospital, Seoul, Republic of Korea.

Genetic factors are known to play an important role in the regulation of bone mineral density (BMD), and the inheritability of BMD has been estimated to lie between 50 - 85%, and to have a strong effect in the axial skeleton. However, the genes responsible for the regulation of bone mass have not yet been defined. The aims of the present study were to evaluate the relationship among the cytosine adenine (CA) polymorphism in calcium sensing receptor (Casr) gene, BMD, and bone responsiveness to hormone replacement therapy (HRT). Casr (CA) polymorphism was analyzed by polyacrylamide-urea gel electrophoretic patterns, genescan and direct DNA sequencing in 502 postmenopausal Korean women. Among these women, 352 women received sequential HRT for 1 year. Serum bone alkaline phosphatase, CrossLaps, osteocalcin, calcitonin, and parathyroid hormone levels were measured by enzyme-linked immunosorbent assay, immunoassay and serum calcium and phosphorus levels by atomic absorptiometry. BMD at the lumbar spine and proximal femur was determined by dual energy X-ray absorptiometry before and after HRT of 1 year. Nine Casr alleles were observed with product sizes ranging between 176-196 base pair (bp), and their distributions were as follows: 188bp 26.2%, 194bp 19.8%, 186bp 18.2 %, 190bp 15.5%.192bp 14.3% etc. No significant differences in basal BMD and annual percentage changes of BMD after HRT were noted among Casr (CA) genotypes. There were no significant differences in the levels of bone turnover markers and their 6 month percentage changes after HRT among Casr (CA) genotypes. The Casr (CA) genotypes were not distributed differently between HRT-responders and HRT-nonresponders (women who lost more than 3 % of bone mass per year) or between women with normal BMD and women with low bone mass. In conclusion, Casr (CA) polymorphism is not associated with BMD and bone responsiveness to HRT in Korean women.

Disclosures: ***J. Kim****, None.*

SU167

Interactions of Calcium Intake with FokI and Androgen Receptor Genotypes in Men. E. A. Krall[1], J. C. Fleet[2], P. S. Vokonas*[3], D. R. Miller*[4], S. E. Rich*[1]. [1]Boston University, Boston, MA, USA, [2]Purdue University, West Lafayette, IN, USA, [3]VA Boston Healthcare System, Boston, MA, USA, [4]VA Center for Health Quality, Outcomes, and Economic Research, Bedford, MA, USA.

Previous studies suggest the associations between bone mineral density (BMD) and polymorphisms of the vitamin D receptor (VDR) are modified by calcium intake, but the results are inconsistent. We examined interactions of calcium intake with the FokI polymorphism and the androgen receptor (AR) in the VALOR study, an observational study of men. Mean age at enrollment was 70 years and 96% of subjects were white. Total body, hip and radius BMD was measured up to 3 times over a mean follow-up of 2 years. Consent for genetic analyses was obtained from 546 men. DNA was isolated from packed red blood and buffy coat cells and analyzed using PCR amplification followed by enzymatic digestion (FokI) or electrophoresis (AR). Dietary and supplemental calcium intakes were assessed by food frequency questionnaire. Total calcium intake was dichotomized at the median (807 mg/day). Distributions of FokI and AR were: 218 FF (41%), 235 Ff (44%), and 81 ff (15%); and 112 (21%) with ≥25 CAG repeats in the AR, 424 (79%) with ≤24 repeats. BMD was analyzed with repeated measures analysis of covariance, controlling for age, body mass index and years of follow-up. Before interactions were examined, only femoral neck BMD was associated with the FokI genotype (p=0.04), and no sites were associated with AR. Significant genotype/calcium interactions were found for both genotypes at all sites. BMD at the femoral neck (p for interaction =0.04) and total radius (p=0.03) was lower in men with ff or Ff genotypes vs. FF if calcium intake was below the median, but comparable if calcium was above the median (table). This trend was also observed at the total body (n=515, p=0.02). Similarly, BMD at the femoral neck (p=0.02), total radius (p=0.04) and total body (p<0.01) was lower in men with ≥25 CAG repeats in the AR vs. ≤24 repeats if calcium intake was low but comparable if calcium was high. These results indicate that environmental factors such as diet influence the attainment of BMD in men and failure to account for environment may attenuate associations of BMD with genotype.

BMD (g/cm^2): mean ± se

		ff or Ff	FF	ff or Ff	FF
		Low Ca	Low Ca	High Ca	High Ca
Femoral Neck	baseline	0.913±0.014	0.977±0.017	0.954±0.016	0.949±0.013
	final	0.908±0.014	0.974±0.017	0.952±0.016	0.949±0.013
	N	94	60	70	106
Total Radius	baseline	0.731±0.008	0.764±0.009	0.762±0.009	0.763±0.007
	final	0.727±0.008	0.766±0.010	0.759±0.009	0.759±0.007
	N	100	67	72	117

Disclosures: ***E.A. Krall****, None.*

SU168

Transmission Disequilibrium Analysis of Polymorphisms of Candidate Genes from Chromosome 1p36 and Bone Mineral Density in Osteoporosis Families. M. Devoto*[1], K. Sol-Church*[1], D. Stabley*[1], C. McKay[1], A. Tenenhouse[2], L. D. Spotila[3]. [1]Nemours Children's Clinic, Wilmington, DE, USA, [2]Montreal General Hospital, Montreal, PQ, Canada, [3]Drexel University, Philadelphia, PA, USA.

Low bone mineral density (BMD) is one of the major risk factors for osteoporosis. Epidemiological studies support the hypothesis that a large part of the variation in BMD is caused by genetic susceptibility factors. In an attempt to identify the specific genes that might influence BMD, and thus osteoporosis, we have performed a whole genome scan for linkage in a total of 40 Caucasian families recruited through a proband with low BMD. After fine mapping, a region on 1p36 near marker D1S214 received support as a candidate locus for femoral neck BMD from both linkage (max lod = 3.53) and linkage disequilibrium analysis ($p < 0.01$). In the present study, we have selected a number of genes based on their location in 1p36 and available information about function and pattern of expression to evaluate as possible candidate genes for femoral neck BMD.

Genotyping of single nucleotide polymorphisms (SNPs) of the selected candidate genes is being performed by either Pyrosequencing using SNPs selected from publicly available databases or on the ABI 7900HT Sequence Detection System using commercially available Applied Biosystems Assays-on-Demand™. Linkage disequilibrium analysis in the sample of 40 families is being carried out using the QTDT software including sex, age and BMI as covariates. Results of this analysis for nine SNPs tested in the guanine nucleotide binding protein (G protein), beta polypeptide 1 gene (GNB1) did not show any significant results (all p-values > 0.1). A second gene, WD repeat-containing protein 8 (WDR8) was selected because experiments in mouse had shown expression in bone and cartilage and in bone forming cells including osteoblasts and chondrocytes during ossification. Among six SNPs tested in this gene, one yielded a nominal p-value of p = 0.006 for association with femoral neck BMD. Additional tests are in progress to confirm this finding and exclude other genes as possible candidates.

Disclosures: ***M. Devoto****, None.*

SU169

Interaction between Vitamin D Receptor and Estrogen Receptor Genotypes does not Influence BMD, Rate of Bone Loss and the Response to Treatment with Calcitriol or Estrogen in Elderly Women. P. B. Rapuri, J. C. Gallagher, V. Haynatzka*. Bone Metabolism Unit, Creighton University, Omaha, NE, USA.

The possibility of an interaction between vitamin D receptor (VDR) and estrogen receptor (ER) polymorphims with bone mass has been investigated with inconsistent results. In the present study, we evaluated the interaction between ER and VDR polymorphisms in relation to bone mineral density (BMD), rate of bone loss and response to treatment with calcitriol, estrogen and combination of both. In a double blind placebo controlled study, 489 elderly women were randomized to 4 treatment groups, calcitriol (0.5 mcg/d), estrogen (CEE 0.625mg/MPA2.5 mg), calcitriol+estrogen and placebo. In this population, we examined whether the interaction between ER and VDR genotypes is related to BMD at baseline (n=489), rate of bone loss in women receiving the placebo treatment (n=96) and response to treatment with calcitriol (n=86) estrogen (n=79) and combination of both (n=76). The women were genotyped for VDR TaqI and ER PvuII and XbaI restriction fragment length polymorphisms. BMD (spine, proximal femur, total body and radius) at baseline and at the end of the study (36 months) was determined by DEXA. The BMD at baseline and the percent change in BMD in various treatment groups was compared between the women with various combinations of VDR and ER genotypes. Statistical analysis was performed by procedure Mixed (SAS) after adjusting for significant covariates like age, weight, calcium intake etc. There were no significant differences in BMD at baseline and rate of change in BMD in treatment groups between the various combinations of VDR and ER genotypes. In conclusion, our results suggest no significant gene X gene interaction effect for the VDR TaqI and ER PvuII or VDR TaqI and ER XbaI polymorphisms, which influenced BMD, rate of bone loss or response to treatment to calcitriol, estrogen or combination of both.

Disclosures: ***P.B. Rapuri****, None.*

SU170

Poly Adenosine Repeat in the Human Vitamin D Receptor Gene Is Associated with Increased Bone Loss in Elderly Women. P. B. Rapuri, J. C. Gallagher, V. Haynatzka*. Bone Metabolism Unit, Creighton University, Omaha, NE, USA.

Polymorphisms at the 3' -end of vitamin D receptor (VDR) gene, ApaI, TaqI and BsmI are in strong linkage disequilibrium with a poly adenosine (A) microsatellite at the VDR 3'UTR, which has been shown to be associated with altered transcriptional activity of endogenous human VDR proteins. However there is no information on whether polymorphism in the poly A microsatellite is associated with bone mineral density (BMD) and rate of bone loss in elderly postmenopausal women. In the present study, we examined the association of VDR polymorphism, the poly A microsatellie with rate of bone loss in a cohort of 78 Caucasian elderly women aged 65-77 years recruited for an osteoporosis intervention trial and receiving placebo treatment for 3 years. The VDR poly A microsatellite localized in the 3' untranslated region from these women was amplified by PCR and the DNA sequence was determined. Based on the length of the A repeat, when the alleles of poly(A) were classified into biallelic system, long (L: A18-22) and short (S: A12-17), the prevalence of SS was 13%, LS 40% and LL was 41% which followed the Hardy-Weinberg equilibrium. These women had previously been genotyped for TaqI and BsmI polymorphism. We observed a strong linkage between S and t/B alleles in this population (SS genotype is equivalent to tt/BB genotypes). BMD (spine, proximal femur, total body and radius) at baseline and end of the study (36 months) was determined by DEXA. Biochemical measurements were made by standard procedures. The percent change in BMD and biochemical variables were compared between the VDR genotypes by procedure Mixed (SAS) after adjusting for significant covariates like age weight etc. Our results suggest that women with SS genotype lost significantly more bone over 3 years at femoral neck compared to women with LL genotype. Even at spine and radius, a similar trend was observed. However, the rate of change in biochemical variables was not different between the three genotypes.

In conclusion, our results demonstrate higher rate of bone loss in elderly women with SS genotype which has been shown to be associated with decreased transcriptional activity of endogenous VDR proteins. Thus variation at this polymorphic site may play a role in VDR functional activity thereby influencing bone.

Rate of change in BMD in relation to VDR poly (A) polymorphism

	Percent Change in BMD (mean±SEM)		
Genotype(N)	FEMORAL NECK	RADIUS-mid	SPINE
LL (34)	0.31±0.62	-2.82±1.09	-0.74±0.76
LS(33)	-0.60±1.03	-2.74±0.71	-1.24±0.67
SS(11)	-3.21±1..63*	-4.02±1.46	-1.46±1.75

* p<0.05 LL Vs SS

Disclosures: ***P.B. Rapuri****, None.*

SU171

Association of Estrogen Receptor-alpha and Vitamin D Receptor Genotypes With Therapeutic Response to Calcium in Postmenopausal Chinese Women. Z. Zhang, Y. Qin*, Q. Huang*, J. He*, M. Li*, Q. Zhou*, Y. Liu*, H. Hu*. Center for preventing and treating osteoporosis, affiliated sixth people`s hospital,Shanghai Jiaotong university, Shanghai, China.

To investigate the correlation between calcium treatment in postmenopausal women and estrogen receptor-alpha (ER-alpha) *Xba* I and *Pvu* II genotype and vitamin D receptor (VDR) *Apa* I genotype. One hundred fifteen postmenopausal Chinese women of Han population were enrolled and treated with Calcichew-D_3 (1000 mg daily as calcium and 400 U daily as vitamin D_3) for 1 year. At entry and after 1 year treatment, the bone mineral density (BMD) at lumbar spine 1-4 (L1-4) and left proximal femur including femoral neck (Neck), trochanter (Troch), serum alkaline phosphatase (ALP), osteocalcin (OC), parathyroid hormone (PTH), 25-hydroxy[25-(OH)] vitamin D, urinary calcium and urinary creatinine-corrected free pyridinoline (PYD) levels were evaluated. DNA was extracted from blood and analyzed with PCR-restriction fragment length polymorphism for *Xba* I and *Pvu* II ER-alpha genotype and *Apa* I VDR genotype. After 1 year of calcium supplementation, a significant increase of BMD in L1-4, Neck and Troch, and a marked reduction in serum ALP and PTH levels, and a significant increase of serum 25-(OH) vitamin D level were observed (P<0.01 or P<0.05). At baseline and after 1 year of treatment, no significant association was found between *Xba* I, *Pvu* II and *Apa* I genotypes and BMD in L1-4, Neck and Troch, and all bone turnover marker levels. However, the percentage of change (median, Q_R) in Neck BMD was significantly different in homozygous XX [-4.1394, (-6.5359 ~ -1.3678)] in comparison with Xx [1.7212, (-1.1198 ~ 3.2039)] (P<0.001) or xx [1.2195, (-1.7408 ~ 3.0560)] *Xba* I ER-alpha genotype (P=0.001). Women with ER-α XX genotype may have a higher risk of relatively fast bone mass loss in femoral neck after menopause than those with the Xx and xx genotype and that they may have a poor responsiveness to calcium supplementation. The changes in BMD are not associated with ER-alpha *Pvu* II genotype and VDR *Apa* I genotype after 1 year of calcium supplementation.

Disclosures: ***Z. Zhang****, None.*

SU172

Association Study and Haplotype Analysis of Twelve Prominent Candidate Genes for BMD Variation in Chinese. S. F. Lei*, M. X. Li*, F. Y. Deng*, D. K. Jiang*, M. Y. Liu*, X. D. Chen*, W. X. Jian*, J. J. Guo*, H. Xu*, Y. B. Wang*, H. W. Deng. College of Life Sciences, Hunan Normal University, Changsha, China.

To evaluate the importance of twelve prominent candidate genes (i.e., the ER-α, VDR, BGP, COL1A1, COL1A2, IL-6, PTH, CASR, IGF-I, TNFR2, PTHR1, and AHSG) on BMD at different skeletal sites in Chinese, we simultaneously tested linkage and/or association of the genes with BMD variation in 401 Chinese nuclear families containing 1,260 subjects.

Each of the nuclear families includes both parents and at least one healthy female offspring aged 19-45with the average 31.4. The mean family size is 3.14 and 349, 50, 2, and 1 families have 1, 2, 3, and 4 children, respectively. Exclusion criteria were adopted to minimize any known potential confounding effects on the study phenotypes of the female offspring. Sixteen markers were genotyped, which are ER-αs *Xba*I, *Pvu*II, and (TA)n, VDR's *Apa*I, BGP's *Hind*III, COL1A1's 1997G/T, COL1A2's *Msp*I and (GT)n, IL-6's *BsrB*I and (CA)n, PTH's *BstB*I, CASR's (AT)n, IGF-I's (CA)n, TNFR2's (CA)n, PTHR1's (AAAG)n, and AHSG's *Sac*I. Hologic QDR 2000+ DEXA scanner was used to measure BMD at the total hip and the L1-4 spine regions. Using QTDT, we tested stratification, within-family association, and total-family association of the above markers and their haplotypes with the hip and spine BMD measured with Hologic.

Table 1 summarizes the most significant results (p values) of the QTDT analysis. Within- or total-family association analyses suggest that the markers or haplotypes of the ER-α, COL1A2, TNFR2, and IL-6 genes are associated with BMD at the hip or spine in our Chinese subjects.

Table 1	**Within-Family Association**		**Total-Family Association**	
	Spine	**Hip**	**Spine**	**Hip**
ER-α: *Xba* I	0.054	-	-	-
ER-α: $(TA)_{21}$	-	-	0.013	0.001
ER-α: *P-x-*$(TA)_{21}$	-	-	0.0007	0.0006
COL1A2: *Msp* I	0.013	0.053	-	-
COL1A2: $(GT)_{17}$	0.0120	0.0108	0.0704	-
COL1A2: *m-*$(GT)_{17}$	0.0040	0.0056	0.0297	0.0789
TNFR2: $(CA)_4$	-	0.015	0.095	0.041
IL-6: *b-*$(CA)_{15}$	-	-	-	0.0262

Our results suggest that the ER-α, TNFR2, COL1A2, and IL-6 genes may play an important role in BMD determination in Chinese, whereas the VDR, BGP, COL1A1, PTH, CASR, IGF-I, PTHR1, and AHSG genes may not contain the QTLs for BMD variation in Chinese. Testing candidate genes for BMD variation in different populations may reveal ethnic peculiarity in BMD determination and confirm genes commonly important to osteoporosis for various ethnic groups.

Disclosures: ***S.F. Lei****, None.*

SU173

Association of Single Nucleotide Polymorphisms in The Low Density Lipoprotein Receptor-related Protein 5 Gene (*LRP5*) with Bone Mineral Density of Adult Women. Y. Ezura[1], T. Urano[2], T. Nakajima*[1], Y. Sudo*[1], H. Yoshida*[3], T. Suzuki[3], T. Hosoi[4], S. Inoue[2], M. Shiraki[5], M. Emi*[1]. [1]Department of Molecular Biology, Institute of Gerontology, Nippon Medical School, Kawasaki, Japan, [2]Dept. Geriatric Medicine, Faculty of Medicine, University of Tokyo, Tokyo, Japan, [3]Department of Epidemiology, Tokyo Metropolitan Institute of Gerontology and Geriatric Hospital, Tokyo, Japan, [4]Department of Internal Medicine, Tokyo Metropolitan Institute of Gerontology and Geriatric Hospital, Tokyo, Japan, [5]Research Institute and Practice for Involutional Diseases, Nagano, Japan.

Low-density lipoprotein receptor related protein 5 (LRP5), a Wnt co-receptor, is an important regulator of the bone development and its maintenance. Recently we identified a correlation between the intronic single nucleotide polymorphism (SNP) and vertebral bone mineral density (BMD) (JBMM 2004, in press), which encouraged us to investigate further the causative genetic ground in this locus for BMD determination. Mutation searches for the selected subjects, as well as scanning searches for functional SNPs correlating with the adjusted BMD were conducted on two independent subject groups of adult Japanese women. The subject group from the initial study was expanded to 387 individuals recruited from the same institute (Group H), and the causative mutation was searched among 12 subjects who had prominently high bone mass (Z-score >3.0). Entire 23 exons and flanking regions were investigated by direct sequencing. Linkage disequilibrium (LD) was analyzed for independently recruited 384 adult Japanese women (Group G) by estimating haplotype frequencies and statistical indices D' and r^2. Genotypic association of 37 SNPs was investigated for adjusted BMD levels among Group G subjects (n=384). Reproducible association was tested for spinal BMD Z-score among the Group H subjects (n=387). Combined effects of the variations were examined by multiple regression analysis. As a result of the mutation search, no rare mutation was detected among the selected 12 individuals. LD analysis on Group G subjects indicated linkage disequilibrium within the entire 132kb region of the LRP5 gene, however a transitional gap around the 7th intron was indicated. The genotypes of two coding-SNPs A1330V (c.3989C>T) and c.2220C>T significantly correlated with radial BMD (Group G: p = 0.019 and 0.021). Multiple regression analyses implied a combined effect of another missense coding-SNP Q89R (c.266A>G). However, reproducible correlation was detected only for A1330V (Group H: p=0.03). Our results indicate the important function of the common genetic variations in LRP5 affecting BMD in adult women, which may contribute to susceptibility of osteoporosis.

Disclosures: ***Y. Ezura****, None.*

SU174

Non-replication in Genetic Studies of Complex Diseases-Lessons Learned from Osteoporosis. H. W. Deng, H. Shen*, Y. J. Liu*, P. Y. Liu*, R. R. Recker. Osteoporosis Research Ctr. and Dept. of Biomedical Sciences, Creighton Univ., Omaha, NE, USA.

Over the past decades, numerous linkage and association studies have been performed to search for genes predisposing to complex human diseases. However, little success has been achieved and inconsistent or controversial results have been accumulated. The 'frustrating' results have led to pessimism about these approaches in gene mapping of complex diseases in general. Reviewers are reluctant to publish or fund such studies. We argue that those non-replication results are not unexpected, given the complicated nature of complex diseases and a number of confounding factors, such as limited statistical power, population stratification, heterogeneity of linkage disequilibrium between marker and QTL, etc. Based on our experience in genetic studies of osteoporosis, we briefly address major potential factors for this inconsistency and provide suggestive remedies. We also point out that with low statistical power, even a 'replicated' finding is still likely to be a false positive. Despite various factors could result in the lack of reproducibility seen in genetic studies of complex diseases, however, this situation does not condemn the approach as being futile, but rather indicate that caution should be take when designing the studies and interpreting the results. We believe that, with rigorous control of study design and interpretation of different outcomes, inconsistency might be largely reduced and the chances of successfully revealing genetic components of complex diseases could be greatly improved.

Disclosures: ***H.W. Deng****, None.*

SU175

Mutation Analysis of the LRP5 Gene in Men with Idiopathic Osteoporosis. P. Crabbe*[1], A. Willaert*[2], I. Van Pottelbergh*[1], P. Coucke*[2], S. Goemaere[1], A. De Paepe*[2], J. Kaufman[1]. [1]Dep. of Endocrinology, Ghent University Hospital, Ghent, Belgium, [2]Dep. of Medical Genetics, Ghent University Hospital, Ghent, Belgium.

The aim of this study was to investigate the role of the low-density lipoprotein receptor-related protein 5 (*LRP5*) gene in male idiopathic osteoporosis (IO). Various mutations in the *LRP5* gene have been associated with different bone phenotypes and a quantitative trait locus for bone mineral density was mapped to the *LRP5* region of chromosome 11. These findings underscore the importance of LRP5 in skeletal regulation and make it a plausible candidate gene for IO.

For this study sixty-six male IO probands were selected on the basis of a BMD Z-score ≤ -2.0 at the lumbar spine (Z_L) or at the proximal femur (Z_{TH}) (Van Pottelbergh et al. 2003, JBMR 18:303-311). All 23 exons and relevant exon-intron boundaries of the *LRP5* gene were amplified by polymerase chain reaction with exon-specific primers. Mutation screening was performed by means of denaturing high performance liquid chromatography and conformation sensitive gel electrophoresis in combination with direct sequencing, restriction enzyme analysis or SNaPshot analysis. Genetic analysis revealed 23 sequence variants, of which 12 had not been reported before. Because of a possible functional aspect, we focused our analysis on the five missense mutations that were detected in the male IO probands. Two of them (1999G>A and 3989C>T) had been reported either as polymorphisms or in association with BMD, the other three (1067C>T, 1364C>T and 4609G>A) were newly detected in this study. These three new missense mutations are all located in highly conserved regions of LRP5. Modeling data showed that mutations 1067C>T and 1364C>T are both located at the surface of the second YWTD-EGF like domain of LRP5 and therefore may disrupt a protein-binding site. None of the three new mutations was found in a control panel and segregation analysis in the respective families could not exclude their possible causality.

Overall, we conclude that for 1999G>A and 3989C>T our results are in agreement with those reported by others and we can assume these are general polymorphisms in the population, while mutations 1067C>T, 1364C>T and 4609G>A are putative disease-causing mutations for male IO. These findings, indicating a possible role of mutations in the *LRP5* gene in a minority of men with IO, warrant further research addressing their prevalence in additional patient populations and efforts to assess their functional role.

Disclosures: ***J. Kaufman****, None.*

SU176

Relation of the XbaI and PvuII Polymorphisms of the Estrogen Receptor Gene and the CAG Repeat Polymorphism of the Androgen Receptor Gene to Peak Bone Mass and Bone Turnover Rate Among Young Healthy Men. V. V. Välimäki*[1], K. Piippo*[2], S. Välimäki*[1], E. Löyttyniemi*[3], K. Kontula*[4], M. J. Välimäki[1]. [1]Division of Endocrinology, Department of Medicine, Helsinki University Central Hospital, Helsinki, Finland, [2]Dept. of Medicine, Helsinki University Central Hospital and Research Program in Molecular Medicine, University of Helsinki, Helsinki, Finland, [3]Department of Statistics, University of Turku, Turku, Finland, [4]Department of Medicine, Helsinki University Central Hospital, Helsinki, Finland.

The genes coding for estrogen receptor-α (ER-α) and androgen receptors (AR) are potential candidates for regulation of bone mass and turnover, which may contribute to both achievement of peak bone mass and bone loss after completion of growth. The present study was aimed at elucidating the role of two restriction fragment length (XbaI and PvuII) polymorphisms of the ER gene and the CAG repeat polymorphism of the AR gene as determinants of peak bone mass in men.

A cross-sectional study, with data on lifestyle factors collected retrospectively, was performed in 234 young men, aged 18.3 to 20.6 years. 184 men were recruits of the Finnish Army, and 50 were men of similar age, who had postponed their military service for reasons not related to health. Bone mineral content (BMC), density (BMD), and scan area were measured in lumbar spine and upper femur by dual-energy X-ray absorptiometry (DXA). Bone turnover rate was assessed by measuring serum procollagen type I N propeptide (PINP) and tartrate-resistant acid phosphatase 5b (TRACP5b) as well as urinary excretion of N-terminal cross-linking telopeptide of type I collagen (NTX-I). After adjusting for age, height, weight, exercise, smoking, calcium and alcohol intake BMC, scan area, and BMD at all measurement sites were similar for the different XbaI and PvuII genotypes of the ER and independent of the number of the CAG repeats of the AR gene. Except for urinary NTX-I which showed a tendency to higher values for the xx (P=0.084) and pp (P=0.10) genotypes of the ER, bone turnover markers were not related to the genotypes studied. The XbaI and PvuII polymorphisms of the ER gene and the CAG polymorphism of the AR gene are not determinants of peak bone mass and bone turnover rate among young Finnish men.

Disclosures: ***V.V. Välimäki****, None.*

SU177

Allelic Imbalance in Human Trabecular Bone Cells: An Approach to Identify SNPs Regulating Gene Expression. E. Grundberg*[1], T. Pastinen*[2], O. Nilsson*[3], T. J. Hudson*[2], H. Brändström*[1]. [1]Department of Medical Sciences, Uppsala University, Uppsala, Sweden, [2]McGill University and Genome Quebec Innovation Centre, Montreal, PQ, Canada, [3]Department of Surgical Sciences, Uppsala University, Uppsala, Sweden.

Osteoporosis is a complex disease characterized by reduced bone mineral density (BMD) and development of fractures of e.g. the spine, hip and wrist. Moreover, BMD is under strong genetic control, demonstrated in numerous family and twin studies.

Several approaches are currently being used to identify the genes underlying the disease, such as genome-wide linkage studies and association studies, using single nucleotide polymorphisms (SNPs) in candidate genes. However, most of the SNPs studied have no functional validation.

We report an approach for investigations of polymorphisms that regulate gene expression in human trabecular bone cells. The detection of a regulatory SNP or allelic imbalance is based on quantitative genotyping of polymorphisms in RNA transcripts derived from heterozygous individuals and comparing the observed allele ratios in corresponding genomic DNA samples, which are assumed to represent 50:50 allele ratios. Genotyping is performed using Fluorescence polarization-single base extension (FP-SBE) to provide quantitative detection of allele-specific transcripts.

To validate the method described herein we examined an imprinted gene, *MEST*, and a gene previously reported to have allelic imbalance in lymphoblastoid cell lines, *BTN3A2*. Human trabecular bone cells from 50 individuals were cultured until confluency and RNA and DNA from each sample were isolated. The polymorphisms were amplified by polymerase chain reaction (PCR) and the relative expression of the two alleles in a heterozygous sample was examined by genotyping of both genomic DNA and cDNA from the same cellular sample by FP-SBE. The study was approved by the local ethic committee.

For *MEST*, 43 % of the samples were heterozygous for the coding SNP and all of them showed mono-allelic expression in the trabecular bone cells. In a total of 13 heterozygous individuals (27 %) for *BTN3A2*, five of them showed allelic imbalance, which are in agreement with previously findings in lymphoblastoid cell lines.

In conclusion, the method offers tools for efficient identification and characterization of allelic variation or imbalance of gene expression in human trabecular bone cells. This promotes identification of regulatory sequence variants in candidate genes for osteoporosis.

Disclosures: ***E. Grundberg****, None.*

SU178

Low DXA and CT Bone Measures in Young Adults with a Simple Sequence Repeat in IGF-I Gene. X. Liu*[1], C. Rosen[2], S. Mora[1], D. Dong*[1], P. Pitukcheewanont[1], V. Gilsanz[1]. [1]Childrens Hospital Los Angeles, Los Angeles, CA, USA, [2]Maine Center for Osteoporosis Research and Education, Bangor, ME, USA.

Several studies have suggested that a polymorphism in a microsatellite within the IGF-I gene is related to decreased bone mass in elderly subjects, although other investigations in premenopausal women have found no such evidence. In the current study, we assessed the possible association between IGF-I genotypes and bone density in 235 healthy white young adults (102 females and 133 males) ages 15 to 20 years, who had achieved sexual and skeletal maturity. Skeletal maturity was assessed by hand and wrist radiographs and sexual maturity by physical examination (attainment of Tanner 5). Areal bone mineral density (BMD) in the spine, hip and total body were obtained by DXA and CT was used to determine volumetric bone density (BD) in the spine and cortical bone area (CBA) and cross-sectional area (CSA) in the femur. Subjects with the 192/192 genotype had lower values for all DXA BMD measurements and lower CT values for BD in the spine and CBA in the femur than subjects with any other IGF-I genotype. Values for CSA were non-significantly lower. These results indicate a relationship between IGF-I genotype and bone mass at sexual and skeletal maturity. This information may contribute to the identification of a subset of the population of normal young adults who may be at risk for developing vertebral fractures later in life, and may ultimately be of value in the planning of early preventive strategies for osteoporosis.

				DXA				CT
Genotype	N (%)	Age yrs	BMI kg/m^2	Spine mg/cm^2	Hip mg/cm^2	Total Body mg/cm^2	Spine BD mg/cm^3	Femur CBA cm^2
192/192	134 (67)	17.4±2.3	24.3±5.2	1.00±0.12	1.11±0.14	1.14± 0.14	298±47	4.72±0.76
Heterozygous	101 (43)	17.3±2.2	24.8±5.4	0.97±0.12	1.06±0.13	1.10± 0.09	284±40	4.52±0.73
t test		p=0.43	p=0.51	p=0.056	p=0.021	p=0.019	p=0.046	p=0.040

Disclosures: ***V. Gilsanz****, None.*

SU179

A Functional $(AAAG)_n$ Polymorphism in the PTHR1 Promoter Is Associated with Height but not with BMD in a Large Cohort of Young Caucasian Women. A. Scillitani*[1], C. Jang*[2], B. Wong*[2], L. Rubin[2], G. Hendy[3], D. Cole[2]. [1]CasaSollievo Sofferenza, San Giovanni Rotondo, Italy, [2]University of Toronto, Toronto, ON, Canada, [3]McGill University, Montreal, PQ, Canada.

The PTHR1 receptor mediates the action of parathyroid hormone and the parathyroid hormone related peptide (PTHrP). Interacting with this receptor, PTHrP contributes to skeletal development through the regulation of chondrocyte proliferation and differentiation, and the P3 promoter of the *PTHR1* gene is the major one in human bone and kidney. Recently, a tetranucleotide repeat - $(AAAG)_n$ - in the P3 promoter has been shown to have functional activity related to size, and homozygosity for $(AAAG)_6$, or the 6/6 genotype, has been associated with greater adult height compared to the 5/5 genotype (J Clin Endocrinol Metab 2002;87:1791). The aim of this study was to evaluate the association of the $(AAAG)_n$ polymorphism with height and bone mineral density (BMD) measured at lumbar spine (LS) and femoral neck (FN) in 565 young Caucasian women aged 18-35 yr recruited from the metropolitan Toronto area. With informed consent, genomic DNA was extracted from whole blood, amplified for the P3 promoter flanking the polymorphism, and genotyped by comparison with sequenced controls following electrophoretic separation on high-resolution polyacrylamide gels. Allele frequencies for $(AAAG)_n$ were: 76.8% (n=5); 20.9% (n=6); 1.8% (n=7); 0.18% (n=8); 0.27% (n=9); 0.08% (n=2), and there was no evidence for Hardy-Weinberg disequilibrium. Univariate analysis of variance showed that subjects bearing one or two of the n=6 allele (6/x & 6/6) had significantly greater mean height (1.656 ± 0.004 m) than all others (x/x, 1.644 ± 0.003 m; p = 0.034). This association was significant after adjusting for multiple covariates - current age, age at menarche, physical activity, smoking status, and intakes of caffeine and calcium. In this multiple regression analysis, the model accounts for 5.5% of the total variance in height, and the *PTHR1* promotor polymorphism for 13.6% of explained variance. Comparison of genotype groups for BMD at LS and FN was not significant (LS: 6/6 & 6/x *vs* x/x, 1.196 ± 0.009 *vs* 1.187 ± 0.007 g/cm^2 p = 0.4 - FN: 1.016 ± 0.008 *vs* 1.002 ± 0.006 g/cm^2, p = 0.2). In conclusion, our data show that the $(AAAG)_5$ allele is the most common allele in our panmictic North American cohort and confirm matching results on smaller Caucasian and Asian populations already described. Moreover subjects bearing one or two $(AAAG)_6$ alleles are taller than subjects without, confirming published results and re-inforcing the notion that *in vivo* variation in promoter activity of the *PTHR1* gene may be a relevant genetic influence on final adult height.

Disclosures: ***A. Scillitani****, None.*

SU180

Effect of the $P2X_7$ Glu496Ala Polymorphism in Osteoclasts and Association to Bone Mass. S. D. Ohlendorff*, S. Petersen*, C. L. Tofteng*, N. R. Jørgensen. 545, Osteoporosis Research Unit, Copenhagen University Hospital Hvidovre, Hvidovre, Denmark.

P2X7 is a ligand-gated cation channel present in many different cells of the immune and hemopoietic system. It is present on the surface of osteoclasts, and is supposedly involved in osteoclast apoptosis and cell death. A Glu496Ala polymorphism has been identified in the human gene coding for the P2X7 receptor. In cells from individuals carrying the CC genotype of this polymorphism, receptor function is partly disrupted. The aim of this study was to determine the association between the presence of the Glu496Ala polymorphism and osteoclast survival *in vitro*. Osteoclasts were cultured from peripheral blood obtained from women (aged 54-69) participating in the Danish Osteoporosis Prevention Study (DOPS), previously genotyped for the Glu496Ala polymorphism. Mature osteoclasts were stimulated with 2 mM adenosine 5'-triphosphate (ATP) for 30 minutes, 1 hour, 4 hours or 24 hours. After incubation supernatant was removed and lactate dehydrogenase (LDH) released from the osteoclasts was measured, as evidence for cell death. Amount of LDH released is calculated as % LDH released by experimental samples in relation to maximum LDH release of controls. Mean percent elevation of LDH release after 24 hours of ATP stimulation in osteoclasts from individuals with the AA genotype was 53,16 % (n=4), compared to 20,84 % (n=4) for the AC and 5,45 % for CC (n=2) genotype. Thus, the cytotoxic effect of ATP on the osteoclasts was dramatically decreased in cells with the CC genotype as compared to AA and AC genotypes. Moreover, osteoclasts from AA individuals were morphologically affected by ATP stimulation after 4 hours. Cells with the AA genotype were granulated and shrinking, signs of beginning cell death. After 24 hours these cells were completely lysed and apoptotic. The osteoclasts from AC individuals showed a delayed apoptosis process compared to osteoclasts from AA individuals, although shrinkage was observed after 4 hours of ATP stimulation. Granulation and lysis was evident after 24 hours of ATP stimulation, though quite a few cells had still survived 24 hours stimulation with ATP. In contrast, osteoclasts from CC individuals were not showing any signs of apoptosis, even after 24 hours of stimulation with 2mM ATP. In conclusion, presence of the C allele of the P2X7 Glu496Ala polymorphism is clearly associated with an increased osteoclast survival *in vitro*, after stimulation with ATP. The lack of apoptosis seen in osteoclasts from individuals with the CC genotype might indicate that the presence of the C allele of the Glu496Ala polymorphism could be associated with increased osteoclast activity and bone resorption *in vivo* leading to bone loss and osteoporosis.

Disclosures: ***S.D. Ohlendorff****, None.*

SU181

Aromatase and Estrogen Receptor Alpha Gene Polymorphisms: Response of the Bone Mineral Density in Post-menopausal Women to HRT. L. Masi, S. Ottanelli*, F. Del Monte*, S. Carbonell*, L. Guazzini*, N. Fossi*, A. Gozzini*, C. Mavilia*, A. Falchetti*, R. Imbriaco*, A. Amedei*, A. Tanini, M. L. Brandi. Internal Medicine, University of Florence, Florence, Italy.

Genetic factors regulate bone mineral density (BMD) and possibly development of osteoporosis. Sex steroids play a pivotal role in maintaining bone. The formation of estrogens from C19 steroids is catalyzed by aromatase in post-menopausal women and men. It is known that polymorphism at the human ERα and at the aromatase genes are associated with low BMD in postmenopausal women. In the present study we evaluated the possibility of interaction between aromatase and ERα genotypes with bone mass and we assessed the response in BMD to HRT in a cohort of postmenopausal women. Subjects consisted of 240 Italian postmenopausal women with a range of age 36-76 years (mean 61.3±8.6). Subjects under HRT received 17β-Estradiol (TTS 50μg/day) and nomegestrol acetate 5mg/day (12 days/month). Vertebral BMD was measured at the baseline and after 1 year. Genomic DNA was isolated from EDTA blood samples by a standard procedure. Pvu II and Xba I

polymorphism of the ERα was determined by PCR and TTTA repeats for the aromatase gene were evaluated by sequence analysis. The capital *P* and *X* and the lower-case *p* and *x* represent respectively the absence and the presence of the restriction site for the ERα. For the TTTA repeats polymorphism the subjects were divided on the basis of the mean TTTA repeats: low (<8) medium (8-10) and high (>10). The genotype distribution for ERα was as follow: XX 41.3%; Xx 44.9%; xx:13.7% (χ2 analysis: p=0.3) and PP: 34.3%; Pp:46.05%; pp: 19.53% (χ2 analysis: p=0.07). For the aromatase TTTA repeats the distribution was as follow: low: 40%; medium 42% and high:18%. The genotype with a low number TTTA repeats was more frequent in osteoporotic and osteopenic subjects in comparison with normal (42.8 and 39.2% vs.17.86%). Ancova analysis did not show any statistical differences in the LS-BMD of various ER alpha genotypes (p=0.6), although LS-BMD tended to be lower in subjects with pp and xx genotypes. During HRT an increase of the LS-BMD was present in all the genotypes suggesting a feeble influence of the polymorphism on the hormone response. The same results were observed for the aromatase gene polymorphism. The absence of difference in the LS-BMD in subjects with or without HRT suggests a low influence of the aromatase gene on the HRT response. In conclusion, ER-alpha and aromatase gene polymorphism do not seem to influence the response to HRT.

Disclosures: ***L. Masi****, None.*

SU182

COL1A1, but not ESR1 or VDR Polymorphisms are Associated with BMD in a Cohort of Spanish Postmenopausal Women. S. Balcells*[1], M. Bustamante*[1], A. Enjuanes*[2], N. Garcia-Giralt*[1], I. Aymar*[2], X. Nogués[2], L. Mellibovsky*[2], A. Díez-Pérez[2], D. Grinberg*[1]. [1]Genetics, Universitat de Barcelona, Barcelona, Spain, [2]Urfoa, IMIM-Hospital del Mar-Universitat Autònoma de Barcelona, Barcelona, Spain.

We have previously identified two polymorphisms in the upstream regulatory region of COL1A1 (-1663indelT and -1997G>T) and showed that they were associated with lumbar spine BMD in Spanish postmenopausal women. We also showed that the sites containing these polymorphisms (PCOL1 and PCOL2) were binding sites for osteoblast nuclear proteins, and that there were affinity differences between the two alleles of each polymorphsim (JBMR 17:384-93;2002). The aim of the present study was to compare the effect of these two polymorphisms on BMD with the effects of polymorphisms of the VDR and ESR1 genes in an enlarged cohort of postmenopausal women.

We have genotyped the following polymorphisms: -1663indelT, -1997G>T and Sp1 of COL1A1; BsmI, ApaI,TaqI and FokI of VDR; and XbaI, PvuII and the promoter (TA)n of ESR1 in a total of 544 DNA samples. The methods employed included SNaPshot, Genescan, RFLP and automatic sequencing. All polymorphisms were found to be in Hardy-Weinberg equilibrium. Haplotypes were obtained using PHASE. BMD was measured by dual-energy X-ray densitometry. Statistical tests (performed with SPSS v. 11.5) were the Chi-square, ANOVA and ANCOVA. Age, body weight, height, and years since menopause were used as covariables for statistic analyses, when appropriate.

None of the polymorphisms was significantly associated with osteoporosis, according to the Chi-square test. A significant association with lumbar spine BMD (LS-BMD) was found only for -1997G>T of COL1A1, when using ANCOVA (p=0.044). We also observed an association (p=0.001) between LS-BMD and the interaction of the two COL1A1 promoter polymorphisms. No other polymorphism gave significant results (or even a hint of association) with BMD in our cohort. Overall, osteoporosis was present in 33.3% of the cases. However, in homozygotes for the T allele of -1997G>T the presence of this condition was almost doubled (62%) and in the group of women carrying two copies of the [-1997T/-1663 8T/Sp1 G] haplotype of COL1A1 the cases with osteoporosis were 75%.

In conclusion, by enlarging the cohort we have found that the association observed previously still holds true, while none of the VDR or ESR1 polymorphisms gave any significant results. Most probably the relatively modest size of this cohort precludes the detection of moderate effects. In this respect, the -1997G>T polymorphism, as well as its interaction with other COL1A1 polymorphisms, may be considered an important genetic factor for BMD determination.

Disclosures: ***S. Balcells****, None.*

SU183

(TAAA)n-Alu Element Polymorphism in Vitamin D Binding Protein Gene and Its Association with Bone Density and Osteoporosis in Men. Z. H. Aloanzi*[1], S. P. Tuck*[2], S. S. Varanasi[1], N. Raj*[3], J. S. Harrop*[4], G. D. Summers*[5], D. B. Cook*[1], R. M. Francis[2], H. K. Datta[1]. [1]School of Clinical & Laboratory Sciences, University of Newcastle, Newcastle upon Tyne, United Kingdom, [2]School of Clinical Medical Sciences, University of Newcastle, Newcastle upon Tyne, United Kingdom, [3]Rheumatology, Derbyshire Royal Infirmary, Derby, United Kingdom, [4]Biochemistry, Derbyshire Royal Infirmary, Derby, United Kingdom, [5]Rheumatology, Derbyshire Royal InfirmarY, Derby, United Kingdom.

In an earlier pilot study in men we found a significant association of BMD with tandem tetranucleotide (TAAA) repeats downstream of intron 8 of vitamin D-binding protein (DBP) gene. Here we present a larger study in men to examine the possible association of DBP gene (TAAA)n polymorphism with plasma DBP concentration and BMD. The subjects were all age-matched English Caucasian, comprising 56 men with idiopathic osteoporosis and 114 male control subjects. The osteoporotic men all had a BMD T score of < -2.5 at either the femoral neck or lumbar spine. The commonest genotype in men with osteoporosis was 8/10, which had a frequency of 30.4%, compared with 13.2% in the control subjects. The predominant DBP-*Alu* genotype in the control subjects was 10/10 (42.1%), whereas the frequency of this genotype in men with osteoporosis was 8.9%. The odds ratio calculated for the commonest genotype in men with osteoporosis compared with control subjects was 10.8 (95% confidence interval 3.4-35.5). In control subjects, the commonest allele *10 was found with a significantly higher frequency than allele *8 (Fisher's exact two-tailed p<0.005). In view of the relative preponderance of 8/10 and 10/10, and relative low frequency and absolute number of the remaining DBP-*Alu* genotypes, the effect of only the main genotypes was studied. The anthropometric indices of the 8/10 and 10/10 DBP-*Alu* genotypes, comprising data from both control subjects and osteoporotic patients, were compared, and no significant differences were seen in age, height, weight and BMI. However, the two genotypes demonstrated a significant difference in BMD; the total femur, femoral neck and lumbar spine BMD being lower for the 8/10 compared with 10/10 DBP-*Alu* genotype. The magnitude of the differences in BMD between the two genotypes was similar at all sites. Higher plasma DBP concentrations were found in men with the 8/10 genotype than the 10/10 genotype (p<0.01). In conclusion, our results suggest that (TAAA)n-Alu polymorphism has an important effect on bone density in men, which may be mediated via an effect on circulating DBP. The observed variation in BMD in different DBP-*Alu* genotypes may also be explained by linkage disequilibrium with other genes located near the DBP locus.

Disclosures: ***S.S. Varanasi****, None.*

SU184

Polymorphisms in the Estrogen Receptor β (*ESR2*) Gene are Associated with Peak Bone Mineral Density in Caucasian Men and Women. S. Ichikawa*[1], D. L. Koller[2], M. L. Johnson*[1], D. Lai*[2], T. M. Fishburn*[1], M. Peacok[1], C. C. Johnston[1], S. L. Hui[1], T. M. Foroud[2], M. J. Econs[1]. [1]Medicine, Indiana University School of Medicine, Indianapolis, IN, USA, [2]Medical and Molecular Genetics, Indiana University School of Medicine, Indianapolis, IN, USA.

Peak bone mineral density (BMD) is a major determinant of osteoporotic fracture and is a highly heritable trait. Recently, we reported several quantitative trait loci (QTLs) for peak BMD identified by 9-cM genome scan. Significant linkage for trochanter BMD in Caucasian and African American sister pairs was found at chromosome 14q (LOD score = 3.5). Follow-up analysis with markers spaced at 5-cM interval confirmed the linkage to 14q in women, where the estrogen receptor β (*ESR2*) gene is located. Analysis of this region including a microsatellite marker with the *ESR2* gene (D14S1026) further confirmed the linkage finding, with a LOD score of 2.0 at the intragenic marker position. Estrogens are necessary for the acquisition of optimal peak bone mass, and functional sequence variations in *ESR2* are likely to influence acquisition of peak bone mass. A recent study in the Framingham cohort suggests that genetic variations in *ESR2* account for up to 4% difference in femoral BMD. To determine whether *ESR2* polymorphisms are associated with peak BMD in our population, we tested ten single nucleotide polymorphisms (SNPs) encompassing the entire *ESR2* gene. Peak BMD at femur and lumbar spine was measured in 190 men (age 20-61) and 588 women (age 21-52) from Indiana. SNP genotyping was performed using matrix-assisted laser disorption/ionization time-of-flight (MALDI-TOF) mass spectrometry of allele-specific primer extension products. We found statistically significant association between *ESR2* alleles and spinal BMD in both men and women. Five of the ten genetic variations reached significance in men, whereas only two reached significance in women (p-value < 0.05). The strongest association in both sexes was found with the allelic variation present in the 5' flanking region of *ESR2* (p-value = 0.004). The alleles may account for up to 2.8% and 0.9% of the spinal BMD variation in healthy men and women, respectively. Further, these results suggest that *ESR2* polymorphisms may be more important in development of bone mass in men than in women.

Disclosures: ***S. Ichikawa****, None.*

SU185

Polymorphisms in the Bone Morphogenetic Protein 2 (*BMP2*) Gene Do Not Affect Peak Bone Mineral Density in Men and Women. S. Ichikawa*[1], D. L. Koller[2], M. L. Johnson*[1], D. Lai*[2], C. C. Johnston[1], S. L. Hui[1], T. M. Foroud[2], M. Peacock[1], M. J. Econs[1]. [1]Medicine, Indiana University School of Medicine, Indianapolis, IN, USA, [2]Medical and Molecular Genetics, Indiana University School of Medicine, Indianapolis, IN, USA.

Peak bone mineral density (BMD) obtained during young adulthood is a major determinant of osteoporotic fracture in later life. Although peak BMD certainly has an environmental component, it is a highly heritable trait. Recently, bone morphogenetic protein 2 (*BMP2*) located at human chromosome 20p12.3 was reported as a susceptibility gene for osteoporosis and BMD variation in Icelandic and Danish populations. To determine whether the *BMP2* gene contributes to peak BMD variation in our Caucasian population, we tested five single nucleotide polymorphisms (SNPs), four of which were determined to be associated with osteoporotic phenotypes in the previous study. SNP genotyping was performed using matrix-assisted laser disorption/ionization time-of-flight (MALDI-TOF) mass spectrometry of allele-specific primer extension products. Peak BMD measurements were taken at the femur and the lumbar spine (L_2-L_4) in 190 men (age 20-61 years) and 588 women from Indiana (age 20-46 years). We observed marginal association with a missense polymorphism in exon 2 (Ser37Ala), which was highly associated with osteoporosis in the Icelandic patients. However, this polymorphism did not reach statistical significance (p-value > 0.1) at the femur neck or spine in either sex. We were also unable to find any association with haplotypes constructed with the five tested SNPs that span the entire *BMP2* gene. Therefore, we conclude that genetic variations in *BMP2* do not substantially contribute to peak BMD variation in our population.

Disclosures: ***S. Ichikawa****, None.*

SU186

Tumor Necrosis Factor Alpha Polymorphism, Bone Strength Phenotypes, and the Risk of Fracture in Older Women. S. P. Moffett*[1], J. M. Zmuda[1], J. I. Oakley[1], T. J. Beck[2], J. A. Cauley[1], K. L. Stone[3], L. Lui[3], K. E. Ensrud[4], T. A. Hillier*[5], M. C. Hochberg*[6], P. Morin*[7], D. Green*[8], G. Peltz*[8]. [1]Epidemiology, University of Pittsburgh, Pittsburgh, PA, USA, [2]Radiology, Johns Hopkins University, Baltimore, CA, USA, [3]Medicine, University of California, San Francisco, CA, USA, [4]General Internal Medicine, Veterans Affairs Medical Center, Minneapolis, MN, USA, [5]Kaiser Permanente Center for Health Research, Portland, OR, USA, [6]School of Medicine, University of Maryland, Pittsburgh, PA, USA, [7]Axys Pharmaceuticals, La Jolla, CA, USA, [8]Roche Molecular Systems, Alameda, CA, USA.

Tumor necrosis factor alpha (TNFα) is a proinflammatory cytokine that promotes osteoclastic bone resorption. Several potentially functional polymorphisms have been identified in the regulatory region of the TNFα gene including a G-308A polymorphism (rs1800629). We evaluated the association between the G-308A polymorphism at the *TNFA* locus and bone mineral density (BMD), bone structural geometry and the risk of fracture in 4402 women aged 65 years and older participating in the Study of Osteoporotic Fractures (SOF). Femoral neck BMD and structural geometry were measured using dual-energy X-ray absorptiometry (Hologic QDR 1000). Incident fractures were confirmed by physician adjudication of radiology reports. Despite similar femoral neck BMD, women with the A/A genotype had greater subperiosteal width (A/A=3.30cm vs G/G=3.21cm, p=0.01) and endocortical diameter (A/A=3.03cm vs G/G=2.95cm, p=0.03) than those with the G/G genotype. The net result of these structural differences was that there was a greater distribution of bone mass away from the neutral axis of the femoral neck in women with the A/A genotype, resulting in greater indices of bone bending strength (cross-sectional moment of inertia: A/A=1.97, G/A=1.90, G/G=1.82, p=0.004; section modulus: A/A=1.18, G/A=1.16, G/G=1.12, p=0.003). There were 376 incident hip fractures during 12.1 years of follow-up. There was a 22% decrease in the risk of hip fracture per copy of the A allele (RR: 0.78; 95% C.I.: 0.63, 0.96). Adjustments for potential confounding factors and adjustments for BMD or bone strength indices had little effect on this association. The G-308A polymorphism was not associated with other fractures (non-spine RR: 0.95; 95% C.I.: 0.86, 1.05). The G-308A substitution in the *TNFA* promoter region may be a novel genetic marker of bone strength and hip fracture susceptibility among older women. These results require confirmation, but suggest a potential role of altered TNFα production and/or signaling in the etiology of osteoporosis.

Disclosures: ***S.P. Moffett****, None.*

SU187

Genetic Polymorphisms of OPG, RANK and ESR1 in Bone Mineral Density in Korean Postmenopausal Women. J. Choi*[1], A. Shin*[1], S. Park*[2], H. Chung[3], S. Cho*[4], C. Shin[4], Y. Chung[5], K. Lee*[1], K. Lee*[1], C. Kang*[6], C. Kang*[6], D. Cho*[7], D. Kang*[1]. [1]Dept. of Preventive Medicine, Seoul National University College of Medicine, Seoul, Republic of Korea, [2]Konkuk University, Chungju, Republic of Korea, [3]Ewha Womans University, Seoul, Republic of Korea, [4]Seoul National University, Seoul, Republic of Korea, [5]Ajou University, Suwon, Republic of Korea, [6]KAIST, Daejeon, Republic of Korea, [7]Clinical Research Institute, Labgenomics Co.,Ltd, Yong-In, Republic of Korea.

To evaluate the association between genetic polymorphisms of OPG, RANK and ESR1 which regulate the osteoclastogenesis and low bone mineral density (BMD), a cross-sectional study was conducted in 752 Korean postmenopausal women. The differences of calcaneus and distal radius BMDs between each genotypes (OPG 163 A>G, 1181 G>C, RANK 421 C>T, 575 T>C, and ESR1 1335 C>T, 2142 G>A) were tested by the analysis of covariance (ANCOVA) adjusted for age, BMI, and years since menopause. In OPG 1181 G>C locus, women with CC genotype have higher BMD at calcaneus and distal radius compared to those with GG genotype; those differences were statistically significant (p=0.003 at calcaneus; p=0.020 at distal radius). No significant association was observed between BMDs and the polymorphisms of RANK and ESR1. The OPG haplotype constructed with 163 A and 1181 G allele was the significant independent predictor of BMD (p=0.037 at calcaneus; p=0.008 at distal radius) in the multiple linear regression model that included other possible predictors of BMD. The association between OPG haplotype and BMD was noted in the subjects carrying RANK 575 TT or ESR1 2142 GG genotypes but this was not significant in those without these genotypes. These results suggested that OPG genetic polymorphisms were related to low BMD in postmenopausal women in Korean.

Disclosures: ***J. Choi****, None.*

SU188

Haplotype Analysis of SNPs of Bone Morphogenetic Proteins (BMPs) and Bone Mineral Density (BMD) in Young Korean Men and Women. J. Choi*[1], H. Chung[2], S. Cho*[1], D. Kim*[3], C. Shin[1], Y. Chung[4], A. Shin*[1], I. Choi*[1], D. Kang*[1]. [1]Seoul National University, Seoul, Republic of Korea, [2]Ewha Womans University, Seoul, Republic of Korea, [3]Kangbuk Samsung Hospital, Seoul, Republic of Korea, [4]Ajou University, Suwon, Republic of Korea.

Bone morphogenetic proteins (BMPs) play critical roles in osteoblast differentiation and were also associated with bone mineral density (BMD). To investigate the association between the single nucleotide polymorphisms (SNPs) of BMPs and BMD, a cross-sectional study was conducted in healthy 270 men and 299 women aged 20-39 in Korea. SNPs of BMP2, BMP4, BMP6, and BMP9 were selected of which allele frequencies were reported more than 10% from NCBI dbSNP and JSNP; BMP2 -1103 C>A, c.584 G>A, IVS1-2744 A>G, c.893 T>A, BMP4 c.712 T>C, IVS1-160 C>T, BMP6 c.1283 G>C, IVS4-6838 A>G, IVS5+24 C>T and BMP9 -305 C>T. All SNPs were determined by the 5'-nuclease assay. Individual haplotypes were estimated by a Bayesian method. The differences of calcaneus and distal radius BMDs between each SNP and haplotype were tested by ANCOVA adjusted for age and BMI. SNPs of BMP2 c.584 G>A and c.893 T>A were significantly associated with BMD of female radius and male calcaneus, respectively. Four SNPs of BMP2 were found to be in strong linkage disequilibrium (LD) (D'0.95), thus four common haplotypes accounted for more than 95%. BMD at distal radius in women significantly decreased with the number of BMP2 A-A-G-A haplotype reconstructed with all variant alleles increased (p=0.030). SNPs of BMP4 c.712 T>C, IVS1-160 C>T were also significantly associated with female radius and male calcaneus BMD. Indicating strong LD between two SNPs of BMP4 (D' ≥0.99), BMD at distal radius in women significantly increased with the number of BMP4 C-C haplotype increased (p=0.042). SNP of BMP6 c.1283 G>C were associated with female calcaneus BMD, however, there was no significant relation between BMP6 haplotypes and BMD. These results suggested that SNPs and haplotypes of BMP2 and BMP4 were associated with BMD in women.

Disclosures: ***J. Choi****, None.*

SU189

The Polymorphisms of the VDR cdx-2 Influence Bone Mineral Density (BMD) in Postmenopausal Women. J. M. Quesada-Gomez[1], A. Casado*[2], R. Cuenca-Acevedo*[1], L. Barrios*[1], C. Diaz-Molina*[1], G. Dorado*[3]. [1]Unidad Metabolismo Mineral, Hospital Reina Sofia, Cordoba, Spain, [2]Sanyres (Grupo PRASA, I+D+I), Cordoba, Spain, [3]Bioquimica y Biologia Molecular, Universidad de Cordoba, Cordoba, Spain.

Genetic factors play an important role in pathogenesis of osteoporosis. The vitamin D endocrine system regulates the bone, mineral metabolism and other physiological processes through the vitamin D receptor protein (VDR). The caudal-related homeodomain protein (*cdx-2*) VDR binding element polymorphism has been recently described in relation to osteoporosis. We have studied the relationship of such polymorphism with bone mineral density in a Spanish cohort of 225 postmenopausal women. We have applied and optimized a DNA pooling approach for large-scale genotyping. Concentration of each individual DNA sample was measured at 260 nm. Samples were diluted to 10 ng/µl and 30 ng of each sample were "pooled". Two different pools were constructed, according to the BMD T score (cutoff at -2,5). Such DNA pools were used to determine the frequencies of the alleles "*A*" and "*G*" by Quantitative Real-Time PCR (QRT-PCR; kinetic PCR). The BMD values obtained for *A* and *G* alleles were significantly different. The A allele showed a protective effect on BMD. A novel allele-specific analysis was performed on an individual scale confirming the DNA pooling. These results were further confirmed by DNA sequencing. The allele-specific genotyping method used involved a quantitative real-time PCR (QRT-PCR). Reactions were carried out as follows: 1 cycle denaturing and *AmpliTaq* Gold (Applied Biosystems) activation at 94 ºC for 7 min; 3 cycles denaturing at 94 ºC for 25 sec, hybridization at 57 ºC for 25 sec and extension at 72 ºC for 20 sec; 3 cycles denaturing at 94 ºC for 25 sec, hybridization at 59 ºC for 25 sec and extension at 72 ºC for 20 sec; and 31 cycles denaturing at 94 ºC for 25 sec, hybridization at 60 ºC for 25 sec and extension at 72 ºC for 20 sec. We have found the following genotypic frequencies: 8% AA (adenine at position -3,731 relative to transcription start site of human *vdr* gene 5-ATAAAAACTTAT-3'), 58% GG (guanine at position -3731 5'-GTAAAAACTTAT-3') and 34% AG. The bone mineral density in this cohort of Spanish postmenopausal women is associated with *cdx-2* polymorphisms at *vdr* gene ($p<0.01$ for GA heterozygotes) and confirms previously reported data. Furthermore, the polymorphism detected could affect the expression of the *vdr* in the small intestine, modulating the bone mineral density response to vitamin D availability.

Acknowledgements: supported by Sanyres XXI (Grupo PRASA, Córdoba), Fondo de Investigación 96/02 and Grupo PAI CTS 413 (Junta de Andalucía), Spain.

Disclosures: ***J.M. Quesada-Gomez****, None.*

SU190

Regulation of mRNA Expression of MEPE/OF45 by FGF2 in Cultures of Rat Bone Marrow-Derived Osteoblastic Cells. G. X. Zhang*, M. Mizuno*, K. Tsuji*, M. Tamura. Department of Biochemistry and Molecular Biology, Graduate School of Dental Medicine, Hokkaido University, Sapporo, Japan.

Matrix extracellular phosphoglycoprotein (MEPE)/ osteoblast/osteocyte factor 45 (OF45) is a factor of osteoblastic phosphatonin and minhibin. It is recently isolated RGD-containing matrix protein that acts as the tumor-derived phosphaturic factor in oncogenic hypophosphatemic osteomalacia. It is also highly expressed by osteoblasts and osteocytes and markedly increased during differentiation and mineralization. The regulation and mechanisms of regulation for MEPE/OF45 gene is unknown in osteoblasts. We examined the regulation of MEPE/OF45 mRNA expression in osteoblastic cells derived from high-density cultures of primary rat bone marrow stromal cells incubated with dexamethasone, ß-glycerophosphate and ascorbic acid.

The level of MEPE/OF45 mRNA in these cells was down-regulated by the addition of fibroblast growth factor 2 (FGF2) for 48 h. These effects were observed in a dose-dependent manner between 2 and 10 ng/ml. To study the mechanism of MEPE/OF45 mRNA was reduced by FGF2, we examined transcription factor Runx2 or osterix mRNA expression and cell proliferation by the addition of FGF2. Runx2 or osterix mRNA expression and cell proliferation were not affected by the addition of FGF2 in these high-density cultures, indicating that regulation by FGF2 may not be dependent on these transcription factors or on the proliferation of cells. Additionally, experiments using actinomycin D indicated that FGF2 decreased the stability of the MEPE/OF45 mRNA. We also added FGF2 with cycloheximide to the cells indicated that down-regulation of MEPE/OF45 mRNA by FGF2 was

independent on de novo protein synthesis. Moreover, inhibition of a specific mitogen-activated protein kinase (MAPK) /extracellular signal-regulated kinase kinase (MEK) by PD98059 blocked FGF2-regulated MEPE/OF45 expressions, indicating that this regulation requires the MAPK pathway. These results suggest that MEPE/OF45 gene is one of the targets of FGF2 and may play an important role during bone formation and calcification.

Disclosures: ***G.X. Zhang****, None.*

SU191

Intraarticular Injection of Basic Fibroblast Growth Factor with Hyaluronic Acid Enhances Osteochondral Repair of the Knee in Rabbits. N. Miyakoshi, M. Kobayashi*, K. Nozaka*, Y. Shimada*, K. Okada*, E. Itoi*. Orthopedic Surgery, Akita University School of Medicine, Akita, Japan.

Growth factors including basic fibroblast growth factor (bFGF) are expected to be the useful tools for enhancing bone and cartilage repair. However, suitable carriers are required to deliver a growth factor to the injury site. This study was to investigate osteochondral repair and potential carrier role of hyaluronic acid (HA) after the intraarticular injection of bFGF with HA. Osteochondral defect was created on the medial femoral condyle of the Japanese white rabbits and received weekly intraarticular injection of bFGF (1 or 10 μg) either alone or combination with HA. Prior to the administration, bFGF was incubated with HA or vehicle-saline for 24 hours at 4 °C. Four weeks after the initial injection, the animals were killed and the defect was evaluated grossly (12-point scale) and histologically (16-point scale). The effect of single intraarticular injection of bFGF (1 μg) with HA was also compared to that of the carrier known as gelatin microspheres (GM) incorporating bFGF. Weekly administration of bFGF alone induced undesirable side effects such as inflammatory responses and osteophyte formation, while administration of HA alone showed moderate osteochondral repair comparing to the vehicle treated control defect but it was still insufficient. On the other hand, weekly administration of 1 μg of bFGF with HA yielded significantly better osteochondral repair than each treatment alone in grossly and histologically with minimal side effects ($p<0.05$). Single administration of 1 μg bFGF with HA but not GM incorporating bFGF showed significantly better osteochondral repair comparing to the vehicle treated control defect ($p<0.05$). Our study showed that low-dose bFGF with HA was effective for osteochondral repair in rabbits. The significant osteochondral repair role of bFGF with HA comparing to GM incorporating bFGF might be explained by the potential carrier role of HA and possible synergistic acts between these two agents during the osteochondral repair. The combination of HA with bFGF significantly reversed the side effects resulted from single use of bFGF.

Disclosures: ***N. Miyakoshi****, None.*

SU192

Stage-Dependent Modulation of MC3T3-E1 Osteoblasts Differentiation by FGF2/FGFR2 Signaling. R. Shozui*, Y. Tanimoto*, K. Moriyama. Department of Orthodontics and Dentofacial Orthopedics, Institute of Health Biosciences, The University of Tokushima Graduate School, Tokushima, Japan.

Fibroblast growth factors (FGFs)/Fibroblast Growth Factor receptors (FGFRs) signaling has been reported to play critical roles in bone formation and resorption. We previously reported the abnormal enhancement of osteoblast differentiation and mineralization in the cells derived from Apert syndrome patients associated by S252W mutation of FGFR2 as well as in MG63 human osteosarcoma cells overexpressing FGFR2 with S252W mutation. Furthermore, we have also shown that a soluble form of FGFR2 with S252W mutation acts as a potent negative regulator for osteoblast differentiation and mineralization induced by the abnormal FGFR2 signaling. In the current study, in order to further elucidate the role of FGF2/FGFR2 signaling in osteoblasts differentiation and mineralization, we examined the expression of osteoblastic marker genes in MC3T3-E1 cells with or without FGF2 (5 ng/ml) administration by Northern blotting. FGF2 transiently inhibited RUNX2 mRNA expression at 24 hours, and it was recovered to the basal level at 48 hours. On the other hand, a stimulation of osteopontin (OPN) mRNA expression was observed after 48 hours of the FGF2 treatment in the subconfluent MC3T3-E1 culture, while a drastic elevation was observed as early as 12 hours of the treatment in the confluent culture. In order to evaluate the effect of FGF2 on matrix mineralization, MC3T3-E1 cells were cultured in a-MEM supplemented with 10-8 M dexamethasone, 10 mM b-glycerophosphate, and 50 mg/ml ascorbic acid with or without FGF2 (5 ng/ml), and the mineralized nodule formation was visualized by alizarin red-S staining. Although there was no difference in mineralized nodule formation with or without FGF2 at the early stage of the culture, FGF2 intensified the nodule formation at the later stage. For better understanding the role of FGF2 in osteoblast, we established three stable clones of MC3T3-E1 cells overexpressing the soluble FGFR2 with S252W mutation (sFGFR2-Ap). All the clones which were confirmed to express sFGFR2-Ap in the conditioned medium by Western blotting showed lower expression of OPN mRNA and significantly higher expression of osteoprotegerin (OPG) mRNA. These results suggested that FGF2/FGFR2 signaling might have not only the stage-specific effect on osteoblast differentiation but also indirect effect on osteoclast differentiation.

Disclosures: ***R. Shozui****, None.*

SU193

Dietary Phosphorus Regulates Serum FGF-23 Concentrations and 1,25(OH)$_2$D Metabolism in Mice. F. Perwad*[1], N. Azam*[2], M. Y. H. Zhang[1], T. Yamashita*[3], H. S. Tenenhouse*[4], A. A. Portale*[1]. [1]Pediatrics, University of California San Francisco, San Francisco, CA, USA, [2]Pediatrics, University of Texas Medical Branch, Galveston, TX, USA, [3]Pharmaceutical Research Laboratories, Kirin Brewery Co. Ltd., Takasaki, Japan, [4]Pediatrics and Human Genetics,, McGill University, Montreal, PQ, Canada.

Fibroblast growth factor-23 (FGF-23) is a novel secreted peptide involved in the regulation of phosphate (Pi) homeostasis and vitamin D metabolism. Excess circulating FGF-23 contributes to hypophosphatemia, renal Pi wasting, and suppression of serum 1,25(OH)$_2$D concentrations in humans and mice. Conversely, FGF-23 gene ablation in mice induces the opposite effects on Pi and vitamin D metabolism. Dietary Pi is known to regulate serum Pi, renal tubular transport of Pi, and synthesis of 1,25(OH)$_2$D independently of PTH, although the mechanisms are unknown. To determine whether serum FGF-23 concentration is regulated by dietary Pi intake, we fed intact C57Bl/6 mice diets containing varying Pi content (0.02, 0.6, 1.0, and 1.65%) for 5 days, and measured serum intact FGF-23 and Pi concentrations, renal mitochondrial 1α-hydroxylase (P450c1α) activity, and P450c1α mRNA abundance. Changes in dietary Pi intake from 0.02% to 1.65% induced significant increases in serum FGF-23 concentrations over a 7-fold range, from 9.8 ± 3.3 to 65.4 ± 15.9 pg/ml, and in serum Pi over a 3-fold range, from 1.2 ± 0.2 to 3.4 ± 0.3 mM. Across the range of dietary Pi, serum FGF-23 concentrations varied directly with those of serum Pi ($r = 0.80$, $p<0.001$). Diet-induced changes in serum FGF-23 concentrations were rapid, occurring as early as 4 hours after the change in dietary Pi. With the low Pi (0.02 and 0.6%) diets, renal 1α-hydroxylase activity and P450c1α mRNA abundance were significantly increased relative to values on the higher Pi (1.0 and 1.65%) diets. The concentrations of FGF-23 correlated inversely with 1α-hydroxylase activity and P450c1α mRNA ($r = -0.6$, $p<0.01$) across all diet groups. To determine whether FGF-23 is regulated by dietary Pi per se or by serum Pi concentration, *Npt2* gene-ablated (*Npt2-/-*) and wild-type (WT) mice were fed the above diets. Under each dietary condition except 0.02% Pi, serum FGF-23 concentrations were significantly lower in *Npt2-/-* mice than in WT mice, but these changes were accounted for entirely by the lower serum Pi levels in *Npt2-/-* mice. The present data demonstrate that dietary Pi intake regulates serum FGF-23 levels in mice and suggest that this effect is mediated by changes in serum Pi concentration. Furthermore, the data support the hypothesis that regulation of renal P450c1α gene expression by dietary Pi is mediated by the direct action of FGF-23 on the kidney.

Disclosures: ***F. Perwad****, None.*

SU194

FGF23: The Counter Regulatory Phosphaturic Hormone For Vitamin D-Mediated Hyperphosphatemia. S. Liu, L. D. Quarles. Internal Medicine/The Kidney Institute, University of Kansas Medical Center, Kansas City, KS, USA.

FGF23 is a pathologic phosphaturic factor in several hypophosphatemic disorders, such as TIO, XLH, ADHR, and McCune Albright disease. The regulation and physiological function of FGF23 have not been defined. Vitamin D increases gastrointestinal absorption of calcium and phosphorus. Calcium balance is restored by suppression of the calcemic hormone PTH, which also reduces renal phosphate excretion. Positive phosphate balance would occur in response to Vitamin D without other mechanisms to enhance renal phosphate excretion. In this study we investigated whether FGF23 is a counter-regulatory hormone for Vitamin D. To assess regulation of FGF23 transcription, we isolated a 3550 base pair of 5' flanking region containing the mouse *fgf23* promoter. The mouse *fgf23* promoter contained a transcription start site, a consensus TATA-box, multiple putative cis-acting regulator elements, and had 67% homology with the human promoter over the first 800 base pairs. We subcloned the 3550 base pair mouse promoter region into pGL3-Basic vector to generate a *fgf23* promoter-luciferase reporter construct, p3.5*fgf23*-luc. We transfected the p3.5*fgf23*-luc construct into ROS17/2.8 osteoblasts and evaluated promoter activity in response to 1,25(OH)$_2$-vitamin D$_3$, calcium and phosphorus. We observed a 6-fold increase of promoter activity of p3.5*fgf23*-luc vs. pGL3-Basic in ROS17/2.8 cells. In addition, we found a dose dependent stimulation of *fgf23* promoter activity in response to 1,25(OH)$_2$-vitamin D$_3$. The maximal increase was 2.1 fold at 10^{-8} M 1,25(OH)$_2$-vitamin D$_3$. In contrast, addition calcium or phosphorus to the media had no effect on *fgf23* promoter activity in Ros 17/2.8 osteoblasts. To evaluate the biological significance of vitamin D regulation of *fgf23* promoter activity *in vivo*, we administrated 1,25(OH)$_2$-vitamin D$_3$ at a dosage of 100 pg/gram body weight to 8-week old C57BLK/6J mice by IP injection. We collected serum samples at 24 hours after injection and measured circulating FGF23 levels by ELISA assay. Serum *fgf23* concentrations increased from a basal level 90.0±8.9 pg/ml to 136.4±8.7pg/ml (Mean±SEM) at 24 hours after a single inject of 1,25(OH)$_2$-vitamin D$_3$ ($p<0.01$). Concomitant changes in serum calcium and phosphorus concentrations were not observed. Our data suggests that FGF23 is a counter-regulatory phosphaturic hormone that maintains phosphate homeostasis in the setting of Vitamin D administration.

Disclosures: ***S. Liu****, None.*

SU195

FGF23 Expression during Osteoblast Development and Matrix Mineralization *In Vitro* and *Vivo* Suggest that FGF23 may be a Local Regulator of Bone Formation. C. Ijuin*[1], H. Wang*[2], K. Tanne*[3], J. E. Audin[4], N. Maeda*[2], Y. Yoshiko[2]. [1]Orthodontics Department, Hiroshima University Hospital, Hiroshima, Japan, [2]Oral Growth and Developmental Biology, Hiroshima University Graduate School of Biomedical Sciences, Hiroshima, Japan, [3]Orthodontics and Craniofacial Developmental Biology, Hiroshima University Graduate School of Biomedical Sciences, Hiroshima, Japan, [4]Molecular and Medical Genetics, University of Toronto, Toronto, ON, Canada.

FGF23 is thought to play important pathophysiological roles in such diseases as autosomal dominant hypophosphatemic rickets, tumor-induced osteomalacia and possibly X-linked hypophosphatemic rickets (XLH). Consistent with this, data from Hyp (the homologue of XLH) mice, from treatment with recombinant FGF23, from transgenic mice over-expressing FGF23 in bone and from FGF23-deficient mice all implicate FGF23 in maintenance of serum phosphate levels and $1,25(OH)_2D$ metabolism. Notably, FGF23-deficient mice also show mineralization defects in bone. Together the data led us to hypothesize that FGF23 may have a direct action on bone metabolism. In northern blotting and semiquantitative PCR, FGF23 mRNA was detected in a wide variety of adult and fetal rat tissues including brain, heart, thyroid, femur and calvaria. Interestingly, FGF23 mRNA levels were higher in young adults compared to fetal femur and calvaria. Immunohistochemistry revealed that FGF23 is localized to mature osteoblasts in both trabecular and membranous bones in young adults. No significant labeling was detected in osteoprogenitors, osteocytes or osteoclasts. However, proliferative and prehypertrophic chondrocytes were labeled. We further assessed FGF23 expression during osteoblast development and bone formation in fetal rat calvaria (RC) cell cultures. FGF23 mRNA and protein (by immunocytochemistry) levels significantly increased during osteoblast differentiation and bone nodule formation. Strikingly, however, FGF23 mRNA levels decreased when β-glycerophosphate was added to mature nodule-containing RC cell cultures to induce mineralization. Our results suggest that FGF23 expression is developmentally regulated during osteoblast differentiation and matrix mineralization. Taken together with the results of cartilage immunohistochemistry, our findings strongly suggest that FGF23 may be involved in both endochondral and intramembranous bone formation independently of its systemic actions.

Disclosures: ***C. Ijuin****, None.*

SU196

The Effects of Dietary Phosphate on the Regulation of FGF-23 in Humans. S. M. Burnett, S. Gunawardene*, F. R. Bringhurst, H. Jueppner, J. S. Finkelstein. Endocrine Unit, Massachusetts General Hospital, Boston, MA, USA.

Serum fibroblast growth factor 23 (FGF-23) levels are elevated in phosphate (PO_4) wasting disorders and are detectable in healthy individuals. Knockout of the FGF-23 gene in mice increases serum $P0_4$ levels suggesting that FGF-23 plays a physiologic role in $P0_4$ regulation. To examine the effects of dietary $P0_4$ on FGF-23 in humans, we randomly assigned 60 healthy males and females, age 18-45, to either a low or a high PO_4 diet intervention for 4 days (days 5-8), after a 4 day control diet. During PO_4 deprivation, the dietary PO_4 was 500mg/day and subjects consumed 2.2g of aluminum and magnesium hydroxide QID. During PO_4 loading, dietary PO_4 was 500 mg/day and subjects consumed an additional 2000mg daily of PO_4 supplements. Calcium, sodium, and caloric intakes were kept constant. Fasting blood and urine samples were collected on days 1, 4, 5, 6, 7, 8, and 9 for PO_4, Ca, FGF-23 and other measures, including the fractional excretion of PO_4 ($FePO_4$). FGF-23 was measured using an immunometric assay detecting intact and C-terminal FGF-23 (Immutopics). 24 hour urine samples were collected on days 4-5 and 8-9 for PO_4, creatinine, Na and Ca. We present data (mean ±SE) from the first 45 of 60 subjects. PO_4 loading increased 24 hour urine PO_4 excretion from 442 ±31 to 1140 ±63 mg/day ($p<0.001$); increased $FePO_4$ from 9 ±0.7 to 17 ±0.8% ($p<0.001$); and decreased urinary Ca excretion from 182 ±24 to 91 ±13 mg/day ($p<0.001$). PO_4 deprivation decreased 24 hour urine PO_4 excretion from 500 ±40 to 69 ±14 mg/day ($p<0.001$); decreased $FePO_4$ from 9 ±0.6 to 2 ±0.4% ($p<0.001$); and increased urinary Ca excretion from 177 ±13 to 216 ±18 mg/day ($p<0.01$). Changes in serum FGF-23 are shown in the figure.

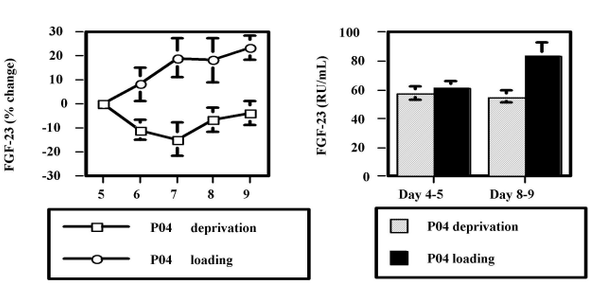

PO_4 loading increased FGF-23 from 61 ±5 to 83 ±10 RU/mL , with an overall 23% increase, ($p<0.02$). PO_4 deprivation had minimal effects on FGF-23 (58 ±4 vs 55 ±4 RU/mL, $p=0.3$). There was, however, a 15% decrease in FGF-23 levels on the 3rd day of PO_4 deprivation. Serum FGF-23 levels and $FePO_4$ correlated weakly ($r = 0.13$). Based on these preliminary data, FGF-23 appears to increase with PO_4 loading, and may promote increased PO_4 excretion. Changes in FGF-23 with PO_4 deprivation are less dramatic and return to baseline over 4 days. FGF-23 may have a greater role in the normal physiologic response to increased dietary PO_4 than the physiologic response to decreased dietary PO_4 .

Disclosures: ***S.M. Burnett****, None.*

SU197

Extra-Skeletal Effects of Systemic Treatment with Basic Fibroblast Growth Factor in Ovariectomized Rats. H. L. Wamsley*, U. T. Iwaniec, T. J. Wronski. Physiological Sciences, University of Florida, Gainesville, FL, USA.

Basic fibroblast growth factor (bFGF) is a pleiotropic mitogen, which, as a potent bone anabolic agent, shows promise as a therapy for osteoporosis. The purpose of this study was to determine systemic side-effects induced by subcutaneous (sc) injection of bFGF. Female Sprague Dawley rats were ovariectomized (ovx) at 3 months of age and left untreated for 2 months to develop osteopenia. The rats were then injected sc for 3 weeks with vehicle (n=9) or with bFGF (n=10) at 1 mg/kg daily. Blood and urine samples were collected for hematologic and biochemical analyses. Kidneys, livers, and proximal tibiae were collected for histology. Data were analyzed using a t-test and expressed as mean ± SD.

SC treatment of ovx rats with bFGF for 3 weeks resulted in a 4-fold increase in osteoblast surface ($P<0.002$) and a 6-fold increase in osteoid surface ($P<0.0004$) compared to vehicle-treated rats. There was no significant difference in body weight between groups, but extra-skeletal effects were detected in bFGF-treated rats. These animals became anemic with a 2.5-fold decrease in packed erythrocyte volume compared to vehicle-treated rats ($P<0.0001$). The bone marrow myeloid:erythroid ratio was higher in bFGF-treated (3.17±1.08) than vehicle-treated rats (1.71±0.23) ($P=0.001$), although there was no significant difference between groups in hematopoietic area of tibial marrow. Hepatic extramedullary hematopoiesis (EMH) that was predominantly myeloid occurred in bFGF-treated rats. There was a 19-fold increase in the number of EMH foci ($P=0.0001$) within the livers of these animals. Glomerular hypertrophy was also found in bFGF-treated rats. The parietal layer of Bowman's capsule was thicker in bFGF-treated (3.42±0.38 μm) than vehicle-treated rats (2.53±0.18 μm) ($P=<0.0001$), and the glomerular diameter was greater in bFGF-treated (114.38±6.28 μm) than vehicle-treated rats (104.24±6.07 μm) ($P<0.003$). However, serum biochemical evidence for renal dysfunction was weak, and there were no urine biochemical signs of dysfunction. There was a small (0.06 mg/dL), but significant ($P<0.05$) increase in serum creatinine in bFGF-treated rats compared to vehicle-treated rats. There were no significant differences between groups in serum albumin, calcium, and phosphorus, nor in urine protein:creatinine ratio. In summary, bFGF-treated ovx rats develop anemia due to a relative increase in myelopoiesis in the bone marrow and liver. The mild glomerular hypertrophy linked with bFGF treatment is not accompanied by strong biochemical evidence for renal dysfunction nor a decrement in general health status. These observations indicate that rats tolerate short-term treatment with bFGF relatively well.

Disclosures: ***H.L. Wamsley****, None.*

SU198

Effect of FGFR3 Anti-sense Oligonucleotides on Bone Growth in an Ex-vivo Long Bone Model and in FGFR3 Mutant Dwarf Mice. M. Liu*[1], Y. Wang*[1], K. Hull*[1], L. Wenrich*[2], C. Reed*[2], S. Davis*[2], J. Siu*[2], H. U. Bryant[1], G. Krishnan[1]. [1]Bone and Inflammation, Eli Lilly and Co, Indianapolis, IN, USA, [2]ISIS Pharmaceutical Inc, Carlsbad, CA, USA.

Achondroplasia (ACH) is the most common form of short-limbed dwarfism in humans. A single gain-of-function point mutation in the FGFR3 (G380R) gene is responsible for 98% of its etiology. Results from various targeting mutations in mice showed that there is a correlation between the mutant FGFR3 expression level and the severity of the dwarfism phenotype. We investigated the bone growth effect of anti-FGFR3 oligonucleotides (ASO) in metatarsal culture, an endochondral ossification model for long bone growth. We are also examining the FGFR3 ASO in a dwarf mouse strain with a mutation in FGFR3. The ASO uptake in metatarsal organ culture was examined using a FITC-labeled ASO. Neonatal rat (P0) metatarsals were cultured with 5 μM of FITC-ASO for 72 hr before processing the image using a fluorescent microscope. Whole-mount imaging indicated there is good cellular uptake of ASO in this metatarsal culture system and the uptake was sustained up to5 days after removal. ASO A is a modified 20-mer targeting rat FGFR3, and ASO B is a control. In vitro assay with ASO A showed dose-dependent target reduction of FGFR3 RNA level with IC50= 20 nM. Pre-natal rat (E20) metatarsals were collected and the mineral deposited on the putative diaphyseal region was measured at the beginning and the end of the treatment. FGFR3 ASO and the control ASO were added to the organs and cultured for 7 days with daily change in media containing treatment agents (n=8). The results indicate that FGFR3 ASO was able to promote mineralization at 10 μM and it is 50% more effective compared to the BMP-4 positive control (25 mg/ml). The FGFR3 ASO also dose-dependently reverses the inhibitory effect of FGF2, a ligand for the FGFR3 signal pathway. In order to examine the growth promoting effect by inhibiting FGFR3 in a genetically altered environment, two 20-mer modified ASOs specific for mouse FGFR3 were designed and characterized. In vitro, they showed a dose-dependent target reduction of FGFR3 RNA with IC50=25 nM. To explore the correlation of bone growth efficacy of ASOs between the ex-vivo model and an in vivo model, studies are designed using a dwarf mouse strain with a FGFR3 point mutation (G369C)**. ** This mouse strain is licensed from Dr. Chu-Xia Deng's laboratory of NIH.

Disclosures: ***M. Liu****, None.*

SU199

Physiological levels of mechanical stress induce *FGF-2* gene and protein expression in MC3T3-E1 osteoblasts. M. Hughes-Fulford[1], C. Li*[2]. [1]Medicine, USCF/ VAMC, San Francisco, CA, USA, [2]Lab of Cell Growth, NCIRE, San Francisco, CA, USA.

Although it is clear that FGF-2 is an important modulator of osteoblast function and bone growth, it's response to normal exercise and it's role in induction of proliferation is not well characterized. In these studies we used short-term physiological g-loading, which results in ERK 1/2 phosphorylation in a dose-dependent manner, with maximum phosphorylation saturating at mechanical loading levels of 120 μstrain (12.g; p< 0.001). We found that a 15-minute pulse of 120 μstrai*n* significantly induced *egr-1, cox-2,* and *fgf-2* over 2-5 fold within 30 minutes with no change in *18S, EP-1* or *TGFβ.* MAPK inhibitors did not affect induction of *fgf-2*, however the induction of *cox-2* and *egr-1* was inhibited by MEK1/2 inhibitor U0126 (p<0.001) but was not affected by MEK1 or p38 MAPK specific inhibitors. We also found that FGF-2 protein and the FGF-2 receptor were significantly increased in osteoblasts after g-loading. Syntheses of all three isoforms of FGF-2 (24kD, 22kD and 18kD) were significantly increased in a 12-g gravity vector (p<0.001). Using immunoflorescence we found that much of the FGF-2 protein was translocated to the nucleus within an hour. The long-term consequence of a single 15-minute gravity pulse was a 200% increase in cell growth (p<0.001) where addition of 2ng of recombinant FGF-2 caused an 80% increase (p<0.01) in proliferation when compared to quiescent cells. These studies suggest that physiological levels of mechanical stress induce immediate-early gene expression and growth in MC3T3-E1 osteoblasts. Induction of *egr-1, cox-2* was primarily mediated through an ERK1/2 mediated pathway, however induction of *fgf-2* was independent of the MAPK signal transduction.

Disclosures: ***M. Hughes-Fulford****, None.*

SU200

TGF-*B* Stimulates Secretion of Cytokines Involved in Bone Destruction from Metastatic Renal Cell Carcinoma. S. Kominsky*, M. Doucet*, K. Weber. Orthopaedic Surgery, Johns Hopkins University School of Medicine, Baltimore, MD, USA.

The TGF-*B* signaling cascade has been implicated in bone metastasis. A vicious cycle of tumor growth and bone destruction has been described in metastatic breast cancer where factors produced by tumor cells enhance osteoclast-mediated bone lysis which, in turn, releases factors that stimulate tumor cell growth. We hypothesized that the TGF-*B* signaling cascade was also important in tumor growth and resultant bone destruction in metastatic renal cell carcinoma (RCC).

Eighteen human samples of RCC bone metastasis were evaluated for the expression of TGF-*B*, TGF-*B*RI, and TGF-*B*RII by immunohistochemistry. Human bone-derived RCC lines, RBM1-IT4, RBM23, and RBM17, were used for western blotting, proliferation studies, and ELISA. For western blotting, cells were probed with antibodies to ERK, phospho-ERK, p38, phospho-p38, Smad2, and phospho-Smad2 with and without the addition of 5 ng/ml of TGF-*B*.

The results revealed that all human tissue samples expressed TGF-*B*, TGF-*B*RI and TGF-*B*RII. There was no significant change in tumor cell proliferation with the addition of 5ng/ml TGF-*B* on MTT studies. Western blotting revealed high constitutive phosphorylation of ERK and p38 that was not affected by TGF-*B*. However, there was a 17- to 62-fold increase in Smad2 phosphorylation that varied by cell line with the addition of 5 ng/ml of TGF-*B*. ELISA revealed very high secreted levels of PDGF-AA (276 pg/10^5 cells) and VEGF (328 pg/10^5 cells) in the RBM1-IT4 cell line that was increased 1.3 to 2-fold with the addition of 2.5 ng/ml of TGF-*B*. Lower levels of IL-6 (1 pg/10^5 cells) were present in two cell lines but could be stimulated 2.3 to 4.6-fold by TGF-*B*. Neutralizing antibodies diminished the effect of TGF-*B*. No TNF-*a* or IL-1*B* secretion was observed.

Based on this preliminary data, we conclude that the TGF-*B* signaling pathway is active in both bone-derived human tissue and cell lines from metastatic RCC. The TGF-*B* dependent stimulation of cytokines known to be involved in angiogenesis and osteoclast-mediated bone destruction may provide targets for future therapy.

Disclosures: ***K. Weber****, None.*

SU201

Inhibition of Endogenous TGF-b Signaling Accelerates Maturation of Osteoblast Differentiation from Mesenchymal Progenitors. S. Maeda[1], M. Hayashi*[1], K. Shirakawa*[1], S. Komiya[2], T. Imamura*[1], K. Miyazono*[1]. [1]Department of Biochemistry, The JFCR Cancer Institute, Tokyo, Japan, [2]Department of Orthopaedic Surgery, Graduate School of Medicine and Dentistry, Kagoshima University, Kagoshima, Japan.

Transforming growth factor-b (TGF-b), one of the most abundant cytokines in bone matrix, has positive and negative effects on bone formation, although the molecular mechanisms of these effects are not fully understood. Bone morphogenetic proteins (BMPs), members of the TGF-b superfamily, induce bone formation in vitro and in vivo. Here, we show that osteoblastic differentiation of mouse C2C12 cells was greatly enhanced by the TGF-b type I receptor kinase inhibitor SB431542. This promotive effect of the compound was prominent after 48 hours of induction. Endogenous TGF-b was found to be highly active and induce expression of inhibitory Smads(Smad6/7) during the maturation phase of osteoblastic differentiation induced by BMP-4. SB431542 suppressed endogenous TGF-b signaling and repressed the expression of inhibitory Smads during this period, while the acceleration of BMP signaling was observed only in SB431542-treated cells. The inhibition of TGF-b signaling and Smad6 by SB431542 seemed to be responsible for the enhancement of BMP signaling, because siRNA of Smad3 and Smad6 mimicked the effect of SB431542. SB431542 also induced production of alkaline phosphatase and bone sialoprotein, and matrix mineralization of human mesenchymal stem cells. Moreover, SB431542 accelerated bone growth in organ culture of mouse embryo metatarsal bones. Thus, signaling cross-talk between BMP and TGF-b pathways plays a crucial role in regulation of osteobtastic differentiation, and TGF-b inhibitors may be invaluable for treatment of various bone diseases by accelerating BMP-induced osteogenesis.

Disclosures: ***S. Maeda****, None.*

SU202

TGFß-induced Osteoblastic Cell Proliferation Is mediated by Prostaglandin-dependent Activation of Extracellular-signal-Regulated Kinase. C. Ghayor*, A. Rey*, J. Caverzasio. Rehabilitation and Geriatrics, Service of Bone Diseases, University Hospital of Geneva, Switzerland.

TGFß is a major coupling factor between bone formation and bone resorption and is known to stimulate osteoblastic proliferation and matrix deposition. The cellular and molecular mechanisms involved in these effects are incompletely understood. Activation of Smad and of mitogen-activated protein (MAP) kinase pathways have been shown to be involved in mediating TGFß effects on osteoblasts but the precise function of each pathway remains unclear.

In the present study, we investigated the role of MAP kinases in mediating cell proliferation induced by TGFß in MC3T3-E1 cells and calvaria-derived primary cultured osteoblasts.

TGFß (2.5 ng/ml) induced activation of the three MAP kinases ERK (extracellular-signal-regulated kinase), p38 and JNK (c-Jun-NH2-terminal kinase) in MC3T3-E1 cells. Surprisingly, whereas activation of Smad2 was rapid and maximal after 15 min incubation, activation of MAP kinases was delayed. p38 stimulation was detected after 1 h exposure whereas activation of ERK and JNK was only detected after 3 h suggesting indirect activation of MAP kinases by TGFß. Associated with this effect, TGFß enhanced cell proliferation by about two fold in both MC3T3-E1 and calvaria-derived osteoblastic cells. Since prostaglandins (PGs) have been reported to mediate some of the TGFß effects on osteoblatic cells, we investigated the influence of indomethacin (indo), a specific PGs synthesis inhibitor, on cell proliferation and signaling induced by TGFß. Indo (10 μM) completely blunted cell proliferation induced by TGFß and markedly reduced activation of MAP kinases without influencing Smad2 phosphorylation. EP4A (5-10 μM), a specific PGE2 receptor antagonist also blunted TGFß-induced osteoblastic proliferation. In addition to these effects, PGE2 (1 μM) rapidly activated MAP kinases in MC3T3-E1 cells (< 15 min) and increased cell proliferation by about 2 fold. The role of each MAP kinases in mediating TGFß- and PGE2-induced cell proliferation was investigated using selective inhibitors. U0126 (10 μM), a specific inhibitor of the ERK pathway, completely blocked both TGFß- and PGE2-induced cell proliferation whereas SB203580 (10 μM) and SP600125 (20μM), which are selective inhibitors of respectively p38 and JNK pathways had no effect.

In conclusion, data presented in this study strongly suggest that activation of the ERK pathway by prostaglandins mediates cell proliferation induced by TGFß in osteoblastic cells.

Disclosures: ***J. Caverzasio****, None.*

SU203

The Role of Smad3 in TGF-ß Inhibition of Adipocyte Differentiation of Marrow Stromal Cells. S. Zhou[1], S. Cao*[2], J. Greenberger[2], M. Epperly*[2], S. Lechpammer[1], J. Glowacki[1]. [1]Orthopedic Surgery, Brigham and Women's Hospital, Boston, MA, USA, [2]University of Pittsburgh Medical Center, Pittsburgh, PA, USA.

Marrow stromal cells (MSCs) have the potential to differentiate to lineages of several mesenchymal tissues, including fat, cartilage, bone, tendon, and muscle. Here, we identified pathways involved in TGF-B inhibition of adipocyte differentiation of MSCs.

Testing different adipocytogenic supplements showed that hMSCs express Smads 2,3,5, and 9; they differentiate to adipocytes; and they express PPARγ2 and lipoprotein lipase (LPL) when cultured in MEM-a, 1% FBS-HI, 1 μM dexamethasone, 0.5 mM 1-methyl-3-isobutylxanthine, ± 10 μg/ml insulin (DM±I). Murine MSCs express PPARγ2 in DMEM, 1% FBS-HI with DM+I. Oil red-O staining, RT-PCR, Western blot, and macroarrays were used to assess TGF-ß effects on adipocytogenesis.

In human MSCs, TGF-ß1 downregulated adipocyte genes (PPARγ2, adipsin, LPL, PI3K, etc) and upregulated TGFß/Smad target genes (PAI-1) and Wnt genes (Wnt2, 4, 5a, 7a, 10a, LRP5). Western blot showed that TGF-ß1 increased the stability of Wnt signal molecule ß-catenin. TGF-ß1 and theWnt-mimetic LiCl synergistically inhibited adipocyte differentiation.

Because of the importance of Smad signaling in TGF-ß's effects, we studied both long-term bone marrow cultures (LTBMC) and MSCs from $Smad3^{+/+}$ and $^{-/-}$ mice. LTBMCs from both achieved confluence of the adherent compartment after 8 w in McCoy's 5A medium (25% FBS). After 22 w, the average number of non-adherent cells in $Smad3^{-/-}$ (2.6 ± 0.5 x 10^6 cells) was 288% greater (p = 0.0316) than in $Smad3^{+/+}$ (0.9 ± 0.3 x 10^6 cells) LTBMCs. The number of hematopoietic CFU-GEMM colonies (d 14) in $Smad3^{-/-}$ cultures (188 ± 8.7) was 1250% greater (p<0.0001) than in $Smad3^{+/+}$ cultures (15.3 ± 2.3). Microscopic inspection at 27 weeks showed that more (16.5%, p<0.001) $Smad3^{-/-}$ adherent cells contained lipid droplets (6.6 ± 0.7%), compared with $Smad3^{+/+}$ adherent cells (0.4 ± 0.2%). Because these findings indicate differences in hematopoiesis between $Smad3^{+/+}$ and $^{-/-}$ LTBMCs, we measured adipocyte differentiation in $Smad3^{+/+}$ and $^{-/-}$ MSCs. There were two notable differences in adipocyte development in isolated MSCs. First, there was more extensive (37-fold) adipocyte differentiation in $Smad3^{-/-}$ than $Smad3^{+/+}$ MSCs; this indicates that Smad3 is a critical inhibitor of adipocyte differentiation. Second, there was a 7-fold attenuation of TGF-ß's inhibition of adipogenesis in cells lacking Smad3

In conclusion, Smad and ß-catenin are involved in the inhibitory effects of TGF-ß on adipocyte differentiation in human and murine marrow stromal cells. Use of $Smad3^{-/-}$ murine MSCs shows a key role of that mediator in TGF-ß inhibition of adipocyte differentiation.

Disclosures: ***S. Zhou****, None.*

SU204

Regulation of MEIS2 Transcription Factors during Estrogen Deficiency, a Potential Mechanism for Regulation of CIITA. N. Kirma, M. N. Weitzmann, K. Dark*, W. Qian, R. Pacifici. Division of Endocrinology, Metabolism and Lipids, Emory University, Atlanta, GA, USA.

We have recently demonstrated that a central event in the initiation of bone destruction during estrogen deficiency is the upregulation of the key regulator of MHCII expression, CIITA. CIITA induction leads to enhanced antigen presentation and expansion of the pool of TNF producing T cells. This enhanced pool of TNF synergizes with amplifies RANKL induced osteoclast formation and activity. The upregulation of CIITA is mediated in part by a decrease in the level of TGF-beta. New lines of evidence suggest that TGF-beta may both stimulate and suppress gene transcription by the recruitment of co-repressors and co-activators to TGF-beta responsive promoters. One such co-repressor is TGIF, while MEIS2 is a transcriptional co-activator that apposes TGIF mediated repression by competing with it for the same DNA binding site. Western blot analyses confirmed the expression of TGIF proteins in bone marrow monocytes (BMM), a population in which CIITA is upregulated in the bone marrow by ovariectomy (ovx). Likewise, DNA-binding isoforms of MEIS2 (c and d) and MEIS2e, an endogenous dominant negative isoform, were detected in BMM by western blotting. To test the effect of estrogen deficiency on the expression of TGIF and MEIS2 isoforms we performed ovx or sham operations on C57BL6/J mice and isolated BMM after 2 week. The data showed a decrease in MEIS2e levels in ovx BMM, suggesting that estrogen deficiency may upregulate the DNA binding activity of stimulatory MEIS2 isoforms by downregulating the levels of inhibitory MEIS2e. No differences in the concentrations of TGIF or MEIS2 c and d isoforms were observed. To test the balance of DNA binding activities between TGIF and MEIS2 in ovx BMM, we performed EMSA and antibody supershift studies using a commercial consensus sequence containing a binding site for TGIF/MEIS2. The data revealed an increased level of MEIS2 complex bound to the consensus probes in ovx relative to sham BMM. No binding of TGIF to the probe was observed under either sham or ovx conditions. Together, the data suggest that in ovx BMM gene transactivation through TGIF/MEIS2 consensus sequences may be stimulated via the enhanced binding of stimulatory MEIS2 species, a consequence of downregulation of the inhibitory isoform MEIS2e.

Disclosures: ***N. Kirma****, None.*

SU205

Role of TGF-b in the Early Steps of Chondrogenesis. S. S. Dong*, H. Seo*, R. Serra. Cell Biology, University of Alabama at Birmingham, Birmingham, AL, USA.

The differentiation of mesenchymal cells into chondrocytes takes place along a multi-step pathway and multiple cytokines are known to influence discrete steps in the pathway. A number of studies suggest that TGFb plays a critical role in the regulation of the cartilage differentiation. To investigate the role of TGFb in regulating chondrogenesis, we generated a recombinant adenovirus containing a truncated TGFb type II receptor (DNIIR) that acts as a dominant negative to block TGFb signaling. Limb bud micromass cultures isolated from E11.5 mouse embryos were infected with DNIIR and rapidly lost their responsiveness to TGFb. DNIIR infection of limb micromass cells caused decreased alcian blue staining and reduced nodule formation in vitro, suggesting that condensation and chondrogenesis require TGFb signaling. Treatment with TGF-b resulted in increased alcian blue staining early and inhibition of alkaline phosphatase activity in later cultures. In addition, we examined whether TGFb modulates Sox9 expression. Sox9 is well known as a potent transcription factor in activating the expression of chondrocyte marker genes. We demonstrate that there are no changes in Sox9 expression or activation in response to TGFb, as measured by RT-PCR and IP/Western analysis. In summary, we conclude that TGFb signaling is an important regulator of chondrogenesis, however, TGFb does not regulate Sox9 expression or activation. The mechanism by which TGFb promotes chondrogenesis is currently unclear. Understanding the early steps of cartilage development should provide valuable insights into mechanisms for regenerating cartilage.

Disclosures: ***S.S. Dong****, None.*

SU206

Connective Tissue Growth Factor (CTGF) Mediates Condensation of Mesenchymal Stem Cells Induced by TGF-β1. J. J. Song*[1], R. A. Kanaan[2], F. F. Safadi[1], S. N. Popoff[1]. [1]Anatomy and Cell Biology, Temple University School of Medicine, Philadelphia, PA, USA, [2]Orthopaedics, University of Pennsylvania School of Medicine, Philadelphia, PA, USA.

Cellular condensation is a stage of skeletogenesis involving the congregation of mesenchymal stem cells and is considered to be a critical step in this process. CTGF is a matricellular protein that has been shown to be highly expressed in cellular condensations by *in situ* hybridization studies during embryonic development. Interestingly, CTGF-deficient mice demonstrated a misshapen skeleton attributed to endoskeletal abnormalities and abnormal cartilage development. CTGF has been found to be highly up-regulated with TGF-β stimulation, and CTGF has also been found to enhance receptor binding of TGF-β. We propose that CTGF may promote condensation through the TGF-β pathway, a known regulator of cellular condensation. In this study, we established high-density micromass cultures using the C3H10T1/2 murine mesenchymal stem cell-line. These cells have been shown to form prechondrocytic nodules following TGF-β1 treatment. C3H10T1/2 cells were micromass cultured in HamF12 media with 10% fetal bovine serum and with 1 ng/ml TGF-β1 treatment. Under these conditions, cellular condensations (nodules) were formed within 72 hours. Next, we down-regulated CTGF expression using an antisense CTGF oligonucleotide, confirming expression levels by RT-PCR and Western blot analyses. Attenuation of CTGF expression was sufficient to inhibit nodule formation induced by TGF-β1 treatment. These results were confirmed using CTGF siRNA, an even more effective method to silence CTGF expression. Knock down of CTGF protein expression was decreased from 40-50% using the antisense oligonucleotide up to 80-90% using siRNA compared to TGF-β1-treated controls. Micromass cultures transfected with CTGF siRNA also showed significant inhibition of cellular condensation induced by TGF-β1. In addition, the levels of fibronectin, an extracellular matrix protein known to play a role in cellular condensation, was down-regulated by CTGF siRNA treatment in micromass cultures. In conclusion, these results demonstrate that CTGF is an important mediator of TGF-β-induced cellular condensation *in vitro*, and supports a role for CTGF in proper skeletal development. The precise nature of the mechanism of action of CTGF in promoting cellular condensation will be elucidated with further experimentation.

Disclosures: ***J.J. Song****, None.*

SU207

Alpha V Beta 3 Integrin Ligands Enhance Volume-sensitive Calcium Influx in Mechanically Stretched Osteocytes. A. Miyauchi[1], M. Gotoh[2], K. Notoya[2], H. Sekiya[3], Y. Takagi[1], K. Jinnai*[1], Y. Yoshimoto[1], T. Sugimoto[4], K. Chihara[4], T. Fujita[5], Y. Mikuni-Takagaki[6]. [1]National Hyogo-Chuo Hospital, Sanda, Japan, [2]Pharmaceutical Research, Takeda Chemical Industries, Osaka, Japan, [3]School of Dental Medicine, Tsurumi University, Yokohama, Japan, [4]Endocrinology/Metabolism, Kobe University Graduate School of Medicine, Kobe, Japan, [5]Ca Research Institute, Kishiwada, Japan, [6]Oral Biochemistry, Kanagawa Dental College, Yokosuka, Japan.

Osteocytes transmit load-induced signals, which result in bone formation. Our previous report illustrated that mechanosensing in rat osteocytes depends on a volume-sensitive calcium influx pathways that is regulated by activation of stretch activated cation channels (SA-Cat), further suggesting that osteocytes utilize contact with the bone matrix upon stretching. $\alpha_V \beta_3$ integrin (vitronectin receptor), highly expressed in osteocytes (Bennett JH et al., 2001), is also reported being upregurated by mechanical strain in osteoblasts (Cavalcant-Adam EA et al., 2002). Therefore, we examined whether specific cell-matrix interaction regulates volume-sensitive calcium influx pathways in osteocytes. Rat osteocytes adhered to the substrates, type I collagen (COL I), fibronectin (FN), osteopontin (OPN), vitronectin (VN), laminin (LN), and thrombospondin (TSP). The cells fully spread on FN, COL I, VN and OPN,and the adhesion to OPN and VN was almost completely inhibited by a GRGDS peptide. Stretch loading by swelling rat osteocytes in hypoosmotic solution (182 mosm, normal 363mosm) induced rapid and progressive increase (100±15nM above basal (n=16)) of cytosolic calcium concentration, $[Ca^{2+}]i$, which was detected by using video-image analysis with fura-2. Cells on FN, LN, TSP-coated coverslips responded less to the hypotonic stimuli (76, 50, and 43% $[Ca^{2+}]i$ increase, respectively) compared to the control cells on Matrigel (MG). In contrast, the cells on OPN, VN, and COL I responded more or equally well (250, 150, and 100% $[Ca^{2+}]i$ increase, respectively) to the hypotonic stimuli. Addition of a soluble GRGDS peptide, not a GRGES peptide at 200 μg/ml prior to the hypotonic stimulation of the cells, enhanced the hypotonic stimulation of $[Ca^{2+}]i$ by 230%. Similarly, specific soluble $\alpha_V \beta_3$ ligand echistatin (10^{-9}M to 10^{-7}M) enhanced hypotonic stimulation of $[Ca^{2+}]i$ by as much as 240%. Perturbation of actin filament by cytochalasin D treatment inhbited hypotonic stimulation of $[Ca^{2+}]i$ by 70%. These data support the notion that the integrin signaling interact with that of mechanosensing to regulate SA function in osteocytes. $\alpha_V \beta_3$ integrin was suggested to play a key role in this process.

Disclosures: ***A. Miyauchi****, None.*

SU208

Cyclooxygenase-2 Inhibitor Suppresses Cancellous Bone Restoration in Tibia in Association with Restriction of Osterix Expression in Reloading Period after Hindlimb Elevation of Mice. K. Nakai*, S. Tanaka*, A. Sakai, M. Tanaka*, H. Otomo*, M. Nagashima*, S. Akahoshi*, T. Mori, T. Takeda*, Y. Katae*, H. Hirasawa*, T. Nakamura. Orthopaedic Surgery, School of Medicine, University of Occupational and Environmental Health, Kitakyusyu, Japan.

To clarify the role of cyclooxygenase-2 (COX-2) in acute recovery of trabecular bone mass during the reloading state after unloading, 108 male C57BL/6J mice, at 8 weeks of age, were divided into two weight-matched groups; ground control (GC) and reloading (RL). The hindlimbs of GC were normal loaded through the experimental period and those of RL were reloaded after 7-day tail-suspension. At the 8th experimental day, GC was divided into three groups; GC baseline, GC+vehicle administration (Veh), and GC+Celecoxib (selective COX-2 inhibitor) administration (Cel). RL was also divided into RL baseline, RL+Veh and RL+Cel. Tibias of GC and RL baseline were harvested at the 8th experimental day, and tibias of other groups were harvested at the15th and 22nd days, and 24 and 48 hours after reloading. Celecoxib was given 30 mg/kg body weight twice a day, and started 3 hours before reloading. At the 8th day, bone volume (BV/TV) of the proximal tibia in RL baseline significantly decreased compared with that in GC baseline. At the 22nd day, BV/TV in RL+Veh was restored to the same level of that in GC+Veh, but that in RL+Cel was not restored. At the 15th day, bone formation rate (BFR/BS) in RL+Veh and RL+Cel increased compared with that in GC+Veh. Even though, there was significant difference in BFR/BS between RL+Cel and RL+Veh. There were no differences in the respective values of the osteoclast surface (Oc.S/BS) and the osteoclast number (Oc.N/BS) among these four groups at the 15th and 22nd days. Quantitative RT-PCR was performed using bone marrow cells of tibias after 24 and 48 hours from reloading. After 24 hours, osterix mRNA expression in RL+Veh showed 2-fold increase compared with GC that in baseline but the expression in RL+Cel did not increased. c-fos expression in RL+Veh showed 8- and 10-fold increase after 24 and 48 hours, respectively, but the expression in RL+Cel did not increased. The expressions of bmp2 and dlx5 in RL+Veh did not change at 24 and 48 hours, and those expressions in RL+Cel increased at 48 hour. These results suggest that COX-2 inhibitor suppresses cancellous bone restoration in tibia in association with restriction of osterix expression and enhances bmp2 and dlx5 expressions.

Disclosures: ***K. Nakai****, None.*

SU209

The Reduced Osteogenic Potential after Skeletal Unloading Relates to the Decreased Expression of PECAM-1 in Bone Marrow Cells in Mice. M. Sakuma-Zenke*[1], A. Sakai[1], S. Nakayamada*[2], N. Kunugita*[3], S. Uchida[1], S. Tanaka*[1], T. Mori[1], Y. Tanaka[2], T. Nakamura[1]. [1]Department of Orthopaedic Surgery, University of Occupational and Environmental Health, Kitakyushu, Japan, [2]First Department of Internal Medicine, University of Occupational and Environmental Health, Kitakyushu, Japan, [3]Department of Health Information Science, University of Occupational and Environmental Health, Kitakyushu, Japan.

Appropriate vascularization is emerging as a prerequisite for bone development and regeneration. We tested the hypothesis that skeletal unloading reduces osteogenic potential by inhibiting angiogenesis and/or vasculogenesis in bone marrow cells. Eight-week-old male mice were assigned to three groups as follows, after acclimatization for one week: ground control (GC), tail-suspension (TS) and reloading after 7-day TS (RL). Bilateral tibial and humeral samples were used for analyses. MC3T3-E1, mouse osteoblastic cell line, and EOMA and ISOS-1, mouse endothelial cell lines, were also used. The flow cytometric analysis revealed that one-week of TS significantly decreased the expression of platelet endothelial cell adhesion molecule-1 (PECAM-1, CD31) in tibial bone marrow cells, but did not those of angiopoietin-1, angiopoietin-2, Flk-1 (vascular endothelial growth factor receptor), and VE-cadherin. The expression of PECAM-1 in tibial marrow cells was significantly reduced at day 3 of TS and thereafter still showed lower level to day 7 of TS, compared to that at day 7 of GC. This decreased expression of PECAM-1 recovered to the GC level by 5-day reloading after 7-day TS. However, the expression of PECAM-1 in humeral marrow cells after TS and RL constantly kept the same level as that of GC. In bone marrow cell culture, the formation of alkaline phosphatase (ALP)-positive colony forming units-fibroblastic was significantly reduced under the medium condition of the supplementation of anti-PECAM-1 antibody, compared under that of immunoglobulin G. ALP production of cultured MC3T3-E1 was enhanced in combination with EOMA, expressing PECAM-1, but not in combination with ISOS-1, unexpressing PECAM-1. The anti-PECAM-1 antibody inhibited the increase in ALP production under the coculture with EOMA. In conclusion, our data demonstrate that the reduced osteogenic potential after skeletal unloading closely relates to the decreased expression of PECAM-1 in bone marrow cells. We speculate that the loss of ostegenic potential due to skeletal unloading may be related to the suppression of PECAM-1 signaling on endothelial cellular surface.

Disclosures: ***M. Sakuma-Zenke****, None.*

SU210

Bio-imaging of Intracellular Nitric Oxide in Single Cells after Mechanical Loading. A. Vatsa*[1], D. Mizuno*[2], T. H. Smit*[3], C. F. Schmidt*[2], F. C. MacKintosh*[4], J. Klein-Nulend[1]. [1]Oral Cell Biology, ACTA-Vrije Universiteit, Amsterdam, Netherlands, [2]Biophysics and Complex Systems, Vrije Universiteit, Amsterdam, Netherlands, [3]Physics and Medical Technology, Vrije Universiteit Medical Centre, Vrije Universiteit, Amsterdam, Netherlands, [4]Theoretical Physics, Vrije Universiteit, Amsterdam, Netherlands.

Osteocytes are the professional mechanosensors of bone. The strain-derived interstitial fluid flow through the lacuno-canalicular porosity seems to mechanically activate them, which may be related to mechanical adaptation of bone. After mechanical loading they produce nitric oxide (NO) that likely affects osteoblasts and osteoclasts. Since the mechanosensitive part of the osteocytes (protrusions or cell body), is unknown, information is needed on the single osteocyte's response to localized mechanical loading. Here we studied intracellular NO production in single MC3T3-E1 osteoblasts after mechanical loading using DAR 4M AM rhodamine.

DAR 4M AM rhodamine loaded, surface-attached MC3T3-E1 cells were subjected to oscillatory mechanical loading (144-560 pN, 0.5-3 Hz, 1 min) through cell-attached colloid particles using optical tweezers. DAR 4M AM is membrane-permeable and traps NO forming a stable, fluorescent compound intracellularly, visible with a rhodamine filter.

Non-loaded cells showed detectable basal NO levels. Mechanical loading increased fluorescence by +21% as compared to the non-loaded fluorescence levels (Fig. 1). Loosely surface-attached cells showed higher deformation and increased fluorescence +25% with lower force (144pN) as compared to firmly-attached cells, which required larger forces (310-560 pN) for deformation showing +18% increase.

NO is essential for loading-induced bone formation, and is a meaningful parameter for measuring bone cell activation after mechanical loading. Its short half-life (0.1-5 s) makes its online detection difficult. Here we show that the NO upregulation in a single bone cell after a localised and quantified mechanical stimulus can be determined using DAR 4M AM rhodamine. This model allows further study on the mechanosensitivity of different parts of a single osteocyte.

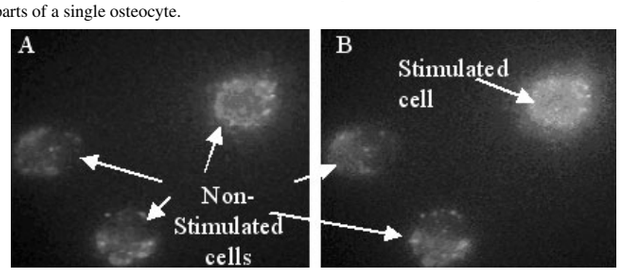

Fig.1. Intracellular NO detection by fluorescence in a single cell, A, before, B, 20 min after mechanical loading

Disclosures: ***A. Vatsa****, None.*

SU211

Agent Based Model of Real-Time Signaling in Osteocytic Networks-Implications for Downstream Mechanotransduction Events. B. J. Ausk*, T. S. Gross, S. Srinivasan. Orthopaedics and Sports Medicine, University of Washington, Seattle, WA, USA.

Recently, we observed that insertion of 10-s rest (unloaded intervals) between each load cycle lowered the threshold strain-magnitude (by 30%) and load cycle numbers (5-fold) required to initiate bone formation. Using approaches uniquely suited for analysis of complex adaptive systems, we explored the cell level basis for our counterintuitive observations. Specifically, we developed agent based models of real-time signaling induced in osteocytic networks by mechanical stimuli. The behavior of osteocytic cells were modeled as follows: 1) a threshold level of stimulus magnitude was required to initiate cell activity, 2) cell-cell signaling initiated cell activity if signals exceeded a threshold, 3) cell activity was modulated based on 'metabolic' stores and the rate at which stores were recovered. In the context of these functions, the response of an osteocytic network to cyclic and rest-inserted (10-s) stimuli was simulated. Network response (average of cell responses) was monitored across time, and over a range of load cycles and stimuli magnitudes. As one reporter of the network signaling, the real-time response was integrated over a specified number of load cycles ('network power'). Real-time network response to cyclic stimuli consisted of a large magnitude transient followed by low-level steady state fluctuations. In contrast, enhanced and sustained responses were elicited by rest-inserted loading (multiple peaks). To relate these distinct real-time signaling events (sec) to *in vivo* bone formation (wks), we assumed that network power in response to 50 cycles of cyclic stimuli would represent the 'threshold' level of signaling required before bone formation events were initiated downstream. Interestingly, and paralleling *in vivo* observations, network power in response to 10 cycles of rest-inserted stimuli was similar (~ 5% increase) to that induced by 50 cycles of cyclic stimuli (i.e., similar response despite 5-fold decrease in load cycles). As well, network power in response to 50 cycles of rest-inserted loading was dramatically enhanced compared with cyclic stimuli (~ 500%). This model observation also mirrored the ability of rest-inserted loading to substantially enhance bone formation *in vivo* (nearly 3-fold compared with identical magnitude/load cycles of cyclic stimuli). Given these relations, and the influence of real-time signaling events (e.g., Ca^{2+} fluctuations) in controlling down-stream gene transcription events, we speculate that the enhanced and sustained real-time signaling induced in osteocytic networks may underlie the osteogenic potency of rest-inserted loading regimens.

Disclosures: ***B.J. Ausk****, None.*

SU212

Evidence That BMD Response To Mechanical Loading (ML) In Vivo Is Caused By Acute Up-Regulation Of Both Bone Formation (BF) Genes And Down Regulation Of Bone Resorption (BR) Genes. C. Kesavan*, S. Mohan, S. Oberholtzer*, D. J. Baylink. JLP VAMC, Loma Linda, CA, USA.

Increase in bone mass in response to skeletal loading is an important adaptive response. It is likely that regulation of both osteoblast (OB) and osteoclast cell functions are involved in producing an optimal response to a given skeletal load. To evaluate the OB and osteoclast cell response to mechanical input, we tested the hypothesis that in vivo ML by 4-point bending leads to acute reduction in the expression of BR genes and a progressive increase in the expression of BF marker genes. We measured expression changes by real time PCR in 12 genes that relate to BF and BR at d2, 4, 8 and 12 of training in 10-wk old C57Bl/6J mice. A 9N load at 2Hz (36cycles) was applied on the right tibia by a 4 point bending device and the left tibia was used as an internal control. 12 days of loading caused a highly significant ($p<0.001$) increase in BMC (33%), volumetric BMD (14%) and total area (26%) as measured by pQCT in the loaded bone compared to corresponding unloaded bone. Measurement of gene expression changes by real time PCR at d2 showed significant ($p<0.01$) change in the down-regulation of BR makers MMP and TRAP by 2 and 4-fold with no change in the expression of BF genes compared to control. 4-days of loading caused down regulation of BR genes MMP-9, TRAP and Sodium-potassium pump by 3, 5, and 2-fold respectively ($p<0.0001$). In contrast, the expression of type-I collagen (Col 1) and bone sialoprotein (BSP) was increased by 2-fold as expected. After 8 days of loading, the expression of TRAP was decreased by 3-fold while expression of Col 1, ALP, BSP, and osteocalcin (OC) was increased by 3-fold. Surprisingly, the expression level of BR marker genes were increased after 12 days of loading (MMP-9 by 12 fold and TRAP by 7.5 fold) which may reflect loading induced increase in remodeling. In contrast, expression of Col 1, BSP, ALP and OC increased by 4.2, 8, 6 and 4 fold respectively ($p<0.001$). In order to determine if gene expression change can be used as a surrogate for bone anabolic response, we determined the correlation between expression levels and BMD changes and found total BMD measured by pQCT showed significant correlation with BSP ($r=0.54$, $p<0.01$) and OC ($r=0.66$, $p<0.01$) expression. Conclusions: 1) ML by 4-point bending increased both size and volumetric BMD after 12 days; 2) The expression levels of BF genes were increased throughout the loading period; 3) This is the first report to demonstrate acute reduction in BR marker genes in response to loading. 4) The increase in expression of BR genes at day 12 may indicate loading induced remodeling of bone. 5) Our findings demonstrate the usefulness of gene expression changes as surrogate marker for bone anabolic response to ML.

Disclosures: ***C. Kesavan****, None.*

SU213

Bone Anabolic Response To A Mechanical Load Is A Complex Trait And Involves Bone Size, Material Bone Density (mBMD) And Volumetric Bone Density (vBMD) Phenotypes. C. Kesavan*, S. Mohan, J. Wergedal, D. J. Baylink. JLP VAMC / LLU, Loma Linda, CA, USA.

Different mouse strains show large variations in BMD in response to the same mechanical load, suggesting that bone response to mechanical loading is genetically regulated. To test the hypothesis that the mechanical load response is a complex trait, we applied 4-point bending to the tibia to evaluate response in six different strains of mice in order to select the two strains with the most different respnse. These were C3H/HeJ (C3), the poor responder, and C57BL/6J (B6), the good responder. These two parents were used to produce 300 F2 mice. The 4-point bending method utilized a 9N load (3500 ue, upper limit of physiological strain) at 2Hz for 36 cycles and was applied for 12 days. Two days after the last load, skeletal changes were evaluated by pQCT. In these F2 mice, all three phenotypes (change in bone size, mBMD and vBMD) showed Gaussian distributions, consistent with complex traits. Heredity indexes ranged from 86-70%. The vBMD data demonstrate that some F2 mice had decreased bone density in response to the load whereas other mice gained as much as 20% in vBMD of the tibia. The other phenotypes ranged from -5 to +5% for mBMD, and -10 to +30% for bone size in the F2 mice. Cortical BMD reflects material bone mineral density (mBMD) since vascular canal volume in our sampling site is too low to alter cortical BMD (less than 1% of the bone volume). Our data on mBMD of bone formed prior to loading indicates for the first time that mechanical loading increases mBMD. We next determined if the magnitude of bone anabolic response to 4-point bending is dependent on body size. None of the three phenotypes were positively correlated with body weight. Furthermore, there was no significant difference betweem the bone size (unloaded bones) and the degree of change in vBMD in response to loading. These data demonstrate that a differential anabolic response cannot be explained by differences of applied mechanical strain in the F2 mice or to differences in body size. Summary: 1) Anabolic response to a standard mechanical load can be divided into at least three different phenotypes (change in bone size, vBMD and mBMD). 2) These three phenotypes show a Gaussian curve in the B6/C3H F2 mice consistent with a complex trait controlled by several genes. 3) Bone size and vBMD changes are dependent upon new bone formation, found to be exceedingly variable in our F2 mice. However, the mBMD phenotype, a measurement of mineral density in preexisting bone, implies that there is a mechanism to increase mBMDmaterial density i.e. the bone quality can adapt to a large mechanical load. Conclusion: This study shows genetic-environmental adaptive interactions in bone of a remarkable magnitude.

Disclosures: ***C. Kesavan****, None.*

SU214

Mechanosensitivity of Human Mesenchymal Stem Cells. R. C. Riddle*, A. F. Taylor*, D. C. Genetos, H. J. Donahue. Department of Orthopaedics and Rehabilitation, Pennsylvania State University College of Medicine, Hershey, PA, USA.

Mechanical signals are clearly important to the maintenance of skeletal homeostasis as both the addition and removal of load are followed by alterations in bone mass. Load-induced oscillatory fluid flow has previously been shown to induce a number of well-defined biochemical responses that are thought to link mechanical signals with cellular responses. However, little is known about the mechanisms by which mesenchymal stem cells respond to mechanical signals and oscillatory fluid flow in particular. The purpose of this study was to determine whether oscillatory fluid flow regulates the behavior of human bone marrow-derived mesenchymal stem cells (hMSCs) in a manner similar to osteoblasts. Exposing hMSCs to physiologic levels of fluid flow that induce shear stresses of 5, 10, and 20 dynes/cm^2 induced a rapid increase in intracellular calcium concentration in 56 ± 2.4%, 87 ± 7.9%, and 89 ± 10.4% (mean ± SD) of cells, respectively. Absolute increases in intracellular calcium in response to these three shear stresses were on the order of 60 ± 20.4, 95 ± 12.5, and 189 ± 30.4nM. Subsequent experiments designed to elucidate the mechanism involved in intracellular calcium increase were performed with a shear stress of 20 dynes/cm^2, as the greatest calcium response was observed in this condition. Treatment with 5μM verapamil and 10μM gadolinum chloride, which antagonize the L-type calcium channel and mechanosensitive cation channel, respectively, did not have a significant effect on either the percentage of cells responding or absolute calcium increase. Treatment with 1μM thapsigargin, which empties intracellular calcium stores, and 10μM U73122, which antagonizes phospholipase C, markedly decreased both the percentage of cells responding and absolute calcium increase suggesting that these responses result from IP_3-mediated calcium release. On a longer time-scale, exposing cells to 20 dynes/cm^2 of fluid shear induced a robust increase in the phosphorylation of the extracellular signal-regulated kinase (ERK), an important regulator of osteoblastic differentiation, at 15, 30, and 60 minutes of flow. Following 120 minutes of flow ERK phosphorylation returned to basal levels. Downstream targets of these responses are currently under investigation. These data suggest that fluid flow not only regulates osteoblastic behavior but also that of hMSCs and imply that a common pathway exists by which mechanical signals are translated to cellular responses.

Disclosures: ***R.C. Riddle****, None.*

SU215

Correlations between DMP1/ MEPE Gene Expression in osteocytes and Axial Strains in an *In-vivo* Model of Overload. S. P. Kotha*[1], J. Gluhak-Heinrich[2], M. Schaffler[3], S. Harris[1], L. F. Bonewald[1]. [1]Oral Biology, University of Missouri, Kansas City, MO, USA, [2]Orthodontics, U of Texas Health Science Center, San Antonio, TX, USA, [3]Mount Sinai School of Medicine, New York, NY, USA.

Alterations of strain in bone are related to different biological responses, with bone loss at low strains, tissue homeostasis at normal strains, modeling at higher strains and the overload response at even higher strains. The osteocyte is believed to play a critical role as mechanotranducer, translating strain magnitude into an appropriate biological response. Using an overload model, where there is both bone formation and resorption, we studied the expression of molecules that are highly expressed in osteocytes, namely, Dentin Matrix Protein 1 (DMP1) and Matrix Extracellular Phosphoglycoprotein (MEPE) and correlated them to axial strains determined from finite element analysis. These molecules may have opposing effects on mineralization, with DMP1 acting as a modulator and MEPE acting as an inhibitor. The right ulna was loaded at 4 Hz with a maximum force of 20N until there was a 30% loss in whole bone stiffness. The left ulna served as contralateral controls and was not subjected to loading. Gene expression of DMP1 and MEPE mRNA was assayed at 2 days by quantitative *in situ* hybridization using P^{32} labeled RNA probes in control and loaded ulnae. Finally, gene expression in all osteocytes that fell along lines with a particular axial strain value were averaged and correlated to local strains as determined from our computational model. The results indicate that loaded ulnae expressed ~2 and 4 times more DMP1 and MEPE gene expression, respectively. The in-plane pattern of gene expression per osteocyte was highly correlated to axial strain magnitude in loaded (DMP1: $r^2= 0.71$; $p< 0.03$; MEPE: $r^2= 0.82$; $p< 0.02$) and control (DMP1: $r^2= 0.64$; $p< 0.05$; MEPE: $r^2= 0.83$; $p< 0.01$) ulnae. The magnitude of expression was similar when considering tensile or compressive strains. At the same strain level, DMP1 to MEPE expression ratios were higher in control bone (~4 times) than in loaded bone (~2 times). The longitudinal pattern of DMP1 and MEPE gene expression, i.e. expression along the length of the ulna, was also highly correlated to peak axial compressive strain at seven cross-sections in both the loaded (DMP1: $r^2= 0.68$; $p< 0.03$; MEPE: $r^2= 61$; $p<0.03$) and control (DMP1: $r^2= 0.65$; $p< 0.05$; MEPE: $r^2= 0.57$; $p<0.05$) ulnae. These findings indicate that DMP1 and MEPE gene expression is higher in regions with higher axial strains within control bone and that gene expression increases when strains are further increased in the loaded bones. This suggests that both molecules may have to be simultaneously expressed in order to regulate the mineralization process.

Disclosures: ***S.P. Kotha****, None.*

SU216

A Novel Mechanical Stress-induced Signaling Pathway Leading to Protein Kinase C Delta-dependent Smad1 Activation in Osteoblasts. S. Kido[1], D. Inoue[1], T. Imamura*[2], K. Miyazono*[3], T. Matsumoto[1]. [1]Medicine and Bioregulatory Sciences, University of Tokushima Graduate School of Medicine, Tokushima, Japan, [2]The Cancer Institute of the Japanese Foundation for Cancer Research, Tokyo, Japan, [3]Department of Molecular Pathology, Graduate School of Medicine University of Tokyo, Tokyo, Japan.

Although mechanical stress to bone plays an important role in maintaining bone mass and strength, the molecular mechanisms by which mechanical loading stimulates bone formation are not fully understood. We have already reported that fluid shear stress (FSS) to primary mouse calvarial osteoblasts (POB) activates Smad1, a critical factor for osteoblast differentiation that mediates BMP actions. In the present study, we further determined the upstream signaling event causing Smad1 activation. Fluid shear stress (FSS) induced Smad1 phosphorylation at S463/S465 in the C-terminal SSXS motif and nuclear translocation with Smad4. Functional and biological significance of these events was confirmed by our observations that FSS induced promoter activity of Smad6, a known target of Smad1, and that FSS increased alkaline phosphatase activity of C3H10T1/2 and C2C12 cells overexpressing Smad1. We found that FSS activation of Smad1 was almost completely inhibited by PKC inhibitors or depletion by long-term treatment with TPA. All the other chemical inhibitors including those for PI-3K, ERK, p38MAPK and PKA had little effect on FSS-induced Smad1 phosphorylation. Surprisingly, PKC inhibition did not affect Smad1 activation by BMP-2, an authentic ligand of ALK3 and 6 receptors known to directly phosphorylate and activate Smad1. Further analysis revealed a critical role for PKCδ, one of the novel PKC isoenzymes, because FSS-induced Smad1 phosphorylation was almost completely inhibited by either selective PKCδ inhibitor (rottrelin) or PKCδ siRNA. We also confirmed that FSS as well as TPA treatment resulted in PKCδ activation. We then tested a hypothesis that Smad1 is a substrate of PKCδ. Consistently, we were able to show direct physical interactions of PKCδ with GST-Smad1 in vitro. Moreover, in vitro kinase assays and LC-mass spectrometry demonstrated that recombinant PKCδ was indeed able to phosphorylate Smad1 by itself. In summary, we have demonstrated that mechanical stress activates Smad1 via a novel PKCδ -dependent signaling pathway distinct from that induced by BMP-2. Further delineation of this pathway will form a molecular basis to better understand the mechanism of mechanical stress-induced bone formation and to identify novel molecular targets for the treatment of immobilization osteoporosis.

Disclosures: ***S. Kido****, None.*

SU217

Differentiation Affects MC3T3-E1 Mechanoresponsiveness and P2Y2 Expression. C. A. Strohbach*[1], D. C. Genetos[2], A. F. Taylor*[1], H. J. Donahue[1]. [1]Orthopaedics and Rehabilitation, Pennsylvania State University College of Medicine, Hershey, PA, USA, [2]Cellular and Molecular Physiology, Pennsylvania State University College of Medicine, Hershey, PA, USA.

Osteoblasts respond to a variety of mechanical stimuli, including strain-induced fluid flow. We, and others, have previously demonstrated that exposure of MC3T3-E1 osteoblasts to oscillatory fluid flow (OFF) induces a rapid and transient increase in cytosolic calcium levels ($[Ca^{2+}]_i$). To our knowledge, all previous studies used the MC3T3-E1 cell line in its undifferentiated state. The aim of this study was to determine the effects of differentiation on OFF-induced Ca^{2+} transients. Cells were grown in αMEM+10%FBS+1%PS for 2 days or 21 days. Alizarin Red staining for calcium incorporation into the matrix, as well as von Kossa staining for phosphate content, confirmed the differentiated phenotype of the cells cultured for 21 days compared to 2 days. MC3T3-E1 cells grown in monolayer for 2 days or 21 days were subcultured onto quartz slides 2 days before Ca^{2+} imaging experiments. On the day of experimentation, cells were loaded with 10μM Fura2/AM and placed in a parallel plate flow chamber. Following a 3min no-flow period, cells were exposed to OFF (20dynes/cm^2, 1Hz) for 3min Cells were considered responsive if the maximum $[Ca^{2+}]_i$ during flow was greater than or equal to the no-flow $[Ca^{2+}]_i$ average plus 4 standard deviations of no-flow $[Ca^{2+}]_i$. There was no significant difference between undifferentiated and differentiated cells in the percentage of cells responding to flow (87% vs 82%, respectively). However, differentiated cells demonstrated a significantly higher resting $[Ca^{2+}]_i$ compared to undifferentiated cells (366nM vs 127nM; $p < 0.0001$). In addition, the maximum Ca^{2+} amplitude during OFF was significantly higher in differentiated cells compared to undifferentiated cells (380nM vs. 100nM; $p < 0.0001$). Because it has previously been demonstrated that activation of the ATP-activated P2Y2 purinergic receptor is required for OFF-induced increases in $[Ca^{2+}]_i$, we examined whether increased P2Y2 expression could be responsible for the increased Ca^{2+} response in differentiated cells. We found higher P2Y2 expression in the differentiated cells compared to undifferentiated cells. These data demonstrate that differentation state affects MC3T3 responsiveness to OFF, perhaps through increased P2Y2 receptor expression.

Disclosures: ***C.A. Strohbach****, None.*

SU218

Effects of Treadmill Exercise on Bone Mass and Bone Metabolism in Ovariectomized Rats. N. Nakamichi*[1], S. Ichimura[2], Y. Aoki*[1], J. Iwamoto[3], Y. Toyama*[4], K. Nemoto*[1]. [1]Orthopaedics surgery, National Defense Medical College, Saitama, Japan, [2]Orthopaedics surgery, Kyorin University, Tokyo, Japan, [3]Sports Clinic of Medicine, Keio University, Tokyo, Japan, [4]Orthopaedics surgery, Keio University, Tokyo, Japan.

Introduction: There are numerous reports on the positive effects of exercise on bone mass in postmenopausal women. In adult animals with estrogen deficiency, there are conflicting reports of a positive effect or no significant effect.Several experimental studies have shown the effect of exercise on bone mass in mature rats, and it has been confirmed that exercise increases bone mass in mature rats. However, a few studies have reported the effect of exercise on bone markers and calciotropic hormones in mature rats. In the present study, we examined the effects of treadmill exercise on bone mass, bone markers, and calciotropic hormones.

Methods: 23 week-old female Wistar rats were divided into 4 groups of 8 animals each; ovariectomy (O), ovariectomy and exercise (OE), sham-operated (S), and sham-operated and exercise (SE). The exercise regimen consisted of treadmill running at 12 m/min, 5°incline, 1hr per day a week, for 12 weeks. Left tibia was used for histomorphometric analysis. Left femur was used for structural analysis by micro-computed tomography. Serum calcium (Ca), inorganic phosphorus (Pi), total alkaline phosphatase (ALP), osteocalcin (OC), PTH and 1,25(OH)2VitD3 were also analysed.

Results: Serum Ca and Pi levels in O and OE groups were significantly lower than S and SE groups. Serum total ALP and OC levels in OE and SE groups were significantly higher than that of O and S groups respectively.12-week exercise increased BV/TV in S (4%) and O (6%) groups and Tb.Th. in the S (6%) and O (11%) groups, and decreased TBPf in S (31%) and O (7.6%), and SMI in S (13%) and O (9%). Therefore, these results suggest that 12-week treadmill exercise protects against the deterioration of microarchitecture in the osteoporotic rat model induced by ovariectomy.

Discussion: It is accepted that exercise promotes a positive calcium balance and increases skeletal mass, largely as a result of an increase in 1,25(OH)2VitD3 and enhancement of intestinal calcium absorption in rats. In the present study, treadmill exercise increased the serum 1,25(OH)2VitD3 level in the OVX rats. It is speculated that treadmill exercise stimulated bone formation and suppressed bone resorption, resulting in an increased demand for minerals that was satisfied by an increase in serum 1,25(OH)2VitD3 level and increased intestinal absorption of calcium.

Disclosures: ***N. Nakamichi****, None.*

SU219

Long-Term Voluntary Exercise Increases Cortical Bone Mass in Male Rats. S. L. Doody*[1], S. Judge*[2], R. R. Arzaga*[1], U. T. Iwaniec[1], T. J. Wronski[1], J. E. Sellman*[2], D. S. Criswell*[2], C. Leeuwenburgh*[2]. [1]Physiological Sciences, University of Florida, Gainesville, FL, USA, [2]Applied Physiology, University of Florida, Gainesville, FL, USA.

Long-term, voluntary mechanical loading in wheel-running animals may provide a sufficient stimulus to prevent osteopenia associated with aging and inactivity. Therefore, the aim of this experiment was to determine the effects of 24 months of voluntary wheel-running exercise on cortical and cancellous bone morphometry of the tibia in Fisher-344 rats. Two-month-old rats were randomly assigned into a wheel-running group (WR; n = 20) and a sedentary control group (S; n = 20). Both groups were 8% calorically restricted throughout the 24 months. WR ran voluntarily within a wheel approximately 1400 m/day during this time. Eleven WR and 12 S rats completed the study. The tibiae were harvested and processed undecalcified for quantitative bone histomorphometry. The cortical bone measurements were performed on the distal tibial diaphyses 1-2 mm proximal to the tibio-fibular junction and the cancellous measurements were performed on the proximal tibial metaphyses using standard methods. Data were analyzed with an independent samples t-test (2-tailed) and reported as mean ± SD.

WR had significantly greater cortical area (4.02 ± 0.20 vs. 3.80 ± 0.20 mm², $p < 0.01$) than S. WR had a significantly smaller endocortical perimeter (3.77 ± 0.21 vs. 3.95 ± 0.20 mm, $p = 0.0514$) and also a smaller medullary area (1.06 ± 0.12 vs. 1.17 ± 0.12 mm², $p < 0.03$) compared to S. In addition, cortical thickness was 7% greater in WR than S ($p < 0.001$). Significant differences between the two groups were not detected in either cortical cross-sectional bone tissue area (cortical area + marrow area; WR = 5.09 ± 0.21 vs. S = 4.97 ± 0.25 mm², $p < 0.2$) or periosteal perimeter (WR = 8.70 ± 0.21 vs. S = 8.61 ± 0.23 mm, $p < 0.36$). There were also no differences between the two groups for cancellous bone volume (WR = 10.84 ± 2.92 vs. S = 9.48 ± 3.52%, $p < 0.32$) or node to terminus ratio, a measure of trabecular connectivity (WR = 0.24 ± 0.15 vs. S = 0.40 ± 0.34), $p < 0.19$). There was a trend for increased trabecular number (2.19 ± 0.56 vs. 1.72 ± 0.54 /mm, $p = 0.0578$) and decreased trabecular separation (436.79 ± 127.34 vs. 590.37 ± 235.63 μm, $p = 0.0688$) in WR compared to S. The results demonstrate that long-term voluntary wheel-running increases cortical bone area and thickness, but not cancellous bone volume or connectivity. Therefore, this experiment provides evidence that bone responds to long-term mechanical loading in a site-specific manner.

Disclosures: ***S.L. Doody****, None.*

SU220

Are Bone Mineral Gains Maintained in Boys One Year following the Cessation of an Intervention? S. L. Manske[1], K. J. MacKelvie[2], A. D. G. Baxter-Jones[3], H. A. McKay[1]. [1]Department of Orthopaedics, University of British Columbia, Vancouver, BC, Canada, [2]Endocrinology and Diabetes Unit, British Columbia Children's Hospital, Vancouver, BC, Canada, [3]College of Kinesiology, University of Saskatchewan, Saskatoon, SK, Canada.

We recently reported a greater increase in bone mineral content at the femoral neck (4.3%) following a 20-month jumping intervention (10 min, 3x/week) in intervention boys compared with controls. The present study served to determine whether the bone mineral accrual advantage was maintained one year after the cessation of the exercise program. We re-assessed a subset of boys (12.74 ± 0.48 years at 1-year follow-up) who had been assigned to intervention (n = 14) or control (n = 21) groups in the original Healthy Bones II Study (n = 64 at the end of 20 months). All boys performed regular activities and PE following cessation of the program. We evaluated proximal femur (PF) and femoral neck (FN) bone mineral content (BMC, g) with DXA (Hologic QDR 4500). We assessed height (cm), weight (kg) and maturity (self-assessed Tanner staging) with standard techniques. Physical activity and calcium intake were assessed by questionnaire. The primary outcome measures were adjusted percent change in BMC at the PF and FN at 1-year follow-up. Data were analyzed using ANCOVA, adjusted for end of intervention (20-month) BMC, change in height and final Tanner stage. In this subset of boys, the 20-month change during the intervention period for the intervention group at the femoral neck was slightly smaller (2.2% greater than control, 95%CI = -4.5% to 8.9%, $p > 0.05$) than the 20-month change reported for the larger cohort (4.3% greater than control, $p < 0.01$). At 1-year follow-up, there was no difference between intervention and control groups for adjusted PF BMC (-1.0%, 95%CI = -6.5% to 4.5%) or FN BMC (-0.2%, 95%CI = -3.2 to 3.7). Results indicate that in boys, bone accrual advantages obtained in an intervention may not be sustained after the cessation of the intervention. Ongoing high-impact activity may be required. Further research should support development of minimal, sustainable interventions.

Disclosures: ***S.L. Manske****, None.*

SU221

High-Frequency Vibrations, in the Absence of Strain, Can Increase Cortical Bone Volume. R. A. Garman[1], L. R. Donahue[2], C. T. Rubin[1], S. Judex[1]. [1]Biomedical Engineering, State University of New York at Stony Brook, Stony Brook, NY, USA, [2]The Jackson Laboratory, Bar Harbor, ME, USA.

Bone's adaptive response to changes in its mechanical loading environment can be used for developing an effective countermeasure of osteopenia. Interestingly, even very small mechanical signals can be anabolic such as low-level vibrations inducing high-frequency (45Hz) but low-magnitude (0.3g) stimuli. We have shown that this stimulus can promote bone formation and increase bone quantity and quality, although the physical basis by which skeletal tissues sense these signals is not well understood. While this specific loading regimen introduces deformations between 5 and 20 microstrain, preliminary data suggest that deformations less than 5 microstrain may also be anabolic. Here, we applied vibratory signals to bone that primarily accelerate the bone and further minimize matrix deformations.

The left hindlimbs of eight female C57BL/6J mice were subjected to high-frequency (45Hz) vibrations at accelerations of either 0.3g or 0.6g for 10min/d. The right hindlimbs served as contralateral controls. After 3 weeks, micro-computed tomography was used to analyze changes in cortical bone of the diaphyseal, metaphyseal, and epiphyseal regions.

Vibratory loading at 0.3g and 0.6g did not alter cortical bone morphology in the diaphysis or metaphysis of the tibia. In contrast, epiphyseal cortical bone displayed greater bone area in the limb vibrated at 0.3g than in the control (+3.2%, p=0.06). Furthermore, loading at 0.6g also induced greater bone area in the vibrated limb (+10%, $p<0.05$) as compared to control. Pooling both vibrated limbs (0.3g and 0.6g) and control limbs revealed a significant difference in bone area between the groups - vibrated limbs were 8.4% greater ($p<0.01$) than the controls.

Although previous low-frequency mechanical loading regimens imply that bone deformations are critical for initiating an anabolic response, this study suggests that bone mass may be increased at strain levels below those typically associated with disuse. This change in bone mass was isolated to the epiphysis, perhaps due to the different anatomical features (spatially more confined, different tissue attachments) found at the proximal tibia as compared to distal regions. Interestingly, vibratory loading at a greater acceleration induced a more pronounced change in bone area than at the lower acceleration, related possibly to differences in shear stress magnitudes on the bone surfaces. In short, this study suggests that acceleration-based vibratory stimuli can increase cortical bone mass and introduces a loading regimen that, with continued development, may lead to a treatment for bedrest and disuse-induced osteopenia.

Disclosures: ***R.A. Garman****, None.*

SU222

Aging Does Not Reduce the Skeletal Sensitivity to Loading. O. Leppanen*, J. Jokihaara*, I. Pajamaki*, H. Sievanen*, P. Kannus*, T. L. N. Jarvinen. Department of Orthopaedics and Traumatology, University of Tampere, Tampere, Finland.

Aging has been shown to decrease the sensitivity of mechanosensory cells of bones to loading-induced stimuli. According to prevailing understanding, this deterioration of the cellular function reduces the capacity of the aged skeleton to adapt to changes in the incident loading, and consequently, results in age-related loss of bone.

To explore the possible modulatory effect of aging on the mechanosensitivity of bones, 100 male Sprague-Dawley rats were randomized into 4 loading (15 animals / group) and 4 control (10 animals / group) groups. The rats in the loading groups were subjected to 14-weeks of progressively intensifying treadmill training at the age of 5-weeks (young), 33-weeks (adult), 43-weeks (old), and 75-weeks (senescent). At the end of the training, the femoral necks were analyzed using peripheral quantitative computed tomography (pQCT) scanning and mechanical testing.

A significant response was observed in the young and senescent rats in the bone cross-sectional area (tCSA) and in the bone mineral content (tBMC), whereas no response was observed in the adult and old rats (A and B, figure below). However, a completely inverse response was observed in the volumetric density (tBMD). Finally, in the structural strength (F_{max}) of the femoral neck, the pattern of response between the different age-groups was virtually identical to the changes seen in tCSA and tBMC, although reaching borderline significance only (p=0.055 and 0.087 in the young and senescent, respectively). In conclusion, the aged bones seem to maintain their capacity to respond to increased loading.

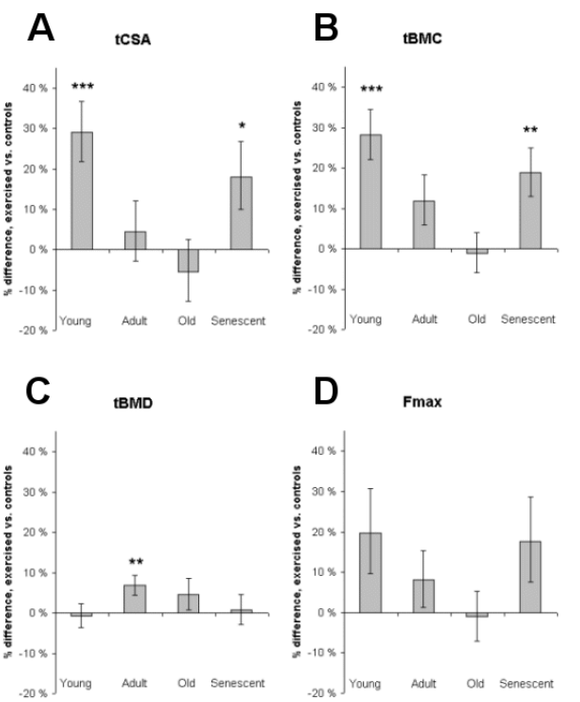

Figure. Effect of exercise on the characteristics of femoral neck in young, adult, old and senescent rats. (A) Total cross-sectional area (tCSA), (B) total bone mineral content (tBMC), (C) total bone mineral density (tBMD), and (D) biomechanical strength (Fmax). Bars represent percent (%) improvements ± the standard errors of the means (SEM) of the loading group compared with corresponding control group at the end of the 14-week exercise period. Significant differences between exercised and controls are indicated: *$p < 0.05$; **$p < 0.01$; ***$p < 0.001$.

Disclosures: ***O. Leppanen****, None.*

SU223

The Correlation between Different Parameters of Physical Fitness and Bone Mineral Content in Hong Kong Adolescents (Preliminary Baseline Results) - The HKABC Study (Adolescent Bone Health Cohort). D. T. K. Choy[1], E. M. C. Lau[1], D. Lo*[1], D. Chan*[1], P. C. Leung*[2]. [1]Jockey Club Centre for Osteoporosis Care and Control, School of Public Health, Chinese University of Hong Kong, Hong Kong, Hong Kong Special Administrative Region of China, [2]Department of Orthopaedics and Traumatology, Chinese University of Hong Kong, Hong Kong, Hong Kong Special Administrative Region of China.

Little is known about the determinants for bone growth in Asian adolescents. The HKABC study is a large scale longitudinal study of Hong Kong adolescents and the objective of this cohort study is to find out the different determinants that will affect bone growth in adolescents e.g., in-utero factors, physical characteristics, nutritional factors and different types of physical activities. We plan to follow up 1000 subjects for 3 years and each subject will have an annual assessment involving a face-to-face interview using a standardized, structured questionnaire. The subjects aged 10 to 13 years old were recruited from different primary schools situated in different areas in Hong Kong. Bone mineral density (BMD) was measured by DEXA (Hologic, Inc). Physical fitness were assessed by standardized methods including 1) Step test, 2) Hand grip and leg strength, 3) one minute sit-up, 4) Sit and reach test. We have analyzed the results of the first 200 subjects. We found that there is a strong positive correlation (Pearson Partial Correlation Coefficients 0.3-0.71, $p<0.0001$) between both the upper and lower limb strength with the bone mineral content at all sites (total hip, spine and whole body) in both sexes. The trunk flexibility of the boys as demonstrated by the sit and reach test also have positive correlations with the BMC at all sites. The VO2 max that is derived from the sub-maximal step test have a

strong inverse correlation (p<0.0001) with the percent body fat in both sexes but there are no correlation with BMC at the different sites. All results were adjusted for pubertal stage. In conclusion, muscle strength is a major determinant of BMC in adolescents but cardiovascular fitness as measured by VO2 max may not have a positive correlation with BMC in adolescents. These preliminary results suggest that different types of physical activities will have different impacts on the bone growth of adolescents.

Disclosures: ***D.T.K. Choy****, None.*

SU224

Genetic Regulation of Mechanotransduction in Mice. A. G. Robling*[1], S. J. Warden[1], K. L. Shultz*[2], W. G. Beamer*[2], C. H. Turner[1]. [1]Indiana University, Indianapolis, IN, USA, [2]Jackson Laboratory, Bar Harbor, ME, USA.

Adequate bone mass and strength are key factors in the prevention of osteoporotic fracture. It is clear that peak bone mass and mineral density are highly heritable traits, with an estimated 50-70% of the variability explainable by genetic composition. However, it is unclear how these genes exert their influence on bone mass. An emerging explanation proposes that a collection of genes modulates bone tissue's sensitivity to routine mechanical loading events, thereby augmenting bone mass through mechanotransduction pathways. The purpose of this study was to assess the contribution of two different genetic loci_one on mouse Chromosome 1 and the other on mouse Chromosome 13_to mechanically stimulated bone formation. Two congenic mouse strains were created in which a region (~40-80 cM) of mouse Chrs. 1 or 13 were moved from C3H/HeJ (C3H) strain to a C57BL/6J (B6) background strain through selective breeding over 9 generations. The regions moved to the B6 background corresponded to two of several quantitative trait loci (QTL) identified for bone size. The resulting congenics were 99% B6 with the remaining genomic DNA comprising the Chr. 1 or 13 QTL of interest. Male and female congenic (1T and 13B) and B6 control mice were subjected to in vivo loading of the right ulna at one of three different load magnitudes. A separate set of animals from each group were strain gauged at the ulnar midshaft to estimate strain at each loading level. Loading was conducted once per day for 3 days (60 cycles/day; 2 Hz). Fluorochrome labels were injected IP 5 and 12 days after loading began. After sacrifice, bone formation rates were measured in loaded (right) and control (left) ulnae. 1T male congenics exhibited significantly lower BFR/BS per unit mechanical strain compared to male B6 controls, but the same comparison among females yielded the opposite result (greater sensitivity in female 1T vs. B6 mice). These results correspond to a sex-specific effect on polar moment of inertia in the femur. The 13B female congenics exhibited a similar bone formation response to loading as the female B6 controls, but the male 13B mice exhibited lower BFR/BS per unit strain than the male B6 controls. Our results indicate that the genetic regulation of mechanotransduction is a real but complex process that involves a number of genes and interactions. Our data might explain why different individuals can engage in similar exercise protocols yet experience different results in terms of bone mass accrual.

Disclosures: ***A.G. Robling****, None.*

SU225

Non-invasive Axial Loading of the Murine Tibia Induces Increases in Cortical Bone Formation Accompanied by Modification in Trabecular Bone Architecture: A Novel Model for in vivo Loading Studies. R. L. de Souza*[1], M. Matsuura*[2], F. Eckstein[3], S. C. F. Rawlinson[1], L. E. Lanyon[1], A. A. Pitsillides[1]. [1]Veterinary Basic Science, Royal Veterinary College, London, United Kingdom, [2]Institute of Anatomy, Ludwig-Maximilians-Universitä, Munchen, Germany, [3]Institute of Anatomy, Paracelsus Medizinische Privatuniversität, Salzburg, Austria.

Systematic study of bones' adaptive responses to loading requires a simple non-invasive model in an appropriate experimental animal where bones' loading may be controlled and the modelling and remodelling of their cortical and cancellous regions quantified. For many purposes the experimental animal of choice is the mouse.

Here we describe validation of a model for in vivo axial loading of the tibia in 14 week old female C57Bl/J6 mice. The peak strains at the tibial midshaft during walking (<300μ) and jumping (<600μ) were measured with longitudinally oriented strain gauges attached to the bone's lateral and medial surfaces. These gauges were also used to determine the strains engendered by external compressive loading between the flexed knee and ankle *ex vivo*. Applied loads between 7 and 12N produced strains of 1200-2000μ, and repetitions of these loads on alternate days for 3 weeks produced significant load magnitude-related increases in periosteal bone formation throughout the one third of the tibia length along which measurements were made. In contrast, increases in endocortical apposition from the tibial midshaft, extending only distally. Micro-CT scans showed significant increases in trabecular bone volume and thickness that contrasted with the decreases in bone volume, trabecular thickness and number, and greater separation of trabeculae following sciatic neurectomy-induced unloading. This model has several advantages over other approaches, including the scope to study the effects of loading in cancellous as well as cortical bone, against a background of disuse or of treatment with osteotropic agents in normal, mutant, and transgenic mice

Disclosures: ***R.L. de Souza****, None.*

SU226

Relation of Neuromuscular Performance to Regional Bone Mineral Density Among Older U.S. Men. K. M. Winters[1], L. Marshall[1], E. Barret-Conner[2], E. Orwoll[1]. [1]Oregon Health & Science University, Portland, OR, USA, [2]University of California, San Diego, San Diego, CA, USA.

Muscle strength has been examined in relation to bone mineral density (BMD) to assess the influence of mechanical loading on bone. However, measures such as muscle power, general mobility and balance that may also reflect loading patterns have not received similar consideration in relation to BMD. Thus it is uncertain whether BMD is related to physical performance among older adults and whether such a relation is independent of lean body mass. To describe the contribution of neuromuscular performance to BMD in the hip and spine, we conducted a cross-sectional analysis with baseline information from 5,940 US men ages ≥ 65 years enrolled in the Osteoporotic Fractures in Men (MrOS) study. Performance measures were: maximal leg power (watts) (Nottingham Power Rig), grip strength (kg) (handheld dynamometer), dynamic leg strength (seconds to complete 5 chair stands), gait (6-m usual pace) (m/s) and balance (20 cm tandem walk pace) (m/s). Performance data included men who were and were not able to perform each test. For each test, performance data were expressed in quintiles among men who completed that test plus a sixth category containing men physically unable to complete the test. BMD at the femoral neck (FN), trochanter (TR), and lumbar spine (LS), as well as total body lean and fat mass, were obtained with DXA. The relation of BMD in the FN, TR and LS with each performance measure was estimated with generalized linear models. We computed partial R^2 values to estimate the amount of variance in each BMD variable that was explained by a performance measure independent of age, race, height, fat mass, and lean mass. FN BMD and LS BMD were not related to any of the performance measures (partial R^2 all <0.001). However, dynamic leg strength was a significant independent predictor of TR BMD (partial R^2=0.011). Adjusted mean TR BMD was 9.0% lower (p<.0001) among men unable to perform the test, compared with men in the quintile with the fastest repeated chair stand times. Among men who completed the 5 chair stands, TR BMD declined significantly with increasing chair stand time (p-trend <.0001). Results from this cross-sectional study suggest that BMD in the hip and lumbar spine is unrelated to neuromuscular performance. The exception was the relation between dynamic leg strength and TR BMD, which was independent of lean body mass and other factors. This observation is consistent with a previous report. Dynamic leg strength may reflect the repeated application of modest forces on bone at the predominantly trabecular trochanter site. Longitudinal data on neuromuscular performance and BMD are needed to better address this issue.

Disclosures: ***K.M. Winters****, None.*

SU227

Bone Loss Following Hindlimb Suspension and Reloading in Mice. M. Xu[1], D. J. Adams[2], M. Barrero*[2], C. C. Pilbeam[1]. [1]Dept. of Medicine, University of Connecticut Health Center, Farmington, CT, USA, [2]Dept. of Orthopaedic Surgery, University of Connecticut Health Center, Farmington, CT, USA.

We are establishing protocols to study the role of cyclooxygensase-2 (COX-2) gene disruption in the bone loss of immobilization, as modeled by hindlimb suspension, and in the subsequent response of bone to reloading. We subjected 6.5 mo old male and female mice in a C57BL/6 x 129 background to hindlimb suspension in specially designed cages modified from the NASA design for rats. Mice were placed in suspension cages and tails were taped 48 h prior to suspension for acclimation. Mice were suspended at a 20~30 degree head-down tilt by taping the outer half of tails and connecting the tape to an overhead rolling bar. Mice had free movement in the rat-sized wire bottom cage with free access to water and standard laboratory chow in a controlled 75 ºF and 12 h/12 h light/dark cycle environment. Ten COX-2 wild type (WT) mice (6 males, 4 females) were suspended for 2 wks and then released from suspension and housed singly in normal cages. Three male WT type mice were housed singly in normal cages as controls. Mice were weighed daily during suspension. Bone mineral density (BMD) of both femora was measured by x-ray densitometry (PIXImus, GE Lunar) and the average BMD for each mouse was used. BMD was measured on the time suspension was initiated (day 0), at the end of 2 weeks of suspension (day 14), and 2 weeks after reloading (day 28). Weights of suspended mice were 6.3 ± 2.0% lower on day 14 than on day 0. Mice regained this weight and more on day 28, being on average 7.1 ± 1.4% heavier than on day 0. Control mice also increased 2-3% in weight over the 4 wks. Femoral BMD in unloaded mice was 7.3 ± 1.0% lower on day 14 than on day 0, a significant decrease compared to control mice (P<0.02). BMD was still 7.9 ± 1.4% lower on day 28, 2 wks after reloading, than on day 0. Three males and 3 female COX-2 knockout (KO) mice, littermates of the COX-2 WT mice, were also unloaded for 2 wks. Weights were 7.0 ± 3.7% lower on day 14 compared to day 0 but were increased 5.3 ± 1.7% compared to day 0 after 2 wks of reloading. Femoral BMD was 8.8 ± 1.6% and 5.7 ± 1.3% lower than BMD on day 0 at day 14 and 28, respectively. Preliminary data indicate that RANKL mRNA was increased and OPG mRNA decreased in hindlimbs by unloading in both COX-2 WT and KO mice. We conclude that tail suspension for 2 wks provides a model to study bone loss in these transgenic mice, that absence of COX-2 expression does not prevent bone loss in this model, and that recovery of bone loss will take more than 2 wks of reloading.

Disclosures: ***M. Xu****, None.*

SU228

Analysis of Trabecular Bone Texture on Magnetic Resonance Imaging of the Distal Radius: Side-to-side Differences in Tennis Players. G. Ducher*[1], S. Même*[2], C. Magni*[3], J. Viala*[4], C. Chappard[1], D. Courteix[1], C. Benhamou[1]. [1]Faculty of Sport Sciences Orléans, ATOSEP, Orleans, France, [2]CNRS Orléans, CBM UPR 4301, Orleans, France, [3]Neuroradiology, Hospital of Orléans, Orleans, France, [4]Radiology, Hospital of Orléans, Orleans, France.

The purpose of this study was to compare the trabecular bone network of the dominant and non-dominant radius in competitive tennis players using magnetic resonance imaging (MRI).

Axial slices were obtained on the dominant and non-dominant distal radius in 20 adult tennis players (10 men and 10 women, age: 23.4 ± 4.8 years) with a spin-echo sequence (TR: 645 ms, TE: 20 ms, field of view: 100×100 mm , pixel size: 195×195 µm , slice thickness: 2 mm) using a 1.5 T MR device (Magnetom Vision, Siemens®). A region of interest (ROI) was manually defined on each slice including the largest trabecular area as possible. To study the intensity and distribution of grey levels of the trabecular network, we selected five methods of texture analysis: grey level histogram, co-occurrence, run length and gradient matrices and wavelets transform. The co-occurrence matrix features the probability distributions of pairs of pixels. The run length method consists in expressing the statistical distribution of the grey level runs in the image. The wavelets transform gives a decomposition of the image in a set of spatially oriented frequency channels. The texture parameters were computed automatically using algorithms (Mazda 3.20 program). Bone mineral density (BMD) was measured at the ultra-distal radius by dual-energy x-ray absorptiometry (Delphi QDR Series, Hologic Inc.®

). The comparison between the dominant and non-dominant radius was performed by a parametric paired t-test.

The "correlation" parameter of the co-occurrence matrices was significantly greater at the dominant radius when compared to its non-dominant counterpart (p=0.02). The non uniformity of the runs, in terms of run length and grey level, was significantly different between both radius (p=0.02). Wavelet analysis revealed a side-to-side difference in the wavelets coefficients for the high frequencies (p<0.05). No difference was observed on the grey level histogram and the gradient matrix. BMD was markedly greater at the dominant radius (0.525 ± 0.080 $g.cm^{-2}$) comparatively to the non-dominant radius (0.488 ± 0.069 $g.cm^{-2}$, p<0.0001), the side-to-side difference reaching 7.4 ± 4.9%.

These data indicate that tennis playing is associated to a higher BMD at the dominant forearm and to significant differences in MRI texture analysis. This study suggests that tennis playing induces not only a higher bone mass but also changes in trabecular bone microarchitecture in the dominant forearm.

Disclosures: ***C. Benhamou****, None.*

SU229

Effects of Isokinetic Muscular Strength Training on Tibial Bending Stiffness and BMD in Young Women. W. G. Herbert[1], C. R. Steele*[2], S. M. Nickols-Richardson[1], W. K. Ramp[3], D. F. Wootten*[1], L. E. Miller*[1], C. E. Callaghan*[1]. [1]Human Nutrition, Foods & Exercise, Virginia Tech, Blacksburg, VA, USA, [2]Mechanical Engineering, Stanford University, Stanford, CA, USA, [3]Health Research Group, Inc, Blacksburg, VA, USA.

Cross-sectional bending stiffness (EI) provides information about structural integrity of bone that is not reflected by bone mineral density (BMD by dual-energy x-ray absorptiometry, DXA). Mechanical Response Tissue Analysis (MRTA) is a technology for assessing EI of the human ulna and tibia in vivo.[1] MRTA applies mechanical vibration (60-1600 Hz) transcutaneously to the bone mid-shaft and utilizes impedance response to predict EI. Our device allows measurement of tibial EI for seated subjects, without rigid clamping of the bone ends. Data are processed with a software model that accounts for mass, stiffness, and damping effects of skin and soft tissue, as well as mass, axial stiffness, and damping of bone, and influences of bone displacement at the proximal and distal ends. We studied adaptations in tibial EI and BMD after 32 weeks of high-intensity isokinetic exercise training. Thirty-two women, 18-25 years, trained by concentric (N=22) or eccentric (N=10) modes, with only the non-dominant leg (knee flexion/extension @ $60^{o}{\cdot}s^{-1}$, 6 reps/set, 5 sets/session, 3 d/week) on an isokinetic dynamometer. Subjects were measured at weeks 0, 16, and 32 for leg muscular strength, tibial EI, and tibial BMD with DXA. Total tibia scans were analyzed with user-defined adaptations to the manufacturer-provided forearm software. Nine measures of EI were taken without repositioning the subject and these results used to compute a single score for each test session. The concentric and eccentric groups increased peak leg torque (composite of four tests) of the trained leg by 19% and 27% (p<0.05), respectively. Strength gains in the untrained leg were minimal (+5-8%) for both groups. Tibial EI of the trained leg increased 21% (p=0.03) in the concentric group, with no change in the untrained leg (-0.3%). In the eccentric group, tibial EI of the trained and untrained legs increased only by 10.9% and 7.6% (p>0.05). Total tibial BMD increased only 1.7% (p=0.05) in the untrained leg of the concentric group, with no change in the concentric group trained leg nor in either tibia of the eccentric group. In conclusion, localized high-intensity muscular resistance training increases tibial EI independent of changes in tibial BMD. Further studies are warranted to investigate MRTA applications in assessing risk for osteoporotic and stress fractures and in evaluating effects of interventions for improving bone status.

[1]Roberts, SG, *et al*. (1996) J Biomech 29(1):91-8.

Disclosures: ***W.G. Herbert****, None.*

SU230

Genetically Modulated Differences in Trabecular Bone Volume and Connectivity Influence the Efficacy of a Catabolic Stimulus. S. Judex[1], L. Xie*[1], A. Parhiz*[1], C. Rubin[1], L. Donahue[2], S. Xu*[1]. [1]Biomedical Engineering, SUNY Stony Brook, Stony Brook, NY, USA, [2]The Jackson Laboratory, Bar Harbor, ME, USA.

Genetic variability is a strong determinant of osteoporosis. The degree by which genetically determined peak bone mass and micro-architecture can influence the rates of bone loss when the skeleton is exposed to a catabolic stimulus is, however, unclear. Here, we subjected a genetically heterogeneous population, displaying large variations in bone morphology, to disuse and hypothesized that indices of baseline bone morphology are related to a differential deterioration of trabecular morphology. Fourty-three female, second generation (F2) BALBxC3H mice were subjected to three weeks of disuse (hindlimb suspension). In vivo micro-computed tomography quantified longitudinal changes in trabecular morphology of the distal femur including bone fractional volume (BV/TV), connectivity density (Conn.D), and trabecular thickness (Tb.Th). Mice were scanned prior to initiating disuse and during each subsequent week. Over the 3-wk experimental period, bone volume fraction diminished by an average of 52%±21% (p<0.001). Supporting the genetic influence on this large variability in bone loss, data were normally distributed with losses ranging from 16%-89%. The average rate of bone loss was similar between the first and second week (20% and 21%) but increased to 29% during the third week. Similarly to bone volume fraction, trabecular connectedness and trabecular thickness decreased significantly by 59%±25% and 20%±9%, respectively (p<0.001). Deterioration of the micro-architecture was also progressive in nature: Conn.D. (Tb.Th) decreased from 20% (6%) in the first week to 25% (6%) in the second week to 36% (8%) in the third week. Changes in bone volume were highly correlated with alterations in connectivity density (r2=0.85) and trabecular thickness (r2=0.75). Baseline bone volume fraction and connectivity density (but not trabecular thickness) were good (inverse) predictors of the change in BV/TV and Conn.D resulting from disuse (r2=0.36-0.46). Similar to data from astronauts that may lose between 0% and 24% of their trabecular bone quantity during 6-mo of space flight, these longitudinal in vivo data describe the large variations in bone loss in a genetically heterogeneous mouse population. The moderately high correlations between baseline bone morphology and the magnitude of bone loss suggest that some genes have simultaneous, if not inverse, influences on both traits. Extrapolated to humans, these data also indicate that people with lower peak bone mineral density may also suffer from higher rates of bone loss during conditions of space flight, bedrest, or aging. Supported by NASA.

Disclosures: ***S. Judex****, None.*

SU231

Loss of Half Cbfa1 Gene Dosage Further Reduces Bone Formation Rate in Tail-Suspended Mice while Loading Totally Resumes Bone Formation Rate to Normal Level In Vivo in The Absence of Half Cbfa1 Gene Dosage. R. Salingcarnboriboon[1], K. Tsuji[1], T. Komori[2], A. Nifuji[1], M. Noda[1]. [1]Dept. of Molecular Pharmacology, Tokyo Medical and Dental University, Tokyo, Japan, [2]Dept. of Molecular Medicine, Osaka University Medical School, Osaka, Japan.

Molecular mechanisms underlying reduction of bone formation in unloaded condition have not yet been fully understood. In in vitro experiments, Cbfa1 has been suggested to be involved in Flexercell-induced stretching stimuli. However, roles of Cbfa1 in unloading induced bone loss in vivo have not yet been known. The purpose of this paper is to examine the roles of Cbfa1 in unloading-induced bone loss and loading-induced bone formation in vivo. Tail-suspension (TS) was conducted using 9-11 wk-old Cbfa1 heterozygous knockout mice (Cbfa1+/-) (HT) and wild-type (WT) littermate. The mice were subjected to TS for two weeks. In the endosteal as well as periosteal surface of the cortical bone in the mid-shaft, TS reduced bone formation rate (BFR) as reported previously. In the absence of Cbfa1 half gene dosage (HT) BFR as well as mineral apposition rate (MAR) were totally suppressed and were almost undetectable. These observations indicate that full Cbfa1 gene dosage is necessary for the maintenance of bone formation even in TS mice. In contrast, BFR as well as MAR were similar between WT and HT mice in the loaded group, indicating that loading totally resume BFR and MAR even in the absence of half Cbfa1 gene dosage. In parallel to these observations in the diaphyseal cortex, cortical bone thickness was reduced by TS in WT mice, while the loss of half Cbfa1 gene further reduced cortical bone thickness after TS. Similar to BFR, loading totally resumed the thickness of the diaphyseal cortex even in the absence of half Cbfa1 gene dosage. RT-PCR analysis of the cortical bone envelope indicated that Cbfa1 mRNA expression was reduced significantly by TS in WT mice. Cbfa1 mRNA levels were about half of the WT in HT mice. In contrast to WT, this Cbfa1 mRNA level was not altered even after TS in HT mice suggesting the presence of unidentified mechanisms downstream to Cbfa1 could be involve in TS induced further suppression of BFR in these mice. Osterix mRNA level was reduced by half again by TS in WT. In HT mice, Osterix mRNA level was also reduced to half even in loaded group and the level was not anymore altered in TS group. Intriguingly, these observations are specific to cortical envelope since in the cancellous bone, basal levels of bone volume in WT and HT mice were similar and TS suppressed similarly the levels of cancellous bone volume in WT and HT mice. These data indicate that Cbfa1 is a critical target of loading stimuli to alter osteoblastic activity and bone formation in adult mice.

Disclosures: ***R. Salingcarnboriboon****, None.*

SU232

Differences in Opposing Hip Bone Density in Patients With Scoliosis. S. M. Strot*, L. Cole*, N. C. Grinnell*, T. M. DeFransisco*, E. A. Mossman, M. R. McClung. Oregon Osteoporosis Center, Portland, OR, USA.

Weight-bearing exercise, activity performed by an individual supporting his or her entire weight, is commonly recommended to slow age-related bone loss and as a general measure to maintain bone strength. Lack of weight-bearing exercise, as in cases of amputation and paralysis, is known to cause bone atrophy and decreased weight-bearing potential. In cases of scoliosis, an individual may preferentially bear their weight on one side or the other, depending on direction and severity of the curvature. This preferential weight-bearing may result in a combination of increased bone formation on preferred weight-bearing side and/or bone loss on the opposite side. The differential effects of this may result in discordant measurements of bone mineral density (BMD) in the hip.

The purpose of this study was to determine if there is a significant difference between BMD measurements of each hip in patients with scoliosis, and to determine if the difference is affected by the degree of spine curvature.

We examined dual-energy X-ray analysis (DXA) scans performed on a Lunar Prodigy densitometer (GE Lunar, Madison, WI) in 205 patients with scoliosis. Six of these were excluded due to biconcave or indeterminate curve direction. Mean age of the remaining 193 females and 6 males was 66.8 years. Hips on the side matching the concave direction of scoliosis were compared against hips on the convex side. Concave-side hips had a significantly higher mean total hip BMD that those on the convex side (0.878 to 0.864, t=3.65, p<0.0005). Degree of spine curvature was determined from the DXA images and categorized as mild, moderate, or severe. Among the mild, moderate, and severe curvature groups, the difference between convex- and concave-side BMDs was 0.012, 0.014, and 0.018g/cm^2, respectively. However, the differences between these groups were not statistically significant by ANOVA (p=0.85). These data suggest that while scoliosis may contribute to a disparity in opposing hip BMD in individual patients, it is not possible to generalize about the magnitude of the side-to-side disparity of hip BMD values based on the presence or severity of scoliosis.

Disclosures: ***S.M. Strot****, None.*

SU233

Regional Bone Loss Following Tibial Stress Fracture and Tibial Stress Syndrome. J. A. Spadaro, E. C. Rust*, T. A. Scerpella*. Orthopedic Surgery, Upstate Medical University, Syracuse, NY, USA.

The loss of regional bone density (BMD) following traumatic injury to bone in the upper or lower extremity is often rapid and dramatic (5-25% in 2-6 months), but has not been studied following repetitive loading injuries. We report results of an initial cross-sectional study of bone density changes in the tibia following tibial stress fracture (TSF) or medial tibial stress syndrome (MTSS, 'shin splints') in running athletes.

BMD of the injured and un-injured tibia was measured in 15 collegiate lacrosse and track athletes with documented unilateral TSF or MTSS (age 18-24, median 20 yr) using dual energy x-ray absorptiometry (DXA)(GE-Lunar DPX-IQ). With IRB approval and informed consent, a measurement was obtained 2-8 months after injury onset in 3 regions surrounding the injury site and the BMD was compared to the corresponding regions in the un-injured side BMD of the un-injured hip BMD was also measured as an indicator of general bone density.

Results showed that all subjects except one had bone loss on the injured relative to the un-injured tibia (mean loss 8.3 ± 5% global, 9.6 ± 7% center, p<0.001). BMD losses in TSF and MTSS subjects were not statistically different as were the losses among males vs. females (table 1). There was no clear difference seen thus far in the effect of time since injury, suggesting a persistence of the loss as found after traumatic fractures. Interestingly, all subjects in this group save one had higher than average hip BMD (mean Z-score: 1.6 ± 0.9) and there was an inverse relation between the amount of the tibial BMD loss and the normal hip Z-score (fig. 1).

We conclude that TSF and MTSS injuries in young healthy individuals appear to be associated with a substantial, rapid and persistent loss of BMD in the injury region. The presence of a unilateral loss after a unilateral injury in athletes with excellent BMD suggests a post-injury etiology, such as hyperemia accelerated resorption, rather than a pre-existing osteopenia.

Table 1: Mean % BMD loss in injured tibia vs un-injured tibia following TSF and MTSS injury. (All p<0.01).

Subject type	N	Proximal Region	At Center	Distal Region	Global Region
TSF	9	-9.2	-17.0	-6.1	-8.0
MTSS	6	-6.1	-10.9	-11.0	-8.6
Females	8	-8.5	-9.2	-6.7	-8.6
Males	7	-6.0	-10.0	-9.5	-7.9
All	15	-7.3	-9.6	-8.0	-8.3

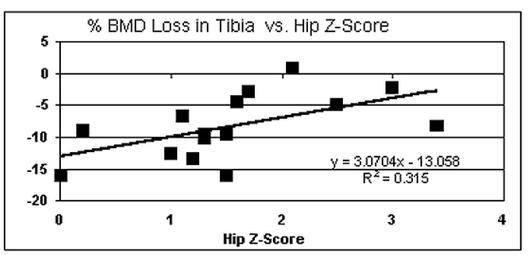

Disclosures: ***J.A. Spadaro****, None.*

SU234

Differentiating the Contribution of Material and Structural Properties to Changes in Bone Mechanical Strength Caused by Disuse Models for Osteoporosis and Antiresorptive Therapies. R. E. Thacker*, T. A. Bateman. Bioengineering, Clemson University, Clemson, SC, USA.

It has been demonstrated that antiresorptive therapies and models for osteoporosis increase and decrease, respectively, the mechanical strength of bone. The aim of this study is to determine the differential contribution of structural and material properties to these changes in strength.

Female Balb/C mice, aged 6 weeks were examined (n = 16/grp). Ten days prior to beginning treatment, calcein was administered to represent extant bone of a known age. A second label was given the day treatment begun. Of the five groups examined, two disuse models for osteoporosis were used (decreasing bone strength) and two antiresorptive therapies (increasing bone strength). The five "treatment" groups were: 1) control (no treatment), 2) hindlimb suspension (HLS), 3) sciatic neurectomy (NX) 4) osteoprotegerin (OPG 20mg/kg) and 5) zoledronate (ZOL 8mg/kg).

Structural properties are being investigated via microCT. Software provided by Scanco, INC. determines cross-sectional area (CSA) as well as the principal moments of inertia (Imax and Imin) for the entire length of the diaphysis (80 9 micron thick slices sampled over the 8mm diaphysis). For analysis of the material component of the bones we performed mineral composition assays (whole bone properties) and microhardness indentation (site specific properties). NS indicates a non significant difference compared to controls.

Structural analysis demonstrates that both CSA and Imin (the most relevant MOI for three point bending) increase at the mid diaphysis of the OPG (3%^{NS}, 5%^{NS}, for CSA, Imin resp) and ZOL (3%^{NS}, 9%) treated mice compared to untreated controls. While for the disuse models both CSA and Imin were negatively affected: HLS (-11%, -12%) and NX (-6%, -10%). Compositional analysis showed an increase in mineral constituents of both the OPG (3.5%) and ZOL (3.0%) treated mice and a decrease for HLS (-1.6%) and NX (-0.4^{NS}). Microhardness indentation of extant bone (indicated by the first calcein label) showed no differences in the hardness values between any of the groups.

It appears that the antiresorptive therapies affect whole bone material properties more than structural properties, and the disuse models affect structural properties more than material properties. Though whole bone percent mineralization was significantly altered for OPG, ZOL and HLS, this did not translate to site specific changes in material properties as measured by microhardness indentation. It is possible that microhardness indentation is not sensitive enough to observe these changes (nanoindentation is in progress). The study was approved by Clemson's Animal Care and Use Committee.

Disclosures: ***R.E. Thacker****, None.*

SU235

Bone Density in Female Rowers. K. Ackerman[1], M. Walcott*[2], N. Glass*[2], M. LeBoff[2]. [1]Medicine, Hospital of the University of Pennsylvania, Philadelphia, PA, USA, [2]Medicine, Brigham and Women's Hospital, Boston, MA, USA.

Female endurance athletes often suffer from the well documented "female athlete triad:" amenorrhea, disordered eating, and osteoporosis. Available data, however, indicate that female athletes who participate in weight-bearing sports (i.e. gymnastics and weightlifting) have higher bone densities than do non-exercising women and women who participate in exercises with less mechanical strain (e.g. running). Although there is increased participation in women's rowing, little is known about the impact of rowing (a sport that includes a high force loading or resistance training) on skeletal health.

To evaluate the effects of rowing on bone density and body composition we recruited 28 rowers age 18-31 years (25 ± 4 yrs) who were trained athletes with 2000 meter ergometer best scores of 6:36 to 7:44 minutes. At the time of enrollment each athlete completed a training, dietary, menstrual, and medication survey, and underwent a DXA scan of the hip, spine, and whole body (Hologic, QDR 4500). Mean total hip Z-score was 0.921, mean hip neck Z-score was 0.507 and mean hip trochanter Z-score was 0.890. Mean spine Z-score was 0.693, and mean total body Z-score was 1.057. In addition, mean body fat composition was 20.41%. Seven women were oligomenorrheic with <9 menses/year either currently or prior to their 18th birthdays. But when these women's values were assessed separately from the larger group, the oligomenorrheic women's Z-scores were not significantly different from the others'. This preliminary data of elite rowers show that rowers have normal bone density compared with age-matched women according to a manufacture's database. Rowing may even have a protective effect on bone density in women with menstrual irregularities. While the total body bone density is greater than age-matched controls, larger ongoing studies that directly compare bone health in rowers versus other athletes will help elucidate the relative benefits of different sports in the maximization of peak bone mass in women.

Disclosures: ***K. Ackerman****, None.*

SU236

Regulation of RANKL Promoter Activity Is Associated with Histone Remodeling in Murine Bone Stromal Cells. X. Fan[1], E. M. Roy*[1], T. C. Murphy*[1], M. S. Nanes[1], S. Kim[2], J. Pike[2], J. Rubin[1]. [1]Medicine, Emory University/VA Medical Center, Decatur, GA, USA, [2]Biochemistry, University of Wisconsin-Madison, Madison, WI, USA.

Receptor activator of NFκ-B ligand (RANKL) is essential for osteoclast formation, function and survival. Although RANKL mRNA and protein levels are modulated by $1,25(OH)_2D_3$ and other osteoactive factors, regulatory mechanisms remain unclear. In this study, we show that transiently transfection with 2kb or 2kb plus exon1 of a RANKL promoter sequence conferred neither $1,25(OH)_2D_3$ response nor tissue specificity. The histone deacetylase inhibitors trichostatin A (TSA) and sodium butyrate, however, strongly increased RANKL promoter activity. A series of 5'-deleted RANKL promoter constructs from 2020 to 110 bp of transcription start site showed at least 4-fold increased activity after TSA treatment. TSA also dose dependently enhanced endogenous RANKL mRNA expression with 50 μM of TSA treatment causing equivalent RANKL expression to that seen with 1 nM $1,25(OH)_2D_3$. Using a chromatin immunoprecipitation (ChIP) assay in the ST2 mouse stromal line, we showed that TSA significantly enhanced the acetylation of both histone H3 and H4 on the RANKL promoter. There was stronger increase in acetylation of histone H4 than that of acetylated histone H3 on the RANKL promoter, 294-fold and 12.5-fold increases respectively. A similar increase in acetylated histone H4 on the RANKL gene locus was seen after $1,25(OH)_2D_3$ treatment. ChIP assay did not, however, reveal localization of VDR/RXR heterodimers on the putative VDRE of the RANKL promoter indicating that $1,25(OH)_2D_3$-receptor does not utilize this sequence. To explore the role of H4 acetylation in $1,25(OH)_2D_3$ stimulated RANKL, we added both TSA and $1,25(OH)_2D_3$ together. While the combination further increased acetylation of H4 on the RANKL locus, surprisingly, TSA inhibited $1,25(OH)_2D_3$-induced RANKL mRNA expression by 70% at all doses of $1,25(OH)_2D_3$ studied. These results suggest that TSA stimulation of endogenous expression of RANKL involves enhanced acetylation of histones on the proximal RANKL promoter. In the $1,25(OH)_2D_3$ stimulated state, however, TSA mediated inhibition of histone deacetylase represses the $1,25(OH)_2D_3$ effect, suggesting that preventing histone deacetylation blocks $1,25(OH)_2D_3$ action on this gene. Chromatin remodeling is therefore involved in RANKL expression.

Disclosures: ***X. Fan****, None.*

SU237

Mechanically Induced Osteocyte Signaling Explains Regulation of Osteoclast Resorption Directionality and Coupling of Formation to Resorption in Cortical Bone Remodeling. R. Ruimerman*[1], R. van Oers*[1], E. Tanck*[2], P. Hilbers*[1], R. Huiskes[1]. [1]Biomedical Engineering, Eindhoven University of Technology, Eindhoven, Netherlands, [2]University of Nijmegen, Nijmegen, Netherlands.

In cortical bone basic multi-cellular units (BMU's) of bone resorbing osteoclasts and bone forming osteoblasts replace old bone by new, forming secondary osteons. The coordination between resorption and formation suggests a coupling mechanism[1] between osteoclasts and osteoblasts, which origin is unknown. Equally unknown is what guides osteoclast resorption in its directionality. The alignment of osteons along the dominant loading direction suggests that mechanical forces are involved.[2] It was hypothesized that osteocytes, serving as mechanosensors, control BMU activities by sending signals through the osteocytic canalicular network.[3]

In this study we tested whether these hypotheses can explain that osteoclasts resorb bone in the main loading direction and that bone formation follows in such a coordinated manner. For that purpose we developed a computational theory, assuming that (1) osteocytes are mechanosensors. Relative to the signal experienced they send biochemical messengers, through the canaliculi, to the internal bone surface. (2) Osteoblasts form bone relative to the strength of the osteocyte signals. (3) Osteoclast activity is inhibited by the osteocyte signals. They resorb bone where low osteocyte signals are received, while they retract from surfaces receiving high osteocyte signals.

We tested this theory in 2-D FEA computer-simulation. The initial configuration consisted of a small piece of compact bone with an initial cutting cone with three osteoclasts. Osteocyte density was set to 1600 mm^{-2}. When the simulation started, the osteoclasts resorbed bone in the principal loading direction, producing a tunnel of 175 μm wide. Osteoblast formation closely followed, forming a new osteon. Reduced external loads on the bone increased the number of osteoclasts active in the cutting cone and the diameter of the osteon formed. Increased loads had the opposite effects. Rotation of the external loads, relative to the longitudinal bone axis, caused the cutting cone to bend accordingly, eventually forming a crooked osteon.

We conclude that the theory describes a cellular-level regulatory mechanism, capable of translating mechanical signals to orient osteoclast resorption in the main loading direction. It also shows that coupling of osteoclast resorption to osteoblast formation through mechanobiological signaling is a viable proposal.

1. Frost, *Bone Biodynamics*. Little Brown, Boston, pp 315-333, 1964.
2. Petryl et al., *J Biomech.* 29, pp 161-169, 1996.
3. Burger et al., *FASEB J.* 13, pp 101-112, 1999.

Disclosures: ***R. Ruimerman****, None.*

SU238

Atorvastatin Stimulates Osteoprotegerin Production by Primary Human Osteoblasts. V. Viereck*[1], C. Grundker*[1], S. Blaschke*[2], K. Frosch*[3], M. Schoppet*[4], G. Emons*[1], L. C. Hofbauer[4]. [1]Gynecology and Obstetrics, Georg-August-University, Goettingen, Germany, [2]Nephrology and Rheumatology, Georg-August-University, Goettingen, Germany, [3]Trauma Surgery, Georg-August-University, Goettingen, Germany, [4]Medicine, Philipps-University, Marburg, Germany.

Recently, HMG-CoA reductase inhibitors (statins) have been shown to exert protective effects on bone metabolism. Because of the widespread use of lipid-lowering statins, prevention of bone loss and fractures would be a desirable side effect. However, the mechanisms how statins affect bone metabolism are still obscure, with some studies showing stimulatory effects on bone formation and others demonstrating inhibition of bone resorption. Here, we evaluated the effect of atorvastatin on osteoblastic production of receptor activator of nuclear factor-κB ligand (RANKL) and osteoprotegerin (OPG), both of which are osteoblast-derived cytokines essential for osteoclast cell biology. While RANKL enhances osteoclast formation and activation and promotes bone loss, OPG acts as a decoy receptor and antagonizes the RANKL effects. In primary human osteoblasts (hOB), atorvastatin increased OPG mRNA levels and protein secretion by hOB by up to 3-fold in a dose-dependent manner with a maximum effect at 10^{-6} M ($P < 0.001$). Time course experiments indicated a time-dependent stimulatory effect of atorvastatin on osteoblastic OPG protein secretion after 24 hrs ($P < 0.001$). Treatment of hOB with substrates of cholesterol biosynthesis that are down-stream of the HMG-CoA reductase reaction such as mevalonate or geranylgeranyl pyrophosphate completely prevented atorvastatin-induced enhancement of OPG production. By contrast, atorvastatin tended to decrease RANKL mRNA levels and protein secretion, although these effect were non-significant. Of note, treatment of hOB cells with atorvastatin enhanced osteoblastic differentiation markers alkaline phosphatase activity and osteocalcin mRNA levels by three- and two-fold, respectively ($P < 0.001$) in a dose- and time-dependent fashion. In summary, our data suggest that atorvastatin enhances the OPG-to-RANKL ratio by primary human osteoblasts which may result in inhibition of osteoclastic bone resorption. Since osteoblastic OPG expression is a positive function of their stage of differentiation, the stimulatory effects of atorvastatin on OPG production may, at least in part, be mediated by promoting their differentiation.

Disclosures: ***V. Viereck****, None.*

SU239

Phosphatidylinositol 3-Kinase Pathway Is Stimulated by Metabolic Acidosis in Bone. N. S. Krieger, K. La Plante*, J. Sullivan*, D. A. Bushinsky. Medicine, University of Rochester, Rochester, NY, USA.

Chronic metabolic acidosis stimulates net calcium (Ca) efflux from bone by alteration of osteoblastic function and stimulation of osteoclastic bone resorption. Acid-induced bone resorption is mediated, in large part, by stimulation of osteoblastic prostaglandin E2 (PGE2) synthesis; however, the subsequent signaling pathways are not known. To determine if PGE2 acts through the EP4 prostaglandin receptor, we incubated neonatal mouse calvariae for 48 h in neutral pH (pH~7.4, [HCO3-] =24 mM, Ntl) or physiologically acid pH (pH~7.1, [HCO3-]=12 mM, Acid) medium in the absence or presence of 1 μM L-161982, a specific antagonist of the EP4 receptor (gift of L. Koch, Merck). Acid medium induced a significant increase in net Ca efflux from bone, which was completely inhibited by L-161982. An inactive isomer (L-161983) had no effect on this Acid induced net Ca efflux. PGE2 binding to the EP4 receptor can lead to activation of phosphatidyl-inositol 3-kinase (PI 3-kinase). To determine the role of PI 3-kinase in acid-induced bone resorption we utilized a specific inhibitor, wortmannin (WTM). Calvariae were incubated in Ntl or Acid medium for 48 h in the absence or presence of 20 nM WTM. Net Ca efflux was stimulated by Acid, compared to Ntl. WTM alone had no effect on Ca efflux in Ntl incubations, but almost completely inhibited the Acid induced Ca efflux. PI 3-kinase is present in both osteoblasts and osteoclasts, thus WTM could be inhibitory in either cell type. Activation of PI 3-kinase leads to the phosphorylation of AKT (pAKT). To determine if activation of PI 3-kinase occurred in the osteoblast, we measured changes in pAKT in primary cells isolated from calvariae, which are almost exclusively osteoblasts. Cells were made quiescent by overnight incubation in Ntl medium in the absence of serum and then medium was changed to Ntl or Acid, each containing 1% serum. At appropriate time points, cells were lysed in denaturing buffer and Western analysis with chemiluminescent detection was performed using a specific antibody to pAKT, followed by normalization using an antibody to total AKT. In response to Acid, pAKT increased at 1 min compared to Ntl. There was no change in total AKT. These results suggest that the acid-induced increase in PGE2 activates the EP4 receptor, which stimulates PI 3-kinase leading to an increase in osteoblastic pAKT which subsequently leads to increased osteoclastic bone resorption.

Disclosures: ***N.S. Krieger****, None.*

SU240

Interleukin-6 Alters the Gene Expression of RANKL and OPG in Response to Titanium Particulate Debris in Osteoblasts. J. T. Ninomiya, K. G. Gilbertson*, J. A. Struve. Department of Orthopaedic Surgery, Medical College of Wisconsin, Milwaukee, WI, USA.

Aseptic loosening remains the principal cause of implant failure following total joint replacement. Despite advances in materials science and engineering, the generation of particulate wear debris leads to bone resorption and impant failure. Recently, two proteins that play a critical role in osteoclast maturation, receptor activator of NFkB (RANK) and its ligand (RANKL), have been described. These two proteins, along with the soluble decoy receptor, osteoprotegerin (OPG), work in concert to modulate osteoclast activity and bone resorption. The addition of wear debris to osteoblasts increases expression and secretion of

RANKL and IL-6, resulting in increased osteoclast maturation and ultimately, osteolysis and implant loosening. However, the relationships between IL-6 and the gene expression of RANKL are not well described. Therefore, we hypothesized that IL-6 secretion modulates the production of RANKL and OPG in response to particulate debris, resulting in increased osteoclast maturation.

The effects of IL-6 and titanium particles on the gene expression and secretion of RANKL and OPG were investigated in murine osteoblastic MC3T3-E1 cells. Exogenous murine IL-6 and titanium particles were added to cultures, and further experiments included the addition of IL-6 neutralizing antibodies. Real-time PCR was used to monitor changes in OPG and RANKL gene expression. Conditioned media and cell lysates were collected and used to determine the effects on osteoclast maturation using a murine marrow cell assay.

Following incubation, the addition of exogenous IL-6 yielded a 3.0-fold induction in RANKL and a 1.4-fold induction of OPG mRNA compared to unstimulated controls. Titanium particles alone increased the expression of both RANKL (3.0-fold) and OPG (1.2 fold) at 24 hours. The addition of anti-IL-6 neutralizing antibody decreased the expression of both RANKL and OPG in comparison to particles alone. Osteoclast maturation was also reduced to control level by the addition of IL-6 antibodies to cultures containing particles (48 hours).

These results demonstrate that IL-6 decreases osteoclast maturation predominantly by decreasing RANKL gene expression and subsequent osteoclast maturation in the presence of titanium particles. Blockade of the effects of IL-6 using IL-6 antibodies decreased the changes in RANKL mRNA levels and inhibited osteoclast maturation. These findings suggest that IL-6 plays an autocrine role in response to particulate wear debris by enhancing osteoclast maturation through an increase in the ratio of RANKL to OPG.

Disclosures: ***J.T. Ninomiya****, None.*

SU241

Study of the Aromatase Cytochrome P-450 Gene (*CYP19*) Promoter Usage in Osteoblast Cells. Effects of vitamin D, dexamethasone, 17β-estradiol and testosterone treatments. A. Enjuanes*[1], N. García- Giralt*[2], D. Grinberg*[2], A. Supervía*[1], S. Ruiz-Gaspà*[1], M. Bustamante*[2], L. Mellibovsky*[1], A. Díez-Pérez[1], X. Nogués[1], S. Balcells*[2]. [1]Urfoa, IMIM-Hospital del Mar, Barcelona, Spain, [2]Departament de Genetica, Universitat de Barcelona, Barcelona, Spain.

Aromatase cytochrome P-450 catalizes the conversion of androgens into estrogens and its presence in bone cells has been documented. Given the potential role of aromatase in osteoporosis and the incomplete understanding of *CYP19* gene regulation in osteoblast cells, we have undertaken a detailed study on the promoter usage of *CYP19* gene and the effect of vitamin D, dexamethasone, testosterone and 17β-estradiol treatments in a cultured human osteoblast cell line.

Several plasmids containing the following *CYP19*-promoter regions upstream of a luciferase reporter gene were constructed: pA) promoter II and exon I.3; pB) promoter II, exon I.3, I.3 promoter region and exon I.6; pC) promoter II, exon I.3 and I.3 promoter region; pD) I.3 promoter region and exon I.3; pE) I.3 promoter region; pF) I.6 promoter region; and pG) I.4 promoter region and exon I.4 and pH) I.4 promoter region. MG-63 cells were grown in DMEM supplemented with 10% FCS. *CYP19* promoter vectors and pSVB-Gal control vector were co-transfected in MG-63 cells at 70 % confluency in DMEM without FCS using FuGene Reagent. Six hours after transfection, MG-63 cells were incubated in DMEM with or without FCS for 24 hours with alternative treatments: 1) 100nM dexamethasone (DEX), 2) 100nM $1,25(OH)_2D_3$ (VitD), 3) 100nM $1,25(OH)_2D_3$ + 100nM DEX, 4) 100nM 17β-estradiol, and 5) 100nM testosterone One day later, cells were lysed and chemiluminescent assays were performed to mesure luciferase and β-galactosidase activities. Both transfection experiments and chemiluminescent assays were duplicated at each experimental step and experiments were repeated at least 4 times. Statistical analysis were performed using the SSPS 11.5 software.

In MG-63 osteoblast cells, FCS inhibit significantly promoter activity in all constructs. Construct pA showed the highest levels of promoter activity, with or without FCS. In this cell line, I.4 promoter region plus exon I.4 mediate the stimulation by DEX, and exon I.4 seems to be important for this stimulation. In contrast, exon I.4 seems to negatively affect the VitD stimulation. Promoter I.3 plus exon I.3 mediate the stimulation by VitD in absence of FCS and the exon I.3 seems to be relevant for this stimulation. Testosterone and 17β-estradiol treatments have no effect on these promoters. Finally, I.6 promoter activity was detected but transcriptional levels were not affected by hormonal treatments.

Disclosures: ***A. Enjuanes****, None.*

SU242

Osteoblast Gene Expression Profiles during Growth of the Immature Skeleton. D. Murray*, C. Farquharson. Gene Function and Developement, Roslin Institute, Midlothian, United Kingdom.

In response to skeletal loading, bones increase their diameter by incorporation and infilling of primary osteons. Comparing chickens with fast (F) and slow (S) growth potential we have previously reported that the tibia of fast growing birds had lowered mechanical properties, likely to be explained by increased cortical porosity. Indirect measurement of osteonal infilling indicated that this process was impaired in the fast strain. The aims of this study were to directly determine the infilling rate of the primary osteons and to compare osteoblastic characteristics of both strains. To quantify the rate of osteon infilling, tibiae were removed from 21-day-old chicks, which had been double labelled with calcein (80 and 8 h before death). The mineral apposition rate was F=11.51μm/day; S=28.16μm/day, P< 0.001 and this data confirms previous histomorphometry results. Osteoblasts were grown and expanded in culture from explants of tibia of 21-day-old birds of both strains (n=4/strain). Osteoblast proliferation was determined by tritiated-thymidine uptake and differentiation by alkaline phosphatase (ALP) activity. At pre-confluency, cell proliferation was higher in the slow growing birds (F=7439dpm; S=11732dpm, P<0.001), but this pattern was reversed at confluency (F=10491dpm; S=1979dpm, P<0.001) and post confluency (F=4564dpm; S=1702dpm, P<0.001) and is a likely consequence of the earlier impairment of proliferation by contact inhibition in the slow growing strain. ALP activity (pNPP hydrol/30 min/mg protein) was only detected at post-confluency and was higher in the fast growing strain (F=1188; S=216, P<0.001). Osteoblastic gene expression was determined by RT-PCR and quantified by densitometry (cnt/mm^2). A higher level of osteopontin (F=382; S=1205, P< 0.01), and BSP (F=33; S=262, P<0.05) expression was observed in the slow growing birds. The serotonin receptor, considered to have a role in mechanoregulation, was more highly expressed in the fast chicks (F=565; S=241, P<0.05) as was Runx2 (F=312: S=72, P<0.001). In conclusion, porosity was confirmed to be due to a lack of infilling within the primary osteons. Osteoblast proliferation was faster in the slow growing birds whereas differentiation was slower. This is in accord with our previous hypothesis that the fast growing birds are characterised by an increase in transit time through the osteoblast lineage, which may be driven by the high levels of Runx2 expression. Osteopontin and BSP are associated with mechanical loading but the significance of the lower expression levels in the fast growing birds requires further study. However, the up regulation of serotonin expression may reflect the greater loads experienced in the fast growing birds in vivo.

Disclosures: ***D. Murray****, None.*

SU243

ATF4 Mediates PTH-dependent Osteocalcin Gene Expression. G. Xiao[1], D. Jiang*[1], H. Boules*[1], C. Ge*[1], Z. Zhao[1], X. Yang*[2], G. Karsenty[2], R. T. Franceschi[1]. [1]Periodontics/Prevention/Geriatrics, The University of Michigan, Ann Arbor, MI, USA, [2]Department of Molecular and Human Genetics and Bone Disease Program of Texas, Baylor College of Medicine, Houston, TX, USA.

Parathyroid hormone (PTH) is an important peptide hormone regulator of bone formation and osteoblast activity. However, its mechanism of action in bone cells is largely unknown. This study examined the effect of PTH on mouse osteocalcin gene expression in MC3T3-E1 preosteoblastic cells and primary cultures of bone marrow stromal cells. PTH increased the levels of osteocalcin mRNA 4- to 5-fold in both cell types. PTH also stimulated transcriptional activity of a 1.3 kb fragment of the mouse osteocalcin gene 2 (mOG2) promoter. Inhibitor studies revealed a requirement for protein kinase A, protein kinase C and mitogen-activated protein kinase pathways in the PTH response. Deletion analysis of the mOG2 promoter identified an essential region for PTH responsiveness between -116 and -34. This region contains a single copy of the previously described osteoblast-specific element, OSE1 (TTACATCA). Deletion and mutation of OSE1 in DNA transfection assays established the requirement for this element in the PTH response. This OSE1 site was recently demonstrated to bind to activating transcription factor 4 (ATF4), a factor which plays a major role in bone formation (Yang et al., 2004, Cell, 117:387-398). Gel mobility retardation shift assays revealed that MC3T3-E1 cells contain ATF4 and that binding of ATF4 to OSE1 DNA was up-regulated by PTH. Furthermore, PTH treatment increased the levels of ATF4 mRNA and protein in osteoblasts. Collectively, these studies indicate that ATF4 mediates PTH-dependent OCN gene expression.

Disclosures: ***G. Xiao****, None.*

SU244

Functional Role of a Zinc Transporter in Osteoblast Differentiation. Z. Tang*, M. A. Khadeer*, A. Gupta. Biomedical Sciences, University of Maryland, Baltimore, Baltimore, MD, USA.

Zinc (Zn) is an essential trace element that has anabolic effects on bone formation, partly through stimulation of osteoblast proliferation and differentiation. Zn deficiency is commonly associated with retardation of bone growth. The mechanisms for Zn uptake into osteoblasts have not previously been examined in detail. There are several families of plasma membrane Zn transporters that have been characterized in mammalian cells, which function in either uptake or efflux of Zn. ZIP1 (*Z*rt, *I*rt-like Protein) is ubiquitously expressed in most cells, and is responsible for plasma membrane Zn uptake. We have examined the role of ZIP1 in differentiation of human mesenchymal stem cells (hMSCs) that can assume an osteogenic phenotype under the appropriate culture conditions. First, we have demonstrated gene and protein expression of ZIP1 in both osteoblast-like cells and hMSCs. Second, subcellular distribution of ZIP1 showed both a plasma membrane and diffuse cytoplasmic localization. Third, ^{65}Zn-uptake was shown to be enhanced in hMSCs cultured under osteogenic conditions when compared to basal (i.e., non-osteogenic) conditions; the protein expression of ZIP1 was also increased when hMSCs became osteogenic. Fourth, we have examined the role of ZIP1 in the differentiation of hMSCs into an osteogenic phenotype. We have proposed that overexpression of ZIP1 in hMSCs can accelerate or enhance the osteogenic differentiation pathway. For this purpose, a highly purified recombinant adenovirus (rAd) encoding for a GFP-tagged ZIP1 was used to infect hMSCs for seven days. The effects of ZIP1 overexpression were examined under both basal and osteogenic (culture) conditions in the presence of 10 μM $ZnCl_2$. For control Ad infections, we have used a rAD encoding for a GFP-tagged NMDA R1 subunit. Our results demonstrated that overexpression of ZIP1 in hMSCs increased both alkaline phosphatase (ALP) activity and mineralization, as assessed by histochemical staining. Our preliminary data suggests that at least one family of Zn transporters, namely ZIP1, plays a role in the differentiation of hMSCs into an osteoblast phenotype. This study provides further insights into the mechanism of the effects of Zn on osteoblast function.

Disclosures: ***A. Gupta****, None.*

SU245

Endothelin-1 and ETRA, via Osterix, Down-Regulate VEGF in Osteoblastic Cells. G. Qu*, H. P. von Schroeder. Dept. of Surgery & Faculty of Dentistry, University of Toronto, Toronto, ON, Canada.

Endothelin-1 (ET-1) is produced by vascular endothelial cells to play an important role during bone development, remodeling and repair. ET-1 promotes osteoblastic cell proliferation and differentiation, but has the unique effect of down-regulating vascular endothelial growth factor (VEGF) and may thereby control angiogenesis during bone production. Our objectives were to identify the intracellular mechanisms by which ET-1 controls VEGF expression during osteoblastic proliferation and differentiation. ET-1-induced osteoblastic differentiation in rat SBMC-D8 osteoblastic cells, but down-regulated expression of VEGF mRNA isoforms (VEGF120, 164 and 188) by 67% as demonstrated by semiquantitative reverse transcription polymerase chain reaction (RT-PCR) with primers designed to hybridize to three different splice variants of the rat VEGF-A gene. ET-1 also resulted in a 41% reduction of activity of a luciferase reporter construct containing the promoter region of the VEGF gene. As a positive control, BMP-2 treatment resulted in an increase in VEGF mRNA. Endothelin receptor A (ETRA) overexpression was achieved by transfection with ETRA. This also resulted in inhibition of VEGF-A levels by 63% as shown by RT-PCR and resulted in a 49% reduction of activity of the luciferase reporter construct containing the VEGF promoter. ET-1 treatment and ETRA transfection resulted in a 52% and 48% increase of the transcription factor osterix (Osx) mRNA respectively. Transfection of SBMC-D8 cells with plasmid containing Osx transcript resulted in a 43% decrease in VEGF mRNA as determined by RT-PCR. RNA silencing with double-stranded RNA of Osx was highly successful in completely eliminating Osx signal and resulted in an increase in VEGF mRNA by 108% as determined by RT-PCR and an increase of 180% of luciferase reporter activity. During Osx mRNA interference, the addition of ET-1 could not re-establish its inhibitory effect. This study supports the novel inhibitory role for ET-1, via Osx, on VEGF synthesis in osteoblastic cells as a mechanism in the temporal and spatial feedback of angiogenesis to bone formation and resorption.

Disclosures: ***H.P. von Schroeder****, None.*

SU246

Involvement of CCAAT Enhancer Binding Protein Transcription Factors In the Activation of Collagenase-3 Transcription. K. Wannemacher*[1], P. Dhawan*[2], X. Peng*[2], N. Selvamurugan*[3], N. Partridge*[3], S. Christakos[2]. [1]Biochemistry, Graduate School of Biomedical Sciences-New Jersey Medical School, Newark, NJ, USA, [2]Biochemistry, University of Medicine and Dentistry of New Jersey, Newark, NJ, USA, [3]Dept. of Physiology and Biophysics, UMDNJ-Robert Wood Johnson Medical School, Piscataway, NJ, USA.

Collagenase-3 (MMP-13) is a member of the matrix metalloproteinase (MMP) gene family which is upregulated in osteoblasts by systemic bone resorbing factors including parathyroid hormone (PTH), prostaglandin E_2 and $1,25(OH)_2D_3$. Matrix degradation by collagenase-3 has been implicated in bone remodeling, bone repair and in PTH and $1,25(OH)_2D_3$ induced bone resorption. CCAAT enhancer binding protein (C/EBP) transcription factors are important in the regulation of differentiation and in the expression of cell type specific genes. Recent studies have indicated the importance of C/EBPs in the regulation of osteoblast gene expression. We recently reported that C/EBPs are targets of $1,25(OH)_2D_3$ in osteoblasts. Similar to the regulation of collagenase-3, not only $1,25(OH)_2D_3$ but also PTH can induce C/EBPβ and δ in osteoblasts. In this study we identified and functionally characterized a C/EBP enhancer element in the proximal promoter of the rat collagenase gene (at -36/-32). We demonstrated by cotransfection experiments and gel mobility shift assay that this element is involved in the inducibility of the collagenase-3 promoter by C/EBPδ. In dose response studies (0.125 - 5 µg C/EBPδ), we found collagenase-3 transcription was maximally induced 5.6 ± 0.2 fold by C/EBPδ. C/EBPβ was also found to activate collagenase-3 transcription. Mutation of the -36/-32 C/EBP site within the wild type -148 promoter reduced basal expression and markedly attenuated the response to the C/EBP proteins. Gel shift analysis indicated the ability of C/EBP β as well as C/EBPδ to interact with this element. Deletion of the Cbfa1 site (-132/-126) did not affect the activation of the collagenase-3 promoter by C/EBPδ or C/EBPβ. Overexpression of Cbfa1 stimulated basal transcription and enhanced C/EBP activation of collagenase-3 promoter activity. Taken together these findings establish for the first time that C/EBP proteins are transcriptional activators of the collagenase-3 gene and suggest interactive effects between Cbfa1 and C/EBP proteins in the regulation of collagenase-3 transcription thus providing new evidence for the importance of these factors in the process of skeletal remodeling.

Disclosures: ***K. Wannemacher****, None.*

SU247

The Runx2 Transcription Factor Is a Positive Regulator of the Murine Bone Sialoprotein Gene in Osteoblasts. H. Roca*, G. Xiao, R. T. Franceschi. Periodontics, Prevention, Geriatrics, University of Michigan School of Dentistry, Ann Arbor, MI, USA.

Bone sialoprotein (BSP) is an important component of the bone extracellular matrix. Expression of Bsp is primarily restricted to mineralizing cells, (e.g. hypertrophic chondrocytes and osteoblasts). We previously identified a homeodomain factor binding site in the proximal Bsp promoter that partially explains the tissue-specific activity of this gene in vitro and in vivo (Benson et al, JBC 275:13907,2000; Gopalakrishnan Conn Tiss Res 44(S1):154,2003). However, this site cannot account for the known requirement for the Runx2 transcription factor in Bsp expression in vivo (Ducy et al., Gen.Dev 13:1025,1999). To clarify this issue, the present study examined the functional involvement of Runx2 in the expression of the murine Bsp gene. Chromatin immunoprecipitation (ChIP) analysis of the Bsp promoter in MC3T3-E1 (clone 4) cells detected Runx2 bound to a chromatin fragment comprising the region from -210 to -1130 bp. In contrast, ChIP analysis of the promoter region near -1335 which contains a site capable of binding to Runx2 in vitro (Benson et al., JBMR14:3,1999) failed to detect fragments within this region that were immunoprecipitated with anti-Runx2 antibody. From the region where Runx2 binds to the promoter in vivo, we identified two consensus Runx2-binding elements present at -81 base pairs (bp) (site B1) and -172 bp (site B2) in the mouse gene. Both sites (B1 and B2) are well conserved in the mouse, rat and human promoters. Runx2 can bind to both sites as demonstrated by electrophoretic mobility shift assay and supershift experiments using nuclear extracts from MC3T3-E1 cells. Competition experiments showed that Runx2 exhibited 4 to 5 fold higher affinity for site B1 than for B2. DNA transfection experiments using C3H10T1/2 mesenchymal cells showed that a 2472 Bsp promoter fragment was able to direct 3 to 4 fold higher levels of luciferase reporter expression when the cells were co-transfected with Runx2 expression plasmid. Mutation in the B1 site reduced promoter activity by approx. 50%, while mutation in site B2 caused only a small drop (about 15 %) in the promoter activity. However, in the osteoblastic cell line MC3T3 E1 (clone 4) each mutation caused a drop in the promoter activity of 50%, while the double mutant further reduced the activity another 15% (to 35% of wild type promoter activity). In summary, our results provide strong evidence that Runx2 is an important direct regulator of the Bsp gene that can account for much of its osteoblast-specific expression.

Disclosures: ***H. Roca****, None.*

SU248

BMP2-Induced Alkaline Phosphatase Expression Is Regulated by Dlx5, which Is Interrupted by Msx2 as a Binding Competition to the Common Response Element. Y. Kim*[1], M. Lee*[1], J. M. Wozney[2], J. Cho*[1], H. Ryoo[1]. [1]Biochemistry, Kyungpook National University, Daegu, Republic of Korea, [2]Wyeth, Inc, Cambridge, MA, USA.

Alkaline phosphatase (Alp) is a widely accepted bone marker. Its expression is stimulated by bone morphogenetic protein (BMP)-2 treatment, the activation of BMP receptors and R-Smads, and the expression of Dlx5 and Runx2. However, how BMP-2 induces Alp expression is not clearly understood. We dissected the murine 1.9 kb Alp promoter and found within it a Dlx5-binding cis-acting element by an electrophoretic mobility shift assays and site-directed mutagenesis of the element. Dlx5 and the product of its target gene, Runx2, stimulated Alp promoter activity in an additive manner. However, since Dlx5 continued to stimulate Alp expression in Runx2-/- cells, the Alp stimulatory activity of Dlx5 is independent of Runx2. We also found that overexpression of Msx2 suppressed Dlx5-stimulated Alp promoter activity by competing with Dlx5 for the cis-acting element in the Alp promoter. Moreover, Msx2 levels are constitutively high in C2C12 myogenic cells but decrease over time after BMP-2 treatment. This may explain why BMP-2 treatment of these cells results in immediate Dlx5 expression yet Alp expression commences only 1-2 days later. In other words, Msx2 in high levels counteracts initially the transcriptional activity of Dlx5 in low levels until a threshold Dlx5:Msx2 ratio is reached to the levels that allow the Alp stimulatory activity of Dlx5 to prevail. Thus, Dlx5 transactivates Alp expression, directly by binding to its cognate response element and/or indirectly by stimulating Runx2 expression, and Msx2 counteracts the direct transactivation of Dlx5.

Disclosures: ***Y. Kim****, None.*

SU249

FLP-mediated Recombinantion to Study Gene Function in Differentiating MSC-like KS483 Cells. G. van der Horst*[1], H. Sips*[1], J. Hoogendam[2], C. Löwik[1], M. Karperien[3]. [1]Endocrinology, LUMC, Leiden, Netherlands, [2]Paediatrics, LUMC, Leiden, Netherlands, [3]Endocrinology & Paediatrics, LUMC, Leiden, Netherlands.

The completion of the human genome project necessiates easy and fast test systems to infer gene function. Genetically engineered KS483 cells made suitable for FLP mediated recombination may provide such a model. KS483 cells have MSC-like characteristics, since they can differentiate into osteoblasts, adipocytes and chondrocytes. To enable easy genetic manipulations, we have stably transfected KS483 cells and integrated 1 copy of a FRT-target site into their genome. This site can be used for insertion of DNA by homologous recombination. We isolated 3 KSfrt clones, which have retained pluripotency.

To test the efficacy of the FRT-targeting procedure, the 3 clones were co-transfected with an FRT-targeting vector driving luciferase expression and FLP recombinase. After two weeks, isogenic KSfrt Luc clones were isolated. In the 3 clones luciferase activity was expressed at a constant level at all stages of osteoblast and adipocyte differentiation, indicating absence of positional effects on activity of the inserted targeting vector.

Next we used this methodology to overexpress RunX2. Two weeks after transfection

isogenic clones were isolated which overexpressed RunX2 at the protein level. In differentiation assays, these clones demonstrated increased osteoblast and chondrocyte differentiation, while adipocyte differentiation was inhibited. To test whether FRT-mediated recombination could be used for an siRNA approach, we created an FRT RNAi vector driving the expression of a 19bp RNA duplex targeting RunX2. In the 3 KSfrt RNAi RunX2 clones, osteoblast differentiation was blocked in contrast to the clones expressing a RNAi mtRunX2 construct having a 2 nucleotide mismatch in the 19 basepair duplex. This indicates that integration of 1 copy of the RNAi vector is sufficient to induce a near complete gene knock down.
Subsequently we tested whether the KSfrt Luc clones could be used *in vivo*, a bone marrow ablation assay was performed in which the cells were injected in the marrow cavity. Cell fate was followed by non-invasive bioluminescent imaging and X-rays. Data suggested that the KSfrt Luc clones were normally incorporated in new bone induced by the ablation. In conclusion, KSfrt cells provide a simple and fast model for testing gene function, either by overexpression or by gene knock down, on differentiation into mesenchymal cell lineages both in vitro and in vivo. Furthermore, these cells may be used for the easy generation of lineage specific reporter cell lines. We are now exploiting this model for the systematic knock down and overexpression of components of the Wnt-signalling pathway.

Disclosures: ***M. Karperien****, None.*

SU250

Transcription Factors Involved in the Regulation of IL-6 in Mouse Calvarial Osteoblasts by Vasoactive Intestinal Peptide. E. Persson*[1], O. Voznesensky[2], C. C. Pilbeam[2], U. H. Lerner[1]. [1]Dept. Oral Cell Biology, Odontology, Umea, Sweden, [2]Dept. Medicine, University of Connecticut Health Center, Farmington, CT, USA.

The skeleton contains an intense network of nerve fibers expressing neuropeptides, including vasoactive intestinal peptide (VIP). We have previously shown that VIP can regulate osteoclast formation and activity. Interleukin-6 (IL-6) and the related cytokines IL-11, leukemia inhibitory factor (LIF) and oncostatin M (OSM) are potent stimulators of osteoclastic bone resorption. In the present study, we have addressed the possibility that the neuropeptide VIP may regulate the production of and/or sensitivity to the IL-6 family of cytokines in mouse calvarial osteoblasts. Using RT-PCR, real-time PCR and ELISA we could show that VIP stimulated the mRNA expression of IL-6 and the release of IL-6 protein in a time- and concentration-dependent manner. The mRNA expressions of IL-11, LIF, OSM, and their cognate receptors were unaffected by VIP. However, the mRNA level of gp130, the signal transducing protein linked to the receptors in the IL-6 family, was decreased by VIP. In cells transfected with the IL-6 promoter coupled to luciferase, VIP increased luciferase activity. All the effects of VIP were potentiatied by cyclic AMP phosphodiesterase inhibitor rolipram, mimicked by forskolin and shared by PACAP-38, but not by secretin, two peptides also belonging to the VIP/secretin family. The facts that PACAP-38 was equipotent with VIP and that secretin was without effect, indicate that the responses were mediated by the VIP type 2 receptor. EMSA demonstrated that the DNA-binding activity of nuclear extracts to C/EBP was increased by VIP, whereas binding to AP-1 was decreased and binding to NF-κB and CREB was unaffected. Gelshift analysis showed that the C/EBP complex consisted of C/EBPβ and C/EBPδ and that the AP-1 complex could be shifted by a combination of antibodies to c-Jun, JunB, c-Fos, and Fra-1 but not by individual antibodies. RT-PCR showed that the mRNA expressions of C/EBPβ, C/EBPδ, C/EBPγ, c-Jun, JunB, c-Fos, Fra-1 and IκBα, and protein level of IκBα were all unaffected by VIP. Immunocytochemical analysis showed that VIP did not affect nuclear translocation of NF-κB (p50, p65), C/EBPβ or C/EBPδ. These observations demonstrate that VIP type 2 receptors stimulate IL-6 production in osteoblasts by a mechanism likely to be dependent on cyclic AMP/protein kinase A activation and also involving regulation of the transcription factors C/EBP and AP-1.

Disclosures: ***E. Persson****, None.*

SU251

Phosphorylation Dependent Enhancement of Vitamin D Receptor Mediated Transcription Is Associated with Phosphorylation of C/EBPβ at Thr[188], Nuclear Accumulation of C/EBPβ and Phosphorylation of CREB-Binding Protein. Y. Liu*, S. Christakos. Biochemistry, Graduate School of Biomedical Science-New Jersey Medical School, Newark, NJ, USA.

We previously reported that okadaic acid (OA), an inhibitor of protein phosphatase 1 and 2A, can enhance the transcriptional activity of WT vitamin D receptor (VDR) as well as the transcriptional activity of mutant VDRs (H305Q, F251C, I268T). The enhancement correlated with increased interaction between DRIP205 and either WT or mutant VDRs. We found that VDR was not phosphorylated in the presence of 50 nM OA. To address the possibility that OA may be acting by enhancing the phosphorylation of another protein involved in VDR mediated transcription, we examined C/EBPβ which is a potent enhancer of VDR mediated 24(OH)ase transcription and contains phosphorylation sites for multiple protein kinases, including a conserved mitogen activated protein kinase (MAPK) consensus site at Thr[188]. Immunoblotting with antibodies against a synthetic phosphopeptide corresponding to residues surrounding Thr[188] of C/EBPβ showed that OA (50 nM) promoted the phosphorylation of C/EBP β in UMR 106 osteoblastic cells at 30 min after OA treatment. Phosphorylation of C/EBP β increased 10 fold after 4h OA treatment. No change in the level of C/EBPβ protein was observed after OA treatment. The MEK inhibitor, U0126 (10 μM), prevented the phosphorylation of C/EBPβ observed at 30 min., suggesting that this phosphorylation involves OA activated MAPK signaling. Studies using immunocytochemistry and fluorescence microscopy indicate that OA (50 nM) can also promote the nuclear accumulation of C/EBPβ in UMR osteoblastic cells 2h after treatment. In addition to phosphorylation and nuclear accumulation of C/EBPβ, we also examined CREB-binding protein (CBP) which cooperates with C/EBPβ in regulating VDR mediated 24(OH)ase transcription and has been reported to be essential for ligand dependent transcription of a number of steroid receptors. Treatment of UMR cells with OA (50 nM) consistently resulted in the appearance of a slower migrating form of CBP as visualized by SDS-PAGE and Western blotting. The slower migrating form was no longer detected after subsequent incubation with phosphatase, providing evidence that OA also results in the phosphorylation of CBP. The phosphorylation of CBP was not induced by $1,25(OH)_2D_3$. These findings suggest that transcriptional activity of WT and mutant VDRs can be enhanced by phosphorylation and this may be mediated by increased coactivator binding and nuclear accumulation and phosphorylation of specific VDR cofactors.

Disclosures: ***Y. Liu****, None.*

SU252

Expression of the Bone-Specific Osteocalcin Gene Requires SWI/SNF Chromatin Remodelling Activity. A. Villagra*[1], M. Villagran*[1], F. Cruzat*[1], L. Carvallo*[1], J. Olate*[1], A. van Wijnen[2], J. Lian[2], G. Stein[2], J. Stein[2], A. Imbalzano*[2], M. A. Montecino[1]. [1]Bioquimica y Biologia Molecular, Universidad de Concepcion, Concepcion, Chile, [2]Cell Biology, University of Massachusetts Medical School, Worcester, MA, USA.

Osteocalcin (OC) is a bone-specific protein that is expressed at late stages of osteoblast differentiation. Transcription of the OC gene is associated with changes in chromatin structure at the promoter region, which are reflected by the presence of two DNase I hypersentive sites (DHS). These DHS span all the key regulatory elements that control basal tissue-specific and vitamin D3-enhanced OC gene transcription. Among the cellular complexes that possess chromatin-remodelling activity, are the SWI/SNF complexes. These complexes include a catalytic subunit containing ATPase activity, which in higher eukaryotes can be either BRG-1 or BRM. Mutations in the ATPase domain of BRG-1 or BRM that abrogate the ability of these proteins to bind ATP, result in the formation of inactive SWI/SNF complexes. To gain understanding into the molecular mechanisms involved in the chromatin remodelling events that are linked to the OC gene transcription, we have stably transfected osteoblastic cells with constructs encoding for Flag-tagged mutated versions of BRG-1 and BRM under the control of an inducible promoter. We found that overexpression of these ATPase mutant proteins results in the formation of inactive SWI/SNF complexes that bind to the OC promoter. This interaction correlates with a significant inhibition of both basal and vitamin D3-enhanced endogenous OC transcription as well as with a marked decrease in nuclease hypersensitivity. Together our results indicate that SWI/SNF complexes have an important role in the chromatin remodelling events that accompany transcriptional activity of the OC gene in osteoblasts.

Disclosures: ***M.A. Montecino****, None.*

SU253

Lef1-Suppression Accelerates Osteoblast Differentiation and Modifies Gene Expression Profiles. R. A. Kahler[1], J. J. Westendorf[2]. [1]Graduate Program in Microbiology, Immunology and Cancer Biology, University of Minnesota, Minneapolis, MN, USA, [2]Department of Orthopaedic Surgery, and The Cancer Center, University of Minnesota, Minneapolis, MN, USA.

Activation of the Wnt signaling pathway via LRP5 Wnt coreceptor increases bone mass. Lef1 is one of the transcription factors responsible for translating the Wnt/ß-catenin signaling cascade into gene expression changes. We recently demonstrated that Lef1 and ß-catenin antagonize Runx2-dependent activation of the osteocalcin promoter. We have also identified multiple Lef1 isoforms in murine osteoblasts that are likely to be products of alternative splicing or alternative promoter usage and may act as dominant negative proteins. Lef1 DNA binding activity decreases during osteoblast maturation. We therefore hypothesize that the regulated expression of specific Lef1 isoforms is crucial for osteoblast maturation. To determine the importance of some of these Lef1 isoforms in osteoblast differentiation, we produced MC3T3-E1 preosteoblast cell lines that express short hairpin RNAs (shRNAs) targeting exon 11 of Lef1 and have reduced Lef1 expression. Lef1-suppressed cells do not grow faster than control cells but they differentiate at a faster rate as they produce alkaline phosphatase, osteocalcin mRNA and mineralized nodules three to four days before control cells expressing an shRNA against firefly luciferase (Ffl). We hypothesize that the reduction of Lef1 expression alters gene expression to promote osteoblast maturation. By probing Affymetrix Mouse Genome 430A gene chip arrays, we identified 48 genes that were differentially expressed by more than two fold in Lef1-suppressed cell lines as compared to the control Ffl line ($p<0.005$). Many genes that were reduced in Lef1-suppressed cells were extracellular matrix genes, including procollagen XI alpha 1 (Col11a1; 6.5 fold), asporin (4.0 fold), fibulin 5 (2.6 fold), and procollagen III alpha 1 (2.1 fold). We confirmed reduced Col11a1 expression in our Lef1 shRNA cells by real-time quantitative PCR. Examination of the promoter revealed three potential Lef1/Tcf binding sites. Lef1 activates the Col11a1 promoter two to three fold and addition of ß-catenin enhances activation in a concentration dependent manner. Mutations in Col11a1 cause both Marshall and Stickler syndromes, which are characterized by craniofacial abnormalities and thickened calvaria. These data suggest that Lef1 regulates osteoblast function by differentially controlling genes such as Col11a1 and osteocalcin.

Disclosures: ***R.A. Kahler****, None.*

SU254

Coactivator PGC-1a Is PTH-Induced and Synergizes with Nurr1 to Regulate Promoter Activity in Osteoblasts. J. Nervina, C. Magyar*, F. Pirih*, I. Ozkurt*, S. Tetradis. UCLA School of Dentistry, Los Angeles, CA, USA.

We have shown that PTH induces expression of the NGFI-B nuclear orphan receptor Nurr1 through cAMP-PKA signaling in bone. Nurr1 induces osteocalcin (OCN) expression through an NGFI-B response element (NBRE)-like site in the proximal promoter. While nuclear receptor transactivation is greatly enhanced by coactivators, no coactivator for Nurr1 is known. PPARg coactivator-1a (PGC-1a) is a promising candidate since it is cAMP-induced and synergizes with nuclear receptors to increase transcription. *We hypothesize that PGC-1α is a PTH-induced primary response gene that synergizes with Nurr1 to induce target gene transcription in osteoblasts.* First, using real time PCR we show that 10 nM PTH for 2 h maximally induced PGC-1α mRNA in primary mouse osteoblasts (MOBs) and calvaria organ culture. PKA activation with 10 μM forskolin induced PGC-1α, while PKC activation with 1 μM PMA and calcium signaling with 1 μM ionomycin did not. Also, 100 nM PTH(3-34), which activates PKC and calcium but not PKA, did not induce PGC-1α. Confirming primacy of cAMP signaling in PGC-1α induction, PTH-induced PGC-1α markedly decreased when PKA but not PKC signaling was inhibited. Protein synthesis inhibition with 3 μg/ml cycloheximide caused superinduction of PTH-induced PGC-1α expression. Next, to investigate PGC-1αs potential function as a Nurr1 coactivator, MOBs were cotransfected with Nurr1 and/or PGC-1α expression vectors and a consensus 3xNBRE-luciferase construct. Nurr1 induced promoter activity 3.5 fold, while PGC-1α had no effect. PGC-1α and Nurr1 together induced promoter activity 10 fold. Then, to examine whether the same transcription factor-coactivator interaction can regulate endogenous promoters, MOBs were transiently cotransfected with Nurr1 and/or PGC-1α expression vectors and the rat (-1050)OCN-luciferase construct. Nurr1 increased OCN promoter activity 3 fold, while PGC-1α had no effect. Importantly, PGC-1α and Nurr1 together increased OCN promoter activity 10 fold. This synergy required Nurr1-DNA binding, since a mutation of the NBRE-like sequence in the proximal OCN promoter abolished both Nurr1- and Nurr1-PGC-1α-induced transactivation. Finally, to test for protein-protein interaction, recombinant Flag-PGC-1α and Nurr-1 proteins were co-incubated. Flag-PGC-1α protein co-immunoprecipitated with Nurr1 antibody, and Nurr1 protein co-immunoprecipitated with Flag antibody. *We conclude that PGC-1α is a PTH-induced coactivator that binds to Nurr1 to synergistically increase OCN promoter activity in osteoblasts.* Taken together with published data, our findings suggest that Nurr1 and PGC-1α may be pivotal mediators of cAMP-induced osteoblast gene expression.

Disclosures: ***J. Nervina****, None.*

SU255

A Novel Secreted, Cell-surface Glycoprotein Containing Multiple EGF-like Repeats and One CUB Domain Is Highly Expressed in Human Osteoblasts. B. Wu*, Y. Su*, M. Tsai*, R. Yang. Institute of Biomedical Sciences, Academia Sinica, Taipei, Taiwan Republic of China.

We have previously identified a novel family of secreted, cell-surface proteins expressed in human vascular endothelium. To date, two family members have been described, sharing a characteristic domain structure including an amino-terminal signal peptide followed by multiple copies of EGF-like repeats, a spacer region and one CUB domain at the carboxyl terminus. Thus, this family was termed SCUBE for Signal peptide-CUB-EGF-like domain containing proteins. Here we described the identification and characterization of one additional member of the SCUBE family named SCUBE3 in humans, sharing an overall 60% protein identity and a similar domain structure with other family members. Real-time quantitative reverse transcriptase-PCR and Northern blot analyses revealed that this gene is highly expressed in human primary osteoblasts. Western blot analysis confirmed that hSCUBE3 protein is expressed in a variety of osteoblast-like cell lines. Consistently, immunofluorescent staining demonstrated that hSCUBE3 is colocalized with type I collagen-positive osteoblasts in mouse skeleton. Overexpression of hSCUBE3 in human embryonic kidney 293T cells resulted in a secreted glycoprotein that can form oligomers, tetherered to the cell-surface. Interestingly, the secreted hSCUBE3 protein can be further proteolytically processed by a serum-associated protease to release the EGF-like repeats from the CUB domain. Moreover, the hSCUBE3 mRNA is down-regulated upon the treatment of lipopolysaccharide in human osteoblast-like SaOS-2 cells. The SCUBE3 gene is mapped to human chromosome 6p21.3, a region that has been linked with the locus for a rare form of metabolic bone disease, Paget's disease of bone 1. Together, this novel secreted, cell-surface osteoblast protein may act locally and/or distantly through a proteolytic mechanism, and may play an important role in bone cell biology.

Disclosures: ***R. Yang****, None.*

SU256

In Vivo **Bone Formation of Bone Marrow-Derived Cells Correlates With CD105, CD166, and Thy1 Cell Surface Markers.** J. E. Dennis[1], K. Renshaw*[2], A. Awadallah*[1], K. Goltry*[2]. [1]Biology, Case Western Reserve University, Cleveland, OH, USA, [2]Aastrom Biosciences, Inc., Ann Arbor, MI, USA.

The purposes of this study were to determine if stromal cell markers correlate with *in vivo* bone formation and to derive optimal culture conditions for the expansion of osteogenic cells.

Identical human bone marrow mononuclear cell aliquots were inoculated into two fully automated, self-enclosed Aastrom RepliCell™ System (ARS) bioreactors and cultured for 12 days with continuous medium perfusion. On day 12, populations of cells were obtained from each bioreactor: A Total Cell Population (TCP) obtained by a standard trypsinization, and an Adherent Cell Population (ACP) obtained by trypsinization after non-adherent cells depletion. Both populations were evaluated by flow cytometry prior to *in vivo* osteogenesis assessment. For *in vivo* bone formation, cells are combined with porous calcium phosphate ceramics and implanted sub-cutaneously into NOD/SCID mice; after 6 weeks, the ceramics were harvested, prepared for histology and scored. Both TCPs and ACPs were tested at ceramic loading concentrations of 5, 10, 25, and 50 million cells/ml. Empty ceramics and mesenchymal stem cell (MSC)-loaded ceramics served as positive and negative controls. A total of 12 mice were used in each experiment (N=6 for each TCP and ACP sample; N = 12 for negative and positive controls);implantation sites were randomized. Three TCP and ACP cohorts and two cohorts comparing two culture conditions (with and without growth factors) were used to derive the correlation values (N=10).

The bone scores showed that ACP consistently showed higher bone scores than the TCP at all four loading dilutions. Empty controls showed only trace amounts of bone and the positive control MSC bone scores were consistently high. To derive the Total Bone Score (TBS), the scores for each cell loading dilution were summed. A graph of the relationship between TBS and selected flow cytometric markers and colony forming units-fibroblastic (CFU-f) are shown in Figure 1. There is a strong correlation between bone scores and the CD-14-/Thy-1+ and CD-166+ (ALCAM) cell populations, and with the CD-105+ (endoglin) population. Interestingly, there was little correlation between total CFU-f and *in vivo* bone scores. The endoglin, Thy1 and ALCAM markers appear to be predictive markers for osteogenic potential in these cell populations.

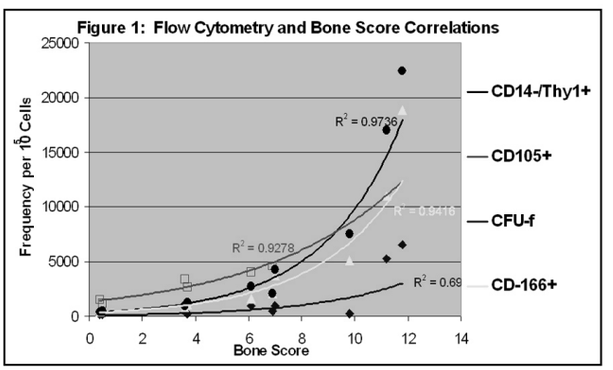

Disclosures: ***J.E. Dennis****, Aastrom Biosciences, Inc. 5.*

SU257

Effects of Bisphosphonate (YM529) on Osteoblastic Function and Differentiation in Bone Regeneration after Drill-Hole Injury in Mice. M. Nagashima*, A. Sakai, S. Uchida*, S. Tanaka*, M. Tanaka*, T. Nakamura. Orthopaedic surgery, University of occupational and enviromental health, Kitakyushu, Fukuoka, Japan.

Recently, bisphosphonates have been shown to have direct effect on osteoblasts, but the effects on bone regeneration in vivo are not elucidated. In this study, we investigated to clarify the effect on osteoblastic function and differentiation at the bone regeneration of drill-hole injury during the bone turnover reduced by bisphosphonate (YM529).

Male C57BL/6N mice, 8 weeks of age, were assigned to two groups with respective dose of 0 (vehicle control; VC group) or 0.1 (YM529 group) mg/kg body weight of the agents, intravenously injected once a week. At 10 weeks of age, six mice each from VC and YM529 groups were sacrificed (day 0). The remaining mice were subjected to drill-hole injury at the diaphysis of bilateral femurs. Femoral specimens were obtained at 7, 10, 14, 21, and 28 days after surgery. Histomorphometric study revealed that, in the YM529 group, the bone volume of the regenerating bone at the injured site did not significantly differ at 7 and 10 days, but the medullary bone mass was larger and the regenerated cortical bone volume was smaller compared to those in the VC group at 21 and 28 days. Expression levels of mRNAs in the regenerating site were evaluated at 0, 3, 5, 7, 10, 14, and 21 days. Osterix, BMP-2, and type I collagen mRNAs in the YM529 group were significantly lower than those in the VC group at day 0. At 3 and 5 days after injury, cbfa1, osterix, BMP-2, type I collagen, and osteocalcin mRNAs in the YM529 group were similar to those in the VC group. At 7 days, osterix, BMP-2, and osteocalcin mRNAs in the YM529 group were significantly higher than those in the VC group. Only osteocalcin mRNA in the YM529 group was significantly lower than that in the VC group at 14 days. Compared to the VC group, RANKL and TRACP mRNAs in the YM529 group were significantly higher throughout the experimental period. To evaluate bone marrow osteogenic capacity, samples taken from femurs at 0 and 5 days after injury were used for CFU-f assay and mineralized nodule formation. In the YM529 group, the numbers of CFU-f and ALP+CFU-f were reduced compared to controls at day 0. At 5 days, the numbers of CFU-f and ALP+CFU-f were similar in both the YM529 and VC groups. At day 0, the area of mineralized nodule formation was significantly smaller in the YM529 group than that in the VC group. At 5 days, there was no significant difference between the YM529 and VC groups.

These data indicate that bisphosphonate does not affect the osteoblastic function and differentiation in initial medullary bone regeneration. But, in the period of cortical bone formation at 14 days and thereafter, bisphosphonate may affect the osteoblastic differentiation.

Disclosures: ***M. Nagashima****, None.*

SU258

Visualizing Levels of Osteoblast Differentiation by a Two Color Promoter-GFP Strategy: Type I Collagen-GFPcyan and Osteocalcin-GFPtpz. I. Bilic-Curcic*[1], M. S. Kronenberg*[1], J. Bellizi*[1], X. Jiang*[1], E. Gardiner*[2], D. W. Rowe[1]. [1]Genetics and Developmental Biology, University of Connecticut Health Center, Farmington, CT, USA, [2]Garvan Insitute, Sydney, Australia.

For understanding cellular and molecular mechanisms of osteoblast differentiation it is necessary to develop visual markers that reflect the progression of cells to full osteoblast differentiation in cell culture that should be readily transferable to in vivo models of bone formation.

The purpose of this study is to show the feasibility of generating transgenic mice containing two promoter constructs driving distinguishable GFP isomers at different stages of osteoblast differentiation to identify cells at different levels of development both in cell culture and intact mouse bone. A 3.9 kb fragment of the human osteocalcin (hOC) promoter and a 3.6 kb fragment of the collagen promoter (Col3.6) linked with visually distinguishable GFP's, topaz and cyan, were used for multiplex analysis of osteoblast lineage progression. Transgenic mice for each construct, identified as pOBCol3.6GFPcyan and hOCGFPtpz, were individually characterized and then crossed. Temporal and spatial expression of both transgenes was analyzed in vitro and in vivo. In marrow stromal and neonatal calvarial cell cultures of crossed transgenic lines the pOBCol3.6GFPcyan low intensity positive cells appeared on day 7 and its expression continued as high intensity GFP positive cells that contributed to the formation of nodules. The hOCGFPtpz transgene expressing cells appeared at day 15 in nodules undergoing mineralization. In the mineralizing nodule we observed the activation of hOCGFPtpz in cells that were originally only cyan positive. The intensity of tpz in double GFP positive cells gradually increased as a concomitant decrease in cyan expression was detected.

In the histological analysis, the double transgenics illustrate a spectrum of osteoblast differentiation. Cells expressing cyan are present in the primary spongiosa and extend a short distance along the cortical bone. Double expressing cells can be found in trabeculae in the secondary spongiosa and lower cortex and along the surface of cortical bone. The majority of cells on the surface of cortical and trabecular bone and osteocytes are only tpz positive.

Thus a spectrum of osteoblast differentiation can be observed in bone nodules in primary culture and within bone. Because genetic disorders of bone may ultimately exert their effect by interfering with the orderly progression of progenitor to fully mature bone cell, this approach may be useful to identify the cellular consequence of a gene mutation as progenitors progress through stages of differentiation in cell culture and intact bone.

Disclosures: ***I. Bilic-Curcic****, None.*

SU259

Bone Nodule Formation Via *In Vitro* Differentiation of Murine Embryonic Stem Cells. S. K. Bronson, K. Dunham*, J. Heaney*, N. Woll*. Cellular and Molecular Physiology, The Penn State University College of Medicine, Hershey, PA, USA.

The process of bone formation can be approximated in vitro, in the form of a mineralized nodule. Osteoprogenitors can be found in fetal and neonatal calvaria, and in the bone marrow. Mesenchymal stem cells (MSCs), the immediate precursor to the osteoprogenitor are found in the marrow, and likely in numerous other sites throughout the organism. These progenitors, when placed into culture, establish colonies that proliferate, differentiate into osteoblasts, and secrete and mineralize matrix over a period of 3 weeks. The overlapping differentiation potential of embryonic stem cells (ESCs) and the MSCs found in adult organisms led us to perform the following experiments. ESCs were allowed to form embryoid bodies (EBs). EBs were disrupted and plated at concentrations as low as 30 cells/cm^2. By 8 days post-plating a significant percentage of the colonies have morphology characteristic of other types of osteoblast cultures. By three weeks in culture these colonies go on to form layered, mineralized nodules as visualized by fixation and staining with the von Kossa technique. Up to 75% of colonies are mineralized. From EBs that range in size from 250-2500 cells approximately 1 in 80 cells is capable of forming a mineralized nodule. We have isolated RNA from entire plates and individual colonies at different stages of the differentiation process and have used QRT-PCR to quantify the expression of genes characteristic of the osteoblast lineage as well as genes characteristic of other lineages and stem/progenitor cells. Runx2, twist 1 and 2, osterix, type I collagen and osteocalcin are all transcriptionally upregulated in the osteoblast culture as differentiation progresses. Gene expression in individual colonies consistently reflects cell and colony morphology. Differentiation of an ESC line with an integrated bacterial artificial chromosome-based osteocalcin-driven GFP reporter was analyzed with confocal microscopy to further document the presence of mature osteoblasts. Differentiation of ES cells into the osteoblast lineage in vitro will be a valuable tool for addressing pertinent questions about the proliferation, differentiation, survival, and intercellular communication between cells of the bone lineage in vitro. In vitro differentiated cells can also provide an important testing ground for therapeutic applications in humans.

Disclosures: ***S.K. Bronson****, None.*

SU260

BMP Regulation of SOST and Osterix Expression During Embryonic Osteogenesis. A. Nifuji, Y. Ohyama*, Y. Maeda*, M. Noda. Molecular Pharmacology, Tokyo Medical and Dental University, Tokyo, Japan.

Sclerostin (SOST), a member of the cystine-knot superfamily, is essential for proper skeletogenesis since loss of function mutation in SOST gene results in sclerosteosis featured with massive bone growth in humans. To understand the function of SOST in developmental skeletal tissue formation, we examined SOST gene expression in embryonic osteogenesis in vitro and in vivo. During osteoblastic differentiation in primary calvarial cells, the levels of SOST expression were increased along with those of alkaline phosphatase activity and nodule formation. In situ hybridization study revealed that SOST mRNA expression was observed in osteogenic front in embryonic 16.5 day postcoitum (E16.5) embryonic calvariae and this expression persisted in the peripheral area of cranial bone in the later developmental stage (E18.5). These temporal and spacial expression patterns in vivo and in vitro were in parallel to those of osterix (Osx), which is a critical transcriptional factor for bone formation. Similar co-expression of SOST and Osx mRNA was observed when the primary osteoblastic calvarial cells were cultured in the presence of BMP2 in vitro. Moreover, endogenous expression of SOST and Osx mRNA was inhibited by infection of noggin-expressing adenovirus into the primary calvarial osteoblastic cells, suggesting that endogenous BMPs are required for these cells to express SOST and Osx mRNA. Thus, expression and regulation of SOST under the control of BMP were closely associated with those of Osx in vivo and in vitro.

Disclosures: ***A. Nifuji****, None.*

SU261

The Effect of Enamel Matrix Derivative (EMD) on Gene Expression in Osteoblasts. S. P. Lyngstadaas*[1], S. Reppe*[2], H. Berner*[1], J. E. Reseland*[1]. [1]Oral research laboratory, University of Oslo, Oslo, Norway, [2]Department of Medical Biochemistry, University of Oslo, Oslo, Norway.

Enamel matrix derivative, obtained from developing porcine teeth, is composed mainly of amelogenin proteins. It is used topically in periodontal surgery to regenerate lost connective tissues and bone. It has been shown that EMD stimulates local growth factor secretion and cytokine expression by periodontal ligament cells. The effect of EMD components on primary bone cells and bone growth, however, is unclear

The effect of EMD(50 µg/ml) on gene expression in primary human osteoblasts were compared to the effect of parathyroid hormone (PTH; 10^{-8}M). Micro array analysis of prepared material was performed using Hu-133A chips containing cDNA oligonuclotides representing more than 22 000 transcripts. Confirmative real-time PCR analysis was performed using the ABI Prism 7900HT Sequence Detection System and the 7900HT Micro Fluidic Card containing 8 ports. The effect of treatments was calculated relative to untreated cells, as signal log ratio.

We found that 254 genes were regulated more than 2 times with both EMD and PTH, and no genes were found to be regulated at least 2 times in the opposite direction by EMD and PTH. A summary of effect of EMD on genes grouped by major biological processes is listed in the table.

A specific effect of EMD on bone formation and enhance osteoblast maturation was found by increased alkaline phosphatase activity in the medium, as well as increased expression and secretion of osteocalcin and collagen type, whereas Runx2 expression was not affected. A possible interactive role of EMD in osteoclastogenesis can be deduced from the observed 16 fold increase in IL-6 and 2.5 fold increase in osteoprotegrein secretion to the media.

Biological Processes	number of genes
Apoptosis	7
Cell to cell signal	10
Transcription	17
Signal tranduction	39
Transport	24
Cell proliferation	51
Metabolism	93

Disclosures: ***J.E. Reseland****, None.*

SU262

Lack of an Effect Of The HIV Protein Tat on Indices of Osteoblastic Cell Function. B. Kang[1], J. Xu*[1], H. Hu*[2], V. Ganapathy*[2], C. M. Isales[3]. [1]Institute of Molecular Medicine and Genetics, Medical College of Georgia, Augusta, GA, USA, [2]Biochemistry and Molecular Biology, Medical College of Georgia, Augusta, GA, USA, [3]Medicine, Medical College of Georgia and the Augusta VA Hospital, Augusta, GA, USA.

Patients infected with HIV have a higher incidence of osteopenia and osteoporosis even prior to the development of opportunistic infections or beginning anti-retroviral therapy. The cause of bone loss in these patients is unknown although measurement of serum markers of bone turnover suggest a problem of increased bone resorption rather than a problem with bone formation. To examine the underlying pathophysiology further, the osteoblastic cell line MC3T3 were transfected with the HIV Tat cDNA to express Tat protein. Tat is a protein encoded by HIV genome that facilitates multiplication of HIV-1 in the host cell. We used a pGEM2-Tat cDNA construct with a 295 bp fragment encoding the first exon of HIV-1 Tat gene and a CMV promoter. Transfected cells were grown in the presence of Geneticin (G418) according to the Lipofectamine (Invitrogen) protocol. The pcDNA3.1 vector by itself was transfected into MC3T3 cells as a control. The expression of Tat in the stably transfected MC3T3 was analyzed by measuring Tat mRNA and protein. Tat protein expression in transfected MC3T3 was assessed by immunocytochemistry using a monoclonal antibody against HIV-1 Tat (obtained through the AIDS Research and Reference Reagent Program, Division of AIDS, NIAID, NIH, contributed by Dr. John Karn). In order to assess whether the expression of the HIV Tat affected indices of osteoblastic function, we measured: RANKL, OPG, alkaline phosphatase, osteocalcin, Cbfa1 and collagen type I expression using real-time PCR light cycler (Roche). Three independent measurements per sample were performed; the specificity was confirmed by melting curve analysis and agarose gel eletrophorosis.
The quantified individual RNA expression levels were normalized for the respective tubulin expression levels. No significant difference was found in gene expression between control and Tat expressing osteoblastic cells.
We conclude that, consistent with the in vivo data, Tat protein expression does not impact indices of osteoblastic cell growth and differentiation and suggests that HIV effects on bone turnover are more likely mediated by effects on bone resorption rather than formation.

Disclosures: ***B. Kang****, None.*

SU263

Imaging GFP Reporters in Frozen Sections of Decalcified and Non-decalcified Mouse Bone. X. Jiang*[1], Z. Kalajzic*[1], P. Mate*[1], A. Braut*[2], J. Bellizzi*[1], M. Mina*[3], D. W. Rowe[1]. [1]Genetics & Developmental Biology, University of Connecticut Health Center, Farmington, CT, USA, [2]Medical and Dental University, Rijeka, Croatia, [3]Dept of Pediatric Dentistry, University of Connecticut Health Center, Farmington, CT, USA.

This is a progress report of the available type I collagen - GFP reporter mice and the implementation of histological techniques to evaluate their expression pattern in sections of mouse bone. Four different colors of GFP (cyan, sapphire, emerald and topaz) have now been studied extensively in bone section to know which colors and filter sets can be used to develop a multiple fluorescent color analysis. Recent transgenic mice suggest that dsRedII is also compatible with healthy mice providing a 5th color that can be multiplexed. Methods for combining GFP imaging with other fluorescent techniques have been developed to allow simultaneous co-localization of the GFP signal to traditional histological methods. Examples include TUNEL, immunofluoresence for surface or intracellular antigens and fluorescent chromatin stains to counter-stain non-GFP expressing cells. Significant progress has been made in preparing frozen non-decalcified section that allow simultaneous imaging of GFP and fluorescent labeling of new matrix formation. Calcein, tetracycline, xylenol orange and alizarin complexone can be used in various combinations with the different GFP colors to assess which population of GFP+ cells are actively depositing new bone. The histology has shown that not all pOBCol3.6GFP+ cells on the bone surface are depositing mineral and regions of mineral deposition do not necessarily have overlying Col3.6GFP+ cells. However essentially all pOBCol2.3GFP+ cells are associated with mineralization. Finally, techniques have been developed to sequentially image for GFP and then process the sample for a histological stain that destroys the GFP signal. The original GFP image is then co-localized with the stained image by overlying the two image files. Examples include chemical stains such as H&E and alizarin red (mineralized section), enzymatic stains such as TRAP, AP or lac Z (for ß-gal expressing transgenic mice) and nucleic acid based procedures such as BrdU and in situ hybridization. The sectioning procedures are based on tape transfer of full longitudinal frozen section of mouse bone. A web site is being developed to provide more detail of the procedures
(http://skeletalbiology.uchc.edu/30_ResearchProgram/304_gap/index.htm, click Lineage in vivo) and examples of the type of histological sections that can reveal a complexity of cellular organization within bone that may not be appreciated by traditional histological methods.

Disclosures: ***X. Jiang****, None.*

SU264

Evidence for Gene Expression of the Neuronal Cell Surface Protein, Neurexin 3ß, in Adult Mesenchymal Stem Cells and Osteoblast-like Cells. B. D. Aggarwal*, S. Kanthala*, K. G. Danielson. Orthopaedic Surgery, Thomas Jefferson University, Philadelphia, PA, USA.

Neurexins comprise a family of neuronal cell surface proteins that serve as neuronal transmembrane cell adhesion molecules and may function in cell signaling and recognition. The neurexin family consists of three neurexin genes that each encode two mRNA forms (a and ß) based on the transcription start site. The a-neurexin proteins are longer with three laminin/EGF-like domains while the ß-neurexins are truncated forms that retain a short signal peptide and ß-neurexin specific sequence followed by the C-terminal portion of a-neurexin domain III. Alpha but not ß-neurexins are highly conserved in mammals with 95% homology and the six primary transcripts (three a and three ß) are subject to extensive splicing. Following detection by differential display of an uncharacterized DNA sequence located 50 kb downstream of a neurexin gene, we hypothesized that adult mesenchymal stem cells (MSCs) or osteoblast-like cells from trabecular bone may express these cell surface proteins and transcriptional activity of these neurexin genes may be modulated during differentiation *in vitro*. A human bone marrow stromal cell line, hMPC32F, previously characterized in our lab was used in these studies and RT-PCR was utilized to monitor gene expression of the neurexin genes. We also utilized human osteoblast-like cell lines, hTBC-1 and hTBC-2, that express low and high alkaline phosphatase activity respectively. Neurexin 3ß was markedly expressed in hMPC32F cells grown in serum free conditions with insulin, transferrin, selenium, (ITS+) in monolayer and this expression was not altered by treatment of cells with 10^{-9} to 10^{-6} M dexamethasone for 6 hr. Identity of the neurexin 3ß amplified fragment was confirmed by sequencing. Neurexin 3a, in contrast, was barely detectable under the same conditions. Gene expression of the neuronal cell surface ligand for ß-neurexins, termed neuroligin, was not detected in hMPC32F cells. In further studies, hTBC-1 osteoblast-like cells derived from trabecular bone did not express neurexin 3ß in monolayer culture or when maintained in chondrogenic conditions as a cell pellet in serum free medium supplemented with TGF ß1 for 26 days. However, the osteogenic hTBC-2 clonal cell expressing high levels of alkaline phosphatase expressed neurexin 3ß transcripts in monolayer culture and this expression was down-regulated when treated with osteogenic supplements for 21 days. Neurexin 3ß may represent a new, previously unrecognized cell surface protein expressed in adult mesenchymal cells that is modulated during cell differentiation.

Disclosures: ***K.G. Danielson****, None.*

SU265

Microarray Validation of Osteoblast Lineage Differentiation by GFP Marker Genes. I. Kalajzic*[1], A. Stahl*[2], W. Yang*[2], R. Gupta*[3], S. Garg*[3], L. Achenie*[3], J. Feyen[2], D. W. Rowe[1]. [1]Department of Genetics and Developmental Biology, University of Connecticut Health Center, Farmington, CT, USA, [2]Bristol Myers Squibb, Princeton, NJ, USA, [3]University of Connecticut, Storrs, CT, USA.

We generated a number of GFP reporter mice to assess lineage progression in vitro and in intact mouse bone. Based on temporal and special expression patterns low intensity signal from the pOBCol3.6GFP transgene marks preosteoblasts, while pOBCol2.3GFP identifies osteoblasts . A comprehensive microarray study was performed to confirm the validity of the GFP assignments. Cultures were established from each transgenic line and harvested at day 7 for low level or absent expression from pOBCol3.6GFP cultures or at day 17 for strong or absent expression from pOBCol2.3GFP cultures. Each culture was separated into positive or negative subpopulations by FACS sorting from which RNA was extracted and used in the Affymetrix hybridizations chips, 74 A, B & C. Three biological replicates were performed for the day 7 and 15 cultures and the pattern of gene expression across the four populations was performed by an adaptive centroid clustering algorithm (Biotechol. Prog. 19:1142,2003). Transition from a 3.6 negative to positive cell is associated with 36 genes with significant down regulation and none that are up regulated. Two patterns were observed: (1) genes that are down regulated in 3.6+ cells and remain low at the later stages of differentiation. Genes characteristic of myofibroblasts populate this group; (2) genes that are down regulated in 3.6+ and 2.3+ cells but which continue to elevate in 2.3- cells. Examples include cell surface expressed genes and adipocytic genes. Two patterns of expression are present in the pOBCol2.3+ cell population. (1) 64 genes with significant up regulation in 2.3+ cells that show limited expression in the other populations. Many are genes associated with osteoblast differentiation although a number were unanticipated. (2) 255 genes that show high expression in both 3.6 cell populations that either begin to fall or remain unchanged in the 2.3- population but are greatly reduce in the 2.3+ population. This group contains a number of gene that are up regulated in microarray studies of total bone cell cultures that in fact are repressed in the osteoblastic population. Thus a low intensity Col3.6GFP+ cell show early evidence of restriction in the progenitor cell differentiation potential relative to the GFP- population suggesting it has progressed toward an osteogenic (and possibly other) fate. Col2.3GFP+ have many markers of a mature osteoblast. This study justifies the continued develop of a wider repertoire of promoter-GFP reporter construct to further deconvolute the osteoprogenitor lineage.

Disclosures: ***I. Kalajzic****, None.*

SU266

Butyltin Compounds Inhibit the Ossification *in vivo* and Differentiation of Osteoblasts *in vitro*. H. Hagiwara[1], Y. Ishihara*[2], T. Sugizaki*[1], Y. Tsukamoto*[3]. [1]Department of Biological Engineering, Toin University of Yokohama, Yokohama, Japan, [2]First Department of Hygiene & Public Health, Tokyo Women's Medical University, Tokyo, Japan, [3]Department of Biological Sciences, Tokyo Institute of Technology, Yokohama, Japan.

Tributyltin is used mainly as antifoulants on ships and fishnets, as wood preservatives, and as biocides for cooling systems, and is an endocrine disruptor for many wildlife species. The formation of bone is easily influenced by the exposure of osteoblasts and osteoclasts to chemical compounds. However, information on the effects and action mechanisms of environmental contaminants in the modeling and remodeling of mammalian bone is not fully available. We examined the effects of butyltin compounds on bone formation. When tributyltin chloride (TBT) (1 mg/kg body weight) was administered subcutaneously to pregnant mice at 10, 12, and 14 days post coitus, fetuses at 17.5 days post coitus revealed the inhibition of calcification of supraoccipital bone. In contrast, monobutyltin trichloride (MBT) did not affect the fetal skeleton. Therefore, we examined the effects of TBT and its metabolites (dibutyltin dichloride, DBT, and MBT) on bone metabolism using rat calvarial osteoblast-like cells (ROB cells). Animals were treated and maintained in accordance with

ethical guidelines and approved by the Tokyo Institute of Technology and Tokyo Women's Medical University animal protocol. The viability of ROB cells was not affected by the exposure of the cells to 10^{-10} M to 10^{-7} M TBT. However, TBT reduced the activity of alkaline phosphatase (ALPase) and the rate of deposition of calcium of ROB cells. In addition, the expression levels of ALPase mRNA and osteocalcin, which are markers of osteoblastic differentiation, were depressed by the treatment with TBT. TBT inhibited ALPase activity and the deposition of calcium to a greater extent than did DBT. MBT had no effect on the osteoblast differentiation of ROB cells. Tributyltin is known to inhibit the activity of aromatase. However, the aromatase inhibitor aminoglutethimide did not reproduce the inhibitory effects of TBT on osteoblast differentiation. In contrast, we found that this compound increased the level of intracellular calcium of osteoblasts. Our findings indicate that TBT might have critical effects on the formation of bone both *in vivo* and *in vitro* although its action mechanism is not clarified.

Disclosures: ***H. Hagiwara****, None.*

SU267

T Cell Cytokines Synergistically Induce Human Mesenchymal Stem Cells Into The Osteoblast Phenotype Via A p38 MAPK Regulated Induction Of Autologous BMP-2. L. Rifas. Department of Pediatrics, Washington University School of Medicine, St. Louis, MO, USA.

T cells have been linked to increased bone formation in inflammatory diseases as well as heterotopic bone formation in fibrodysplasia ossificans progressiva. We tested the hypothesis that human activated T cells (ACT) induce mesenchymal stem cells (BMSC) into differentiated osteoblasts. We have previously demonstrated that ACT conditioned medium (ACTTCM) induces the osteoblast phenotype in BMSC. We now report that ACTTCM induces BMSC to produce BMP-2, a potential autocrine mechanism for the observed differentiation process. ACTTCM induced BMP-2 in a time dependent manner over a 48 hr period. The active principle of ACTTCM was found to be a mixture of four cytokines at physiological levels: TNF-α (120 pg/ml), TGF-β (300 pg/ml), interferon-gamma (IFN-γ, 6 ng/ml) and IL-17 (2 ng/ml) (TTII). TTII, like ACTTCM, induced autologous BMP-2, osteoblast specific genes and mineralization of matrix. Combinations of up to three of the cytokines failed to induce BMP-2 above control levels while a combination of all four cytokines synergistically induced BMP-2 10-fold as assessed by ELISA. IFN-γ appeared to be the key cytokine for synergism. BMSC were pre-incubated in the absence or presence of a specific inhibitor of p38 MAP kinase, SB203580 (1-20μm), prior to 24 hr cytokine(s) treatment. SB203580 completely inhibited BMP-2 production even at the lowest dose. Incubation of BMSC for 21 days in the absence or presence of SB203580 and TTII resulted in induction of alkaline phosphatase and matrix mineralization in only the TTII alone treated cultures. Gene array analysis (Affymetrix U133 Plus 2.0) revealed that BMP-2 gene expression was absent in control cells but was induced by TTII within 24 hrs. Also significantly up-regulated were OSF-2, Wnt5A, osteopontin, osteonectin, osteoprotegerin, collagen type I, cadherin 11, connexin 43, C/EBPβ and interferon responsive genes, including IRF-1 (22-fold), known to enhance cytokine synergistic actions. We demonstrate, for the first time, that four T cell cytokines, TNF-α, TGF-β, INF-γ and IL-17, at physiological levels, can act synergistically to induce BMSC into the osteoblast phenotype via induction of autologous BMP-2. These data indicate that in inflammatory diseases, activated T cell cytokines may initiate accelerated bone formation and/or heterotopic bone formation by inducing mesenchymal stem cells into the osteoblast phenotype.

Disclosures: ***L. Rifas****, None.*

SU268

Ghrelin in Acylated and Unacylated Form Is an Autocrine Stimulator of Osteoblast Proliferation via the MAP- and PI3-kinase Pathways but not via Its Cognate Receptor GHS-R1a. B. C. J. van der Eerden[1], P. J. D. Delhanty*[1], C. Gauna*[1], H. A. P. Pols[1], H. Jahr*[2], H. Chiba*[3], A. van der Lely*[1], J. P. T. van Leeuwen[1]. [1]Internal Medicine, Erasmus MC, Rotterdam, Netherlands, [2]Orthopedics, Erasmus MC, Rotterdam, Netherlands, [3]Pathology, Sapporo Medical University School of Medicine, University of Sapporo, Japan.

Ghrelin is a 28 amino acid growth hormone secretagogue originally identified in the oxyntic mucosa of the stomach. Ghrelin is present in two forms: acylated and unacylated (UAG), the latter of which was formerly supposed to be not active but recently shown to have peripheral actions. Ghrelin acts through its cognate receptor, the growth hormone secretagogue receptor 1a (GHS-R1a) but a variant exists (GHS-R1b) believed to be non-functional. Recent evidence suggests that ghrelin has an effect on bone independent of growth hormone. Therefore, we were interested in the expression of ghrelin and both GHS-R1 subtypes as well as the role of ghrelin in human bone osteoblast growth.

As a first inventory, using real-time PCR, we detected ghrelin and GHS-R1b but not GHS-R1a mRNA in human bone biopsy samples. Next, we measured expression of these genes during dexamethasone-induced differentiation of human osteoblasts (SV-HFO cells) and determined the effect of ghrelin and UAG on proliferation. Differentiation is characterized by maximum alkaline phosphatase activity around day 14 of culture and mineralization thereafter up to day 23. Overall, ghrelin mRNA was expressed at higher levels in differentiating than non-differentiating cells, but was not increased during culture in either group. GHS-R1b mRNA expression was low during the first 19 days of culture, but rose significantly during the last phase of mineralization; in differentiating cells reaching 400% (p=0.004) of initial levels by day 23. GHS-R1a mRNA was not detected in human osteoblasts. Cell proliferation was dose-dependently-stimulated by both ghrelin and UAG with a peak of 155-170% at 1 nM and 182% at 10 nM, respectively. The proliferative response to ghrelin and UAG declined with culture time and state of differentiation. The growth effects of ghrelin and UAG were blocked by the inhibitors of ERK activation U0126 and PD98059 as well as PI3 kinase activation, LY294002.

In summary, ghrelin is expressed in human osteoblasts and stimulates osteoblast proliferation in the absence of its cognate receptor GHS-R1a, indicating the involvement of GHS-R1b or a novel ghrelin receptor signaling via the MAPK and PI3-K pathways. In conclusion, these data provide evidence for new autocrine roles and novel signaling mechanisms for ghrelin and UAG in bone.

Disclosures: ***B.C.J. van der Eerden****, None.*

SU269

Enrichment and Characterization of Primitive Mesenchymal Stem Cells from Rat Bone Marrow Stroma. S. Uchida[1], S. Zhang[1], T. Inoue*[2], D. von der Kooy*[2], J. E. Aubin[1]. [1]Medical Genetics and Microbiology, University of Toronto, Toronto, ON, Canada, [2]Surgery, Division of Anatomy, University of Toronto, Toronto, ON, Canada.

Cells identified as mesenchymal stem cells (MSCs) reside within bone marrow stroma, however, significant enrichment and rapid isolation of these cells remains elusive. The purpose of this study was to isolate and characterize MSCs from young adult rat bone marrow stromal cell populations by using their ability to efflux Hoechst dye, i.e., reside in a side population (SP). Freshly isolated total bone marrow or the stromal fraction pre-cultured for 7 days was incubated with Hoechst 33342, then analyzed and sorted on a Moflo sorter. Sorted cells were divided into three groups: SP, non-SP and total unfractionated population (total). To investigate multilineage potential, sorted fractions were cultured at various densities under osteogenic, chondrogenic, myogenic, adipogenic and neurogenic differentiation conditions and analyzed by histo- and immunohistochemistry and quantitative real time PCR for the expression of lineage related marker genes. A very small proportion of total marrow (0.08±0.02%) or of stromal (0.5±0.34%) cells formed a distinct SP. The SP of total bone marrow did not form CFU-O, CFU-ALP or CFU-F in vitro under any of the conditions tested. However, the stromal cell SP cultured for 4 weeks under osteogenic differentiation conditions formed a much higher number of CFU-O (alkaline phosphatase (ALP) and von Kossa positive; 28±7.7 vs 0.7±0.7 vs 0.9±0.6), CFU-ALP (43±5.2 vs 3.4±1.6 vs 5.2±2.8), and CFU-F (15.6±8.2, vs 3.2±1.7 vs 6±2.5) than the non-SP and Total respectively. The stromal cell SP cultured at high density in micromass cultures with TGF-B1 also formed many more Alcian blue-positive, type II collagen-positive cartilage nodules than did the non-SP and Total (24±5.3 vs 5±2 vs 5.2±2.3 respectively). Similarly, under adipogenic conditions, the stromal cell SP formed many more adipogenic colonies than the non-SP and Total (26±5.3 vs 1.3±0.5 vs 4.5±1.9). Growth under myogenic conditions also resulted in the presence of desmin-positive cells and real time PCR confirmed much higher expression of MyoD and MyH6 in the SP compared to non-SP.. In addition to mesenchymal lineage differentiation, stromal SP cells grown under neurogenic conditions gave rise to cells exhibiting a neuronal-like morphology and expressing bIII tubulin and nestin. These findings suggest that the SP of bone marrow stroma is enriched for putative MSCs compared to the non-SP and Total. In conclusion, Hoechst 33342 dye exclusion may be a useful enrichment stratagem for primitive osteoprogenitors and other multi-lineage precursors in bone marrow stroma.

Disclosures: ***S. Uchida****, None.*

SU270

Effect of Platelet-Rich-Plasma on Bone Marrow Stromal Cell Differentiation. T. R. Meury*[1], L. Kupcsik*[1], T. Stoll*[2], M. Alini*[1]. [1]Cell Biology & Biochemistry, AO-Research Institute, Davos-Platz, Switzerland, [2]Biosurgery, Global Synthes, Bettlach, Switzerland.

Platelets contain many important factors involved in wound healing, including PDGF-AA, -AB, -BB, VEGF, IGF, EGF and TGF-β. Platelet-rich-plasma (PRP) is autologous plasma that has a platelet concentration above baseline (~1Mio platelets/μL vs. ~0.2Mio platelets /μL). PRP can be produced from blood by two simple centrifugation steps. The effect of PRP on bone formation during fracture healing *in vivo* is not clear yet. We performed *in vitro* experiments investigating the effect of PRP on bone marrow stromal cell (BMSC) differentiation towards an osteogenic phenotype.

Human blood samples were obtained with patient consent in CPDA-containing monovettes and were centrifuged at 200g for 15min at RT. The plasma supernatant was transferred to a new tube and was centrifuged at 2'000g for 10min at RT. The top 50% of the supernatant (platelet-poor-plasma, PPP) was removed and PRP was produced by resuspending the pellet in the remaining PPP. In order to release its potent factors, PRP needs to be activated. This was done using one of three different methods: addition of bovine thrombin (100U/mL), repeated freeze-thaw cycles (5x) and sonication. After activation, the PRP was centrifuged at 18'000g for 10min at RT and the supernatant, containing just the released factors (PRF = PRP-released factors) and no more cells or cell debris, was used for our experiments. Human BMSCs, obtained with patient consent, were cultured in IMDM, 10%FBS, nonessential aminoacids, β-glycerophosphate and ascorbic acid. These cells were compared to BMSCs cultured in the same media supplemented with 10%(v/v) PRF. In addition, BMSCs grown in media supplemented with 10mM dexamethasone (Dexa) were used as the positive control. BMSCs proliferation was assessed by measuring the DNA content (Hoechst 33258 assay) and osteogenic differentiation was determined by measuring matrix mineralization ($^{45}Ca^{2+}$ incorporation).

BMSCs grown with the addition of Dexa showed mineralization as soon as after 2 weeks culture time, while BMSCs grown without Dexa showed no mineralization. The addition of 10% PRF to BMSCs grown without Dexa resulted in an up to 40x higher matrix mineralization than BMSCs without Dexa. Cells supplemented with 10% PRF also showed 50-75% higher cell number after 2 weeks than BMSCs grown without PRF. There were no significant differences between the three activation methods.

This data suggests that activated PRP has an osteoinductive effect on BMSCs. Activated autologous PRP could be used to enhance bone healing and may provide an alternative to agents like recombinant growth factors, although in vivo application modalities will require further investigations.

Disclosures: ***T.R. Meury****, Thierry Stoll 3.*

SU271

Activation of Notch Signaling Enhances BMP-2-Induced Osteoblast Differentiation. T. Tsukazaki[1], M. Nobta*[2], A. Shibata*[1], H. Shindo*[2], A. Yamaguchi[3]. [1]Division of Oral Pathology and Bone Metabolism, Nagasaki University Graduate School of Biomedical Sciences, Nagasaki, Japan, [2]Division of Orthopaedic Pathomechanism, Nagasaki University Graduate School of Biomedical Sciences, Nagasaki, Japan, [3]Division of Oral Pathology, Tokyo Medical and Dental University, Nagasaki, Japan.

Notch receptors and their ligands are components of an evolutionarily conserved signaling pathway that plays an important role in a variety of cellular function, including cell proliferation, differentiation and apoptosis. However, functional involvement of Notch in bone development remains obscure. In this study, we investigated the functional property of Notch signaling in the differentiation of the cultured osteoblastic cells. Real-time PCR confirmed the expression of Notch-1, -2, -3, -4 and their ligands, Delta-1, -2 and Jagged-1, -2 in MC3T3-E1, C3H10T1/2, bone marrow- derived mesenchymal cells and calvaria-derived osteoblasts. Immunohistochemical study with confocal microscopy demonstrated that these molecules were coexpressed in the undifferentiated cells and osteoblasts appeared on bone defect in a fracture model. Transient expression of wild-type and constitutive active intra-cellular domain of Notch1, Delta1 or Jagged1 alone did not affect ALP activity, but stimulated BMP-2- induced ALP activity as well as promoter activity of ALP. Overexpression of these molecules also enhanced the expression of osteocalcin, Runx2 and osterix. Similar results were also obtained by recombinant Delta1 and Jagged1 proteins that were precoated on culture plate. In contrast, Notch inhibitor LY-411,575 and dominant- negative extracellular domain of Notch1 resulted in an inhibition of BMP-2- induced osteoblast differentiation. The inhibition of endogenous expression of Notch1 by siRNA also blocked not only ALP activity but also Id-1 promoter activity. These results indicate that Notch/Delta, Jagged signaling system plays an important role for osteoblast differentiation. In particular, Notch signaling appears to be essential for BMP-2- induced osteoblast differentiation.

Disclosures: ***T. Tsukazaki****, None.*

SU272

Expression of the Human Urea Transporter HUT11 in Comparison to the Adipogenic Marker aP2 in Subpopulations of Primary Human Osteoblasts. A. Kluever*, M. L. Ponce*, M. Hüfner*, H. Siggelkow. Gastroenterology and Endocrinology, University Hospital of Goettingen, Göttingen, Germany.

Osteoporosis and age related osteopenia are associated with an increase in marrow adipose tissue that correlates with decreased trabecular bone volume. The Human Urea Transporter HUT11 was identified as a gene expressed in primary human trabecular osteoblast precursors which is downregulated as these cells undergo adipogenesis following combination treatment with dexamethasone and 3-isobutyl-1-methylxanthine. HUT 11 is supposed to mark the switch from the osteoblastic to the adipocytic phenotype.

HUT11 gene expression was investigated in a AP negative subpopulation of primary human osteoblasts isolated by magnetic cell sorting and grown under varying osteogenic differentiating conditions. In all experiments the expression of the adipocytic marker gene aP2 (Fatty Acid Binding Protein) was measured simultaneously. Osteocalcin expression served as a marker of advanced osteogenic differentiation. Cells were grown to preconfluence and stimulated for 2 and 7 days with a combination (OF) of beta-glycerophosphat (2mM), ascorbate (50 g/ml), dexamethasone (10^{-8} M), $1,25(OH)_2D_3$ (10^{-8} M) and either TGF-β 1 (1 ng/ml) or BMP-2 (50 ng/ml). The mRNA expression was determined by semiquantitative RT-PCR using an internal standard. In addition unselected osteoblast-like cells were incubated with single factors for 24 h at day 3 and day 27 in culture.

Under basal conditions HUT11 mRNA was maximally expressed and decreased about 70% under all differentiating conditions. Under control conditions aP2 gene expression was low. OF+BMP-2 after two days stimulated aP2 gene expression maximally when also osteocalcin expression was high. In contrast, the addition of TGF-β inhibited the induction of aP2 gene expression by OF. When testing the single factors for 24 h at day 3 and day 27 of culture HUT11 expression was significantly increased by Vitamin C, TGF-β and BMP-2 at day 4 in culture whereas at day 28 TGF-β showed a significant decrease. aP2 expression was very low under all conditions tested at day 4 but increased maximally at day 28 after Dex stimulation. In conclusion, we can confirm a reciprocal relationship between HUT11 and aP2 mRNA expression in osteoblast-like cells. However, we used osteogenic differentiation conditions in contrast to the adipogenic conditions investigated before. We propose two possible explanations for this phenomenon. 1. there is a heterogeneous behaviour of cells under stimulation developing partly to osteoblasts and partly to adipocytes or 2. aP2 mRNA expression under theses conditions is not representative for an adipocytic phenotype because osteocalcin expression increased in parallel.

Disclosures: ***H. Siggelkow****, None.*

SU273

PTH Simultaneously Inhibits Cell Proliferation and Apoptosis in Early Primary Osteoblast Cultures. Y. Wang, Y. Liu*, D. W. Rowe. University of Connecticut Health Center, Farmington, CT, USA.

Previously we have shown that primary calvarial osteoblast cultures derived from mice transgenic for stage-specific GFP marker genes respond to an early PTH treatment (day 1-7) with an increase in the expression of fluorescent markers and formation of mineralized bone nodules in the end of cultures at day 21. However, results of DNA quantitation showed that DNA content in PTH-treated cultures was not increased and excluded the speculation that this early PTH treatment stimulates cell proliferation. The purpose of present study was to analyze the effect of PTH on cell proliferation and apoptosis in GFP-marked osteoblast cultures during the first 7 days. Calvarial osteoblasts isolated from mice transgenic for pOBCol3.6GFP, which is activated in the preosteoblast stage, were plated on chamber slides or 6-well dishes and cultured with 25 nM PTH for 7 days. Cell proliferation was analyzed in chamber-slide cultures using a fluorescent BrdU-labeling method. Cell viability was visualized by staining of cultures with EthD-1, a red-fluorescent dead-cell indicator with high affinity for DNA and low membrane permeability. Apoptosis was determined by FACS analysis of cells stained with 7-AAD, a DNA dye that is excluded by live cells. 7-AAD not only stains the dead and late apoptotic cells but also penetrates into early apoptotic cells due to alterations in cell membrane integrity. By day 7 of treatment, the intensity of pOBCol3.6GFP signal was decreased in PTH-treated cultures. In agreement with a decrease in DNA content measurement, BrdU-labeling showed a 25% reduction in the number of cells incorporating BrdU in PTH-treated cultures. BrdU-labeled cells were observed in both GFP(+) and GFP(-) subpopulations but whether a difference in the labeling index between GFP(+) and GFP(-) cells is yet to be determined. In PTH-treated cultures, there was less EthD-1 staining associated with a 23% decrease of apoptosis in the FACS analysis of 7-AAD suggesting that an improvement in cell survival compensates for the reduction in cell proliferation. Preliminary data in the concurrent FACS analysis of GFP and 7-AAD revealed that the PTH-mediated inhibition of apoptosis was more prominent in GFP(+) cells. Because a higher proportion of progenitor population acquires the ability to produce a mineralized matrix as a consequence of the early 7-day exposure to PTH, we suggest that a change in differentiation fate is occurring during the treatment period. The increase in cell survival associated with decrease in both GFP intensity and cell proliferation appears to be a manifestation of the reprogramming effect of PTH on the progenitor population to achieve a full osteoblast differentiation.

Disclosures: ***Y. Wang****, None.*

SU274

Molecular Mechanism of Retinoic Acid Stimulation of Osteoblastogenesis and Inhibition of Adipogenesis. K. Hisada*[1], K. Hata*[1], F. Ikeda[1], T. Matubara[1], F. Ichida*[1], H. Yatani*[1], A. Yamaguchi[2], R. Nishimura[1], T. Yoneda[1]. [1]Dept Biochem, Osaka Univ Grad Sch Dent, Suita, Japan, [2]Dept Pathol, Tokyo Medic and Dent Univ Grad Sch, Tokyo, Japan.

Vitamin A has been long implicated in skeletal development and morphogenesis. Deficiency or excess of vitamin A causes skeletal malformations in newborns or increases fracture risk in adults. Previous studies have shown that retinoic acid (RA), which is a physiologically potent metabolite of vitamin A, stimulates osteoblastogenesis and inhibits adipogenesis. Since osteoblasts and adipocytes originate from the common mesenchymal stem cells, these results suggest that RA plays a role in the commitment of the mesenchymal stem cell differentiation. Here, we studied the molecular mechanism responsible for controlling the mesenchymal stem cell differentiation by RA. To approach this, we firstly determined the effects of RA on osteoblastogenesis using the pluripotent mesenchymal cell line C3H10T1/2 which differentiates to osteoblasts by BMP2 treatment. RA alone induced osteoblast differentiation by elevating ALP activity in C3H10T1/2 cells. This action of RA was enhanced in the presence of BMP2, suggesting functional interactions between RA and BMP2. Consistent with this notion, RA-stimulated ALP activity was increased by overexpression of BMP2-specific signaling molecules Smad1 and Smad4 and RA promoted transcriptional activity of these Smads. Since Runx2 is an essential transcription factor for osteoblast differentiation and is a down-stream molecule of the BMP2/Smad signaling, we determined the relationship between RA and Runx2. Contrary to our expectation, RA did not influence the expression and function of Runx2 and a dominant-negative mutant of Runx2 did not affect the osteobalstogenic activity of RA. Furthermore, RA induced ALP activity in Runx2-deficient calvarial mesenchymal cells. We then examined the effects of RA on adipocyte differentiation using the preadipocytic cell line 3T3-F442A which differentiates to mature adipocytes by insulin treatment. Adipocyte differentiation of 3T3-F442A cells by insulin treatment was inhibited by RA. Furthermore, RA markedly inhibited adipocyte differentiation induced by the overexpression of C/EBPβ or PPARγ, both of which are known to play an important role in adipocyte differentiation. RA inhibited the expression of PPARγ and also blocked C/EBPβ-induced PPARγ expression. In conclusion, our data suggest that RA stimulates osteoblastogenesis in cooperation with Smad but independent of Runx2 and inhibits adipogenesis through suppressing C/EBPβ and PPARγ. RA regulates the commitment of mesenchymal stem cell differentiation to osteoblasts and adipocytes at transcriptional levels.

Disclosures: ***K. Hisada****, None.*

SU275

Bone Fetal Cells for Tissue Engineering. M. Montjovent*[1], N. Burri*[2], S. Mark*[3], C. Scaletta*[2], P. Zambelli*[4], D. Pioletti[1], L. Applegate*[2]. [1]Laboratoire de Recherche en Orthopédie, EPFL, Lausanne, Switzerland, [2]Department of Obstetrics, Laboratory of Fetal Medicine, CHUV Lausanne, Switzerland, [3]Ludwig Institute for Cancer Research, Lausanne Branch, University of Lausanne, Epalinges, Switzerland, [4]Hôpital Orthopédique de la Suisse Romande, Lausanne, Switzerland.

For clinical bone transplantations, tissue engineering techniques based on the delivery of cells to the defect using scaffold materials are currently investigated. Part of the project "Lausanne Association for Bone Tissue Engineering" consists of evaluating the possible use of human fetal bone cells for tissue repair. The aim of this work was to characterize these cells biologically with respect to the induction of their osteoblastic phenotype. Results were compared with adult bone cells. Fetal bone cells obtained from a 16 weeks old fetus were treated with ascorbic acid 50µg/ml and β-glycerophosphate 1mM, with or without additional dexamethasone 10^{-8}M and Vitamin D3 10^{-8}M. Proliferation and ALP enzymatic activity were determined during a 12 days time course, and in vitro mineralization was followed every week by von Kossa staining. The generation time of fetal bone cells was estimated to be 27 hours, whereas this value was significantly higher for adult bone cells and clearly age dependent. Fetal bone cells receiving the differentiation mix showed a strong induction of ALP activity after 4-6 days of treatment. This observation was also verified at a higher passage number. Adult cells showed a lower induction of ALP enzymatic activity. Extracellular matrix analysis demonstrated that fetal bone cells were able to mineralize even without treatment, but the differentiation mix did strongly increase this phenomenon. In this study, we showed that human fetal bone cells posses a high proliferate potential and are able to differentiate into osteoblasts. Now, further investigations are necessary to test the possible use of these cells in a bone tissue engineering model.

Disclosures: ***M. Montjovent****, None.*

SU276

1,25(OH)2D3 Regulates Wnt Signaling Pathway in Osteblast-like MC3T3-E1 Cells. Y. Shi*, L. E. Worton*, J. A. Eisman, E. M. Gardiner. Bone and Mineral Research Program, Garvan Institute of Medical Research, Sydney, Australia.

Wnt signaling pathway regulates cell proliferation, differentiation and embryonic development. Recently several lines of evidence indicated that the Wnt pathway is involved in bone biology. Also, 1α,25-dihydroxyvitamin D_3[1,25$(OH)_2D_3$] ,the active metabolite of vitamin D, regulates gene expression through vitamin D receptor (VDR), and has been recently shown to interact with ß-catenin and alter Tcf-mediated transcription in some colon cancer cell lines The present study examined the regulation of the Wnt/ ß -catenin pathway in osteoblast-like MC3T3-E1 cell line.

In this study, Treatment of MC3T3-E1 cells, transiently transfected with a VDR expression vector and the ß -catenin/Tcf responsive TOPFLASH reporter construct, with 1,25$(OH)_2D_3$ caused a dose-dependent repression of ß-catenin/Tcf activity. LiCl (5 to 20mM) activated Tcf activity in a dose-response manner. However, treatment with both 1,25$(OH)_2D_3$ and LiCl reduced Tcf activity even further. In long term mineralizing culture, continuous treatment with 1,25$(OH)_2D_3$(10nM) reduced cell density and slowed cell differentiation, as evidenced by reduced alkaline phosphatase, Von Kossa and Alizarin red staining patterns. Continuous exposure to LiCl also reduced differentiation but, unlike 1,25$(OH)_2D_3$ treatment, was associated with increased cell density. Furthermore, combined treatment with both 1,25$(OH)_2D_3$ and LiCl reduced cell density effect of LiCl, and reduced differentiation compared to either treatment alone. In a 16-day proliferation study, 1,25$(OH)_2D_3$ inhibited cell proliferation dose-responsively in terms of viable cell number and BrdU incorporation, with no change in the proportion of viable cells. LiCl (10mM) had viable cell numbers comparable to vehicle. Surprisingly, combined treatment with 1,25$(OH)_2D_3$ and LiCl brought the viable cell number even lower. Thus our overall results, as previously observed in some colon cancer cell lines, suggest a functional interaction in osteoblasts between 1,25$(OH)_2D_3$ and Wnt response pathways, perhaps through ß -catenin.

Disclosures: ***Y. Shi****, None.*

SU277

TRAIL Regulates Osteocyte-Osteon Structure by Removing Connexons. Y. Li*, C. W. Borysenko, T. Lehmann*, A. Wells*, S. E. Kalla*, V. García Palacios*, H. C. Blair. Pathology, University of Pittsburgh, Pittsburgh, PA, USA.

Bone-synthesizing osteoblasts express Death Receptor-5 (DR5, TRAIL-R2), but do not die when exposed to its ligand, TNF-related apoptosis inducing ligand (TRAIL). Osteoblasts function in multicellular units, osteons, organized by intracellular connections. We previously found that TRAIL markedly reduced intracellular connections in MG63, a human osteosarcoma. Here, we studied how TRAIL affects osteoblast connectivity and cell differentiation in nontransformed osteoblasts. Dye diffusion after microinjection of lucifer yellow showed that serum starvation induced formation of osteon-like cell groups, but that TRAIL eliminated these almost entirely; an osteoblast TNF-family protein, RANKL, and an unrelated cytokine, IL-1, did not affect dye diffusion. The key protein of the gap junction, connexin43 (CX43), forms connexons of hexamers in adjacent cells. Immune localization of CX43 showed increased gap junctions in response to serum starvation, but a dramatic reduction of gap junctions by TRAIL. Doublet-discrimination flow cytometry of cells detached using EDTA showed that physical connectivity was increased by serum starvation but reduced by TRAIL, while control cytokines including TNFα, for which osteoblasts also bear receptors, did not affect connectivity. The osteoblastic actin cytoskeleton was rearranged by starvation, decreasing filamentous actin, although actin quantity was unaffected on Western analysis. However, TRAIL reduced CX43 protein quantity relative to actin. In contrast, real-time PCR showed that CX43 transcription increased with serum starvation; TRAIL and other cytokines did not affect CX43 mRNA. Cell cycle analysis showed that TRAIL decreased cells in S-phase by 80% with a parallel increase in G2, indicating that TRAIL arrests the osteoblast cell cycle. After removal of TRAIL, cells re-established normal morphology and osteoblastic features including alkaline phosphatase per cell, but cell number did not increase as in controls post washout, suggesting that TRAIL terminates osteoblast proliferation. We conclude that DR5 rearranges osteoblast shape with post-transcriptional CX43 degradation, and arrests cell division. TRAIL is expressed in both osteoclasts and osteoblasts, and thus may function during bone degradation, where portions of bone are disconnected for partial degradation of living osteons, of when the bone formation cycle ends.

Disclosures: ***H.C. Blair****, None.*

SU278

Connective Tissue Growth Factor (CTGF) Is a Downstream Mediator of Transforming Growth Factor-Beta 1 (TGF- β1) in Osteoblasts. J. A. Arnott*[1], E. Nuglozeh*[1], M. C. Rico[1], T. A. Owen[2], F. F. Safadi[1], S. N. Popoff[1]. [1]Anatomy and Cell Biology, Temple University School of Medicine, Philadelphia, PA, USA, [2]Pfizer Global Research and Development, Groton, CT, USA.

Connective tissue growth factor (CTGF) is a cysteine rich, extracellular matrix-associated protein that is a member of the CCN family involved in multiple cellular events including skeletogenesis. Recently CTGF was discovered to be highly expressed in bone, specifically osteoblasts. In osteoblast cultures, CTGF acts as a modulator of osteoblast differentiation, regulating proliferation and terminal differentiation. TGF-β1 is a potent multifunctional cytokine that is known to play a major role in bone development and to regulate cellular functions in osteoblasts including proliferation and collagen synthesis. It is well established that TGF-β1 is a potent inducer of CTGF expression in fibroblasts, mesangial cells and chondrocytes. In studies using fibroblasts, CTGF mediates TGF-β1-induced biological activities including proliferation and extracellular matrix (ECM) production. In these systems, SMAD signaling is critical for TGF-β1 induction of CTGF. The relationship between TGF-β1 and CTGF in osteoblasts has not been investigated. This study focuses on CTGF as a downstream mediator of TGF-β1-induced effects in osteoblasts and the requirement of SMAD signaling for this modulation. Using primary osteoblast cultures derived from neonatal rat calvaria, we demonstrated that treatment with TGF-β1 (5ng/ml) increased CTGF expression at the protein and mRNA level during the proliferative (day 7), matrix deposition (day 14) and mineralization (day 21) phases of the culture. This increase in CTGF was time-dependent with maximal CTGF expression occurring at 16 hours post-treatment with TGF-β1. Interestingly, we also observed that the up-regulation of CTGF occurs concurrently with the activation of SMAD-2, and inhibition of SMAD-2 activation significantly decreased up-regulation of CTGF expression. These results link the induction of CTGF expression by TGF-β1 to this SMAD signaling pathway in osteoblasts. RNAi generated against CTGF was able to knock down CTGF expression in TGF-β1-treated osteoblasts by 80-90% as demonstrated by Western blot analysis. Further studies are aimed at; 1) evaluating the levels of activated SMAD-2 in osteoblasts treated with RNAi, and 2) examining the functional consequences of inhibiting CTGF expression with RNAi on TGF- β1-induced osteoblast proliferation and extracellular matrix (ECM) deposition.

Disclosures: ***J.A. Arnott****, None.*

SU279

The Effects of Nicotine on Human Osteoblasts Responding to Implant Materials. L. Li*, A. Jhaveri*, G. Gronowicz, H. Zhang*. University of Connecticut, Farmington, CT, USA.

The use of osseointegrated implants for missing teeth has become the standard of care in prosthetic dentistry. Smoking can impair wound healing and is one of the risk factors in dental implants failure. No studies have been performed on the effects of smoking on osseointegration at a cellular level to understand the mechanisms of failure. Nicotine is one of the major toxic by-products in cigarette smoke. Therefore, we studied the effects of nicotine on the function of osteoblasts on dental implant materials. Saos-2 (human osteosarcoma cells) and primary human osteoblasts (HOBs) from healthy non-smokers were used in the osteoblast/implant in vitro culture system, with and without the presence of nicotine. Based on previous studies, after smoking one cigarette, the human serum nicotine concentration is about 10^{-7} M. Therefore, the dose of nicotine used in this study was 10^{-9} M to 10^{-6} M. Titanium implant disks were used and the surface is the same as clinical implants. Attachment, proliferation, differentiation and mineralization of osteoblasts on implant disks were assessed.

At 4 hr, nicotine treatment (10^{-7} M) significantly increased the number of attached Saos-2 cells on implant surface but had no effect on HOBs. Proliferation rates for both Saos-2 and HOBs were not affected by nicotine treatment (10^{-7} M) over 1-5 days measured by cell number counting. [^{3}H] thymidine incorporation at 24 hr with wider range of nicotine concentrations (10^{-9} to 10^{-6} M) also showed no significant difference between treatment groups and control. Differentiation of human osteoblasts on implant surface was determined by alkaline phosphatase (ALP) activity assay. Nicotine inhibited ALP activity in a dose-dependent manner for both cell types. Long-term (2 wk and 4 wk) mineralization assay demonstrated a decrease in calcium content (about 30% less) in osteoblast/implant cultures with the presence of 10^{-7} M nicotine in the medium. In conclusion, nicotine had some effect on osteoblast attachment to the implant surface, no effect on proliferation but inhibited differentiation and mineralization of osteoblasts on the implant surface. The data suggest that smoking related implant failures might be caused by the nicotine-mediated decreased ability of osteoblasts to differentiate and mineralize on the implant surface.

Disclosures: ***L. Li****, None.*

SU280

Adrenocorticotrophic Hormone Modulates Adipocyte And Osteoblastic Cell Differentiation. S. Sridhar[1], Q. Zhong[2], J. Xu*[1], R. J. Bollag*[1], W. Bollag*[1], C. M. Isales[2]. [1]Institute of Molecular Medicine and Genetics, Medical College of Georgia, Augusta, GA, USA, [2]Medicine, Medical College of Georgia and the Augusta VA Hospital, Augusta, GA, USA.

We have previously demonstrated the presence of melanocortin receptors in osteoblastic-like cells. Melanocortin receptors are activated by peptides derived from processing of a larger prohormone, pro-opiomelanocortin (POMC) which include hormones such as adrenocorticotrophic hormone (ACTH) and melanocyte stimulating hormone (MSH). In addition, we have shown that POMC derived fragments such as ACTH can be synthetized and released from osteoclastic cells which then stimulate osteoblastic cell proliferation. Osteoblasts and adipocytes are derived from the same mesenchymal stem cell precursor, preliminary gene microarray experiments demonstrated an effect of ACTH on multiple genes involved in cell differentiation. In an effort to further define ACTH effects on cell differentiation we utilized an osteoblastic cell line MC3T3 and a pre-adipocytic cell line 3T3-L1. MC3T3 cells in culture were stimulated with either 1 or 100 nM ACTH (1-24) and gene expression for the osteoblastic markers Runx2, osteocalcin and alkaline phosphatase measured sequentially over ten days by RT-PCR and quantitated by comparing to the housekeeping gene GAPDH. At the end of the ten days of culture either 1 or 100 nM ACTH downregulated both Runx2 and osteocalcin by over 50% while there was no effect on alkaline phosphatase. In contrast, when the adipocytic gene markers lipoprotein lipase (LPL) or stearoyl Coa desaturase (SCD) were measured at the end of ten days in MC3T3, either ACTH 1 or 100 nM increased their expression by over four-fold (adipocytic gene markers were initially undetectable in MC3T3). ACTH had no effect on another adipocyte marker, adipsin.

In 3T3-L1, ACTH 1-24 had no effect on the expression of either Runx2 or osteocalcin while upregulating the expression of LPL (two-fold), SCD (two-fold) and adipsin (ten-fold) at the end of ten days. Similarly, if another osteoblastic cell line, MG63, was utilized and incubated with 10 nM ACTH (1-24) for six days there was a large increase in lipid droplet development as assessed by congo red staining.

Taken together these data demonstrate that ACTH facilitates the maturation of the preadipocytic cell line 3T3-L1 into a more mature fat cell phenotype while promoting the conversion of osteoblastic cells into a more adipocytic phenotype.

Disclosures: ***S. Sridhar****, None.*

SU281

Aortic Valve Myofibroblast Cell Undergoes Differentation to an Osteoblast Cell Independent of Osteoclastogenesis. M. Subramaniam[1], H. Hirotani*[2], F. Secreto[1], P. Stern[2], T. C. Spelsberg[1], N. M. Rajamannan[3]. [1]Biochemistry and Molecular Biology, Mayo Clinic, Rochester, MN, USA, [2]Molecular Pharmacology, Northwestern University, Chicago, IL, USA, [3]Cardiology, Northwestern University, Chicago, IL, USA.

Calcific Aortic Stenosis is thought to be a passive phenomena. We hypothesize that the mechanism is not passive but instead an active osteoblast differentiation process. We tested whether in vitro myofibroblast cells can undergo osteoblastogenesis and not osteoclastogenesis as a possible mechanism for mineralization. We isolated porcine aortic valve myofibroblasts expressing alpha actin and tested them with growth factors to determine if these cells develop osteoblast characteristics and form calcified nodules. When these cells were differentiated in culture by the addition of TGFb and dexamethasone, they express osteoblast markers and alkaline phosphatase. Alkaline phosphatase activity increased three-fold over control ($p<0.05$) in the TGBb + dexamethasone cells as compared to the controls. Bone-like nodules developed after 27 days in culture with treatment of TGFb and dexamethasone. Distribution of hydroxyapatite coincided with the area of calcium detected by analyzing nodules with cytochemical Von Kossa staining. Finally, semi-quantitive RT-PCR indentified genes specific to osteoblast differentiation. RT-PCR of the mRNA revealed an increased level of mRNA for osteopontin, bone sialoprotein, osteocalcin and Cbfa1 compared to control myofibroblasts that has been treated with vehicle. The responses of these markers indicate the transformation of myofibroblasts to osteoblast-like cells involved in a calcification process analogous to osteoblastogenesis. To determine if myofibroblast cells have an osteoblast-like ability to support osteoclast precursor differentiation, they were cultured with RAW 264.7 monocyte/macrophage precursor cells. The co-cultures were untreated or treated with 30 nM parathyroid hormone (PTH). Co-culture with RAW cells, with or without PTH, resulted in increased TRAP activity, demonstrating that myofibroblast cells act like osteoblasts by activating RANK on the RAW 264.7 cells. TRAP positive multinucleated cells were not detected in the cultures. Culture of the myofibroblast cells alone, or with PTH, or with M-CSF (20 ng/ml) and RANKL (50 ng/ml) failed to increase TRAP activity. In conclusion, these results suggest that dexamethasone and TGFb promotes osteoblastic differentiation in valve myofibroblast cells and TGFb may play a role in the phenotypic conversion of the myofibroblast cell to an osteoblast-like phenotype.

Disclosures: ***N.M. Rajamannan****, None.*

SU282

Hormonal Regulation Of Melanocortin Receptor Expresssion In Osteoblastic Cells. C. M. Isales. Medicine, Medical College of Georgia and the Augusta VA Hospital, Augusta, GA, USA.

Melanocortin receptors belong to the seven transmembrane domain, G-protein coupled family of receptors and are widely expressed in the body. We have previously reported that all five melanocortin receptors are expressed to varying degrees in osteoblastic cells. These receptors are activated by fragments derived from a larger molecule, pro-opiomelanocortin (POMC) and include: ACTH, alpha, beta and gamma MSH, and beta endorphin. We have further shown that bone-derived osteoclasts have the ability to synthetize, process and secrete POMC-derived fragments including ACTH suggesting the existence of a paracrine loop in the bone.

In an effort to gain an understanding of the regulation of the melanocortin receptors we utilized the osteoblastic-like cells MG63. MG63 cells were grown to confluence and incubated in the presence of estradiol (1 or 100 nM), dexamethasone (1 or100nM), alpha-MSH (1 or100nM), beta-MSH (1 or100nM), gamma-MSH (1 or100nM), beta-endorphin (1 or100 nM) or ACTH (1 or 100 nM) for six hours and melancortin receptor mRNA expression assessed by Northern blots. We found that MC1R message was significantly upregulated by estradiol, dexamethasone, alpha MSH, beta MSH, gamma MSH, beta endorphin and ACTH. In contrast MC2R was upregulated by estradiol, dexamethasone, alpha MSH, ACTH and beta endorphin and MC5R was significantly upregulated by alpha MSH and ACTH. Expression of either MC3R and MC4R was not changed by any of the hormonal manipulations.

Thus, regulation of melanocortin receptors in osteoblastic-like bone cells is a complex process in which the melanocortin receptor(s) appears to be upregulated by its own ligand.

Disclosures: ***C.M. Isales****, None.*

SU283

Transgenic Mice Over-expressing Bone Morphogenetic Protein-2 Inducible Kinase Have Reduced Bone Mass. A. E. Kearns, D. G. Fraser*. Division of Endocrinology, Mayo Clinic, Rochester, MN, USA.

An understanding of mechanisms regulating osteoblast differentiation and function is critical to gain insight into the pathogenesis of osteoporosis. We have previously identified a novel bone morphogenetic protein-2 (BMP-2)-inducible kinase (BIKe) associated with osteoblast differentiation. Over-expression of BIKe inMC3T3-E1 cells decreased alkaline phosphatase activity, osteocalcin expression, and mineralization, which indicates it functions to modulate osteoblast differentiation. We now report the in vivo effect of over-expression of BIKe in osteoblasts of mice. The full coding region of BIKe with an additional FLAG epitope tag on the 3' end was placed under the control of the 3.6-kb alpha1(I)-collagen promoter. Pronuclear injections of the transgene construct into fertilized oocytes of FVB/Cr mice were performed. Transgenic mice were identified among the offspring by Southern blot analysis of mouse tail genomic DNA. All transgenic mice demonstrated germline transmission of the transgene, and appeared normal in growth, weight and fertility. Transgene expression was verified by immunohistochemistry of calvaria using anti-FLAG antibodies. Bone mineral density was measured in adult mice at 20 weeks of age. Transgenic animals had significantly lower bone density of the whole body, vertebrae, and femur by DEXA than wild type animals, although the effect was modest (10-15%). Trabecular bone density was also significantly lower by pQCT measurements. Preliminary data from mice at 10 weeks of age did not show a significant difference between wild type and transgenic animals. Initial bone histomorphometry (n=5 in each group) does not show a mineralization defect. We conclude that over-expression of BIKe in vivo results in modest reduction of bone density by 20 weeks of age, without apparent mineralization defect. This suggests that BIKe over-expression in vivo may affect osteoblast function, as we found with in vitro experiments. The mechanism of this effect requires further investigation.

Disclosures: ***A.E. Kearns****, Merck 2.*

SU284

Lactoferrin - Mechanisms Of Actions In Bone Cells. J. Cornish, A. B. Grey, D. Naot, K. E. Callon*, I. R. Reid. Medicine, University of Auckland, Auckland, New Zealand.

Lactoferrin is an iron-binding glycoprotein that belongs to the transferrin family and is present in milk, other exocrine secretions, and in the circulation. We have previously reported that lactoferrin, at physiological concentrations, stimulates the mitogenesis, differentiation and survival of osteoblasts in vitro. In addition, the local injection of lactoferrin in mice calvaria increases new bone formation in vivo.

We now report that the mitogenic effects of lactoferrin in osteoblast-like cells are mediated through LRP1, a member of the LDL receptor-related family (LRP) of proteins. The specific LRP inhibitor, RAP, inhibits the activation of p42/44 MAPK signalling and the induction of cell proliferation by lactoferrin in primary rat osteoblasts and SaOS2 cells. Lactoferrin-induced osteoblast proliferation is also blocked by an antibody to LRP1. Expression of dominant negative Ras abrogates the ability of lactoferrin to activate p42/44 MAPK signalling in SaOS2 cells. In addition, lactoferrin induces PI3-kinase-dependent phosphorylation of Akt, a critical regulator of cell survival, which may mediate the anti-apoptotic actions of lactoferrin.

Lactoferrin is seen to be endocytosed by primary rat osteoblasts, using confocal laser scanning microscopy. The addition of labelled lactoferrin results in an intracellular vesicular pattern of staining, characteristic of endocytosis. Co-staining with a membrane dye (DiI) reveals co-localisation of lactoferrin with intracellular vesicular structures. Inhibition of endocytosis (using a hypertonic medium or placing the cells at 4°C) results in the absence of intracellular lactoferrin. RAP also blocks lactoferrin endocytosis. Studies using ^{125}I-lactoferrin demonstrate that lactoferrin binds specifically to osteoblastic cells and is internalized by a RAP-sensitive mechanism. However, the signalling and endocytic functions

of LRP1 are independent of each other, since lactoferrin can activate mitogenic signalling in conditions in which endocytosis is inhibited.
In addition to the anabolic effects of lactoferrin in osteoblasts, lactoferrin dose-dependently decreases osteoclastogenesis in mouse bone-marrow cultures, and this is associated with decreased expression of RANKL. We conclude that lactoferrin has powerful anabolic, differentiating and anti-apoptotic effects on osteoblasts, and inhibits osteoclastogenesis. Lactoferrin is a potential therapeutic target in bone disorders such as osteoporosis and may be an important physiological regulator of bone growth.

Disclosures: ***J. Cornish****, None.*

SU285

Cross-Talk Between Cyclic AMP and Intracellular Caclium Signaling Pathways in PTH-responsisve Cells. R. J. Murrills[1], J. J. Matteo*[1], J. L. Andrews*[1], P. Liu*[2], A. Reik*[2], P. D. Gregory*[2], F. J. Bex[1]. [1]Women's Health & Bone, Wyeth Research, Collegeville, PA, USA, [2]Sangamo Biosciences, Richmond, CA, USA.

PTH can activate multiple intracellular signaling pathways in osteoblasts such as the cyclic AMP, intracellular calcium, protein kinase C and MAPK pathways. While the importance of the cyclic AMP pathway is well established, the role of the intracellular calcium pathway, and its relationship with the cyclic AMP pathway is still obscure, particularly at the level of gene transcription. We asked whether activation or inhibition of the cAMP pathway had any influence on PTH's intracellular calcium pathway and also whether the CRE response to PTH and a range of cAMP agonists was enhanced by thapsigargin, a calcium signaling agonist.
We examined intracellular calcium elevation using R45 cells, a 293 cell line stably transfected with an inducible PTH1 receptor, and FLIPR. In these cells thapsigargin (2-10uM) and PTH (100nM) induced a pronounced calcium spike. When cells were pre-incubated for 1 hour with activators or inhibitors of the cAMP pathway, forskolin suppressed the intracellular calcium response to PTH, whereas H-89, a PKA inhibitor, markedly enhanced it. Furthermore, the pattern of calcium influx was modified by H-89, the primary spike being followed rapidly by a secondary spike, suggestive of calcium-induced calcium release. This suggests that PTH1 receptor-mediated intracellular calcium signaling is held under substantial tonic repression by the cAMP pathway.
To examine the effects of calcium signaling on the transcriptional response to cAMP, Saos-2 cells, stably transfected with 15 copies of the CRE linked to a Luciferase reporter, were exposed to test agents overnight, in the presence of thapsigargin, a calcium agonist. While 100nM thapsigargin alone had little effect on the CRE-Luciferase reporter, in combination with all other cAMP agonists, it had a synergistic effect.

cAMP agonist	Fold increase	Fold increase + thapsigargin
Control	1.00	1.8
Forskolin 1uM	15.0	24.9
Forskolin 10uM	27.1	38.8
Rolipram 1uM	4.6	10.2
Rolipram 10uM	8.7	16.6
VIP 1nM	17.7	45.8
Isoproterenol 1uM	18.8	29.9
Isoproterenol 3uM	26.9	34.6

Thapsigargin also had a strong synergistic effect on the CRE response to PTH. From this we conclude that the intracellular calcium signaling pathway synergizes with cAMP agonists on the CRE.
Thus, in contrast to cAMP activation, which has a negative feedback on intracellular calcium signaling by PTH, activation of the intracellular calcium pathway strongly enhances the downstream effects of the cAMP pathway at the level of transcription.

Disclosures: ***R.J. Murrills****, None.*

SU286

Mechanical Stress Induces the Osteoblast Differentiation and Activates Runx2 and Activator Protein-1 through Diverse MAPK Signal Transduction Pathways. T. Kanno*[1], T. Tsujisawa*[2], W. Ariyoshi*[1], T. Koseki*[3], T. Takahashi*[1], T. Nishihara[2]. [1]Sencond Department of Oral and Maxillofacial Surgery, Kyushu Dental College, Kitakyushu, Fukuoka, Japan, [2]Department of Oral Microbiology, Kyushu Dental College, Kitakyushu, Fukuoka, Japan, [3]Department of Life Long Oral Health Science, Tohoku University, Graduate school of Dentistry, Sendai, Miyagi, Japan.

Mechanical stress (MS) plays a fundamental role to maintain the skeletal mineralization by dictating the cellular and metabolic activity of osteoblastic cells. The bone-specific transcription factor, Runx2 and AP-1 have been thought to be critical factors to regulate the many of osteoblast-specific gene expression and subsequent differentiation through binding to the osteoblast-specific element 2 (OSE2) and AP-1-binding sites. Recent findings revealed that MS activates and phosphorylates the Runx2, followed by up-regulating the osteoblast differentiation through Ras-mediated MAPK pathways. The goal of this study was to evaluate the role of Runx2 and AP-1 in the osteoblast differentiation under the MS conditions. MC3T3-E1 and rat calvarial osteoblastic cells were used in this study. MS up-regulated alkaline phophatase activity and the expression of osteocalcin mRNA. The expression and phosphorylation of Runx2 and AP-1 were detected by RT-PCR and Western blot analysis. Phosphorylation of ERK 1/2 and p38 MAP kinase were found to be significantly activated. ERK 1/2 and p38 MAP kinase were evidently blocked by the MAPK selective inhibitors, U0126 and SB203580, respectively. ERK 1/2 selective inhibitor, U0126 completely blocked the Runx2 and AP-1 activation, however, p38 MAP kinase selective inhibitor, SB203580 did not alter Runx2 phosphorylation but blocked AP-1 activation. In addition, the upstream of p38 MAP kinase was interestingly detected to be up-regulated by MS. Furthermore, RNA interference (RNAi) technique was used to clarify the effect of Ras on the activation of Runx2 and AP-1 in MS-activated oosteoblastic cells. RNAi analysis revealed that ERK signal pathway was apparently inhibited, however, p38 MAP kinase pathway was not. Our results suggest that MS regulates osteoblast differentiation through the induction and activation of diverse MAPK signal transduction pathway and transcription factors, Runx2 and AP-1 in osteoblasts.

Disclosures: ***T. Kanno****, None.*

SU287

Regulation of Human Estrogen Receptor Alpha Transcription by a c-Src/PKC-Dependent Mechanism in Osteoblast-like Cells. M. Longo[1], D. Fortunati*[2], V. De Luca*[3], S. Denger*[4], A. Teti[1], S. Migliaccio[5]. [1]Experimental Medicine, University of l'Aquila, L'Aquila, Italy, [2]Histology and Medical Embriology, University "la Sapienza", Rome, Italy, [3]Pediatric Hospital "Bambino Gesù", Rome, Italy, [4]European Molecular Biology Laboratories, Heidelberg, Germany, [5]Department of Medical Physiopathology, University "la Sapienza", Rome, Italy.

The human estrogen receptor alpha (hERα) gene is driven by several promoters, of which the distal E and F promoters appear specifically active, albeit at low levels, in osteoblast cell lines. In order to identify regulatory pathways affecting hERα expression at the transcription level in the bone tissue, we generated a clone of human osteoblast-like cells SAOS-2 stably transfected with a luciferase reporter gene downstream of the F promoter (SAOS.F-Luc). Over-confluence, a condition whereby cultured osteoblasts acquire a more differentiated phenotype, caused a time-dependent increase of promoter activity in these cells. Over-confluence correlated with marked PKCα de-activation, and generic PKC down-regulation in sub-confluent cells, induced by long-term treatments with PMA (Phorbol 12-Myristate 13-Acetate), also resulted in promoter stimulation at similar levels. Furthermore, treatment of cells with PP1, a specific inhibitor of the non-receptor tyrosine-kinase c-Src, showed that impaired c-Src function, previously shown to enhance osteoblast differentiation, caused a remarkable (~three-fold) increase of promoter activity. Consistently, over-expression of wild-type c-Src resulted in partial promoter inhibition. In PP1-treated cells, enhanced promoter activity was not further increased by PMA. Over-expression of exogenous full-length hERα resulted in modest promoter stimulation, which was insensitive to both estrogen and anti-estrogen treatment. Such effect appeared PKC-independent in that total PKCα expression was not affected by exogenous hERα. The F-promoter contains a putative AP-1 site, but AP-1 activation was virtually unremarkable in over-confluent and PP1-treated SAOS.F-Luc cells as compared to PMA-treated counterparts. Moreover, AP-1 inhibition following treatment with the generic kinase inhibitor DMAP (4-DiMethylAminoPyridine) resulted in a dose-dependent further stimulation, rather than inhibition, of promoter activity in PMA-treated cells. Such stimulation matched a dose-dependent decrease of c-Src activating phosphorylation at its Y416 aminoacid residue. These results point to a strongly PKC/c-Src-dependent and estrogen-independent pathway modulating ERα transcription in osteoblasts, perhaps affecting estrogen responsiveness during osteoblast differentiation.

Disclosures: ***M. Longo****, None.*

SU288

Phosphophoryn Regulates Osteoblast Differentiation via Integrin Signaling and MAP Kinase Pathway. J. A. Jadlowiec*[1], H. Koch*[2], L. Zhang*[3], P. Campbell*[4], M. Seyedain*[3], C. Sfeir*[3]. [1]Biological Sciences, Carnegie Mellon University, Pittsburgh, PA, USA, [2]Orthopaedic Surgery, University of Greifswald, Greifswald, Germany, [3]Oral Medicine and Pathology, University of Pittsburgh, Pittsburgh, PA, USA, [4]Institute for Complex Engineered Systems, Carnegie Mellon University, Pittsburgh, PA, USA.

Extracellular matrix (ECM) proteins serve as both a structural support for cells and also as a dynamic bionetwork that directs cellular activities. ECM proteins such as those of the SIBLING family (Small Integrin-Binding LIgand Glycoprotein) could possess inherent growth factor activity. Phosphophoryn (exon 5 of dentin matrix protein 3) is a member of the SIBLING family and has been implicated in biomineralization as a nucleator/modulator of crystal formation. In this study, we demonstrate that PP may also have a signaling role. Quantitative real-time PCR technology was used to demonstrate up-regulation of *Runx2*, *Osx* and *Ocn* in primary human adult mesenchymal stem cells (hMSC), a mouse osteoblastic cell line (MC3T3-E1), and a mouse fibroblastic cell line (NIH3T3). Further, PP increased OCN protein production in hMSC and MC3T3-E1. ALP activity and calcium deposition were enhanced in hMSC. An $\alpha_v\beta_3$ integrin-blocking antibody significantly inhibited rPP-induced expression of *Runx2* in hMSC, suggesting that signaling by PP is mediated through the integrin pathway. Our data further shows that PP signals via the MAP kinase pathway; treatment of hMSC with rPP caused activation of the p38 component. These data demonstrate a novel signaling function for PP in regulating the expression of bone gene markers in addition to its hypothesized role in biomineralization. The implication is that PP could be combined with growth factors in novel tissue-engineered approaches for an enhanced therapeutic effect.

Disclosures: ***J.A. Jadlowiec****, None.*

SU289

Phosphodiesterase Inhibitors Stimulate Osteoclast Formation by Inducing TRANCE Expression in Calvarial Osteoblasts. M. Yim[1], E. Cho*[1], R. Kamijo[2], M. Takami[2]. [1]College of Pharmacy, Sookmyung Women's University, Seoul, Republic of Korea, [2]Department of Biochemistry, Showa University, Tokyo, Japan.

Phosphodiesterases (PDEs) are enzymes that degrade intracellular cAMP. In the present study, 3-isobutyl-1-methylxanthine (IBMX) and pentoxifylline, PDE inhibitors, induced osteoclast formation in cocultures of mouse bone marrow cells and calvarial osteoblasts. These inhibitors induced the expression of the osteoclast differentiation factor TNF-related activation-induced cytokine (TRANCE, identical to RANKL, ODF, and OPGL) in osteoblasts. Induction of TRANCE expression by IBMX was suppressed by a protein kinase A (PKA) inhibitor, H89, an ERK1/2 inhibitor, PD98050, and a p38 MAPK inhibitor, SB203580, suggesting that activation of PKA, ERK and MAPK is involved in TRANCE expression by IBMX. Further, rolipram, a selective inhibitor of PDE4 (a PDE isozyme), also induced osteoclast formation and TRANCE expression. These results suggest that PDE4 is a key regulator of TRANCE expression in osteoblasts, which in turn controls osteoclast formation.

Disclosures: ***M. Yim****, None.*

SU290

Statins Stimulate Phosphatidylinositol 3 Kinase (PI 3 K) Signaling during Osteoblast Differentiation: A Mechanism of New Bone Formation in Osteoporosis. N. Ghosh-Choudhury. Pathology, UTHSC at San Antonio and South Texas Veterans Health Care System, San Antonio, TX, USA.

Recently, statins are shown to induce expression of bone morphogenetic protein-2 (BMP-2), resulting in new bone formation. This action of statin is important in preventing osteoporosis. However, the signaling mechanism by which statins stimulate BMP-2 expression and, therefore, osteoblast differentiation is not known. Incubation of 2T3 mouse osteoblasts and fetal rat calvarial cells with lovastatin or simvastatin increased PI 3 K activity in anti-phospho-tyrosine immunoprecipitates in a dose-dependent manner, indicating association of this enzyme with signaling complex containing tyrosine phosphorylated proteins. One of the downstream targets of PI 3 K is Akt kinase. Lovastatin increased Akt kinase activity as measured by immunecomplex kinase assay of the Akt immunoprecipitates. Ly294002 (Ly), a pharmacologic inhibitor of PI 3 K, blocked lovastatin-induced lipid kinase and also Akt kinase activities, indicating that the PI 3 K regulates lovastatin-induced increase in Akt kinase activity. In order to study osteoblast differentiation, we examined the expression of osteopontin and type I collagen, two late markers of osteoblast differentiation, using Northern analysis. Lovastatin increased expression of mRNAs for both these proteins in 2T3 cells. Treatment of these cells with Ly prior to lovastatin blocked both osteopontin and type I collagen expression. These data represent the first evidence that PI 3 kinase regulates lovastatin-induced osteoblast differentiation. Lovastatin was originally reported to induce BMP-2 in 2T3 cells. We confirmed this observation using RNase protection assay with a BMP-2 specific probe. Ly inhibited expression of BMP-2 in response to lovastatin, indicating that PI 3 K regulates this process. Using transfection assay of BMP-2 promoter-luciferase reporter plasmid, we examined the mechanism of BMP-2 expression. Both lovastatin and simvastatin dose dependently increased transcription of BMP-2 in a decreasing potency, simvastatin > lovastatin. Ly inhibited statin-induced BMP-2 transcription. Together, these data demonstrate for the first time that lovastatin stimulates PI 3 K signaling and that this signal transduction pathway is necessary for expression of osteopontin and type I collagen, two late markers of osteoblast differentiation necessary to form new bone. Furthermore, these data provide the first evidence for a novel mechanism of statin-induced BMP-2 expression and hence osteoblast differentiation involving PI 3 K signaling. Thus design of small molecular mimetics that stimulate PI 3 K signaling may enhance new bone formation in patients with osteoporosis.

Disclosures: ***N. Ghosh-Choudhury****, None.*

SU291

Dynamics of Focal Adhesions in Osteoblastic Cells on Biomaterial Surfaces. A. Diener*[1], B. Nebe*[1], U. Bulnheim*[2], F. Lüthen*[1], P. Becker*[3], H. Neumann*[3], J. Rychly[4]. [1]Department Internal Medicine, University of Rostock, Rostock, Germany, [2]Diagnostik Nord GmbH, Rostock, Germany, [3]DOT GmbH, Rostock, Germany, [4]Experimental Research Center, University of Rostock, Rostock, Germany.

The mechanisms of cell adhesion to the extracellular matrix which are of fundamental importance for function, survival, and growth of cells involve the formation of focal adhesions to facilitate integrin signaling. These adhesions are not stable but move to enable cell migration and extracellular matrix formation. We studied the dynamic behaviour of focal adhesions in stationary osteoblastic MG-63 cells on the surfaces of different biomaterials which are used as permanent or transient bone implants. As a marker for focal adhesions we used GFP-tagged vinculin, a cytoskeletal protein, that was transfected into living cells. On all surfaces that we have tested a mobility of focal adhesions was observed. On collagen coated cover slips the adhesions moved with a speed of 60 nm/min. The speed was reduced on titanium surfaces independently of the roughnesses of the surfaces and was still more restricted on stainless steel. This suggests that the ability of cells to format the extracellular matrix is impaired on these material surfaces but the reduced mobility could strengthen cell adhesion. In contrast, cells on a CaP/SiO xerogel composite which can be used as a degradable carrier for osteoblastic cells to regenerate bone revealed an increased mobility of focal adhesions compared with cells on collagen coated cover slips. To test, whether this increased mobility correlates with biological functions we measured proliferation with DNA cytometry and the expression of three functional proteins in a real time RT-PCR. Proliferation of cells on the xerogel composite was reduced compared with cells on cover slips. In contrast, expression of collagen I, osteopontin, and osteocalcin was distinctly increased on the material. Thus, on the xerogel composite increased mobility of focal adhesions correlated with cell differentiation whereas cell cycle progression was rather inhibited . In conclusion, surface characteristics of implant materials control the dynamics of focal adhesions which correlate with the functional behaviour of osteoblasts. Therefore, analyses of the dynamics of focal adhesions in cells on biomaterials appear to be a suitable approach to evaluate the biological activity of bone implants.

Disclosures: ***J. Rychly****, None.*

SU292

Runx2 Induces Osteoblast and Chondrocyte Differentiation and Enhances Their Migration by Coupling with PI3K-Akt Signaling. T. Fujita*[1], C. A. Yoshida*[2], M. Koida[1], T. Komori[2]. [1]Pharmacol, Setsunan Univ, Hirakata, Japan, [2]Developmental and Reconstructive Medicine, Nagasaki Univ, Nagasaki, Japan.

Runx2 and phosphatidylinositol 3-kinase (PI3K)-Akt signaling play important roles in osteoblast and chondrocyte differentiation. We investigated the relationship between Runx2 and PI3K-Akt signaling. Forced expression of Runx2 enhanced osteoblastic differentiation of C3H10T1/2 cells and MC3T3-E1 cells and enhanced chondrogenic differentiation of ATDC5 cells, whereas these effects were blocked by treatment with IGF-I antibody or LY294002 or adenoviral introduction of dominant negative (dn)-Akt. Forced expression of Runx2 or dn-Runx2 enhanced or inhibited cell migration, respectively, while the enhancement by Runx2 was abolished by treatment with LY294002 or adenoviral introduction of dn-Akt. Runx2 upregulated PI3K subunits (p85 and p110beta) and Akt, and their expression patterns were similar to that of Runx2 in growth plates. Treatment with LY294002 or introduction of dn-Akt severely diminished DNA binding of Runx2 and Runx2-dependent transcription, whereas forced expression of myrAkt enhanced them. These findings demonstrate that Runx2 and PI3K-Akt signaling are mutually dependent on each other in the regulation of osteoblast and chondrocyte differentiation and their migration.

Disclosures: ***T. Fujita****, None.*

SU293

Receptor Tyrosine Kinase Orphan Receptor 2 (Ror2) Binds Notch2 Receptor and Regulates its Transcriptional Activity in Osteoblastic Cells. J. Billiard[1], L. M. Seestaller-Wehr*[1], J. Ross*[2], P. V. N. Bodine[1]. [1]Women's Health Research Institute, Wyeth Research, Collegeville, PA, USA, [2]Protein Technologies, Wyeth Research, Collegeville, PA, USA.

Ror2 is an orphan receptor tyrosine kinase with no known ligand or association with a signaling pathway. To address a possible signaling mechanism of Ror2 receptor, we identified potential Ror2 binding partners by mass-spectroscopy analysis. U2OS human osteosarcoma cells were transiently transfected with flag-epitope-tagged Ror2 or empty vector, and the whole-cell extracts were immunoprecipitated on flag affinity agarose, resolved by SDS-PAGE and analyzed by mass spectroscopy. This approach identified eight potential Ror2 binding partners, including the Notch2 receptor.

Notch2 is a single-span transmembrane receptor that is activated by cleavage and nuclear translocation of its intracellular domain (N2IC). In the nucleus, N2IC activates transcription of target genes, including Hes1. We cloned the human N2IC and confirmed Ror2 interaction with it in U2OS over-expression system by immunoprecipitation studies.

Ror2-N2IC interactions had functional consequences on Notch signaling. Luciferase expression driven by Notch-responsive Hes1 promoter was stimulated 4-fold after co-transfection of U2OS cells with N2IC. In contrast, co-transfection with Ror2 dose-dependently inhibited N2IC-induced activation of this promoter.

Despite its ability to interact with Ror2, N2IC had no effect on Ror2 kinase activity as assessed by *in vitro* Ror2 autophosphorylation, and Ror2 did not phosphorylate N2IC *in vitro* either.

Since both Ror2 and Notch receptor families have been previously implicated in control of osteoblastic differentiation, their physical and functional interactions may have profound consequences on osteoblast development and bone formation.

Disclosures: ***J. Billiard****, Wyeth Research 3.*

SU294

Notch Signaling Is Activated by Binding of Periostin or CCN3 to Notch1 in Osteoblasts. H. Tanabe*[1], I. Kii*[1], N. Amizuka*[2], K. Katsube*[3], A. Kudo[1]. [1]Department of Life science, Tokyo Institute of Technology, Yokohama, Japan, [2]Department of Oral Anatomy, Niigata University, Niigata, Japan, [3]Department of Molecular Pathology, Graduation School of Tokyo Medical and Dental University, Tokyo, Japan.

Periostin, a 90kDa secreted protein, is known to express in periodontal ligament and periosteum in bone. However, the periostin involvement in bone formation remains unclear. To find the periostin function in bone formation, we studied the periostin association with CCN3 (NOV) or Notch1 and the periostin effect in Notch signaling. CCN3 is a 50kDa secreted protein, which associates with Notch1 and activates Notch signaling in the myoblastic cell line. Because Notch signaling plays a fundamental role in osteoblast differentiation, CCN3 is possibly important for osteoblast differentiation. First, using RT-PCR, we detected expressions of periostin, CCN3 and Notch1 in MC3T3-E1, the mouse osteoblastic cell line. Next, we performed immunohistochemistry of an adult mouse tooth. As a result, periostin, CCN3 and Notch1 were shown to co-localize in the periodontal ligament. To investigate interaction of these 3 proteins, we examined whether periostin associates with CCN3 or Notch1. NIH3T3 cells were co-transfected with periostin-HA and CCN3-FLAG or Notch1-FLAG, then immunoprecipitation was performed by using an anti-FLAG antibody. In this experiment, periostin was co-precipitated with Notch1 or CCN3. We also examined the association of periostin with CCN3 in a medium of MC3T3-E1, which is performed by immunoprecipitation using an anti-CCN3 antibody, and revealed that periostin was co-precipitated with CCN3. These results suggested that periostin associates with CCN3 or Notch1 in absence of Notch1 or CCN3. To investigate whether periostin/Notch1 or CCN3/Notch1 association could activate Notch signaling in osteoblasts, we examined the effect of periostin or CCN3 on the promoter activity of Hes1 in TSB13, the mouse osteoblastic cell line, since Hes 1 is a downstream target gene activated by Notch signaling. We observed that both periostin and CCN3 increased the Hes1 promoter activity dose-dependently up to 2 times. Taken together, theses results suggested that interaction of periostin and CCN3 may regulate bone formation through regulating Notch signaling.

Disclosures: ***H. Tanabe****, None.*

SU295

The Wnt Pathway in Human Bone and Bone-Related Cells: Taqman Gene Expression Analysis. L. V. Hale*, D. L. Halladay*, R. J. S. Galvin, J. E. Onyia*, C. A. Frolik. Bone & Inflammation, Eli Lilly/Lilly Research Laboratories, Indianapolis, IN, USA.

The Wnt glycoproteins comprise a highly conserved family of secreted lipid modified signaling molecules. These proteins modulate cell-to-cell interactions and are powerful regulators of cell proliferation and differentiation. The conventional Wnt signaling pathway (canonical) involves proteins that directly participate in gene transcription and cell adhesion. Proteins included in this pathway are the Wnts, Frizzleds (FZDs), Dickkopfs (DKKs), Lipoprotein Related Proteins (LRPs), secreted Frizzled Related Proteins (sFRPs), and Kremens. Recently, several studies have implicated this canonical Wnt pathway in bone formation. It has been shown that mice deficient in LRP5 develop osteopenia while an activating mutation of the LRP5 gene in mice leads to an increase in bone mass. Human LRP5 inactivation similarly reduces bone mass while activation enhances bone density. Finally, deletion of the Wnt antagonist, sFRP-1, enhances trabecular bone formation in adult mice. To identify which of the Wnt pathway genes might be of interest in human bone formation we have employed Taqman Gene Expression Analysis to assess the mRNA from human osteoclasts (cord blood cells treated with RANKL and MCSF), human preosteoclasts (cord blood CFU-GM cells), human adult bone, SaOS-2 osteosarcoma cells, and primary human osteoblasts (hOBs). We have found that genes for FZDs 1-8 are expressed to some degree in all tissues/cells tested. FZD 9 is found only at very low levels in SaOS-2 cells and hOBs. FZD 10 is expressed only in preosteoclasts and osteoclasts and in the bone tissue analyzed. Wnts 2, 3, 3a, 7a, 8a, and 14 are not detected in any tissues/cells tested. Wnt 15 is found only in osteoclasts, Wnt 6 only in SaOS-2 cells, Wnt 4 only in bone, and Wnt 16 only in hOBs. Wnts 1, 5a, 10b, and 11 are prevalent across all or most tissues/cells tested while Wnts 2b, 5b, 7b, 10a, and 16 demonstrate no particular patterning. DKK1 is present only in bone, SaOS-2 cells and hOBs. DKKs 2 and 3 are found in all or most of the samples tested. DKK4 is negative in all tissues/cells. Kremen 1 is expressed in all tissues/cells tested, however, Kremen 2 is negative across the panel. sFRPs 1-3 are relegated to bone and cells of osteoblastic lineage while sFRP-4 is found across the test panel. sFRP-5 is only present in bone. LRP5 and 6 are found in all tissues/cells tested. Although these data do not pinpoint which Wnt pathway genes are involved in regulation of human bone formation, they do indicate that many components of the pathway are present in bone and bone-related cells.

Disclosures: ***L.V. Hale****, None.*

SU296

Bisphosphonates Affect Osteoblast (UMR-106) GTPase Activity. Q. Sun[1], R. W. Katz[2], S. A. Morris[3], X. Fan*[1], J. P. Bilezikian[1]. [1]Division of Endocrinology, College of Physicians and Surgeons, Columbia University, New York, NY, USA, [2]Oral Medicine, College of Dentistry, New York University, New York, NY, USA, [3]Medical Affairs, NPS Pharmaceuticals, Parsippany, NJ, USA.

Bisphosphonates (BPs) are an important class of anti-resorptive medications for the treatment of metabolic bone disease. Although these compounds classically affect the osteoclast, recent studies suggest that bisphosphonates also affect osteoblast function. We previously reported that BPs affect the signal transduction pathways used by teriparatide [(rhPTH(1-34)] . It is not known how teriparatide and BPs could be used for maximal therapeutic effect, therefore our laboratory is interested in identifying possible molecular targets of BP action in osteoblasts. In this report, we characterize the effect of BPs on the prenylation and function of small soluble GTPases and their effect on cell density in-vitro. We hypothesize that BPs inhibit prenylation of GTPases in a representative osteoblast cell line, that this affects GTPase function, and that altered cell viability may be one result. In UMR-106 cells, risedronate reduced the amount of prenylated small GTPases identified by C14-labeled mevalonate to 20% of control levels but alendronate had little effect (63 % of control value). The steady state levels Rho A, Rab-6, and Rap-1 in cell homogenates as measured by immunoblotting was not affected by BP treatment. Overnight incubation of UMR-106 cells with alendronate or risedronate increased total cellular GTPase activity (161 % for alendronate and 172 % for risedronate respectively). Bisphosphonate treatment reduced total protein of harvested cultures by 31% (alendronate) and 36% (risedronate). Similar decreases were noted when total DNA was measured as a reflection of cell density (alendronate was 75% and risedronate was 67% of control values). Cell death, as indicated by propidium iodide influx, increased by BPs (risedronate two-fold greater than alendronate). We conclude that BPs affect GTPase prenylation, the levels of three representative GTPases are unaffected, and that BPs stimulate total GTPase activity. In addition, BPs differentially increase the number of non-viable UMR cells and suppress cell accumulation in overnight culture. The observation that BPs and teriparatide influence osteoblast functions complicates the manner in which these two classes can be used for optimal advantage.

Disclosures: ***Q. Sun****, Alliance for Better Bone Health 2.*

SU297

RANK Ligand Stimulates Cathepsin K Expression via TRAF6 and c-Jun. A. F. Martinez*, M. Pang*, M. Gyda*, W. Balkan*, B. R. Troen. Miami VA GRECC, University of Miami School of Medicine, Miami, FL, USA.

Cathepsin K (CTSK) is a secreted protease that plays an essential role in osteoclastic bone resorption. Receptor activator of NF-κB ligand (RANKL), a member of the TNF superfamily of cytokines, is a critical mediator of osteoclastogenesis that also stimulates CTSK expression in monocytic cells. Little is known about the mechanism whereby RANKL regulates CTSK expression. We have therefore begun to study the regulation of CTSK expression in osteoclast precursors (RAW 264.7 cells), which can be readily differentiated to bone-resorbing osteoclasts by RANKL treatment. Real-time RT-PCR reveals that RANKL stimulates CTSK mRNA expression in a dose- and time-dependent manner. CTSK protein expression is also induced by RANKL. Transfection analysis with CTSK promoter-luciferase plasmids demonstrates that two regions upstream of the transcription initiation site (-1628 to -1089 bp and -698 to -395 bp) are responsible for most of the constitutive activity of the promoter. Both RANKL treatment and a constitutively active TRAF6 expression vector separately stimulate expression of CTSK promoter driven luciferase in transfected cells. In cells stably transfected with the 1628 bp CTSK promoter-luciferase plasmid, RANKL stimulates CTSK promoter activity in a dose-dependent manner. RANKL treatment markedly enhances phosphorylation of both JNK and c-jun. Furthermore, co-transfection of a CTSK promoter-luciferase plasmid with a dominant negative c-jun expression vector inhibits stimulation of CTSK promoter activity by both TRAF6 overexpression and by RANKL treatment. Therefore TRAF6 and c-jun play major roles in the RANKL-mediated regulation of CTSK expression. This model system will permit us to further characterize and identify the specific motifs and nuclear binding factors that regulate CTSK gene transcription.

Disclosures: ***B.R. Troen****, None.*

SU298

Cross-Talk Between RANKL and Interferon Gamma in the Regulation of Cathepsin Gene Transcription in Pre-Osteoclastic Cells. M. Pang*, A. F. Martinez*, J. Jacobs*, W. Balkan*, B. R. Troen. Miami VAMC GRECC, University of Miami School of Medicine, Miami, FL, USA.

Receptor activator of NF-κB ligand (RANKL) and interferon gamma (IFN-γ) are critical and opposing mediators of osteoclastogenesis, exerting stimulatory and inhibitory effects, respectively. Cathepsin K (CTSK) is a secreted protease that plays an essential role in osteoclastic bone resorption. We are examining the role of IFN-γ in the regulation of CTSK expression in the murine monocytic RAW 264.7 cell line, which can be readily differentiated to bone-resorbing osteoclasts upon RANKL treatment. Real-time RT-PCR reveals that RANKL stimulates CTSK mRNA expression in a dose and time-dependent fashion, but that RANKL does not alter the expression of cathepsin L (CTSL) and cathepsin S (CTSS) mRNA. IFN-γ markedly stimulates both CTSL and CTSS expression, but fails to significantly alter CTSK expression. Whereas IFN-γ inhibits the stimulation of CTSK by RANKL, RANKL suppresses the stimulation of CTSL and CTSS by IFN-γ. Transient transfection analysis with a CTSK promoter-luciferase plasmid containing the 1628 bp upstream of the transcription initiation site demonstrates that IFN-γ treatment dramatically suppresses both constitutive CTSK promoter activity and the RANKL stimulation of CTSK promoter driven luciferase expression. Similarly, in stably transfected cells, IFN-γ inhibits CTSK promoter activity and ablates its induction by RANKL. Since IFN-γ does not appear to directly inhibit endogenous CTSK mRNA expression, the suppression of CTSK promoter activity in the transfected cells by IFN-γ alone is likely due to the presence of only the 1628 bp immediately upstsream of the transcription initiation site. In conclusion, IFN-γ and RANKL differentially regulate cathepsin K, S and L gene expression in pre-osteoclastic cells. There appears to be significant cross-talk between the signal transduction pathways mediating the responses to RANKL and IFN-γ. This differential regulation of cathepsin gene expression presents a model system to investigate further the divergent effects of RANKL and IFN-γ upon osteoclastic differentiation.

Disclosures: ***B.R. Troen****, None.*

SU299

Orally Active Cathepsin K Inhibitor, YD-1901, Prevents Bone Resorption *in vitro* and *in vivo* in Rats. M. H. Son*[1], J. I. Lim*[1], J. S. Yang*[1], M. K. Kim*[1], W. Y. Kwak*[1], H. D. Kim*[1], J. H. Park*[1], S. S. Lee*[1], H. J. Kim*[1], H. J. Shim*[1], S. H. Kim*[1], C. H. Lee*[2], J. Y. Shim*[2], N. C. Kim*[2], Y. Huh*[2], T. D. Han*[2], W. Chong*[2], H. Choi*[2], B. N. Ahn*[2], S. O. Yang[3]. [1]Dong-A Pharm. Co., Ltd., Yongin, Republic of Korea, [2]Yuhan Co., Ltd., Kunpo, Republic of Korea, [3]Department of Radiology, Eulji University Hospital, Seoul, Republic of Korea.

Cathepsin K has been shown to play a major role in bone matrix degradation during osteoclastic bone resorption. In this study we disclosed the anti-resorptive activities of a novel candidate *in vitro* and *in vivo*.

YD-1901 is a reversible and potent inhibitor of human and rat cathepsin K with an IC50 of 7.0 and 450 nM, respectively. Also, it inhibited bone resorption by rabbit osteoclasts cultured on bone slice with an IC50 of 37 nM. Pharmacokinetic analysis in the rat revealed YD-1901 to be 85% orally bioavailable when administered as a solution.

For *in vivo* evaluations, YD-1901 was given orally to thyroparathyoidectomized rats. It inhibited PTH-induced bone resorption dose-dependently with an ED50 of 69 mg/kg. When given orally twice daily for 4 weeks to young (3-month-old) ovariectomized (OVX) rats, YD-1901 (50 and 100 mg/kg) completely prevented estrogen deficiency-induced bone loss evaluated by bone densitometry and ashing for the specimen. Furthermore, when old (14-month-old) OVX rats were treated with YD-1901 for 12 weeks, it also prevented bone loss significantly ($p<0.05$) in the femur and vertebra. YD-1901 (50 and 100 mg/kg) decreased the level of urinary DPD/creatinine dose-dependently without affecting elevated serum osteocalcin.

These results suggest that an orally active YD-1901 that inhibits human cathepsin K: 1) blocks bone resorption *in vitro*; and 2) completely prevents estrogen deficiency-induced bone loss in old as well as young rats.We conclude that YD-1901 has the therapeutic potential for the treatment of diseases characterized by excessive bone loss including osteoporosis.

Disclosures: ***M.H. Son****, None.*

SU300

Anti-resorptive Activities and Pharmacokinetic Properties of a Potent Cathepsin K Inhibitor, OST-4510. C. H. Lee*[1], T. D. Han*[1], Y. Hur*[1], J. Y. Shim*[1], N. C. Kim*[1], W. Chong*[1], B. Ahn*[1], M. H. Son*[2], J. S. Yang*[2], M. K. Kim*[2], W. Y. Kwak*[2], S. Y. Sung*[2], H. D. Kim*[2], J. H. Park*[2], S. S. Lee*[2], H. J. Shim*[2], S. H. Kim*[2], H. S. Lee*[3]. [1]Yuhan Research Institute, Yuhan Corp., Gunpo, Republic of Korea, [2]Research Laboratories, Dong-A Pharm. Corp., Ltd., Yongin, Republic of Korea, [3]School of Pharmacy, Wonkwang University, Iksan, Republic of Korea.

Cathepsin K has been shown to play a major role in bone matrix degradation during osteoclastic bone resorption. In this study we investigated the anti-resorptive activities and pharmacokinetic properties of a novel cathepsin K inhibitor, OST-4510, *in vitro* and *in vivo*.

OST-4510 is a reversible and potent inhibitor of human and rat cathepsin K with IC50 values of 1.3 and 150 nM, respectively. It showed highly selective profile against human cathepsin B, L, and S with an IC50 of greater than 400 nM. OST-4510 inhibited bone resorption by rabbit osteoclasts cultured on bone slice with an IC50 of 14 nM. When OST-4510 was given orally to thyroparathyoidectomized rats, it inhibited PTH-induced bone resorption dose-dependently.

OST-4510 (10 mg/kg) had a good oral bioavailability of 40% and showed favorable pharmacokinetic profile in rats. It was also metabolically stable in rat, monkey and human liver microsomes. Furthermore compound B did not inhibit the activities of five major human CYP450s nor induce CYP3A4.

These results suggest that an orally active OST-4510 that selectively inhibits human cathepsin K: 1) blocks bone resorption *in vitro* and *in vivo*; and 2) has favorable pharmacokinetic characteristics. We conclude that inhibition of cathepsin K by OST-4510 is a promising approach to the treatment of osteoporosis and other metabolic bone diseases.

Disclosures: ***C.H. Lee****, None.*

SU301

The Effects of Trypsin-Cleavage and Reduction on the Phosphatase Activity and Reactive Oxygen Species Generating Activity of Human Recombinant Tartrate-Resistant Acid Phosphatase. K. Kaarlonen*[1], H. Ylipahkala*[1], S. L. Alatalo*[1], A. J. Janckila[2], H. K. Väänänen*[1], J. M. Halleen[3]. [1]Institute of Biomedicine, Department of Anatomy, University of Turku, Turku, Finland, [2]Veterans Affairs Medical Center, Louisville, KY, USA, [3]Pharmatest Services Ltd, Turku, Finland.

Tartrate-resistant acid phosphatase (TRACP) is an enzyme with unknown biological function that contains a redox-active iron in its active site. In addition to the acid phosphatase activity, TRACP is also capable of generating reactive oxygen species (ROS). Two forms of TRACP circulate in human blood, a sialic acid-containing form TRACP 5a with a pH-optimum of 5.2 and low specific activity and a non-sialylated form TRACP 5b with a pH-optimum of 5.8 and high specific activity. Serum TRACP 5a is derived from macrophages and serum TRACP 5b from osteoclasts. We produced human recombinant TRACP protein using baculovirus expression system, purified it using cation exchange and gel filtration chromatography, and cleaved the purified enzyme with trypsin. β-mercaptoethanol was used to reduce the disulfide bridge and ascorbate to reduce the redox-active iron. Trypsin cleaved the 35 kD monomeric native recombinant TRACP protein into two subunits of 23 and 16 kD that were linked together with a disulfide bridge. In Western analysis, a monoclonal antibody specific for serum TRACP 5a recognized the non-cleaved protein, but not the cleaved subunits. The cleavage together with reduction by β-mercaptoethanol changed the pH-optimum of the phosphatase activity from 5.4 to 6.2 and activated the enzyme. Thus, antigenic properties and pH-optimum of the phosphatase activity of the non-cleaved reduced recombinant enzyme were similar to those of serum TRACP 5a, and after cleavage similar to those of serum TRACP 5b. Reduction with ascorbate activated both the monomeric and cleaved enzyme. Both trypsin-cleavage and reduction by ascorbate increased the ROS generating activity of TRACP. We conclude that the structure of TRACP contains at least three features that may be important for regulating its activity, the cleavage site for proteases, the disulfide bridge in the polypeptide chain and the redox-active iron in the binuclear iron center. Our results suggest that the osteoclast-derived TRACP 5b circulates in blood in an active cleaved form, and the macrophage-derived TRACP 5a in a less active non-cleaved form.

Disclosures: ***K. Kaarlonen****, None.*

SU302

Monokine Induced by Interferon-gamma (MIG) Is Involved in Osteoclast Adhesion and Migration through STAT1-dependent Pathway. Z. Lee[1], H. Kwak*[1], H. Jin*[1], H. Ha*[2], H. Kim[2]. [1]National Research Laboratory for Bone Metabolism, Chosun University Dental College, Gwangju, Republic of Korea, [2]Department of Cell and Developmental Biology, College of Dentistry, Seoul National University, Seoul, Republic of Korea.

The bone remodeling process is accompanied by complex changes in the expression levels of various genes in osteoclasts. Receptor activator of nuclear factor κB ligand (RANKL) may contribute to this process. We found that monokine induced by interferon-γ (MIG) gene was up-regulated in osteoclast precursors by treatment with RANKL through the cDNA array analysis. MIG is a member of a superfamily of CXC chemokines and is involved in the directed **migration and adhesion in** macrophages, T and B cells that have been implicated in inflammation. The relative abundance of differentially regulated MIG was confirmed by RT-PCR and Western blotting in osteoclast precursors treated with RANKL. RANKL could activate the phosphorylation of Ser727 in STAT1 and p38 MAPK inhibitor suppressed it. And, STAT1 deficient mice did not express the MIG in the response to RANKL in the osteoclast precursors. Therefore, we provide that the first evidence demonstrating that RANKL can activate serine phosphorylation of STAT1 via p38 MAPK pathway to produce the MIG, although NF-kB pathway is involved in the induction of MIG. MIG induced by RANKL could stimulated the migration and adhesion of CXCR3-expressed osteoclast precursors derived by M-CSF with autocrine or paracrine mode. This study provides evidence that MIG carries out the recruitment function of osteoclast precursors to bone remodeling site from bone marrow or peripheral blood.

Disclosures: ***Z. Lee****, None.*

SU303

Osteoclasts Are Essentially Required for Normal Bone Morphogenesis. M. Nakamura[1], H. Horiuchi*[2], M. Mogi*[3], K. Takaoka[4], N. Takahashi[5], N. Udagawa[1]. [1]Biochemistry, Matsumoto Dental University, Shiojiri, Japan, [2]Orthopaedic Surgery, Shinshu University School of Medicine, Matsumoto, Japan, [3]Pharmacology, Aichi Gakuin University, Nagoya, Japan, [4]Orthopaedic Surgery, Osaka City University School of Medicine, Osaka, Japan, [5]Institute for Oral Science, Matsumoto Dental University, Shiojiri, Japan.

Osteopetrosis is an inherited disorder characterized by an increase in bone mass due to reduced bone resorption. It has been reported that the osteoclast deficiency in osteopetrotic op/op mice is due to a mutation in the coding region of the M-CSF gene. Using op/op mice, we explored roles of osteoclasts in ectopic bone formation induced by bone morphogenetic protein (BMP). Collagen sponge disks containing human recombinant BMP-2 were implanted into the dorsal muscle pouches in op/op and wild-type mice for 3 weeks. Bisphosphonate (risedronate) was injected into op/op and wild-type mice every day for 3 weeks. Bone mineral density of each ossicle was measured by single energy x-ray absorptiometry. Quantitative histomorphometric analysis was also performed. Bone mineral density of BMP-induced ectopic bone in op/op mice was about 3-fold higher than that in wild-type mice. Histological examination revealed that BMP induced higher calcified trabecular bone formation in op/op mice than in wild-type mice. Interestingly, the periphery of ectopic bones formed in op/op mice showed extremely rough surface, whereas that in wild-type mice showed smooth ones. Bisphosphonate treatment further enhanced ectopic bone formation in op/op mice. We previously reported that serum levels of RANKL were markedly elevated in osteoprotegerin (OPG)-deficient mice, but were unaffected by bisphosphonate administration. Unexpectedly, serum levels of RANKL in op/op mice were as high as those in OPG-deficient mice, whereas those in wild-type mice were under detectable levels in the RANKL assay. Treatment of op/op mice with bisphosphonate treatment sharply decreased the elevated levels of serum RANKL. These results suggest that BMP-induced ectopic bone formation is accurately enhanced in the absence of osteoclasts, and osteoclasts are involved in normal bone morphogenesis. Our results also suggest that bisphosphonates may be directly involved in bone formation without inhibition of osteoclastic bone resorption. Further studies will elucidate the mechanism of bisphosphonate action in BMP-induced bone formation in osteoclast-deficient mice.

Disclosures: ***M. Nakamura****, None.*

SU304

BMP Tightly Regulates in vivo Osteoclast Formation in OPG-deficient Mice. Y. Yamamoto*[1], S. Matsuura*[2], H. Horiuchi*[3], M. Nakamura*[4], H. Ozawa*[2], T. Noguchi*[1], N. Udagawa*[4], N. Takahashi*[5]. [1]Periodontology, Aichi-Gakuin Univ.,School of Dentistry, Nagoya, Japan, [2]Second Department of anatomy, Matsumoto Dental Univ., Siojiri, Japan, [3]Orthopedic Surgery, Shinshu Univ., Matsumoto, Japan, [4]Biochemistry, Matsumoto Dental Univ., Siojiri, Japan, [5]Institute for Oral Science, Matsumoto Dental Univ, Siojiri, Japan.

OPG is a decoy receptor for RANKL. OPG-deficient ($OPG^{-/-}$) mice exhibit aberrant bone metabolism characterized by accelerated bone resorption and formation. Serum levels of RANKL are shown to be extremely high in patients with OPG-deficient juvenile Paget's disease and in $OPG^{-/-}$ mice. These findings raise a possibility that OPG deficiency may accelerate osteoclast formation inside and outside the bone tissues. Using $OPG^{-/-}$ mice, we examined osteoclast formation in ectopic bone induced by BMP implantation. Collagen disks containing human recombinant BMP-2 or vehicle were implanted into dorsal muscular pouches of $OPG^{-/-}$ and wild-type mice, and recovered at different time points. Osteoclasts and osteoblasts appearing in the collagen disks were detected by enzyme histochemical staining for TRAP and ALP, respectively. Monocytes/macrophages and RANKL-expressing cells were detected by immunohistochemical staining with anti-F4/80 antibody and anti-RANKL antibodies, respectively. TRAP-positive cells and ALP-positive cells appeared simultaneously surroundings of the BMP-containing collagen disks implanted for 1 week into $OPG^{-/-}$ mice and wild-type mice, preceding the onset of calcification. The number of TRAP-positive cells was increased with the increase in periods of implantation, and was significantly higher in the disks harvested from $OPG^{-/-}$ mice than those from wild-type mice. Neither TRAP-positive cells nor ALP-positive cells appeared in BMP-deficient collagen disks implanted even into $OPG^{-/-}$ mice. F4/80-positive macrophages, precursors of osteoclasts, were similarly detected in both BMP-containing and BMP-deficient collagen disks implanted into $OPG^{-/-}$ mice. When collagen disks containing BMP together with OPG were prepared and implanted into $OPG^{-/-}$ mice, ALP-positive osteoblasts and F4/80-positive macrophages appeared in the disks, but TRAP-positive osteoclasts did not. RANKL-expressing cells were detected surroundings of BMP-containing disks but not BMP-deficient disks at 1 week. These results suggest (i) that locally expressed RANKL rather than circulating one is important for osteoclast formation; (ii) that mineralization of bone tissues is not absolutely required for the osteoclast induction; and (iii) that BMP plays important roles in osteoclast differentiation through the induction of osteoclastogenesis-inducing cells.

Disclosures: ***Y. Yamamoto****, None.*

SU305

Study of Osteoclast Apoptosis in a Human Model of Osteoclast Differentiation. S. Roux, P. Lambert-Comeau*, C. Saint-Pierre*. Rheumatology, University of Sherbrooke, Sherbrooke, PQ, Canada.

Survival and apoptosis are of major importance in the osteoclast (Oc) life cycle, and can lead to crucial changes in bone resorption. Although major advances have been made in our understanding of the mechanisms of Oc apoptosis in rodents, little is known about Oc apoptosis in humans.

In the present study, cord blood monocytes (CBMs) were used as the source of human Oc precursors, and were cultured for 3 weeks in presence of M-CSF (25 ng/ml) and RANKL (100 ng/ml). At the end of the cultures, immunohistochemistry was performed to evaluate Oc markers using anti-RANK and anti-CTR antibodies, in addition some experiments were performed on bone slices. After the 3-week culture period, apoptosis was evaluated by a TUNEL-derived method. Finally, TRAIL receptor expression was evaluated by immunohistochemistry, using antibodies directed against TRAIL-R1, -R2, -R3 and -R4.

When cultured in presence of M-CSF and RANKL, CBMs formed multinucleated cells (MNCs) that express RANK and CTR (respectively 72 ±2 and 75 ±4 % of the MNCs, n=5), and these cells were able to resorb bone when cultured on bone slices. At the end of the cultures, apoptosis was evaluated 24 hours after removing RANKL and M-CSF, and in presence of potential apoptosis inducers. The percentage of apoptotic MNCs was 44 ±9 % in control cultures, 47 ±9 % in presence of TRAIL at concentration of 10 ng/ml (ns) and 63 ±9 % at 100 ng/ml (p=0.0012 vs controls), 52 ±9 % in presence of TGFb1 at 0.1 ng/ml (ns), and 63 ±7 % at 1 ng/ml (p=0.0045 vs controls) (n=8). In addition we found that MNCs expressed TRAIL receptors, TRAIL-R1 was expressed in 67 ± 2 %, TRAIL-R2 in 55 ±4 %, TRAIL-R3 in 49 ±6 %, and TRAIL-R4 in 36 ±8 % of the MNCs (n=3).

We have shown that CBMs represent a suitable model of human osteoclast differentiation. In this model, apoptosis was induced by the removal of survival factors (M-CSF, RANKL), and the rate of apoptosis significantly increased in presence of TRAIL and TGFb1. In addition, osteoclast-like cells expressed TRAIL-receptors, both TRAIL-R1 and -R2 that are able to transduce apoptosis, and TRAIL-R3 and -R4 that are decoy receptors. Taken together the results suggest that, at least in part, the TRAIL pathway could be involved in osteoclast apoptosis in humans.

Disclosures: ***S. Roux****, None.*

SU306

Mechanisms of Parathyroid Hormone-Related Protein and Interleukin-1a Induced Expression of Receptor Activator of NF-kB Ligand in Human Periodontal Ligament Cells. H. Fukushima[1], H. Kajiya[2], F. Okamoto*[2], E. Jimi[2], W. Motokawa*[1], K. Okabe[2]. [1]Department of Oral Growth and Development, Fukuoka Dental College, Fukuoka, Japan, [2]Physiological Science and Molecular Biology, Fukuoka Dental College, Fukuoka, Japan.

Physiological root resorption during shedding of human deciduous teeth leads to eruption of permanent teeth and formation of functional occlusion. Root resorption of human deciduous teeth is mediated by osteoclast-like cells (odontoclasts). We examined the effects of PTH-related protein (PTHrP), IL-1a, TGF-b and EGF, which are all secreted from the tooth germ, on tartrate-resistant acid phosphatase positive (TRAP+) cell formation using co-culture of human periodontal ligament (PDL) cells and mouse bone marrow cells. Of these factors examined, only PTHrP and IL-1a promoted TRAP+ cell formation in co-cultures. PTHrP induced receptor activator of NF-kB ligand (RANKL) mRNA expression in PDL cells and slightly reduced osteoprotegerin (OPG) expression. IL-1a up-regulated RANKL and down-regulated OPG mRNA expression. Inhibition of the cAMP/PKA signaling pathways with cAMP/PKA inhibitors Rp-cAMP, H89 or PKI did not affect PTHrP- and IL-1a-induced TRAP+ cell formation. IL-1a- but not PTHrP-induced TRAP+ cell formation was completely blocked by pretreatment with either NS-398, a selective inhibitor of cyclooxygenase (COX)-2 or PD98059, a specific inhibitor of extracellular signal-regulated kinase (ERK). Pretreatment with NS-398 and PD98059 also inhibited both the up-regulation of RANKL and the down-regulation of OPG expression in PDL cells by IL-1a. IL-1a activated ERK phosphorylation and pretreatment with PD98059 greatly inhibited COX-2 mRNA expression in PDL cells by IL-1a. These results suggest that PTHrP and IL-1a released from the tooth germ stimulate odontoclast formation by increasing relative expression level of RANKL versus OPG in PDL cells via separate signaling pathways.

Disclosures: ***H. Fukushima****, None.*

SU307

RANKL Induces The Osteoclast-Specific P3 Calcitonin Receptor Promoter In Stably Transfected RAW 264.7 Cells By Mechanisms Involving NFATc1 and p38 MAPK. N. Kawanabe[1], G. Wang*[2], S. Lee[1], J. A. Lorenzo[1], D. L. Galson[2]. [1]Medicine, University of Connecticut Health Center, Farmington, CT, USA, [2]Center for Bone Biology, Dept. of Medicine, University of Pittsburgh School of Medicine, Pittsburgh, PA, USA.

Calcitonin receptor (CTR) expression is restricted to a spectrum of tissues that include osteoclasts, brain, kidney and reproductive organs. Recently, a murine CTR promoter fragment (P3) was found to enhance the expression of CTR in osteoclasts but not in brain or kidney cells. To characterize this promoter, we established stable RAW 264.7 cell lines, which contain a GFP reporter gene driven by the P3 CTR promoter fragment (P3-GFP RAW cells), and assessed if RANKL-treatment stimulated promoter activity coincident with osteoclast-like (OCL) formation. Using flow cytometry, we found that P3 CTR promoter activity, which was measured as mean GFP fluorescence intensity, was significantly enhanced by RANKL in P3-GFP RAW cells from day 1 to day 4 compared to untreated controls (1.5 fold on day 1, 3.8 fold on day 2, 5.0 fold on day 3 and 4.5 fold on day 4, all $p<.05$). In addition, on day 2 80-90% of the P3-GFP RAW cells had a GFP fluorescence intensity that was above levels in untreated cells. RAW 264.7 cells stably transfected with promoterless GFP constructs had minimal fluorescence in all conditions (>7.4-8.9 fold less than untreated P3-GFP cells). We also compared the mRNA expression of several osteoclast markers (CTR, TRAP, MMP-9) and the transcription factor NFATc1 using RT-PCR. NFATc1, which is an important regulator of osteoclastogenesis, binds and stimulates P3 CTR. RANKL enhanced (> 2 fold) TRAP and NFATc1 mRNA on days 1-4, MMP9 mRNA on days 2-4 and endogenous CTR mRNA on day 3-4. To confirm that RAW 264.7 cells have features of osteoclasts, we performed bone resorption and calcitonin (CT) binding assay. RAW 264.7 cells formed bone resorption pits on bovine bone slices and had calcitonin binding ability after 4 days of RANKL treatment. Cyclosporine A, an inhibitor of NFATc1 activation, blocked both RANKL-induced P3 CTR activity and osteoclastogenesis. Treatment of the cultures with SB202190 (a p38 MAP kinase inhibitor) also blocked RANKL-induced P3 CTR activity.

These results demonstrate that the activity of the P3 CTR promoter fragment is rapidly (< 1 day) stimulated by RANKL in RAW 264.7 cells. Enhancement of this activity was coincident with increases in NFATc1 mRNA expression and blocked by specific inhibitors of NFATc1 and p38 MAPK. These findings imply that RANKL-induced regulation of the P3 CTR promoter in osteoclasts is mediated by NFATc1 and p38 MAP kinase.

Disclosures: ***N. Kawanabe****, None.*

SU308

A Role for the Sodium/Bicarbonate Exchanger, NBCn1 in Colony Stimulating Factor-1 (CSF-1)- Dependent Akalinization and Cell Survival in Osteoclasts. P. Bouyer*[1], T. Itokawa*[1], H. Sakai*[2], W. F. Boron*[1], K. Insogna[1]. [1]Yale University, New Haven, CT, USA, [2]Hamanomachi Hospital, Fukuoka, Japan.

Osteoclasts are short-lived, and increased osteoclast survival plays a role in the pathogenesis of skeletal diseases such as estrogen-deficiency bone loss. CSF-1 promotes osteoclast survival and the mechanism for this effect is currently under study. A rise in cytosolic pH has been linked to inhibition of apoptosis but the effect of CSF-1 on intracellular pH in osteoclasts has not been reported. We therefore measured cytosolic pH in freshly isolated neonatal rat osteoclasts and murine osteoclast -like cells (OCLs), prepared by co-culture on collagen-coated plates, before and after exposure to 2.5 nM CSF-1. Cells were loaded with the pH sensitive dye BCECF to monitor intracellular pH (pHi) and the fluorescence excitation ratio I490/I440 converted to pHi values by using the high-K+ nigericin technique. In the presence of 5% CO_2/22 mM HCO_3^- , CSF-1 caused a significant rise in pHi from 7.14 to 7.36 ($p<0.02$). The alkalinization persisted as long as CSF-1 was present in the solution. In HEPES buffer, the response to CSF-1 was markedly attenuated with pHi only increasing from 7.13 to 7.16. The mean CSF-1-induced increase in pHi was significantly attenuated in HEPES as compared CO_2/HCO_3^- ($p < 0.007$). Changing the sequence in which cells were exposed to the two buffers did not alter the results. OCLs demonstrated responses similar to those seen in freshly isolated osteoclasts. EIPA, an inhibitor of Na-H exchangers and concanamycin A, a proton pump inhibitor, did not attenuate the CSF-1-induced rise in pHi. The rise in pHi induced by CSF-1 was not affected by EIPA (Na-H exchange inhibitor), concanamycin A (proton-pump inhibitor), or DIDS (which inhibits many HCO_3^- transporters), but was completely abolished by the removal of extracellular sodium. This inhibition profile is reminiscent of that for the electroneutral Na/HCO_3 co-transporter, NBCn1. Single-cell RT-PCR in osteoclasts as well as RT-PCR in OCLs demonstrated expression of NBCn1. NBCn1 protein expression was confirmed by immunocytochemical studies in freshly isolated osteoclasts. After 4 hours of serum starvation, CSF-1 reduced the number of apoptotic cells by 45% in CO_2/HCO_3^- buffer but was without effect on cell survival in HEPES buffer. This study provides the first evidence that osteoclasts express a Na/HCO_3 co-transporter, and that the activity of this transporter is regulated by CSF-1. Preventing the activation of NBCn1 markedly attenuated the ability of CSF-1 to prevent osteoclast apoptosis, pointing to a new pathway mediating osteoclast survival.

Disclosures: ***T. Itokawa****, None.*

SU309

CD11c$^+$ Myeloid Dendritic Cells Develop Osteoclastic Phenotype and Function During Immune Activation in Bone Microenvironment. M. Alnaeeli*[1], A. Marleau*[2], B. Singh*[2], J. Penninger*[3], A. Y. Teng*[1]. [1]Microbiology and Immunology, University of Rochester, Rochester, NY, USA, [2]Microbiology and Immunology, University of Western Ontario, London, ON, Canada, [3]Austrian Academy of Sciences, Institute of Molecular Biotechnology, Vienna, Austria.

Bone remodelling is controlled by cytokines, growth factors/hormones, osteoblasts & osteoclasts (OC). OC stem from hematopoietic precursors of monocyte/macrophage lineage; their development & maturation is know to require M-CSF & RANK-RANKL signalling. Professional antigen-presenting cells (APCs), dendritic cells (DCs), can prime naïve T-cells, then activate & regulate the immune response. Activated T-cells express RANKL during immune activation; thus, linking T-cell-immunity to bone remodelling, critical in inflammatory bone disorders like arthritis, periodontitis & osteomyelitis. Periodontitis, the prime cause of alveolar bone loss around teeth in adults (worldwide prevalence >80%). To study the contribution of DCs to bone loss during immune interactions with T-cells, mCD11c$^+$ myeloid DCs were purified from mouse BM (IL-4 & GM-CSF), followed by co-culture with naïve CD4$^+$T cells & *Actinobacillus actinomycetemcomitans,* a key human pathogen (JCI 66: R59, 2000), or mitogen ConA in hydroxyapatide-coated plates. The results of quantitative & clonal analyses show that myeloid CD11c$^+$DCs are activated & develop OC phenotype by expressing tartrate-resistant acid phosphatase (TRAP; $p<0.03$) with significantly elevated bone resorptive activity (lacunae formations; $p<0.02$) and up-regulation of calcitonin receptors on cell surfaces with varying GM-CSF-R levels ($p<0.05$; immunofluorescence & FACS), compared to the controls. Importantly, after adding osteoprotegerin, the natural decoy ligand of RANKL, their OC phenotype & function are abolished ($p<0.02$ & 0.03, respectively). Further analyses of genetically mutated BM-derived precursors indicate that these DCs stem from the myeloid progenitors for OC differentiation, distinct from the classical monocyte/macrophage lineage. In conclusion: **i)** CD11c$^+$myeloid DCs function as professional APCs to prime naïve CD4$^+$T cells for immune activation; in addition, they can develop OC phenotype & function by resorbing bone *in-situ* after receiving RANKL from activated T cells; **ii)** these myeloid DCs may be manifest OC phenotype as OC precursor in the bone microenvironment when appropriately stimulated *in vitro*. Thus, these novel findings will have potentially significant implications on our understanding of the inflammatory bone disorders associated with T-cell-mediated immunity such as periodontitis, arthritis, osteomyelitis and immune surveillance of tumor-associate bone metastasis.

Disclosures: ***M. Alnaeeli****, None.*

SU310

Ara-C Enhanced Osteoclast Differentiation Induced by RANKL Mediated by TRAF-2 Expression. M. Koide*[1], S. V. Reddy[2], S. Fujita*[1], T. Sobue[1], T. Noguchi*[1]. [1]Periodontology, Aichi-Gakuin University, Nagoya, Japan, [2]Medicine/Division of Hematology, University of Pittsburgh, Pittsburgh, PA, USA.

Ara-C (1-β-D-Arabinofuranosylcytosine) is a potent anti-cancer agent used to treat myelogenous leukemia. Ara-C has been shown to induce differentiation of myeloid leukemia cells by NF-κB activation. Although efficacy and toxicity of Ara-C has been evaluated in patients with acute myeloblastic leukemia, the role of Ara-C in associated hypercalcemia of malignancy as well as myeloid cell differentiation is yet unknown. RANK receptor and RANK ligand (RANKL) play a central role in osteoclast differentiation. We show that Ara-C enhanced osteoclast differentiation of RAW 264.7 (RAW) cells induced by RANKL. The other hand, Ara-c did not significantly affect osteoblast proliferation and alkaline phosphatase activity in primary osteoblast cells. Ara-C at high doses (0.1-1 μM) induced NF-κB activation by two fold in these cells. Ara-C also significantly increased AP-1 transcription factor expression in RAW cells. Western blot analysis further demonstrated that Ara-C induced TRAF-2 protein expression, however did not change TRAF-6 protein levels in RAW cells. Therefore, our data suggested that Ara-C has additional effects to enhance osteoclast formation by RANKL. The cellular signaling mechanisms associated with Ara-C effect are mediated through increased expression of TRAF-2 modulating the NF-κB and AP-1 activation during osteoclast differentiation.

Disclosures: ***M. Koide****, None.*

SU311

Toll-Like Receptor 9 Activation on Osteoclastic and Osteoblastic Lineage Cells Modulate Osteoclastogenesis. A. Amcheslavsky*[1], H. Hemmi*[2], S. Akira*[2], Z. Bar-Shavit[1]. [1]Experimental Medicine and Cancer Research, Hebrew University, Jerusalem, Israel, [2]Host Defense, Osaka University, Osaka, Japan.

Bacterial infections cause pathological bone loss by accelerating differentiation/activation of the bone-resorbing cell, the osteoclast. CpG oligodeoxynucleotides (CpG-ODNs), mimicking bacterial DNA, modulate osteoclast differentiation via Toll-like receptor 9 (TLR9) in a complex manner: they inhibit the activity of the physiological osteoclast differentiation factor, RANKL in early osteoclast precursors (OCPs), but markedly stimulate osteoclastogenesis in cells primed by RANKL. The osteoclastogenic effect of TLR9 is mediated by TNF-α. In the current study we use TLR9 deficient mice (-/-) to examine the role of this receptor in osteoclastogenesis. RANKL induces in vitro differentiation of bone marrow derived OCPs in both, -/- and +/+ mice. LPS modulated RANKL-induced osteoclastogenesis in cells derived from -/- mice in a similar manner to its effects in +/+ derived cells. On the other hand, CpG-ODN failed to exert neither stimulatory nor inhibitory effects on -/- derived cells. Intracellular events known to participate in osteoclast differentiation were examined. RANKL and LPS induced TNF-α synthesis, phosphorylation of p38 and ERK, as well as nuclear translocation of NFκB similarly in the wild type and TLR9 deficient mice. CpG-ODN affected normally the wild type mouse, but did not modulate any of the above events in -/-. Finally, we examined the relative contribution of osteoclast and osteoblast (OB) lineage cells in the involvement of TLR9 in osteoclastogenesis. Since both, OCPs and OBs express TLR9, and CpG-ODN induces TNF-α synthesis in these cells, we used co-cultures in the following combinations: 1) OCP(+/+)/OB(+/+); 2) OCP(-/-)/OB(-/-), 3) OCP(+/+)/OB(-/-); 4) OCP(-/-)/OB(T+/+). CpG-ODN increased TNF-α levels in OCP(+/+)/OB(+/+), but not in OCP(-/-)/OB(-/-). The ODN induced TNF-α synthesis in OCP(+/+)/OB(-/-) almost similarly to OCP(+/+)/OB(+/+), but not in OCP(-/-)/OB(+/+). Modulation of osteoclastogenesis by CpG-ODN in the mixed co-cultures mirrored the TNF-α response. No modulation was observed in OCP(-/-)/OB(-/-), while inhibition of the activity by 20% and 50% was observed in OCP(+/+)/OB(-/-) and OCP(-/-)/OB(+/+), respectively. In conclusion, CpG-ODN modulates osteoclastogenesis in TLR9 dependent manner. Activation of TLR9 in OCPs is more crucial to induction of osteoclastogenesis than activation of the osteoblastic TLR9.

Disclosures: ***A. Amcheslavsky****, None.*

SU312

Spontaneous Osteoclastogenesis In Postmenopausal Osteoporosis. P. D'Amelio*[1], A. Grimaldi*[2], C. Tamone*[2], G. P. Pescarmona*[3], G. Isaia[2]. [1]Dpt of Internal Medicine, University of Torino, Torino, Italy, [2]Internal Medicine, University of Torino, Torino, Italy, [3]Dpt of Genetics, Biology and Biochemistry, University of Torino, Torino, Italy.

There are no evidences for increased osteoclast formation in postmenopausal osteoporosis. The aim of the present study is to evaluate a possible increase in spontaneous osteoclast formation from peripheral blood mononuclear cells (PBMC) in postmenopausal osteoporotic women with respect to healthy subjects.

Bone mineral density, markers of bone turnover and cultures of PBMC were performed in 18 women affected by postmenopausal osteoporosis and in 15 controls. PBMC were obtained with Ficoll-Pacque method. All cell incubations were performed in triplicate in 96 well plates [$2x10^5$ cells/well] or on dentin slices [$1x10^6$ cells/well] using αMEM, supplemented with 10% fetal bovine serum, benzyl penicillin (100 IU/ml) and streptomicin (100 μg/ml). In order to verify the cytokine production by PBMC cultures, supernatants were collected at day 3 and 6 and tested for TNF α and RANKL. The data obtained were compared between patients and controls by one-way ANOVA and correlated by Pearson's coefficient. On the 10th day the cells were fixed and stained for Tartrate resistant acid phosphatase (TRAP) and stained immunohistochemically for the expression of vitronectin receptor (VNR). In all the subjects we measured supernatant levels of TNF α and RANKL with ELISA method. On 21st day of culture, dentine slices were stained with toluidine blue and examined by light microscope.

The resorption was as the percentage of surface area reabsorbed.
In patients the number of osteoclasts was 48.21 ± 30 per 10^5 cells, while in the controls it was 10.41 ± 13 (p=0.000). The percentage of bone resorption was higher in patients with respect to controls (9.5±8.5 vs 0.85±5.6, p=0.048). The levels of TNF α and RANKL were higher in patients (Tab.1).
We found inverse correlations between BMD measured at lumbar spine and femoral neck with number of osteoclasts (r=-0.6, p=0.001), RANKL (r=-0.77, p=0.000) and TNF α (r=-0.6, p=0.000); the correlations between cross laps, RANKL (r=0.4, p=0.02) and TNF α (r=0.48, p=0.006) are direct.
Our data demonstrated an increased spontaneous osteoclastogenesis in postmenopausal osteoporosis: this increase may be explained by the higher production of TNF α and RANKL by PBMC cultures of these patients.

	Patients	Controls	p
TNF α (pg/ml) day 3	53±16.3	32.9±6.6	**0.000**
TNF α (pg/ml) day 6	31.9±8.2	33.9±9.5	NS
RANKL (pg/ml) day 3	2±1.4	0.14±0.2	**0.000**
RANKL (pg/ml) day 6	2.4±1.2	0.4±0.6	**0.000**

Disclosures: ***P. D'Amelio****, None.*

SU313

Cyclic AMP/Protein Kinase A Signals Enhance Osteoclastic Differentiation through TAK1 in Osteoclast Precursors. Y. Kobayashi*[1], I. Take*[1], T. Mizoguchi*[1], N. Udagawa[2], N. Takahashi[1]. [1]Institute for Oral Science, Matsumoto Dental University, Shiojiri, Japan, [2]Biochemistry, Matsumoto Dental University, Shiojiri, Japan.

PGE_2 synergistically enhances RANKL-induced osteoclast differentiation of the precursors. Here, we studied the mechanism of synergistic action of PGE_2 on RANKL-induced osteoclast differentiation. Using RT-PCR, mRNA expression of PGE_2 receptor subtypes (EP1, EP2, EP3, EP4) was examined in osteoclast precursors, bone marrow macrophages (BMMϕ) and RAW 264.7 cells (RAW cells). Both BMMϕ and RAW cells expressed EP1, EP2 and EP4 mRNAs. PGE_2 synergistically enhanced RANKL-induced osteoclastic differentiation of BMMϕ or RAW cells. PGE_2 stimulated cAMP production in RAW cells. The synergistic action of PGE_2 on RANKL-induced osteoclastic differentiation of RAW cells was mimicked by dibutyryl cAMP and inhibited by H-89, a PKA inhibitor, suggesting that the synergistic action of PGE_2 is mediated by the cAMP/PKA system through EP2 and EP4 in the precursors. RANKL-induced degradation of IκBα and phosphorylation of MAPKs in RAW cells were enhanced by PGE_2 in a cAMP-dependent manner, suggesting that PGE_2 signals crosstalk with an upper-stream effector(s) of those signaling molecules. We searched the effectors having a consensus sequence (RRXS motif) in RANKL-induced signaling molecules, and found that TGF-β activated kinase 1 (TAK1) possesses the RRXS motif at 409-412. The immuno-precipitation study revealed that the Ser^{412} residue of TAK1 was phosphorylated by PGE_2 in RAW cells. Over-expression of the $S^{412}A$ mutant TAK1 completely inhibited PGE_2-induced phosphorylation of endogenous TAK1 in RAW cells. We then examined whether the Ser^{412}Ala TAK1 serves as a dominant negative mutant in PKA-mediated enhancement of RANK-, TNF receptor- and Toll like receptor 4-induced signals. Forskolin, an activator of adenylyl cyclase enhanced RANKL-, TNFα- and LPS-induced degradation of IκBα and phosphorylation of p38MAPK in RAW cells transfected with mock or wild-type TAK1. However, the synergistic effects of forskolin were completely abolished by the transfection of the mutant TAK1 into RAW cells. Over-expression of the mutant TAK1 also abolished the synergistic effect of PGE_2 on RANKL-induced osteoclastic differentiation of RAW cells. Furthermore, the mutant TAK1 inhibited the synergistic effects of forskolin on both TNFα-induced osteoclastic differentiation and LPS-induced IL-6 production. These results suggest that phosphorylation of the Ser^{412} residue in TAK1 is essential for cAMP/PKA-induced up-regulation of osteoclast differentiation and proinflammatory cytokine production in macrophages of osteoclast precursors.

Disclosures: ***Y. Kobayashi****, None.*

SU314

PGE_2 Storongly Inhibits Human Osteoclast Differentiation. I. Take*[1], Y. Yamamoto*[1], H. Tsuboi*[2], Y. Kobayashi[1], S. Kurihara*[3], N. Udagawa[4], N. Takahashi[1]. [1]Institute for Oral Science, Matsumoto dental University, Nagano, Japan, [2]Department of Orthopaedic Surgery, Osaka University Graduate School of Medicine, Osaka, Japan, [3]Department of Orthodontics, Matsumoto dental University, Nagano, Japan, [4]Department of Biochemistry, Matsumoto dental University, Nagano, Japan.

PGE_2 is proposed to be a potent stimulator of bone resorption in experimental animal models. PGE_2 strongly enhances osteoclast formation induced by RANKL in cultures of mouse bone marrow-derived macrophages or mouse macrophage-like RAW264.7 cells. However, it is well known that administration of cyclooxgenase-2 (COX-2) inhibitors into rheumatoid arthritis patients does not always suppress the bone resorption in the chronic inflammatory lesions. In the present study, we explored the effect of PGE_2 on human osteoclast formation. CD14-positive ($CD14^+$) monocytes were prepared as osteoclast precursors from human peripheral blood, and cultured with RANKL and M-CSF in the presence or absence of PGE_2 and its related products. After culture for 7 days, cells were fixed and stained with anti-vitronectin receptor (CD51) antibody to identify osteoclasts formed in culture. $CD14^+$ cells were also co-cultured with SaOS4/3 cells which were shown to support osteoclastogenesis in response to PTH. mRNA expression of PGE_2 receptor subtypes (EP1-4) was examined in $CD14^+$ cells using RT-PCR. Intracellular cAMP production in $CD14^+$ cells was determined by ELISA. In contrast to murine macrophage cultures, PGE_2 as well as PGE_1 at 10^{-6} M completely inhibited osteoclast formation induced by RANKL and M-CSF in $CD14^+$ cell cultures. A specific EP2/4 agonist (PGE_1 Alcohol) but not an EP1 agonist (17-phenyl-trinor-PGE_2) inhibited human osteoclast formation induced by RANKL and M-CSF. H-89, a PKA inhibitor, rescued the inhibitory effect of PGE_2 on human osteoclast formation, and dibutyryl cAMP, a cell-permeable analogue of cAMP, inhibited it induced by RANKL and M-CSF. $CD14^+$ cells expressed EP2 and EP4 mRNAs. Both PGE_2 and EP2/4 agonist enhanced cAMP production in $CD14^+$ cells. PGE_2 also inhibited osteoclast differentiation induced by TNF-alpha and M-CSF in $CD14^+$ cell cultures. In addition, PGE_2 strongly inhibited osteoclast formation induced by PTH in cocultures of SaOS4/3 cells and $CD14^+$ cells. NS398, a COX2 inhibitor, enhanced PTH-induced osteoclast formation in the co-culture. These results suggest (i) that PGE_2 is a potent inhibitor for human osteoclastogenesis, (ii) that the EP2 and EP4-induced cAMP-PKA pathway is involved in the inhibitory effect of PGE_2 on human osteoclast formation, and (iii) that administration of COX-2 inhibitors to patients with elevated bone resorption may bring the result opposite to the expectation.

Disclosures: ***I. Take****, None.*

SU315

Dimerization of Receptor Activator of Nuclear Factor Kappa B (RANK) Is not Sufficient to Induce Fully Maturated Osteoclasts. T. Miyamoto[1], K. Iwamoto*[1], Y. Sawatani*[1], N. Hosogane*[2], M. Yagi*[1], N. Fujita*[1], Y. Toyama*[2], T. Suda*[1]. [1]Cell Differentiation, Keio University School of Medicine, Shinjuku, Japan, [2]Orthopaedics, Keio University School of Medicine, Shinjuku, Japan.

Osteoclasts are the bone resorbing multinulcear cells derived from hematopoietic stem cells. Two cytokines, macrophage colony stimulating factor (M-CSF) and receptor activator of nuclear factor kappa B ligand (RANKL), a member of the tumor necrosis factor (TNF) ligand family, is essential for osteoclastogenesis. M-CSF induces expression of RANK, and subsequent RANKL binding to RANK transduces signals for differentiation, survival and bone resorption via c-Fos and TRAF6, and this signal selectively induces NFATc1 expression. RANKL likely induces a receptor homotrimer like other family member such as TNFa and CD40 ligand, which transduces an appropriate differentiation signal to osteoclasts; however, whether a differentiation signal can be generated through formation of homodimers is unknown.
To address the signaling mechanism of the RANK receptor, we analyzed the effect of a homodimer inducer RANK-FKBP36v on osteoclastogenesis. The FKBP36v was fused to the C-terminus of RANK lacking the extracellular domain, and the resulting construct was transduced to RAW264.7 cells. The dimerization of this fusion protein was induced by addition of the chemical inducer of dimerization (CID) AP20187. Such treatment resulted in induction of TRAP-activity in a dose dependent manner, with an efficiency equivalent to that of induction by RANKL. Induction of NF-kB activation is comparable between CID-induced and RANKL-induced osteoclasts. However, CID-induced osteoclasts showed a relatively low pit forming activity on the dentine slices and multinucleation. Moreover, the expressions of the calcitonin receptor, cathepsin K and nuclear factor of activated T cells 1 (NFATc1) were low compared with RANKL binding. Thus, signaling induced by RANK-dimer is sufficient to induce TRAP enzymatic activity and NF-kB activation, while it is not enough to generate fully matured osteoclasts through NFATc1.

Disclosures: ***T. Miyamoto****, None.*

SU316

Cloning and Function of a Novel Orphan Seven Transmebrane Receptor Expressed in Osteoclasts. M. Yagi*[1], T. Miyamoto[1], Y. Sawatani*[1], N. Hosogane*[2], N. Fujita*[1], Y. Toyama*[2], T. Suda*[1]. [1]Cell Differentiation, Keio University School of Medicine, Shinjuku-ku Tokyo, Japan, [2]Orthopaedics, Keio University School of Medicine, Shinjuku-ku Tokyo, Japan.

Normal mineral homeostasis, skeletal formation and its maintenance are controlled by the coupled actions of two cell types in bone, osteoblasts and osteoclasts. Osteoclasts are bone resorbing cells, and their control is essential to prevent skeletal abnormalities characterized by osteoporosis or osteopetrosis.
Here we report the identification and characterization of a novel osteoclast specific receptor. This receptor is an orphan seven transmembrane receptor isolated by DNA subtraction method between oteoclasts and macrophages. Osteoclasts and macrophages are derived from common precursor cells (c-Kit+ c-Fms+ [RANK-]), and M-CSF alone induces macrophage whereas M-CSF and RANKL mediate osteoclastogenesis. To isolate osteoclast specific molecules, we have generated two cDNA libraries, and DNA subtraction method was performed. 103 molecules including previously known as osteoclast specific genes such as TRAP(ACP5) and cathepsin K were isolated. Among the molecules, we have identified a novel orphan receptor that specifically expressed in osteoclasts. This receptor has no homological molecules or conserved domain. This molecule has 1492bp cDNA with 4 exons spanning 15kb of genomic DNA, and start codon is located at 2nd exon. The 5' promoter resion of this receptor contains three consensus NFAT bindig motif within 200bp upstream of transcriptional start sight. Reporter assay revealed that an essential transcription factor for osteoclastgenesis NFAT is involved in the transactivation of this receptor. Overexpression of this receptor in RAW264.7 cells represents an abnormal actin ring formation suggesting that this receptor might be involved in the skeletal organization during osteoclastgenesis.
In order to analyze the function of this molecule, we have generated genetically null mouse. We knocked EGFP cDNA in second exon in frame to this molecule at the position of multi-transmembrane lesion located at 2nd exon. The birth rate of this genetically modified mouse follow Mendelian law indicating that no embryonic and perineonatal lethality were observed. Now we analyzed the gross morphological changes and histrogical evaluation of bone morphology in various stages to investigate the effect of this orphan receptor on osteoclastgenesis.

Disclosures: ***M. Yagi****, None.*

SU317

CD69 and Osteoclast Inhibitory Lectin have Similar Effects on Osteoclasts and Their Progenitors. J. M. W. Quinn[1], C. T. Gange*[1], H. Zhou[1], B. J. Jenkins*[2], A. Nakamura*[1], B. A. Cromer*[1], L. E. Purton*[3], C. Ly*[1], D. E. Myers*[4], T. J. Martin[1], K. W. Ng[5], M. T. Gillespie[1]. [1]St. Vincent's Institute of Medical Research, Fitzroy, Victoria, Australia, [2]Ludwig Institute of Cancer Research, Parkville, Victoria, Australia, [3]Peter Macallum Cancer Institute, Melbourne, Victoria, Australia, [4]Dept. Physiology, The University of Melbourne, Parkville, Australia, [5]Dept. Diabetes and Endocrinology, The University of Melbourne, Fitzroy, Australia.

CD69 is a membrane-bound lymphocyte activation marker with a C-type lectin extracellular domain similar to that of osteoclast inhibitory lectin (OCIL), an osteoclastogenesis and bone mineralisation inhibitor and a counter-receptor for the NK cell receptor Nkrp1d. No cellular actions or ligands of CD69 extracellular domain are known. Due to the similarity between CD69 and OCIL we compared their cellular expression in bone-derived cells and the cellular action of recombinant soluble CD69 and OCIL on osteoclast lineage cells (viz. osteoclast formation and survival, and hematopoietic cell colony formation), and compared their respective carbohydrate binding specificities. We identified CD69 and OCIL mRNA expression by murine bone marrow and bone marrow derived macrophages (from which osteoclasts derive) and murine macrophage/osteoclast lineage RAW264.7 cells. Murine osteoblasts expressed OCIL but not CD69 mRNA. CD69 and OCIL dose-dependently inhibited osteoclastogenesis from murine bone marrow cells and human cord blood progenitors (treated with RANKL and M-CSF) but not from RAW264.7 cells. M-CSF- and GM-CSF-dependent hematopoietic colony formation were also reduced by CD69 and OCIL, but formation of multi-lineage colonies was not affected. RANKL-stimulated osteoclast survival was not affected by CD69 or OCIL, but both proteins enhanced osteoclast survival in the absence of exogenous survival factors. Using ELISA methodology we found CD69 and OCIL both bound fucoidan, λ-carageenan, heparan sulphate and chondroitin sulphate but not unsulphated glycosaminoglycans. Thus, CD69 and OCIL show striking similarities in carbohydrate binding and their effects on osteoclast lineage cells. These results are the first demonstration of cellular actions of CD69, and identify new roles for CD69 and OCIL in bone metabolism.

Disclosures: ***J.M.W. Quinn****, None.*

SU318

Single Deficiency of FcRγ Chain, which Is Required for OSCAR (Osteoclast-associated receptor) Singaling Fails to Reveal Bone Phenotype. Y. Saita*[1], S. Ishikawa*[2], K. Kitahara[1], K. Tsuji[1], H. Kurosawa*[3], A. Nifuji[1], H. Arase*[2], T. Saito*[2], M. Noda[1]. [1]Molecular Pharmacology, Medical Research Institute, Tokyo Medical and Dental University, Tokyo, Japan, [2]Molecular Genetics, Chiba University Graduate School of Medicine, Chiba, Japan, [3]Orthopedics, Juntendo University, School of Medicine, Tokyo, Japan.

Bone homeostasis is based on the balance between bone formation and resorption, which are due to the actions of osteoblasts and osteoclasts. The interaction between immune system and skeleton has been observed using mice deficient in molecules required for these systems. Osteoblasts provide RANKL and M-CSF to regulate osteoclastogenesis. OSCAR is expressed specifically in osteoclasts and it is expected to regulate osteoclast differentiation. However, it remained unclear how OSCAR transduces signal for the defferentiation of osteoclasts. Because OSCAR possesses a positively charged amino acid, arginine, within the transmembrane region, OSCAR may associate with ITAM-bearing signal transducing adaptor molecules such as CD3ζ, FcRγ,DAP12 and DAP10. Therefore, the bones of FcRγ-deficient(FcRγ-/-) mice were analyzed. Basal levels of bone volume in FcRγ knockout mice were similar to those in wild type. Bone mineral density, osteoclast number in vivo, and TRAP positive osteoclast-like cell number and the nodule formation in bone marrow cell cultures were all similar between FcRγ-deficient mice compared with wild type mice, in spite of the fact that FcRγ plays a critical role in OSCAR mediated signal transduction. Interestingly, BMP treatment-enhanced alkaline phosphatase level in FcRγknock out mice calvaria derived cells were higher than BMP-treated wild type cells. As recently reported by Koga et al., DAP12 or other accessory molecules would render ITAM-mediated signal to compensate for FcRγ in vivo for osteoclastogenesis.

Disclosures: ***Y. Saita****, None.*

SU319

Osteoclast Differentiation by Distinct Myeloid Lineage Mouse Bone Marrow Cell Populations. T. J. de Vries[1], T. Schoenmaker*[1], B. Hooibrink*[2], W. Beertsen[3], P. J. M. Leenen*[4], V. Everts[5]. [1]Experimental Periodontology, Academic Centre for Dentistry Amsterdam, Universiteit van Amsterdam and Vrije Universiteit, Amsterdam, Netherlands, [2]Cell Biology, Academic Medical Centre, Universiteit van Amsterdam, Amsterdam, Netherlands, [3]Periodontology, Academic Centre for Dentistry Amsterdam, Universiteit van Amsterdam and Vrije Universiteit, Amsterdam, Netherlands, [4]Immunology, Erasmus Medical Centre, Erasmus Universiteit, Rotterdam, Netherlands, [5]Oral Cell Biology, Academic Centre for Dentistry Amsterdam, Universiteit van Amsterdam and Vrije Universiteit, Amsterdam, Netherlands.

Although it has been recognized that osteoclasts can develop from cells of the myeloid lineage at various stages of maturity, little is known about how fast these cell types develop into osteoclasts. Murine bone marrow was fractionated by flowcytometry using CD31 (ER-MP12) and Ly-6C (ER-MP20) expression profiles. Early blasts (ER-MP12^{hi}/20^{-}), myeloid blasts (ER-MP12^{+}/20^{+}) and monocytes (ER-MP12^{-}/20^{hi}) were cultured in the presence of M-CSF and RANKL for 4, 6, 8 and 10 days. Expression of c-Fms and RANK, receptors for M-CSF and RANKL, respectively, was assessed by quantitative real-time PCR and the number of TRAP-positive multinucleated cells was assessed.
Quantitative PCR analysis revealed that all three fractions expressed high levels of c-Fms and RANK. Myeloid blasts developed rapidly into TRAP-positive multinucleated cells and maximal numbers were present after 4 days. At that time point, significantly more osteoclast-like cells developed in this fraction compared to unfractionated bone marrow, early blasts and monocytes. This difference was lost when culturing for a longer period. Osteoclast development by early blasts, monocytes and unfractionated bone marrow reached a maximum at 8 days of culturing. It has previously been shown that cells from the myeloid lineage mature with M-CSF from early blasts to myeloid blasts to monocytes and finally macrophages. To explore further the osteoclastogenic potential of the different cell fractions, each fraction was precultured for 3 days in the presence of M-CSF, followed by an incubation with M-CSF and RANKL for another 4 days. Cells developing from early blasts and monocytes under influence of M-CSF retained their capacity to develop into osteoclasts. In contrast, M-CSF stimulated myeloid blasts lost this potential. These results suggest that within bone marrow myeloid blasts develop fastest in osteoclasts. In contrast to earlier (blasts) and later (monocytes) stages of myeloid differentiation, myeloid blasts loose the capacity to differentiate into osteoclasts when preculured with M-CSF.

Disclosures: ***T.J. de Vries****, None.*

SU320

Proteomic Identification of the Increase in Creatine Kinase Brain Isoform Expression during Osteoclastogenesis. E. Chang*, Z. Lee, H. Kim. Cell and Developmental Biology, Seoul National University School of Dentistry, Seoul, Republic of Korea.

Recently there has been a great development in proteomics technology. Proteomics approach is an efficient way for the identification of proteins showing differential expression levels between targeted cells and tissues and their reference counterparts. Proteomics approaches also have revealed new links of many proteins to previously unexpected biological responses. We have employed the two-dimensional electrophoresis-based proteomics approach to find proteins of which expression is regulated during osteoclast differentiation. Total cellular proteins from Raw264.7 cells and osteoclast-like cells differentiated from Raw264.7 cells were subjected to isoelectric focusing over the pH range of 3-10, second dimensional SDS-PAGE, and silver staining. Protein spots showing differential levels of expression were picked and processed for in-gel digestion with trypsin. The masses of generated peptides fragments were determined using MALDI-TOF and peptide mass fingerprinting was performed. For some protein spots, tandem mass analyses were carried out. By ESI-Q/TOF tandem mass analyses creatine kinase brain isoform was found to be highly increased in differentiated cells. The increase in creatine kinase brain isoform expression was confirmed by RT-PCR and Western blotting experiments in both Raw264.7 cell and bone marrow cell cultures.

Disclosures: ***H. Kim****, None.*

SU321

The Role of Ceatine Kinase Brain Isoform for Osteoclast Differentation and Function. E. Chang*, Z. Lee, H. Kim. Cell and Developmental Biology, Seoul National University School of Dentistry, Seoul, Republic of Korea.

We have found that the expression of brain isoform of ceatine kinase is highly up-regulated during osteoclastogenesis by a 2DE-based proteomics approach. To investigate the functional significance of ceatine kinase brain isoform expression in osteoclasts, we examined the effects of blocking the activity of this enzyme or reducing the expression level on osteoclast differentiation and resorption activity. Ectopic expression of two different kinds of dominant-negative forms of this enzyme resulted in a decrease in multinucleated TRAP-positive osteoclasts. A pharmacological inhibitor of creatine kinase also suppressed multinucleated osteoclast formation. During the generation of actin ring structure, creatine kinase brain isoform became colocalized with actin ring. The creatine kinase inhibitor disrupted this colocalization and the resorption function of osteoclasts. Inhibition of the expression of creatine kinase brain isoform by antisense oligonucleotide or RNAi also showed reduced osteoclast multinucleation and activity. Finally, calvarial implant study with the creatine kinase inhibitor revealed reduced osteoclast activity in vivo under conditions where remodeling was stimulated by IL-1 or RANKL. Taken together, these data demonstrate that the brain isoform of ceatine kinase has important roles in osteoclast differentiation and function.

Disclosures: ***H. Kim****, None.*

SU322

Multiple Nuclei in Osteoclasts Functionally Compartmentalize Gene Regulatory Machinery. L. Saltman*[1], A. Javed[1], S. Hussain*[1], A. J. van Wijnen[1], J. L. Stein*[1], G. S. Stein[1], J. B. Lian[1], Z. Bar-Shavit[2]. [1]Department of Cell Biology and Cancer Center, University of Massachusetts Medical School, Worcester, MA, USA, [2]Experimental Medicine and Cancer Research, Hebrew University, Jerusalem, Israel.

Osteoclasts are multinucleated cells responsible for bone resorption. *In vivo*, these cells can have more than 20 nuclei, but the functional activities of the multiple nuclei are not understood. To address whether these nuclei serve equivalent roles or have distinct functions, we examined the intranuclear organization of the regulatory machinery for gene expression by *in situ* immunofluorescent staining. As in mononuclear cells, we found osteoclast nuclei to be compartmentalized in functional domains for RNA processing, ribosomal RNA synthesis and mRNA transcription, as detected by antibodies against SC35,

B23 and RNA Pol II, respectively. These three components of gene expression are present in all osteoclast nuclei. We further examined the representation and intranuclear localization of the transcription factors Runx1 and NFκB, which are essential for hematopoiesis and osteoclastogenesis, respectively. We demonstrate that each of these regulatory proteins is localized in nuclear matrix-associated punctuate foci, and that all the nuclei of a single osteoclast contain similar levels of protein. RANKL-induced osteoclast differentiation is accompanied by a significant decrease in the intensity of Runx1 foci and an increased intensity of NFκB foci. Biochemical analyses revealed that Runx1 levels decrease by approximately 70% upon osteoclast differentiation in two established models (mouse bone marrow cells and the macrophage cell line RAW264.7). This is seen for both the RNA and protein and occurred within the first twenty-four hours of differentiation. Runx2 and Runx3 proteins were undetectable by western analysis of the osteoclasts, as well as their monocytic precursors, and further analysis by quantitative RT-PCR indicates that Runx2 and Runx3 mRNA levels are up to 50-fold lower than Runx1. In conclusion, these studies have established that all osteoclast nuclei (i) are not only transcriptionally active but appear to be structurally quite similar; (ii) have similar functional activities; and (iii) downregulate Runx1 expression and protein at the early stages of osteoclast differentiation.

Disclosures: ***L. Saltman****, None.*

SU323

TNF Increases Bone Marrow Osteoclast Precursor Numbers by Stimulating Their Proliferation and Differentiation through up-Regulation of c-Fms Expression. Z. Yao*[1], P. Li*[2], Q. Zhang*[1], E. M. Schwarz[2], L. Ma*[2], P. Keng*[3], B. F. Boyce[1], L. Xing[1]. [1]Pathology, University of Rochester, Rochester, NY, USA, [2]Center for Musculoskeletal Research, University of Rochester, Rochester, NY, USA, [3]Cancer Center, University of Rochester, Rochester, NY, USA.

Osteoclasts (Ocls) are derived from myeloid lineage mononuclear bone marrow progenitors, which proliferate and differentiate in response to growth factors and cytokines to become TRAP+ cells that fuse and form mature ocls. Because specific progenitor cell markers are unavailable, the regulation of TRAP- ocl precursor (OCP) formation has been difficult to study in detail, particularly in inflammatory states in which cytokines, such as TNF are increased. Here, we used wt and TNF transgenic (TNF-Tg) mice and FACS analysis to investigate the effects of TNF on bone marrow OCPs. We used CD11b and Gr-1 as myeloid cell surface markers to flow sort various cell populations and cultured sorted cells with M-CSF and RANKL to determine which bone marrow cell populations comprise OCPs. Ocls formed from $CD11b^+/Gr\text{-}1^{-/lo}$ (153+/-16/well) and $CD11b^-/Gr\text{-}1^{-/lo}$ (17+/-9/well) populations, but not from $CD11b^+/Gr\text{-}1^+$ (0/well) cells. TNF-Tg mice have significantly more $CD11b^+/Gr\text{-}1^{-/lo}$ cells (12+/-3%) than wt mice (6.5+/-0.7%) and significantly more $CD11b^+/Gr\text{-}1^{-/lo}$ cells proliferating in S phase (28+/-2% vs 18+/-2%), but similar numbers undergoing apoptosis. Treatment of wt bone marrow cells with TNF and M-CSF *in vitro* for 3d significantly increased the % of CD11b+ proliferating cells. To test if TNF promotes OCP differentiation, we used c-Fms as a cell surface marker for late OCPs. We found that: 1) TNF-Tg mice have increased $CD11b^+/c\text{-}Fms^+$ cells (5% vs 2% in wt mice); 2) TNF-treated wt bone marrow cells have increased % $CD11b^+/c\text{-}Fms^+$ OCPs (40% vs 4% in PBS-treated cells); 3) Increased c-Fms expression by OCPs is directly associated with ocl forming potency in response to TNF (454+/-9 ocl/well vs 47+/-6 in PBS-treated cells); 4) TNF stimulates c-Fms mRNA expression by OCPs. Furthermore, bone marrow cells, but not spleen cells from the TNF-Tg mice have increased expression of M-CSF, suggesting that TNF promotes increased expression of M-CSF by bone marrow stromal cells. We conclude that OCPs are derived from $CD11b^{+/-}/Gr\text{-}1^{-/lo}$ cells; that $CD11b^+/Gr\text{-}1^{-/lo}$ cells are increased in TNF-Tg mice; and that TNF stimulates the expression of c-Fms by OCPs leading to their proliferation and differentiation under the influence of increased M-CSF production. Thus, a major mechanism whereby TNF promotes bone resorption in inflammatory bone diseases may be increasing the number of bone marrow OCP, which can then circulate to inflamed joints and differentiate further into osteoclasts.

Disclosures: ***Z. Yao****, None.*

SU324

Activation of the Wnt Signalling Pathway Inhibits Osteoclast Differentiation and Bone Resorption. T. A. Althnaian, S. P. Allen*, M. Muzylak*, J. G. Mount*, J. S. Price. Basic Sciences, Royal Veterinary College, London, United Kingdom.

The Wnt signaling pathway is now known to be a critical regulator of osteoblast differentiation and function. However, the role of this pathway in the control of osteoclasts has been little studied. We recently immunolocalised activated β-catenin, a component of the canonical Wnt signalling pathway, in regenerating deer antlers at a site where osteoclasts differentiate *in vivo*. This led us to hypothesise that the canonical Wnt signalling pathway may regulate osteoclastogenesis in regenerating bone. Osteoclast differentiation was induced in high density micromass cultures of antler chondrocytes as we have previously described. Cultures were treated for 9 days with LiCl, an activator of β-catenin via GSK inhibition, or Epigallocatechin-3-gallate (EGCG), which antagonises the transcriptional activation of Tcfs. Activation of Wnt signalling by LiCl significantly decreased the numbers of TRAP positive osteoclasts formed (by 30-40%) and the area of dentine resorbed (by 25-40%), as determined by lectin staining and image analysis. RANKL mRNA expression was down regulated in LiCl treated cultures. EGCG (1-25 micromolar) did not change the numbers of osteoclasts formed but at a dose of 6 μM increased the area of dentine resorbed (twofold). ECGC treatment for 24 hours also dose-dependently induced apoptosis in mature osteoclasts. In sections of antler cartilage, RANKL and the active form of β-catenin were immunolocalised in perivascular tissue, a region where TRAP and vitronectin receptor positive cells were also identified.
In conclusion, this study provides evidence that the Wnt signalling pathway regulates the formation, function and survival of osteoclasts in regenerating bone. Since regeneration generally involves recapitulation of developmental signalling pathways these results suggest that the Wnt pathway may control osteoclast function in the wider context.

Disclosures: ***T.A. Althnaian****, None.*

SU325

Formation of Osteoclasts from Human Umbilical Cord Blood Cells Is Regulated by Chondrocytes, Osteoblasts and Fibroblasts. B. Sukhu*[1], I. Rogers*[2], H. C. Tenenbaum[1], J. Sodek*[1], R. F. Casper*[1]. [1]Dentistry, University of Toronto, Toronto, ON, Canada, [2]Research Institute, Mount Sinai Hospital, Toronto, ON, Canada.

Human umbilical cord blood (HUCB) was shown to contain a greater abundance of haematopoietic stem cells when compared to human adult peripheral blood. As such HUCB could serve as an excellent source of osteoclast precursors. Previous work have shown that osteoclast-like cells generated from HUCB express cathepsin K, tartrate resistant acid phosphate (TRAP) and resorb bone. This study was carried out to characterize further osteoclasts-like cells formed from HUBC. When HUBC cells were grown alone in a-MEM containing 20% fetal calf serum multi-nucleated, TRAP-positive cells with actin ring formation and the ability to resorb calcium phosphate-coated slides were identified. The addition of both GMCSF and RANKL to the culture media increased both TRAP activity and the resorptive ability of these cells. In order to assess the influence of other cell types on osteoclasts formation in HUCB, these cells were grown in co-culture with chondrocytes, osteoblasts and fibroblasts. The results showed that when cord cells were grown in contact with chondrocytes and osteoblasts the number of TRAP positive cells increased considerably. However, when these cells were in co-culture but not in contact with each other the TRAP positive cells were almost diminished. On the other hand, co-culture of cord cells with fibroblasts either in contact or not completely inhibited the formation of TRAP positive cells. Furthermore, it was also seen that conditioned media from osteoblasts inhibited TRAP positive cell formation in a dose dependent manner. These results suggest that osteoclast-like cells can be derived from HUCB and that the formation of these cells was determined by neighbouring cells that produce RANKL and OPG, molecules that regulate osteoclast formation. In addition, the results suggest that membrane bound RANKL may have a more potent effect on osteoclast-like cell formation than the soluble form.

Disclosures: ***B. Sukhu****, None.*

SU326

Effect of Nicotine on Osteoclastogenesis in Cultures of Murine Bone Marrow Cells. P. C. Pfeifer*, J. A. Yee. Biomedical Sciences, School of Medicine, Creighton University, Omaha, NE, USA.

Smoking is a risk factor for osteoporosis, but the basis for this relationship is unknown. Although previous studies have examined the effect of nicotine on osteoblasts, few have focused on its effects on osteoclasts. The purpose of this study was to determine if nicotine, a major constituent in tobacco, affected the formation, proliferation, and death of osteoclasts *in vitro*. Cultures were exposed to nicotine at concentrations ranging from 0.05 to 500 μ M, in the absence or presence of 25 nM parathyroid hormone-related peptide (PTHrP). The effect of nicotine on basal and PTHrP-stimulated osteoclastogenesis on days 1-6 was determined by counting the number of TRAP-positive mononuclear cells (pre-osteoclasts), TRAP-positive multinuclear cells (osteoclasts), and the number of nuclei per osteoclast. Effects on cell proliferation were determined by calculating a BrdU labeling index for pre-osteoclasts and TRAP-negative cells. Effects on apoptosis were measured by determining the proportion of TUNEL stained osteoclasts, osteoclast nuclei, pre-osteoclasts, and TRAP-negative cells. Treatment with PTHrP increased the number of pre-osteoclasts and osteoclasts compared to untreated control cultures. Adding nicotine to PTHrP-treated cultures significantly reduced the number of pre-osteoclasts on days 3-6, osteoclasts on days 4-6, and the number of nuclei per osteoclast on day 6. In the absence of PTHrP, nicotine significantly reduced the BrdU labeling index of pre-osteoclasts on day 2, but had no effect on BrdU incorporation in PTHrP-treated cultures. Treatment with nicotine alone or with PTHrP significantly increased the apoptotic labeling index for pre-osteoclasts, osteoclasts, and for nuclei in individual osteoclasts on day 4 and/or day 6. These results demonstrate that nicotine inhibited both basal as well as PTHrP-stimulated osteoclastogenesis *in vitro*. The time-course of the effects of nicotine on the measured endpoints suggests that the decrease in osteoclastogenesis was due to a combination of effects including a decrease in the proliferation of pre-osteoclasts and an increase in the apoptosis of pre-osteoclasts and osteoclasts. These results suggest that bone loss associated with tobacco use may be related to an altered balance between bone formation and resorption.

Disclosures: ***P.C. Pfeifer****, None.*

SU327

Active Caspase 3 Is Required for Osteoclast Differentiation. K. H. Szymczyk*, V. Srinivas, C. S. Adams, I. M. Shapiro, M. J. Steinbeck. Orthopaedic Surgery, Thomas Jefferson University, Philadelphia, PA, USA.

Caspase 3 is an effector enzyme involved in the execution of many apoptotic pathways. Although typically associated with apoptosis, the active form of this enzyme was recently shown to be essential for cell differentiation, fusion, and morphogenesis. It is not known whether osteoclasts, another type of cell that fuses to form multinucleate cells, requires active caspase 3 for differentiation. Thus, the aim of this study was to test the hypothesis that active caspase 3 is required for osteoclast differentiation. To induce differentiation, RAW264.7 cells were treated with 35 ng/mL of receptor-activator of NF-kB ligand (RANKL) for 4 days. Activity of tartrate-resistant acid phosphatase (TRAP), an enzyme highly expressed by mature osteoclasts, and formation of multinucleate cells were used as indicators of differentiation. After 4 days, the cells were found viable as assayed by Neutral red dye uptake and TUNEL staining. Within in one hour of RANKL treatment, active caspase 3 was detected by confocal microscopy using the caspase 3 substrate PhiPhiLux. To determine the importance of active caspase 3 in pre-osteoclast differentiation, we pharmacologically inhibited caspase 3 in pre-osteoclasts with 200 μM Ac-DEVD-CHO or Z-DEVD-FMK for 60 min before and during RANKL treatment. Pre-osteoclasts that had pharmacologically inhibited caspase 3 did not express TRAP and there was a decrease in formation of multinucleate cells. In addition, we created pro-caspase 3 knockdown RAW264.7cell lines using siRNA technology. Clones were isolated and Western blot analysis confirmed the absence of pro- caspase 3. Procaspase-3 knockdown cells also failed to differentiate after RANKL treatment. Our results clearly illustrate that active caspase 3 is essential for osteoclast differentiation. Targeted modulation of caspase 3 activity provides a new pharmacological approach to controlling osteoclast bone resorption in osteoporosis.

Disclosures: ***K.H. Szymczyk****, None.*

SU328

The Role of Bone Matrix in Osteoclast Differentiation and Activation. Z. Shen[1], R. Fajardo*[2], A. Tsay*[1], T. Crotti[1], K. McHugh[3], S. D. Bromme*[4], B. E. Bierbaum*[1], S. R. Goldring[1]. [1]New England Baptist Bone and Joint Institute, Beth Israel Deaconess Medical Center, Boston, MA, USA, [2]Orthopedic Biomechanics Lab, Beth Isreal Deaconess Medical Center, Boston, MA, USA, [3]Orthopedics, Children's Hospital, Boston, MA, USA, [4]Mount Sinai School of Medicine, New York, NY, USA.

Analysis of tissues from patients with rheumatoid arthritis (RA) and bone loss associated with failed orthopedic implants reveals cells with phenotypic features of osteoclasts (OC) localized to the resorption fronts at the interface between the inflammatory tissue and the bone surface. In both conditions there are also cells off the bone surfaces that express Cathepsin K (Cat K) or tartrate resistant acid phosphatase (TRAP). In contrast, expression of the calcitonin receptor (CTR) is confined to cells on the bone surface. The restricted induction of the CTR gene suggests that specific signals are provided by interaction of the OC precursors with the bone substrate that are required for terminal OC differentiation. To directly assess the role of bone matrix in osteoclast recruitment and differentiation, 4 mm discs of murine calvaria were implanted at intramuscular sites in recipient mice. Within several days an inflammatory reaction developed at the circumferential margins of the bone, corresponding with the regions of mineralized bone surface that had been exposed by cutting the discs from the calvarium. The initial cellular response consisted predominantly of macrophage-type cells, as indicated by detection of the lineage specific marker F4/80. Over the next several weeks, Cat K and TRAP expression were induced both in cells on the bone surface, as well as in the immediate surrounding tissue. In contrast, CTR expression was restricted to cells in direct contact with the bone surface, duplicating the pattern of CTR expression in RA and peri-implant tissues. Recent data indicate an essential role of NFATc1 in OC differentiation. A marked up-regulation of NFATc1 was detected on cells associated with the bone surfaces compared with cells distant from the implant. Micro CT imaging revealed a decrease in the disc area over 6 wks consistent with active bone resorption. Pretreatment of calvaria with Type 1 collagenase (Worthington Biochem) resulted in a marked increase in bone resorption area (40.8%). Bone loss associated with CTR, Cat K and TRAP positive cells was noted on both the inner and outer surfaces of the calvaria as well as the cut margins. Removal of the periosteal surfaces by scapel dissection did not enhance resorption. These results indicate the role of the bone substrate in terminal regulation of OC differentiation and provide further evidence that "preparation" of the bone surface contributes to OC-mediated bone resorption.

Disclosures: ***Z. Shen****, None.*

SU329

The Microphthalmia-Associated Transcription Factor (Mitf) Is Required for Proper Bone Development. C. L. Hershey[1], Y. L. Lin[2], D. E. Fisher[1]. [1]Pediatric Oncology, Dana-Farber Cancer Institute, Boston, MA, USA, [2]OHS-Oral Pathology, University of Kentucky, Lexington, KY, USA.

The Microphthalmia-associated transcription factor (Mitf) is a member of the MiT basic/helix-loop-helix/leucine zipper transcription factor family, which includes Mitf, Tfe3, Tfeb and Tfec, and is required for the differentiation and survival of osteoclasts, melanocytes, retinal pigment epithelium and mast cells. We show here that osteoclasts express all 4 members of the MiT family, including at least 7 Mitf isoforms. A dominant negative mutation in murine Mitf ($Mitf^{microphthalmia}$) results in osteopetrosis due to the lack of mature functional osteoclasts. In contrast, mice carrying null alleles of Mitf have been thought to exhibit no osteopetrotic phenotype (Steingrimsson et al., 1994 and Hemesath et al., 1994). This effect has been explained by the observation that Tfe3 (a close relative and dimerization partner of Mitf) is also expressed in osteoclasts (Weilbaecher et al., 1998) and Tfe3/Mitf double null mice exhibit severe osteopetrosis, whereas neither single null does (Steingrimsson et al., 2002). However, we previously identified a deletion in the *Mitf* gene in the *mib* rat that is expected to behave as a null, yet produces age-resolving osteopetrosis. Based on these results, we sought to further study the null $Mitf^{mga\text{-}9}$ mouse to determine if the lack of Mitf in the mouse also causes a bone phenotype. Based on histological analysis of femurs and tibiae, the null $Mitf^{mga\text{-}9}/Mitf^{mga\text{-}9}$ mice have unresorbed primary and secondary spongiosa compared to control littermates, suggesting a mild osteopetrosis. The osteopetrosis is visible in mice ages 2 to 8 months old, with younger and older mice still under investigation. The increase in bone density was visible in nearly every $Mitf^{mga\text{-}9}/Mitf^{mga\text{-}9}$ mouse examined but varied in severity. Micro CT measurements were used to quantitate the bone phenotype and it was observed that the $Mitf^{mga\text{-}9}/Mitf^{mga\text{-}9}$ mice have increased trabecular bone compared to controls, but relatively similar measures of cortical bone. In *in vitro* osteoclast differentiation assays, the $Mitf^{mga\text{-}9}/Mitf^{mga\text{-}9}$ osteoclasts were more sensitive to decreases in RANKL or MCSF concentrations than control osteoclasts as seen by a decrease in the number of multinucleated TRAP+ cells. This sensitivity to limiting growth factor concentrations likely explains part of the decrease in osteoclastic activity in these mice. The results presented here indicate that loss of Mitf produces a bone phenotype that cannot be fully compensated for by Tfe3 or other MiT family members. This places Mitf among the transcription factors that are fundamentally required for osteoclast differentiation and proper bone development.

Disclosures: ***C.L. Hershey****, None.*

SU330

In Vivo **Treatment with Celecoxib, an Inhibitor of COX-2, Suppresses Serum Levels of Bone Resorption but not Bone Formation Markers in Ovariectomized Mice.** Y. Kasukawa[1], N. Miyakoshi[1], A. Srivastava[2], K. Nozaka[1], S. Maekawa[1], D. J. Baylink[2], S. Mohan[2], E. Itoi[1]. [1]Orthopedic Surgery, Akita Univ., Akita, Japan, [2]J.L. Pettis VAMC, Loma Linda, CA, USA.

The importance of prostaglandins as mediators of inflammatory cytokines and growth factors in regulating both bone formation and resorption has been well documented. Prostaglandins are produced by the sequential actions of phospholipase A2 and cyclo-oxygenase (COX) from membrane phospholipids. Celecoxib is a highly selective inhibitor of COX-2 and has been shown to be anti-inflammatory in its action. Furthermore, recent findings have shown that celocoxib inhibited osteoclastogenesis *in vitro* and delayed fracture healing *in vivo* in animals but not in humans. Based on these findings, we proposed that celecoxib could be used to suppress elevated bone resorption that occurs due to sex hormone deficiency. To test this hypothesis, celecoxib (4 mg/kg) or its vehicle was administered orally into ovariectomized (OVX) or sham operated mice and serum levels of bone markers were evaluated. The surgery was performed at 8 weeks of age, and the treatment was started daily by gavage for 4 weeks. Blood samples were collected from retro-orbital sinus at 2 weeks after the treatment under anesthesia and from decapitation at 4 weeks after the treatment. Serum C-telopeptide, which has been shown to reflect degradation products of type I collagen that are generated during osteoclastic bone resorption, and osteocalcin, which is a measure of osteoblast activity, were measured using validated assays. C-telopeptide levels were increased by 37% ($P<0.01$) and 60% ($P<0.01$) in OVX mice compared to those in sham mice at 2 and 4 weeks respectively after treatment with vehicle. Celecoxib treatment significantly decreased the serum C-telopeptide levels in the OVX mice at 2 and 4 weeks after treatment (45% and 41% respectively, $p<0.001$). Furthermore, this treatment also decreased the C-telopeptide levels in sham mice at each time point (21% at 2 weeks and 29% at 4 weeks after treatment, $P<0.05$). Serum osteocalcin level was increased as expected in OVX mice compared to sham mice at 4 weeks (69%, $P<0.01$). However, celecoxib treatment did not suppress the elevated serum osteocalcin levels in the OVX mice at either time point. Conclusions:1) Celecoxib treatment blocked OVX-induced increase in serum C-telopeptide levels and decreased serum C-telopeptide levels in sham mice; 2) Celecoxib had no effect on serum osteocalcin levels either in OVX or in sham mice; 3) The confirmation of the hypothesis that celecoxib inhibits elevated bone resorption but not bone formation in OVX mice would provide therapeutic advantage of this drug in the treatment of bone loss that occurs during postmenopausal period.

Disclosures: ***Y. Kasukawa****, None.*

SU331

Analysis of Bone Remodeling in Neonatal Murine Calvarial Cultures by Laser Scanning Confocal Microscopy. K. Suzuki*[1], S. Takeyama*[2], T. Kikuchi*[2], S. Yamada*[1], J. Sodek*[3], H. Shinoda[2]. [1]Dept. Pharmacol., Sch. Dent., Showa Univ., Tokyo, Japan, [2]Div. Pharmacol., Grad. Sch. Dent., Tohoku Univ., Sendai, Japan, [3]CIHR Group in Matrix Dynamics, Fac. Dent., Univ. of Toronto, Toronto, ON, Canada.

We used laser confocal microscopy to examine the effects of bisphosphonates (BP) on bone remodeling in neonatal murine calvariae *in situ*, which provides a unique system with which to study bone formation and resorption in the absence of systemic influences. Responses were determined by fluorescence staining for TRAP activity, F-actin, β3 integrin, osteopontin, ALPase activity, collagen type I and bone mineral in calvariae cultured in the presence of 10μg/ml LPS or 10^{-8}M PTH and/or BP (1~25μM clodronate or 0.1~2.5μM risedronate) for up to 48 hrs. The morphological abnormalities, including retraction of pseudopods and vacuolization of cytoplasm were observed in non-resorbing osteoclasts in BP-treated calvariae. In calvariae cultured in the presence of PTH and BP, the multinucleated osteoclasts were smaller, displayed severe cytoplasmic vacuolization, and the sealing zone was diffuse compared to osteoclasts in calvariae cultured with PTH alone. Furthermore, the presence of actin, osteopontin and β3 integrin along the edge of resorbing osteoclasts, which is required for cell attachment to the resorption site, was markedly reduced. Serial optical sections above the resorption lacunae revealed ALPase-positive and collagen type I-producing cells with morphological features of osteoblastic cells, which fill the resorbed area and proliferate on top of the resorbed area of bone. From XZ (depth) scans of the calvaria double-stained for actin and mineral after culturing under

various conditions, it was evident that cell proliferation had been stimulated in LPS-treated calvariae, regardless of the presence of BP. In control calvariae and clodronate-treated calvaria, little accumulation of cells with ALPase activity was observed, indicating that the proliferation of bone-forming cells occurs in response to accelerated bone resorption induced by LPS. The area of the remaining bone mineral and proliferation of bone-forming cells were measured from the XZ-images of calvariae stained with Alizarin Red S and Alexa Fluor 488-phalloidin, assuming that the ALPase-positive and collagen-producing cells were bone-forming cells. A negative correlation between the area of mineral remaining and cell proliferation was observed in LPS-treated groups, regardless of the presence of BP. In conclusion, laser scanning confocal microscopy of immunofluorescently labeled calvariae maintained *in situ* provides a valuable approach for evaluating the effects of biological agents on bone remodeling.

Disclosures: ***K. Suzuki****, None.*

SU332

Antisense Oligonucleotides Targeting Mouse RANK and RANKL Inhibit Hypercalcemia and Ovariectomy-Induced Bone Loss. M. Liu*[1], X. Li[2], Y. Wang*[1], D. Halladay*[1], Q. Zeng*[1], C. Thompson*[2], J. Finger*[2], L. Ma*[1], S. Gregory*[2], H. Bryant*[1], R. Galvin*[1], K. J. Myers*[2]. [1]Lilly Research Labs, Indianapolis, IN, USA, [2]ISIS Pharmaceuticals, Carlsbad, CA, USA.

RANK-RANKL-OPG balance is critical for osteoclast activity and bone resorption. We have developed and characterized modified antisense oligonucleotides specific for mouse RANK and RANKL and have evaluated their activity in murine models of hypercalcemia and ovariectomy-induced bone loss. *In vitro*, the RANK and RANKL ASOs were equipotent at reducing targeted mRNAs in transfected cell lines with IC_{50}s in the 50-75 nM range. In a mouse model of PTH-induced hypercalcemia, 2-wk prophylactic treatment with either the RANK or RANKL ASOs reduced the targeted mRNA in bone by as much as 60%. Treatment with either the RANK or RANKL ASOs also provided dose-dependent reductions in serum calcium. Treatment with the RANK ASO at 30 mg/kg/d showed similar efficacy to the positive control calcitonin, while treatment with the RANKL ASO at the same dosage and regimen was about 50% as effective as the RANK ASO. When adult female mice were treated s.c. at 3, 10, or 30/mg/kg/d one week prior to ovariectomy (OVX) and continuing for five weeks after OVX, both the RANK and RANKL ASOs prevented the OVX-induced bone loss in a dose-dependent manner. The BMD of the 30 mg/kg/d RANK or RANKL ASO-treated groups was maintained at the level of sham-operated mice. A histological assessment of bones from the RANK ASO study revealed a reduction in trabecular bone osteoclast numbers, as well as improvements in trabecular area and thickness.

Previous studies have demonstrated that OPG and RANKL antibodies could inhibit bone resorption. Our results, however, are the first to show that antisense oligonucleotides which directly target and downregulate the mRNA of the RANK receptor or its ligand are effective in reducing bone resorption in rodent models. This suggests that antisense oligonucleotides targeting the RANK signaling pathway could prove useful in the treatment of osteoporosis or other bone diseases characterized by increased bone resorption.

Disclosures: ***K.J. Myers****, None.*

SU333

Elucidating Mechanistic Differences in Activation between Large and Small Osteoclasts. D. P. Trebec*[1], K. Li*[2], D. Chandra*[2], J. N. M. Heersche[2], M. F. Manolson[2]. [1]Department of Biochemistry, University of Toronto, Toronto, ON, Canada, [2]Faculty of Dentistry, University of Toronto, Toronto, ON, Canada.

Large osteoclasts (OC) (≥ 10 nuclei) are predominantly observed in diseases associated with excessive bone loss due to increased osteoclastic resorption such as Paget's disease, inflammatory arthritis and periodontal disease [1]. Large OCs were previously shown to resorb more bone than small OCs (≤5 nuclei) [2,3], leading us to hypothesize that size and resorptive activity of osteoclasts are linked, and may result from mechanistic differences in activation. Thus, we have sought to identify factors involved in signaling (c-fms, RANK, TNFR1, IL-1R1, $\alpha_v\beta_3$ SHIP), fusion (SIRPα1), and ion transport (CAII, AE3, V-ATPase) which may differ between large and small OCs. *In situ* hybridization on rabbit OCs demonstrated a 2.7-fold increase in expression of c-fms mRNA in large versus small OCs. Using the differentiated RAW 264.7 cell culture system to examine protein expression by quantitative immunoblotting, we were able to also show an increase (~1.8 ± 0.08-fold) of c-fms protein on large OCs. Significant differences were observed in protein expression of enzymes proMMP9, matMMP9 and pro-cathepsin K (3.8 ± 0.02-, 2.7 ± 0.01- and 2.6 ± 0.08-fold respectively) between large and small OCs. Moreover, increases were noted in expression of receptors on large OCs including: RANK (~2.5 ± 0.3-fold), IL-1R1 (~2 ± 0.6-fold) and TNFR1 (~2.2 ± 0.2-fold). Integrin α_v displayed a 2.8 ± 0.9-fold increase while β_3 was noted to be significantly higher with ~4.5-fold increase in large OCs. In contrast, ~1.5-fold increases in expression of SIRPα1 and IL-1R2 were noted on small OCs as compared to large. Thus, an up-regulation was noted for enzymes MMP-9 and cathepsin K involved in osteoclast resorption as well as for receptors c-fms, IL-1R1, TNFR1, RANK and integrins implicated in osteoclast activity. These findings suggest differences in resorption between the two osteoclast sizes results from a variation in receptor levels with large OCs being more susceptible to activation while small OCs have increased levels of inhibitory (IL-1R2) and fusion receptors. Elucidating specific differences between large and small osteoclasts may result in novel targets for therapeutic intervention to inhibit excessive resorption by larger osteoclasts in a pathological state.

References:
1. Helfrich MH. (2003) Microsc Res Techniq 61: 514-532
2. Lees, R. L. and Heersche, J. N. M (2000) Am J Cell Physiol 279, C751-C761
3. Lees, R. L., Sabharwal, V. K. and Heersche, J. N. (2001) Bone 28, 187-94

Disclosures: ***D.P. Trebec****, None.*

SU334

Risedronate and Other Nitrogen-containing Bisphosphonates Are Selectively Internalized from Bone by Osteoclasts and Inhibit Protein Prenylation *in vitro* and *in vivo*. F. P. Coxon*[1], A. Hughes*[1], F. H. Ebetino[2], M. J. Rogers[1]. [1]Bone Research Group, University of Aberdeen, Aberdeen, United Kingdom, [2]Procter & Gamble Pharmaceuticals, Cincinnati, OH, USA.

Bisphosphonates (BPs) target to bone due to their high affinity for calcium ions. During osteoclastic resorption, BPs appear to be released from the bone surface due to acidification and can then be internalized by osteoclasts, where they act by inhibiting the prenylation of small GTPases essential for osteoclast function. However, it remains unclear whether osteoclasts are the only cells in the bone microenvironment that can take up BPs from the bone surface. We have begun to investigate this using a novel fluorescently-labelled alendronate analogue (FL-ALN) and by examining changes in the prenylation of the small GTPase Rap1A.

Bone marrow cells isolated from rabbits were cultured for 24 hours on dentine slices pre-coated with FL-ALN. Confocal microscopic analysis showed that FL-ALN was internalized by resorbing osteoclasts into intracellular vesicles throughout the cell. This pattern of uptake also occurred with FL-ALN in the absence of dentine, and could be prevented by the presence of molar excess of risedronate or other BPs. Although there was no evidence of uptake by other cells in the cultures on dentine e.g. stromal cells, most bone marrow cells were able to internalise FL-ALN from solution.

To examine uptake of bisphosphonates by bone cells *in vivo*, osteoclasts were isolated from rabbit bone marrow cells using immunomagnetic beads and antibody to the vitronectin receptor (VNR). Prenylation of Rap1A was inhibited in the VNR-positive osteoclast fraction from rabbits that had been injected subcutaneously with 1mg/kg risedronate, alendronate, ibandronate, pamidronate or zoledronic acid, demonstrating that osteoclasts internalise these BPs *in vivo*. However, there was negligible effect on Rap1A prenylation in the general population of non-osteoclast, VNR-negative bone marrow cells. A phosphonocarboxylate analogue of risedronate (NE10790, 45mg/kg), which has lower affinity for bone, also inhibited protein prenylation in VNR-positive osteoclasts but not in the VNR-negative bone marrow population, whereas 0.3mg/kg cerivastatin (lacks affinity for bone) inhibited protein prenylation in both fractions.

These data demonstrate that osteoclasts, but not general bone marrow cells, can take up sufficient BP *in vivo* to cause detectable inhibition of protein prenylation. However, it does not exclude the possibility that minor populations of bone marrow cells or tumour cells could also internalize BPs, or that BPs are taken up by some cells to such a low extent that changes in protein prenylation are not detectable.

Disclosures: ***F.P. Coxon****, None.*

SU335

Degradation of the Organic Phase of Bone by the Osteoclast - a Role for Acidification. K. Henriksen*[1], M. G. Sørensen*[1], S. Schaller*[1], J. Gram*[2], P. Høegh-Andersen*[1], J. Bollerslev*[3], M. A. Karsdal[1]. [1]Nordic Bioscience A/S, Herlev, Denmark, [2]Ribe County Hospital, Esbjerg, Denmark, [3]National University Hospital, Oslo, Norway.

Osteoclasts degrade the inorganic phase of bone by secretion of acid into the resorption lacuna. This process is mediated by the osteoclast specific proton pump (a3), and the chloride channel ClC-7. However, whether these proteins participate in other functions in the osteoclasts has not been clearly demonstrated.

We have developed an assay using decalcified bone slices and isolated human osteoclasts to evaluate the importance of ClC-7 and the proton pump in the osteoclast mediated degradation of a calcium free matrix. Firstly, we characterized the system to assure that osteoclasts are the principal cells degrading this matrix, and accordingly, we found that RANKL dose-dependently induces degradation of the decalcified bone slices. We characterized the cells with respect to morphology and expression of osteoclastic proteins such as cathepsin K and ClC-7. By cytochemistry we found that both cathepsin K and ClC-7 were present but not localized in a gradient towards the resorption pit as on normal bone. By actin staining we found that osteoclasts on decalcified bone did not form actin rings, but instead appeared motile with a large number of podosomes. Furthermore, resorption pits are not formed on decalcified bones, however migratory "tracks" was found by staining for collagen type I fragments.

To assess the role of acidification in the degradation of decalcified bone, we used osteoclasts from ClC-7 deficient (ADOII) patients and matched controls. We found that ADOII osteoclasts ability to degrade the decalcified matrix was reduced by 40%. In contrast, the reduction in resorption on calcified bone was 80%. Furthermore, we tested inhibitors of chloride channels (NS5818), cathepsin K (CK-I), and the proton pump (Bafilomycin) and we found that NS5818, CK-I and bafilomycin dose-dependently inhibited degradation of decalcified bone, with a maximal effect of 40% in controls. Interestingly, the inhibitors had no effect in the ADOII osteoclasts. In contrast, the addition of a matrix metalloproteinase (MMP) inhibitor resulted in 80% inhibition in both ADOII and controls, indicating an acidification independent role for MMPs in this system.

In conclusion, we show that osteoclastic acidification participates in the degradation of the organic matrix. However, attenuation of acidification has a stronger effect on calcified than decalcified bone, showing that the most important role for acidification, and thus ClC-7, in bone resorption is secretion of acid into the resorption lacunae of the osteoclasts.

Disclosures: ***K. Henriksen****, None.*

SU336

Regulation of Osteoclastic Bone Resorption and Bone Mass by the Cannabinoid Receptor 1 Pathway. A. I. Idris*[1], R. J. Van't Hof*[1], I. R. Greig*[1], S. A. Ridge*[1], D. Baker*[2], R. A. Ross*[1], S. H. Ralston[1]. [1]Medicine & Therapeutics, University of Aberdeen, Aberdeen, United Kingdom, [2]Institute of Neurology, University College London, London, United Kingdom.

The endogenous cannabinoid system plays an important role in several physiological processes. In the light of recent data which has shown that neurogenic pathways can play an important role in regulating bone turnover, we studied the role of the endocannabinoids in bone metabolism. The cannabinoid receptor blocking drugs SR144528, SR141617A and AM251 were all potent inhibitors of osteoclast formation and bone resorption *in vitro* with half-maximal inhibitory effects at 5-10μM in osteoblast-bone marrow co-cultures and 0.6-1.0 μM in RANKL stimulated bone marrow cultures. All three compounds caused a 10-15-fold increased in apoptosis of rabbit osteoclasts from basal levels ($p<0.0001$) and inhibited TNF-induced activation of the NFκB pathway (as detected by inhibition of IκB and IKK phosphorylation) and ERK signalling pathway (as detected by inhibition of phospho-ERK). Conversely, the cannabinoid receptor agonist anandamide stimulated osteoclast formation and bone resorption in mouse bone marrow cultures in a dose-dependent manner over the concentration range 1-10μM. Both AM251 and SR144528 (10mg/kg/day for 21 days) prevented ovariectomy (ovx) induced bone loss in mice. Trabecular BMD fell by 12% in ovx/vehicle treated mice, when compared with ovx/sham, whereas ovx mice treated with AM251 lost only 2.5% BMD ($p<0.01$ from ovx) and mice treated with SR144528 gained 2.5% BMD ($p<0.001$ from ovx). Osteoclasts and osteoblasts expressed both CB receptor subtypes (CB1 and CB2), but studies in mice with targeted inactivation of the CB1 receptor showed that this was an important target for osteoclast inhibition. Trabecular BMD was increased by about 10% in CB1 knockouts when compared with wild type mice ($p<0.05$), and osteoclasts generated from RANKL stimulated bone marrow cultures in CB1 knockout mice were significantly resistant to the inhibitory effects of CB antagonists, such that at 0.5μM, AM251 inhibited formation of osteoclasts generated from CB1 knockouts by 5%, compared with 40% inhibition for wild type ($p<0.001$ between groups) . We conclude that cannabinoid receptor antagonist are a new class of antiresorptive drugs and that the endocannabinoid system and the CB1 receptor plays a physiological role in the regulation of bone turnover and bone density.

Disclosures: ***A.I. Idris****, None.*

SU337

Bortezomib, a Novel Proteasomes Inhibitor, Approved for Use in Multiple Myeloma, Inhibits Osteoclast Formation and Function. N. Kawanabe[1], K. Anderson*[2], J. A. Lorenzo[1]. [1]Endocrinology, University of Connecticut Health Center, Farmington, CT, USA, [2]Medicine, Harvard Medical School, Boston, MA, USA.

Bortezomib (Velcade ™, Bzb) is a proteasome inhibitor that is used for the treatment of patients with multiple myeloma (mm). Inhibitors of osteoclast action (i.e. bisphosphonates) are known to prolong survival in mm. We determined if some of the beneficial effects of Bzb in mm patients resulted from its affects on bone resorption. The ability of Bzb to block osteoclast formation and bone resorption was measured in cultures of murine bone marrow cells that were stimulated for 4 days to form osteoclast (OCL) by treatment with RANKL and M-CSF (30 ng/ml for each). Cell viability was assessed by a MTT assay. OCL formation was measured as the number of TRAP + multinuclear cells. Resorption was measured as the number of pits formed by cells cultured on bovine bone slices

In the MTT assay, Bzb suppressed murine bone marrow cell viability only at the concentration of 10 nM or higher. There was no significant effect of Bzb at concentrations of 1nM or less. In contrast, Bzb significantly ($p<.01$) inhibited OCL formation in murine bone marrow culture in a dose-dependent fashion over a concentration rang of 100 fM to 1 nM with a maximum inhibitory effect of about 30% at 1 nM ($P<.05$). Time course studies showed that Bzb (1nM) significantly ($p<.05$) inhibited OCL differentiation when added either during the early (first 2 days) or late stages (last 2 days) of culture. . Furthermore, Bzb (1 nM) decreased pit number by about 50 % revealing that Bzb suppresses OCL bone resorption to a greater degree than OCL formation. Examination of mRNA expression of RANK and NFATc1 in murine primary bone marrow cells treated with RANKL for 24 or 48 h demonstrated no differences between control and Bzb-treated cells.

In conclusion, Bzb suppress OCL formation and resorption in vitro at very low concentrations (100 fM to1 nM), which did not affect cell viability. This effect does not appear to involve regulation of NFATc1 or RANK expression by Bzb. It is possible that the beneficial effects of Bzb in mm patients result from its ability block both bone resorption and mm cell function.

Disclosures: ***J.A. Lorenzo****, None.*

SU338

Antisense Oligonucleotides Targeting RANK and RANKL Both Prevent Bone Loss, But Only RANK ASOs Reduce Inflammation in a Rat Model of Adjuvant Arthritis. M. Liu*[1], K. Hull*[1], H. Cole*[1], Y. Wang*[1], J. Finger*[2], L. Chio*[3], N. Kulkarni*[1], J. Hoover*[1], R. S. Galvin[1], Y. Ma[1], H. U. Bryant[1], K. J. Myers*[2]. [1]Bone and Inflammation, Eli Lilly and Co, Indianapolis, IN, USA, [2]ISIS Pharmaceutical Inc, Carlsbad, CA, USA, [3]Eli Lilly and Co, Indianapolis, IN, USA.

Interrupting RANK signaling by inhibitors such as OPG and RANK-Fc can prevent bone loss in rodent arthritis models. RANK and RANKL, in addition to their normal expression in bone cells, are also expressed in the inflamed and proliferating synovium in rheumatoid arthritis. We have developed and characterized modified antisense oligonucleotides (ASOs) specific for rat RANK and RANKL, and have evaluated their activity in an adjuvant arthritis model. In vitro, both the RANK and RANKL ASOs were equipotent at reducing targeted mRNAs, with IC_{50}s in the 50-75 nM range. ASO uptake in normal and arthritic rats was examined by immunohistochemical analysis, using an antibody specific for modified ASOs. Strong ASO localization was seen in both normal and inflamed rat joints in rats dosed via sc, ip, or oral routes. The RANK and RANKL ASOs were dosed prophylactically in the rat adjuvant arthritis model, with daily subcutaneous dosing at 5, 20, or 40 mg/kg beginning one week prior to lipoidal amine/adjuvant administration, and continuing for another 14 days afterwards. X-ray radiographic analysis indicated that both RANK and RANKL ASOs prevented bone erosion in the ankle joint. However, treatment with the RANK ASOs had an unexpected anti-inflammatory effect, dose-dependently reducing paw swelling in arthritic rats. The RANKL ASOs had no effect on ameliorating paw swelling, even at the highest doses tested. Two separate RANK-specific ASOs were found capable of reducing paw swelling. Oligonucleotide A appeared to be more potent in this regard. A 40 mg/kg daily dose of A reduced paw swelling to the same extent as dexamethasone treatment, while 60 mg/kg of Oligonucleotide B daily was required to produce a similar effect. The potency of the two RANK ASOs in reducing inflammation also correlated with their potency in reducing RANK mRNA in bone as well as reducing osteoclast numbers obtained by histomorphometry. The reduction in paw swelling induced by Oligonucleotide A was accompanied by dose-dependent reductions of the pro-inflammatory cytokines IL-1β and IL-6 in synovial fluid.

Although RANK signaling inhibition by agents such as OPG prevents bone loss in a variety of animal models, these agents have never provided a significant anti-inflammatory effect when tested in arthritis models. Our results with antisense oligonucleotides suggest that a therapeutic advantage may be conferred by inhibiting the receptor (RANK) rather than the ligand (RANKL) in an arthritic condition.

Disclosures: ***M. Liu****, None.*

SU339

Estrogen Regulate Glutathione Reduction in Bone by a Nongenotropic Mechanism of Action: A Requirement for Their Effects on Osteoclastogenesis and on the Apoptosis of Osteoblasts and Osteoclasts. J. R. Chen, L. Han, P. Zimniak*, C. A. O'Brien, T. Bellido, R. L. Jilka, S. Kousteni, S. C. Manolagas. Div. Endocrinol., Center for Osteoporosis and Metabolic Bone Diseases, Central Arkansas Veterans Healthcare System, Univ. Arkansas Med. Sci., Little Rock, AR, USA.

Estrogen may provide protection against oxidative stress in a variety of cell types, including osteoclasts, by increasing glutathione levels and thus dispensing of reactive oxygen species (ROS). Conversely, loss of estrogen may increase osteoclastogenesis and loss of bone by decreasing the levels of glutathione in osteoclasts. We investigated whether anti-oxidant actions of estrogen are mediated via the classical genotropic mechanism of estrogen receptor (ER) action, as opposed to extra nuclear (kinase-mediated) actions of the ER, and whether they play a role in the pro- and anti-apoptotic effects on osteoclasts and osteoblasts, respectively. Osteoclasts were generated from murine bone marrow cultures (devoid of adherent stromal support cells) or the murine macrophage cell line RAW264.7 stimulated with RANKL and M-CSF. We report that L-butathionine-(S,R)-sulphoximine (BSO), a specific inhibitor of glutathione synthesis, at 10^{-5} M, abrogated the suppressive effects of 10^{-8} M estradiol (E_2) or 4-estren-3α, 17β-diol (estren) on osteoclastogenesis. Furthermore, BSO abrogated E_2-or estren- induced osteoclast apoptosis. Strikingly, BSO also abrogated the anti-apoptotic effects of either E_2 or estren on primary cultures of calvaria cells, irrespective of whether apoptosis was induced by the topoisomerase inhibitor etoposide or TNFα. Identical results, i.e. abrogation of the suppressive effects of either E_2 or estren on osteoclastogenesis, the promotion of osteoclast apoptosis and the attenuation of osteoblast apoptosis were obtained when glutathione was depleted using the electrophilic agent diethylmaleate (DEM), at 0.1 mM. Further, E_2 or estren stimulated the activity of glutathione reductase (GR) in osteoclasts and this effect could be completely blocked by the ER antagonist ICI 182,780, as well as by the specific inhibitors of Src or MEK kinase, PP1 and U0126. Estrogen or estren had no effect on the activity of GR in osteoblasts, suggesting that in this cell type an alternative pathway of ROS control is involved. These results demonstrate that not only attenuation of osteoclastogenesis (and perhaps remodeling) but also the stimulation of osteoclast and attenuation of osteoblast apoptosis by estrogen involve nonprotein thiol metabolism. These effects are the result of a nongenotropic mechanism of estrogen action mediated by cytoplasmic kinases and probably downstream transcriptional control of nonprotein thiols.

Disclosures: ***J.R. Chen****, None.*

SU340

The Anti-inflammatory Sesquiterpene Lactone Parthenolide Blocks Lipopolysaccharide Induced Osteolysis via the Suppression of NF-κB Activity. K. H. Yip*[1], M. Zheng[1], H. Feng*[1], J. Steer*[2], D. Joyce*[2], J. Xu[1]. [1]Orthopaedic Surgery, University of Western Australia, Nedlands, Australia, [2]Medicine and Pharmacology, University of Western Australia, Nedlands, Australia.

Osteolysis induced by bacterial infection underlies many bone diseases. Drugs that inhibit LPS-induced osteolysis are critical in the prevention of bone destruction in infective bone diseases. Here we investigated the potential effect of an herbal extract, parthenolide (PAR) on LPS-induced osteolysis.

In this study, the LPS-induced osteolysis in the mouse calvarian model was used to examine the effect of PAR *in vivo*. RANKL-induced osteoclast differentiation from RAW $_{264.7}$ cells and bone resorption were used to assess the effect of PAR *in vitro*. Assays for NF-κB activation, p65 translocation and IκB-α degradation were employed to determine the mechanism of action of PAR in osteoclasts and their precursors. Flow cytometry and confocal microscopic analysis were used to examine cell apoptosis. Semiquantitative RT-PCR

were employed to determine PAR effect on RANK and TRAF6 gene expression
We found that LPS-induced osteolysis in the mouse calvarian (attached figure, panel A showed PBS injeced control and panel B showed LPS injected group) was blocked by PAR (0.5mg/kg and 1mg/kg), injected simultaneously with LPS (25mg/kg) or 3 days later (panel C, D, E, and F respectively in attached figure). *In vitro* studies showed that low concentration PAR (less than 1μM) inhibited *in-vitro* osteoclastogenesis and bone resorption, whilst higher concentrations (greater than 5μM) dose-dependently triggered apoptosis. Furthermore, PAR inhibited LPS-induced NF-κB activation, p65 translocation and IκB-α degradation in both mature osteoclasts and their precursors. In addition, PAR inhibited NF-κB activation induced by osteoclastogenic factors RANKL, IL-1β or TNF-α, and reduced RANK and TRAF6 expression.
In conclusion, the NF-κB pathway is known to mediate both osteoclast differentiation and survival. These findings indicate that PAR blocks LPS-induced osteolysis via the suppression of NF-κB activity; suggests a possible therapeutic value in bacteria-induced bone destruction.

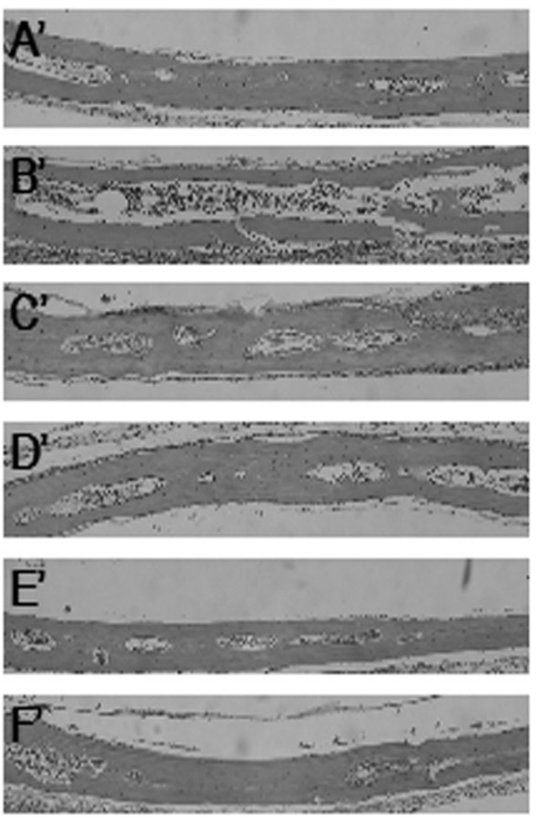

Disclosures: ***K.H. Yip****, None.*

SU341

Osteoclast Apoptosis Is Regulated by the Expression of Immediate Early Genes Egr-1, Egr-2, Egr-3 and Ieg-2 Identified through Microarray Analysis. E. W. Bradley*[1], M. J. Oursler[2]. [1]Cell Biology and Genetics, Mayo Clinic, Rochester, MN, USA, [2]Endocrine Research Unit, Mayo Clinic, Rochester, MN, USA.

Since bone resorption levels depend primarily on the number of osteoclasts present, factors contributing to the survival of osteoclasts increase the amount of bone loss during both normal and pathological bone turnover. In order to better understand the molecular mechanisms by which osteoclasts survive, we have examined *in vitro* generated mouse osteoclast model in which osteoclasts differentiate during co-culture of precursors and stromal cells in the presence of vitamin D and dexamethazone. Removal of the stromal cells from the mature osteoclasts causes apoptosis of about 25% of the osteoclasts and we have explored the signaling pathway by which the surviving osteoclasts repress this apoptosis. We have found that survival of a significant number of osteoclasts is dependant on the activation of the PI3 kinase/MEK/ERK pathway. Inhibition of this pathway using kinase-specific inhibitors as well as inhibition of protein synthesis leads to increased osteoclasts apoptosis. We have further explored expression of downstream targets of the PI3 kinase/MEK/ERK pathway for roles in osteoclast survival following removal of stromal cells. Activation of Elk-1, an Ets transcription factor, was detected five minutes after stromal cell removal. Purified osteoclasts were cultured with and without a MEK specific inhibitor and RNA was isolated for microarray analysis to identify targets of this pathway. Increased transcript levels for several immediate early genes were identified in osteoclasts thirty minutes after stromal cell removal in the absence of MEK inhibition which were not observed in cultures treated with the MEK inhibitor. These genes included the known targets of Elk-1 Egr-1, Egr-2, Egr-3 and Ieg-2 genes, which regulate apoptosis in other cell types. Increased mRNA levels for these genes following stromal cell removal were verified using log phase PCR. Given these results, we hypothesize that activation of the PI3 kinase/MEK/ERK/Elk-1 pathway leads to an increase in the expression of immediate early genes to prolong osteoclast survival, providing new insight into osteoclast survival mechanisms.

Disclosures: ***E.W. Bradley****, None.*

SU342

The Effect of Aryl Hydrocarbons on Osteoclast Differentiation and Function. I. Voronov*[1], J. N. M. Heersche[1], H. C. Tenenbaum[1], R. F. Casper*[2], M. F. Manolson[1]. [1]University of Toronto, Toronto, ON, Canada, [2]Samuel Lunenfeld Research Institute, Mount Sinai Hospital, Toronto, ON, Canada.

Smoking is a risk factor for bone related diseases, bone healing, and endosseous implant failure. The mechanisms responsible for the effects of cigarette smoking are uncertain. Polycyclic aryl hydrocarbons (PAHs) are environmental pollutants present in cigarette smoke, exhaust fumes and furnace gases. Aryl hydrocarbons act through the aryl hydrocarbon receptor (AhR), a nuclear transcription factor. Current evidence suggests that PAHs cause loss of bone mass and bone strength, possibly through inhibition of osteoblast differentiation. Here we test the effect of benzo-a-pyrene (BaP), a representative PAH, on osteoclast (OC) differentiation and function.
OCs derived from newborn New Zealand white rabbits were cultured in the presence of 10^{-7}-10^{-9} M BaP and/or vehicle control. After 48 hours incubation period, the cells were stained for tartrate resistant acid phosphatase (TRAP) and counted. At high OC density (and abundant stromal cells), 10^{-7} M BaP induced a 20% decrease of OC numbers compared to control. At low OC density (and low stromal cell number), 10^{-7} BaP increased OC numbers by 20%, suggesting that cell density of stromal cells, OC precursors, or OCs plays a role in OC differentiation. To eliminate the putative indirect effects of stromal cells on OC differentiation, a mouse macrophage cell line RAW 264.7 was utilized. These cells differentiate into OCs when cultured for 5 days in the presence of the receptor activator of NF-κB ligand (RANKL). Treatment with 10^{-5} M BaP decreased OC differentiation, TRAP activity levels, and resorption of bone-like substrata at 50 ng/mL RANKL, but not at 200 ng/mL. The inhibition was reversed by resveratrol, an AhR antagonist. The observation that either receptor antagonist or high concentrations of RANKL could reverse the BaP effects suggested interacting signaling pathways between RANKL and BaP. To test this hypothesis, RT-PCR was performed on the samples exposed to 10^{-5} M BaP in the presence of different concentrations of RANKL (0, 25 and 200 ng/mL) for 24 hours. The samples were analyzed for the presence of mRNA for cytochrome P450 1B1 (CYP 1B1), a gene commonly activated by BaP. Results indicate presence of CYP 1B1 mRNA in the group exposed to BaP only. The levels decreased either in the presence of resveratrol or increasing concentrations of RANKL. These results confirm the hypothesis that the RANKL and PAH signaling pathways interact, possibly by competing for transcriptional coactivators (SRC-1 or p300/CBP), and demonstrate that the negative effect of PAHs on bone remodeling could, in part, be mediated through inhibition of osteoclastogenesis.

Disclosures: ***I. Voronov****, None.*

SU343

A Peptide Antagonist Mimicking a TNF Contact Site of the TNF-α Receptor Inhibits RANKL-Induced Signaling. C. Itzstein[1], K. Aoki[2], H. Saito*[2], R. Blanque*[3], P. Deprez*[3], M. Ishiguro*[4], W. C. Horne[1], R. Baron[1]. [1]Yale University School of Medicine, New Haven, CT, USA, [2]Tokyo Medical and Dental University, Tokyo, Japan, [3]ProSkelia Pharmaceuticals, Paris, France, [4]Suntory Institute for Bioorganic Research, Osaka, Japan.

The Receptor Activator of NF-κB (RANK), a member of the tumor necrosis factor receptor (TNFR) superfamily, is essential for osteoclast differentiation and activity. Its interaction with its ligand RANKL induces RANK trimerization and stimulates several signaling pathways. Activation of NF-κB, AP-1 (c-Jun and c-Fos) and NFATc1 induce transcriptional activity, while other downstream effectors, (JNK, p38, Erk1/2, Akt and PI3-kinase) affect actin organization, bone resorption and survival. Two cysteine-rich domains (CRD) in the extracellular portions of TNFR superfamily members contain the ligand-binding sites. We previously showed that a cyclized peptide (WP9QY) that mimics a critical TNF-α recognition site on TNFR I (loop 1 of the CRD3) inhibits RANKL-induced osteoclast differentiation and bone resorption, suggesting that WP9QY inhibits RANKL-induced RANK signaling. To confirm this, RAW264.7 cells were stimulated with 2μg/ml of soluble RANKL at 37°C for 20 minutes in the presence or absence of WP9QY (1-50μM) or 0.5μg/ml of OPG. Like OPG, WP9QY blocked RANKL-induced NF-κB activation in a dose-dependent manner, as shown by the inhibition of both the nuclear translocation of p65, a component of NF-κB, and the induction of DNA binding by NF-κB. It also inhibited RANKL-induced activation of Erk1/2 and JNK kinase in a dose-dependent manner. Finally, WP9QY decreased RANKL-stimulated Akt kinase activity. OPG had similar effects on MAP kinase and Akt activity. In contrast to its effects on RANKL-induced signaling, WP9QY had little effect on the binding of RANK to RANKL. By analogy with other TNF/TNFR family members, two contact sites mediate the RANK-RANKL interaction. Mutating the A-A" loop RANKL contact site, which does not bind the RANK CRD3, abolishes the RANK-RANKL interaction (Lam, JCI, 108:971, 2001), suggesting that this site plays the primary role in RANK binding to RANKL. WP9QY would not be expected to affect this contact site. Structural modeling analysis showed that the presence of WP9QY in the CRD3 contact site changes the conformation of the membrane-proximal part of the RANK extracellular domain, apparently affecting the clustering of the RANK intracellular domains that is thought be required for signaling. In conclusion, our results show that WP9QY inhibits RANKL signaling and prevents a consequent increase in osteoclast function, suggesting that RANKL-induced signal transduction depends critically on the contact of RANKL with the first loop of the RANK CRD3.

Disclosures: ***C. Itzstein****, None.*

SU344

The Adaptor and Ubiquitin Ligase Functions of Cbl Have Opposite Effects on Bone Resorption. C. Itzstein, A. Sanjay, T. Miyazaki*, L. Neff*, W. C. Horne, R. Baron. Yale University School of Medicine, New Haven, CT, USA.

Cbl is an adaptor protein involved in the regulation of osteoclast function. $Cbl^{-/-}$ osteoclasts exhibit decreased migration both *in vitro* and *in vivo*. Decreased Cbl phosphorylation in $Src^{-/-}$ osteoclasts (OCs) is associated with a decrease in bone resorption. Downstream of integrins, Cbl forms a tri-molecular complex with Pyk2 and Src in OCs, promoting OC motility and bone resorption. Cbl also acts as an ubiquitin ligase, down-regulating both receptor and non-receptor tyrosine kinases, including the M-CSF receptor (c-Fms) and Src. Although RANK is not itself a tyrosine kinase, it has been suggested that Cbl regulates the surface expression of RANK. However, the structural basis of Cbl's dual functions as an adaptor and an ubiquitin ligase is not fully elucidated. Structurally, the N-terminal half of Cbl includes a tyrosine kinase binding (TKB) domain and a RING finger that is responsible for the ubiquitin ligase activity of Cbl, while the C-terminal half contains a proline-rich region and several regulatory tyrosines that interact with SH3 and SH2 protein-binding domains, respectively. To further investigate the functional roles of various protein binding domains of Cbl, we used the adenovirus system to express myc-tagged wild-type (WT) Cbl, the C-terminal half of Cbl (Cbl-CT) or Cbls containing an inactive TKB domain (CblG306E), a mutated Src SH3 binding site (Cbl6PA) or a mutated PI3-kinase binding site (CblY731F) in murine OCLs, and evaluated their effects on OC cytoskeleton organization and bone resorbing activity. WT Cbl, Cbl-CT, and CblG306E had no effect on actin ring and pit formation. However, over-expression of Cbl6PA or CblY731F disrupted actin organization dramatically and inhibited bone resorption by 25% ($p<0.05$) and 70% ($p<0.001$), respectively, demonstrating that Cbl/Src and Cbl/PI3-kinase interactions play positive roles in OC activity. In contrast, v-Cbl and 70Z-Cbl, which lack ubiquitin ligase activity due to the absence of all or part of the RING finger domain, increased pit formation by 100% ($p<0.001$) and 35% ($p<0.05$), respectively, in $Cbl^{-/-}$ OCLs. These results suggest that Cbl's ubiquitin ligase function is required to down-regulate receptors such as c-Fms or RANK that promote osteoclast formation and activity. Thus, the Src substrate Cbl both promotes osteoclast activity by forming SH2-dependent and SH3-dependent complexes with PI3-kinase and Src, respectively, and reduces osteoclast activity by ubiquitylation-dependent mechanisms.

Disclosures: ***C. Itzstein****, None.*

SU345

Dual Action of Melatonin Signaling Activity in Bone Metabolism. A. Moreau[1], S. Forget*[2], D. Wang*[2], B. Azedine*[2], D. Angeloni*[3], F. Fraschini*[4]. [1]Stomatology & Biochemistry, Research Centre Hôpital Sainte-Justine & Université de Montréal, Montreal, PQ, Canada, [2]Bone Molecular Genetics & Musculoskeletal Laboratory, Research Centre Hôpital Sainte-Justine, Montreal, PQ, Canada, [3]Scuola Superiore Sant' Anna & IFC-CNR, Pisa, Italy, [4]Pharmacology, University of Milan, Milan, Italy.

Hormonal modulation of bone metabolism by melatonin has been proposed to proceed through stimulation of osteoblast differentiation and subsequent osteoclast inhibition. However, little is known concerning melatonin signal transduction in osteoblasts and osteoclasts. Expression analysis of both melatonin receptor subtypes was investigated by RT-PCR using RNA isolated from human osteoblast cell line MG-63 and human osteoclasts derived from PBMCs. Gi proteins interaction with melatonin receptor subtypes were determined by co-immunoprecipitation assays with anti-melatonin receptor antibodies and Western blot analysis with anti-Gi protein antibodies. Melatonin effect on osteoclastic resorption activity was evaluated with the pit resorption assay in presence of melatonin alone or in combination with luzindole, a MT2 melatonin receptor antagonist.

MT2 receptor is the subtype predominantly expressed in both cell types. In human osteoblasts, two distinct forms of Gi proteins were found associated with this receptor subtype: a 43 kDa protein (unphosphorylated, active) and a 60 kDa protein (serine-phosphorylated, inactive), with the following preferential affinity order: $Gi_3 > Gi_2$, while Gi_1 proteins hardly interacted with either melatonin receptors. Addition of melatonin (10^{-7}M) abrogated the interaction of phosphorylated Gi proteins and shifted the affinity order toward $Gi_2 > Gi_3$. In human osteoclasts, MT2 receptor was found to couple almost exclusively with unphosphorylated Gi_3 proteins. However, in absence of melatonin, only tyrosine-phosphorylated Gi_1 proteins were found to interact with MT1 receptor subtype. Melatonin treatment of differentiating osteoclasts abrogated completely the maturation process and inhibited the formation of resorption pits by mature osteoclasts. Addition of luzindole relieves this inhibitory effect indicating that it is mediated through MT2 receptor signaling. Moreover, short-term melatonin treatment almost completely abrogated the expression of RANK by mature osteoclasts, suggesting a direct mechanism of osteoclastogenesis inhibition by melatonin. Taken together those results further strengthen the dual role of melatonin in bone metabolism and aging-associated melatonin decrease could lessen the inhibitory action of melatonin on osteoclastogenesis contributing to the development of osteoporosis.

Disclosures: ***A. Moreau****, None.*

SU346

Synergistic Role of Tyrosine Kinase(s) and the Phosphatase PTP-PEST in the Formation of WASP-Arp2/3 Complex, Actin Ring, and Bone Resorption in Osteoclasts. M. A. Chellaiah[1], R. S. Biswas*[1], D. Kuppuswamy*[2], C. Willies*[2]. [1]Biomedical Sciences, University of Maryland, Baltimore, MD, USA, [2]Cardiology Division, Medical University of South Carolina, Gazes Cardiac Research Institute, Charleston, SC, USA.

Bone resorption is the first step in bone remodeling. Actin ring formation has been shown to be a prerequisite for efficient bone resorption in osteoclasts. We have previously shown that transduction of phosphoinositides binding domain containing gelsolin peptides blocked the formation of WASP-Arp2/3 complex (ASBMR, 2003) and actin ring in the osteoclasts. Despite success in identifying the role of kinases such as, Src, PYK2, and FAK in actin ring formation, the potential target protein of these kinases is poorly understood. Thus, our aim is to identify the target protein involved in actin ring formation. Osteoclasts that were either treated with osteopontin (OPN) or expressing constitutively active Src (CA-Src) by adenoviral-mediated delivery, exhibited an increase in WASP-Arp3 complex formation in the actin ring of osteoclasts. *In vitro* kinase analysis of WASP immunoprecipitates showed OPN stimulated phosphorylation of Src, WASP, PYK2 and three other proteins with molecular masses of 100-110 kDa, 120-130 kDa, 35-40 kDa. These proteins were also found to be phosphorylated in osteoclasts expressing CA-Src but not in kinase negative Src (KN-Src). Biochemical and confocal studies revealed that WASP and PTP-PEST form a complex and are colocalized in OPN-stimulated osteoclasts. Measurement of WASP-associated PTP-PEST phosphatase activity exhibited decreased activity levels both in OPN-treated and in CA-Src expressing osteoclasts. Furthermore, OPN stimulation resulted in serine phosphorylation of WASP associated PTP-PEST. Such increased serine phosphorylation with decreased PTP-PEST phosphatase activity was accompanied by an increased tyrosine phosphorylation of WASP and other associated signaling proteins. Experiments with PTP-PEST inhibitor and antisense ODNs to PTP-PEST further confirmed the involvement of PTP-PEST in the tyrosine phosphorylation levels of proteins, formation of WASP/Arp3 complex, actin ring and bone resorption. Taken together, these results suggest that WASP, which is identified in the actin ring of osteoclasts, associates with Src, PYK2, and PTP-PEST. PTP-PEST and tyrosine kinase(s) coordinate the formation of WASP-Arp2/3 complex and the actin ring.

Disclosures: ***M.A. Chellaiah****, None.*

SU347

Osteocyte Death Can Occur in Young Bone, More Frequently in Black Than in White Women. S. Qiu[1], D. Rao[1], S. Palnitkar*[1], A. Parfitt[2]. [1]Bone & Mineral Research Lab, Henry Ford Health System, Detroit, MI, USA, [2]Division of Endocrinology and Center for Osteoporosis and Metabolic Bone Disease, University of Arkansas for Medical Sciences, Little Rock, AR, USA.

Osteocytes die by apoptosis as bone grows older, leaving empty lacunae in bone matrix. The objective of this study was to determine the frequency of osteocyte death in recently formed bone.

Iliac bone biopsies from 128 healthy women, aged 20-73 years, were used in this study, of whom 34 (16 pre-menopausal and 18 postmenopausal) were blacks and 94 (38 pre-menopausal and 56 postmenopausal) were whites. In the sections stained with Goldner's trichrome, empty lacunae were measured in superficial bone (<25 µm from the bone surface). Empty lacunae in unmineralized osteoid were observed using the sections stained with toluidine blue.

Empty lacunae were found in osteoid tissue (Fig 1), but were not enumerated because too little osteoid was present. In both black and white women, empty lacunae in superficial bone did not significantly increase with age or menopause. However, black women had more empty lacunae than white women in superficial bone ($p < 0.01$), especially when pre-menopausal (Table 1).

The mean age of superficial bone is about 3 years, and the mean age of osteoid is about 2 weeks. The lifespan of osteocytes in cortical bone is about 25 years. The presence of empty lacunae in superficial bone and especially in osteoid indicates that some osteocytes may die very soon after they are formed. A possible explanation is that these fragile osteocytes were differentiated from unhealthy osteoblasts that would have died had they not become osteocytes. The reason for more frequent osteocyte death in black than in white women is unknown.

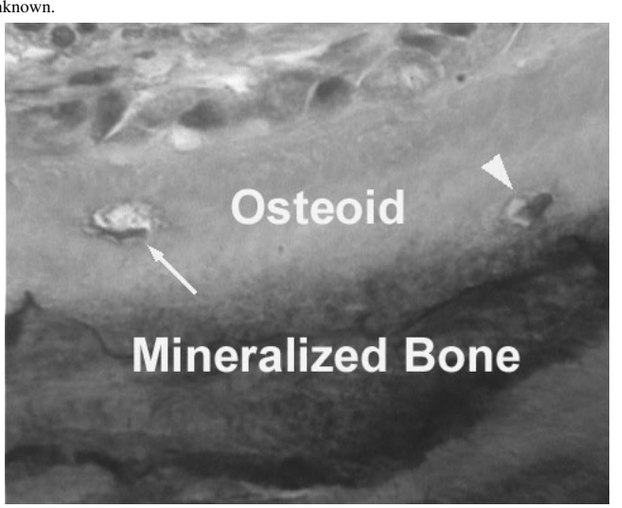

Disclosures: ***S. Qiu****, None.*

SU348

Serotonin and Dopamine Stimulate Prostaglandin Release and Regulate COX-2 Expression in Osteocytic Cells. M. M. Bliziotes, X. Zhang, K. M. Wiren. Medicine, Oregon Health and Science University/Portland VAMC, Portland, OR, USA.

Neurotransmitter regulation of bone physiology is manifested by the osteopenic phenotypes seen in both serotonin (5-HT) and dopamine (DA) transporter knockout mice. The 5-HT transporter (5-HTT) and 5-HT receptors have been identified in both osteoblasts and osteocytes, while DA transporter expression in bone cells has not been documented. We explored the functional consequences of 5-HT and DA treatment of cultured osteocytes using the clonal murine osteocytic cell line MLO-Y4.

We assessed prostaglandin E2 (PGE2) release into culture media from 5-HT and DA treated subconfluent MLO-Y4 cells using an enzyme immunoassay. The expression of two forms of prostaglandin synthase (COX-1 and COX-2) were analyzed by RT-PCR of mRNA isolated from 5-HT and DA treated cells. Finally, expression of connexin 43 (Cx43) was determined by immunoblot using an antibody generated against a synthetic peptide encoding amino acids 252-271 of rat Cx43.

5-HT and DA (both 100 μM) independently stimulated PGE2 release from MLO-Y4 cells. 5-HT increased medium PGE2 levels by 47% and 50% at 5 and 30 min, respectively, while DA increased PGE2 by 150% at both time points. Surprisingly, both 5-HT and DA (100 μM) decreased steady state mRNA levels for COX-2 after 2 hr of treatment (40% for 5-HT and 80% for DA); DA also decreased COX-1 mRNA by 40%. Both neurotransmitters altered connexin 43 protein expression.

In conclusion, the neurotransmitters 5-HT and DA 1) increase PGE2 release rapidly in osteocytic cells, and 2) reduce transcript levels of the inducible PG synthase COX-2 over a more prolonged period. At equimolar doses, DA is more efficacious than 5-HT in regulating COX-2 expression and PGE2 release.We have documented for the first time DA receptor activation in osteocytic cells. These observations suggest potential mechanisms to explain the phenotypic effects on bone induced by in vivo disruption of the DA and 5-HT transporter genes, which alter extracellular concentrations of these neurotransmitters.

Disclosures: ***M.M. Bliziotes****, None.*

SU349

Heat Shock Protein Modulation by Hypoxic Osteocytes. P. Pathare*, T. S. Gross. Orthopaedics and Sports Medicine, University of Washington, Seattle, WA, USA.

Previous studies have indicated that the extracellular matrix protein, osteopontin (OPN) is rapidly upregulated by osteocytes when challenged by disuse (in vivo) or oxygen deprivation (in vitro). In addition to its role in mediating osteoclast attachment and activity, OPN has a broader role in enabling cells to withstand environmental stress. In this context, heat shock proteins (HSP) have been specifically associated with the ability of cells to rapidly respond to and survive biological stress. We therefore hypothesized that HSPs would be upregulated by osteocytes exposed to hypoxia. Following screening studies, we focused on the temporal regulation of HSP90. Osteocyte-like cells (MLO-Y4) were plated at 25% confluence and grown for 24 hr in α-MEM medium containing 2.5% fetal bovine serum and 2.5% calf serum. The cells were exposed to either normal oxygen (19%) or were placed in a commercial hypoxia chamber (< 1% oxygen) and incubated at 37 C for between 4 and 48 hr. As a positive control at each time point, osteocytes were exposed to heat shock (42 C for 20 min) followed by incubation at 37 C. Western blots were performed on whole cell extracts and percent elevation of HSP90 versus control levels was determined using NIH ImageJ. In response to heat shock, we observed a rapid and sustained increase in HSP90 expression (6 hr: 849% elevation, 12 hr: 279% elevation, 24 hr: 80%) that returned to near normal levels only at the 48 hr time point (48 hr: 27% elevation). In response to hypoxia, osteocytes demonstrated upregulation of HSP90 at 12 hr (67% vs control) and 24 hr (43% vs control). HSP90 expression by osteocytes at 4, 8, and 48 hrs did not differ from control levels. In a subsequent experiment, we exposed osteocytes to 0.1 μM of dexamethasone (a synthetic glucocorticoid) for 24 and 48 hr as a means of imposing severe environmental stress upon the cells. We again observed temporal regulation of HSP90, with protein expression was substantially increased at 24 hr (254% vs control) but not at 48 hr (-14% vs control). To our knowledge, this is the first report of HSP modulation in osteocytes. Further, while HSP27 has been implicated as a mediator of the response of osteoblasts to factors such as statins and PGE2, our observations represent the first report of HSP90 modulation by osteoblasts or osteocytes. HSP90 was upregulated in a temporal manner, dependent upon the severity of the imposed stress. Interestingly, HSP90 plays a vital role in the function of the steroid hormone receptor. Given numerous reports of glucocorticoid induced osteocyte apoptosis, it is reasonable to speculate that a condition that induces upregulation of HSP90 (such as hypoxia) would increase the susceptibility of osteocytes to the challenge of glucocorticoids.

Disclosures: ***T.S. Gross****, None.*

SU350

In Vitro Functions of Beta1 Integrins in Mature Cells of the Osteoblast Lineage. J. V. Dovi[1], M. C. H. van der Meulen[2], C. H. Damsky[3], J. B. Kim*[4], E. A. C. Almeida[1], R. K. Globus[1]. [1]Gravitational Biology, NASA Ames Research Center, Moffett Field, CA, USA, [2]Cornell University, Ithaca, NY, USA, [3]University of California, San Francisco, CA, USA, [4]Stanford University, Palo ALto, CA, USA.

Beta1 integrins participate in cellular adhesion of osteoblast lineage cells. However, how beta1 integrins influence the physiology of late stage osteoblasts is not understood. To determine the roles of beta1 integrins in mature osteoblasts and osteocytes, we established primary cell cultures from bones of neonatal and adult wild type (WT) or transgenic (TG) mice, which expressed a function-perturbing fragment of beta1 integrin consisting of its transmembrane and cytoplasmic domain. Expression of this fragment was under the control of the osteocalcin promoter. We also generated stably transfected, MLO-Y4 osteocytic cell lines, using either an empty control vector or a vector encoding for the beta1 fragment under the control of the CMV promoter. Basic cellular functions, including adhesion, proliferation, and differentiation were assessed. MLO-Y4 cells expressing the beta1 fragment displayed fewer cellular processes and were more rounded. Some cells expressing the fragment detached from the type I collagen-coated substrate, but remained viable and were able to reattach. Cells expressing the beta1 fragment migrated more slowly into denuded areas compared to controls. Interestingly, MLO-Y4 cells expressing the beta1 fragment displayed a higher proliferative rate compared to controls. In contrast to the MLO-Y4 cell line expressing the beta1 fragment, primary cells from TG mice proliferated during the logarithmic stage of growth at a rate similar to WT controls, and formed nodules to a similar extent as WT controls. Cells isolated from long bones of both WT and TG adult mice displayed long, interconnecting processes and therefore resembled osteocytes. Despite similar morphological appearances, binding to type I collagen was 10-fold lower in osteocytic cells from TG mice compared to those from WT mice. In conclusion, we have demonstrated that primary cells of the osteoblast lineage expressing the function-perturbing beta1 fragment are able to differentiate, as judged by the formation of mineralized nodules and osteocytic morphology, despite a defect in type I collagen binding. These results raise the possibility that other adhesion molecules are redundant with beta1 integrin function during terminal differentiation of osteoblasts.

Disclosures: ***J.V. Dovi****, None.*

SU351

Dickkopf (Dkk)-1 Is an Osteocyte-expressed and Glucocorticoid-inducible Inhibitor of LRP5 Signaling. V. Kasparcova*, H. Glantschnig, L. P. Freedman, S. Harada. Molecular Endocrinology/Bone Biology, Merck Research Laboratories, West Point, PA, USA.

Both gain of function and loss of function mutations of LDL receptor-related protein 5 (LRP5) in human, leading to reciprocal bone phenotype, have unambiguously documented the role of LRP5 in bone metabolism and bone mass. In Wnt reporter assays, the high bone mass mutant $LRP5_{G171V}$ was found to be resistant to inhibitory effects of Dkk-1. Accordingly, we found that the mutant $LRP5_{G171V}$ failed to interact with Dkk-1, suggesting the role for the potential involvement for Dkk-1 in LRP5 action in bone. To gain insight into the role of Dkks in bone, we evaluated the expression of Dkks known to associate with LRP5. By real-time PCR analysis of RNA isolated from adult rat tissues, Dkk-1 was found to be abundantly expressed in bone tissues with significant expression also observed in placenta, prostate and uterus. In contrast, expression levels of other LRP5 ligands, Dkk-2 and Dkk-4 in bone were minimal with significant expression of Dkk-2 observed in number of tissues such as kidney, eye and esophagus. These reciprocal expression pattern of Dkk-1 and Dkk-2, know to activate wnt signaling, suggests the unique role for Dkk-1 as a bone expressed inhibitor of Wnt signaling. Accordingly, in MC3T3-E1 osteoblastic cells, Dkk-1, but not other Dkks, suppressed osteoblast differentiation induced by Wnt3a. By *in situ* hybridization, expression of Dkk-1 was found predominantly in osteocytes of cortical bone of adult rat tibiae and adult mouse femur with less significant expression observed in osteoblasts on trabecular bone. No expression of Dkk-1 was found in osteoclasts or growth plate chondrocytes. Osteocyte apoptosis has been linked to glucocorticoid-inuduced osteoporosis. Interestingly, expression of Dkk-1 in adult rat diaphysis was markedly induced by treatment with methyl predonisolone in a dose dependent and time dependent fashion with the significant stimulatory effects observed at 4 days. In contrast, expression of osteoblast markers, such as type I collagen and osteocalcin, in diaphysis were suppressed by methyl predonisolone. These results, in combination with recent reports on osteocyte-selective expression of sclerostin, a binding protein of bone morphogenetic proteins, responsible for a high bone mass disease “sclerosteosis”, support the role for osteocytes in bone mass homeostasis by controlling Wnt and BMP signaling in bone.

Disclosures: ***V. Kasparcova****, Merck & Co., Inc. 3.*

SU352

The Contribution of BMD Correlation to Fracture Risk Prediction by Bone Density Measurements at Distant Skeletal Sites. G. M. Blake, I. Fogelman. Nuclear Medicine Department, GKT School of Medicine, London, United Kingdom.

The most reliable BMD measurement for predicting fracture risk at any given site in the skeleton is one made at the fracture site itself. This study examines the hypothesis that fracture prediction by measurements made at sites remote from the fracture site can be explained by BMD correlation. We show that the correlation hypothesis predicts the relationship $\beta_{dist} = r\,\beta_{frac}$, where β is the gradient of the exponential relationship between fracture risk and Z-score, β_{dist} is the β-value for the distant BMD site, β_{frac} that at the fracture site, and r is the correlation coefficient between the Z-scores at the two sites. In practice it is necessary to consider the effect of measurement errors on the relationship between r and β. We show that the effect of the errors at the distant site is to reduce both β_{dist} and r in a way that preserves their original relationship. When the effect of errors at the fracture site is taken into account, the overall effect on the (r, β) plot is for the data point representing the fracture site to lie below the linear trend of the points representing distant sites, thus predicting a characteristic signature for the overall relationship. We tested the correlation hypothesis by using data from the Study of Osteoporotic Fractures to examine the (r, β) plots for hip, spine and forearm fractures. For the hip, the data are consistent with the equation $\beta_{dist} = r\,\beta_{frac}$. This suggests that hip fracture prediction by distant sites is adequately explained by BMD correlation, and that measurements made at distant sites provide no additional information about fracture risk over and above that provided by hip BMD itself. However, for spine and forearm fractures the (r, β) plots are consistent with the expected effects of the BMD measurement errors. This suggests that in the case of these fractures, measurements at distant sites do provide additional information about fracture risk, and that they do this by retaining some of the information about bone that was lost because of the measurement errors at the fracture site. Overall, this study points to the importance of BMD correlation as a key factor in explaining the ability of measurements made at distant sites to predict fracture risk.

Disclosures: ***G.M. Blake****, None.*

SU353

Site-Specific Reductions in Bone Density in Canadian Aboriginal Women: The First Nations Bone Health Study. W. D. Leslie[1], C. J. Metge*[2], H. A. Weiler*[3], C. K. Yuen[1], J. Krahn*[1], M. Doupe*[1], E. A. Salamon[4], P. Wood Steiman*[5], J. D. O'Neil*[1], C. R. Greenberg*[1], L. M. Lix*[1], L. L. Roos*[1], A. Tenenhouse[6]. [1]Faculty of Medicine, University of Manitoba, Winnipeg, MB, Canada, [2]Faculty of Pharmacy, University of Manitoba, Winnipeg, MB, Canada, [3]Human Nutritional Sciences, University of Manitoba, Winnipeg, MB, Canada, [4]Department of Medicine, University of Manitoba, Winnipeg, MB, Canada, [5]Asssembly of Manitoba Chiefs, Winnipeg, MB, Canada, [6]Department of Medicine, McGill University, Montreal, PQ, Canada.

Canadian Aboriginal women are at increased fracture risk compared with the general population (JBMR 18:S151, 2003), but little is known about the burden of osteoporosis in this population. The First Nations Bone Health Study (FNBHS) recruited a random age-stratified (25-39, 40-59 and 60-75) sample of urban and rural Aboriginal women (n=225) and age-matched White women (n=183). All subjects had forearm and calcaneal BMD measured (Lunar PIXI); urban subjects also had BMD measurements of the lumbar spine, hip and total body (Hologic QDR-4500). Aboriginal women had greater weight (80.5±17.7 vs 76.3±18.2 kg, P=0.018) and BMI (30.4±6.3 vs 28.6±6.9 kg/m^2, P=0.005) than Whites due to more adipose tissue (total body fat 3186±1523 vs 2886±1191 g, P=0.039). Weight correlated positively with BMD (r=0.32-0.56, P<0.001 all sites) and could mask an ethnicity effect. Therefore ANCOVA was used to test for an ethnicity effect in Z-scores (controlling for weight and also age if required) and differences in absolute BMD (controlling for weight and age using main effect and interaction terms). There was a significant effect of ethnicity on BMD of the calcaneus, forearm and total body (lower in Aboriginals). Volumetric BMD (BMAD) did not explain this difference as bone area was virtually identical in Aboriginals and Whites. In conclusion, the FNBHS provides the first comprehensive assessment of bone density in Canadian Aboriginal women, and identified significant site-specific differences in age-and weight-adjusted bone density (lower in Aboriginals for the calcaneus, forearm and total body). Central sites (lumbar spine and total hip) were not affected underscoring the importance of a comprehensive assessment of BMD using multiple sites.

Site	Bone Mass as Z-score Predictor: P	Bone Mass as BMD (g/cm^2) Predictor: P
Calcaneus	Ethnicity: 0.0014 Weight: 0.0008	Ethnicity: 0.0008 Age Stratum: 0.0010 Age: 0.0056 Age Stratum*Age: 0.0011 Weight: <0.0001
Distal forearm	Ethnicity: 0.0021 Weight: <0.0001	Ethnicity: 0.0032 Age Stratum: 0.0019 Age: <0.0001 Age Stratum*Age: 0.0027 Weight: <0.0001
Lumbar Spine	Ethnicity: >0.2 Age: <.0001 Weight: <0.0001	Ethnicity: >0.2 Age Stratum: 0.0001 Age: <0.0001 Age Stratum*Age: 0.0004 Weight: <0.0001
Total hip	Ethnicity: 0.14 Age: <0.0001 Weight: <0.0001	Ethnicity: 0.12 Age Stratum: 0.0001 Age: 0.0007 Age Stratum*Age: 0.0004 Weight: <0.0001
Total body	Ethnicity: 0.047 Weight: <0.0001	Ethnicity: 0.030 Age Stratum: 0.0005 Age: 0.0016 Age Stratum*Age: 0.0007 Weight: <0.0001

Disclosures: ***W.D. Leslie****, None.*

SU354

Is Bone Densitometry Appropriate in Women under 50? E. Koshy*, A. L. Dolan*. Rheumatology, Queen Elizabeth Hospital, London, United Kingdom.

Bone densitometry should only be performed if it alters management. The Royal College of Physicians guidelines state that there are no proven treatments available for premenopausal women. This retrospective, cross-sectional, observational study aims to identify if referral of women under 50 years old for densitometry is appropriate and as a consequence establish guidelines for referral indications in this age group.

Women under 50 years old referred to a District Hospital by general practitioners and hospital physicians were identified from the hospital database over a 4 year period. The referral indications and scan outcomes were studied. Risk factors for osteoporosis were also examined.

301 patients were identified. 65% of referrals were requested by GPs and 35% by hospital doctors. 41% of patients had abnormal scans. The most frequent indication for a DXA scan request was 'premature menopause' 27% (43/160) of all the primary request indications and of them 37% were abnormal. Steroid use accounted for 19% (30/160) of exclusive requests and 47% were abnormal. Family history represented 14% (22/160) of the exclusive referrals and 27% were abnormal. Referral based on osteopenia / previous fracture as a primary or co-existing indication, accounted for 37 scans and 54% were abnormal. 11 patients were referred because of amenorrhoea alone and of this group, 64% had abnormal scans. Anorexia nervosa and inflammatory bowel disease were the medical conditions associated with the highest proportion of abnormal scans, 57% and 52% respectively. Low calcium/vitamin D intake, a BMI <20 and amenorrhoea were risk factors associated with a lower BMD in this sample.Focused use of bone densitometry in women under 50 can identify patients with future fracture risk who may merit osteoporosis prevention. When referral for premature menopause, family history, steroid intake or a medical condition are the exclusive indications, approximately a third of scans are abnormal. The medical conditions most associated with a lower BMD are anorexia and inflammatory bowel disease. In premenopausal women treatment options may be predominantly with calcium and vitamin D, but selective DXA does seem to identify a significant number who would benefit from bone pretection

Disclosures: ***A.L. Dolan****, None.*

SU355

Rate of Mammography and Bone Mineral Density Testing in Postmenopausal Women. Y. Chen, P. B. Landsman*, S. K. Brenneman, S. M. Teustch*, L. E. Markson*. Merck & Co., Inc., West Point, PA, USA.

Postmenopausal women (PMW) are at increased risk for breast cancer and osteoporosis-related fractures; about one in two will have an osteoporosis-related fracture and one in eight will receive a diagnosis of breast cancer during her lifetime. Mammography screening and treatment reduces mortality by approximately 16%; BMD screening and treatment can reduce osteoporotic fracture rates by almost half. There have been longstanding evidence-based guidelines by the US Preventive Services Task Force (USPSTF) recommending mammography screening every 1-2 years for women aged 40 and older. More recently, the USPSTF guidelines have recommended routine osteoporosis screening in women 65 years of age and older and in those 60 years and older with risk factors. We sought to describe the utilization of mammography and bone mineral density (BMD) testing in PMW age 50 and older. The 2000 Medstat MarketScan ® Research Databases containing medical claims of employees, retirees, and dependents of over 100 large employers covered by over 300 healthcare plans was used for the analysis. Study sample was women age 50 years and older continuously enrolled in a health plan in 2000. CPT codes for mammography and BMD were used to identify women who had tests performed during the one-year study period. Number of women, not number of tests, was used to calculate testing rate. Rates of mammography (number of women with mammography per 1000 person years) and rates of BMD testing (number of women with BMD testing per 1000 person years) and the ratios of the two rates by age group are shown in Table below.

Age	# women	Rate of mammography	Rate of BMD testing	Ratio
50-54	174,940	448	79	6:1
55-59	140,452	516	112	5:1
60-64	118,325	536	131	4:1
65+	281,230	383	121	3:1

Mammography rates are approximately half the minimum recommended frequency (every other year). No benchmarking is available for assessing BMD testing rates. Compared to mammography, BMD testing appeared to be much less frequently utilized even in women 65 years who are at higher risk for fractures. The lack of clear guidelines on testing frequency may contribute to these findings in this cross-sectional data. Preventive care for osteoporosis in PMW may need more attention.

Disclosures: ***Y. Chen****, None.*

SU356

C-reactive Protein Levels Are Associated with Decreased Bone Mineral Density in Mexican Americans. B. W. Whitcomb*[1], J. M. Bruder[2], R. L. Bauer[2], M. C. Mahaney*[3], R. P. Tracy*[4], C. M. Kammerer[5], B. D. Mitchell[6]. [1]Preventive Medicine and Epidemiology, University of Maryland, Baltimore, Baltimore, MD, USA, [2]Medicine, University of Texas Health Science Center, San Antonio, TX, USA, [3]Genetics, Southwest Foundation for Biomedical Research, San Antonio, TX, USA, [4]Biochemistry, University of Vermont College of Medicine, Burlington, VT, USA, [5]Human Genetics, University of Pittsburgh School of Publ;ic Health, Pittsburgh, PA, USA, [6]Medicine/ Endocrinology, University of Maryland, Baltimore, Baltimore, MD, USA.

Accelerated bone loss is frequently observed in rheumatoid arthritis, Crohn's disease, and other autoimmune diseases suggesting that inflammation may play a role in increased bone resorption. To determine if inflammation contributes to overall levels of bone mineral density (BMD) in a non-selected population, we measured serum levels of C-reactive protein (CRP) and evaluated the correlation with bone mineral density. Study participants (n = 650) ranged from 18 to 96 years of age and were members of 34 large families of Mexican American decent. These families were recruited between 1997-2002 as part of the San Antonio Family Osteoporosis Study, a population-based family study of osteoporosis and cardiovascular disease. Serum CRP levels were measured using a competitive immunoassay (antibodies and antigens from Calbiochem, LaJolla, CA) and BMD was measured at the hip (total and neck), spine (L1-L4), and forearm (ultradistal radius) by dual x-ray absorptiometry (DXA). We performed linear regressions of BMD at each site on CRP, adjusted for age, sex, and body mass index (BMI), using a variance component procedure to account for the familial correlations in BMD between study subjects.

Initial analyses revealed CRP levels to be correlated with increasing age ($p < 0.001$) and increasing body mass index ($p < 0.001$). After adjustment for age, sex, and BMI, serum CRP was significantly associated with BMD at the total hip ($p = 0.03$), femoral neck BMD ($p = 0.01$) and forearm BMD ($p = 0.01$), though not with spine BMD ($p = 0.14$). The impact of CRP levels on BMD was modest, with a one standard deviation unit increase in CRP associated with a decrease of only 0.01 units (95% CI: 0.006, 0.014), or 1.0%, in femoral hip neck BMD. The correlations between CRP and BMD did not differ significantly by sex, nor did they differ significantly between subjects older and younger than age 50. These results are consistent with the hypothesis that systemic inflammation contributes to increased rates of bone resorption and bone loss. Furthermore, systemic inflammation may be a common pathway contributing to the joint occurrence of subclinical atherosclerosis and decreased BMD seen in this and in other populations.

Disclosures: ***B.D. Mitchell****, None.*

SU357

Bone Mineral Density of the Lumbar Spine and Knee Osteoarthritis in Korean: Data from the Korean Arthritis Study Group. I. H. Park*[1], M. S. Park,ES Moon,WI Noh,JM Kim,YG Kim,SH Lee,YJ Cho*[2]. [1]Orthopedic Surgery, Kyungpook University Hospital, Taegu, Republic of Korea, [2]Multicenter, Seoul, Pusan, Chunbuk, Kwangju, Republic of Korea.

A prospective, nation-wide multicenter study was carried out under the title of "Risk factors of knee osteoarthritis(OA) in Korean" by Korean arthritis study group. This study was one of the cross-sectional analysis from those data to evaluate the relationship between bone mineral density(BMD) of the lumbar spine and knee OA. One-hundred sixty-two South Korean from 40- to 64-year-old were eligible. Men were 27, and women were 135. Age was matched between OA and control group. Osteoarthritis of the knee was defined by both OA scales of WOMAC TM 3.01 by professor Bellamy and Kellgren-Lawrence grade III or IV using bilateral standing anteroposterior, lateral and tangential knee radiographs. Erythrocyte sedimentation rate(ESR), cross-reacting protein(CRP), and rheumatoid arthritis(RA) factor were all checked to exclude other arthritis than OA. BMD of the lumbar spine was measured by DXA after adjusting precision error at every center. The results were as Table 1, 2, 3. After adjusting body mass index, there was no statistical significance(p=0.05) between the lumbar spine BMD, T-score and knee OA. However, it seems that OA group showed higher BMD and T-score of the lumbar spine both in men and women in spite of lower mean age than control group. More data would be needed to clear out the possible inverse relationship between knee OA and osteoporosis.

Table 1

Mean Age (years)	Male	Female	Total
OA	56.7	56.1	56.2
Control	55.1	53.7	54.0

Table 2

BMD(gm/cm^2)	Male	Female	Total
OA	1.2127	0.9963	1.0353
Control	1.1097	0.9935	1.0177

Table 3

T-score	Male	Female	Total
OA	0.84	-0.79	-0.38
Control	-0.43	-0.93	-0.79

Disclosures: ***I.H. Park****, None.*

SU358

The Choise of Phantom Is Crucial for Quality Assessment in Longitudinal Studies. N. Emaus*, G. K. R. Berntsen, R. M. Joakimsen*, V. Fønnebø*. Department of community medicine, University of Tromsø, Tromsø, Norway.

Densitometer performance is of ultimate importance in the acquisition of valid data in longitudinal studies. In a longitudinal population based study lasting more than six years, using two single absorptiometry (SXA) devices, we were concerned that densitometer performance could influence bone loss estimates.

We had three sources for evaluation of densitometer influence; data from the aluminium wedge phantom (AWP) provided by the manufacturer, data from the European forearm phantom (EFP), which is a semi-anthropomorphic phantom, and repeated measurements, in 1994-95 and 2001, at the forearm in 3346 women and 2291 men aged 25 to 84 years at baseline.

The AWP measurements were performed daily in both studies. When the EFP became available in 1999, we obtained measurements from both densitometers and we continued to use this phantom throughout the 2001 survey.

Starting the second survey, one of the densitometers underwent a major repair. In addition, both densitometers had the x-ray tube replaced later in the survey. These events were considered equivalent to densitometer changes, giving a total of six participating densitometers and eight possible baseline-follow up densitometer combinations in the study.

The mean follow up time was 6,4 years (SD 0,6). The mean overall crude bone loss was 0,0185 g/cm² or 4,14 % (0,00285 g/cm²/year or 0,64%/year). The population bone loss varied between densitometer combinations from 0,0145 g/cm² to 0,0213 g/cm² (p<0,001). The observed variation in bone loss on the different densitometer combinations was interpreted as differences in densitometers' measurement level, because the population groups did not differ significantly with regard to sex, age and baseline BMD. The EFP measurements revealed that two of the densitometers measured a higher BMD-level than the others. After change of x-ray tube, we registered a significant lowering of one densitometer's measurement level, whereas "wear and tear" over time did not alter densitometer function. The EFP measurements predicted the observed variation between densitometer combinations in the population material. This was in surprising contrast to the producer supplied AWP which did not capture these differences. After adjustment according to the EFP data, the overall crude bone loss was reduced to 0,0174 g/cm² or 3,92 % (0,00269 g/cm²/year or 0,61%/year). We conclude that densitometer performance during longitudinal studies might influence the accuracy of bone loss estimates. As changes in performance are not detected by aluminium wedge phantoms, quality control of BMD measurements in longitudinal studies should be performed with daily measurements of anthropomorphic hydroxyapatite phantoms.

Disclosures: ***N. Emaus****, None.*

SU359

Bone Mineral Markers in South Indian Post Menopausal Women. C. V. Harinarayan*[1], U. V. Prasad*[1], M. Suresh*[1], A. V. Hebbani*[1], P. V. L. Srinivasa Rao*[2], M. Dhananjaya Naidu*[3], P. R. Parthasarathy*[3], E. G. T. Kumar*[1], D. Sudhakar*[1], L. B. Aparna*[2], D. Prasanna Kumar*[1]. [1]Endocrinology and Metabolism, SVIMS, Tirupati, India, [2]Biochemistry, SVIMS, Tirupati, India, [3]SV University, Tirupati, India.

To study the bone mineral markers in serum and urine in south Indian postmenopausal women.

Postmenopausal women (n=437) were evaluated for their dietary intake patterns, bone mineral markers in serum and urine.

The mean ± standard error of mean (SEM) of age (yrs), weight (kg), BMI of the 437 patients were 52±0.4; 62±0.4; 27±0.3 respectively. The serum albumin (gm/dl), creatinine (mg/dl), LH and FSH(IU/l) were 3.96±0.02;0.9±0.01;26±0.8; 65±1.8 respectively. The dietary calcium, phosphorous (mg/day) and phytate/calcium ratio were 322±4; 676±7; 0.56±0.01. The whole group was sub-classified based on 25(OH)D levels into: Group - 1-severe deficiency(<5 ng/ml); Group - 2 moderate deficiency(5-10 ng/ml); Group - 3 -mild deficiency(10-20 ng/ml) and Group - 4 -vitamin D sufficiency(>20 ng/ml). The bone mineral marker parameters of the respective group are depicted in the table below:

Parameter	Group - 1	Group - 2	Group - 3	Group - 4
S.Calcium(mg/dl)	9.63±0.13	9.67±0.05	9.68±0.04	9.76±0.07
S.Phosphorus(mg/dl)	3.4±0.2	3.4±0.05	3.45±0.04	3.57±0.06
S.Alk.Phos(IU/l)	106±15	117±6	106±3.5	107±7.3
S.TRAP(IU/l)	6.5±1.5(4)	5.9±0.4(27)	5.7±0.3(49)	7±0.7(9)
25(OH)D(ng/ml)	4.15±0.2	7.88±0.14	14.86±0.2	26±0.65
PTH ntact (pg/ml)	39±5	25.5±1.7	25±1.2	25±1.5
Ca/Cr ratio	0.16±0.02	0.17±0.01	0.18±0.01	0.18±0.01
PEI	0.03±0.03	0.005± 0.008	-0.02±0.02	-0.01±0.008
Urinary DPC(nmol/mmol of cr)	15.6±6(4)	6.35±0.9(27)	7.9±0.4(51)	8.7±1.9(10)
Urinary OH Proline	4.8±0.09(4)	8.43±1.3(24)	6.6±0.71(47)	5.6±2.3(10)

Values are Mean ± SEM; Parenthesis - patient number

There was no significant difference in the dietary pattern in the subgroups. The dietary calcium intake of the whole group is inadequate compared to the Recommended Daily/ Dietary allowances (RDA) of national guidelines. About 80% of the study group had varying degrees of 25(OH)D deficiency {severe deficiency 4% (19); moderate deficiency 24%(104) and mild deficiency 52% (226)} . Only 20% of the population have normal 25(OH)D levels. Serum PTH negatively correlated with 25(OH)D levels (r -0.2; p <0.01) and positively with SAP (r 0.8; p <0.01). A significant positive correlation (p<0.01) was observed between dietary phytates with SAP (r 0.6); dietary calcium with phytates (r0.75) and SAP (r 0.65).

In all postmenopausal women diet should be enriched with calcium and vitamin D supplemented while considering HRT. The dietary calcium insufficiency and 25(OH)D deficiency could reflect fallaciously as osteopenia in BMD measurements.

Disclosures: ***C.V. Harinarayan****, None.*

SU360

Dietary Determinants of BMD in Hong Kong Chinese Elderly Men and Women - Mr and Ms OS. W. W. Y. Lau*[1], E. M. C. Lau[1], D. T. K. Choy*[1], S. Y. S. Wong[2], J. Leung*[1], L. M. Lee*[1], H. Lynn[2], P. C. Leung*[3]. [1]Jockey Club Centre for Osteoporosis Care and Control, The Chinese University of Hong Kong, Shatin, Hong Kong Special Administrative Region of China, [2]Department of Community and Family Medicine, The Chinese University of Hong Kong, Shatin, Hong Kong Special Administrative Region of China, [3]Department of Orthopaedics and Traumatology, The Chinese University of Hong Kong, Shatin, Hong Kong Special Administrative Region of China.

Not many large cohort studies had been done on the dietary intake of Hong Kong Chinese elderly. Mr OS and Ms OS (Hong Kong) is a large cohort study to address the dietary intake of Chinese elderly in Hong Kong in relation to their bone mineral density (BMD). A total of four thousand men and women, stratified by age and sex, were recruited. They were ambulatory and community dwelling elderly aged 65 to 94 years. A 260 items food frequency questionnaire based on the method of Block food frequency questionnaire with local and Chinese food added was administered at baseline. The results were analyzed by a locally developed nutrients analysis program containing food database from US, UK and China to produce estimation of daily caloric and nutrients intake. BMD in the whole body, total hip and total spine were measure by Dual Energy X-ray Absorptiometry (Hologic QDR 4500W). The mean nutrient intake was higher in men than in women. The mean intake for men was 2102 Kcal, 88 g protein and 68 g Fat whereas women was 1605 kcal, 67 g protein and 49 g fat. In both elderly men and women, the calcium intake was 633 mg and 583 mg respectively, which is much lower than US Dietary Reference Intake of 1200 mg per day. In relation to the total spine BMD, positive association (p<0.05) were found in a multiple regression model (adjusted for age and body weight) with intake of calcium, vitamin A, B1, B2 and phosphorous for women whereas no significant association between BMD and any nutrient intakes in men was found. In relation to the total hip BMD, positive associations were observed with intake of energy, calcium, protein, carbohydrates, vitamin A, B1, B2, C, phosphorous, iron and zinc for elderly women. For men, only intake of calcium was found to have a significantly positive association with total hip BMD.

The results suggested that dietary intake has a larger effect on BMD in elderly women than in men. However, increased calcium intake does play an important role in relationship with higher BMD in both gender although the mean dietary calcium intake in Hong Kong Chinese elderly is still below recommendation level. Further public education may be needed in this area for bone health promotion.

Disclosures: ***W.W.Y. Lau****, None.*

SU361

Assessment of Calcium and Vitamin D Intake Using a Modified Food Frequency Questionnaire in Aboriginal and White Women Residing in Manitoba: The First Nations Bone Health Study. H. A. Weiler*[1], W. D. Leslie[2], E. A. Salamon[3], P. Wood Steiman*[4], C. J. Metge*[5], C. K. Yuen[2], M. Doupe*[2], J. D. O'Neil*[2], C. R. Greenberg*[2], L. M. Lix*[2], L. L. Roos*[2], A. Tenenhouse[6]. [1]Human Nutritional Sciences, University of Manitoba, Winnipeg, MB, Canada, [2]Faculty of Medicine, University of Manitoba, Winnipeg, MB, Canada, [3]Department of Medicine, University of Manitoba, Winnipeg, MB, Canada, [4]Assembly of Manitoba Chiefs, Winnipeg, MB, Canada, [5]Faculty of Pharmacy, University of Manitoba, Winnipeg, MB, Canada, [6]Department of Medicine, McGill University, Montreal, PQ, Canada.

The Canadian Multicentre Osteoporosis Study (CaMos) used a food frequency questionnaire (FFQ) to capture calcium intake from 15 food categories. The assessment of calcium and vitamin D intake in the Manitoba First Nations Bone Health Study (FNBHS) was modified from the riginal CaMos FFQ to include food sources also culturally relevant to Aboriginal women. The FNBHS FFQ included 14 additional foods (commercially available and traditional) identified through 1-on-1 meetings and focus groups with urban and rural Aboriginal women. The objective of this study was to compare dietary calcium and vitamin D intakes obtained using the original CaMos and adapted FNBHS FFQs. Over 2 years, 199 Aboriginal and 139 White women completed a FFQ. The CaMos and FNBHS FFQs correlated well for calcium (r=0.9304, P<0.0001) and vitamin D intake (p=0.856, P<0.0001). In all analyses the FNBHS FFQ gave higher values for calcium and vitamin D intake (see table) than the CaMos FFQ, regardless of ethnicity. Foods making contributions to calcium intake (>20 mg/d) were fortified orange juice, pizza and pizza pops, other cheeses and evaporated milk. Foods making contributions to vitamin D intake (>4 IU/d) were evaporated milk, soy drink, macaroni and cheese dinner, eggs and margarine. Evaporated milk, eggs and margarine were critical for accurately assessing calcium and vitamin D intake in the northern rural Aboriginal group. Calcium intake was similar in Aboriginal and White women (T-test P>0.2), but vitamin D intake was higher in the Aboriginal women (T-test P=0.0157). This work demonstrates the importance of identifying and including food items that are culturally relevant to the study population.

Group - FFQ Used	Calcium Intake (mg/d)	P value between FFQ	Vitamin D Intake (IU/d)	P value between FFQ
All (n=338) - FNBHS FFQ	958±678	<0.001	382±471	<0.0001
All (n=338) - CaMos FFQ	758±594		226±403	
Aboriginal (n=199) - FNBHS	922±746	0.003	433±550	0.001
Aboriginal (n=199) - CaMos	715±629		234±459	
White (n=139) - FNBHS	1010±566	0.0044	308±315	0.0136
White (n=139) - CaMos	820±537		215±307	

Disclosures: ***E.A. Salamon****, None.*

SU362

Low Vitamin K Status Is Associated with Markers of Bone Turnover in Men and Women. K. M. Shedd*[1], D. M. Cheng*[2], C. M. Gundberg[3], G. E. Dallal*[1], D. P. Kiel[4], K. E. Broe*[4], B. Dawson-Hughes[1], S. L. Booth[1]. [1]Tufts University, Boston, MA, USA, [2]BU School of Public Health, Boston, MA, USA, [3]Yale University, New Haven, CT, USA, [4]Hebrew Rehab Center for Aged & Harvard Medical School, Boston, MA, USA.

Low vitamin K status has been associated with reduced bone mineral density and greater hip fracture risk in men and women. Since bone turnover is an independent predictor of fracture, we studied the association between vitamin K status and biochemical markers of bone turnover. Cross-sectional associations between markers of bone formation [Total Osteocalcin (TOC)] and bone resorption [N-telopeptide (NTx)] and biochemical measures of vitamin K status [percent undercarboxylated osteocalcin (%ucOC) and phylloquinone (K1)] were examined in 335 subjects (mean age 56y; female 38%) participating in the Offspring Framingham Heart Study (Study A), and 452 subjects (mean age 68y; female 59%) participating in a vitamin K intervention trial (Study B). In study B, all biochemical measures were made at baseline prior to randomization. In both studies TOC and %ucOC were measured by the same RIA, and K1 was measured by HPLC. In Study A, NTx was measured by RIA in urine; in Study B, NTx was measured in serum. Separate linear regression models were fitted for each marker of bone turnover. Each model included a single biochemical measure of vitamin K status and adjusted for age, weight, triglycerides, sex, and menopausal status (for Study A only as all women in Study B were postmenopausal). K1 was inversely associated with TOC in both Study A (β=-0.040, p=0.02) and Study B (β=-0.010, p=0.05), although the association was marginally significant in Study B. In both studies %ucOC, a marker of poor vitamin K status, was positively associated with NTx (β=0.008, p<0.0001 for Study A and β=0.001, p=0.002 for Study B). However, there was

no association between K1 and NTx in either study (β=-0.009, p=0.54 and β=0.002, p=0.63 for Study A and Study B, respectively). The congruency of the results obtained in these two independent studies suggests that lower vitamin K status may be associated with higher levels of bone turnover markers in men and women, and may contribute to the increased fracture risk observed in persons with lower vitamin K status.

Disclosures: ***K.M. Shedd****, None.*

SU363

Hypovitaminosis D among Healthy Adolescent Girls in the UK. J. L. Berry[1], G. Das*[2], S. Crocombe*[3], M. McGrath*[2], M. Z. Mughal[3]. [1]Vitamin D Research Group, University of Manchester, Manchester, United Kingdom, [2]Central Manchester Primary Care Trust, Manchester, United Kingdom, [3]St Mary's Hospital for Women & Children, Manchester, United Kingdom.

There has been a resurgence of vitamin D deficiency rickets among toddlers in the UK and we have recently observed an increase in the number of adolescents presenting with symptomatic vitamin D deficiency. This cross-sectional study was designed to determine the prevalence of hypovitaminosis D among healthy adolescent schoolgirls. 51 (28%) out of 182 girls [13 white Caucasian and 38 non-white; median(range) 15.3(14.7-16.6) yrs] attending year 10 of an inner city multiethnic girls' school took part in the study. We assessed their serum concentration of 25-hydroxyvitamin D (25OHD) and related it to dietary intake of vitamin D, estimated duration of sunshine exposure and the percentage of body surface area exposed (%SAE). 37 out of 51 (73%) girls were vitamin D deficient (25OHD concentrations <12 ng/ml) and 9 (17%) were severely deficient (25OHD concentrations <5 ng/ml). The median(range) 25OHD concentration of white Caucasian girls (13.2(7.3-29.3) ng/ml) was significantly higher ($p<0.001$) than that of non-white girls (5.9(2.3 to 17) ng/ml). The estimated intake of vitamin D in white Caucasian and non-white groups was 1.9µg/day and was not related to 25OHD concentration. For the whole group, 25OHD concentration was related to the estimated sunshine exposure (r=0.38; p=0.007) and %SAE (r=0.41; p=0.003). In white Caucasian girls the estimated sunshine exposure and %SAE were significantly higher than that of non-white girls, p=0.003 and p=0.001 respectively. Hypovitaminosis D is common among healthy adolescent girls; non-white girls were more severely deficient. Reduced sunshine exposure rather than diet explains the difference in vitamin D status of white Caucasian and non-white girls. Since vitamin D is essential for bone mass accrual during adolescence, vitamin D supplements should to be given to girls with reduced sunshine exposure.

Disclosures: ***J.L. Berry****, None.*

SU364

Fluoride Intake Influences Cortical Bone Characteristics in Young Children. J. M. E. Gilmore*[1], S. M. Levy[1], T. A. Marshall*[1], E. M. Letuchy*[2], T. L. Burns*[3], M. C. Willing[4], K. F. Janz*[5], J. C. Torner*[2]. [1]Preventive and Community Dentistry, University of Iowa, Iowa City, IA, USA, [2]Epidemiology, University of Iowa, Iowa City, IA, USA, [3]Public Heath Genetics, University of Iowa, Iowa City, IA, USA, [4]Pediatrics, University of Iowa, Iowa City, IA, USA, [5]Health and Sports Studies, University of Iowa, Iowa City, IA, USA.

Fluoride intake is thought to affect mineralization of both teeth and bones. Few studies have comprehensively assessed fluoride intake and related findings to bone measures. The aim of this study was to investigate the associations between fluoride intake from birth to age 5 on the cortical bone characteristics of healthy young children measured by peripheral quantitative computed tomography (pQCT) at age 9. The 189 subjects (98F/91M) are participants in the Iowa Bone Development Study, a component of the Iowa Fluoride Study (IFS). Subjects provided detailed questionnaire data 2-5 times per year concerning fluoride intake from water, beverages, selected foods, dentifrice, and dietary supplements. Individuals' multiple water sources and major beverages were assayed for F content. Cortical bone content (CRT_CNT), density (CRT_DEN), area (CRT_A) and wall thickness (CRT_THK_C) at the 20% distal radius were assessed by pQCT using the Norland Stratec XCT 2000 (software version 550, circular ring model) with a voxel size of 0.4 mm, scan speed of 20 mm/sec and a slice thickness of 2.4 mm. Fluoride intakes at 1, 3, 5 years and cumulative 1-5 year intake (AUC) were the focus of this analysis. Fluoride intake at age 5 years, but not at earlier ages was associated with cortical bone characteristics of children at age 9 years. Mean fluoride intake from all sources at age 5 years was 0.77 mg/day (range: 0.18 - 2.50). Intake at 5 years showed an inverse univariate association with CRT_DEN, CRT_A and CRT_THK_C, and a positive association with periosteal (PERI_C) and endosteal (ENDO_C) circumferences ($p < 0.10$, except PERI_C circumference $p > 0.50$). Regression models adjusted for age, gender and body size revealed fluoride intake at 5 years was predictive of CRT_DEN ($p < 0.02$, estimated $\beta = -21.47$), CRT_THK_C ($p < 0.10$, estimated $\beta = -0.12$), PERI_C circumference ($p < 0.01$, estimated $\beta = 1.00$) and ENDO_C circumference ($p < 0.05$, estimated $\beta = 1.78$). Further exploration of dietary fluoride intake and its implications for bone growth and development through adolescence is warranted.

Disclosures: ***J.M.E. Gilmore****, None.*

SU365

A Moderately Low Magnesium Diet Exerts Few Changes in the Leg Bones of Growing Rats. J. M. Welch[1], C. M. Weaver[1], J. E. Sojka*[2]. [1]Foods and Nutrition, Purdue University, West Lafayette, IN, USA, [2]Veterinary Clinical Sciences, Purdue University, West Lafayette, IN, USA.

Dietary intake of magnesium (Mg) by 14-18 year old American girls is estimated to meet only 60% of their Recommended Dietary Allowance (RDA). Although severe Mg deficiencies adversely affect the skeleton, it is unknown if these suboptimal Mg intakes are detrimental. We examined the effects of a moderately low Mg diet on the appendicular skeleton, using growing rats as an experimental model. Female F-344 rats, aged 7 weeks, were assigned to either a low Mg diet (Mg-, 0.02% Mg, n=20) or a control diet containing 100% of the Mg requirement for a rodent (Mg+, 0.05% Mg, n=22) for 8 weeks. Upon completion of the study, rats were euthanized and their leg bones removed. Mechanical strength of the ulnas was measured by axial compression, and metaphyseal and diaphyseal sites on the ulna, radius, humerus, femur, tibia, and fibula were scanned by peripheral quantitative computed tomography (pQCT). Images were analyzed for total, cortical, and trabecular volumetric bone mineral density (BMD); bone area (BA) of total bone as well as cortical, and trabecular fractions; cortical thickness, and periosteal and endosteal circumferences. Final body weight did not differ between groups. The Mg- diet resulted in small decrements in bone length (mean 1.5%) which were only significant in the ulna. Ulnar breaking strength, stiffness, and energy to failure did not differ between groups. The Mg- diet did not result in significant changes in shaft or distal sites of any bones, nor proximal sites of the lower leg bones. In the proximal femur, the Mg- diet resulted in a 4.4% (p=0.04) decrease in total BA and a 2.2% (p=0.04) decrease in periosteal circumference. Additionally, in the proximal humerus, cortical BMD decreased by 1.5% (p=0.04). This study indicates that a diet moderately low Mg, fed to female rats from early puberty through sexual maturation, did not diminish bone strength, and induced few changes in the geometry and density of the appendicular skeleton.

Disclosures: ***J.M. Welch****, None.*

SU366

Risk Factors of Bone Fractures in Bialystok Osteoporosis Study (BOS). J. E. Badurski[1], N. A. Nowak*[1], A. Dobrenko*[1], J. Supronik*[2], J. Lis*[3], S. Daniluk*[1], E. Z. Jeziernicka*[1]. [1]Centre of Osteoporosis & Osteoarticular Diseases, Bialystok, Poland, [2]Departament of Rheumatology, Sniadecki Hospital, Bialystok, Poland, [3]Medical Departament, Eli Lilly, Bialystok, Poland.

In the first part of the Bialystok Osteoporosis Study (BOS) it was proved that 14.8% (out of 727) of the women aged from 46 to 89, mean 59.3 ± 9.4, have their BMD at Femoral Neck (FN) T-score -2.5 and lower (WHO criteria of osteoporosis)[1]. 222 low energy fractures (30.5% out of 727) have been noticed, ¾ of which have affected women with BMD over FN T-score -2.5. The subject of the present analysis was risk factors of fracture influencing the BOS cohort. From among 50 potential risk factors known from other epidemiological studies, statistically significant, BMD - independent impact on increase of fracture risk are that as follow: advanced age, long-term steroid therapy, hematological diseases, poor standard of life, kidney diseases and alcohol abuse. Factors, which decreased fracture risk were: oestrogen use, breast feeding and high body mass index. Also the odds ratio (OR) of fracture was increasing as the bone mass was decreasing, the age increasing as well as hematological and kidney diseases effecting. The fracture risk was decreasing owing to good standard of life and education (using more than one source of information about osteoporosis) and childbirths. Results of our epidemiological studies, as well as Rotterdam Osteoporosis Study [2] and Study of Osteoporosis Fractures [3], lead to a conclusion that over 50% of all fractures appear among persons with FN T-score > -2.5. The generalization of BOS data on whole Polish women population would indicate the following relations between number of fractures, their frequency, bone mass and age: The number of women after menopause living in Poland in 1999 - 6 000 000, the number of women over 45 years old with FN T-score < -2,5 - 900 000 (15%), the number of all fractures among women after menopause - 1 500 000 (25%). The number of fractures appeared to be significantly bigger than the number of persons with osteoporosis according to WHO criteria. It indicates the necessity to distinction osteoporosis and fractures BMD-dependent from that of BMD-independent [4].References: [1]. Nowak NA et al:, Postepy Osteoartrol.2003,14(1):1-5

[2] Burger H, et al. (2000), Am J Epidemiol 147;9:871-879. [3] Cummings SR, et al (1995), N Engl J Med 332:767-773. [4] Badurski JE, (2003) J Bone Miner. Res.

Disclosures: ***J.E. Badurski****, None.*

SU367

The Estimation of the 5-year Probability of Fracture in a General Population of Elderly Women. T. P. van Staa[1], P. Geusens[2], H. Leufkens*[3], S. Gehlbach*[4], C. Cooper[4]. [1]Procter&Gamble Pharmaceuticals, Egham, United Kingdom, [2]Limburg University Center, Diepenbeek, Belgium, [3]Utrecht University, Utrecht, Netherlands, [4]University of Southampton, Southampton, United Kingdom.

The aim of this study was to develop a simple clinical tool for assessing 5-year risks of fractures in elderly women of a large general population.

The study population consisted of all women aged 50+ included in the THIN Research Database (THIN contains computerised medical records of all patients at general practices in the UK, similar to the UK General Practice Research Database). Women currently using oral glucocorticoids were excluded. The period of follow-up was divided into 6-month intervals, with risk factors assessed at each interval. Using Cox proportional hazards models, a risk score, indicating the association to risk, was initially estimated from age, body mass index (BMI), disease and drug history. Routine laboratory data and GP exercise assessment were also used (data available for about 8 and 25% of the records, respectively). The 5-year risk of fracture (survival function) was estimated for each sum of scores. This was done for osteoporotic (O) and hip (H) fractures. Osteoporotic fractures included radius/ulna, humerus, rib, femur/hip, pelvis and clinically symptomatic vertebral fractures.

A total of 388,533 women were included in the study (with 22,832 O and 7184 H fractures) and the average follow-up per person was 7.9 years. The risk scores are summarised in the table:

	O	H
Age 60-69 years	6	12
70-79	11	24
80-89	16	34
90+	19	38
Prior fracture	7	7
Fall history	6	6
BMI < 20	3	6
> 26	-2	-5
Early menopause	0	7
CNS medication	4	6
Hospitalisation chronic disease	4	5
Hemoglobin < 7.5 mmol/l	2	3
Albumin < 33 g/l	0	4
Lack of exercise	1	3

The 5-year risk of osteoporotic fracture for patients with scores of 20, 30, 40, and 50 was 11.1, 23.2, 44.6, and 73.4%, respectively. Hip fracture scores of 30, 40, 50, and 60 corresponded to 5-year hip fracture risks of 2.3, 5.7, 13.7, and 30.6%, respectively. For a 75-year female with low BMI and fracture and fall history, the 5-year risk of osteoporotic fracture was 18.7%. The corresponding hip fracture risk was 7.5%.

In conclusion, this risk score allows for an assessment of an individual's risk of fracture and could be used for targeting patients for further investigation, such as bone densitometry.

Disclosures: ***T.P. van Staa****, None.*

SU368

Quantitative Ultrasound of the Calcaneus but not Biochemical Markers of Bone Turnover Are Associated with Fractures in Frail Older People with Vitamin D Deficiency: The FREE Study. C. Chen*[1], M. Seibel[2], L. March*[1], I. Cameron*[1], R. Cumming*[3], P. Sambrook[1]. [1]Institute of Bone & Joint Research, University of Sydney, Sydney, Australia, [2]ANZAC Research Institute, University of Sydney, Sydney, Australia, [3]Public Health, University of Sydney, Sydney, Australia.

Background: Biochemical markers of bone turnover have been reported to predict fracture risk independent of bone mass in postmenopausal women. We investigated their use in predicting fractures in the frail elderly.

Methods: case-control study of 159 pairs of older people living in residential care facilities who were participants in the Fracture Risk Epidemiology in the Frail Elderly (FREE) study. The cases were the first 159 respondents who had sustained a fracture during study follow-up, where serum samples were available. For each case, a control was selected based on gender, age, institution type and follow-up period. We measured one bone resorption marker (carboxyterminal cross-linked telopeptide of type I collagen, ICTP) and two bone formation markers (bone alkaline phosphatase, BAP, and intact aminoterminal propeptide of type I procollagen, PINP) in serum. Bone ultrasound attenuation (BUA) was measured in the calcaneus using a McCue Cuba II machine.

Results: the mean age of subjects was 86.8 years (range 69.7-110.4; 86% female). 35% were living in nursing homes and 62% of subjects had hypovitaminosis D (25OH D < 31 nmol/L). There was no difference between cases and controls in mean serum 25OH D or PTH. There were significant differences between cases and controls for calcaneal BUA ($p < 0.01$). However, no significant differences were detected for either the resorption marker or the two formation markers between fracture cases and controls (analysed as either total fractures, vertebral or hip fractures). This was also the case after stratifying for age, gender and renal function. Only 12% of BAP values and10.6% of PINP values were above the postmenopausal reference range, however 75% of ICTP values were above the postmenopausal range. For females, significant correlates with increased ICTP, PINP and BAP included higher PTH, lower BUA and older age.

Conclusion: in the frail elderly with a high prevalence of vitamin D deficiency, calcaneal ultrasound but not biochemical markers of bone turnover are useful for predicting fractures. The lack of a biochemical response may be due to the fact that in this vitamin deficient population, bone resorption is already disturbed, possibly confounding the relationship between bone turnover and fractures seen in younger subjects.

Disclosures: ***P. Sambrook****, None.*

SU369

Incidence and Costs of Hip Fractures Compared to Acute Myocardial Infarction in the Italian Population: A 3 Years Study. P. Piscitelli[1], P. Camboa*[1], N. Rosato*[1], V. Dattoli*[1], V. Gigante*[1], E. Viola*[1], F. Fitto*[2], F. Avitto*[3], G. Termini*[4], G. Iolascon*[5], M. Rossini*[6], S. Adami*[6], G. Guida*[5], A. Angeli[7]. [1]AUSL Le/2, Maglie (Le), Italy, [2]Casa di Cura Città di Lecce, Lecce, Italy, [3]EDRA, Milan, Italy, [4]AISO, Palermo, Italy, [5]II University of Naples, Naples, Italy, [6]University of Verona, Verona, Italy, [7]University of Turin, Turin, Italy.

This is the first study aimed to analyze incidence and costs of hip fr. in Italy vs a severe-perceived disease, such as acute myocardial infarction (AMI) in people aged ≥ 45. Since Italy is a country with high life expectancy, it represents an appealing case study for age-related diseases. The study examined 3 years data (1999, 2000, 2001) from the national ICD-9CM diagnosis database. We considered codes 820.0 and 820.1 (cervical hip fr.), 820.2 and 820.3 (intertrochanteric fr.), 820.8, 820.9, 821.1 (other hip fr.) and 410 (AMI). As showed in table 1, the incidence of hip fr. increased with age and was highest in women.

Table 1. Incidence of hip fr/10.000

Age	Hip Fr. **1999**		Hip Fr. **2000**		Hip Fr. **2001**	
	M	F	M	F	M	F
45-64	3.6	4.9	3.7	4.5	3.2	4.9
65-74	13.6	30.1	13.9	29.8	14.2	29.7
75+	72.8	163.9	77.9	165.8	82.2	178.9

The incidence of hip fr. was comparable to the incidence of AMI. We observed 84,188 hip fr. vs 97,913 AMI in 2001; 79,763 hip fr. vs 89,125 AMI in 2000; 78,708 hip fr. vs 86,100 AMI in 1999. To evaluate the costs, we analyzed all the proper DRGs. Table 2 shows that **direct costs of hospitalization for hip fr. in Italy are higher than those for AMI**. Table 3 shows total costs of hip fr. in 2001 including rehabilitation and indirect costs. It confirms an exceedingly high social impact of hip fr., despite unacceptable lack in the perception of their severity.

Table 2. Direct costs (Euros) of hospitalization for hip fr. compared to AMI (overall and ≥ 65 y.o.)

YEAR	Hip Fr. ≥ 45 y.o	AMI ≥ 45 y.o	Hip Fr. >65 y. o.	AMI >65 y. o.
1999	490,800,000	450,175,000	401,800,000	296,595,000
2000	519,300,000	498,667,000	403,300,000	286,515,000
2001	*564,600,000*	*523,463,000*	**438,400,000**	**323,230,000**

Table 3. Total costs of hip fr. in elderly (year 2001)

YEAR 2001	
No. of hip fr. (>65 y.o.)	81,400
Direct costs (hospital. >65 y.o.)	438,400,000 Eur
1 month rehabilitation	416,000,000 Eur
Indirect costs	170,900,000 Eur
Total	**1,025,300,000 Eur**

Disclosures: ***P. Piscitelli****, None.*

SU370

POF1 - Incidence of Peripheral Osteoporotic Fractures Hospitalized in France during 2001. M. Maravic*[1], C. Le Bihan*[1], J. Richard*[1], P. Landais*[1], P. Fardellone[2]. [1]Service de Biostistique et Informatique Médicale, Hôpital Necker Enfants Malades (APHP), Paris cedex 15, France, [2]Service de Rhumatologie, Centre hospitalier universitaire, Amiens, France.

To describe incidence of three peripheral osteoporotic fractures (POF) (upper extremity of humerus and hip, lower extremity of radius and/or ulna) in women and men older than 45 years, hospitalized in France during 2001.

Hospitalizations for each POF in women and men older than 45 years were selected from the dataset of French private and public hospitals in 2001.

Incidence rates (CI 95%) were standardized on age and gender according to the census of French population.We analysed the effect of age (46 to 65 years versus 66 to 80 years versus ≥ 81 years) (Chi-square test, $\alpha = 0.05$) and the existence of a geographical difference between North-South and East-West (Chi-square test, $\alpha = 0.025$) on the incidence of each type of POF.

130 471 hospitalizations for POF (12% humerus, 27% radius and/or ulna et 61% hip, sex ratio 0.27) were registered.

Incidence of POF for 10^6 inhabitants (CI 95%) standardized on age and gender			
Site / gender	**46-65 years**	**66-80 years**	**≥ 81 years**
Humerus / women *	293 (280 - 306)	1366 (1331 - 1402)	3280 (3188 - 3372)
Humerus / men *	238 (226 - 250)	401 (379 - 424)	1083 (1004 - 1163)
Radius / women *	1131 (1106 - 1156)	3541 (3483 - 3598)	4921 (4808 - 5034)
Radius / men	533 (516 - 551)	490 (466 - 515)	789 (721 - 857)
Hip / women *	412 (397 - 427)	4172 (4110 - 4235)	27629 (27364 - 27893)
Hip / men *	445 (429 - 461)	2139 (2087 - 2190)	13740 (13457 - 14022)

* Incidence of POF increased significantly with age (p<0.001). We found a significantly increased of POF in the East of France compared to the West whatever the type of POF or gender and in the South compared to the North in women whatever the type of POF and in men only for hip.

This evaluation was based upon data of the French hospitals during 2001. It describes the hospital incidence rate of POF. We confirmed a significant increase of incidence with age. POF were more incident in women and geographical differences seem to exist. This method could be used for annual follow-up of POF incidence trend in France and for international comparisons.

Disclosures: ***M. Maravic****, None.*

SU371

Hip and Other Osteoporotic Fractures Increase the Risk of Subsequent Fractures in Nursing Home (NH) Residents. K. W. Lyles[1], A. P. Schenck*[2], M. A. Carlson*[1], C. S. Colon-Emeric*[1]. [1]Medicine, Duke University Medical Center, Durham, NC, USA, [2]Medical Review of North Carolina, Inc., Cary, NC, USA.

In community dwelling older adults major risk factors for hip fractures include low bone mass, falls, prior fractures, impaired vision and neurological disease. Osteoporotic fractures are also a major cause of morbidity and mortality in NH residents with a reported annual incidence of 3-6% for hip fractures. We hypothesized that prior hip and other osteoporotic fractures would be risk factors for subsequent fractures in NH residents. Using data from North Carolina Minimum Data Set (MDS) assessments of NH residents, we identified all Medicare enrollees who were in NH in 2000 (N:33,520). Using NH Medicare hospital claims from 1996-2000, we defined subjects with a prior diagnosis of hip fracture or other osteoporotic fracture (N=8667) as the study population. We followed these subjects from their entry into the nursing home until the end of 2002 using Medicare hospital claims to determine which subjects sustained a subsequent hip or osteoporotic fracture (N=4005). Cumulative percents of NH subjects in each group that suffered subsequent fractures are depicted below.

For NH residents with no osteoporotic fracture history, the cumulative percent of fractures is 7.5% over the study period, while 16.7% of NH subjects with a prior non-hip osteoporotic fracture and 25.4% of NH subjects with a prior hip fracture sustain subsequent fractures. For NH residents a prior hip fracture or other osteoporotic fracture appears to be a risk factor for further fractures.

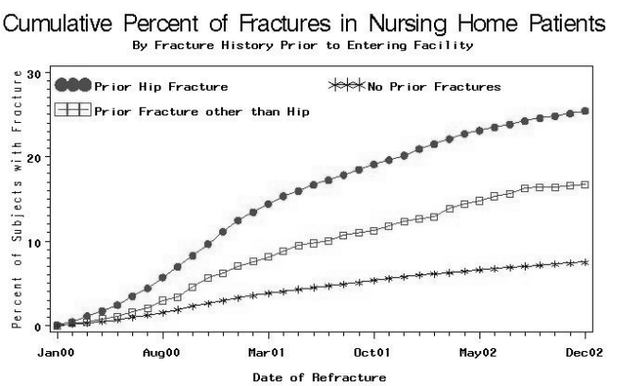

Disclosures: ***K.W. Lyles****, Procter & Gamble 2, 5, 8.*

SU372

Hip Fracture and Ethnicity in Hawaii. F. Singer[1], R. B. Tanaka*[2], F. Lurie*[3]. [1]Endocrinology and Metabolism, Straub Clinic & Hospital, Honolulu, HI, USA, [2]none, None, HI, USA, [3]Straub Foundation, Honolulu, HI, USA.

The state of Hawaii has six different ethnic groups (Black, Chinese, Filipino, Hawaiian, Japanese, and White) of sufficient size as to allow comparative study of hip fracture incidences. The Hawaii Health Information Corporation collects discharge data from all 22 acute care hospitals in the state, which allowed us to obtain information on hip fracture discharges (ICD9 820.X) and ethnicity from 1995-2001. Using available on-line U. S. Census Bureau information from the year 2000, we calculated hip fracture incidences over that period. For each ethnicity, fracture rates were determined separately for females and males in three different age groups: 60-69, 70-79, 80+ years. Using the confidence limits provided by the Census Bureau, differences between ethnicities in the six different matched age/sex categories were tested for significance. Also, we calculated that the pretest probability of one ethnic group having a higher incidence than a second in each of six age/sex-matched comparisons is 1/64. Therefore we considered the appearance of this pattern in the data to be of significance.

Results: The incidence of hip fracture in Whites was higher than each of the five other ethnic groups in each of the six age/sex-matched categories, without exception. The incidence of hip fracture in Japanese was higher than in Chinese in all six age/sex-matched categories. The risk of hip fracture in Whites was three times (p<.05) that of Filipinos, females and males, in the 70-79 year-old age group.

Significance: This study provides comparative hip fracture incidences for the largest number of different ethnic groups observed in a single location during a single time period. It confirms results from other less comprehensive studies and adds new data regarding the Filipino and Hawaiian populations. The consistency of results showing that Whites have a higher hip fracture incidence than each of five other ethnic groups suggests a change in point of view: Rather than asking the question, "Why do Japanese (or Chinese) have a lower incidence of hip fracture than Whites?" for example, we should be asking, "Why do Whites have a higher hip fracture incidence than everbody else?"

Disclosures: ***F. Singer****, None.*

SU373

Fracture Risk in Individuals 65 Years and Older: Association with Season, Snowfall and Sunshine. H. A. Bischoff-Ferrari[1], J. E. Orav*[2], J. A. Barrett*[3], M. Beach*[4], J. A. Baron*[5]. [1]Div. of Aging and Rheumatology, Brigham and Women's Hospital, Boston, MA, USA, [2]Div. of Biostatistics, Brigham and Women's Hospital, Boston, MA, USA, [3]Dept. of Community and Family Medicine, Dartmouth Medical School, Hanover, NH, USA, [4]Dept. of Anesthesiology, Dartmouth Medical School, Hanover, NH, USA, [5]Dept. of Community and Family Medicine and Dept. of Medicine, Dartmouth Medical School, Hanover, NH, USA.

Aims: To investigate seasonal variation and the association of snowfall and sunshine exposure with fracture risk in older persons. To assess seasonal variation of fracture risk in warm and cold climate states, younger and older subjects, and men and women.

Methods: In this population-based analysis, we used Medicare claims for a 5% random sample of the total US Medicare population aged 65 and older to ascertain fractures of the hip (n = 35,007), the distal forearm (n = 16,622), the proximal humerus (n = 9,708) and the ankle (n = 8,520). Weather information was obtained from the US National Oceanic and Atmospheric Administration website (www.noaa.gov). Poisson regression was used to investigate the associations of season and weather factors with fracture risk. All models were adjusted for gender, age (4-year steps) and race/ethnicity.

Results: There was a significant seasonal variation for all of the 4 types of fractures ($p < 0.0001$ for each), with the largest differences occurring between winter and summer months: a 8% increase for the rate of hip fractures, a 19% increase for distal forearm, a 20% increase in proximal humerus fractures, and a 22% increase for ankle fractures. There were winter peaks in both warm and cold climate states for each of the fractures studied and the winter peaks were larger in warm climate states than in colder states. For all fractures, winter peaks were more pronounced in men than in women, and in those younger than 80 than among those who were older. The variability between subgroups was less pronounced for hip fractures than for non-hip fractures.

In winter, snowfall was associated with a reduced risk at the hip (-9% per 10 inches) but an increased the risk of all non-hip fractures (16-34%; $p < 0.05$ at all sites). In summer, sunshine exposure was associated with a decreased risk at the hip (- 6% per week of sunny days) but an increased risk of all non-hip fractures (22%-31%; $p < 0.05$ at all sites).

Conclusion: For each of the fractures, fracture risk was increased in winter compared to summer, and this winter peak was most pronounced in warm states, in men, and individuals between 65 and 80. Our findings are consistent with the idea that hip fractures, which tend to occur indoors among relatively frail individuals, are affected differently by weather factors than the other fractures studied.

Disclosures: ***H.A. Bischoff-Ferrari****, None.*

SU374

Vitamin A Intake and Osteoporotic Fractures. H. E. Meyer*[1], G. B. Smedshaug*[1], E. Kvaavik*[2], J. A. Falch*[3], A. Tverdal*[1], J. I. Pedersen*[2]. [1]Norwegian Institute of Public Health, Oslo, Norway, [2]University of Oslo, Oslo, Norway, [3]Aker University Hospital, Oslo, Norway.

Recent observational studies suggest that moderately increased intake of vitamin A (retinol) increases the risk of osteoporotic fractures. Retinol in oil-based preparations (e.g. cod liver oil) is probably considerably less toxic than retinol in water-soluble, emulsified or solid (i.e. tablets) preparations. A possible adverse effect of retinol could be aggravated by vitamin D deficiency.

We studied the association between retinol intake and fracture risk by using data from a double-blinded randomized controlled trial studying the effect of vitamin D supplementation on fracture risk (1). The study commenced prior to reports of a possible harmful effect of moderately increased intakes of retinol.

The study population consisted of 1144 nursing home residents. The intervention group received ordinary cod liver oil, while the control group received cod liver oil without vitamin D. During the 2 years study period, 76 persons in the control group and 69 persons in the intervention group suffered a nonvertebral fracture, and as previously published there was no difference in fracture incidence between the vitamin D group and the control group (1). The participants were not randomized to different doses of retinol. However, as cod liver oil also contains retinol, both the control group and the vitamin D group received retinol (1.3 mg per daily dose of 5 ml). In addition, around 40 % of the participants took multivitamin supplements at baseline, typically containing around 0.8 mg retinol and 10 µg vitamin D. No attempt was made to stop this supplementation as we found it unethical to do so in this frail population. Those who received retinol both from cod liver oil and supplements thus had an intake of approx. 2.1 mg/d from these sources.

We did not find any difference in fracture risk between those with a moderate intake of retinol and those with a high intake of retinol, irrespective of vitamin D intake from supplements (ranging from 0 to 20 µg/day). For example, the relative risk of any non-vertebral fracture was 1.08 (95% CI 0.67-1.72) in those with a retinol intake of 2.1 mg/day and a vitamin D intake of 10 µg/day compared to those with a retinol intake of 1.3 mg/day and a vitamin D intake of 10 µg/day. Similarly, there was no significant association between retinol intake and hip fracture.

In summary, we did not find any association between a high retinol intake and fracture at two-year follow-up of a cohort of frail elderly.

Ref 1: Meyer HE, Smedshaug GB, Kvaavik E, Falch JA, Tverdal A, Pedersen JI. Can vitamin D supplementation reduce the risk of fracture in the elderly? A randomized controlled trial. J Bone Miner Res. 2002;17:709-715.

Disclosures: ***H.E. Meyer****, None.*

SU375

Recent Trend in the Incidence of Hip Fracture in Tottori, Japan. H. Hagino[1], H. Katagiri[2], T. Okano[2], R. Teshima*[2]. [1]Rehabilitation Division, Tottori University, Yonago, Japan, [2]Department of Orthopedic Surgery, Tottori University, Yonago, Japan.

OBJECTIVE: The purpose of this study was to investigate the recent trend in the incidence of hip fracture in Tottori Prefecture, Japan.

METHODS: Tottori Prefecture is located in mid western Japan and its population was 613,097 in 2001. The percentage of the total population aged 65 years and over was 22.5% in 2001. A survey of all hip fractures in patients 35 years old and over during 1998-2001 was performed in all hospitals in Tottori Prefecture, Japan. Registration information included name, gender, age, place of residence, date of fracture, type of fracture, and treatment. Patients residing in other prefectures were excluded. Duplication of cases was checked by the patients' name and address. The age- and gender- specific incidence rates (per 100,000 person-years) were calculated based on the population of Tottori Prefecture in each year. We compared the data with those in1986-1988 and 1992-1994 when we performed the same survey in Tottori.

RESULTS: Registered numbers in patients were 604, 671, 710 and 729 in 1998, 1999, 2000, and 2001, respectively. The mean age- and gender-specific incidence rates for men in 1998-2001 were 209.0, 449.1, and 780.0 in the age groups of 75-79, 80-84 and over 84, respectively, and those for women were 505.8, 1115.4, and 2066.4, respectively. The incidences age-adjusted to the population structure of 1986 in Tottori Prefecture (≥35 years) for men were 63, 68, 85, 87, 71, 88, 77, 86, 99, and 101, in 1986, 1987, 1988, 1992, 1993, 1994, 1998, 1999, 2000, and 2001, respectively. Those for women were 209, 206, 245, 281, 238, 266, 296, 307, 310, and 309, respectively. The incidence rates for both genders increased significantly from 1986 to 2001; however, the increase was leveled off after 1999.

CONCLUSION: An increase in the incidence rates of hip fractures was observed from 1986 to 2001, but the incidence reached a plateau until 2000 in Tottori Prefecture, Japan.

Disclosures: ***H. Hagino****, None.*

SU376

High Prevalence of Fracture in Young Adults with Cystic Fibrosis. C. C. Kennedy*[1], A. Papaioannou[1], G. Ioannidis*[2], C. Webber*[3], M. Pui*[3], J. O'Neill*[3], R. Hennessey*[2], S. Hansen*[2], A. Freitag*[1], J. D. Adachi[1]. [1]Medicine, McMaster University, Hamilton, ON, Canada, [2]McMaster University, Hamilton, ON, Canada, [3]Radiology, McMaster University, Hamilton, ON, Canada.

Patients with Cystic Fibrosis (CF) may be at increased risk for fracture due to CF-related bone disease. In this multi-year study in a non-transplant CF cohort, changes in bone mineral density (BMD) and fracture were assessed longitudinally. All adult patients ≥18 years who attended the CF Clinic in Hamilton, Ontario during 2002 and had undergone at least one chest radiograph or dual x-ray absorptiometry (DXA) scan were included in the study. Of 56 individuals, 1 was excluded due to no radiographic data, and 3 were excluded due to a past lung transplant. Chest x-rays and DXA scans were reviewed for the remaining 52 patients. BMD was measured using a Hologic QDR 4500A densitometer at the whole body, proximal femur and lumbar spine. Posterior-anterior and lateral chest x-rays were independently reviewed by two radiologists using Genant's semi-quantitative method, and differences resolved by consensus. Relevant laboratory, spirometry and medication variables were abstracted from clinic charts. The mean (standard deviation [SD]) age of the patients at baseline was 25.2 (9.4) years, mean body mass index (SD) was 20.9 (4.4) kg/m^{2}and 54% were women. At baseline, mean (SD) BMD in g/cm^2 at the whole body, left and right proximal femur, and lumbar (1-4) spine was 1.120 (0.097; n=46), 0.908 (0.126; n=42), 0.894 (0.133; n=43), and 0.972 (0.119; n=46) respectively. Over an average (SD) follow-up of 4.01 (1.45) years, the mean BMD % change at the four skeletal sites was -1.66% (n=34), -2.21% (n=30), -2.49% (n=31), and 0.06 % (n=34) respectively. At baseline, chest x-rays indicated that 16.3% (8/49) of individuals had a grade 1 vertebral fracture. After a mean (SD) follow-up of 3.3 (1.4) years, prevalence of Grade 1 fracture increased to 21.3% (10/47). In this population of young adults with CF, we found a high prevalence of Grade 1 fracture. Although there has been evidence that individuals pre and post-transplant have a high prevalence of vertebral fractures, there has been no previous evidence that individuals across the spectrum of illness severity with CF are at risk for vertebral fractures. Further research is needed to understand the pathophysiology and treatment of CF bone disease in this high-risk population.

Disclosures: ***A. Papaioannou****, None.*

SU377

High Incidence of Prevalent Fractures in Patients on Chronic Glucocorticoids Despite Normal BMD. N. Lane[1], S. Goldring*[2], S. Broy*[3], J. Stewart*[4], S. Meeves*[4]. [1]Dept of Med, Univ of California, San Francisco, San Francisco, CA, USA, [2]Rheumatol, Beth Israel Deaconess Med Cen, Boston, MA, USA, [3]Illinios Bone & Joint Institute, Des Plaines, IL, USA, [4]Aventis, Bridgewater, NJ, USA.

The ACTIVATE study is designed to determine if providing patients with information on vertebral fractures by instant vertebral assessment (IVA, Hologic) and bone turnover markers affect compliance with risedronate therapy in patients taking oral glucocorticoids (GCs). This ongoing study enrolled 2 groups: patients taking chronic GCs for at least 6 months (treatment, TREAT) or initiating GC therapy (prevention, PREV). The TREAT group accounts for 76% of patients enrolled (261/344). TREAT patients had a mean age of 60.7 yrs (range 27-85) and received 12.8 mg/d GC (range 4.0-90.0; median 10.0) for 78.3 months (range 1-546; median 34); 53.6% were women. Rheumatoid arthritis (41.5%) and polymyalgia rheumatica (12.4%) were the most common diagnoses. Baseline data were evaluated to assess use of oral calcium (Ca) in patients on chronic GC therapy. Baseline T-scores and vertebral fractures were analyzed for those taking or not taking Ca.

At baseline, T-scores for the TREAT group were in the normal range (total hip -0.73; spine -0.84). By IVA, 19.3% (27/140) of women and 23.1% (28/121) of men in TREAT had at least 1 vertebral fracture at baseline (range 0-8 fractures). T-scores were similar between patients who had or did not have a fracture (lumbar spine fracture: No -0.84±1.49; Yes -0.87±1.59; *P*=0.86; hip fracture: No -0.70 ±1.09; Yes -0.91 ±1.10; *P*=0.14).Older age and rheumatoid arthritis were significant predictors of prevalent baseline fracture.

Patients taking Ca supplements had a slighter build: shorter height (165.4 vs 168.4 cm; *P*<0.05), lower weight (80.0 vs 87.2 kg; *P*<0.05), and smaller wrist circumference (16.4 vs 17.1 cm; *P*<0.05). Despite a similar incidence of prevalent fractures, men were less likely to be taking Ca supplements (40.5% men, 60.7% women, *P*<0.05). Ca supplements were less likely to be taken by rheumatoid arthritis patients (31.3% vs 43.5%; *P*<0.05). Baseline fracture incidence was similar across Ca supplementation subgroups [No Ca 20.8% (30/152); Ca 22.4% (24/107)].

According to current guidelines all patients receiving chronic GCs should receive Ca supplementation. Here, Ca utilization was not balanced, with slighter build patients and women more likely to be taking supplements. Despite normal T-scores, prevalent vertebral fractures were found in 20% of TREAT patients at study entry. These data highlight limitations of BMD T-score cut offs commonly used in postmenopausal osteoporosis to identify patients at risk for fracture on GCs, and the need for better education concerning prevention of fracture.

Disclosures: ***N. Lane****, Aventis 5.*

SU378

Fracture Burden Contributed By Women With Osteopenia: Geelong Osteoporosis Study. J. A. Pasco[1], M. J. Henry*[1], E. N. Merriman*[1], G. C. Nicholson[1], E. Seeman[2], M. A. Kotowicz[1]. [1]Clinical & Biomedical Sciences: Barwon Health, The University of Melbourne, Geelong, Australia, [2]Medicine, The University of Melbourne, Heidelberg, Australia.

The purpose of this study was to quantify fracture risk associated with normal, osteopenic and osteoporotic areal bone mineral density (BMD) based on WHO criteria. This prospective analysis follows 628 postmenopausal women (median age 74.0 yr, range 60-94) who had BMD assessments 1994-7. 37.1% had normal BMD at the total hip, 48.2% were osteopenic and 14.8% osteoporotic. Subjects were followed until the end of 2002, or until sustaining a fracture, death, or migration from the study region. Post-baseline fractures were identified radiologically.

During the study period 66 women died, 25 left the region, 144 sustained at least one fracture and 393 remained fracture-free, alive and residing in the region, generating 3220 person years of follow-up. After 5 years, the proportion of fractures occurring in each category of BMD was 17.0% normal, 54.2% osteopenia and 28.8% osteoporosis. Using Cox proportional hazards models, both decreasing BMD and increasing age contributed

independently to increased fracture risk. Categorizing age into groups 60-69, 70-79 and 80+ yr, and setting 60-69 yr with normal BMD as the referent group, relative risk (RR) for fracture for the osteopenic women was 2.7 (95%CI 1.1-6.6) for 60-69 yr, 4.7 (2.1-10.9) for 70-79 yr and 6.1 (2.7-14.1) for 80+ yr; RRs for the osteoporotic women were 6.1 (1.8-20.8), 6.2 (2.3-16.8) and 9.3 (4.0-21.8), respectively (all p<0.05). Thus, osteoporotic women have the greatest risk for fracture and this risk increases with age. The RR for fracture among osteopenic women is intermediate between osteoporotic and normal women.
Although women with osteoporotic BMD are at greater risk for fracture, they contribute less than a third to the total burden of fractures occurring in the community. Over half of the fractures arise from women with BMD in the osteopenic range who represent approximately 50% of the population at risk.

Disclosures: ***J.A. Pasco****, None.*

SU379

Kyphoplasty Restores More Vertebral Height Than Hyper-extension Positioning Maneuvers Alone. S. V. Bukata, J. Koob*, M. Shindle*, J. M. Lane. Orthopaedics, Hospital for Special Surgery, New York, NY, USA.

Kyphoplasty has been shown to restore vertebral height and sagital alignment. Proponents of vertebroplasty have recently demonstrated that many vertebral compression fractures are mobile and positional correction can lead to clinically significant height restoration. To test the hypothesis that positional maneuvers are statistically inferior to kyphoplastic balloon tamps for the reduction of low energy vertebral compressions fractures, a prospective radiographic analysis of 25 consecutive patients with a total of 43 osteoporotic vertebral compression fractures was performed. Patients were were sequentially evaluated for postural and balloon reduction of their vertebral compression fractures. Preoperative standing and lateral radiographs of the fractured vertebrae were compared with prone cross-table lateral radiographs with the patient in a hyper-extension position and on pelvic and sternal rolls. Following positional manipulation patients underwent a unilateral balloon kyphoplasty. Postoperative standing radiographs were evaluated for percent of height restoration related to positioning and balloon kyphoplasty. In the central portion of the vertebrae, the percent restoration with extension positioning was 10.4%, median=11.1%, and after balloon kyphoplasty was 57.0%, median=62.2 (p<0.001). Thus, kyphoplasty provided an additional 46.6% restoration from the positioning alone. With operative positioning, 51.2% of vertebral compression fractures had >10% restoration of the central portion of the vertebral body as compared with 90.7% after balloon kyphoplasty (p<0.002). Although this study supports the concept that many vertebral compression fractures can be moved with positioning, balloon kyphoplasty enhanced the height reduction >5 fold over the positioning maneuver alone and accounted for over 75% of the ultimate reduction. If height restoration is the goal, kyphoplasty is clearly superior in most cases to the positioning maneuver alone.

Disclosures: ***S.V. Bukata****, None.*

SU380

Low Serum Albumin Levels Predict Incident Vertebral Fractures. J. Finigan[1], A. Chines[2], I. Barton[3], R. A. Hannon[1], R. Eastell[1]. [1]University of Sheffield, Sheffield, United Kingdom, [2]Procter and Gamble Pharmaceuticals, Cincinnati, OH, USA, [3]Procter and Gamble Pharmaceuticals, Egham, United Kingdom.

In an earlier small prospective study, we observed that indicators of frailty such as low serum albumin, low serum thyroid hormone T3 and poor physical strength predicted vertebral fracture but not non-vertebral fracture. This analysis aims to examine the relationship between baseline levels of serum albumin and the incidence of vertebral fractures in a larger cohort.
The subjects were postmenopausal women from the placebo arms of the VERT and HIP trials of risedronate in North America, Europe and Australia. Paired evaluable spinal radiographs at baseline and 3 years were available for 2720 subjects (VERT n=1022, HIP n=1698), mean age 74.1 years. Of these, 2289 had baseline BMD measurements by DXA at the femoral neck. Incident vertebral fractures at T4-L4 were assessed by both quantitative and semi-quantitative methods. Serum albumin was measured at baseline. Data for incident non-vertebral fractures were also available for these subjects and for a further 1636 subjects, of whom 1090 had BMD measurements at the femoral neck. Overall, mean age was 75.5 years (n=4356).
At 3 years, 381 subjects had one or more incident vertebral fractures. The range of albumin values was 29 to 50 g/l (mean 40.9g/l, SD 3.0 g/l). By logistic regression, the unadjusted relative risk of vertebral fracture for each standard deviation decrease in serum albumin was 1.19, 95% CI (1.07, 1.32), p=0.002. In this cohort there was no association between age and incidence of vertebral fracture, but age was inversely related to albumin levels (p=0.028, Spearman's rho = -0.042). Although low femoral neck BMD predicted vertebral fractures (RR=1.89, 95% CI (1.57, 2.27), p<0.001) there was an inverse correlation between femoral neck BMD and serum albumin (p<0.001, r = -0.077). In a multiple stepwise logistic regression, the relative risk of vertebral fracture for each standard deviation decrease in serum albumin, when adjusted for femoral neck BMD, weight and age, was 1.23, 95% CI (1.10, 1.38), p<0.001.
Low serum albumin was not associated with an increased risk of incident non-vertebral fractures in the whole group (n=4356). In the group with data on incident vertebral fractures (n=2720), low serum albumin predicted non-vertebral fracture with an unadjusted relative risk of 1.13, 95% CI (1.01, 1.27), p=0.039. However, when adjusted for femoral neck BMD, weight and age, the association was no longer significant.
We conclude that incident vertebral fractures are predicted by low serum albumin levels. Since serum albumin can be regarded as a marker of frailty, this may indicate that relatively poor health is a risk factor for vertebral fracture.

Disclosures: ***J. Finigan****, None.*

SU381

Validation of Lateral DXA Imaging for Assessment of Vertebral Fractures. C. Wu*[1], H. Genant[1], G. von Ingersleben[1], Y. Chen*[2], C. Johnston*[2], M. Econs*[3], N. Binkley*[4], T. Vokes*[5], T. Fuerst[1], G. Crans*[6], B. Mitlak*[6]. [1]Synarc, Inc., San Fran, CA, USA, [2]UCSF, San Fran, CA, USA, [3]IN Univ., Indianapolis, IN, USA, [4]U of WI, Madison, WI, USA, [5]U of Chicago, Chicago, IL, USA, [6]Lilly Research Labs, Indianapolis, IN, USA.

Standardized visual identification of radiographically depicted vertebral fractures is an established method in osteoporosis research. Lateral spine images from fan-beam dual x-ray absorptiometry (DXA) scanners present an alternative to radiography to detect vertebral fracture. We investigated the utility of lateral DXA imaging combined with visual scoring, Vertebral Fracture Assessment (VFA), by a comprehensive analysis of intra- and inter-reader variation in comparison with radiography.
Study consists of 203 postmenopausal women, enriched for vertebral fractures, each had imaging of lateral spine by DXA using Hologic or GE Lunar scanners and radiography within a short time of each other. Three radiologists expert in vertebral fracture assessment read VFA images and radiographs using Genant semiquantitative method. Assessments were performed independently with radiologists blinded to results when assessing other modality. The radiologists performed second reading of all images 2-3 weeks after the first. Gold standard (GS) readings for each modality were generated. Ability to detect vertebral fracture on VFA images was compared to radiography excluding non-evaluable vertebrae using inter-reader/modality, intra-reader, Kappa statistics, percentage agreement (%), sensitivity (SE), specificity (SP) and positive/negative predictive value (PPV, NPV).
On VFA images 76-89% of vertebral bodies could be assessed while over 98% were evaluable on radiographs. Vertebrae that couldn't be assessed were predominantly at T4-T6 levels. In these 203 women overall prevalence of vertebral fracture was 109/110 (4.1%/4.2%) in the two GS X-Ray, and 82/84 (3.6%/3.6%) in the two GS VFA. Prevalence of only moderate and severe fractures was 51/53 (2.3%/2.3%) in GS X-Ray, and 62/62 (2.8%/2.7%) in GS VFA, respectively.

Inter-Modality, Inter- and Intra-Reader Agreements (1st reading | 2nd reading)

	Inter-Modality		Inter-Reader
VFA Images	0.64-0.69 | 0.65-0.77	0.62-0.74 | 0.63-0.71	0.73-0.88
Radiographic Images		0.75-0.82 | 0.76-0.82	0.81-0.85

Gold Standard VFA versus Gold Standard X-Ray (1st reading | 2nd reading)

	Kappa	Agree (%)	SE (%)	NPV (%)
All fracture grades	0.74 | 0.78	98 | 98	70 | 73	99 | 99
Mod. & Sev. only	0.81 | 0.85	99 | 99	90 | 92	100 | 100

While VFA image quality is inferior to radiography visual detection of vertebral fracture is feasible, and correctly identifies most moderate and severe fractures. For evaluable vertebrae, VFA performance approaches that of radiography. This DXA-based method may provide an important tool for clinical practice and research.

Disclosures: ***C. Wu****, None.*

SU382

Fracture Rate in Perimenopausal Women Is not Dependent on Previous Change in Bone Mineral Density. Preliminary Results from Prospective Population-Based Study. J. Huopio*[1], H. Kroger[1], R. Honkanen[2], S. Saarikoski*[3], E. Alhava*[4]. [1]Department of Surgery, Kuopio University Hospital, Kuopio, Finland, [2]Bone and Cartilage Research Unit, University of Kuopio, Kuopio, Finland, [3]Department of Obstetrics and Gynaecology, Kuopio University Hospital, Kuopio, Finland, [4]Department of Surgery, University of Kuopio, Kuopio, Finland.

Low bone mineral density (BMD) has been shown to predict future fractures in elderly and in perimenopausal women. Thus, the aim of osteoporosis treatment is targeted to elevate BMD in order to reduce the fracture rate. However, there are no prospective data of how well a change in BMD influences the fracture incidence in perimenopausal women. In the present study we followed 2939 perimenopausal women (mean age at the baseline 59.1 yrs, SD 2.9) for a mean follow-up time of 2.9 yrs (SD 0.9) and all fractures during the follow-up were registered by a questionnaire and validated by radiological report perusal. These women had undergone two consecutive BMD measurements (Lunar DPX) of lumbar spine and femoral neck prior the follow-up period. The mean time between BMD measurements was 5.8 yrs (SD 0.5) and the mean percentual changes in lumbar spine and femoral neck BMD were -1.8 (SD 6.5) and -3.0 (SD 5.7) prior the follow-up. The BMD change was positive in 34 percent of women in lumbar spine and in 26 percent in femoral neck. The weight change correlated significantly (p<0.001) with the BMD change. Altogether, a total of 200 fractures were registered during the follow-up period. The first fracture was taken as the end point in the statistical analyses. BMD change prior to follow-up had no effect on subsequent fracture rate. Follow-up fracture rates were 6.3% and 7.0% in women with positive and negative femoral neck BMD change, respectively (p=0.46 between the groups). Similarly, when the study population was divided into four subgroups according to the amount of change in BMD (1= more than -10% change, 2 = change from 0 to -9.9%, 3 = change from 0 to 9.9% and 4 = change more than 10 %) we still could not see any difference in the fracture rate. We conclude that the change in axial BMD is not associated with fracture rate in perimenopausal women during a short follow-up period.

Disclosures: ***J. Huopio****, None.*

SU383

Fragility Fractures in People with Developmental Disabilities: Risk Factor Analysis. B. Roe*[1], K. Dittberner*[2], W. D. Leslie[1]. [1]Medicine, U of Manitoba, Winnipeg, MB, Canada, [2]St. Amant Center, Winnipeg, MB, Canada.

The impact of osteoporotic fractures on morbidity and mortality in the general population is well-described, and there are effective interventions to prevent fractures in individuals at risk. A population at particular risk includes persons with moderate to severe developmental disabilities, where fractures have been described with minimal or no trauma. A review was conducted of 224 persons with developmental disabilities living in a residential care facility, and found that 40 had sustained a low energy fracture. In total, there were 47 fractures documented, and these were confined to the appendicular skeleton. Demographic information, medication use, and other risk factor data was extracted by chart review, and anthropometric measurements were obtained. Univariate analysis demonstrated higher fracture rates associated with Aboriginal ethnicity (p=0.001), use of anti-epileptic drugs (specifically phenobarbital, p=0.004) and triceps skinfold thickness (p=0.059). Logistic regression demonstrated that the strong association between Aboriginal ethnicity and fractures was not accounted for by other measured variables (adjusted odds ratio [OR] 3.03, 95% CI 1.38-6.69). Phenobarbital use was also a strong independent predictor (OR 2.69, 95% CI 1.18-6.12). The association with anti-epileptic drugs including phenobarbital has been described in an ambulatory population, and has been attributed in part to changes in vitamin D metabolism. The basis for the strong association with Aboriginal status is not clear, and will require further study. The recognition of the high rate of fractures in this population as well as these risk predictors, should lead to increased vigilance for screening, consideration of vitamin D supplementation, and targeted interventions for those found to be at highest risk.

Disclosures: ***B. Roe****, None.*

SU384

Relationship between Endogenous Hormones and Calcium Absorption in Older Women. S. Goldman[1], J. A. Cauley[1], J. Zmuda[1], K. Ensrud[2]. [1]Epidemiology, University of Pittsburgh, Pittsburgh, PA, USA, [2]Epidemiology, University of Minnesota, Minneapolis, MN, USA.

Low levels of fractional calcium absorption (FCA) have been linked to increases in hip fractures. FCA declines with increasing age and menopause. Endogenous sex steroids, calcitropic, and thyroid hormones may underlie these observations. In the present analysis, we tested the hypothesis that serum concentrations of endogenous sex steroids, calcitropic hormones, and thyroid stimulating hormone (TSH) are associated with FCA. The study population included 729 randomly chosen Caucasian women age 65 years and older (mean age 76.3 ± 4.5 years) enrolled in the Study of Osteoporotic Fractures. Women who reported use of hormone replacement therapy that included estrogen at the 4th visit were eliminated resulting in a final sample of 595 women. Serum hormones were measured in frozen samples obtained at baseline and FCA concentration was measured at the fourth visit (average time 6 years later) using a 3-hour single isotope (^{45}Ca) technique. After adjustment for age, weight, weight change between visit 1 and 4, daily dietary calcium intake, calcium and vitamin D supplements lower levels of FCA were found associated with TSH levels <0.9 µU/ml and levels ≥ 2.6 µU/ml. Lower FCA levels were found associated with lower levels of 1,25(OH)$_2$D (<31 pg/ml) (Table). No association was found with serum estrogen, total testosterone, free testosterone, parathyroid hormone (PTH), SHBG, or 25(OH)D.
In conclusion, women with lower serum concentrations of 1,25(OH)$_2$D had lower calcium absorption efficiency compared to women with higher concentrations of this hormone. Additionally, an association between TSH and FCA has not previously been reported in humans prior to this. Although our sample size was small, this association warrants further investigation. Finally, it must be recognized that the 6 year average time interval between measurement of the hormones and FCA could affect the relationships noted.

FCA by Hormone Quartile

Hormone	1 (low)	2	3	4 (high)	p [1]
(mean FCA)					
Estradiol(ng/dl)					
(n=495)	0.38	0.38	0.38	0.38	0.99
Tot Test (ng/dl)					
(n=577)	0.37	0.39	0.37	0.38	0.46
Free Test (ng/dl)					
(n=577)	0.37	0.39	0.37	0.39	0.15
SHBG (ug/dl)					
(n=578)	0.39	0.38	0.38	0.37	0.49
TSH (µUml)					
(n=188)	0.34	0.41	0.39	0.36	<0.00
PTH (pg/ml)					
(n=188)	0.36	0.38	0.38	0.39	0.42
25(OH)D(ng/ml)					
(n=187)	0.39	0.38	0.39	0.35	0.19
1,25(OH)$_2$D (pg/ml)					
(n=187)	0.36	0.36	0.37	0.42	0.01

[1] p values represent differences among quartiles

Disclosures: ***S. Goldman****, None.*

SU385

Longitudinal Study of Bone Mineral Density among Postmenopausal Japanese Women. S. Honda[1], M. Tagawa*[2], K. Aoyagi[3]. [1]Radiation Epidemiology, Nagasaki University, Nagasaki, Japan, [2]Nagasaki A-Bomb Casualty Council, Nagasaki, Japan, [3]Public Health, Nagasaki University, Nagasaki, Japan.

Osteoporosis is considered to be a major health problem for postmenopausal women, because osteoporotic fracture can cause substantial limitation of activity of daily living. To investigate the reduction in bone mineral density (BMD) with aging in postmenopausal women, a longitudinal study was conducted among community-dwelling Japanese women. A total of 195 women, aged from 50 to 69 years old, underwent a baseline survey between May 1994 and April 1995. The mean age of study subjects was 60 (standard deviation (SD) 5.4) years old. In the baseline survey, information about lifestyle factors, menopausal status and medical history of osteoporosis were collected. Those who had been treated for osteoporosis were excluded from the subjects. A body mass index (BMI) was calculated as weight (kg) divided by square of height (m). The BMD of anterior-posterior lumbar spine (L2-L4) was measured by dual-energy X-ray absorptiometry (Hologic QDR 2000). We measured BMD repeatedly until April 2004. The mean number of measurements for each subject was 3.1 (SD 1.6) times and the mean length of follow-up was 5.4 (SD 2.8) years. Association of BMD with age, years since menopause and BMI were analyzed by the Spearman's correlation coefficient (r). Distribution of BMD was compared among lifestyle factors by the Wilcoxon rank-sum test. The change of BMD between the baseline and the end of follow-up was analyzed by the signed rank-sum test. The longitudinal change of BMD was analyzed by linear regression model with age, square of age, years since menopause, BMI and lifestyle factors.
At the baseline, BMD correlated negatively with age ($r = -0.29$, $p < 0.001$) and years since menopause ($r = -0.25$, $p < 0.001$), while BMD correlated positively with BMI ($r = 0.22$, $p = 0.002$). BMD was higher in those who took a walk more than an hour regularly compared with those who did not ($p = 0.04$). However, no significant association of BMD with smoking habit, drinking habit and dietary calcium intake was observed. At the end of follow-up, BMD decreased from 0.796 to 0.784. A significant reduction in BMD was observed in those who were aged 50-54 years old at the baseline (from 0.862 to 0.814, $p < 0.001$) and in those who were aged 55-59 (from 0.807 to 0.791, $p = 0.04$), while BMD did not change significantly in those who were aged 60-69. Linear regression analysis confirmed that BMD reduced quadratically with age, however years since menopause, BMI and lifestyle factors did not have significant impact on the reduction in BMD.
In conclusion, BMD reduces significantly in those who were aged 50-55 years old. Further studies about longitudinal change of BMD and life style factors are needed.

Disclosures: ***S. Honda****, None.*

SU386

The Effects of Ovariectomy on Bone Quality of Bax-deficient Mice. L. M. Wise*[1], A. Jurisicova*[1], G. Perez*[2], J. Tilly*[2], M. D. Grynpas[1]. [1]Mount Sinai Hospital and University of Toronto, Toronto, ON, Canada, [2]Massaschusetts General Hospital, Harvard Medical School, Boston, MA, USA.

Bax, a pro-apoptotic member of the Bcl-2 gene family, has been previously implicated in the regulation of ovarian life span. While young Bax-knockout (KO) female mice posses three times as many primordial follicles as do wild-type (WT) mice, they do not exhibit a bone phenotype. Aged KO females retain their ovarian function to advanced chronological age, which is accompanied by elevated Bone Mineral Density (BMD) values in comparison to WT age-matched females. These age-dependent differences are also observed through mechanical testing on excised bones. To determine whether the effects of Bax-deficiency are dependent on ovarian cell function, a group of KO (n=10) and WT (n=7) mice were ovariectomized (OVX) at 3 months and were analyzed and compared to age-matched control KO (n=10) and WT (n=12) mice at 7 months. Dual energy x-ray absorptiometry (DEXA) was performed on all mice to determine BMD and tissue composition. To evaluate mechanical properties, 3-point bending, torsion testing, and femoral neck fracture were performed on the femurs, while unilateral compression was performed on the 5th lumbar vertebrae. Structural parameters were evaluated using histomorphometry on sections of distal femora.
The expected reduction in BMD due to OVX was observed in both the WT (-10.8%) and KO (-11.1%) mice. However, the percent fat mass of the KO mice seemed to be significantly less affected compared to the WT mice (0.5% versus 18.1% change). Failure tests on cortical bone indicate that the OVX reduced some mechanical properties in both WT and KO mice. Nonetheless, the OVX-KO mice still have superior mechanical strength compared to the OVX-WT mice (p=0.02). The OVX caused minimal changes in the mechanical properties of the trabecular bone of both WT and KO mice. Trabecular number (Tb.N) was decreased due to OVX in both WT (-34%) and KO (-28%); however, KO mice had greater Tb.N compared to WT mice, in both control (36%) and OVX (41%) groups. Similarly, trabecular separation was lower in KO mice compared to WT mice, in both control (-35%) and OVX (-49%) groups. While the OVX had similar negative effects in bone of both WT and KO mice, the KO bone maintains superior bone quality. Since the bone phenotype is partially maintained when ovary influence is removed, it appears that Bax may have a direct effect on bone cells. The material properties of bone will be evaluated further through mineralization and collagen analyses. By investigating the interactions between mechanical, structural and material properties of bone, some of the direct effects of deregulated cell death on overall bone quality can be determined.

Disclosures: ***L.M. Wise****, None.*

SU387

Use of Oral Conditions to Screen for Low Bone Mineral Density in Japanese Women. K. Inagaki*[1], Y. Kurosu*[1], N. Yoshinari*[1], T. Noguchi*[1], E. A. Krall[2], R. I. Garcia*[2]. [1]Dept. of Periodontology, Aichi-Gakuin University, Nagoya, Japan, [2]Dept. of Health Policy and Health Services Research, Boston University, Boston, MA, USA.

The relationships between oral disease indicators and bone mineral density at several skeletal sites have been studied by a number of investigators, with mixed and complex results. The purpose of the present cross-sectional study was to evaluate the associations of periodontal conditions and tooth loss with metacarpal bone mineral density (m-BMD) in a large community-based cohort and evaluate the usefulness of tooth count as a potential simple screening tool to detect low BMD. Subjects were 356 Japanese women (171 premenopausal, mean age 37.9 ± 8.0, 185 postmenopausal, mean age 63.3 ± 7.7). Periodontal status was evaluated by the Community Periodontal Index of Treatment Need (CPITN). M-BMD was measured by computed X-ray densitometry. The proportion of subjects with periodontitis (CPITN 3 or 4) increased as m-BMD decreased. The odds ratio of osteopenia or osteoporosis in relation to periodontitis was 3.2 (95% confidence interval (CI) = 2.0 to 5.3). After adjustment for age and menopausal status, the odds ratio was 2.0 (95% CI = 1.1 to 3.7). Among postmenopausal women, those having fewer than 20 teeth were 1.6 times more likely to have low m-BMD compared to those having more than 20 teeth (Chi-square for trend in postmenopausal group = 4.27, $p < 0.05$). ROC analysis indicated that number of teeth remaining or CPITN score had better than 50/50 chance to correctly identify women with osteoporosis or osteopenia, but the areas under the curve (0.72 and 0.67, respectively) are considered only fair screening tools. These results indicate that periodontitis and tooth loss after menopause may be useful indicators of m-BMD loss in Japanese women but more research is needed.

Disclosures: ***K. Inagaki****, AGU High-Tech Research Center Project from the Japanese Ministry of Education, Science, Sports and Culture 2.*

SU388

Postmenopausal Osteoporosis Screening Tool (POST) - Preliminary Data. J. Sirola*[1], M. Tuppurainen[1], J. S. Jurvelin*[1], H. Kröger[2]. [1]Bone and Cartilage Research Unit, University of Kuopio, Kuopio, Finland, [2]Department of Surgery, Kuopio University Hospital, Kuopio, Finland.

The aim was to improve the cost-effectiveness of DXA measurements with Postmenopausal Osteoporosis Screening Tool (POST) that recognises non-osteoporotic women.

The study subjects were selected from the Osteoporosis Risk Factor and Prevention (OSTPRE) Study cohort (13 100 women born in 1932-41), Kuopio, Finland. Random samples were measured with DXA absorptiometry (total neck) at baseline (1989-91) (n=1086 with valid DXA measurement) and 5-year (1994-97) (n=1050 with valid DXA measurement) excluding hysterectomised and biovariectomised women. Mean age of the study subjects was 53 years (48-60 years, baseline) and 59 years (53-66 years, follow-up). Postal inquiries on risk and preventive factors for osteoporosis were collected at the baseline and follow-up. POST was tested in both measurements. Multinomial logistic regressions were performed to identify risk factors for osteoporosis according to which POST was mainly built on. The dependent variable was the three categories WHO classification: BMD over -1 SD normal, -2.5 to -1 SD osteopenic and under -2.5 osteoporotic bone density. Table represents the selected risk factors and their weighting in POST.

Of the present sample 775/632 had normal BMD, 311/383 had osteopenic BMD and 19/33 had osteoporotic femoral neck BMD in baseline/follow-up. POST points varied from 1 to 25 and 3 to 26 in baseline and follow-up. AUROCs for POST in recognizing osteoporotic women were 81 % (95% CI 75 - 87 %, p<0.001) and 82 % (95% CI 77 - 86 %, p<0.001) for baseline and 5-year data, respectively.In OSTPRE population, 42 % (baseline, cut-off POST<13 points) and 38 % (5-year, cut-off POST<14 points) of the total population were determined as non-osteoporotic (BMD >-2.5 SD) with 100 % sensitivity. With baseline criteria (cut-off POST<13 points), 29 % of population were determined as non-osteoporotic (BMD >-2.5 SD) in 5-year measurement with 100% sensitivity.The presented combination of risk factors in POST was more sensitive than any selected risk factor alone or any other possible combination of selected risk factors.

POST may provide useful tool for excluding non-osteoporotic women from DXA measurements thus improving their cost effectiveness. Before adaptation for wider use POST should be validated in other populations.

Postmenopausal Osteoporosis Screening Tool (POST)

Factor	Limits	Points
BMI (kg/m^2)	< 26	10
	26-30	3
	> 30	0
Age (years)	< 49	0
	49-57	1
	57-60	2
	> 60	3
Years since menopause	0	0
	3-6	3
	6-8	6
	> 8	9
Previous fracture	No	0
	Yes	2
Fracture history in mother or sister or both	No	0
	Yes	2

Disclosures: ***J. Sirola****, None.*

SU389

Illness Representations of Osteoporosis among Osteoporotic Men. O. Edelstein*[1], P. Werner*[1], I. Vered[2]. [1]Gerontology, Faculty of Social Welfare and Health Studies, University of Haifa, Haifa, Israel, [2]Endocrinology, Sheba Medical Center, Sackler Faculty of Medicine, Tel Aviv University, Tel Hashomer, Israel.

Research on illness representations suggests that people construct their own representations of an illness in order to understand and deal with it. The Self-Regulation Model (Leventhal & Diefenbach, 1991), proposes that people's illness representations consist of five components that determine emotional and behavioral reactions to illness.

The aim of the present study was to examine illness representations of osteoporosis among 100 osteoporotic men (mean age 63 yr; mean spine t-score = -2.4; 33% had a low-trauma fracture; 20% had glucocorticoid-induced osteoporosis).

Illness representations were assessed using an adapted version of the Illness Perception Questionnaire (Weiman, Petrie, Moss -Morris & Horne, 1996).

Results of the study showed that the identity (i.e., symptoms) of osteoporosis included bending of the back (62%), back pain (59%), loss of height (51%), and general weakness (26%). Participants reported that the main causes of their disease were their own behavior (56%); lack of physical activity (52%), and other diseases or medications (53%). Osteoporosis was perceived as likely to be permanent rather than temporary (86%), and as an illness that will last for a long time (85%).

Participants' perceptions regarding the consequences of osteoporosis were mild: only 38% agreed that their illness is a serious condition, and 39% agreed that the disease had had major consequences on their life. The main consequence related to the economic and financial effects of the illness (47%). Finally, the majority of the participants believed osteoporosis to be a controllable disease: 80% agreed that what they do can determine whether their illness gets better or worse; and 75% agreed that their treatment will be effective in curing their illness.

In sum, findings of this study showed that osteoporotic men perceived their disease as chronic, as having no serious consequences, and as being controllable. These could have important implications in improving the efficacy and adherence to treatment interventions, and in adjustment to a chronic disease.

Disclosures: ***I. Vered****, None.*

SU390

Association of High BMD with the Risk of Benign Breast and Uterine Diseases in Postmenopausal Women. C. Ribot[1], F. Tremollieres[1], V. Cances-Lauwers*[2], J. Pouilles*[1]. [1]Hôpital Paule de Viguier, Menopause Unit, Toulouse, France, [2]CHU Purpan, Department of Epidemiology, Toulouse, France.

Recent studies have underlined the possibility that bone mass may represent a marker of cumulative exposure to estrogen and/or estrogen responsiveness in women. A significant association between high BMD and the increased incidence of breast cancer has been reported in postmenopausal women. In this study, we examined the association between bone mass and the incidence of both benign breast and uterine diseases in postmenopausal women. Between 1992 and 2002, 5847 postmenopausal healthy women who were 45 to 75 years old (mean age : 55.4±4.5 yrs) and had never received ERT/HRT underwent a « menopause check-up » including clinical examination and BMD measurements by DXA. A questionnaire including information on reproductive history was collected and the incidence of past or current both benign breast (including benign lumps and cysts, cystic mastitis and/or microcalcifications) and uterine (including myoma and/or polyps) diseases was recorded. Vertebral and femoral BMDs were measured using DXA (Lunar Rad Corp) in all women. Of the whole population, 1214 (20.8%) and 1597 (27.3%) women reported a history of past or current benign breast and uterine diseases, respectively. After adjustment for age and BMI, the odds ratio for benign breast disease in the third and fourth highest quartiles of vertebral BMD compared to the lowest quartile was significantly higher (1.3 [95% confidence intervalle, 1.1-1.6] and 1.6 [1.3-1.9], respectively). The relation was not significant for femoral BMD. As compared with the women in the lowest quartile, the adjusted odds ratio for benign uterine disease in the highest quartile of BMD was also significantly higher at the femoral neck (1.3 [1.0-1.6]) but not at the lumbar spine. These results suggest that bone mass in postmenopausal women is a good predictor of the risk of benign breast and uterine diseases. The mechanisms underlying this relation may be explained by a cumulative exposure to estrogen and/or estrogen responsiveness.

Disclosures: ***C. Ribot****, None.*

SU391

A Prospective Study to Describe the Feasibility of Case Finding for Osteoporosis in primary care at the Annual over 75 Health Check Using the Black Fracture Score. A. L. Dolan*[1], H. Patrick*[2], S. Mendonca*[2], B. Coutinho*[1], D. Oliver*[3]. [1]Rheumatology, Queen Elizabeth Hospital, London, United Kingdom, [2]Bexley PCT, Kent, United Kingdom, [3]School of Health and Social Care, University of Reading, Reading, United Kingdom.

Fracture prevention services have been established in secondary care in the UK to identify patients with incident fractures and risk of osteoporosis, with high pick up rates (eg 40% of wrist fractures osteoporotic). However, a bone health service also requires case-finding from primary care as many patients with risk factors for osteoporosis may not present to hospital or had previous low impact fractures. There are few data on the feasibility of such case-finding in primary care. This study uses the 'Over 75yr check' to identify such patients and plan preventative management and to assess the effectiveness of the 'Black Fracture risk score' to identify those at high risk of hip fracture. (Black OI 2001). Patients scoring ≥ 5 have a 9% chance of suffering a hip fracture in the next 5 years.

Patients aged 75-80yrs attending for a voluntary annual nurse led check completed the Black score. Those scoring ≥ 5 were offered bone densitometry at the local hospital. Nurses received 2 training sessions on the protocol. Ethics consent was obtained.

558 patients completed assessment from 13 practices, out of a potential population in the age group of 1929. 222 were male, 336 female . 280 had a Black score of 5 or more (50%). Risk factor assessment showed 95 / 558 (17%) had a fracture after 50, 47% used arms to stand, 3% were on steroids, 3.4% had BMI <20. 4.3% had a previous diagnosis of osteoporosis.174 were referred on for DXA (31% of population assessed) but only 139 attended (25%). Scan outcomes are shown below.

	Total	Osteopenic (T <-1)	Osteoporotic (T<-2.5)	Normal
Hip	119	69	13	37
Spine	139	71	21	47

23 patients were osteoporotic at one or more sites (16.5%), 71 osteopenic (51%) and 45 normal (32%). 50 of those with previous fracture received DXA; 30% of these had osteoporotic BMD.

This community screening programme resulted in a low pickup of osteoporosis (23/558 screened). This reflected low up take of check and offer of scan. Those who attended were less osteoporotic than might be expected from population norms, suggesting they may be an unduly fit and compliant group. The Black score was derived to identify hip fracture risk and is weighted by age and frailty so may not be an appropriate tool to identify low bone density. History of fracture may be a better screen.

Disclosures: ***A.L. Dolan****, None.*

SU392

The Relative Importance of Lean and Fat Mass on Bone. C. G. Gjesdal[1], J. I. Halse[2], J. G. Brun*[3], G. S. Tell*[1]. [1]Dept of public health and primary health care, University of Bergen, Bergen, Norway, [2]Clinic of osteoporosis, Oslo, Norway, [3]Dept of Rheumatology, Haukeland University Hospital, Bergen, Norway.

While body weight is one of the strongest predictors of bone mineral content (BMC) and bone mineral density (BMD), it is not clear which attributes of a heavy body (e.g. weight in itself, adiposity, muscularity, body fat distribution or frame size) are most strongly associated with bone measurements. Fat mass (FM), lean mass (LM), as well as both tissues have been reported to be determinants of BMC and BMD. The aim of this study was to evaluate the relative importance of FM and LM on BMC.

The study population consisted of 5117 Norwegian men and women 47-50 and 71-75 years old. BMC of total body and femoral neck as well as soft-tissue body composition were measured by dual X-ray absorptiometry (DXA). In order to assess the effects of fat mass on BMC independently of body weight, quartiles of fat mass in 5-kg strata of weight were plotted against BMC. Only strata with at least 40 persons were included. Analyses of variance were used in each stratum to evaluate the influence of FM.

The general pattern observed was that within each stratum the lowest quartile of FM was associated with the highest BMC indicating that LM is more important than FM within each weight group. The figure shows the results for total body BMC among men. Results were similar for women, although the trends were somewhat weaker among the oldest women. Almost identical results were found for femoral neck BMC. Adjustment for differences in height, age, smoking and level of physical activity did not change the overall pattern.

In summary, FM appeared to be inversely associated with BMC for a given bodyweight. Thus there seems to be an effect of fat mass and lean mass beyond the effect of weight in itself.

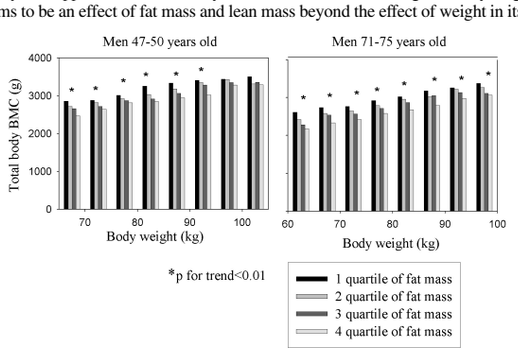

Disclosures: ***C.G. Gjesdal****, None.*

SU393

Performance of a Simple Clinical Tool (FOSTA) for Identifying Japanese Women with Osteoporosis Based upon Quantitative Ultrasound Techniques (QUS) and Vertebral Deformity. K. Aoyagi[1], Y. Abe[1], P. D. Ross[2]. [1]Public health, Nagasaki University, Nagasaki, Japan, [2]Merck Research Laboratories, Rahway, NJ, USA.

The purpose of this study was to evaluate the performance of a simple clinical tool, the Female Osteoporosis Self-assessment Tool for Asians (FOSTA), among postmenopausal Japanese women in a population-based study (the Hizen-Oshima Study) using quantitative ultrasound techniques (QUS) to define osteoporosis (T < -2.5), and vertebral deformity (osteoporotic fracture). The subjects were 523 women ages 43 and older (mean age; 66.1, SD; 8.1 years old) with QUS measurement for calcaneus (stiffness index) and spine radiographs between 1998 and 1999. Lateral spine radiographs were obtained and radiographic vertebral deformities were assessed by quantitative morphometry, defined as vertebral heights more than 3 SD below the normal mean. FOSTA was calculated from the patient's weight and age: FOSTA=0.2 (weight [in kg]-age [in years]), truncated to an integer. Risk categories (high, moderate, and low) were based on previously published criteria. The FOSTA index achieved 96% sensitivity and 29% specificity for osteoporosis (stiffness index T-score < -2.5), which was similar to previous findings using femoral neck and lumbar spine BMD in Japanese women. The index also achieved 99% sensitivity and 22% specificity for vertebral deformity. Using three risk categories, 29% of all women were categorized as high risk (FOSTA<-4). Physicians might be advised to consider treating women with osteoporosis. Among high-risk patients, 73% had osteoporosis and 33% had vertebral deformity. Among women classified as low-risk (18% of all women), only 12% had osteoporosis and 1% had vertebral deformity. Approximately 43% of the moderate risk women had osteoporosis and 12% had vertebral deformity. In summary, the FOSTA index performed well to identify postmenopausal Japanese women with osteoporosis and vertebral deformity. This free and simple risk assessment tool would encourage clinicians appropriate use of BMD measurements for high-risk patients, and initiate appropriate intervention before fractures occur.

Disclosures: ***K. Aoyagi****, Banyu 2.*

SU394

An Evaluation of Osteoporosis Diagnostic Tools for Elderly Caucasian and Chinese Men. H. Lynn[1], E. Lau[1], E. Barrett-Connor[2], M. Nevitt[3], J. Cauley[4], R. Adler[5], E. Orwoll[6]. [1]Chinese University of Hong Kong, Shatin, Hong Kong Special Administrative Region of China, [2]University of California, San Diego, La Jolla, CA, USA, [3]University of California, San Francisco, San Francisco, CA, USA, [4]University of Pittsburgh, Pittsburgh, PA, USA, [5]McGuire Veterans Affairs Medical Center, Richmond, VA, USA, [6]Oregon Health and Sciences University, Portland, OR, USA.

Several osteoporosis screening tools have been shown to be effective for selecting women for dual-energy x-ray absorptiometry (DXA) testing, but such evaluations have not been performed in men. This study assesses the performance of the Osteoporosis Self-assessment tool (OST) and the Male Osteoporosis Screening Tool (MOST) in identifying men for DXA testing. OST is based on body weight and age, while MOST is a function of weight and quantitative ultrasound index (QUI) measurement.

Community-dwelling and ambulatory men 65 years old and above were recruited in the U.S. and Hong Kong for the Osteoporotic Fractures in Men (MrOS) Study. Bone mineral density (BMD) was measured by DXA (Hologic QDR-4500W) and ultrasound measurements by a Sahara sonometer. Osteoporosis was defined as a BMD T-score of < -2.5 using race-specific male normative database. Altogether, 4682 U.S. Caucasians and 1914 Hong Kong Chinese with available BMD, OST and MOST values were included in the current analysis.

The prevalence of osteoporosis at the lumbar spine, total hip, or femoral neck was 10% for Caucasians and 13% for Chinese. The area under the receiver operating characteristic curve (AUC) was 0.680 for OST and 0.779 for MOST among Caucasians (Table 1). Among Chinese, OST had an AUC of 0.763 and MOST, an AUC of 0.811. If body weight alone was used as a diagnostic tool, then the AUC was 0.676 and 0.762 for Caucasians and Chinese respectively. Using the top quartile of MOST as a cutoff score, the resulting test had 95% sensitivity, 24% specificity, and 98% negative predictive value (NPV) in Caucasians, and 95% sensitivity, 28% specificity, and 97% NPV in Chinese.

We conclude that MOST performed better in terms of AUC than body weight alone in Caucasian and Chinese men. Moreover, it is a satisfactory osteoporosis diagnostic tool, adequately screening out those without osteoporosis and possibly saving a quarter of the DXA resources.

Table 1. AUC (standard error) of osteoporosis screening tools

		Osteoporosis (T-score < -2.5)			
		Lumbar spine	Total Hip	Femoral neck	Any site*
Caucasian	Weight	0.653 (0.016)	0.802 (0.021)	0.717 (0.016)	0.676 (0.013)
	OST	0.640 (0.016)	0.824 (0.020)	0.742 (0.015)	0.680 (0.013)
	MOST	0.766 (0.014)	0.883 (0.017)	0.807 (0.014)	0.779 (0.011)
Chinese	Weight	0.735 (0.018)	0.831 (0.019)	0.833 (0.019)	0.762 (0.015)
	OST	0.722 (0.018)	0.855 (0.018)	0.845 (0.019)	0.763 (0.016)
	MOST	0.803 (0.017)	0.864 (0.020)	0.843 (0.023)	0.811 (0.015)

* Any site defined as either lumbar spine, total hip, or femoral neck

Disclosures: ***H. Lynn****, None.*

SU395

Neuromuscular and Sensorimotor Correlates of Gait and Balance in Women with Wrist Fractures. B. J. Edwards[1], C. Langman[2], P. H. Stern[3], K. Martinez*[4], M. W. Rogers*[4]. [1]Medicine, Northwestern University, Chicago, IL, USA, [2]Pediatrics, Northwestern University, Chicago, IL, USA, [3]Molecular Pharmacology and Biological Chemistry, Northwestern University, Chicago, IL, USA, [4]Physical Therapy and Human Movement Sciences, Northwestern University, Chicago, IL, USA.

A wrist fracture is a risk factor for hip fracture. This is only partially explained by low bone density.

Objective: We hypothesized that extra-skeletal effects (neuromuscular and sensorimotor) NMS measures of gait and balance, and functional measures may also play a role.

Methods: We analyzed NMS, and functional measures in women with falls and wrist fracture. Self-reported fractures occurred in the past 10 years. Falls were "an event which results in a person coming to rest inadvertently on the ground or a lower level and not as a result of a major intrinsic event or overwhelming hazard." NMS measures included visual contrast sensitivity (VCS), depth perception (DP), lower limb proprioception, triceps and quadriceps strength, and hand reaction time. Body sway was measured in the frontal (AP) and lateral plane. These measures form part of Lord's Physiologic Profile Assessment (PPA). Functional measures of balance and gait included the Berg Balance Scale, the Dynamic Gait Index (DGI), the Activities of Balance Confidence (ABC Scale), and timed ten-meter walks.

Analysis: Independent samples t tests were conducted. Cohens-d was calculated for effect size.

Results: 26 fractures (age 73.6 ± 9y) and 23 controls (age 69.7 ± 10y)(p=0.26) were evaluated. Fractures had lower visual contrast sensitivity (p=0.002), impairment in static balance measures (BBS) (p=0.043), and lower bone density (p=0.025). A trend toward lower DGI (p = 0.085), sway (p=0.113), and higher vibratory threshold was evident (p= 0.237)

Conclusion: women with wrist fractures exhibit impairments in static and dynamic balance, and visual contrast sensitivity which combined with lower bone density may predispose them to future hip fractures.

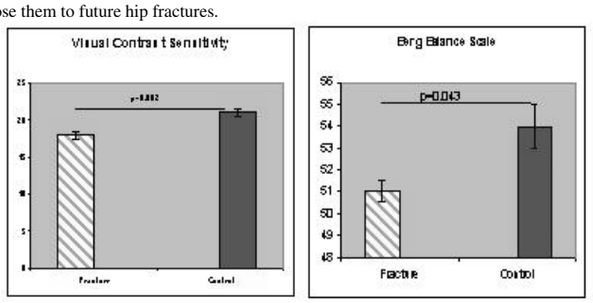

Disclosures: ***B.J. Edwards****, Merck 2, 5; Procter & Gamble 2, 5; Eli Lilly 5.*

SU396

Metabolic Bone Disease among an Ethnically Diverse Cohort of HIV+ Patients with Lipodystrophy. J. R. Curtis*[1], B. Smith*[2], K. Landers*[2], R. Lopez*[1], J. Raper*[1], M. Saag*[1], R. Venkataraman*[1], M. Weaver*[1], K. Saag[1]. [1]University of Alabama Birmingham, Birmingham, AL, USA, [2]University of Maryland, College Park, MD, USA.

Aim: Previous studies report a high prevalence of metabolic bone disease and osteonecrosis among predominantly Caucasian HIV+ patients with lipodystrophy on Highly-Active Anti-Retroviral Therapy (HAART). Given the paucity of data in minorities, we examined the prevalence of these conditions in an ethnically diverse cohort.

Methods: HIV+ patients on HAART with lipodystrophy and hyperlipidemia underwent evaluation for metabolic bone disease including: screening questionnaire and physical exam, 4 day food diary, femoral neck and L2-4 BMD (GE Lunar central DXA) categorized using WHO cutpoints; both hip MRIs (GE 1.5T magnet); and laboratory studies intact-PTH, 25-OH Vitamin D, serum osteocalcin (OC) and urinary N-telopeptide (NTX). Chi-square and t-tests were used for analyses.

Results: 44 patients participated: 23 blacks (10M, 13F), 20 whites (18M, 2F), and 1 Hispanic (1M). Patients were mean age=44.5 (SD=6.7), 66% male, on 3+ drug HAART for 34.1(27.5) months. Blacks had significantly higher femoral neck BMD (1.062 g/cm2) compared with non-blacks (0.948 g/cm2) (p=0.035). Lumbar BMD in blacks (1.272 g/cm2) was not significantly different compared to non-blacks (1.191 g/cm2). Non-blacks appeared more likely to be osteopenic or osteoporotic at any site (59%) compared to blacks (36%) (p=0.050).

Vitamin D deficiency (<34ng/ml) and elevated i-PTH (>65pg/ml) was found in 75% and 23% of patients, respectively. NTX was higher in non-blacks [60.2 (33.9) nM BCE/mM] than in blacks [38.7 (30.9) nM BCE/mM] (p=0.052), suggesting higher bone turnover in non-blacks. No ethnic differences were seen in OC levels. MRI identified 1/32 patients (3%) with bilateral asymptomatic hip osteonecrosis.

Conclusions: The previously-reported burden of bone disease in HIV+ patients with HAART-associated lipodystrophy appears greater in Caucasians compared to Blacks. Future studies to examine genetic and environmental contributions of ethnicity to HAART-associated metabolic bone disease are necessary to devise optimal interventions.

Disclosures: ***J.R. Curtis****, None.*

SU397

Changes in Bone Mineral Density and Body Composition in Lactating Adolescents. J. L. Mansur[1], A. Malpeli*[2], G. Etchegoyen*[2], S. de Santiago*[3], H. Gonzalez*[2]. [1]Center of Endocrinology and Osteoporosis, La Plata, Argentina, [2]IDIP, Hospital de Niños Sor M Ludovica, La Plata, Argentina, [3]Health Dept, Univ Iberoamericana, Mexico DF, Mexico.

Although decreases in Bone Mineral Density (BMD) and Fat Mass (FM) with partial recovery have been observed in adult lactating women, there are not enough data about adolescents. The aim of the work is to evaluate these changes, at a stage when women have not reached the peak of bone mass.

Patients and methods: we study prospectively 14 women exclusively breastfeeding in day 15 and in month 3 and 6 after delivery. Mean age: 15.1 +/-0.7 years. We evaluate weight, height, BMI, body composition by skinfold thickness and by DEXA (FM and Lean Body Mass:LBM), BMD of Lumbar Spine (LS), Total Hip (TH) and Femoral Neck (FN), and Bone Mineral Content (BMC) of Total Body (TB) with Lunar IQ with pediatric software.

Results: weight: 54.9 (5.3), height: 156 (6.4), BMI: 19.3 (4.3). Calcium intake: 643,98 (231) mg/d.

% FM (DEXA) basal vs 6 mo: p=0.03

Conclusions. In 6 months we observe decreases in FN and TH BMD and TB-BMC, and in FM, while LBM is preserved. The lactating adolescents must be under observation because they have not reached their peak of bone mass.

Changes in BMD, BMC and Body Composition

	basal	3 mo	6 mo
BMD-LS %	100	98,8	100,8
BMD-FN %	100	94,3	94,4
BMD-TH %	100	95,2	94,8
BMC-TBody %	100	97,7	96,8
% FM (DEXA)	34,56	32,82	29,98
% FM (Skinfold)	29,47	28,23	27,02
LBM (kg)	32,77	32,40	33,65

Disclosures: ***J.L. Mansur****, None.*

SU398

Bone Response to Lactation: an Important Physiologic Model of Bone Restoration? S. A. Brown[1], D. R. Clemmons*[1], C. J. Rosen[2], A. M. Siega-Riz*[3], M. J. Caminiti*[1]. [1]Endocrinology, University of North Carolina, Chapel Hill, NC, USA, [2]The Jackson Laboratory, Bar Harbor, ME, USA, [3]Maternal Child Health and Nutrition, UNC School of Public Health, Chapel Hill, NC, USA.

Lactation is a unique physiological model of bone remodeling as transient losses of bone mineral density (BMD) are completely restored in most individuals after weaning and therefore may represent a model of optimal conditions for bone formation.

The objective of this study is to prospectively assess the role of anabolic (IGF-I) and anti-resorptive hormones (estradiol) on BMD gain during the skeletal recovery phase after lactation.

We are conducting a prospective observational cohort study with planned recruitment of 120 postpartum women. Spine and hip BMD are measured by DXA, and the radius and tibia are assessed by pQCT at four time points: delivery, 3 months postpartum, resumption of menses and 6 months after menses resume. Serum analysis will include IGF-I, IGF binding proteins, estradiol, PTHrP, 25OH vitamin D, 1,25$(OH)_2$ vitamin D, CTx, osteocalcin, BSAP and calcium. Women complete infant feeding diaries, physical activity and food frequency questionnaires.

To date, 34 women have started the study and 14 have completed the 3-month time point. At 3 months, 10 women were exclusively breast-feeding, 1 was partially breastfeeding and 3 breast-fed less than 5 days. The change in spine BMD from delivery to 3 months was -6.3 ± 5.4% (mean ± SD; P<0.001 by paired t-test) and in total hip BMD was -3.5 ± 2.7% (P<0.001). The 11 lactating women lost BMD (spine: -8.6 ± 2.5%; total hip: -4.1 ± 2.5%; P<0.001) and the 3 non-lactating women had no significant changes in BMD of spine (+2.0 ± 4.7%; P=NS) or total hip (-1.3 ± 2.5%; P=NS).

Six women have completed the third time point at the resumption of menses (mean 6.1 months postpartum). These 6 women almost exclusively breast-fed >5 months and the change in spine BMD from delivery to the resumption of menses was -6.9 ± 1.0% (P<0.01), and total hip BMD was -4.4 ± 1.0% (P=0.01).

Four women have reached the final visit at 6 months post return of menses. Two out of the 4 women breast-fed >5 months and had significant losses of 7.3% at spine and 5.0% at total hip at 3 months which was recovered over a 6 month period from the return of menses to the last visit. The final BMD measurements for all 4 subjects were not significantly different from baseline measured at the time of delivery (spine: -1.4 ± 4.2%; total hip: -2.3 ± 2.3%; P=NS).

As anticipated, women who continue to lactate for an extended period lose bone mineral density. The study is ongoing and data will be forthcoming regarding the role of anabolic and anti-resorptive hormones in skeletal bone recovery after lactation as well as trabecular and cortical changes assessed by pQCT.

Disclosures: ***S.A. Brown****, None.*

SU399

Postural Stability and Physical Performance Tests in Elderly Subjects with Falls. S. M. Logsdon, J. C. Gallagher, R. Satpathy, S. M. Schmitt. Bone Metabolism Unit, Creighton University, Omaha, NE, USA.

Postural instability has been associated with falls in the elderly and 10% of falls result in fracture. Previous measurements of postural stability have been measured under static conditions. In this study, we used a dynamic measurement of postural stability together with standard functional tests. The Biodex Stability System (BSS) measures the angle of deflection (expressed in degrees) to calculate the anterior-posterior stability index (APSI), the medial-lateral stability index (MLSI) and the overall stability index (OSI). We compared this new measure of postural stability with other measures of physical performance in 122 elderly subjects age 65-85 years. Subjects were either classified as fallers, if they had at least 1 fall in the past year, or non fallers if they had no falls in the past 3 years. BSS tests were performed at two platform stabilities. Timed-up-and-go (TUG) was the time it took for them to stand up, walk 3 meters, and return to the chair. The timed rise (TR) was the time it took to stand up and sit down 3 and 5 times and grip strength (GS) was measured using a Jamar Hand Dynamometer at 90deg of shoulder flexion. The results showed mean BMI for female fallers was less than non fallers (p<.02). There was no significant difference in BMI between the male groups. BSS measurements were repeated on 20 subjects two weeks apart; the intra class coefficient was r=0.85. Both female and male fallers had higher mean scores for OSI, APSI (female p<.02) and MLSI than non fallers, (table). Female fallers had significantly higher scores on the TUG, GS and TR (p<0.01) than female non fallers. Male fallers had significantly higher scores on TUG and TR than male non-fallers (p<0.01), but not for GS. In summary, both postural stability and muscle strength were decreased in fallers than non fallers. Although falls are associated with many causes, the significant differences in postural stability, timed up and go, timed rise and grip strength tests between fallers and non fallers indicate these are useful predictors of falls.

Means for fallers and non fallers ±SEM

	FEMALE FALLERS (n=52)	FEMALE NON-FALLERS (n=30)	MALE FALLERS (n=28)	MALE NON-FALLERS (n=12)
AGE	76.08±0.89	73.73±1.09	76.82±1.07	79.92±2.05
BMI	28.83±0.69	26.54±0.75	28.48±0.87	26.71±0.80
OSI (deg)	4.39±0.23	3.68±0.33	5.91±0.38	4.73±0.52
APSI (deg)	3.38±0.20†	2.67±0.23	4.39±0.35	3.57±0.45
MLSI (deg)	2.88±0.16	2.61±0.27	3.99±0.28	3.29±0.30
TUG (sec)	12.42±0.96**	8.59±0.67	12.73±0.94**	8.77±0.59
GS (lbs)	46.86±1.6**	50.71±1.8	68.55±3.03	68.93±5.43
TR3(sec)	9.13±0.57***	6.66±0.37	9.87±0.74*	7.21±0.73
TR5 (sec)	17.9±0.96***	13.08±0.74	19.31±1.4*	14.23±1.23

*p<0.01, **p<0.001, ***p<0.0001, †p<0.02

Disclosures: ***S.M. Logsdon****, None.*

SU400

A National Osteoporosis Awareness Campaign for Older Women. K. M. Cody*, R. Kagan*, E. N. Schwartz. Foundation for Osteoporosis Research and Education, Oakland, CA, USA.

The National Osteoporosis Awareness Campaign seeks to 1) promote awareness among older women and their families and caregivers, 2) improve responsiveness of healthcare professionals to the problem and 3) increase support from policymakers to address awareness and improve services for osteoporosis.

The United States Administration on Aging (AoA) requested an action plan for a national osteoporosis awareness campaign targeting women 65 and older**.** To develop the plan, FORE convened a variety of stakeholders at two summit meetings in 2003. More than 100 individuals from a variety of organizations at local, regional, and national levels participated in the development of core elements of the proposed campaign and implementation plan. This broad participation not only ensured diverse input to the development of the plan, but also established the foundation for future collaboration.

During the planning process, the contributors identified and tested components for a comprehensive communications plan. The final plan incorporates the knowledge-based consensus on messages and methodologies that emerged from the Summits. Summit I focused on understanding the current state of awareness, describing key audiences, and identifying, in general terms, the most important message content to be delivered. Summit II focused on refining the messages for diverse audiences and determining the best strategies for message delivery. Following Summit II, FORE conducted five telephone focus group discussions with experts representing diverse groups, and their feedback was incorporated into the final plan.

The Planning Committee reviewed and prioritized the findings from the summits and focus groups and framed a campaign and implementation strategy that supported best practices, had a significant likelihood of success, and promoted sustainable action. As a final appraisal, nationally recognized experts in osteoporosis and health promotion reviewed the proposed plan to ensure that it addressed salient issues and engaged sound strategies.

The recommended framework for the campaign is to: 1) Implement a sustained (5-year) national awareness campaign to be delivered locally and aimed at all women age 65 and older, 2) Promote awareness -- and action -- by primary health care professionals, family members, and policymakers to support awareness and action, 3) Focus significant effort at reaching diverse, underserved and disadvantaged women, 4) Develop national leadership and an infrastructure to support federal, state, and local efforts, and build collaboration and linkages with partners at all levels, and 5) Assess and evaluate effectiveness of the campaign in achieving desired outcomes.

Disclosures: ***K.M. Cody****, None.*

SU401

Balance in Women with Osteoporosis and Vertebral Fracture: A Funtional Assessment of Kyphotic Posturing. C. B. Ohashi*, A. P. Sansone*, V. L. Szejnfeld, F. F. Ganança*, J. Natour*. Medicine, Federal University of São Paulo, São Paulo, Brazil.

Falling is an increasing hazard for old people, especially for women, who fall twice as often as men. Although multiple factors often contribute to a fall, impaired balance is an important element. The flexed posturing that occurs in people with osteoporotic vertebral fracture may displace the center of gravity and increase the risk of falls. This study was designed to assess balance in osteoporotic women with vertebral fracture and kyphotic posture. Thirteen consecutive patients with vertebral fracture and 22 patients without fracture, from two tertiary medical centers in São Paulo were invited to participate in this study. Patients were 60 years old or older and had osteoporosis (WHO). Patients with comorbidities that can affect balance were excluded. Spine X-ray were taken in all patients and vertebral fracture was identified by a semi-quantitative method. Anthropomorphic measurements were done, kyphosis was measured by Cobb's technique and a questionnaire regarding history of falls in the last year was answered. Berg Balance Scale and *"Time up and go"* test were used to evaluate balance. Vestibular system evaluation including vectonistagmography and audiometry was also performed.The mean age in the patients with fractures was not significantly different from that of patients without fracture (74,3±SD and 72,03±SD years, respectively). Kyphosis was significantly more pronounced in patients with radiographic fracture than in those without (Mean Cobb angle's 48,2° and 29,5°, respectively). Number of falls in the last year (Mean), Berg Balance scores, vestibular evaluation and "*Time up and go"* in patients with vertebral fractures were not significantly different from those without. Our results demonstrate that balance in women with kyphotic posture by osteoporotic fracture is not functionally impaired.

Disclosures: ***C.B. Ohashi****, None.*

SU402

Effect of Physical Activity on Bone, Muscle, and Fat Masses in Collegiate Male Tennis Players and Non-Athletic Controls. J. Ballard*[1], L. S. Wallace[2]. [1]Health and Kinesiology, University of Texas at Tyler, Tyler, TX, USA, [2]Family Medicine, University of Tennessee Graduate School of Medicine, Knoxville, TN, USA.

The purpose of this study was to evaluate the effect of physical activity, upon bone, muscle, and fat masses in 21 male Intercollegiate Tennis Players (mean age=20.9+2.5 yrs) and 20 Controls (mean age=22.5+2.7 yrs) who had not participated in any high school or college athletics. Every subject underwent hydrodensitometry with measured residual volume, anthropometry with Harpenden Skinfold Calipers at 8 sites, and DEXA measurements. The Hologic QDR-2000 was utilized to assess total body composition and the regional bone mass of each arm. "t" tests between the two groups revealed: 1) Tennis Players had significantly (p<.05) less body fat than Controls as determined by skinfolds (mean sum of 8 skinfolds=76.0+24.5 mm vs. 113.1+52.0 mm) by underwater weighing (mean % body fat=11.3+5.1% vs. 18.7+9.1%), and by DEXA (mean % body fat=13.3+4.1% vs. 21.4+7.5%), 2) Tennis Players had more bone and muscle masses then Controls in trunk and legs but not in arms. Two-way ANOVAs (Tennis Players/Controls X Dominant Arm/ Non/Dominant Arm) revealed; 1) Significant (p<.05) interactions with the Dominant Arm of the Tennis Players having more bone mass than the Dominant Arm of the Controls but less bone mass than the Controls in the Non-Dominant Arm for BMC (g) BA cm2 (cm2) and BMC/BA (g/cm2) at the 1/3, mid, ultra distal sites of the radius and ulna. On the basis of these data, it was concluded that the physical activity involved in intercollegiate tennis resulted in less fat, more muscle and greater bone mass in the Tennis Players when compared to the Controls, except in the Non-Dominant Arm where bone mass of the Controls was significantly (p<.05) greater than that of the Tennis Players. It is not known whether the rather low bone mass of the Non-Dominant Arm in these Tennis Players was a result of transferring mineralization to the Dominant Arm or just a lack of development in this extremity due a relatively low level of force exerted by this arm. Further research is needed in younger tennis players during growing years to evaluate the skeletal development of the Dominant and Non-Dominant Arms.

Disclosures: ***J. Ballard****, None.*

SU403

The Mineral Mass and External Dimensions of the Femoral Neck are Dissociated because of the Differing Behaviour of the Periosteal and Endocortical Envelopes. R. M. Zebaze*[1], M. Ghassan[2], E. Seeman[1]. [1]Endocrinology, Austin Health, Melbourne, Australia, [2]Orthopaedic, Balamand University Hospital, Beirut, Lebanon.

Femoral neck apparent volumetric bone mineral density (FN vBMD) is assumed to be independent of the external volume of the FN. This assumption is valid provided that increases in the external dimensions of the FN and the bone mineral content (BMC) within its periosteal envelope are proportional. In 697 women aged 20 to 87 years, assessed using dual energy x-ray absorptiometry, FN BMC correlated with FN volume before ($r = 0.22$, $p < 0.001$), but not after, adjustment for age, height and weight. FN BMC did not increase as FN volume increased so a 1 SD higher FN volume was associated with a 0.67 SD lower apparent vBMD. Height, weight and age had differing effects on FN BMC and FN volume, that was reflected in vBMD. A 1 SD greater height was associated with a 0.15 SD higher FN BMC, but 0.32 SD higher FN volume and so a 0.13 SD lower FN apparent vBMD. A 1 SD higher weight was associated with a 0.36 SD higher FN BMC, and a 0.20 SD higher FN volume and so a 0.15 SD higher apparent vBMD. A 1 SD increase in age was associated with a 0.13 SD increase in FN volume, a 0.36 SD decrease in FN BMC and so a FN apparent vBMD decreased by 0.41 SD . Ex vivo data, derived using QCT and direct mea-

surement on 26 postmortem FN specimens were confirmatory of the dissociation between bone mineral mass and its external dimensions; BMC and FN volume did not correlate (r = - 0.11; NS). vBMD decreased with increasing FN volume (r = - 0.65; p < 0.001). In tubular bones like the femoral neck, BMC and external volume are independent. Apparent vBMD is size dependent and is lower in bigger bones and higher in smaller bones.
Most of the population differences in bone mass, size and so vBMD may reflect the end result of mechanisms that regulate and co-regulate cellular activity on the periosteal and endosteal surfaces to optimize whole bone's tissue mass, size, its tissue mineral density, size, geometry and architecture to regulate strain. Impairment or failure of adaptation by one trait in the face of a developmental abnormality in another trait during growth, or declining function in another trait during aging, may result in bone fragility.

Disclosures: ***R.M. Zebaze****, None.*

SU404

Bone Size at the Distal Radius Is Inversely Correlated with Volumetric Bone Mineral Density. J. S. Walsh, J. A. Clowes, N. F. Peel, R. Eastell. Academic Unit of Bone Metabolism, University of Sheffield, Sheffield, United Kingdom.

The bone mineral content of the distal forearm is often adjusted for bone size by dividing by area or by estimated volume. This study aims to determine the relationship between bone size and bone mineral density of the radius.
We studied 85 healthy premenopausal women ages 18 to 46 years (mean 29.5 years) who underwent measurement by DXA (Osteometer DTX 200) of the distal forearm and pQCT (Stratec XCT 2000) at the 4% forearm site. The non-dominant arm was measured unless it had been previously fractured.
We found cross-sectional area of the radius by pQCT was negatively correlated with volumetric BMD by pQCT (r=-0.581, p<0.01), but it was not correlated with areal BMD by DXA. However, when an estimate of volumetric BMD was made from the DXA measurement by approximating the section of radius to a cube, we observed a negative correlation (r=-0.374, p<0.01). Both cortical (defined as the outer 55% of the cross-sectional area) and trabecular volumetric BMD by pQCT were negatively correlated with cross-sectional area, although cortical volumetric BMD showed a stronger correlation (r =-0.591, 95%CI -0.714 to -0.433) than trabecular volumetric BMD (r=-0.280, 95%CI -0.464 to -0.071). Height, but not age or body mass index, was a predictor of cross-sectional area in this group.
In postmenopausal women ages 55 to 80 years, we found that the inverse correlation between radial cross-sectional area and volumetric BMD by pQCT persists after correction for age (r=-0.478, p<0.01). Volumetric BMD was lower in women with distal forearm fractures (n=69, mean age 67.4 years) than women without forearm fractures (n=380, mean age 68.1 years) (p<0.01), but there was no difference in cross-sectional area between the fracture and non-fracture groups.
This inverse correlation between cortical volumetric BMD and cross-sectional area at the distal radius may represent an adaptive response that results in changes in cortical mass and bone volume to maintain an optimal cross-sectional moment of inertia. In forearm fracture subjects there is a lower volumetric BMD compared to postmenopausal women suggesting volumetric BMD may be more important than bone size in forearm fracture, and that higher volumetric BMD in smaller bones may overcome their mechanical disadvantage.

Disclosures: ***J.S. Walsh****, None.*

SU405

Osteopontin Potent Suppresses PTH Actions in Cancellous and Periosteal Bone and Enhances PTH Actions in Endosteal Bone. K. Kitahara[1], K. Tsuji[1], M. Ishijima[2], S. R. Rittling[3], H. Kurosawa*[2], A. Nifuji[1], D. T. Denhardt[3], M. Noda[1]. [1]Molecular Pharmacology, Tokyo Medical and Dental University, Tokyo, Japan, [2]Juntendo University, Tokyo, Japan, [3]Rutgers University, Piscataway, NJ, USA.

Continuous presence of PTH has been shown to be catabolic in cortical bone while it may be anabolic in cancellous bone. Since PTH regulates expression of osteopontin (OPN) in osteoblasts, OPN could play a certain role in PTH actions in bone. To examine cellular basis for the OPN-deficiency effects on continuous PTH treatment on bone, we subcutaneously implanted osmotic pumps infusing 80 μg/kg/day PTH (1-34) for four weeks into the mice. PTH infusion increased bone formation rate (BFR) as well as mineral apposition rate (MAR) in cancellous bone in wild type mice. In OPN-deficient mice, basal levels of BFR and MAR were similar to the basal levels in wild type mice. However, OPN-deficiency further enhanced PTH-dependent increase of MAR and BFR in the cancellous bone. PTH infusion suppressed periosteal BFR and MAR in the cortex of diaphyseal bone. Mineralizing surface (MS/BS) was also reduced in wild type mice. OPN-deficiency further enhanced the suppressive effects of PTH on periosteal BFR via suppression in MS/BS, while periosteal MAR was not affected by the OPN-deficiency. Contrary to periosteum, PTH infusion enhanced BFR and MS/BS but not MAR in the endosteum in wild type while OPN-deficiency blocked such PTH effects in the endosteum. PTH infusion increased osteoclast number per bone surface as well as osteoclast surface against bone surface in wild type mice. In OPN-deficient mice, these osteoclast parameters were further enhanced compare to wild type mice. Continuous PTH-infusion increased the levels of serum calcium in wild type mice as reported previously. In OPN-deficient mice, PTH-dependent increase in the levels of serum calcium was further enhanced. PTH-infusion similarly increased deoxypyridinoline excretion in urine in wild type as well as OPN-deficient mice. These observations indicated that OPN suppresses PTH-actions in cancellous and periosteal bone while it enhances PTH actions in endosteal bone.

Disclosures: ***K. Kitahara****, None.*

SU406

Comparison of the Effect of Raloxifene on Bone Between Japanese and Caucasian Postmenopausal Women with Osteoporosis. T. Nakamura*[1], T. Matsumoto*[2], M. Fukunaga*[3], S. Watts*[4], K. D. Harper[4], H. Uesaka*[5], M. Tsujimoto*[5], E. Hamaya*[5], K. Sato*[6], A. Tanaka*[6]. [1]University of Occupational and Environmental Health, Kitakyushu, Japan, [2]Tokushima University, Tokushima, Japan, [3]Department of Nuclear Medicine, Kawasaki Medical School, Okayama, Japan, [4]Eli Lilly and Company, Indianapolis, IN, USA, [5]Eli Lilly Japan Co., Ltd., Kobe, Japan, [6]Chugai Pharmaceutical Co., Ltd., Tokyo, Japan.

The bridging concept in clinical development is a method to apply conclusions from the results of clinical trials developed in some region(s) to new region(s). The efficacy of raloxifene (RLX) for the treatment of osteoporosis has been proven in the large randomized multinational 3 year MORE trial (Ettinger et al, JAMA 1999; 282:637-45). A trial of 1year duration (Morii et al, Osteoporosis Int. 2003; 14:793-800) was also conducted with 284 Japanese postmenopausal women, similar to the MORE patient population, to develop a bridging strategy. Both RLX studies had the same treatment groups (placebo, RLX 60 mg/day (RLX60) and 120 mg/day (RLX120)) and all treatment groups received supplements of calcium and vitamin D_3. Because of the study designs, there was a marked difference in the distribution of baseline lumber spine BMD of patients between the two studies (0.468 - 0.741 g/cm^2 in the Japanese study, and 0.412 - 1.449 g/cm^2 in the MORE study). Moreover, the analysis of baseline BMD by tertile in MORE showed that the percent change in BMD was greater in the group with lower baseline BMD. Therefore we used a distribution-adjusted mean of the MORE study population, which is defined as the weighted mean by adding up the mean percent change in each of the 10 divided equal intervals at a width of 0.03 g/cm^2 in the MORE baseline BMD distribution, multiplied by the relative frequency obtained in the Japanese, and then compare this distribution-adjusted mean percent change in BMD to the Japanese study. The percent change in BMD was similar between the two ethnic populations (difference from placebo with 95%CI; RLX60: 3.92 (3.07, 4.77), RLX120: 3.23 (2.39, 4.07) in the Japanese study, and RLX60: 2.77 (1.92, 3.62), RLX120: 3.01 (2.18, 3.83) in MORE study). These results were supported by the absolute BMD gain after RLX treatment being relatively constant (0.016 g/cm^2 to 0.025g/cm^2 in all groups) regardless of baseline BMD values and this trend was similar for both Japanese and MORE studies. This relevant comparison demonstrates that the effect of RLX on bone is similar between Japanese and Caucasian women with osteoporosis and that the dosage is also similar among ethnic populations, supporting the use of RLX for treatment of postmenopausal osteoporosis in Japan with a bridging strategy.

Disclosures: ***T. Nakamura****, Eli Lilly and Company 5.*

SU407

Ethnicity, Plasma 25(OH)Vitamin D, and Calcium Absorption. M. B. O'Connell[1], S. A. Abrams[2], M. Kleerekoper[3], T. Czilli*[1]. [1]College of Pharmacy and Health Sciences, Wayne State University, Detroit, MI, USA, [2]USDA/ARS Children's Nutrition Research Center, Baylor College of Medicine, Houston, TX, USA, [3]School of Medicine, Wayne State University, Detroit, MI, USA.

The purpose of this study was to determine if lower circulating 25(OH)D concentrations in older African Americans women were associated with lower calcium absorptions than in older White women. Study was IRB approved. Nineteen African Americans and 17 White Americans 65 years or older with normal GI function and no calcium absorption-interfering drugs or diseases were enrolled in Fall 2003. Before the absorption study, each woman ingested daily for two weeks 650 units of vitamin D supplements, 500 mg calcium from OsCal, and an additional 700 mg calcium from Tums or diet. After an overnight fast, each woman received 1.2 mg ^{42}Ca (as $^{42}CaCl_2$) intravenously and 20 mcg ^{46}Ca (as $^{46}CaCl_2$) in 8 oz calcium fortified orange juice and a Swanson's Great Start breakfast with 2 slices of buttered toast. Single hip DXA was measured with a Hologic Sahara unit. Food was withheld for 2 hours. Urine was collected for 24 hrs. Thermal ionization mass spectrometry (TIMS) was used for sample analysis. Fractional calcium absorption was calculated as the relative enrichment of the ^{46}Ca vs. the ^{42}Ca in the 24-hour urine. SPSS was used for statistical analysis with significance defined as $P \leq 0.05$. Mean age (range 65 -93 yr old), weight, height, creatinine clearance, plasma 25(OH)D, 24-hr urinary calcium excretion, DXA femoral neck, and DXA total hip were not significantly different between the two ethnic groups. Mean (SD, range) calcium absorption and plasma 25(OH)D concentration for the African Americans were 13.6% (6.3%, 6-24%) and 20.4 ng/ml (9.0, 7-35) and for the White Americans 13.4% (4.3, 6.7-22.1) and 23.8 ng/ml (5.8, 14-36%), respectively. Fifty-eight percent of the African Americans and 18% of the White Americans had hypovitaminosis D (< 20 ng/ml). No significant relationships for the whole group nor within each ethnic group existed between calcium absorption and age, 25(OH)D, urinary calcium excretion, creatinine clearance, DXA femoral neck, or DXA total hip. No ethnic differences between African American and White American seniors for plasma 25(OH)D nor calcium absorption, assessed with the natural isotope method, were observed.

Disclosures: ***M.B. O'Connell****, None.*

SU408

Enhancement of Intestinal Alkaline Phosphatase Gene Expression by Lactose Feeding. N. Sogabe*, R. Maruyama*, L. Mizoi*, M. Goseki-Sone. Food and Nutrition, Japan Women's University, Tokyo, Japan.

Alkaline phosphatase (ALP) hydrolyzes a variety of monophosphate esters into inorganic phosphoric acid and alcohol at a high pH optimum. In humans, studies on the genes related to this enzyme have demonstrated at least four ALP isozymes: tissue non-specific, intestinal, placental and placental-like. The high activity of intestinal ALP, which is localized at the brush border of intestinal epithelial cells, suggests the participation of this enzyme in the transport of nutrients such as inorganic phosphate across the membrane, but little is known about the physiological function of intestinal ALP. It is well known that lactose promotes the intestinal absorption of calcium (Ca) in the paracelluar process and the promotion of Ca absorption seems to be regulated via the passive transport in the small intestine. However, there are few experimental results on the relationships between Ca absorption and ALP expression. In this study, we investigated the effects of lactose on intestinal ALP activity in rats. A total of 64 Sprague-Dawley strain female rats (6-week-old) were divided into three groups: the control, 3% or 10% lactose groups. On day 0, 1 month or 2 months after beginning the experimental diets, rat intestinal segments from the duodenum, jejunum and ileum were obtained immediately after sacrifice. The segments were slit open longitudinally, and the mucosa was scraped and used for enzyme assay. After two months, the levels of intestinal ALP activity in ileum specimens from the 3% lactose group and the 10% lactose group were significantly higher than that from the control group. Two kinds of mRNAs of rat intestinal ALP (RTIN-1 and RTIN-2) were detected by reverse transcription-polymerase chain reaction (RT-PCR). RTIN-1 and RTIN-2 cDNA sequences have 79% homology at the amino acid level. Real-time RT-PCR demonstrated that the level of RTIN-1 mRNA expression in the ileum specimens from the lactose groups was significantly enhanced. This finding was compatible with the findings of enzymatic activity. Further studies on the mechanism of increased intestinal ALP expression induced by lactose would provide useful data on the relationships among lactose, Ca, phosphate and intestinal ALP, and on the physiological function of intestinal ALP.

Time course of ALP specific activity of ileum

Groups	0 time (U/mg protein)	1 month (U/mg protein)	2 months (U/mg protein)
Cont.	0.101±0.015	0.097±0.020	0.215±0.021
Lac. 3%	0.101±0.015	0.170±0.038	0.342±0.030#
Lac. 10%	0.101±0.015	0.195±0.014*	0.361±0.038**

Compared to the control group (# p <0.05, *p <0.05, **p<0.01)

Disclosures: ***N. Sogabe****, None.*

SU409

The Effects of Interaction of Dietary Protein and Calcium on Calcium Retention: A Controlled Feeding Study. Z. K. Roughead[1], L. K. Johnson*[1], G. I. Lykken*[2]. [1]Grand Forks Hum. Nutr. Res. Ctr., USDA-ARS, Grand Forks, ND, USA, [2]University of North Dakota, Grand Forks, ND, USA.

A high protein intake is thought to decrease calcium retention and is often cited as a risk factor for osteoporosis. However, recent findings indicate that a high meat diet, when combined with typically low calcium intakes, does not decrease and may even improve calcium retention. Under controlled feeding conditions, the objective of this study was to characterize the interaction of dietary protein and calcium. In a 2x2 factorial design, healthy postmenopausal women (n=23, age: 45-68 y; body mass index: 26.9 ± 3.8; L1-L4 BMD T-score: -2.4 to1.6) were randomly assigned to either a low calcium (LC, 600 mg/d) or a high calcium (HC, 1500 mg/d) group and consumed low meat and high meat diets [10% and 20% of energy as protein, LP and HP, respectively] for 7 wk each in a randomized crossover design. After 3 wk of equilibration, the menu was extrinsically labeled with ^{47}Ca-radiotracer and its retention was monitored for 28 d by whole body counting. The data were modeled by the two-component exponential equation: $y = \beta_1 \exp(-k_1 t) + \beta_2 \exp(-k_2 t)$, where y is ^{47}Ca retention, as % dose, t time in hours, and coefficients β_1 and β_2 the turnover (%) at rates k_1 and k_2, respectively. (Below are preliminary results; an additional 4 subjects are currently enrolled in the study).

Table: Retention of ^{47}Ca radio tracer[1, 2, 3]

Diet	Model Parameters				Retention, % dose			
	β_1	k_1	β_2	k_2	Day 7	Day 14	Day 21	Day 28
HCHP	87.1	0.03	13.1[a]	0.0009	14.1[a]	9.9[a]	8.5[a]	7.4[a]
HCLP	87.1	0.03	13.2[a]	0.0009	13.7[a]	9.9[a]	8.4[a]	7.3[a]
LCHP	75.0	0.03	25.1[b]	0.0008	23.7[b]	19.1[b]	16.6[b]	14.4[b]
LCLP	77.6	0.03	22.4[c]	0.0009	20.5[c]	16.5[c]	14.2[c]	12.2[c]
Pooled SD	2.2	0.005	2.1	0.0002	1.2	1.3	1.2	1.1
ANOVA Calcium	0.0001	NS	0.0001	NS	0.0001	0.0001	0.0001	0.0001
Protein	0.07	NS	0.06	NS	<0.01	<0.01	<0.01	<0.01
Calcium X Protein	0.06	NS	<0.05	NS	<0.03	<0.01	<0.01	<0.01

[1]Least square means, n=13 in HC and n=9 in LC groups. Data from one subject in LC group were omitted because of poor fit.
[2]Data with a common superscript in a column are not different (P>0.05).
[3]NS: P > 0.08.

The interaction of dietary protein and calcium affected the efficiency of calcium retention such that the fractional calcium retention was highest when calcium intake was low and protein intake was high (P<0.01, Table). As expected, a high calcium intake reduced the fractional calcium retention (by >40%). Protein intake modified calcium retention only when calcium intake was low. In summary, under controlled conditions, no antagonistic effect between dietary protein and calcium was detected on whole body calcium retention. However, when calcium intake was low (~600 mg/d), a high protein intake (~20% of energy) enhanced calcium retention. In conclusion, in healthy postmenopausal women, with a typically low calcium intake, a high protein diet may be beneficial to bone health by improving calcium retention.

Disclosures: ***Z.K. Roughead****, National Cattelemen's Beef Association 2.*

SU410

A Relationship Between Body Composition and Calcium Absorption Efficiency. M. J. Barger-Lux[1], M. S. Dowell*[1], R. P. Heaney[2]. [1]Department of Medicine, Creighton University, Omaha, NE, USA, [2]Creighton University, Omaha, NE, USA.

As part of an ongoing interest in sources of variation in Ca absorption efficiency (CaAbs), we examined its correlates in data collected for another study.

The 56 subjects (23 women and 33 men) were aged 20 to 51 y at entry. All reported ample summer sun exposure and limited non-solar sources of vitamin D. They classified themselves as black (*n*=23), white (*n*=29), or other (*n*=4). Median BMI was 27.1 kg/m^2 (interquartile range, 23.1 to 30.5).

Data were gathered at Visit 1 (after summer sun exposure, Aug. 23 to Sept. 21) and later, at Visit 2 (after winter sun deprivation, Feb. 1 to Mar. 15). We measured body composition (as % body fat by DXA), constitutive skin color (by use of a portable colorimeter with a standard color system), and CaAbs; fasting serum 25(OH)D, vitamin D_3, 1,25$(OH)_2$D, PTH, and Ca; and fasting 2h urine Ca-to-creatinine.

As expected, paired values for CaAbs were strongly related (r = +0.702, P<0.0001). In these data, CaAbs was unrelated to skin color and to 25(OH)D, PTH, and 1,25$(OH)_2$D. However, CaAbs and % body fat were significantly and positively related at both visits, with a stronger relationship after controlling for BMI (r = +0.425, P<0.005 and r = +0.382, P<0.01, respectively).

We conclude that: (1) % body fat may be an important source of variation in Ca absorptive capacity (as an indicator of gut surface area?) and (2) further study is warranted.

Disclosures: ***M.J. Barger-Lux****, None.*

SU411

Short-term Biological Effects of Calcium from Natural Mineral Water in Young Women with Low Calcium Dietary Intakes. P. Fardellone[1], F. Constant*[2], P. Lefauveau*[1], S. Kamel[1], M. Arnaud*[2], J. Aeschlimann*[3], F. Boitte*[1], M. Brazier[1]. [1]Rhumatology, Hospital, Amiens, France, [2]Nestlé Water Institute, Vittel, France, [3]Nestlé Research Center, Lausanne, Switzerland.

Calcium bioavailability from calcium-rich natural mineral waters has been shown as well as its significant contribution to total calcium intakes and its effects on bone turnover. However, it has not been demonstrated whether or not drinking a natural mineral water with moderate calcium content could have similar effects in subjects with a low calcium diet.

The aim of the study was to assess the short-term biological effects of two waters on calcium homeostasis and bone remodeling in a healthy population of 101 young women (aged 18 to 40 years). Spontaneous dietary calcium intakes were assessed by a food frequency questionnaire and ranged from 200 to 600 mg/day. The subjects were under hormonal contraception in order to standardize their hormonal status. They participated to a randomized cross over study comparing the effects of a natural mineral water (Vittel Bonne Source®) containing 91 mg/L calcium with a mineral-free water. Women, distributed between two groups were maintained on their usual diet and drank 1.5l/day of one of the studied waters for a 8-day period. Water was changed after a 20-day washout period. The blood samples were collected at 8 am and 12 am, at baseline (D0) and after 3 (D3) and 8 days (D8) to measure total and ionized calcium, creatinine, intact parathyroid hormone (iPTH), serum C-telopeptidic fragments (CTX), and osteocalcin. On the morning of the sampling, women were asked to drink 250 ml of the studied water each hour for 4 hours and then 500 ml in the afternoon. On D0, D3 and D8, between 8am and 12am it was observed a significant (P<0.003) higher increase of total and ionized calcium and a deeper decrease of serum CTX and iPTH in the women drinking the natural mineral water when compared with mineral-free water. Moreover, a continuous trend in the increase of total and ionized calcium and in the decrease of serum CTX was observed during the 8-day period in the women drinking the natural mineral water.

In conclusion, natural mineral waters with a calcium content close to 100 mg per liter leads to a decrease of bone turnover in women with low calcium intakes and may have beneficial long-term effects.

Disclosures: ***P. Fardellone****, None.*

SU412

Dose Response of Hesperidin, a Citrus Flavonoid, on Bone Mass in Young Intact Rats. M. Horcajada*[1], C. Morand*[1], E. Offord*[2], P. Lebecque*[1], C. Puel*[1], J. Mathey*[1], M. Davicco*[1], V. Coxam[1]. [1]Nutrition, INRA, Saint genès champanelle, France, [2]Nutrition, NRC, Lausanne, Switzerland.

A high consumption of fruit and vegetables has been associated with a positive effect on bone health. An interesting sub-group of flavonoids, flavanones, is present in our diet almost exclusively in citrus fruits. Hesperidin is the main flavanone found in orange fruit (~ 2g/kg), and we have previously reported its ability to affect bone mass and strength in intact and ovariectomized rats. The aim of the current study was to establish the minimum effective dose of pure hesperidin (Hp) which could stimulate bone formation in 3 month-old intact rats.

The dose-response was carried out on 60 young intact Wistar rats, with a time duration of 3 months. The animals were assigned to six groups of ten rats each. One group received a soy-protein-free, semi-purified standard diet (**SH**), while the others were fed the same diet but with added hesperidin at various doses : 0.125% (**SH1**) ; 0.25% (**SH2**); 0.5% (**SH3**); 1% (**SH4**) and 2.5% (**SH5**) of the diet.

Throughout the study period, rats kept growing with the same pattern of body weight evolution in each group and, on day 85, no difference in body composition among groups was detected. At necropsy, femoral mineral density (g/cm²)was significantly increased in SH2 and SH3 (+5% *vs* SH ; $p<0.05$) groups with the same magnitude, this effect was even stronger in SH4 and SH5 groups, when compared to the controls (+6.1% *vs* SH ; $p<0.01$). This impact was achieved in both total and metaphyseal compartments. Diaphyseal femoral density was also increased by Hp consumption starting from the 0.25% dose upwards (SH2 : +4.1% *vs* SH ; $p<0.05$; SH4 : +5.2% *vs* SH ; $p<0.01$). This was paralleled with an enhanced femoral failure load. No differences were observed in BMD or femoral strength, with the lowest dose (0.125%). Plasma osteocalcin concentrations were unchanged in all groups while urinary deoxypyridinolin excretion was significantly decreased in the group from 0.125% - 2.5% (SH1 : -13.3% *vs* SH), indicating a slow down of bone resorption. Plasma hesperetin concentration (aglycone form) increased in a dose dependent manner, each dose inducing a significant difference in plasma level when compared to the lowest dose. A strong correlation with hesperetin intake (24h) was noted ($R^2 = 0.98$) and with urinary DPD excretion ($R^2 = 0.88$).

In conclusion, hesperidin consumption improved both femoral strength and mineral density. This appeared to be linked with a decreased catabolism. The effective dose, in our experimental conditions, was 0.25% hesperidin, corresponding to 1.76µM plasma hesperetin when measured during the post-absorptive period.

Disclosures: ***M. Horcajada****, NESTLE 2.*

SU413

Deflection of Glucocorticoid Action on Osteoclasts from TRAP-11ß-HSD2 Transgenic Mice Abrogates the Antiapoptotic Effects of the Steroid. D. Jia, C. A. O'Brien, S. A. Stewart*, S. C. Manolagas, R. S. Weinstein. Div. of Endo/Metab, Center for Osteoporosis, Central Arkansas Veterans Healthcare System, Univ of Ark for Med Sci, Little Rock, AR, USA.

Glucocorticoid-induced bone loss occurs in two phases in humans and mice: a rapid, early phase in which bone mass is lost due to excessive bone resorption and a slower, chronic phase in which bone is lost due to inadequate bone formation. In vitro and in vivo studies have suggested that glucocorticoids may act directly on differentiated osteoclasts to extend their lifespan. To establish whether the increased bone resorption caused by glucocorticoids excess results from direct actions of glucocorticoids on osteoclasts, we have generated transgenic mice expressing human 11ß-hydroxysteroid dehydrogenase-2 (11ß-HSD2), an enzyme that causes rapid pre-receptor oxidative inactivation of glucocorticoids, under the control of the promoter for mouse tartrate-resistant acid phosphatase (TRAP). Taqman RT-PCR showed that the human 11ß-HSD2 transgene was expressed in bone, but not soft tissue, and immunohistochemistry demonstrated exclusive presence of the human protein in osteoclasts. There was no detectable difference at 5 weeks of age between wild-type and transgenic mice in body weight, femur length or vertebral height, compression strength and cancellous histomorphometry. Furthermore, gender differences were not found in the TG mice. Osteoclast precursor-enriched bone marrow cells from either genotype formed TRAP-positive multinucleated osteoclasts in vitro following 5 days of treatment with the receptor activator of NF-κB ligand (RANKL) and macrophage-colony stimulating factor (M-CSF). Baseline apoptosis, assayed by caspase-3 activity, was reduced by glucocorticoids in cultures of wildtype osteoclasts. This effect was greatly attenuated in osteoclasts from the transgenic animals. Likewise, the ability of glucocorticoids to prevent alendronate-induced osteoclast apoptosis in wildtype cells was abrogated in osteoclasts from the TRAP-11ß-HSD2 mice. These results indicate that glucocorticoids exert at least part of their anti-apoptotic effects on osteoclasts by direct actions. These direct effects may play a role in the rapid, early phase of glucocorticoid-induced bone loss and partially override the pro-apoptotic effects of alendronate. Nonetheless, studies of ours presented elsewhere in this meeting suggest that there are also ancillary indirect effects of glucocorticoids on osteoclasts mediated by an increase in RANKL/osteoprotegerin ratio.

Disclosures: ***D. Jia****, None.*

SU414

Glucocorticoid-Induced Osteopenia at the Axial and Appendicular Bones in Male and Female Mice. J. L. Matthews*[1], V. Shen[2], S. Tellefson*[2], E. Bell*[2]. [1]GlaxoSmithKline Medicines Research Centre, Stevenage, United Kingdom, [2]SkeleTech, Inc., Bothell, WA, USA.

Osteoporosis is a serious side effect of high dose glucocorticoid (GC) treatment in both the male and female populations. There is no commonly accepted GC-induced bone loss animal model that is used to test the safety of new generation GC-like drugs. In this study, we aimed to establish such a model in both male and female animals.

Twenty-seven-week-old male and female Balb/c mice were randomized into treatment groups based on baseline bone area and bone mineral density results. The animals were then given daily subcutaneous injections of vehicle or dexamethasone (DEX, 5 mg/kg). *In vivo* DXA scans were performed pre-dose and after 4, 6 and 8 weeks of dosing. Both axial and appendicular bones were analyzed. DEX administration induced a significant loss in bone mineral density (BMD) at the axial bone, the lumbar spine, and the appendicular bone, the femur, when compared to pre-dose levels. The net BMD loss was about 10% independent of the bone site or gender when examined at 8 weeks. Whereas most of the loss in BMD at the lumbar spine occurred during the last 4 weeks of DEX treatment, the loss of BMD at the femur can be clearly seen at 4 weeks.

In conclusion, we have demonstrated that the use of DEX induced a net bone loss in both the axial and appendicular bones in both genders of mice and that this model can be used as a model for safety testing of new generation GC compounds. The timing of the bone loss differs at these two sites. Based on observed variations in vehicle-treated animals, multiple scans over a longer period of time are recommended to ensure the observation of a net loss of bone.

BMD at Lumbar Spine

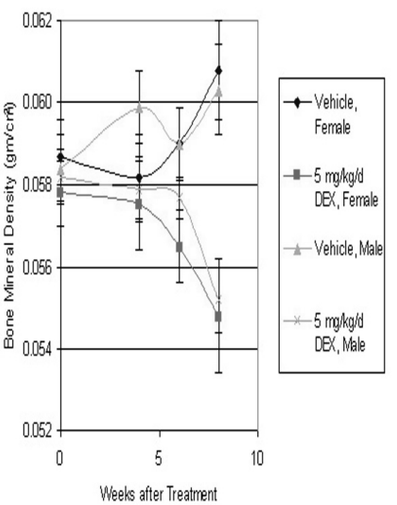

BMD at Femur

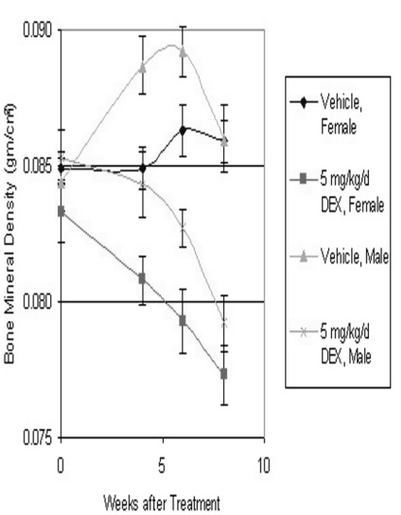

Disclosures: ***V. Shen****, None.*

SU415

Glucocorticoid-Induced Osteoporosis in the Mouse: Reduced Bone Strength Is Associated with Loss of Cortical Bone and Altered Trabecular Bone Structure. J. L. Matthews*[1], V. Shen[2], B. P. Hayes*[1], B. Maschera*[1], G. Wakley[3], K. T. Pun*[1], E. Meldrum*[1], S. N. Farrow*[1]. [1]Asthma Biology, GlaxoSmithKline, Stevenage, United Kingdom, [2]Skeletech Inc, Bothell, WA, USA, [3]Anatomy, BioResults Ltd and University of Bristol, Bristol, United Kingdom.

Glucocorticoid-induced osteoporosis (GIOP) is a serious side-effect of high dose glucocorticoid (GC) treatment leading to increased vertebral and neck of femur fracture risk. The aim of this work has been to develop a mouse model of GIOP reflecting the increased fracture risk seen in man and to elucidate structural and dynamic changes associated with increased fracture risk.

Subcutaneous Dexamethasone (Dex)(0, 1, 3, 5 or 10mg/kg) was administered daily to 27 week old female BalbC mice. DXA scans were performed fortnightly and when dose responsive bone loss was evident, a first intraperitoneal injection of calcein was given. A 2nd dose of calcein was given after a further 8 days followed by cull 2 days later. At termination, bone mineral density (BMD) of the right femur was measured by peripheral quantitative computed tomography (pQCT) before 4 point bend tests were performed to assess bone strength. Structural assessment of the left femur was made using microcomputed tomography (microCT) analysis. Compression tests were performed on L5 vertebrae and bone formation rate (BFR) was measured on the L4 vertebrae using dynamic histomorphometry.

The top 2 doses of Dex induced reductions in femur BMD after 4 weeks and by 6 weeks a clear dose responsive effect was evident so termination was at 8 weeks. PQCT confirmed the reduction in overall BMD, which was mainly due to loss of cortical bone. These reductions correlated with reductions in cortical volume and trabecular bone thickness as assessed by micro CT, and with reduced femur strength. Loss of vertebral BMD also correlated with loss of bone strength and reduced BFR.

In conclusion, we have demonstrated that the major clinical features of GIOP in man are reflected in our mouse model . This model provides a powerful system in which to study the mechanisms regulated by GC's in bone, and to evaluate the potential of novel bone-sparing therapeutic approaches.

Table showing bone measurements of Dex treated mice as a percentage of the vehicle control. * represents significant differences from the vehicle. (P<0.05)

	1mg/kg	3mg/kg	5mg/kg	10mg/kg
Femur BMD (pQCT)	92±0.6*	89±1.6*	90±0.9*	85±1.3*
Femur Cortical thickness	87±1.2*	78±1.5*	80±1.5*	70±2.1*
Femur Trabecular thickness	100±1.1	96±0.8*	97±0.9*	90±1.8*
Femur strength (max load)	83±4.1	69±2.6*	76±4.2*	62±4.1*
Vertebral strength (max load)	102±8.8	95±11.4	76±13.0	54±10.7*
Vertebral BFR	58±20*	24±16.3*	1±1.0*	6±4.3*

Disclosures: ***J.L. Matthews****, None.*

SU416

Osteoporosis Associated with Megestrol Acetate. R. A. Wermers, D. L. Hurley, A. E. Kearns. Endocrinology, Mayo Clinic, Rochester, MN, USA.

Megestrol acetate (Megace) is a progestational agent used in the treatment of metastatic breast and endometrial cancer. It has also been used as an appetite stimulant for patients with human immunodeficiency virus and malignancy, suffering from cachexia and wasting. In addition, it can be beneficial in relieving hot flashes in women and men. Megace has been shown to have a glucocorticoid-like effect and also has been associated with significant suppression of plasma estradiol levels. We describe two postmenopausal women who recently presented to our Metabolic Bone Disease Clinic with severe osteoporosis complicated by multiple vertebral fractures shortly after initiation of high-dose Megace therapy. These patients were shown to have evidence of adrenal axis suppression, but fully recovered after Megace was discontinued. One of the patients manifested clinical features of cortisol excess with facial fullness, abdominal distention, and easy bruising. We speculate that Megace was an important factor in the development of osteoporosis and subsequent fractures, and to our knowledge, this is the first report suggesting such an association. Further study is warranted to clarify the relationship between Megace and its potential for adversely affecting the skeleton.

Disclosures: ***R.A. Wermers****, None.*

SU417

A Histomorphometric Study of the Effects of Steroid Treatment on the Cortical Bone of the Iliac Crest. S. Vedi*[1], S. Elkin*[2], J. E. Compston[1]. [1]Medicine, University of Cambridge, Cambridge, United Kingdom, [2]Cystic Fibrosis, Royal Brompton Hospital, London, United Kingdom.

Long-term administration of glucocorticoids for the treatment of a variety of disorders is associated with increased bone loss and fracture risk. The effects of steroid treatment on cancellous bone remodelling and structure are reasonably well documented but there are no reported histomorphometric studies in human cortical bone. The aim of this study was to investigate the effect of long-term glucocorticoids on iliac crest cortical bone in 14 patients, 9 females and 5 males, aged 18-48 years (mean 34.1 + 8.7 years), using Image Analysis. Results were compared with an age matched control group of 10 premenopausal women with untreated endometriosis and 4 males, aged 22-38 years (mean 30.1 + 4.8 yrs). Although, cortical porosity was significantly higher in patients treated with glucocorticoids (8.4 + 8.9 % ; mean + SD) compared with the untreated group (5.1 + 3.9 %; p=0.03), cortical width and area were similar in the two groups. The Haversian canal number and density were also significantly higher in glucocorticoid treated patients (45.9 + 23.2 vs 31.9 + 24.4 and 13.7 + 9.4 vs 6.7 + 3.3 /mm2; p=0.003 and p=0.00005 respectively), but Haversian canal area did not differ significantly between groups.

The mean wall width of the osteons was significantly lower in the treated patients compared to the untreated group (48.8 + 7.1 microns vs. 59.3 + 12.0 microns; p=0.008). Bone formation rate (microns squared/microns/day) and mineral apposition rate (microns/day) were also both significantly reduced in patients receiving long-term glucocorticoid therapy when compared to the untreated group (0.056 + 0.040 vs. 0.095 + 0.058 and 0.59 + 0.12 vs.0.74 + 0.13; p=0.05 and p=0.01, respectively). The proportion of canals with an eroded surface was lower in the treated group when compared with the untreated control group.

These results demonstrate that there is an increase in cortical porosity in patients treated with long-term glucocorticoid therapy, due to an increase in the number rather than size of Haversian canals. Effects on cortical width were not demonstrated, possibly as a result of the relatively small sample size. Overall, these changes would be consistent with increased resorption during the early stages of glucocorticoid treatment associated with and followed by persistent reduction in bone formation..

Disclosures: ***S. Vedi****, None.*

SU418

The Anabolic Effect of Intermittent PTH on Bone Is Partially Prevented by Simultaneous Glucocorticoid Treatment in Aged Rats. H. Oxlund, G. Ortoft*, T. T. Andreassen. Dept of Connective Tissue Biology, University of Aarhus, Inst of Anatomy, Aarhus, Denmark.

Glucocorticoids (GC) are used for the treatment of a wide spectrum of diseases because of their potent anti-inflammatory and immunosuppressive effects, and they are serious and common secondary causes of osteoporosis. In the present study, the effects of simultaneous parathyroid hormone (PTH) and GC injections were investigated on bone static and dynamic histomorphometry. Twenty-seven-month-old female Wistar rats with ceased linear growth were used. The rats were divided at random into the following groups: baseline, vehicle-injected (Veh), PTH-injected (PTH), GC-injected (GC), PTH+GC-injected. Doses: PTH (1-34) 25 :g/kg body weight daily, GC (methylprednisolone) 2.5 mg/kg body weight daily. The treatment period was 8 weeks. The rats were labelled with fluorochromes 3 times during the experiment: alizarine red 20 mg/kg at day 7, calcein 15 mg/kg at day 42, and tetracycline 20 mg/kg at day 52. Bone sections were cut and studied by fluorescence microscopy. Concerning cancellous bone in the proximal tibia metaphysis, 2 mm distally to the epiphyseal growth plate, the trabecular bone volume (TBV) was markedly increased (2p<0.00001) in PTH-injected rats (41.9 [[Unable to Display Character: "]] 2.5 %, mean [[Unable to Display Character: "]] SEM) compared with the Veh-injected rats (7.5 [[Unable to Display Character: "]] 1.5 %). TBV in the PTH+GC group (26.9 [[Unable to Display Character: "]] 1.8 %) was increased (2p<0.0001), but less pronounced compared with the GC group (10.1 [[Unable to Display Character: "]] 1.5 %). Concerning cortical bone at the tibia mid-diaphysis, the PTH-injections likewise induced a pronounced endocortical formation of new bone, resulting in increased (2p< 0.01) bone cross-sectional area (4.67 [[Unable to Display Character: "]] 0.12 mm^2) compared with the Veh-injected (4.13 [[Unable to Display Character: "]] 0.07 mm^2); and the bone cross-sectional area in the PTH+GC group (4.31 [[Unable to Display Character: "]] 0.10 mm^2) was not significantly increased (2p=0.058) compared with the GC group (4.05 [[Unable to Display Character: "]] 0.09 mm^2). The mid-diaphyseal medullary cross-sectional area of the PTH-injected group (0.92 [[Unable to Display Character: "]] 0.06 mm^2) was reduced (2p=0.0001) compared with the Veh-injected group (1.28 [[Unable to Display Character: "]] 0.05 mm^2). The medullary cross-sectional area of the PTH+GC group (1.08 [[Unable to Display Character: "]] 0.05 mm^2) was reduced (2p=0.041) compared with the GC group (1.29 [[Unable to Display Character: "]] 0.08 mm^2), but to a lesser degree. In conclusion, the pronounced anabolic effect of PTH on endocortical and cancellous bone surfaces was partially prevented by simultaneous treatment with GC in aged rats.

Disclosures: ***H. Oxlund****, None.*

SU419

The Impact of Endogenous Cortisone on Bone: Demonstration of In Vivo 11beta-Hydroxysteroid Dehydrogenase Type 1 Activity. M. S. Cooper[1], H. E. Syddall*[2], P. J. Wood*[3], P. M. Stewart*[1], C. Cooper[2], E. M. Dennison[2]. [1]Division of Medical Sciences, University of Birmingham, Birmingham, United Kingdom, [2]MRC Environmental Epidemiology Unit, University of Southampton, Southampton, United Kingdom, [3]University of Southampton, Southampton, United Kingdom.

Cortisone is an inactive circulating corticosteroid that can be converted to the active corticosteroid cortisol by the enzyme 11beta-hydroxysteroid dehydrogenase type 1 (11b-HSD1). 11b-HSD1 is expressed in osteoblasts and may play a role in age-related and glucocorticoid-induced osteoporosis. The contribution this enzyme makes to endogenous bone metabolism is however unknown. The kinetics of cortisone to cortisol conversion are such that enzyme activity is proportional to cortisone concentration. To examine *in vivo* 11b-HSD1 activity in healthy subjects we have analysed the relationship between serum cortisone, cortisol, markers of bone turnover and BMD in a cohort of women (n=135) and men (n=170) aged 60-75 years at baseline and followed up 4 years later.

0900 serum cortisone levels at baseline were 55±11 nmol/L in women, 55±9 nmol/L in men. Cortisone levels were negatively correlated with serum osteocalcin (r=-0.16, p=0.06 for women; r=-0.20, p=0.01 for men) but not urinary N-telopeptide of type I collagen (NTx)(r=-0.03 women; r=0.03 men, both NS) suggesting enzyme activity within osteoblasts. Negative correlations between serum cortisone and spine BMD were also apparent (r=-0.18, p=0.04 for women; r=-0.14, p=0.07 for men) but cortisone did not predict femoral neck or total hip BMD or changes at any site over 4 years. In analyses adjusted for adi-

posity, osteoarthritis grade and life style variables the significance level did not change substantially (p=0.08 for both men and women). All these relationships were independent of cortisol concentrations. Serum cortisol itself was not associated with levels of bone markers or BMD at any site.
Circulating cortisone appeared to account for a mean 20-27% inhibition of osteocalcin levels and a 12-15% reduction of spine BMD in both men and women. The association of cortisone levels with spine but not hip BMD may reflect increased glucocorticoid sensitivity at the spine or higher 11b-HSD1 activity at this site.
In normal subjects 11b-HSD1 activity occurs within osteoblasts *in vivo* with high cortisone levels associated with suppression of osteocalcin and low spinal BMD. Although an inactive hormone, cortisone appears to have a role in bone physiology.

Disclosures: ***M.S. Cooper****, None.*

SU420

Ultrasound Graphic Trace Analysis At Phalanxes In Men And Women Treated With Glucocorticoid. S. Gonnelli[1], A. Montagnani*[1], C. Cepollaro[1], C. Caffarelli*[1], A. Cadirni*[1], N. Nikiforakis*[2], M. Martino*[2], P. Rottoli*[1], R. Nuti[1]. [1]Department of Internal Medicine, Endocrinologic-Metabolic Sciences and Biochemistry,, University of Siena, Siena, Italy, [2]Department of Clinical Medicine and Immunological Science, Division of Respiratory Diseases, University of Siena, Siena, Italy.

Osteoporosis is one of the major complications of glucocorticoid (GC) therapy. It is well known that for a given BMD value GC treated postmenopausal (PM) women present a higher fracture risk than PM osteoporotic women. This finding suggests that the effect of GCs on bone strength can not be wholly determined by conventional DXA. The use of quantitative ultrasound (QUS) and namely the analysis of the characteristics of the ultrasound graphic trace (UGTA), influenced by both quantitative and qualitative properties of bone, could be useful for the assessment of bone status and of fracture risk in GC treated patients.
This study aimed to evaluate the usefulness of QUS parameters at phalanxes in the evaluation of bone status and fracture risk in patients chronically treated with GCs.
We studied 230 patients (145 women and 85 men, mean age 56.1±13.3 years) on treatment with GCs for at least 6 months, and 230 sex- and age-matched controls. In all subjects QUS parameters were measured at phalanxes by Bone Profilers (IGEA, Italy); the parameters evaluated were: amplitude speed of sound (AD-SOS, m/s) and UGTA parameters, namely bone transmission time (BTT, µs), fast wave amplitude (FWA, mV), speed of sound (SoS, m/s) and signal dynamic (SDy, mV/µs²).
AD-SoS and UGTA parameters resulted significantly reduced in GC treated patients than in controls. Moreover, AD-SoS, BTT, FWA and SoS, but not SDy were significantly lower in fracture than in non fracture GC patients. By dividing the GC patients on the basis of gender, we found that in women both AD-SoS and UGTA were lower in fracture than in non fracture patients; but the statistical significance was reached only for AD-SoS ($p<0.05$), BTT ($p<0.001$)and FWA ($p<0.05$). Whereas, only FWA resulted significantly lower ($p<0.05$) in fracture with respect to non fracture males. ROC analysis showed that FWA was able to discriminate between fracture and non fracture patients both in men (AUC: 0.76) and in women (AUC: 0.63), whereas BTT was a discriminative factor for fracture only in women (AUC: 0.70)
Our findings show that QUS at phalanxes can be useful in the assessment of glucocorticoids-induced bone impairment. Among UGTA, BTT resulted as being a good predictor of fragility fracture in women but not in men, and this finding may be explained by the fact BTT is closely related to the cortical thickness of bone, which strongly differs between men and women, suggesting a possible sex dimorphism in GC effect on bone.

Disclosures: ***S. Gonnelli****, None.*

SU421

Role of Dehydroepiandrosterone, Insulin-Like Growth Factor I and Vitamin D in the Bone Loss of Cystic Fibrosis. C. M. Gordon*[1], E. Binello*[1], H. A. Feldman*[1], M. S. LeBoff[2], M. E. Wohl*[1], C. J. Rosen[3], A. Colin*[1]. [1]Children's Hospital, Boston, MA, USA, [2]Brigham & Women's Hospital, Boston, MA, USA, [3]St. Joseph Hospital, Bangor, ME, USA.

Patients with cystic fibrosis (CF) are at risk for early osteoporosis. Although the mechanisms that mediate bone loss in this group are still being delineated, nutritional and/or hormonal factors likely contribute. Dehydroepiandrosterone (DHEA), a naturally secreted anabolic hormone, has been shown to decrease bone loss in various conditions including the malnutrition related to anorexia nervosa. The aims of this study were to examine whether baseline serum levels of DHEA, insulin-like growth factor I (IGF-I) and vitamin D, as well as measurements of bone density, were low in patients with CF, and to examine if significant correlations existed between these variables. We studied thirty-two patients (18 females), with a mean age (± SD) of 26.2 ± 7.9 yr and a body mass index (BMI) of 21.4 ± 2.6 kg/m^2 (range 16-28). The protocol was approved by the local Committee on Clinical Investigation. Half of the participants (16/32) had a history of fractures. Serum DHEA sulfate (DHEAS) levels were low in 66% of patients: mean 155.8 ± 121.1 µg/dl, range 10-545. The mean serum IGF-I level was low in 62% of patients: 240.0 ± 90.1 ng/mL, range 116-440. The mean serum 25-hydroxyvitamin D level was 20.2 ± 9.5 ng/ml, range <8-39, and twelve patients (38%) met criteria for vitamin D deficiency (25-OHD ≤ 15 ng/ml). Bone mineral density (BMD) measurements by dual energy x-ray absorptiometry (DXA) showed decreased mean lumbar and hip z scores: -1.0 ± 1.3, range -4.0 to 1.5, and -0.62 ± 0.8, range -2.5 to 1.2, respectively. A lumbar Z-score < -1.0 was seen in 16 patients (50%). Spearman correlation analyses revealed a significant positive correlation between serum DHEAS and weight ($r= 0.59$, $p<0.001$), and DHEAS and total hip BMD ($r= 0.39$, $p=0.033$). IGF-I was positively correlated with BMD of both the spine ($r= 0.39$, $p=0.026$) and hip ($r= 0.56$, $p<0.001$). BMI was also positively correlated with total hip BMD ($r= 0.35$, $p=0.048$). In this pilot study of adolescents and young adults with CF, DHEAS and IGF-I levels were low in over half of the subjects and over one-third of the participants were vitamin D-deficient. Furthermore, a spinal bone density was of potential clinical significance (Z- score < -1) in half of the sample. These preliminary findings suggest that a direct correlation may exist between cortical BMD and levels of both DHEAS and IGF-I. As the anabolic effects of DHEA may be mediated through the skeletal IGF-I system, therapeutic supplementation of this hormone should be investigated. These results also replicate previous recommendations that surveillance for vitamin D deficiency is warranted in this group.

Disclosures: ***C.M. Gordon****, None.*

SU422

Abnormal Osteoprotegerin And Rankl Levels In Primary Biliary Cirrhosis. Lack Of Association With Osteoporosis And Biochemical Markers Of Bone Turnover. N. Guanabens[1], A. Pares*[2], L. Alvarez[1], A. Monegal*[1], L. Caballeria*[2], D. Ozalla*[1], P. Peris[1], F. Pons*[1], J. Rodes*[2]. [1]Metabolic Bone Diseases Unit, Hospital Clinic, IDIBAPS, University of Barcelona, Barcelona, Spain, [2]Liver Unit, Hospital Clinic, IDIBAPS, University of Barcelona, Barcelona, Spain.

Background/aims: The pathogenesis of osteoporosis in primary biliary cirrhosis (PBC) is not well understood since both low or high bone turnover have been reported. Osteoprotegerin (OPG) and its ligand (RANKL) regulate osteoclastogenesis, and therefore may influence the development of osteoporosis. However, the clinical utility of circulating OPG and RANKL levels for assessing regulation of bone metabolism in secondary osteoporosis is uncertain.
Patients and Methods: OPG and RANKL levels were assessed in 52 patients with PBC (age: 57 ± 1.5 years) and in an age-matched control group of healthy females. Besides liver function tests, serum bone gla-protein (BGP), as index of bone formation, and urinary amino-terminal telopeptide of collagen I (NTx), as index of bone resorption, were also measured. Bone mineral density of the lumbar spine and femoral neck were assessed for diagnosing osteoporosis (BMD below -2.5 T-score). The overall severity of liver disease was assessed by the Mayo risk score.
Results: OPG levels (pM/l) were significantly higher in PBC (5.5 ± 0.2) as compared to controls (2.9 ± 0.2, $p<0.0001$), whilst RANKL (pM/l) were lower in PBC (0.4 ± 0.1) with respect to controls (1.4 ± 0.3, $p<0.0001$). No correlation was observed between OPG and RANKL. 22 patients (44%) had osteoporosis. No significant differences in OPG and RANKL levels were observed between patients with and without osteoporosis (OPG: 5.9 ± 0.4 vs. 5.2 ± 0.2 pM/l; RANKL: 0.39 ± 0.09 vs 0.44 ± 0.08 pM/l) . OPG was significantly higher in patients with advanced liver disease as defined by high bilirubin levels (OPG: 6.8 ± 0.6 vs. 5.2 ± 0.2 pM/l, $p=0.009$) or by a Mayo score above 4 (OPG: 5.9 ± 0.4 vs 4.9 ± 0.3 pM/l, $p=0.04$). Moreover, a direct correlation was observed between OPG and Mayo score ($p=0.01$). No associations were found between OPG and RANKL with biochemical markers of bone remodeling.
In conclusion, OPG and RANKL are abnormal in patients with PBC, regardless of osteoporosis. The high OPG levels are associated with the severity of the liver disease.

Disclosures: ***N. Guanabens****, None.*

SU423

Dissociation between Global Markers of Bone Remodelling and Direct Measurement of Spinal Bone Formation in Osteoporosis. M. L. Frost[1], G. J. Cook[2], G. M. Blake[1], P. K. Marsden*[3], I. Fogelman[1]. [1]Osteoporosis Unit, Guy's, King's & St Thomas' School of Medicine, London, United Kingdom, [2]Dept of Nuclear Medicine, Royal Marsden Hospital, London, United Kingdom, [3]Clinical PET Centre, Guy's, King's & St Thomas' School of Medicine, London, United Kingdom.

Evaluations of global skeletal metabolism have shown that increased bone turnover is a feature of patients with osteoporosis. The non-invasive functional imaging technique of ^{18}F-fluoride positron emission tomography (PET) allows the direct quantitative assessment of bone metabolism at specific sites in the skeleton, including the lumbar spine. The aim of this study was to compare regional skeletal kinetics in 72 postmenopausal women, with a mean age of 61 years, classified as normal, osteopenic or osteoporotic according to their BMD T-score at the lumbar spine. Each woman had a dynamic PET scan of the lumbar spine after injection of 90 MBq ^{18}F-fluoride ion and measurements of biochemical markers of bone formation and resorption. The arterial plasma input function was derived using aorta arterial activity from the PET image. Time activity curves were obtained by placing regions of interest over the vertebrae. A three-compartmental model was used to calculate bone blood flow (K_1) and the net plasma clearance of tracer to bone mineral (K_i), reflecting regional osteoblastic activity with units of ml min^{-1} ml^{-1}. Rate constants k_2, k_3 and k_4, which describe transport between plasma, the ECF compartment and the bone mineral compartment, were also measured. The net uptake of fluoride to the bone mineral compartment (K_i) was significantly lower in the osteoporotic group compared to both the osteopenic and normal groups, with a mean difference of 0.005 ml min^{-1} ml^{-1} (16.7%). The fraction of the tracer in the extravascular tissue space that underwent specific binding to bone mineral (k_3/k_2+k_3) was also significantly reduced in the women classified as osteoporotic. In contrast, levels of bone-specific alkaline phosphatase (Bs-ALP) were significantly higher in the osteoporotic group compared to the normal and osteopenic groups by 35% and 27% respectively. A significant negative correlation ($r = -0.41$) was observed between levels of Bs-ALP and the fraction of the tracer that underwent specific binding to bone mineral. In conclusion, lower values of K_i, a measurement of regional bone formation activity, were seen in women classified as osteoporotic, while levels of Bs-ALP, a measure of global skeletal metabolism were significantly increased. These findings are suggestive of increased global skeletal bone turnover in women with postmenopausal osteoporosis but with relatively reduced regional bone formation at the predominantly trabecular site of the lumbar spine.

Disclosures: ***M.L. Frost****, None.*

SU424

Methadone Maintenance Therapy Is Associated with Low Bone Mass, Increased Markers of Bone Resorption and Altered Neuroendocrine Axes. A. O. Malabanan, T. Kim*, D. P. Alford*, T. C. Chen, M. F. Holick, J. H. Samet*. Department of Medicine, Boston University School of Medicine, Boston, MA, USA.

Opioid use has acute and chronic neuroendocrine effects, which may adversely affect bone health. To assess the effects of methadone maintenance treatment (MMT) on bone health, we conducted a cross-sectional study of 88 patients attending one methadone program, assessing demographic data, bone pain (McGill Pain Survey), bone mineral density (BMD) of the lumbar spine, proximal femur, and wrist, hormonal profile (free testosterone (fT), estradiol (E2), prolactin (PRL), thyroid stimulating hormone (TSH), follicular stimulating hormone (FSH), and luteinizing hormone (LH)) and metabolic bone profile (25-hydroxyvitamin D (25OHD), serum calcium, intact parathyroid hormone (PTH), serum c-terminal telopeptide (CTX) and osteocalcin (OC)). Eligible patients had attended the clinic for at least 1 month, were able to give informed consent, and were not pregnant.

Subject characteristics were as follows: median age 42 years (range 20-66), 61% female of whom 34% were post-menopausal. Bone pain was present in 64%, and vitamin D insufficiency in 32%, as defined by a 25OHD level < 20 ng/ml. The median duration of MMT was 3 years (1 month to 25 years). BMD in female patients at the lumbar spine (L1-4), femoral neck (FN) and 1/3 wrist site were normal in 58%, 76%, and 78%, osteopenic in 38%, 22%, and 20%, and osteoporotic in 4%, 2% and 2%. BMD in male patients at the LS, FN, and 1/3 wrist site were normal in 38%, 38%, and 44%, osteopenic in 38%, 53% and 34%, and osteoporotic in 25%, 9% and 22%. If all sites except for Ward's area are considered, 78% of the females had either osteopenia (58%) or osteoporosis (20%) and 94% of the males had either osteopenia (31%) or osteoporosis (62%).

Male and female patients with abnormally low FN BMD had lower PRL levels (19.8 ± 19.4 vs 30.9 ± 52.0, $p < 0.001$), higher LH (16.7 ± 52.1 vs 7.9 ± 15.3, $p < 0.001$) and FSH (8.7 ± 23.9 vs 4.3 ± 9.4, $p < 0.001$), lower E2 levels (53.5 ± 28.4 vs 80.4 ± 41.2, $p < 0.05$), higher fT levels (3.8 ± 2.7 vs 2.5 ± 2.0, $p < 0.05$), lower TSH (2.5 ± 5.7 vs 2.9 ± 3.4, $p < 0.005$) and higher CTX (0.287 ± 0.128 vs 0.267 ± 0.073, $p < 0.01$) than those with normal FN BMD. 25OHD, intact PTH and OC did not significantly differ between the two groups. Patients on MMT have a high prevalence of low bone density, associated with increases in markers of bone resorption and altered neuroendocrine and sex hormonal axes. MMT patients should be considered at high risk for low bone mass and should be assessed accordingly. Therapy aimed at decreasing bone resorption or correcting the hormonal aberrations may be useful in preventing further bone loss.

Disclosures: ***A.O. Malabanan****, Merck 8; Procter and Gamble 5; Novartis 5.*

SU425

The Relationship among the Bone Markers, Serum Homocystine and Bone Mineral Density in Korean Postmenopausal Women. D. Byun*, J. Mok*, J. Yoon*, Y. Kim*, H. Park*, C. Kim*, S. Kim*, K. Suh*, M. Yoo*. Endocrinology, Soonchunhyang University Hospital, Bucheon-Si, Republic of Korea.

There are many factors for the pathogenesis of osteoporosis. Considering the high prevalence of osteoporosis in homocysteinemia, abnormal homocysteine metabolism would contribute to the pathogensises of osteoporosis. We investigated the bone markers, serum homocyteine level and bone mineral density(BMD) in 33 Korean postmenopausal women. Serum homocysteine level was increasing associated with aging(r=0.35, p=0.04). Serum alkaline phosphatase level and urine N-telopeptide were correlated with lumbar BMD(r=-0.4, p=0.02 and r=-0.35, p=0.04). But serum homocysteine level was not correlated with bone markers and BMD. These results suggest that homocystein metabolism may be disturbed in the elderly postmenopausal women but the effect of homocysteine metabolism on bone is weak in Korean postmenopausal women.

Disclosures: ***D. Byun****, None.*

SU426

Basal Metabolic Rate Is Related to Lumbar Bone Mineral Density and Body Composition in Pre- and Post-menopausal Women at Korea. S. K. Lee[1], H. J. Choi*[2], Y. C. Kim*[2], H. W. Baik*[3], H. J. Kim*[4], K. J. Ahn*[4], K. S. Park*[4]. [1]Biochemistry/Internal Medicine, Eulji University School of Medicine, Daejeon, Republic of Korea, [2]Family Medicine, Eulji University School of Medicine, Daejeon, Republic of Korea, [3]Biochemistry, Eulji University School of Medicine, Daejeon, Republic of Korea, [4]Internal Medicine, Eulji University School of Medicine, Daejeon, Republic of Korea.

Body weight, fat mass or lean body mass are predictors of bone mineral density (BMD). However, few studies have examined relationships between BMD and basal metabolic rate (BMR) which might be related to body composition. In this study, we investigated the associations of body composition, BMR, lumbar BMD, and serum insulin levels in healthy, osteopenic or osteoporotic but otherwise normal, pre- (n=50; 43±7 years) and post-menopausal (n=60; 60±6 years) women at Korea. Body composition analysis and BMR were performed using the bioelectrical impedance analysis method (InBody, Biospace Co.). BMD (g/cm^2) was determined at the lumbar spine (L_1-L_4) for all subjects with dual-energy X-ray absorptiometry scanner (QDR-1000 plus). BMR was higher in pre-menopausal (1172±93 kcal) than that in post-menopausal (1120±87 kcal) women ($p<0.01$). In premenopausal women, BMR was related to age (r=-0.540, $p<0.01$), BMD (r=0.498, $p<0.01$), height (r=0.794, $p<0.01$), weight (r=0.572, $p<0.01$), and lean body mass (r=0.831 $p<0.01$), but not to fat mass and serum insulin level. In postmenopausal women, BMR was related to BMD (r=0.457, $p<0.01$), height (r=0.692, $p<0.01$), weight (r=0.902, $p<0.01$), fat mass (r=0.712, $p<0.01$), lean body mass (r=0.989, $p<0.01$), and serum insulin level (r=0.549, $p<0.01$), but not to age. In conclusion, BMR was related to lumbar BMD, and body composition in pre- and post-menopausal women. However, BMR was related to fat mass and serum insulin level only in postmenopausal women at Korea.

Disclosures: ***S.K. Lee****, None.*

SU427

Acidification of the Osteoclastic Resorption Compartment Affects Osteoclast Survival and might be of Regulatory Importance for Coupling of Bone Resorption to Bone Formation. M. A. Karsdal[1], K. Henriksen[1], J. Gram[2], S. Schaller*[1], C. Christiansen[1], J. Bollerslev[3]. [1]Nordic Bioscience, Herlev, Denmark, [2]Ribe County Hospital, Esbjerg, Denmark, [3]National University Hospital, Oslo, Norway.

Systematic studies of osteopetrotic mutations in which osteoclast activity is attenuated and osteoblast function seems unaltered may contribute to our understanding of the coupling principle in bone remodelling.

Osteopetrotic patients suffering from deficient acidification of the osteoclastic resorption lacunae either by a defect in the chloride channel ClC-7 or the vATPase have decreased osteoclast resorption with normal osteoblast function in vivo, suggesting that the coupling principle is challenged. In contrast, Cathepsin K deficient patients suffer from both a decrease in bone resorption and bone formation. Interestingly, only the acidification-attenuated patients display an increased numbers of osteoclasts. We speculated that increased numbers of inactive osteoclasts were linked to attenuated acidification, however with unaltered signalling and stimulation of bone formation.

We investigated the effect of acidification on human osteoclast function and life span, and compared this to Cathepsin K inhibition. We used CD14 preparations of human osteoclasts cultured on bone slices with inhibitors of chloride channels (NS3696), the proton pump inhibitor bafilomycin and the Cathepsin K inhibitor E64 and investigated bone resorption and TRAP positive cell-number. We found that bafilomycin and NS3696 dose dependently inhibited acidification of the osteoclastic resorption compartment and bone resorption. Interestingly, the inhibition of acidification by bafilomycin but not cathepsin K inhibition augmented osteoclast survival, which resulted in a 125% increase in multinuclear osteoclasts compared to controls.

To investigate if attenuated acidification in vivo leads to decreased bone resorption with unaffected bone formation, we used the rat OVX model with once daily oral dosing of NS3696 at 50 mg/kg for 6 weeks starting directly after surgery. OVX induced bone loss and strength was inhibited by more than 50 %. As hypothesised, we observed a decrease in resorption 60% (DPYR), increased TRAP levels and no effect on bone formation evaluated by osteocalcin.

We speculate, that attenuated acidification inhibits dissolution of the inorganic phase of bone and results in an increased number of inactive osteoclasts that are responsible for the coupling to normal bone formation. Thus, we suggest that acidification is essential for normal bone remodelling and that attenuated acidification leads to uncoupling with decreased bone resorption and unaffected bone formation.

Disclosures: ***M.A. Karsdal****, Nordic Bioscience 1.*

SU428

Treatment With The TNF-α Antagonist Infliximab Is Associated With Increased Markers Of Bone Synthesis In Patients With Crohn's Disease. M. T. Abreu*[1], L. Y. Kam*[1], E. A. Vasiliauskas*[1], P. Vora*[1], B. Hu*[2], H. Yang*[3], Y. Lin*[3], G. Keenan*[4], J. Gaiennie*[1], C. J. Landers*[1], S. R. Targan*[1], J. S. Adams[2]. [1]Gastroenterology, Cedars-Sinai Medical Center, Los Angeles, CA, USA, [2]Endocrinology, Cedars-Sinai Medical Center, Los Angeles, CA, USA, [3]Pediatrics, Cedars-Sinai Medical Center, Los Angeles, CA, USA, [4]Centocor, Inc., Malvern, PA, USA.

Osteoporosis is a common complication affecting Crohn's disease patients. A principal reason for osteoporosis is glucocorticord use but may also include a detrimental effect of inflammatory cytokines including tumor necrosis factor-alpha (TNF-α). We hypothesized that treatment with the TNF-α antagonist infliximab in patients with active Crohn's disease would result in increased bone formation as measured by surrogate markers of bone turnover. Sera from 38 prospectively-enrolled, Crohn's disease patients were examined for levels of bone alkaline phosphatase (BAP), N-telopeptide of type I collagen (NTX), immunoreactive parathyroid hormone (iPTH), calcium, and inflammatory cytokines at baseline and four weeks postinfliximab infusion. Crohn's Disease Activity Index (CDAI; $p<0.001$) and Inflammatory Bowel Disease Questionnaire (IBDQ; $p<0.001$) results were significantly improved at four weeks. For the 22 patients who were taking glucocorticord at baseline examination, the mean decrease in steroid dose four weeks post-infusion was 7.9 mg ($p<0.001$) or 41% of the baseline dose. Patients steroid-free at baseline remained steroid-free at week 4. Infliximab wass associated with a significant increase in BAP ($p=0.01$); no corresponding increase ($p=0.8$) in NTX was observed. When patients were stratified by baseline steroid use, the increase in BAP was greatest in patients who were taking steroids at baseline ($p=0.05$). In summary, treatment with infliximab was associated with increased markers of bone formation (BAP) without an increase in bone resorption (NTX). This effect may be due to a beneficial effect of TNF-α blockade on bone turnover, a beneficial effect on Crohn's disease activity resulting in decreased glucocorticord dose or both. Longer-term studies should address the effect of infliximab on bone mineral density.

Disclosures: ***J.S. Adams****, None.*

SU429

Possible Pathogenic Mechanisms in a Mouse Model of Type II Diabetes Mellitus with Severe Osteopenia. S. Yakar[1], W. G. Beamer[2], K. M. Delahunty*[2], C. J. Rosen[2], D. LeRoith[1]. [1]Diabetes Branch, National Institutes of Health, Bethesda, MD, USA, [2]The Jackson Laboratory, Bar Harbor, ME, USA.

Several lines of evidence suggest that osteopenia is an important consequence of insulin resistant type 2 diabetes mellitus (DM) although the incidence and pathogenesis of this syndrome have not been clarified. In fact, some studies report no correlation between BMD and HbA1c levels whereas others show a negative relation between DM duration and BMD. In the current study we examined the effects of insulin resistance on BMD in a mouse model of type-II DM. MKR mice express a dominant negative (DN) form of the human IGF-IR under the control of the muscle creatine kinase promoter specifically in muscle on a FVB/N (WT) background. Since the DN IGF-IR forms heterodimers with the endogenous monomers of both the IGF-I and insulin receptors in skeletal muscle, it inhibits the activation of both pathways leading to significant insulin resistance in skeletal muscle and eventually type II diabetes. At 3 weeks of age MKR mice display hyperinsulinemia and dyslipidemia with impaired glucose tolerance. These mice have slightly shorter femurs and weigh significantly less than WT. However, by 8 weeks of age MKR exhibit significant catch up growth such that femur length is identical to WT, and body weight is only 10% lower ($p<0.05$) than WT. At this time MKR demonstrate severe insulin resistance with marked hyperglycemia and lipotoxicity while muscle weight is slightly but not significantly less than WT. BMD measured by pQCT at the pre-diabetic stage (i.e. 3 wk) revealed no significant differences in cortical thickness, periosteal or endosteal circumference, cortical volume or cortical density between MKR and WT($p<0.30$). However, at the frank diabetic stage (i.e. 8 wk), MKR mice display severe osteopenia: results represented as mean±SD (See Table). Taken together these data suggest that type II insulin resistant DM is associated with significant osteopenia. The pathogenic mechanisms responsible for low bone mass in DM include either lipotoxicity and/or glucose toxicity. Further studies are need to delineate the mechanism(s) responsible for impaired peak BMD in DM and to assess whether reduction in hyperglycemia or lipotoxicity rescue the bone phenotype.

Strain -8 week N	FemBMD mg/cc	Cortical thick-mm	Perios Circum-mm
FVB/N- 10	11.66±0.52	0.19±0.01	4.96±0.10
MKR/FVB/N- 12	9.03±0.59	0.16±0.01	4.48±0.13
P value	<0.0001	<0.0001	<0.0001

Disclosures: ***S. Yakar****, None.*

SU430

Systemic Inflammatory Mediators in Calcium and Phosphate homeostasis. M. Pazianas[1], M. Hise*[2], C. Compher*[3], S. Benedict*[4], J. C. Brown*[4], B. Kinosian*[1]. [1]Medicine, Univ of Pennsylvania, Philadelphia, PA, USA, [2]Department of Dietetics and Nutrition, University of Kansas Medical Center, Kansas City, KS, USA, [3]Penn Nursing, Univ of Pennsylvania, Philadelphia, PA, USA, [4]Department of Molecular Biosciences, Univ of Kansas, Lawrence, KS, USA.

Inflammatory bone resorbing cytokines have been implicated in the development of osteoporosis. In patients with home parenteral nutrition (HPN) the inflammatory process could be affected by the reduced gut-associated lymphoid tissue or by the presence of the catheter used for HPN administration.

We studied: 1) systemic inflammatory mediators such as C-reactive protein (CRP), tumor necrosis factor alpha (TNF-α), soluble TNF-α receptor p55 (sTNFR-I) and p-75 (sTNFR-II), and interleukin-6 (IL-6); and T cell function ($CD4^+$and $CD8^+$ lymphocytes and phytohemagglutinin (PHA)-induced T-lymphocyte proliferation) , 2) biochemical bone profile: serum Calcium (Ca), Phosphorus (Pi) Parathyroid hormone (PTH), Alkaline Phosphatase, 25(OH) D and $1,25(OH)_2$ D and 3) bone mineral density (BMD) of the spine and the hip in 9 well nourished , clinically stable patients receiving HPN for >2 years.

Inflammatory mediators IL-6, TNFa and TNFa -RII were significantly correlated with PTH, Pi and Ca; T cell function was negatively correlated with spinal BMD (Table 1). However, none of the systemic inflammatory mediators or T cell function correlated significantly with $1,25(OH)_2$ D or 25(OH) D.

Systemic inflammatory mediators could participate in Ca and Pi homeostasis and chronic inflammation might be considered an additional risk factor for the development of metabolic bone disease.

		Correlation	P
IL-6	PTH	0.748	0.033
IL-6	PO4	-0.751	0.032
TNF-α	Ca	-0.754	0.019
TNFRII	Ca	-0.767	0.016
CD4 (%)	Ca	0.852	0.004
CD4/CD8 (%)	Ca	-0.850	0.007
CD4/CD8(%)	Lumbar BMD	-0.850	0.007

Disclosures: ***M. Pazianas****, None.*

SU431

Severity of Liver Disease Does Not Predict Low Bone Mineral Density in Primary Sclerosing Cholangitis. M. S. Campbell*[1], T. Faust*[1], G. R. Lichtenstein*[1], A. D. Rhim*[1], M. Pazianas[2]. [1]Gastroenterology, Medicine, Univ of Pennsylvania, Philadelphia, PA, USA, [2]Medicine, Univ of Pennsylvania, Philadelphia, PA, USA.

Osteopenia is a complication of chronic cholestatic liver disease. It has been suggested that in primary sclerosing cholangitis (PSC), advanced disease stage may predict advanced bone pathology.

This is a retrospective cross-sectional study. We identified 30 PSC patients who had a DXA (dual energy x-ray absorptiometry) scan. Severity of liver disease was assessed using MELD, Modified Mayo Risk score, presence on the liver transplantation list, and history of hepatic decompensation.

From the 30 patients we studied, nine patients (30%) were osteopenic (T-score between -1 and -2.5), and 1 patient was osteoporotic (T-score less than -2.5). Severity of liver disease was no different between patients with and without osteopenia. BMDs were not different between patients listed or not listed for liver transplantation ($p = 0.49$). Univariate regression showed that MELD ($p = 0.99$) and the Modified Mayo Risk Score ($p = 0.25$) did not predict BMD. A satisfactory multivariate model predicting BMD cannot be constructed from our data.

Our study shows that low BMD cannot be predicted by the severity of liver disease in PSC. The decision to order a DXA scan for a patient with PSC should not be influenced by the severity of liver disease.

Disclosures: ***M. Pazianas****, None.*

SU432

A Single i.v. Injection of Equipotent Doses of Alendronate, Risedronate, Ibandronate and Zoledronic Acid Exerts a Bone Protective Effect of Similar Magnitude and Duration in Ovariectomized Rats. J. A. Gasser, P. Ingold*, J. Green. Bone Metabolism Unit, Novartis Institutes for Biomedical Research, Basel, Switzerland.

There have been suggestions of differences in the terminal half-life between risedronate and alendronate with regard to the duration of antiresorptive action and their elimination from bone (Mitchell et al, Pharm Res 128:166-70, 2001). To address this question we administered the 4 bisphosphonates (BPs) alendronate (AL), risedronate (RI), ibandronate (IB) and zoledronic acid (ZA) given as a single intravenous dose at low, intermediate and high doses to skeletally mature, eight-month old ovariectomized virgin Wistar rats.

The duration of the bone protective effect of the single dose was monitored non-invasively at 4-weekly intervals for 24 weeks at the proximal tibial metaphysis by pQCT (XCT Research SA, cancellous BMD, cortical thickness) and by *in vivo* microCT (vivaCT40, trabecular architecture).

At the low dose, the bone protective effect of 4μg/kg RI, 2μg/kg IB and 0.8μg/kg ZA was significant at 4 and 8 weeks only. With the intermediate doses (AL 40μg/kg, RI 20μg/kg, IB 10μg/kg and ZA 4μg/kg) bone loss was prevented for up to 8 weeks but cancellous BMD, cortical thickness and trabecular bone volume declined thereafter at the same rate regardless of the BP used. With the high dose (AL 200μg/kg, RI 100μg/kg, IB 50μg/kg and ZA 20μg/kg) full protection was achieved for 16 weeks but bone loss occurred thereafter at a similar rate with all 4 compounds.

These results indicate that, after adjustment of the dose to account for the differences in potency (rel. potency versus AL: RI 2x, IB 4x, ZA 10x), the four bisphosphonates show identical duration of action in vivo after a single i.v. dose. Since the antiresorptive effect of the nitrogen-containing BPs is based on their uptake into the mineral phase of bone and their ability to reduce osteoclast activity by inhibiting protein prenylation, our results suggest that the kinetics of their removal from the matrix do not differ between BPs when equipotent doses are directly compared in vivo under the same dosing regimen.

Disclosures: ***J.A. Gasser****, Novartis Pharma AG 3.*

SU433

Use of Differential BMD Thresholds to Assure Adequate Fracture Risk for an International Trial of Zoledronic Acid. E. M. Lau[1], J. A. Cauley[2], J. Caminis[3], T. Rosario-Jansen[3], J. Zhang*[3], S. Farneth*[4], D. M. Black[4]. [1]Prince of Wales Hosp., Shatin, N.T., Hong Kong Special Administrative Region of China, [2]U of Pitt, Pitt, PA, USA, [3]Novartis Pharma, East Hanover, NJ, USA, [4]U of CA, SF, CA, USA.

The HORIZON-PFT is a 3-year, international randomized trial evaluating the effect of once-yearly zoledronic acid on fractures. The two main endpoints are hip and vertebral fractures. Entry criteria include a femoral neck BMD t-score ≤ -2.5, or between -1.5 and -2.5 in the presence of at least 1 vertebral deformity. The design assumed a risk of hip fracture across the entire study of at least 1.8%. Assuring consistent risk across the international cohort to meet that assumption was a priority.

Data published from the Asia Osteoporosis Study revealed that hip fracture risk in Asia is significantly lower than in the US/Europe, despite lower mean BMD. For example, the fracture rate in Hong Kong for women ages 80-84 is about 84% of that in the US; in Thailand it is only 53%. Since both BMD means and hip fracture risk are lower in Asia than in the US and Europe, a lower BMD cutpoint for Asian centers (China, Hong Kong, Korea, Taiwan and Thailand) was necessary to assure adequate hip fracture risk.

For simplicity, we chose to find single cutpoint that could be used in all Asian centers. Reference data for Hong Kong showed a peak mean femoral neck BMD (Hologic) of 0.77 g/cm^2 with a SD of 0.11 g/cm^2. Using this normative data yielded cutpoints for T-scores of -2.5 and -1.5 SD of 0.495 and 0.605 g/cm^2, respectively. These cutpoints were converted to Lunar and Norland values to yield the following BMD entry criterion for Asian sites:

	Non-Asian Countries			Asian Countries		
T score	Hologic BMD cutoff (g/cm^2)	Lunar BMD cutoff (g/cm^2)	Norland BMD cutoff (g/cm^2)	Hologic BMD cutoff (g/cm^2)	Lunar BMD cutoff (g/cm^2)	Norland BMD cutoff (g/cm^2)
T = -1.5	0.683	0.836	0.767	0.605	0.746	0.681
T = -2.5	0.572	0.707	0.644	0.495	0.618	0.559

The study is now fully recruited. The lower BMD thresholds increased the screen failure rate somewhat in Asia where the proportion of screenees ineligible for the study was 67% compared to 58% study-wide. Once the trial is completed in 2006 we will be able to ascertain whether this strategy resulted in a consistent risk of hip fracture across regions.

Disclosures: ***E.M. Lau****, Novartis Pharmaceuticals 2.*

SU434

Significant Reduction of Bone Resorption with Risedronate Treatment in as Soon as One Week. R. Lindsay[1], S. Boonen[2], D. Burgio*[3], T. Johnson*[3], A. Grauer[3], P. Miller*[4]. [1]Helen Hayes Hospital, West Haverstraw, NY, USA, [2]Leuven University Center for Metabolic Bone Disease and Division of Geriatric Medicine, Leuven, Belgium, [3]Procter & Gamble Pharmaceuticals, Mason, OH, USA, [4]Colorado Center for Bone Research, Lakewood, CO, USA.

Risedronate has been shown to reduce vertebral and non-vertebral fractures within 6 months and to preserve parameters of bone micro architecture in postmenopausal women. The objective of this analysis was to monitor the effect of risedronate (RIS) (5mg daily and 35 mg once weekly) on urinary C-telopeptide (u-CTX) over 4 weeks of treatment in healthy postmenopausal women versus placebo. Women were randomised to receive RIS 5 mg/daily (n = 29), RIS 35 mg/weekly (n = 26) or placebo (n = 32). After 4 weeks of treatment, risedronate reduced U-CTX by 53% for the 5mg daily dose and by 49% for 35mg weekly dose compared to baseline (p< 0.001 vs. baseline and vs. placebo). The difference in reduction of turnover was highly significant vs. placebo already at the first follow up measurement at week one for both 5mg RIS (-29.8%, CI -17 to -42%, p<0.0001) and 35mg Ris (-25.1%, CI -14 to -36%, p<0.001) (Fig. 1). Similar changes were observed for serum CTX. Deterioration of micro architecture can be caused by high or unbalanced bone turnover. Risedronate significantly reduces bone turnover as soon as one week after treatment initiation. This may help to explain the preservation of micro architecture and the rapid reduction in vertebral and non-vertebral fractures, experienced during Risedronate treatment.

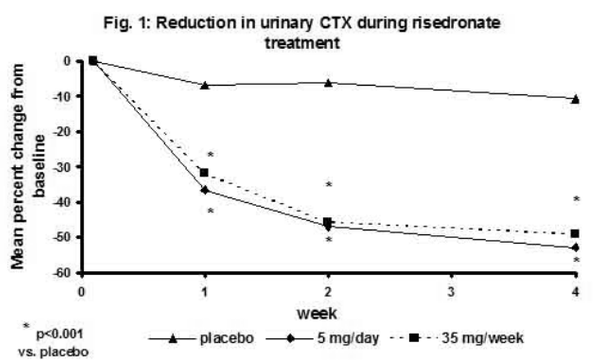

Disclosures: ***R. Lindsay****, Procter & Gamble Pharmaceuticals 5; Aventis Pharmaceuticals 5.*

SU435

Comparison of Risedronate, Calcitonin and Active Vitamin D Treatments in Postmenopausal Osteoporosis. N. Ota, Y. Shibata*, H. Ito*. Orthopedics, Nippon medical school, Tokyo, Japan.

The present study was planned to assess the efficacy of risedronate, calcitonin and active vitamin D treatments on bone mineral density (BMD), bone resorption, and chronic low back pain . A total of 121 postmenopausal women with lumbar spine BMD 2 SD or more below the young adult mean and without any fresh vertebral fractures in lumbar spine were randomly assigned to one of the four groups. 35 patients orally took risedronate 2.5 mg daily (risedronate group), 30 patients were injected with eel calcitonin 20 U intramuscularly once a week (calcitonin group), 25 patients received both risedronate and calcitonin (risedronate-calcitonin group), 20 patients orally received active vitamin D (1-OH-D3) 1 microgram daily (vitamin D group) for four months respectively. BMD of the second metacarpal bone was measured with the digital image processing, urinary cross-linked N-terminal telopeptides of type I collagen (NTx) level was measured with enzyme-linked immunosorbent assay and low back pain was evaluated with a visual analogue scale (VAS). There were no significant differences among these groups in baseline characteristics including age, BMD, NTx and VAS. Low back pain was significantly improved in the risedronate, the calcitonin, the risedronate-calcitonin groups, but not in the vitamin D group. Urinary NTx level was remarkably reduced in the risedronate and the risedronate-calcitonin groups, but not in the vitamin D and the calcitonin groups. BMD was increased in the risedronate and the risedronate-calcitonin groups, representing no significant difference. No serious side-effects were recognized in any of the patients during the follow-up. These results suggest that risedronate and calcitonin have proven to have the same efficacy on chronic low back pain, which does not derive from vertebral fractures.

Disclosures: ***N. Ota****, None.*

SU436

Five Year Risedronate Therapy Normalizes Mineralization: Synchrotron Radiation Micro-Computed Tomography Study of Sequential Triple Biopsies. B. Borah*[1], E. L. Ritman*[2], T. E. Dufresne*[1], S. Liu*[1], P. A. Chmielewski*[1], S. M. Jorgensen*[2], D. A. Reyes*[2], R. T. Turner*[2], R. J. Phipps[1], M. D. Manhart[1], J. D. Sibonga*[2]. [1]Procter & Gamble Pharmaceuticals, Mason, OH, USA, [2]Mayo Clinic College of Medicine, Rochester, MN, USA.

There is a speculation that bisphosphonates cause oversuppression of bone turnover leading to hypermineralization of bone. The goal of this study was to examine the long term effect of risedronate therapy on bone quality, and specifically on the degree of mineralization. The degree of mineralization was measured via Synchrotron μCT in iliac crest bone biopsies taken sequentially at 0, 3 and 5 years from the same patient treated with risedronate (n=7), and in iliac crest biopsies taken from young healthy pre-menopausal women (n=7; mean age 36 years). The high-resolution (4 μm) images obtained from the Synchrotron μCT allowed the detection of small changes in density (g/cc of hydroxyapatite) across trabecular elements. We reported earlier that 3 years of 5 mg daily oral risedronate increased the mean mineralization by 5.1% (p<0.05). After 5 years of continuous treatment with 5 mg daily risedronate, the mean mineralization was significantly higher compared to baseline (p<0.05), but was maintained at the 3 year level, and was comparable to that of young premenopausal healthy women (Figure 1). The mineralization changes in lower and higher mineralization regions were measured independently. The volume ratio of lower to higher mineralized bone was reduced from about 34% at baseline to about 9 - 16% after 3 and 5 year of risedronate treatment (Figure 2) and is consistent with the reduction of bone turnover markers. The ratio of lower to higher mineralized bone in treated patients was comparable to the ratio observed for the young normal group (about 12%, Figure 2). In conclusion, these unique data from the iliac crest biopsies suggest that long term risedronate treatment did not cause hypermineralization and reduced turnover to levels comparable to those found in normal healthy premenopausal women.

Figure 1: Distribution of Mineralization

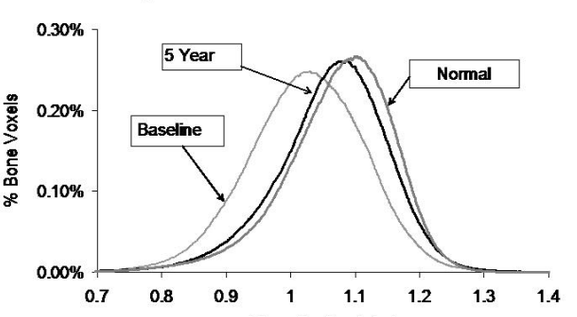

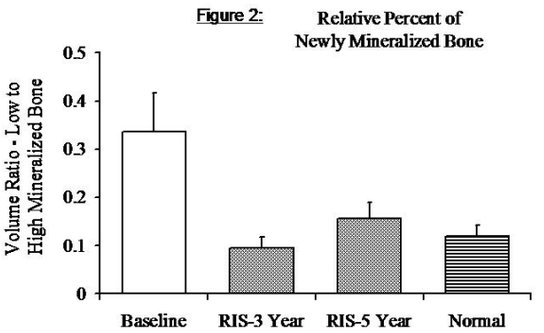

Disclosures: ***B. Borah****, Procter & Gamble Pharmaceuticals 3.*

SU437

Effect of Alendronate in a Murine Model of Estrogen Deficiency. M. A. Gentile*[1], S. Luell*[2], P. Masarachia[1], E. Carballo-Jane*[2], D. B. Kimmel[1]. [1]Bone Biology and Osteoporosis, Merck Research Laboratories, West Point, PA, USA, [2]Pharmacology, Merck Research Laboratories, Rahway, NJ, USA.

The ovariectomized (OVX) rat is the most frequently-used *in vivo* model for testing agents intended to prevent estrogen deficiency bone loss. However, when investigating the relationship of existing agents to genetic alterations in bone-active enzymes or receptors, mice are often more appropriate. We examined the dose response relationship for alendronate (ALN) to prevent OVX-induced bone loss in adult mice.

Female Balb/c mice aged 11 months, weighing ~25g were divided into groups of 11, OVXd, and begun immediately on 2X/wk subcutaneous (SC) ALN (0, 0.03, 0.1, 0.3, or 1 mg/kg/wk), divided in two equal doses/wk) for eleven weeks. A Sham-OVX group was included.

At necropsy, lumbar vertebrae and femurs were placed in 70% ethanol. Bone mineral density (BMD, mg/cm^2) of the femur was measured by pDXA (Norland Corp., Ft. Atkinson, WI USA). Data were analyzed by Kruskal-Wallis non-parametric ANOVA and Student-Neuman Keuls post-hoc testing. Data for distal femur (DFBMD), central femur (CFBMD), and lumbar vertebrae 2-4 (LVBMD) are reported.

Significant OVX-induced bone loss was not detected at any site. Nonetheless, BMD was higher than in untreated OVX rats with ALN in all three sites. DFBMD, a measurement of the bone site in mice where trabecular bone is best evaluated by DXA, was at or above Sham levels in groups given at least 0.1 mg/kg/wk ALN, testing highly significant at 0.3mg/kg/wk. Other sites, with lower portions of trabecular bone, displayed a similar though less marked response.

The SC ALN dose that completely inhibits bone loss in the OVX mouse appears to be 0.1-0.3mg/kg/wk. For comparison, the SC ALN dose that behaves similarly in the OVX rat is 0.03mg/kg/wk. The osteoporosis treatment dose for human (SC equivalent) is 0.07mg/kg/wk. These data suggest that the SC ALN dose that fully inhibits bone loss in the OVX mouse is ~five-fold higher than in the rat. Past experiments with six-month-old Balb/c, C57BL6, and Swiss-Webster mice in our laboratory have consistently shown estrogen-deficiency bone loss in the distal femur by eight weeks post-OVX. These Balb/c mice, aged 11 months at OVX, may already have experienced significant age-related trabecular bone loss that diminished the amount of bone available to be lost post-OVX.

BMD in OVX Mice

ALN(mg/kg/wk)	DFBMD	CFBMD	LVBMD
Sham	62.4±4.0	63.3±2.1	58.8±2.6
OX+0	60.6±4.4	62.9±1.8	58.6±3.5
OX+0.03	60.9±4.4	62.3±3.5	57.8±2.4
OX+0.1	63.6±6.4	65.5±3.3*	60.5±2.4
OX+0.3	66.7±2.5&	65.1±2.6*	60.9±3.4
OX+1	69.1±2.6&	64.4±1.3*	61.7±2.8*

Mean±SD; vs. OX+0: 0.005& .03*

Disclosures: ***D.B. Kimmel****, None.*

SU438

Risedronate 30mg/day Exhibits Renal & Hepatic Safety Over Wide Range of Serum Steady State Concentrations. P. Miller[1], S. Magowan[2], I. Barton*[3], J. Brown[4], E. Siris[5]. [1]Colorado Center for Bone Research, Lakewood, CO, USA, [2]Procter & Gamble Pharmaceuticals, Mason, OH, USA, [3]Procter & Gamble Pharmaceuticals, Egham, United Kingdom, [4]Le Centre Hospitalier Universitaire, Sainte-Foy, PQ, Canada, [5]Columbia University, New York, NY, USA.

Following oral administration, risedronate is primarily eliminated via the kidneys. As such, risedronate serum concentrations are inversely related to renal function (i.e. creatinine clearance). Serum risedronate concentration is also inversely proportional to the volume of distribution (6.3L/kg). This analysis incorporates both these variables to investigate the effect of increasing serum risedronate concentrations on renal and hepatic function in patients with Paget's disease. 276 male and female patients, enrolled in multiple trials for Paget's disease of bone were analyzed after administration of 30 mg/day of risedronate for 2-6 months. Creatinine clearance was estimated using the Cockcroft-Gault methodology. Predicted risedronate steady state concentrations were estimated based on creatinine clearance and the observed body weight using a standard equation. The lowest serum risedronate concentration (i.e. patient with the largest creatinine clearance value and volume of distribution) was arbitrarily assigned a value of 1. The estimated serum steady state concentrations ranged from 1 to a maximum ratio of 13.2. Patients with x13.2 serum steady state concentrations exhibited no change in renal and/or hepatic function from baseline. No correlations were observed between serum steady state concentration and percent change from baseline for serum creatinine, (R^2= 0.02); alanine aminotransferase (R^2<0.01), and aspartate aminotransferase (R^2= 0.001) across the entire range of serum risedronate concentrations. Based on multiple clinical trial experience, this analysis shows that risedronate 30 mg/day exhibits renal and hepatic safety over a wide spectrum of serum steady state concentrations.

Disclosures: ***P. Miller****, Procter & Gamble Pharmaceuticals 5; Aventis Pharmaceuticals 5.*

SU439

Effect of Risedronate Therapy on Serum Osteoprotegerin Levels in Patients with Postmenopausal Osteoporosis. K. H. Baek*, H. J. Tae*, J. H. Han, M. I. Kang, W. Y. Lee*, K. W. Oh*, K. W. Lee*, C. S. Cho*. Internal Medicine, The Catholic University of Korea, Seoul, Republic of Korea.

Bisphophonates are analogs of pyrophosphate with a potent inhibitory effect on bone resorption. They are taken up by osteoclasts and inhibit farnesyl diphosphate synthase, which is essential for osteoclast activity and survival. In addition to the direct effects of bisphosphonates on osteoclasts, there are evidences that these compounds also act on the osteoclasts indirectly through the osteoblasts. In bone remodeling process, RANKL is essential for osteoclasts formation and activation, whereas osteoprotegerin (OPG) neutralizes RANKL. Although OPG is capable of inhibiting bone resorption in vivo, whether bisphosphonates regulate the production of OPG has remained unclear. In this study, we assessed the effects of the risedronate therapy on serum OPG levels in randomized prospective trial. We also investigated the associations of serum OPG levels with various indices of bone metabolism. 111 women (65.8±3.7 years) with postmenopausal osteoporosis were treated with placebo or risedronate (5mg daily) for 6 months and all received 1000mg of calcium and 250 IU of vitamin D. Bone mineral density of lumbar spine were measured before, and 6 months after the treatment. The biochemical markers of bone turnover (sCTx, NTx/Cr and sALP) were measured before the treatment and 1, 3 and 6 months after the treatment. The serum OPG levels were measured before, 1 and 6 months after the treatment. There were negative correlations between the baseline OPG levels and the baseline sALP or sCTx levels(r=-0.22, p<0.05; r=-0.21, p<0.05). A significant correlation was also found between the OPG and lumbar spine bone mineral density at baseline(r=0.26, p<0.05). The women treated risedronate had significant increases in bone mineral density at lumbar spine. Risedronate reduced biochemical markers of bone resorption and bone formation by approximately 50 %. Serum OPG levels were not changed during the treatment period in both risedronate and placebo group. However, in subgroup who showed higher OPG levels initially, OPG levels significantly decreased after risedronate therapy. In conclusion, bisphophonate therapy cause low bone turnover state and this may lead to downregulation of OPG.

Disclosures: ***K.H. Baek****, None.*

SU440

The Effect of Risedronate to Prevent Bone Loss in Men under Androgen-Deprivation Therapy for Prostate Cancer. K. Ishizaka*[1], T. Machida*[1], Z. Ozeki*[1], S. Kobayashi*[1], Y. Mizuno[2], S. Masuda*[3], T. Kamai*[3], K. Arai*[3], M. Honda*[3], K. Yoshida*[3]. [1]Urology, Kanto Central Hospital, Tokyo, Japan, [2]Medicine, Kanto Central Hospital, Tokyo, Japan, [3]Urology, Dokkyo University School of Medicine, Tochigi, Japan.

Androgen-deprivation therapy (ADT) decreases bone mineral density (BMD) and increases the risk of fracture in men with prostate cancer. Bisphosphonate administration is possible treatment modality for male osteoporosis, but the effectiveness on bone loss during ADT has not been established. The clinical benefit of risedronate, a highly potent third generation oral bisphosphonate that is approved for treatment of osteoporosis has been studied. 61 prostate cancer patients with a mean age of 79 ± 6 (± SD) who had been treated with ADT for 42 ± 29 months were enrolled in this study with written informed consent. Patients under ADT were treated with oral administration of 2.5 mg risedronate every day for 6 months. The subjects were not treated with supplemental calcium or vitamin D. Bone mineral density (BMD) was measured in femoral neck, lumbar spine and radius UD by dual energy x-ray absorptiometry (DEXA) with EXPERT-XL Imaging Densitometer (LUNAR Co., Madison, WI, USA). The percent change of BMD from baseline to the end of the study was calculated for primary efficacy variable. Urinary N-telopeptide was examined as the bone resorption marker. T-score of BMD before treatment was -1.5 ± 1.2, -1.1 ± 1.8 and -2.6 ± 2.0 in femoral neck, lumbar spine and radius UD, respectively. BMD was kept stable in femoral neck and in radius UD as shown by the percent change of -0.1 ± 4.8 % (95 % CI: -1.45 - 1.78) and 1.1 ± 7.3 % (-1.30 - 3.48), respectively, by the treatment of risedronate. BMD in lumbar spine was significantly increased from the baseline of 1069 ± 488 mg / cm^2 to 1112 ± 497 mg / cm^2 (P<0.001 by t-test) with the percent change of 4.9 ± 8.9 % (95 % CI: 2.32 - 7.39). Urinary N-telopeptide concentration was decreased from the baseline of 64.9 ± 42.2 nmol BCE / mmol Cr to 37.6 ± 22.4 nmol BCE / mmol Cr (p<0.001) after the treatment of risedronate for 3 months. No significant adverse effect was observed except for 1 patient who quitted the treatment because of appetite loss. Risedronate treatment is safe and effective. Longer follow up is desired.

Disclosures: ***K. Ishizaka****, None.*

SU441

Change in Bone Mineral Density Is Predictive for Fracture Risk Reduction with Ibandronate: Further Insights From a Phase III Study of Intravenous Ibandronate Injection. P. D. Miller[1], S. Epstein[2], H. Huss*[3], K. M. Wilson*[4], R. C. Schimmer[4], R. Wasnich*[5]. [1]Colorado Center for Bone Research, Lakewood, CO, USA, [2]Mt Sinai Medical Center, New York, NY, USA, [3]., Leverkusen, Germany, [4]F. Hoffmann-La Roche Ltd, Basel, Switzerland, [5]Radiant Research, Honolulu, HI, USA.

The relationship between BMD change and fracture risk with bisphosphonates is yet to be fully elucidated. Previously, we examined this relationship with oral daily and intermittent ibandronate (Boniva®) in BONE.[1,2] Logistic regression demonstrated that a 1% increase in total hip (TH) BMD at years 2 and 3 was predictive for a 9.8% (p=0.0026) and 7.9% (p=0.0084) vertebral fracture risk reduction (VF-RR), respectively, at year 3. To examine this relationship further, we analyzed data from a phase III study of intermittent i.v. ibandronate injections. Unlike BONE, which reported lumbar spine (LS) BMD changes approaching the top of the dose response curve for VF-RR, this study reported suboptimal increases in LS BMD, due to suboptimal doses for the between-dose interval.[3] The relationship between TH and LS BMD change and the rate of new VF at year 3 was explored using a moving averages procedure. The logistic regression model employed in BONE was used to quantify the relationship between TH and LS BMD increase and VF-RR (as prospectively specified in the shared data analysis plan). The moving averages analysis demonstrated a reduction in the percentage of patients with VF with increasing BMD. For example, at the TH, ~16% of patients with a BMD change of -3% experienced a VF, versus ~5% of patients with a BMD change of >+4%. Logistic regression revealed that increase in TH BMD at years 1, 2 and 3 was significantly predictive for VF-RR at year 3 (**Table**). Notably, estimates for this parameter were generally higher than those reported in BONE. Increase in LS BMD at years 2 and 3 was also significantly predictive for VF-RR at year 3 (**Table**). These findings further corroborate that ibandronate-related increases in TH and LS BMD are predictive for VF-RR. The variation in the relationship for the current and BONE analyses is likely the result of the disparity in the positioning of the respective BMD changes on the dose response curve for VF-RR with ibandronate.

1. Chesnut CH, et al. J Bone Miner Res (In press).
2. Wasnich R, et al. J Bone Miner Res 2003;18(Suppl. 2):S160 (Abstract SA353).
3. Recker RR, et al. Bone 2004;34:890-9.

Table. Estimated VF-RR at year 3 with a 1% increase in TH or LS BMD

	Total hip		Lumbar spine	
	Risk reduction	p-value	Risk reduction	p-value
Year 1	8.1%	0.0228	4.2%	0.0960
Year 2	9.0%	0.0035	5.9%	0.0104
Year 3	11.6%	<0.0001	6.9%	0.0008

Disclosures: ***P.D. Miller****, F. Hoffmann-La Roche Ltd 2.*

SU442

Effect of Neridronate and Zoledronic Acid on Bone Turnover in Osteopenic Post-menopausal Patients and in Women Affected by Primary Iperpathyroidim. P. Filipponi[1], S. Cristallini*[1], G. Policani*[1], M. Schifini*[1], B. Frediani[2]. [1]Internal Medicine, U.O. Medicina - Ospedale di Umbertide, Perugia, Italy, [2]Rheumatology, University of Siena, Siena, Italy.

We report preliminary data on the effects of a single intravenous infusion of 2 nitrogen containing bisphosphonates (BPs), Neridronate (Ner, Abiogen Pharma, 100 mg) and Zoledronic Acid (Zol, Zometa, Novartis, 4 mg) on bone turnover in 27 post-menopausal osteopenic patients (L1-4 BMD < -1 SD, T-score; Ner = 15; Zol = 12) and in 13 women affected by primary iper-PTH due to parathyroid adenoma (Ner = 6; Zol =7). Bone turnover was assessed by serum bone specific alkaline phosphatase (bAP) and serum Collagen C-terminal Telopeptide (CTx) during a 6-month follow-up.

In iper-PTH both BPs caused a reduction in bone turnover with a nadir between 7 an 15 days. % change from baseline in bAp and CTx (MEAN±SE) was not statistically different between Ner (bAp = -33.3±6.7; CTx = -40.1±5.4) and Zol (bAp = -34.8±9.2; CTx = -44.3±5.4). After 6 months bone turnover returned to baseline values in both Ner (bAp = 4.9±10.4; CTx = -6.2±7.4) and Zol (bAp = -11.3±7.3; CTx = -0.3±7.5) patients.

In post-menopausal women the suppressive effect of Zol was still evident after 6 months (bAp = -37.4±8.6; CTx = -40,6±4.3), when the % reduction in bone turnover was not statistically different from that observed at the nadir, which occurred between 15 and 30 days (bAp = -42.5±4.7; CTx = -45.3±6.3). In the Ner treated postmenopausal women the suppression of bone turnover at the nadir was similar to that observed after Zol; at 6 months, on the contrary, both bAp and CTx have been returned to baseline values.

We conclude that the effect of Zol was still different from that of Ner in subjects where the bone remodeling was not influenced by drivers physiologically not involved in the control of bone biology.

The mechanism/s responsible for the long lasting suppressive effect of Zol in postmenopausal osteopenic women, but not in iper-PTH, requires further investigation.

Disclosures: ***S. Cristallini****, None.*

SU443

Zoledronic Acid Treatment does not Delay The Process of Endochondral Ossification in a Rat Fracture Model. M. M. McDonald*, S. K. Dulai*, D. G. Little*. Orthopaedic Research, The Children's Hospital Westmead, Sydney, Australia.

The process of endochondral ossification of soft callus during fracture repair resembles that of the growth plate. Osteoclasts can contribute to this process, however their role in the invasion and removal of chondrocytes may be redundant. We speculated that while osteoclasts are required for bone remodeling, they may be unnecessary for soft callus removal during fracture repair. We tested this in a closed rat fracture model treated with zoledronic acid (ZA) to specifically target osteoclastic activity.

Three treatment groups were analyzed (n=90): weekly saline (Saline), weekly ZA 0.005mg/kg (Weekly ZA), and a single bolus dose of 0.025mg/kg ZA (Bolus ZA). All doses commenced at 1 week post-op. 10 per group were euthanized at 2, 4 and 6 weeks post-op and subject to analysis by x-ray, QCT scans, histology and histomorphometry.

Plain radiographs revealed no difference in fracture union between groups. At 4 weeks, radiographic fracture union was present in 10% of all samples. By 6 weeks, fracture union was complete in 70% of both Saline and Weekly ZA samples and 90% of Bolus ZA samples.

QCT at 2 weeks showed BMC was increased by 16% in Weekly ZA and 19% in Bolus ZA over Saline ($p<0.01$). By 4 weeks, BMC was increased by 57% and 33%, and at 6 weeks by 80% and 64% respectively ($p<0.01$). Callus volume did not differ between treatment groups at 2 or 4 weeks but was 35% higher for Weekly ZA and 28% higher for Bolus ZA at 6 weeks ($p<0.05$).

At 2 weeks, histomorphometry of the callus showed 8%, 11% and 9% cartilage content for Saline, Weekly ZA and Bolus ZA respectively. At 4 weeks this was reduced to 2% in all groups and by 6 weeks no cartilaginous callus remained. Thus, the percentage of soft callus showed no significant difference at each time point, indicating that ZA treatment did not affect ossification or removal of chondrocytes. However, the ZA groups did show an increase in retention of primitive hard callus, indicating delayed remodeling.

ZA did not delay the process of cartilage removal in endochondral ossification, supporting our hypothesis that osteoclasts are not an absolute requirement for soft callus removal. Moreover, at early time points, ZA treatment led to an increase in callus bone mineral content without an increase in callus size. This may be due to a reduction in the resorption of both primitive hard callus and appositional lamellar bone, thereby providing a scaffold that may be advantageous in some clinical situations. By 6 weeks, there was an increase in callus volume due to ZA treatment. This study indicates that ZA treatment during fracture repair does not delay the phases of endochondral ossification prior to bone remodeling, thus supporting the clinical safety of ZA during fracture repair.

Disclosures: ***M.M. McDonald****, Novartis 2.*

SU444

OP-1 and Zoledronic Acid Act Synergistically to Increase Bone Volume and Strength in a Rat Critical Defect Model. M. M. McDonald*, R. Bransford*, C. Godfrey*, N. Amanat*, D. G. Little*. Orthopaedic Research, The Children's Hospital Westmead, Sydney, Australia.

BMPs induce osteoblast differentiation and bone production. However, BMPs also directly up-regulate osteoclasts through BMP receptors and indirectly via osteoblasts through RANK / RANKL. In some clinical situations this may produce high bone turnover, which could limit the volume of callus produced, or lead to over-remodeled callus in stress-shielded situations. Unwanted host bone resorption may also occur[i] . While this resorption can be controlled by bisphosphonate administration in closed defects[2], we hypothesized that bisphosphonates should act synergistically with BMPs in an uncontained defect to produce increased callus over BMP alone.

A rat 6mm critical size defect model was utilized. 15mg of bovine collagen and carboxymethylcellulose carrier, or carrier containing 50µg OP-1 was placed in the defects. Groups consisted of carrier alone, carrier plus systemic zoledronic acid (ZA), OP-1 alone and OP-1 with ZA either given at surgery or 2 weeks post surgery. ZA 0.1 mg/kg was given as a single parenteral dose. Radiographs, QCT, 3-point bend and histomorphometric analyses were performed.

Carrier alone and carrier ZA groups had not united by 8 weeks. Radiological union occurred in all OP-1 groups. OP-1/ZA group BMC increased in the 6 mm defect by 45% in the ZA at surgery group and 96% in the OP-1/ZA at 2 weeks group over OP-1 alone ($p<0.01$). Callus volume increased by 45% in the OP-1/ZA at surgery group and 86% in the OP-1/ZA at 2 weeks group over OP-1 alone ($p<0.01$). BV/TV was increased 72% in the OP-1/ZA at surgery group and 82% in the OP-1/ZA at 2 weeks group over OP-1 alone ($p<0.01$). This was due to a significant increase in trabecular number of 81% and 106% in OP-1/ZA groups over OP-1 alone ($p<0.01$). The increases in callus volume in the ZA at 2 weeks group translated to increases in strength of 107% and stiffness of 148% ($P<0.05$).

Zoledronic acid significantly increased the mineral content, volume and strength of OP-1 mediated callus in this rat femoral critical size defect at an 8-week outcome time-point. Modulation of the high bone turnover state induced by pharmacotherapeutic doses of OP-1 may optimize the amount and mineral content of callus produced, which could be of clinical benefit in obtaining initial bone union.

[1] Seeherman H, et al. Trans Orthop Res Soc 2000;25;1042
[2] Seeherman H et al J Bone Miner Res 2001;16 Suppl 1:S438

Disclosures: ***M.M. McDonald****, Novartis 2.*

SU445

Efficacy of Risedronate Among Women using Gastric Acid Inhibitors and those at High Risk for Gastrointestinal Side Effects. K. E. Hansen[1], T. D. Johnson*[2], M. V. Gillen*[2], A. Grauer[2]. [1]Medicine, University of Wisconsin, Madison, WI, USA, [2]Proctor and Gamble Pharmaceuticals, Mason, OH, USA.

Women with postmenopausal osteoporosis commonly use proton pump inhibitors (PPI) and H_2-Blockers (H_2B) causing achlorhydria, which could potentially interfere with absorption of bisphosphonates. In addition, patients using PPI/H_2B, NSAIDs, and those with preexisting gastrointestinal (GI) disease are at increased risk of upper GI adverse events. These adverse events may affect compliance and thereby limit clinical effectiveness. Risedronate phase III clinical trials did not exclude such patients, providing an opportunity to examine the anti-fracture efficacy of risedronate among women reporting PPI/H_2B use, and among women at high risk for GI side effects.

We analyzed subgroups of women from the risedronate HIP and VERT phase III studies. Fracture rates were compared for women randomized to placebo, and those randomized to 5 mg risedronate who reported PPI/H_2B use at study entry. Anti-fracture efficacy was also compared in like manner for women with preexisting GI disease, and for women reporting NSAID use who were randomized to risedronate. Fracture incidence was assessed using Kaplan-Meier estimates; relative risk reduction was based on the Cox regression model with adjustment for studies and number of prevalent vertebral fractures; p-values are based on the stratified log rank test.

Subjects were well matched across baseline demographics in terms of age (74 years) femoral neck T-score (-2.5), lumbar spine T-score (-2.5) and prevalent vertebral fractures (58%). Among women randomized to risedronate who reported use of PPI/H_2B, the 1-year reduction in new vertebral fractures was 61%, comparable to the risk reduction for all women randomized to risedronate among individual studies (65% VERT-NA, 61% VERT-MN, 55% HIP). Likewise, among women reporting upper GI disease or NSAID use, fracture risk reduction with risedronate was similar to that obtained among individual studies (see table).

Treatment Group	Incidence*	RR (95% CI)$^+$	Risk Reduction
Patients with Upper GI Disease (n=1,736)			
Placebo	5.8%		
Risedronate 5 mg	2.31%	0.38 (0.22, 0.65)	62%, p<0.001
H_2-Blockers and/ or PPI Users (n=1,258)			
Placebo	7.29%		
Risedronate 5 mg	3.32%	0.39 (0.23, 0.68)	61%, p=0.002
NSAID Users (n=2,870)			
Placebo	6.65%		
Risedronate 5 mg	2.99%	0.41 (0.28, 0.59)	59%, p<0.001

Risedronate provides comparable vertebral fracture protection in women using PPI/H_2B, and among women at high risk for GI side effects, with 1-year fracture risk reductions comparable to all women randomized to risedronate among individual studies.

Disclosures: ***K.E. Hansen****, None.*

SU446

The Effect of Oral Alendronate versus Intravenous Pamidronate on Bone Mineral Density in Patients with Osteoporosis. M. Vis[1], I. Bultink*[2], B. Dijkmans[1], W. Lems[1]. [1]Rheumatology, VU university medical center, Amsterdam, Netherlands, [2]Rheumatology, Slotervaart Hospital, Amsterdam, Netherlands.

Introduction Bisphosphonates are potent inhibitors of osteoclast mediated bone resorption that can be given orally or intravenously. There are no prospective studies comparing the effect on BMD of intravenous versus oral administered bisphosphonates.

Objective: To investigate the effect of 1-year treatment with oral alendronate 10mg/day or intravenous pamidronate 60mg/ 3months on BMD in patients with osteoporosis.

Methods: Since 2000 the Slotervaart Hospital has an outpatient clinic for patients with osteoporosis. We recruited 40 consecutive patients starting treatment for osteoporosis: 20 starting with oral alendronate 10mg/day and 20 starting intravenous pamidronate 60mg/3 months. The first choice bisphosphonate for treatment of osteoporosis was alendronate. Patients with previous treatment with anti-osteoporotic drugs were excluded, except patients who were treated less than one month with an oral bisphosphonate and were stopped because of gastrointestinal intolerance. Pamidronate i.v. was given in patients with gastrointestinal contraindications or intolerance (<1 month) for oral bisphophonates.

BMD was measured on a Hologic 4500 at the lumber-spine (L1-L4) and the total-hip at the start of treatment and after one year.

Results: A total of 40 consecutive patients were enrolled: 20 in the alendronate group and 20 in the APD group. The baseline characteristics of both groups are shown in table 1.

The change in BMD of the vertebral spine and total-hip in both groups was comparable The BMD of the lumbar spine increased +4.0% in the alendronate and +4.0% in the pamidronate group. The BMD of the total-hip increased both in the alendronate group and the pamidronate group, respectively +3.4% and +2.9%. The increases in the BMD (spine and hip) were significant for both groups compared to baseline (p<0.01). There was no significant difference in change in the BMD between the alendronate and pamidronate groups

Discussion: This study shows that in patients, treatment with intravenous pamidronate seems equally as good as treatment with oral alendronate regarding the effect on BMD. Therefore we suggest that i.v. pamidronate is an alternative for patients who do not tolerate or have a gastro-intestinal contra-indication for an oral bisphophonate

Table1: Baseline chracteristics of the pamidronate and alendronate group

		Alendronate Group (n=20)	Pamidronate Group (n=20)	significance
Age	*mean (SD)*	69 (15)	67 (16)	NS
Sex	n (%)	15 (75)	16 (67)	NS
Postmenopausal status	n (%)	14 (93)	15 (88)	NS
BMI	*mean (SD)*	25.9 (5.5)	23.7 (3.2)	NS
History of Fractures	n (%)	11 (55)	8 (40)	NS
History of prednisone use	n (%)	5 (25)	5 (25)	NS
Current prednisone use	n (%)	5 (25)	6 (30)	NS

Disclosures: ***W. Lems****, None.*

SU447

Bone-Specific Gene Signatures Associated with Binge Alcohol and Concurrent Anti-Resorptive Treatment of Adult Rats Identified by Gene Expression Array Analysis. J. J. Callaci*[1], D. Juknelis*[1], M. T. Falduto*[2], F. H. Wezeman[1]. [1]Orthopaedic Surgery, Loyola University Chicago, Maywood, IL, USA, [2]GenUs BioSystems, Chicago, IL, USA.

Chronic alcohol abuse reduces bone mass and strength, increasing fracture risk in alcoholics. Molecular mechanisms underlying this vulnerability have not been identified. Skeletal effects of exposure to high blood alcohol concentrations (BAC's) attained during binge drinking have not been studied. We examined the effects of repeated binge-like alcohol treatment and concurrent risedronate therapy in adult male rats and assayed for effects on bone-specific gene expression profiles using microarray analysis. Our hypothesis was that gene signatures would be identified that were descriptive of both alcohol-induced bone loss and risedronate compensation. A binge alcohol treatment model was developed in our laboratory using intraperitoneal (IP) injection to administer a 20% (vol/vol) alcohol/saline solution (3g/kg, 1X/day) on four consecutive days for 1, 2 or 3 weeks in 400 gram male rats, with and without concurrent weekly risedronate treatment (0.5 mg/kg, 1X/week). Seventy-two Sprague Dawley rats were randomly divided into four groups: control, binge alcohol treated, risedronate treated and alcohol plus risedronate treatment. Total RNA isolated from proximal tibial samples was assessed for global gene expression using the Amersham CodeLink gene array platform representing 10,000 rat genes. We found effects of both treatment (alcohol and risedronate) and time on the expression patterns of both bone formation (26 genes) and resorption-specific (11 genes) gene panels with effects of treatment on many bone-specific genes not previously identified in relation to alcohol-induced bone loss. Unique gene expression profiles were found after 1, 2 and 3 weeks of treatment with either agent or with combined treatment. A unique gene signature (151 genes) was also found comprised of genes that showed 2-fold or greater regulation under ethanol treatment but had expression profiles near control levels with concurrent risedronate treatment. This pattern of gene regulation matches the pattern of biological effects of ethanol and risedronate on parameters of bone health previously identified in our laboratory. Our data provides insights into novel mechanisms of action for both alcohol-induced bone loss and bone sparing effects of risedronate. Bone-specific gene signatures indicative of alcohol-induced bone loss and risedronate prevention have many applications including diagnostics and screening of novel bone-sparing therapeutic agents.

Disclosures: ***J.J. Callaci****, GenUS BioSystems 3.*

SU448

Early Effects and Safety of Alendronate (Fosamax®) 70mg Once Weekly (EASY). M. Djandji*[1], J. S. Sampalis*[2], A. C. Karaplis[3]. [1]Clinical Research, Merck Frosst Inc, Pointe Claire, PQ, Canada, [2]JSS Medical Research Inc, Montreal, PQ, Canada, [3]Medicine, McGill Universty, Montreal, PQ, Canada.

Osteoporosis is a highly prevalent condition in older men and postmenopausal women caused by excessive bone resorption in comparison to bone formation. Alendronate (Fosamax®) is a nitrogen-containing bisphosphonate that selectively inhibits bone resorption. The ultimate goal in the treatment of osteoporosis is to reduce the risk of fractures associated with increased morbidity and mortality in the elderly population. Bone turnover measured by urine NTx values is a valid marker for assessing the rate of bone resorption. The purpose of the current study was to evaluate the effectiveness and safety of alendronate (Fosamax®) in reducing bone resorption in patients with osteoporosis over a period of 13 weeks.

METHODS: This was a prospective, single cohort, open label study. Patients included in the study were postmenopausal women and who had a confirmed osteoporosis (Bone Mass Density < 2.5 SD of normal). Patients were treated with alendronate (Fosamax®) 70mg once weekly for three months. The primary outcome measure of the study was absolute and percent reduction of urine NTx levels as a measure of bone turnover at 5 and 13 week of treatment. The current report presents data on patients that completed five weeks of treatment.

RESULTS: There were 238 patients enrolled in the study. 208 completed five weeks of treatment and are include in this report. One patient withdrew due to an adverse event. The majority were female (85%), 91% were Caucasian. The mean (SD) age was 67(11). The baseline mean (SD) urine NTx (nmol BCE/mmol Cr) was 54.7 (31.7) compared to 31.6 (19.6) after five weeks of treatment. The mean (SD) absolute change of 22.9 (29.9) nmol BCE/mmol Cr and percent change of 36.2% (33.4) in urine NTx were both statistically significant ($P < 0.001$). Significant absolute and percent decreases in urine NTx values were observed for the 186 patients that were compliant with treatment and in the 22 patients that missed one dose or more. There were 21 (10%) patients reporting an adverse event attributed to alendronate by the treating physician. The severity of the adverse events was mild for 11 and moderate for 8.

CONCLUSION: This study demonstrates that, using urine NTx as a surrogate marker. Alendronate is effective in reducing bone resorption within the first five weeks of treatment while being safe and well tolerated. Fosamax® Once weekly has a rapid response reducing bone resorption consequently bone loss in patients with osteoporosis. The rapidity of this response may have important implications for the management of osteoporosis.

Disclosures: ***M. Djandji****, Merck Frosst Inc 3.*

SU449

Long-Term Treatment with a Calcitonin Derivative and Alfacalcidol Reduced the Risk of New Vertebral Fractures. M. Ohama*[1], Y. Honda*[1], Y. Isobe*[1], H. Suzuki*[2], Y. Kato[2], H. Shingu*[1]. [1]Orthopedic Surgery, Seibu Rehabilitation Hospital, Tottori, Japan, [2]Asahi Kasei Pharma Corporation, Tokyo, Japan.

In Japan, combination therapy employing elcatonin (an eel calcitonin derivative) and alfacalcidol is one of the major treatments for primary osteoporosis. However, there is little clinical evidence regarding its long-term use. In this study, we examined data from patients who have been consistently receiving this combination therapy treatment for more than 5 years. All patients selected had been diagnosed with primary osteoporosis according to the guidelines of the Japan Osteoporosis Society and had received the combination therapy of elcatonin 20U i.m. injection (initially, 4 times per month for 3 months and then twice per month) with alfacalcidol 1.0 μg/day oral administration for more than 5 years. Data examined included bone mineral density (BMD: ∑GS/D of CXD), biochemical tests, and radiographs (from Th11 to L5).A total of 17 patients met the profile for inclusion. All were postmenopausal women with an average age of 74.1 years old at the initiation of therapy. The average term of treatment was 6.23 years. BMD increased for four years following the beginning of treatment, and then subsequently decreased. Fresh vertebral fractures occurred in 7 patients (14 vertebral bodies). These fractures occurred during the first two years and after the fifth year in tandem with the BMD decrease. Serum calcium increased during the first two years, and alkaline phosphatase increased after five years had passed. There was no significant change in GOT, GPT, BUN, and creatinine. The combination therapy of calcitonin and alfacalcidol increased BMD during each of the first four years. While new vertebral fractures did occur in the first and second years of treatment, due likely to an insufficient overall effect of treatment, the third and fourth years of treatment showed a complete absence of new vertebral fractures. Thus, for at least the initial four years of treatment, this therapy, on the whole, is effective for primary osteoporosis. In contrast, after more than five years of treatment, BMD decreased from the baseline, leading to vertebral fractures. At the same time, serum alkaline phosphate increased significantly, which may indicate bone turnover was reactivated. These results suggest that after four years, this combination therapy should be replaced by a therapy that reduces bone turnover. The increase of serum calcium during the first two years could have been caused by alfacalcidol, which increases calcium absorption from intestinal tract. This long-term therapy caused no significant change in lung and kidney functions. Thus, this therapy is not only effective but safe for the first four years of treatment.

Disclosures: ***Y. Honda****, None.*

SU450

The Effects of Antiresorptive Agents, Calcitonin and Alendronate, on the Femoral Fracture Healing of Cynomolgus Monkey (Macaca Fascicularis). T. Manabe*, Y. Cao*, S. Mori, T. Mashiba, S. Komatsubara*, Y. Kaji*, H. Norimatsu. Dept. of Orthopedic Surgery, Faculty of Medicine, Kagawa University, Kagawa, Japan.

Antiresorptive agents may disturb the fracture healing because they suppress bone remodeling which is an important process of fracture healing. The effects of antiresorptive agents, calcitonin and alendronate, on the fracture healing were investigated using the fracture model of cynomolgus monkeys (Macaca fascicularis) which have osteonal remodeling same as human beings. Twenty female monkeys aged 18-22 years were divided into CNT(saline vehicle), ELL (elcatonin,Asahi-kasei, Japan,0.5U/kg/day), ELH (elcatonin 5U/kg/day), ALL (alendronate 10ug/kg/day), and ALH (alendronate 100ug/kg/day) groups. Drugs were subcutaneously injected twice a week. After 3 weeks pretreatment, transverse osteotomies were performed at the midshafts of right femora and fixed with AO miniplates. Injection was performed twice a week till the animals were sacrificed at 26 weeks post-fracture. Soft x-ray radiography, contact microradiograph, Micro-CT, biomechanical testing, and histomorphometry were performed on the fractured bone. Endosteal callus area in elcatonin(ECT) and alendronate(ALN) groups was larger than that in CNT, although cross-sectional area and periosteal callus area did not differ among the groups. Fracture Healing Index (FHI) was significantly lower in both ECT and ALN than in CNT. Osteoclast number (N.Oc/BS) in callus was significantly lower in ECT and ALN than in CNT. ALN groups showed lower activation frequency (Ac.f), lamellar bone in callus (lamellar Ar/Ca.Ar), osteoid thickness (O.Th), mineralized surface (MS/BS), and bone formation rate (BFR/BS) compared with CNT. Ultimate load, stiffness, and work to failure of fractured bone were not significantly different among the groups. Although calcitonin and alendronate enlarged endosteal callus, only alendronate significantly suppressed callus remodeling as evidenced by lower lamellar Ar/Ca.Ar.

Disclosures: ***T. Manabe****, None.*

SU451

Six-Month Bone Turnover Marker Results Following Daily Treatment with Fortical® Calcitonin Nasal Spray. N. M. Mehta[1], A. Malootian*[1], E. T. Leary[2], T. Aggoune*[2], T. Carlson*[2], J. P. Gilligan[1]. [1]Unigene Laboratories Inc, Fairfield, NJ, USA, [2]Pacific Biometrics, Inc, Seattle, WA, USA.

Five serum bone turnover markers (BTM) were measured in a 24-week, multicenter, double-blind, parallel design study comparing Fortical® Salmon Calcitonin Nasal Spray and a commercially available positive control. One hundred and thirty four osteoporotic (T score < -2.5) postmenopausal women received 6 months of daily dosing of 200 IU of Fortical or the positive control with calcium and vitamin D supplementation. Two serum markers of bone resorption , C-telopeptide (sCTX, Roche Diagnostics) and N-telopeptide (sNTX, Ostex International) and three serum markers of bone formation, bone specific alkaline phosphatase (BAP, Quidel), osteocalcin (OC, Roche Diagnostics) and procollagen type 1 N propeptide (P1NP, Roche Diagnostics) were measured at baseline, week 4, week 12 and week 24. Serum samples were collected in the fasted state between 8-10 AM. Subjects with accelerated bone turnover were enrolled (i.e. two baseline serum CTX values collected one week apart greater than 0.24 ng/mL). BTM were analyzed in a single batch at the completion of the study. Spine and hip BMD were measured with DEXA at baseline and at six months.

Serum CTX and NTX decreased rapidly following treatment. The Fortical treatment group (n=50) reached -41% and -23 % at 24 weeks from mean baseline values of 0.57 ng/mL CTX and 18.2 nM BCE NTX respectively. The formation markers lagged the resorption markers in response time but not necessarily in magnitude of change. P1NP, OC and BAP decreased by -31%, -25% and -10% from mean baseline values of 55.9 ng/mL, 32.1 ng/mL and 30.6 U/L.

The signal-to-noise ratios of BTM (treatment response at 24 weeks divided by coefficient of variation of markers measured two weeks apart) were greatest for P1NP (5.2), followed by OC (4.2), CTX (3.4), NTX (2.9) and BAP (2.0). Fortical treatment resulted in a modest but statistically significant increase in BMD of 1.3% at the AP spine and 1.1% at the hip at 6 months compared to baseline. The significant decrease in bone resorption and formation markers with Fortical Nasal Spray is greater than that expected from the change in BMD. Serum CTX and P1NP appear to be the most responsive resorption and formation markers respectively.

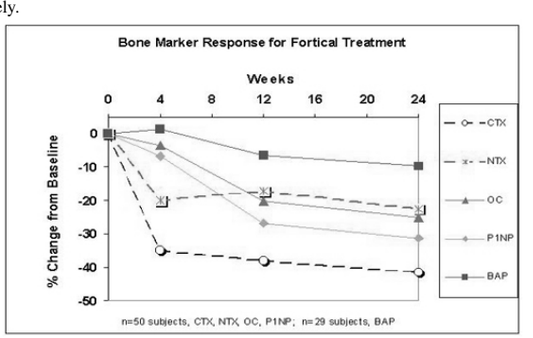

Disclosures: ***N.M. Mehta****, None.*

SU452

Decreased Bone Resorption after Soy Isoflavone Supplementation in Postmenopausal Women (60 - 78 Years of Age). L. Harkness[1], K. Fiedler*[2], A. R. Sehgal*[3], D. Oravec*[4], E. Lerner*[2]. [1]Pediatrics, Case Western Reserve University, Cleveland, OH, USA, [2]Nutrition, Case Western Reserve University, Cleveland, OH, USA, [3]Medicine, Case Western Reserve University, Cleveland, OH, USA, [4]Radiology, Case Western Reserve University, Cleveland, OH, USA.

The purpose of this study was to investigate the effect of soy isoflavone supplementation on bone mineral density and markers of bone turnover in postmenopausal women. For this randomized, placebo controlled clinical trial, we used a crossover design to test the effect of soy isoflavone with known isoflavone composition on bone formation, bone resorption, and bone mineral content (BMC) and density (BMD). Postmenopausal women (n= 19), mean age of 70.6 ± 6.3 years, mean time since menopause of 19.1 ± 5.5 years, were given isoflavone supplements for 6 months. The total isoflavone dosage was 110 mg/day (55 mg in a.m. and 55 mg in p.m.) with an isoflavone composition ratio of 1.3:1.0:0.22 genistein: daidzein: glycitein. We observed a 37% ($p < 0.05$) decrease in urinary concentrations of type 1 collagen α1 chain helical peptide (HP), a marker of bone resorption, during the isoflavone supplementation compared to baseline. In addition, there was a significant difference in mean (SE) HP excretion levels when isoflavone was compared to placebo [43.4(5.2) vs. 56.3(7.2) ug/mmol cr] ($p < 0.05$). After the isoflavone supplementation, mean spine L2 BMC was significantly greater compared to control with a difference between the means of 0.3(0.60) g ($p < 0.05$). Mean BMD at L2 and L3 was greater when treatment was compared to control with a difference between means of 0.03(0.04) g and 0.03(0.04) g ($p < 0.05$), respectively. After isoflavone supplementation, there were non-significant increases from baseline for total spine BMC (3.5%), total spine BMD (1%), total hip BMC (3.6%), and total hip BMD (1.3%). In conclusion, the high rate of bone resorption is a key concern during menopausal bone loss and decreasing bone resorption should be part of any intervention strategy. Soy isoflavone, in isolated form, was effective in this study to significantly decrease bone resorption.

Disclosures: ***L. Harkness****, None.*

SU453

Synergistic Interactions among Calcium, Isoflavone and/or Estradiol Supplementation on Bone Mineral Contents and Serum Estradiol and Vitamin D Hormone Levels in Postmenopasal Osteoporosis Rat Model. Y. Lee*, K. Kim*. Seoul National University, Seoul, Republic of Korea.

This study was conducted to investigate how three factors, dietary calcium, isoflavone supplementation, and estrogen replacement, for prevention and treatment of postmenopausal osteoporosis might be associated with bone mineral increments and bone metabolism-related hormones. Seven weeks old female rats (Sprague-Dawley) were designed as a postmenopausal osteoporosis rat model by ovariectomy and low Ca diet (0.1% Ca in diet) for three weeks. The model rats were divided into eleven groups according to the treatments by alone or by combinations of low Ca diet, Ca (0.5% Ca in diet), isoflavone (80ppm in diet), and estradiol (10μg/kg BW by subcutaneous injection). The groups included two sham contols (three and eleven weeks). The experimental treatments were settled for eight weeks. The ovariectomized osteoporisis model rats were characterized by an increase in weight gain and food intake but a decrease in bone weight, length, breaking force and mineral contents (Ca and P) compared with SHAM control rats. In these model rats, body weight gain and food intake were not affected by dietary calcium and isoflavone supplementation but reduced significantly by estradiol administration. The bone mineral contents, especially calcium contents, were increased significantly by the combination treatments of calcium, isoflavone and estradiol compared to alone treatments. Serum estradiol level was lower with ovariectomy and not affected by calcium addition alone, but significantly elevated by isoflavone supplementation alone and increased to the level of SHAM by estradiol injection alone. The combinations of calcium and estradiol, isoflavone and estradiol, and calcium, isoflavone and estradiol treatments significantly augmented the estradiol level above to the SHAM. Serum 1,25-$(OH)_2D_3$ was significantly higher in the overiectomized model rats than in SHAM rats, but declined by calcium addition alone and estradiol injection alone to the level of SHAM, and more decreased by combination of these two treatments, but not affected by isoflavone supplementation. Reduced uterine weight with ovariectomy was enlarged by estradiol injection but not dietary calcium, isoflavone, and their combination.

In conclusion, the synergistic effects among dietary calcium, soy isoflavone supplementation and/or estradiol injection have been observed on the prevention of bone loss and the maintenance of serum estradiol and activated vitamin D levels in the postmenopausal osteoporosis model rats.

Disclosures: ***Y. Lee****, None.*

SU454

Effects Of Calcium Supplementation On Body Weight And Blood Pressure In Normal Older Women - A Randomized Controlled Trial. I. R. Reid, A. Horne*, B. Mason*, R. Ames*, G. Gamble*. Department of Medicine, University of Auckland, Auckland, New Zealand.

High intakes of calcium are now widely accepted as having a beneficial effect on bone health. Recent epidemiological data suggest that high calcium intakes might also result in decreased body weight, which is potentially of even greater health importance. However, there is little evidence available from randomized controlled trials that addresses this important issue. A further related possible benefit from calcium supplementation is reduced blood pressure, which also lacks definitive trial evidence. We have used data from an ongoing, randomized controlled trial of calcium supplementation (1 g/day vs placebo) in the prevention of fractures, to assess the long-term effects of calcium supplementation on body weight and blood pressure.

Body weight measurements were available in 1203 subjects at 30 months (82% of the initial cohort). Body weight (mean ± SE) decreased by 368 ± 132 g in the calcium group and by 369 ± 134 g in those taking placebo. Each of these changes was significant within the respective group, but the changes over time were not different between-groups ($P = 0.93$ for time-treatment interaction by analysis of variance). When these analyses were repeated using data from subjects still taking study medication and with >80% compliance, the changes in body weight were essentially the same. Fat mass (measured by DXA) did not change significantly in either group (calcium group, +163 ± 146 g; placebo group, +113 ± 145g) and there was no difference between-groups ($P = 0.81$). In contrast, there was a significant loss of lean mass in both groups (calcium, -709 ± 62 g; placebo, -667 ± 61 g) but, again, no significant difference between the treatments ($P = 0.63$). No significant differences were found in the changes in blood pressure between the two groups.

We conclude that calcium supplementation in normal postmenopausal women does not result in biologically significant effects on either body weight or blood pressure.

Disclosures: ***I.R. Reid****, None.*

SU455

Effects of Isoflavone on Bone Loss In Japanese Postmenopausal Women Depend on Bacterio-typing for Equol: A Randomized, Placebo-controlled Trial. J. Wu*[1], J. Oka*[2], M. Higuchi*[2], I. Tabata*[2], M. Fujioka*[1], F. Sugiyama*[1], N. Fuku*[2], T. Toda*[3], T. Okuhira*[3], T. Ueno*[4], S. Uchiyama*[4], K. Urata*[4], H. Cui*[5], K. Yamada*[1], Y. Ishimi[1]. [1]Division of Applied Food Research, National Institute of Health and Nutrition, Tokyo, Japan, [2]National Institute of Health and Nutrition, Tokyo, Japan, [3]Fujicco Co. LTD., Kobe, Japan, [4]Otsuka Pharmaceutical Co. LTD., Saga, Japan, [5]Department of Nutrition and Food Hygiene, Harbin Medical University, Harbin, China.

The objective of this study was to determine the effects of 24 wk of soy isoflavone intake and walking exercise, and their interaction on bone and lipid metabolism in Japanese postmenopausal women. The bioavailability of isoflavone daidzein was also examined to clarify the potential mechanism of bone-protective effects in human. Subjects, who were postmenopausal within 5 years, were randomly assigned into four groups; (1) placebo (n=33); (2) walking exercise (3 times/week) with placebo (n=31); (3) isoflavone intake (75 mg of isoflavone conjugates, Fujiflavone P40) (n=33); (4) isoflavone plus walking exercise (n=31). Furthermore, the subjects were stratified by “bacterio-typing” for equol, which is an intestinal bacterial metabolite of daidzein. The ability responsible for equol production in individuals was determined and the subjects were stratified by “equol producers” or “nonproducers”. The combined intervention of walking and isoflavone intake resulted in an increase in percentage (%) change in HDL-cholesterol concentration and it was significantly higher than those in placebo and isoflavone alone groups. The interventions also decreased fat mass in whole body and legs, and the % changes were significantly different from those in the placebo group. With respect to BMD, there were no significant differences in baseline and after intervention among the groups. However, the % changes in BMD in "equol-producers" were -0.53 and +0.13 in the whole body and total hip regions respectively, which were significantly different compared with -1.35 and -1.77 in "nonproducers" in isoflavone group. These results were related to the serum equol concentration. In contrast, there were no significant differences in % changes in BMD between the "equol-producers" and "nonproducers" in the placebo, walking and walking plus isoflavone groups. These results suggest that the combined intervention of isoflavone and walking exercise exhibited cooperative effects in modifying lipid metabolism and body composition in postmenopausal women. The preventive effects of isoflavones on bone loss depend on the “bacterio-typing” for equol in human.

Disclosures: ***J. Wu****, None.*

SU456

Equol, a Bacterial Metabolite of Isoflavone, Prevents Bone Loss in Ovariectomized Mice. Y. Ishimi[1], M. Fujioka*[1], M. Uehara*[2], J. Wu*[1], H. Adlercreutz*[3], K. Suzuki*[2], K. Kanazawa*[4], K. Takeda*[5], K. Yamada*[1]. [1]Division of Applied Food Research, National Institute of Health and Nutrition, Tokyo, Japan, [2]Tokyo University of Agriculture, Tokyo, Japan, [3]University of Helsinki, Helsinki, Finland, [4]Kobe University, Kobe, Japan, [5]Tokyo University of Science, Chiba, Japan.

Soybean isoflavones have similar structures to estrogen and have received attention as alternatives to hormone replacement therapy for the prevention of postmenopausal osteoporosis. We have reported that isoflavones prevent bone loss in both estrogen- and androgen-deficient osteoporotic model mice Daidzein, a major isoflavone found in soybean, is metabolized to equol by gut microflora, and the metabolite exhibits a stronger estrogenic activity than daidzein. However, there is no direct evidence that equol affects bone metabolism. In this study, we examined the effect of equol on the inhibition of bone loss in ovariectomized (OVX) mice. Eight week-old female mice were assigned to five groups; sham-operated (sham), OVX, OVX+0.1 mg/day equol administration (0.1 Eq), OVX+0.5 mg/day equol administration (0.5 Eq) and OVX+0.03 μg/day 17β-estradiol administration (E_2). Equol and E_2 were subcutaneously administerd, using a mini-osmotic pump. Four weeks after intervention, uterine weight was reduced by OVX and restored by E_2 administration. In contrast, equol at doses used in this study did not affect uterine atrophy in OVX mice. Bone mineral density (BMD) for the whole body measured by dual-energy X-ray absorptiometory (DXA) was reduced in OVX mice, while administration of 0.5 mg/day Eq as well as E_2 maintained it. The BMD of the femur and lumber spine was also reduced by OVX, and treatment with 0.5 mg/day Eq prevented the bone loss. In particularly, the BMD of the proximal femur was the same as that of the sham group. E_2 prevented bone loss from all regions induced by OVX. These results suggest that equol, a major metabolite of daidzein, inhibits bone loss apparently without estrogenic activity in the reproductive organs of OVX mice.

Disclosures: ***Y. Ishimi****, None.*

SU457

Gamma-Glutamyl-Peptide Isolated From Onion by Bioassay Guided Fractionation Inhibits Resorption Activity of Osteoclasts. H. A. Wetli*[1], R. Brenneisen*[2], I. Tschudi*[3], P. Bigler*[4], T. Sprang*[4], S. Schürch*[4], R. C. Muhlbauer[3]. [1]Laboratory for Phytopharmacology, Bioanalytics & Pharmacokinetics and Group for Bone Biology, University of Bern, Bern, Switzerland, [2]Laboratory for Phytopharmacology, Bioanalytics & Pharmacokinetics, Department Clinical Research, University of Bern, Bern, Switzerland, [3]Group for Bone Biology, Department Clinical Research, University of Bern, Bern, Switzerland, [4]Department of Chemistry and Biochemistry, University of Bern, Bern, Switzerland.

The addition of 7% of onion to the diet of rats decreases bone resorption and increases bone mineral content [Nature 401: 343-344, 1999]. This effect is independent of the base excess of onion [J Bone Miner Res 17: 1230-1236, 2002]. Furthermore, an ethanolic extract from onion prevented bone loss in an osteoporosis model and inhibited the resorption activity of osteoclasts in vitro. This suggested that the inhibitory activity of onion on bone resorption could be due to a pharmacologically active compound, prompting us to undertake its isolation and identification.

First, the ethanolic extract was subjected to adsorption column chromatography. Surprisingly, we found no activity in vivo of the flavonoid containing fractions (dose corresponding to 7% onion). Thus, the other, active material was fractionated by reversed phase-medium pressure liquid chromatography and the biological activity of the fractions was tested with the osteoclast pit assay. The active fractions were then further fractionated by normal phase-medium pressure liquid chromatography and finally by semi preparative-reversed phase-high performance liquid chromatography resulting in a single active peak. The structure of this compound was elucidated with high performance liquid chromatography-electrospray ionization-mass spectroscopy and nuclear magnetic resonance.

We found that the single peak is gamma-glutamyl-trans-S-1-propenyl-cysteine-sulfoxide. It has a molecular weight of 306 and inhibits dose dependently the resorption activity of osteoclasts, the minimal effective dose being about 2 mM. As no other peak displayed inhibitory activity it likely is responsible for the effect of onion on bone resorption, a contention that will be confirmed in vivo as soon as sufficient material is available. This will allow to study its mechanism and its role in the activity of the other 25 active vegetable food items we have identified so far.

Disclosures: ***R.C. Muhlbauer****, None.*

SU458

A Randomised Controlled Trial (RCT) of Calcium Supplementation in Pre-Pubertal Gymnasts Versus Controls: Response at the Mid-&-Distal Radial Sites. K. Ward[1], S. Roberts*[2], J. Adams[1], Z. Mughal[3]. [1]Clinical Radiology, Imaging Science & Biomedical Engineering, University of Manchester, Manchester, United Kingdom, [2]Biostatistics Group, CMMCH NHS Trust and University of Manchester, Manchester, United Kingdom, [3]Pediatric Medicine, CMMCH NHS Trust, Manchester, United Kingdom.

The positive effects of physical activity and calcium upon the developing skeleton are well documented. More recently, studies have shown that they may act interdependently upon the bone.

In this double blind RCT we investigated the effects of 12 months supplementation of 500g calcium carbonate (Calcichew™, Shire Pharmaceuticals) or placebo, upon the peripheral and axial skeleton of pre-pubertal gymnasts (G; 14 hrs of weight bearing activity per week) and controls (C; 6 hrs of weight bearing activity per week). Here we present preliminary analyses of the response to calcium supplementation (CaS) at the distal (4%) and mid (50%) radial sites, assessed using the Stratec XCT-2000 pQCT scanner. We hypothesised that CaS in G would result in greater changes in 1) mid-radial bone dimensions and cortical bone mineral density (BMD) and 2) distal radial bone dimensions and trabecular BMD, than C subjects.

Eighty-six subjects (49 females) participated in the RCT (44G: 42C) and 75 subjects completed the trial (45 females, 39G: 36C). Analysis of covariance was used to test differences in response to treatment between CaS and placebo (Pl) groups, including baseline height, gender, weight bearing activity and treatment as covariates; interactions were also tested.

At the mid-radial site, subjects in the CaS group had a greater increase in cortical BMD (12.3mg/cc, p=0.03) but smaller increase in periosteal circumference (-0.54mm, p=0.04) than those in the Pl group. The change in both endosteal and periosteal circumferences appeared to be different in males and females, however when tested, a treatment-gender interaction failed to reach statistical significance.

At the distal radius a significant interaction between treatment and activity was found G + CaS had greater increase in total bone area (10.52mm^2, p=0.04) than C and G+Pl.

At the mid-radius site the CaS group appear to accrue less bone on the periosteum; extra calcium is deposited within the cortex increasing cortical density. In contrast at the distal radius site CaS appears to have resulted in increased change in bone size without an increase in density. In conclusion, these preliminary data suggest that there may be site, activity and gender specific differences in the response of pre-pubertal children to calcium supplementation.

Disclosures: ***K. Ward****, None.*

SU459

Positive Effects on Height Remain One Year after the End of a Calcium Carbonate Intervention in 16-18 Year Old Boys. A. Prentice, F. Ginty, S. Jones*, M. A. Laskey*. MRC Human Nutrition Research, Cambridge, United Kingdom.

We have previously shown that calcium carbonate supplementation of 16-18 year old adolescent boys (1000 mgCa/d for 12 months) led to an increase in bone dimensions, statural height and greater bone mineral content (BMC) at the whole-body, spine and total hip. The aim of this follow-up study (FU) was to determine if these effects persisted beyond the supplementation period, thus indicating a long-term effect on growth and bone mineral accretion, or whether the differences had diminished, thus indicating that tempo of growth had been affected. Of the 143 boys who completed the intervention study, 67 (47%) agreed to return for FU measurements at 15.5 (SD3.3) months after the end of supplementation at a mean age of 19.3 (SD0.4) years. Of those (i.e. the FU responders), 55% (37/67) had been originally allocated to the calcium supplemented group (S) and 45% (30/67) to the placebo group (P). Their baseline characteristics were not significantly different from non-FU responders. There was a significant difference between FU responders and non-responders in reported tablet compliance during the intervention study (S and P together: 68% vs 50%, p=0.0003). The significant effects of the calcium supplement on height and DXA variables remained visible when the intervention data were restricted to FU responders and the differences with the placebo group were more pronounced, possibly reflecting the greater compliance of FU responders.

Between the end of supplementation and FU measurements, the FU responders had significant increases in body weight and in whole body and lumbar spine BMC and bone area (BA) (p<0.001), but not in statural height (p=0.49). Similar patterns were observed in the calcium and placebo groups separately. A significant height differential remained between the S and P groups (S-P at FU corrected for baseline: +0.75 (SE0.20)%, *p*=0.0005), equivalent to a difference of 1.3 cm for boys of average height (180 cm). Significant effects of the supplement also remained for whole body BA (+1.43 (0.69)%, p=0.042), spine BMC (+3.9 (SE1.8)%, p=0.035), spine BMD (+2.40 (1.22)%, p=0.054) and intertrochanteric BMC (+4.3 (SE2.0), p=0.037). These findings suggest there were long-term effects of calcium carbonate supplementation on both bone mineral mass and bone size. A further follow-up in young adulthood is planned, after linear growth has ceased in all individuals.

Disclosures: ***A. Prentice****, None.*

SU460

Effect of Pre- and Probiotics on Isoflavones Bioavailability, Consequences on Bone Metabolism in Postmenopausal Women. J. Mathey*[1], C. Bennetau-Pelissero*[2], M. Davicco*[1], C. Puel*[1], S. Kati-Coulibaly*[1], M. Horcajada*[1], V. Coxam[1]. [1]Nutrition, INRA, Saint-Genès Champanelle, France, [2]Micronutriments, Reproduction, Santé, ENITA, Gradignan, France.

Recently, attention has been focused, as a potential alternative to HRT, on isoflavones (IF), the so-called phyto-oestrogens (occurring in soyfood) that are chemically similar to mammalian estrogens. As bioavailability of these molecules could be improved by modulating intestinal microflora, the present study was undertaken to investigate whether probiotics and fructooligosaccharides (FOS, preobiotics), which are known to modify large bowel flora and metabolism, may exhibit a co-operative bone sparing effect. In that purpose, a two months, randomized, double-blind crossover study was carried out on 39 postmenopausal women without HRT. Volunteers were daily given for one months 100 mg of isoflavones aglycones (powdered soya isoflavones concentrate containing 46.19g/100g total isoflavones (genistin 55%-75%, daidzin 20%-40%, glycitin 1%-5%); Prevastein®HC, Eridania Beghin-Say) introduced in two yoghurts and two cereals bars containing 25 mg of isoflavones each. At the end of the first month, the participants were randomly assigned to three treatments groups all receiving the 100mg/day of isoflavones (IF) for one additional month. Among them, one group received 7g of FOS (FOS, Actilight®, Beghin-Meiji), while the other one was provided with 125 mg of lactic ferments (LF, 50g/100L, lactic bacteria including bifidobacteria, Danone Vitapole). On day 1 (baseline), 30 and 60, blood samples and the 24-h urines were collected in the morning to assess bone alkaline phosphatase (ALP), a marker for

osteoblastic activity and deoxypyridinoline (DPD), a marker of bone resorption, and isoflavones (daidzein, genistein and equol).
In control volunteers (IF), soy consumption was associated with a trend (although non significant) towards lower DPD levels (nM/mMol creatinine) (5.4 ± 0.2 *vs* 4.8 ± 0.2) and higher PAL (microg/l) (13.9 ± 0.5 *vs* 14.7 ± 0.4). On day 60, plasma concentrations of equol, the active metabolite of daidzein, were increased in the probiotics group (LF). This diet was also associated with a trend to an improvement of PAL levels, while DPD concentrations stayed unchanged. On the contrary, as far as prebiotics (FOS) are concerned, a significant decrease in DPD urinary levels was observed, only in early postmenopausal women.
In conclusion, addition of live microorganisms such as bifidobacteria or prebiotics, to an isoflavones-enriched diet may modulate bone turnover by improving bioavailability of those phytoestrogens, although if further longer investigations are warranted.

Disclosures: ***V. Coxam****, Beghin Meiji 2, 3; Danone 2; Nutrition Santé 2.*

SU461

Effects of Vitamin D, Calcium, and Cheese Supplementation on Urinary Calcium Excretion, Serum 25-OH-D and PTH in Pubertal Girls. A. E. Lyytikäinen[1], E. Helkala*[1], S. M. Cheng*[1], M. Suuriniemi[1], C. Lamberg-Allardt[2], A. Koistinen*[3], S. Cheng[1]. [1]Department of Health Sciences, University of Jyväskylä, Jyväskylä, Finland, [2]Department of Applied Chemistry and Microbiology, University of Helsinki, Helsinki, Finland, [3]Central Hospital of Central Finland, Jyväskylä, Finland.

This study was a two-year double-blind, placebo-controlled, randomized intervention to evaluate the effect of calcium (Ca), vitamin D (VD) and cheese supplementation on urinary calcium excretion and on serum 25-OH-vitamin D and parathyroid hormone (iPTH) concentration in pubertal girls. The subjects were Finnish girls aged 10-12 years at Tanner stage I-II with dietary Ca intake <900 mg/day. Altogether 143 completed the intervention (Ca+VD, n=37; Ca, n=33; Cheese, n=37; and Placebo n=36). In the Ca+VD, Ca and Cheese group girls received 1000 mg Ca as Ca carbonate tablets (500 mg x 2/day), or as low-fat cheese (100 g/day). The Ca+D group received vitamin D_3 200 IU/day. Over night fasting blood and 24-h urine was collected at baseline, year 1, and 2 during midwinter (Dec-Feb). Urinary calcium was analyzed by absorption spectrophotometry. Serum 25-OH-D and iPTH were analyzed by immunoenzymometric assays (IDS Inc, OCTEIA). The intake of nutrients was evaluated with a three-day food record. No significant differences were found in the compliance with supplements between the groups (70/74/64/72 % for Ca and 76 % for active VD). The mean weight, height, BMI, maturation status, and U-Ca, 25-OH-D and iPTH were similar among the groups at the baseline. During the two-year trial, all groups increased their Ca intake. The total mean Ca intake from diet and supplements was on average 1627 mg/day in the Ca+VD, 1600 mg/day in Ca, 1406 mg/day in Cheese and 831 mg/day in Placebo group. The corresponding figures for total mean VD intake were 6.3, 2.9, 3.2, and 2.6 µg/day, respectively. We found that a 37 % increase in 25-OH-D (from 41.0 to 52.7 nmol/L) in Ca+VD group caused a concurrent 11 % decrease in iPTH (from 28.7 to 23.2 pg/L) during the first year. Compared to other groups, the changes in Ca+VD group differed significantly for 25-OH-D ($p<0.001$) and there was a trend in iPTH changes compared to the Cheese group ($p=0.05$) and the Placebo group ($p=0.057$). At the second year, the 25-OH-D level did not further increase and iPTH concentration remained similar compared to the first year for all groups. We found a similar increase in the urinary calcium excretions in all groups during the trial (mean for all +83 %). Our results indicate that combined calcium (1000 mg/day) and vitamin D supplementation (200 IU/day) caused an increase in 25-OH-D levels and consequently a decrease in the iPTH levels in pubertal girls. Supplemental calcium alone did not effect iPTH levels.

Disclosures: ***A.E. Lyytikäinen****, None.*

SU462

A Survey of Calcium Concentrations in Bottled and Tap Water and Their Significance for Medical Treatment and Drug Administration. S. Morr*, E. Cuartas*, B. Alwattar*, J. M. Lane. Orthopaedics, Hospital for Special Surgery, New York, NY, USA.

Different forms of water vary in calcium content. High divalent ion (i.e. Ca^{2+}, Mg^{2+} etc.) concentration is deleterious to the efficacy of the bisphosphonate group of drugs in osteoporosis treatment. Water with high calcium concentration may also present an alternate pathway of calcium administration. In either case, knowing the actual concentration is critical. We hypothesize that there is considerable variety in the calcium concentrations in the various water sources. Calcium concentrations in various U.S. cities from different regions, as well as different kinds of bottled water, delineated into purified, spring, and mineral, are conjectured to have varying and somewhat predictable Calcium concentrations. In addition, as water filtration systems have gained popularity within the past years, we hypothesize that the water filter removes a significant amount of mineral, including calcium, from the water. Calcium concentrations in various city tap waters, as well as an assorted number of bottled waters were determined through the direct inspection of scientific data. The effect of filtering was also determined by mineral analysis of mineral water directly before and after filtration. The calcium concentration of water varies across the U.S.A. The average Calcium concentration for the selected group of cities was 50.71 mg/L, ranging from 8.3mg/L in Montgomery, AL to 131.0 in Phoenix, AZ. Upon categorization of the selected cities by regional location, the cities in the Northeast, Midwest, and South present with average values of 41.97 mg/L, 42.10 mg/L, and 42.95 mg/L respectively. The West Coast has an average value of 57.73 mg/L. The South presents with the greatest average value with 81.05 mg/L. Most spring waters were found to have a relatively low calcium concentration, with an average of 21.8 mg/L for the selected group. Purified waters constantly present with a negligible Calcium concentration. Mineral waters, on the other hand, were found to generally present with higher calcium concentrations. The selected group had an average of 208.3 mg/L of Calcium. Filtration was found to remove a considerable amount of calcium from the water, removing 89.42% of the Calcium content on average. Calcium concentration in water varied from, as well as within, different regions in the U.S.A. Different forms of bottled waters presented with varying concentrations of calcium. Certain tap and bottled waters present with concentrations of calcium sufficient to exhibit a deleterious effect on bisphosphonate treatment. Alternatively, certain waters may be used as a source of ingested calcium that may provide over 40% of the daily requirement for calcium ingestion.

Disclosures: ***S. Morr****, None.*

SU463

Design of Compliant Floors to Reduce Impact Forces During Falls on the Hip. A. C. T. Laing*, I. Tootoonchi*, S. N. Robinovitch*. School of Kinesiology, Simon Fraser University, Burnaby, BC, Canada.

Over 90% of hip fractures are due to falls, and fracture risk during a fall depends on the impact force applied to the proximal femur. One strategy for reducing fall impact forces is to decrease the stiffness of the floor, an intervention especially relevant to high-risk environments such as nursing homes or senior centres. Our goals in this study were: (1) to test whether reducing the floor stiffness attenuates peak force during experimental falls on the hip from safe heights; and (2) to develop and use a mathematical (vibratory) model to predict how feasible reductions in floor stiffness reduce peak forces during falls from standing.
Seven young women participated in the experiments (mean age = 23±2(SD) yrs). During the trials, the subject lay on her side, resting her knee and shoulder on rigid side platforms, and her pelvis on a middle platform that was either rigid (having a stiffness of 733 kN/m) or compliant (having a linear stiffness of 18 kN/m, a reasonable lower bound given the known effect of floor compliance on postural stability during standing). A nylon sling and electromagnet was used to lift and instantly release the pelvis from a height of 1.25 or 5.0 cm. Hip contact force was sampled at 960 Hz from a forceplate under the middle platform. We also compared experimental trends to those predicted by a best-fit mass, spring, and damper vibratory model and used the model to predict peak forces during falls from standing.
Peak impact force associated with both floor stiffness ($p<0.001$) and fall height ($p<0.001$), based on repeated-measures ANOVA. In the 1.25 cm fall height condition, average peak forces were 16% lower in the compliant than rigid floor condition (497±81 versus 595±107 N). In the 5.0 cm fall height condition, peak forces were 40% lower in the compliant than rigid floor condition (623±71 versus 1045±88 N). Model predictions of peak force matched experimental data with 14±6% accuracy. Peak forces predicted by the model for falls from standing (with a descent height of 70 cm) were 28% lower for impact on our compliant versus rigid floors (2050 versus 2860 N). The former value is approximately 1.36 standard deviations below the average fracture force of 4100±1510 N for elderly cadaveric femora.
Our results indicate that feasible reductions in floor stiffness may reduce hip impact force during a fall by 28%, to a value that is considerably below the average fracture force. Future work is required to determine the additional benefit provided by damping elements, and to determine threshold values for floor stiffness, below which balance maintenance and recovery is impaired.

Disclosures: ***A.C.T. Laing****, None.*

SU464

Cessation of Training Is Followed by Rapid Loss of Bone Mineral Density, a 8-Year Longitudinal Study in Females. Ö. Valdimarsson, M. K. Karlsson. Orthopeadics, Medicine and Surgery, Malmö, Sweden.

Physical activity at young age increases bone mineral density (BMD) but whether the benefits in BMD are retained with reduced activity level is still controversial. The aim of this study was to evaluate the effect of training and reduced training on BMD in women during an 8-year follow-up. At baseline, dual X-ray absorptiometry (DXA) evaluated BMD (g/cm^2), femoral neck width (cm) and femoral neck volumetric BMD (vBMD; g/cm^3) in 48 active female soccer players with mean age 18.2 ± 4.4 years, in 18 former female soccer players with mean age 43.2 ± 6.2 years and retired since mean 9.4 ± 5.3 years and in 64 age and gender matched controls. The measurements were repeated after mean 8.0 ± 0.3 years when 35 of the at baseline active players had retired since mean 5.3 ± 1.6 years. The at the follow-up still active soccer players had already at baseline a higher BMD in comparison with the matched controls, at the femoral neck (FN) 1.13 ± 0.19 versus (vs.) 1.00 ± 0.13, $p = 0.02$ and at the legs a non significant higher BMD, 1.23 ± 0.12 vs. 1.15 ± 0.11, $p = 0.07$. The yearly gain in BMD during the follow-up was higher in the active players than in the controls, at the leg 0.015 ± 0.006 vs. 0.007 ± 0.012; $p = 0.04$, so that the discrepancy in BMD at follow-up was even larger than at baseline, at the FN 1.20 ± 0.17 vs. 0.99 ± 0.16 and at the legs 1.36 ± 0.10 vs. 1.19 ± 0.09, both $p < 0.001$. The soccer players who retired during the follow-up had at baseline a higher BMD in comparison with the matched controls, at the FN 1.13 ± 0.13 vs. 1.04 ± 0.13, and at the legs 1.28 ± 0.12 vs. 1.20 ± 0.10, both $p < 0.001$. The at follow-up retired players lost whereas the controls gained BMD during the study period, yearly at the FN -0.007 ± 0.01 vs. 0.003 ± 0.02, $p = 0.01$ and at follow-up there was only a discrepancy in BMD at the legs 1.32 ± 0.12 vs. 1.23 ± 0.10, $p = 0.001$. The already at baseline retired soccer players had at study start higher BMD in comparison with the matched controls, in the legs 1.26 ± 0.09 vs. 1.18 ± 0.10, $p = 0.01$. The former players lost whereas the controls gained BMD during the study period, yearly at the trochanter -0.006 ± 0.01 vs. 0.004 ± 0.01, $p = 0.01$. In spite of this, there was still a discrepancy in BMD at follow-up when comparing the players who already at baseline were retired and the controls but at a lesser magnitude, at the legs 1.22 ± 0.10 vs. 1.17 ± 0.10, $p = 0.05$. In summary, this study demonstrates that in girls, intense exercise also after puberty is associated with a higher accrual of BMD and decreased physical activity both in a short term and a long-term perspective is associated with a higher BMD loss. We conclude that physical activity during childhood and adolescence may be used as a prevention strategy of osteoporosis, probably only if the physical activity is advocated lifelong.

Disclosures: ***Ö. Valdimarsson****, None.*

SU465

The Effect of the Multicomponent Exercise on Bone Mineral Density and Fall Risk Factors in Osteoporotic Women. H. Park*[1], S. Park*[2], T. Komatsu*[3], S. Park*[1], T. Kaminai*[3], H. Okuizumi[3], Y. Mutoh*[1]. [1]Department of Physical and Health Education, The University of Tokyo, Tokyo, Japan, [2]Department of Physical Education, University of Dong-A, Busan, Republic of Korea, [3]Department of Orthopedic Surgery and Rehabilitation, Tokyo Kouseinenkin Hospital, Tokyo, Japan.

Osteoporosis-related fractures in older individuals are increasing and become one of the major health problems in Asian world. However, the effects of exercise intervention for preventing fractures in osteoporotic elderly are unknown and controversial. This study assessed that the multicomponent exercise intervention prevents bone loss in weight-bearing bones and improve fall risk factors in women of 65-year-old or older who were diagnosed with osteoporosis by WHO criteria. Sixty-five osteoporotic women were recruited and randomized into the control (CON) group (n=31) and the intervention (INT) group (n=34). The exercise intervention focuses on four components: exercise for fun, aerobic exercise, strengthening exercise, balance and posture training. This supervised exercise intervention performed 50 minutes a day, 4 days a week for 10 months. The control group retained a sedentary life style and joined in Calligraphy, Singing and Oriental checkers class twice a week. Bone mineral densities (BMDs) in both proximal femur and calcaneus by using dual-energy x-ray absorptiometry were measured repeatedly before and after the ten months experiment in both groups. Dynamic balance (tandem walk, timed get-up and go test), static balance (eyes-open one-legged stand time, postural sway), and leg muscle strength and mobility performances (10-meter rapid walking speed, 40-centimeter step up and down, maximal step length) were also measured as fall risk factor. All practitioners were blinded to group assignment. There were no differences in anthropometric variables and menstruation status at baseline. Ninety-four percent of subjects in the INT group and ninety-three percent of subjects in the CON group completed the 9-month follow-up study. BMD measurements revealed bone losses in both groups, but BMD at femoral neck (0.07 vs. 0.02 g/cm^2, p<. 05) and calcaneus (0.08 vs. 0.03 g/cm^2, p<. 05) in the CON group have more lost significantly compared to the INT group. Fall risk factors in the INT group were substantially greater improved than in the CON group. A total of two fractures occurred during the follow-up, including 2 subjects in the CON group. This randomized and prospective study shows that this multicomponent exercise intervention is beneficial for preventing bone loss in weight-bearing bones and ameliorating the fall risk factors in osteoporotic elderly.

Disclosures: ***H. Park****, None.*

SU466

Walking Benefits Bone Mass in Postmenopausal Women. R. A. Brownbill, J. Z. Ilich. School of Allied Health, University Of Connecticut, Storrs, CT, USA.

Studies conflict as to which types of physical activity (PA) best benefit bone mass in postmenopausal women. This study was conducted to determine which types of PA were related to bone mass at various skeletal sites. 136 healthy Caucasian women not taking hormone replacement therapy, mean±SD age 68.6±7.1 (range 57.4-88.64) were enrolled in a 2 1/2 year longitudinal study. PA, bone mineral content (BMC), anthropometrics and diet were assessed every 6 months. BMC of the whole body, femur and lumbar spine were measured with a DPX-MD densitometer. Walks of at least 20 minutes in duration as well as all recreational activities (i.e. aerobics, tennis) were reported as hours per week. Cumulative averages over 2 1/2 years were calculated for PA variables and confounders (age, height, weight, calcium, protein and sodium intake), and used in multiple regression analysis, with BMC measured at 2 1/2 years as the dependent variable. Total hours of walking per week (1.4±1.6) was a significant predictor of whole body BMC, p=0.008, R2 adjusted 61.2. Without age in the model, total hours of walking per week was a significant predictor of femoral neck BMC, p=0.038, R2 adjusted 47.1. Walking was not related to lumbar spine BMC, and recreational activities were not related to any measured bone site. The findings of this study indicate that walking for at least 20 minutes several times per week appears to positively influence bone mass of the whole body and hip and therefore, should be recommended to postmenopausal women.

Disclosures: ***R.A. Brownbill****, None.*

SU467

Lymphatic Flow and Bone Mineral Density. K. J. McLeod[1], J. M. Stewart*[2]. [1]Bioengineering, Binghamton University, Binghamton, NY, USA, [2]Pediatrics and Physiology, New York Medical College, Valhalla, NY, USA.

Recent clinical studies have demonstrated the ability of plantar based vibration to inhibit the loss of bone density in post-menopausal women [1], however, given the very low forces produced by this stimulus, it is unlikely the observed effects would be due to any mechanical loading of the skeleton. Instead, we hypothesized that plantar vibration serves as a neuromuscular stimulus, increasing skeletal muscle pump activity which enhances interstitial (i.e. nutrient) flow to the bone tissue by improving interstitial fluid clearance. Initial studies utilizing strain gage plethysmography to measure microvascular filtration confirmed the ability of plantar vibration to significantly enhance interstitial fluid flow [2]. Here, we tested the third aspect of this hypothesis, that is, whether increased lymphatic flow in the lower limbs was associated with increased bone density.

Strain gauge plethysmography was used to measure calf blood flow, venous capacitance and microfiltration relation in the supine position, in 14 women aged 46-63 years. Hip BMD in these subjects was obtained by DEXA and measurements converted to t-scores. Regression analysis was performed using t-score as the dependent variable, against calf blood flow, filtration coefficient, interstitial pressure, and calculated lymph flow. Hip bone density in this population was not related to blood flow in the lower limbs, however a significant positive correlation between BMD and microfiltration coefficient was observed (R^2 = 0.4). Moreover, a significant positive association between interstitial pressure (threshold pressure for edema) and BMD was also observed (R^2 = 0.44). Further, lower limb lymphatic flow was found to be the strongest correlate of hip t-scores in this perimenopausal population (R^2 = 0.52).

In conclusion, lower limb lymphatic flow can account for over 50% of the variability in femoral neck BMD, consistent with the hypothesis that interstitial fluid flow is a critical factor in mediating bone formation and resorption processes. That therapies such as plantar vibration can significantly enhance interstitial flow in the lower limbs potentially opens the door for preventing and treating bone loss through relatively simple interventions.

1. Rubin CT, Recker R, Cullen D, Ryaby J, McCabe J, and McLeod KJ (2004) Inhibition of post-menopausal bone loss by extremely low magnitude, high frequency mechanical stimuli. J. Bone and Mineral Research 19(3):343-51.

2. Stewart JM, Karman C, Montgomery LD, and McLeod KJ (2004) Plantar vibration improves leg fluid flow in perimenopausal women. FASEB Journal 18:A1213.

Disclosures: ***K.J. McLeod****, Smith & Nephew, Inc. 2, 5.*

SU468

Cortical Bone Density Increases with Resistance and Agility Training: A Six-Month RCT. T. Liu-Ambrose[1], K. M. Khan[2], J. J. Eng*[3], A. Heinonen[4], H. A. McKay[5]. [1]Orthopaedics, University of British Columbia, Vancouver, BC, Canada, [2]Family Practice, Human Kinetics, University of British Columbia, Vancouver, BC, Canada, [3]Rehab Sciences, University of British Columbia, Vancouver, BC, Canada, [4]Health Sciences, University of Jyväskylä, Jyväskylä, Finland, [5]Orthopaedics, Family Practice, University of British Columbia, Vancouver, BC, Canada.

A randomized, controlled, single-blinded 25-week prospective study was conducted to compare the effects of group-based resistance and agility training on bone, as measured by both DXA and pQCT, in older women with low bone mass. The study was approved by the University of British Columbia Clinical Research Ethics Board and the Research Committee of the Children's and Women's Hospital of British Columbia. All participants provided written informed consent. Ninety-eight community-dwelling women aged 75-85 years were randomized to one of three groups: Resistance Training (n = 32), Agility Training (n = 34), or Stretching (sham exercise) (n = 32). Total hip, femoral neck, and trochanteric BMD were measured by a Hologic 4500 DXA. All the DXA scans were analyzed using standard Hologic analysis protocol. Peripheral QCT measurements were performed at the tibia and radius using the Norland/Stratec XCT 540 densitometer. Single 2.5 mm slices were obtained of the left lower leg at (i) the 50% site (i.e., 50% of the tibial length proximal to the distal endplate of the tibia) and (ii) the 10% site. Similar slices were obtained of the left forearm at the 30% and 10% sites of the radius. A voxel size of 0.5 mm was used for all scans. The pQCT outcome measures at the shaft regions were cortical bone content, cortical bone cross-sectional area, cortical bone density, and density-weighted polar section modulus (SSI). The pQCT outcome measures at the distal sites were total bone content, total bone cross-sectional area, and total bone density. An analysis mask was created specifically for each measured site. Different tissues within each slice were separated according to different density thresholds. At trial completion, the Agility Training group significantly increased cortical bone density by 0.5 ± 0.2% (SE) at the tibial shaft compared with a 0.4 ± 0.3% loss in the Stretching group (p = 0.02). The Resistance Training group significantly increased cortical bone density (1.4 ± 0.6%) at the radial shaft compared with a 0.4 ± 0.5% loss in the Agility Training group (p = 0.03). There were no significant differences among the three groups in any of the DXA outcome measures. Future research is needed to determine the mechanism(s) responsible for the observed adaptation of cortical bone to mechanical loading in older adults with low bone mass.

Disclosures: ***T. Liu-Ambrose****, None.*

SU469

Multiexercise Program Reduce Risk Factors for Fractures in 70- to 78-Year Old Women: A Randomized Controlled Trial. A. Heinonen[1], S. Karinkanta*[2], H. Sievänen*[2], K. Uusi-Rasi[2], M. Pasanen*[2], P. Kannus*[2]. [1]Department of Health Sciences, University of Jyväskylä, Jyväskylä, Finland, [2]UKK Institute for Health Promotion Research, Tampere, Finland.

The purpose of this one-year randomized, controlled exercise intervention trial was to evaluate the effects of strength training, balance & agility-jumping training, and combination of strength and balance & agility-jumping training on postural control, muscle strength, and bone mineral mass and geometry in 149 home-dwelling 70 -78-year--old women. The inclusion criteria were no regular exercise or previous bone fractures, no current or previous use of drugs or illness affecting bone metabolism or balance, no contraindication to exercise, and femoral neck T-score ≥ -2.5. The final data could be obtained from 144 women. Femoral neck bone mineral density (BMD) was measured by DXA (Norland XR-26). BMD, total area (TotA), cortical area (CoA) and polar section modulus (SSI) of the shaft and distal part of the tibia were measured with peripheral computed tomography (Stratec XCT 3000). Dynamic balance (agility) was tested by a figure-of-8 running test. Maximal isometric strength of the leg extensors was measured with a leg press dynamometer. All training sessions were supervised and were given 3 times a week for 12 months. Between-group differences were estimated by analysis of covariance using baseline values as covariates. The leg extension strength change was significantly (p<0.05) higher in the strength group (effect: 13%, 95% CI: 3% to 24%) and in the combination group (12%; 2% to 23%) than that in the control group. In addition, the dynamic balance was improved significantly (p<0.05) more in the agility-jumping group (5%; 2% to 7%) and in the combination group (7%; 2% to 11%). In the bone variables, there were no statistically significant differences between the exercise groups and the control group. However,

there was a trend that at the tibial shaft CoA area decreased less in the strength group compared with the control group. This study suggests that 12-month exercise program including muscle strength, balance and jumping training is able to reduce risk factors for fractures among home-dwelling elderly women..Because fluent performance of daily activities and steady postural control require good muscle strength and power, strength training combined with balance & agility-jumping exercises are included in elderly women ´s exercise programs.

Disclosures: ***A. Heinonen****, None.*

SU470

Multiexercise Program to Improve Muscle Strength and Dynamic Balance in Home-dwelling Elderly Women. S. Karinkanta*, A. Heinonen, H. Sievänen*, K. Uusi-Rasi, P. Kannus*. UKK Institute, Tampere, Finland.

Decline in neural and musculoskeletal functions in older adults is associated with the ability to respond abruptly to a loss of balance. Balance and lower limb muscle strength are connected to functional ability. The purpose of this randomized controlled exercise intervention trial was to evaluate the effect of six months strength training, agility-jumping training, and combination of strength and agility-jumping training, on lower limb muscle strength, and dynamic balance and agility in home-dwelling elderly women.

The subjects, 149, elderly women aged 70 to 79 years were randomly assigned into four groups: 1) strength training group (SG) (n=37), 2) agility-jumping training group (AG) (n=37), 3) combination of strength and agility-jumping training group (SAG) (n=38) and 4) control group (CG) (n=37). Progressive, supervised training sessions were given 3 times per week. The maximal isometric strength of the leg extensors was measured with a leg press dynamometer. The dynamic muscle strength of lower limbs was assessed by measuring ground reaction forces with a force platform during common daily activities (sit-to-stand and step-on-a-stair tests). Dynamic balance and agility was assessed by a figure-of-eight running test. The between-group differences were analyzed by analysis of covariance using baseline values as covariates.

The mean increase (95% CI) in the leg extension strength was 11% (2% to 20%) greater both in the SG and SAG than in CG. Further, in the step-on-a-stair test, the mean increase in ground reaction forces (N/kg) improved 13% (1% to 27%) more in the SAG than in the CG. In a sit-to-stand test, improvement in the ground reaction forces were 22% (7% to 40%) greater in the AG compared to the CG and 18% (3% to 35%) greater compared to the SG group. In addition, the agility estimated by the figure-of-eight running time improved by 5% (1% to 9%) in the SAG compared to the CG.

According to this data combined strength and agility-jumping training seems to be an effective way to improve muscle strength of the lower limbs, as well as dynamic balance and agility in home-dwelling elderly women. In these respects, strength or agility-jumping training alone was less effective.

Disclosures: ***S. Karinkanta****, None.*

SU471

Safe Landing During a Fall: Response Time Affects Ability to Avoid Hip Impact During a Sideways Fall. F. Feldman*, S. N. Robinovitch*. Kinesiology, Simon Fraser University, Burnaby, BC, Canada.

Ninety percent of hip fractures are due to falls, and fall severity is at least as important as bone density in determining fracture risk. Of particular importance is whether impact occurs to the hip, which increases fracture risk 30-fold. Previous studies indicate that individuals can avoid hip impact during a sideways fall by rotating the trunk forward or backward during descent. In the present study, we tested whether a critical time window exists for initiating this response after the onset of the fall, in order for it to be effective in preventing hip impact.

Fifteen women participated (mean age=23±4(SD) yrs). In all trials, a sideways fall was initiated by releasing a tether which supported the subject at a 10 deg lean angle. This caused the subject to fall suddenly on a gym mat (average descent time approx. 900 ms). Subjects were instructed to avoid hip impact by rotating backward (BR) or forward (FR) during descent. The instruction was provided as a visual cue (a 1.1x1.6 m image projected in front of them, showing the desired landing configuration) presented either before tether release (by 300, 200, or 100 ms) or after tether release (by 0, 100, 200, or 300 ms). In each trial, we used a 3D motion measurement system to determine the pelvis impact angle. A value of zero deg indicated direct impact to the hip, while 90 deg indicated impact to the anterior or posterior aspect of the pelvis.

From repeated measures ANOVA, we found that the absolute value of pelvis impact angle depended strongly on the time of cue delivery ($p<0.001$; Fig.1), but did not associate with the direction of rotation ($p=0.62$). When the cue was provided 200 ms before release, pelvis impact angles averaged 61.9±22.3 deg for BR and 66.8±12.6 deg for FR. When the cue was provided 200 ms after release, average angles were 19.9±16.0 deg for BR and 13.9±11.9 deg for FR.

Our results indicate that trunk rotation must be initiated early during descent (within 100 ms after loss of balance) to prevent hip impact during a sideways fall. Future studies should examine the sensorimotor and cognitive determinants of response speed, and fracture prevention programs should incorporate safe techniques for enhancing fall protective responses.

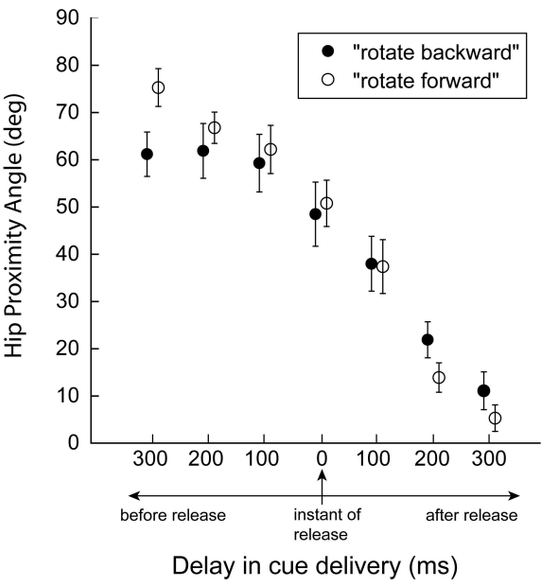

Figure 1: Mean ± S.E. values of pelvis impact angle.

Disclosures: ***F. Feldman****, None.*

SU472

Can Tai Chi Exercise As a Primary Treatment Prevent Osteoporosis And Improve Health Fitness in Seniors? W. Jin*. Shenyang Physical Education University of China, Shenyang, China.

Tai Chi, as a weight bearing form exercise, widely practiced among Chinese, has beneficial effects on cardiorespiratory and musculoskeletal function, posture control capacity, and the reduction of falls experience by elders. However, there have not been enough studies covering the effects of Tai Chi exercise on both preventing bone loss and improving health fitness in seniors. Our objective was to compare the changes of Bone Mineral Density (BMD) and health fitness after six months of Tai Chi exercise in twenty-five healthy seniors (mean age, 65.3+/-5.2y). BMD in the lumbar spine (LS) and femur neck (FN) were measured at baseline and at follow-up by using dual energy x-ray absorptiometry (DXA). Single-stance postural balance, strength, blood pressure and heart rate were also evaluated pre- and post-test. The results showed that there were no significant changes of BMD at LS and FN. Foot COP displacement during stance with eyes open and closed improved +15% ($P<0.01$) and 11% ($P<0.01$). The increases of abdominal muscle and knee muscle strength were +6.4% ($P<0.05$), +22% ($P<0.01$), respectively. The blood pressure (SBP, -11.3%; DBP, -8.8%) decreased significantly but not heart rate (HR, -2.6%). The results indicate Tai Chi exercise as age-appropriate and cost-effective moderate intensity program has benefits on balance, muscle strength, blood pressure in seniors. No significant changes of BMD in this study might be connected with the senior age group and short-term program length. The long term Tai Chi exercise intervention as a primary treatment for preventing osteoporosis should be investigated in further study.

Disclosures: ***W. Jin****, None.*

SU473

Influence of HMG-CoA Reductase Inhibitors on Bone Mass in Postmenopausal Women. Y. J. Kim, S. Y. Lee*, Y. J. Kim*. Family Medicine, Pusan National University Hospital, Busan, Republic of Korea.

Introduction: It is controversial whether use of HMG-CoA reductase inhibitors(statins) is associated with an increased bone mineral density (BMD) in human or not. The purpose of this study was to assess the influence of statins on BMD of postmenopausal women.

Methods: Forty-four postmenopausal women(mean aged 54.3 ± 5.8 years) were included. The statins users(n=24) were adminstered with simvastatin, atorvastatin, pravastatin or lovastatin. The control group (n=20) did not take statins. BMD of the spine was measured by dual energy X-ray absorptiometry. Alkaline phosphatase(ALP) was tested as a bone turnover marker. The data was analysed with two-sample t-test and paired t-test.

Results: The mean annual spinal BMD changes of the study groups were -1.5± 5.6% for statins users and -0.2±4.2% for control group ($P>0.05$ and $P>0.05$). The mean annual ALP changes of the study groups were - 5.6±18.1% for statins users and -0.4±13.9% for the control group($P>0.05$ and $P>0.05$). In each group, the spinal BMD did not change significantly after 1 year($P>0.05$).

Conclusions: Our results suggest that statins do not protect women from postmenopausal bone loss.

Disclosures: ***Y.J. Kim****, None.*

SU474

Vertebroplasty Alters the Structural Behavior of Osteoporotic Vertebrae. R. N. Alkalay*, D. von Stechow*, M. L. Bouxsein. Dept. of Orthopedics, Beth Israel Deaconess Medical Center & Harvard Medical School, Boston, MA, USA.

Percutaneous vertebroplasty and kyphoplasty are gaining acceptance for surgical treatment of vertebral fractures (VF), as they have been shown to alleviate protracted back pain with few complications (1, 2). Yet, several reports suggest a high rate of incident VF following these procedures (3, 4, 5). We hypothesized that this increased rate of VF may be partly attributable to altered mechanical behavior of cement-augmented vertebrae. Our goal was to compare the structural behavior of intact, fractured and cement-augmented osteoporotic vertebrae. We used a multi-axial load cell to measure the strength and stiffness of 19 human thoracic and lumbar vertebrae under combined compression and anterior flexion loading. Each vertebrae was tested to failure (50% reduction in anterior height), allowed to recover unloaded for 30 minutes, retested, then augmented with PMMA cement (3 to 10 cc), and tested again. As expected, fractured vertebrae had a reduced ability to resist loading in compression and anterior bending (Table). Cement augmentation not only increased the load-bearing capacity compared to fractured vertebrae (86 to 489%), but also increased compressive (+125%, $p<0.0001$) and anterior bending strengths (+71%, $p<0.01$) compared to intact vertebrae (Table). In summary, vertebroplasty significantly increased the structural competance of fractured vertebrae. However, the mechanical behavior of cement-augmented vertebrae under combined compression and forward bending loads was markedly altered relative to that of intact vertebrae. Our data indicate that vertebroplasty may change the load transfer pattern between adjacent vertebrae, perhaps increasing their risk of fracture. These findings underscore the need for randomized controlled trials to determine the long-term efficacy and safety of vertebroplasty and kyphoplasty.

	Intact	Fractured	Augmented
Compressive Strength (N)	1581 (44)	1082 (313) a	3552 (961) a,b
Compressive Stiffness (N/mm)	536 (542)	262 (186) a	749 (288) b
Anterior Bending Strength (Nm)	15 (6)	11 (5) a	24 (10) a, b
Anterior Bending Stiffness (Nm/mm)	11 (12)	8 (7) a	15 (6) b
Lateral Bending Strength (Nm)	2 (3)	3 (3)	4 (13) b
Lateral Bending Stiffness (Nm/mm)	-0.1 (1.2)	-0.3 (1.4)	0.7 (3.0)

Mean (sd); a: $p<0.05$ vs intact; b: $p<0.05$ vs fractured.

Refs: 1) Phillips, Spine 2003; 2) Coumans, J Neurosurg 2003; 3) Uppin, Radiology 2003, 4) Grados, Rheumatology 2000; 5) Donovan, JBMR 2004

Disclosures: ***M.L. Bouxsein****, DePuy Medical 2.*

SU475

Does a Distal Forearm Fracture Lead to Evaluation for Osteoporosis? A Retrospective Cohort Study in 147 Danish Women. B. Rud[1], R. Greibe*[2], L. Hyldstrup[1], H. A. Sørensen*[2]. [1]The Osteoporosis Unit, Department of Endocrinology, Hvidovre University Hospital, Copenhagen, Denmark, [2]Department of Internal Medicine, Amager University Hospital, Copenhagen, Denmark.

In postmenopausal women a low trauma distal forearm fracture is a risk factor for osteoporosis and future fracture, which indicates osteoporosis follow-up according to prevailing guidelines. Unfortunately, reports from several countries suggest low compliance with these guidelines.

We decided to determine how often women over 45 years, presenting with a low trauma distal forearm fracture to a Danish emergency department during a one-year period were followed-up for osteoporosis. We excluded women with: 1) dementia or cancer with bone metastases, and 2) avulsion of the styloid process of the ulna.

We performed a retrospective review of hospital records, and we sent the women and their general practitioners pre-tested questionnaires regarding the follow-up undertaken in primary care. Finally, we invited the women for a densitometry of the lumbar spine and the femoral neck. The densitometries were performed on a Norland XR26. T-scores were calculated using a Danish reference material of 103 women aged 20-35 years. We calculated the prevalence of three levels of low BMD using the lowest T-scores measured ($T \leq -2.5$, $T \leq -2.0$, $T \leq -1.5$).

From May 1st, 2001 to April 30th, 2002, 147 women presented with a low trauma distal forearm fracture. According to the review of hospital records none of the women was referred for bone densitometry or spine X-rays. One woman had calcium and vitamin D prescribed and two were recommended to consult their general practitioner for osteoporosis follow-up. As regards primary care we had replies from the women or the GPs for 134 (91%) women. Twelve women were referred for densitometry or spine X-rays and 11 started calcium and vitamin D after the fracture. Women with risk factors for osteoporosis beside the forearm fracture were not more likely to be referred for densitometry or spine X-rays (Fischer's test, $p = 0.10$). Three women started antiresorptive treatment (bisphosponates) following the fracture. The prevalence of $T \leq -2.5$, $T \leq -2.0$ and $T \leq -1.5$ was 24%, 53% and 69%, respectively among the 79 women, who underwent densitometry. Women, who had a densitometry were significantly younger than women, who did not (mean ages 67 and 77 years, respectively) (two sample T-test, $p= 0.0005$).Our study demonstrated a low use of available measures to reduce the risk of future fracture in women with a low trauma distal forearm fracture, and it emphasizes the need to decide on a local level, how to provide osteoporosis follow-up for women with fragility fractures.

Disclosures: ***B. Rud****, None.*

SU476

A Multi-faceted Post-fracture care Model: The Fracture? Think Osteoporosis! Program. A. Papaioannou[1], E. Coker*[1], C. C. Kennedy*[1], J. DeBeer*[2], J. D. Adachi[1]. [1]Medicine, McMaster University, Hamilton, ON, Canada, [2]Orthopaedics, McMaster University, Hamilton, ON, Canada.

Osteoporotic fractures are a significant burden on our health care system. In Ontario alone, the projected number for 2003 was 10,000 wrist fractures and 8700 hip fractures. While it is unknown how many of these fractures were preventable with proper post-fracture care, part of the fracture burden can be attributed to clinicians, patients and health care systems alike not linking fractures to osteoporosis. Canadian studies show that 50-98% of individuals who experience a fragility fracture do not receive treatment for osteoporosis, despite therapeutic options that decrease future fracture risk. The Fracture? Think Osteoporosis! program is a comprehensive, interdisciplinary strategy that will target the entire spectrum of post-fracture care in the Hamilton region and will provide a model for closing the osteoporosis care gap that exists in Canada today. A multi-faceted approach targeting multiple stakeholders, including providers, patients and the overall health system, has been chosen based on knowledge transfer models of dissemination. The primary objective of the *Fracture? Think Osteoporosis* program is to improve diagnosis and treatment of osteoporosis in patients with fragility fractures and to decrease the rate of subsequent fractures by at least 20% in those individuals > 50 who have experienced a fracture. The intervention will span the spectrum of acute care (fracture clinic, orthopedic units and rehabilitation, radiology), primary care and the community (including BMD clinics, community falls prevention clinics). Planned interventions include predisposing strategies to improve practitioner behavior including needs assessment, CME, patient self- assessment and educational materials; enabling strategies such as care maps on orthopedic and rehabilitation units, reminders, and patient-mediated interventions; reinforcing strategies such as practitioner audit and feedback. In addition strategies at the Health Care System Level will include: guidelines and care maps, hospital committees, development of quality indicators, and working across jurisdictions. Over the course of 5-years, these initiatives will be implemented within a continuous feedback model overseen by an advisory board with scheduled evaluations of process and outcome indictors. Partners in the program include all the acute care hospitals in the region, the Public Health Department, and the Osteoporosis Society of Canada and Fitness Centres.

Disclosures: ***A. Papaioannou****, None.*

SU477

See Poster M468B

SU478

Ballon-kyphoplasty in the Treatment of Osteoporotic Vertrebral Compression Fractures (VCF) - Our First Experiences. C. Guenther[1], J. Borgulya*[2], A. Kapner*[1], O. Guenther*[1]. [1]Deutsches Zentrum für Osteoporose, Johannesbad Reha-Kliniken AG & Co. KG, Bad Füssing, Germany, [2]Wirbelsäulenchirurgie, Chriurgisch-Orthopädische Fachklinik Lorsch GmbH & Co. KG, Lorsch, Germany.

To look for pain relief and correction of spinal deformity after ballon-kyphoplasty. In addition to this we were interested in new fractures nearby the operated segments.

All together 85 vertebras were treated in 54 patients (48 women, 6 man, age 72 years). This 85 vertebra can be devided in 49 with acute fractures (AF, operation shorter than four weeks after fracture) and 20 subacute fractures (SAF, four to eight weeks). From this 54 patients had 11 adequate trauma, 15 a non-adequate accident and 28 spontaneous fractures. For pain-estimation we used the VAS-scale, for measurement of kyphosis angle the lateral X-ray of the spine.

AF- group (n=49) showed a improvement kyphosis angle of 11.5 grad postoperative (p.o.). and 10.7grad after four weeks. In the SAF -group we could see an improvement of 1.8/ 1.7grad. Looking to the pain-score the AF showed following VAS- values: 8.8 preoperative, 4.1 postoperative and 3.2 after four weeks. SAF- showed: 8.3, 4.7 and 4.2. In no case we have seen any disturbance wound-heeling. Leakage of cement occured in 12 cases (14% of 85), only in one case a radiculopathy (1.2% from 85 vertebras,1.85% from 54 patients).

1. Fresh osteoporotic vertebral fractures can be good restored within the first 4 weeks after fracture. 2. Subacute fractures don't allow a such good improvement of the kyphosis angle. 3. In both cases a good pain relief is possible. 4. The complications happened within the first month of using of this method, that means within the learning phase. Therefore a good training is necessary. 5. In some cases new fractures happened in the vertebras nearby the operated segment. 6. Our two years experiences show that endangered.

adjacent segments should be treated also. 7. The ballon-kyphoplasty is a very safe therapy option in the treatment of the acute vertrebral fracture. 8. Furthermore, osteoporotic patients, with fractures must also be treated with changes in nutritional behaviour, movement therapy, evidenced bases medical therapy (modern bisphosphonates, serms, parathormon, Calcium and Vitamin D) as well as psychological care.

Disclosures: ***C. Guenther****, None.*

SU479

A Structured Educational Program Improves the Compliance to Osteoporosis Treatment of Patients with Recent Low-trauma Fracture. T. Chevalley[1], M. Schaad*[1], P. Hoffmeyer*[2], R. Rizzoli[1]. [1]Department of Rehabilitation and Geriatrics, Division of Bone Diseases, University Hospitals Geneva, Switzerland, [2]Department of Surgery, Service of Orthopaedic Surgery, University Hospitals Geneva, Switzerland.

Patients with osteoporotic fracture have a 2 to 4-fold higher risk, according to the skeletal sites, to undergo another fracture. These patients represent high risk patients and

deserve high priority diagnostic and prevention procedures for osteoporosis. After acute management by the orthopaedic team, patients with a low-trauma fracture were enrolled in a medical management pathway. A half a day interactive educational program led by a multidisciplinary team was proposed 8 to 12 weeks after fracture and followed by 35% of the patients. Group discussions concern physical activity, fall prevention and available treatments of osteoporosis, nutritional workshops are held, a series of information brochures are made available, ending into the elaboration of a personal habits modifications program. By considering as controls, patients who did not participate to this educational program, we measured its impact on compliance after 6 to 9 months, as evaluated as the percentage of specific anti-osteoporotic drugs still taken on the number of prescribed medications. During a 55-month period, 264 patients (217F/47M, mean age 72.5±10.7 yrs) were evaluated among the 392 (313F/79M, 70.8±12.3yrs) included in this clinical pathway (hip fracture 45%, ankle/tibia 24%, proximal humerus 9%, wrist 7%, spine 6%, pelvis 3% et other sites 13%). A DXA measurement, performed in 80% of the 264 patients, revealed either osteoporosis (55%) or osteopenia (40%) at spine or hip. Among all patients who attended the educational program, compliance was higher (88% vs 71%, $p<0.05$). Among patients who recognized that their fracture was related to bone fragility at the time of the fracture (32%), compliance was also higher among patients who attended the educational program (94% vs 67%, $p<0.05$). Among the patients with a DXA diagnosis of osteoporosis, the educational program increased the compliance (94% vs 74%, $p<0.05$). Likewise, among patients with DXA diagnosis of osteoporosis and who recognized that their fracture was related to bone fragility (32%), compliance was even better among those who participated to the educational program (100% vs 68%, $p<0.05$). By considering the importance of compliance in the treatment of osteoporosis, we conclude that our educational program may improve the long term management of the disease, and possibly contribute to prevent subsequent osteoporotic fracture.

Disclosures: ***T. Chevalley****, None.*

SU480

Targeting Fragility Fractures in an Orthopaedic Treatment Unit: Cost Effectiveness of a Dedicated Coordinator. A. Maetzel*[1], B. Sander*[1], V. I. M. Elliot-Gibson*[2], D. E. Beaton*[2], E. R. Bogoch[3]. [1]Division of Clinical Decision Making and Health Care Research, University Health Network, University of Toronto, Toronto, ON, Canada, [2]Mobility Program Clinical Research Unit, St. Michael's Hospital, University of Toronto, Toronto, ON, Canada, [3]Department of Surgery, St. Michael's Hospital, University of Toronto, Toronto, ON, Canada.

The orthopaedic unit at a university teaching hospital hired an osteoporosis (OP) coordinator to manage a collaborative program to identify fragility fracture patients and arrange for investigation and treatment of OP, and patient education. This analysis evaluates the cost-effectiveness of a coordinator in avoiding inpatient hospitalizations due to further hip fractures from the hospital perspective. A 1-year decision analytic model was developed combining data from the literature and patient-level data from the first year of the program, during which 430 patients entered the study: age 71 years, +/- 14, female n = 333 (77%), index fracture hip (n = 185, 43%), wrist (n = 124, 29%), humerus (n = 72, 17%) and other (n = 49, 11%); OP most likely cause of fracture n = 349 (81%). The decision analysis model calculates the annual incidence of a further hip fracture dependent on type of index fracture (hip, wrist, humerus, other), attribution to OP, age and gender. Referral uptake, initiation of OP treatment and compliance modified the incidence of further hip fractures in the presence of a coordinator. The relative risk of further hip fracture varied from 3.2 to 9.8 depending on the index fracture. Average direct hospital cost of $21,800 for the subset of patients with an index hip fracture were used as a surrogate for the cost of a potential further hip fracture; the cost of a coordinator was $60,000 + 30% benefits. Baseline cost-effectiveness analysis showed that a coordinator who manages 500 patients yearly would reduce further hip fractures from 30 to 21, saving the hospital $104,000. A coordinator was cost-saving: 1) over reasonable cost ranges, 2) if only half of patients initiated treatment and only half complied, 3) if treatment efficacy reduced fractures by as low as 20% and 4) if only 220 patients were seen annually. Employment of a coordinator to manage fragility fracture patients may reduce further hip fractures and is cost-effective from the hospital's perspective. This analysis did not estimate the full benefit of a coordinator on the prevention of other fractures. The results may change, when expanding the model to include all relevant costs from a societal perspective.

Disclosures: ***A. Maetzel****, Merck Frosst Canada and Co. 2.*

SU481

Research Participants' Satisfaction Questionnaire. D. E. Conn*, L. M. Rushforth*, E. E. Steffens*, P. M. Workman*, C. E. Schile*, K. M. Hill*, E. A. Mossman, M. R. McClung. Oregon Osteoporosis Center, Portland, OR, USA.

Research subjects prematurely withdrawing from a clinical trial may substantially impair the quality of data and may even jeopardize the ability to assess the study outcomes. The purpose of this study was to determine which services and activities provided by the Oregon Osteoporosis Center affect the satisfaction of the research participants.

Local institutional review board approval was obtained. In April 2004 a 24-item questionnaire was sent to all current participants in research trials at the Oregon Osteoporosis Center. Participants were asked to rate each item as "not important", "somewhat important", "neutral", "important", "very important" and "not applicable" as it related to influencing their satisfaction with being a research participant. In addition, they were asked to rate their overall study experience satisfaction. Quantitative descriptive statistics were used to analyze the questionnaire responses.

74% of questionnaires were returned (193/260). 93% of respondents rated their overall satisfaction with the study experience as 4 or 5, on a 1 to 5 scale with 5 being extremely satisfied. A skilled phlebotomist, explanation of bone density results by a clinician, and professional staff were all rated as very important (68%, 67% and 57% respectively). In contrast, greeting cards and tote bags/other gifts were rarely rated as very important (8% and 5% respectively). Age of respondents (40-90) and type of trial (prevention versus treatment) did not appear to effect the results.

The vast majority of respondents were very satisfied with their overall experience. In general, the overall services provided by staff were perceived as more important than material items and amenities. Whether or not concentrating on these services would help retention in clinical trials remains to be answered in future studies.

Disclosures: ***D.E. Conn****, None.*

SU482

The Osteoporosis Self-Assessment Tool (OST) Leads to Increased Osteoporosis Evaluation and Therapy in Men. M. I. Williams*[1], V. I. Petkov*[2], D. M. Biskobing[2], R. A. Adler[3]. [1]Endocrinology, McGuire Veterans Affairs Medical Center/Virginia Commonwealth University School of Pharmacy, Richmond, VA, USA, [2]Endocrinology, McGuire Veterans Affairs Medical Center/Virginia Commonwealth University School of Medicine, Richmond, VA, USA, [3]Endocrinology, McGuire Veterams Affairs Medical Center/Virginia Commonwealth University School of Medicine, Richmond, VA, USA.

Osteoporosis (OP) is a silent disorder which, when left untreated, leads to fracture. OP is under-diagnosed, particularly in men. OST, a simple screening tool for stratifying OP risk, is calculated based on age and weight. We tested different modalities using OST over a 12 month period in 3 primary care group practices (GP) at a single VA Medical Center. Through OST, we identified over 5,000 men at high or moderate risk for OP and over 500 were referred for BMD testing (Williams, MI et al. 2003, ASBMR abstract SA 314.) Although no change from baseline was noted in GP1 or 2, GP 3 demonstrated a marked increase (>500%) in the number of DXAs ordered as a result of OST. We hypothesized that OP specific medications and metabolic bone clinic referrals would also increase as a result of the OST implementation.

Specifically, GPs were randomly assigned and providers received: GP1 Education about OST and an OST pocket nomogram only; GP2 Education/nomogram plus a computer desktop OST-index calculator; GP3 Education/nomogram plus an automatic clinical reminder in the electronic patient medical record. GPs assigned to the two interventions were compared to the GP that received education/nomogram only as well as to their baseline.

Metabolic bone clinic referrals increased by 37%, 16% and 275% for GP 1, 2, and 3, respectively. Bisphosphonate prescriptions increased significantly only in GP3 compared to the one-year baseline period. The percent change in calcium prescriptions issued by GP providers was 16%, -3% and 70%, respectively. In conclusion, electronic record reminders for OST resulted not only in an increased number of DXAs ordered but also in an increased number of men referred to a specialized clinic for OP treatment and in prescriptions for OP specific medications. The combination of a simple screening tool (OST) plus an electronic reminder leads to improved patient care through an increase in diagnosis and treatment of osteoporosis.

Disclosures: ***R.A. Adler****, Merck 2.*

SU483

The Influence of Bone Mineral Density Testing on the Initiation of an Osteoporosis-related Pharmacotherapy: A Population-based Analysis. P. A. Caetano[1], W. D. Leslie[2], C. J. Metge*[1]. [1]Faculty of Pharmacy, University of Manitoba, Winnipeg, MB, Canada, [2]Faculty of Medicine, University of Manitoba, Winnipeg, MB, Canada.

The influence of bone mineral density (BMD) assessment on a woman's decision to initiate an osteoporosis-related pharamcotherapy has not been analyzed at the population-level through the use of administrative databases. Through linkage of a BMD database (containing the results of nearly all BMD measurements performed in the province of Manitoba since 1990), we measured the influence of such testing on the likelihood of initiating an osteoporosis-related pharmacotherapy (OSRx) in post-menopausal women. Hospital, physician, pharmaceutical, clinical (bone mineral density results) and demographic data for women continuously residing in Manitoba from 1997 through 2002 were obtained from provincial administrative databases. Outcome variable: Initiation of an OSRx (including hormone replacement therapy [HRT], bisphosphonates, selective estrogen receptor modulators[SERM], and calcitonin). Women with a prescription claim for an OSRx between 1997-1998 were excluded to restrict the analysis to incident users. Explanatory variables: BMD test (yes/no), prior osteoporotic fracture (hip, spine, rib, or vertebral) after age 50, age, income quintile, and urban vs. rural residence. Likelihood of initiating an OSRx was analyzed using the Cox proportional hazards regression. 112,464 women satisfied the inclusion criteria, of which, 7.5% received at least one BMD test and 12.5%(14,031 women) initiated at least one OSRx within the study period (39.8% HRT; 51.9% bisphosphonates; 5.8% SERM; and 2.5% calcitonin). Multivariate-adjusted predictors of OSRx initiation included (but are not limited to): a BMD assessment [RR 9.08 (95%CL: 8.39-9.88)] and, long-term glucocorticoid steroid use [RR 3.77 (95%CI:2.98,4.79)]. Women with BMD results indicating osteoporosis at *either* the spine or hip were more likely to initiate an OSRx [RR 3.89 (95%CI: 3.33,4.55)]. Women with BMD results indicating osteoporosis at *both* the spine and hip were even more likely to initiate an OSRx [RR 15.11 (10.59,21.56)]. Receipt of a BMD assessment drastically increases the likelihood a woman will initiate an OSRx, particularly in those women diagnosed with osteopenia and/or osteoporosis according to their BMD test results.

Disclosures: ***W.D. Leslie****, None.*

SU484

Measuring the Impact of Hip Protector Pads in Mobile Demented Seniors: A Controlled Cohort Study. A. G. Juby*. Medicine, Division of Geriatrics, University of Alberta, Edmonton, AB, Canada.

The prevalence of osteoporosis rises with age, as does the risk of fracture. Hip fractures result in significant morbidity and mortality, and are more frequent in those with increased risk of falls. Mobile, demented nursing home residents are thus at high risk of hip fracture. Hip protector pads have been shown to be efficaceous in preventing hip fracture, but compliance can be an issue.

The purpose of the study was to evaluate the acceptability and efficacy of hip protector pads in preventing hip fracture in mobile, demented, nursing home residents.

Two identical dementia nursing home facilities were chosen within the Capital Care Group in Edmonton, Canada. All residents were independently mobile at baseline. All consenting residents in one facility were provided with hip protector pads (Safehip). All participants (in both facilities) were monitored for cognition (Mini Mental Status Examination), balance (Berg), timed up-and-go and calcaneal ultrasound measurement at baseline. They were followed for three years, and significant falls and fractures recorded.

There were 58 participants (12 men). All had a diagnosis of dementia. The average age was 85 (64-98). At baseline: the average MMSE score was 10/30 (range 0-25); average calcaneal bone mineral density was 0.341g/cm^2 (0.164-0.812gcm^2). 26 participants wore hip protector pads (in a single facility). Over the three year study period, 24 participants died (41%), 12 in each cohort. Multiple falls occurred in 12 participants (>20), 33 participants had falls resulting in injuries. There were 20 fractures in 13 participants 5 of which were hip fractures. 2 of the hip fractures occurred in the hip pad group. In 1 of these the hip pad was on at the time of the fall.

In conclusion, the total number of hip fractures was lower in this high risk cohort than would have been expected. The compliance with pad wearing was high over the three year period. The highly motivated nursing home staff may have accounted for the low fracture rate and high compliance. In those wearing hip pads at the time of the fall, the prevalence of fracture was 20% versus 80% in those without pads.

Disclosures: ***A.G. Juby****, None.*

SU485

Effect of Transdermal vs. Oral Estradiol Treatment on Growth Factors and Markers of Bone Turn-over in Young Adults with Turner Syndrome: A Pilot Study. S. Yigit, M. Onyirimba*, P. Gendreau*, T. Lerer*, K. Rubin. Pediatric Endocrinology, Connecticut Children's Medical Center, Hartford, CT, USA.

Gonadal dysgenesis and subsequent chronic estrogen deficiency is a well-described feature of Turner syndrome(TS) where estrogen replacement is accomplished most commonly using oral estrogen. Recent studies report an increased prevalence of symptomatic osteoporosis in TS. In previous studies comparing transdermal (TD) to oral estradiol (E_2) in postmenopausal women, TD E_2 was shown to stimulate IGF-1 production and increase bone formation markers. This study was designed to compare the short term effects of oral vs. TD E_2 on growth factors and markers of bone turnover in young TS adults.10 young adults with TS , ages 16.6-27.9 years were randomized to receive E_2 patch 100 mcg applied twice weekly(n=5) or oral micronized E_2 (n=5) following a 12 week estrogen wash-out. Duration of treatment was 12 weeks with Provera 5 mg daily instituted during weeks 5,6,11, and 12. E_2, estrone, IGF-1, IGFBP-3, bone specific (bs)-alkaline phosphatase, osteocalcin, PINP, and urine NTx were measured at baseline, 6, and 12 weeks. Changes in levels over time in each group, comparisons between groups, and correlations between growth factors, estrogen levels and bone turn-over markers were analyzed. Higher levels of E_2 were achieved with oral vs TD E_2 reaching significance at 6 weeks(p=0.05). Estrone / E_2 ratio was significantly higher in oral E_2 vs. TD E_2 at 6 and 12 weeks (p=0.002 ,p=0.0007 respectively). An upward trend in IGF-1 in TD E_2 group vs a downward trend in IGF1 in oral E_2 group occurred, although non-significant. IGFBP-3 levels decreased over time with TD E_2 (p=0.01) with no change in the oral E_2 group. NTx levels decreased in both groups, significantly in the oral E_2 group (p=0.02). PINP significantly increased over time in TD E_2 group whereas there was a non-significant decrease in PINP in the oral E_2 group. In the TD E_2 group only, significantly positive correlations were observed between all bone formation markers (Osteocalcin, bs-ALP, PINP) with positive albeit non-significant correlations between IGF-1 and all these markers. These pilot data suggest route-specific effects of TD vs. oral E_2 on IGF-1/ IGFBP3 which impact favorably on markers of bone formation. Similar studies with larger numbers of TS adults are warranted.

Disclosures: ***S. Yigit****, None.*

SU486

Comparison between Testosterone, Biphosphonate and Combination of Both in Males with Decreased BMD. U. Gruntmanis[1], M. Denke*[1], A. Kermani*[1], A. Mello*[2], N. M. Gazmen*[2], B. Welch*[1]. [1]Endocrinology, UT Southwestern and Dallas VA Medical Center, Dallas, TX, USA, [2]Radiology, Dallas VA Medical Center, Dallas, TX, USA.

Both, biphosphonates and testosterone are known to improve BMD in males. To our knowledge, there have been no publications comparing efficacy of testosterone and biphosphonates used separately or in combination. In this study our goal is to evaluate effectiveness of each of three treatment regimens in males with decreased BMD.

We analyzed data on 100 men in retrospective manner. The number of men was predetermined by statistical analysis to have power of .8 and experiment-wise type I error of .05, to find difference in BMD between groups. 40 men were on one of the biphosphonates, 40 men were on testosterone and 20 men on combination of testosterone and biphosphonate. To minimize selection bias, all patients were chosen alphabetically from medical records. The 25-hydroxyvitamin D, PTH, calcium, 24-hour urine calcium and creatinine and AM pooled testosterone were measured in all patients. All patients had two BMDs at least one year apart to be included in analysis. Only patients with hypogonadism were treated with testosterone or combination regimen. All patients were prescribed calcium 500mg and 800 IU vitamin D twice a day. Primary outcome was change in BMD in each of the groups.

At baseline, BMD of the lumbar spine and total hip were 0.837±0.11 and 0.749±0.18 (mean SD) g/cm^2 in biphosphonate, 0.923±0.16 and 0.891±0.13 (mean SD) g/cm^2 in testosterone and 0.827±0.12 and 0.81±0.14 (mean SD) g/cm^2 in combination groups. The mean BMD at the lumbar spine and total hip were statistically different between, testosterone and biphosphonate groups (p=0.04 and p=0.001), and testosterone and combination groups (p=0.03 and p=0.02) at baseline. There were no statistical difference between baseline BMDs in the biphosphonate and combination groups. The baseline median testosterone levels were 3.7ng/ml, 1.55ng/ml and 2.4ng/ml in biphosphonate, testosterone and combination groups respectively (p<0.001). The median percentage per year change in lumbar spine and total hip was 2.6% and 0.97% in biphosphonate, 3.3% and 0.46% in testosterone and 2.3% and 1.27% in combination groups (NS).

We conclude that testosterone has similar efficacy with biphosphonates in increasing BMD in men with hypogonadism. The combination of testosterone and biphosphonate does not appear to be superior to single drug therapy

Disclosures: ***U. Gruntmanis****, Procter&Gamble 8.*

SU487

Effect of Food on the Pharmacokinetics of Lasofoxifene, in Healthy Postmenopausal Women. R. Moller*[1], J. Fisher*[2], A. Taylor*[2], S. Kolluri*[2], M. Gardner*[2]. [1]Worldwide Clinical Development, Pfizer, New York, NY, USA, [2]Global Research and Development, Pfizer, Groton, CT, USA.

The purpose of this study was to determine the effects of food on the bioavailability of lasofoxifene (LASO), a next generation selective estrogen receptor modulator (SERM), in late stage development for the prevention and treatment of osteoporosis, in postmenopausal women.

Sixty-four, postmenopausal women were randomized into this four-armed, parallel design, IRB approved study. Following a 10-hour fast, half the women remained in the fasting state while the other half received a standard high fat breakfast. One fed/fasted group received LASO (0.25 mg) while the other fed/fasted group received 0.5 mg of LASO. Blood samples for LASO pharmacokinetic determinations were collected prior to dosing and at various times during the 96 hours following dosing.

These results indicate that food did not affect the bioavailability of a single 0.25 mg or 0.50 mg dose of LASO relative to the fasting state. The ratio of AUC $_{0\text{-}96}$ for the fed/fasted groups was 98.6% (CI: 90.8-107.1%) and 104.7% (CI: 95.8-114.4%) for the 0.25 and 0.5 mg doses respectively. The ratio of Cmax for the fed/fasted groups were 104.5% (CI: 93.1-117.3%) and 100.5% (CI: 91.6-110.2%) for the 0.25 and 0.5 mg doses respectively. Tmax showed a slight difference between the fed and fasted groups, with the fasted group, reaching peak faster than the fed group.

Food does not affect the relative bioavailability of either the 0.25 or 0.5 mg doses of LASO. Therefore, LASO can be dosed without regard to meals.

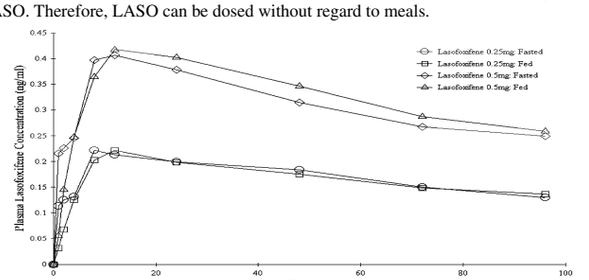

Disclosures: ***R. Moller****, Robert Moller, Jeanine Fisher, Ann Taylor, Sheela Kolluri, Mark Gardner 3.*

SU488

PSK3471 Restores Long Bone Biomechanical Properties in Ovariectomized Mice with Established Osteopenia. P. Clément-Lacroix[1], P. Ammann[2], R. Galien*[1], D. Minet*[1], C. Belleville*[1], N. Bruyniks*[1], M. Resche-Rigon[1], R. Rizzoli[2], R. Baron[1]. [1]ProSkelia, Romainville, France, [2]Univ. Hosp., Geneva, Switzerland.

Among the first generation of selective estrogen receptor modulators (SERMs), Raloxifene (RAL) has proven efficacy in clinic, reducing the risk of vertebral fracture. However, RAL does not significantly prevent non-vertebral fractures. Thus, there is a need for alternative therapy like SERMs, which could prevent bone loss and decrease bone fragility, while preventing breast cancer and lacking side effects on genital tract. PSK3471 displays good safety profile on breast and uterus and efficiently prevents bone loss in ovariectomized (OVX) mice and rat. The present study was conducted to evaluate the effects of PSK3471 on bone strength in OVX mice with established osteopenia. Eight weeks post-ovx osteopenic mice were orally administered PSK3471 (0.03, 0.1, 0.3 mg/kg/d) or RAL (10 mg/kg/d) for 8 weeks or sc injected with PTH (80 µg/kg/d). After 8 weeks treatment, the doses of 1 and 3mg, of PSK3471 not only fully restored OVX-associated bone loss, but also elicited an increase in trabecular bone mass compared to sham mice (+23% and +50% vs. OVX; p<0.001, for PSK3471 0.1 and 0.3 mg/kg/d respectively). RAL (10 mg/kg/d) only partially restored OVX-induced bone loss. MicroCT analysis confirmed that PSK3471 increased cancellous bone volume (+52% to +68% vs. OVX; p<0.01). Again

RAL exhibited only a partial effect (+14% vs. OVX, ns). In terms of micro-architecture, PSK3471 but not RAL, increased trabecular number, but did not change trabecular thickness. PSK3471, and again unlike RAL, also dose-dependently increased cortical BMD of tibia (+2.7% to +3.8% vs. OVX; p=0.031, PSK3471 0.1 and 0.3 mg/kg). Tibia and femur were then evaluated for ultimate strength, stiffness and energy in compression or/and flexion tests, respectively. Ovariectomy significantly decreased ultimate strength at the level of the proximal tibia and of midshaft femora. At the same skeletal site PSK3471 dose-dependently increased ultimate strength and energy, significantly better than RAL and PTH. At cortical site, PSK3471 and PTH treatment increased ultimate strength, but only PTH reached significance. RAL did not exhibit any protection at the level of the midshaft femur. Thus, after 8 weeks of treatment, PSK3471 is able to restore bone mass in mice with established osteopenia, acting at both trabecular and cortical bone, whereas RAL was only acting at trabecular bone. In addition PSK3471 increased dose-dependently bone strength at the level of the proximal tibia.

Disclosures: ***P. Clément-Lacroix****, None.*

SU489

Oxandrolone Acts on Human Osteoblasts by Androgen Receptor. L. X. Bi[1], G. V. Oliveira*[2], G. L. Klein[3], W. L. Buford*[1], E. G. Mainous[4], D. N. Herndon*[2]. [1]Dpts. of Surgery and Orthopaedics & rehabilitation, UTMB, Galveston, TX, USA, [2]Dpt. of Surgery, Shriners Hospitals for Children, Galveston, TX, USA, [3]Dpt. of Pediatrics, UTMB, Galveston, TX, USA, [4]Dpt. of Surgery, UTMB, Galveston, TX, USA.

Use of the anabolic agent oxandrolone in severely burned children has been shown to increase lean body mass at 6 mo and bone mineral content at 1 yr post-burn (Murphy KD et al, Surgery 2004, in press). The mechanism of action of oxandrolone is uncertain. The aim of this study was to determine whether oxandrolone acts directly on the androgen receptor (AR) in bone by stimulating type I collagen synthesis. We examined nuclear translocation of androgen receptor (AR) and expression of type I collagen after treatment of cells with oxandrolone. Human osteoblast cells were cultured in a-minimum essential medium [a-MEM] and 10% fetal bovine serum without or with oxandrolone (15ng, 15ug and 30 ug/ml) for 24 hr, respectively. Immunohistochemistry for Androgen Receptor (Neomarkers, Freemont, CA) and collagen type I (RDI, Flanders, NJ) were performed using indirect immunofluorescence. And images were captured using Confocal Scanning Laser Microscopy. Expression of type I collagen was also confirmed using immunoquantitative assay. AR translocation to the nuclei was observed in stimulated cells compared to control group, suggesting the oxandrolone targets osteoblasts through AR. Increased staining for type I collagen was also observed in osteoblasts stimulated with oxandrolone in higher doses (15 and 30ug/ml) but not in lower doses (15ng/ml). Immunoquantitative assay showed that expression of type I collagen was increased (29%, $P<0.01$) in oxandrolone-treated group (30ug/ml), compared to control group. Conclusion: Thus it appears as if oxandrolone at a dose of 15 and 30ug/ml in cultured human osteoblasts results in nuclear translocation of AR and a subsequent increase of type I collagen immunostaining as well as an increase in cellular production of type I collagen by immunoquantitative assay.

Disclosures: ***L.X. Bi****, None.*

SU490

Raloxifene Prevents Bone Loss Associated with GnRH Agonist Administration in Mice Through a Potentially Different Mechanism of Action from That of Estrogen. Y. Onoe, Y. Miyabara*, R. Yoshikata*, H. Okano, H. Ohta. Obstetrics and Gynecology, Tokyo Wemen's University, Tokyo, Japan.

Marked bone loss due to estrogen deficiency can be prevented by estrogen replacement therapy (HRT). However, HRT has estrogenic effects on the uterus. In contrast, raloxifene, a selective estrogen receptor modulator, has been reported to reduce bone loss without exerting estrogenic effects on the uterus. Likewise, GnRH agonists (GnRHa) decrease the pulsatile gonadotropin secretion and are useful for the treatment estrogen-dependent disease; long-term treatment with GnRHa can lead, however, to bone loss due to associated increased bone resorption. We therefore examined secondary bone loss associated with the use of GnRHa in mice and studied the effect of raloxifene on such bone loss as compared with estrogen.

8 week-old female ddy mice were given an injection of GnRHa (5 mg/kg) every 4 weeks for 4 to 12 weeks. Some of the GnRHa-treated mice also received concurrent raloxifene (1 mg/kg/day) or 17β-estrdiol (1 μg/kg/day) given subcutaneously via an Alzet pump). Control mice underwent ovariectomy (OVX) and received raloxifene or 17β-estradiol.

OVX mice showed a marked decrease in uterine weight due to uterine atrophy. Likewise, GnRHa-treated mice showed a decrease in uterine weight but not to the same degree as in OVX mice. However, serum FSH levels were markedly lower in GnRHa-treated than in OVX mice, suggesting that uterine atrophy was caused by GnRHa administration. Femoral bone mineral density (BMD) levels in GnRHa-treated mice were significantly reduced, and were similar to those in OVX mice. Raloxifene reduced bone loss in GnRHa-treated mice, while it had no effect on uterine weight; in contrast, 17β-estradiol reduced both bone loss and uterine weight. Raloxifene and 17β-estradiol had similar effects on OVX mice. Bone marrow supernatant OPG levels in GnRHa-treated mice were similar to those seen in OVX mice. Both raloxifene and 17β-estradiol decreased OPG levels in GnRHa-treated mice. 17β-estradiol treatment decreased GnRHa-associated increases in bone marrow supernatant sRANKL levels, while raloxifene led to further increases in sRANKL levels. Furthermore, OPG and sRANKL mRNA levels were not changed by GnRHa, raloxifene or 17β-estradiol.

Our results indicate that raloxifene can prevent the bone loss associated with GnRHa treatment without exerting estrogenic actions on the uterus in female mice through a mechanism of action that differs from estrogen.

Disclosures: ***Y. Onoe****, None.*

SU491

Estrens Protect Bone against Ovariectomy-induced Bone Loss in Mice but Fail to be Selective on Reproductive Organs and/or Breast Cancer Cell Lines. R. Galien*[1], S. Windahl[2], P. Clément-Lacroix[1], R. Chiusarolli[2], F. Marsais*[1], D. Minet*[1], L. Lepescheux*[1], C. Jagerschmidt*[1], F. Nique*[1], M. Resche-Rigon[1], R. Baron[1]. [1]ProSkelia Pharmaceuticals, Romainville, France, [2]Orthopaedics and Cell Biology, Yale University School of Medicine, New Haven, CT, USA.

The mechanisms by which androgens and estrogens protect bone are still controversial. Estren α has been reported to act on both receptors and to protect bone while having no effect on reproductive organs in male and female mice. The present study was designed to compare the ability of 4-estren3α-17β-diol (Estrenα) and its isomer 4-estren3β-17β-diol (Estrenβ) to prevent bone loss in adult gonadectomized (GDX) male and female mice and their respective safety profiles on reproductive organs, compared to a classical SERM, PSK3471.

Twelve week-old GDX male and female mice were implanted with slow release pellets delivering either 1/ PSK3471 (30μg/kg/d); 2/ Estrenα (5mg/kg/d); 3/ 17-β-Estradiol (E2; 50μg/kg/d), 4/ DHT (2.5mg/kg/d), or were daily injected with Estrenβ (5mg/kg/d) for 4 weeks. In this model, E2, DHT and PSK3471 not only prevented GDX-induced bone loss, but also elicited an anabolic increase in bone mass compared to sham. In contrast, Estrenα and β, although given at a dose more than 150-fold that of PSK3471, only maintained bone mass at control levels.To assess the safety profile of these compounds, we then measured their impact on uterus and seminal vesicles. As expected from a SERM, PSK3471, but also Estren β, induced very moderate increases in seminal vesicle and uterus weights compared to GDX controls. In contrast, Estrenα had deleterious effects on both uterus and seminal vesicles, similar to E2 and DHT, suggesting that this compound is not selective in its effect on bone versus reproductive organs. We consequently measured the relative binding affinities of Estrenα and β for steroid receptors: unlike PSK3471, these compounds are ligands of both ERs and AR. Both Estrens can stimulate transcription from several estrogen-responsive promoters, and more importantly very efficiently stimulated proliferation of MCF7 cells, whereas PSK3471 did not display agonist activity in these assays but was instead an E2 antagonist. Finally, and again in contrast to PSK3471 or E2, Estrenα and β displayed full agonist activity on the AR, and stimulated strongly ARE-dependent transcription. Given the high concentrations of Estren required *in vivo*, genotropic effects are difficult to exclude. In conclusion, although SERMs and Estrens efficiently prevent bone loss in GDX males and females, the SERM PSK3471 is more efficient on bone and exhibited, in contrast to Estrenα and Estrenβ, a good safety profile on reproductive organs, and breast tissue

Disclosures: ***R. Galien****, None.*

SU492

Psoraleae Semen Prevents Bone Loss in Ovariectomized Rats. H. Ha[1], J. S. Choi*[1], H. Y. Lee*[1], D. Y. Jung*[1], H. Y. Jeong*[1], K. Y. Song*[2], J. H. Lee*[3], C. Kim[1]. [1]Drug Research and Development Team, Korea Institute of Oriental Medicine, Daejeon, Republic of Korea, [2]College of Medicine, Chung-Ang University, Seoul, Republic of Korea, [3]College of Pharmacy, Kyunghee University, Seoul, Republic of Korea.

Psoralease Semen (PS) is the seed of *Psoralea corylifolia* L. (Leguminosae), which has been used in traditional medicine as a tonic and to treat backache and knee pain, *etc.* This study was focused on development of new drug from PS and its ingredients to prevent and treat osteoporosis after menopause without any side effects. The proliferations of osteoblast like cell (Saos-2) induced by PS and its ingredients were analyzed using a tetrazolim salt (MTT) and alkaline phosphatase (ALP) activity. Gene expressions, such as Runx-2, BSP, and OCN were screened by RT-PCR in MC3T3-E1. The inhibition on osteoclast was also studied using the coculture method of mouse bone marrow cells and ST-2 cells. Adult OVX SD rats (10 weeks old) were administrated EtOH extract of PS (5 g herb/kg/day) during 9 weeks. After administration, complete blood cells counted and biomarkers in plasma analyzed biochemical analysis method. Trabecular bone areas (TBAs) of tibia and lumbar were measured by bone histomorphometry. In results, PS increased ALP activity (139.8% of control) on Saos-2. The TBAs of tibia and lumbar in PS group were increased to 141.1% and 135.1% of the control. PS did not induce estrogenic side effects in uterus. In conclusions, PS prevents OVX-induced cancellous bone loss without any adverse estrogenic effects for 9 weeks in OVX rats. (Supported partially by a grant, #03-PJ9-PG6-SO01-0002, from Health Technology Planning & Evaluation Board, Korea)

Disclosures: ***C. Kim****, None.*

SU493

A 12-Month Dose-Response Study of Atorvastatin Effects on Bone in Postmenopausal Women. M. McClung[1], D. Kiel[2], R. Lindsay[3], E. M. Lewiecki[4], M. Bolognese[5], E. Leary[6], H. Bone[7]. [1]Oregon Osteoporosis Center, Portland, OR, USA, [2]Beth Israel Deaconess Medical Center, Boston, MA, USA, [3]Regional Bone Center Helen Hayes Hospital, West Haverstraw, NY, USA, [4]New Mexico Clinical Research & Osteoporosis Center, Albuquerque, NM, USA, [5]Bethesda Health Research, Bethesda, MD, USA, [6]Pacific Biometrics Inc, Seattle, WA, USA, [7]Michigan Bone and Mineral Clinic, Detroit, MI, USA.

Preclinical studies indicate that HMG-CoA reductase inhibitors (statins) may stimulate bone formation and/or inhibit bone resorption. However, this has not heretofore been evaluated prospectively in humans treated with conventional systemic doses. Observational studies and secondary analyses from lipid-lowering trials have yielded inconsistent results regarding the effect of statins on bone mineral density (BMD) and fracture risk.This multicenter, randomized, double-blind placebo-controlled study was designed to determine the effects of a range of doses of atorvastatin on BMD in postmenopausal women. Postmenopausal women (N=626), aged 40-75 yrs, with LDL-cholesterol ≥130 mg/dL and <190 mg/dL, and lumbar spine (LS) BMD -2.5<T-score<0, were randomized to atorvastatin 10 mg, 20 mg, 40 mg, or 80 mg daily or placebo for 52 weeks. All subjects were provided calcium and vitamin D supplements. The primary endpoint was % change from baseline in LS BMD assessed by DXA. Secondary endpoints included additional BMD measurements and changes in biochemical markers of bone turnover (sNTX, sCTX, osteocalcin, BSAP, P1NP and urinary DPD).

On a modified intent-to-treat basis, 482 participants were evaluable. At baseline, the mean age was 59 yrs and mean LS T-score was -1.16. At 52 weeks, there was no significant change from baseline in LS BMD on any dose of atorvastatin or on placebo, and no there was no significant change on any dose vs. placebo. Similar results were obtained for secondary BMD measurements. Changes in biochemical markers of bone turnover did not differ significantly between treatment groups or from baseline within any group. Similar results were observed when the analysis was confined to only the subjects who completed the full 12 months of study. The expected dose-related changes in total cholesterol and LDL-cholesterol were observed. Adverse events across all dose groups were similar to placebo.

Atorvastatin, administered over the range of approved systemic doses, did not affect bone density or turnover in mildly hypercholesterolemic postmenopausal women.

Disclosures: ***M. McClung****, Pfizer 2, 5.*

SU494

Osteopontin Antagonizes Against Bone Formation Induced by EP4 Agonist in vivo Via Specific Suppression of Osteoblastic Activity. N. Kato[1], K. Kitahara[1], K. Tsuji[1], S. R. Rittling[2], H. Kurosawa[3], A. Nifuji[1], D. T.Denhardt[2], M. Noda[1]. [1]Dept of Molecular Pharmacology, Tokyo Medical and Dental University, Tokyo, Japan, [2]Rutgers University, Piscataway, NJ, USA, [3]Juntendo University, Tokyo, Japan.

Bone mass reduction due to osteoporosis increases fracture risk and therefore measures to increase bone formation is to be developed. EP4 agonist (EP4A) has possibility to increase bone in vivo. However, EP4A still is not sufficient since EP4A fails to increase bone mass depending on the background strain of animals due to as yet unidentified reasons. Since osteopontin (OPN) is a molecule which is produced by osteoblasts in response to cytokines and mechanical signals to modulate osteoblastic function as well as osteoclastic function, we examined whether OPN is involved in regulation of bone in response to EP4A (ONO-AE1-329). EP4A was injected three times per day for 5 days a week for 4 weeks subcutaneously into the back of wild type (WT) or OPN deficient (OPN-KO) mice. EP4A significantly enhanced BMD in the distal one fifth of femora in OPN-KO but not in WT. EP4A increased cancellous BV/TV in vertebrae in OPN-KO but not in WT. Subcutaneous EP4A injection in the back did not affect the thickness of calvaria in WT but it was increased significantly in OPN-KO. Mineral apposition rate (MAR) as well as bone formation rate (BFR) were not altered by EP4A in WT but these parameters were both enhanced by EP4A in OPN-KO. In contrast to bone formation parameters, bone resorption parameters were not altered by EP4A in both WT and OPN-KO. Bone marrow cells (BMC) from the femur of OPN-KO treated with EP4A for 4 weeks in vivo significantly increased nodule formation (NF) levels compared to the cells from untreated OPN-KO cells while EP4A treatment in vivo did not alter the NF levels in case of WT. Interestingly, BMC taken from the bone of EP4A-treated OPN-KO but not WT mice showed reduction of osteoclast formation. Systemic injection of EP4A for 4 weeks resulted in increase in alkaline phosphatase (ALP) activity in the cells outgown from the calvaria of these mice. In the EP4A treated OPN-KO-derived cells, there were further increase in ALP activities. OPN-KO enhances ALP activity in the serum of the mice treated with EP4A more than the levels of enhancement of ALP in WT treated with EP4A. Finally, direct EP4A injection onto the calvaria increased new bone formation in WT. However, direct injection of EP4A further enhanced in vivo bone formation on the calvaria in OPN-KO. These data indicated that OPN antagonizes against bone formation induced by EP4A.

Disclosures: ***N. Kato****, None.*

SU495

Inhibin Prevents Orchidectomy-Induced Bone Loss and Is Anabolic in Intact Mice by Increasing Osteoblast Activity. D. S. Perrien, N. S. Akel, M. Bendre, R. A. Skinner*, F. L. Swain*, D. C. Montague, L. J. Suva, D. Gaddy. Physiology and Biophysics and Orthopaedic Surgery, University of Arkansas for Medical Sciences, Little Rock, AR, USA.

Hypogonadism causes a rapid decline in bone mass and strength associated with an increase in turnover favoring resorption over formation. We have previously demonstrated that Inhibin A (InhA) suppresses osteoblast and osteoclast differentiation in primary bone marrow cultures. This led to the hypothesis that Inhibins may suppress bone turnover and maintain bone mass *in vivo* by inhibiting osteoblast and osteoclast development. To test this hypothesis in male mice, the GeneSwitch system of inducible human InhA overexpression was utilized. This system combines liver-specific expression of a mifepristone (MFP)-activated chimeric nuclear receptor (Glvp) and a second Glvp-responsive target transgene encoding linked sequences of the alpha- and beta A-subunits of human InhA. When treated with MFP, mice harboring both transgenes (Glvp/InhA) selectively overexpress InhA from the liver. After reaching peak bone mass (5-6 months), mice underwent either sham operation (Sham) or orchidectomy (Orch) and subcutaneous placement of a time-release pellet containing MFP or vehicle (Veh). All mice were injected with calcein and tetracycline on days 20 and 26, respectively, and were sacrificed on day 28. The mean serum concentration of human InhA in MFP-treated Glvp/InhA mice at the time of sacrifice was 662 pg/ml in Sham-MFP, 808 pg/ml in Orch-MFP, and was undetectable in all Veh treated mice. Treatment of non-InhA expressing Glvp/- mice with MFP had no effect on any measured parameters regardless of gonadal status. Using *ex vivo* microCT and finite element modeling, it was determined that MFP-driven overexpression of InhA prevented Orch-induced loss of trabecular bone volume, microarchitectural parameters, and strength (all $p<0.05$) in the proximal tibia. In addition, InhA improved these measures in intact Sham mice (all $p<0.05$). Systemic bone resorption, measured by serum collagen C-telopeptide crosslinks, was significantly increased by Orch ($p<0.05$ vs Sham) but unaffected by InhA, regardless of gondal status. Histomorphometric analysis of tibial trabecular bone revealed that InhA did not affect the number of osteoclasts or osteoblasts, osteoid thickness, eroded perimeter, osteoclast perimeter, or osteoblast perimeter. In contrast, InhA significantly increased the mineral apposition and bone formation rates in both Sham and Orch mice (all $p<0.05$). Collectively, these data are the first to demonstrate a novel effect of Inhibin A as a potent anabolic agent in intact mice that prevents orchidectomy induced bone loss by increasing bone formation of mature osteoblasts.

Disclosures: ***D.S. Perrien****, Immunogen 1.*

SU496

The Effect Of Oral Dehydroepiandrosterone (DHEA) on Bone in Premenopausal Women Treated with a GnRH Agonist. N. Glass*[1], S. Hurwitz*[1], M. Hornstein*[1], M. Delaney[2], C. Rosen[3], J. Glowacki[1], M. S. LeBoff[1]. [1]Brigham and Women's Hospital, Boston, MA, USA, [2]The Cleveland Clinic Foundation, Cleveland, OH, USA, [3]St. Joseph's Hospital, Bangor, ME, USA.

Use of Gonadotropin Releasing Hormone Agonist (GnRHa) therapy for endometriosis in premenopausal women leads to accelerated bone loss that may not be completely reversible and may compromise peak bone mass. Low-dose estrogen and/or progestin add-back therapy is often used in conjunction with GnRHa to prevent bone loss. The adrenal androgen, DHEA may have an anabolic and antiresorptive effect on bone, and circulating levels may decrease with use of a GnRHa. Using this model of bone loss, we investigated the effects of oral DHEA vs. placebo in women with endometriosis.

Thirty-two women between the ages of 18-40 yrs with endometriosis who elected to undergo a 6-month course of GnRHa were randomized to receive oral, micronized DHEA (12.5 mg/d or 25 mg/d) or placebo in this IRB approved, double-blind study. Lab evaluations included longitudinal tests for bone markers, hormones, and safety parameters. Bone mineral density (BMD) and body composition was measured by Dual X-ray Absorptiometry (DXA) every 3 months.

Baseline data showed normal, mean serum 25-hydroxyvitamin D (26.14 ± 7.62 ng/ml) and PTH levels (28.63 ± 9.92 pg/ml). DHEA sulfate (DHEAS) levels were at the low end of normal range for premenopausal women; 120.48 ± 54.43 µg/dl (normal range 65-380 µg/dl.) Because of no differences between the 12.5 mg and 25 mg DHEA doses, these data were pooled.

Absolute Changes between Baseline and Month 3

Variable	DHEA (mean)	Placebo (mean)	p value
Estrone (pg/ml)	+5.262	-47.374	0.009
Androstendione (ng/ml)	+1.626	-0.448	0.002
DHEAS (µg/dl)	+246.063	-18.000	0.001
SHBG (nmol/L)	-20.375	+5.800	0.012
Osteocalcin (OC) (ng/ml)	-0.854	+3.380	0.010
N-telopeptides (NTX)	+10.286	+12.200	0.611
IGF-1 (ng/ml)	+1.400	-65.200	0.040
BMD Whole Body (g/cm^2)	+0.007	-0.007	0.090

There were no differences in total testosterone, body fat, or weight changes at 3 months. In women treated with DHEA vs. placebo, the positive change in androstendione and DHEAS and reduction in SHBG, indicate predominant androgenic effects of DHEA in estrogen deficient women treated with GnRHa. The positive effect of oral DHEA on IGF-1 compared with placebo suggests an anabolic effect on bone. The positive change in OC in the placebo group may indicate increased bone turnover that was attenuated by DHEA. Although there was a trend for a positive change in the total body BMD with DHEA vs.

placebo, changes in spine or hip BMD were not observed at 3 months. Further studies with long term follow-up or higher doses of DHEA may be necessary to show a skeletal effect in the setting of acute estrogen deficiency.

Disclosures: ***N. Glass****, None.*

SU497

1α,25-dihydroxy-2β-(3-hydroxypropoxy)vitamin D_3 (ED-71) does not Disturb Fracture Healing Process in Rat's Femoral Fracture Model. S. Mori, Y. Cao*, K. Miyamoto*, K. Iwata*, T. Mahiba, T. Akiyama*, S. Komatsubara*, T. Manabe*, H. Norimatsu. Orthopedic Surgery, Kagawa University, Faculty of Medicine, Kagawa, Japan.

While many therapeutic agents are used for the treatment of osteoporosis, osteoporotic patients are prone to fracture. So the question arises whether the drugs should stop or continue when fracture occurred. This study aimed to test whether ED-71 treatment disturb the fracture healing process using rat's femoral fracture model.

160 female SD rats of 6week old were treated either by ED-71 0.025(EDL), 0.05(EDH)) μg/kg, MCT(CNT1) p.o, or alendronate 5(ALL), 10(ALH) μg/kg or saline vehicle (CNT2)s.c. 5 times a week. Four weeks later right femur was fractured and fixed with intramedullary wire. Drug administration was continued and the animals were sacrificed at 6 and 16 weeks post-surgery after double labeling. Fractured femur was assessed by microradiograph, pQCT, 3point bending test and bone histomorphometry. Because no difference was observed, CNT1 and CNT2 were pooled and assumed as CONT for statistical analysis.

At 16weeks after fracture, fracture line disappeared in CNT, ED groups, while it remained in alendronate(ALN)groups. ALN groups showed significantly larger callus area, higher BMC compared to ED groups and CONT. Mechanical test revealed significantly higher ultimate load in ALN groups compared to ED groups and CONT. However % lamellar/callus area was significantly lower in ALN groups (ALL48%,, ALH53%) compared to CONT(99%) and ED groups (EDL99%, EDH98%) at 16 weeks. OC.S/BS was significantly lower in ED and ALN groups compared to CONT. BFR/BS was reduced in ED and ALN groups compared to CONT, while BFR/BS in ALH was the lowest among the groups.

It is considered that the highest mechanical strength of fractured femur in ALN was caused by large callus. However, ALN callus remodeling was delayed as evidenced by lower lamellar bone ratio in the callus. It suggests that strong antiresorptive effect of ALN disturbed the remodeling process of fracture healing. In contrast, ED-71, mild anti-resorptive agent, did not delay callus remodeling, nor disturbed restoration of mechanical strength of the fracture compared to the control. Our results suggest that mild anti-resorptive effect of ED does not disturb fracture healing process.

Disclosures: ***S. Mori****, None.*

SU498

Comparison of Therapeutic Effects on Bone Mineral Metabolism and Soft Tissue Composition between Alfacalcidol and Alendronate. S. Takata[1], M. Takahashi*[1], H. Yonezu*[2], N. Yasui*[1]. [1]Orthopedic Surgery, The University of Tokushima, Tokushima, Japan, [2]Orthopedic Surgery, Shikoku Chuo Hospital, Kawanoe, Japan.

We demonstrated the difference in therapeutic effects of a one-year treatment between alfacalcidol and alendronate on bone mineral metabolism and soft tissue composition in Japanese osteoporotic women. Ninety-two women suffering from primary osteoporosis without osteoporotic fractures, aged 55 to 81 years, were divided into two groups: women treated with alfacalcidol (0.5 microgram/day; alfacalcidol group, n=57) and women treated with alendronate (5 mg/day; alendronate group, n=35). Bone mineral density (BMD) and soft tissue composition were measured using dual energy X-ray absorptiometry. The percentage change in total lean mass of the alendronate and alfacalcidol groups were 98.6±4.0% and 100.0±4.7%, respectively, which was significantly different (p=0.0357). The total fat mass of the alendronate group increased to 106.8±13.7% of the pre-treatment level, whereas that of the alfacalcidol group decreased to 98.1±14.4%. There was a significant difference in total fat mass between these two groups (p=0.0054). The regional lean mass of the alfacalcidol group except for the trunk lean mass was significantly greater than that of the alendronate group. In contrast, the regional fat mass of the alfacalcidol group was significantly smaller than that of the alendronate group. The mean BMD of the 2nd to 4th lumbar vertebrae (L2-4BMD), and regional and total body BMD of the alendronate group were increased after the one-year treatment, whereas those of the alfacalcidol group were maintained at the respective pre-treatment levels. The results showed the difference in therapeutic effects on soft tissue composition and bone mineral metabolism between alfacalcidol and alendronate. These results suggest that one-year treatment by alfacalcidol has extraskeletal effects on the skeletal muscle, maintaining regional and total lean mass, compared with that by alendronate.

Disclosures: ***S. Takata****, None.*

SU499

Does Vitamin D Supplementation to Healthy Danish Caucasian Girls Affect Bone Mineralization? C. Molgaard*[1], C. Lamberg-Allardt*[2], K. Cashman[3], J. Jakobsen*[4], K. F. Michaelsen*[1]. [1]Department of Human Nutrition, The Royal Veterinary and Agricultural University, LMC, Frederiksberg C, Denmark, [2]Department of Applied Chemistry and Microbiology, University of Helsinki, Helsinki, Finland, [3]Nutritional Science, Department of Food Science, Food Technology and Nutrition, University College, Cork, Ireland, [4]Department of Nutrition, Danish Institute for Food and Veterinary Research, Søborg, Denmark.

A few observational studies have shown a relation between serum 25 hydroxy vitamin D (s-25OHD) levels and bone growth. In Scandinavia many pubertal girls have low levels of s-25 OHD during winter time. However, it is not known whether a supplement of vitamin D will affect bone metabolism and result in higher bone accretion during puberty. The purpose of this randomised one-year double-blinded, placebo-controlled study was to examine whether a vitamin D supplement could increase s-25OHD status and furthermore increase bone accretion. From the Danish Central Person Register 11-12 year old healthy Caucasian girls living in a certain area of Copenhagen were selected. About 25 percentage corresponding to 225 healthy girls mean (SD) age 11.4 (0.2) y agreed to participate. The girls were randomised to: group A (n=75): placebo, group B (n=75): 5 μg vitamin D_3 daily or group C (n=75): 10 μg vitamin D_3 daily for one year. The inclusions were evenly distributed over one year. 220 completed the one-year study. The following were registered at baseline and after one year: Weight, height, tanner stages, s-25OHD, whole body and lumbar BMC and BMD (Hologic 1000/W). Vitamin D and calcium intake were recorded at baseline by food frequency questionnaire. Mean (SD) s-25OHD, vitamin D and calcium intake were 43.2 (17.1) nmol/l; 2.6 (1.4) μg/d and 1029 (617) mg/d respectively. 8 percent had s-25OHD below 20 nmol/l. There were no significant differences between groups at baseline (ANOVA, all p>0.15). After one year s-25OHD increased significantly in the supplemented groups compared to placebo. A: -3.1 (9.8) nmol/l; B: +11.0 (10.2) nmol/l and C: +13.3 (10.8) nmol/l (p<0.001 for both B and C vs. A), but the difference between B and C was not significant (p=0.19). However, there were no differences between the three intervention groups in changes in whole body or lumbar BMC or BMD. In conclusion: Vitamin D supplementation to pubertal Danish girls results in higher s-25OHD. However there was no difference in s-25OHD increments between the groups supplemented with 5 and 10 μg vitamin D daily. Vitamin D supplementation did not have an effect on bone accretion in these healthy girls without severe vitamin D deficiency.

Disclosures: ***C. Molgaard****, None.*

SU500

ED-71, 1α,25-dihydroxy-2ß-(3-hydroxypropoxy)vitamin D_3, Is a Potent Inhibitor of Bone Resorption in Aged Estrogen-deficient Rats. S. Takeda*[1], Y. Uchiyama[1], Y. Higuchi*[1], A. Shiraishi*[1], K. Tsunemi*[1], N. Kubota*[1], K. Sato*[1], H. Saito[1], F. Takahashi[1], F. Makishima*[1], N. Kubodera*[1], K. Ikeda*[2], E. Ogata*[3]. [1]Chugai Pharmaceutical Co.,Ltd., Shizuoka, Japan, [2]National Institute for Longevity Science, Aichi, Japan, [3]Cancer Institute Hospital, Tokyo, Japan.

Nutritional vitamin D supplementation is widely accepted to improve intestinal calcium intake as well as to suppress parathyroid hormone (PTH) via normalizing serum 25-hydroxyvitamin D3 in elderly patients with osteoporosis. However, our previous studies suggested that, in addition to the effects above, the main therapeutic effect of active vitamin D was a direct inhibition of bone resorption, which was enhanced by estrogen deficiency.

In the present study, we compared effects of a novel vitamin D analog, ED-71 (1α,25-dihydroxy-2ß-(3-hydroxypropoxy)vitamin D_3) with 1α-hydroxyvitamin D_3 (alfacalcidol) on bone and mineral metabolism of aged ovariectomized rats.

Eight-month-old female Wistar rats were subjected to ovariectomy (OVX) and then treated with ED-71 (0.05-0.2 μg/kg BW) or alfacalcidol (0.1-0.4 μg/kg BW) for 12 weeks. ED-71 increased lumber vertebral bone mineral density (BMD) greater than alfacalcidol, while ED-71 has activities in enhancing calcium absorption and suppressing serum PTH only comparable to those of alfacalcidol. In bone metabolism markers, ED-71 suppressed urinary deoxypyridinoline (DPD) excretion stronger than alfacalcidol, however, both ED-71 and alfacalcidol did not suppress serum osteocalcin. Bone histomorphometry at lumber vertebrae revealed that ED-71 decreased the osteoclast surface (Oc.S/BS), greater than alfacalcidol, while both agents had a same activity in increasing the bone formation rate (BFR/BS). We also observed only four weeks treatment of ED-71 prevented bone loss in aged ovariectomized rats by suppressing bone resorption, however, alfacalcidol did not show its efficacy after four weeks treatment. Reduction of osteoclast surface (Oc.S/BS) became evident within two weeks of ED-71 treatment. These results suggested that both ED-71 and alfacalcidol prevented bone loss, mainly due to suppressing enhanced bone resorption after ovariectomy. And also, ED-71 is a more rapid and strong inhibitor of bone resorption than alfacalcidol *in vivo.* ED-71 may be an attractive candidate for an orally active anti-osteoporosis agent.

Disclosures: ***S. Takeda****, Chugai Pharmaceutical Co.,Ltd. 3.*

SU501

Treatment with ED-71,1α,25-dihydroxy-2ß-(3-hydroxypropoxy) vitamin D_3, for 6 Months Increases Bone Mass in Ovariectomized Cynomolgus Monkey. H. Saito[1], F. Takahashi[1], K. Tsunemi*[1], S. Y. Smith[2], N. Doyle*[2], L. Chouinard*[2], A. Varela*[2], F. Makishima*[1]. [1]Chugai Pharmaceutical Co., Ltd., Gotemba, Japan, [2]CTBR Bio-Research Inc., Senneville, PQ, Canada.

ED-71 (1α,25-dihydroxy-2ß-(3-hydroxypropoxy)vitamin D_3) is a novel vitamin D_3 analog for the treatment of osteoporosis, under Phase 3 clinical trials in Japan. Late Phase 2 clinical trial revealed that 0.5-1.0µg of ED-71 treatment for 48-weeks increased lumber spine bone mineral density (BMD) by 3% as well as femur BMD by 0.62% in patient with osteoporosis. Also, we previously reported that ED-71 dose-dependently increased both BMD and bone strength in vertebrae and femur of ovariectomized rats. The aim of this study is to determine the skeletal effects of ED-71 in ovariectomized (OVX) monkeys, a commonly used bone-remodeling animal model for the osteoporosis drug evaluation.

Adult female cynomolgus monkeys were divided into ovariectomized group (n=9) or ED-71 treated group (n=10). Each animal was orally given either vehicle or 0.3µg/kg of ED-71, daily for 24 weeks. Lumber spine and femur bone mass were measured by dual-energy X-ray absorptiometry, and tibia bone mass was determined by peripheral quantitative computed tomography at 0, 12 and 24 weeks. Serum markers of bone turnover, including bone-specific alkaline phosphatase, osteocalcin, collagen C-telopeptide and urinary collagen N-telopeptide as well as calcitropic hormones, PTH and 1α,25-dihydroxyvitamin D_3 were measured at 0, 12 and 24 weeks. Histomorphometry was carried out in bone sections of lumber vertebrae and proximal femur.

Treatment with ED-71 increased BMD, at lumber spine (OVX: -0.6%; ED-71: 10.2%), femoral neck (OVX: -0.4%; ED-71: 15.5%) and trochanter (OVX: 0.2%; ED-71: 11.8%) following ovariectomy in comparison with vehicle-treated animals. ED-71 significantly increased cortical bone mineral content (OVX: 2.3%; ED-71: 11.9%) and cortical thickness (OVX: 7.1%; ED-71: 13.7%) and also decreased cortical circumferences in tibia diaphysis. Bone histomorphometry revealed that ED-71 decreased bone resorption parameters such as osteoclast surface (Oc.S/BS) and eroded surface (ES/BS) as well as bone formation parameters, mineral apposition rate (MAR) and bone formation rate (BFR/BS) in cancellous bone compared to OVX control, whereas, ED-71 did not affect both periosteal (Ps.BFR/BS) and endocortical (Ec.BFR/BS) bone formation in cortical bone. These results suggested ED-71 increased trabecular bone mass mainly through inhibition of bone resorption, however did not interfere cortical bone formation, which both were enhanced by ovariectomy.

Disclosures: ***H. Saito****, Chugai Pharmaceutical Co., Ltd. 3.*

SU502

Oral Vitamin D3 Supplementation In Postmenopausal African American Women. S. A. Talwar, J. F. Aloia, S. Pollack*, J. Yeh. Bone Mineral Research Center, Winthrop-University Hospital, Mineola, United States, Winthrop University Hospital, Mineola, NY, USA.

BACKGROUND: Vitamin D insufficiency is a major problem among African American (AA)women living at higher latitudes in North America. We conducted a randomized, placebo controlled, double-masked study to test the hypothesis that vitamin D3 supplementation would prevent bone loss in calcium-replete, postmenopausal AA women.

AIM: We hypothesize that Vitamin D supplementation (intended to increase serum 25-OHD to "optimal" levels) would decrease postmenopausal bone loss in calcium-sufficient AA women.

METHODS: 208 healthy black postmenopausal women 50-75 of age, were randomly assigned to receive either placebo or 20 mcg daily of vitamin D3.Calcium supplements were provided to ensure a total calcium intake of 1200-1500mg/d in both groups. After 2 years, the vitamin D3 dose was raised to 50mcg/d in the active group and the study continued for an additional year. Bone mineral density (BMD) of the total body, spine, total hip, and mid radius were measured every 6 months by DXA. Markers of bone turnover, vitamin D metabolites and parathyroid hormone levels were measured in serum.

RESULTS: There were no significant differences in bone mineral density between the active and control groups throughout the study. There was a transient increase in total body, femur, and radial BMD at 6 months in both groups.Over the 3 years, BMD declined at these sites by .26 to .55%/ year. The BMD of the lumbar spine increased slightly in the placebo group and active group, respectively. Serum 25-OHD increased from 47nmol/L to 71 nmol/L at 3 months in the active group and by an additional 20 nmol/L 3 months after the increase in dose to 50 mcg/d. The mean serum 25-OHD levels at the end of the study in Ca+D group was 73.8nmo1/L with about 40% participants still under 80 nmo1/L in spite of supplementation. There were no persistent changes in serum PTH levels or the markers of bone turnover, although there was a transient decline in PTH in both groups at 3 months. No significant adverse events were attributed to vitamin D supplementation.

CONCLUSIONS: There was no effect of vitamin D3 supplementation on bone loss in calcium-replete African-American, postmenopausal women. Further studies are needed to determine if these findings are applicable to other ethnic groups or if higher amounts of vitamin D would have an effect.

BMD changes over 3 years with vitamin D supplementation

BMD site	Ca group (n=104)	Ca+D group (n=104)
Baseline Total Body (TBBMD) (g/m2)	.94(.074)	.934(.095)
Absolute change in TBBMD (g/m2)	-.018(.026)	-.018(.025)
Baseline Total Hip BMD (g/m2)	.946(.116)	.932(.146)
Absolute change in Hip BMD (g/m2)	-.014(.033)	-.012(.036)
Baseline spine BMD (g/m2)	1.005(.142)	.984(.155)
Absolute change in spine BMD (g/m2)	.007(.04)	.006(.039)

Disclosures: ***S.A. Talwar****, None.*

SU503

The Use of Alendronate in the Treatment of Osteonecrosis of the Femoral Head to Reduce Degenerative Osteoarthritis of the Hip. J. G. Hofstaetter*, J. Wang*, M. J. Glimcher. Orthopedic Surgery, Children's Hospital Boston, Boston, MA, USA.

Osteonecrosis (ON) of the femoral head can lead to structural failure and secondary osteoarthritis (OA) of the hip. We evaluated the effects of Alendronate (ALN), a potent bone resorption inhibitor, on microarchitecture and mineralization of trabecular and compact bone during the repair of the osteonecrotic femoral head and subsequent OA of the hip using micro-Quantitative Computer Tomography (16 microns), radiography and histology. ON of the left femoral head was surgically induced in 60 adult male NZW rabbits. Animals were randomized into four groups of 15 each and treated either with ALN (150µg/kg/day, s.c., 3x per wk) or saline, starting one month post-surgery. Rabbits were sacrificed 6 and 12 month post-surgery and contra-lateral hips of the saline groups served as controls. Two osteonecrotic femoral heads from the saline-group were collapsed at 12 months, whereas no collapse was observed in either ALN group. Repair of necrotic trabecular bone resulted in significant increases in volumetric bone mineral density (vBMD) and bone volume fraction (BVF) when compared to controls. Inhibition of resorption of necrotic trabecular bone by ALN led to marked increases in vBMD and BVF when compared to the saline-treated ON groups. Resorption of the necrotic subchondral bone was inhibited by ALN. In the saline-treated OA acetabulum, subchondral bone resorption was markedly increased at 6 and 12 month post-surgery, which was almost completely inhibited by ALN. The subchondral bone of the saline-treated OA acetabulum had a significantly higher porosity, lower vBMD and lower degree of mineralization than healthy controls. The OA subchondral bone of the ALN group was found to have an even higher vBMD and degree of mineralization than controls, and no change in porosity was observed. Bone volume and vBMD was significantly increased, but mineralization was decreased in the subchondral trabecular region of the OA acetabulum when compared to controls. In the ALN treated OA-group the increase of subchondral trabecular bone volume was less, but the bone had an even higher degree of mineralization than normal bone, which resulted in an overall increase in vBMD in this region. ALN reduced the histological Mankin score ($p<0.05$) of cartilage damage during OA progression in the acetabulum. These results strongly suggest that ALN effectively inhibits resorption of trabecular and subchondral compact bone in the ON femoral head without impairing new bone formation and thus preventing structural failure. Furthermore, this demonstrates that ALN reduces subchondral bone resorption in OA, and slows down the progression of OA.

Disclosures: ***J.G. Hofstaetter****, None.*

SU504

Coumadin Therapy Is Associated with Bone Formation in Aortic Valves Excised for Aortic Valve Stenosis. S. W. Ing[1], E. R. Mohler*[2], M. Putt*[3], M. Leonard[4]. [1]Internal Medicine, Geisinger Health System, Wilkes-Barre, PA, USA, [2]Internal Medicine, University of Pennsylvania, Philadelphia, PA, USA, [3]Center for Clinical Epidemiology and Biostatistics, University of Pennsylvania, Philadlelphia, PA, USA, [4]Pediatrics, Childrens Hospital of Philadelphia, Philadelphia, PA, USA.

Ossification has been described in a number of vascular areas, including cardiac valves, and attributed to an inflammatory endochondral pathway of osteogenesis. The objective of this study was to identify determinants of aortic valve ossification in a series of 207 valves; 30 contained ossification. Medical records were reviewed for (1) factors associated with skeletal bone: age, sex, race, age, height, weight, BMI, cigarette smoking, serum creatinine, calcium, phosphate, and use of statins, warfarin, bisphosphonate, systemic glucocorticoids, estrogen, calcium, and multivitamin; and (2) additional factors associated with the development of aortic valve calcification or stenosis: hypertension, diabetes mellitus, elevated cholesterol, mitral regurgitation and left ventricular hypertrophy. Univariate analysis was performed using chi-square tests for dichotomous variables, and Student t-test or Wilcoxin rank-sum test for continuous variables. Multivariate analysis was performed using step wise logistic regression. Five variables were associated with valvular ossification (using a higher p-value cutoff of <0.1) for inclusion into multivariable analysis. The univariate odds ratios (OR, 95% C.I.) for these factors were: warfarin use- OR 5.3 (1.59, 17.72), p = 0.004; African American race (vs. Caucasian) - OR of 6.1 (1.56, 23.7), p = 0.006; female gender - OR 0.46 (0.2, P=1.07), p = 0.07, taller stature (taller median height) - OR 2.43 (1.09, 5.43), p = 0.03; and diabetes - OR=0.4, p=0.07. Warfarin use was not associated with race, sex, or diabetes. Inclusion of these factors in a step-wise logistic regression model revealed that warfarin use and African America race were independently associated with valvular ossification while female gender and diabetes were marginally associated with valvular ossification: warfarin use- OR 5.7 (1.5, 21.1), p=0.010; p=0.009; African Americans- OR=8.3 (1.8, 38.8), p=0.007; female gender- OR 0.39 (0.15, 0.98), p=0.044; and diabetes- OR=0.34 (0.11, 1.00), p=0.049. Further studies are needed to explore these associations, and the role of warfarin-induced inhibition of matrix Gla protein function in the development of valvular ossification.

Disclosures: ***S.W. Ing****, None.*

SU505

The Effect of Growth Hormone Replacement on Serum FGF-23 and Various Phosphate Indices in Adult GH Deficiency. B. H. Durham[1], H. D. White*[2], A. M. Ahmad*[2], J. P. Vora*[2], W. D. Fraser[1]. [1]Clinical Biochemistry & Metabolic Medicine, Royal Liverpool University Hospital, Liverpool, United Kingdom, [2]Endocrinology, Royal Liverpool University Hospital, Liverpool, United Kingdom.

We have measured FGF-23 in fasting serum from growth hormone deficient adults [GHD] 12 male, 8 female, average age 55 yr [range 24-72] prior to, and at 1,3,6 and 12 months of GH replacement [GHR]. We also measured phosphate [PO4] and creatinine in serum and a 24 hour urine; from these we calculated the ratio of PO4 clearance to creatinine [PCl], PO4 excretion index [PEI] and the percentage of tubular reabsorbed PO4 [TRP]. After one month GHR, FGF-23 increased by > 25% in 15/20 [75%] and >50% in 10/20 [50%]. Maximum concentration was reached at 3 months in 6 [3m, 3f] and at 6 months in 5 [3m, 2f], in the remaining 9 [6m,3f] the concentration FGF-23 was still increasing 12 months after the commencement of GHR. The PO4 indices were calculated in the samples from the month when FGF-23 reached a maximum [or in the case of the nine who did not reach a maximum, the 12month sample]. Prior to GHR the median [range] values were: FGF-23 121 RU/L [49 to 324], serum PO4 1.08 mmol/L [0.73 to 1.33], total 24 hr urinary PO4 excretion [TuPO4] 23.8 mmol/24hr [7.7 to 46.1], PCl 0.22 [0.08 to 0.37], TRP 78.2 [63.2 to 91.6] and PEI 0.11 [-0.09 to 0.31]. Post GHR the values were: FGF-23 289 [82 to 1925], serum PO4 1.23 [0.71 to 1.38], TuPO4 26.9 [11.0 to 67.5], PCl 0.19 [0.12 to 0.41], TRP 80.6 [58.6 to 88.0], PEI 0.11 [-0.04 to 0.27]. The increases in FGF-23 and serum PO4 were significant [p= 0.05] and the percentage change in FGF-23 correlated significantly [p= 0.05] with those for serum PO4 and TRP. Although there was no significant correlation between the change in FGF-23 and that for TuPO4 the percentage change in TuPO4 correlated positively with the percentage change of PCl [p=0.05] and PEI [p=0.01] and negatively with that for TRP [p=0.01]. Therefore the increase in FGF-23 in GHR could be a mechanism to counteract the increase in circulating PO4 which occurs during GHR by altering the renal handling of PO4 and increasing phosphaturia.

Disclosures: ***B.H. Durham****, None.*

SU506

A Vanadium-based Anti-diabetic Drug Affects Bone Cells and Bone Mineral In a Rat Model of Diabetes. D. Facchini*[1], V. Yuen*[2], M. Battell*[2], J. McNeill*[2], M. Grynpas[1]. [1]Mount Sinai Hospital & University of Toronto, Toronto, ON, Canada, [2]University of British Columbia, Vancouver, BC, Canada.

Vanadium-based drugs have an insulin-like glucose lowering ability, and oral vanadium drugs are being tested as alternatives to insulin injections for diabetes. Vanadium accumulates in bone where, in the form of vanadate, it replaces phosphate in the apatite lattice of bone mineral. The purpose of this study is to determine if incorporated vanadium affects bone quality in normal and diabetic bone. Nine to 12 month old, sham-operated and streptozotocin-induced diabetic Wistar rats were given BEOV, a vanadium-based anti-diabetic drug, in drinking water for 12 weeks. Non-diabetic rats were divided into groups of 10 to receive 0, 0.25 or 0.75 mg/mL BEOV. Groups of diabetic rats were either left untreated (n=12) or treated with 0.25-0.75 mg/mL BEOV as necessary to lower blood glucose in each rat (n=22). In diabetic rats, this treatment resulted in 2 groups: 1) a controlled glucose group (n=10), simulating well-managed diabetes, and 2) an uncontrolled glucose group (n=12), simulating poorly managed diabetes. BMD was assessed by DEXA. Mechanical properties were determined by femoral bending, vertebral compression and femoral neck fracture. Degree of mineralization was determined by density fractionation, mineral crystal size by x-ray diffraction and mineral chemistry by instrumental neutron activation analysis. Trabecular architecture and connectivity were assessed by image analysis and bone remodeling parameters by static and dynamic histomorphometry. In non-diabetic bone, BEOV increased vanadium content, degree of mineralization, osteoid volume (>+55% for both doses) and bone formation rate (>+140% for both doses). Diabetes decreased BMD (-16% in femurs, -21% in vertebrae) and mechanical strength (-16% in bending, -38% in compression, -22% in femoral neck). The diabetic bone was less mineralized, and this bone mineral had shorter crystals (-8%). Diabetes also decreased bone volume (-45%) and connectivity (-56% Number of Nodes). Controlling glucose with BEOV increased vanadium content, and improved bone properties. Increases in BMD of femurs (+10%), mechanical strength (+12% in bending, +19% in compression) and degree of mineralization were observed. There were also increases in osteoid volume (+91%) and bone formation rate (+220%), but no changes in bone volume or connectivity. The uncontrolled glucose state increased vanadium content, but did not improve bone properties. The results suggest that BEOV improves diabetes-related bone dysfunction. This may be due to a direct action of BEOV on bone cells, the incorporation of vanadate into bone mineral and the improvement by BEOV of the diabetic state.

Disclosures: ***D. Facchini****, None.*

SU507

Tobacco Smoking Effects on Bone Biomechanical Properties. M. P. Akhter, A. D. Lund*, S. Morgan*, D. J. Wells*, D. M. Cullen. Medicine, Creighton University, Omaha, NE, USA.

Tobacco use is associated with decreased bone mass and increased fracture risk. Based on a study of twin pairs discordant for cigarette use, women who smoke one pack of cigarettes per day throughout life will have 5 to 8% less bone than nonsmokers. The purpose of the current study was to evaluate the effects of high concentration tobacco smoke on bone strength in estrogen-replete (intact) and estrogen-deplete (ovariectomized) rats. Adult (6-month-old) Sprague dawley female rats were divided into 4 groups. Intact rats (n=24) and ovariectomized (OVX, n=24) were subjected to either sham or tobacco/cigarette (1R4F University of Kentucky research) smoke exposure. A steady state concentration of 126±4mg (mean± sem) smoke TSP/m^3 was maintained in the chamber during exposure of the rats to smoke. Exposures were given for 2hrs each week day and 1 hr on weekends (total of 12hrs/week) for 12 weeks. At the time of necropsy, femurs were collected and frozen in saline for subsequent structural and biomechanical evaluations. Specimens were allowed to reach room temperature before structural and strength evaluation. Using a micro computed tomography device (μCT20, Scanco Medical AG, Bassersdorf, Switzerland), femoral necks were scanned (9 micron resolution with an integration time of 80 milliseconds) to determine cancellous/trabecular structural properties in terms of bone volume (BV/TV), trabecular thickness, and spacing. After scanning, the mid-shaft femur was subjected to a 3-point bending test (along anterior-posterior direction) and femoral neck tested in bending. All tests were performed at rate of 3mm/minute. Structural strength parameters (ultimate/yield load, stiffness) were obtained from the load-displacement diagram. The apparent material strength (ultimate/yield stress, modulus) was calculated. Tobacco smoke exposure- and ovariectomy-related differences in all the measured variables were tested using two-way ANOVA at a significance level of P<0.05, followed by a Tukey HSD post-hoc test. While tobacco exposure effects on biomechanical properties were not detected, the ovariectomy caused a significant decline in most of the structural and biomechanical properties in the femoral shaft and femoral neck (Table, only the affected variables are listed).

Table. Biomechanical Properties (Mean ± SD)	Intact Sham	Intact Smoke Exposed	OVX Sham	OVX Smoke Exposed
FS Ultimate Load (N)	160±11	168 ± 15	142 ± 14 [b]	144 ± 18 [b]
FS Stiffness (N/mm)	336±17	332 ± 37	312 ± 26 [b]	306 ± 34 [b]
FS Ultimate Stress (N/mm^2)	259±25	258 ± 16	232 ± 29 [b]	245 ± 31 [b]
FN BV/TV	0.85±0.05	0.84 ± 0.08	0.73 ± 0.05 [b]	0.74 ± 0.04 [b]
FN Trabecular thickness	0.32±0.03	0.34 ± 0.06	0.26 ± 0.02 [b]	0.26 ± 0.02 [b]
FN Ultimate Load (N)	108±13	114 ± 18	98 ± 11 [b]	93 ± 7 [b]
FN Stiffness (N/mm)	368±55	377 ± 76	331 ± 75 [b]	345 ± 30 [b]

[b] Differences due to ovariectomy (OVX) (P < 0.05) FS= femur shaft, FN= Femoral Neck

Disclosures: ***M.P. Akhter****, None.*

SU508

Changes in Biochemical Bone Markers and Bone Mineral Density after Parathyroidectomy in Primary Hyperparathyroidism: A Three-Year Follow-up Study. F. Debiais[1], J. Kraimps*[2], M. Bounaud*[3], R. Marechaud*[4], P. Ingrand*[5], I. Azais*[1], R. Brault*[1], M. Alcalay*[1]. [1]Departments of Rheumatology, La Miletrie Hospital, Poitiers, France, [2]Endocrine Surgery, La Miletrie Hospital, Poitiers, France, [3]Biophysic, La Miletrie Hospital, Poitiers, France, [4]Endocrinology, La Miletrie Hospital, Poitiers, France, [5]Biostatistics, Faculty of Medicine, Poitiers, France.

Primary hyperparathyroidism may be associated with bone involvement. The aim of this study was to determine the changes in biochemical bone markers and to investigate long-term bone mineral density (BMD) changes at both trabecular and cortical sites after parathyroidectomy.

Serum levels of osteocalcin and bone alkaline phosphatase as markers of bone formation and excretion of urinary deoxypyridinoline as a marker of bone resorption were measured at baseline, 3 days, 1 month, 6, 12, 24 and 36 months. Measurements of BMD of lumbar spine (L2-L4), hip (femoral neck, trochanteric region and total hip), distal radius (proximal third, Mid, ultradistral and total) and whole body were obtained by dual energy X-ray absorptiometry (Hologic QDR 2000). BMD was measured before and after parathyroidectomy at 6 months (42 patients), 12 months (40 patients), 24 months (31 patients) and 36 months (27 patients). Mean age of the patients (10 men, 10 premenopausal women, 22 postmenopausal) was 57.4 ± 12.9 years. Before surgery, patients had increased serum calcium concentrations (Mean : 2.83 ± 0.21 mmoles/l ; normal range : 2.20-2.60 mmoles/l) and parathormone levels (Mean : 126.7 ± 84.1 pg/ml ; normal range : 15-60 pg/ml), and 28 patients had a low BMD with a T-score <-2.5 at least at one of the studied sites.

Following parathyroidectomy, the three biochemical markers, compared to baseline, decreased significantly within 6 months, with no major changes during the following 2.5 years. Increases in BMD were significant within 6 months in the spine (p<0.0001), the total hip (p<0.0001), the trochanteric region (p<0.0001), the femoral neck (p<0.05), and the whole body (p<0.001). In the radius, bone density rose more slowly and increases were significant within 1 year (mid, ultradistal, total) or 2 years (proximal third). At 3 years, the more pronounced increases were in the spine (6.6% + 5.7%) and in the trochanteric region (7.6% + 5.1%)

These results show that, following parathyroidectomy, bone turnover decreases and BMD increases at both cancellous and cortical sites, but with a slower and more modest increase in the radius.

Disclosures: ***F. Debiais****, None.*

SU509

Vitamin D Replacement in Patients with Concomitant Primary Hyperparathyroidism and Vitamin D Deficiency - A Safe Option. V. Eshed[1], E. Segal*[2], G. Tsvetov[1], C. Benbasat*[1], S. Ish-Shalom[3]. [1]Endocrinology and Metabolism, Rabin medical center, PetahTikva, Israel, [2]Metabolic bone diseases, Rambam Medical Center, Haifa, Israel, [3]Bruce Rapaport Faculty of Medicine, Technion Israel Institute of Technology, Haifa, Israel.

The prevalence of vitamin D deficiency/insufficiency in patients with primary hyperparathyroidism is more than 50%. Data from the literature support the notion that vitamin D deficiency may contribute to the severity of primary hyperparathyroidism. The aim of our work was to asses the effect of vitamin D replacement on calcium metabolism, in such patients. We followed 20 consecutive patients with a combination of primary hyperparathyroidism and $25(OH)D_3$ levels below 15 ng/ml. Sixteen (80%) of the patients were women and 4 (20%) were men. The mean age was 60.3 ± 21.01. All patients were hypercalcemic at their baseline test. Baseline and post treatment levels of serum and urinary calcium, serum phosphorus, alkaline phosphatase, $25(OH)D_3$ and PTH are shown in the table. All patients had normal serum creatinine levels. Patients were treated with 400-1000 units/day of vitamin D. Serum level of $25(OH)D_3$ significantly increased, to a mean of 17.04 ng/ml ($p<0.0001$) after a mean time of 4.2 ± 2.3 months. No significant changes in serum calcium, phosphorus, alkaline phosphatase, PTH and 24 hours urine secretion of calcium were observed.

Mean levels	Vitamin D depleted	Vitamin D repleted
25 hydroxyvitamin D (ng/ml)	7.8 ± 3.5	17.04 ± 6.7
PTH (pg/ml)	104.4 ± 78	99.3 ± 49.9
Serum calcium (mg/dl)	10.6 ± 0.4	10.55 ± 0.6
24 hours urine calcium (mg)	298 ± 163.9	249 ± 100.5
Alkaline phosphatase (u/l)	99.99 ± 38.38	89.75 ± 31.32
Phosphorus (mg/dl)	3.06 ± 0.7	2.91 ± 0.48

We conclude that treatment of patients with concomitant primary hyperparathyroidism and vitamin D deficiency/insufficiency with 400-1000 IU of vitamin D daily is safe and leads to improvement of vitamin D status.

Disclosures: ***V. Eshed****, None.*

SU510

Impact of Autoimmune Polyendocrinopathy-Candidiasis-Ectodermal Dystrophy (APECED) on Bone Health: Findings in 25 Adult Patients. O. Mäkitie*[1], E. Sochett[2], S. Bondestam*[3], J. Perheentupa*[1]. [1]Pediatric Endocrinology, The Hospital for Children and Adolescents, Helsinki University Hospital, Helsinki, Finland, [2]Division of Endocrinology, The Hospital for Sick Children, Toronto, ON, Canada, [3]Department of Radiology, Helsinki University Hospital, Helsinki, Finland.

Autoimmune polyendocrinopathy-candidiasis-ectodermal dystrophy (APECED) is an autosomal recessive disorder characterized by chronic mucocutaneous candidiasis and autoimmune destruction of endocrine organs. The resulting endocrinopathies and their treatment may impact bone health in patients with APECED.

The purpose of our study was to assess bone health and its correlates in adult patients with APECED.

Twenty-five adults (12 males) with APECED, followed at the Helsinki University Hospital, were prospectively assessed. Data on their previous medical history was collected from hospital records. Areal BMD (aBMD) for the lumbar spine (L1-L4) and femoral neck as well as volumetric BMD (vBMD) for the lumbar spine (L2-L4) were measured with dual-energy x-ray absoptiometry (DXA, Hologic Discovery A); the aBMDs were transformed into z-scores using age- and sex-specific reference data for the equipment.

Mean age at study assessment was 38 years (range 21-59 years). All patients had 1-4 autoimmune endocrinopathies (median 2) and other manifestations. The most common endocrinopathies were Addison's disease (AD, 20 patients), hypoparathyroidism (HPT, 18), hypogonadism (10) and diabetes mellitus (6). The mean age at the onset of AD was 13.2 years (5.5 - 28.1 years) and of HPT, 5.8 years (1.6 - 18.9 years). The median aBMD z-scores were for the lumbar spine -0.3 (-2.3 - +3.3) and for the femoral neck, -0.1 (-2.2 - +2.0). The median volumetric BMD was 0.23 g/cm^3 (0.17-0.31 g/cm^3). The patients with HPT had significantly higher BMDs than the patients with normal parathyroid function: the mean aBMD z-scores were for the lumbar spine +0.4 *vs* -1.2 (P=0.016) and for the femoral neck, +0.2 *vs* -0.6 (P=0.094), respectively, and the vBMD, 0.24 g/cm^3 *vs* 0.21 g/cm^3 (P=0.008), respectively. Of the four patients with a lumbar spine aBMD z-score >+1.5 all had HPT and only one had AD. In contrast, of the four patients with a z-score <-1.5 all had AD and only one had HPT. The prevalence of fractures was higher among those with normal parathyroid function (4/7) than among those with HPT (4/18).

Our study suggests that despite the complex endocrine problems the overall prevalence of osteopenia and osteoporosis is low among adults with APECED. Normal parathyroid function may have a positive and AD a negative impact on bone health in patients with APECED.

Disclosures: ***O. Mäkitie****, None.*

SU511

Gene Expression in Primary and Secondary Hyperparathyroidism : Phosphate-Induced Genes in Human Parathyroid Tissue in Organ Culture. K. Sato, K. Nakajima*, K. Takano*, T. Obara*. Insitute of Clinical Endocrinology, Tokyo Women's Medical University, Tokyo, Japan.

To investigate the mechanism of phosphate-induced parathyroid cell proliferation, human parathyroid tissues were cultured in low and high phosphate medium, and mRNAs induced by high phosphate medium were analyzed using DNA microarray (Agilent), which can analyze 17000 - 41000 genes in a single run.

Hyperplastic parathyroid glands obtained from patients with primary hyperparathyroidism (N = 4), secondary hyperparathyroidism (N =4), and parathyroid carcinoma (N=1) were cut into pieces (1x1x0.5mm), placed on collagen-coated nylon mesh, and cultured in 10cm dishes. Culture medium containing 10% bovine serum and various concentration of Ca (4 - 11mg/dl) was prepared so that final phosphate concentrations were 2.5mg/dl (low P) or 10mg/dl (high P). After 5 - 30 days of culture, the conditioned medium was taken for measurement for PTH. Data were expressed as ng intact PTH/microg DNA.

Intact PTH secretion continued for a prolonged period (>30 days). PTH secretion was inhibited in Ca concentration-dependent manner, particularly at total calcium concentration between 5.8 - 7.4mg/dl (Ca++ 1.2 - 1.4mmol/L). When parathyroid tissues were cultured in low and high P medium, intact PTH secretion (basal level 5-10ng/microg DNA/16h) nearly doubled in the high P medium. [3H]-thymidine incorporation also increased in the high P medium. This phenomenon was not observed in parathyroid carcinoma. Oligo-DNA microarray analysis revealed that mRNAs of PTH, chromogranin A, CaSR, and VDR were highly - moderately expressed. Among growth factors, TGFbeta1, FGF1, FGF2, and FGF3 were substantially expressed but not modulated by the high P medium. Little or no mRNA for FGF23 was detected. More than 30 genes (e.g. cytochrome P450 retinoid metabolizing protein, etc) were expressed more than 100% in the high P medium. In addition, a number of mRNAs for proteins with unknown function increased nearly by 100%, although they were different in primary and secondary hyperparathyroid tissues.

In summary, we have established parathyroid organ culture system in which human parathyroid tissue maintained its patho-physiological features for a prolonged period. Although genes expressed in primary and secondary hyperparathyroidism are substantially different, genes which constantly increased in high P medium are under investigation.

Disclosures: ***K. Sato****, None.*

SU512

See Plenary Poster number F497

SU513

Human Chorionic Gonadotropin: A Potential Tumor Marker for Parathyroid Carcinoma. M. R. Rubin, S. Birken*, J. P. Bilezikian, S. J. Silverberg. Columbia University College of Physicians & Surgeons, New York, NY, USA.

Differentiating between parathyroid carcinoma (PTHCa) and severe non-malignant primary hyperparathyroidism prior to surgery is difficult. A tumor marker for PTHCa could identify the disease preoperatively and increase the likelihood of surgical cure. In patients with established PTHCa, it could also possibly quantify tumor burden and be useful in monitoring therapy. Human chorionic gonadotropin (hCG) is a glycoprotein hormone, well established as a tumor marker in trophoblastic cancers such as choriocarcinoma, germ cell tumors and non-trophoblastic malignancies. Moreover, a hyperglycosylated isoform of hCG that normally comprises 10% of total urinary hCG excreted by pregnant women is excreted at much higher levels in patients with hCG-secreting malignancies. We observed elevated serum hCG levels (72 ± 20; nl <25 mIU/mL) in 3 non-pregnant women with PTHCa who were being evaluated for treatment with the calcimimetic agent cinalcalcet HCl. We hypothesized that hCG could be a tumor marker in both men and women with PTHCa and that hCG levels might correlate with changes in tumor burden.

hCG was measured in a first morning urine specimen in 8 patients (5 men, 3 women) with PTHCa. Several immunometric two-site assays were used to measure urinary β core metabolites of hCG and hLH as well as a hyperglycosylated isoform of hCG and total hCG and β subunit. In 5 patients with the highest PTH values (1106 ± 274 pg/ml), 3 had markedly elevated levels of urinary hCG metabolite (621 ± 286, nl 10-50 fmol/mg Cr) with a predominance of the malignant-associated isoform of hCG, while 2 had normal levels of hCG metabolite (23 ± 7, nl 10-50 fmol/mg Cr), consistent with pituitary-derived hCG. However, 1 of the 2 with normal hCG metabolite levels had a subsequent rise of hCG with cinacalcet of 1400% (16 to 226 fmol/mg) with a predominance of the malignant isoform. This change in hCG was associated with a 45% increase in PTH after cinacalcet. In the patients with lowest PTH values (262 ± 49 pg/ml; n=3) urinary hCG metabolite levels (pituitary-derived hCG) were normal (7 ± 2, nl 10-50 fmol/mg Cr). hCG subsequently increased by 1900% (7 to 136 fmol/mg Cr) in 1 patient. The increase was due to the appearance of the malignant isoform and was associated with a post cinacalcet increase in PTH of 50%.

In summary, hCG levels (predominantly the malignant isoform) are elevated in men and women with PTHCa who have severe disease. The levels of hCG were associated with higher PTH concentrations. The post cinacalcet rise in hCG in some patients might signal the presence of a more aggressive form of PTHCa than those individuals whose hCG levels did not rise after cinacalcet. The results suggest that hCG might become a useful biochemical marker for PTHCa.

Disclosures: ***M.R. Rubin****, None.*

SU514

A Molecular Form of PTH Distinct from PTH (1-84) Is Produced in Parathyroid Carcinoma. M. R. Rubin[1], P. D'Amour[2], J. H. Brossard[2], T. Cantor[3], J. P. Bilezikian[1], S. J. Silverberg[1]. [1]Columbia University College of P& S, New York, NY, USA, [2]Centre de recherche du CHUM, Montreal, PQ, Canada, [3]Scantibodies Lab Inc, Santee, CA, USA.

Circulating PTH is composed of bioactive PTH (1-84) and fragments of varying lengths. In normal (nls), primary (PHPT) and secondary hyperparathyroid (SHPT) subjects, there are large C-terminal fragments (CTF) which arise from parathyroid gland secretion and peripheral metabolism . The "intact" PTH IRMA (iPTH) detects both PTH(1-84) and CTF. The newer Scantibodies assay (wPTH) uses an Ab which binds only if the first amino acid is present, making it specific for the complete molecule, PTH(1-84). Since the iPTH assay detects CTF and PTH(1-84), iPTH levels are generally higher in PHPT, SHPT, and nls than wPTH levels. An N-PTH molecular form has been reported in a minority of patients (pts) with PHPT. We observed that in pts with parathyroid carcinoma (PTHCa) treated with the calcimimetic cinacalcet HCl, serum calcium (S Ca) falls yet iPTH is unchanged or rises. We investigated the existence of different types of PTH species in PTHCa and how cinacalcet might alter these measurements.

We measured iPTH and wPTH in 5 pts with PTHCa at baseline and after cinacalcet. The mean S Ca concentration of the pts (50 ± 6 yr; 3 M, 2 F) was 15.8 ± 1 mg/dl. We found an unusually high amount of wPTH relative to iPTH in all pts. In 3 pts with the most severe disease (S Ca 17.3 ± 2 mg/dl) wPTH was 1.4 times higher than iPTH (wPTH 1047 ± 154, iPTH 755 ± 64 pg/ml), the reverse of the typical pattern. In 2 pts with less severe disease (S Ca 13.6 ± 1 mg/dl), iPTH was greater than wPTH, as is usual, but CTF made up only an average of 24% of circulating PTH (wPTH 225 ± 35, iPTH 302 ± 77 pg/ml), a lower percentage than is usually seen. The ratio of wPTH to iPTH did not change in any of the pts over time with cinacalcet treatment.

A serum HPLC profile was obtained in one patient with wPTH > iPTH. wPTH was made up of 2 immunoreactive peaks. The first 45% coeluted with standard PTH (1-84) and was recognized equally by both PTH assays. The other 55% of PTH immunoreactivity was detected only by the wPTH assay. It was less hydrophobic, and migrated in front of PTH(1-84). An additional peak of immunoreactivity corresponding to N-truncated fragments was detected by the iPTH assay.

In summary, a new form of PTH in PTHCa is detected by the wPTH assay but not the iPTH assay. This new PTH form is distinct from PTH(1-84) and contains the first amino acid of native PTH (1-84). Posttranslational modification in site(s) not detected by iPTH but detected by wPTH are consistent with these findings. More information about this molecular variant of PTH including its structure, bioactivity, source and regulation will give new insights about PTHCa and the PTH molecule itself.

Disclosures: ***M.R. Rubin****, None.*

SU515

Parathyroidectomy Improve Bone Mineral Density in Mild Asymptomatic Primary Hyperparathyroidism of Post-menopausal Women. E. Hagstrom*, E. Lundgren*, H. Mallmin, J. Rastad*, P. Hellman*. Dept. of Surgical Sciences, Uppsala, Sweden.

Bone mineral density (BMD) in truly mild primary hyperparathyroidism (pHPT) and controls, and the effects on BMD of surgery vs surveillance over five years of time is reported.

A population-based screening of 5202 post-menopausal women identified 87 overtly asymptomatic women with mild pHPT. The 5-year follow-up included 49 cases subjected to parathyroidectomy and 20 individuals who were only surveilled, each assigned an age-matched control. BMD of lumbar spine (L2-L4), femoral neck and total body was measured with DXA at inclusion and at follow-up. The pHPT diagnosis was confirmed in 98% of the cases.

At inclusion in the study cases had s-calcium of 2.57±0.12 mmol/l and s-PTH 53.6±22 ng/l (controls: 2.36±0.07 and 29.5±9.7, respectively). At study entry BMD was 5-6% lower in L2-L4 and femoral neck in cases compared to matched controls ($P<0.05$). During follow-up BMD increased in L2-L4 with 2.9% ($P<0.01$) in the parathyroidectomized cases and remained stable in the femoral neck. In contrast, BMD in surveilled cases decreased 3.9% in neck during follow-up ($P<0.01$), but had no change in L2-L4. Controls decreased in BMD in femoral neck with 2.5% ($P<0.05$), but not in L2-L4.

In accordance with recent NIH guidelines of pHPT treatment, the level of BMD per se in the investigated group of patients justifies parathyroidectomy in almost half of the cases with truly mild pHPT. Surgery could be expected to preserve femoral neck BMD and increase BMD in L2-L4 to the level of controls, while surveilled cases continues to decrease in BMD.

Disclosures: ***E. Hagstrom****, None.*

SU516

Inappropriate Levels of Parathyroid Hormone in Relation to Serum Calcium in a Pre-menopausal Population - an Indication of Early Primary HPT? H. Siilin*[1], Ö. Ljunggren[2], E. Lundgren*[1]. [1]Dep. of Surgery, University Hospital, Uppsala, Sweden, [2]Dep. of Internal Medicine, University Hospital, Uppsala, Sweden.

Primary hyperparathyroidism (pHPT) in elderly females, the individuals most prone to develop pHPT, have been explored in recent studies, while less is known of the disease in younger females. The progress of the disease is slow and although the estrogen deficiency after menopause might be one underlying cause, pHPT could exist years before this period. The prevalence of inappropriate high parathyroid hormone in relation to serum calcium, maybe in accordance with early pHPT, in a pre-menopausal population is reported.

Altogether 1888 pre-menopausal women, between the ages of 40 and 50 years, participating in a mammography health survey during one year, were included in the study. All subjects with total serum (s-) calcium at or above 2.50 mmol/L (n=553; 29 %) were invited for subsequent fasting tests of s-creatinine, intact parathyroid hormone (iPTH) and total s-calcium.

Mean age in the screening cohort was 44.9 years and mean s-calcium 2.45 mmol/L (2.08-2.89 mmol/L). In those 553 individuals, who were asked back for further investigations, mean age was 45 years and mean total s-calcium was 2.57 mmol/L (2.50-2.89 mmol/L). Altogether 548 women (five additional drop outs) had fasting values of mean s-calcium 2.48 mmol/L (2.22-2.79 mmol/L), and mean iPTH value of 47 ng/L (1.38-164 ng/L). Only one individual had slightly elevated s-creatinine (119µmol/L). The prevalence of assumed mild pHPT, or inappropriate iPTH value in relation to total s-calcium, was estimated to be 13% (n=245).

These data suggest that primary HPT is probably more prevalent in pre-menopausal females than previously suggested, but diagnostic criteria must be tested in each age interval separately. The significance of these biochemical criteria for premenopausal women must be investigated further in prospective studies.

Disclosures: ***H. Siilin****, None.*

SU517

Regulation of Plasma Fibroblast Growth Factor 23 Level by Calcium in Primary Hyperparathyroidism. K. Kobayashi*[1], Y. Imanishi[1], A. Miyauchi*[2], N. Onoda*[3], T. Kawata*[1], K. Nakatsuka[1], H. Tahara[1], T. Miki[4], E. Ishimura*[5], T. Sugimoto[6], T. Ishikawa*[7], M. Inaba[1], Y. Nishizawa[1]. [1]Department of Metabolism, Endocrinology and Molecular Medicine, Osaka City University Graduate School of Medicine, Osaka, Japan, [2]National Hyogo Chuo Hospital, Hyogo, Japan, [3]Department of Oncology, Osaka City University Graduate School of Medicine, Osaka, Japan, [4]Department of Geriatrics and Neurology, Osaka City University Graduate School of Medicine, Osaka, Japan, [5]Department of Nephrology, Osaka City University Graduate School of Medicine, Osaka, Japan, [6]Department of Clinical Molecular Medicine, Kobe University Graduate School of Medicine, Osaka, Japan, [7]Department of Surgical Oncology, Osaka City University Graduate School of Medicine, Osaka, Japan.

While the importance of FGF-23 is established in the pathogenesis of phosphate wasting disorders, little is known about the regulatory mechanism of its circulating level. To investigate the role of parathyroid hormone (PTH) in FGF-23 metabolism, we examined plasma FGF-23 levels on 50 patients of primary hyperparathyroidism (PHPT) and 52 controls. All subjects provided written informed consent before participation in this study, which were approved by institutional ethics committee and conducted in accordance with the principles endorsed by the Declaration of Helsinki. The FGF-23 was significantly elevated in PHPT compared with those in controls. When analyzed together with PHPT patients and healthy controls, log FGF-23 levels were significantly correlated in a positive manner with creatinine-clearance, serum corrected-calcium, inorganic phosphate, and log intact PTH levels, among which creatinine-clearance and corrected-calcium were factors independently associated. To assess the significance of corrected-calcium on FGF-23 levels, time course of changes were monitored in 5 PHPT patients after parathyroidectomy (PTX). Under minimum calcium loading, corrected-calcium levels were significantly decreased by 1 h after PTX, which was followed by a reduction in plasma FGF-23 levels. Serum phosphate levels increased and 1,25-dihydroxyvitamin D did not change appreciably after PTX. Under steady-state levels of these parameters which was attained by 6 h after PTX, FGF-23 level on next day morning on 15 PTX patients was significantly correlated positively with corrected-calcium, supporting serum calcium as one of major regulators of FGF-23. The absent expression of FGF-23 on surgically resected parathyroid glands by both RT-PCR and immunohistochemistry indicated that parathyroid glands were not major sources of circulating FGF-23.

In conclusion, serum calcium could regulate plasma FGF-23 levels in primary hyperparathyroidism.

Disclosures: ***K. Kobayashi****, None.*

SU518

HRPT2 Gene Alterations in Sporadic and Familial Primary Hyperparathyroidism. C. Marcocci, E. Pardi*, S. Borsari*, E. Ambrogini*, L. Cianferotti, E. Vignali, A. Pinchera*, F. Cetani. Endocrinology & Metabolism, University of Pisa, Pisa, Italy.

We investigated the involvement of *HRPT2* gene by loss of heterozygosity (LOH) analysis and direct sequencing in a kindred with hyperparathyroidism-jaw tumor syndrome (HPT-JT) and three kindreds with isolated primary hyperparathyroidism (FIHP). Seven patients with sporadic parathyroid cancers and 35 with parathyroid adenomas with no family history of primary hyperparathyroidism or HPT-JT were also studied. A novel germline heterozygous substitution G to A was found in the donor splice site of intron 1 in one of the three FIHP families. No mutations were identified in the HPT-JT kindred. A somatic *HRPT2* mutation was found in six of seven patients with parathyroid cancers, two of which were novel frame shift mutations (195insT and 195insA) in exon 2. Unexpectedly, two of the six mutations found in parathyroid cancer were germ-line mutations. Four adenomas showed LOH at 1q24-32, whereas a somatic *HRPT2* mutation was found in one. In conclusion, we provide further evidence for a strong association between *HRPT2* gene mutations and sporadic parathyroid cancer. The finding that two of the six patients with sporadic parathyroid cancer carried a *HRPT2* germ-line mutation suggests that they might have occult HPT-JT. Our results also confirm the need for testing *HRPT2* gene in FIHP families.

Disclosures: ***C. Marcocci****, None.*

SU519

Continued Higher Secretion of PTH after Curative Parathyroidectomy (PTX) In Patients with Primary Hyperparathyroidism (PHPT): Implications for Pathogenesis and Treatment of Mild Asymptomatic PHPT. D. Rao[1], N. Parikh*[1], T. Eskridge*[1], E. Phillips*[1], G. B. Talpos*[2]. [1]Bone & Mineral Research Laboratory, Henry Ford Hospital, Detroit, MI, USA, [2]Surgery, Henry Ford Hospital, Detroit, MI, USA.

It is generally assumed that PTH secretion returns to normal after curative PTX in PHPT, but very little data exists to support this notion. Furthermore, it is well known that age related bone loss is attenuated after PTX, mild untreated PHPT does not cause continued bone loss and continued BMD gain occurs long after PTX. Collectively, these data imply that an anabolic stimulus is present in such patients. We hypothesized that serum PTH levels after PTX may remain mildly elevated because of change in set-point of the remaining apparently "normal" glands.

We studied 53 of the 237 well characterized patients who were "cured" by removal an adenoma. To reduce the influence of confounders the study was restricted to women with both pre and post-operative PTH levels measured by the same method. We excluded 110 patients without post PTX-PTH levels and 38 men. There were no systematic differences between the 53 included and the excluded patients. Mean duration after PTX was 24.4 ± 19.8 months. The relevant data are in the Table:

In comparison to healthy subjects the 53 patients had significantly higher PTH levels, 14 of whom had values above the 2SD for healthy controls. However, no differences in various pre-PTX variables between these two PHPT groups except for higher age and pre-PTX-PTH levels in the latter group. There was no correlation between post-PTX-PTH levels and the time after PTX, serum 25-OHD or age.

PHPT patients continue to secrete higher than normal PTH levels after "curative" PTX possibly due to altered set point. Because of very low parathyroid cell proliferation, a second adenoma (as could be predicted from our proposal) is uncommon in the remaining life expectancy of most patients. This continued higher PTH secretion might explain the observed anabolic effects on bone both of post-PTX and in untreated mild PHPT. We propose that a PTH level of <100 pg/ml is anabolic to bone and this cut off level should be used to recommend PTX in PHPT. Further studies of steady state and dynamic PTH levels are needed to confirm or refute our hypothesis.

VARIABLE	PATIENTS	CONTROLS	p VALUE
Age (Years)	63 ± 12	58 ± 9	0.017
Serum Ca (mg/dl)	9.27 ± 0.54	9.40 ± 0.31	0.055
Serum Cr (mg/dl)	0.81 ± 0.15	0.79 ± 0.19	ns
Serum PTH (pg/ml)	50 ± 22	36 ± 12	<0.001

Disclosures: ***D. Rao****, None.*

SU520

Temporary Brittle Bone Disease (TBBD): Analysis of an Additional 39 Cases Associated with Fetal Immobilization. M. Miller*. Department of Pediatrics, Wright State University, Dayton, OH, USA.

TBBD was described in 1993 by Paterson as an intrinsic bone disorder with unexplained fractures in the first year of life. In 1999 the analysis of 26 cases of TBBD suggested fetal immobilization from intrauterine confinement (IUC) as a cause of this transient brittle bone state [Calcif Tissue Intl 64:137-143]. Most child abuse experts believe that TBBD does not exist and that it is a ruse for child abuse. Herein is the analysis of an additional 39 cases of TBBD associated with fetal immobilization in which allegations of child abuse were made against the parents. Cases of unexplained fractures in infants were considered TBBD associated with fetal immobilization if the following were found: (1) parents deny wrongdoing, (2) no significant bruising or internal organ injury, (3) no history of antecedent injury, (4) no radiographic or laboratory evidence of biochemical bone disease such as rickets or OI, and (5) history/clinical evidence of decreased fetal movement or IUC. The average age of presentation with the fractures was 9 weeks (1 sd = 5 weeks, range = 2-24 weeks). The average number of fractures was 12 (1 sd = 7 fractures, range = 3-26 fractures). The basis of the fetal immobilization was the following: (1) Cephalopelvic disproportion- 20 cases (2) Maternal use of drugs during pregnancy that cause fetal immobilization (opiates, beta-blockers)- 7 cases. (3) Twins- 7 cases (4) Breech presentation- 2 cases (5) Large maternal fibroids- 1 case. Umbilical cord length was available in 7 cases, and in all 7 it was extremely short, a finding consistent with decreased fetal movement. The striking, early presentation of TBBD is consistent with a prenatal onset etiology. The large number of fractures (average = 12) without bruising or other extraskeletal injury suggests this is not child abuse. The results confirm the previous association of TBBD with fetal immobilization with the new observation that the fetal immobilization can also result from maternal use of medications that cause decreased fetal movement. These overall findings support the concept that fetal bone loading is an important determinant of fetal bone strength, and that fetal immobilization is the primary risk factor for TBBD. This hypothesis is in accord with the contemporary model of bone physiology and bone strength as posited by Frost in the Utah paradigm (Anat Rec 262:398-419) and explains the transient nature of TBBD.

Disclosures: ***M. Miller****, None.*

SU521

Ibandronate Decreases Femoral Head Deformity Following Ischemic Osteonecrosis of the Femoral Head in Immature Pigs. H. K. W. Kim[1], T. S. Randall[1], H. Bian[1], J. Jenkins*[1], A. Garces*[1], F. Bauss*[2]. [1]Shriners Hospital for Children, Tampa, FL, USA, [2]Roche Diagnostic GmbH, Penzberg, Germany.

Development of femoral head deformity (FHD) is the most serious sequela of Legg-Perthes disease, a juvenile form of osteonecrosis of the femoral head. The deformity can produce premature osteoarthritis. The predominance of bone resorption during repair of the osteonecrotic femoral head has been shown to contribute to the development of FHD. The purpose of this study was to test the hypothesis that inhibition of bone resorption during repair will preserve the trabecular framework and minimize FHD. To test this hypothesis, the effects of a potent anti-resorptive agent, ibandronate, was investigated in a well-established animal model of Legg-Perthes disease. The study was approved by the local institutional animal care and use committee. Ischemic osteonecrosis of the femoral head was produced in 24 piglets by surgically placing a ligature tightly around the femoral neck. Animals were divided into 3 groups; saline, prophylactic ibandronate treatment, and post-ischemia ibandronate treatment groups. At 8 weeks, the femoral heads were assessed for deformity using radiography and for trabecular bone indices (trabecular bone volume, trabecular number, and trabecular separation) using histomorphometry. Radiographic assessment showed that the saline group had the greatest deformity. The epiphyseal quotient, a ratio of the maximal femoral head height over diameter, was lowest in the saline group. The epiphyseal quotient was significantly better preserved in the prophylactic ($p<0.001$) and the post-ischemia ibandronate treatment ($p=0.02$) groups compared to the saline group. Histomorphometric assessment also showed that the trabecular bone indices were significantly better preserved in the prophylactic and the post-ischemia ibandronate treatment groups compared to the saline group ($p<0.01$). The total number of osteoclast per tissue area was significantly higher in the saline group compared to the ibandronate treatment groups. In conclusion, ibandronate preserves the trabecular framework and minimizes FHD during the study period in the piglet model. The results support the hypothesis that therapeutic strategies to inhibit bone resorption in the early phase of Legg-Perthes disease will prevent the development of FHD.

Disclosures: ***H.K.W. Kim****, Roche 2.*

SU522

Ilial Histomorphometry in Children with Osteoporosis Secondary to Chronic Illness. L. M. Ward[1], F. T. Rauch[2], C. A. White*[1], F. H. Glorieux[2]. [1]Pediatrics, University of Ottawa, Ottawa, ON, Canada, [2]Pediatrics, McGill University, Montreal, PQ, Canada.

Osteoporosis is a potentially debilitating consequence of chronic illness among children and adolescents. In this study we characterized the bone tissue abnormalities of 16 children with symptomatic secondary osteoporosis. The study population comprised 8 patients with steroid-induced osteoporosis (S-O; mean age 13.3 yrs, range 7.4 to 17.6; 4 girls), and 8 patients with osteoporosis secondary to neuromuscular disorders (NM-O; mean age 13.8 yrs, range 10.2 to 17.3; 7 girls). Fracture distribution varied with diagnosis. Atraumatic lower limb fractures had occurred in 7 patients with NM-O, but in only 1 S-O patient, whereas vertebral compression fractures were present in 7 patients with S-O and only in 2 patients with NM-O. The age- and sex-matched z-score for volumetric bone mineral density of the lumbar spine averaged -1.8 (range -3.0 to 0.0) in the S-O group and -2.9 (range -5.0 to -1.9) in patients with NM-O. Results of iliac bone histomorphometry are given below as the median of the raw value for each parameter and as the percentage of the age-specific healthy average result.

	S-O	NM-O
Structural		
Core Width (mm)	6.8 (79%)	4.5 (56%)
Cortical Width (μm)	618.0 (62%)	598.0 (59%)
Bone Volume per Tissue Volume (%)	17.9 (70%)	14.1 (57%)
Formation		
Osteoid Thickness (μm)	4.5 (68%)	5.1 (79%)
Osteoid Surface per Bone Surface (%)	12.0(60%)	13.0 (53%)
Mineralizing Surface per Bone Surface (%)	8.7 (74%)	6.4 (64%)
Mineral Apposition Rate (μm/d)	0.9 (94%)	0.8 (93%)
Resorption		
Osteoclast Surface per Bone Surface (%)	0.5 (44%)	0.9 (78%)

These observations highlight the potential severity of osteoporosis in childhood due to steroid use and neuromuscular disorders. The bone mass deficit in S-O and NM-O is due to a combination of small bone size, thin cortices and a low amount of trabecular bone. Bone turnover tends to be low in both types of secondary osteoporosis.

Disclosures: ***L.M. Ward****, None.*

SU523

The Effects of Type 1 Diabetes on the Metabolism and Density of Bone in Korean Children. K. Won[1], H. Lee*[1], H. Shon*[2], H. Yoon*[2], E. Jung*[3], I. Lee*[3]. [1]Internal Medicine, Yeungnam University, Daegu, Republic of Korea, [2]Internal Medicine, Catholic University of Daegu, Daegu, Republic of Korea, [3]Internal Medicine, Keimyung University, Daegu, Republic of Korea.

Background: The effects of type 1 diabetes mellitus on the metabolism and density of bone in children are still controversial. The aim of this study was to evaluate the effects of type 1 diabetes on markers of bone metaboism and BMD in children by analyzing BMI, HbAlc, biochemical markers, sex hormones, bone metabolism and BMD related factors. Methods: We compared 36 patients (15 males, 21 females) with type l diabetes mellitus to 167 healthy children (84 males, 83 females) who lived in South Korea. We measured FBS, serum calcium, phosphorus, HbAlc, osteocalcin, testosterone and estradiol for analyzing the factors which influence on bone metabolism and BMD. BMD was measured at lumbar spine, femur and total body by DEXA. Results: The BMI and serum level of osteocalcin were not different in both groups. Serum calcium level was significantly lower in the diabetic group than that of control group. BMD had no difference in both groups. There was no correlation between BMD and glycemic control (HbAlc) or duration of diabetes. There was good correlation (r=0.78, p<0.01) between serum testosterone level and BMD in male patient group. There was negative correlation (r=-0.4) between serum osteocalcin level and BMD. There was significant correlation (male: r=0.76, female: r=0.66) between lean body mass and BMD in both group. Conclusion: The BMD was not decreased significantly and bone turn-over was normal in children with noncomplicated type 1 diabetes mellitus, and BMD was not influenced by the duration or degree of metabolic control of diabetes. But, we need further study including other risk factors that have influences on BMD and bone metabolism in Korean type 1 diabetes mellitus.

Disclosures: ***K. Won****, None.*

SU524

Effect of Vitamin D and Calcium on Percent True Calcium Absorption and Bone Mineralization in Children with Cystic Fibrosis. L. S. Hillman[1], J. D. Robertson*[2], B. J. Higgins*[2], F. Chanetsa*[1], M. F. Popescu*[1]. [1]Child Health, U. of Mo., Columbia, MO, USA, [2]Chemistry, Mo Research Reactor, U. of Mo., Columbia, MO, USA.

Bone mineralization is documented to be reduced in children with Cystic Fibrosis (CF). Because of the known fat malabsorption in CF there is concern that both calcium and vitamin D absorption may be decreased but supporting data is limited.This study was designed to assess the effects of supplemental calcium and vitamin D on calcium absorption and bone mineralization in children with CF. The study was approved by the U.of Mo. Health Sciences IRB. Eighteen children age 9.1±2.3 years with CF not treated with steroids were randomized to four sequences of treatments with each child getting all four treatments: P, 400 IU vitamin D and placebo calcium; Ca, 400 IU vitamin D plus 1gm calcium; D, 2000 IU vitamin D and placebo calcium and D+Ca, 2000 IU vitamin D plus 1gm calcium. Each treatment lasted 6 months followed by a 3 month washout period. Biochemical assays at 6 months and DEXA measurements (Hologic QDR 1000) at 9 months (period plus washout) were analyzed for significant change from period baseline. Calcium absorption was measured at 6 months by a dual stable isotope method using IV ^{48}Ca and PO ^{46}Ca measured in a 24 hr urine referenced to ^{42}Ca by HR-ICP-MS. The Kruskal-Wallis Test saw no order effect so all results for each treatment were combined. Serum and urine Ca, Mg, and P were unchanged by any treatment with mean serum Ca (9.0±0.3 mg/dl) remaining below normal values (10.1±0.6 mg/dl). 2000 IU of vitamin D did not increase 25-OHD or 1,25$(OH)_2$D over the study period and there were no differences in 25-OHD or 1,25-(OH)2D between treatments in this vitamin D sufficient population (study baseline 25-OHD 38±13 ng/ml, 1,25$(OH)_2$D 49±10 pg/ml). BMC and BMD of the whole body, hip, spine, and arm significantly increased with age but there were no differences between treatments. Bone markers were unchanged and not different by treatment. Calcium absorption was within the normal range for prepubertal and early pubertal children. There were no differences in percent true calcium absorption by treatment: P, 37±14%; Ca, 38±23%; D, 36±11%; Ca+D, 46±26%. We conclude that percent true calcium absorption is normal in children with CF and not significantly altered by 1gm calcium and/or 2000 IU vitamin D. Oral absorption of vitamin D may be reduced due to fat malabsorption in children with CF and, in children who are already vitamin D sufficient, 2000 IU/day does not increase serum 25-OHD , serum calcium, BMC, or markers of bone turnover. Studies using higher doses of vitamin D are warranted in this population. However, factors other than calcium and vitamin D may play major roles in the decreased mineralization seen in children with CF.

Disclosures: ***L.S. Hillman****, None.*

SU525

Osteopenia in Children With Inflammatory Bowel Disease Is Due to Persistent Decrease in Bone Formation. F. A. Sylvester[1], J. S. Hyams*[1], P. M. Davis*[1], N. Wyzga*[1], T. Lerer*[2], A. M. Griffiths*[3]. [1]Digestive Diseases & Nutrition, Connecticut Children's Medical Center, Hartford, CT, USA, [2]Research, Connecticut Children's Medical Center, Hartford, CT, USA, [3]Gastroenterology & Nutrition, The Hospital for Sick Children, University of Toronto, Toronto, ON, Canada.

Decreased BMD has been reported in patients with inflammatory bowel disease (IBD) due to increased bone resorption, but most studies examined corticosteroid-treated patients years after diagnosis and who may also have had age-related or post-menopausal bone loss. We hypothesized that children with IBD have decreased BMD secondary to decreased bone formation. Furthermore, we proposed that bone remodeling becomes activate in response to clinical improvement, with rapid accrual of bone calcium. To examine these questions, a 2-year prospective observational study was conducted in newly diagnosed children with IBD. We measured BMD in total body and lumbar spine by DXA, serum 25-hydroxyvitamin D (vit D), intact parathyroid hormone, interleukin (IL)-6, insulin growth factor (IGF)-1, sex steroids, and serum and urinary parameters of bone remodeling. BMD was performed yearly and laboratory evaluation every 6 months. BMD comparisons were adjusted for height-age and bone age in growth-retarded children. Disease severity was estimated using standard clinical scores. The control group consisted of age- and sex-matched healthy children from the same community. We studied 59 children with Crohn disease (CD) (20 F), 18 with ulcerative colitis (UC) (7 F), and 52 controls (CL) (23 F). Children with IBD had moderate-to-severe disease activity at diagnosis, and improved significantly with treatment. Age at diagnosis was (means ± SD, in yr), CD 12.8 ± 2.7, UC 11.8 ± 2.5, and CL 12.8 ± 2.7. Tanner stage and serum sex steroids were consistent with early puberty in all groups. BMD spine Z-score at diagnosis was -0.80 ± 1.02, -0.24 ± 1.14, -0.13 ± 1.12, respectively ($p < 0.01$, CD vs. CL); 10 CD children had Z-scores <-2. Patients with IBD exhibited low bone turnover at diagnosis that partially recovered with clinical improvement. However, Z-scores were stable over the course of the study. Calcium accretion by bone was lower than normal in IBD. At baseline, serum IL-6, IGF-1, vit D, and body mass index were significantly different in children with CD compared to CL, but no single parameter predicted decreased mineralization. We conclude that decreased BMD is common in newly diagnosed children with IBD, especially in the lumbar spine of CD children, and is probably due to decreased bone formation. Although clinical improvement is associated with increased bone remodeling, calcium incorporation into bone is slower than in healthy children up to 2 years after diagnosis.

Disclosures: ***F.A. Sylvester****, None.*

SU526

SHP-2 Mutations in Noonan Syndrome Lead to Increased MAPK Activation: A Possible Mechanism of Short Stature. N. Namba[1], E. Ogura*[2], K. Ozono[1], Y. Seino[3], H. Tanaka[2]. [1]Pediatrics, Osaka University Graduate School of Medicine, Suita, Osaka, Japan, [2]Pediatrics, Okayama University Graduate School of Medicine and Dentistry, Okayama, Japan, [3]Pediatrics, Osaka Koseinenkin Hospital, Osaka, Japan.

Noonan syndrome (NS) is an autosomal dominant disorder characterized by unusual facial features, proportionate short stature, skeletal anomalies, and congenital heart defects. Though the molecular basis of this disease has been elusive, Tartaglia and coworkers have recently identified mutations in the PTPN11 gene, which encodes the protein tyrosine phosphatase SHP-2, in about 50% of the patients. Mutations have also been identified in LEOPARD syndrome and juvenile myelomonocytic leukemia (JMML).

SHP-2 is a ubiquitously expressed protein composed of two tandemly arranged SH2 domains at the amino-terminus (N-SH2 and C-SH2) followed by a protein tyrosine phosphatase (PTP) domain. Most of the known mutations cluster in the interacting portions of the N-SH2 domain and the PTP domain and are postulated as gain-of-function changes. Previous studies have also shown that SHP-2 is required for activation of the Ras/Erk cascade. However, despite intensive study, the underlying molecular mechanisms are not completely understood.

Since MAPK has been shown to influence chondrocyte proliferation and differentiation, we evaluated phosphatase activity, intracellular distribution, and EGF induced MAPK activity in SHP-2 mutants found in NS patients. COS-1 cells were transfected with wild type (WT) or mutated FLAG-tagged SHP-2. Cell lysates were subsequently immunoprecipitated and tested for phosphatase activity using phosphorylated poly(Glu, Tyr) random peptides as substrate. N58K SHP-2 exhibited a 3.2-fold increase in phosphatase activity compared to WT SHP-2, which was comparable to that of E76K, a mutation commonly found in JMML. In contrast, P491T SHP-2 had less phosphatase activity than that of WT SHP-2. This coincided with the observation that N58K and E76K were partially membrane associated while WT and P491T were distributed in the cytosol. However, when the cells were stimulated with EGF, both NS mutations and E76K displayed increased Erk1/2 activation compared to WT.

In conclusion, NS mutants show increased MAPK activation in response to EGF stimulation, while basal phosphatase activity is not necessarily elevated. Increased MAPK activation in chondrocytes could lead to the skeletal anomalies and short stature seen in NS.

Disclosures: ***N. Namba****, Novo Nordisk 2.*

SU527

Increased Early Resorption Activity and Alterations of Morphology in Osteoclasts Derived from the oim/oim Mouse Model of Osteogenesis Imperfecta (OI). H. Zhang[1], C. Hughes[2], C. Raggio*[1], D. W. Dempster[2], N. P. Camacho[1]. [1]Research Division, Hospital for Special Surgery, New York, NY, USA, [2]Regional Bone Center, Helen Hayes Hospital, West Haverstraw, NY, USA.

Histologic and histomorphometric studies have established that patients with the collagen-based disease osteogenesis imperfecta (OI) have increased bone turnover, which may be linked to abnormal osteoclast activity. To date, there have been no studies on isolated osteoclasts from either OI patients or animal models of OI. The goal of the current study is to determine if there are alterations in osteoclasts derived from oim/oim mice, an established animal model of moderate-to severe OI. Bone marrow cells from oim/oim and +/+ mice were cultured on bovine bone slices in the presence of macrophage colony-stimulating factor (M-CSF, 20ng/ml) and (RANKL, 60ng/ml), and studied at days 1, 4, and 7 of culture. Tartrate-resistant acid phosphatase (TRAP) staining was used to identify multinucleated osteoclast-like cells (MNCs). Confocal microscopy was used to evaluate formation of resorption pits and to study the cytoskeletal organization with fluorescein-labeled phalloidin staining for F-actin and Topro-3 staining for nuclei. At day 1 culture, only mononuclear cells were present on the bone slices, but the oim/oim slices had a greater percentage of those cells associated with resorption pits compared to +/+ bone slices (43.4$\pm$6.0 % vs 21.9$\pm$11.0%, $p<0.05$). Although a similar number of TRAP positive MNCs were present on both oim/oim and +/+ bone slices at days 4 and 7, the oim/oim MNCs had obvious cytoskeletal differences compared to the +/+ MNCs. The overall diameter and area of the oim/oim MNCs were larger compared to the +/+ MNCs (87.3$\pm$ 9.4 nm vs 61.8$\pm$7.4 nm, $p<0.05$, and 4399.0$\pm$558.6 nm^2 vs 2262.8 $\pm$ 746.1 nm^2, $p<0.05$). In addition, the number of nuclei per MNC were greater for the oim/oim vs +/+ derived cells (21.9 $\pm$3.0 vs 6.64 $\pm$ 1.57, $p<0.01$). Overall, this study demonstrates that there is an increase of early resorption activity in the oim/oim-derived osteoclasts, and that they are also morphologically different from wildtype osteoclasts in this in vitro culture system. These findings may yield insight into the basis of the increased bone turnover in OI patients and animal models of OI.

Disclosures: ***H. Zhang****, None.*

SU528

Bisphosphonate Binding in the Infarcted Piglet Femoral Head. T. S. Randall*[1], M. V. Sanders*[1], H. Bian[1], A. H. Garces*[1], F. Bauss[2], H. K. W. Kim[1]. [1]Shriners Hospitals for Children, Tampa, FL, USA, [2]Roche Diagnostics GmbH, Penzberg, Germany.

Recent studies have shown that bisphosphonate (BP) therapy may prevent the development of femoral head deformity following osteonecrosis by inhibiting bone loss during repair. These studies raise questions regarding the most appropriate time for commencement of BP treatment, and also regarding the delivery and distribution of systemically administered BPs into the infarcted femoral head. The purpose of this study was to investigate the optimal time to begin BP treatment following the induction of osteonecrosis and also the distribution of BP within the femoral head as it undergoes repair.

Sixteen piglets had ischemic necrosis surgically induced. One, 3 and 6 wks following the induction surgery the animals were injected with 14C labeled ibandronate. The animals were euthanatized 24 hrs after the injection and the level of radioactivity in the infarcted femoral heads was assayed by liquid scintillation. Autoradiographic assessment was performed on undecalcified sections to determine the distribution of ibandronate in the infarcted head in relation to the areas of revascularization and repair.

One-wk post surgery, the level of radioactivity was not increased above background in the infarcted femoral head either by liquid scintillation or by autoradiography. There was also no evidence of revascularization. In contrast, 6 wks following the induction of ischemia the level of radioactivity was significantly increased above background ($p<0.01$). Autoradiographic assessment of the infarcted femoral heads revealed a strong level of binding in areas with renewed bone growth. Within the areas of revascularization, ibandronate was bound to the necrotic bone, although not as heavily as on live bone. Areas of the head that were not revascularized at six weeks showed increased ibandronate binding compared to back ground, but less than was seen in revascularized areas. All femoral heads showed large areas of revascularization, with the presence of fibrovascular tissue and resorption of trabecular bone. Renewed endochondral ossification was also observed.

The findings from this study indicate that the most appropriate time to start BP treatment following osteonecrosis is when revascularization has begun in the infarcted head. Given this finding a bone scan or a perfusion MRI scan may be indicated to confirm blood flow, prior to initiating BP therapy in patients with osteonecrosis of the femoral head.

Disclosures: ***T.S. Randall****, None.*

SU529

Altered Bone Mineral Metabolism in Children at Time of Diagnosis of Inflammatory Bowel Disease. M. Harpavat*[1], D. J. Keljo*[1], D. Bowen*[2], S. L. Greenspan[3]. [1]Pediatrics, University of Pittsburgh, Pittsburgh, PA, USA, [2]Radiology, University of Pittsburgh, Pittsburgh, PA, USA, [3]Medicine, University of Pittsburgh, Pittsburgh, PA, USA.

Recent studies suggested that bone mineral metabolism is altered in children with Inflammatory Bowel Disease (IBD). The cause of these alterations is unclear, but often attributed to corticosteroid use. The purpose of this study was to examine biochemical markers of bone turnover in a cohort of children newly diagnosed with IBD before initiation of steroid therapy.

We studied 23 otherwise healthy, corticosteroid-naive children within 3 weeks of initiation of therapy for IBD. We assessed serum aminoterminal propeptide of type I collagen [(P1NP) a marker of bone formation] and urine N-telopeptide crosslinked collagen type 1 [(NTx) a marker of bone resorption]. Bone mineral content (BMC) and bone mineral density (BMD) were obtained by Dual Energy X-ray Absorptiometry (DXA, Lunar DPX-L). Z-scores were calculated based on age and gender. Data analysis was performed by Mann Whitney U and Spearman rank-order correlation.

Of the 23 newly diagnosed children (12 girls, 11 boys), 18 had Crohn's disease, 4 had ulcerative colitis, and 1 had indeterminate colitis. Mean age at diagnosis was 12.5 years with a range of 5.5 to 16.8 years. Five of the 23 patients (22%) had a total body BMD Z-score of less than -1, with 1 patient having a Z-score of less than -2. Twelve (52%) subjects had vertebral BMD Z-scores of less than -1, with 3 children having Z-scores of less than -2. IBD patients had significantly reduced mean lumbar spine BMD Z-scores (-0.90 ± 1.1, $p=0.001$). IBD patients also had significantly reduced mean serum P1NP Z-scores (-1.8 ± 1.2; $p=0.0006$). Mean urine NTx Z-scores were not altered. Correlation coefficients between P1NP Z-scores and DXA measurements ranged from 0.49-0.72 (see Table, *all $p<0.05$).

We conclude that children newly diagnosed with IBD have significantly reduced vertebral BMD and decreased bone formation, as reflected by significantly low P1NP Z-scores. P1NP Z-scores correlate positively with BMC and BMD. Bone resorption, as reflected by normal urine NTx Z-scores, does not appear to be altered. Low bone formation with normal bone resorption may explain alterations in bone mineral metabolism in steroid naïve children newly diagnosed with IBD.

Correlation Between BMD and BMC with P1NP Z Scores

DXA	P1NP
Whole body BMC (g)	0.63*
Whole body BMD (g/cm^2)	0.54*
Femoral neck BMC (g)	0.49*
Femoral neck BMD (g/cm^2)	0.51*
Trochanter BMC (g)	0.59*
Lumbar spine BMC (g)	0.70*
Lumbar spine BMD (g/cm^2)	0.72*

Disclosures: ***S.L. Greenspan****, None.*

SU530

A Phase 1, Single-Dose Study of ABX10241, a Fully Human Monoclonal Antibody to Parathyroid Hormone Secondary Hyperparathyroidism (SHPT) Patients. G. M. Bell*[1], S. Swan*[2], K. J. Martin[3], T. Shamp*[2], W. B. Smith*[4], M. Sack*[5], R. H. Arends*[1], M. R. Wyres*[1], L. Roskos*[1], A. Young*[2], N. Raie*[1], S. Huang*[1], D. Shoback[6]. [1]Abgenix, Inc., Fremont, CA, USA, [2]Hennepin County Medical Center and DaVita Clinical Research, Minneapolis, MN, USA, [3]Saint Louis University, St. Louis, MO, USA, [4]New Orleans Center for Clinical Research, New Orleans, LA, USA, [5]Radiant Research, Austin, TX, USA, [6]Endocrine Research Unit, VAMC, University of California - San Francisco, San Francisco, CA, USA.

ABX10241 is a high affinity monoclonal antibody directed against the 1-34 region of human parathyroid hormone (PTH). ABX10241 is specific for human and non-human primate PTH. In primate and rodent models of hyperparathyroidism induced by continuous administration of PTH, ABX10241 reverses the metabolic consequences of hyperparathyroidism in a dose-dependent manner. In the primate model, a single 4 mg/kg dose of ABX10241 produced a sustained reduction in plasma unbound PTH (non-antibody complexed PTH measured with the Nichols Intact Assay) and normalized serum Ca for up to two weeks relative to control animals. On the basis of these results, a randomized, double-blind, single-dose, dose-escalation study in hemodialysis patients with SHPT was initiated. Eligibility criteria include plasma PTH > 300 pg/mL (Nichols Intact Assay), serum corrected Ca $\geq$9 mg/dL, and a Kt/V $\geq$ 1.2. Vitamin D or vitamin D analogs, oral phosphate binders, and cinacalcet were permitted provided the doses were stable for at least 2 weeks prior to treatment. Planned dose cohorts include 30, 100, 200, and 300 mg of ABX10241; the starting dose of 30 mg was less than the no-effect level in preclinical studies. Within each cohort subjects are randomized 3:1 to ABX10241 or placebo. ABX10241 is administered by IV push after hemodialysis and patients are monitored in a Phase 1 unit for 3 days post treatment. Four patients were randomized in the 30 mg dose cohort. Mean baseline PTH was 442 pg/ml (range 319 - 632 pg/ml). Twenty-four hours post-dose the mean reduction in plasma unbound PTH was 45% in the ABX10241-treated group compared with a 12% reduction following placebo treatment. Consistent with the decrease in PTH, the ABX10241-treated group had an average 6.9% reduction in iCa compared with 0% change following placebo treatment 24 hours post-treatment. Both PTH and iCa returned to baseline within 72 hours post treatment. The transient (< 72 hour) PTH suppression following the 30 mg dose was consistent with in silico modeling simulations that predict higher doses of ABX10241 may suppress PTH to within the desired normal uremic range (100- 250 pg/ml) for up to 7 days after a single dose. Based on the safety of the 30 mg cohort, higher dose levels will be explored and reported.

Disclosures: ***M.R. Wyres****, None.*

SU531

OPG, RANK-L, Bone Metabolism and BMD in Patients on Haemodialysis and Continuous Ambulatory Peritoneal Dialysis. E. Wittersheim*[1], M. Mesquita*[2], A. Demulder[1], M. Guns*[1], O. Louis*[3], M. Dratwa*[2], P. Bergmann[4]. [1]Laboratory of Haematology, Brugmann University Hospital, Brussels, Belgium, [2]Nephrology Departement, Brugmann University Hospital, Brussels, Belgium, [3]Departement of Radiology, Brugmann University Hospital, Brussels, Belgium, [4]Laboratory of Experimental Medicine, Brugmann University Hospital, Brussels, Belgium.

Patients with end-stage renal failure (ESRF) on dialysis develop hyperparathyroid bone disease; PTH acts on bone resorption through the cytokines osteoprotegerin (OPG) and Receptor Activator of Nuclear κB-Ligand (RANK-L).

We evaluated serum OPG and RANK-L in 79 patients with ESRF undergoing hemodialysis (HD, n=58) or continuous ambulatory peritoneal dialysis (CAPD, n=21) and assessed their relation with hyperparathyroidism (circulating iPTH), bone turnover rate (βCrossLaps, CL, and the carboxyterminal extension peptide of type I procollagen, PICP), bone densitometry (BMD, Hologic QDR 4500) and hand radiography. A group of 65 healthy subjects matched for sex and age was used as control. Bone densitometry was performed at the lumbar spine, left and right hip and right forearm. An X-ray of the right hand was obtained.

In our control group, there was no sex difference for OPG nor RANK-L; OPG increased slightly with age, significantly for men; RANK-L and the RANK-L/OPG ratio did not change with age.

OPG and RANK-L were higher in patients with ESRF than in controls (3.7 vs 1.8 ng/ml, and 1.2 vs 0.14 pg/ml respectively), particularly in the HD group than in controls ($p<0.001$ and <0.05); RANK-L was higher in HD than in CAPD ($p<0.001$). None of the parameters varied with the duration of dialysis. OPG levels were higher in women undergoing HD ($p<0.001$) and increased significantly with age ($p<0.0001$), particularly in men. RANK-L and the ratio RANK-L/OPG did not change with age nor sex. Nor OPG neither RANK-L depended on iPTH levels. Serum CL and PICP were significantly higher in ESRF than in controls ($p<0.001$), but they did not correlate with OPG, RANK-L or RANK-L/OPG ratio. BMD did not differ significantly between HD and CAPD; as opposed to PTH and CL, nor OPG neither RANK-L correlated significantly with BMD. OPG was significantly higher in patients with cortical demineralization at X-Ray (3.0 vs 4.3 ng/ml); CL was lower in patients with calcifications (3.1 vs 3.9 ng/ml). Conclusions: 1) PICP and CL are significantly increased in ESRF and BMD is low. 2) BMD correlates negatively with serum iPTH and CL. 3) Serum OPG increases with age in control and ESRF subjects. OPG and RANK-L serum levels are significantly higher in ESRF. 4) Serum OPG, RANK-L or RANK-L/OPG ratio do not correlate with serum iPTH levels nor BMD. Thus, circulating OPG and RANK-L do not reflect bone status in ESRF.

Disclosures: ***E. Wittersheim****, None.*

SU532

Osteoprotegerin Is a Bone Protective Agent in a Rat Model of Chronic Renal Insufficiency and Hyperparathyroidism. V. Shalhoub, J. Padagas*, M. Colloton*, E. Shatzen*, S. Morony, P. Kostenuik, C. R. Dunstan, D. L. Lacey, D. Martin. Department of Metabolic Disorders, Amgen, Inc., Thousand Oaks, CA, USA.

Osteoprotegerin (OPG) is a novel antiresorptive agent that plays a critical role in the physiological regulation of bone resorption. OPG acts by neutralizing RANKL, the dominant mediator of osteoclast differentiation, activation and survival. OPG is non-toxic to kidney cells, and may thus represent a novel and safe approach to treating bone loss in patients with renal insufficiency. Renal insufficiency is also associated with hyperparathyroidism, which leads to significant cortical osteopenia. OPG effectively blocks the catabolic effects of PTH, so we examined whether OPG could prevent or reverse bone loss in a rodent model of secondary HPT. Secondary HPT was induced in young growing male SD rats (250-275 g) by performing 5/6 nephrectomy (Nx). One week post-surgery, sham and Nx rats (n=6-10) were fed a 1.2% P/ 0.6% Ca^{2+} diet, and treated with vehicle or OPG (3 mg/kg, IV), every 2 weeks for 9 weeks. Prior to treatment (baseline) and at 3, 6 and 9 weeks, BMD was assessed by DEXA and blood was taken for PTH and ionized calcium levels. Nx resulted in dramatic increases in serum PTH at all timepoints, reaching a maximum of 912 pg/ml at 9 weeks (vs. 123 pg/ml in shams at 9 weeks). Nx rats also had significant osteopenia at all skeletal sites compared to shams. Treatment of either Nx or sham rats with OPG-Fc caused rapid and progressive increases in BMD at all skeletal sites. At the earliest timepoint (3 weeks), the mean percent changes from baseline (±SEM) in Nx OPG compared with Nx vehicle are shown in the table below. OPG had no significant effect on serum PTH or blood ionized calcium levels in Nx or sham animals. Histologically, OPG augmented the thickness of trabeculae in both Nx and shams at 9 weeks in the primary spongiosa of the distal femur and/or proximal tibia. This study demonstrates that the RANKL antagonist OPG effectively restores BMD in a rat model of HPT and chronic renal insufficiency. The data also confirm that OPG is capable of blocking the catabolic effects of PTH on cortical and cancellous bone, even when PTH is continuously elevated for sustained periods. This suggests that RANKL may be an important therapeutic target for protecting bone in patients with HPT and/or chronic renal insufficiency.

	Veh Nx	SEM	OPG Nx	SEM
wbBMC	7.3	1.2	15.7	2.3
wbBMD	-1.7	0.9	6.0	1.1
legBMD	0.8	1.4	9.3	1.1
femBMD	-2.2	1.6	9.0	1.3
lumBMD	-4.8	1.9	8.5	1.5
L3BMD	0.2	2.5	11.3	2.8

Disclosures: ***V. Shalhoub****, Amgen Inc 3.*

SU533

PTH-Stimulated Signaling Molecules that Are Involved in the Endocytosis of NaPi-IIa Phosphate Transporter Are Compartmentalized and Activated in Caveolae-Like Microdomains. Y. Taketani, T. Takeichi*, K. Nashiki*, H. Yamamoto, N. Sawada*, M. Ichikawa*, H. Arai*, E. Takeda. Department of Clinical Nutrition, Institute of Health Biosciences, University of Tokushima Graduate School, Tokushima, Japan.

Phosphate homeostasis is maintained by regulating the renal type IIa sodium-dependent phosphate transporter (NaPi-IIa). Parathyroid hormone (PTH) is a potent inhibitor of NaPi-IIa activity by leading endocytosis from brash border membrane of renal proximal tubular cells. We have demonstrated caveolae-like microdomains (CM) and actin play an important role in the apical targeting and regulation of NaPi-IIa endocytosis in response to PTH, though their precise role has not been clarified. To clarify the role of CM in the translocational regulation of NaPi-IIa by PTH, we investigated the effect of PTH on the activation of PKA and PKC and their substrate phosphorylation in biochemically isolated CM fraction from opossum kidney cells. PTH activated both PKA and PKC-alpha in CM through PTH receptor also localized in CM. Inactive PKA is widely distributed in the cells, but was only strongly activated in CM by PTH. On the other hand, inactive PKC-alpha is localized in cytosol, and was translocate to CM in response to PTH. Both PKA and PKC activation increased the phosphorylation of 80 kDa and 250 kDa substrates observed by anti-phospho-PKA or PKC substrate antibody. Resulted from protein sequence analyses, 80 kDa substrate was identified as ezrin that is a ERM (ezrin-radixin-moesin) family protein, and is a linker protein between brash border membrane and actin cytoskeleton. Previous studies demonstrated that NaPi-IIa can bind to NHERF-1/EBP-50 that associates with ezrin-actin complex, and this interaction is necessary for apical targeting of NaPi-IIa in proximal tubular cells. Ezrin is also phosphorylated by many protein kinases to interact with target proteins. This study suggests that ezrin can be phosphorylated by PKA or/and PKC in response to PTH in proximal tubular cells, and the phosphoryation would also play an important role in the actin-dependent NaPi-IIa endocytosis, probably that may be involved in reorganization of actin directly or indirectly. CM appear to be important for the regulation of NaPi-IIa endocytosis in proximal tubular cells by compartmentalizing signal transduction and cytoskeletal molecules.

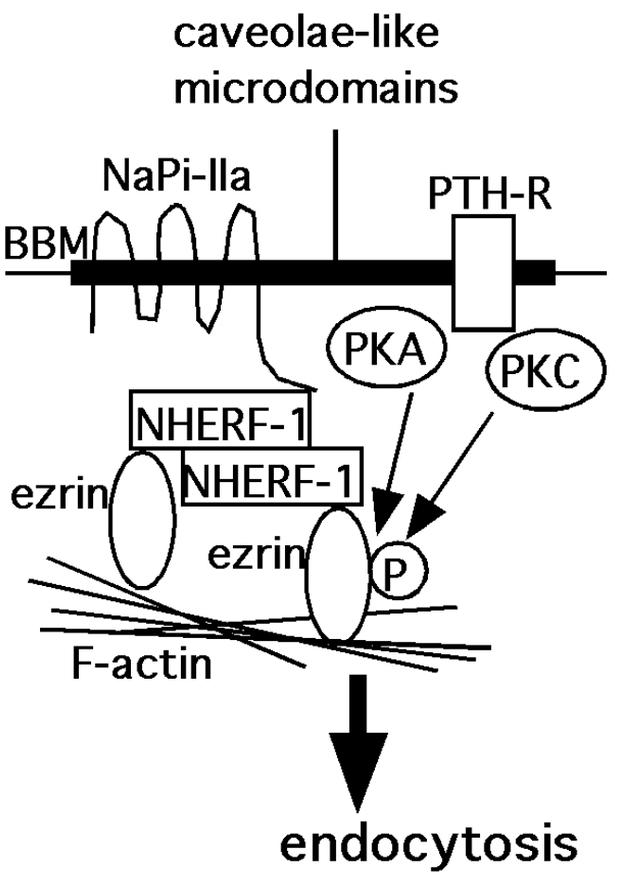

Disclosures: ***Y. Taketani****, None.*

SU534

Impact of Parathyroidectomy for Renal Hyperparathyroidism on the Endocortical Surface, the Juxtaendocortical Resorption Spaces and Cancellous Bone. A. Yajima[1], Y. Ogawa*[2], Y. Tominaga*[3], T. Tominaga*[4], T. Inou*[1], O. Otsubo*[1], S. Yagi*[1]. [1]Nephrology, Towa Hospital, Tokyo, Japan, [2]Urology, University of the Ryukyus, Naha, Japan, [3]Surgery, Nagoya Second Red Cross Hospital, Nagoya, Japan, [4]Urology, Mitsui Memorial Hospital, Tokyo, Japan.

Purpose: Impact of parathyroidectomy (PTX) for renal hyperparathyroidism on the endocortical surface (A), and the juxtaendocortical resorption spaces (B) were compared with that on cancellous bone (C). Methods: Iliac bone biopsies were performed before and at 1 week after PTX in Group 1 (n=13), and before and at 4 week in Group 2 (n=10). Oc.S/BS and O.Th were measured in both Groups before and after PTX, and BFR/BS was also measured in Group 2 only after surgery Results: Group 1; Oc.S/BS significantly decreased after PTX in (A)-(C), but that in (B) was higher than that in (C) after surgery; 1.2 ± 1.3 vs 0.1 ± 0.5 % ($p<0.05$). Ob.S/BS increased from 18.1 ± 17.1 to 35.6 ± 20.8 % ($p<0.001$) in (C). O.Th increased from 13.4 ± 3.5 to 17.6 ± 6.0 µm ($p<0.005$) in (C), but these two values in (A) and (B) did not. Group 2; Oc.S/BS decreased to 0 after PTX in (C), but to 0.1 ± 0.2 in (A) and 0.9 ± 1.8 % in (B). BFR/BS in (B) tended to be higher than that in (C); 0.012 ± 0.0018 vs 0.003 ± 0.005 mm^3/mm^2/year ($p=0.06$).Conclusion: An increase in BMD of cortical bone was estimated to be smaller than that of cancellous bone because bone turnover was higher in cortical bone even after PTX.

Disclosures: ***A. Yajima****, None.*

SU535

Disassociation of the Anabolic, Catabolic and Fibrotic Response to Parathyroid Hormone. R. T. Turner, S. Lotinun. Orthopedic Research, Mayo Clinic, Rochester, MN, USA.

Intermittent increases in parathyroid hormone (iPTH) are highly anabolic in regards to bone formation, whereas continuous increases (cPTH) are generally considered to be catabolic. We tested this latter belief by performing detailed time course (1-7d) studies in which the effects of PTH administered continuously (40 µg/kg/d) using a s.c. implanted osmotic pump were compared to hormone given by daily s.c. injection. PTH induced impressive increases in osteoblast number and mRNA levels for bone matrix proteins. The response to the two treatments were virtually identical indicating that the method of PTH administration had little effect on the measured osteoblast parameters. However, iPTH resulted in an ~2 fold increase in osteoclast number with no change in serum calcium and no bone marrow fibrosis while cPTH resulted in an ~8 fold increase in osteoclast number, severe hypercalcemia and extensive peritrabecular fibrosis (~70% of trabecular surface covered by fibroblasts), changes similar to osteitis fibrosa seen in patients with parathyroid bone disease. These findings suggest that the effects of PTH on osteoblasts are mediated by signaling pathways that differ from the catabolic and fibrotic responses and that these differences are partially (bone resorption) or fully (fibrotic) disassociated by reducing the duration of exposure to elevated PTH levels. Over expression of platelet derived growth factor-A by mast cells has been implicated as having a causal role in the development of parathyroid bone disease. In this regard, cPTH treatment of mast cell deficient W/Wv mice increased bone formation but did not cause hypercalcemia, increase osteoclast number or induce peritrabecular bone marrow fibrosis. The importance of PDGF-A signaling is supported by additional studies in which we demonstrated that antagonism of receptor tyrosine kinase activity with gleevec greatly reduced peritrabecular bone marrow fibrosis in cPTH-treated rats but did not diminish the bone anabolic response to the hormone. Taken together, these results suggest that PDGF-A signaling mediates PTH-induced bone marrow fibrosis but not the PTH-induced increase in osteoblast number and activity.

Disclosures: ***R.T. Turner****, None.*

SU536

Most Renal Transplant Patients have Primary or Active Secondary Hyperparathyroidism. A. Räkel*[1], J. H. Brossard[1], L. Rousseau*[1], G. St-Louis*[2], M. Pâquet*[2], T. Cantor[3], P. D'Amour[1]. [1]Hôpital Saint-Luc, Centre de recherche du CHUM, Montreal, PQ, Canada, [2]Hôpital Notre-Dame, Centre de recherche du CHUM, Montreal, PQ, Canada, [3]Scantibodies Laboratory Inc., Santee, CA, USA.

Carboxyl-terminal PTH/Total-PTH ratio values differ in various hyperparathyroid states. When the parathyroid function is stimulated, C-PTH/T-PTH ratio values are similar or lower than those observed in normal individuals but when the parathyroid function is suppressed, C-PTH/T-PTH values are usually increased. To see whether hyperparathyroidism after renal transplant reflects a stimulated parathyroid function or suppressed persistent hyperplasia, we have measured total (T) and carboxyl-terminal (C) PTH as well as total corrected calcium (Ca_{tc}), phosphate (PO_4), alkaline phosphatase (AP) and creatinine levels in 225 receivers of a renal graft (RTP) over a period of 30 years, 71 normals individuals (N) and 14 patients with primary hyperparathyroidism (PHP). The RTP were subdivided in 3 groups according to Ca_{tc} and T-PTH levels. Results are means ± SD and were compared with a non parametric ANOVA. Serum creatinine levels were similar in each RTP groups (110±33 to 119±36 mmol/L) and higher than in N or PHP (66±17 and 76±26 µmol/L, $p<0.05$). Phosphorus levels were higher in N (1.12±0.14 mmol/L, $p<0.05$) than in the four other groups. Group 1 included 61 RTP with normal Ca_{tc} (<2.55 mmol/L) and T-PTH levels (<6.5 pmol/L). Compared to N, these patients had slightly higher Ca_{tc} (2.37±0.10 vs 2.42±0.09 mmol/L, $p<0.05$), C-PTH (7.0±21.8 vs 12.9±4.5 pmol/L, $p<0.05$) and T-PTH levels (3.1±1.2 vs 5.1±1.2, $p<0.05$) and a similar C-PTH/T-PTH ratio (2.5±0.8 vs 2.7±1.1). The 102 RTP of group 2 had normal Ca_{tc} (2.42±0.08 mmol/L) but high T-PTH levels. Their C-PTH (21.6±10.4 pmol/L) and T-PTH levels (11.8±5.8 pmol/L) were higher than the two previous groups but similar to values observed in PHP or RTP group 3. Group 2 patients had a lower C-PTH/T-PTH ratio (1.9±0.5) than the four other groups ($p<0.05$). Group 3 was composed of 62 hypercalcemic RTP with similar characteristics to PHP patients: elevated Ca_{tc} (2.62±0.07 and 2.74±0.24 mmol/L), increased C-PTH (25.0±14.2 and 38.5±27.8 pmol/L) and T-PTH (11.1±6.8 and 16.9±14.7 pmol/L) but normal C-PTH/T-PTH ratio (2.5±0.9 and 2.6±0.8). Thus, 27% of RTP have a PTH profile typical of classical primary hyperparathyroidism with a set point defect, 45% have significant increase in PTH levels with low C-PTH/T-PTH ratio suggestive of an active secondary hyperparathyroidism, and the remaining 28% have slightly elevated PTH levels compatible with an ongoing state of PTH resistance. This work was supported by a grant from CIHR.

Disclosures: ***A. Räkel****, None.*

SU537

Low Prevalence of Osteoporosis Among Pediatric Patients With Juvenile Idiopathic Arthritis - Protective Influence of Anti-Rheumatic Drug Combinations? H. Valta*[1], P. Lahdenne*[1], K. Aalto*[1], O. Mäkitie[2]. [1]Pediatric Rheumatology, The Hospital for Children and Adolescents, Helsinki University Hospital, Helsinki, Finland, [2]Pediatric Endocrinology, The Hospital for Children and Adolescents, Helsinki University Hospital, Helsinki, Finland.

Patients with juvenile idiopathic arthritis (JIA) are at increased risk of secondary osteoporosis because of chronic inflammation and frequent use of glucocorticoids (GC). Previous studies have reported high prevalence of osteopenia and fractures even in pediatric patients with JIA.

The aim of this study was to assess bone health and its correlates in an unselected cohort of GC treated pediatric patients with JIA.

The study included 35 consecutive patients (24 females) followed at the Pediatric Rheumatology clinic, Helsinki University Hospital, with a history of systemic GC treatment for at least 3 months. Patients were assessed clinically and their charts reviewed for medical history. Blood biochemistry was obtained for S-Ca, Pi, PTH and 25-OH-Vitamin D (25-OHD). Bone mineral density (BMD) of the lumbar spine (L1-L4) and femoral neck was assessed with DXA (Hologic Discovery A); age- and sex adjusted z-scores were used for analysis.

The disease onset was polyarticular in 51%, oligoarticular in 43% and systemic type in 6% of the patients. The mean age at study assessment was 11.3 yrs (4.6-17.9 yrs) and the mean disease duration 6.3 yrs (2.4-14.8 yrs); 16 patients (46%) had an ongoing GC treatment. The median duration of GC treatment was 820 days (170-3920 days) and the median cumulative dose (as prednisolone) was 3.3 g (0.5-21.2 g). In addition to systemic GCs, all patients had been treated with methotrexate, 97% with intra-articular GCs, 63% with hydroxychloroquine and 40% with TNF-α antagonists. Other less frequently used medications included sulphasalazin, azathioprine and cyclosporin A. Two patients had a positive fracture history.

The median BMD z-score for the lumbar spine was -0.1 (-2.4 - +1.3) and for the femoral neck, -0.2 (-2.1-+1.4). Only four patients (11%) had a BMD z-score below -1.5. The BMD z-score tended to be lower in patients with longer disease duration ($P=0.001$) and higher absolute ($P=0.007$) and weight-adjusted ($P=0.07$) cumulative GC dose. None of the biochemical parameters correlated with the BMD z-scores; ten patients (29%) had vitamin D-deficiency (S-25-OHD <37 nmol/l).

We suggest that with the presently used anti-rheumatic drug combinations and increasing use of TNF-α antagonists resulting in reduced GC use, secondary osteoporosis is not as common as previously reported among pediatric patients with JIA. The high frequency of vitamin D deficiency suggests that preventive measures of osteoporosis are often neglected.

Disclosures: ***H. Valta****, None.*

SU538

Selective COX-2 Inhibitor suppresses the Increased Bone Resorption Associated with Collagen-Induced Arthritis in Mice. T. Taketa*, A. Sakai, S. Akahoshi*, M. Nagashima*, T. Mori, K. Nakai*, T. Nakamura. Orthopeadic surgery, university of occupational and environmental health, Fukuoka, Japan.

Type II collagen-induced arthritis (CIA) has been established as a possible model of rheumatoid arthritis (RA). We have already demonstrated that trabecular bone mass of tibia is reduced as a result of increased bone resorption in CIA mice. And there is a study that celecoxib, selective cyclooxygenase-2 (COX-2) inhibitor, inhibited bone resorption which was elicited by the inflammatory cytokines in vitro. The aims of this study are to clarify whether selective COX-2 inhibitor (celecoxib) suppresses theincreased bone resorption associated with collagen-induced arthritis, and also to discriminate differences of actions on bone resorption among celecoxib, a selective COX-1 inhibitor (SC-58560) and indomethacin, which inhibits both COX-1 and -2. DBA/1J male mice, 8 weeks in age, were divided into 6 groups of 5 animals each as follows: no-treated (1 group) and collagen-induced (5 groups) mice. CIA mice were administered celecoxib orally at doses of 0 (vehicle control), 16, 75 mg/kg body weight in contrast to SC-58560 (1.0mg/kg) and indomethacin (0.5mg/kg). All mice were killed at 6 weeks after commencement of oral administration. At the end of the experiment, serum osteocalcin and urinary deoxypyridinoline (DPD) were measured. Histomorphometrical analyses were also performed on the undecalcified sections of the proximal tibia. The DPD values in CIA were significantly higher than those in vehicle control. Celecoxib suppressed the increased DPD in CIA to the control level. In bone histomorphometry, trabecular bone volume (BV/TV) in CIA mice decreased compared to that in vehicle control mice. BV/TV in high dose celecoxib group significantly increased compared to that in CIA mice. Osteoclast number (Oc.N/BS) in CIA mice increased compared to that in vehicle control. Oc.N/BS in celecoxib groups decreased compared to that in CIA mice. On the other hand, there were no significant differences in DPD and any parameters of bone histomorphometry among SC-58560, indomethacin and CIA mice. Celecoxib administration suppresses the increased bone

resorption and trabecular bone loss in collagen-induced arthritis mice. The inhibitory effect of celecoxib on bone resorption in arthritis miceis remarkable compared to that of SC-58560 or indomethacin.

Disclosures: ***T. Taketa****, None.*

SU539

Effect of Alendronate on Radiographic Progression in Rheumatoid Arthritis. T. Shuto, T. Kuwano*, Y. Nakashima*, H. Yamada*, K. Okazaki*, T. Mawatari*, T. Maeda*, Y. Iwamoto*. Orthopedics, Kyusyu university, Fukuoka, Japan.

Objective. Because bone erosion in patients with rheumatoid arthritis (RA) is mainly formed by accelarated osteoclastic bone resorption, it is possible that bisphosphonate retards the progression of bone destruction in RA patients. We previously reported that amino-bisphosphonate inhibits bone and joint destruction in established adjuvant arthritis (Matsuo et al, J Rheumatol, 30: 1280, 2003). The aim of this study is to examine if oral administration of alendronate retards the radiographic progression in RA patients.

Methods. Twenty five patients with RA who were administered alendronate (AL) for the treatment of osteoporosis were examined as AL group. The Sharp's score (erosion score, joint space narrowing score), serum C-reactive protein (CRP), RAHA, erythrocyte sedimentation rate (ESR), and the excretion of urinary deoxypyridinoline/creatinine (DPD/Cre) were measured before and after the AL treatment. We also evaluated yearly radiographic progression before (estimate-Sharp score) and after (delta-Sharp score) the treatment. As a control, 25 patients with RA who had not been administered bisphosphonate including alendronate were randamly selected (control group).

Results. The mean score of delta-Sharp with respect to erosion significantly decreased compared to that of estimate-Sharp in AL group. However, there was no significant difference between the mean erosion score of delta-Sharp and that of estimate-Sharp in control group. The mean of delta/estimate ratio of erosion was significantly lower in AL groups compared to control group. On the other hand, the delta-Sharp score with respect to joint space narrowing (JSN) was significantly lower than that of estimate-Sharp in both AL and control groups. There was no significant difference with respect to the delta/estimate ratio of JSN between both groups. In laboratory analysis, the urinary DPD/Cre value decreased significantly by AL treatment, however, significant change of the ESR and CRP level was not observed between before and after AL treatment.

Discussion & Conclusion. This is the first report demonstrating significant retardation of radiographic progression of bone erosion after alendronate treatment in RA patients. Although it is unclear if alendronate has benefical effect on either articular cartilage destruction or inflammatory reaction, alendronate could have the inhibitory effect on progressive bone destruction in RA patients.

Disclosures: ***T. Shuto****, None.*

SU540

Nurse-like Cells from Patients with Rheumatoid Arthritis Support Survival of Osteoclast Precursors via Macrophage-Colony Stimulating Factor Production. H. Tsuboi*[1], N. Udagawa[2], J. Hashimoto*[1], H. Yoshikawa[1], N. Takahashi[3], T. Ochi*[4]. [1]Orthopaedic surgery, Osaka University, Suita, Japan, [2]Department of Biochemistry, Matsumoto Dental University, Shiojiri, Japan, [3]Institute for Dental Science, Matsumoto Dental University, Shiojiri, Japan, [4]National Hospital Organization Sagamihara National Hospital, Sagamihara, Japan.

Osteoclasts play an important role in the bone destruction of rheumatoid arthritis (RA). In RA synovium, synovial fibroblasts are thought to support osteoclastogenesis. This study was performed to elucidate the role of nurse-like cells (NLCs), which were established from RA synovium, in bone destruction with progressive synovial expansion. CD14-positive monocytes (CD14+s) were cocultured with NLCs for 4 weeks and collected as NLC-supported CD14+s (NCD14+s). To determine the ability of NCD14+s to differentiate into osteoclasts, NCD14+s were further cultured with macrophage colony-stimulating factor (M-CSF) together with receptor activator of nuclear factor-kB ligand (RANKL) or tumor necrosis factor a (TNFa). NCD14+s were also cocultured with SaOS-4/3 cells, which were shown to support osteoclastogenesis in response to parathyroid hormone (PTH). Furthermore, CD14+s were cocultured with SaOS-4/3 cells to elucidate how SaOS-4/3 cells and NLCs supported CD14+s for a long period in the coculture. Synovial expansion adjacent to bone in RA patients was examined immunohistochemically to detect osteoclast precursors like NCD14+s. In results, NLCs supported the survival of CD14+s for 4 weeks. NCD14+s as well as CD14+s differentiated into osteoclasts in the presence of M-CSF together with RANKL or TNFa. NCD14+s also differentiated into osteoclasts in PTH-treated cocultures with SaOS-4/3 cells. SaOS-4/3 cells supported the survival of CD14+s for 4 weeks in the presence but not in the absence of PTH. Treatment of SaOS-4/3 cells with PTH up-regulated M-CSF mRNA expression. Neutralizing antibodies against M-CSF inhibited the NLC-supported survival of CD14+s. In immunohistochemical stains of tissue sections from RA patients, CD68-positive monocytes and M-CSF-positive fibroblast-like synoviocytes were co-localized in the regions adjacent to bone destruction with progressive synovial expansion. The present study suggests that NLCs are certainly involved in RA-induced bone destruction through maintaining osteoclast precursors via M-CSF production.

Disclosures: ***H. Tsuboi****, None.*

SU541

The Determinants of the Bone Mineral Density in Korean Patients with Rheumatoid Arthritis. The Focus on the Use of the Glucocorticoids. W. Park*, B. H. Park*, J. S. Song*, S. B. Hong. Medicine, Inha University Hospital, Incheon, Republic of Korea.

There are more risk factors of osteoporosis in rheumatoid arthritis (RA) than in general population including the use of the glucocorticoid(GC). We evaluated the effect of the daily and cumulated glucocorticoid dose, duration of the disease, markers of disease activity, and menopausal status on the bone mineral density (BMD), and markers of bone metabolism in RA patients.

Sixty-three patients with RA (disease duration of 4.9, range 0.5-32 years), aged 21~72 years (9 men, 26 premenopausal and 28 postmenopausal women) who met the American College of Rheumatology classification of RA were randomly enrolled in the study between 1999 and 2001. Depending on the daily prednisolone (PD) doses, patients were divided into D1 (5.0 mg or less, mean 3.7 mg) and D2 (7.5 - 15 mg, mean 8.3 mg) groups. According to cumulated PD doses, they were divided into C1 (less than 5.0 gm, mean 3.68 gm) and C2 (more than 5.0 gm, mean 10.30 gm) groups. They were also divided into 2 groups by the limit of 3 years disease duration, ESR 20mm/hr, and CRP 0.5mg/dL. BMD was measured at lumbar spine and femur neck by DEXA. Serum osteocalcin (OC) and urinary deoxypyridinoline (DPD) level were measured.

The results are 1) The BMD T-score in total patients were -1.85, -1.81 and -2.13 in L-spine, total femoral neck and Ward's triangle respectively. The femoral neck BMD was lower in postmenopausal female patients, the patients with more than 3 years of the disease duration, the patients with ESR more than 20mm/hr, and C2 group. The lumbar BMD were lower in postmenopausal female patients and patients with ESR more than 20mm/hr. 2) Urinary excretion of DPD tended to be higher, while serum OC level was within normal limit in most of the RA patients (normal, 3.0-7.4 nM/mM creatinine). 3) Urinary DPD was neither different between D1 and D2 groups(7.7 ± 4.78, and 9.4 ± 6.51 nM/mM creatinine, respectively, p=0.066) nor between CI and C2 groups(7.7 ± 5.55, and 8.9 ± 5.69 nM/mM creatinine, respectively, p=0.147). 4) Serum OC was neither different between D1 and D2 groups(7.68 ± 4.14, and 6.00 ± 2.74 ng/ml, respectively, p=0.152) nor between CI and C2 groups(7.49 ± 2.93, and 6.76 ± 4.25 ng/ml, respectively, p=0.259). 5) The independent predictors of bone mass by linear regression analysis were ESR, cumulated GC dose, disease duration, and menopausal state.

Conclusively, RA patients generally have an imbalance in bone metabolism markers. But the imbalance was not GC dose dependent in the low dose range(less than 15 mg PD daily). The BMD was lower in RA patients in postmenopausal state, with long disease duration, higher cumulated GC dose, and high ESR.

Disclosures: ***W. Park****, None.*

SU542

Positive Effects of Infliximab Therapy on Bone Metabolism in Patients with Rheumatoid Arthritis. T. Thomas[1], P. Garnero[2], A. le Henanff*[3], F. Debiais[4], X. Le Loet*[5], C. Roux[6], J. Sany*[7], D. Wendling[8], C. Zarnitsky*[9], P. Ravaux*[3]. [1]Rheumatology, INSERM 0366, Saint-Etienne, France, [2]SYNARC, Lyon, France, [3]Epidemiology, Biostatistics and Clinical Research, Hôpital Bichat, Paris, France, [4]Rheumatology, University Hospital of Poitiers, Poitiers, France, [5]Rheumatology, University Hospital of Rouen, Rouen, France, [6]Rheumatology, Hôpital Cochin, Paris, France, [7]Immuno-Rheumatology, Hôpital Lapeyronie, Montpellier, France, [8]Rheumatology, University Hospital of Besançon, Besançon, France, [9]Rheumatology, Groupe Hospitalier du Havre, Le Havre, France.

Rheumatoid arthritis (RA) is characterized by a progressive destruction of joint structures. The RA-related bone loss is mediated by cytokines, including TNFa, which are produced within the synovitis. Therefore we proposed the working hypothesis that administration of anti-TNFa drugs in the treatment of RA would also slow down bone remodeling. We present here a prospective study of a multicentric cohort of 48 women, mean age 54.2±12.1 years old, with a severe RA for 11.4±7.8 years, who started infliximab after failure of other disease-modifying antirheumatic drugs. The objective of the study was to evaluate bone metabolism under infliximab by measuring type I procollagen N-terminal propeptide (PINP), a marker of bone formation, and serum C-terminal cross-linked telopeptide of type I collagen (S-CTX), a marker of bone resorption at 0, 6 and 22 weeks. In addition, bone mineral density (BMD) was assessed at baseline and after 6 months by DEXA both at the lumbar spine and hip.

Only 12.5% of patients were current smokers, 62.5% were postmenopausal women and 77% were under oral glucocorticoids (mean daily dose: prednisone 10 mg/d). Two patients had a previous clinical vertebral fracture. No patient received bisphosphonates. Patients had a total dose of infliximab 1002.6±262.5 in 4.6±0.6 infusions during the course of the study.

The S-CTX levels rapidly and significantly decreased by 19% and 28% after 6 and 22 weeks, respectively ($p<0.001$) whereas PINP levels remained stable with -9% and -13% decrease after 6 and 22 weeks of infliximab, respectively (NS). Prior treatment, BMD values expressed in T-score, were -0.65±1.53 and -0.66±1.63 at the spine and total hip, respectively. After 6 months, BMD did not change at both sites.

In conclusion, the 20% improvement in the formation/resorption balance observed after 6 months of therapy demonstrated beneficial bone effects of infliximab in patients with RA. These effects could partly explain the prevention of structural joint lesions observed with anti-TNFa therapy. Moreover, these results suggest that modulating TNFa pathway could be a potential therapeutic avenue in the treatment of osteoporosis.

Disclosures: ***T. Thomas****, None.*

SU543

Serum from Children with Juvenile Rheumatoid Arthritis (JRA) Inhibits the Differentiation and Increases Apoptosis of Human Osteoblasts in Culture. V. F. Caparbo*, C. A. A. da Silva*, R. M. R. Pereira. Rheumatology Division, University of São Paulo, São Paulo, Brazil.

Background: Bone demineralization is common in Juvenile Rheumatoid Arthritis and it has been associated with activity and severity of disease. The decrease of bone mineral density has been related to decrease of bone turnover, mainly with low bone formation. Decrease of osteocalcin, alkaline phosphatase has been described in the serum of these patients suggesting that the bone formation is compromised in JRA patients.
Objective: To examine the effects of JRA serum on the proliferation, differentation, and fate of human osteoblast cells (hOb) culture up to 17 days after confluence.
Methods: The human osteoblast cells were cultured in presence of 10% serum from JRA patients (n=10) and from healthy controls (n=10), 100 ug/mL ascorbic acid and 5 mmol/L beta-glycerophosphate and the medium was changed every 3 or 4 days. No JRA patient were using glucocorticoid at least one month before the study or another drug that can affect bone mineral metabolism and all patients were on disease activity. DNA synthesis was assessed by measuring the incorporation of H^3 thymidine into acid-precipitable material. The osteoblast cells differentation was examined by alkaline phosphatase activity and ostecalcin secretion. Serum from each control and JRA patient was tested in 8 indepedent cultures for alkaline phosphatase, osteocalcin and DNA synthesis assays and in 3 hOb osteoblasts cultures for DNA fragmentation.
Results: There is a decrease of alkaline phosphatase activity and secretion of osteocalcin, boths markers of mature osteoblasts, in hOb cultured with the serum of JRA compared with controls. No effect statistically significant was observed in DNA proliferation in hOb cultured with JRA serum. Apoptosis of hOb was present in cells cultured with JRA serum, but not with controls sera, detected by DNA fragmentation.

	JRA	Healthy controls	p
1. Celular differentation			
Alkaline phosphatase activity, µmol	16.93 ± 4.54	22.75 ± 5.08	0.015*
Osteocalcin synthesis, ng/well	1.30 ± 0.023	1.33 ± 0.022	0.023*
2. Celular proliferation			
DNA synthesis, dpm/well	955.3 ± 155.63	1078.6 ± 310.8	NS
3. DNA quantification, µg/culture	10.7 ± 7.4	27.8 ± 4.0	0.002*

Conclusion: JRA serum decrease the differentiation of human osteoblast cells but not the DNA proliferation. There is also an increase of apoptosis in human Osteoblasts cultured with JRA serum. A lot of cytokines has be implied in physiopathology of JRA bone loss that can explain these results. Understanding better the role of these cytokines in bone formation is fundamental to find a drug to prevent and treat the osteoporosis and fractures that occur in JRA patients.

Disclosures: ***R.M.R. Pereira****, None.*

SU544

Catabolic Effects of Continuous Infusion of Human PTH1-34 Fragment in C57BL/J6 Mice. A. Iida-Klein[1], S. S. Lu[1], R. Kapadia[2], M. Burkhart*[2], D. W. Dempster[1], R. Lindsay[3]. [1]Regional Bone Center, Helen Hayes Hospital, West Haverstraw, NY, USA, [2]Scanco Inc., USA, Wayne, PA, USA, [3]Clinical Research Center, Helen Hayes Hospital, West Haverstraw, NY, USA.

Parathyroid hormone (PTH) stimulates bone resorption as well as bone formation in vivo and in organ culture. Catabolic actions of PTH have been recognized in patients with hyperparathyroidism, whose serum PTH levels are continuously elevated. However, it is often difficult to create a condition of hyperparathyroidism in mice. The goal of the present study was to determine whether continuous infusion of N-terminal human PTH1-34 fragment (hPTH1-34) could be catabolic in mice, and whether its catabolic action could be confirmed by biochemical markers, and by changes in bone mineral density (BMD) and microarchitecture. Ten-week-old female C57BL/J6 mice were continuously treated with hPTH1-34 for 2 weeks, using the Alzet osmotic pumps containing either hPTH1-34 (8.1 pmoles/0.25 µl/hr, equivalent to 40µg/kg/day, n=7) or vehicle (n=9). BMD was measured weekly, and bone and blood samples were collected at euthanasia. Serum levels of total calcium, hPTH1-34, mouse intact PTH1-84 (mPTH1-84) and mouse tartrate acid phosphatase activity (mTRAP) were measured. As expected, hPTH1-34 was undetectable in control mice, while the hPTH1-34 level was significantly elevated in the PTH-infused mice (79.79 $\pm$ 20.31 pM, $p<0.02$). Infusion of hPTH1-34 markedly suppressed endogenous intact mPTH1-84 (0.73 $\pm$ 0.25 pM for infused vs. 2.40 $\pm$ 0.55 pM for control, $p<0.02$), and significantly increased total calcium (2.64 $\pm$ 0.13 mM vs. 2.04 $\pm$ 0.07 mM, $p<0.005$). In one of two pilot experiments, infusion of hPTH1-34 increased serum TRAP activity (28.26 $\pm$ 0.78 vs. 10.78 $\pm$ 3.8 U/L, $p<0.002$) by ~3 fold. Finally, µCT analysis of the right femur revealed that infusion of hPTH1-34 decreased trabecular connectivity density by 40% ($p<0.05$, n=4 for vehicle and n=5 for PTH) as compared to vehicle infusion. This pilot study clearly showed that infusion of hPTH1-34 induces catabolic effects on bone with increased serum calcium and TRAP activity accompanied by decreased trabecular connectivity density. Infusion of hPTH1-34 in mice may be a good model to study the catabolic actions of PTH on the mammalian skeleton and to contrast these from a mechanistic standpoint with the anabolic effect seen with daily PTH injections

Disclosures: ***A. Iida-Klein****, None.*

SU545

Survival After Parathyroidectomy In Patients With End-stage Renal Disease And Severe Hyperparathyroidism. A. Trombetti*[1], F. Herrmann*[1], C. Stoermann*[2], J. Robert*[3], P. Pennisi*[1], P. Y. Martin*[2], A. Spiliopoulos*[3], R. Rizzoli[1]. [1]Department of Rehabilitation and Geriatrics, University Hospital, Geneva, Switzerland, [2]Department of Internal Medicine, University Hospital, Geneva, Switzerland, [3]Department of Surgery, University Hospital, Geneva, Switzerland.

Patients with end-stage renal disease (ESRD) are at high risk of cardiovascular morbidity and mortality. Secondary hyperparathyroidism (SHPT) is considered as a contributing factor. Whether parathyroidectomy (PTX) influences long-term survival of patients with ESRD and severe SHPT is not known.
Between 1977 and 2002, 63 patients (mean age ± SD, 46.7 ± 13.7 years) with ESRD and severe SHPT underwent PTX. Their survival was compared to those of 752 ESRD patients treated at the same institution during the same period. Follow-up began either at the date of the first dialysis, at birth or at PTX, and continued until death or censoring (March 1st 2003). The observed survival curves were compared using a log-rank test. A Cox proportional hazards model was used to estimate the influence of patients' characteristics on mortality rate. Independent variables evaluated were gender, age at first dialysis, time on dialysis, and the presence of functioning renal graft.
Because of secondary or tertiary HPT, PTX was performed in 3% before onset of dialysis, in 68% during dialysis, and in 29% after kidney transplantation. The mean time between the first dialysis and PTX was 6.6 ± 5.0 years. Three PTX patients (4.8%) and 24 ESRD controls (3.2%) were lost to follow up (not significant). Taking into consideration the follow-up since time of first dialysis, PTX was associated with a significantly lower mortality rate than in non-operated ESRD controls (hazard ratio (HR): 0.33, 95% CI 0.22-0.50). However, the age at first dialysis (40.3 ± 14.6 vs 57.5 ± 16.6, $p < 0.001$), the proportion of patients with renal transplants (54.0 vs 32.1%, $p < 0.0001$) and the time on dialysis (8.6 ± 6.7 vs 3.9 ± 5.0 years, $p< 0.001$) markedly differed between PTX patients and controls. Adjustment for these factors negated the difference (HR: 0.98, 95% CI 0.64-1.52). Life expectancy at birth was not different between the two groups. Finally, to compare survival after PTX, we randomly selected 3 controls for each PTX case within the same 5-year age strata at time of first dialysis and who had the mean duration between first dialysis and PTX. Survival tended to be longer in PTX patients in the first 8 years after surgery (not significant). Censoring at time of first renal transplantation did not change the results. In conclusion, although patients who underwent PTX seemed to be very different from non-operated controls, PTX may protect against early death in patients with ESRD and severe SHPT.

Disclosures: ***A. Trombetti****, None.*

SU546

Signaling and Transcriptional Regulation of Matrix Gla Protein by Parathyroid Hormone in MC3T3-E1 Osteoblast-like Cells. S. Suttamanatwong*[1], R. T. Franceschi[2], R. Gopalakrishnan[1]. [1]Oral Sciences, University of Minnesota, Minneapolis, MN, USA, [2]Periodontics/Prevention/Geriatrics, University of Michigan, Ann Arbor, MI, USA.

The inhibition of osteoblast-mediated mineralization is one of the major catabolic effects of parathyroid hormone (PTH). We have previously shown that matrix gla protein (MGP) is a key regulator of PTH-mediated inhibition of mineralization (*Endocrinology,* 142:4379-4388, 2001). To further understand the mechanism of this regulation, we investigated the effect of PTH on the 748 bp murine *Mgp* promoter activity in MC3T3-E1 osteoblast-like cells. Transient transfection of *Mgp*-luciferase reporter construct (pMGP-luc) in MC3T3-E1 cells showed that PTH (10^{-7} M) induced Mgp promoter activity in a time-dependent manner. Induction was noted as early as 3 hours, with maximal induction at 6 hours (~ 3 to 4-fold) and a return to baseline levels 24 hours after PTH treatment. The time course of pMGP-luc activation by PTH correlated with earlier published results for MGP mRNA induction. Using activators and inhibitors of various signaling pathways, we determined that protein kinase A (PKA) is one of the major pathways required for regulation of MGP by PTH. A specific PKA inhibitor, H-89, suppressed both PTH-induced pMGP-luc activity and MGP mRNA levels in a dose-dependant manner. Promoter deletion analysis of the pMGP-luc promoter revealed that PTH activation dramatically decreased when the region between position -173 and -49 was deleted, suggesting that a PTH-responsive element lies in this region of the promoter. We are currently investigating the transcriptional element/s contained between -173 to -49 of the promoter, which may be necessary for PTH responsiveness. The results described here indicate that PTH transcriptionally regulates MGP in MC3T3-E1 cells and this regulation, at least in part, requires a PKA-dependent mechanism.

Disclosures: ***S. Suttamanatwong****, None.*

SU547

Continuous And Intermittent Treatment Of Zebrafish With Recombinant Human Parathyroid Hormone (1-34) Have Opposite Effects On The Growing Fish Skeleton. A. Fleming*[1], M. Sato[2]. [1]DanioLabs, Cambridge, United Kingdom, [2]Bone and Inflammation, Lilly Research Labs, Indianapolis, IN, USA.

Skeletal effects of continuous and intermittent rhPTH (1-34) were evaluated in zebrafish (Danio rerio). Zebrafish larvae in embryo media were incubated in a 96 well plate format from 3 to 9 days d.p.f., either in the continuous presence of PTH or for 2 hr every other day. Viability of zebrafish was unaffected by the continuous presence of the highest dose of PTH (100 ng/ml) evaluated. PTH had no effect on the length of zebrafish, as evaluated up to 30 ng/ml, whether administered continuously or intermittently. Mineralization was measured by image processing of the head after alizarin red staining at 10 d.p.f., and evaluated as pixel number above a threshold and analysis of the pixel histogram

(integrated optical density, IOD). A dose dependent inhibition of bone formation activity was observed with continuous PTH, leading to a significant, dose-dependent 40% reduction in mineralization (pixel number) at 30 ng/ml, after 6 days treatment. Image processing showed that not all mineralized structures in the head respond equally to PTH treatment. Specifically, otoliths did not respond reproducibly to PTH; so exclusion of otoliths from mineralization analyses improved the coefficient of variation to about 8%. IOD analysis by the latter method showed up to 83% suppression with 30 ng/ml, that was significant at all doses. By contrast, intermittent PTH induced a significant, dose-dependent 16% and 17% increase in mineralization for 10 and 30 ng/ml, respectively. These data show that PTH has effects on the growing zebrafish skeleton, not unlike the catabolic and anabolic skeletal effects described previously for continuous and intermittent PTH treatment in rats and primates. However, not all of the effects may be identical, as intermittent PTH did not significantly enhance longitudinal growth, as has been observed for the growing rat skeleton.

Disclosures: ***A. Fleming****, DanioLabs Ltd 3.*

SU548

Time-course of PTH-Regulated RANKL and OPG Expression in SaOS-2 Cells. J. L. Glover*, A. B. Hodsman, L. J. Fraher, P. H. Watson. Medicine, Lawson Health Research Institute, University of Western Ontario, London, ON, Canada.

Receptor activator of NF-kappaB ligand (RANKL) and osteoprotegerin (OPG) are important factors in the regulation of osteoblast to osteoclast communication during bone remodelling. Parathyroid hormone (PTH) is a key regulator of bone remodelling and affects osteoblastic expression of these molecules. It is well known that clinical use of PTH (1-34) in daily intermittent doses is highly anabolic while continuous exposure is catabolic to bone. Recently, PTH (1-31) and its derivatives have also shown promise as selective bone anabolic agents. Understanding the time course involved in PTH analogue regulation of OPG and RANKL protein expression should aid us to better understand the actions of PTH. SaOS-2 cells were grown to 70% confluence on cover slips and serum starved for 24 hours prior to treatment. The cells were treated with 10nM PTH 1-34 or PTH 1-31 and thereafter fixed at 0, 1, 2, 4, 8 and 24hours. Control cells for each time period were incubated with serum free media. Expression of OPG and RANKL protein was studied by immunofluorescence. Initial experiments have shown that after treatment with either PTH analogue there is an overall decrease in the apparent fluorescence for OPG. Treatment of SaOS-2 cells with 10 nM PTH 1-34 resulted in increased RANKL fluorescence localizing to the cell surface and in the golgi after 8 hrs. Treatment with 10 nM PTH 1-31 resulted in RANKL accumulation around the nucleus after 8 hrs. In time-course experiments with PTH 1-34, RANKL immunofluorescence was seen to change over a 24hour period. RANKL fluorescence was limited to the golgi after 1 and 2 hours of treatment. At 4 hours, most RANKL immunofluorescence was seen on the surface of the cell. RANKL fluorescence was uniformly dispersed throughout the cytoplasm at the later time points and was negligible after 24 hours. These studies demonstrate a clear pattern of RANKL subcellular localization throughout a 24 hour period in the presence of 10 nM PTH 1-34. Maximal presentation of RANKL on the cell membrane was seen after 4-8 hrs of PTH 1-34 exposure which may, in part, explain the catabolic action of this analogue. Although increased immunofluorescence for RANKL was seen in SaOS-2 cells after treatment with PTH 1-31, this fluorescence was limited to the perinuclear region. No RANKL was seen on the cell membrane which is a necessary step for osteoclast activation, providing a possible explanation for the more selectively anabolic activity of the PTH 1-31 analogue.

Disclosures: ***J.L. Glover****, None.*

SU549

Serum Parathyroid Hormone (PTH) Levels Obtained with an "Intact" In House Monoclonal-Antibody Based Assay that Shows a 50% Cross-Reactivity with PTH-(7-84). Comparison with Two Commercial Assays. J. G. Vieira[1], S. K. Nishida*[1], M. T. Camargo*[1], L. H. Obara*[1], I. S. Kunii*[2], M. N. Ohe*[2], O. M. Hauache*[1]. [1]Endocrinology, Laboratório Fleury, São Paulo, Brazil, [2]Endocrinology, EPM/UNIFESP, São Paulo, Brazil.

Immunometric assays for serum PTH supposedly measure only the intact PTH-(1-84) circulating form. A series of studies published in recent years showed that some long carboxyl terminal forms, as PTH-(7-84), were also present in serum and were measured by these assays "intact" PTh assays (2nd generation). New assays (3rd generation), based on amino-terminal antibodies directed against the first amino acids, provide serum values that are significantly lower. We developed a monoclonal-antibody based immunofluorometric assay (IFMA) that presents a 50% cross-reaction with PTH-(7-84). The analytical sensitivity is 2.7 ng/dL, and the interassay CV <10%. The two commercial assays used were an electrochemiluminescent assay (ECLIA, Roche Diagnostics) and an immunochemiluminometric assay (ILMA, Nichols Institute). Both assays show 100% cross-reactivity with PTH-(7-84). Two sets of serum samples from our diagnostic service were used for the study. One comprising 135 samples was measured with the IFMA and the ECLIA; a second set of 252 samples were measured using the IFMA and the ILMA. In the first set, the results using the IFMA showed a median of 35.0 ng/L, with a range from 4.0 to 1579.0 ng/L, and the results using the ECLIA a median of 51.0, with a range from 6.0 to 1900.0 ng/L, values that were significantly higher (P<0.0001, Wilcoxon). Spearman correlation (rs) was 0.961 (P<0.0001). In the second set of samples, the IFMA showed a median of 36.0 ng/L, with a range from 3.0 to 1524.0 ng/L, and the ILMA a median of 45.5 ng/L, with a range from 5.0 to 1795.0 ng/L, values that were significantly higher (P<0.0001, Wilcoxon). Spearman correlation (rs) was 0.883 (P<0.0001). In both sets of samples the results obtained with our in house assay were significantly lower, as expected by the specificity of the amino-terminal antibody employed. Our data support the need of a precise description of the specificity of the amino-terminal antibodies employed in "intact" PTH assays (2nd generation) in order to better compare results and define normal ranges.

Disclosures: ***J.G. Vieira****, None.*

SU550

IL-6 Is Not Required for Parathyroid Hormone Stimulation of RANKL Expression, Osteoclast Formation, and Bone Loss in Mice. C. A. O'Brien, R. L. Jilka, Q. Fu, S. Stewart*, R. S. Weinstein, S. C. Manolagas. Internal Medicine/Endocrinology, Univ. Arkansas for Medical Sciences, Little Rock, AR, USA.

Sustained elevation of parathyroid hormone (PTH) stimulates osteoclast formation and net bone loss; and PTH regulation of the RANKL/OPG ratio is thought to play an important role in this process. However, previous studies have shown that PTH also stimulates the production of IL-6 and the increased bone resorption caused by PTH infusion was blunted in IL-6-deficient mice. The goal of these studies was to determine whether chronic elevation of endogenous PTH alters IL-6 gene expression in vivo and whether IL-6 is required for bone loss associated with this condition. To allow accurate quantitation of IL-6 gene activity in vivo, we generated transgenic mice harboring a luciferase reporter gene under the control of IL-6 gene regulatory regions. Serum PTH was elevated by feeding adult mice a calcium-deficient diet for 7 days. Secondary hyperparathyroidism did not alter IL-6-luciferase transgene expression in bone or any of the other tissues examined. However, RANKL mRNA expression was elevated in bone tissue from these mice. These results suggested that IL-6 gene expression was not altered by chronic elevation of endogenous PTH. However, it remained possible that elevation of IL-6 expression in a tissue that we did not examine is nonetheless required for PTH-induced osteoclast differentiation and bone loss. Alternatively, a tonic level of IL-6 expression may be required for PTH actions on bone. To address these issues, bone loss and compression strength were compared in 6 month old wild type and IL-6-deficient C57Bl/6 mice after 7 days of dietary calcium deficiency. Dietary calcium deficiency induced significant bone loss in the hind limbs and spine of both wild type and IL-6-deficient mice. Consistent with the loss of spinal BMD, loss of vertebral compression strength and increase in cancellous osteoclast perimeter were similar in wild type and IL-6-deficient mice. We, therefore, compared the ability of PTH to regulate RANKL and OPG mRNA in bone marrow cultures from wild type and IL-6-deficient mice. Consistent with the loss of bone mass in vivo, there was no difference in the stimulation of RANKL, or suppression of OPG, mRNA by PTH in bone marrow cultures from wild type and IL-6-deficient mice. This was reflected in equivalent osteoclast formation in response to PTH in cultures from wild type and IL-6-deficient mice. These results demonstrate that chronic elevation of endogenous PTH stimulates osteoclast formation and bone loss via a mechanism that does not require IL-6; instead it requires changes in the RANKL/OPG ratio.

Disclosures: ***C.A. O'Brien****, Nuvios 1, 2, 5.*

SU551

Parathyroid Hormone Injection Induces Cyclooxygenase-2 in Bone, Kidney and Muscle *In Vivo*. M. Xu, O. S. Voznesensky*, L. G. Raisz, C. C. Pilbeam. Dept. of Medicine, University of Connecticut Health Center, Farmington, CT, USA.

Intermittent parathyroid hormone (PTH) is used as an anabolic agent to treat patients with osteoporosis. Since PTH is a potent inducer of cyclooxygenase-2 (COX-2) in osteoblastic cells in vitro, we examined the PTH induction of COX-2 in vivo. We used CD-1 mice transgenic for 371 bp of the murine COX-2 promoter fused to a luciferase reporter. Total RNA was extracted from freshly isolated tissues and COX-2 mRNA and GAPDH mRNA were measured by Northern analysis. Cell lysates from the same tissues were analyzed for luciferase activity, normalized to total protein. COX-2 is a transiently inducible gene and little COX-2 mRNA is detectable by Northern analysis in freshly isolated bone under basal conditions. After injection of PTH (human PTH 1-34) 30 μg/kg subcutaneously bilaterally above each calvaria, COX-2 mRNA in the calvariae peaked at 1 h and returned to basal levels at 6 h. Because multiple tissues have been reported to express PTH/PTHrP receptors, we injected PTH (160 μg/kg) intraperitoneally and examined tissue samples from femur, tibia, kidney, muscle, brain, lung, heart, spleen and liver at 1 and 3 h after injection. Basal luciferase activity was highest in brain (brain > femur, tibia, muscle > heart, lung > kidney, spleen, liver). PTH increased luciferase activity 7-fold in tibia, 5-fold in femur, 3.5-fold in kidney, and 1.6-fold in muscle (all P<0.01) at 3 h. There was no increase in luciferase activity in the other tissues. PTH induced COX-2 mRNA, normalized to GAPDH mRNA, in femoral and tibial bone by 5 to 6-fold at 1 h with levels decreasing at 3 h. Smaller increases were seen in kidney (2-fold) and muscle (1.6-fold). At 3 h but not 1 h, serum calcium was significantly increased in PTH injected mice compared to controls (10.3 ± 0.2 *vs.* 9.3 ± 0.1, P<0.01) and serum phosphorus was decreased (10.6 ± 0.3 *vs.* 12.3 ± 0.2, P<0.01). Since increased extracellular calcium can induce COX-2, some of the effects of PTH might be due to increased serum calcium. However, the increase in calcium occurred later than the peak in COX-2 mRNA levels. This study suggests that exogenous PTH induces COX-2 mRNA rapidly and transiently in vivo, and that the induction is transcriptionally mediated. Bone has the greatest COX-2 response to PTH, but other tissues can also respond.

Disclosures: ***M. Xu****, None.*

SU552

Connexins and PTH Regulation of the Osteocalcin Promoter. A. De Marzo, J. P. Stains, R. Civitelli. Bone and Mineral Diseases, Washington University in St. Louis, St. Louis, MO, USA.

It has been previously shown that the effect of PTH on cAMP production and in vitro mineralization are curtailed when gap junctional communication is disrupted. We have demonstrated that expression of chick connexin45 (cCx45) in ROS 17/2.8 and MC3T3-E1 cells, which express abundant endogenous connexin43 (Cx43), decreases the permeability of gap junctional channels and down-regulates osteocalcin (OC) and collagen α1 (I) promoters. We tested whether PTH regulation of OC gene transcription is altered by dominant negative inhibition (cCx45 expression) of Cx43 mediated gap junctional communication. Different fragments of the rat OC proximal promoter were used in a luciferase (LUC) reporter system and transiently co-transfected with cCx45 into ROS 17/2.8 or MC3T3 cells. Incubation (16-24 h) of either cell line with 10^{-8}M rat PTH (1-34) induced circa 1.8-fold increase of -637OCLUC (containing -637 to +32 promoter fragment) and -199OCLUC (containing -199 to +32 promoter fragment) reporter activities. Co-transfection with cCx45 reduced both basal and PTH stimulated luciferase activities, although the degree of PTH stimulation relative to basal activity was similar in the presence or in the absence of cCx45 for either reporter. A shorter, 5' truncated promoter fragment, -92OCLUC was minimally responsive to PTH and yet retained sensitivity to Cx45 overexpression. Since the OC promoter fragments tested encompass both a cAMP response region (ROCRR) and a connexin response element (CxRE), these data argue against a role of these regulatory regions in connexin sensitivity of PTH responsiveness observed in osteoblastic cells. Consistent with this hypothesis, cCx45 did not alter PTH stimulation of a heterologous promoter-luciferase construct containing 2 copies of ROCRR; and PTH did not stimulate a CxRE-LUC reporter. Further, while forskolin (10^{-5}M) did not affect OC gene transcription in ROS 17/2.8 cells, it did induce on average a 3-fold activation of -637OCLUC in MC3T3-E1 cells, as did 8Br-cAMP (10^{-3}M). This stimulation was not altered by co-expression of cCx45, arguing against a role of cAMP in cCx45 modulation of the OC promoter's responsiveness to PTH. In fact, cCx45 consistently exhibited synergistic activation of a canonical cAMP response element (CRE) when co-transfeted with a CRE-LUC reporter in either ROS 17/2.8 or MC3T3-E1 cells. These data suggest that interference with gap junctional communication by cCx45 expression reduces basal OC promoter activity, but does not abolish PTH activation of the promoter. Modulation of cAMP mediated responses does not seem to be involved in the mechanism by which gap junctional communication modulates OC gene transcription.

Disclosures: ***A. De Marzo****, None.*

SU553

Receptor Structural Determinants for Extracellular Signal-Regulated Kinases (ERK) Activation by PTH. A. Rey*, D. Manen*, J. Caversazio, R. Rizzoli, S. L. Ferrari. Division of Bone Diseases, Geneva University Hospital, Geneva, Switzerland.

PTH/PTHrP receptor (PTH1R) activation by cognate agonists triggers intracellular signaling through the adenylate cyclase (AC)-cAMP and phospholipase C (PLC)-IP3/Ca pathways. In addition, PTH has been reported to activate ERK1/2 (ERK) through PTH1R, but the signal transduction mechanisms responsible for this activation remain uncertain. Moreover, it is currently unknown whether activation of the PTH receptor type 2 (PTH2R) by cognate agonists, PTH and TIP39, triggers ERK signaling. We investigated PTH1R and PTH2R structural requirements for ERK activation by evaluating ERK phosphorylation using immuno-western blotting in HEK293 cells transiently expressing wild type (WT), mutant or chimeric receptors.

In PTH1R expressing cells, ERK activation increased 60 fold over baseline (by ImageQuant analysis) 5 min. after exposure to PTH(1-34) (100nM), and quickly declined thereafter. In cells expressing the Jansen's PTH1R mutant H223R, which constitutively activates cAMP but is deficient for PLC-IP3 signaling, ERK activation by PTH was similar to WT. In contrast, AC-cAMP activation by forskolin did not activate ERK. In PTH2R expressing cells, ERK was activated by TIP39 (100nM), but not by PTH. Moreover, a PTH2R chimeric receptor carrying the N-term and 3rd extracellular loop of PTH1R, which we had previously shown to improve PTH-stimulated Gq-mediated signaling compared to WT PTH2R, did not mediate PTH activation of ERK. Altogether, these data indicated that cAMP is not sufficient whereas PLC signaling is not required for ERK activation by PTH. To further investigate the PTH1R determinants for ERK activation, sequential PTH1R C-terminus deletions were carried out. A juxta-membrane deletion of PTH1R C-term (aa472) abolished PTH activation of ERK . On the opposite, with a more distal C-term deletion (aa501), ERK activation was 2 fold higher after 5min. and was sustained at 15min. compared to WT PTH1R. Moreover, compared to WT PTH1R , PTH-mediated ERK activation was significantly increased in cells expressing a chimeric PTH1R carrying the distal C-term of PTH2R.

In summary, ERK is selectively activated by PTH through PTH1R and by TIP39 through PTH2R. Distinct structural determinants in PTH1R C-term, rather than Gs- or Gq-mediated signaling, appear to mediate PTH-stimulation of ERK. Indeed, PTH1R proximal C-term harbors activating sequences whereas the distal C-term, which shares the least homology with PTH2R C-term, harbors inhibitory sequences for ERK activation. These findings suggest that PTH-stimulated MAPK signaling is regulated by interactions of PTH1R C-term with cytoplasmic molecules, which remain to be identified.

Disclosures: ***S.L. Ferrari****, None.*

SU554

Role of Angiogenesis in the Anabolic Effect of Parathyroid Hormone. Y. Rhee[1], Y. Kim[2], S. Lee*[1], J. Lee*[1], S. Kim*[1], J. Byoun*[1], R. Hwang*[1], S. Jun*[1], J. An*[1], S. Lim[1]. [1]Brain Korea 21 Project of Medical Science, Internal Medicine, College of Medicine, Yonsei University, Seoul, Republic of Korea, [2]Internal Medicine, NHIC Ilsan Hospital (National Health Insurance Corporation Ilsan Hospital), Seoul, Republic of Korea.

In vivo osteogenic responses to anabolic stimuli are expected to be accompanied by angiogenesis as well as in the process of development of bone. One of the strongest pharamacologic osteogenic stimuli take place with the administration of parathyroid hormone(PTH). Consequently, angiogenesis might play an important role in mediating this bone forming stimulating effect of PTH. To investigate this relationship, actively growing young Sprague-Dawley rat were used. All animals were treated in accordance with the guidelines and regulations for the use and care of animals of Yonsei University, Seoul, Korea. The analogue of TNP-470 inhibitor, one of the angiogenesis inhibitor(AI) was administered concomitatntly to show the role of angiogenesis in the effect of PTH. The groups(n=7, each) were divided as (1) vehicle(VEH), (2) recombinant human PTH(1-84) (PTH84) [80 mcg/kg, sc, 5 days a week], (3) angiogenesis inhibitor alone (AI) [1 mg/kg, sc, 5 days a week] (4) PTH(1-84) + AI concomitatntly with same dosage as group 2 and 3(AI84). The duration of the treatment took 5 weeks. The dual x-ray absorptiometry(Hologic QDR 4500 A, small animal program) of right femur were taken. The bone mineral density(BMD) of PTH84 was higher than VEH by 6.3% ($p<0.05$) and the gain of bone mass was attenuated by 2.5% in AI84($p<0.05$). However more significant attenuation by concomitant use of AI was shown in the 3-point bending test. The maximal failure load was increased as much as 14.8%($p<0.05$) in PTH85 than VEH, but it was diminished by 24.3%($p<0.05$) by concurrent use of AI. Moreover, the toughness showed similar significant changes($p<0.05$). The BMD or the biomechanic data of AI group were similar with the VEH suggesting the minimal effect on the normally modeling phase of the growing rat. In contrast, the angiogenesis seemed to be quite important in completing the anabolic effect of PTH.

Disclosures: ***Y. Rhee****, None.*

SU555

Protein Profiling in the Parathyroid Hormone-treated Bone Marrow Cell by Proteomics. S. Jun*, E. Lee*, R. Hwang*, S. Kim*, J. An*, S. Lee*, Y. Rhee, S. Lim. Brain Korea 21 Project of Medical Science, Internal Medicine, College of Medicine, Yonsei University, Seoul, Republic of Korea.

Parathyroid hormone (PTH) plays a major role in the balance between bone formation and bone resorption. While prolonged exposure to PTH cause increased bone resorption, intermittent injections of PTH have an anabolic effect on bone. The ability of PTH to enhance bone formation has recently been exploited in the treatment of osteoporosis. However, despite the large body of evidence that intermittent administration of PTH is strongly anabolic and increases bone mass in humans, little is known of the mechanism by which it stimulates bone formation. Therefore, in this study, protein profiling in the intermittent PTH-treated bone marrow cells were evaluated by using proteomics. Daily treatment for 5 days consisting of subcutaneous (sc) injection of either 150 μg/kg per day of mouse PTH (1-84) or vehicle (0.9% normal saline) was performed to the ICR mouse. At the end of the treatment period, the animals were killed 6 hour after last treatment and bone marrow cells were extracted from mouse tibiae and femur. Bone marrow cells were separated with marrow plasma by centrifugation, and red blood cells were removed. Bone marrow cells were washed with PBS 2 times and homogenized by urea lysis buffer. Proteins were separated in 2-dimensional-electrophoresis and visualized by clumsier blue staining. Gel images were analyzed by PDquest software and a total of 7 known proteins and 1 unknown protein were found to have at least 2-fold expression changes after PTH treatment. Four known proteins were newly synthesized and 4 known proteins and 2 unknown proteins disappeared after PTH treatment. Newly expressed or increased proteins in PTH-treated cell are related to signaling, cell cycle proteins and Ca2+ ion regulation. Structural proteins like vimentin and putative beta-actin decreased or disappeared in PTH-treated cell. Proteins related in energy metabolism eg, mitochondrial or endoplasmic reticulum ATPase were down regulated. These results could be helpful to understand the physiological function of PTH in bone marrow cells.

Disclosures: ***S. Jun****, None.*

SU556

The Effects of Intermittent but not Continuous Parathyroid Hormone (PTH) on Mineralation are Mediated through Hemichannels. P. Cherian[1], X. Wang*[1], L. F. Bonewald[2], J. X. Jiang[1]. [1]Biochemistry, University of Texas Health Science Center, San Antonio, TX, USA, [2]Oral Biology, School of Dentistry, University of Missouri, Kansas City, MO, USA.

Sustained elevation of PTH as in hyperparathyroidism, stimulates bone resorption, whereas intermittent administration stimulates bone formation. Even though $PTH_{(1-34)}$ is now used clinically for the treatment of osteoporosis, the mechanism whereby PTH mediates these opposing effects depending on timing of administration is not understood. Intermittent, but not continuous, treatment by $PTH_{(1-34)}$ has been demonstrated to stimulate osteoblast proliferation and differentiation. It has also been shown that inhibitors of gap junction function can block PTH induced osteoblast differentiation. We sought to determine the role that Cx43 as a component of gap junctions plays in the effect of $PTH_{(1-34)}$ on osteoblast mineralization. The cell line MLO-A5 that rapidly mineralizes in culture within 3-6 days was used. Intermittent PTH enhances mineralization of MLO-A5 cells, whereas continuous PTH inhibits this process. The stimulation of mineralization by intermittent PTH was significantly inhibited by the gap junction inhibitor 18 β-glycyrrhetinic acid

which is also known to block hemichannels. Cx43 is abundantly expressed intracellulary in MLO-A5 cells with minor expression on the cell surface. When the cells are treated with 10^{-8} M $PTH_{(1-34)}$ continuously for 48 h, the expression level of Cx43 mRNA increased significantly; however, there was no obvious change in the cell surface expression. In contrast, when the cells are subjected to intermittent treatment (4 h-treatment per 24 h culture) of 10^{-8} M $PTH_{(1-34)}$ for a total of 48 hrs, the majority of the intracellular Cx43 migrates to the cell surface even though overall total protein expression of Cx43 is unchanged. Interestingly, gap junction function was stimulated to the similar extent by both intermittent as well as continuous $PTH_{(1-34)}$. This work emphasizes the importance of not only examining the regulation of mRNA and protein expression, but also protein migration and localization. We propose that Cx43 in the form of hemichannels, instead of gap junctional channels, is likely to modulate the effect of intermittent PTH on the mineralization process.

Disclosures: ***J.X. Jiang****, None.*

SU557

Differential Short Term Responses of the Mouse Skeleton to the Same Daily Amount of hPTH1-34 Delivered Either Intermittently or Continuously: Effects of Bone Density and Biochemical Markers. S. S. Lu, D. W. Dempster, R. Lindsay, A. Iida-Klein. Regional Bone Center, Helen Hayes Hospital, West Haverstraw, NY, USA.

Intermittent parathyroid hormone (PTH) treatment has an anabolic action on the skeleton, but PTH can also be catabolic when administered continuously. The mechanisms underlying those diverse actions are poorly understood. We investigated the response of mouse bone to the same daily amount of human PTH1-34 fragment (hPTH1-34) given either intermittently(iPTH)or continuously (cPTH). Female C57BL/6J mice at 10 weeks of age were treated with hPTH1-34 (40μg/kg/day, n=6) or vehicle (n=6) by subcutaneous injection, or were implanted with osmotic pumps releasing hPTH1-34 (33.3 ng/hr/0.25 μL, equivalent to 40μg/kg/day,n=6) or vehicle (n=6) for 14 days. Another 6 mice were sacrificed on day 0 as a basal group. Bone mineral density (BMD) was measured by PIXImus at 0, 7 and 14 days. Serum was obtained at autopsy for the measurement of hPTH1-34, mouse intact PTH (mPTH1-84), mouse tartrate resistant acid phosphatase (mTRAP) and total calcium. iPTH treatment induced a 9% increase in femoral BMD (from 0.0581 to 0.0636 g/ cm^2, $p<0.01$); an 80% increase in mTRAP (from 9.0 to 16.2 U/L, $p< 0.01$); but no change in serum calcium. cPTH treatment for 2 weeks reduced femoral BMD by 5% (from 0.0570 to 0.0547 g/ cm^2, $p<0.01$); increased mTRAP (from 8.5 to15.2 U/L, $p<0.05$) and calcium (from 9.4 to14.6 mg/dl, $p<0.01$) by 80% and 57%, respectively. Neither treatment changed BMD in tibia or vertebrae ($p>0.05$), but compared to cPTH treatment, iPTH treatment had both higher femoral BMD (0.0636 *vs* 0.0547 g/cm^2, 16%, $p<0.01$) and tibial BMD (0.0449 *vs* 0.0414 g/cm^2, 9%, $p<0.05$). Serum mTRAP was increased, and endogenous mPTH1-84 was reduced to the same extent by both treatments. However, exogenous hPTH1-34 was only detected with cPTH administration. Although both modes of administration increased a resorption marker, only cPTH induced hypercalcemia without increased bone mass, while iPTH increased BMD with no change in serum calcium. We conclude that 1) the two modes of administration of the same daily amount of hPTH1-34 produce distinctly different outcomes in serum total calcium and long bone BMD , 2) exogenous hPTH1-34 stays high when infused continuously but is metabolized rapidly when injected daily , and 3) short-term intermittent or continuous treatment of mice with hPTH1-34 represents a good model to study the dual actions of PTH on the skeleton .

Disclosures: ***S.S. Lu****, None.*

SU558

Overexpression of G Protein-coupled Receptor Kinase 2 (GRK2) in Osteoblasts Decreases Bone Mass and Reduced the Anabolic Effects of PTH(1-34). L. Wang*, P. Flannery*, R. F. Spurney. Medicine, Duke Medical Center, Durham, NC, USA.

G-protein coupled receptor (GPCR) systems are important regulators of bone remodeling. The osseous effects of GPCR systems are likely to be modulated by the rate of receptor desensitization in osteoblasts. GPCR desensitization is largely mediated by phosphorylation of GPCR proteins by a family of enzymes termed GRKs. To investigate the role of GRKs in regulating bone formation in vivo, we overexpressed the potent GPCR regulator GRK2 in bone using the osteocalcin gene 2 (OG2) promoter to target expression to osteoblasts. Previous studies (JBMR 8(suppl 2):S38, 2003) found that GRK2 transgenic (TG) mice demonstrated a significant reduction in whole body bone mineral density (BMD) compared to non-TG littermate controls at 6 weeks of age. To investigate the age-dependent effects of GRK inhibition, we monitored BMD in TG mice and in controls at 6-week, 3-month and 6-month time points. Consistent with our previous findings, whole body BMD was decreased in TG mice compared to controls at the 6-week time point. The decrease in BMD was most prominent in trabecular rich lumbar spine and was less pronounced in cortical bone of the femoral shaft. A similar pattern was seen in animals at the 3 and 6 months time points although the difference decreased over time and remained statistically significant only in lumbar spine at 6 months of age (64.3 ± 1.2 mg/cm2 [non-TG] vs. 59.2 ± 0.9 mg/cm2 [TG]; P=0.003). To determine if the GRK2 transgene inhibited the effects of an anabolic GPCR agonist, 6-month-old mice were treated with PTH (1-34) for 4 weeks. Data was expressed as a percent increase in BMD above baseline to reduce the effect of the difference in baseline BMD. We found that PTH(1-34) increased whole body BMD to a greater extent in non-TG mice compared to TG animals (8.0 ± 0.9% [non-TG] vs. 3.4 ± 1.7% [TG]; P=0.025). A more pronounced effect of the GRK2 transgene on PTH(1-34) responsiveness was seen in trabecular rich lumbar spine (14.6 ± 3.2% [non-TG] vs. 6.9 ± 1.8% [TG]; P=0.038). PTH(1-34) treatment increased femoral shaft BMD to a similar extent in TG mice and non-TG controls (7.5 ± 1.9% [non-TG] vs. 7.4 ± 2.0% [TG]; P=NS). Taken together, these data suggest that enhancing GRK activity in osteoblasts causes a decrease in bone mass and reduction in the anabolic response to the bone-forming GPCR agonist PTH(1-34). We conclude that GRKs play a key role in regulating PTH responsiveness in bone.

Disclosures: ***L. Wang****, None.*

SU559

PTH Receptor Activation but not Internalization Is Required for MAPK Stimulation. P. A. Friedman[1], J. Ba*[2]. [1]Depts. of Pharmacology and of Medicine, University of Pittsburgh School of Medicine, Pittsburgh, PA, USA, [2]Dept. of Pharmacology, University of Pittsburgh School of Medicine, Pittsburgh, PA, USA.

The Type 1 PTH receptor (PTH1R) activates multiple signaling pathways, including mitogen-activated protein kinase (MAPK, ERK), in a cell- and ligand-specific manner. In previous work we showed that PTH stimulated ERK1 and ERK2 in kidney distal tubule cells. Blockade of MAPK inhibited PTH-stimulated calcium transport. Emerging evidence points to a requirement for internalization of some G protein-coupled receptors, such as the ß2 adrenergic receptor, for induction of MAPK activity. In the present work we determined the role of PTH1R endocytosis in MAPK stimulation by taking advantage of PTH peptide fragments that are either capable of activating the PTH1R without internalizing it, or internalizing the PTH1R without antecedent activation. PTH(1-34) activated the PTH1R with 20x cAMP formation and 2x inositol phosphate accumulation, and promoted receptor desensitization and internalization. MAPK activation was measured by phosphospecific immunoblotting. Results were normalized to total MAPK. In distal tubule kidney cells harboring 10^6 PTH receptors/cell, PTH(1-34) stimulated ERK2 in a time-dependent manner, with maximal 3-fold activation at 10 min. Therefore, the effects of other PTH peptide fragments were examined after a 10-min stimulation. PTH(1-31) stimulated adenylyl cyclase and PLC caused receptor desensitization. However, PTH(1-31) does not internalize the PTH1R. PTH(1-31) stimulated 2.5-fold activation of ERK2. PTH(7-34) does not activate or desensitize the PTH1R but promotes efficient PTH1R internalization in these cells. PTH(7-34) had no effect on ERK2. We conclude that MAPK activation in distal kidney cells requires PTH1R activation but not internalization.

Disclosures: ***P.A. Friedman****, None.*

SU560

Functional Studies of the Nuclear Localization Sequence of the PTH Receptor. E. K. Patterson*[1], P. H. Watson[1], A. B. Hodsman[1], G. N. Hendy[2], F. R. Bringhurst[3], L. J. Fraher[1]. [1]Medicine, Lawson Health Research Institute, University of Western Ontario, London, ON, Canada, [2]Medicine, McGill University, Montreal, PQ, Canada, [3]Medicine, Harvard University, Boston, MA, USA.

In previous studies presented to this society, we attempted to demonstrate the function of the putative nuclear localization sequence (NLS) we identified in the PTH receptor. Initial immunocytochemical studies demonstrated the unexpected result that the PTH1R is apparently able to localize to the nucleus of cells in the gut, ovary, testes, liver and kidney in rat. Further studies in the monoclonal cell line MC3T3-E1, demonstrated that this localization to the nucleus occurs in a cell-cycle dependent manner, moving into the nucleus just before S-phase. An analysis of the amino acid sequence of all available PTH1Rs revealed a putative NLS of the bipartite type first described in nucleoplasmin. We began studies using green fluorescent protein (GFP) tagged constructs of the PTH1R, as a whole, lacking the NLS or the NLS alone to determine the function of the putative NLS. The PTH1R-GFP constructs showed the receptor on the plasma membrane as would be expected, but the NLS deletion construct, collected in a ring around the nucleus, possibly due to an inability to be transported away from the endoplasmic reticulum. The construct with the putative NLS alone tagged with GFP, collected in the cytoplasm, but did not enter the nucleus. This suggested the 18 amino acid sequence identified as the NLS was not able on its own to direct GFP to the nucleus. Since phosphorylation has been shown to be important for the import of other proteins into the nucleus and we have identified probable phosphorylation sites surrounding the NLS, we decided to create a construct including regions surrounding the NLS. A construct was produced including 15 amino acids upstream of the NLS down to the C-terminus of the PTH receptor, which was tagged on the N-terminus with the FLAG epitope, and on the C-terminus with the c-myc epitope. LLC-PK1 cells were transiently transfected with this construct and the fusion protein was detected with immunofluorescence. Nuclear localization of the fusion protein was detected in a large number of cells using an anti-C-myc primary antibody, as compared to untransfected controls. These results suggest that sequences in the C-terminal cytoplasmic tail of the PTH1R are capable of targeting proteins to the nucleus and support the concept of PTH1R translocation to the nucleus.

Disclosures: ***E.K. Patterson****, None.*

SU561

Loss-of-function Mutations in Exons 2 through 13 of GNAS Impair Signalling through both Human Gs-alpha and XL-alpha Proteins. A. Linglart*, H. Jüppner, M. Bastepe. Endocrine Unit, Massachusetts General Hospital and Harvard Medical School, Boston, MA, USA.

The α-subunit of stimulatory G-protein ($G\alpha_s$) and its variant $XL\alpha_s$ share identical C-terminal domains encoded by exons 2-13 of *GNAS,* but both differ in their N-termini. $G\alpha_s$ is ubiquitously and mostly biallelically expressed, whereas $XL\alpha_s$ expression seems to be restricted to neuroendocrine tissues and occurs only from the paternal allele. Rat-$XL\alpha_s$ couples to typical $G\alpha_s$-coupled receptors in transfected cells that endogenously lack $G\alpha_s$ and $XL\alpha_s$ ($Gnas^{E2-/-}$ cells). To investigate the putative signalling function of human-$XL\alpha_s$ ($hXL\alpha_s$), which diverges from its rat homolog in the N-terminal domain, we transfected $Gnas^{E2-/-}$ cells with cDNAs encoding both wild-type and mutant forms of $hXL\alpha_s$ and $G\alpha_s$. In $hXL\alpha_s$ transfected $Gnas^{E2-/-}$ cells, cholera toxin treatment (inhibiting the intrinsic GTPase activity) and stimulation of the endogenous β-adrenergic receptor by Isoproterenol (Iso) raised cAMP levels from 6.5±5.2 to 36±11.5 pmol/well and 75.5±12.1 pmol/well, respectively, indicating that $hXL\alpha_s$ can function as a signalling protein. Mutations (Y391X, and H362P) identified in patients with pseudohypoparathyroidism (PHP) Ia and Ic were introduced into $hXL\alpha_s$ and $G\alpha_s$ cDNAs. These $hXL\alpha_s$ and $G\alpha_s$ mutants showed diminished basal cAMP accumulation and no evidence for Iso-stimulated second messenger formation. Compared to our previous study of wild-type $XL\alpha_s$ and $G\alpha_s$ that increase cAMP accumulation after PTH(1-34) or TSH treatment, the Y391X and the H362P mutant failed to increase the agonist-stimulated cAMP formation when $Gnas^{E2-/-}$ cells were co-transfected with cDNAs encoding the PTH/PTHrP or the TSH receptor (table).

cAMP (pmol/well); n= 4 to18; mean±SEM

	Y391X-$G\alpha_s$	**Y391X-$XL\alpha_s$**	**H362P-$G\alpha_s$**	**H362P-$XL\alpha_s$**
Basal	1.6±0.7	0.8±0.2	0.6±0.2	0.5±0.3
Isoproterenol	1.7±0.4	0.4±0.0	1±0.3	2.4±0.3
PTH	0.8±0.1	0.7±0.3	1.1±0.0	0.5±0.1
TSH	1.8±0.2	0.6±0.1	1.1±0.6	0.5±0.3
Cholera Toxin	6.3±3.2	31±15.5	1±0.5	0.8±0.4

Cholera toxin treatment of $hXL\alpha_s$ or $G\alpha_s$ with the Y391X mutation, but not with the H362P mutation yielded cAMP accumulation similar to that observed with wild-type $G\alpha_s$ and $hXL\alpha_s$. In summary, $hXL\alpha_s$ mediated ligand-dependent cAMP accumulation is indistinguishable from that of $G\alpha_s$ when expressed in $Gnas^{E2-/-}$ cells. These data suggest that 1) defective $hXL\alpha_s$ signaling may contribute to the phenotypes of diseases associated with *GNAS* mutations in exons 2-13, especially when inherited paternally; 2) the Y391X mutation affects coupling of $G\alpha_s$ and $hXL\alpha_s$ to different G protein-coupled receptors, likely explaining the PHP-Ic phenotype of the patient in whom this mutation was identified.

Disclosures: ***A. Linglart****, None.*

SU562

A Specific High-Affinity Carboxy-Terminal Parathyroid Hormone Receptor Is Present In Vascular Endothelial Cells And Utilizes a Calcium-Dependent Signaling Pathway. C. M. Isales[1], K. H. Ding[1], P. Divieti*[2], F. R. Bringhurst[3]. [1]Medicine, Medical College of Georgia and the Augusta VA Hospital, Augusta, GA, USA, [2]Medicine, Massachusets General Hospital, Boston, MA, USA, [3]Medicine, Massachussets General Hospital, Boston, MA, USA.

We previously reported that human umbilical vein endothelial cells (HUVEC) contain PTH1R and respond to PTH 1-84(intact) with increased cellular proliferation. However, we found that carboxy-terminal PTH (C-PTH) fragments 53-84, 70-84 and 73-84 increased intracellular calcium and proliferation to the same extent as intact PTH, while PTH 1-34 and 28-48 had no effect on either response. To define the specificity and signaling pathways utilized by intact vs. C-PTH molecules we used the intracellular calcium chelator BAPTA. BAPTA at concentrations of 1 μM and above was more effective in abolishing thymidine incorporation in PTH 1-84 stimulated cells PTH1-84(10-12M)+BAPTA(10-6M): 183+11 vs. 108+2.2; PTH73-84(10-12M)+BAPTA(10-6M): 185+10 vs. 139+8.3 %change/control+SEM. There was no effect of PKC inhibition on C-PTH stimulated proliferation, PTH1-84(10-12M)+Go6850(10-6M): 184+4.9 vs. 177+5; PTH73-84(10-12M)+ Go6850(10-6M): 186+8.5 vs. 182+6.5 %change/control+SEM. However, C-PTH stimulated proliferation was much more sensitive to inhibition by CAM kinase II inhibitor (KN93) compared to intact PTH: PTH 1-84(10-12M)+KN93(10-7M): 183+1.8 vs. 197+15.4; PTH 73-84+KN93(10-7M):188+3.5 vs. 153+0.5 10-12M: %change/control+SEM, p<0.01 PTH 1-84+KN93 vs. PTH 73-84+KN93. To assess the specificity of C-PTH fragment binding to the HUVEC we utilized alanine substituted PTH analogs (PTH53-84) in which the EDN sequence at 55-57 is replaced with alanine(s), the single alanine substituted analog (M9.1) binds CPTHR with equal affinity as PTH53-84 while the triple alanine substituted analog (M9) does not bind to the C-PTH receptor. We found that the triple alanine substituted PTH M9 (in contrast to the M9.1 analog) does not significantly stimulate HUVEC proliferation PTH53-84 M9(10-12M) vs. PTH53-84M9.1(10-12M): 116+3.5 vs. 156+8.7 %change/control+SEM.

In an effort to assess the downstream effects of the C-PTH fragments on HUVEC function we performed gene microarray studies. PTH 1-84 (10-11M) altered the expression of 222 genes of which 166 genes were upregulated and 56 down-regulated. In contrast PTH 73-84 (10-11M) altered the expression of 1621 genes of which 922 genes were upregulated and 699 down-regulated.

Taken together, these data demonstrate the existence of a specific high-affinity C-PTH receptor in endothelial cells that preferentially uses a calcium-CAM kinase II signaling pathway to stimulate endothelial cell proliferation.

Disclosures: ***C.M. Isales****, None.*

SU563

PTH Receptor Activates Wnt/β-catenin Signaling Pathway in Growth Plate Chondrocytes ex vivo. J. Guo, F. R. Bringhurst, H. M. Kronenberg. Endocrine Unit, Massachusetts General Hospital and Harvard Medical School, Boston, MA, USA.

Wnt/β-catenin-signaling pathway plays an important role in many processes of development. Activation of the Wnt family of proteins leads to translocation of β-catenin into the nucleus and the formation of transactivation-competent Lef/Tcf-β-catenin complexes. To examine whether the canonical Wnt/β-catenin signaling pathway is regulated by the PTH/PTHrP receptor (PTHR) in chondrocytes, we treated cultured E14.5 tibia and femur isolated from mice expressing the TOPGAL transgene, and then assessed reporter β-galactosidase activity by in situ staining using X-gal. In TOPGAL transgenic mice the LacZ gene is expressed under the control of regulatory sequence consisting of three consensus Lef/Tcf-binding motifs upstream of a minimal c-fos promoter. The transgene expression is dependent upon stabilized β-catenin and is comparably responsive to Tcf3 and Lef1 in vitro. Here we show that TOPGAL is weakly active mostly at the boundary of proliferative and prehypertrophic chondrocytes after treatment with vehicle for three days, whereas treatment with hPTH (100 nM) dramatically induced transgene expression in chondrocytes at the center of the rudiments. At the same time, PTH treatment greatly suppressed chondrocyte hypertrophy, as assessed histologically and by in situ hybridization for type X collagen mRNA. These observations raise the question of the role of PTHrP-induced Wnt signaling in the growth plate.

Disclosures: ***J. Guo****, None.*

SU564

Signaling Characteristics of the PTH Type-1 Receptor can not be Transferred to the Type-2 Receptor by Mimicking the Type-1 Cytosolic Interface Using Receptor Chimeras. E. Blind, U. Heindel*, T. Wobbe*. Medicine - Endocrinology, University of Wuerzburg, Wuerzburg, Germany.

Activation of the phospholipase C (PLC) pathway upon stimulation with PTH is unique to the PTH-1 receptor (P1R) and is virtually absent in the PTH-2 receptor (P2R). The sites of P1R mutations known to reduce PLC signaling may achieve this indirectly by disturbing coupling at other sites. We therefore chose a more stringent approach and attempt to reestablish PLC signaling in the closely (70%) related P2R by gradually adapting the P2Rs cytosolic interface to a P1R-like sequence by engineering hybrid P1R/P2R constructs. Key differing regions of the P1R´s second loop (DT272-273:EK), third loop (IW344-345:LR), and C-terminal tail (T440-end: K-end) were put into the P2R. A fourth chimeric P1R/P2R receptor, combining all these changes, thus had a > 90% sequence identity with the cytosolic interface of the P1R. All mutants were expressed on the cell surface of stably transfected HEK 293 cells, using a radioreceptor assay with [125I]-Nle8,21-Tyr34-rat PTH(1-34), with a similar density of 1.1 to 2.5 mio receptors/cell. Activation of the PLC pathway was assessed by: 1) accumulation of total inositol phosphates in myo[3H]-inositol-prelabeled cells. No increase was detectable in the P2R or any of the receptor chimeras, even after enhancing the possible response by blockade of protein kinases A and C, despite an up to 13-fold increase with the P1R upon PTH stimulation. 2) Similarly, a PTH-induced increase in intracellular calcium (detected by fluo-3) of the wildtype P1R with as little as 1 nM hPTH(1-34) was completely absent in all mutants as well as in the P2R. The PTH-induced max. response of the cyclic AMP pathway was virtually identical for the P1R and P2R. However, the max. response of the mutant with the P1R tail sequence was reduced to only 35% (PTH) and 26% (TIP39) of the P2R response. Surprisingly, this signaling loss could be overcome by introducing more P1R sequence into the second and third cytoplasmic loop of this P1R/P2R hybrid receptor thus regaining a max. cAMP response of 64% (PTH) and 85% (TIP39). Presumably, an interaction of P1R sequences seems to result in a more effective coupling to the cAMP signaling pathway. In conclusion, these results suggest that the activation of the IP / intracellular calcium signaling pathway by the P1R is highly dependent on a P1R-like intracellular contact interface, which can not be mimicked easily even in the presence of > 90% of P1R sequence in the cytosolic interface of the P2R.

Disclosures: ***E. Blind****, None.*

SU565

Expression, Purification and Characterization of Human Parathyroid Hormone Receptor 1 from a Stable HEK293S Cell Line. L. Gan*, J. M. Alexander, M. Rosenblatt. Department of Physiology, School of Medicine, Tufts University, Boston, MA, USA.

In order to further explore the structural basis of the interaction between human parathyroid hormone (hPTH) and human parathyroid hormone receptor 1 (hPTHR1) by comparative methods such as photoaffinity crosslinking, X-ray crystallography or NMR, we aimed to purify milligram quantities of receptor. To accomplish this, a HEK293S GnTI$^-$ cell line stably expressing recombinant hPTHR1 with a 9 amino acid rhodopsin tag at its C-terminus has been constructed. The inactivity of N-acetylglucosaminyltransferase I in this cell line is hypothesized to enable the production of receptor with homogeneous N-glycan at its four N-glycosylation sites. Transfection of the stable HEK293S GnTI$^-$ cell lines with CRE-luc plasmid resulted in robust increase in luciferase activity in response to hPTH(1-34), indicating the expressed hPTHR1_rho is fully functional (EC_{50} = 2.4 nM). The receptor was expressed in large-scale cell culture grown in a bioreactor. It was solubilized with dodecyl maltoside and subsequently purified to homogeneity by affinity and gel filtration chromatography. The purified receptor will allow us to accurately identify the contact sites in the ligand-receptor complex by structural analysis.

Disclosures: ***L. Gan****, None.*

SU566

G protein Dependent Binding of a PTH(1-15) Analog Radioligand to the Juxtamembrane Portion of the PTH/PTHrP Receptor. T. Dean*, A. Linglart, M. Bastepe, M. Mahon, J. T. Potts, H. Jueppner, T. J. Gardella. Endocrine Unit, Massachusetts General Hospital, Boston, MA, USA.

PTH(1-34) is thought to bind to the PTH/PTHrP receptor (PTHR) via a two-site mechanism that involves high-affinity interactions between the ligand's C-terminal domain and the receptor's amino-terminal extracellular (N) domain, and lower-affinity interactions between the ligand's amino-terminal domain and the receptor's juxtamembrane (J) region, comprised of the extracellular loops and seven transmembrane helices. It is further hypothesized that the J domain interactions promote G protein coupling, and, reciprocally, that G protein coupling stabilizes the ligand/J domain complex. We explored this hypothesis using ^{125}I-PTH(1-34) as a radioligand that binds to both N and J domains, and ^{125}I-PTH(1-15) (^{125}I-[Aib^{1,3},Gln^{10},Har^{11},Ala^{12},Trp^{14},Tyr^{15}]ratPTH(1-15)NH$_2$) as a radioligand that binds selectively to the J domain. In membranes prepared from LLC-PK1 (HKRK-B7) cells that stably express the hPTHR, ^{125}I-PTH(1-34) and ^{125}I-PTH(1-15) exhibited similarly high binding affinities (K_ds ~1 nM) and maximum binding values (B_{max}s ~ 5 picomoles/mg protein). The binding of ^{125}I-PTH(1-34) was only marginally (~10%) inhibited by GTPγS (IC_{50} > 100,000 nM), whereas, in contrast, the binding of ^{125}I-PTH(1-15) was nearly completely (~95%) inhibited by GTPγS (IC_{50} = 10 nM). The rates of dissociation of both the ^{125}I-PTH(1-34)/ and ^{125}I-PTH(1-15)/PTHR complexes formed in HKRK-B7 cell membranes were slow ($t_{1/2}$s ~ 100 minutes). In the presence of GTPγS, most (~75 %) of the bound ^{125}I-PTH(1-34) remained in a slowly dissociating form, while a minor fraction (~25%) dissociated rapidly ($t_{1/2}$ ~3 min.). In contrast, nearly all (~95%) of the bound ^{125}I-PTH(1-15) dissociated rapidly ($t_{1/2}$ < 3 min.) in the presence of GTPγS. Since the PTHR signals most strongly via the cAMP pathway, we tested the hypothesis that Gαs might be the principal G protein determinant of ^{125}I-PTH(1-15) binding affinity. To test this, we used a line of fibroblast cells (Gnas$^{E2-/-}$ cells) derived from Gαs gene-knock-out mouse embryos, and transduced these, via an adenovirus/shuttle vector system, to transiently express the hPTHR. ^{125}I-PTH(1-34) bound to these cells as well as it did to HKRK-B7 cells; in sharp contrast, ^{125}I-PTH(1-15) bound only poorly. The overall results show that the binding of PTH(1-15) to the PTHR, but not that of PTH(1-34), is strongly dependent on coupling of the receptor to G protein, and that the G protein modulates specifically the affinity of the J domain ligand-binding site.

Disclosures: ***T.J. Gardella****, None.*

SU567

The Skeletal Response to Estrogen Is Impaired in Female but not in Male Steroid Receptor Coactivator-1 Knock Out Mice. U. I. Moedder[1], A. Sanyal[1], J. Xu*[2], B. W. O'Malley*[2], T. C. Spelsberg[1], B. L. Riggs[1], S. Khosla[1]. [1]Mayo Clinic, Rochester, MN, USA, [2]Baylor University, Houston, TX, USA.

Steroid Receptor Coactivator (SRC)-1 is an important nuclear receptor coactivator that enhances estrogen (E) action in a number of tissues. We previously demonstrated (Endocrinol 145:913, 2004) that SRC-1 knock out (KO) female mice have a defect in E action in cancellous, but not in cortical bone. Here we report findings in the 3 month old male littermates of the female mice that were treated concurrently either with sham surgery, orchiectomy (orch) plus vehicle (V), or orch plus estradiol (E_2) replacement (0.25 μg/d) (n = 10/group) by slow release pellets for 60 days. The Figure below shows, for reference, our previous data on changes in the spine (which contains predominantly cancellous bone) BMD, measured by DXA, in the wild type (WT) and SRC-1 KO female mice (panel A) as well as the comparable new data on spine BMD changes in the male WT and SRC-1 KO mice (panel B). While the 0.25 μg/d dose of E_2 was entirely ineffective in preventing spine bone loss following ovariectomy in the female SRC-1 KO mice (Panel A; overall P-values are for within strain ANOVAs), the same dose of E_2 was equally effective in the male WT and SRC-1 KO mice in preventing spine bone loss following orch (Panel B).

We have previously also demonstrated (J Endocrinol 176:349, 2003) that in osteoblastic cells, SRC-1 potentiates the activity of co-expressed ER-α/β or ER-β alone, with little or no potentiation of ER-α. Based on this, we hypothesized that the defect in E action in cancellous bone in the female SRC-1 KO mice could be due to the presence of both ER-α and -β in cancellous bone versus the predominant expression of ER-α in cortical bone (Endocrinol 145:913, 2004; JCEM 86:2309, 2001). Of interest, using ER-α KO mice, Sims et al. (JCI 111:1319, 2003) have recently demonstrated that whereas ER-β plays no role in E action on bone in male mice, it does partially mediate E effects on bone in female mice. Thus, our current findings of a lack of a defect in E action in male SRC-1 KO mice are consistent with this gender difference in ER-β action on bone in male versus female mice. These findings also provide further support for our hypothesis that the defect in E action predominantly in cancellous bone in the SRC-1 KO female mice may be due to differential interactions of SRC-1 with ER-β versus ER-α in cancellous and cortical bone.

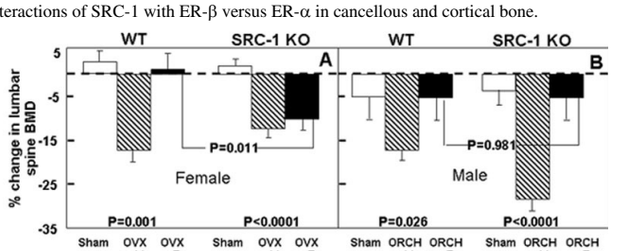

Disclosures: ***S. Khosla****, None.*

SU568

Loss of Signaling Through Classical EREs Leads to Osteopenia and Paradoxical Responses to Estrogen in Cortical Bone. F. A. Syed*[1], A. Sanyal[1], D. Fraser*[1], A. Krust*[2], P. Chambon*[2], L. Jameson*[3], T. C. Spelsberg[1], B. L. Riggs[1], S. Khosla*[1]. [1]Mayo Clinic, Rochester, MN, USA, [2]Institut de Genetique et de Biologie Moleculaire et Cellulaire (IGBMC), Illkirch, France, [3]Northwestern University, Chicago, IL, USA.

The ER can act either via classical EREs or through non-classical pathways that do not require binding to an ERE (eg AP-1 sites). Generation of mice with a wild type ERα allele (ERα+) and an ERα allele with a knock-in mutation abolishing ERE binding [non-classical ER knock-in, NERKI (Mol Endo 16:2188, 2002)] presents a unique opportunity to unravel the roles of classical vs non-classical pathways of E signaling in bone. However, while heterozygous male NERKI mice are fertile, heterozygous females are infertile, making it difficult to generate homozygous NERKI/NERKI mice. To circumvent this problem, we crossed heterozygous ERα+/NERKI male with ERα+/ERαKO (-) female mice and compared skeletal phenotypes and E action in ERα+/ERα+ mice versus littermates with one deleted ERα and one NERKI allele (NERKI/ERα-). Due to the presence of only the NERKI receptor in the NERKI/ERα- mice, they can transduce E signals solely through non-classical pathways. Trabecular BMD (tibial metaphysis) was similar in ERα+/ERα+ and NERKI/ERα- mice; however, cortical BMD at the tibial mid-shaft was reduced by 6.2% in the NERKI/ERα- mice (P < 0.001). To further assess E signaling in the NERKI/ERα- mice, 3 month old ERα+/ERα+ and NERKI/ERα- mice underwent sham surgery, ovx plus vehicle (V) pellet, ovx plus a 0.25 μg/d E_2 pellet ($E_{0.25}$), or ovx plus a 1 μg/d E_2 pellet ($E_{1.0}$) (n = 10-12/group). All treatments were for 2 months. As shown in the Figure, the pattern of changes in tibial cortical BMD was the exact opposite in the NERKI/ERα- as compared to the ERα+/ERα+ mice (P < 0.001 for a treatment/genotype interaction). Thus, relative to the sham mice, ovx'd NERKI/ERα- mice gained more bone (not less, as in the ERα+/ERα+ mice), and E dose-dependently suppressed this increase (while augmenting it in the ERα+/ERα+ mice).

These data thus demonstrate that E signaling solely through non-classical pathways results in osteopenia and paradoxical responses to E in cortical bone. Defining the molecular mechanisms responsible for these changes in the NERKI/ERα- mice may provide fundamental, novel insights into the role of classical vs non-classical signaling pathways in transducing E effects on bone.

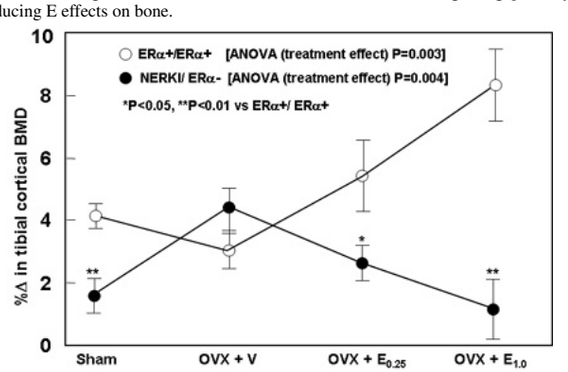

Disclosures: ***S. Khosla****, None.*

SU569

Estrogen regulation of TNF-α -induced expression of cytokine mRNA in U2OS human osteosarcoma cells transfected with estrogen receptor α. T. Guo*[1], E. Lamminen*[2], K. Väänänen*[2], P. Härkönen*[2], T. Hentunen[2]. [1]Institute of Hematology, Union Hospital, Huazhong University of Science and Technology, Wu han, Hubei, China, [2]Medicity Research Laboratory and Department of Anatomy, Institute of Biomedicine, University of Turku, Tykistökatu 6, 20520, Turku, Finland.

Osteoblasts are capable of producing a wide array of cytokines and growth factors that can potentially act as autocrine and paracrine regulators of bone cell function. To investigate the action of estrogen on TNF-α induced cytokine production in osteoblast-derived cells we first stably transfected estrogen receptor -negative U2OS human osteosarcoma cells with human estrogen receptor α or an empty control vector. Expression of estrogen receptor α in transfected U2OS cells was confirmed by RT-PCR, western blotting and immunocytochemistry. Reporter gene assays were further used to confirm that estrogen receptor α was functional in these cells. We then used these cell lines to study the effect of TNF-α on expression of TNF-α and IL-6 mRNA using RT-PCR analysis of the cells treated with or without estrogen. Treatment of U2OS cells with TNF-α for one hour led to a strong induction of IL-6 and TNF-α mRNA in both estrogen receptor a expressing and non-expressing cells. Pretreatment of the cells with 17-β-estradiol for 24 hours before a one-hour incubation with TNF-α blocked the TNF-α induction of IL-6 and TNF-α mRNA in estrogen receptor α expressing U2OS cells but had no effects on the increase of IL-6 and TNF-α mRNA levels in estrogen receptor α -negative control cells. - Our results demonstrate that ectopic expression of estrogen receptor α in estrogen receptor -negative U2OS human osteosarcoma cells can render them estrogen responsive. The results further show that in these osteoblast-derived cells 17-β-estradiol represses expression of IL-6 and TNF-α mRNA by interacting with estrogen receptor α.

Disclosures: ***T. Guo****, None.*

SU570

Creation of Estrogen-Resistance in vivo by Transgenic Overexpression of the Heterogeneous Nuclear Ribonucleoprotein (hnRNP)-Related Estrogen Responsive Element Binding Protein. H. Chen[1], W. D. Stuart*[2], L. Nguyen*[1], B. Hu*[3], G. Huang*[1], T. L. Clemens[4], J. S. Adams[1]. [1]Division of Endocrinology, Cedars-Sinai Medical Center, Los Angeles, CA, USA, [2]Surgery, University of Cincinnati, Cincinnati, OH, USA, [3]Pathology, Cedars-Sinai Medical Center, Los Angeles, CA, USA, [4]Pathology, University of Alabama, Birmingham, AL, USA.

Trans dominant-negative-acting proteins in the hnRNP family are now thought to be a proximal cause of steroid/sterol hormone resistance in both non-human and human primates. Estrogen resistant New World primate cells demonstrate constitutive overexpression of an hnRNPC-like protein that competes with the estrogen receptor (ER) for binding to the estrogen responsive element (ERE). In order to verify that it is this hnRNPC-like protein, coined the ERE-binding protein or ERE-BP, that legislates estrogen-resistance in vivo, we generated five transgenic mouse lines that overexpressed ERE-BP only in breast tissue under the control of whey acidic protein (WAP) gene promoter. Despite the detection of equivalent levels of transgene in the breast of male and female ERE-BP +/- mice, there was distinct sexual dimorphism at the level of expression of the product of the transgene. At the protein level, ERE-BP was encountered only in breast of female transgenic mice. Low-to-high ERE-BP overexpression did not alter expression of ER in the breast of transgenic mice. Both male and female founder mice were viable and fertile. Female transgenics in all lines gave birth to pups, but the ability to nurse offspring was variable. Mothers with low or intermediate levels of ERE-BP expression in the breast were able to lactate and nurse pups to weaning in a fashion similar to that observed for wild-type pups. Mothers from the high ERE-BP-overexpressing line were unable to lactate, and none of their pups survived to weaning unless were fostered to a normally-lactating mother. This maternal nursing phenotype were recapitulated in all subsequent generations of the "high" ERE-BP line. Mice with a low ERE-BP transgene expression had a mammary phenotype similar to wild-type. However, mice expressing the high level of ERE-BP demonstrated both impaired mammary gland differentiation and lactation; whole-mount and histological analyses showed only rudimentary duct formation, aborted alveolar generation and near absence of milk-containing lumina. In summary, relatively high overexpression of ERE-BP leads to the development of a lactation-deficient mouse incapable of undergoing adolescent "estrogen priming" of mammary tissue. It is our plan to employ this animal model of estrogen resistance to antagonize estradiol-ERalpha-ERE directed breast cancer growth and development in vivo.

Disclosures: ***H. Chen****, None.*

SU571

From Non-genomic Androgen Action to phosphatidylinositol 3-Kinase/Akt Signaling Pathway in Osteoblasts. H. Kang*[1], K. Huang*[2], K. Huang*[1]. [1]Graduate Institute of Clinical Medical Sciences, Chang Gung University, Kaohsiung, Taiwan Republic of China, [2]Department of Biological Science, National Sun Yat-sen University, Kaohsiung, Taiwan Republic of China.

Androgens have important effects on the human skeleton in both males and females. However, the mechanism of androgen action on bone cell growth remains unclear. The aims of this current study were to determine the effect and mechanism of androgen action on the osteoblast cells. Here we demonstrated that 5α-dihydrotestosterone (DHT) accelerates cell growth of MC3T3-E1 cell line in a time and dose dependent manner. The specific phosphatidylinositol 3-kinase (PI 3-kinase) inhibitor LY294002 and kinase-deficient Akt mutant can repress the androgen effect on MC3T3-E1 cells. Western blot analysis showed that DHT, 17β-estradiol and testosterone (T) induce a rapid and transient phosphorylation of Akt in MC3T3-E1 cells. This activation reached to a plateau after 15 min and gradually diminished after 60 min of DHT treatment. Fluorescence microscopy showed a distinct increase in immunostaining intensity in the nuclear interior after androgen treatment but no change in the subcellular distribution of Akt when the cells were pretreated with hydroxyflutamide (HF) or LY294002. In addition, small interfering RNA against androgen receptor (siRNA-AR) prevented DHT-induced Akt phosphorylation and cell growth. In addition, G-proteins, phospholipase C (PLC), Src kinase and intracellular calcium mobilization are essential for androgen-mediated Akt activation. These findings strongly suggest that this androgen non-genomic action mediated by AR and androgen-induced Akt activation represents the first physiological finding to indicate how steroid hormones such as androgens can mediate the nuclear localization of Akt/PKB in osteoblasts that has previously mainly been linked to growth factor-induced events occurring at the plasma membrane level.

Disclosures: ***H. Kang****, None.*

SU572

Effects of Phytoestrogens and Their Metabolites on estrogenic activity and Osteoclast Formation. C. Hwang*[1], Y. Kang[1], I. Moon*[1], C. Yim*[2], H. Yoon[2], I. Han*[2], H. Hur*[3], K. Han[2]. [1]Laboratory of Endocrinology, Samsung Cheil Hospital and Women's Healthcare Center, Sungkyunkwan University School of Medicine, Seoul, Republic of Korea, [2]Medicine, Samsung Cheil Hospital and Women's Healthcare Center, Sungkyunkwan University School of Medicine, Seoul, Republic of Korea, [3]Department of Environmental Science and Engineering, Gwangju Institute of Science and Technology, Gwangju, Republic of Korea.

Phytoestrogens are plant-derived compounds with estrogen-like biological activity. Although there are many convincing data on the bone-sparing effects of soy isoflavonoes such as genistein and daidzein, the exact effects and mechanisms of phytoestrogen action remain elusive. In this study, we investigated the estrogenic activity of phytoestrogens and their metabolites in competition binding assays with ERα or ERβ protein, and in a transient gene expression assay by co-transfection of ERα or ERβ cDNA with estrogen dependent reporter plasmid. Also, we examined the effect of phytoestrogens on the $1,25(OH)_2D_3$-induced osteoclast formation. phytoestrogens and metabiltes; GTN(genistein), DIH-GTN(dihydrogenistein), DDZ(daidzein), DIH-DDZ(dihydrodaidzein), T-DDZ(tetrahydrodaidzein), Eqoul, O-DMA(O-desmethyl-angolensin). Saturation ligand-binding analysis of hERα and β protein for [^{3}H]-17β-estradiol(E_2) revealed a K_d of 0.054nM for ERα and 0.078nM for ERβ. Relative binding affinities(RBA) of phytoestrogen metabolites are 100-1000-fold lower than that of E_2 and they bound more stronger to ERβ than to ERα. The phytoestrogens and their metabolites stimulated the transcriptional activity of both ER subtypes in co-transfection analysis using MCF-7, MC3T3E1 and 293 embryonic kidney cells. The ranking of binding affinity is, E2>RAL>>GTN>EQOUL>>DDZ>T-DDZ>O-DMA>DIH-GTN>DIH-DDZ for ERα, and E2>RAL>>GTN>EQOUL>>T-DDZ>DDZ=O-DMA>DIH-GTN>DIH-DDZ for ERβ. Transactivation assay using cells showed similar degrees to the binding affinities. The phytoestrogens and metabolites induced cell proliferation 2-6-fold higher in MCF-7 than control, but not in MC3T3E1 cell line. E_2(10^{-8}M-10^{-5}M), raloxifene(10^{-8}M-10^{-5}M), tamoxifen(10^{-6}M-10^{-5}M) and genistein(10^{-6}M-10^{-5}M) clearly inhibited the $1,25(OH)_2D_3$-induced osteoclast formation, but not with others metabolites. In transactivation analysis using 293 cell and $1,25(OH)_2D_3$-induced osteoclast formation in the presence of E_2 or raloxifene, genistein did not enhance the activity of E_2 or raloxifene. These results demonstrate that the estrogenic activity of phytoestrogens is substantially weak compared to E_2, and phytoestrogens did not show a synergistic action on the activity of E_2

Disclosures: ***C. Hwang****, None.*

SU573

Ginsenoside Rg1 Induce Human Breast Cancer Cell Proliferation and IGF-I Receptor Expression via Tyrosine Kinase- and MEK-Dependent Pathways. W. Lau*, W. Chen*, R. Y. Chan*, M. Wong. Department of Applied Biology and Chemical Technology, Central Laboratory of the Institute of Molecular Technology for Drug Discovery and Synthesis,The Hong Kong Polytechnic University, Hong Kong, Hong Kong Special Administrative Region of China.

Ginsenoside Rg1, an active ingredient commonly found in ginseng root, was previously demonstrated to be a novel class of phytoestrogen as it can stimulate the growth of human breast cancer (MCF-7) cell as well as to activate the estrogen response element-luciferase activity in HeLa cells. Interestingly, the action of Rg1 is estrogen receptor alpha (ERa)-dependent but it does not interact directly with this receptor. Therefore, we hypothesize that Rg1 may mediate its estrogen-like actions in MCF-7 cell via its cross-talk with IGF-I receptor (IGF-IR) mediated pathway. The present study aims to investigate if Rg1 alter signaling proteins expressions in the IGF-IR mediated pathway and to determine if tyrosine kinase and the downstream signaling molecule MEK are involved. In order to investigate the roles of tyrosine kinase and MEK in the action of Rg1, MCF-7 cells treated with 1 pM Rg1 were cotreated with either 50 μM genistein (tyrosine kinase inhibitor) or 50 μM PD98059 (MEK inhibitor). After treatment of MCF-7 cells for 48h, their effects on cell proliferation was determined by MTS assay and their effects on protein expression of IGF-IR, src-homology-collagen (Shc) and ERa were measured by western blotting analysis. Our results showed that Rg1 could increase the expression of IGF-1R protein significantly ($p<0.05$) but did not alter the expression of Shc and ERa. When MCF-7 cells were cotreated with 50 μM genistein, the proliferative effects of Rg1 and its induction of IGF-1R protein expression were completely abolished. Similarly, the effects of Rg1 on MCF-7 cells could also be abolished by 50 μM PD98059. These results showed that the proliferative effect of Rg1 in MCF-7 cells is at least in part mediated by the induction of IGF-I receptor expression and its action involved both tyrosine kinase- and MEK- dependent pathways. These data provide new evidence to support our hypothesis that Rg1 may mediate its estrogen-like actions in MCF-7 cell via the cross-talk with IGF-I receptor mediated pathway.

Disclosures: ***W. Lau****, None.*

SU574

Proteome Analysis for the Identification of Estrogen Regulated Proteins in Bone. R. Pastorelli*[1], D. Carpi*[1], L. Airoldi*[1], C. Chiabrando*[1], R. Bagnati*[1], R. Fanelli*[1], S. Moverare[2], C. Ohlsson[2]. [1]Department of Environmental Health Sciences, Institute of Pharmacological Research, Milan, Italy, [2]Department of Internal Medicine, Centre for Bone Research at the Sahlgrenska Academy, Gotenburg, Sweden.

Estrogen deficiency results in a reduced bone mass, which can be prevented by treatment with estrogen. However, the detailed cellular and molecular mechanisms underlying these effects remain poorly understood.

In this study, the *in vivo* effects of estrogens on global bone protein expression have been investigated by comprehensive differential display analysis and mass spectrometry, in a murine model of osteoporosis induced by ovariectomy followed by treatment with 17-beta estradiol (E2).

To our knowledge, this is the first report of a proteomic analysis of bone *in vivo*. Humerus proteome profiles were examined in three experimental mice groups: (i) sham-operated with normal ovarian functions (sham), (ii) ovariectomized with osteoporosis induced by ovariectomy (ovx), and (iii) ovx mice treated with 17-beta estradiol. (ovx+E2). Bone proteins were separated by 2-D electrophoresis and visualized by the Coomassie colloidal staining. Approximately 300 spots in each averaged (n=3) gel image were detected and quantitated using the Progenesis Workstation software (Nonlinear Dynamics, UK). Differential expression analysis among the three experimental groups showed statistically significant changes for fourteen proteins, which were subsequently identified by mass spectrometry (MALDI-TOF-MS and LC-MS/MS). Our results indicate that ovariectomy causes a broad spectrum of metabolic perturbations in a nonreproductive tissue like bone,

and suggest possible interactions among various proteins in estrogen depletion. Our data also suggest that some proteins, related to cytoskeleton and to energy pathways, are involved in the mechanism behind the bone sparing effect of estrogens.
In conclusion, the identification of several differential expressed proteins, as described in this study, might represent an important starting point for the search of novel aspects of the pleiotropic effects of estrogens on bone.

Disclosures: ***C. Ohlsson****, None.*

SU575

Estrogen Receptor α and β Heterodimers Have Unique Effects on Estrogen- and Tamoxifen-Dependent Gene Expression. D. G. Monroe[1], F. J. Secreto[1], B. J. Getz*[1], B. L. Riggs[2], S. Khosla[2], T. C. Spelsberg[1]. [1]Biochemistry and Molecular Biology, Mayo Clinic, Rochester, MN, USA, [2]Endocrine Research Unit, Mayo Clinic, Rochester, MN, USA.

Estrogen (E) exerts its genomic effects largely through two distinct estrogen receptor (ER) isoforms, ERα and ERβ, which function as dimers and are found individually or in combination. The presence of both isoforms in osteoblasts (OBs) can potentially lead to either homodimer formation or ERα heterodimer formation in response to ligand binding. Virtually no information exists in the literature concerning the functions of the ERα heterodimer on gene expression. Therefore, we have developed osteoblastic U2OS cell lines, stably expressing ERα, ERβ or both ERα and ERβ. Western blot analysis demonstrates that the U2OS-ERα line expresses the receptors in a 1:4 ratio (ERα :ERβ). Using a combination of CoIP and an ERα-specific agonist (PPT), we have identified functional ERα heterodimers. To understand the contribution of ERα in ligand-dependent gene expression, we first performed duplicate microarray analysis in the ERα which were treated with E2 for 24 hrs using the U2OS-ERα and -ERβ lines as controls. Microarray analysis identified 270 genes regulated by E2 (< > 2-fold) in the ERα line with 90 (33 %) regulated exclusively in the ERα line (compared to the ERα and ERβ lines). These results indicate that ERα heterodimers specifically regulate the expression of a unique pattern of genes. Since the SERM, 4OH-tamoxifen (4HT) has effects on osteoblasts and is clinically relevant, we performed identical microarray analysis using 4HT as the ligand. Significantly less genes (140), when compared to E2, were 4HT-regulated (< > 2-fold) in the ERα line. Interestingly, 95 (68 %) were regulated exclusively in the ERα line, again demonstrating that 4HT bound to the ERα heterodimer generates specific patterns of gene regulation. Relatively few genes are commonly regulated in the ERα, ERβ and ERα by both E2 and 4HT (9 %, 12 %, 10 %, respectively), citing important differences that the actions of the ER isoforms and the SERMs have on ER-dependent gene expression. To more stringently examine the genes specifically regulated by 4HT, we identified those genes regulated by 4HT (< > 2-fold) that were unaffected by E2 treatment (within 20 % of control). We found 23, 24, and 31 genes (in ERα, ERβ, ERα) that fit this stringent criteria, demonstrating that 4HT can effect gene expression on a unique set of genes not affected by E2. Collectively our data clearly show that the ERα heterodimer, as well as ERα and ERβ homodimers, have specific and unique effects on ligand-dependent transcription in OBs. Furthermore, E2 and 4HT also have unique effects on gene expression through each of these isoforms.

Disclosures: ***D.G. Monroe****, None.*

SU576

Comparative Analysis of Bone Tissue Histomorphotherapy in the Ovariectomized (OVX) Rats under Replacement Hormonal Therapy and a Phytoestrogen. A. Kandilyotu, F. Gafurova*, L. Nugmanova*, V. Vorojeikin*. Institution of Endocrinology, Tashkent, Uzbekistan.

Aim- to study effect of a phytoestrogen (ferutinin) on the ovariectomized rat bone tissue and to compare the effect with the one of a replacement hormonal therapy (estradiol valerat+levonorgestrel). 3-month old white rats-virgins with body mass of 120-150g were divided into 5 groups. The 1st control group (n=10)-intact animals, the 2nd one - sham OVX rats (n=10), the 3rd one - OVX untreated rats (n=20), 4th - 10 OVX rats receiving estradiol valerat + levonorgesterl (*per os* 0.5 mg)and 5th - 10 OVX rats receiving ferutinin (*per os* 1,2 mg). The 3rd group was subdivided into two subgroups, 10 rats decapitated a month after castration and 10 rats- two month after castration, respectively. Ferutinin is an ester of terpenoid alcohols obtained from a Central Asian plant *Ferula L* possessing estrogenic activity. Thighbones were prepared; their proximal metaphyses underwent histomorphometry. Histomorphometry of sham OVX rats was similar to the one in the control structure. The 3rd group rat bone histomorphometry "a month after castration" showed marked signs of osteoporosis. Thighbone mass reduction in female rats by 24% is the leading sign. The process is caused by both cortical layer and trabeculae thickness reduction. In the 3rd group rat bones "2 months after castration" revealed reduction in mass of non-calcified thighbone by 32% of the initial one, decrease of cortical layer area by 30%, the highest (35%) reduction being observed in trabecular area. The trabeculae are thin and "trabecular nodes", their connection zones, are practically absent. Histomorphometry of the 4th group rat bones showed: the bone resorption intensity decrease. Though thighbone mass is 0.9% lower than the one in the condition "a month after castration", it is 10.7% higher than that in the condition "two months after castration". The increase of cortical layer area by 6.5% in the average and the one of trabecular apparatus by 15.7%, are the evidence for the fact. Thinning of the trabeculae is less marked; they have few connective nodes. In the5th group rats:highbone mass reduction by 5.4% as compared with the one under condition "a month after castration" and its increase by 5.6% as compared with the one under condition "two months after castration". Cortical layer area increased by 3.7% in the average, the one of trabecular apparatus by 9%. Hormonal therapy stimulated osteogenesis, stabilized resorption and sustained it on the level of "a month after castration" condition. Ferutinin caused poor stimulation of osteogenesis, the cortical layer and trabecular resorption continuing with less speed and not reaching "a month after castration" condition.

Disclosures: ***A. Kandilyotu****, None.*

SU577

Transcriptional Profiling of Cell-type and Tissue Selective Agonism of an Osteoanabolic SARM. S. Harada[1], W. J. Ray[1], D. B. Kimmel[1], C. Bai*[1], F. Chen*[1], P. V. Nantermet*[1], V. Kasparcova*[1], H. Zhang*[1], R. L. Vogel*[1], S. Rutledge*[1], M. E. Duggan*[2], S. P. Sahoo*[2], R. L. Phillips*[3], G. A. Rodan[1], L. P. Freedman[1], A. Schmidt[1]. [1]Molecular Endocrinology/Bone Biology, Merck Research Laboratories, West Point, PA, USA, [2]Medicinal Chemistry, Merck Research Laboratories, West Point, PA, USA, [3]Molecular Profiling, Merck Research Laboratories, West Point, PA, USA.

Tissue and cell-type agonisms have been documented for nuclear receptor ligands. We have identified a selective androgen receptor modulator (SARM), SA-766, that is anabolic to bone and muscle with limited effects on prostate and uterus. In osteopenic OVX rats, SA-766 (10 mg/kg/day) stimulates periosteal bone formation and increases cortical bone and lean body mass similar to the effects of 5α-dihydro-testosterone (DHT, 3 mg/kg/day). In the same animals, SA-766 had no effects on uterus while DHT treatment induced significant enlargement. In castrated rats, SA-766 exhibited minimal effects on prostate weight and antagonized the effects of testosterone, confirming the tissue selective androgen receptor (AR) partial agonism of SA-766. In cell-based transcription assays, SA-766 exhibits context-dependent AR agonism by repressing the MMP-1 promoter, while having no effects on AR-AF2 activity in 22RV1 prostate cancer cells where DHT acts as an AF2 agonist. To gain additional insight into the molecular mechanisms underlying tissue-selective AR agonism by SA-766, transcriptional profiles of uterus and bone were analyzed by microarray using DNA chips containing 25,000 rat genes. Analysis of RNA isolated from uterus identified strong DHT specific gene signatures, including IGF-I and uterocalin that were also induced by estrogens but not by SA-766. In addition, significant but less prominent signatures were induced by both DHT and SA-766 in uterus, supporting the notion that differential effects of DHT and SA-766 on uterus are mediated by tissue-selective and promoter-specific AR agonism. Aalysis of RNA from tibia identified rather weak signatures induced modestly by both DHT and SA-766. These signatures are distinct from known androgen-responsive signatures found in uterus and prostate, suggesting that androgen effects on bone are mechanistically distinct. Accordingly, DHT pellets implanted in tibia failed to document the local stimulatory effects on bone, suggesting that anabolic action of androgens could be mediated at least in part via AR expressed in extra-skeletal tissues. Taken together, transcriptional profiling of androgen target tissues uncovered the distinct mode of action of androgens in reproductive tissues versus bone that could account for tissue-selective AR agonism of SARMs.

Disclosures: ***S. Harada****, Merck & Co., Inc. 3.*

SU578

Bone Density and Body Composition in Mice with Defective Classical Signaling through the Estrogen Receptor Alpha. O. K. Oz[1], A. Thomas*[1], J. L. Jameson*[2]. [1]Radiology, UT Southwestern Medical Center at Dallas, Dallas, TX, USA, [2]Medicine, Northwestern University Medical School, Chicago, IL, USA.

Estrogens regulate accrual of peak bone mass and bone remodeling by acting through estrogen receptor (ER) α or β. The signaling may occur through the classical pathway in which the ER bound to an agonist regulates gene transcription by binding directly to DNA. The ER also regulates gene transcription through protein-protein interactions, a pathway known as the nonclassical pathway. Recent studies have shown that ERα is the major mediator of estradiol's protective effects on trabecular bone mass but that signaling through ERβ is partially protective in females only (1). Recently a nonclassical estrogen receptor knock-in mouse (NERKI) model has been created (2). Homozygous NERKI females are infertile. The phenotypes of the reproductive tissues from heterozygous females have been described (2) but the bone phenotype of neither gender has been reported. The purposes of this study were to determine if the NERKI mice have abnormalities in bone mass, body composition, and skeletal response to estradiol after ovariectomy. Heterozygous NERKI males were mated to WT 129 females to produce NERKI heterozygotes and WT littermates. The whole body bone mineral density (BMD) and body composition of WT and NERKI mice, aged 8-12 months, were compared by DEXA (GE Lunar PIXImus). Following ovariectomy female mice were treated with a water soluble form of estradiol (20μg/mouse) 3 times per week for 1 month. DEXA was performed weekly. NERKI males had significantly lower BMD than WT males (52.7±2.3, n=9 vs. 58.9±3.4, n=10, p<0.001). The BMD of NERKI females was also significantly lower (54.5±3.8, n=7 vs. 61±3.4, n-15, p=0.003). There was no significant difference in percentage body fat between NERKI and WT mice. Estradiol was less protective of spinal BMD in NERKI females following ovariectomy. There was a13% decrease compared to baseline for NERKI versus 3% for WT. Therefore, an imbalance in classical and non-classical signaling is sufficient to decrease bone mass in both genders. In contrast to other models of estrogen resistance or deficiency body composition does not seem to be affected.
References:
1. Sims et al. J. Clinical Invest. 111: 1319, 2003
2. Jakacka et al. Molec. Endocrinol. 16:2188, 2002.

Disclosures: ***O.K. Oz****, None.*

SU579

Androgen Responsive Genes Identified in Orchidectomized Mice through Affymetrix Microarray Analysis. A. Jackson*, P. Clément-Lacroix, T. Garcia*, W. Newell*, R. Galien*, M. Resche-Rigon, C. Robin-Jagerschmidt*, R. Baron. Proskelia, Romainville, France.

Despite limited clinical data on the role of androgens in bone mass maintenance, several studies have shown that DHT prevents the increase in bone turnover and the decrease in bone mass in orchidectomized (ORX) rats and mice, thereby demonstrating direct effect of androgens mediated via androgen receptor. However little is known regarding the mechanisms of action of androgens on bone cells and androgen regulated genes. The present experiment was therefore designed to determine the genes that are modulated by androgens in bone marrow cells of C57Bl/6 mice. Bone marrow cells were collected from twelve week-old sham and ORX mice which had been treated with vehicle and DHT 2.5 mg/kg/d (pellet) for 7, 10 and 14 days. Total RNA from 3 animals in each group were pooled, labeled by *in vitro* transcription and hybridized to Affymetrix Murine Genome MU74Av2 arrays, which interrogate 12488 full-length genes and EST clusters. Analysis has been completed to discover genes differentially regulated between sham or DHT treated-ORX groups and ORX mice (2-fold regulation with pvalue < 0.05). In addition, Chi2 statistical filtering of the data was performed to determine the genes most significantly regulated based on their profiles. Comparing expression profiles allowed identification of four clusters of differentially regulated genes. Among those clusters were found genes involved in the Wnt-signaling pathway such as Lef-1. In addition, Inpp5d (SHIP) is strongly repressed by ORX at d10 and its repression is prevented by DHT. Inpp5d is known to negatively regulate osteoclast formation and function. Another example is Wdr5 (BIG-3) that is induced by ORX at d14, an effect prevented by DHT treatment. Wdr5 is known to be induced by BMP-2 treatment and to increase osteoblast differentiation. These results are consistent with *in vivo* results since ORX in mice induces an increase of bone turnover, indicated by increased osteoclast number, osteoblast surface and mineral apposition rate as well as elevated urinary deoxypyridinolin and serum osteocalcin levels. It therefore appears that androgens normally maintain the expression of a number of genes capable of down regulating bone turnover. ORX suppresses this regulation and allows a marked increase in turnover with a negative balance.

Disclosures: ***A. Jackson****, None.*

SU580

Vitamin D Insufficiency Is Common in Obese Patients Prior to Bariatric Surgery. J. Fleischer[1], M. Bessler*[2], N. Restuccia*[2], L. Olivero-Rivera*[2], D. J. McMahon*[1], S. J. Silverberg[1]. [1]Medicine, Columbia University, New York, NY, USA, [2]Surgery, Columbia University, New York, NY, USA.

Bariatric surgery has become one of the most effective means to treat and prevent the complications of morbid obesity. Several procedures are available, some of which greatly alter the gastrointestinal tract and its absorptive capacity. While there are limited data regarding the effects of bariatric surgery on skeletal health, there is growing recognition that these procedures may be associated with the development of metabolic bone disease. One of the main concerns and a proposed mechanism of post-operative bone disease is vitamin D malabsorption. Obesity itself has also been associated with lower serum 25-hydroxyvitamin D (25D) levels, which has been attributed to both decreased sun exposure and decreased bioavailability of vitamin D_3 from its deposits in body fat. Since obesity itself and the surgical procedures available for its treatment may be associated with altered vitamin D metabolism, it is essential to know the vitamin D status of obese patients prior to bariatric surgery.

We conducted a retrospective chart review study of 120 patients (21 men, 99 women; (mean ± SD) age: 41.4 ± 11.5 yrs, BMI: 49.6 ± 8.2 kg/m^2) evaluated by a single bariatric surgeon over a 3-month period. Mean serum calcium (Ca) was 9.3 ± 0.4 mg/L; albumin 4.1 ± 0.3 g/dL; BUN 15 ± 4 g/dL and creatinine (Cr) 0.8 ± 0.2 mg/dL. Severe vitamin D deficiency (25D <10 ng/mL) was present in 31 patients (26%). Fifty-three patients (44%) had 25D levels between 10-20 ng/dL, 27 (22%) had 25D levels between 20-30 ng/dL and only 9 (8%) had 25D levels >30 ng/mL. Parathyroid hormone (PTH) concentration was 39 ± 17 pg/mL (normal range: 10-65 pg/ml). 25-Hydroxyvitamin D levels were negatively correlated with both BMI (R= -0.18, <0.05) and PTH concentration (R= -0.55, p=0.006). No association was observed between 25D and serum Ca or Cr.

In summary, vitamin D deficiency or insufficiency (25D ≤ 20 ng/ml) was documented in 70% of young obese individuals evaluated prior to bariatric surgery. Serum 25D levels were negatively correlated with BMI and PTH. These data suggest that post-operative vitamin D insufficiency, often attributed to the malabsorptive effects of the surgery itself, may in fact be a reflection of poor pre-existing vitamin D stores. We conclude that standard of care should include assessment of 25D levels in patients prior to bariatric surgery, so that appropriate treatment can be initiated.

Disclosures: ***J. Fleischer****, None.*

SU581

Vitamin D Deficiency Is Associated with Diminished Quality of Life: Insights from Qualeffo-41 Questionnaire Analysis. P. Sapountzi*, P. M. Camacho. Endocrinology and Metabolism, Loyola University of Chicago, Maywood, IL, USA.

Vitamin D deficiency leads to accelerated bone loss, fractures, bone pain, and muscle weakness . Vitamin D deficient individuals who are treated with vitamin D frequently report an improvement in the general feeling of well-being and mood, however, the impact of vitamin D deficiency on patients' quality of life has not been systematically analyzed and quantified. We describe the partial results of an ongoing prospective study that aims to determine the effect of vitamin D deficiency on health-related quality of life based on the Qualeffo-41 questionnaire. Qualeffo-41 is a quality of life questionnaire designed by the International Osteoporosis Foundation specifically for patients with osteoporosis. It contains questions in five domains: pain, physical function, social function, general health perception, and mental function. Each domain score and Qualeffo total scores are expressed on a 100-point scale, with 0 corresponding to the best health related quality of life.

Individuals being evaluated for low bone mineral density at the Loyola Osteoporosis and Metabolic Bone Disease Center were screened for vitamin D deficiency. Patients with 25 OH Vitamin D level < 20 ng/ml were asked to participate in the study.

The study group was composed of 24 individuals with vitamin D deficiency (21 females and 3 males). The mean age was 60 years +/-, 25 OH Vitamin D level was 14 ng/ml +/- 4.97, and intact PTH level was 65.5 pg/ml +/-32.28. The mean lumbar spine T score was -1.1+/-2.06 and the femoral neck T score was -1.7 +/-1.14.

The mean Qualeffo-41 score of the cohort was 39.8 +/-15.8. These scores showed a negative correlation with 25OH Vitamin D levels (r=-0.25). No correlation was seen with the severity of osteoporosis or parathyroid hormone levels.

The total score seen in our cohort is higher than the score previously reported in osteoporotic patients with and without vertebral fractures (36 +/- 17 and 26 +/- 14) . Our scores will further be compared to age-matched controls and will be presented at the meeting.

Thus, it appears that Vitamin D deficient individuals suffer from diminished quality of life. Future results of this ongoing study will determine if correction of the deficiency will lead to an improvement in these patients' quality of life.

Disclosures: ***P.M. Camacho****, None.*

SU582

Prevalence of Vitamin D Insufficiency in an Osteoporosis Population in Southern California. E. M. Blau*[1], S. K. Brenneman[2], A. L. Bruning*[1], Y. Chen[2]. [1]Kaiser Permanente, Southern California, San Diego, CA, USA, [2]Merck & Co., Inc., West Point, PA, USA.

Vitamin D is an important factor for bone mineralization, prevention of osteomalacia, muscle strength and balance. The reported ideal level of vitamin D is 30 ng/mL or greater as measured by serum 25-hydroxyvitamin D (25 (OH)D). A primary source of Vitamin D is conversion in the skin through sun exposure; therefore, vitamin D deficiency/insufficiency may be perceived as less of an issue in southern latitudes. However, few data have described the vitamin D distribution in the sunnier latitudes, and among those who are osteoporotic. We report the prevalence of vitamin D insufficiency/deficiency in an osteoporosis population living in Southern California. Study sample were consecutive community-dwelling women referred to an osteoporosis clinic in Southern California from November 2003 to April 2004 following fragility fracture (37%) or with a bone mineral density T-score less than -2.5 (63%). Vitamin D levels were assessed by measuring serum 25 (OH)D levels at a central laboratory (Quest Diagnostic Lab: Diasorin radioimmunoassay [RIA]). Blood specimen was collected at the time of assessment, prior to any treatment for osteoporosis. Demographics were obtained by patient self-report. Results of 25(OH)D levels were available for 252 women and are included in the current analysis. Patients were Caucasian (78%), Asian (8%), Hispanic (4%) and African American (2%) with mean age 71 (range 45 - 91). The mean 25 (OH)D level was 29 ng/mL (SD 13) with a range of 5 - 70 ng/mL. 53% of the patients had 25 OHD levels <30 ng/mL: 42% ≤ 25 ng/mL, 29% ≤ 20 ng/mL, 13% ≤ 15 ng/mL, and 4% ≤ 9 ng/mL. Mean 25 OHD levels were not significantly different between women under 65 years (mean 29.0, SD 12.7) and women 65 years and older (mean 29.4, SD 13.1) or between Caucasian (mean 29.9, SD 13.4) and non-Caucasian (mean 27.3, SD 11.5) women. About one-half of the osteoporotic women in this study located in southern California were vitamin D insufficient (< 30 ng/mL), including 4% with deficiency (≤ 9 ng/mL). Women with osteoporosis warrant special attention to ensure adequate and persistent vitamin D intake to prevent further bone loss and fractures.

Disclosures: ***E.M. Blau****, Merck & Co., Inc. 2.*

SU583

Vitamin D Insufficiency Is Highly Prevalent among North American Women Treated For Osteoporosis. M. F. Holick*[1], E. Siris*[2], N. Binkley*[3], M. K. Beard*[4], A. A. Khan*[5], J. Sackarowitz*[6], E. Chen*[6], A. E. de Papp[6]. [1]Boston University, Boston, MA, USA, [2]Columbia University, New York, NY, USA, [3]University of Wisconsin, Madison, WI, USA, [4]University of Utah, Salt Lake City, UT, USA, [5]McMaster University, Oakville, ON, Canada, [6]Merck & Co., Inc., West Point, PA, USA.

Vitamin D (D) is an essential component of osteoporosis therapy. However, D insufficiency may be overlooked by clinicians, leading to inadequate D supplementation in patients diagnosed with osteoporosis. Serum 25-hydroxyvitamin D (25(OH)D) levels greater than 30 ng/mL have been recommended to maximize intestinal calcium absorption and prevent secondary hyperparathyroidism. This cross-sectional observational study was designed to measure the distribution of serum 25(OH)D levels in postmenopausal women currently receiving antiresorptive or anabolic therapies to treat or prevent osteoporosis.

We enrolled 1554 postmenopausal women from 61 North American sites between November 2003 and March 2004. A serum 25(OH)D and biointact PTH (both using the Nichols Advantage System) and blood chemistry panel were obtained. A patient questionnaire was administered to obtain fall and fracture history, and information on factors that influence 25(OH)D.

1536 subjects, mean age 71 years (range 47-103), 92% Caucasian, completed the study. 35% resided at a latitude ≥ 42° N (Boston, Massachusetts) and 24% resided below 35° N (Memphis, Tennessee). The majority were ambulatory, community dwelling women seen in primary care offices. 84% reported good to excellent health. 51% had either some college education or a post-graduate degree. 66% reported previously discussing the importance of vitamin D for bone health with their physician and 59% reported taking at least 400 IU of vitamin D supplementation daily. 18.7% reported a low trauma fracture since

age 45 and 18.5% reported a fall resulting in a fracture within the past 5 years. The mean (SD) serum 25(OH)D was 30.4 (13.2) ng/mL, median 29 ng/mL (range 7-212 ng/mL). 1.1% had 25(OH)D <9 ng/mL, 8.1% < 15 ng/mL, 18% < 20 ng/mL, 36% < 25 ng/mL and 52% < 30 ng/mL. 16.5% had evidence of secondary hyperparathyroidism as defined by a normal serum calcium and an elevated PTH. The prevalence of D insufficiency (25(OH)D < 25 ng/mL) was significantly higher in subjects who took less than 400 IU of D supplementation daily compared with those who took at least 400 IU daily (47% vs 28% respectively, p<0.001).

This study demonstrates that approximately 50% of North American women currently receiving treatment for osteoporosis have suboptimal 25(OH)D levels. Despite routine recommendations for OTC vitamin D supplementation by physicians, D insufficiency is highly prevalent even among women diagnosed and treated for osteoporosis.

Disclosures: ***A.E. de Papp****, Merck & Co., Inc. 1, 3.*

SU584

Clinical Assessment of Vitamin D Status: An Imposing Dilemma. D. M. Gemar*, N. Binkley, D. Krueger, J. Engelke*, M. K. Drezner. University of Wisconsin, Madison, WI, USA.

Recent studies suggest that vitamin D (D) inadequacy is common in patients with osteoporosis and contributes to bone loss and fracture. Thus, adequate D supplementation is critical to assure optimal osteoporosis treatment and, appropriately, clinicians have focused on developing strategies for accurate assessment of D stores. These attempts include assay of serum 25OHD levels by commercially available methods and theoretically, use of elevated serum parathyroid hormone (PTH) levels to confirm the presence of inadequate D reserves. However, our previous studies suggest that commercially available chemiluminescent 25OHD assays do not define D status similarly to HPLC. Thus, radioimmunoassay (Diasorin) or HPLC techniques appear essential for accurate clinical 25OHD measurement. Unfortunately, use of radioisotopic assays in clinical laboratories has become less frequent and few commercial laboratories are equipped for high volume HPLC assays. Thus, the necessary means for accurate clinical evaluation of 25OHD status are limited. In the present study, we examined if a newly available chemiluminescent technology, the Diasorin Liaison, provides accurate assessment of serum 25OHD and if PTH measurement confirms a D insufficiency state. We obtained blood from 183 healthy young (mean age 23.8, range 18.1-39.5 years) male and female subjects having normal serum calcium and creatinine. Measurements of Liason-determined 25OHD were compared with that obtained by Diasorin RIA. Additionally, assays of whole and intact PTH by Scantibodies, Diasorin and Liaison methodology were performed. Liason determined serum 25OHD significantly correlated with that determined by RIA (r^2=0.78; p < 0.001). However, the Liason-determined values had a consistent bias, systematically underestimating serum 25OHD by an average of 9.8 ng/ml. As the mean 25OHD measured by RIA was 34.4 ng/ml, this under read is ~30% of the observed concentration. Moreover, whole and intact PTH measurements did not reveal a trend to elevated levels at concentrations of 25OHD <30 ng/ml. Indeed, in all cases correlation between the serum 25OHD and PTH levels was not significant. These observations reaffirm that currently available assays do not produce interchangeable serum 25OHD values. Thus, a single value cannot be widely utilized to define D insufficiency. Moreover, clinical reliance on serum PTH measurement to confirm suboptimal D status has no factual basis. Hence, the clinically attractive approach of a single 25OHD value to define D status is not currently feasible. As such, given the apparent epidemic of D insufficiency, standardization of 25OHD assays is essential unless definitions of insufficiency/deficiency are established for each assay.

Disclosures: ***D.M. Gemar****, None.*

SU585

Evaluation of Precision and Accuracy of Nichols Advantage 25-Hydroxyvitamin D Assay for 25-Hydroxyvitamin D_2 and 25-Hydroxyvitamin D_3: Comparison to Four Other Assay Methods Including Liquid Chromatography-Mass Spectrometry. M. F. Holick[1], T. C. Chen[2], D. Jamieson*[2], Z. Lu*[2], J. Mathieu*[2]. [1]Department of Medicine, Boston University School of Medicine, Boston, MA, USA, [2]Medicine, Boston University School of Medicine, Boston, MA, USA.

The serum assay for 25-hydroxyvitamin D [25(OH)D] is used to determine the vitamin D status of patients. The serum 25(OH)D assay measures both $25(OH)D_2$ and $25(OH)D_3$. The automated Nichols Advantage 25(OH)D assay is based on chemiluminescence detection and vitamin D binding protein (DBP) for competitive displacement. To determine how efficient and accurate the Nichols Advantage chemiluminescence assay was for detecting both $25(OH)D_2$ and $25(OH)D_3$, as compared to other methods, serum samples were obtained from healthy adults and from patients who were treated for several months with pharmacologic doses of vitamin D_2. The serum was divided into aliquots and numbered. Frozen samples were provided in a blinded fashion for analysis by five different methods including: (1) high performance liquid chromatography (HPLC), (2) liquid chromatography-mass spectrometry (LC-MS), (3) DBP binding assay, (4) radioimmunoassay, and (5) the Nichols Advantage System. These samples were tested at several independent laboratories. The amount of $25(OH)D_2$ and $25(OH)D_3$, was determined from results obtained by LC-MS and HPLC. A comparison of all the assays suggests that there are precision and accuracy differences among the various methods. The DBP binding assay, radioimmunoassay and the Nichols Advantage assay were able to detect $25(OH)D_2$ and $25(OH)D_3$.

Disclosures: ***M.F. Holick****, Consultant at Nichols Institute 5.*

SU586

Prevalence of Vitamin D in Post Menopausal Women and its Relevance to i-PTH in the Central Jersey. G. Kulkarni*, C. Guerard*, A. Wilson*, S. J. Wimalawansa. Dept. Medicine, Div. Endocrinology, Robert Wood Johnson Medical School, New Brunswick, NJ, USA.

Introduction: The incidence of osteoporosis is rising in the US due to aging of the population. More than 90% of all the fractures in the elderly are associated with osteoporosis. Osteoporosis lead to spine and hip fractures, which is a major source of morbidity and mortality. Treatment options available are although effective, are costly and associated with significant adverse effects.

Methods: In the present study on prevention of postmenopausal bone loss, using Nitroglycerine as an Option: Value in Early Bone Loss (NOVEL study), a baseline data obtained from 123 postmenopausal women (ages ranging from 40- 60 years) who qualified out of 248 pre-screened for the study were analyzed. Several biochemical tests were performed and the data from serum 25(OH) Vitamin D, i-PTH, and spine and hip BMD data presented.

Results: The results obtained were analyzed by ANOVA. Depend on the age, women were classified into (i) 40 - 55 years (n=57), (ii) > 55 years (n=66). The overall correlation between i-PTH vs. vitamin D showed a statistically significance inverse relation as observed in previous studies (r = -0.31 and P = 0.0005). Serum i-PTH levels were higher in the age group >55, compared to the age group 40-55 years (Fig 1). Spine and hip BMD showed a strong correlation with each other [r = 0.478 and p = >0.001]. The body surface area (BSA) strongly correlated with height and weight as expected (height: r =0.525 and P = >0.0001; weight: r = 0.981 and p = >0.0001), while the spine and hip BMD values correlated well with BSA p <0.05 level (spine BMD: r = 0.192; p = 0.034 and hip BMD: r = 0.184; p = 0.041).Conclusion: We can conclude that serum i-PTH increases with age and strongly correlated with vitamin D status inversely. Vitamin D insufficiency is common, and needs to be identified (incidence of ~12% in this population) and corrected to avoid secondary hyperparathyroidism in postmenopausal women, especially in the elderly, prior to embark on any anti-osteoporosis therapy.

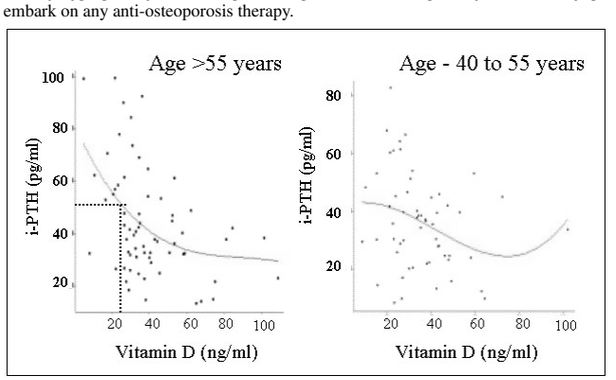

Disclosures: ***S.J. Wimalawansa****, Alliance of Better Bone Health 5; Norvatis 5; Lilly 8.*

M001

The Effect of Physical Activity on Bone Mass After Puberty in Men: A Eight-year Longitudinal Study. A. Nordstrom*[1], P. Nordstrom[2]. [1]Department of Surgical and Perioperative Sciences, Sports Medicine, Umeå, Sweden, [2]Department of Community Medicine and Rehabilitation, Geriatric Medicine, Umeå, Sweden.

Background: A high peak bone mass from physical activity could reduce the risk of osteoporosis if the benefits are retained with reduced activity. The long term effect of physical activity on bone mass after puberty to peak bone mass has not been studied.

Material and Methods: At baseline, bone mineral density (BMD, g/cm^2) of the total body, total hip, femoral neck, and spine were measured in 63 athletes (mean age 17.2 years) and 27 controls (mean age 17.1 years). Follow ups were made after a mean of 27, 68, and 94 months. The aim was to investigate the effect of physical activity on BMD after puberty in men, and evaluate whether a high BMD from physical activity is sustained with reduced activity.

Results: At baseline, the athletes were found to have significantly higher BMD at all sites compared to controls (total body 2.5%, femoral neck 7.7%, total hip 9.0%, spine 2.6%, p<0.05 for all). During the whole study period the 23 athletes that remained active increased significantly more at all BMD sites compared to controls (total body 3.6%, femoral neck 10.2%, total hip 7.8%, spine 5.2%, p<0.05 for all). Between the first and second follow up 27 athletes stopped their active career. During the same time period these athletes lost significantly more BMD compared to the still active athletes in the femoral neck (7.8%, p<0.001) and total hip (5.5%, p=0.009), but not compared to the control group. From the second to the third follow up period the former athletes did not loose BMD compared to any other group. At the final follow up the former athletes still had higher BMD compared to the controls at the femoral neck (10.6%, p=0.007) and total hip (9.1%, p=0.02).

Conclusion: The results of the present study suggest a high sensitivity to physical loading after puberty in men. Reduced activity is associated with bone mass losses only the first three years, and a sustained benefit from previous physical activity is seen five years after cessation of active career. Thus, previous physical activity up to the time of peak bone mass may decrease the risk of osteoporosis.

Disclosures: ***A. Nordstrom****, None.*

M002

Comparison of Two DXA Software Versions for Assessment of Whole Body Bone Mineral Density and Body Composition in Pediatric Population. B. Fan[1], M. Sherman*[1], L. Borrud*[2], A. Looker*[2], J. Shepherd[1]. [1]Radiology, University of California San Francisco, San Francisco, CA, USA, [2]National Center for Health and Statistics/CDC, Washington DC, WA, USA.

Objective: To compare three Hologic software versions for assessment of BMD and body composition analysis of whole body scans in children. Dual-energy X-ray absorptiometry (DXA) has been widely used in pediatric populations for assessment of bone density as well as body composition. However, when using an adult algorithm to assess pediatric bone density, it often fails to recognize small bones . To address this issue, the manufacturer (Hologic Inc., Bedford, MA) offers a pediatric analysis option (QDR Pediatric Whole Body, version 8.26a) for whole body scans. Recently, Hologic updated its pediatric analysis software (Discovery Software, version 12.1). Which has a variable bone density threshold that automatically adjusts for differing body sizes.

Methods: We compared the QDR Adult, QDR Pediatric, and Discovery whole body algorithms, using106 pediatric subjects aged 7 to 21 years old (mean = 14 ± 4 yrs) who participated in the NHANES 1999-2004 pilot study. The children were measured on one of three QDR-4500A DXA densitometers. Scans were analyzed by a single operator using all three analysis options. To evaluate how well each algorithm identified true bone area, we developed the Bone Area Score and applied it to each region of interest as follows: 0 = too little bone (< 50% true area) identified, 1 = accurate bone (50% < bone area < 100%) identified, and 2 = too much bone (>100% of true bone area) identified.

Results: The results of BMD and body composition from the three analysis options were highly correlated, with R square values ranging from 0.923 to 0.997. The table below shows the percentage of scores in different body parts for each algorithm.

	QDR Adult Analysis			QDR Pediatric Analysis			Discovery Analysis		
	0 (low)	1 (accurate)	2 (too high)	0 (low)	1 (accurate)	2 (too high)	0 (low)	1 (accurate)	2 (too high)
Hand	64.15	35.85		2.83	96.23	0.94	33.96	66.04	
Forearm		100			92.45	7.55		100	
Pelvis	10.38	89.62			80.19	19.81	3.77	94.34	1.89
Femur		100			88.68	11.32		100	
Foot	39.62	60.38			99.06	0.94	11.23	88.68	

Our data shows that the adult algorithm failed to identify the bone area in small bones half of the time. The pediatric algorithm increased sensitivity in finding lower density small bones; however, in the axial region and large bones it often defined lean mass.

The Discovery algorithm identified more of the bone area in small bones than the adult algorithm without the tendency to identify lean tissue as bone in the axial and large bones.

Conclusions: The Discovery software was more accurate in identifying bone area than either the adult or pediatric options.

Disclosures: ***B. Fan****, None.*

M003

Osteoporosis Resulting From Deficient Acquisition of Peak Bone Mass: the SAMP6 Mouse Model. J. Ophoff*, S. Boonen, E. Van Herck*, R. Bouillon, D. Vanderschueren. K.U.Leuven, Leuven, Belgium.

The SAMP6 (P6) mouse model is characterized by spontaneous fractures and is considered an animal model of senile osteoporosis. In line with human findings in hip fracture patients, P6 mice show thinner but wider bone cortices. Presently, it is unclear when and how these structural abnormalities of the bone cortex develop.

This *in vivo* study was designed to monitor acquisition of peak bone mass longitudinally in (male and female) P6 and control SAMR1 (R1) mice. To this end, serial peripheral computed tomography (pQCT) and dual-energy X-ray absorptiometry (DEXA) measurements were performed from 4 weeks till 20 weeks of age. At week 4 also urinary deoxypyridinoline (DPD) and serum osteocalcin (oc) levels were determined.

Peak bone mass acquisition in the tibia of R1 was characterized by greater cortical thickness in males than females. Male R1 showed 39% periosteal expansion, compared to only 18% at the endocortical site; females had less periosteal (24%) and no endocortical expansion. In both genders, total-body bone mineral content (tBMC) and polar moment of inertia (pCSMI) correlated with body weight (r^2= 0.59 and r^2=0.74 respectively, p<0.0001). Even after adjusting for differences in body weight, males had a higher pCSMI compared to females. Adjusting for lean body mass gave similar results.

Compared to R1 mice, P6 mice showed evidence of impaired cortical bone mass acquisition due to an early acceleration of endocortical expansion. It was observed in both genders (22% endocortical expansion in P6 females, 28% in P6 males), was already present at 4 weeks and reached its maximum around 8 weeks. This was confirmed by higher DPD (a marker for bone resorption) and lower oc (marker for bone formation) levels at week 4 in SAMP6 mice compared to R1 mice. In female P6 mice, endocortical expansion was partly compensated by additional periosteal bone apposition (7% more than in female R1 mice). Male P6, however, did not show such extra periosteal bone expansion and, consequently, experienced excessive cortical thinning. As a result, a decrease in pCSMI and lower pCSMI/weight and tBMC/weight ratios were observed in both genders of P6, but particularly in male animals.

In conclusion, SAMP6 mice show deficient peak bone mass acquisition as a result of an early, gender-neutral acceleration of endocortical bone expansion. Additional periosteal apposition compensates for the endocortical bone expansion in female P6 mice but not in male P6 mice. These findings support the concept that osteoporosis and osteoporotic fracture may partly result from deficient peak bone mass acquisition during skeletal development.

Disclosures: ***J. Ophoff****, None.*

M004

Bone Mass has Reached its Peak in the Spine and Hip but Continues to Increase in the Cortices of the Long Bones in 18-20-Year-Old Men. M. Lorentzon[1], D. Mellström[2], C. Ohlsson[1]. [1]Dept. of Internal Medicine, Center for Bone Research at the Sahlgrenska Academy (CBS), Gothenburg University, Gothenburg, Sweden, [2]Department of Geriatric Medicine, Gothenburg University, Gothenburg, Sweden.

In men, peak bone mass is believed to be achieved by the end of the second decade in life. The aim of the present study was to determine if the peak bone mass, at different localities, is reached in 18-20-year-old men. The *G*othenburg *O*steoporosis and *O*besity *D*eterminants (*GOOD*) study consists of 1075 men, age 18.9±0.6 yrs, and was initiated with the aim to find environmental and genetic determinants for bone and fat mass. Questionnaires were used to collect information about physical activity, dairy product intake and smoking. Bone parameters were measured using DXA and pQCT.

DXA measurements demonstrated that age was correlated to areal BMD of the radius (r=0.16; p<0.001) and the ulna (r=0.15; p<0.001) but not to the total body, femoral neck, or lumbar spine. pQCT measurements revealed that age was correlated to cortical BMC in both the radius and tibia (p<0.05). Age was found to be an independent predictor (in a multiple linear regression analysis including height, weight, physical activity, and smoking) of both the cortical volumetric BMD (radius β=0.29, p<0.001; tibia β=0.14, p<0.001) and the cortical thickness (radius β=0.15, p<0.001; tibia β=0.08, p<0.01) in the long bones. Trabecular volumetric BMD of the radius (β=0.08, p<0.05) but not of the tibia was associated with age.

These results demonstrate that in 18-20-year-old men peak bone mass has been attained in the femoral neck and lumbar spine, but not yet in the cortical bone of the long bones.

Disclosures: ***M. Lorentzon****, None.*

M005

Bone Mineral Density in Healthy School Children in North India. N. Tandon*[1], R. K. Marwaha*[2], H. K. Reddy*[1], R. Aggarwal*[2], B. Saluja*[3], M. A. Ganie*[1]. [1]Endocrinology, All India Institute of Medical Sciences, New Delhi, India, [2]Endocrinology, Institute of Nuclear Medicine and Allied Sciences, Delhi, India, [3]Dentistry, Instiute of Nuclear Medicine and Allied Sciences, Delhi, India.

Preliminary studies suggest that ethnic Asian Indians have a lower bone mass compared with white Caucasians. Clinical observations also suggest that osteoporosis is more prevalent in this ethnic group, occurs at an earlier age and affects males more frequently than that described in whites. One possible mechanism could be poor accrual of peak bone mass. In this study we have measured bone mineral density of apparently healthy school children from North India.

Bone mineral density of forearm and calcaneum was measured by pDXA in a total of 745 school children, aged 10-18 years, hailing from lower (Group 1; N=443) and higher (Group 2; N = 302) socio-economic groups. Dental fluorosis was observed in 213 children from Group 1 and 38 children from Group 2. Serum concentrations of calcium, phosphorus, alkaline phosphatase, 25 hydroxy vitamin D and iPTH were measured in fasting blood samples.

The mean BMD at the forearm and calcaneum in the total cohort was 0.373 ± 0.07 g/cm^2 and 0.482 ± 0.09 g/cm^2. There was a significant positive correlation between BMD at both forearm and calcaneum with BMI. There was a significant negative correlation between BMD at both sites with serum alkaline phosphatase. Children from Group 1 had a significantly lower BMD than Group 2 at both forearm and calcaneum. Males had significantly higher BMD at both forearm and calcaneum than females in both socio-economic groups. There was a progressive increment in the mean BMD at both sites with age. Interestingly, the mean BMD at both sites was significantly lower in children with dental fluorosis than those without fluorosis.

The significantly lower BMD in children belonging to the lower socio-economic group suggests that nutrition plays an important role in the accrual of bone mass and could be contributory in the lower bone mass in Asian Indians compared with other ethnic groups.

This study will also help establish norms for bone mineral density in the age group 10-18 years in North India.

Disclosures: ***N. Tandon****, None.*

M006

Physical Activity Level and Peak Bone Mass in 737 Young Adult Women. M. Callréus*, K. Ringsberg*, K. Akesson*. Malmö University Hospital, Dept of Orthopedics, Malmö, Sweden.

Introduction: The level of peak bone mass is most likely one of the key factors for later risk of osteoporosis. Peak bone mass is largely genetically determined and reached between age 20-30. External factors, such as physical activity, are contributing, but the relative significance is not evaluated in young adult women at the age of peak.

Materials and methods: 737 women, all 25 yrs (25.0-25.9), were included in this population-based study to evaluate factors of importance for peak bone mass.

Bone mineral density (BMD) was measured at the total body (TB), femoral neck (FN), trochanter (Troch) and spine (LS). Muscle strength was measured with isokinetic, concentric peak torque of the hamstrings and quadriceps together with handgrip strength. A questionnaire was completed for different variables of physical activity and lifestyle.

Physical activity was assessed by the subjects own scoring, recreational activity level (RAL) and objectively for impact load by the peak strain activity (PSA) score, a model based on ground reaction forces related to the type of activity. A combination of the RAL and PSA scores (COMB-RP) was also constructed. The scores were dichotomized into high and moderate/low.

Results: Young adult women reporting higher physical activity level, had significantly higher peak BMD at most sites, compared to those with lower physical activity. This was most pronounced for those (n=229) scoring high in both domains (COMB-RP), with also an increase in TB BMD 1.1% ($p<0.05$). Body weight, height and BMI were similar between groups.

High vs Low	Troch	FN	LS	p-levels
RAL (recreational activity)	3.6 %	2.9 %	1.8 %	0.044-0.007
PSA score (peak strain activity)	2.6 %	1.7 %	2.0 %	0.027-0.0002
COMB-RP (combined scores)	4.0 %	3.0 %	2.5 %	0.008-0.0002

Knee flexion and extension strength correlated with hip BMD (r^2=0.22-0.27, $p<0.0001$) and COMB-RP ($p<0.0001$), but not with handgrip strength. Women with high COMB-RP enjoyed to a greater extent scheduled physical exercise already in school (36% vs 23%) and were less likely to decrease their activity level compared to those with low combined activity.

Conclusion: This is the first study demonstrating the effect of physical activity on peak bone mass in the average 25-year-old woman. Physically active young women, particularly those involved in recreational activities with high impact, have a significantly higher peak bone mass at the hip, spine and total body. It also indicates that in order to achieve the beneficial effect, it is important to establish a behavioral pattern where physical activity is enjoyed already in the early school years.

Disclosures: ***M. Callréus****, None.*

M007

The Effect of Ethnicity and Gender on the Growth of the Axial and Appendicular Skeleton in Children. L. H. Nyati*[1], S. A. Norris[1], N. Cameron*[2], J. M. Pettifor[1]. [1]MRC Mineral Metabolism Research Unit, Department of Paediatrics, University of the Witwatersrand, Johannesburg, South Africa, [2]Department of Human Biology, University of Loughborough, Loughborough, United Kingdom.

Ethnic and gender variations in the growth of the axial and appendicular skeleton have been explored to determine their effects on bone mass. The heterogeneity in growth of one region in relation to another and the disparity in the size and mass of the same region are suggested to predispose to differential susceptibility to bone fracture. However, the influence of the differential axial and appendicular growth on the expression of bone mineral content is not yet established. Data assessing axial and appendicular growth and bone mass is largely drawn from the developed world and there is paucity of data describing these trends in the developing world where patterns may differ. Hence the aim of this study was to investigate (i) ethnic and gender differences in axial and appendicular dimensions of South African prepubertal children (ii) and the influence of regional bone length on the expression of site-specific bone mass. Anthropometric measurements of stature, weight, sitting height and limb lengths were taken on 369 black and white, male and female 9 yr old children. DXA scans of the ulna; radius; hip and spine were also obtained. An ANCOVA was performed to assess stature independent differences of limb lengths. A multiple regression was also performed to assess significant predictors of site-specific bone mass.

White children of both sexes were significantly taller than black children. Similarly sitting height was significantly greater in white children than black children of both sexes. However sub-ischial, humerus, ulna and calf lengths were similar between the ethnic and gender groups. Black girls had longer thighs than black boys. White boys were also heavier than black boys but no gender difference was observed.

Stature adjusted means of limb lengths show that black boys have longer legs and humerus but shorter trunks than white boys. In addition, black children have longer forearms than white children and girls have longer thighs than boys. This pattern is similar to those observed in the African American and Caucasian American populations. Bone mineral content at all sites with the exception of the hip, was predicted better by regional bone length than stature. However, using regional bone length as compared to stature to adjust for the effect of size on bone mass only had a marginal effect on the significance level of ethnic and gender differences.

Disclosures: ***L.H. Nyati****, None.*

M008

Association Between Central Bone Mineral Density and Biochemical Bone Markers in Japanese Young Women. H. Ohta[1], Y. Onoe[1], Y. Miyabara*[1], R. Yoshikata*[1], H. Okano[1], T. Kuroda*[2]. [1]Obstetrics and Gynecology, Tokyo Wemen's University, Tokyo, Japan, [2]Public Health Research Foundation, Tokyo, Japan.

The relationship between the status of central bone mineral density (BMD) and bone metabolism in young Japanese women remains unclear. To establish the status of peak bone mass in these women, we investigated BMD and biochemical bone markers.

The study subjects comprised healthy 139 women aged between 19 to 25 years of age (mean, 21.1 years), and those receiving treatment for any disease affecting bone mass or on diet and/or exercise therapy were excluded from the study. Subject background data surveyed included age, weight at birth, age at menarche, and current menstrual status. Measurements included height, body weight, lumbar vertebrae 2-4 BMD (L 2-4 BMD), and total BMD of the proximal femur (QDR 4500). Biochemical variables examined included serum levels of calcium, phosphorus, and albumin. To investigate the bone metabolism milieu in these women, serum levels of intact-osteocalcin, cross-linked N-telopeptides (NTX), bone specific alkaline phosphatase (BAP), osteoprotegerin (OPG) and soluble RANKL (sRANKL) were also measured.

The mean BMD at the lumbar spine (L2-4) and the total of proximal femur was 0.99 ± 0.10 and 0.90 ± 0.10 g/cm^2, respectively. There were no statistically significant differences in BMD (peak bone mass) in the subjects aged between 19-25 years of age. Furthermore, the mean BMD was lower than the YAM established previously by the JSBMR. The mean serum levels of NTX and BAP were 13.5 + 4.14 nmol BCE/L and 22.1 + 7.1 U/L, respectively. These levels were higher than the mean previously reported for those aged 30-44 years old, and were similar to those seen in older women. Serum BAP levels showed a significant (r = -0.22, p = 0.01) negative correlation with age, and serum NTX levels also indicated a negative correlation with age. Moreover, there was a significantly (r = 0.39, p = 0.0001) positive correlation between serum OPG and sRANKL levels.

In Japanese young women between 19-25 years of age, bone metabolism was shown to be of high turnover type where bone resorption exceeded bone formation. However, during these ages, the BMD at the lumbar spine and the total BMD of the proximal femur was not shown to peak. Further investigation in subjects in a wider age range is required to determine the age at which bone mass peaks in these women, as well as their peak BMD values.

Disclosures: ***H. Ohta****, None.*

M009

Proximal Femur Bone Bending Strength Is Appropriately Adapted to Muscle Mass in Overweight Children and Adolescents. M. A. Petit[1], T. J. Beck[2], J. Shults*[3], B. Zemel[4], B. J. Foster*[4], M. B. Leonard[5]. [1]Health Evaluation Sciences, Penn State University, Hershey, PA, USA, [2]Dept. of Radiology, Johns Hopkins University, Baltimore, MD, USA, [3]Biostatistics and Epidemiology, Univeristy of Pennsylvania School of Medicine, Philadelphia, PA, USA, [4]Pediatrics, University of Pennsylvania School of Medicine, Philadelphia, PA, USA, [5]Pediatrics; Biostatics and Epidemology, University of Pennsylvania School of Medicine, Philadelphia, PA, USA.

It is unclear whether bones of overweight children are appropriately adapted to their skeletal loads. The objective of this study was to compare cross-sectional bone geometry and strength in 40 overweight (body mass index [BMI] > 85th percentile) and 94 normal weight (BMI ≤ 85th percentile) subjects, aged 4-20 yr. Proximal femur, dual energy x-ray absorptiometry (DXA, Hologic QDR 4500) scans were analyzed at the femoral shaft (FS) and narrow neck (NN) by the Hip Structure Analysis Program. Subperiosteal width and indices of axial and bending strength (bone cross sectional area - CSA - and section modulus - Z) were measured from bone mass profiles and cortical thickness was estimated using models. Log transformed regressions were used to determine percent differences in bone parameters in overweight compared with controls. After adjusting for height, maturation and gender, Z was 11 [95% C.I. 5, 19] and 13 [7, 20] % higher at the FS and NN, respectively, in overweight subjects ($p \leq 0.001$). At the NN, higher Z was due to greater subperiosteal diameter (4% [2, 7]) bone CSA (10% [5, 16]) and thicker cortices (9% [3, 15]) and at the FS, to higher bone CSA (10% [5, 16]). Differences for all bone variables became non-significant ($P > 0.22$) after adjusting for lean mass, with the exception of NN subperiosteal width (+3%, [0, 6], $p = 0.04$). Fat mass did not contribute significantly to any model. In summary, proximal femur bone strength in overweight children is appropriately adapted to their lean body mass and height, but greater weight in the form of fat mass does not have an independent effect on bone bending strength. These geometric adaptations are consistent with the mechanostat hypothesis where bone strength adapts to skeletal loads dominated by muscle forces, but not to static loads represented by body weight.

Disclosures: ***M.A. Petit****, None.*

M010

The Relationship Between Continued Periosteal Apposition and Bone Fragility. J. E. Bird*[1], P. Nasser*[1], S. M. Tommasini[2], D. Casagrande[1], K. J. Jepsen[1]. [1]Mt Sinai School of Medicine, New York, NY, USA, [2]CUNY Graduate School, New York, NY, USA.

Continued periosteal apposition (CPA) has the benefit of maintaining bone strength during age-related endocortical bone loss. Recent cross-sectional data segregating Caucasian females based on fracture history revealed evidence of CPA at the distal radius of females without a history of fracture but not in those with a history of fracture [1]. Because Lazenby [2] showed that the degree of CPA varies with bone size, we tested whether differences in CPA between the fracture (fx) and non-fracture (n-fx) groups could be explained by differences in initial bone size.

Morphological parameters of the distal radius were obtained for Caucasian females (age < 50 yrs) with and without a history of fracture in an IRB approved clinical evaluation using plain film radiographs. All data were age-corrected. To determine the degree of periosteal apposition needed to maintain a constant moment of inertia or strength throughout life, we derived an equation for CPA or periosteal apposition rate (dR/dt) as a function of endocortical resorption rate (dr/dt) assuming the radial diaphysis has a circular cross-section (R = periosteal radius, r = endosteal radius): $CPA = dR/dt = (r/R)^3 * dr/dt$.

For both fracture groups, r/R increased linearly with R. This means that individuals with small bones (small R) have a small r/R ratio or proportionally thicker cortices. Based on our equation, individuals with small bones would need a much smaller dR/dt to maintain bone strength when compared to individuals with large bones (note: r/R is raised to the 3rd power). No differences in any morphological traits were observed between the two groups ($r = 3.0 \pm 0.6$ mm n-fx, 3.2 ± 0.9 mm fx; $R = 6.2 \pm 0.8$ mm n-fx, 6.3 ± 0.7 mm fx; $r/R = 0.48 \pm 0.06$ n-fx, 0.5 ± 0.11 fx). In addition, no difference in endosteal resorption rate (dr/dt) was observed between the two groups (0.017 mm/yr n-fx and 0.019 mm/yr fx). Given these parameters, the predicted degree of CPA was similar for the two fracture groups (dR/dt = 0.0031mm/yr n-fx, 0.0036 mm/yr fx). However, this was not observed clinically; dR/dt had a positive slope in the non-fracture group and zero slope in the fracture group. Thus, the difference in CPA (dR/dt) between the two groups could not be explained on the basis of initial bone size. This data indicated that the fracture group failed to add the appropriate amount of bone to maintain bone strength.

The derived equation may be used prospectively to predict the amount of CPA necessary to maintain bone strength on an individual basis. These findings have important clinical implications for providing novel diagnostic measures for the prevention of fragility fractures. [1] Bird et al, Trans.ORS 2004 [2] Lazenby, 1990 Amer J Phys Anthr 82.

Disclosures: ***K.J. Jepsen****, None.*

M011

Demineralized Bone Promotes Chondrocyte or Osteoblast Differentiation of Human Marrow Stromal Cells Cultured in Collagen Sponges. S. Zhou, K. E. Yates, K. Eid*, J. Glowacki. Orthopedic Surgery, Brigham and Women's Hospital, Boston, MA, USA.

Demineralized bone implants are used for many osseous reconstruction procedures. Demineralized bone powder (DBP) induces chondrogenesis of human dermal fibroblasts (hDFs) in a DBP/collagen culture system. Here, we test the hypothesis that human marrow stromal cells (hMSCs) can be stimulated by DBP to differentiate to chondrocytes or to osteoblasts, depending upon the culture conditions. First, we confirmed that hMSCs became chondrocytes when treated with TGFß. Second, we found that DBP induced chondrogenesis in hMSCs in 3-D sponges (serum-free MEM-a with 1% ITS^{+1}, 10^{-8} M dexamethasone, 50 µg/ml ascorbate-phosphate), assessed by metachromasia and induction of chondrocyte-specific genes *COL II and COL X*. Third, hDFs were used to define mechanisms of chondroinduction because unlike hMSCs they have no inherent chondrogenic potential. *In situ* hybridization revealed that hDFs vicinal to DBPs express chondrocyte-specific genes *Aggrecan* or *Col II*. Macroarray analysis showed that there was convergence and divergence in DBP and rhBMP-2 regulation of genes in the TGFß/BMP signaling pathway in 3-D hDFs cultures. Smad target genes were the predominant group of DBP or rhBMP-2 regulated genes. Several genes (*IGF-BP3*, *ID2*, and *ID3*) responded similarly to DBP and rhBMP-2. In contrast, many genes that were greatly upregulated by DBP, such as *TGFBI/ßig-h3* (1260% vs collagen sponges), *Col3A1* (1400%), *Col1A2* (1770%), *TIMP1* (250%), *p21/Waf1/Cip1* (260%) etc., were barely affected by rhBMP-2. On basis of Smad target gene changes, we conclude that DBP acts through both AR and BR Smads. Although BMP-2 was originally isolated as a putative inductive factor in DBP, rhBMP-2 alone and DBP do not affect all the same genes or in the same ways. Finally, DBP induced hMSCs to express osteoblast genes *Alkaline Phosphatase* and *Osteocalcin* when cultured in MEM-a with 10% FBS-HI, 10^{-8} M dexamethasone, 5 mM ß-glycerophosphate, 50 µg/ml ascorbate-phosphate. In summary, we show that culture conditions influence the differentiation pathway that human marrow stromal cells follow when stimulated by DBP. Second, our results show that DBP activates TGFß/BMP signaling pathway genes. The mechanism of induction by DBP is very complex and is not mimicked by TGFß or by rhBMP-2. Understanding the interactions of the various growth and differentiation factors in bone matrix will be important to determine the mechanisms of DBP's action and its effects on chondroinduction or osteoinduction.

Disclosures: ***S. Zhou****, None.*

M012

Mechanisms of Osteoblast Differentiation by BMP-7 in Human Bone Marrow Osteoprogenitor Cells. L. R. Chaudhary, K. A. Hruska. Pediatrics, Washington University School of Medicine, St. Louis, MO, USA.

Bone remodeling is complex biological process which involves osteoprogenitor commitment, differentiation, expression of osteogenic genes, synthesis of matrix proteins and mineralization resulting in new bone formation. Although BMP-7 is a potent stimulator of human osteoprogenitor differentiation and mineralization accompanied by induction of alkaline phosphatase (ALKP) activity and BSP gene expression, its mechanism of action remains unknown. Human bone marrow stromal (HBMS) progenitors although positive for CBFA1 do not progress to osteoblast differentiation without positive stimulation suggest that the processes of osteoblast commitment and differentiation require additional osteoblast specific factors. Here this hypothesis was tested in HBMS treated with BMP-7 (40 ng/ml), FGF-2 (20 ng/ml), dexamethasone (DEX, 10-7 M) or PTH (10-7 M) for 1, 2, 3, and 4 weeks in the alpha-MEM medium containing 50 µg/ml ascorbic acid and 10 mM β-glycerophosphate. RNA was analyzed by conventional and Real-Time RT-PCR. BMP-7 stimulated alkaline phosphatase activity and hydroxyapatite crystal deposition. CBFA1 expression was observed throughout the osteoblast differentiation without significant change in response to BMP-7 and other factors. Osterix gene expression was stimulated only by BMP-7 as the cells were undergoing differentiation program, and only stimulation of Osterix correlated with osteoprogenitor differentiation. PTH had no effect on ALKP activity, osterix gene expression and biomineralization. DEX did not affect osterix or OPGL gene expression. Interestingly, FGF-2 increased the expression of OPGL at 2, 3, and 4 weeks indicating a role in osteoclastogenesis. FGF-2 did not stimulate ALKP activity and inhibited BMP-7 stimulated ALKP and biomineralization. Results suggested that CBFA1 might be important in early commitment to the osteoblast phenotype, but osterix is a key regulatory factor in the differentiation of osteoprogenitor cells and biomineralization. Our results demonstrate that BMP-7 acts as a potent stimulator of osteoprogenitor cell differentiation and this process is mediated by osterix.

Disclosures: ***L.R. Chaudhary****, None.*

M013

Autoregulation of Endogenous BMP Expression Mediates Osteogenic Differentiation of Murine Marrow Stromal Cells in Culture. C. M. Edgar, V. Chakarvarthy*, G. L. Barnes, L. C. Gerstenfeld, T. A. Einhorn. Orthopaedic Surgery Research Laboratory, Boston University Medical Center, Boston, MA, USA.

Bone Morphogenetic Proteins (BMPs) are key morphogenetic regulators of skeletal tissue development and are necessary proteins in both the developmental and post-developmental regulation of stem cell differentiation. Previous studies show a temporal expression pattern for multiple BMPs during fracture repair and pre-natal bone development, suggesting that skeletal tissue development and repair is regulated through the coordinated actions of multiple BMPs. The goals of these experiments were to determine if the osteogenic differentiation of adherent murine MSCs, in an *ex vivo* system is dependent on the endogenous expression of multiple BMPs, characterize their interactions within this network, and determine if the network is autonomously regulated by specific BMP expression. Murine bone marrow stromal cells (MSCs) were prepared from 10 week old male mice and grown in osteogenic media for 21 days. Osteogenic differentiation was characterized by development of mineralizing nodules, AlkPase activity, and the assessment of mRNA expression. During the normal differentiation of MSCs in culture, increased expression of Dlx5 and Runx2 was accompanied by commensurate decreases in the expression of specific AP1 transcription factor family members. These changes were associated with sequential temporal increases in Col1α1, OPN, BSP and OC expression, and the unique up-regulation the expression of BMPs 2, 4, 5, 6, 8A and 3. Noggin treatment inhibited nodule counts by 50%-70% with an accompanied reduction in the expression of osteo-inductive transcription factors, matrix gene mRNA expression and the expression of BMPs 8A, 2, 5, and 3, in contrast BMP-4 and 6 demonstrated an increased expression. The addition of rhBMP-7, or 2 increased nodule counts by 30%-50% and the expression of osteogenic extracellular matrix markers and at 21 days, transcription factors Dlx5 and Runx2 expression was twice that of control cultures. Interestingly, the addition of rhBMP-7 or 2 inhibited the endogenous expression of BMP-4, 6, and 3b while enhancing the expression of BMP-8a,and 3. Culture treatment with a specific blocking antibody to BMP-2 had identical effects to noggin, and the inhibition of differentiation could be rescued by competitive addition of BMP-2 back to the media. In conclusion, these data suggest that the *ex vivo* MSCs system relies on the expression of certain endogenous BMPs during osteogenic differentiation which is regulated in a dynamic network which appears to be largely controlled through the action of BMP-2.

Supported by NIH/NIAMS P01-AR049920-01

Disclosures: ***C.M. Edgar****, None.*

M014

The Comparison of Lentiviral- and Adenoviral-mediated BMP-2 Gene Transfer in the Repair of Segmental Femoral Defects in Rats. W. Hsu*, O. Sugiyama*, B. Feeley*, N. Liu*, L. Krenek*, J. Lieberman*. UCLA Medical Center, Los Angeles, CA, USA.

Our laboratory has previously demonstrated that lentivirus-mediated gene transfer into rat bone marrow stromal cells (RBMSC) induced BMP-2 production *in vitro* for up to 12 weeks after transduction. We have also shown through previous studies that adenoviral-mediated BMP-2 gene transfer is capable of robust bone formation *in vivo*. This study compares the bone repair potential of lentiviral and adenoviral vectors in an immunocompetent rat femoral defect model.

Lentiviral-mediated gene transfer (LGT) via Lenti-RhMLV-BMP2 and adenoviral-mediated transfer (AGT) using Adv-cmyc-BMP2 vectors were used. A total of 50 8-mm femoral defects were created in five groups of Lewis rats: Group 1 - 5 x 10^6 BMP-2-producing RBMSC generated through LGT; Group 2 - 5 x 10^6 BMP-2-producing RBMSC created through LGT implanted 8 weeks after transduction; Group 3 - 5 x 10^6 GFP-producing RBMSC created through LGT; Group 4 - 5 x 10^6 BMP-2-producing RBMSC generated through AGT; Group 5 - 5 x 10^6 RBMSC alone. A compression resistant matrix comprised of both calcium phosphate ceramic and type I bovine collagen was used as a carrier for all groups. All specimens were harvested 8 weeks after surgical implantation and underwent plain radiographs, manual palpation, histological evaluation, and biomechanical testing.Table 1 summarizes results seen 8 weeks after treatment based on plain radiographs and manual palpation. ELISA results for BMP2 production *in vitro* for the following groups were measured: Group 1: 131 ng BMP-2/day/mg cell protein, Group 2: 84.5 ng BMP-2/day/mg cell protein, and Group 4: 29.2 ng/mL.

BMP2-producing RBMSC from LGT can heal a segmental rat femoral defect *in vivo*. Furthermore, we concluded that in an immunocompetent rat model, the use of LGT offers superior results in the induction of bone formation of a segmental defect when compared to AGT. The safety profile of lentiviruses has been recently improved by genetic alterations allowing study in experimental animal models. All animals in our study survived until the 8-week endpoint without observed side effects. Furthermore, because lentiviral vectors are less immunogenic, provide a high rate of transduction efficiency, and offer stable, long-term production of BMP2, they show promise in the future treatment of orthopaedic conditions which require bone repair.

Group	Treatment	N	N Fused
1	Lentiviral-BMP2-transduced 5 mil RBMSC	9	9
2	Lentiviral-BMP2-transduced 5 mil RBMSC 8-wk old	8	4
3	Lentiviral-GFP-transduced 5 mil RBMSC	13	0
4	Adenoviral-BMP2-transduced 5 mil RBMSC	8	4
5	5 mil RBMSC alone	12	0

Disclosures: ***W. Hsu****, None.*

M015

Repair of Intercalated Long Bone Defect with Biodegradable β-Tricalcium Phosphate Added by a New Delivery System for Recombinant Human Bone Morphogenetic Protein-2. M. Yoneda*, H. Terai, S. Miyamoto, K. Takaoka. Orthopaedic Surgery, Osaka City University Graduate School of Medicine, Osaka, Japan.

To create a new absorbable biomaterial with osteo-inducing capacity equivalent to autogenous bone-graft, we combined recombinant human bone morphogenetic protein (rhBMP-2, Yamanouchi Pharmaceutical. Co., Ltd.) with its delivery system and absorbable osteo-conductive biomaterial. In this study, porous β-tricalcium phosphate (β-TCP, Olympus. Co., Ltd.) cylinder blocks were coated with a block copolymer composed of poly-D,L-lactic acid with random insertion of p-dioxanone and polyethylene glycol (PLA-DX-PEG, Taki Chemical. Co., Ltd.) containing rhBMP-2 at the concentration of 0.02%. Twenty Japanese white rabbits were used for this study A longitudinal critical bone defect (15 mm in length) were filled with three β-TCP cylinder blocks coated with PLA-DX-PEG containing rhBMP-2 in the experimental group (n=10). Five rabbits recieved the same implants without rhBMP-2 as a control group. The critical defects left empty in 5 rabbits as another control. All critical defects were fixed with external fixators until 8 weeks after surgery. The animals were examined every two weeks by radiographs. At 8 weeks after surgery, half of the experimental group (n=5) and both control groups (n=5 each) were sacrificed and the both femurs were harvested for histological and mechanical examinations. The rests of experimental group (n=5) were fed up to 24 weeks.

On radiological examination of the femurs in the experimental group, the calcified image became more evident at 4 weeks and the newly formed bone connected both ends of the defect, appeared to be remodeled into the cortical bone with bone marrow cavity at 8 weeks. Image analysis and mechanical testing performed at 24 weeks revealed the complete anatomical restoration of defects with cortical bone and marrow space without the residual of β-TCP blocks.

On histological sections of the femurs in the experimental group, the newly formed bone in the defect was remodeled and cortical bone was clearly recognized with regenerated hematopoietic marrow like tissue. In 24 weeks, cortical bones were remodeled into the original anatomical shape with marrow like tissue without the the residual of β-TCP.

Our experimental results indicated that porous β-TCP combined with rhBMP-2 with its delivery system have osteogenic capacity equivalent to autogenous bone grafts. This newly developed material is effective for the repair of large bone defects without leaving implants in the defects.

Disclosures: ***M. Yoneda****, None.*

M016

A Combinatorial Approach to Craniofacial Regeneration in Wounds Compromised by Radiation Therapy. Z. Wang*, B. Nussenbaum*, P. H. Krebsbach. School of Dentistry, University of Michigan, Ann Arbor, MI, USA.

Functional and aesthetic restoration of craniofacial defects is challenging. One practical obstacle is the exposure to radiation that is characteristic of patients with head and neck malignancies. A potential strategy for overcoming the negative effects of radiation includes the use of anabolic dosing of parathyroid hormone (PTH), which effectively augments bone formation during stem cell directed osteogenesis. We hypothesized that a combination of molecular medicine and gene therapy could successfully overcome the negative effects of radiation in skeletal regeneration. Two weeks prior to surgery, 200 gm rats received no radiation or a single 12 Gray radiation dose delivered to the calvarium. The radiated (n=32) and non-radiated (n=32) rats were divided into 4 groups of 8 animals: inlay calvarial bone graft, non-transduced dermal fibroblasts, transduced dermal fibroblasts plus vehicle injections, and transduced dermal fibroblasts plus PTH injections. For the gene therapy treated groups, fibroblasts were transduced ex vivo with an adenoviral vector containing the BMP-7 cDNA. Transduced cells were loaded into a gelatin scaffold and were placed into 9 mm critical-sized calvarial defects. PTH treated groups were given daily injections of rhPTH [1-34] (80 mg/kg) and the controls received 0.9% sodium chloride. Bone regeneration was evaluated by micro-computed tomography (μCT) and histomorphometry. Non-transduced dermal fibroblast groups revealed fibrous union without any bone formation independent of radiation exposure. Micro-CT analysis in the non-radiated rats demonstrated significantly increased percent bone volume/total defect volume when comparing gene therapy plus anabolic-PTH to gene therapy plus vehicle (75 ±12.7 versus 63.0 ± 12.1, $p< 0.05$). Radiation therapy significantly limited tissue regeneration by transduced cells. This was demonstrated by comparing bone growth for the gene therapy plus vehicle treated rats that did or did not receive radiation (63.0 ± 12.1 versus 37.7 ± 15.6, $p< 0.05$). However, bone regeneration was significantly enhanced in the radiated defects by the combination of gene therapy plus anabolic-PTH compared to gene therapy plus vehicle (54.9 ± 13.9 versus 37.7 ± 15.6, $p< 0.05$). In fact, there was no significant difference when comparing the non-radiated gene therapy plus vehicle treated group to the radiated gene therapy plus anabolic-PTH group (63.0 ± 12.1 versus 54.9 ± 13.9, $p=0.67$). Bone mineral density was also significantly increased by the addition of PTH treatment. Anabolic dosing of PTH can augment bone regeneration induced by BMP-7 ex vivo gene therapy and overcome the negative effects of radiation therapy in cranial defects.

Disclosures: ***P.H. Krebsbach****, None.*

M017

Role of ERK Activation in the Osteogenic Actions of BMP-2. S. Fukayama, J. M. Owens, J. M. Wozney. Women's Health and Bone, Wyeth Research, Cambridge, MA, USA.

BMP-2 is a well-known osteogenic factor and is used clinically as a bone-inductive agent. It has been shown that BMP-2 signals not only via Smad activation but also via activation of a variety of kinases such as extracellular signal-regulated kinase (ERK) and p38. BMP-2 activates these kinases either in Smad-dependent or -independent fashion. For example, recent evidence suggests that BMP-2 activates ERK and p38 via activation of Ras. Using a neonatal mouse (ICR) calvaria organ culture assay, we have explored the role of activation of these kinases in the action of BMP-2. In this assay model, incubation with 500 ng/ml BMP-2 for 7 days did not increase total bone area although the same treatment resulted in an increase in the number of osteoblasts by up to 100%. Continued incubation with BMP-2 stimulated bone resorption as well, as assessed by measuring calcium release from calvaria into the medium. However, withdrawal of BMP-2 from culture after a brief treatment (~3 days) resulted in an increase in total bone area by up to 30% after 7 days incubation (brief exposure model). In contrast, the stimulatory effect of BMP-2 on the number of osteoblasts often was reduced in the brief exposure model. In the brief exposure model, BMP2-induced bone resorption was no longer evident at the end of organ culture (day 7) although it was still enhanced on day 4. Using this brief exposure model, we examined the roles of ERK and p38 kinase in the osteogenic action of BMP-2. The stimulatory effect of 500 ng/ml BMP-2 on total bone area was almost completely blunted in the presence of 1 μM U-0126 (MEK inhibitor). Incubation with 1 μM SB-203580 (p38 kinase inhibitor) did not alter the stimulatory effect of BMP-2 on total bone area. Incubation with either U-0126 or SB-203580 alone was without effect on total bone area. This argues against nonspecific inhibitory effects of U-0126 on bone formation. Similar results were obtained when calvaria were incubated with 30 μM PD-98059, another MEK inhibitor. In contrast, bone resorption stimulated by BMP-2 was not altered either by MEK or p38 inhibitors when examined on day 4, suggesting differences in BMP2-induced signaling pathways responsible for bone formation and resorption. We conclude that ERK activation, but not p38 activation, is involved in BMP2-induced bone formation but not resorption in this organ culture model.

Disclosures: ***S. Fukayama****, None.*

M018

Role of SFRP-1 in the Osteogenic Effects of BMP-2. S. Fukayama[1], J. M. Owens[1], P. V. N. Bodine[2], J. M. Wozney[1]. [1]Women's Health and Bone, Wyeth Research, Cambridge, MA, USA, [2]Women's Health and Bone, Wyeth Research, Collegeville, PA, USA.

Several recent lines of evidence suggest that Wnt(s) are involved in the action of bone morphogenetic protein (BMP)-2. Secreted frizzled-related protein (SFRP)-1, a secreted receptor for Wnt(s), binds Wnt(s) and modulates their action. In immortalized human osteoblastic HOB cells, BMP-2 down-regulates expression of SFRP-1. SFRP-1 knockout (KO) mice (C57B/6J) exhibit increased trabecular bone density, increased osteoblast differentiation and mineralization, and decreased apoptosis of osteoblasts and osteocytes. Deletion of the SFRP-1 gene also stimulates osteoclast (OC) differentiation from bone marrow progenitor cells *in vitro*. Using a neonatal mouse calvaria organ culture assay, we have examined the possible functional role of SFRP-1 in the action of BMP-2. We used calvaria harvested from 32 littermates [14 wild-type (WT) and 18 KO]. In control (WT) calvaria, treatment with 500 ng/ml BMP-2 significantly increased the total bone area and number of osteoblasts in 9 of 14 littermates by up to 30-40% and 100%, respectively. BMP-2 also stimulated cartilage formation in the peripheral region of the calvaria in all the littermates examined. Total bone area in the control groups was not significantly different between WT and SFRP-1 KO. In calvaria harvested from SFRP-1 KO mice, the increase in total bone area by BMP-2 was largely blunted in 17 of 18 littermates, although the stimulatory effect on the number of osteoblasts in 14 of 18 littermates and cartilage formation in all littermates were not altered. However, histological analysis revealed that bone remodeling (both bone formation and resorption) stimulated by BMP-2 was enhanced in SFRP-1 KO calvaria. This suggests that the lack of a stimulatory effect of BMP-2 on total bone area may be due to accentuation (rather than loss) of the BMP-2 effects in SFRP-1 KO calvaria since bone remodeling was increased. Finally, there was no significant effect of BMP-2 on OC differentiation or activation in either WT or SFRP-1 KO bone marrow cells. Our findings are most consistent with the hypothesis that the osteogenic effect of BMP-2 involves, at least in part, up-regulation of Wnt(s) signaling, via down-regulation of SFRP-1.

Disclosures: ***S. Fukayama****, None.*

M019

δEF1 Represses BMP-2-induced Osteoblast Differentiation of C2C12 Cells. S. Yang*[1], M. Petrey*[2], P. Stevens*[2], N. Jaiswal*[2], D. Chai*[1], H. Yang*[1], T. Zhu*[1], X. Ji[2], G. Sabatakos[2]. [1]Nankai University Medical College, Tianjin, China, [2]Skeletal Research, Procter and Gamble Pharmaceuticals, Mason, OH, USA.

Osteoblasts are derived from mesenchymal precursor cells which acquire their phenotype following distinct stages of proliferation, maturation and mineralization. In an attempt to identify novel regulators of osteoblast differentiation, human mesenchymal stromal cells were subjected to osteoblastic differentiation in the presence of BMP-2 and the expression profile of regulated genes was analyzed by READS analysis. δEF1, a member of the zinc finger-homeodomain family was identified in this manner as a repressor of osteoblast differentiation as its expression was downregulated in time courses in response to BMP-2. Since deletion of δEF1 in vivo resulted in profound skeletal effects, we sought to elucidate the molecular mechanism by which δEF1 regulates osteoblast differentiation. For this purpose, δEF1 or mutants lacking the C- or N-terminal zinc finger domains were stably transfected in C2C12 cells and their effect was analyzed in response to BMP-2. Overexpression of δEF1 or the truncated mutants resulted in a decrease in the mRNA levels of early osteoblast marker genes including osterix and collagen type I. This inhibitory effect was further confirmed by decreased alkaline phosphatase activity levels in cells overexpressing all δEF1 proteins, suggesting that neither of the zinc finger domains is critical for δEF1 function in osteoblast differentiation. In an effort to determine whether the repressive function of δEF1 was mediated via interactions with the Smad transcriptions factors, we performed co-immunoprecipitation studies with Smad1, Smad6 and Smad4 in the presence of BMPRIA. Neither δEF1 nor the zinc finger domain mutants were able to interact with any of the Smad factors analyzed. However, it was observed that Smad1 protein levels were downregulated in cells co-transfected with δEF1. In order to identify additional pathways that are regulated by δEF1, stable cell lines overexpressing δEF1 were co-transfected with constructs containing a variety of promoter elements and their responses were analyzed using the Mercury Pathway Profiling System. Consistent with its role as an inhibitor of osteoblast differentiation, δEF1 overexpression resulted in the downregulation of AP-1 responses in response to BMP-2. In contrast, in similar time courses the NFkB, NFAT and HSE pathway responses were significantly increased, suggesting that the effect of δEF1 in osteoblast differentiation could be mediated via these pathways. In conclusion δEF1 is a potent inhibitor of osteoblast differentiation that functions by differentially regulating a variety of essential signaling pathways.

Disclosures: ***S. Yang****, None.*

M020

Plasma Amino-Terminal proCNP: A Putative Marker of Growth Plate Activity. T. C. R. Prickett*[1], G. K. Barrell*[2], M. Wellby*[2], A. M. Lynn*[3], R. J. Kaaja*[4], V. A. Cameron*[1], E. A. Espiner*[1], A. M. Richards*[1], T. G. Yandle*[1]. [1]Department of Medicine, Christchurch School of Medicine & Health Sciences, Christchurch, New Zealand, [2]Animal & Food Sciences Division, Lincoln University, Canterbury, New Zealand, [3]Department of Pediatrics, Christchurch Hospital, Christchurch, New Zealand, [4]Department of Obstetrics and Gynecology, Helsinki University, Helsinki, Finland.

Recent evidence from rodents and humans shows that C-type natriuretic peptide (CNP) plays an essential role in endochondral bone growth. Like other members of the natriuretic peptide family, the biologically active (carboxy-terminal) forms of CNP are processed from a precursor (proCNP), and are subject to rapid degradation by clearance receptors (NPR-C) and enzyme hydrolysis. We have recently identified a stable product of proCNP, amino-terminal proCNP (NT-proCNP), which unlike CNP is readily measurable in human and ovine plasma. Further, despite reports of low CNP gene expression (and peptide levels) in growth plates, we have identified NT-proCNP in growth plate tissues of lambs at concentrations exceeding those in plasma. Hypothesising that plasma NT-proCNP concentrations reflect in part CNP synthesis within growth plates of rapidly growing cartilage, we have studied levels of CNP forms in both children and growing lambs and related these to age, growth velocity and biochemical markers of bone turnover.

NT-proCNP concentration (RIA) in umbilical venous plasma (246 ± 17 pmol/L, mean ± sem, n=13) greatly exceeded levels in children aged 5-18y (46.6 ± 1.7 pmol/L, n=58) and fully mature adults aged 20-80y (19.2 ± 0.4 pmol/L, n=117). Highly significant positive associations were found in children between plasma NT-proCNP and height velocity ($r=0.57$, $p<0.005$), alkaline phosphatase (ALP) ($r=0.55$, $p<0.001$) and Type 1 collagen C telopeptide ($r=0.33$, $p<0.013$). Plasma NT-proCNP concentrations were 10-50 fold those of CNP irrespective of age. In longitudinal animal studies, elevated plasma concentration of NT-proCNP in 1 week old lambs (61.7 ± 1.9 pmol/L, n=24) fell progressively to mature adult levels (26.7 ± 0.9 pmol/L, $p<0.001$) at age 27 weeks. Plasma NT-proCNP showed a highly significant positive association with ALP ($r=0.94$, $p<0.001$) and metacarpal growth velocity ($r=0.55$, $p<0.001$). Glucocorticoids (dexamethasone 0.25mg/kg/d for 15 days) - a treatment known to inhibit cartilage proliferation - reduced metacarpal growth elongation ($P<0.001$) in 4 week old lambs and markedly lowered circulating NT-proCNP levels ($p<0.001$).

In summary, NT-proCNP levels in blood show a strong association with growth velocity and markers of bone formation and may well serve as a useful marker of growth plate activity in humans and other mammals.

Disclosures: ***T.C.R. Prickett****, None.*

M021

Withdrawn

M022

Canonical Wnt Signaling Promotes Chondrogenic Differentiation and Hypertrophy. F. Yano*[1], S. Ohba*[1], F. Kugimiya*[1], T. Ikeda[1], N. Ogata[1], T. Ogasawara[1], T. Takato*[1], K. Nakamura[2], H. Kawaguchi[2], U. Chung[1]. [1]Tissue Engineering, University of Tokyo, Tokyo, Japan, [2]Orthopaedic Surgery, University of Tokyo, Tokyo, Japan.

Although several pieces of evidence in mouse genomics have implicated the involvement of Wnt signaling pathways in cartilage development, its direct action remains unknown. To better understand the role of the canonical Wnt pathway in cartilage development, we constructed adenoviral vectors expressing a constitutively active form (ca) and a dominant negative form (dn) of T-cell factor/lymphoid enhancer factor-1 (TCF/LEF-1), the main nuclear effecter of the pathway. To analyze its effect on chondrogenic differentiation, we transfected undifferentiated mesenchymal cell line C3H10T1/2 with caTCF/LEF-1 or dnTCF/LEF-1, and examined early differentiation markers of cartilage such as type II collagen, aggrecan and chondromodulin-1 by real-time RT-PCR analysis. caTCF/LEF-1 induced expression of these markers, and treatment with LiCl, an activator of the canonical Wnt pathway by inhibiting GSK3ß, also up-regulated them. In contrast, dnTCF/LEF-1 down-regulated the markers, and silencing of ß-catenin, an essential signaling molecule of the canonical Wnt pathway, through RNA interference also suppressed them. We further investigated the role of the pathway in hypertrophic differentiation of chondrocytes using a three-dimensional culture of mouse embryo rib chondrocytes. caTCF/LEF-1 induced expression of type X collagen, a marker of hypertrophy, whereas dnTCF/LEF-1 suppressed it. These results suggest that the canonical Wnt pathway promotes cartilage development at both early and late stages.

Disclosures: ***F. Yano****, None.*

M023

Growth Factors Capable of Suppressing Chondrocyte Hypertrophy Arrest Collagen Cleavage in Human Osteoarthritic Cartilage. E. V. Tchetina*, A. R. Poole. Joint Diseases Laboratory, Shriners Hospitals for Children, McGill University, Departments of Surgery and Medicine, Montreal, PQ, Canada.

Articular cartilage degeneration in idiopathic osteoarthritis (OA) involves excessive degradation of extracellular matrix, including type II collagen and aggrecan. It is also characterized by chondrocyte differentiation (hypertrophy). We hypothesised that destruction of the collagen network in OA involves mechanisms that include chondrocyte terminal dif-

ferentiation. If this hypothesis is correct, collagen degradation in OA may be inhibitable by agents that suppress hypertrophy. We show in cultured explants of human OA articular cartilage that collagenase-mediated collagen cleavage measured by ELISA is downregulated in about half the cases by the combined action of the growth factors TGFbeta2, FGF-2 and insulin. These have previously been shown to suppress hypertrophy, maintaining a prehypertrophic phenotype. Examination by semi-quantitative RT-PCR of the expression profiles of genes involved in chondrocyte differentiation revealed that the decrease in collagen cleavage induced by these growth factors was accompanied by the downregulation of terminal differentiation related genes namely, COL10A1, MMP-13, MMP-9, Indian hedgehog, caspase 3, as well downregulation of genes related to early chondrocyte differentiation (proliferation) such as TGFbeta2, PTHrP, FGF-2, cyclin B2. Downregulation of the cytokines IL-1beta and TNFalpha was also observed. In contrast the expression of aggrecan and TGFbeta1 was upregulated. The analysis of the effect of individual growth factors on collagen cleavage showed two types of response. In some OA articular cartilage explants FGF-2 or insulin did not downregulate collagen cleavage activity. In contrast TGFbeta2 downregulated collagen cleavage activity in all OA cartilage explants tested and is likely to be most potent molecule that can suppress type II collagen cleavage. These observations suggest that chondrocyte differentiation may play a role in cartilage collagen resorption in OA and that a combination of growth factors described above or TGFbeta2 alone can suppress cartilage matrix damage.

Disclosures: ***E.V. Tchetina****, None.*

M024

Estrogen Receptor-Related Receptor Alpha, ERRa, Regulates Cartilage Formation and Is dysregulated in Inflammatory Arthritis. E. Bonnelye[1], N. Laurin*[1], P. Jurdic[2], D. Hart*[3], J. Aubin[1]. [1]Department of Molecular and Medical Genetics, University of Toronto, Toronto, ON, Canada, [2]Laboratoire de Biologie Moleculaire et cellulaire, Ecole Normale Superieure de Lyon, Lyon, France, [3]Department of Surgery, McCaig Center for Joint Injury and Arthritis Research, University of Calgary, Calgary, AB, Canada.

The estrogen receptor related receptor alpha, ERRa, has been shown to be expressed by osteoblasts and play a functional role in bone formation. We now report the expression of ERRa in fetal and adult rat chondrocytes in growth plate and articular cartilage and the rat chondrogenic cell line C5.18 cells in vitro. ERRa mRNA and protein were expressed from proliferating chondrocytes to mature chondrocytes with the exception of fetal hypertrophic chondrocytes. To assess a functional role for ERRa in chondrocyte proliferation and differentiation, we blocked its expression by antisense oligonucleotides in C5.18 cell cultures and found significant inhibition of cell growth with concomitant downregulation of Sox9 and Ihh (Indian Hedgehog), both master genes in cartilage formation and cyclinD1, a cell cycle marker. We also found a proliferation-independant inhibition of cartilage formation and accelerated maturation of proliferating chondrocytes into hypertrophic chondrocytes in vitro. Semi-quantification of expression of cartilage markers showed a dramatic decrease in expression of Sox9, Ihh, Aggrecan, Link, and Col2a1 compared to control. Consistent with the decrease of Sox9 and Ihh, the hypertrophic chondrocyte markers Col10a1 and PTHrP receptor increased and the anti-apoptotic marker Bcl2 decreased. We therefore next asked whether ERRa dysregulation may play a role in conditions in which cartilage integrity is lost such as joints undergoing destruction as seen in inflammatory arthritis. Erosive arthritis was induced by injection of type II collagen into the joints of DBA-1 mice. Semi-quantitative RT-PCR of RNA from joints 7 weeks after injection revealed a dramatic decrease in expression of ERRa and mature chondrocyte markers; the decreases were even more striking when mice were boosted 5 weeks after the first injection. Notably, expression of ERRa and markers of bone formation was also decreased in the subchondral bone of the same treated mice. Taken together, these results suggest that ERRa plays a role in cartilage formation and integrity with a functional role in maturation of proliferating chondrocytes into hypertrophic chondrocytes. They also suggest that agonists and antagonists of ERRa may be useful as therapeutic agents in a wide variety of bone and cartilage metabolic and other diseases affecting these two tissues.

M025

ATF-2 Directs BCL-2 Expression in the Growth Plate. Q. Ma*[1], M. L. Brown*[1], Y. Li*[2], F. Beier*[3], P. LuValle[1]. [1]Anatomy and Cell Biology, University of Florida, Gainesville, FL, USA, [2]University of Calgary, Calgary, AB, Canada, [3]University of Western Ontario, London, ON, Canada.

Activating transcription factor-2 (ATF-2) is expressed ubiquitously, but in the endochondral growth plate it is restricted to chondrocytes in the resting and proliferating zones. Mice that are deficient in ATF-2 demonstrate ataxia, hyperactivity, diminished hearing and a hypochondroplasia-like dwarfism characterized by shortened limbs and disorganized growth plates. ATF-2 targets the cyclic AMP response element (CRE) in several genes in growth plate chondrocytes, including cyclin D1, cyclin A, pRb, p107, p130, c-fos, and c-jun in order to activate their expression. Bcl-2, an inhibitor of cell death that functions in the regulation of apoptosis, is also targeted by ATF-2. The bcl-2 promoter contains a CRE at approximately 1550bp upstream of the translation start. Bcl-2 is expressed within the growth plate in proliferative and prehypertrophic chondrocytes, but its expression is decreased in hypertrophic chondrocytes (Amling; et al. J Cell Biol. 134: 205-213, 1997). We employed western blot analyses, transient transfection assay, immunohistochemistry, in situ hybridization and apoptosis assay (TUNEL) to determine the consequences of ATF-2 deficiency on bcl-2 expression and activity. Bcl-2 protein levels and promoter activity are significantly reduced (~ 50%) in growth plate chondrocytes from ATF-2 deficient mice. Bax/Bcl-2 ratios in growth plate chondrocytes are increased in the absence of ATF-2. The growth plates themselves display a severely truncated hypertrophic zone, consisting of only one or two layers of hypertrophic chondrocytes. The number of hypertrphic chondrocytes expressing type X collagen in ATF-2 deficient mice growth plates is less than in wild type mice. Apoptotic activity is significantly increased in the few hypertrophic-appearing chondrocytes of these mice. One possibility for this interesting phenotype is that the hypertrophic chondrocytes are undergoing apoptosis prior to their complete maturation. These results suggest that bcl-2 expression and activity in the growth plate requires optimal ATF-2 expression and activation, in order to provide adequate longitudinal growth and endochondral ossification.

Disclosures: ***Q. Ma****, None.*

M026

EphrinB2, an Arterial Endothelial Cell Marker, Is Expressed in Avascular Chondrocyte and Is Regulated by Sp1. N. Hosogane*[1], T. Miyamoto[2], M. Yagi*[1], N. Fujita*[1], Y. Toyama*[1], T. Suda*[2]. [1]Orthopaedics, Keio University School of Medicie, Shinjuku-ku, Japan, [2]Department of Cell Differentiation The Sakaguchi Laboratory, Keio University School of Medicie, Shinjuku-ku, Japan.

EphrinB2 is a transmembrane ligand for Eph receptor tyrosine kinases. They are presumed to regulate cell-cell interactions, and the major consequence of activation of Eph receptors and ephrin ligands is cell repulsion. EphrinB2 is specifically expressed in arterial endothelial cells and is known to be involved in angiogenesis. Mice deficient for ephrinB2 die at E9.5 with severe cardiovascular defect. Recently, by using ephrinB2 LacZ knock-in mice, we found that ephrinB2 is expressed in proliferating chondrocyte in the developing stage, where vascularization does not occur. EphrinB2 expression is promoted by Notch1 in arterial endothelial cells, however, the constitutive active Notch1 and adeno-Notch1-IC did not stimulate ephrinB2 expression in chondrogenic cell line ATDC5. Thus, we analyzed the regulatory elements of its promoter by luciferase assay to elucidate the regulatory mechanisms of ephrinB2 expression using ATDC5. First, the transcriptional start site was determined by primer extension method, and it was located at 628bp up-stream of ATG start codon and 31bp down-stream of TATA box.

Deletion mutants of the promoter containing 5'UTR region were fused to promoter-less firefly luciferase gene. The -107/+629 fragment was required for maximum promoter activity which contained two CCAAT boxes and a specificity protein 1(Sp1) site. The luciferase activity reduced to 40% when two CCAAT boxes were deleted(-56/+629), and to basal level by further deleting Sp1 site(-42/+629). Also, we found that the co-localized expression of ephrinB2 and Sp1 in chondrocytes of E17.5 embryo by immunohistochemical studies. These results indicate that Sp1 is involved in the expression of ephrinB2 in chondrocytes.

Nuclear factor Y(NFY), which can also bind to CCAAT box, up-regulated the promoter activity when three isoforms(A, B and C) were co-transfected together. Moreover, NFYs and Sp1 synergistically up-regulated the promoter activity. Thus, NFY and Sp1 coordinately regulate the expression of ephrinB2 in chondrocytes.

To elucidate the function of ephrinB2 in chondrocytes in vivo, we are now generating chondrocyte specific deletion mice using typeXI collagen-Cre transgenic mice and ephrinB2 loxP mice. This chondrocyte specific ephrinB2 deficient mice will clarify the function of ephrinB2 on the regulation of angiogenesis in chondrocytes.

Disclosures: ***N. Hosogane****, None.*

M027

Characterization of Growth Plate Abnormalities in Rachitic Mouse Models. Y. Sabbagh[1], T. O. Carpenter[2], M. Demay[1]. [1]Endocrine Unit, Massachusetts General Hospital and Harvard Medical School, Boston, MA, USA, [2]Department of Pediatrics, Yale University, New Haven, CT, USA.

Rickets is seen in association with vitamin D deficiency and vitamin D receptor (VDR) mutations, suggesting that the actions of vitamin D are required for a normal growth plate. Studies in VDR null mice have demonstrated that the expansion of the late hypertrophic chondrocyte layer, characteristic of rickets, is secondary to impaired apoptosis of these cells. Since mutations in the VDR or vitamin D deficiency lead to hypocalcemia, hypophosphatemia and secondary hyperparathyroidism, the underlying pathogenesis of the impaired apoptosis and subsequent rachitic changes is uncertain. The observation that normalization of mineral ion homeostasis in VDR null mice normalizes PTH levels and prevents rachitic changes, suggests that rickets is secondary to hypocalcemia, hypophosphatemia or hyperparathyroidism, rather than impaired VDR action. To determine which of these abnormalities leads to impaired chondrocyte apoptosis and subsequent rachitic changes, two additional models were examined: diet induced hypophosphatemia and hypophosphatemia secondary to mutations in the Phex gene. The former model is associated with hypercalcemia and suppressed PTH levels as a consequence of elevated levels of 1,25-dihydroxyvitamin D. The latter model demonstrates normal calcium and PTH levels, but 1,25-dihydroxyvitamin D levels that are inappropriately low for the degree of hypophosphatemia.

Histological sections of the tibial growth plate were examined in mice fed chow and littermates fed a phosphorus restricted (0.02%) diet from day 18 to 24, as well as from 24 day old mice with mutations in the Phex gene (Hyp mice) and their wild type littermates. For evaluation of chondrocyte apoptosis, TUNEL staining was performed on adjacent tissue sections. Our studies demonstrate that hypophosphatemia, regardless of circulating PTH, 1,25-dihydroxyvitamin D, or calcium levels, leads to a rachitic growth plate secondary to impaired apoptosis of the hypertrophic chondrocytes. These data demonstrate that normal phosphorus levels are required for growth plate maturation and implicate a critical role for a phosphorus regulated apoptotic signaling pathway in endochondral bone formation.

Disclosures: ***Y. Sabbagh****, None.*

M028

Wnt Expression Induces Chondrocyte Maturation through β-Catenin-mediated Signaling: Modulation by TGF-β. Y. Dong, M. Chen*, M. J. Zuscik, D. Chen, E. M. Schwarz, R. N. Rosier, H. Drissi, R. J. O'Keefe. Orthopeadics, University of Rochester, Rochester, NY, USA.

Wnt secreted factors are expressed during limb morphogenesis yet their role and mechanism of action remains unclear during cartilage development. We used a chick embryonic cell culture model to assess the role of Wnt expression and signaling and its interaction with TGF-β during chondrocyte differentiation. Several wnt transcripts, including *wnt4*, *wnt8* and *wnt9a* were upregulated during the spontaneous differentiation of chick embryonic sternal chondrocytes in cell culture, while *wnt5a*, expression was slightly increased. TGF-β, which blocks chondrocyte maturation, inhibited the increase in *wnt* expression. Over-expression of β-catenin, Wnt8 and Wnt9a stimulated the expression of the chondrocyte maturation specific genes, *colX* and *alkaline phosphatase*, while Wnt5a inhibited expression of these markers. We found that activation of the β-catenin pathway potently enhanced chondrocyte maturation while wnt-mediated activation of calcium pathways repressed differentiation. Over-expression of β-catenin and/or its nuclear co-factor TCF/LEF caused a 20-30 fold induction of transcription of the ABC-640 chick type X collagen promoter. Induction of this promoter by β-catenin signaling was dramatically repressed by TGF-β indicating a cross talk between TGF-β and the β-catenin-dependant Wnt signaling pathways. TGF-β also inhibited β-catenin mediated induction of *colX*. To further assess the effect of TGF-β on TCF/LEF-β-Catenin signaling transfection assays were performed using the β-catenin/TCF/LEF-responsive reporter, Topflash. TGF-β blocked Topflash induction in chondrocytes transfected with β-catenin and/or TCF/LEF, indicating a direct inhibition of the β-catenin transcriptional complex. Potential interactions between Smad signaling and -β-catenin was investigated by immunoprecipitation, which showed co-immunoprecipitation of β-catenin with Smad3, with an increase observed with activation of β-catenin or TGF-β signaling. Altogether we demonstrate that Wnt/β-catenin signaling induces chondrocyte maturation, but is modified by activation of TGF-β/Smad signaling.

Disclosures: ***Y. Dong****, None.*

M029

High-Throughput Modelling Of Bone Disease In Zebrafish. A. Fleming*, P. Goldsmith*. DanioLabs Ltd, Cambridge, United Kingdom.

The optical clarity, speed of development, and fecundity of zebrafish have made them a popular vertebrate model for the study of developmental biology and more recently as an animal model to study disease processes. Larval stages are viable in 96-well plates for the first 10 days of life and the optical clarity of the tissue at these stages allows the use of vital dyes to mark discrete tissues and observe disease changes in the living animals and in post-mortem studies. The entire skeleton of the zebrafish larva can be visualized *in vivo* by the administration of a fluorescent dye such as calcein and tetracycline to the embryo medium or on fixed tissue using alizarin red. Staining not only provides a rapid method for visualizing the skeleton but also allows measurement of the labeled area or the intensity of staining in particular elements that can then be used to quantify bone size and density. Having optimized staining protocols for skeletal analysis in zebrafish larvae, we examined whether we could induce and detect bone loss in zebrafish larvae by administration of the glucocorticoid prednisolone. When exposed to 30 uM prednisolone from 5 d.p.f. to 10 d.p.f., staining in the head skeleton is markedly reduced compared to control (untreated) samples of the same age. Using digital image analysis, we have measured the amount of stained, mineralized tissue to quantify the OP-inducing effects of prednisolone at a range of doses. A dose-dependent decrease in the amount of stained tissue was observed with increasing doses of prednisolone, with statistically significant changes observed at 3, 10 and 30 uM (24%, 36% and 49% decrease in stained area, respectively). This bone loss is partially rescued in a dose-dependent manner by co-administration with etidronate. These staining and quantification methods can also be applied to anabolic bone agents to determine the relative anabolic effects of compounds. In the zebrafish larva, we have detected statistically significant anabolic bone effects with estradiol, PTH and calcitriol. We are now performing compound screens in 96 well plate format to identify novel compounds for both the rescue and prevention of bone loss.

Disclosures: ***A. Fleming****, None.*

M030

Fibrin-sealant Thrombin Promotes Proliferation, Cytosolic Ca^{2+} Elevation and Survival of Human Chondrocytes via Activation of Protease-Activated Receptors. M. Zheng[1], R. Han*[2], L. Kirilak*[2], N. Asokananthan*[3], G. Stewart*[3], A. J. Bakker*[3], P. Henry*[4], D. Wood[1]. [1]Orthopaedic Surgery, University of Western Australia, Perth, Australia, [2]University of Western Australia, Perth, Australia, [3]Department of Microbiology, University of Western Australia, Perth, Australia, [4]Pharmacology, University of Western Australia, Perth, Australia.

Fibrin sealants have recently been recommended to be used as tissue glue for autologous chondrocyte implantation. However, it is not clear that the effect of fibrin sealants on the proliferation and migration of human chondrocytes. In this study, we investigated the possible inovlvement of protease-activated receptors in the effect of fibrin sealant thrombin on the proliferation and migration of human chondrocytes. Thrombin at a concentration ranged from 0.11 to U/ml to 1 U/ml was shown to signifigantly promote proliferation of human chonrocytes in vitro. The maximum effect on stimulating proliferation was achieved at a concentration of 0.5 U/ml of thrombin. Fibrin glue (thrombin) also promoted migration of human chondrocytes co-cultured with collagen membrane from the membrane to fibrin glue within two weeks. Many of thrombin effects have been attributed to activation of protease-activated receptors (PARS). In this study, we also found that PAR-1 through PAR-4 were expressed by human chondrocytes. Thrombin and PAR-1 agonist peptide induced a fast intracellular Ca2+ response in human condrocytes. Taken together, these data suggest thrombin promotes proliferation and migration of human chondrocytes at least in part by stimulating PAR-1

Disclosures: ***M. Zheng****, None.*

M031

Repression of Glycogen Synthase Kinase Inhibits Chondrocyte and Perichondrial Osteoblast Differentiation. R. Kapadia*, M. C. Naski. Pathology, University of Texas Health Science San Antonio, San Antonio, TX, USA.

Glycogen synthase kinase 3 (GSK3) is an essential regulator of cell differentiation in diverse organisms and cell-types. Unlike many kinases, GSK3 has constitutive enzymic activity that is regulated by repressor pathways. To understand how the regulation of GSK3 influences osteoblast and chondrocyte differentiation, we inhibited GSK3 in mouse metatarsal bone rudiments using the specific inhibitors, lithium and SB216763. Repression of GSK3 caused a dramatic inhibition of both chondrocyte and perichondrial osteoblast differentiation. Chondrocyte differentiation was completely inhibited as evidenced, by 1) a histological absence of hypertrophic chondrocytes and 2) dramatic repression of chondrocyte-specific gene expression including type II collagen and aggrecan. The differentiation of perichondrial osteoblasts was also repressed as demonstrated by the absence osteoid synthesis and diminished assembly of a chain of terminally differentiated osteoblasts linked via adherens junctions. Interestingly, inhibition of GSK3 caused a reduction in chondrocyte proliferation, whereas perichondrial cell proliferation was increased. The effects of GSK inhibition were accompanied by an increase in the expression of fibroblast growth factors (FGFs). Significantly, the effects of GSK3 inhibition on chondrocytes and osteoblasts were phenocopied by treatment of metatarsals with FGF. These results indicate that GSK is an important regulator of FGF expression and that effects of GSK3 on bone and cartilage cells may be mediated by FGFs.

Disclosures: ***M.C. Naski****, None.*

M032

Maturation of the Epiphyseal Chondrocyte:Survival-Death Decisions at the HIF-PHD Axis. S. P. Terkhorn*, M. Ohashi*, C. S. Adams, I. M. Shapiro, V. Srinivas*. Orthopaedic Surgery, Thomas Jefferson University, Philadelphia, PA, USA.

During long bone growth, activated chondrocytes undergo a series of temporal and spatial changes that lead to hypertrophy and the induction of the terminally differentiated phenotype. Since the cartilage is avascular, it is hypothesized that the low pO_2 induces apoptosis of the hypertrophic chondrocytes. Indeed, previous studies have shown that the transcription factor, HIF-1 is required for cell survival in this oxygen limited microenvironment. The purpose of this study was to examine the impact of the environmental pO_2 on HIF expression and chondrocyte apoptosis. N1511 chondrocytes were cultured under hypoxic conditions and subsequently challenged with either staurosporin or FasL. Surprisingly, at low pO_2, the cells were refractory to staurosporin-mediated apoptosis. In contrast, almost 100% of the cells were killed when challenged with 50 nM FasL under hypoxic conditions. We noted that in 2% pO_2 there was upregulation of Fas receptor expression. To examine the mechanism of sensitization, we evaluated by Western blot and RT-PCR analysis the expression of both pro- and anti-apoptotic members of the Bcl-2 gene family. We noted enhanced Bcl2 and Nip3 expression was temporally correlated with the downregulation of survival signals in terminally differentiated chondrocytes. To further explore the O_2 sensitivity to apoptosis, we modulated the expression of the cellular PHD oxygen sensors using siRNA technology. Down regulation of the PHDs resulted in an increased resistance to staurosporin-mediated apoptosis. This observation lends support to our hypothesis that inhibition of apoptosis at low pO_2 is mediated by the HIF signaling pathway. Once growth plate cells are terminally differentiated, the hypoxic chondrocytes are highly sensitized to FasL mediated apoptosis. Based on these observations, we suggest that the rise in pO_2 that accompanies the invasion of vascular elements in the growth plate, serves to increase the sensitivity of terminally differentiated chondrocytes to apoptogens such as FasL.

Disclosures: ***V. Srinivas****, None.*

M033

Post-irradiation Recovery of Growth Plate Function Is Driven by Expansions of Regenerative Clones. J. A. Horton, B. S. Margulies*, J. A. Strauss*, T. A. Damron*, J. A. Spadaro. Orthopedic Surgery, SUNY Upstate Medical University, Syracuse, NY, USA.

Radiation therapy used to treat pediatric malignancies may result in a disruption in the progression of chondrocytes through proliferation and maturation in the growth plate, which can impact longitudinal growth. In the present study we compare growth plate cell-cycle kinetics between the normal and irradiated growth plates following their functional and morphologic nadir until the appearance of regenerative clones. We hypothesize that growth rate, while initially reduced in the irradiated limb, would partially recover, and correlates with the expansion in size and number of the regenerative clones.Under IACUC approval, the right knees of 27 weanling male rats were exposed to a 17.5 Gy X-ray exposure, with the left limb used as an internal control. Six days following treatment animals were injected with oxytetracycline (OTC). On day seven bromodeoxyuridine (BrdU) was injected. Proximal tibiae were sampled 1,2, 4, 12, 24, 48, 72, 96, and 120 hours following BrdU injections and prepared for histomorphometry. Indices of BrDU labeling, matrix area fraction (Aa), growth plate zonal height, and numeric density of clones (Nv) were calculated from digital images at 10x magnification. Analysis of BrdU indices revealed one mitotic cycle per 24-48 hours in the normal

growth plate. After irradiation there were fewer BrdU positive proliferative cells in irradiated tibiae; however, they were cycling at the same rate as the cells in unirradiated growth plates. The label progresses through the strata, peaking in the transitional and hypertrophic zones of both tibiae at 72 and 96 hours, respectively. Nv increased at a rate of $2x10^{-4}$ clones/mm^3/day (R^2=0.94), and Aa decreased in the proliferative, transitional, and hypertrophic zone during this period. Increases in Nv were correlated (R^2=0.92) to increases in daily growth by OTC labeling. Growth in the unirradiated limb proceeded at a constant rate within the period observed.

In previous work, irradiation of the growth plate lead to cell death and accelerated maturation of proliferative chondrocytes. In the present study proliferating cells were lost at a faster rate than they were replenished, thus fewer cells were available to progress into hypertrophy resulting in the observed growth arrest. The lack of differences in reserve zone BrDU labeling between normal and irradiated limbs suggests that this population of slowly cycling relatively radio-resistant cells may seed the proliferative zone with progenitor cells that expand to become regenerative clones. Thus, restoration of the proliferative pool via expansion of regenerative clones appears to initiate functional recovery in the irradiated growth plate.

Disclosures: ***J.A. Horton****, None.*

M034

Impaired Fracture Healing in Diabetes May Be Due To Enhanced Chondro/osteoclast Activity. D. V. Tsatsas*[1], K. Wang*[2], C. Edgar*[2], C. Leone*[1], L. C. Gerstenfeld*[2], D. T. Graves[1]. [1]Department of Periodontology and Oral Biology, Boston University School of Dental Medicine, Boston, MA, USA, [2]Orthopedic Surgery Research Laboratory, Boston University Medical Center, Boston, MA, USA.

Patients with diabetes type I exhibit significant problems with fracture healing due to delayed or inadequate bone formation. We investigated fracture repair in a mouse model examining several histomorphometric endpoints. The underlying hypothesis was that alterations in cartilage lead to subsequent deficits in bone formation associated with diabetes. In the experimental group mice were rendered diabetic by multiple low dose streptozotocin treatment, which induces diabetes via an autoimmune response in the pancreas. Results were compared to a control group that was treated with vehicle alone, citrate buffer. Closed simple standardized tibial fractures were generated by blunt trauma and mice were sacrificed at 12, 16 and 22 days post-fracture. Samples were prepared for histomorphometric analysis. The area of new bone and cartilage formation and number of chondro/osteoclasts were determined using Van Gieson, saffranin-O and TRAP staining, respectively. New bone formation in the diabetic group was significantly less on day 12 and 22 compared to non-diabetic controls ($p<0.05$). The area of cartilage was similar on day 12 but was reduced ~50% in the diabetic compared to normoglycemic group by day 16 and absent from both groups on day 22. This coincided with chondro/osteoclast numbers on days 12 and 16 that were significantly higher in the diabetic group ($p<0.05$). These results indicate that diabetes may affect fracture healing by increased formation of chondro/osteoclasts that cause more rapid removal of cartilage thereby impairing the ultimate formation of bone within the healing callus. Supported in part by DE11254 and AR47045.

Disclosures: ***D.T. Graves****, None.*

M035

Negative Regulation of TGF-β Signaling by Smurf2 in Growth Plate Chondrocytes. M. K. Mulcahey*, M. Pirri*, Y. Dong*, Q. Wu, E. M. Schwarz, J. E. Puzas, R. J. O'Keefe, H. Drissi, R. N. Rosier, M. J. Zuscik. Orthopaedics, University of Rochester, Rochester, NY, USA.

Growth plate chondrocyte (GPC) differentiation involves a series of maturational events that are tightly regulated by several factors including TGF-β, a potent suppressor of hypertrophic differentiation. The signaling mechanisms that facilitate this suppressive function of TGF-β include phosphorylation of Smad proteins (Smads 2 and 3) which directly, or in concert with other transcription factors, affect target gene expression. Negative regulation of these signaling events occurs via several mechanisms including the Smad ubiquitin regulatory factor-2 (Smurf2), an E3 ubiquitin ligase which is known to promote degradation of Smad2 by the proteasome. Based on the ability of Smurf2 to block Smad2/TGF-β signaling, we hypothesize that it acts to relieve the suppressive constraint of the TGF-β pathway on GPC maturation, thereby inducing progression of these cells toward terminal maturation. We tested this hypothesis by performing Smurf2 gain of function experiments in GPCs to assess the signaling and phenotypic impact of this gene. To establish that Smurf2 inhibits Smad2/TGF-β signaling, we performed Western analyses to measure ubiquitination of Smad2 along with P3TP promoter-luciferase reporter assays to assess TGF-β signaling. Western analyses of ubiquitinated Smad2 in empty vector- and Smurf2-transfected cells indicated that Smurf2 enhanced ubiquitination of endogenous Smad2. This degradative effect was even more pronounced in cells treated with 5 ng/ml TGF-β. Corellating with these findings, TGF-β signaling on the P3TP reporter was reduced in cells transfected with Smurf2. Having confirmed the function of this gene in GPCs from a signaling perspective, we proceeded to assess the effect of Smurf2 overexpression on chondrocyte phenotype. As expected, Smurf2-transfected cells displayed a more hypertropic phenotype based on increased expression of type X collagen and alkaline phosphatase, two markers of chondrocyte hypertrophy. Given the signaling and phenotypic effects of Smurf2 in GPCs, we next examined the regulation of Smurf2 expression by factors that are known to alter GPC phenotype. Of the factors tested, PTHrP, another potent inhibitor of chondrocyte maturation, strongly enhanced expression of Smurf2 mRNA and induced a concommittant decrease in TGF-β signaling on the P3TP reporter. These findings suggest a novel interaction between PTHrP and TGF-β signaling that involves Smurf2-induced degradation of Smad2. This novel interaction may represent an important regulatory mechanism in the progression of GPC maturation.

Disclosures: ***M.J. Zuscik****, None.*

M036

SP Transcription Factors and Histone Deacetylases Regulate Alpha 2 Type XI Collagen Gene Expression in Saos-2 Human Osteosarcoma-Derived Cells. T. Goto*[1], Y. Matsui*[1], K. Yukata*[1], T. Kubo*[1], H. A. Chansky*[2], L. Yang*[2], D. R. Eyre[2], N. Yasui*[1]. [1]Orthopaedics, The University of Tokushima, Tokushima, Japan, [2]Orthopaedics and Sports Medicine, University of Washington, Seattle, WA, USA.

Type XI collagen, composed of three chains, alpha 1 (XI), alpha 2 (XI) and alpha 3 (XI), is crucial for collagen fibril formation and skeletal morphogenesis. It was previously reported that the mouse alpha 2 (XI) collagen gene (*Col11a2*) is regulated by modular arrangement of cartilage- and neural tissue-specific cis-elements in the promoter region. Several lines of evidence revealed that *Col11a2* is expressed by osteoblastic cells in mice, rats and humans. Although the mechanisms by which *Col11a2* is transactivated in chondroblastic cells have been well documented, those in osteoblastic cells remain unclear. We therefore analyzed Saos-2 cells, osteosarcoma-derived human osteoblastic cells, in which we found the alpha 2 (XI) collagen gene (*COL11A2*) expression. RT-PCR analysis showed that Saos-2 cells expressed a range of splicing variants of *COL11A2*. The mouse *Col11a2* promoter sequence from -742 bp to +380 bp, from the transcriptional start site, was activated in Saos-2 cells when transiently transfected and assayed for luciferase activity. Deletion of cartilage- and neural tissue-specific cis-elements did not affect promoter activity. Further deletion analysis identified a minimum sequence for promoter activity between +133 bp and +380 bp. The evolutionally conserved human *COL11A2* promoter construct H149, containing the sequence from -149 bp to +27 bp, from the transcriptional start site, showed activity in Saos-2 cells. Deletion and mutation analysis of H149 construct revealed that at least two SP1 sites were critical for the promoter activity. Electrophoretic mobility shift assay demonstrated physical interaction between the SP1 sites in the *COL11A2* promoter and SP1/3 proteins in the Saos-2 nuclear extract. Inhibition of the histone deacetylases (HDACs) using trichostatin A enhanced the *COL11A2* promoter activity in Saos-2 cells. This enhancement was abolished when the SP1 sites were mutated, suggesting that the binding of SP1/3 proteins to the *COL11A2* promoter mediated the action of HDACs. Together, our results indicate that *COL11A2* collagen gene is transactivated via functional interaction between SP transcription factors and HDACs in Saos-2 osteoblastic cells.

Disclosures: ***Y. Matsui****, None.*

M037

Temporal Gene Expression Profiles in Cartilage Development. C. James*[1], T. Appleton*[1], V. Ulici*[1], T. M. Underhill[2], F. Beier[1]. [1]Physiology and Pharmacology, CIHR Group in Skeletal Development and Remodeling, University of Western Ontario, London, ON, Canada, [2]Anatomy and Cell Biology, University of British Columbia, Vancouver, BC, Canada.

Endochondral ossification occurs through the coordinated expression of genes that regulate the formation of a cartilaginous template, which is ultimately replaced by bone. Microarray analysis of primary mouse mesenchymal cells undergoing chondrocyte differentiation in high-density micromass cultures was performed using Affymetrix MOE430A arrays containing 14 000 genes. Bioinformatics approaches were employed to characterize temporal gene regulation during cartilage differentiation. Data analysis using Microarray Suite 5.0 algorithms and GeneSpring 6.1® filtering parameters identified approximately 3300 expressed transcripts. Among the expressed probe sets, 1772, 481 and 249 demonstrated minimum two-fold, five-fold and 10-fold changes over a 15-day time course, respectively. The temporal expression patterns of selected markers identified in the array such as Cartilage link protein were confirmed with RT-PCR. Parallel filtering criteria employed in GeneTraffic 3.0® generated similar, albeit reduced numbers of differentially expressed genes. K-means clustering was used to identify pervasive gene expression patterns, namely genes that are either upregulated or downregulated towards the end of the culture period. Functional categorization of the probe sets used in this analysis according to GeneOntology terms revealed differentially expressed growth factors, receptors, transcription factors and extracellular matrix molecules among others.

Several genes identified in these microarray analyses were stably overexpressed in the mouse chondrogenic cell line ATDC5 for functional characterization. Specifically, overexpression of Activating Transcription Factor 3 (ATF-3), a transcriptional repressor that was shown to be upregulated in hypertrophic chondrocytes in our microarrays, results in decreased proliferation and cyclin A promoter activity as well as accelerated differentiation of ATDC5 cells. These data support a role of ATF-3 in cartilage hypertrophy. Similarly, overexpression of various RGS (regulator of G-protein signalling) proteins also accelerates chondrocyte hypertrophy.

The amalgamation of bioinformatics and functional studies will lead to a comprehensive view of important genetic regulatory mechanisms and signalling cascades that mediate skeletal development. Ultimately, this work will contribute to a better understanding of the pathophysiology of chondrodysplasias and other degenerative bone diseases.

Disclosures: ***C. James****, None.*

M038

Reduced Bone Mineral Density in Adult Heterozygous *Sox4*$^{+/-}$ Mice. L. S. H. Nissen-Meyer*[1], V. T. Gautvik*[1], S. Reppe*[1], F. P. Reinholt[2], K. M. Gautvik[3], R. Jemtland*[4]. [1]Dept. of Biochemistry, Institute of Basic Medical Sciences, University of Oslo, Oslo, Norway, [2]Institute of Pathology, Rikshospitalet University Hospital, Oslo, Norway, [3]Dept. of Biochemistry, Institute of Basic Medical Sciences, University of Oslo, Ullevål University Hospital and Lovisenberg Hospital, Oslo, Norway, [4]Endocrine Section, Dept. of Medicine, Rikshospitalet University Hospital, Oslo, Norway.

The aim of the study was to examine how deletion of a single allele of the PTH-regulated transcription factor *Sox4* gene affected bone mineral density (BMD) and gene expression in mice. Sox4 is vital for normal fetal development, as knock-out mice (*Sox4*$^{-/-}$) die *in utero* from circulatory failure. We have previously shown that PTH regulates Sox4 in osteoblastic and osteosarcoma cells. *Sox4* is also expressed in hypertrophic chondrocytes in mouse embryos. A potential role for Sox4 in osteoblast differentiation has recently been suggested (Billiard et al 2003, J Cell Biochem 89, 389-400). Heterozygous mice appear phenotypically normal. We have determined peak bone mass in the *Sox4*$^{+/-}$ animals compared to wildtypes (wt), and characterised age-related changes in BMD, biochemical and morphological parameters. Gene expression was studied in limbs of *Sox4*$^{-/-}$ embryos compared to wildtypes.

BMD was measured in *Sox4*$^{+/-}$ and wt mice by DEXA (Dual energy X-ray absorptiometry) at regular time intervals. Regions of interest (ROI) include total body, 3 lumbar vertebrae, right femoral neck, femoral shaft and proximal tibia. Blood samples were collected for serum analysis of biochemical bone turnover parameters. *Sox4*$^{+/-}$ and wt mice (180 days) tibiae were fixed immediately after dissection, and embedded in an epoxy resin for subsequent morphologic analysis using light and electron microscopy. Hindlimbs from *Sox4*$^{-/-}$ and wt embryos (embryonic day 14) were subjected to gene expression analysis using the MOE430A array (Affymetrics).

Time curves show a maximal BMD for all groups around 180 days, the *Sox4*$^{+/-}$ males exhibiting significantly lower total body BMD (minus 5.1 %; SE=1.7 %) than wt males ($p<0.05$). In the femoral neck the difference is 15.9 % (SE=3.3 %, $p<0.001$), and similar changes are found in other ROIs. At 180 days, female *Sox4*$^{+/-}$ have slightly lower total BMD than wt females, and significant differences are seen in femoral and lumbar ROIs. Gene expression analysis in embryonic hindlimbs demonstrated changed expression of several genes related to skeletal development.

Our results show that mice with only one functional *Sox4* allele have impaired ability to reach peak BMD and maintain normal bone mass, suggesting a role for Sox4 in normal bone turnover.

Disclosures: ***L.S.H. Nissen-Meyer****, None.*

M039

Transgenic Mice Constitutively Expressing Histone H4 Gene Display Increased Trabecular Bone Mass Mediated By Histone H4 Alternative Translation. T. Noh*[1], E. Smith*[1], T. E. Myerrose*[1], T. Kohler*[2], M. Namdar-Attar*[3], N. Bab*[3], O. Lahat*[3], J. A. Nolta*[1], R. Müller*[2], I. Bab[3], B. Frenkel[1]. [1]University of Southern California, Los Angeles, CA, USA, [2]Swiss Federal Institute of Technology and University of Zurich, Zurich, Switzerland, [3]The Hebrew University of Jerusalem, Jerusalem, Israel.

The evolutionary conserved *histone H4* genes encode at least two peptides: the 103 amino acid H4 protein and a 14 amino acid circulating mitogen Osteogenic Growth Peptide (OGP). OGP is synthesized *de novo* from H4 mRNA by leaky ribosomal scanning through the imperfect H4 AUG initiator and alternative translation starting at codon 85, a perfect AUG initiator. To test the functionality of *H4* alternative translation *in vivo*, we engineered transgenic mice that ubiquitously and constitutively express a mutant H4 mRNA, *H4tTG1*, which exclusively encodes OGP. Quantitative micro-computed tomographic analysis of femora from 8, 17 and 34 week-old mice revealed marked increases in trabecular bone volume density at all ages. Cortical bone density did not exhibit a significant change. The observed effect on trabecular bone was particularly strong in females, which exhibited a significant 2-fold increase in trabecular bone density compared to wild-type controls. The enhancement of trabecular bone density was accompanied by increased trabecular number and connectivity, parameters that contribute to bone strength. Dynamic histomorphometric analysis demonstrated a significant 35% increase in the percentage of trabecular surface engaged in bone formation and a significant 23% increase in the mineral appositional rate in females. Osteoclast number was not significantly altered. No adverse effects of OGP over-expression were noticeable in transgenic mice up to 18 months of age. Thus, continuous OGP over-expression throughout life results in a specific augmentation of trabecular bone without noticeable effects on cortical bone or extra-skeletal tissues. In summary, transgenic expression of H4 mRNA lacking the upstream initiation codon in post-mitotic cells results in increased trabecular bone accrual.

Disclosures: ***T. Noh****, None.*

M040

Identification of Adiponectin Receptor-1, 2 in Osteoblast-like Cell Lines, MG-63 Cells. W. Lee[1], E. Rhee*[1], S. Kim*[1], S. Kim*[1], K. Oh[2], K. Baek[3], M. Kang[3]. [1]Department of Internal Medicine, Sungkyunkwan University School of Medicine, Seoul, Republic of Korea, [2]Department of Internal Medicine, Hallym University, College of Medicine, Chunchon, Republic of Korea, [3]Department of Internal Medicine, The Catholic University of Korea, College of Medicine, Seoul, Republic of Korea.

Recent clinical study by Lenchik L *et al.* suggested that adiponectin is a novel determinant of bone mineral density and visceral fat in adults. If adiponectin could influence bone metabolism, it could be mediated by adiponectin receptor. Recent reports displayed that adiponectin receptors are found in liver, muscle, pancreas cells, etc. Although the expression of adiponectin was reported in human bone marrow, the expression of adiponectin receptor in osteoblasts has not been reported. Here, we found the expression of adiponectin receptor in MG-63 cells, thus report it. A human osteoblast-like cell line (derived from a human osteosarcoma), MG-63, was purchased from Korean cell line bank. Cells were maintained in Eagle's minimal essential medium, supplemented with 10% fetal calf serum. Total cellular RNA was prepared using the Trizol reagent kit. After quantification by spectrophotometry, it was reverse transcribed and cDNAs were made. PCR was done in a Perkin-Elmer 9600 thermocycler in a 50 ul reaction volume containing cDNA, dNTPs, $MgCl_2$, appropriate oligonucleotide primers of each gene, and AmpliTaq Gold DNA polymerase. The following primers were used: human adiponectin receptor-1, sense 5′-TTC TTC CTC ATG GCT GTG ATG T-3′, anti-sense 5′-AAG AAG CGC TCA GGA ATT CG-3′; human adiponectin receptor-2, sense 5′-ATA GGG CAG ATA GGC TGG TTG A-3′, anti-sense 5′-GGA TCC GGG CAG CAT ACA-3′.

The reaction products were then separated on a 2% agarose gel in Tris borate EDTA buffer. Sequencing of PCR product revealed that it was compatible to human adiponectin-R1 and R2, respectively (using NCBI nucleotide-nucleotide BLAST). We found that human adiponectin-R1 and R2 were expressed in MG-63 cells. It suggests that adiponectin could affect bone metabolism via adiponectin receptors in human.

Disclosures: ***W. Lee****, None.*

M041

Hypoxia Stimulates Chondrogenesis by Human Fibroblasts Chondro-induced in vitro by Demineralized Bone. S. Mizuno[1], C. Wykoff*[2], J. Glowacki[1]. [1]Orthopedic Surgery, Brigham and Women's Hospital, Boston, MA, USA, [2]Harvard Medical School, Boston, MA, USA.

In vivo, endochondral osteogenesis induced by demineralized bone powder (DBP) initiates the formation of cartilage and its replacement by bone. *In vitro*, chondroinduction can be modeled by exposing human dermal fibroblasts (hDFs) to DBP contained within a porous collagen sponge [1]. Given that cartilage is a relatively hypoxic tissue, we tested the hypothesis that low pO2 promotes chondroinduction in this system. In this study, we compared chondrogenesis by hDFs in DBP/collagen sponges ± medium perfusion at 5% (hypoxia, Hypo) or 19% O2 (normoxia, Norm).

1 million human dermal fibroblasts (hDFs) was seeded onto porous collagen sponges ± DBP [2] and precultured at Norm for 3 days in DMEM with 10% FBS. The sponges were divided to four culture conditions: Hypo or Norm without/with perfusion of medium (0.33 ml/min). Hypo and Norm were achieved by auto-regulating nitrogen and carbon dioxide inflow in an incubator. At intervals, sponges were harvested for histological and for biochemical evaluation. Sponges were fixed and stained with toluidine blue-O or immunohistologically with prolifering cell nuclear antigen, PCNA. Other sponges were extracted in 4 M guanidine-hydrochloride and ethanol precipitates were used for measurement of chondroitin 4-sulfate (Ch4-S) proteoglycan by ELISA. Other sponges were extracted in urea for Western immunoblot using an antibody for hypoxia inducible factor-1α (HIF) in order to validate hypoxic condition.

Either with/without perfusion, hDFs around and on DBPs were surrounded by fibrous and granular metachromatic matrix. In Hypo, densest fibrous metachromatic matrix was frequently seen near the DBPs. In the DBP/sponges, Hypo significantly enhanced Ch4-S accumulation both without (165%, $p < 0.05$) and with perfusion (160%, $p < 0.05$) compared to Norm. Analysis of PCNA+ cells showed that Hypo did not inhibit proliferation. HIF was not expressed in Norm with perfusion, but was expressed at a low level in Norm without perfusion; this suggests that some cells within the sponge were in fact exposed to low oxygen. HIF was dramatically upregulated by Hypo with/without perfusion, as expected.

In sum, DBP induced chondrogenesis in hDFs; this was significantly increased by Hypo. Thus, exposure to DBP renders hDFs sensitive to hypoxia.

[1] Exp Cell Res 227:89,1996; [2] Biomater 17:1819,1996.

Disclosures: ***S. Mizuno****, None.*

M042

$1,25(OH)_2D_3$ Differentially Regulates Osteoblast Expression of Integrin Beta-1 and Its Partners Alpha-2 and Alpha-5 in a Substrate Dependent Manner. L. Wang[1], P. Raz*[2], D. M. Ranly*[1], C. H. Lohmann*[3], J. Turner*[1], B. D. Boyan[1], Z. Schwartz[1]. [1]Biomedical Engineering, Georgia Institute of Technology, Atlanta, GA, USA, [2]Periodontics, Hebrew University Hadassah, Jerusalem, Israel, [3]Orthopaedics, University of Hamburg-Eppendorf, Hamburg, Germany.

$1,25(OH)_2D_3$ decreases osteoblast proliferation and increases osteoblast differentiation. This transition is accompanied by a shape change in vivo and in vitro, suggesting that changes in integrin expression may occur as well. Microrough substrates also induce osteoblast differentiation, and this effect is synergistic with $1,25(OH)_2D_3$. Here we tested the hypothesis that changes in integrin expression over time in culture and regulation of integrin expression by $1,25(OH)_2D_3$ are substrate dependent. Human MG63 osteoblast-like cells were grown for 4, 6, and 8 days on tissue culture plastic and on Ti disks with smooth and rough microtopographies. Cells were treated with $1,25(OH)_2D_3$ [10^{-8}-10^{-9}M] and the expression of beta-1, alpha-2, alpha-5, beta-3, and alpha-v integrins, as well as of the differentiation marker osteocalcin, was determined by real time PCR. Messenger RNAs for osteocalcin, beta-1, and alpha-2 were increased on Ti compared to plastic. $1,25(OH)_2D_3$ increased osteocalcin expression on all surfaces at 4 and 6 days but levels were reduced at day 8. $1,25(OH)_2D_3$ increased alpha-2 and beta-1 expression on plastic and further increased the expression on Ti surfaces compared to plastic. This effect was pronounced at day 8. Levels of alpha-5 mRNA were significantly decreased on Ti surfaces and upon addition of $1,25(OH)_2D_3$ at all time points. Levels of alpha-v mRNA were reduced in response

to $1,25(OH)_2D_3$ on Ti surfaces and on plastic at 6 and 8 days whereas beta-3 expression was not sensitive to time of culture, surface chemistry or topography, or $1,25(OH)_2D_3$ treatment. These results confirm prior studies showing that integrin expression is substrate dependent and show for the first time that they are differentially regulated by $1,25(OH)_2D_3$ and that the effect of $1,25(OH)_2D_3$ is sensitive to physicochemical characteristics of the surface. (Supported by GTEC and the ITI Foundation).

Disclosures: ***L. Wang****, None.*

M043

Digit Tip Regeneration and Global Gene Expression Profiling in the MRL Super-Healer Mouse. R. B. Chadwick*, L. M. Bu*, H. Yu*, Y. Hu*, R. Sachdev*, Q. W. Tan*, J. E. Wergedal, S. Mohan, D. J. Baylink. Molecular Genetics, Musculoskeletal Disease Center, Loma Linda, CA, USA.

The MRL mouse is the only known strain of mouse that shows complete healing of an ear punch without scarring. Additionally, the MRL mouse can regenerate cardiac lesions. The present study sought to test the hypothesis that the MRL mouse also shows superior regeneration properties in the digit tip amputation model. The control mouse was the DBA mouse that exhibited only moderate healing in ear-punch experiments.

Immediately after birth, right paw digit tips of neonatal mice were dissected, with the left front paws as uncut controls. The amount of tissue amputated was measured and consecutive x-ray images were captured of the left and right paws at 7, 14, 21 and 28 days post amputation. Additionally, at four days post dissection, total RNA from the MRL and DBA regenerating digit tips was isolated. Microarray expression profiling was undertaken of this RNA in comparison to RNA from control tissue collected at the time of surgery.

At 14 days post amputation both mouse strains were found to regenerate, however the regeneration rate of the MRL digit tips was greater in comparison to the DBA strain ($p=0.016$). Over 500 genes out of 15,000 on the microarray were significantly differentially expressed ($p < 0.05$) in MRL and DBA mice at day four in comparison to control tissue at day zero. Of these, 170 genes were upregulated and 280 were downregulated in both mouse strains. About 50% of these genes represent ESTs and unknown genes. Pathway analysis reveals that genes in the BMP/TGF pathway are differentially expressed in both mouse strains (BMP-1, Actr2, Smad 4, TGFb1i4, Fstl3, Twsg1, TSC22), thus implicating the BMP/TGF signaling pathway in regulation of digit tip regeneration ($p < 0.05$). Multiple differences between MRL and DBA strains were found in transcription factors that are implicated in embryogenesis, including Mesp2 (involved in Notch signaling and somitogenesis, upregulated 2.8 fold), Net1 (highly expressed in neurons and involved in gastrulation, upregulated 1.7 fold), Bola-like transcription factor (upregulated 4.1 fold) and EST Mm. 270291 (DNA binding zinc-finger protein, upregulated 3.0 fold). We conclude that 1) MRL mice show greater regenerative capacity to heal digit tips compared to DBA mice; 2) The BMP/TGF signaling pathway is involved in digit tip regeneration; 3) Increased regenerative capacity of the MRL mouse may be due to strain specific increased expression of transcription factors that function in embryogenesis and development.

Disclosures: ***R.B. Chadwick****, None.*

M044

Regulation of Gene Expression in *ank/ank* Mouse Tooth Root Cells by Phosphate and Pyrophosphate. B. L. Foster*[1], E. C. Swanson*[1], F. H. Nociti, Jr.*[1], J. E. Berry*[2], F. Boabaid*[1], M. J. Somerman[1]. [1]School of Dentistry, University of Washington, Seattle, WA, USA, [2]School of Dentistry, University of Michigan, Ann Arbor, MI, USA.

A cementum phenotype has been described for animals with mutations in genes/proteins that regulate the level of extracellular pyrophosphate, *e.g. ank* transmembrane PP_i transporter, plasma cell membrane glycoprotein-1 (PC-1), and tissue nonspecific alkaline phosphatase (TNAP). Here, we isolated cell populations from the tooth root region of *ank/ank* mutant and wild-type (WT) mice, and compared *in vitro* gene expression with phosphate or pyrophosphate treatment.

Cells were harvested from *ank/ank* and WT mice, and cementoblast/PDL cell populations were immortalized using WT SV40 large TAg to create *ank/ank* mutant (SVAT) and WT (SVWT) cells. Cells were treated with inorganic phosphate (P_i) (1, 5, 10mM) or pyrophosphate (PP_i) (0.01, 0.1, 1mM) for 24 hours, and total RNA was isolated. Gene expression was analyzed by real time RT-PCR for bone sialoprotein (BSP), osteocalcin (OCN), osteopontin (OPN), dentin matrix protein-1 (DMP1), matrix Gla protein (MGP), PC-1, and TNAP.

SVAT and SVWT cells contrasted in the basal expression of several genes, including regulators of mineralization (BSP, OCN, OPN, DMP1, MGP) and regulators of P_i/PP_i metabolism (PC-1, TNAP). While SIBLING (Small integrin-binding ligand N-linked glycoprotein) family member BSP was expressed more highly in SVAT mutant cells, two other SIBLING transcripts, OPN and DMP1, were at much lower levels in SVAT cells compared to SVWT cells. SVWT and SVAT also diverged in their response to P_i and PP_i treatments, *in vitro*. SVAT cells were more sensitive than SVWT to up-regulation of OPN by both P_i (20,000% vs. 300% increase) and PP_i (300% vs. 100% increase). DMP1 transcripts in SVAT cells were increased by P_i and PP_i from undetectable levels to higher expression than equivalently treated SVWT cells. Mineralization regulator MGP was up-regulated 150% in SVAT cells by both P_i and PP_i, but was not regulated in SVWT cells. Inversely, TNAP was down-regulated in SVWT cells by P_i (down 65%) and PP_i (down 50%), but was not regulated in SVAT cells.

The cells from *ank/ank* mutant mice have an impaired ability to export PP_i from the intracellular space, resulting in low extracellular PP_i and inflated intracellular PP_i. These studies show that in addition to differences in basal levels of several genes, these cells react differently to P_i and PP_i exposure. Genes involved in regulation of mineralization and P_i/PP_i handling were regulated differently in SVWT and SVAT cells, indicating that altered gene expression may contribute to the hypermineralizing cementum phenotype of *ank/ank* mice, in addition to decreased extracellular PP_i.

Disclosures: ***B.L. Foster****, None.*

M045

Repair of Large Bone Defects in Sheep with Allografts Augmented with Loading of Bone Marrow Stromal Cells. M. B. C. Fernandes*[1], J. S. N. Reis*[1], H. S. H. Martins*[1], P. C. M. Lopez*[1], A. Balduíno*[1], M. L. Aceto*[2], C. E. Ambrósio*[2], A. C. F. Pinto*[2], F. N. Rodrigues*[2], M. A. Miglino*[2], R. Borojevic*[1], M. E. L. Duarte[1]. [1]Histology and Embriology, UFRJ, Rio de Janeiro, Brazil, [2]College of Veterinary Medicine, USP, São Paulo, Brazil.

Repair of large bone defects is a major problem in orthopedic surgery since autologous bone grafts are not available in large amounts and harvest is often associated with donor-site morbidity. In contrast, bone allografts are readily available in different shapes and sizes and, tissue-processing and sterilization procedures have virtually eliminated the risk of infectious disease transmission. Bone marrow stromal cells (BMSC) are responsible for the maintenance of bone turnover through life and can be considered as a mesenchymal progenitor. The purpose of the current study was to verify if cultured autologous BMSC loaded onto allografts would elicit a more effective bone repair at the site of a large segmental defect in the sheep tibia. Three weeks before surgery, 20-30mL marrow aspirates were harvested from the iliac crest. Marrow samples were washed twice in DMEM, filtered through a 40µm cell strainer, suspended in DMEM supplemented with 10% FCS and antibiotics and plated at the density of $6x10^7$ in 150 cm² culture flasks. The medium was changed after 24 hours and then twice a week. Cultures reached confluence 21-27 days after the initial plating. Segmental bone defects, 30 mm in length, were created in the left tibial diaphysis of eight mature female sheeps. Four animals were treated with $1,4x10^7$-10^8 *ex-vivo* expanded autologous BMSC loaded onto a cortical allograft previously packed with cancellous chips. Allografts were harvested from two donors of the same breed as the receptor sheep, sterilized by γ-radiations (25 000 gray), kept frozen at -80º C and thawed immediately before use. The healing response was evaluated histologically and by computed tomography at 6, 10, 14 and 18 weeks after surgery and compared with four control animals treated with cell-free allografts. Union was established more rapidly at the interface between the host bone and allografts that had been loaded with BMSC. In cell-loaded allografts a larger osseous callus had developed around the periphery and along the adjacent host bone. In retrievals from animals treated with cell-loaded allografts healing at the cortical-cortical junctions took place by bridging external callus from the host bone and extended on the surface of the allograft. Our results indicated a significant advantage in the healing of the segmental bone defects when BMSC were delivered together with the bone allograft. In all time points, bone integration as well as functional recovery was more conspicuous in allografts loaded with BMSC.

Disclosures: ***M.E.L. Duarte****, None.*

M046

Effect of Dietary Magnesium Reduction to 25% of Nutrient Requirement on Bone and Mineral Metabolism in the Rat. R. K. Rude. Keck School of Medicine, University of Southern California, Los Angeles, CA, USA.

Previous studies have demonstrated that severe Mg deficiency results in osteoporosis in rodent models. We now report the effects of more moderate dietary Mg restriction (25% of nutrient requirement (NR)) on bone and mineral metabolism in the rat. At 2, 4, and 6 months, serum Mg, Ca, PTH, and $1,25(OH)_2D$ were measured in control and Mg deficient animals. Femurs and tibias were collected for mineral content, histomorphometric, and immunocytochemical analyses. As shown below, serum and bone Mg were significantly reduced by 2 months and continued so through 6 months. sCa did not differ between groups. sPTH became lower in Mg depleted animals at 4 and 6 months. Serum 1,25-D was significantly reduced by 4 and 6 months of study. Histomorphometry demonstrated decreased bone volume and trabecular thickness. This was confirmed by micro-CT which also showed that trabecular volume, and number were significantly lowered ($p<.02$; data not shown).

	2 months		4 months		6 months	
	Control	Mg def	Control	Mg def	Control	Mg def
sMg, mg/dl	1.9±0.2	01.1±0.2*	1.8±0.2	01.2±0.2*	1.6±0.2	0.9±0.2*
sCa, mg/dl	9.2±0.6	8.9±0.7	8.9±0.3	9.1±0.3	8.5±0.6	9.2±0.6
sPTH, pg/ml	201±109	202±137	564±364	329±181*	320±146	134±116*
1,25-D, pg/ml	57±57	37±24	38±11	14±11#	18±13	8±4#
Ash Mg, %	.74±.09	.59±.03*	.77±.03	.61±.05*	.77±.04	.56±.05*
BV/TV (%)	22±3	17±2	25±5	14±3	19±5	14±4#
TTh (um)	42±3	38±4	46±5	39±3	42±5	41±3@

Data are means ± SD. *p<.001, #p<.01, @p<.02

TNFα immunocytochemical localization in osteoclasts was increased 138% of controls at 2 months, 138% at 4 months and 150% at 6 months. Increased TNFα may be due to increased substance P which was increased to 313% of control at 2 months and 179% at 4 months and 432% at 6 months. These data demonstrate that Mg intake of 25% NR in the rat causes bone loss which may be secondary to increased release of substance P and TNFα.

Disclosures: ***R.K. Rude****, None.*

M047

Modulation of Morphological and Mechanical Properties in Distraction Osteogenesis by Minodronic Acid. M. Takahashi*, K. Yukata*, Y. Matsui, S. Takata, A. Abbaspour*, N. Yasui*. Orthopedic, Tokushima University, Tokushima, Japan.

The limb lengthening procedure using an external fixator is an excellent treatment to rebuild the functional limbs for many troublesome cases. However, it has several problems such as persistent treatment until removal of external fixator, and mechanical fragility of regenerated bone. These problems were related to the high activity of bone resorption in distraction gap. The characteristic zonal structure is detected radiographically in a rabbit model of distraction osteogenesis, where the sclerotic zone has been absorbed from each original cortex. We hypothesized that the regenerated bone was sufficient to sustain the load if it was not remodeled. To prove this we administered potent third-generation bisphosphonate to rabbit undergoing distraction osteogenesis.

A lengthening protocol is composed of a 3-week of distraction at a rate of 0.7 mm/day after one-week waiting period, and a 4-week consolidation period. Fifteen immature rabbits were divided into the following three groups; group 1 was administered only saline as a control, group 2 and group 3 were administered weekly doses of 0.004 mg/kg and 0.4 mg/kg of minodronic acid for 6 weeks from the operation, respectively. Radiological examination was performed with an aluminum wedge that allowed quantifying radiographic bone density of the zonal structure in distraction gap. Although group 1 showed zonal patterns according to respective time points during the consolidation, group 3 showed neither remodeling zone nor tubular structure in distraction gap at any time point. In bone density study, group 2 demonstrated same zonal patterns as group 1, but showed wider sclerotic zones than group 1. In distal remodeling zone, both group 1 and 2 indicated same bone density value (3 mm Al-thickness). In group 3, the whole bone densities in the distraction gap have gained over 5 mm Al-thickness uniformly at last. After extraction, lengthened tibiae were examined the mechanical properties by three-point bending test. Group 3 was significantly stronger in all of mechanical properties than others.

In conclusion, bisphosphonate modulated the remodeling in distraction osteogenesis and strengthened the mechanical property of regenerated bone.

Disclosures: ***M. Takahashi****, None.*

M048

Effects of Calcitonin on Subchondral Trabecular Bone Changes and on Osteoarthritic Cartilage Lesions following Acute Anterior Cruciate Ligament Deficiency. D. H. Manicourt*[1], C. Behets*[2], D. Chappard[3], M. Azria[4], J. P. Devogelaer[1]. [1]Rheumatology Unit, St-Luc University Hospital, Brussels, Belgium, [2]Human Anatomy Research Unit, St-Luc University Hospital, Brussels, Belgium, [3]Lab Histology-Embryology, Faculty Medicine Angers, Angers, France, [4]Research Department, Novartis Pharma Inc, Basel, Switzerland.

As subchondral bone remodeling may contribute to cartilage breakdown in osteoarthritis (OA), we evaluated to what extend calcitonin (CT) might affect cartilage and bone changes in the early stages of canine experimental OA. Twelve dogs underwent transection of the anterior cruciate ligament (ACLT) of the right knee. After ACLT, each animal received a daily nasal spray delivering either 400 units of CT (CT-treated group; n = 6) or a placebo (PL-treated group; n = 6). At day 84 postsurgery, animals were sacrificed, and cartilage changes were graded. Bone mineral density (BMD) and volume fraction (BVF) were assessed by pQCT in different regions of interest (ROIs) of the subchondral cancellous bone of tibial plateaus (TP).Statistics included a 2x2 factorial analysis with CT + or - as one factor and ACLT + or - as the other. Non-operated (N-OP) knees were normal in both groups. In PL-treated group, ACLT knees all exhibited OA changes which predominated in the medial knee compartment. Further, when compared to N-OP knees, the BMD and BVF of ACLT joints were both markedly reduced in medial TP ($p < 0.001$) but not in lateral TP. In contrast, in CT-treated group, cartilage OA lesions of ACLT knees were significantly reduced ($p < 0.001$) and there was no difference in BMD and BFV between N-OP and ACLT knees. These findings suggest that the loss of subchondral trabeculae contributes to cartilage breakdown, possibly by enhancing cartilage deformation upon joint loading. By counteracting bone loss, CT reduced cartilage OA lesions and, thus, might be useful in the treatment of OA in cruciate-deficient dogs.

Disclosures: ***J.P. Devogelaer****, Novartis Pharma Inc. 2.*

M049

In Vivo Over-expression of Circulating Dlk1/Pref-1 Protein Using Hydrodynamic-based Gene Transfer Leads to Lower Bone Mass with Marked Effects on Trabecular Bone Micro-architecture. B. M. Abdallah*[1], M. Ding*[1], C. Jensen*[2], N. Serakinci*[1], B. Teisner*[2], F. Dagnæs-Hansen*[3], M. Kassem[1]. [1]Endocrinology Department, OUH, Odense, Denmark, [2]Institute of Medical Immunology, SDU, Odense, Denmark, [3]3Department of medical Microbiology and Immunology, AU, Aarhus, Denmark.

Dlk1/Pref-1 (delta like1/preadipocte factor-1) is an imprinted gene encoding a transmembrane protein that belongs to EGF-like repeats protein family. We have recently identified Dlk1/Pref-1 as negative regulator for differentiation of human mesenchymal stem cells into osteoblasts and adipocytes (Abdallah BM, et. al., JBMR, May,19(5):841-852, 2004). To further investigate the in vivo effect of Dlk1/Pref-1 on bone, we generated mice expressing high serum levels of FA1 (biological soluble form of Dlk1) using the hydrodynamic-based gene transfer procedure. Full length of mouse Pref-1 cDNA was subcloned under human ubiquitin promoter and rapidly injected via tail vein into BALB/cA male mice (16 weeks old, n =15) every 2 weeks over a period of 2 months. DNA, mRNA analysis, immunohistology and ELISA for FA1 were assayed to identify the expression of the transgene. Bone mass and structure were determined by PIXImus (Lunar^R) and micro-CT (Scanco^R) respectively. We could only localize the plasmid in the liver and no complications were detected due to transgene expression. Serum levels of FA1 in Dlk1 injected mice (Dlk1$^+$mice) was elevated by more than 15 folds compared to control saline injected mice (control) (198.0 ± 74.3 ng/ml vs 13.4 ± 1.1 ng/ml, $p<0.001$, respectively). Dlk1$^+$mice displayed lowered body weight and reduced total fat mass (13.5%, $p< 0.05$ and 17.8%, $p< 0.05$ respectively). Interestingly, Dlk1$^+$mice displayed (16.6 %, $p<0.005$) lowered total bone mineral density (BMD) compared to controls and BMD was negatively correlated with the circulating levels of FA1. Micro-CT analysis revealed significantly decreased micro-architectural parameters of trabecular bone in the distal femur and proximal tibia of the Dlk1$^+$mice compared to controls (see table).

Naked DNA delivery by hydrodynamic injection is a simple and safe procedure for evaluating the effect of genes on bone phenotype in vivo. Our data suggest that Dlk1/Pref-1 is a novel regulator of bone mass.

Groups (n=8)/ Measurments	BV/TV	TbTh (µm)	TbSp (µm)	TbN (1/mm)	CD (1/mm^3)
Distal femur	0.34 ±0.11	0.07±0.01	0.19±0.03	5.80±1.10	155.1±37.4
Control group					
Dlk+ group	0.19 ±0.06	0.06±0.00	0.24±0.04	4.60±0.84	113.3±37.8
Proximal Tibia	0.20±0.07	0.07 ±0.01	0.24±0.04	4.60±0.57	98.6±21.27
Control group					
Dlk+ group	0.14±0.03	0.06 ±0.01	0.25±0.02	4.26±0.42	75.5±25.7

P<0.05 for all tested parameters

TbTh , Sp ,N=trabecular thickness, space, number, CD=connectivity

Disclosures: ***B.M. Abdallah****, None.*

M050

Evaluation of Quality of Life Criteria According to the Severity of Vertebral Osteoporosis: The Act'Os Study. J. Fechtenbaum[1], C. Cropet*[2], R. Said*[1], S. Kolta[1], O. Madi*[3], P. Orcel[4], C. Roux[1]. [1]Rheumatology, Cochin hospital, Paris, France, [2]MAPI - CRO, Lyon, France, [3]Aventis, Paris, France, [4]Rheumatology, Lariboisière hospital, Paris, France.

Introduction: osteoporotic vertebral fractures are responsible for back pain and for the reduction of mobility and functions. These different factors are determining of quality of life, and a specific questionnaire concerning osteoporosis has been validated (QUALEFFO).

Aim of the study: to evaluate de quality of life of women having vertebral fractures according to the severity of the disease.

Patients and methods: 629 menopausal osteoporotic patients having at least one vertebral fracture according to the investigator have been included.The QUALEFFO 41 questionnaire that covers 5 aspects (pain, physical activity, social activity, perception of general health and mental health) and has a total score, has been used in the study. Spine X-rays have been done in standardized conditions and analyzed centrally. Fracture analysis was done according to the semi-quantitative method (in 4 grades).

Results: analysis was done on 588 patients (in 41 patients, diagnosis was not possible due to the presence of some non legible or missing vertebrae with the remaining vertebrae considered as non fractured). The diagnosis of fractured patients was confirmed in 548 cases. Patients having at least one vertebral fracture had QUALEFFO scores greater than other patients (i.e. a worse quality of life) in two aspects: physical activity ($p = 0.055$) and social activity ($p = 0.027$). The scores were worse with increasing number of fractures for 3 aspects: physical activity ($p = 0.001$), social activity ($p = 0.002$) and total score ($p = 0.027$). The same results were obtained when the severity of the disease was defined as the sum of the grades of fractures or by an index calculated by the sum of the grades and the number of fractures.

The variation of pain and mental health scores was never significant.

Conclusion: the quality of life evaluated by a specific questionnaire is altered in menopausal patients having vertebral osteoporotic fractures compared to patients of the same age without fracture. A pain score was not significantly different in this evaluation. The quality of life is significantly worse with the severity of the disease. This is important to be considered in order to start treating women as soon as the first fracture is diagnosed.

Disclosures: ***J. Fechtenbaum****, None.*

M051

Collagen Bundle Distribution along the Radial Direction of Human Secondary Osteons. M. Ascenzi, A. Lomovtsev*. Orthopaedic Surgery, UCLA, Los Angeles, CA, USA.

Collagen orientation distribution within so-called bright and extinct lamellae, secondary osteons' building blocks, is observed along the previously unexplored osteon radial direction.

70±3µm thick cross-sections were cut from femoral mid-shafts, aged 19-40, pathology-free. 22 fully-calcified lamellar specimens, 11 per type identified as bright or extinct on transverse section under circularly polarized light, were then isolated and gently flattened (Ascenzi M-G et al., J. Struct. Biol. 141: 22, 2003). A Leica TCS-SP confocal microscope (krypton laser, 63x Planapochromat lens) scanned wet specimens each 0.5µm through thickness. Natural fluorescence shows as green pseudo-color. Images were observed at 1575x and 3000x magnification with Image-I. Collagen bundles appear as bright elements on dark background of mucopolysaccharides and glycoproteins. Long portions of canaliculae appear to follow local collagen orientation. Domains were identified as 3D regions whose collagen bundle orientation varies up to ±7.5° within and across adjacent scans.

Collagen orientation within domain was measured relative to original osteon axis.
Bright lamellae show characteristic collagen distribution somewhat transverse to the original osteon axis within the middle thickness (Fig. a) becoming gradually oblique towards approximately ±45º with respect to the osteon axis. Extinct lamellae show characteristic collagen distribution whose orientation makes up to approximately ±22.5º angle relative to original osteon longitudinal axis (Fig. b).
Results conform to findings by different methods (Ascenzi M-G et al., J. Struct. Biol. 141: 22, 2003), mechanical significance of bone shaft collagen orientations (Ascenzi A, J. Biomech. Eng. 110: 357, 1988), and skeletal adaptation to mechanical function (Frost, Calc. Tissue Int. 45: 145, 1987). Results are integrated in high-accuracy hierarchical bone models (Ascenzi M-G, Scanning, 26: 25, 2004) which use the super-computer capability to test hip prostheses virtually.

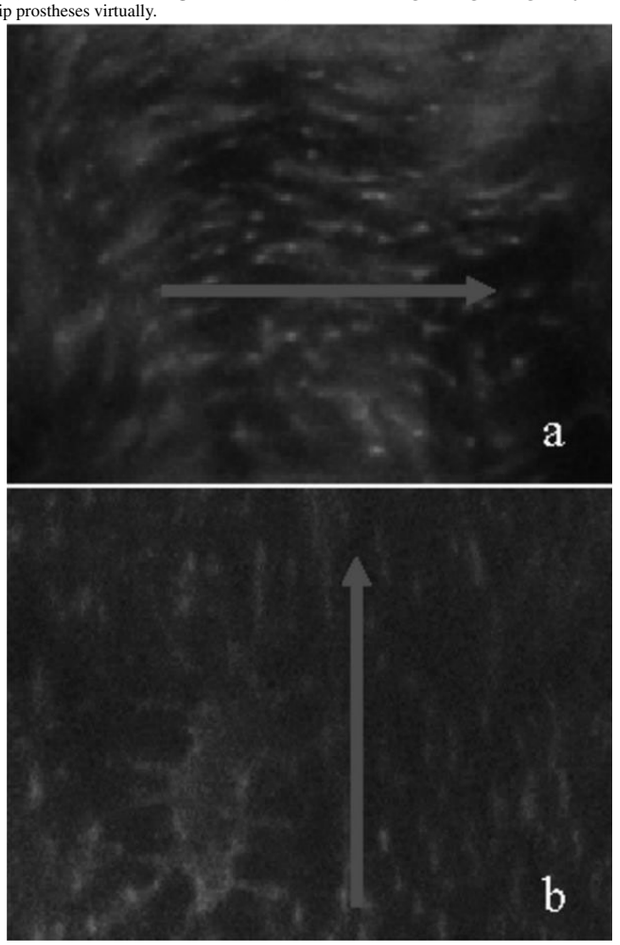

Disclosures: ***M. Ascenzi****, None.*

M052

Localisation of Beta Catenin in Regenerating Bone Supports a Role for the Canonical Wnt Pathway in Regulating Progenitor Cell Function, Intramembranous Ossification and an Interrelationship with PTHrP. J. G. G. Mount*, S. P. Allen*, M. Muzylak*, T. Althnaian, J. S. Price. Basic Sciences, Royal veterinary college, London, United Kingdom.

Mutations in Lrp5 reveal a critical role for the Wnt pathway in the acquisition of bone mass and Lrp5 is known to signal through β-catenin, a component of the canonical Wnt pathway that regulates osteoblast differentiation. In this study we used the deer antler to explore the hypothesis that the Wnt signalling pathway will be recapitulated when bone regenerates in an adult. Antlers elongate at an unparalleled rate by an endochondral process from an extensive 'growth zone' of multi-potential progenitors and increase in diameter by intamembranous ossification. Immunocytochemistry was used to localise the dephosphorylated, activated form of β-catenin (^{a}βCAT) in antler tissues and this was related to the localisation of PTHrP, which is widely expressed in antlers and is known to interact with the Wnt pathway in some developing systems. Compared to PTHrP, ^{a}βCAT staining had a restricted localisation; staining was associated with proliferating cells in hair follicles and in sebaceous glands but no immunoreactivity was seen in the epidermis, dermis, perichondrium, in hypertrophic chondrocytes or in osteoblasts at sites of endochondral bone formation. However, ^{a}βCAT was localised in cellular periosteum and in osteoblasts in intramembranous bone. Of particular note was intense ^{a}βCAT staining in progenitor cells in the antler's growth zone; these cells are not highly differentiated and have a high rate of division (21.7±5.5% of cells) and apoptosis (63.9±9.2% cells). Con-focal microscopy revealed that PTHrP and ^{a}βCAT co-localise in these progenitor cells. To identify the functional role of the Wnt pathway, cells from the growth zone were cultured with LiCl, which activates β-CAT, and EGCG, which inhibits Tcf transcription. LiCl inhibited ($p<0.001$) whereas EGCG increased alkaline phosphatase activity ($p<0.05$). LiCl and PTHrP had no effect on cell growth, whereas both EGCG and PTHrP induced apoptosis. However, Western blot analysis showed that PTHrP did not regulate ^{a}βCAT expression.
In conclusion, this study provides evidence that the canonical Wnt signalling pathway regulates progenitor cell differentiation and survival in regenerating bone. Results also suggest that there is an interaction between the PTHrP and Wnt pathways in controlling progenitor cell function, although PTHrP does not appear to signal through β-catenin. This study also shows that β-catenin's role in regulating osteoblast differentiation may be site specific.

Disclosures: ***J.G.G. Mount****, None.*

M053

Human Osteoblast Proteomics: Implications for Drug Discovery. K. J. MacLeod*[1], K. Shopbell*[1], B. L. Allen*[2], M. R. Pisano*[2], M. W. Long[1]. [1]Velcura Therapeutics, Inc., Ann Arbor, MI, USA, [2]Proteomic Research Services, Ann Arbor, MI, USA.

We hypothesized that a proteomics drug discovery platform utilizing primary human osteoblasts would produce physiologically relevant information important to the therapy of bone diseases such as osteoporosis. To develop such a platform, we postulated that 2-dimensional gel electrophoresis (2-DGE) analyses of osteoblast protein expression, averaged over a number of bone-cell donors, would identify specific protein expression patterns (i.e., protein maps). We utilized osteogenic growth-factors (OGFs) to model whether human osteoblast protein maps would be indicative of osteoblast responsiveness. Such maps are representative of induced "cellular activation states" and potentially useful in the identification of drug candidates that stimulate bone formation. We report that protein mapping using primary human osteoblasts distinguishes specific protein patterns for individual OGFs, or synergistic combinations thereof. The 2-D gels for TGF-β1 (100 pM), BMP2 (50 pM), or PTH (200 pM; cells cultured in serum-free, chemically defined media) were compared to control gels to identify differentially modulated proteins. Composite 2-DGE profiles, averaged across all donors (n = 8), were then generated showing differentially modulated protein patterns, or maps, that are unique to the effects of each cytokine. We also analyzed human osteoblasts nuclear phosphorylation and identified specific patterns in which several new phosphoproteins appear in the nucleus, reflecting either newly phosphorylated proteins, or phosphoproteins translocated to the nucleus. Finally, we utilized mass spectrometry (MALDI-TOF or LC/MS/MS) to identify 110 proteins from the OGF-composite protein maps. These include proteins relevant to bone formation such as annexin, and type I collagen, as well as several proteins (alpha tubulin, vimentin, actin) indicative of cytoskeletal rearrangement in differentiating osteoblasts. As well, concordant modulation of these proteins is seen among sub-cellular fractions. For example, we detected up-regulation of annexin V in membrane fractions and a coordinate increase in the cytoplasm of a calcium binding protein known to be critical for annexin-membrane association. We conclude that these results constitute an important proof of concept that proteomic analysis can distinguish specific patterns of responsive proteins in human osteoblasts. The use of such "cellular activation state" maps in drug discovery has important implications in developing bone disease therapies.

Disclosures: ***K.J. MacLeod****, None.*

M054

The Effect of Rosiglitazone, an Anti-diabetic PPAR-γ Agonist, on Bone Mass and Architecture in Growing, Adult, and Aged Mice. B. Lecka-Czernik[1], O. P. Lazarenko*[1], S. O. Rzonca*[1], K. Teng*[1], L. J. Suva[2]. [1]Geriatrics, UAMS, Little Rock, AR, USA, [2]Orthopedic Surgery, UAMS, Little Rock, AR, USA.

Rosiglitazone represents an oral anti-diabetic agent that is FDA-approved for the treatment of type 2 diabetes; a disease which affects individuals of all ages. Mechanistically, rosiglitazone sensitizes cells to insulin *via* the specific activation of PPAR-γ. PPAR-γ activated with rosiglitazone acts as a dominant inhibitor of osteoblast differentiation and phenotype. *In vivo,* PPAR-γ activation induces bone loss whereas PPAR-γ insufficiency leads to increased bone formation. Since bone and bone progenitor status changes with normal aging, we investigated the effect of rosiglitazone on bone of young, adult and aged mice. C57BL/6 mice (young - 1 mo, adult - 6 mo, aged - 24 mo old) were fed a rosiglitazone (young: 15 μg/g body weight/day; adult and aged: 20 μg/g body weight/day) supplemented diet for 8 weeks. Bone mineral density (BMD) and bone mineral content (BMC) were measured at the beginning and end of the experiment, and the tibiae were analyzed by microCT and histomorphometry. Administration of rosiglitazone to adult and aged mice produced a significant decrease in global BMD and BMC, with the expected changes in bone microarchitecture. Histomorphometric analysis revealed that rosiglitazone administration to adult mice simultaneously decreased osteoblast number and activity by 3-fold and increased osteoclast number and their activity by 4-fold. Surprisingly, in aged animals rosiglitazone did not appear to affect any osteoblast parameters but increased osteoclast parameters similarly as in adults. These changes were accompanied by increased serum levels of C-telopeptide. In contrast, rosiglitazone administration to 1-mo old growing mice did not affect global BMD, but it decreased global BMC, however serum markers of bone formation and resorption remained unchanged. These results demonstrate that the skeletal response to rosiglitazone differs with aging and may reflect the status of the osteoblast and osteoclast progenitors targeted by this drug. If confirmed in humans these data suggest that anti-diabetic rosiglitazone therapy should be accompanied by therapies specifically designed for patient age that would target either the prevention of bone resorption or the stimulation of bone formation, or both.

Disclosures: ***B. Lecka-Czernik****, None.*

M055

Delayed Fracture Healing in iNOS Knockout Mice. F. F. Safadi[1], T. A. Freeman*[2], J. L. Castaneda*[1], I. Arango*[1], S. N. Popoff[1], J. M. Daly*[2], P. P. Stapleton*[3]. [1]Anatomy and Cell Biology, Temple University School of Medicine, Philadelphia, PA, USA, [2]Microbiology and Immunology, Temple University School of Medicine, Philadelphia, PA, USA, [3]Surgery, Temple University School of Medicine, Philadelphia, PA, USA.

Inducible nitric oxide synthase (iNOS) is expressed in osteoblasts and is detected in the initial stages of fracture healing with expression localized to cells within the intra-membranous region of the fracture callus. In this study, we examined fracture healing in iNOS knockout (KO) and wild type (WT) mice with injury consisting of an open femur fracture. iNOS KO and WT mice (n=10/group) were subjected to femur fracture under anesthesia. Histological and x-ray analyses as well as expression of osteoblast-related genes, such as osteoactivin, type I collagen and osteocalcin were performed using RT-PCR analysis. Histological analysis of normal, non-fractured femurs from WT and iNOS mice showed an increase in trabecular bone volume in iNOS KO compared with WT littermates. At one and three weeks-post fracture, x-ray analysis showed a marked delay in fracture callus formation in iNOS KO compared with WT mice. These results were confirmed by histological analysis. In non-fractured femurs, osteoactivin, type I collagen and osteocalcin were over-expressed in iNOS KO compared with WT mice. In fractured femurs, osteoactivin, type I collagen, and osteocalcin expression were highly up-regulated in WT but not in iNOS KO mice. These data suggest that increased bone formation occurs after fracture in iNOS KO mice and furthermore, that iNOS regulates osteoblast development and function. These data suggest that iNOS might play an important role in fracture healing and mediate ostoeblast differentiation and function.

Disclosures: ***F.F. Safadi****, None.*

M056

Impaired Cartilage Regeneration with Aging in the MRL Mouse Regeneration Model: Evidence for Blunted Growth Factor Expression. G. L. Masinde*, S. Mohan, H. Klamut*, M. Covarubias*, D. J. Baylink. Mdc, J.L. Pettis VAMC, Loma Linda, CA, USA.

The MRL strain of mouse has the unique capacity to regenerate completely an earhole punch. Because cartilage is a major component in the ear tissue, this model provides a means to characterize the molecular mechanisms involved in cartilage regeneration. We sought to test the hypothesis that during aging, the healing of an earhole punch, even in the MRL mouse, would decline. A 2 mm through and through hole was punched in the ear of 14 week and 1 year old mice and the rate of cartilage regeneration measured by the extent of ear healing as a function of time (up to 28 days) after ear punch. The rate of cartilage regeneration was 15% per week in the 1 year old MRL mouse compared to 23% per week in the 14 week old MRL mouse ($P<0.01$). To identify the molecular mechanism that contribute to impaired cartilage regeneration in the old mice compared to the young MRL mice, we performed microarray analysis of over 5,000 genes using RNA extracted from healing ear tissue at 4 hours (inflammatory stage), 14 days (proliferation stage) and 28 days (remodeling stage). Microarray analysis was performed using RNA from three replicate pools (RNA pooled from 3-5 mice for each pool) and data analyzed using GeneSpring software. We found that 318, 356 and 252 numbers of genes were differentially expressed in the ear tissue of 14 week old mice compared to 1 year old mice up to 28 days respectively. Of 30 ontological gene categories, the largest differences in gene expression between the young and old MRL mice were in cell growth and maintenance, signal transduction and inflammation for each category ($P<0.001$)(see table). Conclusions: 1) The impairment of healing in the older MRL mouse is associated with down regulation of several growth factor genes.

Growth factors upregulated in the young MRL mouse as compared to 1 year old MRL mouse

GENE	FOLD CHANGE	P-VALUE
FGF1	6	0.001
FGF6	7	0.000002
FGF8	9	0.0009
FGF7/KGF	10	0.0005
TGFB	11	0.000007
PDGF	6	0.000004

Growth Factors upregulated in the young MRL as compared 1 year old mouse

GENE	FOLD CHANGE	P-VALUE
IGF-II	7	0.000002
BP-5	10	0.0001
BP-2	9	0.0001

Disclosures: ***G.L. Masinde****, None.*

M057

Histological Evaluation of a Calcium Sulfate-Carboxymethylcellulose Bone Graft Binder in a Critical Size Defect Model. M. A. Reynolds[1], J. D. Kassolis*[1], M. E. Aichelmann-Reidy*[1], H. S. Prasad*[2], M. D. Rohrer*[2]. [1]Periodontics, University of Maryland, Baltimore, MD, USA, [2]Oral Pathology, University of Minnesota, Minneapolis, MN, USA.

Carboxymethylcellulose (CMC) has been recently shown to enhance the handling properties medical grade calcium sulfate (CS) when used as a binder for particulate bone grafts. Few controlled studies, however, have examined the potential influence of CMC on bone regeneration. The purpose of this study, therefore, was to examine the osseous healing of critical size calvarial defects in rats grafted with demineralized bone allograft in combination with a CS:CMC (9:1 wt.) binder. Using a paired design, two separate 5 mm critical size defects were created using a trephine in the calvarium of 24 Wistar rats (350 g). Defects in each animal were randomly assigned to treatment with rat demineralized bone matrix (DBM) in combination with CS or CS:CMC binder, together with a CS barrier. The ostoinductive activity of the DBM was verified using a nude mouse model. Six animals each were sacrificed at 7, 14, 21 and 28 days. Calvarial specimens were dehydrated, infiltrated, and embedded in resin for undecalcified sectioning, staining, and blinded histomorphometric analysis using computer assisted image analysis. Statistical analysis was made using an analysis of variance. Histological findings consistent with a brisk cellular response were observed in essentially all specimens, with all defects demonstrating significant new bone formation, often in close apposition to recalcifying DBM. Evidence of inflammatory wound healing was evident in specimens, consistent with the post-surgical period; however, the lymphocytic and plasmacytic response was minimal. At 28 days post-grafting, differences between defects (CS and CS:CMC, respectively) were insignificant with respect to the proportion (%) of new bone (31.7 ± 9.5 versus 33.7 ± 12.9), fibrous tissue/marrow (54.2 ± 8.3 versus 53.0 ± 10.8), and residual DBM particles (8.3 ± 6.8 versus 10.1 ± 6.3). Comparable levels of residual binder were found in the CS and CS:CMC treated defects at 28 days (5.5 ± 4.6 versus 3.7 ± 3.5, respectively; $p \geq 0.05$). The results of this critical size defect model indicate that CMC and CS, when combined with particulate DBM graft, support osseous healing similar to that obtained with CS and allograft alone.

Disclosures: ***M.A. Reynolds****, LifeCore Biomedical, Inc. 2.*

M058

Role Of Architecture And Collagen Cross-linking on Trabecular Bone Mechanical Properties. T. M. Keaveny[1], E. K. Wong*[1], S. M. Daugherty*[1], S. Majumdar*[2], A. Burghardt*[2], N. Sakkee*[3], F. van der Ham*[3], J. deGroot*[3]. [1]Mechenical Engineering, University of California at Berkeley, Berkeley, CA, USA, [2]Radiology, University of California at San Francisco, San Francisco, CA, USA, [3]Gaubius Laboratory, TNO Hospital, Leiden, Netherlands.

While bone density plays a dominant role in the strength and stiffness properties of trabecular bone, it is widely believed that trabecular "bone quality" _ such as measures of cross-linking and architecture _ may also be an important aspect of bone integrity. The goal of this study was report on the combined role of architecture and collagen cross-linking, including non-enzymatic glycation, on the mechanical properties of aged human vertebral trabecular bone. Twenty-nine cylindrical specimens from the thoracolumbar spine were obtained from 29 radiographically normal cadaver spines (age 54-94; mean ± SD = 75.4 ± 11.7; 16F, 13 M). Specimens were imaged using micro-computed tomography and from the architecture was quantified. Mechanical tests were used to measure tensile strength. After testing, sections of the specimen were removed and both enzymatic and non-enzymatic cross-links were measured using reversed-phase HPLC. Results indicated that in terms of strength and stiffness, volume fraction dominated the behavior, architecture had some independent effects, and cross-linking had no effects. Multiple regression on ultimate strength showed effects of BV/TV, Tb.Th.SD, Conn-Dens, and DA, in that order of importance (adjusted R2=0.90, n=29). Regarding ultimate strain, only Tb.Th and Tb.Th.SD had any effect ($p<0.008$ both cases), and were negatively correlated with ultimate strain. While collagen cross-linking had no effect of any of these mechanical properties, it did have an effect on yield strain: Hyl was positively correlated with yield strain ($r=0.45$, $p=0.025$) whereas pentosidine was negatively correlated ($r=-0.44$, $p=0.027$). None of the collagen parameters were correlated with age. We conclude that while collagen cross-linking may have subtle effects on the mechanical behavior of trabecular bone, vertebral bone strength and stiffness are dominated by bone volume fraction and architecture.

Disclosures: ***T.M. Keaveny****, None.*

M059

Measurement of the Oxemic Status of the Intervertebral Disc Using a 2-Nitroimidizole Derivative. D. C. Lee*[1], S. M. Evans*[2], C. J. Koch*[2], I. M. Shapiro[1], T. J. Albert*[1], C. S. Adams[1]. [1]Orthopaedic Surgery, Thomas Jefferson University, Philadelphia, PA, USA, [2]Radiation Oncology, University of Pennsylvania, Philadelphia, PA, USA.

Previous work suggests that cells of the intervertebral disc have a limited vascular supply. As a result, it has been assumed that the pO_2 in the nucleus pulposus is low and the cells are in a hypoxic state. To test the hypothesis that the cells are hypoxic, we utilized a non-invasive technique to monitor the disc's oxemic status. Eight-week old (200 g) rats were injected with EF5, a 2-nitroimidazole derivative. This agent is metabolized by oxygen-sensitive nitroreductases that cleave EF5; these adducts can then be detected in tissues using monoclonal antibody techniques. We assayed the cleaved adducts by immunohistochemistry in both longitudinal and transverse sections of lumbar intervertebral discs. In addition, we used HPLC to measure both metabolized and unmetabolized drug in tissue extracts. We noted that there was a low level of EF5 staining in the nucleus pulposus suggesting that the pO_2 was insufficient to inhibit nitroreductase activity. Pharmacological distribution of the drug was similar to that of glucose and was approximately 50% of the serum concentration. As the level of drug binding to the nucleus pulposus was low the results suggested that there was minimal nitroreductase activity. Thus, to assess enzyme activity we artificially inducing hypoxia in vivo. Accordingly, discs were collected from a hypoxic animal following injection of EF5 and the oxemic status again determined. Since cells in these discs bound and metabolized EF5, it was clear that this enzyme system was active in the nucleus pulposus. This finding confirms the pharmacological analyses indicated above and indicates that the cells of the intervertebral disc contain an active nitroreductase system that metabolizes EF5. Since there was minimal EF5 binding in vivo, it is concluded that while the vascular supply is limited, the cells are adapted to a low pO_2 and do not exhibit signs of hypoxia.

Disclosures: ***D.C. Lee****, None.*

M060

Hyperparathyroidism Secondary to Vitamin D Depletion Stimulates Phex Expression in Rat Tibiae Independently of Serum Phosphate Concentrations. N. Dion[1], G. Mailhot*[1], M. Gascon-Barré[1], V. Lascau-Coman*[1], A. C. Karaplis[2], L. G. Ste-Marie[1]. [1]Hôpital Saint-Luc, CHUM Research Centre, Université de Montréal, Montréal, PQ, Canada, [2]Department of Medicine, McGill University, Montréal, PQ, Canada.

Mutations of the PHEX/Phex gene (phosphate-regulating gene with homologies to endopeptidases on the X-chromosome) in humans and mice are responsible for X-linked hypophosphatemic rickets, a renal phosphate-wasting disorder associated with defective bone mineralization. Recently, H.S. Tenenhouse's group showed that Phex expression in bone obtained from rats with chronic renal insufficiency is positively correlated with serum parathyroid hormone (PTH) levels (Brewer AJ et al., Am J Renal Physiol 286:F739-F748, 2004). Previously, our group used a non-rachitogenic rat model [low calcium (Ca)-vitamin D (D) depleted (Ca-D-) diet] to study bone mineralization and endochondral ossification defects. These rats had high serum parathyroid hormone (HPTH) concentration secondary to hypocalcemia and D depletion with increased serum levels and urine excretion phosphate (P). To better dissect the relationship between Phex expression and serum PTH, Ca and P, Ca-D- rats were repleted for 14 days with diets presenting various Ca/P ratios. Five groups were studied with Ca/P ratios of: 1.11/1 (Ca-D-); 4/1.5 (P+); 4/3 (P++); 2.25/1 (Ca+) and the same 2.25/1 ratio but repleted with D (Ca+D+). Rats paired for age and fed a regular rat chow diet served as controls. Compared to Ca-D-, P+ and P++ remained HPTH and hypocalcemic but normalized their serum P. However, Ca+ normalized both their serum Ca and P but remained HPTH. Ca+D+ normalized their serum Ca, P and PTH. Immunohistochemistry technique (IHC) was used to localize Phex protein on proximal tibiae sections. In all groups with HPTH, Phex was highly expressed in fibrosis surrounding trabecular bone at the primary and secondary spongiosa. Strong staining for Phex was also detected in osteoblasts, osteocytes and in some bone marrow cells. In Ca+D+, expression of Phex was decreased to a level similar to that of the controls. It was restricted to some osteoblasts, lining cells, osteocytes and few bone marrow cells. No major between-group difference was observed for the IHC of NEP which belongs to the same metallopeptidase family as Phex. Taken together, these results support the hypothesis that PTH or/and D is/are involved in the regulation of Phex expression in bone independently of serum phosphate concentrations. At present, the precise functions of Phex are not known and its potential role as an enzyme controlling the local action of PTH in bone or of still yet other unidentified anabolic factor(s) will require additional investigations.

Disclosures: ***N. Dion****, None.*

M061

Synergistic Catabolic Effects of TNFα and RANKL in Articular Chondrocytes. L. Ma*[1], P. Li*[1], E. P. Paschalis*[2], A. L. Boskey[2], R. J. O'Keefe[1], E. M. Schwarz[1], H. Drissi[1]. [1]Orthopeadics, University of Rochester, Rochester, NY, USA, [2]The Hospital for Special Surgery, New York, NY, USA.

Extensive research on RANK-RANKL in inflammatory arthritis has clearly defined its critical role in erosive pathology and its lack of involvement in inflammation. However, the role of RANK signaling in osteoclast-independent cartilage catabolism remains controversial base on several studies, which showed that the articular surface of inflamed joints are protected from degradation and proteoglycan loss as a result of RANK blockade. Here we tested the hypothesis that TNF and RANK signals in articular chondrocytes synergize to exacerbate cartilage catabolism. First we performed immunohistochemistry on surgically retrieved tissues to formally demonstrate that RANK expression is up-regulated in chondrocytes at sites of articular cartilage erosion, suggesting a potential role in catabolism. Next, we performed histomorphometry on toluidine blue stained knee sections from wild-type, TNF-transgenic mice (TNF-Tg), TNF-Tg treated with RANK:Fc and TNF-Tg x RANK-/- mice. The results showed that both biologic and genetic disruption of RANK signaling completely prevents proteoglycan loss in TNF-induced arthritis. We further quantified this chondroprotective effect in mice with collagen induced arthritis treated with placebo or RANK:Fc. Infrared microscopy showed that RANK:Fc sustained the [pyr/dHLNL] and [proteoglycan/collagen] ratios in articular cartilage. To investigate the downstream mechanisms of these effects, we compared the gene expression profiles of primary murine articular chondrocytes before and after treatment with TNFα or RANKL alone or in combination. Microarray analysis showed that of all the MMPs and TIMPs, MMP3 and MMP13 are significantly induced, and TIMP3 expression is dramatically decreased, by TNFα in comparison to untreated controls. While RANKL alone had no effects, its addition significantly enhanced the TNFα effects. Validation real time RT-PCR studies confirmed that RANKL alone has no effects, but synergies with TNFα to potently induce MMP3, 13 expression and TIMP3 down regulation. Taken together, our results indicate that TNFα and RANKL have a synergistic effect on articular cartilage catabolism and provide a novel explanation for the chondroprotective effects of RANK blockade in inflammatory arthritis.

Disclosures: ***H. Drissi****, None.*

M062

Inhibition of Osteoblastic Matrix Metalloproteinases (MMPs) Positively Affects Anabolic Action of Parathyroid Hormone (PTH) In Vivo. V. Geoffroy*, D. Merciris*, N. Legoupil*, C. Marty*, M. C. de Vernejoul. Hôpital Lariboisière, INSERM U606, Paris Cedex 10, France.

Our aim was to evaluate whether inhibition of osteoblastic MMPs can affect the anabolic action of PTH using transgenic mice over expressing the TIMP-1 (tissue inhibitor of MMPs) specifically in osteoblastic cells. We have shown previously that these mice present an increase in bone mineral density and bone mass resulting from an overall decreased bone turnover reminiscent of the changes induced by pharmaceutical agents such as bisphosphonates. In this study, 10-week-old wild-type (WT) and transgenic (TG) females were treated with PTH at 40 µg/kg/day for 1.5 months. DEXA analysis was performed before and after treatment and histomorphometric and molecular analysis at the end of the experiment.

The densitometric analysis showed an increase in bone mineral density (BMD) and bone mineral content (BMC) in PTH-treated animals at the femur and the vertebrae. Only measurements of BMD and BMC at the femurs showed a significative positive interaction between genotype and treatment.

The histomorphometric analysis indicated that anabolic PTH treatment induced an increase of bone volume and trabecular thickness (Tr.Th.) in both genotypes. Only Tr. Th. was further increased in TG compared to WT mice. WT mice presented an increase in mineralizing surfaces and bone formation rate under PTH treatment. In contrast, matrix apposition rate (MAR) appears to be increased only in TG mice. Resorption parameters in cancellous bone (osteoclastic surfaces and trabecular separation) remain unchanged under PTH treatment. Interestingly, an increase of cortical thickness due to the expansion of the external perimeter was observed in TG mice. We observed an increase in intracortical osteoclastic surfaces and cortical porosity that was identical in WT and TG mice.

Molecular analysis performed on long bones indicated that expression of MMP-13, collagene type I and TRAP was increased by the PTH treatment. Only osteocalcin expression was shown to be affected in the WT bones but not in TG bones. This result corroborate the increase in MS and BFR observed only in WT mice. In conclusion, the interaction between transgene and treatment observed when measuring BMD and BMC at cortical sites is in accordance with the measurement of cortical thickness by histomorphometry. Furthermore, we showed that treatment of TG mice with PTH leads to an increase in MAR and therefore in trabecular thickness without affecting osteoblastic number as illustrated by osteocalcin expression. Our data suggest that in vivo inhibition of MMPs that induces a low bone turnover can potentiate the anabolic effect of low dose of PTH both at trabecular and cortical sites.

Disclosures: ***V. Geoffroy****, None.*

M063

Extracellular Matrix Remodeling by MMP13 in the Developing Mouse Bone. D. J. Behonick*, D. Stickens*, Z. Werb*. Anatomy, University of California, San Francisco, San Francisco, CA, USA.

This study asked whether extracellular matrix (ECM) remodeling by the protease MMP13 (collagenase-3) is criticial for endochondral ossification. Generation of transgenic mice, including MMP13-null and cell type-specific MMP13-null animals, and histological and cellular analyses of tissues from these animals identified two significant yet transient phenotypes in the developing endochondral bones. MMP13-null mice show reduced type II collagen cleavage and an expanded hypertrophic cartilage zone, as well as reduced type I collagen cleavage and increased trabecular bone density. These phenotypes are ameliorated by as yet unidentified processes after 5 weeks of age. Preliminary studies in cell-type specific null mice generated by Cre/Lox-mediated gene ablation suggest that MMP13 - which is expressed and secreted by hypertrophic chondrocytes in the growth plate and osteoblasts in the trabecular bone - acts locally, and create new opportunities for further investigation of this vital remodeling process during endochondral ossification. We conclude that MMP13 activity is critical for proper endochondral ossification; however, it is also clear that other ECM remodeling enzymes (possibly other MMPs) are active in this process.

Disclosures: ***D.J. Behonick****, None.*

M064

Pretreatment with Cathepsin K Inhibitor but not Alendronate Demonstrated Further Increases in Bone Mineral Density in Ovariectomized Rats Followed by Add-on Treatment with Parathyroid Hormone. Y. Ochi*, N. Kawada*, H. Yamada*, H. Mori*, R. Kayasuga*, M. Tanaka*, A. Hatayama*, K. Ohmoto*, K. Kawabata*. Minase Research Institute, ONO Pharmaceutical Co., Ltd., Osaka, Japan.

Cathepsin K, a cystein protease highly expressed in osteoclasts, is capable of degrading bone type I collagen. Recently, cathepsin K inhibitors have drawn much attention as novel therapeutic agents for treatment of impaired bone turnover including osteoporosis. However, the therapeutic potential of these inhibitors has not been fully elucidated, especially when used in combination with other treatments such as anabolic parathyroid hormone (PTH). A thorough evaluation of combination treatments for osteoporosis is essential, since bisphosphonates fail to demonstrate additive or synergistic effects with PTH in human clinical trials (Path study). In this study, we examined the effects of an α-amino acid derivative of cathepsin K inhibitor, given alone or in combination with PTH, on bone mineral density (BMD) in ovariectomized rats, and compared them to those of alendronate, a powerful bone anti-resorptive bisphosphonate, also given alone or in combination with PTH. In vitro studies showed that this compound potently inhibited human and rat cathepsin K with Ki values of 1.1 and 3.1 nM, respectively. In addition, this compound concentration-dependently inhibited the release of C-terminal telopeptide of type I collagen (CTX) from bovine bone slices incubated with rabbit bone cells. In ovariectomized rat model of osteoporosis, this inhibitor, given orally for 3 months, increased BMD, in a way dependent on its inhibition of CTX release, without affecting the level of osteocalcin. Furthermore, when ovariectomized rats were orally treated with this inhibitor for 2 month followed by a combination with PTH for 1 month, a further increase in BMD was observed. This increase in BMD was higher than that induced by the inhibitor or PTH alone, and most importantly, was not observed following combination therapy with alendronate and PTH. These results suggest that cathepsin K inhibitors have therapeutic potential not only by themselves alone but also in combination with anabolic agents in osteoporosis, and that the beneficial effects of this combination therapy are not reproducible with a combination of alendronate and PTH.

Disclosures: ***Y. Ochi****, None.*

M065

Maspin, a Serine Protease Inhibitor, Regulates the Bone Matrix Maturation by Enhancing the Accumulation of Latent TGF-beta. R. Tokuyama*, K. Satomura, E. Maeda*, E. Kitaoka*, K. Kume*, M. Nagayama*. Department of Oral and Maxillofacial Surgery, Graduate School of Health Biosciences, The University of Tokushima, Tokushima, Japan.

Maspin, a 42-kDa serine protease inhibitor originally isolated from mammary carcinomas, has been considered to have tumor suppressive and antiangiogenic activities. Despite of the huge amount of data concerning the expression pattern of maspin and its relevance to the biological properties of human breast and prostate cancer cells, little is known on maspin expression in skeletal tissues. This study was performed to elucidate a possible role of maspin in bone formation. First, the expression of maspin in endochondral ossification of tibiae of 1-week-old rats was immunohistochemically investigated. Gene and protein expression of maspin in ROS 17/2.8 and rat primary osteoblasts isolated from femora of 4-week-old rats were analyzed by reverse transcription-polymerase chain reaction (RT-PCR), immunocytochemistry and Western blotting. Besides, to elucidate the biological role of maspin in bone matrix formation and maturation in the cultures of ROS 17/2.8, the gene expression of bone matrix proteins such as type I collagen, bone sialoprotein and osteocalcin was examined by RT-PCR in the presence or absence of anti-maspin antibody. TGF-beta content in extracellular matrix was also examined by ELISA in the same culture condition. Moreover, the effect of maspin on the TGF-beta accumulation into extracellular matrix and serine protease activity of ROS 17/2.8 was analyzed by transfecting maspin expression vector or by repressing maspin mRNA using gene silencing methods with siRNA or antisense RNA. As a result, immunohistochemistry revealed that active osteoblasts in primary spongiosa beneath the growth plate of tibiae strongly expressed maspin. Moreover, RT-PCR, immunocytochemistry and Western blotting showed that ROS 17/2.8 expressed maspin in mRNA and protein levels. In addition, latent TGF-beta content in extracellular matrix decreased in the presence of anti-maspin antibody and under the condition in which maspin mRNA was repressed. In contrast, latent TGF-beta content in extracellular matrix was noted to increase in the culture of ROS 17/2.8 which overexpressed maspin. Moreover, serine protease activity decreased in ROS 17/2.8 which overexpressed maspin, while the activity increased in ROS 17/2.8 in which maspin mRNA expression was repressed. These findings suggest that maspin expressed in active osteoblasts was considered to play an important physiological role in bone matrix maturation, particularly in the accumulation of latent TGF-beta into the extracellular matrix.

Disclosures: ***R. Tokuyama****, None.*

M066

Endothelin-1 Promotes Extracellular Matrix Degradation via Matrix Metalloprotease Induction in Human Osteosarcoma Cells. M. Felx*[1], F. Shipkolye*[1], M. Isler*[2], J. Doyon*[3], R. Turcotte*[4], A. Moreau[1], F. Moldovan*[1]. [1]Dentistry Medecine, Ste-Justine Hospital Research Center, Montreal, PQ, Canada, [2]Surgery, Maisonneuve-Rosemont Hospital, Montreal, PQ, Canada, [3]Pathology, Maisoneeuve-Rosemont Hospital, Montreal, PQ, Canada, [4]Surgery, McGill University, Montreal, PQ, Canada.

Degradation of extra cellular matrix (ECM) in many tumours including osteosarcoma is an essential step to promote cell invasion and malignancy. Matrix metalloproteases (MMPs) and endothelin-1 (ET-1) are among the factors contributing to ECM destruction and they are potential target in cancer therapy. This study investigates the effect of ET-1 and its precursor, Big ET-1, on MMP-2 and MMP-9 synthesis and activity in osteosarcoma (MG63) and chondrosarcoma (SW1353) cell using Western Blot, zymography, RT-PCR and Northern Blot. First, we showed that ET-1 and its two receptors (ETA and ETB) are constitutively expressed in osteosarcoma and chondrosarcoma cells. Then, we demonstrated that both ET-1 and Big ET-1 markedly induce synthesis and enzymatic activity of MMP-2 and that enzymatic activity is significantly increased when compared to MMP-9. Furthermore, inhibition of NF-κB activation (by PDTC) blocked MMP-2 production and activity indicating the involvement of NF-κB, a ubiquitous trancription factor playing a central role in the differentiation, proliferation and malign transformation processes. Similarly, inhibition of Big ET-1 maturation by the furin convertase inhibitor, abrogated MMP-2 synthesis and enzymatic activity. These findings demonstrate that ET-1 acts as an autocrine mediator through the induction of MMP-2 and MMP-9 synthesis and activity and could contribute to the tumour cells growth promotion and malignancy.

Disclosures: ***M. Felx****, None.*

M067

Interaction of MMP-13 and its Specific Receptor with Low Density Lipoprotein Receptor Related Protein-1. I. Choudhury*, S. Williams*, N. C. Partridge. Physiology and Biophysics, Robert Wood Johnson Medical School - UMDNJ, Piscataway, NJ, USA.

An endocytotic receptor mechanism for matrix metalloproteinase-13 (MMP-13) removal in osteoblastic cells, fibroblasts and chondrocytes has been identified previously. MMP-13 internalization and subsequent inactivation in these cells proceeds through a dual receptor mechanism, involving high affinity binding to a specific MMP-13 receptor followed by interaction with the low-density lipoprotein receptor related protein-1 (LRP1). In the present study, the specific MMP-13 receptor purified from rat primary osteoblastic cells and LRP1 purified from rat liver and rat primary osteoblastic cells were used in solid phase binding assays. The available ligand binding sites in the specific receptor are higher than that in LRP1. However, mMMP-13 binding to the specific receptor is augmented in the presence of LRP1. The MMP-13 specific receptor associates with LRP1 independent of MMP-13. There is no competition of binding of MMP-13 and LRP1 with the MMP-13 specific receptor, suggesting that different domains of MMP-13 bind to each of these. To identify the binding domain in LRP1 for MMP-13, the receptor associated protein (RAP) and α2 macroglobulin (α2M) were used as competitors. In the solid phase binding assay, RAP does not compete with MMP-13 for binding sites on LRP1, but α2M competes for binding in a dose dependent manner. RAP binds to three different clusters (II, III and IV) of ligand binding repeats in LRP1, α2M binds mainly in cluster I and possibly cluster II of LRP1. Binding and internalization of MMP-13 apparently requires co-operative participation of the specific receptor and LRP1. Soluble mini receptors representing each of the putative ligand binding domains (I, II, III and IV) of LRP1 as well as the transmembrane domain and cytoplasmic tail, termed mLRP1, mLRP2, mLRP3 and mLRP4 respectively, were stably expressed in CHO cells that lack endogenous LRP1. These cells were used for MMP-13 binding and internalization studies. MMP-13 binds to all of these cells but internalizes primarily in mLRP2 cells. The results suggest that i) MMP-13 binds to both specific receptor and LRP1 independently, ii) the recognition site in LRP1 for MMP-13 is localized in cluster I and /or II and iii) the recognition site on LRP1 for MMP-13 is different from that for the specific receptor.

Disclosures: ***I. Choudhury****, None.*

M068

Acidic Microenvironment Created by Osteoclasts Causes Bone Pain Associated with Tumor Colonization. M. Nagae*, T. Hiraga, T. Yoneda. Biochemistry, Osaka University Graduate School of Dentistry, Osaka, Japan.

Bone pain is one of the most common and devastating complications in cancer patients with bone metastases. Although the mechanism of cancer-induced bone pain is poorly understood, previous results that inhibitors of osteoclastic bone resorption such as bisphosphonates (BPs) reduce bone pain in cancer patients indicate a critical role of osteoclasts that are increased in number and activated in bone metastases. These osteoclasts destroy bone to facilitate tumor colonization by secreting protons, thereby making adjacent microenvironment acidic. Since acidosis is a well-known cause of pain, it is plausible that an acidic microenvironment created by osteoclasts may cause bone pain associated with cancer colonization in bone. To test this notion, we studied an animal model in which inoculation of the MRMT-1 rat breast cancer cells into the tibial bone marrow cavity in female rats induced hyperalgesia. Radiographical analyses demonstrated that MRMT-1 cells caused aggressive bone destruction and histological observations revealed numerous TRAP-positive osteoclasts in the lesions. Behavioral analyses including the plantar, foot stamp and force grip test showed that rats exhibited hyperalgesia in tumor-inoculated legs as tumor grew, while non-tumor-inoculated legs had no hyperalgesia. Subcutaneous injections of the BP zoledronic acid (ZOL) (250 μg/kg/day) significantly reduced the cancer-

induced hyperalgesia and bone destruction. To investigate a role of acidosis, mRNA expression of acid-sensing receptors including the acid-sensing ion channels (ASICs) and the transient receptor potential channel-vanilloid subfamily member 1 (TRPV1) in the dorsal root ganglions (DRGs) was determined by RT-PCR. The expression of ASIC1a and ASIC1b mRNA was increased in the ipsi-lateral DRGs, whereas TRPV1 expression was not changed. Of note, ZOL reduced the expression of ASIC1a and ASIC1b in the DRGs. In addition, immunohistochemical examinations revealed that the expression of c-Fos, which is a widely-used marker of neural activity in response to noxious stimuli of primary sensory neurons, in the ipsi-, but not contra-lateral, lamina I-II and V-VI neurons in spinal cord was increased in association with hyperalgesia. ZOL decreased these c-Fos-positive neurons. In conclusion, our data suggest that an acidic microenvironment created by proton release by osteoclasts, at least in part, contributes to the induction of hyperalgesia through up-regulating ASICs expression. Our results also suggest BPs reduce cancer-induced bone pain through preventing the development of acidic microenvironment by inhibiting osteoclasts, which in turn down-regulates ASICs and c-Fos expression.

Disclosures: ***T. Hiraga****, None.*

M069

2-Methoxyestradiol-mediated Cell Death Is Dependent on Protein Kinase PKR in Osteosarcoma Cells. A. Maran, K. L. Shogren*, R. T. Turner. Orthopedics, Mayo Clinic, Rochester, MN, USA.

Osteosarcoma is the most common primary bone tumor and most frequently develops during adolescence. 2-Methoxyestradiol (2-ME), a naturally occurring mammalian metabolite of 17β-estradiol induces interferon gene expression, cell cycle arrest, and cell death by apoptosis in human osteosarcoma cells. PKR is an interferon-inducible serine-threonine protein kinase that plays a role in regulation of cell growth, differentiation and apoptosis and mediates the anti-proliferative and anti-cancer activities of interferon. To test a cause and effect relationship we determined the effect of 2-ME and protein kinase inhibitors on PKR protein and cell death in MG63 human osteosarcoma cells. Western blot analysis showed that PKR protein level was increased by 2 fold in 2-ME (10 μM) treated cells, whereas 17β-estradiol, 4-hydroxy- and 16-hydroxyestradiol, estrogens which do not induce cell death, had no effect on PKR protein levels. Flow cytometric analysis of 2-ME treated cells showed an increase in PKR staining compared to the vehicle control. SB203580, a general serine-threonine kinase inhibitor and 2-aminopurine, a specific PKR inhibitor blocked 2-ME-mediated cell death in MG 63 cells. These results suggest that 2-ME-mediated activation of interferon signaling is transduced by PKR protein, resulting in anti-growth and apoptosis in osteosarcoma cells.

Disclosures: ***A. Maran****, None.*

M070

Osterix Inhibits RANKL and IL-1α in Osteosarcoma Cells Resulting in Decreased Bone Destruction and Tumor Growth. Y. Cao*, Z. Zhou*, E. S. Kleinerman*. Pediatrics, UT MD Anderson Cancer Center, Houston, TX, USA.

Osteosarcoma is a malignant tumor that originates and grows within bone resulting in bone destruction. This destruction is thought to be mediated by osteoclasts. Osterix (osx) is a new zinc finger-containing transcription factor required for osteoblast differentiation and bone formation. We previously demonstrated that osx expression was absent in mouse K7M2 osteosarcoma cells. In addition, osx expression was low or absent in TC71 human Ewing's sarcoma cells, PC3-MM2 human prostate cancer cells and RBM1 human renal cancer cells all of which cause osteolytic bone lesions when injected *in vivo*. Replacement of osx in K7M2 cells inhibited tumor incidence following bone injection and decreased osteolysis. The purpose of these studies was to investigate possible mechanisms by which K7M2 cells cause bone destruction and how osx inhibits osteolysis. Osteolytic bone lesions (detected radiographically) developed 35 days following intraosseous injection of K7M2 cells. Histologic examination demonstrated TRAP+ multinucleated giant osteoclasts in the interface between tumor cells and bone cortex. Using an *in vitro* osteoclast formation assay, we found that K7M2 cells stimulated significant osteoclasts formation in the presence of stromal osteoblasts. K7M2 cells co-cultured with normal MC3T3 mouse osteoblasts for 5 days resulted in increased RANKL (Receptor activator of NF-κB ligand) expression as quantified by RT-PCR. By contrast, osteoprotegerin (OPG) expression was unchanged. Two stable osx-transfected K7M2 cell lines (K7M2-osx1 and K7M2-osx2) and a control transfected cell line (K7M2-neo) were generated to determine the effect of osx on tumor development, growth and morphology. Intraosseous injection of K7M2-osx1 and K7M2-osx2 cells resulted in a lower tumor incidence. Tumors that did develop were significantly less osteolytic as judged by x-ray, histology and TRAP staining. Co-culturing K7M2-osx1 or K7M2-osx2 cells with MC3T3 cells did not stimulate RANKL expression as seen when MC3T3 cells were co-cultured with either K7M2 or K7M2-neo control cells. In addition, IL-1α expression was significantly decreased in both K7M2-osx transfected cells. We demonstrated that IL-1α protein increased MC3T3 RANKL expression. These data indicate that the suppression of RANKL by osx may be mediated by an effect on IL-1α. Our results also indicate that K7M2 cells disrupt the RANK/OPG balance in normal osteoblasts leading to increased RANKL expression and bone destruction. We, therefore, conclude that osx inhibits IL-1α leading to a reduction in RANKL, which subsequently inhibits osteolysis and invasion of the tumor cells into the bone cortex thereby reducing tumor growth.

Disclosures: ***Y. cao****, None.*

M071

Zoledronic Acid and Calcitriol in Malignancies with Bone Involvement - A Pilot Trial. G. M. A. Palmieri, L. S. Schwartzberg*, R. E. Imseis*. The West Clinic, P.C., Memphis, TN, USA.

Calcitriol has anticancer effects by stimulating cell differentiation and inhibiting proliferation and angiogenesis. Its major drawback is stimulation of osteoclasts with liberation of cancer growth factors from bone and hypercalcemia. Aminobisphosphonates inhibit osteoclasts and correct hypercalcemia of malignancies. We reported bone healing with calcitriol + pamidronate in 2 multiple myeloma patients (pts) (AmJMedSci, 1999). We are reporting ongoing findings from a 12 month (m) pilot trial with zoledronic acid (Z) + calcitriol (C) in 11 pts (5 women, 6 men), with bone metastases from various tumors (4 breast, 5 prostate, 2 myeloma). Patients on cancer therapy received Z, 4 mg i.v./m + C (Calcijex), 1 μg i.v., 2/week x 2 weeks, followed by C (Rocaltrol) 0.25 μg po/tid + Ca 1,500 mg/d. Chemistries, calciotropic factors, bone turnover markers, skeletal MRI and bone mineral density (BMD) by DEXA were determined at 1 - 3 m. Of 11 pts so far recruited, 2 died of cancer in the first 2 m, 4 are in the study and 5 have completed the 12 m of the pilot trial. So far Z and C were well tolerated. One patient developed transient hypercalcemia (11.6 mg/dl) and hypercalciuria that responded to temporary reduction of the dose of C. In the 5 pts who completed this trial we observed stable skeletal MRI at 3 m intervals in 3 pts and new lesions in 2 pts; serum PTH fell by 64% in 4 of 5 pts; serum C remained within the normal range in most pts; variable results were observed in bone alkaline phosphatase; urinary NTX fell in 4 or 5 pts by 62% and BMD, measured every 3 m for 1 year, increased in 5 of 5 pts (total hip 11%, lumbar spine 15%, whole body 6%). The ongoing data suggest: 1. Z + C were well tolerated. 2. Skeletal metastases did not progress in some pts. 3. PTH and NTX fell by 60%. 4. Bone density increased in multiple sites. These results are encouraging and support the continuation and completion of this study.

Disclosures: ***G.M.A. Palmieri****, Novartis 2.*

M072

Reciprocal Regulation of Osteoclast and Dendritic Cell Differentiation from Monocytes by Myeloma Cells: A Role for MIP-1. T. Hashimoto*, M. Abe, Y. Tanaka*, E. Sekimoto*, T. Oshima*, H. Shibata*, S. Ozaki*, S. Kido, D. Inoue, T. Matsumoto. Department of Medicine and Bioregulatory Sciences, University of Tokushima Graduate School of Medicine, Tokushima, Japan.

Multiple myeloma (MM), a malignancy of plasma cells, generates a devastating bone destruction by osteoclasts (OCs). We and others reported that macrophage inflammatory protein (MIP)-1alpha and beta are among major OC activating factors secreted by MM cells. In contrast to OCs, dendritic cells (DCs) decrease in number and their function is defective in MM, leading to tumor escape and susceptibility to infection. Because OCs and myeloid DCs are derived from the same monocytic precursor cells, we hypothesized that differentiation into the two cell lineages are reciprocally regulated and that MM cells modulate the lineage determination process. In this study, we examined roles for MIP-1 as well as MM cells in OC and DC induction from human peripheral blood monocytes. OCs were formed from monocytes spontaneously or by exogenous M-CSF and soluble RANKL. Interestingly, addition of anti-MIP-1alpha and beta antibodies in combination inhibited OC formation with a concomitant increase of RANK-negative macrophages. Culture supernatants of thus formed OCs revealed MIP-1alpha and beta immunoreactivity, suggesting an autocrine action of MIP-1 in the OC induction. We next investigated a role for MM cell-derived MIP-1 in OC induction from monocytes. When the MIP-1- and RANKL-expressing MM cell line TSPC-1 was co-cultured with adherent populations of monocytes on dentine slices, formation of TRAP-positive multinucleated cells as well as pits were enhanced. Again, anti-MIP-1alpha and beta in combination abrogated these enhancement, suggesting a critical role for MM cell-derived MIP-1 in enhancement of monocyte-derived OC formation and function. In sharp contrast to the OC induction, non-adhesive co-cultures with MIP-1-producing MM cell lines as well as primary MM cells inhibited the induction of CD83+ mature DCs from monocytes in the presence of GM-CSF plus IL-4, followed by TNF-alpha. However, the DC maturation impaired by MM cells was not restored by addition of anti-MIP-1alpha and beta in combination, suggesting that soluble factors other than MIP-1 may be responsible for inhibition of DC maturation. These results suggest that MIP-1 may play a critical role in the commitment of OC lineage as well as OC maturation and activation and that MM cells may affect the reciprocal regulation of differentiation into OC and DC lineages, thereby enhancing bone resorption and concomitantly inhibiting antigen-presenting capacity of DCs.

Disclosures: ***T. Hashimoto****, None.*

M073

5T2MM Murine Myeloma Cells and CD138+ve Human Myeloma Cells Promote Osteoclastic Activity Rather Than Osteoclast Formation *In Vitro*. G. S. Mueller*[1], K. Vanderkerken*[2], R. G. G. Russell[1], P. I. Croucher[3]. [1]Botnar Research Centre, Nuffield Department of Orthopaedic Surgery, Oxford University, Oxford, United Kingdom, [2]Department of Hematology and Immunology, Free University Brussels, Brussels, Belgium, [3]Division of Clinical Sciences, University of Sheffield School of Medicine, Sheffield, United Kingdom.

A major clinical feature in multiple myeloma (MM) is the development of osteolytic bone disease. Increased osteoclastic bone resorption is responsible for bone disease; however, it is unclear whether this is mediated by increased osteoclast recruitment and differentiation, or increased osteoclastic activity, or both. The aim of the present study was to determine whether 5T2MM murine myeloma cells or human myeloma cells isolated from patients with myeloma could promote osteoclast formation and osteoclastic bone resorption, in vitro, in a stromal cell independent manner.

5T2MM murine myeloma cells were injected intravenously into C57BL/KaLwRij mice. All mice developed a serum paraprotein and the growth of 5T2MM cells in the bone marrow (BM). Radiographic and histological analysis demonstrated the presence of lytic bone lesions and an increase in the number of TRAP+ve osteoclasts cells lining bone surfaces. 5T2MM murine myeloma were purified by density gradient centrifugation and incubated with murine peripheral blood mononuclear cells in the presence or absence of soluble RANKL (sRANKL). 5T2MM caused a significant reduction in the formation of TRAP+ve cells when compared to control. However, when cultured on dentine slices, those osteoclasts that formed, created large resorption 'trails', rather than the smaller pits seen in the absence of 5T2MM cells suggesting that resorption activity was increased. In contrast, 5T33MM cells, which in vivo do not promote osteoclastic resorption, inhibited osteoclast formation and resorption of dentine slices. To determine whether this was specific to the 5T2MM murine cells, human myeloma cells were isolated from the bone marrow of patients with MM by density gradient centrifugation and purified by immunomagnetic separation using an antibody to CD138 to identify the myeloma cells. CD138+ve human myeloma cells did not affect TRAP+ve osteoclast formation when cultured with human peripheral blood mononuclear cells, but did promote an increase in the proportion of dentine slices undergoing resorption and induced the formation of resorption 'trails' rather than the pits seen in the absence of myeloma cells. In all cases, sRANKL was required to induce osteoclastic bone resorption. These data are consistent with 5T2MM murine myeloma cells and CD138+ve human MM cells promoting osteoclast activity and/or survival rather than osteoclast formation.

Disclosures: ***G.S. Mueller****, None.*

M074

Clinical Study Using Urine NTX in Patients with Metastatic Spine Tumors. S. Ichimura[1], T. Miyamoto*[1], H. Maruno*[1], T. Asazuma*[2], J. Ogawa*[1], K. Satomi*[1]. [1]Orthopaedic Surgery, Kyorin University, Tokyo, Japan, [2]Orthopaedic Surgery, National Defense Medical College, Tokorozawa, Japan.

We investigated the utility of bone resorption marker (NTX) for metastatic spine tumors. This study included 101 patients (male: 45, female: 56) with various malignancies who ranged in age from 42 years to 87 years (mean 64). Twenty-four patients had breast cancer, 14 had prostate cancer, 13 had lung cancer, 11 had gastric cancer, 7 had renal cancer, 6 had colon cancer, and 26 had various other malignancies. Of the 53 patients with spine metastasis, 49 had not been treated and 4 treated with radiation therapy or spine surgery for spine metastasis. Forty-eight patients had no spine and bone metastasis. We classified bone metastasis into 3 Grades. Grade - had no bone and spine metastasis (n:48), and Grade + had only one spine metastasis (n:10), and Grade ++ had multiple spine and bone metastasis (n:43). Urinary NTX was measured by second-void urine samples. Urinary NTX level in patients with Grade ++ was greater than in patients with Grade + and - (129 nM BCE/mM Cr vs. 58 nM BCE/mM Cr and 53 nM BCE/mM Cr; $p < 0.01$), and no significant difference was observed in urinary NTX level between Grade + and -. We were able to follow the clinical course in 13 patients with conservative treatment (mean: 11.4 months) and in 15 patients with spine surgical treatment (mean: 7.8 months). There was a temporary reduction of urinary NTX level by mean 33% after Radiation therapy. However, the levels of urinary NTX were gradually increased and the prognosis was poor in patients with Grade ++ in both treatment groups. On the other hand, in patients with Grade + in both groups, the levels of urinary NTX were not changed and there was no death during observation period. The measurement of urine NTX appeared to be more useful to monitor the clinical course in patients with spine metastasis than to diagnose spine metastasis.

Disclosures: ***S. Ichimura****, None.*

M075

Heparanase Supports Tumor Metastasis to Bone. Y. Yang*, M. Bendre, Y. Huang*, L. Joseph*, V. Macleod*, A. M. Theus*, T. Kelly*, R. Sanderson*, L. J. Suva. Orthopaedic Surgery, Pathology and Arkansas Cancer Research Center, UAMS, Little Rock, AR, USA.

Bone is a common site for cancer metastasis. Skeletal metastases connote a dramatic change in the prognosis for the patient and significantly increase the morbidity associated with disease. Relatively little is known regarding the mechanisms that control myeloma metastasis, although widespread skeletal dissemination is an important step in disease progression. Understanding the complex interactions contributing to the metastatic behavior of cancer cells is essential for the development of effective therapies. The myeloma microenvironment is replete with heparan sulfate, an important component of the extracellular matrix and vascular basement membrane, where it can serve as a physical barrier to tumor cell metastasis and interaction with normal tissue. In addition, heparan sulfates on the cell surfaces and within the extracellular matrix bind to, and regulate the activity of, numerous factors that control myeloma growth and angiogenesis (e.g., IL-8, HGF, FGF-2). In the present study, the enhanced expression of human heparanase-1 (HPSE1) *in vivo* dramatically upregulates spontaneous metastasis of myeloma cells to bone. HPSE1 is the primary mammalian enzyme responsible for cleaving heparan sulfate chains into 10-20 residue fragments that are biologically active. Promotion of metastasis by HPSE1 is an early event, occurring before primary tumors reach a large size. In addition, HPSE1: (i) greatly enhances whole body tumor burden compared to controls, and (ii) has a dramatic impact on both the number and size of microvessels within the primary tumor, suggesting an important role for heparanase in myeloma tumor angiogenesis. Similarly, preliminary studies indicate that breast cancer cells expressing HPSE1 growing in the mammary fat pad are more capable of dissemination to bone than non-HSPE1 expressing cancer cells. The process correlates with a dramatic increase in serum C-telopeptide collagen cross-links, demonstrating increased bone resorption. These data, from two distinct tumor types, indicate that HPSE1 is an important determinant of cancer dissemination in bone. In addition, these studies reveal a novel experimental animal model for examining the spontaneous metastasis of bone-homing tumors. This novel model of bone metastasis provides a unique opportunity to study the entire metastatic cascade *in vivo*, and may provide insight into new therapeutic modalities.

Disclosures: ***L.J. Suva****, GlaxoSmithKline 1; Procter and Gamble 5; Wright Medical 2.*

M076

Regulation of PTH-rP Expression and Osteolysis by Human Breast Cancer Cells by Gli2 and Gli 3. J. A. Sterling, B. O. Oyajobi, M. Zhao, A. Gupta*, M. Banerjee*, B. Grubbs*, G. R. Mundy. Cellular and Structural Biology, University of Texas Health Science Center at San Antonio, San Antonio, TX, USA.

Osteolysis associated with breast cancer is due to the tumor peptide parathyroid hormone-related peptide (PTH-rP). The molecular mechanisms responsible for PTH-rP expression by breast cancer cells are clearly important, since PTH-rP is the causative factor in osteolysis, inhibition of PTH-rP transcription by small molecules reduces bone lesions and tumor burden (Gallwitz et al., 2002), and there is evidence for differential expression of PTH-rP by breast cancer cells in different organ sites. However, the mechanisms responsible for increased PTH-rP expression by breast cancer cells are unknown. We hypothesize that the Gli family of transcriptional regulators is responsible for regulating PTH-rP transcription in breast cancer. The rationale for this concept is that PTH-rP expression in the growth plate is controlled physiologically by hedgehog signaling, and the Gli family mediates hedgehog signaling in vertebrate cells. Furthermore, Gli2 is overexpressed in some human carcinomas. To investigate this hypothesis, we transfected breast cancer cells with PTH-rP promoter luciferase constructs and expression vectors for the Gli family. We found that Gli2 specifically increased PTH-rP promoter activity by greater than 2-fold, while Gli3 and Gli1 did not significantly affect basal promoter activity. We and others have shown that Gli3 is processed in the proteasome to a truncated form (trGli3). This proteasomally processed form of Gli3 suppressed the Gli2 stimulated-PTH-rP transcription in human MDA-MB-231 breast cancer cells. Furthermore, when MDA-MB-231 human breast cancer cells stably overexpressing Gli2 were inoculated into the left cardiac ventricle of athymic nude mice, enhanced osteolysis was observed when compared with mice injected with the empty vector control. We examined the relationship between expression of Gli2 in human and murine breast cancer cells and PTH-rP expression and osteolysis, and found Gli2 was expressed in cells that also express PTH-rP (MDA-MB-231, RWGT2, PC-3, and 4T1), but not in cells that do not (MCF-7, ZR-75, and T47D). Taken together, these data indicate that the Gli family of transcriptional factors regulates PTH-rP expression and subsequent tumor-induced osteolysis. The activities are distinct and uncoupled, with Gli2 acting as a stimulator and truncated Gli3 as a repressor of PTH-rP transcription. This family represents possible targets for drug development to retard osteolytic bone metastases associated with breast cancer.

Disclosures: ***J.A. Sterling****, None.*

M077

Bone-Specific Microenvironment and Epithelial-Mesenchymal Transition Contribute to the Increased Bone Metastatic Potential of Human Prostate Cancer Cells. V. A. Odero-Marah*[1], J. Xu*[1], Y. Cui*[1], M. N. Weitzmann[2], L. W. K. Chung*[1], H. Y. E. Zhau*[1]. [1]Urology, Emory University School of Medicine, Atlanta, GA, USA, [2]Division of Endocrinology & Metabolism & Lipids, Emory University School of Medicine, Atlanta, GA, USA.

The propensity of human prostate cancer to metastasize to the skeleton and elicit osteoblastic and osteolytic reactions has been the subject of intense investigation. In our laboratory, we proposed that acquisition of osteomimetic properties by human prostate cancer cells is essential for human prostate cancer growth, survival, and invasion in bone. In addition, the epithelial-mesenchymal transition (EMT) whereby epithelial cancers undergo morphological changes to become more mesenchymal and migratory has a known role in cancer invasiveness and metastatic potential. In this study, we developed a novel ARCaP human prostate cancer bone metastasis model to evaluate the role of osteomimicry and EMT in experimental bone metastasis. The ARCaP cell line was derived from a patient with highly metastatic prostate cancer. When injected into athymic mice, it mimics clinical behaviors as seen in patients, including the development of bone metastasis, formation of ascites fluid, expression of neuroendocrine factors, androgen receptor and prostate-specific antigen. We further derived two morphologically and behaviorally stable and distinct ARCaP subclones, 1A8 and 1F11, which share a common genetic background. We have evaluated a wide range of genes expressed by these subclones using RT-PCR, IHC, and western blots and tested their tumorigenicity and metastatic potential in athymic mice using an intracardiac injection protocol. The results of

these studies showed that 1A8, a cell line with spindle-like morphology, expressed mesenchymal markers and was more aggressive than 1F11, which exhibited a cobblestone morphology and expressed epithelial markers. The data suggests that 1A8 could be the mesenchymal derivative of 1F11 through the process of EMT. Secondly, skeletal metastatic variants from 1A8 and 1F11 subclones gained highly aggressive bone metastatic potential with higher incidences and shorter latency periods after intracardiac administration, compared to their respective parental subclones. Thirdly, 1A8 and 1F11 cells that metastasized to bone generated both osteoblastic and osteolytic lesions. We observed a marked elevation of osteomimicry-related genes, osteopontin and osteocalcin, but not RANKL in bone metastatic tissue specimens, compared to these same variants grown subcutaneously. Thus, our data suggest an important role for EMT in the acquisition of tumor aggressiveness and the inductive role of the bone microenvironment for prostate cancer homing to bone.

Disclosures: ***V.A. Odero-Marah****, None.*

M078

An Immune-Intact Murine Model of Bone Metastasis for Prostate Cancer. M. T. Moser*, X. Wang*, B. A. Foster. Pharmacology & Therapeutics, Roswell Park Cancer Institute, Buffalo, NY, USA.

Prostate cancer is the most commonly diagnosed cancer in men in the United States and is second only to lung cancer as the leading cause of death from cancer in men. The terminal stages of prostate cancer frequently metastasize to bone resulting in osteoblastic lesions. In men who died of prostate cancer greater than 70% had bone metastases. However, relatively little is understood about the underlying molecular mechanism of prostate cancer initiation, progression, as well as, why prostate cancer preferentially metastasizes to bone and elicits an osteoblastic response. This is in part due to the lack of animal models that recapitulate the full spectrum of the human disease. Recent studies suggest that species-specific factors may limit the ability of human cancers to colonize rodent bone. This may be one explanation for the scarcity of human prostate cancer cell lines that metastasized to bone in severe combined immunodeficient (SCID) mice.

We have established cell lines from a spontaneously occurring boney metastasis in the transgenic adenocarcinoma of mouse prostate (TRAMP) model of prostate cancer. A C57/FVB (50:50) TRAMP animal presented with hind leg paralysis. Upon examination a large tumor mass was observed engulfing the spine. Histological analysis indicated that the spinal cord contained poorly differentiated prostate cancer with both osteolytic and osteoblastic features. Three plates of cells were established from this tumor tissue, designated TRAMP-BC1, -BC2 and -BC3. RT-PCR analysis indicates the TRAMP-BC cell lines express bone markers such as cbfa1/RUNX, bone alkaline phosphatase, osteopontin, osteocalcin, bone sialoprotein II and procollagen type I. The tumorigenicity of the parental TRAMP-BC cells has been characterized by injection of cells into immune-intact, syngeneic hosts. Three routes of injection have been investigated; 1) subcutaneous; 2) intrafemoral and 3) intracardiac. TRAMP-BC cells were tumorigenic and metastatic by all three routes of injection. Radiographic analysis of the femurs showed thickening of the bone consistent with an osteoblastic response. Furthermore, TRAMP-BC cells have be reisolated from the femurs of host animals following intracardiac injection, indicating TRAMP-BC cells can home to bone and induce an osteoblastic response.

These cell lines can be used to further our understanding of prostate cancer-bone interactions leading to better treatment and prevention of bone metastasis in the clinical disease. These cell lines can also be used as a preclinical model to test new therapies for bone metastases in prostate cancer, including immune-based therapies.

Disclosures: ***B.A. Foster****, None.*

M079

Protein Profiling of Highly Osteolytic MDA-231 Breast Cancer Expressing High Gelatinase Activity versus Poorly Osteolytic MDA-231 Breast Cancer with Low Gelatinase Activity. P. A. Veno*[1], J. Guthrie*[2], J. Zhao*[1], M. R. Dallas*[1], J. Bonewald*[1], D. Dinakarpandian*[1], N. Gopathi*[1], L. F. Bonewald[1], S. L. Dallas[1]. [1]Univ. of Missouri, Kansas City, MO, USA, [2]Midwest Research Institute, Kansas City, MO, USA.

Breast cancer frequently metastasizes to bone, causing bone destruction with complications of hypercalcemia, fracture and nerve compression. Although breast cancer metastasis to bone is often associated with formation of osteolytic lesions, osteoblastic lesions can also occur. While comparing a panel of human breast cancer cell lines that either cause osteolytic or osteoblastic lesions in nude mice, we noted that osteolytic cell lines showed higher expression of the gelatinases (matrix metalloproteinases 2 and 9) compared to osteoblastic lines. To test the hypothesis that gelatinases may be a determinant for osteolytic bone metastasis, parental MDA-MB-231 cells were cloned by limiting dilution and screened for high or low gelatinase expression by zymography. Individual clones maintained their gelatinase expression phenotype for a minimum of 3 months in culture and also when cultured on bone extracellular matrix. High and low MMP9 expressing clones were evaluated in a mouse model of bone metastasis. X-ray analysis showed significantly higher osteolytic lesion area in the high MMP9 expressing clone compared to the low expressing clone in long bones of both fore and hind limbs. Histomorphometric analysis confirmed significantly higher tumor volume and lower bone volume with the high MMP9 expressing clone. To identify proteins causing or associated with the osteolytic phenotype, protein profiles were obtained from whole cell lysates of high and low MMP9 expressing clones using 2D gel electrophoresis, peptide mass mapping (MS) and selected peptide sequencing (MS/MS). Approximately 700 protein spots were detected, of which 34 were assigned to the MDA-231 proteome. 8 protein spots were identified that are differentially expressed in high versus low MMP9 clones, several of which have been shown to be associated with cancer. To identify activated signaling pathways, 2D gels were stained for phosphorylated proteins. 171 positively stained spots were detected, of which three have been identified. The differentially expressed phosphorylated proteins are currently being identified. An informational database cataloging the proteome of parental and high vs low MMP9 expressing MDA-231 clones has been created to help identify new protein targets that may be involved in breast cancer metastasis to bone. These studies will provide important insights into the role of gelatinases in bone metastatic breast cancer and may highlight novel targets for treatment of osteolytic bone disease.

Disclosures: ***P.A. Veno****, None.*

M080

Osteoporosis and Spinal Fractures in Men with Prostate Cancer: Risk Factors and the Effects of Androgen Deprivation Therapy. T. H. Diamond[1], J. Bucci*[2], J. H. Kersley*[2], P. Aslan*[3], C. Bryant*[4]. [1]Endocrinology, St George Hospital Campus and University of New South Wales, Sydney, NSW, Australia, [2]Radiation Oncology, St George Hospital Campus, Sydney, NSW, Australia, [3]Urology, St George Hospital Campus, Sydney, NSW, Australia, [4]Radiology, St George Hospital Campus, Sydney, NSW, Australia.

To determine the risk factors for osteoporosis and spinal fractures in men with prostate cancer receiving androgen deprivation therapy.

We performed a retrospective analysis of 87 consecutive men with prostate cancer receiving androgen deprivation therapy and who were referred for evaluation of osteoporosis. Data comprised of lateral thoraco-lumbar radiographs, bone densitometry, serum biochemistry and a detailed assessment of osteoporotic risk factors. Multivariate regression analysis was used to determine the major risk factors for osteoporosis and spinal fractures.

There were 38 (44%) men aged 74.5 years who had radiographic evidence of spinal fractures. They had an initial mean PSA value of 52.8 ng/mL and had received androgen deprivation therapy for a mean of 39.6 months (95% confidence interval, 28.7 to 50.4 months). Their mean spinal (quantitative computed tomography t-score = -4.2) and femoral neck bone mineral densities (dual energy x-ray absorptiometry t-score = -2.1) were significantly lower than men without spinal fractures ($P<0.001$ for all measurements). In the regression analysis, the duration of androgen deprivation therapy ($P=0.002$), serum 25 hydroxyvitamin D levels ($P=0.003$), and a history of alcohol excess (defined as more than 4 standard drinks per day) ($P=0.04$) were the main determinants of spinal fractures.

Prolonged androgen deprivation therapy, low serum 25 hydroxyvitamin D levels and a history of alcohol excess are important risk factors for osteoporosis and spinal fractures in men with prostate cancer.

Disclosures: ***T.H. Diamond****, None.*

M081

Methylation of Urokinase (uPA) Promoter Results in Blocking Prostate Cancer Cells Invasion, Growth and Metastases *in Vitro* and *in Vivo*. N. Shukeir*, P. Pakneshan*, M. Szyf*, S. A. Rabbani. Departments of Medicine, Oncology and Pharmacology, McGill University, Montreal, PQ, Canada.

Prostatic adenocarcinoma is among the leading hormone-dependent cancers with a high propensity to develop skeletal metastases. Urokinase, a member of the serine protease family, has been implicated in the progression of several malignancies including prostatic cancer. uPA mRNA is undetectable in normal (PrEC) and low invasive (LNCAP) human prostate cancer cells. In contrast uPA mRNA is abundantly expressed by highly invasive prostate cancer cells PC-3 due to the demethylation of the uPA promoter. This epigenetic mechanism regulating gene transcription is controlled by balanced activity of DNA methyltransferase and demethylase (MBD2).

In order to evaluate the role of uPA promoter methylation in prostate cancer, PC-3 cells were treated with the universal methylating agent S-adenosylmethionine (SAM) and an anti-sense oligonucleotide directed against MBD2 (AS). Scrambled oligonucleotide was included as a control (S). Both SAM and MBD2-AS resulted in a dose and time dependent inhibition in uPA production and tumor cell invasive capacity as determined by Matrigel invasion assay. For *in vivo* studies male Balbc nu/nu mice were inoculated with control and experimental cells into the right flank. Animals inoculated with control cells exhibited tumors of progressively increasing size as compared to animals inoculated with PC-3 cells treated with SAM (500μM for 6 days) or MBD2-AS (200nM for 3 days). To determine the effect of SAM treatment on the development of skeletal metastases, male Fox-Chase SCID mice were inoculated directly into the tibia with control and SAM (500μM) treated PC-3 cells. Large lesions were observed in the tibia of mice inoculated with control PC-3 cells upon X-ray analysis using Faxitron. Majority (90%) of experimental animals inoculated with PC-3 cells pretreated with SAM failed to develop any radiological evidence of skeletal metastases. In 10% of remaining animals these lesion were of markedly smaller area. Bone histomorphometric analysis of tibia where no radiological lesions were observed showed the presence of microscopic tumor cells in the tibia of animals inoculated with SAM treated PC-3 cells. Control and experimental tibias are being evaluated by immunohistochemical analysis to determine the levels of uPA production and markers of bone turnover. The results obtained from these studies will establish the role of uPA methylation status in prostate cancer in promoting tumor growth and metastasis. Additionally these studies will provide valuable insight into developing novel therapeutic strategies against this common disease, which target the demethylation machinery.

Disclosures: ***N. Shukeir****, None.*

M082

The Relationship between Bone Mineral Density and Breast Cancer in Hispanic and Non-Hispanic White Postmenopausal Women - An Ancillary Study of the Women's Health Initiative. L. Arendell*, D. Deshpande*, R. Bruhn*, T. Bassford*, M. Maricic, Z. Chen. University of Arizona, Tucson, AZ, USA.

Previous studies among primarily non-Hispanic white populations have found that women with higher bone density are more likely to develop breast cancer. The purpose of this study was to investigate the association between bone mineral density (BMD) and breast cancer in both Hispanic and non-Hispanic white postmenopausal women. We hypothesize that our study will confirm this association among both ethnic groups.

This is a matched case-control study. Seventy-two newly diagnosed breast cancer cases (56% Hispanic) were recruited from physician's offices in Southern Arizona. We selected 288 age and ethnicity matched women from the Women's Health Initiative Observational Study as controls. BMD was measured using dual energy x-ray absorptiometry (DXA). Conditional logistic regressions were used to compute odds ratios (OR) for univariate and multivariate analyses and to test for an interaction of ethnicity and BMD.

Cases and controls did not differ significantly on age at menarche, pregnancy status, Hormone Therapy (HT) use, or family history of breast cancer. Cases were significantly heavier. In the unadjusted models, the OR of breast cancer among those in the highest tertile of whole body BMD compared to the lowest tertile was 2.7 (95% CI: 1.4, 5.3) and the OR of breast cancer for those in the highest tertile of hip BMD compared to the lowest tertile was 2.1 (1.1, 4.2). Interactions of ethnicity and BMD were indicated in these models, so analyses stratified by ethnicity were conducted. The ORs of breast cancer for those in the highest versus lowest tertile of whole body BMD were 1.2 (0.5, 2.9) among Hispanic women and 7.7 (2.4, 24.8) among the non-Hispanic white women. The ORs of breast cancer for those in the highest versus lowest tertile of Hip BMD were 1.2 (0.5, 2.9) and 4.8 (1.5, 14.8) among the Hispanic and non-Hispanic white women, respectively. Additional analyses support these findings after adjustment for potential confounders, including age at menarche, BMI, HT use, family history of breast cancer and pregnancy.

These data support an association between BMD and breast cancer. In this small sample the association between BMD and breast cancer appears to differ in the two ethnic groups. Since the groups were not population-based samples representative of the two ethnic groups, conclusions cannot be made about the ethnic differences; however, these data suggest that further studies of the relation between BMD and breast cancer are needed in Hispanic women.

Disclosures: ***L. Arendell****, None.*

M083

BMP-7 in Prostate Cancer Bone Metastases. L. G. Brown*, T. E. Pitts*, A. M. Odman*, R. L. Vessella*, E. Corey. Urology, University of Washington, Seattle, WA, USA.

Metastases of prostate cancer result in osteoblastic reactions in bone. Mechanisms that are involved in the increased bone formation under these conditions are not fully understood at present. Understanding of mechanisms responsible for development of the osteoblastic reaction might lead to identification of potential treatment targets. Bone morphogenetic proteins (BMPs) regulate many developmental processes and are involved in bone formation. BMP-7 has been reported to be upregulated in prostate cancer bone metastases. The objective of this study was to evaluate effects of over-expression of BMP-7 in C4-2 cells *in vitro* and on the character of bone metastases *in vivo.*

Treatment with recombinant BMP-7 inhibited proliferation of LNCaP cells *in vitro* (35.6%, p=0.0029) while androgen-independent prostate cancer cells C4-2 and C4-2B were not affected, suggesting alteration of BMP signaling accompanying development of androgen independence. To evaluate effects of BMP-7 expression on C4-2, androgen-independent prostate cancer cells, the ORF of BMP-7 was amplified, cloned into pcDNA3.1, and used to transfect C4-2 cells using the AMAXA system. BMP-7-transfected cells express ~30 times higher levels of BMP-7 mRNA than pcDNA3.1-transfected C4-2 cells, as determined by real-time PCR. BMP-7 protein was detected in conditioned media of BMP-7-C4-2 cells but not in the conditioned media of pcDNA3.1-C4-2 cells. BMP-7-transfected cells secreted 4.8 ng BMP-7/ml/10^6 cells in a 3-day period. Real-time PCR analysis of transfected cells revealed altered expression of various transcription factors involved in BMP signaling, including SMAD-1, znf-8, and smurf-2. To determine effects of BMP-7 overexpression on C4-2 CaP tumors *in vivo* the BMP-7- and pcDNA3.1-transfected C4-2 cells were injected subcutaneously and intratibially in SCID male mice. *In vivo* studies are underway.

Further investigation of the effects of BMPs on CaP cells are warranted to delineate the signal transduction pathways activated in CaP cells and to elucidate more fully the role of BMPs in CaP bone metastases.

Disclosures: ***L.G. Brown****, None.*

M084

Effect of 17 Beta-estradiol on the Metastasis-related Gene Transcription in Estrogen Receptor-positive Human MCF7 Breast Cancer Cells. S. Kim*, H. Chung*, J. Byoun*, R. Hwang*, J. An*, S. Jun*, Y. Rhee, S. Lim. Brain Korea 21 Project of Medical Science, Internal Medicine, College of Medicine, Yonsei University, Seoul, Republic of Korea.

While hormone replacement therapy (HRT) has proven to be effective in relieving many of the uncomfortable symptoms of menopause such as osteoporosis, its use remains highly controversial. Recently, numerous studies have demonstrated the potential health risks surrounding HRT. Of foremost concern is the possibility that women on HRT are particularly susceptible to blood clots, heart attack, stroke, gallbladder disease and breast cancer. Therefore, in this study, we evaluated the effect of 17beta-estradiol on the metastasis-related gene transcription in estrogen receptor (ER)-positive human MCF7 breast cancer cells with poor metastatic potential. MCF7 cells were cultured until 70% confluency in alpha-Minimum Essential Medium (MEM) containing 10% Fetal Bovine Serum (FBS) and then rendered quiescent by incubating cells in alpha-MEM medium containing 0.1% FBS for 24h. After the starvation, cells were treated by 17beta-estradiol for 4 days. Total RNAs were isolated for semi-quantiative RT-PCR and total proteins were prepared for Western blotting. Cell culture media were collected, filtrated and concentrated for the analysis of metalloproteinases (MMPs). 17beta-estradiol (10 nM) significantly induced the proliferation of MCF7 cells, and induced the mRNA expression levels of angiogenesis-related gene, vascular epithelial growth factor (VEGF) and invasion-related gene, MMP-1, in a dose-dependent manner. The induced mRNA expression levels of MMP-9 and tissue inhibitor of metalloproteinase (TIMP)-2 by the treatment of 17beta-estradiol were also observed, but these were not in a dose-dependent manner. Several metastasis-related genes such as angiopoietin-2, tumor growth factor-beta, cyclin E, and TIMP-1 were also evaluated, but not induced by 17beta-estradiol. In addition, MMP-2 activity and the protein expression of ER were evaluated by gelatin zymography and Western blotting, respectively, but both were not changed by 17beta-estradiol. Considering that 17 beta-estradiol highly induced the mRNA expression levels of both VEGF and MMP-1, which have been well known to be related with the metastasis process, in human MCF7 breast cancer cells, it could increase the metastatic potential of breast cancer cells via the selective induction of the metastasis-related gene transcription.

Disclosures: ***S. Kim****, None.*

M085

Bisphosphonates Decrease Telomerase Expression in Prostate Cancer Cells In Vitro. M. Valenti*[1], L. Dalle Carbonare*[1], G. Azzarello*[2], E. Balducci*[2], A. Fracalossi*[1], S. Zenari*[1], O. Vinante*[2], F. Bertoldo*[1], V. Lo Cascio[1]. [1]Dpt. of Biomedical and Surgical Sciences, Medicina Interna D, Verona, Italy, [2]Dpt. of Oncology and Hematologic Oncology, Noale Hospital, Noale, Italy.

Telomerase is a cellular ribonucleoprotein reverse transcriptase responsible for elongation of the telomere that prevents the loss of sequence from chromosome ends to avoid replicative senescence. Telomerase expression is increased in many cancers. Bisphosphonates play an important role in the management of tumors with a secondary involvement of bone. Recent findings have suggested an effect of these drugs on primary tumor burden, too.

We studied the direct effects of alendronate at different concentrations (from 10^{-6} M to 10^{-4} M) on PC-3 human hormone-resistant prostate cancer cell line. In particular, we investigated the effect on viability, and on quantitative telomerase expression. We used real-time reverse transcriptase-polymerase chain reaction to quantify mRNA expression of the catalytic subunit of telomerase (hTERT gene) vs the housekeeping gene GAPDH with gene specific, dual labeled fluorescence probes.

Alendronate induced a dose-dependent inhibition of viability of prostate cancer cells (-27% and -32% vs controls at concentration of 10^{-5} and 10^{-4} M, respectively; $p<0.0001$) as expressed by XTT-test. In addition, treatment with alendronate showed a significant decrease in telomerase expression with respect to control group in PC-3 cells as analyzed through the real-time RT-PCR by two tube comparative Ct method. In conclusion: our preliminary data on alendronate showed that bisphosphonates are able to inhibit PC-3 prostate cancer cell growth. In addition, they reduce the telomerase expression. This is a new finding that suggests an alternative explanation of the direct effect of bisphosphonates on prostate tumor cells.

Disclosures: ***M. Valenti****, None.*

M086

The RalGEF Pathway Promotes Prostate Cancer Metastasis to Bone. J. Yin, M. D. Oberst*, M. K. Chock*, Y. Ward*, K. Kelly*. NIH/NCI, Bethesda, MD, USA.

Although conflicting results have been reported regarding the involvement of oncogenic mutation of Ras in prostate cancer carcinogenesis, functional activation of Ras has been shown to correlate with prostate cancer progression and metastases. Ras is a multi-effector signaling molecule that activates the Raf/MEK/MAPK, PI3 kinase, and RalGDS pathways. Previous work done in this lab has shown that the Ras effector pathway mediated by the Ras(12V,37G) mutant increased the invasiveness of both epithelial cells and fibroblasts by activating the RalGEF pathway. To determine if RalGEF pathway activation is essential for prostate cancer-related bone metastasis, Ras(12V,37G) was expressed in the DU145 prostate cell line. We then studied the metastatic capacity using a mouse bone metastasis model. Vector-transfected DU145 cells (DU145/EV) were only weakly metastatic, whereas cells expressing Ras (12V,37G) induced multiple metastases in long bones and vertebral bodies 6-8 weeks after injection. Ras (12V,37G) bearing mice had decreased survival compared with DU145/EV control. Interestingly, DU145/Ras (12V,37G) caused cortical bone metastases in which tumor cells grew between periosteal and cortical bone.

These metastases destroyed cortical bone before invading the bone marrow cavity. Cortical bone metastases are mostly seen in bronchogenic carcinoma, and have also been reported in other cancers. To investigate the mechanism responsible for the increased metastastic property, we compared the gene expression profiles of DU145/EV and DU145/ Ras(12V,37G) cells using oligonucleotide arrays. DU145/Ras(12V,37G) expresses a distinct set of genes including 3 upregulated genes (CD24, CTGF and HAS3) and 2 down-regulated genes (E-cadherin and Hsp 27) that may determine the metastastic property of these cells. Since TGFβ has been shown to promote bone metastasis, the growth rate and gene expression in response to TGFβ (2ng/ml) treatment were also compared between these two cell lines. DU145/EV cells were growth inhibited by TGFβ, while DU145/ Ras(12V,37G) cells were not. 13 genes were up-regulated in DU145/ Ras(12V,37G) after TGFβ treatment. Several genes such as angiopoietin-like 4, PDGFB, and CTGF encode angiogenic factors and growth factors that may promote tumor invasion and metastasis. We are currently validating these gene expression changes using real-time RT-PCR and Western blotting, and will charaterize the biological significance of these changes using the *in vivo* bone metastasis model. Prostate cancer bone metastasis is a multifactor process, and our results indicate that Ral-GDS pathway activation may be important in promoting the development and progression of bone metastasis.

Disclosures: ***J. Yin****, None.*

M087

Induction of PTHrP mRNA Expression in Human Lung Carcinoma at Sites of Bone Metastasis in Nude Mice. X. Deng*, S. Tannehill-Gregg*, P. Nadella*, E. He*, A. Levine*, T. Rosol. Veterinary Biosciences, Ohio State University, Columbus, OH, USA.

PURPOSE AND BACKGROUND: Parathyroid hormone-related protein (PTHrP) plays an important role in inducing bone resorption at sites of bone metastases. However, it is still unclear how the expression of PTHrP messenger RNA is regulated during the process of bone metastasis. We hypothesized that various isoforms of PTHrP would be regulated differentially in bone metastases compared to subcutaneous neoplasms. METHODS: Human lung squamous cell carcinoma HARA cells (1 x 10^5) were injected into the left ventricle (intracardiacally, IC) or subcutaneously (SQ) into nude mice (8 for IC and 5 for SQ). In addition, in vitro experiments with MDA-231 human breast cancer cells were performed. MDA-231 cells were cultured overnight in the presence of medium conditioned with neonatal mouse calvaria. Total RNA were prepared from mouse bone metastases and SQ tumors or cultured cells. Quantitative real-time RT-PCR was performed to measure the expression of the various isoforms of human PTHrP (139, 141 and 173) mRNA. Human GAPDH mRNA expression served as the normalization control.

RESULTS: Intracardiac injection of HARA cells resulted in bone metastases in the femurs, tibias, and humeri 6 - 8 weeks after inoculation; whereas subcutaneous tumors formed in the SQ-injected mice. Bone metastases were confirmed by radiography and histological examination. PTHrP (139), PTHrP (141), and PTHrP (173) mRNA expression were increased 4-, 14-, and 7-fold, respectively, in bone metastases compared to the subcutaneous tumors ($P < 0.05$). In vitro co-culture of MDA-231 cells with mouse calvaria-conditioned medium resulted in a 3.6-fold increase in PTHrP (139) mRNA expression.

CONCLUSIONS: All three isoforms of human PTHrP messenger RNA were induced in bone metastases in vivo, but the effect was greatest for PTHrP (141). PTHrP (139) was induced in MDA-231 cells co-cultured with mouse calvaria-conditioned medium. PTHrP induction may be an important step in the pathogenesis of bone metastasis by some human cancers.

Disclosures: ***T. Rosol****, None.*

M088

Type I Collagen Receptor ($\alpha_2\beta_1$) Signaling Promotes the Growth of Human Prostate Cancer Cells within the Bone. C. L. Hall*[1], J. Dai*[1], E. T. Keller[1], M. W. Long[2]. [1]Urology, University of Michigan, Ann Arbor, MI, USA, [2]Velcura Therapeutics, Inc., Ann Arbor, MI, USA.

Bone is the most frequent site of distant metastases in human prostate cancer (CaP). Selective binding to organ specific factors may facilitate organ specific metastasis of cancer cells. Therefore, we tested whether bone metastasis of CaP cells is mediated by binding to Type I collagen, a factor that comprises 90% of the total protein within the bone. To examine the role of collagen binding, human LNCaP cells, that routinely fail to bind to Type I collagen, were selected for collagen binding by serial passage on Type I collagen. These collagen-selected cells ($LNCaP_{col}$) were compared to parental LNCaP cells, and the highly metastatic, isogenic CaP variants LNCaP-LN3 and C4-2B. The data show that $LNCaP_{col}$ cells bound collagen equivalent to that of bone metastatic C4-2B cells (34 ± 2%, n=3). In sharp contrast, the non-metastatic parental LNCaP and lymph node metastatic LN3 cells were incapable of collagen binding. FACS analysis demonstrated that both C42B and $LNCaP_{col}$ express equivalent levels of the integrin $\alpha_2\beta_1$, a known collagen receptor. Antibodies to $\alpha_2\beta_1$ or GRGDTP peptide inhibited C42B and $LNCaP_{col}$ binding to collagen thus confirming that integrins mediate the attachment. Importantly, both $LNCaP_{col}$ and C4-2B cells had an increased ability to migrate towards collagen I compared to parental LNCaP cells and $\alpha_2\beta_1$ blocking antibodies prevented this migration. To directly test whether $\alpha_2\beta_1$ dependent collagen binding contributes to the bone metastatic phenotype, the ability of $LNCaP_{col}$ and parental LNCaP cells to grow within the bone was evaluated following intratibial injection into nude mice. After 9 weeks, 7 of 13 mice (53%) injected with $LNCaP_{col}$ had mixed lytic/blastic bone tumors; whereas, 0 of 8 mice injected with parental LNCaP cells had evidence of bony lesions. We conclude that binding type I collagen through $\alpha_2\beta_1$ induces motility programs in human CaP cells that promote growth within the bone and may explain the high prevalence of CaP metastasis to this site.

Disclosures: ***C.L. Hall****, None.*

M089

Assessment of Total Body Percent Fat from Regional Spine and Femur DXA Measurements. H. S. Barden, W. K. Wacker*, K. G. Faulkner. GE Healthcare, Madison, WI, USA.

Body composition studies usually rely on total body scans using full sized DXA (dual-energy x-ray absorptiometry) systems. Regional assessment of soft tissue composition, however, is a requirement for accurate DXA bone mineral measurements at the spine and femur. In this study, we determined whether regional body composition estimates from spine and femur DXA data could be used to predict total body fat percentage.

We evaluated the ability of soft tissue measurements (tissue %fat and thickness) available from spine and femur scans, along with height, weight and body mass index (BMI), to predict total body soft tissue %fat. We examined results from 161 female subjects (mean age 55;range 22-91 years) whose spine, femur, and total body were measured concurrently with the Lunar Prodigy densitometer (GE Healthcare). Percent fat and tissue thickness for spine and femur scans were available from scan printouts and were stored in the database. A best subset regression analysis fitting the residuals from an initial regression of total body %fat on BMI found that a regression equation using spine thickness, femur %fat, spine %fat, spine %fat x spine thickness, and height provided the best prediction of total body %fat ($R^2 = 0.85$, $r = 0.93$). Three subjects who fell more than 3 SEE from the regression line were excluded.

Regression of measured on predicted total body %fat gave a slope and intercept not significantly different from one and zero, respectively (Figure 1). The median absolute deviation was 1.6 %fat, with 62% of predicted values within 2 %fat of measured values. This regression might be improved with the addition of thin (<20%fat) and very heavy subjects. We conclude that data obtained from spine and femur scans, in combination with anthropometric information, provide a good estimate of total body fat and fat-free body composition. On systems that do not offer total body measurements, regional body composition information derived from spine and femur scans can be used to estimate total body fat percentage.

Figure 1. Prediction of Total Body %Fat

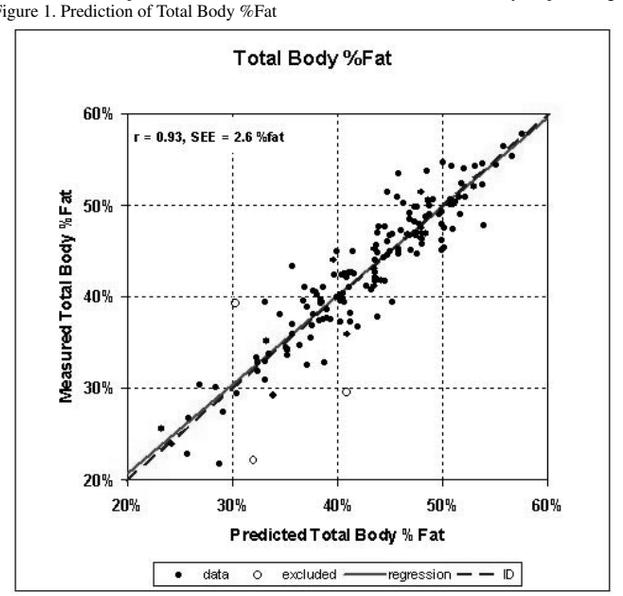

Disclosures: ***H.S. Barden****, None.*

M090

Comparison of Spine BMD Measurements from DXA With and Without Leg Elevation. C. Simonelli[1], L. Del Rio[2], N. Binkley[3]. [1]HealthEast Clinics, Woodbury, MN, USA, [2]CETIR Centre Medic, Barcelona, Spain, [3]UW Osteoporosis Clinical Center and Research Program, Madison, WI, USA.

Measurement of lumbar spine BMD using DXA traditionally requires hip flexion and elevation of the legs onto a positioning block. This flattens the lumbar curve with the intent of producing more accurate and precise BMD measurement. We determined if not elevating the legs affected BMD accuracy and precision.

Ninety-six women (54 ± 12 years, 70 ± 12 kg) had spine scans using Lunar Prodigy or Bravo (GE Medical) densitometers. One center[3] scanned 30 subjects with Prodigy, once using standard positioning (legs elevated on the manufacturer's spine positioner) and once without the spine positioner (legs flat on the table, feet secured with the dual-femur positioner). Two other centers[1,2] scanned 40 subjects with Prodigy and 26 with Bravo 3 times legs-up and 3 times legs-down. The RMS CV was determined for BMD values measured in triplicate. Single-scan results[3] were pooled with first-scan results from the other centers. L1-L4 BMD for both positions were compared using paired T-tests.

There were no obvious visual differences in disc spaces or vertebral bodies between the two positions. There was a small, but statistically significant, difference of 1.3% (0.014 g/cm^2) in measured L1-L4 BMD, with higher BMD in the legs-down position ($p<0.001$). Bland-Altman analysis showed no significant bias with mean BMD. Precision (~1% CV) was excellent in both positions. Linear regression analysis showed BMD was highly correlated (r = 0.99), with slope near unity (0.97), intercept near zero (0.02) and SEE=0.021 g/cm^2. Given the high correlation, a mathematical correction factor was derived to produce comparable T-scores between the two measurements. After adjustment, there was no significant difference (<0.01 T) in mean T-scores ($p=0.65$). We conclude that measured spine BMD differences with legs-down are small and there is no effect on precision. Adjusted T-scores for the legs-down position are equivalent to the legs-up position.

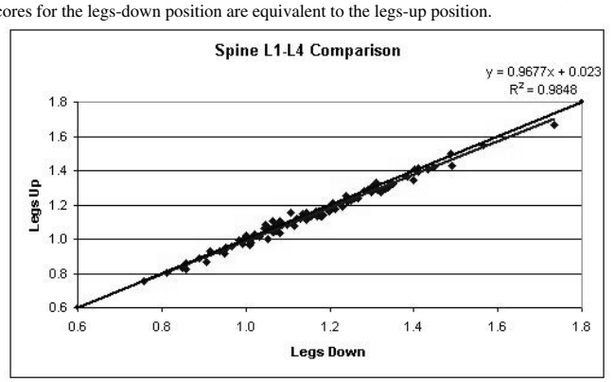

Disclosures: ***C. Simonelli****, GE Healthcare 2.*

M091

The Threshold of Vertebral Fracture Determined by Bone Mineral Density in Secondary Osteoporosis Caused by Glucocorticoid Treatment and Primary Hyperparathyroidism. M. Yamauchi, T. Sugimoto, T. Tobimatsu*, J. Naito, M. Iu*, R. Nomura*, Q. Chen*, H. Sowa, H. Kaji, K. Chihara*. Division of Endocrinology/Metabolism, Neurology and Hematology/Oncology, Kobe University Graduate School of Medicine, Kobe, Japan.

Although the vertebral fracture (VFx) risk has good relationship with bone mineral density (BMD) in primary osteoporosis, it remains uncertain whether the same relationship exists in secondary osteoporosis. Glucocorticoid(GC) excess as well as primary hyperparathyroidism (pHPT) are classically listed as important causes of secondary osteoporosis. Thus, we analyzed the cut-off values of BMD in the incidence of VFx in patients with GC treatment and pHPT, and compared these values with those in control subjects. One hundred and thirty-six female patients with GC treatment for more than 6 months (Mean: age 50yr; daily dose of predonisolone 10.1mg; treatment duration 7yr; VFr+ 34), 116 pHPT female patients (age 60yr; serum Ca 11.7 mg/dl; intact PTH 206 pg/ml; VFx+ 14) and 716 female controls (age 61yr; VFx 158) participated in this study. BMD measurement was performed by DXA at sites of lumbar spine, femoral neck and distal one third of radius. VFx was assessed on lateral radiographs of thoracic and lumbar spines. The cut-off values of BMD for the discrimination of VFx were obtained from ROC analysis, that is, the points where the sensitivity curve intersects the specificity curve, as the optimal VFx thresholds. As for comparison of BMD Z scores between VFx+ and VFx-, values at any site were significantly lower in VFx+ in controls. In contrast, values only at femoral neck were significantly lower in VFx+ in patients with GC treatment and no significant differences were found at any site in pHPT patients. At lumbar spine, the cut-off values of BMD (g/cm2) as well as their sensitivity/spefcificity (%) were 0.716; 71, 0.807; 67 and 0.676; 62 in controls, patients with GC treatment and pHPT patients, respectively. At femoral neck, they were 0.581; 75, 0.611; 71 and 0.556; 62, respectively. At radius, they were 0.477; 73, 0.592; 62 and 0.398; 60, respectively. Cut-off values of BMD at any site were higher and lower in patients with GC treatment and pHPT patients, respectively, compared with controls. Sensitivity/specificity was lower in both groups, compared with controls. In conclusion, the present findings suggest that GC excess and endogenous PTH excess induce more accelerated and less deteriorative vertebral fragility than that estimated from BMD, respectively. Although BMD is a good predictor of bone fragility in primary osteoporosis, it is rather difficult to assess bone fragility from BMD value in secondary osteoporosis.

Disclosures: ***M. Yamauchi****, None.*

M092

Predicting the Risk of Fracture at Any Site in the Skeleton: Are All BMD Measurements Equally Effective? G. M. Blake[1], K. M. Knapp[1], T. D. Spector[2], I. Fogelman[1]. [1]Imaging Sciences, Guy's, King's and St Thomas' School of Medicine, London, United Kingdom, [2]Twin Research and Genetic Epidemiology Unit, St Thomas' Hospital, London, United Kingdom.

The ability to assess a patient's risk of fracture is fundamental to the clinical role of bone densitometry. Fracture discrimination is quantified by the relative risk (*RR*) defined as the increased risk of fracture for a 1 standard deviation decrease in bone mineral density (BMD). The larger the value of *RR*, the more effective measurements are at identifying patients at risk of fracture. The data available suggests that if the objective is to predict the risk of fracture at *any* skeletal site then all types of BMD measurement are equally effective. In this study we show theoretically that the observation that *RR* values for predicting the risk of any fracture are comparable for all types of measurement is a consequence of two other observations: (1) that fracture risk prediction at BMD sites distant from the fracture site is quantitatively explained by the correlation of the BMD measurements; (2) that the correlation coefficients between distant BMD sites are all comparable with values in the range $r = 0.55$-0.65. Although both these observations are only approximations, they nevertheless provide useful insight into the potential for improving the clinical effectiveness of bone densitometry. In particular, they point to the importance of the correlation coefficient between different types of measurement as a key index that is predictive of the ability of new types of measurement to discriminate fracture risk. It is the narrow range of values of the correlation coefficient between BMD measurements in the central and peripheral skeleton that leads to the conclusion that such measurements should all have comparable power to predict fracture risk. The ability of peripheral bone densitometry to predict fracture risk could be improved by the development of new techniques that correlate better with BMD measurements in the central skeleton, for example by reducing the accuracy errors due to variations in soft tissue composition. Conversely, those techniques that correlate poorly with central BMD, for example some types of ultrasound measurement, are likely to prove less effective at predicting fracture risk.

Disclosures: ***G.M. Blake****, None.*

M093

DXA and QUS Can Comparably Dicriminate Patients with Osteoporotic Hip Fractures from Matched Controls. P. Hadji, M. Gottschalk*, V. Ziller*, E. Mann*, G. Esser*, U. Wagner*. Endocrinology and Osteoporosis, Clinic of Gynokology and Obstretics of Philipps- University, Marburg, Germany, Marburg, Germany.

Introduction: The aim of this pilot study was to evaluate the ability to discriminate patients with hip fracture from healthy controls using DXA and QUS in postmenopausal women.

Material and Methods: We included 22 Patients mean age 76,5 ± 5,4 years with an incident osteoporotic hip fracture and 22 age and BMI matched controls. Women in the control group with a history of Osteoporosis or with a fracture or diseases or treatments known to effect bone metabolism were excluded from the study. BMD was measured by DXA (Prodigy, GE/Lunar) at the spine and hip. QUS was performed at the Os Calcaneus using the Achilles + device as well as the Insight device (GE/Lunar).

Results: DXA results of women with hip fractures at the femoral neck showed statistically significant lower T-score of -2.6 and Z-score of - 0.8 compared to T-score of -1.7 and a Z-score of 0.1 in healthy controls (p= 0,008 and p= 0,01). In women with hip fracture, DXA results of the Spine (L1-L4) showed an insignificant difference in T- and Z-score compared to age and BMI matched controls. In accordance to QUS results, measurement at the Os Calcaneus (Achilles + and Insight) showed significant differences between the groups. The T-score was -3.3 and -2.6 in women with hip fracture compared to a T-score of -2.3 and -1.6 (p= 0,01) in controls. The Z-score was -0.9 and -0.3 in women with hip fracture compared to 0.1 and 0.8 (p= 0.01 and p= 0.005) in controls.

Conclusion: The results of our pilot study confirm the capability of DXA and QUS to discriminate patients with prevalent hip fracture from healthy controls. This significant difference could be observed by DXA at the hip and both QUS devices measuring at the Os calcaneus but not for DXA of the spine. Further large scale longitudinal studies are needed to evaluate the diagnostical capabilitys of DXA and QUS.

Disclosures: ***P. Hadji****, None.*

M094

Association between Current Bone Metabolism Parameters and the Progression of Vascular Calcification in Men and Women. M. Naves-Diaz*, J. B. Díaz-López*, C. Gómez, A. Rodríguez-Rebollar*, M. Rodríguez-García*, J. B. Cannata-Andía. Bone and Mineral Research Unit, Hospital Universitario Central de Asturias, Oviedo, Spain.

In the elderly population it has been found that low bone mass is associated with a higher prevalence of vascular calcification (VC). The aim of this study was to find out the association between bone metabolism parameters and the progression of aortic VC in men and women from a non-selected Spanish population.

A cohort of 156 men and 164 women participated in this study. Two lateral dorsal and lumbar radiographs and lumbar and hip bone densitometry were performed at baseline and again 4 years later. The progression of aortic VC was defined by an increase in the severity -with a semi quantitative scale- of the VC in the second radiograph compared with the radiograph performed at baseline. In addition, the presence of a new aortic VC was also determined. Bone metabolism parameters selected were analysed in a fast serum sample. All those subjects who had undergone any previous osteoporosis treatment were excluded from the analysis.

Progression of aortic VC was found in 56% of men and in 33% of women. The incidence of aortic VC was 26% in men and 15% in women. The univariate analysis showed that in men, those with VC progression showed a significant reduction in lumbar spine bone mineral density (BMD) compared with those without VC progression (-1.94±4.4% vs. 0.66±4.7% respectively, p=0.006). In addition, in men with VC progression, the serum calcium was significantly higher 9.5±0.3 mg/dl and the osteocalcin lower 5.0±1.5 ng/ml compared with those without VC progression, 9.3±0.3 mg/dl and 5.9±2.3 ng/ml respectively, p<0.05).
Women with VC progression showed also a significantly reduction in lumbar spine BMD compared with those without VC progression (-0.58±5.8% vs. 2.06±4.9%, p=0.035). Serum calcitriol was higher in women with new VC (43±15 vs. 37±11 pg/ml, p=0.047).
In men, using logistic regression adjusting by age and smoking, increments in serum calcium [RR=3.46; (95% CI)=1.17-10.20], increments in osteocalcin levels [0.75; (0.61-0.92)] and the rate of reduction in lumbar spine BMD [1.14; (1.03-1.25)] were independently associated with progression of VC.
In women, only serum calcitriol was positively associated with the incidence of VC [1.04; (1.00-1.09)]. The rate of change in BMD at lumbar spine was not independently associated, either with the progression or the incidence of VC.In summary, in men higher serum calcium and a reduction in lumbar spine BMD were independent risk factors for the aortic VC progression, whereas higher levels of osteocalcin were a protective factor. In women, higher serum calcitriol was the only risk factor associated with the appearance of a new aortic VC.

Disclosures: ***M. Naves-Diaz****, None.*

M095

Wider Limits of Acceptable Change in Projected Vertebral Areas Between Serial Scans Still Renders Many Serial DXA Interpretations Invalid. G. Kline*, D. A. Hanley. Medicine, University of Calgary, Calgary, AB, Canada.

The ISCD recommends vertebral projected areas should differ by < 2% to avoid measurement error due to apparent change in bone size. This strict criterion is rarely achieved in clinical practice. We re-analyzed 103 consecutive pairs of DXA reports to determine the frequency and magnitude of serial differences in vertebral area.
Scans were performed at qualified community radiology sites and included if free from any technical errors, artifacts or rotation. We calculated the proportion of paired scans having at least 2 vertebrae differing in area by <2%, <3%, <4% or <5%. Using the differing sets of validity criteria, vertebrae not meeting the areal standard were removed from the analysis and the overall change in BMD recalculated. The new, recalculated BMD was compared to the original report to determine the frequency and magnitude by which the re-analysis would change the final report.
Of the paired scans, 5%, 16%, 27% and 35% had all 4 vertebrae differ in area by less than 2%, 3%, 4% and 5% respectively. When only 2 vertebrae were required to meet acceptability criteria, 51%, 73%, 85% and 89% of scans met the 2%, 3%, 4% and 5% difference criteria. 11% of scans were non-comparable by even the least stringent criteria of 2 vertebra differing by <5% between scans.
Re-analysis of BMD change in each group differed from the reported change by 0.012 to 0.015 g/cm2. However, this amount was sufficient to change a clinical report from "significant change" to " non-significant change" in 26%, 27%, 21% and 20% of scans in each of the four validity groups using a least significant change of 0.025 g/cm2. Between 11%-17% of scans differed in the recalculated BMD change by an amount greater than the least significant change of 0.025 g/cm2.
Fewer serial BMD results were classified as non-acceptable when using the broader validity criteria of <5% area difference, but when corrected for areal differences, a similar and large proportion of scans would have a major change in the clinical interpretation of BMD change. These results do not change the interpretation of population BMD change in randomized trials but highlight the need for more caution in data analysis of serial densitometry results when used to make individual patient management decisions.

Disclosures: ***G. Kline****, None.*

M096

Variation in the Location of the Ward's Triangle Region in the Norland Femur Study. J. M. Wang*[1], J. C. Liu*[2], T. V. Sanchez[3]. [1]Research and Development, Norland--a CooperSurgical Company, Beijing, China, [2]Department of Nuclear Medicine, PLA 304th Hospital, Beijing, China, [3]Research and Development, Norland--a CooperSurgical Company, Socorro, NM, USA.

Variations in distribution of femur head bone mineral have been reported as a major component to bone fragility by a number of investigators. In addition to other femur regions, DXA allows assessment of an area reported as the Ward's Triangle region. When using the Norland scanner to locate the Ward's region, the analysis program searches for a region with the lowest density along a fixed area located near the crosshair formed by the femur neck cursor and the trochanteric boundary cursor. While the Ward's region is usually located very near this crosshair region, on occasion the search program locates the lowest density region somewhere deeper into the femur neck region or the trochanteric region. This study examines these substantially "off-line set" Ward's regions in a population referred for DXA evaluation.
Femur studies using the Norland XR-36 were performed on an ambulatory population of 3,000 subjects referred for DXA to the Department of Nuclear Medicine at the PLA 304th Hospital. All studies were reviewed by a factory trained operator (JMW) to insure that all scans had been properly performed and analyzed. Of the 3,000 studies examined, 207 (6.9%) subjects showed "off-line set" Ward's regions--70 (2.3%) being off-line set in the femur neck region and 137 (4.6%) being off-line set in the trochanteric region. Examining those studies with the "off-line set" Ward's located in the femur neck area showed bone density was 84% that found in the normally located Ward's region. Similarly, bone density in the "off-line set" Ward's located in the trochanteric region was about 80% that in the normally located Ward's region.
The survey shows that, when compared to the bone density in the normally located Ward's region, a number of subjects show significantly lowered densities within the "off-line set" Ward's located deeply within the femur neck or trochanteric regions. Finding these significantly reduced bone densities within biomechanically stressed areas may serve to identify subjects especially prone to femoral neck or trochanteric fracture.

Disclosures: ***J.M. Wang****, Norland--a CooperSurgical Company 3.*

M097

Finite Element Analysis of DXA Images (FEXI) for the Prediction of Osteoporotic Fractures - Experimental Validation. C. M. Langton*[1], J. A. Thorpe*[2], M. J. Fagan*[3]. [1]Centre for Metabolic Bone Disease, University of Hull, Hull, United Kingdom, [2]Centre for Metabolic Bone Disease, Hull & East Yorkshire Hospitals, Hull, United Kingdom, [3]Engineering, University of Hull, Hull, United Kingdom.

The preferred method of assessing the risk of an osteoporosis related fracture is currently a measure of bone mineral density (BMD) by dual energy X-ray absorptiometry (DXA). We know however that other factors contribute to the overall risk of fracture including anatomical geometry and the spatial distribution of bone. The purpose of this study was to compare the abilities of plane radiograph- and DXA-derived finite element analysis (FEXI), along with BMD, to predict experimentally derived mechanical stiffness and yield load of the porcine proximal femur.
The FEXI analysis procedure simulates a mechanical compression test, providing a measure of stiffness (N mm^{-1}), being inherently sensitive to the external shape and internal structure of a bone.
DXA scans and digital plane radiography were performed on 23 excised porcine femurs, with BMD recorded for the proximal third. Following addition of resin support platens over the greater trochanter and femoral head, compressive mechanical testing provided stiffness and yield load data. The DXA and plane radiograph images were converted into bitmap format (256 grey levels). Simulated support platens were manually added to the images. A bespoke computer program converted the images into a finite element model whereby the grey level of each image pixel was converted into a corresponding Young's modulus value. 2D plane stress finite element analysis was performed, from which the stiffness of the bone image was derived.
BMD showed a good correlation with both experimentally determined stiffness and yield load (R^2=0.65 and 0.71 respectively). FEXI stiffness derived from DXA images demonstrated higher correlation with stiffness and yield load (R^2=0.61 and 0.71 respectively) than did plane radiograph-derived FEXI (R^2=0.53 and 0.63 respectively). BMD correlated highly with DXA derived FEXI (R^2=0.83), but less so with plane radiograph FEXI (R^2=0.45). FEXI utilising the two X-ray modalities were highly correlated (R^2=0.65).
These findings confirm that both BMD and DXA-derived FEXI predict the stiffness and yield load of bone, the poorer performance of plane radiograph derived FEXI being attributed to variability in X-ray exposure. The porcine proximal femur exhibits a short and wide neck, a large greater trochanter, and lower variation in hip angle and hip axis length. It is therefore feasible that the ability of FEXI to predict mechanical integrity may be higher in human than porcine bones.

Disclosures: ***C.M. Langton****, McCue plc 5, 7.*

M098

Assessment of Criteria for Lateral Morphometry in over 65 Year Olds Attending for Bone Densitometry. A. L. Dolan*, J. Wilkinson*, B. Coutinho*. Rheumatology, Queen Elizabeth Hospital, London, United Kingdom.

The presence of vertebral fractures increases the risk of subsequent fracture fourfold and supports the need for more potent treatments such as bisphosphonates or PTH, yet many are undetected clinically. Lateral vertebral morphometry is now widely available on modern densitometry machines an can identify such fractures. There is now a need to define those patients in whom the technique is most appropriate.
Patients were selected for lateral vertebral morphometry if they were over 65 years and satisfied one of the following criteria: previous low impact fracture, kyphosis, height loss > 2", height loss seen at DXA or BMD <-2.5 and non of above. Scans were performed on a Hologic 4500c DXA Bone Densitometer with an upgraded 'Discovery' software package and Instant vertebral assessment. Ethics committee consent was obtained.
268 patients (36 males, 232 females) satisfied one or more criteria and received lateral morphometry, out of 363 patients over 65 years of age (74%) referred to an open access bone densitometry service at Queen Elizabeth Hospital, Woolwich over a 4 month period. Of these 160 patients (60%) had satisfied criteria for morphometry because of low impact fracture, 77 (29%) had kyphosis, 84 (31%) showed height loss >2", 56 (21%) had height loss observed at DXA and 40 (15%) had solely low BMD values. 152 patients had one or more vertebral fractures (57%) identified. A total of 338 vertebral fractures were identified in these patients of which 79 (23%) were severe, 149 (44%) moderate and 110 (32%) mild according to Genant criteria. 76/152 patients (50%) with vertebral fracture were osteoporotic at either hip, spine or forearm (6 males, 70 females). 99/152(65%) patients were osteopenic (9 male, 90 female).
Lateral morphometry at DXA identified a significant number (57%) of patients with vertebral fracture when they were selected according to high risk criteria. This is an important intervention since it may imply need of more potent osteoporosis treatment. This is especially so for those with vertebral fracture but osteopenia 99/268 (37% of those receiving morphometry) where treatment should be upgraded following their morphometry results.

Disclosures: ***A.L. Dolan****, None.*

M099

The Femoral Neck Is Ellipsoid: the Assumption of Circularity or Parallelepipedal Shape Introduces Errors in Volume and Volumetric Bone Mineral Density. R. M. Zebaze*[1], F. Welsh*[2], S. Iuliano-Burns[1], A. Evans*[1], E. Seeman[1]. [1]Endocrinology, Austin Health, Melbourne, Australia, [2]University of Aberdeen, Aberdeen, United Kingdom.

Comparisons of femoral neck dimensions, volumetric BMD and bone strength between sexes, races, patients with and without fractures use estimates derived from bone densitometry. Calculation of FN external volume, medullary diameter, cortical thickness, volumetric BMD, sectional modulus assume that the FN approximates a cylindrical structure in which 60% of the mineral is in the cortex, the rest is medullary in location, and that the tissue mineral content is constant with age (1.05 g/cc). These assumptions are untested. Volumetric BMD assumes the FN is a parallelepipedal structure and computed as BMC/ area2 (vBMDe1) or a cylinder computed as BMC/*(W/2)2*h (BMDe2), h being the height of the bone scan region. We used DXA in 26 Caucasian female cadavers mean age of 69.2 ± 3.2 years (range 29 to 85 years) and directly measured FN dimension using a caliper and Archimedes principle. FN diameter measured by DXA as an average FN 3.37 ± 0.4 or mid-FN value 3.37 ± 0.1 were no different from FN width measured in vitro 3.51 ± 0.13 cm. Femoral axis length and neck shaft angle measured by DXA and directly did not differ (9.61 ± 0.2 vs 9.65 ± 0.22 cm and 123.5 ± 0.21 vs 123.6 ± 0.19 degrees respectively). However, FN depth was always lower than the width by 25% (from 14 to 36%). Thus, DXA underestimated FN vBMD by 41% for BMADe1 (0.214 ± 0.02 vs 0.364 ± 0.03 g/cm3) to 20% for BMADe2 (0.272 ±0.01 vs 0.364 ± 0.03 g/cm3). Smaller bones were more circular, bigger bones were ellipsoid so the bigger the bone, the worse the vBMD under-estimate. Adjustments of the DXA estimates assuming that the FN was ellipsoidal (BMADe3) with the bigger axis being the FN width and the smaller axis being the depth (0.75 depth/width) result in no difference between BMADe3 (0.359 ± 0.02 vs BMAD 0.364 ± 0.03 g/cm3). We infer that DXA overestimates volume, and underestimates estimates FN vBMD and this may have an impact on fracture prediction. (ii) Estimates assuming a cuboidal structure should be abandoned in favour of an ellipsoidal structure.

Disclosures: ***R.M. Zebaze****, None.*

M100

Bone Mineral Density and the Risk of Peripheral Arterial Disease: Mr Os, Hong Kong. S. Y. S. Wong[1], E. M. C. Lau[2], H. Lynn[1], J. Woo*[1], P. C. Leung*[3]. [1]Department of Community and Family Medicine, Chinese University of Hong Kong, Shatin, Hong Kong Special Administrative Region of China, [2]Jockey Club Centre for Osteoporosis Care and Control, Chinese University of Hong Kong, Shatin, Hong Kong Special Administrative Region of China, [3]Department of Orthopedics and Traumatology, Chinese University of Hong Kong, Shatin, Hong Kong Special Administrative Region of China.

Previous studies have demonstrated an association between peripheral vascular disease and bone mineral density in women but not in men. In a large prospective cohort of 2000 Chinese men aged 65 to 92 years of age in Hong Kong (Mr Os, Hong Kong), the association between peripheral vascular disease and bone mineral density was explored.

Demographic and lifestyle information were obtained from face to face interviews using standardized questionnaire. These include demographic information, medical history, smoking and alcohol history and physical activity. Physical examination measurements include anthropometry and tibial and brachial systolic blood pressures. The ratio of the posterior tibial and brachial systolic blood pressures, the ankle/arm index, was used as a measure of peripheral arteriosclerosis in the lower extremities. Bone mineral density at the total hip and spine (L_1 - L_4) was measured by Hologic QDR-4500W densitometers (Hologic, Inc., Waltham, MA).

In this cross-sectional analysis, the ankle brachial index was positively associated with BMD at the total hip but not the spine. A decrease in index of 2 standard deviations (SD) was associated with a decrease of 3.6 % in hip BMD. In multiple regression analysis, the effect size at the hip decreased from 3.6% to 1.4% when adjustment was made for smoking, body mass index, history of hypertension and diabetes, and physical activity (Table 1).

Table 1. Summary of multivariate analysis of bone mineral density (g/cm^2) at the total hip expressed as the percent difference (95% Confidence Interval) in BMD per unit change of the predictor variables (N=2000)

Variable	Mean (SD)/ prevalence	Unit (2SD)	Percent difference (95% CI)
Age	72.4(5)	10	**-2.4(-3.6, -1.2)**
BMI	23.4(3.1)	6	**13.2(12, 14.2)**
Current smoker	11.9%	Yes/no	-1.2(-2.9, 0.6)
Hypertension	41.8%	Yes/no	-0.2(-1.4, 1)
PASE score	97.3(50.3)	100	**1.2(0, 2.4)**
A history of diabetes mellitus	14.7%	Yes/no	**4(2.4, 5.7)**
Ankle-arm index	1.1(0.13)	0.26	**1.4(0.4, 2.6)**
			R^2=0.268

Bold numbers indicate statistical significance at the p<0.05 level.

Our study shows that in addition to women, peripheral arteriosclerosis in the lower extremities may also be associated with decreased bone mineral density in men. This shows that in addition to the previously suggested role of abrupt estrogen decrease in explaining the association between peripheral arterial disease and osteoporosis, other factors must also be involved.

Disclosures: ***S.Y.S. Wong****, None.*

M101

Significant Malnutrition And Osteopenia In Gaucher Type I Patients Despite Enzyme Replacement Therapy. B. Oliveri, M. Parisi*, G. Goldstein*, A. Bagur. Sección Osteopatías Médicas, Hospital de Clínicas, Universidad de Buenos Aires, Buenos Aires, Argentina.

Gaucher patients (GP) have a deficit in Beta glucocerebrosidase activity, which in turn leads to accumulation of glucocerebroside in the macrophages of various organ systems (spleen, liver, lung, kidney, bone and bone marrow). Eighty % of Type I GP present skeletal involvement. In a previous cross-sectional study we reported that GP receiving enzyme replacement therapy (ERT) (ASBMR2003) had diminished bone mass associated with unbalanced bone metabolism due to higher resorption than formation. Hypermetabolism (higher resting energy expenditure) was described in GP, and found to improve partially and to varying extents with ERT. The aim of the present study was to evaluate whether GP patients receiving ERT presented alterations in body composition (BC) (fat and lean mass), and the relationship between body composition and bone mass. The study population comprised 10 patients (5 women, 5 men) aged (X± SD) 26.1± 7.0 years (range (r):19-43) with a BMI of 19.4.±1.7 kg/m2 (r:16.5-22.9). Six patients were splenectomized and 5 had hepatomegaly. All patients had been receiving ERT (imiglucerase) in a dose of 50.8±14.0 IU/kg/2weeks (r:30-71) during 4.9±3.7 years. Bone Mineral Density and Content (BMD and BMC) of Total Skeleton (TS) and fat and lean mass were measured by DXA (Lunar DPX-L) and compared with age/sex matched controls, to calculate Z score and percentage of diminution.

Age and height of GP were similar to controls but the following parameters were significantly diminished: weight, fat. and lean mass Zs were: -1.84 (p<0.05), -1.6 (p<0.001) and -1.13 (p<0.05) respectively and TS BMD, BMC and total calcium Zs were: -1.69 (p<0.001), -1.65 (p< 0.001) and -1.67 (p<0.001), respectively .When GP were grouped according to sex: both males and females had a high diminution in TS BMC (-19%,p<0.05) and fat mass (-40%,p<0.01) but only males showed a significant diminution in lean mass (-12%,p<0.05).

When divided according to ERT dose, the patients receiving <60IU/ kg/2w had lower: TS BMD: Zs -2.5 vs -1.1 (p<0.04), BMI 18 vs 20 (p<0.067), and fat mass Z: -2.0 vs -1.3 (p<0.067), than those receiving >60IU/kg/2w. No differences in BC were observed in patients with hepatomegaly or splenectomy. The only positive significant correlation was between Z of TS BMC and lean mass. CONCLUSION: GP present severe malnutrition (mainly due to diminished fat mass) and present significant osteopenia, which is probably due to multifactorial causes rather than to fat mass diminution. Although ERT was not sufficient to prevent body composition alterations, patients receiving higher ERT doses tended to present fewer alterations.

Disclosures: ***B. Oliveri****, None.*

M102

A Randomized Study to Evaluate Strategies to Improve Osteoporosis Detection and Treatment in Elderly Women. B. Muma*[1], J. Lafata*[1], B. McCarthy*[2], D. Kolk*[1], E. Peterson*[1], D. Rao[1], T. Weiss[3], Y. Chen*[3]. [1]Henry Ford Health System, Detroit, MI, USA, [2]Alina Medical Group, Minneapolis, MN, USA, [3]Merck & Co., Inc., West Point, PA, USA.

Current estimates are that only 20% women age 65 and older have received a bone mineral density (BMD) test, despite recommendations from the US Preventive Services Task Force and the National Osteoporosis Foundation. Thus, a large number of women are at risk of avoidable late-stage osteoporosis. We report preliminary findings of a randomized prospective study to evaluate strategies to enhance the quality of care for osteoporosis.

We identified women aged 65-89 that received primary care from 15 ambulatory care clinics of a large medical group in southeast Michigan between 4/1/2001 and 3/31/2003. The clinics were stratified by size and BMD availability, and randomized to one of 3 study arms: (1) usual care; (2) patient mailing (BMD reminder letters + educational material); and (3) patient mailing plus physician reminder prompts for BMD testing. Women that previously received a BMD test, a diagnosis for osteoporosis, or a prescription drug claim for an osteoporosis-specific therapy (alendronate, risedronate, raloxifene, or calcitonin) were excluded. A total of 10,565 eligible women were included in the study: 3,110 women in strategy (1) clinics; 3,368 in strategy (2) clinics; and 4,087 in strategy (3) clinics. Preliminary analysis of BMD testing rates were calculated for each study arm for a six-month window starting in August 2003. Differences between groups in BMD testing rates were evaluated using generalized estimating equations. To adjust for different intervention start times, we matched the usual care group to each of the intervention groups separately by starting time. Statistically significant differences in BMD testing rates between groups were evaluated using generalized estimating equation approaches.

Preliminary analysis adjusted for intervention start date indicate differences in BMD screening rates between the usual care and patient mailed reminders (2% vs. 13%); and the usual care and the patient mailing plus PCP prompt (5% vs. 27%).

Differences between usual care and patient mailing strategies were significant (p<.001). The use of a patient mailing plus physician prompts lead to significant improvements in BMD testing compared to both usual care and patient mailing alone (p<.001). Results did not change with adjustments for clinic, race, and age.

Preliminary results indicate that the use of mailed patient reminders alone or in combination with physician prompts can lead to significant increases in osteoporosis screening rates compared to usual care, with the combination intervention (patient mailing + PCP prompt) showing the greatest effect.

Disclosures: ***D. Rao****, None.*

M103

In-vivo and Phantom Bone Mineral and Body Composition Calibration of DXA. D. Pearson*[1], B. Horton*[1], D. J. Green*[1], C. G. Miller[2], S. A. Jackson[2]. [1]Nottingham City Hospital NHS Trust, Nottingham, United Kingdom, [2]Bio-Imaging Technologies Inc, Newtown, PA, USA.

The purpose of this study was to obtain in-vivo and phantom cross calibrations for bone mineral and body composition studies using DXA.

21 subjects (18F, 3M mean age 55, range 31-80) had whole body scans on GE Lunar Prodigy (P) and Hologic QDR2000 (H) scanners. The Bio-Imaging Variable Composition Phantom (VCP) is a lightweight DXA phantom for cross calibration for body composition. It consists of a stack of 4 rectangular plastic blocks 13cm thick, with an aluminium head to simulate the skull. Three different kinds of plastic sheet are used in different combinations to simulate low (10%), medium (24%) and high (48%) fat content, but it has no bone mineral content (BMC). The VCP has a simulated body weight of about 9.5kg and was scanned on both machines 4 times with each percentage fat (%fat) . The calibrations were calculated using a standardised principal components analysis. The BMC, fat mass (FM), lean body mass (LBM) and %fat were compared using a Bland & Altman plot to calculate the mean difference and limits of agreement (LA).

The mean weight of subjects was 65kg (range 43-92kg), providing a good range of body composition values for cross calibration. There was good correlation between FM, LBM and %fat measured on the two instruments (r=0.97). The mean difference in BMC was 364g (P - H) and the LA were 91g to 638g compared to a mean BMC of 1712g on the QDR2000 ($p<0.01$). For FM the difference was -1.5kg (-4.3kg to 1.3kg mean 26kg $p<0.01$). For LBM the difference was -0.6kg (-3.6kg to 2.6kg mean 39kg). For %fat difference was -1.3% (-5.5% to 2.8% mean 38.7% $p<0.01$). The mean differences in FM, LBM and %fat using the VCP were -0.4kg, 0.2kg and -3.3% respectively. Figure 1 shows the in-vivo and VCP calibrations for %fat. The in-vivo calibration equation for LBM is H = 1.034P - 709 g (± 1587g), for FM is H=1.038P+562 g (±.1364g), for BMC is H = 0.83P-11 g (±111g) and for %fat is H = 1.099P + 0.72 (±2.1).

There is a consistent difference in BMC, %fat, FM and LBM between the Prodigy and QDR2000. The VCP gives an adequate cross calibration for %fat, FM and LBM despite it being necessary to extrapolate to higher values of FM and LBM. The limits of agreement are acceptable for cross calibration in the context of a cross sectional study, but would not be acceptable in longitudinal measurements to allow individuals to transfer between DXA instruments.

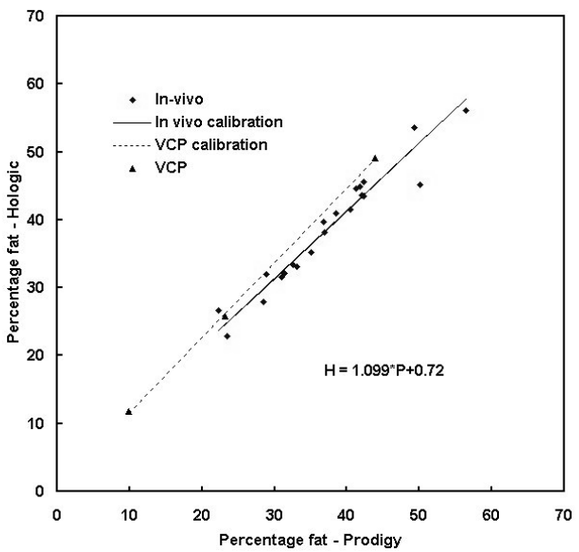

Disclosures: ***D. Pearson****, GE Lunar 2; Bio-Imaging Technologies Inc 2.*

M104

Inter-observer Variation of Vertebral Morphometry Using Two Different DXA Methodologies: Expert vs Prodigy. D. Pearson*[1], B. Horton*[1], D. J. Green*[1], D. J. Hosking[1], A. Goodby*[2], S. A. Steel*[2]. [1]Nottingham City Hospital NHS Trust, Nottingham, United Kingdom, [2]Hull Royal Infirmary, Hull, United Kingdom.

The purpose of this study was to compare inter-observer variation and vertebral morphometry on a supine lateral DXA scanner (GE Lunar Expert) and decubitus lateral scanner (GE Lunar Prodigy).

25 patients (19F, 6M, mean age 68, range 50 to 84) were recruited. Morphometry was carried out on each machine. Patients completed a questionnaire on comfort during scanning. The scans from each machine were analysed by two operators. Both completed a questionnaire on image quality.

One patient had an unsatisfactory scan on the Prodigy because of the presence of pins and plates in the lumbar spine. There was no significant difference between the scanners in terms of patient comfort. 19/25 reported that comfort was very good or better on the Expert compared with 17/25 on the Prodigy. There was no significant difference between the scanners in perceived image quality or in the ability to identify osteophytes or aortic calcification. The image quality was significantly worse in the thoracic (median 4, range 1-6) compared to the lumbar spine (median 5, range 2-6, $p<0.001$). T4 was the highest vertebra assessed in 71% of cases on the Expert compared to 46% of cases on the Prodigy ($p=0.08$). Inter-observer coefficients of variation (CV) ranged from 4% in the lumbar region to 13% for the posterior height in the upper thoracic region. The limits of agreement on vertebral height were ±3.5mm. Posterior height CVs were higher than anterior or mid height CVs. In the inter-machine comparison, mid and posterior heights were significantly higher (0.5mm) on the Expert ($p<0.001$) and the limits of agreement were ±3mm. The Expert identified 10 wedge fractures, 3 in a patient not scanned on the Prodigy and 2 further not seen on the Prodigy. The Expert identified 7 biconcave fractures and the Prodigy identified 9, all at different sites.

There are no qualitative differences between the Expert and Prodigy in patient comfort or image quality. Whilst the mean difference between machines in vertebral height measurements, A/P ratio, M/P ratio and Z-scores were small, the limits of agreement were wide. The inter-observer limits of agreement were the same size as the inter-machine limits of agreement suggesting that this is representative of underlying precision of MXA rather than differences in patient positioning or scanner used. There was reasonable agreement between the two machines on the identification of wedge fractures, although the number of fractures identified was small. The number of biconcave fractures, and the lack of agreement between the two systems requires further study, although it is unsurprising given the limits of agreement.

Disclosures: ***D. Pearson****, GE Lunar 2.*

M105

A Strategy for DXA Cross Calibration during Equipment Upgrade. D. Pearson*[1], B. Horton*[1], D. J. Green*[1], C. G. Miller[2], S. A. Jackson[2]. [1]Nottingham City Hospital NHS Trust, Nottingham, United Kingdom, [2]Bio-Imaging Technologies Inc, Newtown, PA, USA.

The purpose of this study was to develop a cross calibration strategy for replacing three old DXA scanners (GE Lunar DPXL, GE Lunar Expert, Hologic QDR2000) with two new GE Lunar Prodigy scanners.

Each of the old scanners was paired with one of the new scanners, e.g. patients scanned on the Expert or QDR2000 would be transferred to Prodigy 1 and only scanned on that machine in future. A cohort of patients was recalled for each old scanner, and up to 30 patients had lumbar spine and hip scans on the old scanner and the appropriate new scanner. An in-vitro calibration was carried out using a Bona Fide Phantom (BFP) scanned on each scanner on the days when calibration scans were carried out. Calibrations were fitted using a standardised principal components method. A Bland & Altman plot was used to calculate the mean difference and limits of agreement (LA) between scanners. Standardised BMD (sBMD) was calculated as an alternative method of calibration and compared with the in-vivo calibration.

A range of calibrations was generated, e.g. for Expert to Prodigy 23 patients (mean age 70, range 50-84) were scanned. There was a good range of lumbar spine BMD (mean 1.086g.cm^{-2} range 0.753-1.460 g.cm^{-2}). The calibration equation was P = 1.014 E -0.044 (see = 0.046 g.cm^{-2}) where P and E are Prodigy and Expert BMD respectively (Figure 1). Without calibration, the mean difference was 3% with LA of 0.063 to -0.122 g.cm^{-2}. Applying the calibration, the LA were ±0.047g.cm^{-2}. There was no significant difference between the in-vivo an in-vitro calibration. As expected, Prodigy BMD was about 15% higher than Hologic BMD. Following calibration the LA were ±0.064g.cm^{-2}. Using sBMD to calibrate gave a mean difference of 3% with LA of 0.115 to -0.045 g.cm^{-2}. There was good correlation at spine and hip for all pairs of scanner (r=0.95 to 0.98).

The LAs following calibration are clinically significant so it is not possible to apply a calibration to an individual patient for trending purposes, as the error is similar to the expected annual change in BMD. The calibrations can be used for group data in clinical trials. The in-vivo calibration gives better agreement than using sBMD to transfer patients between scanners. The BFP calibration was close to the in-vivo calibration. When introducing a new scanner, a new baseline BMD has to be obtained for each patient.

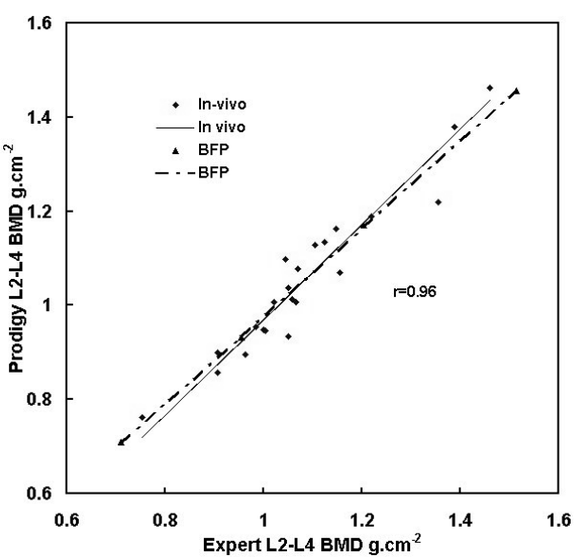

Disclosures: ***D. Pearson****, GE Lunar 2; Bio-Imaging Technologies Inc 2.*

M106

Regional Trabecular Bone Volume Ratio Predicts Failure of Thoracic Vertebrae under a Posteroanterior Load. M. M. Sran[1], K. M. Khan[1], D. M. Cooper*[2], S. K. Boyd[3], R. F. Zernicke[4], T. R. Oxland*[1]. [1]Division of Orthopaedic Engineering Research, Medicine, UBC, Vancouver, BC, Canada, [2]Archaeology, UofC, Calgary, AB, Canada, [3]Engineering, UofC, Calgary, AB, Canada, [4]Engineering, Medicine, UofC, Calgary, AB, Canada.

Failure load of thoracic cadaveric vertebrae under a posteroanterior (PA) load (where fracture occurred at the base or middle of the spinous process), and which may be linked to fracture during spinal mobilization, is not predicted by lateral or AP DXA or geometry of the spinous process or vertebral body.[1] We hypothesized that this may be due to BMD being an integrated measure of the entire vertebra, whereas these particular fractures occur in the largely cortical spinous process.[1] Thus the objective of this study was to: a) measure trabecular bone volume ratio (BV/TV) using µCT in four regions of thoracic vertebrae and to correlate those measures with PA failure load, and b) compare trabecular BV/TV of the spinous process base with the central lamina and middle spinous process regions, as a possible determinant of the fracture site.

We measured failure load and failure site in 11 T5-8 cadaveric spine segments (mean age 77 yr) when a PA load was applied at the spinous process of T6 using a servohydraulic material testing machine (Instron 8874), simulating a commonly used spinal mobilization technique. The T7 vertebra was dissected and sectioned to produce regional samples of the spinous process, the central lamina, and a central vertebral body core (8mm diameter). Each sample was scanned with µCT (Skyscan 1072, 15µm nominal isotropic resolution). We segmented four trabecular regions (spinous process base, spinous process middle, central lamina, and vertebral body centrum) and determined BV/TV in each region. We correlated PA failure load (N) with BV/TV for each region and compared BV/TV of the spinous process base with the middle spinous process and central lamina regions (paired t-test).

BV/TV at the base or middle of the T7 spinous process (fracture sites) showed a strong significant correlation with PA failure load of T6 (base: r=0.74, p=0.01; middle: r=0.73, p=0.01). The relations between BV/TV of the vertebral body centrum (r=0.44, p=0.1) or central lamina (r=0.57, p=0.07) and PA failure load were not significant. There was a significant difference between BV/TV in the spinous process base and the central lamina (p=0.03).

These novel data supported the findings of our previous study where AP and lateral BMD measures by DXA did not predict failure load of the spinous process.[1] However, BV/TV of the base and middle regions of the spinous process predicted failure at those sites, and lower BV/TV at the base (compared with the lamina) may have influenced the site of fracture.

1. Sran et al Spine 2004 in press

Disclosures: ***M.M. Sran****, None.*

M107

Dual Femur Densitometry - Effect on Diagnosis and Treatment Decisions. R. E. Cole. Osteoporosis Testing Center, Brooklyn, MI, USA.

The proximal femur is the best site for predicting hip fracture risk; a decrease of 1 T-score in hip BMD corresponds to ~3-fold increase in hip fracture risk. Recent technology enhancements allow rapid scanning of both hips in one acquisition, eliminating time-consuming repositioning and providing BMD results for individual and combined hips. While significant right vs. left BMD asymmetry is not the norm, discordance does exist in some patients. Bilateral scanning improves patient management by avoiding a potential missed diagnosis from scanning only one of two discordant femora.

Dual femur results from 537 women (mean age 61.2 years; SD 10.5, range 32 to 90 years) were evaluated for right and left BMD discordance that caused a difference in diagnosis (Dx) or treatment (Tx) recommendation. Subjects were classified as osteoporotic (T ≤-2.5), osteopenic (-2.5< T≤-1.0), or normal (T >-1.0) using WHO guidelines. A threshold of T-score ≤-2.0 was used for Tx recommendation. Chi square tests determined the significance of discordance in Dx and Tx recommendations between women under and over 65 years old.

Average femur BMD was ~1% higher on the left vs. right; there was no relation to hand dominance. Dx (normal, osteopenia, osteoporosis) differed with right vs. left femora in 29% of subjects at one or more sites, and in 14%, 15% and 10% of subjects for neck, trochanter and total femur, respectively. About 1% of women below age 65 showed Dx discordance between osteopenia and osteoporosis at neck and total femur, but 5% to 6% showed discordance after age 65.

Disagreement between right and left femora (any site) in Tx recommendation occurred in 7% (37/537) of subjects. Most subjects with Tx discordance were over 65 years old: 4% (14/349) were under 65 and 12% (23/188) were over 65 ($p<0.01$). When Tx agreement was defined as agreement at each left and right site (neck, trochanter, and total) 14% (74/537) of subjects showed Tx disagreement, while 6% to 7% showed disagreement at any one site. In subjects with discrepancy at an individual site, Tx discordance was 9% (31/349) for subjects under 65 and 23% (43/188) for subjects over 65 years old ($p<0.001$). In conclusion, dual femur scans showed right vs. left diagnosis differences in 10-15% of subjects and treatment differences in 7% of subjects, with significantly greater discordance (12%) in women over 65 years. Dual femur scanning enhances accurate clinical decision-making, especially in women over age 65.

Age-related Percentage of Subjects with Left-Right Femur Discordance

	Neck			Trochanter			Total Femur		
	<65	>65	All	<65	>65	All	<65	>65	All
Normal vs. Osteopenic	12.3%	10.7%	11.7%	12.0%	10.7%	11.5%	8.0%	7.5%	7.8%
Normal vs. Osteoporotic	0.0%	0.5%	0.2%	0.3%	0.0%	0.2%	0.0%	0.0%	0.0%
Osteopenic vs. Osteoporotic	0.9%	5.9%***	2.6%	2.6%	5.9%	3.7%	1.4%	4.8%*	2.6%
Treatment vs. no Treatment	3.7%	12.3%***	6.7%	4.6%	11.2%**	6.9%	4.6%	9.6%*	6.3%

* $p<0.05$ ** $p<0.01$ *** $p<0.001$

Disclosures: ***R.E. Cole****, None.*

M108

TACT Study: Spinal Pain and Height Loss: Diagnostic Value for Screening of Osteoporotic Vertebral Fractures in Women over 65 Years of Age. J. Fechtenbaum[1], C. Roux[1], C. Benhamou[2], P. Ravaud*[3], S. Brin*[4], F. Coriat*[4], S. Horlait*[5]. [1]Rheumatology, Cochin Hospital, Paris, France, [2]Rheumatology, Porte Madeleine Hospital, Orléans, France, [3]Biostatistics and Clinical Epidemiology, Bichat Hospital, Paris, France, [4]Aventis, Paris, France, [5]Procter et Gamble, Neuilly sur Seine, France.

Introduction : Two thirds of osteoporotic vertebral fractures are thought to be asymptomatic. These fractures are associated with increased risk of future vertebral and non-vertebral fractures. Several treatments have demonstrated a clear benefit in postmenopausal women presenting with such fractures. Therefore, it is useful to specify the indications and usefulness of spinal x-rays in screening for vertebral fractures. The aim of this study was to evaluate the sensitivity and specificity of recent spinal pain and its location, on one hand, and height loss >3 cm, on the other hand, in ambulatory women over 65 years of age, for the diagnosis of osteoporotic vertebral fractures. Patients and methods : Female patients who consulted a rheumatologist in private practice regardless of the reason and who presented with an episode of thoracic or upper lumbar pain (TULP) or lower lumbar pain (LLP) within the previous six months were recruited. Female patients with documented fractures were excluded. Patients in the two groups (TULP and LLP) were matched for age. Standardized x-rays of the thoracic and lumbar spine were performed on each patient, with centralized reading. Patients' height was measured and compared to height reported at age 25 years. Results : 114 female patients (57 per group) 74 ± 5 years of age were enrolled. In this ambulatory patient population, at least one vertebral fracture was noted in 23.7 % of the patients. In the TULP group, 26.3 % presented with one vertebral fracture; this percentage was 21.1 % in the LLP group. Sensitivity and specificity of localization of pain were 56 % and 52 % respectively (Likelihood ratio 1:15 ; 95 % CI 0.77-1.72). Among the female patients who lost > 3 cm, 27.5 % had at least one vertebral fracture, versus 13.8 % in those whose height remained stable. The sensitivity of height loss was 85 % while the specificity was 30 % (LR 1 :21 ; 95% CI % 0.98-1.50). Conclusion : The prevalence of vertebral fractures in ambulatory women over 65 years of age, who presented with spinal pain within the previous six months, and who consulted a rheumatologist regardless of the reason was 23.7%. Localization of pain (thoracic or lumbar spine) has no diagnostic value. This study confirms the good sensitivity of height loss for screening of vertebral fractures in such a population.

Disclosures: ***C. Roux****, None.*

M109

The Number of Canadian Men and Women Needed to be Screened to Detect a Case of Osteoporosis: A Population-Based Study from the Canadian Multicentre Osteoporosis Study (CaMos). A. M. Sawka[1], L. Thabane*[2], A. Papaioannou[3], A. Gafni*[2], G. Ioannids[4], D. A. Hanley[5], E. Papadimitropoulos[6], L. Pickard[4], J. D. Adachi[4], C. Investigators*[7]. [1]Endocrinology, McMaster University, Hamilton, ON, Canada, [2]Clinical Epidemiology and Biostatistics, McMaster University, Hamilton, ON, Canada, [3]Medicine, McMaster University, Hamilton, ON, Canada, [4]Rheumatology, McMaster University, Hamilton, ON, Canada, [5]Endocrinology, University of Calgary, Calgary, AB, Canada, [6]Eli Lilly, Toronto, ON, Canada, [7]Canadian Multicentre Osteoporosis Study, Hamilton, ON, Canada.

The Osteoporosis Society of Canada has recommended routine screening of men and women ≥65 years of age for osteoporosis by measurement of bone mineral density (BMD) at the spine and hip. However, the efficiency of routine population-based screening of Canadians of both genders is not known. Our goal was to determine the number of Canadian men and women age ≥65 years as well as those age 55-64 years needed to be screened by BMD in order to detect a case of osteoporosis, using prevalence estimates from CaMos. CaMos is prospective population-based cohort study involving 9 sites across Canada. Regional participants were randomly recruited (stratified by age and gender). 5883 participants ≥55 years of age (1645 men and 4238 women) who underwent standardized baseline measurements of BMD at the hip (trochanter and femoral neck) and lumbar spine (L1-L4) using DXA were included in this study. The diagnosis of osteoporosis was based on a T-score ≤ 2.5 at any site. Of the participants studied, 2143 people (36.4%) were age 55-64 years and 3740 (63.8%) people were ≥65 years of age). The prevalence of osteoporosis in men was as follows: age 55-64 years - 3.9% (95% confidence interval [CI], 2.6, 5.8) (24/612), age ≥65 years - 9.0% (95% CI, 7.4, 10.9) (93/1033). The prevalence of osteoporosis in women was as follows: age 55-64 years - 12.3% (95% CI, 10.7, 14.0) (188/1531), age ≥65 years - 25.9% (24.2, 27.5) (700/2707). The number of men needed to be screened by BMD measurement in order to detect one case is: age 55-64 years - 25 men (95% CI, 17, 38), age ≥65 years - 11 men (95% CI, 9, 14). The number of women needed to be screened in order to detect one case is: age 55-64 years - 8 women (95% CI, 7, 9), age ≥65 years - 4 women (95% CI, 4,4). In conclusion, screening of women ≥65 years by measurement of BMD of age is the most efficient. The efficiency of BMD screening of men age ≥65 years and women age 55-64 years is similar but inferior to screening of older women.

Disclosures: ***A.M. Sawka****, None.*

M110

A Population-based Study of Osteoporosis Testing and Treatment Following Introduction of a New Bone Densitometry Service. W. D. Leslie[1], L. Lix*[2], L. MacWilliam*[2], G. Finlayson*[2], P. A. Caetano*[3]. [1]Faculty of Medicine, University of Manitoba, Winnipeg, MB, Canada, [2]Manitoba Centre for Health Policy, University of Manitoba, Winnipeg, MB, Canada, [3]Faculty of Pharmacy, University of Manitoba, Winnipeg, MB, Canada.

Bone density measurement plays a key role in the initial diagnostic assessment of osteoporosis and for targeting pharmacologic therapies. However, the impact of access to dual x-ray absorptiometry (DXA) on physician prescribing habits remains unclear. The objective of this study was to directly evaluate the change in physician osteoporosis testing and prescribing following the introduction of a DXA testing service in a geographic region that previously had very limited access. Manitoba has a provincially-based bone density testing program and maintains a population-based bone density database that can be linked with other provincial health databases. Manitoba was geographically partitioned into the urban and rural health regions serviced by the new DXA (URBANnew and RURALnew) and compared to health regions which had relatively unchanged DXA access during this period (URBANcontrol and RURALcontrol). Regression models of DXA testing rates and osteoporosis prescription rates were created for all women over 50 years of age in these regions. There was a statistically significant increase in bone density testing and BMD-guided osteoporosis treatment in the URBANnew and RURALnew regions after introduction of the DXA testing service relative to the control regions. There were no significant changes in overall prescribing rates for any group. When analysis was limited to non-hormonal agents a significant reduction in preventive and empiric post-fracture treatment emerged in some subgroups of women. Access to bone density testing led to an increase in both testing and BMD-guided osteoporosis treatment initiation, with a decrease in the use of newer non-hormonal osteoporosis agents for preventive and empiric treatment in some subgroups. This would be expected to translate into more cost-effective targeting of treatment, particularly for newer, more expensive agents.

Disclosures: ***W.D. Leslie****, None.*

M111

The Prevalence of Osteoporosis in Japan - A longitudinal Cohort Study in Tottori, Japan. H. Katagiri*[1], H. Hagino*[2], R. Teshima*[1]. [1]Orthopedic Surgery, Tottori University, Yonago, Tottori, Japan, [2]Rehabilitation Division, Tottori University, Yonago, Tottori, Japan.

As the elderly population increases, osteoporosis has become an increasingly serious problem. It is well known that age-related bone loss has a great influence on development of osteoporosis. Early diagnosis of bone loss is important to prevent osteoporosis and osteoporosis related fractures. However, there have been few longitudinal studies of bone mineral density (BMD) in Japan. This study investigated the change in bone mass with aging and predicted the magnitude of age-related bone loss and the prevalence of osteoporosis (defined as calcaneus BMD <70% of the young adult mean) in a sample of Japanese men and women.

We examined BMD and age-related bone loss of the calcaneus in a cohort of Japanese men and women living in Tottori, Japan. The longitudinal studies included 160 men aged from 30-85 and 385 women aged 29-83 who had two bone mass measurements during 3 years. The bone measurement was performed using single X-ray absorptiometry (SXA).

In men calcaneal bone loss rate remained essentially constant from the forties. The loss rate among women in their fifties were greater than those in their forties and sixties. The longitudinal reduction in calcaneus BMD among women in their forties and seventies was similar to the men's data.

The prevalence rates of osteoporosis increased progressively with age. Eleven of the 160 males were diagnosed with osteoporosis. As for females, 185 of the 385 subjects were diagnosed with osteoporosis.

The prevalence rate diagnosed at the calcaneus seemed to be higher in the present study than that diagnosed by the spine BMD. This study suggests that the different definitions of osteoporosis should be established for the different skeletal sites.

Prevalence of osteoporosis in Japan

	Men		**Women**	
Age group	N	%	N	%
40-49	0/4	0	0/24	0
50-59	0/22	0	14/80	17.5
60-69	3/68	4.4	86/162	53.1
70-79	4/45	8.9	79/98	80.6
total	11/160	6.9	185/385	48.1

Disclosures: ***H. Katagiri****, None.*

M112

Hip, Spine and Total Body BMD Measurements in Children Using the Lunar Prodigy. H. Fors*, D. Swolin Eide*, S. Valdimarsson*, I. Bosaeus*, K. Albertsson Wikland*. GP-GRC, Institute of the Health of Women and Children, Sahlgrenska Academy of Göteborg University, Göteborg, Sweden.

Measurement of bone mineralisation in children has become important in clinical endocrinology and endocrine research. At the Göteborg Pediatric Growth Research Center children and adolescents with growth hormone disorders and diabetes are frequently measured with a DXA (Dual-energy X-ray absorptiometry) system to monitor their bone density and body composition. Recently, we purchased a new bone densitometer, the Lunar Prodigy, together with a new pediatric software package that takes into account biological/developmental age of the child. In addition, the femur program automatically adjusts the size of the neck, trochanter and shaft regions of interest (ROI) depending on the child's height.

In this study we evaluated the performance of this new pediatric software and the accuracy of the new Lunar Prodigy in comparison to our previously used Lunar DPX-IQ.

Thirty nine children (29 boys and 10 girls) with ages ranging from 6 to 20 years had a AP-spine and total body BMD measurement with both the Lunar Prodigy and the Lunar DPX-IQ (GE Healthcare). Fifty children (37 boys and 13 girls) with ages ranging from 3 to 20 years had a femur scan with the Lunar Prodigy using the new pediatric femur software. Accuracy was determined with linear regression analysis to compare Prodigy vs. DPX-IQ results. Bland-Altman plots were used to detect any systematic differences between Prodigy and DPX-IQ measurements.

Very strong correlations were obtained for the BMD measurements with the Prodigy and the DPX-IQ at the spine and total body (r=0.99) with small SEE values (0.019 g/cm^2 and 0.015 g/cm^2 respectively). Bland Altman plots showed no significant biases with mean BMD. The automatic adjustment of the femur ROI with subject height performed well: e.g. the width of the neck ROI changes from 1.0 cm for subjects smaller than 91cm (3 feet) to 1.5 cm for subjects taller than 152 cm (5 feet, see figure). The three new graphs that report in centile the subject's height for age, BMC for bone area, and bone area for height are useful in identifying those children with potential developmental problems.

We conclude that the new pediatric software on the Prodigy performed well for measuring BMD at the hip, spine and total body in children with a wide range of ages.

Automatically resized pediatric femur ROI as a function of the child's height

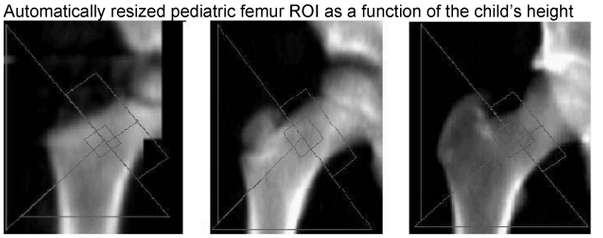

Girl 88 cm tall
Width neck box =1.0 cm

Boy 125 cm tall
Width neck box =1.28 cm

Boy 174 cm tall
Width neck box =1.5cm

Disclosures: ***H. Fors****, None.*

M113

Screening Men 70 Years and Older for Osteoporosis: Are We Missing Osteoporosis in Younger Men? R. A. Adler[1], V. I. Petkov*[1], P. S. Via*[2], M. I. Williams*[3]. [1]Endocrinology, McGuire Veterans Affairs Medical Center/ Virginia Commonwealth University School of Medicine, Richmond, VA, USA, [2]Endocrinology, McGuire Veterans Affairs Medical Center, Richmond, VA, USA, [3]Endocrinology, McGuire Veterans Affairs Medical Center/ Virginia Commonwealth University School of Pharmacy, Richmond, VA, USA.

The International Society of Clinical Densitometry (ISCD) recommends that men 70 years and older should be routinely screened for osteoporosis by dual energy X-ray absorptiometry (DXA). The purpose of this study was to compare the prevalence of osteoporosis and osteopenia in men who were referred for bone density testing because of high or moderate osteoporosis risk as determined by the Osteoporosis Self Assessment Tool (OST). OST, calculated by the simple formula 0.2 X [age - weight (kg)], identifies subjects likely to have low bone mass. We compared using OST to using age $\geq$ 70 to screen asymptomatic men.

We analyzed data from an interventional trial on improving osteoporosis diagnosis in Primary Care Clinics at a Veterans Affairs Medical Center. Men (N = 410) who had a BMD test due to high (< -2) or moderate (-2 to 3) OST risk score were categorized by age (< 70 and $\geq$ 70 years). Proportions of osteoporotic and osteopenic patients were compared using two-sided Fisher's exact test.

The mean age was 61.5 (8.0) and 76.7 (11.3) years for the younger and older group. The younger group had significantly lower weight (73.7 vs. 77.6 kg). T-scores were similar in the hip, significantly higher at the lumbar spine in the older group (-0.4 vs. -0.8), but lower at the forearm (-1.4 vs. -1.0).

In both age groups, about 1/3 had osteoporosis and about 1/2 had osteopenia. Thus, using only age as a criterion for DXA referrals in men leads to substantial under-diagnosis. Adding weight by using the OST formula identifies both younger and older men with osteoporosis, particularly if forearm measurements are also considered.

Table. Osteoporosis classification in men by age group

	Age < 70 (N=132) %	*Age $\geq$ 70 (N=278) %*
TH, FN, Troch, or LS		
Osteoporosis (T-score $\leq$ -2.5)	27.7	24.1
Osteopenia (T-score -1 to -2.49	48.8	56.8
Normal (T-score > -1)	23.5	19.1
TH, FN, Troch, LS or FA*		
Osteoporosis	33.3	35.3
Osteopenia	45.5	51.0
Normal	21.2	13.7

* TH = total hip, FN = femoral neck, Troch = trochanter, LS = lumbar spine, FA = forearm

Disclosures: ***R.A. Adler,*** *None.*

M114

Comparison of BMD and %Fat in Adults and Children with the DPX-L and Prodigy Densitometers. P. Kooij*[1], F. Rivadeneira[2], M. Zillikens*[2], J. Sluimer*[1], E. Krenning*[1], H. Pols[2]. [1]Department of Nuclear Medicine, Erasmus MC, Rotterdam, Netherlands, [2]Departments of Internal Medicine and Epidemiology & Biostatistics, Erasmus MC, Rotterdam, Netherlands.

Replacing older densitometer systems with newer and better performing ones is a big obstacle for the assessment of bone mineral density (BMD) and body composition in both the clinical and research setting. At the Erasmus Medical Center, two older generation pencil-beam densitometers (Lunar DPX-L, GE Healthcare) have been used: one system (DPX1) for the study and evaluation of adult and pediatric patients and another (DPX2) used for research within the Rotterdam study (a population-based prospective study of disease and disability in elderly men and women age 55 years and over). Moreover, a large local pediatric reference database has been collected on the DPX1. Recently, both DPX-L systems have been replaced by Lunar Prodigy systems (a new generation narrow fan beam densitometer). Therefore, this study aimed to evaluate the cross-calibration of the Prodigy and DPX-L systems, in order to allow comparison of follow-up data across densitometers and to implement the pediatric reference database in the new system.

For the DPX1 and Prodigy1 systems, AP spine and femur scans were measured in 96 adults, and AP spine and total body scans were measured in 30 children. For the DPX2 and Prodigy2 cross-calibration, a random sample of 105 participants of the Rotterdam study had AP spine and femur scans measured on both systems. Cross-calibration methods included linear correlations and Bland-Altman comparisons.

Results correlated very well for all BMD sites in adults and children (table). In both comparisons, the highest correlation was observed at the lumbar spine. Femoral neck correlations were comparatively lower in the DPX2 - Prodigy2 than in the in the DPX1 - Prodigy1 comparison. Pediatric body composition (fat %) also observed a high correlation.

We conclude that BMD results from DPX-L and Prodigy systems can be cross-calibrated across pediatric, adult and elderly populations. Furthermore, based on this calibration the local Rotterdam pediatric reference database for BMD and fat% can be adapted for the Prodigy system.

	Scan site	Subjects F / M		Age (in years)	Pearson Correlation	Slope	Intercept
DPX1 vs. Prodigy1	AP-spine (29 children + 96 adults)	72	53	C: 9.1 (± 3.6) A: 50.1 (± 15.8)	0.991	0.987	-0.012
	Femur Neck (adults)	59	35	50.6 (±15.6)	0.972	0.976	0.040
	Total body BMD (children)	13	16	9.1 (± 3.6)	0.991	1.000	-0.018
	Total body % fat (children)	13	16	9.1 (± 3.6)	0.970	1.050	0.031**
DPX2 vs. Prodigy2	AP-spine	67	37	77 (± 6)	0.978	0.998	0.015
	Femur Neck	67	33		0.953	0.889 *	0.103**
	Femur Trochanter	67	34		0.956	0.939 *	0.002

*Slope significantly different from unity
**Intercept significantly different from zero

Disclosures: ***M. Zillikens****, None.*

M115

Bone Mineral Density of Healthy Premenopausal Women of South India. U. Sriram*. Endocrinology, EV Kalyani medical center, Chennai, India.

Bone mineral density of apparently healthy south premenopausal women were studied. This study was undertaken to both establish the reference data for peak bone mass and to document the bone density in the pre and perimenopausal years. we rcruited women from the community between the ages of 20 and 49 with no prior history of metabolic bone disease and not on any treatmnet with bisphosphonates, selective estrogen receptor modulators, Teriparatide, Calcitonin or hormone replacement therapy. The women were recruited through corporate offices, the southern railways employee labor union and their relatives. Some were recruited by word of mouth.

BMD was measured in the spine, left hip and forearm using Hologic DXA. The results obtained are shown in a table. There were 249 women who were part of this study. The number of women between the ages of 20- 29 was 75, between 30-39 was 76 and between 40-49 was 98. The BMD of the peak adult bone mass group [20-29] was 0.93328 in the spine and 0.807213 in the hip. The BMD for the 30-39 group was 0.9614 in the spine and 0.879786 in the hip. The BMD for the 40-49 age group was 0.935112 in the spine and 0.7815 in the hip.

This study documents the normative data for healthy premenopausal women of South India.

BMD of premenopausal women

Age	Number	Spine BMD	Hip BMD
20-29	75	0.93328	0.80721
30-39	76	0.9614	0.8276
40-49	98	0.923487	0.7815

Disclosures: ***U. sriram****, None.*

M116

Bone Mineral Density of Healthy Men and Women of South India between the Ages of 20 and 50. U. Sriram*. Endocrinology, EV Kalyani medical center, Chennai, India.

Bone mineral density was studied in apparently healthy women of South India . This study was undertaken both to establish refence data base for peak bone mass and to study the effect of age on BMD. We recruited women from the community between the ages of 20 and 49 with no history of metabolic bone disease and not on any treatment with bisphosphonates, selective estrogen receptor modulators, teriparatide , calcitonin or hormone replacement therapy. The women were recrited through corporate offices, the Southern railways office labor union and their relatives and by word of mouth..

BMD was measured at the left hip, spine and forearm using Hologic DXA. The results obtained have been shown in a table. The total number of women studied were 259 . Between the ages of 20-29 there were 75 women, 76 between the ages of 30-39, 98 betwen the ages of 40-49. The BMD of the peak adult bone mass age group [20-29] was 0.93328 in the spine and 0.807213 in the hip. The BMD for the 30 -39 age group was 0.9614 in the spine and 0.879786 in the hip. The BMD for the 40-49 age group was 0.935112 in the spine and 0.7815 in the hip.

This study documented normative data for healthy premenopausal south Indian women.

BMD of women 20-49 years

Age	Number	Spine BMD	Hip BMD
20-29	75	0.93328	0.80721
30-39	75	0.9614	0.8276
40-49	98	0.923487	0.7815

Disclosures: ***U. sriram****, None.*

M117

Are Tissue Facsimile Bags Necessary for DXA Measurements? N. C. Grinnell*, T. M. DeFrancisco*, S. M. Strot*, L. Cole*, E. A. Mossman, M. R. McClung. Oregon Osteoporosis Center, Portland, OR, USA.

DXA of the hip and lumbar spine is commonly accepted as the standard technique for measuring bone mineral density to aid in the diagnosis of osteoporosis, help assess fracture risk, and monitor therapy. The analysis software used by DXA instruments distinguishes bone from the surrounding tissue using algorithms designed to detect the edges of the bone. In measurements of the hip where there is insufficient soft tissue surrounding the bone, air spaces, commonly referred to as air points, between the patient and the instrument can cause errors in these algorithms. In the past when such errors occurred, tissue facsimile bags (TFB) were placed under the hip to eliminate these spaces and the scan was repeated. The manufacturers of modern DXA instruments currently claim that air points appearing in the analysis in areas of tissue will be labeled as artifact in the instrument software, and that tissue facsimile bags are unnecessary. It is unclear what effect not using the tissue facsimile bags has on measured BMD values. This study was designed to determine if there is a systematic difference in measured BMD between simply allowing the air points to be labeled as artifact in the DXA software and re-scanning the hip using tissue bags.

We analyzed electronic records from patients referred to our clinic for DXA testing who had a hip DXA scan on a single Lunar Prodigy densitometer (GE Lunar, Madison, WI) repeated with tissue facsimile bags due to the presence of air points in the first hip image. A total of 31 women and 19 men were included in the analysis. Average age at the time of the scan was 65.8 years. Mean total hip (TH) BMD for the first scan in which the air points appeared and were labeled by the DXA software as artifact was 0.778 g/cm^2, and mean TH BMD for the second scan using tissue facsimile bags was 0.774 g/cm^2. These differences were not significant by paired t-test ($p=0.235$). However, when the results were analyzed by gender, the BMD values in men were significantly lower with tissue facsimile bags than without (mean difference 0.10 g/cm^2, $t=3.99$, $p<0.001$). The BMD values in women were not significantly affected by the use of the tissue bags ($p=0.479$). These results suggest that the use of tissue facsimile bags may be still be appropriate for some patients, even on newer densitometers.

Disclosures: ***N.C. Grinnell****, None.*

M118

Gene Expression Regulated by Physical Contact between Prostate Cancer Cells and Osteoblasts in a Heterotypic Co-culture System. J. Wang*, A. S. Levenson*, K. E. Thurn*, L. A. Simons*, R. L. Satcher. Department of orthopaedic surgery, Northwestern University, Chicago, IL, USA.

Bone is the most common target of prostate cancer metastasis. The molecular mechanisms of bone metastases involve in bi-directional interactions between prostate cancer cells and bone cells. In addition to interaction mediated by soluble factors, physical contact is an important step in metastasis formation and progression.

Several in vitro co-culture models were used to study the interaction between cancer cells and osteoblasts, such as cell culture with conditioned medium or co-culture with inserts (bi-compartmental culture system). These models can only detect the effects of soluble factors. In order to identify factors that are regulated in response to physical contact between cancer cells and osteoblasts, we established a heterotypic co-culture system containing prostate cancer cells PC-3 and primary osteoblasts derived from rat bone marrow. PC-3 cells were labeled with Vybrant CFDA SE fluorescent reagent before they were co-cultured with osteoblasts. Different ratios (1:100, 1:10, 1:1 and 10:1) between PC-3 cells and osteoblasts mimicked the different stages of metastasis development. The proportion of co-cultured cells was quantified with flow cytomytric analysis to explore the regulation of proliferation. In order to detect the effects of physical contact on gene expression, PC-3 cells and osteoblasts were co-cultured with inserts (bi-compartmental) or without inserts (heterotypic). The cells in heterotypic co-culture system were then re-separated with mag-

netic-activated cell sorting (MACS). Epithelial cell-derived PC-3 cells were positively selected by magnetic microbeads conjugated with antibody against human epithelial antigen (HEA). Differential gene expression in MACS-separated prostate cancer cells and osteoblasts was analyzed by Northern blot.
The results showed that proliferation of PC-3 cells in heterotypic co-culture was interrupted at ratios 1:100 and 1:10, which represented early stage of metastasis. Proliferation of BMSC was suppressed at ratio 10:1, which mimicked late stage of metastasis. The peak expression level of uPA in PC-3 cells was found at ratio 1:1. The expression of insulin growth factor binding protein-3 was down-regulated in bi-compartment co-culture, while it is much lower in heterotypic co-culture. In contrast, the expression of osteopontin and osteonectin in osteoblasts was not effected by physical contact. This heterotypic co-culture system set a fundamental to identify factors in response to physical contact.

Disclosures: ***J. Wang****, None.*

M119

Assessment of Vertebral Fractures in Post-Meopausal Women by Topological Analysis of High Resolution MRI of the Distal Radius in 2D and 3D Using Bone Mineral Density and Linear Texture Measures as a Standard of Reference. H. F. Boehm*[1], T. M. Link[2], R. A. Monetti*[3], D. Mueller*[1], E. J. Rummeny*[1], G. Morfill*[3], C. W. Raeth*[3]. [1]Radiology, TU-Munich, Munich, Germany, [2]Radiology, UCSF, San Francisco, CA, USA, [3]Institut fuer Extraterrestrische Physik, Max-Planck-Society, Garching, Germany.

Topological texture measures based on the Minkowski Functionals (MF) in 2D and 3D have successfully been employed to predict the mechanical competence of trabecular bone in-vitro.
In this in-vivo study, the MF in 2D and 3D are used to characterize the micro-structure of the distal radius in post-menopausal women as depicted by high-resolution magnetic resonance imaging (HRMRI) for identification of patients with vertebral fractures. Results are compared with bone mineral density (BMD) and standard texture measures in 2D, i.e. apparent trabecular separation (app.Tb.Sp) and apparent trabecular bone volume fraction (app.BV/TV).
HRMRI of the distal radius in 36 age-matched post-menopausal women (age 66 +/- 6 yrs) were obtained at 1.5 T using a 3D gradient-echo sequence with a spatial resolution of 195 x 195 x 500 µm. 23 of the women had vertebral fractures as diagnosed on lateral radiographs of the spine. BMD was measured by quantitative computed tomography in the lumbar spine.
From the image data, the MF in 2D {3D} corresponding to area, perimeter, and Euler-Number {volume, surface, mean integral curvature, and the Euler Number} were obtained as a function of gray-level threshold. In order to assign a scalar quantity to each image set, an optimised filtering procedure using two independently sliding windows of variable width was employed. As a standard of reference, linear texture measures in 2D were extracted from the image data.
The predictive potential of BMD, the linear and the topological texture measures was expressed using the receiver operator characteristic (ROC), validation of results was achieved by leave-one-out (LOO) analysis.
Mean values of BMD, linear and topological measures significantly differed for the fracture group and the controls ($p < .05$). When employing ROC-analysis for identification of fracture patients, an area-under-the-curve (AUC) of .73 was found for BMD, AUC for the linear measures ranged from .60 (app.BV/TV) to .65 (app.Tb.Sp), whereas the topological measures resulted in an AUC of .78 (2D) and .79 (3D).
In conclusion, topological descriptors are well suited to identify patients with vertebral fractures by texture analysis of HRMRI of the distal radius. Texture measures based on the MF in 2D and 3D are equally reliable. The diagnostic performance of topological analysis is superior to bone densitometry and linear texture measures.

Disclosures: ***H.F. Boehm****, None.*

M120

Monitoring of Changes in Structural Cancellous Bone Parameters over Time with the Novel vivaCT40 in Anesthetized Rodents. J. A. Gasser[1], P. Ingold*[1], B. Koller*[2], G. Schett*[3]. [1]Musculoskeletal Research, Novartis Institutes for Biomedical Research, Basel, Switzerland, [2]Scanco Medical AG, Bassersdorf, Switzerland, [3]University of Vienna, Vienna, Austria.

Characterization of trabecular bone structures requires necropsy of animals followed by a labor intense histomorphometric or *ex vivo* microCT analysis. We tested the novel *in vivo* microCT vivaCT40 from SCANCO Medical AG (Bassersdorf, Switzerland), which allows to monitor such changes at a maximal resolution of 10µm and a total acquisition time of less than 15 minutes repeatedly in anaesthetized rats and mice. The scanner allows to accurately measure trabecular architecture with a reproducibility better than 0.2%.
Postmenopausal Osteoporosis: In 8 month old ovariectomized (OVX) rats, the vivaCT40 was capable to pick up the decrease in trabecular bone volume, the trabecular thinning as well as the decrease in the number of trabecular elements as a function of time at 0, 1, 2, 4, 8, 12, and 16 weeks post OVX. The bone anabolic effects of parathyroid hormone [hPTH(1-34)] as well as the bone protective effect of the two antiresorptive agents zoledronic acid and 17-α ethinylestradiol were detected correctly with the vivaCT40.
Imaging & Rheumatoid Arthritis: Imaging of subtle erosive lesions such as those occurring in subchondral bone and around the growth plate in the proximal tibia of TNFα-transgenic mice was easily possible. We were also able to detect trabecular bone loss caused by periarticular inflammation in a rat model of adjuvans arthritis and demonstrate the bone protective effect of dexamethasone on structural integrity.
Tumor Osteolysis: The vivaCT40 allowed monitoring of the osteolytic response caused by the local administration of 4T1luc2000 tumor cells into the tibia metaphysis of nude mice. The potent protective effect of zoledronic acid on tumor osteolysis was demonstrated. The new vivaCT40 is capable to monitor the effects of known agents and diseases such as osteoporosis, inflammatory arthritis and tumor invasion on 3D-trabecular microarchitecture accurately, repeatedly, reliably and quickly in more than 25 anaesthetized rats and mice per day. The scanner represents a breakthrough for large scale non-invasive imaging and 3D-structural measurements in anesthetized small rodents.

Disclosures: ***J.A. Gasser****, None.*

M121

Modelling Trabecular Changes using Cellular Automata. C. Raeth[1], R. Monetti*[1], D. Mueller*[2], T. Link[3], H. Boehm*[2]. [1]Theory Division, CIPS/MPE, Garching, Germany, [2]Radiology, TU-Munich, Munich, Germany, [3]Radiology, UCSF, San Francisco, CA, USA.

Cellular automata (CA) have intensively been employed to model nonlinear phenomena by numerically solving differential equations governing the underlying (bio-)physical processes of the system. We propose a novel approach to simulate bone remodelling processes using probabilistic CAs. Bone remodelling processes including the effects of mechanical forces on the adaptation of form in trabecular bone can be described by nonlinear rate equations, which model the effects of osteoclasts and osteoblasts on the local change of the relative bone density (Huiskes et al., Nat., 405, 704). The differential equations can be solved numerically using CAs. CAs are discrete dynamical systems whose behaviour is specified in terms of local relations. Space is represented by a uniform grid and time advances in discrete steps. The physical laws expressed in the differential equations are transformed to local rules with which at each step each cell computes its new state from that of its close neighbours. A two-dimensional realization of a CA for bone remodelling processes is presented: Bone pixels are defined by applying a threshold to the bone density distribution. Within the bone pixels the loaded skeleton, i.e. the connected lines, which transfer the forces, is determined and the local strain is calculated. Bone resorption (spatially random) and bone formation (strain-dependent) at the bone surface is simulated. Various configurations (e.g. different direction of the external force) for the CA and the effects of (slight) changes in the control parameters (e.g. sensitivity of osteoblasts to local strain) are studied. We show that trabecular structures emerge from a uniform distribution whereby the alignment of the trabeculae follows the direction of the forces acting on the bone (Wolff's law). The configuration is stable with a mean relative bone density of mrbd=.42 (arbitrary units). Slightly decreasing the sensitivity of osteoblasts to local strain results in a new stable configuration with lower bone density (mrbd= .36) and rarefied trabecular structure. Recently introduced texture measures (e.g. scaling indices and Minkowski Functionals) can account for the structural changes. The variations of them are comparable to those observed in vitro and in vivo. Bone remodelling processes can well be described within the framework of CAs. They can account for trabecular changes induced by variation of control parameters. Therefore these models offer the possibility to investigate drug-effects 'in silicio' and to analyse systematically the sensitivity of texture measures to slight changes in the bone structures.

Disclosures: ***C. Raeth****, None.*

M122

Three-dimensional Analysis of Trabecular Bone Structure of Human Vertebra in Vivo Using Image Data from Multi-detector Row Computed Tomography-correlation with Bone Mineral Density and Ability to Discriminate Women with Vertebral Fractures. M. Takada[1], K. Kikuchi*[2], S. Imai*[2], K. Murata*[1]. [1]Radiology, Shiga University of Medical Science, Otsu, Japan, [2]Orthopaedic Surgery, Shiga University of Medical Science, Otsu, Japan.

We developed a system to perform three-dimensional (3D) analysis of trabecular bone structure of human vertebra in vivo using image data from multi-detector row computed tomography (MDCT). The purpose of this study was to evaluate whether 3D structural parameters correlate with bone mineral density (BMD) of human vertebra, and whether they can discriminate women with vertebral fractures. We studied 20 women with no vertebral fractures (67±8 years old) and 27 women with vertebral fractures (74±7 years old). They underwent lumbar examinations by MDCT and dual x-ray absorptiometry (DXA). L3 was scanned using MDCT, Somatom Plus 4 Zoom (Siemens, Erlangen, Germany) at 140Kv and 170mAs by a slice thickness of 0.5mm and L2-4 BMD was assessed using Lunar DPX-L (General Electrics, Milwaukee, WI, USA). The CT images were reconstructed using a field of volume of 50mm x 50mm with 0.2mm interval, and were resulted in a spatial resolution of 0.097mm x 0.097mm on x-y axes with overlap of 0.3mm along z-axis. The CT image data was imported into software of 3D analysis for trabecular bone structure, TriBON (Ratoc System Engineering, Tokyo, Japan) and a 3D image was constructed. A cubic region of interest for analysis was extracted after the images containing the upper and lower endplates were excluded. The following 3D parameters were calculated; trabecular bone volume fraction (BV/TV), trabecular thickness (Tb.Th), trabecular number (Tb.N), trabecular separation (Tb.Sp), trabecular bone pattern factor (TBPf), structure model index (SMI), and Fractal dimension (FD). L3 BMD was used for data analysis. Correlation between structural parameters and BMD was evaluated by linear regression analysis, and discrimination between women with and without vertebral fractures was evaluated by student t' test. A p-value of less than 0.05 was considered significant. The BMD was significantly correlated with the values of BV/TV, Tb.Sp, TBPf, SMI and FD with correlation coefficients of 0.30, 0.32, -0.46, -0.44 and 0.36, respectively. The values of TBPf, SMI and FD significantly differed between the two groups with t-values of 2.6, 3.2, and 2.4, respectively, but the L3 BMD did not differ. The results suggested that trabecular bone structure correlated with BMD and that the trabecular bone structural analysis could discriminate women with vertebral fracture better than lumbar DXA in this population. This technique appears to be useful for assessing osteoporosis in human vertebra in vivo.

Disclosures: ***M. Takada****, None.*

M123

A Model Based Anaysis to Study Mechanical Properties of Bone and to Identify Non-invasive Diagnostics for Bone Strength. G. H. Gunaratne[1], M. Liebschner*[2], S. Wimalawansa[3]. [1]Physics, University of Houston, Houston, TX, USA, [2]Bioengineering, Rice University, Houston, TX, USA, [3]Medicine, Robert Wood Johnson Medical School, New Brunswick, NJ, USA.

Aging induces several types of architectural changes in trabecular bone including thinning, increased levels of anisotropy, and perforation. It has been determined, on the basis of analysis of mathematical models, that reduction in fracture load caused by perforation is significantly higher than those due to equivalent levels of thinning or anisotropy. This analysis has also provided an expression which relates the fractional reduction of strength to the fraction of elements that have been removed from a network. Further, it was proposed that the ratio of linear responses of a sample to uniform loading and high-frequency driving can be used as a surrogate for bone strength.

Unfortunately, experimental validation of these predictions requires following architectural changes in a given sample of trabecular bone; such a process cannot be implemented in human or animal studies with current technology. Instead, we use computer models constructed from digitized images of bone samples for the purpose. Images of healthy bone are subjected to successive levels of synthetic degradation via erosion of voxels that lie on the surface. Computer models constructed from these images are used to calculate their fracture load and other mechanical properties. Results from these computations validate predictions derived from the analysis of mathematical models.

Disclosures: ***G.H. Gunaratne****, None.*

M124

Orientation of Load Force Influences Mechanical Stability in the Human Scaphoid: Implications for Traumatic Fractures. D. S. Perrien, R. R. Bindra*, L. J. Suva. Departments of Orthopaedic Surgery and Physiology and Biophysics, University of Arkansas for Medical Sciences, Little Rock, AR, USA.

Fractures of the wrist occur most frequently in the scaphoid and account for approximately 70% of all carpal fractures. The scaphoid is composed of three anatomical regions: proximal pole, waist, and distal pole. Despite the high incidence of fracture in this bone, little information regarding the structural and mechanical properties of these three regions that may contribute to the differing fracture rates is known. The current study used microCT and finite element modeling (FEM) to investigate the hypothesis that inferior micro-architectural properties in the waist of the scaphoid were responsible for the high incidence of fracture in this region. Ten (10) intact scaphoids obtained from adult cadavers were scanned by microCT with a voxel size of 37 μm. Using 3-dimensional reconstructions of the whole bone, three 5-mm-thick regions of interest (ROIs) corresponding to the waist and proximal and distal poles were extracted from each specimen. In five of the bones, the ROI's were extracted perpendicular to the long axis of the bone and parallel to one another. For the other five bones, the ROIs were extracted at angles that were perpendicular to the natural curvature of the bone within the respective region. Standard three-dimensional morphometric analysis of the trabecular structure in all 30 ROI's demonstrated that BV/TV and trabecular number were highest in the proximal pole and lowest in the waist. To determine the mechanical integrity of each ROI, FEM was used to simulate a 'high-friction' compression test in which 500 N of compressive force was applied, and the displacement and tissue level strains were calculated. This analysis revealed that when the ROIs were taken at right angles to the natural curve of the bone, the waist consistently experienced the greatest displacement and tissue level strain during compression. In contrast, if the ROI's were taken at right angles to the long axis, the distal pole experienced the greatest displacement and strain. These results demonstrate that regardless of ROI orientation, the waist of the scaphoid consistently displays inferior micro-architectural properties. However, in spite of the poor architecture, mechanical insufficiency in the waist or distal pole appears to be dependent on the direction of the force applied. Hence, the mechanics of the trauma, in addition to microarchitecture, likely play an important role in determining the location of the scaphoid fracture. This analysis provides information critical for evaluating implant fixation, vascularity and mechanisms of fracture in the human scaphoid.

Disclosures: ***D.S. Perrien****, None.*

M125

Changes In Sublesional Bone Mineral Density/ Bone Architecture Amongst Women With Spinal Cord Injury: A Twin Study. B. C. Craven*[1], L. Giangregorio*[2], C. E. Webber[3]. [1]Medicine Toronto Rehab, University of Toronto, Toronto, ON, Canada, [2]Kinesiology, McMaster University, Hamilton, ON, Canada, [3]Nuclear Medicine, Hamilton Health Sciences, Hamilton, ON, Canada.

This study measured changes in bone mineral density (BMD), bone geometry and muscle cross-sectional area (CSA) in two sets of homozygous female twins, where one of each twin pair had a spinal cord injury (SCI). Twin Pair 1 (TP1) was premenopausal and 32 years of age. Twin pair 2 (TP2) was postmenopausal and 47 years of age. The SCI twin (TP1) had C7 tetraplegia and was 7 years post injury. The SCI twin (TP2) had T6 paraplegia and was >20 years post injury. BMDs of the proximal femur, distal femur, proximal tibia, and spine were measured using dual-energy x-ray absorptiometry (DXA). Computed tomography was used to measure volumetric BMDs, bone geometries and muscle CSAs of the thigh (mid-femur) and calf (proximal-tibia). Dramatic differences were noted when the SCI twin and non-SCI twin were compared. For TP1, the SCI twin's BMD of the total proximal femur, distal femur, proximal tibia and spine BMDs were 59.5%, 46.6%, 53.1% and 93.3% of their non-SCI twin. For TP2, the corresponding values for the SCI twin were 36.2%, 35.9%, 39.2% and 62.2% of their non-SCI twin. Average thigh and calf muscle CSAs of the SCI twins were 31.2±2.3% and 31.0±6.1% of the values for their non-SCI twins, indicating that muscle CSAs were reduced by almost 70%. Amongst the SCI twins, average volumetric BMD at the mid-femur and tibias were 83% and 87% of the values of their non-SCI twins. Maximum moments of inertia (I_{max}) at the mid-femur site were reduced in the SCI twins; 73.8±1.5% of the values for their non-SCI twins. In TP1, tibia I_{max} values in the right and left legs of the SCI twin were 67.6% and 79.7% of the non-SCI twin. For TP2, the SCI twin tibia I_{max} values were 97.9% and 88.4% of the non-SCI twin. Similarly, bone cross-sectional areas at the mid-femur site of the SCI twin were 66.8±0.1% of their non-SCI twin, whereas at the tibia site the differences were larger in TP1 than in TP2. The bone areas in the right and left legs of the SCI twin of TP1 were 62.3% and 67.5% of those of their non-SCI twin. In TP2, the corresponding values were 88.1% and 83.7%. Similar observations were noted for minimum and polar moments of inertia. Muscle atrophy and declining BMD are common consequences of SCI. This study reveals that important changes in bone geometry occur after SCI. The magnitude of these changes may depend on patient-specific variables such as lesion level, age at injury, time post injury or bone site measured.

Disclosures: ***B.C. Craven****, None.*

M126

Advances in Mechanical Response Tissue Analysis of the Human Tibia. C. E. Callaghan*[1], C. R. Steele*[2], S. M. Nickols-Richardson[1], W. K. Ramp[3], D. F. Wootten*[1], L. E. Miller*[1], W. G. Herbert[1]. [1]Virginia Tech, Blacksburg, VA, USA, [2]Stanford University, Stanford, CA, USA, [3]Health Research Group, Blacksburg, VA, USA.

Mechanical response tissue analysis (MRTA) provides a noninvasive means for estimating the cross-sectional bending stiffness (EI) of long bones utilizing impedance response to low frequency (60-1600Hz) vibration. Cross-sectional bending stiffness of a long bone is predictive (R^2>0.9) of the maximum breaking strength of the bone [Roberts *et al. J Biomech* 1996 Jan; 29(1):91-8]; thus, in vivo measurement of EI can be used to assess bone quality. MRTA has demonstrated good reliability (coefficient of variation: CV = 3-5%) in laboratory settings for measurement of the human ulna and monkey tibia, but due to the more complex geometry of the human tibia, reliability of in vivo measurements has been problematic. The purpose of this study was to evaluate sources of variability in EI estimation for the human tibia and explore methods of controlling this variability. The current MRTA prototype supports the foot and thigh, allowing for measurement while both proximal and distal ends of the tibia are free to vibrate within the joints without external restraint. Computer algorithms fit prediction curves to the raw impedance response data of the tibia and use these curves to estimate EI. The algorithm rejects measurements if the root mean square error between the prediction curve and the raw data is > 9%, indicating that the measurement was inadequate for accurate prediction estimates. To identify sources of variability in EI, data from 110 females (age 20.2 ± 1.8 yr, height 163.3 ± 5.9 cm, weight 60.7 ± 9.3 kg) were evaluated. Nine sequential MRTA measurements from the right and left tibiae of each subject were taken without repositioning. The initial algorithm yielded a within-trial CV of 11.2%. Analysis of these results revealed that some measurements were acceptable, although the EI values were unrealistic and that repeated measurements without repositioning could yield a wide range of EI values. These errors are partially based upon variability in curve fitting due to noise in the raw data at the upper frequency range, which can send the iterative algorithm toward an unrealistic bone mass and resonant frequency. Based upon the lower frequency data, there are five possible prediction curves for the upper frequency range. Our refined algorithm now allows for iteration through all five possible upper frequency prediction curves and incorporates realistic estimates of mass and resonant frequency into the selection and rejection of these curves. These refinements have allowed for improvement in within-trial reliability of EI estimation to a CV of 3.7%.

Disclosures: ***C.E. Callaghan****, None.*

M127

Variability of pQCT Measurement at the Distal Forearm: Influence of Voxel size, Region of Interest and Analysis Software. M. Ashe*, K. M. Khan, N. White*, P. Guy*, H. A. McKay. Orthopaedics/Family Practice, University of British Columbia, Vancouver, BC, Canada.

Peripheral quantitative computed tomography (pQCT) is a safe and precise technique to differentiate cortical from trabecular bone and assess both bone geometry and density. Currently, pQCT data acquisition and analysis protocols are seldom reported and there are no universal standards. Smaller voxel size (and slower scan speed) enhances scan resolution but increases scan time, radiation exposure and movement. The default voxel size is .4mm and .5mm. However, in a compromised skeleton where cortices are thin, lower resolution scans may result in an inability to detect the outer edge and analysis failure. Thus, the purpose of this investigation was to: 1) determine the effect of voxel size (and scan speed) on the determination of bone structure at the distal radius (4%) and 2) to compare the difference between the two most common pQCT software programs (XCT 550 and Geanie 2.1 Bonalyse). We obtained ten fresh-frozen right female radial cadaveric specimens (mean age 79 ± 6 years). Specimens were sealed in a plastic tube with normal saline for scanning. Bone measurements were performed with the Norland/Stratec XCT 2000 pQCT. Three contiguous 2.5mm slices were obtained at the 4% site of the radius using .2mm, .3mm, .4mm and .5mm voxel sizes. Scan speeds were 10 mm/sec for .2mm voxel; 15mm/sec for .3mm; 20mm/sec for .4mm voxel and 25mm/sec for the .5mm voxel. Scans were analyzed using XCT 550 (with 2 different region of interest (ROI) techniques; rectangular and automatic) and Geanie 2.1 Bonalyse software analysis programs. We used ANOVA to compare total bone area across voxel sizes and between analysis software. We experienced a mean analysis failure rate of 43% of the scans at the 4% (distal radius) using the standard rectangular ROI. This significantly improved to 24% using a custom automatic ROI (chi-square p<.01). Table shows total bone area at the 4% site using XCT 550 and Geanie 2.1 Bonalyse software. The lower resolution (.5mm voxel) had significantly more failures overall. Dif-

ference between the two software programs was 23%, on average. There was a difference between the software programs across voxel sizes. There is a need to establish standard reporting procedures for pQCT data acquisition and analysis protocols as results vary significantly depending on the acquisition, ROI and software.

Total Bone Area 4% site (mm2)

Voxel Size	XCT 550 (Custom ROI)	Bonalyse
.2mm	310.74±103.25	241.30±84.69
.3mm	307.26±97.71	246.80±87.52
.4mm	303.63±103.02	250.60±95.83
.5mm	277.88±133.46	254.70±101.18

Disclosures: ***M. Ashe****, None.*

M128

Use of Micro-CT in Comparison with DEXA for Rat Osteoporosis. E. M. Johnson*[1], C. G. Ambrose[2], H. Hogan[3], D. D. Cody[1]. [1]Imaging Physics, M.D. Anderson Cancer Center, Houston, TX, USA, [2]Orthopaedics, UTHSC Medical School, Houston, TX, USA, [3]Mechanical Engineering, Texas A&M University, College Station, TX, USA.

The aim of this study was to determine if Micro-CT could significantly improve the DEXA analysis of the OVX rat osteoporosis model**,** by evaluating BMD distribution and trabecular structure.

16 female rats 9 months old were randomly divided into two groups: OVX (n=6) and SHAM control (n=8). The proximal and distal regions of the right femur of each animal were scanned *in-vivo* using DEXA at baseline and 8 weeks post-OVX just prior to sacrifice.

The right femurs were excised and scanned using a Micro-CT at 27 μm voxel size. Trabecular bone architecture parameters and BMD values were evaluated within distal and proximal cancellous 3D regions of interest. Mechanical tests included three-point bending, femoral neck shear test, and distal cancellous bone compression. A third set of femurs was used for correlation of conventional histomorphometry to Micro-CT architectural data (trabecular thickness [TbTh], bone volume fraction [BVF], and bone surface to bone volume ratio [BS/BV]).

No DEXA parameters separated the OVX group from the SHAM group; however, Micro-CT was able to detect differences in cancellous bone architecture that were not apparent from DEXA. Statistical differences were observed between the OVX and SHAM groups for isolated distal cancellous bone architecture and mechanical compression strength variables. Cortical bone-influenced mechanical tests were not significantly different between the SHAM and OVX groups. Significant correlations were found between the mechanical tests and DEXA and Micro-CT imaging parameters. Regression models to predict mechanical properties had more significant predictive value when both Micro-CT and DEXA variables were included, as opposed to DEXA parameters alone. There was no significant difference between histomorphometric and Micro-CT-derived average TbTh or BS/BV results. Although BVF was significantly different among the paired values, this difference was due to sampling issues. Despite small sample sizes, mature rats, and only 8 week period between OVX and sacrifice, the overall hypothesis of this study was proven. *Ex vivo* Micro-CT imaging improved the discrimination of the OVX and SHAM femur characteristics over *in-vivo* DEXA examination alone. Although the OVX femurs, based on DEXA and cortical-influenced mechanical test results, did not appear to become osteoporotic, the two groups were definitively separated by distal cancellous material and Micro-CT measures. This may indicate that the distal cancellous is sensitive to a hormone-deficient state and could serve as an early marker for developing osteoporosis in the OVX rat model.

Disclosures: ***E.M. Johnson****, None.*

M129

Effect of Alendronate on Human Osteoporotic Spine Induced by Glucocorticoid -3D Microarchitectural Analyses in Vivo. T. Mawatari[1], H. Miura*[2], S. Hamai[2], T. Shuto*[2], Y. Nakashima*[2], R. L. Smith*[1], Y. Iwamoto*[2]. [1]Orthopaedics, Stanford University, Stanford, CA, USA, [2]Orthopaedics, Kyushu University, Fukuoka, Japan.

Disruptions of the cancellous bone architecture may be the earliest and most damaging skeletal lesions of osteoporosis and will produces a disproportionate loss of strength. The purpose of this study was to evaluate the effect of alendronate on 3D microarchitecuture of the human osteoporotic lumber spine in rheumatoid arthritis patients in vivo by using high-resolution computed tomography (HRCT). 18 postmenopausal rheumatoid arthritis (RA) patients (mean 61.8 years) who are receiving long-term glucocorticoid therapy (prednisone equivalent of >=5mg/day) and vertebral bone mineral density (BMD) T-score is below -1 measured by dual-energy x-ray absorptiometry were enrolled in this study and the whole body of the third lumber vertebra was scanned by HRCT at a spatial resolution of 351 x 351 x 500 micron. All the gray-value slice images were then noise-eliminated, segmented, and transformed to binary images. Preliminary experiments on the cadaveric human lumber spine were designed specifically to select the correct threshold value by using histologic sections. Finally, from the reconstructed 3D volume data, arbitrary-shaped volume which cover the whole trabecular space were extracted. A parametric analysis was carried out using bone-volume fractions (BV/TV, %), the fractal dimension (FD) as the measure of complexity calculated by the 3-D box-counting method, and the connectivity density (CD, the first Betti number / total volume (/mm3)) as determined by topological analysis. Randomly selected subjects (alendronate group; n=9) commenced 5mg of oral alendronate once daily and continued taking it for the duration of the study, while the rest of the patients were remain untreated (control; n=9). All patients were re-evaluated after 6 months or more and change rate per 6 months were calculated. HRCT provided satisfactory in vivo assessment of consecutive slice images, even though an effective resolution of 351 micron seems to be the lowest resolution level available for human trabecular bone. In control, BMD, the BV/TV, FD, and CD decreased significantly after six months. Alendronate significantly increased vertebral trabecular bone mass, however the effect on CD were not statistically significant. Once connectivity loss occurs, it seems more difficult to restore connectivity, and only possible to increase the thickness of the remaining trabeculae. Since deterioration of connectivity may limit the potential benefit to be derived from the agents that increase bone mass, appropriate therapeutic intervention should be initiated before the connectivity has been lost.

Disclosures: ***T. Mawatari****, Japan Osteoporotic Foundation (2003) 2; Grants-in-Aid for Scientific Research, Ministry of Education, Culture, Sports, Science & Technology, Japan (2003) 2; The Japanese Society of Clinical Pharmacology and Therapeutics 2.*

M130

The Correlation with between Background Variables and Urine NTX Levels and Bone Mineral Density in Japanese Osteoporosis Patients. H. Matsuo*. Internal Medicine, Matsuo Hospital, Fukuoka, Japan.

In 397 patients diagnosed as having osteoporosis (348 females and 49 males), NTX level (a representative marker of bone metabolism) was measured, and its relationship to background variables (age, height, body weight, BMI, time of menopause and bone mineral density) was analyzed statistically. Furthermore, effects of Risedronate (Actonel®), a new bisphosphonate preparation, on NTX level were evaluated.

When the distribution of NTX in each range was analyzed for the 397 patients, its 50-percentile level (median) was 45.7 nmol BCE/mmol Cr. Its mean ± SD was 53.2 ± 30.91 nmol BCE/nmol Cr.

In the analysis of correlation of NTX level to background variables of the 397 patients (age, height, body weight, BMI, time of menopause and bone density), NTX level did not correlate with age ($R2 = 0.0000$) but it showed a negative correlation with height ($R2 = 0.0333$), body weight ($R2 = 0.0748$), BMI ($R2 = 0.0464$) and bone density ($R2 = 0.0898$). That is, NTX level tended to raise as height, body weight, BMI and bone density decreased. Furthermore, a weak positive correlation was noted between NTX level and time of menopause ($R2 = 0.0012$).

Of the 397 patients with osteoporosis, 36 were treated with Risedronate after the diagnosis of the disease. The time course of NTX level was followed in these 36 patients. The mean decrease in NTX level in the Risedronate treatment group (n = 36) was 40.5%. When analyzed for each category of individual background variables, the decrease in NTX level following Risedronate treatment was not large enough to be rated as statistically significant ($P < 0.10$) for the category "male" (n = 3) and the category "bone density over 70" (n = 6), but the decrease was statistically significant ($P < 0.05$) for the other categories of background variables.

Disclosures: ***H. Matsuo****, None.*

M131

Bone Turnover Markers Predict Changes Over Three Years in Pubertal, But Not Prepubertal Females. E. M. Laing[1], K. H. Yurman*[1], C. M. Modlesky[2], D. B. Hall*[3], A. R. Wilson*[4], R. D. Lewis[1]. [1]Foods and Nutrition, The University of Georgia, Athens, GA, USA, [2]Health, Nutrition and Exercise Sciences, The University of Delaware, Newark, DE, USA, [3]Statistics, The University of Georgia, Athens, GA, USA, [4]Campbell Soup Company, Camden, NJ, USA.

The purpose of this study was to examine the relationships of the bone turnover markers serum osteocalcin (OC), urinary pyridinoline (PYD) and deoxypyridinoline (DPD) with changes in bone area (BA), bone mineral content (BMC), and areal bone mineral density (aBMD) over three years in prepubertal females. Bone turnover markers, bone properties and sexual maturation (i.e., breast stage rated by a physician) were assessed annually in 32 prepubertal females, four to eight years of age. OC was determined using radioimmunoassay, PYD and DPD by high performance liquid chromatography and bone measures by dual-energy x-ray absorptiometry (DXA). By the end of three years, 13 participants progressed to breast stages 2/3 (early puberty), whereas 19 remained in breast stage 1 (prepuberty). Regression models with random subject effects were used to determine predictors of bone turnover markers. Canonical correlation and multiple regression analyses were employed to determine relationships between bone turnover markers and DXA measures of bone. OC, BA, BMC, and aBMD at all skeletal sites increased significantly over time ($p < 0.0001$). Significant predictors for annual increments in bone turnover markers were: annual increments of body weight for OC (slope = 0.305, p = 0.002), BMI and height for PYD (slope = 27.2, p = 0.002 and slope = 17.5, p = 0.046, respectively), and BMI for DPD (slope = 3.52, p = 0.019). Using canonical correlations, changes in all bone turnover markers were found to be more strongly correlated to changes in DXA measures of bone in those participants in breast stages 2/3 compared to those remaining in stage 1 ($R = 0.80$ vs. 0.38, total body; $R = 0.63$ vs. 0.39, lumbar spine; $R = 0.62$ vs. 0.38, proximal femur; $R = 0.82$ vs. 0.39, radius). The results suggest that OC, PYD and DPD may be useful in predicting changes in bone in early pubertal children. Assessment of additional bone turnover markers and bone properties may be necessary to elucidate relationships between markers and changes in bone in prepubertal females.

Disclosures: ***E.M. Laing****, None.*

M132

Change of Biochemical Markers of Bone Turnover of General Residents in a Rural Japanese community, 1993-2003: The Taiji Study. N. Yoshimura[1], K. Nakatsuka[2]. [1]Department of Public Health, Wakayama Medical University School of Medicine, Wakayama, Japan, [2]The 2nd Department of Internal Medicine, Osaka City University Medical School, Osaka, Japan.

Biochemical markers of bone turnover were measured over a ten-year period in a cohort study in the town of Taiji, Wakayama Prefecture, Japan, to provide information on change of biochemical marker levels in the mature and elderly population. Four hundred subjects were selected by sex and age decade from the full list of residents born in 1913-1952 and aged 40-79 years at the end of 1992, with 50 men and 50 women in each age decade. Baseline BMD of the lumbar spine and the proximal femur was measured using dual energy X-ray absorptiometry (DXA) in 1993, 1996, 2000 and 2003. Blood samples of all participants were examined to obtain values for N-mid osteocalcin (NmidOC) as a bone formation marker, and C-telopeptide of type I collagen (CTX) as a bone resorption marker in 1993 and 2003.

The evaluation of changes in biochemical markers of bone turnover over ten years was completed for 322 of the 400 participants initially recruited (80.5%: 153 men, 169 women). There was no significant difference among age groups in the mean values of bone metabolic markers in men both at the first survey and 10 year-follow-up survey. In women, the mean values of NmidOC(ng/ml; SD) in 1993 and 2003, respectively, were 14.8(5.8) and 19.2(7.1) in their 40's, 28.1(8.9) and 23.7(9.5) in their 50's, 30.9(9.2) and 23.4(7.7) in their 60's, 29.3(10.8) and 23.0(10.1) in their 70's. The mean values of CTX(ng/ml; SD) in 1993 and 2003, respectively, were 0.10(0.07) and 0.20(0.11) in their 40's, 0.25(0.12) and 0.26(0.23) in their 50's, 0.29(0.13) and 0.27(0.14) in their 60's, 0.30(0.16) and 0.29(0.16) in their 70's. In women, there was a significant difference ($P<0.001$) of both serum NmidOC and CTX levels between in their 40s and in their 50s and older at the initial survey. The mean values of NmidOC and CTX in their 40's increased significantly over ten-year-period (NmidOC:$P<0.01$, CTX:$P<0.001$). In women in their 50's, 60's and 70's, NmidOC levels decreased significantly ($P<0.05$), while there was no significant difference of serum CTX levels during 10 years in their 50's, 60's and 70's. Furthermore, we found evidence of differences in biochemical marker levels for given age strata between birth cohorts. The mean values of NmidOC and CTX in women in the birth cohort of 1943-52, when they reached the age stratum 50-59, was significantly lower ($P<0.001$) than that of the older cohort born in 1933-42 when in the same age stratum.

Disclosures: ***N. Yoshimura****, None.*

M133

Anabolic Index (Serum Osteocalcin/Urine NTX) Predicts Bone Mineral Density. O. S. Indridason*[1], L. Franzson*[2], G. Sigurdsson[1]. [1]Medicine, University Hospital, Reykjavik, Iceland, [2]Laboratory Medicine, University Hospital, Reykjavik, Iceland.

The usefulness of bone turnover markers in osteoporosis has been controversial. The aim of this study was to assess the association between BMD and bone turnover markers and examine if the ratio of a bone formation marker to a bone resorption marker might be useful.

This was a cross-sectional study of 70 year old Icelandic women who were invited for BMD measurement (DXA, Hologic QDR 2000+ scanner, Hologic, Waltham, MA, USA) at the hip, lumbar spine and total body. All subjects answered a thorough questionnaire on health and medication use. For the current analysis we excluded women with diseases or taking medications affecting mineral metabolism. Serum osteocalcin (OC) was measured using an immunoradiometric assay (Nichols Institute, San Juan Capistrano, CA, USA). Cross-linked N-telopeptides of type I collagen (U-NTx) was measured in urine with a competitive enzyme linked immunosorbent assay (Osteomark, Ostex International, Seattle, WA, USA) and expressed as a ratio to urinary creatinine concentration. Anabolic index (AI) was defined as the ratio of OC to U-NTx (OC/U-NTx). We used Spearman´s correlation coefficient and multivariable linear regression to assess the relationship between BMD, AI and other variables. Where needed, we used natural logarithm to obtain normal distribution for variables used in the regression analysis.

Of 418 women invited, 308 participated but after exclusion, 248 remained for analysis. There was a strong correlation between OC and U-NTx ($r=0.61$, $p<0.0001$). BMD at lumbar spine, hip and total body correlated negatively with OC ($r=-0.22$, $p<0.001$; $r=-0.24$, $p<0.001$; $r=-0.33$, $p<0.001$, respectively) and U-NTx ($r=-0.25$, $p<0.001$; $r=-0.26$, $p<0.001$; $r=-0.30$, $p<0.001$, respectively) but positively with AI ($r=0.18$, $p=0.006$; $r=0.18$, $p=0.01$; $r=0.17$, $p=0.01$, respectively). After adjusting for important covariates, including leanweight, fat-mass and serum iPTH, there remained a significant negative relationship between OC or U-NTx and BMD at all sites, whereas the relationship between the AI and BMD remained positive for all BMD sites (standardized beta coefficients: $r=0.14$, $p=0.03$; $r=0.18$, $p=0.002$; $r=0.12$, $p=0.05$, for lumbar spine, hip and whole body, respectively).

In contrast to OC, a marker of bone formation and Urinary-NTx, a marker of bone resorption, both of whom are negatively associated with BMD, the ratio between the two, the anabolic index, is positively associated with BMD in elderly women. Its usefulness in predicting BMD and changes in BMD should be evaluated in other studies.

Disclosures: ***O.S. Indridason****, None.*

M134

Variation of Bone and Connective Tissue Turnover Markers with Age, Gender, BMI and Ethnicity in Elite Athletes. A. E. Nelson[1], M. J. Seibel[2], C. J. Howe*[3], T. V. Nguyen[4], J. de Winter*[2], K. Leung*[4], G. J. Trout*[3], R. C. Baxter*[5], D. J. Handelsman*[6], M. Irie*[7], R. Kazlauskas*[3], K. K. Ho*[1]. [1]Pituitary Research Unit, Garvan Institute of Medical Research, Sydney, Australia, [2]Bone Research Program, ANZAC Research Institute, Sydney, Australia, [3]Australian Sports Drug Testing Laboratory, Sydney, Australia, [4]Garvan Institute of Medical Research, Sydney, Australia, [5]Kolling Institute of Medical Research, Sydney, Australia, [6]ANZAC Research Institute, Sydney, Australia, [7]TOHO University, Tokyo, Japan.

The aim of this study was to determine the effect of the demographic factors age, gender, BMI and ethnicity on bone and connective tissue turnover markers in elite athletes, in order to establish reference ranges. As these markers are responsive to growth hormone (GH) and remain elevated following withdrawal of exogenous GH, they may be useful as indirect indices of GH doping. Reference ranges are essential to develop a test for GH doping based on these indirect markers.

Serum samples were obtained from 1087 elite athletes aged 22 ± 5 years from 14 countries, representing the following ethnic groups: Caucasian (53%), Asian (32%), African (10%) and Oceanian and other (5%). Bone and connective tissue markers were measured in duplicate by radioimmunoassay: N-terminal propeptide of type I procollagen (PINP), a marker of bone formation; N-terminal propeptide of type III procollagen (PIIINP), a marker of connective tissue collagen synthesis; C-terminal cross-linked telopeptide of type I collagen (ICTP), a marker of bone resorption. Statistical analysis was performed by random-effects analysis of variance.

There was a highly significant inverse relationship between all three markers with age. All three markers were significantly higher in males than in females, and were negatively correlated with BMI. Multiple regression analysis indicated that age, gender, BMI and ethnicity accounted for 32 - 48% of the total variability of serum PINP, ICTP and PIIINP. Age exerted the greatest effect (PINP: 27%, ICTP: 42%, PIIINP: 27% of the variability), then gender (PINP: 7.6%, ICTP: 4.6%, PIIINP: 2% of the variability). BMI (1.3%, 0.6% and 0.9% respectively) and ethnicity (0.7%, 0.01% and 2% respectively) both had modest contribution to the variability of PINP, ICTP and PIIINP.

In conclusion, reference ranges for the GH-sensitive bone and connective tissue markers PINP, ICTP and PIIINP should take into account demographic factors such as age and gender. For these markers, however, reference ranges can be established without needing to account for BMI and ethnicity.

Disclosures: ***M.J. Seibel****, None.*

M135

Does Impaired Renal Function in the Elderly Influence Serum Concentration of Bone Biochemical Markers? M. Healy*[1], M. Casey*[2], C. Walsh*[3], D. Coakley*[4], G. Cox*[1], C. Cunningham*[4], V. Crowley*[1], J. B. Walsh[4]. [1]Biochemistry Department, St James's Hospital, Dublin, Ireland, [2]Falls/ Osteoporosis Service, St James's Hospital, Dublin, Ireland, [3]Statistics Department, Trinity College, Dublin, Ireland, [4]Mercer's Institute for Research on Ageing, St James's Hospital, Dublin, Ireland.

The purpose of this study was to examine the effects of impaired renal function on the analysis of serum bone biochemical markers in an elderly population group.

245 patients referred from the St James's Hospital Care of the Elderly Service for DEXA bone scanning were recruited. All patients had calculated creatinine clearance (Cockcroft Gault), a marker of bone resorption (serum CTx), a marker of bone formation (serum osteocalcin), parathyroid hormone (PTH), and 25-hydroxyvitamin D (25OHD) assessed. The relationship between renal function and bone markers was examined. Bone markers and PTH were measured on a Roche 2010 analyser. 25OHD was analysed by radioimmunoassay (Diasorin Inc).

36 patients were male and 209 were female. Means and ranges for the variables are illustrated in the table. Statistics were calculated using Datadesk 6.1.

No correlation was found between creatinine clearance and CTx in the group as a whole and osteocalcin was only weakly correlated ($r = -0.183$). However, below a cut-off of 45 ml/min creatinine clearance an inverse relationship between renal function and markers became apparent (CTx v CrCl $r = -0.391$ $p < 0.0001$; OC v CrCl $r = -0.402$ $p < 0.0001$). This result indicates that declining renal function is associated with elevated marker concentrations.

In conclusion, care needs to be taken when interpreting biochemical markers of bone turnover in the elderly given the prevalence of renal impairment in this population. Creatinine clearance should be estimated to avoid misinterpretation

Table: Data for variables included in the study

N=245	Mean (+/- SE)	Range	Reference Intervals
CTx ng/ml	0.49 (0.02)	0.032-2.25	0.01-1.0
OC µg/ml	27.3 (1.3)	3.2-126	11-50
PTH ng/ml	41.7 (1.9)	4.9-181	10-65
25OHD ng/ml	23.9 (1.0)	2.5-67	>20
CrCl ml/min	47.5 (1.4	16-107	~1ml/min yearly decline after 3rd decade
Age years	78.8 (0.7)	50-97	

Disclosures: ***M. Healy****, None.*

M136

Can Multiple Measurements or Pooled Measurements Reduce Within-subject Variability? J. A. Clowes, N. F. A. Peel, A. Blumsohn, F. Gossiel*, R. Eastell. Clinical Sciences (North), University of Sheffield, Sheffield, United Kingdom.

A decrease in bone turnover markers in response to therapy predicts fracture risk reduction; therefore monitoring may assist clinicians in determining an individual's therapeutic response. However, variability (noise) in the bone marker measurements frequently limits the ability to detect a statistically significant response (signal). We hypothesized that performing more then one measurement would reduce within-subject variance (SD_i) by the square route of the number of measurements performed. Thus if 4 measurements were made we might expect to reduce the SD_i by a factor of two (50%), since n=4 (calculated multiple sample approach). Increasing the number of measurements increases cost, therefore we examined whether a pooled sample obtained by taking a fixed volume aliquot from the 4 separate urines could reduce variance by a similar magnitude (pooled approach).

Twenty five postmenopausal women (age 50-80 years) were recruited as a control group for a randomized control study. Subjects attended at baseline, 1 and 24 weeks. At each visit subjects provided 4 urine samples, 3 from the preceding 3 mornings and 1 on the morning of the visit. Samples were stored at 4 ºC. Measurements of urine N telopeptide of type I collagen were performed in replicate in a batched analysis using an automated immunoassay (Vitros ECi). We calculated short term (1 week) and long term (24 weeks) analytical variability (CV_a) based on replicate assays and within-subject coefficient of variation (CV_i) after accounting for CV_a. Components of variance were assessed by nested ANOVA. We compared either 4 separate measurements (calculated multiple sample approach) or a pooled measurement (pooled approach) to a single measurement (global individual).

The calculation approach reduced the within-subject SD by between 27% and 35%. The pooled approach reduced the SD_i by between 20% and 61%. The calculation and pooled approach had a greater effect on short-term variance (35 to 61%) then long-term variance (20 to 27%). This may be because day-to-day variability is a significant part of short-term variance with additional sources of variability arising with long-term variance e.g. seasonal effect. In conclusion, multiple measurements and pooled samples reduce variance by up to 61%, which may be of benefit when monitoring response to therapy in an individual.

	Analytical SD_a	Analytical CV_a	Within-subject SD_i	Within-subject CV_i
Short-term, global individual	1.4	2.7	11.2	21.3
Short-term, pooled	2.2	4.4 (3.6-5.2)	4.4	12.1 (8.7-16.0)
Short-term calculated multiple	-	-	7.3	13.7 (8.9-19.0)
Long-term, global individual	1.9	3.6	9.9	18.8
Long-term, pooled	1.8	3.6 (2.9-38)	7.9	15.5 (0.0-18.2)
Long-term calculated multiple	-	-	7.2	13.6 (9.9-17.6)

Disclosures: ***J.A. Clowes****, None.*

M137

The Degree of Isomerization of Collagen Type I C-telopeptide in Postmenopausal Women: A Potential Biochemical Index of Bone Quality. I. Byrjalsen*[1], P. A. Cloos*[1], P. Qvist[1], C. Christiansen[2]. [1]Nordic Bioscience A/S, Herlev, Denmark, [2]Center for Clinical & Basic Research, Ballerup, Denmark.

The main protein component of the extracellular bone matrix is collagen type I of which the C-telopeptide motif of CTX is released during osteoclastic bone resorption. Newly synthesized bone matrix contains the α-form of CTX, but with aging the motif spontaneously isomerizes to the β-form. The α/β ratio has been reported to be high in trabecular bone and low in cortical bone (Cloos 2000), and it has been suggested to be an index of bone quality.

Purpose: To provide reference data in healthy pre- and postmenopausal women, and to investigate the effect of various antiresorptive therapies on the α/β ratio.

Methods: The native α-CTX, and the age-related isomerized β-CTX type I collagen C-telopeptide fragments were measured in fasting second void morning urine of healthy premenopausal (*n*=76; 40-50 years of age) and postmenopausal women (*n*=446). The postmenopausal women were from cohorts of women participating in placebo-controlled double-blind antiresorptive treatment studies, and samples were obtained at baseline, after 6, 12, and 24 months of therapy.

Results: Early postmenopausal women, mean age of 53 years and less than 5 years since menopause, had a significant ($p<0.0001$) two-fold increase in the bone resorption markers of urinary α-CTX and β-CTX as compared to premenopausal women. In contrast the ratio between the two markers were unaffected by change in menopausal status (geometric mean ratios of 0.202 and 0.213 for pre- and post, respectively, *p*-value=0.31). In postmenopausal women, the index of the α/β ratio showed a highly significant ($p<0.0001$) increase of 1.41% per menopausal year, and it was found that the index was independent of the rate of bone resorption as assessed by urinary β-CTX ($r=0.03$; $p=0.50$).

The antiresorptive therapies had different effects on the index of the α/β ratio with the time-averaged mean relative change from the baseline values during the two year study period of -35% (p<0.01), and -50% (p>0.0001) for two bisphosphonate treatments, -20% (p<0.01) for oral HRT, -10% (NS) for cutaneuos HRT, +12% (p<0.05) for nasal HRT, -11% (p<0.01) for SERM, and +1% (NS) for placebo.

Conclusion: The association between the increasing ratio of α- and β-CTX and the duration of the menopause, and the fact that the ratio in itself is independent on the rate of bone resorption, suggests that the α/β-ratio could provide information on the quality of the skeleton. The different responses of the index of the α/β-ratio caused by the various antiresorptive therapies may reflect different treatment effects between trabecular and cortical bone in the prevention of bone loss.

Disclosures: ***I. Byrjalsen****, Nordic Bioscience A/S 3.*

M138

Bone Turnover Response to Feeding and infusion of Gut Hormones Peptide YY_{3-36}, Pancreatic Polypeptide and Oxyntomodulin. F. Gossiel*[1], C. W. Le Roux*[2], R. L. Batterham*[2], M. A. Cohen*[2], S. R. Bloom*[2], A. Blumsohn[1]. [1]Bone Metabolism Unit, University of Sheffield, Sheffield, United Kingdom, [2]Department of Metabolic Medicine, Imperial College, London, United Kingdom.

Mechanisms underlying the apparent change in bone turnover in response to feeding or in relation to time-of day in humans are uncertain, but may relate to a change in skeletal blood flow or a direct effect of a gastrointestinal peptide on the skeleton. Several peptides are secreted in the postprandial phase, and it is possible that one or more of these peptides could influence bone turnover. It is important to examine the response to these peptides at physiological dose.

Peptide YY_{3-36} (PYY_{3-36}), Pancreatic polypeptide (PP) and Oxyntomodulin (OXM) are secreted following meals, and infusion of these peptides reduces appetite and food intake in humans. The aim of this study was to investigate the effect of physiological-dose infusion of these peptides on bone turnover. Healthy volunteers were infused with placebo/PYY_{3-36} (0.8 pmol/kg/min, n=12), placebo/OXM (3.0 pmol/kg/min, n=13) or placebo/PP (10 pmol/kg/min, n=10) in a double blinded placebo crossover study for each peptide. Serum samples were collected at regular time points prior to peptide infusion, after cessation of peptide infusion and following a weighed buffet meal provided at t_{210} (PYY_{3-36} and PP infusion) and t_{75} (OXM infusion). We assessed the effect of peptide infusion and subsequent food ingestion on the serum concentration of the respective peptides, serum C-telopeptide of type I collagen (sβCTX), procollagen type 1 N-propeptide (P1NP), osteocalcin and parathyroid hormone (PTH). There was no significant effect of these peptides on bone turnover at physiological dose in comparison with saline infusion (all P>0.2, AUC analysis or repeated measures ANOVA). The decrease in sβCTX in response to subsequent food intake was 69±3%SEM (PYY study), 61±3 % (PP study) and 57±3% (OXM). There was no substantial effect of prior peptide infusion on the sβCTX response to feeding (although food intake was influenced by peptide infusion). Food intake resulted in increased serum PYY_{3-36} , OXM and PP of magnitude similar to that achieved with parenteral peptide. There was no significant effect of any peptide on serum PTH, PINP or OC versus placebo (all P > 0.05). In summary we were unable to establish an effect of any of these three food-stimulated peptide hormones on bone resorption when administered at physiological dose. Other peptides such as GLP-2 may be relevant.

Disclosures: ***A. Blumsohn****, None.*

M139

Serum Markers of Bone Remodeling Following Total Knee or Hip Arthroplasty. R. L. Illgen*, L. M. Bauer*, T. M. Forsythe*, M. Hagenauer*, A. K. Franta*, T. R. Enright*, W. B. Valhmu*, J. P. Heiner*. Orthopedics and Rehabilitation, University of Wisconsin-Madison, Madison, WI, USA.

Pre-radiographic detection would be a valuable diagnostic of periprosthetic osteolysis, a major mode of failure after total hip (THA) and knee arthroplasty (TKA).[1] Osteolysis is often asymptomatic and radiologically undetectable until periprosthetic loosening or fracture occur. Serological markers of bone remodeling have been identified as a candidate approach.[2,3] This study defines the natural history of 2 serum markers following arthroplasty.

IRB approval and patient consent were obtained. Patients diagnosed with osteoarthritis or osteonecrosis scheduled for THA or TKA were recruited. Exclusion criteria included osteoporosis, rheumatoid arthritis, anti-resorptive agent prescriptions, or multiple joint arthroplasties within 1 year. Serum was collected at selected time points and stored at -80°C. Time points collected were at days 0 (preop and postop), 14, 28, 42; and 3, 6, 12, and 24 months. Serum was assayed using commercial enzyme-linked immunosorbent assay (ELISA) kits, measuring concentrations of the bone resorption marker, N-Telopeptide (NTx) (Ostex International, Seattle, WA) and bone formation marker, Bone-Specific Alkaline Phosphatase (BAP) (MetraBiosystems, Mountainview, CA). Multivariate analysis was performed using analysis of variance (ANOVA).

Sixty-nine patients were followed for 1 year after THA (N=32) or TKA (N=37). Of these, 33 were followed to 2 years (17 THA, 16 TKA). Pre-menopausal women were not analyzed due to small sample size (N=9).

ANOVA revealed significant serum elevations of NTx and BAP at 28 days (Fig. 1). NTx returned to preop levels, whereas BAP may have established a new baseline by 6 months. ANOVA for NTx and BAP didn't reveal effects ($\rho<0.05$) due to gender, THA versus TKA, surgeon, implant fixation (cemented or hybrid TKA), nor time from 6 months to 2 years.

These data suggest serum markers of bone remodeling change in predictable patterns after THA and TKA. This supports further investigation into whether patients developing periprosthetic osteolysis will display a significant deviation from these expected profiles prior to radiographic evidence of osteolysis.

1. Harris WH et.al., *Clin. Orthop.* 1995; 311: 46-53
2. Watts N et.al.; *Clin. Chem.* 2000; 45(8): 1359-683. Looker A et.al., *Osteoporosis Int.* 2000; 11(6): 467-80

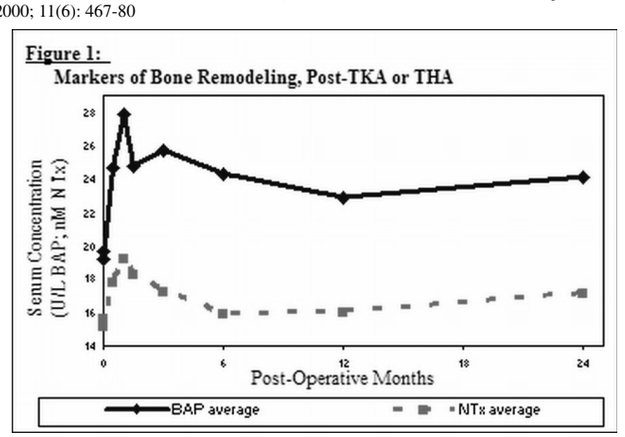

Disclosures: ***L.M. Bauer****, None.*

M140

Quantitative Ultrasound Bone Measurements in Healthy American Adolescents. K. J. Loud, H. A. Feldman*, K. C. DePeter*, A. A. Pettinato*, C. M. Gordon. Children's Hospital, Boston, MA, USA.

Quantitative ultrasound (QUS) bone measurements are appealing in young adolescents because of the absence of ionizing radiation. A limitation of their use in the United States is the lack of pediatric normative data. The purposes of this study were to develop reference distributions for speed of sound (SOS) measurements of the radius and tibia via QUS among American adolescents and to evaluate relationships between SOS and specific demographic and lifestyle variables.

Eighty-six (86) otherwise healthy adolescents and young adults aged 11-26 years were recruited during routine visits to an urban medical center adolescent clinic. The protocol was approved by the Committee on Clinical Investigation at Children's Hospital Boston. Participants completed a confidential semi-structured interview for demographic information and health history as well as self-administered, validated exercise and nutritional questionnaires. Weight, height, and sexual maturity ratings (SMR) were also recorded. The main outcomes, SOS at the distal third of the radius and mid-shaft of the tibia, were measured on the non-dominant limb using the Omnisense 7000P QUS (Sunlight Medical Ltd., Tel-Aviv, Israel).

The age of participants was 17.2 $\pm$ 2.5 years (mean $\pm$ SD). Forty-six (53%) were female. Self-reported ethnicities were 49% African-American, 24% Hispanic, 17% Caucasian, 6% Asian, and 3% other. Fifty-nine (69%) of the participants had achieved SMR 5; 96% of the females were post-menarcheal, with age at menarche of 12.4 $\pm$ 1.4 years. Daily dietary intakes of calcium and vitamin D were 1155 $\pm$ 710 mg and 242 $\pm$ 179 IU, respectively.

There were moderate correlations between age and SOS at the radius, with a correlation coefficient (r) of 0.59 ($p < 0.0001$), and at the tibia, $r = 0.58$ ($p < 0.0001$). Participants who had achieved SMR 5 had a significantly higher SOS than those who were less mature at both the radius ($p < 0.0001$) and tibia ($p = 0.002$). There were no significant relationships found between SOS and self-reported ethnicity, BMI, intake of calcium or vitamin D, age at menarche, or activity levels. In multiple linear regression controlling for these factors, age remained significantly associated with SOS at the distal radius ($p < 0.0001$) and mid-shaft tibia ($p < 0.0001$).

These findings suggest that skeletal QUS measurements follow similar age distribution patterns to bone mineral density (BMD) determinations by dual-emission x-ray absorptiometry (DXA) among healthy American adolescents. Youth in our sample did not, on average, meet the recommended daily allowances (RDA) for calcium or vitamin D. More data are needed to establish reference distributions in this population and to provide sufficient power to identify other modulating factors.

Disclosures: ***K.J. Loud****, None.*

M141

Ultrasound Bone Mineral Density of Os Calcis - Its Relationship with Bone Mineral Markers and 25(OH)D in Endemic Flurotic and Non-flurotic Villages. C. V. Harinarayan*, T. Ramalakshmi*, A. V. Hebbani*, U. V. Prasad*, E. G. T. Kumar*, D. Sudhakar*, D. Prasanna Kumar*, M. Suresh*. Endocrinology and Metabolism,, SVIMS, Tirupati, India.

OBJECTIVES: To study the relationship between the nutritional status, serum bone mineral markers, 25(OH)D levels and ultrasound bone mineral density of Os Calcis (USBMD) in endemic flurotic and non-flurotic villages.

METHODS: Sixty-four subjects from flurotic and 79 subjects from non-flurotic villages were studied for their dietary habits, biochemical parameters of bone mineral markers, 25(OH)D levels and correlated with stiffness index (SI) measured using USBMD (Achilles).

RESULTS: The results are depicted in table as mean $\pm$ SEM. (* $p< 0.001$; @ $p < 0.05$)

Table - 1 Dietary parameters

Parameter	Flurotic village	Non-flurotic village
Water fluoride(PPM)	> 1.5	<1
Age(yrs)	43$\pm$2	48$\pm$1
Energy(Kcal/day)	1763$\pm$46*	1398$\pm$10
Dietary Calcium(mg/day)	241$\pm$3	272$\pm$1.34*
Dietary Phosp(mg/day)	433$\pm$6	553$\pm$5*
Phytate/Calcium ratio	0.7$\pm$0.01	0.7$\pm$0.01
Dietary Proteins(mg/day)	26$\pm$0.28	37$\pm$0.54*

Table - 2 Biochemical parameters

Parameter	Flurotic village	Non-flurotic village
S. Calcium(mg/dl)	10$\pm$0.01	10.1$\pm$0.07
S. Phosphorus(mg/dl)	2.68$\pm$0.03	3.07$\pm$0.06*
S. Alk. Phos(IU/l)	65$\pm$2.4*	41.7$\pm$1.94
S. Protein(gm/dl)	6.5$\pm$0.04	6.76$\pm$0.03
25(OH)D(ng/ml)	20.3$\pm$0.94	22.6$\pm$0.71@
Serum fluoride(SF)(PPM)	0.13$\pm$0.005*	0.05$\pm$0.001
Young Adult(YA)(SI)	85.17$\pm$2.41@	76.44$\pm$2.58
Age Matched (AM)(SI)	94.78$\pm$2.74	88.81$\pm$1.58

Dietary calcium intake in both the villages is far below the recommended daily allowances (RDA) by Indian Council of Medical Research (ICMR), India for Indian population. 25(OH)D correlated positively with energy intake (r 0.7;p<0.001); dietary calcium(r 0.5;p<0.001); and negatively with phytate/calcium ratio(r 0.02;p<0.001), in the fluortic village. There was no similar correlation in non-flurotic village. For comparable levels of serum calcium, subjects in non-flurotic villages were more osteopenic than the flurotic counterparts. USBMD did not correlate with 25(OH)D in the flurotic and non-flurotic subjects.

CONCLUSIONS: Monitored food fortification program is required to correct the inadequate dietary calcium of both the populations. USBMD does not indicate the 25(OH)D status of an individual. Fluoride forms fluroappatite in the bone which is hyper dense and can fallaciously produce increased bone density. USBMD should not be used for screening osteoporosis in areas endemic for flurosis.

Disclosures: ***C.V. Harinarayan****, None.*

M142

Heel Ultrasonometry as a Tool for Identifying Women at High and Low Risk for Osteoporosis. M. Gambacciani, B. Cappagli*, M. Ciaponi*, A. Genazzani*. Department of Obstetrics and Gynecology, University of Pisa, Pisa, Italy.

Not all people at high risk for future fracture have access to DXA bone density measurements. Inexpensive methods selecting high-risk patients could therefore improve healthcare delivery. Quantitative ultrasound of the os calcis is accepted as an effective, low-cost method to identify women likely to have osteoporosis at the hip or spine as measured by DXA. In this study, we wished to determine T-score cutpoints for the Achilles bone ultrasonometer to identify women at high and low risk for osteoporosis.

A total of 272 women aged 40 to 83 years (mean age 58 ± 7 years) had DXA measurements of the spine and hip using a Lunar DPX (GE Healthcare) and a heel ultrasound measurement using the Achilles InSight. The Achilles InSight is an imaging heel ultrasonometer with 8-10 second measurement time; the complete examination takes 3-5 minutes. Osteoporosis was diagnosed if the lowest DXA T-score at spine (L1-L4) or hip (total femur) was ≤ -2.5. Using the binormal fit to the ROC data, InSight T-score cutoffs for 90% sensitivity (patients at low risk) and 90% specificity (patients at high risk) were determined. For the different InSight T-score cutoffs the likelihood ratios for a positive test (LR+) and a negative test (LR-) at spine or hip were also calculated.

From the DXA results, 54 of 272 subjects were classified as osteoporotic. The InSight T-score cutoffs were found to be -0.8 and -2.3 for 90% sensitivity and 90% specificity, respectively. Women with InSight T-scores ≤ -2.3 are at high risk, and could be potential candidates for treatment and DXA monitoring measurements. Women with InSight T-scores ≥ -0.8 could be considered at low risk and scheduled for retesting in future depending on risk factors. Women with an InSight T-score between -2.3 and -0.8 should be referred for DXA assessment.

We conclude that the Achilles bone ultrasonometer can be used as a valid screening tool for identifying those patients who should be considered for spine and hip bone density assessment.

InSight T-score	Sensitivity	Specificity	LR+	LR-
-0.80	90%	41%	1.52	0.25
-2.34	45%	90%	4.51	0.61

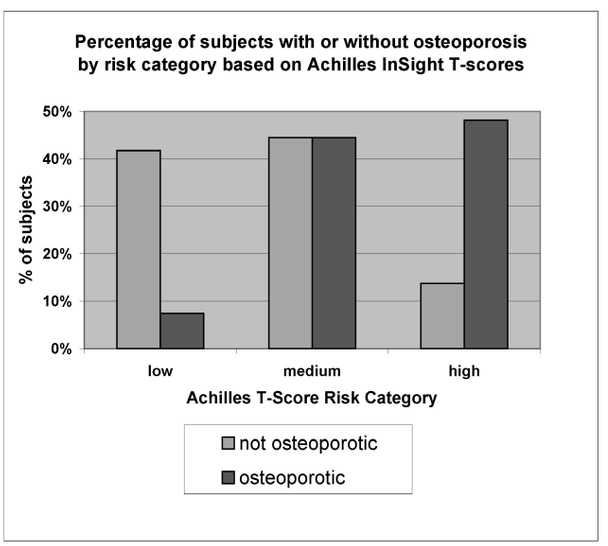

Disclosures: ***M. Gambacciani****, None.*

M143

The Usefulness of Quantitative Ultrasound at Calcaneus in the Detection of the Different Types of Non-traumatic Fracture in Chinese Men. S. K. AU*[1], E. M. C. Lau[1], D. T. K. Choy[1], S. Wong*[2], J. Leung*[1], F. W. K. Chan*[1], H. Lynn*[2], J. Woo*[2], P. C. Leung*[3]. [1]Jockey Club Centre For Osteoporosis Care & Control, The Chinese University of Hong Kong, Hong Kong, Hong Kong Special Administrative Region of China, [2]Department of Community & Family Medicine, The Chinese University of Hong Kong, Hong Kong, Hong Kong Special Administrative Region of China, [3]Department of Orthopedics & Traumatology, The Chinese University of Hong Kong, Hong Kong, Hong Kong Special Administrative Region of China.

To determine the discrimating ability of QUS at calcaneus between individuals with and without non-traumatic fractures in elderly Chinese men.

A total of 1708 men, aged 65 years or above, have their heel QUS measured by Sahara Sonometer (Hologic) in our centre from Aug 2001 to Feb 2004. Subjects are either recruited by public announcements or from Orthopedics out-patient clinic, Prince of Wales Hospital. Details on history of fracture were obtained, and subjects were divided into controls without fractures (n=1456) and with non-traumatic prior fractures (n=252). The fractured group was divided into hip, vertebral and forearm fractures subgroup. Statistical significance of difference between Quantitative Ultrasound Index (QUI) of each group was assessed by ANOVA (adjusted for age, weight, height and BMI).

The clinical characteristics and QUS values of the participants are summarized in table below.

	Control	All	Hip	Vertebral	Forearm
N	1456	252	10	44	56
Age	72.7 (5.1)	73.8 (5.7)	78.5 (4.1)	74.8 (6.3)	75.1 (5.5)
Weight (Kg)	62.1 (9.3)	61.0 (10.3)	58.8 (12.2)	58.2 (10.7)	62.0 (9.2)
Height (cm)	163.2 (5.7)	162.3 (8.4)	161.4 (8.8)	158.7 (15.6)	162.2 (5.5)
QUI	89.7 (16.2)	84 (17.9)	64.3 (14.8)	77.9 (18.9)	81.5 (18.3)

* Data in mean (SD)

QUI of each of the 3 fracture subgroups was significantly lower ($p<0.001$) than the normal controls.

The sensitivity & specificity of QUI T-score (local normal range) were also assessed in 2 different cut-off values (-2.5 and -1). Specificity of using -2.5 as cut-off was 0.88 and sensitivity were 0.25, 0.7, 0.45 & 0.32 for "All", "Hip", "Vertebral" & "Forearm" fracture group, respectively. In contracts, the specificity of using -1 as cut-off was 0.70 and sensitivity were 0.77, 1.0, 0.86 & 0.82 for "All", "Hip", "Vertebral" & "Forearm" fracture group, respectively.

Result shows Calcaneus QUS can discriminate between healthy individuals and subjects with previous fractures. In addition, T-score cut-off at -1 will greatly increase the sensitivity of QUS assessment, compared to the conventional -2.5 cut-off, with only a slight decrease in specificity.

Disclosures: ***S.K. Au****, None.*

M144

In Vivo Performance Evaluation Of The Achilles Insight QUS Device. C. Cepollaro, S. Gonnelli, A. Montagnani*, S. Martini*, A. Cadirni*, C. Caffarelli*, R. Nuti. Internal Medicine, Endocrine-Metabolic Sciences and Bichemistry, Internal Medicine, Siena, Italy.

Quantitative ultrasound (QUS) of the os calcis is increasingly accepted as an effective method to assess osteoporotic fracture risk. However, not all heel ultrasonometers have equivalent clinical utility; in fact they differ for technology, coupling, measurements time, precision and relationship to axial measurements. GE Achilles plus (A+) is widely used worldwide since 1990 and for its ability to predict fragility fractures, may be considered a reference standard among QUS devices. As a water-bath system, A+ has obvious practical drawbacks such as the need for draining and filling water, cumbersome size, no portability. Achilles Insight (AI) is a new generation device that uses inflatable membranes and an alcohol spray to couple the measurement transducers to the heel, and gives QUS parameters in less than a minute providing also real time imaging of the os calcis. The aim of this study was to evaluate the in vivo performance of AI in comparison with A+. The precision was evaluated in 30 healthy subjects who underwent QUS measurements (A+ and AI) twice in the same day, with repositioning. We also studied 102 postmenopausal women, 33 with and 69 without osteoporotic fractures. The difference between the QUS device were assessed using a comparison approach described by Bland and Altman. The precision, calculated by dividing the RMS SD by the mean of all subjects and express as a percentage, showed a CV of 1.9% for Stiffness obtained by A+ and 1.4% for Stiffness obtained by AI. Linear regression analysis showed a significant correlation between SOS ($r=0.83$, $p<0.001$), BUA ($r=0.81$, $p<0.001$) and Stiffness ($r=0.92$, $p<0.001$) obtained with the two devices. The evaluation of the areas under Receiver Operating Characteristic (ROC) curves showed a similar ability for A+ and AI in discriminating patients with or without vertebral fractures. The values of areas under ROC curves were 0.89, 0.80 and 0.86 for SOS, BUA and Stiffness obtained with A+, and 0.88, 0.80 and 0.86 for the same parameters obtained by AI.

We can conclude that:

the better precision of the AI with respect to A+ could be explained by the fact that the measurement with AI needs less time and gives a consequent reduction in motion artefacts. The high correlation and the similar ability to identify postmenopausal women with vertebral fracture suggest the possibility of using the database of A+ for AI.

Disclosures: ***C. Cepollaro****, None.*

M145

Quantitative Ultrasound of the Calcaneus in the Evaluation of Bone Mass in Liver and Cardiac Transplantation Patients. G. Martinez*, A. Escalona*, E. Jódar*, E. García*, S. Azriel*, L. Gil-Fraguas*, J. Meneu*, E. Moreno*, F. Hawkins. University Hospital 12 de Octubre, Madrid, Spain.

Bone loss is one of the most common complications following solid-organ transplantation, and severely affects quality of life in these patients. Although DXA is the gold standard for bone mass measurement, QUS has some potential advantages over DXA. However, only a few studies have investigated the utility of this technique in transplanted patients, mainly kidney transplantation.

The purpose of this study was to determine the usefulness of QUS in comparison with DXA to identificate liver and cardiac transplanted patients with osteoporosis.

We have cross-sectionnally evaluated one hundred and forty patients (109 males/31 females; 85 liver/55 cardiac transplantation), mean age 53,6 ± 12,5 years, time since transplantation 67,9 ± 53,3 months. BMD was assessed with DXA (Hologic 4500 QDR) at lumbar spine and hip. In addition, QUS measurements at the heel were obtained at the same time with a Sahara Clinical Sonometer (Hologic Inc, MA, USA) . The quantitative ultrasound index (QUI) and the estimated heel BMD were calculated from speed of sound (SOS, m/s) and broadband ultrasonic attenuation (BUA, dB/MHz) as has been described elsewhere. QUI T-score and BMD T-score (spine & hip) were obtained from Spanish normative data.

Results: According WHO criteria, 53% of the patients had osteopenia and 17% had osteoporosis. Calcaneal QUS parameters (BUA, SOS, QUI) correlated significantly with DXA values: QUI was positively correlated with lumbar BMD (r= 0.356 , p<0.001), femoral neck BMD (r=0.351, p<0.001) and trocanteric BMD (r=0.441, p<0.001). Heel BMD was positively correlated with lumbar BMD (r= 0.356 , p<0.001), femoral neck BMD (r=0.351, p<0.001) and trocanteric BMD (r=0.441, p<0.001). ROC analysis were performed to investigate the ability of QUS to correctly identificate patients with densitometric osteoporosis (Table 1). To obtain a 5% of false-negative, QUI T-score cutoff should be -0.6 SD but specificity drops to 42%; conversely, to obtain a 5% of false-positive, QUI T-score cutoff should be -2.1 SD.

Table 1. QUS parameters. ROC analysis

QUS Parameter	Area under curve (AUC)	95% Confidence Interval (CI)	p
SOS	0.805	0.707-0.903	<0.001
BUA	0.742	0.625-0.859	<0.001
T-score QUI	0.777	0.669-0.886	<0.001

Conclusion: A positive correlation exists between lumbar and femoral BMD and QUS parameters in liver and cardiac recipients. QUS could be recommended for screening in transplanted patients.

Disclosures: ***G. Martinez****, None.*

M146

Axial and Transverse Transmission Quantitative Ultrasound may Selectively Assess Material and Structural Properties of Bone. G. M. Kiebzak[1], C. G. Ambrose[2]. [1]St. Luke's Episcopal Hospital, Houston, TX, USA, [2]Orthopaedics, UT Health Science Center at Houston, Houston, TX, USA.

Fracture resistance is dependent on both material properties (collagen cross-linking, mineral content, etc) and structural properties (bone size, trabecular patterns, etc). Axial quantitative ultrasound (QUS) measurements, dependent on elastic modulus and mineral density, may reflect mainly material properties (assuming bone width > wavelength) whereas transverse QUS may better reflect overall bone strength. We compared ulnar QUS (Sunlight Omnisense, speed of sound, SOS, m/s, measured at the 33% region) and heel QUS measurements (GE Lunar Achilles Express, stiffness, which combines SOS and ultrasound attentuation) to ulnar size, bone mineral content (BMC, g/cm) and area density (BMD, g/cm^2, a variable partially corrected for bone size) for total ulna (entire distal third of ulna) and 33% region using dual-energy x-ray absorptiometry (DXA) and in vivo cross-sectional bending strength (EI, Nm^2, at midshaft) using MRTA (a low-frequency mechanical vibrational test; J Clin Densitometry 2(2): 143, 1999) in 138 women (18-86 yrs). EI, considered the most direct measure of whole bone strength, was significantly correlated with total ulna area (from DXA) r = +0.478, P<0.0001, and BMC, r = +0.597, P<0.0001. SOS was significantly correlated with total ulna BMC, r = +0.309, P=0.0002, but not area, r = +0.05. Correlation with 33%BMD was better for SOS, r = +0.438, P<0.0001, than for EI, r = +0.361, P<0.0001. EI and SOS were significantly correlated, r = +0.218, P= 0.01. SOS and total ulna BMD were used to estimate elastic modulus, which correlated with EI, r = +0.377, P<0.0001. Ulnar EI (r = +0.288) but not SOS (r = +0.06) was significantly correlated (P=0.0007) with heel stiffness. Heel stiffness (r = +0.303), but not SOS (r = +0.167), significantly correlated (P=0.0003) with the estimated maximum axial force to failure (derived using EI). These weak correlations may be related to the imperfect development of the MRTA technology and/or use of the ulna instead of a direct weightbearing bone. Alternatively, given the composite nature of the MRTA and QUS measurement systems (being dependent on multiple bone properties), perhaps only weak correlations should be expected. The general lack of significant correlations between SOS and variables reflective of bone size suggest that SOS was primarily measuring material properties of bone. The correlation between variables from different bones, heel and ulna, suggests that the heel measurement may provide a better assessment of global skeletal status whereas SOS may be a better site-specific measurement. Combined use of MRTA technology and QUS may expand options for in vivo bone assessment.

Disclosures: ***C.G. Ambrose****, None.*

M147

Effects of Leptin and IGF-1 on Bone Mineral Density in Long-Term Survivors after Allogeneic Stem Cell Transplantation for Hematological Malignancies. L. Tauchmanova*[1], B. Serio*[2], C. Carrella*[3], T. Musella*[1], G. Maziotti*[3], G. Mossetti[4], G. Lombardi*[1], B. Rotoli*[2], A. Colao*[1], C. Selleri*[2]. [1]Dept of Molecular and Clinical Endocrinology and Oncology, University of Naples Federico II, Naples, Italy, [2]Unit of Hematology, University of Naples Federico II, Naples, Italy, [3]Dept of Internal Medicine, II University of Naples, Naples, Italy, [4]Dept of Internal Medicine, University of Naples Federico II, Naples, Italy.

Previously we and others have described a persistent decrease in femoral and phalangeal bone mineral density (BMD) after allogeneic stem cell transplant. The transplant procedure, gonadal failure and immunosuppression were pointed out as principal risk factors for bone loss, however, they influence mostly trabecular bone and the cause of persistent BMD decrease at cortical bone is not clear. This study investigated the effects of two factors: leptin and IGF-1, known to influence bone mass in physiological conditions, but not considered important in transplant recipients. Thirty six patients (15 F; age, 32±10.2 yrs; BMI, 24.6±3 kg/m^2; time from transplant, 18±15 mos) were enrolled and compared to 36 controls matched for age, gender and BMI. DEXA technique was used to determine BMD at lumbar spine and femoral neck; quantitative ultrasonometry was used at proximal phalanges and amplitude-dependent speed of sound (AdSoS) was considered. Serum leptin, IGF-1, INF-γ, cortisol and gonadal status were determined. BMD was lower in patients than in controls at all skeletal sites considered (p<0.01). Serum leptin was higher (p<0.05) and IGF-1 lower (p<0.05) in patients than in controls. IGF-1 was lower also in the patients without growth hormone deficiency, likely mirroring their poor metabolic state. Leptin correlated with BMI in controls (r=0.73; p<0.005) but not in the patients (r=-0.057; p=0.8). In these latter leptin levels correlated with INF-γ (r=0.4; p<0.05), produced by activated Th1 lymphocytes. Femoral BMD correlated positively with IGF-1 in the patients (p<0.05) and with leptin values in females (p<0.05). A negative correlation was found between leptin and lumbar BMD in males (p<0.05). A negative correlation was observed between leptin and AdSoS in both females and males and between INF-γ and AdSoS in females (p<0.05). Neither leptin nor IGF-1 were correlated with age, period of time elapsed from transplant, cortisol and gonadal function. In conclusion, both increased leptin and decreased IGF-1 levels have important influence on bone density in long-term survivors after allo-SCT. Quantitative ultrasonometry is likely influenced throughout immune system derangement**.** However, further investigations are needed to better clarify this relationship.

Disclosures: ***L. Tauchmanova****, None.*

M148

Correlation Between Quantitative Ultrasound Parameters and Physical Performance Ability in Children. H. Kudo*, I. Owan, H. Horizono*, H. Arakaki*, F. Kanaya*. Orthopedic Surgery, University of the Ryukyus, Nishihara, Okinawa, Japan.

The purpose of this study was to determine whether physical performance ability in children was reflected by quantitative ultrasound parameters. We measured calcaneal broadband ultrasound attenuation (BUA) and velocity of sound (VOS) in 697 children aged 6 to 12, 347 boys and 350 girls, using a CUBA Clinical Paediatric device. Basic anthropometric data (body weight, height, foot length and septum of heel) and total scores from physical performance ability tests were collected. The physical performance ability tests comprised 8 tasks including grip strength, trunk extension, sitting flexion, side step, 50 meter run, standing long jump, ball throw, and 20 meter shuttle run. Subject age, weight, height, and scores strongly correlated with BUA, and age and height, and scores weakly correlated with VOS. Multiple regression analysis showed that weight, VOS, and septum of heel were the best predictors of BUA (R2=0.711 for boys, R2=0.684 for girls), and BUA, septum of heel, and scores were the best predictors of VOS (R2=0.527 for boys, R2=0.440 for girls). In conclusion, physical performance ability affects VOS more than BUA indicating that increase ability of physical strength influence the quality of bone more than bone mineral density or bone structure in children.

Disclosures: ***H. Kudo****, None.*

M149

Osteoporosis Screening: Comparison of Heel Ultrasound Measurement to Calculated Risk Assessment Tools. S. Poriau*[1], P. Geusens[2], F. Van den Bosch*[1], F. De Keyser*[1]. [1]Locomotorisch Centrum, Sijsele-Damme, Belgium, [2]Biomedical Research Institute, Diepenbeek, Belgium.

Quantitative ultrasound of the os calcis is accepted as an effective, low-cost method to assess osteoporotic fracture risk. Recently the International Society for Clinical Densitometry (ISCD) recommended the use of peripheral densitometry to identify patients who might have osteoporosis and should therefore undergo BMD testing at the hip and spine. This recommendation requires the use of a device specific T-score cutpoint on the peripheral device that detects 90% of individuals with osteoporosis at either the spine or hip. In this study, we wished to determine the 90% sensitivity cutpoint that could be used with the Achilles bone ultrasonometer. We also compared the performance of this ultrasonometer as a screening tool to a calculation-based osteoporosis risk assessment screening tool (OST). A total of 1087 women aged 50 years and older (mean age 68 ± 10 years) had DXA measurements of the spine (L1-L4) using a Lunar Prodigy (GE Healthcare) or a Lunar DPX-NT, as well as a heel ultrasound measurement using Achilles Solo. The OST ((weight in kg - age)*0.2) was calculated for each subject. From the ROC analysis the AUC values were determined for heel T-score and OST as well as the heel T-score cutpoint with 90% sensitivity for identifying subjects with osteoporosis (T-score ≤ -2.5) at the spine.

From the DXA results, 332 out of the 1087 subjects were classified as osteoporotic at the spine. A heel T-score of -1.4 demonstrated 91% sensitivity and 38% specificity in identifying osteoporotic subjects. Higher specificity of nearly 50% could be obtained with a T-score cutpoint of -1.8, which has a sensitivity of 85%.

ROC AUC for Osteoporosis at the AP Spine

Diagnostic Variable	AUC (95% Confidence Interval)
Stiffness Index T-Score	0.758 (0.727 - 0.790)
OST Risk Assessment Tool	0.747 (0.715 - 0.778)
Combined: T-score & OST	0.790 (0.761 - 0.819)

Comparison of ROC AUCs

Comparison	AUC Difference	p
T-Score - OST	0.011	0.543
Combined Risk - T-Score	0.032	0.0009
Combined Risk - OST	0.043	<0.0001

We conclude that the Achilles bone ultrasonometer can be used as a valid screening tool for osteoporosis according to ISCD recommendations. The Achilles Stiffness Index T-Score and OST provide independent assessment of risk for osteoporosis at the spine. Combining these risk factors yields better diagnostic performance than either used separately. However, a similar study using both hip and spine measurements for identifying subjects with osteoporosis showed that heel T-score performs better as a diagnostic tool than OST (M. Gambacciani *et al.*, 2004, presented at the World Congress Osteoporosis, Rio de Janeiro).

Disclosures: ***S. Poriau****, None.*

M150

Autosomal Dominant Pattern of Inheritance in an Australian Family with Low Bone Mineral Density. C. Meier[1], M. Kennerson*[2], G. Nicholson*[3], M. J. Seibel[1]. [1]Bone Research Program, ANZAC Research Institute, University of Sydney, Concord NSW, Australia, [2]Neurobiology Laboratory, ANZAC Research Institute, University of Sydney, Concord NSW, Australia, [3]Molecular Medicine Laboratory, Concord Hospital, Concord NSW, Australia.

Low bone mineral density (BMD) is a major risk factor for osteoporotic fractures. Based on family and twin data it is estimated that 60-80% of the variance in BMD is attributable to genetic factors.

We have identified a family of Anglo-German derivation (21 members, 3 generations, aged 19-86 years) in which 14 members are affected by low BMD at the spine and/or the femoral neck. The 1st generation consists of a female patient aged 86 yrs presenting with multiple low trauma fractures, a lumber spine BMD (LSBMD) T-Score of -4.1 SD (Z-Score -2.2 SD) and a femoral neck BMD (FNBMD) T-Score of -7.4 SD (Z-Score -5.5 SD). In the 2nd generation, all four members (2 females, 2 men, median age 58.2 yrs) are affected by low BMD (LSBMD: median T-score -3.1 SD, median Z-Score -2.8 SD; FNBMD: T-Score -1.8 SD, Z-Score -1.2 SD). Two members presented with prevalent fragility fractures. In the 3rd generation, 9 members (56%, 3 females, 6 males, age 30.7 yrs) had low BMD (LSBMD: T-Score -1.7 SD, Z-Score -1.4 SD; FNBMD: T-Score -1.3 SD, Z-Score -1.0 SD), whereas 7 individuals (3 females, 4 males; age 26.6 yrs) had normal BMD (LSBMD: T-Score -0.4 SD, Z-Score -0.3 SD; FNBMD: T-Score -0.1 SD, Z-Score -0.1 SD). One member of the 3rd generation was diagnosed with a fragility fracture. Secondary causes of osteoporosis were excluded in all affected individuals. Segregation of low BMD in this family is consistent with an autosomal dominant mode of inheritance.

In simulation studies using the SIMLINK program and four allele markers (n=450) a theoretical mean maximum logarithm of odds (LOD) score of 5.34 was obtained at a recombination fraction (θ) of 0.0. Simulation data also indicated the family had the power to exclude 10.2 cM on either side of an unlinked marker. Two-point linkage analyses excluded mutations in the genes for *COL1A1* (D17S1795, LOD score -2.91, θ of 0.10) and *COL1A2* (D7S3050, LOD score -3.29, θ of 0.10). In addition, the *LRP5* gene has been excluded by linkage analysis (D11S987, LOD score -2.16, θ of 0.5). Based on the autosomal dominant inheritance pattern of low BMD it seems likely that in this family, accrual and maintenance of BMD is under the predominant control of a single gene. A 10 cM genome wide screen is presently under way.

In summary, the study of this family has the statistical power to define a locus on a single chromosome demonstrating that an individual gene produces the observed phenotype.

Disclosures: ***C. Meier****, None.*

M151

Identification of Novel Genetic Loci for Bone Size and Mechanosensitivity in an ENU Mutant Exhibiting Decreased Bone Size. A. K. Srivastava, S. Kapur*, G. Masinde*, S. Kapur*, R. Chadwick*, J. Wergedal, S. Mohan, D. J. Baylink. JLP VAMC / Loma Linda Univ Dept Med, Loma Linda, CA, USA.

Using the ENU mutagenesis approach to reveal gene function, we have identified a mutant with reduced bone size in a dominant screen in C57BL/6J mice. Data from 16-week old progeny from this mutant showed that total body bone area was 10-14% lower and mean periosteal circumference was 4-8% lower at femur and tibia mid-diaphysis, as compared to WT B6 mice. Interestingly, the phenotype was mainly expressed in males while <5% females showed decreased bone size phenotypes. Since periosteal bone expansion is involved in bone adaptive response to mechanical loading, we predicted that genes regulating bone size could also be sensitive to mechanical loading. We used an in-vitro model of mechanical loading, a fluid flow induced shear stress, to study the effect of loading on periosteal osteoblasts isolated from tibia and femur (n=3) of mutant and wild type mice by collagenase digestion. Osteoblasts from wild type animals show a 70-80% increase in cell proliferation in response to shear stress, which was reduced by 60-70% ($p<0.01$) in cells from mutant mice. These observations suggest that in addition to bone size regulation, the mutant gene may be involved in modulating response to mechanical stress. In addition, the periosteal osteoblasts from mutant mice showed significantly reduced cell proliferation ($p<0.01$) and increased apoptosis ($p<0.01$), as compared to wild type controls (n=3), indicating a potential cellular mechanism for reduced bone size. To determine the chromosomal location of the mutation, we bred mutant B6 mice with C3H in an intercross breeding to generate B6C3H F2 mice (n=69 males) for a low-resolution (46-50 markers) QTL mapping. By using interval mapping, a mutant locus was identified in Chr 4 with a LOD score of 7.6 with genome wide significance of $p<0.001$. Based on the findings that genetic alleles from B6 contributed to low bone size and that a similar locus regulating bone size could not be identified in F2 mice generated from non-mutagenized C3HB6F2 (n=75 males), we consider this to be a mutant locus. In addition, this locus (7.5-12.1 cM) is novel since no QTL regulating bone size has been identified in this region of Chr 4 in any other crosses. In conclusion, an ENU mutant with decreased bone size was identified, the phenotype of mutant includes an impaired response of osteoblasts isolated from mutant mice to proliferation and mechanosensitivity, and QTL mapping indicates involvement of a new locus on chromosome-4 in regulating the bone size phenotype. Fine mapping is potentially more rapid for ENU mutations than a QTL gene.

Disclosures: ***A.K. Srivastava****, None.*

M152

QTL Mapping Of Blood Levels Of Alkaline Phosphatase In F2 Population Of MRL/SJL Mice Indicate Loci That Cosegregate With Bone Density And Bone Size. A. Srivastava, G. Masinde*, H. Yu*, D. J. Baylink, S. Mohan. JLP VAMC / Loma Linda Univ Dept Med, Loma Linda, CA, USA.

To examine the hypothesis that serum alkaline phosphatase (ALP) levels have a heritable component, we analyzed blood from two inbred strains of mice, MRL/MpJ and SJL, which exhibit 90% difference in total serum ALP activity (268±26 *vs.* 140±15 U/L, respectively, $P<0.001$). A genome-wide scan was carried out using 137 polymorphic markers in 518 F2 female mice. Serum ALP activity in the 7-week old F2 progeny showed a normal distribution with an estimated heritability of 56%. Genome-wide scan for co-segregation of genetic marker data with serum ALP activity revealed five significant quantitative trait loci (QTL), one on chromosomes 2 (LOD score 3.8), three on chromosome 6 (LOD scores, 6.5, 12.0, 5.8), and one on chromosome 14 (LOD score 3.7). In addition, one suggestive QTL on chromosome-2 exhibited LOD score of 3.3. Combined together, these QTLs explain 34.3% of the F2 variance in serum ALP levels. Serum ALP showed a moderate (Pearson r=0.12, p=0.0108) but significant correlation with body weight adjusted total body bone mineral (measured by DEXA) in F2 mice. The chromosome-6 locus harboring the major serum ALP QTL also contains a major BMD and bone size QTL identified earlier in the F2 population of these two strains of mice. In addition, this QTL is also close to locus that regulates IGF-I levels (LOD score 8-9) in C3HB6 F2 mice. Three additional QTLs of Chromosome 2 and 14 also harbor QTLs for BMD and bone size. Presences of these common QTLs indicate that the observed difference in ALP, BMD, and bone size may be regulated by the same loci (or genes). Osteoblast cells isolated from femur and tibia of MRL mice showed significantly higher number of ALP +ve cells/colony and higher ALP activity ($p<0.05$) as compared to the cells isolated from SJL mice, thus suggesting that differences in serum ALP between MRL and SJL mimic expression of osteoblasts from bone of these strains of mice. These data suggest that serum ALP levels are genetically determined and correlate with cellular mechanisms that differentiate BMD accrual in these two strains of mice. The findings that ALP and BMD traits share the same loci on chromosome-6 indicate a role for genetic determinants of bone formation in overall BMD accretion. To our knowledge this is the first study describing QTLs that regulate variation in serum levels of alkaline phosphatase among inbred strains of mice.

Disclosures: ***A. Srivastava****, None.*

M153

Genetic Linkage Exclusion of Six Candidate Loci for the Gene Causing Idiopathic Multicentric Osteolysis. W. Balemans*[1], E. Van Hul*[1], T. J. L. de Ravel*[2], E. Cleiren*[1], J. P. Fryns*[2], W. Van Hul[1]. [1]Dept. Medical Genetics, University of Antwerp, Antwerp, Belgium, [2]Centre for Human Genetics, UZ Gasthuisberg, Leuven, Belgium.

Idiopathic multicentric osteolysis (IMO) or Thieffry-Kohler syndrome is a rare, progressive bone disorder which mostly occurs as an autosomal dominant trait, but a number of isolated cases have been described and an autosomal recessive mode of inheritence has also been suggested. The condition presents already in early childhood with pain and swelling of peripheral joints. Radiographically, destructive bone lesions are observed starting at the carpal and tarsal bones, and spreading to the adjacent bones. Affected individuals may have distinct facial abnormalities with frontal bossing, protruberant eyes and micrognathia. Variable renal involvement has been described predominantly in isolated cases. We have studied a three-generation family with nine affected members showing the radiological and clinical features of IMO. The pedigree shows an autosomal dominant mode of inheritence. Previous linkage analysis (de Ravel et al., J. Med. Genet. 2000;37:E34) already excluded a region on chromosome 18q22.1 in which the gene encoding the receptor activator of nuclear factor kappaB (RANK) is located, the gene mutated in familial expansile osteolysis (FEO). Our objective was to carry out a linkage study on a number of other candidate loci. We investigated three regions harbouring a functional candidate gene: the osteoprotegerin (OPG) gene on chromosome 8q24, the gene encoding receptor activator of nuclear factor kappaB ligand (RANKL) on chromosome 13q14 and the matrix metalloproteinase 2 (MMP2) gene located on chromosome 16q13. These regions were studied because OPG and RANKL share a common pathway with RANK and mutations in MMP2 have been found in patients with multicentric osteolysis and arthritis syndrome. Additionally, three regions on chromosome 2q36, 5q35 and 10p13 for which suggestive linkage with familial Paget disease of bone has been reported, were investigated. Analysis of microsatellite markers for the six candidate loci, a haplotype study and two-point LOD score calculations did not reveal linkage with any of these regions. Therefore, we can conclude that the IMO phenotype segregating in our family is not linked to any of the six regions analyzed. In a further effort to localize the disease-causing gene in IMO we are currently performing a genome wide linkage study with microsatellite markers covering the entire genome.

Disclosures: ***W. Balemans****, None.*

M154

Fine Mapping Provides Further Evidence of Linkage for Bone Mineral Density to 3p21. S. G. Wilson[1], P. W. Reed*[2], T. Andrew*[3], M. Langdown*[4], R. L. Prince[5], T. D. Spector[3]. [1]Sir Charles Gairdner Hospital, Nedlands, Australia, [2]SignaGen, Rotorua, New Zealand, [3]St Thomas' Hospital, London, United Kingdom, [4]Sequenom Inc., San Diego, CA, USA, [5]University of Western Australia, Nedlands, Australia.

Low bone mineral density (BMD) is a major risk factor for osteoporotic fracture. Studies of BMD in families and twins have shown that this trait is under strong genetic control. We previously performed genome screens in two populations of Caucasian women in an attempt to localize the position of quantitative trait loci that regulate BMD (1). In that study we found evidence for linkage of lumbar spine BMD to markers on chromosome 3p, which was replicated in both genome screens. The aim of this study was to confirm and refine our previous linkage results for chromosome 3 by genotyping an expanded number of highly polymorphic microsatellite markers in available samples.

We studied a cohort of highly selected, extreme discordant and concordant sib pairs (1098 individuals). Lumbar spine and total hip BMD were determined using dual x-ray absorptiometry (QDR 2000, Hologic Inc, MA, USA). Laboratory analysis involved the genotyping of thirty additional microsatellite markers in the 3p region using standard fluorescence-based genotyping methodologies and ABI 377 automated sequencers (Applied Biosystems, CA, USA). At the conclusion of the study the average marker spacing in the region of interest (50cM - 111cM) was 2cM. Nonparametric multipoint linkage (NPL) analysis was undertaken for age adjusted lumbar spine and total hip BMD using MAPMAKER/SIBS. The maximum evidence of linkage defined by this analysis was LOD 3.6 for age-adjusted spine BMD at 68cM (Genethon linkage map). This is approximately the same position highlighted in the initial analysis. NPL analysis of age adjusted total-hip BMD provided a LOD <2.0. Average information content in the region increased to 0.6 and the -1 LOD support interval was reduced to 17cM. PTHR1 is positioned at approximately 67cM and continues to be a strong candidate for the QTL. Other positional candidate genes include MST1, MST1R and TNA.

The data further supports the presence of a gene(s) regulating BMD at 3p21 by providing an improved linkage map of the region in this cohort and by removing reliance of the linkage on a small number of widely spaced markers. This study provides strong support for the validity of our initial findings (1) and contributes to the goal of localizing and identifying QTL that regulate BMD.

1. Wilson SG *et al.*, 2003 Am. J. Hum. Genet. 72:144-155.

Disclosures: ***S.G. Wilson****, None.*

M155

Androgen Receptor CAG Repeat Polymorphism and Bone Density: A Family and Case-control Association Study in Men with Primary Osteoporosis. P. R. Ebeling[1], Z. Hussein*[1], J. Ellis*[2], A. Lamantia*[2], K. Greenland*[3], S. Yeung*[1], Z. Y. H. Wong*[2], J. D. Zajac[4], S. Harrap*[2]. [1]Diabetes and Endocrinology, The Royal Melbourne Hospital, Parkville, Australia, [2]Physiology, The University of Melbourne, Parkville, Australia, [3]Centre for Hormone Research, Murdoch Children's Research Institute, Parkville, Australia, [4]Medicine, Austin Hospital, The University of Melbourne, Heidelberg, Australia.

Androgens are important modulators of bone mass in men. The CAG trinucleotide repeat length in exon 1 of the AR gene is inversely associated with its transcriptional activity and may affect bone metabolism. Previous studies in normal men have yielded conflicting results on the role of AR CAG repeat polymorphisms on bone density (BMD).

We therefore investigated the association between the AR CAG repeat length, by DNA sequencing of exon 1 of the AR gene, and BMD in men with primary osteoporosis, their first-degree relatives and in normal men. Lumbar spine (LS), proximal femur and total body BMD was measured by DXA.

Forty-nine pedigrees were recruited and 38 sib-pairs were available for linkage analysis. From the family studies, hereditability was 0.74 (0.11) at the lumbar spine and 0.56 (0.17) at the femoral neck. Standardised bone density (Z-score) were mean z-LS = -1.35; and mean z-FN = -0.91. The CAG repeat length effect was equivalent to 0.3 SDs per 5 base pair difference in CAG repeat length at the lumbar spine, but not at the femoral neck.

Two association studies were also performed. The first was a case-controlled study of 81 men with primary osteoporosis and spinal fractures (mean age 55.6 years, mean LS T-score -2.53 and mean FN T-score -2.93) and 25 normal men (mean age 44.7 years, mean LS T-score 0.46 and mean FN T-score -0.14). Median AR CAG repeat length for the osteoporotic group was 20 (SD 3.2) versus 21.0 (SD 2.4) for the control group. Each group was also dichotomised with regards to with regards to short (less than 22) or long (greater than 22) repeat lengths. BMD was similar at all sites in men with either short or long CAG repeat length. The second study comprised 157 unrelated men (mean age 54.3 years, mean LS T-score -1.60, mean FN T-score -2.11 and median CAG repeat length of 20) who were subdivided according to genotypes of different AR CAG repeat lengths (range 6-29). BMD was then compared using one-way ANOVA. No associations were seen between CAG repeat length and BMD in either study.

Hereditability of BMD in families of men with spinal fractures is high and greater for the spine than proximal femur or total body sites. CAG repeat length in the androgen receptor has a small effect on spinal, but not femoral neck BMD. Other genetic factors are therefore likely to be more important.

Disclosures: ***P.R. Ebeling****, Roche 2; Aventis 5; merck 8.*

M156

Genome Screen for Femoral Structure QTLs in Men. D. L. Koller[1], S. L. Hui[2], C. C. Johnston[2], M. J. Econs[2], T. Foroud[1], M. Peacock[2]. [1]Medical and Molecular Genetics, Indiana University School of Medicine, Indianapolis, IN, USA, [2]Medicine, Indiana University School of Medicine, Indianapolis, IN, USA.

Femoral structure contributes to bone strength and predicts hip fracture risk independently of BMD. We previously reported an autosomal genome screen for femoral structure phenotypes in Caucasian premenopausal sister pairs (JBMR 16:985-91, 2001). Several of these loci were confirmed in an expanded sample of sister pairs (JBMR 18:1057-65, 2003). Reports in mice suggest that genes regulating BMD may be sex-specific. Thus we collected a sample of 257 healthy Caucasian brother pairs (age 18-61) to compare with our sister pairs and test the hypothesis that genes underlying normal variation in femoral structure are sex-specific. Pelvic and femur axis lengths, and widths of femur head, neck and femur midshaft were measured from radiographs. A genome screen using 392 microsatellite markers was completed on the brother pairs. Multipoint quantitative linkage analysis was performed using Mapmaker/SIBS. All chromosomal positions (cM) reported here correspond to the Marshfield map coordinates.

The most significant linkage finding in this study was for pelvic axis length, with a LOD score of 4.1 at position 70 cM on chromosome 4p. Pelvic axis length also produced a suggestive linkage finding (LOD > 2.2) on chromosome 17q (LOD=2.8 at 85 cM). The other LOD score exceeding 3.0 was for femoral head width on chromosome 15q (LOD=3.11 at 66 cM). Head width also demonstrated suggestive linkage on distal chromosome 11q (LOD=2.3 at 109 cM). We also found evidence of linkage of femur midshaft width to chromosome 14q (LOD=2.7 at 72 cM). There is no overlap between the linkage regions identified in men with the femoral structure linkages in women that we have previously reported. This suggests that different genes underlie the observed variability in femoral structure among healthy men and women.

Disclosures: ***D.L. Koller****, None.*

M157

Genome-wide Scan for QTL Underlying Normal Variation in Calcaneal Quantitative Ultrasound Measures: The Fels Longitudinal Study. S. A. Czerwinski*, M. Lee, A. C. Choh*, E. W. Demerath*, W. C. Chumlea*, S. S. Sun*, R. M. Siervogel*, B. Towne*. Community Health, Wright State University School of Medicine, Kettering, OH, USA.

Despite increasing knowledge of the genetics of osteoporosis in recent years, identifying the specific genes influencing osteoporosis risk factors has remained an elusive task. Calcaneal quantitative ultrasound (QUS) measures are correlated with bone mineral density, yet they also independently predict risk for fracture. In order to identify genes influencing susceptibility to osteoporosis, we performed quantitative trait linkage analysis on calcaneal QUS measures collected in a sample of nuclear and extended families participating in the Fels Longitudinal Study. A total of 453 participants ranging in age from 18-91 years had at least one calcaneal QUS assessment and genetic marker data. Each of these individuals were genotyped for 377 autosomal markers spaced approximately every 10 cM along the genome. Three calcaneal QUS measures were obtained from each participant including speed of sound (SOS), broadband ultrasound attenuation (BUA), and quantitative ultrasound index (QUI) using the Sahara ® bone sonometer (Hologic, Inc., Waltham, MA). Using a variance-components based maximum likelihood method (SOLAR) for pedigree data, we calculated initial heritability estimates (h^2) and identified quantitative trait loci (QTL) influencing variation in the three calcaneal QUS measures. In this sample, each of the QUS measures were highly heritable ranging from h^2=0.49 to 0.72 ($p<0.000001$) after adjusting for the effects of age, sex, age^2, age-by-sex, and age^2-by-sex. Preliminary results of the quantitative trait linkage screen revealed several chromosomes with LOD scores > 1 including regions of chromosomes 1, 11, 12, 13, and 20. The strongest evidence for linkage (maximum LOD = 2.12) was found at chromosome 4p15 near marker D4S419, a region identified in a previous study to influence variation in forearm bone mineral density.

Disclosures: ***S.A. Czerwinski****, None.*

M158

Associations Between Genetic Variation in the IL-1 Gene Cluster and Risk of Vertebral Fractures in Elderly Women. L. Lui[1], J. Rogus*[2], J. M. Zmuda[3], K. Kornman*[2], G. W. Duff*[4], K. Martha*[2], M. C. Nevitt[1], K. L. Stone[1]. [1]UCSF, San Francisco, CA, USA, [2]Interleukin Genetics, Waltham, MA, USA, [3]University of Pittsburgh, Pittsburgh, PA, USA, [4]University of Sheffield, Sheffield, United Kingdom.

Cytokines such as interleukin-1 (IL-1) are known to play a role in bone metabolism. Several studies have found polymorphisms of the IL-1 receptor antagonist gene (IL-1RN) to be associated with bone mineral density and spine bone loss in postmenopausal women. To test the hypothesis that genetic markers in the IL-1 gene cluster influence risk of vertebral fractures, we conducted a case-control study within a prospective study of 9,704 community-dwelling non-black women aged 65 years and older.

Whole blood samples were collected on filter paper at the second examination (1988-9). Prevalent and incident vertebral fractures were determined by morphometry using X-rays collected at baseline and an average of 3.5 years later. In 2003, polymorphisms in the IL-1 gene cluster on chromosome 2 (IL-1A +4845, IL-1B -511, IL-1B -3737, IL-1B +3954, IL-1RN +2018) were determined by PCR analysis. Polymorphisms were compared among 1237 women who had either a baseline prevalent or incident vertebral fractures and 1290 controls using logistic regression. Odds ratio (OR) and 95% confidence interval (CI) are reported. All models were adjusted for age, modified body mass index (using knee-height), age at menopause, and hormone use (ever vs. never use).

Overall, there was a modest 30% increase in risk of vertebral fracture among women with IL-1B (-511) 2.2 genotype compared to those with type 1.1 (OR=1.3; 95% CI 1.0 - 1.8; p=0.07). Similarly, those with IL-1RN type 2.2 were more likely to suffer a vertebral fracture than those with type 1.1 (OR=1.3; 0.9-1.9; p=0.10). Among women who had never used hormone replacement, these results were more pronounced. Never users of hormone replacement with IL-1B (-511) 2.2 genotype were at 60% increased risk of vertebral fractures compared to those with type 1.1 (OR=1.6; 95% CI 1.1-2.3; p=0.02), while those with IL-1RN genotype 2.2 were at 80% increased risk of fracture compared to type 1.1 (OR=1.8; 1.1-2.8; p=0.01). We found no consistent pattern of association for other polymorphisms of the IL-1 gene cluster and risk of vertebral fracture. Genetic variation in the IL-1 gene cluster may influence risk of vertebral fracture in elderly women, particularly among those who have never been treated with hormone therapy. Further study is needed to explain differences in patterns of association.

Disclosures: ***L. Lui****, None.*

M159

Vitamin D Receptor Polymorphisms and the Risk of Prostate Cancer. E. T. Jacobs[1], M. R. Haussler[2], M. E. Reid*[3], A. R. Giuliano*[1], E. Panczyk*[2], G. K. Whitfield[2], J. R. Marshall*[3], M. E. Martinez*[1]. [1]Arizona Cancer Center & Mel and Enid Zuckerman Arizona College of Public Health, University of Arizona, Tucson, AZ, USA, [2]Biochemistry & Molecular Biophysics, University of Arizona, Tucson, AZ, USA, [3]Roswell Park Cancer Institute, Buffalo, NY, USA.

In the United States, prostate cancer has the highest incidence rate of all cancers in males, with few known modifiable risk factors. The hormonal form of vitamin D, 1,25-dihydroxyvitamin D_3 (1,25D), has been shown to exert antiproliferative and prodifferentiating effects on prostate cancer cell lines via interaction with the vitamin D receptor (VDR). Alterations in the concentration or activity of this receptor could have a significant impact on the functions of the 1,25D ligand within the cell. The human VDR exhibits polymorphic variation, with two common unlinked variants identified via *FokI (F/f)* and *TaqI (T/t)* restriction enzymes. Data indicate that the *F* VDR allele generates an intrinsically more transcriptionally potent receptor, whereas the *T* haplotype (tightly linked to an *L* singlet (A) repeat allele) is associated with enhanced total VDR activity. The role of these VDR gene variants in the incidence of cancer is not well understood; therefore, we sought to determine whether the *FokI* and *TaqI* VDR polymorphisms were associated with the risk of prostate cancer among participants from the Nutritional Prevention of Cancer trial. In a nested case-control design with 92 prostate cancer cases and 174 controls matched for age, treatment group, and clinic site, we calculated the adjusted odds ratios for each VDR genotype. Compared to the *ff* genotype, the adjusted odds ratios (95% CI) for *Ff* and *FF* were 1.07 (0.52-2.20) and 1.34 (0.67-2.65), respectively. Although not statistically significant, this trend supports a recent result that the *F* VDR allele tends to enhance the risk of prostate cancer. For the *TaqI* polymorphism, the odds ratios were 0.73 (0.32-1.69) and 0.63 (0.27-1.45) for *Tt* and *TT,* respectively, compared to *tt*. Although not statistically significant, this trend is contrary to previous reports that the *T* VDR haplotype imparts a 4-fold increase in the risk of prostate cancer. Exploratory analyses of the combined VDR genotypes did not reveal any significant trends with respect to the incidence of prostate cancer. Therefore, in contrast to bone mineral density and fracture prevention, where the biochemically more active *F* and *T(L)* VDR alleles appear to be beneficial and additive, the incidence of prostate cancer appears to be influenced independently by the *F/f* and *T/t* variants in an opposing fashion. These data may explain the contradictory nature of reported individual VDR polymorphism correlations with the risk of prostate cancer.

Disclosures: ***E.T. Jacobs****, None.*

M160

Lack Of Association Between Androgen Receptor Polymorphisms And Bone Mineral Density Or Physical Function In Older Men. A. M. Kenny[1], D. McGee*[2], C. Joseph*[1], C. Abreu*[3], L. G. Raisz[3]. [1]Geriatrics, UConn Health Center, Farmington, CT, USA, [2]Biostatitics, Florida State University, Tallahassee, FL, USA, [3]Clinical Research Center, UConn Health Center, Farmington, CT, USA.

Individuals whose androgen receptors have short polyglutamine tracts (CAG repeats) exhibit greater transcriptional activation of the androgen receptor. Studies of the impact of this polymorphism on bone density have been conflicting and frequently lack a control group. We, therefore, evaluated the association between bone mineral density and the number of CAG repeats in older men with normal,osteopenic or osteoporotic femoral neck bone mineral density (FN BMD) and with or without a history of femoral fracture.

The number of CAG repeats was determined in 42 men with a history of a hip fracture in the preceding 3 years (FX), 33 men with no fracture but FN BMD T score -1.0 (C). In addition we measured bioavailable testosterone (BioT) and several measures of physical performance, including walking speed, chair rise time and standing balance as well as self-reported physical activity (PASE).

Mean age of the men was 76 + 7 years and body mass index was 27 + 4 kg/m2, with no difference among the groups. FN BMD t scores were -2.16 + 1.08 (FX), -2.26 + .74 (OP), and -0.20 + 0.40 (C) ($p<.001$). CAG repeats ranged from 17-29 and mean length was 21.9 + 2.7 (FX), 22.5 + 2.4 (OP), and 22.3 + 2.9 (C) ($p=.63$). The correlation between CAG and FN BMD was $r=.06$ ($p=.55$). Further, no significant correlations were found between CAG and bioavailable testosterone levels ($r=.02$, $p=.82$) or physical performance including walking speed ($r=.07$, $p=.52$), hand grip strength ($r=-.06$, $p=.63$), chair rise time ($r=.09$, $p=.40$) or composite physical performance (CPP) score ($r=.08$, $p=.44$). BioT levels were 66 + 36 ng/dl (FX), 63 + 32 ng/dl (OP), and 115 + 36 ng/dl (OC) ($p<.001$). Eight foot walk times were 3.4 + 1.3 s (FX), 2.8 + 1.0 s (OP) and 2.6 + .2 s (C) ($p=.046$). CPP scores were 8.0 + 3.0 (FX), 9.7 + 2.0 (OP), and 11.3 + .9 (C) ($p<.001$). PASE scores were 91 + 66 (FX), 122 + 66 (OP), and 200 + 55 (C)($p<.001$).

Thus in this cross-sectional study no association was found between the number of CAG repeats and FN BMD in older men with normal or low bone mineral density or with femoral fracture. Men with osteoporosis had significantly lower bioavailable testosterone levels than the control group. Further, physical performance and physical activity were lower in men with osteoporosis. The impact of BioT and physical activity and performance on BMD was substantial. These results do not rule out effects of CAG repeats and androgen receptor activity on age-related bone loss and changes in physical function, which need to be analyzed in longitudinal studies.

Disclosures: ***A.M. Kenny****, None.*

M161

Genetic and Environmental Determinants of Bone Mineral Density in Chinese Women. H. H. L. Lau[1], M. Y. M. Ng*[1], A. Y. Y. Ho[1], K. D. K. Luk*[2], A. W. C. Kung[1]. [1]Medicine, The University Of Hong Kong, Hong Kong, Hong Kong Special Administrative Region of China, [2]Orthopaedic Surgery, The University Of Hong Kong, Hong Kong, Hong Kong Special Administrative Region of China.

Genetic and Environmental Determinants of Bone Mineral Density in Chinese Women
BMD is a complex trait determined by genetic and lifestyle factors. To assess the genetic and environmental determinants of BMD in southern Chinese women, we studied a community-based cohort of 531 pre- and postmenopausal southern Chinese women and assessed the influence of 12 candidate gene loci and lifestyle risk factors on spine and hip BMD. The candidate genes studied include estrogen receptor alpha (ESR1) and beta (ESR2), calcium sensing receptor (CASR), vitamin D receptor (VDR), collagen type Iα1 (COLIA1) and LDL receptor-related protein 5 (LRP5). Social, medical, reproductive history, dietary habits and lifestyle factors were determined using a structured questionnaire. Single nucleotide polymorphisms (SNPs) of the COLIA1 and LRP5 gene in Chinese were determined by direct sequencing. Nucleotide (nt) -1363C/G and -1997 G/T of COLIA1, nt 266A/G, 2220C/T and 3989C/T of LRP5 gene were analyzed.
Using stepwise multiple linear regression analyses, body weight was the strongest predictor for BMD in premenopausal women (n=262), which accounted for 15.9% of the variance at the spine, 20% at femoral neck, 17.1% at trochanter, 24.3% at total hip and 10.9% at the Ward's triangle. Other significant predictors were ESR1 Ivs1 -397T/C genotype (2.2% at the spine); LRP5 2220C/T genotype (1.3% at the spine, 1.6% at the trochanter); LRP5 266A/G genotype (1.1% at Ward's triangle); age at menarche (1.3% at trochanter) and age (2.0% at Ward's triangle). As for postmenopausal women (n=269), body weight (~25% at various sites) and age (~16% at femoral neck, trochanter, total hip and Ward's triangle sites) were the strongest predictors of BMD. Other significant predictors were age at menarche (4.4% at spine, 0.7% at femoral neck, 1.4% at trochanter, and 1.4% at Ward's triangle); weight bearing physical activity (2.1% at trochanter and 1% at total hip); calcium intake (1.1% at femoral neck, 0.9% at trochanter, and 1.7% at total hip) ; height (0.7% at trochanter); and ESR2 1082A/G genotype (0.8% at trochanter). We conclude that BMD at various sites and at different time span of a woman is modified by different genetic and lifestyle factors, suggesting that BMD is highly dependent on gene-environmental interactions.

Disclosures: ***H.H.L. Lau****, None.*

M162

Association of Single Nucleotide Polymorphisms in The Promoter Region of Pro-opiomelanocortin Gene (*POMC*) with Low Mineral Density of Adult Women. Y. Sudo*[1], Y. Ezura[1], H. Yoshida*[2], T. Hosoi[2], S. Inoue[3], M. Shiraki[4], H. Orimo[2], H. Ito*[5], M. Emi*[1]. [1]Molecular Biology, Nippon Medical School, Institute of Gerontology, Kawasaki, Japan, [2]Tokyo Metropolitan Institute of Gerontology and Geriatrics Hospital, Tokyo, Japan, [3]Department of Geriatric Medicine, University of Tokyo, Faculty of Medicine, Tokyo, Japan, [4]Research Institute and Practice for Involutional Diseases, Nagano, Japan, [5]Orthopaedics, Nippon Medical School, Tokyo, Japan.

Osteoporosis, a multi-factorial common disease, results from interplay of multiple environmental and genetic factors, including the corticoid actions on bone mineral status. To investigate the genetic susceptibility of primary osteoporosis in adult women, we focused on a gene encoding the pro-opiomelanocortin (*POMC*), one of whose processing products adrenocorticotrophic hormone (ACTH) is a key regulator of the serum corticoid level. Association study was conducted on 384 adult Japanese women, whose bone mineral density (BMD) on distal radius was measured by DXA, and was adjusted for age and body mass index. Correlation between the adjusted BMD and the numerically categorized genotypes was tested by analysis of variance and the linear regression test as a post hoc test. Eight single nucleotide polymorphisms (SNPs) were investigated, including -2353G>A, -2345G>A, and -2313A>C. Linkage disequilibrium between every combination of the two SNPs was investigated by calculating indices of D' and r^2. Significant correlation between the genotypes and the BMD was detected for three promoter variations -2353G>A, -2345G>A and -2313A>C, among which the most significant correlation was detected for -2353G>A ($r = -0.16$, $p = 0.002$). The homozygous carriers of the major G-allele (G/G) had the highest BMD (mean ± SD = 0.405 ± 0.054 g/cm^2), the heterozygous carriers (G/A) had the intermediate (0.390 ± 0.053 g/cm^2) and the homozygous A-allele carriers (A/A) had the lowest (0.369 ± 0.048 g/cm^2). These three promoter variations appeared to be in strong LD at the level of almost complete LD ($D' \geq 0.978$, $r^2 \geq 0.856$). No significant correlation was detected for the other covariates (age, body weight, height, BMI, adjusted serum levels of cholesterols and triglyceride), except the significant association between -2313A>C and the adjusted total-cholesterol levels ($r = -0.12$, $p = 0.019$). Sequential consensus binding motif analysis of this promoter to the transcription factors revealed that two of the correlated SNPs were within the consensus binding-sites for known transcription factors (-2353G>A for GATA-1 or GATA-2 site, -2345G>A for the AML-1a site). These results suggested that variation of POMC might be one of the important determinants for postmenopausal osteoporosis.

Disclosures: ***Y. Sudo****, None.*

M163

Aromatase CYP19 Genetic Polymorphism Is Associated with Adult Stature, Androgen Levels, and Bone Mineral Density in 18-20-year-old Swedish Males. M. Lorentzon, C. Swanson, A. Eriksson, C. Ohlsson. Department of Internal Medicine, Center for Bone Research at the Sahlgrenska Academy (CBS), Gothenburg University, Gothenburg, Sweden.

Peak bone mass is to a large extent genetically determined and believed to be a predictor of future risk of osteoporosis. Androgens and estrogens are key regulators of skeletal growth and maturation in males. The aromatase CYP19 enzyme catalyzes the biosynthesis of estrogens from androgens.
The aim of the present cross sectional study was to determine if a tetranucleotide repeat polymorphism $(TTTA)_n$ in intron 4 of the aromatase CYP19 gene was associated with circulating androgen levels, adult stature, and bone mineral density (BMD) in 18-20-year-old Swedish males, currently included in The *G*othenburg *O*steoporosis and *O*besity *D*eterminants (*GOOD*) study.
941 men (age 18.9±0.6) were genotyped and classified according to the amplified fragment length, where fragments ≥182 and <182 bp, where coded L (long allele) and S (short allele), respectively. Subject homozygous for LL (n=141) where found to have 7.6 % higher serum levels of testosterone (p=0.008), 10.6 % higher free androgen index (FAI; p=0.015), and 1.4 cm higher stature (p=0.028) than their SL heterozygote and SS homzygote counterparts (n=800). Bone parameters were measured using both DXA and pQCT.
The aromatase CYP19 repeat polymorphism was found to be an independent predictor (in a multivariate analysis including present physical activity, age, height, weight, smoking, and calcium intake) of areal BMD of the lumbar spine as measured by DXA (p=0.03). To determine the associations between the aromatase CYP19 repeat polymorphism and the different bone compartments pQCT was utilized, demonstrating that this genetic polymorphism was an independent predictor of the radius cortical volumetric BMD (p<0.05), but not of the trabecular volumetric BMD. In conclusion, we demonstrate that the aromatase CYP19 repeat polymorphism is associated with adult stature and bone mineral density in young Swedish men, and propose that this association might be explained by the genotype specific differences in circulating levels of androgens.

Disclosures: ***M. Lorentzon****, None.*

M164

Cytochrome P450c17α (*CYP17*) Gene Polymorphism Indirectly Influences on Bone Density through Their Effects on Endogenous Androgen in Postmenopausal Japanese Women-Are the Effects of Age and Body Mass Index Greater than Those of Endogenous Sex Steroids? I. Gorai[1], M. Inada*[2], H. Morinaga*[2], Y. Uchiyama*[2], H. Yamauchi*[2], O. Chaki[2], F. Hirahara*[2]. [1]Obstetrics and Gynecology, International University of Health and Welfare Atami Hospital, Atami, Japan, [2]Obstetrics and Gynecology, Yokohama City University School of Medicine, Yokohama, Japan.

We aimed to assess whether circulating sex steroid hormones influence bone measured as bone density and biochemical markers, and whether some part of this influence can be explained by genetic variation measured as polymorphisms in candidate genes influencing circulating hormone levels in 250 postmenopausal Japanese women aged 46 yr and over who had been followed for eight years. Bone mineral density (BMD) at lumbar spine, femoral neck, total hip and distal radius was measured by DXA method every year and endogenous sex steroid hormone levels are determined at the start of the study. We investigated the polymorphisms of estrogen metabolizing enzyme genes, *CYP17*; estrogen biosynthesis (high activity, A2/A2), *CYP1A1*; hydroxylation (high inducibility, vt/vt) and *COMT*; inactivation (low activity, L/L) with PCR-based restriction fragment length polymorphism assays. The *CYP17* has both 17α-hydroxylase and 17, 20-lyase activities and catalyzes two distinct steps in steroid hormone production. There were significant correlations between the levels of androstenedione (AND) or dehydroepiandrosterone (DHEA), and bone densities at all sites examined. AND levels significantly correlated with annual bone loss in lumbar spine. After the adjustments of sex steroid levels with age and body mass index (BMI), all the significant associations between endogenous androgens and BMD or bone loss have disappeared. Women with A2/A2 genotype had significantly higher level of DHEA than that with A1/A1 or A1/A2 genotypes (DHEA P=0.0021 and P=0.0013, respectively). There was no significant difference between estrogen levels and *CYP17* genotype. We could not find any significant correlations between sex steroid hormone levels and *CYP1A1* or *COMT* gene polymorphism. There were no significant differences in bone density and annual changes of BMD at each site examined among each *CYP17*, *CYP1A1* or *COMT* genotypes except in bone loss at distal radius. The results suggest *CYP17* gene polymorphisms may have some indirect influences on bone density through their effects on endogenous androgen and these effects might be overcome by both ages and BMI.

Disclosures: ***I. Gorai****, None.*

M165

Functional Genomics of Tissue-nonspecific Alkaline Phosphatase. M. Goseki-Sone[1], N. Sogabe*[1], M. Fukushi-Irie*[1], L. Mizoi*[1], H. Orimo*[2], T. Suzuki[3], H. Nakamura*[4], H. Orimo[5], T. Hosoi[6]. [1]Food and Nutrition, Japan Women's University, Tokyo, Japan, [2]Biochemistry and Molecular Biology, Nippon Medical School, Tokyo, Japan, [3]Tokyo Metropolitan Institute for Gerontology, Tokyo, Japan, [4]Chemistry, Gakushuin University, Tokyo, Japan, [5]Health Science University, Tokyo, Japan, [6]Tokyo Metropolitan Geriatric Medical Center, Tokyo, Japan.

Alkaline phosphatase (ALP) is present mainly on the cell membrane in various tissues and hydrolyzes a variety of monophoshate esters into inorganic phosphoric acid and alco-

hol at a high optimal pH (pH8-10). Human ALPs are classified into four types: tissue nonspecific, intestinal, placental, and placental-like types. Based on studies of hypophosphatasia, which is a systemic skeletal disorder resulting from a tissue-nonspecific ALP (TNSALP) deficiency, TNSALP was suggested to be indispensable for bone mineralization. However, the polymophisms of TNSALP gene have not been studied as a possible determinant for the variation of bone mineral density or as a genetic predisposing factor for osteoporosis. We explored the possibility that the TNSALP gene may contribute to age-related bone loss in humans by examining the association between TNSALP gene polymorphisms and bone mineral density (BMD) in 501 Japanese post-menopausal women. We genotyped two single nucleotide polymorphisms (787T>C [Tyr246His] and 876A>G [Pro275Pro]), and these two polymorphisms were proved to be in complete linkage disequilibrium. There was a significant difference in BMD and Z score among haplotypes (p=0.041): lowest among 787T/876A homozygotes, highest among 787T>C/876A>G homozygotes, and intermediate among heterozygotes. In subgroups divided by age, haplotypes were significantly associated with BMD in aged postmenopausal women (>74 years; p=0.001), but not in younger postmenopausal women (≤74 years; p=0.964). Expression of the 787T>C TNSALP gene using COS-1 cells demonstrated that protein translated from 787T>C had ALP specific activity similar to that of 787T. Interestingly, the Km value for TNSALP in cells transfected with the 787T>C TNSALP gene was decreased significantly compared to that of cells bearing the 787T gene, reflecting the higher affinity. These results suggest that variation of TNSALP may be one of the important determinants of age-related bone loss in humans and that the phosphate metabolism pathway may provide novel targets for prevention and treatment of osteoporosis.

Disclosures: ***M. Goseki-Sone****, None.*

M166

The Cannabinoid CB2 Receptor: A Potential Target for the Diagnosis and Treatment of Osteoporosis. M. Karsak*[1], O. Ofek*[2], M. Fogel*[2], K. Wright*[3], J. Tam*[2], Y. Gabet[2], R. Birenboim*[2], M. Attar-Namdar*[2], R. Müller[4], M. Cohen-Solal[5], M. de Vernejoul[5], E. Shohami*[6], R. Mechoulam*[7], A. Zimmer*[1], I. Bab[2]. [1]Psychiatry, University of Bonn, Bonn, Germany, [2]Bone Laboratory, Hebrew University of Jerusalem, Jerusalem, Israel, [3]Pharmacology, University of Bath, Bath, United Kingdom, [4]Institute for Biomedical Engineering, ETH and University Zürich, Zürich, Switzerland, [5]Unite de Recherche 349, INSERM, Paris, France, [6]Pharmacology, Hebrew University of Jerusalem, Jerusalem, Israel, [7]Medicinal Chemistry, Hebrew University of Jerusalem, Jerusalem, Israel.

Endocannabinoids signal via G-protein coupled central CB1 and peripheral CB2 cannabinoid receptors. Although both receptors were discovered more than a decade ago, the physiologic function of the CB2 receptor remains obscure. Here we report the presence of CB2 receptors in trabecular, diaphyseal and MC3T3 E1 osteoblasts as well as osteoclasts. Reminiscent of post-menopausal osteoporosis in humans, the skeletal phenotype of CB2 deficient mice, which are otherwise normal, is characterized by a low trabecular bone mass, cortical expansion and increases in bone formation rate and osteoclast number. To extrapolate these findings to the human scenario, we performed genetic association studies in a case-control approach typing single nucleotide polymorphisms covering a region of about 100 kb. We found a highly significant difference of allelic and genotypic distributions, strongly arguing for a causative involvement of this locus with human osteoporosis. In line with the low trabecular bone mass phenotype of *CB2* knockout mice we found that HU-308, a specific CB2 agonist, stimulated dose dependently the number and activity of primary and MC3T3 E1 osteoblastic cells. Using the same dose range, HU-308 also restrained osteoclast differentiation of bone marrow derived monocytes. Most importantly, HU-308 attenuated ovariectomy-induced bone loss mainly by inhibiting osteoclast number. Collectively these results assign a skeletal regulatory role for CB2 signalling and offer a new molecular target for the diagnosis and treatment of osteoporosis.

Disclosures: ***M. Karsak****, None.*

M167

Interleukin 1ß -511 C/T Polymorphysm Is Related to the Response to Bisphosphonate Treatment in Paget Disease of Bone (PDB). J. del Pino-Montes*[1], L. Corral-Gudino[2], R. Gonzalez-Sarmiento*[3], C. A. Montilla*[1], I. Pastor*[2], J. García-Aparicio*[2]. [1]Medicine. Rheumatology, University Hospital. Universidad de Salamanca, Salamanca, Spain, [2]Medicine, University Hospital. Universidad de Salamanca, Salamanca, Spain, [3]Medicine, Universidad de Salamanca, Salamanca, Spain.

Bisphosphonates (BP) are used frequently for the treatment of PDB. BP suppress bone resorption by inhibiting both osteoclast (OCL) proliferation and activity, and inducing OCL apoptosis. The interleukines 1ß and 6 (IL-1ß, IL-6) play a role in OCL formation and activity so they could influence the response to BP treatment.

We evaluated whether genetic variability at the IL-1ß and the IL-6 loci are associated with the response to BPS in PDB.

We analysed single-nucleotide polymorphisms (SNP) in the promoter region of IL-1 ß gene (-511 C/T), exon 5 of IL-1 ß gene (3953 T/C), IL-1 receptor gene (IL-1 R1), IL-1 receptor antagonist gene (IL-1 RN) and promoter region of IL-6 gene (-174 G/C). Genotypes were tested for an association with the percentage of successful responses to BSP treatment (% SRB) in a group of 96 patients with sporadic non familial PDB: Tiludronate (n = 42), Etidronate (n = 34), Risedronate (n =22), Clodronate (n = 11), Pamidronate (n = 2) and Alendronate (n = 1). We considered a successful response to treatment when a decrease of, at least, 50% of the levels of total serum alkaline phosphatase (SAP) previous to the treatment were achieved at six months. Moreover we tested the skeletal extension (Renier anatomic index) and the clinical activity (AP) (number of times that SAP is over the upper normal limit at diagnosis). ANOVA test and Tukey Post Hoc Multiple comparison test were used for continuous variables.

The IL-1ß promoter region genotype was significantly associated with the response to BSP treatment. The multiple comparison with the genotype A1/A1 was statistically significant (A2/A2-A1/A1 p value 0,05, A1/A1-A1/A2 p value < 0,01, A2/A2-A1/A2 p value 0,82).

There were no differences in the extension and activity of the PDB between the different genotypes. ANOVA test for the comparison of Renier index according to exon 5 of IL-1 ß gene was statistically significant but Tukey test did not show any significance.

In conclusion, the A2 allele of the -511 C/T IL-1ß polymorphism could be a marker of favourable outcome to the BSP treatment in PDB patients. This observation still needs to be clarified through further study.

Disclosures: ***J. del Pino-Montes****, None.*

M168

Faster Bone Growth During Puberty Contributed by the COL1A2 Polymorphism - A Benefit or Risk? M. Suuriniemi*[1], A. Mahonen*[2], A. Lyytikäinen*[1], V. Kovanen*[1], M. Alén*[3], S. Cheng[1]. [1]University of Jyväskylä, Jyväskylä, Finland, [2]University of Kuopio, Kuopio, Finland, [3]PEURUNKA - Medical Rehabilitation Center, Jyväskylä, Finland.

We have previously found an association between the COL1A2 polymorphism and fractures in pre- and early pubertal Finnish girls. The purpose of this study was to search for possible explanations behind the increased fracture risk of the *PP* genotype from the rate of growth in bone mass. The subjects were 10-13 yr-old girls (n=218) with Tanner stage I-III, who participated in an intervention study (the CALEX-study). Measurements were made at baseline, year 1, and year 2. Genotyping of the COL1A2 locus at the *PvuII* polymorphic site was performed. Bone properties of the total body (TB), total proximal femur (TF), femoral neck (FN), and lumbar spine (L2-L4) were measured by DXA (Prodigy, GE Lunar). Our results showed that girls with different genotype were evenly distributed into the different intervention groups. Bone properties were similar at baseline between the genotypes. There were no significant differences among the genotypes in Tanner stage during the trial or in 2-yr changes (%) of weight, height, body mass index, and bone areas of the measured bone sites. However, girls with the *PP* genotype had significantly greater increases (%) of bone mineral content (BMC, g) [*PP* (28±11) vs. *Pp* (24±10), p=0.031, and *pp* (23±9), p=0.023] and areal bone mineral density (aBMD, g/cm^2) [*PP* (17±7) vs. *Pp* (13±7), p=0.004, and *pp* (14±6), p=0.023] of FN, compared to the others. They also tended to have greater increases (%) of BMC [*PP* (38±13) vs. *Pp* (33±11), p=0.086, and *pp* (33±11), p=0.080] and aBMD [*PP* (17±8) vs. *Pp* (14±6), p=0.052, and *pp* (14±7), p=0.094] of TF. Compared to the others, the increments of BMC and aBMD of TB and L2-L4 were 2-4% and 1-2% higher in the *PP* girls, respectively, but the differences did not reach statistical significance. Interestingly, girls with the *PP* genotype tended to be taller (cm) at birth than girls with the *pp* genotype [*PP* (50.3±2.0) vs. *pp* (49.6±1.8), p=0.098]. Fathers of the *PP* girls were taller (cm) as well compared to those of the *pp* girls [*PP* (179.4±6.4) vs. *pp* (176.8±6.0), p=0.034]. Our results suggest that the COL1A2 polymorphism may contribute to acquisition of bone mass during puberty. The rapid growth in bone matrix of the *PP* girls may exceed the capacity of mineralization, leading to an increase in bone fragility and fracture risk. In addition, the COL1A2 polymorphism may affect skeletal growth during fetal period of rapid growth. Whether the increased incidence of fractures due to fast growth of the *PP* girls is just a price that has to be paid in order to maximize bone accumulation during growth, or a real risk for osteoporotic fractures in older age, needs to be clarified.

Disclosures: ***M. Suuriniemi****, None.*

M169

LRP5 **Gene Polymorphisms Predict Bone Mass and Incident Fractures in Elderly Australian Women.** J. Bollerslev[1], S. G. Wilson*[2], I. M. Dick*[2], A. F. M. Islam*[2], T. Ueland*[1], A. Devine*[2], R. L. Prince*[2]. [1]Rikshospitalet University Hospital, Oslo, Norway, [2]University of Western Australia, Nedlands, Australia.

Postmenopausal osteoporosis and bone mass are influenced by multiple factors including genetic variance. The importance of LDL Receptor-Related Protein 5 (*LRP5)* for the regulation of bone mass has recently been established, where loss of function mutations is followed by severe osteoporosis and gain of function related to increased bone mass. The aim of this study was to evaluate the role of polymorphisms in the *LRP5* gene for bone mass and prospective fracture frequency in a well described, large cohort of normal, ambulatory Australian women. A total of 1301 women were genotyped for 7 different single nucleotide polymorphisms (SNPs) within the *LRP5* gene and related to basal biochemistry, calcaneal Quantitative Ultrasound measurements (QUS) and osteodensitometry of the hip. Two SNPs were found to be associated with fracture rate and bone mineral density. The two SNPs were in strong LD, the LD block spanning from exon 15 to intron 19. Homozygous mutation of rs556442 was associated with significant reduction in bone mass at most femoral sites. The difference in total hip BMC was 3.4%, (P< 0.037), in femoral neck BMC 3.9% (P = 0.012), femoral neck BMD 3.9% (P = 0.005), in trochanter BMC 4.4% (P = 0.033), and in BUA 1.4% (P = 0.038). In the 5 years follow-up period, 227 subjects experienced a total of 290 fractures which were radiologically confirmed. The incident fracture rate was significantly increased in subjects homozygous for the polymorphism (RR of fracture = 1.61, 95% CI [1.05 - 2.44], P = 0.027). After adjusting for total hip BMD, the fracture rate was still increased (RR = 1.67 [1.02 - 2.78], P = 0.045), indicating factors other than bone mass are of importance for bone strength. In conclusion, genetic variance of *LRP5* seems to be of importance for regulation of bone mass and osteoporotic fractures.

Disclosures: ***J. Bollerslev****, None.*

M170

Insulin-Like Growth Factor I (IGF-I) Gene Microsatellite Repeat Polymorphism and Its Relation to Hyperthyroidism and Thyroid Hormone-stimulated Bone Loss. E. Bajnok*, A. Tabak*, I. Takacs, P. L. Lakatos*, C. Horvath, Z. Nagy, G. Speer, P. Lakatos. First Department of Medicine, Semmelweis University, Budapest, Hungary.

The knowledge and understanding of the molecular and genetic mechanisms that generate toxic adenoma (TA) producing hyperthyroidism, and resulting in thyroid hormone-stimulated bone loss are far from complete. In this study we investigated the previously described IGF-I gene CA microsatellite repeat polymorphism, located 1 kb upstream from the IGF-I gene transcription start site. These gene variants are involved in the influence of different serum IGF-I concentrations, tumorgenesis and bone metabolism. We studied the possible functional contribution of this gene polymorphism to the pathogenesis of hyperthyroidism and bone loss as a consequence of TA.

Allele and genotype frequencies for the IGF-I gene and bone mineral density (BMD) values were determined among 182 postmenopausal women: 68 patients with TA (TA, mean age: 57.03 ± 9.15 [40-70] years) and 114 healthy controls (C, mean age: 54.21 ± 5.38 [40-68] years). The polymorphic regions of IGF-I gene were amplified by PCR technique using genomic DNA isolated from blood. BMD of the lumbar spine, femoral neck and distal radius was measured by DEXA and SPA, respectively. For statistical analysis SPSS for Windows 9.0.0 was applied.

We have found the allele “192” (67.03%) and “194” (18.14 %) to be the most common gene variants in our population. We have demonstrated the higher presence of the noncarrier subjects of allele “192” in the TA group compared to the controls (p =0.028). Studying subjects by BMD, “192/192” genotype was found to be exhibited more frequently in TA patients having normal BMD compared to TA subjects with osteoporosis and to healthy controls (p=0,0267). This polymorphism of IGF-I gene was also correlated with BMD in TA group. Z-score values at the radius, as being among the sites affected by hyperthyroidism, were higher in the subjects homozygous for “192” allele compared to that be heterozygous or noncarrier of it (p=0,025).

This is the first study reporting the possible functional contribution of IGF-I gene promoter polymorphism in the pathogenesis of TA. Based on our observations we suppose that the absence of “192” allele might predispose for the susceptibility of toxic adenoma and thyreogen bone loss in postmenopausal women. Extension and confirmation of these preliminary data are needed.

Disclosures: ***E. Bajnok****, None.*

M171

Association between Collagen Type I Alpha1 (COL1A1) Gene Sp1-, Calcium-sensing Receptor (CaSR) Gene A986S-, Interleukin-1 Receptor Antagonist (IL-1LN) Gene VNTR Polymorphisms and Osteoporosis; Their Impact in Prediction of Osteoporotic Bone Fracture. E. Bajnok*, G. Lakatos*, A. Tabak*, I. Takacs, C. Horvath, J. Kosa*, G. Speer, E. Madarasz*, Z. Nagy, P. Lakatos. First Department of Medicine, Semmelweis University, Budapest, Hungary.

Osteoporosis (OP) is the most common bone disease. The disabilities, which result from osteoporotic fractures (OPF), have enormous impact on the health of individuals, societies and economies. Twin and family studies have shown that genetic factors play an important role in regulating bone mineral density (BMD) as well as contributing to the development of OPF itself. The genes responsible for these effects are incompletely defined and require a multi-gene approach. Based on the results of former studies, our aim were to investigate the importance of the COL1A1 gene G1245T Sp1-, the CaSR gene A986S- and the IL-1RN gene 86 bp VNTR polymorphism in BMD, and their possible functional contribution to the susceptibility to OPF in Hungarian postmenopausal women.

Frequencies of genotypes and BMD values were determined among 180 postmenopausal women [40-70 yrs]: 90 subjects with serious OP (sOP, mean age: 60.79 ± 8.75 yrs*)* and 90 healthy controls (C, mean age: 54.2 ± 4.83 yrs). BMD of the lumbar spine, femoral neck and distal radius was measured by DEXA and SPA, respectively. Patients were enrolled in the study if the BMD value was below -4 t-score at any measured site. Prevalent fractures were estimated by obtaining a fracture history from each subject. OPF was diagnosed if it was occurred after the age of 40 years and was due to minimal trauma included at the femoral neck-, thoracolumbal vertebral region or at the wrist.

The ss genotype of COL1A1 gene- and the AS/SS genotypes of CaSR gene were found to be more frequent in patient with sOP compared to C subjects (p=0.028/p=0.04). We have found significant correlation between BMD and COL1A1/CaSR genotypes (p=0.05/0.021). No clinical significance of these polymorphisms on OPF was proved. There was no association between the IL-1RN gene polymorphism and BMD. On the other hand, in the sOP group the A2A2/A1A2 genotypes were more frequent in patients with OPF than in the subject without it.

Our results affirm that certain genotypes of COL1A1 gene Sp1 and CaSR gene A986S polymorphisms might predispose to postmenopaual osteoporosis and might also be a prognostic marker of the disease. We could not prove any clinically significance of these gene variants on bone fracture. Based on our observation we conclude that IL-1RN VNTR polymorphism may not play an essential role in the determination of BMD in postmenopausal osteoporosis; however, our data support a hypothesis that it may influence the bone fracture risk, independent of BMD.

Disclosures: ***E. Bajnok****, None.*

M172

Polymorphisms in the Osteoclast-associated Receptor Gene Are Associated With Risk of Osteopenia and Osteoporosis. J. Koh[1], E. Park[2], G. Kim[1], H. Shin*[3], S. Kim[4]. [1]Department of Endocrinology and Metabolism, University of Ulsan School of Medicine, Seoul, Republic of Korea, [2]Skeletal Diseases Genome Research Center, Kyungpook National University Hospital, Daegu, Republic of Korea, [3]Department of Genetic Epidemiology, SNP Genetics, Inc, Seoul, Republic of Korea, [4]Department of Orthopedic Surgery, Kyungpook National University Hospital, Daegu, Republic of Korea.

Osteoclast-associated receptor (OSCAR) is expressed specifically in preosteoclasts or mature osteoclasts. and has been suggested that it may be an important bone-specific regulator of osteoclast differentiation.

Despite the important role as bone regulator of the OSCAR, little is known concerning the genetic study of this gene. The human OSCAR (alternatively, MIM 606862), located on chromosome 19q13.4, has two Ig-like domains.

In an effort to discover polymorphisms in OSCAR gene, we scrutinized the single nucleotide polymorphisms (SNPs) in OSCAR as a potent candidate gene for osteoporosis by direct sequencing in 24 Korean individuals. Ten sequence variants were identified: 2 in 5' flanking region, 1 in intron 1, 1 in 5'UTR, 3 in exon 4, 2 in exon5, and 1 in exon 6. Five of these polymorphisms were selected for a large scale genotyping (n=683) by considering their allele frequencies, haplotype-tagging status, and linkage disequilibrium coefficiencies (LDs) among polymorphisms. Using statistical analyses for association of *OSCAR* polymorphisms with bone mineral density (BMD), no significant signals were detected. However, in case-control analysis, one polymorphism in 5' flanking region, *OSCAR-2322A>G,* and two haplotypes (*OSCAR-ht1* and *-ht4*) were associated with the risk of osteopenia and osteroporosis.

In conclusion, we identified ten genetic polymorphisms in the OSCAR gene and *OSCAR-2322A>G, -ht1*, and *-ht4* were significantly associated with the risk of osteopenia and osteoporosis, although no significant associations of OSCAR variants with the change of BMDs were detected. OSCAR variation/haplotype information identified in this study will provide valuable information for future association studies of other genetic diseases.

Disclosures: ***E. Park****, None.*

M173

Effect of CYP450 Gene Polymorphisms on Estrogen Metabolism and Bone Density. N. Napoli, S. Mumm, S. Sheik*, G. B. Rini, R. C. Villareal. Medicine, Washington University School of Medicine, St. Louis, MO, USA.

Polymorphisms of the CYP450 enzymes that metabolize estrogen are linked to hormone-related disorders, but little is known on their effect on estrogen metabolism in-vivo, and on bone density (BMD). The objective of this study, is to evaluate the effect of polymorphisms of the CYP1A1, CYP1A2, CYP1B1 and CYP3A4 on estrogen metabolism and BMD. We previously reported that the A allele of the CYP1A1 C4887A polymorphism is associated with a profile of accelerated estrogen catabolism, and lower femoral BMD. Here, we report new findings from this ongoing study which, to date, enrolled 193 postmenopausal women and 74 men ≥ 50 years old. Genotyping was done by restriction fragment length polymorphism and pyrosequencing. BMD of the lumbar spine and femur were measured by dual energy X-ray absorptiometry, and urinary metabolites [2-hydroxyestrone ($2OHE_1$), 2-methoxyestrone ($2MeOE_1$), 16α-hydroxyestrone ($16\alpha OHE_1$), and estriol (E_3)] by enzyme immunoassay. Our latest findings indicate that women with the C allele (GC+CC) of the G1294C polymorphism of the CYP1B1 gene have higher urinary metabolites and lower BMD of the spine and femur. Women subjects were further stratified into 3 composite genotypes for CYP1A1 C4887A and CYP1B1 G1294C polymorphisms. Group1: no genes “affected” i.e. CC for CYP1A1 and GG for CYP1B1; group 1: one gene “affected”, "affected" CYP1A1 (CA or AA) and "unaffected" CYP1B1 (GG), or “unaffected” CYP1A1 (CC) and “affected” CYP1B1 (GC or CC); and group 3: where both genes are “affected” i.e. CA or AA for CYP1A1 and GC or CC for CYP1B1. Group 3 have the highest levels of individual and total metabolites (Figure, Panel A) group 1 the lowest, and group 2 levels intermediate groups 1 and 3. In contrast, spine and femoral BMD (Figure, Panel B) were lowest in group 3, highest in group1, and group 2 values intermediate groups 1 and 3. Serum estradiol were comparable among the groups. In conclusion, the C allele of the CYP1B1 G1294C polymorphism is associated with increased estrogen catabolism and lower BMD. A combination of the A allele (CYP1A1 C4887A) and the C allele (CYP1B1 G1294C) resulted in an augmented rate of estrogen catabolism, and much lower BMD relative to those with none or only one of these alleles are present. These polymorphisms may represent as genetic risk factors for osteoporosis.

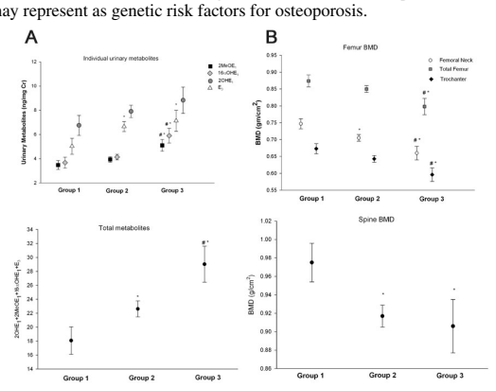

Disclosures: ***N. Napoli****, None.*

M174

Polymorphisms in the IGF-II Gene are Associated with Body Weight and Bone Mass. B. L. Langdahl, L. B. Husted*, L. Stenkjaer*, M. Carstens*. Endocrinology, Aarhus University Hospital, Aarhus C, Denmark.

Insulin-like growth factor (IGF)-I and -II stimulate proliferation of osteoblast-like cells in vitro. With this role in the control of bone development and osteoblast activity the IGFs have been suggested as candidate genes for genetic control of bone mass and fracture risk. We therefore examined the 9 exons with surrounding intron sequences and the four promoter regions of the IGF-II gene for polymorphisms by sequencing in 50 osteoporotic patients and 50 normal controls. We found 6 polymorphisms, of which some have been reported earlier. We here report the analyses of the effects of one polymorphism in the first promoter: 6815delAGGGC, one polymorphism in exon 3: 1252T-C, two polymorphisms in the third promoter (intron 4): 1543C-T and 1981C-T and one polymorphism in the 5'UTR: 266C-T on prevalence of osteoporotic fractures, bone mass and bone turnover in 409 osteoporotic patients and 340 normal controls.

The 6815delAGGGC polymorphism has previously been reported as a SNP: 6815A-T, however, sequencing revealed that the polymorphism was a deletion of 5 bases. This polymorphism has previously been found to be associated with BMI in middle-aged men.

In the present study, the C allele of the 1252T-C polymorphism in exon 3 was associated with reduced weight in normal men: 75.5±10.2 kg vs. 82.8±12.5 kg ($p<0.05$), none of the other examined polymorphisms was significantly associated with BMI, height or weight in neither osteoporotic patients or in normal controls.

None of the examined polymorphisms was significantly associated with osteoporosis either defined by the presence of osteoporotic fractures or BMD T-score of the spine or hip less than -2.5.

The 3'UTR polymorphism 266C-T was significantly associated with BMD at the hip sites. In women with the CC, CT and TT genotypes, femoral neck BMD were: 0.739±0.119 g/cm^2, 0.762±0.092 g/cm^2 and 0.891±0.104 g/cm^2, respectively, $p<0.05$. At the total hip the corresponding values were: 0.846±0.142 g/cm^2, 0.869±0.136 g/cm^2 and 1.042±0.025 g/cm^2, respectively, $p<0.05$. The 266C-T was not associated with biochemical markers of bone turnover. None of the other polymorphisms was associated with bone mass or bone turnover.

In conclusion: We have identified 6 polymorphisms in the IGF-II gene and we have found that a polymorphism in the first promoter: 6815delAGGGC is associated with body weight and that a polymorphism in the 3'UTR: 266C-T is associated with increased bone mass at the hip.

Disclosures: ***B.L. Langdahl****, None.*

M175

A DNA Variant Correlated to Lactose Intolerance Interacts with VDR Gene Variants to Determine Height, Bone Geometry and BMD. J. van Meurs[1], C. Zillikens*[1], Y. Fang*[1], H. Zhao*[1], J. van Leeuwen[1], A. Hofman*[1], B. Obermayer-Pietsch*[2], H. Pols[1], A. Uitterlinden[1]. [1]Internal Medicine, Erasmus Medical Center, Rotterdam, Netherlands, [2]Internal Medicine, Karl-Franzens Hospital, Graz, Austria.

Adult-type lactose intolerance affects about half of the world's population. It is caused by developmental down-regulation of the lactase-phlorizin hydrolase (LPH) gene in the small intestinal epithelial cells. Lactose intolerance may affect calcium supply and, thus, might influence bone strength and risk for osteoporosis. Recently, the C-allele of a functional T/C substitution at position -13910 bp upstream of the LPH-gene was found to be expressed >4-times lower in intestinal biopsies, and was found associated with lactose intolerance. We therefore examined whether this variant is associated with dietary habits, calcium levels, bone characteristics, and fracture risk. Since calcium absorption is regulated by vitamin D, we also studied interaction between the LPH variant and polymorphisms at the 3'end of the VDR gene, as previously defined by haplotype tagging SNPs, encompassing the 3'UTR. We determined LPH and VDR genotype in a population-based sample of 6,464 Dutch Caucasian elderly men and women who participated in a large prospective follow-up study. BMD data were available for 5321 subjects while 957 incident fractures were validated.

We found the LPH C-allele (31% allele frequency) to be associated in an allele-dose dependent way with lower calcium-intake ($p<0.001$), lower serum calcium levels ($p=0.005$), smaller stature ($p<0.001$), and smaller bone size ($p=0.003$). These associations were present in both men and women and were independent of age. The associations with stature and bone size were not dependent on calcium-intake or calcium serum levels. The LPH SNP was not associated with BMD or with fracture risk.

For analysis of interaction with VDR polymorphisms, subjects were divided by carrier status for VDR haplotype allele 1. We observed that only in carriers of VDR haplotype 1 (n= 4,581), the LPH C-allele was associated with lower height, smaller bone size, and with lower BMD. We detected significant interaction between both genetic variants with respect to height (p interaction term = 0.02), bone size ($p=0.01$), BMD at the femoral neck and lumbar spine ($p=0.04$). We could not detect an interaction for fracture risk.

In conclusion, variation at the VDR- and LPH-gene interact to determine height, bone geometry and bone mineral density, but not fracture risk. The biological mechanism underlying this interaction probably involves calcium-absorption. Further research will focus on interaction of dietary components and the vitamin D system with the LPH polymorphism.

Disclosures: ***J. van Meurs****, None.*

M176

Intragenic Interaction of VDR Haplotype Alleles Determines Fracture Risk. Y. Fang*, J. van Meurs, H. Y. Zhao*, J. van Leeuwen, H. Pols, A. Uitterlinden. Internal Medicine, Erasmus Medical Center, Rotterdam, Netherlands.

Polymorphisms of the vitamin D receptor (VDR) gene have been found associated with complex diseases, including osteoporosis. Most studies have used polymorphisms at the 3'end or in exon 2, but information on other polymorphism across the VDR gene is scarce. In 15 Caucasians, we sequenced 22 kb genomic VDR sequence, including the 3'untranslated region (3'UTR), all coding exons and the 6 promoter exons 1f - 1c. We determined linkage disequilibrium (LD; pair-wise D') between single nucleotide polymorphisms (SNPs) across and flanking the VDR gene in 234 Caucasians, 107 Asians and 58 African Americans. We performed association studies with "haplotype tagging" SNPs (htSNPs) and fracture risk in 6535 elderly Caucasians from the Rotterdam Study. 5819 subjects had BMD measurement, and 950 osteoporotic fractures and 356 vertebral fractures were validated in 7.4 follow-up years. Dietary calcium intake was assessed by food frequency questionaire.

We identified 62 polymorphisms, of which 22 SNPs (40%) are new. In the promoter region, 14 polymorphisms change the putative recognition sequences of transcription factors, 4 SNPs are located in destabilizing elements in the 3'UTR. LD analysis of common SNPs (frequency ≥ 5 %) revealed 4 - 8 haplotype blocks ($D' > 0.8$) which are conserved among Caucasians and Asians, but more fragmented in Africans. Haplotype blocks in the VDR gene show no or low linkage to other genes nearby, and 15 htSNPs were used for the association study. The 1e - 1a promoter haplotype block 2 (containing the Cdx-2 SNP), was associated with 32 % increased risk for vertebral fracture ($p = 0.03$). Haplotype block 5 (including the 3'UTR) was associated with 26 % increased risk of osteoporotic fracture ($p = 0.004$). The combined risk alleles showed 46% increased risk for vertebral fracture ($p = 0.03$) and 34% increased risk for osteoporotic fracture ($p = 0.01$) with adjustment for age, gender, height and weight. Overall, no or small genotype effects on BMD were observed. Dietary calcium intake is positively correllated with BMD ($r = 0.10$; $p < 0.001$), but this correlation (r) was absent and non-significant in carriers with promoter and 3'UTR VDR risk haplotype alleles (n = 204) vs. non-carriers (n = 2818): $r = -0.001$; $p = 0.98$ vs. $r = 0.11$; $p < 0.001$.

This "whole gene" analysis demonstrates intragenic interaction of VDR polymorphisms in the promoter region and in the 3'UTR to significantly contribute to fracture risk. We found differential VDR genotype-dependent effects on the influence of dietary calcium intake on BMD. Our finding suggests these risk alleles to encode a "less-sensitive" VDR, probably by encoding lower numbers of VDRs on target cells.

Disclosures: ***Y. Fang****, None.*

M177

Genetic Variation in *LRP5, RANKL, RANK, OPG* and *VDR* Gene Is Associated with BMD. Y. Hsu[1], T. Niu*[1], X. Xu*[1], Y. Feng[1], H. Terwedow*[1], T. Zang*[2], D. Wu*[2], G. Tang*[2], Z. Li*[2], X. Hong*[2], B. Wang*[1], M. L. Bouxsein[3], J. Brain*[1], C. Rosen[4], X. Xu[1]. [1]Program for Population Genetics, Harvard School of Public Health, Boston, MA, USA, [2]Anhui Medical University. Institute of Medicine, Anhui, China, [3]Beth Israel Deaconess Medical Center, Boston, MA, USA, [4]Maine Center for Osteoporosis Research and Education, St. Joseph Hospital, Bangor, ME, USA.

The variation of BMD is influenced by both genetic and environmental factors. The purpose of this study was to assess the contribution of *LRP5 (low density lipoprotein receptor-related protein 5), RANKL (tumor necrosis factor ligand superfamily, member 11), RANK (tumor necrosis factor receptor superfamily, member 11a, activator of NFκB), OPG (osteoprotegerin, tumor necrosis factor receptor superfamily, member 11b)* and *VDR* (*vitamin D receptor*) polymorphisms to the population-based variation in BMD among Chinese. For each candidate gene, we selected SNPs in exon (nonsynonymous SNPs), 5' flanking region, and 3' UTR region and intron haplotype tagSNPs with minor allele frequency larger than 5% in Chinese population. Forearm BMD was measured by pDEXA in 540 men and women aged 20-80 among residents of Anhui Province, China. Multivariate regression models were performed to access the association with adjusting for age, gender, body mass index and other confounders. The table below showed the result with significant level. For each SNP, the β coefficient was calculated by compared the genotype of minor allele homozygosity to the genotype of major allele homozygosity. Haplotype analysis also showed significantly associated with forearm BMD for LRP5, OPG, VDR and RANKL gene. In summary, we found polymorphisms in LRP5, OPG, RANKL, RANK and VDR gene were strongly associated with forearm BMD in Chinese population. An ongoing large scale case control study will be used to confirm these result. Supported by NIAMS grant R01 AR045651

Gene (SNPs)	Substitution	Region	Minor allele frequency	Distal BMD β coefficient	Distal BMD p-value	Proximal BMD β coefficient	Proximal BMD p-value
OPG (8q24.1)							
A163G	A - > G	5' flanking	16.5%	0.4691	0.0004	0.4849	0.0002
T245G	T - > G	5' flanking	16.2%	0.5057	0.0002	0.5264	<0.0001
rs2875845	A - > G	Intron	12.0%	0.5727	0.0015	0.3084	0.0247
RANK (18q22.1)							
Ala192Val	T - > C	Exon7	33.7%	0.1211	0.0123	0.1310	0.0050
RANKL(13 q14)							
rs2277438	G - > A	5' UTR	31.1%	0.2310	0.0007	0.1323	0.014
VDR (12q12-q14)							
rs739837	C - > A	3' UTR	30.1%	0.2443	0.0018	0.2160	0.0040
LRP5 (11q13.4)							
Gln89Arg	A - > G	Exon2	8.6%	-0.1601	0.0345	-0.1784	0.0022
Asn740Asn	C - > T	Exon11	20.4%	-0.1099	0.003	-0.0724	0.0370
Ala1330Val	C - > T	Exon19	21.5%	-0.1350	0.0002	-0.1538	0.0003

Disclosures: ***Y. Hsu****, None.*

M178

Genetic Variation in *ALOX15, BMP2, PPARr* and *IGF1* Gene Is Associated with BMD. Y. Hsu[1], Y. Zhang[1], X. Xu*[1], Y. Feng[1], H. Terwedow*[1], T. Zang*[2], D. Wu*[2], G. Tang*[2], Z. Li*[2], X. Hong*[2], B. Wang*[1], M. L. Bouxsein[3], J. Brain*[1], C. Rosen[4], X. Xu[1]. [1]Program for Population Genetics, Harvard School of Public Health, Boston, MA, USA, [2]Anhui Medical University. Institute of Medicine, Anhui, China, [3]Beth Israel Deaconess Medical Center, Boston, MA, USA, [4]Maine Center for Osteoporosis Research and Education, St. Joseph Hospital, Bangor, ME, USA.

The variation of BMD is influenced by both genetic and environmental factors. The purpose of this study was to assess the contribution of *ALOX15 (arachidonate 15-lipoxygenase), BMP2 (bone morphogenetic protein 2), PPARr (peroxisome proliferative activated receptor, gamma) a*nd *IGF1 (insulin-like growth factor 1)* polymorphisms to the population-based variation in BMD among Chinese. For each candidate gene, we selected SNPs in exon (nonsynonymous SNPs), 5' flanking region, and 3' UTR region and intron haplotype tagSNPs with minor allele frequency larger than 5% in Chinese population. Hip BMD was measured by DXA in 6743 men and women aged 25-65 among residents of Anhui Province, China. The subjects were then grouped into men, post-menopausal women and pre- (or peri-) menopausal women. For each group, a multiple linear regression model including age, BMI, weight and lifestyle factors was used to calculate the hip BMD residual. Subjects with hip BMD residual below the 10th and above the 90th percentile of the reference distribution were defined as extreme low BMD case and extreme high BMD control, respectively. We genotyped 547 cases and 547 controls. (53% were men, 18% post-menopausal women). The table below showed a partial result. For each SNP, the OR was calculated by compared genotypes to the reference genotype (homozygosity of major allele). In summary, this study has identified several novel associations between genetic variation and the BMD in Chinese population. The genetic effect seems not contribute the same way between men, pre- (peri-) menopausal and post-menopausal women. An ongoing cross-sectional study will be used to confirm these results. Supported by NIAMS grant R01 AR045651

Gene (SNPs)	Region	Genotype	Men OR (p-value)	Pre- (Peri-) menopausal women	Post-menopausal women
ALOX15(17P13. 3)					
rs2664592	5' flanking Malt box	CC	1	1	1
		CG	0.82	0.60	0.59 (0.04)
		GG	2.37	3.55	0.65
IGF1 (12q22-q23)					
rs6220	Exon6UTR	CC	1	1	1
		CT	0.57 (0.020)	0.92	0.48 (0.020)
		TT	0.55 (0.001)	0.89	0.62
rs5742657	Intron 3	AA	1	1	1
		AG	0.78	4.09	1.29
		GG	1.23	4.14 (0.010)	1.23
BMP2 (20p12)					
Arg190Sel	Exon4	TT	1	1	1
		TA	2.58	0.53	0.53
		AA	2.01	0.57 (0.03)	0.46
PPARγ (3p25)					
rs2960422	Intron 4	GG	1	1	1
		GA	0.93	0.58 (0.04)	0.94
		AA	0.79	0.67	0.46

Disclosures: ***Y. Hsu****, None.*

M179

A VNTR in the *CLCN7* Gene Influences Bone Density in Patients with Autosomal Dominant Osteopetrosis (ADO) Type II and in Post-menopausal Women. U. Kornak*[1], S. Branger*[2], A. Ostertag*[2], M. C. de Vernejoul*[2]. [1]Research Group Development and Disease, Max Planck Institute for Molecular Genetics, Berlin, Germany, [2]Inserm u 606, Hôpital Lariboisière, Paris, France.

The ClC-7 chloride channel is crucial for bone resorption as it is part of the osteoclast acid secretion mechanism. Heterozygous mutations in ClC-7 are responsible for autosomal dominant osteopetrosis type II (ADOII), a disorder characterized by a highly variable phenotype even within the same family. We hypothesized that polymorphisms in the *CLCN7* gene could be associated with the variability of bone density in ADO II and in the general population. We therefore investigated a large family with a mild variant of ADO II caused by the heterozygous mutation 2423DelAG in *CLCN7*. The penetrance was exceptionally low with 9 affected and 8 non-affected mutation carriers. Instead of sandwich vertebrae, some affected carriers only showed a diffuse osteosclerosis at the spine that is more typical for other high bone mass traits, e.g. ADO type 1. We investigated the non-coding SNP 126C/T in exon 1, the coding SNP 1252A/G in exon 15 and a VNTR in intron 8 that ranges between 2 and 10 repeat units. No association between the phenotype of the carriers and the SNPs was observed. All the affected carriers, however, had 3 repeat units in intron 8 of the allele without mutation, whereas the corresponding number in 5 of 8 non-affected carriers was higher than 3 (p=0.002). We therefore investigated if the length of the intron 8 VNTR could be associated with a higher bone density in 394 post-menopausal women with an average age of 64+5 years. Women with 3 repeat units on both alleles (17%) had a higher BMD at the femoral neck (0.78+0.14 vs. 0.74+0.12 mg/cm2 (p<0.009) than individuals with higher repeat numbers. The difference between both groups persisted when the BMD was adjusted for age, height, weight, years since menopause and hormone replacement therapy.

In conclusion, a VNTR polymorphism in intron 8 of *CLCN7* has a small impact on BMD in ADO II and in the normal population. In both cases the allele containing 3 repeat units is associated with a higher bone density, presumably because of a reduced osteoclast activity.

Disclosures: ***U. Kornak****, None.*

M180

LRP5 Amino Acid Substitutions: Ethnic Differences in Allele Frequencies and Association with Bone Density and Structure in Afro-Caribbean Men. J. I. Oakley[1], S. P. Moffett*[1], N. Petro*[2], J. A. Cauley[1], T. J. Beck[3], C. H. Bunker*[1], A. L. Patrick*[4], V. W. Wheeler*[4], R. E. Ferrell*[2], J. M. Zmuda[1]. [1]Epidemiology, University of Pittsburgh, Pittsburgh, PA, USA, [2]Human Genetics, University of Pittsburgh, Pittsburgh, PA, USA, [3]School of Medicine, Johns Hopkins University, Baltimore, MD, USA, [4]Tobago Health Studies Office, Scarborough, Trinidad and Tobago.

Recent studies have indicated that the low-density lipoprotein (LDL) receptor related protein 5(LRP5) gene located on chromosome 11q12-13 in humans is a major contributor to bone mass and morphology. Mutations within the gene have been linked to both high bone mass syndromes and low bone mass disorders like osteoporosis-pseudoglioma. We investigated the association of two amino acid substitutions in the LRP5 gene with bone mineral density (BMD) and structural geometry in men of African ancestry age 38-90 years (mean, 57) from Tobago.

BMD was measured at the hip by dual-energy X-ray absorptiometry (DXA; Hologic QDR 4500). Bone structural geometry was assessed at the femoral neck and shaft by hip structural analysis on hip DXA scans. Men were genotyped for two SNPs that altered the amino acid sequence of the protein by missense substitution. At exon 9 a G to A substitution changes the amino acid from valine to methionine at codon 667 (V667M) and at exon 18 a C to T substitution changes the amino acid from arginine to valine at codon 1330 (A1330V).

We sequenced the first 171 men for the V667M polymorphism and only found two heterozygotes (G/A) and 169 homozygotes (G/G). The minor allele frequency (MAF) was 0.006, considerably less than that reported in Caucasians (MAF, 0.06); thus we did not genotype any additional individuals.

Of the 778 men genotyped by fluorescence polarization for the A1330V polymorphism the majority were homozygous (C/C) and only 5% heterozygous (C/T). The genotypes were in Hardy-Weinberg Equilibrium. The minor allele frequency was 0.02 which is considerably less than that reported in Caucasians and Asians (MAF, 0.15 and 0.21 respectively). Despite sufficient sample size to detect modest genotype related differences we found no significant association between the A1330V polymorphism and femoral neck and shaft BMD, cortical thickness, or biomechanical indices of bone strength (p=0.35-0.90).

Since lower BMD in Caucasians and Asians has been found in other studies to be associated with the A1330V polymorphism, our non-significant association to BMD in this Afro-Caribbean cohort parallels ethnic differences seen in bone mass across these ethnicities. We conclude that ethnicity may influence the impact of the A1330V polymorphism on bone mass and morphology.

Disclosures: ***J.I. Oakley****, None.*

M181

Nuclear Receptor Coactivator-3 (*NCOA3/AIB1/SRC3*) Alleles are a Strong Correlate of Bioavailable Testosterone and Vertebral Bone Mass in Older Men. J. M. Zmuda[1], J. A. Cauley[1], R. E. Ferrell[2]. [1]Epidemiology, University of Pittsburgh, Pittsburgh, PA, USA, [2]Human Genetics, University of Pittsburgh, Pittsburgh, PA, USA.

Nuclear receptor coactivator-3 (*NCOA3/AIB1/SRC3*) is a member of the steroid receptor coactivator family that interacts with nuclear hormone receptors to enhance their transcriptional activator functions. The protein encoded by this gene has histone acetyltransferase activity and recruits p300/CBP-associated factor and CREB binding protein as part of a multi-subunit coactivation complex. We describe a novel and strong association between genetic variation at this locus, androgenic hormone levels, and bone mass among older men. We analyzed the association between alleles at this locus and bone mineral density (BMD) (Hologic QDR) in 263 community-dwelling Caucasian men (age 66±7 yrs, mean±SD; range, 51-84 yr). Men were genotyped for a CAG repeat polymorphism of *NCOA3* which encodes a polyglutamine tract of variable length in the C-terminus of the encoded protein. We found a significant monotonic decrease in lumbar spine BMD with increasing copies of the 224 bp allele (Table). Men with two copies of this allele had 7% or 0.5 standard deviations (SD) greater spine BMD than men without this allele, and *NCOA3* genotype explained 3.5% of the phenotypic variation in spine BMD independent of age, weight and height. Serum levels of bioavailable testosterone and sex hormone binding globulin paralleled genotype related differences in spine BMD. In contrast, there was no significant association between *NCOA3* alleles and hip BMD. An association with spine, but not hip, BMD raises the possibility that *NCOA3* alleles act in a bone compartment (trabecular *vs* cortical) and/or skeletal site specific (spine *vs* hip) manner. We conclude that allelic variation at the *NCOA3* locus may contribute to the genetic regulation of androgenic hormones and vertebral bone mass among older men.

Table. NCOA3 224 bp Alleles

	0	1	2	*P*-Value
Number of Men	67	112	84	
Bioavailable Testosterone (ng/dl)	140 (38)	122 (48)	124 (43)	0.01
Sex Hormone Binding Globulin (ug/dl)	1.09 (0.36)	1.18 (0.51)	1.35 (0.63)	0.003
Lumbar Spine BMD (g/cm^2)	1.10 (0.16)	1.08 (0.16)	1.02 (0.16)	0.006
Total Hip BMD (g/cm^2)	0.96 (0.15)	0.95 (0.13)	0.94 (0.15)	0.54

Disclosures: ***J.M. Zmuda****, None.*

M182

Estrogen Receptor-a Genotype and Hip Fracture Risk in Older Women: Evidence for a Strong Interaction with Body Mass Index. J. M. Zmuda[1], J. A. Cauley[1], L. Lui[2], D. R. Greene*[3], J. Li*[3], K. Walker*[3], K. L. Stone[2], K. E. Ensrud[4], T. A. Hillier[5], G. Peltz*[6], S. R. Cummings[7]. [1]Epidemiology, University of Pittsburgh, Pittsburgh, PA, USA, [2]Epidemiology, University of California, San Francisco, CA, USA, [3]Roche Molecular Systems, Alameda, CA, USA, [4]University of Minnesota, Minneapolis, MN, USA, [5]Kaiser Permanente Center for Health Research, Portland, OR, USA, [6]Roche Palo Alto, Palot Alto, CA, USA, [7]California Pacific Medical Center, San Francisco, CA, USA.

Women with low levels of endogenous estrogen have an increased risk for hip fracture. Adipose tissue is a major source of endogenous estrogen among older women and obesity is inversely related to hip fracture risk. In the current study, we analyzed the independent and joint effects of an estrogen receptor alpha (*ESR1*) polymorphism (IVS -401 T→C) which has been shown to enhance estrogen sensitivity and body mass index (BMI) on the risk of hip fracture among 6177 women aged 65 years and older in the Study of Osteoporotic Fractures. *ESR1* genotype was determined by the TaqMan 5' exonuclease assay. A total of 522 hip fractures occurred over an average of 10 years. *ESR1* genotype was not associated with the risk of hip fracture in the total cohort (Relative Risk, 0.97 per C allele; 95% CI: 0.86, 1.10). However, the relationship between *ESR1* genotype and fracture risk was modified by BMI (*P*=0.009 for interaction). For example, among women with BMI above the median (25.6 kg/m^2), the RR per C allele for hip fracture was 0.74 (95% CI: 0.61, 0.91) vs. 1.15 (95% CI: 0.98, 1.34, p=0.08) for those with BMI above the median. Among women with BMI below median, the RR of hip fracture for those with the C/C genotype compared to T/T was 0.47 (95% CI: 0.30, 0.76). Results were adjusted for age, use of hormone therapy, hip bone mineral density, and clinical center. These findings suggest a role of the *ESR1* locus in the genetic susceptibility to hip fracture among a subgroup of older women. The decreased risk of hip fracture among heavier women with the *ESR1* C allele might be explained by an increased sensitivity to endogenous estrogen in this subgroup of women.

Disclosures: ***J.M. Zmuda****, None.*

M183

Effects of PGE2 EP4 Receptor Agonist on Distraction Osteogenesis. F. Chang*, H. Mishima, H. Akaogi*, T. Ishii*, N. Ochiai*. Department of Orthopaedic Surgery, Institute of Clinical Medicine,University of Tsukuba, Tsukuba,Ibaraki, Japan.

As a bone remodeling factor, PGE2 exerts the effects mainly via the EP4 receptor. It is reported that the EP4 receptor agonist stimulated bone formation both in vivo and in vitro. In present study, we examined whether EP4 selective agonist enhanced the bone consolidation during distraction osteogenesis.

First, rats were operated to make the distraction osteogenesis models in left femur. The lengthening protocol included a seven-day latency period, followed by twice daily incremental lengthening of 0.25 or 0.5 mm (Tab 1). Normal saline, EP4 selective agonist (ONO-4819-CD) 3, 10, 30 μg /kg were delivered by subcutaneous injection twice daily. Lengthening and injection were performed until animals were sacrificed. This protocol was approved by the ethics committee of Tsukuba University.

Tab 1 Experimental groups

	0.5 mm/day			0.25 mm/day
	10 day	17 day	21 day	21 day
30μg /kg	3	3	5	6
10μg /kg			6	6
3μg /kg			5	6
normal saline	3	3	6	6

To evaluate the results, hardness, soft X-ray and histological examination were performed. The hardness of the middle parts of distraction area was measured. Using soft X-ray photo, bone mineral density was determined by Scion Image.

As a result, bone mineral density was higher in EP4 agonist injection group in both 0.25 mm and 0.5 mm (fig 1, 2) lengthening groups ($P<0.05$). As to hardness examination, EP4 agonist injection group was harder than control group ($P<0.05$). Both effects were dose dependent. In histological section, compare to the abundant fiber tissue in control group, there was more bone like tissue in EP4 agonist injection group.

In conclusion, subcutaneous injection of EP4 receptor agonist stimulated the regenerate ossification and increased bone mineral density during distraction osteogenesis.

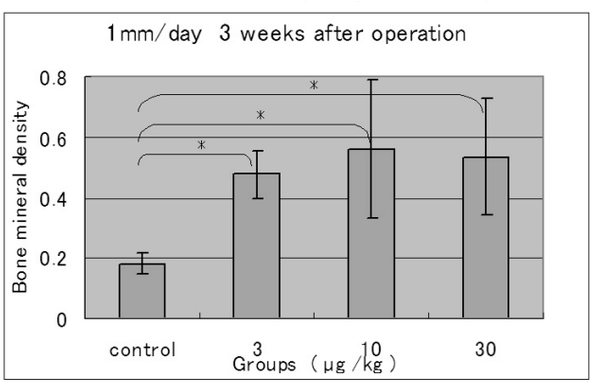

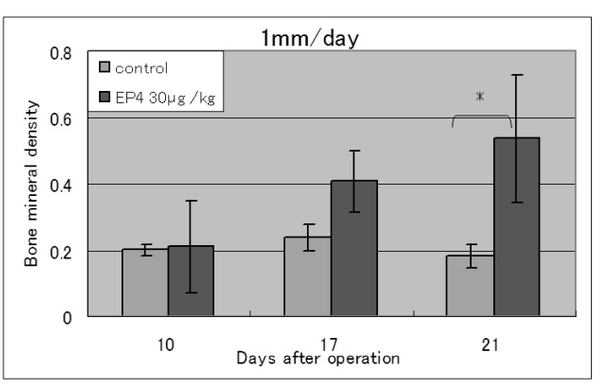

Disclosures: ***F. Chang****, None.*

M184

Osteoinduction of Human Mesenchymal Stem Cells by Adenovirus-Mediated ALK-2 Gene Therapy. S. Moon, H. Kim*, U. Kwon*, K. Lee*, J. Jeon*, J. Jahng, K. Yang*, H. Lee*, S. Park*. Department of Orthopaedic Surgery, Yonsei Univesity College of Medicine, Seoul, Republic of Korea.

Human mesenchymal stem cells (hMSCs) from the bone marrow represent a potential source of pluripotent cells for autogenous bone tissue engineering. Various growth factors, chemicals, and signaling molecules were utilized to facilitate osteogenic differentiation of hMSC. Transforming growth factor-betas (TGF-betas) and bone morphogenetic proteins (BMPs), members of a TGF-beta superfamily, are known to play an important role in osteogenic cell differentiation and consequently bone formation. Activin-receptor-like kinase-2 (ALK-2) has osteogenic activity through phosphorylation by BMP-2 induced TGF-beta type II receptor. In this study, osteogenic activity of hMSC through overexpression of ALK-2 was tested. hMSC were harvested from bone marrow and cultured. Type 5 adenovirus-ALK-2 gene constructs (Ad/ALK-2) were engineered and amplified in 293 cells. hMSC cultures were transfected by Ad/ALK-2 with an multiplicity of infection (MOI) of 150 and 300 with or without BMP-2 (20ng/ml). Then cultures were incubated for 3, 7, 14 days in 5% serum added medium. Immunohistochemistry and ELISA for osteocalcin, stains for alkaline phosphatase, von Kossa, alizarin-red S were performed. RT-PCRs and Western blot analysis for ALK-2, Smad8, and osteocalcin were also performed. hMSC cultures with Ad/ALK-2 showed positive stain for alkaline phosphatase, von Kossa, alizarin red-S, and increased expression of osteocalcin at 7 and 14 days compared control. hMSC culture with Ad/ALK-2 also demonstrated increased expression of ALK-2, Smad8, and osteocalcin in mRNA and protein level in dose dependent manner. hMSC cultures with Ad/ALK-2 (150 MOI) and BMP-2 (20ng/ml) showed synergistic effect in osteogenic differentiation compared to those of Ad/ALK-2 alone. However, hMSC with BMP-2 alone did not show osteogenic differentiation. In summary, overexpression of ALK-2 rendered osteogenic differentiation of hMSC, which effect was synergistic with low dose of BMP-2. In conclusion, ALK-2 gene therapy to MSC provides a feasible option for osteoinduction and osteogenesis.

Disclosures: ***S. Moon****, Brain Korea 21 Project 2.*

M185

A Crucial Role of Membrane-bound Prostaglandin E Synthase (mPGES) in Inflammatory Bone Loss. C. Matsumoto*[1], S. Uematsu*[2], S. Akira*[2], C. Miyaura[1]. [1]Biotechnology and Life Science, Tokyo University of Agriculture and Technology, Tokyo, Japan, [2]Research Institute for Microbial Disease, Osaka University, Osaka, Japan.

Prostaglandin E2 (PGE2) is produced by osteoblasts and acts as a potent stimulator of bone resorption. We have found that the production of PGE2 by osteoblasts is induced by lipopolysaccharide (LPS), and regulated by the release of arachidonic acid (AA) from membranous phospholipids by cytosolic phospholipase A2, the conversion of AA to PGH2 by COX-2, and the synthesis of PGE2 by membrane-bound PGE synthase (mPGES). However, the relationship between mPGES-dependent PGE synthesis and inflammatory bone loss is not known. In this study, using mPGES-null mice, we examined the role of mPGES in PGE2 synthesis by osteoblasts, and LPS-induced bone loss in femur and mandibular alveolar bone. To examine the role of mPGES in PGE2 synthesis by osteoblasts, bone marrow cells were collected from mPGES-null and wild-type (WT) mice, and cultured for 2 weeks to obtain osteoblastic stromal cells. LPS greatly stimulated PGE2 production by the osteoblastic stromal cells in WT mice, but not in mPGES-null mice. When mPGES-null and WT mice were injected with LPS intraperitoneally, we detected the reduced bone mineral density (BMD) in femur in WT mice, but not in mPGES-null mice. In histological sections of distal femoral metaphysis, LPS administration induced osteoclastic bone resorption in femoral cancellous bone in WT mice, but not in mPGES-null mice. To examine the role of mPGES in bone loss associated with an experimental periodontitis, LPS was injected into gingiva in mPGES-null and WT mice, and alveolar bone was collected from mouse mandible to measure the BMD. LPS injection into gingiva markedly reduced alveolar bone mass with increased osteoclasts in WT mice, but not in mPGES-null mice, suggesting the role of mPGES in inflammatory bone loss associated with periodontitis. In conclusion, our results indicate that mPGES-dependent PGE synthesis is essential to LPS-induced bone loss in femur and mandibular alveolar bone in mice, and suggest a possible new approach to inflammatory bone destruction including periodontal diseases by inhibiting mPGES.

Disclosures: ***C. Miyaura****, None.*

M186

Platelet-Derived Growth Factor-D (PDGF-D) Is a Novel Osteogenic Factor. S. Topouzis*, K. Lum*, D. Thompson*, M. Holdren*, J. Shin*, C. Birks*, A. Haran*, R. Kuestner*, H. Ren*, D. Gilbertson*, T. Palmer*, D. Dong*, S. Hughes*, E. Moore. ZymoGenetics Inc., Seattle, WA, USA.

We describe the in vivo and in vitro bone anabolic properties of a new member of the PDGF family, PDGF-D. PDGF-D is elaborated as an inactive precursor dimer, PDGF-DD-Full-Length (PDGF-DD-FL). Proteolytic cleavage releases the bioactive C-terminal moiety, PDGF-DD-Growth-Factor-Domain (PDGF-DD-GFD), which selectively binds to the PDGF receptor-beta.

PDGF-B has been previously reported to possess bone-anabolic properties. For this reason, we compared the effects of PDGF-B and PDGF-D on the skeleton by bolus delivery of adenoviral constructs expressing human PDGF-BB (hPDGF-BB) or hPDGF-DD-FL into two-month-old female mice (8 mice per group). ELISA analysis of sera showed that circulating PDGF-BB and PDGF-DD protein levels peaked around 10-15 days post virus treatment and had returned to basal by 4-6 weeks. Histopathological evaluation of multiple bones including the femur, humerus and vertebrae revealed extensive formation of mineralized endosteal bone within the marrow cavity as early as 2 weeks after treatment with

either hPDGF-BB or hPDGF-DD-FL adenoviral constructs but not with a parental adenoviral construct. The newly formed bone persisted with some signs of remodeling for at least 8 weeks post-treatment.
In order to elucidate the underlying mechanism of action, we tested the effect in vitro of recombinant factors on marrow-derived human Mesenchymal Stem Cells (huMSC) from 2 independent donors. Both PDGF-BB and PDGF-DD-GFD induced 8- to 10-fold increases in thymidine incorporation. When huMSC were maintained in an adipogenic medium, both growth factors abrogated adipogenic differentiation, as assessed by the appearance of lipid droplet-filled cells. In contrast, when huMSC were maintained in an osteogenic medium, treatment with PDGF-BB or PDGF-DD-GFD resulted in increased mineralization at 3 weeks, as assessed by von Kossa staining and calcium content. In addition, immunocytochemical analysis showed that treatment with either protein enhanced the nuclear accumulation of the osteoblast-specific marker Osf2/CBFA-1. Finally, both PDGF-BB and PDGF-DD-GFD induced increases of steady-state mRNA levels of the osteogenic differentiation markers osteocalcin and osteopontin at day 9 of differentiation.
These observations are consistent with a positive effect of PDGF-B and PDGF-D on osteoblast differentiation from multipotential precursors and may explain their dramatic effects on trabecular bone in vivo. In combination, the present results support the notion that PDGF-D, like PDGF-B, has significant bone anabolic potential and may be clinically useful in bone regeneration.

Disclosures: ***S. Topouzis****, None.*

M187

Adiponectin Is Expressed in Human Osteoblasts. J. E. Reseland*[1], H. Berner*[1], M. Monjo*[1], L. Thommesen*[2], C. Drevon*[3], U. Syversen*[4], S. P. Lyngstadaas*[1]. [1]Oral research laboratory, University of Oslo, Oslo, Norway, [2]Department of Physiology & Biomedical Engineering, University of Science and Technology, Trondheim, Norway, [3]Department of Nutrition, University of Oslo, Oslo, Norway, [4]Department of Intra-Abdominal Diseases, University of Science andTechnology, Trondheim, Norway.

Adiponectin is a recently discovered adipokine, which is highly expressed in adipose tissue. Body weight is associated with increased bone mineral density and decreased risk of fractures. The mechanisms explaining this relation are, however, not completely understood. Here we provide information to the link between adipokines and bone homeostasis by demonstrating transcription, translation and secretion of adiponectin, as well as expression of its receptors, AdipoR1 and AdipoR2, in bone forming cells. We also show that adiponectin and the receptors are expressed in primary human osteoblasts from femur and tibia. The phenotype of the cells was characterized by the expression levels of alkaline phosphatase, collagen type 1, osteocalcin and CD44, and formation of mineralization nodules. The expression of adiponectin and AdipoR1 was also confirmed in murine osteoblast cells (MC-3T3-E1). Immunostaining with monoclonal antibodies demonstrated the presence of adiponectin in human osteosarcoma cells and normal osteoblasts. Both expression of mRNA and secretion of adiponectin to the medium increased during differentiation of human osteoblasts.
How adiponectin is regulated is still obscure. We observed higher adiponectin mRNA level for cells cultured 24 h with dietary fatty acids (0.5 mM palmitic acid), and dexamethasone (1 μM) compared to untreated control.
Administration of recombinant adiponectin enhances the proliferation of MC-3T3-E1, indicating a functional role for adiponectin in bone homeostasis.
The present findings of adiponectin expression and secretion from bone forming cells demonstrate that adiponectin is not adipocyte-specific, but may have other important functions related to bone growth and maintenance. Furthermore, the expression of adiponectin in bone cells appears to be regulated, suggesting that also in these cells, this factor can be influenced by external stimuli known to regulate adipokines. The regulation of bone metabolism is complex, and the observed expression and secretion of adipokines by bone forming cells add to the complexity, to this intriguing tissue.

Disclosures: ***J.E. Reseland****, None.*

M188

Inhibition of Stem Cell Factor Activity Modulates Proliferation and Differentiation Patterns in Human Dental Pulp Cells. E. Gagari*[1], L. Suri*[2], P. D. Damoulis[3]. [1]Oral and Maxillofacial Pathology, Tufts University, Boston, MA, USA, [2]Orthodontics, Tufts University, Boston, MA, USA, [3]Periodontology, Tufts University, Boston, MA, USA.

Stem cell factor (SCF), an important growth factor typically produced by stromal cells, affects primarily hematopoietic cells that bear its receptor, c-kit. Human dental pulp (HDP) cells are of mesenchymal origin and co-express SCF and c-kit. However, the functional role of SCF in these cells is unclear. The purpose of this project was to explore the effects of inhibiting SCF bioactivity on cell proliferation and differentiation in mineralizing HDP cultures. Cells were cultured in αMEM supplemented with ascorbic acid and β glycerol phosphate for 38 days, with media changes every 3 days starting on d2. Assays were performed every 6 days, starting on d14. Inhibition of SCF activity was achieved with the addition of an anti-SCF neutralizing antibody (A) or an anti-c-kit receptor antibody (B). Addition of the respective antibody was performed with every media change, starting either on d8 (at confluence, gr. 1), or d20 (when soluble SCF [sSCF] typically peaks, gr. 2). Cell growth was assessed by DNA and total protein content, whereas cell viability was monitored through LDH release. Alkaline phosphatase (AlP) activity and alizarin red staining for mineralization were also measured. sSCF was measured by ELISA. Control cultures showed a gradual increase in DNA and protein content until d26, with a sharp drop on d32, coinciding with peak AlP activity and initiation of mineralization. At the same time, a significant drop in sSCF and increased LDH release were observed. Inhibition of SCF bioactivity produced a variety of phenotypic changes, which greatly depended on the timing of antibody addition. The mechanism of inhibition (A vs B) also resulted in some qualitative and quantitative differences. The most striking observation was that late inhibition of SCF (gr. 2, both A and B) caused a sharp drop in cell growth on d26 accompanied by a decrease in sSCF, increased LDH release and acceleration of mineralization. In contrast, gr.1 showed higher cell growth on d14 and d20, but changes at the later time points varied depending on the mechanism of inhibition. Addition of anti-c-kit receptor antibody in gr. 1 showed the highest variability from control, resulting in a more gradual decline in cell growth after d26, with a sSCF peak and a concomitant decrease in mineral content on d32. Taken together, these findings implicate SCF as an important regulator of cell growth and mineralization potential in HDP cultures. Establishing a role for SCF as a negative regulator of mineralization is an intriguing proposition, which could provide more insight in our understanding of bone formation.

Disclosures: ***E. Gagari****, None.*

M189

Regulation of SDF-1 (CXCL12) Production by Osteoblasts in the hEmatopoietic Microenvironment- A Mechanism for Stem Cell Homing. Y. Jung*[1], J. Wang*[1], A. Schneider[1], Y. Sun*[1], A. J. Koh-Paige*[1], N. I. Osman*[2], L. K. McCauley[1], R. S. Taichman[1]. [1]Periodontics,Prevention,Geriatrics, University of Michigan Dental School, Ann Arbor, MI, USA, [2]Anesthesiology, University of Michigan Medical School, Ann Arbor, MI, USA.

SDF-1 controls many aspects of stem cell function including stem cell trafficking and development. Previously we demonstrated that DNA-damaging agents such as irradiation, cyclophosphamide, or 5-fluorouracil caused an increase in the expression of SDF-1 in the marrow of mice or in cultured osteoblastic cells. Recently transgenic mice expressing constitutively active PTH/PTHrP receptors were found to have increased numbers of hematopoietic stem cells recovered from the animals bone marrow. Here we evaluated SDF-1 secretion by ELISA in response to cytokines known to be particularly important in bone physiology in primary human osteoblasts (HOBs), mixed marrow stromal cells (BMSCs), MG-63 and SaOS-2 human osteosarcoma cell lines, the murine MC3T3-E1 clone 4 cells and the rat osteosarcoma ROS 17/2.8 cell line. Examination of SDF-1 synthesis vs time *in vitro* revealed that SDF-1 secretion is a feature of early osteoblastic induction, which can be modulated *in vitro* and in response to a variety of cytokine and hormonal signals. In particular, TNF-α, IL-1ß, VEGF, PDGF-BB and PTH all increased SDF-1 synthesis while TGF-$ß_1$ decreased secretion. Subsequent examinations of the medium or cell/extracellular matrix lysates from either BMSCs or MG-63 cells demonstrated an equal distribution of SDF-1 between all fractions. Surgical transplantation of mixed BMSCs into 4- to 6-week-old male mice (N:NIH-bg-nu-xid) and subsequent daily administration of 40 μg/kg PTH (1-34) or vehicle for 21 days increased the expression of SDF-1 mRNA in developing ossicle implants but not in endogenous bone. Interestingly, SDF-1 protein levels were significantly decreased in the serum (24%) of the PTH-treated animals (Vehicle: 408±25 Vs. PTH 308±20 SDF-1 pg/ml). These data suggest a possible mechanism for localizing stem cells into a developing marrow. Increased expression of SDF-1 in the local marrow environment along with decreased SDF-1 in the serum may create a homing gradient for the localization of hematopoietic stem cells to developing bone marrow.

Disclosures: ***R.S. Taichman****, None.*

M190

Leukemia Inhibitory Factor has Biphasic Effects on Bone Formation In Vivo. D. Falconi[1], J. E. Aubin[2]. [1]Department of Medical Biophysics, University of Toronto, Toronto, ON, Canada, [2]Department of Medical Genetics and Microbiology & Department of Medical Biophysics, University of Toronto, Toronto, ON, Canada.

Members of the gp130 family of cytokines elicit both anabolic and catabolic effects on bone, either directly or as mediators of at least some of the actions of factors such as PTH, IL-1 α and TNF α. Previously, we showed that leukemia inhibitory factor (LIF) has differentiation stage-specific inhibitory effects in rat calvarial (RC) cell cultures, but biphasic effects in the rat bone marrow (RBM) stromal cell model, with stimulation of osteogenesis during proliferation phase in the RBM model and inhibition at late osteoprogenitor-preosteoblast stages in both models. To determine whether LIF may elicit similar effects in vivo, we treated one-day-old neonatal Wister rats with increasing doses (1, 5 and 15 μg/kg in a volume of 20 μl) of mouse recombinant LIF or its vehicle (PBS), once a day for five consecutive days, by subcutaneous injections over the calvaria along the sagittal suture. The animals (12-16 per group) were sacrificed on the sixth day and the calvariae dissected for analyses. Hematoxylin-eosin staining revealed no significant differences in cell morphology in the suture or bones. Histomorphometric analyses indicated a biphasic effect of LIF on sagittal suture width, with a trend towards narrowing of the suture at 1 and 5 μg/kg but widening of the suture at 15 μg/kg (n=8; $p<0.05$) in LIF-treated compared to PBS-treated animals, suggesting respectively stimulation or inhibition of bone formation at the osteogenic front. The biphasic effect of LIF was also seen in calvaria width, measured at three sites (250, 500 and 750 μm from the middle of the suture), with bone width greatest at 5 μg/kg and least at 15 μg/kg compared to control. By real-time PCR, expression of ALP was slightly decreased with LIF at 1 μg/kg and 5 μg/kg but increased at 15 μg/kg. Levels of Osx and BSP were not significantly affected but OCN levels were slightly reduced by LIF. However, Runx2 levels were decreased at 1 μg/kg (2X), but were increased at the higher doses (5>15 μg/kg) compared to PBS. OPG and RANK expression levels were not significantly affected by LIF at the doses tested. RANKL levels were decreased in calvariae from mice treated with 1 μg/kg LIF, but increased with 5 μg/kg of LIF (6.5X) and 15 μg/kg (2X), a pattern mimicking the expression changes in Runx2, confirming Runx2 regulation of RANKL and consistent with increased osteoclastogenesis at higher LIF doses. Taken together, our results suggest that LIF effects in vivo are biphasic, with stimulation of bone formation and remodeling at low doses but inhibition of bone formation and stimulation of resorption at higher doses.

Disclosures: ***D. Falconi****, None.*

M191

High-throughput Quantification of Femoral Bone Strength in Murine Inbred Strains. G. H. van Lenthe[1], T. Kohler*[1], R. Voide*[1], L. R. Donahue[2], R. Müller[1]. [1]Institute for Biomedical Engineering, ETH, Zurich, Switzerland, [2]The Jackson Laboratories, Bar Harbor, ME, USA.

The gold standard to determine bone strength is experimental biomechanics. However, it has its limitations, as it is a destructive test, laborious, and prone to errors, especially when testing small bones. Therefore, we recently used microstructural finite element (μFE) analysis to determine bone strength directly from bone structure. We have applied this technique to femora of two murine growth-hormone deficient inbred strains (B6-*lit/lit* and C3.B6-*lit/lit*), and found that although having higher bone volume and higher cortical thickness, C3.B6-*lit/lit* had lower femoral strength than B6-*lit/lit* (Table 1).

Phenotypic data on two murine inbred strains [mean(SD), all data p<0.0001]

Location	Parameter		B6-*lit/lit* N=17	C3.B6-*lit/lit* N=19
Whole femur	Total Volume	[mm^3]	17.9 (1.23)	15.9 (1.27)
	Bone Volume	[mm^3]	8.41 (0.87)	9.96 (1.06)
	App.Vol.Dens	[%]	46.9 (2.63)	62.7 (3.62)
Cortex,1 mm slab	Ct.Th	[mm]	0.11 (0.01)	0.21 (0.02)
	Total Volume	[mm^3]	1.08 (0.06)	0.82 (0.06)
Neck	Strength	[N]	2.28 (0.21)	1.87 (0.19)

To further investigate the genetics causing these differences, an F2 population of 2,000 mice was produced. Genetic loci can be identified when genomic markers as well as bone strength have been assessed for all these animals. However, although huge progress has been made in fast acquisition of genomic data, fast characterization of bone strength is not well developed. Therefore, the aim of the present study was to implement high-throughput μFE analyses for bone strength assessment. 100 femora of the F2 population were μCT scanned using a 20 μm resolution. After automated alignment, μFE models were created from which strength was calculated. As expected, we found large variations in strength between femora. Interestingly, the present data suggest that there is a shift towards stronger femora (Fig. 1), indicating that the combination of high bone mass (C3.B6-*lit/lit*) and favorable geometry (B6-*lit/lit*) often works towards a stronger bone. We conclude that high-throughput characterization of murine femoral bone strength is now possible, allowing scanning, morphometric and functional analysis of 70 femora per day, depending on computational resources; it will allow the location of genetic loci directly for bone strength, rather than for surrogate markers of bone strength, such as bone volume or other architectural parameters.

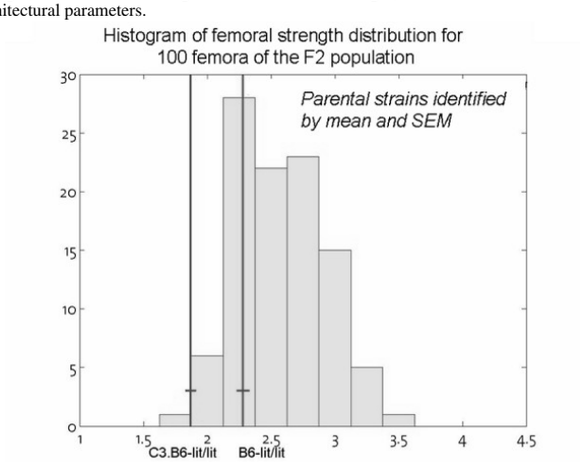

Disclosures: ***G.H. van Lenthe****, None.*

M192

Does Increased Bone Formation Associated to Decreased Adipogenesis Participates to Mechanical Loading-Induced Bone Adaptation? V. David*, M. Lafage-Proust, S. Peyroche*, A. Guignandon*, A. Rattner*, L. Vico. Lbto, Inserm, St Etienne, France.

Osteoblasts and adipocytes develop from common bone marrow mesenchymal precursors. Aging and unloading inhibit bone formation and increase adipogenesis. It is not known whether mechanical loading has the ability to reverse such situation. Pluripotent C3H10T1/2 cells and bovine primary marrow stromal cells, cultured on a permissive osteoblastic and adipocytic medium (DMEM, 10% SVF, 10μg/ml insulin, 0.5mM IBMX, and dexamethasone, ascorbic acid, retinoic acid, at 10^{-8}M) were expended 72 hours on type I collagen-coated-silicone membranes then daily submitted to cyclic strain (10 min, 0.5%, 1Hz; FLEXCELL FX-3000 unit). C3H10T1/2 growth in stretched cells (S) was not affected after 3, and 7 days, and slightly decreased thereafter. After 14 days, osteoblastic markers measured in cell lysates increased in S as compared to non stretched cells (NS): alkaline phosphatase (ALP) activity by 49%, osteocalcin (OC) and Runx2 (sandwich ELISA) by 37% and 63%, respectively. At this time, we observed a 74% decrease in the adipogenic determining factor PPARγ2 (sandwich ELISA). Levels of mRNA were assessed by real time PCR for osteoblastic and adipogenic markers. The expression of Runx2, Msx2 and OC showed dramatic increases after 3 days in S vs. NS (4-fold, 7-fold, and 60-fold, respectively) which lowered thereafter; those for GAPDH, PPARγ2, and cytoplasmic retinoic acid binding protein 1 (CRABP1) decreased after 7 and 14 days (all more than 80%). After 14 days, alkaline phosphatase positive cells (osteoblasts) are more numerous in S than in NS (+18%) whereas the contrary is seen for red oil positive cells (adipocytes) (-46%). As for primary bovine cells, stretch induced cell growth increase during the first 3 days only. After 14 days of stretching, protein evaluation showed that ALP activity and OC increased by 147% and 76%, respectively. After 3 days of stretching, Runx2 increased by 67% then reached NS level. At 14 days, osteoblasts are more numerous in S (+35%). At 14 days, PPARγ2 decreased by 80%, glyceraldehyde-3-phosphate dehydrogenase (GAPDH) decreased by 50 % and adipocytes are less numerous (-65%) in S as compared to NS. We demonstrated that cyclic strain enhances osteoblastogenesis and decreases adipogenesis in vitro suggesting that this reciprocal fate can be manipulated in order to improve bone formation.

Disclosures: ***L. Vico****, None.*

M193

Estrogen Modulates Osteoclast Responsiveness To Mechanical Strain By Altering Glutamate Receptor Subtype Expression. K. M. Black*[1], B. Theriault*[2], G. I. Anderson[3]. [1]Pharmacology, Dalhousie University, Halifax, NS, Canada, [2]Surgery, Dalhousie University, Halifax, NS, Canada, [3]Surgery, Flinders University, Adelaide, Australia.

Glutamate receptors (gluRs) of both the ionotropic and metabotropic subytpes are expressed in osteoblasts and osteoclasts of the long bones of rat, rabbit, and mouse. Glutamate receptors are sensitive to mechanical stimulation, a major driving force for the maintenance of bone density. Glutamate signalling in the central nervous system is involved in the processes of learning and memory: we postulate that gluRs mediate mechanical stimulation in bone cells to increase bone density in a manner analogous to their role in mediating CNS synaptic plasticity. In our mixed murine marrow-derived cultures, gluR antagonists MK801 and NBQX inhibit osteoclast differentiation and function, implying that these glutamate receptors are functional. We have also shown by RT-PCR and western analysis that mechanical stimulation appears to decrease the expression of NMDAR1 and NMDAR2B, but increase expression of NMDAR2A, AMPAR1, and AMPAR3. These changes in glutamate receptor subtype expression suggest that mechanical stimulation of osteoclasts appears to precipitate a shift in the balance of ionotropic receptor function from NMDA receptor-mediated pathways (calcium entry, calmodulin kinase II) to AMPA receptor-mediated pathways(sodium entry, MAP kinase). The endpoint effect of this shift is to decrease osteoclast activity to low levels in the presence of mechanical stimulation. Since estrogen levels are known to be important in in vivo bone balance, we wished to characterize the effects of estrogen on gluR mechanosensitivity in our cultured osteoclasts. Bone marrow cells from femora and tibiae of 7-week old female CD1 mice were seeded onto collagen-I coated silastic membranes, and grown for 8 days with mechanical stimulation on days 4, 5, and 6 (1 Hz, 900 cycles) and or 1x10E-6 M 17-beta estradiol doses added on days 1, 4, & 6. Mature osteoclasts were partially purified from harvested cells using anti-RANK coated immunomagnetic beads and total RNA or total protein was isolated. Using RT-PCR, and Northern and Western analyses, we showed that estrogen effects glutamate receptor subtype expression and therefore modulates the sensitivity of osteoclasts to mechanical strain. We did not detect by RT-PCR the expression of estrogen receptor subtype alpha or beta mRNA in osteoclast-enriched fractions that may suggest that the actions of estrogen are mediated either through paracrine signalling from osteoblast-lineage cells or via a non-genomic mechanism directly on osteoclasts. Studies are ongoing to further understand the mechanisms by which estrogen modulates glutamate receptor-mediated mechanotransduction in osteoclasts and ultimately how these mechanisms might contribute to the maintenance of bone density.

Disclosures: ***G.I. Anderson****, None.*

M194

Fluid Shear Stress Induces Cyclooxygenase-2 Via Activation of Protein Kinase D in Murine Primary Osteoblasts. M. Mehrotra, C. B. Alander*, O. S. Voznesensky*, L. G. Raisz, C. C. Pilbeam. Medicine, University of Connecticut Health Center, Farmington, CT, USA.

Protein kinase D (PKD), also known as protein kinase Cμ (PKCμ), is a novel serine threonine kinase that is distinct from PKCs in structure and substrate specificity. However, PKD can be activated by phorbol esters in parallel with PKCs or downstream of PKC phosphorylation, and inhibitors of PKCs may also inhibit PKD. PKD has a potentially important role in growth factor and stress-induced signaling pathways, the same pathways that may mediate responses of bone to mechanical loading. Mechanical loading is transmitted to bone cells via the action of fluid shear stress (FSS) on cell surfaces. Cyclooxygenase (COX-2) is induced by FSS in osteoblasts and osteocytes and is thought to mediate some of the anabolic effects of loading on bone. We examined the role of PKD in the FSS induction of COX-2 in primary murine calvarial osteoblasts obtained from CD-1 mice. Cells were obtained by sequential digestion of calvariae. Populations 2-5 were pooled, grown to confluence, and replated on type I collagen-coated glass slides and grown to near-confluence for experiments. Cells were subjected to a FSS of 10 dynes/cm^2 in medium with 1% FCS for 1 h or maintained in stationary culture in the same medium (no flow controls). Induction of COX-2 mRNA was measured by Northern analysis. Treatment with GF109203X (1.25 μg/ml), which inhibits both conventional and novel PKC isoforms and also inhibits PKD at the dose used, reduced the FSS induction of COX-2 mRNA by 60%. Another PKC/PKD inhibitor, Go6976 (1 μM), which inhibits conventional isoforms of PKC as well as PKD at the dose used, reduced the FSS induction of COX-2 mRNA by 50%. However, Go6983 (1 μM), which inhibits conventional, novel and atypical PKC isoforms but does not inhibit PKD at the dose used, had no effect on the FSS induction of COX-2 mRNA. Western analysis was performed using antibodies specific for phosphorylated serine residues Ser744 and Ser748, transphosphorylation sites located in the activa-

tion loop of PKD; antibodies specific for Ser916, the autophosphorylation site located at the C-terminal of PKD; and antibodies for total PKD. PKD was constitutively expressed. Phosphorylation of PKD at both Ser744/748 and Ser916 sites was induced by 40 min of FSS. These data suggest that FSS activates PKD in calvarial osteoblasts and that activation of PKD plays a role in the FSS induction of COX-2.

Disclosures: ***M. Mehrotra****, None.*

M195

Fluid Shear Stress Induces RANKL Expression in Primary Osteoblastic Cells. M. Mehrotra, S. K. Lee, M. Saegusa, C. B. Alander*, L. G. Raisz, C. C. Pilbeam. Medicine, University of Connecticut Health Center, Farmington, CT, USA.

Expression of receptor activator of nuclear factor kappa B ligand (RANKL) on osteoblastic cells is critical for osteoclast formation and activity. The activity of RANKL is opposed by osteoprotegerin (OPG), a decoy receptor for RANKL. There is conflict in literature regarding the effects of mechanical forces on RANKL expression. Decreased expression of RANKL has been observed in murine bone marrow stromal cells subjected to biaxial 0.2-2% strain (J Biol Chem 278: 34018, 2003; J Bone Min Res 17:1452, 2002; Am J Physiol Cell Physiol 278: C1126, 2000). On the other hand, continuous compressive forces up-regulated RANKL expression in periodontal ligament cells and this effect was dependent on PGE_2 production (J Bone Min Res 17: 210, 2002). We used a parallel plate flow apparatus to apply laminar fluid flow, equivalent to a fluid shear stress (FSS) of 10 dynes/cm^2, to primary calvarial osteoblasts plated on collagen-coated glass slides and grown to about 90% confluence. Cells were subjected to FSS for 1 h and subsequently cultured under static conditions (post FSS) for varying lengths of time up to 24 h. Because FSS induces cyclooxygenase-2 (COX-2) expression and because this induction results in PGE_2 production that can induce RANKL, experiments were performed in the presence of NS398 (0.1 μM), an inhibitor of COX-2 activity, to block production of prostaglandins. Little or no RANKL mRNA was seen by Northern analysis in control (no flow) cultures, but RANKL mRNA was detectable in these cultures by RT-PCR. RANKL mRNA was induced at 1 h post-FSS, levels peaked at 4 h post FSS and declined thereafter. By real-time quantitative PCR, RANKL mRNA was induced up to 20-fold at 4 h following 1 h of FSS. Five min of FSS was sufficient to induce the expression of RANKL mRNA at 4 h post FSS to the same level as observed 4 h post 1 h FSS. On the other hand 4 h of continuous FSS decreased RANKL mRNA to lower levels than seen in the control cultures. There was little change in OPG mRNA levels under any conditions. On Western blot analysis, RANKL protein was undetectable in no-flow cultures, slightly elevated at 2 and 4 h post 1 h of FSS, and strongly induced at 8 h post FSS. A role of a protein kinase C (PKC) pathway in the FSS regulation of RANKL expression in primary osteoblasts is suggested by the observation that GF109203X (1.25 μg/ml), an inhibitor of the PKC pathway, decreased the FSS induction of RANKL mRNA by 60-90% at 2 h post FSS. We conclude that 1 h of FSS induces RANKL mRNA and protein expression in primary calvarial osteoblasts and that this induction is independent of PGE_2 production and may occur via a PKC pathway..

Disclosures: ***M. Mehrotra****, None.*

M196

Activation Of The Mechanosensitive Channel And Intracellular Ca^{2+} Response To Mechanical Stimulation In Osteoblasts Is Regulated By Actin Filament Length. J. Zhang*, J. A. Bethel*, K. D. Ryder*, R. L. Duncan. Orthopaedic Surgery, Indiana University School of Medicine, Indianapolis, IN, USA.

Osteoblasts respond to mechanical stimulation with a rapid increase in intracellular free Ca^{2+} ($[Ca^{2+}]_i$) that is dependent on activation of the mechanosensitive, cation-selective channel (MSCC). We have recently shown that parathyroid hormone significantly enhances both the $[Ca^{2+}]_i$ response to mechanical stimulation and the activity of the MSCC. Since PTH has been shown to alter the organization of the actin cytoskeleton, we postulated that the effects of PTH on the MSCC and $[Ca^{2+}]_i$ resulted from actin cytoskeletal reorganization. Using both UMR-106.01 and MC3T3-E1 osteoblast-like cells, we examine the effects of disorganizing actin filaments to varying degrees using three actin cytoskeletal poisons; cytochalasin D (cyto D), latrunculin A (lat A) and jasplakinolide (jasplak). Previous studies have shown that cyto D severs actin filaments into short-length chains, but does not alter the insoluble fraction of actin in MC3T3-E1 cells. Lat A increases the solubilized fraction of actin to 68% of total actin while jasplak increases solubilized actin to 98%. Fura-2 Ca^{2+} imaging demonstrated that pretreatment with 1-5 μM cyto D for 30 min significantly increased the peak $[Ca^{2+}]_i$ response to fluid shear or hypotonic challenge approximately 2.5 fold over the peak $[Ca^{2+}]_i$ response to mechanical stimulus alone in either cell type. This increase in peak $[Ca^{2+}]_i$ was similar to that induced by PTH pretreatment and addition of the MSCC blocker, $GdCl_3$, significantly inhibited the $[Ca^{2+}]_i$ response to both PTH and cyto D . Pretreatment for 30 min with 1 μM lat A did not significantly alter the peak $[Ca^{2+}]_i$ response compared to mechanically-stimulated controls. Jasplak (1 μM) produced varied patterns of $[Ca^{2+}]_i$ response to mechanical stimulation. Using patch clamp analyses, we examined the effects of cyto D and lat A on MSCC activity in response to mechanical stimulation in UMR-106.01 cells. We have previously shown that when MSCC's are activated by negative pressure applied to the patch pipette, PTH increases MSCC activity (NP_O) 3.5 fold. This increase was negated when the actin cytoskeleton was stabilized with phalloidin. We found that cyto D produced a similar increase in MSCC NP_O, but that lat A decreased suction-induced MSCC NP_O. These data would suggest that actin reorganization into short-chained actin filaments increases MSCC activity resulting in an increased $[Ca^{2+}]_i$ response to mechanical stimulation, but that more complete disruption of actin filaments reduces these responses. These data also suggest that the synergistic response of PTH and mechanical loading may be mediated through the actin cytoskeleton.

Disclosures: ***J. Zhang****, None.*

M197

$P2X_7$ Purinergic Receptor Activation Modulates Prostaglandin Synthesis And Release From Osteoblasts In Response To Fluid Shear. D. Liu[1], J. Li[2], C. H. Turner[1], R. L. Duncan[1]. [1]Orthopaedic Surgery, Indiana University School of Medicine, Indianapolis, IN, USA, [2]Anatomy and Cell Biology, Indiana University School of Medicine, Indianapolis, IN, USA.

We have shown that ATP is rapidly released from osteoblasts in response to fluid shear stress (FSS), suggesting that purinergic (P2) receptor activation may be involved in mechanotransduction in bone. Recently, $P2X_7$ receptor knockout mice have been shown to be less responsive to mechanical loading than wild type mice. To examine the mechanisms associated with FSS-induced $P2X_7$ activation, we used $P2X_7$ antagonists and antibody to examine changes in the response of MC3T3-E1 osteoblasts to FSS. MC3T3-E1 cells, grown on type I collagen-coated glass slides, were pretreated with $P2X_7$ antagonists for 10-30 min prior to, and during, application of 12 dynes/cm^2 fluid shear. Distinct from other P2 receptors, activation of $P2X_7$ receptors results in insertion of membrane pores capable of conducting large (<900 Da) molecules. We found that 30 min of FSS significantly increased the number of cells that incorporated YO-PRO-1, a 630 Dalton dye (46.9 ± 10. 7%, p<0.001), indicating that a mechanical stimulus causes membrane pore formation. The uptake of YO-PRO-1 was completely blocked by hydrolysis of ATP with apyrase (6.4 ± 4.5%) or with the P2X7 inhibitor, Brilliant Blue G (BBG) (7 ± 3.42%). Activation of P2X7 receptors in static, non-flowed MC3T3-E1 cells resulted in an increase in PGE_2 release, whereas addition of apyrase nearly abolished the FSS-induced increase in PGE_2 release. BBG also significantly reduced PGE_2 release in response to shear. To determine the specificity of the P2X7 receptor in the release of PGE_2, we added antibody against the extracellular domain of this receptor to the cells 10 min prior to flow. PGE_2 release as reduced by 75% (P<0.01) during block of the P2X7 receptor. To determine if COX-2 protein production was affected by ATP signaling, we examined COX-2 production in the presence of apyrase. FSS-induced COX-2 production was decreased by 90% (P<0.01) when extracellular ATP was hydrolyzed. Neutralization of the $P2X_7$ receptor with antibody produced a similar decrease in COX-2. These data indicate that the $P2X_7$ receptor plays an important role in prostaglandin synthesis and release in response to FSS and may be essential for the complete response of bone to mechanical loading.

Disclosures: ***D. Liu****, None.*

M198

NO-Dependent Decreased Expression of eNOS Following Pulsatile Fluid Flow. J. L. Picconi, M. L. Johnson. Osteoporosis Research Center, Creighton University Medical Center, Omaha, NE, USA.

Mechanical stimulation of osteogenic cells activates the production of NO that is immediate and sustained throughout stimulation. Previous *in vitro* studies have shown eNOS mRNA to be increased in bone cells in response to mechanical stimulation. Following fluid flow, we found decreased eNOS mRNA levels immediately after the cessation of flow that later increased. We hypothesize this is the result of NO-induced destabilization of eNOS mRNA followed by later increases due to eNOS gene transcription. A major target of NO is guanylate cyclase (GC). Activation of GC increases cGMP production, which is known to downregulate the mRNA stabilizing protein HuR and results in the destabilization of a number of mRNA species. Analysis of the 3' UTRs of human and bovine eNOS mRNAs revealed the presence of conserved elements known to be important in the stabilization in COX-2 and VEGF mRNAs by HuR. 2T3 clonal preosteoblast-like cells were subjected to pulsatile fluid shear stress of 4.0 ±; 0.6 dynes/cm^2 for 2 hours followed by post-flow incubation for 0 to 24 hours. Total RNA was extracted and quantified for eNOS, COX-2, VEGF, and HuR mRNAs by real time PCR. Following fluid flow, eNOS mRNA was immediately decreased to 20% of controls and was increased 4 hours later. Pretreatment with the GC inhibitor methylene blue prevented this flow-dependent decrease, while the NO donor SNP mimicked this response in control cells. Following fluid flow, VEGF and HuR mRNA levels were unchanged from controls, while COX-2 mRNA was increased. Pretreatment with methylene blue in the presence of flow dramatically increased COX-2 and VEGF mRNA levels and mildly increased HuR mRNA levels. From these results, we conclude that the decreased eNOS mRNA levels immediately following fluid flow are the result of flow-induced NO but the mechanism mediating this feedback remains unknown. It is clear, however, that the decrease in eNOS mRNA is not the result of decreased stabilization by HuR. One possibility is this is the result of activation of destabilizing proteins such as AUF1, TTP, or KSRP.

Gene Expression in 2T3 Cells in Response to Fluid Flow

	eNOS Mean (±;SEM)	COX-2 Mean (±;SEM)	VEGF Mean (±;SEM)	HuR Mean (±;SEM)
Static Control	1.15 (0.20)	1.03 (0.07)	1.01 (0.04)	1.01 (0.04)
0 Hours Post Flow	0.20 (0.06)	2.42 (0.13)	1.00 (0.05)	1.04 (0.05)
2 Hours Post Flow	1.68 (0.37)	2.83 (0.32)	1.55 (0.11)	0.80 (0.06)
4 Hours Post Flow	38.96 (1.80)	1.58 (0.31)	2.70 (0.36)	0.70 (0.09)
Methylene Blue	1.40 (0.02)	0.46 (0.07)	0.68 (0.02)	0.95 (0.01)
Static Flow	1.13 (0.49)	23.75 (1.72)	27.12 (2.68)	1.89 (0.06)
SNP	0.30 (0.05)	ND	0.38 (0.02)	0.63 (0.06)
Static Flow	0.37 (0.18)	ND	0.63 (0.04)	0.73 (0.08)

Disclosures: ***J.L. Picconi****, None.*

M199

Biphasic Expression of COX-2 in Response to Pulsatile Fluid Flow. J. L. Picconi, M. L. Johnson. Osteoporosis Research Center, Creighton University Medical Center, Omaha, NE, USA.

The hypothesis of this project is the magnitude of fluid shear stress to which bone cells are exposed determines their osteogenic response. *In vivo* experiments have shown lamellar bone formation in response to moderate mechanical loads that is prevented by pretreatment with COX-2 specific inhibitors. In contrast, exogenous administration of PGE_2 is synergistic in combination with moderate loads for woven bone formation. A biphasic production of PGE_2 or cAMP in primary bone cells subjected to increasing magnitudes of mechanical strain or fluid shear stress was shown in 2 previous studies. To further explore this pattern, clonal 2T3 preosteoblast-like and MLO-Y4 osteocyte-like cells were subjected to fluid flow regimens of 2, 4, 8, 16, 24, or 32 dynes/cm^2 with pulses of 0.6 dynes/cm^2 at a frequency of 5 Hz for 2 hours and then incubated in flow medium for 0 or 24 hours (n=6/group). Total RNA was extracted and COX-2 mRNA quantitated by real time PCR. In response to pulsatile fluid flow, both 2T3 and MLO-Y4 cells demonstrated biphasic induction of COX-2 expression at both 0 and 24 hours post-flow. The magnitude of the first peak was significantly less than the second and occurred over a much narrower range (2-8 dynes/cm^2 in both cell types) than the second peak (16-32 dynes/cm^2 in 2T3 cells and 8-24 dynes/cm^2 in MLO-Y4 cells). These patterns are similar to previous studies and support the hypothesis that the response of osteogenic cells is dependent on the magnitude of stimulation. Additionally, MLO-Y4 cells responded and recovered rapidly to changes in stimulation, while 2T3 cells were still increasing COX-2 expression at 24 hours, supporting the role of osteocytes as the mechanosensors in bone. It is tempting to compare the biphasic expression of COX-2 in bone cells to the lamellar and woven bone formation responses observed *in vivo*, although further studies are needed. Regardless, it is clear that the osteogenic response of bone cells does not follow a linear dose response or logarithmic pattern and this should be considered when interpreting current or future studies.

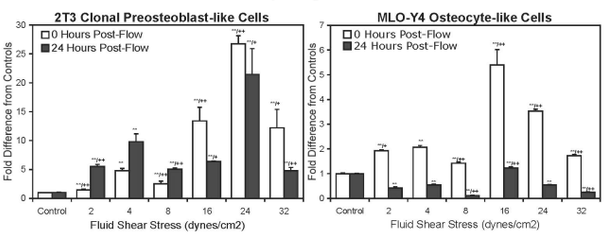

Disclosures: ***J.L. Picconi****, None.*

M200

Protein Kinase C Modulates Mechanical Load-Induced $[Ca^{2+}]_i$ Changes and Prostaglandin E_2 Production in MC3T3-E1 Osteoblasts. V. Fomin, D. Liu, J. Lincoln*, B. Chelladurai*, R. L. Duncan. Orthopaedic Surgery, Indiana University School of Medicine, Indianapolis, IN, USA.

Osteoblasts respond to mechanical stimulation with a rapid increase in intracellular free calcium ($[Ca^{2+}]_i$) and activation of a number kinase cascades that culminates in prostaglandin-dependent bone formation at the tissue level. Several reports have indicated that protein kinase C (PKC) alters osteoblastic responses to mechanical stimulation leading us to postulate that activation of PKC would enhance the $[Ca^{2+}]_i$ response to load. Using fura-2 loaded MC3T3-E1 preosteoblastic cells grown on glass coverslips, we examined changes in the $[Ca^{2+}]_i$ response when PKC was acutely activated (≤ 10min) with 4β phorbol 12 myristate 13 acetate (PMA). Acute activation of PKC produced a 3.4 fold increase in peak $[Ca^{2+}]_i$ response to hypotonic swelling as well as a significant increase in the rise slope of the response. Inhibition of PKC with 1 μM GF109203X (GFX) for 10 min decreased the peak $[Ca^{2+}]_i$ response below the hypotonic swelling control levels (65% of the control). As in other tissues, we found that chronic PMA (1μM) stimulation for more than 6 hours completely downregulated PKC protein in MC3T3-E1 cells. Interestingly, when PKC levels were abolished with chronic PMA treatment, the peak $[Ca^{2+}]_i$ response and rise slope to hypotonic swelling was again increased (6 and 22 fold, respectively) over hypotonic control levels, suggesting two mechanisms for PKC regulation of this response. Examination of the effects of acute and chronic activation of PKC on prostaglandin production found that acute PKC activation significantly increased arachidonic acid (AA) release in static MC3T3-E1 cells and potentiated the release of AA in response to mechanical stimulation. This increase in AA release by PKC activation was mirrored by release of PGE_2 in both static and fluid sheared (12 dynes/cm^2) MC3T3-E1 cells. Inhibition of PKC with GFX significantly blocked the release of AA and PGE_2 during mechanical stimulation. However, cyclooxygenase-2 (Cox-2) production in response to fluid shear was not enhanced with acute PKC stimulation. These data would suggest that acute PKC activation may be stimulating phospholipases, such as PLA_2, to increase the substrate for prostaglandin synthesis. Chronic downregulation of PKC with PMA also stimulated AA and PGE_2 release, suggesting that the control of the $[Ca^{2+}]_i$ response by PKC is important in prostaglandin release, but that this control may be mediated through two different mechanisms.

Disclosures: ***V. Fomin****, None.*

M201

A Novel Alginate Carrier System to Evaluate Osteoblast Apoptosis in Vector-averaged Gravity using Rotating Wall Vessels. M. A. Bucaro*[1], A. M. Zahm*[1], M. V. Risbud*[1], P. S. Ayyaswamy*[2], K. Mukundakrishnan*[2], M. J. Steinbeck[1], I. M. Shapiro[1], C. S. Adams*[1]. [1]Thomas Jefferson University, Philadelphia, PA, USA, [2]University of Pennsylvania, Philadelphia, PA, USA.

It has been hypothesized that an elevated rate of osteoblast apoptosis contributes to the osteopenia that occurs during spaceflight, possibly due to a loss of gravitational forces at the cellular level. We have evaluated apoptosis in osteoblasts subjected to vector-averaged gravity using a novel system in which MC3T3-E1 osteoblast-like cells are encapsulated in alginate carriers and cultured in a high aspect ratio vessel (HARV). The encapsulated cells retained a well defined osteoblast phenotype in static culture, maintaining expression of osteopontin and osteocalcin and exhibiting increased expression of Runx2/Osf2 relative to cells cultured on tissue culture plastic. Two types of carriers that could be co-cultured in the HARV were developed to ensure that the effects observed in simulated microgravity were not due to shear stresses or other factors characteristic of the HARV culture system: "nonpolar" carriers that spun with the HARV's rotation, were used to expose cells to vector-averaged microgravity, and "polar" carriers that remained vertically oriented throughout the HARV's rotation served as controls. Video microscopy of the carriers in the HARV confirmed that the polar carriers maintained a stable vertical orientation (unit gravity) while nonpolar carriers underwent clinorotation, exposing cells to time-averaged gravitational accelerations of 0.99g and 0.05g, respectively. To determine if simulated microgravity induced osteoblast apoptosis, MC3T3-E1 cells in polar and nonpolar carriers were cultured together in the same HARV at 3/15 rpm for 24 h, and then sorted. In contrast to other studies which used cells in static culture as unit gravity controls, no difference in viability was detected between cells cultured in the polar and nonpolar carriers. Furthermore, we investigated the hypothesis that cells exposed to vector-averaged gravity would exhibit increased sensitivity to apoptosis when treated with staurosporine, relative to control cells. While our results using static culture controls indicated that vector-averaged gravity sensitized the cells to apoptosis, we consistently found no difference in viability using the polar and nonpolar carriers. We conclude that the use of alginate carriers in the HARV is an optimal system for evaluating apoptosis of osteoblasts in simulated microgravity. Moreover, the use of polarized carriers accounts for the unique environment of the HARV, providing a tightly controlled system for evaluating the direct effects of vector-averaged gravity on cellular behavior.

Disclosures: ***M.A. Bucaro****, None.*

M202

High Salt Intake Promotes Urinary Loss of Vitamin D Metabolites by Dahl Salt-Sensitive Rats in a Space Flight Model. M. Thierry-Palmer[1], S. Cephas*[1], P. Sayavongsa*[1], T. Cleek*[2], S. B. Arnaud[3]. [1]Biochemistry, Morehouse School of Medicine, Atlanta, GA, USA, [2]Life Sciences Division, NASA Ames Research Center, Moffett Field, CA, USA, [3]Life Sciences Division, NASA Ames Research Center, Moffett Field, CA, USA.

Vitamin D metabolism in the Dahl salt-sensitive (S) rat, a model of salt-induced hypertension, differs from that in the Dahl salt-resistant (R) rat. We have demonstrated that female S rats are more vulnerable than female R rats to decreases in plasma 25-hydroxyvitamin D (25-OHD) and 1,25-dihydroxyvitamin D (1,25-$(OH)_2$D) concentrations during hind limb unloading (a space flight model). We report here on the response of the vitamin D endocrine system of S and R rats to hind limb unloading during high salt intake. Dahl female rats (2.4-month-old) were tail-suspended (hind limb unloaded) for 28 days, while fed a diet containing twice the salt in standard rat chow (2 % sodium chloride). Control rats were fed the same diet, but were not hind limb unloaded. Vitamin D metabolites were analyzed by HPLC and radioimmunoassay kits from Diasorin. Significantly higher amounts of 25-OHD ($P < 0.001$) and 24,25-$(OH)_2$D ($P < 0.05$) were excreted into urine by S rats, compared with R rats, and excretion by S rats was increased by hind limb unloading ($P < 0.05$). The consequence was lower plasma concentrations of these two metabolites in S rats than in R rats ($P < 0.05$). Plasma parathyroid hormone concentration was twice that of rats fed a low salt diet (0.3 %) in previous experiments and was similar in all four groups of rats. Urinary calcium was increased ($P < 0.001$) by salt sensitivity. Urinary 25-OHD binding activity and protein of S rats were greater ($P < 0.001$) than that of R rats and were increased by hind limb unloading of S rats ($P < 0.05$). These data suggest that plasma 25-OHD and 24,25-$(OH)_2$D concentrations of S rats are lower that that of R rats during hind limb unloading, because of urinary excretion of protein-bound vitamin D metabolites. Urinary 25-OHD, 25-OHD binding activity, and protein were increased by hind limb unloading of S rats during 2 % salt intake, but not during 0.3 % salt intake (earlier study). This suggests that low salt intake can prevent the increased urinary loss of vitamin D metabolites by S rats that is related to hind limb unloading.

Disclosures: ***M. Thierry-Palmer****, None.*

M203

Loss of Myostatin (GDF8) Function Attenuates the Osteogenic Response Observed with Exercise. M. Hamrick[1], C. Pennington*[1], C. Byron[1], D. Xie[2], C. M. Isales[2]. [1]Cellular Biology & Anatomy, Medical College of Georgia, Augusta, GA, USA, [2]Institute of Molecular Medicine & Genetics, Medical College of Georgia, Augusta, GA, USA.

Mice lacking myostatin (GDF8) show a significant (40-100%) increase in muscle mass compared to normal mice, and our previous research also indicates that these mice have significantly greater bone mineral density (BMD) in their femora compared to normal mice. The goal of this study was to determine if BMD in exercised normal mice is comparable to that of sedentary myostatin-deficient mice. We also sought to determine if exercise

further increased BMD in myostatin-deficient animals beyond that observed in exercised normal mice. We exercised 12 week-old female normal and myostatin-deficient mice (n=12 per group) for 30 minutes a day, 5 days per week, for four weeks. Mice were run on a motorized treadmill at a speed of 12 m/min. Whole-bone mineral content and density were measured in the femur using DEXA (PIXImus system) and cross-sectional slices from the femur midshaft and metaphysis were taken using pQCT. Results indicate that quadriceps muscle mass did not increase significantly in either group of exercised mice compared to sedentary controls. Exercised wild-type mice show significantly greater periosteal expansion, measured as periosteal circumference, at both the midshaft and metaphysis (+15%, P<.01) compared to exercised myostatin-deficient mice. The increase in bone size with exercise in the normal mice is mostly in the mediolateral direction, so that the area (*Iyy)* and polar (*J)* moments of inertia are significantly (20%, P<.01) greater in the exercised wild-type mice. Furthermore, exercised wild-type mice show significantly greater (20%, P<.01) trabecular BMC and BMD at the metaphysis than exercised myostatin-deficient mice. These data suggest that mice lacking myostatin may be less responsive to the effects of exercise than normal mice. Furthermore, these data indicate that the positive effects of regular exercise on bone mass and density are not necessarily dependent upon marked increases in muscle mass.

Disclosures: ***M. Hamrick****, None.*

M204

Estrogen and an ERα Agonist Suppress the Osteogenic Response to Exercise. L. K. Saxon*, C. H. Turner*. Orthopaedic Surgery, IUPUI, Indianapolis, IN, USA.

It is well established that exercise has the potential to increase bone density and strength. It has been proposed that estrogen enhances the osteogenic response to exercise, particularly through estrogen receptor α (ERα). The aim of this study was to determine the combined effect of exercise and estrogen or PPT (an ERα agonist) on bone formation. Forty-three young (8 wks) male Sprague-Dawley rats were randomized to one of following groups: 1) high dose 17-α ethynylestradiol (High EE_2), 2) low dose 17-α ethynylestradiol + mechanical loading (Low EE_2), 3) propyl pyrazole triol + mechanical loading (PPT), 4) vehicle treated + mechanical loading (control) or 5) baseline control. Low EE_2 was selected to undergo mechanical loading because this dose closely reflects physiological levels of serum estrogen. An axial load was applied to the right ulna for 120 cycles, at 17N, 3 days/wk for 5 weeks. Calcein labels were given on days 5 and 12 of the experiment allowing histomorphometric measurement of bone formation rates of the midshaft ulnae. At the end of the 5 week intervention, High EE_2 and PPT showed reduced gains in body weight, longitudinal growth and cortical area ($p<0.05$). In contrast, High EE_2 also increased trabecular vBMD at the lumbar spine and distal femur ($p<0.05$) but PPT did not. Five weeks of mechanical loading increased cortical area and polar moment of inertia (Ip) in the control group, and only partially increased cortical area in the Low EE_2 and PPT groups. Exercise increased BFR/BS of the loaded ulna, however the response was reduced in the Low EE_2 and PPT groups versus controls (Figure 1). In conclusion, High EE_2 inhibits gains in longitudinal growth and cortical area, but also increases trabecular bone density. When combined with exercise, Low EE_2 and PPT decrease the osteogenic response to exercise by inhibiting periosteal bone formation.

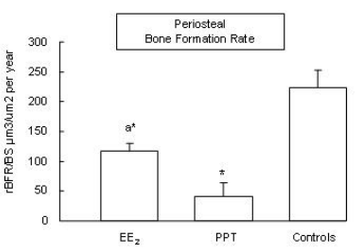

Figure 2. The effect of exercise and Low EE_2, PPT or vehicle (control) treatment on periosteal bone formation rate (loaded verus nonloaded ulna) after 1-2 weeks of mechanical loading in growing male rats. *p<0.05 vs controls, a p<0.05 vs PPT

Disclosures: ***L.K. Saxon****, None.*

M205

Three-Dimensional Mandible Bone Architectures Simulated by a Reaction-Diffusion Bone Remodeling Model. K. Tezuka[1], T. Takeda*[1], Y. Wada*[2], A. Takahashi*[2], M. Kikuchi*[2]. [1]Dept. Tissue and Organ Development, Gifu University Graduate School of Medicine, Gifu, Japan, [2]Dept. Science and Technology, Tokyo University of Science, Noda, Japan.

Bone is a complex system with adaptation and repair functions. Therefore, simulation of bone remodeling under various mechanical conditions will be very useful to understand patho-physiological state of bone from structural information. To understand how bone cells can create a structure adapted to the mechanical environment, we proposed a simple bone remodeling model, iBone, based on a reaction-diffusion system (JBMR 2003, vol. 18 suppl. 2, pp. S220). To analyze three-dimensional models, we constructed a PC cluster system with 11 Pentium4 desktop computers, and adapted finite element analysis and reaction-diffusion softwares for parallel computation. A three-dimensional mandible bone model consisting of approximately 1.4 million elements was constructed from sequential CT images of a 14-year old female. Both teeth and bone were modeled with isoparametric voxel elements with Young's Modulus = 20GPa and Poisson's ratio = 0.3. Both heads of mandible were fixed allowing rotation and horizontal movement. Teeth were fixed vertically allowing horizontal movements. Incisor, right or left group, and right or left molar biting conditions were simulated by fixing corresponding teeth. The locations and directions of masseter, temporalis, and medial pterygoid muscles, and their muscle forces were predicted from the CT images. Remodeling simulation was performed by 10 sets of finite element analysis, reaction-diffusion calculation, and remodeling simulation to obtain internal structure adapted to each loading condition.

As a result, major part of the corpus of the simulated mandible bone showed similar internal structures under different biting conditions. Moreover, these simulated structures resembled that of real mandible bone. On the other hand, some regions of the simulated bone, for example mentum, showed different shape under each biting condition, and any single loading condition could not give the real bone structure. These results suggest that part of the internal structure of mandible bone can be simulated by relatively simple modeling method and remodeling simulation. However, some regions which shows different shapes under different loading conditions will require combination of multiple conditions for shape simulation.

Disclosures: ***K. Tezuka****, None.*

M206

Does Marathon Training Influence Calcaneal BUA. I. P. Drysdale, H. J. Hinkley*, D. Bird*, N. J. Walters*. British College of Osteopathic Medicine, London, United Kingdom.

Physical activity has been shown to be associated both positively and negatively with bone mineral density. Marathon running requires the athlete to participate in strenuous activity if they are to complete the 26.2 mile distance. The purpose of this study was to determine the BUA of the calcaneus of participants in the 2004 Flora London Marathon and make comparisons with age matched normative data from a population of non-marathon runners. Caucasian athletes (n=408) aged 18-75 gave informed consent for ultrasound (McCue CUBA Clinical) determination of BUA of the calcaneus. Prior to running in the marathon, duplicate readings were made of right and left BUA of both calcanei. Participants also completed a questionnaire in order that their recent training history could be evaluated. We have previously reported age categorised normative data for males and females aged 20-75 years. Statistical differences (t score,% males=6.2; females=&7.3 in a two-tailed t-test, $p<0.0001$) were observed between the marathon runners and normative data for both males and females. When the age grouped data from this study were compared with normative data using one-way ANOVA, significant differences ($p<0.01$) were observed in the 40-49 and 50-59 years of age groups for both male and female subpopulations with mean BUA being higher in all marathon runners independent of age or gender. The data for BUA was split at the 4 hrs completion time threshold (at ~9min/mile pace) and an unpaired two-tailed t-test performed which showed significant difference ($t=2.9$;$P<0.0035$). It is suggested that those who train and complete a marathon at moderate, or better, running pace intensities display a higher BUA than those who train and complete at a slower pace.

Disclosures: ***I.P. Drysdale****, British Naturopathic & Osteopathic Association 2.*

M207

Retired Collegiate Artistic Gymnasts Retain Higher Bone Mass: A 10-Year Follow-Up. N. K. Pollock*, E. M. Laing, R. D. Lewis. Foods and Nutrition, The University of Georgia, Athens, GA, USA.

Fifteen years after cessation of the sport, we found that retired collegiate artistic gymnasts (GYM; n=18) had higher measures of areal bone mineral density (aBMD; g/cm^2) at all skeletal sites compared to nongymnast controls (CON; n=15) of similar age (years), height (cm) and body weight (BW; kg). It is unknown, however, if the aBMD differences in GYM and CON observed at that time are maintained into the years approaching menopause. A 10-year follow-up study was conducted to compare aBMD in GYM (n=16; age=44.8± years) and CON (n=13; age=44.2 years) and the changes over time. Total body fat mass (kg), percent fat (%FAT), fat-free soft tissue (FFST; kg) and aBMD of the total body, lumbar spine, non-dominant proximal femur (PF), femoral neck and Ward's triangle were assessed using dual-energy X-ray absorptiometry (DXA; Hologic QDR-1000W). Past physical activity was estimated using a self-report, study-designed questionnaire. Independent samples *t*-tests were employed to compare aBMD in GYM and CON at baseline and at the 10-year follow-up. Analysis of covariance was used to compare the changes (Δ) in aBMD between GYM and CON and to quantify the magnitude of the effects (i.e., partial eta-squared; η^2; where 0.06 and 0.13 are medium and large effects, respectively). GYM had significantly lower BW, fat mass and %FAT ($p<0.05$; $\eta^2>0.14$), and higher measures of FFST/BW and aBMD at all skeletal sites compared to CON ($p<0.05$; $\eta^2>0.14$) at both time points. Over time, changes in GYM and CON did not differ significantly with respect to BW ($p=0.12$; $\eta^2=0.09$), %FAT ($p=0.92$; $\eta^2<0.01$), or aBMD at any skeletal site ($p>0.05$; $\eta^2<0.08$), except the PF, where CON had greater gains than GYM (3.27 ± 2.45% vs. -3.22 ± 1.57%; $p=0.03$; $\eta^2=0.16$). CON also had greater gains in FFST than GYM (8.68 ± 1.80% vs. 3.22 ± 0.92%; $p=0.01$; $\eta^2=0.23$). When controlling for changes in FFST, statistically significant differences in PF aBMD between groups no longer existed. There were no significant differences in the total minutes of physical activity per week reported over the past 10 years between groups. In conclusion, the higher aBMD observed in GYM compared to CON fifteen years after the cessation of the sport, was maintained over the following 10 years. While loading activity in GYM is clearly less than when competing, it is possible that a minimal defined level of physical activity is needed in the years following retirement to sustain the high aBMD.

Disclosures: ***N.K. Pollock****, None.*

M208

Marrow and Bone Responses in the SAMP6 Osteoporotic Mouse Following *in vivo* Mechanical Loading. M. D. Brodt*, M. Ko*, W. J. Hucker*, M. J. Silva. Orthopaedic Surgery, Washington University, St. Louis, MO, USA.

Senile osteoporosis is characterized by low rates of bone formation. A contributing factor may be an age-related reduction in skeletal responsiveness to mechanical loading, perhaps due to a reduced ability of the marrow to support osteogenesis. The senescence accelerated mouse SAMP6 is a model of senile osteoporosis with reduced marrow osteogenic potential and endocortical bone formation (vs. control SAMR1 mice). Our aim was to characterize the mechano-responsiveness of SAMP6 mice by assessing marrow and endocortical osteogenesis after increased mechanical loading *in vivo*. Male SAMP6 and SAMR1 (control strain) mice (4-5 mo) were subjected to three-point tibial bending. Prior to *in vivo* experiments, finite element models of tibias were generated from μCT scans and used to simulate bending. The predicted ratio of peak endocortical:periosteal strain was 0.6 for both SAMP6 and SAMR1. Strain gages were used to record periosteal strains for 4-24 N bending force (n = 6). From the combined data we estimated the forces to produce 1000 and 2000 microstrain (με) on the endocortical surface at the mid-shaft. Due to their larger size, SAMP6 tibiae require 20% higher force vs. SAMR1. Right tibiae of anesthetized mice were then loaded daily for two weeks using a rest-inserted protocol (60 cycles/day, 10 s rest interval); left tibiae (contralateral control) were not loaded. Calcein was injected on days 5 and 12; mice were killed on day 15. Bone marrow cells were cultured under osteogenic conditions and stained for alkaline phosphatase (ALP) and alizarin red on days 14 and 28. There were no significant changes in ALP or alizarin staining in cultures from loaded limbs vs. controls ($p > 0.05$), indicating that bending did not increase the osteogenic potential of the marrow. Based on histomorphometry, SAMR1 mice exhibited a dose-response, with increases in the relative values of bone formation indices in proportion to endocortical strain (Table). In contrast, SAMP6 osteoporotic mice did not exhibit a dose-response and were less responsive than SAMR1 in terms of double-labeled bone surface and mineral apposition rate ($p < 0.05$). In conclusion: 1) SAMP6 osteoporotic mice have impaired responsiveness to loading, 2) tibial bending *in vivo* does not upregulate the *in vitro* osteogenic potential of the bone marrow, which suggests that it acts primarily on mature osteoblasts.

Endocortical Bone Formation (n=3-4/group) *SAMP6 different from SAMR1 ($p<0.05$)

Relative (r) Formation Indices (R,Loaded - L,Control)	1000 με SAMR1	1000 με SAMP6	2000 με SAMR1	2000 με SAMP6
r_dLS/BS (%) *	16 ± 15	6 ± 7	40 ± 18	1 ± 2
rMS/BS (%)	7 ± 13	27 ± 6	30 ± 23	0 ± 19
rMAR (μm/day) *	0.92 ± 0.87	0.78 ± 0.58	1.80 ± 0.71	0.16 ± 0.28
rBFR/BS (μm/day)	0.37 ± 0.40	0.43 ± 0.39	0.93 ± 0.52	0.04 ± 0.07

Disclosures: ***M.J. Silva****, None.*

M209

Transient Muscle Paralysis Rapidly Induces Bone Loss in Mice. S. E. Warner[1], D. A. Sanford*[1], B. A. Becker*[1], S. D. Bain[2], C. Lin*[2], H. C. Zheng*[2], S. Srinivasan[1], T. S. Gross[1]. [1]Orthopaedics & Sports Medicine, University of Washington, Seattle, WA, USA, [2]SkeleTech, Inc, Bothell, WA, USA.

A murine model in which bone loss was primarily achieved by bone resorption would hold substantial potential for elucidating the role of mechanical stimuli in the maintenance of bone mass. Given the integral role of muscle action in mechanical loading of the skeleton, we therefore hypothesized that transient hindlimb muscle paralysis would rapidly induce bone loss in the mouse. To test this hypothesis, we developed a murine model of disuse in which hindlimb extensor muscle action was transiently paralyzed via intramuscular (IM) injections of Botulinum neurotoxin type A (Botox). Twenty female C57B6 mice (16 wk) were randomized into four groups (n=5 each): 1) 3 wk Botox, 2) 3 wk saline, 3) 6 wk Botox, and 4) 6 wk saline. At day zero all animals received IM injections of either saline or Botox in both the calf and quadriceps of the right leg. The 6 wk mice received a second injection on d 21. Calcein was injected 8 and 2 d prior to sacrifice. Alterations in tibia metaphyseal trabecular bone (0.8 mm volume distal to the growth plate) and cortical bone (1 mm volume centered 1.7 mm proximal to the tib-fib junction) were assessed by micro-CT. Static and dynamic histomorphometry was then performed at the metaphyseal site. Differences are presented as a percent of saline control values. Botox treatment significantly diminished both calf (3 wk: -54%, 6 wk: -64%) and quadriceps (3 wk: -34%, 6 wk: -62%; all $p < 0.001$) wet weights. Trabecular BV/TV loss observed by 3 wk (-33%) progressed to a near total removal of trabeculae by 6 wk (-80%, $p < 0.001$), which was achieved mostly by trabecular thinning (3 wk: -20%, $p < 0.01$; 6 wk: -27%, $p < 0.001$). Cortical bone volume was significantly reduced at both 3 wk (-9%, $p < 0.01$) and 6 wk (-22%, $p< .001$), primarily via endocortical expansion (3 wk: +12%, 6 wk: +23%, $p < 0.01$) as periosteal volume was unchanged (3 wk: 0.4%, 6 wk: -5.0%). Trabecular osteoclast surface was elevated (+55%), but bone formation rate (BFR) was not (+1%). By 6 wk, both osteoclast surface (-25%) and BFR (-16%) were reduced in Botox mice. We conclude that our model demonstrated rapid muscle atrophy and bone degradation, with the bone loss achieved primarily via osteoclastic resorption. It is likely that the transient muscle paralysis induced by Botox altered both low magnitude, high frequency strains typically induced by muscle and higher magnitude, lower frequency strains induced by joint contact during gait. As such, this model holds substantial promise to enable mechanistic exploration of fundamental, yet poorly understood, interactions between muscle and bone.

Disclosures: ***S.E. Warner****, None.*

M210

Bone Size and Strength Is Related to Long-Term Impact Sports Participation in Older Men. R. M. Daly, S. L. Bass*, S. Kukuljan*. School of Exercise and Nutrition Sciences, Deakin University, Melbourne, Australia.

Lifetime loading history is thought to be a significant determinant of bone strength in old age. However, little is known about the effects of long-term participation in impact sporting activities during different stages of the lifespan on bone strength in older adults. Thus, we asked in men aged 50+ yrs (61.3 ± 7.4 yrs), does participation in moderate-high impact sports during adolescence and/or adulthood enhance bone strength? We assessed FN, L2-4, and UD radial BMD by DXA (n=159), and femoral mid-shaft total (ToAr), cortical (CoAr) and medullary area (mm^2), and the polar moment of inertia (Ip, mg/cm) by QCT (n=105). Current (50+ yrs) and past hours of sports participation during adolescence (13-18 yrs) and adulthood (19-50 yrs) were assessed by questionnaire. Because load magnitude and frequency are more important than duration for stimulating an osteogenic response, an osteogenic index (OI) for mod-high impact sports was then calculated for each participant at each time period by adapting the formula developed by Turner and Robling (Ex Sports Sci Rev 31:45-50, 2003). Regression analysis was used to examine the relationship between each bone trait and the OI after adjusting for age, height, weight, smoking, calcium and alcohol intake, and lifetime non-low impact sports activity (hours). A greater lifetime OI (13-50+ yrs) was associated with a greater femoral ToAr (adj. ß ± SE; 0.50 ± 0.21, $p<0.05$), CoAr (0.32 ± 0.17, $p=0.06$), and Ip (1.19 ± 0.46, $p<0.05$). Similarly, a greater OI in adulthood (19-50 yrs) was related to greater femoral ToAr, CoAr and Ip ($p<0.05$), but no association was found between adolescent (13-18 yrs) OI scores and bone size or strength. Furthermore, no relationship was detected between OI scores at any time with DXA BMD at any site. Subjects were then categorised into either a high (H) or low/non-impact (L) group according to their OI scores in adolescence and adulthood. Four groups were then formed to reflect impact categories during adolescence and adulthood: LL (n=28), LH (n=7), HL (n=40) and HH (n=32). Regression analysis revealed that compared to the LL group, femoral ToAr and Ip were 7-14% ($p=0.05$) higher in the HH and 11-21% ($p<0.01$) higher in the LH group of older men. No significant differences were detected between the LL and HL groups; nor were there any differences between groups for DXA BMD. In summary, lifetime participation in impact sports was a determinant of bone size and strength (not BMD) in older men. We conclude that: 1) regular impact loading in men led to an increase in bone strength due to an increase in bone size and not BMD, and 2) continued participation in weight-bearing impact exercise throughout life is important for reducing the risk of low bone strength in old age.

Disclosures: ***R.M. Daly****, None.*

M211

Differences in DXA Body Composition Observed in Active and Inactive Populations. C. Maes*[1], B. Jacobs*[1], A. Ferdinande*[2], S. Poriau*[2]. [1]Medical Centre for Sports, Business and Related Research MENSANA, Sijsele-Damme, Belgium, [2]Locomotorisch Centrum, Sijsele-Damme, Belgium.

While the value of total body BMD as measured by DXA is well recognized, less is known of the assessment of fat and lean soft tissue from these measurements. Differences in total fat as well as regional fat distribution between men and women, and between athletes and non-athletes, may provide insight to physiological changes with age, disease, or fitness programs. In this study we examined if there are differences in fat mass distribution as a function of the level and type of sports activity.

Total body DXA measurements of 348 men and 80 women were performed on the Lunar Prodigy (GE Healthcare). Body composition results for total body, android (A), and gynoid (G) regions (figure), as well as the A/G fat ratio were calculated automatically by the software. In some obese subjects manual adjustment of android and gynoid regions was necessary. Subjects who didn't participate in sports were defined as inactive while active subjects participated in sports.

The average percentage of total body fat (% TB Fat) for the 80 women was 28.5 ± 8.6% while the average A/G fat ratio was 0.73 ± 0.20. For the 348 men the average % TB Fat was 17.4 ± 8.2% while their average A/G fat ratio was 1.06 ± 0.27. Inactive men had significantly higher %TB Fat (23.4%) compared to men who were active in sports (18.9%, $p<0.005$) while the A/G fat ratio was not significantly different. Significant differences in %TB fat ($p<0.001$) were also observed when comparing the different types of sports (running, biking, mountain biking, duathlon, triathlon , fitness and survival) while there was again no significant difference ($p = 0.17$) for the A/G fat ratio. Percent TB fat of male professional athletes (14.7%), amateur competitors (17.4%) and recreational sports enthusiasts (20.6%) were significantly different ($p < 0.001$). Although there was no difference in A/G fat ratio between professionals and amateur competitors, the recreational sports men had a significantly higher A/G fat ratio ($p = 0.001$).

In conclusion, we observed a significant difference in %TB fat between active and inactive male subjects, but the A/G fat ratio showed no differences. In active men, % TB fat was significantly different depending on type and level of sports; and the A/G fat ratio was significantly higher in men participating in recreational vs. competitive sports.

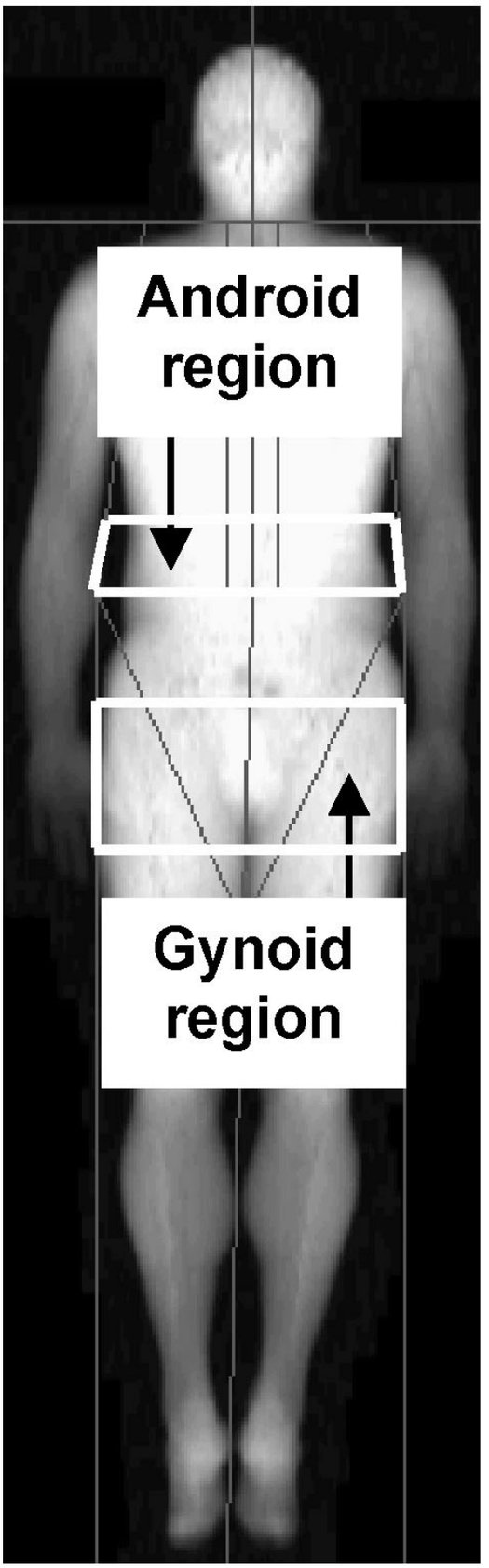

Disclosures: ***C. Maes****, None.*

M212

Level of Physical Activity and Vitamin D Modify the Effectiveness of Calcium Supplementation in Bone Mass Accrual during Rapid Growth: A 2-year Randomized Trial. S. Cheng[1], A. Lyytikäinen[1], Q. Wang*[1], M. Alen*[2], H. Suominen[1], A. Koistinen*[3], R. Korpela*[4], C. Lamberg-Allardt[5], H. Kröger[6]. [1]Jyväskylä Univ, Jyväskylä, Finland, [2]PEURUNKA, Jyväskylä, Finland, [3]Central Hospital, Jyväskylä, Finland, [4]Valio, Helsinki, Finland, [5]Helsinki Univ, Helsinki, Finland, [6]Kuopio Univ, Kuopio, Finland.

This two-year double-blind (dairy was blind for researchers), placebo-controlled and randomized trial (the CALEX-study) was to evaluate whether vitamin D (VD) supply and level of physical activity (PA) modify the effectiveness of calcium (Ca) supplementation on bone mass accrual during rapid growth. Normal healthy girls aged 10-12 years (n=195) at Tanner stage I-II with dietary Ca intake <900 mg/day were first stratified into two groups by their PA level and then randomly assigned into four groups: 1) Placebo (Ca and VD pla, Pla, n=48); 2) 1000 mg Ca carbonate + 5µg VD daily (Ca+VD, n= 49); 3) 1000 mg Ca carbonate daily + VD pla (Ca, n=49); 4) 1000 mg Ca from dairy products (mainly low fat cheese, Che, n=49). Altogether 159 girls completed the trial. Bone mineral content (BMC), bone area (BA) and area bone mineral density (BMD) of the total body (TB), femoral neck and lumbar spine were assessed using DXA (Prodigy, GE Lunar). There were no significant differences among the groups at baseline in any of the variable studied. The compliance in taking the supplements was 70%, 74%, 64% and 72 % for Ca and 76 % for active VD, respectively. Girls in the Che group gained on average 3% more BMC of the TB than other groups. However, after adjusting for growth speed using multilevel analysis, no significant difference in bone gain was found at any measured bone site between the intervention groups. While girls with high initial level of PA had consistently higher BMC and BMD in all measured bone sites after adjusting for growth speed. At the menarche, the high PA group were on average 176 g higher in BMC of the TB than the low PA group ($p<0.01$). No significant difference was found in BA between the low and high PA groups. When comparing the percentage change over the two-year period between low and high PA within the intervention groups (controlled for baseline), we found that in the Ca+VD group, those with high PA gained 1.1% more BMC of the TB than those with low PA, but the difference did not reach statistic significance. On the contrary, girls with high PA in the Ca, Che and Pla groups gained less compared to the low PA girls (-3.4%, -5.7% and 1.4%, respectively). Our results indicate that during the rapid growth period, Ca intakes exceeding 800 mg/day (diary or tablets) has no significant effect on bone mass accrual. Vitamin D plus high physical activity may, however, modify the effectiveness of calcium supplementation on bone mass accrual during rapid growth.

Disclosures: ***S. Cheng****, None.*

M213

Relationship Between Daily Impacts and BMD. T. J. Jämsä*[1], A. Vainionpää*[1], R. Korpelainen*[2], E. Vihriälä*[1], A. Rinta-Paavola*[3], J. Leppäluoto*[4]. [1]Department of Medical Technology, University of Oulu, Oulu, Finland, [2]Oulu Deaconess Institute, Oulu, Finland, [3]Newtest Ltd, Oulu, Finland, [4]Department of Physiology, University of Oulu, Oulu, Finland.

Osteoporosis has become one of the major health problems in developed countries. It has been suggested that regular exercise, especially high-impact activities, contributes to development of high peak bone mass and deceleration of bone loss. However, there have been no quantitative data on the exercise needed for strengthening bone. Here we studied the effect of daily impacts at different acceleration levels on BMD. We performed a population-based randomized intervention study with 80 women (35-40 years). The subjects carried an activity monitor (Pat.WO03/055389A1, Newtest Ltd, Oulu, Finland) daily for 12 months for individual quantification of their daily physical activity. Half of the subjects were assigned to an exercise group with high-impact exercise training, while the others continued their normal life. The average number of daily impacts was defined at 33 acceleration levels from 0.3g to 9.9g. The numbers were normalized by the mean values of the controls and analysed in four acceleration regions, 0.3-1.7g, 1.9-3.3g, 3.6-5.7g and 6.1-9.3g. The relationship between the physical activity data and percentage changes of different bone parameters were evaluated using linear regression analysis, adjusted for percentage weight change, smoking and calcium intake. The BMD change was related to the physical activity data. The relative number of daily impacts at the acceleration levels of 3.6-5.7g and 6.1-9.3g had a significant relationship with femoral BMD, accounting for up to 20% of the annual change in BMD. The calcaneal ultrasound measurements showed a significant exercise-induced increase in speed of sound (SOS) and quantitative ultrasound index (QUI) even at the low acceleration levels, while broadband ultrasound attenuation (BUA) was correlated only with the number of high-acceleration impacts. We conclude that the acceleration level of daily impacts is a significant determinant of the changes in BMD.

Correlation coefficients between BMD change and number of daily impacts at different g levels.

	0.3-1.7	1.9-3.3	3.6-5.7	6.1-9.3
Femoral Neck	ns	ns	0.391**	0.394**
Ward's Triangle	ns	ns	0.356*	0.414**
Trochanter	ns	ns	0.410**	0.451***
BUA	ns	ns	0.317*	0.334*
SOS	0.322*	ns	ns	ns
QUI	0.344*	0.334*	0.342*	0.334*

Disclosures: ***T.J. Jämsä****, Newtest Ltd 4.*

M214

Characteristics of Mechanical Strain Engendered in the Rodent Femur by Planar Orbital Shaking and Hindlimb Suspension. D. J. Adams, D. K. Sung*. Orthopaedic Surgery, University of Connecticut Health Center, Farmington, CT, USA.

A new noninvasive rodent model of skeletal loading, planar orbital shaking, has been reported to stimulate immature osteoblasts in the mouse skeleton. To characterize the magnitudes and temporal features of skeletal loading engendered in rodents by orbital shaking relative to physiologic activities, uniaxial mechanical strain gages with a sensing grid of 0.15 mm^2 were bonded to the anterolateral surface of the femur mid-diaphysis in adult Sprague-Dawley rats. Strain signals were recorded during volitional wheel running and cage activities to provide comparisons to physiologic loads, and with the animals' hindlimbs unloaded via tail suspension as a comparison to disuse. The animals were also subjected to in-plane orbital shaking at incremental speeds up to 220 rpm, using a laboratory shaker with a ¾-inch diameter circular path. Videographic archival of all activities provided for matching strain signals to specific activities involving the instrumented femur. Strain magnitudes, strain rates, and dynamic frequencies were compared between volitional activities, hindlimb suspension, and orbital shaking. Longitudinal strain magnitudes recorded on the anterolateral surface of the femur ranged up to 200-300 microstrain (με), corresponding closely to strain magnitudes measured at this femoral site in other rat studies. Volitional wheel running produced the largest femoral strain magnitudes among physiologic activities (127 ± 29 με), demonstrating characteristic footstrike frequencies of approximately 2 Hz. Strain magnitudes engendered by orbital shaking increased with orbital velocity in an exponential manner ($p<0.05$, $R^2=0.96$), and reflected the characteristic frequency of orbital velocity from 0 to 220 rpm (i.e., only one pulse of mechanical strain per revolution). However, maximum strain amplitudes associated with orbital shaking at 220 rpm (85 ± 34 με) did not exceed those for volitional wheel running. Strain magnitudes were negligible during hindlimb suspension when the animals remained stationary, but were substantial when the animals forcefully moved their freely suspended hindlimbs (50-100 με). These results suggest that planar orbital shaking engenders mechanical signals on the anterolateral femur that are not larger in magnitude than those associated with physiologic activities. Surprisingly, exertions of suspended hindlimbs were sufficient to cause substantial strain magnitudes, suggesting that the tail suspension model may not provide a temporally uniform model of disuse as is often assumed.

Disclosures: ***D.J. Adams****, None.*

M215

Inbred Mouse Strains Exhibit Variations In The Skeletal Adaptive Response to 4-Point Bending: Evidence For Involvement Of Different Genetic Mechanisms. C. Kesavan*, D. J. Baylink, J. E. Wergedal, S. Mohan. JLP VAMC / Loma Linda Univ Dept Med, Loma Linda, CA, USA.

A fundamental feature of skeletal tissue is its adaptive response in the amount of bone tissue present and the configuration of this tissue in response to mechanical loads. The present study was undertaken to test the hypotheses that: 1) different inbred strains of mice would show variable responses to a given mechanical load; and 2) within these mouse strains, the mechanisms involved in these adaptive interactions to mechanical loads would be variable. We compared bone anabolic response to 4 point bending in four different, commonly used inbred strains of mice (C57BL/6J [B6], DBA, C3H/HeJ [C3] and Balb/c). A 9N load (except for Balb/c in which 8N was used since 9N caused fractures) at 2Hz for 36 cycles was applied for 12 days on right tibia and left tibia was used as internal control. Two days after last loading, skeletal changes were evaluated by pQCT. A dramatic 15.7% and 10.8% increase in total vBMD ($P<0.0001$) was seen in C57BL and DBA mice after 12 days of loading. While vBMD increased by 3% ($P<0.05$) in Balb/c, no increase in vBMD was seen in C3H mice (-0.5%) after the same duration of training. We subsequently performed dose response studies (6, 7, 8 and 9 N load) using B6 as good responder and C3H as poor responder strain. While 4 point bending caused a dose-dependent increase in BMD in B6, it did not cause a BMD increase in C3 mice at any of the four loads tested. The lack of BMD response in C3H mice cannot be explained on the basis of differential mechanical strain since strain gage measurements revealed a slightly higher mechanical strain in C3 mice compared to B6 mice at all four loads tested. 4 point bending increased endosteal circumference in a dose-dependent manner in both B6 and C3 mice in a similar manner with no difference in slopes (B6=y:5.891x -34.44,C3H- y:5.859x -32.44,$p>0.05$). On the contrary, the increase in periosteal circumference in response to 4 point bending was greater in B6 mice compared to C3 mice (B6=y:5.3x-29.58, C3H=y:2.98x-14.23, $p<0.05$). Conclusions: 1) the increase in BMD by 4-point bending is variable in four strains tested, from no response to 15.7% increase in BMD after 2 weeks; 2) in B6 mice, 4 point bending increased both periosteal and endosteal circumference in a dose-dependent manner; 3) in C3 mice, there was an impaired periosteal response, but the magnitude of increase at the endosteum was similar to that of the B6 mice; 4) because the C3 mice responded as well as the B6 mice to the endosteum, it follows that the impairment in responsiveness to C3 mice is not due to an overall decrease in detection of the mechanical signal and accordingly, different genetic mechanisms may regulate periosteal and endosteal responses to mechanical loading.

Disclosures: ***C. Kesavan****, None.*

M216

Comparison of Skeletal Disuse Models in Mice: Spaceflight Versus Hindlimb Suspension. J. R. Milstead*[1], S. J. Simske*[2], T. A. Bateman[1]. [1]Bioengineering, Clemson University, Clemson, SC, USA, [2]Bioserve Space Technologies, University of Colorado, Boulder, CO, USA.

The effects of microgravity have been examined in rats on several occasions, and a ground based model, hindlimb suspension (HS), has been developed to mimic the skeletal unloading aspects of spaceflight (SF) on the hindlimbs. However, because STS-108 was the first Space Shuttle flight to examine the skeletal system of mice, a direct comparison of HS and SF has never been examined in mice. The objective of this research was to closely repeat the STS-108 profile, with HS replacing SF, to determine the degree to which HS predicts the effects SF on the murine skeleton.

10-week-old female C57/BL6J mice (n=12/group) were flown on STS-108 for a 12-day spaceflight (HS was repeated for the same duration). Mass and age-matched vivarium housed (VC) mice were used as controls. The effects of SF and HS on the skeletal system of mice were investigated using four different assays: micro-computed tomography, dynamic histomorphometry, mechanical testing, and compositional analysis. *Denotes significant difference between SF and HS groups ($p<0.05$).

MicroCT analysis of the proximal tibia determined that trabecular bone volume was decreased in both SF (18%) and HS (42%*) when compared with vivarium ground controls. Trabecular thickness was decreased in SF groups (8%) as well as HS (15%*). Histomorphometry determined that SF resulted in a 50%* decrease in periosteal bone formation rate (BFR), whereas there was no significant effect from suspension. SF also resulted in a 60% decrease in endocortical BFR, and HS resulted in a 40%* decrease in endocortical BFR. Average mineral apposition rate was decreased by 52% in SF groups, and 21%* in HS groups. Mechanical strength was reduced by 8% by SF and 15%* by HS. Compositional analysis determined that whole bone percent mineral composition was reduced by 4%* in HS groups, whereas SF reduced mineral composition by 3%.

In general, results showed that both SF and HS result in osteopenia. However, each method reduces bone quantity and quality to differing degrees. HS appears to have a greater effect on trabecular bone than SF. HS reduces bone strength to a greater degree than SF, with mineral composition and BFR differentially contributing to strength changes in each model.

This study was approved by Clemson University's Animal Care and Use Committee (ARC protocol# 40002).

Disclosures: ***J.R. Milstead****, None.*

M217

Ulna Loading Response Altered by the HBM Mutation. D. M. Cullen, M. P. Akhter, M. L. Johnson, S. Morgan*, R. R. Recker. Osteoporosis Research Center, Creighton University, Omaha, NE, USA.

The G171V substitution in the human LRP5 gene is a naturally occurring mutation that results in extremely high bone mass (HBM) in humans. An HBM heterozygote mouse HBM model has been constructed by inserting the human LRP5 G171V gene into C57Bl6 (WT)mice. HBM mice tibiae are overadapted to daily loads since body mass is the same as WT but tibial bone size and strength are much greater. This study confirms structural differences in the ulna and tests the ulna response to in vivo compression loading. Adult female HBM and WT mice (23.9 +/- 1.6) were randomized into 3 load groups (n=15/grp). Loads were adjusted for each genotype to achieve three strain levels: Low (1000με), Medium (1350με), and High (1950 με). The right ulna was loaded in compression for 99 cycles, at 2Hz, 3 d/wk for 3 weeks. Right and left ulna were fixed in 70% EtOH, embedded in MMA, and cortical sections taken from the midshaft for histomorphometry. The loading response is reported as difference between loaded and non loaded ulna for midshaft periosteal mineralizing surface (MS/BS)and bone formation rate (BFR). The nonloaded, proximal ulna bone mass and structure were measured by micro computed tomography at 9micron resolution and 50 msec integration time (μCT20, Scanco Medical AG, Bassersdorf, Switzerland). The scan region extended from 0.8 to 1.3 mm from the proximal end and the results are the average of 60 continuous 2D sections (proximal total area, cortical area, and trabecular BV/TV). Similar to the tibia, the HBM bones were larger and contained more bone tissue. In fact the proximal tibial cancellous bone was densely packed. Loading increased midshaft periosteal formation but differences in WT were not seen until 1950 με while formation began at lower strains in HBM ulna. While the pattern resembles that of the tibia, the ulna is much less sensitive to new loads. Tibial responses in WT mice are routinely seen with 1300 με and only 36 cycles. The higher forces required for the ulna may be a result of a more physiological loading pattern that medial to lateral bending in the tibia. The histology data represents the average of three sections (70μm) per bone, but there was considerable variability within bone. More precise localization of section or more sections should be considered for future studies to decrease variability between bones.

Genotype (με)	WT (1000 1350 1950)	HBM (1000 1350 1950)
Mid.MS/BS (%)	0.83 1.44 9.63[2]	6.53 2.78 13.46[2]
Mid.BFR (μm/d)	6.71 3.61 26.44 [2]	21.20 13.66 42.36[2]
MidTot.Ar (mm)	0.278 [1]	0.460
ProxTot.Ar (mm)	0.83 [1]	1.01
Prox.CoAr (mm)	0.30 [1]	0.37
Prox.BV/TV (%)	51.1 [1]	93.3

[1] HBM greater than WT, [2] load reaponse greater than 1350

Disclosures: ***D.M. Cullen****, American Home Products 2.*

M218

Low-Level Mechanical Vibrations Reduce Bone Resorption in the Growing Skeleton. L. Xie*[1], E. Choi*[1], L. Donahue*[2], C. Rubin[1], S. Judex[1]. [1]Biomedical Engineering, State University of New York at Stony Brook, Stony Brook, NY, USA, [2]The Jackson Laboratory, Bar Harbor, MN, USA.

Extremely small magnitude but high-frequency (>25Hz) mechanical stimuli can increase trabecular bone formation rates in the adult skeleton of a variety of species including mice. We have further demonstrated that these extremely low-level whole body vibrations can enhance bone morphology in the growing skeleton. Exposing the skeleton of 8wk old mice to 15 min/d of vibrations led to significantly enhanced trabecular bone volume fraction and thicker trabeculae over a 6wk period. The mechanism by which these morphologic changes were achieved was not immediately clear. Here, we investigated the influence of low-magnitude vibrations on the *resoptive* activity in trabecular bone of the growing skeleton. Eight-week old male BALB/cByJ (BALB) mice were randomly divided into three groups; baseline control (n=8), age-matched control (n=10), and mice that were vibrated at 45Hz (0.3 g) for 15 min/d (n=10). After the 3-wk experimental protocol, trabecular bone volume fraction, bone surface, and trabecular thickness of the tibial metaphysis were quantified via standard histomorphometry. Tartrate resistant acid phosphatase (TRAP) staining was used to determine bone resorptive activity by measuring osteoclast surface (Oc.S/BS) of the metaphyseal trabecular bone surface. Normal growth within the 3-wk period did not significantly alter activity levels of osteoclasts or produce architectural changes in the metaphysis of the tibia. Superimposing subtle vibrations onto the skeleton for 15 min/d, however, significantly decreased trabecular Oc.S/BS by 31% ($p<0.01$). No significant changes in bone morphology were observed over the 3-wk mechanical loading period. These results demonstrate, for the first time, that extremely small levels of vibrations are not only capable of stimulating bone's anabolic activity but can also decrease levels of bone resorption. Thus, this biomechanical countermeasure, in contrast to current pharmacologic interventions, may be able to increase peak bone mass and decrease the incidence of osteoporosis later in life by exertting positive effects on both bone formation and resorption. This work was supported by the Army.

Disclosures: ***L. Xie****, None.*

M219

Nutrient Artery Hypertrophy Induced by Cyclic Intramedullary Fluid Flow Loading. H. Lam*[1], P. Brink*[2], C. Rubin[1], Y. Qin[1]. [1]Biomedical Engineering, Stony Brook University, Stony Brook, NY, USA, [2]Biophysiology, Stony Brook University, Stony Brook, NY, USA.

Bone fluid flow induced by intramedullary pressure (ImP) has been demonstrated to mediate bone modeling in the absence of mechanical strain. To further evaluate the potential mechanism of this fluid flow effect on altering the nutrient supply, we hypothesize that fluid flow generated by ImP oscillation will generate nutrient vasculature adaptation which may trigger bone modeling. Thus, our objective is to investigate the relationship between cyclic hydraulic stimulation in the marrow cavity and nutrient blood vessel adaptation. We have previously demonstrated that the cross-sectional vessel wall area increased up to 50% at 3Hz loading and up to 60% at 30Hz with various intramedullary pressures applied. We are now interested in determining the contributions toward this increase in vessel wall area. Using an avian model, cyclic hydraulic stimuli was applied to the left ulnae, 10 minutes per day, with magnitude of 50-90mmHg at 3Hz and 30Hz for 2, 3, & 4 weeks (n=32), while the right ulnae were left unloaded as sham control. Four additional birds were used as age-matched control, in which both left and right ulnae were unloaded. After euthanasia, the nutrient arteries were dissected, embedded in paraffin wax, sectioned to ~8μm and stained with H&E. The average vessel wall thickness, lumen perimeter and smooth muscle cell (SMC) layer number were assessed. The lumen area was calculated from the measurement of lumen perimeter. Our data showed that the loaded side, increased in average vessel wall thickness and SMC layer number, yet decreased in lumen area. For instance, loading at 3Hz, 90mmHg for 3 weeks produced 29% increase in wall thickness and 45% in SMC layer number. Loading at 3Hz, 70mmHg for 3 weeks and 90mmHg for 4 weeks showed a lesser increase in wall thickness, 13%, and SMC layer number, 2% and 10% repetitively, but a stronger decrease in lumen area, 26% and 31% respectively. Likewise, similar trends were seen for loading at 30Hz, up to 19% increase in wall thickness, 29% in SMC layer number, and 50% decrease in lumen area. In conclusion, the results strongly suggested cyclic hydraulic stimulation does affect the adaptive response of the nutrient artery. More specifically, these repetitive ImP loading leads to nutrient artery hypertrophy, by thickening of the vessel wall with increased SMC layer and/or reducing of the lumen area. This study strongly implies that ImP fluid loading could further influence the blood supply to bone and trigger remodeling in bone tissue, which may contribute to certain skeletal diseases. Future targets will be focused on cellular level changes within the nutrient artery and along with modeling the nutrient supply to bone.

Disclosures: ***H. Lam****, None.*

M220

Identification and Characterization of the Ubiquitin-Proteasome Pathway-Targeting Molecular Chaperone, Valosin-Containing Protein (VCP/p97) in Untransformed Osteoblast-Like Cells. K. Behnam*[1], S. S. Murray*[2], E. J. B. Murray[2]. [1]Physiological Sciences, University of California, Los Angeles, CA, USA, [2]GRECC/Medicine, VAGLAHS/University of California, Sepulveda/Los Angeles, CA, USA.

Valosin-containing protein (VCP or p97) is a member of the AAA ATPase family (ATPases associated with a variety of cellular activities) that acts as a molecular chaperone that targets polyubiquitinylated proteins to the 26 S proteasome for degradation. VCP also mediates Golgi, ER (endoplasmic reticulum), and nuclear membrane fusion; ER-mediated protein degradation; protein transport from the ER to the cytoplasm; and cellular proliferation. High constitutive levels of VCP gene and protein expression are associated with enhanced degradation of phosphorylated inhibitor of NF-kappa B-α, persistent activation of the NF-kappa B transcription factor, suppression of apoptosis, and high pulmonary metastatic potential in osteosarcoma cells. The purpose of this study was to determine the occurrence and distribution of VCP protein expression in untransformed MC3T3-E1 osteoblast-like cells. Cellular protein was separated by 2D IEF/SDS-PAGE. An abundant spot with a M_r of 94 kDa and acidic pI of 5.4 was definitively identified as VCP by MALDI/ToF MS and peptide mass fingerprint analysis. Constitutive expression of VCP in subconfluent and confluent resting and mildly physiologically stressed MC3T3-E1 cells was confirmed by Western blotting. Under resting conditions, indirect immunofluorescent staining indicated that VCP is abundant in the cytoplasm, perinuclear Golgi, and nuclei of MC3T3-E1 cells, while mild physiological stress sufficient to stimulate the ubiquitin-proteasome pathway was associated with reduced diffuse cytoplasmic and enhanced nuclear immunofluoresence. In conclusion, VCP is an abundant protein in untransformed osteoblast-like cells under all conditions tested. It is not simply a marker for high metastatic potential in osteosarcomas. VCP may play previously unrecognized roles in normal osteoblast-like cell functions, such as protein turnover, membrane fusion, and mitosis.

Disclosures: ***E.J.B. Murray****, None.*

M221

Wnt Signaling Prevents Apoptosis of Both Uncommitted Osteoblast Progenitors and Osteoblasts through Src, ERK, PI3K and β-catenin Pathways. M. Almeida, L. Han, A. D. Warren*, V. G. Lowe*, S. Kousteni, S. C. Manolagas. Div. Endocrinol., Center for Osteoporosis and Metabolic Bone Diseases, Central Arkansas Veterans Healthcare System, Univ. Arkansas Med. Sci., Little Rock, AR, USA.

Genetic studies in humans and mice with mutations in LRP-5 and secreted Frizzled-related protein-1 (SFRP-1) have revealed an important role of the Wnt signaling pathway in the regulation of bone formation and mass, resulting from potent effects on the control of osteoblast progenitor proliferation, commitment, differentiation and perhaps osteoblast apoptosis. To establish the linkage between Wnts and osteoblast survival and elucidate the molecular pathways that link the two we have utilized three cell models: the uncommitted bipotential C2C12 cells, the pre-osteoblastic cell line MC3T3-E1 and bone marrow-derived OB-6 osteoblasts. We report that in cultures of all three cell types withdrawal of serum from the medium induced apoptosis within six hours, as assayed by an average of 3-fold increase in caspase 3 activity. The induction of apoptosis in all three models was reversed by the addition of 50 ng/ml of purified Wnt3A (R&D) protein. The protective effect of Wnt signaling against apoptosis was not restricted to Wnt3A, as MC3T3-E1 cells transfected with expression plasmids carrying wnt1 or wnt5A were also protected from serum withdrawal-induced apoptosis. As expected, transfection of MC3T3-E1 cells with Dkk1, a secreted inhibitor of Wnt signaling, abrogated the anti-apoptotic effect of Wnt3A. Furthermore, the anti-apoptotic effect of Wnt3A was abolished in MC3T3-E1 cells transfected with a dominant negative mutant of β-catenin. Treatment of MC3T3-E1 cells with Wnt3A protein induced phosphorylation and nuclear accumulation of ERKs within 2 min; and this effect was transient. The anti-apoptotic effect of Wnt3A was abrogated by expressing dominant negative MEK as well as Src or PI3 kinases or by the addition of cycloheximide into the culture medium. Further, Wnt3A induced phosphorylation of the glycogen synthase kinase 3β (GSK-3β), and the effect of Wnt3A was inhibited by the MEK kinase-specific inhibitor PD98059. Likewise, PD98059 inhibited Wnt3A-induced transcription of Wnt/β-catenin as measured in C2C12 cells carrying a TCF-luciferase reporter. Finally, Wnt3A induced an increase (2-fold) in the expression of the anti-apoptotic protein Bcl-2 in MC3T3-E1 cells. These results demonstrate for the first time that Wnt signaling prolongs the survival of osteoblast progenitors and their progeny via activation of both the canonical pathway and ERKs, with GSK-3β representing at least one convergence point between the two signaling cascades. Src and PI3 kinases are evidently also involved.

Disclosures: ***M. Almeida****, None.*

M222

ERK and p38 MAPKs Activation Contribute Synergistically to Osteoblast Survival in Etoposide-Induced Apoptosis. N. Ibargoyen*, A. Patiño*, M. San Julián*, L. Sierrasesúmaga*, F. Lecanda. Center of Applied Biomedical Research, University of Navarra, Pamplona, Spain.

Mitogen-activated protein kinase (MAPK) signaling pathways are key transduction cascades mediating cell proliferation, differentiation in response to various growth factors and cell survival. The three classical MAPK cascades include ERK (extracellular signal-regulated kinase) induced by mitogens, and the stress-stimulated kinases p38 and JNK (c-Jun N-terminal kinase). The aim of this study was to examine the contribution of each of the MAPK pathways to cell survival and apoptosis. For this purpose, we have established a low passage chemonaive tumoral cell line (OS-491) from a pediatric osteogenic sarcoma and a normal osteoblastic cell line (N-491) from the same patient. OS-491 displayed constitutive activation of the three MAPK pathways compared to N-491 and other osteoblastic primary cell lines. Treatment of OS-491 cells with specific p38 inhibitor SB 203580, ERK inhibitor U0126, and JNK II inhibitors led to a decreased phosphorylation of the three MAPK pathways. Phenotypic characterization by RT-PCR revealed decreased expression of osteocalcin, osteopontin and bone sialoprotein in OS-491 compared to N-491 cells. No differences were found in collagen type I. Inmmunocytochemical alkaline phosphatase staining was slightly reduced in OS-491 compared to N-491. Serum-induced proliferation was similar in both OS and N cells in a 5-day MTT assay. Resistance to apoptosis was measured by treatment with etoposide Interestingly, OS-491 cells were more resistant to etoposide-induced apoptosis than N-491 cells during the 5-day treatment period. Another osteosarcoma cell line, OS-500, with non-activated MAPK, showed no differences in cell survival compared to normal osteoblastic cell line N-500, by either serum depletion or etoposide-induced apoptosis in MTT assay. Specific inhibition of ERK, p38 or JNK in constitutive active MAPK OS-491 cells or non-activated MAPK OS-500 cells did not affect apoptotic rate after etoposide treatment compared to vehicle treated cells. Similarly, dual inhibition of JNK with either p38 or ERK inhibitors did not have any effect on apoptosis in any of the cell lines compared to vehicle-treated cells. However, concomitant inhibition of p38 and ERK pathways in OS-491 cells led to a dramatic increase in the apoptotic rate compared to vehicle treated cells, suggesting that p38 and ERK activation contribute synergistically to osteoblastic cell survival. Taken together, these data suggest that MAPK cascades could play important roles in osteoblast survival and drug resistance. Simultaneous inhibition of p38 and ERK may be required to reach a therapeutic effect.

Disclosures: ***F. Lecanda****, None.*

M223

PTHrP Control of the Cell Cycle Machinery in Differentiating Osteoblasts. N. S. Datta, C. Chen*, J. E. Berry*, L. K. McCauley. Perio/Prev/Geriatrics, University of Michigan, Ann Aror, MI, USA.

PTHrP has been implicated in the control of bone cell turnover but the mechanisms underlying its effect on osteoblast proliferation and differentiation have not been clearly defined. To establish the role of PTHrP, cell cycle analysis was performed in proliferating and differentiating MC3T3-E1 cultures with and without PTHrP (0.1μM) treatment. Flow cytometric analysis found 82% of differentiating MC3T3 cells in G0/G1 phase compared to 58% of proliferating osteoblasts. PTHrP significantly decreased S-phase cells (12 to 2%) and increased cells in G0/G1 (80 to 95%) suggesting PTHrP causes growth arrest. Cell cycle progression is dependent on periodic and phase specific abundance and activity of cyclin-cell division kinase (CDK) complexes. Western blot analyses of total cellular extracts from PTHrP or vehicle treated differentiated MC3T3 cells indicated that cyclin D1 (a G1 progression cyclin) was dramatically reduced (5-10 fold) in PTHrP treated cells. In contrast, cyclins E, A (responsible for G1/S transit and S-phase progression) or B (G2/M progression) were unchanged. Among the CDKs, the catalytic subunit of the protein kinase complexes, only the relative protein abundance of CDK1 was down regulated. Cell cycle progression is also controlled by CDK inhibitors (CDKIs) which negatively regulate the cell cycle machinery by forming complexes with CDKs. PTHrP induced p16 (INK4) CDK inhibitory protein abundance. No significant differences were noted in p19 (the alternative spliced form of p16), p21 (CIP1), or p27 (KIP1) protein abundance between vehicle and PTHrP treated MC3T3 cells. Cyclin D1- CDK complex formation was assessed by measuring the presence of CDK4/CDK6 and CDKIs in immunoprecipitations performed using antibodies to cyclin D1. Analysis of immunoprecipitates from whole cell lysates revealed a decrease in CDK4/CDK6 and an increase in p16, p21, and p27 association with cyclin D1 following PTHrP induction. In addition, the functional role of the kinase complexes were determined by *in vitro* kinase assays using either GST-Rb (for CDK4/6) or H1-histone (for CDK1, CDK2) as substrates. PTHrP down-regulated cyclin D1-CDK4/CDK6 as well as CDK1 kinase activities in differentiating MC3T3 osteoblasts. Finally, expression of JunB, an AP-1 transcription factor known to regulate cyclin D1 and p16 transcription, was found to be significantly up regulated via western, ELISA, and northern blot analysis implying involvement of JunB in PTHrP mediated growth arrest of MC3T3 cells. These data suggest cell cycle control may be a mechanism through which PTHrP impacts the life span and bone forming activity of osteoblasts.

Disclosures: ***N.S. Datta****, None.*

M224

Regulation of Human Osteoblast Survival and Differentiation by Death Receptor-3. C. W. Borysenko, V. García Palacios, A. P. Brunskill*, Y. Li*, W. F. Furey*, H. C. Blair. Pathology and Physiology & Cell Biology, University of Pittsburgh and Veteran's Affairs Medical Center, Pittsburgh, PA, USA.

Background: Several growth factors are known to be necessary for osteoblast differentiation, but no mechanism that specifically regulates the decision to secrete bone matrix has been reported. We demonstrate in this study that Death Receptor-3 (DR3) can regulate this transition in MG63 human osteoblast-like cells. DR3, a TNF-receptor family member, was discovered as a regulator of immune cell survival, but its occurrence in bone was unknown.
Methods and Results: Western analysis, cDNA cloning, and flow cytometry demonstrate expression of alternatively spliced soluble (blocking) and full length transmembrane (signaling) isoforms of DR3 in human osteoblasts and in MG63 cells. Transmembrane DR3 was activated in MG63 by antibody crosslinking and effects on cell survival and osteoblast differentiation were determined. In low density (10^3/cm^2) MG63 cultures, anti-DR3 crosslinking reduced cell survival, studied by tetrazolium dye reduction and nuclear labeling, via an apoptotic mechanism as shown by annexin V labeling. Conditioned media from high-density cultures, containing soluble DR3, was protective against apoptosis. In high-density cultures ($3x10^4$/cm^2) under conditions allowing bone nodule formation, DR3 crosslinking prevented bone formation, shown by absence of mineral deposition, reduced alkaline phosphatase activity, and increased MMP-2 secretion. Three-dimensional comparative modeling of the ligand-binding domain predicts reduced structural integrity for a variant of DR3 linked to rheumatoid arthritis, further supporting the role of DR3 in normal bone physiology.
Conclusions: DR3 is expressed in osteoblasts in soluble forms that may prevent apoptosis and in a transmembrane form, which in isolated cells can mediate apoptosis, but in high density cells is a direct regulator of osteoblast matrix production. Thus, these results establish a direct role for DR3 in controlling survival and regulating whether human osteoblast-like MG63 cells grow in a mesenchymal cell-like form or differentiate to synthesize bone matrix. That bone-forming cells express functional DR3 suggests that the RA-linked mutations in DR3 may contribute to pathology, beyond its role in T cell regulation, by affecting the response of bone cells directly.

Disclosures: ***C.W. Borysenko****, None.*

M225

Bioactive Peptides IPP and VPP have Multifunctional Properties on UMR-106 Osteoblastic Cells. M. M. Huttunen*, M. E. Ahlström*, M. Pekkinen*, J. Loponen*, C. J. E. Lamberg-Allardt. Department of applied chemistry and microbiology, University of Helsinki, Helsinki, Finland.

Protein accounts for 30% of bone mass, making bone one of the most protein-dense tissues of the body. Continuous dietary intake of protein is essential for bone turnover and matrix formation since large amount of bone collagen amino acids cannot be reutilized. In the digestive tract dietary protein is hydrolyzed by proteolytic enzymes into shorter amino acid chains. Some of these peptides possess biological functions in addition to bone matrix formation. Such bioactive peptides must be resistant to further proteolysis and absorb efficiently into blood in order to reach their target. These peptides are typically 2-5 amino acids in length and often they have a proline residue in the C-terminus. This structure is common among food-derived angiotensin converting enzyme (ACE) -inhibitory peptides such as Ile-Pro-Pro (IPP) and Val-Pro-Pro (VPP). Both of these peptides are shown to lower blood pressure in spontaneously hypertensive rats. High blood pressure is associated with abnormalities in calcium metabolism and increased bone loss. Agents interfering the renin-angiotensin-system (RAS), such as ACE-inhibitors, might also affect bone metabolism. ACE-inhibitors are good candidates since they hinder the formation of angiotensin II, the major effector peptide of the RAS. However, the effect of food-derived ACE-inhibitory peptides on bone cells *in vitro* has not been studied.
The aim of this study was to investigate if IPP and VPP have an effect on UMR-106 osteoblastic cell proliferation, differentiation, mineralisation and apoptosis. Cell proliferation was assessed by thymidine incorporation after 24 h treatment with 5, 50 and, 500 μM IPP or VPP. The effect of IPP and VPP on proliferation was biphasic, peaking at 50 μM with IPP and at 5 μM with VPP. Alizarin red S was used to assess mineralised nodule formation. As the proliferation increased, the formation of mineralised nodules decreased. Cell differentiation was assessed by measuring alkaline phosphatase (ALP) activity but neither IPP nor VPP had any effect on ALP. Preliminary results indicate that 50 μM IPP prevents etoposide-induced apoptosis in UMR-106 cells, whereas VPP has no such effect.
As a conclusion ACE-inhibitory peptides IPP and VPP possess *in vitro* osteoblast effects. Especially IPP increases UMR-106 cell proliferation and has anti-apoptotic properties and therefore it can be referred to as multifunctional peptide.

Disclosures: ***M.M. Huttunen****, None.*

M226

Enhanced Apoptosis Associated with Anabolic Actions of Androgens in AR-Transgenic Mice: Requirement of Reduced Bcl-2/Bax Ratio. K. Wiren, A. Toombs*, X. Zhang. VA Medical Center, Oregon Health & Science Univ, Portland, OR, USA.

Like estrogen, non-aromatizable androgens have significant beneficial effects on skeletal homeostasis. Estrogen has been shown to protect osteocytes from apoptosis but the effects of androgen are still poorly understood. We demonstrated that prolonged androgen signaling leads to reduced osteoblast viability, mediated via inhibition of the extracellular signal regulated kinase (ERK) cascade in both primary cultures and in an osteoblastic model with enhanced androgen responsiveness: MC3T3-E1 cells stably transfected with androgen receptor (AR) under the control of the 3.6-kb α1(I)-collagen promoter (colAR-MC3T3). Based on this evidence, we sought to elucidate the effects of 5α-dihydrotestosterone (DHT) on osteoblast apoptosis in colAR-MC3T3 cultures. In addition, recently characterized AR-transgenic mice with AR overexpression in the osteoblast lineage provide an enhanced model to examine in vivo relevance of androgen signaling. ColAR-MC3T3 cultures were treated with DHT and the effects on osteoblast apoptosis were assessed by three independent assays: accumulation of cytoplasmic mono- and oligonucleosomes, caspase-3 activity using DEVD cleavage, or changes in mitochondrial membrane potential. In proliferating cultures, apoptosis was induced by treatment with the topoisomerase II inhibitor etoposide (50μM; 18h). Continuous treatment with DHT (10^{-8}M DHT; 5 days) enhanced apoptosis over two-fold ($P<0.001$), but as expected similar treatment with 17ß-estradiol (E2) inhibited apoptosis. In highly confluent osteocytic cultures (day 29) apoptosis was induced by serum withdrawal. In osteocytic cultures continuous DHT treatment also enhanced ($P<0.001$) while E2 inhibited apoptosis. The involvement of apoptotic regulators bcl-2 (antiapoptotic) and bax (proapoptotic) was characterized by qRT-PCR and Western analysis. Bcl-2 mRNA levels were unchanged and Bax was modestly elevated with DHT treatment by qRT-PCR. The ratio of Bax to Bcl-2 was increased by Western analysis. Overexpression of bcl-2 or knockdown of bax expression with siRNA abrogated the effect of DHT to enhance osteoblast apoptosis. The physiologic relevance of androgen regulation of osteoblast apoptosis was evaluated in vivo in calvaria from male AR-transgenic mice. TUNEL staining demonstrated increased apoptosis in areas of new bone growth and in osteocytes. These results are consistent with the hypothesis that apoptosis is important during bone growth to make room for new bone. Collectively, these findings demonstrate that androgen signaling through the AR in bone directly influences osteoblast survival and offers valuable insight into the role of androgen in bone homeostasis.

Disclosures: ***K. Wiren****, None.*

M227

Menin Inhibits Osteoblast Maturation by Antagonizing Osteoblast Differetiation Induced by JunD in Mouse Osteoblastic Cells. J. Naito*[1], H. Kaji[1], H. Sowa[1], G. N. Hendy[2], T. Sugimoto[1], K. Chihara*[1]. [1]Endocrinology/Metabolism, Neurology and Hematology/Oncology, Kobe university graduate school of medicine, Kobe, Japan, [2]Medicine,Physiology and Human Genetics, McGill University, Montreal, PQ, Canada.

Menin, the product of the multiple endocrine neoplasia type 1 gene, is ubiquitously expressed.Homozygous menin knockout mice exhibit cranial and facial hypoplasia, suggesting a role for menin in bone formation. Menin interacts with the bone morphogenetic protein (BMP)-2 signalling molecules Smad1/5, and the key osteoblast transcriptional regulator, Runx2, and is required for the commitment of multipotential mesenchymal stem cells
into the osteoblast lineage. However, menin inhibits the later differentiation of committed osteoblasts by unknown mechanisms. The AP-1 transcription factor, JunD, is expressed in osteoblasts and has been shown to interact with menin in other cell types. In the present study, we examined the consequences of menin-JunD interaction on osteoblast differentiation in mouse osteoblastic MC3T3-E1 cells. JunD,
assessed by immunoblot, gradually increased during osteoblast differentiation. Stable expression of JunD enhanced expression of differentiation markers, Runx2, type 1 collagen and osteocalcin, and
alkaline phosphatase (ALP) activity and mineralization. Hence JunD promotes osteoblast differentiation. In MC3T3-E1 cells in which menin expression was reduced by stable menin antisense cDNA transfection,
JunD levels were increased. When JunD and menin were co-transfected in MC3T3-E1 cells, they co-immunoprecipitated. JunD overexpression increased the transcriptional activity of an AP-1 reporter construct
and this activity was reduced by co-transfection of menin. Therefore, JunD and menin interact both physically and functionally in osteoblasts. Furthermore, menin overexpression inhibited the ALP activity induced by JunD. In conclusion, these findings suggest that menin suppresses osteoblast maturation by inhibiting the bone anabolic actions of JunD.

Disclosures: ***J. Naito****, None.*

M228

The Effect of Parathyroid Hormone (1-34) on Angiopoietin-1 Expression in Human Osteoblast-like Cells. J. Park*, J. Kim*. Division of Endocrinology and Metabolism, Department of Internal Medicine, Chonbuk National University Medical School, Chonju Chonbuk, Republic of Korea.

The effect of parathyroid hormone on osteoporosis has been established. However, the mechanism is not fully known. To elucidate the molecular mechanism in related to anabolic action of parathyroid hormone, we investigated the effect of PTH (1-34) on angiopoietin-1 expression in primary-cultured human oseoblast-like cells. Quiescent cultures of osteoblasts were exposed to PTH (1-34) or vehicle for 24 or 48 hours. Reverse transcription-polymerase chain reaction (RT-PCR) analysis showed that mRNA expressions of angiopoietin-1 (Ang-1) were increased in PTH-treated osteoblasts compared to vehicle-treated one. Western blotting showed the similar pattern with mRNA expression at 24 or 48 hours. The adenylate cyclase activator forskolin induced the increase of Ang-1 mRNA expression, the protein kinase A inhibitor H-89 inhibited the increase of Ang-1 mRNA by PTH (1-34). These data indicate that PTH (1-34) increase Ang-1 expression in osteoblasts by protein kinase A dependent pathway, and may be a mechanism of anabolic action of PTH (1-34) on bone through the improvement of vascularity.

Disclosures: ***J. Park****, None.*

M229

Runx2 as a Transcriptional Repressor of Steroid Hormone Receptors. H. Kawate*[1], Y. Wu*[1], K. Ohnaka*[1], H. Nawata*[2], R. Takayanagi*[1]. [1]Department of Geriatric Medicine, Kyushu University, Fukuoka, Japan, [2]Department of Medicine and Bioregulatory Science, Kyushu University, Fukuoka, Japan.

Purpose: Both steroid hormone receptors and Runx2 are transcription factors and play a crucial role in the skeletal development and maintenance. We have examined the functional relationship between Runx2 and steroid hormone receptors.
Methods: Runx2 and one of the steroid hormone receptors (androgen receptor (AR), estrogen receptor (ER) or glucocorticoid receptor (GR)) were expressed in osteoblastic cells, MC3T3-C1. Luciferase assay was performed to evaluate the effect of Runx2 on the transactivation mediated by steroid hormone receptors. Green fluorescent protein (GFP)-tagged polypeptides were used for observation of the intracellular localization of the proteins under the confocal laser scanning microscopy.
Results: Luciferase assay using promoters carrying the hormone-responsive elements revealed that Runx2 suppressed the ligand-dependent transcriptional activation mediated by all three steroid hormone receptors. Coexpression of Cbfb, which is a transcriptional cofactor for Runx2, enhanced the Runx2-mediated repression. We previously observed that after the treatment of ligands steroid hormone receptors were translocated from the cytoplasm into the nucleus and produced the intranuclear foci. In this study, we have identified that Runx2 was located in the nucleus and showed foci formation and were colocalized with the steroid hormone receptors. Moreover, one of the nuclear receptor coactivators, TIF2, was colocalized with Runx2 and steroid hormone receptors after adding the ligands.
Conclusions: These data indicate that Runx2 plays an important role in the regulation of steroid hormone receptor-mediated transcriptional activation in the osteoblasts.

Disclosures: ***H. Kawate****, None.*

M230

Large Scale Transcriptional Profiling Across the Time Course of Fracture Healing. K. H. Wang*[1], V. Prashanth*[2], G. Eichler*[2], C. M. Edgar[1], T. Smith*[2], L. C. Gerstenfeld[1]. [1]Orthopaedic Surgery Research Laboratory, Boston University Medical Center, Boston, MA, USA, [2]Department of Biomedical Engineering, Boston University School of Engineering, Boston, MA, USA.

Skeletal tissue regeneration occurs through the recapitulation of many aspects of the original endochondral developmental process that formed the osseous skeleton during embryogenesis. The repair process that is initiated in response to fracture entails the complex interaction of multiple cell types and cellular processes and is reflected in the complexity of the transcriptional expression that occurs during fracture healing. The transcriptional expression of ~13,000 genes was assessed over the first 21 days of fracture healing. Standard mid-diaphyseal tibia fractures were generated in C57B6 murine tibiae. The profile of transcriptional expression of ~13,000 genes was carried out across the time course of fracture healing using 75mers covalently linked onto oligo-nucleotide microarray chips. Ribonuclease protection analysis was used for a small number of candidate genes, to verify the time course of chondrogenic and osteogenic gene expression and validate the accuracy of the predictive values of the micro array analysis. The data that were obtained from these experiments were analyzed using a novel algorithm called a Gene Expression Dynamics Inspector (GEDI) that produces self organizing maps of the expressed genes, which are graphically presented as colored coded mosaics that enables individual clusters of genes to be identified, easily visualized and associated with various temporal stages of fracture healing. Using unfractured bone tissue as the reference and ln 2 fold greater or lesser from the reference, ~1000 mRNAs within ~13,000, were identified that varied across the time course of healing. These data identified the heat shock (HSP) gene family to be tightly expressed immediately after injury at day 3 and is the first demonstration that this family of stress related genes, which is activated in response to burn or chemical toxicity is also activated as a consequence of mechanical trauma. On the other hand a sub family of genes within the metalloproteinase (MMP) family was identified as having a complex pattern of expression during the chondrogenic and osteogenic phases of fracture healing. Showing both excluded expression during chondrogenesis MMP8 and elevated expression during endochodnral resorption (MMP2,9,13 and 14). In conclusion these data demonstrate the potential uses of a global transcriptional profiling approach to identify complex networks of gene interactions that are regulated over the time course of fracture healing.
Supported by DOD/DAMD 170310576

Disclosures: ***K.H. Wang****, None.*

M231

NFAT Negatively Regulates Osteoblast Differentiation. H. Yeo*, M. Zayzafoon, J. M. McDonald. Department of Pathology, University of Alabama at Birmingham, Birmingham, AL, USA.

Nuclear Factor of Activated T cells (NFAT) is a family of transcription factors which play a key role in regulating expression of several genes. Protein phosphatase 2B (PP2B), also known as calcineurin, dephosphorylates and activates NFAT by allowing it to translocate to the nucleus and bind to a specific DNA consensus sequence. In addition, it has been reported that NFAT binds synergistically with transcription factors of activator protein-1 (AP-1 : fos/jun) on a composite DNA element which contains an NFAT and an AP-1 binding site. This highly stable ternary complex regulates the expression of many genes. The purpose of this study is to examine the expression of NFAT in osteoblast-like cells (MC3T3-E1) and to elucidate its role in osteoblast differentiation. Here we show by RT-PCR and Western blot analysis that NFAT c1, c2 and c3 are expressed in osteoblasts. Immunofluorescence staining and Western blotting of osteoblast nuclear proteins demonstrate that NFAT c1 and c3 are found in the nucleus and in the cytoplasm, while NFAT c2 is only present in the cytoplasm. To determine the role of NFAT in osteoblast differentiation, we used Cyclosporin A (CsA), a pharmacological inhibitor of PP2B, that is known to prevent NFAT dephosphorylation and nuclear translocation. CsA inhibits PP2B activity between 10nM - 100nM in a dose dependent manner. Interestingly, at these concentrations, CsA induces osteoblast differentiation, in a dose-dependent manner, demonstrated by increases in alkaline phosphatase (ALP) and Von Kossa (VK) staining. This increase in osteoblast differentiation was confirmed by demonstrating an increase in the expression of osteoblastic gene markers, ALP, collagen I and osteocalcin, in response to treatment with PP2B inhibitor by semi-quantitative RT-PCR. In addition, using a mouse calvaria *in vivo* model, we demonstrate that treatment with CsA increases bone thickness, osteoblast numbers and mineralization. To elucidate the mechanism by which NFAT inhibition induces osteoblast differentiation, we examined the effect of CsA on the DNA binding activity of AP-1 by EMSA. Inhibition of NFAT by CsA is associated with increased Fra2 and JunD binding to the AP-1 consensus sequence and decreased binding of c-Jun and c-Fos. These novel findings suggest that NFAT negatively regulates osteoblast differentiation by increasing c-Jun and c-Fos binding to AP-1.

Disclosures: ***H. Yeo****, None.*

M232

1,25(OH)$_2$D$_3$ Suppresses cbfa1 Gene Expression Transcriptionaly: Identification of Regulatory Elements. K. Hasegawa*[1], Y. Seino*[2], H. Tanaka*[1]. [1]Okayama University Graduate school of medicine and dentistry, Okayama, Japan, [2]Osaka Kosei Nennkinn Hospital, Osaka, Japan.

Cbfa1 is an essential regulator of bone specific cell differentiation.

We have shown increased expression of cbfa1 mRNA in vitamin D receptor knock out mice compared with wild type mice by the bone transplantation experiment and the organ culture experiment. To clarify the mechanism of suppressive effect of 1,25(OH)$_2$D$_3$(D3) on cbfa1 gene expression, we performed reporter gene assay using distal promoter of cbfa1 gene, which contains 17 E-box like sequences and 1 typical DR3 sequence (DR3:-98 /-84) near the transcription start site.

Materials and Methods We cloned the distal promoter region of mouse cbfa1 gene (-4579 /-8) into pGL3-Luciferase vector (Promega). Based on this sequence, several truncation mutant constructs (-168/-8, -1825/-8, -2165/-8, -2269-8) were generated. Vector was transfected to MC3T3E1 cell by FuGENE6 (Roche). Cells were treated with D3(1x10-8M) for 12 hours and measured luciferase activities at 48 hours after transfection.

Results While shorter constructs (-168/-8, -1825/-8) showed no repression activities by D3 treatment, D3 induced repression (30%) was observed only in longer constructs (-1927/-8, -2165/-8, -2269/-8). Thus D3 seemed to suppress cbfa1 gene expression thorough 100bp sequence between -1825 and -1927. For this construct, PKA activation by Forskolin did not exert any effects on basal luciferase activity in contrast to the negative VDRE in vitamin D 1 a-hydroxylase gene.

To delineate the function of DR3 motif located at -98 /-84, we next introduced a mutation into the DR3 motif to abrogate its binding activity to liganded VDR/RXR. This mutation enhanced the repression activity of D3 from 30% to 50%.

Conclusions From these results, we conclude that D3 suppresses cbfa1 gene expression transcriptionally thorough the sequence between -1825 to -1927. The DR3 sequence located at -98 /-84 is positive VDRE and this may interfere repressive activity of D3.

Disclosures: ***K. Hasegawa****, None.*

M233

Expression Pattern of Core Binding Factor-β in Skeletal Tissues. H. Kim[1], M. Hwang*[1], M. Han*[1], A. Javed[2], B. Lee*[1], R. Park*[1], S. Kim[3], H. Ryoo[3], J. L. Stein*[2], A. V. Wijnen[2], J. B. Lian[2], G. S. Stein[2], J. Choi[1]. [1]Dept.of Biochemistry, Kyungpook Natl. Univ. School of Medicine, Daegu, Republic of Korea, [2]Dept.of Cell Biology, UMASS Medical School, Worcester, MA, USA, [3]Skeletal Diseases Genome Research Center, Daegu, Republic of Korea.

Core binding factor-β (Cbf-β) is a partner protein of RUNX family transcription factor. Recently, knock-in and rescue mice of Cbf-β result in skeletal abnormalities. However, exact expression of Cbf-β has not been studied in skeletal tissues. To determine the expression pattern of Cbf-β in bone, we performed cDNA cloning, Cbf-β purification, antibody production, and immunohistochemical staining in mice skeletal tissues. Open reading frame of Cbf-β cDNA isolated from rat osteoblasts showed 188 amino acids. Anti-Cbf-β antibody was produced using recombinant Cbf-β protein. The expression of Cbf-β during osteoblast and chondrocyte differentiation was determined by Northern and Western blot analysis in MC3T3-E1 and ATDC5 cell culture system, respectively. Cbf-β and its mRNA were gradually increased during osteoblasts or chondrocytes differentiation. This pattern was similar in primary cultured osteoblast differentiation system. The expression of Cbf-β on growth plates was observed in osteoblasts, articular chondrocytes, and hypertrophic chondrocytes from both embryonic day 15 and postnatal 2 weeks mice long bones. Collectively, the expression patterns of Cbf-β from both *in vivo* growth plates and *in vitro* bone cell culture systems suggest that Cbf-β may play an important role in skeletal growth and differentiation.

Disclosures: ***J. Choi****, None.*

M234

Ectopic Overexpression of Adipogenic Transcription Factors Induced Transdifferentiation of MC3T3-E1 Osteoblasts. S. W. Kim*[1], S. J. Her*[2], T. J. Cho[3], D. H. Kim*[4], S. Y. Kim*[4], C. S. Shin[4]. [1]Department of Internal Medicine, Seoul National University Boramae Hospital, Seoul, Republic of Korea, [2]Clinical Research Institute, Seoul National University Hospital, Seoul, Republic of Korea, [3]Department of Orthopedic Surgery, Seoul National University College of Medicine, Seoul, Republic of Korea, [4]Department of Internal Medicine, Seoul National University College of Medicine, Seoul, Republic of Korea.

Osteoblasts and adipocytes originate from a common mesenchymal progenitor cells and it has been shown that the differentiation to a particular lineage has been associated with reciprocal inhibition of differentiation to the other pathways. We have investigated whether MC3T3-E1 cells - the committed osteoblast originated from mouse calvarial cells - can be induced to transdifferentiate into mature adipocytes by the ectopic expression of two adipogenic transcription factors, PPARγ, C/EBPα, or both. In osteoblastogenic culture condition, the alkaline phosphatase activity was decreased by retrovirus-mediated overexpression of PPARγ whereas its activity was slightly increased by retroviral overexpression of C/EBPα. Overexpression of both PPARγ and C/EBPα had a neutral effect. Under conditions for promoting adipogenesis by treatment with insulin, dexamethasone and IBMX, cells overexpressing PPARγ alone or PPARγ and C/EBPα showed transdifferentiation to mature adipocytes expressing molecular markers of this lineage. Cells expressing both PPARγ and C/EBPα showed more robust phenotype of adipocytes than the cells expressing PPARγ. Overexpression of C/EBPα alone did not result in adipogenesis. Taken together, these results suggest that PPARγ is a key molecular switch for the transdifferentiation to adipocytes whereas C/EBPα differentiate MC3T3-E1 cells into osteoblasts as well as adipocytes.

Disclosures: ***S.W. Kim****, None.*

M235

Expression Profiles of Osteogenesis Related Genes in Calvarial Bone Development. J. Cho*[1], W. Lee*[1], H. Kim*[1], H. Shin[2], H. Ryoo[1]. [1]Biochemistry, School of Dentistry, Kyungpook National University, Daegu, Republic of Korea, [2]Pathology, School of Dentistry, Kyungpook National University, Daegu, Republic of Korea.

Understanding of osteogenesis-related gene profile is very important in the development of a new regimen for the osteopenic conditions. Developing calvaria undergoes typical intramembranous bone forming process. In embryonic day 15.5 of mouse, the parietal bones are clearly separable from the overlying skin, the underlying dura mater. Moreover, the intervening sutural mesenchyme that includes osteoprogenitor cells could be clearly demarcated from the bone tissue. To identify genes related to osteoblast differentiation, we isolated total RNAs from parietal bones and sutural mesenchyme, and analyzed a comprehensive gene expression profile of each tissue by oligo-based Affymetrix microarrays containing 22,690 probes. About 2100 genes with “Present” calls showed more than 2-fold higher signals in bones compared to sutures and 73 out of them showed more than 8-fold higher. Some of them are already known as bone-related biomarkers; VitD receptor, bone sialoprotein, osteocalcin, osteopontin, MMP13, etc, or already reported their differential gene expression patterns in the same tissue by *in situ* hybridization. Ten genes were selected and subjected to confirmation by quantitative real-time RT-PCR analyses. All the genes tested showed higher expression in bones, ranging 5 to 140-folds. Several of these genes are ESTs and the others are already known but their functions in osteogenesis are still unknown. These results suggest that all the processes, including tissue isolation, RNA preparation, microarray hybridization and Genechip scanning were properly executed. Our data imply the result is so convincing that it can be used as a good standard for the mining of osteogenesis-related genes.

Disclosures: ***J. Cho****, None.*

M236

FK506 Modulates Osteoblast-specific Transcription Factors Cbfa1 and Osterix Gene Expression in ROS 17/2.8 Cells. S. S. Varanasi, H. K. Datta. School of Clinical &Laboratory Sciences, University of Newcastle, The Medical School, Newcastle upon Tyne, United Kingdom.

FK506 like other immunosuppressants binds to an abundant cytosolic immunophilin called FK506 binding protein 12 (FKBP12). Although acute osteoporosis is one of the prominent and debilitating side effects on osteoblast differentiation and function, the direct effect of FK506 on osteoblast specific transcription factors, Cbfa1 and Osterix, has never been investigated. In the present study we have characterised FKBP12 by using RT-PCR, immuno-localisation and Western blotting and investigated the effect of FK506 on expression of osteoblast-specific transcription factors in ROS 17/2.8 cells. Western blotting extracts of ROS17/2.8 cells revealed the 12 KDa isoform, which was immuno-localized

predominantly in the cytosol. The transient exposure of serum-starved ROS17/2.8 cells to H_2O_2 (100 µmol/L) was found to elevate FKBP12 mRNA after 10 min and increase protein expression after 24h. Interestingly, both PTH (0.1 µmol/L) and 1,25 $(OH)_2D_3$ (1 nmol/L) suppressed FKBP12 protein expression. The fact that different osteoblast proliferating agents had dissimilar effect on an ubiquitous but important cytosolic protein FKBP12 led us to examine possible functional significance of this observation. Therefore, we studied the regulation of osteoblast-specific transcription factors Cbfa1 and osterix by FK506 in ROS 17/2.8 cells. Our study showed a marked inhibition of Cbfa1 isoforms II/III and osterix gene expression in serum-starved ROS 17/2.8 cells by therapeutic level of FK506. The exposure of these cells to FK506 (50 µmol/L) for 0, 30 ad 240 min was found to lead to inhibition of both Cbfa1 isoforms II/III and osterix mRNA expression. The inhibition of Cbfa1 expression was evident both at 30 min and 240 min, whereas osterix mRNA expression was found to be more inhibited after 240 min. The dose-dependant inhibition of osterix in these cells, carried out using 2.5, 25 and 250 µmol/L of FK506, showed maximal inhibition at 2.5 µmol/L; the extent of inhibition remaining similar at higher concentrations. Interestingly, Cbfa1 isoforms II/III were also maximally inhibited at 2.5 µmol/L, however the inhibition became less marked at 25 and 250 µmol/L. alkaline phosphatase, FKBP12 and GAPDH mRNAs levels were unaffected both in the time-course and dose-response studies. In conclusion, this study characterises FK506-binding proteins in osteoblasts and suggests a possible involvement of immunophilins in directly mediating osteoblast-specific transcription factor gene regulation. The results of this study thus suggest that FK506-induced osteoporosis may also be accentuated by the inhibition of osteoblast differentiation and function.

Disclosures: ***H.K. Datta****, None.*

M237

Dlx5 Knock Out Calvaria Cell Cultures Have Decreased Osteoblast Differentiation. H. Li*[1], M. S. Kronenberg[1], M. Stover*[1], M. J. Depew*[2], J. R. Rubenstein*[2], A. C. Lichtler[1]. [1]Genetics and Developmental Biology, University of Connecticut Health Center, Farmington, CT, USA, [2]Nina Ireland Laboratory of Developmental Neurobiology, University of California at San Francisco, San Francisco, CA, USA.

Previous studies have shown that Dlx5 induces osteoblast differentiation of calvarial osteoblasts and bone marrow stromal cells. Dlx5 knockout mice have defective calvarial development. Lentivirus delivered RNAi targeting both Dlx5 and Dlx3 blocked osteoblast differentiation in calvarial cell cultures. To better understand the role of Dlx5 in regulating osteoblast differentiation, we did in vitro studies on Dlx5 knock out mice. The mice were in 129J, CD1 and C57BL/6J mixed background. Dlx5 heterozygous mutant mice were crossed and embryos were collected at stage E18.5 because the Dlx5 homozygous knock out mice were neonatal lethal. Calvaria were isolated and maintained in culture media temporarily while genotyping was being done. Calvaria with the same genotype were pooled and cultures were made from serial digestions with trypsin and collagenase. Cells were kept in DMEM until they became confluent (day 6-8) and were then switched into aMEM supplemented with ß-glycerophosphate and ascorbic acid. Cell cultures were taken down at different time point from day 11 to day 20 and Northern blot and quantitative RT-PCR were carried out to study the expression levels of key markers of osteoblast differentiation. The expression levels of alkaline phosphatase in Dlx5 homozygous knock out calvaria cell culture decreased about 40%-50%, bone sialoprotein decreased about 15% to 40%, and osteocalcin decreased about 40% to 50% compared to wild type and heterozygous Dlx5 mutant cell cultures. The decreases in osteoblast marker expression were most pronounced at the earlier time points of the cell cultures. Dlx3 expression was not changed significantly, and its expression may partially compensate for the absence of Dlx5. Our studies support the concept that Dlx5 has a positive regulatory role in osteoblast differentiation.

Disclosures: ***H. Li****, None.*

M238

Abnormal Transdifferentiation Associated with Delayed Fracture Healing in Older Rats. M. H. Meyer, R. A. Meyer. Department of Orthopaedic Surgery, Carolinas Medical Center, Charlotte, NC, USA.

Formation of bone to bridge the fracture gap of healing skeletal fractures slows with age in rats and humans. While six-week-old rats reach radiographic union in four weeks following mid-shaft femoral fracture, adult 26-week-old rats need 10 weeks, and older 1-year-old rats need in excess of 6 months. To explore factors related to this delayed healing, microarray analysis was employed. Simple, transverse, mid-shaft femoral fractures with intramedullary rod fixation were induced in intact female Sprague-Dawley rats at 6, 26 and 52 weeks of age. At 0, 0.4, 1, 2, 4, and 6 weeks after fracture, the fracture site, including the external callus, cortical bone, and marrow elements, was harvested. Total RNA was extracted and pooled between pairs of rats of the same age and time after fracture, and cRNA was prepared and hybridized to 54 Affymetrix U34A microarrays (3/age/time point) with 8,700 genes on each array. GenBank entries are shown for each gene in parentheses. The average for each gene for each of the 18 treatment groups was calculated from the 3 arrays per group and analyzed by the SOM (self-organizing map) algorithm in the Data Mining Tool (3.0, Affymetrix). Several clusters contained genes with greater up-regulation in the older rats than in the young rats following fracture. Biomechanical data, bone morphogenetic protein expression, and expression of types II and X collagen suggested similar rates of formation of soft callus in young and older rats. However, two genes suggested delayed progression to calcification. ACLP (AEBP1, AA799755) and mesenchyme homeobox 2 (Meox2, Z17223) were increased more and longer in the older rats than in the younger rats. These two genes are up-regulated in cells differentiating towards mature osteoblasts. The failure of these two genes to down-regulate in the older rats suggests a failure of the osteoblasts to finish the maturation process. Also found to be up-regulated more and longer in the older rats were additional genes that are known to be up-regulated as stem cells undergo maturation towards the osteoblast and chondrocyte lineage. These genes include alpha smooth muscle actin (AA866452, AI104567, and X80130) and sarcomeric myosin heavy chain (K03467 and K03468). In conclusion, these changes suggest a stronger stimulus in the older rats for differentiation of precursor cells towards chondrocyte and osteoblast formation. However, the continued expression of ACLP and Meox2 suggest that the osteoblasts failed to fully mature and were thus slower to make bone in their fracture callus.

Disclosures: ***M.H. Meyer****, None.*

M239

PTHrP Mediation of AP-1 Signaling in Mesenchymal (Cementoblast) Cells. J. E. Berry*[1], E. L. Ealba*[1], L. R. McCabe*[2], L. K. McCauley[1]. [1]Periodontics/Prevention/Geriatrics, University of Michigan, Ann Arbor, MI, USA, [2]Michigan State University, East Lansing, MI, USA.

The major components of the AP-1 family of transcription factors include the Fos members (c-Fos, Fra-1, Fra-2, FosB) and Jun members (c-Jun, JunB, JunD). These transcriptional regulators form heterodimers (Fos/Jun) or homodimers (Jun/Jun) to interact with sites (CRE or TRE) in a large number of genes important in bone. Skeletal hormones and growth factors such as PTH and PTHrP have been found to regulate AP-1 proteins and suggest these regulators may be instrumental in determining effects of anabolic agents in bone. The purpose of this study was to examine the impact of PTHrP on gene expression and nuclear protein levels of AP-1 family members in a mesenchymal cell line derived from mouse cementum (OCCM). Cells lining the tooth root from day 41 (birth at day 19) transgenic OC-TAg mice were isolated, and a clonal population that expresses markers of mineralization, including osteocalcin and bone sialoprotein, were utilized. Timed studies with PTHrP (0.1 µM) for 0, 60, 120 min. and 6 h. were performed. Northern blot analysis revealed that PTHrP rapidly increased mRNA for c-*fos* (peak at 60 minutes of 5-fold), *fra*-1 (peak at 120 minutes of 2.5-fold), *fra*-2 (peak at 60-minutes of 2-fold) and *fos*B (peak at 60-minutes of 1.5-fold). PTHrP also increased mRNA for *jun*B (peak at 60 minutes of 4-fold) but did not alter c-*jun* or *jun*D expression. Levels of Fos and Jun proteins were determined from nuclear extracts using an ELISA-based protein assay at the same time points. Levels of c-Fos peaked at 120-minutes and were the most highly elevated (12-fold) in response to PTHrP. Levels of Fra-1 peaked at 6-hours and were 2-fold elevated. Fra-2 levels peaked at 120 min and were 3-fold elevated. Levels of FosB peaked at 120-minutes and were elevated 2-fold. JunB was the only Jun family member significantly elevated at the protein level (peak at 120-minutes and 2.5-fold increase). Protein levels for phosphorylated c-Jun were reduced with PTHrP treatment at 120-minutes, and JunD levels were unchanged. Similar results for AP-1 member RNA and protein levels were obtained for MC3T3-E1 osteoblastic cells treated with PTHrP. Since JunB has been reported to be a key regulator of bone formation in osteoblasts, these data suggest that PTH and PTHrP may exert anabolic actions in bone via AP-1 heterodimerization containing one of the Fos family members and JunB. Furthermore, these data with a cementoblastic cell line suggest that PTHrP may have effects on cementum development through its action on AP-1 containing genes.

Disclosures: ***J.E. Berry****, None.*

M240

Oncofetal Fibronectin Correlates with Decreased Markers of Bone Formation in vivo and Modulates Osteoblast Proliferation and Differentiation in vitro. I. Nakchbandi, P. Feick*, A. Geursen*, M. Singer*. Department of Medicine II, University of Heidelberg at Mannheim, Mannheim, Germany.

Hepatic osteodystrophy, a disease associated with significant morbidity, results mainly from decreased bone formation. Three observations suggest that abnormal production of fibronectin (FN) may be involved in the development of hepatic osteodystrophy. First, patients with liver disease exhibit altered FN production. Second, treatment of liver stellate cells with carbontetrachloride results in the production of fibronectin isoforms not normally produced by these cells. Third, FN is important for the survival and differentiation of osteoblasts in vitro.

Circulating oncofetal fibronectin (oFN), an isoform of FN, was found to be elevated in patients with cholestatic liver disease (4.0±0.5 µg/ml, n=20) compared to age-, sex-, and BMI-matched controls (2.9±0.2 µg/ml, n=20), p=0.056. Circulating oFN correlated negatively with osteocalcin in the whole group (r= -0.39, $p<0.05$, n=40) and in the patients (r= -0.49, $p<0.05$, n=20). Next, the effect of oFN on proliferation and mineralisation of cultured human osteoblasts was examined. Treatment of osteoblasts with increasing doses of oFN resulted in a small increase in proliferation (peak response 1.32-fold induction with 10 µg/ml, $p<0.05$, n=5). Simultaneous addition of GRGDSPK and oFN showed no significant decrease in proliferation compared to oFN alone, suggesting that the oFN effect is not mediated by RGD-binding integrins. Treatment of osteoblasts in mineralising conditions with increasing doses of oFN showed that the area of mineralised nodules (determined by von Kossa staining) was decreased in oFN-treated cultures. At 100 µg/ml mineralisation was maximally reduced by 69% as compared to control (n=5, $p<0.01$).

The data show that oFN correlates with decreased bone formation markers in patients with liver disease, and that oFN modulates osteoblast proliferation and differentiation in vitro. This effect seems unrelated to RGD-signalling. Since oFN promotes proliferation, it may indirectly inhibit differentiation. In conclusion, the increase in oFN production by the liver and its release into the circulation influences osteoblasts and hence may contribute to the decreased bone formation seen in chronic cholestatic liver disease.

Disclosures: ***I. Nakchbandi****, None.*

M241

Computer Simulations Support the Regulatory Role of the Matrix in Bone Formation. M. J. Martin, J. C. Buckland-Wright*. Applied Clinical Anatomy Research, King's College, London, London, United Kingdom.

The development of pharmaceutical treatments for bone disease can be enhanced by mathematical models that predict their effects on formation during cancellous bone remodeling.

The amount of bone formed and the duration of the formation phase at one micro-site on the surface of cancellous bone was simulated by, the number of mature osteoblasts and changes in rates of osteoblast activity. The number of mature osteoblasts at the start of osteoid formation was simulated by a relationship that describes the proliferation of muscle stem cells in the presence of growth factors (Deasy et al., 2002). Osteoblast activity was described by Michaelis-Menten enzyme kinetic equations adapted to describe cellular activity.

The model incorporated four negative feedback effects on the rate of bone formation:

- the reduction in size of mature osteoblasts with differentiation, which limited the maximum capacity of cellular osteoid-forming activity;
- the reduction in osteoblast cell numbers due to osteocyte formation;
- the apoptosis of surplus osteoblasts that are not required for lining cell or osteocyte formation;
- and, as mineralization progresses, the limited availability of osteoid substrate.

The model was parameterised by fitting simulations to data of changes in absolute osteoid seam thickness and it's depth of formation and mineralization, together with relative changes in rates of osteoid formation and calcification (Eriksen et al., 1984).

Simulated depth of new bone formed was increased by 12.2% and 6.4% by a 2% increase in mitotic fraction, and a 2% decrease in division time, respectively. The duration of formation was increased by 2.6% with a 2% increase in maximum capacity of osteoid-forming activity. A 2% change in other input variables produced less than 2% changes in depth and duration.

The high sensitivity of bone formation to mitotic fraction supports the potential role played by the matrix in mediating cell number, not only by embedded mitogenic growth factors, but also by the amount of surface area of matrix that is available for cell attachment. The bone matrix factors that control the mitotic fraction and division time of pre-osteoblasts during proliferation are therefore suggested to be potentially useful areas for future pharmaceutical research.

Disclosures: ***M.J. Martin****, None.*

M242

Tartrate-Resistant Acid Phosphatase Deficient Mice Have Defective Osteoblast Function And Increased Mineralization. H. C. Roberts*[1], L. Dufaur*[1], T. M. Cox*[2], M. J. Evans*[3], A. R. Hayman[1]. [1]School of Clinical Veterinary Science, University of Bristol, Langford, Bristol, United Kingdom, [2]Medicine, University of Cambridge, Cambridge, United Kingdom, [3]School of Biosciences, University of Cardiff, Cardiff, United Kingdom.

Tartrate-resistant acid phosphatase (TRAP) is an iron-containing protein expressed by osteoclasts, macrophages and dendritic cells. The enzyme is secreted by the osteoclast during bone resorption and serum TRAP activity correlates with the level of resorptive activity in diseases of bone metabolism. Although its precise role is unknown, we have shown using 'knockout' mice that TRAP is essential for the normal mineralization of cartilage in developing bones and the maintenance of the adult skeleton. Mice lacking TRAP were shown to have a skeletal phenotype characterised by developmental deformities of the limbs and axial skeleton. These bones were wider and shorter than normal with thickened cortices and disorganised, enlarged growth plates. An increase in mineralization density was also observed. Osteoclasts isolated from TRAP knockout animals demonstrated a defect of bone resorption in vitro which over time may have resulted in the increased bone density observed. However, osteoblast function could also be affected in the animals lacking TRAP and contribute to the altered bone density. We now demonstrate studies on osteoblast function in vitro.

The development of the osteoblast phenotype normally involves three distinct phases: a proliferative phase, a matrix development and remodelling phase followed by a mineralization phase. Osteoblasts were isolated from the bone marrow of 6 week old TRAP deficient and normal (wild-type) mice and cultured in α-MEM medium containing 10%FCS and antibiotics. The cell growth rate was determined spectrophotometrically by measuring the activity of living cells via mitochondrial dehydrogenase activity. In the proliferative phase cell growth for osteoblasts isolated from wild-type mice was approximately 55% higher than osteoblasts lacking TRAP. To evaluate the ability of osteoblasts to form and mineralize bone nodules in vitro, wild-type and knockout osteoblasts were cultured in media supplemented with ascorbic acid (50μg/ml), using β-glycerophosphate (10mM) as the phosphate source. At selected time points, the cultures were fixed and stained with von Kossa. The number of mineralized nodules was significantly greater in the osteoblast cultures from the TRAP knockout mice.

We conclude from these studies that the growth of cells is reduced in osteoblasts deficient in TRAP and that mineralization is increased. This suggests that TRAP plays a role in the regulation of bone formation and its mineralization.

Disclosures: ***H.C. Roberts****, None.*

M243

Parathyroid Hormone Related Peptide (1-36) Decreases Bone Nodule Formation and Reduces Bone Sialoprotein mRNA during Intramembranous Ossification by Neonatal Rat Calvarial Cells. S. A. Kamel*, J. A. Yee. Biomedical Sciences, Creighton, Omaha, NE, USA.

The appearance of neonatal mice that develop in the absence of parathyroid hormone-related peptide (PTHrP) established that the peptide is necessary for normal development and growth of the skeleton. The shortening of appendicular bones in knockout mice is explained by an effect of PTHrP on endochondral bone growth where it functions to inhibit the hypertrophy of chondrocytes in the epiphyseal growth plate. Whether or not PTHrP influences intramembranous ossification is less clear. The purpose of this study was to examine the expression of PTHrP and its receptor (PTH1R) by osteogenic cells involved in intramembranous ossification *in vitro* and to determine the effect of exogenous PTHrP on this process. Cells isolated from calvariae of neonatal rats were plated at 75 cells /cm^2 so that individual cell colonies could be studied over a period of 3 weeks. Continuous and intermittent treatment with PTHrP (1-36) was compared to address whether the pattern of exposure to PTHrP influenced the response by rat calvarial cells. PTHrP and PTH1R were localized by immunohistochemistry and alkaline phosphatase (AP) was detected by enzyme histochemistry. Staining was visualized by confocal microscopy. Calvarial cells were exposed to 100 nM PTHrP (1-36) continuously or for the first 1 or 6 hrs of each 48 hr incubation interval (intermittent treatment). The effects of PTHrP on proliferation, apoptosis and gene expression were measured using BrdU incorporation, TUNEL staining and real time RT-PCR respectively. It was found that PTHrP and PTH1R were co-localized in cell colonies as early as day 3 while AP was not detected until day 6. During the course of bone nodule development PTHrP and its receptor were co-localized in pre-osteoblasts, osteoblasts, and osteocytes. By comparison, the AP activity exhibited by pre-osteoblasts and osteoblasts disappeared in osteocytes. Both continuous and intermittent exposure to PTHrP (1-36) caused a reversible inhibition in bone nodule formation. Treatment with PTHrP (1-36) had no effect on AP activity, cell proliferation, apoptosis, or the level of osteopontin mRNA. However, bone sialoprotein (BSP) mRNA was reduced by > 90% compared to control. These results suggest that PTHrP may be function as an autocrine/paracrine factor for cells in the osteoblast lineage involved in intramembranous ossification. Since PTHrP inhibited bone nodule formation and reduced BSP gene expression, we conclude that PTHrP may influence bone mineralization by controlling the production of BSP.

Disclosures: ***S.A. Kamel****, None.*

M244

Therapeutic Touch Affects Proliferation and Bone Formation in Vitro. A. P. Jhaveri*[1], M. B. McCarthy*[1], Y. Wang*[2], G. Gronowicz[1]. [1]Orthopaedic Surgery, UCONN Health Center, Farmington, CT, USA, [2]Statistics, UCONN, Storrs, CT, USA.

Pioneered and developed by Dr. Dolores Krieger and Dora Kunz, modern-day Therapeutic Touch (TT) is a highly disciplined and orchestrated 5-step process by which a practitioner can promote healing. TT is performed by holding hands 5-10 cm away from the patient or the culture dish. Our goal was to determine if TT had an effect on the growth and differentiation of bone cells *in vitro*. Human osteoblasts (HOBs) obtained from orthopaedic procedures, and an established osteoblast-like cell line originally dervived from a human osteosarcoma (SaOs-2) were used. Cells were plated into 6-well culture dishes at 10,000 cells/cm^2/$2ml^{-1}$ and incubated at 37°C, saturated humidity for 2 days prior to treatment. To test the effects of TT on cells, the culture plates were removed from the incubator for 10 minutes twice per week and divided into the following treatment groups; 1. qualified TT practitioners, 2. non-TT practitioner (an individual unfamiliar w/TT) and 3. untreated. Results were statistically analyzed with the Wilcoxon Rank Sum test.

At 1 and 2 weeks, cell proliferation was determined by [^{3}H]-thymidine incorporation and by immunocytochemistry for Proliferating Cell Nuclear Antigen (PCNA) (Zymed Laboratories Inc., San Fransisco, CA). No significant differences were found in proliferation assayed by [^{3}H]-thymidine incorporation at 1 or 2 weeks for SaOs-2 cells and 1 week of TT for HOBs. However, TT significantly ($p=0.01$) increased HOB proliferation after 2 weeks. PCNA staining confirmed these data. At 2 and 4 weeks, calcium content was measured biochemically (Eagle Diagnositics, De Soto, TX) and was visualized by fluorescent microscopy with calcein and phalloidin. No calcium content increase was observed in HOB or SaOs-2 cells at one week, but mineralization increased significantly in HOBs ($p=0.002$) and significantly decreased in SaOs-2 ($p=0.004$) after 2 weeks of TT, which was confirmed by calcein/phalloidin staining. Northern blots were performed to determine the expression of mRNA levels (Qiagen Inc., Valencia, CA) of Type I collagen, bone sialoprotein and alkaline phosphatase. Northern blots indicated an increase in mRNA expression for bone matrix proteins in HOBs and a decrease for SaOs-2 cells at 2 and 4 weeks of culture.

In conclusion, Therapeutic Touch increases human osteoblast proliferation, differentiation and bone mineralization, and decreases differentiation and mineralization in human osteosarcoma-derived cells. This is the first demonstration of TT being able to affect osteoblast proliferation and differentiation, and is the first to demonstrate statistically significant effects of TT *in vitro*.

Disclosures: ***A.P. Jhaveri****, None.*

M245

In Vitro Assessment of Demineralized Bone Matrix on Murine Mesenchymal Stem Cell Differentiation. J. L. Fitch*[1], D. Knaack*[2], T. A. Einhorn[1], L. C. Gerstenfeld[1]. [1]Orthopaedic Surgery Research Laboratory, Boston University Medical Center, Boston, MA, USA, [2]Osteotech, Inc, Eatontown, NJ, USA.

In 1965, Marshall R. Urist demonstrated that implantation of demineralized bone matrix (DBM) at extraskeletal sites induced *de novo* formation of cartilage and bone. While it is assumed that BMPs are the primary inductive factors in DBM, the bone matrix contains many other morphogens, cytokines and mitogens. However, few comparative studies of DBM and BMPs have been performed. The purpose of our investigation was to develop an in vitro system to assess the effects of DBM treatment on skeletal cell differentiation. Specifically, we wanted to determine the duration of bioactivity within DBM, its dose dependency and the underlying molecular mechanisms by which it effects differentiation. Initial experiments examined the inductive activities of DBM on C3H10T1/2 murine mesenchymal stem cells. Previous studies using C3H10T1/2 cells have shown that they would undergo an endochondral sequence of cellular differentiation when exposed to BMPs. Comparison of the gene expression of cells treated with BMP-2 and DBM indicated that, while both induce expression of collagen-α1 type X, collagen-α1 type II and osteopontin, the inductive effects of BMP-2 were four times greater than that of the highest dose of DBM. However, the known concentrations of BMP in this quantity of DBM would be ~50 fold less than the added BMP. Interestingly, treatment with high doses of DBM induced expression of bone sialoprotein while BMP-2 treated C3H10T1/2 cultures never showed the induction of this gene. Noggin is a demonstrated antagonist of BMPs. We applied Noggin to the media of C3H10T1/2 cell cultures treated with DBM in a dose previously demonstrated by our laboratory to inhibit the effects of BMPs on C3H10T1/2 cells. These results indicated that Noggin did not have an antagonistic effect on DBM's bioactivity. Qualitatively, the ability of DBM to induce bone sialoprotein and its resistance to antagonism by Noggin suggest that there are other bioactivities in DBM than simply BMPs. These data suggest that DBM appears to promote a fuller range of osteogenic gene activity in the C3H10T1/2 cells than BMP alone.

Disclosures: ***J.L. Fitch****, Osteotech 2.*

M246

Polyphenols in the Extract of Greens+™ Herbal Preparation Have Effects on Cell Proliferation and Differentiation of Human Osteoblast Cell Line SaOS-2. B. Balachandran*[1], V. Rao*[2], T. Murray[1], L. Rao[1]. [1]Medicine/Division of Endocrinology & Metabolism, St.Michael's Hospital, Toronto, ON, Canada, [2]Nutritional Sciences, University of Toronto, Toronto, ON, Canada.

Postmenopausal osteoporosis is a condition resulting from an abnormality in bone remodeling. There is evidence to implicate oxidative stress in the pathophysiology of osteoporosis. Epidemiological studies associate polyphenol intake with increased bone mineral density. Polyphenols are a natural component of plants that have potent antioxidant properties. greens+™ is a commercially available herbal preparation that is an important source of antioxidant polyphenols. The purpose of this study was to determine the effects of antioxidant polyphenols in the extract of greens+™ on the cell proliferation and differentiation of human osteoblast cell line SaOS-2 and to compare these effects with those of a standard pure phenolic compound**,** epicatechin. The total content of polyphenolics in Greens+ ™ was found to be 1.396 ± 0.29 mg of expressed as gallic acid equivalents/100g. The SaOS-2 cells were cultured in supplemented Ham's F-12 medium in the absence or presence of greens+™ extracts containing various concentrations (0.4, 0.8, 1.2, 1.6, 2.0mg/ml) of greens+ extract corresponding to 5.6, 11.7, 16.8, and 22.3, 27.9ng/ml of total polyphenol expressed as gallic acid equivalents/ml respectively. Control cultures received the vehicle extract. greens+™ extracts were added at day 8 and at every medium change thereafter. The cultures were stopped and the cell numbers determined after 2, 4, 7 and 9 days of treatment using the Methylene Blue Assay. Our results showed that the cell numbers increased significantly ($p<0.05$) compared to vehicle control after 2 and 4 days of treatment. The effects on cell proliferation of greens+™ extracts containing free polyphenol of 5.6 to 27.9 ng gallic acid equivalent/ml were found to be greater and more potent than those of the standard pure polyphenolic compound, epicatechin, at concentrations of 11.6 and 116.4 ng/ml. However, the cell numbers were reduced significantly after 7 days of treatment with greens+™ extract. Treatment with greens+™ extract from day 13 to the end of culture period resulted in **a** significant ($p<0.05$) inhibition of alkaline phosphatase activity in a time ($p< 0.0001$) and dose dependent ($p<0.0001$) manner. In conclusion, our results showed that greens+™ extract influenced human osteoblasts in a manner consistent with its effects on the proliferation and subsequent differentiation of osteoprogenitors towards progression to a bone-forming stage. Our data suggest that greens+™ may have beneficial effects on bone formation.

Disclosures: ***B. Balachandran****, None.*

M247

MMP-13 Negatively Regulates Osteoblast Activity. J. M. Owens[1], P. S. Chockalingam*[1], J. J. Wu*[2], J. M. Wozney[1], S. Fukayama[1]. [1]Womens Health & Bone, Wyeth Research, Cambridge, MA, USA, [2]Chemical & Screening Sciences, Wyeth Research, Cambridge, MA, USA.

Matrix metalloproteinase-13 (MMP-13/Collagenase-3) plays an important role in extracellular matrix remodeling. MMP-13 is expressed in osteoblasts and hypertrophic chondrocytes and specific cell-surface receptors for MMP-13 have been cloned from rat osteoblastic UMR-106 cells. Although it has recently been reported that MMP-13 knockout mice have increased bone volume, (Inada et al ASBMR 2002), the functional role of MMP-13 in bone remodeling remains unclear. We used the neonatal mouse calvaria organ culture to examine the action of an MMP-13 inhibitor on bone remodeling. This inhibitor was active at 3nM against MMP-13, with more than 10,000 fold selectivity over MMP-1 and MMP-14. Incubation of calvaria with MMP-13 inhibitor for 7 days was without effect on either total bone area or number of osteoblasts. MMP-13 inhibitor was also without effect on basal or fibroblast growth factor-2 (FGF-2)-induced bone resorption, as assessed by measuring calcium release from calvaria into the medium. However, the osteoblasts surrounding the calvaria became cuboidal after treatment with MMP-13 inhibitor, suggesting that they were activated. These findings suggest that MMP-13 plays a role in regulating osteoblastic function. To investigate this we examined the effect of MMP-13 inhibitor on two well-established osteoblastic cell lines. First, we confirmed that human osteoblastic SaOS-2 cells produce MMP-13 by fluorometric analysis of cell lysates and conditioned media. Incubation with MMP-13 inhibitor for 72 hours significantly increased alkaline phosphatase (ALP) activity in these cells. Osteocalcin expression was also up-regulated following treatment with MMP-13 inhibitor, as assessed by RT-PCR. On the other hand, treatment with 1nM MMP-13 enzyme, significantly inhibited ALP activity in UMR-106 cells. Incubation with other MMPs, such as MMP-2, MMP-9 or aggrecanase, did not significantly alter ALP activity in these cells. In addition, neutralization of MMP-13 enzyme activity with MMP-13 inhibitor did not reverse the inhibitory effect of MMP-13 enzyme on ALP activity in these cells. These findings argue against the possibility that the action of MMP-13 is mediated via its enzymatic interaction with extracellular matrix proteins. We also examined the effect of MMP-13 inhibitor on osteoclast differentiation and activity. Multinucleated TRAP-positive cell number and pit number were not significantly altered by the inhibitor, in mouse bone marrow cultures treated with M-CSF and RANKL. Together, our data are consistent with the hypothesis that MMP-13 negatively regulates osteoblastic function possibly via its specific receptor on osteoblasts.

Disclosures: ***J.M. Owens****, None.*

M248

Differentiating Human Adipocytes Reduce Osteoblast Function and Survival through the release of Fatty Acids: Senile Osteoporosis as a Lipotoxic Disease. G. Duque. Medicine/Geriatrics, McGill University, Bloomfield Centre for Aging Studies, Montreal, PQ, Canada.

BACKGROUND: The increasing bone marrow adipogenesis in aging bone is a consequence of the dysdifferentiation of mesenchymal adipocyte-like default cells which release large amounts of fatty acids that could affect osteoblast proliferation, action and survival. Although previous studies using mature adipocytes in co-cultures with osteoblasts have shown that secreted fatty acids affect osteoblast proliferation without affecting survival, no studies have looked at pre-differentiated adipocytes which are the predominant cells in the aging bone marrow.

AIM: To determine the influence of differentiating adipocytes on the proliferation and activity of human osteoblasts *in vitro*.

METHODOLOGY: Human primary osteoblasts (Cambrex, Pittsburgh, PA) were co-cultured with adipogenic differentiating mesenchymal stem cells (MSC) for three weeks being separated by a porous membrane (0.4 μm). Osteoblasts were seeded either in the upper or the lower side of the membrane. Osteoblasts cultured under the same conditions but without the presence of MSC were used as a control. After three time intervals (first, second and third week) cell proliferation and viability were assessed using MTS-Formazan and trypan blue staining respectively. In addition, alkaline phosphatase and mineralization staining were used as markers of osteoblastic activity. Finally, cerulenin, a known inhibitor of fatty acid oxidation, was used to potentially reverse the toxic effect of fatty acids and to assess the potential mechanism.

RESULTS: Although at all time intervals all parameters were significantly lower, a more significant effect was found on proliferation (-32±4%, $p<0.005$) and viability (-70%± 4%,$p<0.01$) of human osteoblasts at one week as compared with the control. In addition, the proportion of alkaline phosphatase and mineralization expressing cells was significantly lower in co-cultured osteoblasts than in the control (42%±4 vs. 86%± 3,$p<0.01$). Finally, the addition of cerulenin (10 μg/ml) induced a recovery in osteoblast function and viability at all three time points.

CONCLUSION: We found that both pre-adipocytes and differentiated adipocytes not only inhibited osteoblast proliferation but also affected their survival and activity. The potential mechanism involves the release of fatty acids by adipocytes more significantly in their early stages of differentiation. The regulation of the presence of pre-adipocytes in bone marrow might constitute a new approach for the treatment and prevention of age-related bone loss.

Disclosures: ***G. Duque****, None.*

M249

Knockdown of Chordin Using siRNA Induces Osteoblastic Differentiation in MC3T3-E1 Preosteoblastic Cells. W. Huang, G. Rudkin*, K. Ishida*, D. T. Yamaguchi, T. A. Miller*. Plastic Surgery, VA Greater Los Angeles Healthcare System, Los Angeles, CA, USA.

Signaling of bone morphorgenetic proteins (BMPs) is regulated at multiple levels: intracellularly, at the membrane site and extracellularly. Chordin is one of major extracellular antagonists of BMPs. In order to better understand the role of chordin in BMP-2 induced osteoblastic differentiation, we silenced expression of chordin in MC3T3-E1 cells using small interfering RNA and studied the effect of silencing of chordin on osteogenic differentiation in targeted cells. Among the four double-stranded siRNAs designed for targeting chordin, one of them was effective in silencing chordin when transiently transfected into MC3T3-E1 cells. Transfected cells demonstrated a decrease of approximately 70% in steady state chordin mRNA accompanied by an about 80% decrease in chordin protein secreted into culture medium. Those cells also exhibited drastic increases (>100-fold) in the mRNA expression of osteocalcin and alkaline phosphotase. Protein expression of alkaline phosphatase was significantly increased as measured by its enzymatic activity. The effect of chordin siRNA on osteoblastic differentiation can last up to 7 days. Comparison of mineralization showed little effect after 10 days of siRNA transfection. These data indicate that a decrease in chordin expression results in an increase in osteoblastic differentiation. The chordin siRNA is a potent enhancer of osteoblastic differentiation. It has an implication in the development of therapeutic agents that increase bone formation.

Disclosures: ***W. Huang****, None.*

M250

Co-culture of Human Umbilical Vein Endothelial Cells (HUVEC) with Human OsteoProgenitors (HOP): Effects on Osteoblastic Differentiation and/or Neoangiogenesis. B. Guillotin*, R. Bareille*, C. Bourget*, L. Bordenave*, J. Amedee. Gironde, INSERM U 577, Bordeaux, France.

Osteogenesis relies on a balance between bone formation and bone resorption, and occurs in striking interaction with neoangiogenesis. In this tightly regulated process, cell-to-cell communication supported by Connexin-43 in bone plays a pivotal role. Assuming that endothelial cells are located in very close vicinity to bone formation sites, we have been interested for several years in the potential role of endothelial cells and Connexin-43 in osteoprogenitor differentiation.

Our previous work has detailed an immunomagnetic-based method to separate primary HUVEC from primary HOP after a time of co-culture. Thus, molecular effects of HUVEC could be specifically studied on the HOP and reciprocally. The aim of our study was to identify bone specific markers as well as extracellular matrix (ECM) proteins which are regulated by the co-culture.

We first focused on the analysis of the temporal expression of osteogenic markers such as Alkaline phosphatase (ALP), CBFA1 and Osteocalcin (OC) in HOP co-cultured with HUVEC up to 48 hours. The results, as assessed by RT- real time quantitative PCR (RT-QPCR) have confirmed previous work showing an up regulation of ALP in the co-cultured HOP compared to HOP alone. Surprisingly, we also showed that the co-culture induced a 2 fold down regulation of CBFA1 in the HOP, and a 4 to 5 fold down regulation of OC.

Second, we took advantage of macroarrays to study the effects of the co-culture on the expression pattern of osteogenesis markers in the HOP. This global study revealed that genes implicated in ECM remodelling were regulated in co-cultured HOP as compared to steady-state expression in controls. HSP47, which participates in fibrillar Collagen (type I and type V) assembly, was 2 fold up-regulated in co-cultured HOP. A 4 fold up-regulation of type V Collagen was also observed. Timp-1, an inhibitor of metalloproteinase was also up-regulated whereas MMP-2 (type 2 metalloproteinase) was 2 fold down-regulated. Finally, preliminary microscopic observations indicate that the co-culture induces tube formation by the HUVEC in our model, to which ECM synthesis and remodelling could partly contribute.

Put together, our results suggest that osteoblast/endothelial cells communication modulate osteoblast differentiation and ECM synthesis. This should have some significance for bone remodelling or/and neoangiogenesis.

Disclosures: ***B. Guillotin****, None.*

M251

Exploring the In Vitro Proteome of Differentiating Osteoblasts. S. C. Verberckmoes, A. Hufkens*, L. Oste*, G. J. Behets*, M. E. De Broe*, P. C. D'Haese*. Nephrology-Hypertension, University of Antwerp, Wilrijk, Belgium.

Primary osteoblast cultures isolated from rat bone marrow have widely been used as a model of in vitro osteogenesis. The effects of various culture conditions on the protein expression of this model has been investigated in the past by others using classical protein analysis techniques such as ELISA and Western blotting. One of the major drawbacks of these techniques is the very limited number of proteins that can be analyzed in each experiment. Recently, methods such as differential proteome analysis based on two-dimensional polyacrylamide gel electrophoresis (2D-PAGE) have become available allowing the comparison of the expression of many proteins simultaneously. To the best of our knowledge, no reports on the osteoblast proteome have been reported so far. Therefore we have used the 2D-PAGE technique to construct a reference proteome map of the rat osteoblast under standard mineralizing in vitro conditions.

Bone marrow was flushed from the femoral cavity of five 22 week-old rats. The released cells were collected in five 75 cm^2 flasks and grown until confluence in alpha-MEM medium supplemented with 10 % fetal calf serum, 50 µg/ml ascorbic acid and 10^{-9} M dexamethasone. At confluence the cells were passed into 6-well plates after which the experiment was started. From confluence in the 6-well plates the medium was further supplemented with 2 mM beta-glycerolphosphate after which the cultures were further cultivated for 2 weeks. Medium samples for the analysis of alkaline phosphatase (ALP) activity and Ca-incorporation were taken from 3 different parallel experiments during medium refreshments 3 times per week. Cell samples for proteome analysis were taken from 3 independent cultures at the time of confluence, 1 and 2 weeks post-confluence to build up a time evolution map of the differentiating osteoblast proteome.

ALP activity, Ca-incorporation and nodule development showed a normal time-evolution characteristic for the in vitro osteoblast differentiation as reported in literature. The 2D-PAGE profiles showed 326 ± 42, 450 ± 133 and 1082 ± 183 individual spots at confluence, 1 and 2 weeks post confluence respectively. Differential analysis of the protein profiles was performed based on a spot intensity ratio threshold of 2 and revealed an up-regulation of 755 spots and a down-regulation of 9 spots over time.

Identification of these spots using MALDI tandem mass spectrometry is ongoing and will allow us to further complete the construction of an osteoblast proteome database. In the near future this proteome database will be used as a reference for the detection of changes in osteoblast protein expression in response to a large range of physiological and pathophysiological stimuli.

Disclosures: ***S.C. Verberckmoes****, None.*

M252

The Transcription Factor Osterix Controls Both Osteoblast Proliferation and Osteoblast Differentiation. C. Zhang, K. Sinha*, X. Zhou*, K. Nakashima*, B. de Crombrugghe*. Department of Molecular Genetics, University of Texas M. D. Anderson Cancer Center, Houston, TX, USA.

Osterix (Osx) is an osteoblast-specific transcription factor required for bone formation and osteoblast differentiation. Indeed, in Osx-null embryos, which completely lack both endochondral and intramembranous bone formation, preosteoblasts are arrested in their differentiation and fail to express many osteoblast marker genes, despite normal expression of the transcription factor Runx2 in these cells. To determine whether Osx plays a role in control of osteoblast proliferation, we now compared proliferation rates of primary calvarial cells isolated from wild type and Osx-null E18.5 embryos. BrdU incorporation in Osx-null cells was increased compared to wild type cells. We also generated C2C12 cells in which expression of a stably integrated Osx DNA could be induced using the Tet-off system. Induction of Osx expression inhibited cell proliferation. To begin to examine possible mechanisms by which Osx could control osteoblast proliferation, we used microarrays to compare the RNA expression profiles of wild type and Osx-null calvarial cells from E18.5 embryos. These experiments have revealed the broad repertoire of genes that constitute the genetic program of osteoblasts controlled by Osx, and strongly support the view that Osx is a major effector of the osteoblast program. Among the differentially expressed genes, expression of a Wnt inhibitor, Dkk1, which is high in wild type osteoblast, was abolished in calvarial cells of Osx-null embryos. In addition, expression of several Wnt target genes such as c-Myc and cyclin D1 increased in Osx-null calvarial cells. These results are consistent with the notion that Osx could control osteoblast proliferation through the Wnt pathway, a pathway that has been implicated in several human bone genetic diseases. We hypothesize that Osx coordinates both osteoblast differentiation and proliferation.

Disclosures: ***C. Zhang****, None.*

M253

Downstream Mitogenic Signaling of Osteogenic Growth Peptide C-Terminal Pentapeptide Involves Transcriptional Activation of MAP Kinase-Activated Protein Kinase 2. S. San-Miguel*, M. Attar-Namdar*, I. Bab*. Bone Laboratory, Hebrew University of Jerusalem, Jerusalem, Israel.

The osteogenic growth peptide (OGP) is a 14-mer bone cell mitogen that reverses ovariectomy-induced bone loss and enhances fracture healing. Its active derivative comprises the C-terminal pentapeptide, OGP(10-14). Mitogenic signaling by OGP(10-14) involves G_i-protein and MAP kinase activation. To further explore the downstream signaling activated by OGP(10-14) we examined its effect on phosphorylation of the MAP kinases ERK1, ERK2 and p38 in murine osteoblastic MC3T3 E1 cells. Immunoblot analysis using antibodies against the phosphorylated forms of these MAP kinases showed dose-dependent activation of ERK1 and ERK2, but not p38, 5-15 min after a challenge with OGP(10-14). The optimal OGP(10-14) concentration, 10^{-13} M, is also the dose with the highest OGP(10-14) mitogenic activity in these cells. In line with these results, the ERK1/2 inhibitor PD98059, but not the p38 inhibitor SB203580, inhibited the OGP(10-14) stimulation of BrdU uptake. We then subjected RNA from OGP(10-14)-treated MC3T3 E1 cells to microarray analysis using a cDNA array designed to interrogate the MAP kinase pathway. Of the genes encoding nuclear proteins, only the expression of MAP kinase -activated protein kinase 2 (Mapkapk2) was changed, showing >2-fold increased mRNA levels in cells treated with OGP(10-14) for 4-8 hours. Real-time RT-PCR analysis showed 3- to 96-fold OGP(10-14)-induced increase in mRNA levels in three independent experiments. The increase in Mapkapk2 mRNA was associated with a vast increase in Mapkapk2 total protein after 8-24 h exposure to OGP(10-14), as demonstrated by immunoblot analysis. This was accompanied by a moderate inhibition of Mapkapk2 phosphorylation. Collectively, these data suggest that the OGP(10-14) mitogenic activity is mediated by ERK1/2 activation, resulting in increased Mapkapk2 levels and thus overall activity. Mapkapk2, in turn, was previously shown to phosphorylate CREB that has an important role in osteoblastic cell proliferation and differentiation.

Disclosures: ***S. San-Miguel****, None.*

M254

The Effect Of Oxygen Tension On The Colony Formation Of Human Connective Tissue Progenitor Cells. S. M. Villarruel*, C. A. Boehm*, K. A. Powell*, M. Pennington*, G. M. Muschler. Biomedical Engineering, Cleveland Clinic Foundation, Cleveland, OH, USA.

Bone marrow (BM) contains connective tissue progenitor cells (CTPs) that can be activated to form new tissues. Proliferation of CTP progeny can be characterized using a colony-forming unit (CFU) assay. The number of CFUs found in a population reflects both the number of CTPs in the population and the activation efficiency of these cells under the culture conditions. Proliferation can be assayed in each colony, based on the number of cells in each colony at a fixed time. Optimization of the use of CTPs in therapeutic cellular grafts requires an improved understand of the bone healing environmental condition of hypoxia on CTPs.

BM derived cells were cultured to promote an osteoblastic phenotype for 6 days under oxygen levels: 20%, 10%, 5%, and 1% and then fixed and DAPI stained. CTP cultures were imaged using a Quantix K6303E 12 bit digital camera attached to a Leica DMXRA motorized microscope controlled by Metamorph . Individual images were collected at 512 x 768, 8-bit gray level, using a 10x objective and then montaged together to create one image of the cell culture well (2cm x 2cm). The image analysis software used for quantitative characterization of CTPs was developed using algorithms written in the C/C++ and Motif X-Windows TM environment.

In fifteen patient donors, a total of 9,174 colonies containing a total of 367,418 cells were assayed. The colony forming efficiency, based on the median number of colonies at each oxygen tension was increased at all lower oxygen tensions when compared to CTPs cultured at 20%. Oxygen tension 5% is sixty percent more efficient than the baseline value of 20% O_2 with a p-value<0.0001. In addition both 1% O_2 and 10% O_2 are also higher than the baseline. This is also reflected in that the median colony formation increased at lower oxygen tensions. All oxygen tensions possess a similar cells per colony distribution trend, but both 5% and 10% O_2 are markedly greater than oxygen tensions 1% and 20%, which themselves are comparable. Cycles of proliferation was significantly greater at all lower oxygen tensions than at 20% O_2 (p-value < 0.0002) despite large variation between individual CFUs at all oxygen tensions.

Using the CFU assay we have demonstrated that low oxygen tension conditions, even down to 1% O_2 may actually increase CTP activation and also increase the proliferation of progenitor cells in colonies. These features may enhance the CTPs capacity to survive and compete with other local cells in the wound healing environment or other transplantations. These findings have important implications in the biological response and survival of CTPs and also influence the design of delivery systems for CTPs in tissue engineering applications.

Disclosures: ***S.M. Villarruel****, None.*

M255

Bisphosphonates Differentially Affect Osteoblast Survival In Vitro. R. W. Katz[1], Q. Sun[2], J. P. Bilezikian[2]. [1]Oral Medicine, College of Dentistry, New York University, New York, NY, USA, [2]Medicine, College of Physicians and Surgeons, Columbia University, New York, NY, USA.

Bisphosphonates (BPs) have had a major impact on the management of osteoporosis and other metabolic bone diseases. Their actions have generally been ascribed to a direct inhibitory action on mature osteoclasts. Recent studies have suggested that BPs may also act directly on cells in the osteoblast lineage. Previously, we have shown that BPs affect signaling pathways utilized by the bone forming agents, parathyroid hormone and teriparatide. We intend to test the hypothesis that BPs affect osteoblast proliferation and survival. Several osteoblast cell lines were examined for their ability to grow in-vitro for 48-72 hours in the presence of BPs with a fluorometric assay of total DNA from harvested cell cultures. SaOS-2 cells displayed a 30% decrease in total DNA at 48 hours in the presence of 10-4 M risedronate (RIS) or alendronate (ALE) and at 72 hours, an even greater reduction in DNA was noted with ALE (65% of control values). The normal increases in cellular DNA of UMR-106 cultures was also inhibited significantly at 48 hours, with RIS being more potent than ALE (50% reduction with RIS compared to 30% with ALE). By 72 hours of culture, both BPs strongly inhibited cell accumulation. In experiments utilizing normal diploid rat calvarial osteoblast cultures, the effects of BPs was striking, with only minor (20-50%) increases in total DNA at 48 and 72 hours compared to initial starting values. In contrast, control calvarial cultures showed 3-4 fold increases in DNA content at 48-72 hours. To determine whether the inhibition of culture growth was due to increased cell death, the proportion of propidium iodide positive cells was examined by FACs. In UMR-106 cultures, treatment overnight with 10-6 M RIS led to a 2-3 fold increase in cell death over that seen with ALE-treated cultures. In SaOS-2 cultures, both BPs increased the percentage of dying cells three-fold over control cultures. In summary, our results indicate that BPs differentially affect osteoblast survival and cell accumulation in-vitro. Further studies are needed to understand how, under what circumstances, and by what mechanisms, BPs affect osteoblasts. These observations have key relevance to concepts of BP action, with particular reference to their potential use with bone forming agents, like teriparatide.

Disclosures: ***R.W. Katz****, Alliance for Better Bone Health 2; College of Physicians and Surgeons, Columbia University 5.*

M256

The PKA Inhibitor PKIγ, Is a Potent Regulator of Osteoblast Differentiation. L. Zhao*[1], S. Yang*[1], M. Petrey*[2], P. Stevens*[2], N. Jaiswal*[2], T. Zhu*[1], X. Ji[2], G. Sabatakos[2]. [1]Nankai University Medical College, Tianjin, China, [2]Skeletal Research, Procter and Gamble Pharmaceuticals, Mason, OH, USA.

In an effort to identify novel bone anabolic therapeutic targets we performed extensive genomic studies that evaluated the expression profile of regulated genes during osteoblastic differentiation of human mesenchymal stromal cells. Protein kinase inhibitor γ (PKIγ) was identified as a putative target as its expression was significantly downregulated in the presence of BMP-2. In order to elucidate the mechanism by which PKIγ regulates osteoblast differentiation we generated stable transfectants of PKIγ in C2C12 cells. Analysis of the effect of PKIγ overexpression in response to BMP-2 demonstrated a decrease in the expression of the early osteoblast markers osterix and Collagen type I. Furthermore the decrease in the mRNA levels of osteoblast marker genes in cells expressing PKIγ correlated with a decrease in alkaline phosphatase activity that was comparable to the response of control cells. In order to determine whether the inhibitory effect of PKIγ is mediated via effectors of the BMP/Smad pathway, we compared the activation of phosphorylated Smad1 between control and PKIγ overexpressing cells. Although pSmad1 levels were induced in control cells in response to BMP-2, no changes were observed in the PKIγ stable transfectants, suggesting that the effect of PKIγ could be mediated through alternative pathways. In order to investigate possible synergism between the PKA and BMP-2 pathways, C2C12 cells were treated with the PKA activator 8-Br-cAMP or inhibitor KT5720 and the alkaline phosphatase activity of the cells was determined in the presence of BMP-2. Although the alkaline phosphatase levels of the cells were not affected by treatment with either the PKA activator or inhibitor alone, co-administration of BMP-2 resulted in a synergistic increase or decrease in alkaline phosphatase activity, respectively. Having demonstrated that PKA and BMP-2 can synergistically regulate osteoblastic responses, we investigated whether the inhibitory effect of PKIγ on BMP-2 induced osteoblast differentiation was mediated via the PKA pathway. For this purpose, we studied the ability of PKIγ to modulate the activity of the cAMP-response element (CRE) using the Mercury Profiling Pathway System. As expected, BMP-2 induced AP-1 responses were inhibited by PKIγ overexpression. More importantly, PKIγ overexpression inhibited BMP-2 induced CRE responses. In conclusion our data suggest that the osteoblastic potential of C2C12 cells could be regulated by a mechanism that involves synergistic co-operation between the BMP-2 and PKA pathways and identify PKIγ is a potent inhibitor of osteoblast differentiation.

Disclosures: ***X. Ji****, None.*

M257

Intermittent Exposure to Vitamin D Analog (Analog V) Stimulates Mineralized Bone Nodule (MBN) Formation and Alkaline Phosphatase Activity in Cultures of Human Osteoblasts SaOS-2 Cells. L. G. Rao[1], L. J. Liu*[1], S. Reddy[2], M. S. Uskokovic*[3]. [1]Medicine/Div Endocrinology & Metab, University of Toronto & St. Michael's Hospital, Toronto, ON, Canada, [2]Chemistry, Brown University, Providence, RI, USA, [3]Hoffman-LaRoche, Nutley, NJ, USA.

Although 1α,25$(OH)_2D_3$ is used in some countries for the treatment of osteoporosis, its worldwide approval has not yet been achieved because of its narrow therapeutic window of safety in terms of dose and time duration of administration due to the toxic side effects of hypercalcemia and hypercalciuria. We previously demonstrated that 1α,25$(OH)_2D_3$ and a number of vitamin D analogs, including the noncalcemic analog, 1α,25$(OH)_2$-16-ene,23-yne-D_3 (analog V), had differential effects on normal human osteoblasts and clonal SaOS-2 cells. In this study, we tested the effect of analog V on MBN formation and alkaline phosphatase activity in long-term cultures of human osteosarcoma SaOS-2 cells. SaOS-2 cells were initially cultured in HAM's F-12 supplemented with 10 nM dexamethasone (Dex). 50 ug/ml ascorbic acid phosphate important for matrix formation and 10 mM β[[Unsupported Character - ]]-glycerophosphate needed for mineralization were added at day 8 of culture. Varying concentrations of analog V were added intermittently on day 8 for the first 30 min, 1hr 6 hr or 24 hrs, the medium replaced fresh without the hormone and the cultures continued for 48-hr. The 48-hr cycle was repeated until day 17. The cells were then fixed, stained with von Kossa and the MBN areas and MBN numbers quantitated by an image analyzer, or the cells sonicated for determination of alkaline phosphatase activity. Results were as follows: One way ANOVA analysis showed that 0.1 pM analog V significantly stimulated MBN number ((p<0.05), MBN area (p< 0.05) and alkaline phosphatase activity (p<0.05) in a time-course dependent manner after 30 min and 1 hr, but not after 6 hrs and 24 hrs of incubation. In conclusion, our data provide evidence for a stimulatory effect of analog V on mineralized bone nodule formation and differentiation via its effect on early progenitor cells. The results of our studies may prove that analog V, with its bone forming activity and low calcemic index, is a good candidate for the prevention and treatment of osteoporosis without the hypercalcemic and hypercalciuric toxicity.

Disclosures: ***L.G. Rao****, None.*

M258

Tumor Necrosis Factor Inhibition of the Osterix Promoter. X. Lu, X. He*, J. Rubin, M. S. Nanes. Medicine, Emory University, VA Medical Center, Decatur, GA, USA.

Tumor necrosis factor-alpha (TNF) is a potent suppressor of osteoblast (OB) differentiation and a mediator of bone loss after menopause. Factors shown to support the commitment of pluripotent precursor cells toward the OB phenotype are potential targets of TNF inhibition. The nuclear protein osterix (OSX) is needed for OB differentiation since mice deficient in OSX have cartilaginous skeletons and lack sufficient functional osteoblasts to form mineralized bone. We considered that OSX might be a target of TNF suppression. To test this hypothesis, we measured the TNF regulation of OSX steady state mRNA and promoter activity. OSX mRNA was measured by real time PCR (preliminary data, ASBMR 2003). The OSX promoter was cloned from murine genomic DNA using PCR primers that amplified a 1.3 kB fragment, including a portion of the 5'-untranslated region. This was subsequently cloned into pGL basic to create a luciferase reporter. MC3T3-E1 cells were grown in media supporting differentiation (ascorbate, beta-glycerophosphate) and treated with TNF at doses previously shown to completely inhibit differentiation (0.1-10 ng/ml). Real time PCR at 0, 4, 8, and 18 hours after TNF treatment (10 ng/ml) showed that TNF suppressed OSX mRNA 95% by 24 hours. The effect of TNF was dose dependent and not prevented by co-treatment with cycloheximide, suggesting that new protein synthesis was not required for TNF suppression of mRNA. TNF had no effect on OSX half-life. Transient transfection studies using the pOSX-pGL-luciferase reporter revealed that TNF treatment for 18 hours inhibited basal transcription by 71%. BMP-2, which can be shown to increase OSX mRNA and protein, increased promoter activity only slightly (28%). Suppression of promoter activity by TNF occurred independent of BMP-2 stimulation. The OSX promoter had regions of high homology for binding of numerous transcription factors including NfkB, MSX, RUNX2, DLX, TCF/LEF-1, SOX, SMAD3 and 14 repeats of a Myf5 bHLH site. To identify genes activated or suppressed by TNF in association with the inhibition of OB differentiation, MC3T3-E1 cells were treated with TNF for 4, 8, or 18 hours and mRNA was isolated for Affymatrix analysis using a chip set that included >7000 genes. Subtraction analysis of mRNA expression between differentiated (untreated) or undifferentiated (TNF-treated) cultures revealed 188 genes that were differentially regulated by TNF (>2-fold change, sustained for more than one time point). These included increased expression of NfkB precursors, RelB, JunB and down regulation of RUNX2, DLX-1, DLX-5, SOX6, and Tbx2 among others. Further analysis of the OSX promoter will be required to determine the critical factors that regulate OSX transcription.

Disclosures: ***X. Lu****, None.*

M259

Osteoblast-targeted ICER Expression Leads to Impaired Osteoblast Differentiation. T. K. Chandhoke*[1], Y. Huang[2], D. J. Adams[3], B. E. Kream[1]. [1]Medicine, UConn Health Center, Farmington, CT, USA, [2]Molecular Medicine, UConn Health Center, Farmington, CT, USA, [3]Orthopaedic Surgery, UConn Health Center, Farmington, CT, USA.

Inducible cAMP early repressor (ICER), a member of the CREM transcription factor family, is encoded by the P2 promoter of the CREM gene. ICER protein contains a basic leucine zipper region that serves as a site for DNA binding and dimerization, rendering ICER a dominant negative regulator of cAMP-dependent gene transcription. Prior studies have shown ICER mRNA and peptide to be induced by PTH through the cAMP-PKA signaling cascade in cultured osteoblasts and in calvariae *in vivo*. To dissect the role of ICER in osteogenesis, a transgene was developed to overexpress ICER in osteoblasts *in vivo* by cloning ICER cDNA with an N-terminal FLAG epitope downstream of a bone selective 3.6 kb fragment of the rat Col1a1 promoter (pOBCol3.6-ICER). The Col3.6 promoter targets ICER expression to nearly all cells of the osteoblast lineage. Our previous data showed that transgenic mice expressing pOBCol3.6-ICER showed lower body weight than wild type animals, decreased bone formation rate and markedly decreased trabecular bone volume. The aim of the present study was to further evaluate the role of ICER in bone remodeling by evaluating femoral bone morphometry and the effect of the transgene on osteoblast differentiation. X-ray microcomputed tomography (microCT) analysis of femurs from 8-week-old mice showed significant changes in bone microarchitecture, including an almost complete absence of trabecular bone volume in the most affected line. To determine the effect of the ICER transgene on osteoblast differentiation, hemizygous pOBCol3.6-ICER mice were bred with homozygous pOBCol2.3-GFP mice in which GFP cDNA is driven by the Col2.3 promoter. This GFP transgene is activated in mature osteoblasts and serves as a real time marker of osteoblast differentiation. Bone marrow stromal cells from 6-8-week-old ICER/GFP progeny were cultured for up to 21 days in the presence of ascorbate and ß-glycerophosphate. At days 14 and 21, ICER/GFP cells showed reduced GFP expression by fluorescence microscopy and fluorimager analysis compared to WT/GFP cells, suggesting that the ICER transgene inhibited osteoblast differentiation. Sex-matched cultures of bone marrow stromal cells from ICER/GFP mice showed the reduction in GFP expression to be conserved between males and females. Bone marrow cultures observed at day 14 and day 21 showed reduced mRNA expression of several markers of osteoblast differentiation, including bone sialoprotein and osteocalcin. In summary, these data show that overexpression of ICER led to impaired bone microarchitecture, osteoblast differentiation and osteoblast function.

Disclosures: ***T.K. Chandhoke****, None.*

M260

Mechanism of Glucocorticoid-TGF-β antagonism: Inhibition of Smad3 Transcriptional Activity by Glucocorticoid Receptor. X. Shi, L. Yang*, X. Shen*, X. Cao. Pathology, University of Alabama at Birmingham, Birmingham, AL, USA.

Glucocorticoid (GC)-induced osteoporosis affects more than 30 million Americans. However, the molecular and cellular mechanism responsible for GC-induced bone disorder is largely unknown. TGF-β and GC have important, but directly opposing effects on bone metabolism. TGF-β is one of the most abundant of the known growth factors stored within the bone. During the remodeling cycle, osteoclasts resorb bone, TGF-β is released and it stimulates osteoblast proliferation and new bone formation. GCs, on the other hand, inhibit proliferation, induce the death of osteoblast and osteocytes, and result in osteoporosis and bone fractures. To determine the molecular mechanisms of GC- TGF-β antagonism in osteoblast differentiation, we examined the cross-talk between glucocorticoid receptor (GR) and TGF-β. We found that GR interacts with Smad3, a TGF-β signaling transducer, and the interaction inhibits Smad3 transcriptional activity by blocking Smad3 DNA-binding ability. Consistent with the binding studies, transient transfection and promoter activity assays showed that dexamethasone (Dex) suppressed TGF-β induced promoter reporter activity of 3TP-Lux, a TGF-β sensitive luciferase reporter, in Mv1Lu cells. We then examined the effects of GC on TGF-β regulated osteoblast differentiation marker gene expression, we treated 2T3 preosteoblast cells with TGF-β, Dex, and both TGF-β and Dex, the expression levels of alkaline phosphatase (ALP) and Rux2/Cbfa1 mRNA were determined by real-time RT-PCR. The results showed that TGF-β inhibited the expression of ALP; Dex increased the mRNA expression of ALP. Finally, we examined the effects of GC and TGF-β in osteoblast differentiation. In consistent with the real time RT-PCR experiment, ALP staining of the Dex treated 2T3 cells showed an increased number of ALP positive cells, and this increase is blocked when the cells were treated with Dex and TGF-β together. From these studies, we conclude that GC antagonizes TGF-β action in osteoblast proliferation, the GC-TGF-β antagonism is mediated by GR-Smad3 interaction and the subsequent inhibition of Smad3 DNA-binding by GR. As we know, TGF-β couples bone resorption and formation by stimulating bone marrow mesenchymal cell proliferation. Pharmacological dosage of GC could cause bone disease by uncoupling bone resorption and formation through inhibition of TGF-β function. This finding may provide an opportunity to develop a tissue specific drug target for controlling GC-induced bone loss.

Disclosures: ***X. Shi****, None.*

M261

Marked Improvement of Bone Allograft Incorporation and Vascularization by Tissue Engineer of Live Periosteum on Devitalized Cortical Bone Graft. X. Zhang[1], C. Xie*[1], H. Ito[1], A. Lin*[2], R. E. Guldberg*[2], R. J. O'Keefe[1], E. M. Schwarz[1]. [1]Center for Musculoskeletal Research, University of Rochester, Rochester, NY, USA, [2]Georgia Institute of Technology, Atlanta, GA, USA.

There is an increasing demand for large cadaveric structural bone allograft for reconstruction of critical defects. However, the lack of osteogenic and angiogenic potential of devitalized bone graft results in poor long term outcomes. We have developed a 4mm segmental femur cortical bone grafting model in mice. Using this model we have showed that the preservation of periosteum on bone graft leads to superior graft incorporation and repair. Periosteal donor cell fate and its cellular contribution to cortical bone graft healing were further examined using live donor bone isografts from Rosa26 mice that constitutively express b-gal. Histological analysis using X-gal stained tissue sections demonstrated the expansion of b-gal positive periosteal mesenchymal cells from day 3 to day 7 post-op, which was largely confined to donor bone graft. By day 10, at the peak of endochondral and intramembranous bone formation, 73% of chondrocytes, 50% of osteocytes and 30% of osteoblasts on donor graft were positive for b-gal staining (n=5). The graft-derived cartilage and bone tissue were rapidly replaced through host dependent remodeling. By day 28, only a few cells at the graft site remained positive for b-gal. These results further underscore the vital role of live osteogenic stem cells for bone graft incorporation and suggest a novel approach to improve healing via engraftment of osteogenic stem cells on devitalized bone grafts. To this end, we infected bone marrow stromal cells derived from Rosa 26 mice with adenovirus BMP-2, loaded the cells onto collagen gel foam and wrapped it around devitalized bone allograft. Radiographic and MicroCT analysis of the cellular bone graft healing showed the formation of completely bridged new bone callus around devitalized bone grafts 9 weeks following surgery. Quantitative measurement of the new bone around the grafts showed a 3.7-fold increase compared to the control group without cell engraftment (n=4). MicroCT vascular imaging of the grafted femur was acquired following vascular perfusion of Microfil and bone decalcification. The results indicated that total vessel volume was significantly increased at the cortical bone junction and areas surrounding the graft upon bone marrow cell engraftment. Histologic examination further confirmed the osteointegration of donor cell derived bone on devitalized bone graft. Collectively, our studies demonstrated an effective alternative to improve devitalized allograft incorporation and neovascularization via tissue engineering and stem cell engraftment.

Disclosures: ***X. Zhang****, None.*

M262

Concentration Of Bone Marrow Derived Connective Tissue Progenitor Cells Onto Implantable Matrix Scaffolds. C. A. Boehm*[1], K. Kumagai*[1], J. Wright*[2], L. G. Griffith*[3], G. F. Muschler[4]. [1]Biomedical Engineering, Cleveland Clinic Foundation, Cleveland, OH, USA, [2]Biological Engineering Division, Massachusetts Institute of Technology, Cambridge, MA, USA, [3]Chemical and Biological Engineering Division, Massachusetts Institute of Technology, Cambridge, MA, USA, [4]Biomedical Engineering and Orthopaedic Surgery, Cleveland Clinic Foundation, Cleveland, OH, USA.

Methods for concentration and/or selection of osteoblastic connective tissue progenitors (CTPs) from bone marrow can be used to improve the outcome of bone grafting procedures. One effective method is Selective Retention, which requires a chemical surface that provides a binding site for a desired cell type, similar in concept to an affinity column. This study evaluated the highly porous polycaprolactone matrix fabricated using three dimensional printing (3DP) as a substrate for selective retention and evaluated the performance of the resulting cell-matrix composite grafts in an established canine femoral defect model. Heparinized bone marrow was aspirated from the proximal humerus. Implants were prepared as 9.5 mm diameter x 10mm cylinders with a pore size of 1000 microns and a wall thickness of 500 microns. Marrow was passed through the matrix at a constant linear flow rate of 25mm/min.. Aliquots of initial and effluent marrow were collected. Cell counts and CTP assays were performed on all samples. Four loading concentrations were compared; no marrow, 1X, 4X and 16X, based on marrow:matrix volume ratio. Loaded matrices were implanted into the 1.0 cm diameter cylindrical defects in the femur. After four weeks, the tissue in the defect was assayed for bone formation using microCT and then undecalcified histomorphometry. Mineral density and the area fraction of bone formation were primary outcome parameters.

Cell retention in the implants was 68 % +/- 1.1, 40 % +/0.6, and 28 % +/- 9, for [1X], [4X] and [16X], respectively. CTP efficiency for cells loaded onto matrix was 81%, +/- 11, 74 % +/- 14, and 71 % +/-1 8, for [1X], [4X] and [16X], respectively. The selection ratio for these concentrations was 1.16, 2.42 and 3.32, for [1X], [4X] and [16X], respectively. This represented nearly a 12 fold increase in overall CTP concentration in the 16X group compared to the 1X group. Analysis of bone formation and histologic data from 48 implants (12 per group) is pending.

These data confirm that a synthetic PCL-based 3DP matrix material can be used as an affinity column to concentrate and select bone marrow-derived CTPs. We believe that this method for harvest and transplantation of CTPs has important implications for tissue engineering strategies to repair or regenerate bone and other tissues.

Disclosures: ***C.A. Boehm****, None.*

M263

Wnt10b Expression in Bone Marrow Stromal Cells are Regulated by Sex Steroids. T. Hayashi*[1], S. kido*[2], D. Inoue[2], T. Ishikawa*[1], T. Matsumoto[2], R. Okazaki[1]. [1]Third Department Medicine, Teikyo University, Chiba, Japan, [2]Medicine and Bioregulatory Science, University of Tokushima, Tokushima, Japan.

Bone marrow stromal cells (BMSCs) are the common progenitors for bone forming osteoblasts and adipocytes. We previously reported that their differentiation into osteoblasts and adipocytes is promoted and inhibited, respectively, by estrogen. Because it has recently shown that the Wnt10b-mediated signaling pathway facilitates osteoblastic differentiation and hampers adipocytic differentiation, we have examined the effects of estrogen and other sex steroids on this pathway. We used the following mouse stromal cell lines: MC3T3/PA6 cells, wild-type ST2 cells, and ST2 cells stably overexpressing human estrogen receptor (ER)α or ERβ. Cells were treated with 17β-estradiol (E2), dehydroepiandrosterone(DHEA), and 5α-dihydrotestosterone(DHT) in the presence or absence of bone morphogenetic protein (BMP)-2 and/or troglitazone, and Wnt10b mRNA levels were assessed by RT-PCR. In PA6 cells, Wnt10b expression was increased and decreased by BMP-2 and troglitazone, respectively. Similarly, in ST2 cells, Wnt10b mRNA was induced by BMP-2. In both ST2ERα and ST2ERβ cells, Wnt10b expression was up-regulated by BMP-2, E2, DHEA and DHT, and was reduced by troglitazone. These results suggest that regulation of BMSC differentiation by sex steroids may be mediated at least in part by the Wnt10b signaling pathway.

Disclosures: ***T. Hayashi****, None.*

M264

Runx2 Gene Transfer in Marrow Stromal Cells Stimulates Osteoblast Differentiation and Bone Formation. Z. Zhao*, M. Phimphilai*, M. Zhao*, G. Xiao, R. Franceschi. Periodontics, Prevention, Geriatrics, University of Michigan School of Dentistry, Ann Arbor, MI, USA.

Bone marrow stromal cells (MSCs) have the potential to differentiate into multiple cell types including osteoblasts, chondrocytes, myoblasts and adipocytes. If MSCs are to be successfully used to regenerate bone, methods must be developed to optimally stimulate the differentiation of these cells to osteoblasts. The objective of this study was to examine the feasibility of using ex vivo Runx2 gene transfer to stimulate osteoblast differentiation in MSCs. Primary MSCs harvested from 6-week old male C57BL6 mice were transduced with adenoviral vectors encoding b-galactosidase (lacZ) or Runx2 and assayed for osteoblast differentiation and mineralization. Cells transduced with Ad-Runx2 expressed Runx2 protein in a dose-dependent manner and underwent osteoblast differentiation as measured by increases in alkaline phosphatase, osteoblast marker mRNA expression and mineralization. Detailed time course studies revealed that Runx2 protein was highest 1 d after transduction and declined below the limits of detection by 15 d. Osteocalcin and bone sialoprotein mRNA levels paralleled Runx2 levels. In contrast, Runx2-dependent mineralization persisted for the duration of the experiment. In addition to stimulating osteoblast differentiation, Ad-Runx2 transduction increased BMP responsiveness of both MSCs and C3H10T1/2 mesenchymal cells. Runx2 transduction also increased autocrine BMP synthesis in C3H10T1/2 cells. This BMP activity was necessary for osteoblast differentiation in that effects of Runx2 transduction could be blocked by Noggin, a BMP antagonist. To assess in vivo osteogenic activity, Ad-Runx2 transduced and control MSCs were suspended in type I collagen hydrogels and subcutaneously implanted into C57BL6 mice. Cells expressing Runx2 formed approximately twice the amount of bone formed by control cells. Taken together, these studies indicate that Runx2 gene transfer may be an effective route to enhance the osteogenic potential of MSCs.

Disclosures: ***Z. Zhao****, None.*

M265

GNAS Is an Osteoblast Fate Suppressor Gene in Soft Connective Tissue. R. A. Kanaan*[1], W. S. Kuo*[1], F. S. Kaplan[1], R. J. Pignolo[2], E. M. Shore[3]. [1]Orthopaedic Surgery, University of Pennsylvania, Philadelphia, PA, USA, [2]Medicine, University of Pennsylvania, Philadelphia, PA, USA, [3]Orthopaedic Surgery and Genetics, University of Pennsylvania, Philadelphia, PA, USA.

Progressive osseous heteroplasia (POH) is an autosomal dominant disorder characterized by heterotopic ossification of skin and subcutaneous adipose tissue during infancy, followed by disabling and wide spread ossification within skeletal muscle and deep connective tissue as the disease progresses. Previously, we demonstrated that POH is caused by heterozygous inactivating mutations in the GNAS gene, which encodes a G protein alpha subunit (Gsα). G proteins mediate transmembrane signaling from a diverse group of cell surface receptors to effectors that include phospholipase C, adenylyl cyclase and ion channels. We investigated the expression of Gsα in bone and fat by immunohistochemistry of mouse tissues. Normal bone (femur) was weakly positive for Gsα in osteoblasts lining bony trabeculae as well as in osteocytes. By contrast, intense staining of Gsα occurred in adipocytes within subcutaneous fat. Stromal stem cells from processed lipoaspirates (PLA) that are isolated from mouse subcutaneous fat tissue can be induced to differentiate to several cell fates, including osteoblasts and adipocytes. To examine the effect of reduced murine Gnas expression on stem cell differentiation to osteoblasts, PLA cells were transfected with Gnas siRNA. GFP siRNA was used as a negative control. Real time RT-PCR analysis to detect osteoblast markers (alkaline phosphatase, collagen type I, and osteopontin) revealed that Gnas siRNA enhanced osteoblast differentiation markedly, where as GFP siRNA had no effect. These data suggest a reciprocal relationship in the expression of Gsα in adipocytes (high) and osteoblasts (low) *in vivo*, and further support that Gnas acts as an osteoblast fate suppressor gene in soft connective tissue. [All animal studies followed IACUC approved protocols.]

Disclosures: ***R.A. Kanaan****, None.*

M266

Parathyroid Hormone Treatment Improves Survival after Bone Marrow Transplantation and Increases Osteoblastic Expression of the Notch Ligand Jagged1. J. M. Weber*[1], G. B. Adams*[2], M. L. Guzman*[3], C. T. Jordan*[3], D. T. Scadden*[2], L. A. Milner*[4], L. M. Calvi[1]. [1]Endocrine Unit, University of Rochester School of Medicine, Rochester, NY, USA, [2]Center for Regenerative Medicine and Technology, Massachusetts General Hospital, Boston, MA, USA, [3]Wilmot Cancer Center, University of Rochester School of Medicine, Rochester, NY, USA, [4]Pediatrics, University of Rochester School of Medicine, Rochester, NY, USA.

In the bone marrow, immature hematopoietic stem cells (HSC) are found in close proximity to osteoblasts. We recently showed that Parathyroid Hormone (PTH), through activation of the PTH/PTHrP receptor (PPR) in osteoblastic cells results in expansion of HSC. When PTH was administered intermittently after myeloablative bone marrow transplantation using limiting numbers of donor cells, mice had dramatically improved survival at 28 days (100%) compared to vehicle-treated mice (27%). Histological analysis of hind limbs from the two groups showed a striking increase in bone marrow cellularity with decreased adipocytes in the PTH-treated mice.

We had shown that activation of the Notch signaling pathway is necessary to mediate the PTH-induced expansion of HSC. This pathway plays a fundamental role in HSC self-renewal through cell-cell interactions. Since primary murine stromal cells treated with PTH (1-34) had improved ability to support HSC, we analyzed by immunocytochemistry the protein level of the Notch ligand Jagged1 in these cells. A small subpopulation of PTH-treated primary murine cells had a dramatic increase of Jagged1 protein, while this subpopulation was not identified in vehicle-treated stromal cells. Since real time PCR analysis of total RNA from primary stromal cells showed no changes in Jagged1 message in PTH compared to vehicle-treated cells, UMR106 cells were chosen to study osteoblastic cells. A 10-fold time and dose-dependent increase in Jagged1 expression was measured by real time PCR in RNA from UMR106 cells treated with PTH compared with vehicle. Western blot analysis confirmed the PTH-dependent increase in Jagged1 protein. Treatment with forskolin also increased Jagged1 message, suggesting that activation of adenylate cyclase downstream of the PPR was sufficient to reproduce this PTH-dependent effect.

In summary, PTH treatment alters dramatically the bone marrow microenvironment and improves survival from bone marrow transplantation in mice. Osteoblastic cell treatment with PTH increases expression of the Notch ligand Jagged1. UMR106 cells provide a useful model to study the molecular mechanisms underlying osteoblastic PTH-dependent increases in Jagged1 levels, which are likely to play an important role in the PTH-induced enhanced osteoblastic support of HSC.

Disclosures: ***L.M. Calvi****, None.*

M267

Sp1 and Sp3 Regulate Basal Transcription of RANKL Gene in Osteoblasts and Stromal Cells. J. Liu*, Z. Shi, X. Cao*, X. Feng. Pathology, Univ. of alabama at birmingham, Birmingham, AL, USA.

RANKL and its receptor RANK have been shown to play to pivotal role in bone homeostasis. In bone, RANKL is expressed by osteoblasts/stromal cells and mediates osteoclast differentiation and function by binding RANK expressed on osteoclast precursors and mature osteoclasts. Since the unraveling of the RANKL/RANK system, it has been established that many osteotropic hormones and cytokines regulate osteoclast formation and function through modulating RANKL expression by osteoblasts/stromal cells. However, the molecular mechanism by which RANKL gene expression is regulated in osteoblast/stromal cells largely remains unclear. To investigate the molecular mechanisms by which gene expression is regulated in osteoblasts/stromal cells, in the current study we characterized the molecular mechanism underlying the basal transcription of RANKL gene in osteoblast/stromal cells. To this end, we cloned 1.1-kb murine RANKL promoter (from -953 to +150, relative to the transcription start site) and showed that this promoter fragment is highly active in both transfected osteoblasts and stromal cells. To locate the promoter region required for the basal transcription of RANKL gene, we constructed 7 deletion mutants of the 1.1-kb RANKL promoter: RL(-753)Luc, RL(-553)Luc, RL(-403)Luc, RL(-253)Luc, RL(-153)Luc, RL(-103)Luc and RL(-53)Luc. These mutants contain RANKL promoter regions starting from different 5' positions (indicated by the numbers in parentheses) and ending at the same 3' site (+150). Using these mutants, we identified a 100-bp RANKL promoter region (-154 to -54) critical for the basal transcription of RANKL gene. We then synthesized 4 overlapping oligos (Oligo I, II, II, and IV) spanning the 100-bp promoter region. Gel shift assays using these oligos showed that Oligo I and Oligo II specifically bound the nuclear proteins with high affinity from both osteoblasts and stromal cells. Computer analysis of these two oligos indicated that both oligos contain a putative Sp1-binding sequence, suggesting that these oligos may utilize members of the Sp1 family in regulating the basal transcription of RANKL gene. Supershift assays with antibodies Sp1 and Sp3 confirmed that the nuclear proteins binding to Oligo I and II are Sp1 and Sp3. Importantly, the mutation of Sp1-binding site in Oligo I profoundly reduced the basal promoter activity while the mutation of Sp1 site in Oligo II gave rise to a slight reduction in the basal promoter activity. Moreover, the mutation of both sites totally abrogated the basal promoter activity of RANKL gene. Token together, our current study revealed that Sp1/Sp3 play a key role in the basal transcription of RANKL gene in osteoblasts and stromal cells.

Disclosures: ***J. Liu****, None.*

M268

A Modulatory Role for Adenosine in an Osteoprogenitor Cell Line and in Primary Human Bone Marrow Cells. B. A. J. Evans[1], C. Elford*[1], K. Francis*[2], J. Ham*[2]. [1]Child Health, University of Wales College of Medicine, Cardiff, United Kingdom, [2]Medicine, University of Wales College of Medicine, Cardiff, United Kingdom.

Adenosine has a wide range of actions in many tissues, but there is little information on its role in bone physiology. We have demonstrated the presence of the four adenosine P1 receptor subtypes in HCC1 (human osteoprogenitor) cells, and shown that adenosine and adenosine receptor agonists (NECA, CCPA, and IB-MECA) stimulate the release of IL-6 from these cells. CGS2180 had no effect. Furthermore, adenosine, NECA, CGS2180 and CCPA, but not IB-MECA, inhibited the production of osteoprotegerin. RT-PCR and immunocytochemical methods showed that primary adult human bone marrow stromal (BMS) cells also expressed the four receptor subtypes. α-MEM with ribonucleosides and deoxyribonucleosides is used for routine culture of such BMS cells in many laboratories. We showed that basally secreted IL-6 concentrations by BMS in this medium were very high. Furthermore, adenosine and adenosine receptor agonists increased IL-6 secretion by these cells, but only when they were maintained in α-MEM not containing ribonucleosides and deoxyribonucleosides. RT-PCR and immunocytochemical methods showed that both cell types expressed enzymes (adenosine deaminase, adenosine kinase, ecto 5′ -nucleotidase) responsible for the synthesis and metabolism of adenosine. In addition, mineralisation studies with BMS cells either i) in medium with or without ribonucleosides and deoxyribonucleosides, or ii) in medium without ribonucleosides and deoxyribonucleosides, but with or without adenosine or adenosine receptor agonists, further demonstrated the ability of these compounds to modulate osteoprogenitor cell function. Other work showed that both HCC1 and BMS cells express IL-6 receptor and the gp130 subunit needed for IL-6 signalling. Collectively, our results indicate that adenosine modulates (possibly via IL-6) osteoprogenitor cell function and differentiation. These effects might be especially important in conditions such as rheumatoid arthritis, where high levels of adenosine due to inflammation may influence the progression of bone disease.

Disclosures: ***B.A.J. Evans****, None.*

M269

Human Marrow-Isolated Adult Multilineage Inducible (MIAMI) Cells Require NT-3 to Differentiate to Functional Neurons. G. D'Ippolito*[1], S. Diabira*[1], G. A. Howard[1], A. Valeyev*[2], J. Hackman*[2], P. Menei*[3], C. Montero-Menei*[3], B. A. Roos*[1], P. C. Schiller*[1]. [1]Medicine, GRECC & Research Service VAMC and University of Miami, Miami, FL, USA, [2]Neurology, Research Service VAMC and University of Miami, Miami, FL, USA, [3]INSERM ERIT-M 646, Angers, France.

We have isolated a novel population of non-transformed pluripotent human cells from bone marrow after a unique expansion/selection procedure. Based on their unique molecular characteristics and unparalleled differentiation properties, we refer to them as Marrow-Isolated Adult Multilineage Inducible cells, or MIAMI cells. Colonies of cells were expanded as single-cell derived colonies or multicolony pools on fibronectin treated substrates at low density, low oxygen tension, and 2% FBS. MIAMI cells express high levels of CD29, CD63, CD81, CD122, CD164, cMet, BMPR1B, and NTRK3, and are $CD34^-$, $CD36^-$, $CD45^-$, $CD117^-$, and $HLA\text{-}DR^-$. The embryonic stem cell markers SSEA4, Oct-4, Rex-1, and hTeRT were expressed in all cultures examined. Cells have been expanded more than 50 population doublings. This primitive population of cells was isolated from men and women of ages ranging from 3 to 72 years old. They have been differentiated to mesodermal-derived lineages including osteoblasts, cartilage-forming chondrocytes, and adipocytes. The cells were also grown as attachment-independent spherical clusters expressing genes associated with pancreatic islets, including insulin and glucagon, indicating their capacity for differentiation to endodermal-derived lineages.

Unlike other human stromal cell populations, the MIAMI cells have been differentiated to neuroectoderm-derived phenotypically mature neuronal cells expressing numerous neuronal markers including tyrosine hydroxylase and exhibiting a resting membrane potential of -70 mV as well as inward and outward ion currents. Since bone tissue is extensively innervated, these novel results open the possibility that marrow stromal cells may contribute to the motor and/or sensory neural cellular network critically important for adequate bone and skeletal function.

Early passage MIAMI cells independently differentiated into mature neurons under defined and specific treatment conditions requiring neurotrophic factors, without the need for coculture with any other type of cells in order to develop a functionally mature phenotype. MIAMI cells were found to engraft in several tissues and were not tumorigenic. In conclusion, MIAMI cells represent a novel and unique population of non-transformed human post-natal cells with a plasticity and expansion capacity resembling that of embryonic stem cells and represent the ideal candidate for cellular therapies of inherited or degenerative diseases.

Disclosures: ***P.C. Schiller****, None.*

M270

The Thiazide Diuretic Metolazone Directly Stimulates Osteoblast Function. M. M. Dvorak*[1], G. Gamba*[2], D. Riccardi*[1]. [1]School of Biological Sciences, University of Manchester, Manchester, United Kingdom, [2]Instituto de Investigaciones Biomedicas, Universidad Nacional Autonoma de Mexico, Mexico City, Mexico.

Thiazide diuretics are commonly used in the management of hypertension. There is also plethora of studies correlating such therapy with an increase in bone mineral density. It has been proposed, but not unequivocally proven, that this may be a result of increased availability of circulating calcium, due to the action of thiazides on the thiazide-sensitive sodium-chloride cotransporter (NCC) in the kidney.

We have previously reported the expression of the NCC mRNA and protein in the cells of osteoblastic origin in freshly frozen undecalcified preparations of human and rat bone, as well as in tissue culture models of osteoblasts [1]. Here we studied the effects of metolazone, a potent thiazide diuretic, on proliferation, differentiation and production of mineralised nodules in human and rat freshly isolated osteoblasts. We observed that metolazone dose-dependently attenuates BrdUrd incorporation (n=6; $p<0.05$) indicating an inhibition of osteoblast proliferation. On the other hand, metolazone increased osteoblast differentiation, evident from an increase in expression of markers such as *Runx2,* observed by western blotting (n=3; $p<0.05$) and an increase in the production of mineralised nodules quantified by von Kossa staining (n=6; $p<0.05$). These findings were specific to thiazide diuretics and were not reproduced using the loop diuretic bumetanide.

These results provide evidence for direct action of thiazide diuretics on bone, acting on the thiazide-sensitive sodium-chloride cotransporter expressed by osteoblasts. We therefore support the view that thiazides should be considered as diuretics of choice in elderly osteoporotic patients.

[1] Dvorak MM, Carter DH, Riccardi D. (2002) Thiazide-Sensitive Sodium Chloride Co-Transporter (NCC) in Cryosections of Rat and Human Bone. J. Bone Miner. Res. 17:SA194 Suppl.1.

Disclosures: ***M.M. Dvorak****, None.*

M271

Eosinophil Chemotactic Factor-L (ECF-L) Enhances Osteoclast Formation by Blocking the Suppressive Effects of IL-12 on Osteoclast (OCL) Formation. H. Y. Chung[1], S. J. Choi[1], G. D. Roodman[2]. [1]Medicine-Hematology/Oncology, University of Pittsburgh, Pittsburgh, PA, USA, [2]Medicine-Hematology/Oncology, University of Pittsburgh and Dept. of Veterans Affairs Medical Center, Pittsburgh, PA, USA.

OCL formation and bone destruction is increased in inflammatory conditions such as rheumatoid arthritis (RA). This bone destruction occurs even though known inhibitors of OCL such as IL-12, IFN-γ and IL-4 are produced by activated T-cells in the affected joints. It is our hypothesis that other factors produced in RA joints block the activity of these inhibitors of OCL formation. Recently, we identified ECF-L as a novel autocrine stimulator of OCL produced by. monocytes/macrophages and OCL, and showed that ECF-L production is increased by IL-4. Therefore, we determined if ECF-L could block the inhibitory effect of IL-12 on OCL formation. Purified ECF-L Fc fusion protein was added to murine bone marrow cultures in the presence or absence of IL-12. ECF-L increased OCL-like cell formation in a dose-dependent manner in mouse marrow cultures compared to control cultures and blocked the inhibitory effects of IL-12 on OCL formation. To further investigate the mechanism responsible for these observations, the effects of ECF-L on IL-12, and IL-12 receptor production and IL-12 receptor signaling were examined using PHA-stimulated non-adherent spleen cells as a source of lymphocytes. ECF-L decreased IL-12p40 levels by 50% in spleen cell conditioned media compared to control cultures, as determined by Western blot analysis. Furthermore, ECF-L markedly decreased IL-12 R beta1 mRNA

expression by 80% and decreased IL-12 R beta1 protein expression by 40% in PHA-activated spleen cells compared to control treatments. This decrease in IL-12 receptor expression resulted in a 70% decrease in IL-12-induced IFN-γ mRNA expression in spleen cells, as assessed by RT-PCR. Although STAT4 signaling was not decreased by simultaneous treatment of PHA activated spleen cell cultures with ECF-L and IL-12, STAT4 signaling was decreased by 30% when the cultures were pretreated with ECF-L for 24 hrs. To further investigate the mechanism responsible for ECF-L effect on IL-12 receptor expression, we determined if ECF-L increased cox-2 mRNA levels. Wu et al. (J Immunol 161, 1998) previously reported that PGE2, a major cox-2 metabolite, inhibited IL-12 receptor expression and IL-12 responsiveness. Treatment of mouse marrow cultures with ECF-L increased cox-2 mRNA and protein expression by 50% and 30% respectively. These results suggest that ECF-L may enhance OCL formation through decreases both in IL-12 and IL-12 receptor expression and that this effect may in part be mediated by increasing cox-2 metabolites such as PGE2.

Disclosures: ***G.D. Roodman****, Novartis 8; SCIOS, Inc. 5.*

M272

Bone Loss in Inflammatory Arthritis Is Associated with a Local and Systemic Decrease in Parameters of Bone Formation. M. Stolina*[1], G. Schett*[2], B. Bolon*[1], S. Middleton*[1], H. Brown*[1], L. Zhu*[1], S. Adamu[3], F. Asuncion*[3], P. Kostenuik[3], U. Feige*[1], D. Zack*[1]. [1]Inflammation, Amgen, Thousand Oaks, CA, USA, [2]Medical University of Vienna, Division of Rheumatology, Vienna, Austria, [3]Metabolic Disorders, Amgen, Thousand Oaks, CA, USA.

Purpose: Chronic inflammatory arthritis leads to accelerated bone loss. Vanishing of bone is only possible if bone resorption outweighs bone formation. Since osteoclasts are present in inflamed joints, bone resorption is regarded as a predominant factor for bone loss in inflammatory arthritis. It is unclear, however, whether bone formation attempts to balance bone resorption or is even downregulated and aggravates bone loss. To address this question we performed a time-dependent analysis of systemic and local bone metabolism in two rodent models of inflammatory arthritis.

Methods: Lewis rats were challenged with 0.5 mg heat-killed mycobacteria suspended in mineral oil to induce adjuvant arthritis (AdA) or 1 mg porcine collagen type II emulsified in Freund's incomplete adjuvant to produce collagen-induced arthritis (CIA). Animals were sacrificed at the day of disease onset (d0), or at 10 different time points up to d27 after disease onset. Paw sections were assessed for osteoclasts and osteoblasts using immunohistochemistry for cathepsin K and in situ hybridization for osteocalcin, respectively. In addition, serum was analyzed for tartrate-resistant acid phosphatase (TRAP) and TRAP-5b as well as alkaline phosphatase and osteocalcin.

Results: In both AdA and CIA structural skeletal damage rapidly increased from d4 and peaked on d10. Osteoclast activity, as shown by the expression of cathepsin K, was dramatically increased at d4 and d1 in the paws of AdA and CIA, respectively. In contrast, osteoblast activity, as shown by expression of osteocalcin decreased after disease onset and reached its nadir on d4 in both models. Osteoblast activity partially returned after d10 when formation of osteophytes was observed. Systemic bone metabolism showed very similar kinetics with peaking of osteoclast markers, TRAP and TRAP-5b, on d4 and d2 in AdA and CIA, respectively. Concomitantly, both osteoblast markers, alkaline phosphatase (d4 for AdA, d3 for CIA) and osteocalcin (d3 for AdA, d1 for CIA) reached their nadirs. Thus, the phase of rapid bone loss in inflammatory arthritis coincides with lowered bone formation.

Conclusion: These data suggest that blunted bone formation even accelerates inflammatory bone loss. Fostering of bone formation may therefore be an additional attractive therapeutic option to counteract skeletal damage in arthritis.

Disclosures: ***M. Stolina****, None.*

M273

Effect of Exogenous and Endogenous Prostaglandin E_2 on Osteoclastogenesis in the RAW 264.7 Macrophage Cell Line. H. Kaneko[1], S. Lee[1], J. A. Lorenzo[1], Y. Toyama*[2], C. C. Pilbeam[1], L. G. Raisz[1]. [1]Medicine, University of Connecticut Health Center, Farmington, CT, USA, [2]Orthopaedic Surgery, Keio University School of Medicine, Tokyo, Japan.

Prostaglandins can enhance osteoclast formation by effects on both the hematopoietic and osteoblastic lineages. PGE_2 increases osteoclast like cell (OCL) formation in spleen cells that are cultured with M-CSF and RANKL and in the RAW 264.7 macrophage cell line (RAW cells) cultured with RANKL. We examined the ability of exogenous PGE_2 to stimulate OCL formation in RAW cells as well as the role that endogenous PGE_2 has in the response of RAW cells to LPS and TNF-α. Exogenous RANKL increased the number of OCL, defined as TRAP (+) multinucleated cells, in a dose-dependent fashion from 1 to 30 ng/ml with no difference between 30 and 100 ng/ml. Therefore, all further experiments were performed at 30 ng/ml. In the presence of RANKL, exogenous PGE_2 increased OCL number by 60 ± 6% at 1 μM and 37 ± 6% at 0.1 μM ($P<0.01$) in the RAW cells. LPS (100 ng/ml) increased OCL number by 31 ± 12% ($P<0.05$) and TNF-α (10 ng/ml) increased OCL number by 54 ± 4% ($P<0.01$). To determine the role of endogenous prostaglandin synthesis in these responses, we used NS-398 (0.1 μM), a specific COX-2 inhibitor. NS-398 did not affect the response to RANKL but significantly ($P<0.05$) decreased responses to PGE_2, LPS and TNF-α by 60%, 64% and 74%, respectively. Treatment of RAW cells for 1 h with PGE_2 or LPS, followed by washing, increased endogenous PGE_2 production 4 h later from 1 nM to 72 and 48 nM respectively. These results demonstrate that both exogenous and endogenous PGE_2 can directly augment the ability of myeloid precursor cells to form OCL. Furthermore, it appears that endogenous production of PGE_2 enhances osteoclastogenic responses of RAW cells to LPS and TNF-α as well as to PGE_2 itself.

Disclosures: ***H. Kaneko****, None.*

M274

Interleukin-1 Is an Essential Component of TNF-α-induced Osteoclastogenesis. S. Wei, H. Kitaura, P. Zhou, F. P. Ross, S. L. Teitelbaum. Pathology and Immunology, Washington University in St. Louis, St. Louis, MO, USA.

TNF and IL-1 are pro-osteoclastogenic inflammatory cytokines but their relationship in the osteoclastogenic process is not understood. Reflecting sequential signaling of the two cytokines, we find that TNF-α induced RANKL synthesis by bone marrow stromal cells is abolished by IL-1 receptor antagonist (IL-1Ra) or deletion of the type I IL-1 receptor (IL-1RI) gene. Furthermore, TNF-α induces expression of IL-1 and its functional receptor. These data suggest TNF-α regulates the RANKL gene, in stromal cells, via IL-1 and therefore IL-1 plays a role in TNF-α-induced periarticular osteolysis. Consistent with this posture, TNF-α-stimulated osteoclastogenesis is blunted approximately 50% by IL-1Ra in a model in which osteoclasts are generated by co-culture of marrow stromal cells and TNF receptor deficient macrophages. The same results obtain when TNF is added to osteoclastogenic cultures containing stromal cells derived from IL-1RI deficient mice. Importantly, TNF-induced osteoclastogenesis, in vivo, is also dampened 50% in IL-1RI-/- mice. IL-4, an anti-osteoclastogenic cytokine, arrests IL-1-induced RANKL expression, an event associated with blunted p38 activity. Confirming TNF-α and subsequently, IL-1 regulates osteoclastogenesis via this MAP kinase, stromal cell expression of RANKL stimulated by these cytokines is blocked by the specific p38 inhibitor, SB 203580. Like TNF-α, short exposure to IL-1 can also directly stimulates marrow macrophages to commit to the osteoclast phenotype in the presence of sub-osteoclastogenic concentrations of RANKL, an event accompanied by upregulation of IL-1RI and inhibition of the decoy receptor, IL-1RII. Thus, IL-1 mediates the osteoclastogenic effect on TNF-α by enhancing stromal cell expression of RANKL in a p38 MAP kinase dependent manner and by directly stimulating differentiation of osteoclast precursors. The interdependency of the two inflammatory cytokines in the generation of osteoclasts lends credence to the observation that their combined blockade is most effective in preventing the periarticular bone loss of inflammatory arthritis.

Disclosures: ***S. Wei****, None.*

M275

Role of IGF-IR in Osteoclast Biology and Differentiation. S. Avnet, G. Quacquaruccio*, A. Lamolinara*, D. Granchi*, A. Giunti*, N. Baldini*. Laboratory for Pathophysiology, Istituti Ortopedici Rizzoli, Bologna, Italy.

Although IGF-1 and 2 and their receptor IGF-IR play a key role in osteoblast biology and in normal skeletal growth, only fragmentary data are available on their contribution to bone resorption. IGFs are synthetized by osteoblasts and stored in the skeletal matrix, therefore interacting with pre-osteoclasts and mature osteoclasts after being released as a consequence of bone resorption. By using monocyte-monoblast-like models (human FLG29.1 and murine RAW264.7 cell lines), by Western blot and RT-PCR we demonstrated that IGF-IR is expressed in osteoclast precursors. After exposure to an anti-IGF-IR blocking MAb (alpha-IR3, 1 mg/ml), or to suramin (500 mg/ml), a drug that is known to interfere with IGF binding to their receptor, a growth inhibition (doubling time: 34.5 h vs 23.4 h of controls) was recorded in FLG29.1 cells. A similar effect was observed in human monocytes from peripheral blood that were induced to differentiate to osteoclasts by RANK-L (30 ng/ml) and MCS-F (25 ng/ml) exposure. In fact, treatment with alpha-IR3 or suramin inhibited cell viability and TRAP activity (day 4) of osteoclast precursors, resulting in a net reduction of in vitro bone resorption (day 10). Furthermore, IGF-IR phosphorilation was found to be very low at cell seeding, greatly increased on day 2, almost null on day 4, and again increased in multinucleated osteoclasts (day 7), as shown by Western blot . In mature osteoclasts IGF-IR immunolocalization was also demonstrated by fluorescence microscopy. By Real-Time PCR we verified that the blockage of IGF-IR activity by alpha-IR3 treatment is followed by an increased synthesis of IGF-IR mRNA (Figure), further supporting the functional role of IGF-IR in osteoclast differentiation. These data show that IGF-IR acts at different times during the committment and differentiation of osteoclasts. IGF-IR-mediated signaling may therefore be considered as a fundamental pathway for osteoclast biology in addition to its well-established role in osteoblasts.

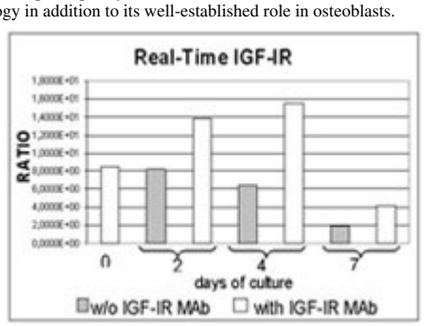

Disclosures: ***S. Avnet****, None.*

M276

Osteoblast Specific Overexpression of Human Interleukin-7 Increases Femoral Trabecular Bone Mass in Female Mice and Inhibits *in Vitro* Osteoclastogenesis. S. Lee[1], J. F. Kalinowski*[1], D. J. Adams[2], H. L. Aguila*[3], J. A. Lorenzo[1]. [1]Medicine, University of Connecticut Health Center, Farmington, CT, USA, [2]Orthopaedic Surgery, University of Connecticut Health Center, Farmington, CT, USA, [3]Center for Immunotheraphy, University of Connecticut Health Center, Farmington, CT, USA.

Interleukin-7 is a potent stimulator of B and T lymphocytes and a direct inhibitor of *in vitro* osteoclastogenesis in murine bone marrow cultures. To explore the role of IL-7 in bone, we generated 3 transgenic mouse lines (A, B and C) in a C57BL/6 background (Tg) that used the 2.3 Kb rat collagen 1A1 promoter to selectively express human IL-7 in osteoblasts.

Measurable human IL-7 levels were detected by ELISA in the medium of neonatal calvarial cultures from all three lines. Line C (high Tg) produced the highest level of IL-7 while line B (low Tg) had levels that were 470 fold lower. Line A was intermediate. There was an increase in early B cells ($B220^+/IgM^-$) in the bone marrow of high Tg mice (WT = 29.1%, high Tg = 47.5%), which is a known effect of IL-7. In contrast, low Tg mice had normal bone marrow B-lymphopoiesis. hIL-7 was minimally detectable in the serum of all Tg lines. μCT analysis of high Tg mice demonstrated increased (15%, p<.05) trabecular bone mass in females but not in males at 7.5 weeks. Low Tg mice had no changes in trabecular bone mass. CFU-GM, an assay of osteoclast precursors, showed decreased colonies in high Tg females (by 44%, p<.01) but no effect of Tg on males. To investigate if locally produced IL-7 had effects on OCL formation *in vitro*, we cultured bone marrow from high Tg and WT littermates with M-CSF and RANKL (both at 30 ng/ml) for up to 7 days. OCL formation peaked at day 5 and declined thereafter. OCL formed in female bone marrow cells was greater than in male bone marrow cells (by 92% at day 4 and 26% at day 5, P<.01). Bone marrow cultures from high Tg mice showed decreased osteoclast formation on day 4 and day 5 in cells from both males and females (30% to 50% inhibition, p<.01) compared to WT littermate cells. However, at day 6 only male high Tg bone marrow cells showed decreased OCL formation (38% inhibition, p<.01). 1,25 $(OH)_2$ vitamin D_3 (10^{-8} M) treatment of bone marrow cells from high Tg and WT littermates produced a significant inhibition of OCL formation at day 6 in both male and female high TG cells (36% and 23%, respectively, p<.01) compared to WT and no significant differences at day 7.These findings demonstrate that female IL-7 high Tg mice have increased trabecular bone mass *in vivo* and decreased osteoclast formation *in vitro* compared to WT littermates. Increased bone mass in high Tg female mice likely reflects both a direct inhibitory effects of IL-7 on osteoclastogenesis and differences in responses to IL-7 between females and males.

Disclosures: ***S. Lee****, None.*

M277

Mechanism of Repression of Human Cu/Zn Superoxide Dismutase-1 Expression by the Pro-Inflammatory Cytokine TNF-α. V. Afonso*, G. Santos*, P. Collin*, A. Lomri. Lariboisiere Hosp., INSERM U-606, Paris 10, France.

Activation of macrophages leads to the secretion of cytokines that control the inflammatory response and increase the production of reactive oxygen species. Copper/zinc superoxide dismutase (SOD-1) is one of the major cellular defense enzymes that perform a vital role in protecting cells against the toxic effect of superoxide radicals. Over-expression of SOD-1 in monocytes renders them resistant to the toxic effect of TNF-α, indicating that TNF-α mediated growth inhibition of hemopoïetic cells occurs via the production of superoxide radicals. In this study, we evaluated the effect of TNF-α on SOD-1 transcription, and investigated the molecular & cellular mechanisms by which TNF-α regulates SOD-1 gene in the U937 and U2OS cells. Promoter deletions and mutations, over-expression experiments and specific chemical inhibitors indicate that TNF-α acts via the Sp-1 transcription factor binding sites located between -60 and -38 in the SOD-1 promoter to suppress gene expression. Electrophoretic mobility shift assays show that Sp-1 proteins constitutively bind to this consensus sequence and TNF treatment decreases Sp-1 binding to SOD-1 promoter. Promoter inhibition by TNF was associated with AP-1 activation. In contrast the anti-inflammatory curcumin, a selective c-jun/activator protein (AP)-1 inhibitor enhanced SOD-1 basal activity and suppressed AP-1 activation and SOD-1 down-regulation induced by TNF. Over-expression of Sp-1 enhances SOD-1 expression in contrast TNF inhibitory effect was repressed. Inhibition of protein synthesis with cycloheximide failed to prevent TNF inhibition of SOD-1 transcription, suggesting that a newly translated protein did not mediate the TNF effect and this effect involves post-translation modifications. In agreement with the transfection results, endogenous SOD-1 mRNA was suppressed by TNF-α (-41%) after 7 h of treatment. We also investigated the signaling pathway that mediates the effect of TNF. MEK inhibitor PD98059 inhibits SOD-1 promoter activity and mimics TNF effect, suggesting that ERK activity protects SOD-1 gene from the inhibitory effect of TNF. Furthermore, inhibition of JNK/AP-1 pathway by SP600125 prevented SOD-1 inhibition by TNF. Taken together, our results suggest that Sp-1 dephosphorylation and JNK/Ap1 activation by TNF-α are the key pathways involved in the down-regulation of SOD-1 transcription. Knowledge of the mechanisms of gene transcription in inflammation could lead to the development of novel therapies based on the pharmacological manipulation of the production of this important antioxidant gene in inflammation.

Disclosures: ***A. Lomri****, None.*

M278

Regulation of Human Osteoclast Activity by Rearrangement of Attachment Proteins via Phosphorylation of VASP by cGMP-dependent Protein Kinase I. B. B. Yaroslavskiy, S. E. Kalla*, V. García Palacios, Y. Li*, H. C. Blair. Pathology and Physiology & Cell Biology, University of Pittsburgh and Pittsburgh Veteran's Affairs Medical Center, Pittsburgh, PA, USA.

Osteoclasts resorb bone by acid secretion into an extracellular compartment defined by an αvβ3 integrin ring, which organizes cytoplasmic F-actin. Bone attachment is reversible and detachment can be initiated with nitric oxide (NO) via guanosyl cyclase and cGMP-dependent Protein Kinase I (PKG-I); how PKG-I modifies attachment was unknown. We studied this using human osteoclasts differentiated, on bone and glass, from CD14-isolated circulating monocytes. An integrin-binding actin-organizing protein, VASP, was identified in osteoclasts by gene screening. Western analysis showed VASP in NO-activated and control osteoclasts in similar quantity, although VASP is phosphorylated, mainly on ser239 (pVASP), by PKG-I. NO donors increased pVASP with maximum 1-2 h after a pulse, 50-100 μM, of the non-hydrolysable cGMP analog 8-pCPT-cGMP, after which pVASP returned to baseline. In a blocking cGMP analog, Rp-cGMPS, immune labeling localized VASP strongly to the bone attachment and pVASP was essentially undetectible. NO donors reduced membrane and increased cytoplasmic VASP, although pVASP at the leading edge of the cytoplasm was detectible, and co-localized with PKG-I. Actin expression changed from a polymerized ring to short branched actins after activation by 8-pCPT-cGMP, with a distinct cellular polarity. Polarity corresponed to onset of migration by micro-cinematography. Transfection with siRNAs that reduced VASP or PKG-I expression modified the attachment structure, and impaired but did not abolish acid secretion. In low-VASP osteoclasts, bone attachment was unimpaired but the actin ring was broken, the cytoskeleton disordered, and these cells did not move in response to 8 pCPT-cGMP, although cGMP still caused transient membrane ruffling. In osteoclasts with low PKG-I, actin bundles were seen instead of actin rings; cells did not move in response to cGMP or NO. We conclude that VASP and PKG-I are required for NO-dependent reorganization of the osteoclastic attachment and motility, and probably are necessary for efficient bone degradation.

Disclosures: ***B.B. Yaroslavskiy****, None.*

M279

Estrogen and Phytoestrogens Inhibit Osteoclast Formation by Distinct Mechanisms. V. García Palacios, L. J. Robinson*, C. W. Borysenko, S. E. Kalla*, H. C. Blair. Pathology and Physiology & Cell Biology, University of Pittsburgh and Veteran's Affairs Medical Center, Pittsburgh, PA, USA.

We compared estradiol and phytoestrogen effects on growth and differentiation of Raw 264.7 cells, which express ERα and β and form TRAP positive osteoclast-like cells in RANKL, Genistein 3 μM, daidzein 3 μM, and β-estradiol 10 nM were compared in growth medium (DMEM with basal CSF-1) and in RANKL, 30 ng/ml, and CSF-1, 10 ng/ml over 5 d. Estradiol activates ERα and β; genistein is an ERβ inhibitor that also inhibits Y-kinases including Src; daidzein is a nonspecific estrogen analog. In media without RANKL, estrogen and both phytoestrogens reduced proliferation, although the genistein effect was 15-20% smaller. Estrogen, genistein, and daidzein all decreased Src phosphorylation, in contrast to expectations genistein did not have a larger effect. Fluorescent localization showed RANKL translocation of NF-κB. P65 showed greater phosphorylation in genistein, but nuclear/cytoplasmic NF-κB was unaltered relative to RANKL and CSF-1 alone. Estrogen and daidzein reduced nuclear NF-κB, but genistein did not. ERα or β siRNA suppression did not alter this, suggesting a non-ER mechanism. Erk kinase was inhibited ~50% at 1 h and stimulated 2-3 fold at 2 d by estrogen, daidzein, or genistein in the absence of RANKL and CSF-1. However, in RANKL and CSF-1, estrogen or phytoestrogens had no effect on Erk, suggesting that some estrogen and phytoestrogen effects are limited to pre-osteoclasts. However, estrogen, genistein, and daidzein all decreased multinucleated cells in RANKL at 2 d, with daidzein and estrogen more efficient (60-70% inhibition) than genistein (35%). Flow cytometry showed 80% reduction in S-phase RAW cells in estrogen, a smaller effect of genistein (40%), and no effect in daidzein. On the other hand, daidzein reduced apoptosis in G_0-G_1 cells ~20%; genistein and estrogen had no effect relative to RANKL and CSF-1. We conclude that estrogen, genistein, and daidzein regulate osteoclastogenesis under a balance between Erk and p65 pathways with a probable dominance of ER α mechanisms. Tyrosine kinase-antagonist properties of genistein appeared to be unimportant. Estrogen and phytoestrogens all increased Erk phosphorylation, but without added effect in the presence of CSF-1 and RANKL. Daidzein and estrogen shared important similarities, including reducing nuclear localization of NF-κB. Nuclear localization was unaffected with the ERβ agonist genistein, and thus it is probably an ERα-dependent estrogen effect.

Disclosures: ***V. García Palacios****, None.*

M280

Plasticity of a Myeloid Progenitor with Increased Osteoclasts from Pax5 Deficient Mice. M. Horowitz[1], D. Pflugh*[1], Y. Xi[1], J. Lorenzo[2], A. Bothwell*[1]. [1]Yale School of Medicine, New Haven, CT, USA, [2]University of Connecticut, Farmington, CT, USA.

Pax5 is a member of the paired box transcription factors and its expression is required for normal B cell development. We have demonstrated that Pax5 is also required for normal osteoclastogenesis. Loss of Pax5 results in a 5-fold increase in the number of osteoclasts (OC) in the bone of Pax5-/- mice, which are severely osteopenic. With the exception of red cells and megakaryocytes, bone marrow (BM) derived $B220^+$ pro-B cells from Pax5-/- mice can differentiate into all of the hematopoietic cell lineages including OC. Culture of Pax5-/- spleen cells results in the emergence of an adherent, $Fc\gamma R^+$, Mac-1^+, c-fms^+ macrophage-like cell line (SCL). Interestingly, these cells grow continuously in vitro, without

added growth factors, for more than 5 weeks. Addition of M-CSF and RANKL induces the rapid formation of numerous OC. Thus, it was the purpose of this work to determine if the SCL had similar plasticity of differentiation as the Pax5-/- pro-B cells.
To test this, SCL were treated with cytokines selected to induce specific lineage differentiation. Differentiation was determined by morphological changes, the expression of cell surface markers measured by flow cytometry and functionally by phagocytosis and T cell co-stimulation. Cellular proliferation was also measured.
The SCL proliferated to the cytokines in a hierarchical manner with GM-CSF>M-CSF>IL-3>IL-4. LPS also induced proliferation. The cells did not respond to IL-7 or G-CSF. Treatment of the cells with M-CSF caused no morphologic changes but induced a modest increase in FcR and Mac-1 expression. In contrast, cells treated with GM-CSF took on a marked dendritic appearance, associated with a dramatic increase in FcR, Mac-1 and CD45 expression. MHC class II expression also increased. The cells became $CD11c^+$ (dendritic cell marker), and $CD80^+$ (co-stimulatory molecule). Activation with LPS caused expression of CD40 and CD80. Cells treated with IL-4 also had increased expression of FcR, Mac-1, CD11c and CD80 but did not increase class II. In addition, the cells did not have a dendritic appearance but rather were elongated and larger than untreated cells. G-CSF caused no changes in morphology or determinant expression. Phagocytosis increased with M-CSF or GM-CSF treatment. Untreated SCL were potent co-stimulators of T cell activation.
These data indicate that the loss of Pax5 causes the appearance of a myeloid progenitor in the spleens of Pax5-/- mice. These cells can be induced to form functional macrophages, dendritic cells and OC but not granulocytes. The SCL is similar to the Pax5 BM pro-B cell in that both cells are progenitors however, the SCL is more differentiated and restricted to the myeloid lineage.

Disclosures: ***M. Horowitz****, None.*

M281

Stimulation of Resorption in Cultured Mouse Calvarial Bones by the Thiazolidinedione, Ciglitazone. A. M. Schwab*[1], B. N. Wilkes*[1], U. H. Lerner[2], H. H. Conaway[1]. [1]Physiology and Biophysics, University of Arkansas for Medical Sciences, Little Rock, AR, USA, [2]Department of Oral Cell Biology, University of Umeå, Umeå, Sweden.

Thiazolidinedione drugs are PPARγ ligands used to treat Type 2 diabetes. Recent studies have suggested that PPARγ ligands may have effects on bone cells. In the current investigation, a natural PPARγ ligand, 15-deoxy-Δ12, 14-prostaglandin J2 (15d-PG-J2), and a thiazolidinedione, ciglitazone, were evaluated for their ability to stimulate resorption in neonatal mouse calvarial bones.
No stimulation was noted with 15d-PG-J2, but dosage-dependent release of ^{45}Ca from prelabeled mouse calvariae was observed following treatment with ciglitazone. Release of ^{45}Ca by ciglitazone was unaffected by the PPARγ antagonist GW 9662, by the mitotic inhibitor hydroxyurea, and by the cyclooxygenase enzyme inhibitor indomethacin. In contrast, significant inhibitions of ^{45}Ca release elicited by ciglitazone were noted in the presence of the carbonic anhydrase enzyme inhibitor acetazolamide, the hormone inhibitor calcitonin (CT), a bisphosphonate, 3-amino-1-hydroxypropylidene-1, 1-bisphosphonate (AHPrBP), the anti-inflammatory cytokine interleukin-4 (IL-4) and the decoy receptor osteoprotegerin (OPG). Real-time, quantitative polymerase chain reaction (PCR) analysis demonstrated enhanced expression of receptor activator of NFκB ligand (RANKL) mRNA and decreased OPG mRNA in ciglitazone treated calvarial bones. ELISA measurements of RANKL and OPG were in good agreement with the mRNA measurements, revealing an increase in RANKL protein and a decrease in OPG protein in bone explants exposed to ciglitazone. Real-time PCR analysis showed that expression of the transcription factor NFAT2 and osteoclast markers, tartrate resistant acid phosphatase (TRAP) and cathepsin K, were also increased by ciglitazone treatment of calvariae.
The data indicate that stimulation of osteoclast differentiation and activity by ciglitazone occurs by a non-PPARγ dependent pathway that does not require cell proliferation, is sensitive to inhibition by the decoy receptor, OPG, is sensitive to the osteoclast inhibitors, acetazolamide, CT, AHPrBP and IL-4 and is associated with an increased RANKL/OPG ratio.

Disclosures: ***U.H. Lerner****, None.*

M282

α-Lipoic Acid Suppresses Osteoclastogenesis Despite of Increased RANKL/OPG Ratio in Bone Marrow Stromal Cells. J. Koh[1], E. S. Kim*[2], E. Chang*[3], H. Kim*[3], H. Kim*[3], G. S. Kim[1]. [1]Division of Endocrinology and Metabolism, Asan Medical Center, University of Ulsan College of Medicine, Seoul, Republic of Korea, [2]Department of Internal Medicine, Ulsan University Hospital, University of Ulsan College of Medicine, Ulsan, Republic of Korea, [3]Department of Cell and Developmental Biology, Dental Research Institute, and Brain Korea 21 Program, College of Dentistry, Seoul National University, Seoul, Republic of Korea.

Growing evidence has shown a biochemical link between increased oxidative stress and reduced bone density. α-Lipoic acid (ALA) has gained considerable attention due to its roles as an outstanding biological thiol antioxidant, however, its effect on bone cells has not been addressed. In this study, ALA did not have significant effects on proliferation and differentiation of human bone marrow stromal cells (BMSC, HS-5 cell), based on cell counting, cell death ELISA and alkaline phosphatase activity. However, we found six differentially expressed proteins in the conditioned media from HS-5 cells by ALA treatment using proteomic analysis. Of them, receptor activator of NF-κB ligand (RANKL) was significantly up regulated, which was confirmed by immoblotting with anti-RANKL antibody. ELISA assay revealed that ALA stimulated RANKL production in conditioned media and cellular extracts up to 4.8-fold and 22.9-fold, respectively, and did not affect osteoprotegerin secretion. However, ALA markedly suppressed osteoclastogenesis in a dose-dependent manner both in co-culture system of mouse bone marrow cells and osteoblast, and in mouse bone marrow cell culture system. These results suggest that ALA suppresses osteoclastogenesis directly, not mediated by RANKL acting.

Disclosures: ***J. Koh****, None.*

M283

Epigenetic Regulation of Mouse Receptor Activator NF-kappaB Ligand (RANKL) Gene. R. Kitazawa, K. Mori*, T. Kondo, S. Kitazawa. Molecular Pathology, Kobe University Graduate School of Medicine, Kobe, Japan.

To clarify the epigenetic regulation mechanism of RANKL gene expression, we analyzed the mouse RANKL gene promoter that contains three Runx2-binding sites, one CRE shared by vitamin D responsive element (VDRE), and two CpG clustering regions: one around the transcription and translation start sites (-65/+350) and the other downstream of the VDRE (-920/-800). Comparison of the two subpopulations of mouse stromal ST2 cells, P9 which expresses RANKL in response to vitamin D and P16 which does not, has revealed higher CpG methylation of the -65/+350 RANKL promoter region in P16 than in P9. Western blotting, showed the same VDR expression level in P9 and P16 cells, and EMSA, with nuclear extracts from P9 and P16 cells, showed specific binding to the oligonucleotide containing VDRE, suggesting that RANKL gene suppression in P16 cells is not due to VDR deterioration. By ChIP assay using anti-H3, -H4 antibodies and pairs of primers designed to amplify -950/-680 (containing VDRE) and -250/+10 (containing the transcription start site), in response to vitamin D, H3, H4 histone acetylation in both regions was observed in P9 cells but not in P16 cells. To determine how CpG methylation suppresses RANKL gene transcription, we examined the effect of in vitro methylation on RANKL gene promoter activity. The RANKL promoter-luciferase reporter construct pGL3-1005 was methylated with SssI methylase (as pGL3-m1005) and transfected into ST2 cells. The basal activity of pGL3-m1005 was only 20% of that of pGL3-1005, and pGL3-m1005 did not increase the promoter activity in response to vitamin D whereas pGL3-1005 did. We then examined the effect of demethylating agent 5-Aza-dC on RANKL expression in P9 and P16. Assessed by RT-PCR and Western blotting, expression of RANKL mRNA and protein in response to vitamin D in P16 cells was significantly restored by 5-Aza-dC pretreatment. Immunohistochemically, RANKL protein in cultured cells was heterogeneously distributed, reflecting the heterogeneity of CpG methylation and of RANKL gene activation. Our data suggest that CpG methylation of the RANKL promoter suppresses gene activation by vitamin D. The epigenetic mechanism may cause the heterogeneity and diversity of stromal/osteoblastic cells in response to bone-resorbing stimuli.

Disclosures: ***R. Kitazawa****, None.*

M284

Protease-Activated Receptor-1-Mediated Osteoclast Differentiation. S. Sivagurunathan*[1], P. D. Campbell*[2], R. Smith*[2], C. N. Pagel*[1], R. N. Pike*[2], E. J. Mackie[1]. [1]School of Veterinary Science, University of Melbourne, Victoria, Australia, [2]Department of Biochemistry and Molecular Biology, Monash University, Victoria, Australia.

The serine protease thrombin is well known to have a central function in the blood coagulation process but it also exerts specific hormone-like effects on cells, including bone cells. Thrombin has been shown to stimulate osteoclastic bone resorption in organ culture, however little is known about the mechanism of thrombin's effect and whether it is exerted on osteoclast differentiation or activity of mature osteoclasts. It has previously been shown that two known thrombin receptors are expressed by mouse osteoblasts, protease-activated receptor (PAR)-1 and PAR-4. The aim of the current study was to investigate whether thrombin can regulate osteoclastic differentiation, and if so, whether it is mediated by PAR-1. Mouse bone marrow cultures were used to investigate thrombin's effect on osteoclast differentiation. Thrombin markedly stimulated the formation of multinucleated tartrate-resistant acid phosphatase-positive cells (TRAP+ MNC). A specific PAR-1 activating peptide (AP) was also shown to enhance the formation of TRAP+ MNC. A concentration of 100 nM thrombin stimulated a maximal increase in the number of TRAP+ MNC, and the number of TRAP+ MNC formed in response to thrombin was at least 70% of the number formed in response to 10 nM parathyroid hormone (PTH). The numbers of nuclei per osteoclast in thrombin-treated cultures (7 ± 0.60) and PAR-1 AP-treated cultures (5 ± 0.24) were lower than in PTH-treated cultures (18 ± 0.37). In bone marrow cultures prepared from PAR-1-null mice, neither thrombin nor the PAR-1AP was able to stimulate osteoclast differentiation. These results suggest that thrombin stimulates osteoclastic differentiation and that the effect is mediated by PAR-1.

Disclosures: ***S. Sivagurunathan****, None.*

M285

Muramyl Dipeptide Synergistically Enhances Osteoclast Formation Induced by lipopolysaccharide, interleukin 1 and Tumor Necrosis Factor-α through Nod2-mediated Signals in Osteoblasts. S. Yang*[1], N. Takahashi[2], M. Takahashi*[1], M. Mogi*[3], T. Uematsu*[1], Y. Kobayashi[2], Y. Nakamiti[2], H. Takada*[4], K. Takeda*[5], S. Akira*[5], K. Furusawa*[1], N. Udagawa[6]. [1]Department of Oral and Maxillofacial Surgery, Matsumoto Dental University, Shiojiri, Japan, [2]Institute for Oral Science, Matsumoto Dental University, Shiojiri, Japan, [3]Department of Pharmacology, Aichi Gakuin University, School of Dentistry, Nagoya, Japan, [4]Department of Microbiology and Immunology, Tohoku University School of Dentistry, Sendai, Japan, [5]Research institute for Microbial Disease, Osaka University, Suita, Japan, [6]Department of Biochemistry, Matsumoto Dental University, Shiojiri, Japan.

Muramyl dipeptide (MDP), the essential structure responsible for the immunoadjuvant activity of peptidoglycan, exists in gram-positive and -negative bacterial walls. As well as bone-resorbing factors such as 1 α,25$(OH)_2D_3$ and PGE_2, IL-1 α and LPS stimulated osteoclast formation in mouse co-cultures of primary osteoblasts and hemopoietic cells. MDP alone could not induce osteoclast formation in the co-culture, but synergistically stimulated it induced by LPS and IL-1 α but not by 1 α,25$(OH)_2D_3$ or PGE_2. MDP failed to enhance osteoclast formation from osteoclast progenitors induced by RANKL and M-CSF. MDP up-regulated RANKL expression in osteoblasts treated with LPS but not with 1 α,25$(OH)_2D_3$. Recently, it was proposed that nucleotide-binding oligomerization domain (Nod) 2, a member of the Apaf1/Nod protein family, is an intracellular sensor of MDP. A frameshift mutation of Nod2, which results in deficiency in MDP-mediated NF-κB activation, is involved in the susceptibility to Crohn's disease, a chronic inflammatory disorder of the intestinal tract. Nod2 mRNA was undetectable in untreated osteoblasts, but it was strongly expressed in osteoblasts treated with LPS and IL-1 α but not with 1 α,25$(OH)_2D_3$. TNF- α also stimulated expression of Nod2 mRNA in osteoblasts. Indeed, MDP synergistically enhanced TNF- α induced both osteoclast formation in the co-culture and RANKL mRNA expression in osteoblasts. Induction of Nod2 mRNA expression by LPS but not by TNF- α in osteoblasts was TLR4 (a signal-transducing receptor for LPS) and MyD88 (an adaptor molecular of TLR4) dependent. Osteoclasts rapidly died due to apoptosis. LPS and RANKL stimulated the survival of osteoclasts, which was not enhanced by MDP. These results suggest that MDP synergistically enhances osteoclast formation induced by LPS, IL-1 α and TNF- α through RANKL expression in osteoblasts, but not the survival of osteoclasts supported by LPS and RANKL. Nod2-mediated signals appear to be involved in the MDP-induced RANKL expression in osteoblasts.

Disclosures: ***S. Yang****, None.*

M286

MyD88 but not TRIF Is Essential for Osteoclastogenesis Induced by Lipopolysaccharide, Diacyl Lipopeptide and IL-1. N. Sato*[1], N. Takahashi[2], K. Suda*[3], Y. Kobayashi[2], S. Akira*[4], K. Shibata*[5], T. Noguchi*[1], N. Udagawa[6]. [1]Periodontology, School of Dentistry, Aichi-Gakuin Univ., Nagoya, Japan, [2]Institute for Oral Science, Matsumoto Dental Univ., Shiojiri, Japan, [3]Biochemistry, Showa Univ., Tokyo, Japan, [4]Osaka Univ., Suita, Japan, [5]Hokkaido Univ., Sapporo, Japan, [6]Biochemistry, Matsumoto Dental Univ., Shiojiri, Japan.

LPS is a potent stimulator of bone resorption in inflammatory diseases caused by bacteria. Bacterial lipoprotein/lipopeptides are also pathogen-specific molecular patterns. Toll-like receptor 4 (TLR4) is identified as the signaling receptor for LPS. The complex of TLR6 and TLR2 recognizes diacyl lipopeptide. The signaling cascade of TLR is similar to that of IL-1 receptors, because both TLR and IL-1 receptors use MyD88 as a common signaling molecule. Toll-IL-1 receptor domain-containing adapter inducing interferon-β (TRIF)-mediated signals are also shown to be involved in LPS-induced MyD88-independent pathway. Using MyD88-deficient ($MyD88^{-/-}$) mice and TRIF-deficient ($TRIF^{-/-}$) mice, we examined roles of MyD88 and TRIF in osteoclast differentiation and function. LPS, diacyl lipopeptide (DL) and IL-1 stimulated osteoclastogenesis in co-cultures of osteoblasts and hemopoietic cells obtained from $TRIF^{-/-}$ mice but not $MyD88^{-/-}$ mice. LPS, DL and IL-1 stimulated RANKL mRNA expression in $TRIF^{-/-}$ osteoblasts but not $MyD88^{-/-}$ osteoblasts, suggesting that only MyD88-mediated signal in osteoblasts was important for RANKL expression in response to those factors. This finding was particularly interesting, because both MyD88-dependent and TRIF-dependent pathways are essential for LPS-induced cytokine production in macrophages. Indeed, LPS failed to stimulate IL-6 production in $TRIF^{-/-}$ bone marrow macrophages. But, LPS could stimulate IL-6 production in $TRIF^{-/-}$ osteoblasts. LPS and IL-1 enhanced the survival of $TRIF^{-/-}$ osteoclasts but not $MyD88^{-/-}$ osteoclasts. TRIF-related adaptor molecule (TRAM) was shown to be essentially involved in the TRIF-mediated signaling pathway. Interestingly, macrophages expressed both TRIF and TRAM mRNAs, while osteoblasts and osteoclasts expressed only TRIF mRNA. The fact that TRIF-mediated signals are not required for LPS-induced RANKL and IL-6 expression in osteoblasts and for osteoclast survival may be related to the lack of TRAM expression in osteoblasts and osteoclasts. Bone histomorphometry showed that $MyD88^{-/-}$ mice exhibited low turnover osteoporosis with reduced bone resorption and formation. These results suggest that the MyD88-mediated signal is essential for the osteoclastogenesis and function induced by IL-1 and TLR ligands, and that MyD88 is physiologically involved in bone turnover.

Disclosures: ***N. Sato****, None.*

M287

Novel Fluorescent Activated Cell Sorting Method for in vitro Analysis of Matured Osteoclast Differentiation Rate. C. Herath, S. Wimalawansa. Dept. Medicine, Div. Endocrinology, Robert Wood Johnson Medical School, New Brunswick, NJ, USA.

The molecular basis of age-related imbalance in bone cell coupling is complex. These include enhanced osteoclast differentiation, life span, and increased bone resorption. The procedures currently used are based on counting multi-nuclear cell formation in osteoclast cultures; but this is laborious, and adds random counting field errors. We developed a dual-color Florescent Activated Cell Sorting (FACS) method to assay the differentiation rate of mature multi-nucleated osteoclast from mono-nucleated osteoclast progenitors based on osteoclast marker RANK receptors (RANK-R) expression, and osteoclast nuclear density.
Bone marrow cells were cultured on glass cover slips to obtain >98% pure osteoclast progenitors cells. Cells were harvested at 48, 72, 96 and 192 hrs, and their differentiation rates were analyzed on reference to their expression of RANK-R protein (immuno-labeling of RANK-R using goat-anti-mouse RANK-R Ab, and secondary labeling with Green fluorochrome Labeled-rabbit anti-goat IgG). RANK-R labeled cells were stained with Propidium Iodide for simultaneous analysis of nuclear density.
Samples were analyzed using Cytomic FC 500 flowcytometer and scatter plot obtained with intensities of green fluorescents and red fluorescent exhibited phenotypically distinct sub populations of osteoclasts. Percentage of cells gated into sub population (gate 0) having high RANK-R expression and nuclear density was analyzed. Osteoclast formation rates were examined at same time points by counting multi-nucleated vs. mono nucleated cells on randomly selected 16 fields after staining with Hoechet nuclear stain in a fluorescents microscopy. Each experiment was repeated three times to obtain the average values.
The new method was accurately separate distinct sub-population of high nuclear density and RANK-R expressing mature osteoclast cells. Linearity of the method and its' simplicity allowed us to accurately measure the osteoclast cell differentiation rates per unit time (i.e., slope of the graph). The new FACS method is currently used in our laboratory to analyze osteoclast differentiation rates from bone marrow cells, osteoblast mediated regulation on osteoclasts, and to analyze the effect of novel therapeutic agents on rates of osteoclast differentiations.

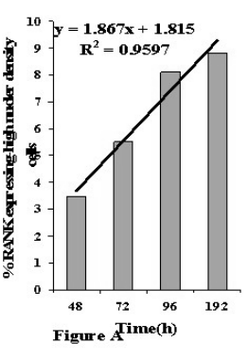

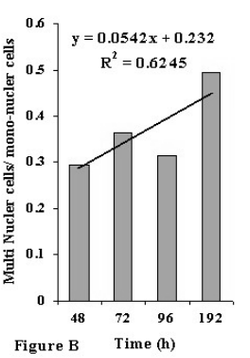

Figure A: Differentiation rates of RANK-R expressing & high nuclear density OCs by FACS method Figure B: Multi- nuclear OCs formation rate by nuclear counting.

Disclosures: ***S. Wimalawansa****, None.*

M288

Multiple Mechanisms Contribute to Stimulation of Osteoclastogenesis by Ascorbate. R. M. Kadlcek*, A. A. Ragab*, E. M. Greenfield. Orthopaedics, Case Western Reserve University, Cleveland, OH, USA.

We have previously shown that ascorbate is required for osteoclastogenesis (JBMR 13:970-77, 1998). In other cell types, the primary mechanism of action of ascorbate is to promote collagen crosslinking and extracellular matrix (ECM) assembly. To determine whether this mechanism contributes to osteoclastogenesis, we provided exogenous ECM by performing *in vitro* osteoclastogenesis assays on dentin or ivory slices. For this purpose, splenocytes were co-cultured with ST2 cells in the presence and absence of 0.284 mM ascorbate plus 10 nM 1,25-D3 and 100 nM dexamethasone. We found that exogenous ECM completely ablated the ascorbate requirement for formation of both TRAP-positive MNCs and resorption lacunae. Moreover, ECM digestion by either pronase or collagenase completely blocked the ability of dentin to overcome ascorbate deficiency. These experiments document the importance of ECM during osteoclastogenesis. Otsuka et al. (Endocrinology 141:3006-11, 2000) found that ascorbate upregulates RANKL mRNA levels and suggested that ascorbate-dependent ECM assembly increases RANKL production, thereby allowing for osteoclastogenesis. To test this possibility, we added exogenous RANKL [0.3-30.0 ng/ml] and found that RANKL partially overcomes ascorbate deficiency. Thus, RANKL dose-dependently stimulated osteoclastogenesis with maximal effects ~40% of that induced by ascorbate. Similar conclusions were obtained in experiments with highly purified osteoclast precursors cultured in the absence of mesenchymal cells. In this case, RANKL (with 10 ng/ml M-CSF) dose-dependently stimulated osteoclastogenesis in both the presence and absence of ascorbate. However, maximal osteoclastogenesis in the absence of ascorbate was ~25% of that induced in the presence of ascorbate and required 10-fold more RANKL. The primary mechanism of action of ascorbate other than ECM assembly is to regulate the intracellular redox state. To determine whether this mechanism also contributes to osteoclastogenesis, we examined the effect of N-acetyl cysteine, a reducing agent that does not promote collagen crosslinking. 2.5mM N-acetyl cysteine maximally stimulated osteoclastogenesis with effects ~40% of that induced by ascorbate.

Taken together, these results demonstrate that multiple mechanisms contribute to stimulation of osteoclastogenesis by ascorbate. These include redox regulation, direct effects on osteoclast precursors, and indirect effects through ST2 support cells (ECM assembly and RANKL upregulation).

Disclosures: ***R.M. Kadlcek****, None.*

M289

Spontaneous Osteoclastogenesis in Solid Tumours with Bone Involvement. I. Roato*[1], M. Grano*[2], G. Brunetti*[2], S. Colucci*[2], R. Ferracini*[3]. [1]CeRMS, A.S.O. S.Giovanni, Turin, Italy, [2]Human anatomy histology, University of Bari, Bari, Italy, [3]Orthopaedic surgery, A.S.O. S.Giovanni, Turin, Italy.

We studied the mechanisms of bone osteolytic metastases in solid tumours (breast, lung, kidney, prostate). Osteoclasts (OCs), cells deriving from granulocitic-macrophagic lineage, are responsible for osteolysis, which is usually associated with severe bone pain and fragility. By inhibiting OCs formation and activity osteolysis may be reduced.

Human peripheral blood mononuclear cells (PBMCs) isolated from cancer patients with or without osteolytic metastases, healthy donors and purified $CD14^+$ cells were cultured in presence or absence of M-CSF and RANKL. TRAP staining and Vitronectin Receptor (VR) immunofluorescence were performed to characterize OCs. Flow Cytometry was utilized to identify OC precursors (OCPs) circulating by staining with anti-human CD11b, CD14, CD51/CD61. OC resorbing-activity was evaluated by analyzing the percentage area of resorption pits on dentine slices. RNA was extracted from OCs and cDNA was prepared. The expression of mRNA for OCs markers was analysed by reverse transcriptase-polymerase chain reaction (RT-PCR).

We report here that cancer patients with bone involvement have an increase in OCPs compared to those from healthy controls and cancer patients without bone metastases. PBMC from patients carrying osteolytic lesions showed osteoclastogenesis without adding RANKL and M-CSF (OCs were $TRAP^+$ and VR^+). On the other side, these factors are necessary for generating OCs from healthy donors, not osteolytic patients PBMC and purified $CD14^+$ cells. OCs derived from cancer patients showed more resorption pits than OCs derived from healthy donors, and expressed genes involved in osteoclastogenesis.

Our data show that spontaneous osteoclastogenesis occurs in patients affected by osteolytic lesions, and may be sustained by factors released by T lymphocytes, which could give a priming to OCPs and promote osteoclastogenesis. In fact, $CD14^+$ cells cultured alone do not differentiate to OCs without adding M-CSF and RANKL. However, we did not obtain a higher number of OCs by increasing RANKL doses in cultures, and OCs and lymphocytes mRNA were positive for TNF-α but not for RANKL. Furthermore we observed an inhibition of osteoclastogenesis adding anti-TNF-α in culture. These data infer the existence of specific mechanisms promoting osteoclastogenesis in solid tumours with bone involvement. Our results suggest that TNFα may be responsible for osteoclastogenesis in these tumours.

Disclosures: ***I. Roato****, None.*

M290

Chemokines Acting Through CCR1 or CCR5 Differentially Promote Osteoclast Recruitment, RANKL Development, and Function. X. Yu, Y. Huang*, P. A. Collin-Osdoby, P. A. Osdoby. Department of Biology, Washington University, St. Louis, MO, USA.

Chemokines are the primary signals controlling cell trafficking and are important in the differentiation, function or survival of many cells. However, our knowledge of osteoblasts (OBs) or osteoclasts (OCs) as sources or targets of specific chemokines in normal or pathological conditions is limited at present. Recently, we investigated chemokine and chemokine receptor mRNA expression and responses in murine RAW 264.7 and primary marrow (MA) mononuclear cells during their RANKL development into bone-resorptive OCs. CCR1 was the major receptor of the beta-chemokine subfamily expressed by differentiated OCs, and both RAW and MA precursor cells expressed CCR1 and responded to ligands (MIP-1 alpha, RANTES, MCP-3) that engage CCR1 by dose-dependently increasing chemotaxis and transmatrix migration. This led to greater OC formation upon RANKL development of migrated cells. MIP-1 alpha, RANTES, and MCP-3 also directly and strikingly enhanced RANKL mediated OC formation in MA cultures, but not in RAW cells. This unexpected finding was notable because RAW cells expressed only CCR1 mRNA, whereas MA cells also expressed other CCRs including CCR5, which can bind these same chemokines. Thus, we hypothesized that CCR1 might mediate the chemotactic, and CCR5 the OC developmental, actions of these chemokines. To test this, we compared transwell chemotaxis and RANKL-mediated OC development of MA cells from wild-type (wt) vs. CCR5-/- mice in response to these chemokines. We also analyzed the ability of MIP-1beta, which binds CCR5 but not CCR1, to augment RANKL induced OC formation. Consistent with our hypothesis, MIP-1α was equally able to dose-dependently stimulate chemotaxis of MA cells from either wt or CCR5-/- mice, indicating that CCR5 is not essential for this chemotactic response. However, RANKL-mediated OC formation and bone pit resorption were dramatically decreased in MA cells cultured from CCR5-/- mice compared to wt mice, both in the presence or absence of exogenous MIP-1alpha, RANTES, or MCP-3 addition. These data suggest that CCR5 has an important role in mediating the dramatic stimulatory effects of these chemokines on RANKL induced OC formation and, further, that endogenous levels of one or more of these chemokines may help regulate normal RANKL mediated OC development. Together with the ability of these chemokines to chemoattract OC precursors and stimulate their matrix migration, our findings indicate that inflammatory raised levels of these chemokines may significantly contribute to localized bone loss through stimulating multiple mechanisms that include enhanced recruitment, differentiation and migration of bone-resorptive OCs.

Disclosures: ***P.A. Osdoby****, None.*

M291

Tannin Compound Suppresses Receptor Activator of Nuclear Factor-*k*B Ligand-induced Osteoclast Differentiation and Function by Inhibiting p38 Mitogen Activated Protein Kinase, c-Jun N-terminal Kinase and Aactivating Protein-1 Pathways. E. Park[1], M. Kim*[1], S. Lee*[2], T. Kim*[1], I. Lee*[3], J. Jung*[4], J. Woo[5], S. Kim[6]. [1]Skeletal Diseases Genome Research Center, Kyungpook National University Hospital, Daegu, Republic of Korea, [2]Department of Pharmacy, Yeungnam University, Daegu, Republic of Korea, [3]Department of Food Science and Technology, Keimyung University, Daegu, Republic of Korea, [4]Department of Biology, Kyungpook National University, Daegu, Republic of Korea, [5]Department of Biological Chemistry, Chubu University, Aichi, Japan, [6]Department of Orthopedic Surgery, Kyungpook National University Hospital, Daegu, Republic of Korea.

Recently polyphenolic compounds have been implicated in suppression of osteoclast differentiation/function and prevention of bone diseases. However, the effects of hydrolizable tannins of polyphenolic compounds on bone metabolism have not been elucidated. In this study, we screened hydrolizable tannins and found that K16, an ellagitannin, markedly decreases the differentiation into osteoclasts in both murine bone marrow mononuclear (BMM) cells and RAW264.7 cells as revealed by the reduced number of tartrate resistant acid phosphatase (TRAP)-positive multinucleated cells and TRAP activity. K16 appears to target the early stage of osteoclastic differentiation while having no cytotoxic effect on those cells. Furthermore, K16 also reduced resorption pit formation in osteoclasts. Analysis of inhibitory mechanisms of K16 revealed that it inhibits the receptor activator of nuclear factor-*k*B ligand (RANKL)-induced activation of p38 mitogen-activated protein kinase (p38MAPK), c-Jun N-terminal kinase (JNK), and activating protein-1 (AP-1). Taken together, these results demonstrate that naturally occurring K16 has an inhibitory activity on both osteoclast differentiation and function through a mechanism involving inhibition of the RANKL-induced p38MAPK, JNK, and AP-1 activation.

Disclosures: ***S. Kim****, None.*

M292

Novel Genes Regulated by Microphthalmia Transcription Factor in Macrophages and Osteoclasts. N. A. Meadows*[1], G. Faulkner*[1], C. Wells*[1], T. Ravasi*[1], D. Hume*[1], U. Sankar*[2], R. Hu*[2], M. Ostrowski*[2], A. Cassady[1]. [1]Institute for Molecular Bioscience, University of Queensland, Brisbane, Australia, [2]Department of Molecular Genetics, Ohio State University, Columbus, OH, USA.

Microphthalmia transcription factor (Mitf) is a member of the helix-loop-helix leucine zipper family of transcription factors. Mitf is a key regulator of osteoclast differentiation and regulates its target genes by binding as a homo- or heterodimer to an E-box consensus sequence (CANNTG). The macrophage cell line, RAW264.7, which has the potential to differentiate into osteoclast-like cells, has been used to generate stable transfectant cell lines expressing the Mitf-A (RAW/Mitf-A) and *mi* (RAW/*mi*) isoforms. The RAW/Mitf-A and RAW/*mi* cell lines were used to identify the effect of modulating Mitf activity on selected macrophage- and osteoclast-specific promoters and to identify novel Mitf target genes.

Western blotting established that the recombinant Mitf-A and *mi* protein are present and immunofluorescence identified that proteins are localized in the nucleus. Real time PCR validated the effect of modulating Mitf activity by identifying changes in the expression of known Mitf targets including TRAP and cathepsin K. Microarray expression profiling on the 22,000 element murine Compugen array of RAW/Mitf-A and RAW/*mi* cell lines was performed before and after induction of osteoclast differentiation with RANKL. This identified Mitf-responsive genes on macrophage and osteoclast phenotypic backgrounds. Complementary experiments using primary bone marrow-derived osteoclasts from C57BL6 mice and *mi/mi* mice using an Affymetrix array identified a similar set of genes.

A bioinformatic analysis was undertaken in parallel to identify candidate E-box-containing genes that may be Mitf targets. A large-scale Blast technique has been developed to download 5kb of DNA sequence 5' of the translation start site for all the genes on the Compugen cDNA array. These promoter regions have been searched for the presence of the E-box and a subset of potential Mitf target genes has been compiled and compared with targets generated from the microarray analysis. Of the generated targets an Ikaros family member, Eos, was shown to possess an E-box and microarray and real time PCR data has shown that it is down-regulated in osteoclasts derived from *mi/mi* spleen cells. Eos is a Zn-finger transcription factor, which has previously been shown to have a role in lymphocyte differentiation. Real time PCR also showed Eos to be up-regulated in the RAW264.7 cell line over-expressing Mitf. The data indicates that a combined bioinformatic and microarray approach can be successful in defining a specific list of possible Mitf targets.

Disclosures: ***N.A. Meadows****, None.*

M293

Oxidative Stress Accelerates Human Osteoclast Differentiation: Possible Role of Thioredoxin. M. A. Chacksfield*, N. Zimmerman*, J. M. Hodge*, C. J. Aitken*, M. Constable*, C. M. Lopez*, G. C. Nicholson. Clinical and Biomedical Sciences: Barwon Health, The University of Melbourne, Geelong, Australia.

Redox-sensitive cell signaling regulates many cell functions including proliferation, activation, growth inhibition and apoptosis. Signaling pathways important for osteoclast differentiation, including NF-kappaB and AP-1 can be modulated the endogenous redox-sensitive thiol, thioredoxin.

We have used a human osteoclastogenesis model employing CFU-GM precursors treated with M-CSF and soluble RANKL for 7-14 days to investigate the effects of the ROS-donor H_2O_2 on differentiation and function of osteoclasts. In this model, proliferation, differentiation and fusion of precursors occurs in the first week of culture, and resorption in the second week.

In the presence of a high concentration of RANKL (125 ng/mL), H_2O_2 treatment increased osteoclast number and osteoclast size by 70-80% at 7 days, with 1 nM producing a maximum effect. Resorption of dentine was increased by 140% with maximum effect at 10 nM. In the presence of a lower concentration of RANKL (31 ng/mL), 100 nM H_2O_2 was required to produce maximum effects on formation (+170%) and resorption (+200%) and there was no enhancement of osteoclast size. Time-course studies showed that it was only necessary for H_2O_2 to be present for the first 24 hours of culture to achieve a maximum stimulatory effect on M-CSF/RANKL-induced osteoclastogenesis. In contrast, it was necessary for RANKL to be present for the first 6-7 days of culture for significant osteoclast generation to occur. In cultures extended for 14 days, continuous treatment with 100nM H_2O_2 had a variable effect on ultimate formation and resorption, depending on control osteoclastogenic activity. Delayed treatment after the first day of culture had no significant effect on osteoclast formation or resorption. Treatment of CFU-GM precursors with 10 mM H_2O_2 produced a 4-fold increase in thioredoxin mRNA at 12 hours (real-time PCR).

Our results show that oxidative stress induced by H_2O_2 accelerates very early RANKL-induced differentiation events in human osteoclast precursors, but does not enhance resorption by mature osteoclasts. The model used does not possess unlimited potential for osteoclast generation because of the finite number of precursors present. However, in the presence of a regenerating progenitor pool (eg in vivo), oxidative stress is likely to produce a steady-state of increased osteoclasts. The stimulatory effect of H_2O_2 is much more sensitive in the presence of a low concentration of RANKL, suggesting a common molecular mechanism. Up-regulation of thioredoxin is likely to facilitate RANKL/RANK signalling and may mediate the pro-osteoclastogenic effect of H_2O_2.

Disclosures: ***G.C. Nicholson****, None.*

M294

Functional Validation of Osteoclast-Specific Genes in RAW264.7 Cells by RNA Interference. G. B. Tremblay, R. Sooknanan*, A. Kalbakji*, D. Bergeron*, M. Sasseville*, M. Filion*. Target Validation, Alethia Biotherapeutics, Montreal, PQ, Canada.

The ability to maintain bone strength is controlled through bone remodeling which involves concomitant bone formation by osteoblasts and bone degradation by osteoclasts (OC). In diseases such as osteoporosis, the balance between these two processes is shifted in favor of increased bone resorption resulting in a reduction in bone mineral density. In many cases, this is due to an increase in the number or activity of OCs. Although current treatments are somewhat effective in treating osteoporosis, these are associated with many side effects. Thus, new molecular targets for treating this disease would be beneficial for developing new drugs and preventing bone loss in post-menopausal women. Using the mouse RAW264.7 (RAW) cell line as a model for osteoclastogenesis, we utilized RNA interference (RNAi) to knock-down the expression of several OC-specific genes to test whether they were required for OC differentiation or activation.

We have identified 556 genes that were upregulated in response to RANK ligand in RAW OCs and 70 of these were found to be highly specific to OCs in terms of their expression pattern. Although some of the genes were previously described, most were uncharacterized functionally. Plasmids expressing short inhibitory (si) RNAs specific for 29 of these were transfected into RAW cells and selected with G418. These cell lines were tested for osteoclastogenesis where TRAP staining and OC number was assessed and compared to cell lines transfected with the empty plasmid. OC activity was tested by growing the RAW-derived OCs on calcium phosphate and determining their ability to resorb the substrate. In addition, the RNAi effect was monitored by Northern blot and, where possible, by Western blot. To date, 10 of the 29 knocked-down genes appear to be required for OC function. We have detected three phenotypic categories: reduced OC differentiation, increased OC differentiation, and perturbed OC function. For example, one of the genes, designated AB0440, encodes an uncharacterized OC-specific protease and is required for formation of mature OCs. Cell lines containing siRNAs targeting AB0440 also display reduced expression of the OC markers TRAP and Cathepsin K. RNAi of another gene, AB0351, that encodes a protein containing a predicted membrane-anchoring domain, exhibited a similar phenotype and showed significant reduction in OC markers. These new targets, and others we have identified, have the potential to serve as the basis for the development of novel therapeutic drugs to treat osteoporosis and other bone-related diseases.

Disclosures: ***G.B. Tremblay****, None.*

M295

A New Hormonal Upstream Factor in the RANKL/OPG System? Effects of the Thyroid Stimulating Hormone TSH in Humans. H. P. Dimai, A. Fahrleitner*, C. Piswanger-Soelkner*, S. Ramschak-Schwarzer*, B. Obermayer-Pietsch*, G. Leb. Internal Medicine, University Hospital, Graz, Austria.

In vitro evidence indicates a possible involvement of the human thyroid stimulating hormone (TSH, thyrotropin) in the regulation of bone metabolism. Recently, a highly purified recombinant human TSH alpha (THYROGEN) has been registered for diagnostic purposes. Patients with carcinoma of the thyroid gland usually are thyroidectomized, and in addition, they are on TSH suppressive thyroid hormone therapy, in order to avoid endogenous TSH production. Administration of THYROGEN without interrupting suppressive thyroid hormone therapy provides an excellent opportunity to study the effects of TSH without changes in the serum levels of free thyroid hormones. We therefore saught to investigate the effects of THYROGEN on markers of bone metabolism and the osteoprotegerin (OPG)/receptor activator of NF-kB ligand (RANK-L) system.

We investigated 25 patients who underwent total thyroidectomy because of well-differentiated thyroid cancer. All patients received suppressive thyroid hormone therapy. THYROGEN was administered at a dosage of 0.9mg IM daily on two consecutive days. Blood samples were drawn right before the first injection, 120 minutes thereafter, and 24hrs (i.e right before the second injection), 48 hrs, and 72 hrs after the first injection. All patients continued receiving their usual dosage of thyroid hormone.

TSH (microU/mL): 0.14 ± 0.07; 100.8 ± 10.8 ($p < 0.0001$); 141.9 ± 6.7 ($p < 0.0001$); 141.8 ± 7.4 ($p < 0.0001$); 58.6 ± 7.9 ($p < 0.0001$); Interleukin-6 (pg/mL): 1.95 ± 0.36; 2.54 ± 0.47 ($p < 0.01$); 2.28 ± 0.42; 2.05 ± 0.39; 1.98 ± 0.43; Osteocalcin (ng/mL): 21.8 ± 2.6; 21.1 ± 2.6; 22.9 ± 2.6 ($p < 0.05$); 23.1 ± 2.4 ($p < 0.01$); 21.3 ± 1.7; CrossLaps (pmol/L): 3593 ± 676; 3609 ± 710; 4514 ± 673 ($p < 0.05$); 4465 ± 716 ($p < 0.001$); 3709 ± 541; RANKL: 1.65 ± 0.61; 1.78 ± 0.70; 1.64 ± 0.61; 1.76 ± 0.66; 1.54 ± 0.71. OPG: (fig.)

These data indicate that the (recombinant human) thyroid stimulating hormone is affecting bone metabolism in terms of increasing bone turnover. This effect may involve the OPG/RANK-L system which has been shown to determine the pool size of active osteoclasts. Our findings also may explain accelerated bone loss in hyperthyroidism associated with elevated serum TSH-receptor antibodies (e.g. Graves' disease).

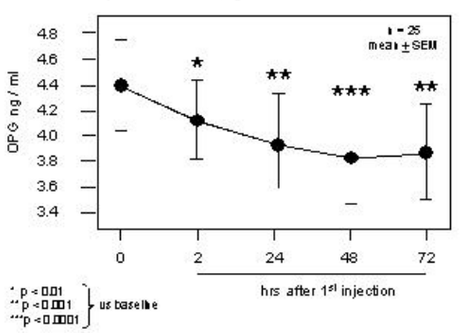

Disclosures: ***H.P. Dimai****, None.*

M296

GSK-3 Inhibitors Block Bone Marrow Cell Proliferation and Osteoclast Differentiation. R. J. S. Galvin[1], T. Fuson*[1], D. L. Halladay*[1], J. E. Onyia*[2], W. C. Roell*[2], A. Kriaucionas*[2]. [1]Bone and Inflammation, Eli Lilly and Company, Indianapolis, IN, USA, [2]Integrative Biology, Eli Lilly and Company, Indianapolis, IN, USA.

Recent studies have demonstrated the important role of the Wnt/Frizzled (Fzd) pathway in bone. Wnt activation of Fzd receptor results in inhibition of GSK-3β activity that stabilizes β-catenin. Accumulated β-catenin translocates to the nucleus and activates gene expression. Since previous studies have focused on the role of this pathway in osteoblasts, the present study evaluated the effects of GSK inhibitors on osteoclast differentiation and function. Osteoclast differentiation was studied in 2 different models: A) co-cultures of Balc cells (calvarial-derived cell line) and bone marrow cells stimulated with $1,25(OH)_2D_3$, and B) murine bone marrow or murine spleen cells stimulated with soluble rhRANKL and mM-CSF. Osteoclast differentiation was evaluated by counting the number of tartrate-resistant acid phosphatase (TRAP)-positive multinucleated cells or evaluating TRAP activity on day 6. Bone resorption was evaluated in murine calvariae stimulated with PTH (1-38) and the Cytostar T assay was used to evaluate bone marrow cell proliferation. Northern analysis of mRNA from differentiated murine osteoclasts demonstrated abundant expression of GSK-3β mRNA. LiCl, an inhibitor of GSK-3, completely blocked osteoclast differentiation from RANKL and M-CSF stimulated murine bone marrow cells (IC_{50} = 9.6 mM). Likewise, genistein (general tyrosine kinase inhibitor that inhibits GSK-3 activity) blocked osteoclast differentiation with an IC_{50} of 1.2 μM. A bisaryl maleimide (BAM) GSK-3α/β dual inhibitor also suppressed osteoclast differentiation with an IC_{50} of 17.4 nM. CTR-positive mononuclear cells, as well as, multinuclear cells were decreased in the spleen cell model by BAM. Bone marrow cell proliferation studies demonstrated that BAM decreased mM-CSF induced proliferation. Calvarial bone resorption was also suppressed by BAM in a concentration dependent manner. In summary, inhibition of GSK-3 results in decreased osteoclast differentiation and calvarial bone resorption. The inhibitory effects may be mediated in part by decreased proliferation of the progenitor cells.

Disclosures: ***R.J.S. Galvin****, None.*

M297

Identification of Osteoclast-Specific Genes using Subtractive Transcription Amplification of mRNA (STAR). R. Sooknanan*, J. Hitchen*, A. Fortin*, V. Gagné*, L. Lapointe*, C. Straccini*, G. B. Tremblay, M. Filion*. Expression Genomics and Target Identification, Alethia Biotherapeutics Inc., Montreal, PQ, Canada.

Imbalance in bone remodeling from increased osteoclast activity (bone resorption) *versus* osteoblast activity (bone formation) leads to osteoporosis. Although the role of osteoclasts is better understood, many of the factors involved remain uncharacterized. Thus, current therapeutics for osteoporosis is only somewhat effective. Improved understanding of the biology of both osteoclast and osteoblast will likely unveil better therapeutic targets and new treatments for osteoporosis.

Gene expression analysis in order to identify genes unique to osteoclastogenesis was performed using the mouse cell line model (RAW 264.7) and human CD34+ progenitors differentiated into osteoclasts in the presence of RANK ligand. The approach that we have taken for gene expression analysis uses our core patented (US 5,712,127) STAR (Subtractive Transcription Amplification of mRNA) technology, which also enriches for rare mRNA sequences that are often missed by DNA microarrays. Additionally, STAR has the potential to discover novel sequences since it is not limited by hybridization to predetermined arrayed sequences. The differential expression patterns of sequences contained in the "STAR library" were confirmed using customized micro- and macroarrays. A "STAR library" representing 5d-osteoclast mRNA subtracted with precursor mRNA was prepared for the RAW 264.7 cell model and 1536 clones were sequenced. Amongst these clones were 744 unique sequences representing a redundancy of ~50% with 18.5% novel sequences. Following microarray analysis using subtracted cDNA probes, 556 (~75%) sequences appeared to be upregulated in osteoclasts compared to only 21% using standard cDNA probes. The use of subtracted cDNA probes markedly increased the detection of low abundance differentially expressed sequences. However, when these clones were used as probes on macroarrays comprising RNA from multiple osteoclast differentiation experiments and normal tissues from mouse, only 70 were found to be highly osteoclast-specific, most of which are as yet uncharacterized functionally. To date, validation studies using RNAi has been completed on 29 of these 70 clones. Concomitantly, the human orthologues for some of these 70 clones were used as probes, which confirms upregulation in human osteoclasts as well. Overall, STAR appears to be a robust tool for gene expression analysis yielding specific and often novel sequences as observed for the osteoclastogenesis model.

Disclosures: ***R. Sooknanan****, None.*

M298

A Putative Role for the Adipocyte Peptide Hormone Resistin in Bone Metabolism. L. Thommesen*[1], A. Stunes*[1], K. Grøsvik*[1], E. Kjøbli*[2], U. Syversen[1]. [1]Department of Cancer Research and Molecular Medicine, Norwegian University of Science and Technology, Trondheim, Norway, [2]Norwegian University of Science and Technology, Department of Medical Laboratory Technology, Sør-Trøndelag University College, Trondheim, Norway.

Resistin was recently identified as a hormone secreted by adipocytes and is postulated to be an important link between obesity and insulin resistance in rodents. However, some studies failed to find a corresponding link in humans, indicating that this area is still in its beginning, and that other biological effects should be explored. Resistin belongs to a novel class of cystein-rich secreted proteins termed the RELM/FIZZ (found in inflammatory zone) family.

We have previously shown the expression of the adipocyte hormone leptin in osteoblasts. The aim of the present study was to examine if resistin is expressed in osteoblasts and osteoclasts, and whether resistin influences differentiation and proliferation of osteoblasts and osteoclasts, using cell cultures (the preosteoblast MC3T3-E1, and preosteoclast RAW 264.7 cell lines) and human peripheral blood mononuclear cells.

We found the expression of resistin mRNA in both MC3T3-E1 and RAW 264.7 cells. Western blot analysis showed the presence of resistin in differentiated MC3T3-E1 cells and in differentiated RAW264.7 and 3T3-L1 cells. Resistin increased MC3T3-E1 proliferation in a dose-dependent manner, but had no proliferative effect on RAW 264.7 cells. Moreover, resistin increased IL-6 release from MC3T3-E1 cells in a dose-dependent manner with 1800 pg/ml after 72 hrs. Resistin showed no effect on osteoprotegerin release in these cells.

Human peripheral blood mononuclear cells were treated with resistin in addition to RANKL, MCSF and dexamethasone. The number of TRAP (tartrate resistant acid phosphatase) positive cells increased with 50% compared to control.

In conclusion, these data indicate that resistin may play a role in bone metabolism by stimulating osteoclast differentiation both directly and indirectly.

Disclosures: ***U. Syversen****, None.*

M299

NK Cells Support Osteoclast Formation in Vitro. S. Owen*, L. Danks*, U. Sarma*, M. Feldmann*, F. Brennan*, N. Horwood. Kennedy Institute of Rheumatology, London, United Kingdom.

Bystander-activated lymphocytes have been shown to contribute to inflammation by inducing pro-inflammatory cytokine production by cells of the monocyte/macrophage lineage. Cytokine-stimulated T cells (Tck's) were prepared from elutriated human peripheral blood mononuclear cells by stimulation with TNF, IL-2 and IL-6, or by stimulation with IL-15 alone, for up to 8 days. When co-cultured with primary monocytes in varying ratios, these cells are potent inducers of TNF production. We and others (1) have shown that Tck's are able to support osteoclast formation in-vitro. Cells were stimulated for up to 8 days before fixing in gluteraldehyde and co-culturing with adherent primary human monocytes for a further 10-14 days. Osteoclasts were identified by TRAP+ staining and the ability to resorb calcified matrix. Fixed cells were able to induce osteoclast formation however non-fixed cells were inhibitory. This is most likely due to the production of IFN-γ by these cells although they no longer make IL-10 and TGF-β, unlike antigen-stimulated T cells.

Tck's proliferated over the 8 day period however the T cell numbers remained constant whilst the NK population increased up to 3-fold. To further characterise the cell population(s) responsible for the osteoclast supporting activity, we FACS sorted the Tck's using CD3 as a marker of T cells and CD56 for NK cells. These cells were then used in cocultures as previously described and both subpopulations were able to support osteoclastogenesis. We also examined the ability of the NK cell line, NK92, to support osteoclast formation. Cells were stimulated and fixed as described prior to co-culturing with monocytes for 10 days. Likewise these cells were able to support osteoclast formation in-vitro. Taqman analysis and Western blotting showed that RANKL expression was elevated during the culture period and by day 8 the CD56+ NK population was expressing 10-20 fold higher mRNA levels for RANKL than the CD3+ T cell population. These findings indicate that NK cells are able to support osteoclast formation and further work is being carried out to identify the role of different subsets within the NK population.

(1) O'Gradiagh et al. Rheumatology 2003:42 (Suppl1):15

Disclosures: ***N. Horwood****, None.*

M300

Coupling of Bone Resorption and Bone Formation: A Comparison of a RANKL Antagonist (OPG) and Bisphosphonates in Mice. P. J. Kostenuik, F. Asuncion*, K. Warmington*, S. Morony, H. Tan, M. Grisanti*, S. Adamu. Metabolic Disorders, Amgen, Inc., Thousand Oaks, CA, USA.

Bone resorption and formation are physiologically and pharmacologically coupled. Antiresorptive therapy typically results in some suppression of bone formation, but the mechanisms and extent of this coupling are poorly understood. If physiological and pharmacologic coupling are similar, suppression of bone resorption should result in a proportional decrease in formation markers that is similar across therapeutic classes. To test this hypothesis, we studied the kinetic response of bone resorption and formation markers after treating mice with antiresorptive agents with bisphosphonates or with the RANKL antagonist OPG-Fc.

Normal young mice (4-5 weeks old) were treated once (SC) with either PBS, or human OPG-Fc, or zoledronic acid (ZOL, 5 mg/kg) or pamidronate (APD, 5 mg/kg). Groups of mice (5-10/group/drug) were sacrificed at regular intervals and serum was analyzed for calcium, PTH, TRAP-5b (a novel osteoclast-specific resorption marker), total TRAP, and osteocalcin (OC, an osteoblast-specific formation marker).

OPG-Fc caused the most rapid (6 h) suppression of bone resorption (based on serum TRAP-5b), followed by ZOL (24 h) and APD (24 h). The rapid antiresorptive effect of OPG-Fc was also associated with a greater serum PTH response compared to ZOL or APD. Serum calcium remained within the normal range in all groups throughout the study. OPG-Fc maintained >90% suppression of TRAP-5b through 21 days after a single treatment, while ZOL and APD maintained significant TRAP-5b suppression for 14 days and 3 days, respectively. While OPG-Fc caused the greatest suppression of bone resorption, ZOL caused significantly greater suppression of bone formation (i.e. serum OC) compared to OPG-Fc or APD. We attempted to quantify the coupling between resorption and formation by determining the ratio of serum OC:TRAP-5b in individual animals at each timpoint. Despite significant differences in potency, ZOL and APD treatment resulted in similar ratios of OC:TRAP-5b. In contrast, OPG-Fc treatment resulted in significantly greater OC:TRAP-5b ratios at all timepoints compared to other treatments. All antiresorptives caused significant reductions in serum markers of bone resorption and formation. OPG-Fc caused the greatest suppression of bone resorption (TRAP-5b), while ZOL caused the greatest suppression of bone formation (osteocalcin). These data suggest a difference between RANKL antagonism and bisphosphonate therapy in terms of the coupling between bone resorption and formation.

Disclosures: ***P.J. Kostenuik****, None.*

M301

Effect of Bisphosphonate on Odontoclasts in Dental Root Resorption. R. Putranto*, Y. Oba*, K. Kaneko*, A. Shioyasono*, K. Moriyama. Orthodontics and Dentofacial Orthopedics, The University of Tokushima Graduate School, Tokushima, Japan.

Dental root resorption is a common complication during orthodontic treatment, but the regulation of root resorption remains clinically unsolved. Odontoclasts, which have been recognized as the principal cells in dental root resorption, show characteristic features of osteoclasts responsible for bone resorption. To examine the effects of bisphosphonates on the root resorption by increasing odontoclast formation due to mechanical forces, we topically administrated etidronate, alendronate, and pamidronate in rat with experimental tooth movement. A rubber elastic was inserted to the interproximal space between the maxillary first and second molars of male SD rats (7-8 weeks old) to create a mechanical force. Each bisphosphonate was subperiosteally injected (2.5 mg/kg BW) one day before the elastic rubber insertion, and the injection was continued every three days until the end of the experiment. Control groups injected with vehicle were similarly processed. At day 3, 7 and 14, the molar-bearing segments were dissected and processed for scanning electron microscope and histological examination. At day 3, the treatment with etidronate and alendronate significantly increased the number of odontoclasts and subsequent pit formation on the dental root compared with control group, and then the enhancement of root resorption in alendronate-treated group was observed until day 7. At day 14, the treatment with all three bisphosphonates reduced the number of odontoclasts and completely blocked the root resorption. Furthermore, the number of osteoclasts on the bone surface was significantly decreased at day 14 in treatment with these bisphosphonates. These results demonstrate that the short-term treatment with etidronate and alendronate cause the induction of odontoclastogenesis, suggesting that odontoclasts appear to show a different response from osteoclasts to the effect of bisphosphonate under mechanical forces.

Disclosures: ***R. Putranto****, None.*

M302

GLP-2 Reduces Bone Resorption In Vitro Via the Osteoclast GLP-2 Receptor. M. A. Karsdal[1], J. J. Holst*[2], D. Henriksen[3]. [1]Nordic Bioscience A/S, Herlev, Denmark, [2]Department of Medical Physiology, University of Copenhagen, Copenhagen, Denmark, [3]Sanos Bioscience A/S, Herlev, Denmark.

The receptor for the gastrointestinal hormone, glucagon like peptide-2 (GLP-2), has recently been found to be expressed by osteoclasts both in human and rodents. GLP-2 is thought to serve in the regulation of absorption of ingested nutrients and has been suggested to be involved in the acute postprandial reduction of bone resorption.

We assessed the direct effect of GLP-2 on human osteoclastic resorption by using monocytes isolated from peripheral blood differentiated into mature human osteoclast on bovine cortical bone slices in the presence of 25ng/mL M-CSF and 25ng/mL RANKL. After culture for 14 days, the mature human osteoclasts were exposed to GLP-2 for 24 hours at different concentrations increasing from 0 to 160 µg/mL. The treatment was followed for a further 24-hour period without GLP-2 to monitor reversibility. The release of c-terminal type I collagen fragments (CTX) from the bone slices was assessed by the CrossLaps for culture ELISA kit (Nordic Bioscience Diagnostics). The level of CTX release during the incubation period with GLP-2 from each individual well was correlated to the basal level measured at day 14.

In a different ex vivo setup, bone resorption was evaluated in cultures of mouse tibia by measuring the release of 45Ca and collagen fragments in the culture media. Culture media were replaced every day, and collected for measurements of release of 45Ca, and CTX (RatLaps, Nordic Bioscience Diagnostics). The demineralization of the bone explants during the cultures was expressed as percentage of total amount of radioactivity.

We found that GLP-2 reduces bone resorption (CTX) in a dose related manner in the human osteoclast study and that the osteoclastic bone resorption reverts to same level as the untreated cultures if GLP-2 is removed. GLP-2 treatment of the mouse tibia cultures resulted in a similar dose related decrease in CTX as was seen for the human osteoclasts. The reduction in bone resorption correlated to the 45Ca release, which was decreased as a dose related function of increasing concentration of GLP-2. The cell number was assessed by TRAP positive cell counting and was unchanged.

We provide for the first time functional data for the GLP-2 receptor on osteoclasts. Recently, subcutaneous injections of GLP-2 in human subjects have been shown to result in a significant and acute reduction of the bone resorption in a dose dependent manner. Taken together, our in vitro and ex vivo results strongly suggest that the reduction of bone resorption seen in these human studies most likely is mediated via the activation of the osteoclast GLP-2 receptor.

Disclosures: ***D. Henriksen****, Sanos Bioscience 3.*

M303

Nitric Oxide Directly Inhibits Mature Osteoclast Bone Resorption Through Decreasing TRAP and V-ATPase Expression and Actin Ring Formation by cGMP Dependent and Independent Mechanisms. H. Zheng, X. Yu, P. Collin-Osdoby, P. A. Osdoby. Department of Biology, Washington University, St. Louis, MO, USA.

High nitric oxide (NO) levels are well known to inhibit osteoclast (OC) development, function, and survival in vivo or in vitro. In OC development, NO prevents RANKL induction of multiple OC characteristics that must be acquired for the essential resorptive function of OCs. However, the exact mechanisms by which NO directly inhibits bone resorption by mature OCs are not well defined. To resorb bone, OCs form a tightly sealed compartment into which they secrete acid (via V-ATPase in the ruffled border membrane) and proteases (especially cathepsin K) to degrade the mineral and organic components of bone, respectively. Both V-ATPase and cathepsin K, in addition to actin ring formation, are necessary for OC bone resorption. Here, we have used highly purified preparations of differentiated OCs generated by RANKL from RAW 264.7 cells (RAW-OCs) or primary murine marrow cells (MA-OCs) from normal or mutant mice to examine the effects of a nontoxic NO donor, NOC-12, on mature OC function. NOC-12 (150uM) inhibited TRAP mRNA expression and enzymatic activity, expression of the essential a3 (ATP6i) subunit of V-ATPase, and actin ring formation in both purified RAW-OCs and MA-OCs. In contrast, neither cathepsin K nor MMP-9 mRNA expression or enzymatic activity were affected by NOC-12. Addition of the cGMP inhibitor 1H-[1,2,4]oxadiazolo-[4,3-alpha]quinoxalin-1-one (ODQ) prevented the inhibition of ATP6i expression and actin ring formation due to NOC-12, while reduced TRAP expression and activity were not recovered. Furthermore, NOC-12 caused fewer and shallower pit excavations by purified RAW-OCs cultured on ivory, whereas the inclusion of ODQ abrogated such inhibition. In other studies we have shown that RANKL induced iNOS mRNA and NO production in RAW-OCs and MA-OCs, and that an iNOS selective inhibitor, L-NIL, blocked such autocrine NO production in parallel with increasing OC bone resorption. Consistent with this, a reduction in NO levels, either by L-NIL treatment of normal MA-OCs or by generating MA-OCs from iNOS-/- mice, caused higher APT6i expression and increased bone pit resorption relative to normal MA-OCs. Therefore, we conclude that NO inhibits mature OC bone resorption through cGMP-mediated inhibition of V-ATPase and actin ring formation, while NO suppresses TRAP mRNA and activity via cGMP-independent mechanisms and does not alter cathepsin K or MMP-9 in mature OCs (although NO inhibits their developmental expression). NO therefore sensitively regulates both the development of bone-resorptive OCs and their mature function through differential paracrine and autocrine mechanisms.

Disclosures: ***H. Zheng****, None.*

M304

TNFRI Mediated RANK/RANKL Signaling Plays Dominant Roles in Osteoclastogenesis in Lipopolysaccharide Induced Bone Loss. Y. Asou[1], N. Okuda[2], K. Shinomiya*[3], T. Muneta*[2], S. Itoh*[1]. [1]Human Genes and Science Center, Tokyo Medical and Dental University, Division of Molecular Tissue Engineering, Tokyo, Japan, [2]Devision of Bio-Matrix, Graduate School Tokyo Medical and Dental University, Section of Orthopeadic Surgery, Tokyo, Japan, [3]Tokyo Medical and Dental University, Department of Orthopaedic Surgery, Tokyo, Japan.

Lipopolysaccharide (LPS), a major constituent of Gram-negative bacteria, has been suggested to stimulate bone loss in ostemyelitis. LPS was reported to play roles in proliferation and differentiation of osteoclasts directly or indirectly via TNFα/TNFR1 and/or RANK/RANKL. However, the hierarchy of LPS function in bone metabolism in vivo remains to be elucidated. The purpose of this study was to investigate the role of RANK-RANKL pathway and TNFα -TNFR1 pathway in LPS induced bone loss in vivo. C57BL6 background wild type mice or TNFR1-/- mice were injected LPS (20mg/kg, s.c.) with or without OPG (0.05-5mg/kg, i.p.) and sacrificed 48 hours after the injection. Histological observation in wild type mice (tibial trabecular bone 200um apart from growth plate) indicated that BV/TV was suppressed by LPS injection about 40% in wild type mice. OPG administration dose dependently reversed the LPS induced bone loss. Oc.S/BS and Oc.N/BS were increased in LPS treated wild type mice. In addition, there were many TRAP positive cells apart from bone surface in bone marrow of LPS treated mice. The increase in Oc.N/BS, Oc.S/BS and the number of TRAP positive cells in bone marrow induced by LPS injection were suppressed by OPG administration in dose dependent manner. As for bone formation, Ob.S/BS and ALP positive area were increased by LPS injection, suggesting that LPS induced high turn over osteopenia 2days after the injection. OPG treatment also reduced these parameters to basal levels. To investigate the roles of TNFα and RANKL in LPS signaling, TNFR1-/- mice were injected LPS with or without OPG. BV/TV was reduced significantly in LPS injected TNFR1-/- mice two days after injection. The reduction in bone volume was reversed partially by OPG treatment. As for osteoclastogenesis, administration of LPS and OPG had less effect on Oc.N/BS or Oc.S/BS in TNFR1-/- mice compared with wild type mice. Interestingly, Ob.S/BS was remarkably reduced in LPS injected TNFR1-/- mice, this parameter was increased in LPS injected wild type mice, suggesting that TNFR1 mediated signaling might support survival of osteoblasts in acute phase of inflammation. From these observations, we concluded that TNFR1 mediated RANK/RANKL signaling played dominant roles in LPS induced osteoclastogenesis. Our data suggested that OPG could rescue bone loss in the region of infection such as osteomyelitis and periodontitis.

Disclosures: ***Y. Asou****, None.*

M305

Secretion of Tartrate-Resistant Acid Phosphatase 5b from Human Osteoclasts Treated with Antiresorptive Agents. H. Ylipahkala*[1], J. Rissanen[2], S. Suutari*[2], H. K. Väänänen*[1], J. M. Halleen[2]. [1]Institute of Biomedicine, Department of Anatomy, University of Turku, Turku, Finland, [2]Pharmatest Services Ltd, Turku, Finland.

We have studied secretion of tartrate-resistant acid phosphatase isoform 5b (TRACP 5b) from human osteoclasts *in vitro* in the presence and absence of antiresorptive agents. In the culture system, osteoclast precursors cells (Poietics™, Cambrex, East Rutherford, NJ, USA) were cultured on bovine bone slices for 9 days in the presence of M-CSF, RANKL and TGF-β_1. After the culture period, TRACP-positive multinucleated osteoclasts were counted under microscope. Medium TRACP 5b was determined with an in-house immunoassay and medium C-terminal cross-linked telopeptides of type I collagen (CTX) with a commercial assay (CrossLaps® for culture, Nordic Bioscience, Herlev, Denmark). Cytotoxicity was determined using the ToxiLight® assay (Cambrex). The cells were cultured without added compounds and with osteoprotegerin (OPG), the cysteine protease inhibitor E64, and sodium azide. OPG was added at day 0, and the cultures were stopped at day 7. E64 and azide were added after changing the culture medium at day 7, and the cultures were stopped at day 9. OPG decreased dose-dependently osteoclast number, TRACP 5b and CTX without toxic effects. E64 did not affect osteoclast number but decreased dose-dependently both TRACP 5b and CTX without toxic effects. Azide caused toxic effects and decreased dose-dependently osteoclast number, TRACP 5b and CTX. In the presence of OPG and azide, TRACP 5b correlated significantly with both osteoclast number and CTX, but the correlation was slightly better with osteoclast number. However, in the presence of E64, TRACP 5b correlated significantly with CTX, but not with osteoclast number. As a summary: 1) Medium TRACP 5b correlated with osteoclast number during osteoclast differentiation (based on OPG results); 2) In cultures of actively resorbing osteoclasts, TRACP 5b correlated with osteoclast activity but not with osteoclast number (based on E64 results); 3) TRACP 5b was not released as an active enzyme from dying cells (based on azide results). These results suggest that TRACP 5b is released from osteoclasts by two different mechanisms, one operating during osteoclast differentiation and the other during resorption. We conclude that TRACP 5b is a useful marker of osteoclast number in *in vitro* osteoclast cultures during osteoclast differentiation, and a useful marker of osteoclast activity in cultures of resorbing osteoclasts.

Disclosures: ***H. Ylipahkala****, None.*

M306

Molecular Identification and Electrophysiological Properties of Cl-Channels Expressed in Mouse Osteoclasts. F. Okamoto*, H. Kajiya, E. Jimi, H. Fukushima, K. Okabe. Physiological Science and Molecular Biology, Fukuoka Dental College, Fukuoka, Japan.

CLC-7 Cl- channels are important for osteoclastic bone resorption since disruption of these channels can lead to severe osteopetrosis. However, the functional roles and expression of Cl- channels other than CLC-7 in osteoclasts are still obscure. In this study, we identified the molecular types of chloride channels expressed in osteoclasts generated from co-cultures of mouse bone marrow and osteoblastic cells and examined the properties of Cl- currents through the osteoclast cell membrane. Furthermore, we examined the effects of antisense oligonucleotides for CLCs on bone resorbing activity. RT-PCR analysis showed that mouse osteoclasts express mRNAs for CLC-3, -4, -5, -6, and -7. Although these CLC mRNA were also detected in mouse osteoblastic cells, expression level of CLC-3 mRNA was higher in osteoclasts than in osteoblasts. An outwardly rectifying Cl- current was identified using the whole-cell patch-clamp technique in osteoclasts plated on glass coverslips. This current was reversibly blocked by Cl- channel blockers DIDS and NPPB and its anion permeability sequence was I- > Cl-. When osteoclasts were seeded on calcium phosphate-coated coverslips, most of these cells formed resorption pits. Regardless whether pit-forming or not, outwardly rectifying Cl- current was observed in all osteoclasts examined. However, the current density of Cl- current (current magnitude/cell capacitance) recorded from pit-forming cells was significantly greater than that recorded from cells not forming pits. Pretreatment of osteoclasts with antisense oligonucleotides targeted for CLC-3 and CLC-7 suppressed bone resorbing activity as estimated from the total pit area on bone slices. As a control, no change in bone resorbing activity was observed when osteoclasts had been treated with sense oligonucleotides for CLC-3 and CLC-7. Bone resorbing activity was also inhibited by DIDS and NPPB. These results suggest that osteoclasts express not only CLC-7 but also other CLCs and that Cl- channels with outwardly rectifying properties are involved in osteoclastic bone resorption.

Disclosures: ***F. Okamoto****, None.*

M307

Reveromycin A, which Induces Apoptosis Specifically in Functional Osteoclasts, Inhibits Bone Resorption *in vitro* and *in vivo*. J. Woo[1], M. Kawatani*[2], M. Kato*[1], H. Yonezawa*[1], N. Kanoh*[2], T. Shinki[3], M. Takami[3], H. Osada*[2], P. Stern[4], K. Nagai*[1]. [1]Chubu University, Kasugai, Japan, [2]RIKEN, Wako, Japan, [3]Showa Universiry, Tokyo, Japan, [4]Northwestern University, Chicago, IL, USA.

Osteoclasts, which are multinucleated cells that play a crucial role in bone resorption, are formed by the fusion of mononuclear osteoclasts derived from osteoclast precursors of the monocyte/macrophage lineages. Compounds are targeted specifically to functional osteoclasts would be ideal candidates as anti-resorptive agents for clinical application. We have found that reveromycin A (RMA), a natural low molecular weight acidic compound with three carboxyl groups, inhibits bone resorption through inducing apoptosis specifically in functional osteoclasts. RMA induces apoptosis in functional multinucleated osteoclasts, but not in their progenitor cells, mononuclear osteoclasts, non-functional multinucleated osteoclasts or osteoblastic cells. The cell death induced by RMA is accompanied by nuclear condensation, DNA fragmentation, induction of caspase 3-like activity and the release of cytochrome c from mitochondria into the cell cytoplasm. The inducible effect of RMA is prevented by disruption of acidic microenvironment by addition of concanamycin B, a specific V-ATPase inhibitor, and is increased in acidic culture condition. The apoptotic effect of RMA was decreased by the methylation of the carboxyl groups. RMA inhibited both pit formation on dentine slices and pre-labeled ^{45}Ca release stimulated by PTH in long bone cultures. RMA decreased the increased calcium level in blood elicited by PTH injection in TPTX rats, and prevented the decrease of bone density induced in rats by OVX. The observations indicate that the specificity of the effect of RMA on functional osteoclasts is due to their acidic environment, which may increase the permeability of RMA by suppressing dissociation of protons from carboxyl groups, and that the inhibitory effect of RMA bone resorption in vitro and in vivo is caused by apoptosis of functional osteoclasts. The findings suggest that RMA could be a valuable tool for distinguishing activated osteoclasts in a population of mixed osteoclasts, and thus would be a unique anti-resorptive agent for the treatment of bone diseases such as osteoporosis.

Disclosures: ***J. Woo****, None.*

M308

Minodronic Acid (YM529/ONO-5920) Distributed on Bone Surfaces Inhibits Osteoclastic Bone Resorption in Nude Rats with Bone Metastases. S. Tanaka*[1], K. Nakano*[2], A. Nii[2], S. Kawamura*[2], S. Fukushima*[1], M. Sasamata*[1]. [1]Pharmacology Lab., Yamanouchi Pharmaceutical Co., Ltd., Tsukuba-shi, Japan, [2]Safety Research Lab., Yamanouchi Pharmaceutical Co., Ltd., Itabashi-ku, Japan.

To evaluate the interaction between osteoclasts and bisphosphonate minodronic acid in bone, the localization of ^{14}C-minodronic acid and the effects on osteoclasts were studied in nude rats with osteolytic metastases induced by A375 human melanoma cells. Metastases were induced by intracardiac injection of A375 cells into nude rats. Minodronic acid was intravenously given to nude rats after osteolytic metastases were radiologically defined. Histological examination confirmed that numerous TRAPase-positive cells (osteoclasts) appeared on the bone surfaces near the tumors. Intravenous administration of minodronic acid reduced the number of osteoclasts and the ratio of osteoclast surface to bone surface at each tumor site in a dose dependent manner. The effects of minodronic acid were statistically significant at dose of 0.1 mg/kg i.v. Under light microscopy autoradiography, silver grains were seen on bone surfaces near the tumors at 2 hr after the administration. Then, they were selectively seen above the osteoclasts. In addition, structural examination of osteoclasts showed abnormalities of morphology, such as round-shaped osteoclasts and degeneration. These findings suggest that osteoclasts interact with minodronic acid distributed on bone surfaces and that the bone-resorbing activity of osteoclasts are inhibited by these interactions, resulting in inhibition of the tumor-induced osteolysis.

Disclosures: ***S. Tanaka****, None.*

M309

Immature Dendritic Cells Transdifferentiation into Osteoclasts: A Novel Pathway Sustained by the Rheumatoid Arthritis Microenvironment. M. M. P. Mazzorana*[1], A. Rivollier*[2], J. Tebib*[3], M. Piperno*[4], T. Aitsiselmi*[5], C. Rabourdin-Combe*[2], P. Jurdic[1], C. Servet-Delprat*[2]. [1]LBMC, UMR CNRS 5161, Lyon, France, [2]INSERM U503, Lyon, France, [3]Service de Rhumatologie, Centre Hospitalier Lyon-Sud, Lyon, France, [4]Centre Hospitalier Lyon-Sud, Lyon, France, [5]Centre Livet, Lyon, France.

Dendritic cells - the mononuclear cells which initiate immune response - and osteoclasts - the multinucleated bone-resorbing cells - are hematopoietic cells derived from monocyte/macrophage precursor cells. GM-CSF and M-CSF reciprocally regulate the differentiation of both lineages in mouse. Using *in vitro* generated human monocyte-derived dendritic cells, we show that immature dendritic cells transdifferentiate into functional osteoclasts in the presence of M-CSF and RANKL. These dendritic cell-derived osteoclasts resorb dentine and display characteristic markers of monocyte- or bone-derived osteoclasts and classical organization of podosomes in belts localized at the periphery of the cells. Transdifferentiation operates through fusions of intermediate adherent bipolar fusiform mononuclear cells expressing CD14 and CD1a, RANKL and able to to induce RANKL-positive T cells proliferation. Surprisingly, *in vitro* dendritic cell-derived osteoclast formation is faster and more efficient than monocyte-derived osteoclast formation. The transdifferenciation process we report here comforts the existence of a high cellular plasticity within differentiated myeloid phagocytes. Importantly, this process is greatly enhanced by rheumatoid arthritis synovial fluid and involves pro-inflammatory cytokines such as IL-1 or TNF-α as well as fragments of some components of the extracellular matrix such as hyaluronic acid. These data suggest that dendritic cell-derived osteoclasts may be directly involved in the osteolytic lesions observed in human inflammatory bone diseases such as rheumatoid arthritis or in particular forms of Langerhans Cell Histiocytosis, characterized by accumulation of immature skin dendritic cells and chronic lytic bone lesions.

Disclosures: ***M.M.P. Mazzorana****, None.*

M310

Establishment and Characterization of Pre-osteoclastic Cells Lines Derived of Osteosclerotic Mice oc / oc. C. Blin-Wakkach*[1], V. Breuil[2], J. Esdaile*[3], C. Bagnis*[4], L. Euller-Ziegler[5], G. F. Carle[6]. [1]Fre 2720 - ifr 50, CNRS UNSA, Nice, France, [2]Fre 2720 , ifr 50, CNRS - UNSA, Nice, France, [3]Fre 2720 - ifr 50, CNRS - UNSA, Nice, France, [4]EFS Alpes Maritimes Méditerranée, Department of Cellular Therapy and Genetics, Marseille, France, [5]Rheumatology, University Archet Hospital, Nice, France, [6]Fre 2720 ; ifr 50, CNRS - UNSA, Nice, France.

Infantile malignant osteopetrosis. (IMO) is a rare autosomal recessive disease, leading to death during childhood. IMO is characterized by a lack of bone resorption due to a defect in osteoclast function. Among the models of osteopetrosis, the oc/oc mouse displays a phenotype very similar to the human disease. The mutation involved is a deletion of 1.6 kb in the Tcirg1 (T cell immune regulator 1) gene encoding for the 116 kDa a3 isoform subunit of the V-ATPase pump. This protein is essential, during acidification of the resorption lacuna, for the dissolution of mineral matrix and also for enzymes activities involved in the degradation of the organic bone matrix. For the majority of IMO patients, mutations in the TCIRG1 gene have been described. The oc/oc mouse model is particularly suited to study this pathology and to develop new therapeutic approaches. We are particularly interested in cellular therapy to rescue the oc mutation in osteoclasts precursors of these animals.

To verify in vitro if this complementation of the oc mutation in pre-osteoclasts is feasible, we established several oc/oc and wildtype mouse preosteoclastic cell lines. We crossed Tcirg1 +/oc mices with p53+/- mices. Indeed, p53 is involved in the control of cell proliferation and p53-/- animals develop tumors, mostly lymphoma and osteosarcoma, around the age of 5 months. These animals have been used to obtain cell lines from various organs.

We cultured bone marrow of Tcirg1oc/ocp53-/- and Tcirg1+/oc p53-/- animals. Several oc/oc or wildtype cell lines have been obtained and characterized by RT-PCR and flow cytometry for osteoclastic and myelomonocytic markers. The cell lines display monocytic features and express among others the RANK and c-FMS receptors. In the presence of M-CSF and RANKL, these precursors are able to differenciate in cells presenting osteoclast's characteristics, including multinucleation, TRAP activity and calcitonin receptor expression.

A lentivirus encoding for the GFP gene (Green Fluorescent Protein)was used to determine the transduction conditions in these osteoclast precursors cell lines.The transduction efficiency was close to 65 % and the cells transducted kept their capacity to differenciate into osteoclasts. These pre-osteoclastic cell lines represent a new approch to investigate the role and the regulation of the Tcirg1 gene, in normal and pathological conditions.

Disclosures: ***V. Breuil****, None.*

M311

Identification of Multiple Osteoclast Precursor Populations by Flow Cytometry in Murine Bone Marrow. C. Jacquin*[1], S. Lee[2], J. A. Lorenzo[2], H. L. Aguila*[1]. [1]Cicid, UConn Health Center, Farmington, CT, USA, [2]Medicine, UConn Health Center, Farmington, CT, USA.

The lineage of osteoclast precursors is not clearly defined. To characterize osteoclast progenitors in murine bone marrow, we fractionated cells by fluorescence activated cell sorting (FACS) and cultured them with M-CSF and RANKL (30 ng/ml) for 2 to 6 days in 96 well plates. Osteoclast-like cells (OCLs) were identified as TRAP+ multinucleated cells. Initially, cells were separated by surface expression of B220 (CD45R), a B lymphoid lineage marker and Mac-1 (CD11b), a myeloid lineage marker.

Single sorted populations of B220+Mac- (B+) cells (99.0% pure) were able to form abundant OCLs in vitro whereas, double FACS separated B+ (99.8% pure) failed to do so. Double FACS separated Mac-1+B220- (M+) cells (99.9% purity) differentiated into OCLs with low efficiency (5,000 M+ cells produced 4 ± 1 OCL on day 4 and 33 ± 6 OCLs on day 6). Unexpectedly, double negative Mac-1- B220- (DN) cells differentiated into OCLs efficiently and rapidly (5,000 DN cells produced 184 ± 36 OCLs on day 3 and 474 ± 29 OCLs on day 4). The number of OCLs in M+ and DN fractions was proportional to the number of plated cells. Additional fractionation of the DN population found the OCL progenitor activity entirely within the mono-myeloid population since it did not separate with markers for T lymphocytes (CD3) or erythrocytes (Ter119). Enrichment of DN cells (CD3-, Ter119-) for those highly (hi) expressing the M-CSF receptor (c-fms) increased the rate of OCL formation by about 2 fold on day 3. Analysis of the DN c-fms negative to low fraction (CD3-, Ter119-), showed little osteoclast formation on day 3 (5,000 cells plated), but abundant OCL formation on day 4 (298 ± 51). Interestingly, by day 4 a large number of OCLs generated from the DN c-fms(hi) cells appeared to have died. Finally, OCLs derived from the DN (CD3-, Ter119-) fraction formed resorption pits on bovine cortical bone in vitro and were positive for the calcitonin receptor.

These results demonstrate that there are multiple populations of bone marrow cells that can differentiate into osteoclasts. DN c-fms(hi) cells are the most highly enriched for late OCL precursors since they differentiated most rapidly but survived in vitro for only 1-2 days. DN, c-fms negative to low cells appeared less mature since they took longer to form OCL in vitro. M+ cells were the least enriched and took the longest time to form OCL in vitro. Previous demonstration of OCL formation in B+ murine bone marrow cells appears to result from contamination of these populations by small numbers of mono-myeloid precursors.

Disclosures: ***C. Jacquin****, None.*

M312

Src Induces Translocation of SHIP1 to Focal Adhesion. K. Yogo*[1], M. Mizutamari*[1], N. Ishida*[1], T. Sasaki*[2], T. Takeya*[1]. [1]Graduate school of Bilogical Sciences, Nara Institue of Science and Technology, Ikoma, Japan, [2]The 21st Century Center of Excellence (COE) Program, Akita University School of Medicine, Akita, Japan.

c-Src, a family of non-receptor tyrosine kinase, plays an essential role for osteoclastogenesis by regulating cytoskeletal organization and survival pathway through PI3K. To understand this mechanism, we screened and identified 10 proteins as c-Src binding partners using RANKL-induced differentiation system of RAW264 cells. Among them, SH2-containing inostol phosphatase 1 (SHIP1) was included. Although SHIP1 has been shown as a binding protein to Src family kinases and *SHIP1* knock out mice are known to cause osteoporosis, the functional relationship between c-Src and SHIP1 has been largely unknown.

First, we confirmed the direct association of c-Src and SHIP1 using pull down assay *in vitro*. We then examined the effect of Src kinase activity on their association and phosphorylation state of SHIP *in vivo*. SHIP1 could be immunoprecipitated with c-Src and its phosphorylation level was found to be increased in SrcY527F-overexpressing 293 cells. We identified two tyrosine residues, Y917 and Y1020, as major phosphorylation sites in SHIP1 by Src. Next, we examined the effect of Src kinase activity on intracellular localization of SHIP1 in HeLa cells. Immunohistochemical study showed that the localization of SHIP1 was shifted from cytoplasm to focal adhesion (FA) in the presence of SrcY527F. When PP1, a specific Src family kinase inhibitor, was administered, peripheral (presumably podosome) localization of SHIP was reduced in osteoclasts as well as HeLa cells.

To understand the mechanism of the translocation more precisely, we prepared three kinds of truncated mutants of SHIP1: SHIP1-457, SHIP401-866 and SHIP739-1190. When these mutants were introduced into HeLa cells together with SrcY527F, SHIP1-457 and SHIP739-1190 were localized in FA while SHIP 401-866 which contains the phosphatase domain remained in the cytoplasm, suggesting that the inositol phosphatase activity may not be required for this translocation. We further introduced point mutations into the SH2 domain of SHIP1-457 and Tyr917/1020 of SHIP739-1190, respectively. The resulting SHIP 1-457 R34L which lost the binding activity to phosphor-tyrosine could not be translocated to FA, whereas SHIP1 Y917F/Y1020F still could be translocated. Taken together, these results suggest that Src kinase activity induces the translocation of SHIP1 to FA and that the NH2- and C-terminal region of SHIP1, respectively, are regulated in independent manners for the translocation.

Disclosures: ***K. Yogo****, None.*

M313

Evidence for Involvement of PYK2-Mediated Signaling in Calcitonin-Induced Sealing Zone Detachment in Osteoclasts Microinjected with Fluorescent G-Actin. J. Shyu[1], C. Lin*[2], H. Chen*[1], H. Tsung*[1], C. Shih[1]. [1]Biology and Anatomy, National Defense Medical Center, Taipei, Taiwan Republic of China, [2]Microbiology and Immunology, National Yang-Ming University, Taipei, Taiwan Republic of China.

Bone resorption is primarily carried out by osteoclasts. The osteoclastic bone resorption starts with adhesion to the bone matrix, leading to cytoskeletal reorganization that is important for the migration of these cells to and between the resorption sites and their polarization during the resorption process. It has been well studied that, the calcitonin induced quiescent and retraction effects in osteoclasts which involved PKA and PKC pathways, respectively. However, the detailed mechanism is still unknown. Recently, effects of calcitonin on the turnover of podosome and function of PYK2 had been reported. Therefore, this signaling molecule in podosome could be the potential targets for the calcitonin-induced signaling. Using immunoprecipitation and immunofluorescent microscopy methods, our previous results showed that decreased tyrosine phosphorylation and redistribution of PYK2 in osteoclasts upon calcitonin stimulation. Though the effects of calcitonin on PYK2 in osteoclasts are clear, evidence for involvement of PYK2-mediated signaling in calcitonin-induced podosome reorganization was still lacking. To address this issue, microinjection of fluorescent G-actin into authentic living osteoclasts cultured on collagen-I coated Petri dish was performed. In real time, we observed the formation of actin ring and its association of PYK2 in resorbing osteoclasts. The addition of calcitonin induced reorganization of the podosomes, disruption of the actin ring, and redistribution of PYK2 in these cells. In the same cell, calcitonin also induced dephosphorylation of Tyr402, which is the autophosphorylation site of PYK2. In conclusion, we developed a model of microinjection system in isolated living rabbit osteoclasts in which the involvement of PYK2-mediated signaling in calcitonin-induced acting ring disruption was demonstrated.

Disclosures: ***J. Shyu****, None.*

M314

P2X7 Nucleotide Receptors Act through Two Distinct Mechanisms to Regulate Osteoclast Survival. J. Korcok*, S. M. Sims*, S. J. Dixon. CIHR Group in Skeletal Development and Remodeling, Dept. Physiology & Pharmacology, University of Western Ontario, London, ON, Canada.

Extracellular nucleotides signal through P2X (ATP-gated ion channels) and P2Y (G protein-coupled) receptors. Osteoclasts express multiple P2 receptors including P2X7, which can induce formation of membrane pores in the presence of low concentrations of divalent cations. P2X7 receptor knockout (KO) mice show enhanced trabecular bone resorption associated with increased osteoclast numbers. Osteoclastogenesis was similar in cultures of bone marrow from wild-type (WT) and KO mice, suggesting that osteoclast survival is prolonged in KO mice. The aim of this study was to examine whether P2X7 receptors regulate osteoclast survival. Osteoclasts were isolated from long bones of new-

born WT and KO mice. Acute cell death was assessed by ethidium bromide uptake in medium containing a low concentration of divalent cations. Benzoylbenzoyl-ATP (BzATP 300 μM, P2X7 receptor agonist) increased ethidium bromide uptake in WT but not in KO osteoclasts. To assess survival under more physiological conditions, osteoclasts were counted following isolation (time 0) and at 12 h, in medium containing divalent cations. Apoptosis was quantified by counting Hoechst-stained osteoclasts showing condensed and fragmented nuclei. In the absence of exogenous nucleotides, higher numbers of WT than KO osteoclasts were apoptotic at 6 h. Consistent with this observation, fewer WT osteoclasts survived at 12 h. Interestingly, BzATP had no additional effect on either apoptosis or survival. Control experiments revealed that WT and KO osteoclasts were equally susceptible to apoptosis induced by the proapoptotic agent staurosporine. Brilliant blue G (P2X7 antagonist) decreased apoptosis and increased survival of WT osteoclasts, providing additional evidence for involvement of the P2X7 receptor. To determine if P2X7 receptors induce cell death in a ligand-independent manner or are activated by constitutively released nucleotides, WT osteoclasts were treated with alkaline phosphatase (AP) to hydrolyze endogenous nucleotides. AP increased survival of WT osteoclasts to levels comparable to KO osteoclasts. These data indicate that P2X7 receptors act through two mechanisms to regulate osteoclast survival. First, activation of the receptor by high concentrations of nucleotides induces membrane pore formation leading to acute cell death. Second, under physiological conditions, activation of P2X7 receptors by low concentrations of constitutively released nucleotides induces apoptosis. Thus, the P2X7 receptor reduces bone resorption by decreasing osteoclast survival and represents a potential target for the development of antiresorptive drugs.

Disclosures: ***J. Korcok****, None.*

M315

Evidence of Reciprocal Regulation between the High Extracellular Calcium and RANKL Signal Transduction Pathways in RAW Cell Derived Osteoclasts. J. Xu*[1], C. Wang*[1], R. Han*[1], N. Pavlos*[1], T. Phan*[1], J. H. Steer*[2], A. J. Bakker*[3], D. A. Joyce*[2], M. H. Zheng[1]. [1]Orthopaedic Surgery, The University of Western Australia, Nedlands WA, Australia, [2]Pharmacology, The University of Western Australia, Nedlands WA, Australia, [3]Physiology, The University of Western Australia, Nedlands WA, Australia.

During osteoclastic bone resorption, osteoclasts are exposed to high Ca^{2+} concentrations (up to 40 mM). High concentrations of Ca^{2+} haveextracellular Ca^{2+} has been shown to trigger a cytosolic Ca^{2+} increase, inhibit resulting in inhibition of osteoclastic bone resorption and induce induction of osteoclast apoptosis. In this study, we show that receptor activator of NF-κB ligand (RANKL) enhances osteoclast tolerance to high extracellular Ca^{2+} by protecting the cell from high extracellular Ca^{2+}-induced cell lossdeath in a dose dependent manner. We have providedshown evidence that RANKL does this by attenuating high extracellular Ca^{2+}-induced Ca^{2+} elevations. Moreover, we have found that high extracellular Ca^{2+}-induced cell death was partially inhibited by a caspase-3 inhibitor, suggesting that a caspase-3-mediated apoptosis is involvedis involved.. Conversely, using reporter gene assays and western blot analysis, we have demonstrated that high extracellular Ca^{2+} desensitizes the RANKL-induced activation of NF-κB and c-Jun N-terminal kinase (JNK), and inhibitedinhibits constitutive and RANKL-stimulated ERK phosphorylation, indicating a negatively feed-back mechanism via specific RANKL signaling pathways. Taken together, our studies providethis study provides evidence for a reciprocal regulation between high extracellular Ca^{2+} and RANKL signaling in RAW cell derived osteoclasts. Our data suggest a mechanism of extracellular Ca^{2+} on osteoclast survival through the regulation of RANKL.

Disclosures: ***M.H. Zheng****, None.*

M316

Activation of the Rho-GTPase by *Pasteurella Multocida* Toxin (PMT) in Osteoclasts Reveals Contrasting Roles in Differentiation and Activation. N. W. A. McGowan*[1], D. Harmey[2], J. E. Dunford*[3], M. J. Rogers[3], A. E. Grigoriadis[1]. [1]Craniofacial Development, Kings College London, London, United Kingdom, [2]The Burnham Institute, La Jolla, CA, USA, [3]Bone Research Group, Institute of Medical Sciences, University of Aberdeen, Aberdeen, United Kingdom.

Rho family GTPases are well-known regulators of the cell cytoskeleton, cell migration and differentiation. We have recently demonstrated that the unique bacterial toxin, *Pasteurella Multocida* toxin (PMT), which activates the heterotrimeric G-protein, G_q, leading to stimulation of Rho and actin rearrangements, as well as activation of phospholipase C, protein kinase C and the Ras/MAP kinase pathway, inhibits osteoblast differentiation and bone nodule formation via activation of Rho and Rho kinase (ROK). However, PMT also targets osteoclastic cells, since the main *in vivo* effect of PMT is the porcine bone resorbing disease, atrophic rhinitis, resulting in pathological bone resorption. Since Rho proteins play an important role in the rapid cytoskeletal rearrangements during bone resorption, the effects of PMT on osteoclast differentiation and activity were investigated.

In RANKL- and MCSF-based cultures of human PBMCs or murine bone marrow cells PMT inhibited osteoclast differentiation and resorption in a dose-dependent manner. Molecular analysis revealed that PMT had no effect on RANK or *c-fms* gene expression, but inhibited the expression of the specific osteoclast markers calcitonin receptor and cathepsin K. Biochemical studies demonstrated that 6h incubation with PMT induced a 4-fold increase in the levels of active GTP-bound Rho, with no significant increase in the levels of GTP-bound Rac or Cdc42. Furthermore, PMT also induced a sustained activation of the MAP kinase pathway as shown by an increase in the levels of pERK 1 and 2. Using specific pathway inhibitors to investigate the relevance of these signalling mechanisms, treatment of murine or human osteoclast precursors with the ROK inhibitor, Y-27632, partially rescued the inhibition of osteoclast differentiation, whereas the MEK inhibitor PD98059 failed to rescue the PMT effect. In contrast to the inhibitory effects on differentiation, PMT appeared to promote resorption and survival of the mature osteoclast as addition of PMT to human osteoclast cultures at day 10 increased the proportion of F-actin ring-containing, vitronectin receptor-positive osteoclasts, with a concomitant increase in resorption. Overall, these data suggest an important inhibitory role for the Rho-ROK pathway in osteoclast differentiation and we are currently investigating how the divergent effects of PMT on osteoclast differentiation and activity may converge to produce the bone loss observed *in vivo*.

Disclosures: ***N.W.A. McGowan****, None.*

M317

Inhibition of Src Kinase Activity Decreases M-CSF-Induced Cell Survival in Human Osteoclasts. R. J. S. Galvin[1], T. Fuson*[1], A. Regmi*[1], A. Bansal*[2]. [1]Bone and Inflammation, Eli Lilly and Company, Indianapolis, IN, USA, [2]Integrative Biology, Eli Lilly and Company, Indianapolis, IN, USA.

M-CSF prolongs cell survival in fully differentiated osteoclasts. However, the mechanisms by which M-CSF blocks apoptosis have not been extensively evaluated. This study evaluated the pathways involved in the regulation of caspase activity by M-CSF in differentiated human osteoclasts. Osteoclasts were generated from human cord blood cells, which had been maintained in Delta Culture for 7-9 days. The Delta culture cells were treated with rhM-CSF and shRANKL for 7 days. The differentiated cultures contained predominately large tartrate-resistant acid phosphatase (TRAP)-positive multinucleated osteoclasts. The cells were treated with various factors and caspase 3 activity was determined by measuring z-VAD-FMK cleavage. rhM-CSF inhibited caspase activity in a time dependent manner with 24-30 h significantly reducing caspase activity. RANKL also blocked caspase activity, but the effects were small compared to the effects of M-CSF. M-CSF blocked caspase activity in a concentration dependent manner. The src kinase inhibitor PP2, but not the control PP3, reversed the suppression of caspase activity seen with M-CSF in a concentration-dependent manner with a maximal effect at 20 uM. To further define the mechanism of apoptosis we evaluated the effects of M-CSF on AKT-phosphorylation in human osteoclasts and found that it was enhanced by 3 ng/ml and greater concentrations of M-CSF at 5 min. The effects of M-CSF on caspase activity were blocked by the phosphoinositol 3-Kinase (PI3K) inhibitor, LY294002, but not by the MEK inhibitor PD980592 or the p38 MAP kinase inhibitor SB203580. In summary these studies demonstrate that M-CSF blocks the increase in caspase activity that is seen with its removal and that these effects are reversed by treatment with src kinase inhibitors and PI3K inhibitors.

Disclosures: ***R.J.S. Galvin****, None.*

M318

Fas Binding to Calmodulin (CaM) Regulates Apoptosis in Osteoclasts. X. Wu[1], E. Ahn*[2], M. A. McKenna[1], H. Yeo*[1], J. M. McDonald[1]. [1]Pathology, University of Alabama at Birmingham, Birmingham, AL, USA, [2]University of California, San Diego, San Diego, CA, USA.

CaM, the major intracelluar Ca^{2+} receptor, is an important signaling modulator in osteoclasts, modulating not only osteoclastogenesis but also bone resorption. TFP, a CaM antagonist, rescues bone loss in ovariectomized mice (Endocrinology, Vol.144, p4536). Whether CaM plays a role in regulating osteoclast survival has not been investigated. CaM interacts with Fas, the death receptor, in Jurkat cells. This interaction has been implicated in regulating Fas-mediated apoptosis (J Biol Chem Vol.279, p5661). Whether CaM binds Fas and the significance of this binding in osteoclasts is unknown. Apoptosis in osteoclasts, derived from mouse primary monocyte/macrophage progenitors, is measured by nuclear staining and fluorescent caspase-3 activity assay. The interaction between Fas and CaM in osteoclasts is analyzed by CaM-Sepharose pull-down, coimmunoprecipitation, and ^{125}I-CaM overlay. After three-hour treatment with the CaM antagonists, tamoxifen (TMX) and trifluoperazine (TFP), osteoclasts undergo apoptosis dose-dependently. TMX, 10 μM, and TFP, 10 μM, induce a 7.3 ± 1.5-fold and a 5.3 ± 1.3-fold increase in osteoclast apoptosis, respectively. Both TFP and TMX activate caspase-3 dose-dependently, as detected by Western blotting. Importantly, in osteoclasts, CaM binds Fas. A point mutation in the death domain of the human Fas molecule (V254N) reduces binding to CaM *in vitro*. A similar mutation (I225N) in the Lpr^{cg} mouse renders Fas inactive, and osteoclasts, derived from Lpr^{cg} mouse bone marrow, have markedly diminished Fas/CaM binding. Interestingly, osteoclasts derived from Lpr^{cg} mice are more sensitive to CaM-antagonist-induced apoptosis than osteoclasts from wild type (wt) mice. TMX, 10μM, induces 42 ± 6 % of Lpr^{cg} osteoclasts to undergo apoptosis compared with 27 ± 2.2 % in wt osteoclasts. Similarly, 10μM TFP induces 37 ± 0.8 % of Lpr^{cg} osteoclasts to undergo apoptosis in comparison with 24 ± 2.8 % in wt osteoclasts. Results are confirmed using a fluorescent caspase-3 activity assay. Furthermore, when osteoclasts, derived from RAW264.7, a macrophage cell line, are treated with 10 μM TFP for 0-60 min, the binding between Fas and CaM is dramatically decreased at 15 min and gradually recovers over 60 min. In summary, in osteoclasts, CaM antagonists induce apoptosis and activate caspase-3 dose-dependently by a mechanism that involves interfering with CaM binding to Fas. The involvement of CaM in regulating osteoclast survival and specifically the effects of Fas/CaM binding on CaM-antagonist-induced apoptosis may open a new avenue for therapeutics.

Disclosures: ***X. Wu****, None.*

M319

PI3 Kinase Has Divergent Impacts on Osteoclast Survival Depending on TGF-β Levels During Differentiation. A. Gingery[1], M. J. Oursler[2]. [1]Biochemistry and Molecular Biology, University of Minnesota, Duluth, MN, USA, [2]Endocrine Research Unit, Mayo Clinic, Rochester, MN, USA.

Modulating osteoclast survival can alter bone resorption levels by changing osteoclast numbers. We have therefore studied the mechanisms by which osteoclast survival is regulated. PI3 kinase (PI3K) is a component of osteoclast survival signaling since inhibition leads to apoptosis of 100% of the cells within 3 hours of treatment. PTEN, a known tumor suppressor inactivates PI3K when phosphorylated, there by regulating PI3K activity. To elucidate a possible role of PTEN regulation of PI3K in osteoclasts, levels of PTEN and phospho-PTEN (pPTEN) in osteoclasts generated by co-culture of marrow precursors and ST2 cells were examined.

Mature osteoclasts from which ST2 cells were removed contained high levels of pPTEN, with the resultant decrease in PI3K activation of survival pathways. This is in concordance with PI3K inhibition increasing osteoclast apoptosis. TGF-β addition increased pPTEN, PI3K activity was decreased and increased osteoclast apoptosis. Thus, PTEN regulation of PI3K is important in osteoclast survival and targeting PTEN is one mechanism by which TGF-β increases osteoclast apoptosis.

Since TGF-β is present in high levels during periods of elevated bone resorption, it is important to discover the impact of osteoclast differentiation in the presence of TGF-β on osteoclast survival. In contrast to TGF-β-mediated osteoclast apoptosis induction in cells differentiated without TGF-β addition (naïve cells), TGF-β-induced osteoclasts had elevated apoptosis following TGF-β removal from mature cells while continued TGF-β treatment reduced apoptosis. These data support that TGF-β-induced osteoclast survival is dependent on TGF-β.

We also examined whether PTEN is likely to be involved in regulating apoptosis of TGF-β-induced osteoclasts. Levels of PTEN are high in both un-induced and TGF-β induced osteoclasts, indicating regulation of PI3K activity. When TGF-β-induced osteoclasts were cultured without TGF-β, pPTEN levels increased, resulting in increased osteoclasts apoptosis. TGF-β maintenance during culture resulted in a dramatic decrease in pPTEN and increased survival. We therefore propose that PI3K is mediating survival in naive osteoclasts and TGF-β induced osteoclasts. Therefore osteoclasts may have divergent signaling pathways downstream of PTEN/PI3K that are dependent on the presence or absence of TGF-β during osteoclast differentiation.

Disclosures: ***A. Gingery****, None.*

M320

Tyrosine 559 and 807 in c-Fms Regulate M-CSF Dependent Signaling and Proliferation of Osteoclast Precursors. S. Takeshita[1], R. Faccio[1], J. Chappel*[1], J. D. Weber*[2], S. L. Teitelbaum[1], F. P. Ross[1]. [1]Pathology, Washington University, St. Louis, MO, USA, [2]Cell Biology, Washington University, St. Louis, MO, USA.

We studied how M-CSF stimulates proliferation of osteoclast (OC) precursors. Bone marrow macrophages (BMMs) were tranduced with a chimeric erythropoietin receptor (EpoR)/c-Fms receptor that transmits intracellular signals following exposure to Epo, enabling us to define the role of individual Y residues in c-Fms signaling in authentic M-CSF responsive cells. Following transduction and cytokine treatment, all Epo-generated data were normalized to results from cells exposed to M-CSF. We first confirmed that cell proliferation is identical in M-CSF treated cells expressing endogenous c-Fms or in Epo-treated cells expressing a chimera containing the wild type (WT) c-Fms cytoplasmic tail. Next, we examined the impact on cell division of mutating individual Y residues to phynylalanine (F) in the chimeric c-Fms tail and established that Y559 and Y807 and, to a lesser extent, Y697 each play regulate proliferation. Turning to signal transduction, we analyzed the first step of M-CSF signaling, namely auto-phosphorylation of the receptor and determined that the mutants Y559F and Y 697F both strongly inhibit phosphorylation of Y807. The finding that Src family members bind Y559 suggests that they phosphorylate Y807. Confirmation of this hypothesis is provided by the observation that the src family kinase inhibitor PP2 inhibits phosphorylation of Y807. Furthermore, the src family member Lyn, but not c-Abl, phosphorylates Y807 in an vitro kinase assay. Attesting to specificity, both Lyn and c-Abl phosphorylate Y721. We next turned to the role of c-Fms Y559, Y697 and Y807 on activation of ERKs and Akt and expression of cyclin D, the central regulator of the cell cycle. By expressing both single and combined point mutations we find that Y559F, but not Y697F, strongly suppresses phosphorylation of the two kinases, down-regulates cyclin D1 levels and decreases cell proliferation. Surprisingly, cells expressing Y807F exhibit enhance both autophosphorylation of c-Fms Y721 and cyclin D 1 expression, but are hypo-proliferative. Next, we expressed in BMMs a series of add-back EpoR/c-Fms chimeras, each containing one or more specific Y residues, with all others mutated to F. The triple add-back Y559/Y697/Y807 is sufficient to promote ERK and Akt activation and cell proliferation, confirming data obtained with mutational analysis. In summary, tyrosines 559 and 807, and to a lesser extent Y697, in c-Fms regulate M-CSF-dependent signaling and proliferation of OC precursors.

Disclosures: ***S. Takeshita****, None.*

M321

The Associations between Body Composition, Muscle Strength and Bone Mineral Density in Postmenopausal Women: A Cross-sectional Study. T. P. Rikkonen*[1], J. Sirola[1], H. Kröger*[2], M. Tuppurainen[3], J. Jurvelin*[4], R. Honkanen[1]. [1]University of Kuopio, Bone and Cartilage Research Unit, Kuopio, Finland, [2]Kuopio University Hospital, Department of Surgery, Kuopio, Finland, [3]Kuopio University Hospital, Department of Ostetrics and Gynecology, Kuopio, Finland, [4]University of Kuopio, Department of Applied Physics, Kuopio, Finland.

Objective: The aim of this study was to examine relationships between muscular strength, body composition and bone mineral density in postmenopausal women. Subjects and methods: A population based cohort of 414 Finnish postmenopausal females (Mean age 68, 4 years; SD ± 1, 8 years). BMD at the proximal femur, lumbar spine (L2-L4) and total body was assessed by dual energy X-ray absorptiometry (DXA) (GE Lunar Prodigy). Total body composition, fat mass index (FI) (Fat/Height²) and lean mass index (LI) (Lean/Height²) variables were obtained from the total body scan. Strength measurements included handgrip dynamometer (Jamar) and isometric knee extension by sitting in bench (Metitur). Study population was divided into 3 groups by WHO osteoporosis criteria, according to femoral neck value with normal (N=189), osteopenia (N=204) and osteoporosis (N=21) status. Results: There were significant differences between osteoporotic and normal subjects in lean mass index (P<0.001), grip strength (P<0,001) and knee extension strength (P=0.007) but not in fat mass index (P>0.05). Grip Strength was 18% (p<0.001) and quadriceps strength was 19 % lower (p<0.001) in osteoporotic women compared to women with normal BMD status. In our results fat mass alone explained 85% and lean mass 32% of BMI variation. Both variables together predicted 87%. After adjusting for age, BMI, use of medications, diseases, alcohol consumption and smoking with logistic regression model, grip strength remained as an independent determinant for osteoporosis at the proximal femur (Adjusted OR=1.36; CI95% 1.13 - 1.54; P<0,001) and lumbar spine BMD (Adjusted OR= 1.20; CI95% 1.09 - 1.32; P<0,001) (AUROC 75% for FN and 67 % for LS respectively). Quadriceps strength measurements showed similar trend with these results. Conclusions: BMI and strength measurements are independently associated with postmenopausal BMD. Grip strength measurement is simple, useful and moderately sensitive tool for osteoporosis risk assessment patterns. Keywords: Muscle strength, body composition, postmenopausal, bone mineral density.

Disclosures: ***T.P. Rikkonen****, None.*

M322

Correlates of Osteoporosis Screening, Diagnosis and Treatment in Women with Arthritis at High Risk for Osteoporosis. S. M. Cadarette, D. E. Beaton*, M. A. M. Gignac*, S. B. Jaglal, G. A. Hawker. University of Toronto, Toronto, ON, Canada.

The purpose of this study was to examine predisposing, enabling and need factors related to osteoporosis screening (bone mineral density (BMD) testing), diagnosis and treatment (bisphosphonate, raloxifene or calcitonin) among community-dwelling women with arthritis at high risk for osteoporosis. A convenience sample of women participating in a longitudinal study of arthritis were consecutively recruited into the current study, N=425. Those at low risk for osteoporosis or residing in long-term care were excluded (N=6). Descriptive statistics were summarized as means or proportions. Correlates were grouped by type of factor as predisposing, enabling or need. Chi-squared analyses and unadjusted logistic regression were used in bivariate analyses. Correlations within and between the groups of factors were used to identify collinearity between variables before adjusted modeling began. Multivariable logistic regression was used in adjusted analyses. Overall, 55%, 24% and 15% reported to have been screened, have a diagnosis and were being treated respectively. Correlates of osteoporosis treatment included higher perceived calcium benefits (OR=1.04, 95%CI=1.01-1.07) and the following need factors: prior fragility fracture (OR=3.4, 95%CI=1.6-6.9), BMD testing (OR=9.5, 95%CI=3.1-29), osteoporosis diagnosis (OR=9.8, 95%CI=4.8-20), and long-term prednisone use (OR=9.7, 95%CI=3.0-31). Controlling for need factors, more frequent physician visits (OR=1.05, 95%CI=1.01-1.09) and having less than secondary school education (OR=1.9, 95%CI=1.06-3.4) were independently associated with a diagnosis of osteoporosis. Few need factors were associated with having a BMD test (fragility fracture, OR=1.7; and kg body weight, OR=.98). Rather, enabling factors such as living in metropolitan Toronto vs. a county with large rural areas (OR=2.2, 95%CI=1.3-3.6), and predisposing factors (lower general health status, fewer non-osteoporosis related conditions, younger age, fewer exercise barriers and higher perceived seriousness of osteoporosis) were independently associated with osteoporosis screening. Therefore, while need factors such as a diagnosis of, or major risk factors for osteoporosis, were correlated with osteoporosis treatment, several enabling and predisposing characteristics were found to be associated with BMD testing. These data suggest problems in access to osteoporosis screening by BMD testing, and subsequent unmet needs for osteoporosis prevention/management in asymptomatic women.

Disclosures: ***S.M. Cadarette****, None.*

M323

Prevalence of Low Bone Density in Older Italian Adults from the ESOPO Study. G. Crepaldi[1], S. Maggi*[1], D. de Feo[2], S. Adami[3], O. Di Munno*[4], S. Giannini[5], G. Isaia[6], L. Sinigaglia*[7], P. Filipponi[8]. [1]CNR Aging Center, Padua, Italy, [2]Procter & Gamble, Rome, Italy, [3]Rheumatology, Valeggio Hospital, Verona, Italy, [4]Rheumatology, Pisa university, Pisa, Italy, [5]Internal Medicine, Padua University, Padua, Italy, [6]Internal Medicine, Turin University, Turin, Italy, [7]Rheumatology, Gaetano Pini, Milan, Italy, [8]Internal Medicine, Umbertide Hospital, Umbertide, Italy.

Most estimates of osteoporosis in older Italians have been based on its major complications, such as hip and vertebral fractures. In the present study, quantitative ultrasound measurements were carried out with the Lunar Achilles Express apparatus in a random sample of 11,011 women 40-80 years old and 4,981 men aged 60-80 years, participating in the ESOPO Study (Epidemiological Study on the Prevalence of Osteoporosis) to estimate the prevalence of the disease in the older Italian population. Low BMD levels were defined in accordance with WHO criteria. For women, estimates indicate 22%, or 3.5 million, have osteoporosis (i.e., BMD > 2.5 standard deviations [SD] below the mean of young women) and 42%, or more than 6 million, have osteopenia (BMD between 1 and 2.5 SD below the mean of young women). For men, the prevalence rates of osteoporosis and osteopenia are 14% (about 1 million) and 34% (about 2 million) respectively. Based on this measurements and the history of fractures, we were able to calculate the OR for fractures in different sites for individuals with osteopenia and osteoporosis versus normal bone density. For hip fractures, for examples, the OR were respectively 10.8 and 28.3 in women and 2.9 and 6.6 in men and they remained highly significant even after adjusting for age. Therefore, most of the older Italians adults with low bone density are women, but the prevalence among men is substantial and their increased risk of fractures should be a major public health concern

Disclosures: ***S. Maggi****, None.*

M324

Association between Baseline Bone Mineral Density and the Risk of a Future Osteoporostic Fracture in Elderly Women: Results from the PERF Study. Y. Z. Bagger, L. B. Tankó, P. Alexandersen, C. Christiansen. Center for Clinical and Basic Research, Ballerup, Denmark.

To investigate the relationship between the first bone mineral density (BMD) at the different skeletal sites, prevalent fractures, age and incidence of osteoporotic fractures, we have followed 5800 Danish postmenopausal women for a mean period of 10 years. BMD at the forearm, spine or hip were assessed at baseline by DEXA. Women were then stratified into normal, osteopenic and osteoporotic BMD groups according to WHO criteria. Vertebral fractures were assessed on digitalized lateral X-rays of the thoracic and lumbar spine. A more than 20% reduction of the vertebral height was considered as a radiological fracture. Non-vertebral fractures were collected by questionnaire. The mean age of women at follow-up was 71±6.5 years old. In this population, 4.1% of women had prevalent vertebral fractures detected at baseline, and 15.3% had reported prevalent non-vertebral fractures before study entry. Thus, 17.6% of women had experienced a new vertebral fracture, and 14.2% had a new non-vertebral fracture during the follow-up period. Women with BMD value of 2.5 SD below the normal mean of young adults at the spine, hip, or forearm were at significantly higher risk of osteoporotic fractures with odds ratios (OR) 2.36, 3.63, and 3.66, respectively (all p values <0.001)after adjustment for age and BMI. For any given T-score of baseline BMD measured at the different skeletal sites, the relative risk of vertebral fracture increased with increasing age. As shown in Figure 1, the risk of vertebral fracture in women between the ages of 50 and 80 years increased by 1.5 to 3.5-fold depending on T-score of BMD at the spine. Similar trends of the increased risk for vertebral fracture with increasing age were also observed at the hip and forearm BMD. Women with a prevalent fracture at baseline had a significantly increased risk for a new vertebral fracture (OR: 2.36, 95% confidence interval: 2.01-2.75, p<0.001) by the end of follow-up. In conclusion, this study further illustrates the utility of bone mass measurement at the different skeletal sites for the prediction of future fracture with slightly higher sensitivity of the peripheral sites. The results also emphasize that patients with a prevalent fracture should be instantly referred for treatment to reduce the risk of further incidences.

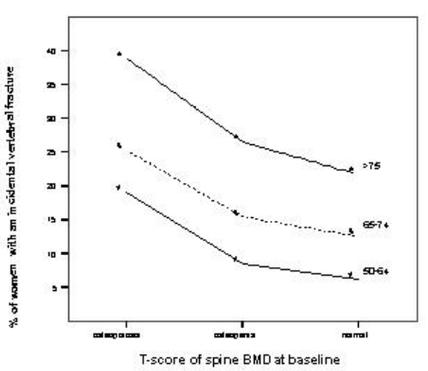

Disclosures: ***Y.Z. Bagger****, None.*

M325

Major Determinants of Bone Mineral Density (BMD) at Multiple Skeletal Sites in Chinese. Y. Hsu[1], C. Chen*[1], Y. Feng[1], H. Terwedow*[1], T. Zhang*[2], D. Wu*[2], G. Tang*[2], Z. Li*[2], X. Hong*[2], B. Wang*[1], M. L. Bouxsein[3], J. Brain*[1], S. Cummings[4], C. Rosen[5], X. Xu[1]. [1]Program for Population Genetics, Harvard School of Public Health, Boston, MA, USA, [2]Institute of Medicine, Anhui Medical University, Anhui, China, [3]Beth Israel Deaconess Medical Center, Boston, MA, USA, [4]San Francisco Coordinating Center, UCSF, San Francisco, CA, USA, [5]Maine Center for Osteoporosis Research and Education, St. Joseph Hospital, Bangor, ME, USA.

The purpose of this study was to identify major environmental determinants of BMDs at different skeletal sites in Chinese population.

We conducted a community-based cross-sectional study among residents of Anhui Province, China. Body mass composition, whole body and total hip BMD were measured by DXA in 3439 men and 3304 women aged 25-65 years from 1843 families. Information on lifestyle, occupation, disease history, physical activity, reproductive characteristics was collected by standardized questionnaires. Generalized estimating equation (GEE) models were performed to access the major determinants of BMD with adjusting for potential confounders and inter-correlation within family members. Among women, 38% are postmenopausal, and 368 (11.2%) and 171 (5.2%) had a T-score less than -2.5 at whole body and total hip, respectively. Men have significantly lower percentage body fat than females (13.2%, 27.9% and 27.4% for men, pre-menopausal and post-menopausal women). The table below showed the amount of variability in BMD explained by age, weight and percentage body fat; and also showed the regression coefficient of other determinants of BMDs with significant level at least in one of the three populations (men, pre- and post-menopausal women). Our findings suggest the percentage body fat, heavy physical activity, tofu and tea consumption as well as the age, gender, body weight and cigarette smoking are important determents of BMD. Supported by NIAMS grant R01 AR045651.

	Men		Pre-menopausal women		Post-menopausal women	
	Whole Body	Hip	Whole Body	Hip	Whole Body	Hip
	R^2	R^2	R^2	R^2	R^2	R^2
Age	2.8%	4.4%	0.01%	0.04%	13.8%	10.0%
Body weight	23.9%	9.8%	16.8%	10.2%	18.7%	15.2%
Body fat %	9.5%	3.2%	8.5%	4.2%	10.0%	7.7%
Age and body weight	24.6%	12.5%	16.8%	10.3%	30.1%	23.4%
Multivariate regression models	β (SE)	β (SE)	β (SE)	β (SE)	β (SE)	β (SE)
Body fat %	-0.078 (0.030)**	-0.189 (0.049)**				
Heavy physical activity	0.008 (0.003)*	0.015 (0.006)**				
Cigarette smoking		-0.014 (0.006)*		-0.048 (0.023)*		
Tea consumption		0.014 (0.005)*				
Tofu consumption			0.009 (0.004)*			

The adjusting variables for regression models included age, BMI, body weight and occupation. *:p < 0.05; **:p < 0.01

Disclosures: ***Y. Hsu****, None.*

M326

BMD and Structure at the Proximal Femur Measured by CT in Men and Women and Blacks and Whites. M. Peacock[1], S. A. Persohn*[2], J. L. Rankin*[2], M. J. Econs[1], S. Hui[1], K. A. Buckwalter*[2]. [1]Medicine, Indiana University, Indianapolis, IN, USA, [2]Radiology, Indiana University, Indianapolis, IN, USA.

Women have higher hip fracture incidence than men and whites have higher hip fracture incidence than blacks. It is considered that these differences are due in part to men having higher BMD than women and blacks higher BMD than whites as measured by DXA. However, DXA measures areal density (aBMD). It does not provide volumetric density (vBMD). Further it cannot measure density of cortical and trabecular bone separately. Thus it is not clear which aspect of bone is responsible for sex and race differences in BMD. Similarly, differences in bone geometry at the hip between blacks and whites are considered to account for part of the difference in incidence of fracture between whites and blacks. However, bone structure from both radiographs and DXA is subject to variability from patient positioning and magnification. To overcome these problems we have used CT of proximal femur to measure and compare vBMD and structure in a sample of women and men.

325 healthy premenopausal white women, age 26-52, and 110 healthy white men, age 20-62, and 70 black men, age 20-60, were studied. Spiral CT of the lower pelvis and upper femur was performed on a multi-slice helical CT machine (MX 8000, QUAD Philips Medical Systems) with a QCT 4 bar calcium hydroxyapatite standard (Image Analysis) placed behind the proximal femur. Images of the upper femur were displayed on an image analysis work station (Philips Medical Systems). Proximal femur geometry including head width, neck width, shaft width and femoral axis length was measured from multiplanar reformatted images created from the axial images. vBMD(G/cm^3) of femoral shaft cortex and femoral neck were calculated from the Hounsfield Units corrected to the standard.

Results show that vBMD G/cm^3 was higher in white women than white men and higher in black men than white men. Women had lower values for femoral geometry. There was no difference in the femoral geometry variables between white and black men.

In conclusion a higher volumetric cortical density at the femur shaft and femur neck accounts for the difference in aBMD between white and black men. Women have a smaller skeleton than men. However, the volumetric cortical density at femur shaft and femur neck was higher in white women than white men.

group	shaft cortex vBMD	neck cortex vBMD	neck cancellous vBMD
white women	1303[a]	731[a]	315[a]
white men	1281	666	302
black men	1321[b]	698[b]	320[b]

[a] p<0.005 white women v white men [b] p<0.001 black men v white men

Disclosures: ***M. Peacock****, None.*

M327

Bone Density Measurement Followed by Osteoporosis Education Leads to Sustained Improvement in Osteoporosis Prevention Habits. C. S. Cowgill, S. Ma*, D. Krueger, S. Zeldin*, N. Binkley. University of Wisconsin, Madison, WI, USA.

Bone mineral density (BMD) measurement identifies individuals at increased risk for osteoporotic fracture. Osteoporosis education may, or may not, be provided when BMD measurements are performed. Studies suggest that BMD measurement may favorably alter health behaviors of women. However, the long-term effects of BMD measurement with subsequent education on skeletal health behaviors are limited. We hypothesized that postmenopausal women would maintain bone preserving activities implemented as a result of BMD measurement and education.

During the months of January-March 2003, free central DXA BMD screening was offered through newspaper advertisement to postmenopausal women not receiving osteoporosis treatment. At that time, 203 women received proximal femur and lumbar spine BMD measurement utilizing GE Lunar DPX-IQ or Prodigy densitometers. All participants immediately discussed their test results with one of four physicians or a nurse practitioner specializing in osteoporosis and received counseling regarding lifestyle changes or appropriate treatment options that might maintain or improve bone health. Three months later, women who agreed to be contacted were mailed a survey that contained 25 questions about osteoporosis-related lifestyle and overall health habits before and after their BMD test. Subsequently, one year after their initial BMD measurement, those 185 participants who responded to the initial questionnaire were mailed a six-question survey that asked what lifestyle changes had been maintained. Results from 130 completed surveys received from 160 women indicate that lifestyle changes had been maintained by 92% of respondents. Specific interventions included increasing calcium intake (58%), increasing exercise (53%), using handrails to go up and down stairs (49%) increasing vitamin D (48%) and taking safety precautions at home (32%).

In conclusion, bone density screening immediately followed by osteoporosis education and individualized counseling is effective in motivating 92% of postmenopausal women to implement and maintain lifestyle changes to preserve their skeletal health. Postmenopausal women can be positively influenced by BMD testing with immediate individualized counseling.

Disclosures: ***C.S. Cowgill****, None.*

M328

Food Group Intake and Bone Mineral Content (BMC) during Growth from Childhood to Adolescence. H. Vatanparast*[1], S. Whiting[1], A. Baxter-Jones*[2], R. Faulkner[2], D. Bailey[2]. [1]College of Pharmacy and Nutrition, University of Saskatchewan, Saskatoon, SK, Canada, [2]College of Kinesiology, University of Saskatchewan, Saskatoon, SK, Canada.

Nutrition is an important modifiable factor in the development and maintenance of bone mass particularly during peak bone mass development. The purpose of this study was to determine the role of consumption of different levels of food groups on the total body-bone mineral content (TB-BMC) accrual in boys and girls after the age of peak height velocity (PHV). Six-year longitudinal data were used from 85 boys and 67 girls (8-20 y). Biological age was defined by the age of PHV. Nutritional intake was assessed via serial 24-hour recalls. Food group intakes were classified into three levels, mostly as low, adequate and high. TB-BMC was the indicator of bone mass. The majority of subjects consumed an adequate level of milk product with more boys at the highest level than girls. In contrast, most boys and girls consumed vegetables and fruit less than the recommended amounts. As age increased, TB-BMC increased with higher magnitude in boys than girls. There was a significant difference in TB-BMC between very low and adequate levels of vegetables and fruit intake in girls (P<0.05), which was not significant after adjusting for height. Our data could not demonstrate the effect of milk product intake on bone mass during adolescence.However our subjects had an appropriate intake of milk products and consequently substantial calcium accrual during the critical years of maturity and their bone accrual data have been used as the basis for calculating calcium requirements of adolescents. Therefore, in this cohort, we are not surprised to find a lack of the effect of calcium intake on bone accrual. The data on the effect of vegetables and fruit intake on bone mass in girls should encourage continuing research on this topic.

Disclosures: ***H. Vatanparast****, None.*

M329

Dietary Influences on Bone Mineral Density in Chinese Men and Women. P. A. Zalloua*[1], Y. Hsu*[2], H. Terwedow*[2], T. Zang*[3], D. Wu*[3], G. Tang*[3], Z. Li*[3], X. Hong*[3], B. Wang*[2], M. Bouxsein*[4], J. Brain*[5], S. Cummings*[6], C. Rosen*[7], X. Xu*[2]. [1]Internal Medicine, American University of Beirut, Beirut, Lebanon, [2]Harvard School of Public Health, Boston, MA, USA, [3]Anhui Medical University, Anhui, China, [4]Beth Israel Deaconess Medical Center, Boston, MA, USA, [5]Environmental Health, Harvard School of Public Health, Boston, MA, USA, [6]San Francisco Coordinating Center, UCSF, San Francisco, CA, USA, [7]Maine Center for Osteoporosis Research and Education, St Joseph Hospital, Bangor, ME, USA.

Diet choices and nutrition have proven in the last decade to be one of the major modulators of BMD in both men and women. The objectives of this study were to explore the possible environmental determinants, specifically dietary habits, of BMD by using multiple regression models in Chinese women and men living in a rural area. BMDs were measured at the hip and total body in 2127 men and 2673 women, aged 35-65. Dietary and supplement intakes were assessed by a food-frequency questionnaire. Another questionnaire was used to collect information on the subject's age, disease history, smoking, alcohol consumption, diet, physical activity as well as women's menstrual status and reproductive history. Regression models were used to assess the relationships among dietary variables and BMD, after adjusting for age, BMI, weight, occupation, smoking status and alcohol consumption. Milk consumption did not show a significant effect on BMD. Seafood consumption was significantly associated with greater BMD in both sexes (p= 0.006 for men, p=0.001 for women). Fruit consumption was also associated with higher BMD (p=0.005). High vegetables consumption, however, did not seem to positively impact BMD and, on the contrary, showed a significant association with lower BMD in pre-perimenopausal women (p=0.001). Greater consumption of preserved food was found to be associated with lower BMD in pre- and postmenopausal women (p=0.005). Finally, there was no significant association between vitamin D supplementation and greater BMD, but this lack of association may be due to the relatively small number (1.5%) of participants who took Vitamin D supplementation. Our results highlight the importance of several dietary variables as significant determinants of BMD. These results emphasize the role of dietary intake in general and show that specific foods such as fruits and seafood can positively impact BMD. This study with its large population size proves highly beneficial in identifying preventive measures, as well as some risk factors, involved in bone loss and osteoporosis. Supported by NIAMS grant R01 AR045651.

Disclosures: ***P.A. Zalloua****, None.*

M330

Association of Apolipoprotein E Genotypes with Bone Mineral Density and Bone Loss in Early Postmenopausal Scottish Women: No Evidence of Gene Nutrient Interaction with Dietary Vitamin K or Fat. H. M. Macdonald, F. E. McGuigan*, S. H. Ralston, D. M. Reid. Medicine and Therapeutics, University of Aberdeen, Aberdeen, United Kingdom.

We previously found an association between APOE polymorphism and bone mineral density (BMD) in women from the Aberdeen Prospective Osteoporosis Screening Study (APOSS) with carriers of E4 having lower BMD and greater bone loss compared to carriers of E2. Whether the effect of APOE is mediated through vitamin K transport, interaction with dietary fat or is independent is unknown. Gene nutrient interactions have been found between polyunsaturated fatty acids (PUFA) and APOA1 and between alcohol and APOE genotype on lipoprotein levels in subjects from the US.

A total of 3883 women from APOSS underwent bone densitometry in 1990-3 (mean ± SD

age: 48.5 ± 2.4 y) and again 6.3 ± 0.9 y later. 3239 women completed a food frequency questionnaire at the 2nd visit of whom 2481 were genotyped for APOE by DNA sequencing. Allele frequencies were: E3 78.1%; E4 14.5%; E2 7.4%. Genotypes in Hardy Weinberg equilibrium were as follows: E3/E3 1517 (61.1%), E3/E4 562 (22.7%), E2/E3 280 (11.3%), E2/E4 59 (2.4%), E4/E4 48 (1.9%), E2/E2 15 (0.6%). Subjects with E2/E4 were excluded for this analysis. We found weak positive associations between vitamin K intake and BMD at hip (FN) and spine (LS) and between alcohol intake, BMD and BMD change. There was a non-significant negative trend relating PUFA and bone loss. We found no evidence of nutrient gene interaction for APOE with either PUFA or vitamin K. The trend for BMD increasing (and bone loss decreasing) with APOE alleles 34/44 <33< 22/23 was confined to alcohol drinkers and was significant after adjustment for confounders (age, weight, height, smoking, menopausal status and HRT use) for bone loss (table). Median alcohol intake for drinkers was 7.3 g/d (range 1.2 to 79.4 g/d). We did not observe a significant interaction between alcohol consumed and APOE genotype on BMD.

APOE	Drinkers (n 1779)			Non-drinkers (n 642)		
	n	FN BMD (g/cm2)	FN BMD change (%/y)	n	FN BMD (g/cm2)	FN BMD change (%/y)
22/23	212	0.858 ± 0.124	-0.57 ±1.06	83	0.821 ± 0.131	-0.79 ± 1.01
33	1117	0.840 ± 0.121	-0.73 ±1.10	396	0.827 ± 0.121	-0.83 ± 1.10
34/44	448	0.833 ± 0.121	-0.81 ±1.00	163	0.823 ± 0.126	-0.81 ± 0.94
P		0.055	0.029		0.883	0.942
P adjusted		0.072	0.023		0.781	0.815

Characteristics of non-drinkers may differ from alcohol consumers, which may partly explain the differences in results. Since the effect size of nutrient variables on BMD is small, the power to detect gene nutrient interaction is limited. However, these data suggest it is unlikely that the effect of APOE genotype on BMD is influenced by intake of vitamin K or fat in healthy early postmenopausal women. The influence of alcohol requires further research.

Disclosures: ***H.M. Macdonald****, None.*

M331

Vitamin D Insufficiency in Canadian Aboriginal Women: The First Nations Bone Health Study. W. D. Leslie[1], J. Krahn*[1], H. A. Weiler*[2], C. J. Metge*[3], C. K. Yuen[1], M. Doupe*[1], E. A. Salamon[4], P. Wood Steiman*[5], J. D. O'Neil*[1], C. R. Greenberg*[1], L. M. Lix*[1], L. L. Roos*[1], A. Tenenhouse[6]. [1]Faculty of Medicine, University of Manitoba, Winnipeg, MB, Canada, [2]Human Nutritional Sciences, University of Manitoba, Winnipeg, MB, Canada, [3]Faculty of Pharmacy, University of Manitoba, Winnipeg, MB, Canada, [4]Department of Medicine, University of Manitoba, Winnipeg, MB, Canada, [5]Assembly of Manitoba Chiefs, Winnipeg, MB, Canada, [6]Department of Medicine, McGill University, Montreal, PQ, Canada.

Canadian Aboriginal women are at increased fracture risk compared with the general population (JBMR 18:S151, 2003), but the factors related to this are unknown. Obesity, insulin resistance and type 2 diabetes are also endemic in this population. The First Nations Bone Health Study (FNBHS) recruited a random age-stratified (25-39, 40-59, and 60-75) sample of Aboriginal and age-matched White women. 364 subjects underwent fasting assessments of 25OH-vitamin D (25OHD), PTH, total calcium (albumin corrected), CTX, and osteocalcin. Measures of glucose metabolism were also evaluated including serum glucose, insulin, C-peptide, IGFBP-1, IGFBP-3, and HbAlc. Aboriginal women had lower 25OHD values and higher PTH; 25OHD and PTH were negatively correlated (r=.24, P<.001). Markers of bone resorption (osteocalcin) and formation (CTX) were similar for Aboriginal and White women, but correlates of insulin resistance were all greater in Aboriginal women. 25OHD was positively correlated with IGFBP-1 (r=.24, P<.001) and IGFBP-3 (r=.17, P=.003); negatively correlated with BMI (r=-.24, P<.001), insulin (r=-.18, P=.002); C-peptide (r=-.26, P<.001), and HbAlc (r=-.12, P=.039). ANCOVA showed that ethnicity differences in 25OHD persisted after adjustment for BMI and markers of glucose metabolism. In summary, our findings show reduced vitamin D levels in Canadian Aboriginal women. Greater BMI and markers of insulin resistance (also more common in Aboriginal women) were associated with lower 25OHD levels as previously reported (JCEM 2004;89:1196), but this did not explain the ethnic difference. Further work is needed to understand the nature of the interrelationship between vitamin D metabolism and glycemic control in this population.

	Aboriginal(N=185)	White (N=179)	P
25OH-Vit D (mmol/L)	52.8±24.8	72.8±31.8	0.000001
PTH (ng/L)	57.0±25.1	46.5±21.4	0.000007
Calcium corrected (mmol/L)	2.24±0.20	2.27±0.19	0.14
Osteocalcin(ng/mL)	23.6±10.5	25.6±11.6	0.056
CTX (ng/mL)	0.31±0.18	0.31±0.17	>0.2
HbAlc (%)	6.4±1.8	5.9±1.0	0.00012
BMI (kg/m^2)	30.5±6.2	28.7±6.9	0.0078

Disclosures: ***W.D. Leslie****, None.*

M332

Relationship between Vitamin D Status and Plasma Parathyroid Hormone Level in Healthy Japanese Women; Evaluation of Age-related Vitamin D Requirement. N. Tsugawa*[1], M. Shiraki*[2], K. Tanaka*[3], T. Okano[1]. [1]Department of Hygienic Sciences, Kobe Pharmaceutical University, Kobe, Japan, [2]Research Institute and Practice for Involutional Diseases, Nagano, Japan, [3]Department of Nutrition, Kyoto Women's University, Kyoto, Japan.

Vitamin D is an important factor for prevention of osteoporosis and bone fracture. Subclinical vitamin D insufficiency is enhanced risk of osteoporotic fracture. Vitamin D insufficiency is characterized by mild secondary hyperparathyroidism and thus requirement for vitamin D is thought to vary with age. In the present study, in order to evaluate age-related vitamin D requirement, we measured plasma levels of 25-hydroxyvitamin D (25-OH-D) and PTH in 432 healthy Japanese women, aged 30-88 yr. Serum 25-OH-D was measured by RIA kit (DiaSorin Inc.). Serum PTH was measured by 2 immunoradiometric assays, intact PTH (1-84 and 7-84) assay and the new CAP (1-84) assay (Scantibodies Laboratory, Inc.). Data were classified into three age categories; 30-49 yr, 50-69 yr, and 70 and older than 70 yr. As the results, no correlation was observed between age and 25-OH-D level. CAP PTH and intact PTH levels correlated positively with age (r^2=0.010, p=0.0351 or r^2=0.011, p=0.024, respectively). Plasma 25-OH-D levels correlated negatively with CAP PTH (r^2=0.035, p<0.0001) and intact PTH (r^2=0.034, p<0.0001) levels in every stratified age group. Data were further classified into five subgroups according to plasma 25-OH-D level; less than 25, 25 to <37.5, 37.5 to <50, 50 to <75, 75 and more than 75 nmol/L. When plasma 25-OH-D levels were lower than 50 nmol/L, PTH levels increased significantly in any group of ages. The result suggests that 50 nmol/L of 25-OH-D is thought to be the cut-off value for vitamin D insufficiency in elderly women. PTH levels of 50-69 yr group and 70 and older than 70 yr group were significantly higher than that of the youngest group even in more than 50 nmol/L of 25-OH-D. These results suggest that 50 nmol/L of 25-OH-D is thought to be vitamin D sufficient for women younger than 50 yr, but not for women elder than 50 yr to prevent elevation of plasma PTH level, resulting in bone loss.
We conclude that Japanese elderly women might require more vitamin D and calcium intakes from diets or supplements.

Disclosures: ***N. Tsugawa****, None.*

M333

Impact of Calcium Vitamin D Supplementation on Cardiovascular Parameters in Osteoporosis. G. Rajzbaum*[1], C. Chaignaud*[2], P. Bréville*[1], F. Roux*[1], M. Chauffert*[3], Y. Bézie*[2]. [1]Rheumatology, Fondation hôpital Saint-Joseph, Paris, France, [2]Pharmacie, Fondation hôpital Saint-Joseph, Paris, France, [3]Biochimie, Fondation hôpital Saint-Joseph, Paris, France.

High doses of vitamin D3, calcium and nicotine induce severe vascular calcifications in rats. Daily supplementation with calcium and vitamin D is often prescribed to osteoporotic patients to prevent fractures. Nevertheless this treatment, as in experimental pharmacology, might also have an impact on the occurrence of vascular calcification. Our aim was to investigate association of calcium vitamin D supplementation with abdominal calcifications in osteoporotic postmenopausal women.
We studied 317 post menopausal consecutive outpatients consulting for osteoporosis evaluation in a French general hospital. Presence of abdominal aortic calcifications was assessed on profile lumbar X-rays. Were noted osseous and cardiovascular parameters : age of menopause, calcium intake, osteoporotic fractures, osteodensitometry, phosphocalcic and bone turnover biochemical parameters, systolic, mean and pulse pressure, tobacco, hypercholesterolemia, previous and current treatments.
Demographic characteristics of women treated by calcium vitamin D (n=109) was not different from the controls (n=218). The treated population was characterized by a lower lumbar and femoral T score (respectively -2.51± 0.14 vs -2.05± 0.10 SD, p<0.05, and -2.17± 0.09 vs -1.86± 0.07 SD, p<0.05) associated with a higher 25OHD3 plasmatic concentration (20.5± 0.8 vs 13.1± 0.6 µg/L ; p<0.00001) and calciuria (0.46± 0.03 vs 0.36± 0.02 mmol/mmol cr ; p=0.003). The percentage of patients with abdominal aortic calcifications was identical between the two groups (45.7± 7.3 vs 53.6± 5.5 %). Nevertheless, patients treated with calcium and vitamin D were characterised by a lower aortic stiffness compared with non supplemented patients as indicated by their lower pulse pressure (51.7± 1.5 vs 55.2± 1.1 mm Hg, p=0.05).
Our results indicate that supplementation of calcium and vitamin D in osteoporotic patients is not associated with aortic calcifications, suggesting that toxic effects shown in experimental pharmacology are not relevant at therapeutic dosages in women. The lower pulse pressure observed with calcium vitamin D suggests a beneficial impact on arterial stiffness, which is an independent predictor of cardiovascular mortality in hypertensive patients.

Disclosures: ***G. Rajzbaum****, None.*

M334

Is Diversity More Important Than Quantity of Physical Activity In Maintaining The Fracture Resistance of The Proximal Femur? S. Kaptoge, N. Dalzell*, R. W. Jakes*, N. J. Wareham*, K. T. Khaw*, N. Loveridge, J. Reeve. Public Health & Medicine, Cambridge University, Cambridge, United Kingdom.

Hip fractures occur as a direct consequence of cortical bone instability. Biomechanical principles suggest that larger bones would have greater bending resistance as measured by the section modulus (Z), which increases in direct proportion to the bone's diameter. However, structural stability, least for the lateral/superior cortex, and measured as critical buckling stress is compromised if the bone's cortices are either thinner or located further away (d-lat) from the section's centre of gravity. We hypothesised that aging, anthropometry and physical activity may conserve Z through distribution of bone tissue, to result in an optimal placement of the bone's centre of gravity for Z rather than cortical stability.

Hip structural analysis software was used to derive structural measurements from DXA scans on 1,359 men and women in the EPIC-Norfolk population-based prospective study. Up to 4 repeat DXA scans were done in 8 years of follow-up: 2 scans(n=954, 2.9y); 3 scans(n=722, 5.4y) and 4 scans(n=78, 7.5y). Weight, height and activities of daily living (ADL) were assessed on each occasion. A standard physical activity and lifestyle questionnaire was administered at baseline. The distance from the lateral bone surface to the centroid was measured on three narrow cross-sections; narrow neck(NN), intertrochanter(IT) and shaft(S). A linear mixed model was used to assess associations with predictors.

There were significant differences in the distance to the centroid in the 3 regions (greatest at IT and smallest at S, P<0.0001). Men had greater d-lat than women (0.075cm difference, P<0.0001). Aging was associated with medial shifting of the centroid that was greater in women NN (F&M=0.010cm/y), IT (F=0.011cm/y, M=0.005cm/y) and S (F=0.003cm/y, M=0.001cm/y) P<0.0001. Increasing weight and height were associated with greater d-lat (P<0.0001). Among physical activity variables, lifetime activity (P=0.036), walking/cycling for more than 1hr/day (P=0.001), weekly time spent on weight bearing activity (P=0.009), and FEV1 (P=0.016) were associated with higher d-lat. Interestingly after adjusting for these variables, ADL scores as a measure of current activity and weekly time spent on low impact activities were associated with shorter d-lat (P<0.019). We conclude that diversity of physical activities may be superior to stereotypic walking activity in maintaining proximal femur structural stability.

Disclosures: ***S. Kaptoge****, None.*

M335

Dietary Factors and Physical Activity in Low-Income Postmenopausal Osteoporotic Women. P. S. Genaro*[1], G. A. P. Pereira*[1], M. M. Pinheiro*[2], V. L. Szjenfeld[2], L. A. Martini[1]. [1]Nutrition, Sao Paulo University, Sao Paulo, Brazil, [2]Rheumatology, UNIFESP, Sao Paulo, Brazil.

Osteoporosis and related fractures represent major public health problem that are expected to increase dramatically as the population ages. Dietary risk factors and physical activity are particularly important. In a low-income population diet and physical activity could be inadequate since there is a tendency to obesity with over consumption of carbohydrates and fats, low mineral and vitamin intakes and absence of physical activity. The aim of the present study was evaluate nutrient intakes, physical activity and body composition in osteoporotic women, before nutritional advice and drug therapy. Twenty-four postmenopausal women, mean age (64 ± 7 years old) and BMI (26 ± 3 Kg/m²) assisted at São Paulo Hospital osteoporosis outpatients clinic were invited to participate. Body composition analysis was performed in all participants using DEXA technique (Lunar DPx). Diet and physical activity was assessed using three days dietary records and the Beacke questionnaire, respectively. Bone metabolism was evaluated by serum and urinary calcium. Results are presented as mean ± SD. Energy intake was 1293 ± 487 Kcal/day. Protein, total fat, carbohydrate and phosphorus intakes were 1.09 ± 0.5 g/Kg/day, 35 ± 16 g/day, 185 ± 76 and 901 ± 76 mg/day, respectively, all in accordance with proposed DRI's. However, mean calcium intake (663 ± 320 mg/day) was significantly lower than the value for this age group (1200 mg/day). Eighty-four percent of the participants had low calcium intake according to the Food and Nutrition Board (1997). Serum ionized calcium (1.19±0.10 mg/dl), total calcium (9.06±0.42) and calcium/creatinine ratio in the urine (215±128 mg/24hs) were normal. Body composition analysis demonstrated that 83% of the participants were classified as obese (mean body fat 38.0±7.8 % and mean lean mass 32±4 Kg). Most of the patients had low physical activity levels. The results demonstrate high prevalence of obesity, low calcium intake and sedentary pattern in our population. This study emphasizes the importance of proper nutritional and physical evaluation and advice in patients with osteoporosis in order to optimize adjuvant interventions to their pharmacological management.

Disclosures: ***P.S. Genaro****, None.*

M336

Fracture Prevalence and Treatment with Bone-Sparing Agents: Are there Urban-Rural Differences? A Population-Based Study in Ontario, Canada. S. M. Cadarette, S. B. Jaglal, G. A. Hawker. University of Toronto, Toronto, ON, Canada.

A census of persons aged 55 or more years residing in two regions of Ontario, Canada (East York, a borough of Toronto, and Oxford County), was completed between 1995 and 1998, response rate=77%. Information including self-reported physician diagnosed osteoporosis, height loss, fracture history and treatment by a physician with bone-sparing agents (calcium, vitamin D, etidronate, fluoride and estrogen) were ascertained. The objectives of this study were to estimate the prevalence of self-reported osteoporotic fractures (arm, hip, rib, pelvis or vertebrae since age 40 years in women or 50 years in men) and the use of bone-sparing agents, and to examine if region of residence is associated with fracture or treatment prevalence. Region was coded by record linkage of residential postal codes to 1996 Canadian Census data into 4 groups: East York (urban core), and Oxford County subdivided into: urban core, small urban and rural. Respondents were excluded if they resided outside the regions of interest or were missing fracture data (5%). A total of 26,839 persons (15,541 women) were studied, of whom half resided in East York. Among those living in Oxford County, 30% lived in a rural area. Nearly 3 times as many women as men reported having had an osteoporotic fracture (14% vs. 5%), with 31% and 8% of these women and men respectively taking bone-sparing agents. Controlling for age, a diagnosis of osteoporosis, number of osteoporotic fractures and height loss, women residing in East York were more likely (OR=1.2, 95%CI=1.0-1.4) to be taking a bone-sparing agent other than estrogen, but less likely to be taking estrogen (OR=0.8, 95%CI=0.7-0.9) compared to those living in rural areas. No regional differences were observed in fracture prevalence, treatment amongst those with an osteoporotic fracture, or use of a bone-sparing agent among men. Further research should examine if regional differences in osteoporosis prevention continue to exist among women in Ontario, and if applicable, to separate physician practice patterns from individual characteristics, such as willingness to begin treatment with bone-sparing agents.

Disclosures: ***S.M. Cadarette****, None.*

M337

Elderly Women Whose Mothers Lived to Extreme Old Age Have a Lower Risk of Hip and Non-spine Fractures than Women with Shorter-Lived Mothers. P. M. Cawthon[1], S. R. Cummings[1], T. L. Blackwell*[1], J. Zmuda*[2]. [1]Research Institute, California Pacific Medical Center, San Francisco, CA, USA, [2]University of Pittsburgh, Pittsburgh, PA, USA.

Background: We have previously shown that older women (age_65) whose parents survived to extreme old age have a survival advantage compared to women with shorter-lived parents, among participants in the Study of Osteoporotic Fractures (SOF). Additionally, these women appear to have better health overall.

Research Question: In the current analyses, we tested the hypothesis that women with long-lived parents (age ≥90 or age ≥95) experience fewer non-spine and hip fractures, and report fewer falls, than women with shorter-lived parents.

Methods: SOF women with parental death information and DXA data (N=7,862) were included in these analyses, of whom 1299 (16.6%) had mothers live past 90; 398 (5.2%) had mothers live past 95; 639 (8.1%) had fathers live past 90; and 168 (2.1%) had fathers live past 95 years of age. Fractures were adjudicated by x-ray report. Proportional hazards models were used for all analyses. Multivariate results were adjusted for age, bmd, smoking and years of education.

Results: Mothers who lived to ≥90 or ≥95 years of age had a small but significantly decreased risk of incident hip and non-spine fractures (table), compared to women whose mothers did not live as long, in age and multivariate adjusted models. In contrast, father's age at death was not significantly related to risk of fracture in age- or multi-adjusted models. Parental age at death was not significantly related to falling during follow-up (results not shown).

Conclusion: Our results suggest that there is a familial resemblance between maternal longevity and fracture resistance in women. Older maternal age at death is associated with not only extended, but also healthier survival.

Risk of Non-Spine, Hip Fracture by Parental Age at Death

Hazard Ratios (95% CI)	Non-Spine Fracture		Hip Fracture	
Parental Age at Death	Age-Adjusted	Multi-Adjusted	Age-Adjusted	Multi-Adjusted
Mother ≥ 90	**0.91 (0.83, .99)**	**0.89 (0.81, 0.99)**	**0.83 (0.69, 0.99)**	**0.77 (0.64, 0.94)**
Father ≥ 90	0.95 (0.84, 1.08)	0.93 (0.81, 1.07)	1.02 (0.82, 1.28)	1.03 (0.81, 1.31)
Mother ≥ 95	**0.83 (0.70, 0.97)**	**0.8 (0.67, 0.96)**	**0.69 (0.50, 0.95)**	**0.7 (0.49, 0.99)**
Father ≥ 95	1.11 (0.88, 1.39)	1.16 (0.91, 1.48)	0.71 (0.44, 1.15)	0.68 (0.4, 1.15)

Disclosures: ***P.M. Cawthon****, None.*

M338

Reduced Fracture Risk in Current Users of Thiazide Diuretics. L. Rejnmark, P. Vestergaard, L. Mosekilde. Dept of endocrinology and metabolism C, Aarhus Amtssygehus, Aarhus, Denmark.

Thiazide diuretics (TD) reduce the renal calcium excretion and may increase bone mineral density. A reduced fracture risk in subjects treated with TD has been reported in some but not all studies. The aim of the present study was to assess fracture risk in users of TD. Design: a nation-wide population-based pharmaco-epidemiological case-control study with any fracture in year 2000 as outcome and use of TD during the previous five years as exposure variable. Individual use of TD was derived from the Danish National Pharmacological Database and related to fracture data from the National Hospital Discharge Register. These data were combined with information on use of other drugs, social status, working status, income (from tax authorities), educational status (National Bureau of Statistics), contacts to general practitioners, practising specialists (The National Health Register), and comorbidity (The Charlson Index). 64,699 cases aged 40 years or more that sustained a fracture during year 2000 were compared to 194,111 age- and gender-matched controls. TD was used by 15,316 (23.7%) of the cases and by 42,647 (22.0%) of the controls (crude odds ratios (OR), 1.10; 95%CI, 1.08-1.12). However, after adjustment for potential confounders, ever use of TD was associated with a 13% (95%CI, 10%-15%) reduced risk of any fracture and a 17% (95%CI, 12%-21%) reduced risk of a forearm fracture. In current users of TD who had redeemed prescriptions for more than 1000 defined daily dosages (DDD), risk of any fracture was reduced by 29% (95%CI, 12%-42%) and risk of hip fracture was reduced by 39% (95%CI, 9%-59%). Conversely, use of less than 1000 DDD was associated with an increased fracture risk in current users. In former users, fracture risk was increased for all dosages groups. No important differ-

ences were found between men and women in either the crude or the adjusted analysis upon age- and gender-stratification. Thus, current use of TD is associated with a significantly reduced fracture risk. The reason for the reduced fracture risk in current long-term users needs further elucidation. Large long term randomized controlled studies on effects of TD on fracture risk are warranted.

Disclosures: ***L. Rejnmark****, None.*

M339

Profile of Care for Hip Fracture Patients In Italy. S. Maggi*, D. Bianchi*, P. Gallina*, C. Marzari*, M. Noale*, G. Crepaldi. Aging, Italian Research Council, Padua, Italy.

Hip fracture is one of the most important causes of death and disability among older people. In spite of the increasing interest at international level, due to the clinical and functional sequelae, in Italy only limited epidemiological data are available about the incidence of hip fractures. These data vary widely across the Italian regions.

Primary aim of the present study was to ascertain the profile of hospital care for hip fractures in different geographic areas of Italy. The secondary

objectives were to determine the availability of access to community services in different regions and to evaluate the completeness and the accuracy of coding of hip fractures using ICD9 codes. The centers included in the study were in Veneto (Padova), Emilia Romagna (Parma), Liguria (Genova), Campania (Napoli), and Basilicata (Matera). The same general approach to data collection was used in all areas. Patients with pathological fractures were excluded from the study, as well as multiple hospital discharges for the same event. The frequency of hip fractures ranges from 65-75/10.000 individuals aged 65+. The accuracy of hip fractures coding using ICD9 codes is high, and the coding mistakes irrelevant. The profile of care and the availability of community services present a high variability among the different geographic areas of Italy. In particular, the timing of surgery after hospital admission varies from 2,2 ± 2,4 days in Parma to 6,2 ± 4,0 days in Napoli (mean ± standard deviation) and the percentage of patients undergoing surgery varies from 45% in Matera to about 90% in Padova and Parma. 80% of patients are discharged at home in Napoli, versus 40% in Genova, while only 1% is istitutionalized in Parma and Matera, versus 19% in Genova.

These results suggest the need for creating a national registry for hip fractures to collect data from different areas and to build the basis for standardized care in Italy.

Disclosures: ***S. Maggi****, None.*

M340

Osteoporosis Is Significantly Underdiagnosed and Undertreated - a Nationwide Study from Denmark. P. Vestergaard, L. Rejnmark, L. Mosekilde. The Osteoporosis Clinic, Aarhus Amtssygehus, Aarhus, Denmark.

Aim: To assess the number of patients actually diagnosed with osteoporosis in Denmark with the number expected to have osteoporosis based on normative BMD data. The number of subjects with osteoporotic fractures was also assessed.

Subjects and methods: All patients diagnosed with osteoporosis and/or with osteoporotic fractures between 1995 and 1999 were retrieved from the National Hospital Discharge Register, which covers all in- and outpatient contacts to the hospitals. Based on normative values for BMD in Danish subjects and the NHANES-III data, the expected number of subjects aged 50 years or more with osteoporosis according to the WHO definition (T-score <-2.5) was calculated. The population in 1999 was 5.3 million.

Results: The estimated prevalence of osteoporosis (T-score <-2.5) was 30.7% in the hip and 27.5% in the lumbar spine (If the two sites were combined 40.8% had a T-score <-2.5 in either one or both sites) among women aged ≥50 years and 16.0% in the hip and 4.3% in the spine (combined 17.7%) among men aged ≥50 years based on normative Danish BMD values. Using the NHANES III data only 16.4%of women and 3.6% of men were expected to have a T-score <-2.5 in the hip. The expected annual incidence was 58,658/mio/yr in women ≥50 years and 23,648/mio/yr in men ≥50 years. However, the observed incidence was only 4,823 and 862/mio/yr respectively (8.2 and 3.6% of the expected). In 1999, a total of 34,691 hip, spine and forearm fractures were reported in subjects ≥50 years, and of these 18,566 were potentially attributable to osteoporosis (14,240 fractures in women and 4,326 in men equaling an incidence of 14,976 and 5,297/mio/yr, i.e. also much higher than the number diagnosed with osteoporosis). Only 0.3% of men ≥50 years were receiving a bisphosphonate while 2.2% of women received a bisphosphonate or raloxifene. Among women ≥50 years 27.7% received hormone replacement therapy.Conclusions: Osteoporotic fractures are rather frequent in Denmark, but the diagnosis of osteoporosis is rarely used. It seems that osteoporosis is markedly underdiagnosed and undertreated in Denmark as probably also elsewhere. This may have significant implications for the prevention of osteoporotic fractures.

Disclosures: ***P. Vestergaard****, None.*

M341

Fracture Incidence in the City of Glasgow: Analysis by Age, Sex and Socioeconomic Deprivation. S. J. Gallacher[1], I. Baxter*[2], A. McLellan[3], C. McQuillian*[1], M. Fraser*[3], A. Gallagher*[1], F. Lovell*[4]. [1]Medical Unit, Southern General Hospital, Glasgow, United Kingdom, [2]Department of Public Health, Greater Glasgow Health Board, Glasgow, United Kingdom, [3]Department of Medicine and Therapeutics, Western Infirmary, Glasgow, United Kingdom, [4]Medical Unit, Royal Infirmary, Glasgow, United Kingdom.

The Fracture Liaison Service assesses all patients over the age of 50 presenting with an incident fracture at any site for osteoporosis risk. This service uses Nurse Specialists to link with Orthopaedic Services to identify and assess all such patients (using DXA scanning). This service covers the whole of the City of Glasgow. Glasgow has a relatively stable population of approximately 1 million people. Since the population is relatively stable and since the whole population is covered a denominator is available in order to define annual fracture incidence. This work describes all fracture incidence over the calendar year 2002 by age and sex and further describes the effects of socioeconomic deprivation on this fracture incidence. A total of 4659 fractures presented through 2002. Crude fracture rates as a percentage of the population by age group and sex are presented below.

Age	50-54	55-59	60-64	65-69	70-74	75-79	80-84	85+
Male	0.65	0.81	0.87	0.83	1.02	1.37	1.61	2.62
Female	0.92	1.44	1.73	1.92	2.54	2.87	3.91	5.03

From the above it can be seen that around 1% females age 50-54 present in 1 year with fracture compared with over 5% at age 85+. As expected incidence rates for males are lower but also increase with age - especially over age 75. Socioeconomic deprivation was then assessed for this population using UK National Census data. This allocates individuals into one of seven categories (DepCat) with DepCat 1 being the most affluent and DepCat 7 the most deprived populations. These were then grouped 1&2 (least deprived), 3,4,5 (intermediate) and 6,7 (most deprived). The effect of deprivation on fracture incidence is shown below.

Age	50-54	55-59	60-64	65-69	70-74	75-79	80-84	85+
Least Deprived	0.41	0.79	0.98	1.02	1.50	1.78	2.63	4.02
Intermediate	0.74	1.00	1.24	1.41	1.80	2.16	3.14	3.55
Most Deprived	1.02	1.39	1.53	1.62	2.15	2.61	3.42	5.28

This table demonstrates the strong relationship between deprivation and fracture incidence. This relationship was especially strong in males with fracture incidence being especially high in the most deprived group (data not shown)

Disclosures: ***S.J. Gallacher****, None.*

M342

Prior Foot Fracture, Current Foot Pain and Physical Function in Men and Women of the Framingham Foot Study. M. T. Hannan[1], K. E. Broe[1], M. Rivinus*[1], M. Hogan*[1], J. Murabito*[2]. [1]Hebrew Rehabilitation Center for Aged, Boston, MA, USA, [2]NHLBI Framingham Study, Framingham, MA, USA.

Despite the relatively common occurrence of foot fractures, it is not known whether a prior foot fracture (FootFx) affects physical function and foot pain. Thus, we examined the cross-sectional association of prior foot fracture with physical function and foot pain in a population-based sample. The Framingham Foot Study (2002-2006) queried participants about previous toe, ankle or foot fracture, current foot pain (e.g., present on most days in a month), and self-reported physical function (limitations using the Nagi items of walking, standing, and stair-climbing, and timed gait and chair stands). Body mass index (BMI) was calculated from measured weight and height. We used logistic regression to examine the relation of prior FootFx with current foot pain or physical function adjusting for sex, age and BMI, producing odds ratios (OR) and 95% confidence intervals (CI).

Participants included 568 men and 750 women of the Framingham Foot Study who were ambulatory and cognitively intact. Mean (±sd) age was 68y ±12 (range 40-100), and mean BMI was 28 kg/m^2 (range 17-52). FootFx was reported by 391 of the 1318 subjects (28% of men, 31% of women). 48% of those with FootFx reported that shoes hurt their feet (39% of those without FootFx, p=0.002). When shown a picture of the foot, participants with FootFx more frequently reported pain at the toes, hindfoot, forefoot, and arch than those without fracture (table). Presence of heel pain did not differ for those with and without FootFx. There were no differences between the two groups in walking or stair-climbing limitations of (p>0.42), or timed gait and chair stand items (p>0.84), however, those with FootFx more often reported limitations in ability to stand for 15 minutes than those without FootFx (table).

Foot pain remained more frequent in those with FootFx even after adjusting for effects of sex, age & BMI (table) as did difficulty in standing for 15-minutes. Timed gait and chair stands as well as limitations in walking or stair-climbing remained unassociated with prior FootFx.

Self-report of prior FootFx is associated with current foot pain and difficulty in standing but not other physical function measures in this population-based sample even after controlling for age and BMI. FootFx may have a lasting influence upon the presence of foot pain.

Prevalence of foot pain and physical function measure and adjusted OR for FootFx

(Presence/absence)	FootFx	no FootFx	adjusted OR (95%CI)
Current foot pain	31%	22%	1.4 (1.06, 1.92)
Toe pain	23%	14%	1.8 (1.28-2.50)
Hindfoot pain	14%	8%	2.0 (1.36-3.15)
Forefoot pain	14%	8%	1.6 (1.04-2.45)
Arch pain	12%	6%	1.7 (1.05-2.64)
Difficulty in standing	40%	34%	1.3 (1.01, 1.78)

Disclosures: ***M.T. Hannan****, None.*

M343

The Incidence of Fractures at All Skeletal Sites Is Highest Among the Socioeconomically Deprived. A. R. McLellan[1], I. Baxter*[2], S. J. Gallacher*[3], M. Fraser*[1], F. Lovell*[4], C. McQuillian*[3]. [1]Division of Cardiovascular Sciences & Medicine, Western Infirmary, Glasgow, United Kingdom, [2]Department of Public Health, Greater Glasgow Health Board, Glasgow, United Kingdom, [3]Medical Unit, Southern General Hospital, Glasgow, United Kingdom, [4]Division of Medicine, Royal Infirmary, Glasgow, United Kingdom.

The impact of socioeconomic deprivation (SED)on fracture incidence is unclear; we have previously reported a possible association between SED and fracture incidence at some skeletal sites (McLellan et al JBMR2003; 18suppl.2S245abstSU275).

The Fracture Liaison Service (FLS) is a clinical service that routinely offers post-fracture assessment for osteoporosis (and treatment, where necessary) to all women and men over 50yr presenting with new fractures(McLellan et al O.I.2003;14:1028-1034); the aim is to effect optimal secondary prevention of osteoporotic fractures. Established in 1999, since 2002 the FLS has provided a unified service covering the entire City of Glasgow's urban population of ~900,000. The FLS is a unique resource for observing the epidemiology of fractures, and in particular the impact of factors such as SED on fracture incidence.

To investigate the association between SED and fracture incidence the entire cohort of 4659 women and men over 50yr who presented with fractures in 2002 were included. SED is classified according a validated 7 point scoring system (DepCat)(Carstairs 1991)based on UK National Census data linked to postcode of residence; DepCat 1 is the most affluent, & DepCat 7 the most deprived.

Annual % age/sex standardised fracture incidence rates

Depcat	Wrist (1324)	Hip (919)	Humerus (716)	Ankle (496)
1	0.38	0.27	0.21	0.15
2	0.35	0.29	0.17	0.10
3	0.5	0.24	0.24	0.17
4	0.39	0.20	0.24	0.15
5	0.53	0.33	0.21	0.24
6	0.46	0.36	0.26	0.15
7	0.62	0.47	0.36	0.25

The most deprived (DepCat 6-7) compared to the least deprived (DepCat 1-2) have age/sex standardised fracture incidence rates that are higher at all skeletal sites; the extent of the increase in fracture rates with SED ranges from 26% at hand / foot (data not shown) to 47% at the humerus. SED, however, also impacts on rates of acceptance of the offer of osteoporosis assessment by the FLS. While ~92% of patients accept assessment by the FLS after hip fracture irrespective of DepCat, for all other fracture sites there is a substantially higher refusal rate of 30% among those from Depcat 6-7 versus 19% among those from DepCat 1-2. SED is associated with higher fracture rates at all skeletal sites, and apart from after hip fracture, with higher rates of refusal to undergo assessment for the secondary prevention of osteoporotic fractures.

Disclosures: ***A.R. McLellan****, None.*

M344

Measurements from Heel Bone Ultrasounds Predict Future Non-spine Fracture among Men as Well as Women. S. Fujiwara[1], T. Sone[2], K. Yamazaki[3], N. Yoshimura[4], K. Nakatsuka[5], K. Kushida[3], M. Fukunaga[2]. [1]Clinical Studies, Radiation Effects Research Foundation, Hiroshima, Japan, [2]Kawasaki Medical School, Kurashiki, Japan, [3]Hamamatsu University School of Medicine, Hamamatsu, Japan, [4]Wakayama University, School of Medicine, Wakayama, Japan, [5]Osaka City University Medical School, Osaka, Japan.

Quantitative ultrasound (QUS) is widely adopted for screening patients at risk of osteoporosis because it is an ionizing radiation-free, low-cost, simple and portable method. Although QUS measures were not well correlated with bone mineral density (BMD) by dual X-ray absorptiometry (DXA), a number of prospective studies have demonstrated that measures of QUS could predict future fracture risk in the US and Europe. To our knowledge, there has been no report based on longitudinal study if measures of QUS predict the subsequent fracture risk in Japanese, and very few studies have evaluated QUS measures in fracture prediction among men even in the US and Europe. A multi-center longitudinal study was performed to investigate the relationship between baseline heel QUS measurements and bone fracture risks.

The subjects of this study are 4,989 individuals (1,200 males and 3,789 females), 66 ±10 years (mean ± SD) of age, who underwent heel QUS (A-1000 [Lunar] and AOS-100 [Aloka]) measured at the five centers between 1993 and 2000, and responded to the questionnaire survey in 2002. In the survey they were asked their history of fracture after undergoing QUS. Average follow-up period was 5 years. The two heel QUSs measured speed of sound (SOS), and the A-1000 measured broadband ultrasound attenuation (BUA). The SOS by either QUS and BUA by A-1000 predicted self-reported hip, radius, and the other fracture except spine fracture. The relative risk (RR) of 1 standard deviation (SD) decrease of SOS by A-1000 for the fracture other than spine fracture was 1.8 (95% Confidence Interval 1.3-2.3) for women and 1.7 (95% CI 1.3-2.3) for men, and that for BUA was 1.4 (95% CI 1.2-1.7) for women and 1.6 (95% CI 1.1-2.3) for men. The RR was similar between men and women. The RR of 1SD decrease in QUS measures for the fracture was similar to that of 1SD decrease in BMD by DXA. In conclusions, SOS and BUA obtained from heel QUS predicted future fracture other than spine in both Japanese men and women with similar relative risk (RR) to that obtained from previous reports in Caucasian women.

Disclosures: ***S. Fujiwara****, None.*

M345

Risk Factors for Osteoporotic Fractures in Older Women: the Leisure World Cohort. S. White[1], A. Paganini-Hill*[2], S. Service*[3], K. Atchison*[1], A. Nattiv*[3], J. Gornbein*[3]. [1]UCLA School of Dentistry, Los Angeles, CA, USA, [2]USC School of Medicine, Los Angeles, CA, USA, [3]Geffen School of Medicine at UCLA, Los Angeles, CA, USA.

Our purpose was to identify risk factors for osteoporotic fractures in older women. The Leisure World Cohort is a population-based cohort including 8,877 women from a California retirement community. The residents are mostly Caucasian and upper-middle socioeconomic class. Subjects joined the cohort by completing a questionnaire mailed to all residents in 1981-85. This survey included basic demographic information, medical history, personal habits (exercise, smoking, intake of alcohol, coffee, milk, sodas, and vitamin supplements), and menstrual/reproductive history including menopausal estrogen use. Fracture information came from follow-up surveys, hospital records, or death certificates. Subjects were followed from completion of baseline survey to date of either fracture, last follow-up survey, or, for hip fracture, death. Data were analyzed separately for fractures of hip, leg, arm, wrist, and spine. Clinical variables were first analyzed univariately to assess their influence on fracture risk. All statistically significant ($p<0.05$) variables plus those with a hazard ratio <0.8 or >1.2 were then analyzed jointly using Cox proportional hazards model and backwards elimination procedure to identify significant variables.

The mean age (SD) of women at entry was 74 (7.4) years. Risk factors and hazard ratios, in order of importance by bone, are shown in the table. For the binary variables, the hazard ratio represents the change in fracture rate for having the condition in question, compared to a person without the condition in question. For continuous variables, the hazard ratio represents the change in the fracture rate for a person at the third quartile of the variable compared to a person at the first quartile of the data. Hazard ratios >1.0 represent an increased fracture rate, hazard ratios <1.0 represent a decreased fracture rate, compared to the reference group.

Risk factors and hazard ratios for fracture by bone

Hip		Wrist		Arm		Leg		Spine	
930 fractures 6,709 subjects		376 fractures 6,391 subjects		415 fractures 7,183 subjects		339 fractures 8,237 subjects		527 fractures 6,878 subjects	
Risk Factor	Hazard Ratio	Risk Factor	Hazard Ratio	Risk Factor	Hazard Ratio	Risk Factor	Hazard Ratio	Risk Factor	Hazard Ratio
Age	2.39	Previous fracture	2.42	Previous fracture	2.41	Previous fracture	2.38	Age	2.32
Diabetes	1.69	Heart attack	1.60	Diabetes	2.32	Heart attack	0.65	Previous fracture	1.67
Current smoker	1.44	Hysterectomy	0.75	Age	1.53	Diabetes	1.31	Current smoker	1.54
Previous fracture	1.40	Age	1.27	Rheumatoid arthritis	1.36	Ever pregnant	0.81	Blood pressure meds	1.37
Body mass index	0.76	Alcohol use	0.81	Passive indoor exercise	0.80	Attitude	0.83	Active outdoor exercise	0.73
Glaucoma	1.27	Body mass index	0.84	Attitude	0.81	Age	0.84	Body mass index	0.73
Ever pregnant	0.83	Vitamin A supplements	1.15	Current smoker	0.89			Pain meds	1.28
Attitude	0.90	Cola use	0.92					Attitude	0.81
Vitamin A supplements	1.07	Diabetes	1.04					Glaucoma	0.86
Smoking pack years	1.07							Smoking pack years	1.07
								Active indoor exercise	0.94

No. of subjects vary due to missing values for some variables.

The most important risk factors for osteoporotic fracture are history of fracture after age 40, age at entry into study, diabetes, previous heart attack, and smoking. Body mass index, exercise, ever pregnant, and a positive attitude are protective.

Disclosures: ***S. White****, None.*

M346

Fracture in Stroke: Influence of BMD and Balance. M. W. J. Davie, N. J. Bainbridge*, M. J. Haddaway*. Charles Salt Centre, Robt Jones and Agnes Hunt Hospital, Oswestry, United Kingdom.

Patients with stroke are at increased risk of fracture, but many studies have used fit subjects as controls and not taken into account balance problems of stroke patients. To investigate the effect of balance and bone density on fracture risk, stroke patients were compared with subjects without stroke, but sufficiently unfit to require care in an institution (controls). Stroke subjects were matched for age and sex with controls. An “age at stroke” for a control was determined from the age at stroke of the matched stroke patient allowing comparison of fracture incidence over the same period of time. Bone density (BMD) was measured at the R and L heel with a PIXI densitometer and each subject had a Tinetti balance assessment (TBA) [range 0-16]. Dichotomous variables were compared by Chi squared, other data by ‘t’ tests or Mann-Whitney U tests and correlation by Kendall’s tau. The study was passed by the local research ethics committee.

23 female and 16 male subjects were matched (strokes age 77yr, controls age 78yr). Median time since stroke was 5.3yr (all >1yr post-stroke). No difference between R and L heel BMD for either group, nor between groups (stroke (R) 0.41: Control 0.43g/cm^2) was found. TBA was lower in stroke(med. score = 6) than controls(med. score = 9)($p<0.05$). Fractures occurred with median time post-stroke of 3.3yr in stroke subjects and 1.3yr in controls, in 33.3% of the stroke patients 12.8% of controls (p=ns). Fracture patients were

therefore pooled. TBA for stroke subjects without fracture(SNF) was lower than either control subjects without fracture(CNF) ($p<0.01$) or all subjects with fracture ($p<0.05$). Fracture subjects scored particularly badly at the 360^0 turn ($p< 0.05$ cf controls)component of TBA. Fracture subjects had lower BMD (0.34 g/cm^2) than either SNF (0.45, $p<0.01$) or CNF subjects(0.44, $p<0.01$). To investigate fracture incidence according to Tinetti score, all patients were allocated to one of 4 TBA score groups (TBA score[no. in group: no. with fracture]: 0-4[14:2]; 5-8[35:8]; 9-12[23:7];>12[6:1]). No difference in fracture incidence was evident. No relationship between TBA and BMD was found in either the stroke or control group. BMD was lower in subjects with fracture compared with non fracture patients for all Tinetti bands.

Stroke patients were not found to be at greater risk of fracture compared with institutionalised subjects. SNF subjects had the worst TBA suggesting that more active stroke patients were at greater risk of fracture. Nevertheless BMD at all Tinetti scores was lower in the subjects having fractures. Low BMD is probably more important in fracture risk than instability and should be measured in stroke patients.

Disclosures: ***M.W.J. Davie****, None.*

M347

Characteristics of 252 Community-Dwelling Men and Women with Hip Fracture. A. E. Kearns[1], M. E. Bolander[2], L. A. Fitzpatrick[3]. [1]Division of Endocrinology, Mayo Clinic, Rochester, MN, USA, [2]Department of Orthopedic Surgery, Mayo Clinic, Rochester, MN, USA, [3]Global Development, Amgen, Thousand Oaks, CA, USA.

Hip fracture results in significant mortality and morbidity in both men and women. However, few data have compared the gender differences. We evaluated 252 community-dwelling patients admitted after a hip fracture. Patients with pathologic fracture and significant trauma were excluded. Patients were tracked through the surgical register and cases confirmed by operative reports. Baseline demographics and clinical characteristics were collected by chart review and bedside interview. There were 175 women and 77 men. On average, the men were significantly younger (77.1 ± 12.6 years) than the women (81.5 ± 9.2 years) ($p<0.002$). 25% (n=44) of women and 6% (n=5) of men had a prior diagnosis of osteoporosis ($p<0.0001$). 34 out of the 44 women who had a prior diagnosis of osteoporosis were taking antiresorptive medication (17 estrogen, 11 calcitonin, 4 alendronate, 2 raloxifene), whereas 4 out of the 5 men who had a prior diagnosis of osteoporosis were taking antiresorptive medication (2 calcitonin, 2 alendronate) at the time of the current hip fracture. Previous fracture (vertebral, ankle, pelvis, wrist, or hip) was common with 65 women (36%) and 23 men (29%) having had a prior fracture. Interestingly, in none of the men with a hip fracture prior to the current one (n= 6) had a diagnosis of osteoporosis been made as a result of the first hip fracture. In women 9 of 23 (39%) with a previous hip fracture carried a diagnosis of osteoporosis. 5 women and 6 men were taking oral glucocorticoids at the time of the fracture, but none of the 5 women and only 2 of the 6 men were taking antiresorptive medication. One third of patients had dementia/delirium/altered mental status and were unable to complete interviews during the acute hospitalization. Of those completing interviews, only 18% of women but 36% of men reported being active, 40% of both were sedentary. Only one person was bedridden. Medical conditions potentially causing balance problems were common in both men and women (36%). These data indicate that men and women in the community who sustain a hip fracture share certain characteristics but men are much less likely to be diagnosed with osteoporosis prior to the fracture. A large number of both sexes had prior fracture and highlight the many missed opportunities for earlier intervention.

Disclosures: ***A.E. Kearns****, Merck 2.*

M348

Identification of Women at High Risk for Primary Prevention of Osteoporotic Fracture: Geelong Osteoporosis Study. M. J. Henry*[1], M. A. Kotowicz[1], J. A. Pasco[1], K. M. Sanders*[1], E. Seeman[2], G. C. Nicholson[1]. [1]Clinical & Biomedical Science, The University of Melbourne, Geelong, Australia, [2]Endocrinology, The University of Melbourne, Melbourne, Australia.

Low BMD and previous fracture are independent predictors of subsequent fracture risk. Osteoporosis trials targeting women with osteoporotic BMD and prevalent fracture have confirmed that treatment of this high-risk group is cost-effective. The aim of this case-control study was to determine T-score thresholds among women with no previous fracture that are associated with equivalent fracture risk to those with a previous fracture and femoral neck or lumbar spine BMD ≤ -2.5 (FracOP). From a low trauma fracture cohort (n=668), 291 women (mean age 72yr, range 50-93yr) were identified with fractures of the proximal femur, spine, humerus and distal forearm who had BMD measurements (median time since fracture 59 days). Controls (n=823, median age 70yr, range 50-94yr) were drawn from a random population-based sample recruited concurrently. BMD was measured at the femoral neck and spine using a Lunar DPX-L densitometer, self-reported history of fractures in adult life associated with low trauma was recorded. Optimal cut-points for fracture within the NoFrac group, stratified by age and BMD, were determined by discriminant analysis and fracture risk scores were calculated. Logistic regression determined the fracture risk score threshold that produced an equivalent odds for fracture to that of the FracOP group.

Table 1: T-Scores of equivalent fracture risk (NoFrac *vs* FracOP)

	50-54yr	55-59yr	60-64yr	65-69yr	70-79yr	≥ 80yr
Spine	-4.6	-4.2	-3.9	-3.5	-2.8	-2.0
Femoral Neck	-5.1	-4.7	-4.4	-4.0	-3.2	-2.5

Women with BMD below these thresholds without previous fracture are likely to be at high risk of fracture. Osteoporosis therapy may prove to be cost-effective in this population.

Disclosures: ***M.J. Henry****, None.*

M349

Fractures of the Proximal Femur, Vertebrae, Distal Forearm and Proximal Humerus: Association with Bone Size, Geometry and Strength. C. M. Smith*[1], J. A. Clowes[2], N. F. A. Peel[2], R. Eastell[2]. [1]Research and Development, Barnsley District General Hospital, Barnsley, United Kingdom, [2]Bone Metabolism Group, University of Sheffield, Sheffield, United Kingdom.

We have examined the strength of association between different types of osteoporotic fracture and measurements of bone size and geometry at the proximal femur. We consecutively recruited women (age 55 - 80 years) who had sustained a distal forearm (n = 78), humeral (75), hip (53) or vertebral (73) fracture. These were compared to a population-based sample of 500 postmenopausal women from the Sheffield centre of the Osteoporosis and Ultrasound Study (OPUS study).

Total hip DXA (Hologic QDR4500A) bone mineral content (BMC) and bone area (BA) were measured. We calculated estimated bone volume (BV) using the formula BV = (BA^2 x 3.14)/4, and bone mineral apparent density (BMAD) using BMAD = BMC/BV (Henry YM et al. OI 2004). Hip strength analysis was used to measure parameters of bone size and strength in 498 women (Beck TJ, Johns Hopkins University, USA). Mean Z scores, corrected for age, height and weight were calculated using control data from the population-based postmenopausal women. The difference between fracture syndromes was compared using 1-way ANOVA with a Bonferroni correction for multiple comparisons (Table * P <0.05).

After adjusting for age, height and weight all fracture syndromes had reduced BMC and BMAD however only hip fractures had increased BV. Hip structural analysis of the narrow neck demonstrated a decreased cortical thickness, cross-sectional moment of inertia and section modulus (data not shown) and an increase in buckling ratio in vertebral and hip fractures. Only the hip fracture syndrome demonstrated an increased endocortical diameter. There was no difference in the subperiosteal diameter between fracture syndromes (data not shown).

All fracture syndromes had reduced BMC and BMAD however the pattern of structural changes at the hip differs in the different fracture syndromes. Thus both vertebral and hip fractures had a decrease in section modulus (bending strength) and an increase in buckling ratio (cortical stability) although only in hip fracture syndromes was this related to an increased endocortical diameter. These data suggest hip and vertebral fracture patients may be more at risk of subsequent hip fractures then patients with either humeral or distal forearm fractures.

	Fracture Syndrome			
Variable	Forearm	Humeral	Vertebral	Femoral
BMC ZSc	-0.53*	-0.31*	-0.79*	-0.46*
BV ZSc	-0.05	-0.07	0.12	0.54*
BMAD ZSc	-0.46*	-0.37*	-0.83*	-0.76*
Cortical Thickness ZSc	-0.37	-0.29	-0.84*	-0.75*
Buckling Ratio ZSc	0.28	0.12	1.05*	1.35*

Disclosures: ***C.M. Smith****, None.*

M350

Assessment of Bone Status and Calcium Intake in Children with Minor Trauma Fractures Using Quantitative Ultrasound Measurement at the Radius and The Tibia. S. Ish-Shalom*[1], A. Brecher*[2], G. S. Rozen*[3], N. Ish-Shalom*[4]. [1]Bone and Mineral Metabolism Unit, Rambam Medical Center, Haifa, Israel, [2]Deparment of Pediatrics, Carmel Medical Center, Haifa, Israel, [3]Department of Clinical Nutrition, Rambam Medical Center, Haifa, Israel, [4]Department of Pediatrics, Carmel Medical Center, Haifa, Israel.

Fractures are very common among children. A previous fracture is an independent risk factor for future fractures in osteoporosis. Very few studies examined the bone status in children with fractures.

The purpose of this study was to evaluate the bone status and the calcium intake of pediatric population with fractures due to minor trauma and to assess the relationship between family history of osteoporosis and low impact fractures in children.

Seventy one children that sustained wrist or forearm fractures due to minor trauma were included in our study. Patients with fractures due to a vehicle accident or falling from height were excluded. A detailed medical history was obtained including previous fractures and a family history of osteoporosis and fractures. Weight, height and BMI (body mass index) were determined. Calcium intake was calculated from a 3-days-eating diary reported by the children and their parents. Bone status at the radius and at the tibia was evaluated using a quantitative ultrasound device Sunlight Omnisense (Sunlight Medical Ltd., Tel Aviv, Israel). The measurements were compared with aged matched controls. Mean and SD for the Z-score of the radius and the tibia was -0.5±-1.1 and -2.2±-1.8 respectively. No significant differences were observed between boys and girls. Twenty one (29.6%) patients have sustained more than one fracture. A significant correlation ($r=0.43$, $p<0.001$) was observed between Z-score of the radius and Z-score of the tibia. No significant correlation was found between Z scores of the radius or tibia and the corrected BMI. Multiple fractures were more frequent in children with a family history of osteoporosis ($r=0.3$ $p<0.02$). Thirty six children completed the food diaries. The average calcium intake was 504mg/day ± 232 mg/day. None of the children reached the recommended daily intake adjusted for age, with an average deficiency of 59.3% ± 19.8%. Protein intake was 66.3 ± 20.4 gram/day, with an average excess of 14.6% ± 31.7%.

We conclude that children with a history of low trauma fracture revealed slight decrease in bone mass of the radius and marked decrease at the tibia. Children with a history of low trauma fracture consumed low calcium and a high protein diet. Multiple low trauma fractures were more frequent in children with family history of osteoporosis.

Disclosures: ***S. Ish-Shalom****, None.*

M351

Osteoporotic Fracture Prevalence in an Area of Barcelona (Spain). Relationship with Peripheric Densitometry and Risk of Fracture Questionnary. M. Ciria*[1], L. Perez-Edo[1], J. Blanch*[1], M. Coll*[1], J. Carbonell*[1], I. Gonzalez*[2], J. Fernandez*[3], [1]Rheumatology, Institut Municipal d'Asisténcia Sanitària, Barcelona, Spain, [2]Abs baix guinardo, ICS, Barcelona, Spain, [3]Abs besos, ICS, Barcelona, Spain.

Aims: To assess the prevalence of osteoporosis (OP) and fractures in women over 65 years in an urban area through the use of AccuDEXA. To test the use of accuDEXA and the "FRACTURE" questionnaire to discriminate between patients with bone fragility fractures.

Patients and methods: Prospective population based study. Universe: women over 65 years-old attended in an Primary Care center. Data recorded: height, weight, past fractures, calcium intake, use of tobbacco and alcohol, osteopenizing drugs, maternal hip fracture, years of menarchy and menopause, use of antiresortive drugs.

The FRACTURE questionnaire was applied with no inclusion of bone density (FR1). Also, FRACTURE questionnaire was applied without the question regarding past history of fragility fractures (FR2). The cut-off point in FRACTURE score for "high risk" was 4. Bone density assessment was performed with accuDEXA. Two BMD diagnosis thresholds for OP were defined: (OP1: -2,5 SD, T-score; OP2: -1,65 SD, T-score).

Results: Target population:1.390 women. Noticed of the study:1.077. Enrolled:789. Declined to participate:75. Died:11. Unable to walk:201. Censal errors:82. Age:72.9+/-6 y.; Weight:67.8+/-11 kg; Height:1.52+/- 0.06 m; BMI:29+/-4.5; Menarchy:13.6+/-2 y.; Menopause:48.6+/-5.7y.; calcium intake:0.848+/-0.34 gr/d; BMD:0.439+/-0.076 gr/cm2; T-score:-1.25+/-1.3 SD; OP prevalence:OP1:18.3%; OP2:37.5%; Previous clinical Fx:21.9%: Colles 10.5%, humerus:4.6%, vertebrae:3.4%, ribs:1.8%, hip:1.6%. Odds ratio for fractures through diagnosis of OP (OP1 and OP2) are shown in TABLE 1. FRACTURE scores FR1 and FR2 and their Odds ratio for fracture are shown in TABLE 1. Use of antiresortive therapy:8.9%. No patients with hip fracture were treated; vertebral Fx treated:22%, Colles fracture treated:9%.

Conclusions: Prevalence of fractures was of 21.9%. A great number of patients with fractures were not treated with antiresortive drugs. AccuDEXA was able to discriminate population with a greater risk of fracture. The FRACTURE questionnaire discrimine patients with fractures to the population, also in case of excluding the previous fracture question of the FRACTURE score.

TABLE 1: CORRELATIONS WITH FRACTURES

	OP1	OP2	FR1	FR2
All Fractures	2.4 (1.8-3.2)	1.8 (1.5-2.2)	2.6 (2.1-3.1)	1.5 (1.1-1.9)
Colles Fractures	2.4 (1.8-3.3)	1.9 (1.6-2.3)	1.9 (1.5-2.4)	NS
Ribs Fractures	2.4 (1.3-4.5)	1.7 (1.2-2.6)	2.05 (1.3-3.2)	1.88 (1.1-3.43)
Humerus Fractures	NS	1.4 (1.1-2)	2.2 (1.7-2.9)	NS
Hip Fractures	2.6 (1.4-4.7)	NS	2.8 (2.2-3.7)	2.87 (1.9-4.2)
Vertebral Fracture	2.1 (1.3-3.5)	1.7 (1.3-2.3)	2.23 (1.6-3.01)	1.74 (1.1-2.78)

Disclosures: ***M. Ciria****, AVENTIS 5.*

M352

Predictors of Incident Appendicular Fractures in Men and Women. G. R. Haynatzki, M. R. Stegman*, R. R. Recker, R. P. Heaney. Osteoporosis Research Center, Creighton University, Omaha, NE, USA.

A rural population sample, 50+ years of age, was randomly selected for a prospective observational study (The Saunders County Bone Quality Study), consisting of 899 women and 529 men, followed for an average of 3.66 and 3.62 years, respectively. At each visit, they were measured by QUS at the patella and by SPA at distal radius and ulna, and completed a questionnaire on current and past medical history, medication use, dietary calcium intake, alcohol and caffeine consumption, cigarette smoking, fall and fracture history. Here we report the most current results from the low-trauma fracture, independently assessed by two MDs (RPH and RRR). The Cox proportional hazard model (Cox regression) was used to reveal the effect of different predictors on time to fracture. The table below shows the number of first reported low-trauma appendicular fractures (i.e. the unit is a fractured person). The analyses revealed that sex, age, radius BMD, smoking were significant predictors of time to low-trauma fracture while, for example, thyroid problem was marginally significant, at level of significance 0.05. The statistical package SAS was used in all analyses.

Low-Trauma Fracture Reported Site	**Female**	**Male**
Wrist	14	2
Hand	4	2
Ribs	4	3
Pelvis	2	0
Shoulder & Clavicle	4	1
Humerus & Elbow	6	0
Hip	9	0
Femur (distal) & Patella	3	1
Fibula (distal) & Ankle	10	2
Foot	11	3
Total Persons	67	14

Disclosures: ***G.R. Haynatzki****, None.*

M353

Hip Fracture Trends from 1990-2001: Indirect Evidence of Improved Diagnosis and Treatment. N. Goel[1], C. H. Orces*[2], S. Lee*[3]. [1]Internal Medicine, University of Texas Medical Branch, Galveston, TX, USA, [2]South Texas Veterans Health System, Laredo, TX, USA, [3]South Texas Veterans Health System, Laredo and San Antonio, TX, USA.

As the US population ages, hip fracture rates are expected to rise. This rise may be counteracted by increasing awareness of the osteoporosis disease state as well as the availability of more diagnostic and therapeutic options. The purpose of this study is to examine trends in hip fracture hospitalization rates among persons 50 and over in the US.

Data from the National Hospital Discharge Survey were obtained covering the years 1990-2001. Only short-stay or general specialty hospitals with 6 or more staffed beds were included in the survey. Of these, only 6-8% of all eligible hospitals were represented, selected by weighted randomization based on hospital size, to represent an acute sample of the US hospitalized population. All hospital discharges among persons aged 50 years and older with a listed ICD-9 code of 820.0-820.9, corresponding to femoral neck fracture, were included. Annual hospitalization rates by age and gender were determined and then age-standardized and adjusted against the year 2000 US census data.

A total of 985,054 men and 3,014,409 women aged 50 years and older were hospitalized with a hip fracture during 1990-2001. Analyzing overall trends, the estimated number of hip fracture admissions rose 22.3% in women from 217, 813 in 1990 to 266,447 in 2001. In men they rose by 29.5% from 69, 355 in 1990 to 89, 887 in 2001. Looking at yearly data, there was evidence of an interim rise and then fall in hip fracture hospitalizations, with women reaching a peak incidence of 289,127 hospitalizations in 1996 and men, 102,541 hospitalizations in 1998. Examining age-specific rates, hip fracture hospitalization rates did not start to decline in women 65-74 and 75-84 years old until 1996 (R^2=0.52 and 0.95, respectively) and in women 85 and over until 1999 (R^2=0.93). Women under 65 experienced a slight decrease in hospitalization rates over the entire time interval (R^2=0.79). The age adjusted rates in men demonstrated a continued rise in those 65-74 (R^2=0.87), a peak in rates for those 75-84 in 1997 (R^2=0.95), and a peak in rates in those 85 and older in 1998, with a sharp decline from 1999 onwards (R^2=0.93).

Hip fracture hospitalization rates rose until the mid to late 1990's in both women and men. The subsequent decline in overall rates may speak to the Bone Mass Measurement Act and increased availability and use of densitometry and non-pharmacologic and pharmacologic therapies in this time frame. Ageism towards both genders as well as diminished awareness of the occurrence of osteoporosis-related hip fractures in men may help to explain the delay in rate downturn seen in these populations.

Disclosures: ***N. Goel****, Procter & Gamble Pharmaceuticals 1, 2, 3.*

M354

Study Design of the Canadian Quality Circle (CQC) Pilot Project in Osteoporosis. M. Doupe*[1], G. Ioannidis[2], A. Papaioannou[2], A. Katz*[1], B. Kvern*[1], A. Hodsman[3], A. Baldwin*[4], D. Johnstone*[5], S. Glezer*[6], J. D. Adachi[2]. [1]University of Manitoba, Winnipeg, MB, Canada, [2]McMaster University, Hamilton, ON, Canada, [3]University of Western Ontario, London, ON, Canada, [4]St. Boniface Hospital, Winnipeg, MB, Canada, [5]Procter & Gamble Pharmaceuticals Inc, Toronto, ON, Canada, [6]Aventis Pharma, Toronto, ON, Canada.

While the Osteoporosis Society of Canada (OSC) guidelines recommend evidence-based management of osteoporosis, recent studies have estimated the proportion of untreated patients in North America to be as high as 80%. A partnership of stakeholders, including the OSC, the Ontario College of Family Physicians, the University of Manitoba and Bone Metabolism Board members, initiated the CQC Project to assess the utilization of these guidelines by primary care physicians (PCP). The primary objectives are to (1) document current PCP practices of fracture prevention treatments in women at risk of osteoporosis and (2) to monitor changes in PCP practices after their participation in accredited educational interventions within a quality circle (QC) framework. This abstract highlights the unique attributes of the CQC interventions, and discusses their potential to optimize PCP care management of osteoporosis.

The CQC Pilot Project is a one year, integrated disease management project designed to assess and monitor changes in PCP's practice patterns as compared to the OSC 2002 guidelines. The 52 PCPs who participated in this initiative formed 7 quality circle (CQ) groups. Each CQ group was lead by a CQ Champion (PCP) and an Expert (specialist). Each member conducted chart reviews and completed standardized data collection forms on 30 patients during the baseline period. Patient inclusion criteria were women age 55 years and over with at least two visits to the PCP in the previous 24 months. PCPs documented their awareness of patient risk factors, and rates of BMD testing and treatment modalities. A total of 1505 data collection forms were faxed to a central database, where PCP specific practice profiles were developed, along with comparative data for each quality circle and project sample. Practice profiles were returned to each PCP, who in turn attended a CME osteoporosis workshop designed to help them understand and improve on their personal and group results. CQ members are in the process of collecting data on 30 additional patients. A second set of profiles will be developed to inform PCPs of changes in their practice patterns since the baseline period.

Disclosures: ***M. Doupe****, None.*

M355

The Association between Osteoporosis and Oral Bone Loss in Postmenopausal Women. J. Wactawski-Wende[1], E. Hausmann*[2], K. Hovey*[1], S. Grossi*[2], R. Genco*[2], M. Trevisan*[1]. [1]Social and Preventive Medicine, University at Buffalo, Buffalo, NY, USA, [2]Oral Biology, University at Buffalo, Buffalo, NY, USA.

Epidemiological evidence supporting association between osteoporosis and oral bone loss is limited. This study investigated that association in a large cohort of postmenopausal women.

A cross-sectional cohort of 1,341 postmenopausal women aged 53 to 85 were assessed for alveolar crestal bone loss (ACH) and bone density. ACH was determined from oral radiographs with subjects dichotomized on disease severity (none/low vs. moderate/severe). Bone density was assessed using Dual Energy X-ray Absorptiometry (DXA), with severity categories determined by worst T-score measured (Normal >-1.00; Low -1.00 to -2.00; Moderate -2.01 to -2.49; Osteoporotic ≤-2.5).

Compared to subjects in the normal T-score group, the odds worse ACH increased by 39%, 59% and 330% for those with low, moderate and osteoporotic T-scores, respectively. After adjustment for weight, education, hormone use, calcium or vitamin D supplementation and smoking, the association between T-score and ACH remained appreciably unchanged. Further adjustment for age attenuated the association with osteoporotic subjects having twice the odds of being in the worst ACH group (OR=1.90; 95%CI 1.19-3.05). After age stratification, in women <70 there was a significant trend by decreasing T-score category (P<0.02). However, those in the osteoporotic group were significantly associated with worse ACH (OR=1.95; 95%CI 1.20-3.17). However, in women aged 70 and older, the odds of ACH loss was 2.5 to 4.6 fold increased for decreasing T-score category. After adjusting for all factors and age, the odds ratios (and 95% CI) for the low, moderate and osteoporotic groups were 2.66 (1.12-6.29), 2.31 (0.89-6.01) and 3.57 (1.42-8.97), respectively (P for trend=0.026).

This study is the largest to date support the finding that in postmenopausal women, there is a strong and consistent association between worsening T-score and loss of ACH, and that increasing age is an important modifier of that association.

Disclosures: ***J. Wactawski-Wende****, None.*

M356

A Meta-analysis of Milk Intake and Fracture Risk. J. A. Kanis, H. Johansson*, A. Oden*, C. De Laet*, O. Johnell, J. A. Eisman, E. V. McCloskey, D. Mellstom, H. Pols, J. Reeve, A. Silman, A. Silman. Centre for Metabolic Bone Diseases, University of Sheffield, Sheffield, United Kingdom.

WHO Collaborating Centre for Metabolic Bone Diseases, University of Sheffield Medical School, Beech Hill Road, Sheffield S10 2RX, UK

A low intake of calcium is widely considered to be a risk factor for future fracture. The aim of this study was to quantify this risk on an international basis and to explore the effect of age, gender and bone mineral density (BMD) on this risk.

We studied 39,563 men and women (69% female) from 6 prospectively studied cohorts comprising EVOS/EPOS, CaMos, DOES, the Rotterdam study, the Sheffield study and a cohort from Gothenburg. Cohorts were followed for 152,000 person-years. The effect of calcium intake as judged by the intake of milk on the risk of any fracture, any osteoporotic fracture and hip fracture alone was examined using a Poisson model for each sex from each cohort. Covariates examined were age and BMD. The results of the different studies were merged by using the weighted β-coefficients.

A low intake of calcium (less than 1 glass of milk daily) was not associated with a significantly increased risk of any fracture, osteoporotic fracture or hip fracture. There was no difference in risk ratio between men and women. When both sexes were combined there was a small but non-significant increase in the risk of osteoporotic and of hip fracture. There was also a small increase in the risk of an osteoporotic fracture with age which was significant at the age of 80 years (RR = 1.15; 95% CI = 1.02-1.30) and above. The association was no longer significant after adjustment for BMD. No significant relationship was observed by age for low milk intake and hip fracture risk.

We conclude that a low intake of milk is not associated with any marked increase in fracture risk and that the use of this risk indicator is of little or no value in case-finding strategies.

Disclosures: ***J.A. Kanis****, None.*

M357

Parental Hip Fracture Predicts Falls, Fractures and Low Bone Density in Early Postmenopausal Women. R. J. Honkanen, H. Kröger, M. Tuppurainen*. Bone and Cartilage Research Unit, University of Kuopio, 70211 Kuopio, Finland.

Family history predicts fractures but only part of the effect seems to go through low bone mineral density (BMD). Our purpose was to determine this effect in middle-aged women and to evaluate if it is related to falling risk or bone density.

We examined the role of parental history of hip fracture in the occurrence of fractures and falls in Finnish women from a defined geographic area. The population-based cohort consisted of 11074 OSTPRE (Osteoporosis Risk Factor and Prevention Study) women born in 1932-41 who responded to three postal enquiries in 1989, 1994 and 1999. Eight hundred and seventy-eight women reported a parental hip fracture in the 1994 enquiry. Fractures during 1989-99 reported by 1915 women were validated by perusal of patient records. 4695 women reported a fall within the last 12 months either at 1994 or 1999.

Women with a history of parental hip fracture had a 29 % higher fracture risk (p=0.004) and a 22 % higher falling risk (p=0.005) than women without such a history. Adjustments did not affect these relationships. Parental hip fracture predicted also fractures (N=932) sustained after the acquisition of exposure information (+39 %; p=0.003) but did not predict subsequent falls (+14 %; p=0.119). Adjusting for age, height, weight, HRT, calcium intake, smoking, fracture history or falling at 1994 affected only slightly the association between parental fracture and fracture during 1994-1999.

In a random sample of 1244 of these women, femoral and spinal BMDs, measured thrice during the 10-year follow-up, were 3-4 % lower (p values ranging from 0.005 to 0.031) in the 105 women with a history of parental hip fracture than BMDs in other women. Adjusting for baseline age, menopausal status, height, weight, calcium intake and fracture history as well as for HRT ad 1994 and falling at 1994 slightly decreased the difference. This subsample was too small to study the effect of parental fracture on fracture incidence.

We conclude that parental fracture is a moderate predictor early postmenopausal fracture. Falling history does not considerably modulate this relationship.

Disclosures: ***R.J. Honkanen****, None.*

M358

Improved Diagnostic Precision by Modifying 4 Decision Rules Replacing Weight by Body Mass Index (BMI) to Identify Chilean Women with Low Bone Mineral Density (BMD). C. Campusano*[1], C. Rodriguez*[1], M. Cabezas*[1], P. Viviani*[2], O. Contreras*[3], R. Pruzzo*[4], H. Amaral*[4], G. Gonzalez[1], J. Lopez*[1], E. Arteaga*[1]. [1]Endocrinology, Pontificia Universidad Catolica de Chile, Santiago, Chile, [2]Public Health, Pontificia Universidad Catolica de Chile, Santiago, Chile, [3]Radiology, Pontificia Universidad Catolica de Chile, Santiago, Chile, [4]Nuclear Medicine, Clinica Alemana, Santiago, Chile.

Decision rules developed in North America to identify women who require BMD testing have high false positive rates leading to an excess of normal subjects tested, which raises the cost of osteoporosis screening. The value of including height to improve their usefulness has not been evaluated, especially in a lower height population as the Chilean . Aim: To compare 4 international rules, modified by considering BMI instead of weight to identify low BMD Chilean postmenopausal women. Subjects and Methods: A questionnaire was performed in a cohort of postmenopausal Chilean women, followed by bone densitometry (DXA, LUNAR). Subjects using bone sparing drugs other than calcium or estrogens were excluded. We calculated scores for the following rules: National Osteoporosis Foundation (NOF), Osteoporosis Risk Assessment Instrument (ORAI), Age, Body Size, No Estrogen (ABONE) and Simple Calculated Osteoporosis Risk Estimation (SCORE), in which a 10 point cut level was used due to the absence of black race in our country. Obtained scores were analyzed versus BMD at lumbar spine and hip. Sensitivity, specificity, positive predictive value(PPV), negative predictive value(NPV) and area under the receiver operating characteristic curve (AUROC) were calculated. Subgroup analysis was performed in <65y. Results: 737 women, mean age 60.4±9.2years, were classified according to spine and/or hip BMD as osteopenic (45.5%), osteoporotic (17.2%) and below treatment threshold (T score <-2) (32.2%). Thirty nine percent were taking calcium preparations and 62% were current or former estrogen users. Diagnostic precision of classic and modified $_{(m)}$ decision rules is presented in %:

	NOF/ NOF(m)	ORAI/ ORAI(m)	SCORE/ SCORE(m)	ABONE/ ABONE(m)
Sensitivity	80.2 / 84.3	80.9 / 66.9	76.9 / 62.2	40.5 / 58.5
Specificity	35.9 / 27.5	50.5 / 70.5	31.0 / 73.2	69.3 / 73.5
PPV	19.7 / 18.6	24.3 / 30.8	17.9 / 30.7	20.6 / 29.6
NPV	90.2 / 89.5	93.1 / 91.6	83.4 / 91.0	85.6 / 90.3
False Positive	80.3 / 81.4	75.7 / 69.2	82.1 / 69.3	79.4 / 70.4
False Negative	16.4 / 10.1	6.9 / 8.4	12.6 / 15.9	14.4 / 9.7
AUROC(m) (CI)	0.58 (0.54-0.61)	0.72 (0.69-0.75)	0.73 (0.69-0.76)	0.69 (0.66-0.73)

Conclusions: In this cohort, replacement of weight by BMI in decision rules improves specificity, allowing better discrimination in whom not to test. ORAI, SCORE and ABONE had better diagnostic precision than NOF. In the subgroup of <65y ORAI and ABONE had the best specificities (data to be shown).

Disclosures: ***C. Campusano****, None.*

M359

Predictors of Osteoporosis in Young Women - a Case Population-based Control Study from BC CaMOS. J. C. Prior, C. Hitchcock*, F. Kirson & YOW*. UBC, Van Hosp CeMCOR, Vancouver, BC, Canada.

The population-based bone studies in premenopausal women show osteopenia related to age, weight, menarche, milk and lower progesterone [1-3]. Fractures occur in amenorrhea and anorexia. Cognitive dietary restraint (Restraint), perception of limiting food intake to prevent weight gain [4], is associated with lower DXA [5], higher cortisol levels [6] and ovulation disturbances [7]. The purpose of this secondary analysis from a participatory study (Young Osteoporosis Women, YOW) was to compare Restraint and reproductive variables in young women with self-identified low bone density (cases=YOW) to a similar age-stratified population-based sample with normal DXA (controls=CaMOS). YOW participants had osteoporosis (15) osteopenia (9) and 11 reported fractures (4 hip). YOW researchers met monthly, created an interviewer-administered questionnaire (IAQ) that also included items from the CaMOS IAQ [8] and interviewed 24 women. All YOW interviews were taped, blinded and transcribed. Of 123 women 25-49 years old in BC CaMOS, 44 were excluded for menopause (5/123) and DXA $\leq$-1SD (39/123) [9]. Variables include age, skipped 3 cycles (Y/N), # periods skipped (continuous), menarche age, family osteoporosis history (FHO, Y/N), Restraint (0-3 scale; assessed using 3 items from the 21-item restraint subscale of the Three-Factor Eating Questionnaire[4]) and molimina (Y/N = usually able to tell the period is coming based on axillary breast tenderness). Results compared 24 YOW cases and 79 CaMOS controls. Data reported as mean [95% confidence intervals]. The groups were similar in age (41.6 vs. 40.4), parity (0.50 vs. 0.58) and menarche (12.7 vs. 12.7). Skipped periods occurred in 46% of YOW with a mean of 12.7 [1.9,23.5] and 10% of CaMOS mean 5.4 [-0.39,11.3]. FHO was present in 76% (n=17) YOW and 14% of CaMOS participants, and Restraint scores were 1.58 [1.10,2.06] and 1.18 [0.94,1.41]. Backward stepwise logistic regression analysis of YOW including all variables except age and FHO showed that skipped periods (P=0.005) and Restraint (P=0.024) stayed in the model and explained 17.3% of the variance. This case-population control study suggests young women skipping 3 or more cycles and having higher cognitive dietary restraint are more likely to have osteoporosis and fractures than women in the general population.

1.Sowers M *J.Bone Min.Res.* 1998;**13**:1191-202. 2.Hawker G, Forsmo S *Am.J.Epidemiol.* 2002;**156**:418-27. 3.Bainbridge K *Am.J.Epidemiol.* 2002;**156**:410-7. 4. Stunkard A *J.Psychosomatic.Res.* 1985;**29**:71-83.5.McLean J *Med.Sci.Sports Exerc.* 2001;**33**:1292-6. 6.McLean J *Am.J.Clin.Nutr.* 2001;**73**:7-12.7. Barr SI *Am.J.Clin.Nutr.* 1994;**60**:887-94. 8.Kreiger N *Can.J.Aging* 1999;**18**:376-87. 9.Tenenhouse A *Osteoporos.Int.* 2000;**11**:897-904.

Disclosures: ***J.C. Prior****, None.*

M360

Association of Increased LDL-cholesterol Levels with Osteoporosis in Postmenopausal Women. F. Tremollieres[1], J. Fillaux*[2], J. Pouilles*[1], V. Cances-Lauwers*[2], C. Ribot[1]. [1]Hôpital Paule de Viguier, Menopause Unit, Toulouse, France, [2]CHU Purpan, Department of Epidemiology, Toulouse, France.

Several studies suggest that osteoporosis is associated with increased cardiovascular morbidity and mortality in postmenopausal women. The aim or this study was to assess the relationship between BMD, bone remodeling markers and plasma lipid profile in a large cohort of early menopausal women. We selected 1961 women aged 45 to 65 years old who attended our menopause clinic for a general « menopause check-up ». According to the menstrual status and serum FSH and estradiol levels women were classified as early perimenopausal (PM), late PM or postmenopausal women. All women were free of past or current cardiovascular diseases and none had ever received ERT/HRT, lipid lowering drugs or drugs affecting bone metabolism. Fasting blood and urine samples were collected for determination of plasma lipids and lipoproteins and bone remodeling markers (osteocalcin, bone alkaline phosphatase and urinary C-telopeptide of type I collagen). Vertebral and femoral BMD were measured using DXA (GE Lunar).The relationship between BMD (categorized as normal, osteopenia and osteoporosis) and the lipid and bone remodeling variables were tested using multiple logistic regression analyses. According to the WHO classification, 914 women were considered as osteopenic (op) and 214 as osteoporotic (OP). All bone remodeling markers were significantly increased both in op and OP women ($p<0.001$) as compared to normals. Mean total cholesterol (CT) and LDL-cholesterol (LDL-C) plasma levels were also significantly increased in OP as compared to normals, but not in op women. In multiple regression analyses, all bone remodeling markers, menopausal status, time since menopause, LDL-C and BMI were independently and significantly associated with the prevalence of osteoporosis. Women with LDL-C levels $\geq$ 1,30 g/l had an odds ratio of 1.71 [95% CI 1.12-2.62] to be classified as OP compared with women with LDL-C < 1,30 g/l. The results or this study show that women with increased LDL-C levels have a greater risk of being OP compared with women whith normal LDL-C levels. Because bone remodeling markers were also significantly increased in women with increased LDL-C levels compared to women with normal LDL-C levels, it could be hypothesized that LDL-C might increased bone turnover which in turn would contribute to osteoporosis. Additional studies are needed to clarify this hypothesis.

Disclosures: ***F. Tremollieres****, None.*

M361

Do Differences in Body Fat Contribute to Variation in 25-hydroxyyvitamin D Values by Age and Race in Women? A. C. Looker. National Center for Health Statistics, CDC, Hyattsville, MD, USA.

Obesity has been linked to lower serum 25 hydroxyvitamin D values, but whether this relationship is the same across age and race is not clear. To explore this question, the relationship between 25(OH)D and percent body fat (%BF) was examined by race and age in 6042 women from the third National Health and Nutrition Examination Survey (NHANES III, 1988-94). The sample consisted of 3567 non-Hispanic white and 2475 non-Hispanic black females ages 12+ years. 25(OH)D values were measured with an RIA kit (DiaSorin, Stillwater MN), while %BF estimates were calculated from bio-electrical impedance analysis. Results were compared before and after adjusting for several confounding factors: month of blood collection, dietary vitamin D intake, supplement use, milk or breakfast cereal consumption, urban/rural residence, smoking, hormone use and physical activity. Regression analyses revealed a significant age*race*body fat interaction with 25(OH)D values ($p<0.0000$). %BF was significantly negatively related to 25(OH)D levels in white females across the age range, but among blacks the relationship was significant only in the younger groups. The strength of the relationship was stronger in whites (e.g., regression coefficients were ~4 times greater on average) than in blacks within the same age group. Within race, the relationship was stronger in younger than older individuals (e.g., on average regression coefficients were ~3 times greater in those under age 50). Adjusting for confounders reduced, but did not remove, the differences in relationship strength. Differences in mean 25(OH)D by race before vs. after adjusting for %BF were also only slightly affected: 1.63 vs. 1.55 times higher in whites, respectively. In conclusion, the relationship between body fat and 25(OH)D in women varies both by age (more pronounced in younger than older persons), and race (more pronounced in whites than blacks). Differences in obesity appear unlikely to play a major role in explaining variation in 25(OH)D by age or race.

Disclosures: ***A.C. Looker****, None.*

M362

Contribution of Hip Strength Indices to Hip Fracture Risk in Elderly Women and Men. H. G. Ahlborg, N. Nguyen, T. V. Nguyen, J. R. Center, J. A. Eisman. Bone and Mineral Research Program, Garvan Institute of Medical Research, Sydney, Australia.

This study was designed to characterize the association between hip strength indices and hip fracture risk in relation to bone mineral density (BMD) in an elderly population. From the prospective, population-based Dubbo Osteoporosis Epidemiology Study, 1902 subjects that had baseline measurements of BMD by dual energy x-ray absorptiometry (Lunar DPX-L) at the femoral neck were analysed. Of these, 71 women and 25 men aged 60 and above, sustained a hip fracture during the study period of 1989-2003. These subjects were randomly matched for age with 142 women and 50 men (ratio of case:control; 1:2) who had not sustained any fracture. Hip strength indices, including femoral neck diameter (FND), cross-sectional moment of inertia (CSMI), section modulus (Z), cross-sectional area (CSA) and compressive stress (Cstress) were estimated by reanalysis of the image files using hip strength analysis software. The association between these measures and hip fracture risk were considered in a multiple conditional logistic regression model. A Bayesian approach was used to estimate the odds ratio for each risk factor in men.

BMD-adjusted odds ratio for hip fracture for each SD difference in each parameter.

	BMD-adjusted odds ratio (95% CI)		
	Women	Men	Men (Bayesian analysis)
FND	**1.6 (1.0, 2.7)**	1.3 (0.7, 2.4)	**1.5 (1.0, 2.3)**
CSMI	**1.8 (1.0, 3.2)**	1.3 (0.6, 2.5)	**1.6 (1.0, 2.5)**
Z	**2.3 (1.1, 5.1)**	2.3 (0.95, 6.3)	**2.3 (1.4, 3.9)**
CSA	2.2 (0.7, 6.9)	1.3 (0.4, 4.6)	1.5 (0.8, 2.8)
Cstress	1.3 (0.7, 2.3)	1.7 (0.5, 5.2)	1.4 (0.91, 2.3)

In women, after adjustment for BMD, smaller FND, lower CSMI or Z were each significantly associated with hip fracture risk. In men none of these hip strength indices was significant. However, using the results in women as a prior distribution, it was estimated that the BMD-adjusted odds ratio for FND, CSMI or Z were each significantly associated with hip fracture risk in men. In the logistic regression model, BMD alone accounted for 32% and 16% of the variance of fracture liability, in women and men respectively. The addition of FND, CSMI or Z to the model increased the respective variance proportion to 34% and 19%.

These data suggest that smaller FND, lower CSMI or Z are independent risk factors for hip fracture in both women and men. However, the contribution of these measures to hip fracture prediction independent of BMD was modest in this long term prospective study in elderly women and men.

Disclosures: ***H.G. Ahlborg****, None.*

M363

Smoking as a Major Osteoporosis Risk Factor Among Iranian Australian Women. A. Baheiraei[1], N. A. Pocock[1], J. E. Ritchie*[2], J. A. Eisman[1], T. V. Nguyen[1]. [1]Bone and Mineral Research Program, Garvan Institute of Medical Research, St Vincent's Hospital,University of New South Wales, Sydney, Australia, [2]School of Public Health and Community Medicine, University of New South Wales, Sydney, Australia.

While the prevalence and risk factors of osteoporosis in Caucasian populations have been well documented, such a profile has not been studied in Iranian Australian women. The present study was designed to estimate the prevalence and lifestyle risk factors of osteoporosis among Iranian women in Sydney, Australia.

Ninety women aged 35 years and older were recruited via a media campaign and community invitation. All subjects completed a questionnaire on socio-demographic background and lifestyle factors, including dietary calcium intake, cigarette smoking , alcohol consumption, and physical activity. Weight and height were recorded and body mass index (BMI) was calculated. Bone mineral density (BMD) was measured at the lumbar spine and femoral neck using dual-energy X-ray absorptiometry. A BMD T-score of less than -2.5 using the Australian reference database was considered as osteoporosis.

The average age of the women was 48 years, with 42% being postmenopausal. Approximately 37% of women were considered obese (body mass index $\geq$ 30 kg/m^2). Of all the anthropometric and lifestyle risk factors considered, advancing age, lower body weight and smoking were independently associated with lower BMD. These factors collectively accounted for 30 % and 38% variance of lumbar spine and femoral neck BMD, respectively. The proportion of women with osteoporosis was 12.2% at the lumbar spine and 2% at the femoral neck. These data, for the first time, indicate that the prevalence of osteoporosis in the Iranian women is comparable to Caucasian women, and more importantly, cigarette smoking is a major modifiable lifestyle risk factor of osteoporosis in this population.

Disclosures: ***A. Baheiraei****, None.*

M364

Effects of Age and Gender on Bone Histomorphometry of Iliac Crest Biopsies from 89 Healthy Individuals. J. D. Sibonga[1], S. S. Cha*[2], D. E. Jewison*[1], R. T. Turner[1]. [1]Orthopedics, Mayo Clinic, Rochester, MN, USA, [2]Biostatistics, Mayo Clinic, Rochester, MN, USA.

There are few published studies investigating the effects of age and gender on bone histomorphometry in healthy humans. We performed such an analysis on 89 archived iliac crest biopsies obtained from subjects (46 women and 43 men), who were recruited specifically as healthy controls for 3 IRB-approved protocols (1981-1990). The median ages for the men and women were 48 and 56 years, respectively. Static and fluorochrome-based dynamic measurements were performed on newly prepared biopsy tissue slides. Gender-specific differences between age-adjusted means (ANCOVA, F-test) were determined for 19 indices. Gender data were correlated to age to elucidate temporal changes for each index. The effect of menopausal status was also evaluated in female data (Wilcoxon Rank Sum Test). All reported differences and correlations have p values <0.1 with significance considered at p<0.05

The age-adjusted means for osteoid width, osteoblast-osteoid interface and osteoid maturation were lower and mineralization lag time higher in men. Women had greater age-adjusted means for eroded surface, labeled surfaces (single and double), bone formation rates (surface and volume referents) and adjusted appositional rate. There was no gender difference in cancellous bone volume but trabecular separation was greater in men.

The following indices in male biopsies were negatively correlated with age: cancellous bone volume, trabecular number, osteoclast number, mineral apposition rate, adjusted apposition rate and bone formation rates (surface and volume referents). The age effect was greatest on mineral apposition rate (p<0.005). Additionally, there was a positive correlation between trabecular separation and age in men. In women, a positive correlation with age was noted for osteoid surface and volume, osteoclast number, double-labeled surfaces and trabecular thickness; there was a negative correlation with cortical thickness.

Post-menopausal women (n=33) had greater numbers of osteoclasts but reduced eroded surfaces than pre-menopausal women (n=13).

Histomorphometry suggested that sex differences in iliac crest bone biopsies were partly due to gender-specific changes in bone turnover and bone balance. Age-related bone loss seen in men was due to an unbalanced reduction in matrix production and mineralization, while an increased but balanced bone turnover maintained bone mass in the healthy women. These results indicate the importance of gender- and, to a lesser extent, age-matched reference values when using iliac crest histomorphometry to diagnose abnormalities in bone architecture, quality and turnover.

Disclosures: ***J.D. Sibonga****, None.*

M365

Is Nullyparity a Risk for Post-menopausal Fracture? L. M. del Rio, S. Di Gregorio*, J. Rosales*. Bone densitometry, CETIR.Centre Medic, Barcelona, Spain.

Reproductive history may affect bone mass in post menopausal women. Several authors have correlated the nulliparity with a lower bone mineral density in post menopausal women.

The aim of this study was to evaluate the parity effect on fracture incidence in post menopausal women

We included 2926 nulliparous women (61 ± 7.5 year of age) and 3306 multiparous women, who had given birth to ≥ 3 children, (60 ± 7 years of age). Lumbar spine and femoral bone mineral density were measured by DEXA (GE-Lunar). Fracture history, age of menarche, age of menopause, physical activity, smoking status and calcium intake were evaluated by a questionnaire.

T- test was used to compare means between nulliparous and multiparous group. A multiple regression test was used to determine correlations between both groups.

All results showed statisticaly differences between groups. Nulliparous women had a lower BMD in lumbar spine (0.947 g/cm2 vs 0.977g/cm2; p<0.001), femoral neck (0.787g/cm2 vs 0.822g/cm2; p<0.001), trochanter (0.656g/cm2 vs 0,694g/cm2 p< 0.001), and total femur (0.843g/cm2 vs 0.890g/cm2;p<0.001). Nulliparous and multiparous had the similar osteoporotic fracture incidence (577 vs 544), but the hip fracture incidence was higher in nulliparous women (58 vs 29) while the incidence of vertebral (213 vs 202) and wrist (306 vs 303) fracture was similar. To explain this results we studied another variables (Weight, BMI; BMD). We founded a statistical significant difference in weight, and BMD in, lumbar spine, femoral neck and total femur between both groups: nulliparous women weighing less, and had a lower BMD.

In conclusion, the nulliparity is related with a high risk to hip fracture in postmenopausal women perhaps due to physical changes related to morphological changes in femur that could explain the difference in fracture incidence only in this skeletal site.

Disclosures: ***S. Di Gregorio****, None.*

M366

Prevalence of Risk Factors for Osteoporosis and Rate of Bone Density Testing Among Young Menopausal Women. M. T. Connelly*[1], S. Oddleifson*[2], L. Bernstein*[2], J. Frampton*[2], J. Gifford*[2], T. Ireland*[2], M. Kelly*[2], M. Levy*[2], K. Salvato*[2], R. Shames*[2], D. Tafone*[2]. [1]Ambulatory Care and Prevention, Harvard Medical School and Harvard Pilgrim Health Care, Boston, MA, USA, [2]Women's Health Lead Team, Harvard Pilgrim Health Care, Boston, MA, USA.

The purpose of this study was to determine the prevalence of risk factors for osteoporosis among women age 50-64 who were members of a large managed care organization in New England and to evaluate the rate of bone mineral density (BMD) testing among those with risk factors. Risk factors for osteoporosis included discontinuation of hormone therapy, exposure to steroids or anti-seizure medications, fracture of bones other than skull, face, fingers, or toes, or evidence of tobacco use. Women with these risk factors who were continuously enrolled in the health plan between 2000 and 2003 were identified from the automated data systems. For the evaluation of BMD testing rate, women were excluded from the analysis if they had, between 2000-2002, a BMD test, use of medication for osteoporosis, or diagnosis of osteoporosis. The outcome of interest was proportion completing a BMD test at 6 months and 12 months after 2002. Of the 39,110 women who were members from 2000-2003, 6,852 (18%) had documentation of at least one of the risk factors of interest. Of those with risk factors, 3,371 (49%) had not had BMD testing, diagnosis of osteoporosis or treatment for osteoporosis between 2000-2002. Among these 3,371 women, evidence of tobacco use was found in more than half (53%). The second most common risk factor was fracture (26%). In the first 6 months of 2003, 454 (13.5%) of the women with risk factors had a BMD; an additional 390 (11.5%) completed a BMD test by the end of 2003. In total, 25% (844/3371) of the young menopausal women age 50-64 with risk factors for osteoporosis and no testing for, diagnosis of, or treatment of osteoporosis in the prior 2 years had a BMD during the one year window of evaluation. We conclude that strategies for improving testing among high-risk women are needed to optimize care for this population.

Disclosures: ***M.T. Connelly****, Eli Lilly 2; Procter and Gamble 2, 5.*

M367

Height Loss: A Predictor of Low Forearm Bone Mineral Density, but not of Bone Loss in Postmenopausal Women. The Health Study of Nord-Trøndelag (HUNT), Norway. S. Forsmo[1], H. M. Hvam*[2], M. Larssen*[2], A. Langhammer*[1]. [1]Dept. of Public Health and General Practice, Norwegian University of Science and Technology, Trondheim, Norway, [2]Faculty of Medicine, Norwegian University of Science and Technology, Trondheim, Norway.

Height loss is a predictor of osteoporosis and fractures. This particularly counts for spine fractures, but has also been shown for other fractures. Less is known concerning the relation between height loss and appendicular bone loss. The purpose of this study was to investigate the association between height loss and forearm bone mineral density (BMD) and bone loss in postmenopausal women. In 1984-86 (HUNT I) and 1995-97 (HUNT II) all inhabitants in the county of Nord-Trøndelag aged >19 years (about 92,000) were invited to the HUNT study, a multipurpose health survey. Among 2749 women born between 1924 and 1941 having participated in HUNT I, a total of 2151 underwent forearm BMD measurement in HUNT II and 1390 in a follow-up study in 2001 (mean interval 4.6 years). Baseline BMD data of 2148 (mean age 65.8) and longitudinal data of 1383 postmenopausal women (mean age 68.9) were eligible for analysis. BMD measurements were performed by single X-ray absorptiometry (Osteometer DTX 100) at the distal and ultradistal non-dominant forearm. Weight (kg) and height (cm) were measured at all three occasions with light clothing and without shoes. Mean height loss during the 11.3 years between HUNT I and HUNT II was 1.30 cm (95% CI: 1.24; 1.36), and 1.42 cm at the follow-up study (interval of 15.9 years). Age was a significant determinant of height loss, 20% of the women aged >69 at HUNT II had lost 3 cm or more compared to 5% of women <60 years ($p<0.001$). At baseline in HUNT II there was a statistically significant negative association between forearm BMD and height loss (HUNT I-HUNT II) adjusted for age, weight, smoking, years since menopause (YSM) and hormone therapy (HT). Odds ratio (OR) for forearm T-score 3 cm compared to those with height loss of 1-2 cm, (adjusted for age, weight, YSM, smoking, HT and height at HUNT I). Mean reduction in distal forearm BMD during the 4.6 years was 19 mg/cm2 (4.9%), this loss was not associated to age. No statistically significant association was found between bone loss and height loss from HUNT I to follow-up. Statistically significant predictors of forearm bone loss were weight (negative), smoking (positive), HT (negative) and BMD at baseline (positive).
In conclusion, height loss is a strong predictor of low forearm BMD in postmenopausal women. In this study, with rather short follow-up time, no association between forearm bone loss and height loss was found.

Disclosures: ***S. Forsmo****, None.*

M368

Two Cases of Obese Women With Atraumatic Fractures Associated with Normal BMD and Low Bone Turnover with Hypomineralization. T. J. Vokes[1], P. Roschger*[2], A. Nader*[3], P. Fratzl*[4], K. Klaushofer[2]. [1]Medicine/endocrinology, University of Chicago, Chicago, IL, USA, [2]Ludwig Boltzmann Institute of Osteology, 4th Med. Dept., Hanusch Hospital & UKH-Meidling, Vienna, Austria, [3]Institute for Pathology, Hanusch Hospital, Vienna, Austria, [4]Department of Biomaterials, Max Plank Institute of Colloids and Interfaces, Potsdam, Germany.

In post-menopausal women the fracture risk is increased by low BMD and high bone turnover. We encountered two subjects with extreme bone fragility and clinical presentation different form the usual patients with postmenopausal osteoporosis. A 58 year old woman with high BMI (48.1), no risk factors for osteoporosis and normal BMD (T-score +3.5 at the spine and -0.6 at the left femoral neck, but +3.3 at the right femoral neck prior to its fracture) had atraumatic fractures of the right femoral neck, left femoral shaft, 3 ribs and several stress fractures of the feet. The second patient, a 66 year old woman (BMI=30.9) with early menopause (age 38) but no other risk factors for osteoporosis, had 2 vertebral fractures with a fall at age 58 and was despite having a normal BMD started on alendronate. In the subsequent 7 years she fractured both femoral shafts and multiple ribs without trauma. In both patients serum values of calcium, Vit D and PTH were normal while the biochemical markers of bone turnover (serum osteocalcin and urinary NTx) were in the normal premenopausal range. The patients underwent tetracycline labeled transiliac bone biopsy. Histomorphometric evaluations of undecalificed 5 micron sections of plastic embedded bone biopsies revealed normal bone volume (BV/TV= 15.6 and 15.2 %, respectively), but extreme low static parameters of bone formation and resorption. The dynamic bone parameters of bone formation could not be obtained, because tetracycline labeling was undetectable. A quantitative backscattered electron imaging (qBEI) method was used to assess the bone mineralization density distribution (BMDD) and revealed a reduction on degree of mineralization of the bone matrix (CaPeak= -4.3% and -3.4%) to healthy controls (n=52). This was accompanied by a broadening of the distribution peak (CaWidth= +18.2% and +17.1%) indicating a more heterogeneous mineralization. The moderate reduction in degree of mineralization may contribute, but is not likely to account alone for the high bone fragility observed. These results suggest that some patients with extreme bone fragility may have a yet unclassified disorder characterized by a combination of low bone turnover and hypomineralization often misclassified as established osteoporosis. Recognizing this disorder may be clinically important for treatment decision.

Disclosures: ***T.J. Vokes****, None.*

M369

Localization of the Cancellous Bone inside the Human Lumber Vertebra. S. Hamai*, T. Mawatari*, H. Miura*, T. Shuto*, Y. Nakashima*, H. Yamada*, K. Okazaki*, T. Kawano*, N. Tsukamoto*, Y. Iwamoto*. Department of Orthopaedic Surgery, Graduate School of Medicine, Kyushu University, Fukuoka, Japan.

Clinical evaluation of bone mineral density (BMD) is commonly performed in the lumber vertebra by dual x-ray absorptiometry (DXA), however the localization of the cancellous bone inside the lumber vertebra cannot be taken into consideration. The purpose of this study was to evaluate postmenopausal women by high-resolution computed tomography (HRCT) in vivo. We examined 20 osteoporosis subjects including 12 rheumatoid arthritis (RA) and 8 non-RA subjects and 20 non-osteoporosis subjects including 15 RA and 5 non-RA subjects. A total of those 40 (mean 61.0 years) were examined by DXA, and the whole body of the third lumber vertebra was scanned by HRCT at a spatial resolution of 351x 351 x 500 micron. All the gray-value slice images were then noise-eliminated, segmented. Preliminary experiments on the cadaveric human third lumber spine were designed specifically to select the correct threshold value. Finally, from the reconstructed 3-dimensional (3-D) volume data, arbitrary-shaped trabecular bone volume that is then divided into six parts (upper anterior, upper posterior, middle anterior, middle posterior, lower anterior, lower posterior) was extracted. Bone volume fraction (%) of each part was calculated, and 3-D image reconstruction was done. A total of those 40 were divided into four groups (Osteoporotic RA group, Osteoporosis group, RA group, and Control group). Average standard deviation of BMD by DXA were -3.162 ± 0.61, -3.158 ± 0.478, -1.379 ± 0.341, and -1.606 ± 0.853, at Osteoporotic RA group, Osteoporosis group, RA group, and Control group, respectively. In the Osteoporotic RA group, the upper and the lower anterior parts were significantly lower than the middle posterior part. In the RA group, the upper and the lower anterior were significantly lower than the upper and the middle posterior and the lower posterior was significantly lower than the middle posterior. In the Osteoporosis group and the Control group, relatively low-density areas were found in the anterior parts and the lower posterior, but the difference didn't reach statistical significance. Our study had three major findings. First, systematic density patterns inside the vertebral body were classified as the inhomogeneous pattern and the relatively homogeneous pattern. Second, regardless of the degree of osteoporosis, degree of the localization of the cancellous bone inside the vertebral body for RA subjects was more inhomogeneous than for non-RA subjects. Third, relatively low-density areas were found in the anterior parts and the lower posterior of the vertebral body.

Disclosures: ***S. Hamai****, Japan Osteoporotic Foundation (2003) 2; Grants-in-Aid for Scientific Research, Ministry of Education, Culture, Sports, Science & Technology, Japan (2003) 2.*

M370

Premenopausal Women with Idiopathic Osteoporosis Have Histomorphometric Evidence of Decreased Bone Formation. M. A. Donovan[1], H. Zhou*[2], D. McMahon*[1], D. Dempster*[2], E. Shane[1]. [1]Medicine, College of Physicians and Surgeons, Columbia University, New York, NY, USA, [2]Regional Bone Center, Helen Hayes Hospital, West Haverstraw, NY, USA.

Most young people with osteoporosis (OP) have an identifiable cause. Others have an idiopathic form for which no contributory etiology can be found. We have previously reported that men with idiopathic osteoporosis (IOP) have histomorphometric evidence of decreased bone formation and osteoblast dysfunction. The pathogenesis of IOP in young women is unclear. Our aim was to characterize the histomorphometric features of IOP in otherwise healthy premenopausal women. Nine such women, who presented to our clinic with OP and fragility fractures, underwent tetracycline labeled transiliac bone biopsies after secondary causes of OP were excluded by history and biochemical testing. All women were Caucasian. Mean age at diagnosis and menarche was 32.7 and 13.7 yrs respectively. Mean BMI was 21.9 kg/m^2. All had ≥1 fragility fractures and 4 had sustained hip fractures. Three were on oral contraceptives and 5 were taking calcium. Three reported a family history of OP. Mean T-score (±SD) was -2.1±1.0 at the spine and -1.7±1.3 at the hip. Compared to biopsies of age, sex and race matched controls (n=18), significant differences in bone structure and turnover were identified, particularly in cancellous bone. Although cancellous bone volume did not differ, there was a trend toward lower trabecular number (1.7±.2 *vs* 1.9±.2; p=.11) and increased separation (428.6±59.1 *vs* 387.6±73.2um; p=.16) in women with IOP. In cancellous bone, although there was no increase in osteoid thickness or surface, IOP patients had lower bone formation parameters including a 12% reduction in wall width (46.5± 4.0 *vs* 41.1±5.5 um; p<.01), an 18% decrease in mineral apposition rate (0.67±0.11 *vs* 0.82±0.09um/day; p<.01) and a 42% reduction in mineralizing surface (3.8±1.7 *vs* 6.5±3.1%; p=0.02). Similarly, the bone formation rate was 52% lower (.026±0.01 *vs* .054±.03um/um^2/day; p<.01) and the activation frequency was 38.5% lower (0.32±0.30 *vs* 0.52±0.24 cycle/year; p=.07) in IOP patients. Conversely, bone resorption was increased among IOP patients, as reflected by a markedly longer resorption period (RP) (134.2±103.9 *vs* 38.1±23.8 days; p=0.02) and increased eroded surface (ES) (5.5±2.1 *vs* 4.1±1.6%; p=.059). Similarly, wall width and mineralizing surface were significantly lower in endocortical bone and RP and ES were higher in intracortical bone. In summary, women with IOP have evidence of increased bone resorption and decreased bone formation. We conclude that women with IOP have uncoupling of resorption and formation and, like men with IOP, have evidence of relative osteoblast dysfunction.

Disclosures: ***M.A. Donovan****, None.*

M371

Is a Bolster Necessary to demonstrate the Dynamic Mobility of Vertebral Fractures? F. E. McKiernan, R. Jensen*. Center for Bone Diseases, Marshfield Clinic, Marshfield, WI, USA.

Dynamic mobility (DM) is a change in vertebral compression fracture (VCF) configuration between standing and supine cross-table lateral radiographs (vertebroplasty series; VpS). DM may be correlated with greater fracture severity, the presence of intravertebral clefts and predilection for the thoracolumbar junction. DM may be a mechanism by which vertebral height is restored during percutaneous vertebroplasty (PV). The best radiographic method to demonstrate DM is unknown. The purpose of this study is to determine whether an extension bolster is necessary to demonstrate DM when performing VpS.

This IRB approved protocol enrolled consecutive consented adult subjects undergoing VpS as part of their evaluation for possible PV. VpS was performed according to previously published protocol. Standing lateral X-rays centered on the index VCF were taken as usual. Supine cross table lateral X-rays were taken both before and after inflation of a sphygmomanometer bolster placed under the patient in the supine position beneath the level of the index VCF. Bolster inflation ceased when inflation pressure reached 100 mmHg or at patient request. X-rays were evaluated for the presence of DM and intravertebral clefts and manually digitized using centralized PACS system software. Dynamic mobility (DM) was said to be present when change in anterior vertebral height (ΔHa) exceeded our in vivo precision error for this measurement by 2 SD (thus, DM ≥ 0.8 mm). Using a 10-point visual analogue scale (VAS) subjects rated their fracture pain immediately before and immediately after bolster inflation.

37 subjects with 44 VCFs were enrolled. DM was demonstrated in 25/37 subjects and 28/44 VCFs prior to bolster inflation. ΔHa > 2 mm was seen in 19 and between 5 and 12.6 mm in 5/25 subjects. Bolster inflation induced or further enhanced ΔHa >0.8mm in 29/44 and > 2mm (2.1-4.5 mm) in 12/29 VCF. In 10/29 VCFs DM was only appreciated after bolster inflation (1-4.5 mm). Intravertebral clefts were appreciated in 10/37 subjects prior to bolster inflation. 3 clefts increased in size following bolster inflation. One cleft became apparent only after bolster inflation. In 4 VCF Ha decreased after bolster inflation (-0.9 to -1.6 mm). VAS in the supine position was 3.5 immediately prior to bolster inflation and rose to 6.6 immediately after bolster inflation.

Bolster inflation frequently and sometimes substantially enhances DM during VpS. Occasionally DM and rarely clefts are elicited only after bolster inflation. Bolster inflation adds minimal complexity but can add significant discomfort to the VpS. The potential significance of DM is uncertain but opportunities for pain relief and vertebral height restoration at PV may be missed if DM is not appreciated.

Disclosures: ***F.E. McKiernan****, None.*

M372

Spatial and Temporal Differences in Bone Loss Due to Aging and Ovx in the Tibiae of Rats. J. H. Waarsing*[1], J. S. Day*[1], A. G. H. Ederveen*[2], H. Weinans[1]. [1]Erasmus MC, Rotterdam, Netherlands, [2]N.V.Organon, Oss, Netherlands.

During the later years of life, bone mass slowly decreases. In women this loss is accelerated after menopause. In-vitro techniques like histology and conventional micro-CT have been used extensively to study bone loss. Because of limitations of the cross-sectional study design inherit to in-vitro methods it is still not clear how bone loss proceeds in space and over time. The aim of this study was to follow the process of bone loss in the tibiae of aging and ovariectomised rats in a longitudinal study using in-vivo micro-CT

Ten female 10-month old Wistar rats were divided in a sham operated and an ovariectomised group. Over one year post-operation, the right proximal tibiae of the rats were scanned at various time-points, using a prototype in-vivo micro-CT scanner (Skyscan 1076). The animals were scanned at week 0, prior to surgery, and at week 4, 14, 34 and 54. The Animal Ethics Commity approved all animal procedures.

All data sets were repositioned to exactly match the scan at week 0, using image registration software. For the metaphysical trabecular bone, we calculated volume fraction (BV/TV) and trabecular thickness (Tb.Th).

After 4 weeks BV/TV rapidly decreased by 31% in the OVX animals, which gradually proceeded to 83% after 54 weeks. Besides bone loss, also new bone formation was observed at the endosteal cortex. Non-resorbed trabecula increased in thickness (from 139 μm to 153 μm) for all animals (figure 1) and even complete new trabecular structures were formed.

In the sham operated rats, BV/TV slowly decreased at all time points reaching a loss of 37% at week 54, while the thickness of the remaining trabecula increased, again for all animals.

The changes in bone structure for both groups followed a similar pattern. Decrease in bone volume was followed by an increase in trabecular thickness. The similarity between age related bone loss and bone loss caused by OVX might indicate that similar mechanisms are at work, and that estrogen depletion resulted in an increase in the speed at which these mechanisms inflict changes in the OVX group.

The fact that some trabecula increase in thickness while at the same time their neighbors are being resorbed raises questions on how bone cells sense spatial differences. The well-known mechanical responsiveness of bone might make it plausible that the mechanism at work is an ongoing mechanical adaptation of the bone.

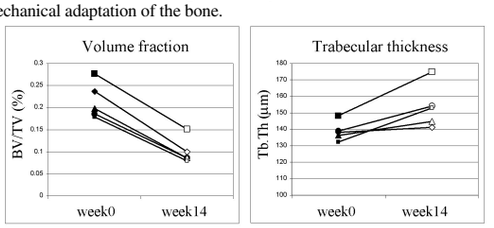

Disclosures: ***J.H. Waarsing****, None.*

M373

A High Prevalence of Vitamin D Insufficiency/Deficiency in a Minimal Truama Fracture Population. C. Simonelli[1], J. A. Morancey*[1], L. Swanson*[2], K. K. Killeen*[2], K. A. Grimm*[3], T. Weiss*[4], Y. Chen[4]. [1]Osteoporosis Services, HealthEast Clinics, Woodbury, MN, USA, [2]Department of Nursing, St. Joseph's Hospital, St. Paul, MN, USA, [3]Department of Research, HealthEast Medical Research, St. Paul, MN, USA, [4]Merck & Co., West Point, PA, USA.

Ideal vitamin D level is reported to be >30 ng/mL to allow for normal mineralization of bone, optimization of calcium absorption, and to prevent osteomalacia and secondary hyperparathyroidism. Low vitamin D is a risk factor for osteoporotic fractures that may be independent of osteoporosis by directly affecting bone mineralization, muscle strength and balance. This bone qualitative defect can only be corrected by adequate vitamin D replacement. We report the prevalence of vitamin D insufficiency/deficiency in a population of adults with non-traumatic fractures.

To evaluate the impact of nurse-practitioner consultation, 82 adults (ages 52-97 with 63% age 80+) consecutively hospitalized with hip and extremity fractures between August 2001 and January 2002 were recruited from two St. Paul, MN hospitals (latitude 42 degrees). Patients came from independent living and assisted living facilities. Demographics, medical history, and vitamin D supplementation were obtained by self-report. Blood specimens were collected during hospitalization within 48 hours of admission. Serum 25-hydroxyvitamin D [25 (OH)D] levels were performed using Diasorin 25-hydroxyvitamin D radioimmunoassay kit (RIA; normal values are 8-30 ng/mL determined in wintertime in Rochester, MN) at Mayo Clinic, Rochester, MN. Results of 25(OH)D levels were available for 78 patients and are included in the current analysis.

Patients were 99% Caucasian, 63% ≥80 years and 78% female. On admission, 9% reported using at least 800 IU per day of vitamin D through supplements (including multivitamins) and 12% were on osteoporosis medication (3 estrogen, 5 alendronate, 1 etidronate, 1 raloxifene). The mean 25 (OH)D level was 14.2 (SD 6.6) with a range of 5-39 ng/mL. The cumulative distribution of 25 (OH)D levels is shown in Figure below.

The majority (82%) of the patients had 25 (OH)D levels ≤20 ng/mL, including 19.2% < 8 ng/mL and 97.4% of patients had 25 (OH)D levels < 30 ng/mL. Mean 25(OH)D levels were not substantially different by gender, age, or osteoporosis medication use. Patients who reported vitamin D supplementation ≥800 IU/day had significantly greater mean 25 (OH)D level, albeit suboptimal, compared to those did not (19.0 vs. 13.7; p = 0.04).

Vitamin D insufficiency/deficiency is common in hospitalized fracture patients, even those who reported sufficient supplementation. Significant opportunity exists to ensure adequate and persistent vitamin D intake in patients at risk for fractures.

Disclosures: ***C. Simonelli****, Merck & Company 2, 5, 8; Alliance For Better Bone Health 5, 8; Eli Lilly & Company 2, 5, 8; Novartis 2.*

M374

Serum Insulin-like Growth Factor Binding Protein-2 (IGFBP2): A Nutrient-responsive Marker of Catabolism after Hip Fracture. R. E. Rizzoli[1], P. Ammann[1], J. Burgess*[2], L. R. Donhaue*[2], C. J. Rosen[2]. [1]Div. Bone Diseases, University Hospital, Geneva, Switzerland, [2]St Joseph Hospital, Bangor, ME, USA.

Insulin-like growth factor binding protein-2 (IGFBP2) is a ubiquitous 30 kilodalton IGF binding protein which circulates in relatively high concentrations (300-500 ng/ml) and has strong binding affinity for extracellular matrices and hydroxyapatite. High levels of serum IGFBP2, inversely related to IGF-I, have been reported in catabolic states such as metastatic disease, protein calorie undernutrition, anorexia nervosa and growth hormone deficiency, although the regulatory determinants of IGFBP2 are unknown. Since hip fracture and the immediate postoperative period is a highly catabolic state, and nutritional supplementation has been shown to accelerate healing and improve functional parameters, we postulated that IGFBP2 would be increased after hip fracture, and then reduced by nutritional supplementation. We thus studied men and women (n=50) who had fracture of the hip (FH) within 10 days of surgery, and elderly unfractured controls (UC, n=28). At time of sampling FH subjects had twice the IGFBP2 concentrations as UC (1119+99 ng/ml vs 586+50 ng/ml; x±SEM, p<0.001). IGF-I was decreased in FH patients (77.1±3.7 vs 126.5±7.5 ng/ml, p<0.001), as were serum prealbumines (172±7 vs 297±7 ng/ml, p<0.001). At 6 and 12 months post surgery, IGFBP2 decreased by 14.7±5.1 and 14.9±4.7 %, respectively (p<0.05 for both). Patterns of serum IGFBP2 6 and 12 months post FH were the opposite of serum IGF-I. This suggests a marked reduction in the bioactivity of IGF-I during the immediate post FH period. Then, to further address the nutrient responsiveness of IGFBP2, we studied adult rats on a normal or an isocaloric low protein (LP) diet followed by essential amino acid supplementation (EAA) using a newly developed RIA for serum IGFBP2. Serum IGFBP2 levels were 183+25 ng/ml in controls, while those in LP fed rats were 230+36. Rats on a LP diet but supplemented either with 2.5% or 5% EAA, had a return of serum IGFBP2 concentrations to baseline (174±19 and 172±14 ng/ml, respectively) together with an overcorrection of IGF-I. In conclusion, high serum IGFBP2 is a marker of the catabolic status during and after surgery for hip fractures. Renutrition is associated with a reduction in IGFBP2. These data illuminate another mechanism whereby nutritional supplementation of hip fracture patients can positively affect functional outcome measures.

Disclosures: ***R.E. Rizzoli****, None.*

M375

Skeletal Effects of Long-Term Marginal Zinc Supply in Aged Rats. R. G. Erben[1], K. Lausmann*[1], W. Windisch*[2]. [1]Institute of Animal Physiology, University of Munich, Munich, Germany, [2]Department of Animal Science, Animal Nutrition, Technical University Munich, Freising, Germany.

A deficient Zn supply has been implicated as a risk factor for osteoporosis in humans. The aim of the current experiment was to investigate the long-term effects of an insufficient zinc (Zn) supply on bone metabolism in aged rats, and to explore further the role of Zn in the pathogenesis of osteoporosis. Nine-month-old female Fischer-344 rats were divided into 8 weight-matched groups with 8 animals each. At the beginning of the experiment, all rats were adapted for one month to restrictive feeding (7.5 g/animal) of a semi-synthetic diet containing 8 g/kg sodium phytate and 64 ppm Zn. Thereafter, 8 animals were killed as baseline controls. For the whole duration of the experiment, control animals were pair fed to account for possible decreases in food intake in the Zn deficient rats. During the 1-month depletion phase, control animals received the Zn replete diet with 64 ppm Zn, whereas the Zn deficient rats were fed the same diet, but with a Zn content of 2.2 ppm. Eight rats in each group were killed after the depletion phase. Subsequently, the 2-month marginal phase began in which the rats on the diet with 2.2 ppm Zn received an additional daily Zn supplement of 75 µg Zn/rat by gavage. At the end of the marginal phase, 1 control and 1 Zn deficient group were killed. In the following repletion phase, 1 marginal group was switched to the Zn replete diet, while 1 group each was maintained on marginal Zn supply or on the Zn replete control diet. All remaining rats were killed after this phase. The Zn-depleted and also the Zn marginal rats showed a significant reduction in the serum concentration of Zn. Serum alkaline phosphatase was decreased by 44% relative to control animals after the depletion phase, and by 28% after the marginal phase. Zn repletion normalized the serum Zn concentrations. Bone Zn content showed a significant reduction in Zn deficient rats not before the end of the marginal phase, and did not reach control levels after the repletion phase. Using biochemical bone markers, bone histomorphometry and pQCT analysis, we found distinct age-related changes in bone metabolism and in bone mass of the appendicular skeleton during the course of the study. However, Zn deficient animals did not show decreased cancellous or cortical bone mass, increased bone resorption, reduced bone formation, or structural changes in bone architecture relative to control rats at any time point. Thus, the current study strongly suggests that Zn does not play an essential role in bone metabolism in adult rats. Based on our findings, it appears questionable whether Zn deficiency is a risk factor for osteoporosis or other bone diseases.

Disclosures: ***R.G. Erben****, None.*

M376

The Effects of Binge Drinking on Bone Turnover. K. C. Westerlind[1], R. Strange*[1], R. Story*[1], G. Evans[2], R. Turner[2]. [1]AMC Cancer Research Center, Denver, CO, USA, [2]Orthopedic Research, Mayo Clinic, Rochester, MN, USA.

Chronic alcohol (ETOH) consumption has repeatedly been shown to result in generalized decreased bone formation and locally increased bone resorption. The prevalence of binge drinking (≥ 5 drinks/session) is increasing at an alarming rate particularly in young individuals but its effect on the bone is not well studied. The purpose of this study in rats was 1) to determine whether gavaging ETOH resulted in elevated blood alcohol concentrations comparable to those in humans and 2) determine the effects of a brief period of binge drinking on histomorphometric indices of bone turnover Thirty-six 6-mos old male Sprague Dawley rats were stratified by weight and randomized to a baseline, binge drinking (gavage-fed 1.2 g ETOH/kg bw, 2x/wk on consecutive days for 2 wks), or control (gavage-fed kcal substitute, 2x/wk on consecutive days for 2 wks). Serum was collected 1 hr post-gavage. Calcein labels (10 mg/kg/bw) were given 5 and 14 days prior to sacrifice. Blood alcohol content (BAC) averaged 56 mg/dL for the binge group vs 3 mg/dL for the controls. This level is significantly lower than that observed in humans who binge drink. Despite low BACs, a significant increase in medullary area (p=0.008) was noted in the binge group (1.23mm^2) compared to controls (1.10 mm^2) and baseline (1.06 mm^2). Cortical area also tended to be reduced [4.64 mm^2 (binge) vs. 5.01 mm^2 (control) and 5.18 mm^2 (baseline); p=0.09]. No change in periosteal bone formation rate was observed. In the cancellous bone, 4 episodes of binge drinking over 2 wks resulted in no difference in mineral apposition rate but non-significant reductions in LS/BS (9.1% vs. 12.7%; p=0.10) and BFR/BS (0.13 µm^3/µm^2/d vs. 0.19 µm^3/µm^2/d; p=0.13) in the binge group compared to controls. The data suggest that binge drinking has a significant effect on bone turnover, specifically increased endocortical resorption and decreased cancellous bone formation. These effects were noted in animals with moderate BAC levels and after only 4 episodes of binge drinking. Longer-term binge drinking behavior with significantly greater concentrations of ETOH could be expected to have more deleterious skeletal effects.

Disclosures: ***K.C. Westerlind****, None.*

M377

Effect of Food Restriction and Hindlimb Unloading on Serum Leptin and Histomorphometric Measures of Cancellous Bone. K. Baek*, A. Currado*, M. Allen*, S. Bloomfield. Texas A&M, College station, TX, USA.

Leptin is a potential candidate responsible for linking energy metabolism to bone mass. Because astronauts are commonly in negative energy balance during spaceflight, this study was designed to assess independent effects of simulated microgravity and food restriction on bone mass and serum leptin. Male Sprague-Dawley rats (6-mo-old, skeletally mature) were randomly assigned to 4 groups (n=12 each). One group was subjected to hindlimb unloading (HU) and fed 100% of their food requirement (HU100), while another HU group was fed 70% of their food requirement (HU 70). Two cage-activity control groups were fed 100%(Con100) and 70%(Con70) of their requirement. On day 0 and day 28, peripheral computed tomography (pQCT,Stratec XCT Research M;Norland) was used to assess bone mineral density(BMD) and serum was collected to measure leptin levels by ELISA (Crystal Chem. Chicago, IL). Fluorochrome labels were given 9 and 2 days prior to sacrifice. Femurs were embedded in plastic, sectioned at 4µm and distal femoral metaphysis was analyzed, using standard histomorphometric techniques for kinetic measures (% mineralizing surface, mineral apposition rate(MAR), and bone formation rate (BFR) and static measures of bone volume (%BV/TV) and forming and resorbing surfaces. All procedures were approved by institutional animal use committee. Con 100 rats gained body weight (BW), whereas all other groups lost BW, the loss was great in HU70 vs CON70 & HU100 ($p<0.05$). We previously reported a decrease in serum leptin was observed after 28days in Con70 and HU100 (-60% and -27%,repectively) and was nondetectable in HU70 rats [Baek et al., JBMR 18:S333,2003].The change in total BMD at the proximal tibia was moderately correlated with the change in serum leptin values over 28d (r^2=.48, $p<0.01$). Percent forming surface in Con 70 and HU100 was significantly lower than that of CON100 (8.66%, 8.90% vs 10.65%, respectively; $p<0.05$) and this decrease was more pronounced in HU70 (3.33%). BFR of CC70 and HU100 was significantly lower than that of CC100 (12.2, 12.1 vs 39.4 [mm^3/mm^2/day], respectively; $p<0.0001$). MAR of CC70 and HU100 was significantly lower than that of CC100 (1.5, 1.6 vs 2.1 [µm/day], respectively; $p<0.05$) The change in BFR was strongly correlated with the change in serum leptin value over 28d (r^2=.73 $p<0.002$). We conclude that moderate caloric restriction could cause bone loss to a similar degree as does the unloading effect of microgravity. Serum leptin might be a key endocrine regulator contributing to this change in bone metabolism.

Disclosures: ***K. Baek****, None.*

M378

The Acute Effects of Different Dietary Phosphate Sources on Calcium and Bone Metabolism in Young Women. H. J. Karp*, K. P. Vaihia*, C. J. E. Lamberg-Allardt. Department of Nutrition, University of Helsinki, Helsinki, Finland.

A high-phosphate intake together with low calcium intake has been shown to elevate the serum parathyroid hormone concentration which causes bone resorption and increased bone turnover. The most important dietary sources of phosphate are meat, milk and grain products. Phosphate salts are commonly used as additives by food industry. Therefore, phosphate is easily achieved in a typical Western diet, and its intake exceeds the recommended amounts 2-3 fold. Dietary phosphate is considered to be easily absorbed in the small intestine. However, there have been only few studies concerning the bioavailability and metabolic consequences of dietary phosphate from different food sources.

The aim of this study was to evaluate the acute effects of dietary phosphate from three different foodstuffs and a phosphate supplement on calcium and bone metabolism. Sixteen female volunteers aged 20-30 participated in the study at five separate 24-hour sessions. At the control session both calcium and phosphate intakes were low (ca. 250 mg/day of Ca, 500 mg/day of P). At the other four sessions phosphate intake was 1500 mg/day, and 1000 mg of it was taken in from meat, cheese, wholegrains or a phosphate supplement, respectively. The foods served were exactly the same at the phosphate sessions and the control sessions, with the exception of the phosphate sources. The order of the days was randomized.

Calcium and bone metabolism was monitored for 24h by measuring the concentrations of serum ionized calcium (S-iCa), serum phosphate (S-P), serum intact parathyroid hormone (S-PTH), and the activity of serum bone specific alkaline phosphatase (S-BALP). The excretions of urinary phosphate (U-P) and urinary calcium (U-Ca) were also measured.

Compared with the control session, the S-P rose at all phosphate sessions (p=0.006-0.001). The S-P level was highest after ingesting cheese compared to all the other sessions (p=0.0001). The U-P was higher during the meat and phosphate supplement sessions as compared to the sessions when grain or cheese were given (p=0.013 and 0.0001, respectively). The S-iCa (p=0.0001) and U-Ca (p=0.003-0.0001) increased at the cheese session as compared with all the other sessions. Compared to the control day, the S-iCa declined after the phosphate supplement (p= 0.026). Due to the high calcium intake, the S-PTH was lower when cheese was given as compared with the control session (p=0.031). The S-BALP activity was higher at the meat than at the control or wholegrain sessions (p<0.045). In conclusion, there were differences in the metabolic response of phosphate from different foods. Phosphate additives had a more unfavourable effect on bone than the foods containing phosphates naturally.

Disclosures: ***H.J. Karp****, None.*

M379

Glucocorticoids Induce Changes Around the Osteocyte Lacunae That Reduces Bone Strength and Bone Mineral Content Independent of Apoptosis: Preliminary Data From A Glucocorticoid-Induced Bone Loss Model in Male Mice. N. E. Lane, M. Balooch*, J. Zhou, Y. Jiang, W. Yao. Medicine, University of California in San Francisco, San Francisco, CA, USA.

Gluococorticoids (GC) excess frequently leads to osteoporosis, with an increased fracture risk. The purpose of this study was to assess cellular, trabecular microstructure and bone strength changes within the trabecular bone of GC treated and GC naïve mice. METHODS: We administered 1.4 mg/kg prednisolone or placebo to 6 mo. old Swiss-Webster mice for 21 days. Serum was collected to assess osteocalcin (OST) by ELISA at day 21. The 5th lumbar vertebrae (LVB) was imaged by µCT for trabecular structure, and then processed for histomorphormetric assessment of bone turnover. Atomic Force Microscopy (AFM) was then used to assess elastic modulus around the osteocytes (OC) lacunae. Apoptotic osteocytes were identified by the TUNEL assay. MicroRaman spectroscopy was performed on trabecular bone of the vertebrae to assess mineral/organic peak ratio around OC lacunae.

Results: Mice treated with GCs had decreased serum OST (79%) and BV/TV (18%) in the LVB compared to GC naïve mice. These changes in GC treated mice were accompanied by decreased bone formation (35%) and increased OC apoptosis compared to GC naïve

(56%). Compared to GC naïve mice and estrogen deficient mice, elastic modulus accessed across trabecular bone regions was significantly reduced in a 40μm^2 area of around all OC lacunae in GC treated mice (67%), independent of OC apoptosis. The ratio of phosphates/ organic content around OC lacunae was significantly reduced (36%) in GC treated mice compared to GC naïve. (all comparisons $p < 0.05$).

In conclusion, we found that GC excess induced loss of trabecular bone mass and bone strength in mice. Accumulation of apoptotic OC may partly contribute to the deterioration of bone strength and structure. However, reduction on elastic modulus and changes in the mineral/collagen content was reduced independent of OC apoptosis. These findings suggest that GC-induced bone fragility arises from changes that occur around the OC lacunae that alters bone strength, independent of apoptosis and in addtion to changes in microarchitecture.

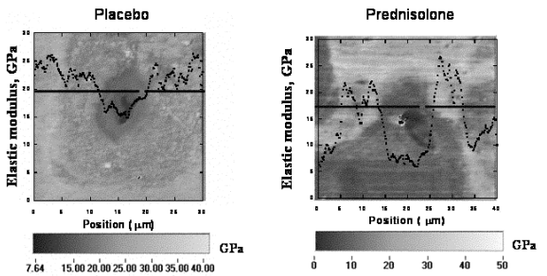

FIGURE ON ELASTIC MODULUS

Disclosures: ***N.E. Lane****, None.*

M380

Transient Stimulation of RANKL and Persistent Inhibition of Osteoprotegerin Expression by Glucocorticoid Administration in Mice: Molecular Correlates of Glucocorticoid Effects on Vertebral Osteoclast Numbers. R. S. Weinstein, D. Jia, C. A. O'Brien, S. A. Stewart*, S. C. Manolagas. Div. of Endo/Metab, Center for Osteoporosis, Central Arkansas Veterans Healthcare System, Univ of Ark for Med Sci, Little Rock, AR, USA.

The adverse effects of glucocorticoid excess on bone result from suppression of osteoblastogenesis and osteoclastogenesis as well as promotion of osteoblast and attenuation of osteoclast apoptosis. In vitro studies indicate that these steroids act directly on differentiated osteoclasts to extend their lifespan, however, it is unknown whether effects of glucocorticoids on other cells also contribute to changes in osteoclast number in vivo. Here, we have studied the temporal relationships among a) the number of osteoclasts and osteoblasts; b) the prevalence of osteoblast apoptosis; c) mRNA expression of RANKL, osteoprotegerin (OPG) and osteocalcin (OCN); and d) the number of osteoblast and osteoclast progenitors in bone taken from mice treated with prednisolone for 3, 7, 10 and 27 days. After 3 days of prednisolone, vertebral cancellous osteoclasts decreased by 50%, as compared to placebo controls; and this change was accompanied by a 45% decrease in osteoclast progenitors. However, the decrease in cancellous osteoclasts was transient as by day 7, osteoclast number increased to 60% above controls while osteoclastogenesis remained low, suggesting that the increase was probably due to prevention of osteoclast apoptosis. Nonetheless, by day 10, cancellous osteoclasts were only 11% above controls and declined further to 60% below controls by day 27. Taqman RT-PCR of mRNA from vertebra showed increased RANKL expression on day 3, preceding the increase in cancellous osteoclasts, but in accord with the osteoclast number, RANKL returned to control levels by day 7 and 10. OPG expression, however, was decreased on day 3 and remained low. Cancellous osteoblasts were profoundly decreased to 8% of controls by day 3 and remained suppressed, due to both reduced production of progenitors and increased apoptosis of mature osteoblasts. OCN expression decreased to 2% of controls by day 3 and remained low, corresponding to the decrease in osteoblast number as indicated by a tight correlation between these two measurements ($r = 0.94$, $P < 0.0001$). The transient increase in osteoclast number and RANKL expression, in spite of a sustained decrease in osteoblast number and osteocalcin expression, strongly suggests that glucocorticoids increase osteoclast number not only by direct actions on osteoclasts but also indirectly by increasing the pro-survival effects of an increased RANKL/OPG ratio and that the cells expressing RANKL are not mature osteoblasts.

Disclosures: ***R.S. Weinstein****, Nuvios 1, 2, 5; P & GP, Novartis, Aventis, Roche 2; Merck 5.*

M381

Species Specific Differences in Bone Metabolism and Osteoprotegerin Regulation During Glucocorticoid Treatment. E. G. Vajda, K. N. Griffiths*, W. Y. Chang*, L. Wang*, A. L. Hogue*, F. J. López*, O. H. Viveros*. Pharmacology, Ligand Pharmaceuticals, Inc., San Diego, CA, USA.

In humans, glucocorticoids (GCs) induce osteoporosis through two mechanisms, a transient elevation of bone resorption leading to an acute rapid loss of bone, followed by a phase of slower bone loss due to a chronic deficit in bone formation. Recent clinical studies suggest that the increase in resorption induced by GCs is the result of decreased serum levels of osteoprotegerin (OPG), an inhibitor of osteoclastogenesis. In these studies, we investigated the actions of dexamethasone and prednisolone (14 day treatment) in male Swiss-Webster mice on serum concentrations of osteocalcin (OC), OPG, and RANKL. Both dexamethasone and prednisolone significantly reduced serum levels of OC (79% and 53% reduction, respectively), increased serum OPG (72% and 35%), and decreased serum levels of free-soluble RANKL (30% and 33%) in a dose dependent manner. Subsequently, the effects of prednisolone on bone mass were examined in a 28 day treatment regimen. Prednisolone produced similar alterations in biochemical markers as observed in the shorter treatment period. In contrast, prednisolone treatment did not reproducibly decrease total body or spinal bone mineral density assessed by dual energy x-ray absorptiometry. Microcomputed tomography scans of the distal femur and histomorphometric analysis of the lumbar spine confirmed no statistically significant treatment-related decrease in trabecular bone volume. Dynamic histomorphometric analysis, however, revealed dramatically reduced lumbar spine trabecular bone formation rates (vehicle = 0.28 ± 0.05 μm^2/μm/day; prednisolone = 0.04 ± 0.02 μm^2/μm/day; $p<0.001$). Retention of fluorochrome labels administered prior to treatment, a measure of bone resorption, was increased by prednisolone, indicating suppression of bone resorption. These results clearly show that glucocorticoids dramatically suppress bone formation in mice, consistent with the findings in humans. Unlike humans, however, rapid dramatic loss of bone was not observed in the mouse. The absence of GCs effects on bone resorption in mice is probably explained by increased production of OPG and consequent reduction in bone resorption. These data suggest that the early rapid bone loss observed in humans, but not in mice, after treatment with GCs is the result of species specific differences in the regulation of the OPG/RANKL pathway.

Disclosures: ***E.G. Vajda****, Ligand Pharmaceuticals 3.*

M382

Histomorphometric Analysis of Osteopenia Induced by Immunosuppressive Drugs in Rats. Effects of Risedronate. L. Dalle Carbonare*[1], S. Giannini[2], S. Zordan*[2], M. Valenti*[1], F. Bertoldo*[1], G. Realdi*[2], G. Crepaldi[3], V. Lo Cascio[1]. [1]Biomedical and Surgical Science, Internal Medicine D, University of Verona, Verona, Italy, [2]Internal Medicine, University of Padua, Padua, Italy, [3]CNR Aging Center, Padua, Italy.

Osteopenia is an important complication after transplantation. Corticosteroids is one of the most important pathogenic factors, while more contrasting data have been reported about the effects on bone metabolism of cyclosporin A. Bisphosphonates are a powerful therapeutic option to prevent osteoporosis and related fractures.

The aims of this study based on the rat model were: 1. to verify structural alterations on bone induced by immunosuppressive therapy with glucocorticoids (GC) and ciclosporin A (CsA); 2. to establish the efficacy of Risedronate (Ris) in the prevention of these effects.

We studied 70 female Sprague-Dawley rats, maintained at the same standard diet. The rats were divided randomly into 7 groups of treatment (10 rats each) as follows:

1.Control group: CsA vehicle + vehicle of Methyl Prednisolone (MP) + vehicle of Risedronate (Ris);
2. *Group MP*: 7 mg/Kg 3 times a week s.c. + CsA vehicle + vehicle of Ris;
3. *Group CsA*: CsA 3 mg/Kg 3 times a week s.c. + vehicle of MP + vehicle of Ris;
4. Group CsA + MP + vehicle of Ris;
5. Group CsA + Ris 5 mg/Kg body weight 3 times a week + vehicle of MP;
6. Group MP + Ris + CsA vehicle;
7. Group CsA + MP + Ris.

All the rats were weighed once a week to adjust the dose of drugs to body weight and they were treated for 30 days. Then, the rats were sacrificed. Histomorphometric evaluations on the right tibiae of 42 rats showed a reduction of bone volume (BV/TV) with a thinning of the trabeculae (TbTh), associated with decreased osteoblastic activity (BFR/TV) in GC treated group with respect to controls (BV/TV: 33±1 vs 36±1%, $p < 0.05$; TbTh: 43 vs 50mm, $p < 0.01$; BFR/TV: 15.8 vs 22.1%/y; $p < 0.01$). Risedronate seemed to counteract the effects of GC on bone (BV/TV 38±3%, $p <0.05$ vs group 2; TbTh: 53±2mm, $p < 0.01$ vs group 2; BFR/TV: 23.2 ±2.4%/y, $p < 0.01$ vs group 2). In addition, risedronate was able to preserve microarchitecture, expressed as the number of nodes (NdN/TV) and Marrow Star Volume (MSV), (NdN/TV: 27±5 #/mm^3; MSV 0.04±0.01 mm^3, $p < 0.01$ vs GC).

In conclusion, preliminary histomorphometric data of this pre-clinical rat model of secondary osteopenia, highlighted that risedronate was able to preserve bone quality in 30 days, whereas GC treated group showed that bone quality was readily deteriorated.

Disclosures: ***L. Dalle Carbonare****, None.*

M383

Bone Loss Is More Severe In Primary Adrenal Than In Pituitary-Dependent Cushing's Syndrome. M. Minetto*, G. Reimondo*, G. Osella*, M. Ventura*, A. Dovio*, M. Terzolo*, A. Angeli. Department of Clinical and Biological Sciences, University of Turin, Orbassano, Italy.

Exogenous or endogenous glucocorticoid (GC) excess is an established cause of osteoporosis and fractures. As many as 50% of patients with Cushing's syndrome suffer from osteoporosis. It is presently unknown if Cushing's disease (CD) sustained by a pituitary ACTH-producing adenoma and adrenal-dependent Cushing's syndrome (ACS) sustained by an adrenocortical adenoma have a different potential of inducing osteopenia. Aim of the present study was to retrospectively analyze bone mineral density (BMD) in 26 patients with CD (4 men, 22 women, aged 14-79 years), 12 patients with ACS (4 men, 8 women, aged 32-79 years) and 38 healthy subjects carefully matched for sex, age and body mass index (BMI). Measurement of BMD was performed by dual energy x-ray absorptiometry (DXA) using the Hologic QDR 4500 W instrument. Data were analyzed using absolute BMD values (g/cm^2), t-score and z-score referred to the manufacturer's normative data for the lumbar spine and to the NHANES III dataset for the hip. The patients with CD and ACS were comparable for age, BMI, estimated duration of disease, urinary free cortisol (UFC) levels, midnight serum cortisol and gonadal function. Lumbar DXA values were significantly different among the three groups. They were more reduced in patients with ACS (BMD, 0.76 ± 0.03 g/cm^2; t-score, -2.78 ± 0.28; z-score, -2.25 ± 0.30) while patients with CD (BMD, 0.87 ± 0.02 g/cm^2; t-score, -1.74 ± 0.24; z-score, -0.99 ± 0.32) showed DXA values between the first group and controls (BMD, 1.02 ± 0.02 g/cm^2; t-score, -0.35 ± 0.19; z-score, 0.33 ± 0.16). The difference in BMD at the spine remained statistically significant (p=0.04) after adjustment for the non-significant differences in age, UFC and fat mass between CD and ACS. Conversely, femoral DXA values were not significantly different between patients with ACS and CD, even if they were reduced with respect to controls. In patients with ACS, we observed a reduction of DHEA-S levels, expressed as standard score (z-score) to circumvent the pronounced effect of gender and age on such hormone (DHEA-S z-score: ACS -0.88 ± 1.4 vs. CD 2.25 ± 2.35, p=0.0001). DHEA-S z-score values were significantly correlated with lumbar BMD (r=0.41, p=0.02) and femoral BMD (r=0.43, p=0.01). DHEA-S z-score values were also significantly correlated with osteocalcin levels (r=0.45, p=0.01). Our data suggest that bone loss is greater in ACS than in CD. A plausible explanation comes from the reduced DHEA-S level in ACS since DHEA-S has well known anabolic actions on bone. However, this hypothesis needs to be confirmed in large, prospective series of patients with Cushing's syndrome of different etiology.

Disclosures: ***M. Minetto****, None.*

M384

Cortical Bone Is Superior to Trabecular as an Indicator of Glucocorticoid-induced Vertebral Osteoporosis in a Murine Model. P. L. Salmon[1], O. Baeyens*[1], D. Souza*[2]. [1]Application Research, Skyscan, Aartselaar, Belgium, [2]Pharmaceutical R&D, Boehringer Ingelheim Inc., Ridgefield, CT, USA.

Glucocorticoid induced osteoporosis (GIO) has proved difficult to reproduce in a mouse model. Mice frequently gain increased trabecular relative volume in response to steroids. However murine vertebral cortical bone may be superior to vertebral trabecular bone as a model of GIO, since the cortical volume and thickness changes are in the right direction and dose-dependent. Mice were treated by injection with either vehicle or the steroid prednisolone for five weeks. Lumbar vertebral morphometry was assessed post-mortem by micro-CT. The response to prednisolone of the lumbar vertebral body volume was biphasic - first a decrease then an increase in total vertebral size with increasing prednisolone dose. Trabecular bone relative volume (BV/TV) at the mouse lumbar vertebral body showed small changes which were also biphasic, mirroring vertebral volume. BV/TV significantly increased in the group receiving 10 mg/kg prednisolone, while higher doses showed decreasing BV/TV. Bone structure thickness showed a more unidirectional response. There was a consistent dose-dependent reduction in thickness in both trabecular and cortical vertebral bone, in response to prednisolone, which was more pronounced and significant for cortical bone. The trabecular thickness decrease however was accompanied by an increased trabecular number (the density of trabecular structures) with the overall result that there was either no significant change, or a slight increase in relative trabecular volume. Structure model index also showed biphasic outcome in trabecular bone, with a decrease at low to medium doses of prednisolone reversed to no effect at high dose. By contrast, cortical thickness and volume showed dose-dependent decrease in response to steroid over the whole dose range. Thus cortical bone appears to be superior to trabecular bone, in the mouse vertebra, as a model indicator of the osteopenia in humans caused by the sharp reduction in bone formation rate resulting from glucocorticoid administration.

Disclosures: ***P.L. Salmon****, None.*

M385

Lack of Significant Low Bone Density in Many Glucocorticoid Treated Children. R. P. Green. Pediatrics, Washington University School of Medicine, St. Louis, MO, USA.

Purpose: Glucorticoid treated children followed by a variety of subspecialty groups were evaluated longitudinally to characterize the natural history of glucocorticoid (GC) mediated bone disease in childhood, and as part of an effort to recruit children for a GC-induced bone disease treatment protocol.

Methods: Pediatric patients from various subspecialties, including lung transplant, pulmonary, rheumatolgy and GI clinic, who had used or were anticipated to use suprphysiologic doses of a glucocortiocid medication were invited to participate. Each participant underwent BMD assessment at approximately 6 month intervals. Because of the effect of size on BMD, both chronologic age Z scores and height age (HA) adjusted Z scores were determined at hip and spine on each scan using a Hologic QDR4500 scanner and a Hologic Research Database with gender specific normals.

Results: Based on all BMD measurements, GC treated children had bone density Z scores below the population expected mean for both chronologic age and height age [spine mean -1.19 SDS (CI -1.57 to -0.81), height age spine mean -0.64 SDS (CI -1.0 to -0.28), hip mean -1.12 SDS (CI -1.43 to -0.81), height age hip mean -0.66 SDS (CI -0.92 to -0.4). Despite this, when using -2 SD below the mean BMD for height age to define low BMD, less than 10% of BMD measurements in GC treated children met the criteria for low BMD. 4 children had clinical evidence of osteoporosis (vertebral fracture or low trauma extremity fracture). These children had BMDs significantly below children without clinical evidence of osteoporosis (spine mean Z score -3.14 vs -0.96; hip mean Z score -2.0 vs -1.0).

Conclusion: Many GC treated children do not have DEXA evidence of significantly low BMD. Children in this population who had clinical evidence of osteoporosis based on fracture did have BMDs significantly below the remainder of the population. Further research is needed to define whether DEXA BMD can be used in the clinical setting to identify those GC treated children at risk of fracture.

Disclosures: ***R.P. Green****, None.*

M386

See Plenary Poster number F396

M387

Low Dose Estradiol Rapidly Increases Osteoblastic Procollagen Production in Postmenopausal Women. P. Y. Liu*, K. L. Mielke*, K. A. Hoey*, J. D. Veldhuis*, S. Khosla. Endocrine Research Unit, Mayo Clinic, Rochester, MN, USA.

The acute effects of estradiol on procollagen type 1 formation in postmenopausal women are controversial. Eighteen pre- and 12 postmenopausal women received two consecutive i.m. injections of 3.75 mg leuprolide acetate three weeks apart to block endogenous ovarian steroidogenesis. Transdermal estradiol therapy commenced on the night of the second leuprolide injection in an incremental stepwise fashion, with each dose of 0.05, 0.10, 0.15 and 0.20 mg per day administered for 4 consecutive days, to mimic the estradiol changes typifying the follicular phase of the menstrual cycle. Blood aminoterminal propeptide of type I procollagen (PINP), intact osteocalcin (OC), carboxyterminal crosslinked telopeptide of type I collagen (CTx) and estradiol were measured before, and then every 4 days during estradiol therapy. In the postmenopausal women, serum estradiol concentrations significantly increased from 7.1 ± 0.9 (SEM) to 150 ± 25 pg/mL (P<0.001). Furthermore, as illustrated, PINP increased by 5.7 ± 2.7 µg/L (P<0.03) from baseline after 4 days of low-dose estradiol therapy, continued to rise and remained significantly above baseline for the entire 17 day duration of estradiol therapy. Whilst PINP increased, CTx and OC did not change. Similar, but muted, alterations were seen in premenopausal women. The relationship between the changes in estradiol and PINP was further explored by multilinear regression. This demonstrated a highly significant association (P=0.001), which differed between pre- and postmenopausal women (P=0.015).

We conclude that low dose estradiol rapidly increases osteoblastic collagen synthesis in postmenopausal women at a time when collagen degradation is stable. Further analysis of the data being collected will dissect any difference in estradiol's effects on serum markers of bone turnover in pre- vs postmenopausal women.

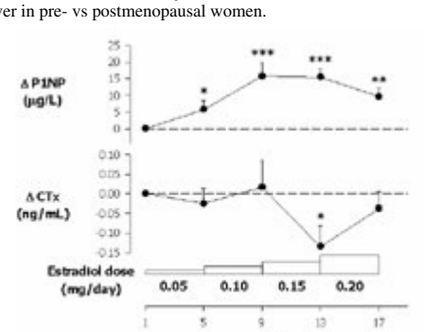

Disclosures: ***P.Y. Liu****, None.*

M388

Characterization of the Changes on Trabecular, Endocortical and Periosteal Bone in Senescence Accelerated Mouse (SAMP6) and the Effects of Testosterone. H. Z. Ke, G. Xu*, H. A. Simmons, H. Qi, D. T. Crawford*, L. C. Pan, M. Li. Pfizer Global Research and Development, Groton, CT, USA.

The SAMP6 strain (P6) has been investigated as a model of senile osteoporosis. It has been reported that P6 has lower trabecular bone mass and bone formation due to a defective osteoblastogenesis. However, the changes on different bone surfaces in P6 have not been fully characterized. The purposes of this study were to (a) characterize the changes on trabecular, endocortical and periosteal bone in P6 as compared with normal control (R1) mice in both sexes, and (b) test whether testosterone propionate (TP) can increase bone mass in P6 males and females. Ten male and 10 female R1 control mice, and 8 male and 10 female SAMP6 at 5.5 months of age were treated with vehicle, while another 8 male and

11 female SAMP6 were treated by s.c. injection with TP at 10 mg/kg/d for 8 weeks. Compared with male R1 controls, male P6 had significantly lower total mineral content (-15%), total mineral density, trabecular density, cortical content and cortical thickness, and a significantly higher marrow cavity area in the distal femoral metaphysis (DFM) by PQCT analysis. Micro-CT analysis of DFM showed male P6 had a 33% lower trabecular bone volume, while trabecular bone histomorphometry showed that male P6 have a lower mineral apposition rate and mineralizing surface. In FS, a significantly lower total mineral density (-15%) and cortical thickness with a significantly higher total bone area, marrow area (+43%), periosteal and endocortical circumferences were observed in male P6. These data indicate that the male P6 had lower bone mass on trabecular and endocortical compartments due to a lower bone formation. However, male P6 had increased cross-sectional area and marrow cavity area of long bone, indicating higher bone resorption on endocortical surface and higher bone formation on periosteal surface. TP treatment in male P6 significantly increased bone mass by further reducing bone turnover in trabecular compartment but had no effect on endocortical and periosteal compartments. Similarly, a lower bone mass in trabecular and endocortical compartments and increased cross-sectional area of long bone were found in female P6 compared with female R1 controls. However, TP failed to increase bone mass in neither trabecular, endocortical nor periosteal compartments in female P6. These results reveal that both male and female P6 had lower trabecular and endocortical bone mass due to a lower bone formation, thus can be used as senile osteoporosis models. Testosterone increases trabecular bone mass but fails to increase endocortical and periosteal bone mass in male P6, while it has no effect on female P6.

Disclosures: ***H.Z. Ke****, Full Time Employee of Pfizer Inc. 3.*

M389

Free Serum Estradiol Levels Correlate with both Trabecular and Cortical Volumetric Bone Mineral Density in Young Adult Swedish Men. M. Lorentzon, A. Eriksson, C. Ohlsson. Department of Internal Medicine, Center for Bone Research at the Sahlgrenska Academy (CBS), Gothenburg University, Gothenburg, Sweden.

Estrogens regulate skeletal growth and mineralization in males. The aim of the present study was to determine the associations between serum levels of estradiol (E_2) and skeletal size and mineralization in young adult males. The *G*othenburg *O*steoporosis and *O*besity *D*eterminants (*GOOD*) study consists of 1075 men, age 18.9±0.6 yrs, and was initiated with the aim to find both environmental and genetic determinants for bone and fat mass. Bone parameters were measured using both DXA and pQCT. Serum levels of SHBG and E_2 were measured using RIA and free E_2 (fE_2) levels were calculated.

Regression models using physical activity, smoking, age and fE_2 as covariates showed that fE_2 was an independent predictor of areal BMD in the total body, the total femur, the femoral neck and the trochanter ($p<0.01$) but not in the spine as measured by DXA. pQCT analysis demonstrated that fE_2 was an independent predictor of both trabecular (radius β=0.13, *p<0.001;* tibia β=0.11, *p<0.001*) and cortical (radius β=0.10, *p<0.001;* tibia β=0.12, *p<0.001*) volumetric BMD but not of cortical periosteal circumference or cortical cross sectional area. The subjects with the highest tenth percentile of fE_2 (n=107) had 9.5 % ($p<0.01$) higher trabecular volumetric BMD in the radius than the subjects with the lowest tenth percentile of fE_2 (n=108). These findings demonstrate that fE_2 is a predictor of both the trabecular and the cortical volumetric BMD but not of the size of the cortical bone in young adult Swedish men.

Disclosures: ***M. Lorentzon****, None.*

M390

Serum Leptin and Resistin Levels are associated with Lumbar Spine Bone Mineral Density in the Middle-aged Men. K. Oh*[1], C. Park*[1], S. Ihm*[1], S. Park*[1], E. Rhee*[2], W. Lee[2], K. Baek[3], M. Kang[3]. [1]Internal Medicine, Hallym University, Anyang, Republic of Korea, [2]Internal Medicine, Sungkyunkwan University School of Medicine, Seoul, Republic of Korea, [3]Internal Medicine, The Catholic University of Korea, Seoul, Republic of Korea.

Fat mass is an important determinant of bone mineral density (BMD), but the mechanism involved in this relation is uncertain. Several lines of evidence have suggested that the effects of fat mass on BMD may be mediated by hormonal factors, with the principal candidates being serum sex hormone, insulin, leptin, and adiponectin. Thus, the aim of this study was to investigate the relationship between serum adipocytokine and ghrelin levels, and BMD in men. Subjects were eighty men aged 42~70 (mean age, 54.5 yr). Serum concentrations of leptin and ghrelin were measured with RIA, adiponectin with ELISA, and resistin with EIA. Serum concentrations of estradiol, total testosterone, and biochemical markers of bone turnover were measured by standard methods. BMD at lumbar spine and femoral neck were measured by dual energy x-ray absorptiometry. Serum leptin levels were correlated to body mass index (BMI), waist to hip ratio (WHR), blood pressure, fasting blood sugar, serum fasting insulin, total cholesterol, triglyceride, and calcium levels. Although serum leptin levels were not significantly correlated to serum estradiol levels, but there was a weak trend in it. Serum adiponectin levels were correlated to BMI, WHR, and serum fasting insulin levels; resisitin to serum total cholesterol and low density lipoprotein cholesterol levels; ghrelin to age, WHR, and serum triglyceride levels. We observed a significant negative correlation between serum resistin levels and lumbar spine BMD. Also, there was a significant negative correlation between serum leptin levels and lumbar spine BMD. The above correlation was observed only when BMI, serum estradiol and insulin levels were included, as an independent variable, in the regression analysis model. Serum adiponectin levels were not significantly correlated with BMD, either in the presence or absence of BMI and serum insulin levels. We observed that the serum adipocytokine levels are partly associated with BMD in men. So, these data suggest that leptin and resistin may play a role on the bone mineral metabolism in men. Further studies are needed to clarify this relationship.

Disclosures: ***K. Oh****, None.*

M391

Hypomineralization of Bone Matrix in Male Patients with Idiopathic Osteoporosis and Fragility Fractures. S. Poetter-Lang*[1], P. Roschger[2], A. Nader*[3], P. Fratzl*[4], H. Resch*[1], K. Klaushofer[5]. [1]2nd Med.Dept., St. Vincent Hospital, Vienna, Austria, [2]Ludwig Boltzmann Institute of Osteology, 4th Med. Dept., Hanusch Hospital and UKH-Meidling, Vienna, Austria, [3]Institute for Pathology, Hanusch Hospital, Vienna, Austria, [4]Max Planck Institute of Colloids and Interfaces, Dept. Biomaterials, Potsdam, Germany, [5]Ludwig Boltzmann Institute of Osteology, 4th Med. Dept., Hanusch Hospital, Vienna, Austria.

Transiliac bone biopsies from male patients (n=24, mean age: 47 ±12) with idiopathic osteoporosis and fragility fractures (vertebral and non vertebral) were investigated for microarchitecture and bone mineralization density distribution (BMDD) to elucidate their contribution to fracture risk. Microarchitecture was described by trabecular bone volume (BV/TV), trabecular thickness (Tb.Th) and trabecular connectivity (N.Bf./B.Ar.). Mean calcium content (CaMean), the variation of calcium content (CaWidth) and the percentage of low mineralized matrix (CaLow) measured by quantitative backscattered electron imaging (qBEI) were used to characterize BMDD. The data were compared to published normative data. The clinical chemical parameters and the results of osteodensitometry (BMD measured by DXA) were compared to those of a healthy male control group (n=35, mean age: 49±9).

The clincal parameters and the biochemical markers of bone turnover of the patients did not differ from the control group. The mean value of T-score (neck: -2.2±0.8 SD, spine: -2.7±1 SD, n=24) of the patient group was significantly ($P<0.001$) different from that of the control group (neck : -0.7±1.1 SD, spine: -0.2±0.9 SD, n=35). The analysis of the biopsies revealed that patients with fragility fractures were characterized at the tissue level by reduced Tb.Th.(-12.9 %) and at the material level by decreased CaMean (-5.8 %, $P<0.0001$), increased CaWidth (+15.9 %, $P<0.0001$) and increased CaLow (+27 %). No correlation was found between BMD of lumbar spine or hip and number of clinical fractures. In contrast multiple fractures were significantly correlated ($r=0.8$; $p<0.001$) to connectivity.

We conclude from these data, that hypomineralization at the material level but not BMD is linked to fracture risk in idiopathic male osteoporosis.

Disclosures: ***S. Poetter-Lang****, None.*

M392

Sex Hormone Binding Globulin in Primary and Secondary Osteoporosis in Men. E. Legrand, T. Couchouron*, P. Insalaco*, D. Chappard, M. Baslé*, M. Audran. Service de Rheumatologie, CHU et Inserm-EMI 0335, Angers, France.

Background: We have shown that Sex Hormone Binding Globulin (SHBG) serum concentration was increased in men with osteoporosis (OP) and was correlated with hip bone mineral density. However the cause of high serum SHBG has not been investigated (*Legrand, Bone 2001, 29: 90-95*). .

Aim: To compare SHBG and bioavailable steroids serum levels in men with primary or secondary OP.

Methods: 341 men (mean age 57.1 years) with a spine or a hip low BMD (T-score< -2) and 50 controls were included in a cross sectional and prospective study. Age, BMI and risk factors for osteoporosis were checked. Fasting serum samples were assayed for total and free testosterone, total and bioavailable estradiol and SHBG. Men without risk factors and with normal total testosterone (n= 137) were categorized as Primary OP. Spinal X rays films were analysed independently by 2 trained investigators and vertebral fracture was defined as a reduction of at least 20% in the anterior, middle or posterior vertebral height.

Results: In the total cohort, SHBG concentration was higher (38.8 vs 24.4 nmol/l, p< 0.001) and bioavailable estradiol (75.5 vs 128.2 %) and testosterone (14.7 vs 25.4%) were lower in patients compared with controls. After adjusting for age and BMI, there was no significant difference between primary and secondary OP for SHBG, total and bioavailable estradiol. Furthermore, SHBG and bioavailable estradiol levels were not correlated with tobacoo smoking, alcohol consumption or corticosteroids use. In contrast, total testosterone (4.2 vs 4.9 microg/l, p< 0.01) and bioavailable testosterone(12.9 vs 17.23 %) were lower and LH (6.1 vs 4.4 IU/l) was higher in men with secondary OP.

After adjusting for BMI, total testosterone and estradiol, hip BMD was correlated with SHBG in primary OP (r = 0.34, p< 0.001) and in secondary OP (r = 0.17, p< 0.01). Finally, logistic regression analysis showed that after adjusting for BMI, SHBG was strongly associated with the presence of vertebral fracture in men with primary OP (1SD increase, Odds ratio = 2.4, CI 1.3-4.5) or secondary OP (1SD increase, Odds ratio = 2.2, CI 1.4-3.5)

Conclusions These results confirm that SHBG serum level is higher in men with OP, correlates with hip BMD and vertebral fracture, *independently* of classical risk factors such as tobacco smoking, alcohol abuse or corticosteroid therapy. In contrast these factors inhibit the secretion of testosterone, which could worsen bone loss. Family and genetic studies are needed to elucidate the over expression of SHBG in men with low BMD.

Disclosures: ***E. Legrand****, None.*

M393

Rapid Bone Loss at the Hip in HIV-infected Postmenopausal Women. M. T. Yin*, J. Dobkin*, V. Addesso, J. Zadel*, K. Brudney*, E. Shane. Medicine, Columbia College of Physicians & Surgeons, New York, NY, USA.

Low bone mineral density (BMD), a complication of HIV infection and antiretroviral therapy (ART), has been reported both in HIV-infected men and premenopausal women, although increased rates of bone loss have not been observed consistently in these groups. The incidence of HIV infection is increasing among postmenopausal (PM) women, in whom the risk for fractures and the need for intervention may be much greater. In this regard, we have reported that that the prevalence of osteoporosis (T<-2.5) at the lumbar spine (LS) was significantly greater in Hispanic and African-American HIV+ than HIV- PM women (41% vs 22%; p< 0.05). HIV status remained a significant predictor of LS BMD after controlling for age, body mass index (BMI) and ethnicity.

Hypothesizing that rates of bone loss would be more rapid in HIV+ than normal PM women, we measured BMD by DXA and biochemical indices of mineral metabolism in 32 HIV+ PM women at baseline and 1 year. Because comparable data have not been published for African-American and Hispanic women, annual % change in BMD in the HIV+ women was compared with data from healthy white PM women after stratification for early (<5 years) and late (>5 years) after menopause. Correlates of annual % change in BMD were evaluated by t-tests and simple regression. Data are reported +/- SEM.

Subjects were aged 56 +/- 2 and were PM by 10 +/- 2 yrs. 72% were Hispanic and 28% African American. Time since HIV diagnosis was 8 +/- 2 yrs; 79% were currently on ART and of those, the mean duration of ART was 5 +/- 1 yrs. Annual % change in femoral neck BMD was -2.5 +/- 0.9% in the early menopause group (N=10) and -2.7 +/- 1.6% in the late group (N=19), both higher than the upper limit of annual rates reported in healthy PM women (-0.6%). Annual % change in total hip (TH) BMD was positively correlated with time since HIV diagnosis (r=0.38, p=0.04), and baseline levels of bone turnover markers: osteocalcin (r=0.51, p<0.01), bone specific alkaline phosphatase (r=0.43, p=0.02), and N-telopeptide (r=0.41, p=0.04). Annual % change in TH BMD was not significantly correlated with age, time since menopause, BMI, nadir CD4, duration or class of ART, or serum levels of 25-OH vitamin D. Annual % change in lumbar spine BMD was within the range reported for healthy women.

In summary, the higher prevalence of osteoporosis in PM Hispanic and African American PM women with HIV is also associated ongoing bone loss that is greater than expected at the hip and associated with biochemical evidence of increased bone remodeling. We conclude that Hispanic and African American PM women with HIV may be at increased risk for hip fracture and should be evaluated and treated for osteoporosis.

Disclosures: ***E. Shane****, None.*

M394

OPG Polymorphism, Serum RANKL, Serum OPG and Bone Metabolism in Men. D. Merlotti, L. Gennari, G. Martini, A. Calabrò*, V. De Paola*, N. Dal Canto*, S. Salvadori*, R. Valenti*, B. Franci*, S. Campagna*, B. Lucani*, R. Nuti. Dept. of Internal Medicine Endocrine Metabolic Sciences and Biochemistry, University of Siena, Siena, Italy.

Osteoprotegerin (OPG) is a soluble decoy receptor that binds to the receptor activator of NF-kB ligand (RANKL), the final effector molecule for osteoclastogenesis. Both OPG and RANKL are present in the circulation in detectable amounts, however their relationship with bone mass and bone turnover in men has not been completely established. We conducted a study aimed at evaluating serum OPG and RANKL levels and their correlation with OPG polymorphism (C/T), bone turnover markers, cytokine levels, sex hormones and BMD in 100 elderly men. Serum OPG levels increased with age (r=0.26; p<0.05), while RANKL levels did not significantly varied with age (r=-0.02). OPG correlated inversely with serum bioavailable testosterone (r=-0.28; p<0.05) and estradiol levels (r=-0.26; p<0.05) and positively with LH levels (r=0.31; p<0.01). In contrast, there was no correlation between OPG or RANKL and biochemical markers of bone turnover. RANKL levels were positively correlated with circulating IL-6 (r=0.39; p<0.01) and TNF-alpha (r=0.23; p<0.05), while no relationships between OPG and cytokine levels were observed. Interestingly, even though no correlations were observed with baseline BMD (lumbar spine and femoral neck) or quantitative ultrasound (QUS) parameters at calcaneous and phalanxes, both OPG and RANKL levels appeared slightly and negatively correlated with rates of bone loss at the femoral neck (r=-0.20 and r=-0.23, respectively; p<0.05). No major differences were observed in markers of bone turnover, baseline BMD, QUS or rates of bone loss in subjects grouped according to either serum OPG or RANKL above or below the median value. However, subjects with serum RANKL levels below the median value showed higher bioavailable estradiol levels and lower IL-6 and TNF-alpha levels. Even though osteoporotic subjects showed higher OPG and RANKL levels with respect to non osteoporotic subjects these differences were not statistically significant. Finally, no significant differences in bone turnover markers, BMD and rates of bone loss were observed according to the C/T polymorphism in the OPG gene, except for OPG levels that were higher in men homozygous for the C allele. In conclusion, our data confirm that age and sex hormones are important determinant of serum OPG levels in men. While the increase in circulating RANKL may reflect an increase in bone remodeling, the rise in circulating OPG could represent an homeostatic mechanism to limit bone loss.

Disclosures: ***D. Merlotti****, None.*

M395

Posturographic Evaluation of the Effects of Alfacalcidol and Active Absorbable Algal Calcium (AAA Ca) on Sway Parameters with Eyes Opened and Closed. T. Fujita[1], S. Nakamura*[2], M. Ohue*[2], Y. Fujii[1], A. Miyauchi*[3], Y. Takagi*[3], H. Tsugeno*[4]. [1]Calcium Research Institute, Kishiwada, Japan, [2]Katsuragi Hospital, Kishiwada, Japan, [3]National Sanatorium Hyogo Chuo Hospital, Sanda, Japan, [4]Tsuyama Chuo Hospital, Tsuyama, Japan.

Swaying and postural in stability frequently seen in elderly subjects representing one of the risk factors has been difficult to evaluate accurately until the introduction of computerized posturography. In view of the effects of vitamin D derivatives and active absorbable algal calcium (AAA Ca) preventing fracture in addition to moderately increasing bone mineral density (Journal of Bone and Mineral Metabolism 22: 32-38, 2004), 30 subjects without specific disorders of mineral metabolism or neurological disorders were randomly selected and divided into 3 groups of 10 subjects each. After baseline posturography, group A was given 1μg alfacalcidol daily, group B 900 mg calcium as AAA Ca and group C nothing in addition to continued daily food. Mean age (61± 2, 62 ± 2 and 63 ± 2 years in groups A, B and C respectively) and lumbar bone mineral density was indistinguishable among these groups. After 2 months, posturography was repeated. Paired t-test before and after treatment revealed significant decrease of the area covered by the tract of the center of gravity indicating the extent of sway (p=0.0039) and significant increase of the tract density per unit area indicating sway-control efficiency (p=0.0054) in group A but not B and C, with eyes opened. With eyes closed, however, significant decrease of sway area (p=0.0169) and significant increase of tract density (p=0.0245) occurred only in group B and not in A and C. Analysis of variance with multiple comparison by Fisher's PLSD method of after/ before ratio of sway area revealed significant decrease in both A and B but not C. With eyes closed, only B showed significant increase of tract density. Both alfacalcidol and AAA Ca alleviated swaying, the former especially with eyes opened and the latter with eyes closed, suggesting a difference in the mechanism of action.

Disclosures: ***T. Fujita****, None.*

M396

Immobilization Induces a Widespread Loss of Bone Integrity and Impaired Sensory Neurohumoral Signaling. W. S. Kingery[1], S. Offley*[1], T. Guo*[1], T. Wei*[1], D. Lindsey*[2], C. Jacobs[2]. [1]PM&R service (117), VAPAHCS, Palo Alto, CA, USA, [2]Rr&d, VAPAHCS, Palo Alto, CA, USA.

Recently we observed that unilateral sciatic nerve transection in rats caused a reduction in cancellous bone density and substance P content in the contralateral intact hindlimb. Chronic administration of a substance P receptor antagonist after sciatic section further enhanced bone loss in the intact contralateral hindlimb, therefore we postulated that reduced neuropeptide release in bone could contribute to the remote bone loss. It has long been recognized that immobilization alone can cause a loss of trabecular mass, structure, and strength, but the remote effects of immobilization alone have not been previously investigated. In the current study we tested the hypothesis that prolonged unilateral limb immobilization has deleterious effects on cancellous bone and neuropeptide signaling in the contralateral limb. The right hindlimbs of skeletally mature Sprague Dawley male rats were casted for 4 weeks. Immobilization caused a reduction in bone mineral density (measured by DXA scanning at 4 weeks after cast removal) in the metaphyses of the ipsilateral and to a lesser extent contralateral femur. There was no effect on diaphyseal bone density in either limb. Microcomputed tomography (μCT) in the distal femur demonstrated bilateral loss of trabecular bone volume and connectivity after unilateral immobilization. On biomechanical testing bone strength was also reduced bilaterally. No changes were observed in body weight or 24-hour grid-crossing activity at 4 weeks after immobilization and there was no reduction in weight bearing or gastrocnemius and soleus muscle mass in the non-immobilized left hindlimb, data indicating that skeletal unloading did not contribute to the loss of cancellous bone integrity the contralateral femur. Substance P and calcitonin gene-related peptide (CGRP) levels in the sciatic nerve were reduced bilaterally after unilateral immobilization. Sciatic nerve stimulation evoked extravasation responses were also diminished bilaterally after immobilization. These results support the hypothesis that the remote osteoporotic effects of unilateral limb immobilization are a consequence of impaired sensory neurohumoral signaling in the cancellous bone.

Disclosures: ***W.S. Kingery****, None.*

M397

In Postmenopausal Women, Femoral Neck BMD Is Positively Correlated to Circulating Levels of Soluble RANKL and Negatively Correlated to Levels of IL-7. S. Walker*, M. B. Finch*, D. Marsh*, G. Li. Trauma Research Group, Queen's University Belfast, Belfast, United Kingdom.

Increased T cell expression of receptor activator of nuclear factor-κB ligand (RANKL) and its binding to receptor activator of nuclear factor-κB (RANK) on osteoclasts and their precursors plays a major role in osteoclastogenic bone loss in mice. IL-7, a potent stromal cell derived cytokine, can also stimulate T cell RANKL expression and induce osteoclastogenesis in murine models.

We investigated the relationship of plasma soluble RANKL (sRANKL) and IL-7, and T cell RANKL expression in 60 post-menopausal women: 30 with osteoporosis and 30 with 'normal' BMD. BMD measurement by DXA (Lunar DPX), giving T score readings at the femoral neck and L2-L4, enabled categorisation. Osteoporosis was defined as a T score of ≤ -2.5 at femoral neck or L2-L4 or both. Plasma from each subject was banked and levels of each cytokine were determined using commercially available ELISAs. Applying a whole blood technique, mononuclear cells were dual-labelled with FITC-conjugated CD3 antibody (Dakocytomation, UK) and RPE-conjugated RANKL antibody (R&D Systems,

Europe). The percentage of CD3+RANKL+ cells was calculated using flow cytometry (EPICS Elite, Beckman Coulter).
Between the osteoporotic and non-osteoporotic groups, there was no difference in the mean plasma levels of either sRANKL or IL-7, or RANKL positive T cells (using student's t test after log transformation). However, a significant negative correlation was seen between the hip BMD and IL-7 (Pearson r = -0.24, p=0.034) which persisted after adjustment for age (r = -0.19, p = 0.043). There was a significant positive correlation between hip BMD and sRANKL (r = 0.4, p= 0.03) which persisted after adjustment for age (r=0.33, p=0.05).There was no correlation between spinal BMD and either sRANKL or IL-7 levels. When the subjects were divided into two groups; those with hip T score ≤ -2.5 and those with hip T score > -2.5, the mean sRANKL between the groups was significantly different (0.055 pmol/l v 0.125 pmol/l respectively, p = 0.008). There were no significant correlations between RANKL positive T cells and sRANKL, IL-7, hip or spinal BMD. In summary, sRANKL levels are significantly lower in those with femoral neck T scores ≤ -2.5; T cell RANKL expression does not appear to be correlated to either hip or spinal BMD, nor to plasma sRANKL or IL-7 levels. Plasma IL-7 is positively and significantly correlated with hip BMD.
In conclusion, these results suggest sRANKL and IL-7 are altered in post-menopausal femoral neck bone loss. Low levels of plasma sRANKL and high levels of IL-7 may prove useful tools in identifying those with femoral neck osteoporosis and preventing future hip fractures.

Disclosures: ***S. Walker****, None.*

M398

Institutionalized Elderly Type II Diabetics Have Higher Bone Mass, Lower Bone Turnover Markers and PTH Levels Compared to Non-diabetics: Evidence for Decreased Calcium Sensing by Parathyroid Glands. M. Roth*, A. Fahrleitner*, C. J. Piswanger-Sölkner*, B. Obermayer-Pietsch*, A. Tiran*, G. Leb*, E. Maier*, H. Dobnig. Internal Medicine, Medical University Graz, Graz, Austria.

Introduction: There is evidence that patients with type I diabetes mellitus (DM) have low and those with type II DM higher BMD levels when compared to controls. Little is known whether bone status and calcium regulation of elderly type II diabetics differ from non-diabetics.
Patients and methods: We compared 301 female residents with DM with 1398 non-diabetic individuals living in 95 homes for elderly. Patients´ age was between 70 and 100 years. Exclusion criteria were known malignancies, hypercalcemia and predefined significant impaired liver- and kidney function. We performed quantitative bone ultrasound measurements at the calcaneus, radius and the proximal third phalanx. Biochemical measurements included among others osteocalcin, serum cross laps (sCTX), PTH and vitamin D levels in 177 patients as well as PTHrP and amylin concentrations in a smaller subgroup. Patients were prospectively followed for the occurrence of fractures over two years. All analyses were performed after adjustment for age, BMI and renal function.
Results: Patients with DM had significantly higher BUA and SOS readings at the calcaneal- (0.5 SD in Z-score, p<0.0001) and radial site (0.3 SD, p<0.01). In diabetic subjects serum PTH, osteocalcin and sCTX levels were significantly *lower* and protein-normalized serum calcium levels *higher* when contrasted with non-diabetic patients. These differences were seen in all three decades. For defined serum calcium categories mean PTH levels were consistently lower by 15% in diabetic individuals when compared to non-diabetic patients. There was no difference in serum amylin and PTHrP levels between the two groups. A total of 110 prospective hip- and 242 non-vertebral fractures occurred. Incidence rates for non-vertebral fractures were 15% (DM) and 14% (non-DM) and for hip fractures 6% (DM) and 7% (non-DM), respectively. None of these differences were significant.
Conclusion: Bone ultrasound measurements were significantly higher in elderly residents with DM throughout all age groups. This difference was likely attributable to lower PTH secretion due to impaired calcium-sensing by the parathyroids and consecutive decreased bone turnover rates in patients with DM. This beneficial change in bone metabolism was, however, not reflected by fracture rates and may have been offset by a higher propensity of falls in diabetic residents.

Disclosures: ***H. Dobnig****, None.*

M399

Decreased Cortical Bone Mineral Density in Type2 Diabetes Mellitus. K. Tanaka[1], K. Shide*[2], K. Ishida*[1], S. Tsugawa*[1], S. Kido*[1], Y. Seino*[2]. [1]Kyoto Women's University, Kyoto, Japan, [2]Kyoto University Hospital, Kyoto, Japan.

Although type1 diabetes is associated with decreased BMD, it is controversial whether type2 diabetes causes decreased BMD or not. Obesity is common in type2 diabetes, and body weight greatly affects BMD at weight-bearing sites such as lumbar spine and hip, but not at non-bearing sites such as radius. These facts, however, do not seem to be fully taken into account by the previous researchers, which is likely to be responsible for the large discrepancies on the effects of type2 diabetes on BMD.
Fortytwo hospitalized patients with type2 diabetes were recruited in the study (62 +/- 12 years old). BMD was measured at lumbar spine, hip, radius, and whole body using QDR2000 (Hologic). As shown below, more than half of the patients had T score above -1SD at lumbar spine and total hip according to the WHO criteria. In contrast, two third of the patients were considered osteoporotic at distal one third of radius.

DXA Results at Various Skeletal Sites

	L2-4	Total Hip	Radius (distal one third)	Radius (ultradistal)
Normal	23	31	6	15
Osteopenia	15	11	8	12
Osteoporosis	4	7	28	15

Next, the patients were classified according to the skeletal site showing the lowest T score. As shown below, T score was the lowest at distal one third of radius in most of the patients.

Skeletal Site Showing the Lowest T Values

	L2-4	Total Hip	Radius (distal one third)	Radius (ultradistal)
Number of Patients	2	0	35	5

Our results suggest that type2 diabetes is associated with decreased BMD, which is obscured at weight-bearing sites. Preferential decrease of BMD at distal one third of radius suggests that BMD is decreased at cortical bone, and suggests that the pathogenesis of osteoporosis in type2 diabetes is different from that in postmenopausal osteoporosis.

Disclosures: ***K. Tanaka****, None.*

M400

Chronic Bone Pain Following Femur Fracture in the Rat: Modeling the Osteoporotic Pain Experience. M. P. Roudier, J. S. Wiley*, T. L. Panzitta*, M. D. Brot*, S. D. Bain. SkeleTech, Inc., Bothell, WA, USA.

Chronic bone pain associated with osteoporotic fractures is a commonly encountered clinical problem. However, there are no established preclinical models to investigate the nature and source of the enduring pain observed in osteoporotic patients. In order to explore this question, we have evaluated nociceptive responses in a rat bone fracture model. Experimentally, male Sprague-Dawley rats received either a closed fracture of the right femur stabilized by an intramedullary pin (IM pin) or a sham procedure which involved insertion of the IM pin only. An untreated control group was also included. Pain associated with the bone fracture was determined beginning 3 weeks post-fracture using tests for thermal and mechanical hyperalgesia. The test of thermal hyperalgesia measures the withdrawal latency when a heat source is directed at the hind paw, while mechanical hyperalgesia uses Von Frey filaments to assess somatosensory responses to pressure stimuli. Testing for thermal and mechanical hyperalgesia continued until the rats were sacrificed at 6 weeks post-fracture. Compared to intact and IM pin controls, the analyses of the thermal and mechanical hyperalgesia revealed that the animals experienced significant pain in the fractured limb (p<0.01), which, in the case of the mechanical hyperalgesia, persisted for the duration of the 6-week experiment (p<0.01). Furthermore, the mechanical hyperalgesia was inhibited dose-dependently by gapapentin, an agent prescribed for neuropathic pain, but not by salmon calcitonin or the non-specific cyclo-oxygenase inhibitor, ketorolac. Finally, immunostaining of the dorsal horn of the spinal cord for the astrocyte marker, glial fibrillary acidic protein (GFAP) revealed a significant upregulation of GFAP immunostaining in the ipsilateral cord that was at least partially abrogated by gabapentin treatment. In summary, the persistent mechanical hyperalgesia and GFAP upregulation in the spinal cord observed post-fracture is indicative of chronic pain conditions. Moreover, the inhibition of persistent pain by gabapentin but not by calcitonin or ketorolac suggests that the fracture pain in this model may be neuropathic in nature. Therefore, these findings demonstrate the potential of this model to investigate and characterize the mechanisms associated with the development of chronic bone pain following fracture.

Disclosures: ***S.D. Bain****, None.*

M401

Association between 8-Hydroxydeoxyguanosine Levels in Bone Marrow and Bone and Mineral Metabolism. M. I. Kang, K. H. Baek*, H. J. Tae*, J. H. Han, W. Y. Lee*, K. W. Oh*, C. S. Cho*, H. S. Kim*, K. W. Lee*. Internal medicine, The catholic University of Korea, Seoul, Republic of Korea.

Reactive oxygen species (ROS) have been shown to be responsible for the aging process and osteoporosis. Several lines of evidence have found a tight association between oxidative stress and pathogenesis of osteoporosis. We studied the relationship between oxidative stress in the bone marrow and bone and mineral metabolism. Little is known about the oxidant status in the bone marrow, and its direct measurement from the bone marrow may establish the effect of oxidative stress on the local milieu of the bone metabolism within the bone microenvironment. The main aim of this study is to investigate whether oxidative stress in bone marrow may have an impact on bone metabolism and bone mass. Oxidative stress was evaluated in bone marrow serum by measurement of 8-hydroxy-2'-deoxyguanosine (8-OHdG) in 39 patients (48.2±13.5 years, 24 men, 15 women). The biochemical markers of bone formation (bone specific ALP) and resorption (ICTP) were measured from the same specimen. Bone mineral density (BMD) of the lumbar spine, and proximal femur were measured by dual energy X-ray absorptiometry. In the age-, sex-, weight- and smoke status- adjusted model, the marrow 8-OHdG level showed a positive correlation with marrow ICTP level (r=0.36, p<0.05). Although statistically not significant, the 8-OHdG levels tended to be negatively associated with the BMD at lumbar spine and proximal femur. Taken together, theses results suggest for the first time that increased oxidative stress in bone marrow could be involved in negative balance in the bone metabolism

Disclosures: ***M.I. Kang****, None.*

M402

Osteoprotegerin and RANKL Serum Levels in Primary and Secondary Osteoporosis. G. Martini, S. Salvadori*, L. Gennari, R. Valenti*, B. Franci*, S. Campagna*, A. Avanzati*, B. Galli*, D. Merlotti, B. Lucani*, R. Nuti. Dept. of Internal Medicine Endocrine Metabolic Sciences and Biochemistry, University of Siena, Siena, Italy.

Osteoprotegerin (OPG), a secreted member of tumor necrosis factor superfamily, has been identified as an osteoblast-derived regulator of bone resorption: it acts neutralizing the receptor activator of nuclear factor κβ ligand (RANKL), a cytokine required for osteoclast formation and activation. The aim of the study was to evaluate both age-dependent changes of these cytokines with age in healthy women and men and their relationships with bone mass and bone metabolism. Moreover we examined the behaviour of serum OPG and RANKL in patients with postmenopausal osteoporosis or chronic glucocorticoid treatment.
The population studied was: 150 healthy women aged 59.9±10.2 years, 87 healthy men aged 68.4±8.7 years, 103 women with postmenopausal osteoporosis aged 65.2±8.5 years, and 36 subjects with myastenia (18 females and 18 males aged 61.8±18.1) on glucocorticoid treatment for at least one year.
Sera were assayed for OPG and RANKL using a sandwich enzyme immunoassay (Osteoprotegerin and RANKL, Biomedica, Austria). Precision intra and interassay was lower than 10%. Bone metabolism was evaluated by serum cross linked C-telopeptides of type I collagen (sCTX, Serum CrossLaps, Osteometer, Denmark), serum parathyroid hormone (PTH intakt MTPL, Germany, and vitamin D status (25-OH RIA Kit, DiaSorin, USA).
Osteoporotic women and patients on glucocorticoid showed significantly higher values of OPG (7.6±4.8 pmol/L and 8.6±6.1 pmol/L, respectively) compared to healthy women and men (6.5±3.4 pmol/L and 5.4±3.2 pmol/L, respectively). High levels of RANKL were found in steroid-osteoporosis (7.04±4.4 pmol/L) while in the other groups RANKL ranged from 0.97 pmol/L to 1.24 pmol/L. Serum OPG was positively correlated to bone mass expressed as T-score in all the studied population except in osteoporotic women. The only significant relationship regarding bone turnover was found between RANKL and CTX in healthy women ($r=0.22$, $p<0.01$). No correlations were found as regards OPG, RANKL, PTH and 25-OHD. We conclude that OPG increase with age both in women and men. The high values of OPG in primary and secondary osteoporosis suggest an attempt to counteract the increased rate of remodeling although serum levels of OPG and RANKL were unrelated to bone turnover, parathyroid function and vitamin D status. The increase of RANKL in steroid-induced osteoporosis have to be better clarified.

Disclosures: ***G. Martini****, None.*

M403

Iliac Crest Biopsy Chemical Composition Differentiates Fractured from Non-fractured Women and Exhibits Change with Age. B. R. McCreadie[1], T. Chen*[2], D. S. Rao[3], M. D. Morris*[2]. [1]Orthopaedic Surgery, University of Michigan, Ann Arbor, MI, USA, [2]Chemistry, University of Michigan, Ann Arbor, MI, USA, [3]Bone and Mineral Research Laboratory, Henry Ford Hospital, Detroit, MI, USA.

It is currently unclear whether chemical composition of bone tissue changes with age or influences osteoporotic fracture risk.
Archival iliac crest biopsies from subjects without fractures (n=10, mean age 56 y, range 43-70 y) and patients with osteoporotic fractures (n=5, mean age 63 y, range 50-72 y) were studied. Separate regions 220 x 330 microns were scanned in trabecular and cortical regions of each specimen using Raman spectroscopy, resulting in datasets of 18,900 pixels each. From pixels containing bone, average carbonate/phosphate and phosphate/amide I band area ratios were obtained separately for trabecular and cortical regions of each specimen. No corrections were made for multiple comparisions.
Both carbonate/phosphate ratio and phosphate/amide I ratio were higher in cortical than trabecular bone for all specimens ($p=0.005$ and $p=0.01$, respectively, paired t-tests). This suggests that mineralized matrix chemistry differs between bone types. Whether this is a fundamental difference or a result of differing average tissue age is unclear.
Chemical composition of cortical bone mineralized matrix changes with age, as demonstrated by a decrease in phosphate/amide I ratio ($p=0.005$, linear regression model). Neither carbonate/phosphate ratio in cortical bone nor any measure in trabecular bone showed significant change with age.
The phosphate/amide I ratio in non-fractured subjects was greater in cortical than trabecular bone until age 55 (in all 6 subjects), but greater in trabecular bone in those 55 y or older (in all 4 subjects). In all 5 fractured patients, the phosphate/amide I ratio was greater in cortical bone. Thus, fractured patients demonstrated the pattern seen in younger (under 55) non-fractured subjects, as opposed to the pattern of non-fractured subjects of similar age. It is possible that failure to alter mineralized matrix chemistry results in increased fracture risk.
Comparing fractured to non-fractured individuals, trabecular bone from fractured patients had lower phosphate/amide I ratio ($p=0.03$, t-test). No differences were found in cortical bone or in carbonate/phosphate ratio in trabecular bone. This lower mineral/matrix ratio (decreased mineral) in trabecular bone suggests a systemic increase in remodeling prior to or following fracture, and is likely demonstrated more clearly in trabecular bone because of its more rapid turnover. If this increase in remodeling occurs prior to fracture, chemical composition from iliac crest biopsy specimens may improve fracture risk assessment.

Disclosures: ***B.R. McCreadie****, Potential commercialization 7.*

M404

A Comparison of Estrogen, Calcitriol or Both Therapies on the Relationship between Serum Parathyroid Hormone and 25 Hydroxy Vitamin. J. C. Gallagher, P. B. Rapuri, G. Haynatzki*. Bone Metabolism Unit, Creighton University, Omaha, NE, USA.

Estrogen deficiency , decreased serum calcitriol and secondary hyperparathyroidism have been implicated in the pathogenesis of osteoporosis.It has been proposed that estrogen prevents the age-related increase in parathyroid hormone (PTH) either directly or indirectly by suppressing PTH secretion. In the present study, we compared the effects of calcitriol and conjugated estrogens or the combination of both on the relation between PTH and 25OHD. In a double blind, placebo randomized study, 489 elderly women were randomized to HRT, CEE.625 mg +MPA2.5mg daily (ERT only in hysterectomized), calcitriol 0.25 mg. b.i.d., HRT & calcitriol, or placebo for 3 years .Serum 25OHD levels were measured by competitive protein binding assay and serum intact PTH was measured with an Allegro immunoradiometric assay both at baseline and end of study (36 months). The differences between slopes and intercepts between the regression lines of serum 25OHD and PTH in the four treatment groups was compared by SAS. There was no significant difference between the regression slopes of placebo and the hormone therapy/estrogen therapy ($p=0.77$) groups. However there was a significant ($p<0.006$) difference between the placebo ($y=65.78-0.81x$) and the calcitriol ($y=39.6-0.32x$) treatment groups.
After 3 years treatment with estrogen there was no decrease in serum PTH and no change in the relationship between serum 25OHD and PTH whereas calcitriol treatment significantly decreased serum PTH by sixty percent compared to placebo.In estrogen treated women serum 25OHD remains the primary determinant of serum PTH. In contrast on calcitriol treatment there was no significant relationship between serum 25OHD and PTH.In summary,calcitriol is more effective than estrogen in reducing secondary hyperparathyroidism in elderly women.

Disclosures: ***J.C. Gallagher****, Wyeth, Roche 2.*

M405

Valproic Acid Inhibits Osteoblast and Osteoclast Activity in Therapeutic Dose Ranges. B. L. Gracious*[1], R. P. Bossert*[2], J. Puzas[3]. [1]Psychiatry and Orthopedics, University of Rochester Medical Center, Rochester, NY, USA, [2]University of Rochester Medical Center, Rochester, NY, USA, [3]Orthopedics, University of Rochester Medical Center, Rochester, NY, USA.

Cross-sectional studies have demonstrated reduced bone mineral density in children or adults receiving anticonvulsant treatment with valproic acid (VPA). Mechanisms for such action have not been determined. We examined direct effects of VPA on osteoblast viability, proliferation, and activity and on osteoclast cell function.
Osteoblasts from neonatal mouse calvaria were isolated and plated in standard solution. Media from the cells was replaced with plating media +/- VPA in 1:5 dilutions from 1000-0.32µg/ml in triplicate. Exposure concentrations for all components of the study were 0.0µg/ml, 0.32µg/ml, 1.6µg/ml, 8µg/ml, 40µg/ml, and 200µg/ml. Cells were harvested after 24 or 48 hours in VPA media for determinations of viability, proliferation or alkaline phosphatase activity evaluation. Viability was assessed using an MTT assay system with absorbance measured at 595nm. Proliferation was measured via de novo DNA synthesis after incorporation of radiolabeled thymidine. Radioactivity was determined by liquid scintillation spectrometry. Alkaline phosphatase activity was measured after adding p-nitrophenylphosphate solution for up to 30". Absorbance was read at 410nm. Osteoclast function was measured by lacunae formation on bovine bone wafers incubated for 14 days with neonatal rat osteoclast cells at concentrations of either no VPA or 0.32µg/ml - 200µg/ml VPA in 1:5 dilutions. Number and area of osteoclast lacunae were quantified with Osteometrics software.
Osteoblast alkaline phosphatase activity decreased significantly at 48 hours at VPA levels from 4-200ug/ml corrected for viability ($p < 0.05$ for VPA at 8, 40, and 200ug/ml). Osteoblast viability and proliferation were unaffected by VPA through 200ug/ml with evidence of decreased proliferation at 1000ug/ml. Osteoclast lacunae formation trended downward as VPA concentration increased.
Human therapeutic ranges of VPA (50-100µg/ml) appears to inhibit osteoblast alkaline phosphatase activity in a rodent cell model. Osteoclast lacunae formation may decrease as valproic acid concentration increases. Replication of these findings, determination of the specific cellular/genetic pathways of inhibition, and an animal model to examine for potential histologic and clinical changes are needed.

Disclosures: ***B.L. Gracious****, Bristol Myers Squibb 2; National Alliance for Research in Schizophrenia and Affective Disorders 2.*

M406

The Rate That Family Physicians Prescribe Pharmacological Treatment to Their Patients: Canadian Quality Circles (CQC) Project. B. Kvern*[1], G. Ioannidis[2], M. Doupe*[1], A. Katz*[1], A. Papaioannou[2], A. Hodsman[3], A. Baldwin*[4], D. Johnstone*[5], M. Baranci*[6], J. D. Adachi[2]. [1]University of Manitoba, Winnipeg, MB, Canada, [2]McMaster University, Hamilton, ON, Canada, [3]University of Western Ontario, London, ON, Canada, [4]St. Boniface Hospital, Winnipeg, MB, Canada, [5]Procter & Gamble Pharmaceuticals Inc, Toronto, ON, Canada, [6]Aventis Pharma, Laval, PQ, Canada.

The CQC Pilot Project is a one year, integrated disease management project to improve family physicians' adherence to the OSC 2002 guidelines through the use of standardized documentation and sequential quality QC meetings. There were 449 family physicians approached to participate. Among these, 52 formed 7 quality circles. The 52 physicians conducted chart reviews for a total of 1505 patients. These patients were women age 55 years and over, were known to the physician and had attended at least 2 visits in the past 24

months. Data were gathered using the quality circle project data collection form.
Our baseline analysis examined the rate that family physicians prescribe drug treatment to their patients depending on the likelihood that they had osteoporosis. A patient likely to have osteoporosis was one who was perceived by the physician to have the disease or the physician interpreted the patient's BMD test results as osteoporosis. A patient not likely to have osteoporosis was one who was perceived by the physician not to have the disease or the physician interpreted the patient's BMD test results as not osteoporosis. We examined rates of drug therapy for patients likely and not likely to have osteoporosis. For those patients who received drug therapy, we evaluated the rate that physicians were prescribing their drug of choice.
Results indicated that of those patients who were likely to have osteoporosis, 70% were and 30% were not treated for the condition. Of the patients not likely to have osteoporosis, 11% were and 89% were not given therapy. For those patients that received therapy, approximately 73% of patients were taking the physician's drug of choice. The reasons why some patients were not taking the physician's drug of choice included the price of medication to the patient, treatment side effects, formulary restrictions, patient refused treatment, and patient compliance.
In conclusion, a high proportion of patients with osteoporosis are being treated, much higher than has previously been reported. However, 30% of patients that were eligible for treatment did not receive therapy. In addition, a portion (27%) of patients on therapy are not taking the physician's drug of choice. Future research should focus on education approaches that address the barriers identified by family physicians in prescribing therapy to their patients with osteoporosis.

Disclosures: ***B. Kvern****, None.*

M407

Alendronate Treatment Prevents Periprosthetic Bone Loss Following Total Hip Arthroplasty. G. M. Blake[1], A. I. A. Rahmy*[2], A. Tonino*[3], I. Fogelman[1]. [1]Nuclear Medicine Department, GKT School of Medicine, London, United Kingdom, [2]Nuclear Medicine Department, Atrium Medical Centre, Heerlen, Netherlands, [3]Orthpaedics Department, Atrium Medical Centre, Heerlen, Netherlands.

Historically periprosthetic bone losses of up to 25% have been reported in patients undergoing total hip arthroplasty (THA). We report a pilot study to investigate whether treatment of THA patients with alendronate (70 mg once a week) starting before their operation can prevent these losses. Twenty-eight consecutive patients (23F,5M) (mean age 62 y, range 41-77 y) undergoing THA with a cementless hip prosthesis (ABG2, Howmedica International, Rutherford, NJ) commenced alendronate treatment one month before surgery. Twenty-six untreated patients (14F,12M) (mean age 62 y, range 48-69 y) also receiving the ABG2 prosthesis served as a control population. Both groups were operated on by the same team of surgeons and followed an identical regime after THA. Postoperative DXA scans were performed to measure BMD in periprosthetic bone at 10 days (treated as baseline for the subsequent follow-up), 6 weeks, 3 months and 6 months in the 7 Gruen zones (GZ) and the total periprosthetic region of interest (total ROI). For the total ROI the mean percentage change (SEM) in BMD at 6 months was +0.7 (1.3) % in alendronate treated patients compared with -5.2 (1.2) % in untreated patients ($p = 0.002$). The trend for alendronate treatment to prevent postoperative bone loss was found in both female (+0.9 (1.7) % vs -4.6 (1.7) %, $p = 0.032$) and male patients (+0.2 (1.1) % vs -5.7 (1.7) %, $p = 0.051$). A repeated measures ANOVA test showed a highly statistically significant treatment effect in the total ROI ($p = 0.002$), GZ1 ($p = 0.002$), GZ2 ($p = 0.014$), GZ3 ($p = 0.010$), GZ4 ($p = 0.001$) and GZ5 ($p = 0.008$), but not GZ6 ($p = 0.60$) or GZ7 ($p = 0.59$). In conclusion, alendronate treatment was effective in preventing periprosthetic bone loss in patients undergoing THA with the ABG2 prosthesis in the total periprosthetic ROI and in 5 out of 7 Gruen zones.

Disclosures: ***G.M. Blake****, None.*

M408

Bisphosphonate Effects on the Program of Gene Transcription During Osteoclastogenesis. L. Sun*[1], G. Gross*[2], A. Varbanov*[2], R. Phipps*[2], M. Zaidi[1], B. R. Troen[3]. [1]Mount Sinai School of Medicine, New York, NY, USA, [2]Procter & Gamble, Cincinatti, OH, USA, [3]Miami VAMC GRECC, University of Miami School of Medicine, Miami, FL, USA.

To investigate the impact of bisphosphonates upon gene expression during osteoclast formation, we performed micro array transcriptional profiling of osteoclast precursors (RAW 264.7 cells) *in vitro*. We analyzed the 5-day time point following induction of osteoclastogenesis with RANK ligand (RANKL), with or without risedronate (RIS) (10^{-6} M) or alendronate (ALN) (10^{-7} M). Cells were also treated with RIS or ALN alone, without RANKL. cRNA was prepared from duplicate samples of each treatment condition and hybridized to Affymetrix U74Av2 mouse genome arrays. Eliminating probe sets with absent calls across all conditions removed 5678 of the 12422 probe sets on the chip. Of the remaining 6744, the probe sets where the NLOGP values were >3 (NLOGP=log10(P-value)) were considered differentially expressed. Of a total of 629 differentially expressed probe sets identified through this analysis, RANKL versus untreated cells exhibited 479, and RANKL + RIS versus control exhibited 523. In contrast, RIS versus untreated, and RANKL + RIS versus RANKL exhibited only 17 and 2 differentially expressed probe sets, respectively. The addition of RIS to RANKL thus resulted in only 2 differentially expressed genes in comparison to RANKL alone, indicating a minimal effect of RIS on transcription during osteoclastogenesis. Initial analyses suggested that ALN did alter transcription, but we cannot, at this point, exclude the possibility of technical artifacts resulting from "bright chips". RANKL treatment expectedly stimulated the expression of osteoclastic genes, including MMP-9, calcitonin receptor, TRAP, cathepsin K, integrin β3, and carbonic anhydrase, but inhibited cathepsins L, S, C, and B. Genes such as VEGF-C, chemokine receptor 1, and M-Ras, were newly identified as RANKL inducible. Interestingly, RANKL potently suppressed expression of a large group of interferon-γ regulated genes, including interferon-γ-induced proteins with tetratricopeptide repeats 1 and 2 and IFN regulatory factor 7. Quantitative real-time RT-PCR of a subset of genes confirmed the transcriptional profiling data. Thus, utilizing powerful transcriptional profiling technology, we demonstrate (a) the divergent regulation of cathepsin, interferon-γ-regulated, and growth factor (VEGF-C and IGF-1) genes, and (b) that the potent bisphosphonate, risedronate, at least *in vitro*, appears to act by mechanisms other than by altering gene transcription during osteoclast formation.

Disclosures: ***B.R. Troen****, Procter and Gamble 2.*

M409

Evaluation of BMD in Patients with Graves' Disease and Its Change during Anti-thyroidal and Aminobisphosphonate (Alendronate or rIsedronate) Therapy. S. Wada[1], S. Yasuda*[2], M. Kogawa*[2], S. Kamiya*[1], S. Katayama*[2]. [1]Dept of Clinical Science, Josai International University, Chiba, Japan, [2]Dept of Endocrinology and Metabolism, Saitama Medical School, Saitama, Japan.

It is recognized that loss of bone mineral density (BMD) and risk of fractures are associated with endocrine disturbances. Although hyperthyroidism has been considered as one of the risk factors for osteoporosis, it is not well established whether hormone excess due to Graves' disease (GD) actually reduces BMD or whether effective treatment can reverse the decrease of BMD in these patients. The aim of this study was, therefore, to evaluate BMD in GD, and its change by treatment. We examined 44 GD patients (14 males and 30 females), and 45 with Hashimoto's disease (HD), as a reference. GD patients were treated with anti-thyroidal drugs, radioisotope, or subtotal thyroidectomy and patients of HD were treated with lT4. In patients with GD, BMD did not correlate solely with duration of disease, body mass index, the titers of TSH receptor antibodies, or the amounts of anti-thyroidal drugs. There was no significant difference between BMD in premenopausal GD women or women with HD. In postmenopausal women treated for GD, however, lumbar BMD was reduced significantly in comparison with healthy controls and with the HD patients. The age of disease onset correlated significantly with BMD ($p<0.01$, $r=-0.88$), suggesting that the age of onset could be an important factor in the eventual loss of BMD or development of osteoporosis. We further examined the changes of BMD during the treatment of hyperthyroidism in 26 patients (4 males and 22 females). 22 out of 26 patients were successfully treated and regained euthyroid status; their lumbar BMD increased in response to therapy (T score -0.72 vs. -0.26). In contrast, patients whose treatment was unsuccessful lost ~5% of lumbar BMD over ~2yr . After the follow up period (when BMD was largely unchanged), GD patients with low BMD (<-2.5SD) received alendronate (5mg/day) or risedronate (2.5mg/day). This medication effectively increased lumbar BMD by 6.95±7.33%/yr. Although bone loss associated with hyperthyroidism is regarded as a transient event, this study indicates that patients who develop hyperthyroidism after menopause hardly ever retain BMD. GD could be a significant risk for osteoporosis, but effective therapy for this, as well as aminobisphosphonate administration, can significantly increase BMD in these patients.

Disclosures: ***S. Wada****, None.*

M410

Risedronate Therapy reduces the Risk of New Vertebral Fractures by 60% in Osteoporotic Men with osteoporosis within 1 year. J. Ringe[1], H. Faber*[1], M. Salem*[1], A. Grauer[2], G. Möller[3]. [1]Medizinische Klinik IV, Klinikum Leverkusen, University of Cologne, D-51375 Leverkusen, Germany, [2]Medical Affairs, Procter & Gamble Pharmaceuticals USA, Mason, OH, USA, [3]Medical Affairs, Procter & Gamble Pharmaceuticals Germany GmbH, D-65824 Schwalbach, Germany.

Background: In postmenopausal osteoporosis clinical studies with Risedronate have shown rapid fracture reduction at vertebral and non-vertebral sites after only 6 months of treatment. Rapid reduction of vertebral fracture risk with Risedroante has also been shown in glucocorticoid-induced osteoporosis and interestingly, the risk reduction observed in male and female subgroups was not different. Purpose of the study: In the current study, we examine the effects of Risedronate on vertebral fractures and BMD mean change in lumbar spine, femoral neck and total hip BMD only in men with primary and secondary osteoporosis. Secondary endpoints include non-vertebral fractures, height loss, pain, safety, and tolerability. Methods: In this single center, open label, prospective, conrolled trial, patients were randomized by stratum. 316 male patients were recruited with T-score values of lower than -2.5 SD at lumbar spine (LS) and lower than -2.0 SD at the femoral neck (FN) with or without prevalent vertebral fractures (vert-fx). Patients in Group A (n=158; 81 with, 77 without prevalent vert-fx) received Risedronate 5 mg plus calcium 1000 mg and 800 IU Vit. D daily. Group B comprised equally 158 men. Those with a prevalent vert-fx (subgroup B1 n=81) were treated with alfacalcidol 1 mg plus calcium 500 mg daily, whereas patients without prevalent vert.-fx (subgroup B2, n=77) were treated with 800 IU plain vitamin D plus calcium 1000 mg daily. In group A 64 patients (41%) and in group B 66 (42%) had secondary osteoporosis. BMD measurements and x-rays were performed at baseline and 12 months thereafter. Results: After this first year of treatment men receiving Risedronate showed a mean LS-BMD increase of 4.7% compared to a mean increase of 1.0% in Group B patients ($p<0.001$). The mean change of total hip BMD was 2.7% and 0.4% for groups A and B, respectively ($p<0.001$). Corresponding changes at the FN were 1.8% and 0.3% for the respective groups ($p<0.001$). During the 12 months of therapy in 5% (8/158) of patients of Group A and in 12.7% (20/158) of Group B new vert-fx were recorded (RR 0.4, Fisher' exact test; $p<0.028$). The corresponding incidences for patients with new non-vert-fx were 10 and 17, (RR 0.59, n.s due to insufficient power). Both therapies were well tolerated. Conclusions: We conclude that Risedronate therapy within one year reduces the risk of new vertebral fractures by 60% and significantly increases BMD at all measurement sites in men with osteoporosis.

Disclosures: ***G. Möller****, Procter & Gamble Pharmaceuticals Germany GmbH 3.*

M411

Effects of Continuous Combined HRT and Clodronate on Bone Mineral Density in Osteoporotic Postmenopausal Women: 5-Year Follow-Up. K. Hänninen*[1], M. Tuppurainen[1], M. Komulainen*[1], J. Jurvelin*[2], H. Kröger[3], E. Alhava*[3], S. Saarikoski*[1]. [1]Obstetrics and Gynecology, Kuopio University Hospital, Kuopio, Finland, [2]Clinical Physiology and Nuclear Medicine, Kuopio University Hospital, Kuopio, Finland, [3]Surgery, Kuopio University Hospital, Kuopio, Finland.

Recent Studies suggest, that adding bisphosphonates to hormone replacement therapy (HRT) may improve the antiresorptive effects of HRT. In this 5-year randomized study we examined the effects of HRT with or without bisphosphonate. In the Kuopio Osteoporosis Study (OSTPRE) a sample of 3200 women were selected for BMD measurement by Lunar DPX in 1995-97. In all 167 women aged 61±2.7 years (11±4.9 years postmenopausal), with a T-score ≤ -2.5 SD at either the lumbar spine or femoral neck were recruited. They were randomized to receive daily estradiol hemihydrate (E2) 2mg + noretisterone acetate (NETA) 1mg (Kliogest®, Novo Nordisk, Denmark) + Boneplac, which consisted of either 800mg clodronate (Bonefos®, Leiras Ltd, Finland) (n=48) or placebo(n=47). In case of contraindications or refusal from HRT, the women were offered clodronate 800mg/day (n=50). The multivariate ANOVA analyses for repeated measurements were used. The results are based on an intention to treat analyses.BMD was measured at 0,1,3 and 5-year intervals. The baseline characteristics were similar in all treatment groups, including BMD. After one year treatment the lumbar BMD increased in all treatment groups: 4.9%±3.4% in the HRT group, 4.6%±4.5% in the combination group and 1.8%±4.3% in the clodronate group. After three years the HRT and combination groups showed increases of 2.9%±4.3% and 2.1%±5.5% from the baseline, while the clodronate group showed a decrease of -3.4%±4.6% ($p<0.001$). After 5-years lumbar BMD had increased by 3.9±5.1% in the HRT group and by 4.2±7.0% in the combination group. The clodronate group showed a decrease of -1.4±5.3% ($p<0.01$).In the femoral neck, after one year, the HRT and combination groups showed increases in BMD of 3.0%±2.9% and 3.1%±3.8% respectively, while BMD in the clodronate group decreased by -0.08%±4.6% . After three years the HRT and combination groups increased 2.7%±5% and of 2.3%±5.6%, while the clodronate group decreased -2.9%±5.2%. After five years, BMD benefit was 1.2%±12.9% and 2.8±5.9% in the HRT and combination groups, while net loss of BMD in the clodronate group was -3.3±5.7% ($p<0.01$).In conclusion, E2 2mg combined with NETA 1mg increased spinal and femoral BMD in postmenopausal women with severe primary or secondary osteoporosis.The addition of clodronate 800mg did not further increase the BMD values in combination with HRT. In contrast, clodronate 800mg /day could not preserve BMD in five years.

Disclosures: ***K. Hänninen****, None.*

M412

Effect Of Bisphosphonate In Insufficiency State Of Vitamin D. Preliminary Experimental Study. S. N. Zeni[1], S. R. Mastaglia*[1], P. Mandalunis*[2], M. C. Degrandi*[1], M. B. Oliveri[1], J. Somoza*[1]. [1]Sección Osteopatías Médicas, Hospital de Clínicas, University of Buenos Aires, Buenos Aires, Argentina, [2]Catedra de Fisiología, School of Dentistry, University of Buenos Aires, Buenos Aires, Argentina.

It is known that vitamin D insufficiency or deficiency has negative effects on skeletal metabolism. Experimental bone loss is achieved by ovariectomy (OVX) in rats by increasing bone turnover. Bisphosphonates (BPs) are useful antiresortive agents to inhibit resorption in several bone diseases. Hypothetically vitamin D insufficiency could affect bisphosphonate therapy. The aim of the present preliminary study was to investigate whether bone mass recovery due to olpadronate (OPD) treatment is affected by Vitamin D status- i.e. normal or insufficiency, using OVX rats with established osteopenia. A total of 16 female Wistar rats (280-300 g) were OVX: 8 rats were fed a synthetic diet that covered all adequate requirements (+VitD); 8 rats were housed under red light and fed the same synthetic diet lacking of Vitamin D (-VitD). During 60 days rats lost approximately 15% of bone mass, after that (To) 8 rats of +VitD group and all rats of -VitD group received during a 45-day period (Tf) 16ug OPD/100g rat weekly. Simultaneously, 8 OVX and 8 SHAM rats were fed the synthetic diet throughout the study and only received placebo treatment. Bone mineral density (BMD) (mg/cm2), 25OHvitamin D (ng/ml), bone alkaline phosphate (mUI/ml) and serum CTX (ng/ml) were assessed at To and Tf and tibia histomorphometry was made at Tf. (Table).Different letters indicated a $p<0.05$. Bone recovery by OPD treatment was greater in +VitD than in -Vit D. At Tf sCTX was lower and 25OHVitD was higher than in -VitD group. The +VitD group presented greater bone volume and lower erosive surface than -VitD group. Conclusion: These results suggest that OPD effects may be less beneficial in vitamin D deficient state.

Delta: Changes (Tf-To) in total skeleton (TE) and lumbar spine (LS).

	OPD+VitD	OPD-VitD	SHAM+VitD	OVX+VitD
DeltaBMD(TE)	12±4 a	5±3 a	10±3 a	-1±2 b
DeltaBMD(LS)	3.3±3.0 a	1.8±2.0 b	2.5±1.9 a	-5.3±2.4 b
Tf sCTX	99±10 a	138±11 b	181±13 c	204±13 d
Tf 25OHD	59.0±3.5 a	9.2±0.8 b	62.1±2.9 a	46.5±3.9 a
BV/BS%	29.9±5.6 a	19.7±8.1 b	28.2±8.4 a	12.6±5.1 b
ES/BS%	19.8±2.2 a	26.5±1.9 b	17.5±3.4 a	28.5±3.2 b

Disclosures: ***S.N. Zeni****, None.*

M413

The Point-Of-Care Device and Actonel® (risedronate) Once-a-Week Dosing Satisfaction Trial (POWER). W. P. Olszynski[1], A. Jovaisas*[2], W. Bensen*[3], S. Morin*[4], J. Stewart*[5], M. Baranci*[5], K. S. Davison[3]. [1]Medicine, University of Saskatchewan, Saskatoon, SK, Canada, [2]Med., Univ. of Ottawa, Ottawa, ON, Canada, [3]Med., McMaster Univ., Hamilton, ON, Canada, [4]Int. Med., McGill Univ. Health Centre, Montreal, PQ, Canada, [5]Aventis Pharma Inc., Laval, PQ, Canada.

The Point-of-Care device and Actonel® Once-a-Week dosing satisfaction trial (POWER) is a 24-week, multi-centre, prospective, open-label, randomized, controlled community practice-based study. The primary objective was to determine whether feedback on response to therapy using bone resorption results will improve subject satisfaction with therapy, a surrogate measure of persistence. Secondary objectives included: (1) comparing subject satisfaction of those previously treated for osteoporosis with those who were treatment-naïve; (2) documenting the response of bone turnover markers to Actonel (risedronate) 35mg Once-a-Week after 12 weeks of treatment; and (3) evaluating the correlation between subject satisfaction on Actonel 35mg Once-a-Week and bone turnover marker results after 12 weeks of treatment.

Patients (mean age of 63-71 yrs) were enrolled from 556 primary care centres in Canada and included postmenopausal women with osteoporosis, stratified into two groups: (1) osteoporosis treatment-naïve (n=1341); or (2) treated for osteoporosis within the past two years with either alendronate (n=157), etidronate (n=552), hormone replacement therapy (n=136), or calcitonin (n=33), but discontinued prior to enrolment due to lack of effect or intolerance.

All patients received Actonel 35mg Once-a-Week and were randomly assigned to either the bone turnover marker (n=1065) or no bone turnover marker group (n=1154). For the bone turnover marker group, urinary NTX was assessed at baseline and after 12 weeks using Osteomark® NTX Point-of-Care devices, which are registered by Health Canada as a rapid, one-step, in-office, disposable medical device for this purpose. Feedback and interpretation on response to therapy will be provided to patients in the bone turnover marker group at 12 weeks. Patients in the no bone turnover marker group will receive standard care at both time points. Patient satisfaction will be measured in both groups at 24 weeks with a self-administered questionnaire.

The POWER trial will help determine whether feedback on response to therapy using bone resorption results will improve subject satisfaction with therapy, a surrogate measure of persistence, and will describe the effect of Actonel 35 mg Once-a-Week on the level of bone turnover markers at 12 weeks of treatment.

Disclosures: ***W.P. Olszynski****, Alliance for Better Bone Health, a collaboration agreement between Procter & Gamble Pharmaceuticals and Aventis Pharma 5.*

M414

Differential Gene Expression in Bone Tissue of Postmenopausal Osteoporotic and Healthy Women. I. Takacs[1], J. P. Kosa*[1], G. Speer*[1], A. Tabak*[1], Z. Nagy[1], J. Kiss*[2], P. Lakatos[1]. [1]I.st Department of Medicine, Semmelweis University, Budapest, Hungary, [2]Department of Orthopedics, Semmelweis University, Budapest, Hungary.

The central role of estrogen deficiency in the pathogenesis of osteoporosis in postmenopausal women is well established, however, its effect on gene expression is not fully understood. The recently developed DNA macroarray technique allows analysis of changes in expression of genes related to bone metabolism. In this study, we examined the difference in bone-related gene expression of 9 osteoporotic (age range: 75-88) and 5 healthy (age range: 58-78) postmenopausal women. The bone samples were collected in the course of total hip arthroplasty. The bone samples were cryo-grinded, and total RNA was isolated by a column-based method. Following cDNA synthesis, biotin labeling by linear polymerase reaction and hybridization were carried out. Gene expression values were normalized to GAPDH and analyzed by unpaired Student's t-test. Among the 96 genes examined, the expression patterns of five genes were significantly different in the osteoporotic and healthy postmenopausal groups. The expression of matrix metalloproteinase 10 (MMP-10) and platelet-derived growth factor alpha polypeptide (PDGFα) genes was increased while the collagen type I receptor (CD36), insulin-like growth factor 2 (IGF-II), and transforming growth factor beta receptor I (TGFβR1) genes exhibited a decreased expression in osteoporotic subjects compared to that of the control group. These results may provide further insight into the pathomechanism of postmenopausal osteoporosis.

Disclosures: ***I. Takacs****, None.*

M415

Alendronate Is More Effective than Alphacalcidol in Preventing Glucocorticoid-induced Osteoporosis. R. de Nijs*[1], J. Jacobs*[1], A. Algra*[1], E. Buskens*[1], A. Huisman*[1], R. Laan*[2], C. de Laet*[3], W. Lems*[4], J. Bijlsma, on behalf of the STOP study group[1]. [1]University Medical Center, Utrecht, Netherlands, [2]University Medical Center, Nijmegen, Netherlands, [3]Erasmus Medical Center, Rotterdam, Netherlands, [4]Free University Hospital, Amsterdam, Netherlands.

Treatment with glucocorticoids (GCs) is associated with bone loss initiated already early in therapy, causing an increased fracture risk. The most important mechanism is decreased bone formation. Alendronate blocks bone resorption, but alphacalcidol stimulates bone formation.

The aim of the study: to determine which treatment is the most effective in prevention of glucocorticoid-induced osteoporosis.

We performed a randomized, double-blind, double-placebo clinical trial of 18 months dura-

tion in patients with a rheumatic disease, starting treatment with GCs in a dosage of 7.5 mg prednisolon equivalent daily or higher for 6 months or longer. Patients were allocated to treatment with either alendronate 10 mg and alphacalcidol-placebo daily or alphacalcidol 1 microgram and alendronate-placebo daily. In case of insufficient dietary calcium intake patients received calcium 500 mg daily and whenever vitamin D deficiency existed suppletion with inactive vitamin D 400 IU daily. Primary outcome was change of bone mineral density (BMD) of the lumbar spine (LS) in 18 months. Secondary outcomes were change of BMD in 18 months of the hips and symptomatic vertebral fractures. Evaluation of the incidence of vertebral deformities will take place at a follow-up of 3.5 years after start of the study.

Included were 201 patients in 23 outpatient departments of rheumatology in the Netherlands. One hundred patients received alendronate, 101 alphacalcidol; 163 patients completed the study. The BMD of the LS in the alendronate group increased with 2.3 ± 4.6%, in the alphacalcidol group the BMD decreased with 1.9 ± 5.7%. After 18 months the difference between both groups was 4.2% (95% confidence interval (CI) 2.6 to 5.8). In the alendronate group the BMD of the total hip increased with 0.7 ± 5.9%, in the alphacalcidol group it decreased with 2.5 ± 6.3%. After 18 months the difference in BMD between both groups was 3.2% (95% CI 1.0 to 5.5). No new symptomatic vertebral fractures were reported in the alendronate group, but in the alphacalcidol group 6 new symptomatic vertebral fractures occurred in 3 patients. Two non-vertebral fractures in 2 patients occurred in the alendronate group and 3 in 3 patients in the alphacalcidol group. No serious side effects were observed. We concluded that in this 18-month study concerning patients with rheumatic diseases treated with GCs, alendronate was more effective in preserving bone than alphacalcidol.

Disclosures: ***R. de Nijs****, None.*

M416

One-year Follow-up of 27 Patients With Osteoporosis Treated With a Single Intravenous Dose of Zoledronate. G. J. Paz-Filho*[1], C. A. M. Kulak[1], J. Kaminski*[1], S. C. Radominski[2], J. P. Bilezikian[3], V. Z. C. Borba[1]. [1]Endocrinology, SEMPR, Curitiba, Brazil, [2]Division of Rheumatology, UFPR, Curitiba, Brazil, [3]Departments of Medicine, College of Physicians & Surgeons, Columbia University, New York, NY, USA.

Zoledronate is a potent intravenous bisphosphonate with potential to be effecticious in postmenopausal women and men with osteoporosis. We studied the effects of zoledronate on bone mineral density in 27 patients (6 men and 21 women, aged 59±17 years) with osteoporosis (mean T score, -3.18±1.4). Thirty-three percent of the subjects had history of at least one fragility fracture. All subjects received 4 mg of intravenous zoledronate in a single dose. Lumbar-spine and total hip bone mineral density were measured at baseline , 6 months (T6) and 12 months (T12) after drug administration. At T6, mean lumbar-spine bone density increased from 0.699±0.149 g/cm^2 to 0.727±0.104 g/cm^2, a mean increase of 4%. Mean total hip density increased from 0.643±0.147 g/cm^2 to 0.659±0.136 g/cm^2, a mean increase of 2.4%. At T12, nineteen patients, evaluated so far, showed a 6.3% increase in lumbar-spine density and a 4.6% increase in total hip density, as compared to baseline. These changes in bone mineral density were not statistically significant because not all patients had yet completed the protocol. Adverse effects were limited to mild and self-limited myalgias, pyrexia and paresthesias. No one developed clinical hypocalcemia. Biochemical markers of bone resorption and formation were obtained at baseline and T12. The plan for this study is to continue to follow these patients for at least 2 years after the single dose of zoledronate in order to answer a key question: how long does a single dose of zoledronate maintain reduced indices of bone turnover? The answer to this question, not previously available from other cohorts, will help to guide an approach to the use of this agent in women and men with osteoporosis.

Disclosures: ***G.J. Paz-Filho****, None.*

M417

Early Changes in Urinary Cross-linked N-terminal Telopeptides of Type I Collagen Level Predict One-year Response of Lumbar Bone Mineral Density to Alendronate in Japanese Elderly Women with Osteoporosis. J. Iwamoto[1], T. Takeda*[1], M. Uzawa*[2]. [1]Department of Sports Medicine, Keio University, Tokyo, Japan, [2]Department of Orthopaedic Surgery, Keiyu Orthopaedic Hospital, Gunma, Japan.

The purpose of this study was to determine whether the early changes in urinary cross-lined N-terminal telopeptides of type I collagen (NTX) level would predict the one-year response of lumbar bone mineral density (BMD) to alendronate in Japanese elderly women with osteoporosis. One hundred and five postmenopausal women with osteoporosis, 54-88 years of age, were treated with alendronate (5 mg daily) for 12 months. Urinary NTX level was measured by enzyme-linked immunosorbent assay at the baseline and months 3, 6, and 12, and lumbar (L1-L4) BMD was measured by dual energy X-ray absorptiometry using a Hologic QDR 1500W instrument (Bedford, MA, USA) at the baseline and month 12. The mean percent reduction in urinary NTX level at months 3, 6, and 12 was 36.8 %, 49.5 %, and 49.0 %, respectively, with a more significant reduction at months 6 and 12 than at month 3, and the mean percent increase in lumbar BMD at month 12 was 8.2 %. Single regression analysis showed a significant correlation between the percent reductions in urinary NTX level at months 3, 6 and 12 and the percent increase in lumbar BMD at month 12 (r=0.200, P<0.05; r = 0.341, P<0.001; and r = 0.338, P<0.001, respectively). Thirty percent of patients were thought to be poor responders at month 3, with a reduction in urinary NTX level of less that minimum significant change (MSC), and 61 % of them showed a greater reduction in urinary NTX level exceeding MSC at month 6. These results suggest that the change in urinary NTX level at 3 and 6 months after the start of alendronate treatment at 5 mg daily could be a predictor of the one-year response of lumbar BMD, followed by a steady state level of urinary NTX after 6 months of treatment, in Japanese elderly women with osteoporosis.

Disclosures: ***J. Iwamoto****, None.*

M418

Comparative Study of Bone Turnover and BMD Responses to Treatment with Risedronate, Vitamin D, or Vitamin K in Japanese Osteoporosis Patients: Results of a 24-Week Interim Analysis. H. Iwata*, S. Yamada*, H. Takagi*. Rheumatism and Prosthesis Center, Nagoya Kyoritsu Hospital, Nagoya, Japan.

The Japanese have the world's longest average life span (84 years for women, 77 years for men) and the elderly population of Japan is rapidly rising. Measures to counter diseases specific to the elderly, particularly osteoporosis, are important. We compared changes in bone turnover markers and BMD with the administration of risedronate (RIS), the latest bisphosphonate treatment available in Japan, with those of vitamin D and vitamin K, currently the most common treatments for osteoporosis in Japan.

120 Japanese patients with primary osteoporosis (11 men, 79.5 yrs; 109 women, 70.7 yrs; overall age, 71.7 yrs) were enrolled at Nagoya Kyoritsu Hospital between May 2002 and May 2003 and were randomly assigned to one of three treatment groups (n=40/arm). They received 2.5 mg/d of oral risedronate (Actonel®, RIS), 1.5μg/d of vitamin D3 (Alfarol®, VD_3), or 45 mg/d of vitamin K (Glakay®, VK_2).

The mean (SD) changes in bone turnover markers and BMD from baseline to 24 weeks are shown in the table below:

Variables	% Change from Baseline			*P*-value	
	RIS	VD_3	VK_2	RIS vs VD_3	RIS vs VK_2
Urinary NTX	-43.8 (28.9)	1.3 (83.1)	6.2 (59.4)	0.006	<0.001
Serum NTX	-32.4 (14.4)	-20.5 (21.8)	-6.6 (22.2)	0.033	<0.001
Urinary DPD	-28.4 (35.4)	-2.5 (43.8)	1.2 (36.2)	0.013	0.003
Serum OC	-37.9 (23.4)	-12.4 (26.6)	14.8 (48.6)	<0.001	<0.001
Serum BAP	-26.3 (24.0)	-24.7 (18.4)	-4.3 (44.7)	0.772	0.029
BMD	4.7 (2.48)	1.7 (4.97)	0.5 (4.89)	0.029	0.001

NTX = cross-linked N-telopeptides of type I collagen; DPD = deoxypyridinoline; OC = osteocalcin; BAP = bone alkaline phosphatase; BMD = bone mineral density.

The decreases from baseline in urinary and serum NTX, and urinary DPD were significantly greater with RIS compared with both VD_3 and VK_2, from 4 weeks (data not shown) to 24 weeks of drug administration. RIS resulted in a greater reduction from baseline in serum OC than both vitamin groups. For serum BAP, similar decreases were observed for RIS and VD_3; the decrease was greater for RIS compared with VK_2. At 24 weeks, the BMD increase was significantly greater with RIS compared with both VD_3 and VK_2.

After 24 weeks of treatment in Japanese patients, risedronate is a more effective treatment for osteoporosis than VD_3 or VK_2 alone.

Disclosures: ***H. Iwata****, None.*

M419

Role of Alendronate in Therapy of Post-Traumatic Complex Regional Pain Syndrome I of the Lower Limb. D. H. Manicourt*, J. P. Brasseur*, Y. Boutsen, G. Depresseux*, J. P. Devogelaer. Rheumatology Unit, St-Luc University Hospital, Brussels, Belgium.

Introduction: As complex regional pain syndrome I (CRPS I) is associated with regional osteoclastic over-activity, the effect of the anti-resorbing agent alendronate (ALN) at the daily oral dose of 40 mg was evaluated in patients with post-traumatic CRPS I of the lower limb.

Methods: Forty patients were enrolled in this 8-week randomized, double-blind, placebo-controlled study with an optional 8-week open extension (week-12 to week 20) with ALN after a non therapeutic time period of 4 weeks. Clinical parameters included joint mobility (JM), limb edema as well as pressure tolerance (PT) and spontaneous pain (SP). Urinary levels of type I collagen N-telopeptides (NT x) were assessed by using an ELISA. Patients were examined at week-4, -8, -12, -16, -20 and -24. Statistical analysis included two-way factorial ANOVA.

Results and conclusions: In contrast to placebo-treated patients (n = 20), all patients of the ALN-treated group (n = 19) exhibited a marked and sustained improvement in SP, PT and JM as well as a significant reduction in urinary NT x levels at week-4 and -8. The improvement was maintained at week-12. Twelve patients from the ALN-treated group and 12 patients from the placebo-treated group volunteered for the 8-week open trial and they all responded positively to ALN, therefore supporting the use of oral ALN in post-traumatic CRPS I . By reducing local bone accelerated remodeling, ALN might relieve pain by effects on nociceptive primary afferents in bone and pain associated changes in the spinal cord, and also possibly through a central mechanism.

Disclosures: ***J.P. Devogelaer****, None.*

M420

Osteoporosis Treatment Using Reinforcement With Bone Turnover Marker Data Reduces Fracture Risk: The IMPACT Study. P. D. Delmas*[1], B. Vrijens*[2], C. Roux*[3], A. Le-Moigne-Amrani*[4], R. Eastell*[5], A. Grauer*[6], N. B. Watts*[7], H. A. P. Pols*[8], J. D. Ringe*[9], L. van de Langerijt*[10], D. Cahall[11]. [1]INSERM Research Unit 403, Lyon, France, [2]AARDEX Ltd, Zug, Switzerland, [3]University René-Descartes, Paris, France, [4]Aventis Pharmaceuticals, Bridewater, NJ, USA, [5]University of Sheffield, Sheffield, United Kingdom, [6]Procter & Gamble Pharmaceuticals, Mason, OH, USA, [7]University of Cincinnati, Cincinnati, OH, USA, [8]Erasmus University, Rotterdam, Netherlands, [9]Klinikum Leverkusen, Leverkusen, Germany, [10]Aventis Pharmaceuticals, Hoevelaken, Netherlands, [11]Aventis Pharmaceuticals, Bridgewater, NJ, USA.

With effective agents available for treatment of postmenopausal osteoporosis, patient persistence with treatment is necessary to sustain beneficial results. The IMPACT study assessed the effect of physician reinforcement using bone turnover marker (BTM) data on persistence with risedronate treatment. Eligible patients included postmenopausal women aged 65-80 years with spine/hip T-score ≤-2.5 or T-score ≤-1.0 with a low-trauma fracture after age 45 years. All subjects received risedronate 5 mg/d for 1 year and were pretreated with calcium 500 mg/d and vitamin D 400 IU/d for 20 days (median) prior to BTM baseline and initiation of risedronate. Centers were randomized into either reinforcement (RE+; verbal feedback based on urinary N-telopeptide of type I collagen [NTX] change from baseline) or nonreinforcement (RE-) groups. Electronic monitoring caps were used to assess daily compliance. Persistence was defined as the number of days from first dose intake until treatment discontinuation. A total of 2302 women from 171 centers in 21 countries were enrolled into the study. Lumbar and thoracic spine X-rays were performed at baseline and at 52 weeks for assessment of vertebral fractures and assessed using semi-quantitative techniques. Of these, vertebral fracture data were available for 1317 patients (RE+ n=676, RE- n=641). A total of 390 (30%) women had a prevalent vertebral fracture at baseline. Treatment was associated with a low incidence of new vertebral fractures during treatment (1.9%). In total, 8 (1.2%) new vertebral fractures were observed in the RE+ group compared with 17 (2.7%) in the RE- group (p=0.049). In summary, reinforcement of osteoporosis treatment using BTM data correlated with increased benefits on fracture reduction. This benefit could be explained partially by the significant increase in persistence observed in the subgroup of patients that was reinforced with a positive message based on a ≥30% decrease of urinary NTX. We conclude that reinforcement of osteoporosis treatment using BTM data might be beneficial for obtaining optimal fracture reduction.

Disclosures: ***P.D. Delmas****, Aventis 2.*

M421

Increased Osteoclast Number and Size in C57bl Mice with Calcium Deprivation and Treatment with a Single Dose of Zoledronic Acid. C. Gaudin*, H. Libouban*, M. Moreau*, M. F. Basle*, M. Audran, D. Chappard. LHEA Faculté de Médecine, INSERM EMI 0335, Angers, France.

The objective of this study is to evaluate the efficacy of a single dose of zoledronic acid (ZOL) in preventing bone loss and the associated mechanism in a calcium deprived mice. ZOL dosage was calculated to mimic the annual dose regimen used in human.

In animals, a low calcium diet induces: a significant increase in bone remodeling markers, an increase in osteoclast (Oc) number, and a reduction in the bone mineral density. Histomorphometric studies have confirmed that both trabecular and cortical bone are altered in animals fed with a low calcium diet. Recently, a single annual zoledronic acid (ZOL) infusion was reported to be as efficient as daily oral dose of bisphosphonate in the treatment of osteoporotic patients. Similar to other bisphosphonates ZOL has been shown to reduce Oc activity and induce Oc apoptosis.

Thirteen groups of nine C57BL mice (6-10 weeks old) were given laboratory food (either standard or calcium deprived), and water ad libitum (either tap or distilled). ZOL+ animals received at day 0, a single injection of ZOL in the tail vein (78µg/kg) and were fed with either a low calcium (ZOL+Ca-) or a normal diet (ZOL+Ca+); animals used as control (ZOL-Ca+) or fed with a low calcium diet (ZOL-Ca-) received a single saline injection by the same route. Animals were euthanized at 0, 2, 4 and 8 weeks and the effect on bone of calcium deficiency with/without ZOL was quantified by X-ray microcomputed tomography. Oc were histochemically identified by TRAcP staining.

Calcium diet induced a rapid trabecular bone loss in Zol-Ca- mice with reduced Tb.N and increase in Tb.Sp. ZOL+Ca- animals had an increased bone volume and preserved Tb.N. Surprisingly, Oc number was dramatically increased in ZOL+Ca- animals with calcium-deficient diet. This was associated with an increased of the Oc length in ZOL+Ca- mice (45.1 ± 2.1 µm vs. 17.9 ± 1.1 µm A normal calcium diet seemed to be required to induce Oc apoptosis by ZOL although Oc activity was impaired as evidenced by the preserved bone mass.

In conclusion, ZOL has been efficacious in preventing bone loss in calcium deprived mice through a significant reduction in Oc activity while their number increased.

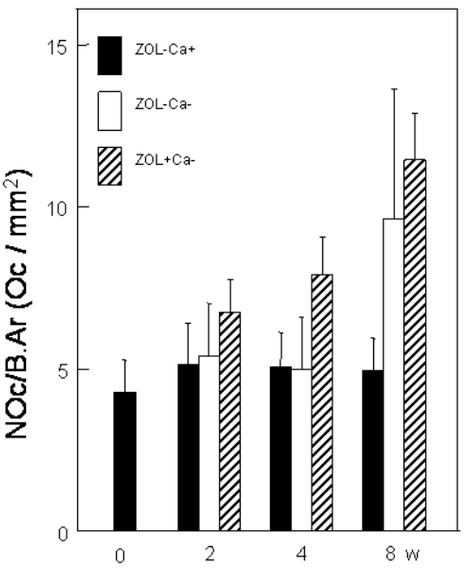

Disclosures: ***D. Chappard****, Novartis Pharma 2.*

M422

Effect of Alendronate in a Lapine Model of Estrogen Deficiency. B. Pennypacker, T. Cusick*, P. Masarachia, D. B. Kimmel. Bone Biology and Osteoporosis, Merck Research Laboratories, West Point, PA, USA.

The adult ovariectomized (OX) rat is the most oft-used *in vivo* model for testing agents to prevent estrogen deficiency bone loss. Despite its cancellous bone remodeling, the adult rat lacks Haversian remodeling of cortical bone. The smallest, most ubiquitous adult animal with significant Haversian remodeling, that develops OX-induced bone loss, is the rabbit. We further characterized the OX rabbit by evaluating bone remodeling after OX and the minimum dose of the anti-resorptive, alendronate (ALN) that fully blocks OX-induced bone loss.

Two experiments are reported. In #1, adult (7.5 months old, 3.9kg) rabbits were OX'd (N=22) or Sham-OX'd (N=11) during early June. 11 OX rabbits were given ALN (0.2mg/kg; subcutaneous (SC), 3X/wk) for 27 weeks. After in vivo dual calcein labeling, all were necropsied. Lumbar vertebrae (LV) 2-4 were fixed in 70% ethanol. Bone mineral density (BMD, mg/cm^2) of LV3 was determined (DXA); LV4 was embedded in methacrylate, sectioned parasagitally (6µm), and analyzed for cancellous (c) mineralizing surface. 100µm sections of the mid-femur were analyzed for endocortical (e) and periosteal (p) mineralizing surface (MS/BS; double+half-single, %), and number of labeled Haversian systems (HS)/mm^2. In #2, adult rabbits were OX'd (N=44) or Sham-OX'd (N=11) during early July. OX rabbits (11/grp) were given ALN (0, 0.03, 0.1, or 0.3mg/kg; SC, 2X/wk) for 13 weeks and necropsied. BMD of LV2-4 was determined ex vivo. Kruskal-Wallis plus Student-Neuman-Keuls post-hoc testing was applied.

OX-induced bone loss (9-13%) occurred in the LV of both experiments. In #1, bone loss was accompanied by increased formation rate at all four measured sites. ALN (0.6mg/kg/wk) completely blocked OX-induced bone loss in both experiments. In #2, ALN (0.2mg/kg/wk, LVBMD=409±29) was fully efficacious, while ALN (0.06mg/kg/wk, LVBMD=389±19) was partially efficacious for blocking bone loss.

These results suggest that the OX rabbit is an accurate, though seasonal, model of OX-induced bone loss, when considering behavior of bone mass and bone formation rate. These results also show that ALN inhibits bone formation at the cancellous, endocortical, and Haversian surfaces, but not at the periosteal surface. They further indicate that the minimum dose of ALN that fully inhibits vertebral bone loss in the OX rabbit is 0.2mg/kg/wk SC.

BMD and Bone Turnover

ALN (mg/kg/wk) Endpoint (Exp#)	Sham	OX+0	OX+0.6
LVBMD1	325±40[&]	288±32	320±33[&]
cMS/BS #1	10.4±7.8*	21.8±13.7	9.1±7.2*
eMS/BS #1	10.2±11.7*	18.0±9.7	10.4±12.3*
pMS/BS #1	1.6±1.5*	8.2±7.0	9.4±7.7
Labeled HS #1	0.0±0.0*	4.5±4.1	0.3±0.9*
LVBMD#2	409±32[&]	372±35	405±37[&]

vs. OX+0: 0.01[&] ; .05*; .1[+]

Disclosures: ***D.B. Kimmel****, None.*

M423

Impact of Non-Compliance and Non-Persistence With Daily Bisphosphonates on Longer-Term Effectiveness Outcomes In Patients With Osteoporosis. R. J. Sebaldt*[1], L. G. Shane*[2], B. Z. Pham*[2], R. J. Cook*[3], L. Thabane*[1], A. Petrie*[4], W. P. Olszynski[5], D. A. Hanley[6], J. Brown[7], J. D. Adachi[1], T. Murray[8], R. Josse[8], A. Papaioannou[1]. [1]McMaster University, Hamilton, ON, Canada, [2]Outcomes Researcher, Toronto, ON, Canada, [3]University of Waterloo, Waterloo, ON, Canada, [4]Research Associate, Hamilton, ON, Canada, [5]University of Saskatchewan, Saskatoon, SK, Canada, [6]University of Calgary, Calgary, AB, Canada, [7]University of Laval, Quebec, PQ, Canada, [8]University of Toronto, Toronto, ON, Canada.

This study aims to measure the impact of patient non-compliance and non-persistence with daily-regimen bisphosphonate treatment on longer-term treatment effectiveness outcomes, including changes in BMD and fracture rates.

We studied patients with OP treated with daily BP regimens in routine clinical care. All patients were being treated by tertiary care specialists collaborating in a systematic, prospective, observational, clinical data collection program. We report program follow-up rates and inconsistent use of BP therapy i.e. early discontinuation of BP or self-report of taking BP less than 80% of the time over the follow-up interval. We compared longer-term clinical outcomes between patient groups who reported inconsistent and consistent use of BP therapy: change in BMD (analysis of covariance) and incidence of fracture (Poisson regression).

From 1990 to 2002, 4,405 patients with OP (t-score < -2.5) (mean age 64, 86% female) were treated with BP. Cumulative follow-up rates in the program after 1, 2, and 3 years were 78%, 63% and 52%, respectively. Complete data for analysis of longer-term clinical outcomes were available for 1,041 patients (23.6%). This subset excludes patients who did not return for follow-up and is considered significantly enriched for patients who adhere to therapeutic advice rather than representative of the average patient population. In consistent BP users (CU) (n = 920, 88%), lumbar spine BMD increased significantly from baseline after 1, 2 and 3 years: 3.3% (95% CI: 0.6%, 6.1%), 4.9% (2.2%, 7.7%) and 6.5% (3.7%, 9.3%), respectively. In inconsistent BP users (IU) (n = 121, 12%), no significant improvement in BMD occurred until Year 3, at which time a modest gain of 3.2% (0.03%, 6.3%) was achieved relative to baseline (p = 0.002). The differences in BMD increase between the CU and IU were statistically significant after 1, 2 and 3 years: 1.4% (0.5%, 2.3%), 2.4% (1.2%, 3.6%) and 3.3% (1.5%, 5.2%), respectively. In addition to BMD, there was a trend of a 27% greater 10-year fracture risk in IU compared with CU (adjusted relative risk 1.27 (0.9, 1.8), p = 0.18).

This study demonstrates that patients who use BP inconsistently do not attain the proven clinical benefits of BP therapy.

Disclosures: ***R.J. Sebaldt****, Procter&Gamble 2; Aventis 2; Merck Frosst 2; GlaxoSmith-Kline 2.*

M424

New Approach to Simplify Osteoporosis Treatment Regimen for Bisphosphonate and Calcium. J. D. Ringe[1], S. van der Geest*[2]. [1]Klinikum Leverkusen, Leverkusen, Germany, [2]Procter & Gamble Pharmaceuticals, Geneva, Switzerland.

All large bisphosphonate trials have added calcium in amounts ranging from 500 to 1000 mg/day above individual dietary intake. Accordingly, calcium supplements or calcium/vitamin D combinations are recommended today as co-medication to antiresorptive therapy in all recently published national or international guidelines on the care strategy for osteoporosis. This consistent use of calcium may be hampered and impaired by several factors in the individual patient: low prescription rate or advice to purchase calcium; reduced compliance due to complex regimen; incorrect administration (e.g. calcium together with bisphosphonates). Therefore, treatment can be simplified by offering the two compounds in an integrated package, developed to facilitate the intake of this complex regimen. A new blister strip was developed containing one tablet of risedronate 35mg and 6 calcium carbonate tablets for a week of therapy. The package contained dosing instructions for the two products on one patient information leaflet. In a cohort of 164 patients, mean age 68.5 years, we studied in a cross over design, the impact of the new pack versus separate packages on the patients understanding of intake instructions. The understanding of five instructions was tested: intake of risedronate 35mg in the morning, only with water, without food, without other medication, separate from calcium. Adherence to all 5 instructions increases the likelihood of obtaining maximal therapeutic response to bisphosphonate treatment. Analysis of cross-over data (n=164) showed high understanding of instructions for the separate packaging (70%, n=115) but improved significantly with the combination pack (82% n=134) (p<0.05). In this cohort, 83% of participants preferred the new combination pack over separate packs (p<0.05). Reasons for this preference are shown in table 1.

TABLE 1

Reasons for preference*(n=164)	%
Prefer one pack over two packs	49
Easy/convenient to use/ practical handy	39
Easy to understand/less confusion	36
Easier to remember/ less likely to forget	19

* multiple reasons possible

These data support that the integrated combination packaging of risedronate with calcium can lead to simplification of therapy. Simplification of therapy can lead to improved adherence to treatment and consequently the likelihood to meet therapeutic goals of the therapy.

Disclosures: ***J.D. Ringe****, Procter & Gamble Pharmaceuticals 5; Aventis Pharmaceuticals 5.*

M425

Zoledronic Acid Counteracts Bone Loss in the Spinal Cord Injury Model of Microgravity. J. R. Shapiro[1], T. J. Beck[2], B. Mustapha*[3], C. B. Ruff*[4], P. Ballard*[5], J. Caminis[6]. [1]Medicine, Uniformed Services University, Bethesda, MD, USA, [2]Radiology, Johns Hopkins University, Baltimore, MD, USA, [3]Neuroscience Research, National Rehabilitation Hospital, Washington, DC, USA, [4]Cell Biology, Johns Hopkins University, Baltimore, MD, USA, [5]Spinal Cord Injury, National Rehabilitation Hospital, Washington, DC, USA, [6]Novartis Pharmaceutical, East Hanover, NJ, USA.

Although mechanical consequences are not well known, exposure to microgravity causes significant lower-limb bone loss; similar patterns have been seen in tetra- or paraplegic spinal cord injury (SCI). In a double-blind placebo-controlled randomized study, we evaluated effects of intravenous 4 or 5 mg of zoledronic acid on SCI bone loss. Subjects included 12 males and 3 females (8 placebo, 7 zolendronate) evaluated within 10 weeks of injury and followed for 1 year. SCI lesions were located between C-5 and T-12 and were classified as ASIA A or ASIA B depending on motor/sensory deficit. DXA scans of the LS spine and hip were obtained at 0, 6 and 12 months using Hologic QDR 1000 and GE Lunar Prodigy densitometers standardized with a special phantom. Hip Structure Analysis was used to derive BMD, cross sectional area (CSA), periosteal diameter, section modulus (Z), and estimates of endocortical diameter, mean cortical thickness and buckling ratio. Zoledronic acid maintained femoral neck CSA and had significant positive effects (p= <0.05) on BMD, CSA, periosteal diameter, Z, and buckling ratio in the intertrochanteric region. Overall, treatment effects were most evident at the shaft. Compared to placebo, treatment significantly reduced the decline in BMD, CSA, Z, and cortical thickness and attenuated the increase in endosteal diameter, and buckling ratio. Lumbar spine BMD rose 13.3 % in controls and 5.2% in treatment group: each group sat erect daily. Urinary n-telopeptide excretion was decreased following treatment. SCI, as a model for microgravity exposure, causes major losses in bone mass and structural strength at the proximal femur. Despite the small sample size, this study showed that zoledronic acid had significant positive effects on some structural parameters of the femoral neck and intertrochanteric region, and on all structural parameters in the femoral shaft, thus counteracting the negative effects of non-weight-bearing, and potentially that of microgravity, on BMD and bone strength.

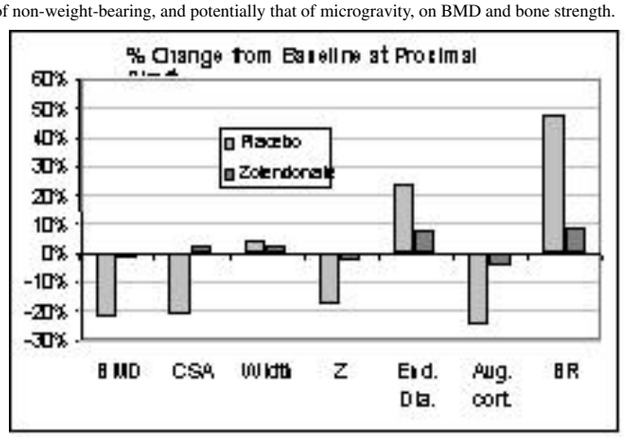

Disclosures: ***J.R. Shapiro****, Novartis Pharmaceutical 5.*

M426

Bone Mineral Density Response to Pamidronate in Adult Osteogenesis Imperfecta. J. R. Shapiro[1], C. Hickman*[1], M. Shindle*[1], K. BrintzenhofeSzoc*[2], P. Sponseller*[3]. [1]Osteogenesis Imperfecta Program, Kennedy Krieger Institute, Baltimore, MD, USA, [2]School of Social Service, Catholic University, Washington, DC, USA, [3]Orthopedic surgery, Johns Hopkins University, Baltimore, MD, USA.

We report the response to treatment with pamidronate in adults with osteogenesis imperfecta (OI). Pamidronate is reported to induce a robust increase in bone mineral density and a significant decrease in fracture rate in children with OI. An assessment of pamidronate treatment for one year in adults with type IA OI was reported to improve bone biopsy morphology, with positive, but statistically non-significant, increases in bone density.

Factors influencing treatment results in adults include: fracture incidence, is significantly less than in children, bone turnover is lower, adults are less compliant with treatment and testing schedules, the presence of rodding, scoliosis and greater limb deformity alters DXA readings.

This cohort includes 59 patients, 17 males and 42 females having OI types I (n = 34) , III (n=18) and IV (n=7) between the ages of 16-64 years. 24 patients were treated with IV bisphosphonate. Bisphosphonate treatment regimens in 35 patients included: IV pamidronate (n=24) : 1.5 mg/kg body wt. to a maximum of 60 mg every 3-4 months. 24 patients were non treatment controls. 11 subjects received oral bisphosphonate (data not included). Diets were supplemented with calcium, 800-1200 mg/day and 400 U vitamin D daily. DXA scans were obtained at 6-12 month intervals on the same machine and are reported comparing baseline to months 12 and 18.

After treatment of type I OI for18 months, mean L1-L4 BMD changed from 0.830 gm/cm2 to 0.805 gm/ cm2 (p=>0.10) total hip changed from 0.739 gm/cm2 to 0.808 gm/cm2(p > 0.10). In type III OI, L1-4 changed from 0.607 gm/cm2 to 0.648 gm/cm2, total hip changed from 0.804 to 0.652 gm/cm2 (p=>0.01) . In type IV patients mean L1-L4 changed from 0.671 gm/cm2 to 0.697 gm/cm2, total hip changed from 0.423 to 0.558 (n=1, p=> 0.10). For treated type I patients, urine NTX (nMBCE/mM creatinine) was 49, at baseline, 28 at 6 mo., and 33 at 12 mo. For treated type 3 patients, urine NTX (nMBCE/mM creatinine)= 98 at baseline, 93 at 3 mo., 82 at 6 mo., 87 at 9 mo. and 103 at 12 mo.

Bisphosphonate treatment of adults with mild or severe OI for 18 months has non-significant effects on BMD in the lumbar spine or proximal femur. Patients may show a small increase in spine BMD after 1 year of treatment, which then plateaus. Adult OI patients treated with bisphosphonates remain susceptible to sporadic fractures particularly with mild trauma. Urine NTX values decline in treated type I patients but not in treated type 3 patients. Bone morphology is required to assess treatment effects in the individual patient.

Disclosures: ***J.R. Shapiro****, Novartis 5.*

M427

Evaluation of Alendronate Therapy in a Murine Model of Male Idiopathic Osteoporosis. J. E. Zerwekh, R. Millsaps*, A. Thomas*, E. Simpson*, O. Oz. Center for Mineral Metabolism and Clinical Research, University of Texas Southwestern Medical Center at Dallas, Dallas, TX, USA.

Up to 50% of men with osteoporosis have no identifiable etiology and are defined as having primary or idiopathic osteoporosis (IO). Clinical trials have shown such men respond favorably to bisphosphonate treatment, an antiresorptive agent, despite the low bone-turnover remodeling pattern that is usually seen in male IO. These observations raise the possibility of an anabolic effect of bisphosphonate in male IO. In order to clarify the mechanism(s) of bisphosphonate action in low turnover states of bone remodeling, we evaluated the effect of alendronate therapy on bone density, histomorphometry, biochemical markers of turnover, and ex-vivo osteoprogenitor cell studies in 12 adult male aromatase-deficient mice (ArKO) and compared the response to that in 12 placebo-treated ArKO male mice and 12 placebo-treated wild-type littermates. This murine model has been found to have a similar histological and biochemical presentation as seen for men with IO. Following 1 month of alendronate therapy (70 µg/kg, twice per week), lumbar BMD increased by 7.7% in ArKO males (p=0.00002) but decreased by 0.9% and 3.2% in placebo-treated ArKO and wild-type animals, respectively. Both bone histomorphometry and biochemical markers of bone turnover disclosed further reductions in bone turnover following alendronate treatment. Placebo-treated ArKO males had significant reductions in cancellous bone volume, trabecular thickness, osteoid volume and surface, and osteoblastic surface as compared to wild-type mice. Alendronate administration to ArKO males further reduced eroded surface and mineralizing surfaces as compared to ArKO-placebo, resulting in a significant reduction in bone formation rate. Alendronate also resulted in a significant decline in 24 hr urinary calcium, deoxypyridinoline and in serum osteocalcin when compared to the pre-treatment baseline values. Compared to wild-type littermates, ArKO mice had significant reductions in the number of bone marrow osteoprogenitors. Alendronate treatment did not affect osteoblast progenitor number or the number of osteoblasts undergoing apoptosis. Taken together, these findings suggest that alendronate's ability to raise bone density in males with idiopathic osteoporosis is the result of further reduction of bone turnover and that there is no apparent effect on osteoblastogenesis.

Disclosures: ***J.E. Zerwekh****, Merck 2.*

M428

Predictive Value of Biochemical Markers of Bone Turnover in the Treatment of Japanese Postmenopausal Women with Alendronate. K. Kurasawa*[1], O. Chaki[1], K. Mochizuki*[1], Y. Arata*[1], H. Yoshikata*[1], R. Kikuchi[1], I. Gorai[2], F. Hirahara*[1]. [1]Obstetrics and Gynecology, Yokohama city University School of Medecine, Yokohama, Japan, [2]Obstetrics and Gynecology, International University of Health and Welfare Atami Hospital, Atami, Japan.

We aimed to evaluate the effect of alendronate on bone density and biochemical markers of bone turnover in postmenopausal Japanese women with osteoporosis or osteopenia.Sixty eight postmenopausal Japanese women (64.9+/-7.1 years old) diagnosed as osteopenia or osteoporosis were enrolled in this study. After giving informed consent, the subjects were treated with arendronate 5mg per day. Lumbar and femoral neck bone mineral density(BMD) were determined at the start of this study and every six months. Biochemical markers of bone formation were measured intact osteocalcin (IOC) after 1, 3, 6,12,18,24 months. And biochemical markers of bone resorption were measured urinary deoxypyridinoline (DPD) and crosslinked N-telopeptide of type I-collagen (NTX) after 1, 3, 6,12,18,24 months. The predictive value of biochemical markers of bone turnover for bone density was evaluated by using the minimum significant change (MSC). Lumbar spine BMD was increased by 6.76+/-4.95% 2 years after treatment. Femoral neck BMD was increased by 4.21+/-4.90% 2years after treatment. The percent changes of each biochemical marker at 3 and 6 months after treatment were significant as compared with baseline values; DPD -24.9% and -26.0%, IOC -25.0 and 34.4%, NTX -32.0% and -34.4%. In addition, the percent changes of NTX at 1 month after treatment were greater than MSC. The results suggest that treatment alendronate 5mg daily significantly increased lumbar BMD and reduced biochemical markers, especially IOC and NTX are useful for predicting the effect of alendronate in postmenopausal Japanese women. In addition, it was recognized that an effect of treatment with alendronate continued during an observation period.

Disclosures: ***K. Kurasawa****, None.*

M429

Monthly Oral Ibandronate Is Well Tolerated in Women with Postmenopausal Osteoporosis: 1-Year Results from MOBILE. E. M. Lewiecki[1], P. D. Miller[2], R. Lorenc[3], C. Hughes*[4], B. Bonvoisin[4], M. R. McClung[5]. [1]New Mexico Clinical Research & Osteoporosis Center, Albuquerque, NM, USA, [2]Colorado Center for Bone Research, Lakewood, CO, USA, [3]The Children's Memorial Institute, Warsaw, Poland, [4]F. Hoffmann-La Roche Ltd, Basel, Switzerland, [5]Oregon Osteopor**osis Center, Portland, OR, USA.**

As with other chronic, asymptomatic conditions, adherence to osteoporosis therapies is poor. Adverse events (AEs) are often cited as a reason for treatment discontinuation. A convenient, monthly-dosed oral bisphosphonate with good safety and tolerability may enhance adherence, thereby optimizing therapeutic outcomes in postmenopausal osteoporosis (PMO). Ibandronate (Boniva®) is a potent, nitrogen-containing bisphosphonate. In a recent clinical study, oral ibandronate, administered daily or intermittently with an extended between-dose interval of more than 2 months, significantly reduced the risk of new vertebral fractures (3-year vertebral fracture risk reduction: 52% and 50%, respectively).[1] A safety profile similar to placebo was also reported, independent of the administration schedule. The MOBILE study is investigating the efficacy and safety of a convenient monthly oral ibandronate regimen. MOBILE is a randomized, double-blind, phase III, non-inferiority study comparing monthly oral ibandronate (100mg given as 50mg per day on two consecutive days, 100mg, or 150mg) with 2.5mg per day in 1,609 women with PMO. The safety and tolerability of ibandronate was assessed at 1 year, with a confirmatory analysis after 2 years. The 1-year safety analysis showed oral ibandronate to be well tolerated, with no numerical imbalances between arms in the overall number of AEs or overall number of AEs by body system. Importantly, no difference in the incidence of upper gastrointestinal AEs was observed in the 50/50mg, 100mg, 150mg monthly oral regimen, compared with daily arm (15.9%, 21.7% and 16.9% vs 18.0%, respectively). More specifically, the incidence of dyspepsia was similar across the study arms (6%, 9% and 6% vs 7%, respectively). In conclusion, monthly oral ibandronate was well tolerated with no apparent unexpected safety concerns. By providing greater patient convenience and excellent tolerability, monthly oral ibandronate may enhance therapeutic outcomes in PMO through improved long-term therapeutic adherence.

1. Chesnut CH, et al. J Bone Miner Res (In press).

Disclosures: ***E.M. Lewiecki****, F. Hoffmann-La Roche Ltd 2.*

M430

Evidence for a Specific Recognition Step Involved in Cellular Uptake of Bisphosphonates. K. Thompson, M. J. Rogers, F. P. Coxon*, J. C. Crockett*. Medicine & Therapeutics, University of Aberdeen, Aberdeen, United Kingdom.

The exact mechanism by which bisphosphonates (BPs) are internalised into cells remains unclear. Cellular uptake of BPs has been shown to be dependent on calcium in RAW264 macrophages. We have previously shown that the non-nitrogen-containing BP (non-N-BP) clodronate (CLO) antagonises the effects of nitrogen-containing BPs (N-BPs) in J774 macrophages *in vitro* and postulated that BP uptake takes place via a membrane-bound transport protein. To investigate this further, we synthesised a fluorescently-labelled analogue of alendronate (FL-ALN).

Using confocal microscopy, uptake of FL-ALN by J774 macrophages was detected in intracellular vesicles within 5 minutes of treatment. We compared the pattern of uptake of

FL-ALN to specific markers of fluid-phase endocytosis (TRITC-dextran), adsorptive endocytosis (wheat germ agglutinin-TAMRA) and receptor-mediated endocytosis (transferrin-TAMRA). Only TRITC-dextran showed a marked degree of co-localisation with FL-ALN, suggesting that a major component of BP uptake is mediated by fluid-phase endocytosis.

Using flow cytometry, J774 cells were found to markedly accumulate FL-ALN within 4 hours. Consistent with our previous findings, molar excess of the non-N-BP CLO dramatically inhibited the vesicular uptake of 100μM FL-ALN. Co-treatment of J774 cells with FL-ALN and 250μM CLO inhibited uptake of FL-ALN by 90%. This inhibitory effect of CLO was not due to inhibition of fluid-phase endocytosis, since CLO did not affect the uptake of FITC-dextran.

Since BPs are non-hydrolysable analogues of pyrophosphate (PP_i) we hypothesised that PP_i may also compete with BPs for cellular uptake. Co-treatment of J774 cells with 250μM PP_i decreased FL-ALN uptake by 76%. Due to the high affinity of BPs for divalent ions (such as Ca^{2+}), we investigated whether the inhibitory effect of CLO or PP_i was due to Ca^{2+} chelation. Whilst molar excess Ca^{2+} ions stimulated FL-ALN uptake, 500μM EGTA (a Ca^{2+} chelator) inhibited FL-ALN uptake by 96%, which was reversed in the presence of 2mM Ca^{2+}. Supplementation of 250μM CLO or PP_i with molar excess (1mM) Ca^{2+} partially prevented the inhibitory effect of CLO, but not PP_i, on FL-ALN uptake.

These observations show that cellular uptake of BPs can occur by fluid-phase endocytosis. However, there appears to be a specific recognition step prior to endocytosis that is dependent on Ca^{2+} and can be blocked by competition with PP_i or other BPs, such as CLO.

Disclosures: ***K. Thompson****, None.*

M431

Fluvastatin Prevents Bisphosphonate-Induced Vγ9Vδ2 T-Cell Activation and Proliferation *In Vitro*. K. Thompson, M. J. Rogers. Medicine & Therapeutics, University of Aberdeen, Aberdeen, United Kingdom.

An acute phase response is the major adverse effect of intravenously-administered nitrogen-containing bisphosphonates (N-BPs) and is associated with the activation (TNFα and IFNγ release) and proliferation of the major subset of γ,δ-T cells in humans ($Vγ9Vδ2^+$ subset). We, and others, have recently reported that the stimulatory effects of N-BPs on γ,δ-T cell proliferation in cultures of human PBMCs are most likely due to inhibition of FPP synthase, an enzyme in the mevalonate pathway. By this mechanism, N-BPs cause the accumulation of upstream isoprenoid lipids such as IPP, which then directly activate $Vγ9Vδ2^+$-T cells. N-BPs, such as zoledronic acid (ZOL), stimulate γ,δ-T cell proliferation in human PBMC cultures with a similar order of potency to the order of potency for inhibition of FPP synthase. Mevastatin, by inhibiting HMG-CoA reductase, can abrogate the stimulatory effects of N-BPs on γ,δ-T cells by preventing the N-BP-induced accumulation of IPP.

Treatment of PBMC cultures with 1μM ZOL for 7 days caused an ~8-fold increase in the proportion of γ,δ-T cells in the $CD3^+$ population. This proliferative effect of ZOL was decreased by >75% when PBMCs were simultaneously treated with 1μM fluvastatin (FLU). Consistent with this, 1μM ZOL caused a marked increase in the proportion of $Vγ9Vδ2^+$-T cells in the γ,δ-T cell population from ~70% (+/-9.1%) in naïve cultures to 98.6% (+/-1.6%) after 7 days treatment. Simultaneous treatment with FLU reduced the ZOL-induced increase in the proportion of $Vγ9Vδ2^+$-T cells to 86% (+/- 2.9%). The inhibitory effect of FLU could be abolished by replenishing cells with mevalonate, suggesting that FLU prevents $Vδ2^+$-T cell proliferation by inhibiting HMG-CoA reductase and preventing ZOL-induced accumulation of IPP.

Although the concentration of ZOL used in this study is similar to the C_{max} following intravenous administration to patients *in vivo* (1μM), plasma concentrations decrease rapidly with a $t_{½}$ of <2hrs. Therefore, the effectiveness of a short pulse of ZOL for inducing IFNγ release in PBMC cultures was investigated. A 2hr pulse of 1μM ZOL induced a 10.3-fold (+/-0.7) increase in IFNγ release from PBMCs after 48hrs. A simultaneous 2hr pulse with 1μM FLU markedly decreased ZOL-induced IFNγ release by >70%. When FLU was present for the entire 48hr period, FLU was only slightly more effective at preventing the ZOL-induced IFNγ release than when present only for the 2hr ZOL pulse, suggesting that sufficient FLU is internalised by PBMCs within a 2hr period to prevent the accumulation of IPP resulting from a clinically relevant exposure to ZOL. Co-administration of FLU with intravenous N-BPs may therefore provide a means for preventing the acute-phase response *in vivo*.

Disclosures: ***K. Thompson****, Novartis Pharma AG 2.*

M432

Once Monthly Dosing Increases the Proportion of Patients who Respond to Oral Ibandronate: 1-Year Results from MOBILE. R. Emkey[1], D. Felsenberg[2], J. J. Stepan[3], C. Hughes*[4], E. Dumont*[5], P. Van der Auwera*[4], R. R. Recker[6]. [1]Radiant Research, Wyomissing, PA, USA, [2]Charite - Campus Benjamin Franklin, Berlin, Germany, [3]Charles University, Prague, Czech Republic, [4]F. Hoffmann-La Roche Ltd, Basel, Switzerland, [5]GlaxoSmithKline, Collegeville, PA, USA, [6]Creighton University, Omaha, NE, USA.

Studies of antiresorptive agents indicate that 1-year threshold values for treatment-induced increases in BMD and decreases in BCM predict for antifracture efficacy.[1] Ibandronate (Boniva®) is a potent, nitrogen-containing BP with antifracture efficacy when given daily or intermittently.[2] A 2-year, randomized, double-blind, phase III, non-inferiority study (MOBILE) is comparing the efficacy and safety of 50/50mg (single doses on consecutive days), 100mg (single day) and 150mg (single day) monthly oral ibandronate with oral daily ibandronate (2.5mg; 3-year vertebral fracture risk reduction: 52%) in 1,609 women with PMO. After 1 year, a prespecified analysis examined the proportion of patients in each arm achieving increases in: lumbar spine (LS) BMD above baseline or 6%; total hip (TH) BMD above baseline or 3%; both LS and TH BMD above baseline. The proportion of patients achieving decreases in sCTX below defined threshold values was also examined. After 1 year, the majority of patients achieved increases in LS or TH BMD above baseline (**Table**). Compared with the daily arm, significantly more patients achieved increases above baseline in the 150mg arm for LS BMD and the 100mg and 150mg arms for TH BMD. Likewise, more patients in the 100mg and 150mg arms achieved substantial increases in LS BMD (>6%) and TH (>3%) BMD than in the daily arm. In addition, most participants achieved increases in both LS and TH BMD above baseline ($p \leq 0.001$ for 100mg and 150mg vs 2.5mg). In the analysis of sCTX, a significantly greater proportion of patients in the 150mg arm consistently achieved decreases in sCTX of >30%, >50% and >70%, respectively, compared with the daily arm. In summary, a larger proportion of women receiving 100mg and 150mg monthly oral ibandronate achieve increases in LS and/or TH BMD after 1 year versus those receiving daily ibandronate. Moreover, compared with daily, significantly more patients receiving 150mg ibandronate achieve threshold values for sCTX.

1. Hochberg MC, et al. J Clin Endocrinol Metab 2002;87:1586-92.
2. Chesnut CH, et al. J Bone Miner Res (In press).

Table. Proportion (%) of participants considered responders to daily or monthly ibandronate.

	Daily ibandronate	Monthly ibandronate		
Relative change (%) in BMD	2.5mg (n=318)	50/50mg (n=330)	100mg (n=315)	150mg (n=327)
LS BMD >baseline	84.0	87.8	86.5	91.3*
LS BMD >6%	24.2	30.5	32.2*	35.3*
TH BMD >baseline	76.7	81.9	87.1†	90.0†
TH BMD >3%	34.9	38.0	43.4*	48.4†
LS BMD + TH BMD >baseline	65.7	73.2*	77.7†	83.9†

*p<0.05 vs 2.5mg
†p≤0.001 vs 2.5mg

Disclosures: ***R. Emkey****, F. Hoffmann-La Roche Ltd 2.*

M433

Relative Change in Bone Mineral Density Is a Valid Surrogate for Antifracture Efficacy with Ibandronate. S. Epstein[1], H. Huss*[2], K. M. Wilson*[3], R. C. Schimmer[3]. [1]Mt Sinai Medical Center, New York, NY, USA, [2]., Levekusen, Germany, [3]F. Hoffmann-La Roche Ltd, Basel, Switzerland.

Predefined statistical analyses of the findings from recent antifracture studies of oral and intravenous ibandronate in postmenopausal osteoporosis demonstrate a reduction in risk of vertebral fracture that is significantly associated with improvements in BMD.[1,2] In light of these positive findings, an additional statistical analysis[3] was performed to validate relative change (%) from baseline in BMD as a surrogate marker for predicting 3-year VF RR with ibandronate (using total hip and lumbar spine BMD after 1, 2 and 3 years). The following criteria were used to evaluate surrogacy: (1) BMD is affected by treatment; (2) fracture incidence is affected by treatment; (3) BMD is prognostic for fracture; and (4) the proportion (ρ) of the 3-year antifracture effect explained by relative change (%) from baseline in BMD at each time point. For criteria 1-3, parameter estimates were produced using simple logistic regression models. When the studies were considered separately, findings were variable due to the small sample sizes. However, when the data were pooled, robust findings were reported. Notably, the criteria for surrogacy (outlined above; 1-3) were fulfilled for all analyzed surrogate endpoints for 3-year VF RR (**Table**). In addition, values for ρ (criterion 4) indicated that relative change (%) from baseline in total hip and lumbar spine BMD after 2 and 3 years explained a substantial proportion of the 3-year antifracture effect with ibandronate (**Table**). Importantly, values were similar to those obtained for other widely accepted surrogate endpoints. In summary, while not providing a complete explanation for antifracture efficacy, these findings highlight the utility of using relative change (%) from baseline in total hip and lumbar spine BMD after 2 and 3 years as surrogate markers for 3-year VF RR with ibandronate.

1. Wasnich R, et al. J Bone Miner Res 2003;18:S160 (Abstract SA353).
2. Miller P, et al. ASBMR 2004 (In submission).
3. Prentice RL. Stat Med 1989;8:431-40.

Table. Proportion of 3-year antifracture effect explained by relative change (%) in BMD

Surrogate	Year	Proportion of antifracture effect explained by surrogate
Relative change (%) from baseline in total hip BMD	1	14%*
	2	24%*
	3	37%*
Relative change (%) from baseline in lumbar spine BMD	1	6%*
	2	23%*
	3	27*

*Endpoints fulfilling criteria for surrogacy

Disclosures: ***S. Epstein****, F. Hoffmann-La Roche Ltd 5.*

M434

Does Dosing Regimen Impact Persistence With Bisphosphonate Therapy Among Postmenopausal Osteoporotic Women? J. A. Cramer*[1], M. M. Amonkar*[2], A. Hebborn*[3], N. Suppapanya*[2]. [1]Yale University, West Haven, CT, USA, [2]GSK, Collegeville, PA, USA, [3]Roche, Nutley, NJ, USA.

Although bisphosphonates are effective in the management of osteoporosis, patients often omit doses or discontinue treatment for a variety of reasons. This study assessed treatment adherence with daily and weekly bisphosphonates among postmenopausal osteoporotic women. Administrative claims data (from 1997-2002) from 30 health plans were used to identify postmenopausal osteoporotic women (>45 years) newly-prescribed (no bisphosphonate Rx at least 6 months prior) a once-weekly (QW - alendronate 35 or 70 mg) or once-daily (QD - alendronate 5 or 10 mg or risedronate 5 mg) bisphosphonate. The QW and QD cohorts were followed for 12 months from the date of fill of the index prescription. Medication possession ratio (MPR) was used to estimate compliance and cumulative bisphosphonate exposure during follow-up while persistence was calculated as the number of days from the initial prescription to a lapse of >30 days after completion of the previous refill. A total of 2741 women met the inclusion criteria (alendronate QW = 731; alendronate or risedronate QD = 2010). Mean age was 63.7 years. Overall MPR was 60.6% but QW users had a significantly higher MPR than QD users (69.2% vs 57.6%, t = -7.51, p<0.0001). Overall treatment persistence during the 12 months of follow-up was 196 days but significantly longer persistence was observed for QW users when compared with QD users (227 vs 185 days to discontinuation, respectively, log-rank X^2 = 30.3, p<0.0001). Kaplan-Meier analysis (Fig. 1) showed that at the end of 12 months, 44.2% of women on the QW regimen and 31.7% of women on the QD regimen persisted with therapy. Median duration of persistence was substantially higher in the QW cohort than the QD cohort (269 vs 134 days respectively). Also, 31% of QD users had ≤2 fills as compared to 21% of QW users (X^2= 23.11, p < 0.0001). Results indicate that postmenopausal osteoporotic women prescribed a weekly bisphosphonate regimen had significantly higher rates of compliance and longer persistence compared with those taking a more frequent, daily dosing regimen. However, rates for both regimens were less than desirable in terms of MPR, time to discontinuation and refill rates. These data demonstrate that less frequent dosing increases persistency, which is needed to obtain maximal long-term therapeutic benefits.

Figure 1: Time to discontinuation

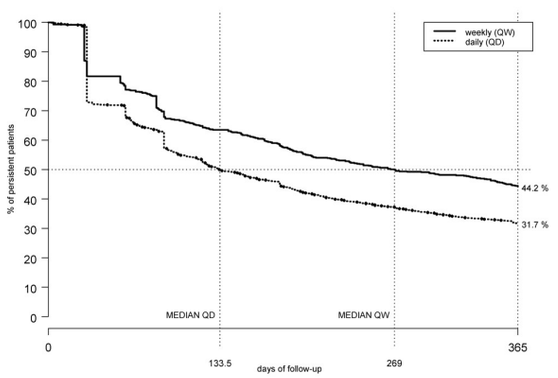

Disclosures: ***J.A. Cramer****, Roche 7.*

M435

The Response to Bisphosphonates and No Treatment Varies on the Concave and Convex Sides of the Scoliotic Spine. R. H. Routh*[1], A. L. Burshell[1], E. A. Nauman*[2]. [1]Endocrinology, Ochsner Clinic Foundation, New orleans, LA, USA, [2]Department of biomedical engineering, Tulane University, New orleans, LA, USA.

Adult scoliosis is estimated to be present in 5-10% of the population and its etiology may be related to adolescent scoliosis, degenerative disease or osteoporosis. Previous studies from our laboratory showed that the lumbar spine Z-Score is +1.5 S.D. greater than the femoral neck and the concave side is 15-20% denser than the convex side (SPINE, 2004).
The higher BMD on the concave side may be related to compression of the vertebrae, accretion of bone on the concave side, or greater bone loss on the convex side. In order to differentiate between these possibilities, we compared the repeat BMD to the original BMD in patients with scoliosis taking no therapy (N) or a bisphosphonate (B).
Scoliosis was identified by a single certified BMD interpreter and included in the study if they had a previous BMD scan and were taking either no N or B using the Hologic Delphi DXA. There were 35 patients in the N group and 27 patients in the B. The average time between scans was approximately 2 years. The L1-L4 vertebrae were divided vertically in two equal areal segments. The BMD of the concave and convex sides was determined.
The concave BMD increased significantly more than the convex side in the N group (See Figure). Similarly, the concave BMD increased more than the convex in the B group. The B group density was greater than the N on both the concave and convex sides. There did not appear to be any change in the angles of deformity between the repeat and baseline DXA scans.
This is the first study to show in scoliosis that the concave BMD increases without therapy. Bisphosphonates increase the lumbar BMD in both the concave and convex scoliotic spine, but greater on the concave. Finally, at least some of the increase in lumbar concave BMD is due to new bone formation.

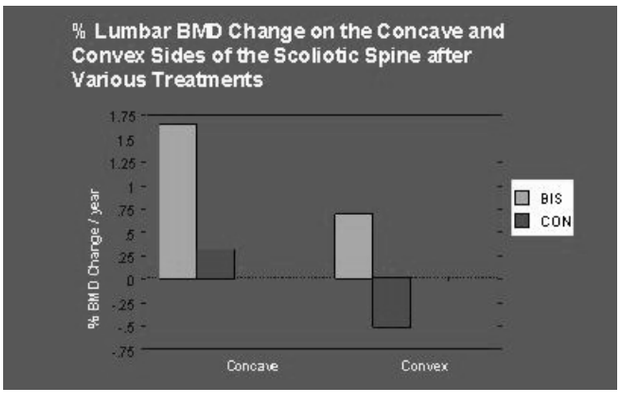

Disclosures: ***A.L. Burshell****, Eli Lilly 2, 5, 8; Merck 5, 8; Proctor & Gamble 2.*

M436

Improving Compliance with Oral Bisphosphonate Therapy in a Pharmacist-managed Osteoporosis Clinic. E. N. Griffin*[1], V. I. Petkov*[2], M. I. Williams*[1], R. A. Adler[2]. [1]Endocrinology and Bone Metabolism, McGuire VA Medical Center/Virginia Commonwealth University School of Pharmacy, Richmond, VA, USA, [2]Endocrinology and Bone Metabolism, McGuire VA Medical Center/Virginia Commonwealth University School of Medicine, Richmond, VA, USA.

Bisphosphonates (BIS) are effective for osteoporosis. Patients discontinue therapy due to adverse events, cost, or problems with administration. Pharmacists can play a significant role in compliance. We hypothesized that a Bone Pharmacotherapy Clinic (BPC) could improve compliance with osteoporosis treatments.
In a single Veterans Affairs Medical Center we compared compliance with oral BIS in BPC patients to those followed by other providers (OTH). Compliance was calculated as the cumulative months of oral BIS prescribed divided by the months the BIS prescription was actually refilled. A retrospective electronic medical record review was conducted of 63 patients who had ≥ 4 visits to the BPC and 63 patients monitored by OTH, matched by BIS start date (± 3 months).
The 2 groups had similar age, weight, body mass index, gender, race, and fracture history distribution. BPC patients had significantly shorter exposure to oral BIS because 12 (19%) were switched to intravenous formulations. A greater proportion of BPC patients had follow-up BMD tests and documented adverse events than OTH patients. Compliance with oral BIS was greater in the BPC patients as compared to OTH patients. Alendronate had a compliance rate of 82.6 % vs. 70.1 % (p-value 0.016) while risedronate had a rate of 71.8 % in the pharmacotherapy group as compared to 62.3% in the OTH group (p-value NS). The difference in alendronate compliance remained significant after adjusting for the length of treatment, BMD test follow-up, and treatment related adverse events. Least square means from the ANCOVA model were 80.1% [74.9, 89.2] for BPC patients and 70.7% [63.1, 78.2] for OTH patients. A larger number of OTH patients (n=16) discontinued therapy as compared to BPC patients (n=10). Characteristics of patients who discontinued therapy in both groups were not significantly different with respect to age, BMI, gender, race, BMD follow up, fracture history, length of treatment or the number of active medications, but 37% of patients who discontinued therapy had a documented fracture (27.3% of BPC and 43.8% of OTH). Only 30% of patients who discontinued therapy had documented side effects from BIS.
In the BPC patients, factors associated with continued therapy were older age and having a recent BMD test follow-up (logistic regression model). Patients enrolled in a Bone Pharmacotherapy Clinic are more likely to be compliant with oral BIS therapy as compared to those patients followed by other healthcare providers.

Disclosures: ***E.N. Griffin****, None.*

M437

Effect of Change in Dietary Acid-base Balance on Bone Turnover and Urine Calcium Excretion. R. Jajoo*[1], L. Song*[2], H. Rasmussen*[3], B. Dawson-Hughes[2]. [1]Division of Rheumatology, Tufts-New England Medical Center, Boston, MA, USA, [2]Bone Metabolism Laboratory, JM USDA Human Nutrition Research Ctr on Aging at Tufts University, Boston, MA, USA, [3]Metabolic Research Unit, JM USDA Human Nutrition Research Ctr on Aging at Tufts University, Boston, MA, USA.

We conducted this study to determine whether net acidity of the diet influences the rate of bone turnover and urinary calcium excretion. Forty subjects, age 50 years and older, with low usual protein and calcium intakes, were given supplemental protein at 0.75g/kg, 600 mg of elemental calcium and 400 IU of vitamin D3 daily. They were randomly assigned to fruit and vegetable supplements to neutralize the acid load from the added protein or to supplements containing carbohydrates and fat that were isocaloric to the fruits and vegetables. Net endogenous acid production was assessed by 24-hour urine net acid excretion (NAE). Urinary NAE, N-telopeptide (NTX) and calcium excretion and serum PTH and osteocalcin were measured at baseline, day 30 and day 60. Neither group had a significant change in weight during the study. This study was approved by the Investigation Review Board. There were no significant differences in NAE or in markers of bone turnover or urinary calcium excretion in the two groups by ANOVA. However, in all sub-

jects, baseline NAE was significantly correlated with 24-hour urine NTX (r = 0.428, P = 0.006). Baseline NAE was not significantly associated with serum PTH (r = 0.264, P = 0.100), serum osteocalcin (r = -0.017, P = 0.917), or urine calcium excretion (r = 0.281, P = 0.079). An increase in NAE from baseline to day 60 was significantly associated with an increase in urine NTX (r = 0.367, P = 0.020), and adjustment for change in serum PTH modestly altered this correlation (rp = 0.304, P = 0.060). Change in NAE was also significantly correlated with change in serum PTH (r = 0.358, P = 0.023); however, there was no association between change in serum PTH and change in urine NTX (r = 0.260, P = 0.106). Change in NAE was not significantly associated with change in serum osteocalcin (r = -0.128, P = 0.431) or with change in urine calcium excretion (r = 0.231, P = 0.152). We conclude that in healthy elderly men and women, a diet-induced increase in NAE over 60 days was significantly associated with an increase in urine NTX, indicating that acidogenic diets promote bone resorption. This association appears to be partially mediated by PTH. Increasing diet acidity did not appear to alter serum osteocalcin or urine calcium excretion. Because there was no difference in NAE between groups, it was not surprising to see no group difference in markers of bone turnover or urine calcium excretion.

Disclosures: ***R. Jajoo****, None.*

M438

Influence of Iron and Calcium on Change in Bone Mineral Density Differs by HRT Status in Postmenopausal Women. J. Maurer*[1], M. Harris*[2], T. Lohman[3], V. Stanford*[1], E. Cussler*[3], S. Going*[1], L. Houtkooper*[1]. [1]Nutritional Sciences, University of Arizona, Tucson, AZ, USA, [2]Pediatrics, Center for Applied Research and Evaluation, University of Arkansas, Little Rock, AR, USA, [3]Physiology, University of Arizona, Tucson, AZ, USA.

Hormone Replacement Therapy (HRT) has been used to prevent osteoporosis related bone mineral loss, yet, little research is known about how HRT may influence the nutrient-bone mineral density (BMD) interaction. This study was conducted to determine if dietary iron (iron) and dietary plus supplemental calcium (calcium) were associated with 1 year changes in BMD of postmenopausal women and if HRT use influenced these associations. Subjects were healthy nonsmoking postmenopausal women (n =228, mean age 55.6 ±4.6 years) from the Bone, Estrogen, Strength Training (B.E.S.T.) Study who completed the first year of this partially randomized clinical trial were examined. Women were stratified by HRT use status (HRT n =116, No HRT n =112). BMD was measured at five sites (lumbar spine L_2-L_4, trochanter, femur neck, Ward's triangle and total body) using dual energy X-ray absorptiometry (DXA) at baseline and 1 year. Mean nutrient intakes were assessed using 8-day diet records. All women received 800 mg a day of elemental calcium as calcium citrate. Regression analyses were conducted examining the effects of iron and calcium on BMD change adjusting for the effects of years past menopause, baseline BMD, weight change, exercise, and energy intake. Further associations of iron and BMD change adjusting for the same covariates and calcium were also examined, and vice versa. Tertiles were created for iron and calcium intake and then graphed against estimated marginal mean change in BMD to assess the interaction of iron with calcium on BMD change. Iron was associated ($p \leq .05$) with greater positive change in BMD at the trochanter and Ward's triangle in women taking HRT. Calcium was associated ($p \leq .05$) with change in BMD at the trochanter and femur neck for women not taking HRT. In women taking HRT in the lowest tertile of calcium intake (900-1400 mg), change in femur neck BMD increased linearly as tertile of iron intake increased. Conversely, in women not taking HRT, increase in BMD was seen only in the women in the highest tertile of calcium intake (1600-2600 mg). For both groups combined, change in BMD at the trochanter and Ward's triangle increased with increasing intakes of dietary iron in women at the lowest tertiles of calcium intake (HRT: 900-1400 mg; No HRT: 500-1300 mg). We concluded that HRT influences the associations of iron and calcium on change in BMD.

Supported by National Institutes of Health grant AR39559 and Mission Pharmacal

Disclosures: ***J. Maurer****, None.*

M439

Calcaneal Ultrasound Change Rates In Girls From Age 10 To Age 13. K. M. Davies, J. M. Lappe, G. Lypaczewski*, J. Stubby*. Osteoporosis Research Center, Creighton University, Omaha, NE, USA.

Two cohorts of girls aged between 9 and 10 were recruited for longitudinal studies of the effects of calcium nutrition and exercise on bone acquisition from 9 to 13. Those with more than 3 sessions/wk in organized sports were excluded. At semiannual visits, heel speed of sound (SOS) and attenuation (BUA) were measured by the Osteometer DTU-One. Graphs of group averages of these variables by visit or age appeared linear, so linear regressions over visits covering age 10 through 13 were done for individuals to obtain rates of change of SOS and BUA relative to baseline. In the CalKids study, participants were randomized into "normal diet" as controls and "calcium" with diet enhanced by foods richer in or supplemented with calcium. In the ExKids study, the groups were controls "C", 3 times a week exercise sessions "EX", and exercise sessions with more calcium food intake "EXHC". There was no difference between the studies in baseline values. Pooled for the 58 CalKids and 102 Exkids in this analysis, they are: SOS 1551.8 (SD 6.5) m/s and BUA 37.3 (SD 4.8) dB/MHz. In each study there was no difference between groups for the rates, but for the ExKids the rates were not different from zero, while for the CalKids they were positive: SOS 0.07%/y, P <0.002; BUA 3.3%/y, P < 0.0001. We believe the difference may be due to the effect of menarche. In the CalKids study, 37 of 58 girls (64%) had menarche within the interval of analysis, while for the ExKids only 44 of 102 (43%) had menarche. Conclusion: Hormonal status affects the change of calcaneal Ultrasound SOS and BUA in girls age 10 through 13.

Disclosures: ***K.M. Davies****, None.*

M440

Effects of Calcium-fortified Soy Milk Supplementation on Bone Mineral Density in Chinese Adolescent Girls Aged 14-16. S. C. Ho[1], G. Guldan*[2], J. Woo*[3], R. Yu*[1], M. Tse*[2], A. Sham*[1], J. Cheng*[4]. [1]Community & Family Medicine, Chinese University of Hong Kong, HK, Hong Kong Special Administrative Region of China, [2]Food & Nutritional Sciences Programme, Department of Biochemistry, Chinese University of Hong Kong, HK, Hong Kong Special Administrative Region of China, [3]Department of Medicine & Therapeutics, Chinese University of Hong Kong, HK, Hong Kong Special Administrative Region of China, [4]Department of Orthopaedics & Traumatology, Chinese University of Hong Kong, HK, Hong Kong Special Administrative Region of China.

Purpose: We aim to study the effect of calcium-fortified soy milk supplementation on change of bone mineral density (BMD) and content (BMC) in Chinese adolescent girls aged 14-16 y. **Methods:** This one-year study was conducted in 210 adolescent girls recruited from 6 secondary schools with comparable academic status, and assigned randomly to the intervention or control groups. Girls of the intervention group were supplied daily with 375 ml of calcium fortified soymilk (Calciplus) supplementation containing 142.5 kcal, 6.75 g protein, 4.1 g fat, 600 mg Ca and 54 mg isoflavones. At baseline, all participating subjects were ascertained the pattern of dietary intake based on 3-day self-administered food diary. BMD was measured at baseline and at 12 months with a Delphi QDR series, Hologic Dual-energy X-ray densitometre (Walthan, MA) at the spine (L1-L4), and hip (femoral neck, trochanter, and intertrochanter, and total hip). We compare the percentage change in BMD/BMC of the spine and hip region between the intervention (N=104) and control group (N=95). **Results:** The mean percentage changes of BMD/C and standard deviation (SD) over the followup for the intervention and control groups are: neck of femur BMD 2.7± 2.94%, 1.8±3.49% (p = 0.08); trochanter BMD 3.3±3.27%, 1.6±2.94% (p = <0.001); intertrochanter BMD 3.6±3.05%, 2.32±2.95% (p = 0.002); total hip BMD 3.1±2.39%, 2.05±2.22% (p = 0.001); total hip BMC 3.8±3.05%, 2.6± 2.96% (p = 0.006). The percent difference between the two study groups [100x (soymilk-control)/control] ranged from 45% to 113%. We observed no difference in the spine BMD/C between the two groups. Analysis of covariance controlling individually for height, weight, growth stage, dietary energy, calcium from usual diet yielded similar results. Stepwise multivariate regression analysis also showed that the supplementation group was significantly associated with increase in % BMD/C at the hip after simultaneously controlling for the covariates. **Conclusion:** 375 ml calcium fortified soymilk supplementation is among the effective strategies in increasing hip BMD and BMC and the optimization of peak bone mass in Chinese adolescent girls.

Disclosures: ***S.C. Ho****, None.*

M441

Effect of Choline Stabilized Orthosilicic Acid on Bone Density in Ovariectomized Rats. M. Calomme[1], J. Sindambiwe*[1], P. Cos*[1], C. Vyncke*[2], P. Geusens[3], D. Vanden Berghe*[1]. [1]Pharmaceutical Sciences, University of Antwerp, Antwerp, Belgium, [2]Bio Minerals nv, Destelbergen, Belgium, [3]Limburg University Center, BIOMED, Limburg, Belgium.

Silicon (Si) deficiency in animals results in bone defects. Orthosilicic acid is a bioavailable form of Si and was found to stimulate collagen type 1 synthesis[1] in human osteoblast-like cells. Choline stabilized orthosilicic acid (ch-OSA) was reported to increase the femoral BMD in chicks[2].

The effect of ch-OSA supplementation on bone loss was investigated in mature ovariectomized rats. The study was approved by the local Ethical Committee. Female Wistar rats (n=58, age: 9 months) were randomly divided in 3 groups. One group was sham operated (SHAM, n=21) and bilateral ovariectomy (OVX) was performed in the other 2 groups. One group (OVX1, n=20) was supplemented orally with ch-OSA (1 mg Si/kg BW) starting immediately after OVX whereas rats in the second group (OVX0, n=17) were controls. Rats were pair fed a standard diet and were sacrificed after 30 weeks supplementation. BMC and BMD were analyzed by DEXA. Scans were recorded for total femur, 4 regions of interest in the femur (H1: midshaft, H2, H3, H4: distal metaphysis), and lumbar vertebrae. Si concentration was measured by ETAAS. Comparison between groups was evaluated with the Mann-Witney U test.

The serum Si concentration of supplemented rats (mean: 253 µg/l) was significantly higher compared to SHAM (113 µg/l, p<0.0001) and OVX controls (147 µg/l, p=0.001). The 24 hour urinary Si excretion of supplemented OVX rats (165 µg) was significantly higher compared to SHAM (120 µg, p=0.001) and OVX controls (94 µg, p<0.0001).

Bone mineral content was significantly decreased by OVX in the femur (-15 %, SHAM vs. OVX0, p=0.0001) and spine (-17 %, SHAM vs. OVX0, p<0.0001). Ch-OSA supplementation increased significantly the femoral BMC in the distal region (H3: +9.4 %, OVX1 vs. OVX0, p=0.01) and total femoral BMC (+6.4 %, OVX1 vs. OVX0, p=0.025). Lumbar BMC was marginally increased by ch-OSA supplementation (+3.5%, vs. OVX0, p=0.17).

OVX significantly decreased bone mineral density in the femur (-15 %, SHAM vs. OVX 0, p<0.0001) and spine (-14 %, SHAM vs. OVX0, p=0.0005). Ch-OSA supplementation increased significantly the femoral BMD at two sites in the distal region (H2: +4.2 %, H3: +7.2 %, OVX1 vs. OVX0, p<0.05). Total lumbar BMD was marginally increased by ch-OSA supplementation (+4.6 %, vs. OVX0, p=0.11).

In conclusion, ch-OSA supplementation partially but significantly prevents femoral bone loss in the aged ovariectomized rat model. These results confirm earlier studies suggesting an essential role of Si in bone metabolism.

[1] Reffitt DM et al., Bone. 32 :127, 2003.
[2] Calomme M et al., Calcif Tissue Int, 70:292, 2002.

Disclosures: ***M. Calomme****, Bio Minerals nv 2.*

M442

An Investigation into the Effects of Calcium Carbonate Supplementation on Markers of Pubertal Status and Leptin in 8-12 Year Old Gambian Girls. F. Ginty[1], A. Prentice[1], L. McKenna*[1], J. Bennett*[1], B. Dibba*[2]. [1]MRC Human Nutrition Research, Cambridge, United Kingdom, [2]MRC, Keneba, Gambia.

It has been suggested that menarcheal age may be inversely associated with calcium intake, but the mechanistic basis for this remains uncertain. The aims of the present study were to investigate, in a population where delayed puberty is common, whether calcium supplementation of prepubertal Gambian girls aged 8-12 years modified markers of pubertal status including, luteinising hormone (LH), follicle-stimulating hormone (FSH), and sex-hormone binding globulin (SHBG). Since dietary calcium has been postulated to indirectly affect fat mass, which in turn may modify the rate of pubertal development, leptin was also measured. Eighty girls were randomised, double-blind to receive either 714 mg/d of supplemental calcium (as calcium carbonate (Calcichew)) or a matching placebo for 12 mo. Fasting blood samples were collected from all subjects at baseline and at the end of the intervention period. Plasma from sixty subjects (n=28 and 32, respectively, for calcium and placebo groups) was analysed for LH, FSH and SHBG by Immulite immunoassay analyser (DPC, UK). Leptin was analysed by enzyme-linked immunoassay (Quantikine Human Leptin R&D Systems, UK). At baseline, the majority of subjects were in Tanner stage 1, with the exception of two subjects from the placebo group, who were at Tanner stage 2. No significant differences were found between groups for any of the markers. Conditional regression analysis was conducted to determine differences between groups at the end of the supplementation period, after adjustment for baseline value, age, body weight, height and number of supplementation days. At the end of the study, two subjects from the calcium group and three subjects from the placebo group had moved from Tanner stage 1 to 2. There were two further subjects in the placebo group who had moved to Tanner stage 3. There was a non-significant trend for higher LH (+28.7 (SE 20.2)%, p=0.16) and FSH (+39.1 (23.9)%, p=0.11) in calcium-supplemented subjects. Significant differences were not found for SHBG (+1.8 (8.9) %, p=0.84) or leptin (-13.0 (11.0)%, p=0.60). A significant difference in body weight was not found (+1.23 (1.26)%, p=0.37 for calcium vs placebo subjects), nor was there a significant difference in triceps skinfold measurement (-5.88 (4.76)%, p=0.22). These findings do not provide convincing evidence that calcium supplementation of prepubertal Gambian girls modifies markers of pubertal status or leptin. This may be due to the slower maturation rate of Gambian children compared to Caucasians. Further research is required to investigate the mechanisms by which calcium might affect the rate of pubertal maturation.

Disclosures: ***F. Ginty****, None.*

M443

Evaluation of the Clinical Use of Vitamin K Supplementation in Postmenopausal Women with Osteopenia (The EKCO Trial): Study Design and Baseline Data. A. Cheung[1], L. Tile*[1], Y. Lee*[1], G. Hawker*[2], L. Thompson*[3], R. Vieth*[4], P. Massicotte*[5], T. Murray*[6], R. Josse*[6]. [1]University Health Network, Toronto, ON, Canada, [2]Sunnybrook and Women's Health Sciences Centre, Toronto, ON, Canada, [3]University of Toronto, Toronto, ON, Canada, [4]Mount Sinai Hospital, Toronto, ON, Canada, [5]University of Alberta, Edmonton, AB, Canada, [6]St. Michael's Hospital, Toronto, ON, Canada.

In recent years, vitamin K has been postulated to play an important role in bone health. Epidemiologic studies suggest that fracture patients have lower serum vitamin K levels when compared to non-fracture controls. As well, those with low vitamin K intake are at higher risk of fractures.

We are currently conducting a 2-year double-blind placebo-controlled randomized trial of 5mg oral vitamin K_1 daily supplementation in 430 postmenopausal women with osteopenia. Our primary hypothesis is that 5mg of vitamin K_1 daily will attenuate the natural BMD loss in postmenopausal women with osteopenia. We included postmenopausal women with T-scores between -1 and -2 in the lumbar spine (L1-L4), total hip, and femoral neck. We excluded women with osteoporosis, Paget's or other metabolic bone disease, and those on chronic oral steroids, coumadin, antiresorptive medications in the past 3 months, or megadoses of vitamin A or E. All women will have baseline, 1-year and 2-year measurements of BMD, as well as bone turnover markers. Each has a dietary assessment for calcium and vitamin D intake and is supplemented to 1500mg of calcium and 800IU of vitamin D a day. This protocol was approved by the ethics review boards of all participating centers, and informed consent is obtained prior to participants enrolling in the study.

As of May 2004, we have screened 729 women, and 386 have been randomized. Mean age at baseline was 59 years. Natural menopause was at age 50, and surgical menopause was at age 43. Mean height was 161.7 cm, mean weight was 68.4 kg, and mean BMI was 26.1. Mean BMD for lumbar spine (L1-L4) was 0.923 g/cm^2 (T-score = -1.2), total hip was 0.869 g/cm^2 (T-score = -0.6), and femoral neck was 0.712 g/cm^2 (T-score = -1.2). 88.6% of participants were Caucasian, 2.3% African-Caribbean, 6.2% Asian and 2.8% other. 55.8% were married or cohabiting. 35.0% had a family history of osteoporosis. 65.8% used some alcohol. 6.2% are current smokers, 46% ex-smokers, and 47% never smoked. 66% rated their health as very good or excellent, and 34% good or fair. Overall, our participants are relatively healthy.

The ECKO trial is one of three ongoing large-scale randomized trials to examine the effect of vitamin K supplementation on bone health in North America. We expect to complete this study by 2006.

Disclosures: ***A. Cheung****, None.*

M444

Dose-dependent Effects of Vitamin E on Bone in an Orchidectomized Rat Model of Osteoporosis. S. Chai*[1], E. A. Lucas[1], B. J. Smith[1], A. Patade*[1], L. Devareddy*[1], D. Y. Soung[1], K. Korlagunta*[1], C. Wei*[1], D. Marlow*[2], B. H. Arjmandi[1]. [1]Nutritional Sciences Department, Oklahoma State University, Stillwater, OK, USA, [2]Laboratory Animal Resources, Oklahoma State University, Stillwater, OK, USA.

In a previous study we demonstrated that a moderately high dose of vitamin E in the diet improves biomechanical and biochemical properties of bone in old male mice. The present study was conducted to evaluate whether vitamin E can exert bone-sparing effects on osteopenic male bone. Forty 12-mo old male Sprague-Dawley rats were either sham-operated (sham) or orchidectomized (orx) and fed a control diet for 120 days to establish bone loss. Thereafter, rats were assigned to their corresponding treatment groups (n=10): Sham + 75 IU vit E; ORX rats received 75, 250, or 500 IU vit E per kg diet for 90 days. To date, whole body as well as 4th lumbar and femoral bone mineral density (BMD) and content (BMC) have been evaluated using dual energy x-ray absorptiometry. Data are presented below:

Parameters	Sham + 75 IU vit E	Orx + 75 IU vit E	Orx + 250 IU vit E	Orx + 500 IU vit E
BMC, *g*				
Whole Body	15.863±0.26 [a]	14.548±0.25[b]	14.709±0.25 [b]	14.432±0.25 [b]
Femur	0.717±0.017 [a]	0.625±0.016 [b]	0.635±0.016 [b]	0.608±0.016[b]
BMD, *g/cm^2*				
4th Lumbar	0.203±0.005[a]	0.1733±0.005 [b]	0.1658±0.005[b]	0.1632±0.005[b]
Whole Body	0.187±0.002 [a]	0.177±0.002 [b]	0.174±0.002 [b]	0.174±0.002 [b]
Femur	0.277±0.004[a]	0.249±0.004[b]	0.252±0.004[b]	0.242±0.004[b]
4th Lumbar	0.256±0.004[a]	0.223±0.004 [b]	0.224±0.004[b]	0.219±0.004[b]

Values presented are mean ± SE. Within each row, values with different superscript letters are significantly different from each other (P<0.05).

Although vitamin E has been shown to have some osteoprotective properties in other animal models, the findings of the present study indicate that vitamin E is unable to restore bone mass once the loss has occurred in this rat model of male osteoporosis.

Disclosures: ***E.A. Lucas****, None.*

M445

Does Vitamin E Affect Microarchitectural Properties of Osteopenic Female Rats? E. A. Lucas[1], D. A. Khalil[1], B. J. Smith[1], L. Devareddy*[1], D. Y. Soung[1], V. Peddireddy*[1], S. Juma[2], M. P. Akhter[3], D. Chakkalakal*[4], B. J. Stoecker[1], B. H. Arjmandi[1]. [1]Nutritional Sciences Department, Oklahoma State University, Stillwater, OK, USA, [2]Department of Nutritional Sciences, University of Cincinnati Medical Center, Cincinnati, OH, USA, [3]Osteoporosis Research Center, Creighton University, Omaha, NE, USA, [4]Department of Orthopedic Surgery, Creighton University Medical Center, Omaha, NE, USA.

In the present study, the dose-dependent effects of vitamin E in improving bone microarchitectural properties was investigated using osteopenic ovariectomized rat model. Seventy-five 12-month old female SD rats were divided into 5 groups and were either ovariectomized (ovx; 4 groups) or sham-operated (1 group). Rats were fed standardized laboratory diet (AIN-93M) containing 75 mg vitamin E per kg diet for 120 days to allow occurrence of significant loss in bone mineral density (BMD) due to ovx. Thereafter, the diet of rats in sham and one ovx group was maintained on the 75 mg vitamin E per kg diet while three ovx groups was supplemented for 100 days with one of the vitamin E dose: 300, 525, or 750 mg vitamin E per kg diet. Animals that received 750 mg vitamin E had enhanced 4th lumbar vertebral bone quality as evident by improved yield force and yield stress in comparison with ovx controls. However, neither histomorphometric (proximal tibia) nor micro-structural (5th lumbar vertebra) data indicated that vitamin E supplementation results in higher bone volume over total volume (BV/TV), an index of bone mass. Additionally, micro-computed tomography (μCT) findings including finite element analysis showed no effects of vitamin E on trabecular region of 5th lumbar vertebral bone. The improvement in biomechanical properties of 4th lumbar may not be due to enhanced trabecular bone mass or micro-structural properties.

Disclosures: ***E.A. Lucas****, None.*

M446

Effects of Soy Isoflavones on Bone Mineralization and Milk Mineral Concentration in Lactating Rats. C. A. Peterson*, J. Schnell*, L. Hillman. Nutritional Sciences, University of Missouri-Columbia, Columbia, MO, USA.

Although research has shown that soy isoflavones increase bone density during periods of chronic estrogen deficiency (e.g. surgical or natural menopause), scarce data exists on the skeletal effects or safety of soy isoflavone intake during acute estrogen deficiency (e.g. lactation). Our hypothesis is that soy isoflavone consumption will attenuate the bone loss associated with lactation. Further, we want to determine if isoflavones affect milk quality or quantity. Immediately after parturition, lactating rats were randomly assigned to one of four nutritionally complete diets (n=12/group) in which casein-based diets were supplemented with different levels of soy isoflavone extracts (ADM Novasoy, Decatur, IL): 0, 2, 4, or 8 mg total aglycone isoflavone/g protein. At day 12-15 of lactation, milk was col-

lected once from each dam. At weaning (day 21), bones and serum were harvested from 6 animals per group (lactation groups). The remaining 6 rats from each group continued on their respective diets for 4 weeks when bones and serum were collected (recovery groups). There were no differences in dam age or weight among all groups. Animals consumed significantly more food during the lactation phase than during the recovery phase. Serum genistein concentration was higher in lactating, high isoflavone diet dams; likewise, milk genistein concentration was higher in high isoflavone diet dams. Histomorphometry revealed that lactation results in losses in cancellous bone volume, mineralized bone volume, trabecular thickness and growth plate volume and thickness. Isoflavone treatment had no effect on any of these indices. Despite a trend for increased total tibia calcium in animals receiving the high isoflavone diet (p=0.1), isoflavone treatment did not affect milk calcium or phosphorus concentration or litter weight. This is the first report on the bone effects of isoflavone intake using an intact lactating rat model. Results provide support that consumption of soy isoflavones, in levels that can be readily attained through moderate consumption of soy foods, have neither protective effects on bone nor deleterious effects on milk quality or quantity during lactation.

Disclosures: ***C.A. Peterson****, Mead Johnson Nutritionals 5.*

M447

Dried Plum Prevents Bone Loss in Animal Model of Male Osteoporosis. B. J. Smith[1], M. Franklin*[1], E. A. Lucas[1], E. A. Lancaster*[1], D. Y. Soung[1], L. Devareddy[1], D. Bellmer*[2], D. Marlow*[3], B. H. Arjmandi[1]. [1]Nutritional Sciences, Oklahoma State University, Stillwater, OK, USA, [2]Food & Agricultural Products Research & Technology Center, Oklahoma State University, Stillwater, OK, USA, [3]Laboratory Animal Resources, Oklahoma State University, Stillwater, OK, USA.

Among the dietary approaches for improving skeletal health, dried plum has been found to both prevent and reverse bone loss in female rat models. The effectiveness of dried plum in preventing bone loss in males, however, has not been examined. Therefore, the present study was undertaken to investigate the osteoprotective effects of dried plum in a male model of osteoporosis. Sixty, 6-month old male Sprague Dawley rats were either sham-operated (Sham=1 group) or orchidectomized (ORX=4 groups) and randomly assigned to dietary treatments: standard semi-purified diet (Control) with either LD=5%, MD=15%, or HD=25% (w/w) dried plum for 90 days. All diets were isocaloric, isonitrogenous, and had similar calcium and phosphorus content. Both the MD and HD dried plum completely prevented the ORX-induced decrease in whole body, femur, and 4th lumbar vertebra bone mineral density (BMD). Biomechanical testing of the femur mid-diaphysis indicated that ultimate load values for the MD and HD groups were also similar to that of the Sham group. Analyses of the distal femur metaphysis revealed that compared to the ORX-Control group, trabecular bone volume (BV/TV) was increased by the HD, while trabecular number (TbN) and separation (TbSp) were improved by all doses of dried plum. We conclude that that dried plum can prevent osteopenia in male rats of gonadal hormone deficiency, similar to that observed in females. Further studies are planned to investigate the bone-sparing mechanisms of dried plum and its bioactive components, e.g. polyphenols.

Disclosures: ***B.J. Smith****, None.*

M448

Low Adherence with External Hip Protectors Due to Both Hip Protector Itself and Garment. T. Koike, H. Toyoda*, R. Sugama*, M. Tada*, Y. Orito*, K. Takaoka. Orthopaedic Surgery, Osaka City University Medical School, Osaka, Japan.

External hip protectors appear effective for preventing hip fracture in nursing home residents with osteoporosis. However, compliance with use of hip protectors has been poor. The following factors may negatively influence compliance: cerebral disorders; adverse effects such as skin irritation; hip protector experienced as too hot in summer, uncomfortable in bed or necessitating assistance with toilet functions. We have therefore designed a new hip protector using softer porous materials, which is “open” so as to not interfere with toilet functions. To assess the benefits of this newly designed garment, a cluster randomized intervention-control design was used to examine the acceptability of hip protectors worn by residents at high-risk of falls (n=140) in nursing homes for 6 months. No previous studies have used sham hip protectors. Participants were divided into four groups: conventional garment with hip protector (Safehip, n=27); conventional garment without protector (n=27); open garment with protector (n=44); and open garment without protector (n=42). The four groups were alike in age (mean 81.3 y), body weight (45,7 Kg), body height (145.7 cm), and activities of daily living. Only one hip fracture occurred in the group of open garment without protector and no fracture in other groups. Compliance with hip protectors was very low for both garment types (Table). We accepted the use of hip protectors only during the daytime, and defined it as full adherence. Although compliance was slightly higher for conventional garments than for open garments, low compliance was largely attributable to the use of a hip protector in itself. Furthermore, we were surprised at low adherence with use of garments without protector. To achieve adequate adherence with use of external hip protector, we should reform not only the protectors but also hip protector underwear.

Month	0	3	6
Open garment w/ protector	44 (100%)	7 (15.9%)	5 (11.4%)
Open garment w/o protector	42 (100%)	24 (57.1%)	14 (33.3%)
Conventional garment w/ protector	27 (100%)	5 (18.5%)	6 (22.2%)
Conventional garment w/o protector	27 (100%)	15 (55.6%)	15 (55.6%)

Disclosures: ***T. Koike****, None.*

M449

Factors Related to Spinal Mobility in Patients with Postmenopausal Osteoporosis. N. Miyakoshi, M. Hongo, S. Maekawa, Y. Ishikawa*, E. Itoi*. Orthopedic Surgery, Akita University School of Medicine, Akita, Japan.

We have shown that the quality of life (QOL) in patients with spinal osteoporosis is impaired by the spinal mobility. However, factors related to the spinal mobility in these patients are still unclear. We evaluated the possible factors affecting spinal mobility in patients with postmenopausal osteoporosis. A total of 128 postmenopausal women with osteoporosis aged over 50 years (mean, 70 years) were included in this study. The thoracic and lumbar kyphosis angles and range of motion (ROM) of the total spine (thoracic and lumbar spine) were measured in the upright position and at maximum flexion/extension with a computer-assisted device (SpinalMouse®) for determination of shape and mobility of the spinal column. The paravertebral muscle (PVM) thicknesses of thoracic and lumbar spine in upright position were measured using ultrasound. The number of vertebral fractures was evaluated with lateral radiographs of the spine. Isometric back extensor strength was evaluated with a dynamometer in 91 patients. Age (r=-0.412), lumbar kyphosis angle (r=-0.284), back extensor strength (r=0.369), PVM thickness at lumbar spine (r=0.227), and the number of vertebral fractures (r=-0.260) showed significant correlations with total spinal ROM ($p<0.05$). However, no significant correlations were observed between the total spinal ROM and PVM thickness at thoracic spine (r=-0.069) or thoracic kyphosis angle (r=-0.138). Multiple regression analysis revealed that the back extensor strength was the most significant contributor to the total spinal ROM. We conclude that the back extensor strength is an important factor to maintain spinal mobility in patients with postmenopausal osteoporosis. The present study suggests a possible effect of back extensor exercise on maintaining the QOL in patients with postmenopausal osteoporosis.

Disclosures: ***N. Miyakoshi****, None.*

M450

Bone Density, Bone Biomarker and Serum IGF-1 Responses to 80 Weeks of Resistance Training in Older Adults. D. Bemben, M. Bemben*, I. Palmer*, J. Baker*. Health and Exercise Science, University of Oklahoma, Norman, OK, USA.

The purpose of this study was to examine the effects of 80 weeks of resistance training on bone metabolism and serum IGF-1 levels in older men (n=15) and women (n=25), 57-70 years of age. The training programs involved 3 sets of 12 isotonic resistance exercises performed either 2 or 3 days per week, at low (40%1RM) or high (80% 1RM) intensities. Muscular strength was assessed at 5 week intervals to determine progression. Dual Energy X-Ray Absorptiometry (GE Lunar DPX-IQ, version 4.7b) was used to measure BMD at the lumbar spine, proximal femur and total body sites at baseline, 40 and 80 weeks of training. Serum levels of bone-specific alkaline phosphatase (BAP, Metra Biosystems) and cross-linked N-telopeptide of Type I collagen (NTx, Ostex International) were measured at the same time points using ELISA kits. IGF-1 and IGF Binding Protein 3 (BP3) levels were measured by RIA kits (Diagnostic Systems Laboratory). Significant increases in BMD ($p<.05$) from baseline to 80 weeks of training were observed for the spine, trochanter, and total hip sites. Total body BMD showed a transitory increase ($p<.05$) from baseline to 40 weeks of training. There were significant ($p<.05$) trial x training group effects for the trochanter and total body BMD sites. There were gender differences in the bone biomarker responses to training as BAP significantly increased ($p<.05$) approximately 20% from baseline to 40 weeks in men and NTx significantly decreased ($p<.05$) 18% in women from baseline to 80 weeks. There were significant ($p<.05$) trial, gender, trial x gender, and trial x training group effects for serum IGF-1. Men had significant increases ($p<.05$) in IGF-1 from baseline to 40 weeks and the high intensity training groups showed the same pattern of response. BP3 significantly decreased ($p<.05$) from baseline to 80 weeks of training in both men and women. In conclusion, resistance training significantly improved BMD in men and women with the high intensity programs exerting greater effects at the trochanter and total body sites. The bone biomarker responses suggest the mechanisms for increasing BMD may differ between men and women. The decrease in the BP3 indicates that there may be greater bioavailability in circulating IGF-1 by the end of the 80 weeks of resistance training.

Disclosures: ***D. Bemben****, None.*

M451

Treadmill Exercise on the International Space Station: The Effects of External Loading. K. O. Genc*[1], C. C. Maender*[2], A. J. Rice*[1], R. S. Ochia*[3], J. G. Snedeker*[4], P. R. Cavanagh[1]. [1]The Cleveland Clinic Foundation, Cleveland, OH, USA, [2]NASA-Johnson Space Center, Houston, TX, USA, [3]Rush Presbyterian-St. Luke's Medical Center, Chicago, IL, USA, [4]ETH, Zurich, Switzerland.

Providing Earth-like gravity replacement loads (GRL) during exercise on long duration space missions may be critical to the maintenance of bone mass. Two devices are currently used on the International Space Station (ISS) to provide a restoring force to return the astronaut to the treadmill surface during treadmill exercise: a subject load device (SLD) and various bungee cord (BC) configurations. In this experiment, the loads on the feet during treadmill exercise on the ISS were measured while all combinations of GRLs were used. The results were compared to similar exercise protocols on Earth. In-shoe forces were monitored using modified Pedar insoles (Novel Gmbh, Munich, Germany) placed inside the shoes of a single astronaut, who gave his informed consent to participate in the IRB-approved experiment. Data were recorded at 128 Hz on a wearable computer and downlinked via satellite. Thirty seconds of exercise data during 10 different loading conditions on orbit were collected and low-pass filtered using a 50 Hz cutoff frequency. All on-orbit loading profiles showed a marked decrease in peak ground reaction force when compared to 1g loading. The mean push off force (MPF) was significantly larger in 1g compared to 0g (Fig. 1). Daily load stimulus (DLS), a mathematical model used to relate changes in bone mineral density to daily loading histories, was also calculated from the force data for each loading condition using an exponent, m, of 5. During treadmill running the ratio of DLS for a 30 second period of activity in 0g to that in 1g varied from 0.50 to 0.78 over the range of loading configurations. Thus, treadmill exercise in space provided a maximum of only approximately 75% of the stimulus to bone experienced during typical exercise on Earth.

Figure 1: The mean push off force (MPF) from 30 seconds of walking and running at varying loading configurations on earth (1g) and on-orbit (0g). The dashed lines are used to illustrate the difference in MPF in 1g compared to 0g. All Running MPFs are significantly different from one another ($p < 0.05$) and all walking MPFs are significantly different from one another except for SLD 170 and 1Bungee ($p<0.05$).

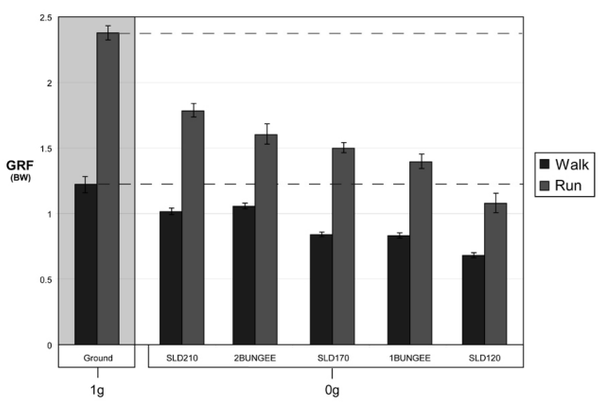

Disclosures: ***K.O. Genc****, None.*

M452

Stimulation of Cortical Bone Formation Using Extremely Low-Level, High-Frequency Mechanical Signals. S. Judex[1], L. Karim*[1], R. Garman[1], L. Donahue[2], C. Rubin[3]. [1]Biomedical Engineering, State University of New York at Stony Brook, Stony Brook, NY, USA, [2]The Jackson Laboratory, Bar Harbor, ME, USA, [3]Center for Biotechnology, State University of New York at Stony Brook, Stony Brook, NY, USA.

The osteogenic potential of mechanical signals indicates that a biomechanical modality, if it can be applied safely, would constitute a unique, non-pharmacologic intervention for osteoporosis. While preliminary work demonstrates that trabecular bone can be augmented by low-level, high frequency loads, the response in cortical bone remains unclear. Eighteen adult (4m), female, BALB/cByJ mice were randomly assigned to one of two groups: Loaded (10min/d of 45Hz @ 0.3g, induced non-invasively using a vibrating platform) and Long-Term Control. Bone labels were administered on days 10 & 20, and histomorphometric parameters measured at the diaphyseal midshaft of the tibia. Following a 21d experimental period, mineralizing (periosteal) surface (MS/BS) in loaded animals was 25% greater than controls (p=0.19), with a 33% increase at the endosteal surface (p=0.17). Loading increased mineral apposition rate (MAR) by 46% (p=0.03) and bone formation rates (BFR/BS) by 93% (p=0.06).

	Endocortical MS/BS (%)	Periosteal MS/BS (%)	Periosteal MAR (μm/d)	Periosteal BFR/BS (μm/y)
Control (Mean ± sd)	36.0 ± 16.4	37.7 ± 17.5	0.41 ± 0.10	61.2 ± 38.3
Load (Mean ± sd)	48.0 ± 18.0	47.1 ± 24.2	0.60 ± 0.19	118.0 ± 91.5
% Difference	33%	25%	46%	93%
p-value	0.17	0.19	0.03	0.06

These data indicate that extremely low-level mechanical signals, inducing cortical strains well below ten microstrain, can effectively augment cortical bone formation. When considered together with the ability of such signals to stimulate trabecular bone, it suggests that an amalgam of high-frequency signals may help regulate both cortical and trabecular bone physiology. As these strain levels are two orders of magnitude below those generated by functional activity, they may represent a safe and efficacious means of augmenting bone quantity and quality in the clinic. This work supported by NSBRI.

M453

Long-Term Changes in Body Composition Predicts Bone Change in Postmenopausal Women. J. Choi*, E. C. Cussler*, S. B. Going, L. L. Metcalfe*, H. G. Flint-Wagner*, T. G. Lohman. Department of Physiology, University of Arizona, Tucson, AZ, USA.

The aim of this study was to examine changes in bone mineral density (BMD) in relation to 4-yr changes in weight and body composition in exercising postmenopausal women at four bone sites: femoral trochanter and neck, lumbar spine, and total body. Both lean tissue mass and percent body fat were assessed. One hundred sixty-six postmenopausal women, 45-66 yr old, who completed annual 4-yr dual-energy x-ray absorptiometry (DXA) and anthropometric measurements were included in the analyses of this study. At baseline, subjects were blocked into hormone replacement therapy (HRT) or no-HRT groups and randomized into exercise or no-exercise groups. Exercise training involved 3 days per week completing two sets of 6 to 8 repetitions in resistance exercises at 70-80% of one repetition maximum. During the four years of data collection, 32.9% in no-HRT crossed over to take HRT and 72.7% in no-exercise crossed over to participate in exercise. Therefore, the variables used in 4-yr analyses were years on HRT during the four years of the study and mean exercise attendance. Using multivariate linear regression, change in body weight was a significant predictor of change in BMD at all four bone sites; it was the strongest predictor of BMD at the femoral trochanter and neck bone sites. Mean exercise attendance was also a significant predictor of BMD, stronger at the lumbar and femoral trochanter bone sites. Multivariate regression models including changes in lean tissue mass and percent body fat showed both were significant predictors of BMD. Femoral trochanter BMD was associated most strongly with change in lean tissue mass ($p < 0.01$). Subgroup analyses included covariance analysis (ANCOVA) among tertiles of change in lean tissue mass. Changes in BMD among the tertiles were only significant at the femoral trochanter bone site, where the reduced BMD seen in the lowest tertile was significantly different from gains in BMD within the middle and highest tertiles ($p < 0.01$). We conclude that there is a positive relationship between long-term change in body weight and change in BMD. Long-term change in lean tissue mass, change in percent body fat, and mean exercise attendance are all significant predictors of BMD in postmenopausal women. Lean tissue mass changes had the greatest effect at the femoral trochanter bone site.

Disclosures: ***J. Choi****, None.*

M454

Change in Walking Endurance Among Women with Prevalent Vertebral Fractures: Associations with Concurrent Change in Impairment, Functional Status, and Disability. K. M. Shipp[1], C. F. Pieper*[2], D. T. Gold[3], K. W. Lyles[4]. [1]Community and Family Medicine, Duke University, Durham, NC, USA, [2]Biostatistics and Bioinfomatics, Duke University, Durham, NC, USA, [3]Psychiatry and Behavioral Sciences, Duke University, Durham, NC, USA, [4]Medicine, Duke University, Durham, NC, USA.

Osteoporotic vertebral fractures are associated with functional limitations and disability. We tracked changes in functional performance (walking endurance as measured by six minute walk [SMW] distance) over six months in 142 older women (age 80.9 ± 5.6 years) with prevalent vertebral fractures (number=2.4 ± 1.8) who were subjects in an exercise/coping skills clinical trial. Although the exercise intervention did not target endurance walking, and, therefore, did not significantly improve SMW distance, we conducted exploratory analyses to determine whether a change in SMW over six months was related concurrently to change in other parameters along the disability model.

Using Spearman's correlation coefficients, change in SMW was correlated significantly ($p < 0.05$) to change in 7 parameters, including impairment: trunk rotation range of motion 0.24, psychiatric symptoms -0.20, confidence in mobility 0.29; functional performance: gait velocity 0.59; functional status: Functional Status Index (FSI) -0.22, MOS-36 physical function subscale 0.25; and disability: MOS-36 physical role subscale 0.25. Linear regression analyses, controlling for age and number of vertebral fractures, estimated that 33% of the variance in change in SMW distance was explained by change in the impairments and gait velocity. In turn, change in SMW distance accounted for 9% (FSI) and 7% (MOS-36 physical function subscale) of the variance for change in functional status and 4% of the variance for change in role disability (MOS-36 physical role subscale).

Walking endurance, the construct measured by the SMW, has been shown to improve with targeted exercise in older adults with chronic medical problems. The results presented here support the premise that an exercise regime that targets and improves walking endurance could lead to better functional status and less disability in older women with prevalent vertebral fractures.

Disclosures: ***K.M. Shipp****, None.*

M455

Weight Lifted in Strength Training Predicts Four-Year Bone Changes in Postmenopausal Women. E. C. Cussler*, S. B. Going, H. G. Flint-Wagner*, R. B. Blew*, J. Choi*, T. G. Lohman. Physiology, University of Arizona, Tucson, AZ, USA.

The aim of this study was to examine the relationship between weight lifted over four years of progressive strength training and change in bone mineral density (BMD) in a group of calcium-replete, postmenopausal women.

As part of a large clinical trial, 89 calcium-supplemented postmenopausal women (55.4±4.5 years), randomized to a progressive strength training program, were followed for four years. Fifty-four percent of the women were using hormone replacement therapy. Three times weekly, subjects were asked to complete two sets of six to eight repetitions in eight core exercises at 70-80% of one repetition maximum. Women recorded weights and repetitions of all exercises throughout the four years. Total and regional BMD was measured at baseline and thereafter annually using dual-energy x-ray absorptiometry (DXA). Hormone replacement therapy (HRT) use was calculated as continuous years on HRT through the fourth year.

Women using HRT (48) and not using HRT (41) had similar baseline age, body mass index, percent fat, and lean soft tissue(LST). HRT users had fewer years past menopause and had higher initial lumbar spine BMD ($p<.01$ and $p<.05$, respectively) than non-users. Exercise compliance averaged 75.2±18.3%, 54.3±33.9%, 38.9±33.8%, and 33.2±32.8% for sequential years. The mean weight lifted in the dumbbell or military press (MP), used as a surrogate for exercise compliance, was 26,223.8±17,734.1kg over four years. In multiple linear regression, increases in lumbar spine(LS), total body(TB), and ulna(U) BMD were positively and significantly related to weight lifted in the military press after adjusting for age, baseline BMD and weight, HRT use, and weight and LST change. LS BMD increased 0.016g/cm^2 (1.6%) ($p<.01$), TB, 0.006g/cm^2 (0.6%) ($p<.01$), and U, 0.003g/cm^2 (1.5%) ($p<.05$) for every standard deviation of weight lifted in the MP. While hips sites (femur neck, trochanter, and wards) and ultradistal radius models did not reach significance, gains at all these sites were found with higher levels of weight lifted. Only TB BMD change was independently associated with HRT use ($p<.01$). No interaction was found between HRT use and weight lifted.

Evidence of an independent, linear relationship between regional and total BMD change and weight lifted in the military press during a four-year strength training program supports the positive, long-term usefulness of this type of exercise for the prevention of osteoporosis in postmenopausal women.

Disclosures: ***T.G. Lohman****, None.*

M456

Adapting a Vibration-Based Countermeasure for Bone Loss for use in Microgravity Conditions. X. Lei*, Y. Qin, W. Lin, S. Judex, C. T. Rubin. Biomedical Engineering, SUNY Stony Brook, Stony Brook, NY, USA.

Osteoporosis, the progressive loss of bone density and strength, is both common and severe in astronauts subjected to long-term space flight; yet effective countermeasures have proven elusive. Recent work has shown that brief exposure to 30Hz, 0.3g whole-body vibration can effectively inhibit disuse osteopenia, and thus potentially applicable in microgravity conditions. The device consists of a base plate which uses an electromagnetic actuator to drive the top platen, which remains coupled via connecting springs. Due to the absence of gravity, an elastic restraint secures the subject to the vibration platform, and thus transmits the loads from the shoulders through to the weight bearing skeleton. To avoid disrupting other experiments, the base plate cannot be fixed to the space station, and thus it must be determined if the mechanical signal, in the free floating system, will reach regions of interest (i.e., hip), a challenge which was not anticipated in a previous ground-base model of transmissibility [Fritton et al. 1997]. The objective of this study is to determinate the appropriate parameters needed to produce sufficient but not excessive vibrations to the hip. A simple mass-spring-dashpot model with 3 degrees of freedom was first applied to study the system responses to harmonic excitations. The mass of the base plate and the stiffness of the support spring were considered as major design parameters. Noting that the rigid-body mode is not of concern, the two natural frequencies of the system were analytically obtained. The preliminary results reveal that the higher natural frequency of the system can be dramatically altered by adjusting the above two design parameters, while the lower natural frequency is relatively unaffected.

In a first-order approximation, a 50% body weight restraint and an 8kg device weight, an 18N, 30Hz load applied to an 80kg astronaut in microgravity will deliver 4.4N to the femoral neck. Displacement of the plate would be less than 1mm. Mechanical responses can be modulated by optimizing the base plate and connection springs as shown in the figure. The results using the vibration models found to match ground-base experimental data reasonably. The model predictions provide a better understanding of human body responses to vibration treatment in the weightless environment and a guideline for an optimal design of the vibration apparatus as well. This work was supported by NASA.

Disclosures: ***X. Lei****, None.*

M457

Post Study Follow up in a Group of Women Completing Osteoporosis Treatment Drug Trials. K. M. Hill*, E. A. Mossman, M. R. McClung. Oregon Osteoporosis Center, Portland, OR, USA.

Little is known regarding follow-up care of participants completing osteoporosis treatment research trials. The purpose of this study was to determine if participants completing such trials at our center saw a health care provider at study end and if osteoporosis medications were prescribed.

Local institutional review board approval was obtained. Questionnaires were sent to all women completing osteoporosis treatment trials at the Oregon Osteoporosis Center between April 2002 and January 2004. One reminder telephone call was made to non-responders. Quantitative descriptive statistics were used to analyze the questionnaire responses.

49% of questionnaires were returned (91/187). 39% (16/41) of initial non-responders returned the questionnaire after a reminder call. 58% of respondents (53/91) saw their health care provider at study end and 74% (39/53) of those were given a prescription for osteoporosis medication. Of those given a prescription, 90% (35/39) filled the prescription, and 80% (28/35) were still taking the medication at the time of this study. The majority of respondents were prescribed a bisphosphonate when a prescription was written. Of those not seeing a provider at study end, 24% (7/29) indicated inability to afford medication, 17% (5/29) indicated they didn't think they needed the medication, 3% (1/29) listed no provider, 3% (1/29) listed concerns regarding side effects, and 41% (12/29) listed a variety of other reason with no trend identified in these responses.

Following participation in an osteoporosis drug treatment trial, just over half of questionnaire respondents had a follow up visit with their health care provider. Of those, the majority received an osteoporosis medication prescription, filled the prescription and continued taking the medication up to 2 years post study. Our results indicate the need to determine ways to better promote post study follow up care.

Disclosures: ***K.M. Hill****, None.*

M458

Analysis of First Events vs. Multiple Outcomes. A. L. Oberg*, E. J. Atkinson*, S. J. Achenbach*, L. J. Melton. Mayo Clinic, Rochester, MN, USA.

There is controversy in the clinical trial literature about the appropriateness of considering multiple outcomes. While a single endpoint (e.g., death or recurrence) may be reasonable in cancer trials, it makes less sense for studies of osteoporosis treatments where patients are at risk of multiple fractures of diverse types. The traditional time-to-first event Cox models have been extended by Anderson & Gill to permit evaluation of time-to-multiple events (A-G). We undertook to determine what is gained or lost in the assessment of fracture risk when using all fractures experienced by each patient rather than just the first one. We analyzed the risk of additional fractures at multiple sites among 225 postmenopausal women from an age-stratified sample of Rochester, MN residents gathered in 1980 with median follow-up of 16.2 years. Altogether, 110 subjects subsequently had at least one moderate trauma fracture and 245 moderate trauma fractures were observed in total. We used Cox and A-G analyses to examine age, baseline femoral neck BMD, and dietary protein as predictors of subsequent fracture. The information gain was assessed by examining the ratio of standard errors (SE) of the parameter estimates from the two models. If each subsequent fracture provides completely new information (is independent), first and subsequent fractures would contribute equal amounts of information. However, the assumption of complete independence is generally not met. In this sample, 135 additional fractures were actually worth 31, 73, and 14 first fractures, respectively, for age, BMD and dietary protein. The table indicates the detectable hazard ratio (HR) in a study with risk factor prevalence of 50%. With proportions of first and subsequent fractures approximately equal, as is true in this study, and subsequent fractures worth 45% of a first fracture, the detectable HR with 90% power is improved by 9%-14%. The largest gain is realized for the smaller sample sizes.

Expected # 1st fractures (fxs)	Expected # subsequent fxs	%Worth, subsequent fxs	Detectable HR 80%/90% power
50	50	0%*	2.21/2.51
		15%	2.10/2.36
		30%	2.01/2.24
		45%	1.94/2.15
100	100	0%*	1.76/1.92
		15%	1.69/1.84
		30%	1.64/1.77
		45%	1.60/1.72
200	200	0%*	1.49/1.59
		15%	1.45/1.54
		30%	1.42/1.50
		45%	1.39/1.47

* Results for Cox analyses.

Although it remains to be determined whether the worth of additional subsequent fractures is consistent across differing study populations and/or variable types, including multiple fractures per subject allows use of all information from a patient and permits sample size or follow-up time to be decreased at substantial cost savings.

Disclosures: ***A.L. Oberg****, None.*

M459

Outcome of Balloon Kyphoplasty with PMMA and Calcium Phosphate Cement in Patients with Painful Vertebral Fractures due to Primary Osteoporosis: A Comparative Prospective Controlled Trial. C. Kasperk[1], I. Grafe*[1], K. DaFonseca*[2], U. Liegibel*[1], U. Sommer*[1], U. Hilscher*[1], G. Noeldge*[3], M. Libicher*[3], P. Nawroth*[1], P. Meeder*[2]. [1]Endocrinology and Metabolism, University of Heidelberg, Heidelberg, Germany, [2]Trauma Surgery, University of Heidelberg, Heidelberg, Germany, [3]Radiology, University of Heidelberg, Heidelberg, Germany.

Medical treatment of primary osteoporosis does not entirely solve the clinically severe complications of osteoporosis: pain and impaired mobility due to vertebral fractures. This study analyses changes in radiomorphology, pain, mobility, number of new vertebral fractures and health care utilization one year after augmentation of vertebral fractures by balloon kyphoplasty.

60 patients with primary osteoporosis and more than 12 months old painful vertebral fractures were included in this cohort study selected by an interdisciplinary team of osteologists/endocrinologists, trauma surgeons and radiologists. 40 patients were treated with balloon kyphoplasty (20 received PMMA and 20 calcium phosphate cement) while 20 served as controls. The groups were analyzed prior to treatment and 3 and 6 months later. All patients received standard medical treatment (1g calcium, 1000 IE vitamin D3, standard dose of an oral aminobisphosphonate, pain medication, physical therapy).

Balloon kyphoplasty increased midline vertebral height of the treated vertebral bodies by 12.1 % while in the control group vertebral height decreased by 8.2 % (p=0.001). Augmentation and internal stabilization by balloon kyphoplasty resulted in a 70 % (p=0.007) reduction of back pain, while mobility increased by 24 % (p=0.031). There is no significant change in control patients with regards to pain and mobility during the 6 months follow up. The number of back-pain-related doctor visits within the 6 months follow up period decreased significantly after kyphoplasty compared to controls: 3.3 visits/patient in the balloon kyphoplasty group and 8.6 visits/patient in the control group. There is no significant difference with regards to the clinical outcome between the patients treated with PMMA or calcium phosphate cement.

Balloon kyphoplasty improves quality of life for elderly patients with primary osteoporosis suffering from chronic pain caused by vertebral fractures. Therefore, balloon kyphoplasty appears to be a promising addition to evidence-based medical osteoporosis treatment in selected patients with chronic pain due to old vertebral fractures.

Disclosures: ***C. Kasperk****, None.*

M460

The Effect of anti-TNFa Therapy on Spinal Bone Mineral Density in Patients with Crohn's Disease. A. D. Rhim*[1], G. R. Lichtenstein*[1], A. M. Weinberg*[1], C. Su*[1], M. Pazianas[2]. [1]Gastroenterology, Medicine, Univ of Pennsylvania, Philadelphia, PA, USA, [2]Medicine, Univ of Pennsylvania, Philadelphia, PA, USA.

Pro-inflammatory cytokines might be, at least partially, responsible for the development of osteopenia or osteoporosis in Crohn's Disease. We investigated whether anti-TNF therapy for Crohn's Disease could have any positive skeletal impact. Hence, we studied the effects of Infliximab, a monoclonal antibody against TNFa without or with bisphosphonates, on spinal bone mineral density (BMD). The effect of corticosteroids was also analyzed. A retrospective cohort analysis was performed on 61 patients with Crohn's and low BMD. Twenty three (23) patients were on Infliximab and 36 patients were on bisphosphonates. Mean duration between DXA scans was 2.2 $\pm$ 0.99 years. After controlling for corticosteroid use, patients with concurrent Infliximab and bisphosphonate treatment exhibited a greater increase in BMD compared to those on bisphosphonates alone (+6.7%/y vs +4.46%/y, $p<0.05$); corticosteroids inhibited this effect ($p<0.05$). However, Infliximab alone had no effects on BMD. Patients receiving bisphosphonates showed a significant increase in lumbar spine BMD compared to those not on bisphosphonates (+3.97% change in T-score/y vs -3.68%/y, $p<0.001$). Concurrent corticosteroid use significantly inhibited this effect. Concurrent Infliximab use may confer an additional benefit to that already documented for bisphosphonate use alone; bisphosphonates are beneficial in the treatment of low BMD in patients with Crohn's disease, though corticosteroids may partially inhibit this effect.

Disclosures: ***M. Pazianas****, None.*

M461

A Practical Stepwise Flow Sheet for Pharmacologic Treatment of Low Energy Fractures in a Department of Orthopaedic Surgery. H. Christoffersen[1], S. N. Holmegaard*[2]. [1]Orthopaedic, Thisted Hospital, Thisted, Denmark, [2]Department of medicine, Thisted Hospital, Thisted, Denmark.

Patients with low energy fractures (LEF) are at high risk for new fractures, but orthopaedic surgeons primarily focus attention on operative procedure and ignore preventive measures of established value.

Adequate prevention is especially important in the elderly patient with LEF of the hip, in whom a new fracture carriers a considerable risk of fatal consequences. However, only 5-25% of patients with LEF are evaluated and treated for osteoporosis. This state can probably only be improved by standardized and automatically initiated procedures for evaluation and pharmacologic treatment of LEF where the patients primarily are treated. We have therefore developed a stepwise strategy for clinical evaluation and appropriate pharmacologic treatment of patients with LEF.

For patients admitted to the orthopaedic department due to LEF of the hip, screening tests for secondary osteoporosis are done immediately after admission and all patients are started on treatment with 1200 mg calcium and 20 mcg vitamin D daily.

Patients with positive screening tests are referred for evaluation by an endocrinologist. The remaining majority is evaluated for propensity to fall, estimated life expectancy and for males palpation of the testes.

When fall is the dominant problem, possible contributory factors in the home and effects of drug treatment, e.g. glucocorticoids, sedatives and antihypertensive drugs, are evaluated.

All patients are discharged with calcium and vitamin D (1200mg/20 mcg), and if estimated life expectancy is > 2 years therapy with biphosphonate (Alendronate 70 mg once weekly) started before discharge.

Patients with LEF seen in the OPD are also treated with calcium and vitamin D, given information about the possible relation between LEF and osteoporosis and encouraged to contact their general practitioner for screening tests and measurement of BMD.

This simple program can increase awareness amongst orthopaedic surgeons, general practitioners and patients about prevention of new osteoporotic fractures in a high risk population.

Disclosures: ***H. Christoffersen****, None.*

M462

Drug Compliance in Glasgow: A Year Following Hip Fracture. A. P. Gallagher*, S. J. Gallacher, C. A. McQuillian*, M. Harkness*. Medical Unit Southern General Hospital, Glasgow, United Kingdom.

As the population ages, orthopedic surgeons worldwide are seeing an increasing number of hip fractures. Our Fracture Liaison Service was introduced in November 2000 to put in place a system which would identify and treat, automatically, all hip fractures following admission to the orthopedic unit.

More than 1200 fractured neck of femur patients have been identified to date.

An osteoporosis treatment algorithm was integrated into the hip fracture pathway.

To audit compliance with the medications prescribed, and to assess the incidence of side effects experienced, a postal survey was undertaken in 112 patients (aged over 70 and with AMT>7) who had been commenced upon osteoporosis therapy a year earlier.

65 questionnaires were returned complete: 20% male and 80% female.

1.5% were recommended calcium/vitamin D alone however 15.4% were commenced upon this.

27.5% were recommended bisphosphonate alone however only 21.5% received this.

71% were recommended bisphosphonate and calcium/vitamin D although it was only prescribed in 56.9%.

Thankfully 95% of patients were given some form of osteoporosis medication.

90% stated medication was being taken as directed (10% leaving this question blank).

7.8% of patients experienced side effects (bisphosphonates being the main source), 4.7% stopped the medication whilst the other 3.1% stopped and restarted.

This simple study emphasizes the very high continuance rates in all osteoporosis drug therapies following hip fracture.

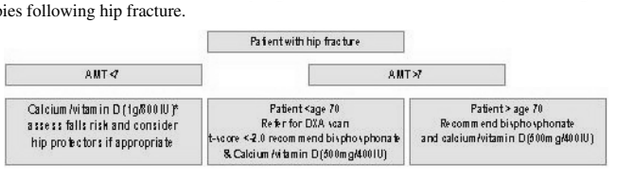

recommended medication / which medication are you taking (crosstabulation)

		which medication are you taking				
		ca/vit D	bisph	bisph+ca/vitD	none given	Total
recommended medication	calcium/vitamin D	1	0	0	0	1
		1.5%	0%	0%	0%	1.5%
	bisphosphonate	3	14	1	0	18
		4.5%	21.5%	1.5%	.0%	27.5%
	bisphosphonate and calcium/vitamin D	6	0	37	3	46
		9.4%	0%	56.9%	4.6%	71.0%
Total		10	14	38	3	65
		15.4%	21.5%	58.4%	4.6%	100.0%

Disclosures: ***A.P. Gallagher****, None.*

M463

Barriers to Effective Management of Osteoporosis in Minimal and Moderate Trauma Fractures: A Prospective Study. D. Bliuc*, C. R. Ong, J. A. Eisman, J. R. Center. Bone and Mineral, Garvan Institute of Medical Reasearch, St Vincent's Hospital, University of NSW, Sydney, Australia.

Osteoporosis is suboptimally investigated and treated even in high-risk people with a history of prior fracture. In addition, there is some evidence that individuals with moderate trauma fracture have a lower bone density and are at higher risk of subsequent fracture. The aim of this study was to define the factors influencing the management of individuals at risk of osteoporosis and the risk profile of individuals with minimal and moderate trauma fractures. Consecutive fracture patients (n=218) treated in the outpatient fracture clinic of a teaching hospital in Sydney over an 18 month period (February 2002-July 2003) were interviewed. Risk factors for osteoporosis, type and circumstance of fracture, prior investigation and treatment for osteoporosis were collected and participants were contacted by telephone 3 months after enrolment to ascertain follow up.

Risk factors for osteoporosis including family history, low dietary calcium intake, glucocorticoid use and conditions associated with bone loss occurred with similar frequency in the minimal and moderate trauma groups and between the sexes. Overall, half of the participants (50% of women and 48% of men) had had a prior fracture independent of whether their current fracture was due to minimal or moderate trauma. Even among those with a prior fracture, only 37% had a bone density scan, and 14% were on specific osteoporosis

treatment. There was only a minimal (5%) increase in the rates of investigation and treatment after 3 months. The proportion of people investigated and treated was lower in the moderate trauma group and particularly in males. In multivariate analysis, independent predictors for being investigated for osteoporosis were age over 50, presence of prior fracture and female gender. The only independent factors influencing treatment were age over 50 and having been investigated.
This study has confirmed the low rates of investigation and treatment of low trauma fractures even in the group who already have suffered a prior fracture. Osteoporosis is even more poorly managed in males and in those under the age of 50. People with moderate trauma fractures have the same risk factors for fracture as those with minimal trauma fractures including a similarly high proportion of prior fractures. These findings support the concept that people with moderate trauma fractures are at higher subsequent fracture risk, yet are neither investigated nor treated. This study highlights the need for further exploration of barriers to appropriate osteoporosis management.

Disclosures: ***D. Bliuc****, None.*

M464

Osteoporosis Identification and Treatment After Fragility Fracture in an Inner City Orthopaedic Unit. E. R. Bogoch[1], V. I. M. Elliot-Gibson*[2], D. E. Beaton*[2], S. A. Jamal[3], R. G. Josse[3], T. M. Murray[3]. [1]Department of Surgery, St. Michael's Hospital, University of Toronto, Toronto, ON, Canada, [2]Mobility Program Clinical Research Unit, St. Michael's Hospital, University of Toronto, Toronto, ON, Canada, [3]Department of Medicine, St. Michael's Hospital, University of Toronto, Toronto, ON, Canada.

The orthopaedic unit at St Michael's Hospital, a university hospital in Toronto, Ontario, has a program to identify, educate, refer, treat, and evaluate fragility fracture patients for osteoporosis (OP). An OP Exemplary Care Program was designed to address system and individual barriers to identification and treatment of OP. System modifications included coordination between the orthopaedic, endocrinology and nuclear medicine units to provide a continuum of care for fragility fracture patients with suspected OP. Individual barriers were addressed through ongoing education of physicians, staff and patients to increase knowledge and awareness of OP. A coordinator is responsible for daily program operations. Criteria for inclusion into this program were: male ≥ 50; female ≥ 40; fracture resulting from low trauma; fracture sites: distal radius, proximal humerus, proximal femur, vertebrae. Increased awareness of OP among surgeons led to the additional inclusion of patients with suspected OP but were either below age criteria, sustained a high trauma fracture, and/or had an atypical fracture site. Data presented is from the period December 1, 2002 to November 30, 2003 (n = 430).

	Inpatients n = 154		**Outpatients n = 276**	
	Female n = 123	Male n = 31	Female n = 210	Male n = 66
Mean age	80.36	72.55	67.70	65.47
Fracture Site: Hip	95	29	48	13
Wrist	2	0	96	26
Shoulder	11	0	42	19
Vertebra/Other#	15	2	24	8
Previous Dx/Rx of OP	43	6	88	9
Referral or Rx initiated#	72 of 80	18 of 25	103 of 122	51 of 57
No referral or rx intiated*	8 of 80	7 of 25	19 of 122	6 of 57

*# Minimum Rx initiated was vitamin D and calcium. *No referral/rx due to refusal, contraindications, death, normal BMD.*

Over 90% of fracture patients received appropriate OP attention demonstrating a positive change in clinical behaviour by physicians and staff and unprecedented success in OP care. Anticipated outcomes are an increase in preventive health behaviours in fracture patients and a decreased rate of subsequent fractures and related health care costs. Six-month follow-up will be completed for all patients to assess compliance with referral and medications which may demonstrate those groups most amenable to treatment. An orthopaedic leader, motivated staff, an assigned OP coordinator and stable resources are required to maintain an intensive clinical program.

Disclosures: ***V.I.M. Elliot-Gibson****, None.*

M465

Temporal Trends in Prevention of Glucocorticoid-Induced Osteoporosis. K. G. Saag*[1], S. H. Gehlbach*[2], J. R. Curtis*[1], K. Worley*[3], T. E. Youket*[3], J. L. Lange*[3]. [1]University of Alabama at Birmingham, Birmingham, AL, USA, [2]University of Massachusetts at Amherst, Amherst, MA, USA, [3]Procter & Gamble Pharmaceuticals, Mason, OH, USA.

The 1996 American College of Rheumatology (ACR) recommendations for prevention and treatment of glucocorticoid-induced osteoporosis (GIOP) suggest bone mass measurement (BMM) and anti-resorptive medications for at risk patients. We investigated changes in the proportion of chronic glucocorticoid (GC) users who received these tests or medications from 1996 - 2001. The data source was a random sample from a medical and pharmaceutical claims database (Protocare), representing a health plan with 7 million covered lives in 20 states. The study population (denominator) included patients initiating chronic oral GCs (average > 7.5 mg/day prednisone equivalent for > 6 months) in a biennial period. Numerators were patients receiving BMM within 12 months before and after initiating GC therapy and those who received a non-estrogen anti-resorptive pharmaceutical (bisphosphonate, calcitonin, raloxifene) within 12 months after initiating GC therapy. 3,125 adults initiated chronic GC therapy over 1996-2001 and were: 62% women; 18 - 49 years old: 30%, 50-64: 23%, 65+: 47%. The proportion of women ages 50+ who received BMM increased from 10% in 1996-7 to 19% in 2000-2001. Anti-resorptive pharmaceutical use similarly increased from 7% to 23%. In contrast, among all men and women ages 18 - 49, the proportions receiving BMM and/or anti-resorptives were less than 6% for all biennial periods. Besides demographics, factors that increased the likelihood of receiving BMM were prior fracture in the 12 months before GC therapy (OR 2.5, 95% CI 1.0 - 2.5) and treating physician specialty (OR 1.8 specialist vs. generalist; 1.0 - 3.4). Factors associated with increased likelihood of receiving anti-resorptive medications included prior fracture (OR 6.0; 3.3 - 10.9), physician specialty (OR 2.2 specialist vs. generalist; 1.3 - 3.8), and cumulative dose of GC (OR 1.7 for highest tertile of use compared to lowest; 1.0-1.9). In contrast to the 1996 ACR recommendations for prevention and treatment of GIOP, the proportion of patients initiating chronic GC therapy between 1996 and 2001 who received BMM or non-estrogen anti-resorptive pharmaceutical was low. However, trends seem to be improving somewhat over time, especially among post-menopausal women.

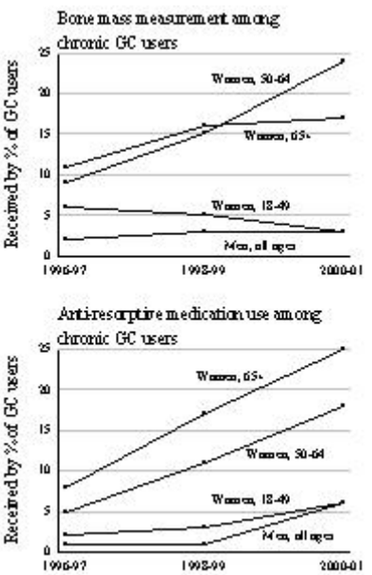

Disclosures: ***K.G. Saag****, None.*

M466

Beta-blocker Use, Bone Mineral Density and Fracture Risk in Older Women: Results from the EPIDOS Prospective Study. R. Levasseur[1], P. Dargent-Molina*[2], J. P. Sabatier*[3], C. Marcelli*[1], G. Bréart*[2]. [1]Rheumatology CHU, Caen, France, [2]INSERM U149, Villejuif, France, [3]Nuclear Medicine CHU, Caen, France.

Recent experimental studies in mice suggest that beta-blocker use may be associated with a reduced risk of osteoporosis (Takeda et al. Cell 111:305, 2002). To verify this hypothesis, we assessed the association between non cardio selective beta-blocker use and both bone mineral density (BMD, g/cm²) and fracture risk in a large cohort of elderly French women who participated to the EPIDOS (Epidemiologie de l'Osteoporose) study. BMD was measured by DXA (Lunar DPX-Plus) at the hip (femoral neck, ward triangle, trochanter) and total body. Out of the 7598 women (mean age 80.5 ± 3.8 years) included in the cohort, 283 (3.7%) were taking a beta-blocker at baseline. The average duration of use was 13.9 (± 10.1) years.The drugs most frequently used were sotalol (n=97) and propranolol (n=93). All beta-blocker users were taking the drug 5 to 7 days a week. Women who were taking a beta-blocker were slightly younger than non users (79.8 vs 80.6 years; p=0.0002). Women were asked how they would judge their health compared to other women of their age. Compared to non-users, beta-blocker users declared more often that they were as healthy as other women of their age (69.9 vs 60.9%), and less often that they were either in worse health (26.1 vs 32.5%) or in better health (4.0 vs 6.6%) than other women of their age (p=0.009). There were no significant difference in mean weight between beta-blocker users and non users (60.7 vs 59.8 kg, p=0.18). After adjustment for age and subjective health status, there was no significant difference in hip or total body BMD between beta-blocker users and non users. During an average of 3.6 (± 1.2) years of follow-up, 1311 women suffered at least one non-vertebral osteoporotic fracture. After adjustment for age and health status, there was no significant association between beta-blocker use and risk of fracture (hazard ratio = 1.2; 95% CI: 0.9 - 1.5). We conclude that beta-blocker use is not associated with a reduced risk of osteoporosis in older women. Thus, there is a controversy about the beta-blocker effect on bone between animal studies and human studies and between human studies that show the same results than our study (Reid et al. JBMR 18(Suppl2):SU327 2003) and other that show a positive effect on BMD and fracture risk (Pasco et al. JBMR 19:19 2004).

Disclosures: ***R. Levasseur****, None.*

M467

AC-100, a Fragment of MEPE, Promotes Fracture Healing in a Femoral Closed Fracture Model in Rats. M. Lazarov*[1], M. Shih*[2], A. Negron*[2], R. Blacher*[1], Y. Kumagai[1], D. M. Rosen[1]. [1]Acologix, Inc, Emeryville, CA, USA, [2]Skeletech, Bothell, WA, USA.

MEPE, a protein originally cloned from tumors associated with hypophosphatemic osteomalacia, increases renal phosphate excretion and is expressed in normal human bone cells. **AC-100 (Dentonin)**, a central 23-amino acid fragment of MEPE, conserved among species, contains motifs that are important in regulating cellular activities in the bone microenvironment including an integrin-binding, a glycosaminoglycan-binding, and a calcium binding motif and has demonstrated potent anabolic activity on osteoblast precursor cells *in vitro*. Here we report that AC-100 exhibits bone anabolic activity *in viv*o as well as *in vitro* and promotes fracture healing in a femoral closed fracture model in rats.

Methods: Sprague Dawley female rats, approximately 3 months old, were randomly assigned to different treatment groups (n=12 per group) by body weight at the commencement of the study. All rats received a unilateral closed fracture femoral defect created in the right femur. Radiographs were taken to confirm the fracture. Following the fracture, all animals received daily local subcutaneous injections (approximately 0.3 mL) of saline (vehicle control) or the treatment compound at or near the fracture site. The positive control group received subcutaneous injections of PTH. After euthanasia using carbon dioxide asphyxiation, the right and left femurs were excised and tested by a mechanical device for strength in 3-point bending. In addition, histopathological assessments were performed on the toluidine blue stained sections of the femoral defect region without knowledge of treatment group.

Results: By comparison of the biomechanical properties, AC-100, 5 mg/mL showed significantly higher ($p < 0.05$) normalized (value from the test side divided by value from the intact side) absorbable strain energy (improved material properties) from the 3-point bending test, as compared to the vehicle control group. By histopathology evaluation on the amount of callus and its mineralization (calcein labeling), the AC-100 5 mg/mL group was significantly greater ($p < 0.05$) than the vehicle control group, and not significantly different from the PTH-treated group (positive control).

Conclusion: These data suggest that AC-100 does promote fracture healing in this experimental model and may have potential as an anabolic drug to increase bone mass.

Disclosures: ***M. Lazarov****, Acologix, Inc 3.*

M468A

Treatment Initiation after Osteoporosis Screening Varies by Skeletal Site of Diagnosis and Disease Severity. R. M. Brennan, J. Wactawski-Wende, K. M. Hovey*. Social and Preventive Medicine, University at Buffalo, Buffalo, NY, USA.

The objective of this study was to assess variations in treatment initiation among postmenopausal women determined to have osteoporosis. Dual-energy x-ray absorptiometry (DXA) screening was conducted as part of a larger study of osteoporosis and periodontal disease. Copies of DXA results were provided along with a summary cover sheet reporting T-scores for the lateral spine, antero-posterior spine, femoral neck, and total forearm. Subjects were followed after one year to assess treatment initiation. The study was approved by the Health Sciences Institutional Review Board at the University at Buffalo. Subjects included in this analysis (n = 230) had no previous knowledge of their bone density, were newly determined at screening to have osteoporosis (T-score <= -2.5), reported discussing DXA results with a health care provider, and were not missing data on study variables. Overall, 129 (56.1%) women initiated new treatment for osteoporosis. Ninety-four (55.6%) women with osteoporosis at the lateral spine, 51 (62.2%) women with osteoporosis at the antero-posterior spine, 40 (71.4%) women with osteoporosis at the femoral neck, and 55 (61.1%) women with osteoporosis at the total forearm initiated new treatment. Many women had osteoporosis at more than one skeletal site, with 68 (67.3%) initiating new treatment. In univariate logistic regression analyses, osteoporosis at the femoral neck (OR = 2.39; 95% CI: 1.25, 4.58), more than one skeletal site with osteoporosis (OR = 2.30; 95% CI: 1.34, 3.94), and T-score of -3.0 or less (OR = 2.57; 95% CI: 1.50, 4.40) compared with greater than -3.0 were significant predictors of treatment initiation. Other skeletal sites of diagnosis and other risk factors for fracture (age, hormone therapy use, previous fracture, family history of fracture, and body mass index) were not significant univariate predictors of treatment initiation. After stratifying by osteoporosis at the femoral neck, multivariate modeling showed that severity of disease (T-score of -3.0 or less) only predicted treatment initiation for those without osteoporosis at the femoral neck (OR = 2.13; 95% CI: 1.13, 4.03), and number of sites with osteoporosis was not statistically significant for either group. Treatment after osteoporosis screening was more likely for postmenopausal women determined to have osteoporosis at the femoral neck compared to other skeletal sites. Among women who did have osteoporosis at other skeletal sites, those with more severe disease were more likely to be treated.

Disclosures: ***R.M. Brennan****, None.*

M468B

Diagnosis and Treatment of Osteoporosis in Vertebral Fracture Patients Who Have Undergone Vertebroplasty or Kyphoplasty: The Importance of Clinical Pathways. A. Fang*[1], A. Abdelmalek*[2], M. Weisman*[3], S. L. Silverman[4]. [1]Cedars-Sinai, Los Angeles, CA, USA, [2]Kaiser Permanente West Los Angeles, Los Angeles, CA, USA, [3]Cedars-Sinai, Beverly hills, CA, USA, [4]Cedars-Sinai/UCLA/OMC, Los Angeles, CA, USA.

Osteoporosis is often underdiagnosed and undertreated in hospitalized patients with hip fracture. We studied the diagnosis and treatment of osteoporosis in hospitalized patients with acute vertebral compression fracture who underwent vertebroplasty (VP) or kyphoplasty (KP) in two different institutions in Los Angeles: a closed model HMO (Kaiser West Los Angeles) and a community academic hospital (Cedars-Sinai Medical Center or CSMC).

We performed a retrospective chart review of patients admitted with a primary diagnosis of vertebral fracture to CSMC in May and June 2003 and to the HMO from January 2002 to April 2003. Cases were identified by diagnostic codes for osteoporosis, fracture and vertebral body augmentation (VBA).We excluded vertebral fracture associated with significant trauma, malignancy or bone disease. Patients hospitalized for reasons unrelated to vertebral fractures were also excluded from this study.

At CSMC we identified twenty patients . Of these twenty patients all underwent a VBA procedure: ten patients had KP and ten patients had VP. Only 1/20 of the patients had a DXA during hospital stay. At hospital admission, 6/20 patients were on an osteoporosis treatment medication other than calcium. At discharge 9/20 of the patients were on osteoporosis medication.

At the HMO we identified 32 patients: 20 female ,12 male with vertebral fracture who received VP. The HMO has a mandatory clinical pathway requiring a physical medicine consultation prior to surgical authorization.30/32 patients were on an osteoporosis medication other than calcium prior to discharge. 8/32 had a DXA during hospitalization.

In summary, our data show marked differences in OP diagnosis and treatment between an HMO and a community academic hospital for patients with surgically treated osteoporotic vertebral fracture. We conclude that patients with vertebral fracture who are surgically treated may not have a DXA or treatment during hospitalization. Our data suggests that clinical pathways may be helpful in increasing diagnosis and treatment of osteoporosis in surgically treated patients with vertebral compression fracture.

Disclosures: ***A. Fang****, None.*

M469

A Single-Dose Pharmacokinetic Study of Lasofoxifene in Japanese and Caucasian Postmenopausal Women. M. Gardner*[1], Y. Nishizawa*[2], G. Wei*[1], L. Dogolo*[1], A. Calcagni*[1]. [1]Pfizer Inc, Groton, CT, USA, [2]Pfizer Inc, Tokyo, Japan.

Lasofoxifene, a next generation selective estrogen receptor modulator (SERM), is in late stage development for the treatment of osteoporosis. Lasofoxifene is extensively metabolized via both oxidative and conjugative pathways in the liver. Since ethnic differences in drug metabolism between Asian and Western populations have been reported for other drugs, the pharmacokinetics (PK) of lasofoxifene in postmenopausal women of Japanese (J) heritage were compared to those of Caucasians (C).

This was a double-blind, placebo controlled, parallel group, single oral dose study. Twelve J subjects living in the West and 12 age-matched (within 5 years) C subjects were studied at the projected therapeutic dose of 0.25 mg. Six of the J subjects were first-generation (FG) and six were second-generation (SG). At the 0.1 mg and 0.5 mg dose levels, 6 J and 6 age-matched C subjects were studied. The J subjects at these doses were a mixture of FG and SG. Lasofoxifene was administered after an overnight fast. Serial plasma samples for determination of lasofoxifene PK were obtained up to 480 hours postdose. ANOVA was used to calculate 90% confidence intervals (CI) for the ratios of least-squares mean Cmax and AUC(0-∞) values (based on log transformation). PK comparisons were made between first generation and second generation Japanese subjects at the 0.25 dose and between Japanese (FG & SG) and Caucasians at all doses.

All subjects completed the study and the treatments were well tolerated. Lasofoxifene PK in FG subjects were similar to those of SG subjects at the 0.25 mg dose. The SG/FG treatment ratio (90% CI) of log-transformed Cmax and AUC(0-∞) was 96% (83% to 111%) and 94% (73% to 122%), respectively. Lasofoxifene was absorbed and eliminated slowly in both groups with the mean Tmax and t½ values of approximately 11 and 150 hours, respectively. Overall the PK of lasofoxifene was similar for J and C subjects. The J/C treatment ratio of log-transformed Cmax and AUC(0-∞) at the 0.25 mg dose was 105% (93% to 118%) and 100% (85% to 119%), respectively. Exposure to lasofoxifene increased predictably with dose in both populations over the range of 0.1 to 0.5 mg. Differences in body weight between J and C subjects did not affect exposure to lasofoxifene.

Lasofoxifene PK in Japanese and Caucasian postmenopausal women are similar, with predictable increases in exposure following single doses ranging from 0.1 to 0.5 mg.

Disclosures: ***M. Gardner****, Pfizer Inc. 3.*

M470

Effect of Toremifene on Orchiectomy-Induced Osteopenia in the Male Rat. S. Raghow*[1], J. Okolicany*[2], V. Shen[3], K. Veverka*[2], M. Steiner*[2]. [1]GTx, Inc., Memphis, TN, USA, [2]GTx, Inc, Memphis, TN, USA, [3]SkeleTech, Inc., Bothell, WA, USA.

Osteopenia, osteoporosis and bone fractures are common complications of androgen deprivation therapy (ADT) in men with prostate cancer. Selective estrogen receptor modulators (SERMs) are known to reduce bone loss in females and may prevent osteoporosis and fractures in males as well. We tested the efficacy of a SERM, toremifene (Tor), to prevent bone loss in the orchiectomized (Orx) male rat. In a 12-wk study, fifty skeletally mature male rats were either sham-operated or orchiectomized (Orx) and divided into 5 groups (n=10) as follows: Sham + vehicle, Orx + vehicle, Orx+Tor (5mg/kg/d), Orx+Tor (10 mg/kg/d) and Orx+Estradiol (E, 0.2mg/kg/ml control). Treatment was initiated at castration via s.c. pump. Calcein fluorochrome was administered by injection at 12 and 2 days before necropsy for static and dynamic histomorphometric analysis. Serum bone biomarkers osteocalcin (OC) and C-terminal telopeptides (CTX) were measured at 0, 1.5, 4, 6 and 12 wks by ELISA. Prostate was weighed at necropsy. Lumbar vertebrae (LV4 and LV5) were excised at the end of the treatment period. LV5 was subjected to DXA scan for bone mineral density and LV4 was fixed in buffered formalin for histology and histomorphometry. Prostate weight of the Orx rats was 22% of the sham controls. Orx increased OC levels significantly and both E and Tor reversed this effect. Serum CTX levels showed no mean-

inful difference between groups. Orx induced reductions in bone mineral density of L5 and trabecular bone volume (TBV) in L4 of male rats due to significantly elevated bone turnover as evidenced by increase in BFR and osteoclast surface and number. Tor prevented the Orx-induced loss in BMD and preserved TBV at the lumbar vertebral body. The mechanism of action of Tor appears to be anti-resorptive in nature as Tor reduced BFR and osteoclast parameters significantly ($p < 0.05$) below the sham-operated animals. The use of estradiol similarly exerted an anti-resorptive effect on Orx rats and the protection of bone mass in the lumbar vertebrae was quite evident. Tor had no effect on prostate weight in the Orx rat. In conclusion, both estrogen and toremifene were able to combat androgen deficiency-induced bone loss in male rats and their protective effects on bone microarchitecture appeared to be due to suppression of bone turnover. Our studies suggest the possibility that toremifene may prevent vertebral bone loss, protect bone quality and prevent vertebral fractures in prostate cancer patients treated by androgen-deprivation therapy.

Disclosures: ***S. Raghow****, GTx, Inc. 1, 3.*

M471

Raloxifene Modulates IL-6 and TNF-alpha Synthesis in vivo: Results from a Clinical Pilot Study. S. Migliaccio. Fisiopatologia Medica, University La Sapienza, Rome, Italy.

Walter Gianni1, Andrea Ricci2, Paola Gazzaniga3, Marina Brama2, Maria Pietropaolo4, Sergio Votano5, Francesco Patanè3, Anna Maria Aglianò3, Stefania Falcone6, Giovanni Spera6, Vincenzo Marigliano4, Sergio Ammendola2, Donato Agnusdei7, Roberto Scandurra2 and Silvia Migliaccio6 Unità Geriatria Oncologica, INRCA, Rome; Departments of 2Biochemical Sciences, 3Experimental Medicine, 4Geriatrics, 6Medical Physiopathology, University of "La Sapienza", Rome; 5Hospital San Carlo-IDI Sanità, Rome; 7University of Siena & Eli Lilly & Company, Italy.

Raloxifene (RAL), a selective estrogen receptor modulator, is indicated for prevention and treatment of postmenopausal osteoporosis. RAL, by decreasing bone turnover, prevents bone loss and microarchitecture damage, significantly reducing the incidence of osteoporotic fractures. Our previous in vitro data demonstrated that RAL modulates osteoclast activity by, at least in part, an Interleukin-6 (IL-6) and Tumor Necrosis Factor-alpha (TNF-alpha)-dependent mechanism. In this study we evaluated the effects of RAL treatment (60 mg/day) on these two cytokines circulating levels in 14 postmenopausal women with osteoporosis. Lumbar bone density (DEXA), IL-6 and TNF-alpha blood levels were measured before and, after 6, and 24 months of therapy. In this small group of postmenopausal women RAL, 60 mg/day for 24 months, induced a significant increase in lumbar bone mineral density as compared to baseline before therapy (Tscore -2.8 ± 0.1 baseline vs Tscore -2.57±0.1 after 6 months and Tscore -2.0±0.1 after 24 months), as previously demonstrated in larger cohort of postmenopausal women. IL-6 and TNF-alpha expression, elevated before tratment, significantly decreased (50% and 30%, respectively) after 6 months. This effect was sustained up to the end of the treatment period (75% and 35% respectively). Thus, our data show that RAL treatment can significantly modulate circulating levels of cytokines involved in osteoclastogenesis and bone resorption, suggesting that the modulation of soluble factors could play a pivotal role in the mechanisms of the osteoprotective effect of RAL.

Disclosures: ***S. Migliaccio****, None.*

M472

Significant Bone Loss Following Cessation of Estrogen Replacement Therapy in Postmenopausal Women. S. B. Broy, L. G. Jankowski*. Center for Arthritis and Osteoporosis, Illinois Bone and Joint Institute, Park Ridge, IL, USA.

Since publication of the Women's Health Initiative (WHI), many women have discontinued estrogen replacement therapy (ERT). Review of 2 large national databases estimated a 66% national decline in Prempro prescriptions 1 year following the July 2002 publication of WHI[1]. The NORA study suggests that women who have recently discontinued estrogen have an increased risk for hip fracture compared to women who have never taken estrogen[2].

The purpose of this study was to evaluate the effect of estrogen cessation on bone mineral density (BMD). Bone densitometry (Hologic 4500A) records from 1/1/2000 - 5/1/2004, in a large rheumatology/orthopedic practice and osteoporosis center, were reviewed. Postmenopausal women who had been on ERT for at least 2 years and then discontinued ERT for 6 months to 5 years were included and divided into Group I: patients on no osteoporosis medication, Group II: patients who continued ongoing (>1 year) osteoporosis medication and Group III: patients who began a new osteoporosis medication when ERT was discontinued. Patients in renal failure or on >5mg prednisone were excluded. Change in BMD was considered significant if it exceeded the least significant change in the spine, total hip or femoral neck.

Group I: 52 patients, age 49-83 (mean 64), no osteoporosis medication.

44/52 patients (84.6%) lost bone, 4 gained and 4 had stable BMD.

Bone loss ranged from 2.6-14.9% in the spine (SP), 2.4-12.4% in the total hip (TH) and 3.0-13.3% in the femoral neck (FN). Mean change was -2.9% ±4.5 SP, -3.3% ±3.3 TH and -3.4% ± 4.5 FN. Bone loss was seen whether patients had stopped ERT for 6-12 months (11 of 12), 1-2 years (17 of 22) or 2-5 years (15 of 18).

Group II: 7 patients, age 61-86 (mean 74), continued osteoporosis medication, alendronate (4), risedronate (3).

6/7 patients lost bone (up to 8.7% SP, 10.6% TH, 10.4% FN), 1 had stable BMD.

Group III: 16 patients, age 40-79 (mean 65) who started raloxifene (5), alendronate (7) or risedronate (4).

6/16 patients lost bone (up to 10.7% SP, 7.6% TH, 9% FN), 7 gained, 3 had stable BMD.

This study documents that significant bone loss is common when ERT is discontinued. Without other therapy, most patients (84.6%) lost a statistically significant amount of bone in at least one area whether ERT was discontinued 6 months, or up to 5 years previously. Even patients on medication for osteoporosis can loose bone: 6/7 (85.7%) who continued ongoing therapy for osteoporosis and 6/16 (37.5%) who began a new osteoporosis medication lost bone. Women who discontinue estrogen at any age should be carefully monitored following cessation of ERT.

[1] Hersh et al JAMA 2004; 294:47-53

[2] Yates et al Obstet Gynecol 2004; 103:440-6

Disclosures: ***S.B. Broy****, Merck & Co, Inc. 2, 5, 8; Procter & Gamble 2, 5, 8; Novartis 2, 5, 8; Eli Lilly and Company 2, 5, 8.*

M473

Patients Profile on Hormonal Replacement Therapy and Raloxifene to Treat Post Menopausal Osteoporosis: Are There Any Clinical Differences? The Switch from Hormonal Replacement Therapy to Evista Study; The SHE Study. J. Oliveira*[1], M. Kayath[1], M. Escander*[2], P. Beltrame*[3], R. Bertazzo*[4], W. Weissheimer*[5], P. Basso*[1], O. L. Bracco*[1]. [1]Medical Division, Eli Lilly Brazil, São Paulo, Brazil, [2]No disclosure, Campo Grande, Brazil, [3]No disclosure, Santa Maria, Brazil, [4]No disclosure, São José do Rio Preto, Brazil, [5]No disclosure, Chapecó, Brazil.

The Women's Health Initiative (WHI) Study publication has raised concern about the indication and length of estrogen replacement therapy. Raloxifene is an option to prevent and treat osteoporosis in women with postmenopausal osteoporosis. The Switch from Hormonal Replacement Therapy to Evista (SHE) Study was an observational study designed to evaluate tolerability and treatment satisfaction associated with raloxifene treatment after hormone replacement therapy in postmenopausal women in a naturalistic setting in Brazil. Twenty-nine gynecologists participated in the study. The study involved two groups of patients, both previously on HRT: one group maintained HRT to prevent or treat osteoporosis (Group 1, n=70), while the second group switched to raloxifene from HRT (Group 2, n=164) after a 4-8 week washout period, each according to the gynecologist's recommendation. Twice as many patients were included in the raloxifene group according to the protocol. We present data regarding the clinical features of both groups. Student t-test or Mann-Whitney was used for statistical analyses, and results are expressed as mean ± standard deviation.Statistical significance was set at $p \leq 0.05$. Results: Patients advised to maintain HRT were significantly younger than patients who switched to raloxifene; the chronological age was 58.3 ± 5.1 vs 62.7 ± 6.3, respectively, $p<0.001$. Time since menopause was shorter in group 1 than group 2 (9.2 ± 5.7 years vs 12.7 ± 6.9 years, respectively, $p=0.001$). Mineral bone density measurement was the most common clinical reason to switch from HRT to raloxifene (95.7% of patients). Only 1.2% of the patients who stopped HRT presented vasomotor symptoms during the "wash-out" period. There was no difference between the 2 groups regarding presence of vasomotor symptoms. In conclusion, Brazilian physicians prescribe raloxifene to treat postmenopausal osteoporosis for older women with a longer time since menopause, in comparison to women in whom they continue HRT. Physicians reported raloxifene's bone efficacy as the most common reason to switch from HRT. The transition from HRT to raloxifene did not result in significant vasomotor symptoms. Raloxifene, due to its bone efficacy, is an important option to prevent or treat postmenopausal osteoporosis after HRT in a naturalistic setting in Brazil.

Disclosures: ***J. Oliveira****, Eli Lilly Brasil 3.*

M474

Vitamin K2 and Raloxifene Combine to Improve the Femoral Neck Strength of Ovariectomized Rats. J. Iwamoto*[1], J. Yeh[2], A. Schmidt*[3], E. Rowley*[3], T. Takeda*[1], M. Sato[3]. [1]Orthopaedic Surgery, Keio University School of Medicine, Tokyo, Japan, [2]Dept. Medicine, Winthrop University Hospital, New York, NY, USA, [3]Bone and Inflammation, Lilly Research Labs, Indianapolis, IN, USA.

We evaluated the skeletal effects of two therapies available in Japan, vitamin K2, raloxifene, as well as the vitamin K2 plus raloxifene combination, in a rat model of post-menopausal osteoporosis. Six-month-old rats were ovariectomized, except for sham-ovariectomy controls (Sham), and dosed orally with vehicle, 30 mg/kg vitamin K2 (K), 1 mg/kg raloxifene (Ral), or the combination of K+Ral for 6 weeks following surgery.K had no effect on serum estrogen, low-density lipoprotein cholesterol (LDL-C), or urinary deoxypyridinoline (DPD) levels, but slightly increased osteocalcin (OC) compared to Ovx. Ral lowered total cholesterol, LDL-C, OC, and urinary DPD levels to below Ovx levels, while having no effect on estrogen levels. Ral, but not K, prevented ovariectomy-induced loss of bone in the distal femoral metaphysis and proximal tibial metaphysis, as did the K+Ral combination. Ral, but not K, partially prevented loss of vertebral vBMD, while K+Ral had vBMD greater than Ovx. K increased bone formation rate (BFR/BS) to above Ovx, while Ral and K+Ral reduced BFR/BS to Sham levels. K had no effect on eroded surface (ES/BS) compared to Ovx, while Ral and K+Ral reduced ES/BS to Sham levels. Groups were not different in the vBMD of femoral midshaft; however K was observed to increase periosteal mineralizing surface (MS/BS) of the tibial shaft to above Ovx, while Ral reduced periosteal MS/BS toward Sham levels. Femoral neck strength was not different between groups, except K+Ral was reproducibly stronger than Ovx or Sham. Ral, but not K, partially prevented loss of lumbar vertebra strength; but K+Ral was not different from Sham or Ovx. Therefore, K and Ral had complementary effects on bone formation and resorption activities, respectively, resulting in a reproducible, additive improvement of femoral neck strength. These rat data suggest interesting therapeutic possibilities that may require clinical verification.

Disclosures: ***J. Iwamoto****, None.*

M475

Preliminary Infra-Red Analysis of Biopsies from the MORE Study. D. Faibish*[1], S. M. Ott[2], A. L. Boskey[1]. [1]Mineralized Tissues Laboratory, Hospital for Special Surgery, New York, NY, USA, [2]Medicine, Division of Metabolism, University of Washington, Seattle, WA, USA.

The selective estrogen receptor modulator raloxifene reduced the risk of vertebral fracture in postmenopausal women with osteoporosis in a large clinical trial (Multiple Outcomes of Raloxifene Evaluation - MORE) conducted in 7705 post-menopausal women [Ettinger et al., JAMA 282:637, 1999]. Quantitative microradiographic analyses of bone biopsies from this trial showed an increase in mineral content with treatment. It was hypothesized that the changes in the bone mineral content reflect changes in the "quality" of bone in patients treated with raloxifene.

Randomly selected iliac crest biopsies from 3 groups of patients (n=5 per group) enrolled in the MORE study were analyzed; 2 experiment groups, treated with 60 or 120mg of raloxifene, and a placebo group. All were given calcium and vitamin D. Biopsies, obtained at baseline and two years after treatment were embedded in polymethyl methacrylate (PMMA) and cut in two µm-thick sections (Microm) and scanned using a FTIRI spectrometer (Spotlight, Perkin Elmer). For each biopsy, spectra from six 200 X 200 µm regions were collected, 3 in the cortical bone and 3 in the trabecular at a spectral resolution of $8cm^{-1}$. The spectra were linearly baselined and the contribution of the embedding media spectrally subtracted (Isys, Spectral Dimensions). Spectroscopic parameters examined were previously established as sensitive to bone quality: mineral to matrix peak area ratio (ash weight), 1660/1690 cm^{-1} peak intensity ratio (collagen maturity), 1030/1020 cm^{-1} peak intensity ratio (mineral crystallinity). The change in pixel population means for each of the parameters was compared with one-way ANOVA**.**

All three groups showed increases in the mineral-to-matrix ratio in trabecular and cortical bone, but no significant changes were found in the examined parameters. Collagen maturity and crystallinity did not vary significantly from baseline in any of the groups.

In conclusion, two-year treatment did not show a marked improvement in the bone quality as determined by infra-red analyses in the group analyzed. Both longer term studies and a larger sample size might be needed to detect any effect of raloxifene on bone quality.

Disclosures: ***D. Faibish****, None.*

M476

Influences of Intermittent Administration of Human Parathyroid Hormone on Bone Marrow Cells after Cancellous Bone Osteotomy in Ovariectomized Rats. K. Nozaka, N. Miyakoshi, Y. Kasukawa, S. Maekawa*, E. Itoi. Orthopedic Surgery, Akita University School of Medicine, Akita, Japan.

Osteosynthetic surgeries for patients with osteoporosis frequently results in delayed or non union. It is well known that intermittent administration of human parathyroid hormone (hPTH) acts on osteoblasts and their precursor cells and exerts anabolic effects on bone in osteopenic animals and humans. We therefore hypothesized that intermittent hPTH administration would facilitate osteosyntesis in patients with osteoporosis. To test this hypothesis, proximal tibial osteotomy was created in mature osteopenic rats induced by ovariectomy (OVX) and effects of intermittent administration of hPTH on bone marrow at the surgery site were evaluated. After OVX or sham-operation, hPTH(1-34) 100µg/kg or its vehicle solution was administered subcutaneously once a week for four weeks. The animals were killed one week after the last injection, and their tibiae were harvested. Conventional bone histomorphometry and the measurements of adipocyte number and size were performed using the decalcified hematoxylin and eosin stained sections. Furthermore, using the immunohistochemical technique, the percentages of proliferating cell nuclear antigen (PCNA) positive cells in bone marrow cells were evaluated. OVX-vehicle group showed high turnover osteopenia compared to sham-vehicle group. PTH increased bone volume per tissue volume (BV/TV) compared to vehicle treatment both in sham-operated and OVX rats by increasing bone formation. The quantity of adipocyte and the number of adipocyte per marrow volume (AV/MV and N.A/MV) were significantly increased in OVX-vehicle group and decreased in OVX-PTH group compared to those in sham-vehicle group. The percentages of PCNA positive cells were increased in sham-PTH and OVX-PTH groups compared to those in corresponding vehicle treated groups. These results support the view that intermittent administration of hPTH could exert the anabolic effects on bone by differentiating marrow stromal cells to osteoblasts more than adipocytes. The increased PCNA positive cells in bone marrow at the osteotomy site revealed that the PTH might have a potential role of affecting cell kinetics at osteotomy site.

Disclosures: ***K. Nozaka****, None.*

M477

Once-weekly Sustained-Duration PTH (PTH-Fc) Exerts Potent Anabolic Effects on Bone by Activating ß-arrestin2. S. L. Ferrari[1], D. Manen*[1], P. J. Kostenuik[2], M. L. Bouxsein[3], R. Rizzoli[1], D. Pierroz[1]. [1]Division of Bone Diseases, Geneva University Hospital, Geneva, Switzerland, [2]Amgen Inc., Thousand Oaks, CA, USA, [3]Orthopedic Biomechanics Laboratory, Beth Israel Deaconess Med Center, Harvard Med School, Boston, MA, USA.

Twice-weekly injections of a fusion molecule of PTH(1-34) with human IgG-Fc fragment (PTH-Fc), which confers sustained duration to PTH, increases bone mass in rodents (1). However, the mechanisms of action of PTH-Fc remain to be elucidated. PTH activity is normally regulated by ß-arrestin2 (ß-arr2), a cytoplasmic protein interacting with the PTH/PTHrP receptor (PTH1Rc). Thus, we hypothesized that PTH-Fc anabolic activity could depend on ß-arr2 activation. We characterized ß-arr2-GFP and PTH1Rc-GFP trafficking in HEK293 cells, as well as cAMP signaling in response to PTH-Fc. Moreover, we compared bone mineral density (BMD, by pDXA) and skeletal micro-architecture (by µCT) in ovariectomized (OVX) wild-type (WT) and ß-arr2 KO adult female mice (n=4-11/group) treated with PTH-Fc once weekly (150 nmol/kg/wk, equivalent to PTH(1-34) 80 mg/kg/wk), daily PTH(1-34) (80 mg/kg/d) or vehicle (VEH) s.c for 4 wks.

PTH-Fc recruited ß-arr2-GFP from the cytoplasm to the membrane and internalized PTH1Rc-GFP within minutes, a pattern indistinguishable from cells exposed to PTH(1-34). Maximal acute cAMP response to equimolar concentrations of PTH-Fc and PTH(1-34) was similar, but residual cAMP accumulation 2 hrs after exposure to agonist was significantly higher (2x) with PTH-Fc compared to PTH(1-34). Yet, rechallenge with either agonist induced a maximal cAMP response, indicating that PTH-Fc did not cause major desensitization. In OVX WT mice, vertebral trabecular bone volume fraction (Tb.BV/TV) and trabeculae thickness (Tb.Th) were significantly higher with PTH-Fc compared to both VEH and PTH(1-34) (all $p<0.0001$). Moreover, PTH-Fc was slightly superior to PTH in increasing cortical thickness (C.Th.) ($p=0.048$, and $p<0.0001$ vs VEH). In OVX ß-arr2 KO mice, PTH-Fc was also marginally better than PTH in increasing C.Th. ($p=0.08$, and $p<0.0001$ vs VEH) and vertebral Tb.Th ($p=0.017$, and $p<0.0001$ vs VEH). In contrast, PTH-Fc failed to significantly increase Tb.BV/TV (NS vs either PTH or VEH) and it decreased Tb. number compared to PTH ($p=0.05$). Altogether, total body BMD gain with either PTH or PTH-Fc was greater in WT than ß-arr2 KO mice, and significantly better with PTH-Fc in WT ($p=0.04$ vs PTH), but not in ß-arr2 KO mice.

These data indicate that PTH-Fc activity is normally regulated by ß-arr2, which allows for the potent anabolic effects of PTH-Fc on cancellous bone despite its prolonged circulating half-life.

(1) P Kostenuik et al., J Bone Miner Res 2003, 18 (suppl 2), S385

Disclosures: ***S.L. Ferrari****, Amgen Inc., Thousand Oaks, CA 2.*

M478

DANCE: Direct Analysis of Non-vertebral Fracture in the Community Experience Study Overview. P. D. Miller[1], S. L. Silverman[2], D. T. Gold*[3], P. Chen*[4], K. A. Taylor[4], R. B. Wagman[4]. [1]Colorado Center for Bone Research, University of Colorado Health Sciences Center, Lakewood, CO, USA, [2]OMC Clinical Research Center and the Department of Medicine, University of California Los Angeles, Los Angeles, CA, USA, [3]Duke Aging Center, Duke University Medical Center, Durham, NC, USA, [4]Lilly Research Laboratories, Indianapolis, IN, USA.

The Fracture Prevention Trial established that Forteo® [rhPTH (1-34); generic name, teriparatide] treatment substantially reduced the risk of vertebral and non-vertebral fractures after a median 19 months of therapy (Neer et al., 2001). Overall, vertebral fracture risk was reduced by 65%. Non-vertebral fragility fracture risk, measured at over six sites (including wrist, rib, and hip), was reduced by 53%. The experience in randomized placebo-controlled clinical trials may differ from that in community practice. The DANCE study is a prospective observational study designed to evaluate the long-term effectiveness, safety, and tolerability of FORTEO in a larger, more diverse patient population than studied in clinical trials. The primary objective is to evaluate the occurrence of non-vertebral fragility fractures in subjects treated with FORTEO for up to 24 months. Secondary objectives include determination of clinical vertebral fractures, serious adverse events, new or worsening pain and back pain, adherence to therapy, bone mineral density changes, and criteria used to initiate FORTEO therapy. Subjects will be followed through a course of FORTEO therapy for up to 24 months and for an additional 24 months after cessation of treatment (Figure). Therefore, subjects may participate in this study for up to 48 months. All aspects of patient care, including diagnostic and therapeutic interventions, will be chosen and conducted at the discretion of the participating study physician according to their clinical judgment and the local standard of medical care.

DANCE Study Design: Summary

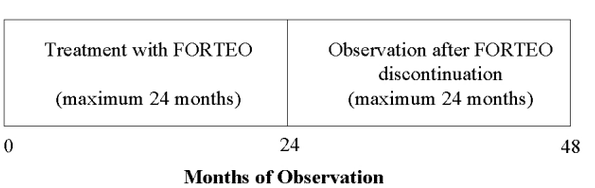

Two study periods:

1) FORTEO treatment phase, maximum 24 months

2) Post-treatment phase, maximum 24 months

Approximately 200 sites, 4000 subjects

Disclosures: ***P.D. Miller****, Eli Lilly and Company 2, 8.*

M479

Defining the Maximal Tolerable Does of PTH-related Protein(1-36) in Humans. M. J. Horwitz, M. Tedesco*, S. Sereika*, A. Bisello, A. Garcia-Ocana*, A. F. Stewart. U Pittsburgh, Pittsburgh, PA, USA.

Once daily hPTHrP(1-36) administered subcutaneously to postmenopausal women with osteoporosis in very high doses (6.56 ug/kg or ~ 400 ug/day) causes a rapid (3 months) and marked (4.7%) increase in lumbar spine density. These results compare favorably to those reported for PTH. However, PTHrP differs from PTH in that whereas markers of bone formation are increased with both PTH and PTHrP, markers of bone resorption increase with PTH, but do not change with PTHrP. Thus, PTHrP appears to have pure anabolic effects. Surprisingly, despite the 20-fold higher doses of PTHrP vs. PTH employed {20 ug/d for hPTH(1-34) vs. 400 ug/d for PTHrP(1-36)}, subjects receiving PTHrP experienced no acute or subacute hypercalcemia, hemodynamic changes, or other objective or subjective adverse effects.

Given this absence of dose-limiting adverse effects or toxicity, the current study was designed to explore the maximal tolerable dose of PTHrP given as a single one-time injection to healthy young adults. Thus, hPTHrP(1-36) was given under close observation to healthy young (22-35 y.o.) volunteers, in groups of three, in escalating (approximately 30%) doses of 9 ug/kg, 12 ug/kg and 16 ug/kg (or approximately 600 ug, 900 ug and 1.2 mg). These doses correspond to 30, 45 and 60 times the approved dose for hPTH(1-34). Despite the large doses and meticulous objective and subjective monitoring for the 10 hours following administration of the dose, no adverse effects have been identified. Orthostatic pulse and blood pressure, serum calcium, serum ionized calcium, and serum creatinine were all completely normal. The highest serum calcium observed was 9.9 mg/dl in one subject.

To confirm that the hPTHrP(1-36) employed was fully active, its structure was confirmed using amino acid analysis and mass spectroscopy, and its biological activity was confirmed using adenylyl cyclase assay in human SaOS-2 osteosarcoma cells. Finally, when administered intravenously to normal volunteers in far lower doses, prompt increases in serum calcium were observed.

Thus, despite employing doses of hPTHrP that are some 60 times higher than those tolerated for PTH, no hypercalcemia or other adverse effects have been observed, and further dose escalation continues. These studies suggest that while the 4.7%, 3 month increment in lumbar BMD described in earlier studies is appealing, the maximal therapeutic dose, and maximal efficacy of PTHrP have not been defined. Further studies are in progress to define the maximal tolerable dose, the pharmacokinetics that underlie these observations, and longer term efficacy. Given the tolerability of large doses and the anabolic efficacy of smaller doses, once or twice per week dosing of PTHrP may be a therapeutic option.

Disclosures: ***M.J. Horwitz****, Merck and Co 8; Eli Lilly 8.*

M480

hPTH (1-34) Treatment Increased Serum FGF2 Levels in Glucocorticoid Induced Osteoporosis Patients. M. M. Hurley[1], W. Yao[2], C. D. Arnaud[2], N. E. Lane[2]. [1]Medicine, University of Connecticut Health Center, Farmington, CT, USA, [2]Medicine, University of California at San Francisco, San Francisco, CA, USA.

Basic fibroblast growth factor (bFGF or FGF2) is a potent bone anabolic agent in experimental animals in vivo and Fgf2-/- mice develop low bone mass with aging (Montero et al, JCI 2000). Although intermittent administration of parathyroid hormone (PTH) stimulates new bone formation in rodents and humans, the mechanism of this effect is not established. Previous studies showed that PTH increased FGF2 mRNA and protein expression in osteoblasts and that the hypercalcemic and anabolic effects of PTH are diminished in Fgf2-/- mice. We therefore assessed whether PTH modulated FGF2 in humans. Daily injections with hPTH (1-34) are associated with increases in both biochemical markers of bone formation and bone resorption (JCI 1998). In addition, previous studies showed that changes in levels of biochemical markers predicted increases in bone mass associated with hPTH (1-34) treatment (Lane et al, OST. Int 2000). We determined the changes in the serum level of FGF2 in patients treated with hPTH (1-34) for 12 months and at 12 months off treatment. All studied subjects (n=51) had post-menopausal osteoporosis, were treated chronically with glucocorticoid + estrogen (HRT) and were randomized to hPTH (1-34) 40 mg/d (n=28) or a control group (n=23). In addition, all study subjects were also treated with 1000 mg/d calcium and 800 IU/d vitamin D3. Biochemical markers of bone formation [osteocalcin (OST), and bone-specific alkaline phosphatase (BSAP)] and FGF2 (ALPCO Diagnostics, Windham, NH) were monitored at the baseline, every 3 months for 18 months and at 24 months. All of these were assayed by ELISA in duplicate. In the hPTH (1-34) group, osteocalcin increased by more than 150% above baseline at 3 month ($p<0.05$ from time 0) and was maintained at this level throughout the treatment period. BSAP increased more than 80% over the baseline level at 3 months and was maintained at 90% above baseline for the next 9 months ($p<0.05$). FGF2 levels increased at a slower rate than OST and BSP, with an increase of about 45% by 3 month, an increase of 60% above baseline from 6 to 9 months ($p<0.05$) and increased more than 90% from baseline by 12 months ($p<0.05$). In the control group, no significant changes were observed in any biochemical markers of bone formation or FGF2 levels. In summary, we found that daily hPTH (1-34) injections increase FGF2 levels. These results support the hypothesis that hPTH (1-34) daily injections increases osteoblast activity by stimulating osteoblast production of FGF2.

Disclosures: ***M.M. Hurley****, None.*

M481

Effects of PTH on Bone Architecture and Bone Mass in Orchidectomized Rats. S. Gomez*[1], M. Diaz-Curiel[2], C. de la piedra[3], d. serfaty*[4], M. Lefort*[3], M. Montero*[3], F. Perez Martinez*[5], S. Luna*[6], J. Garcia*[7]. [1]Facultad de medicina, Universidad De Cadiz, Cadiz, Spain, [2]Medicina interna, Fundacion Jimenez Diaz, Madrid, Spain, [3]Fisiopatologia Ósea, Fundacion Jimenez Diaz, Madrid, Spain, [4]Fisiopatología Ósea, Fundacion Jimenez Diaz, Madrid, Spain, [5]Medicina Experimental, Fundacion Jimenez Diaz, Madrid, Spain, [6]Facultad de Medicina, Universidad De Cadiz, Cadiz, Spain, [7]Facultad de Medicina, Universidad De Granada, Granada, Spain.

The aim of this work was to determine the effects of PTH administration (1-34 rat PTH, SIGMA, $4x10^{-6}$ g/kg/day, subcutaneous daily injection) to rats, in order to avoid the development of osteopenia due to orchidectomy. Twenty-four nine month-old male Wistar rats were orchidectomized: 12 were treated with PTH during 72 days (OQX+PTH) and 12 were untreated (OQX). Twelve age- and sex-matched rats were sham operated (SHAM). After that time, rats were sacrificed. Bone mineral density in lumbar spine (L2-L4) was measured by DEXA. Bone Volume/Total Volume (BV/TV), Trabecular Thickness (Tb.Th), Trabecular Separation (Tb.Sp), Trabecular Number (Tb.N) in L4. The following results were respectively found in SHAM, OQX and (OQX+PTH) groups: BMD (0.311+/-0.019; 0.308+/-0.022; 0.331+/-0.008 g/cm2); BV/TV (29.3+/-3.7; 22.7+/-2.4; 36.1+/-8.1 %); Tb.Th (124.2+/-49.3; 127.3+/-48.2; 145+/-60 microm); Tb.Sp (263.2+/- 155; 337.2+/-277; 260.8+/-166 microm); Tb.N (2.35+/-0.29; 1.78+/- 0.19; 2.48+/-0.55 number/mm).

In summary, orchidectomy produced a significant decrease on bone mass (expresssed by BV/TV) in male rats, due to a decrease in the number of bone trabecula with a higher separation between them, but with the same thickness than those of control rats. PTH treatment, not only avoid bone mass decrease development in OQX rats, but also increase BMD in treated rats with respect to SHAM group. This fact was due to a significant increase in trabecular thickness without changes in number or trabecular separation. BMD determination by DEXA was not enough sensitive to detect changes between SHAM and OQX rats after 72 days from orchidectomy, but it was able to detect the BMD increase produced by the PTH treatment to OQX rats.

Disclosures: ***M. Diaz-curiel****, Spanish Institute of Health 2.*

M482

Should the National Guidelines for Mineral and Vitamin D Supplements Be Modified for Patients Using Teriparatide: Some Clinical Observations. D. A. Licata. Endocrin, Cleve Clinic, Cleveland, OH, USA.

Teriparatide has opened a new modality for treatment of primary osteoporosis and has so far proven to safe and effective. No long lasting metabolic alterations in mineral metabolism are found in the original pivotal study. In its clinical use, however, unexpected changes were found in mineral metabolism of some patients. The present report describes results from a retrospective survey undertaken to understand the mechanism of these observations. The study evaluated changes in mineral metabolism in patients(n=12) using teriparatide for 3-6 months. Serum calcium, PTH, 25 vitamin D, 1,25 vitamin D, bone turnover markers (serum osteocalcin [OSC], and urinary NTX) were measured using standard clinical procedures. Patients were using supplemental calcium and vitamin D per standard published guidelines. The average daily calcium supplement was 1080 mg and the vitamin D 2025 IU. During treatment, serum calcium increased 5-6% and PTH decreased 16-17% ($p<0.05$). All changes, however, were within the normal reference interval. Seventy-five percent of calcium values were between 10 and 10.5 mg/dL. OSC and NTX increased 3.5 ($p<0.05$) and 4.2($p<0.1$) -fold, respectively. 25 vitamin D did not significantly change. 1,25 vitamin D increased 2-3 fold ($p<0.05$) from baseline. Sixty-six percent of values were greater than the 95% reference value (upper reference cutoff 66 pg/mL vs. patients average 98.8 pg/ml). Patients experienced no symptoms during this period of treatment. Adjustment of the daily mineral supplement corrected the serum calcium changes when seen. Comparing these patients and those with documented hyperparathyroidism showed several interesting differences. Higher calcitriol levels and lower PTH levels were noted in the treated osteoporotic patients. Summary: teriparatide increases serum 1,25 vitamin D and calcium, the later change reflecting the amount of daily mineral supplement used. Conclusion: For patients using teriparatide, clinicians may need to adjust the mineral and vitamin D doses recommended in published guidelines.

Disclosures: ***D.A. Licata****, eli lilly 8.*

M483

Intermittent PTH and Propranolol Have Synergistic Effects on Vertebral Trabecular Bone in Ovariectomized Mice. D. D. Pierroz[1], M. L. Bouxsein[2], V. Glatt*[2], R. Rizzoli[1], S. L. Ferrari[1]. [1]Div of Bone Diseases, University Hospital, Geneva, Switzerland, [2]Orthopedic Biomechanics Laboratory, Harvard Medical School, Boston, MA, USA.

Adrenergic system stimulation decreases bone mass, and adrenergic blockade with propranolol has been shown to prevent ovariectomy-induced bone loss in mice. Intermittent PTH administration increases bone formation and resorption, resulting in improved bone mass and architecture. We thus hypothesized that propranolol and PTH could have synergistic effects on bone. For this purpose, 15 wk-old mice were ovariectomized (OVX) and were pair-fed to a non-ovariectomized group (Sham). Propranolol (PRO, 0.5 g/L in drinking water) was immediately administered to one group of OVX mice, whereas another group remained untreated. After 4 weeks, mice with and without PRO were further assigned to daily hPTH(1-34) (80 µg/kg/d) or vehicle VEH for 4 weeks (n=5-7/group). Changes in total body bone mineral density (TB BMD) were evaluated by pDXA, trabecular (Tb) and cortical (Cort) bone architecture were measured by µCT at the end of the experiment. Osteocalcin (OC) and a bone resorption marker (TRAP) were also evaluated.

As expected, OVX significantly reduced TB BMD gain compared to Sham (P=0.014). Intermittent PTH significantly increased TB BMD gain compared to VEH (P<0.0001) in OVX mice. More specifically, PTH increased femur Cort thickness (Th) and vertebral Tb Th compared to VEH (both P<0.0001), whereas vertebral Tb Number (N) and Tb bone volume fraction (BV/TV) did not significantly change with PTH alone. PRO significantly increased TB BMD gain (P=0.01), vertebral Tb Th and Tb N (both P=0.007), and Tb BV/TV (p=0.001) compared to OVX mice without PRO, but did not affect Cort Th. Most importantly, the combined treatment of PRO plus PTH significantly increased TB BMD over PTH alone (P=0.003). This synergistic effect was seen particularly on Tb BV/TV (+17%, P=0.0025 vs PTH), Tb N (+11%, P=0.01), and marginally on Tb Th (+4%, P=0.05), but not on Cort Th. PTH significantly increased OC (+46% vs VEH, P<0.0001), whereas PRO did not modify OC levels in the PTH or VEH groups. In contrast, PRO decreased TRAP levels significantly compared to VEH (-53%, P=0.03) and marginally compared to PTH (-18%, ns).

Altogether, these data confirm that propranolol confers some protection against OVX-induced bone loss, particularly in trabecular bone, and this possibly by inhibiting bone resorption. Moreover, propranolol and PTH in combination exert a synergistic anabolic action on trabecular bone. In contrast, cortical bone remodeling does not appear to be prominently affected by adrenergic blockade. Hence, the development of combined therapies might be of interest for the treatment of osteoporosis.

Disclosures: ***D.D. Pierroz****, None.*

M484

Administration of ThPTH to Humans Using Macroflux® Transdermal Technology Results in the Rapid Delivery of Biologically Active PTH. V. Gopalakrishnan*[1], S. Hwang*[1], H. Loughrey[2], B. Alexandre*[2], D. Desai*[1], L. Haiying*[1], T. Abribat*[2], L. Vachon*[2], P. Daddona*[1]. [1]Alza Corporation, Mountain View, CA, USA, [2]Theratechnologies Inc, St Laurent, PQ, Canada.

Purpose of Study: The objective of this first-in-human study was (i) to evaluate the general safety, and (ii) to determine the pharmacokinetic (PK) and pharmacodynamic (PD) profile of Macroflux-PTH transdermal patch delivery.

Clinical Trial Design: In this 2-part crossover study, a total of 31 female subjects (age range 20 to 40) received a single 1-hour application of a 2 cm^2 Macroflux-PTH patch in the upper arm and a subcutaneous (SC) injection of teriparatide (FORTEO®) into the thigh. Macroflux patches were loaded with 30 µg of synthetic human PTH (1-34) and the comparator teriparatide doses used were 20 and 40 µg in part I and part II respectively. Human PTH (1-34) was measured over a 24 h period using an optimized commercially available enzyme immunoassay (EIA) that was shown by the vendor to have 100 % cross reactivity with hPTH (1-34) and 0 % cross reactivity with hPTH (1-84). Urinary biomarkers (cyclic AMP (cAMP) and phosphate), and plasma biomarkers (total and ionized Ca^{++} and phosphate levels) were measured over an 8-hour and 24-hour period respectively.

Results: The preliminary results indicate that the 30µg Macroflux-PTH patch delivered hPTH (1-34) at blood levels in the range of that obtained with a 40 µg teriparatide dose. The plasma PK profiles of hPTH (1-34) were comparable for both SC and Macroflux delivery (see Figure). Urinary cAMP increased markedly within two hours for both routes of administration indicating that the delivered hPTH (1-34) was biologically active. Changes in plasma biomarkers were also comparable between the two routes of administration. On the whole the frequency of adverse events (AE) reported between the two groups were comparable and typical of those seen with teriparatide. No serious AE's were reported and the majority of AE's were mild in severity.

Conclusion: The results of this proof-of-concept study in humans demonstrate the feasibility for the efficient transdermal delivery of hPTH (1-34) by Macroflux technology. This delivery approach warrants further development and investigation as a convenient alternative to SC administration of hPTH (1-34) for osteoporotic patients.

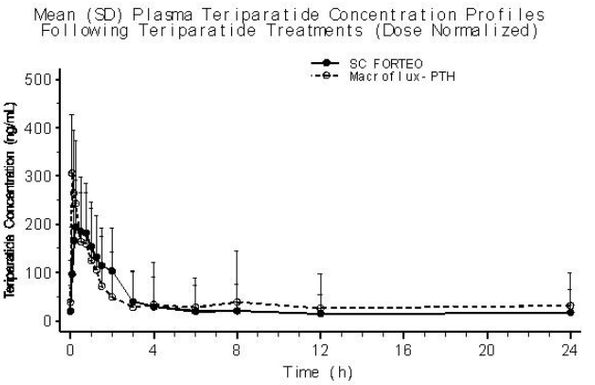

Disclosures: ***V. Gopalakrishnan****, Alza Corporation 3.*

M485

Parathyroid Hormone and 1,25-Dihydroxyvitamin D_3 Exert Independent but Co-operative Effects on Bone Anabolism. D. S. Miao, Z. L. Zhang*, R. Samadfam*, J. R. Li*, I. Bolivar*, Q. W. Xia*, G. N. Hendy, D. Goltzman. Medicine, McGill University, Montreal, PQ, Canada.

Parathyroid hormone (PTH) is required for bone anabolism in the fetus and is a potent stimulus for bone formation when administered intermittently to post-natal animals. We previously reported that when mice with targeted deletion of the 25-hydroxyvitamin D 1α hydroxylase [1α-(OH)ase$^{-/-}$] are fed a "rescue" diet (2% calcium, 1.25 % phosphorus, 20% lactose), they normalize their serum calcium and PTH levels and exhibit reduced bone volume. Consequently, 1,25-dihydroxyvitamin D [1,25-$(OH)_2$D] is required for optimal bone formation. To determine the requirement for 1,25-$(OH)_2$D for the anabolic effect of exogenous PTH, we administered PTH-(1-34), 40 µg /kg body weight subcutaneously, either once daily or three times-a-day to 1α-(OH)ase$^{-/-}$ mice fed a rescue diet and to wild-type (WT) animals on the same diet. PTH administration was begun at three months of age and continued for 1 month. Animals were examined at 4 months. In vehicle-treated animals serum calcium and PTH levels were not significantly different in 1α-(OH)ase$^{-/-}$ and in WT. On the rescue diet, however, bone mineral density (BMD), bone volume and osteoblast numbers were reduced in vehicle-treated 1α-(OH)ase$^{-/-}$ versus WT controls. Administration of once daily or thrice daily PTH did not significantly raise serum calcium above vehicle-treated levels in either group. Serum PTH levels were slightly increased in both groups after once daily administration and markedly increased after injection three times-a-day. Serum 1,25-$(OH)_2D_3$ levels were undetectable in 1α-(OH)ase$^{-/-}$ mice and raised slightly by once daily PTH and more dramatically by thrice daily injections in the WT mice. BMD, bone volume, osteoblast numbers and IGF-1 immunoreactivity in osteoblasts were increased in both mutant and WT mice after once daily PTH administration but these anabolic indices remained lower in the 1α(OH)ase$^{-/-}$ mice than in the WT. Thrice daily PTH administration produced even greater increases in trabecular and cortical bone in both WT and 1α-(OH)ase$^{-/-}$ mice but the levels reached were still slightly lower in 1α-(OH)ase$^{-/-}$ than in WT mice. The results: 1) Confirm that 1,25-$(OH)_2D_3$ exerts an anabolic effect on bone 2) Show that PTH, even when given three times-a-day to murine models, produces a strong anabolic effect 3) Show that the anabolic effect of exogenous PTH can occur in the absence of 1,25-$(OH)_2D_3$ and 4) Show that both hormones are required for optimal bone anabolism.

Disclosures: ***D.S. Miao****, None.*

M486

PTH Increases Bone Mineral Density and Resistance to Mechanical Load in a Rat Model of Osteoporosis. Z. Henriksen*[1], C. Thorkildsen*[2], J. E. B. Jensen[1], N. R. Jørgensen[1]. [1]The Osteoporosis and Bone Metabolic Unit, Departments of Endocrinology and Clinical Biochemistry, Copenhagen University Hospital, Hvidovre, Denmark, [2]Zealand Pharma A/S, Glostrup, Denmark.

Parathyroid hormone (PTH) is an anabolic agent that stimulates cancellous and compact bone formation and reduces fractures in patients with osteoporosis. Thereby PTH represents an important new advance in the therapy of osteoporosis. In this study we looked at the effects of PTH on bone in mature female rats.

Six months old female nullipara Fisher rats were ovariectomized (ovx) or sham operated (sham). Three months after the operation, ovx rats were randomized to 4 month of treatment with either saline (veh) or PTH 40 µg/kg/day 5 days a week. At the end of the dosing period, blood was collected for measurement of the following markers of bone formation: alkaline phosphatase (ALP) and osteocalcin (OCN) as well as the bone resorption marker C-telopeptide collagen type I fragment (RatLaps). Right femur and tibia were collected for measurement of bone mineral density (BMD) and left femur was collected for bone strength (max-load) measurements. Data were analyzed by one-way ANOVA followed by Fisher's LSD for posthoc comparison.

	veh/sham (n=21)	veh/ovx (n=20)	PTH/ovx (n=19)
Femur BMD (g/cm2)	0.199±0.002**	0.167 ±0.001	0.254 ± 0.003**§§
Femur max-load (Newton)	108 ± 2**	89 ± 1.	154 ± 3**§§
ALP (nmol/ml)	193 ± 7**	245 ± 11	303 ± 12**§§
OCN (ng/ml)	136 ± 6 $^{p=0.07}$	178 ± 8	453 ± 20**§§
RatLaps (ng/ml)	15.1 ±1.4*	20.1 ± 1.4	24.1 ± 1.1*§§

Values are mean ±SEM. *: p<0.05, **p<0.001 relative to veh/ovx treated animals, §§: p<0.001 relative to veh/sham treated animals

PTH treatment dramatically increased femoral BMD and bone strength as compared to both ovx/vehicle and sham/vehicle treated animals. In addition, all measured bone markers were significantly increased in PTH/ovx rats compared to veh/ovx rats and veh/sham. Thus, the ovx induced bone loss was not only reversed by the PTH treatment, but the ovx/PTH treated group also had significantly stronger bones than the sham-operated group.

In conclusion PTH treatment results in a dramatically increased bone formation as well as an increased bone resorption, indicating an increased bone turnover. The data demonstrates a net bone formation leading to increased BMD and bone strength.

Disclosures: ***Z. Henriksen****, None.*

M487

Optimizing Patient Selection for Recombinant Parathyroid Hormone Therapy. M. Casey*, J. Walsh*, M. Healy*, N. Maher*, C. Kirby*, C. Connolly*, C. Cunningham*, D. Coakkey*. St. James Hospital, Dublin, Ireland.

Introduction: The recent availability of anabolic therapies for osteoporosis necessitates a thorough investigation for this treatment to our rule the recognised contra indications as well as potential complicating factors such as idiopathic hypercalcuria which substantially increased the patients' risk of renal calculi whilst on PTH therapy.

Methods: We review the first 84 patient referrals to a specialist osteoporosis clinic for PTH therapy and we report the results of a comprehensive clinical investigation of these subjects.

Results: The mean age of the referrals was 74.9 ± 11 years with 71 females and 12 males. All had severe osteoporosis and 70% had addition of vertebral fractures (≥1). Nine patients were excluded from PTH Therapy because of monoclonal gammopathy and / or Bence Jones Proteinuria. One was also excluded because of a history of breast cancer with radiotherapy. Four males with elevated PSA could not immediately commence PTH and were referred for Prostatic biopsy. Two patients were in advanced CRF (creatinine clearance of < 30mls / min). Five patients had hypercalcuria (24 hours U. Ca of > 7.5mmol) and this is under active management at present prior to PTH. On patient was treated for thyrotoxicosis and two for coeliac disease prior to commencing PTH Therapy. Six patients were unable / unwilling to self inject.

Conclusion: In older age groups there is a high prevalence of secondary causes for osteoporosis and these must be thoroughly investigated prior to consideration for PTH Therapy

Disclosures: ***M. Casey****, None.*

M488

Basic FGF Increases Trabecular Bone Connectivity and Improves Bone Strength in the Lumbar Vertebral Body of Osteopenic Rats. W. Yao[1], T. Hadi*[1], J. Zhou*[1], Y. Jiang[1], T. J. Wronski*[2], N. Lane[1]. [1]University of California in San Francisco, San Francisco, CA, USA, [2]University of Florida, Gainesville, FL, USA.

Recently, basic fibroblast growth factor (bFGF) has been found to increase trabecular bone mass (BV/TV) and connectivity (CD)in the proximal tibial metaphyses (PTM) in osteoporotic rats. The purpose of this study was to determine the bone anabolic effects of bFGF in the lumbar vertebral body (LVB), a less loaded skeletal site with a lower rate of bone turnover than the PTM.

METHODS: 6-month old female SD rats were ovariectomized (OVX) or sham-operated and untreated for 8 weeks to induce osteopenia. Then G 1 (Sham) and G2 (OVX) were treated SC with vehicle and OVX; G 3 and G4 were treated SC with PTH [hPTH (1-34) at 40ug/kg, 5×/wk] and bFGF (1 mg/kg daily, 5×/wk), respectively, for 8 wks. At sacrifice, the 5th LVB was removed, subjected to μ-CT for determination of trabecular bone structure, and then processed for histomorphometry to assess bone turnover. The 6th LVB was used for mechanical compression testing (MTS, Bionix 858). The data were analyzed with the Kruskal Wallis test followed by post-hoc testing as needed.

RESULTS: After 16 wks of estrogen deficiency, there were significant reductions in BV/TV, trabecular thickness (Tb.Th), and bone strength. Treatment with either bFGF or hPTH (1-34) increased BV/TV in OVX animals. However, hPTH (1-34)-treated animals had a significant increase in BV/TV, and trabecular and cortical thickness compared to bFGF-treated animals. Treatment of OVX rats with hPTH (1-34) also significantly increased bone strength compared to OVX + Vehicle animals (maximal load and stiffness). Treatment with bFGF increased Tb.N more than hPTH (1-34). Basic FGF also significantly increased Tb.Th, and maximum load compared to OVX + Vehicle animals.

SUMMARY. These results suggest that both anabolic agents increase trabecular bone volume in the LVB of osteopenic rats. However, they alter trabecular structure differently with hPTH(1-34) predominantly increasing trabecular thickness whereas bFGF increases trabecular number and connectivity density. Although both anabolic agents improved bone strength by compressive testing compared to OVX + Vehicle animals, hPTH (1-34) appeared to be more potent at this skeletal site.

Treatment Groups	N	BV/TV (%)	CD (1/mm^3)	Tb.N (1/mm)	Tb.Th (μm)	Max. Load (N)	Stiffness (10^{2}N/mm)
1. Sham + Vehicle	12	37.6 ± 5.0	51.3 ± 12.7	3.8 ± 0.2 ^{d}	98.5 ± 11.1	266 ± 47 ^{c}	7.9 ± 3.7 ^{c}
2. OVX + Vehicle	12	29.9 ± 7.4^{a}	42.0 ± 13.2	3.4 ± 0.4	88.2 ± 10.6^{a}	212 ± 50^{a}	5.0 ± 2.1
3. OVX + PTH	12	40.6 ± 4.6^{b}	26.3 ± 6.3^{bc}	3.0 ± 0.3^{b}	130.2 ± 10.1^{e}	349 ± 91	10.9 ± 5.0^{bc}
4. OVX +bFGF	12	34.3 ± 4.6	46.5 ± 13.7	3.7 ± 0.4	99.5 ± 7.9	260 ± 82	6.3 ± 2.2

a= p < 0.05 from groups 1,3,4; b= p < 0.05 from group 4; c= p < 0.05 from group 2; d= p < 0.05 from groups 2,3; e= p<0.05 from groups 1,2,4

Disclosures: ***W. Yao****, None.*

M489

Administration of Vitamin K2 (Menatetrenone: MK4) Improves Bone Strength by Promoting Bone Formation in Diabetic Rats. S. Wada[1], S. Yasuda*[2], M. Kobayashi*[3], K. Omura*[3], K. Hara*[3], M. Kogwa*[2], Y. Akiyama*[3], S. Katayama*[2]. [1]Dept of Clinical Science, Josai International University, Chiba, Japan, [2]Dept of Endocrinology and Metabolism, Saitama Medical School, Saitama, Japan, [3]Eisai Co. Ltd, Tokyo, Japan.

A subanalysis of large-scale clinical studies demonstrated that not only type 1 but type 2 diabetes showed an increased incidence of fractures. To examine the underlying mechanisms for bone fragility in type 2 diabetes, we have studied the effects on bone of chronically elevated serum glucose levels in Goto-Kakizaki (GK) rats. The results suggested that continuous elevation of serum glucose leads to skeletal fragility and that administration of MK4 partially protects against the decline of bone strength. In the present extensive analysis, we focused on skeletal morphology to identify the factors involved in these processes. The experimental animals included 111 GK rats and 44 non-diabetic Wistar rats. The rats, eight weeks of age at the start of the experiment, were fed a normal diet until they were 40 weeks of age, during which time their blood glucose and HbA1c levels and body weight were measured every two weeks. At 40 weeks of age, they were divided into two groups: those to be given MK4 (30 mg/kg b.w./day) and those to receive no active drug treatment; and were further fed for an additional 24 weeks. The results of vertebral compression tests showed increased bone elasticity and stiffness of lumbar vertebrae in the MK4 group (elasticity: 240±12.5 N/mm2 in the control diet vs. 326.9±16.3 N/mm2 in the MK4, p<0.01; stiffness: 538±29 in the control diet vs. 669±34 N/mm in the MK4, p<0.01). These beneficial effects were further assessed by bone histomorphometry, where significantly increased new bone formation was recognized in the MK4 group with respect to the following measurements: BV/TV (4.75±0.39% in the control diet vs. 6.49±0.49% in the MK4, p<0.01) and Tb.N (0.76±0.06/mm in the control diet vs. 1.00±0.07/mm in the MK4, p<0.05). The Ob.S/BS was 2.04±0.25% in the control diet and 4.85±0.46% in the MK4 (p<0.01) and Oc.S/BS was 2.73±0.20% in the control diet and 3.42±0.27% in the MK4 (p<0.05). The MAR, an index reflecting bone formation obtained by double labeling with calcein, was significantly higher in the MK4 group (0.512±0.076 micro m/day in the control diet vs. 0.716±0.066 micro m/day in the MK4, p<0.05). Similar effects of MK4 on skeletal morphology were observed in Wistar rats. These findings suggest that administration of MK4 ameliorated low bone turnover and remodeling in diabetes and that this treatment increased bone formation and improved bone strength. These results provide evidence that support the usefulness of MK4 in the treatment of diabetic osteopathy.

Disclosures: ***S. Wada****, None.*

M490

A Selective EP4 Agonist Stimulates Fracture Healing. Y. Shinagawa*, T. Maruyama, H. Oida*, K. Sakata*, A. Seki*, H. Yoshida*, K. Oda*, M. Naka*, K. Kondo*. Research and Development Headquarters, ONO Pharmaceutical Co., Ltd, Osaka, Japan.

The morbidity and mortality associated with impaired/delayed fracture healing remain high. Since fracture healing requires reparative phase and remodeling phase, prostaglandin E_2 (PGE_2), which has been reported to stimulate both bone formation and resorption, seems to be an appropriate intervention for fracture healing. However, due to side effects, PGE_2 is an unacceptable therapeutic option. We have recently demonstrated that the bone anabolic action of PGE_2 is mimicked by the activation of EP4 receptor, which is a subtype of PGE_2 receptor, and that the selective EP4 agonist ONO-4819·CD restores bone mass and strength in rats subjected to ovariectomy or immobilization at doses without severe side effects (*). The aim of this study was to examine the effect of ONO-4819·CD on fracture healing in rats at tolerable doses. Rats were prepared by making a surgical osteotomy on the fibula and sacrificed at 21 days after surgery. The strength and bone mineral content of the callus area in the fibula was assessed by means of three-point biomechanical testing and radiographic analysis. ONO-4819·CD was injected intravenously for 2 hours twice a day from the day after the surgery until the end of the experiments. In vehicle-treated animals, the strength of the fractured fibula recovered around 50% compared with the untreated fibula at 21 days after osteotomy. Administration of ONO-4819·CD enhanced the strength of the callus area in a dose dependent fashion. In addition, the radiographic analysis revealed that bone mineral contents and closure of fracture line in the callus area was more pronounced in rats treated with ONO-4819·CD than those obtained with vehicle. These results indicate that ONO-4819·CD enhanced the fracture healing by the activation of both bone formation and bone remodeling. Since no obvious adverse effect was observed in rats treated with ONO-4819·CD in this study, the activation of EP4 receptor with ONO-4819·CD may be a therapeutic intervention for fracture healing. Its usefulness in patients will be clarified by clinical trial on-going in Japan.

*: Proc Natl Acad Sci U S A. 2002 99(7):4580-5

Disclosures: ***Y. Shinagawa****, None.*

M491

A Single Intraosseous Injection of rhBMP-2/CPM Improves Structure and Strengthens the Distal Radius of Ovariectomized Nonhuman Primates in 6 Months. H. J. Seeherman, E. A. Smith-Adaline, J. D. Parkington*, X. J. Li, J. M. Wozney. Women's Health and Bone, Wyeth Research, Cambridge, MA, USA.

Recombinant BMP-2 (rhBMP-2) is a potent osteoinductive factor with the potential to lower fracture risk in osteoporotic patients by inducing anabolic bone formation following local injection. This study evaluated intraosseous (IO) delivery of 0.2 mL of 1.5 mg/mL rhBMP-2 administered in a calcium phosphate matrix (CPM, ETEX Corporation, Cambridge, MA) into one distal radius of 11 adult female cynomolgus monkeys that had been ovariectomized 5 years previously. The contralateral radii remained untreated. Animals were euthanized at 1 month (n = 1) and 3 months (n = 1) for histologic evaluation and 9 animals were euthanized at 6 months either for histology (n=3) or pQCT and biomechanics (n=6).

Radiographs demonstrated new bone formation as early as 2 months after treatment. The majority of the carrier appeared to be resorbed by 3 months. At 6 months, there was substantial new bone formation leading to an increase in the circumference of the distal radius. At 1 month, histology demonstrated increased marrow cellularity, vascularity, appositional and new trabecular bone formation, along with an increase in endosteal and periosteal bone formation compared to the untreated limb. Marrow activation and anabolic bone formation persisted at 3 months and was still ongoing at 6 months. Ex-vivo pQCT analysis at 6 months demonstrated BMP/CPM significantly increased cross-sectional area (17 ± 12%, p = 0.015), trabecular bone area fraction (23 ± 14%, p = 0.013) and cortical thickness (23% ± 17%, p = 0.05) in the radial metaphysis (paired t-test). Cross-sectional area of the distal radial shaft increased (25% ± 28%, p = 0.08) and cortical thickness remained unchanged. BMP/CPM increased maximum compressive load (23% ± 22%, p = 0.05), yield load (45% ± 25%, p = 0.01) and energy (68% ± 64%, p = 0.069), but not stiffness.

In summary, a single IO administration of BMP/CPM resulted in a marked and rapid increase in cortical and trabecular bone in the distal radius leading to increased mechanical properties at 6 months. The anabolic effect of BMP/CPM was still present at 6 months. The combination of rhBMP-2/CPM represents a promising anabolic therapy for prevention of osteoporotic fractures, particularly for patients undergoing surgical treatment for vertebral or contralateral wrist or hip fractures.

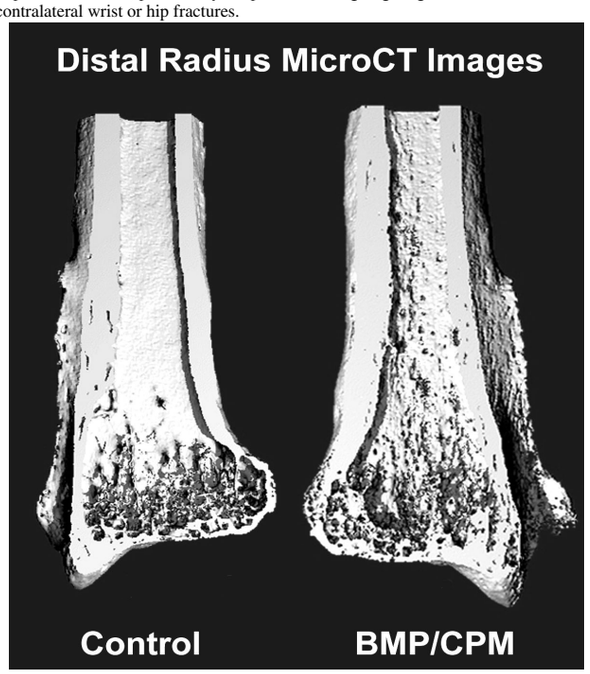

Disclosures: ***H.J. Seeherman****, Wyeth Research 3.*

M492

Glucose-Dependent Insulinotropic Peptide Regulates Bone Turnover In Vivo. D. Xie[1], K. H. Ding[2], M. Hamrick[3], A. L. Mulloy[2], K. Insogna[4], C. M. Isales[2]. [1]Institute of Molecular Medicine and Genetics, Medical College of Georgia, Augusta, GA, USA, [2]Medicine, Medical College of Georgia and the Augusta VA Hospital, Augusta, GA, USA, [3]Cellular Biology and Anatomy, Medical College of Georgia, Augusta, GA, USA, [4]Medicine, Yale University School of Medicine, New Haven, CT, USA.

Glucose-dependent insulinotropic peptide (GIP) is an incretin hormone whose release from the small intestine is stimulated by nutrient ingestion. We previously reported that GIP receptors are present in osteoblastic cells and GIP increases collagen type I synthesis and alkaline phosphatase activity in isolated osteoblasts. To further define GIP's role as an anabolic hormone in vivo we utilized two genetically altered mouse models, a transgenic mouse over-expressing GIP under the control of the metallothionein promoter (Tg+/+) and a GIP receptor knockout mouse (GIPR -/-). Tg +/+ mice were fed zinc (25 mM) in their drinking water beginning at one month of age and all measurements were taken at five months of age and compared to age-matched wild-type (C57/Bl6) and GIPR -/- mice. Tg +/+ mice had significantly higher mean GIP levels (wild-type: 251 pM, Tg +/+: 606 pM, GIPR -/-: 261 pM, (n=26 animals, p<0001 control vs. Tg +/+). Tg+/+ animals also had a significant increase in markers of bone formation (serum alkaline phosphatase activity, wild-type: 104 U/L, Tg+/+: 136 U/L, GIPR -/-: 86 U/L, (n=30 animals, p<0.003 control vs. Tg+/+) and a decrease in pyridinoline (GIPR -/-: 1.9, Tg+/+: 1.3 nM; n=26 animals, p<0.001 GIPR -/- vs. Tg +/+). Consistent with these biochemical data, GIP transgenic mice had a significant increase in bone density and GIPR -/- mice a significant decrease when compared to wild-type by PIXImus (wild-type: 0.0492, Tg+/+: 0.0534, GIPR -/-: 0.0480 g/cm2, n=30 animals, p<0.007 wild type vs. Tg+/+; p<0.028 wild type vs. GIPR -/-).

These data are consistent with the conclusion that: 1. GIP inhibits bone breakdown and stimulates bone formation. 2 Loss of GIP signaling results in significant bone loss. Since GIP receptor is known to be downregulated in humans with increasing age, our data suggest that attenuation of the GIP signal in bone may contribute to aging-related bone loss.

Disclosures: ***D. Xie****, None.*

M493

The Novel Vitamin D Analog ED-120 Inhibits Bone Resorption and Stimulates Periosteal Apposition in Overiectomized Rats. Y. L. Ma, Q. Zeng*, S. Smith*, H. W. Cole*, H. U. Bryant, M. Sato. Bone and Inflammation, Eli Lilly and Company, Indianapolis, IN, USA.

Skeletal effects of ED-120, an oral vitamin D analog, were examined in ovariectomized (Ovx) rats. In study 1, ED-120 (provided by Chugai) at 0.008, 0.04 or 0.1μg/kg/d was given to 6 month old rats for 6 weeks starting at two weeks post-Ovx. ED-120 significantly increased serum calcium over Ovx controls (up to 7%) at 0.04 and 0.1μg/kg/d doses; but micro-CT analysis showed that all 3 doses of ED-120 increased bone mineral density (BMD) of the distal femur relative to Ovx controls (13-73%). Histomorphometry analysis showed that trabecular area of the proximal tibiae in the two highest dose groups was greater than Ovx (89% and 168%, respectively) and not different from Sham. In study 2, ED-120 at 0.03, 0.1 or 0.3 μg/kg/d (po) and PTH (1-38) 40 μg/kg/d sc were given for 3 months to 7 month-old rats that were permitted to lose bone for 1 month prior to treatment. Compared with Ovx, ED-120 significantly increased serum calcium (up to 15%) at 0.1 and 0.3 μg/kg/d, but ED-120 completely restored BMD at 0.03μg/kg/d, and increased BMD over Sham at 0.1 and 0.3μg/kg/d in vertebrae L-5. Trabecular area in the proximal tibia was 280% and 502% higher than Ovx controls, respectively. The bone mass increase was accompanied by thickening trabeculae and increased trabecular connectivity. The high dose effect was not different from PTH 40μg/kg/d treatment. ED-120 also significantly increased mid-femur BMD and tibial shaft cortical area over both Ovx and Sham controls at 0.1μg/kg/d or higher. The efficacy of ED-120 was due to lower bone resorption and reduced turnover rate on trabecular and endocortical surfaces, with increasing mineralizing surface, mineral appositional rate and bone formation rate on the periosteal surface. To determine the bone efficacy of ED-120 in the absence of intestine or renal effects, ED-120 was given through a cannulae into the tibial marrow cavity of Ovx rats daily for 10 days. Up to 50% more new bone formation was seen in ED-120 treated tibiae compared to vehicle controls. These data suggest that ED-120 compares favorably to PTH in restoring lost bone due to Ovx in rats and could have therapeutic potential for the treatment of osteoporosis, if hypercalcemia is monitored closely.

Disclosures: ***Y.L. Ma****, Eli Lilly Company 3.*

M494

A Higher Dose of Vitamin D Reduces the Risk of Falls in Nursing Home Residents: A Randomized, Placebo-Controlled, Multiple Dose Study. D. P. Kiel[1], K. E. Broe[1], T. C. Chen*[2], L. A. Cupples*[3], H. Bischoff-Ferrari[4], M. F. Holick*[2]. [1]Hebrew Rehab Ctr for Aged & Harv Med Sch, Boston, MA, USA, [2]Boston Med Ctr, Boston, MA, USA, [3]BU Sch Pub Hlth, Boston, MA, USA, [4]Brigham & Women's Hosp, Boston, MA, USA.

Although a recent meta-analysis of randomized, controlled trials reported that vitamin D (vit D) supplementation reduced the incidence of falls, there was insufficient data to formally test which dose of vit D would be most beneficial. Therefore we analyzed results of a five-arm, double-blinded, placebo-controlled trial involving 125 residents (89 women, 36 men) from a 725-bed long-term care facility in Boston, MA. Eligible residents had none of the following: severely limited mobility; fx within past 6 mo; use of glucocorticoids or anti-seizure drugs; disorders associated with abnormal calcium metabolism; use of pharmacologic doses of vit D; expected death within the next five mo. These 125 residents were randomly assigned to one of four dose groups of daily vit D supplementation (200, 400, 600, or 800 IU) or placebo from January-May, 1995. At baseline, subjects were evaluated for age, wt, ht, 25 hydroxy vit D (ng/ml), functional and cognitive status, falls in prior year, and facility multivitamin use (400 IU of vit D). Falls were ascertained using the facility's computerized incident reporting system.

We examined risk of falls across all intent to treat dose groups using Cox proportional hazards adjusting for age and multivitamin use (y/n) and then compared the risk of falls in the 800 IU group to the other four groups combined. Additionally we looked at multiple falls using negative binomial regression and repeated these across quintiles of total vit D supplement intake (study tablet + multivitamin).

Of the 125 participants, 72% were female, mean age 89±6 years, 63% were taking a daily multivitamin, and 115 completed the trial. There were no baseline differences across groups with the exception of age. The number of falls over the 5 mo period in the placebo, 200, 400, 600, and 800 IU groups were 31, 37, 33, 41, and 9 respectively. The percentage of participants with > one fall during follow up were 32%, 42%, 36%, 36%, and 9% respectively.

Compared to the 800 IU group, participants in the other groups had a 3 to 4-fold increase in the hazard ratio (HR) for first fall. Participants in the 800 IU group had a 71% reduction in the risk of falls (HR 0.29; 95% CI: 0.11-0.72) compared to the other four groups combined. Similar results were obtained when considering all falls or when using quintiles of total vit D

intake.
In conclusion, nursing home residents taking at least 800 IU of vit D daily have a lower risk of falls than those taking lower daily doses. To maximally reduce the risk of falls in nursing homes, vit D doses of 800 IU or higher may be needed.

Disclosures: ***D.P. Kiel****, None.*

M495

Importance of the Understanding of the 25-hydroxyvitamin D Status for the Alendronate Treatment of Postmenopausal Osteoporosis. M. Yamanaka*[1], M. Ishijima[1], A. Tokita[2], K. Kitahara[1], F. Enomoto*[3], M. Sawa*[3], M. Nozawa*[3], H. Kurosawa*[1]. [1]Dept. of Orthopaedics, Juntendo Univ. School of Medeicine, Tokyo, Japan, [2]Dept. of Pediatrics, Juntendo Univ. School of Medeicine, Tokyo, Japan, [3]Orthopaedic Surgery, Juntendo Tokyo-Kouto Geriatric Medical Center, Tokyo, Japan.

The aim of this study is to investigate the relationship between the vitamin D status and the effect of the treatment of alendronate in postmenopausal osteoporotic Japanese women. Seventy-eight Japanese women who were all outpatients for our hospital were included in this study. Subjects were ranged from 52 to 82 years of age. Serum levels of 25(OH)D3, 1,25(OH)2 D3, intact-PTH and bone specific alkaline phosphatase (BAP) and urinary levels of NTX were measured at the first medical examination and every three months thereafter. In those, eighteen patients who were diagnosed as primary osteoporosis were treated with alendronate (5mg, daily). BMD of the lumber spine was measured every six months. Serum levels of 25(OH)D3 at the first medical examination were correlated negatively with that of intact-PTH (intact PTH=64.8-0.87*25(OH)D, r=-0.29, p=0.01). Insufficient levels of 25(OH)D3 (<15 ng/ml) at the first medical examination were recognized in nine patients (12%). In addition, five patients (7.2%) in residual 69 patients were increased in levels of intact-PTH (>65 pg/mL) at the first medical examination. One of those patients was diagnosed with primary hyperparathyroidism. In eighteen patients who were treated with alendronate for primary osteoporosis, insufficient levels of 25(OH)D3 at the first medical examination were recognized in five patients. In two of them the levels of 25(OH)D3 were not improved after six months from the first examination despite of dietary education. The increase in the BMD in lumber spine and the decrease in urinary levels of NTX of the two patients after six months of alendronate treatment was insufficient compared to those of residual sixteen patients. These results indicate that patients with secondary hyperparathyroidism are not rare in postmenopausal outpatients. In addition, insufficiency of vitamin D status in postmenopausal osteoporotic women may inhibit the effect of alendronate that suppresses osteoclastic bone resorption. Therefore, understandings of the vitamin D status in postmenopausal women are really important not only to understand their nutritive status but also to obtain a satisfactory effect using alendronate for treatment of osteoporosis.

Disclosures: ***M. Yamanaka****, None.*

M496

Bone Histomorphological Examination Reveals ED-71, 1α,25-dihydroxy-2ß-(3-hydroxypropoxy)vitamin D_3, and Human PTH(1-34) Activate Bone Formation in A Different Way in Aged Ovariectomized Rats. K. Tsunemi*, S. Takeda*, A. Sugita*, F. Takahashi, H. Saito, N. Kubodera*, F. Makishima*. Chugai Pharmaceutical Co.,Ltd., Gotemba, Japan.

ED-71 (1α,25-dihydroxy-2ß-(3-hydroxypropoxy) vitamin D_3) is a novel orally active vitamin D analog for the treatment of osteoporosis, currently under Phase 3 clinical trials in Japan. We previously reported ED-71 dose-dependently increased both bone mineral density (BMD) as well as bone strength of both lumber vertebrae and femur in aged ovariectomized (OVX) rats. In present study, we examined effects of ED-71 on bone formation by bone histomorphometry in compared with human parathyroid hormone (hPTH(1-34)) in aged OVX rats. Seven-month old female rats were ovariectomized and kept untreated to lose bone mass for three months prior to the treatment. OVX rats were given either vehicle, ED-71 (0.08μg/kg) or hPTH (1-34) (20 nmol/kg), five times a week. Sham-operated animals were given vehicle. Rats were sacrificed at day 7, day 14, day 28 and day 56. In all groups, serum calcium was within normal range. Both ED-71 and hPTH(1-34) restored lumber spine BMD comparable to Sham group at day 28, and continued to increased BMD to overcome the Sham group at day 56. ED-71 increased serum osteocalcin, however, did not affect serum alkaline phosphatese. ED-71 decreased urine deoxypyridinoline throughout the treatment period.
In bone histomorphometry, both ED-71 and hPTH(1-34) groups restored bone volume (BV/TV) comparable to the Sham group at day 28 and day 56. The ED-71 group maintained high mineral apposition rate (MAR), bone formation rate (BFR/BS), and obteoblast surface (Ob.S/BS) as observed in OVX group, however, significantly decreased eroded surface (Er.S/BS), osteoclast surface (Oc.S/BS) and osteoclast number (Oc.N/BS). On the other hand, hPTH(1-34) significantly activated both bone formation (MAR, OV/BV, Ob.S/BS, BFR/BS) and bone resorption (ES/BS, Oc.S/BS, Oc.N/BS) compared to OVX group.
Bone histomorphological analysis revealed that both ED-71 group and hPTH(1-34) group had thick trabecular bones, in which lamellar bones were added to the trabeculaes, observed at day 7 and day 14. After reaching Sham level, ED-71 started to form convexed shape of trabecular contour and increased trabecular connectivity, without showing any bone resorption figures, which observed at day 28 and day 56. On the other hand, hPTH(1-34) still continued to add lamellar bones to trabecularae as well as activating bone resorption at day 28 and day 56. These data suggested that both ED-71 and hPTH(1-34) increased bone mass, however the time-course and the way of bone formation of the two agents were not identical.

Disclosures: ***K. Tsunemi****, Chugai Pharmaceutical Co., Ltd. 3.*

M497

Effect of Long Term Antiepileptic Therapy on Bone Density and Response to Different Doses of Vitamin D: Two Randomized Trials in Children and Adults. M. Mikati*[1], L. Dib*[2], B. Yamout*[2], R. Sawaya*[2], G. El-Hajj Fuleihan[2]. [1]Pediatrics Department, American University of Beirut, Beirut, Lebanon, [2]Internal Medicine Department, American University of Beirut, Beirut, Lebanon.

Antiepileptic drugs (AEDs) are risk factors for low bone density[1], possibly due to a deleterious effect on vitamin D metabolism. To date, there are no randomized trials assessing the efficacy of vitamin D supplementation on bone parameters in patients on AEDs.
We conducted two parallel randomized controlled trials, both in adults and children, to test the efficacy of vitamin D supplementation over one year in maintaining bone mineral density. The two doses were a maintenance dose (400 IU vitamin D/day) versus a higher dose (2000 IU/day for children and 4000 IU/day for adults); a placebo was not used for ethical reasons. The adult study group included 78 subjects, 40 women and 33 men, age 28.7±9.7 years, duration of AED therapy 10.8±9.5 years. The pediatrics group included 78 subjects, 41 boys and 37 girls, age 13.2± 2 years, duration of AED therapy 5.2± 4.6 years. Serum 25 hydroxy vitamin D (25 OHD) and spine hip and forearm BMD in adults and spine and total body BMD/bone mineral content (BMC) in children were measured at baseline and at one-year.

Vitamin D levels in study groups before and after study entry

	Adults		Children	
	Low Dose	High Dose	Low Dose	High Dose
Baseline 25 (OH)D (ng/ml)	13.4 (6.4)	13.7 (8.0)	18.2 (7.1)	18.0 (9.1)
One year 25(OH)D (ng/ml)	17.5 (7.3)*	26.3 (8.9)*	21.2 (8.5)*	22.9 (8.4)*

*Implies significant changes compared to entry values, p< 0.05.

At baseline, bone density in epileptic adults, but not in children, was significantly lower than that of age, gender and ethnic-matched controls[2] at the spine and hip in men (p=0.05 and p=0.023 respectively) and women (p=0.038 and p=0.013). At one-year, no significant difference in percentage change BMD/BMC was observed between the two treatment arms, both in the adult and in the pediatric studies. When compared to a longitudinal study of age, gender and ethnic-matched healthy controls, epileptic boys, but not girls, had significantly lower total body BMC increments at one year (10.9±11.2% versus 15.8±8.4%, p=0.016), with a trend for lower increments at the spine.
Adults, but not children, on AED had lower BMD compared than age-gender and ethnic matched controls, as we previously reported[1].Particular attention to skeletal health is warranted in ambulatory subjects on chronic antiepileptic therapy. Although Vitamin D supplementation seems to maintain BMD, the optimal dose is however still unclear and necessitates larger dose-ranging multicenter trials.
1. Farhat G. Neurology 2002; 58:1348-1353 .
2. El-Hajj Fuleihan G. Bone 2002; 31:520-528.

Disclosures: ***G. El-Hajj Fuleihan****, None.*

M498

One-year Vitamin D Supplementation of Adolescent Girls Influenced only Serum 25-hydroxyvitamin D. H. T. Viljakainen[1], A. Natri*[1], M. M. Huttunen[1], A. Palssa*[1], J. Jakobsen*[2], K. D. Cashman*[3], C. Mølgaard*[4], C. Lamberg-Allardt[1]. [1]Department of Applied Chemistry and Microbiology, division Nutrition, University of Helsinki, Helsinki, Finland, [2]Danish Institute for Food and Veterinary Research, Söborg, Denmark, [3]Department of Food and Nutritional Sciences, Cork, Ireland, [4]Research Department of Human Nutrition, The Royal Veterinary and Agricultural University, Frederiksberg C, Denmark.

Exposure to sunlight is the major source of vitamin D for adolescent girls in the summer, even in Finland, a country with hardly any UVB-light in the winter. However, body stores of vitamin D with inadequate dietary intake do not maintain serum 25-hydroxyvitamin D (s-25-OHD) concentrations through out the winter, which leads to increased parathyroid hormone (s-iPTH) secretion and may sabotage bone mineral accretion.
The purpose of this one-year study was to determine in a randomised, double-blinded, placebo-controlled setting the effect of vitamin D3 supplementation on s-25-OHD, s-iPTH concentration and bone markers in adolescent girls.
Altogether 225 girls, mean aged (SD) 11.4 (0.4) y, participated the study between September 2001 and March 2002. They were randomly assigned into three groups receiving 0, 5, or 10 μg of vitamin D3. Subjects with a compliance of at least 80% were included in the final analysis. Fasting blood and second void urinary samples were collected during month 0, 6 and 12 of the intervention. S-25-OHD was measured by a HPLC method, S-iPTH by OSTEIA assay and s-osteocalcin by ELISA. Deoxypyridinole from urine samples was analysed by HPLC. Statistical analyses were performed by ANOVA by SPSS.
At baseline, mean S-25-OHD concentration was 47.8 (17.3) nmol/L and median dietary intake of vitamin D and calcium was 4.4 (4.0) μg and 1230 (540) mg, respectively. S-25-OHD was influenced by supplementation (p<0.0001) and season (p=0.008), and an interaction of these two (p=0.03). The concentration of S-25-OHD increased in groups receiving 5 and 10 μg by 5.7 (15.7) nmol/L and 12.4 (13.7) nmol/L, respectively, over the year, while it decreased by 6.7 (11.3) nmol/L in the control group. Increase in S-25-OHD differed between groups (p<0.001). Supplementation influenced neither S-iPTH nor the bone markers, but higher concentrations of all bone markers were seen in autumn than in winter (p=0.04), indicating an effect of season.
In conclusion, there is an interaction between season and vitamin D supplementation in determining the variation of S-25-OHD. Serum 25-OHD concentration was maintained only in the group receiving 10 μg throughout the year. The total dietary vitamin D intake (including supplement) in this group was 14.8 μg, which is more than the DRI.

Disclosures: ***H.T. Viljakainen****, None.*

M499

Bone Mineral Density Determinations by DXA in the Management of Marfan Syndrome Patients. Some Factors Which Affect the Measurement. P. F. Giampietro*[1], M. G. E. Peterson*[2], R. Schneider*[3], J. G. Davis*[4], C. Raggio*[5], E. Myers*[6], S. W. Burke*[5], O. Boachie-Adjei*[7], C. M. Mueller*[8]. [1]Medical Genetic Services, Marshfield Clinic, Marshfield, WI, USA, [2]Center for Clinical Outcome Research, Hospital for Special Surgery, New York, NY, USA, [3]Radiology, Hospital for Special Surgery, New York, NY, USA, [4]Pediatrics, Weill Medical College, New York, NY, USA, [5]Pediatric Orthopedics, Hospital for Special Surgery, New York, NY, USA, [6]Biomechanics, Hospital for Special Surgery, New York, NY, USA, [7]Adult and Pediatic Spine Surgery, Hospital for Special Surgery, New York, NY, USA, [8]Nutrition Services, Weill Medical College, New York, NY, USA.

The purpose of this study was to statistically compare bone mineral densities (BMD) in a series of 30 patients with Marfan syndrome to those patients reported in the literature. We hypothesized that agreement between values, hence the degree of osteoporosis or osteopenia reported, was dependent on the instrumentation used. Dual-energy x-ray absorptiometry (DXA) was performed using a pencil-beam Lunar DPXL instrument on a sample of 30 adult patients with diagnosed Marfan syndrome from 1993-2000. The results were compared with those of studies studies published from 1993-2000 that used either Lunar or Hologic bone densitometry instrumentation. The differences of our results compared with those made on other Lunar machines were not statistically significant, but did differ with statistical significance with published results from Hologic machines. Before progress can be made in the assessment of BMD and fracture risk in Marfan patients, and in the evidence-based orthopedic management of these patients, standardization of instrumental bone density determinations will be required along with considerations of height, obesity, age and sex.

Disclosures: ***P.F. Giampietro****, None.*

M500

Effect of 3 Years of Pamidronate on the Functional, Radiographic, Densitometric and Biochemical Outcomes of Infants with Severe Osteogenesis Imperfecta. C. F. J. Munns, F. Rauch, F. H. Glorieux. Genetics, Shriners Hospital for Children, Montreal, PQ, Canada.

In children with severe osteogenesis imperfects (OI), cyclical intravenous pamidronate treatment may be of greatest benefit when started at a very young age. We evaluated 29 children with OI types I (n=3), III (n=14) or IV (n=12) who started pamidronate therapy at 2 years of age or less (mean 0.7 ±SD 0.6 years), and had completed 3 years of treatment. They were compared to an historical control group of 29 untreated children with severe OI matched for OI type and age at the three year time point. The total annual pamidronate dose was 9 mg/kg. At analysis, the mean age of the pamidronate and control cohorts were similar (3.6 vs 3.7 years; p>0.05, paired t-test). The pamidronate cohort were heavier (12.1 vs 10.7 kg; p=0.05) but were of similar height (84.1 vs 80.1 cm; p>0.05). Bone age did not differ significantly between the pamidronate and control groups (3.7 vs 3.2 years; p>0.05). Morphometry of L1-4 vertebral bodies showed a significant improvement of vertebral shape (p<0.05). There was no difference in the incidence of popcorn epiphysis or scoliosis (p>0.05 by chi squared test). The age at the first lower limb rodding procedure was significantly lower in the pamidronate cohort (2.5 vs 4.0 years; p=0.003), suggesting that they were pulling to stand at a younger age. Insufficient data was available to allow for meaningful comparisons of fracture incidence. Serum parathyroid hormone levels did not differ significantly between the groups. The table summarizes other significant findings.

Clinical feature	Pamidronate	Control	P
PEDI gross motor score	36.2 ±13.1	23.9 ±12.3	<0.001
Mobility score	2.3 ±0.9	0.8 ±1.0	<0.001
2nd metacarpal cortical thickness (mm)	0.86 ±0.09	0.67 ±0.28	0.02
Volumetric BMD (mg/cm^3)	88 ±12	45 ±11	<0.001
Ionized calcium (mmol/l)	1.29 ±0.05	1.31 ±0.04	0.05
Alkaline phosphatase (U/l)	185 ±45	274 ±63	<0.001
Urine NTx (μmol/min/l)	339 ±132	850 ±301	<0.001

This study, in infants with severe OI, demonstrates that 3 years of cyclical pamidronate is safe with regards to growth, bone age advancement and calcium homeostasis, while decreasing bone turnover. More over, it was associated with significant improvements in gross motor function, vertebral morphometry, cortical thickness and volumetric BMD. Further follow-up is required to evaluate its effects on scoliosis, popcorn epiphysis and final height.

Disclosures: ***C.F.J. Munns****, None.*

M501

Musculoskeletal Manifestations of Mild Osteogenesis Imperfecta in the Adult. F. E. McKiernan. Center for Bone Diseases, Marshfield Clinic, Marshfield, WI, USA.

The musculoskeletal manifestations of mild Osteogenesis Imperfecta (OI) in the adult are not well described. Scant available literature suggests variable hypermobility, rare tendon rupture, occasional Reflex Sympathetic Dystrophy (RSD), infrequent fracture and little overall disability.

The objective of this study is to better characterize the musculoskeletal manifestations of mild OI in adults and to estimate their degree of impairment. An anonymous, 32-question survey designed to meet the study objective was hosted on the OI Foundation (OIF) web site for 6 weeks ending 4/9/04. Unduplicated adult respondents constituted the registry. IRB analysis determined that registry analysis was exempt from their review.

111 respondents (33M /78F) were of mean age 42.1yM/40.2yF (range 20-70). 73.9% considered their OI mild, 23.4% moderate and 2.7% severe. Fracture number and morphometrics did not differ among these 3 groups and all fit the descriptive term mild. Peak height was 65.6"M/61.1"F. 91% of sclera were blue or not white. 49%M/87.2%F considered bruising abnormal. 48.8% M/87.2%F considered dental health abnormal. There were 3410 lifetime fractures; 27.6% of these occurred after age 18y. 44.4% reported an established diagnosis of "arthritis". Of those, 66.7% reported osteoarthritis, 37.5% unknown arthritis, 6.25% fibromyalgia, 4.2% inflammatory arthritis. Pain and stiffness scores dominated at the low back and large weight bearing, lower extremity joints. 82.7% reported some functional impairment based on articular issues; 46.3% requiring some assistance with ADL. 65.7% reported hypermobility, 55.8% prior joint dislocation and 38.9% prior tendon rupture. Instability dominated at the knees. 52% reported some functional impairment based on ligament and tendon issues. Back pain was reported to be common in 70.1%. 72.5% reported some impairment from back pain. 46.8% reported scoliosis. 5.5% reported RSD. In spite of this 60.9 % rated overall physical health as good or excellent. 72% had previously used NSAID/COX II-inh, 47% anti-remodeling agents and 24% systemic/IM/articular steroids.

In conclusion, the majority of adults with mild OI report some functional impairment due to musculoskeletal concerns. 30-50% require some assistance with ordinary ADL. 5-15% require assistance with light physical tasks and personal ADL. Pain and stiffness were dominant in the low back and large weight bearing LE joints. Instability was dominant at the knees. Tendon rupture was not uncommon. RSD was rare and may be over-represented in the literature. This population frequently uses NSAID/COX II-inhibitors, glucocorticoids and anti-remodeling agents. This and fluoroquinolone use may be of some concern for these persons.

Disclosures: ***F.E. McKiernan****, None.*

M502

X-Linked Hypophosphatemia: Favorable Outcome of Joint Replacement. M. P. Whyte. Center for Metabolic Bone Disease and Molecular Research, Shriners Hospitals for Children, St. Louis, MO, USA.

X-linked hypophosphatemia (XLH) is the most common heritable form of rickets (prevalence ~ 1:20,000). Affected children are treated with 1,25-dihydroxyvitamin D_3 and inorganic phosphate (Pi) supplementation during childhood to overcome renal Pi wasting and to prevent skeletal deformity and to improve stature. Whether medical treatment should continue during the adult years is considered on an individual patient basis. Radiographic surveys have shown that osteoarthritis (OA), especially in the knees but also in the hips, is a common complication of XLH during adulthood reflecting the previous eras of suboptimal medical treatments (Medicine 68: 336 '89). The likelihood and severity of OA in the knees correlates positively with the degree of bowing of the lower limbs. However, the utility of joint replacement for XLH, and whether patients should be receiving perioperative medical therapy, is uncertain.

Having treated 186 children with XLH during the last 20 years, we have also encountered a significant number of affected adults with this X-linked dominant disorder. To assess the outcome of joint replacement for XLH in adults, we contacted all 10 patients known to us who have undergone either knee or hip replacement. The 10 patients had 12 knees and 3 hips replaced by different surgeons at different medical centers. Age at surgery ranged from 41 - 65 years. Only 5 of these individuals received medical therapy [1,25$(OH)_2D_3$ and Pi] perioperatively. Postoperative follow-up ranged from 1-20 years.

None of the patients reported a complication from surgery. One individual had reduced flexion after knee replacement. All experienced considerable reduction in pain and improvement in mobility.

Knee or hip replacement for adults with XLH, with or without perioperative medical treatment, is well tolerated and associated with significant clinical improvement including reduction in pain and increase in mobility.

Disclosures: ***M.P. Whyte****, None.*

M503

High Bone Mass Disease with Fragile Dentition In A Kentucky Kindred: A New Autosomal Dominant Disorder. D. Wenkert[1], S. Mumm[2], W. H. McAlister*[2], M. P. Whyte[1]. [1]Shriners Hospitals for Children, St. Louis, MO, USA, [2]Washington University School of Medicine, St. Louis, MO, USA.

Genetic analyses of high bone mass phenotypes in patients have revealed critical mechanisms for human skeletal remodeling. Examples are activating mutations of exons 2-4 of *LRP5* leading to benign or symptomatic osteosclerosis and hyperostosis and defects in genes that regulate acidification by osteoclasts causing osteopetrosis.

We have studied 10 affected individuals of a 4-generation kindred from Kentucky with a unique high bone mass disease with prominent dental manifestations. Clinical and laboratory features are distinct from Albers-Schönberg disease ("benign" osteopetrosis) and from LRP5 high bone mass phenotypes. Family members recognize affected individuals in infancy by their head shape (high forehead and squared-off parietal occipital region). Later, and more striking, there is eruption of small translucent primary teeth. Affected teenagers and adults develop mandibular prominence and bone aches and pains.

Growth: Linear growth is normal. Pre-adolescents appear proportional in weight although BMI percentiles can be elevated perhaps due to high bone mass. Excessive weight gain and hyperlipidemia begin in adolescence.

Neurologic: Affected individuals first complain of severe "migraine" headaches in their teens. Some have early impaired hearing and one developed tunnel vision.

Teeth: Primary and secondary teeth are small, brittle, abscess-prone, and have translucent edges. Both are generally "lost" early through wear, although prolonged retention of pri-

mary teeth affected one patient. Worn secondary teeth are removed due to uncontrollable abscesses. Most affected adults are edentulous by age 30.
Bone: Small facial sinuses lead to frequent sinusitis beginning in childhood. In some patients, progressive bone pain becomes intermittently incapacitating in adulthood. Dentists and surgeons describe the teeth and skeleton as hard but brittle. X-rays show neither the rugger-jersey spine nor the basilar skull sclerosis characteristic of Albers-Schönberg disease. Furthermore, iliac crest biopsy of one affected woman (age 39) showed no cartilage bars.
Biochemistry: Screening for *LRP5* mutations in exons 2, 3 and 4 was negative. Fasting serum phosphate levels were normal in children, however, 3 affected adults had low concentrations (2.2-2.3 mg/dl) yet a normal level of 1, 25-dihydroxyvitamin D. Serum calcium, magnesium, bone alkaline phosphatase, osteocalcin, serum tartrate resistant acid phosphatase and creatine kinase fractionation (brain isoform) and urinary NTX were unremarkable.
The chromosomal location and gene defect causing this unique disorder of bone and teeth are as yet unknown.

Disclosures: ***M.P. Whyte****, None.*

M504

Vertebral Morphometry During Pamidronate Treatment for Pediatric Osteogenesis Imperfecta. S. Sahebjam*, C. Munns, F. Rauch, F. H. Glorieux. Shriners Hospital, Montreal, PQ, Canada.

There is anecdotal evidence that long-term treatment with intravenous pamidronate improves vertebral shape in children and adolescents with osteogenesis imperfecta (OI), but detailed analyses are lacking. In this study we measured the height of vertebral bodies L1 to L4 of patients with moderate to severe OI before and during pamidronate treatment. Anterior, posterior and midpoint height was determined on lateral lumbar spine X rays and results were related to the length of the vertebral bodies in the antero-posterior direction. Before pamidronate treatment, there was evidence of continued compression of vertebral bodies L1 to L3, where mid-height decreased significantly during an average follow-up period of 3.3 years (n = 22 patients). After an average of 3.3 years of pamidronate treatment, the height of all vertebral bodies had increased significantly at all measurement sites (n = 46 patients). This reshaping of vertebral bodies continued during the fourth and fifth year of treatment. Thus, vertebral bodies have a tendency to progressively crush in untreated children with moderate to severe OI. During pamidronate treatment considerable reshaping of vertebral bodies occurs.

Disclosures: ***F. Rauch****, None.*

M505

Restoration of Bone Resorption Causes Down-Regulation of CTGF Expression in Osteopetrotic Rats. R. A. Aswad*[1], C. A. MacKay*[2], J. M. Aubin*[2], P. R. Odgren[2], F. F. Safadi[1], S. N. Popoff[1]. [1]Anatomy and Cell Biology, Temple University School of Medicine, Philadelphia, PA, USA, [2]Cell Biology, University of Massachusetts Medical School, Worcester, MA, USA.

The mammalian osteopetroses represent a pathogenetically diverse group of skeletal disorders characterized by excess bone mass resulting from reduced osteoclastic bone resorption. Connective tissue growth factor (CTGF) is a secreted, extracellular matrix-associated signaling protein that regulates diverse cellular functions. We have previously shown that CTGF expression was highly (8- to 10-fold) over-expressed in bone in the rat mutation, *osteopetrosis* (*op*), when compared to normal rat bone. In addition, much of the CTGF in bone is produced and secreted by osteoblasts. In this study, we examined CTGF expression in bones in the *incisors-absent* (*ia*) and *toothless* (*tl*) osteopetrotic mutations. All osteopetrotic mutants share the skeletal characteristics of osteopetrosis including; lack of bone marrow spaces and unerupted teeth. They nevertheless have dramatically different phenotypes when considering osteoclasts. In *ia* rats, osteoclasts are two to three times more abundant than normal, they are small and non-functional; they slowly normalize over the first postnatal month. In *tl* rats, there is a profound lack of osteoclasts but an abundant pool of mononuclear osteoclast precursors. In *tl* rats, osteoclast function can be restored only in response to CSF-1 treatment. Here, we examined CTGF expression at different ages (1, 2 and 4 weeks) in bones from *ia* and *tl* mutant and normal rats. CTGF expression was up-regulated in *ia* mutants at 1 and 2 weeks of age, while the expression level was normalized by 4 weeks of age. However, in *tl* rats, CTGF expression was up-regulated at all ages examined (1, 2 and 4 weeks). CTGF expression levels were normalized only when mutants treated with CSF-1 when compared to untreated or CSF-1-treated normal littermates. Down-regulation of CTGF expression was also associated with an increase in TRAP positive osteoclasts and MMP-9 expression in *tl* rats. These data suggest that restoration of osteoclast resorptive function is positively correlated with normalization of CTGF expression in osteopetrotic bone. Future studies will examine the role of CTGF as an extracellular matrix protein that promotes osteoclast-mediated bone resorption.

Disclosures: ***R.A. Aswad****, None.*

M506

Ascorbic Acid Supplementation, Urinary Oxalate and Risk of Kidney Stone Disease. L. Massey[1], S. Kynast-Gales*[1], M. Liebman*[2]. [1]Human Nutrition, Washington State University, Spokane, WA, USA, [2]Family and Consumer Sciences, University of Wyoming, Laramie, WY, USA.

Endogenous conversion of ascorbic acid (AA) to oxalate contributes to urinary oxalate so AA supplementation may potentiate calcium oxalate stone risk. This study determined the effect of a divided dose of 2 g AA/d on oxalate absorption and excretion, and Tiselius risk index (TRI) for calcium oxalate precipitability.

Twenty-nine stone formers (SF) and 19 age and gender matched non-stone formers (NS) participated in a randomized crossover controlled diet study, 6 days consuming 1 g AA with each breakfast and dinner (treatment A), vs. 6 days without AA (treatment N). The study periods included two free-living adaptation days on self-selected low oxalate diet, followed by three free-living days on a controlled low oxalate diet provided by the investigators, and concluded with 25 hours in a metabolic unit during which participants were given 131 mg C^{13} labeled oxalate with a controlled low oxalate diet.
Mean oxalate absorption for all 48 subjects was not different A vs. N (13.2% vs. 12.2%), but was greater for SF on A vs. N (14.9% vs. 12.4%, p = 0.02), and SF vs. NS on A (14.9% vs. 10.6%, p = 0.002). Mean 24 h total oxalate excretion (n = 48) was increased on A vs. N (0.61 $\pm$ 0.16 vs. 0.54 $\pm$ 0.11 mmol/d, p = 0.002), and during metabolic unit collections from 2 to 4 h and 6 to 8 h after oxalate load (0.10 $\pm$ 0.04 vs. 0.08 $\pm$ 0.03 mmol/d, p = 0.02; 0.06 $\pm$ 0.04 vs. 0.04 $\pm$ 0.02 mmol/d , p < 0.001, respectively). Urine volume, calcium and magnesium were not different over 24 h A vs. N, while 24 h citrate (60.4+22.5 vs. 56.3+20.1 mmol/d) approached significance (p = 0.06).
Though 24 h mean (n=48) TRI increased on A vs. N (0.64 $\pm$ 0.4 vs. 0.56 $\pm$ 0.3), significance was not reached (p = 0.08). TRI was greater for SF vs. NS on both A and N (0.76 $\pm$ 0.41 vs. 0.45 $\pm$ 0.32, p = 0.02, and 0.66 $\pm$ 0.31 vs. 0.42 $\pm$ 0.32, p = 0.008, respectively). Mean TRI was greater during metabolic unit collections A vs. N from 6 to 8 and 8 to 11 h after oxalate load (0.68 $\pm$ 0.63 vs. 0.49 $\pm$ 0.33, p 0.01 and 0.61$\pm$ 0.37 vs. 0.49 $\pm$ 0.37, p = 0.01, respectively). 19 of 48 participants were identified as responders, defined as increased 24 h oxalate excretion $\geq$ 10% on A vs. N. Eleven responders were SF and 8 NS. Responders (n=19) had increased 24 h TRI on A vs. N (0.76 $\pm$ 0.46, vs. 0.52 $\pm$ 0.29, p=.008).
Consumption of 1 gm AA twice a day results in a distinct bimodal response in this population, with 40% of individuals experiencing increases in 24 h urinary oxalate of $\geq$ 10% and 38% of individuals having increases in TRI of $\geq$ 20%. . As individual urinary oxalate response to AA supplementation is not predictable, supplementation should be considered cautiously by both SF and NS.

Disclosures: ***L. Massey****, None.*

M507

Importance of the Bone in Severe Absorptive Hypercalciuria. H. J. Heller, J. E. Zerwekh*, C. Y. C. Pak. Internal Medicine, Center for Mineral Metabolism and Clinical Research, UT Southwestern Medical Center at Dallas, Dallas, TX, USA.

Absorptive hypercalciuria (AH), a stone-forming condition in which calcium is excessively absorbed from the intestine, is paradoxically associated with low bone mass. We hypothesized that in patients with severe AH, bone formation is impaired and the relative excess bone resorption contributes to hypercalciuria. Nine stone-formers (age 28 to 53; no other causes of bone loss) underwent bone biopsy at the iliac crest after tetracycline labeling. They were placed on a stone-prevention diet for 3 weeks followed by baseline inpatient evaluation on a constant metabolic diet. On the same diet, alendronate (**A:** 10 mg/d X 2 weeks) was used to probe the contribution of excess bone resorption to urinary calcium.

Cancellous Bone Parameters	AH (6 men, 3 women)	AH (Z-score)	Normal Men (n=43)	Normal Women (n=42)
BV/TV, %	14.8±4.7	-1.0	20.3±7.3	24.5±7.2
Tb. Th, mcm	95±16	-5.2	147±7	140±23
OV/TV, %	0.82±1.03 (0.51±0.31)*	-0.7 (-1.1)*	1.47±0.85	1.93±1.33
Ob.S/BS, %	2.0±2.2 (1.4±0.8)*	-0.6 (-0.9)*	3.4±2.1	4.2±3.0
BFR/BS, $mcm^3/mcm^2/yr$	0.009±0.013 (0.005±0.004)*	-0.1 (-0.8)*	0.009±0.007	0.013±0.007
ES/BS, %	3.1±1.3	-1.0	6.4±3.3	6.5±3.0
Oc.S/BS, %	0.4±0.2	-1.5	1.1±0.4	0.6±0.7

*(not including single outlier with high bone formation)

Bone volume, by histomorphometry, was markedly decreased (equal to that of postmenopausal women with osteoporosis) and out of proportion to the osteopenia demonstrated by bone mineral densitometry. Relative to the historical controls, we found low bone turnover in AH patients and there was no evidence of osteomalacia. Baseline serum CTX correlated with change in urinary calcium after **A** (r=0.75) suggesting that bone resorption was an important source of urinary calcium. The mean fall in urinary calcium with **A** was 53 mg/d; however, results were dichotomous. Urinary Ca fell in responders by 112 mg/day (n=4), but there was a nonsignificant increase (5 mg/day, n=4) in nonresponders. In the nonresponders, the source of urinary calcium changed with increased input from the intestine (intestinal calcium absorption increased by dual stable isotope method) and decreased contribution from the bone (markers of bone resorption decreased). There was no change in markers of bone formation. We conclude that 1) severe AH is associated with impaired bone quality associated with low bone turnover and 2) treatment with **A** may lower urinary calcium and, by increasing intestinal calcium absorption while decreasing bone resorption, may improve calcium balance.

Disclosures: ***H.J. Heller****, None.*

M508

Balloon Kyphoplasty Is Effective in Deformity Correction of Osteoporotic Vertebral Compression Fractures. G. Voggenreiter*. Department of Trauma Surgery, University Hospital Mannheim, Ruprecht-Karls University of Heidelberg, Mannheim, Germany.

Introduction: Kyphoplasty (KP) is a minimally invasive treatment for osteoporotic vertebral compression fractures (VCFs) designed to address the fracture (Fx)-related pain and spinal deformity. Fx mobility has not been taken into account but it has to be considered when performing vertebral augmentation and when reporting and interpreting the significance of vertebral height restoration. The aim of this study was to determine the spontaneous reduction of deformity in prone position, the subsequent correction by the inflatable bone tamp (ITB), and the overall correction after deposition of the cement in VCFs.

Materials and Methods: 25 osteoporotic VCFs were treated in 20 patients (pt) by KP. Fractures (Fx) were classified according to Faciszewski et al. (JBJS 17:185, 2002). Radiographs were analyzed at six different time points. (1) Preoperative (preop) standing AP. During the KP procedure 4 consecutive radiographs were obtained (2) after placing the patient in prone, (3) after inflation of the ITB, (4) after deflation of the ITB, and (5) after deposition of the cement. (6) Standing AP radiographs were taken after the procedure (postop). All Fx were analyzed for improvement in sagittal alignment [Cobb angle; Kyphosis angle (Ka); anterior (Ha), medial (Hm), posterior vert. height (Hm)], complications and reduction of pain (VAS). Statistical analysis was performed by paired T-test and regression analysis.

Results: The morphology was wedge in 18 and crush in 7 Fx. Fx were acute in 17 and chronic in 3 pt. The mean duration of symptoms was 8.2 (range 1 to 24) weeks. Violation of the posterior vertebral cortex was present in 21 (84%) of VCFs with a mean narrowing of the medullary canal of 20 (range 0 to50)%. Placement of the pt in prone position displayed a significant spontaneous reduction in deformity with significant further reduction after inflation of the ITB (Table). After deflation and removal of the ITB and placement of cement no change occurred. Postop all parameters improved significantly compared to preop. Cement leaks occurred in 6 of 25 Fx. All pt subjectively reported immediate relief of their pain. The VAS-score significantly improved from 8.2 ± 2.0 preop to 2.1 ± 1.0.

Conclusion: The restoration of height in kyphoplasty is attributed to dynamic fracture mobility as well as to the expansion of the ITB.

Spinal deformity and vertebral body height during the kyphoplasty procedure

	preoperative	prone	Inflation of ITB	postoperative
Cobb angle	15.8 ± 7.9	9.6 ± 7.5	6.3 ± 7.4	10.3 ± 8.4
Ka	12.1 ± 5.5	8.0 ± 6.0	3.7 ± 5.0	4.8 ± 5.0
Ha	0.55 ± 0.22	0.67 ± 0.17	0.83 ± 0.15	0.79 ± 0.16
Hm	0.55 ± 0.18	0.65 ± 0.17	0.77 ± 0.15	0.76 ± 0.15
Hp	0.78 ± 0.13	0.85 ± 0.11	0.86 ± 0.10	0.86 ± 0.09

Disclosures: ***G. Voggenreiter****, Dr G. Voggenreiter 5.*

M509

An Effective Treatment for Localized Transient Osteoporosis: Intravenous Ibandronate Injection. J. D. Ringe. University of Cologne, Leverkusen, Germany.

Localized transient osteoporosis (LTO; bone marrow edema) is a rare condition characterized by acute onset of disabling bone pain, which typically occurs at a single skeletal site, without prior trauma. Although its etiology is unknown, LTO has been linked to pregnancy and prolonged periods of exercise. Current treatment options are limited in number and provide inadequate efficacy. Ibandronate (Boniva®) is a potent, nitrogen-containing bisphosphonate that produces significant increases in bone mineral density (BMD),[1,2] significant decreases in bone turnover and, most importantly, significant reductions in vertebral fracture risk[2] when given as an intermittent intravenous (i.v.) injection. Patients were enrolled into a 6-month, open label, observational study to investigate the effect of i.v. ibandronate on LTO. BMD at the lumbar spine and hip was measured at baseline and thereafter, at 1, 2, 3 and 6 months. Pain was assessed at the same time intervals using a visual analogue scale (VAS; 1-10). Initial treatment consisted of a 4mg i.v. ibandronate administration. An optional 2mg i.v. ibandronate injection was administered after 3 months. All participants received daily calcium (1g) and vitamin D (800IU) supplementation. Five men and seven women who had a pain duration of 2-15 weeks and mean age of 45 years (range: 29-61) participated in the study. The most frequently affected skeletal site was the hip (7/12 patients). At study onset, patients were classified as having normal BMD (n=4), osteopenia (n=5) or osteoporosis (n=3). The mean lumbar spine BMD T-score at baseline was -1.64 (range: -2.83 to +0.10). Following 6 months of treatment, the mean VAS pain score decreased from 9.3 (at baseline) to 0.5. The robust effect on pain after the initial administration of ibandronate was rapid in most patients, as indicated by individual VAS pain scores. Relative to baseline, mean lumbar spine BMD increased by 4% (range: -0.8 to +7.7% in the overall population) after 6 months of treatment. In participants with LTO in the hip region, the mean difference in BMD between affected and unaffected areas decreased from 10.1% to just 2.6% within 6 months. Improvements in mobility and QoL were also observed. In summary, i.v. ibandronate was shown to be highly effective in reducing pain, restoring BMD and improving mobility and QoL in patients with LTO.

1. Adami S, et al. Bone 2004;34:881-9.2. Ringe JD, et al. Osteoporos Int 2003;14:801-7.

Disclosures: ***J.D. Ringe****, F. Hoffmann-La Roche Ltd 5.*

M510

Skeletal Fluorosis and Instant Tea. M. P. Whyte[1], K. Essmyer*[2], F. H. Gannon[3], W. R. Reinus*[4]. [1]Division of Bone and Mineral Diseases, Washington University School of Medicine, St. Louis, MO, USA, [2]Center for Metabolic Bone Disease and Molecular Research, Shriners Hospitals for Children, St. Louis, MO, USA, [3]Orthopedic Section, Armed Forces Institute of Pathology, Washington, DC, USA, [4]Mallinckrodt Institute of Radiology, Washington University School of Medicine, St. Louis, MO, USA.

Skeletal fluorosis occurs in various regions of Asia where inferior quality "brick" tea is especially rich in fluoride. A middle-aged American woman with axial bone pain and osteosclerosis developed these features of skeletal fluorosis while reportedly drinking 1-2 gallons of double-strength instant tea each day throughout her adult life. Dual energy x-ray absorptiometry revealed bone density Z-scores of + 9.9 and + 1.7 in her lumber spine and hip, respectively. Urine fluoride levels were distinctly elevated, but corrected after she stopped consuming this beverage. Bone density, however, was unchanged 5 years later. No explanation for high bone mass other than fluorosis was disclosed. Ion-specific electrode studies of brand name instant teas, made regular strength in distilled water, showed substantial fluoride levels (up to 6.5 parts per million).

Bone densitometry is now commonly used to screen for low bone mass. We find that chronic ingestion of instant tea could account for skeletal fluorosis if prepared extra-strength or consumed in excess (e.g., hot climates) -- especially if made with fluoride-containing or contaminated water. Skeletal fluorosis from instant tea should be considered when dense, achy skeletons are encountered. Increasingly, antioxidant flavonoids and other components in tea are said to benefit health. We suggest that further understanding of the fluoride levels in different commercial preparations of instant tea is warranted.

Disclosures: ***M.P. Whyte****, None.*

M511

Effects of Thyroid Status on TNF-alpha and Vascular Endothelial Growth Factor (VEGF) Production by Peripheral Blood Mononuclear Cells (PBMCs): Potential Involvement in Bone Remodelling. S. Subesinghe*[1], E. Meade*[1], S. E. M. Clarke*[2], H. K. Mohan*[2], Y. T. Mak*[1], G. Hampson[1]. [1]Chemical Pathology, St Thomas' Hospital, London, United Kingdom, [2]Nuclear Medicine, Guy's Hospital, London, United Kingdom.

Thyroid hormone (T_3) plays an important role in skeletal remodelling. T_3 promotes bone resorption by stimulating the production of pro-resorbing cytokines by osteoblasts, although the exact mechanisms are still unclear. Cytokine production by mononuclear cells has been implicated in bone turnover. The aim of the study was to assess whether changes in thyroid status are associated with changes in cytokine production by PBMCs. We studied 11 subjects aged (mean [SEM] years) 53.1 [5.2] with newly diagnosed hypothyroidism (Group 1), 6 patients aged 46.5 [5.1] with Graves' disease undergoing radio-iodine ablation (Group 2) and a control group of 11 euthyroid subjects. Thyroid function tests were measured at baseline and at 6, and 12 weeks following thyroxine replacement in Group1, at baseline and at 6 weeks in Group 2 and the control group. Serum CTX and VEGF was also measured. PBMCs were isolated at the same time points and cultured for 4 days. TNF-alpha and VEGF were assayed in the conditioned medium by ELISA to assess the constitutive production of these cytokines. Euthyroid status was restored in Groups 1 and 2 following treatment (Group 1 baseline Free T_4 9 [0.9] pmol/L, Free T_3 3.1 [0.3] pmol/L, TSH 71.8 [14.5] m U/L, 6 weeks : Free T_4 14.9 [0.9], Free T_3 4.2[0.1], TSH 18.4 [6.5], 12 weeks : Free T_4 13.6 [1.2], Free T_3 4.0 [0.2], TSH 20 [8.1]. Group 2 baseline : Free T_4 20.7 [4.3], Free T_3 7.7 [1.6], TSH 0.9 [0.3], 6 weeks : Free T_4 12.8 [1.9], Free T_3 4.1 [0.45], TSH 5.8 [3.5]). Serum CTX increased following thyroxine replacement in Group1 (baseline : 0.2175 [0.027] ng/ml, 6 weeks : 0.3342 [0.036] p = 0.01, 12 weeks : 0.3737 [0.017] p = 0.02) and decreased in Group 2 following treatment (baseline : 0.5902 [0.018], 6 weeks : 0.4473 [0.147] p = 0.07). Serum VEGF increased significantly at 12 weeks in Group 1 only (baseline : 394 [56.2] ng/L, 6 weeks : 429 [59], 12 weeks : 487 [77] p = 0.01). TNF-alpha and VEGF in the cell culture supernatant increased at 6 weeks in Group 1 (TNF-alpha/protein ratio baseline : 0.38 [0.05], 6 weeks : 1.01 [0.22] p = 0.04, 12 weeks : 0.35 [0.06], VEGF baseline : 14.8 [3.2], 6 weeks : 21.7 [3.5] p = 0.06, 12 weeks : 20.2 [9.2]). A reduction in TNF-alpha was seen in Group 2 (baseline : 8.4 [4.05], 6 weeks : 0.6 [0.12] p = 0.001). VEGF production increased in Group 2 (baseline : 6.5 [2.75], 6 weeks : 11.6 [2.32] p = 0.04). No significant change in TNF-alpha or VEGF production was observed in the control group. These data suggest that PBMCs may play a role, at least partly, in mediating the effects of thyroid hormone on bone remodelling.

Disclosures: ***S. Subesinghe****, None.*

M512

Prevalence and Evaluation of Metabolic Bone Disease in Inflammatory Bowel Disease. B. Sinnott, A. Licata. Department of Endocrinology, Cleveland Clinic Foundation, Chicago, IL, USA.

The purpose of our study was to determine the prevalence and the degree of bone loss in IBD (Inflammatory Bowel Disease) patients, by evaluating bone mineral density and indices of bone and mineral metabolism in CD (Crohns Disease) and UC (Ulcerative Colitis) patients.

This was a retrospective study of data from patients seen at the metabolic bone clinic database at the Cleveland Clinic Foundation from 1995-2001. Our study consisted of 30 patients with CD and 18 patients with UC. Dual energy x-ray absorptometry was performed to determine Bone Mineral Density (BMD) at the lumbar spine and femoral neck. Serum calcium, phosphorus, parathyroid hormone (PTH), Vit D 25OH, Vitamin D1,25OH and urinary N-telopeptide cross linked collagen type 1 (NTX) levels were studied.

Based on WHO T score definitions of bone loss, in the IBD group as a whole, 46.8% had

osteopenia and 25.5% had osteoporosis at the lumbar spine; at the femoral neck, 54.4% had osteopenia and 30.4% had osteoporosis. CD patients had evidence of a higher prevalence of bone loss (combined osteopenia and osteoporosis values) at the hip and spine compared to UC patients. The prevalence of bone loss was greater at the femoral neck compared to the lumbar spine in both the CD and the UC groups. Secondary hyperparathyroidism, defined as a PTH level >55 pg/mL, was seen in one third of IBD patients. Fifty percent of our CD patients had secondary hyperparathyroidism, in contrast to 7% UC patients. IBD patients with secondary hyperparathyroidism had a more pronounced reduction in BMD at the femoral neck compared to patients with normal PTH levels. There was evidence of a negative correlation between PTH levels and femoral neck T scores (p = 0.06) and a positive correlation between PTH and lumbar spine Z scores, in the IBD group as a whole.

	UC	CD	
BONE MARKERS	Mean (SD)	Mean (SD)	P value
CALCIUM (mg/L)	9.5(0.8)	9.0(0.6)	0.042
NTX (nmol/mmol Cr)	30.7(12.4)	42.6(24.3)	0.057
PO4	3.7(0.9)	3.7(0.7)	0.88
PTH (pg/mL)	35.1(15.5)	57.7(27.1)	0.001
Vit D 25 OH (ng/mL)	30.0(18.7)	24.0(14.3)	0.36
Vit D 1,25 OH (pg/mL)	29.6(17.0)	52.4(20.4)	0.074

Metabolic bone disease is common in IBD. There is a higher prevalence of bone loss in CD patients compared to UC patients, with evidence of a higher prevalence of bone loss at the femoral neck compared to the lumbar spine in both groups. The mechanism of bone loss appears to be different in each disease entity. In contrast to UC, bone loss in CD appears to be mediated via Vitamin D deficiency and secondary hyperparathyroidism.

Disclosures: ***B. Sinnott****, None.*

M513

High Skin Blood Flow of the Feet in Patients with Severe Peripheral Neuropathy Is Associated with Elevated Foot BMD. K. A. Witzke[1], A. I. Vinik*[2]. [1]Health, Physical Education, Exercise Science, Norfolk State University, Norfolk, VA, USA, [2]Strelitz Diabetes Institutes, Eastern Virginia Medical School, Norfolk, VA, USA.

Peripheral neuropathy (PN) is a complication in type 2 diabetes which causes a variety of sensory, motor, and autonomic deficits. Charcot neuroarthropathy is a severe manifestation of PN which leads midfoot collapse and deformity, and is thought to indicate low bone mass. Patients with impending Charcot present with painless inflammation of the foot which resolves with progression of the condition. Using a laser doppler system (Perimed Periflux 5000) to quantify skin blood flow, we have observed elevated skin blood flow in patients with impending Charcot, which we believe may be indicative of an attempt to heal microtrauma and microfractures. Using a novel DXA technique to measure foot BMD (Lunar DPX-IQ), we sought to examine the relationship between foot BMD and skin blood flow in patients with severe PN. A retrospective analysis of 52 foot bone scans (28 female feet, 24 male feet) and 38 skin blood flow curves from 30 different patients (age 66.5 y Â±10.5y) was conducted. Each foot was classified into one of three groups based on skin blood flow data (BF) or the physician's notes if BF was not available: established Charcot neuroarthropahy (C), no Charcot (N), and transitional (T), characterized by BF > 15,000 BF units and/or presence of a "hot foot". A Standard Least Squares linear regression model revealed a significant gender ($p<0.0001$) and group effect ($p<0.017$) on foot BMD ($r2 = 0.38$, $p< 0.0001$). Specifically, the transitional (T) group displayed significantly HIGHER foot BMD and BF than the other two groups, which were not significantly different from one another. It appears that the presence of severe peripheral neuropathy accompanied by high skin BF is not only indicative of impending Charcot neuroarthropathy, but also a transient increase in bone density. Although foot inflammation has previously thought to accompany an increase in osteoclastic resorption, it may actually indicate increased bone formation in an attempt to heal microtrauma. Prospective studies should clarify the role of blood flow in bone dynamics of Charcot development and the events which immediately follow.

BMD and Skin Blood Flow for C, N, T

		Foot BMD (g/cm2)	Skin Blood Flow (BF units)
Charcot (C) (n=8)	Male	.688+/-.050	5120+/-0
	Female	.560+/-.045	17798+/-0
Non-Charcot (N) (n=19)	Male	.692+/-.076	12343+/-348
	Female	.610+/-.053	10986+/-8624
Transitional (T) (n=25)	Male	.825+/-.078*	27706+/-951**
	Female	.646+/-.092*	23763+/-5215**

Disclosures: ***K.A. Witzke****, None.*

M514

Osteopontin Mediated Regression of Ectopic Calcification. R. M. Rajachar*, E. Tung*, C. M. Giachelli*. Bioengineering, University of Washington, Seattle, WA, USA.

Ectopic calcification is the leading cause of failure in bioprosthetic heart valves. The purpose of this study was to quantitatively determine the details of an ectopic mineral regression mechanism in vascular tissues by attempting to create an *in vivo* calcification regression rescue model. Osteopontin (OPN) is thought to regulate mineralization by inhibiting apatite crystal growth and promoting osteoclast function. OPN is not found in normal arteries, but is abundant at sites of vascular calcification. In our lab we have been able to show that OPN acts as an inducible inhibitor of vascular calcification. We have also developed a subcutaneous mouse implantation model, in which we have been able to show significant increases in calcification of gluteraldehyde-fixed implants in OPN deficient mice (OPN-/-). More interestingly, OPN+/- mice showed early calcification of implants with subsequent regression that correlated with the accumulation of OPN. In these studies we have been able to show OPN mediated inhibition and regression of ectopic calcification, details of the mechanism however still need to be determined. Building on these previous experiments, we tested several candidate materials to use as an *in vivo* implantation substrate to measure resorption pitting, a physical marker of mineral resorption. We induced *in vitro* osteoclast formation and resorption with bone marrow derived macrophages stimulated with M-CSF and RankL, and were able to detect resorption pitting on polished bovine cortical bone, dentin and OPN-coated hydroxyapatite (HA) substrates using scanning electron microscopy (SEM). Of the three materials we achieved maximum osteoclast formation on polished bovine cortical bone, but more importantly we also detected osteoclast formation on OPN-coated HA discs. Using the pure mineral HA discs in our model, we may be able to quantitatively measure mineral regression by local verification of resorption pitting with SEM. We are currently testing OPN-coated HA discs as a substrate for our *in vivo* calcification regression rescue model.

Disclosures: ***R.M. Rajachar****, None.*

M515

Frequency of Sequestosome 1 (SQSTM1) Mutations in Hereditary and Sporadic Paget's Disease of Bone in the United States. E. C. Rhodes*[1], T. L. Johnson-Pais[2], J. Wisdom*[1], E. Lin*[3], H. G. Bone[4], F. R. Singer[3], R. J. Leach[1]. [1]Department of Cellular and Structural Biology, University of Texas Health Science Center, San Antonio, TX, USA, [2]Department of Pediatrics, University of Texas Health Science Center, San Antonio, TX, USA, [3]John Wayne Cancer Institute, St. John's Health Center, Santa Monica, CA, USA, [4]Michigan Bone and Mineral Clinic, Detroit, MI, USA.

Paget's disease of bone (PDB) is a metabolic bone disease characterized by excessive bone resorption and formation due to overactive osteoclasts. This disease is distinguished by focal areas of increased and disorganized bone turnover, resulting in bone pain and fractures. One to 3 million Americans have PDB, making it the second most common metabolic bone disease. Classic familial PDB is characterized by late onset, autosomal dominant segregation, genetic heterogeneity and incomplete penetrance. Seven genetic loci (PDB1-PDB7) have been reported for late onset PDB. However, PDB3 is the only locus where a gene, SQSTM1, has been identified. S*equestosome 1* (SQSTM1/p62) plays a key role in osteoclast differentiation through its involvement in the RANK signal transduction pathway and has been implicated in both sporadic and hereditary PDB. A total of 6 mutations have been reported in SQSTM1 and all affect the ubiquitin binding domain. Previous studies suggest that the SQSTM1 mutation, P392L, is responsible for 46% of familial and 16% sporadic PDB in French-Canadians and 19% of familial and 9% of sporadic PDB in patients of British origin.

The purpose of this study was to determine the mutation frequency of SQSTM1 amongst PDB patients in the United States. Blood samples were obtained from a total of 60 PDB patients, 33 sporadic, 21 hereditary and 5 familial. We have defined hereditary PDB patients as having a documented family history and familial patients as having a suspected but not documented family history. DNA was extracted from blood samples and PCR and sequencing was performed on exons 7 and 8 of SQSTM1. Mutations were found in 8/21 (38%) of hereditary patients, 0/5 (0%) of familial patients and 0/33 (0%) of sporadic patients. P392L mutations were found in four hereditary PDB patients representing both Caucasians and African Americans.

These preliminary findings suggest a role for SQSTM1 in hereditary PDB. Interestingly, our study finds no evidence that SQSTM1 is implicated in sporadic PDB in the United States. We are in the process of analyzing more blood samples from PDB patients the United States. The information we obtain will help determine the role of SQSTM1mutations in PDB in the United States population.

Disclosures: ***E.C. Rhodes****, None.*

M516

Pagets Disease in the Black Community in South East London. C. Moniz[1], R. Chandra*[1], B. Bowden*[2], T. Mangion*[1]. [1]Clinical Biochemistry, Kings College Hospital, London, United Kingdom, [2]Medical School, Guys Kings Thomas, London, United Kingdom.

Paget's cases described are predominantly in caucasians and epidemiological studies suggest a decrease in prevalence. Changing migratory patterns of communities and alternative diagnostic tests warrants a review. Using biochemical testing of requests from patients over age 50 yrs, seen in primary care for non-bone diseases, who had an isolated raised total alkaline phosphatase (ALP), in the presence of a normal liver function profile (AST, GGT) were further investigated for a possible metabolic bone disease. Those with a reported diagnosis of carcinoma, diabetes, osteomalacia or recent fracture, known causes of raised ALP, were excluded. Following consent by the general practitioner and patient to further investigate, a repeat blood test, bone scintigraphy and where appropriate X rays were performed prior to a clinical consultation. Over a period of 24 months, 152 cases were identified with an isolated raised ALP with a cut-off of >200 IU/L (ref range upto 120 IU/L). 88 had a explainable diagnosis and 64 cases were further investigated of which 52 (34%) had Paget's disease of bone confirmed by scintigraphy and appropriate X-Rays of affected sites. Of the remaining 12, two had unrecognised osteomalacia, 1 had primary hyperparathyroidism, 1 had unrecognised diabetes and 8 were unexplained. Of the Paget's cases 28 were female, mean age (yrs) was 76 (60-89) and 24 were male, mean age 79.8 yrs (range 67-89). The mean ALP female to male ratio was 265:291 IU/L and symptoms were in 91: 96% of cases. The commonest site affected in females were pelvis>skull>limbs> spine, whereas in males the pattern was different: pelvis> spine>limbs> skull. Ten of the 52 cases (19%) were Black, either of West Indian or West African origin, in a local community where the black to white ratio is 1:4 and the prevalence of the disease appears to be high in this ethnic minority group. Most of these patients had repeated blood tests in the past, but none had Paget's as a primary diagnosis and the findings were serendipitious. Pagets may not be decreasing in the community and reported low rates of diagnosis could be due to low thresholds for identification. Appropriate laboratory testing and recognition of findings has helped to diagnose a disease, which hitherto has gone unrecognised.

Disclosures: ***C. Moniz****, None.*

M517

Severe Hypocalcemia in a Patient with Paget's Disease of Bone (PD) Treated with Bisphosphonate. H. E. Whitson*[1], B. Lobaugh[2], K. W. Lyles[2]. [1]Medicine, VA Medical Center, Durham, NC, USA, [2]Duke University Medical Center, Durham, NC, USA.

A 53yo African-American woman with polyostotic PD diagnosed twelve years earlier reported pain in her skull, right arm, and left hip. She had never received any treatment for her PD. Physical exam showed obesity, BMI of 46, enlarged skull with a warm, prominent area near the hairline, limited range of motion of her spine. PD was confirmed with bone scan and radiographs, and audiometry confirmed hearing loss. Laboratory studies: alkaline phosphatase 1899 U/L [30-135], calcium 9.3 mg/dL [8.7-10.2], PTH 14 pg/mL [12-72], creatinine 0.8 mg/dL [0.7-1.4], and 25(OH) vitamin D 13ng/mL [8-38]. She received vitamin D (100,000 IU daily) and serum 25(OH) vitamin D level rose to 19ng/mL. She was enrolled in a blinded, randomized, placebo-controlled trial of PD in which she was allocated to receive oral risedronate 30mg daily for two months.Ten days after enrollment, she developed altered mental status, slurred speech, and myoclonus. Serum calcium was 5.4 mg/dL with an ionized calcium of 0.63 mmol/L [1.12-1.32]. She was hospitalized in an ICU and received IV calcium and supportive care. She was discharged eight days later in good condition with normal serum calcium levels.

We hypothesize that hypocalcemia resulted from PTH suppression caused by longstanding PD associated with elevated bone remodeling. PTH suppression is suggested by the low PTH level (14 pg/mL) in the setting of a low 25(OH) vitamin D level (13 ng/mL), which should cause a higher PTH level. We believe that Risedronate blocked bone resorption, but osteoblast activity continued without sufficient parathyroid reserve to maintain normal serum calcium. The patient fully recovered, but she continued to suffer from symptomatic PD. She received s.c. calcitonin 50 units 5 days per week for 6 weeks (30 doses) then risedronate 5mg every other day for a month (16 doses), then 30mg every other day for two weeks (5 doses), then 30mg daily for 2 months (55 doses). Throughout this course, serum calcium levels were normal and most recent laboratory findings reveal calcium 9.3 mg/dL, ionized calcium 1.22 mmol/L, PTH 65 pg/mL, and alkaline phosphatase 599 U/L. She reports that her current pain level is 0/10 on most days and never higher than 3.5/10. Reports suggest that bisphosphonates may cause hypocalcemia in patients with PD and hypoparathyroidism, as well as in patients with vitamin D deficiency (*JBMR* Stuckey B 2001, *NEJM* Rosen C 2003). This case suggests that patients in states of high bone turnover from PD may be at risk due to suppressed parathyroid function resulting in relative hypoparathyroidism.

Disclosures: ***K.W. Lyles****, Procter & Gamble 2, 5, 8; Novartis 2, 5, 8.*

M518

Mutations of *p62/Sequestosome1* Gene (*SQSTM1*) in an Italian Series of Patients Affected by Paget's Disease of Bone (PDB). A. Falchetti*[1], F. Marini*[1], F. Del Monte*[1], D. Strigoli*[1], A. Gozzini*[1], A. Tanini[1], L. Masi[1], M. Di Stefano*[2], G. Isaia*[2], G. B. Rini*[3], M. L. De Feo*[4], S. Maddali*[5], M. Matucci Cerinic*[1], M. Benucci*[6], G. Marin*[6], A. Matucci*[6], V. Ferioli*[7], F. M. Ulivieri*[7], S. Giannini[8], L. Sartori[8], V. Braga*[9], S. Adami[9], L. Di Matteo*[10], M. L. Brandi[1]. [1]Internal Medicine, University of Florence, Florence, Italy, [2]Internal Medicine, University of Turin, Turin, Italy, [3]Internal Medicine, University of Palermo, Palermo, Italy, [4]Azienda Ospedaliera Careggi, Florence, Florence, Italy, [5]Critical Care, University of Florence, Florence, Italy, [6]Rheumatology Unit, Asl 10, Florence, Florence, Italy, [7]Servizio Di Radiologia, Ospedale Maggiore Di Milano Ircss, Milan, Italy, [8]Medical and Surgical Sciences, Clinica Medica 1, University of Padua, Padua, Italy, [9]Rheumatology Unit, Valeggio S/M, University of Verona, Verona, Italy, [10]Division of Rheumatology, University of Pescara, Pescara, Italy.

PDB is a genetically heterogeneous disorder and mutations in p62/*SQSTM1* gene on chromosome 5q35-qter account for most of the sporadic and familial forms of PDB reported in literature. Exons 7 and 8, encoding the ubiquitin protein-binding domain, represent a mutational hot spot area. A study on French Canadian PDB patients identified the P392L mutation at exon 8 and the same mutation has been also reported, together with two different mutations, in 18 PDB families of British descendent: exon 8 P392L in 13 families (19.1%), exon 8 T insertion at position 396 in 4 families (5.8%) and a splice donor site mutation in intron 7 in 1 family (1.5%). Moreover, P392L mutation has been reported in 8.9% of the sporadic PDB cases. Recently, 3 novel mutations have been also reported in 4/5 PDB families from the United States:1210delT, 1215delC at exon 8 and a C to T transversion (P387L) at exon 7. We previously reported mutations of exon 7 and exon 8 of *SQSTM1* gene in 62 sporadic Italian PDB patients: P392L was found in only 1/62 PDB patients. Moreover, in 2 different patients we found two novel mutations, A>G and G>A transitions, at exon 8 both consisting of amino acid changes, respectively M404V and G425R substitutions. DNA analysis from 100 healthy control subjects failed to detect such mutations. Then, we extended the mutational analysis to other 132 PDB patients, reaching a total of 194 PDB subjects. We detected the following mutations: P386L at exon 7, P392L, S396A, M404V and G425R. Our findings, compared to those on predominantly British descent PDB patients, suggest an involvement of *p62/SQSTM1* gene of 7.2% vs. 8.9% in the pathogenesis of sporadic and familial Italian PBD cases, confirming the important role that *p62/SQSTM1* gene may play in conferring a genetic susceptibility to develop PDB.

Disclosures: ***A. Falchetti****, None.*

M519

Mutations of *p62/Sequestosome1* Gene (*p62/SQSTM1*) in 4 Italian Families Affected by Paget's Disease of Bone (PDB). A. Falchetti*[1], M. Di Stefano*[2], F. Marini*[1], F. Del Monte*[1], L. Masi[1], R. Imbriaco*[1], A. Tanini[1], N. Fossi*[1], S. Carbonell Sala*[1], L. Guazzini*[1], G. Leoncini*[1], G. Isaia[2], M. L. Brandi[1]. [1]Internal medicine, University of Florence, Florence, Italy, [2]Internal medicine, University of Turin, Turin, Italy.

We performed mutational analysis of *p62/SQSTM1* gene in 194 PDB Italian cases. Consequently, it has been possible to identify 4 Italian families affected by PDB (F1, F2, F3 and F4). Specifically, we analyzed 21 members from F1, originating from Central Italy, and we found 11 M404V mutant carriers, 5 of which with the clinical diagnosis of PDB; 10 members from F2, originating from Lucania (Southern Italy) and we found 6 G425R mutant carriers, 2 of which with the clinical diagnosis of PDB; 7 members from F3, originating from Northern Italy, where we found 6 insT;E396X mutant carriers, 3 of which with the clinical diagnosis of PDB; and 5 members from F4, originating from Lucania (Southern Italy), where we found 3 G425R mutant carriers, 1 of which with the clinical diagnosis of PDB. Interestingly, F2 and F4 families, exhibiting the same G425R mutation, originate from Lucania (Southern Italy), nearby Potenza, the capital town of this small region (total surface equals to 3,3% on the national territory, 9.992 squared Km), strongly suggesting the existence of a founder effect. Actually, only for the M404V mutation (F1) has been possible to hypothesize a genotype/phenotype correlation. Twelve subjects were potentially affected and all the 5 clinically ascertained PDB cases carried out the M404V mutation and exhibited the polyostotic form of PDB, but one patient with a X-rays assessed monostotic localization. Six unaffected subjects showed to bear the M404V mutation, representing asymptomatic gene carriers. The presence of these mutations at exons 7 and 8 of the *p62/SQSTM1* gene in sporadic and familial Italian PDB patients confirms the evidence of a clustered mutation area at this level in this disorder, supporting the role of the UBA domain in the biological properties of p62/SQSTM1 protein. Biochemical and clinical evaluation of the asymptomatic mutant carriers from the four families have been performing. *p62/SQSTM1* gene analysis is at the moment extended to other sporadic Italian cases and to first-degree relatives of patients in order to detect new genetic carriers in potentially familial forms of PDB and to study the co-segregation of such DNA variants with the PDB phenotype. All together these studies could open new possibilities in the prevention and therapy of PDB and of other metabolic bone disorders.

Disclosures: ***A. Falchetti****, None.*

M520

Absence of Evidence of Paget's Disease of Bone in Subjects who Harbor Sequestosome 1 Mutations. F. R. Singer[1], E. Lin*[1], D. S. B. Hoon*[2], T. L. Johnson-Pais*[3], R. J. Leach*[3]. [1]Skeletal Biology, John Wayne Cancer Institute, Santa Monica, CA, USA, [2]Molecular Oncology, John Wayne Cancer Institute, Santa Monica, CA, USA, [3]Department of Cellular and Structural Biology, University of Texas Health Science Center, San Antonio, TX, USA.

Familial Paget's disease of bone has been found to be associated with six unique mutations in the sequestosome1 (SQSTM1) gene in some families with Paget's disease. We have found this to be the case in 5 families of heterogeneous ethnic background. The mutations include P389L, P392L, 1210delT and 1215delC. However, we have observed that some of the family members who have the family-specific mutations do not have discernable Paget's disease. In each of the five families at least one individual was demonstrated to have a SQSTM1 mutation, no physical evidence of Paget's disease and no elevation of serum alkaline phosphatase activity (18 subjects). Nine of the subjects had a technetium-99m MDP bone scan and in no case was there evidence of abnormal uptake indicative of Paget's disease. The patients were up to 63 years of age with many ranging in age from 30 to 50 years. These observations suggest that SQSTM1 mutations in members of families with Paget's disease are not sufficient to cause Paget's disease, but that the mutations confer susceptibility to the disease. It is likely that environmental factors such as viral infections or additional somatic events may be important in the pathogenesis of the disease.

Disclosures: ***F.R. Singer****, None.*

M521

Alendronate in the Treatment of Low Bone Mass in Steroid-treated Boys with Duchenne Muscular Dystrophy. G. A. Hawker[1], R. Ridout[2], V. A. Harris*[3], C. C. Chase*[4], L. F. Fielding*[4], W. D. Biggar*[5]. [1]Osteoporosis Clinical Research Program, Women's College Campus of Sunnybrook & Women's College Health Sciences Centre, Toronto, ON, Canada, [2]Toronto Western Hospital, University Health Network, Toronto, ON, Canada, [3]Bloorview Mac Millan Children's Centre, Toronto, ON, Canada, [4]Osteoporosis Clinical Research Program, Women's College Campus of Sunnybrook and Women's College Health Sciences Centre, Toronto, ON, Canada, [5]Paediatrics, Bloorview Mac Millan Children's Centre and The Hospital for Sick Children, Toronto, ON, Canada.

The objective of this study was to examine alendronate's side effect profile and affect on bone mineral density (BMD) in deflazacort-treated boys with Duchenne Muscular Dystrophy (DMD) and low BMD.

The study design was a before-after trial. Participants were recruited from the Neuromuscular Clinic at Bloorview MacMillan Children's Centre in Toronto, Canada between 1999 and 2000. The study included all consenting boys with DMD who had z-scores < -1.00 (spine and/or total body) and in whom BMD testing was feasible. Boys received 0.08 mg/kg/day alendronate orally with daily calcium 750 mg and vitamin D 1,000 I.U. BMD, height, weight, physical activity, Tanner stage, and adverse effects were followed for two years.The main outcome measure was BMD z-scores at the lumbar spine (L1 - L4) and total body.

Of the 42 eligible boys assessed, 23 had low BMD; for 16/23, future BMD testing was feasible. Mean age was 10.8 years (6.9 - 15.6 years). Mean baseline z-scores at the total body and spine were -0.80 and -1.94, respectively. At two years, mean z-scores were unchanged. Furthermore, alendronate response varied by baseline age. In multivariable analysis, improvement in total body and spine z-scores was associated with younger age at baseline (p=0.01 for both). Based on these results we concluded, in deflazacort-treated boys, alendronate had a positive effect on BMD z-scores; the effect was greatest when given early in the course of disease.

Disclosures: ***R. Ridout****, None.*

M522

Functional Analysis of OPG Mutations That Cause Idiopathic Hyperphosphatsia; Relationship Between Genotype and Phenotype. C. A. Middleton-Hardie, H. R. Cundy*, I. R. Reid, J. Cornish, T. F. Cundy, D. Naot. Medicine, University of Auckland, Auckland, New Zealand.

Familial Idiopathic Hyperphosphatasia (FIH) is a rare, congenital bone disease characterised by increased bone turnover. There is considerable phenotypic variation: from presentation in infancy with severe progressive deformity, through to presentation in late childhood with minimal deformity. The link between mutations in OPG and FIH has recently been established by genetic studies. Eight of the ten mutations reported are restricted to single families. The aim of our study was to investigate any relationship between the mutant genotypes, OPG production and function and the corresponding patient's disease severity. The patients were grouped into mild, intermediate and severe phenotype according to clinical, biochemical and radiographic data**.**

We have produced constructs corresponding to 4 identified mutations in the cysteine-rich domain of OPG: OPGΔD182 has a deletion of an aspartate residue, OPGC65R and OPGC87Y have missense mutations resulting in substitution of cysteine residues, and OPGF117L has a missense mutation causing the substitution of a phenylalanine residue. When expressed in HEK293 cells, the constructs have similar levels of transcription, but different levels of OPG protein are secreted into the medium. While OPGF117L has comparable expression to wtOPG, OPGC65R and OPGC87Y have much lower yields, with OPGΔD182 having an intermediate yield. We are using confocal microscopy to follow the expression of wtOPG and the OPG mutants to ascertain if an increased level of intracellular degradation is responsible for the reduced yield of OPGΔD182, OPGC65R and OPGC87Y. For functional analysis of the mutant proteins we are utilising the surface plasmon resonance technology of BIAcore, to investigating the RANKL-binding ability of all the OPGmutants. Also, as we have previously shown OPGΔD182 has reduced activity in the murine bone marrow osteoclastogenesis assay, we are investigating the ability of the OPG mutants to inhibit osteoclast formation.

Our investigations show that missense mutations in cysteine residues, predicted to cause major disruption to the structure of OPG, significantly lower the levels of OPG secretion from the cell. These mutations were associated with a severe FIH phenotype.

Disclosures: ***C.A. Middleton-Hardie****, None.*

M523

Uncoupling of Bone Formation and Resorption Following a Thermal Injury. J. Shea, S. Miller. Radiobiology, University of Utah, Salt Lake City, UT, USA.

Severe burns result in long-term growth retardation in children and osteopenia among children and adults. The development of osteopenia is accompanied by profound disturbances in calcium metabolism including: hypocalcemia, hyper and hypoparathyroidism, and low vitamin D levels. The first goal of the current study was to determine if there were alterations to bone formation, bone resorption, and serum parathyroid hormone (PTH) levels 3, 5, and 7 days post burn. The second goal was to examine the progression of the skeletal changes in the burn group during the same time frame.

Adults male Balb/c mice at 3 months of age were divided into time control, sham-burned, and burned groups with 8 animals per group. The time controls were included on days 3 and 7. A 20% total body surface area burn was applied following a previously published protocol. Calcein, was given to all groups a day before the thermal injury and tetracycline was given one day prior to necropsy. The left proximal tibia was embedded in methylmethacrylate and utilized for dynamic histomorphometric analysis. The serum was also taken for subsequent PTH analysis (Immutopics Inc., San Clemente, Ca). Statistics were done using an ANOVA followed by a Tukey HSD post hoc test for days 3 and 7 and a t-test for day 5.

There were no differences between the time control, sham-burned, and burned groups on day 3 at the proximal tibia in measures of percent double label (p=0.49), mineral apposition rate (p=0.74), bone formation rate (p=0.59), or percent eroded surface (p=0.42). On both days 5 and 7 the burn group had reduced measures of percent double label (p=0.0005, p<0.0001 respectively) and bone formation rate (p=0.002, p=0004) and increased percent eroded surface (p=0.01, p=0.003) compared with the time control and sham-burned groups. PTH was significantly elevated in the burn groups on days 3, 5, and 7 compared with the time controls and sham-burned groups (p<0.0001, p=0.04, p=0.0002). Comparisons of the burn groups revealed that Day 5 and 7 were less than day 3 for measures of percent double label (p=0.0005) and bone formation rates (p<0.0001) and higher for percent eroded surface (p=0.01). PTH levels were not different in the burn groups on days 3,5, or 7 (p=0.73).

The current study suggests that the uncoupling of bone formation and resorption occur in less than a week in the cancellous bone of the proximal tibia in a thermal injury mouse model. These skeletal changes were preceded by an increase in PTH. The increase in PTH along with the uncoupling of bone remodeling might be a response to disturbances in calcium regulation, perhaps due in part to the reported disregulation of the calcium receptor.

Disclosures: ***J. Shea****, None.*

M524

Serum Osteoprotegerin (OPG) and Receptor Activator of Nuclear Factor κB Ligand (RANKL) in Healthy United States Children and in Children with Cystic Fibrosis. H. E. Price*, C. B. Langman, A. Arwady*, S. McColley*, K. Lyons*. Department of Pediatrics, Feinberg Medical School, Northwestern University, Chicago, IL, USA.

The morphogenesis and remodeling of bone requires the synthesis and ossification of bone matrix by osteoblasts and its coordinated resorption by osteoclasts. Osteoprotegerin (OPG), as an inhibitor of the differentiation and activation of osteoclasts is balanced by RANKL, which promotes active osteoclast resorption and embryogenesis. Abnormalities in the balance of RANKL/OPG system may lead to disturbances of bone that underlie osteoporosis, Paget's disease, bone loss in metastatic cancers, and rheumatoid arthritis. The purpose of this study was to measure serum OPG and RANKL in healthy US children to establish a normal range, and then compare the established normal range to children with cystic fibrosis (CF), a disease in which bone density is reduced. OPG and RANKL were measured in the serum of 80 healthy children (37 males, 43 females). The age range was 1-17 years (X=10.3 y), and self-reported Tanner stages ranged from 1 to 5. Seven children were African-American, three were Asian; the remainder were Caucasian. Levels of OPG and RANKL were determined using an enzyme immunoassay (ALPCO Diagnostics, Windham, NH). The assays were performed in duplicate and results are reported in pg/mL. To determine a normal reference range in children, the mean and standard deviation of measured OPG and RANKL values were calculated ($X \pm \sigma$ = 69.1 ± 20.3 and 7.5 ± 8.4 pg/mL, respectively). The normal range was assigned as the mean ± 2SD, resulting in normal ranges for OPG and RANKL = 25.8-109.7 and 0-24 pg/mL, respectively. There were no differences in healthy children of either OPG or RANKL based on ethnicity or pubertal status within a narrow age range. However, there was an inverse relationship between measured OPG and chronological age. Serum OPG and RANKL were measured in 20 children with CF (8 males, 12 females), age range 6-14 years (X=8.6 y), all Tanner stage 1, and whose mean DXA lumbar BMD Z-score was -0.22. There were increases in RANKL (X=17.5 pg/mL, p<0.01), and decreases in OPG (X=56.3 pg/mL, p<0.01) when compared to healthy children. As a result, the RANKL/OPG ratio was elevated. In conclusion, we established a normal value set for OPG and RANKL in the blood of US children, and have applied it to understand better the mechanisms of bone disease in children with CF. These data support our hypothesis that inappropriate osteoclast activation occurs in children with cystic fibrosis, leading, in part, to diminished bone mass. We will evaluate the blood OPG/RANKL ratio in the therapeutic response to recombinant human growth hormone and/or anti-resorptive therapies in the care of the bone disease in such children.

Disclosures: ***H.E. Price****, None.*

M525

Skeletal Assessment In Duchenne Muscular Dystrophy Using New DXA Pediatric Tools. J. D. Landoll*[1], H. S. Barden*[2], W. King*[3], J. T. Kissel*[3], K. G. Faulkner*[2], V. Matkovic[1]. [1]Bone and Mineral Metabolism Laboratory, The Ohio State University, Columbus, OH, USA, [2]GE Healthcare, Madison, WI, USA, [3]Department of Neurology, The Ohio State University, Columbus, OH, USA.

Dual-energy x-ray absorptiometry (DXA) provides rapid, low dose assessment of total body bone in children, but the areal measurement of bone mineral density (BMD, g/cm^2) is influenced by body size. Recently, GE Healthcare introduced software with pediatric body-size ratios (height for age, bone area for height, and bone mineral content (BMC) for bone area) for assessing bone status in children with developmental disabilities.

We assessed bone status using DXA (Lunar Prodigy) in 22 male children age 6 to 17 y (mean 11.5 y) with Duchenne Muscular Dystrophy (DMD). Children were evaluated for BMD, height for age, BMC for bone area, and bone area for height Height-for-age Z-scores were calculated using USA Center for Disease Control data. BMC-for-area and area-for-height Z-scores were calculated from normal male children in the Lunar pediatric database with SEEs that varied with age.

Subjects with DMD had a substantial deficit in BMD (Z= -1.3), but were normal for BMC for bone area (Z= 0.04). The BMD deficit appeared to result from short stature (height-for-age Z = -1.2) and small (narrow) bone area for height (Z= -2.8). Both BMD and height-for-age Z-scores decreased with subject age, mirroring the progressive nature of this disease.

The head region contribution to total body BMC in normal subjects decreased from 45% at age 5 to 15% at age 19 years. Z-scores for total body BMC for area with and without the head were 0.0 and -1.6, respectively (p<0.001). Z-scores for BMD for age with and without the head were -1.3 and -2.2, respectively (p<0.001). Head BMC for area and BMD for age were positive, Z = 0.5 and 0.3, respectively.

Adjustments for body size provide a more complete representation of bone status than BMD alone in children with developmental abnormalities. Exclusion of the head region may enhance the ability of the BMC-for-area ratio to detect deficits at total body and regional sites. Total body BMD and BMC-for-area Z-scores including the head were significantly higher than Z-scores excluding the head. DMD boys had negative Z-scores for total body and regional BMD, as well as for BMC-for-area Z-scores for arms, legs and, trunk, but not the head.

Total body and regional Z-scores for boys with DMD

	BMC for Area	BMD for Age	Bone Area for Height	Height for Age
Total Body with Head	0.0	-1.3	-2.8	-1.2
Total Body without Head	-1.6*	-2.2*		
Arms	-0.4	-1.7		
Legs	-0.6	-2.6		
Trunk	-2.1	-1.8		

* With and without head difference significant at p<0.001

Disclosures: ***V. Matkovic****, None.*

M526

Withdrawn

M527

Vitamin D Insufficiency Is Common Among Pediatric Subjects Participating in an Osteoporosis Treatment Trial: A Glaser Pediatric Research Network Study. E. von Scheven*[1], C. M. Gordon*[2], K. Gallagher*[3], M. Wertz*[1], L. Bachrach[4]. [1]Pediatrics, UCSF, San Francisco, CA, USA, [2]Pediatrics, Harvard, Boston, MA, USA, [3]Pediatrics, UCLA, Los Angeles, CA, USA, [4]Pediatrics, Stanford, Stanford, CA, USA.

Background: We screened subjects with inflammatory disorders for a double-blind placebo-controlled trial of alendronate at four US University Hospitals. Eligibility included baseline vitamin D (25OHD) levels > 20 ng/mL.

Objective: To determine the prevalence of 25OHD deficiency and hyperparathyroidism in pediatric patients at risk for osteoporosis secondary to inflammatory disease and glucocorticoid therapy.

Methods. Sixty-one patients (69 % female, 34% Caucasian, 25% Hispanic, 21% Asian, 8% African-American and 12 % mixed), age 13.7 ±3.5 yrs, with inflammatory disease (30% lupus, 28% dermatomyositis, 13% Crohn's, 11% vasculitis, 7% systemic JRA, 2% mixed connective tissue disease) were consented and screened. Inflammatory disease duration was 0.7 - 12 yrs (mean 4.3). Medications included biologic agents (41%), cyclophosphamide (18%), Cellcept (13%), Imuran (7%), and Azacol, Azulphidine, 6MP, Thalidamide, and MTX or Arava (each 5%). Forty-eight (77%) of subjects were taking systemic steroids (mean prednisone dose 0.22 mg/kg/d [SD 0.24]) at screening. Only 25 % of subjects were taking vitamin D supplements (mean dose for those taking was 445 IU/d ±122). Vitamin D level (competitive protein binding radioassay) and intact PTH concentration (immunochemiluminometry) were determined at a commercial laboratory.

Results. Serum 25OHD levels ranged from 0-38 ng/mL (mean 20.7) and were <20 ng/mL in 46% of subjects. PTH concentration ranged from 0-70 pg/mL (mean 33.0). Increased 25OHD levels were associated with younger age (beta -1.0, p= 0.001), vitamin D supplements (beta 0.01, p=0.009) and lower PTH (beta -0.49, p=0.03). 25OHD levels did not correlate with underlying diagnosis, ethnicity, disease duration, or current prednisone dose. Twelve subjects diagnosed with vitamin D insufficiency were supplemented with varying vitamin D regimens (2,000 IU po QD (6 subjects), 50,000 IU po Q week (4 patients) and 100,000 IU IM per dose (5 patients)). This resulted in 7 of 12 subjects achieving a 25OHD level >20 ng/mL after 1-14 months.

Conclusion. Vitamin D deficiency was observed in nearly half of these subjects receiving glucocorticoids for childhood inflammatory diseases. Furthermore, 25OHD levels were inversely associated with PTH concentrations, suggesting compensatory hyperparathyroidism. These data suggest a need to monitor for vitamin D deficiency in this clinical setting and to establish the optimal regimen for vitamin D supplementation.

Disclosures: ***E. von Scheven****, None.*

M528

Predicting Low Bone Mineral Density in Childhood Inflammatory Diseases: Experience from a Glaser Pediatric Research Network Alendronate Trial. E. von Scheven*[1], C. M. Gordon*[2], K. Gallagher*[3], M. Wertz*[1], L. Bachrach[4]. [1]Pediatrics, UCSF, San Francisco, CA, USA, [2]Pediatrics, Harvard, Boston, MA, USA, [3]Pediatrics, UCLA, Los Angeles, CA, USA, [4]Pediatrics, Stanford, Stanford, CA, USA.

Background Subjects with inflammatory disorders were screened for low bone mineral density (BMD) in a controlled trial of alendronate at 4 University Hospitals. Steroid exposure inclusion criteria were employed to enhance recruitment of low BMD subjects.

Objective To determine frequency and correlates of low BMD in pediatric subjects receiving glucocorticoids for inflammatory diseases screened for an osteoporosis treatment trial.

Methods Sixty-one patients (69 % female, 34% Caucasian, 25% Hispanic, 21% Asian, 8% African-American and 12 % mixed), mean age 13.7 ±3.5 yrs, with inflammatory disorders (30% lupus, 28% dermatomyositis, 13% Crohn's disease, 11% vasculitis, 7% Systemic JRA, 2% mixed connective tissue disease) were consented and screened. The underlying inflammatory disease duration ranged from 0.7 - 12 yrs (mean 4.3). Medications included biologic agents (41%), cyclophosphamide (18%), cellcept (13%), imuran (7%), and azacol, azulphidine, 6MP, thalidamide, and MTX or arava (each 5%). 77% of subjects took systemic steroids (mean dose 0.22 mg/kg/d [SD 0.24]). Age-adjusted lumbar spine BMD Z-scores (BMD Z-score) were determined by DXA (Hologic 4500, Hologic Research Upgrade software).

Results 33% of screened subjects were eligible for randomization. BMD Z-scores ranged from -3.2 to 2.2 SD (mean -1.3) and only 41% met the diminished BMD inclusion criteria (BMD Z-Score <-1.5 SD). 46% of subjects failed to meet the vitamin D (25OHD) inclusion criteria of > 20 ng/mL. A multivariate linear regression model for predicting low BMD Z-score included diagnosis, age at diagnosis, disease duration, gender, ethnicity, prior year average prednisone dose (mg/m^2/d), family history of osteoporosis, 25OHD level, and intact PTH concentration. It revealed a protective effect for African American's (beta 1.9, p=0.003) and increased risk for prednisone exposure (beta -0.025, p=0.046). However, this model explained only a small portion of the Z-score variance (adj R^2= 13).

Conclusion Less than half the patients treated with Glucocorticoids for inflammatory disorders were eligible for this trial due to unexpected vitamin D insufficiency and BMD Z-scores above -1.5. The weak association between BMD Z-score and risk factors suggests unmeasured factors, a highly multifactorial process, or unanticipated resilience of the pediatric skeleton. Furthermore, these data suggest that osteoporosis risk assessment is difficult in young patients and prophylactic bisphosphonate therapy should be approached cautiously.

Disclosures: ***E. von Scheven****, None.*

M529

A Longitudinal Study of Tibial Speed of Sound and Lower Limb Length in Preterm Infants: Relationship with Biochemical Markers of Bone Turnover. J. May*[1], J. Dutton*[2], J. Morris*[3], W. D. Fraser[2], A. J. B. Emmerson*[1], M. Z. Mughal[4]. [1]Neonatal Medicine, St Mary's Hospital for Women & Children, Manchester, United Kingdom, [2]Clinical Biochemistry, Royal Liverpool Hospital, Liverpool, United Kingdom, [3]Medical Statistics, University of Manchester, Manchester, United Kingdom, [4]Paediatric Medicine, St Mary's Hospital for Women & Children, Manchester, United Kingdom.

In healthy singleton infants between 31 to 42 weeks gestation, we showed that the tibial speed of sound (SOS; m/s) measured at median age of 2.1 days after birth increased with gestational age (*Yiallourides et al. Biol Neonate. 2004;85(4):225-228.*). The tibial SOS is known to be influenced by cortical thickness and bone mineral density (*Prevrhal et al. Osteoporos Int 2001;12 (1):28-34*).

In this longitudinal study we measured the tibial SOS using the Sunlight Omnisense quantitative ultrasound device (Sunlight Medical Ltd., Israel) and the knee-heel limb length (mm) using an electronic neonatal knemometer (FORCE Institutes, Denmark), in the same limb, in 58 preterm infants. The median (range) gestation and birth weight of infants was 26.4 weeks (23 to 34.4 weeks) and 928 grams (506 to 1499 grams), respectively. The measurements were performed weekly; median period of 4 weeks (2 to 14 weeks). As shown in figure 1, there was a significant decrease (within-subject correlation, r = -0.15; p=0.011) in tibial SOS with postnatal age. In contrast, as shown in figure 2, the lower limb length increased significantly (r = +0.96; p<0.001) with postnatal age.

In a subgroup of 24 infants, changes in serum concentration of bone specific alkaline phosphatase (BSALP; a marker of bone formation) and urinary excretion of urinary deoxypyridinoline (DPD; a non-reducible cross link of collagen that is a marker of bone resorption) were measured on the same day and around the same time as tibial SOS and lower limb length measurements. The serum concentration of BSALP (r = +0.44; p=0.001) and urinary DPD/creatinine (r = +0.24; p=0.033) increased with postnatal age.

The observed increase in lower limb length during the early neonatal period is consistent with a rapid tibial growth, whereas the decrease in tibial SOS during this period might either be due to a lag in tibial cortical mineralization or cortical thinning. Preliminary results also suggest that bone turnover increases progressively during the early neonatal period.

Fig 1

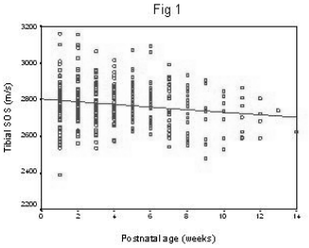

Fig 2

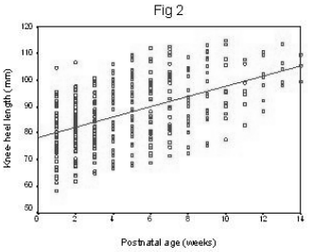

Disclosures: ***J. May****, None.*

M530

Bone Histomorphometry in Children with Suspected Secondary and Idiopathic Juvenile Osteoporosis. E. Sochett[1], O. Mäkitie*[2], A. Doria*[3], M. G. Mendes*[4], K. Pritzker*[5]. [1]Pediatric Endocrinology, The Hospital for Sick Children, University of Toronto, Toronto, ON, Canada, [2]Pediatric Endocrinology, The Hospital for Children and Adolescents, Helsinki University Hospital, Helsinki, Finland, [3]Radiology, The Hospital for Sick Children, University of Toronto, Toronto, ON, Canada, [4]Pathology, Mount Sinai Hospital,, University of Toronto, Toronto, ON, Canada, [5]Pathology and Laboratory Medicine, Mount Sinai Hospital, University of Toronto, Toronto, ON, Canada.

The Bone health clinic at the Hospital for Sick Children, Toronto is evaluating an increasing number of patients with severe chronic illnesses for osteoporosis. In many this appears likely given the chronic nature of the illness and the prolonged use of medications, such as high dose glucocorticoids. In addition an increasing number of patients with symptomatic Idiopathic juvenile osteoporosis (IJO) are being referred for bisphosphonate therapy. Areal bone mineral density (aBMD), the most commonly used investigative tool in adults, is limited in children because of the confounding effects of short stature and delayed puberty, common characteristics of chronically ill children. Ancillary tests such as bone turnover markers and spinal X-rays often suggest but are not diagnostic of osteoporosis.

To address these developments, we now undertake transcortical iliac crest biopsies before bisphosphonate therapy, in those with a high probability of osteoporosis and report here bone histomorphometry, aBMD, and spinal X-ray results in 7 patients.

Mean age was 14.2 years (range 10.0-16.6 yrs). Underlying medical conditions included rheumatological diseases (3), cerebral palsy (1) and leukemia (1); two patients had IJO. Mean aBMD z-score was -3.1 (range -1.6 - -4.8). Moderate to severe spinal compression fractures were documented in 6/7 patients. Serum calcium, phosphate, 25-OH-Vit D and PTH were normal in all subjects. Table 1 details the key static structural, formation and resorption bone morphometric findings.

Iliac crest bone histomorphometric parameters confirm the clinical assessment of osteoporosis in approximately 40% of this group and suggest an adynamic form of the disease. Overall resorption appears to be consistently suppressed with variable decrease in formation. Further studies will be required to fully characterize the various forms of osteoporosis in childhood.

Bone histomorphometric findings in 7 children with osteoporosis. N, normal; L, low; I, increased

Patient	Trabecular Bone Volume (%)	Osteoid Volume (%)	Mean Mineralized Trabecular width (ug)	Eroded Trabecular Surface (%)
1	19 = L	0 = L	163 = N	4 = L
2	26 = N	0 = L	241 = I	6 = L
3	27 = N	1 = N	134 = N	3 = L
4	17 = L	0 = L	126 = N	0 = L
5	16 = L	2 = N	175 = N	0 = L
6	19 = N	0 = L	146 = N	3 = L
7	21 = N	2 = N	142 = N	1 = L

M531

The Novel Bone Alkaline Phosphatase Isoform B1x and Bio-Intact (1-84) Parathyroid Hormone in Children with Renal Failure. P. Magnusson[1], S. Hansson*[2], L. Larsson[1], D. Swolin-Eide[2]. [1]Division of Clinical Chemistry, Faculty of Health Sciences, Linköping, Sweden, [2]Department of Pediatrics, Queen Silvia Children's Hospital, Göteborg, Sweden.

Children with renal failure are at high risk developing metabolic bone disease with long-term consequences as growth retardation and low peak bone mass. This study focused on novel markers of bone and mineral metabolism in pediatric patients since these markers are of potential value for diagnosis and monitoring of renal osteodystrophy. The study group was comprised of 31 patients, 3 - 20 years of age, with different kidney diseases of which 18 patients had acquired and 13 congenital disease. We measured parathyroid hormone (PTH), bio-intact (whole 1-84) PTH, and osteoprotegerin (OPG), and bone formation by serum type I procollagen intact amino-terminal propeptide (PINP), osteocalcin, total alkaline phosphatase (ALP), and four bone ALP (BALP) isoforms B/I, B1x, B1, and B2. Bone resorption was assessed using serum CrossLaps (CTX), derived from the carboxy-terminal telopeptide of type I collagen, and tartrate-resistant acid phosphatase isoform 5b (TRACP5b). There was a significant correlation between PTH and bio-intact PTH, r = 0.83, with 19 (61%) and 20 (65%) patients above the reference interval, respectively. However, we observed, on average, 50% higher levels of PTH vs. bio-intact PTH demonstrating non-(1-84) PTH fragments detected by the PTH assay. Increased activities were found in five, three, and four patients for total ALP, B1, and B2, respectively. However, 17 (55%) patients had increased B/I levels of which 13 had a glomerular filtration rate (GFR) <70 ml/min/1.73 m^2. The BALP isoform B1x was identified in two (6%) patients. B1x has previously only been detected in (60%) adults with chronic renal failure on dialysis but not in healthy individuals or in other bone diseases. The two children with B1x had OPG levels in the higher range independently of age, GFR, and bio-intact PTH. One boy, 9 years, with identified B1x was monitored during one year of growth hormone (GH) treatment. B1x was identified prior to and after 9 days of GH therapy, however, not after 1, 3, 6, and 12 months. In conclusion, our study demonstrate that: 1) The BALP isoform B1x is expressed in children with renal failure (and not only in adults) and should be further evaluated as a marker of adynamic renal bone disease; 2) There are selective differences between the BALP isoforms in children with renal failure; 3) The BALP isoforms, PINP and TRACP5b are useful markers of bone turnover in renal bone disease since their clearance is independent of renal function; and 4) Children with renal failure have increased levels of circulating non-(1-84) PTH fragments.

Disclosures: ***P. Magnusson****, None.*

M532

Assessing Fracture Risk in Patients with Renal Failure. S. A. Jamal[1], P. MacFarlane*[1], D. Pearce*[2], S. V. Jassal*[3]. [1]Medicine, St. Michael's Hospital, University of Toronto, Toronto, ON, Canada, [2]Diagnostic Imaging, St. Michael's Hospital, University of Toronto, Toronto, ON, Canada, [3]Medicine, The University Health Network, University of Toronto, Toronto, ON, Canada.

Men and women with dialysis dependent renal failure have a high prevalence of fractures. To assess if bone mineral density (BMD) measurements and/or tests of muscle strength were associated with fractures we studied 37 men and 15 women, 50 years and older, who had been on hemodialysis for at least one year. We excluded patients with prior renal transplants and women taking hormone replacement therapy. We inquired about risk factors for fractures and low trauma fractures since starting dialysis. A chart review gave the most recent laboratory tests. Subjects underwent BMD testing at the lumbar spine and total hip with a Lunar DPX-L densitometer. Tests of muscle strength included: timed up and go (TUG), six minute walk, functional reach, and grip strength. We obtained radiographs of the thoracic and lumbar spine and identified prevalent fractures by morphometry. We used logistic regression to examine the relationships between fracture (prevalent vertebral, self-reported low trauma and/or both) and BMD, and fracture and muscle strength tests. Results are adjusted for age and weight and reported as Odds Ratios (OR) per standard deviation increase in the dependent variable. The mean age of subjects in our study was 65.9 ± 8.9 years, the mean weight was 72.8 ± 15.2 kg, and most (35 of 52 subjects) were Caucasian. The average duration of dialysis was 3.9 ± 2.5 years. The most common cause of renal failure was diabetes (17 subjects). The mean levels of calcium, phosphate, and alkaline phosphatase were normal. The mean level of PTH was 42.1 ± 41.8 pmol/L. There were no differences by gender or between subjects with and without fractures. Of the 52 subjects, 12 had prevalent vertebral fractures, 20 reported a low trauma fracture since starting dialysis, and 27 subjects had either a vertebral fracture or low trauma fracture. Just under half of the subjects (24) reported having at least one fall in the past year. Mean lumbar spine BMD was 1.1 ± 0.2 g/cm^2 and total hip BMD was 0.8 ± 0.2 g/cm^2. Mean grip strength was 21.5 ± 9.3 kg, mean TUG was 19.7 ± 25.9 seconds, mean functional reach was 17.3 ± 10.9 cm, and mean six minute walk 108.8 ± 58.1 meters. There was no association between fractures, falls in the past year, hip BMD, spine BMD, or grip strength. Fractures were associated with the six minute walk (OR = 0.1; p = 0.001), functional reach (OR = 0.3; p =0.005), and TUG (OR = 6.9; p = 0.004). Adjusting for spine or hip BMD did not change our results. Simple, inexpensive tests of muscle strength may identify subjects with renal failure at increased risk for fractures.

Disclosures: ***S.A. Jamal****, None.*

M533

Nutritional Assessment in Renal Osteodystrophy Patients Submitted to Parthyroidectomy. B. S. E. Peters*[1], V. Jorgetti[2], R. M. A. Moyses*[2], L. A. Martini[1]. [1]Nutrition, Sao Paulo University, Sao Paulo, Brazil, [2]Medicine, Sao Paulo University, Sao Paulo, Brazil.

Its recognized that undernutrtion is frequent in patients with renal osteodysthrophy with elevated parathyroid hormone (iPTH). The elevated iPTH induce nutritional abnormalities in these patients, such as loss of appetite, abnormal food taste, protein catabolism and weight loss. These complications could be relived by parathyroidectomy (PTX). This study was undertaken in order to evaluate the nutritional status of Chronic Renal Failure patients (CRF) with Renal Osteodystrophy six months after parathyroidectomy. The study was carried out in a renal osteodystrophy outpatient clinic from the São Paulo University. Fifteen patients, mean age 42 ± 11 years old, participated in the study. All of them completed a 3 days dietary records (energy, protein calcium and phosphorus), anthropometric measurements (body mass index - BMI, skinfold thickeness, midarm muscle circunference and body fat), and biochemical indices (serum calcium and phosphorus, total protein and albumin, alkaline phosphatase, and iPTH), before and six months after the PTX. The results are presents as mean ± SD. The iPTH was negatively correlated with weight and fat mass (r= -0.53 and r= -0.55 respectively; p<0.05) before the PTX. The mean energy, carbohydrate, protein, lipid and phosphorus intake, increased after the surgery with no statistical significance. Only the calcium intake significantly increased after PTX (397 ± 189 mg to 676 ± 401 mg, p<0.05). There are no significant differences in body composition, six months after the PTX. However, the biochemical indices of nutritional status, serum total protein (g/dl) and albumin (g/dl) increased significantly (6.9 ± 0.9 to 7.6 ± 0.6 g/dl and 3.8 ± 0.4 to 4.2 ± 0.6 g/dl p<0.05, respectively). As expected, the serum total calcium (mg/dl), phosphurus (mg/dl), alkaline phosphatase (U/l), iPTH (pg/ml) significantly decreased after PTX (9.5 ± 1.2 to 8.4 ± 1.2 mg/dl; 6.5 ± 1.8 to 4.5 ± 1.4 mg/dl; 689.9 ± 789.0 to 155.4 ± 108.6 U/l; 1516.14 ± 841.7 to 449.8 ± 753.7 pg/ml, p<0.05 respectively). In conclusion, the present study confirm the evidence that high iPTH levels have deleterious effects on the nutritional status of CRF patients, and based on biochemical indices of nutritional status, the PTX could have beneficial effects on nutritional status.

Disclosures: ***B.S.E. Peters****, None.*

M534

Long Term Bone Health In Male Renal Transplant Patients. A. H. Khan*[1], N. Bhargava*[1], R. Chandra*[1], P. Kon*[2], C. Moniz[1]. [1]Clinical Biochemistry, Kings College Hospital, London, United Kingdom, [2]Renal Unit, Kings College Hospital, London, United Kingdom.

Metabolic bone disease is a recognised complication following renal transplantation, but whether this persists several years after transplantation was investigated. We studied consecutively 43 male patients with renal transplantation, on average 13 yrs post transplantation (range 2- 38 yrs). A fracture risk assessment including risk questionnaires, second void urine samples for bone turnover markers and morning serum samples and BMD of the lumbar spine and femoral neck was undertaken. The mean age of patients was 49 years (range 25-75). All were on steroids with a mean daily cumulative dose of 6.8 mg, although individuals' doses varied from year to year. At the lumbar spine, osteopenia and osteoporosis seen in 9 (21%) and 7 (16%) cases with a mean T score BMD of -1.57 and -3.18 respectively. At the femoral neck, osteopenia was present in 13 cases (30%) with a mean T score -1.65 and osteoporosis in 7 cases (16%) with mean T score of -2.96, 12 cases 28% reported low trauma fracture. Mean BMDs with pre-existing fractures were T score spine -1.67 and femur -1.96. Gonadal status was within normal limits (mean testosterone 14.2 nmol/L; reference range 10-30). Serum adjusted calcium homeostasis was within normal limits, with secondary hyperparathyroidism (mean PTH 135 pmol/L (14-1670), and vitamin D, mean 19.9 ug/L (range 7-38). Mean Urine deoxypyridinoline (DPD) was 6.2 nmol/mmol creatinine (range 2.2-13.8; reference range 7.8-9.4). 79% of cases had low DPD (mean 4.8 nmol/mmol creatinine) and only three cases had DPD above the reference range. This study shows that fractures occur at a higher BMD and long-term fracture risk persist in male post renal transplant patients. Our data also demonstrates low DPD despite hyperparathyroidism indicating low bone turnover persists which might restrict the use of antiresorptive agents in the treatment and prevention of osteoporosis

Disclosures: ***A.H. Khan****, None.*

M535

Bone Quality and Fractures or Osteonecrosis in Renal Transplant Recipients. S. M. Ott, S. Kuehner*, D. J. Sherrard. University of Washington, Seattle, WA, USA.

Recipients of solid organ transplants suffer a high incidence of skeletal complications. These are not consistently predicted by bone density measurements, which suggests that other aspects of bone quality contribute to bone strength. One such factor could be the mineralization density (MinDen) of the bone, which reflects how tightly mineral crystals are packed into the bone matrix. We examined bone biopsies from a prospective study of 34 hemodialysis patients who underwent living-related kidney transplantation from 1985-89. Mean age was 33 ± 12 yrs, duration of dialysis 16 mo, and none had previous glucocorticoid use. Tetracylcine-labeled bone biopsies, bone density, and magnetic resonance imaging were done at transplant and repeated after 20 ± 4 mo in 21 patients. Bone density was measured using single and dual photon absorptiometry. MinDen was measured using backscattered electron imaging. Images were analyzed with the NIH Image program, and results expressed in grey-scale values.

After transplantation 5 patients had experienced fractures, 9 had osteonecrosis and 7 no bone symptoms. In the entire group, bone density did not change significantly (-2.0 ± 5%/yr at radius and -1.0 ±7.9%/yr at spine). Baseline bone density was slightly but not significantly lower in the fracture group, with no difference in change of bone density among the three groups. Those with fractures had higher aluminum surface (AlS), higher MinDen, lower mineralizing surface (MS/TA), less decrease in PTH and less decrease in fibrosis (Fib) compared to those without fractures. Osteoid area, bone area, and eroded surfaces were not different. The MinDen showed significant inverse correlation with the mineralizing surface (r = -.55) and with area of fibrosis (r = -.46). The total prednisone dose was similar among groups, but the dose in the first month was higher in the osteonecrosis group.

These data show that changes in bone quality affect the risk of fractures in the transplant patients. Those who had fractures had lower bone formation. The MinDen was probably increased because low bone turnover allowed longer time for mineral crystals to accumulate in the bone matrix. The bone formation rates increased after transplantation (possibly because aluminum was removed), with decrease in MinDen. In the patients with osteonecrosis, bone formation rates did not increase, possibly a result of the glucocorticoids.

Data at transplant and after 20 months; * p<.05 baseline values; # p<.05 change after Tx

	Fracture (5)	No Fracture (7)	Osteonecrosis (9)
AlS* %	30 - 4	7 - 1	21 - 5
MinDen* units	124 - 116	113 - 117	117 - 118
MS/TA* µm/mm2	241 - 707	1050 - 936	620 - 652
PTH# pg/mL	60 - 39	79 - 19	38 - 18
Fib# %	0.4 - 0.08	1.1 - 0.04	0.15 - 0.17
SPA g/cm2	0.49 - 0.48	0.58 - 0.54	0.54 - 0.54

Disclosures: ***S.M. Ott****, None.*

M536

Pamidronate Shows a Novel, Renal-Insufficiency-Specific Deposition of Mineral on the Endosteal Bone Surface. J. Jokihaara*[1], P. Koobi*[2], P. Jolma*[3], M. Feng*[2], I. Porsti*[4], T. L. N. Jarvinen[1]. [1]Department of Orthopaedics and Traumatology, University of Tampere, Tampere, Finland, [2]Department of Pharmacology, University of Tampere, Tampere, Finland, [3]Department of Neurology, University of Tampere, Tampere, Finland, [4]Department of Medicine, University of Tampere, Tampere, Finland.

To characterize the structural effects of Pamidronate (PAMI), an intravenously administered bisphosphonate, on healthy and diseased bone, 30 twelve-wk-old rats were subjected to either SHAM-surgery or 5/6 nephrectomy (NTX). After a 4-wk disease-progression period, the rats were further randomized into placebo or PAMI groups for 8 wks. At the end of the intervention, the cross-sectional characteristics of the femoral midshaft and distal femur were analysed using pQCT scanner.

In the femoral midshaft, a cortical bone region, the only NTX-effect was a significant reduction in total and cortical bone mineral density (**A-B**), whereas PAMI had a clearly more pronounced effect on the tBMD (p=0.001). This general PAMI-effect also appeared specific to the NTX (+11%, p=0.002), as there was no effect in the SHAM rats (+3%, NS) (**A-B**). A general PAMI-effect was also observed on the cortical wall thickness (p=0.01) (**C**). However, a more detailed assessment showed that identically to the situation with the tBMD, the PAMI-effect was highly specific to the NTX'd rats. PAMI-treatment also resulted in significant reduction of bone size (tCSA) irrespective of the renal function (p=0.02, **D**), an apparent consequence of the PAMI-induced deposition of mineral and the resulting increase in bone stiffness. A significant interaction was also observed between PAMI-treatment and NTX: In the SHAM rats, the PAMI-treatment had no effect on the cortical (not shown) or total BMC (**E**) or cortical CSA (**F**), but resulted in a significant increase in all of these parameters in the NTX rats. Finally, in the distal femur, a mainly trabecular region, NTX had no effect at all, while the PAMI-treatment resulted in increased total BMC (+27%, p=0.000) and BMD (+30%, p=0.000) (not shown).In conclusion, the NTX-induced deleterious effects on bone appear to concern mainly the cortical bone, while pamidronate has a clear preference on the trabecular bone. However, an intriguing interaction was found between NTX and PAMI in the femoral midshaft, as a clear PAMI-induced endocortical deposition of mineral was observed.

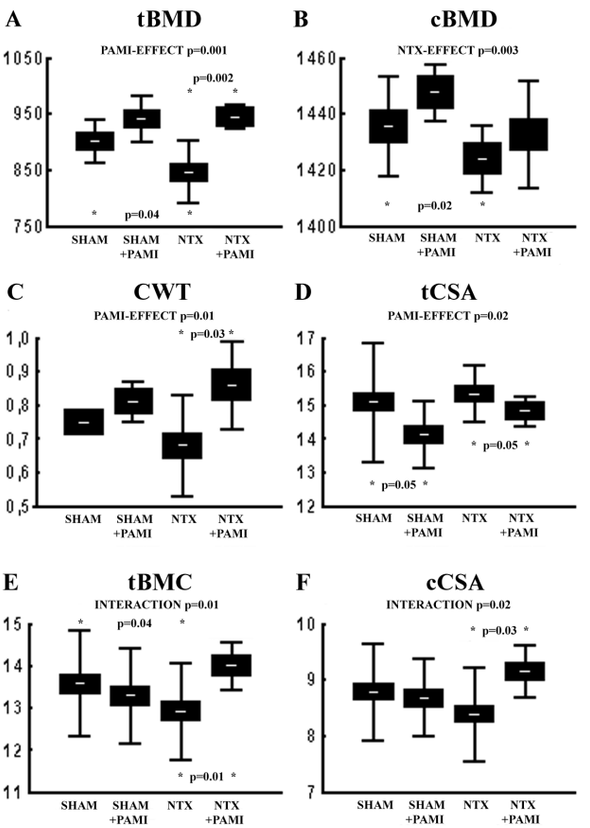

Disclosures: ***J. Jokihaara****, None.*

M537

CKD Induces an Adynamic Bone Disorder and Vascular Calcification Amenable to Skeletal Anabolism in the Metabolic Syndrome. R. J. Lund[1], M. R. Davies*[2], S. Mathew*[3], G. Saab*[2], K. A. Hruska[3]. [1]Internal Medicine, Washington University, St. Louis, MO, USA, [2]Internal Medicine, Washington University, St. louis, MO, USA, [3]Pediatrics, Washington University, St. louis, MO, USA.

In low density lipoprotein receptor null (LDLR-/-) mice, a model of the metabolic syndrome, we have shown that vascular calcification (VC) is worsened by chronic kidney disease (CKD) and ameliorated by Bone Morphogenetic Protein -7 (BMP-7), an efficacious agent in treating renal osteodystrophy (ROD). Here, LDLR-/- animals without CKD had significant reductions in bone formation rates, associated with increased VC and hyperphosphataemia. Superimposing CKD resulted in the adynamic bone disorder (ABD), while VC worsened and hyperphosphataemia persisted. This supports a pathological link between abnormal bone mineralization and VC. BMP-7 treatment corrected the ABD, ameliorated CKD-induced VC and corrected hyperphosphataemia, compatible with BMP-7-driven stimulation of skeletal phosphate deposition reducing plasma phosphate and thereby removing a major stimulus to VC.

To examine the mechanisms underlying osteogenic insufficiency induced by high fat feeding, we analysed the proliferation and differentiation of pluripotent bone marrow stromal cells (BMSC) that include osteoblast lineage precursors. LDLR-/- BMSC proliferated more than wild type cells, but LDLR-/- cells from high-fat fed animals proliferated less than wild type, a finding reversed and further stimulated by BMP-7 treatment. Since LDLR-/- adaptatively upregulates the Lrp family of proteins, we examined the function of Lrp5, a high bone mass gene, in LDLR-/- BMSC. Lrp5 was induced by LDLR-/-, but its function was diverted from Wnt signalling to lipid metabolism by high fat feeding. Thus, a putative mechanism of high fat feeding induced deficiency in bone formation was discovered. BMP-7 markedly induced Lrp5 restoring skeletal precursor proliferation and differentiation in vitro and bone formation in vivo.

Thus in the metabolic syndrome with CKD, a reduction in bone forming potential of osteogenic cells leads to the ABD producing hyperphosphatemia and VC, processes ameliorated by the skeletal anabolic agent BMP7, in part through deposition of phosphate and increased bone formation.

Disclosures: ***K.A. Hruska****, None.*

M538

Curcuminoid-Enriched Turmeric Extract Prevents Arthritis in Lewis Rats. J. L. Funk, G. Chen*, G. McCaffrey*, G. Stafford*, J. A. Beischel*, J. Wilson*, R. C. Lantz*, A. M. Solyom*, S. D. Jolad*, B. N. Timmermann*. Arizona Center for Phytomedicine Research, University of Arizona, Tucson, AZ, USA.

Turmeric, the ground dried rhizome of the herb *Curcuma longa* L. (Zingiberaceae) that contributes flavor and lively yellow color to curries and mustard, has also been used for centuries in Ayurvedic medicine for the treatment of inflammation. Turmeric has been found to be a rich source of phenolic compounds (besides essential oil, the second major component of turmeric) commonly referred to as curcuminoids. Botanical dietary supplements, including turmeric extracts, are increasingly being used by the public in the United States for the treatment of chronic diseases, such as rheumatoid arthritis. However, scientific data regarding the clinical efficacy of these chemically complex botanical extracts are lacking. Studies were therefore undertaken to test the effect of an essential oil-free, curcuminoid-enriched extract of turmeric (curcuminoid extract) on joint inflammation and destruction in streptococcal cell wall (SCW)-induced arthritis, an animal model of rheumatoid arthritis (RA). Female Lewis rats were treated with: (1) vehicle alone; (2) curcuminoid extract (45 mg curcuminoids/kg/d ip); (3) SCW (25 mg/kg ip); (4) SCW + curcuminoid extract. Extracts were administered via intraperitoneal injection 5-7 days/week beginning 4 days prior to SCW injection. SCW-treated animals rapidly developed an acute phase of joint swelling, as assessed clinically by daily arthritic index, and subsequent nadir in disease activity, followed by a persistent chronic phase of joint swelling that is associated with joint destruction. Treatment with the curcuminoid extract profoundly inhibited joint swelling, a statistically significant effect that was seen as early as day 3 and persisted throughout the subsequent course of acute and chronic arthritis. Indeed, arthritis incidence was reduced to 20% by curcuminoid extract treatment (vs. 100% in SCW alone). Bone destruction was also significantly inhibited, as determined by measurement of osteoclast number in the distal tibia and BMD (Piximus, GE Lunar) of the distal femur. Curcuminoid extract also prevented the increase in circulating leukocytes that occurs during SCW-induced inflammation. In addition, ex vivo treatment of LPS-stimulated bone marrow or spleen cells with curcuminoid extract inhibited TNF-α secretion. The marked inhibitory effect of this turmeric extract on inflammatory cells and inflammatory mediator production in association with a profound inhibition of joint inflammation and destruction in SCW-induced arthritis suggests that essential oil-free extracts of turmeric may be efficacious in the treatment of RA.

Disclosures: ***J.L. Funk****, None.*

M539

The Effect of of Multiple Sclerosis on Bone Metabolism. A. Cranney[1], L. Ruhland*[2], W. Hopman*[2], V. McBride*[2], T. Anastassiades[2], D. Brunet*[2]. [1]Medicine, University of Ottawa, Ottawa, ON, Canada, [2]Medicine, Queen's University, Kingston, ON, Canada.

Previous studies have noted that Multiple Sclerosis (MS) subjects have a higher prevalence of osteopenia, vitamin D deficiency and more frequent fractures. The purpose of this study was to determine the proportion of MS subjects with low bone mass, vitamin D deficiency, and identify potential predictors of low BMD in an MS population. In a cross-sectional study we identified 100 subjects who attended a tertiary care MS clinic. The study population involved men and women > age 25 years with a neurologist-confirmed diagnosis of MS. Bone density, serum calcium, TSH, vitamin D, PTH and biochemical markers were measured. BMD (DXA Hologic) results were compared to a healthy age and sex-matched population. A questionnaire with details on duration, type of MS, medications, osteoporosis risks and dietary calcium intake was administered. The degree of walking disability was evaluated with the Kurtzke EDSS (1-10) with higher scores indicating greater disability. The Katz Comorbidity Index and an Osteoporosis Knowledge Questionnaire (OPQ) were completed. Mean age of the sample was 47.2 yrs (range 27-70), mean weight 76.1 kg (SD 17.8) and height 168.5 cm (SD 8.0). 65% were female and 38% were postmenopausal. 69% had relapsing remitting (RR) MS, 14% had primary progressive (PP) and 17% secondary progressive (SP). The mean EDSS was 3.3 (SD 1.9) and mean duration of MS was 11.4 (SD 8.8 years). 54% of subjects were on disability and 84% had a comorbidity score of zero. 25% reported having a prior BMD, 8% had been told they had osteoporosis and 9% had received osteoporosis counseling. 38% were taking ≥400 IU vitamin D and 22% had received IV glucocorticoids. 26% of the sample reported having a prior fracture after age 25 and 67% reported falling during the previous year. Mean femoral neck BMD (FN) was 0.77 g/cm^2 for females and 0.76 g/cm^2 for males. Mean total hip BMD was 0.89 and 0.92 g/cm^2 and mean lumbar spine BMD was 1.01 and 1.00 g/cm^2 for females and males, respectively. Twenty-three percent of subjects had a Z score ≤ -1.0 at the lumbar spine, 31% had Z score ≤ -1.0 at the FN and 25% at the total hip. Total hip BMD was 0.92g/cm^2 for (RR), 0.87 g/cm^2 for (PP) and 0.83 g/cm^2 for Secondary Progressive MS subjects. Total hip BMD was lower in those with an EDSS ≥ 5.5, ($p<0.05$). Mean vitamin D level was 92.0 nmol/l (46.8) and mean PTH 4.08 pmol/l (2.0). The mean score on the OPQ (max of 20) was 9.58 (4.64). There was a significant negative correlation between duration and type of MS with hip BMD. The prevalence of low BMD is not as high as noted in other hospital-based studies of MS subjects, which may reflect the lower level of disability seen in our population.

Disclosures: ***A. Cranney****, None.*

M540

A Novel Macromolecular System to Image and Therapeutically Target Inflammatory Diseases In or Near Bone. B. Anderson*[1], D. Wang*[2], S. C. Miller[1], M. Sima*[2], P. Kopeckova*[2], J. Kopecek*[2]. [1]Radiobiology, University of Utah, Salt Lake City, UT, USA, [2]Pharmaceutics and Pharmaceutical Chemistry, University of Utah, Salt Lake City, UT, USA.

Inflammatory diseases can cause substantial localized and regional bone loss and skeletal dysfunction. A macromolecular delivery system has been developed that may improve the ability to image inflammatory foci in and near bone. In addition, this same technology may be used to enhance the delivery and retention of therapeutic agents to these sites. For these studies, the rat adjuvant-induced arthritis (AIA) model was used to induce inflammation-mediated skeletal disease. The macromolecular delivery system is synthesized based on N-(2-hydroxypropyl)methacrylamide (HPMA) copolymers. The localization and retention of the polymers to inflammatory sites was first demonstrated by magnetic resonance imaging (MRI) using a gadolinium (Gd) polymer complex. The injected polymer-Gd complex had preferential uptake and a prolonged retention in the inflammatory regions in skeletal and associated soft tissues as demonstrated by MRI and confirmed by histopathology. To demonstrate the utility for using this system in therapeutics, AIA rats with established inflammation were treated with 4 continuous daily injections of dexamethasone (Dex) or one injection of a polymer-Dex conjugate with an equivalent dose of Dex. The inflammation in the Dex-treated animals was transiently reduced, but returned within several days after the 4 doses of Dex treatment. The inflammation in the animals treated with polymer-Dex was suppressed for a longer period. Local bone mass and density measured by pDXA was significantly greater with the polymer-Dex treatment compared with Dex treatment alone. Histomorphometry of the tarsal bones showed that the osteoclast and resorption parameters were substantially reduced in the animals treated with polymer-Dex compared with Dex alone. These results demonstrate the utility of a novel macromolecular imaging and therapeutic delivery system that may prove advantageous in the diagnosis and treatment of inflammatory diseases that affect skeletal tissues and joints.

Disclosures: ***B. Anderson****, None.*

M541

Assessment of 3D Cortical and Trabecular Bone Microstructure and Erosion on Micro CT Images of a Murine Model of Arthritis. Y. Jiang[1], J. J. Zhao[1], R. Mangadu*[2], S. Medicherla*[2], A. A. Protter*[2], H. K. Genant[1]. [1]Osteoporosis and Arthritis Research Group, University of California San Francisco, San Francisco, CA, USA, [2]Scios Inc., Fremont, CA, USA.

The study of inflammatory arthritis lacks reliable 3D imaging indices of disease activity and treatment response to direct the development of specific therapies. Due to the wide availability of various genetically altered mice in genomics research, drug discovery and development, a murine model may be useful for studying inflammatory arthritis. We evaluated 3D bone microstructure and erosion in such a model. Male DBA-1 Lac/J mice were immunized with collagen in complete Freund's adjuvant, boosted with collagen II in incomplete Freund's adjuvant on day 21. The paws were collected on days 33 (n=6) and 53 (n=14). Naïve paws were also harvested (n=3). They were scanned using a Scanco µCT with isotropic resolution of 16 µm. 3D cortical and trabecular structure were directly measured in the distal radius and the scaphoid, the distal tibia and the talus. The specimens were re-scanned and -measured 2-month later. 3D images were displayed from different angles to demonstrate integrity of bone surfaces. Bone erosion was independently scored by 2 experienced readers using a method adapted from a radiologic grading method used in epidemiological studies and clinical drug trial for rheumatoid arthritis. The readers were blinded to ID and scored twice with an interval of 2-month, according to an 8 point scale with 0.5 increments, from 0 as normal to 3.5 as severe worse. In the frontal paw, 8 joints were examined: metacarpo-phalangeal of digits I to V, combination of all carpometacarpal and intercarpal joints, distal radius, and distal ulna. Maximum score is 28. In the rear paw, 14-joint were examined: bases of metatarsals I to V, cuneiforms I to III, cuboid, navicular, calcaneus, talus, distal fibula, and distal tibia, with maximum score of 49. The root mean square coefficient of variation was 1.8% for bone volume fraction, 2.9% for thickness, 2.1% for separation. Intraclass correlation coefficients were 0.98 and 0.99 (intra-reader), and 0.98 (inter-reader). The images demonstrated mild changes on day 33 to moderately advanced disease on day 53. The erosion score was over 2-fold greater on day 53 than on day 33 (p=0.01). Thus, assessment of 3D cortical and trabecular microstructure and bone erosion in a murine model of inflammatory arthritis provides highly reproducible results. The 3D bone microarchitecture imaging system and the animal model may find application testing anti-inflammatory arthritis agents and anti-osteoporotic agents and investigating pathophysiology of inflammatory arthritis and arthritis-induced osteoporosis.

Disclosures: ***Y. Jiang****, Scios Inc. 2.*

M542

Factors Associated with Knee Osteoarthritis among Japanese Women. T. Hashikawa*[1], K. Aoyagi[2], S. Yoshida*[3], P. D. Ross[4]. [1]Orthopaedics, St.Francis Hospital, Nagasaki, Japan, [2]Public Health, Nagasaki University, Nagasaki, Japan, [3]Orthopaedics, Suga Orthopaedic Hospital, Isahaya, Japan, [4]Merck Research Laboratories, Rahway, NJ, USA.

Several studies have been conducted to determine the risk factors for knee osteoarthritis (OA) in western counties, but there are no population-based reports in Japan.
We studied 582 community-dwelling Japanese women ages 40 to 89 years (mean age = 64.2, SD = 9.6 years). Radiographs were obtained of bilateral knees (antero-posterior weight bearing), and were graded according to the criteria described by Kellgren-Lawrence (K/L). Definite OA was defined as K/L grade 2 or higher, present in at least one joint. Height (m) and weight (kg) were measured, and body mass index (BMI) was calculated as weight (kg) /height (m^2). Occupation and history of knee injury were obtained from questionnaire. Daily intake of vitamin C and carotene were estimated by a self-administered semiquantitative food frequency questionnaire.
In univariate analyses, women with knee OA were significantly older and weighed more than those without. Women engaging in farming had higher prevalence of knee OA. Women with history of knee injury had significantly higher prevalence of knee OA than those without. There was no significant difference in daily intake of vitamin C and carotene between women with and without knee OA. Multivariate logistic regression analysis showed that older age (per 5 years increase, odds ratio [OR]; 1.8, 95% confidence interval [CI]; 1.6-2.1), greater BMI (per 5-unit increase, OR; 2.2, 95% CI; 1.7-3.0) and history of knee injury (yes/no, OR; 3.1, 95% CI; 1.7-5.6) were significantly associated with knee OA. Daily intakes of vitamin C and carotene were not associated.
Our findings suggest that aging, obesity and previous knee injury are important risk factors for development of knee OA among Japanese women, which is consistent with previous reports among Caucasian populations.

Disclosures: ***T. Hashikawa****, None.*

M543

Systemic Bone Loss Induced by Local Inflammation Is Associated with Greatly Increased Mast Cell Number in Bone Marrow. G. L. Evans*[1], N. H. Bell[2], R. T. Turner[1]. [1]Orthopedic Research, Mayo Clinic, Rochester, MN, USA, [2]Dept. of Medicine, Medical University of South Carolina, Charleston, SC, USA.

Prostaglandins can produce either pro- or anti-inflammatory actions depending upon their route of administration. We previously reported that subcutaneous implantation of prostaglandin E_2 (PGE_2) results in local inflammation and systemic bone loss in normal and ovariectomized (OVX) rats. Others reported that circulating 17ß-estradiol (E_2) inhibits inflammation, whereas PGE_2 induces local mast cell differentiation. Mast cells accumulate in the marrow cavity following OVX and treatment with estrogen suppresses the release of the osteolytic cytokines TNFα and IL-6 by mast cells. The purpose of this study was to determine the effects of local PGE_2 and circulating E_2 on cancellous bone mass and bone marrow mast cell number in growing OVX rats. Drugs and carrier were delivered by use of 7.5 mg PGE_2 pellets, 0.5 mg E_2 pellets and placebo pellets after s.c. implantation onto the back of 7-w-old OVX rats. Histological analysis of the proximal tibial metaphysis was performed 3 w later. The results are shown in the Table (values are mean ± SE; N=5-7).

Measurement	Control	PGE_2	E_2	E_2 + PGE_2	PGE_2 P Value	E_2
BV/TV (%)	14.4 ± 6.5	6.9 ± 2.1	42.1 ± 5.6	26.0 ± 13.3	0.026	0.0001
Mast cells (#/mm^2)	12.0 ± 4.6	143 ± 21	12.6 ± 1.7	38 ± 10	0.0001	0.0001

PGE_2 produced local inflammation at the site of implantation without increasing circulating PGE_2 values. E_2 increased uterine weight indicating that serum E_2 values were increased. PGE_2 decreased, whereas E_2 increased cancellous bone volume. There was a 13-fold increase in mast cell number in bone marrow following PGE_2 treatment compared to only a 3-fold increase when E_2 was administered concomitantly. These findings demonstrate a strong association between local inflammation-induced systemic bone loss and accumulation of mast cells in bone marrow. The results provide evidence that mast cells mediate inflammation-induced bone loss.

Disclosures: ***G.L. Evans****, None.*

M544

Decreased Bone Strength in HLA-B27 Associated Ankylosing Spondylitis. M. P. Akhter[1], A. D. Lund*[1], M. Wing*[2], L. K. L. Jung*[2]. [1]Medicine, Creighton University, Omaha, NE, USA, [2]Pediatrics, Creighton University, Omaha, NE, USA.

Ankylosing spondylitis is an inflammatory disorder which involves the spine, peripheral joints and entheses. Patients with this disorder often develop osteopenia /osteoporosis. The exact etiology of the osteopenia/osteoporosis is not clear. Possible causes include corticosteroid use and the underlying inflammatory disease. This project investigated the nature of osteopenia/osteoporosis in this disorder using the histocompatibility leukocyte antigen (HLA)-B27 transgenic rat model of ankylosing spondylitis. HLA-B27 transgenic rats and their littermates were purchased from Charles River Laboratories at 6 - 8 weeks of age. The animals were housed individually and sacrificed at the peak of their disease (8-month-old). The spine and femurs were removed and stored at -20ºC in saline until analysis. The bone structure and strength were determined using a micro computed tomography device (µCT20, Scanco Medical) and mechanical testing (Instron 5543). Vertebral bodies were scanned (17 micron resolution with an integration time of 50 milliseconds) to determine trabecular structural properties in terms of bone volume (BV/TV), trabecular thickness, and spacing. After scanning, the mid-shaft femur was subjected to a 3-point bending test (along anterior-posterior direction), the femoral neck was tested in bending, and vertebral bodies (L4) were tested in compression. All tests were performed at a rate of 3mm/minute. Structural strength parameters (ultimate/yield load, stiffness) were obtained from the load-displacement diagram. The apparent material strength (ultimate/yield stress, modulus) was calculated. Genotype-related differences in all the measured variables were tested using one-way ANOVA at a significance level of $P<0.05$. B27-trangenic rats had poor biomechanical strength and structural properties at every site (Table). All the measured parameters (Table) were significantly lower ($P<0.05$) in the B27 transgenic rats as compared to control littermates. Micro-CT data suggest that the transgenic animals had lower BV/TV and trabecular thickness in their vertebral bodies. The poor trabecular structure in B27 rats is consistent with the poor biomechanical strength properties in the vertebral bodies. In conclusion, the HLA-B27 genotype contributes to the bone fragility in ankylosing spondylitis.

Table. Biomechanical Properties (Mean ± SD)	Control littermate [n=5]	Transgenic (B27) [n=8]
FS Ultimate Load (N)	141±27	110 ± 21 [a]
FN Ultimate Load (N)	103±28	76 ± 21 [a]
Vert Ultimate stress(N/mm^2)	36±6	18 ± 7 [a]
Vert Yield stress (N/mm^2)	29±5	14 ± 6 [a]
Vert BV/TV	0.67±0.11	0.55 ± 0.04 [a]
Vert TbTh	0.18±0.02	0.14 ± 0.02 [a]

[a] Differences due to genotype (P < 0.05) FS= femur shaft, FN= Femoral Neck, Vert=L4 vertebral body

Disclosures: ***M.P. Akhter****, None.*

M545

Combination Therapy With Ibandronate and Calcitriol Is Effective in Patients Following Liver Transplantation: A Three Year Prospective Controlled Study. A. Fahrleitner-Pammer[1], G. Prenner*[2], D. Kniepeiss*[2], K. Tschelissnigg*[2], G. Leb*[1], C. J. Piswanger-Sölkner*[1], B. M. Obermayer-Pietsch*[1], H. Dobnig[1]. [1]MedUnivKlinik, Endocrinology, Graz, Austria, [2]ChirUnivKlinik, Transplantation, Graz, Austria.

Due to improved long term survival rate, transplantation bone disease is of growing importance as a potential serious late complication following liver transplantation (LTX).
Aim of the present study was to evaluate the influence of 2mg ibandronate iv. every 3 mos in combination with oral calcitriol in 15 LTX patients (f/m 5/10) with osteoporosis (OPO). Results were compared to respective baseline evaluations as well as contrasted to 8 LTX recipients (f/m 2/6) with normal bone mineral density (BMD) and bone metabolism receiving 1200mg Calcium and 800 IU cholecalciferol as controls. Median age of the patients was 55±2 years and average time since TX was 27±4 mos. All patients were on immunosuppressive therapy and none of them had received any specific osteoporosis treatment prior to study entry. The study was conducted over 3 years; scheduled BMD measurement at the hip, spinal x-ray and laboratory analysis for bone metabolism were performed every year. Baseline Z-score values were -1.64±0.26 at the neck and -1.67±0.27 at the trochanteric region in the treatment group as compared to +0.17±0.29 and -0.09±0.43 in the control group. Furthermore bone markers (iPTH, TRAP 5b, sCTX, bALP and Osteocalcin) were significantly higher (p<0.05) among OPO patients than in controls.
After 3 years BMD of the ibandronate/calcitriol treated group had significantly increased by 17±3% at the neck (p<0.0001) and 14±3% at the trochanter (p=0.0002). Although most of the increase (+11% and +7% respectively, p<0.05) was evident in the first year of treatment, during the second and third year BMD continued to increase significantly. Control patients revealed a total bone loss of -4.8±3% at the neck and -3±1% at the trochanteric region compared to baseline (p<0.05). In the OPO patients` group bone markers decreased significantly (p<0.001) and stayed low throughout therapy.
Study results clearly indicate that a combination therapy with ibandronate and calcitriol is an effective and well tolerated treatment option in patients following LTX.

Disclosures: ***A. Fahrleitner-Pammer****, None.*

M546

Bone Density After Renal Transplantation in Relation to Immunosuppressive Therapy: a Follow-Up Study. C. Ejersted*[1], J. D. Jensen*[2], B. Jespersen*[3], C. Bistrup*[3], J. Carstens*[4], T. Torfing*[5], L. Lund-Olesen*[6], L. Mosekilde[7], K. Brixen[1]. [1]Dep. of Endocrinology, University Hospital of Odense, Odense, Denmark, [2]Dep. of Nephrology, University Hospital of Aarhus, Aarhus, Denmark, [3]Dep. of Nephrology, University Hospital of Odense, Odense, Denmark, [4]Dep. of Nephrology, University Hospital of Aarhus, Aarhus, Denmark, [5]Dep. of Radiology, University Hospital of Odense, Odense, Denmark, [6]Dep. of Radiology, University Hospital of Aarhus, Aarhus, Denmark, [7]Dep. of Endocrinology, University Hospital of Aarhus, Aarhus, Denmark.

After renal transplantation (RTx) a decline in bone mass has been described and is thought to be due to the use of immunosuppressive agents especially glucocorticoids.
In this study, bone mineral density (BMD) of lumbar spine and femoral neck where measured by dual energy x-ray absorptiometry (DEXA) at 0, 3, 6, and 12 months after RTx. Patients were included from 2 cities in Denmark having the same criteria for RTx but using different immunosuppressive therapy: in Odense a combination of cyclosporine and mycophenolate (group I, n=37) and in Aarhus a combination of prednisolone, azathioprine and cyclosporine (group II, n=29). The purpose of the study was to evaluate differences in BMD between the 2 groups.
In both groups, vertebral BMD in percent of baseline value (mean±SEM) decreased at 3, 6, and 12 months: group I:, 100±0, 96.7±0.6 *, 95.1±1.5*, 97.5±1.2*, group II: 100±0, 98.6±1.5, 94.9±1.9*, 94.8±1.8* whereas femoral neck BMD only decreased in group II (mean±SEM at 0, 3, 6, 12 months: group I:100±0, 98.9±0.6*, 98.5±0.8, 98.5±1.4, group II: 100±0, 97.9±0.5*, 96.7±0.6*, 97.1±0.7*). No BMD differences were found between the groups.
Excluding patients given anti-rejection therapy with high dose prednisolone (group I: n=9/37, group II: n =4/29) vertebral BMD decreased more in group II than group I 1 year after RTx (mean±SEM at 0, 3, 6, 12 months: group I: 100±0, 97.2±0.6 *, 97.3±1.0*, 99.4±1, group II: 100±0, 98.4±1.6, 94.9±1.9*, 94.4±2.0*#). No differences between the groups were found concerning femoral neck BMD but femoral neck BMD decreased only in group II (mean±SEM at 0, 3, 6, 12 months: group I: 100±0, 98.9±0.7, 98.7±1.0, 99.5±1.7, group II: 100±0, 98.1±0.6*, 97.0±0.7*, 97.8±0.7*).
In conclusion, BMD decreased within the first year after RTx and BMD tended to be lower in the prednisolone treated group II. However, this was only significant for vertebral BMD. (*:p<0.05 compared to baseline value, #p<0.05 group I compared to group II)

Disclosures: ***C. Ejersted****, None.*

M547

Bone Turnover Markers, Bone Mineral Density and Vitamin D-Calcium-phosphate Homeostasis before and after Liver Transplantation. E. Karczmarewicz*. ZBiMD, IPCZD, Warsaw, Poland.

Introduction: Bone disorders, frequently with fractures, are common in children with end stage liver diseases, especially associated with cholestasis. Abnormal hepatocyte function, disturbed vitamin D-Ca-P homeostasis, malnutrition and immunosupressive treatment are potential factors of bone pathology before and after transplantation.
Aim of the study: The aim of the study was to investigate bone turnover, bone mineral density, vitamin D-Ca-P homeostasis in children qualified for liver transplantation (Ltx) and during 6,9,12 and 24 months after transplantation.
Material and methods: 24 children aged 1,3 to5 years before performed living related liver transplantation were enrolled into the study. Serum levels of bone formation marker (osteocalcin - OC), bone resorption marker (CTX), densitometric bone mineral density (TB BMD -total body BMD) and BMI (body mass index) were analyzed. All patients were supplemented with 25OHD (1-2 µg/kg body weight). After transplantation immunosupressive treatment was introduced with tacrolimus (to keep the serum level 8-19 ng/dl) and prednison (0,1 mg/kg body weight). Vitamin D-Ca-P homeostasis was monitored with serum levels of 25(OH)D, Ca and P.
Results: Six months after transplantation. Marker of bone formation has increased two-fold: bone formation (OC: 60±39/141±58 ng/ml; p=0,000075) as well as bone resorption (CTX: 0,68±0,37/1,22±0,55 ng/ml, p=0,000187) reflecting pronounced stimulation of bone growth process. In the same time a twofold increase in serum PTH (20±15/39±14,0 pg/ml; p=0,000549) and 1,25$(OH)_2$D (36±14/63±20 pg/ml: p=0,000123) were observed. Increased serum levels of OC, CTX, PTH and 1,25$(OH)_2$D after 6 months continued up to 2 years of observation after transplantation. The velocity of bone growth after transplantation measured as densitometric total body bone mineral density changes per year (TB BMD/ year) was twofold increased in comparison to control group. BMD before and after transplantation was positively correlated with nutritional status (BMI). Stable levels of serum 25(OH)D, Ca and P during whole period of observation documented balanced vitamin D-Ca-P homeostasis.
Conclusions: Successful transplantation in cholestatic children with balanced vitamin D-Ca - P homeostatis triggered pronounced bone growth manifested by increased bone turnover and velocity of TB BMD changes. The role and mechanism of concomitant increase in 1,25$(OH)_2$D and PTH need further investigations.
Financial support KBN PB 98/P05/2001/20

Disclosures: ***E. Karczmarewicz****, None.*

M548

Calcitriol and Alendronate Do Not Affect Immunological Status in Cardiac Transplant Recipients. S. Xydas*[1], R. Rosen*[1], V. K. Topkara*[1], V. Addesso[2], E. M. Burke*[1], D. M. Mancini*[2], Y. Naka*[1], S. Itescu*[1], S. Maybaum*[2], M. C. Oz*[1], E. Shane[2]. [1]Surgery, Columbia University College of Physicians & Surgeons, New York, NY, USA, [2]Medicine, Columbia University College of Physicians & Surgeons, New York, NY, USA.

Calcitriol (CAL) and Alendronate (ALN) have been shown to have immunomodulatory effects in *in vitro* and *in vivo* experimental models. A recent study reported lower immunosuppression doses in cardiac transplant (CTX) recipients receiving CAL for osteoporosis prevention. We therefore examined the effects of CAL and ALN on immunological status, exposure to immunosuppressive drugs, and rates of rejection and transplant coronary artery disease (TCAD) after CTX.
We followed 211 patients who participated in a trial comparing CAL and ALN for prevention of bone loss during the first year after CTX. Patients randomized to CAL (n=71, 0.5 mcg/d) or ALN (n=70, 10 mg/d) were compared to a concurrently transplanted reference group (n=70, REF). Immunological data were analyzed retrospectively by intention-to-treat. Panel reactive antibody (PRA) and lymphocyte growth assays (LGA) were performed at the time of endomyocardial biopsies and if rejection was suspected. The presence of anti-HLA antibodies was defined as >10% panel reactivity. Outcome variables included: PRAs, LGAs, medication regimen dosages, rejection history, and TCAD incidence.
The mean age was 53.3 ± 11.2 years. Patients were predominantly male (n=175, 83%) and evenly split between ischemic (n=115, 55%) and non-ischemic (n=97, 46%) cardiomyopathy. Actuarial survival was 96% and 89% at 1 and 5 years, respectively. The mean number of rejection events was 0.86 ± 0.96 per year of followup. There were no pre-study differences between the CAL, ALN, and REF groups in age, gender, race, heart failure etiology, cross-match status, HLA class A, B, and DR matches, or PRA levels. After CTX, there were no differences among the groups in the proportion of patients with post-transplant anti-HLA IgG class I (CAL: 29%, ALN: 32%, REF 26%; p = 0.73) or class II (CAL: 34%, ALN: 38%, REF 40%; p = 0.80) antibodies or growth on LGA (CAL: 55%, ALN: 58%, REF 49%, p = 0.58). The groups did not differ in daily immunosuppressive doses at 2, 6, 9, or 12 months for prednisone, cyclosporine, FK506, azathioprine, or mycophenolate mofetil. There were no differences in the rejection rate (CAL: 1.1 ± 1.4, ALN: 1.0 ± 1.0, REF 1.0 ± 1.1 events per patient year; p = 0.61) or time-free from TCAD over a follow-up of 4.6 ± 1.7 years.
Our results revealed no clinically signficant changes in the immunological status of CTX patients treated with CAL or ALN. Patients receiving calcitriol or alendronate for the prevention of bone loss after CTX are unlikely to sustain immunological benefits from these therapies.

Disclosures: ***E. Shane****, Merck and Co. 2.*

M549

Bone Status in 52 Patients after Kidney Transplantation with and without Bisphosphonates Treatment. P. Guggenbuhl[1], S. Dupeux*[1], J. D. Albert*[1], G. Chalès*[1], P. Le Pogamp*[2], S. Werner-Leyval*[1], V. Joyeux*[2]. [1]Rheumatology, University Hospital, Rennes, France, [2]Nephrology, University Hospital, Rennes, France.

Bone loss and osteopenia are frequent complications after kidney transplantation. Many factors can explain this osteopenia, particularly the pre-existing bone renal disease and the immunosuppressive treatments. Nevertheless, treatment of osteopenia after kidney transplantation is not well established. Bisphosphonates'use after transplantation has to be validated. We retrospectively studied 52 unselected patients with kidney transplantation regularly followed in a nephrology department. There were 18 females and 34 males with a mean age of 50.4±14.5 years; all patients received immunosuppressive treatment (most of them ciclosporin) and low doses of corticoseroids. At the time of the first BMD measurement with DEXA, the median delay from transplantation was 9 months, with a mean of 68±90.5 months (0-331). A second measurement was available in 32 patients at 19±9.6 months (3-43) from the first BMD. Among them, twelve had been treated with bisphosphonates (BP): 11 with pamidronate (30 mg/3 months) and 1 with alendronate (10 mg/day) during 19.7±5.2 months (11-28). At baseline, the lumbar spine BMD was 0.775±0.167 g/cm² and the femoral neck BMD was 0.655±0.09 g/cm² ; 51/52 patients had an osteopenia (T score<-1 SD) and 34/52 an osteoporosis (T score<-2.5 SD) according to WHO criteria. Before treatment, BP patients group differed from untreated patients group only by a significantly lower T score at lumbar spine (+ 3.6 vs -1.7%*) and at femoral neck (-2.8 vs -2.11 SD*) and a higher serum creatinine level (154.17 vs 124.05 µmol/l*). The BMD annualized mean variation between the two BMD measurement, showed a significant increase at lumbar spine in the BP group (+ 3.6 vs -1.7%*) but not at femoral neck (+1.1 vs +1.4%). There was a non significant decrease of annualized variation of bone alkaline phosphatase (-9.8 vs +0.15%) and osteocalcin (-3 vs +35%) in the BP group. **Conclusion**: Osteopenia and osteoporosis are frequent after kidney transplantation. Bisphosphonates significantly increase lumbar spine BMD in patients with low BMD.
*statistically significant difference

Disclosures: ***P. Guggenbuhl****, None.*

M550

Urinary Calcium Excretion after Renal Transplant Is Inversely Associated with Bone Mineral Density. P. S. Coates[1], W. H. Lim*[2], G. R. Russ*[2], P. T. H. Coates*[2]. [1]Burnside Diabetes Centre, Rose Park, Australia, [2]Renal Unit, The Queen Elizabeth Hospital, Woodville, Australia.

Kidney transplantation is the preferred treatment for end stage renal disease. However, patients are at significantly increased risk for osteoporosis and fracture. To investigate calcium metabolism and bone turnover after renal transplant and the effects on the skeleton, we studied all stable renal transplant patients at our outpatient clinic over 3 months. Data are shown as mean ± SD (reference range). Calcium metabolism, bone turnover and bone mineral density were assessed in 31 male and 28 female patients, 10 ± 8 years post transplant, serum creatinine 133 ± 37 umol/l (50-120). All patients were treated with calcineurin inhibitors and 55 patients were also taking prednisone 10 mg daily. No patients took either thiazides or calcium supplements. Total serum calcium was 2.37 ± 0.18 mmol/l (2.10-2.55), albumin 39 ± 3.8 g/l (34-48). Intact parathyroid hormone was elevated at 11.4 ± 8.5 pmol/l (0.8-5.5*),P*<0.01*;* 25 hydroxy vitamin D 68 ± 28 nmol/l (desirable 60-160); 1,25 dihydroxyvitamin D 103 ± 41 pmol/l (50-160). Urinary calcium excretion was significantly reduced compared to the reference range at 2.8 ± 2.2 mmol/24 hours (2.5-7.5), *P*<0.01; urine creatinine 12.9 ± 4.7 mmol/24 hours (6.0-16.0). Urine deoxypyridinoline: creatinine (DPD/Cr) was 24 ± 18 nmol/mmol (<23); pyridinoline: creatinine (PYD/Cr) was 66 ± 40 nmol/mmol (<77). L1-L4 BMD (Lunar) was 1.211 ± 0.210 g/cm2 (male), 1.059 ± 0.146 g/cm2 (female). Total hip BMD was 1.004 ± 0.215 g/cm2 (male), 0.861 ± 0.109 g/cm2 (female). In a multiple stepwise regression model, independent determinants of BMD were age, bone resorption (PYD/Cr), 24 hour urine calcium and log PTH. We hypothesize that low urine calcium after renal transplant, due to a combination of dietary insufficiency and persistent secondary hyperparathyroidism contributes to loss of bone mass at clinically relevant sites. Longitudinal studies are needed to confirm this.

Disclosures: ***P.S. Coates****, None.*

M551

Osteoprotegerin Levels in Cirrhotic Patients Referred for Orthotopic Liver Transplantation. A. Monegal[1], N. Guañabens[1], M. Navasa*[2], L. Alvarez[3], D. Ozalla*[4], P. Peris[1], J. Rodes*[2]. [1]Rheumatology, Hospital Clinic, Barcelona, Spain, [2]Liver Unit, Hospital Clinic, Barcelona, Spain, [3]Biochemistry, Hospital Clinic, Barcelona, Spain, [4]IDIBAPS, Barcelona, Spain.

Aim: The purpose of the study was to analyse osteoprotegerin (OPG) levels and it's relationship to bone disease in cirrhotic patients referred for orthotopic liver transplantation.

Patients and Methods: A prospective study was carried out in 22 cirrhotic patients (13 m/9 f) (age: 54±12 years) referred for orthotopic liver transplantation. Biochemical parameters of bone mineral metabolism, standard liver function tests, urinary N-terminal cross-linking telopeptide of type I collagen (uNtx), serum levels of procollagen type I N propeptide (sPINP), serum parathyroid hormone (PTH), 25-hydroxyvitamin D levels (25OHD) and serum OPG were measured in all patients. OPG results were compared to those obtained in 29 healthy controls of similar age and sex. Bone mineral density (BMD) of the lumbar spine and proximal femur was measured by DXA and spinal X-rays were performed to detect vertebral fractures.

Results: OPG levels were higher in cirrhotic patients than in controls (6.4±2 vs 2.7±0.7; p=0.000). Ten patients had osteoporosis (45%) and only two patients (9%) had normal BMD. Moreover, 45% of cirrhotic patients showed skeletal fractures. No differences were found in OPG levels between patients with and without osteoporosis by densitometric criteria. In addition, patients with or without fractures showed similar OPG values. Negative correlations were found between OPG levels and femoral neck (R -0.46; p= 0.03) and total hip BMD (R -0.48; p= 0.025). By contrast, OPG values were not related to markers of bone turnover.

Conclusion: OPG values are elevated in patients before liver transplantation, particularly in those with reduced femoral BMD.

Disclosures: ***A. Monegal****, None.*

M552

Post-transplantation Hypogonadism: A Reflection of Sex Steroids Deficiency due to Previous Congestive Heart Failure or an Immunosuppressive Side Effect? J. Stief*, R. Gaertner, P. Ueberfuhr*, K. Theisen*, H. Stempfle. Cardiology, Med. Poliklinik Innenstadt, LMU, Munich, Germany.

Background: Hypogonadism might play an important role in the multifactorial pathogenesis of the immunosuppressant-induced bone loss. We recently demonstrated that cardiac transplants with hypogonadism reveal a significant decrease in bone mineral density compared to normogonadal patients. It remains unclear, however, if the post-transplantation hypogonadism reflects only a sex steroid deficiency due to previous congestive heart failure (CHF) or a side-effect of the immunosuppressive therapy.

Methods: The following longitudinal study examined the role of hypogonadism in the evolution of bone loss in 20 male patients before and after heart transplantation (HTx). Immunosuppressive therapy included calcineurin phosphatase inhibitors, antiproliferative agents and corticosteroids. Total serum testosterone (T ng/dl), sex hormone binding globulin, serum free testosterone, as well as gonadotropins: luteinizing hormone (LH U/l) and follicle stimulating hormone (FSH U/l) were measured in fasting patients before and six months after HTx.

Results: The mean testosterone level decreased significantly after transplantation (433ng/dl vs. 314ng/dl; p = 0,024). 6 of the 20 (30%) patients with CHF showed an hypogonadism with a mean testosterone level of 239±35 ng/dl and inadequately low gonadotropins (LH 5U/l±5,7, FSH 6,4U/l±7) indicating a hypogonadotropic hypogonadism. Six month after HTx, all six patients remained hypogonadal. Additionally three transplant patients developed a new hypogonadism within the study period (T 202ng/dl±74, LH 7,8U/l±1,8, FSH 8,9U/l±2,7). Therefore 45% (9 of 20) of patients after HTx demonstrated a sex hormone deficiency followed by a decrease in bone mineral density.

Conclusions: Hypogonadism is frequently seen in patients with CHF. After HTx, however, a significant decrease in gonadal hormones is observed probably due to the immunosuppressive therapy. Furthermore hypogonadal patients showed no recovery of gonadal function within six months. To prevent rapid bone loss, truly hypogonadal patients might profit from testosterone replacement after HTx. The role of replacement therapy in patients with CHF remains still unclear.

Disclosures: ***J. Stief****, None.*

M553

Bone-Protective Therapy after Kidney and Kidney Pancreas Transplantation. G. J. Elder, C. Moy*. Department of Renal Medicine, Westmead Hospital, Sydney, Australia.

After transplantation, immunosuppressives and residual changes of osteodystrophy influence bone strength. Kidney pancreas transplant recipients may be at particular risk. Eighty-three kidney and 49 kidney pancreas recipients were assessed before and 2 weeks, 3 and 12 months after transplantation. One-year data is available on 38 kidney and 19 kidney pancreas recipients. BMD was assessed by dual-energy X-ray absorptiometry at baseline and 12 months. Patients with diabetes spent fewer months on dialysis (21±17 vs. 38±37, p=0.005), had lower body mass index (BMI) (24.7±2.8 vs. 26.5±4.9 kg/m^2, p<0.05) and levels of 25-hydroxyvitamin D (49±24 vs. 70±30 nmol/l, p=0.0003). Patients without type 1 diabetes had normal Z scores at the lumbar spine (0.1±1.5) femoral neck (-0.2±1.3) and wrist (0.5±2). Patients with type 1 diabetes had lower BMD at the lumbar spine (p<0.05), femoral neck (p<0.0001) and wrist (p<0.02) but BMD was normal except at the femoral neck (Z score -1.4±0.9). Prevalent vertebral fracture was present in 31% but did not differ for patients with or without diabetes. After transplantation, patients commenced standard therapy (calcium plus ergocalciferol or calcitriol as required). Patients with osteoporosis and/or prevalent fracture added bisphosphonates. Treatment did not differ with transplant type. Baseline iPTH of 6.9±6.7 fold the assay upper range, reduced to 2.4±2.9 fold at 2 weeks and 1.4±1 fold at 1 year. Deoxypyridinoline/creatinine ratios fell from 2 weeks to 1 year (p=0.005) but levels remained at or above the upper range. Serum osteocalcin in the mid-normal range was lower in kidney pancreas recipients (p<0.05 at 2 weeks). BMD did not change significantly within either group (paired t-test) but between groups, lumbar spine BMD for kidney recipients increased by 5±2% (mean±SEM) vs. -1±2% for kidney pancreas recipients (p<0.05). Patients treated with bisphosphonate or standard therapy did not differ in outcome. In conclusion, with targeted therapy, BMD loss was not detected in the first year after kidney or kidney pancreas transplant. Bone turnover markers suggest hyperparathyroidism and elevated bone resorption are present in both groups. Kidney pancreas recipients have additional risk factors, including lower baseline BMD and 25-hydroxyvitamin D levels.

Disclosures: ***G.J. Elder****, None.*

M554

The Type I PTH/PTHrP Receptor Associates with Karyopherins in Cultured Osteoblast-like Cells. B. W. Pickard*, L. J. Fraher, A. B. Hodsman, P. H. Watson. Medicine, Lawson Health Research Institute, University of Western Ontario, London, ON, Canada.

Parathyroid hormone regulates bone turnover via its interaction with the type 1 PTH receptor (PTH1R) present on osteoblasts. Our studies have demonstrated that PTH1R is not only found on the cell membrane, but also in the nucleus, thus providing a new avenue for the exploration of the mechanisms behind the action of PTH. Proteins destined for the nucleus contain intrinsic nuclear localization signals (NLS). Such a signal is present in the PTH receptor carboxy-terminus region (rat/mouse:471-487) which is highly conserved across all known PTH1R sequences. Receptors are targeted to the nucleus through the interaction of their NLS with proteins of the karyopherin (Kap) family of transport regulatory molecules. To determine the identity of individual members of the Kap family in the regulation of nuclear transport of PTH1R, rat osteosarcoma (ROS 17/2.8), mouse non transformed osteoblast cell line (MC-3T3-E1), and human osteosarcoma (SaOS-2) were cultured under standard conditions for use in assays. Cells were grown on cover slips and probed with antibodies to the C-terminal domains of PTH1R, Kap apha2 and Kap beta1 by immunofluorescence. Immunoprecipitation and western blots were used to investigate the interaction between the karyopherins and PTH1R. PTH1R, Kap alpha2/beta1 were immunoprecipitated with antibodies to the C-terminal domains with protein G Sepharose 4 Fast Flow beads. Immunoprecipitations were then separated by SDS-PAGE and probed with antibodies to the N-terminal domain of PTH1R and Kap beta1 and antibodies to the C-terminal domain of Kap alpha2. Blots were also probed with biotinylated hPTH(1-84) (ligand blots) to confirm the presence of PTH1R in immunoprecipitates. Immunoprecipitation and western blots have identified karyopherin alpha2 and beta1 as proteins that associate with PTH1R. Biotinylated PTH 1-84 recognized a 66.3 KD band on blots of samples immunoprecipitated with each of the 3 antibodies, thus confirming the Western blot results. Immunofluorescence has confirmed the presence of PTH1R and Kap alpha2/beta1 in three osteoblast like cell lines as well as demonstrated the spatial overlap of these proteins. Studies on the co-localization of these proteins in rat liver tissue add additonal support these results. These studies have demonstrated that PTH1R associates with Kap alpha2 and beta1 suggesting a role for the karyopherins in the regulation of PTH1R transport to the nucleus. Future studies on the function of PTH1R in the nucleus will identify candidate genes potentially involved in the anabolic response of bone to PTH or novel genes involved in the PTH regulation of bone metabolism.

Disclosures: ***B.W. Pickard****, None.*

M555

Mechanism of Concanavalin A on PTH Receptor Down-regulation on Cell Membrane. Q. Sun[1], R. W. Katz[2], X. Fan*[1], J. P. Bilezikian[1]. [1]Division of Endocrinology, College of Physicians and Surgeons, Columbia University, New York, NY, USA, [2]Oral Medicine, College of Dentistry, New York University, New York, NY, USA.

Stimulation of PTH receptors in intact cells causes, first, rapid functional uncoupling from its G-protein complex, and, second, a somewhat slower sequestration of receptors to internal compartments. We have previously reported that pretreatment of EW-29 cells with hPTH(1-34) down-regulates the PTH receptor. The present study addresses the hypothesis that concanavalin A, which has been used in some cell lines to block receptor sequestration, will impair PTH-receptor down-regulation. Exposure of EW-29 cells to 10-7M hPTH(1-34) caused a time-dependent receptor internalization. Maximal internalization of labeled PTH was reached by 3 hours. After 3 hours exposure to 10-7 M hPTH(1-34), PTH-dependent adenylyl cyclase (ACA) and phospholipase C (PLC) activities were suppressed by 25% and 84%, respectively, and membrane PTH receptor labeling was 31% of untreated control cells. Pretreatment with concanavalin A and hPTH(1-34) resulted in complete recovery of ACA and only 40% suppression of PLC compared to untreated control cultures. Surprisingly, concanavalin A pretreatment with hPTH increased PTH receptor internalization by 20%, increased the amount of surface receptor two-fold, but did not alter receptor recycling rate to the surface. This study indicates that concanavalin A recovery of homologous down-regulation of PTH-dependent ACA and PLC activity is independent of receptor internalization. The mechanism by which PTH receptor function is protected by concanavalin A in this model may provide information on how to extend the activity of PTH analogues through modulation of receptor down-regulation.

Disclosures: ***Q. Sun****, None.*

M556

The Sodium/Proton Exchanger Regulatory Factor Type I (NHERF1/EBP50) Regulates PTH(7-34) but not PTHrP(7-34)-induced Type I PTH Receptor (PTH1R) Internalization. W. B. Sneddon. Dept of Pharmacology, University of Pittsburgh School of Medicine, Pittsburgh, PA, USA.

Internalization of the Parathyroid Hormone Type I Receptor (PTH1R) is regulated in a cell- and ligand-specific manner. We have previously demonstrated that the presence or absence of the sodium/proton exchanger regulatory factor type 1 (NHERF1) is pivotal in determining the range of peptides that are capable of internalizing the PTH1R. For example, PTH(7-34), which binds to, but does not activate the PTH1R, internalizes the PTH1R in kidney distal tubule (DT) cells, where NHERF1 is not expressed. Introduction of NHERF1 into distal tubule cells blocks PTH(7-34)-induced PTH1R internalization. Similarly, PTH(7-84), a secreted C terminal fragment, internalizes the PTH1R in a NHERF1-dependent manner. Very little is known, however, about PTH1R internalization in response to PTH-related protein (PTHrP) fragments. We, therefore, examined a series of synthetic PTHrP fragments for their ability to induce PTH1R internalization. PTH1R internalization was examined using real time confocal fluorescence microscopy of mouse DT cells stably expressing an EGFP-tagged PTH1R. PTHrP(1-36), which binds and activates the PTH1R, internalized the PTH1R 50% after 15 min. PTHrP(7-34), a PTH1R antagonist, internalized the PTH1R 80% after 15 min. This is similar to the level of PTH1R endocytosis observed in response to PTH(7-34). In contrast to PTH(7-34), however, PTHrP(7-34)-stimulated PTH1R internalization was not inhibited by overexpression of NHERF1. This effect of a synthetic PTHrP fragment, while not physiological, is informative in terms of how PTH1R levels can be exogenously regulated. Under pathophysiological circumstances such as renal failure, PTH(7-84) levels are elevated and may contribute to PTH resistance by selectively downregulating the PTH1R in specific tissues such as renal distal tubules, where NHERF1 is absent. If a less selective downregulation of the PTH1R is desirable, synthetic peptides could be designed to remove the NHERF1-dependence of this process and promote PTH1R internalization in a broader range of cells and tissues.

Disclosures: ***W.B. Sneddon****, None.*

M557

A role for Src Family Kinases in PTH Activation of ERK1/2 Mitogen Activated Protein Kinases. H. A. Tawfeek*, A. B. Abou-Samra. Endocrine Unit, Massachusetts General Hospital, Boston, MA, USA.

Our previous results suggested that PTH/PTHrP receptor phosphorylation and internalization are not required for PTH activation of ERK1/2 mitogen-activated protein (MAP) kinases. The goal of the current study was to investigate the role of Src family non-receptor tyrosine kinases in PTH activation of ERK1/2 MAP kinases and to examine whether these signaling pathways are involved in PTH regulation of P90RSK ribosomal kinase, CREB/ATF-1 and c-fos. PTH increased phosphorylation of Hck Src kinase in LLCPK-1 stably expressing PTH/PTHrP receptor. To study the role of Src family kinases, we used a combination of pharmacological and biochemical inhibitors. PP2, a specific Src family kinase inhibitor, caused a remarkable decrease in PTH activation of ERK1/2. Furthermore, stable over-expression of a c-terminal Src family kinase (CSK), a physiological down-regulator of Src kinases activity, in LLCPK-1 cells attenuated ERK1/2 activation in response to PTH treatment. PTH increased phosphorylation of P90RSK and CREB/ATF-1 and induced transcription of c-fos. U0126, a specific inhibitor of ERK1/2 pathway, and PP2 Src family kinase inhibitor did not significantly affect PTH activation of CREB/ATF-1. Both U0126 and PP2, however, significantly reduced PTH phosphorylation of P90RSK. Additionally, U0126 decreased PTH stimulation of c-fos expression. Taken together, these data suggest that Src family kinase(s) are involved in PTH activation of ERK1/2 MAP kinases and P90RSK but not in PTH activation of CREB/ATF-1 and that ERK1/2 MAP kinases play a role in PTH-stimulation of c-fos expression.

Disclosures: ***H.A. Tawfeek****, None.*

M558

Defining the Entry Point of Parathyroid Hormone (1-34) into the PTH1 Receptor. A. Wittelsberger[1], M. Corich*[1], B. Lee*[1], B. E. Thomas*[1], A. Ahmad*[1], M. Chorev[2], D. F. Mierke[3], M. Rosenblatt[1]. [1]Department of Physiology, Tufts University School of Medicine, Boston, MA, USA, [2]Laboratory for Translational Research, Harvard Medical School, Cambridge, MA, USA, [3]Department of Chemistry and Molecular Pharmacology, Brown University, Providence, RI, USA.

Parathyroid hormone (PTH) 1-34 contains two a-helical domains associated with specific functions: the N-terminal helix is required for activation of its G protein-coupled receptor, and the C-terminal helix is responsible for receptor binding. We recently focused on the role of the mid-domain of PTH. The region from residue 14-15 to residue 19-21 was found to be unstructured in solution by NMR studies. Whereas distinct contact sites between N-terminal and C-terminal residues of PTH and the receptor had been identified by photoaffinity crosslinking studies and could be used for molecular modeling of the ligand-receptor complex, little information was available on interactions of the hormone mid-region. In particular, it was not known at what site of the helix bundle the mid-region of PTH traversed to connect the N-terminal activation domain in contact with the top of transmembrane helix (TM) VI and the C-terminal binding domain interacting with the N-terminal extracellular domain (N-ECD) of the receptor. Recently, we introduced the photoreactive p-benzoylphenylalanine singly at positions 11, 15, 18, and 21 in a series of PTH-(1-34) analogs. By digestive mapping of the crosslinked conjugates, we then identified receptor regions [165-189], [183-189], [189-240], and [165-189] as respective contact sites. Molecular dynamics simulations, using the crosslinking regions of the mid-region in addition to previously identified contact sites as distant restraints, showed a refined model of the PTH ligand-receptor complex in which the ligand traverses between the top of TM's I and II. This finding prompted us to propose an intermediate step in the ligand-receptor interaction: after binding of the N-terminal ligand domain to the N-ECD of the receptor, extensive contacts in the mid-region anchor the hormone in the correct orientation for the N-terminal domain to reach, in the third step, the binding groove within the helix bundle, leading to receptor activation. Our current work investigates several routes to test the important role we propose for the mid-region of the hormone. Primarily, using point mutations within the [165-189] region of the receptor for introduction of additional cleavage sites and/or probing for important side-chain contacts, we are aiming at a higher resolution model of the entry point of PTH-(1-34) into the receptor's 7 transmembrane helical bundle.

Disclosures: ***A. Wittelsberger****, None.*

M559

PTH1R Endocytosis and G_q Signaling Independently Contribute to the Activation of the Mitogen-activated Protein Kinases ERK1 and ERK2. C. A. Syme*, A. Bisello. Department of Medicine/Division of Endocrinology and Metabolism, University of Pittsburgh, Pittsburgh, PA, USA.

Agonist-mediated activation of the type 1 parathyroid hormone receptor (PTH1R) results in several signaling events, and receptor endocytosis. It is well documented that arrestins contribute to desensitization of both G_s- and G_q-mediated signaling and mediate PTH1R internalization. However, whether PTH1R trafficking directly contributes to PTH1R signaling remains unclear. To begin addressing this, we investigated the role of PTH1R trafficking in cAMP signaling and ERK1/2 activation in HEK-293 cells. Dominant-negative forms of dynamin (K44A) and β-arrestin2 (319-418) abrogated PTH1R internalization but had no effect on cAMP signaling: neither acute cAMP production by PTH, nor desensitization and resensitization of cAMP signaling were affected. Identical observations were made in either the absence or presence of cyclohexamide. Therefore, PTH1R trafficking is not necessary for regulation of cAMP signaling. ERK1/2 activation by PTH(1-34) peaked at 5 min (average 4.8-fold ± 1.3, n=15). A PTHrP-based analog (Bpa[1]-PTHrP-(1-36)) that selectively activates the G_s/cAMP/PKA without inducing PTH1R endocytosis, failed to activate ERK1/2, indicating that G_q-signaling and/or PTH1R internalization are required for ERK1/2 activation. Inhibition of PTH1R endocytosis by K44A-dynamin dampened ERK1/2 activation in response to PTH(1-34) by 45%. For wild-type PTH1R, ERK1/2 activation occurred only in response to the full agonist PTH(1-34) but not to PTH(7-34). In contrast, a mutant PTH1R (M593A-PTH1R) which does not require activation for endocytosis was able to induce ERK1/2 phosphorylation in response to both PTH(1-34) and PTH(7-34). Collectively, these data indicate that PTH1R trafficking and G_q (but not G_s) signaling independently contribute to ERK1/2 activation. Together with previous reports, these findings underlie the complexity of the molecular mechanisms leading to PTH-stimulated ERK1/2 activity, which may involve G_q-mediated ERK1/2 activation, transactivation of EGF receptors and PTH1R trafficking.

Disclosures: ***C.A. Syme****, None.*

M560

Specific Activation of Type I or C-Terminal PTH Receptors Regulate Gap-Junctional Communication Among Bone-Derived Cells Expressing or Lacking PTH1R. P. C. Schiller*[1], G. D'Ippolito*[1], P. Divieti[2], F. R. Bringhurst[2], G. A. Howard[1]. [1]Medicine, University of Miami/VAMC, Miami, FL, USA, [2]Endocrine Unit, Massachusetts General Hospital, Boston, MA, USA.

We and others have reported that gap-junctional communication (GJC) plays a critical role in bone physiology. A potential part of the mechanism of that role is the fact that parathyroid hormone (PTH) can increase cell-to-cell GJC among bone cells via activation of the type 1 PTH/PTHrP receptor (PTH1R). In other studies we have shown that long fragments of PTH, lacking the N-terminal portion of the hormone, are able to bind to a receptor distinct from the PTH1R and specific for the C-terminal region of PTH, the CPTH receptor (CPTHR). To assess if CPTHR activation is involved in cell-to-cell communication, we studied GJC in bone cells lacking PTH1Rs but expressing CPTHRs. Quantification of GJC was determined in PTH1R-null osteoblastic (F1-14) and osteocytic (OC14) cell lines as well as in MC3T3-E1 mouse and ROS 17/2.8 rat osteoblastic cells expressing functional PTH1Rs. Specifically, fluorescent dye transferred from loaded PTH1R-null F1-14 and OC14 cells, as well as from MC3T3-E1 and ROS 17/2.8 cells to F1-14 and OC14 cells. Similarly, F1-14 and OC14 cells transferred pre-loaded dye to MC3T3-E1 and ROS 17/2.8 cells, demonstrating that PTH1R expression is not required for GJC. We then investigated whether PTH fragments, with different C termini, could modulate the extent of GJC among PTH1R-null bone cells and PTH1R-expressing osteoblastic cells. We quantitatively assayed GJC in the presence and absence of PTH(1-34), PTH(53-84) or PTH(1-84). Interestingly, PTH(1-84) and PTH(53-84) significantly increased GJC among PTH1R-null cells, while PTH(1-34) had no effect in these cells. PTH(1-84) also increased GJC between ROS 17/2.8 and OC14 or F1-14 cells. In those experiments PTH(1-34) also had a stimulatory effect similar to that of PTH(1-84). Finally, PTH(53-84) increased GJC between MC3T3-E1 cells and OC14 or F1-14 cells. Our results demonstrate that PTH1R-null cells not only form functional GJ channels among themselves but also with cells expressing PTH1Rs. In addition, activation of CPTHR not only increases GJC between PTH1R-null cells but also with PTH1R-expressing osteoblasts. Our data strongly suggest that CPTHRs may play a critical role in regulating cell-to-cell communication and maintaining bone homeostasis independent of the PTH1R.

Disclosures: ***P.C. Schiller****, None.*

M561

Parathyroid Hormone Activates a Galpha12/Galpha13-RhoA-Phospholipase D Signaling Pathway in Osteoblastic Cells. A. T. K. Singh[1], A. Gilchrist*[2], T. Voyno-Yasenetskaya*[3], P. H. Stern[1]. [1]Molecular Pharmacology and Biological Chemistry, Northwestern University, Chicago, IL, USA, [2]Molecular Pharmacology and Biological Chemistry, Cue BIOtech, Chicago, IL, USA, [3]Pharmacology, University of Illinois, Chicago, IL, USA.

Parathyroid hormone (PTH) interaction with its receptor in osteoblasts activates signaling through heterotrimeric G proteins. We have shown that PTH activates phospholipase D (PLD) in both UMR-106 osteoblastic cells and primary osteoblasts, however the G protein mediating this response, and the intermediate signaling events between G protein activation and PLD are not yet established. To determine the involvement of specific Gα subunits, UMR-106 cells were transfected with minigenes coding for expression of small peptides antagonistic to specific G protein alpha subunits, prior to 30 minute treatment with 10 nM bPTH 1-34. PLD was measured by transphosphatidylation. Minigenes coding for antagonists to Gα12 and Gα13 prevented the effect of PTH, whereas those coding for Gαs and Gαq were ineffective. The lack of effect of Gαs supports previous findings that PTH stimulation of PLD does not require PKA. We previously found that PTH activates RhoA, and that RhoA is essential for PTH stimulation of PLD in UMR-106 cells. The role of RhoA in Gα12 and Gα13-stimulated PLD activation was evaluated. Transfection with dominant negative RhoA prevented PLD activation by constitutively active Gα12 and Gα13. PTH-stimulated PLD is inhibited by the statin, mevastatin, and the aminobisphosphonate, alendronate. Since RhoA is activated by isoprenylation, the effects of these agents on PLD could be due to their inhibition of the formation of isoprenyl groups in the cholesterol biosynthesis pathway. To investigate this, intermediates in cholesterol biosynthesis were tested. Mevalonate, the product of HMGCoA reductase, prevented the inhibitory effect of the statin, but not of the bisphosphonate on PTH-stimulated PLD activity. Squalene, which acts at a step beyond the generation of isoprenyl groups, failed to prevent the effects of either inhibitor. However, the geranylgeranyl group donor, geranylgeranylpyrophosphate, which would bypass the steps at which both statins and bisphosphonates inhibit the pathway, prevented the inhibitory effects of both compounds on PLD. The current findings demonstrate that Gα12 and Gα12-containing heterotrimeric G proteins, and subsequent RhoA activation, mediate the effects of PTH on PLD in osteoblastic cells. The results further suggest that effects of statins and aminobisphosphonates on isoprenylation mediate their inhibitory effects on PTH-stimulated PLD activity, which could lead to their modulation of differentiated functions of osteoblasts.

Disclosures: ***A.T.K. Singh****, None.*

M562

Pelvic Sexual Dimorphism Is Generated through Opposite Functions of Sex Hormone Receptors in Mice. S. Tanaka*[1], T. Matsumoto*[1], T. Yamada[2], K. Yoshimura*[1], H. Shiina*[1], J. Miyamoto*[1], Y. Yamamoto*[1], T. Sato*[1], A. Krust*[3], P. Chambon*[3], S. Kato[1]. [1]IMCB, Univ. of Tokyo, Tokyo, Japan, [2]Dept. of Orthopedic Surgery, Faculty of Medicine, Univ. of Tokyo, Tokyo, Japan, [3]IGBMC, ULP, Strasbourg, France.

Sexual dimorphism in bone patterning, mineral density and size is well known in mammals. Particularly, the sexual dimorphism of humans is evident in pelvic patterning. The pelvic cavity in female is larger than that in male. Although a number of morphometric analyses have been performed, the molecular basis for the generation of such sexual dimorphism remains largely unknown. To address this issue, we established the analysis model of pelvis in growing mice for genetic identification of factors, that generate sexual dimorphism. In the present study, we found that opposite functions of sex hormone receptors define the sexual dimorphism of the pelvis.

Pelvic patterning was examined in 9-week-old wild-type (WT) mice. In female mice, the pubis was about 50% longer than that in male mice, and accordingly the cavity area of pelvis was also about 50% larger. The analyses of 2 to 9-week-old WT mice revealed that the sex difference of these parameters could be detected at the age of 4 weeks, and became marked before sexual maturation, thus implicating sex hormone actions.

To investigate this possibility, we analyzed androgen receptor knockout (ARKO) and estrogen receptor α/β knockout (ERα/βKO) mice. The pelvic cavity in either male ARKO mice or female ERαKO mice was clearly altered, and both of them exhibited an almost identical intermediate volume.

Gonadectomy of mice at the age of 2 weeks grew up in both adult male and female WT mice with an intermediate type pelvis. Treatment with 5α-dihydrotestosterone (DHT) reduced the intermediate type pelvis into the narrow male type pelvis in both male and female gonadectomized WT mice. Conversely, treatment with 17β-estradiol (E2) enlarged the intermediate type pelvis into female wider type pelvis in both male and female gonadectomized WT mice. However, such hormonal actions were not seen in mice deficient in the cognate receptor.

To further investigate the molecular basis of the hormonal actions in the pelvis, we performed morphological and histological analyses of the pelvis of growing mice. We identified growing chondrocyte layers at the distal end of the pubis, that is presumed to support bone growth. A BrdU incorporation experiment showed that the rate of proliferation of the proliferating chondrocyte layer in female pubis was higher than that in male, while such a sex difference was not seen in receptor KO mice.

From these studies, we conclude that the sexual dimorphism of the pelvic pattering is generated through opposite functions of sex hormone receptors, but not genetic sex.

Disclosures: ***S. Tanaka****, None.*

M563

Bone and Muscle Protection and Prostate-Sparing Effects of the Selective Androgen Receptor Modulator (SARM) 7α-Methyl-19-Nortestosterone: Evidence from the Aged Orchidectomized Male Rat Model. K. Venken*[1], S. Boonen[1], E. Van Herck*[1], L. Vandenput*[1], N. Kumar*[2], R. Sitruk-Ware*[2], K. Sundaram*[2], R. Bouillon[1], D. Vanderschueren[1]. [1]K.U. Leuven, Leuven, Belgium, [2]Center for Biomedical Research, Population Council, New York, NY, USA.

The synthetic androgen 7α-methyl-19-nortestosterone (MENT™) is a selective androgen receptor modulator (SARM) which is not converted to a dihydroderivative by 5α-reductase in the prostate. This study reports its bone protective potential as assessed in the aged orchidectomized male rat model. Male, 13-month old Wistar rats were either sham-operated (sham) or orchidectomized (orch). Groups of orchidectomized rats were treated with different doses of MENT (4, 12 or 36 µg/day) subcutaneously for 16 weeks via mini-osmotic pumps. Analysis of the effects of androgen deficiency versus MENT replacement was performed using quantitative computed tomography (pQCT), dual energy X-ray absorptiometry (DEXA), and biochemical markers of bone turnover. At the end of the study period, prostate weight in orchidectomized rats treated with low- (4 µg/day) or mid-dose (12 µg/day) MENT

remained significantly lower compared to the sham-operated animals (-47% and -25%, respectively, $p < 0.05$). High-dose MENT (36 µg/day), on the other hand, induced prostate hypertrophy (+21%, $p < 0.05$). Low-, mid-, and high-dose MENT were found to be effective in suppressing the acceleration of bone remodelling following orchidectomy, as assessed by osteocalcin (-25%, -44% and -53% respectively, $p < 0.05$) and deoxypyridinoline (-45%, -66% and -79% respectively, $p < 0.05$) and in preventing orchidectomy-induced bone loss at the spine, femur, and total-body, as evaluated by DEXA and, at the femur, as evaluated by pQCT (+ 76%, + 75% and +67% respectively, $p < 0.05$). Compared to sham-operated animals, the low- and mid-dose MENT groups showed no decline in lean body mass and no muscle atrophy (as measured by m. quadriceps weight) at 16 weeks, whereas high-dose MENT was associated with a significant decline in lean body mass (-8.5%, $p < 0.05$) and quadriceps weight (-10.6%, $p <0.05$). MENT behaves as a SARM in orchidectomized aged rats as low- and mid-doses have full bone and muscle protective effects while not inducing prostate hypertrophy. Our findings support the need for human studies to explore the potential of MENT as an option for androgen replacement in aging men.

Disclosures: ***K. Venken****, None.*

M564

Estrogen Stimulates Periosteal Expansion in Male Mice, Even in the Context of Depressed Systemic Levels of Insulin-Like Growth Factor-I. K. Venken*[1], S. Boonen[1], M. Lindberg*[2], N. Andersson*[2], S. Movérare*[2], J. Svensson*[2], R. Bouillon[1], C. Ohlsson[2], D. Vanderschueren[1]. [1]K.U. Leuven, Leuven, Belgium, [2]Gothenburg University, Gothenburg, Sweden.

Based on animal research in ovariectomized animal models, estrogen is generally considered to inhibit, not stimulate skeletal growth. This concept, however, was not supported by recent observations of ongoing radial skeletal growth during estrogen treatment in a young man with aromatase deficiency (R. Bouillon et al., unpublished data). The current study in male orchidectomized mice was designed to address the question as to whether estrogen is able to stimulate periosteal bone formation and, if so, to what extent this stimulatory action involves interaction with systemic insulin-like growth factor-I (IGF-I). To this end, periosteal bone formation was assessed by dynamic histomorphometry following estradiol (E_2) replacement (0.05 µg/day via subcutaneous silastic implants) in 3-month-old orchidectomized (orch) male mice with Cre-loxP-induced liver-specific IGF-I gene inactivation (LI-IGF-I KO) and corresponding WT mice. Mice were treated for 5 weeks. Results are expressed as % gain or loss compared to orch and analysed via two-factor ANOVA. As shown in the figure, periosteal bone formation (Ps.BFR/B.Pm.) increased significantly, not only in E_2-treated orch WT (+114%) but also in E_2-treated orch Li-IGF-I KO mice (+46%). In the latter, periosteal bone apposition was induced despite severely reduced serum IGF-I levels (-79%). E_2 activated both osteoblast number (+93% and +37%, respectively) and activity (+18% and +8%, respectively) at the periosteal site in WT and Li-IGF-I KO. Periosteal bone apposition resulted in significant thickening of the femoral cortical area, both in WT (+22%) and Li-IGF-I KO (+23%). Moreover, E_2 upregulated cortical (+5% and +9% in WT and Li-IGF-I KO, respectively) and trabecular (+38% and +40%, respectively) bone mineral density, as measured by pQCT. In addition, polar moment of inertia, a non-invasive marker of bone strength, was higher in E_2-treated animals (21% and 38%, respectively).We conclude that estrogen is able to stimulate periosteal expansion in male orchidectomized mice, even in the context of depressed systemic IGF-I levels.

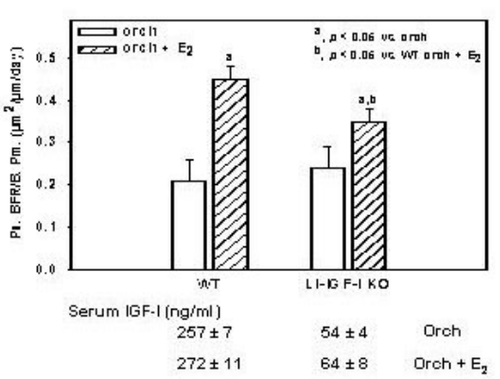

Disclosures: ***K. Venken****, None.*

M565

Effect of OVX and E2 Treatment on Bone in Aged ERKO Mice. Z. Peng, H. Väänänen*, P. Härkönen*. Department of Anatomy, Institute of BioMedicine, Turku, Finland.

In order to understand the role of estrogen receptors in bone metabolism we studied effects of ovariectomy (OVX) and estradiol (E2) treatment on bone in aged estrogen receptor alfa knockout (ERKO) mice. Over one year old ERKO and wild type mice were ovariectomized and half of them were implanted with subcutaneous E2 pellets for four weeks. Bone analysis included pQCT, bone histomorphometry and mechanical testing. Results from OVX and E2 treatment groups were compared to age matched control groups of wild type (WT) and ERKO animals. pQCT measurements showed that E2 treatment significantly increased trabecular bone density at proximal tibia and distal femur of both WT-OVX and ERKO-OVX animals. In histomorphometry both OVX-WT and OVX-ERKO groups showed increased area of bone marrow cavity, which was prevented by E2 treatment in both groups. Dynamic histomorphometry revealed highly elevated mineral apposition rate (MAR) and bone formation rate (BFR) at periosteum of the femoral shaft in both OVX groups. This increase was more efficiently inhibited by E2 in WT than in ERKO mice. OVX did not have a clear effect on endocortical MAR or BFR but E2 treatment markedly elevated MAR. E2 stimulation of BFR was, however, more enhanced in the WT than in the ERKO group. TBV was higher in ERKO than WT mice. It was decreased by OVX and strongly increased by E2 treatment in both groups. However, the maximal load of the bending strength was decreased in WT-OVX-E2 group compared to WT-OVX or WT group. This difference was not seen in ERKO groups. Histological appearance of E2-increased trabecular bone was roughly similar in WT and ERKO mice indicating a typical high turnover situation with an increased number of active osteoblasts and osteoclasts. These results suggest that aged female ERKO mice are almost as sensitive as WT mice to E2 treatment and arouse interesting questions concerning possible age dependent functions of different estrogen receptors.

Disclosures: ***Z. Peng****, None.*

M566

SRC-2 Associates Preferentially with ERα. F. J. Secreto[1], D. G. Monroe[1], S. K. Dutta*[1], B. L. Riggs[2], S. Khosla[2], T. C. Spelsberg[1]. [1]Biochemistry, Mayo Clinic, Rochester, MN, USA, [2]Endocrine Research Unit, Mayo Clinic, Rochester, MN, USA.

Nuclear co-activators (NCo-A) and co-repressors (NCo-R) play a critical role in mediating the ability of nuclear receptors to effect gene expression in a tissue specific manner. Although some NCo-A/NCo-R proteins are required for estrogen receptor (ER) mediated gene transcription in many tissue types (ex. SRC-1), others are not as ubiquitous in their tissue distribution. AIB-I (SRC-3) is a carcinoma specific NCo-A, virtually undetectable in human osteoblasts. Further, the various SERMS and pure ER antagonists profoundly effect the recruitment of co-activator proteins. Since estrogen (E2) regulates many key processes involved in bone homeostasis, we wanted to extend our studies of NCo-A/NCo-R beyond SRC-1, which our lab and others have found to be an essential component of ER mediated gene expression in osteoblasts. We choose to examine SRC-2 (NCo-A), a co-activator that has not been thoroughly investigated in osteoblasts to date. Although SRC-2 has been studied at the protein level in other tissues, we have had limited success with commercial antibodies recognizing the protein. Therefore, we developed polyclonal antibodies to SRC-2 using a specific peptide epitope. Using nuclear extract isolated from human fetal osteoblast cells (hFOb), U2OS cells, and COS-7 cells, immunoblots showed that SRC-2 was present, and the signal was successfully reduced using antibodies pre-incubated with an excess of the corresponding immunoreactive peptide. Nuclear extract pull-down assays using GST-ERα C-terminal domain (AF-2) fusion proteins pre-incubated with either E2, 4'OH-Tamoxifen (4HT), or ICI, showed that SRC-2 binding to the AF-2 domain of the ERα increased with E2 treatment. SRC-2 binding was nearly absent in ICI and 4HT treated samples, comparable to control levels. Interestingly, minimal binding of SRC-2 was seen in pull-down assays using similarly treated GST-ERβ fusion proteins, regardless of the source of nuclear extract on the bound ligand. This isoform specificity may explain the preferential enhancement of gene expression we observed in osteoblasts co-transfected with SRC-2 and ERα compared to similarly treated cells co-expressing SRC-2 and ERβ. Future experiments, including the use of Si-RNA targeted to both SRC-1 and SRC-2, will be used to elucidate E2-dependent gene expression differences that exist between cells expressing ERα and ERβ .

Disclosures: ***F.J. Secreto****, None.*

M567

Growth Plate Chondrocytes Respond to Estrogen with Sex Specific Increases in IP3 and Intracellular Ca^{++} Signaling via a Capacitative Entry Mechanism. Z. Schwartz[1], J. Ekstein*[2], E. Nasatzky*[2], A. Ornoy*[2], B. D. Boyan[1]. [1]Biomedical Engineering, Georgia Institute of Technology, Atlanta, GA, USA, [2]Periodontics, Hebrew University, Jerusalem, Israel.

17-Beta-estradiol (E_2) regulates growth plate chondrocyte differentiation through two interacting pathways: via classic nuclear receptors ERα and ERβ, and through membrane associated signaling. E_2's effects are gender-specific and cell-maturation-dependent. This study examined the role of intracellular calcium concentration (ICCC) in determining cell response and the mechanisms involved. Resting zone (RC) and growth zone (GC) chondrocytes were isolated from costochondral cartilage of male and female rats. ICCC was measured using a fluorescent probe, Flou-4. Chondrocytes were treated with E_2 or 17-alpha-estradiol in the presence of high and low extracellular Ca^{++}. Changes in fluorescence were recorded every 5 sec for 500 sec. To examine the source of Ca^{++} responsible, Ca^{++} pumps on the endoplasmic reticulum were inhibited with 3 uM thapsigargin and Ca^{++} channels on the cell membrane were inhibited with 1 uM verapamil. External Ca^{++} was removed using EGTA. We monitored the levels of two products of phospholipase C (PLC) action: diacylglycerol (DAG) and inositol 1,4,5-trisphosphate (IP3). DAG is a regulator of protein kinase C (PKC), which is activated by E_2 in a sex-specific manner and IP3 is known to control ICCC in other systems. E_2 increased ICCC only in the cells from female rats. The effect was stereospecific; it was found in RC and GC chondrocytes but it had a greater magnitude in RC cells. The increase was rapid and peaked at approximately 140 seconds; the entire event was over within 300 seconds. Low Ca^{++} media did not abolish the E_2-dependent ICCC elevation, nor did verapamil. However, thapsigargin reduced the effect of E_2 on ICCC. E_2 caused increased IP3 and DAG only in female cells. IP3 was generated within 10 seconds and the greatest increases were in RC cells. These results indicate that E_2 increases ICCC via membrane-associated mechanisms mediated by PLC-dependent production of IP3. The effect on ICCC is rapid and sex-specific and cell maturation-dependent. The source for this Ca^{++} was almost exclusively from the endoplasmic reticulum. The results indicate that the entity responsible for sex-specific responses to E_2 is upstream from PLC activation.

Disclosures: ***Z. Schwartz****, None.*

M568

Adhesion and Apoptosis Are Regulated by 17β-estradiol in Differentiating and Mature Murine Osteoclasts. D. Saintier*, V. Khanine*, M. de Vernejoul, M. E. Cohen-Solal. 606, INSERM, Paris, France.

Estrogen deficiency induces enhanced bone resorption which might be responsible for osteoporosis. The mechanism of action of estradiol in the inhibition of osteoclastic bone resorption is still unknown. We have previously shown that in vitro estradiol exerts a direct inhibitory effect on osteoclast activity in human osteoclast progenitors that was associated with decreased β3 integrin expression. Therefore, this study was designed to evaluate the effect of estradiol on both adhesion and apoptosis in differentiating or mature murine osteoclasts. We used RAW 264.7 cells which were differentiated for 3 days (D3, differentiating osteoclasts) or 5 days (D5, mature osteoclasts) in phenol red free αMEM supplemented with 10% FCS and RANKL (30 ng/ml) in the presence (E+) or absence (C) of 10^{-8}M 17β estradiol. At D5, estradiol reduced the number of TRAP+ multinuclear cells by 50 % compared to controls (3.1±0.9 vs 6.1±0.4/mm^2, p<0.01), as well as TRAP+ mononuclear cells (237.6±20.7 for E+ vs 306.4±12.6 /mm^2, p<0.01). Moreover, estradiol decreases TRAP+ multinuclear/mononuclear cells ratio, indicating that estradiol decreased the fusion of osteoclast precursors.The effect of estradiol on cell adhesion in vitronectin pre-coated plates was tested by crystal violet method. Exposure for 2 hours with estradiol decreased adhesion time of mature osteoclasts by 35% compared to controls (1.01±0.35 vs 1.33±0.83 AU respectively).

Apoptosis was then investigated through the caspase 3 and 8 activities at D3 and D5 after 24 and 48h exposure of estradiol using fluorescence spectrometry method. Caspase 3 and 8 activities were not changed by 24 hour-treatment with estradiol. However 48 hour-exposure with estradiol promoted caspase 3 activity by 34 % in differentiating cells and by 59% in mature osteoclasts compared to controls. Caspase 8 activity was enhanced by estradiol as well. These effects were reversed by estrogen receptor antagonist ICI 182-780.

Moreover differentiating and mature osteoclasts were cultured with estradiol for 48 hours in the presence of caspase 8 inhibitor for the measurement of caspase 3 activity. Caspase 8 inhibitor induced a lower caspase 3 activity in both cultures. However estradiol had no effect on caspase 3 in mature osteoclasts cultured with caspase 8 inhibitor. These data suggest that estradiol might act upstream caspase 8 pathway.In conclusion, 17β estradiol decreased osteoclast resorption through decreased fusion of precursors and adhesion of osteoclasts. Apoptosis was promoted in differentiating and mature osteoclasts after 48 hours indicating the involvement of several pathways in direct inhibition of bone resorption by estradiol.

Disclosures: ***D. Saintier****, None.*

M569

Correlations between *in Vi*vo Activities of Estrogens and Their Differential Effects on ERα-Controlled Repression of MMP-1 Promoter Activity. A. Schmidt[1], A. Scafonas*[1], P. J. Masarachia*[1], G. J. Sedor*[1], E. T. Birzin*[1], S. Kim*[2], H. Y. Chen*[2], Q. Tan*[1], H. A. Wilkinson*[1], X. S. Hou*[3], F. DiNinno*[2], S. P. Rohrer*[1], J. M. Schaeffer*[4], M. L. Hammond*[2], G. A. Rodan[1], D. A. Towler[5], D. B. Kimmel[1]. [1]Molecular Endocrinology, Merck Research Laboratories, West Point, PA, USA, [2]Medicinal Chemistry, Merck Research Laboratories, Rahway, PA, USA, [3]Biometrics Research, Merck Research Laboratories, West Point, PA, USA, [4]External Scientific Affairs, Merck Research Laboratories, Rahway, PA, USA, [5]Bone and Mineral Diseases, Washington University School of Medicine, St. Louis, MO, USA.

Estrogen receptors (ER), ERα and ERβ, are ligand-dependent transcription factors that bind to specific DNA sequences and regulate gene expression. Genetic studies in mice and man suggest that ERα controls bone, uterus, and breast effects of estrogen. To date, the mode of action of estrogen and SERMs (selective estrogen receptor modulators) on bone is not fully understood. Furthermore, no *in vitro* assays that show agonist actions of estrogenic agents can predict their agonist activities *in vivo*. We report the development of a transrepression assay in which ERα controls the activity of an AP-1 transcription factor binding site in the MMP-1 promoter. In this assay, ICI-182780, raloxifene, 4-hydroxytamoxifen, estradiol, and SERAMs 4-D and 5 (selective estrogen receptor alpha modulators) exhibit differential agonistic activities by repressing the MMP-1 promoter by 20 to 80%. MMP-1 transrepression efficacy and potency not only correlates positively with uterotrophic activity (R^2=0.98), but also predicts their osteoprotective potential in the ovariectomized rat (R^2=0.98). Using structure-function analysis of ERα, we determined that raloxifene repression is predominantly controlled by the amino terminal region, while that of estradiol is controlled by both the amino- and carboxy-terminal regions of ERα. Introducing the AF-2 mutation L540Q to the ER does not influence the ability of raloxifene to repress MMP-1. However, L540Q increases the repression of MMP-1 by ICI-182870 to the level of raloxifene and decreases that of estradiol to the level of raloxifene. These results suggest that estradiol and selective and non-selective osteoprotective SERMs display agonistic activity in transcription, controlled by ERα via protein-protein interaction that correlates with their actions in vivo in bone and uterus. AP-1 transrepression via ER-alpha is a multi-step process that may be responsible for the differential actions of various ER ligands.

Disclosures: ***A. Schmidt****, Merck & Co. 1, 3.*

M570

Expression Levels of ERα in Different Compartments of Proximal Tibia and the Effect of Ovariectomy. G. Zaman*[1], R. F. L. Suswillo*[1], A. Pitsillides[1], T. Arnett[2], L. E. Lanyon[1]. [1]Basic Sciences, The Royal Veterinary College, London, United Kingdom, [2]Anatomy & Developmental Biology, University College London, London, United Kingdom.

A number of *in vitro* and *in vivo* studies have highlighted the role of Estrogen Receptor alpha (ERα) in bone's adaptive response to loading. A number of recent reports have described the distribution of ERα in human bone. Braidman et al. [1] (using 6F11 monoclonal antibody to the recombinant human full-length sequence of ERα, Novocastra Laboratories, Newcastle-upon-Tyne, UK) have reported that only about 14% of the osteocytes express ERα in human and rat bones. Using the same antibody Hoyland et al. [2] reported that the proportion of osteocytes with immunodetectable ERα decreases from 25% in hormone replete women to 12% in women with ovarian steroid deficiency. Conversely, Ankrom et al. [3] (using ERα-EIA, Abbott Laboratories Chicago, IL, USA) have reported that older women have higher levels of ERα than younger women. Somewhat conflicting patterns of ER expression reported may possibly be due to methodological variations, such as different antibodies used and the methods employed for antigen retrieval. We have used two antibodies (HC-20 and MC-20, purchased from Santa Cruz, CA, USA) both directed specifically against the carboxy terminus of ERα having no cross reactivity with ERβ. Immunocytochemistry was performed on sections from fixed and decalcified rat tibiae mounted on poly-lysine coated slides. Deparaffinated and re-hydrated sections were immunostained for ERα using an indirect immunoperoxidase method as described previously [4]. Semi-quantification analysis of ERα protein expression per cell was performed using a Vickers M85 microdensitometer. Using this methodology ERα was expressed in over 90% of the osteocytes. ERα expression levels per cell were higher in osteoblasts than in osteocytes. Expression levels of ERα per cell varied in different compartments of the proximal tibia with the strongest immunostaining seen in osteocytes within the mid-shaft. The epiphysis and primary spongiosa had equal ERα expression but the levels were lower than mid-shaft osteocytes. The secondary spongiosa expressed by far the lowest levels of ERα. Ovariectomy significantly reduced the ERα expression levels per cell in the midshaft osteocytes suggesting that ERα number is regulated by circulating estrogen levels. The variation of ERα expression levels in different compartments of the bone may reflect the potential for loading related osteogenic response.

1. Braidman IP et al. 2000 Bone 26: 423-27.
2. Hoyland JA et al. 1999 J Pathol 188: 294-303
3. Ankrom MA et al 1998 Biochem J 333: 787-94
4. Bord S et al. 2001 J Clin Endocrinol Metab 86(5): 2309-14

Disclosures: ***G. Zaman****, None.*

M571

Bone-Sparing and Cholesterol Lowering Effects of Non-Uterotropic, Selective Estrogen Receptor Alpha Modulators (SERM-αs). A. A. Reszka[1], S. Adamski*[1], J. E. Fisher[1], E. T. Birzin*[2], L. Lipfert*[1], S. Kim*[3], H. Y. Chen*[3], Q. Tan*[3], F. DiNinno*[3], S. P. Rohrer*[2], J. M. Schaeffer*[2], M. L. Hammond*[3], G. A. Rodan[1], L. P. Freedman*[1], D. B. Kimmel[1]. [1]Molecular Endocrinology and Bone Biology, Merck Research Laboratories, West Point, PA, USA, [2]Molecular Endocrinology and Bone Biology, Merck Research Laboratories, Rahway, NJ, USA, [3]Medicinal Chemistry, Merck Research Laboratories, Rahway, NJ, USA.

Two isoforms of the estrogen receptor (ER), ERα and ERβ bind equally well to the natural ligand, 17β-estradiol. In the present study, we tested the hypothesis that transcriptional activation of ERα *in vivo* was sufficient to protect against ovariectomy (OVX)-induced bone loss and to suppress serum cholesterol without substantially increasing uterine wet weight in the rat. We selected eight SERM-αs from the chromane and dihydrobenzoxathiin platforms to test for *in vivo* effects on bone and lipids and in comparison to 17α-Ethinyl Estradiol (EE) and/or raloxifene. SERM-αs were competitive inhibitors for the binding of 17β-estradiol to ERα with IC50s of 0.21-1.8 nM. Selectivity for ERα vs. ERβ was between 10 and 48-fold (5.6-fold for raloxifene). In the immature rat, SERM-α-induced uterotropism was equal to or less than that of raloxifene and far below that of EE. In six-month old, newly-OVX rats, urinary deoxypyridinoline/creatinine rose ≥two-fold at two weeks. Treatment with the SERM-αs suppressed this by 59-86% (replete to sham), while raloxifene and EE suppressed by 83% and 100%, respectively. To directly assess effects on bone mass, we measured the ratio of bone mineral density of the distal femoral metaphysis and central femur (DFM/C ratio). The OVX control lost 11-12% of DFM/C vs. sham six weeks post-OVX. All SERM-αs maintained DFM/C at 56-100% replete to sham. DFM/C was 64% replete with raloxifene and 86-100% with EE. In three day OVX-rat assays, all SERM-αs significantly reduced total serum cholesterol by 27-45% vs. baseline, comparable to the 37% suppression by raloxifene (all at 1.5 mg/kg/d, p.o.). After six weeks of treatment of the OVX rat, cholesterol suppression was 29-62% vs. 49% with raloxifene. EE (0.6 mg/kg/day, p.o.) induced 85-90% suppression of serum cholesterol over three days, but only 48-56% by six weeks. Together, these data suggest that ERα-selective ligands can elicit similar desirable effects to those of EE and raloxifene on endpoints related to bone and lipids. Similar to the less ERα-selective SERM, raloxifene, the SERM-αs maintain bone mass and reduce serum total cholesterol without inducing substantial uterotropism. This suggests that SERM-αs can achieve the same desirable effects of non-receptor specific SERMs on bone and lipids while avoiding ERβ antagonism.

Disclosures: ***A.A. Reszka****, None.*

M572

Sex Specific Responses of Growth Plate Chondrocytes to Testosterone Require Metabolism to Dihydrotestosterone by Steroid 5-Alpha Reductase Type 1. P. Raz*[1], E. Nasatzky*[1], B. D. Boyan[2], Z. Schwartz[1]. [1]Periodontics, Hebrew University Hadassah, Jerusalem, Israel, [2]Biomedical Engineering, Georgia Institute of Technology, Atlanta, GA, USA.

Growth plate chondrocytes exhibit sex-specific responses to testosterone. Only cells from male rats exhibit testosterone-dependent changes in proliferation and differentation, although testosterone receptors are present in both male and female cells, indicating that mechanisms other than those mediated by nuclear receptors may be involved. In male cells testosterone is preferentially metabolized to dihydrotestosterone (DHT), suggesting that DHT may play a role. Here we tested the hypothesis that the sex-specific response to testosterone requires further metabolism of the hormone to DHT. Rat costochondral resting zone (RC) and growth zone (GC) cartilage cells from male and female Sabra strain rats were treated with 10^{-11} to 10^{-7} M testosterone or DHT for 24 h. Measurement of [^{3}H]-thymidine incorporation in quiescent, preconfluent cultures and alkaline phosphatase specific activity in cell layer lysates of confluent cultures showed that testosterone and DHT has comparable effects in GC cells. Both parameters were increased in cells from male rats. Testosterone decreased DNA synthesis in male RC cells but DHT had no effect. Moreover, neither testosterone nor DHT affected alkaline phosphatase specific activity of male RC cells. Female GC and RC chondrocytes had no response to testosteroneT or DHT. Inhibition of steroid 5α-reductase activity with finesteride (1, 5 or 10 μg/ml) reduced the response of male GC cells to testosterone in a dose-dependent manner, indicating that metabolism to DHT was required. RT-PCR showed that both male and female cells expressed mRNAs for steroid 5α-reductase type 1 but lacked mRNAs for the type 2 form of the enzyme. These observations indicate that the sex-specific response of rat growth plate chondrocytes to testosterone is maturation-state dependent and requires the further metabolism to DHT. Failure of female chondrocytes to respond to the hormone may reflect differences in testosterone metabolism, since these cells possess the ability to aromatize testostoerone to estradiol. (Supported by GTEC)

Disclosures: ***P. Raz****, None.*

M573

Identification and Characterization of Androgen Response Elements on the Rat IGF-1 Promoter. B. C. Yaden*, H. Bullock*, K. Chen*, T. Moore*, G. Krishnan*. Eli Lilly, Indianapolis, IN, USA.

Insulin-like growth factors are critical for normal growth and development of the organism. IGF1, has been shown to positively regulate cell proliferation, DNA replication, RAS protein signal transduction, muscle development, skeletal development, cell motility, and signal transduction. Androgen receptor (AR) belongs to the nuclear receptor family of DNA-binding transcriptional activator proteins. Binding of the natural steroid hormone ligands testosterone or dihydrotestosterone (DHT) to AR causes the protein to translocate from the cytoplasm to the nucleus where it binds to the promoters of androgen target genes and has been shown to have anabolic effects in various tissues such as muscle and bone. IGF1 has also been shown to induce myotube formation in myoblastic cell lines. The myoblast lines L6 and C2C12 were treated with R1881 (methyl trienolone) and IGF1 expression was measured. No significant changes were identified, but when a newly developed cell line LA-20 (rat striated levator ani muscle cells) was treated with R1881, IGF1 protein and mRNA levels increased. To further elucidate the mechanism of AR-mediated changes in IGF1, the rat IGF1 5' prime upstream region (+1 being the first nucleotide in the start codon, -4915/-37) was cloned into a luciferase reporter. The IGF1 promoter/upstream region has no defined TATA, CAAT homologies or a region that is GC rich, however it contains an imperfect Inr sequence at the -185 position. In addition several proximal response elements (AP1, CRE, GATA1 etc…) were found in this region. Transient transfections were performed using this construct in LA-20 cells. After treatment with R1881 for 48 hr, reporter expression was increased to 4.5 fold when compared to vehicle control. Deletion constructs were designed (-1716/-155 and -478/-145) to identify the potential ARE within this region. However, the truncated 333bp promoter continued to show maximal androgen-responsiveness in the reporter assay. From the data obtained in the deletion experiments three atypical androgen response elements were found at the 5' end of the proximal promoter construct. Detailed characterization of the androgen response element using ChIP assays suggests that it androgen-bound AR mediates its action on IGF-1 gene expression by targeting this element.

Disclosures: ***B.C. Yaden****, None.*

M574

1-alpha, 25-dihydroxycholecalciferol Reduces ApoA1 Expression. K. R. Wehmeier*, M. J. Haas*, A. E. Beers*, A. D. Mooradian*. Division of Endocrinology, Diabetes and Metabolism, Department of Internal Medicine, Saint Louis University School of Medicine, St. Louis, MO, USA.

Daily Vitamin D intake over 30 mcg has been correlated with higher myocardial infarction events. In addition, supplemental cholecalciferol in women taking estrogens blunts the elevation of HDL-cholesterol. Members of the steroid receptor superfamily are known to alter the transcription of the major apoprotein of HDL cholesterol, ApoAI. To assess the effect of a ligand to the vitamin D receptor (VDR) on ApoAI, we investigated the effect of 1-alpha, 25-dihydroxycholecalciferol (1,25 OH2D3) on ApoAI protein, mRNA, and transcriptional activity in the human hepatoma cell line HepG2. ApoAI secretion was suppressed in a dose-dependent manner in HepG2 cells treated with 1,25 OH2D3. ApoAI protein levels were 166+/-10.0, 155.5+/-10.5, 130.5+/-8.5 and 89+/-7.0, arbitrary units (AU) in cells treated with 0, 10, 50, and 250 nM 1,25 OH2D3, achieving statistical significance in the 250 nM range (P<0.02). In order to determine if the effect of 1,25 OH2D3 occurs at the transcriptional level, HepG2 cells were transfected with a chloramphenicol acetyltransferase (CAT) reporter gene plasmid containing the full-length apoAI promoter, and after 24 h, treated with 1,25 OH2D3. CAT activity was suppressed by the VDR ligand 19.2+/-1.0% acetylation in control cells vs. 12.0+/-0.9% (P<0.005) and 6.3+/-1.1% acetylation (P<0.001) in cells treated with 50 and 250 nM 1,25 OH2D3, respectively. Therefore, the VDR activation by 1,25 OH2D3 suppressed ApoA1 expression at the transcriptional level in a dose dependent manner. These studies suggest that various ligands for the VDR may regulate apoAI gene expression. Further studies are needed to define implications of vitamin D supplementation on cardiovascular risk.

Disclosures: ***K.R. Wehmeier****, None.*

M575

1,25(OH)$_2$ D$_3$ Is an Important Regulator in Organogenesis of Bone. K. Hasegawa*[1], Y. Seino*[2], S. Kato*[3], H. Tanaka*[1]. [1]Department of Pediatrics, Okayama university graduate school of medicine and dentistry, Okayama city, Japan, [2]Department of Pediatrics, Osaka Kosei Nennkinn Hospital, Osaka city, Japan, [3]Tokyo University, Tokyo, Japan.

Vitamin D plays an important role in bone metabolism. The role of Vitamin D to the bone is considered indirect, and there is little evidence that Vitamin D has direct effect to the bone. We have shown that 1,25(OH)$_2$D$_3$ (D3) may directly suppress the bone formation by bone transplantation experiments and organ culture system of femur of Vitamin D receptor Knock Out Mice(VDRKO). To clarify the direct effect of D3 on the membranous bone formation, we performed the organ culture calvaria which was removed from neonate of VDRKO .

There were no significant difference in the thickness of parietal bone between WT and VDRKO before the culture (20±2 VS20±1micrometer). After the culture, the thickness decreased compared with before the culture (20±2 to 12±2 micrometer) in WT. Contrary to WT, thickness of parietal bone didn't change before and after the culture in the VDRKO. Before and after the 5 days culture, there was no significant difference in the osteoclast number between VDRKO and WT. This shows that vitamin D directly suppresses the bone formation.

Next, to assess the difference of ossification during the organogenesis, we examined the whole skeletal preparation of VDRKO and WT (+/+ and +/-). Calcificated bone was stained red with alizalin red and cartilage was stained blue with alcian blue in the skeleton. Calcification of parietal bone in VDRKO began as early as at 13.5 d.p.c. while it began at 14.5 d.p.c. in WT (+/+) mouse. Skeletal findings in WT(+/-) were apparently middle between in VDRKO and in WT(+/+).

From these results, we conclude that vitamin D directly suppresses membranous bone formation of neonate. Moreover, the findings in whole skeletal preparation indicate that vitamin D is an important organogenesis regulator of bone.

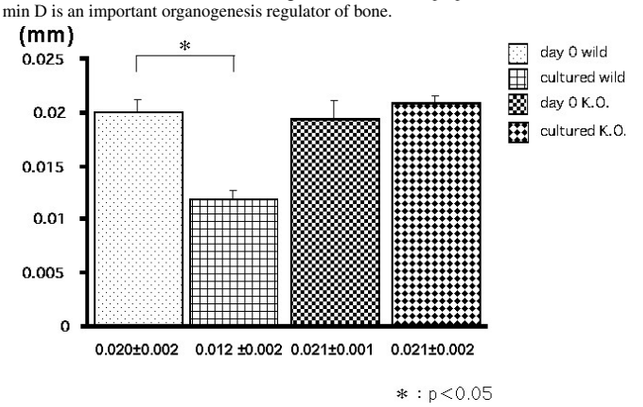

Disclosures: ***K. Hasegawa****, None.*

M576

Attentuation of Disuse-Induced Bone Loss by Estrogen and Vitamin D Receptor Ligands in Unloaded and Ambulatory Female Rats. R. Narayanan*[1], C. Seng*[1], N. L. Weigel[1], S. A. Bloomfield[2], C. L. Smith[1]. [1]Molecular and Cellular Biology, Baylor College of Medicine, Houston, TX, USA, [2]Health and Kinesiology, Texas A&M University, College Station, TX, USA.

Decreased mechanical usage as experienced during spaceflight, bedrest, and hindlimb unloading (HU) induces bone loss. Two estrogen receptor (ER) ligands, estradiol (E2) and raloxifene (RAL; a selective estrogen receptor modulator), and two vitamin D receptor (VDR) ligands, 1,25-dihydroxyvitamin D3 (1,25D) and EB1089 (a less calcemic analog of 1,25D, Leo Pharmaceuticals) were tested previously for prevention of bone loss in HU male rats. In this study RAL and EB1089, alone and in combination, were assessed for their ability to prevent bone mineral density (BMD) loss during 28d HU in 6-mo-old virgin female Sprague-Dawley rats in comparison to E2 or 1,25D (n=10-12 animals/group). Estradiol (12 μg/d) and RAL (535 μg/d) were administered by time-release pellets (Innovative Research of America), while 1,25D (0.03 μg/kg BW) and EB1089 (0.3 μg/kg BW) were administered by Alzet osmotic pump; appropriate vehicle (VEH) controls were employed. Peripheral quantitative computed tomography scans (pQCT; Stratec XCT Research M) for BMD and geometry were taken *in vivo* at the proximal tibial metaphysis on d0 and after 28d of HU and hormone treatment. Administration of EB1089 alone (+1.6%) or together with RAL (-0.4%) prevented the loss of total BMD (-5.8%) observed for the VEH group, in comparison to d0 values, while E2 treatment attenuated BMD loss. Individually, neither RAL nor 1,25D were effective. Both EB1089 and EB1089+RAL prevented endocortical bone loss, blocking the increase in marrow area observed in VEH rats (+9.2%), and instead reduced marrow area by 5.1 and 3.1%, respectively. EB1089 and EB1089+RAL increased cancellous BMD over d0 values (9.8 and 3.9%, respectively), while the BMDs of VEH animals were reduced by 6.2%. Increased serum osteocalcin in EB1089 relative to VEH groups was consistent with EB1089 effects on bone. No significant changes in serum calcium were detected relative to VEH controls. In ambulatory animals, 28 d of treatment with EB1089, EB1089+RAL, E2 or 1,25D increased total BMD over baseline values by up to 7.3%, and this was reflected in increased cancellous BMD of up to 20.4%. In the case of EB1089 and EB1089+RAL, BMD alterations were accompanied by reductions in marrow area of 13.0 and 8.8%, respectively. Taken together, these results indicate that EB1089 effectively counteracts the deleterious effects of HU on bone in mature female rats. Our previous work suggested that in HU male rats, 1,25D more effectively prevented loss of BMD than EB1089, and future experiments will address the gender-based differences in response to EB1089 and 1,25D.

Disclosures: ***C.L. Smith****, None.*

M577

The Vitamin D Receptor (VDR) Coactivators, DRIP/205, SRC/1 and 3, and TAF_{II}-17 Are Differentially Involved in VDR Mediated Transactivation during Pagetic Osteoclasts (OCL) Differentiation. N. Kurihara[1], S. Onate*[2], A. Hidalgo*[2], M. Ito[1], G. D. Roodman[3]. [1]University of Pittsburgh, Pittsburgh, PA, USA, [2]Roswell Park Cancer Institute, Buffalo, NY, USA, [3]University of Pittsburgh & VA Med Ctr, Pittsburgh, PA, USA.

OCL in Paget's disease (PD) are abnormal and characterized by expression of the measles virus nucleocapsid protein (MVNP) gene, increased levels of TAF_{II}-17 and hyperresponsivity to 1,25-$(OH)_2D_3$. The basis for the hyper-responsivity to 1,25-$(OH)_2D_3$ is unclear. It is our hypothesis that MVNP induces enhanced VDR mediated gene transcription by increasing expression of VDR coactivators in pagetic OCL precursors. To test this hypothesis, we determined the expression levels of known coactivators of VDR in OCL isolated from normal individuals and from PD patients, and in MVNP transfected human OCL precursors or empty vector (EV) using PCR, Western blot analysis and immunocytochemistry. We then used the chromatin immunoprecipitation (ChIP) assay with NIH3T3 cells stably transfected with EV or MVNP to examine the recruitment of these coactivators to the VDR response element (VDRE) occurred in the 24-(OH)-ase gene promoter. Increased levels of DRIP205 were detected in early OCL precursors from PD patients or normal precursors transfected with MVNP compared to EV transfected cells. DRIP205 levels decreased as PD OCL precursors differentiated. After 14 days of culture, SRC-1 and SRC-3, and TAF_{II}-17 were increased as DRIP205 decreased in MVNP transfected and PD OCL precursors. ChIP analysis demonstrated that in MVNP transduced cells the association of un-liganded VDR with its corepressor SMRT was significantly decreased. MVNP transduced cells also had increased recruitment of DRIP205/TRAP220 and SRC-1 to the VDRE in the 24-OHase promoter, in a ligand-dependent manner. Furthermore, when CFU-GM transduced with MVNP were cultured for 14 days in the presence or absence of a DRIP205 antisense oligonucleotide (AS-DRIP205) and treated with 10^{-11}-10^{-7} M 1,25-$(OH)_2D_3$ to induce OCL formation, AS-DRIP205 inhibited OCL formation about 20% ($P < .05$) compared to mismatch sense oligonucleotide (MS) treated control cultures. AS-TAF_{II}-17 also significantly inhibited OCL formation by 40% ($P < .01$) compared to MS-ODN treated control cultures. These results indicate that DRIP205 is initially upregulated in PD OCL precursors followed by SRC1, 3, and TAF_{II}-17, and suggest that these coactivators may be involved in the enhanced VDR mediated gene expression that occurs in PD.

Disclosures: ***N. Kurihara****, None.*

M578

Molecular and Functional Characterization of the 1α,25$(OH)_2$-Vitamin D_3-Sensitive Chloride Channel in Osteoblasts. L. P. Zanello, W. Smith*, H. L. Henry, A. W. Norman. Biochemistry, University of California-Riverside, Riverside, CA, USA.

Osteoblasts are a major target for the steroid hormone 1α,25$(OH)_2$-vitamin D_3 [1,25D]. 1,25D deficiency leads to impaired osteoblastic functions and decreased bone formation. 1,25D mechanisms of action comprise genomic (modulation of gene expression via a nuclear 1,25D receptor) and non-genomic pathways. The latter include rapid intracellular calcium elevation, signal transduction activation, and ion channel potentiation. Osteoblasts express a 1,25D-sensitive anion (Cl^-) current that is significantly enhanced by nanomolar concentrations of the hormone within 1-5 min (Zanello and Norman, J.Biol.Chem. 1997). This Cl^- conductance is responsible for a local repolarization of the osteoblast, and couples to secretion (Zanello and Norman, Bone 2003, Proc.Natl.Acad.Sci. 2004). We characterized the biophysical properties of this voltage-gated Cl^- channel by means of whole-cell patch-clamp recordings on rat osteosarcoma ROS 17/2.8 cells. The specific Cl^- channel blocker 4,4'-diisothiocyanatostilbene 2,2'-disulfonic acid (DIDS, 200 μM) partially reduced (up to 50%) 1,25D-enhanced Cl^- conductance at depolarizing potentials (80 mV). This blockade developed in a voltage and time-dependent manner. The 1,25D-sensitive channel is permeable to $I^- > Cl^- > F^-$ > glutamate > gluconate. With the purpose to study the molecular identity of this Cl^- channel, we investigated at the mRNA level the expression of different types of Cl^- channels of the ClC gene family of voltage-gated Cl^- channels. For RT-PCR experiments, we used primers designed from previously cloned rat Cl^- channels whose sequences are available in data banks. We found that ROS 17/2.8 cells express transcripts of the outward rectifier, DIDS-sensitive ClC-3 gene, but not the ubiquitous swelling-activated ClC-2 or the intracellular ClC-7 channel found in osteoclasts. This agrees with our pharmacological and electrical studies. We conclude that the 1,25D-sensitive Cl^- channel in osteoblasts appears to be the ClC-3 type. We have thus identified a potential therapeutic target for the treatment of bone pathologies associated with 1,25D deficiency and characterized by decreased bone mass and insufficient mineralization.

Disclosures: ***L.P. Zanello****, None.*

M579

1,25-Dihydroxyvitamin D Regulates Soluble RANKL and OPG Release from Bovine Vascular Endothelial Cells. K. J. Lamb*[1], J. L. Berry[1], C. E. Evans*[2], A. E. Canfield*[3], A. P. Mee[1]. [1]Vitamin D Research Group, University of Manchester, Manchester, United Kingdom, [2]LMAG, University of Manchester, Manchester, United Kingdom, [3]School of Biological Sciences, University of Manchester, Manchester, United Kingdom.

Recent evidence has suggested a role for the receptor activator of nuclear factor kappa beta (RANK) system in modulating vascular calcification. 1,25-dihydroxyvitamin D (1,25D) is produced in extra-renal sites, and vascular endothelial cells can both synthesise and respond to 1,25D. Therefore, the purpose of this study was to investigate the effects of 1,25D on soluble RANK Ligand (RANKL) and osteoprotegerin (OPG) production by vascular endothelial cells. Bovine aortic endothelial cells were incubated in standard medium, in the absence of fetal calf serum, with varying doses of 1,25D (10^{-7}, 10^{-9}, 10^{-11}M) for 6, 24 and 48 hours. Control cells were incubated in the absence of 1,25D. OPG and RANKL levels were assessed by ELISA. Both dose- and time-dependent effects were seen in OPG and RANKL production. At all time points examined, 1,25D stimulated OPG production, with the effect being greatest at 10^{-11}M 1,25D. The maximum effect was seen after 24hrs with 10^{-11}M 1,25D (4.1±1.2pmol/l cf. 0.95±0.05 in control medium). RANKL secretion showed a more phasic response; using 10^{-11}M 1,25D the response was greatest at 24hrs and was reduced at 6 and 48hrs, whereas at 10^{-9} and 10^{-7}M, there was an increase at 6hrs, with a decrease at 24hrs and then a dramatic increase after 48hrs. The maximum response was seen after 48hrs at 10^{-7} M 1,25D (0.92±0.14pg/ml cf. 0.04±0.08pg/ml). This study has confirmed both a dose-dependent and duration-associated secretion profile of RANKL and OPG in response to 1,25D. Interestingly, the maximum effect on OPG secretion was seen after 24hrs at a low dose of 1,25D, with a corresponding decrease in RANKL secretion, whereas the maximum effect on RANKL was seen at 48hrs with a high dose of 1,25D, with a corresponding decrease in OPG. These findings clearly demonstrate that 1,25D, produced locally, is a candidate to modulate the effects of RANK, RANKL and OPG within the vascular system, which may have profound effects on vascular calcification.

Disclosures: ***A.P. Mee****, None.*

M580

Bone Anabolic Effects of 1,25(OH)$_2$ Vitamin D3 Are Detected Only in the Presence of a Powerful Antiresorptive. A. A. Reszka, S. Pun*, G. A. Rodan, L. P. Freedman*, D. B. Kimmel. Molecular Endocrinology and Bone Biology, Merck Research Laboratories, West Point, PA, USA.

Controversy exists concerning the in vivo skeletal response to pharmacologic levels of 1,25(OH)$_2$ vitamin D3 (1,25D3). We hypothesize that feedback loops that involve the regulation of the bone remodeling system influence the outcome of experiments with 1,25D3. The purpose of this experiment was to assess the effect of 1,25D3 on the skeleton of estrogen deficient, osteopenic adult rats.

Three month-old Sprague-Dawley rats were ovariectomized (OVX) three months prior to treatment with alendronate (ALN; 10 µg/kg, s.c., 3X/wk). At that time, rats were also given 0, 0.01, 0.03, or 0.1µg/kg/d 1,25D3, p.o., or PTH (80 µg/kg. s.c., 3X/wk). Non-ALN-treated rats given 1,25D3 (0 or 0.1 µg/kg/day, p.o.) were also included. Treatment continued for eight weeks. *In vivo* dual calcein labeling was used to assess directly lumbar vertebral body cancellous bone formation rate (BFRBS, based on double label). Osteoclast surface (OcSBS), urine calcium (UCa), urinary DPD (uDPD/Cre), and lumbar vertebral bone mineral density (LVBMD) were also measured.

Tx (ug/kg/d)	UCa	uDPD/Cre	LVBMD	BFRBS	OcSBS
Veh	196±93	102±15	196±20	6.1±3.38	1.8±1.2
1,25D3 (0.1)	735±254vo	40±17v	227±22v	2.6±1.8vo	0.3±0.2vo
Veh + ALN	135±77v	37±9v	216±20v	0.1±0.1v	0.9±0.4v
1,25D3 (0.01) + ALN	511±124vo	26±6vo	225±15v	0.2±0.3v	0.4±0.2vo
1,25D3 (0.03) + ALN	666±114vo	19±7vo	220±19v	0.6±0.4vo	0.3±0.3vo
1,25D3 (0.1) + ALN	818±108vo	16±3vo	222±14v	2.4±1.6vo	0.2±0.2vo
PTH (80) + ALN	221±93	32±8v	243±25vo	1.3±0.6vo	1.0±0.6v

Mean ± S.D.; v- diff from vehicle (P<.05); o- diff from Veh + ALN (P<.05)

Despite equivalent reductions of uDPD/Cre by ALN and 1,25D3, lumbar vertebral cancellous bone formation rate was reduced by different degrees, suggesting an uncoupled response to 1,25D3. In the presence of the powerful anti-resorptive, ALN, the ability of 1,25D3 to stimulate cancellous bone formation after eight weeks treatment was clearly demonstrated. Together, these data show that 1,25D3 increases bone formation both when administered alone and in the presence of ALN. These anabolic effects of 1,25D3 occurred despite significant decreases in osteoclast activity, suggesting an independent effect of 1,25D3 on osteoblast function/activity. We hypothesize that the net decrease in cancellous bone formation rate seen with 1,25D3 monotherapy is a combination of its direct effect to stimulate bone formation and an indirect effect of antiresorptive-mediated coupling associated with cancellous bone remodeling.

Disclosures: ***A.A. Reszka****, None.*

M581

Assessment of Total and 'Free' Circulatory 25-hydroxyvitamin D and 1, 25-dihydroxyvitamin D$_3$ Status in Men with Osteoporosis. Z. H. Al-Oanzi*[1], S. S. Varanasi[1], S. P. Tuck*[2], R. M. Francis[2], H. K. Datta[1]. [1]School of Clinical & Laboratory Sciences, University of Newcastle, Newcastle upon Tyne, United Kingdom, [2]School of Clinical Medical Sciences, University of Newcastle, Newcastle upon Tyne, United Kingdom.

The clinical assessment of vitamin D$_3$ status often relies upon measuring total circulatory levels. The metabolites 25OHD$_3$ and 24,25(OH)$_2$D circulate in blood at concentration about 1000 times higher than those of 1,25(OH)$_2$D$_3$, but because of the remarkably high concentration of DBP in relation to the vitamin D metabolites, many binding sites are still available for 1,25(OH)$_2$D$_3$ and the percentage of free hormone is very low. Therefore the concentration of the free rather than total forms of 1,25(OH)$_2$D$_3$ and 25OHD$_3$ are likely to provide a better assessment of the vitamin D status. The present study was carried in of male control subjects (n=114) and men with osteoporosis (n=56), with a view to determine the relationship of free 25OHD$_3$ and 1,25(OH)$_2$D[[Unsupported Character - Codename]]$_3$ concentrations with total plasma 25OHD$_3$, 1,25(OH)$_2$D$_3$, vitamin D-binding protein (DBP) and albumin levels. The total plasma DBP was determined using monospecific polyclonal goat anti-human DBP antibody. The assay used for 25OHD$_3$ and 1,25(OH)$_2$D$_3$ in human plasma was carried out using commercially available kit. 'Free' 25OHD$_3$ and 1,25(OH)$_2$D$_3$ levels were inferred from plasma 25OHD$_3$, 1,25(OH)$_2$D$_3$, DBP and albumin levels, using the following equation: [F] = [T] / (1 + Ka$_{ALB}$ [ALB] + Ka$_{DBP}$ [DBP]). [T] and [F] are the total and free vitamin levels respectively, whereas Ka$_{ALB \text{ and}}$ Ka$_{DBP}$ are the association constants for albumin and DBP. Our data shows that whilst there were no differences between men with osteoporosis and male control subjects in total plasma 25OHD$_3$ (44.7±21 nmol/L (n=56) vs. 43.3±17 nmol/L (n=114)), and 1,25(OH)$_2$D$_3$ (90±37 pmol/L (n=50) vs.103 ± 39 pmol/L (n=50)). However, calculated free plasma 25OHD3 levels were significantly lower (p<0.00001) in the osteoporotic men (6.1±3.1 pmol/L) than in the control subjects (9.1±4.4 pmol/L). Calculated free plasma 1,25(OH)$_2$D$_3$ was also significantly lower (p<0.00001) in osteoporotic men (77±37 fmol/L) than in the control subjects (142±58 fmol/L). The mean ±SD plasma level of DBP was significantly higher (p<0.001) in men with osteoporosis (224 ± 62 mg/L; n=56) than in the control subjects (143 ± 34 mg/L; n=114). Whilst there was no correlation between total plasma 25OHD$_3$ and 1,25(OH)$_2$D$_3$ levels, the calculated free plasma 25OHD$_3$ and 1,25(OH)$_2$D$_3$ showed positive correlation (r=0.614, p<0.01). These results suggest the measurement of plasma DBP and the ratio of total vitamin D metabolites to plasma DBP may provide a useful index of the biological activity of the vitamin.

Disclosures: ***S.S. Varanasi****, None.*

M582

ED-71, a Novel Vitamin D Analog, Promotes Bone Formation and Inhibits Bone Resorption after Bone Marrow Ablation. N. Okuda[1], S. Takeda*[2], K. Shinomiya*[3], T. Muneta*[1], S. Itoh*[4], Y. Asou[4]. [1]Section of Orthopeadic Surgery, Department of Molecular Regulation of Supportive Tissue, Graduate School Tokyo Medical and Dental University, Tokyo, Japan, [2]Chugai Pharmaceutical Co., LTD., Tokyo, Japan, [3]Section of Orthopeadic Surgery, Tokyo Medical and Dental University, Tokyo, Japan, [4]Division of Molecular Tissue Engineering, Human Genes and Science Center, Tokyo Medical and Dental University, Tokyo, Japan.

A novel vitamin D analog 1α,25-dihydroxy-2β-(3-hydroxypropoxy)vitamin D$_3$ (ED-71) had reported to have greater activity than vitamin D in preventing bone loss in ovariectomized rat, and the effect of promotion in bone formation and reduction in number of osteoclast. However, the effect of ED-71 on acute phase of bone remodeling remains to be elucidated. Bone marrow ablation causes vigorous new bone formation within the first week and then subsequent rapid bone resorption in the second week to regenerate bone marrow with normal levels of trabecular bones. It is a highly reproducible in vivo assay to evaluate bone remodeling. The purpose of this study was to evaluate the effect of ED-71 on bone remodeling in vivo by using mice bone ablation model. ICR mice were divided into ED-71 treatment and control groups, and all the femoral bone marrow were ablated by using K-wire . First, ED-71 (0.8µg/kg body weight) was injected intraperitoneally once the day after surgery to elucidate the effect of ED-71 on rapid bone formation during bone remodeling. Histological examination showed that ablated bone marrow in ED-71 treatment group were filled with more abundant matrix compared with control 3 and 5 days after surgery. As trabecular bone volume reaches at its maximal level 7 days after surgery, more abundant and thicker newly formed trabecular bones were observed in ED-71 treatment group by histological and micro CT analysis. Osteoblast surface (Ob.S/BS) was increased in ED-71 treatment group, whereas osteoclast number (Oc.N/BS) was not significantly affected by ED-71 possively because of reduced bone resorption activity at the time of ED-71 injection . Second, to elucidate the effect of ED-71 on bone resorption, ED-71 was injected once 8 days after surgery. Bone volume were 50 % more in ED-71 treatment group 14 days after surgery. Interestingly, Ob.S/BS was increased and Oc.N/BS was reduced significantly in ED-71 treatment group 2 days after administration. These results indicated that ED-71 administration at the period of trabecular bone maturation raised trabecular bone volume through both increase in osteoblast number and reduction in osteoclast number. We concluded that ED-71 promote bone formation and inhibit bone resorption in the region of rapid bone turn over after bone marrow ablation.

Disclosures: ***N. Okuda****, Chugai Pharmaceutical Co., LTD., Tokyo, Japan 2.*

M583

In vivo Actions of a Novel Vitamin D Analogue, ED-71, Mediates VDR. Y. Yamamoto*[1], K. Yoshimura*[1], T. Nakamura*[1], K. Takeyama*[1], H. Saito*[2], S. Kato[1]. [1]Institute of Molecular and Cellular Biosciences, The University of Tokyo, Tokyo, Japan, [2]Pharmaceutical Research Dept. II, Chugai Pharmaceutical Co., Ltd., Gotemba, Japan.

Most of vitamin D actions are believed to be exerted through VDR-mediated transcriptional control of target genes. The physiological impact of VDR in bone remodeling and formation have been well documented by generating VDR deficient mice (VDRKO) mice with features typical of vitamin D-dependent type II rickets, but only after weaning.

A variety of vitamin D analogues has been developed with characteristic actions derived from diverse biological actions of 1α,25(OH)$_2$D$_3$. ED-71 [1α,25-dihydroxy-2β-(3-hydroxypropoxy)vitamin D$_3$] is an analog of 1α,25-dihydroxyvitamin D$_3$ [1α,25(OH)$_2$D$_3$]. Clinical studies in osteoporotic patients demonstrated that the ED-71 treatment increased bone mass in a dose-dependent manner without causing sustained hypercalcemia or hypercalciuria, through serving as a tissue-selective vitamin D agonist. However, the molecular basis of the bone-selective agonistic action of ED-71 in terms of VDR activation in intact animals remains to be studied.

To address the VDR function in the ED-71 actions in vivo, we assessed the ED-71 activity in the VDR KO mice. Even excess doses of ED-71 given to the VDR KO mice caused no hypocalcemia and hypophosphatemia, confirming the indispensable function of VDR in the ED-71 actions. Currently, to more characterize the bone-selective ED-71 actions, we analyzing the ED-71 actions in osteoblast-spcific VDRKO (Ob-VDRKO) mice generated through a Cre/loxP system.

Disclosures: ***Y. Yamamoto****, None.*

M584

Transcriptional Effects of a Shortened Side Chain Vitamin D Analog 2-Methylene-19-Nor-(20S)-Bishomopregnacalciferol in Bone and Intestinal Cells. M. Watanuki, N. K. Shevde, L. A. Plum, H. F. DeLuca, J. W. Pike. Biochemistry, University of Wisconsin- Madison, Madison, WI, USA.

A major role of 1,25-dihydroxyvitamin D3 (1,25(OH)2D3) is to maintain calcium and phosphorus homeostasis through direct actions on gene expression in intestine, kidney and bone. 1,25(OH)2D3 also regulates growth and differentiation, providing the impetus for the development of synthetic analogs of this hormone that might be useful therapeutically in psoriasis, immune suppression, renal osteodystrophy or cancer. A significant limitation of many of these analogs, however, is their tendency to increase serum calcium levels due entirely to the homeostatic actions described above. In this report, we explore the actions of 2-methylene-19-nor-(20S)-bishomopregnacalciferol (2MbisP) on gene expression in bone and intestinal cells. Importantly, 2MBisP is unable to induce hypercalcemia at high doses in vivo relative to 1,25(OH)2D3. Interestingly, 2MBisP induced the expression of marker genes equally well in both osteoblast and intestinal cell lines, displaying a potency that was slightly less than that of 1,25(OH)2D3 and consistent with its affinity for the vitamin D receptor (VDR). Surprisingly, 2MBisP was also capable in osteoblasts of inducing the expression of RANKL and suppressing the expression of OPG, gene products involved in osteoclast-mediated bone calcium mobilization. As a consequence, 2MBisP was nearly equivalent to 1,25(OH)2D3 in inducing osteoclastogenesis in coculture assays. Equally surprising was the observation that 2MBisP was fully efficacious in inducing the expression in Caco2 cells of the calcium channel gene TRPV6 and the calcium "transporter" gene calbindin D9K. In keeping with these findings, 2MBisP also promoted the localization of VDR/RXR to the promoters of several of these genes as analyzed by chromatin immunoprecipitation assay. 2MBisP was also similar in its ability to promote VDR interaction with RXR as well as with coactivators such as SRC-1 and -2 and DRIP205, as assessed in GST pull-down and in mammalian 2-hybrid assays in both bone and intestinal cell backgrounds. These studies indicate that 2MBisP is fully able to activate the expression of genes involved in calcium homeostasis. Thus, the inability of 2MBisP to induce bone calcium mobilization or to stimulate intestinal calcium absorption in vivo may be independent of the molecular mechanisms essential to the activation of gene expression by this compound.

Disclosures: ***M. Watanuki****, None.*

M585

Molecular and Apoptotic Mechanisms of 25-hydroxyvitamin D_3 Analogs in Prostate Cancer Cells. J. Lambert*[1], S. Sarkar*[2], R. Ray*[2]. [1]Pathology, University of Colorado Health Sciences Center, Denver, CO, USA, [2]Medicine, Boston University School of Medicine, Boston, MA, USA.

Recently we described that 25-hydroxyvitamin D_3-3-bromoacetate (25-OH-D_3-3-BE), a non-toxic and vitamin D receptor (VDR)-cross-linking analog of 25-hydroxyvitamin D_3 (25-OH-D_3) strongly inhibited the proliferation of LNCaP, PC-3, DU-145 and LAPC-4 prostate cancer cells and induced apoptosis. In the present study we synthesized 25-hydroxyvitamin D_3-3-epoxide (25-OH-D_3-3-Epoxide), another VDR-cross-linking analog of 25-OH-D_3 that is stable towards esterases. We observed that 25-OH-D_3-3-Epoxide strongly inhibited the proliferation of PC-3 cells, similar to 25-OH-D_3-3-BE. In LNCaP cells both 25-OH-D_3-3-BE and 25-OH-D_3-3-Epoxide induced the expression of prostate derived factor (PDF), a protein that is implicated in the vitamin D activity in prostate cancer cells, similar to 1,25-dihydroxyvitamin D_3 (1,25$(OH)_2D_3$). In a growth-assay with ALVA-31 prostate cancer cells and a VDR-antisense ALVA-31 clone, 25-OH-D_3-3-BE and 25-OH-D_3-3-Epoxide showed growth-inhibitory effect similar to1,25$(OH)_2D_3$. Earlier we showed that 25-OH-D_3-3-BE induced apoptosis in PC-3 cells by fragmenting nuclear DNA and enhancing caspases 3,8 and 9 activities. In this study we probed the apoptotic behavior of 25-OH-D_3-3-BE and 25-OH-D_3-3-Epoxide in PC-3 cells, and observed that both the compounds activated AKT-phosphorylation. In summary results described in this communication strongly suggested that antiproliferative property of 25-OH-D_3-3-BE and 25-OH-D_3-3-Epoxide in prostate cancer cells is mediated by 1,25$(OH)_2D_3$-signaling pathway, and the apoptotic behavior involves AKT-mediated pathway.

Disclosures: ***R. Ray****, None.*

WORKING GROUP ON MUSCULOSKELETAL REHABILITATION IN PATIENTS WITH OSTEOPOROSIS ABSTRACTS

WG1

Introduction of a New Concept to Assess Quality of Life in Patients with Osteoporosis. H. W. Minne, C. Hinz, M. Pfeifer, Institute of Clinical Osteology "Gustav Pommer" and Clinic "DER FÜRSTENHOF", Bad Pyrmont, Germany.

The morbidity of osteoporosis is caused by fractures. Vertebral fractures lead to pain and disability and a decrease in quality of life. Over the last 15 years several important parameters have been identified, which determine quality of life in patients suffering from vertebral fractures in postmenopausal osteoporosis. Besides the degree of kyphosis and deformity [1,2], especially time since last fracture [3] and sense of coherence [4] are important predictors of health-related quality of life (HRQoL).

In order to estimate quality of life, several questionnaires have been developed. Starting with generic instruments such as the Nottingham Health Profile and the Short Form 36, which provide a general estimate of health perception, we introduced more and more disease-specific questionnaires [2,3], which agree better with grade of disease and which are usually more sensitive to change in parallel with improvement or deterioration of disease. Together with clinicians and other quality of life specialists from eight European countries, we validated the so-called "QUALEFFO" in two multi-center studies [5]. This questionnaire contains 41 questions in 5 domains: pain (5), physical function (17, divided over subdomains : activities of daily living, jobs around the house, mobility), social function (7), general health perception (3), and mental function (9). Most of this 41 questions were specifically designed for this questionnaire, but a few were taken from the MEDOS and EVOS questionnaires.

QUALEFFO has been shown to discriminate between patients with osteoporotic fractures and control subjects and the contents of the questions were derived from complaints and common problems of patients with osteoporosis. Clinical experience, however, indicate that the degree of disease specificity is not high enough to reveal the whole picture of osteoporosis and to reflect the burden of the disease in its complexity and various appearances in different patients. We, therefore, undertook the task to create a new assessment tool with the aim to reflect function, handicap, impairment and disability of patients after vertebral fractures more accurate than previous questionnaires. In its first and crude version, our instrument consisting of 103 questions now entered the validation phase to test for within-subject reproducibility, internal consistency and construct validity. Preliminary results suggest a good reproducibility and a discrimination between patients and controls.

References:

1) Leidig G, Minne HW et al. A study of complaints and their relation to vertebral destruction in patients with osteoporosis. Bone Miner 1990;8:217-29.
2) Leidig-Bruckner G, Minne HW et al. Clinical grading of spinal osteoporosis: quality of life components and spinal deformity in women with vertebral osteoporosis. J Bone Miner Res 1997;12:663-75.
3) Begerow B, Pfeifer M et al. Time since vertebral fracture: an important variable concerning quality of life in patients with postmenopausal osteoporosis. Osteoporos Int 1999;10:26-33.
4) Scholz MG, Minne HW. Spinal deformity, disability, and quality of life in osteoporotic patients. Curr Opin Orthoped 1998;9:V21-27.
5) Lips P, Cooper C et al. Quality of life as outcome in the treatment of osteoporosis : the development of a questionnaire for quality of life by the European Foundation for Osteoporosis. Osteoporos Int 1997;7:36-38.

WG2

Effects of Whole Body Vibration on Bone Density and Muscle Function. S. Boonen, S. Versheuren. Leuven University Center for Metabolic Bone Diseases and Division of Geriatric Medicine, Katholieke Universiteit Leuven, Leuven, Belgium.

High-frequency mechanical strain has been shown to stimulate bone strength in different animal models. However, the effects of vibration exercise on the human skeleton have hardly been studied. Particularly in postmenopausal women – who are most at risk of developing osteoporosis – randomized controlled data on the safety and efficacy of vibration loading are lacking. The aim of this randomised controlled trial was to assess the musculoskeletal effects of high-frequency loading by means of whole-body vibration in postmenopausal women.

Seventy volunteers (age, 58-74 years) were randomly assigned to a whole-body vibration training group (WBV, *n*=25), a resistance training group (RES, *n*=22), or a control group (CON, *n*=23). The WBV-group and the RES-group trained three times weekly during 24 weeks. The WBV-group performed static and dynamic knee-extensor exercises on a vibration platform (35-40 Hz, 2.28-5.09 g), mechanically loading the bone and evoking reflexive muscle contractions. The RES-group trained knee-extensors by dynamic leg press and leg extension exercises, increasing from low (20RM) to high (8RM) resistance. The CON-group did not participate in any training. Hip bone density was measured using DXA at baseline and after the 6-month intervention. Isometric and dynamic strength were measured by means of a motor-driven dynamometer. Data were analysed by means of repeated measures ANOVA.

No vibration-related side effects were observed. Vibration training improved isometric and dynamic muscle strength (+15% and +16%, respectively, $p<0.01$), but also significantly increased BMD of the hip (+0.93%, $p<0.05$). No changes in hip BMD were observed in women participating in resistance training or age-matched controls (-0.60% and –0.62%, respectively, NS). Serum markers of bone turnover did not change in any of the groups.

These findings suggest that WBV training may be a feasible and effective way to modify well-recognized risk factors for falls and fractures in older women, and support the need for further human studies.

WG3

Assessment of the Risk of Falls.E. Preisinger. Physical Medicine and Rehabilitation, Krankenhaus Lainz, Vienna, Austria

Approximately 30% of people over 65 years of age and living in the community fall each year; the number is higher in institutions. 1 in 10 falls results in a fracture or in another serious injury. Therefore, to prevent fractures in the elderly reduction of the risk of falling is as important as the augmentation of bone quality. Although few falls have a single cause, the majority result from interactions between long-term and short-term predisposing factors and short-term precipitating factors in a person's environment. Each of the following conditions has been shown to increase the subsequent risk of falling in two or more observation studies: arthritis; depressive symptoms; orthostasis; impairment in cognition, vision, balance, gait or muscle strength; and the use of four or more prescription medications. Furthermore, the risk of falling consistently increases as the number of these risk factors increases. The risk of falling increased in a cohort of elderly persons living in the community, from 8% among those with no risk factors to 78% among those with four or more risk factors.[1] Also it is suggested that risk factors for indoor and outdoor falls are different.[2]

A risk assessment of falls should include the number of falls in the past, current diseases or chronic conditions and medications, as well as an investigation of balance and some activities of daily living (ADL), such as getting up from chair and walking. Tinnetti has been summarized the clinical approach to the prevention of falls among elderly persons living in the community in an algorithm:[1]

Ask all patients ≥75 years old about falls,→no falls→preventive exercising:

balance or gait difficulties → Two or more falls or balance or gait difficulties

no balance orbalance, strength gait difficultiestraining → One fall and no balance or gait difficulties → ↑ → →

↓

Assessment of predisposing and precipitating factors, followed by interventions suggested by the results of detailed assessment

Balance assessment tools could be divided in high tech assessment tools and clinical assessments. The basic requirements of such high tech equipments have a forceplate or platform the patient stands on which has sensors embedded in it. Data of measurements, i.e. excursions of body's center of gravity (static posturography), were calculated by a computer. In a previous study Nguyen et al. reported that body sway was an important predictor of osteoporotic fractures.[3] Clinical assessments of balance, for example, are the Romberg Test, One-Legged Stance Test, Postural Stress Test, the Berg Balance Scale, Timed Get Up and Go Test and Tenetti Index. These clinical tools can be used for screening. They are simple, but mainly not extensively tested. In a prospective cohort trial Guralnik et al. demonstrated that objective measures of lower-extremity function were highly predictive of subsequent disability in the elderly.[4] It is well known that functional deficits in the lower-extremities increase the risk of falling. Therefore, in view of the literature and in my opinion physicians should ask their elderly patients about any falls and ask about and look for any difficulties with balance or gait. Brief clinical screens followed by assessments providing more specific information about balance or gait abnormities should be included. A comprehensive assessment of risk for falls should prepare the way for further strategies to prevent osteoporotic fractures in the elderly.

[1] Tinetti. NEJM 2003 ;348 :42.
[2] Bergland A, et al. Aging-Clin-Exp-Res 2003 ; 15 :43-50.
[3] Nguyen et al. BMJ 1993 ;307 :1111.
[4] Guralnik at al. NEJM 1995;332:556.

WG4

Effects of Vitamin D on Musculoskeletal Health. M. Pfeifer, H. W. Minne. Institute of Clinical Osteology "Gustav Pommer" and Clinic "Der Fürstenhof", Bad Pyrmont, Germany.

We have found in a first prospective, randomized, placebo-controlled trial that short-term supplementation with vitamin D and calcium reduced body sway and the mean number of falls during a one-year period of follow-up in women 70 years of age or older who were vitamin D deficient (mean serum 25OHD level: 23 nmol/liter) with a mean calcium intake of 560 mg per day and living at a latitude of 52°N [1]. Compared with calcium monotherapy, supplementation with vitamin D and calcium in women with vitamin D insufficiency resulted in a decrease in plasma PTH of 18% ($p = 0.0435$), and a decrease in body sway of 9% ($p = 0.0435$). The mean number of falls during one year of single-blinded follow-up was 0.47 for the calcium monotherapy group and 0.24 for the vitamin D and calcium group ($p = 0.0346$) [1]. These results support the concept that hypovitaminosis D impairs neuromuscular coordination, as measured by body sway, and thus increases the risk of falling and fall-related fractures. In an other randomized, controlled trial Bischoff *et al.* demonstrated a reduction in falls after treatment with vitamin D and calcium in elderly institutionalized women [2]. The women with a mean age of 85 ± 7 years received either 1200 mg of elemental calcium or 1200 mg of elemental calcium plus 800 IU of vitamin D [2]. Mean fall incidence rate – the number of falls before treatment subtracted from the number of falls during treatment period – was 2.4 in the calcium group and 0.9 in the calcium and vitamin D group ($p = 0.04$).

This effect of cholecalciferol on fall risk was confirmed by Larsen *et al.* (2004) in 9,605 community-dwelling residents aged 65 years and over (females 5,771, males 3,834; median age 74.0 years; range 65-103 years) in the municipality of Randers in Denmark. The participants were offered a daily supplement of 1,000 mg of elemental calcium as calcium carbonate and 400 I.U. of cholecalciferol. During 3½ years of follow-up, female residents fell more rarely (RR: 0.9; $p<0.05$), whereas both males and females had a reduced risk of osteoporotic fractures (RR: 0.8; $p<0.025$), [3].

In veiled Arab women living in Denmark, Glerup *et al.* [4] found that muscle power as determined by maximal voluntary contraction (MVC) significantly correlated to serum levels of 25OHD ($r = 0.34$; $p < 0.01$) but not to $1,25(OH)_2D$ ($r = -0.14$; NS) [4]. Compared with Danish controls maximal voluntary knee extension as measured with a strain gauge dynamometer was reduced by 34% in 55 vitamin D deficient Arab women (serum 25OHD < 20 nmol/liter). Treatment with intramuscular injections of ergocalciferol 100,000 IU per month and an oral supplementation of 1200 mg calcium and 400 IU ergocalciferol per day resulted in an increase in mean MVC of 13% after 3 months and 24% after 6 months [4].

Gallagher *et al.* demonstrated in a randomized double blind placebo-controlled trial in 489 postmenopausal women that treatment with 0,25 µg calcitriol twice daily reduced the number of falls [5]. The three-year incidence rate for falls was 0.43 on placebo compared to 0.29 on calcitriol ($p<0.001$), [5]. Concerning another vitamin D metabolite, Dukas *et al.* showed in a prospective, placebo-controlled study among 191 women and 187 men 70 years of age or older that alfacalcidol ($1(OH)D_3$) reduces fall risk (OR: 0.69; 95% C.I.: 0.41-1.16), [6]. Over 36 weeks of treatment, 1 µg alfacalcidol reduced not only mean number of falls (OR: 0.46; 95% C.I.: 0.22-0.99; $p=0.045$) but also mean number of fallers (OR: 0.45; 95% C.I.: 0.21-0.97; $p=0.042$) among participants with a mean nutritional calcium intake above 512 mg per day [6] This study highlights the importance of calcium in mediating the effects of vitamin D on parameters of muscle function, because study subjects with a mean calcium intake below 512 mg per day did not show a fall reduction [6].

References

1. Pfeifer M, Begerow B, Minne HW, Abrams C, Nachtigall D, Hansen C. Effects of a short-term vitamin D and calcium supplementation on body sway and secondary hyperparathyroidism in elderly women. J Bone Miner Res 2000;15:1113-1118.
2. Bischoff HA, Stähelin HB, Dick W et al. Effects of vitamin D and calcium supplementation on falls: a randomized controlled trial. J Bone Miner Res 2003:18:343-51.
3. Larsen ER, Mosekilde L, Foldspang A. Vitamin D and calcium supplementation prevents osteoporotic fractures in elderly community dwelling residents: a pragmatic population-based 3-year intervention study. J Bone Miner Res 2004;19:370-8.
4. Glerup H, Mikkelsen K, Poulsen L et al. Hypovitaminosis D myopathy without biochemical signs of osteomalacic bone involvement. Calcif Tissue Int 2000;66: 419-24.
5. Gallagher JC, Haynatzki G, Fowler S. Effect of estrogen, calcitriol or the combination of both on falls and non vertebral fractures in elderly women. J Bone Miner Res 2002; 17(Suppl.1): abstract F 381.
6. Dukas L, Bischoff HA, Lindpaintner LS et al. Alfacalcidol reduces the number of fallers in a community-dwelling elderly population with a minimum calcium intake of more than 500 mg daily. J Am Geriatr Soc 2004;52:230-6.

WG5

Proprioceptive Dynamic Program for Osteoporotic/Kyphotic (O/K) Individuals. M. Sinaki[1], R. Brey[2], C. Hughes[3], D. Larson[4] K. Kaufman[3]. [1]Physical Medicine and Rehabilitation; [2]Vestibular Laboratory; [3]Biomechanics and Motion Analysis Laboratory; [4]Biostatistics, Mayo Clinic, Rochester, MN, USA.

Falls are multifactorial; therefore, multifaceted approaches are required to prevent falls. Imbalance and posture sway are two important risk factors for falls. Controlling sedative pharmacotherapy decreases iatrogenically affected alertness and can reduce falls in the geriatric population. Axial muscle strength decreases about 50% from age 30 to 80.[1] Axial bone mass also decreases approximately 50% in women and 30% in men by age 80.

This study was designed to investigate the influence of kyphosis on postural sway, gait unsteadiness and falls in osteoporotic individuals. Age, height, weight, gait, muscle strength and balance were objectively evaluated in 13 osteoporotic/kyphotic (OK) women with thoracic kyphosis (Cobb angle between 50 to 60 degrees)[2] and 13 healthy controls of comparable age. Isometric lower extremity strength data was collected using a Quantitative Muscle Assessment (QMA) system (The Computer Source, Gainesville, GA). Isometric back extensor strength was measured using the BID-2000 back dynamometer. Gait was studied during unobstructed level walking and while stepping over obstacles of four different heights randomly assigned (2.5, 5, 10 and 15% of the subject's height). Repeated measures ANOVA was used for the statistical analysis with the significance level set at $p < 0.05$. Balance was objectively assessed using Computerized Dynamic Posturography (CDP), (Neurocom, Clackamas, Oregon). A composite score of the Sensory Organization Test (SOT) component was used for this study. Each subject also completed a Dizziness Handicap Inventory and falls efficacy test prior to inclusion in the study. Statistical analysis was done using a student t-test.

O/K subjects had lower muscle strength than the controls in the lower extremities and back extensors ($p<0.05$). Gait analysis showed a significant difference in the anterior/posterior (A/P) and medial/lateral (M/L) displacements and velocities. The OK subjects had less A/P displacement, greater M/L displacement and reduced A/P velocity when compared to the control subjects. This was true for all conditions of unobstructed and obstructed level walking. Also, there was a significant effect of obstacle height on all center of mass (COM) parameters. CDP test showed that the OK subjects had statistically significantly greater balance abnormalities compared to the control group ($p<0.001$).

Following baseline evaluations, the 13 O/K subjects began a specific 4-week home based proprioceptive dynamic program.[3] At the end of the study period, lower extremity strength was unchanged; however, balance improved significantly. Gait parameters also showed statistically significant improvement compared to baseline evaluations.

1. Sinaki M. Nwaogwugwu NC. Phillips BE. Mokri MP. Effect of gender, age, and anthropometry on axial and appendicular muscle strength. *Am J Phys Med Rehabl. 80(5):330-8, 2001 May.*
2. Itoi E. Roentgenographic analysis of posture in spinal osteoporotics. *Spine. 16(7):750-6, 1991 Jul.*
3. Sinaki M. Lynn SG. Reducing the risk of falls through proprioceptive dynamic posture training in osteoporotic women with kyphotic posturing: a randomized pilot study. *Am J Phys Med Rehabl. 81(4):241-6, 2002 Apr.*

WG6

Back Exercise for Management of Osteoporosis. E. Itoi[1], M. Hongo[1], N. Miyakoshi[1], M. Sinaki[2]. [1]Department of Orthopedic Surgery, Akita University School of Medicine, Akita, Japan. [2]Department of Physical Medicine and Rehabilitation, Mayo Clinic, Rochester, USA.

Increased thoracic kyphosis is a typical postural deformity observed in patients with osteoporosis. Disadvantages of increased thoracic kyphosis are chronic back pain, decreased vital capacity, reflux esophagitis, increased risk of fall, and deteriorated QOL. Falls may cause a new vertebral fracture, which in turn aggravates the kyphotic deformity. In order to stop this vicious circle, prevention and treatment of malposture is required. We have demonstrated that back strengthening exercise is effective not only in increasing the back extensor strength but also in reducing the risk of vertebral fractures in healthy postmenopausal women. Another potential benefit of back strengthening exercise is to increase or maintain the spinal mobility. Recently, we have demonstrated that QOL is affected by the spinal mobility and that the back extensor strength is the most significant contributor to the spinal mobility. However, the safety and effectiveness of back strengthening exercise in patients with osteoporosis have not been clarified. Last year, we reported that reducing each of the weight of the backpack, repetition times, or frequency of the exercise resulted in reduction in the amount of obtained strength of the back extensors. From the view point of reducing the risk of vertebral fractures, it seemed reasonable to reduce the amount of weight rather than reducing the repetition times or frequency. We further investigated the relationship between the reduction of the weight of the backpack and the back extensor strength in healthy young female volunteers. Even without a backpack, the subjects obtained an average 17% increase in back extensor strength in 4 months compared with 5% increase in the control group. Based on this preliminary study, we started a prospective randomized study to determine the effect of back strengthening exercise on posture, spinal mobility, and QOL of patients with osteoporosis. We will share the preliminary results of this ongoing clinical trial.

PEDIATRIC BONE AND MINERAL WORKING GROUP ABSTRACTS

WG7

Rheumatologic Manifestations of Pediatric Forms of Hypophosphatasia. D. Wenkert[1], S. Mumm[2], J. Zerega[1], W. H. McAlister[2], M. P. Whyte[1]. [1]Shriners Hospitals for Children, St. Louis, MO, USA;[2]Washington University School of Medicine, St. Louis, MO, USA.

Hypophosphatasia (HPP), an inborn-error-of-metabolism characterized biochemically by subnormal serum levels of alkaline phosphatase (ALP), is caused by deactivating mutations in the gene which encodes the tissue-nonspecific ALP isoenzyme (TNSALP). Radiographs in "childhood" HPP typically show rickets, including "tongues" of lucency that project from physes into metaphyses in major long bones and sometimes, areas of metaphyseal osteosclerosis. Yet children with the most mild form, odontoHPP, have no skeletal radiographic abnormalities and seek medical attention for early tooth loss.

Purpose: To define the prevalence of joint and bone pain with various pediatric forms of HPP and to highlight two patients with presentations mimicking *chronic recurrent multifocal osteomyelitis* (CRMO).

Methods: We reviewed 111 HPP patient charts. Nearly all have completed molecular diagnoses. 11 had infantile HPP, 64 had childhood HPP, and 36 had odontoHPP. Patients with complex phenotypes (ie. more than one disease),a marrow transplant recipient, and patients less than 2.5 years at last evaluation were excluded.

Results: Among patients who met inclusion criteria: Significant joint and skeletal pain troubled 8 of 8 children (100%) diagnosed with infantile HPP. Of 58 patients with childhood HPP, 72% complained of pain varying from mild to incapacitating (sometimes with morning stiffness) often following physical activity. All reported lower extremity pain. 20% had upper extremity pain as well. Of 32 patients with odontoHPP, 59% complained of pain in their lower extremities and/or back. Hence, joint and or bone pain occur often in each pediatric form of HPP. These, symptoms may often be attributable to obvious rickets, but pain also troubled patients with early tooth loss as their only HPP manifestation.

Two of our HPP patients presented with an unusual syndrome of periarticular pain and bone edema mimicking CRMO: A 13-year-old boy without premature loss of deciduous teeth, had life-long a stiff-legged gait and joint pains twice considered elsewhere as possible CRMO. Additionally, he had distal tibial metaphyseal expansion worsening over 2 years that is atypical for HPP. Serum ALP was 94 (133-347 IU/L). Study of the *TNSALP* gene showed a mutation (Asp361Val) in one allelle.

At age 11 years, a girl with infantile HPP (and a history of morning stiffness and joint and bone pain) developed bilateral, incapacitating leg pain and bone edema (detected by MRI) consistent with CRMO on MRI after an epiphyseal stapling procedure to correct knock knee deformity. Serum ALP was 39 (mutational analysis revealed compound heterozygosity: Ala34Ser; Thr117His).

Conclusions: Causes of pediatric joint pain are numerous and sometimes are unexplained. Premature tooth loss (less than 5 years of age) and careful assessment for low serum levels of ALP using age-appropriate norms should be included in the differential diagnosis of puzzling pediatric joint and bone pain syndromes.

Disclosures: ***D. Wenkert****, None.*

WG8

Parathyroid Carcinoma and Atypical Adenoma Associated with Germline *HRPT2* Mutation in Familial Isolated Hyperparathyroidism. T. Kelly[1*], T. Shattuck[2*], M. Reyes-Mugica[1*], B. Kinder[1*], A. Arnold[2], T. Carpenter[1] [1]Yale Univ., New Haven, CT, USA, [2]University of Connecticut, Farmington, CT, USA

Familial isolated hyperparathyroidism (FIHP) is a rare cause of parathyroid (PT) tumors without other neoplasms or endocrinopathies. Mutations in *CASR*, *MEN1* and rarely, *HRPT2*, a putative tumor suppressor, have been identified in kindreds with FIHP. *HRPT2* mutations may be enriched in FIHP families with PT carcinoma, underscoring the importance of identifying causative mutations. Unsuspected germline *HRPT2* mutations occur in sporadic PT carcinoma, and genetic testing of such patients has been advocated.

A 13-year-old boy developed hematuria, hypercalcemia (12.6 mg/dL) and elevated serum PTH (93 pg/mL). Ultrasound demonstrated nephrolithiasis with no other renal pathology. His father had died three years earlier from complications of PT carcinoma. Ultrasound identified a left superior PT mass, which was removed surgically with the ipsilateral inferior PT gland. Aggressive histological features of the tumor included fibrous trabeculae, mitoses, and microscopic capsular infiltration; the inferior gland had normal histology. PTH levels corrected intra-operatively after extirpation of the adenoma, and serum calcium normalized post-operatively. Serum prolactin and calcitonin, and urinary catecholamine excretion were normal. Two years later hematuria, hypercalcemia, and elevated PTH levels recurred. Ultrasound and MRI indicated no recurrent disease in the left neck. An enlarged right inferior PT gland was identified and removed surgically; histology was typical of a benign adenoma. Serum PTH corrected intra-operatively, and serum calcium normalized following surgery. Leukocyte DNA analysis revealed a 5 bp deletion at nucleotide 138 of *HRPT2* (leading to an early frameshift at parafibromin amino acid 46). The initial tumor manifested the expected germline *HRPT2* mutation, plus a distinct somatic mutation (4 bp deletion at nucleotide 60 causing frameshift at amino acid 20), consistent with the Knudson "two hit" concept of biallelic inactivation of a tumor suppressor gene.

Germline mutations in *HRPT2* occur in the hyperparathyroid-jaw tumor syndrome (HPT-JT), in which ossifying fibromas of the jaw and renal lesions occur. These features were not present in our patient, however as they usually appear in the 2nd or 3rd decade of life, HPT-JT remains a possible diagnosis. Genetic screening of the patient's 7 siblings (ages 11-28) is planned, however all have been normocalcemic. Thus, despite the reported rarity of *HRPT2* mutations in FIHP, a personal or family history of PT carcinoma in FIHP mandates serious consideration of a germline *HRPT2* mutation that would affect diagnosis and management.

WG9

Toward a Molecular Understanding of Bone Sarcoma Formation and Malignancy: Implication of a Poly(ADP-ribose) Polymerase-1 Pseudogene. A. Moreau[1, 2], D.S. Wang[1], J. Doyon[3], M. Isler[4], R. Turcotte[5].[1]Bone Molecular Genetics & Musculoskeletal Malformations Laboratory, Research Centre, Hôpital Sainte-Justine; [2]Department of Stomatology and Biochemistry, Université de Montréal, Montreal, Canada; [3]Department of Pathology, Hôpital Maisonneuve-Rosemont; [4]Orthopedic Division, Hôpital Maisonneuve-Rosemont & Hôpital Sainte-Justine Hospital; [5]Orthopedic Division, Montreal's General Hospital & McGill University, Montreal.

Bone cancer is the fourth most common cancer in people under 25 years of age. These skeletal cancers in children are serious and highly fatal conditions while in adolescents and adults, they can have devastating consequences for the life and the limb of the patient. Very little is known about the etiology and the molecular mechanisms involved in skeletal cancerogenesis due to the heterogeneous nature and unpredictable behavior of that disease, which results in controversy as its cause and progression. In the course of studying the role of different factors in bone sarcomas, we serendipitously discovered two transcripts of a PARP-1 pseudogene located to 13q33-qter (PARP-1p), one corresponding to the common A allele and the other to the less common B allele harboring a 193-bp deletion. Poly (ADP-ribose) polymerase 1 is a nuclear enzyme and a DNA binding protein that catalyzes the synthesis of ADP-ribose polymers from NAD+ and their attachment to a variety of nuclear proteins and enzymes. Transcription factors that are ribose modified by poly (ADP-ribose) loose their ability to bind DNA. The PARP-1 gene has been mapped to human chromosome 1q42 and two PARP-1 pseudogenes to 13q33-qter (PARP-1p) and 14. A two-allele PARP-1p polymorphism has been originally detected resulting from a 193-bp deletion of part of the PARP-1p pseudogene at chromosome 13. It has been suggested that PARP-1p polymorphism may be linked to a predisposition to certain cancers. Interestingly, the expression of both alleles were detected only in severe and malignant osteosarcomas (high grade), which contrasted with benign tumors like Giant Cell Tumors or low grade osteosarcomas (grade 2 or less) expressing only the A allele. Moreover, the B allele of PARP-1p was detected only in severe and malignant bone sarcomas and in tumorigenic cancer cell lines. Taken together these results showed for the first time that PARP-1p pseudogene is expressed in human malignant bone sarcomas and co-expression of its B allele could be used as a molecular marker for the early identification in children of skeletal tumors exhibiting a high tumorigenic and malignant potential for whose better pharmacological approaches could be designed.

WG10

Longitudinal Pediatric Reference Standards for the Assessment of Bone Mineral Content. A.D.G. Baxter-Jones[1], R.L.Mirwald[1], M. Petit[2], T. Lloyd[2], L. Bachrach[3], H.A. McKay[4]. [1]College of Kinesiology, University of Saskatchewan, SK, Canada, [2]Department of Health Evaluation Sciences, Penn State University, PA, [3] Department of Pediatrics, Stanford University School of Medicine,[4]Department of Orthopaedics, University of British Columbia, BC, Canada.

There are a number of childhood diseases that can deleteriously affect bone mineral accrual during the growing years. Further, with current bone assessment tools children can easily be misclassified with low bone mass based on small size. Thus, appropriate normative data are needed to accurately determine children at risk for low bone mass and to monitor the effects of intervention designed to enhance bone mass. The present study developed an anthropometry-based prediction model for the assessment of bone mineral content (BMC) in children and adolescents aged 8 to 19 years. Data from 4 longitudinal studies, across 3 sites were collapsed. Healthy boys and girls from four ethnic groups (Caucasian, African-American, Asian and Hispanic) were measured annually for a minimum of four consecutive years. The studies were: the Saskatchewan Pediatric Bone Mineral Accrual Study (BMAS) (239 subjects; 1341 observations), UBC Healthy Bones Trials (1021 subjects; 1964 observations); Penn State Young Women's Health Study (217 Subject; 1113 observations) and Stanford's Bone Mineral Accretion (BMA) Study (325 subjects; 758 observations). Dual-energy X-ray absorptiometry (DXA) (Hologic 4500) was used to measure total body (TB), total proximal femur (PF), femoral neck (FN) and lumbar spine (L1-L4) (LS) bone mineral content (BMC). Data were analyzed using random effects models and gender and site-specific models were created. Models were built in a stepwise procedure with predictor variables added one at a time, using the loglikelihood ratio statistic to determine if one model was a significant improvement over the previous one. The initial models were based on the BMAS data and were verified in the other two data sets. The data were then combined for the final models and variance between predicted and actual data was investigated using the Bland-Altman procedure. The coefficients that best predicted BMC were age, height, weight and their interactions. Ethnic differences were also found, for example when compared to Caucasians, African-Americans and Hispanics had significantly greater FNBMC 0.39 (± 0.06) and 0.34 (± 0.07) g respectively ($p<0.05$), once the confounders of age and size had been controlled. In contrast Asians had 0.20 (± 0.03) g less FNBMC than Caucasians ($p<0.05$). The Bland-Altman graphs of boys FNBMC indicated that the difference between actual and predicted values was less than 1.0 g in 95% of the cases and in girls less than 1.5 g, 95% of the time. Similar results were found for the other sites. In conclusion we have produced a series of longitudinal growth models that predict BMC by accounting for sex, body size and ethnicity. Our findings suggest that the prediction models provide a useful clinical tool to determine potential bone mineral deficits in pediatric populations.

WG11

Vitamin D Deficiency Among Children Living in Canada: Results of a National Disease Surveillance Program. L.M. Ward[1], C.A. White[1], S. Zlotkin[2]. [1]Department of Pediatrics, University of Ottawa, Ottawa, Ontario, Canada, [2]Departments of Pediatrics and Nutritional Sciences, University of Toronto, Toronto Ontario, Canada.

The incidence of Vitamin D deficiency rickets is rising in many countries worldwide. Our experience suggested Canada may be no exception, despite the Canadian Paediatric Society position statement that all breast-fed infants receive daily, oral vitamin D (400 IU). We sought to determine the disease incidence through the Canadian Paediatric Surveillance Program (CPSP), a national network which provides regular, written contact with 2,300 pediatricians across the country. Between July 2002 and March 2004, there were 71 confirmed cases of vitamin D deficiency rickets among children living in Canada. The mean age at diagnosis was 1.45 years (SD 0.94; range 0.10-6.34), 44% of confirmed cases were female, and half were from Ontario. The ethnicity profile was as follows: 34% Black, 14% First Nations, 13% Middle Eastern, 10% Inuit, 10% Caucasian, and 1% Asian (not indicated in the remaining 18%). The mean maternal age at delivery was 29 years (SD 6.2; range 18-39). Eighty-six percent of cases were intermediate- or dark-skinned, and 85% had been breast-fed (the feeding status was not indicated in the remaining 15% of cases). The vast majority (86%, 61/71) of cases had not received vitamin D prior to diagnosis. In the remaining 14%, vitamin D was either unreliably administered or supplementation data was not available. Only 16% of mothers received vitamin D during pregnancy, a number which fell to 6% following delivery, and the majority of mothers did not drink milk. Milk allergies and sunscreen use among children were not significant risk factors for developing the disease, as both were documented in less than 5% of cases. Significant morbidity was present at diagnosis, including skeletal deformity (48%), seizures (14%), failure to thrive (13%), fractures (10%) and delayed developmental milestones (3%). The remaining 12% of cases presented with an incidental discovery of rickets on x-rays. The mean alkaline phosphatase level at diagnosis was 1,381 U/L (range 296 to 6,067), while the 25-hydroxyvitamin D level prior to treatment was a mean of 21.0 nmol/L (SD 14.7; range 1-58). Though it is not surprising that children with the greatest number of risk factors for vitamin D deficiency were the most frequently diagnosed, it is surprising that the condition is frequently detected in a country with ready access to vitamin D and a clear recommendation for prevention from the country's national paediatric organization. These results highlight an urgent need for heightened awareness among health care providers and the general public for prevention of vitamin D deficiency among children in Canada.

ADULT BONE AND MINERAL WORKING GROUP ABSTRACTS

WG12

Prevalence of High Incidences of Secondary Causes of Osteoporosis in Men and Women. S. Wimalawansa Department of Medicine, Division of Endocrinology, Robert Wood Johnson Medical School, New Brunswick, NJ, USA.

Osteoporosis is a disease with continuous loss of bone and, therefore, artificial division into type I and type II (e.g. senile) is not logical. Simple classification of primary and secondary osteoporosis is more practical and useful in their management. Osteoporosis affects ~10% of the World's population, and 3-4% of these patients have treatable secondary causes leading to, or aggravating, this most common metabolic bone disease which is neglected in many instances.

We have examined the incidence of secondary causes of bone loss in 1,000 consecutive patients referred to a tertiary osteoporosis referral clinic. 72% of these patients were female, and 90% of these women were postmenopausal.

The percentages reported with secondary osteoporosis vary with referral patterns. For example, Francis et al. have reported figures of 20% and 35%, and Mayo Clinic reported figures of 40% and 55% for females and males respectively. Current study shows 46% of females and 75% of males referred to this tertiary osteoporosis clinic had treatable secondary causes of bone loss. Since these reported data are from highly selected populations, the true incidence of secondary causes leading to osteoporosis in the community is likely to be much lower.

Table: Incidence of secondary causes of osteoporosis (numbers* and percentages) in 1,000 consecutive patients referred to a tertiary osteoporosis clinic.

Disease / Ailment	Females (n = 720)		Males (n = 280)		Mean Incidence
	Number	Percentage	Number	Percentage	%
Glucocorticoid	89	12.4	28	10.0	11.7
Other medications	45	6.3	17	6.1	6.2
Smoking/alcohol abuse	62	8.6	25	8.9	8.7
Cytotoxic drugs/ radiotherapy	37	5.1	10	3.6	4.7
GI problems	53	7.4	17	6.0	7.0
Malignancy/myeloma	29	4.0	12	4.3	4.1
Hyperthyroidism	19	2.6	6	2.1	2.5
Hyperparathyrodism	36	5.3	9	3.2	4.5
Vitamin D deficiency	65	9.0	16	5.7	8.1
Miscellaneous causes	67	9.3	19	6.8	8.6
Idiopathic hypercalciuria	60	8.0	28	10.0	8.8
Hypogonadism	Excluded	0	42	15.0	---

* Some patients had more than one identifiable/treatable secondary cause.

Environmental factors and habits, such as excessive cigarette smoking and/or alcohol abuse, poor diet and other causes leading to osteomalacia (e.g., malabsorption, gastric surgery, drug interference, etc), and various medications especially glucocorticoids lead to bone loss. Other secondary causes include hypogonadism, GnRH therapy, hyperparathyroidism, hyperthyroidism (i.e., sub-clinical or biochemical hyperthyroidism, excessive intake of thyroxin), hypopituitarism, chronic liver disease, myeloma, conditions associated with immobilization and paralysis including hemiplegia.

In addition to a good history, physical examination and biochemical markers, non-routine tests such as 24 hour urine calcium; serum intact PTH, 25 (OH) vitamin D, sex-steroid hormone levels are useful in identifying these secondary causes. It is essential to identify and treat the underlying secondary causes aggravating further bone loss prior to embarking on anti-osteoporosis therapy.

WG13

Prevalence and Seasonal Variation of Vitamin D in ESRD Patients on Hemodialysis. M. Padda[1], D. S. Rao[2], G. Zusuwa[3], M. Goggins[3], S. Bhat[3], A. Gupta[1]. [1]Division of Nephrology, University of California at Los Angeles and Charles R. Drew University Schools of Medicine and Science, Los Angeles, CA, USA, [2]Bone and Mineral Research Laboratory, Henry Ford Hospital, Detroit, MI, USA, [3]Division of Nephrology, Henry Ford Hospital, Detroit, MI, USA.

Seasonal and racial differences in vitamin D levels have been studied extensively in the general population but not in patients with end stage renal disease (ESRD).

We measured serum 25-hydroxyvitamin D levels in chronic hemodialysis patients at the end of the summer and again at the end of the winter, and determined the prevalence and risk factors for vitamin D deficiency.

Serum 25-hydroxyvitamin D level was measured at the end of summer (September) in 142 patients and again at the end of winter (April) in 73 of these 142 patients. The prevalence of vitamin D depletion, defined as serum 25-hydroxyvitamin D level less than 20 ng/mL, was 54% at the end of summer and further increased to 85% by the end of winter (P <0.001 summer *versus* winter).

Vitamin D depletion is present in about half of ESRD patients with marked seasonal variations. Patients with ESRD should have more frequent assessment of their vitamin D nutrition by serum 25-hydroxyvitamin D levels and vitamin D supplementation should be routinely prescribed, which may prevent many of the complications related to vitamin D deficiency and secondary hyperparathyroidism.

WG14

Osteitis Fibrosa Cystica: An Unusual Manifestation of Primary Hyperparathyroidism and Its Relationship to Vitamin D Nutrition. F. Cheema, M.G. Lagman, D.S. Rao, H.D. Nair, M.W. Lee, M.R. Ansari, G.B. Talpos. Henry Ford Hospital, Detroit, MI. USA.

Osteitis fibrosa cystica was an important diagnostic clue to the presence of hyperparathyroidism in the past. Over the last 50 years, its prevalence declined dramatically in the US, following fortification of milk with Vitamin D. We report four cases of hyperparathyroidism in whom osteitis fibrosa cystica was present, and explore its relationship to vitamin D nutrition.

A total of 565 cases of hyperparathyroidism presented to the bone and mineral clinic of Henry Ford Hospital over a period of 12 years (1989-2001). We reviewed relevant history, diagnostic evaluation, radiographic findings, parathyroid pathology, and response to treatment. The estimated prevalence of osteitis fibrosa cystica is 0.70%, 4 out of 565 patients with hyperparathyroidism seen during this time period. Two patients had primary hyperparathyroidism, one patient developed hyperparathyroidism 12 years after renal transplantation, and another patient with cystic fibrosis and severe vitamin D depletion developed autonomous hypercalcemic hyperthyroidism. On thorough chart review of the remaining 561 patients, a total of 98 patients had alkaline phosphatase > 120 IU/L. The alkaline phosphatase elevation was associated with other causes (such as fractures and elevated liver enzymes). None of these 98 patients were observed to have radiographic lytic lesions consistent with osteitis fibrosa cystica.

Among the patients with osteitis fibrosa cystica, the mean duration of hypercalcemia was 3 years (range 2-4 years), mean serum 25-hydroxyvitamin D level was 11 ± 9 ng/mL, and mean parathyroid gland weight was 6.7 g (range 2.8-10.6 g). The mean gland weight in these 4 patients was approximately 5-fold larger than in 147 patients without osteitis fibrosa cystica (1.27 ± 1.61 g) and in each case, the parathyroid gland weight was at or above the 95% CI predicted for the level of serum 25-Hydroxyvitamin D level. Parathyroidectomy resulted in resolution of bone lesions in each patient.

We conclude that osteitis fibrosa cystica is an unusual manifestation of modern day hyperparathyroidism in the US and is associated with larger parathyroid tumors. Based on the relationship between parathyroid gland weight and serum 25-hydroxyvitamin D level, we believe that vitamin D nutrition plays an important role not only in parathyroid tumor growth but also contributes to development of osteitis fibrosa cystica through increased PTH secretion. There appeared to be a significant delay in the diagnosis of osteitis fibrosa cystica primarily because of the rarity of its occurrence and an apparent lack of awareness by physicians of this specific bone disease.

WG15

Acute Renal Failure, Hypercalcaemia and Cytokine Profiles in Human T-Cell Lymphotropic Virus Type 1 Associated Adult T-Cell Leukaemia/ Lymphoma. J.H. Wang[1], J.B. Eastwood[1], F. Harris[1], W.D. Fraser [2], M. Pazianas[3]. [1] Renal Unit, St. George's Hospital, London, United Kingdom.

A 52-year-old Guyanese man presented with lethargy, severe renal failure, thirst and polyuria having recently started a thiazide for hypertension. Plasma HTLV-1 test was positive and immunophenotyping confirmed Adult T-Cell Leukaemia/Lymphoma (ATLL). His plasma creatinine was 248 umol/l (2.8mg/dl) and calcium was raised at 5.12 mmol/l (20.4mg/dl) and was resistant to therapy. Hand radiographs showed widespread bone resorption with subperiosteal erosions. 25-hydoxyvitamin D_3 and Alkaline Phosphatase levels were in the normal range but 1,25-$(OH)_2$vitamin D_3 was low and PTH levels were suppressed. PTHrP level was greatly raised. Also, IL-6 was elevated, the Receptor activator of nuclear factor kB ligand (RANKL) reported at upper limit values and Osteoprotegerin was raised. TNFa levels were suppressed. Soluble TNF Receptor-1 (sTNFR-1) levels were extremely high. Therefore, the low TNFa levels may not reflect true values in the face of markedly raised sTNFR-1 levels. Interestingly, for such severe hypercalcaemia both RANKL and TNF levels were low in the presence of high OPG & sTNFR-1 levels. However, since the assay only measures the free fraction of molecules it may be that the bound portions of RANKL & TNF were far greater. This case highlights the complexity of the pathophysiology of the humoral hypercalcemia of malignancy and physicians will need to be aware of this particular cause of calcium imbalance.

	Units	Patient Values	Reference Range
Adjusted Calcium (ACa)	mmol/l	5.1	2.2-2.6
Phosphate (PO_4)	mmol/l	1.7	0.75-1.5
Parathyroid Hormone (PTH)	pmol/l	0.3	0.5-5.5
25-OH Vitamin D_3	nmol/l	29	>50
1,25-$(OH)_2$vitamin D_3	nmol/l	38	43-144
Parathyroid Hormone Related Peptide (PTHrP)	pmol/l	6.3	< 1.8
Interleukin-6 (IL-6)	pg/ml	4.6	< 3
Receptor activator of nuclear factor B Ligand (RANKL)	pmol/l	1.3	0.7-1.2
Osteoprotegerin (OPG)	pmol/l	8.3	2.7-3.2
Tumour Necrosis Factor (TNF)	pg/ml	2.9	< 15.6
Soluble TNF Receptor-1 (sTNFR-1)	pg/ml	3787	512-1739

WG16

A Randomized Study to Evaluate Strategies to Improve Osteoporosis Detection and Treatment in Elderly Women. B. Muma[1], J. Lafata[1], B. McCarthy[2], D. Kolk[1], E. Peterson[1], D. Rao[1], T. Weiss[3], Y. Chen[3]. [1] Henry Ford Health System, Detroit, MI, USA, [2] Alina Medical Group, Minneapolis MN, USA, [3]Merck & Co., Inc., West Point, PA, USA.

Current estimates are that only 20% women age 65 and older have received a bone mineral density (BMD) test, despite recommendations from the US Preventive Services Task Force and the National Osteoporosis Foundation. Thus, a large number of women are at risk of avoidable late-stage osteoporosis. We report preliminary findings of a randomized prospective study to evaluate strategies to enhance the quality of care for osteoporosis.

We identified women aged 65-89 that received primary care from 15 ambulatory care clinics of a large medical group in southeast Michigan between 4/1/2001 and 3/31/2003. The clinics were stratified by size and BMD availability, and randomized to one of 3 study arms: (1) usual care; (2) patient mailing (BMD reminder letters + educational material); and (3) patient mailing plus physician reminder prompts for BMD testing. Women that previously received a BMD test, a diagnosis for osteoporosis, or a prescription drug claim for an osteoporosis-specific therapy (alendronate, risedronate, raloxifene, or calcitonin) were excluded. A total of 10,565 eligible women were included in the study: 3,110 women in strategy (1) clinics; 3,368 in strategy (2) clinics; and 4,087 in strategy (3) clinics. Preliminary analysis of BMD testing rates were calculated for each study arm for a six-month window starting in August 2003. Differences between groups in BMD testing rates were evaluated using generalized estimating equations. To adjust for different intervention start times, we matched the usual care group to each of the intervention groups separately by starting time. Statistically significant differences in BMD testing rates between groups were evaluated using generalized estimating equation approaches.

Preliminary analysis adjusted for intervention start date indicate differences in BMD screening rates between the usual care and patient mailed reminders (2% vs. 13%); and the usual care and the patient mailing plus PCP prompt (5% vs. 27%).

Differences between usual care and patient mailing strategies were statistically significant (p<.001). The use of a patient mailing plus physician prompts lead to significant improvements in BMD testing compared to both usual care and patient mailing alone (p<.001). Results did not change with adjustments for clinic, race, and age.

Preliminary results indicate that the use of mailed patient reminders alone or in combination with physician prompts can lead to significant increases in osteoporosis screening rates compared to usual care, with the combination intervention (patient mailing + PCP prompt) showing the greatest effect.

WG17

Bone Mineral Density (BMD) in Healthy Indian Women: Development of a Reference Database and Implications for Diagnosis of Osteoporosis in Indian Women. S. Nangia, P. Reddy, N. Ramaswamy, A. Mithal, U. Sriram, Indraprastha Apollo Hospital, New Delhi, Sanjay Gandhi Post Graduate Institute of Medical Sciences, Lucknow, and Apollo Specialty Hospital, Chennai, India.

Genetics and ethnicity are the two most important determinants of peak adult bone mass, thereby necessitating the need for a separate reference databases for different ethnic groups. We sought to establish the first BMD reference database for Asian Indian women so that appropriate comparisons can be made in evaluating individuals of Asian Indian origin for osteoporosis.

Seventy five women from Lucknow, North India and 65 women from Chennai, South India, and aged 20-29 years were recruited to develop a reference database to facilitate calculation of ethnic-specific T-scores. BMD was measured at the lumbar spine, proximal hip, and non-dominant forearm by Hologic 4500 DEXA. Height, weight, BMI, age at menarche and the estimated dietary calcium intake were determined in all subjects.

BMD in Asian Indians was significantly lower than that of the U.S. white women at all relevant measurement sites and at both centers (p<0.001 for all). The peak adult BMD for Indian women was 0.927 ± 0.097 g/cm^2 at the spine (L1-L4), 0.788 ± 0.10 g/cm^2 at the femoral neck, 0.839 ± 0.095 g/cm^2 at the total hip, and 0.555 ± 0.050 g/cm^2 at the forearm (distal 1/3 radius). Compared to the U.S. white women, peak BMD was about 11% lower at the left femoral neck and total hip; 12% lower at the lumbar spine; and 35% lower at the distal forearm. Dietary intake of calcium in this reference group was 556.3 ± 253.2 mg/day. The spine BMD was slightly higher (p=ns) and femoral neck and forearm BMDs were slightly lower (p=0.018 and p<0.001 respectively) in Chennai women compared to Lucknow women. This difference could be explained by higher BMI and lower calcium intake in Chennai women.

At all measurement sites, BMD was significantly lower in Asian Indian women from two large cities in India, as compared to U.S. white women, although the lower BMI, calcium intake, and vitamin D nutrition might explain some or most of this difference between the two racial groups. Nevertheless, until the BMD-fracture relationship is established in this ethnic group, we recommend the use of the peak adult BMD from this study to calculate T-scores for Asian Indian women.

WG18

Phosphate and 1,25 Vitamin D Interaction Expressed in the Context of PHEX, FGF_{23}, and MEPE. R.S. Fredericks. Endocrine Associates. Reno, NV, USA

Molecular genetic exploration of syndromes involving phosphate metabolism has identified key mediators influencing phosphate homeostasis. 1,25 D has a fundamental role in metabolism as a signal of environmental phosphate deficiency. We have previously demonstrated that bisphosphonate signals are capable of modulating an unusual presentation of dysmetabolic syndrome X. Through extensive use of an N of 1 research strategy we have reported on regional regulation of skeletal mineralization as influenced by evolutionary constraints, where competition for environmental phosphate and energy is the fundamental organizing principle informing the models developed. Organic pyrophosphate functions as a primary signal of the adequacy of energy and phosphate. In the course of evaluating patients with subjective complaints in energy metabolism, we have utilized bone density results as a record of individual physiology. Two cases recently evaluated appear to demonstrate findings consistent with a disruption in the signaling of 1,25 D, Phex, FGF_{23} and MEPE. The bone phenotype is restricted to the ultra distal forearm where there appears to be less of a negative influence of 1,25 D on Phex, and the models would predict a decrease in MEPE. This process appears to be inherited as an autosomal dominant trait. The 2nd case presents as a disruption in the ability of FGF_{23} to decrease serum 1,25 D. These cases are supportive of the concept that the fundamental role of 1,25 D is best understood as it influences phosphate metabolism, with the influence on calcium homeostasis being manifestations of an integrative function developing in more complex biological systems.

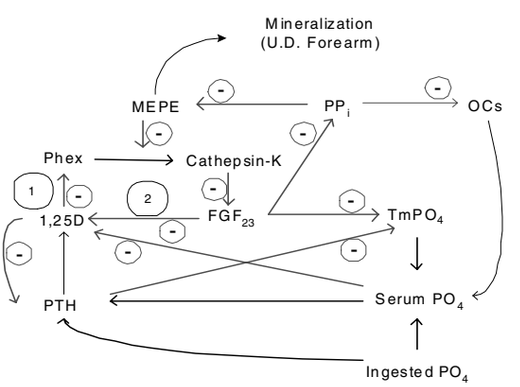

WG19

Fanconi's Syndrome and Osteomalacia. M.A. Cameron, O.W. Moe, K. Sakhaee. UT Southwestern Medical Center, Dallas TX

Osteomalacia (OM) is a metabolic bone disease with diverse etiologies. In adults, the commonest acquired and genetic causes are vitamin D deficiency and X-linked hypophosphatemic rickets, respectively. We present a case of OM in an adult subject with characteristics distinctive of Fanconi's syndrome.

A 36 year old African American male was evaluated for bone pain present for three years. The pain originated in his feet, progressed to his legs, and significantly impaired ambulation. He suffered spontaneous fractures of the metatarsal and ankle bones. The physical examination was remarkable for a waddling gait and tender extremities. X-rays showed pseudofractures in the hips.

Plasma	Values	Normal
Creatinine	2.2 mg/dL	0.9 - 1.1 mg/dL
Total CO_2	16 mEq/L	22 – 28 mEq/L
Anion Gap	10	10 - 12
Phosphorus	2.0 mg/dL	2.4 – 4.4 mg/dL
Glucose	106 mg/dL	70 – 105 mg/dL
1,25 $(OH)_2$ vitamin D_3	16 pg/mL	8-42 pg/mL
Alkaline Phosphatase	308 U/L	20-225 U/L
PTH	24 pg/mL	10-65 pg/mL

24 hour Urine	Values	Normal
pH	6.87	Variable
Glucose	9.2 g/24 hours	None
Protein	2.382 g/24 hours	< 0.15 g/24 hours
Aminoacids	Present	Absent
TmP/GFR	0.75 mg/dL	> 2.38 mg/dL

In conclusion, it is important to recognize that patients with congenital or acquired forms of Fanconi's syndrome are at risk for OM. Fanconi's syndrome can cause OM by multiple mechanisms: including phosphate wasting, calcitriol deficiency, and metabolic acidosis.

WG20

The Latent Mobility of Osteoporotic Vertebral Compression Fractures. F. E. McKiernan, Center for Bone Diseases, Marshfield Clinic, Marshfield, WI, USA.

Dynamic mobility (DM) is a property of some osteoporotic vertebral compression fractures (VCFs) that is being recognized with increasing frequency. DM is defined as a measurable change in vertebral body configuration between standing lateral and supine crosstable lateral radiographs (vertebroplasty series). DM can be harnessed to result in restoration of vertebral body height and reduction of sagittal kyphosis during the course of percutaneous vertebroplasty (PV). Recent experience, exemplified by this case report, reveals an important new dimension of DM.

A 74 yo woman experienced back pain 2 days after vigorous housework. 2 weeks later X-ray showed mild new T7+T8 VCFs. In spite of comprehensive medical management she worsened and was hospitalized 4 wks after pain onset. X-ray then showed moderate T7 VCF, T8 vertebra plana and a severe sagittal deformity. MR confirmed the acute nature of both VCFs. No intravertebral cleft was seen in either vertebra. She was transferred to our institution 5 wks after pain onset for possible PV. PE revealed a severe, painful thoracic kyphosis and a normal neurologic exam. Vertebroplasty series showed insufficient DM to permit safe PV at T8. PV at T7 was recommended for partial pain relief and prevention of further vertebral T7 collapse. After strict overnight confinement to the supine position the T8 vertebra plana increased to 80% of its original height and revealed a typical intravertebral cleft. Successful PV of both T7 and T8 resulted in vertebral height restoration, reduction of the sagittal deformity and pain relief.

The absence of DM in a mid T-spine VCF was not surprising since DM is more common at the thoracolumbar junction. But mature osseous union of T8, sufficient to preclude DM, seemed unlikely within 2 wks of catastrophic vertebral collapse. We postulated that DM was hindered by hemorrhage, soft tissue scarring or muscle contraction. After 12 hrs in the supine position the "latent mobility" (LM) of this VCF became apparent and led to a favorable symptomatic, functional and biomechanical outcome. We speculate that the current vertebroplasty series underestimates the prevalence and magnitude of DM since patients only assume the supine position for a brief period of time. Furthermore, vertebral height restoration achieved during PV might be further enhanced if patients were kept supine for some period of time preoperatively.

Both DM and LM raise important questions about vertebral injury response, fracture healing, vertebral morphometry and care of patients. Failure to recognize and incorporate these simple observations into clinical practice and PV outcomes research *a priori* may result in missed opportunities for pain relief, invalidated study designs and flawed study conclusions.

WG21

Cervical Spine Anomalies in Patients with Fibrodysplasia Ossificans Progressiva: Clues from the BMP Signaling Pathway. A.A. Schaffer,[1,6,7] F.S. Kaplan,[1,2,3,6] M.R. Tracy,[6,7] M.L. O'Brien,[6,7] J.P. Dormans,[2,6] E.M. Shore,[1,2,4] R.M. Harland,[8] and K. Kusumi.[5,6,7] [1]The Center For Research In FOP & Related Disorders, The University of Pennsylvania, Philadelphia, PA, USA, [2]The Departments of Orthopaedic Surgery, [3]Medicine, [4]Genetics and [5]Pediatrics, The University of Pennsylvania School of Medicine, Philadelphia, PA, USA, [6]The Divisions of Orthopaedic Surgery, and [7]Genetics, The Children's Hospital of Philadelphia, Philadelphia, PA, USA, and [8]The Department of Molecular and Cell Biology, The University of California, Berkeley, CA, USA.

Minor developmental features of diseases can often provide seminal clues to underlying etiologies and pathophysiologic pathways. While progressive replacement of connective tissue with heterotopic bone is the most dramatic and disabling feature of fibrodysplasia ossificans progressiva (FOP), less severe phenotypic anomalies of the normotopic skeleton often receive minimal attention. After noting generalized neck stiffness and decreased range of motion of the cervical spine in nearly all children with FOP prior to the formation of heterotopic bone at that anatomic site, we reviewed available plain films in 70 FOP patients and found characteristic anomalies including large posterior elements, tall narrow vertebral bodies, and fusion of the facet joints between C_2 and C_7 while the occiput-C_2 levels were ubiquitously spared. Most notably, the characteristic anomalies of the cervical spine in patients with FOP were distinctly different from those of the Klippel-Feil syndrome and were nearly identical to those seen in mice with homozygous deletions of the gene encoding Noggin, a potent BMP antagonist. While the Noggin gene is not mutated in patients who have FOP, our findings provide strong support for the role of the BMP signaling pathway in the morphogenesis of the vertebrate cervical spine and extend a growing body of evidence implicating overactivity of the BMP4 signaling pathway in the molecular pathogenesis of FOP.

WG22

Ectopic Production of PTH by a Neuroendocrine Carcinoma of the Pancreas. N. Yu, J. VanHouten, L. Ardeshirpour, D. Rimm, R. Udelsman, J. Wysolmerski. Yale University Medical School, New Haven, CT, USA.

A 74 y/o female presented to an outside hospital and was found to have a serum calcium level of 15.3mg/dL. CT scanning revealed a 2.2cm hypodense mass in the liver and a pancreatic mass. However, a PTH level of 399 pg/mL (10-65) suggested the diagnosis of primary hyperparathyroidism. She was transferred to our hospital where her calcium was 18.0mg/dL (ionized Ca 10.5mg/dL). Repeat intact PTH level was 2,310pg/mL. A sestamibi scan revealed uptake in the lower pole of the left thyroid bed. She was taken to the operating room and a left-sided mass was resected that proved to be a thyroid nodule. Subsequently a thymic parathyroid was also resected and 4 other parathyroid glands appeared normal. Right and left internal jugular intra-operative PTH levels were similar to peripheral levels, suggesting a source of PTH outside the neck. The patient underwent CT-guided liver and pancreatic biopsies. Histology revealed high-grade neuroendocrine carcinoma, which stained for PTH. The PTHrP level also returned elevated at 11.7pg/L (<1.3). The patient's hypercalcemia could not be controlled and she died several days later.

An autopsy revealed neuroendocrine carcinoma of the pancreas with metastases to the liver, mesenteric, periaortic, and peripancreatic lymph nodes. Tumor cells from these sites stained for PTH. Expression of PTH mRNA in the tumor was documented by real-time RT-PCR analysis of RNA prepared from the pancreatic primary and the liver metastasis. Uninvolved pancreas and liver tissue from the patient was negative. Interestingly, the tumor tissue was negative for GCMB expression. Primary cell lines have been established from malignant ascites, the liver metastasis and the pancreatic primary. The tumor cell lines are all positive for PTH and PTHrP mRNA and conditioned media from the cells contained 15-80 pM PTH (1-84) and 5-25 pM PTHrP (1-86).

In summary we report a patient with "parathyroid crisis" that was caused by the rare ectopic production of PTH and PTHrP by a poorly differentiated neuroendocrine tumor of the pancreas. This case is instructive in several ways. First, it demonstrates the utility of the intra-operative PTH assay in suggesting the possibility of ectopic PTH production. Second, it demonstrates that GCMB expression is not absolutely necessary for PTH gene expression. Third, the tumor tissue and cell lines harvested from the patient will be valuable for the study of the molecular mechanisms underlying ectopic hormone production by tumors as well as the study of PTH gene expression.

WG23

Hypocalcemia as the Presenting Manifestation of Metastatic Prostate Cancer. E. Gonzalez-Feldman, Y. Hmadeh. D.S. Rao. Department of Internal Medicine and Bone & Mineral Metabolism, Henry Ford Hospital, Detroit, MI, USA

Hypercalcemia is a well known complication of several types of cancer, but symptomatic hypocalcemia is less frequently reported. We report two such unusual cases.

Case 1: A 70 y old African American man without any previous medical problems was admitted to the medicine service with a 3 month history of persistent hiccups and 20 pound weight loss. He was severely anemic and complained of right hip pain. His serum calcium was 5.6 mg/dl but Chevostek and Trousseau signs were absent. In spite of normalizing serum 25-hydroxyvitamin D levels (which was 9 ng/ml) with vitamin D and continuous calcium supplementation, his serum calcium level remained low. Only after pharmacologic doses of Calcitriol (5 ug/d for several weeks) his serum calcium normalized.

Case 2: A 79 y old African American man was admitted to the emergency service after having a generalized seizure. His serum calcium was low (4.3 mg/dl) despite normal serum 25-OHD (28 ng/ml) and 1,25-dihydroxyvitamin D (30 pg/ml) levels. Continuous iv and oral calcium supplements were given over two weeks, but serum calcium remained persistently low. Only after starting pharmacologic doses of Calcitriol (4 ug/d) his calcium normalized.

Relevant laboratory are shown in the Table

	calcium mg/dl	iCa mmol/L	PTH pg/ml	creatinine mg/dl
Case 1	5.6	0.7	268	2.2
Case 2	4.3	0.56	175	4.3

DISCUSSION: True hypocalcemia is an uncommon manifestation of prostate cancer. Apparent hypocalcemia is more prevalent is most often due to low serum albumin. A prevalence of 16 % has been noted in a series of 143 patients with bone metastasis from different kinds of cancers, all asymptomatic, but ionized calcium was not measured. In another report, the prevalence of hypocalcemia was 23% in patients with bone metastasis, but only one patient had low ionized calcium. Various theories have been proposed to explain hypocalcemia including "hungry bone" syndrome with quantum of uptake of calcium with rapid growth of osteoblastic metastasis.

In spite of baseline high levels of 1,25-DHCC and correction of 25-OHD, our patients continued to have hypocalcemia. We believe that our patients were resistant to vitamin D from an unknown cause, perhaps from an antivitamin D factor produced by the neoplastic cells.

WG24

Unusual Femoral Shaft Fractures Following Long Term Bisphosophonate Therapy. S. Levy[1], C. Odvina[2], S.Palnitkar[1], D.S. Rao[1]. [1]Bone & Mineral Research Laboratory, Henry Ford Hospital, Detroit, MI, and [2]University of Texas, Southwestern Medical School, Dallas, TX.

There has been a growing concern about long term effects of bisphosphonate therapy. We previously reported 6 patients with unusual fractures while on long term bisphosphonates. Now we present 4 additional cases.

A 68 y white man had metatarsal stress fractures at the age 60 y. A BMD of the spine at the time was T score -0.27 and femoral neck T score -1.32. Alendronate 10mg/d was begun and changed later to once weekly. In Jan 2003 he stepped off a step in his garage and sustained fracture of the left femoral shaft. He underwent open reduction and internal fixation (ORIF). Recovery was uneventful. He was well until January 2004, while walking down a corridor he felt a snap and fell sustaining fracture of the right femoral shaft again requiring ORIF. Most recent BMD: spine T score +1.3 and femoral neck T score -1.1.

A 52 y white woman with a history of ovarian cancer had surgery and chemotherapy in 1994. She was prescribed alendronate 10 mg/d in 1995 primarily to prevent postmenopausal bone loss, and was changed to 70 mg once a week. In August, 2003 while vacationing on a cruise she turned around, felt a snap and fell suffering a left femoral shaft fracture requiring ORIF. The patient discontinued alendronate in October, 2003. A BMD in 1991 was normal, as was one in 1998.

A 67 y white woman with osteopenia in 1998 was started on alendronate therapy. She had been on estrogen, calcium and vitamin D. Breast cancer was diagnosed in 2002, estrogen was stopped and Arimidex was started in 2003. In May 2003, she developed spontaneous fractures of both femoral shafts requiring intramedullary rods. BMD in 2001: spine T-score +1.38 and femoral neck T-score +0.23, and a repeat BMD of the spine T-score in 2003 was +1.7.

A 74 y white woman with a history myasthenia gravis and steroid osteoporosis was started on alendronate in 1995. Her BMD prior to treatment was T score -4.5 in the lumbar spine and T score -2.4 in the femoral neck. In 2003 she heard a snap and then she fell sustaining a right femoral fracture requiring ORIF. Her BMD in 2002: spine T score -2.8 and femoral neck T score -2.4.

A transiliac bone biopsy following tetracycline labeling in 3 of the 4 patients showed severely suppressed bone turnover.

Femoral shaft fractures are rare even in patients with osteoporosis. Therefore, the occurrence of femoral shaft fractures in our four patients on long term bisphosphonate therapy raises the possibility that such treatment may be associated with spontaneous unusual fractures.

WG25

Bisphosphonate-Induced Hypocalcemia. N.M. Maalouf, P.J. Kim, H.J. Heller, K. Sakhaee. Center for Mineral Metabolism, U.T. Southwestern Medical Center, Dallas, TX, U.S.A.

Bisphosphonates (BPs) are pyrophosphate analogs that are potent inhibitors of osteoclast-mediated bone resorption. Although BPs are widely used in the treatment of osteoporosis and of hypercalcemia of malignancy, it is important to carefully consider the limitations and risks of these drugs. We hereby present two patients who developed severe symptomatic hypocalcemia following BP administration.

Patient #1 is a 56 year-old man who presented with facial tingling. He had received a single dose of intravenous pamidronate and one round of chemotherapy with vincristine, adriamycin, and dexamethasone for multiple myeloma and was discharged a week prior to his admission. His laboratory information is presented in the table below, and was consistent with severe hypocalcemia, vitamin D insufficiency and secondary hyperparathyroidism.

Patient #2 is a 75 year-old woman who had a history of Crohn's disease, requiring glucocorticoid use and 4 bowel resection surgeries. She also was taking phenytoin for a seizure disorder. Due to the finding of a low bone mineral density, she was started on alendronate 10 mg daily three months prior to her admission with severe paresthesias and weakness. At presentation, she had a positive Trousseau's sign and profound hypocalcemia and vitamin D deficiency (see table).

Patient #	1	2	Normal Range
Presenting serum calcium, corrected for albumin (mg/dl)	6.5	5.6	8.4-10.2
Ionized serum calcium (mg/dl)	3.2	2.1	4.7-5.1
Serum phosphorus (mg/dl)	2.2	1.8	2.4-4.4
Serum magnesium (meq/l)	1.4	0.6	1.3-1.9
Presenting serum PTH (pg/ml)	313	94	10-65
Presenting serum 25-OH-vitamin D (ng/ml)	20	3	"20-60"
Serum Creatinine (mg/dl)	1.3	0.7	0.6-1.2

Bone resorption constitutes a major protection against hypocalcemia of various etiologies. Since BPs are very potent inhibitors of osteoclastic bone resorption, this defense mechanism is blunted in BP-treated patients. Cases of BP-induced hypocalcemia have previously been described, mostly in patients with undiagnosed hypoparathyroidism. In the two patients described, hypoparathyroidism was not the cause of the hypocalcemia.

Rather, a decreased intestinal absorption of calcium due to underlying vitamin D deficiency likely contributed to the severe symptomatic hypocalcemia.

In addition to their indications for the treatment of osteoporosis, BPs are increasingly used in the therapy of patients with various malignancies. This factor, along with the high prevalence of occult vitamin D deficiency among medical patients, will likely lead to an increase in the incidence of symptomatic hypocalcemia in BP-treated patients. Thus, patients at risk for vitamin D deficiency should have an evaluation of their vitamin D reserve prior initiation of treatment with BPs.

PHYSICAL ACTIVITY WORKING GROUP

WG26

Vitamin D and Physical Function in the Older Population. H. A. Bischoff-Ferrari. Brigham and Women's Hospital, Boston, MA, USA.

The protective effect of vitamin D on fractures has been primarily attributed to the established moderate benefit of vitamin D on calcium homeostasis and bone mineral density[1]. However, an alternative or complementary explanation might be that vitamin D affects factors directly related to muscle strength and function, thus reducing fracture risk through fall prevention. Muscle weakness is a prominent feature of the clinical syndrome of vitamin D deficiency. A physiologic explanation for the beneficial effect of vitamin D on muscle strength is that 1,25-dihydroxyvitamin D (1,25(OH)2D), the active vitamin D metabolite, binds to a highly specific nuclear receptor in muscle tissue leading to improved muscle function and reduced risk of falling[2]. In older persons there is some support in the literature for higher 25-OHD levels being preferable to lower levels in regard to musculoskeletal function. The positive associations between vitamin D and musculoskeletal function observed in cross-sectional studies are supported by two recent randomized controlled trials (RCTs)[3, 4], where vitamin D supplementation improved musculoskeletal function and body sway in older women. However, most of this literature has been collected in populations at risk for vitamin D deficiency, such as institutionalized elderly persons or ambulatory elderly residing in Europe, where food is not fortified with vitamin D. Still, in a large US survey, we found that in both active and inactive ambulatory individuals age 60 and older, 25-OHD levels above 40nmol/l and as high as 90 nmol/l, the upper end of the reference range, are associated with better musculoskeletal function in the lower extremities. This association was consistent across two lower extremity function tests, the timed 8-foot walk and the timed repeated sit-to-stand test. Given the high prevalence of low 25-OHD levels and inactivity in this national survey and the positive association between 25-OHD and lower extremity function, vitamin D supplementation may offer a way to improve lower extremity function in both active and inactive subjects 60 years and older. This recommendation is supported by a recent meta-analysis of RCTs on the risk of falling, where, vitamin D reduced a persons' risk of falling by more than 20%[5].

References:
1. Dawson-Hughes B, Harris SS, Krall EA, Dallal GE: Effect of calcium and vitamin D supplementation on bone density in men and women 65 years of age or older. N Engl J Med 1997; 337(10): 670-6.
2. Bischoff-Ferrari HA, Borchers M, Gudat F, Durmuller U, Stahelin HB, Dick W: Vitamin D receptor expression in human muscle tissue decreases with age. J Bone Miner Res 2004; 19(2): 265-9.
3. Pfeifer M, Begerow B, Minne HW, Abrams C, Nachtigall D, Hansen C: Effects of a short-term vitamin D and calcium supplementation on body sway and secondary hyperparathyroidism in elderly women. J Bone Miner Res 2000; 15(6): 1113-8.
4. Bischoff HA, Stahelin HB, Dick W, et al.: Effects of vitamin D and calcium supplementation on falls: a randomized controlled trial. J Bone Miner Res 2003; 18(2): 343-51.
5. Bischoff-Ferrari HA, Dawson-Hughes B, Willett CW, et al.: Effect of vitamin D on falls: a meta-analysis. JAMA 2004; 291(16): 1999-2006.

WG27

Mechanical Loading Responses in Genetically Engineered Mice. C. Turner. Department of Orthopaedic Surgery, Indiana University School of Medicine, Indianapolis, IN, USA.

Mechanical loading provides an anabolic stimulus for bone. More importantly the mechanosensing apparatus in bone directs osteogenesis to where it is most needed for improving bone strength. The biological processes involved in bone mechanotransduction are poorly understood and further investigation of the molecular mechanisms involved might uncover drug targets for osteoporosis. One characteristic of the mechanosensing apparatus that has only recently been studied is the important role of desensitization. Experimental protocols that insert "rest" periods to reduce the effects of desensitization can double anabolic responses to mechanical loading. Several pathways are emerging from current research, including membrane ion channels, ATP signaling, and second messengers such as prostaglandins and nitric oxide. Some key molecular targets include the L-type calcium channel (alpha 1C isoform), a gadolinium-sensitive stretch-activated channel, P2Y2 and P2X7 purinergic receptors, EP2 and EP4 prostanoid receptors, and the parathyroid hormone receptor.

WG28

What Types of Exercise Work in Fall Prevention (The FaMe Study). D. Skelton. University of Manchester, Manchester, United Kingdom.

Nearly half of nursing home admissions in the UK are due postural instability (1) and older people themselves fear hip fracture and subsequent nursing home admission (2). Frequent fallers have poor outcomes. In one trial, 27% of people who fell 3 or more times in a year were admitted to hospital, transferred to nursing homes or died at one year follow-up (3). Although there is evidence that exercise alone can help prevent falls, there is still concern over safety and effective types and intensities of exercise for those who already have a history of falls (4).

To investigate the effectiveness of a 9 month group Exercise intervention (FaME), compared with a control intervention to reduce falls and injuries, frequent fallers were recruited. 100 community dwelling, independent women aged 65 years and over with a history of three or more falls in the previous year were enrolled into the study and randomly allocated (blind) into Exercisers (n=60) or Controls (n=40). 43 Exercisers and 27 Controls completed full diary returns, for the entire duration of the trial (30 months) with a (mean age 72.6 (SD 5.5 years)). 5 Exercisers dropped out of the intervention and 7 were lost to follow up (ill, health, death). The frequent fallers completed fortnightly fall diaries for 36 weeks as a prospective Baseline fall history, 36 weeks during their Intervention and 36 weeks in the Follow- up period. Those not allocated to group exercise (Controls) performed home-based seated flexibility training. Exercisers attended weekly one hour tailored dynamic balance and strength exercise classes (taken by qualified, advanced exercise instructors) and performed home exercise twice-weekly for nine months.

Poisson regression models suggest that Exercisers had half the risk (RR 0.53, 95% CI 0.38 to 0.73) of a fall compared to the Controls during the Follow-up period. Although women with a history of frequent falls increased their risk of falls during this exercise Intervention (relative risk 1.19, 95% CI 0.86 to 1.66) they were less likely to sustain injurious falls (relative risk 0.51, 95% CI 0.21 to 1.23) than those who did not exercise and were much less likely to sustain an injurious fall during the Follow-up period (relative risk 0.39, 95% CI 0.16 to 0.93). A nine-month specific, progressive group exercise programme (FaME) is effective at reducing further falls and injuries in community dwelling women with a history of falls. Group balance exercise should be a referral option for any evidence-based interdisciplinary falls prevention programme. The challenge is to effectively deliver these classes within the "health" setting, ensuring balance specificity, tailoring, adequate duration and intensity, sufficient progression, education and telephone support.

3T3-L1. SEE *Adipocytes*

A

ABX10241, SU530, 1201, SA498
AC-100 (Dentonin), M467
Accelerator mass spectrometry, SA034
Achondroplasia, SU198, 1045. SEE ALSO *Dwarfism*
Acid-base balance, dietary, M437
Acidification, bone resorption and, SU335
Acidogenic diet, SA331
Acidosis, metabolic, SA505, SU239
Actin filament length, M196
Actin ring, SU346
Activating transcription factor 2 (ATF-2), M025
Activating transcription factor 4 (ATF-4), SU243
Activator protein-1 (AP-1), SU286, M239
Activin-receptor-like kinase-2 (ALK-2), M184
Adeno-associated virus, recombinant (rAAV), F066**,** SA066, SU011
Adenosine, M268
Adipocytes, SU280, F061, SA061
Adipogenesis
- Cyclic strain effects on bone formation and, M192
- Human MSCs and, SA236
- Hypoxia inhibition of, F168, SA168
- MC3T3-E1 cells transdifferentiation and ectopic overexpression of, M234
- Msx2 inhibition of, 1120
- PPARγ and, SA247
- Retinoic acid inhibition of, SU274
- Senile osteoporosis and, M248
- TGFβ inhibition of, SU203

Adiponectin, M187, SA146, 1021
Adiponectin receptors-1, 2, M040
Adipose-derived stem cells, SU044
A disintegrin and metalloproteinase-8 (ADAM8), SA281, F513, SA513
Adolescents. SEE ALSO *Puberty*
- BMC and physical fitness in, SU223
- BMD and oral contraceptives in, F396, M386, SA396
- BMD measurements using DXA in healthy, SA103, 1048
- BMD reference values in Latin American, SU117
- Calcium carbonate and height of male, SU459
- DXA *versus* CT vertebral BMD measurements in, F102, SA102
- Hypovitaminosis D in healthy girls in UK, SU363
- Inflammatory bowel disease and BMD in, SA387
- Lactation and BMD, body composition changes in, SU397
- Lifestyle intervention effects on BMD in girls, 1044
- Mechanical adaptation to weight gain in, 1046
- Overweight, femur bending strength and muscle mass in, M009
- QUS bone measurements in, M140
- Racial differences in calcium retention in girls, SA418
- Site-specific bone mineral accrual in, SA006
- Vitamin D, bone metabolism in perinatally HIV-infected, SA501
- Vitamin D supplementation and musculoskeletal parameters in, 1047
- Vitamin D supplementation one-year effects in girls, M498

Adrenal-dependent Cushing's syndrome, M383
Adrenalectomy, SU068
β-Adrenergic receptor, 1008, 1122, 1121
β-Adrenergic receptor antagonist, SA021
Adrenocorticotrophic hormone (ACTH), SU280
Adrenomedullin, 1093
Adynamic bone disorder, M537
Affymetrix Murine Genome MU74Av2 arrays, SU579
Aged. SEE ALSO *Osteoporosis, postmenopausal; Postmenopausal women*
- Bone markers and impaired renal function, M135
- Fall risk assessment, WG3
- Fracture risk and adipocyte hormones, 1021
- Genetic fracture liability, SU151
- Hypovitaminosis D and musculoskeletal health in sunny country, 1186
- IGFBP-2 and bone turnover prediction, SA161
- Rosiglitazone and bone mass, architecture, M054
- Seasonal modulations for fracture risk, SU373
- Secondary osteoporosis risk factors, 1185
- Vitamin D_3 and calcium effect on fall risk, 1221
- Vitamin D and physical function in, WG26

Aged (animal models)
- BMP responsiveness and bone loss during disuse in, SU009
- Cartilage regeneration impairment with, M056
- Intervertebral disc degeneration and, SU045
- Self-renewal in senescence-associated bone loss, SU004
- SPARC and disc degeneration in, SU060

Aged, 80 and over, SA452, 1219
Age factors
- Bone densitometry measures and, SU354
- Bone histomorphometry of iliac crest biopsies and, M364
- Cortical bone cross-sectional structure and mineralization, SA015
- Delayed fracture healing, abnormal transdifferentiation and, M238
- Dietary fish oil and bone loss in middle-aged male rats, SU003
- DXA of BMD, trabecular bone structure and, SA115
- Femoral neck differences and, SA018
- Fracture risk in postmenopausal women and, F339, SA339
- IGF-I receptor up-regulation, IGF-1 down-regulation and, SA019
- Iliac crest biopsies chemical composition in women and, M403
- Knee osteoarthritis in Japanese women and, M542
- Medial minimum joint space width in knees and, SU022
- Pediatric calcaneal SOS, SA121
- Pediatric DXA precision, SU124
- Quantitative genetic analysis in hand skeleton of, SA130
- Skeletal sensitivity to loading and, SU222
- Spatial and temporal bone loss differences due to ovariectomy and, M372
- 3D volumetric analysis of cortical porosity in femur, SU006
- Trabecular and cortical bone loss in proximal femur and, SU010
- Zinc skeletal effects in rats, M375

AIDS. SEE *HIV*
Akt, 1194
Albumin, SU380
Alcohol drinking, SA432, M376, SA447
Aldosteronism, primary, SA476
Alendronate
- Administration and dosage, SU432, SU448
- Alfacalcidol *versus,* M415, SU498
- Basal bone metabolism, SA411
- Boys with Duchenne muscular dystrophy, M521
- Complex regional pain syndrome I, M419
- Cost-effectiveness for fracture reduction in Spain, SA409
- Early NTx response in Japanese osteoporotic elderly women, M417
- Estrogen deficiency (murine model) and, SU437

Alendronate (Continued)
- Femoral fracture healing of cynomolgus monkeys, SU450
- Hip fracture risk reduction, F410, SA410
- 25-Hydroxyvitamin D status in postmenopausal osteoporosis, M495
- Immunological status after heart transplantation, M548
- Long term effects, 1174, 1173
- Low BMD in children with inflammatory diseases, M528
- Male solid organ transplantation recipients, SA405
- Murine model of male osteoporosis, M427
- NTx baseline measures in treatment-naïve *versus,* SU144
- Ossicle formation in rat vascularized bone formation model, SA023
- Osteogenesis imperfecta and, 1043
- Osteonecrosis of femoral head in hip osteoarthritis and, SU503
- Pamidronate *versus,* SU446, F466, SA466
- Periprosthetic bone loss after total hip arthroplasty, M407
- Placebo in femoral neck strength increases *versus,* F400, SA400
- Predictive value of bone remodeling markers, M428
- PTH combination and bone turnover in osteoporotic men, 1172
- PTH(1-84) heterogeneity in skeletal response *versus,* F429, SA429
- PTH(1-84) treatment followed by, 1098
- Radiographic progression in rheumatoid arthritis and, SU539
- Rheumatoid arthritis and, SA403
- Risedronate *versus,* F412, SA412
- Skeletal response to PTH in osteoporotic postmenopausal women, F439, SA439
- Spinal microarchitecture in glucocorticoid-induced osteoporosis, M129

Alfacalcidol
- Alendronate *versus,* M415, SU498
- Fast bone losers and, SA458
- Low creatinine clearance, fall risk and, F415, SA415
- Posturographic evaluation on effects of, M395
- Risedronate combination therapy with, SA457
- Vertebral fracture risk with long-term calcitonin derivative and, SU449

Alkaline phosphatase
- B1x isoform in children with kidney failure, M531
- Lactose feeding and enhanced intestinal expression of, SU408
- Msx2 interruption of DLx5 transactivation and expression by, SU248
- QTLs in mice of serum levels of, M152
- Skeletal involvement of younger persons with Paget's disease and, SA487
- Up-regulation in PC-1 mutant periodontal cells, SU034
- Vitamin D analog in human osteoblast cultures and, M257

Alkaline phosphatase staining, SA567
Alkaline phosphatase, tissue-nonspecific, M165, F474, SA474
Alopecia, SA551
Alveolar crestal bone , M355
AMG 162, 1072
Androgen deprivation therapy, M080, M470, SU440
Androgen receptor
- BMD and CAG repeat polymorphism of, M155
- BMD or physical function in older men and polymorphisms of, M160
- Dietary calcium, FokI and male genotypes of, SU167
- IGF-I gene expression and, M573
- Osteoclast-specific knockout mice, 1006

Androgen receptor (Continued)
Oxandrolone and, SU489
Peak bone mass, bone turnover rate in young healthy men and polymorphisms of, SU176
Trabecular bone activation in ovariectomized rats, estrogen and, SA397
Androgen replacement, M563
Androgens, SU571, SA206, SU579, M226, M584, M164
Androstene immune regulation hormones, SA203
Angiogenesis, SA261, F147, SA147, SU554
Angiopoietin-1, M228
Angiotensin converting enzyme (ACE) inhibitors, M225
***ank/ank* mouse tooth root cells,** M044
Ankylosing spondylitis, SA361, M544, SA108
Anterior cruciate ligament deficiency, M048
Anticonvulsants, F367, SA367
Antiepileptic agents, SA475, M497
Antiresorptive agents, SA307, SU234. SEE ALSO *specific agents*
Antisense oligonucleotides, SU332, SU338
Aortic stenosis, calcific, SU281. SEE ALSO *Vascular calcification*
AP-2, SA273
aP2 (fatty acid binding protein), SU272
APC, 1001
ApoA1, M368
Apolipoprotein E, 1208, M330
Apoptosis
Androgens in androgen-receptor transgenic mice and, M226
Calcium and phosphate-induced osteoblast, SA197
COX-2 gene expression in osteoblasts and, SA195
COX-2 overexpression and, SA196
Estrogen-induced osteoclastic, cadmium and, SA319
Fas/calmodulin binding and osteoclastic, M318
GFP reporter system for, SA193
Osteoblastic, IGF-II and, F194, SA194
Osteoblastic, Runx2, continuous PTH and, 1066
Osteoclastic, human model of, SU305
Osteoclastic, immediate early genes expression and, SU341
1-β-D-Arabinofuranosylcytosine, SU310
Arachidonate 12-lipoxygenase (ALOX12), 1081
Arachidonate 15-lipoxygenase (ALOX15), M178, 1081
Archeological studies, F336, SA336
Arkadia gene, SU012
Aromatase, SA398, SU181
Arrestin, 1229
β-Arrestin2, M477
Arterial calcification. SEE *Vascular calcification*
Arteriosclerosis, peripheral, M100
Arthritis, SU338, SA065, M322, SA451, SA303. SEE ALSO *Osteoarthritis; Rheumatoid arthritis*
Arthritis (animal models), SA030, M541, M538, SU538, M540
Arthritis, inflammatory, SA510, M272, F313, SA313, M024, SA289
Arthritis, juvenile idiopathic, 1138, SU537, SA512
Ascorbate, M288
Ascorbic acid, M506
Asthma, SA122
Athletes, M134. SEE ALSO *specific sports*
Atorvastatin, SU238, SU493
ATP-binding cassette (ABC) membrane transporter genes, 1202
ATP release, fluid flow-induced, SU136
Autoimmune polyendocrinopathy-candidiasis-ectodermal dystrophy (APECED), SU510

B

Back extensor strength, M449, SA422, WG6. SEE ALSO *Bone strength*
Bacterial artificial chromosomes (BACs), SA258
Balance, SU356, SA419, SU399, SU401
BALBxC3H mice, SA190
Basal metabolic rate, SU426
Basic fibroblast growth factor, SU191, SU197, M488
Bcl-2, M025
Bcl-2/Bax ratio, M226
Bed rest studies, 1145
Bending tests, SA035, M215, SU213, SU229
Beta-blockers, M466
Bialystok (Poland) Osteoporosis Study, SU366
Biglycan, 1078, SU070
Bim, 1194
Bioinformatics, F224, SA224
Biopsy, bone core, SA241
Biopsy, transiliac bone, SA111
Bioreactor systems, SU036, SU081
Bisphosphonates. SEE ALSO *Alendronate; Clodronate; Etidronate; Ibandronate; Minodronic acid; Neridronate; Pamidronate; Risedronate; Zoledronate; Zoledronic acid*
Antitumor mechanisms *in vivo* of, 1094
Bone regeneration after drill-hole injury in mice, SU257
Bone response to systemic therapy for prostate cancer metastasis and, SA089
Bone status after kidney transplantation with and without, M549
Calcium packaged with, M424
Cellular uptake of, M430
Cost-effectiveness of bone protection from glucocorticoid therapy with, SA454
Dosing regimen and compliance with, M434
Gene transcription during osteoclastogenesis and, M408
Growth factors effects on prostate cancer cells and, SU097
GTPase activity in osteoblasts and, SU296
Hip fracture risk reduction and, F410, SA410
Hypocalcemia induced by, WG25
IL-1β C/T polymorphism and Paget's disease response to, M167
Long-term, femoral shaft fractures with, WG24
Mechanism of action studies, SA305
Medication persistence with weekly, SA407
Molecular actions on osteoblasts by, SA225
Nitrogen-containing, protein prenylation inhibition *in vitro* and *in vivo* by, SU334
Noncompliance, non-persistence and effectiveness of, M423
Odontoclasts in dental root resorption and, M301
OPG *versus,* M300
Osteoblast survival *in vitro* and, M255
Osteonecrosis of femoral head and, SU528
Pharmacist-managed osteoporosis clinic and compliance with, M436
PTH effects on bone tissue quality *versus,* SA384
Scoliosis response to, M425
Separately or combined with testosterone for hypogonadism, SU486
Severe hypocalcemia in Paget's disease treated with, M517
Telomerase *in vitro* expression in prostate cancer and, M085
Vitamin D insufficiency and, M412
Black cohosh, SA210
Blood-derived adherent cells (BdACs), 1135
Blood, peripheral, 1136
Blood pressure, SU454
Body composition
Basal metabolic rate in women and, SU426
Bone change in postmenopausal women and, M453
Calcium absorption efficiency and, SU410
DXA images in active and inactive populations, M221
Muscle strength, BMD in postmenopausal women and, M321
Newborn twins *versus* singletons, SA004
Postmenopausal hormone therapy and, 1154
Regional spine and femur DXA measurements, M089
Sex differences in skeletal development and, 1084
Total skeleton evaluation of BMD, EE2 and, SU116
In vivo and phantom cross calibrations using DXA, M103
Body fat, M361, M089, 1080, M221. SEE ALSO *Obesity*
Body mass, SU392, M182
Body weight, SU454, M174, SA490, SU121. SEE ALSO *Weight gain; Weight loss*
Bone allografts, M045, SU011. SEE ALSO *Bone grafts*
Bone and cartilage stimulating peptide-1 (BCSP-1), SU061
Bone and cartilage stimulating peptide-7 (BCSP-7), SA442
Bone biomechanical properties, SU488, SU507, F131, SA131, SU155, M151, M123
Bone formation. SEE ALSO *Bone tissue engineering; Distraction osteogenesis; Fracture healing*
Apolipoprotein E and, 1208
BMD *in vivo* response to loading, SU212
BMP-2 and BMP-6 effects, 1038
BMP-2 and FGF2 induced, β-adrenergic receptor antagonist and, SA021
BMP4 effects, 1049
Burns and uncoupling of bone resorption from, M523
Butyltin compounds and, SU266
Caloric restriction and, F388, SA388
Cathepsin K null mice and, 1082
Circulating osteogenic cells in, 1135
Col3.6-p20C/EBPβ transgenic mouse model, SA231
Cyclic strain effects on osteoblastogenesis and, M192
$1,25(OH)_2D_3$ and, SA583
Endochondral, differently modified Sonic hedgehog and, 1127
EphrinB2-EphB4 bi-directional signaling, 1051
Estrogen-receptor-related receptor α and, 1117
FGF23 and regulation of, SU195
Glutamate signaling and, SU032
GSK3 α/β dual inhibitor and, 1218
Hemichannels and intermittent *versus* continuous PTH for, SU556
Idiopathic osteoporosis in premenopausal women, M370
IGF-I supplementation to rest-inserted loading and, 1146
Indian hedgehog mutation and, 1060
Intermittent hPTH after osteotomy in ovariectomized rats and, M476
Isometric mechanical loading and, SA192
Leukemia inhibitory factor *in vivo* and, M190
Low-level, high-frequency mechanical signals and, M452
Mathematical models, M241
Mdm2 oncogene and runx2 expression during, 1015
Mechanical loading, $P2X_7$ nucleotide receptor and, 1032
Mechanically-induced osteocyte signaling, SU237

Bone formation. SEE ALSO *Bone tissue engineering; Distraction osteogenesis; Fracture healing* (Continued)
MSCs derived from human embryonic stem cells and, F246, SA246
Myostatin and exercise-induced, M203
Osteoclasts and, SU303
Osterix regulation of osteoblast proliferation, differentiation, M252
Phosphatidylinositol transfer protein-α and defects in, SA257
Platelet-derived growth factor-D and, M186
Prostanoid receptor EP4 agonist with rhBMP-2 and BMP-induced, SA238
PTHrP and cell cycle control in osteoblast differentiation, M223
SOST and PTH-induced, 1166
Spinal, bone turnover markers in osteoporosis and, SU423
Sympathetic nervous system and unloading effects on, F191, SA191
TRAP control at remodeling sites of, SA201
Vitamin D analog in human osteoblast cultures and, M257
In vitro differentiation of murine MSCs and, SU259
In vivo monitoring with near-infrared fluorescence imaging, 1069
Bone geometry, 1153, SU008, M175, SA492, M125
Bone grafts, SA276, F066, SA066, M261, M057, SA023. SEE ALSO *Bone allografts*
Bone implants, SU279, SU328, SA032, SU015
Bone markers. SEE ALSO *Bone remodeling markers*
Alendronate and, 1174
BMD in Japanese young women and, M008
BMD in systemic lupus erythematosus and, SA514
Collagen-induced rat-model arthritis and, SA030
Multiple *versus* pooled measurements and within-subject variability of, M136
OPG polymorphisms as, SA128
Parathyroidectomy in primary hyperparathyroidism and, SU508
PTH in perimenopausal women and, SA117
Renal function in elderly and, M135
Resistance training in older adults and, M450
Serum homocystine, BMD in Korean postmenopausal women and, SU425
South Indian postmenopausal women, SU359
Bone marrow
Adipogenesis and BMD in thyroid hormone receptor-deficient mice, 1126
Connective tissue progenitors aspiration from, SA241
ED-71 and bone formation after ablation of, M582
IGF-1 and adiposity in, 1080
Inflammation and mast cells in, M543
mRNA analysis of lysyl hydroxylases in, SU141
Oxidative stress in, M401
PTH anabolic actions and compartments in, 1062
RWV bioreactor system for cartilage tissue regeneration from, SU036
T cell TNF production in dendritic cells of ovariectomized mice, and antigen presentation in, 1059
Bone marrow, murine, 284, SA292
Bone marrow stromal cells
Biglycan, fibromodulin and ossification in tendon of, SU070
Bone allografts in sheep and, M045
Danshensu effects on, SA274
Demineralized bone powder and chondrocyte or osteoblast differentiation from, M011
Heparanase effects on, 1211
Bone marrow stromal cells (Continued)
Mesenchymal stem cells from rat, SU269
Noggin and, SU020
Osteoblast differentiation and Runx2 gene transfer in, M264
Platelet-rich plasma and differentiation of, SU270
TNF-α-induced inflammatory arthritis, osteoclastogenesis and, SA289
Wnt10b expression regulation by sex steroids in, M263
Bone marrow stromal cells, human, M012
Bone marrow stromal cells, murine, M013
Bone marrow transplantation, SA276, M266. SEE ALSO *Stem cell transplantation*
Bone mass. SEE ALSO *High bone mass disease*
β-Adrenergic receptor knockout mice, 1122, 1121
BMP-2 overexpression and, SU283
Breast cancer metastasis to bone and, SA098
Cardiovascular mortality and, SA352
Children with sickle cell disease, SA504
Dlk1/pref-1 protein regulation of, M049
ED-71 in osteoporosis, SA460
ED-71 in ovariectomized cynomolgus monkeys and, SU501
FGF2 exported 18kDa isoform and, 1042
Genetic regulation of mechanotransduction in mice and, SU224
Hesperidin effects in young intact rats, SU412
IGF-II gene polymorphisms and, M174
IL-7 inhibition of osteoclastogenesis and, M276
Juvenile idiopathic arthritis and, SA512
LRP5 gene polymorphism in elderly women and, M169
NCOA3 alleles in men and vertebral, M181
$P2X_7$ receptor Glu496Ala polymorphism in osteoclasts and, SU180
Physical activity in post-pubertal males and, M001
QUS in school-aged children, SA011
Retired collegiate artistic gymnasts, M207
Sex differences in, F362, SA362
Trends in women over 30 years, 1188
Voluntary long-term exercise and cortical bone in male rats, SU219
Walking by postmenopausal women and, SU466
Bone mass, peak
Attainment of, F002, SA002
Childhood cancer, estrogen and, SU085
Diet, physical activity in young Japanese women and, SA010
ER and AR polymorphisms in young healthy men and, SU176
Men, M004
NOS-1α and, 1036
Physical activity in young adult women and, M006
Bone matrix, SU328, 1132. SEE ALSO *Bone geometry*
Bone metastasis
Adrenomedullin from prostate cancer and, 1093
Breast cancer, nucleotide-bisphosphonates and, F095, SA095
Cell-surface carbohydrate expression in breast cancer and, SU099
Early *in vivo* detection using GFP expressing melanoma cells, SA080
ET-1 regulation of Dkk1 expression and, SA148
Gelatinases and osteolytic, M079
Heparanase support of, M075
Hypocalcemia in prostate cancer and, WG23
$\alpha_v\beta_3$-Integrin agonist and, F090, SA090
PTHrP induction and, M087
Radiation therapy for breast cancer and, SA096
RalGEF pathway in prostate cancer and, M086
Renal cell carcinoma, TGF-β and cytokines secretion in, SU200
Bone metastasis (Continued)
Runx2 regulation of gelatinases transcription and, SA091
Bone microarchitecture
Alendronate for 10 years and, 1173
Axial and transverse QUS in assessment of, M146
Osteoporotic fractures and, M349
Sex differences in congenic mice, 1083
Strontium ranelate and, SA448
3D high resolution pQCT, SU132
3D images in arthritis, M541
3D images in osteoporosis, SU133
3D mandible bone remodeling reaction-diffusion model simulation, M205
Vitamin E effects in osteopenic female rats, M445
X-ray micro-computed tomography of trabecular, SA110
Bone mineral content (BMC), SU392, F185, SA185, SU112, SU223, WG10
Bone mineral density (BMD)
Adolescent reference values in Latin America, SU117
Age, gender-specific, body size of children, SU112
Age-related bone loss at calcaneus in Japan, M111
Alendronate treatment and, 1174
Anti-thyroidal and aminobisphosphonate therapy for Graves' disease and, M409
Autosomal dominant pattern of low, M150
Basal metabolic rate in women and, SU426
BMP4 overexpression in transgenic mice and, SA028
Body composition, muscle strength in postmenopausal women and, M321
Bone markers in Japanese young women and, M008
Bone markers in systemic lupus erythematosus and, SA514
Breast and uterine disease risk in postmenopausal women and, SU390
Calcaneal QUS and genetic links to, SU164
Calcium homeostasis in systemic lupus erythematosus and, SA515
Calcium supplementation and, SA416
Canadian Aboriginal women, site-specific reductions, SU353
Cardiovascular disease and volumetric, areal, 1189
Cathepsin K inhibitors pretreatment after PTH in ovariectomized rats, M064
Chemotherapy for breast cancer and, SU090
Clinically-defined frailty in older women and, F323, SA323
C-reactive protein in Mexican Americans and, SU356
CYP450 gene polymorphisms and, M173
Daily impact exercise and, M213
Daughters of women with osteoporosis and low, SU157
Decision rules for assessment of low, M358
DEXA of age-related changes in trabecular bone and, SA115
Dietary vitamin A in multiethnic cohort of midlife women, F328, SA328
Digital imaging *versus* film-based radiographic absorptiometry, SA107
Elderly Italians, M323
Environmental determinants at different skeletal sites of Chinese, M325
Familial aggregation of osteoporosis and, SU160
Female rowers, SU235
Femoral neck external dimensions *versus* volumetric, SU403
Femoral neck geometry and, M099
Fluoride effects on bone mineral markers, $25(OH)_2D$ and, SU359

Bone mineral density (BMD) (Continued)
Fragility fractures and, 1153
Gene candidates for variation in Chinese of, SU172
Genetic and environmental determinants in Chinese women of, M161
Genetic association in Chinese with, SU159
Genome-wide linkage analysis in inbred rats of femoral neck, SA132
Haplotype analysis of single nucleotide polymorphisms of BMPs and, SU188
Healthy people in South India between 20 and 50, M116
Healthy women in South India, M115
Hemodialysis, continuous ambulatory peritoneal dialysis and, SU531
Heritability in male osteoporosis, SA129
High-dose steroid therapy in male SARS patients and, SA322
High sensitivity C-reactive protein and, SA372
IGF-I genotypes in healthy young adults and, SU178
Immunosuppressive therapy after kidney transplantation and, M546
Labyrinthectomy and rat femoral metaphysis, 1155
Lasofoxifene protection of, F426, SA426
Lean *versus* fat body mass and, SU392
Lifestyle intervention effects in adolescent girls on, 1044
Liver transplantation in children and, M547
Long-term acute lymphoblastic leukemia survivors and, SU083
LRP5 and single nucleotide polymorphisms in adult women and, SU173
Lymphatic flow and, SU467
Methadone maintenance therapy and, SU424
Multicomponent exercise effects in osteoporotic women on, SU465
Multiple sclerosis and, M539
Neurologically active medications and, F367, SA367
Norwegian natives and Pakistani immigrants, SA342
NTx levels, individual characteristics of osteoporosis patients and, M130
Opposing hip, in scoliosis, SU232
Oral contraceptives and, SA395
$P2X_7$ receptor mutation and variability in inbred mice of, SU152
Parathyroidectomy in primary hyperparathyroidism and, SU508
Peripheral arteriosclerosis risk and, M100
Peripheral neuropathy and elevated foot, M513
Postmenopausal Japanese women, SU385
Postmenopausal mammography and testing of, SU355
Primary sclerosing cholangitis severity and, SU431
QTL for regulation of, M154
QTL with pleiotropic effects in baboons for, SA133
Raloxifene for 7 years and maintenance of increases in, 1215
Reference database for Indian women, WG17
Reference data for 4-year-olds, SA101
Resistance training in older adults and, M450
Sclerostin regulation of adult, 1217
Selective serotonin reuptake inhibitors in men, 1024
Serial differences in DXA vertebral area and, M095
SERM-αs effects on, M571
Serum leptin in baboons and, SA134
Serum osteocalcin/urine NTx ratio and, M133
Sex differences in areal *versus* volumetric, SU111
Sex differences in skeletal development and, 1084
Skeletal site differences in, M092, SU352

Bone mineral density (BMD) (Continued)
Sox4 gene and, M038
Spinal DXA measurements with and without leg elevation, M090, SU122
Systemic lupus erythematosus in women and, SA516
Testing in young menopausal women, M366
Testing prompts for eldery women, WG16
L-Thyroxine suppressive therapy in women, SU120
Total lymphocyte count in postmenopausal women and lumbar, SU114
Total skeleton evaluation of body composition, EE2 and, SU116
Trends in women over 30 years, 1188
Urbanization and, SU104
Urinary calcium excretion after kidney transplantation, M550
Vascular pressure in lower limbs, 1190
Vertebral fracture threshold in secondary osteoporosis, M091
In vivo and phantom cross calibrations using DXA, M103
WIF-1 overexpression and, 1115
Bone mineral density, peak, 1181, 1081, SU184
Bone mineralization, SA038, SU102, F039, SA039, M535, SA508
Bone morphogenetic protein-2
BMD and genetic variation in, M178
Bone formation and, 1037
Bone formation, BMP6 and, 1038
Bone regeneration, β-tricalcium phosphate and, M015
ERK and osteogenic actions of, M017
FGF2 and anabolic response to, F026, SA026
Fibronectin, osteoblast mineralization and, SU063
Functional analysis of 395-kilobase region surrounding, 1115
Gli2 and osteogenic effects of, 1176
Heparin, heparin sulfate proteoglycans and, SU021
Intraosseous injection in ovariectomized cynomolgus monkeys, M491
Lentivirus-mediated transduction by, SA022
Lentivirus- *versus* adenovirus-mediated gene transfer of, M014
Noggin inhibition in prostate cancer of, F084, SA084
Notch signaling and osteoblast differentiation induced by, SU271
OPG and RANKL regulation during chondrogenesis by, SA057
Osteoactivin expression regulation and, SA078
Overexpression, bone mass and, SU283
Peak BMD and polymorphisms of, SU184
Prostate cancer metastasis inhibition and, F085, SA085
SFRP-1 and osteogenic effects of, M018
Bone morphogenetic protein-2/calcium phosphate matrix, SU017
Bone morphogenetic protein-2/transforming growth factor β, 1175
Bone morphogenetic protein-4, SU014, 1049, 1037, SA028, WG21
Bone morphogenetic protein-6, 1038
Bone morphogenetic protein-7, M012, SA509, M083
Bone morphogenetic protein binding peptide, SA074
Bone morphogenetic protein receptors, SU052, SU016
Bone morphogenetic protein receptor type 1a, 1039, 1177
Bone morphogenetic proteins (BMPs)
BMD and haplotype analysis of single nucleotide polymorphisms of, SU188
Bone loss during disuse in aged animals and, SU009

Bone morphogenetic proteins (BMPs) (Continued)
Chondrocyte differentiation, maturation and, F049, SA049
FGF signaling antagonism to signaling by, 1179
Gene expression in distraction osteogenesis, SA027
Osteoclast formation in OPG-deficient mice and, SU304
Osteogenic differentiation and autoregulation of, M013
Osteogenic differentiation through Cbfb regulation by, SA249
Prostate cancer cell growth and, F092, SA092
Sclerostin and osterix regulation during osteogenesis by, SU260
Smads anchor for receptor activation and, 1041
Twisted gastrulation and, 1178, F024, SA024
Bone morphology, SA385, SU230, SU155
Bone quality
Architecture, collagen cross-linking and mechanical properties in, M058
Bone vasculature as marker for, SU153
Intra-individual heterogeneity index of, SA038
Kidney transplantation and, M535
Ovariectomized Bax-deficient mice and, SU386
Stress fractures and, SA385
TGF-β and, SA169
Bone regeneration. SEE ALSO *Fracture healing*
Bisphosphonates and osteoblastic function and differentiation for, SU257
BMP-2 delivery with β-tricalcium phosphate for, M015
Bone sialoprotein and, SU071
β-Catenin regulation of Wnt signaling, PTHrP in, M052
Digit tip, in MRL mouse, M043
Hyaluronic acid with bFGF in, SU191
Hypoxia-inducible-factor 1α and, SA062
Lactation model, SU398
Lentivirus- *versus* adenovirus-mediated BMP-2 gene transfer for, M014
Bone remodeling
Alendronate and basal metabolism of, SA411
Binge alcohol drinking and, M376
*Bsm*I and *Fok*I effects on response to raloxifene, SA138
^{41}Calcium for direct measurement of, SA034
Dietary acid-base balance and, M437
ER and AR polymorphisms in young healthy men and, SU176
Feeding and infusion of gut hormones and, M138
Gene expression in postmenopausal osteoporotic *versus* healthy women of, M414
Glucose-dependent insulinotropic peptide and *in vivo* regulation of, M492
Hemodialysis, continuous ambulatory peritoneal dialysis and, SU531
IGFBP-2 and predictions in elderly of, SA161
Juvenile idiopathic arthritis and, SA512
Lactation and, SU398
Laser confocal microscopy of neonatal murine, SU331
Mechanically-induced osteocyte signaling and, SU237
Osteoactivin/Gpnmb gene and, 1016
Osteoclast-derived factor and, 1143
Oxytocin and, SA204
Peripheral blood mononuclear cells and, M511
Pinealectomy in sheep and, SA391
Point-of-care device for measurement of urinary NTx, SU147
Probabilistic cellular automata simulation, M121
PTH/PTHrP receptor and OPG modulation of, 1164
PTH range and, SA327

Bone remodeling (Continued)
Reaction-diffusion model simulation of 3D mandible bone architecture, M205
Resveratrol effects on myeloma cells and, 1091
Risedronate and vitamin D status in nursing home residents, SA399
Serotonin transporter role in, F068, SA068
Serum osteocalcin assay by Elecsys 2010, SU148
Urokinase receptor and, SA076
Bone remodeling markers
Alendronate treatment and predictive value of, M428
Athletes' variations in, M134
Bisphosphonates in Pagetic patients with skull involvement and, SA485
Changes for general residents in rural Japanese community, M132
Daily calcitonin nasal spray and, SU451
Fracture prediction in older people with vitamin D deficiency, calcaneal ultrasound *versus,* SU368
Glucocorticoid-induced bone loss in multiple sclerosis, SU142
γ-Glutamyl transpeptidase as, SU146
Kidney transplantation in men and, M534
Liver transplantation in children and, M547
Menopausal status and changes in, SA116
Osteoporosis treatment reinforcement using data from, M420
PTH levels in Pakistani *versus* Norwegian natives, SA376
Pubertal *versus* prepubertal females and, M131
Spinal bone formation in osteoporosis and, SU423
Tibial speed of sound in preterm infants and, M529
Total knee or hip arthroplasty and, M139
Urinary osteocalcin, SU143
Vitamin K status and, SU362
Bone resorption
Acidification and, SU335
Bisphosphonate-induced hypocalcemia and, WG25
BMD *in vivo* response to loading and, SU212
BMPR1a signaling in osteoblasts and, 1039
Burns and uncoupling of bone formation from, M523
Cadmium-induced, SA060
Cannabinoid receptor 1 pathway and, SU336
Cbl proteins and, 1198
Cbl ubiquitin ligase functions and, SU344
Chemokines differential actions in, M290
ED-71 inhibition in estrogen-deficient rats of, SU500
GLP-2, GLP-2 receptor and, M302
Hypercalcuria and, M507
LIGHT (TNFSF14) and, 1030
Lower limb loading during long-duration spaceflight and, F421, SA421
Low-level mechanical vibration in growing skeleton and, M218
Male osteoporosis and, F354, SA354
Mathematical model of markers in rats, SU026
Membrane-bound prostaglandin E synthase 1 and, F511, SA511
Methadone maintenance therapy and, SU424
Muscle paralysis in mice and, M209
Nitric oxide inhibition of, M303
Nox4, superoxide production and, SA314
Nude rats with bone metastasis, minodronic acid and, M308
Oral squamous cell carcinoma and, SU086
P2X7 nucleotide receptors and, M314
p38 MAP kinase signaling cascade and, 1272
Postprandial, gastrointestinal signaling and, F390, SA390
PYK2 signaling in calcitonin-induced actin ring disruption and, M313
Reveromycin A inhibition of, M307
Bone resorption (Continued)
Risedronate effects, SU434
Soy isoflavones in postmenopausal women and, SU452, SA414
Species specific differences during glucocorticoid treatment and, M381
Strontium ranelate and, SA302
T cell stimulation of B cell production of OPG and, F144, SA144
Thyroid-simulated, IGF-I polymorphism and, M170
Vitaxin blockage of osteoclast attachment and, SA284
Wnt signaling and, SU324
YD-1901 and, SU299
Bone sialoprotein, M243, SU247, SU034, SU071
Bone size, M349, 1124, SU404, M151, M210
Bone strength. SEE ALSO *Back extensor strength*
β-Adrenergic receptor knockout mice, 1122
Asymptomatic primary hyperparathyroidism and, SA492
Breast cancer metastasis to bone and, SA098
Computer models from digitized bone sample images to calculate, M123
Continued periosteal apposition and lack of, M010
Femoral neck torsional strength indices and, SU139
Fragility fractures and, 1153
Genetic regulation of, F127, SA127
Genome-wide linkage analysis in inbred rats of femoral neck, SA132
GIP and PTH-induced increases in, SA447
Glucocorticoid-induced osteoporosis in mouse and, SU415
Hip fracture risk in elderly, M362
Hips of female twins, 1183
HLA-B27-associated ankylosing spondylitis and, M544
Long-term impact sports participation by older men and, M210
Lumbar vertebrae of osteopenic rats, bFGF and, M488
Material *versus* structural properties of mechanical, SU234
Microstructural finite element analysis in inbred mice, M191
Osteoporotic fractures and, M349
Post-translational modifications of collagen and, SU067
QTLs in inbred mice for, F131, SA131
Risedronate and EP4 agonist effects on bone strength and, SA446
Scaling vector analysis of high-resolution MRI of proximal femur, SU129
Side-to-side difference in chronic stroke population of, SU131
TNFα polymorphism in older women and, SU186
Virtual osteoporotic simulation, finite element analysis of, SU080
Bone tissue engineering. SEE ALSO *Bone regeneration; Demineralized bone matrix; Organ culture model*
Bone marrow-derived connective tissue progenitors for, M262
Cbfa1 overexpression and, SA245
Devitalized cortical bone for, M261
Dual IgG domain containing cell adhesion family molecules, SU055
Fetal cells for, SU275
Focal adhesion in osteoblastic cells on biomaterial surfaces, SU291
Lentivirus-mediated BMP-2 transduction and, SA022
MAPK pathways in Cbfa1 phosphorylation in HOP onto cyclo-RGD peptide, SA271
Mineralization in nano-fibrous scaffolds, SU029
Msx2 transduction for, SA240
Bone tissue engineering. SEE ALSO *Bone regeneration; Demineralized bone matrix; Organ culture model* (Continued)
Phosphophoryn and, SU288
Bone turnover. SEE *Bone remodeling*
Bone vasculature, SU153
Bortezomib (Bzb), SU337
Boys, SU220. SEE ALSO *Adolescents; Children*
Brachydactyly B, SU050
Breast cancer
BMD in Hispanic *versus* non-Hispanic postmenopausal women and, SA093
Bone mass, strength and bone metastasis in, SA098
Bone metastasis and osteoblasts in, SU092
Bone metastasis, nucleotide-bisphosphonates and, F095, SA095
Cadherin-11 and metastasis of, F087, SA087
Cell-surface carbohydrate expression and bone metastasis in, SU099
Chemotherapy and BMD, QUS in, SU090
Chemotherapy and bone loss in, SU101
c-Src inhibition and bone metastases from, SU091
CYP27B1 expression in, SA094
IL-1 expression in bone metastasis of, SU094
Lysophosphatidic acid and bone metastasis from, 1092
Osteonecrosis of maxilla, mandible and metastatic, SU092
Osteonection derived from bone *versus,* SU093
Radiation therapy effects on bone metastasis in, SA096
Breast cancer cells, M076, SU098, SU100. SEE ALSO *MCF-7 cells*
Broadband ultrasound attenuation (BUA), SU130, M206
Brtl mice, G349C mutation and viability of, 1205
Buckling ratio, baseline, F383**,** SA383. SEE ALSO *Bending tests*
Burns, M523
Butyltin compounds, SU266

C

C2C12 cells, M221, M019
C-3 epimerization, SA583
C3H10T1/2 (mesenchymal progenitor) cells, 1129
C3H/HeJ mice, 1083, F264, SA264
C57BL/6J mice, SU544, 1083, F264, SA264
C57bl mice, M421
CAAT/enhancer-binding protein α (C/EBPα), SA247. SEE ALSO *CCAAT/enhancer-binding protein α (C/EBPα)*
CAAT/enhancer-binding proteins (C/EBP) homologous, F214, SA214, 1164
N-Cadherin, F248**,** SA248, 1193
Cadherin-11, F087, SA087
Cadmium, SA060, SA319
Caffey disease, 1102
Calcilytics, SA547
Calcineurin, F316, SA316
Calcinosis, tumoral, 1160, SA469
Calcitonin, M048, SA518, SU435, SU449, SU450
Calcitonin gene-related peptide (CGRP), SA517, SA519
Calcitonin, nasal, SU451, SA469
Calcitonin receptor P3 promoter, SU307
Calcitriol, M545, M404, M548, M071. SEE ALSO *Alfacalcidol*
Calcium. SEE ALSO *Calcium, dietary; Calcium, extracellular; Calcium, intracellular; Calcium supplementation; Sodium/calcium exchangers*
Bisphosphonates and, M424
Body composition and absorption of, SU410
Dietary acid-base balance and urinary excretion of, M437

Calcium. SEE ALSO *Calcium, dietary; Calcium, extracellular; Calcium, intracellular; Calcium supplementation; Sodium/calcium exchangers* (Continued)
Dietary protein and retention of, SU409
Dietary protein-induced absorption of, 1156
Different dietary phosphate sources in young women and, M378
Endogenous hormones and absorption in older women of, SU384
Ethnicity, plasma vitamin D and absorption of, SU407
Hip fracture and absorption of, SU140
Inflammation and phosphate homeostasis with, SU430
Liver transplantation in children and, M547
Osteoblast apoptosis induced by, SA197
Pediatric thyroidectomy and PTH impact on, SA003
Posturographic evaluation on effects of active absorbable algal, M395
Protein kinase C and mechanical load-induced changes in, M200
Racial differences by adolescent girls in retention of, SA418
Regulation in institutionalized elderly type II diabetics, M398
Systemic lupus erythematosus, BMD and, SA515
Urinary excretion after kidney transplantation, M550
Vitamin D receptor regulation in mouse renal cells by, SA561
^{41}Calcium, SU145, SA034
^{45}Calcium, SU026
Calcium carbonate, F507, SA507, M442, SU459
Calcium channels, voltage-dependent, SA536
Calcium channels, voltage sensitive L-type, SA254
Calcium channels, voltage sensitive T-type, SA254
Calcium, dietary. SEE ALSO *Calcium supplementation*
Calcitonin for tumoral calcinosis and restriction of, SA469
Canadian Aboriginal *versus* white women, SU361
Children with trauma fractures, M350
Concentrations in bottled *versus* tap water, SU462
FokI and androgen receptor genotypes in men, SU167
Hormone replacement therapy and BMD influence by, M438
Natural mineral water effects in young women, SU411
Supplementation in postmenopausal osteoporosis rat model, SU453
Vitamin D requirement and, SA579
Zoledronic acid, osteoclasts in C57bl mice and, M421
Calcium, extracellular, M315, SA292, SA045, SA494
Calcium, intracellular, M196, SA279, SU285, M567
Calcium phosphate, SA067
Calcium phosphate cements, M459
Calcium, placental, F523, SA523
Calcium-promoted Ras inactivator (CAPRI), F199, SA199
Calcium receptor, SA546
Calcium-sensing receptor (CASR)
BMD, bone responsiveness to HRT and polymorphism in, SU166
Calcimimetics in osteoblasts, SA265
Chondrocyte up-regulation in osteoarthritis, SA549
Dietary calcium absorption and, 1156
Genetic predispostion to disease and mutation in, SA542
Calcium-sensing receptor (CASR) (Continued)
IL-1β and *in vivo* expression of, SA544
Lactation and, 1163
Osteoporotic bone fracture and polymorphisms of, M171
Salinity-dependence in Mozambique tilapia, SA545
Calcium-sensing receptor antagonists, SA547
Calcium sulfate-carboxymethylcellulose binder for bone grafts, M057
Calcium supplementation. SEE ALSO *Calcium, dietary*
BMD outcomes with, SA416
Body weight, blood pressure in normal older women and, SU454
Bone mass accrual during rapid growth and, M212
ER-α, VDR association ìn postmenopausal women with, SU171
Falls reduction, vitamin D combination with, 1222, WG4
Osteoporotic fracture prevention with, 1007
Teriparatide and national guidelines for, M482
Vascular calcification in osteoporosis and, M333
Vertebral deformity and vertebral fracture outcomes with, F417, SA417
Calmodulin, M318
Calmodulin-dependent protein kinase II, SA259
Caloric restriction, F388, SA388, SA165
Cancellous bone, F431, SA431, SA436, M369, SU534, M377
Cancer, SA540. SEE ALSO *specific types*
Canine distemper virus, SU300
Cannabinoid receptor 1 pathway, SU336
Cannabinoid receptor 2, M166
Cardiovascular disease, 1189, F377, SA377, SU033, SA352
Cardiovascular events, 1055
Cartilage, articular, SA043, SU043, SU046, M023, SU075
Cartilage cells, F044, SA044, SU048. SEE ALSO *Chondrocytes*
Cartilage link protein, SU062
Cartilage markers, SA030
Cartilage tissue, SU036, M037, F047, SA047, M024, SU064, SA130
Caspase 3, SU327
Catechol-o-methyltransferase (COMT), F139**,** SA139
Catechol-o-methyltransferase (COMT) val158met, SA140
β-Catenin, 1001, F277, SA277, 1002, M052, SA155, F558, SA558. SEE ALSO *Wnt/β-catenin signaling*
Cathepsin, SU298
Cathepsin K, SU297, SU299, SU300, 1196, F118, SA118, 1082
Caudal-related homeodomain VDR binding element polymorphism, SU189
Caveolae-like microdomains, SU533
Cbfa1/Runx2. SEE *Runt domain factor 2/core binding factor 1*
Cbl proteins, 1198, SU344
Cbl-Src-Pyk2 signaling, F283, SA283
CCAAT/enhancer-binding protein α (C/EBPα), F251, SA251. SEE ALSO *CAAT/enhancer-binding protein α (C/EBPα)*
CCAAT/enhancer-binding protein β (C/EBPβ), SA532, SA221, SU251, 1085
CCAAT/enhancer-binding protein transcription factors, SU246
CCN3, SU294
CCR4-associated factor 1 (Caf1), F056, SA056
CD4+ T cells, 571
CD8+ T cells, 571
CD11c^{+} myeloid dendritic cells, SU309
CD14+ monocytes, SA298
CD38, SA291
CD44, F2029, SA299
CD69, SU317
CD105, SU256
CD157, SA291
CD166, SU256
Celecoxib, SU330, SU538
Cementoblasts, M239, SU054, 1177
Cementum, SA463
c-Fms Y559, F285, SA285, F253, SA253
c-Fms Y807, F253, SA253
c-Fos, F053, SA053
***c-fos*,** SA259
Charlie Chaplin (CC), 1209
Chemokines, M290
Chemotherapy, SA089, SU101
Chickens, SU242, SU156
Children. SEE ALSO *Boys; Girls; Osteogenesis imperfecta; Skeletal growth*
Age, gender-specific, body size BMD and BMC for, SU112
Age variations in DXA precision, SU124
BMC and physical activity, F185, SA185
BMD and fracture risk, 229
BMD in glucocorticoid-treated, M385
BMD in healthy N. Indian, M005
BMD measurements using DXA in healthy, SA103, 1048
BMD reference data in 4-year-old, SA101
Bone histomorphometry for osteoporosis, M530
Bone metabolism at inflammatory bowel disease diagnosis, SU529
Bone metabolism, density in diabetes type 1, SU523
Bone status, calcium intake with trauma fractures, M350
Calcium supplementation in gymnasts, SU458
Cancer, estrogen, and peak bone mass, SU085
Cortical bone and fluoride intake, SU364
Crohn's disease and bone, muscle mass, Φ503, ΣA503
Crohn's disease and cortical bone strength, SA499
Cystic fibrosis and supplemental calcium, vitamin D absorption, SU524
Cytokines in juvenile rheumatoid arthritis, SU543
DXA measurements of hip, spine, total body BMD, M445
DXA *versus* CT vertebral BMD measurements, F102, SA102
DXA whole body scans for software comparison, M002
Ethnicity and gender effects on skeletal growth, M007
Fragility fractures, radial volumetric BMD and, F343, SA343
Growth plate recovery of function after radiation therapy, M033
Inflammatory bowel disease and BMD, SA387
Inflammatory bowel disease and osteopenia, SU525
Inflammatory diseases and BMD, M528
Long-term BMC reference standards, WG10
Maturity, sex-related changes in bone, muscle during growth, F007, SA007
Overweight, femur bending strength and muscle mass in, M009
PARP-1p pseudogene and osteosarcoma in, WG9
pQCT of tibia, SU113
PTH and calcium, vitamin D supplementation after thyroidectomy, SA003
QUS and physical performance ability, M148
QUS of bone mass, SA011
Rheumatoid manifestations of hypophosphatasia, WG7
School-curriculum based exercise and bone mineral accrual, 1147
Secondary osteoporosis severity, SU522
Sex- and age-related changes in calcaneal SOS, SA121

Children. SEE ALSO *Boys; Girls; Osteogenesis imperfecta; Skeletal growth* (Continued)
Sex differences in functional muscle-bone units at different skeletal sites, F012, SA012
Sickle cell disease and bone deficits, SA502, SA504
Vitamin D, bone metabolism in perinatally HIV-infected, SA501
Vitamin D deficiency among Canadian, WG11
Vitamin D insufficiency from secondary osteoporosis, M527
Chloride channels, M306, M578
Cholangitis, primary sclerosing, SU431
Cholesterol, M360, F426, SA426, M571
Chondrocytes. SEE ALSO *Cartilage cells; Growth plate chondrocytes*
BMP signaling and differentiation, maturation of, F049, SA049
BMP signaling and Smad 3-deficient, 1180
β-Catenin and proliferation, maturation of, 1002
c-Fos overexpression, BMP-induced differentiation and, F053, SA053
Dishevelled molecule and, 1131
EphrinB2 expression in, M026
Epiphyseal, HIF-PHD axis and maturation of, M032
GSK3 and differentiation of, M031
Hypertrophic, dietary phosphate and, SU035
Nkx3.2/Bapx1 and maturation of, 1128
Radiation therapy effects *in vitro* on, SU038
Rheumatoid arthritis and apoptosis of, SA050
Thrombin and implantation of, M030
TNFα, RANKL catabolism in, M061
Chondrodysplasia, Jansen metaphyseal, F042, SA042
Chondrodysplasia, Schmid metaphyseal, 1130
Chondrogenesis
CTGF/Hcs24/CCN2 and, SU046
Cycle GMP protein kinase II, Sox9 function and, 1050
Extracellular calcium, PTHrP signaling and pace of, SA045
FGF signaling, $p57^{Kip2}$ suppression and, SU049
Hypoxia and, F047, SA047
Nkx3.2 repression of runx2 gene activity and, 1129
Rhoa/ROCK signaling pathway and, SA052
Runx1/Cbfa2 induction in mouse limb bud cells of, F058, SA058
TGF-β in early stages of, SU205
Transcription factors activated during, SA069
Wnt signaling and, M022
Chordin, M249
Chorionic gonadotropin, human, SU513
Chromatin immunoprecipitation (ChiP) display, F216, SA216, SU262
Chromatin remodeling, SU252, 1086
Chromosome 1, 1206
Chromosome 1p36, SU168
Chromosome 2, SA467
Chromosome 3p21, M154
Chromosome 9, SA467
Chromosome 11q12-13, SA133. SEE ALSO *Lipoprotein-related protein-1*
Ciglitazone, M281
CIITA, SU204, 1086
Cimicifuga racemosa (black cohosh), SA210
Cinacalcet HCl, SA470, F497, SA497, SU512, SA546, F495, SA495, SA548, SA491
Circadian rhythm, F364, SA364, F390, SA390
c-jun, SU297
***CLCN7* gene,** M179, SA467
Clinical trials, M457, M458, SU433, SU481
Clodronate, M411
CMP1, 1216
***Col1a2*^{oim} mice,** F464, SA464
Collagenase 3, SU057. SEE ALSO *Matrix metalloproteinase-13*
Collagen bundles, M051
Collagen fiber orientation, SU079
Collagen hydrolysate, SU048
Collagen triple helix repeat containing gene (Cthrc1), 1132
Collagen type I, SU061, M387
Collagen type Iα1, SU182, 1102
Collagen, type I-GFPcyan, SU258
Collagen type I receptor, SA100
***Collagen type Xa1* gene,** 1130
Collagen type XIα2, M036
Colony-stimulating factor-1 (CSF-1), F290**,** SA290, SU308, SA209
Computational imaging, dynamic, 1073
Computed tomographic microscopy
Dual X-ray absorptiometry of rat osteoporosis *versus,* M128
3D images of age-related cortical porosity changes in femur, SU006
3D images of bone microstructure and erosion in arthritis, M541
3D images of bone microstructure in osteoporosis, SU133
3D images of cortical bone porosity, SA029
3D images *versus* mechanical analysis of cortical bone, SU024
Trabecular bone microarchitecture assessment, SA110
VivaCT40 monitoring of cancellous rodent bones, M120
Computed tomography, F102, SA102
Computed tomography, high resolution quantitative, F104, SA104, SU132
Computed tomography, high resolution spiral, SA386
Computed tomography, multi-detector, M122
Computed tomography, quantitative, 1124, M127
Concanavalin A, M555
Connective tissue, SA033
Connective tissue growth factor (CTGF), M505, SU278, SU206
Connective tissue growth factor/hypertrophic chondroctye-specific gene product 24/ CCN family member 2 (CTGF/Hcs24/ CCN2), SU046
Connective tissue progenitors (CTPs), SA241, M254, M262
Connexin43, 1106, SA440
Connexins, SU552
Constitutively-active-mutant estrogen receptor α (CAMERA), F207, SA207
Contraceptives, oral, SA395, F396, M386, SA396
Core binding factor α 1 (Cbfa1), SA245, SA223, M236, F070, SA070, M232, SU231
Core binding factor β (Cbfb), SA249, M233
Correlation metrics, SU155
Cortical bone
Age-related loss in proximal femur, SU010
Aging, cross-sectional structure and mineralization, SA015
Bone matrix strain at osteocyte lacunae, F175, SA175
Diabetes mellitus type II and, M399
Exercise in young adult men, SA184
Fluoride intake in young children, SU364
Formation stimulation using low-level, high-frequency mechanical signals, M452
Glucocorticoid-induced vertebral osteoporosis and, M384
Glucocorticoid signaling disruption in Col2.3-HSD2 transgenic mice, 1115
High-frequency vibrations and volume of, SU221
Nanonindentation measures *versus* Young's mechanical properties modulus for, SU077
OPG-Fc in cynomolgus monkeys and, 1071
Partial volume effects in pediatric pQCT of, SU106
Post-translational modifications of collagen and toughness of, SU067
Cortical bone (Continued)
PTH in combination with glucocorticoids, SA436
Resistance, agility training and density of, SU468
Sex differences in genetic regulation in congenic mice strains, SU163
Steroid treatment and, SU417
3D computed tomographic microscopy of, SA029
3D computed tomographic microscopy *versus* mechanical analysis of, SU024
3D volumetric analysis of age-related change in porosity in femur of, SU006
Voluntary long-term exercise by male rats and, SU219
Corticosteroids, SA568, F345, SA345. SEE ALSO *Glucocorticoids*
Cortisone, SU419
Coumadin, SU504
Craniofacial skeleton, SU039, 1078, M016
Craniosynostosis, SA157, 1134
Cre, SA166. SEE ALSO *Cre recombinase*
C-reactive protein, SA372, SU356
Creatine kinase brain isoform, SU320, SU321
Creatinine clearance, F415, SA415
CREB-binding enhancer, 1104
Cre recombinase, SA310
Crohn's disease, M460, SU428, SA499, F503, SA503
Csk, F309, SA309
c-Src, M312, SA279, F309, SA309, SU091
Cushing's syndrome, M383
CXC chemokines, SA145
CXCL12 chemokine, SA286
Cyclic AMP, SU285
Cyclic AMP/protein kinase A, SU313
Cyclic AMP response element modulator (CREM) gene, 1061
Cyclic GMP protein kinase II, 1050
Cyclin D1, SA048, F493, SA493
Cyclin-dependent kinase 6 (CDK6), SA048
Cyclooxygenase-2
Anterior-cruciate-ligament transection model of osteoarthritis and, SA046
Apoptosis from oxidative stress by overexpression of, SA196
Biphasic expression with pulsatile fluid flow, M199
Bone loss recovery in mice after unloading and expression of, SU227
Decreased acid-induced bone resorption and, SA505
Fluid shear stress and induction in MC3T3 cells of, SA176
Gene expression and apoptosis in osteoblasts, SA195
PGE_2, elevated bone resorption and, SU314
Protein kinase D in osteoblasts and fluid shear stress-induced, M194
PTH *in vivo* induction of, SU551
Serotonin, dopamine and osteocytic expression of, SU348
Cyclooxygenase-2 inhibitor, SA143, SU538, SU208
Cyclo-RGD peptide, SA271
CYP2C11, SA581
***CYP2R1*,** SA584
***CYP17*,** M164
***CYP19*,** SU241, M163
***CYP24*,** F586, SA586
CYP27B1 (cytochrome P450), SA094, SA589
CYP450 gene polymorphisms, M173
Cysteine-rich domains, SU343
Cystic fibrosis, SU376, SU421, SU137, M524, SU524
Cytokines, SU569
Cytoskeleton, SU073

D

Daidzein, SA208
Danshensu (TSU), SA274
DAP12, 1195
Death receptor-3, M224
Decorin, 1078
δEF1, M019
Dehydroepiandrosterone (DHEA), SU421, SU496
Delivery of health care, SA348
Delta-like 1/preadipocyte factor-1 (Dlk1/pref-1) protein, M049
Demineralized bone matrix, SU014, M245, SA069, SU031
Demineralized bone powder, M011, M041
Dendritic cells, M309, SU309, 1059
Denmark, underdiagnosis, undertreatment of osteoporosis in, M340
Densitometers
- Anthropomorphic phantoms for cross-calibration of, SU127
- BMD, percentage fat cross-calibration with Lunar DPX-L and Prodigy, M114
- Cross calibration during equipment upgrades, M105
- Fan-beam, precision errors with, SU126
- Inter-observer vertebral morphometry variation using Expert *versus* Prodigy, M104
- Phantom choice for longitudinal studies using, SU358
- Tissue facsimile bags and, M117
- *In vivo* and phantom BMD, body composition calibration of, M103

Densitometry, SU354, F106, SA106, M107, M110. SEE ALSO *Dual X-ray absorptiometry*
Dental pulp cells, SA235, M188
Dentin, SA463
Dentin matrix protein-1 (DMP-1), 1004, 1035
Dentin matrix protein-1/matrix extracellular phosphoglycoprotein, 1105, SU215, F182, SA182
Dentinogenesis imperfecta, F464, SA464
Depot medroxyprogesterone acetate (DMPA), F396, M386, SA396
Developmental disabilities, SU383
Dexamethasone, SA562, SA563
Diabetes mellitus
- Calcium sensing in institutionalized elderly with type II, M398
- Cortical bone density in type 2, M399
- Fall risk and physical performance changes in older adults with, 1110
- Falls by older men with, SA355
- Fracture healing in, M034
- Type 1, bone metabolism, density in Korean children, SU523
- Type II mouse model with severe osteopenia, SU429

Diabetes mellitus (animal models), M489, SU506
Dickkopf-1 (Dkk-1)
- Collagen 1 α promoter and, 1018
- ET-1 regulation of, SA148
- Fra-1 and, F253, SA253
- Glucocorticoid-induced osteoporosis and, F565, SA565
- Glucocorticoid-inducible LRP5 signaling inhibition by, SU351
- LRP5/6 interactions with, F270, SA270
- LRP5/6-Wnt-TCF-signaling and C-terminal 21 amino acids of, F262, SA262
- Osteoporosis and, 1017
- Proteaosome inhibitor in multiple myeloma, 1011

Diet. SEE ALSO *Caloric restriction*
- BMC during childhood to adolescence growth, M328
- BMD in Chinese elderly, SU360, M329

Diet. SEE ALSO *Caloric restriction* (Continued)
- Low-income postmenopausal osteoporotic women, M335
- Magnesium reduction to 25% of nutrient requirement, M046
- Peak bone mass in young Japanese women, SA010
- Postmenopausal osteoporosis and, SA389
- Renal osteodystrophy before parathyroidectomy, M533

Dihydrotestosterone, M572
1,25 Dihydroxyvitamin D, SU193, M579, F471, SA471, F234, SA234, SA584, SA560
25 Dihydroxyvitamin D, M581
1,25 Dihydroxyvitamin D_2, SU585
1,25 Dihydroxyvitamin D_3
- ApoA1 expression and, M368
- Bone anabolic effects of, M580
- Bone formation and, SA583
- Cbfa1 gene expression and, M232
- Endochondral bone formation and postnatal survival, PTH and, SA576
- HIF1α, VEGF gene expression and, SA575
- Male osteoporosis, total, free circulatory $25OHD_3$ and, M581
- Nicholas Advantage 25-Hydroxyvitamin D Assay evaluation, SU585
- Osteoblast expression of integrins and, M042
- Osteoporotic hip fractures, sunlight, and serum levels of, SA338
- PTH and anabolic actions on bone by, M485
- Renal type IIa sodium-dependent phosphate cotransporter regulation by, F154, SA154
- TRPV6 and intestinal cells response to, 1088
- VDR gene polymorphisms impact on, SA552
- Wnt signaling in MC3T3-E1 cells and, SU276

1,25 Dihydroxyvitamin D_3-1α-hydroxylase (CYP27B1), SA094
1,25 Dihydroxyvitamin D_3-membrane associated, rapid response steroid-binding (1,25D_3-MARRS) protein, SA550, SA572
Diosgenin, SA261
Dioxin, SA472
Dishevelled (Dvl) molecule, 1131
Distraction osteogenesis, SA150, M183, SA027, M047
Disuse osteoporosis, SU234
Dlx3, 1144
Dlx5, M237, 1108, F218, SA218, SU248
Dopamine, SU348
DRIP/205, M577
Dual IgG domain containing cell adhesion family molecule (DICAM), SU055
Dual X-ray absorptiometry (DXA). SEE ALSO *Densitometers; Densitometry; Ultrasound, quantitative*
- Age variations in pediatric precision of, SU124
- BMD in healthy children and adolescents, SA103
- BMD in Marfan syndrome, M499
- BMD of hip regions of interest, SU109
- Cost-efficient postmenopausal osteoporosis screening, SU388
- Discordant spine and hip measurements, SU128
- Finite element analysis of, M097
- Lateral morphometry of vertebral fractures, M098, SU381
- Leg elevation and spine BMD, M090, SU122
- Micro-computed tomography of rat osteoporosis *versus,* M128
- Pediatric, Duchenne muscular dystrophy assessment and, M525
- Peripheral, UK National Osteoporosis Society on, SU110
- QDR Adult, QDR Pediatric, and Discovery whole body algorithms comparison, M002
- QUS diagnosis of hip fractures *versus,* M093

Dual X-ray absorptiometry (DXA). SEE ALSO *Densitometers; Densitometry; Ultrasound, quantitative* (Continued)
- Radiographic absorptiometry in postmenopausal Middle Eastern women *versus,* SU103
- Radius *versus* total forearm in men, SU125
- Serial differences in vertebral area, M095
- 3D scaling index method *versus,* SA031
- Tissue facsimile bags and, M117
- Vertebral BMD in children and adolescents, F102, SA102
- Ward's triangle region location in femoral neck variations, F333, SA333

Dual X-ray and laser of calcaneus (DXL), SU107, SA105
Dwarfism, SA048, SU198, F042, SA042, 1018
Dynamin, F283, SA283

E

E11/gp38, F173, SA173
Early region 1A (E1A) proteins, SU089
ED-71 (1α,25-dihydroxy-2β-(3-hydroxypropoxy) vitamin D_3)
- Bone formation after bone marrow ablation by, M582
- Bone mass increases in ovariectomized cynomolgus monkeys, SU501
- Bone mass in osteoporosis, vitamin D status and, SA460
- Bone resorption inhibition in estrogen-deficient rats, SU500
- Fracture healing and, SU497
- PTH(1-34) bone formation *versus,* M496
- *In vivo* mediation of VDR by, SA569

ED-120, M493
EF5 (2-nitromidizole derivative), M059
Egr2/Krox20, SA564
Elecsys 2010, SU148
Enamel matrix derivative (EMD), SU261
Endocrinopathies, autoimmune, SU510
Endothelial cells, human microvascular, SA298
Endothelial cells, human umbilical cord, M250
Endothelin-1, SU245, SA148, M066
Endothelin receptor A (ETRA), SU245
Energy metabolism, SA570
Environmental factors, M161
Enzyme-linked immunosorbent assay (ELISA), F118, SA118
Eos, M292
Eosinophil chemotactic factor-L (ECF-L), M271
EP4 agonist. SEE *Prostaglandin E_2 receptor subtype EP_4 receptor agonist*
EphB4, 1051
EphrinB2, 1051, M026
Epidermal growth factor receptor, 1096
Epilepsy, SA475
Epithelial-mesenchymal transition (EMT), M077
Equol, SU455, SU456
ERK1/2 MAP kinases, M557
Estradiol
- Fracture risk in older men, 1019
- IGF-I synthesis in liver, 1167
- Osteoblastic procollagen production in postmenopausal women and low dose, M387
- Ovariectomized ER knockout mice, M565
- Skeletal size, mineralization in young men, M389
- Supplementation in postmenopausal osteoporosis rat model, SU453
- Transdermal *vs.* oral, for Turner syndrome, SU485
- Volumetric BMD and bone size in older men, 1152

17β-Estradiol, M568, M084
Estradiol 2, endogenous, SU116

Estren(s), 1119, 1118, SU491
Estrogen receptor, SU169, SU176
Estrogen receptor-α. SEE ALSO *Constitutively-active-mutant estrogen receptor α*
BMD response in postmenopausal women to gene polymorphisms of, SU181
Body mass, hip fracture risk in older women, M182
Bone density and body composition in mice with defective signaling through, SU578
Calcium supplementation in postmenopausal women and VDR association with, SU171
Loading, and expression in ovariectomized rat tibia, SA188
Ovariectomy and expression in tibia, M570
Raloxifene and, SA392
Smad3-induced apoptosis and, F097, SA097
SRC-2 gene expression in osteoblasts, M566
Transcription regulation by c-Src/PKC-dependent mechanism, SU287
Estrogen receptor-α agonist (PPT), M204
Estrogen receptor-β, SA392, SU184
Estrogen-receptor-related receptor α (ERRα), 1117, M024
Estrogen receptors, SA205
Estrogen response elements (EREs), SU568
Estrogen response elements binding protein, SU570
Estrogens. SEE ALSO *Hormone replacement therapy*
Bone sensitivity to loading and, F187, SA187
Calcitriol effects on serum PTH and $25(OH)_2D$ relationship *versus,* M404
CD4+ T cells, CD8+ T cells, and bone loss in deficiency of, 571
Childhood cancer, peak bone mass and, SU085
CYP450 gene polymorphisms and, M173
Disuse-induced bone loss and, M576
ERα and ERβ effects on gene expression by, SU575
ERα-controlled MMP-1 promoter repression and *in vivo,* M569
Fracture risk after progestin discontinuation and, 1100
Glutamate receptors and osteoclast responsiveness to mechanical strain, M193
Glutathione regulation in bone, SU339
Hydrogen peroxide induction of TNF-α, SA393
Male *versus* female steroid receptor coactivator-1 skeletal response to, SU567
MHC class II transactivator control *in vivo,* 1086
Osteogenic response to exercise and, M204
Periosteal expansion stimulation in orchidectomized mice, M564
Phytoestrogens and, SU572
Phytoestrogens' osteoclast formation inhibition *versus,* M279
Proteomic analysis of *in vivo* effects in bone, SU574
TGF-β signaling, T cell activation and, 1191
Trabecular bone activation in ovariectomized rats, androgen receptor and, SA397
Transcriptional inhibition by vitamin D and, 1089
Etanercept, SA303
Ethnic/racial groups
Amino acid substitutions in LRP5, M180
Bending stiffness of ulna, tibia and, SA109
BMD and fracture prediction in African American women, 1056
BMD in Asian men, SU115
BMD in Canadian Aboriginal women, SU353
BMD in healthy N. Indian children, M005
BMD in men, SA363
BMD in Norwegian natives and Pakistani immigrants, SA342
Bone turnover markers and PTH levels in Pakistani *versus* Norwegian natives, SA376
Ethnic/racial groups (Continued)
Calcium and vitamin D intake in Canadian Aboriginal women, SU361
Calcium retention in adolescent girls and, SA418
Chinese American bone densitometry database, SU108
Diet and BMD in Chinese elderly, SU360, M329
Environmental determinants of Chinese BMD, M325
Female osteoporosis self-assessment tool for Asians, SU393
Femur BMD and structure measured by computed tomography, M326
Fracture prevalence and BMD in Mayan women, SA342
Gene candidates for BMD variation in Chinese, SU172
High BMD in men of African descent and prostate cancer risk, SA100
Hip fractures in Hawaii, SU372
Knee osteoarthritis and lumbar spine BMD in Korea, SU357
Leg length of Chinese *versus* Caucasians, SA382
Osteocyte death in young bone, SU347
Osteomalacia in immigrants, SA368
Osteoporosis diagnostic tools evaluation for elderly Caucasian and Chinese men, SU394
Paget's disease in south east London, M516
Plasma 25(OH) vitamin D and calcium absorption, SU407
Quality of life in Canadian Aboriginal women, SA456
Raloxifene and Japanese *versus* Caucasian postmenopausal women, SU406
Skeletal growth in children, M007
Smoking among Iranian Australian women and osteoporosis risk, M363
Vertebral deformities in men, F360, SA360
Vitamin D insufficiency in Canadian Aboriginal women, M331
Vitamin D supplementation for African American postmenopausal women, SU502
Etidronate, SU144, SA473
Exercise. SEE ALSO *Loading; Vibration exercise*
Anabolic bone response to low dose PTH, SA534
BMC in young children, F185, SA185
BMD and daily impact, M213
BMD, bone markers, and IGF-1 responses to isometric, M450
BMD, fall risk in osteoporotic women, SU465
BMD in female rowers, SU235
BMD loss in females with cessation of, SU464
Bone accrual in boys after cessation of, SU220
Bone mass after puberty in men, M001
Bone mass, bone metabolism in ovariectomized rats and treadmill, SU218
Bone mineral accrual in children with school-curriculum based, 1147
Bone, muscle, fat masses in male tennis players, SU402
Calcium supplementation, bone mass accrual during rapid growth, M212
Cortical bone density and, SU468
Cortical bone size, volumetric density in young adult men, SA184
Estrogen, ERα agonist and osteogenic response to, M204
Fall prevention, WG28
Femur structural stability and diversity *versus* quantity of, M334
Fracture risk in 70- to 78-year old women, SU469
Low-income postmenopausal osteoporotic women and, M335
LRP5 polymorphisms, BMD and, F136, SA136
Exercise. SEE ALSO *Loading; Vibration exercise* (Continued)
Marathon training effects on calcaneal BUA, M206
Muscle strength in 70- to 79-year old women, SU470
Myostatin and bone formation induced by, M203
Osteoporosis risk with lifetime recreational gymnastics, SU002
Peak bone mass in young adult women, M006
Peak bone mass in young Japanese women, SA010
Reduced-intensity back-strengthening, SA422
Spinal mobility in postmenopausal osteoporosis, M449, WG6
Tai Chi as osteoporosis prevention treatment, SU472
Tibial bending stiffness in young women and isokinetic, SU229
Voluntary long-term, cortical bone mass in male rats, SU219
Walking endurance of women with prevalent vertebral fractures, M454
Weight lifting by postmenopausal women, M455
Exon A/B methylation, 1203
Exostoses, abdominal and hand, SA040
Extracellular matrix
Ascorbate, osteoclastogenesis and, M288
Dynamic computational imaging in living osteoblasts, 1073
Endothelial cells, osteoblast differentiation in synthesis of, M250
Endothelin-1 in human osteosarcoma cells and, M066
Fourier-transformed infrared spectroscopy, SU030
MMP-13 remodeling of, M063
Morquio A disease and, SU064
PHOSPHO1 expression during embryonic development and, F037, SA037
SPARC and structural integrity of, SU060
Extracellular signal-regulated kinase (ERK), SU202, M017, SU553
Extracellular signal-regulated kinase 1/2 (ERK1/2), M559
Extracellular signal-regulated kinase (ERK) signaling, 1106, M222

F

Factor inhibiting ATF4-mediated transcription (FIAT), 1052
Fall index, F112, SA112
Fall prevention, SU463, SA420, WG28
Fall risk
Assessment tool, WG3
Chronic stroke and, SA325
Hip fracture prediction, 1184
Multicomponent exercise in osteoporotic women and, SU465
Reduction in osteoporotic women, SA419
Vitamin D_3, calcium in elderly and, 1221
Vitamin D for nursing home residents and, M491
Falls
Alfacalcidol treatment of low creatinine clearance and, F415, SA415
Cataract surgery and, 1109
Elderly postural stability and physical performance tests, SU399
Older diabetic men, SA355
Older diabetics, prediabetics and, 1110
Safe landing during, SU471
Vitamin D and calcium supplementation effects on, 1222, WG4
Vitamin D supplementation for residential care subjects to prevent, F459, SA459

Familial expansile osteolysis, SA308
Family physicians, M406
Fan-beam densitometers, SU126, SU138
Fanconi's syndrome, WG19
Fas, M318
FAT cells, SA245
Fat, dietary, M330
Fatty acids, M248, SA557
FcRγ chain, SU318
Femoral head deformity, SU521, SU528
Femoral neck
- Bone geometry, bone mineral in cystic fibrosis at, SU137
- Bone mass loss and gastric lap-banding weight loss, SA374
- Fracture prediction in Caribbean men, SA359
- Genome-wide linkage analysis of density and strength in inbred rats of, SA132
- Geometric effects of aging and osteoporosis, SU008
- Geometry, BMD volume measurements and, M099
- *Mif* promoter and BMD of, SA135
- Mineral mass and external dimensions in, SU403
- Torsional strength indices, SU139
- Ward's triangle region location variations, F333, SA333
- Young-elderly differences in, SA018

Femoral shaft failure load (animal models), SU161
Femoral shaft fractures, WG24
Femur, SU141, M326, SU156, M334, M009
Fetal bone cells, SU275
Fetal development, F037, SA037, SU028, SU520
FHL2, 1029
Fibrillin 1 gene, F075, SA075
Fibroblast growth factor, SU049, 1179
Fibroblast growth factor 2
- Anabolic response to BMP-2 and, F026, SA026
- Bone mass in mice and exported 18kDa isoform of, 1042
- Gene and protein expression in osteoblasts, SU199
- MEPE/OF45 gene expression in bone marrow-derived osteoblasts and, SU190
- Osteoblast survival induced by, SA155
- PTH(1-34), glucocorticoid-induced osteoporosis and serum levels of, M480
- Signaling in osteoblast differentiation, SU192

Fibroblast growth factor 23
- Bone formation and, SU195
- Calcium regulation in primary hyperparathyroidism of plasma, SU517
- Dietary phosphate and, SU196
- Dietary phosphorus and, SU193
- Genetic dissection of phosphate- and vitamin D-regulated circulation of, 1162
- G protein signaling and gene expression by, SA151
- Growth hormone replacement in adult GH deficiency and, SU505
- NHERF-1 and internationalization of NaPi-2a cotransporter by, F156, SA156
- Phosphate, vitamin D metabolism and, 708, WG18
- Phosphorus levels, advanced malignant ovarian tumors and, SA083
- Phosphorus levels, small cell and squamous cell lung cancer and, SA082
- Physiological role and expression *in vivo* of, 1133
- Primary hyperparathyroidism and *in vivo* expression of, SA153
- Surgically-treated primary hyperparathyroidism and, SA488
- Tumoral calcinosis and, 1160
- Vitamin D-mediated hyperphosphatemia and, SU194

Fibroblast growth factor receptor 1, 1005
Fibroblast growth factor receptor 2, SU192, F226, SA226, 1005, SA157, 1134
Fibroblast growth factor receptor 3, SU198
Fibroblasts, M041, SU020
Fibrodysplasia ossificans progressiva, SU016, WG21
Fibromodulin, SU070
Fibronectin, SU063, M240, SA054
Fibrous dysplasia, 1157
Finite element analysis, M097, SU080, M191
Fish oil, dietary, SU003
FK506, M236
Floors, compliant, SU463
Flow cytometry, M311
FLP recombinase, SU249
Fluid flow, SU136, M219
Fluid shear stress. SEE ALSO *Oscillatory fluid flow*
- Biphasic expression of COX-2 and, M199
- Bone formation in C3H *versus* B6 mice and, F264, SA264
- COX-2 in MC3T3 cells and, SA176
- IGF-I, osteoblast proliferation and, SA263
- MMP-13 in osteoblasts and, SA177
- Nitric oxide production and, M198
- $P2X_7$ purinergic receptor, prostaglandin synthesis and release from osteoblasts and, M197
- Protein kinase D activation in osteoblasts and COX-2 induced by, M194
- RANKL expression in osteoblasts and, M195

Fluorescence imaging, 3-D volumetric, SU023
Fluorescence scanning system, small animal molecular imager, SA080
Fluorescent activated cell sorting (FACS) method, M287
Fluorescent color analysis, SU263
Fluoride, SU359, SU364
^{18}Fluoride ion, 1150
Fluorosis, skeletal, M510
Fluvastatin, M431
FokI, SU167
Foot fractures, M342
Footwear, Yaktrax, SA420
Forearm, SA353, M367, SU475, M127, SU125
Forteo. SEE *Teriparatide*
ΔFosB, 1142
Δ2ΔFosB, 1142
Fra-1, F253, SA253
Fracture healing
- Abnormal transdifferentiation in older rats and delayed, M238
- AC-100 (Dentonin) and, M467
- Alendronate *versus* calcitonin in cynomolgus monkeys, SU450
- BMP receptors and hepatocyte growth factor in, SU052
- Chondro/osteoclast activity in diabetes, M034
- ED-71 therapy, SU497
- iNOS knockout mice, M055
- Integrated care model, SA348
- Meox2 and, SU506
- Multifaceted care model, SU476
- Placental growth factor and, F147, SA147
- Pleitrophin and, SU506
- Selective prostaglandin EP_4 agonist stimulation of, M490
- TP508 promotion of, 1201
- Transcriptional profiling across, M230
- Zoledronic acid and endochondral ossification in rat model, SU443

Fracture prediction
- BMD in African American women, 1056
- BMD measurements at different skeletal sites, M092, SU352
- Calcaneal ultrasound of men and non-spinal, M344
- CTx measure of bone collagen quality, 1068
- DXA and QCT at hip and spine in men, 1067
- Effectiveness of easily measurable risk factors, F371, SA371

Fracture prediction (Continued)
- Fall index, F112, SA112
- Finite element analysis of DXA images, M097
- High resolution quantitative CT of distal radius or tibia, F104, SA104
- Hip/spine BMD in men, 1009
- Limb, prior rib fractures, 1111
- *LRP5* gene polymorphism in elderly women, M169
- Older people with vitamin D deficiency, SU368
- Parental hip fracture in postmenopausal women, M357
- Previous BMD change during perimenopause, SU382
- Prior fractures by nursing home residents, SU371
- Quantitative calcaneal ultrasound analysis, F123, SA123
- Retinol and retinyl esters in osteoporotic elderly women, 1020
- Rural residents, M352
- Serum albumin and vertebral, SU380
- Vertebral, baseline buckling ratio, F383, SA383

Fracture risk
- Adipocyte hormones in elderly, 1021
- Age/BMD effects in postmenopausal women, F339, SA339
- Aged, seasonal modulations, SU373
- Alfacalcidol, calcitonin derivative and vertebral, SU449
- Annual intramuscular vitamin D_3 supplementation, 1220
- Asymptomatic vertebral deformities, 1112
- Baseline BMD in elderly women, M324
- Beta-blocker use, M466
- BMD change with ibandronate and, SU441, M433
- BMD in children, 229
- Bone loss in postmenopausal women, F380, SA380
- Calcium supplementation clinical trial, 1007
- Cataract surgery and, 1109
- Chinese American bone densitometry database, SU108
- Elderly women with longer- *versus* shorter-lived mothers, M337
- ER-α, body mass in older women, M182
- Estrogen plus progestin discontinuation, 1100
- Family history of fracture, F375, SA375
- Five-year probability in elderly women, SU367
- Hip strength in elderly, M362
- Inhaled corticosteroids, F345, SA345
- Intragenic interaction of VDR polymorphisms, M176
- Kidney failure, M532
- Knee pain and knee osteoarthritis, F335, SA335
- Lifetime recreational gymnastics, SU002
- Milk intake, M356
- Multiexercise program of 70- to 78-year old women, SU469
- ORACLE assessment, F341, SA341
- Osteoporotic, high risk women, M348
- Osteoporotic, in older women, M345
- Raloxifene effects after 8 years on nonvertebral, F428, SA428
- Reduction during teriparatide treatment of, 1170
- Reproductive history and postmenopausal, M365
- Teriparatide and increasing osteoporotic fractures, 1070
- Testosterone, estradiol in older men, 1019
- Thiazide diuretics, M338
- TNFα polymorphism in older women, SU186

Fractures. SEE ALSO *Hip fractures; Vertebral fractures*
- Absence of osteoporotic treatment for men, 1113
- Bone pain in animal model, M400
- Direct analysis of non-vertebral fracture in community experience study, M478

Fractures. SEE ALSO *Hip fractures; Vertebral fractures* (Continued)
DXL in postmenopausal women with and without prior, SA105
Elderly genetic liability for, SU151
Glucocorticoid, normal BMD and, SU377
Iliac crest biopsies chemical composition in women and, M403
Long-term bisphosphonates and, WG24
Low energy, pharmacologic treatment plan for, M461
Low-impact risks for men with ankylosing spondylitis, SA361
Low trauma, education program for treatment compliance after, SU479
Mechanical homeostasis in elderly women with osteoporotic, F017, SA017
Obesity, hypomineralization, and atraumatic, M368
Osteopenic women *versus* total osteoporotic, SU378
Osteoporotic, bone size, geometry, and strength association, M349
Osteoporotic, urban Spanish women, M351
Peripheral osteoporotic, in France, SU370
Quantitative calcaneal ultrasound in elderly Chinese men for, M143
Risedronate, osteopenic postmenopausal women and, F404, SA404
Risk factors in Bialystok Osteoporosis Study, SU366
Sex differences in, F362, SA362
Socioeconomic deprivation and, M341, M343
Stroke influence on BMD, balance and, M346
Traumatic, osteoporosis management and, M463
Vitamin A and osteoporotic, SU374
Vitamin D insufficiency with minimal trauma, M373
Young adults with cystic fibrosis, SU376
Fractures, fragility
Bone density, geometry, strength indices and, 1153
Coordinator to manage investigation, treatment of, SU480
Developmental disabilities and, SU383
Hypomineralization in male idiopathic osteoporosis and, M391
Osteoporosis diagnosis and treatment after, M464
Osteoporosis evaluations in Denmark after, SU475
Pediatric, radial volumetric BMD and, F343, SA343
Frailty, F323, SA323
Fructooligosaccharides, SU460

G

Gait, SU356
Galectin-2, SA041
Gap junctions, 1106, M560
Gastrointestinal tract, F390, SA390, SA401, SU445
Gaucher's disease, M101
Gelatinases, M079, SA091. SEE ALSO *Matrix metalloproteinase 9*
Gender differences. SEE *Sex differences*
Gene chip microarray analysis
Anabolic response of bone to mechanical strain in mice *in vivo,* F180, SA180
Bone profiles of binge alcohol drinking and antiresorptive treatment, SA447
Cadmium-induced bone loss, SA060
Candidate genes for vitamin-D-dependent proteins in mouse kidney, SA577
Cartilage tissue development, temporal gene expression profiles in, M037
Gene chip microarray analysis (Continued)
Circulating monocytes in postmenopausal low *versus* high BMD women, SU150
Enamel matrix derivative gene expression in osteoblasts, SU261
Gene expression within discrete growth plate compartments, SU059
Osteoblast lineage differentiation validation by GFP marker genes, SU265
PTHrP target genes in chondrocytes using, SU040
Tbx3 mediation of growth hormone effects on bone, F160, SA160
Gene Expression Dynamics Inspector (GEDI), M230
Gene profiles, osteogenesis-related, M235
Gene therapy, M184
Genetic predisposition to disease, F375, SA375, M150, M161, M153, M503
Genetic studies, SU174
Genistein, SA208
GFP marker genes, SU265
GFP reporter imaging, SU263
Ghrelin, SU268, SA163
Giant cell tumor stromal cells, SU084
Ginsenoside Rg1, SU573
Girls. SEE ALSO *Children*
BMD loss with exercise cessation by, SU464
Bone growth in pubertal, F009, SA009
Bone mineralization and vitamin D supplementation, SU499
Bone remodeling markers in pubertal *versus* prepubertal, M131
Calcaneal QUS from age 10 to 13, M439
Calcium-fortified soy milk and BMD in Chinese adolescent, M440
COL1A2 polymorphism and skeletal growth during puberty, M168
COMT and bone growth during puberty, F139, SA139
Seasonal variation in lumbar spine, hip BMC in early-puberty, SA013
Vitamin D, calcium, cheese supplementation effects on PTH in pubertal, SU461
Gli2, 1176, M076
Gli3, M076
Glitazones, SA171
Gli transcription factors family, F044, SA044
Globin activator of transcription (GATA-1), SA556
Glucagon-like peptide-2 (GLP-2), M302, F390, SA390
Glucocorticoids. SEE ALSO *Corticosteroids; Osteoporosis, glucocorticoid-induced*
Anabolic effect of intermittent PTH, SU418
BMD and bone strength in postmenopausal women, SA379
BMD in children, M385
BMD in rheumatoid arthritis, SU541
Cortical bone and, SU417
Cost-effectiveness of bone protection, SA454
Human osteoblastic differentiation rapid assay, SA567
IL-11 gene transcription inhibition, SA569
Normal BMD and fracture incidence with chronic, SU377
Osteocalcin transcription in osteoblasts, SA564
Osteocyte death, 1074
PTH in combination with, SA436
RANKL stimulation and OPG inhibition by, M380
RANK, OPG, and RANKL regulation by, SA566
Rat osteocalcin, lumbar bone and, SU068
Sex differences in ultrasound graphic trace analysis at phalanxes and, SU420
Signaling disruption in Col2.3-HSD2 transgenic mice, 1115
Species specific differences in bone metabolism, OPG regulation, M381
Glucocorticoids. SEE ALSO *Corticosteroids; Osteoporosis, glucocorticoid-induced* (Continued)
TGF-β antagonism, M260
TRAP-11β-HSD2 deflection from osteoclasts, SU413
Glucosamine, N-butyrylated, SA065
Glucose-dependent insulinotropic peptide (GIP), M492, SA447
Glutamate receptors, M193
Glutamate signaling, SU032, 1033
γ-Glutamyl peptide, SU457
γ-Glutamyltranspeptidase, 1125, SU146
Glutathione, SU339
Glycogen synthase kinase 3 (GSK3), M031, F445, SA445
Glycogen synthase kinase 3 α/β dual inhibitor, 1218
Glycogen synthase kinase 3β (GSK-3β), 1057, M296
GNAS gene, SA126
GNAS gene mutations, M265, SU561, 1157
Gonadotropin-releasing hormone agonist (GnRHa), SU490, SU496
GPR54 gene, F394, SA394
G protein, SA151, SU566
G protein α, M265, SU561, M561
G protein-coupled receptor kinase 2 (GRK2), SU558
G protein q, M559
Graves' disease, M409
Green fluorescent protein cells, SU258, SA193, F061, SA061
Greens+ herbal preparation, M246
Growth hormone, F160, SA160, SA444, SU505
Growth hormone receptor/binding protein, SA165, SU007
Growth plate, M020, SA043, SU059, M027, M033
Growth plate chondrocytes, SU041, M018, SU563, M567, M572. SEE ALSO *Chondrocytes*
GTPase activity, SU296
Gymnastics/gymnasts, SU002, M207, SU458

H

Hairless gene product (Hr), SA551, F555, SA555
Hand, SA130, SA040
HCC1 (osteoprogenitor) cells, M268
Health care costs, F402, SA402, SU480, SA409
Health education, SU400, M327. SEE ALSO *Patient compliance*
Hearing impairment, SA461
Heart transplantation, M552, M145, M548
Heat shock factor-2, F228, SA228
Heat shock proteins, SU349, SA535
Heel, SU130, M142, SA114
Height, SU179, M175, SU459
Height loss, M108, M367, SA453, SU379, SA332, F333, SA333, SA334
HEK293S cells, SU565
Hematopoietic markers, SU084
Hematopoietic stem cells, 1116
Hemodialysis, SU025, SU531, WG13
Heparanase, 1211, SU042, M075
Heparin, SU021
Heparin binding growth factor (HBGF), SU042
Heparin sulfate proteoglycans (HSPGs), SU021
Hepatic osteodystrophy, M240
Hepatocyte growth factor, SU052
Herpes simplex virus-1, SA258
Hes-1, F230, SA230
Hesperidin, SU412
Heterogeneity index, intra-individual, SA038
High bone mass disease, F268, SA268, F468, SA468, M503, M217

Hip(s)
DXA in region of interest of femoral neck, SU109
DXA measurement discordance of spine *versus,* SU128
Geometry, medieval *versus* modern, F336, SA336
Nerve function and BMD, 1022
Safe landing during fall, SU471
Scoliosis and side-to-side BMD differences, SU232
Serotonin receptor inhibitors and bone loss, F369, SA369
Serotonin transporter intron-2 polymorphism and BMD, SA142
Hip arthroplasty, M407, M139, M502
Hip fractures
Bisphosphonates and risk of, F410, SA410
Calcium absorption and, SU140
Care profile in Italy, M339
Drug compliance after, M462
Dual femur densitometry, diagnosis and treatment, M107
DXA *versus* QUS diagnosis, M093
Elderly aged 90 years and over, SA452
Ethnicity in Hawaii, SU372
Fall index, F112, SA112
Fall-related fractures as prediction of, 1184
IGFBP-2 as catabolism marker after, M374
Increased mortality after acute, 1187
Leg length of Chinese *versus* Caucasians and, SA382
Myocardial infarction incidence/costs *versus,* SU369
Osteoporotic, sunlight, $25(OH)_2D_3$ levels and, SA338
Primary care screening in UK, SU391
Seasonal presentation of osteoporotic, SA337
Sex differences in community-dwelling patients, M347
Trends from 1990–2001 in U.S., M353
Trends in Tottori, Japan, SU375
Walking as protection against, SU005
Hip protectors, M448, SU484
Hip structural analysis, 1183, SU158
Histocompatibility leukocyte antigen (HLA)-B27 transgenic rats, M544
Histone deacetylases (HDACs), SA229, M036, SU236
Histone H4 gene, M039
HIV, SU262, SU396, M393, SA501
HMG-CoA reductase inhibitors. SEE *Statins*
Homocystine, SU425
Hormone replacement therapy
BMD response in postmenopausal women, SU181
Body composition and postmenopausal, 1154
Bone loss after cessation in postmenopausal women of, M472
Calcium-sensing receptor polymorphism and, SU166
Clodronate combination, BMD in postmenopausal women and, M411
Dietary iron and calcium influence on BMD, M438
NTx baseline measures in treatment-naïve *versus,* SU144
Phytoestrogen combination for ovariectomized rats, SU576
Raloxifene for postmenopausal osteoporosis *versus,* M473
Hoxc8, SA215
***HRPT2* gene,** SU518
***HRPT2* gene mutation,** WG8
Human T-cell lymphotropic virus type 1, WG15
Hyaluronic acid, SU191
Hybridization, in situ (ISH), SA162
Hydrogen peroxide, SA393
^{3}Hydrogen-tetracycline, SU026
Hydroxyapatite, SA305
8-Hydroxydeoxyguanosine, M401
1α-Hydroxylase, SA556, 1085, SU588
11β-Hydroxysteroid dehydrogenase, SA568
11β-Hydroxysteroid dehydrogenase type 1, SU419
25-Hydroxyvitamin D, M495
25-Hydroxyvitamin D-1-hydroxylase, SA580
1α-Hydroxyvitamin D_2, SA570
25-Hydroxyvitamin D_3, M019
Hypercalcemia, SU332, SA470, 1201, F495, SA495, WG15
Hypercalcemia, familial hypocalciuric, SA542
Hypercalcuria, idiopathic, 1077
Hypercalcuria, severe absorptive, M507
Hyperostosis, autosomal dominant infantile cortical, 1102
Hyperparathyroidism, SU532, M060, 1165, SA530, SU545, SU511, SU534
Hyperparathyroidism, familial isolated, WG8
Hyperparathyroidism, neonatal severe, SA542
Hyperparathyroidism, primary
Apoptosis of osteoblasts with preserved cancellous bone in, SA496
Asymptomatic, bone geometry, bone strength and, SA492
Body weight and, SA490
Bone markers, BMD changes after parathyroidectomy in, SU508
Calcium regulation of plasma FGF23 in, SU517
Cinacalcet HCl and PTH secretion in, SA548
Elderly women and, F489, SA489
FGF23, PTH, and $1\alpha,25(OH)_2D$ in surgically-treated, SA488
HRPT2 gene alterations in, SU518
Osteitis fibrosa cystica and, WG14
Parathyroidectomy and BMD of postmenopausal women with asymptomatic, SU515
Premenopausal women and, SU516
PTH and *in vivo* FGF23 expression in bone, SA153
PTH secretion after parathyroidectomy, SU519
Vitamin D replacement with vitamin D deficiency, SU509
Hyperparathyroidism, secondary, SA368, SA476, SU530, F477, SA477, SA494, SU536
Hyperphosphatasia, M522
Hyperphosphatemia, SU194
Hyperthyroidism, M170
Hypocalcemia, bisphosphonate-induced, WG25
Hypocalcemia, severe, M517
Hypogonadism, M552, SU486
Hypomineralization, M368, M391
Hypophosphatasia, SA463, WG7. SEE ALSO *Paget's disease*
Hypophosphatemia, X-linked, M502
Hypopituitarism, SA444
Hypovitaminosis D, 1186, SU363
Hypoxia, SA227, M254, SU349, F047, SA047, F168, SA168
Hypoxia-inducible-factor 1 (HIF-1), M032, F272, SA272
Hypoxia-inducible-factor 1α (HIF1α), F072, SA072, 1054, SA062, SA575

I

Ibandronate
Administration and dosage, F408, SA408, M429, M432
BMD change and fracture risk, SU441, M433
Bone resorption in postmenopausal osteoporosis, F406, SA406
Combination therapy with calcitriol after liver transplantation, M545
Duration of action after single dose, SU432
Femoral head deformity, SU521
Localized transient osteoporosis and, M509
Id1, F212, SA212
IκB kinase a, 1027
IKK complex, F313, SA313
Ile-Pro-Pro (IPP), M225
Iliac crest biopsies, M364, M403
Immediate early genes, SU341, SA522
Immunity, T-cell-mediated, SU309
Immunoglobulin-like domain, SU055
Immunoreceptor tyrosine-based activation motif (ITAM), F297**,** SA297
Immunosuppression, M382
Importin 4, F553, SA553
Indian hedgehog, SU051, M028, SU039, F051, SA051, 1060
Inducible cAMP early repressor (ICER), M259, 1061
Infants, newborn, SA059, SA004
Infants, newborn, preterm, M529
Inflammation, M543, SU430, M540, SU075, M528. SEE ALSO *Arthritis; Arthritis, inflammatory*
Inflammatory bowel disease, M512, SA387, SU525, SU529
Infliximab, SU428, SU542
Infrared spectroscopy, Fourier-transformed, SU030
Inhibin, SU495
Inositol 1,4,5-triphosphate (IP3), M567
Insulin-like growth factors, SA188
Insulin-like growth factor I (IGF-I)
Aging and, SA019
Androgen receptor and gene expression by, M573
BMD after allogenic stem cell transplantation, M147
BMD and genetic variation in, M178
Bone loss in cystic fibrosis, SU421
Cre-driven targeted disruption in mature osteoblasts of, SA166
Fluid shear stress, osteoblast proliferation and, SA263
Gene expression localization in rat tibiae, SA162
Liver-derived, ovariectomy-induced bone loss and, 1168
Liver synthesis of, estradiol and, 1167
Low BMD in young adults with simple sequence repeat in, SU178
Mineralization during fetal development, SU028
OP-1 gene enhanced osteoblastic cell differentiation, SA025
Osteoblast differentiation, body and marrow adiposity, 1080
Resistance induced by skeletal unloading, F178, SA178
Resistance training in older adults, M450
Rest-inserted loading and bone formation, bone mass in aged, 1146
Insulin-like growth factor II (IGF-II), SA159, M174
Insulin-like growth factor binding protein 2 (IGFBP-2), SA164, SA161, M374
Insulin-like growth factor binding protein 5 (IGFBP-5), 1181, SA273
Insulin-like growth factor binding protein 5 interacting protein (IGFBP5-IP), SA158
Insulin-like growth factor II (IGF-II), F194**,** SA194
Insulin-like growth factor I receptor, M275, SA019, F531, SA531, SA263
Insulin receptor substrate-1 (IRS-1), SA430
$\alpha_9\beta_1$-Integrin, SA281
$\alpha_v\beta_3$-Integrin, SA279, SA284, SA321, SU207, F090, SA090
β_3-Integrin, F304, SA304
Integrins, SU350, F077, SA077, M042, F178, SA178
Interferon γ, SU298, SU302, SU013
Interleukin-1, M274, SU094

Interleukin-1β, SA544
Interleukin-1β C/T polymorphism, M167
Interleukin-1 gene cluster, M158
Interleukin-1 receptor agonist, M171
Interleukin-3, SA079
Interleukin-6, SU240, SU250, 1138, SU550, M471
Interleukin-7, M276, 1116, M397
Interleukin-11, SA569
Interleukin-12, M271
Intervertebral discs, SA055, SU045, M059
Intramedullary pressure fluid flow, M219
Intranuclear informatics, SA217
Iron, dietary, M438
Ischemia and perfusion injury, SA073
Isoflavones. SEE *Soy isoflavones*
Isoproterenol, 1008
Italy/Italians, M339, M323

J

Jagged1, M266
Joint prosthesis, SA033. SEE ALSO *Hip arthroplasty*
JunD, M227

K

K16 (tannin compound), M291
Karyopherins, M554
Kidney, SA577, M135. SEE ALSO *Opossum kidney cells*
Kidney disease, end-stage, SU545, WG13
Kidney failure, SA509, M532, M533, F507, SA507, M531
Kidney failure, chronic (animal models), SA506, SA508, SA480
Kidney insufficiency, SU532, M536
Kidney-pancreas transplantation, M553
Kidney stones, M506
Kidney transplantation
- Bisphosphonates and bone status, M549
- BMD and urinary calcium excretion, M550
- Bone-protective therapy, M553
- Bone quality and fractures or osteonecrosis, M535
- Fracture risk in men, M534
- Immunosuppressive therapy and BMD, M546
- Secondary hyperparathyroidism, SU536

Klotho proteins, SA020
Knee arthroplasty, M139, M502
Knee osteoarthritis, SU357, F335, SA335, M542
Knees, SU022
Knock-in mice, SA538, SU578
Knockout mice
- β-Adrenergic receptor, 1122, 1121
- N-Cadherin, F248, SA248
- Caf1, F056, SA056
- Cathepsin K, 1082
- *Chop,* 1164
- COX-2, SA505
- ERα, M565
- ERα male, 1118
- Growth hormone receptor/binding protein, SU007
- Heat shock factor-2, F228, SA228
- HIF-1α in osteoblasts, 1054
- Lrp5, 1149
- NOS-1α, 1036
- *Ocil,* 1025
- Oc/oc, M310
- OPG, SU304
- *Op/opfit-ITK,* F287, SA287
- Orphan seven-transmembrane receptor expressed in osteoclasts, SU316
- Osteoclast-specific androgen receptor, 1006
- $P2X_7$, M197
- Pax5, M280

Knockout mice (Continued)
- Periostin, 1076
- PERK, SA059
- PTH and 1α-OHlase, F537, SA537
- *PTHrP,* F433, SA433
- Pyk2, F311, SA311
- Rachitic, M027
- *Runx*2-II, F220, SA220
- Seven in absentia homolog proteins, F266, SA266
- Sox8, 1140
- *Thbs3,* SU069
- TRAP, M242
- Twist-1 (Charlie Chaplin), 1209

KO240 (vitamin D receptor) cells, SA554
Kremen proteins, F270, SA270
KS483 cells, SU249
Kudzu, SA016
Kyphoplasty, M508, M459, M468B, SU478, SA351, SU379. SEE ALSO *Vertebroplasty*
Kyphosis, SU401, WG5

L

Labyrinthectomy, 1155
Lactase-phlorizin hydrolase gene, M175
Lactation, SA518, SA524, 1163, SU398, SU397, M446
Lactoferrin, SU284
Lactose, SU408
Lactose intolerance, M175
Lanthanum carbonate, F507, SA507, SA506
Laser ablation inductively-coupled plasma mass, SA033
Lasofoxifene, M469, F424, SA424, SA423, SU487, F426, SA426
Latin America, vertebral fractures prevalence in, F340, SA340
Lef1, SU253
Legg-Perthes disease (animal model), SU521
Leptin
- BMD after allogenic stem cell transplantation, M147
- BMD in baboons and circulating, SA134
- Calcium carbonate supplementation in Gambian pubertal girls, M442
- Food restriction, unloading in cancellous bone histomorphometry, M377
- Fracture risk in elderly, 1021
- Lumbar spine BMD in middle-aged men, M390
- Neuropeptide Y Y1 receptor deletion, 1123
- Neuropeptide Y Y4 receptor, 1101
- Osteoarthritis, SA252
- Osteogenesis *versus* adipogenesis, F275, SA275

Leptin receptors, SA239
Leukemia, acute lymphoblastic, SU083
Leukemia inhibitory factor (LIF), M190
Leukemia/lymphoma, adult T-cell, WG15
LIGHT (TNFSF14), 1030
Limb fracture, 1111
Limbs, lower, 1190, SA325, SU162, M419, SU467, F421, SA421
LIMD1, F486**,** SA486
Lining cells, F527, SA527
Lipodystrophy, SU396
α-Lipoic acid, M282
Lipopolysaccharides, M304
Lipoprotein-related protein-1 (LRP1), M067
Lipoprotein-related protein-5 (LRP5)
- BMD in Chinese and genetic polymorphisms of, M177
- Bone anabolic effects of PTH, F525, SA525
- Bone density, limb deformities and mutations in, 1214
- Dkk-1 inhibition of signaling by, SU351
- Ethnic differences with amino acid substitutions, M180
- Genetic polymorphisms predict bone mass, fractures in elderly women, M169

Lipoprotein-related protein-5 (LRP5) (Continued)
- High bone mass disease, F468, SA468
- Mechanotransduction pathways, 1149
- Mutation analysis in idiopathic male osteoporosis, SU175
- Osteoporosis-pseudoglioma and compound heterozygous mutations, SA125, SA465
- Physical activity, BMD and polymorphisms of, F136, SA136
- PTH stimulation of bone formation in mice, 1064
- Single nucleotide polymorphisms, BMD of adult women, SU173
- Wnt signaling and bone mass accrual, 1001
- Wnt signaling and OPPG-causing missense mutations, F268, SA268

Lipoprotein-related protein-5/6 (LRP5/6), F262**,** SA262, F270, SA270
Lipoprotein-related protein-6 (LRP6), 1214
Liquid chromatography-mass spectrometry, SU585
Liver, SU025
Liver cirrhosis, biliary, SU422, M551
Liver transplantation, M547, M545, M145
Loading. SEE ALSO *Exercise; Pressure, hydrostatic; Stress, mechanical*
- Aging and bone adaptation, M192
- Aging and skeletal sensitivity, SU222
- Bio-imaging of intracellular NO in single cells, SU210
- BMD *in vivo* response, SU212
- DMP1 and MEPE expression in osteocytes, 1105
- DMP-1/MEPE gene expression, F182, SA182
- DMP-1 role in osteocyte function, 1004
- E11/gp38 and *in vitro, in vivo,* F173, SA173
- Estrogen and sensitivity of bones, F187, SA187
- Ex-vivo bioreactor bone organ culture chamber, SU081
- ^{18}Fluoride ion imaging of fatigue, 1150
- Genetic-environmental adaptations, SU213
- IGF, ER-α expression in ovariectomized rat tibia, SA188
- Inbred mouse strains with various skeletal adaptations, M215
- Mechanical properties and bending direction, SA035
- Microgravity and external, M451
- Murine high bone mass model and ulna response, M217
- NASA rat studies, SA186
- Osteoblastic memory, 1033
- Osteogenic response to isometric, SA192
- Oxygen tension and inflammation in articular cartilage, SU075
- $P2X_7$ nucleotide receptor and osteogenesis, 1032
- Pressure modulation of trabecular bone, SA183
- Rest inserted, genetically-engineered mice response, WG27
- Rest inserted, IGF-1 supplementation, 1146
- Rest inserted, osteoblast increases from *in vitro,* SA181
- Rest inserted, real-time signaling model in osteocytic networks, SU211
- SAMP6 mouse marrow and bone response, M208
- Sciatic denervation and bone formation, 1148
- Sex differences in long bone fatigue rat model, SU076
- Thoracic vertebrae failure prediction, M106
- *In vivo* axial model of murine tibia, SU225
- Wnt signaling, 1014
- Zetos organ culture model, SU074

Long-term potentiation mechanisms, 1033
Lumbar spine, SU068, SU357, SU135, M369
Lumbar spine fusion (animal model), SU015
Lunar Prodigy densitometers, M104, M103, M105, M114, SU127, M117, M445

Lung cancer, SA082
Lung cancer cells, SA571
Lupus erythematosus, systemic, SA516, SA514, SA515
Lymphatic flow, SU467
Lymphocytes, SU114
Lysophosphatidic acid (LPA), 1207, 1092
Lysyl hydroxylase, SU141
Lysyl oxylase, 1200

M

Macrophage-colony stimulating factor (M-CSF), SU540, M317, F285, SA285, F287, SA287
Macrophage inflammatory protein (MIP)-1α (MIP-1α), M072
Macrophage migration inhibitory factor (MIF) gene promoter region polymorphism, SA135
Macrophages, SA300
Magnesium, dietary, M046, SU365
Magnetic resonance imaging, SU102, SU228
Magnetic resonance imaging, high-resolution, M119, SU129, SA114
Malnutrition, M101
Mammalian target of rapamycin (mTOR), 1194
Mammography, SU355
Mandible, SU141, SU165, M205, SU092
MAP kinase pathway, 1210, SA271, 1175, SU559, SU526. SEE ALSO *specific types*
Marfan syndrome, M499
Marrow-isolated adult multilineage inducible (MIAMI) cells, M269
Maspin, M065
Mathematical models, M241, M121, SU026
Matrix extracellular phosphoglycoprotein (MEPE), F479, SA479, 1161, WG18. SEE ALSO *Dentin matrix protein-1/matrix extracellular phosphoglycoprotein*
Matrix extracellular phosphoglycoprotein (MEPE)/osteoblast/osteocyte factor 45 (OF45), SU190
Matrix gla protein (MGP), SU546
Matrix metalloproteinase 1, M569
Matrix metalloproteinase 9, SA286, 1196. SEE ALSO *Gelatinases*
Matrix metalloproteinase-13, M247, SU246, M063, F063, SA063, M067, SU047, SA177
Matrix metalloproteinases, M062
Maxilla, SU092
MC3T3 cells, SU280, M220, SA176
MC3T3-E1 cells
- Adiponectin and proliferation of, M187
- Cannabinoid receptor 2 stimulation, M166
- Differentiation by FGF2/FGFR2 signaling, SU192
- 1,25 $(OH)_2D_3$ and Wnt signaling, SU276
- Ectopic overexpression of adipogenic factors induced transdifferentiation, M234
- FGF2 gene and protein expression, SU199
- Heparanase and, 1211
- Mechanoresponsiveness and P2Y2 expression, SU217
- MMP-13 induction by fluid shear stress, SA177
- NFAT negative regulation, 1140
- Osteoactivin overexpression and, SU053
- Proliferation and differentiation in low passage, SA237
- PTH and differentiation, SA255
- Wnt signaling and survival of, M221

MC-33 (zinc-finger containing protein), 1142
MCF-7 (human breast cancer) cells, SU573, M084
MDA-MB-231 (breast cancer) cells, SU095, SA079, 1095
Mdm2 oncogene, 1015
Measles virus nucleocapsid protein (MVNP), 1010, 1159
Mechanical homeostasis, F017, SA017
Mechanical response tissue analysis, M126
Mechanical signals, low-level, high-frequency, M452
Mechanical strain. SEE *Stress, mechanical*
Mechanotransduction, SU224
Megakaryocytes, SA294
Megalin, SA541, SA478
Megestrol acetate, SU416
MEIS2 transcription factors, SU204
MEK simulated phosphorylation, 1210
Melanocortin receptor, SU282
Melanoma cells, SA080
Melatonin, SU345
Men. SEE ALSO *Osteoporosis, male; Sex differences*
- Alendronate in solid organ transplantation recipients, SA405
- Amino acid substitutions in LRP5, ethnicity and, M180
- Androgen receptor polymorphisms and BMD or physical function, M160
- Aromatase CYP19 genetic polymorphism, adult stature, BMD, and androgens in young, M163
- Beer intake and BMD, F330, SA330
- BMD in Asian, SU115
- Bone size, strength and long-term impact sports participation, M210
- Calcaneal ultrasound, non-spinal fracture prediction, M344
- Circadian rhythm and BMD, F364, SA364
- COMT val158met polymorphism and BMD in young, SA140
- Densitometric vertebral fracture assessment, F106, SA106
- DXA of radius *versus* total forearm, SU125
- Falls by older diabetic, SA355
- Femoral neck geometry in Caribbean, SA359
- Fracture prediction with DXA and QCT at hip and spine, 1067
- Fracture risk after kidney transplantation in, M534
- Genome screen for femoral structure QTLs, M156
- High-dose steroid therapy and BMD, SA322
- Leptin, resistin and lumbar spine BMD in middle-aged, M390
- Low-impact fracture risks with ankylosing spondylitis, SA361
- Neuromuscular performance and regional BMD in older U.S., SU226
- OPG polymorphism, sRANKL, sOPG, and bone metabolism, M394
- Osteoporosis screening by age group, M113
- Osteoporosis self-assessment tool, SU482
- Peak bone mass, M004
- Quantitative calcaneal ultrasound for fractures, M143
- QUS prediction of hip and non-spine fractures, 1023
- Racial/ethnic differences in BMD, SA363
- Selective serotonin reuptake inhibitors and lower BMD, 1024
- Serum estradiol levels and skeletal size, mineralization, M389
- Sex steroids and BMD, 1058
- Sex steroids and vBMD/structural parameters, F356, SA356
- Sex steroids, weight loss, and hip bone loss in older, F358, SA358
- Silent osteoporosis in veterans, SA365
- Vitamin D insufficiency, SA326
- Volumetric BMD/bone size and estradiol/testosterone levels, 1152

Menaquinone-4 (MK-4), SA449
Menatetrenone (MK4), M489
Menin, M227
Menopause, M366. SEE ALSO *Perimenopause; Postmenopausal women; Premenopause*
Meox2, SU506
Mesenchymal stem cells. SEE ALSO *Stem cells*
- Bone-marrow-derived, adipogenic and osteogenic differentiation from, SA236
- CTGF and TGF-β-induced condensation of, SU206
- ELR^+ CXC chemokines in human, SA145
- Enrichment and characterization from rat bone marrow stroma of, SU269
- Human embryonic stem cells, bone formation by, F246, SA246
- Mechanosensitivity of human, SU214
- Msx2, paracrine Wnt-Dkk signals and, 1141
- Neurexin 3β gene expression in, SU264
- Regeneration of rat mandible marrow, SA071
- Self-renewal in senescence-associated bone loss, SU004
- T cells and differentiation of, SU267

Mesenchymal stem cells, human, M184, SA239
Mesenchymal stem cells, murine, M245, SU259
Metabolic syndrome with chronic kidney disease, M537
Metals, trace, SU025
Methadone, SU424
2-Methoyxestradiol, M069
7α-Methyl-19-nortestosterone (MENT), M563
2-Methylene-19-nor-(20S)-bishomopregnacalciferol (2MbisP), M584
Metolazone, M270
MG-63 cells (osteoblastic cells), SA539, SA208, M224, SU282, SU291, M040
MHC class II transactivator (CIITA). SEE *CIITA*
MIAMI (marrow-isolated adult multilineage inducible) cells, M269
Microarray analysis. SEE *Gene chip microarray analysis*
Microcracks, SU027
Microgravity, M456, SU073, M451, F272, SA272, M201. SEE ALSO *Bed rest studies; Spaceflight; Unloading*
Microphthalmia transcription factor (Mitf), M292, SU329
Microscopy, laser confocal, SU331
Milk, dietary, M356
Mineralization. SEE *Bone mineralization*
Minodronic acid, M047, M308
MLO-Y4 cells, SU350
MNAR (scaffolding protein), F573, SA573
Monoclonal-antibody-based immunofluorometric assay, SU549
Monoclonal gammopathy of undetermined significance, SU088
Morquio A disease, SU064
Mortality, 1187, SA353, 1112
MPC32F cells, SU264
MRL123, F450, SA450
MRL mouse, M043, M056
MRL/MpJ and SJL mice, F2 population of, M152
mSin3a, SA229
Msx2, 1120, 1141, SA240, SU248, 1097
Msx2-interacting-nuclear-matrix-target (MINT) protein, F232, SA232
Multiple myeloma, 1011, SA079, 1091, SU088. SEE ALSO *Myeloma cells*
Multiple sclerosis, M539, SU142
Muramyl dipeptide, M285
Muscle paralysis, M209
Muscle performance, SU226, WG2
Muscle strength, M321, SU121, SU470
Muscular dystrophy, Duchenne, M521, M525
MyD88, M286
Myeloid blasts, SU319
Myeloma cells, F081, SA081, M072, M073, SU087
Myocardial infarction, acute, SU369
Myofibroblasts, SU281
Myostatin (GDF8), M203

N

αNAC coactivator, SA213
Nacre, SA296
Nano-computed tomography scanner, SU027
Nano-fibrous scaffolds, SU029
Nanonindentation measures, SU077, F063, SA063
National Health and Examination Survey (NHANES), SU118
Natriuretic peptide, plasma amino-terminal pro C-type, M020
Natriuretic system, 1075
NE10790, SU087
Near-infrared fluorescence imaging (NIRF), quantitative, 1069
***Nell-1*,** F070, SA070
NEMO-binding domain peptide, F313, SA313
Neonates. SEE *Infants, newborn*
Neridronate, SU442
Nerve function, 1022
Neurexin 3β, SU264
Neuroendocrine carcinoma of pancreas, WG22
Neurologically active medications, F367, SA367
Neuropeptide Y (NPY) Y1 receptor, 1123
Neuropeptide Y (NPY) Y4 receptor, 1101
Neurospecific enolase (NSE) promoter, 1138
Nicotine, SU279. SEE ALSO *Smoking*
NIK, 1028
Nitric oxide, M303, SU210, SA526
Nitric oxide synthase, SA235, M198
Nitric oxide synthase-1α, 1036
Nitric oxide synthase, inducible, M055, F272, SA272
NK cells, M299
Nkx3.2 (homeodomain protein), 1129
Nkx3.2/Bapx1, 1128
Noggin, SU020, F084, SA084, F085, SA085
Nonsteroidal anti-inflammatory drugs (NSAIDs), SA401, SA473
Noonan syndrome, SU526
Notch 1, SU065
Notch2 receptor, SU293
Notch intracellular domain (NotchIC), F244, SA244
Notch signaling, SU271, SU294
Nox4, SA314
NPS-568, SA265
Nuclear factor activated T cells (NFAT), 1140
Nuclear factor activated T cells 1/nuclear factor activated T cells c2 (NFAT1/NFATc2), 1026
Nuclear factor activated T cells 2 (NFAT2), F295, SA295
Nuclear factor activated T cells c1 (NFATc1), 1027, 1003
Nuclear factor-κ B (NF-κB), F318**,** SA318, 1028, F293, SA293, 1003, SU018, SU100
Nuclear receptor coactivator-3 alleles, M181
Nucleoside triphosphate pyrophosphohydrolase (NPP1), F039, SA039
Nucleotide-bisphosphonates, F095**,** SA095
Nurr1, SU254
Nurse-like cells, SU540
Nursing home residents, SU371
Nutrition. SEE *Diet*

O

OB-6 cells (osteoblasts), M221
Obesity, M368, M376, SU580, M542. SEE ALSO *Body fat; Weight loss*
Odontoblasts, 1177
Odontoclasts, M301, SU306
Onions, SU457
Opossum kidney cells, SA520
ORACLE (osteoporosis assessment tool), F341**,** SA341
Orbital shaking, planar, M214
Orchidectomy (animal models), M564, M481, SU495, M444, SA064, M470
Organ culture model (Zetos), SU074
Organ transplantation, SA405
Orthopedic surgeons, M461
Orthosilicic acid, M441
Oscillatory fluid flow, SA174, SU214, SU217. SEE ALSO *Fluid shear stress*
Ossification, SA473, SU504
OST-4510, SU300
Osteitis fibrosa cystica, WG14
Osteitis fibrosa, PTH-induced, 1200
Osteoactivin, SU053, SA078
***Osteoactivin/Gpnmb* gene,** 1016
Osteoarthritis. SEE ALSO *Arthritis; Knee osteoarthritis*
- Age relationship to medial minimum joint space width in knees, SU022
- Alendronate and osteonecrosis of femoral head, SU503
- Calcitonin and acute cruciate ligament deficiency, M048
- Cartilage-specific overexpression of Smurf2, 1040
- Chondrocyte CASR and PTHrP up-regulation, SA549
- COX-2 inhibitor and anterior-cruciate-ligament transection model, SA046
- Galectin-2 and, SA041
- Growth factors and collagen cleavage of cartilage, M023
- Leptin and cartilage degradation, SA252
- Quality of life, SA350
- Runx2 effects under mechanical stress, 1012

Osteoblast-derived lectin (OCIL), SU317
Osteoblastogenesis
- *BMP2* and *BMP4* for, 1037
- Glitazones and, SA171
- GSK3 and, M031
- Knockdown of chordin by siRNA and, M249
- PKIγ regulation of, M256
- TGF-β signaling and, SU201
- Twisted gastrulation and, F024, SA024

Osteoblast proteome, M251, M053, SA225
Osteoblasts. SEE ALSO *C2C12 cells; MG-63 cells; OB-6 cells; SaOS-2 cells; UMR-106 cells*
- Apoptosis evaluation in high aspect ratio vessel vector-averaged gravity system, M201
- Apoptosis in primary hyperparathyroidism, SA496
- BCSP-1 and collagen type 1 expression, SU061
- Bisphosphonates and differential *in vitro* survival, M255
- Breast cancer bone metastasis, SU092
- *CYP19* gene regulation, SU241
- $1\alpha,25(OH)_2D_3$-sensitive chloride channels, M578
- Estren, 1119
- Estrogen-deficiency bone loss and CSF-1, SA209
- Fluid flow-induced signals by osteocytes, 1031
- Gene expression regulated by physical contact of prostate cancer cells, SU101
- GSK3 α/β dual inhibitor and differentiation, 1218
- IGF-1, 1080
- IGFBP5-IP, SA158
- Inducible cAMP early repressor, M259
- Integrin ligands and focal adhesion assembly, signaling, F077, SA077
- Multiple myeloma cells, F081, SA081
- Notch 1 and aberrant maturation in osteonectin-null, SU065
- PTH anabolic actions, 1062
- PTH and cell cycle progression from G1 to S phase of, F521, SA521
- Tartrate resistant acid phosphatase, SA198
- Valproic acid inhibition, M405
- Vitamin D metabolism, SA587
- Vitamin D receptor, 1099

Osteocalcin
- Adrenalectomy and glucocorticoid replacement, SU068
- ATF4 mediation of PTH-dependent gene expression, SU243
- BMD and urine NTx ratio, M133
- Gene expression and SWI/SNF chromatin remodeling, SU252
- Glucocorticoids and transcription in osteoblasts of, SA564
- αNAC coactivating function, SA213
- Serum assay by Elecsys 2010, SU148
- Serum Gla type and glucocorticoid-induced osteoporosis, SA120
- TRAP and *in vitro* expression in cementoblasts, SU054
- Urinary, as bone metabolism marker, SU143

Osteocalcin-GFPtpz, SU258
Osteocalcin promoter, SU552
Osteoclast-associated receptor (OSCAR), SU318, M172
Osteoclast-derived factor (ODOF), 1143
Osteoclast inhibitory lectin (OCIL), 1025
Osteoclast inhibitory peptide 1 (OIP-1) gene expression, F306, SA306
Osteoclast-like cells, M311
Osteoclastogenesis
- Ascorbate and, M288
- Bisphosphonates and gene transcription, M408
- Bone matrix role, SU328
- Calcineurin and, F316, SA316
- Caspase 3 and, SU327
- CD44, presenilins and stimulation of, F299, SA299
- Creatine kinase brain isoform expression, SU320, SU321
- FHL2 suppression of TRAF6-mediated, 1029
- Fluorescent activated cell sorting for *in vitro* analysis, M287
- Gene expression analysis, M297
- γ-Glutamyltranspeptidase and, 1125
- GSK-3β and, M296
- Human umbilical cord cells, SU325
- Immunoreceptor tyrosine-based activation motif, F297, SA297
- α-Lipoic acid suppression, M282
- Marrow stromal cells in TNF-α-induced, SA289
- Mitf and, SU329
- Muramyl dipeptide enhancement, M285
- Myeloid lineage mouse bone marrow cells, SU319
- Nacre water soluble matrix and cell culture models, SA296
- Paget's disease, 1159
- Phytoestrogens and, SU572
- RANK cytoplasmic motifs, F301, SA301
- RANK dimerization, SU315
- Resistin and, M298
- Smoking and, SU342, SU326
- Spontaneous, in postmenopausal osteoporosis, SU312
- Spontaneous, in solid tumors with bone involvement, M289
- STAT6 inhibition of JNK-mediated, SA312
- TIEG expression, 1197
- Time point for TGF-β lineage diversion, SA167
- TNF-α-induced, IL-1 and, M274
- TREM2 and DAP12, 1195

Osteoclast precursors, SU323, F320, SA320, F253, SA253, SA303, 1204
Osteoclasts
- Acidic microenvironment in cancer-induced bone pain, M068
- Adhesion and apoptosis regulation by 17β-estradiol, M568
- Androgens in AR-transgenic mice, M584
- Apoptosis, human model of, SU305
- Bone formation and, SU303
- Bortezomib and, SU337

Osteoclasts (Continued)
Chloride channels in, M306
IGF-IR and, M275
Large *versus* small, mechanistic differences in, SU333
Microtubule maturation and podosome organization, SA282
Multiple nuclei, SU322
Oral squamous cell carcinoma and differentiation by, SU086
Orphan seven-transmembrane receptor, SU316
Osteogenesis imperfecta morphology, SU527
PTH1R expression by, SA317
Renal cell carcinoma metastasis, 1096
Sympathetic nervous system and unloading effects, F191, SA191
TRAP-5b secretion from, M305
Valproic acid inhibition, M405
In vitro activity *versus* formation in multiple myeloma cells of, M073
In vitro antiresorptive agents testing on human, SA307
Osteocrin, 1075
Osteocytes
Apoptosis preceding bone resorption in murine unloading model, SA172
Bone matrix strain in cortical bone at lacunae, F175, SA175
Death in young bone of black *versus* white women, SU347
DMP-1 dual role, 1004
DMP-1 gene expression and mechanical signals, 1035
Fluid flow-induced signals to osteoblasts, 1031
Glucocorticoid-induced changes around lacunae of, M379
Glucocorticoids and cell detachment-induced apoptosis, 1074
Integrin signaling and mechanosensing stretch-activated cation channels, SU207
Lacunar wall permeability after ischemia and perfusion injury, SA073
Mechanically-induced signaling, SU237
Nano-computed tomography scans, SU027
Osteoblasts in hyperparathyroidism and, 1165
Rest-inserted loading and real-time signaling model, SU211
TRAIL regulation, SU277
Osteogenesis imperfecta
Adult and BMD response to pamidronate, M426
Alendronate for, 1043
Alendronate *versus* pamidronate for, F466, SA466
Increased early resorption in, SU527
Musculoskeletal manifestations in adults, M501
Osteopotentia gene and, 1077
Pamidronate for, F462, SA462, M500, M504
Viability of Brtl mice with G349C mutation, 1205
Osteogenic growth peptide (10-14), M253
Osteogenic protein-1 (OP-1), SU444, SA025
Osteolysis, SU340
Osteolysis, idiopathic multicentric, M153
Osteomalacia, SA368, SA480, WG19
Osteomalacia, tumor-induced, F479, SA479
Osteonecrosis of femoral head, SU503, SU528
Osteonectin, SU093
Osteons, SU277, M051, SU079
Osteopenia
Cbl proteins and, 1198
Diabetes mellitus type II mouse model, SU429
Enzyme replacement therapy for Gaucher's disease, M101
Estrogen signaling loss through classical ERE pathways, SU568
Fracture burden for women, SU378
Histomorphometric analysis of risedronate, M382
Indian hedgehog mutation, 1060
Inflammatory bowel disease, M512
Osteopenia (Continued)
Mechanoreactivity in LRP5-mutant mice and site-specific, 1149
OSCAR polymorphisms, M172
Postmenopausal women without prior fracture, cost-effectiveness of drug therapy for, F402, SA402
Screening and characterization in middle-aged women, SU001
Vitamin K supplementation in postmenopausal women, M443
Osteopenia, glucocorticoid-induced, SU414. SEE ALSO *Glucocorticoids; Osteoporosis, glucocorticoid-induced*
Osteopetrosis, F311, SA311, M310, M505
Osteopetrosis, autosomal dominant type II, M179, SA467
Osteopontin, SU054, SA050, SU066, SU405, SA221, SU494, M514
Osteoporosis. SEE ALSO *Osteoporosis self-assessment tool; specific types*
Alkaline phosphatase polymorphisms, M165
Androgens and corticosteroid-induced, SA206
Arthritis in women and screening, diagnosis, and treatment for, M322
Assessment method comparisons, SA378
BMD and education for lifestyle changes with, M327
BMD in daughters of women with, SU157
BMD reference database for Indian women, WG17
BMD testing effects on pharmacotherapy initiation for, SU483
Bone histomorphometry for children with, M530
Bone microstructure monitoring and predicting in, SU133
Burden and management in Manitoba of, M340
Calcium, vitamin D supplementation and vascular calcification in, M333
Canadian family physicians diagnosis and therapy, M406
Cannabinoid receptor 2 and, M166
Cardiovascular disease risk factors in women, SU033
Chinese American bone densitometry database, SU108
Chronic medical conditions *versus,* SA455
Daily nasal spray of hPTH(1-34) and bone mass in, 1171
Decision rules for low BMD assessment, M358
Detection, treatment strategies in elderly U.S. women, M102
Education program for treatment compliance, SU479
Familial aggregation of BMD, SU160
First events *versus* multiple outcomes analysis, M458
Follow-up after hip fracture, M462
Follow-up after treatment research trials, M457
Fragility fractures and diagnosis, treatment, M464
Ghrelin levels, SA163
High risk women for primary fracture prevention, M348
Japanese prevalence, M111
Kyphosis and proprioceptive dynamic posture training, WG5
Localized transient, intravenous ibandronate for, M509
Megestrol acetate and, SU416
Melatonin dual action signaling, SU345
Multifaceted post-fracture care model, SU476
National awareness campaign, SU400
NHANES standard deviation recalculation and prevalence of, SU118
Non-replication in genetic studies of complex diseases and, SU174
OPG and RANKL serum levels, M402
OSCAR polymorphisms, M172
Osteoporosis. SEE ALSO *Osteoporosis self-assessment tool; specific types* (Continued)
Peripheral fractures, in France, SU370
Predictors in young women, M359
Primary care physician practice profiles, M354
QUALEFFO assessment tool, WG1
Raloxifene and short-term hormonal profile, OPG-RANKL system in, 1104
Risk factors and BMD testing in young menopausal women, M366
Routine population-based screening of Canadians, M109
Secondary cause incidences in men and women, WG12
Secondary causes in older men and women, 1185
Secondary, juvenile idiopathic arthritis and, SU537
Secondary, patient selection for rPTH therapy and, M487
Secondary, severity in children, SU522
Secondary, vertebral fracture threshold in, M091
Severity of vertebral, quality of life and, M050
Smoking among Iranian Australian women and risk of, M363
Transiliac bone biopsy, SA111
Treatment after secondary cause identification, WG12
Treatment initiation after diagnosis of, M468
Treatment reinforcement using bone remodeling marker data, M420
Underdiagnosis, undertreatment in Denmark, M340
Virtual simulation and finite element analysis, SU080
Vitamin D insufficiency and, SU582
Vitamin D insufficiency in N. American women treated for, SU583
Osteoporosis (animal models). SEE ALSO *Ovariectomy*
^{41}Calcium assay, SU145
Calcium, isoflavone and/or estradiol supplementation, SU453
Dkk-1 overexpression, 1017
Gene profiles fo, M235
Immobilization and impaired sensory neurohumoral signaling, M396
Pleurotus eryngii extracts and, SA443
SARMs and bone remodeling, 1216
Transgenic dwarf rat strain, SA014
Osteoporosis, glucocorticoid-induced
Alendronate effect on spine, M129
Alendronate *versus* alfacalcidol for prevention of, M415
Bone strength in mouse, SU415
Dkk1 expression in osteoblasts, F565, SA565
GlaOC, OPG, urinary NTx as markers in, SA120
Prevention trends over time, M465
PTH(1-34) and serum FGF2 levels, M480
Screening and treatment, 1114
Vertebral, cortical bone and, M384
Osteoporosis, male. SEE ALSO *Men; Orchidectomy*
Absence of treatment for men with fractures, 1113
Age factors in screening for, M113
Alendronate therapy in murine model, M427
Androgen receptor CAG repeat polymorphism, M155
BMD heritability in idiopathic, SA129
BMD with vertebral fractures, SU123
Bone resorption and, 129
Diagnostic tools evaluation for elderly Caucasian and Chinese, SU394
Dried plum prevention of bone loss, M447
Hip/spine BMD and fracture prediction, 1009
Hypomineralization and fragility fractures, M391
Illness representations, SU389

Osteoporosis, male. SEE ALSO *Men; Orchidectomy* (Continued)
LRP5 mutation analysis in idiopathic, SU175
Osteoporosis self-assessment tool, SU482
Prostate cancer and, M080
PTH, alendronate or combination and bone turnover, 1172
Risedronate and vertebral fractures, M410
Self-assessment *versus* risk-factor questionnaire, SA357
Sex hormone binding globulin serum concentration, M392
Silent, among veterans, SA365
Total and free circulatory $25(OH)_2D$ and $1,25(OH)_2D_3$ status, M581
Vertebral deformities and racial differences, F360, SA360
Vitamin D binding protein gene polymorphism and, SU183
Osteoporosis, postmenopausal. SEE ALSO *Ovariectomy*
Cardiovascular disease and, F377, SA377
Clinical risk in elderly women and treatment for, F373, SA373
Cost-efficient DXA screening, SU388
Diet, physical exercise in low-income, M335
Early BMD response to teriparatide, F441, SA441
Early NTx response to alendronate, M417
Fall risk reduction, SA419
Gene expression in healthy bone tissue *versus,* M414
Gene expression profiling *in vivo,* SU150
HRT *versus* raloxifene, M473
Ibandronate administration and dosage, F408, SA408, M429, M432
Ibandronate and bone resorption, F406, SA406
Increased LDL-cholesterol, M360
Infrared analysis of raloxifene, M475
Latent mobility in vertebral compression fractures, WG20
MRL123 and bone remodeling markers, BMD, F450, SA450
Nutritional assessment, SA389
OPG-RANK-RANKL gene expression in osteoblast cultures, SA250
RANKL circulating levels, SA119
Risedronate effects on serum OPG, SU439
Single-dose lasofoxifene pharmacokinetics, M469
Single nucleotide polymorphisms in promoter region of pro-opiomelanocortin gene, M162
Spinal mobility factors in, M449
Spontaneous osteoclastogenesis in, SU312
Treatment for women 80 and over, 1219
Osteoporosis-pseudoglioma syndrome (OPPG), 1057, F268, SA268, SA125, SA465
Osteoporosis self-assessment tool
Elderly Chinese and Caucasian men, SU394
Female, for Asians, SU393
Interviewer-assisted risk assessment, physician-supplied data *versus,* SA378
Male, SU482
Male risk-factor questionnaire *versus,* SA357
Men younger than 70 and, M113
Postmenopausal, SU388
Quantitative calcaneal ultrasound *versus,* M149
Osteoporosis, senile, 1057, M248, SA014
Osteopotentia (Opt), 1077
Osteoprotegerin (OPG)
Androstene immune regulation hormones and, SA203
Atorvastatin and osteoblastic production of, SU238
Bisphosphonates *versus,* M300
Black cohosh stimulation and production of, SA210
BMD in Chinese and genetic polymorphisms of, M177
Osteoprotegerin (OPG) (Continued)
BMD, serum OPG and polymorphisms in, SA128
Bone metabolism in men, M394
CGRPand expression in human osteoblast-like cells of, SA519
Children with cystic fibrosis *versus* healthy children and, M524
Chronic renal insufficiency, hyperparathyroidism and, SU532
Cirrhotic patients referred for liver transplantation, M551
$1,25(OH)_2D$ regulation of release from vascular endothelial cells by, M579
Gene expression by steroid hormones, SA563
Glucocorticoid-induced osteoporosis, SA120
Glucocorticoid regulation, SA566
Glucocorticoids and RANKL ratio to, M380
Hemodialysis, continuous ambulatory peritoneal dialysis and, SU531
Hydrostatic pressure and, SU072
Idiopathic hyperphosphatasia and mutations of, M522
Juvenile Paget's disease/familial hyperphosphatasia and, F500, SA500
Low BMD in postmenopausal women and genetic polymorphisms of, SU187
Megakaryocytes regulation, SA294
Multiple myeloma *versus* monoclonal gammopathy of undetermined significance and, SU088
Oscillatory fluid flow and expression of, SA174
Osteoporosis serum levels, M402
Primary biliary cirrhosis and, SU422
PTH/PTHrP receptor and bone remodeling modulation, 1164
RANKL shedding by osteoblasts, activated T cells and, 1192
Retinoic acid and BMP-2 regulation during chondrogenesis, SA057
Rheumatoid arthritis susceptibility, joint erosion and variations in, F141, SA141
Risedronate effects in postmenopausal osteoporosis, SU439
Species specific differences during glucocorticoid treatment, M381
T cell stimulation of B cell production of, F144, SA144
Thyroid stimulating hormone, M295
Time-course in SaOS-2 cells of PTH-regulated, SU548
Osteoprotegerin-Fc (OPG-Fc), 1071
Osteosarcoma, WG9
Osteosarcoma cells, M069, M070, M066
Osteostatin, SA539
Osterix, SU245, SU260, M236, M252, SA233, SU208, M070
Osterix promoter, M258
Osx, SA211
Ovarian tumors, advanced, SA083
Ovariectomy (animal models). SEE ALSO *Osteoporosis (animal models)*
Alendronate effects on rabbits, M422
Alendronate effects on rats, SU437
Anabolic effects of BCSP-7, SA442
Antigen presentation in bone marrow, 1059
Aromatase bone expression, SA398
Binge alcohol and bone loss, SA432
Bone mass preservation in Caf1-deficient mice, F056, SA056
Bone quality of Bax-deficient mice, SU386
Cathepsin K inhibitors pretreatment, PTH treatment and BMD increases, M064
Celecoxib and bone remodeling, SU330
E2 treatment and bone in aged, M565
ED-120 and bone loss, M493
ER-α expression in tibia, M570
ER and AR activation in trabecular bone, SA397
Estrens protections, SU491
Ovariectomy (animal models). SEE ALSO *Osteoporosis (animal models)* (Continued)
Extraskeletal effects of systemic bFGF treatment, SU197
GSK3 and bone formation, bone mass, F445, SA445
HRT and phytoestrogen combination, SU576
Intermittent PTH and propranolol synergy on vertebral trabecular bone, M483
Intraosseous BMP-2 injection and bone strength, structure, M491
Liver-derived IGF-I and bone loss from, 1168
Orthosilicic acid effects, M441
PSK3471 and bone biomechanical properties with osteopenia, SU488
PSK3471 for bone strength loss, SA427
Psoralease semen prevention of cancellous bone loss, SU492
PTH bone effects, M486
Raloxifene and bone marrow stromal stem cells, SA278
RANK/RANKL-targeted antisense oligonucleotides, SU332
Soy isoflavones effects on osteoblast-specific gene products in, SU058
Spatial and temporal bone loss differences from aging, M372
T cell TNF production in dendritic cells, 1059
Tibolone protection of lumbar spine bone tissue, SU135
Treadmill exercise, bone mass, bone metabolism, SU218
Vitamin K2 and raloxifene combination, M474
Oxalate, urinary, M506
Oxandrolone, SU489
Oxyntomodulin, M138
Oxysterols, SA223
Oxytocin, SA204

P

P2 receptors, SA269, SU136
$P2X_7$ receptor, 1207, M197, M314, SU152, SU180, 1032
P2Y2 receptor, SU217
p27, F005**,** SA005
p30, F251**,** SA251
p38 MAP kinase, M222, 1272, F293, SA293, SU037, SU100
$p57^{Kip2}$, SU049
p62/sequestosome 1, F486, SA486
p65, SU018
Paget's disease
Bisphosphonates and bone remodeling markers, SA485
Bisphosphonates and IL-1β C/T polymorphism, M167
Bisphosphonates and severe hypocalcemia, M517
Canine distemper virus and osteoclast precursors, SU300
Characteristics and familial aggregation in Italy, SA483
Ethnic minorities in south east London, M516
Measles virus nucleocapsid gene, 1010
Measles virus nucleocapsid protein, 1159
Sequestosome 1 IVS7+1 G-A mutation, SU154
Sequestosome 1 M404V mutation, M519
Sequestosome 1 mutations and absence of, M520
Sequestosome 1 mutations in hereditary and sporadic, M515
Sequestosome 1 P392L mutation, 1204, M518
Skeletal involvement of younger persons with, SA487
VDR coactivators and osteoclast differentiation, M577
Wildtype and ubiquitin-associated domain sequestosome 1 mutations, F484, SA484

Paget's disease (Continued)
Zoledronic acid *versus* risedronate, F482, SA482
Paget's disease, juvenile/familial hyperphosphatasia, F500, SA500
Pain, M108, M400, M419, SU082, M068, WG20
Pamidronate
Administration and dosage, SA413
Alendronate *versus,* SU446, F466, SA466
Intervertebral disc, endplate and, SA055
Osteogenesis imperfecta, M426, F462, SA462, M500, M504
Renal-insufficiency-specific mineral deposition on endosteal bone surface, M536
Pancreas, neuroendocrine carcinoma of, WG22
Pancreatic polypeptide, M138
Parafibromin, F493**,** SA493
Parathyroid adenomas, 1202
Parathyroid carcinoma, F497, SA497, SU512, SU513, SU514, F495, SA495, SA498, WG8
Parathyroid cells, F533, SA533
Parathyroidectomy, SU545, M533, SU508, SU515, SU534, SU519, SU149
Parathyroid gland, SA494
Parathyroid hormone (1-15), SU566
Parathyroid hormone (1-34). SEE ALSO *Teriparatide*
Aging, connexin43 and intermittent, SA440
Angiopoietin-1 expression in osteoblast-like cells, M228
Bone architecture and bone mass in orchidectomized rats, M481
Bone mass increases with daily nasal spray, 1171
Catabolic effects of continuous infusion in C57BL/J6 mice, SU544
Continuous and intermittent, SU547
ED-71 bone formation *versus,* M496
Entry point into PTH1R of, M558
GRK2 overexpression in osteoblasts, SU558
IRS-1 and bone anabolic function, SA430
Osteoblast differentiation via PLC-independent PKC pathway, 1158
PTHrP haploinsufficiency and bone effects, F433, SA433
Serum protein and responders *versus* non-responders to, SA438
sFGF2 levels in glucocorticoid-induced osteoporosis, M480
Short term responses to daily intermittent or continuous, SU557
Parathyroid hormone (1-36), M479
Parathyroid hormone (1-84), F429, SA429, F431, SA431, 1098, F435, SA435, M531
Parathyroid hormone (PTH). SEE ALSO *Teriparatide*
Achondroplastic bone growth in mice and, 1045
Administration by transdermal patch, M484
Akt/PKB regulation in opossum kidney cells, SA520
Alendronate and skeletal response in osteoporotic postmenopausal women to, F439, SA439
Alendronate combination and bone turnover in osteoporotic men, 1172
Angiogenesis and anabolic effect of, SU554
ATF4 mediation of osteocalcin gene expression, SU243
Bioinformatics for signaling network dissection in osteoblasts, F224, SA224
Bisphosphonates effects on bone tissue quality *versus,* SA384
BMD gain with raloxifene combination and later withdrawal of, F437, SA437
Bone effects in LRP5 transgenic high bone mass mice, F525, SA525
Bone effects in ovariectomized female rats, M486
Parathyroid hormone (PTH). SEE ALSO *Teriparatide* (Continued)
Bone health markers in perimenopausal women, SA117
Bone marrow cells in ovariectomized rats and intermittent, M476
Bone turnover markers in Pakistani *versus* Norwegian natives, SA376
Bone turnover variations, SA327
Calcilytics and parathyroid glands release of, SA547
Calcium-regulated mRNA stability in parathyroid cells of, F533, SA533
cAMP and intracellular calcium signaling crosstalk, SU285
C/EBPβ induction, SA532
Cell proliferation, apoptosis in early primary osteoblast cultures, SU273
Collagenase 3 transcriptional activation, SU057
Connexins and regulation of osteocalcin promoter, SU552
COX-2 induction in bone, kidney, muscle *in vivo,* SU551
CREM/ICER and anabolic effect on bone mass of intermittent, 1061
$1,25(OH)_2D_3$ and anabolic actions on bone, M485
Disassociation of anabolic, catabolic, and fibrotic response to, SU535
Ectopic production, WG22
Endochondral bone formation and postnatal survival, $1,25(OH)_2D_3$ and, SA576
Exercise level and anabolic bone response to low dose, SA534
Glucocorticoids and anabolic effect of intermittent, SU418
Hemichannels and intermittent *versus* continuous, SU556
IGFBP-5 transcriptional regulation through AP-2, SA273
IGF-I receptor and anabolic actions on bone, F531, SA531
IL-6 and osteoclast formation stimulation, SU550
Immunometric assays of serum levels, SU549
Intermittent, lining cells and, F527, SA527
LRP5, bone formation in mice and, 1064
Matrix gla protein regulation, SU546
Megalin regulation of secretion, SA541
MMPs and anabolic action *in vivo,* M062
Molecular form in parathyroid carcinoma, SU514
NO and skeletal anabolic effect, SA526
Osteoblast cell cycle progression from G1 to S phase, F521, SA521
Osteoblast differentiation, SA255
Osteoblastic *versus* bone marrow cellular compartments, 1062
Osteopontin and actions in bone of, SU405
Patient selection for osteoporosis therapy, M487
Placental calcium transfer, F523, SA523
Protein profiling of bone marrow cells, SU555
PTHrP stimulation of $1,25(OH)_2D$ production in humans *versus,* F471, SA471
Runx2-regulated genes suppression from continuous, 1066
Selective activation of ERK, SU553
SFRP-1 and bone anabolic effects, 1063
Skeletal mineral lost during lactation, SA524
SOST and bone formation, 1166
Temporal profile in humans of subacute skeletal anabolic response to, 1065
Vertebral trabecular bone in ovariectomized mice, propranolol and intermittent, M483
Vitamin D, calcium, cheese supplementation effects in pubertal girls on, SU461
Vitamin D in Japanese women and plasma levels of, M332
Vitamin D receptor regulation in mouse renal cells by, SA561
Parathyroid hormone (PTH). SEE ALSO *Teriparatide* (Continued)
Wnt/β-catenin signaling, F529, SA529
Parathyroid hormone-Fc (PTH-Fc), M477
Parathyroid hormone fragments, amino-terminal, SA530
Parathyroid hormone receptor, SU559, SU560, M555, 1229, SU563. SEE ALSO *Parathyroid hormone type 1 receptor*
Parathyroid hormone receptor, carboxy-terminal, SA536, SU562, M560, F435, SA435
Parathyroid hormone-related peptide (PTHrP)
Cell cycle control in differentiating osteoblasts, M223
Expression regulation and osteolysis by human breast cancer cells by Gli2, Gli3, M076
Gli family regulation of cartilage cells expression by, F044, SA044
Indian hedgehog in chondrocytes, MAP kinases and, F051, SA051
Knockout mice, bone anabolic effects of PTH (1-34) and, F433, SA433
Mediation of AP-1 signaling in mesenchymal (cementoblast) cells, M239
Production in cancer cells, vitamin D analogues' effects on, SA571
PTH and 1α-OHlase knockout mice and, F537, SA537
PTH stimulation of $1,25(OH)_2D$ production in humans *versus,* F471, SA471
Target genes identification in chondrocytes using cDNA microarray, SU040
Temporal profile in humans of subacute skeletal anabolic response to, 1065
TREK stretch-activated potassium channels and gene expression in osteoblasts by, SA179
Parathyroid hormone-related peptide (PTHrP) (1-36), M243
Parathyroid hormone-related peptide (PTHrP) (107-139). SEE *Osteostatin*
Parathyroid hormone-related peptide-lacZ allele mice, SA538
Parathyroid hormone-related protein (PTHrP)
Cell differentiation of mouse growth plate chondrocytes and signaling, SA045
Chondrocyte up-regulation in osteoarthritis, SA549
DNA repair mediation in cancer, SA540
E1A oncogene repression of gene expression in prostate cancer cells, SU089
HSP-70 and binding *in vitro* to, SA535
IL-1a-induced RANKL expression in periodontal ligament cells, SU306
Lung carcinoma bone metastasis, M087
p27 and vascular protection after arterial angioplasty, F005, SA005
Parathyroid hormone type 1 receptor (PTH1R). SEE ALSO *Parathyroid hormone receptor*
ERK1 and ERK 2 activation and endocytosis, M559
Gap junction communications, M560
Karyopherins and, M554
Mimicking signaling characteristics in PTH2R, SU564
NHERF1 and, M556
Osteoclast expression, SA317
PTH (1-34) entry point, M558
Purification from HEK293S cells, SU565
Parathyroid hormone type 2 receptor (PTH2R), SU564
Parity, M365
Parthenolide, SU340
Particulate wear debris, SU240
***Pasteurella multicoda* toxin (PMT),** M316
Patient compliance. SEE ALSO *Health education*
Bisphosphonates dosing regimen, M434
Bisphosphonates effectiveness, M423
BMD testing and initiation of osteoporosis-related pharmacotherapy, SU483

Patient compliance. SEE ALSO *Health education* (Continued)
Drug treatment following hip fractures, M462
Hip protectors, M448, SU484
Osteoporosis education program, SU479
Pharmacist-managed osteoporosis clinic, M436
Weekly bisphosphonates, SA407
Pax5, M280
PC3 (prostate cancer cells), 1095
Peptide YY_{3-36}, M138
Perimenopause, SU382
Periodontal ligament, 1076, 1177
Periodontal ligament cells, SU306
Periodontal tissue, SA071
Periodontitis, SU387
Periostin, SU294, 1076
Peripheral blood mononuclear cells, M511
Peripheral neuropathy, M513
Peripheral quantitative computed tomography (pQCT), SA458, SU106, SU113. SEE ALSO *Computed tomographic microscopy*
PERK eIF2 kinase, SA059
Peroxisome proliferator-activated receptor α (PPARα), SA247, SU041
Peroxisome proliferator-activated receptor γ (PPARγ), SA247, M178
Peroxisome proliferator-activated receptor γ coactivator-1α (PGC-1α), SU254
Phalanxes, SU420
PHD oxygen sensors, M032
Phex. SEE *Phosphate-regulating gene with homologies to endopeptidases on X chromosome*
Phosphatase, SU301
Phosphate
Gastrointestinal-kidney axis modulation of vitamin D metabolism, SA582
Gene expression in hyperparathyroidism, SU511
Gene expression regulation in *ank/ank* mouse tooth root cells, M044
Growth hormone replacement in adult GH deficiency, SU505
Inflammation and calcium homeostasis, SU430
Liver transplantation in children, M547
Osteoblast apoptosis and, SA197
Serum FGF23 and, 1162
Transport in chick duodenum and $1,25(OH)_2D_3$-MARRS, SA550
Vitamin D and, 708, WG18
Phosphate, dietary, SU035, M378, SU196
Phosphate-regulating gene with homologies to endopeptidases on X chromosome (Phex), M060, F234, SA234, F154, SA154, 1161, WG18
Phosphatidylinositol 3 kinase (PI3K), SU290, SU239, M319, SA155, SA575
Phosphatidylinositol 3 kinase (PI3K)-Akt signaling, SU292, SU571
Phosphatidylinositol transfer protein-α (PITP-α), SA257
PHOSPHO1, F037, SA037
Phosphodiesterase inhibitors, SU289
Phospholipase A2 activating protein, SA572
Phospholipase D, M561
Phosphophoryn, SU288
Phosphorus, dietary, SU193, SA589
Phylloquinone (PK), SA449
Physical activity. SEE *Exercise*
Physical performance, SU399, WG26
Phytoestrogens, SU572, M279. SEE ALSO *Daidzein; Genistein; Ginsenoside Rg1; Resveratrol*
Pinealectomy, SA391
Pituitary-dependent Cushing's syndrome, M383
Placebo, F400, SA400, SA159
Placental growth factor, F147, SA147
Plasma cell membrane glycoprotein-1 (PC-1), SU034
Plasma, platelet-rich, SU270, SA143
Plasmid gene transfer, SA067
Plasminogen activator system, SA076
Platelet-derived growth factor-A (PDGF-A), SU535, 1200
Platelet-derived growth factor-D (PDGF-D), M186
Platelet endothelial cell adhesion molecule-1 (PECAM-1), SU209
Pleitrophin, SU506
***Pleurotus eryngii* extracts,** SA443
Plum, dried, M447
PMMA, M459
Point-of-care device, M413
Polycyclic aryl hydrocarbons, SU342
Poly(ADP-ribose) polymerase-1 pseudogene, WG9
Postmenopausal women. SEE ALSO *Osteoporosis, postmenopausal*
Acidogenic diet and fractures, SA331
African American, oral vitamin D_3 supplementation in, SU502
AMG 162 and BMD increases, 1072
Atorvastatin dose-response and bone effects, SU493
Baseline BMD and osteoporotic fracture risk, M324
BMD among Japanese, SU385
BMD and OPG-RANKL gene expression of osteoblast cultures from, SA250
BMD association with breast and uterine disease risk, SU390
BMD test prompt strategies, WG16
Body composition and bone change, M453
Bone loss after cessation of estrogen replacement therapy, M472
Bone marker changes and menopausal stage, SA116
Bone mineral markers in south Indian, SU359
Breast cancer, BMD in Hispanic *versus* non-Hispanic, SA093
Calcium absorption and endogenous hormones, SU384
Cdx-2 VDR binding element polymorphism and BMD, SU189
Col1a1 polymorphisms and BMD, SU182
CTx degree of isomerization and bone quality, M137
ER-α, VDR and calcium supplementation, SU171
Female osteoporosis self-assessment tool for Asians, SU393
Femoral neck BMD, IL-7 and sRANKL, M397
Five-year probability of fractures, SU367
Fracture burden of osteopenic, SU378
Fracture risk and age, F339, SA339
Fracture risk and bone loss rate, F380, SA380
Glucocorticoid effects on BMD and bone strength, SA379
Height loss as bone loss predictor, M367
HIV-infected, bone loss at hip, M393
Longer- *versus* shorter-lived mothers and fracture risk, M337
Low dose estradiol and osteoblastic procollagen production, M387
Mammography and BMD testing, SU355
Mayan, fracture prevalence and BMD, SA342
OPG genetic polymorphisms and low BMD, SU187
Oral bone loss and osteoporosis, M355
Osteopenic without prior fracture, drug therapy cost-effectiveness for, F402, SA402
Osteoporosis as cardiovascular event risk, 1055
Osteoporosis treatment based on clinical risk, F373, SA373
Osteoporotic fracture risk, M345
Osteoporotic fractures in urban Spanish, M351
Parental hip fracture, M357
Quality of life with or without subclinical vertebral fractures, SA344
Recent fracture and quality of life, F349, SA349
Postmenopausal women. SEE ALSO *Osteoporosis, postmenopausal* (Continued)
Reproductive history and bone mass, M365
Soy isoflavone supplementation and bone resorption, SU452
Statins and bone mass, SU473
Vitamin D status and i-PTH, SU586
Vitamin D status variability, SA578
Vitamin K supplementation for osteopenic, M443
Walking effects on bone mass, SU466
Weight lifted in strength training and bone changes, M455
Whole body vibration effects on BMD and muscle function, WG2
Wine intake and BMD, F330, SA330
Posture, M395, WG5. SEE ALSO *Kyphosis*
Potassium channels, TREK stretch-activated, SA179
Pregnancy, SA001
Premenopause, M359, M116, M115, M370, M376, SU001, SU516
Presenilins, F299, SA299
Pressure, hydrostatic, SU072
Primary care physicians, M354, SU391, SA334, M102
Probiotics, SU460
Procollagen type I N-terminal propeptide, SA434
Progestin, 1100
Progressive osseous heteroplasia, M265, SA126
Promoter region of pro-opiomelanocortin gene, M162
Propranolol, SA021, M483
Prostaglandin E_2, M200, SU314, M273, SU348
Prostaglandin E_2 receptor subtype EP_2 receptor, 1013
Prostaglandin E_2 receptor subtype EP_4 receptor, 1013, M490
Prostaglandin E_2 receptor subtype EP_4 receptor agonist, M183, SA446, SU494
Prostaglandin E synthase 1, membrane-bound, F511**,** SA511
Prostaglandin E synthase, membrane-bound, M185
Prostaglandins, SA237, M197, SU202, SU136
Prostanoid receptor EP4 agonist, SA238
Prostate cancer
Adrenomedullin and bone metastasis, 1093
Bisphosphonates reduction of telomerase *in vitro* expression, M085
BMP-7 in bone metastasis, M083
BMP/Smad1 inhibition of cell growth, F092, SA092
Bone response to systemic therapy for metastasis, SA089
Collagen receptor type 1 signaling in bone metastasis, SA100
High BMD in men of African descent and risk of, SA100
Hypocalcemia in metastatic, WG23
Immune-intact murine model of bone metastasis, M078
Noggin inhibition of BMP-2, F084, SA084, F085, SA085
Osteoporosis and spinal fractures, M080
RalGEF pathway and bone metastasis, M086
Risedronate and androgen-deprivation therapy, SU440
VEGF121 fusion toxin and bone metastasis, F099, SA099
VEGF and bone microenvironment, SU096
Vitamin D receptor polymorphisms and risk of, M159
Prostate cancer cells
Bisphosphonates and growth factors effects, SU097
E1A oncogene repression of PTHrP gene expression, SU089

Prostate cancer cells (Continued)
Gene expression regulated by physical contact by osteoblasts, SU101
25-Hydroxyvitamin D_3 molecular and apoptotic mechanisms, M019
Metastatic potential, M077
RANKL effects on RANK-expressing, 1095
Urokinase promoter methylation, M081
Vitamin D analogues' effects on PTHrP production, SA571
Prostate cells, SA585
Prostate-specific antigen (PSA), SA093
Protease-activated receptor-1 (PAR-1), M284, M030
Proteasome inhibitors, 1011. SEE ALSO *Bortezomib*
Protein, dietary, SU409
Protein kinase 2, M253
Protein kinase C, M200, 1158
Protein kinase C α, SA279
Protein kinase C/c-Src, SU287
Protein kinase C-δ, SU216
Protein kinase D, M194
Protein kinase I, M278
Protein kinase inhibitor γ (PKIγ), M256, SA522
Protein kinase R, M069
Protein, serum, SA438
Protein-tyrosine phosphatase, F318, SA318
Proteomics, SU574. SEE ALSO *Two-dimensional gel electrophoresis; Two-dimensional polyacrylamide gel electrophoresis*
Pseudohypoparathyroidism, autosomal dominant Ib, 1203
PSK3471, SU488, SA427
Psoralease semen, SU492
***PTHR1* promoter polymorphism,** SU179
PTP-PEST, SU346
Puberty, M001, F394, SA394, M168, SA008, M442. SEE ALSO *Adolescents; Girls*
Pyk2, M313, F311, SA311. SEE ALSO *Cbl-Src-Pyk2 signaling*
Pyrophosphate, M044

Q

QUALEFFO (osteoporosis assessment tool), WG1
Quality of life
Back exercise for osteoporosis management, WG6
Canadian Aboriginal women, SA456
Osteoporosis assessment tool, WG1
Postmenopausal women with or without subclinical vertebral fractures, SA344
Recent fracture in postmenopausal women, F349, SA349
Spinal mobility in postmenopausal osteoporosis, M449
Vertebral deformities, osteoarthritis, and chronic diseases, SA350
Vertebral osteoporosis severity, M050
Vitamin D deficiency, SU581
Quantitative trait loci
BMD regulation, M154
BMD regulation in chromosome 1, 1206
Bone quality mapping using nanonindentation technology, F063, SA063
Bone size and mechanosensitivity in ENU mutant, M151
Bone strength, biomechanical properties in inbred rats, F131, SA131
Bone strength regulation, F127, SA127
DEXA-based osteoporosis phenotypes for hip structural analysis, SU158
Femoral shaft failure load (animal models), SU161
Gene candidates for BMD variation in Chinese, SU172
Quantitative trait loci (Continued)
Genetic association with BMD in Chinese, SU159
Genome screen for male femoral structure, M156
Genome-wide scan for calcaneal quantitative ultrasound variation, M157
Serum alkaline phosphatase in mice, M152

R

Rab7, SA315
Rabbits, ovariectomized, M422
Rac1, SA315, F290, SA290
Radiation therapy, M016, M033, SU038, SA096
Radiographic absorptiometry, SU103, SA107, SA124
Radiographs, SU531
Radius, SU404. SEE ALSO *Forearm*
RalGEF pathway, M086
Raloxifene
BMD gain with PTH combination and later PTH withdrawal, F437, SA437
BMD maintenance after 7 years, 1215
Bone loss and GnRH agonist administration in mice, SU490
Bone marrow stromal stem cells in ovariectomized rats, SA278
*Bsm*I and *Fok*I effects on bone turnover, SA138
Estrogen receptors' expression and, SA392
Extraskeletal effects of lasofoxifene *versus,* SA423
HRT for postmenopausal osteoporosis *versus,* M473
IL-6 and TNF-α synthesis *in vivo,* M471
Infrared analysis of postmenopausal osteoporotic bone biopsies, M475
Japanese *versus* Caucasian postmenopausal women, SU406
Lasofoxifene for bone loss prevention in postmenopausal women *versus,* F424, SA424
Nonvertebral fracture risk after 8 years, F428, SA428
Short-term hormonal profile and OPG-RANKL system in osteoporosis, 1104
Teriparatide combination and teriparatide-induced bone resorption stimulation, 1169
Vitamin K2 combination for ovariectomized rats, M474
H-Ras, 1034
RAW 264.7 cells, M273, M294, F306, SA306
RAW264 cells, F295, SA295
Reactive oxygen species, SU301, M401
Receptor activator of NFκB (RANK)
Antisense oligonucleotides targeting signaling in arthritis, SU338
BMD in Chinese and genetic polymorphisms, M177
Cbl proteins and, 1198
Dimerization and osteoclastogenesis, SU315
Glucocorticoid regulation, SA566
Hydrostatic pressure, SU072
Osteoclastogenesis and cytoplasmic motifs, F301, SA301
Self-assembly in 293T cells, SA308
Receptor activator of NFκB ligand (RANKL)
Androstene immune regulation hormones, SA203
BMD in Chinese and genetic polymorphisms, M177
Bone destruction in inflammatory arthritis (rat models), SA510
Bone grafts and, F066, SA066
Bone metabolism in men, M394
Calcitonin receptor P3 promoter expression, SU307
CAPRI-ΔCAPRI and Ras pathways, F199, SA199
Receptor activator of NFκB ligand (RANKL) (Continued)
Cathepsin gene transcription and IFN-γ crosstalk, SU298
CREB-binding enhance and stromal/osteoblast-specific control of transcription by, 1104
Cystic fibrosis in children *versus* healthy children, M524
$1,25(OH)_2D$ regulated release from vascular endothelial cells, M579
Dominant negative N-cadherin inhibition, 1193
Epigenetic regulation of gene expression, M283
Femoral neck BMD in postmenopausal women, M397
Fluid shear stress-induced expression in osteoblasts, M195
Glucocorticoid regulation, SA566
Glucocorticoids and OPG ratio to, M380
Hemodialysis and continuous ambulatory peritoneal dialysis, SU531
H-Ras isoform and mechanical strain inhibition, 1034
Hydrostatic pressure and, SU072
Mouse expression in growth plate and articular cartilage, SA043
Multiple myeloma *versus* monoclonal gammopathy of undetermined significance, SU088
OPG regulation, 1192
Oscillatory fluid flow and, SA174
Osteoclast formation and histone deacetylase inhibitors, SU236
Osteoporosis serum levels, M402, SA119
Primary biliary cirrhosis, SU422
RANK-expressing human cancer cells, 1095
Retinoic acid and BMP-2 regulation during chondrogenesis, SA057
Runx2 regulation in mature *versus* less mature osteoblasts, SA200
Signal transduction in osteoclasts and high extracellular calcium concentrations, M315
Sp1 and Sp3 regulation of basal transcription in osteoblasts, stromal cells, M267
Synergistic catabolic effects in articular chondrocytes, M061
Thyroid-stimulating hormone, M295
Time-course in SaOS-2 cells of PTH-regulated, SU548
Receptor-associated protein, SA478
Receptor tyrosine kinase orphan receptor 2 (Ror2), SU293
Regucalcin, 284
RelB complexes, 1028
Renal cell carcinoma, SU200, 1096
Renal cells, mouse, SA561
Resistin, M298, M390
Resveratrol, SA208, 1091
Retinoic acid, SA057, SU274
Retinol and retinyl esters, 1020
Reveromycin A, M307
Rheumatoid arthritis
Alendronate and radiographic progression, SU539
Chondrocyte apoptosis, SA050
CXCL12 chemokine and bone resorption, SA286
Dendritic cells' transdifferentiation into osteoclasts, M309
Glucocorticoid use and BMD, SU541
Infliximab and bone metabolism, SU542
Nurse-like cells, M-CSF and bone destruction by, SU540
OPG genetic variants, F141, SA141
Synovial fluid macrophages and osteoclast differentiation, SA300
TNF protection of osteoclasts from alendronate-induced apoptosis, SA403
Rheumatoid arthritis, juvenile, SU543
Rheumatoid arthritis pannus, F513, SA513

RhoA, M561, SU073
Rhoa/ROCK signaling pathway, SA052
Rho-GTPase, M316
Rho/mDIA2/HDAC6 pathway, SA282
Rickets, autosomal dominant hypophosphatemic, 1123
Rickets, hypophosphatemic, SU035
Rickets, X-linked hypophosphatemic, F479, SA479, 1161, SA461
Risedronate. SEE ALSO *Bisphosphonates*
Administration and dosage, M413, SU438
Alcohol-induced bone loss and, SA447
Alendronate effects on BMD, bone turnover markers *versus,* F412, SA412
Alfacalcidol combination therapy in ovariectomized osteoporosis model, SA457
Analogs and antitumor mechanisms *in vivo,* 1094
Androgen-deprivation therapy for prostate cancer, SU440
Bone remodeling and BMD responses to vitamin K, vitamin D *versus,* M418
Bone resorption, SU434
Breast cancer cells' growth, SU098
Calcitonin, vitamin D treatment of postmenopausal osteoporosis *versus,* SU435
Calcium packaged with, M424
Duration of action after single dose, SU432
EP4 agonist effect on bone strength, SA446
Fracture reduction in osteopenic postmenopausal women, F404, SA404
Hip fracture risk reduction, F410, SA410
Histomorphometric analysis of osteopenia, M382
Mineralization analysis after 5 years, SU436
NE10790 effects on human myeloma cells *versus,* SU087
NSAIDs and upper gastrointestinal tolerance for high dose oral, SA401
Protein prenylation inhibition *in vitro* and *in vivo,* SU334
Serum OPG in postmenopausal osteoporosis, SU439
Vertebral fractures in osteoporotic men, M410
Vitamin D status, bone turnover in nursing home residents, SA399
Women on gastric acid inhibitors with risk for gastrointestinal side effects, SU445
Zoledronic acid for Paget's disease *versus,* F482, SA482
RNA interference, M294
***Ror2*^{W749X} gene,** SU050
ROS 17/2.8 cells, M236, 1106
Rosiglitazone, M054
Running, M206
Runt domain factor 1 (Runx1), F058, SA058
Runt domain factor 2 (Runx2)
BMP2/TGFβ, MAPK signaling in osteogenic differentiation, 1175
Bone sialoprotein regulation, SU247
Chondrocyte maturation and Nkx3.2/Bapx1 repression, 1128
Continuous PTH and osteoblast apoptosis, 1066
Dlx3 and, 1144
Dominant-negative, bone mass accrual and, F222, SA222
Gelatinases transcription in metastatic cancer cells, SA091
Gene transfer in bone marrow stromal cells, osteoblast differentiation, and bone formation, M264
Genomic sites in osteoblasts, F216, SA216
Hes-1 regulation of $1,25(OH)_2D_3$-induced OPN transcription, F230, SA230
Hypoxia and osteoblast, osteocyte gene expression, SA227
Mdm2 oncogene during skeletogenesis, 1015
Runt domain factor 2 (Runx2) (Continued)
mSin3a and multiple HDACs' regulation, SA229
Osteoarthritis and, 1012
Osteoblast development and RIP regulation, 1139
Osteoblast differentiation regulation, SU286, 1120
Osteogenic differentiation through Cbfb regulation, SA249
PI3K-Akt signaling and osteoblast, chondrocyte differentiation, SU292
RANKL regulation in mature *versus* less mature osteoblasts, SA200
Steroid hormone receptors' repression, M229
Subnuclear organization and osteogenic function, SA217
Trps1 transcription factor regulation, 1107
Wnt signaling, 1213
Runt domain factor 2/core binding factor 1 (Runx2/Cbfa1) gene P1 promoter, SU262
Runt domain factor 2-interacting protein (RIP), 1139
Runt domain factor 2 (Runx2) type-II, F220, SA220, 1108
Rural residents, M352. SEE ALSO *Urban-rural difference*

S

S^{752}P (β_3-integrin mutant), F304, SA304
SA-766, SU577
Saethre-Chotzen syndrome, SA243, F226, SA226
Salinity, SA545
Salmon, Atlantic, SU051
Salt, dietary, M202
SaOS-2 cells, M246, SA269, SA196, SU548, M036
Scanning small angle X-ray scattering study, SA032
Scaphoid, M124
Sciatic denervation, 1148
Sclerostin (SOST), SU260, F270, SA270, 1166, 1165, 1217, 1079
Scoliosis, M425, SU232
SDF-1, M189
Seasonal modulations, SA337, SU373, SA013, WG13
Secreted frizzled related protein-1 (SFRP-1), F260, SA260, M018, 1063
Secreted frizzled related protein-2 (SFRP-2), F081, SA081
Secreted phosphoprotein-24 (SPP-24), SA074
Secreted protein, acidic, and rich in cysteine (SPARC), SU060
Selective androgen receptor modulators (SARMs), 1216. SEE ALSO *7α-Methyl-19-nortestosterone; SA-766*
Selective estrogen receptor α modulators (SERM-αs), M571
Selective estrogen receptor modulators (SERMs). SEE *Lasofoxifene; PSK3471; Raloxifene*
Selective serotonin reuptake inhibitors (SSRIs), 1024
Senescence accelerated mouse 6 (SAMP6), M388, M208, M003
Sequestosome 1 mutations, F484, SA484, M515, 1204, SU154, M518, M519, M520
Serotonin, SU348
Serotonin receptor inhibitors, F369, SA369
Serotonin transporter, SA142
Serotonin transporter (5-HTT), F068, SA068
Serum calcification factor, SU031
Sestamibi imaging, 1202
Seven in absentia homolog-1a (Siah1a) protein, F266, SA266
Severe acute respiratory syndrome (SARS), SA322
Sex differences
Areal *versus* volumetric BMD, SU111
BALBxC3H mice skeletal sensitivity to unloading, SA190
Bone mass and fractures, F362, SA362
Cortical bone characteristics across puberty, SA008
Dioxin/sucrose effects in bone tissue, SA472
Femur BMD and structure measured by computed tomography, M326
Functional muscle-bone units at different skeletal sites in children, F012, SA012
Genetic regulation of trabecular and cortical bone in congenic mice strains, SU163
Glucocorticoid treatment and ultrasound graphic trace analysis of phalanxes, SU420
Hip fractures in community-dwelling patients, M347
IGFBP-2 genetic regulation, SA164
Long bone fatigue in rat model, SU076
Muscle-bone relationship in lower skeleton, SU162
Pediatric calcaneal SOS, SA121
Routine population-based osteoporosis screening of Canadians, M109
Skeletal development, 1084, M007
Twin study of body composition components, BMD, SA370
Vertebral compression fracture presentation and outcome, SA351
Sex hormone binding globulin, M392
Sex hormone receptors, M562
Sex hormones, SU424, 1151
Sex steroids, M263, 1058, F356, SA356, F358, SA358
Sexual bimorphism, pelvic, M562
SH2-containing inositol phosphatase (SHIP), F320, SA320
SH2-containing inositol phosphatase 1 (SHIP1), M312
Shin splints, SU233
SHP-2 mutations, SU526
Sickle cell disease, SA502, SA504
Side populations, SU269
Signal peptide-CUB-EGF-like domain containing proteins-3 (SCUBE3), SU255
Single nucleotide polymorphisms, SU168, M162, SU173, SU177
Single X-ray absorptiometry (SXA), SU358
Skeletal growth
Cinacalcet HCl in juvenile dogs, SA491
COL1A2 polymorphism in pubertal girls, M168
Dietary magnesium and rat leg bones, SU365
Ethnicity and gender effects, M007
Food group intake and BMC during childhood to adolescence, M328
Hepatic IGF-I synthesis, 1167
Juvenile idiopathic arthritis and stunted, 1138
Maturity and sex-related changes in bone, muscle, F007, SA007
Osteoblast gene expression profiles, SU242
Osteoblast lineage cells circulation and pubertal, 1136
Osteoporosis in SAMP6 mouse model from deficient peak bone mass, M003
Pubertal girls, F009, SA009
Rosiglitazone and bone mass, architecture, M054
Site-specific bone mineral accrual from adolescence to adulthood, SA006
Skin blood flow, M513
Skull, SA485
Smad 1, F218**,** SA218, SU216, F092, SA092
Smad3, 1180, F168, SA168, SU203, SU095, SA562
Smad4, F097**,** SA097
Smad pathways, SU037
Smads, F214**,** SA214, SU013

Smads anchor for receptor activation (SARA), 1041
Smoking, SU342, SU326, M363, SU507
Smurf1, SU012
Smurf2, 1040, M018
Socioeconomic deprivation, M341, M343
Sodium/bicarbonate exchanger (NBCn1), SU308
Sodium phosphate cotransporter, type IIa (NaPi-IIa), F156, SA156, SU533, F154, SA154
Sodium/proton exchanger regulatory factor type 1 (NHERF1), M556
Sonic hedgehog, SU051, 1127
***Sox4* gene,** M038
Sox8, 1140
SOX9, SU062
Sox9, 1050
Soy isoflavones. SEE ALSO *Equol*
- Bone matrix protein synthesis and osteoblast activity in male rat osteoporosis model, SA064
- Bone mineralization, milk mineral concentration in lactating rats, M446
- Bone resorption in postmenopausal women, SU452
- Dose response in postmenopausal women of bone resorption, SA414
- Kudzu reductions of bone loss in ovariectomized rats, SA016
- Osteoblast-specific gene products in postmenopausal rat osteoporosis model, SU058
- Postmenopausal walking women, SU455
- Probiotics and prebiotics effects on bioavailability, SU460
- Supplementation in postmenopausal rat osteoporosis model, SU453

Soy milk, M440
Sp1 (specificity protein 1), M267, M026, M171
Sp3, M267
Spaceflight, F421, SA421, M216. SEE ALSO *Microgravity*
Spinal cord injury, M125
Spinal curvature irregularity index, SU134. SEE ALSO *Vertebral deformities*
Spine, SU128, M074. SEE ALSO *Lumbar spine; Vertebral fractures*
Spondyloepimetaphyseal dysplasia, F063**,** SA063
SP transcription factors, M036
Squamous cell carcinoma, oral, SU086
SRC 1, 3, M577
SRC-2, M566
Src kinases, M317, M557. SEE ALSO *Cbl-Src-Pyk2 signaling*
SRp40, SA054
STAT1-dependent pathway, SU302
STAT6, SA312
Statins, SU290, SU473. SEE ALSO *Atorvastatin; Fluvastatin; Osteostatin*
Stem cell factor, M188
Stem cells, M189. SEE ALSO *Adipose-derived stem cells; Mesenchymal stem cells*
Stem cell transplantation, M147. SEE ALSO *Bone marrow transplantation*
Steroid 5α-reductase, M572
Steroid hormone receptors, M229
Steroid receptor coactivator-1, SU567
Steroids, SA122
Stress fractures, SA385, SU233
Stress, mechanical. SEE ALSO *Loading; Oscillatory fluid flow*
- Actin filament length and osteoblastic response, M196
- Bone matrix strain at osteocyte lacunae in cortical bone, F175, SA175
- DMP-1/MEPE gene expression in osteocytes and axial strains in overload model, SU215
- FGF2 gene and protein expression in MC3T3-E1 osteoblasts, SU199

Stress, mechanical. SEE ALSO *Loading; Oscillatory fluid flow* (Continued)
- Global genetic analysis of bones *in vivo,* F180, SA180
- Glutamate receptors and estrogen modulation of osteoclasts, M193
- H-Ras isoform and RANKL inhibition, 1034
- Osteoblast differentiation regulation, SU286
- Planar orbital shaking *versus* hindlimb suspension, M214
- Protein kinase C-δ-dependent Smad 1 activation in osteoblasts, SU216

Stress, oxidative, M293, SU045
Stress syndrome, medial tibial, SU233
Stroke, M346
Stroke, chronic, SA325, SU131
Stromal cell markers, SU256
Stromal cells. SEE *Bone marrow stromal cells*
Strontium ranelate, SA302, SA448
Substance P, SA517
Subtractive transcription amplification of mRNA (STAR), M297
Sucrose, SA472
Sunlight, SA338
Surface-enhanced laser desorption/ionization time-of-flight mass spectroscopy (SELDI-TOF MS), SA093
SWI/SNF complex, SU252
Syk, SA321
Sympathetic nervous system, 1148, F191, SA191
Synovial fibroblasts, SU037
Synovial fluid macrophages, SA300
Synovial joint articular cartilage, SU043
***Syntaxin16* 3-kb deletion,** 1203

T

T47D (breast cancer cells), SA079
TAF_{II}-17, M577
Tai Chi, SU472
Tamoxifen, SU575
Tannins, M291
Taqman gene expression analysis, 986
Tartrate resistant acid phosphatase (TRAP), M242, SA201, SA198, SU301, SU054
Tartrate resistant acid phosphatase-5b (TRAP-5b), SA510, M305, SU082
Tartrate resistant acid phosphatase-11β-hydroxysteroid dehydrogenase-2, SU413
Tat protein, SU262
Tbx3, F160, SA160
T cell immune regulator 1 gene, M310
T cells, SU267, F144, SA144, M431, 1191, 1116
T cells, cytokine-stimulated, M299
TCF signaling, F262, SA262
Tea, instant, M510
Telomerase, M085
C-Telopeptide (CTx), 1068, M137
N-Telopeptide (NTx), SU144, M130, M133, SA120, SU147, M074
Temporary brittle bone disease, SU520
Tennis players, SU402, SU228
Teriparatide (rhPTH (1-34)). SEE ALSO *Parathyroid hormone (1-34)*
- Aortic Msx2/Wnt gene regulatory programs *in vitro* and *in vivo,* 1097
- Direct analysis of non-vertebral fracture in community experience, M478
- Fractal analysis of calcaneus radiograph texture, SA113
- Fracture risk reduction, 1170
- Fracture risk with increasing osteoporotic fractures, 1070
- IGF-II expression in human bone, placebo *versus,* SA159
- National guidelines for mineral and vitamin D supplements, M482
- Postmenopausal osteoporosis and early BMD response, F441, SA441

Teriparatide (rhPTH (1-34)). SEE ALSO *Parathyroid hormone (1-34)* (Continued)
- Procollagen type I N-terminal propeptide responder algorithm, SA434
- Raloxifene combination and bone resorption stimulation, 1169

Testosterone, 1019, 1152, M388, SU486, M181
Therapeutic touch, M244
Thiazide diuretics, M270, M338
Thiazolidinediones, M281, SA451
Thioredoxin, M293
3T3-L1. SEE *Adipocytes*
3-D volumetric fluorescence imaging, SU023. SEE ALSO *Bone microarchitecture; Computed tomographic microscopy*
Thrombin, M284, M030
Thrombospondin 3 (TSP3), SU069
Thy1, SU256
Thyroidectomy, SA003
Thyroid hormone receptor, 1126
Thyroid stimulating hormone (thyrotropin, TSH), SA288, M295
L-Thyroxine suppressive therapy, SU120
Tibia, M126, SA109, SU225, SU233, SU113. SEE ALSO *Bending tests*
Tibolone, SA205, SU135
Tight skin mice, Skeletal overgrowth in, F075, SA075
Toll-IL-1 receptor domain-containing adapter inducing interferon β (TRIF), M286
Toll-like receptor 9, SU311
Toll-like receptors, F295, SA295
Tooth loss, SU387, M503
Topological analysis, M119
Toremifene, M470
TP508, 1201
Trabecular bone
- Adiponectin and age-related loss, SA146
- Age-related loss in proximal femur, SU010
- Architecture, collagen cross-linking and mechanical properties, M058
- bFGF and lumbar vertebrae of osteopenic rats, M488
- Caloric restriction, F388, SA388
- DEXA of age-related changes in BMD, SA115
- Disuse-induced transcriptional changes *versus* morphologic changes in male, SA189
- Finite element analysis of virtual osteoporotic simulation, SU080
- Fractal analysis of calcaneus radiograph texture with teriparatide, SA113
- Genetically-modulated differences in bone volume, connectivity, SU230
- Glucocorticoid-induced vertebral osteoporosis, M384
- Histone H4 gene, M039
- Pressure modulation during loading, SA183
- Probabilistic cellular automata simulation of remodeling, M121
- rhBMP-2/CPM and, SU017
- Sex differences in congenic mice vertebral fraction, 1083
- Sex differences in genetic regulation of congenic mice, SU163
- SNPs regulating gene expression, SU177
- Spinal site and vertebral region for high resolution spiral-CT, SA386
- 3D-structural analysis, M122
- Vhlh effects on, F072, SA072
- VivaCT40 monitoring in anesthetized rodents, M120

Trabecular bone, human, SA219
Transforming growth factor β
- Bone mechanical properties, SA169
- Early chondrogenesis, SU205
- Glucocorticoid receptor inhibition of Smad3 transcriptional activity, M260
- Maspin and bone matrix maturation, M065

Transforming growth factor β (Continued)
Metastatic renal cell carcinoma bone destruction and cytokines secretion, SU200
Osteoblast differentiation from mesenchymal progenitors, SU201
PI3K impact on osteoclast survival, M319
Smurfs and Arkadia regulation, SU012
TIEG and gene expression in osteoblasts, F170, SA170
Time point for lineage diversion towards osteoclastic phenotype, SA167
Transforming growth factor β1, SA054, SU278
Transforming growth factor β2, SU047
Transforming growth factor β activated kinase 1 (TAK1), SU313
Transforming growth factor β inducible early gene (TIEG), 1197, F170, SA170
Transgenic mice
3.6Col1a1-tk, F527, SA527
Adenoma of mouse prostate, M078
β1 integrins, SU350
BMP-2 overexpression, SU283
Col1a1-CreERT2, SA233
Col3.6-p20C/EBPB, SA231
Cthrc1, 1132
Dkk-1, 1017
Dominant-negative Runx2, F222, SA222
ERE-BP, SU570
Expressing Cre recombinase in osteoclasts, SA310
FGF23(R176Q), 1123
FIAT and bone mass accrual in, 1052
LRP5 high bone mass, F525, SA525
MOG2 promoter, 1210
NSE/hIL-6, 1138
Promoter-GFP reporter, SA276
TIMP-1, M062
TOPGAL, 1014
TRAP-11β-HSD2, SU413
Transient receptor potential vanilloid type 6 (TRPV6) promoter, 1088
Transplant osteoporosis. SEE *Bone marrow transplantation; Heart transplantation; Kidney transplantation; Liver transplantation; Organ transplantation*
Trauma, M463
β-Tricalcium phosphate, M015
Triggering receptor expressed in myeloid cells-2 (TREM2), 1195
***Trps1* transcription factor,** 1107
Tumor necrosis factor, SU323, SA403
Tumor necrosis factor-α
Bone strength and fracture risk in older women, SU186
Catabolic effects in articular chondrocytes, M061
CD38 and CD157 regulation, SA291
Estrogen deficiency through hydrogen peroxide induction, SA393
IL-1 and osteoclastogenesis, M274
Osterix promoter inhibition, M258
Raloxifene and *in vivo* synthesis, M471
Spinal BMD in Crohn's disease, M460
Tumor necrosis factor axis, SA288
Tumor necrosis factor receptor 1 (TNFR1), M304
Tumor necrosis factor receptor-associated factor-2 (TRAF2), SU310
Tumor necrosis factor receptor-associated factor-6 (TRAF6), SU297, 1029
Tumor necrosis factor-related activation induced cytokine (TRANCE), SU289
Tumor necrosis factor-related apoptosis-inducing ligand (TRAIL), SU277
Tumor necrosis factor SF 14 (LIGHT), 1030
Tumors, M289. SEE ALSO *Bone metastasis; specific neoplasms*
Turmeric extract, curcuminoid-enriched, M538
Turner syndrome, SU485
Twin studies, SA370, 1183, M125, SA004
Twist, F226**,** SA226
Twist-1, 1209
***TWIST1* mutations,** SA243
Twisted gastrulation (Tsg), 1178, F024, SA024
Two-dimensional gel electrophoresis (2-DGE), M053, SU320, SU555
Two-dimensional polyacrylamide gel electrophoresis (2D-PAGE), M251
Tyrosine kinase, SU346

U

U20S human osteosarcoma cells, SU569
Ubiquitin ligase. SEE *Seven in absentia homolog-1a protein*
Ubiquitin-proteasome pathway, M220
Ulna, SA109
Ultrasound, quantitative
Adolescent bone measurements, M140
Axial and transverse transmission assessment of bone microarchitecture, M146
Bone mass in school-aged children, SA011
DXA diagnosis of hip fractures *versus,* M093
Fracture prediction in older people with vitamin D deficiency *versus* calcaneal, SU368
Hip and non-spine fracture prediction in men, 1023
Physical performance ability in children, M148
Sex- and age-related changes in pediatric calcaneal SOS, SA121
Vertebral deformities *versus* nonspine fractures in Japanese women, SA124
Ultrasound, quantitative calcaneal
Achilles Insight Device *in vivo,* M144
BMD and genetic links to, SU164
Bone mass evaluation in liver and cardiac transplantation patients, M145
Calculated risk assessment for osteoporosis *versus,* M149
Changes in girls from age 10 to 13, M439
Fetal bone accrual and maternal calcaneal, SA001
Fracture detection in elderly Chinese men, M143
Fracture risk prediction, F123, SA123
Genome-wide scan for QTL in normal variations of, M157
Nerve function and, 1022
Non-spinal fracture prediction in men, M344
Osteoporosis risk screening, M142
Umbilical cord cells, human, M250, SU325
UMR-106 (osteoblastic) cells, SU296, M225
Unloading. SEE ALSO *Microgravity; Spaceflight*
Bone integrity and sensory neurohumoral signaling, M396
Bone loss recovery in mice, SU227
Cbfa1 and bone formation in adult mice, SU231
Estrogen and VDR ligands' attenuation of bone loss, M576
Genetically-modulated differences in trabecular bone, SU230
IGF-I resistance, F178, SA178
NASA rat model, SA186
NOS-1α and bone response, 1036
Osteocyte apoptosis preceding bone resorption in murine model, SA172
PECAM-1 and reduced osteogenic potential, SU209
Sex differences in BALBxC3H mice skeletal sensitivity, SA190
Spaceflight *versus* hindlimb suspension in mice, M216
Transcriptional *versus* morphologic changes in male skeleton, SA189
Zoledronic acid and bone loss in spinal cord injury model, M425
Urban-rural difference, M336, SU104, SU105, M110
Urea transporter 11, human (HUT11), SU272
Urokinase promoter, M081
Urokinase receptor, SA076

V

Vacuolar H^+-ATPase (V-ATPase), SA280
Valosin-containing protein (VCP/p97), M220
Valproic acid, M405
Val-Pro-Pro (VPP), M225
Vanadium-based antidiabetic drugs, SU506
Van Buchem disease (mouse model), 1079
Vascular calcification, M094, SU033, F474, SA474, SA040, M333, M514, M537. SEE ALSO *Aortic stenosis, calcific*
Vascular endothelial cells, SU562
Vascular endothelial growth factor, SU245, F066, SA066, SA575, SU096
Vascular endothelial growth factor-121 fusion toxin, F099, SA099
Vascular endothelial growth factor receptor, SA150, 1096
Vascular endothelial growth factor receptor-1 tyrosine kinase, F287, SA287
Vascular pressure, 1190
Vascular smooth muscle cells, SA036
Vascular smooth muscle cells, aortic, SU066
Vasoactive intestinal peptide, SU250
Vasopressin, SA036
VASP, M278
Velcade. SEE *Bortezomib*
Vertebral column defects, SU051
Vertebral deformities, SA350, 1112, F417, SA417, SA124
Vertebral endplate, SA055
Vertebral fractures. SEE ALSO *Fractures*
Absence of radiological collapse, SU531
Balloon kyphoplasty for compression-type, M508, SU478
BMD analysis in ankylosing spondylitis, SA108
BMD in male osteoporosis, SU123
Bolster inflation of dynamic motility evaluation, M371
Calcium supplementation, F417, SA417
Compression, sex differences in presentation and outcome, SA351
Diagnositic discrepancies, SU119
Genetic variation in IL-1 gene cluster and elderly women risk, M158
Historical height loss, SA332
Historical height loss and multiple, F333, SA333
Latent mobility in osteoporotic compression, WG20
Lateral DXA imaging, SU381
Lateral morphometry assessment criteria, M098
Latin American prevalence, F340, SA340
Osteoporosis diagnosis and treatment, M468B
Osteoporotic, diagnostic value of spinal pain and height loss, M108
Postanterior loading and regional trabecular bone volume ratio prediction, M106
Radiographic image resolution of fan-beam densitometers, SU138
Spinal curvature irregularity index, SU134
3D scaling index method *versus* DXA detection, SA031
3D-structural analysis of trabecular bone, M122
Threshold in secondary osteoporosis, M091
Walking endurance among with women with prevalent, M454
Vertebral morphometry, M104, M504
Vertebroplasty, SA453, SU474, M468B, M371. SEE ALSO *Kyphoplasty*
Vγ9vδ2 T cells, M431
Vibration exercise, M456, SU221, 1145, M218, WG2
Vitamin A, SU374, F328, SA328

Vitamin D. SEE ALSO *1,25 Dihydroxyvitamin D; 1,25 Dihydroxyvitamin D_3; ED-71; Hypovitaminosis D; Vitamin D receptor; Vitamin D supplementation*
Auto/paracrine action in bone, SU588
Bone loss in cystic fibrosis, SU421
Bone remodeling and BMD responses to vitamin K, risedronate *versus,* M418
Bone remodeling and risedronate in nursing home residents, SA399
Calcitonin, risedronate for postmenopausal osteoporosis *versus,* SU435
Calcium combination and falls reduction, 1222, WG4
Calcium supplementation, bone mass accrual during rapid growth and, M212
Canadian Aboriginal *versus* white women and dietary, SU361
Clinical assessment, SU584
Deficiency, in Canadian children, WG11
Deficiency, minimal trauma fractures and, M373
Deficiency, primary aldosteronism, secondary hyperparathyroidism and, SA476
Deficiency, primary hyperparathyroidism and replacement of, SU509
Deficiency, quality of life and, SU581
Dietary salt and urinary loss of, M202
Ethnicity, calcium absorption and plasma, SU407
Fall risk in nursing homes, M491
sFGF23, 1162
Gastrointestinal-kidney axis modulation by phosphate, SA582
Insufficiency, bisphosphonates and, M412
Insufficiency in Canadian Aboriginal women, M331
Insufficiency in men, SA326
Insufficiency in obese patients prior to bariatric surgery, SU580
Insufficiency in osteoporosis population, SU582
Insufficiency in pediatric secondary osteoporosis, M527
I-PTH in postmenopausal women, SU586
Liver transplantation in children, M547
Metabolism in human osteoblasts, SA587
N. American women treated for osteoporosis, SU583
Osteitis fibrosa cystica, WG14
Osteomalacia in immigrants, SA368
Phex expression, M060
Phosphate interaction, 708, WG18
Physical function in elderly, WG26
Plasma PTH in Japanese women, M332
Prophylaxis for fall prevention in residential care centers, F459, SA459
Prostate cancer prevention, SA585
Protein partners in intracellular binding and transport, SA574
Seasonal modulation in ESRD patients on hemodialysis, WG13
Transcriptional inhibition by estrogen, 1089
Variability in postmenopausal women, SA578
Vitamin D_3, SA583, 1220
Vitamin D_3 receptor, F573, SA573
Vitamin D analog, M257. SEE ALSO *ED-71; ED-120*
Vitamin D binding protein gene, SU183
Vitamin D-24-hydroxylase, SA581
Vitamin D-25-hydroxylase, SA581
Vitamin D receptor
Alternative ligand binding site for docking genomic and non-genomic agonists, 1090
BMD and ER polymorphisms interactions with, SU169
BMD in Chinese and genetic polymorphisms of, M177
Bone loss in elderly women and poly adenosine repeat in, SU170
Vitamin D receptor (Continued)
β-Catenin signal transduction crosstalk in $1,25(OH)_2D_3$ tissues with, F558, SA558
C/EBPβ and phosphorylation-dependent transcription enhancement, SU251
$1,25(OH)_2$-mediated events in mouse intestine, SA560
Dissection of functional domains, SA554
Disuse-induced bone loss and, M576
ED-71 mediation, SA569
ER-α association with calcium supplementation in postmenopausal women, SU171
Essential unsaturated fatty acids, SA557
Fracture risk and polymorphisms intragenic interaction, M176
GATA-1 and, SA556
Gene polymorphisms and postmenopausal female mandibular trabecular bone, SU165
Gene polymorphisms impact on $1,25(OH)_2D_3$, SA552
Hairless gene product repression, SA551, F555, SA555
Importin 4 and ligand-independent translocation, F553, SA553
Nuclear localization in ligand-mediated protection, 1087
Osteoblastic function, 1099
Prostate cancer risk, M159
PTH and calcium differential regulation in mouse renal cells, SA561
Vitamin D receptor B1, SA559
Vitamin D supplementation
Adolescent girls for one-year, M498
Adolescent musculoskeleton, 1118
Antiepileptic agents, M497
Bone mineralization in girls, SU499
Calcium intake effect on requirement for, SA579
Pediatric thyroidectomy and PTH impact, SA003
Teriparatide and national guidelines for, M482
Vascular calcification in osteoporosis, M333
Vitamin D insufficiency in African American postmenopausal women, SU502
Vitamin E, M444, M445
Vitamin K, SU362, M418, M443, M330. SEE ALSO *Menaquinone-4; Phylloquinone*
Vitamin K2, M474
Vitaxin, SA284
VivaCT40, M120
Von Hippel Lindau (VHL) tumor suppressor protein, F072, SA072
Von Kossa staining, SA567

W

Walking, SU455, SU466, SU005
Warfarin, SU504
WASP-Arp2/3 complex, SU346
Water, SU411, SU462
Weight gain, 1046
Weight lifting, M455
Weight loss, F358**,** SA358, SA374
Wnt3a, F212, SA212
Wnt9a bacterial artificial chromosome transgenes, SU043
Wnt10b, M263
Wnt/β-catenin signaling, F529**,** SA529, 1103, SU563
Wnt/Dkk signaling, F232, SA232
Wnt-inhibitory factor-1 (WIF-1), 1115
Wnts, SA027, 1097
Wnt signaling
Apoptosis prevention of uncommitted osteoblast progenitors, M221
Bone mass, 1014
Chondrogenic differentiation and hypertrophy promotion, M022
CHOP overexpression, F214, SA214
Wnt signaling (Continued)
$1,25\ (OH)_2D_3$, SU276
Dkk-1 C-terminal 21 amino acids and glycosylation, F262, SA262
Fra-1 and osteoblast differentiation, F253, SA253
Human trabecular bone maintenance, SA219
NotchIC overexpression, F244, SA244
Osteoblast development, M028
Osteoclastic differentiation and bone resorption, SU324
Runx2 expression regulation and runx2 P1 promoter activation, 1213
SFRP-1 as antagonist of, F260, SA260
Taqman gene expression analysis of, 986
Women. SEE ALSO *Osteoporosis, postmenopausal; Perimenopause; Postmenopausal women; Premenopause; Sex differences*
Aging, cortical bone cross-sectional structure and mineralization, SA015
Asthmatic, inhaled steroids and, SA122
BMD and systemic lupus erythematosus, SA516
$25(OH)_2D$ variations by age and race, M361
Isokinetic muscular strength training and tibial bending stiffness, SU229
Poly adenosine repeat in VDR and bone loss in elderly, SU170
Rowing effects on BMD, SU235
Sex hormones and proximal femur diameter, 1151
Young-elderly differences in femoral neck, SA018
WP9QY, SU343
Wrist fractures, SU356, M124
WT145 (vitamin D receptor) cells, SA554

X

XL-α proteins, SU561

Y

$Y^{747/759}$ (β_3-integrin mutant), F304**,** SA304
Yaktrax walker, SA420
YD-1901, SU299
Young's cortical bone modulus, SU077

Z

Zebrafish, SU547, M029
Zinc, SU244, M375
ZIP1, SU244
Zoledronate, M416
Zoledronic acid
Bone loss in spinal cord injury model of microgravity, M425
Bone volume and strength increases with OP-1, SU444
Calcitriol in malignancies with bone involvement, M071
Differential BMD thresholds for once-yearly dose trials, SU433
Duration of action after single dose, SU432
Endochondral ossification in rat fracture model, SU443
Neridronate combination effects on bone remodeling, SU442
Osteoclasts in C57bl mice with calcium deprivation, M421
Risedronate for Paget's disease *versus,* F482, SA482

A

Aalto, K. SU537
Abbas, S. F313, SA312, SA313
Abbaspour, A. M047
Abdallah, B. Mohamed 1091, M049
Abdelmagid, S. A. SA078
Abdelmalek, A. M468B
Abe, E. F316, SA288, SA291, SA316
Abe, M. F081, M072, SA081
Abe, Y. SA124, SU393
Abou Samra, R. SA381
Abou-Samra, A. B. M557
Abrams, E. SA501
Abrams, S. A. SU407
Abreu, C. M160
Abreu, M. T. SU428
Abribat, T. M484
Abu-Amer, Y. F313, SA289, SA312, SA313
Aburatani, H. SA240
Abuzahra, H. 1102
Aceto, M. Lorenzoni M045
Achenbach, S. J. SA161, M458
Achenie, L. SU265
Achyutharao, R. SA582
Ackerman, J. L. SU102
Ackerman, K. SU235
Ackert-Bicknell, C. L. 1080, F127, SA127
Adachi, J. D. F371, M109, M354, M406, M423, SA332, SA366, SA371, SA455, SU022, SU376, SU476
Adami, S. 1219, F406, M323, M518, SA401, SA406, SU369
Adamo, M. L. 1080
Adamopoulos, I. SA300
Adams, C. S. M032, M059, M201, SA197, SU327
Adams, D. J. 1061, 1115, M214, M259, M276, SU227
Adams, G. B. M266
Adams, J. F012, SA012, SU458
Adams, J. S. F586, SA574, SA580, SA586, SU428, SU570
Adamski, S. M571
Adamu, S. 1017, M272, M300, SA510
Addesso, V. M393, M548
Adebanjo, O. F316, SA316
Adler, R. A. M113, M436, SA365, SU125, SU394, SU482
Adlercreutz, H. SU456
Aeschlimann, J. SU411
Afonso, V. M277
Afzal, F. 1175
Agarwal, S. K. F493, SA493
Aggarwal, B. D. SU264
Aggarwal, R. M005
Aggoune, T. K. SU148, SU451
Aguila, H. Leonardo M276, M311
Aguirre, J. Ignacio 1074, SA172
Ahlbom, A. SU151
Ahlborg, H. G. 1188, M362
Ahlström, M. E. B. M225
Ahmad, A. M558
Ahmad, A. M. SU505
Ahn, B. N. SU299, SU300
Ahn, E. M318
Ahn, K. Jeong SU426
Ai, C. Mei. SA274
Ai, M. 1057, 1149, 1214, F268, SA268
Aichelmann-Reidy, M. E. M057
Aickin, M. 1044, 1113
Ainola, M. F513, SA513
Airoldi, L. SU574
Aitken, C. J. M293
Aitsiselmi, T. M309
Akahoshi, S. SU208, SU538
Akaogi, H. M183
Akel, N. S. SU009, SU495
Akeno, N. 1054
Akesson, K. M006, SU143
Akhouayri, O. SA213
Akhter, M. P. M217, M445, M544, SU507
Akira, S. F511, M185, M285, M286, SA511, SU311
Akiyama, T. SU497
Akiyama, Y. M489
Al-Dayeh, L. SA107
Al-Oanzi, Z. H. M581, SU183
Al-Regaiey, K. SA165
Alam, I. F131, SA131, SA132
Alander, C. A. 1013
Alander, C. B. M194, M195
Alatalo, S. SA198
Alatalo, S. Leena. SU301
Albert, J. David. M549
Albert, T. J. M059
Albertsson Wikland, K. M112, SA101
Alcalay, M. SU508
Alén, M. F009, M168, M212, SA009
Alexander, J. M. F207, SA207, SU565
Alexandersen, P. F377, M324, SA377
Alexandre, B. M484
Alfonso, C. F123, SA123
Alford, D. P. SU424
Algan, C. SA368
Algra, A. M415
Alhava, E. M411, SU382
Alhawagri, M. 1028
Ali, A. Afshan 1066, 1165, F527, SA527
Ali Shiri, G. SU103
Alicknavitch, M. SA254
Alini, M. SA391, SU270
Alkalay, R. N. SU474
Allan, E. H. 1025
Allen, B. L. M053
Allen, K. M. F262, SA262
Allen, M. M377
Allen, M. J. SA096, SA098, SU038
Allen, M. R. SA035
Allen, S. Paul M052, SU324
Allison, J. 1114
Allison, S. J. 1101, 1123, SA559
Alliston, T. N. SA169
Almagor, O. SA514, SA515, SA516
Almeida, E. A. C. SU350
Almeida, M. 1119, M221
Almstedt, H. C. SA395
Alnaeeli, M. SU309
Aloia, J. Francis SU502
Alon, U. S. SA461
Alonso, G. SA119, SA425
Alonso, R. F441, SA441
Alonso, V. SA208, SA539
AlRegaiey, K. SU007
Althnaian, T. A. M052, SU324
Alvarez, L. M551, SA485, SU422
Alver, K. SA324
Alwattar, B. SU462
Amaar, Y. SA158
Amanat, N. SU444
Amantea, C. M. SA223
Amaral, H. M358
Ambartsoumian, G. 1052
Ambrogini, E. SU518
Ambrose, C. G. M128, M146
Ambrósio, C. Eduardo M045
Amcheslavsky, A. SU311
Amedee, J. M250, SA271
Amedei, A. SU181
Ames, R. SU454
Amin, S. SA161
Amizuka, N. 1076, F433, SA433, SU294
Amling, M. 1140, 1208
Ammann, P. M374, SA384, SA427, SA448, SU488
Amonkar, M. SA407, M434
Amoui, M. F318, SA318
Amr, D. SA559
An, D. SA022
An, J. M084, SU554, SU555
Anagnostopoulos, I. F053, SA053
Anandarajah, A. P. SA303
Anastassiades, T. M539, SA065
Andersen, T. Levin. 1091
Anderson, B. M540
Anderson, C. 1049
Anderson, F. 1220, F335, SA335
Anderson, G. I. M193
Anderson, J. SA281
Anderson, K. SU337
Anderson, M. G. 1016
Anderson, N. F. 1181
Anderson, P. H. SA587
Andersson, L. SU156
Andersson, N. 1168, M564, SA140
Ando, T. SA288
Ando, W. SA146
Andrade, S. Caixeta. SA542
Andreassen, T. T. SA436, SU418
Andrew, J. Glynne SU072
Andrew, T. M154
Andrews, J. L. SU285
Angeli, A. M383, SU369
Angeloni, D. SU345
Anisowicz, A. F262, SA262
Aniteli, T. M. SA389
Ansari, M. R. WG14
Aoki, K. F311, SA311, SU343
Aoki, Y. SU218
Aoyagi, K. M542, SA124, SU385, SU393
Aparna, L. B. SU359
Applegate, L. SU275
Appleton, T. M037
Aquino, J. 1219
Arabi, A. 1186
Aragaki, A. SA331
Arai, H. F154, SA154, SU533
Arai, K. SU440
Arai, T. SA121
Arakaki, H. M148
Arango, I. M055
Arase, H. SU318
Arata, Y. M428
Araujo, A. B. SA326, SA327, SA363
Araya, K. 1160
Arden, N. K. F335, F336, SA001, SA335, SA336
Ardeshirpour, L. 1163, WG22
Arendell, L. M082
Arends, R. H. 1201, SA498, SU530
Arends, R. J. SA255
Ariyoshi, W. SU286
Arjmandi, B. H. M444, M445, M447, SA064, SU058
Armbrecht, H. J. SA589
Armstrong, A. P. 1027 1095
Armstrong, V. J. SA181
Arnaud, C. D. M480
Arnaud, M. SU411
Arnaud, S. B. M202, SA109
Arnett, T. M570, SA317
Arnold, A. SA153, SA548, WG8
Arnold, A. P. 1084
Arnott, J. A. SU278
Arpadi, S. SA501
Arquitt, A. B. SU058
Arrington, S. Ann SA096, SA098
Arteaga, E. M358
Artigas, S. SA103
Arwady, A. M524
Arzaga, R. R. 1064, SU219
Asadi, F. SU089
Asazuma, T. M074
Ascenzi, M. M051
Ashby, R. F012, SA012
Ashe, M. M127, SU131
Aslan, P. M080
Asokananthan, N. M030
Asou, Y. M304, M582
Aspelund, T. 1124
Asuncion, F. 1071, M272, M300, SA510
Aswad, R. A. M505
Atchison, K. M345
Athanasou, N. 1030, SA300
Atkins, G. J. SA587
Atkinson, E. J. 1153, F356, M458, SA356
Atkinson, J. 1071
Attar-Namdar, M. M166, M253
Au, S. Ki. M143
Aubin, J. M024, M190, SA247, SU269
Aubin, J. M. M505
Audin, J. E. SU195
Audran, M. F441, M392, M421, SA441
Aulchenko, Y. SU158
Auluck, J. SA442
Ausk, B. J. SU211
Avanzati, A. M402, SA483
Avery, G. SU138
Avitto, F. SU369
Avnet, S. M275
Awad, H. F220, SA220
Awada, H. 1186
Awadallah, A. SU256
Aya, K. SA151, SA289
Aymar, I. SA250, SU182
Ayyaswamy, P. S. M201
Azais, I. SU508
Azam, N. SU193
Azedine, B. SU345
Azria, M. M048
Azriel, S. M145
Azulay-Parrado, J. SA346
Azzarello, G. M085

B

Ba, J. SU559
Bab, I. 1211, M039, M166, M253
Bab, N. M039
Babbar, R. SU108
Bachrach, L. M527, M528, SU137, WG10
Backenroth, R. 1160
Baddoura, R. 1186
Badell, I. SA403
Badenhop-Stevens, N. E. F343 SA343
Badurski, J. E. SU366
Bae, S. 1108
Bae, S. SA372
Baek, D. SA443
Baek, J. SU029
Baek, K. Hyun M040, M377, M390, M401, SU439
Baeyens, O. M384
Bagger, Y. Z. F377, M324, SA377
Bagnati, R. SU574
Bagnis, C. M310
Bagur, A. M101, SU116
Baheiraei, A. M363
Bai, C. SU577

Bai, S. 1029, SA215
Bai, X. Ying F433, F477, SA433, SA477
Baik, H. Woon SU426
Baile, C. A. F275, SA275
Bailey, D. A. F002, M328, SA002, SA006
Bain, S. D. M209, M400
Bainbridge, N. J. M346
Bajnok, E. M170, M171
Bajwa, A. SA556, SA561
Baker, D. SU336
Baker, J. M450
Bakker, A. J. M030, M315
Bakshi, S. SA501
Balachandran, B. M246
Balcells, S. SU182, SU241
Baldassano, R. N. 1137
Baldini, N. M275
Baldock, P. A. 1101, 1123
Balducci, E. M085
Balduíno, A. M045
Baldwin, A. M354, M406, SA366
Balemans, W. M153
Balkan, W. SU297, SU298
Ballanti, P. 1138
Ballard, J. SU402
Ballard, P. M425
Ballesta, A. SA485
Ballock, R. Tracy. SU041
Balooch, G. SA169
Balooch, M. M379, SA169
Bamji, M. SA501
Bandyopadhyay, A. 1037
Banerjee, M. 1011, F044, M076, SA044
Bank, R. SU064
Banovac, K. SA473
Bansal, A. M317
Baptist, M. 1079
Baqi, L. SU120
Bar-Shavit, Z. SU311, SU322
Baranci, M. M406, M413, SA366
Barbe, M. F. SA078
Barbuto, N. F437, SA437
Barclay, C. 1102
Barden, H. S. M089, M525, SU126
Bare, S. 1173, F431, SA431
Bareille, R. M250, SA271
Barger-Lux, M. Janet SU410
Barisic, T. F075, SA075
Barker, M. Elizabeth 1020
Barletta, F. F573, SA573
Barnes, G. L. M013
Barnes, S. SA414
Barnett, B. SA305
Baron, J. A. SU373
Baron, R. 1057, 1117, 1118, 1142, 1198, F090, F283, F311, SA090, SA279, SA283, SA311, SA427, SU343, SU344, SU488, SU491, SU579
Barrauld, S. SA384, SA448
Barrell, G. K. M020
Barrero, M. SU227
Barrett, J. A. SU373
Barrett-Connor, E. 1019, 1058, 1185, F339, F349, F358, F400, SA339, SA349, SA355, SA358, SA400, SU226, SU394
Barrios, L. SU189
Barski, A. F216, SA216
Barsony, J. SA020
Barth, A. SA391
Barthe, N. SA115
Barthel, T. K. F555, F558, SA551, SA555, SA557, SA558
Bartke, A. SA165, SU007
Barton, I. SU380, SU438
Barton, I. P. F404, SA404
Barzel, U. S. SA331
Basillais, A. SA029, SA110, SU024
Baslé, M. M392, M421
Bass, S. L. M210
Basse-Cathalinat, B. SA115
Bassford, T. 1154, M082
Bassin, S. SA109
Basso, N. SA186
Basso, P. M473
Bastepe, M. 1102, 1203, SU561, SU566
Bateman, T. A. M216, SU234
Battaglino, R. A. F068, SA068
Battell, M. SU506
Batterham, R. L. M138
Bauer, D. 1009, 1019, 1021, 1023, 1058, 1185, 1189, F362, F369, SA362, SA369
Bauer, J. S. SA386
Bauer, L. Marie M139
Bauer, R. L. SU356
Bauss, F. SU521, SU528
Baxter, I. M341, M343
Baxter, R. C. M134
Baxter-Jones, A. D. G. F002, M328, SA002, SA006, SU220, WG10
Bayat, N. SU103
Baylink, D. J. 1181, 1206, F127, F160, F180, F264, F318, M043, M056, M151, M152, M215, SA127, SA158, SA160, SA166, SA180, SA258, SA263, SA264, SA318, SU056, SU212, SU213, SU330
Beach, M. SU373
Beamer, W. G. 1080, 1206, F127, SA127, SA164, SU078, SU163, SU224, SU429
Beamer, W. J. 1083
Beard, M. K. SU583
Beaton, D. E. M322, M464, SU480
Beattie, K. A. SU022
Beck, T. J. 1046, 1151, 1183, F017, F383, M009, M180, M425, SA017, SA359, SA383, SA499, SU005, SU008, SU158, SU186
Becker, A. 1114
Becker, B. A. M209
Becker, P. SU291
Beckman, M. J. SA203, SA556, SA561
Bedini, J. SA485
Bédouet, L. SA296
Beerli, R. SA547
Beers, A. E. M574
Beertsen, W. SA198, SA463, SU319
Begerow, B. 1222
Behets, C. M048
Behets, G. J. M251, SA480, SA506, SA508
Behnam, K. M220, SA074
Behonick, D. J. M063
Behringer, R. R. 1039, 1179
Beier, F. M025, M037, SA052
Beischel, J. A. M538
Beke, D. SU088
Bekker, P. J. 1072
Belenkov, A. SA080
Belflower, R. Marie F058, SA058
Belknap, J. K. SU161
Bell, E. SU414
Bell, G. M. 1201, SA498, SU530
Bell, N. H. M543, SA581
Belleville, C. 1057, 1117, SU488
Bellido, T. 1066, 1074, 1119, 1165, SA172, SU339
Bellizi, J. SU258, SU263
Bellmer, D. M447
Bellows, C. G. SA186
Beltrame, P. M473
Bemben, D. M450
Bemben, M. M450
Benasciutti, E. 1086
Benavides, P. F123, SA123
Benbasat, C. SU509
Bencsik, M. F529, SA529
Bendre, M. M075, SU099, SU495
Benedict, S. SU430
Beneton, M. F489, SA489
Benhamou, C. M108, SA029, SA110, SA113, SU024, SU228
Benjamin, I. J. F228, SA228
Bennetau-Pelissero, C. SU460
Bennett, J. M442
Bensamoun, S. SA029, SU024
Bensen, R. F371, SA371
Bensen, W. G. M413, SA401, SU144
Bentley, C. 1046
Benucci, M. M518
Berg, A. SU051
Bergeron, D. M294
Bergmann, P. SU531
Bergow, C. SA494
Bergwitz, C. 1205
Berlanga, E. SA337, SA338
Berner, H. M187, SU261
Berni, S. 1138
Bernstein, L. M366
Berntsen, G. K. Rosvold SU358
Berridge, B. R. F445, SA445
Berry, J. E. M044, M223, M239
Berry, J. L. M579, SU072, SU363
Berryhill, S. B. SA172
Bertazzo, R. M473
Bertin, T. 1107
Bertoldo, F. M085, M382
Bervoets, A. R. SA480, SA506, SA508
Besenbacher, F. SA032
Bessette, M. 1075
Bessler, M. SU580
Bethel, J. A. M196
Bex, F. J. 1063, F525, F262, SA262, SA525, SU285
Beynon, O. SA128
Bézie, Y. M333, SU033
Bezler, M. F077, SA077
Bhargava, N. M534
Bhat, B. M. F262, SA262
Bhat, R. A. F260, SA260
Bhat, S. WG13
Bhattacharya, R. K. SU130
Bhattacharyya, M. H. SA060
Bhattacharyya, S. SA093
Bhudhikanok, G. S. SU137
Bi, L. X. SU489
Bi, X. SA107
Bi, Y. 1078, SU070
Bialek, P. E. 1209
Bian, H. SU521, SU528
Bianchi, D. M339
Bianco, P. 1157
Bierbaum, B. E. SU328
Biggar, W. Douglas M521
Bigler, P. SU457
Bijlani, R. 1084
Bijlsma, J. M415
Bikle, D. D. F178, F531, SA178, SA531, SU028
Biko, J. SA003
Bilezikian, J. P. 1098, 1199, F429, F495, F497, M255, M416, M555, SA429, SA495, SA496, SA497, SU085, SU108, SU296, SU512, SU513, SU514
Bilgin, Y. SA368
Bilic-Curcic, I. SU258
Billiard, J. SU293
Billings, P. C. 1135, SU016
Bindra, R. R. M124
Binello, E. SU421
Binkley, N. F106, M090, M327, SA106, SA342, SA399, SU118, SU381, SU583, SU584
Bird, D. M206
Bird, J. E. M010
Birenboim, R. M166
Birken, S. SU513
Birks, C. M186
Birzin, E. T. M569, M571
Bischoff, D. S. SA145
Bischoff-Ferrari, H. 1221, M494, SU373, WG26
Bisello, A. 1065, F471, M479, M559, SA471
Bishop, J. E. 1090
Biskobing, D. M. SU482
Bistrup, C. M546
Biswas, R. S. SU346
Blacher, J. SU033
Blacher, R. M467
Black, A. J. SA117
Black, D. M. 1009, 1067, 1098, 1174, F362, F400, F429, SA362, SA400, SA429, SU433
Black, K. Melissa M193
Blackwell, T. F369, M337, SA369
Blair, H. C. F316, M224, M278, M279, SA316, SU277
Blake, G. M. M092, M407, SU110, SU352, SU423
Blanch, J. M351, SA250
Blank, R. D. F464, SA464, SU077
Blankenstein, M. A. SA162
Blanque, R. SU343
Blanton, C. A. SA442
Blaschke, S. SA210, SU238
Blasi, F. SA076
Blau, E. M. SU582
Blesius, A. SA302
Blew, R. B. M455
Blin-Wakkach, C. M310
Blind, E. SU564
Bliuc, D. M463
Bliziotes, M. 1024, SA142, SU348
Block, G. F328, SA328
Bloom, S. R. M138
Bloomfield, S. M377, M576
Blottner, D. 1036
Blumsohn, A. 1020, M136, M138, SA128, SU147
Boabaid, F. M044
Boachie-Adjei, O. M499
Bodine, P. V. N. 1063, 1213, F260, F525, M018, SA260, SA525, SU293
Body, J. J. SU097
Boehm, C. A. M254, M262, SA241
Boehm, H. M119, M121, SA031, SA114, SU129
Bogoch, E. R. M464, SA348, SU480
Boileau, C. SA041
Boissy, P. 1091
Boitte, F. SU411
Boivin, G. SA038
Bolander, M. E. M347
Boling, E. P. SU103
Bolivar, I. M485

Bollag, R. J. SU280
Bollag, W. SU280
Bolland, M. J. SA490
Bollerslev, J. M169, SU335, SU427
Bolognese, M. A. 1072, 1199, F424, F426, SA424, SA426, SU493
Bolon, B. M272, SA510
Boltz, M. Ann SA589
Bondestam, S. SU510
Bone, H. G. M515, SU493
Bonewald, J. M079
Bonewald, L. F. 1004, 1035, 1105 1177, F173, F175, F182, M079, SA028, SA173, SA175, SA179, SA182, SU215, SU556
Bonfield, W. SU005
Bonkowski, M. S. SA165, SU007
Bonnelye, E. M024
Bonnet, N. SA110
Bonnick, S. F412, SA412
Bonny, A. F396, M386, SA396
Bonvoisin, B. F408, M429, SA408
Boonen, S. 1167, 1219, M003, M563, M564, SU434WG2
Booth, S. L. SU362
Borah, B. SU436
Borba, V. Zeghbi Cochenski M416
Bordenave, L. M250
Bordet, J. 1092
Boreham, J. Victoria SU147
Borel, O. SU067
Borgström, F. SA409
Borgulya, J. SU478
Bornstein, P. SU069
Borofsky, M. A. 1199
Borojevic, R. M045
Boron, W. F. SU308
Borrud, L. M002
Borsari, S. SU518
Borysenko, C. W. M224, M279, SU277
Bosaeus, I. M112
Boskey, A. L. M061, M475
Bossert, R. P. M405
Bothwell, A. M280
Bothwell, M. SA157
Botolin, S. SA227
Botta, R. SA541
Boucharaba, A. 1092
Boucher, N. SU020
Boudignon, B. 1036
Boudouscq, V. SA115
Bouhelal, R. SA547
Bouillon, R. 1167, F147, M003, M563, M564, SA147
Boules, H. SU243
Boulet, J. SU082
Boulos, P. SU022
Boumah, C. E. SU057
Bounaud, M. SU508
Bouralexis, S. SA540
Bourget, C. M250
Boutsen, Y. M419
Bouvet, M. SA535
Bouxsein, M. L. 1001, 1054, 1080, 1083, 1121, 1122, 1153, 1214, F429, M177, M178, M325, M329, M477, M483, SA429, SU139, SU160, SU474
Bouyer, G. 1196
Bouyer, P. SU308
Bowden, B. M516
Bowe, E. A. 1033, SU032
Bowen, D. SU529
Bowtell, D. D. L. F266, SA266
Boyan, B. D. M042, M567, M572, SA572
Boyce, B. F. 1003, SA403, SU323
Boyd, S. K. M106, SU133
Boyer, B. SU089
Boyer, M. SA030
Bracco, O. Luís M473
Bracke, M. F345, SA345
Bradley, E. W. SU341
Braga, V. M518
Brain, J. M177, M178, M325, M329, SU160
Brandao-Burch, A. SA317
Brandi, M. Luisa M518, M519, SA552, SU181
Brändström, H. SU177
Branger, S. M179
Bransford, R. SU444
Branstetter, D. 1095
Brasier, M. SA296
Brasil, R. Rezende Oliveira SA444
Brasseur, J. Pierre M419
Brault, A. L. 1008
Brault, R. SU508
Braun, M. SA418
Braun, W. SA109
Braut, A. SU263
Bravenboer, N. SA162, SA188
Brazier, M. SA088, SA302, SU411
Bréart, G. F373, SA373, M466
Brecher, A. M350
Breitwieser, G. SA547
Brennan, F. M299
Brennan, K. J. SA568
Brennan, R. M. M468A
Brenneisen, R. SU457
Brenneman, S. K. F339, F349, SA339, SA349, SU355, SU582
Brenner, K. SU088
Bretzel, R. SA368
Breuil, V. M310
Bréville, P. M333, SU033
Brey, R. SA419, WG5
Breyer, M. D. 1013
Brin, S. M108
Bringhurst, F. Richard 1018, 1158, M560, SA536, SU196, SU560, SU562, SU563
Brink, P. M219
Brinskelle-Schmal, N. F118, SA118
Brinton, B. T. SA546
BrintzenhofeSzoc, K. M426
Brismar, T. B. SA105, SU107
Bristol, D. SU082
Brixen, K. M546
Broadus, A. E. SA179, SA538
Brodt, M. D. M208
Broe, K. E. M342, M494, SU362
Broeckmann, E. SU081
Brommage, R. 1064, F394, SA394
Bromme, S. D. SU328
Bronson, S. K. SU259
Brossard, J. SA530, SU514, SU536
Brot, C. SA578
Brot, M. D. M400
Broughton, K. M. SA243
Brown, A. J. F533, SA533
Brown, A. Joy. SU042
Brown, E. 1163
Brown, H. M272
Brown, J. F371, F482, M423, SA371, SA482, SU438
Brown, J. C. SU430
Brown, J. Keenan SU010
Brown, L. G. M083
Brown, M. A. F141, SA128, SA141
Brown, M. Lesley M025
Brown, S. A. SU398
Brown, T. A. 1008, 1216
Brownbill, R. A. SU466
Broy, S. F412, M472, SA412, SU138, SU377
Bruder, J. M. SU356
Brudney, K. M393
Brudzinski, E. SA342
Bruhn, R. M082
Brun, J. G. SU392
Brunell, R. F426, SA426
Brunet, D. M539
Brunet-Imbault, B. SA029, SA110, SU024
Brunetti, G. M289
Bruning, A. L. SU582
Brunner, A. SU061
Brunskill, A. P. M224
Bruynick, N. SA427, SU488
Bruzzaniti, A. F283, SA283
Bryan, J. SU044
Bryant, C. M080
Bryant, H. U. 1218, F445, M493, SA445, SU198, SU332, SU338
Bryant, R. J. SA418
Bu, L. M. M043
Bucala, R. SA135
Bucaro, M. A. M201
Bucci, J. M080
Buckbinder, L. SA567
Buckendahl, P. SU068
Buckland-Wright, J.Christopher M241
Buckle, K. L. SA524
Buckner-Berguis, B. D. 1214
Buckwalter, K. A. M326
Buford, W. L. SU489
Bugnard, F. SU119
Buhl, T. SA547
Buison, A. SA502
Bukata, S. V. SA351, SU379
Buki, K. G. SA315
Bula, C. M. 1090
Bullock, H. M573, SA200
Bulnheim, U. SU291
Bultink, I. SU446
Bünger, M. Hauge SA032
Bungum, A. O. SA082
Bunker, C. M180, SA100, SA359
Burckhardt, P. F104, SA104
Burford, J. H. SU032
Burgess, J. M374
Burghardt, A. F531, M058, SA531, SU028
Burgio, D. SU434
Burke, E. M. M548
Burke, J. F. SU059
Burke, P. K. F112, SA112
Burke, S. W. M499
Burkhart, M. SU544
Burleson, J. A. SA135
Burnett, S. M. SU196
Burnham, J. M. 1137, SA499
Burns, T. L. F185, SA185, SU364
Burri, N. SU275
Burshell, A. F468, M435, SA468
Burton, D. W. SA034, SA549, SA535, SA571, SU145
Bushinsky, D. A. SA505, SU239
Buskens, E. M415
Busque, S. 1156
Bussiere, J. SA491
Bustamante, M. SU182, SU241
Buurman, C. J. SA588
Byoun, J. M084, SU554
Byrjalsen, I. M137
Byrne, M. H. F063, SA063
Byron, C. M203
Byun, D. SU425

C

Caballeria, L. SU422
Cabezas, M. M358
Cáceres, E. SA250
Cadarette, S. M. M322, M336, SA348
Cadirni, A. M144, SU420
Caetano, P. A. M110, SU483
Caffarelli, C. M144, SU420
Caglilyan, A. SA108
Cahall, D. M420
Cai, G. SA134
Calabrò, A. 1060, M394, SA483
Calcagni, A. M469
Callaci, J. J. SA432, SU447
Callaghan, C. E. M126, SU229
Callon, K. E. SU284
Callréus, M. M006
Calomme, M. M441
Calvi, L. Maria M266
Camacho, N. P. F039, F464, SA039, SA464, SU030, SU527
Camacho, P. M. SU581
Camargo, M. Tereza SU549
Cambell, G. SU123, SU123
Camboa, P. SU369
Camerino, C. SA204
Cameron, I. SU368
Cameron, M. A. WG19
Cameron, N. M007
Cameron, V. A. M020
Caminis, J. M425, SU433
Caminiti, M. J. SU398
Camp, J. F356, SA356
Campagna, S. M394, M402
Campbell, M. J. SA094
Campbell, M. S. SU431
Campbell, P. SA211, SU288
Campbell, P. D. M284
Campo, D. A. SU093
Campusano, C. M358
Canaff, L. SA544
Canalis, E. 1053, 1178, F024, F214, F244, SA024, SA214, SA244, SU013, SU050
Cances-Lauwers, V. M360, SU390
Canfield, A. E. M579
Cann, C. E. SU010
Cannata-Andía, J. B. M094, SA392
Cantor, P. 1169
Cantor, T. SU149, SU514, SU536
Cao, J. 1212
Cao, J. J. SA019
Cao, S. SU203
Cao, X. 1041, F092, F097, M260, M267, SA092, SA097, SA215
Cao, Y. M070
Cao, Y. SU450, SU497
Caparbo, V. Falco SU543
Capozza, R. SA003
Cappagli, B. M142
Caralis, P. 1100
Carballo-Jane, E. SU437
Carbonell, J. M351
Carbonell, S. M519, SU181
Cárcel Trullols, J. SU099
Carle, G. F. M310
Carlos, A. S. SU161
Carlson, M. A. SU371
Carlson, T. SU148, SU451
Carlsson, Å. SA409
Carlsten, H. 1168
Carmeliet, G. F147, SA147
Carmeliet, P. F147, SA147
Carnes, D. L. 1161
Carnevale, V. SA344
Carnevalli, C. M. Z. SA389
Carney, D. SA149
Caron, R. SU016
Carpenter, T. O. M027, WG8
Carpi, D. SU574
Carr, C. 1133
Carran, J. Richard SA065

Carrella, C. M147
Carrillo-López, N. SA392
Carroll, J. SA348
Carson, D. SU042, SU096
Carstens, J. M546
Carstens, M. M174
Carter, E. J. 1181
Carvajal, R. SU117
Carvalho, R. S. SA027, SA150
Carvalho, S. M. T. SU101
Carvallo, L. SU252
Casado, A. SU189
Casado, E. SA337, SA338
Casagrande, D. M010
Casebeer, L. 1114
Casey, M. M135, M487
Cashman, K. D. M498, SA013, SU499
Casper, R. F. SU325, SU342
Cassady, A. M292, A310
Castañeda, J. L. 1016, M055
Castro, C. H. M. SA352
Cattley, R. 1017
Cauley, J. 1009, 1019, 1021, 1022, 1023, 1024, 1056, 1058, 1100, 1110, 1154, 1174, 1189, F323, F358, F362, M180, M181, M182, SA100, SA323, SA355, SA358, SA359, SA362, SU186, SU384, SU394, SU433
Cavalcanti-Adam, E. A. F077, SA077
Cavanagh, P. R. F421, M451, SA421
Cavener, D. SA059
Caversazio, J. SU202, SU553
Cawthon, P. M. 1009, F362, M337, SA355, SA362
Ceccarelli, E. SA483
Celil, A. B. SA211
Cenci, S. 1086
Center, J. R. 1112, 1184, F354, M362, M463, SA354, SU121
Cephas, S. M202
Cepollaro, C. M144, SU420
Cerchio, K. F450, SA450
Cerna, Z. SU083
Cetani, F. SA541, SU518
Cha, S. S. M364
Chacksfield, M. A. M293
Chadha, A. B. SA514, SA515, SA516
Chadwick, R. B. F160, F180, M043, M151, SA160, SA180, SU056
Chaffer, S. SU082
Chagin, A. SA397
Chagnaud, C. SA346
Chai, D. M019
Chai, S. M444
Chaignaud, C. M333
Chaisson, M. 1027, 1095
Chakarvarthy, V. M013
Chaki, O. M164, M428
Chakkalakal, D. M445
Chalès, G. M549
Chalouni, C. F299, SA299
Chambers, T. J. SA393
Chambon, P. 1006, M562, SU568
Champsaur, P. SA346
Chan, B. K. S. 1009, 1024, 1067
Chan, C. 1102
Chan, D. SU223
Chan, F. M143, SA322
Chan, R. Y. K. SU573
Chan, V. SA125, SU159
Chandhoke, T. K. M259
Chandler, R. L. 1182, SU043
Chandra, D. SU333
Chandra, R. M516, M534
Chanetsa, F. SU524
Chang, E. M282, SU320, SU321
Chang, F. M183
Chang, S. SA443
Chang, W. SA045, SA292, SA545
Chang, W. Y. M381
Chansky, H. A. M036
Chappard, C. SA029, SA110, SA113, SU024, SU228
Chappard, D. M048, M392, M421, SA451
Chappel, J. F285, M320, SA285
Charlesworth, D. F489, SA489
Charlton-Kachigian, N. 1097, 1141, SU066
Chase, C. C. M521
Chasseraud, M. SA088
Chaudhary, L. R. M012
Chauffert, M. M333, SU033
Chavida, F. F123, SA123
Chavoshi, T. 1168
Cheema, F. WG14
Chelladurai, B. M200
Chellaiah, M. A. SU346
Chen, C. M223
Chen, C. M325
Chen, C. SU368
Chen, D. 1176, 1180, M028
Chen, E. F412, SA412, SU583
Chen, F. SU577
Chen, G. M538
Chen, H. F097, M313, SA097, SU570
Chen, H. Y. M569, M571
Chen, I. S. Y. SA022
Chen, J. 1029
Chen, J. Ran SU339
Chen, K. M573
Chen, L. 1134
Chen, M. M028
Chen, P. 1170, M478
Chen, P. SA434
Chen, Q. M091
Chen, Q. SU063
Chen, S. SA280
Chen, T. 1205, M403
Chen, T. C. M494, SA326, SA327, SA585, SU424, SU585
Chen, T. H. SA045, SA292
Chen, V. SU029
Chen, W. SA261
Chen, W. SU573
Chen, X. SA179, SA538
Chen, X. SA522
Chen, X. Dong 1066, F224, SA224
Chen, X. D. SU172
Chen, Y. 1130, 1139, WG16
Chen, Y. F339, F349, M102, M373, SA339, SA349, SU355, SU582
Chen, Y. SU381
Chen, Z. 1100
Chen, Z. 1154, M082
Cheng, D. M. SU362
Cheng, E. 1173
Cheng, J. M440
Cheng, S. 1141, 1193, F248, SU248
Cheng, S. F009, M168, M212, SA009
Cheng, S. SU461
Cheng, S. Li 1097, F232, SA232
Cheng, S. Mei SU461
Chenu, C. C. 1148
Cheong, J. M. K. SA414, SU026
Cherian, P. SU556
Cherman, N. 1157
Cheskis, B. J. F573, SA573
Chesnut, C. H. 1072
Chesterfield, A. K. F253, SA253
Cheung, A. M443, SU076
Cheung, E. Y. N. SU115
Cheung, J. SA206
Cheung, P. T. SA125
Cheung, W. M. W. SU159
Chevalley, T. SU479
Chiabrando, C. SU574
Chiba, H. SA588, SU268
Chihara, K. M091, M227, SA562, SU207
Chikazu, D. SA143
Chikuda, H. 1038, 1050, SU037
Chines, A. SU380
Chio, L. SU338
Chirgwin, J. M. 1093, SA148
Chiu, H. SU078
Chiu, R. F070, SA070
Chiu, W. Sze Maria SA310
Chiusaroli, R. 1057, 1117, 1118, 1164, 1198, F072, SA072, SU491
Chmielewski, P. A. SU436
Cho, C. Soo M401, SU439
Cho, D. SU187
Cho, E. SU289
Cho, J. 1108, F218, M235, SA218, SU248
Cho, S. SU187, SU188
Cho, T. Joon M234
Cho, Y. J. SU357
Chock, M. K. M086
Chockalingam, P. S. M247
Choh, A. C. M157, SU164
Choi, E. M218
Choi, H. F275, SA275
Choi, H. SA116
Choi, H. SU299
Choi, H. Jeong SU426
Choi, I. SU188
Choi, J. M233
Choi, J. M453, M455
Choi, J. SU055
Choi, J. SU187, SU188
Choi, J. Sook SU492
Choi, S. Jin F513, M271, SA079, SA281, SA513
Choi, Y. SU166
Chong, W. SU299, SU300
Chorev, M. M558
Choucair, M. 1047
Choudhary, S. SA195, SA196
Choudhury, I. M067
Chouinard, L. SA030, SU501
Chow, J. W. M. SA526
Choy, D. Tak Kee M143, SU223, SU360
Christakos, S. F230, SA221, SA230, SA532, SU246, SU251
Christian, R. C. SA405
Christiansen, C. 1055, 1068, F377, F390, M137, M324, SA377, SA390, SU067, SU427
Christie, P. T. F063, SA063
Christoffersen, H. M461
Chu, K. SA467
Chumlea, W. Cameron M157, SU164
Chumley, A. F336, SA336
Chun, R. F. SA574, SA580
Chung, D. SA440
Chung, H. M084
Chung, H. SU187, SU188
Chung, H. Yeon M271
Chung, L. W. K. M077, SU096
Chung, U. 1012, 1038, 1050, 1128, M022, SA249
Chung, U. Il F042, SA042
Chung, Y. SA166
Chung, Y. SA372
Chung, Y. SU187, SU188
Churchill, G. A. F127, SA127
Cianferotti, L. SA541, SU518
Ciaponi, M. M142
Ciolfi, V. SU061
Ciria, M. M351
Civitelli, R. 1106, 1193, F248, F277, F424, SA248, SA277, SA424, SA440, SU552
Clark, P. F340, SA340
Clark, S. H. F075, SA075
Clarke, B. L. SA488
Clarke, S. E. M. M511
Clarke Anderson, H. F039, SA039, SU030
Cleek, T. M202
Cleiren, E. M153
Clemens, T. L. 1001, 1054, F272, F531, SA166, SA272, SA531, SU570
Clement, J. SU005, SU006
Clément-Lacroix, P. 1057, 1117, 1118, F090, SA090, SA427, SU488, SU491, SU579
Clemmons, D. R. SU398
Clézardin, P. 1092, 1094, F090, SA090
Cliby, W. A. SA083
Cliffe, J. F489, SA489
Cline, G. SA401
Clines, G. A. SA148
Cloos, P. A. M137, SA485
Clopton, P. SA571
Clor, J. L. SU050
Clowes, J. A. M136, M349, SA138, SU404
Coakkey, D. M487
Coakley, D. M135
Coates, P. S. M550
Coates, P. Toby Hewlett M550
Cock, T. SA559
Cody, D. F253, M128, SA253
Cody, K. M. SU400
Coffin, J. D. 1042, F026, SA026
Cohen, M. A. M138
Cohen-Solal, M. M166, M568, SA129
Cointry, G. SA003
Coker, E. SU476
Colaianni, G. F285, SA204, SA285
Colao, A. M147
Cole, D. SU179
Cole, H. M493, SU338
Cole, J. A. SA520
Cole, J. H. SU137
Cole, L. M117, SU127, SU128, SU232
Cole, R. E. M107
Cole, T. J. SU112
Cole, W. G. 1102
Coleburn, V. E. F262, SA262
Colin, A. SU421
Coll, M. M351
Collet, C. SU154
Collin-Osdoby, P. A. M277, M290, M303, SA298
Collins, J. F. F234, SA234, SA582
Colloton, M. SA470, SU532
Colon-Emeric, C. S. SU371
Colston, K. W. SA094
Colucci, S. M289, SA204
Coluci, A. SA491
Compher, C. SU430
Compston, J. Elizabeth SU417
Comuzzie, A. G. SA134
Conaway, H. H. M281, SA566
Conceição, F. Lucia SA444
Conn, D. E. SU481
Connelly, M. T. M366
Connolly, C. M487
Cons Molina, F. F340, SA340
Constable, M. M293

(Key: 1001-1222 = Oral, F = Friday Plenary poster, SA = Saturday poster, SU = Sunday poster, M = Monday poster, WG = Working Group Abstract)

Constant, F. SU411
Contreras, O. M358
Convery, J. SA149
Conway, T. SU150
Cook, D. B. SU183
Cook, G. J. SU423
Cook, J. L. SU089
Cook, R. J. M423
Cooper, C. 1220, F335, F336, F345, F406, SA001, SA335, SA336, SA345, SA406, SA454, SU367, SU419
Cooper, D. SA109
Cooper, D. M.L. M106, SU006
Cooper, M. S. SU419
Corey, E. 1093, M083
Coriat, F. M108
Corich, M. M558
Corley-Mastick, C. SA570
Cornélis, F. SU154
Cornish, J. M522, SU284
Cornuz, J. F104, SA104
Corr, M. F293, SA293, SU100
Corral-Gudino, L. M167
Corvisier, J. 1155
Cos, P. M441
Coschigano, K. 1167
Cosenza,, M. E. SA491
Cosman, F. F437, SA317, SA437
Costessi, A. SA225
Couchouron, T. M392
Coucke, P. SU175
Couper, R. 1102
Courteix, D. SU228
Coutinho, B. M098, SU391
Couzens, M. 1101
Covarubias, M. M056
Cowgill, C. S. M327
Cox, A. G. SA033, SU025
Cox, D. A. 1055
Cox, G. M135
Cox, K. 1037
Cox, T. Martin M242
Coxam, v. SU412, SU460
Coxon, F. P. M430, SU334
Cozar-Castellano, I. F005, SA005
Crabbe, P. SU175
Cramer, J. A. M434
Crandall, C. F328, SA328
Crandall, L. F246, SA246
Cranney, A. M539, SA455
Crans, G.
Crans, G. SU381
Crans, G. C. 1070
Crans, G. G. 1170, F383, F428, SA383, SA428
Craven, B. Catharine M125
Crawford, D. T. 1008, 1216, M388
Crepaldi, G. M323, M339, M382
Cristallini, S. SU442
Cristino, S. SA286
Criswell, D. S. SU219
Crockett, J. C. M430
Crocombe, S. SU363
Cromer, B. F396, M386, SA396
Cromer, B. A. SU317
Cropet, C. M050
Crotti, T. SU328
Croucher, P. I. M073
Crowley, C. SU144
Crowley, V. M135
Crozier, S. F335, SA001, SA335
Crozier, S. R. 1220
Crumley, G. SU082
Cruzat, F. SU252
Cuartas, E. SU462
Cuenca-Acevedo, R. SU189
Cui, H. SU455
Cui, L. SA274
Cui, W. F299, SA299
Cui, Y. M077
Cullen, D. M. M217, SU507
Cumming, R. SU368
Cummings, S. 1009, 1019, 1021, 1055, 1056, 1067, 1110, 1215, 1174, F017, F340, F362, F428, M182, M325, M329, M337, SA017, SA340, SA362, SA428, SU160
Cundy, H. Richard M522
Cundy, T. F500, M522, SA500
Cunningham, C. M135, M487
Cunningham, M. E. SA023
Cunningham, M. L. SA243
Cupples, L. Adrienne F136, F330, M494, SA040, SA136, SA330
Currado, A. M377
Curtis, D. SA219
Curtis, J. R. 1114, M465, SU396
Cusick, T. M422
Cussler, E. M438, M453, M455
Czerwinski, S. A. M157, SU164
Czilli, T. SU407
Czirok, A. 1073

D

D'Amelio, P. SU312
D'Amour, P. SA530, SU514, SU536
D'Angelo, M. SU047
D'Erasmo, E. SA344
D'Haese, P. C. M251, SA480, SA506, SA508
D'Ippolito, G. M269, M560
D´Souza-Li, L. F. SA542
da Silva, C. Arthur Almeida SU543
Daddona, P. M484
DaFonseca, K. M459
Dagnæs-Hansen, F. M049
Dai, J. M088
Dai, J. C. SA522
Dai, S. F313, SA312, SA313
Daigo, Y. SU141
Dal Canto, N. M394
Dale, K. SA512
Dallal, G. SA579, SU362
Dallas, M. F173, M079, SA173
Dallas, S. L. 1073, M079, SU063
Dalle Carbonare, L. M085, M382
Dalstra, M. SU135
Daly, J. M. M055
Daly, R. M. M210
Dalzell, N. 1151, M334
Dam, T. L. SA355
Dambacher, M. SU132
Dambacher, M. A. F104, SA104, SA458
Damoulis, P. D. M188, SA235
Damron, T. A. M033, SA096, SA098, SU038
Dams, G. SA480
Damsky, C. H. SU350
Danielson, K. G. SU264
Daniluk, S. SU366
Danks, L. M299
Dann, P. 1014, F471, SA471
Daphtary, M. M. F017, SA017, SU008
Dard, M. SA271
Dargent-Molina, P. F373, M466, SA373
Dark, K. 1059, 1191, SU204
Darnay, B. G. F099, SA099
Darwanto, A. SA043
Das, G. SU363
Datta, H. K. M236, M581, SU183
Datta, N. S. M223
Dattoli, V. SU369
Daugherty, S. M. M058
Davey, R. Ann SA310
Davey, T. 1143
Davicco, M. SU412, SU460
David, V. M192, SU074
Davidson, J. F500, SA500
Davie, M. W. J. M346
Davies, J. SA393, SA526
Davies, K. Michael M439
Davies, M. R. M537
Davies, T. SA288
Davis, D. SA348
Davis, H. E. SA491
Davis, J. G. M499
Davis, P. M. SU525
Davis, S. SU198
Davis, S. I. 1162
Davison, K. S. M413, SU144
Daws, M. R. 1195
Dawson, J. L. F555, SA551, SA555
Dawson-Hughes, B. 1221, M437, SA579, SU362
Day, J. SU123
Day, J. S. M372
Dayer, R. SA448
De Benedetti, F. 1138
De Broe, M. E. M251, SA480, SA506, SA508
De Camilli, P. F283, SA283
de Crombrugghe, B. M252, SA233
de Feo, D. M323, SA225
De Feo, M. Laura M518
De Geronimo, S. SA344
de Gortázar, A. SA208, SA539
De Keyser, F. M149
de la Higuera, M. SA119, SA425
De La Piedra, C. M481, M415, SA375
De Luca, V. SU287
De Marzo, A. SU552
de Nijs, R. M415
De Paepe, A. SU175
De Paola, V. 1060, M394, SA483
De Paoli, A. F500, SA500
de Papp, A. E. F412, SA412, SU583
de Ravel, T. J. L. M153
de Rekeneire, N. 1022, 1110
de Santiago, S. SU397
de Souza, R. L. SU225, 1148
de Vernejoul, M. M062, M166, M179, M568, SA113, SA129
de Vries, F. F345, SA345
de Vries, T. J. SU319
de Winter, J. M134, SA568
Deal, C. 1169
Dean, T. SU566
Debanne, S. M. F396, M386, SA396
DeBar, L. 1044
DeBeer, J. SU476
Debiais, F. SA155, SU508, SU542
DeChiara, T. M. SU050
DeFrancisco, T. M. M117, SU127, SU128, SU232
Deftos, L. J. SA034, SA535, SA549, SA571, SU145
Degrandi, M. C. M412
deGroot, J. M058
Del Monte, F. M518, M519, SU181
del Pino-Montes, J. M167
Del Rio, L. F112, M090, SA103, SA112
del Rio, L. Miguel M365
Delahunty, K. M. SU163, SU429
Delaisse, J. Marie 1091
Delalandre, A. SA252
Delaney, J. D. SA192, SA231
Delaney, M. SU496
Delany, A. M. SU065
Deleze, M. F340, SA340
Delhanty, P. J. D. SU268
Della Badia, M. SU108
Della-Fera, M. Anne F275, SA275
Delling, G. SA111, SU084
Delmas, P. 1068, 1170, F380, F408, M420, SA113, SA353, SA380, A408, SU067, SU132
DeLuca, H. F. M584
DeMarini, S. SA004
Demay, M. 1162, M027
Demerath, E. W. M157, SU164
Demers, C. SA584
Demidchik, Y. SA003
Demir, E. SA368
Demiralp, B. 1062
Dempster, D. 1010, M370, SA317, SA496, SU527, SU544, SU557
Demulder, A. SU531
Deng, C. 1134
Deng, F. Y. SU172
Deng, H. W. SU150, SU172, SU174
Deng, L. 1054
Deng, X. M087
Denger, S. SU287
Denhardt, D. T. F191, SA050, SA191, SU405
Denise, P. 1155
Denke, M. SU486
Dennis, J. E. SU256
Dennison, E. SA001, SU419
Denton, J. F507, SA033, SA507, SU025
DePalmer, S. 1102
DePeter, K. C. M140
Depew, M. J. M237
Depresseux, G. M419
Deprez, P. SU343
Deregowski, V. 1178, F024, F214, F244, SA024, SA214, SA244
Derynck, R. SA169
Desai, D. M484
Deshpande, D. M082
deSilva, J. F207, SA207
Destaing, O. F283, SA282, SA282, SA283
deTakats, D. F489, SA489
Devareddy, L. M444, M445, M447, SA064, SU058
Devine, A. 1007, F417, M169, SA416, SA417
Devogelaer, J. Pierre M048, M419
Devoto, M. SU168
Dhaliwal, S. S. 1007, F417, SA416, SA417
Dhananjaya Naidu, M. SU359
Dhawan, P. SA221, SA532, SU246
Dhillon, H. 1122
Di Benedetto, A. SA204
Di Giacinto, C. 1138, SA279, SU091
Di Gregorio, S. M365, SA103
Di Matteo, L. M518
Di Munno, O. M323
Di Stefano, M. M518, M519
Diabira, S. M269
Diamond, T. H. M080
Diaz-Curiel, M. M481
Díaz-López, J. B. M094
Diaz-Molina, C. SU189
Dib, L. M497, SA381
Dibba, B. M442
Dick, I. M. 1007, F417, M169, SA416, SA417
Dickins, R. A. F266, SA266
Diem, S. 1173, F369, SA369
Diener, A. SU291
Díez-Pérez, A. F428, SA250, SA428, SU182, SU241
Dijkmans, B. SU446

Dillard, E. SA520
Diller, L. SU085
Dilzer, C. SU113
Dimai, H. P. M295
DiMeglio, L. A. F466, SA466
DiMuzio, M. T. SU109
Dinakarpandian, D. M079
Ding, K. Hong M492, SA447, SU562
Ding, M. M049, SU135
DiNinno, F. M569, M571
Dinulescu, D. C. 1084
Dion, N. M060, SU035
Dittberner, K. SU383
Divakara, V. P. 1073
Divieti, P. M560, SA536, SU562
Divine, G. W. SA492
Dixon, S. Jeffery 1207, M314
Djandji, M. SU448
Dobkin, J. M393
Dobnig, H. 1222, M398, M545
Dobrenko, A. SU366
Dobrolecki, L. E. SA438
Dodds, R. A. SA509
Doetschman, T. 1042, F026, SA026
Dogolo, L. M469
Dolan, A. Louise M098, SU354, SU391
Dominguez, L. 1074
Donahue, H. 1031, SU136, SU214, SU217
Donahue, L. 1080, 1083, 1206, M191, M218, M374, M452, SA189, SA164, SA190, SU153, SU163, SU221, SU230
Donehower, L. SU004
Dong, D. M186
Dong, D. SU178
Dong, S. S. SU205
Dong, Y. F058, M028, M035, SA058
Donley, D. W. SA159
Donovan, L. M. 1064
Donovan, M. A. M370, SU108
Donovan, S. M. SU001
Doody, S. L. SU219
Dorado, G. SU189
Doria, A. M530
Dormans, M. L. WG21
Dosy, J. SU001
Doty, S. SA023, SA149
Doucet, M. 1096, SU200
Dougall, W. 1027, 1095
Doupe, M. M331, M354, M406, SA366, SA456, SU353, SU361
Dousevich, V. SA028
Dovi, J. V. SU350
Dovio, A. M383
Dowell, M. Susan SU410
Dowsett, M. 1151
Doyle, D. SU123
Doyle, N. F435, SA030, SA435, SU501
Doyon, J. M066, WG9
Dratwa, M. SU531
Drevon, C. M187
Dreyer, B. E. SA538
Drezner, M. K. F408, SA408, SA582, SU118, SU584
Drinka, P. SA399
Drissi, H. 1040, 1180, F058, M028, M035, M061, SA058, SA201
Drozd, V. SA003
Drysdale, I. P. M206
Du, X. 1134
Duan, Y. SA382
Duarte, M. Eugenia Leite M045, SA074, SA444
Duboeuf, F. F380, SA380, SU067
Ducher, G. SU228
Ducy, P. SA200
Dufaur, L. M242
Duff, G. W. M158
Dufresne, T. E. SU436
Duggan, M. E. SU577
Dukas, L. C. F415, SA415
Dulai, S. K. SU443
Dumble, M. SU004
Dumon, J. C. SU097
Dumont, E. F406, M432, SA406
Duncan, E. L. SA128
Duncan, R. L. 1032, M196, M197, M200, SU136
Dunford, J. E. M316
Dunham, K. SU259
Dunlop, D. D. SA514, SA515, SA516
Dunn, D. M. SU003
Dunn, N. 1206
Dunstan, C. R. SA568, SU532
Duong, L. T. SA046
Dupeux, S. M549
Dupin-Roger, I. SA302
Duplat, D. SA296
Dupont-Versteegden, E. E. SU009
Dupuis, J. F136, SA136
Duque, G. M248
Durham, B. H. SU505
During, M. 1123
Duryea, J. SU022
Dusevich, V. 1177
Dusso, A. 1085
Dutta, S. K. M566
Dutto, D. SA109
Dutton, J. M529
Dvorak, M. M. M270
Dvornyk, V. SU150

E

Eagleton, A. C. SU147
Ealba, E. Lynn 1062, M239
Eastell, R. F428, F441, M136, M349, M420, SA128, SA138, SA428, SA434, SA441, SU147, SU380, SU404
Eastwood, J. B. WG15
Easwaran, V. F253, SA253
Ebeling, P. R. M155
Ebert, D. F253, SA253
Ebert-McNeill, A. SA060
Ebetino, F. H. 1094, SA305, SA442, SU087, SU098, SU334
Ebisu, S. F251, SA251
Eckstein, E. C. C. SU078
Eckstein, F. SA386, SU225
Economides, A. N. 1178, SU050
Econs, M. J. 1081, F131, M156, M326, SA131, SA132, SA467, SU184, SU185, SU381
Edderkaoui, B. 1206
Edelstein, O. SU389
Ederveen, A. G. M372, SA255, SU135
Edgar, C. M. M013, M034, M230
Edwards, B. J. SU395
Edwards, C. J. F336, SA336
Edwards, J. 1030
Egeland, T. SA512
Egermann, M. SA391
Eghbali-Fatourechi, G. Z. 1136
Ehrlich, L. A. 1010, SA079
Eichhorst, K. SA557
Eichler, G. M230
Eick, D. 1177, SA028
Eid, K. M011
Einhorn, T. A. M013, M245, SA027, SA150
Eiriksdottir, G. SU162
Eisman, J. A. 1112, 1184, F354, F375, F410, M356, M362, M363, M463, SA354, SA375, SA410, SA559, SU105, SU121, SU276
Ejersted, C. M546, SA436
Ekstein, J. M567
El Hajj Dib, I. SA088
El-Hajj Fuleihan, G. 1047, 1186, M497, SA381
ElAlieh, H. Z. F178, F531, SA178, SA531, SU028
Eldeiry, L. SA288
Elder, G. J. M553
Elford, C. M268
Elkin, S. SU417
Elliot-Gibson, V. I. M. M464, SU480
Elliott, D. 1044
Elliott, M. Elizabeth SA405
Ellis, J. M155
Elmer, P. 1044, 1113
Elmessadi, N. SU059
Elmore, D. SA414
Emaus, N. SU358
Embree, M. 1078
Emi, M. M162, SU173
Emkey, R. M432, SA423
Emmerling, P. SA305
Emmerson, A. J. B. M529
Emons, G. SA210, SU238
Ench, Y. M. F484, SA484
Eng, J. J. SA325, SU131, SU468
Engelke, J. SU584
Engelson, E. SA501
Engler, T. A. 1218, F445, SA445
Enjuanes, A. SA250, SU182, SU241
Enomoto, F. M495
Enright, T. R. M139
Enriquez, R. F. 1101, 1123
Ensrud, K. 1009, 1021, 1023, 1024, 1056, 1058, 1098, 1173, 1174, 1185, F323, F358, F362, F369, F402, F429, M182, SA323, SA358, SA362, SA369, SA402, SA429, SU186, SU384
Epperly, M. SU203
Epstein, S. F316, M433, SA316, SU441
Erben, R. G. 1133, M375, SA494
Erclik, M. S. SA273
Ergan, S. SA108
Eriksen, E. F. 1169, F383, SA159, SA383
Eriksson, A. F139, M163, M389, SA139, SA140
Erkal, M. Ziya SA368
Erlacher, K. SA032
Esbrit, P. SA208, SA539
Escalona, A. M145
Escander, M. M473
Escobar-Jimenez, F. SA119, SA425
Esdaile, J. M310
Eshed, V. SU509
Eskridge, T. SU519
Esparza, X. 1011
Espiner, E. A. M020
Esser, G. M093
Essmyer, K. M510
Esteban, L. 1085
Esteban, L. M. SA559
Estilo, C. L. SU092
Estores, I. SA473
Etard, O. 1155
Etchegoyen, G. SU397
Ettinger, M. F426, SA423, SA426
Euller-Ziegler, L. M310
Evans, A. M099
Evans, B. A. J. M268, SA206
Evans, C. E. M579, SU072
Evans, G. M376
Evans, G. L. M543, SA534
Evans, M. J. M242
Evans, S. M. M059
Everts, V. SA198, SU064, SU319
Ewing, S. 1023
Eyre, D. R. M036
Ezura, Y. M162, SU173

F

Fabbro, D. SU091
Faber, H. M410
Facchini, A. SA286
Facchini, D. SU506
Faccio, R. F285, M320, SA285, SA321
Faciszewski, T. SA453
Fagan, M. John M097
Fahrleitner, A. M295, M398
Fahrleitner-Pammer, A. M545
Faibish, D. M475
Faiman, C. F495, SA495
Fajardo, R. F207, SA207, SU328
Falch, J. A. SA324, SA376, SU374
Falchetti, A. M518, M519, SU181
Falconi, D. M190
Falduto, M. T. SU447
Fan, B. F360, M002, SA360, SU124
Fan, X. 1034, SU236
Fan, X. M555, SU296
Fan, Z. SU078
Fanelli, R. SU574
Fang, A. M468B
Fang, Y. M175, M176
Farach-Carson, M. SA254, SA550, SU042, SU096
Fardellone, P. SA113, SU370, SU411
Farhat, G. N. 1189
Farias, M. F. SA444
Farley, J. SA517
Farneth, S. SU433
Farquharson, C. F037, SA037, SU242
Farrell, F. X. SA509
Farrerons, J. F441, SA441
Farrow, S. Neville SU415
Faugere, M. 1001, 1054
Faulkner, G. M292
Faulkner, K. G. F112, M089, M525, SA112, SU126
Faulkner, R. A. F002, M328, SA002, SA006
Faust, T. SU431
Fechtenbaum, J. M050, M108, SU119
Fedarko, N. S. F479, SA479
Feeley, B. T. F084, F085, M014, SA022, SA084, SA085
Fehling, P. C. SU131
Feick, P. M240
Feige, U. M272, SA510
Feingold, K. R. 1110
Feldman, D. SA552
Feldman, F. SU471
Feldman, H. A. M140, SU421
Feldmann, M. M299
Feldstein, A. C. 1113
Felsenberg, D. 1145, M432
Felson, D. T. SA040
Felx, M. M066
Feng, H. SU340
Feng, J. Q. 1004, 1035, 1049, 1177, F173, SA028, SA173
Feng, M. M536
Feng, X. F301, M267, SA257, SA301
Feng, Y. F486, SA486
Feng, Y. M177, M178, M325

(Key: 1001-1222 = Oral, F = Friday Plenary poster, SA = Saturday poster, SU = Sunday poster, M = Monday poster, WG = Working Group Abstract)

Feng, Y. SU160
Ferdinande, A. M211
Ferguson, D. SA300
Ferioli, V. M518
Ferm, H. SU151
Fermor, B. SU075
Fernandes, J. C. SA252
Fernandes, M. Bernardo Cury M045
Fernandez, D. SA119, SA425
Fernández, E. SA337, SA338
Fernandez, J. M351
Fernández, M. SA239
Ferracini, R. M289
Ferrari, S. L. 1121, 1122, F136, M477, M483, SA136, SU553
Ferrell, R. E. M180, M181
Ferreri, S. SU080
Ferretti, J. SA003
Feyen, J. SU265
Fiaschi-Taesch, N. M. F005, SA005
Fiedler, K. SU452
Fielding, L. F. M521
Filion, M. M294, M297
Filipponi, P. M323, SU442
Fillaux, J. M360
Finch, M. B. M397
Findlay, D. Malcolm SA587
Finger, J. SU332, SU338
Finigan, J. SU380
Fink, H. A. 1009, 1058, 1185, F358, F362, SA358, SA362
Finkelstein, J. S. 1172, F439, SA439, SU196
Finlayson, G. M110
Fiori, J. L. SU016
Fischbeck, M. SA386
Fishburn, T. SA467
Fishburn, T. M. F131, SA131, SA132, SU184
Fisher, D. E. SU329
Fisher, J. SU487
Fisher, J. E. M571
Fishman, G. SA461
Fitch, J. L. M245
Fitto, F. SU369
Fitzgerald, R. L. SA034, SU145
Fitzpatrick, L. A. M347
Fjelldal, P. SU051
Flanagan, J. L. SA559
Flanagan, J. N. SA585
Flannery, P. SU558
Flaster, E. SA475
Flatø, B. SA512
Flavell, R. A. 1191
Fleet, J. C. SA560, SU167
Fleischer, J. SU580
Fleming, A. M029, SU547
Fleming, N. J. SA570
Flicker, L. F459, SA459
Flint-Wagner, H. G. M453, M455
Flores, A. 1011
Flores, R. H. F360, SA360
Fogel, M. M166
Fogelman, I. M092, M407, SA206, SU110, SU352, SU423
Foltz, I. 1201
Fomin, V. M200
Fong, C. SA559
Fønnebø, V. SU358
Foote, I. P. 1104
Ford, L. F466, SA466
Forget, S. SU345
Foroud, T. F131, M156, SA131, SA132, SA467
Foroud, T. M. SU184, SU185
Foround, T. M. 1081
Førre, Ø. SA512
Fors, H. M112
Forsberg, M. F139, SA139
Forsmo, S. M367
Forsythe, T. Michael M139
Fortin, A. M297
Fortunati, D. SU091, SU287
Foss, A. 1109
Foss, M. SA032
Fossi, N. M519, SU181
Foster, B. SU034
Foster, B. A. M078
Foster, B. J. M009
Foster, B. L. M044
Foster, B. Lee SU054
Foster, M. SA549
Fournier, P. G. 1094
Fox, J. F431, F435, SA431, SA435
Fox, S. W. SA167
Fracalossi, A. M085
Fraher, L. J. M554, SU548, SU560
Frampton, J. M366
Franceschi, R. T. 1210, SU243, M264, SU247, SU546
Franci, B. M394, M402
Francis, K. M268
Francis, R. M. M581, SU183
Frank, A. SA059
Franklin, M. M447
Franta, A. K. M139
Franzson, L. M133
Fraschini, F. SU345
Fraser, D. 1136, SU568
Fraser, D. G. SU283
Fraser, M. M341, M343
Fraser, W. F482, SA482
Fraser, W. D. M529, SA117, SU505, WG 15
Fratzl, P. 1173, F462, M368, M391,
Fratzl-Zelman, N. F462, SA462
Frederick, M. M. 1048, F102, SA102
Fredericks, R. S. SA570, WG18
Frediani, B. SU442
Fredrick, M. SU124
Fredriksson, R. SU156
Freedman, L. P. F270, M571, M580, SA270, SU351, SU577
Freeman, T. A. M055
Freemont, A. J. F507, SA507
Freitag, A. SU376
Frenkel, B. F216, M039, SA216, SA564
Fretz, J. A. F246, SA246
Frew, I. J. F266, SA266
Frick, K. K. SA505
Friedman, P. A. SA528, SA561, SU559
Froelich, C. F293, SA293, SU100
Fröhlich, L. F. F042, SA042
Frolik, C. A. 1218, F445, SA445, SU295
Frosch, K. SA210, SU238
Frost, M. L. SU423
Fryns, J. P. M153
Fu, H. F477, SA477
Fu, Q. 1066, 1104, 1165, SU550
Fuchs, E. 1014
Fudge, N. J. F523, SA523, SA524
Fuerst, T. SU381
Fujii, Y. M395, SA460
Fujioka, M. SU455, SU456
Fujita, N. M026, SU045, SU315, SU316
Fujita, S. SU310
Fujita, T. 1089, 1160, F152
Fujita, T. F222, SA222
Fujita, T. M395
Fujita, T. SA152
Fujita, T. SU207
Fujita, T. SU292
Fujiwara, S. M344
Fukayama, S. M017, M018, M247
Fuku, N. SU455
Fukuda, T. 1006, 1039, 1099
Fukumoto, S. 1160, F152, SA152
Fukunaga, M. M344, SA460, SU406
Fukushi-Irie, M. M165
Fukushima, H. M306, SU018, SU306
Fukushima, S. M308
Fukuyama, R. F222, SA222
Fulde, F. SU061
Fullman, R. SA355
Funahashi, T. SA146
Funari, A. 1138
Fung, E. B. SA504
Funk, J. L. M538
Funk, S. SU060
Furey, W. F. M224
Furlan, F. SA076
Furuichi, T. F222, SA222
Furusawa, K. M285
Fuson, T. M296, M317

G

Gabet, Y. 1211, M166
Gacad, M. A. SA574
Gaddy, D. SU009, SU495
Gadois, C. SA113
Gaertner, R. M552
Gafni, A. M109, SA455
Gafurova, F. SU576
Gagari, E. M188, SA235
Gagel, R. F. SA518
Gagné, V. M297
Gagnon, J. 1015
Gaiennie, J. SU428
Galien, R. 1117, 1118, SU488, SU491, SU579
Gallacher, S. J. M341, M343, M462
Gallagher, A. M341
Gallagher, A. P. M462
Gallagher, J. C. 1070, M404, SU169, SU170, SU399
Gallagher, K. M527, M528
Gallagher, R. SA407
Gallet, M. SA088, SA296
Galli, B. M402, SA483
Gallina, P. M339
Galson, D. L. SU307
Galvin, R. M296, M317, SU295, SU332, SU338
Gamba, G. M270
Gambacciani, M. M142
Gamble, G. SU454
Gamble, G. G. SA490
Gamradt, S. SA022
Gamradt, S. C. F084, SA084
Gamse, R. SA547
Gan, L. SU565
Ganança, F. Freitas SU401
Ganapathy, V. SU262
Gange, C. T. 1025, SU317
Ganie, M. Ashraf M005
Gannon, F. H. M510
Gant, T. G. 1216
Gao, Y. 1191
Garces, A. SU521
Garces, A. H. SU528
García, E. M145
Garcia, J. M481
Garcia, M. SU162
Garcia, R. I. SU387
Garcia, S. SU081
Garcia, T. SU579
García Palacios, V. M224, M278, M279, SU277
García-Aparicio, J. M167
García-Giralt, N. SU182, SU241
Garcia-Ocana, A. 1065, F471, M479, SA471
Gardella, T. J. SU566
Gardi, J. SA163
Gardiner, E. M. 1101, 1123, SA559, SU258, SU276
Gardner, M. M469, SU487
Gardsell, P. 1147
Garg, S. SU265
Garimella, R. F039, SA039, SU030
Garman, R. M452
Garman, R. A. SA190, SU221
Garnero, P. 1068, SU067, SU542
Garrett, I. R. 1011, 1161, 1176
Garton, M. F341, SA341
Gascon-Barré, M. M060, SA584, SU035
Gasser, J. A. M120, SA219, SU133, SU432
Gaudin, C. M421
Gauna, C. SU268
Gaur, T. 1213
Gautvik, K. M. M038
Gautvik, V. T. M038
Gavin, D. SU017
Gay, C. V. SA086, SU093
Gazmen, N. M. SU486
Gazzerro, E. 1178, F024, F244, SA024, SA244, SU050
Ge, C. 1210, SU243
Gebauer, M. 1208
Gehlbach, S. SU367
Gehlbach, S. H. M465
Gehron Robey, P. 1157
Geibel, J. 1156
Geiger, M. Jane 1055
Gelb, B. 1196
Gemar, D. M. SU584
Genant, H. 1070, 1077, F360, F433, M541, SA360, SU381, SU433
Genaro, P. Souza M335
Genazzani, A. M142
Genc, K. O. F421, M451, SA421
Genco, R. M355
Gendreau, P. SU485
Genetos, D. C. SU136, SU214, SU217
Geng, Y. SU049
Gennari, L. 1060, M394, M402, SA483
Gensure, R. C. 1102
Gentile, M. A. 1039, SU437
Geoffroy, V. M062
George, V. 1114
Gerdhem, P. SU143
Gerhardt, C. SA391
Gersch, R. 1131
Gerson, A. SA183, SU081
Gerstenfeld, L. C. M013, M034, M230, M245, SA027, SA150
Getz, B. J. SU575
Geursen, A. M240
Geusens, P. M149, M441, SA454, SU367
Gevers, E. 1126
Ghasemzadeh, A. SU103
Ghassan, M. SU403
Ghayor, C. SU202
Ghishan, F. K. F234, SA234, SA582
Ghosh-Choudhury, N. SU290
Giachelli, C. M. M514
Giacomelli, T. SA541
Giambernardi, T. A. 1214
Giampietro, P. F. M499
Giangregorio, L. M125
Giannini, S. M323, M382, M518
Gibson, C. W. SU054
Gibson, K. 1172

(Key: 1001-1222 = Oral, F = Friday Plenary poster, SA = Saturday poster, SU = Sunday poster, M = Monday poster, WG = Working Group Abstract)

Gifford, J. M366
Gigante, V. SU369
Gignac, M. A. M. M322
Gil-Fraguas, L. M145
Gilbertson, D. M186
Gilbertson, K. G. SU240
Gilchrist, A. M561
Gill, M. F507, SA507
Gillen, M. V. SU445
Gillespie, M. T. 1025, F266, SA266, SA540, SU317
Gilligan, J. P. SU451
Gilmore, J. M. F185, SA185
Gilmore, J. Mae Eichenberger SU364
Gilquin, B. SA282
Gilsanz, V. 1048, F102, SA102, SU124, SU178
Gineyts, E. SU067
Gingery, A. M319
Ginty, F. M442, SU459
Giordano, N. 1060
Giuliano, A. E. 1202
Giuliano, A. R. M159
Giunti, A. M275
Gjesdal, C. G. SU392
Glantschnig, H. F270, SA270, SU351
Glaser, D. L. SU021
Glass, E. V. 1169
Glass, N. SU235, SU496
Glatt, V. 1121, 1122, M483
Glesne, D. A. SA060
Glezer, S. M354
Glimcher, M. SU102
Glimcher, M. J. SU071, SU503
Gliniak, C. SA560
Globus, R. K. SU350
Glorieux, F. H. 1043, F462, M500, M504, SA462, SU522
Glover, J. L. SU548
Glowacki, J. F168, M011, M041, SA168, SU203, SU496
Gluhak-Heinrich, J. 1035, 1105, F182, SA182, SU215
Glynn, J. SU020
Goater, J. Jeffery F066, SA066, SU011
Godfrey, C. SU444
Godfrey, K. SA001
Godin, C. SA302
Goel, N. M353
Goemaere, S. F428, SA428, SU175
Goggins, M. WG13
Going, S. M438
Going, S. B. M453, M455
Gold, D. T. M454, M478
Goldman, S. SU384, SU377
Goldring, S. R. SU328
Goldsmith, C. F371, SA371
Goldsmith, P. M029
Goldstein, G. M101
Goldstein, S. A. 1205
Goll, J. H. SU130
Goltry, K. SU256
Goltzman, D. F433, F477, F537, M485, SA433, SA477, SA537, SA576
Gómez, A. SA337, SA338
Gómez, C. M094, SA392
Gomez, S. M481
Gomi, N. SA015
Gong, J. 1217
Gonnelli, S. M144, SU420
Gonzalez, G. M358
Gonzalez, H. SU397
Gonzalez, I. M351
González-Carcedo, A. SA392
Gonzalez-Feldman, E. WG23
González-Macías, J. F123, SA123
Gonzalez-Sarmiento, R. M167
Goodby, A. M104
Goodpaster, B. 1022
Gopalakrishnan, R. SU546
Gopalakrishnan, V. M484
Gopathi, N. M079
Gorai, I. M164, M428
Gordon, A. SU082
Gordon, C. L. SU022
Gordon, C. M. M140, M527, M528, SU421
Gornbein, J. M345
Gorny, G. F170, SA170
Gorny, G. Anna 1197
Goseki-Sone, M. M165, SU408
Gossiel, F. 1020, M136, M138, SA138
Göthe, S. 1126
Goto, T. M036
Gotoh, M. SU207
Gottesdiener, K. F450, SA450
Gottschalk, M. M093, SU090
Gottshall, S. SU082
Goussous, R. Y. SA579
Govoni, K. F160, SA160, SA166
Gozzini, A. M518, SU181
Gracious, B. L. M405
Grafe, I. M459
Graham, E. Ann SA572
Graham, J. 1219
Graham, L. SU102
Gram, J. SU335, SU427
Gramoun, A. SA284
Granados, J. F123, SA123
Granchi, D. M275
Grano, M. M289, SA204
Grassi, F. 1059, 1116, SA286
Gratacòs, J. SA337, SA338
Grauer, A. F404, M410, M420, SA404, SU434, SU445
Graves, D. F068, SA068
Graves, D. T. M034
Green, D. SU186
Green, D. John M103, M104, M105
Green, J. SU432
Green, P. 1063, F525, SA525
Green, R. P. M385
Green, S. B. 1154
Greenberg, C. R. M331, SA456, SU353, SU361
Greenberger, J. F168, SA168, SU203
Greendale, G. A. F328, F400, SA328, SA400
Greene, D. R. M182
Greene, S. F. SA491
Greenfield, E. M. M288, SA522
Greenland, K. M155
Greenspan, S. 1098, F429, SA429, SU130, SU529
Greenwald, M. SA107
Greep, N. 1100, 1202
Gregersen, P. K. SA135
Gregory, P. D. SU285
Gregory, S. SU332
Gregson, R. 1109
Greibe, R. SU475
Greig, I. R. SU336
Gremlich, H. 1069
Grey, A. B. SA490, SU284
Griffin, E. N. M436
Griffin, J. SU123
Griffin, T. L. SA034
Griffith, L. G. M262
Griffiths, A. M. SU525
Griffiths, K. N. M381
Grigoriadis, A. E. F053, M316, SA053
Grigoryan, M. F360, SA360
Grimaldi, A. SU312
Grimm, K. A. M373
Grinberg, D. SU182, SU241
Grinnell, N. C. M117, SU127, SU128, SU232
Grisanti, M. 1017, M300
Groener, J. E. M. SU064
Gronowicz, G. 1061, 1205, F194, M244, SA194, SU094, SU279
Gross, G. M408
Gross, T. S. 1146, M209, SU211, SU349
Grossi, S. M355
Grøsvik, K. M298
Grubbs, B. M076
Gruber, B. SU080
Gruber, H. E. SU060
Grumley, J. F141, SA141
Grundberg, E. SU177
Grundker, C. SA210, SU238
Gruntmanis, U. SU486
Grynpas, M. SA065
Grynpas, M. SU506
Grynpas, M. D. SU076, SU386
Grzesiak, J. J. SA535
Gu, J. SU115
Gu, W. SU078
Guañabens, N. M551, SA485, SU422
Guazzini, L. M519, SU181
Gubrij, I. 1066, 1165, F527, SA527
Gudmundsson, A. 1124
Gudnason, V. 1124
Guénou, H. F226, SA226
Guenther, C. SU478
Guenther, O. SU478
Guerard, C. SU586
Guévremont, M. SA041
Guggenbuhl, P. M549
Guglielmi, J. 1092, F090, SA090
Guida, G. SU369
Guido, V. SA164
Guido, V. E. 1080
Guidobono, F. SA519
Guignandon, A. M192, SU074
Guilak, F. F220, SA220, SU075
Guillotin, B. M250
Guise, T. A. 1093, SA148
Guldan, G. M440
Guldberg, R. E. 1191, M261, SU011
Gunaratne, G. H. M123
Gunawardene, S. SU196
Gundberg, C. M. 1065, SA294, SU362
Gunnarsson, U. SU156
Guns, M. SU531
Guo, D. 1035, 1049, SA028
Guo, J. 1018, 1158, F042, SA042, SU563
Guo, J. J. SU172
Guo, M. D. 1199
Guo, T. M396, SU569
Gupta, A. 1011, F044, M076, SA044, SU244, WG13
Gupta, J. 1174
Gupta, R. SU265
Gurevich, M. F558, SA557, SA558
Guth, S. SA219
Guthrie, J. M079
Gutierrez, G. 1176
Gutierrez, G. E. 1161
Guy, M. SA094
Guy, P. M127
Guzman, M. L. M266
Gyda, M. SU297
Gyuris, T. 1017

H

Ha, E. F343, SA343
Ha, H. SU302, SU492
Haas, M. J. M574
Haberland, M. 1140
Hackman, J. M269
Haddaway, M. J. M346
Haddock, L. F340, SA340
Hadi, T. M488
Hadji, P. M093, SU090
Hadjiargyrou, M. 1131, SA062
Haemmerle, S. SU132
Hagenauer, M. M139
Hagino, H. 1171, M111, SA460, SU375
Hagiwara, H. SU266
Hagstrom, E. SU515
Hahn, T. J. SA223
Haiying, L. M484
Hale, L. V. SU295
Hall, C. L. M088
Hall, D. B. M131
Hall, N. F558, SA557, SA558
Halladay, D. SU332
Halladay, D. L. 1218, M296, SA200, SU295
Halleen, J. Marko M305, SA307, SU301
Halleux, C. SA219, SA547
Hallgrímsson, B. SU006
Halloran, B. P. F178, F531, SA019, SA178, SA531
Halpern, J. SU092
Halse, J. I. SU392
Ham, J. M268
Hamada, N. SA460
Hamai, S. M129, M369
Hamaya, E. SU406
Hamlin, N. J. SU031
Hammond, M. L. M569, M571
Hammond, V. SA538
Hampson, G. M511, SA206
Hamrick, M. F275, M203, M492, SA275, SA447
Han, F. SA054
Han, I. SU572
Han, J. Ho M401, SU439
Han, K. SU572
Han, L. 1119, M221, SU339
Han, M. M233, SU055
Han, R. 1143, M030, M315
Han, T. D. SU299, SU300
Handelsman, D. J. M134
Handoko, G. SA463
Haney, E. M. 1024, SA142
Hangartner, T. N. F343, SA343
Hankenson, K. D. SU069
Hanley, D. F371, SA371
Hanley, D. Arthur M095, M109, M423, SA455
Hanley, E. N. SU060
Hannan, M. T. M342
Hänninen, K. M411
Hannon, R. A. SU147, SU380
Hansen, K. SA405
Hansen, K. E. SU445
Hansen, N. M. 1202
Hansen, S. SU376
Hansen, T. SU051
Hansson, S. M531
Hara, K. M489
Harada, A. SA010
Harada, D. 1045
Harada, S. 1039, F202, F270, SA202, SA270, SU351, SU577
Haran, A. M186
Harba, R. SA113

(Key: 1001-1222 = Oral, F = Friday Plenary poster, SA = Saturday poster, SU = Sunday poster, M = Monday poster, WG = Working Group Abstract)

Harding, G. SA206
Hardisty, J. F. F435, SA435
Harfe, B. 1037
Harinarayan, C. V. M141, SU359
Harkness, L. SU452
Harkness, M. M462
Härkönen, P. M565, SU569
Harland, R. M. WG21
Harmey, D. F039, F474, M316, SA039, SA474
Harpavat, M. SU529
Harper, K. D. F383, SA383, SU406
Harrap, S. M155
Harris, F. 1021, WG15
Harris, M. 1049, M438
Harris, M. A. 1035, 1105
Harris, S. 1049, SA028, SU215
Harris, S. E. 1035, 1105, F182, SA182
Harris, S. S. SA326, SA327, SA363
Harris, S. T. 1215, F428, SA428
Harris, T. 1021, 1189, SU162
Harris, T. B. 1022, 1110, 1124
Harris, V. A. M521
Harrison, J. R. 1115, SA231
Harrop, J. S. SU183
Hart, D. M024
Hartmann, B. F390, SA390
Hartmann, L. C. SA083
Hartzell, D. F275, SA275
Harvey, N. SA001
Harwood, R. 1109
Hasegawa, H. F152, SA152
Hasegawa, K. M232, M575
Hasegawa, T. SA247
Hashikawa, T. M542
Hashimoto, J. SA146, SU540
Hashimoto, T. F081, M072, SA081, SA460
Hashimoto, Y. SA478
Hassan, M. Q. 1144
Hastings, R. H. SA571
Hata, K. 1026, 1120, F251, F309, SA251, SA309, SU274
Hatakeyama, S. SA583
Hatano, H. SA247
Hatayama, A. M064
Hatch, N. E. SA157
Hauache, O. M. SU549
Haug, E. SA376
Haugen, M. SA512
Hausmann, E. M355
Haussler, C. A. F555, F558, SA551, SA552, SA555, SA557, SA558
Haussler, M. R. 1087, F234, F555, F558, SA234, SA551, SA552, SA555, SA557, SA558
Haussler, M. Robert M159
Havill, L. M. SA133, SA134
Havrdova, E. SU142
Hawa, G. F118, SA118, SU088
Hawker, G. A. M322, M336, M443, M521, SA348
Hawkins, F. M145
Hayakawa, N. SA036, SA457
Hayami, T. SA046
Hayashi, M. SU012, SU201
Hayashi, T. M263
Hayashi, Y. SA460
Hayashida, K. SA146
Hayes, A. 1172, F439, SA439
Hayes, B. Peter SU415
Hayman, A. R. M242
Haynatzka, V. SU169, SU170
Haynatzki, G. M352, M404
He, E. M087
He, J. SA231
He, J. SU157, SU171
He, X. M258
Healy, M. M135, M487
Heaney, J. SU259
Heaney, R. P. M352, SU410
Heaton, W. L. SA546
Hebbani, A. Vardhan M141, SU359
Hebborn, A. M434
Heersche, J. N. M. SA186, SA284, SU333, SU342
Hefferan, T. E. SA534
Heickendorff, L. SA578
Heindel, U. SU564
Heiner, J. P. M139
Heinonen, A. SU002, SU143, SU468, SU469, SU470
Heitmann, C. SU090
Helgason, C. D. F320, SA320
Helkala, E. F009, SA009, SU461
Heller, H. J. M507, WG25
Hellman, P. SU515
Helvering, L. M. 1218
Hemmi, H. SU311
Hendy, G. N. F537, M227, M485, SA537, SA543, SA544, SA576, SU179, SU560
Henn, H. F311, SA311
Hennessey, R. SU376
Henriksen, D. M302
Henriksen, D. B. F390, SA390
Henriksen, K. SU335, SU427
Henriksen, Z. M486, SA269, SU152
Henry, H. L. M578
Henry, M. J. M348, SU378
Henry, P. M030
Hens, J. R. 1014
Hentunen, T. SU569
Her, S. J. 1193
Her, S. Joo M234
Herath, C. M287
Herbert, A. G. F136, SA136
Herbert, W. G. M126, SU229
Hermann, P. 1139
Herndon, D. N. SU489
Herold, D. A. SA034, SU145
Herrmann, F. SU545
Hershey, C. L. SU329
Herskovitz, R. M. 1137
Herson, M. 1113
Hertel, C. A. SA365
Herzog, H. 1101, 1123
Hess, F. J. F270, SA270
Hess, J. Fred 1214
Hess, R. SA239
Hewison, M. F586, SA094, SA586
Heyden, N. 1043
Heymann, R. E. SA352, SA361
Hickey, R. J. SA438
Hickman, C. M426
Hickok, N. J. SA054
Hidalgo, A. M577
Higano, C. S. SA089
Higgins, B. J. SU524
Higuchi, M. SU455
Higuchi, Y. SU500
Hikita, A. F199, SA199
Hilbers, P. SU237
Hill, D. 1017
Hill, K. M. M457, SU481
Hill, R. J. 1216
Hillegonds, D. J. SA034, SU145
Hillier, T. F323, SA323
Hillier, T. A. M182, SU186
Hillion, F. SU025
Hillman, L. M446
Hillman, L. S. SU524
Hilscher, U. M459
Hilton, M. J. 1002
Hines, E. R. F234, SA234
Hinkley, H. J. M206
Hinz, C. WG1
Hiraga, T. F087, M068, SA087
Hirahara, F. M164, M428
Hiramatsu, K. 1125
Hirao, M. F047, SA047
Hiraoka, H. SU037
Hirasawa, H. SU208
Hirayama, T. F313, SA312, SA313
Hirota, T. SA460
Hirotani, H. SU281
Hirouchi, T. F295, SA295
Hisada, K. 1120, SU274
Hise, M. SU430
Hishiya, A. SA240
Hitchcock, C. M359
Hitchen, J. M297
Hmadeh, Y. WG23
Ho, A. Y. Y. M161, SU115
Ho, K. K. M134
Ho, S. C. M440
Ho Ba Tho, M. SA029, SU024
Hochberg, M. C. 1056, F323, F360, F412, SA323, SA360, SA412, SU186
Hock, J. M. SA438
Hockman, E. M. SA004
Hodge, J. M. M293
Hodsman, A. M354, M406, SA366
Hodsman, A. B. M554, SU548, SU560
Hodson, T. SU125
Hoeben, K. A. SU064
Høegh-Andersen, P. SU335
Hoey, K. A. M387
Hofbauer, L. C. SA210, SU088, SU238
Hoff, A. O. SA518
Hoffmann, K. 1017
Hoffmeyer, P. SU479
Hofman, A. M175
Hofstaetter, J. G. SU071, SU503
Hogan, B. 1049
Hogan, H. M128
Hogan, H. A. SA035
Hogan, M. M342
Hogue, A. L. M381
Holdren, M. M186
Holick, M. F. M494, SA326, SA327, SA363, SA585, SU424, SU583, SU585
Holliday, L. Shannon SA280
Hollinger, J. O. SA211
Hollis, B. F471, SA471
Holloway, D. L. 1072
Holloway, L. SA475
Holmäng, A. SA397
Holmbeck, K. 1157
Holmegaard, S. Nistrup M461
Holmen, S. L. 1214
Holmen, S. Lynn 1001
Holst, J. Juul F390, M302, SA390
Holt, M. SA033
Holvik, K. SA376
Honda, M. SU440
Honda, S. SU385
Honda, Y. SU449
Hong, S. SA278
Hong, S. Bin SU541
Hong, X. M177, M178, M325
Hong, X. M329
Hong, X. SU160
Hongo, M. M449, SA422, WG6
Honkanen, R. M321, M357, SU382
Honsawek, S. SU014
Hoogendam, J. SU040, SU249
Hooibrink, B. SU319
Hoon, D. S. B. 1202, M520
Hoover, J. F445, SA445, SU338
Hopman, W. M539, SA455
Hopper, J. L. F459, SA459
Horakova, D. SU142
Horard, B. 1117
Horcajada, m. SU412, SU460
Horiuchi, H. SU303, SU304
Horizono, H. M148
Horlait, S. M108
Horlick, M. 1048, F102, SA102, SA501, SU124
Hormuzdi, S. SU069
Horne, A. SU454
Horne, W. C. 1118, 1142, SU343, SU344
Horne, W. CT. 1198
Horner, A. 1033, SU032
Hornstein, M. SU496
Horowitz, M. 1014, 1080, M280, SA294, SU140
Horreard, F. SU025
Horton, B. M103, M104, M105
Horton, J. A. M033, SU038
Horton, W. SU044
Horvath, C. M170, M171
Horwitz, M. J. 1065, F471, M479, SA471
Horwood, N. M299
Hoshi, K. 1012, SA249
Hoshino, M. SU015
Hosking, D. J. F482, M104, SA482
Hosogane, N. M026, SU045, SU315, SU316
Hosoi, T. M162, M165, SU173
Hosseini M., S. SU103
Hosterman, M. SA401
Hou, X. S. M569
Houghton, A. F253, SA253, SA442
Houtkooper, L. M438
Houwing-Duistermaat, J. J. SU158
Hovey, K. M355
Hovey, K. M. M468A
Hovhannisyan, H. F256, SA256
Howard, G. A. M269, M560
Howard, K. M. 1137
Howe, C. J. M134
Hruska, K. A. 1194, M012, M537
Hruzikova, P. SU120
Hsieh, G. SA551
Hsieh, J. 1087
Hsieh, J. C. F555, F558, SA551, SA555, SA557, SA558
Hsu, W. M014
Hsu, W. K. F084, F085, SA084, SA085
Hsu, Y. M177, M178, M325
Hsu, Y. M329
Hsu, Y. Hsiang SU160
Hu, B. SU428
Hu, B. SU570
Hu, H. 1103
Hu, H. SU171
Hu, H. SU262
Hu, R. M292
Hu, Y. F180, M043, SA180
Hu, Y. SU157
Huang, A. F464, SA464
Huang, D. Chao SA080
Huang, G. SU570
Huang, J. SA438
Huang, K. SU571
Huang, K. SU571
Huang, M. F328, SA328
Huang, Q. SU157, SU171
Huang, S. SA498, SU530
Huang, W. M249
Huang, Y. M075, M259
Huang, Y. M290
Huang, Z. SU044
Huard, J. F084, F085, SA084, SA085
Hucker, W. J. M208

(Key: 1001-1222 = Oral, F = Friday Plenary poster, SA = Saturday poster, SU = Sunday poster, M = Monday poster, WG = Working Group Abstract)

Hudis, C. SU092
Hudson, T. J. SU177
Hue, T. 1098
Hufkens, A. M251
Hüfner, M. SU272
Hughes, A. SU334
Hughes, A. C. SA509
Hughes, C. F406, F408, M429, M432, SA406, SA408, SA419, SU527
Hughes, S. M186
Hughes-Begos, C. SA317
Hughes-Fulford, M. SU199
Huh, Y. SU299
Hui, D. SA322
Hui, S. M326
Hui, S. L. M156
Hui, S. Lui. 1081, SU184, SU185
Huiskes, R. SU237
Huisman, A. M415
Hukkanen, M. F513, SA513
Hull, K. SU198, SU338
Hulley, P. A. SU087
Hume, D. M292
Humphrey, M. B. 1195
Humphries, R. K. F320, SA320
Hung, I. H. 1005
Hunzelman, J. 1172
Huopio, J. SU382
Hur, H. SU572
Hur, Y. SU300
Hurd, J. SA164
Hurley, D. L. SU416
Hurley, M. M. 1042, F026, M480, SA026
Hurley, M. P. SU053
Hurtel-Lemaire, A. SA302
Hurwitz, S. SU496
Huryn, J. M. SU092
Huss, H. M433, SU441
Hussain, S. SU322
Hussein, Z. M155
Husted, L. B. M174
Huttunen, M. M. M225, M498
Huynh, H. T. SA109
Hvam, H. Midtbø M367
Hvid, I. SU135
Hwalla, N. SA381
Hwang, C. SU572
Hwang, H. SA443
Hwang, M. M233
Hwang, R. M084, SU554, SU555
Hwang, S. M484
Hyams, J. S. SU525
Hyldstrup, L. SU475
Hyodo, S. SA545

I

Ibañez, L. SA103
Ibargoyen, N. M222
Ichida, F. 1120, F309, SA309, SU274
Ichikawa, M. SU533
Ichikawa, S. 1081, SU184, SU185
Ichimura, S. M074, SU218
Idris, A. I. SU336
Igarashi, T. 1160
Ihm, S. M390
Iida-Klein, A. SA317, SU544, SU557
Iinuma, H. 1171
Ijuin, C. SU195
Ikeda, F. 1026, 1120, F251, F309, SA251, SA309, SU274
Ikeda, K. 1125, F287, F388, SA240, SA287, SA388, SU500
Ikeda, S. SA460
Ikeda, T. 1050, M022, SA249
Ikegawa, S. SU062
Ilich, J. Z. SU466
Ilievska, N. SA540
Illgen, R. Lynn. M139
Imai, N. SA457
Imai, S. M122
Imai, Y. SU052
Imamovic, A. F136, SA136
Imamura, S. SA036
Imamura, T. SU012, SU037, SU201, SU216
Imanishi, Y. SA153, SA411, SA548, SU517
Imbalzano, A. SU252
Imbriaco, R. M519, SU181
Imseis, R. E. M071
Inaba, M. SA153, SA411, SA548, SU517
Inada, M. F063, M164, SA063
Inagaki, K. SU387
Indridason, O. S. M133
Ing, S. W. SU504
Ingold, P. M120, SU432
Ingrand, P. SU508
Inou, T. SU534
Inoue, D. F081, M072, M263, SA081, SA569, SU216
Inoue, S. M162, SU173
Inoue, T. 1076, SU269
Insalaco, P. M392
Inskip, H. M. SA001
Insogna, K. 1156, F290, M492, SA209, SA290, SU308
Inui, M. F297, SA297
Investigators, C. M109, SA455
Ioannidis, G. F371, M354, M406, SA332, SA366, SA371, SA455, SU376
Ioannids, G. M109
Iolascon, G. SU369
Iqbal, J. F316, SA288, SA291, SA316
Ireland, T. M366
Irie, M. M134
Irie, N. 1051
Irwin, R. SA227
Isaia, G. M323, M518, M519, SU312
Isales, C. M. M492, SA447, SU262, SU280, SU282, SU562
Isales, C. Miguel M203
Ish-Shalom, N. M350
Ish-Shalom, S. M350, SU509
Ishida, K. M249
Ishida, K. M399
Ishida, N. F295, M312, SA295
Ishida, Y. SA452
Ishiguro, M. SU343
Ishihara, Y. SU266
Ishii, T. M183
Ishijima, M. M495, SA050, SU405
Ishikawa, H. 1051
Ishikawa, I. F056, SA056
Ishikawa, S. SU318
Ishikawa, T. M263, SA548, SU517
Ishikawa, Y. M449
Ishimi, Y. SU455, SU456
Ishimura, E. SA153, SA548, SU517
Ishiwata, Y. SA036
Ishizaka, K. SU440
Islam, A. F. M. M169
Isler, M. M066, WG9
Ismail, A. A. 1111
Isobe, Y. SU449
Itakura, H. SA460
Itescu, S. M548
Ito, H. F066, SA066, SU011
Ito, H. M162
Ito, H. M261
Ito, H. SU435
Ito, M. 1125
Ito, M. 1159, F228, F306, SA079, SA228, SA306
Ito, M. F388, SA388, SA446, SA457
Ito, M. M577
Ito, M. SA458
Ito, N. 1160
Ito, Y. SA569
Itoh, M. SA036
Itoh, S. M304
Itoh, S. M582
Itoi, E. M449, M476, SA422, SU191, SU330, WG6
Itokawa, T. SU308
Itzstein, C. SU343, SU344
Iu, M. M091, SA562
Iuliano-Burns, S. M099
Ivaska, K. Karoliina SU143
Iwamoto, J. M417, M474, SU218
Iwamoto, K. SU315
Iwamoto, M. SU039
Iwamoto, Y. M129, M369, SU539
Iwaniec, U. T. 1064, SU197, SU219
Iwata, H. M418
Iwata, K. SU497
Iyer, D. SA556

J

Jaakkimainen, L. SA348
Jackman, L. A. SA418
Jackson, A. SU579
Jackson, G. S. SA414
Jackson, R. D. 1100, 1154
Jackson, S. A. M103, M105
Jacob, A. 1005
Jacobs, B. M211
Jacobs, C. M396
Jacobs, C. R. SA174
Jacobs, E. T. M159
Jacobs, J. M415, SU298
Jacobsen, C. SA461
Jacobsen, K. SA027, SA150
Jacobson, G. SA492
Jacobson, P. S. SA546
Jacquin, C. M311
Jadlowiec, J. A. SU288
Jagerschmidt, C. SU491
Jagger, C. J. SA393, SA526
Jaglal, S. M322, M336, SA348
Jahng, J. M184, SA055
Jahr, H. SU268
Jain, A. F479, SA479
Jaiswal, N. M019, M256
Jajoo, R. M437
Jakes, R. W. M334
Jakob, F. SA236
Jakobsen, J. M498, SA013, SU499
Jalava, T. F489, SA489
Jamal, S. A. M464, M532
James, C. M037
Jameson, J. Larry SU578
Jameson, L. SU568
Jamieson, D. SU585
Jämsä, T. J. M213
Jan de Beur, S. M. F156, F479, SA156, SA479
Janckila, A. J. SU301
Jang, C. SU179
Jankowski, L. G. M472, SU138
Janz, K. F. F185, SA185, SU364
Järvinen, T. L. N. 1188, F187, M536, SA187, SU222
Jassal, S. Vanita M532
Javaid, M. K. SA001
Javed, A. 1144, 1175, 1213, M233, SA217, SU322
Jee, W. S. S. F445, SA445
Jeker, H. 1166
Jemtland, R. M038
Jen, H. F333, SA333
Jenkins, B. J. SU317
Jenkins, J. SU521
Jensen, C. M049
Jensen, J. SA076
Jensen, J. D. M546
Jensen, J. Erik Beck M486
Jensen, R. M371, SA453
Jenson, N. H. SU079
Jeon, J. M184, SA055
Jeon, T. SU122
Jeong, H. Yun SU492
Jeong, J. SU055
Jeppesen, P. Bekker F390, SA390
Jepsen, K. J. 1196, M010, SA385, SU155
Jeske, A. SU084
Jespersen, B. M546
Jewison, D. E. M364
Jeziernicka, E. Zofia SU366
Jhaveri, A. SU279
Jhaveri, A. P. M244
Ji, X. M019, M256
Jia, D. M380, SU413
Jian, W. X. SU172
Jiang, D. 1210, SU243
Jiang, D. K. SU172
Jiang, J. SA280
Jiang, J. X. SU556
Jiang, X. F061, SA061, SA276, SU258, SU263
Jiang, Y. 1077, F433, M379, M488, M541, SA433
Jiang, Z. SA418
Jiao, X. SU021
Jiao, Y. SU078
Jilka, R. L. 1066, 1165, F224, F527, SA224, SA527, SU004, SU339, SU550
Jimi, E. M306, SU018, SU086, SU306
Jin, H. SU302
Jin, L. Yan SA125
Jin, W. SU472
Jinnai, K. SU207
Joakimsen, R. M. SU358
Jódar, E. M145
Joe, M. F068, SA068
Johansson, H. F375, M356, SA375
John, M. R. SA219
John, S. W. M. 1016
Johnell, O. 1147, 1188, F375, M356, SA375, SA409
Johnson, E. M. M128
Johnson, K. SA549
Johnson, K. C. 1189
Johnson, L. K. SU409
Johnson, M. L. 1081, M198, M199, M217, SU184, SU185
Johnson, R. S. 1054
Johnson, T. 1028
Johnson, T. SU434
Johnson, T. D. SU445
Johnson-Pais, T. L. F306, F484, M515, M520, SA306, SA484
Johnston, C. Conrad 1081, M156, SU184, SU185, SU381
Johnstone, D. M354, M406, SA366
Jokihaara, J. M536, SU222
Jolad, S. D. M538
Jolette, J. F435, SA435
Jolma, P. M536
Jonart, L. F095, SA095
Jonczyk, A. SA271
Jones, C. F507, SA507
Jones, D. SU074

Jones, D. B. SA183
Jones, D. B. SU081
Jones, J. 1095
Jones, M. D. F234, SA234
Jones, S. SU459
Jones, S. N. 1015
Jonsdottir, B. 1124, SU162
Jönsson, B. SA409
Jordan, C. T. M266
Jorgensen, N. SA076
Jorgensen, N. R. SA269
Jørgensen, N. Rye SU152, SU180, M486
Jorgensen, S. M. SU436
Jorgetti, V. M533
Joseph, C. M160, SA135
Joseph, L. M075
Josse, R. F371, M423, M443, SA371
Josse, R. G. M464
Jougleux, J. SU001
Journé, F. SU097
Jouzeau, J. Yves SA451
Jovaisas, A. M413, SU144
Joyce, D. SU340
Joyce, D. A. M315
Joyce, K. SA018
Joyeux, V. M549
Juby, A. G. SU484
Judex, S. M218, M452, M456, SA189, SA190, SU221, SU230
Judge, S. SU219
Jueppner, H. SA536, SU196, SU566
Juknelis, D. SA432, SU447
Julesz, J. SA163
Juma, S. M445, SA064
Jun, J. SU029
Jun, S. M084, SU554, SU555
June, H. H. SU031
Jung, D. SA443
Jung, D. Young SU492
Jung, E. SU523
Jung, J. M291
Jung, L. K. L. M544
Jung, M. SU055
Jung, Y. M189
Jung, Y. SU055
Jüppner, H. 1102, 1133, 1203, F042, SA042, SU561
Jurdic, P. M024, M309, SA282
Jurisicova, A. SU386
Jurutka, P. W. F234, F555, F558, SA234, SA551, SA552, SA555, SA557, SA558
Jurvelin, J. M321, M411
Jurvelin, J. S. SU388
Jussi, H. SA198
Justice, M. 1209

K

Kaabeche, K. F226, SA226
Kaaja, R. J. M020
Kaarlonen, K. SU301
Kacena, M. A. SA294
Kaczmarska, M. J. SA552
Kadlcek, R. M. M288
Kado, D. F400, SA400
Kadowaki, T. SA430
Kagan, R. F412, SA412, SU400
Kahler, R. A. SU253
Kaiser, E. A. SU084
Kaji, H. M091, M227, SA562
Kaji, Y. SA015, SU450
Kajiya, H. F228, F306, M306, SA228, SA281, SA306, SU018, SU306
Kakita, A. SA036
Kakitani, M. F152, SA152
Käkönen, S. SU143
Kaku, M. SA280
Kalajzic, I. 1035, F061, SA061, SU020, SU265
Kalajzic, Z. SA276, SU263
Kalbakji, A. M294
Kalinowski, J. F. M276
Kalkwarf, H. 1048, F102, SA102, SU112, SU124
Kalla, S. E. M278, M279, SU277
Kalli, K. R. SA083
Kam, L. Y. SU428
Kamai, T. SU440
Kamao, M. SA583
Kamei, D. F511, SA511
Kamekura, S. 1012, 1038, SA249, SA430, SU037
Kamel, S. SA088, SA296, SA302, SU411
Kamel, S. A. M243
Kamijo, R. SU289
Kaminai, T. SU465
Kaminski, J. M416
Kamiya, N. 1039, 1177
Kamiya, S. M409
Kammen, B. SA504
Kammerer, C. M. SU356
Kan, J. F053, SA053
Kanaan, R. A. M265, SU206
Kanatani, N. F222, SA048, SA222
Kanaya, A. 1021
Kanaya, F. M148
Kanazawa, H. 1005
Kanazawa, K. SU456
Kandilyotu, A. SU576
Kane, R. L. F402, SA402
Kaneko, H. M273
Kaneko, K. M301
Kang, B. SU262
Kang, B. M. SA116
Kang, C. SU187
Kang, C. SU187
Kang, D. SU187, SU188
Kang, H. SU571
Kang, M. M040
Kang, M. M390
Kang, M. Il M401, SU439
Kang, Y. SU572
Kanis, J. F489, SA489
Kanis, J. A. F375, M356, SA375
Kann, P. H. SA111
Kanno, J. 1076
Kanno, T. SU286
Kannus, P. F187, SA187, SU002, SU143, SU222, SU469, SU470
Kanoh, N. M307
Kansagor, J. N. SU161
Kanthala, S. SU264
Kantor, S. 1183
Kapadia, R. M031, SU544
Kaplan, F. S. 1135, M265, SA126, SU016, SU021, WG21
Kapner, A. SU478
Kaptoge, S. 1111, 1151, M334
Kapur, S. F264, M151, M151, SA263, SA264
Karaplis, A. C. F433, F477, F523, F537, M060, SA433, SA477, SA523, SA524, SA537, SA576, SU448
Karasik, D. F136, SA040, SA136
Karczmarewicz, E. M547
Karim, L. M452
Karinkanta, S. SU469, SU470
Karlamangla, A. F328, F400, SA328, SA400
Karlin, J. 1144
Karlsson, M. 1147
Karlsson, M. K. 1188
Karlsson, M. Karl SU464
Karnik, K. SU147
Karp, H. J. M378
Karpeisky, M. F095, SA095
Karperien, M. SU040, SU249
Karsak, M. M166
Karsdal, M. A. M302, SU335, SU427
Karsenty, G. 1099, 1209, F191, F523, SA191, SA523, SU243
Kartsogiannis, V. 1025
Kasparcova, V. 1039, F202, F270, SA202, SA270, SU351, SU577
Kasperk, C. M459
Kassem, M. 1091, M049
Kassolis, J. D. M057
Kasugai, S. SA067
Kasukawa, Y. 1181, F160, M476, SA160, SU330
Katae, Y. SU208
Katafuchi, M. SU141
Katagiri, H. M111, SU375
Katagiri, M. SA143
Katagiri, T. F212, SA212, SU018
Katayama, S. M409, M489
Kati-Coulibaly, S. SU460
Kato, M. M307
Kato, N. SU494
Kato, S. 1006, 1099, M562, M575, M583, SA560
Kato, T. SA036
Kato, Y. SU449
Katsube, K. SU294
Katz, A. M354, M406, SA366
Katz, R. W. M255, M555, SU296
Kaufman, J. 1219
Kaufman, J. SA129, SU175
Kaufman, K. SA419, WG5
Kaur, A. SU020
Kawabata, K. M064
Kawada, N. M064
Kawaguchi, H. 1012, 1038, 1050, F511, M022, SA048, SA143, SA177, SA249, SA430, SA511, SU037
Kawamura, S. M308
Kawanabe, N. F306, SA306, SU307, SU337
Kawano, H. 1099
Kawano, T. M369
Kawata, T. SA153, SA548, SU517
Kawatani, M. M307
Kawate, H. F565, M229, SA565
Kawchak, D. SA502
Kayasuga, R. M064
Kayath, M. M473
Kazakia, G. J. SU023
Kazlauskas, R. M134
Ke, H. F299, SA299
Ke, H. Z. 1008, 1032, 1216, M388
Kearns, A. E. M347, SU283, SU416
Keaveny, T. M. M058, SU023
Keenan, G. SU428
Keljo, D. J. SU529
Keller, B. 1130
Keller, E. T. M088
Keller, H. 1166
Keller, H. J. 1079
Kelly, K. M086
Kelly, M. F394
Kelly, M. M366
Kelly, M. SA394
Kelly, P. L. SA231
Kelly, T. M075, wg8
Kelly, T. L. SU112
Kelsey, C. SU123
Kempf, H. 1128
Kendler, D. L. F406, SA406
Keng, P. SU323
Kenko, T. SA548
Kenmotsu, S. F228, SA228
Kennedy, A. M. F063, SA063
Kennedy, C. C. SU376, SU476
Kennerson, M. M150
Kenny, A. M. M160, SA135
Kent, K. SU137
Kermani, A. SU486
Kerrad, S. 1069
Kersley, J. H. M080
Kerstetter, J. 1156
Kesavan, C. F180, M215, SA166, SA180, SA258, SU212, SU213
Kessler, C. SU065
Key, L. SA314
Keyak, J. SU139
Keyak, J. H. SA379
Khadeer, M. Abdul SU244
Khairalla, T. S. H. SA492
Khalil, D. Agha M445, SA064, SU058
Khan, A. A. SU583
Khan, A. H. M534
Khan, K. SA008
Khan, K. M. F007, M106, SA007, SU468
Khan, K. Miran M127
Khan, M. F479, SA479
Khang, Y. SA372
Khanine, V. M568
Kharode, Y. 1063, F525, SA525
Khaw, K. 1151
Khaw, K. Tee M334
Kheddoumi, N. SU097
Khochbin, S. SA282
Khokhar, A. SA564
Khosla, S. 1136, 1153, F356, M387, M566, SA161, SA356, SU567, SU568, SU575
Kibe, L. W. SU106
Kida, N. SU036
Kido, S. F081, M072, M263, M399, SA081, SA569, SU216
Kieber-Emmons, T. SU099
Kiebzak, G. M. M146, SU118
Kiel, D. SU493
Kiel, D. P. F136, F330, M494, SA040, SA136, SA330, SU362
Kiela, P. R. F234, SA234
Kiely, D. K. SA040
Kii, I. 1076, SU294
Kikuchi, K. M122
Kikuchi, M. M205
Kikuchi, R. M428
Kikuchi, T. SU331
Killeen, K. K. M373
Killinger, Z. SU120
Kilts, T. SU070
Kim, B. F218, SA218
Kim, B. SU111
Kim, C. SU425
Kim, C. SU492
Kim, C. Hyun SA174
Kim, D. SU188
Kim, D. H. 1193
Kim, D. Hee M234
Kim, E. Sook M282
Kim, G. M172
Kim, G. SU029
Kim, G. SU111
Kim, G. Su M282, SA372
Kim, H. M184
Kim, H. M233
Kim, H. M235
Kim, H. M282
Kim, H. M282
Kim, H. SA055
Kim, H. SA055
Kim, H. SA443
Kim, H. SU302, SU320, SU321

(Key: 1001-1222 = Oral, F = Friday Plenary poster, SA = Saturday poster, SU = Sunday poster, M = Monday poster, WG = Working Group Abstract)

Kim, H. D. SU299, SU300
Kim, H. J. SU299
Kim, H. Jin SU426
Kim, H. K. W. SU521, SU528
Kim, H. S. 1193
Kim, H. Soo M401
Kim, I. SU055
Kim, J. M228
Kim, J. SA233
Kim, J. SU166
Kim, J. A. 1193
Kim, J. B. SU350
Kim, J. G. 1193
Kim, J. M. SU357
Kim, K. SU453
Kim, M. M291
Kim, M. K. SU299, SU300
Kim, N. C. SU299, SU300
Kim, P. J. WG25
Kim, S. 1088
Kim, S. M040
Kim, S. M040
Kim, S. M084
Kim, S. M172, M233, M291
Kim, S. M569, M571
Kim, S. SA443
Kim, S. SU055
Kim, S. SU055
Kim, S. SU111
Kim, S. SU166
Kim, S. SU236
Kim, S. SU425
Kim, S. SU554, SU555
Kim, S. H. SU299, SU300
Kim, S. W. 1193
Kim, S. Wan M234
Kim, S. Y. 1193
Kim, S. Yeon M234
Kim, T. M291
Kim, T. SU424
Kim, Y. F218, SA218
Kim, Y. SA278
Kim, Y. SU248
Kim, Y. SU425
Kim, Y. SU554
Kim, Y. Chul SU426
Kim, Y. G. SU357
Kim, Y. Joo SU473
Kim, Y. Jin SU473
Kim, Y. K. SU114
Kimmel, D. B. 1082, 1173, M422, M569, M571, M580, SU437, SU577
Kimura, T. F295, SA295
Kindblom, J. M. 1126
Kinder, B. WG8
Kindle, L. SA298
Kindmark, A. SU156
King, C. 1201
King, K. A. 1146
King, W. M525
Kingery, W. S. M396
Kinjo, M. F367, SA367
Kinosian, B. SU430
Kirby, C. M487
Kirby, H. 1217
Kirilak, L. M030
Kirma, N. SU204
Kirn-Safran, C. SU042
Kiroff, G. K. SA374
Kirson & YOW, F. M359
Kishimoto, K. SA043
Kiss, J. M414
Kissel, J. T. M525
Kissling, R. F104, SA104, SA458, SU132
Kitagawa, M. SU034
Kitahara, K. F191, M495, SA191, SU318, SU405
Kitahara, K. SU494
Kitajima, S. 1076
Kitaoka, E. M065
Kitaura, H. M274, SA289
Kitazawa, R. 1193, M283, SA043, SA563
Kitazawa, S. M283, SA043, SA563
Kiyoshi, K. SA308
Kjøbli, E. M298
Klakamp, S. 1201
Klamut, H. M056
Klaushofer, K. 1173, F462, M368, M391, SA462
Kleerekoper, M. SU407
Klein, G. L. SU489
Klein, R. F. 1081, 1084, SU161
Klein-Nulend, J. SU210
Kleinerman, E. S. M070
Klibanski, A. SU085
Kline, G. M095
Kloosterboer, H. J. SA205
Kluever, A. SU272
Knaack, D. M245
Knapp, K. M. M092
Kneissel, M. 1069, 1079, 1166, SA547
Kneuer, R. 1069
Kniepeiss, D. M545
Knight, M. C. 1164, F072, SA072
Ko, J. F521, SA521
Ko, M. M208
Ko, S. SA443
Ko, S. SU029
Kobayashi, J. SU165
Kobayashi, K. SA153, SA548, SU517
Kobayashi, M. M489
Kobayashi, M. SU191
Kobayashi, S. SU440
Kobayashi, T. F049, SA049
Kobayashi, Y. 1192, M285, M286, SU313, SU314
Kobyliansky, E. SA130
Koch, C. J. M059
Koch, H. SU288
Kodama, I. SU146
Koedam, M. SA588
Koefoed, M. F066, SA066, SU011
Koesoebjono, M. SA188
Koga, T. F297, SA297
Kogawa, M. M409
Kogwa, M. M489
Koh, A. J. 1062
Koh, J. M172, M282, SA372
Koh-Paige, A. J. M189
Kohara, S. Keiko SA542
Kohler, T. F068, M039, M191, SA068
Kohli, M. SA093
Koida, M. SU292
Koide, M. SU310
Koike, T. M448
Koistinen, A. M212, SU461
Kojima, H. SA245, SU036
Kolarz, G. F118, SA118
Kolek, O. I. F234, SA234
Kolk, D. M102, WG16
Koller, B. M120
Koller, D. L. 1081, F131, M156, SA131, SA132, SA467, SU184, SU185
Kolluri, S. SU487
Kolta, S. M050, SU119
Komatsu, D. E. SA062
Komatsu, T. SU465
Komatsubara, S. SU450, SU497
Komeda, K. 1050
Kominsky, S. SU200
Komiya, S. SU201
Komm, B. S. 1213, F573, SA573
Komori, T. 1012, F222, SA048, SA222
Komori, T. SU231
Komori, T. SU292
Komulainen, M. M411
Kon, P. M534
Kon, S. SA050
Konaka, A. SA446
Kondo, H. F191, SA191
Kondo, H. SA067
Kondo, K. M490
Kondo, T. M283, SA043, SA563
Kondou, H. SA478
Konttinen, Y. Tapio F513, SA513
Kontula, K. SU176
Kontulainen, S. SA008
Kontulainen, S. A. F007, SA007
Koo, W. W. K. SA004
Koob, J. SA351, SU379
Koobi, P. M536
Kooij, P. M114
Kopchick, J. 1167
Kopecek, J. M540
Kopeckova, P. M540
Korcok, J. M314
Korlagunta, K. M444
Kornak, U. M179
Kornman, K. M158
Korpela, R. M212
Korpelainen, R. M213
Kosa, J. M171
Kosa, J. P. M414
Koseki, T. SU286
Koshy, E. SU354
Kostenuik, P. J. 1017, 1071, 1164, 1217, M272, M300, M477, SA510, SU532
Kosulwat, V. SU104
Kotevoglu, N. SA108
Kotha, S. 1004, F182, SA182, SU215
Kotowicz, M. A. M348, SU378
Kottler, M. SA398
Kotzki, P. SA115
Kou, I. SU062
Koufany, M. SA451
Koumo, T. SA411
Kousteni, S. 1119, M221, SU339
Kovac, S. H. 1114
Kovacs, C. S. F523, SA518, SA523, SA524
Kovanen, V. M168
Koyama, E. SU039
Kozloff, K. M. 1205
Krahn, J. M331, SU353
Kraimps, J. SU508
Krall, E. F364, SA364, SU167, SU387
Kram, V. 1211
Krane, S. M. F063, SA063
Krapcho, K. J. SA546
Krause, P. SA399
Kream, B. E. 1013, 1015, 1049, 1061, 1115, M259
Krebsbach, P. H. M016
Kreder, H. SA348
Krege, J. H. 1070, 1169, SA434
Kremer, A. SA080
Kremer, R. SA080
Krenek, L. F084, F085, M014, SA084, SA085
Krenning, E. M114
Kriauciunas, A. 1218, M296
Krieg, M. F104, SA104
Krieger, N. S. SA505, SU239
Krishnan, G. M573, SU198
Krishnan, V. SA200
Kriss, M. SA298
Krits, I. F533, SA533
Kröger, H. M212, M321, M357, M411, SU382, SU388
Kronenberg, H. M. 1018, 1128, F049, SA049, SU059, SU563
Kronenberg, M. S. F061, M237, SA061, SU258
Krueger, D. F106, M327, SA106, SA399, SU118, SU584
Krueger, W. SU020
Krust, A. M562
Krust, A. SU568
Krystal, G. F320, SA320
Ku, S. SU166
Kubo, T. M036
Kubodera, N. M496, SA583, SU500
Kuboki, T. SU046
Kubota, N. SA457, SU500
Kubota, S. SU046
Kuchel, G. A. SA135
Kudlacek, P. SU088
Kudo, A. 1076, SA308, SU294
Kudo, H. M148
Kudo, I. F511, SA511
Kuehner, S. M535
Kuestner, R. M186
Kugimiya, F. 1038, 1050, M022, SA249
Kuhn, A. SU133
Kukreja, S. C. SU089
Kukuljan, S. M210
Kulak, C. Aguiar Moreira M416
Kulessa, H. 1049
Kulkarni, G. SU586
Kulkarni, N. SU338
Kulkarni, N. H. 1218
Kulkarni, P. M. 1215
Kullenberg, R. SA101
Kumagai, K. M262
Kumagai, Y. M467
Kumar, E. G. T. M141, SU359
Kumar, N. M563
Kumar, R. SA082, SA083, SA488
Kume, K. M065
Kung, A. W. C. M161, SA125, SU115, SU159
Kunii, I. S. SU549
Kunugita, N. SU209
Kuo, M. SA261
Kuo, W. S. M265
Kupcsik, L. SU270
Kuppuswamy, D. SU346
Kuran, B. SA108
Kurasawa, K. M428
Kurihara, N. 1010, 1159, 1204, F306, M577, SA281, SA306
Kurihara, S. SU314
Kurimoto, P. S. SA019
Kuroda, S. SA067
Kuroda, T. M008, SA010
Kuroki, Y. SA460
Kurosaka, M. SA043
Kurosawa, H. M495, SU037, SU318, SU405, SU494
Kurosu, Y. SU387
Kushibiki, T. SU046
Kushida, K. M344
Kusumi, K. WG21
Kutilek, S. SA387, SU083
Kuwano, T. SU539
Kvaavik, E. SU374
Kvern, B. M354, M406, SA347, SA366, SA378
Kvetnansky, R. SU068
Kwak, H. SU302
Kwak, W. Y. SU299, SU300
Kwan, E. Y. W. SA125

Kwok, S. SU095
Kwon, T. SU055
Kwon, U. M184, SA055
Kynast-Gales, S. M506

L

La Plante, K. SU239
Laan, R. M415
Lacey, D. L. 1017
Lacey, D. L. 1217
Lacey, D. L. SU532
LaCroix, A. Z. 1100, 1154
Lad, B. F141, SA141
Lafage-Proust, M. 1036, M192
Lafata, J. M102, WG16
Lafer, E. M. 1161
Lafforgue, P. SA346
Lafreniere, F. 1075
Lagman, M. G. WG14
Lagneaux, L. SU097
Lahat, O. M039
Lahdenne, P. SU537
Lai, C. Fang SU066
Lai, D. 1081
Lai, D. SA467
Lai, D. SU184, SU185
Lai, L. P. F051, SA051
Lai-Huang, C. F248, SA248
Laing, A. C. T. SU463
Laing, E. M. M131, M207
Lajeunesse, D. SA252
Lakatos, G. M171
Lakatos, P. M170, M171, M414
Lakatos, P. Laszlo M170
Lal, A. SA504
Lam, H. F262
Lam, H. M219
Lam, H. SA262
Lam, K. F. SU115
Lamantia, A. M155
Lamb, K. J. M579
Lamberg-Allardt, C. M212, M225, M378, M498, SA013, SU461, SU499
Lambert, J. M585
Lambert, L. 1019, 1024, 1084
Lambert, L. F358
Lambert, L. SA142
Lambert, L. SA358
Lambert, L. C. 1152
Lambert-Comeau, P. SU305
Lammers, J. F345, SA345
Lamminen, E. SU569
Lamolinara, A. M275
Lamsam, J. 1136
Lancaster, E. A. M447
Lanctot, C. 1075
Landais, P. SU370
Landers, C. J. SU428
Landers, K. SU396
Landoll, J. D. F343, M525, SA343
Landsman, P. B. SU355
Lane, J. SA149
Lane, J. M. SA023, SA351, SU379, SU462
Lane, N. E. M379, M480, M488, SA379, SU377
Lang, T. SA018, SU139
Lang, T. F. 1067, 1098, 1124, 1152, SA379, SU162
Langdahl, B. L. M174, SA032
Langdown, M. M154
Lange, J. L. M465
Langerwerf, P. Eli J. SA255
Langhammer, A. M367
Langley, R. 1096
Langman, C. SU395
Langman, C. B. M524, SA514, SA515, SA516
Langton, C. M. M097
Languino, L. SA091
Lankford, J. F175, SA175
Lanske, B. 1133
Lantz, R. C. M538
Lanyon, L. E. 1148, M570, SA181, SU225
Laplanche, J. SU154
LaPlante, K. SA505
Lapointe, L. M297
Lappe, J. M. 1048, F102, M439, SA102, SU124
LaPres, J. SA227
Laroche, N. 1036, SU074
Larrosa, M. SA337, SA338
Larsen, K. I. 1127
Larson, D. SA419, WG5
Larson, E. A. 1084
Larssen, M. M367
Larsson, L. M531
Lascau-Coman, V. M060, SU035
Laskey, M. Ann SU459
Lasmoles, F. SA155
Lassar, A. B. 1128
Latham, J. A. 1217
Lau, E. SA322
Lau, E. SU394
Lau, E. M. C. M100, M143, SU223, SU360, SU433
Lau, H. H. L. M161, SA125, SU159
Lau, K. H. W. F264, F318, SA263, SA264, SA318, SU056
Lau, K. S. SA125
Lau, W. SU573
Lau, W. Wan Yee SU360
Laudier, D. M. 1196
Lauridsen, A. L. SA578
Laurin, N. M024
Lausmann, K. M375
Lavigne, J. R. SA530
Lazarenko, O. P. M054, SA171
Lazarov, M. M467
Lazebnik, R. F396, M386, SA396
Lazell, R. SA501
Lazure, C. SA530
Le Bihan, C. SU370
le Henanff, A. SU542
Le Loet, X. SU542
Le Mée, S. F226, SA155, SA226
Le Pogamp, P. M549
Le Roux, C. W. M138
Le-Capling, T. SA546
Le-Moigne-Amrani, A. M420
Leach, R. J. F484, M515, M520, SA484
Lean, J. M. SA393
Leary, E. SU493
Leary, E. Teng SU148
Leary, E. T. SU451
Leavey, J. Kraft 1059
Leb, G. M295, M398, M545
Lebecque, p. SU412
LeBoff, M. S. 1154, SA331, SU235, SU421, SU496
Lecanda, F. M222
Lechpammer, S. F168, SA168, SU203
Lecka-Czernik, B. M054, SA171
Leclerc, N. SA564
Leder, B. Z. 1172
Lederman, S. 1072
Ledgard, F. 1205
Lee, A. F424, F426
Lee, A. SA135
Lee, A. SA423, SA424, SA426
Lee, B. 1107, 1130, 1139
Lee, B. M233
Lee, B. M558
Lee, B. SA278
Lee, B. SA443
Lee, C. SA514, SA515, SA516
Lee, C. H. SU299, SU300
Lee, D. SU111
Lee, D. C. M059
Lee, E. SU555
Lee, H. M184, SA055
Lee, H. SU523
Lee, H. S. SU300
Lee, H. Young SU492
Lee, I. M291
Lee, I. SU523
Lee, J. 1021
Lee, J. SU554
Lee, J. C. SA025
Lee, J. Hyun SU492
Lee, J. J. SU023
Lee, K. F333
Lee, K. M184, SA055
Lee, K. SA333
Lee, K. SU187
Lee, K. SU187
Lee, K. K. SU115
Lee, K. Woo M401, SU439
Lee, L. Man SU360
Lee, M. 1108
Lee, M. M157, SU164
Lee, M. SU248
Lee, M. W. WG14
Lee, S. 1061
Lee, S. F160
Lee, S. M273, M276
Lee, S. M291
Lee, S. M311
Lee, S. M353
Lee, S. SA160
Lee, S. SU307
Lee, S. SU554, SU555
Lee, S. H. SU357
Lee, S. Kyeong M195
Lee, S. Keun SA166
Lee, S. Kyu SU426
Lee, S. S. SU299, SU300
Lee, S. Yeoup SU473
Lee, T. SU008
Lee, W. M040
Lee, W. M235
Lee, W. M390
Lee, W. Young M401, SU439
Lee, Y. M443
Lee, Y. SU453
Lee, Z. SU302, SU320, SU321
Leenen, P. J. M. SU319
Leese, G. F341, SA341
Leeuwenburgh, C. SU219
Lefauveau, P. SU411
Lefevre, G. SA155
Lefker, B. A. 1216
Lefort, M. M481
Legoupil, N. M062
Legrand, E. M392
Lehmann, T. SU277
Lei, S. F. SU172
Lei, X. M456
Leman, E. S. F529, SA529
Lemineur, G. SA113, SU024
Lemonnier, J. SA155
Lems, W. M415, SU446
Lengner, C. J. 1015, 1129, F256, SA256
Leonard, M. SU504
Leonard, M. B. 1137 M009, SA499, SA502, SU106, SU112, SU113
Leoncini, G. M519
Leone, C. M034
Leontovich, A. A. 1200
Lepescheux, L. SU491
Leppäluoto, J. M213
Leppanen, O. SU222
Lepper, C. 1129
Lerer, T. SU485, SU525
Lerger, S. SA046
Lerner, E. SU452
Lerner, U. H. M281, SA566, SU250
LeRoith, D. SA166, SU429
Leroux, J. SA115
Leslie, W. D. M110, M331, SA347, SA378, SA456, SU353, SU361, SU383, SU483
Lespessailles, E. SA113
Letuchy, E. M. SU364
Leufkens, H. F345, SA345, SA454, SU367
Leung, J. M143, SU360
Leung, K. M134
Leung, P. SA322
Leung, P. Chung M100, M143, SU223, SU360
Levasseur, R. 1155, M466, SA398
Levenson, A. S. M118
Levine, A. M087
Levine, M. J. SA575
Levis, S. 1174
Levy, M. M366
Levy, S. WG24
Levy, S. M. F185, SA185, SU364
Lewiecki, E. M. 1072, M429, SU118, SU493
Lewis, C. F358, SA358
Lewis, C. B. 1185
Lewis, C. E. 1100
Lewis, J. S. 1150
Lewis, R. D. M131, M207
Lewis, S. SU072
Li, C. 1134
Li, C. 1196
Li, C. SU199
Li, F. 1003
Li, G. M397
Li, H. F061, M237
Li, H. SA032
Li, H. SA061
Li, J. 1017
Li, J. 1032, 1149
Li, J. F525
Li, J. M182
Li, J. M197
Li, J. SA525
Li, J. R. F477, M485, SA477
Li, K. SU333
Li, L. 1177
Li, L. SU017
Li, L. SU279
Li, M. 1008
Li, M. 1076
Li, M. 1216, M388
Li, M. SU157, SU171
Li, M. X. SU172
Li, P. M061, SU323
Li, Q. N. F097, SA097
Li, T. 1180
Li, T. Fang F513, SA513
Li, X. F521
Li, X. SA149
Li, X. SA215
Li, X. SA521
Li, X. SU017
Li, X. SU332
Li, X. Jian M491
Li, Y. F144, M025
Li, Y. M224, M278
Li, Y. SA144
Li, Y. SU277
Li, Z. M177, M178, M325
Li, Z. M329
Li, Z. SU160

Lian, J. B. 1015, 1129, 1144, 1175, 1213, F256, M233, SA091, SA217, SA256, SU252, SU322
Lian, K. SA379
Liang, M. 1201
Liang, M. T. C. SA109
Libicher, M. M459
Libouban, H. M421
Licata, A. M512
Licata, A. A. 1170
Licata, D. A. M482
Lichtenstein, G. R. M460, SU431
Lichtler, A. 1049, M237, SA249
Liddle, C. SA559
Lieberman, J. M014
Lieberman, J. R. F084, F085, SA022, SA084, SA085
Liebman, M. M506
Liebschner, M. M123
Liegibel, U. M459
Lien, G. SA512
Lim, J. I. SU299
Lim, S. M084, SU554, SU555
Lim, W. H. M550
Lin, A. M261, SU011
Lin, A. S. P. 1191
Lin, C. M209
Lin, C. M313
Lin, D. 1123
Lin, E. M515, M520
Lin, H. 1046
Lin, L. F493, SA493
Lin, W. M456
Lin, Y. SA011
Lin, Y. SU428
Lin, Y. Ling SU329
Linares, G. F160, SA160
Lincoln, J. M200
Lind, P. Monica SA472
Lindberg, M. M564
Lindberg, M. K. 1126, 1168
Linden, C. 1147
Lindner, V. 1132
Lindsay, R. F437, SA317, SA437, SA496, SU434, SU493, SU544, SU557
Lindsey, D. M396
Linglart, A. 1203, SU561, SU566
Lingle, W. F095, SA095
Link, T. M121, SU129
Link, T. M. M119, SA031, SA114, SA386
Linkhart, T. SA517
Lipfert, L. M571
Lips, P. SA162, SA188, SA350
Lipton, A. SU098
Lis, J. SU366
Lisi, S. SA541
Lisignoli, G. SA286
Little, D. Graham SU443, SU444
Liu, C. F248, SA248, SA440
Liu, D. 1032
Liu, D. M197
Liu, D. M200
Liu, F. 1061
Liu, G. 1064, F394, SA394
Liu, G. SU108
Liu, J. F400
Liu, J. M267
Liu, J. SA400
Liu, J. Chang M096
Liu, L. F131, SA131, SA132
Liu, L. J-F. M257
Liu, M. 1218, SU198, SU332, SU338
Liu, M. Y. SU172
Liu, N. F084, F085, M014, SA084, SA085
Liu, N. Q. SA022
Liu, P. SA276
Liu, P. SU285
Liu, P. Y. M387
Liu, P. Y. SU174
Liu, S. F220, SA220, SU194
Liu, S. SU436
Liu, W. F301, SA301
Liu, X. 1066, 1165
Liu, X. F102, SA102
Liu, X. SU178
Liu, Y. SA276
Liu, Y. SA532
Liu, Y. SU157
Liu, Y. SU171
Liu, Y. SU251
Liu, Y. SU273
Liu, Y. J. SU174
Liu, Y. Yu. SA274
Liu, Y. Z. SU150
Liu-Ambrose, T. SU468
Livshits, G. SA130
Lix, L. M110
Lix, L. M. M331, SA456, SU353, | SU361
Ljunggren, Ö. SU516
Lloyd, N. SA546
Lloyd, T. 1046, WG10
Lo, D. SU223
Lo Cascio, V. M085, M382
Lobaugh, B. M517
Loewy, A. 1141
Loewy, A. P. 1097
Loewy, A. P. F232, SA232
Loewy, A. P. SU066
Logsdon, S. Mary SU399
Lohman, T. M438
Lohman, T. G. M453, M455
Lohmann, C. H. M042
Lombardi, A. 1043, 1173, 1174
Lombardi, G. M147
Lomovtsev, A. M051
Lomri, A. M277
Long, F. 1002, 1103
Long, M. W. M053, M088
Longmore, G. F486, SA486
Longo, M. SU287
Looker, A. M002, M361
Loots, G. G. 1079
Lopez, C. M. M293
Lopez, E. SA296
López, F. J. M381
Lopez, J. M358
Lopez, P. Cunha Moreno M045
Lopez, R. SU396
Lopez Franco, G. E. F464, SA464, SU077
Loponen, J. M225
Lorenc, R. M429
Lorentzon, M. M004, M163, M389, SA140, SA184, SA566
Lorenzo, J. M280
Lorenzo, J. A. M273, M276, M311, SU307, SU337
Loretz, C. A. SA545
Loria, R. M. SA203
Lotinun, S. 1200, SU535
Loud, K. John M140
Loughrey, H. M484
Louis, O. SU531
Lovell, F. M341
Lovell, F. M343
Loveridge, N. 1151, M334, SU005
Lovett, F. A. 1181
Lovibond, A. Clare SA167
Low, L. SA125
Lowe, V. G. 1119, M221
Löwik, C. SU040, SU249
Lowndes, C. F459, SA459
Löyttyniemi, E. SU176
Lu, H. 1201
Lu, S. SA317
Lu, S. S. SU544, SU557
Lu, X. M258
Lu, Y. 1035
Lu, Y. SA018
Lu, Y. SU150
Lu, Z. SU585
Lucani, B. M394, M402
Lucas, E. A. M444, M445, M447, SA064, SU058
Luell, S. SU437
Luetters, C. F328, SA328
Lui, L. M158
Lui, L. M182
Lui, L. SU186
Lui, L. Y. 1056
Luk, K. D. K. M161, SU159
Lum, K. M186
Luna, S. M481
Lund, A. D. M544, SU507
Lund, R. J. M537
Lund-Olesen, L. M546
Lundeberg, J. SU156
Lundgren, E. SU515, SU516
Lundy, M. W. 1094, SA442
Luong, K. Vinh Quoc SA476
Lurie, F. SU372
Lüthen, F. SU291
LuValle, P. M025
Luz, K. SA361
Ly, C. SU317
Lykken, G. I. SU409
Lyles, K. F482, SA482
Lyles, K. W. M454, M517, SU371
Lyngstadaas, S. Petter M187, SU261
Lynn, A. M. M020
Lynn, H. M100, M143, SU360, SU394
Lyons, K. M524
Lyons, K. M. 1179, F049, SA049
Lypaczewski, G. M439
Lyritis, G. F441, SA441
Lyytikäinen, A. F009, M168, M212, SA009, SU461

M

Ma, G. SA080
Ma, L. M061, SU323
Ma, L. SU332
Ma, P. X. SU029
Ma, Q. M025
Ma, S. M327
Ma, Y. SU338
Ma, Y. L. 1218, F445, M493
Ma, Y. L. SA159
Ma, Y. L. SA445
Maalouf, G. SU134
Maalouf, J. 1047
Maalouf, N. SU134
Maalouf, N. M. WG25
Maaswinkel, P. SU064
MacCosbe, P. SA407
Macdonald, H. SA008
Macdonald, H. M. F007, M330, SA007
Macdonald, H. Margaret SA117
MacFarlane, P. M532
Machida, T. SU440
MacInnis, R. J. F459, SA459
MacKay, C. A. M505
MacKelvie, K. J. SU220
MacKelvie-O'Brien, K. J. F007, SA007
Mackie, E. J. M284
MacKintosh, F. C. SU210
MacLeod, K. J. M053
Macleod, V. M075
MacWilliam, L. M110
Madarasz, E. M171
Maddali, S. M518
Madi, O. M050, SU119
Madureira, M. M. SA389
Maeda, E. M065
Maeda, K. SA146
Maeda, N. SA247, SU195
Maeda, S. SA043, SA563
Maeda, S. SU012, SU201
Maeda, T. 1076
Maeda, T. SU539
Maeda, Y. SU260
Maekawa, S. M449, M476, SU330
Maender, C. C. F421, M451, SA421
Maes, C. F147, M211, SA147
Maetzel, A. SU480
Maggi, S. M323, M339
Magni, C. SU228
Magnusson, P. M531
Magowan, S. SU438
Magyar, C. SU254
Mahaney, M. C. SA133, SA134
Mahaney, M. C. SU356
Mahboubi, S. 1048, F102, SA102, SU124
Maher, N. M487
Mahiba, T. SU497
Mahon, M. SU566
Mahon, M. J. SA536
Mahon, P. F336, SA336
Mahonen, A. M168
Maier, E. M398
Mailhot, G. M060, SU035
Mainous, E. G. SU489
Maire, T. SA451
Maitzen, S. F118, SA118
Majumdar, S. F531, M058, SA031, SA114, SA531, SU028, SU129
Mak, Y. SA206
Mak, Y. T. M511
Makhijani, N. SA145
Makishima, F. M496, SU500, SU501
Mäkitie, O. 1102, M530, SU510, SU537
Makovey, J. SA370
Malabanan, A. O. SU424
Malhotra, S. F445, SA445
Malkin, I. SA130
Mallmin, H. SU515
Malloy, P. J. SA552
Malootian, A. SU451
Malpeli, A. SU397
Manabe, T. SA015, SU450, SU497
Manalo, D. J. SA062
Mancini, D. M. M548
Mandalunis, P. M412
Mandelin, J. F513, SA513
Mandella, R. C. SA491
Manen, D. M477, SU553
Mangadu, R. M541
Mangion, T. M516
Manhart, M. D. SU436
Manicourt, D. H. M048, M419
Mann, E. M093
Mann, K. A. SA096, SA098
Manness, L. SA347, SA378
Männistö, P. T. F139, SA139
Manolagas, S. 1066, 1074, 1104, 1119, 1165, F224, F527, M221, M380, SA172, SA224, SA527, SU004, SU339, SU413, SU550
Manolson, M. F. SA284, SU333, SU342
Mansi, J. L. SA094
Manske, S. SA008

Manske, S. L. SU220
Mansur, J. L. SU397
Mao, S. Y. SA284
Maran, A. M069, SA205
Maranghi, M. SA344
Maravic, M. SU370
Marcelli, C. M466, SA398
March, L. SU368
Marchand, F. SA353
Marchetti, D. SU042
Marciniak, S. J. 1053
Marcocci, C. SA541, SU518
Marechaud, R. SU508
Margolis, K. L. 1154
Margulies, B. S. M033, SA096, SA098, SU038
Maricic, M. M082
Marie, P. J. F226, SA155, SA226
Marín, F. F123, F441, SA123, SA441
Marin, G. M518
Marini, F. M518, M519
Marini, J. C. 1205
Marinò, M. SA541
Mark, S. SU275
Markson, L. E. F349, SA349, SU355
Marleau, A. SU309
Marlow, D. M444, M447
Marriott, T. B. F435, SA435
Marsais, F. SU491
Marsden, P. K. SU423
Marsh, D. M397
Marshall, G. 1065, F471, SA471
Marshall, G. W. SA169
Marshall, J. R. M159
Marshall, L. 1019
Marshall, L. 1058
Marshall, L. SA142, SU226
Marshall, L. M. 1152
Marshall, S. J. SA169
Marshall, T. A. F185, SA185, SU364
Martel-Pelletier, J. SA041
Martha, K. M158
Martin, B. R. SA414, SA418, SU026
Martín, D. F123, SA123
Martin, D. SA265
Martin, D. SA470
Martin, D. SU532
Martin, K. J. SU530
Martin, M. J. M241
Martin, P. Yves SU545
Martin, T. J. 1218
Martin, T. John 1025, SA540, SU317
Martinez, A. 1093
Martinez, A. F. SU297, SU298
Martinez, G. M145
Martinez, K. SU395
Martinez, M. SA129
Martinez, M. Elena M159
Martini, G. 1060, M394, M402, SA483
Martini, L. A. M335, M533, SA389
Martini, S. M144
Martino, M. SU420
Martins, H. Saramago Hermann L. M045
Marty, C. M062
Maruno, H. M074
Maruyama, R. SU408
Maruyama, T. M490, SA446
Maruyama, Z. 1012, SA048
Marvi, U. F529, SA529
Marwaha, R. Kumar M005
Marx, S. J. F493, SA493, SA543
Marzari, C. M339
Masaki, H. SA411
Masarachia, P. 1173, M422, M569, SU437
Masatomo, S. SA176, SA177
Mascarelli, F. SA155
Maschera, B. SU415
Mashiba, T. SA015, SU450
Masi, L. M518, M519, SU181
Masinde, G. M056, M151, M152
Maskow, C. SU090
Maslin, P. F335, SA335
Mason, B. SU454
Masse, P. G. SU001
Massey, L. M506
Massicotte, P. M443
Mastaglia, S. R. M412, SU116
Masternak, M. M. SA165, SU007
Mastro, A. M. SA086
Masud, T. 1109
Masuda, S. SU440
Matan, Y. SU019
Mate, P. SU263
Mathew, S. M537
Mathey, j. SU412, SU460
Mathieu, J. S. SA585, SU585
Matkovic, V. F343, M525, SA343
Matsubara, T. 1026, 1120, F251, F309, SA251, SA309
Matsui, Y. M036, M047
Matsumoto, C. M185
Matsumoto, K. SU052
Matsumoto, M. F295, SA295
Matsumoto, T. 1006
Matsumoto, T. 1171, F081, M072, M263
Matsumoto, T. M562
Matsumoto, T. SA036
Matsumoto, T. SA081, SA460, SA569, SU216, SU406
Matsuo, H. M130
Matsuo, K. 1003, 1051
Matsuura, M. SU225
Matsuura, S. SU304
Matsuura, T. SU141
Matsuzawa, M. SA201
Matteo, J. J. SU285
Matthews, J. L. SU414, SU415
Mattioli, P. M. SU047
Mattmann, C. SU133
Mattos, A. 1062
Matubara, T. SU274
Matucci, A. M518
Matucci Cerinic, M. M518
Maugars, Y. SU154
Maurer, J. M438
Mavilia, C. SU181
Mawatari, T. M129, M369, SU539
May, J. M529
Maybaum, S. M548
Mayer, J. SA030
Mayhew, P. SU005
Mays, S. F336, SA336
Maziotti, G. M147
Mazor, Z. F415, SA415
Mazzorana, M. M. P. M309
Mbalaviele, G. F248, F277, SA248, SA277
McAlister, W. H. M503, SA469, WG7
McBride, D. SA465
McBride, V. M539
McCabe, G. P. SA414, SA418
McCabe, L. R. M239, SA227
McCaffrey, G. M538
McCarthy, B. M102, WG16
McCarthy, M. F194, SA194
McCarthy, M. Beth M244
McCary, L. C. 1199
McCauley, L. Kay 1062, M189, M223, M239
McClintock, C. F466, SA466
McClintock, R. F466, SA466
McCloskey, E. V. 1020, F375, F375, F489, M356, SA375, SA375, SA489
McClung, M. 1072, F404, F412, F424, M117, M429, M457, SA404, SA412, SA423, SA424, SU493, SU127, SU128, SU232, SU481
McColley, S. M524
McCreadie, B. R. M403
McDermott, K. J. 1182, SU043
McDonald, J. M. F272, M231, M318, SA259, SA272, SU073
McDonald, M. M. SU443, SU444
McDorman, K. 1212
McGee, D. M160
McGowan, J. A. 1098, SA331
McGowan, N. W. A. M316
McGrath, B. SA059
McGrath, M. SU363
McGuigan, F. E. M330
McGurk, C. F489, SA489
McHugh, K. SU328
McIntosh, L. SA080
McIsaac, W. SA348
McKay, C. SU168
McKay, H. A. F007, M127, SA007, SA008, SU131, SU220, SU468, WG10
McKenna, L. M442
McKenna, M. A. M318
McKenny, J. SA423
McKiernan, F. E. F468, M371, M501, SA420, SA453, SA468, WG20
McKinlay, J. Bruce SA326, SA327, SA363
McKinstry, M. B. SA193
McLellan, A. M341, M343
McLeod, K. J. 1190, SU467
McMahon, A. P. F049, SA049
McMahon, D. M370, SA501, SU108
McMahon, D. J. SU580
McManus, J. Frances SA310
McNabb, M. 1055
McNeill, J. SU506
McQuillian, C. M341, M343, M462
Mead, K. E. F459, SA459
Meade, E. M511
Meadows, N. A. M292
Mechoulam, R. M166
Medich, D. L. SU130
Medicherla, S. M541
Mee, A. P. M579, SA481, SU072
Meeder, P. M459
Meeves, S. SU377
Meganck, J. A. SU069
Mehrotra, M. M194, M195, SA176, SA177
Mehta, N. M. SU451
Meier, C. F354, M150, SA354
Meldrum, E. SU415
Melhus, H. SU151
Mellibovsky, L. SA250, SU182, SU241
Mello, A. SU486
Mellström, D. F375, M004, M356, SA140, SA184, SA375
Melton, L. J. 1153, F356, F375, F402, M458, SA161, SA356, SA375, SA402
Même, S. SU228
Menaa, C. F293, SA293, SU100
Mendes, M. G. M530
Mendonca, S. SU391
Menei, P. M269
Meneu, J. M145
Mentaverri, R. SA302
Mercer, R. R. SA086
Merciris, D. M062
Merdes, M. 1069
Merlotti, D. 1060, M394, M402, SA483
Merriman, E. N. SU378
Mertens, A. C. SU085
Mesenbrink, P. F482, SA482
Mesquita, M. SU531
Meta, M. SA018, SU162
Metcalfe, A. J. F435, SA435
Metcalfe, L. L. M453
Metge, C. J. M331, SA347, SA378, SA456, SU353, SU361, SU483
Metz, M. SU140
Metzger, D. 1006
Meunier, P. J. SA038
Meury, T. R. SU270
Meyer, H. E. SA324, SA376, SU374
Meyer, M. H. M238, SA577
Meyer, R. A. M238, SA577
Meyer, S. SA111
Meyers, V. E. F272, SA272, SU073
Mezquita-Raya, P. SA119, SA425
Miao, D. S. F433, F477, F537, M485, SA433, SA477, SA537, SA576
Miao, Y. F070, SA070
Miccoli, P. SA541
Michaelsen, K. Fleischer SU499
Michaëlsson, K. SU151
Michienzi, S. 1157
Michigami, T. F553, SA478, SA553
Michou, L. SU154
Miclea, R. SU040
Middleton, S. M272, SA510
Middleton-Hardie, C. A. M522
Mielke, K. L. M387
Mierke, D. F. M558
Miettinen, H. M. SA472
Migliaccio, S. M471, SU287
Miglino, M. Angélica M045
Miholic, J. F390, SA390
Mikati, M. M497
Miki, T. SA153, SA411, SA460, SA548, SU517
Mikuni-Takagaki, Y. SU207
Miles, L. J. F141, SA128, SA141
Milet, C. SA296
Millan, J. L. F039, F474, SA039, SA474
Miller, C. G. M103, M105
Miller, D. R. F364, SA364, SU167
Miller, J. SU082
Miller, L. E. M126, SU229
Miller, M. SU520
Miller, M. A. F431, SA431
Miller, P. F412
Miller, P. F482
Miller, P. SA412
Miller, P. SA482
Miller, P. SU434, SU438
Miller, P. D. 1072, F339, F349, F408, M429, M478, SA339, SA349, SA408, SU118, SU441
Miller, R. 1095
Miller, S. M523
Miller, S. C. M540
Miller, T. A. M249
Miller-Hansen, D. SA461
Millham, M. L. SA567
Milligan, C. 1063, F525, SA525
Millsaps, R. M427
Milner, L. A. M266
Milstead, J. R. M216
Mimura, K. SA121
Mina, M. SU263
Minet, D. 1118, F090, SA090, SU488, SU491
Minetto, M. M383
Minisola, S. SA344

(Key: 1001-1222 = Oral, F = Friday Plenary poster, SA = Saturday poster, SU = Sunday poster, M = Monday poster, WG = Working Group Abstract)

Minne, H. F441, SA441, WG1, WG4
Minugh-Purvis, N. SU039
Mirwald, R. L. F002, SA002, SA006, WG10
Mishima, H. M183
Mishina, Y. 1039, 1177, 1179
Misurski, D. A. 1170
Mitchell, B. D. 1215, SU356
Mitchell, J. F051, SA051
Mitchell, J. A. SA273
Mithal, A. WG17
Mitlak, B. SU381
Mitlak, B. H. 1170
Mittra, E. SU080
Mittre, H. SA398
Miura, H. M129, M369
Miyabara, Y. M008, SA010, SU490
Miyakoshi, N. M449, M476, SA422, SU191, SU330, WG6
Miyamoto, J. 1006, M562
Miyamoto, K. SU497
Miyamoto, S. M015
Miyamoto, S. SU015
Miyamoto, T. 1051, M026
Miyamoto, T. M074
Miyamoto, T. SU045, SU315, SU316
Miyauchi, A. M395, SU207, SU517
Miyauchi, M. SU034
Miyauchi, Y. F553, SA553
Miyaura, C. M185
Miyazaki, T. F311, SA311, SU344
Miyazono, K. SU037, SU201, SU216
Mizoguchi, T. SU313
Mizoi, L. M165, SU408
Mizuno, D. SU210
Mizuno, K. SA240
Mizuno, M. SU190
Mizuno, S. M041
Mizuno, Y. SU440
Mizutamari, M. M312
Mizwicki, M. T. 1090
Mobley, S. L. F343, SA343
Mochizuki, K. M428
Modin, G. W. SA379
Modlesky, C. M. M131
Moe, O. W. WG19
Moedder, U. I. SU567
Moermans, K. F147, SA147
Moffatt, P. 1075
Moffett, A. 1072, F424, SA424
Moffett, S. P. M180, SU186
Moffett, Jr., A. H. F426, SA426
Mogi, M. 1192, M285, SU303
Mohamedali, K. F099, SA099
Mohammad, K. S. 1093, SA148
Mohan, H. K. M511
Mohan, S. 1181, 1206, F160, F180, M043, M056, M151, M152, M215, SA158, SA160, SA166, SA180, SA258, SU056, SU212, SU213, SU330
Mohler, E. R. SU504
Mohr, A. 1077
Moir, J. M. 1052
Mok, J. SU425
Moldovan, F. M066, SU035
Mølgaard, C. M498, SA013, SU499
Möller, G. M410
Moller, R. SU487
Monegal, A. M551, SA485, SU422
Monetti, R. M121, M119, SA031, SA114, SU129
Moniz, C. M516
Moniz, C. M534
Monjo, M. M187
Monllau, J. Carlos SA250
Monroe, D. G. F170, M566, SA170, SU575
Montagnani, A. M144, SU420
Montague, D. C. SU495
Montecino, M. 1144, SU252
Montero, M. M481
Montero-Menei, C. M269
Montilla, C. A. M167
Montjovent, M. SU275
Moon, E. S. SU357
Moon, I. SU572
Moon, S. M184, SA055
Moon, S. SU166
Moon, Y. SU114
Moonga, B. F316, SA316
Mooradian, A. D. M574
Moore, A. 1217
Moore, E. M186
Moore, T. M573
Mora, S. SU178
Moran, C. SA517
Morancey, J. A. M373
Morand, c. SU412
Moranda, L. Morgan SA231
Morasso, M. I. 1144
Moravits, D. M. F175, SA175
Moreau, A. M066, SU345, WG9
Moreau, I. SA030
Moreau, M. M421
Morello, R. 1107, 1139
Moreno, E. M145
Moreno, L. D. SU076
Morey-Holton, E. SA534
Morfill, G. M119, SU129
Morgan, S. M217, SU507
Mori, G. SA204
Mori, H. M064
Mori, K. M283
Mori, S. SA015, SU450, SU497
Mori, T. SU208, SU209, SU538
Morii, H. SA121
Morin, P. SU186
Morin, S. M413, SU144
Morinaga, H. M164
Moriyama, K. M301, SU192
Moro, L. SA225
Morony, S. 1017, 1212, 1217, M300, SA510, SU532
Morr, S. SU462
Morrell, M. SA475
Morris, H. A. SA587
Morris, J. M529
Morris, M. D. 1205, M403
Morris, S. A. SU296
Mortlock, D. P. 1182, SU043
Morton, H. SA465
Morvan, F. 1057, 1117, 1142
Mosekilde, L. M338, M340, M546, SA578
Moser, M. T. M078
Mosher, D. F. SU063
Mossetti, G. M147
Mossman, E. A. M117, M457, SU127, SU128, SU232, SU481
Motokawa, S. SA014
Motokawa, W. SU306
Mount, J. G. SU324
Mount, J. G. Gavin M052
Mourao Netto, M. SU101
Mouton, C. P. 1100
Movérare, S. 1126, 1167, 1168, M564, SA397, SU574
Moy, C. M553
Moyer-Mileur, L. J. SU112
Moyses, R. M. A. M533
Mrak, E. SA076, SA519
Mravec, B. SU068
Mueldner, C. 1140
Mueller, C. M. M499
Mueller, D. M119, M121, SA031, SA114, SA386, SU129
Mueller, G. S. M073
Mughal, M. Z. M529, SU363
Mughal, Z. F012, SA012, SU458
Muhlbauer, R. C. SU457
Muir, C. SU096
Mukherjee, A. 1001, 1054
Mukundakrishnan, K. M201
Mulcahey, M. K. 1040, M035
Mulder, J. E. SU085
Mullaney, S. SA034
Müller, R. 1211, F068, M039, M166, M191, SA068, SU133, SU153
Mulloy, A. Lysander M492, SA447
Muma, B. M102, WG16
Mumm, S. F468, M173, M503, SA468, WG7
Münch, C. 1208
Mundy, G. R. 1011, 1161, 1176, F044, M076, SA044
Muneta, T. M304, M582
Munivez, E. 1139
Munns, C. M500, M504
Munoz, F. 1068, F380, SA353, SA380
Muñoz-Torres, M. SA119, SA425
Murabito, J. M342
Murakami, A. SA449
Murakami, M. F511, SA511
Murata, K. M122
Muresan, M. M. SA451
Murphy, M. F450, SA450
Murphy, R. 1072
Murphy, T. C. 1034, SU236
Murray, D. SU242
Murray, E. J. B. M220, SA074
Murray, S. Scott M220
Murray, S. S. SA074
Murray, T. F371
Murray, T. M246
Murray, T. M423, M443, SA371
Murray, T. M. M464
Murrills, R. J. SU285
Murtaugh, L. Charles 1128
Murthy, S. SA438
Muschler, G. F. M262, SA241
Muschler, G. M. M254
Musella, T. M147
Mustapha, B. M425
Mutoh, Y. SU465
Muzylak, M. M052, SU324
Muzzin, P. 1121
Myerrose, T. E. M039
Myers, D. E. SU317
Myers, E. M499
Myers, E. R. SA023
Myers, K. J. SU332, SU338
Myers, S. L. 1169
Myoui, A. F047, F087, SA047, SA087

N

Nabeshima, Y. SA020
Nabizadeh, F. SU108
Nabulsi, M. 1047
Nadeau, J. H. SU155
Nadella, P. M087
Nader, A. M368
Nader, A. M391
Nagae, M. M068
Nagai, K. M307
Naganathan, V. SA370
Naganawa, T. 1042
Naganawa, T. F026, SA026
Nagano, N. SA548
Nagashima, M. SU208, SU257, SU538
Nagashima, Y. SU141
Nagayama, M. M065
Nagy, Z. M170, M171, M414
Nair, H. D. WG14
Naito, J. M091, M227, SA562
Naka, H. SA411
Naka, M. M490
Naka, Y. M548
Nakai, K. SU208
Nakai, K. SU538
Nakajima, A. 1198
Nakajima, K. SU511
Nakajima, T. SU173
Nakamichi, N. SU218
Nakamichi, Y. 1006, 1192
Nakamiti, Y. M285
Nakamoto, C. SA241
Nakamoto, T. SU165
Nakamura, A. 1025, SU317
Nakamura, H. M165
Nakamura, H. SU015
Nakamura, K. 1012, 1038, 1050, F199, F511, M022, SA048, SA177, SA199, SA249, SA430, SA511, SU037
Nakamura, M. 1192, SU303, SU304
Nakamura, M. C. 1195
Nakamura, N. SA146
Nakamura, S. M395
Nakamura, T. 1006, 1099
Nakamura, T. 1171
Nakamura, T. F056
Nakamura, T. M583
Nakamura, T. SA056
Nakamura, T. SA460
Nakamura, T. SU052
Nakamura, T. SU208, SU209, SU257, SU406, SU538
Nakano, K. M308
Nakano, T. SA460
Nakao, K. SU046
Nakashima, A. F212, SA212
Nakashima, K. M252, SA233
Nakashima, Y. M129, M369, SU539
Nakatsuka, K. M132, M344, SU517
Nakayama, K. 1160
Nakayama, K. SA446
Nakayamada, S. SU209
Nakchbandi, I. M240
Nam, M. SA278
Namba, N. F320, SA320
Namba, N. SU526
Namdar-Attar, M. M039
Namikawa, T. SU015
Nampei, A. SA146
Nancollas, G. H. SA305
Nanes, M. S. 1034, M258, SU236
Nangia, S. WG17
Nantermet, P. V. SU577
Naot, D. M522, SU284
Napierala, D. 1107, 1130
Napoli, N. M173
Nappo, L. SA361
Narayanan, R. M576
Naressi, M. SU117
Nasatzky, E. M567, M572
Nashiki, K. SU533
Naski, M. Chester M031
Nasser, P. M010
Nasser, P. SA385
National Repository F141, SA141
Natour, J. SU401
Natri, A. M498, SA013
Nattiv, A. M345
Naujoks, R. SU094
Nauman, E. A. M435

Navasa, M. M551
Naves, M. SA392
Naves-Diaz, M. M094
Nawata, H. F565, M229, SA565
Nawroth, P. M459
Nebe, B. SU291
Need, A. G. SU140
Neer, R. 1172, F439, SA439
Neff, L. 1142, F283, F311, SA283, SA311, SU344
Neff, M. F104, SA104, SA458, SU132
Negron, A. M467
Nelson, A. E. M134
Nelson, T. 1080
Nemere, I. SA550
Nemeth, E. F. SA546
Nemoto, K. SU218
Nenonen, A. SU143
Nervina, J. SU254
Nest, L. SA399
Netter, P. SA451
Neubort, S. SA317
Neumann, H. SU291
Neuner, J. M. 1100
Nevitt, M. 1019, 1058, SU394
Nevitt, M. C. 1110, M158
Newell, W. SU579
Newitt, D. SU129
Newitt, D. C. SA031
Newman, A. 1021
Newman, A. B. 1022, 1189
Newman, M. K. F431, SA431
Ng, K. Wah 1025, SA179, SU317
Ng, M. Y. M. M161
Nguyen, C. V. 1087
Nguyen, D. Ngoc Pham SA476
Nguyen, H. 1017
Nguyen, L. F586
Nguyen, L. SA574, SA580
Nguyen, L. SA586
Nguyen, L. SU570
Nguyen, L. Thi Hoang SA476
Nguyen, N. M362
Nguyen, N. Dinh. 1112, 1184
Nguyen, N. D. F410, SA410
Nguyen, N. Dinh. SU121
Nguyen, P. F529, SA529
Nguyen, T. V. F354, SA354
Nguyen, T. V. M134, M362
Nguyen, T. V. M363
Nguyen, T. V. SU104, SU105
Nguyen, T. Van 1112, 1184, F410, SA410, SU121
Ni, R. 1196
Nicholella, D. 1004, 1004
Nichols, G. 1113
Nicholson, G. M150
Nicholson, G. C. M293, M348, SA374, SU378
Nicholson, P. F009, SA009
Nicholson, T. F441, SA441
Nickelsen, T. N. F441, SA441
Nickols-Richardson, S. M. M126, SU229
Nicolella, D. P. F175, SA175
Niehof, A. SA463
Niemeier, A. 1208
Niemi, E. C. 1195
Nieves, J. F437, SA317, SA437
Nifuji, A. F056, F191, SA050, SA056, SA191, SU231, SU260, SU318, SU405, SU494
Nii, A. M308
Niida, S. 1125, F287, SA287
Nikiforakis, N. SU420
Nilsson, O. SU177
Nimura, Y. 1125
Ninomiya, J. T. SU240
Nique, F. SU491
Nishida, S. F178, F531, SA178, SA531
Nishida, S. K. SU549
Nishida, T. SU046
Nishihara, T. SU286
Nishimori, S. SU059
Nishimura, R. 1026, 1045, 1120, F251, F309, SA251, SA309, SU274
Nishiwaki, T. 1051
Nishiwaki-Yasuda, K. SA036
Nishizawa, Y. M469
Nishizawa, Y. SA153, SA411, SA548, SU517
Nissen-Meyer, L. Sofie H. M038
Nissenson, R. A. F529, SA529
Nistala, H. SU050
Niu, T. M177
Noale, M. M339
Nobta, M. SU271
Nocea, G. SA409
Nociti, Jr., F. Humberto M044
Noda, M. F056, F191, SA050, SA056, SA191, SU231, SU260, SU318, SU405, SU494
Noda, T. F056, SA056
Noeldge, G. M459
Noeth, U. SA236
Noguchi, T. M286, SU304, SU310, SU387
Nogués, X. SA250, SU182, SU241
Noh, T. M039, SA564
Noh, W. I. SU357
Nolan, J. R. SA414
Noll, J. SA575
Nolta, J. A. M039
Nomura, R. M091
Nomura-Furuwatari, C. SU052
Nonaka, K. SA121
Nordgarden, U. SU051
Nordin, B. Edgar Christopher SU140
Nordstrom, A. M001
Nordstrom, P. M001
Norimatsu, H. SA015, SU450, SU497
Norman, A. W. 1090, M578
Norris, S. Anthony M007
Norton, P. A. SA054
Noseworthy, C. S. F523, SA523
Notini, A. Jill. SA310
Notomi, T. 1033
Notomi, T. SU032
Notoya, K. SU207
Novack, D. V. 1028, F304, SA304
Novakova, I. SU142
Nowak, N. Anna SU366
Nowson, C. 1183
Nowson, C. A. F459, SA459
Nozaka, K. M476, SU191, SU330
Nozawa, M. M495
Nuglozeh, E. SA078, SU053, SU278
Nugmanova, L. SU576
Nussenbaum, B. M016
Nuti, R. 1060, M144, M394, M402, SA483, SU420
Nyári, T. SA163
Nyati, L. Howard. M007
Nyberg, C. SA105
Nyman, J. A. F402, SA402

O

O'Brien, C. A. 1066, 1104, 1165, F527, M380, SA527, SU339, SU413, SU550
O'Brien, M. L. WG21
O'Brien, T. 1040
O'Connell, M. B. SU407
O'Donnell, G. F573, SA573
O'Keefe, R. J. 1040, 1180, F058, F066, M035, M261, SA058, SA066, SA201, SU011
O'Loughlin, P. Damian SU140
O'Malley, B. W. SU567
O'Malley, J. P. 1216
O'Neil, J. D. M331, SA456, SU353, SU361
O'Neill, J. SU022, SU376
O'Neill, T. W. 1111
O'Sullivan, M. Jo 1100
O'Donnell, C. J. SA040
O'Keefe, R. J. M028, M061
Oakley, J. I. M180, SU186
Oba, Y. M301
Obara, L. H. SU549
Obara, T. SU511
Oberg, A. E. F356, SA356
Oberg, A. L. 1153, M458, SA161
Oberholtzer, S. SU212
Obermayer-Pietsch, B. M175, M295, M398, M545
Oberst, M. D. M086
Obrant, K. 1147
Obrant, K. J. SU143
Ochi, T. SU540
Ochi, Y. M064
Ochia, R. S. F421, M451, SA421
Ochiai, N. M183
Ochs, P. F441, SA441
Oda, H. F199, SA199, SU037
Oda, K. M490, SA238
Oda, N. SA036
Oddleifson, S. M366
Oden, A. F375, M356, SA375
Odero-Marah, V. A. M077
Odgren, P. R. M505
Odman, A. M. M083
Odvina, C. WG24
Oesser, S. SU048
Ofek, O. M166
Offley, S. M396
Offord, E. SU412
Ogasawara, T. M022, SA143, SA249
Ogata, E. SU500
Ogata, N. M022, SA430
Ogawa, J. M074
Ogawa, T. F295, SA295
Ogawa, Y. SU534
Ogston, S. F341, SA341
Ogura, E. SU526
Oh, K. M040
Oh, K. M390
Oh, K. Won. M401, SU439
Ohama, K. SU146, SU165
Ohama, M. SU449
Ohashi, C. SA352
Ohashi, C. Barros SU401
Ohashi, M. M032
Ohba, S. M022, SA143, SA249
Ohe, M. N. SU549
Ohene-Frempong, K. SA502
Ohlendorff, S. D. SU152, SU180
Ohlsson, C. 1126, 1167, 1168, F139, M004, M163, M389, M564, SA139, SA140, SA184, SA397, SU574
Ohmoto, K. M064
Ohnaka, K. F565, M229, SA565
Ohshima, H. F228, SA228
Ohta, H. M008, SA010, SU490
Ohtsuka, M. SU165
Ohue, M. M395
Ohya, K. SA067
Ohyama, Y. SU260
Oida, H. M490
Oikawa, K. F056, SA056
Oiso, Y. SA036
Oka, J. SU455
Okabe, K. M306, SU018, SU086, SU306
Okada, K. SU191
Okada, M. F309, SA309
Okamoto, F. M306, SU018, SU306
Okamoto, S. SA460
Okano, H. M008, SA010, SU490
Okano, T. M332, SA449, SA583
Okano, T. SU375
Okazaki, K. M369, SU539
Okazaki, R. M263
Okazaki, T. 1089
Okolicany, J. M470
Okuda, N. M304, M582
Okuhira, T. SU455
Okuizumi, H. SU465
Olate, J. SU252
Older, D. SA035
Oliva, L. 1086
Oliveira, G. V. SU489
Oliveira, J. M473
Oliveira, K. R. B. SA352
Oliver, D. SU391
Oliveri, B. M101, SU116
Oliveri, M. B. M412
Olivero-Rivera, L. SU580
Olson, D. A. 1084
Olson, K. A. F495, SA495
Olszynski, W. F371, SA371
Olszynski, W. P. M413, M423, SU144
Omizo, M. 1169, F424, SA424
Omura, K. M489
Onate, S. M577
Ong, C. R. M463
Ong, D. Bee-Bee SA181
Ono, T. SA146
Ono, Y. SA036
Onoda, N. SA548, SU517
Onoe, Y. M008, SA010, SU490
Onyia, J. E. 1218, M296, SU295
Onyirimba, M. SU485
Oostra, B. SU158
Opdenakker, G. 1196
Ophoff, J. M003
Opotowsky, A. SU108
Orav, J. E. 1221, SU373
Oravec, D. SU452
Örberg, J. SA472
Orcel, P. M050, SU119, SU154
Orces, C. H. M353
Orellana, S. A. SA522
Orimo, H. M162
Orimo, H. M165
Orimo, H. M165
Orito, Y. M448
Ornitz, D. M. 1005, 1045
Ornoy, A. M567
Orrù, L. SA279
Ortoft, G. SA436, SU418
Orwoll, E. 1009, 1019, 1023, 1024, 1044, 1058, 1067, 1081, 1084, 1113, 1152, 1185, F358, F362, SA142, SA355, SA358, SA362, SU226, SU394, SU161
Ory, S. SA282
Osada, H. M307
Osborn, F. 1109
Osdoby, P. A. M290, M303, SA298
Osella, G. M383
Oshima, H. SA120
Oshima, T. F081
Oshima, T. F152
Oshima, T. M072, SA081
Oshima, T. SA152
Osman, N. I. M189

(Key: 1001-1222 = Oral, F = Friday Plenary poster, SA = Saturday poster, SU = Sunday poster, M = Monday poster, WG = Working Group Abstract)

Oste, L. M251, SA480, SA506, SA508
Ostertag, A. M179, SA129
Ostrowski, M. M292
Ota, N. SU435
Otomo, H. SU208
Otsubo, O. SU534
Ott, S. M. M475, M535, SA089
Ottanelli, S. SU181
Oursler, M. 1197, F170, M319, SA170, SU341
Ovadia, S. SA209
Owan, I. M148
Owen, S. M299
Owen, T. A. SU053, SU278
Owens, J. M. M017, M018, M247
Oxland, T. R. M106
Oxlund, H. SA436, SU418
Oyajobi, B. O. 1011, 1176, F044, M076, SA044
Oz, M. C. M548
Oz, O. M427, SU578
Ozaki, S. F081, M072, SA081
Ozalla, D. M551, SU422
Ozawa, H. SU304
Ozeki, S. SU086
Ozeki, Z. SU440
Ozkurt, I. SU254
Ozono, K. F553, SA478, SA553, SU526

P

Pacifici, M. SU039
Pacifici, R. 1059, 1116, 1191, F144, SA144, SU204
Pack, A. M. SA475
Padagas, J. SU532
Padda, M. WG13
Padrino, J. 1219
Paganini-Hill, A. M345
Pagel, C. N. M284
Paglia, F. SA344
Paine, M. L. SU054
Pajamaki, I. F187, SA187, SU222
Pak, C. Y. C. M507
Pakbaz, Z. SA504
Pakneshan, P. M081
Palacios, C. SA418
Palermo, L. 1067, 1098, F340, F429, SA340, SA429
Pallu, S. SA271
Palmer, I. M450
Palmer, T. M186
Palmieri, G. M. A. M071
Palnitkar, S. SA073, SU347, WG24
Palssa, A. M498, SA013
Pamenter, R. SA165, SU007
Pan, H. SU112
Pan, L. Codetta F061, M388, SA061
Pan, W. SA011
Panayiotou, E. SU110
Pancaldi, P. F104, SA104
Panczyk, E. M159
Pande, S. F533, SA533
Pang, M. SU297, SU298
Pang, M. Y. C. SA325
Panici, J. A. SA165
Pantschenko, A. G. SU094
Pantsulaia, I. SA130
Panupinthu, N. 1207
Panzitta, T. L. M400
Papadimitropoulos, E. M109, SA455
Papaioannou, A. F371, M109, M354, M406, M423, SA366, SA371, SA455, SU376, SU476
Pâquet, M. SU536
Pardi, E. SU518
Pares, A. SU422
Parfitt, A. SA073, SA172, SU004, SU347
Parhami, F. SA223
Parhiz, A. SU230
Parikh, N. SU519
Parisi, M. M101
Park, B. Hyoung SU541
Park, C. M390
Park, D. SU059
Park, E. M172, M291
Park, H. 1108, F218, SA218
Park, H. SU425
Park, H. SU465
Park, H. Moo. SA116
Park, I. H. SU357
Park, J. M228
Park, J. H. SU299, SU300
Park, K. Seo. SU426
Park, M.D. SU357
Park, R. M233
Park, S. M184
Park, S. M390
Park, S. SA055
Park, S. SU187
Park, S. SU465
Park, S. SU465
Park, W. SA278, SU541
Parker, A. 1130
Parkington, J. D. M491
Parlevliet, E. SU040
Paro, R. 1138
Partanen, J. M. 1005
Parthasarathy, P. R. SU359
Partridge, N. C. F521, M067, SA521, SU057, SU095, SU246
Pasanen, M. SU469
Paschalis, E. P. M061
Pasco, J. Anne M348, SU378
Pastinen, T. SU177
Pastor, I. M167
Pastorelli, R. SU574
Paszty, C. 1212, 1217
Patade, A. M444
Patano, N. SA204
Patel, R. SU110
Paterson, A. D. SU159
Pathare, P. SU349
Patiño, A. M222
Paton, L. M. 1183
Patrick, A. SA359
Patrick, A. L. M180, SA100
Patrick, H. SU391
Patrick, K. SA581
Patterson, E. K. SU560
Paul, C. 1071
Paulhamus, D. SU113
Pavlos, N. M315
Payer, J. SU120
Payes, M. SA250
Paz-Filho, G. J. M416
Pazianas, M. M460, SU430, SU431, WG15
Peacock, M. 1072, 1081, 1199, F466, F495, M156, M326, SA414, SA418, SA466, SA495, SU185, SU184
Pearce, D. M532
Pearson, D. M103, M104, M105
Pecherstorfer, M. SU088
Pecheur, I. F090, SA090
Peddireddy, V. M445
Pedersen, J. SA032
Pedersen, J. I. SU374
Pedersen, N. SU151
Peel, N. F. SU404
Peel, N. F. A. M136, M349, SA138
Pekkinen, M. M225
Peleg, S. 1087
Pell, J. M. 1181
Pelletier, J. SA041
Peltz, G. M182, SU186
Peng, X. SA221, SA532, SU246
Peng, Y. F316, SA288, SA316
Peng, Z. M565
Penninger, J. SU309
Pennington, C. F275, M203, SA275
Pennington, M. M254
Pennisi, P. SU545
Pennypacker, B. 1082, M422
Pepe, J. SA344
Pereira, G. A. P. M335
Pereira, R. C. 1053, F214, SA214, SU050
Pereira, R. M. SA389, SU543
Pérez, C. F340, SA340
Perez, G. SU386
Pérez, J. F123, SA123
Perez, S. G. SA198
Perez Martinez, F. M481
Perez-Edo, L. M351
Perheentupa, J. SU510
Peris, P. M551, SA485, SU422
Perrien, D. S. M124, SU009, SU032, SU495
Persohn, S. A. M326
Persons, K. S. SA585
Persson, E. SU250
Perwad, F. SU193
Pescarmona, G. Piero SU312
Peters, B. S. E. M533
Peters, D. M. Pesciotta SU063
Petersen, S. SU180
Peterson, C. A. M446
Peterson, E. M102, WG16
Peterson, M. G. E. M499
Peterson, W. J. SA237
Petit, M. 1046, WG10
Petit, M. A. M009, SA499
Petkov, V. I. M113, M436, SA365, SU125, SU482
Petley, G. F336, SA336
Petrey, M. M019, M256
Petrie, A. F371, M423, SA371
Petro, N. M180
Petruschke, R. A. F412, SA412
Pettersson, I. SA472
Pettifor, J. Morley M007
Pettinato, A. A. M140
Peyrin, F. SU028
Peyroche, S. M192, SU074
Peyruchaud, O. 1092
Pfeifer, M. 1222, WG1, WG4
Pfeifer, P. Charles SU326
Pflugh, D. M280
Pham, B. Z. M423
Pham, T. SA346
Phan, T. 1143, M315
Philbrick, W. 1142, SA538
Phillips, E. SA492, SU519
Phillips, R. L. SU577
Phimphilai, M. M264
Phipps, R. M408, SU436
Pi, M. SA265
Piacentini, A. SA286
Piault, S. F373, SA373
Picconi, J. L. M198, M199
Pickard, B. W. M554
Pickard, L. M109, SA455
Pickarski, M. SA046
Pidasheva, S. SA543
Pieper, C. F. M454
Pierroz, D. M477
Pierroz, D. D. 1121, M483
Pignolo, R. J. 1135, M265
Piippo, K. SU176
Pike, J. SU236
Pike, J. W. 1088, F246, M584, SA246
Pike, R. N. M284
Pilbeam, C. C. 1013, M194, M195, M273, SA176, SA177, SA195, SA196, SU227, SU250, SU551
Pinchera, A. SA541, SU518
Pines, A. SA225
Pinette, K. V. F383, SA383
Pinheiro, M. M. M335, SA352, SA361, SU101
Pino, A. María SA239
Pinto, A. C. Fonseca M045
Pioletti, D. SU275
Piperno, M. M309
Pirih, F. SU254
Pirri, M. M035
Pisano, M. R. M053
Piscitelli, P. SU369
Pisetsky, D. S. SU075
Piswanger-Soelkner, C. M295, M398, M545
Pitner, N. Douglas 1149
Pitsillides, A. M570
Pitsillides, A. A. 1148, SU225
Pitts, T. E. M083
Pitukcheewanont, P. F102, SA102, SU178
Plavetic-Chee, K. SA317
Plawinski, E. SA442, SU061
Plesner, T. 1091
Plesums, K. SA109
Ploeg, H. SA183, SU081
Plotkin, L. I. 1074, 1165, SA172
Plum, L. A. M584
Poblenz, A. T. F099, SA099
Pocock, N. A. M363
Poetter-Lang, S. M391
Pohl, G. SU088
Poirier, F. SA041
Policani, G. SU442
Pollack, S. SU502
Pollak, M. 1163
Pollina, C. SA545
Pollock, N. K. M207
Pols, H. F375, M114, M175, M176, M356, M420, SA375, SA454, SA588, SU158, SU268
Pomonis, J. SU082
Ponce, M. Laura SU272
Pongchaiyakul, C. 1112, 1184, SU104, SU105
Pons, F. SA485, SU422
Poole, A. Robin M023
Popescu, M. F. SU524
Popoff, S. N. 1016, M055, M505, SA078, SU053, SU206, SU278
Poriau, S. M149, M211
Porsti, I. M536
Portale, A. A. SU193
Porter, J. SA219
Porter, J. Anne SU147
Portman, D. SA423
Possmayer, F. 1207
pothuaud, L. SA115
Potrel-Burgot, C. 1155, SA398
Potts, J. T. SU566
Poueymirou, W. T. SU050
Pouilles, J. M360, SU390
Powell, D. R. F394, SA394
Powell, J. F330, SA330
Powell, K. SA241
Powell, K. A. M254
Powers, H. J. 1020
Powers, R. M. SU014
Pozuelos, J. F123, SA123
Prahalad, A. K. SA438

(Key: 1001-1222 = Oral, F = Friday Plenary poster, SA = Saturday poster, SU = Sunday poster, M = Monday poster, WG = Working Group Abstract)

Prasad, H. S. M057
Prasad, U. V. M141, SU359
Prasanna Kumar, D. M141, SU359
Prashanth, V. M230
Pratap, J. 1175, SA091
Pratt, S. SA545
Pregizer, S. Karl F216, SA216
Preisinger, E. WG3
Prenner, G. M545
Prentice, A. M442, SU459
Prestwood, K. M. SA135
Pretorius, J. 1212
Price, H. SA514, SA515, SA516
Price, H. E. M524
Price, J. Susan M052, SA181, SU324
Price, P. A. SU031
Prickett, T. C. R. M020
Priemel, M. 1140, 1208
Priest, L. F244, SA244
Prince, R. L. 1007, F417, M154, M169, SA416, SA417
Prior, J. C. M359
Pritzker, K. M530
Protter, A. A. M541
Provot, S. 1128
Prud'homme, J. 1052
Pruzzo, R. M358
Puel, c. SU412, SU460
Puentes, F. SA447
Puffenberger, E. SA465
Pui, M. SU022, SU376
Pujuguet, P. F090, SA090
Pun, K. Tao. SU415
Pun, S. M580
Purton, L. E. F266, SA266, SU317
Putranto, R. M301
Putt, M. SU504
Puzas, J. M405
Puzas, J. Edward 1040, F058, M035, SA058, SA201
Pyagay, P. 1132

Q

Qi, H. 1008, 1216, M388
Qian, N. F394, SA394
Qian, W. 1059, 1116
Qian, W. 1191
Qian, W. F144, SA144, SU204
Qiao, M. 1176
Qiao, N. F330, SA330
Qin, L. F521, SA521
Qin, Y. M219, M456, SU080
Qin, Y. SU157, SU171
Qiu, S. SA073, SU347
Qiu, T. F092, SA092
Qiu, W. 1017
Qu, G. SU245
Qu, Y. 1215
Quacquaruccio, G. M275
Quandt, S. 1174
Quarles, L. D. F220, SA220, SA265
Quarles, L. Darryl SU194
Quélo, I. SA213
Quesada-Gomez, J. Manuel SU189
Quibria, N. F207, SA207
Quinn, J. M. W. 1025, F266, SA266, SU317
Quinn, R. H. SU094
Qvist, P. 1068
Qvist, P. M137

R

R. Rittling, S. SU494
Rabaia, N. A. 1146
Rabbani, S. A. M081
Rabourdin-Combe, C. M309
Radominski, S. Cesar M416
Raejntroph, N. SA344
Raeth, C. M121, SA031, SA114, SU129
Raeth, C. W. M119
Ragab, A. A. M288
Raggio, C. M499, SU527
Raghow, S. M470
Ragi, S. F112, F340, SA112, SA340
Rahmaniyan, M. SA581
Rahmy, A. I. A. M407
Rahnert, J. 1034
Raie, N. 1201, SA498, SU530
Raisz, L. G. 1013, M160, M194, M195, M273, SA176, SA195, SU551
Raj, N. SU183
Rajachar, R. M. M514
Rajamannan, N. M. SU281
Rajatanavin, R. SU104, SU105
Rajendren, G. F316, SA316
Rajkumar, R. F180, SA180
Rajzbaum, G. M333, SU033
Räkel, A. SU536
Ralston, S. H. M330, SU336
Ramalakshmi, T. M141
Ramaswamy, N. WBG17
Ramos, J. SU117
Ramp, W. K. M126, SU229
Ramschak-Schwarzer, S. M295
Ramsey-Goldman, R. SA514, SA515, SA516
Randall, T. S. SU521, SU528
Rankin, J. L. M326
Ranly, D. M. M042
Rao, D. M102, M403, SA073, SA492, SU347, SU519
Rao, D. S. WG13, WG14, WG16, WG23, WG24
Rao, H. SA281
Rao, L. M246
Rao, L. G. M257
Rao, V. M246
Raper, J. SU396
Raphael, H. F335, SA335
Raphael, H. M. 1220
Rapuri, P. B. M404, SU169, SU170
Rasmussen, H. M437
Rasmussen, K. F170, SA170
Rastad, J. SU515
Ratisoontorn, C. SA243
Rattner, A. M192
Rauch, F. 1043, F462, M500, M504, SA462
Rauch, F. T. SU522
Ravasi, T. M292
Ravaud, P. M108
Ravaux, P. SU542
Rawadi, G. 1057
Rawlinson, S. C. F. SU225
Ray, R. M585
Ray, W. J. SU577
Raz, P. M042, M572
Raz, R. SU050
Realdi, G. M382
Reaney, L. F489, SA489
Réber, A. 1155
Reboul, P. SA041
Recchia, I. SU091
Recker, R. 1173, F406, F431, F450, M217, M352, M432, SA406, SA407, SA431, SA450, SU150, SU174
Reddy, H. Kishore M005
Reddy, P. WG17
Reddy, S. V. 1010, 1026, 1159, 1204, M257, F228, F306, SA228, SA306, SA314, SU310
Reddy, V. SA492
Reed, C. SU198
Reed, P. W. M154
Reeve, J. 1111, 1151, F375, M334, M356, SA375, SU005
Reginster, J. 1219
Reginster, J. Y. F408, SA408
Regmi, A. M317
Regunathan, A. SA060
Rehman, Q. SA379
Reid, D. F341, SA341
Reid, D. M. M330
Reid, D. MacCauley. SA117
Reid, I. F482, SA482
Reid, I. Reginald. M522
Reid, I. R. SA490, SU284, SU454
Reid, M. Ellen M159
Reijnders, C. M. A. SA162
Reik, A. SU285
Reimondo, G. M383
Reiners, C. SA003
Reinholt, F. P. M038
Reinholz, G. F095, SA095
Reinholz, M. M. F095, SA095
Reinus, W. R. F468, M510, SA468
Reis, J. Sérgio Nobre. M045
Reith, W. 1086
Rejnmark, L. M338, M340, SA578
Ren, H. M186
Ren, S. F586, SA586
Renieri, A. 1060
Renshaw, K. SU256
Reppe, S. M038, SU261
Resau, J. H. 1214
Resch, H. M391
Resche-Rigon, M. 1117, 1118, SU488, SU491, SU579
Reseland, J. E. M187, SU261
Resnick, H. E. 1022, 1110
Restuccia, N. SU580
Reszka, A. A. M571, M580
Rey, A. SU202, SU553
Reyes, D. A. SU436
Reyes, R. SA425
Reyes-Mugica, M. WG8
Reynolds, M. A. M057
Rhee, E. M040
Rhee, E. M390
Rhee, Y. M084, SU554, SU555
Rhim, A. D. M460, SU431
Rho, J. SU078
Rhodes, E. Copes M515
Ribot, C. M360, SU390
Riccardi, D. M270
Rice, A. J. F421, M451, SA421
Rich, S. F364, SA364
Rich, S. E. SU167
Richard, J. SU370
Richards, A. Mark M020
Richardson, J. A. SA223
Rickels, M. F468, SA468
Rico, M. C. 1016, SU053, SU278
Riddle, R. C. SU214
Ridge, S. A. SU336
Ridout, R. M521
Riera, G. S. SU117
Ries, W. SA314
Ries, W. L. F228, SA228
Rifas, L. SU267
Riggs, B. L. 1136, 1153, F356, M566, SA161, SA356, SU567, SU568, SU575
Rigon, H. J. SU101
Rikkonen, T. P. M321
Riminucci, M. 1157
Rimm, D. WG22
Ringe, J. M410, M420, M424, M509
Ringsberg, K. M006
Rini, G. B. M173
Rini, G. Battista M518
Rink, J. SA319
Rinta-Paavola, A. M213
Rios, H. F. 1004
Ríos, S. SA239
Risbud, M. V. M201
Rissanen, J. M305, SA307
Ritchie, J. E. M363
Ritchlin, C. T. SA303
Ritenbaugh, C. 1044, SA331
Ritman, E. L. SU436
Ritter, C. Sue F533, SA533
Rittling, S. R. F191, SA050, SA191, SU066, SU405
Rittweger, J. 1145
Rivadeneira, F. M114, SU158
Rivinus, M. M342
Rivollier, A. M309
Rizzoli, R. 1121, 1219, M374, M477, M483, SA384, SA427, SA448, SU132, SU479, SU488, SU545, SU553
Roato, I. M289
Robb, R. F356, SA356
Robbins, D. J. 1127
Robbins, J. A. 1100
Robbins, P. F084, SA084
Robert, J. SU545
Roberts, H. Christina. M242
Roberts, S. SU458
Roberts, S. J. F037, SA037
Robertson, J. D. SU524
Robin-Jagerschmidt, C. SU579
Robinovitch, S. N. SU463, SU471
Robinson, L. J. M279
Robinson, M. 1217
Robison, L. L. SU085
Robling, A. G. 1105, 1149, SU224
Roca, H. SU247
Rocha, J. S. SA165, SU007
Rodan, G. A. M569, M571, M580, SA046, SU577
Rodes, J. M551, SU422
Rodrigues, F. Nogueira M045
Rodriguez, C. M358
Rodriguez, J. Pablo SA239
Rodriguez, L. SA045, SA292
Rodríguez-García, M. M094
Rodríguez-Rebollar, A. M094
Rodríguez-Rodríguez, A. SA392
Roe, B. SU383
Roell, W. C. M296
Roelofs, A. Jozefien SU087
Roemer, F. 1077
Rogers, A. SA138
Rogers, I. SU325
Rogers, J. SA133, SA134
Rogers, M. J. M316, M430, M431, SU087, SU334
Rogers, M. W. SU395
Rogus, J. M158
Rohe, B. SA550
Rohrbach, J. F253, SA253
Rohrer, M. D. M057
Rohrer, S. P. M569, M571
Romagnoli, E. SA344
Roman Roman, S. 1057
Romanello, M. SA225
Rome, E. F396, M386, SA396
Ron, D. 1053
Rongish, B. J. 1073
Roodman, D. 1204
Roodman, G. D. 1010, 1159, M271, M577, SA079, SA281
Roos, B. A. M269
Roos, L. L. M331, SA456, SU353, SU361
Rosales, J. M365
Rosario-Jansen, T. SU433

(Key: 1001-1222 = Oral, F = Friday Plenary poster, SA = Saturday poster, SU = Sunday poster, M = Monday poster, WG = Working Group Abstract)

Rosato, N. SU369
Roschger, P. 1173
Roschger, P. F462, M368
Roschger, P. M391
Roschger, P. SA462
Rose, M. SA035
Rosen, C. 1065, 1080, 1083, 1098, F412, F429, M177, M178, M325, M329, M374, SA164, SA412, SA429, SU160, SU163, SU178, SU398, SU421, SU429, SU496
Rosen, D. M. M467
Rosen, R. M548
Rosen, V. 1037
Rosenblatt, M. M558, SU565
Rosenblum, M. G. F099, SA099
Rosier, R. N. 1040, 1180, M028, M035, SA201
Roskos, L. 1201, SA498, SU530
Rosol, T. M087
Ross, F. P. 1029, F285, F304, F320, F486, M274, M320, SA285, SA289, SA304, SA320, SA321, SA486
Ross, J. SU293
Ross, P. D. M542, SU393
Ross, R. A. SU336
Rossini, G. 1011, 1176
Rossini, M. SU369
Roth, M. M398
Rothe, L. SA298
Rotoli, B. M147
Rottoli, P. SU420
Roudier, M. P. M400, SA089
Roughead, Z. K. SU409
Rousseau, E. SA149
Rousseau, L. SA530, SU536
Routh, R. H. M435
Roux, C. 1219, M050, M108, M420, SU119, SU542
Roux, F. M333, SU033
Roux, S. SU305
Rowe, D. SU020
Rowe, D. W. 1035
Rowe, D. W. SA276, SU258, SU263
Rowe, D. W. SU265, SU273
Rowe, D. Whitney F061, SA061, SA192, SA193
Rowe, P. S. N. 1161
Rowley, E. M474
Roy, E. M. SU236
Roy, M. C. SU042
Royer, M. SU116
Rozen, G. S. M350
Rubenstein, J. R. M237
Rubin, C. M218, M219, M452, SA189, SA190
Rubin, C. SU156
Rubin, C. SU230
Rubin, C. T. M456, SU221
Rubin, E. M. 1079
Rubin, J. 1034, M258, SU236
Rubin, K. SU485
Rubin, L. SU179
Rubin, M. R. F495, F497, SA495, SA497, SU512, SU513, SU514
Rubinacci, A. SA076, SA519
Rucci, N. 1138, SA279, SU091
Rud, B. SU475
Rude, R. K. M046
Rudkin, G. M249
Rueger, J. Maria 1140, 1208
Ruegg, C. E. F445, SA445
Ruff, C. B. F017, M425, SA017
Ruhland, L. M539
Ruimerman, R. SU237
Ruiz-Gaspà, S. SA250, SU241
Ruiz-Requena, M. SA119, SA425
Rummeny, E. SU129
Rummeny, E. J. M119, SA031, SA114, SA386
Rundle, C. H. SU056
Ruppe, M. D. F156, SA156
Rushforth, L. M. SU481
Russ, G. R. M550
Russell, R. G. G. M073, SU087
Rust, E. C. SU233
Rutledge, S. SU577
Rutlin, J. R. 1150
Ryaby, J. T. SA149, SU056
Ryan, M. 1116
Ryan, P. SU123
Rybak-Feiglin, A. 1174
Rychly, J. SU291
Ryder, K. D. M196
Rydziel, S. F214, SA214
Ryoo, H. 1108, F218, M233, M235, SA218, SU248
Rzonca, S. O. M054

S

Saab, G. M537
Saag, K. SU396
Saag, K. G. 1114, M465
Saag, M. SU396
Saarikoski, S. M411, SU382
Saavedra, P. SA122
Sabatakos, G. F253, M019, M256, SA253
Sabatier, J. SA398
Sabatier, J. Pierre 1155, M466
Sabbagh, Y. 1162, M027
Sabokbar, A. 1030, SA300
Sachdev, R. M043
Sack, M. SU530
Sackarowitz, J. SU583
Saegusa, M. F511, M195, SA511
Safadi, F. F. 1016, M055, M505, SA078, SU053, SU206, SU278
Safar, M. SU033
Safford, S. E. SA550
Safran, K. SA281
Saga, Y. 1076
Sage, E. Helene SU060
Sage, M. 1209
Saha, R. SU099
Saha, S. 1020
Sahebjam, S. M504
Sahoo, S. P. SU577
Said, R. M050, SU119
Sainsbury, A. 1101, 1123
Saint-Pierre, C. SU305
Saintier, D. M568
Saita, Y. SU318
Saito, H. M496, M583
Saito, H. SU343
Saito, H. SU500, SU501
Saito, T. SU318
Sajjan, S. F339, F349, SA339, SA349
Sakai, A. SU208, SU209, SU257, SU538
Sakai, H. SU308
Sakari, M. 1006
Sakata, K. M490, SA446
Sakhaee, K. WG19, WG25
Sakkee, N. M058
Sakuma-Zenke, M. SU209
Salamon, E. A. M331, SA456, SU353, SU361
Salamoun, M. 1047, 1186
Salatto, C. T. 1216
Salazar, V. S. F277, SA277
Salem, M. M410
Salih, D. A. 1181
Salih, E. SU071
Salingcarnboriboon, R. SU231
Salmeron, J. F340, SA340
Salminen, H. SA105
Salmon, P. SA397
Salmon, P. L. M384, SU027
Salome, M. SA506
Saltel, f. SA282
Salter, E. D. 1216
Saltman, L. SU322
Saluja, B. M005
Salvadori, S. M394, M402, SA483
Salvato, K. M366
Samadfam, R. M485
Sambrook, P. SA370, SU368
Samet, J. H. SU424
Sampalis, J. S. SU448
San Julián, M. M222
San-Miguel, S. M253
Sanada, M. SU146, SU165
Sanchez, T. V. M096
Sandell, L. SU044
Sander, B. SU480
Sanders, K. Margaret M348, SA374
Sanders, M. SU094
Sanders, M. V. SU528
Sanderson, R. M075
Sanford, D. A. M209
Sanjay, A. 1198, F283, F311, SA283, SA311, SU344
Sankar, U. M292
Sansone, A. Paula SU401
Santos, G. M277
Sany, J. SU542
Sanyal, A. SU567, SU568
Sapountzi, P. SU581
Sarkar, P. SA520
Sarkar, S. M585
Sarma, U. M299
Sarosi, I. 1017, 1217
Sartori, L. M518
Sasaki, S. SA010
Sasaki, T. M312
Sasamata, M. M308
Sasaoka, R. SA238
Sasov, A. Y. SU027
Sasseville, M. M294
Satcher, R. L. M118
Sato, A. 1100
Sato, H. SU141
Sato, K. SU406
Sato, K. SU500
Sato, K. SU511
Sato, M. 1218, F445, M474, M493, SA445, SU547
Sato, N. M286
Sato, S. SU034
Sato, T. 1006
Sato, T. 1085
Sato, T. F154
Sato, T. M562
Sato, T. SA154
Satomi, K. M074
Satomura, K. M065
Satpathy, R. SU399
Satterfield, S. 1174
Saulnier Blache, J. 1092
Saunders, M. 1031
Saunders, N. SU123
Saunders, R. SA197
Sauter, N. SU092
Sävendahl, L. SA397
Savolainen, P. SU156
Sawa, M. M495
Sawada, N. SU533
Sawakami, K. 1149
Sawatani, Y. SU315, SU316
Sawaya, R. M497
Sawka, A. M. M109, SA455
Saxon, L. K. M204
Sayavongsa, P. M202
Scadden, D. T. M266
Scafonas, A. M569
Scaletta, C. SU275
Scerpella, T. A. SU233
Schaad, M. SU479
Schacht, E. F415, SA415, SA458
Schaeffer, J. M. M569, M571
Schaeublin, M. SA219
Schafer, B. W. SU008
Schaffer, A. A. WG21
Schaffler, M. SU215
Schaffler, M. B. 1196, F182, SA182
Schall, J. I. SA502
Schaller, S. SU335, SU427
Schelling, D. F268, SA268
Schenck, A. P. SU371
Scherer, S. C. F459, SA459
Schett, G. M120, M272, SA510
Schifini, M. SU442
Schile, C. E. SU481
Schiller, P. C. M269, M560
Schilling, A. F. 1140, 1208
Schilling, T. SA236
Schimmer, R. C. F406, M433, SA406, SU441
Schinke, T. 1140, 1208
Schipani, E. 1164, F072, SA072
Schlessinger, J. F311, SA311
Schmidt, A. F445, M474
Schmidt, A. M569
Schmidt, A. SA445
Schmidt, A. SU577
Schmidt, C. F. SU210
Schmidt, K. 1140
Schmitt, S. M. SU399
Schneeweiss, S. F367, SA367
Schneider, A. M189
Schneider, E. SA391
Schneider, P. SA003
Schneider, P. SU153
Schneider, R. M499
Schneidereit, J. SA236
Schnell, J. M446
Schoeberl, T. F462, SA462
Schoenmaker, T. SA198, SU319
Schoonmaker, J. E. SA096, SA098
Schoppet, M. SA210, SU238
Schousboe, J. T. F402, SA402
Schroeder, T. M. SA229
Schuetze, N. SA236
Schürch, S. SU457
Schut, H. A. SU064
Schwab, A. M. M281
Schwanauer, L. E. F495, SA495
Schwartz, A. 1174
Schwartz, A. V. 1022, 1110
Schwartz, E. N. 1169, SU400
Schwartz, Z. M042, M567, M572, SA572
Schwartzberg, L. S. M071
Schwarz, E. SA303
Schwarz, E. M. 1040, 1180, F058, F066, M028, M035, M061, M261, SA058, SA066, SA201, SA403, SU011, SU323
Schwarz, P. M. 1161
Scillitani, A. SU179
Scott, R. K. SU047
Screen, J. SA440
Scumpia, S. 1199
Sebaldt, R. F371, SA371
Sebaldt, R. J. M423
Secreto, F. SU281
Secreto, F. J. M566, SU575
Sedor, G. J. M569

Seeherman, H. J. M491, SU017
Seeman, E. 1219, M099, M348, SA382, SU134, SU378, SU403
Seestaller-Wehr, L. 1063
Seestaller-Wehr, L. M. SU293
Segal, E. SU509
Sehgal, A. R. SU452
Seibel, M. J. F354, M134, M150, SA354, SA568, SU368
Seidman, J. 1102
Seifert, J. SU048
Seino, Y. 1045, M232, M399, M575, SA151, SU526
Seki, A. M490
Sekimoto, E. F081, M072, SA081
Sekimoto, T. F553, SA553
Sekiya, H. SU207
Selim, A. SA536
Selleri, C. M147
Sellin, K. 1075
Sellman, J. E. SU219
Sellmeyer, D. E. 1110, 1185, F429, SA429
Selvaag, A. Marit SA512
Selvamurugan, N. SU057, SU095, SU246
Semanick, L. 1183
Semanick, L. M. F383, SA359, SA383
Semeao, E. SA499
Semenza, G. L. SA062
Semler, J. 1219
Sen, S. Sankar SA409
Seng, C. M576
Seo, H. SU205
Seo, S. SU029
Seo, S. Hyung SA116
Serakinci, N. M049
Sereika, S. 1065, F471, M479, SA471
Sereika, S. M. SU130
Serey, S. H. F234, SA234
Serfaty, D. M481
Serio, B. M147
Serra, R. 1127, SU205
Serrano de la Pea, L. SU016
Serre, C. 1092
Servet-Delprat, C. M309
Service, S. M345
Seto, H. SU037
Seto, M. SA157
Seto, M. L. SA243
Setoguchi, S. F367, SA367
Seton, M. SA487
Seuwen, K. SA219, SA547
Sewing, A. SA271
Seya, T. F295, SA295
Seyedain, M. SU288
Sfeir, C. SU288
Shaaf,, S. SU099
Shabbout, M. SU113
Shah, R. SA093
Shalhoub, V. SU532
Sham, A. M440
Shames, R. M366
Shamp, T. SU530
Shane, E. M370, M393, M548, SA475, SA501
Shane, L. G. M423
Shao, J. 1141
Shao, J. Su 1097, F232, SA232, SU066
Shao, Y. SA254
Shao, Y. SU041
Shapiro, I. M. M032, M059, M201, SA197, SU327
Shapiro, J. R. M425, M426
Sharma, A. F068, SA068
Shattuck, T. WG8
Shatzen, E. SA470, SU532
Shea, J. M523
Shea, M. SU161
Sheafor, M. 1146
Shedd, K. M. SU362
Sheik, S. M173
Shelton, R. S. SA172
Shen, C. SU003
Shen, H. SU150, SU174
Shen, J. F256, SA256
Shen, Q. F230, SA230
Shen, V. M470, SU414, SU415
Shen, X. M260
Shen, Z. SU328
Sheng, M. H-C. F127, SA127
Sheng, X. SA059
Shepherd, J. M002
Shepherd, J. A. 1048, F102, SA102, SU112, SU118, SU124
Sher, L. B. 1115
Sherman, A. SA473
Sherman, M. M002, SU124
Sherrard, D. J. M535
Shetty, S. SA498
Sheu, T. Jen SA201
Shevde, N. K. 1088, F246, M584, SA246
Shi, K. SA146
Shi, W. 1041
Shi, X. F097, M260, SA097
Shi, Y. SU276
Shi, Z. M267
Shibata, A. SU271
Shibata, H. F081, M072, SA081
Shibata, K. M286
Shibata, Y. SU435
Shibuya, M. F287, SA287
Shide, K. M399
Shih, C. M313, SA071
Shih, M. M467
Shiina, H. 1006, M562
Shim, H. J. SU299, SU300
Shim, J. Y. SU299
Shim, J. Y. SU300
Shimada, T. F152, SA152
Shimada, Y. SA422, SU191
Shimoda, K. 1051
Shimokawa, I. SA014
Shin, A. SU187, SU188
Shin, C. SU187, SU188
Shin, C. S. 1193
Shin, C. Soo M234
Shin, H. F218
Shin, H. M172
Shin, H. M235, SA218, SU055
Shin, J. M186
Shinagawa, Y. M490, SA446
Shindle, M. M426, SU379
Shindo, H. SU271
Shingu, H. SU449
Shinki, T. M307
Shinoda, H. SU331
Shinoda, Y. SA430
Shinomiya, K. M304, M582
Shinotsuka, C. SA240
Shioyasono, A. M301
Shipkolye, F. M066
Shipman, C. 1030
Shipman, C. M. SU087
Shipp, K. M. M454
Shiraishi, A. SA457, SU500
Shirakawa, K. SU201
Shiraki, M. 1171, M162, M332, SA010
Shiraki, M. SA460
Shiraki, M. SU173
Shiva, K. F173, SA173
Shivdasani, R. 1107
Shoback, D. M. 1199, F495, SA045, SA292, SA495, SA498, SA545, SU530, W>G21
Shogren, K. L. M069, SA205
Shohami, E. M166
Shon, H. SU523
Shopbell, K. M053
Shore, E. M. 1135, M265, SA126, SU016, SU021
Shorr, R. 1022
Shorr, R. I. 1110
Short, G. F. SU059
Shoup, M. E. SU130
Shozui, R. SU192
Shukeir, N. M081
Shults, J. M009
Shults, J. SA499
Shultz, K. 1206
Shultz, K. L. 1080, 1083, SU163, SU224
Shuto, T. M129, M369, SU539
Shyu, J. M313
Shyu, J. SA071
Sibonga, J. D. M364
Sibonga, J. D. SU436
Siddhanti, S. R. 1215
Siega-Riz, A. Maria SU398
Siegel, E. SA093
Sierra, O. L. F232, SA232
Sierrasesúmaga, L. M222
Siervogel, R. M. M157, SU164
Sievanen, H. F187, SA187, SU002, SU222, SU469, SU470
Siggeirsdottir, K. SU162
Siggelkow, H. SU272
Sigler, R. E. 1001
Sigurdsson, G. 1124, M133, SU162
Sigurdsson, S. SU162
Siilin, H. SU516
Silman, A. M356, M356
Silman, A. J. 1111, F375, SA375
Silva, E. Maria. Carvalho SA444
Silva, J. D. P. SA074
Silva, L. F364, SA364
Silva, M. J. 1150, M208
Silver, J. 1160
Silverberg, S. J. F495, F497, SA495, SA496, SA497, SU512, SU513, SU514, SU580
Silverman, S. L. 1187, M468B, M478, SA107
Sima, M. M540
Siminoski, K. F333, SA332, SA333, SA334
Simmons, H. A. 1008, 1216, M388
Simoes, E. F441, SA441
Simonds, W. F. F493, SA493, SA543
Simonelli, C. F112, M090, M373, SA112
Simonet, S. 1217
Simonet, S. S. 1017
Simons, L. A. M118
Simpson, E. M427
Sims, N. A. 1025, F266, F311, SA266, SA311
Sims, S. M. 1207, M314
Simske, S. J. M216
Sinaki, M. SA419, SA422, WG5, WG6
Sindambiwe, J. M441
Sindrey, D. R. SA442
Sindrey, D. R. SU061
Singer, F. 1202, 1204, F484, M515, M520, SA484, SU372
Singer, M. M240
Singh, A. T. K. M561
Singh, B. SU309
Singh, R. J. SA082, SA083, SA488
Singhal, V. K. SA461
Sinha, K. M252
Sinigaglia, L. M323
Siniscalchi, A. R. SU101
Sinnott, B. M512
Sipe, J. SU030
Sipe, J. B. F039, SA039
Sips, H. SU249
Siris, E. S. 1215, F339, F349, F404, F428, SA339, SA349, SA404, SA428, SU438, SU583
Sirjani, N. B. F234, SA234
Sirola, J. M321, SU388
Sisk, J. M. F555, SA551, SA555
Sitara, D. 1133
Sitruk-Ware, R. M563
Siu, J. SU198
Sivagurunathan, S. M284
Sivakumar, P. 1073, SU063
Skarnes, W. C. 1077
Skedros, J. G. SA357, SU079
Skelton, D. WG28
Skerry, T. 1033, 1148, SU032
Skinner, R. A. SU009, SU495
Sklar, C. A. SU085
Skoumal, M. F118, SA118
Slater, S. A. F555, SA551, SA555
Slatopolsky, E. F533, SA533
Sliney, J. F497, SA497, SU512
Sluimer, J. M114
Smallridge, R. F495, SA495
Smedshaug, G. B. SU374
Smets, N. F147, SA147
Smit, J. H. SA350
Smit, T. H. SU210
Smith, B. SU396
Smith, B. B. SA491
Smith, B. Jane SA064, SU058, M444, M445
Smith, B. J. M447
Smith, C. L. M576
Smith, C. M. M349
Smith, D. H. 1113
Smith, D. K. SA125
Smith, E. M039, SA564
Smith, E. SU081
Smith, E. L. SA183, SU074
Smith, H. F335, SA335
Smith, H. E. 1220
Smith, J. SA407
Smith, P. 1043
Smith, R. M284
Smith, R. Lane M129
Smith, S. 1071
Smith, S. M493
Smith, S. B. SA505
Smith, S. Y. F435
Smith, S. Y. SA030
Smith, S. Y. SA435, SU501
Smith, T. M230
Smith, W. M578
Smith, W. B. SU530
Smith-Adaline, E. F525, M491, SA525
Smuts, V. 1143
Snead, M. L. SU054
Sneddon, W. B. M556, SA528
Snedeker, J. G. F421, M451, SA421
Snow, C. M. SA395
Snyder, R. SA467
Soares, D. Vieir. SA444
Sobue, T. SU310
Sochett, E. M530, SU510
Sock, E. 1140
Sode, M. SU139
Sodek, J. SU325, SU331
Söderpalm, A. SA101
Sofaer Derevenski, J. F336, SA336
Sogaard, A. Johanne SA324, SA376

(Key: 1001-1222 = Oral, F = Friday Plenary poster, SA = Saturday poster, SU = Sunday poster, M = Monday poster, WG = Working Group Abstract)

Sogabe, N. M165, SU408
Sohaskey, M. L. 1077
Sojka, J. E. SU365
Sol-Church, K. SU168
Solberg, H. SA485
Solgaard, M. SA269
Solomon, D. H. F367, SA367
Solyom, A. M. M538
Somayaji, V. F424, F426, SA423, SA424, SA426
Somerman, M. SU034
Somerman, M. Joan M044, SU054
Sommer, U. M459
Somoza, J. M412
Son, J. SU111
Son, M. H. SU299, SU300
Sone, T. M344
Song, J. F428, SA428
Song, J. J. SU206
Song, J. Soo. SU541
Song, K. Young SU492
Song, L. M437, SA579
Song, Y. SA560
Soo, C. F070, SA070
Sooknanan, R. M294, M297
Sørensen, H. Ancher SU475
Sørensen, M. Grøndahl SU335
Sorensen, O. 1219
Sorenson, S. M. SU079
Sornay-Rendu, E. 1068, F380, SA380
Sorocéanu, M. Alexandra F433, SA433
Sørskaar, D. SA512
Sosa, M. SA122
Sosnoski, D. SU093
Soung, D. Yu M444, M445, M447, SA064, SU058
Souza, D. M384
Sowa, H. M091, M227, SA562
Spadaro, J. A. M033, SU233
Späte, U. F068, SA068
Spathis, R. 1190
Spatz, J. Pius F077, SA077
Specker, B. L. SU112
Spector, T. 1219
Spector, T. D. M092, M154
Speer, G. M170, M171, M414
Spelsberg, T. 1197, F095, F170, M566, SA095, SA170, SA205, SU281, SU567, SU568, SU575
Spettell, C. 1114
Spica, E. 1138
Spies, S. SA514, SA515, SA516
Spiliopoulos, A. SU545
Spina, L. Diniz Carneiro SA444
Sponseller, P. M426
Spotila, L. D. SU168
Sprague, S. F293, SA293, SU100
Sprang, T. SU457
Spurney, R. F. SU558
Squire, M. E. SA189, SA190
Sran, M. M. M106
Sridhar, S. SU280
Srinivas, V. M032, SU327
Srinivasa Rao, P. V. L. N. SU359
Srinivasan, S. 1146, M209, SU211
Sriram, U. M115, M116, WG17
Srivastava, A. M152, SU330
Srivastava, A. K. M151
St-Arnaud, R. 1052, SA213
St-Louis, G. SU536
Stabley, D. SU168
Stadmeyer, L. 1178, SU050
Stafford, G. M538
Stähelin, H. B. F415, SA415
Stahl, A. SU265
Stains, J. P. 1106, F277, SA277, SA440, SU552
Stakkestad, J. A. F408, SA408
Stallings, V. A. SA502
Stallings, V. A. SU113
Stampanoni, M. SU153
Stanford, V. M438
Stanley, J. SU099
Stapleton, P. P. M055
Starbuck, M. W. 1039
Starnes, C. SA470
Stashenko, P. F068, SA068
Stauffer, B. F260, SA260
Ste-Marie, L. G. M060, SU035
Steel, S. A. M104
Steele, C. R. M126, SU229
Steer, J. SU340
Steer, J. H. M315
Steer, S. F141, SA141
Stefanick, M. 1058, 1100, 1154
Steffens, E. E. SU481
Stegman, M. Ruth M352
Stein, G. S. 1015, 1129, 1144, 1175, 1213, F256, M233, SA091, SA217, SU252, SA256, SU322
Stein, J. SU252
Stein, J. L. 1129, 1144, 1175, 1213, F256, M233, SA091, SA217, SA256, SU322
Stein, M. S. F459, SA459
Steinbeck, M. J. M201, SU327
Steiner, M. M470
Steinman, H. A. 1015
Stempfle, H. M552
Stenkjaer, L. M174
Stenova, E. SU120
Stepan, J. J. M432, SU142
Stephens, P. 1217
Sterling, J. 1011
Sterling, J. A. 1176, F044, M076, SA044
Sterling, T. M. SA550
Stern, P. H. M307, M561, SU281, SU395
Sternfeld, B. F328, SA328
Stevens, P. F253, M019, M256, SA253
Steward, S. A. SA172
Stewart, A. F341, SA341
Stewart, A. F. 1065, F005, F471, M479, SA005, SA471
Stewart, A. J. F037, SA037
Stewart, C. F500, SA500
Stewart, G. M030
Stewart, J. M413, SU144
Stewart, J. SU377
Stewart, J. M. SU467
Stewart, M. SU049
Stewart, P. M. SU419
Stewart, S. SU550
Stewart, S. A. F224, M380, SA224, SU413
Stickens, D. M063
Stief, J. M552
Stoch, S. F450, SA450
Stock, J. L. 1215
Stockmans, I. F147, SA147
Stoecker, B. J. M445
Stoermann, C. SU545
Stolina, M. M272, SA510
Stoll, T. SU270
Stone, D. S. SU077
Stone, K. 1056
Stone, K. SA142
Stone, K. L. F017, M158, M182, SA017, SU186
Story, R. M376
Stover, M. M237
Straccini, C. M297
Stracke, H. SA368
Strange, R. M376
Strauss, J. A. M033
Streeten, E. A. SA465
Streichert, T. 1208
Strigoli, D. M518
Strohbach, C. A. SU217
Strot, S. M. M117, SU127, SU128, SU232
Strotmeyer, E. 1021, 1022, 1110, 1189
Struve, J. A. SU240
Stuart, W. D. SU570
Stubby, J. M439
Studer, A. 1166
Stunes, A. M298
Su, C. M460
Su, H. F433, SA433
Su, J. SA261
Su, N. 1134
Su, Y. SU255
Suarez, E. F340, SA340
Subesinghe, S. M511
Subler, M. 1010, 1204
Subramaniam, M. 1197, F170, SA170, SU281
Suda, K. M286
Suda, R. K. 1135
Suda, T. 1051, M026, SU045, SU315, SU316
Sudhakar, D. M141, SU359
Sudo, Y. M162, SU173
Suei, Y. SU165
Suematsu, A. F297, SA297
Sugama, R. M448
Sugatani, T. 1194
Sugimoto, T. M091, M227
Sugimoto, T. SA460
Sugimoto, T. SA562, SU207, SU517
Sugita, A. M496
Sugiyama, F. SU455
Sugiyama, O. M014, SA022
Sugizaki, T. SU266
Suh, C. SU166
Suh, K. SU425
Suhara, Y. SA449
Sukhu, B. SU325
Sullivan, J. SU239
Summers, G. D. SU183
Sun, C. 1041
Sun, L. F316, M408, SA291, SA316
Sun, Q. F131
Sun, Q. M255, M555
Sun, Q. SA131, SA132
Sun, Q. SU296
Sun, S. 1030
Sun, S. S. M157
Sun, S. S. SU164
Sun, Y. M189
Sun, Y. SA315
Sundaram, K. M563
Sung, D. Katherine M214
Sung, S. Y. SU300
Suominen, H. F009, M212, SA009
Supervía, A. SU241
Suppan, K. 1222
Suppapanya, N. M434
Supronik, J. SU366
Suresh, M. M141, SU359
Suri, L. M188, SA235
Suriyapperuma, S. P. SU020
Survice, S. K. SU165
Susa, M. SU091
Suswillo, R. Frater Lawrence M570, SA181
Suter, A. 1069
Sutherland, M. K. 1217
Suttamanatwong, S. SU546
Sutton-Tyrrell, K. 1189
Suuriniemi, M. F009, M168, SA009, SU461
Suutari, S. M305, SA307
Suva, L. J. M054, M075, M124, SA093, SU009, SU032, SU099, SU495
Suzuki, A. SA036
Suzuki, E. SU015
Suzuki, H. SU449
Suzuki, K. SA460
Suzuki, K. SU331
Suzuki, K. SU456
Suzuki, T. M165
Suzuki, T. SA021
Suzuki, T. SU173
Svensson, J. 1168, M564
Swafford, J. A. SA442
Swain, F. L. SU009, SU495
Swan, S. SU530
Swanson, C. M163, SA566
Swanson, E. Christine M044, SU054
Swanson, L. M373
Swenson, J. 1083
Swolin Eide, D. M112, M531, SA101
Syberg, S. SU152
Sybrowsky, C. L. SA357
Syddall, H. E. SU419
Syed, F. A. SU568
Sykora, J. SA387
Sylvester, F. A. SU013, SU525
Sylvia, V. SA572
Syme, C. A. M559
Syversen, U. M187, M298
Szejnfeld, V. L. M335, SA352, SA361, SU101, SU401
Szulc, P. M. SA353
Szyf, M. M081
Szymczyk, K. H. SA197, SU327

T

T.Denhardt, D. SU494
Taaffe, D. 1189
Tabak, A. M170, M171, M414
Tabata, I. SU455
Tabata, Y. SU046
Tabin, C. J. 1037
Tachiki, K. SA145
Tada, M. M448
Tada, T. SU018, SU086
Tae, H. Jung M401, SU439
Tafone, D. M366
Tagawa, M. SU385
Taguchi, A. SU165
Taguchi, T. SU036
Tague, S. F039, SA039
Tahara, H. SA548, SU517
Taichman, R. S. M189
Taiwo, Y. O. F253, SA253, SA442
Takacs, I. M170, M171, M414
Takada, H. M285
Takada, M. M122
Takagi, H. M418
Takagi, Y. M395, SU207
Takahashi, A. M205
Takahashi, F. M496, SU500, SU501
Takahashi, M. F152
Takahashi, M. M047
Takahashi, M. M285
Takahashi, M. SA152
Takahashi, M. SU498
Takahashi, N. 1192, M285, M286, SU303, SU304, SU313, SU314, SU540
Takahashi, T. SU286

Takai, T. F297, SA297
Takaiwa, M. SA151
Takami, M. M307
Takami, M. SU289
Takane, K. K. F005, SA005
Takano, K. SU511
Takaoka, K. M015, M448, SA238, SU015, SU052, SU303
Takasu, H. 1125, F388, SA388
Takata, S. M047
Takata, S. SA460
Takata, S. SU498
Takata, T. SU034
Takato, T. M022, SA143, SA249
Takayanagi, H. F297, SA297
Takayanagi, R. F565, M229, SA565
Take, I. SU313, SU314
Takeda, E. F154, SA154, SU533
Takeda, K. M285
Takeda, K. SU456
Takeda, S. F191
Takeda, S. M496, M582
Takeda, S. SA191
Takeda, S. SU500
Takeda, T. M205
Takeda, T. M417, M474
Takeda, T. SU208
Takegoshi, Y. F511, SA511
Takei, Y. SA545
Takeichi, T. SU533
Takeshita, S. F285, F320
Takeshita, S. M320
Takeshita, S. SA285
Takeshita, S. SA289
Takeshita, S. SA320
Taketa, T. SU538
Taketani, Y. F154, SA154, SU533
Takeuchi, K. 1076
Takeuchi, Y. 1160, F152, SA152
Takeya, T. F295, M312, SA295
Takeyama, K. M583
Takeyama, S. SU331
Takigawa, M. SU046
Takita, H. SA021
Talpos, G. B. SA492, SU519, WG14
Talwar, S. A. SU502
Tam, J. M166
Tam, S. SU115
Tamai, N. F047, SA047
Tamim, H. 1047
Tamma, R. SA204
Tamone, C. SU312
Tamura, D. F087, SA087
Tamura, M. F212, SA021, SA212, SU190
Tan, H. M300
Tan, Q. M569, M571
Tan, Q. W. M043
Tan, X. SA028
Tanabe, H. SU294
Tanaka, A. SU406
Tanaka, H. 1045, M232, M575, SA151, SU526
Tanaka, I. SA120
Tanaka, J. SU036
Tanaka, K. M332, M399
Tanaka, M. M064
Tanaka, M. SU208, SU257
Tanaka, R. B. SU372
Tanaka, S. 1006
Tanaka, S. F199
Tanaka, S. M308
Tanaka, S. M562
Tanaka, S. SA199, SU037
Tanaka, S. SU208, SU209, SU257
Tanaka, Y. F081, M072, SA081
Tanaka, Y. SU209
Tanck, E. SU237
Tandon, N. M005
Tang, G. M177, M178, M325
Tang, G. M329
Tang, Z. SU244
Tanigawara, Y. SA460
Taniguchi, H. F565, SA565
Taniguchi, T. F297, SA297
Tanimoto, K. SU165
Tanimoto, Y. SU192
Tanini, A. M518, M519, SU181
Tanko, L. 1055
Tankó, L. B. F377, M324, SA377
Tanne, K. SA247, SU195
Tannehill-Gregg, S. M087
Tao, J. H. SA241
Tao, Z. SA054
Tapia, B. SA158
Targan, S. R. SU428
Tateishi, K. SA146
Tatsumi, S. 1125, F388, SA388
Tauchmanova, L. M147
Tawfeek, H. A. M557
Taylor, A. SU487
Taylor, A. F. 1031, SU214, SU217
Taylor, B. 1058
Taylor, B. F358, SA358
Taylor, B. C. 1185
Taylor, K. A. M478
Taylor, P. F336
Taylor, P. SA001
Taylor, P. SA336
Tchetina, E. V. M023
Tebben, P. SA082, SA083, SA488
Tebib, J. M309
Tedesco, M. 1065, F471, M479, SA471
Teegarden, D. SA575
Teh, R. 1183
Teilmann, J. SU152
Teisner, B. M049
Teitelbaum, S. L. 1029, F285, F304, F320, F486, M274, M320, SA285, SA289, SA304, SA320, SA321, SA486
Tell, G. SA225, SU392
Tellefson, S. SU414
Tenenbaum, H. C. SU325, SU342
Tenenhouse, A. F375, M331, SA375, SA456, SU168, SU353, SU361
Tenenhouse, H. S. SU193
Teng, A. Y-T. SU309
Teng, K. M054, SA171
Terai, H. M015, SA238, SU015, SU052
Terauchi, Y. SA430
Terkeltaub, R. F039, SA039, SA549
Terkhorn, S. P. M032
Termini, G. SU369
Terryberry, J. W. SU061
Terwedow, H. M177, M178, M325, M329, SU160
Terzolo, M. M383
Tesfai, J. SU056
Teshima, R. M111, SU375
Teta, M. SA059
Teti, A. 1138, SA279, SU091, SU287
Tetradis, S. SA223, SU254
Teustch, S. M. SU355
Tezuka, K. M205
Thabane, L. M109, M423, SA455
Thacker, R. E. SU234
Thakker, R. V. F063, SA063
Thatcher, M. L. F555, SA551, SA552, SA555
The CaMOS Research Group SA332
The GIUMO Study Group SA122
The LAVOS Group F340, SA340
Theisen, K. M552
Theriault, B. M193
Theus, A. M. M075
Thibault, X. SU028
Thierry-Palmer, M. M202
Thomas, A. M427, SU578
Thomas, B. Elizabeth M558
Thomas, C. David L. SU006
Thomas, D. SU005
Thomas, G. P. 1075
Thomas, J. F459, SA459
Thomas, T. SU542
Thomas-Mudge, R. J. SA540
Thommesen, L. M187, M298
Thompson, C. SU332
Thompson, C. C. F555, SA555
Thompson, C. M. SA551
Thompson, D. M186
Thompson, D. D. 1216
Thompson, K. M430, M431
Thompson, L. M443
Thompson, V. SU123
Thomson, J. A. F246, SA246
Thorkildsen, C. M486
Thorpe, J. Adrian M097
Thurn, K. E. M118
Ticha, V. SU142
Tile, L. M443
Tilly, J. SU386
Timmermann, B. N. M538
Ting, K. F070, SA070
Tiran, A. M398
Tivesten, Å. SA397
Tobimatsu, T. M091
Toda, T. SU455
Toft, L. I. M. SU107
Tofteng, C. Landbo SU180
Tokita, A. M495
Tokuyama, R. M065
Tomakidi, P. F077, SA077
Tometsko, M. 1095
Tometsko, M. E. 1027
Tomin, E. SA149
Tomin, E. A. SA023
Tominaga, T. SU534
Tominaga, Y. SU534
Tomita, M. SA014
Tomizuka, K. F152, SA152
Tommasini, R. SU061
Tommasini, S. M. M010
Tommasini, S. M. SA385
Toneguzzi, S. SA286
Tonino, A. M407
Toombs, A. F202, M226, SA202
Tootoonchi, I. SU463
Topkara, V. K. M548
Topouzis, S. M186
Toraldo, G. F144, SA144
Torbay, N. SA381
Torfing, T. M546
Torner, J. C. F185, SA185, SU364
Towler, D. A. 1097, 1141, F232, M569, SA232, SU066
Towne, B. M157, SU164
Townsend, K. SA094
Toyama, Y. M026, M273, SU045, SU218, SU315, SU316
Toyoda, H. M448, SA238, SU015
Toyosawa, S. F222, SA222
Tracy, J. Kathleen F323, F360, SA323, SA360
Tracy, M. R. WG21
Tracy, R. P. SU356
Travaglini, L. 1157
Trebec, D. P. SA284, SU333
Tremblay, G. Bernard M294, M297
Tremollieres, F. M360, SU390
Trendelenburg, V. SA219
Trevisan, M. M355
Tripathi, G. 1181
Troen, B. R. M408, SU297, SU298
Trofimov, S. SA130
Troiano, N. SA209
Trombetti, A. SU545
Tromp, A. M. SA188
Trout, G. J. M134
True, L. D. SA089
Truong, T. F070, SA070
Tsai, M. SU255
Tsaih, S. F127, SA127
Tsatsas, D. V. M034
Tsay, A. SU328
Tschelissnigg, K. M545
Tschudi, I. SU457
Tse, M. M440
Tsiridis, E. SA027, SA150
Tsuboi, H. SA146, SU314, SU540
Tsuchiya, Y. SA050
Tsuda, M. SU146, SU165
Tsugawa, N. M332
Tsugawa, S. M399
Tsugeno, H. M395
Tsuji, K. 1037, F056, F191, SA050, SA056, SA191
Tsuji, K. SU190
Tsuji, K. SU231, SU318, SU405, SU494
Tsuji, M. F154, SA154
Tsujimoto, M. SU406
Tsujisawa, T. SU286
Tsukamoto, N. M369
Tsukamoto, Y. SU266
Tsukazaki, T. SU271
Tsumaki, N. F047, SA047
Tsunemi, K. M496, SU500, SU501
Tsung, H. M313
Tsutsumi, K. F388, SA388
Tsvetov, G. SU509
Tu, C. SA045
Tu, S. SA011
Tu, S. SA571
Tuan, R. S. SA054
Tuck, S. P. M581, SU183
Tucker, K. L. F330, SA330
Tullai, J. A. SA509
Tung, E. M514
Tunick, S. SU092
Tuppurainen, M. M321, M357, M411, SU388
Turcotte, R. M066, WG9
Turner, A. SA363
Turner, C. WG27
Turner, C. H. 1032, 1105, 1149, F131, M197, M204, SA131, SA132, SU224
Turner, J. M042
Turner, R. M376
Turner, R. T. 1200, M069, M364, M543, SA205, SA534, SU436, SU535
Turner, S. A. 1199, F495, SA495
Tverdal, A. SU374
Tyblova, M. SU142
Tylavsky, F. 1021, 1022

U

Uchida, S. SU209, SU257, SU269
Uchiyama, S. SU455
Uchiyama, Y. M164, SU500
Udagawa, N. 1192, M285, M286, SU303
Udagawa, N. SU304
Udagawa, N. SU313, SU314, SU540
Udelsman, R. WG22
Ueberfuhr, P. M552
Ueda, K. 1045
Ueda, M. F251, SA251
Uede, T. SA050
Uehara, M. SU456

(Key: 1001-1222 = Oral, F = Friday Plenary poster, SA = Saturday poster, SU = Sunday poster, M = Monday poster, WG = Working Group Abstract)

Ueland, T. M169
Uematsu, S. F511, M185, SA511
Uematsu, T. M285
Uemura, T. SA245, SU036
Ueno, T. SU455
Uesaka, H. SU406
Uitterlinden, A. M175, M176, SU158
Ulici, V. M037
Ulivieri, F. Massimo M518
Underhill, T. Michael M037
Urakawa, I. F152, SA152
Urano, T. SU173
Urata, K. SU455
Urban, N. Hairrell SA203
Uskokovic, M. S. M257
Usui, M. F056, SA056
Uthgenannt, B. A. 1150
Uusi-Rasi, K. SU002, SU143, SU469, SU470
Uveges, T. E. 1205
Uzawa, M. M417

V

Väänänen, H. M565
Väänänen, H. Kalervo M305, SA315, SU143, SU301
Väänänen, K. SU569
Vääräniemi, J. SA315
Vachon, L. M484
Vaculik, S. SA035
Vaihia, K. Pauliina M378
Vainionpää, A. M213
Vaira, S. F024, SA024
Vaisman, M. SA444
Vajda, E. G. M381
Valdimarsson, Ö. SU464
Valdimarsson, S. M112
Valenti, M. M085, M382
Valenti, R. M394, M402
Valenzuela, D. M. SU050
Valeyev, A. M269
Valhmu, W. B. M139
Välimäki, M. Juhani SU176
Välimäki, S. SU176
Välimäki, V. Valtteri SU176
Valkusz, Z. SA163
Vallarta-Ast, N. F106, SA106, SA405
Valles, A. SU089
Valrance, M. E. SA554
Valta, H. SU537
van Beuningen, M. SA255
van de Klundert, T. M. C. SA255
van de Langerijt, L. M420
Van den Bosch, F. M149
Van der Auwera, P. M432
van der Eerden, B. C. J. SU268
van der Geest, S. M424
van der Ham, F. M058
van der Horst, G. SU249
van der Lely, A. SU268
van der Meulen, M. C. H. SU137, SU350
van Driel, M. SA588
van Duijn, C. M. SU158
van Duin, M. SA255
van Essen, H. W. SA188
Van Herck, E. M003, M563
Van Hoof, V. O. SA480
Van Hul, E. M153
Van Hul, W. M153
van Leeuwen, J. M175, M176
van Leeuwen, J. P. T. SA588, SU268
van Lenthe, G. H. M191
Van Looveren, R. F147, SA147
van Meurs, J. M175, M176
van Oers, R. SU237
Van Pottelbergh, I. SA129, SU175
Van Poznak, C. H. SU092
Van Schoor, N. M. SA350
van Staa, T. F345, SA345
van Staa, T. P. SA454, SU367
van Wijnen, A. J. 1129, 1144, 1175, 1213, F256, SA091, SA217, SA256, SU322, SU252
Van't Hof, R. J. SU336
Vanacker, J. 1117
Vanden Berghe, D. M441
VandenBos, T. SA463
Vandenput, L. M563
Vanderkerken, K. M073
Vanderschueren, D. 1167, 1168, M003, M563, M564, SA397
VanHouten, J. 1163, WG22
Varanasi, S. S. M236, M581, SU183
Varbanov, A. M408
Varela, A. SA030
Varela, A. SU501
Varghese, S. SU013
Varin, S. SU154
Vashi, S. SA091
Vasiliauskas, E. A. SU428
Vatanparast, H. M328
Vatsa, A. SU210
Vayssière, B. 1057
Vedi, S. SU417
Veith, R. 1047
Velasquez, G. SU117
Veldhuis, J. D. M387
Vellas, B. 1219
Venkataraman, R. SU396
Venken, K. 1167, 1168, M563, M564, SA397
Vennström, B. 1126
Veno, P. A. M079
Ventura, M. M383
Verbalis, J. G. SA020
Verberckmoes, S. C. M251, SA480, SA506
Verbruggen, N. 1043
Vered, I. SU389
Vernizeau, M. SA271
Versheuren, S. WG2
Vessella, R. L. 1093, M083, SA089
Vestergaard, P. M338, M340, SA578
Veverka, K. M470
Via, P. S. M113, SU125
Viala, J. SU228
Vichinsky, E. SA504
Vico, L. 1036, M192, SU074
Vidal-Sicart, S. SA485
Vieira, J. G. SU549
Viereck, V. SA210, SU238
Vieth, R. M443
Vignali, E. SU518
Vignery, A. F299, SA299
Vihriälä, E. M213
Vila, J. F123, SA123, SA250
Vilela, R. SA361
Viljakainen, H. T. M498, SA013
Villa, I. SA076, SA519
Villagra, A. SU252
Villagran, M. SU252
Villareal, R. C. M173
Villarruel, S. M. M254
Viluksela, M. SA472
Vinante, O. M085
Vinik, A. I. 1022, M513
Vinje, O. SA512
Viola, E. SU369
Virgen, A. M. 1016
Vis, M. SU446
Vittinghoff, E. 1110
Viveros, O. Humberto M381
Viviani, P. M358
Vlodavsky, I. 1211
Vogel, J. SA034
Vogel, P. F394, SA394
Vogel, R. L. SU577
Vogels, I. SA198
Voggenreiter, G. M508
Voide, R. M191
Vokes, T. SU381, M368
Vokonas, P. S. SU167
von der Kooy, D. SU269
von Ingersleben, G. SU381
von Scheven, E. M527, M528
von Schroeder, H. Peter SU245
von Stechow, D. SU474
Vora, J. P. SU505
Vora, P. SU428
Vorojeikin, V. SU576
Voronov, I. SU342
Voyno-Yasenetskaya, T. M561
Voznesensky, O. SU250
Voznesensky, O. S. M194, SA196, SU551
Vrijens, B. M420
Vujevich, K. T. SU130
Vuohelainen, T. F187, SA187
Vuori, I. SU002
Vyas, K. 1074, SA172
Vyncke, C. M441
Vyskocil, V. SA387, SU083

W

Waarsing, J. H. M372
Wacker, W. K. F112, M089, SA112
Wactawski-Wende, J. M355, M468A
Wada, M. SA548
Wada, S. M409, M489
Wada, Y. M205
Wadhwa, S. 1078
Wagman, R. B. 1170, M478
Wagner, J. M. SU130
Wagner, U. M093, SU090
Wagoner, W. J. SU161
Wainman, D. S. SA065
Wakley, G. SU415
Walcott, M. SU235
Walker, K. M182
Walker, K. SU082
Walker, S. M397
Walkley, C. R. F266, SA266
Wallace, C. SU017
Wallace, L. S. SU402
Wallace, R. 1174
Walsh, C. M135
Walsh, J. M487
Walsh, J. Bernard M135
Walsh, J. S. SU404
Walters, N. J. M206
Wamsley, H. L. SU197
Wan, M. SA215
Wang, B. M177, M178, M325
Wang, B. M329
Wang, B. SU160
Wang, C. M315
Wang, C. SA129
Wang, D. M540
Wang, D. SU345
Wang, D. S. WG9
Wang, G. SA052
Wang, G. SU307
Wang, H. 1202
Wang, H. SA149, SU056
Wang, H. SU195
Wang, J. 1041
Wang, J. 1134
Wang, J. 1169
Wang, J. M118
Wang, J. M189
Wang, J. SU503
Wang, J. H. WG15
Wang, J. Mei M096
Wang, K. M034
Wang, K. H. M230
Wang, L. M042
Wang, L. M381
Wang, L. SA276
Wang, L. SA572
Wang, L. SU041
Wang, L. SU558
Wang, N. F097, SA097, SA215
Wang, Q. 1132
Wang, Q. F009, M212, SA009
Wang, S. SA065
Wang, X. M078
Wang, X. SA382
Wang, X. SU050
Wang, X. SU556
Wang, X. N. 1216
Wang, Y. 1017
Wang, Y. F058, SA058
Wang, Y. F178, SA178
Wang, Y. M244
Wang, Y. F531, SA531, SU028
Wang, Y. SU038
Wang, Y. SU198
Wang, Y. SU273
Wang, Y. SU332, SU338
Wang, Y. B. SU172
Wang, Z. 1093
Wang, Z. M016
Wang-Fischer, Y. SA509
Wang_, J. SU071
Wannemacher, K. SU246
Ward, K. F012, SA012, SU458
Ward, L. M. 1043, SU522, WG11
Ward, Y. M086
Warden, S. J. 1149, SU224
Wareham, N. J. M334
Wargelius, A. S. SU051
Wark, J. D. 1183, F459, SA459
Warman, M. 1057, 1149, 1214, F268, SA268
Warmington, K. 1212, 1217, M300
Warner, S. 1146
Warner, S. E. M209
Warren, A. D. 1119, M221
Warshawski, R. F333, SA333
Wasnich, R. SU441
Wass, J. A. SA128
Watanabe, K. SA240
Watanabe, T. 1006
Watanuki, M. 1088, M584
Watson, P. H. M554, SU548, SU560
Wattel, A. SA302
Watts, N. B. 1100, M420
Watts, S. SU406
Weaver, C. M. SA414, SA418, SU026, SU365
Weaver, M. SU396
Webber, C. SU376
Webber, C. E. M125, SU022
Weber, J. D. M320
Weber, J. M. M266
Weber, K. 1096
Weber, K. SA494
Weber, K. SU200
Weber, M. F462, SA462
Wegner, M. 1140
Wehbe, J. SU134
Wehmeier, K. R. M574
Wei, C. M444
Wei, G. M469
Wei, J. SA059
Wei, S. M274, SA289
Wei, T. 1218
Wei, T. M396
Weigel, N. L. M576

Weiler, H. A. M331, SA456, SU353, SU361
Weiler, S. SA547
Weinans, H. M372, SU135
Weinberg, A. M. M460
Weinberg, J. Brice SU075
Weinstein, R. S. F527, M380, SA172, SA527, SU413, SU550
Weisman, M. M468B
Weiss, S. F424, F426, SA424, SA426
Weiss, T. M102, M373, WG16
Weissheimer, W. M473
Weissman, N. 1114
Weitzmann, M. N. 1059, 1116, 1191, F144, M077, SA144, SU204
Welch, B. SU486
Welch, D. SA086
Welch, J. M. SU365
Welch, M. J. 1150
Wellby, M. M020
Welldon, K. SA587
Wells, A. SU277
Wells, C. M292
Wells, D. J. SU507
Wells, D. S. F435, SA435
Welsh, F. M099
Welsh, J. Ellen SA554
Wendling, D. SU542
Wenkert, D. M503, SA469, WG7
Wenrich, L. SU198
Werb, Z. M063
Wergedal, J. 1206, M151, SU213
Wergedal, J. E. 1181, F127, M043, M215, SA127
Wermers, R. A. SU416
Werner, P. SU389
Werner-Leyval, S. M549
Wertz, M. M527, M528
Weryha, G. SA113, SA451
Wesolowski, G. SA046
Westendorf, J. J. SA229, SU253
Westerlind, K. C. M376
Westfall, A. 1114
Wetli, H. A. SU457
Weynand, L. S. SU126
Wezeman, F. H. SA432, SU447
Wheeler, V. SA359
Wheeler, V. W. M180, SA100
Whitcomb, B. W. SU356
White, C. A. SU522, WG11
White, H. D. SU505
White, K. E. 1162
White, N. M127
White, S. M345
White, S. C. SU165
Whitfield, G. K. F555, F558, M159, SA551, SA552, SA555, SA557, SA558
Whiting, S. M328
Whitlatch, L. W. SA585
Whitson, H. E. M517
Whyte, M. SA463
Whyte, M. P. F063, F468, M502, M503, M510, SA063, SA468, SA469, WG7
Widler, L. SA547
Wiemann, B. SA470
Wigertz, K. SA418
Wijnen, A. van M233
Wilde, J. SA368
Wilde, J. SU150
Wiley, J. S. M400
Wilker, C. E. F435, SA435
Wilkes, B. N. M281
Wilkie, S. 1114
Wilkinson, H. A. M569
Wilkinson, J. M098
Willaert, A. SU175
Williams, B. Owen 1001
Williams, B. O. 1214
Williams, C. J. SA054
Williams, M. I. M113, M436, SA365, SU125, SU482
Williams, S. M067
Williams, S. SA532
Williams, T. SU092
Williamson, M. K. SU031
Willies, C. SU346
Willing, M. C. F185, SA185, SU364
Wilson, A. SU586
Wilson, A. K. SA319
Wilson, A. R. M131
Wilson, J. M538
Wilson, K. 1014
Wilson, K. M. M433, SU441
Wilson, P. W. F. SA040
Wilson, S. G. M154, M169
Wimalawansa, S. M123, M287, WG12
Wimalawansa, S. J. SA413, SU586
Winata, T. SA438
Windahl, S. SU491
Windahl, S. H. 1118
Windisch, W. M375
Windle, J. J. 1010, 1204, F306, SA306
Winer, K. 1048, F102, SA102, SU124
Wing, M. M544
Winkler, D. G. 1217
Winters, K. M. SU226
Wiren, K. F202, M226, SA202, SU348
Wirsching, J. 1166
Wisdom, J. M515, F484, SA484
Wise, L. M. SU386
Wit, J. SU040
Wittelsberger, A. M558
Witters, L. SU098
Wittersheim, E. SU531
Witzke, K. Anne M513
Wobbe, T. SU564
Wohl, M. Ellen SU421
Wolf, R. M. SA547
Wolfinbarger, L. SU014
Woll, N. SU259
Woloszczuk, W. F118, SA118
Won, K. SU523
Wong, B. SU179
Wong, E. K. M058
Wong, M. SU573
Wong, N. SA109
Wong, S. M143
Wong, S. Y. S. M100, SU360
Wong, Z. Y. H. M155
Woo, J. M100
Woo, J. M143
Woo, J. M291
Woo, J. M307
Woo, J. M440
Woo, K. SU029
Wood, D. M030
Wood, P. J. SU419
Wood Steiman, P. M331, SA456, SU353, SU361
Woodard, G. E. F493, SA493
Woodrow, J. P. SA518
Woods, A. SA052
Woodson, G. 1072
Woon, P. Y. SA128
Wootten, D. F. M126
Wootten, D. F. SU229
Wordsworth, P. SA300
Workman, P. M. SU481
Worley, K. M465
Worton, L. Elizebeth SU276
Wozney, J. M. M017, M018, M247, M491, SU017, SU248
Wren, T. A. L. F102, SA102
Wright, J. M262
Wright, K. M166
Wronski, T. J. 1064, M488, SU197, SU219
Wu, A. SA322
Wu, B. SU255
Wu, C. SU381
Wu, D. M177, M178, M325
Wu, D. M329
Wu, J. SA209
Wu, J. SU455
Wu, J. SU456
Wu, J. J. M247
Wu, L. F097, SA097
Wu, M. 1142
Wu, M. F450, SA450
Wu, Q. 1040, M035
Wu, S. SA580
Wu, T. SA274
Wu, X. M318
Wu, Y. F097
Wu, Y. M229
Wu, Y. SA097
Wu, Y. SU102
Wuelling, M. SU084
Wykoff, C. M041
Wyland, J. 1172, F439, SA439
Wylie-Rosett, J. SA331
Wynne, R. A. 1165, F527, SA527, SU004
Wyres, M. SA498, SU530
Wysolmerski, J. 1014, 1163, F471, SA471, WG22
Wyzga, N. SU013, SU525

X

Xi, Y. M280
Xia, Q. W. F477, M485, SA477
Xiao, G. 1210, M264, SU243, SU247
Xiao, L. 1042
Xiao, L. F026, SA026
Xiao, Z. F220, SA220
Xie, C. M261
Xie, D. M203, M492, SA447
Xie, L. M218, SA190, SU230
Xie, Y. 1004
Xie, Y. 1177
Xing, L. 1003, SA403, SU323
Xing, W. F180, SA180, SA258
Xing, Y. SA582
Xiong, W. SA257
Xu, D. F301, SA301
Xu, D. L. SA509
XU, G. 1008, M388
Xu, H. SU172
Xu, J. 1143
Xu, J. M077
Xu, J. M315
Xu, J. SU262, SU280
Xu, J. SU340
Xu, J. SU567
Xu, M. SA126
Xu, M. SU227, SU551
Xu, S. SA190, SU230
Xu, X. M177
Xu, X. M177, M178
Xu, X. M178, M325
Xu, X. M329
Xu, X. SU160
Xu, X. SU160
Xu, Z. SA195, SA196
Xue, J. SA280
Xue, Y. B. F537, SA537, SA576
Xuenong, Z. SA032
Xydas, S. M548

Y

Yacoby-Zeevi, O. 1211
Yaden, B. C. M573, SA200
Yaffe, K. F369, SA369
Yagami, K. SA057
Yagi, M. M026, SU045, SU315, SU316
Yagi, S. SU534
Yajima, A. SU534
Yakar, S. SU429
Yamada, H. M064
Yamada, H. M369, SU539
Yamada, K. SU455, SU456
Yamada, S. M418
Yamada, S. SU331
Yamada, T. 1099, M562
Yamagata, M. F553, SA478, SA553
Yamaguchi, A. 1120, SU271, SU274
Yamaguchi, D. T. M249, SA145, SA237
Yamaguchi, M. SA430
Yamakawa, K. F511, SA511
Yamamoto, H. F154, SA154, SU533
Yamamoto, K. SU141
Yamamoto, T. F056, SA056
Yamamoto, T. SA121
Yamamoto, Y. 1006, 1099, M562, M583
Yamamoto, Y. SU304
Yamamoto, Y. SU314
Yamana, K. F222, SA222
Yamanaka, M. M495
Yamanaka, Y. 1045, SA151
Yamashita, T. 1160, F152, SA152, SU193
Yamauchi, H. M164
Yamauchi, M. M091
Yamazaki, K. M344
Yamazaki, Y. 1160, F152, SA152
Yamout, B. M497
Yancopoulos, G. D. SU050
Yandle, T. G. M020
Yang, D. 1158
Yang, H. M019
Yang, H. SA257
Yang, H. SU078
Yang, H. SU428
Yang, J. 1085
Yang, J. S. SU299, SU300
Yang, K. M184, SA055
Yang, L. M036
Yang, L. M260
Yang, Q. Fen. SA193
Yang, R. SU255
Yang, S. M019, M256
Yang, S. M285
Yang, S. SA314
Yang, S. SU122
Yang, S. O. SU299
Yang, T. 1084
Yang, W. 1035, 1049
Yang, W. SU265
Yang, W. Mona 1105
Yang, X. SU243
Yang, X. Fang SA080
Yang, Y. M075
Yano, F. M022, SA249
Yao, G. SA209
Yao, W. M379, M480, M488
Yao, Z. SU323
Yaroslavskiy, B. B. M278
Yasuda, H. F199, SA199
Yasuda, S. M409, M489
Yasui, N. M036, M047, SU498
Yatani, H. 1120
Yatani, H. SU274
Yates, K. E. M011, SA069

Yaworsky, P. F262, F525, SA262, SA525
Ye, L. 1004
Ye, L. 1177, F173, SA173
Yee, J. A. M243, SU326
Yeh, J. M474, SU502
Yeh, J. K. SU003
Yeh, L. Caroline SA025
Yen, M. SA261
Yeo, H. M231, M318
Yeung, S. M155
Yigit, S. SU485
Yim, C. SU572
Yim, M. SU289
Yin, J. M086
Yin, L. 1134
Yin, M. T. M393
Yip, K. H.M. SU340
Ylipahkala, H. M305, SA307, SU301
Yogendran, M. SA347
Yogo, K. F295, M312, SA295
Yoh, K. SA121
Yokoyama, A. SA021
Yoneda, M. M015
Yoneda, T. 1026, 1120, F087, F095, F251, F309, M068, SA087, SA095, SA251, SA309, SU274
Yoneda, Y. F553, SA553
Yonezawa, H. M307
Yonezu, H. SU498
Yong, J. SA016
Yoo, M. SU425
Yoon, B. Seob 1179
Yoon, H. SU523
Yoon, H. SU572
Yoon, J. SU425
Yoshida, C. SA048
Yoshida, C. A. SU292
Yoshida, H. M162
Yoshida, H. M490
Yoshida, H. SU173
Yoshida, K. SU440
Yoshida, S. M542
Yoshii, I. 1179
Yoshikata, H. M428
Yoshikata, R. M008, SA010, SU490
Yoshikawa, H. F047, F087, SA047, SA087, SA146, SU540
Yoshiko, Y. SA247
Yoshiko, Y. SU195
Yoshimoto, Y. SU207
Yoshimura, K. 1006, M562, M583
Yoshimura, N. M132, M344
Yoshinari, N. SU387
Yoshizawa, T. 1099
Youket, T. E. M465
Young, A. SU530
Young, B. SU039
Young, D. SA217
Young, M. 1078
Young, M. F. SU070
Young, M. V. SA585
Yu, H. F160, F180, M043, M152, SA160, SA180, SU056
Yu, K. 1005
Yu, N. WG22
Yu, K. F290, SA290
Yu, R. M440
Yu, V. Wing Chi. 1052
Yu, X. 1162
Yu, X. M290, M303
Yuan, B. SA582
Yuen, C. K. SA347, SA378
Yuen, C. Kin M331, SA456, SU353, SU361
Yuen, V. SU506
Yukata, K. M036, M047
Yumoto, K. SA050
Yurman, K. H. M131

Z

Zack, D. M272, SA510
Zadel, J. M393
Zahm, A. M. M201
Zahradnik, R. J. SA530
Zaidi, M. F316, M408, SA288, SA291, SA316
Zaidi, S. K. SA217
Zajac, J. D. M155, SA310
Zaka, R. SA054
Zallone, A. F316, SA204, SA316
Zalloua, P. A. M329
Zaman, A. 1109
Zaman, G. M570, SA181
Zambelli, P. SU275
Zanchetta, J. F428, SA428
Zanello, L. P. 1090, M578
Zang, T. M177, M178
Zang, T. M329
Zang, T. SU160
Zannettino, A. C. W. SA587
Zarnitsky, C. SU542
Zayzafoon, M. F272, M231, SA259, SA272, SU073
Zcharia, E. 1211
Zebaze, R. M. M099, SU403
Zeitz, U. SA494
Zeldin, S. M327
Zemel, B. 1137, 1048, F102, SA102, M009, SA499, SA502, SU106, SU112, SU113, SU124
Zenari, S. M085
Zeng, Q. F445, M493, SA445, SU332
Zeng, Q. Q. SA159
Zeni, S. N. M412
Zerega, J. WG7
Zernicke, R. F. M106
Zerwekh, J. E. M427, M507
Zezabe, R. SU134
Zhan, P. 1013
Zhang, C. M252
Zhang, G. X. SU190
Zhang, H. F144
Zhang, H. F194
Zhang, H. F270
Zhang, H. SA144
Zhang, H. SA194
Zhang, H. SA270
Zhang, H. SU279
Zhang, H. SU527
Zhang, H. SU577
Zhang, J. 1049
Zhang, J. 1142
Zhang, J. 1177
Zhang, J. 1196
Zhang, J. F299, SA299
Zhang, J. M196
Zhang, J. SA028
Zhang, J. SA091
Zhang, J. SU433
Zhang, K. F173, SA173
Zhang, L. SU288
Zhang, M. 1200, SA205, SA534
Zhang, M. Y. H. SU193
Zhang, Q. SA403
Zhang, Q. F445, SA445
Zhang, Q. SU323
Zhang, S. 1177
Zhang, S. SU269
Zhang, T. M325
Zhang, W. F194, SA194
Zhang, X. F070, SA070
Zhang, X. F468, SA468
Zhang, X. M226
Zhang, X. M261
Zhang, X. F202, SA202
Zhang, X. SU011
Zhang, X. SU348
Zhang, Y. M178
Zhang, Y. SA314
Zhang, Z. SU157, SU171
Zhang, Z. L. F537, M485, SA537
Zhao, C. 1051
Zhao, H. F304, F486, M175 SA304, SA486
Zhao, H. Y. M176
Zhao, J. 1077
Zhao, J. M079
Zhao, J. J. F433, SA433
Zhao, J. J. M541
Zhao, L. 1134
Zhao, L. M256
Zhao, M. 1011, 1176, F044, M076, M264, SA044
Zhao, X. F290, SA290
Zhao, Y. Dan SU026
Zhao, Z. M264, SU243
Zhau, H. Y. E. M077
Zheng, H. M303
Zheng, H. C. M209
Zheng, M. M030
Zheng, M. SU340
Zheng, M. H. 1143, M315
Zheng, Q. 1107, 1130, 1139
Zhong, N. 1131
Zhong, Q. SU280
Zhou, G. 1107, 1130, 1139
Zhou, H. 1010
Zhou, H. 1025
Zhou, H. M370, SA496
Zhou, H. SA568
Zhou, H. SU071
Zhou, H. SU317
Zhou, J. M379, M488
Zhou, P. F320, M274, SA289, SA320
Zhou, Q. 1201
Zhou, Q. SU157, SU171
Zhou, S. F168
Zhou, S. M011
Zhou, S. SA168
Zhou, S. SU203
Zhou, X. M252
Zhou, Z. 1031
Zhou, Z. M070
Zhou, Z. SA257
Zhu, J. SA145
Zhu, L. M272
Zhu, T. M019, M256
Zhuo, Y. SA046
Ziegler, J. F396, M386, SA396
Zikan, V. SU142
Ziller, V. M093, SU090
Zillikens, C. M175
Zillikens, M. M114
Zillikens, M. Carola SU158
Zimmer, A. M166
Zimmerman, N. M293
Zimniak, P. SU339
Zingmond, D. 1187
Zion, M. F437, SA437
Zlotkin, S., WG11
Zmuda, J. M337
Zmuda, J. SA142
Zmuda, J. SU384
Zmuda, J. M. 1021, 1056, 1185, M158, M180, M181, M182, SA100, SA359, SU186
Zordan, S. M382
Zou, L. Yi. SA274
Zou, W. SA321
Zuck, P. D. F270, SA270
Zuo, J. SA280
Zuscik, M. J. 1040, 1180, M028, M035, SA201
Zusuwa, G. WG13
Zylstra, C. R. 1001, 1214
Zysset, P. SA384